iJERGS International Journal of Engineering Research And General Science

Journal which deals with research, Innovation and Originality

International Journal Of Engineering Research and General Science

ISSN 2091 - 2730

Table of Content

CHIEF EDITOR BOARD

Message from Associate Editor In Chief

Let me first of all take this opportunity to wish all our readers a very happy, peaceful and prosperous year ahead.

This is the Fifth Issue of the Third Volume of International Journal of Engineering Research and General Science. A total of 143 research articles are published and I sincerely hope that each one of these provides some significant stimulation to a reasonable segment of our community of readers.

In this issue, we have focused mainly on the students innovation and ongoing challenging trends. We also welcome more research oriented ideas in our upcoming Issues.

Author's response for this issue was really inspiring for us. We received many papers from many countries in this issue but our technical team and editor members accepted very less number of research papers for the publication. We have provided editors feedback for every rejected as well as accepted paper so that authors can work out in the weakness more and we shall accept the paper in near future. We apologize for the inconvenient caused for rejected Authors but I hope our editor's feedback helps you discover more horizons for your research work.

I would like to take this opportunity to thank each and every writer for their contribution and would like to thank entire International Journal of Engineering Research and General Science (IJERGS) technical team and editor member for their hard work for the development of research in the world through IJERGS.

Last, but not the least my special thanks and gratitude needs to go to all our fellow friends and supporters. Your help is greatly appreciated. I hope our reader will find our papers educational and entertaining as well. Our team have done good job however, this issue may possibly have some drawbacks, and therefore, constructive suggestions for further improvement shall be warmly welcomed.

Er. Pragyan Bhattarai,

Associate Editor-in-Chief, P&R,

International Journal of Engineering Research and General Science

E-mail -Pragyan@ijergs.org

International Journal of Engineering Research and General Science Volume 3, Issue 5, September-October, 2015
ISSN 2091-2730

Comparative Study of Data Mining Classification Techniques over Soybean Disease by Implementing PCA-GA

Dr. Geraldin B. Dela Cruz

Institute of Engineering, Tarlac College of Agriculture, Philippines, delacruz.geri@gmail.com

Abstract— Data mining is a relatively new approach in the field of agriculture that can be used in the extraction of knowledge and discovery of patterns and relationships in agricultural data. Classification techniques in data mining are used to discover patterns and knowledge agricultural datasets, however, the accuracy of these classification techniques depends on the quality of data that are used as inputs in the data mining process. In this paper, an efficient data mining methodology based on PCA-GA is applied as a data pre processing technique, to reduce the dimensionality of the soybean dataset. The mechanism draws improvements to classification problems by applying Principal Components Analysis (PCA) and subsequently applying Genetic Algorithm (GA) to further reduce the dimensionality of the dataset, and selecting the best representative subsets, thereby improving the performance of classifiers. Different data mining classification techniques are applied to the resulting reduced dataset and classification metrics are compared. This approach is to asses classification rates on the PCA-GA reduced soybean dataset. The learning and validation experiment was performed using WEKA, a workbench containing implementations of the k-NN, Naïve Bayes, J4.8 and MLP classification algorithms, including the PCA and GA. Classification accuracy was validated using 10-folds cross validation..

Keywords—classification, data mining, genetic algorithm, optimization, PCA-GA, soybean,

INTRODUCTION

Databases not only store and provide data but also contain hidden knowledge which can be very important however, human ability to analyze and understand these massive datasets lags far behind his ability to gather and store data in databases. Data in the agricultural domain are robust, comes in different formats, complex, multidimensional and contains noise. Interesting patterns can be mined in this space in discovering knowledge, revealing solutions to specific domain problems [1]. Extraction of the useful set of features is usually unknown from these volumes of data [2], considering every single feature of an input pattern in a large feature set makes classification and knowledge discovery computationally complex. Also, the inclusion of irrelevant or redundant features in the data mining model results in poor predictions and interpretation, high computational cost and high memory usage [3], [4].

In general, it is desired to keep a number of features as discriminating and as small as possible in order to reduce computational time and complexity in the data mining process [5], [6]. This can be addressed by dimensionality reduction [7] method that improves data mining classification and facilitates visualization and data understanding. It is a process that creates a set of features based on transformations or combinations of the original dataset, thereby reducing it into a smaller representative dataset.

The focus of this study is to implement an efficient mechanism based on the combination of Principal Component Analysis (PCA) and Genetic Algorithm (GA) [8], [9] as a data preprocessing method, to reduce the dimensionality of the data by keeping a number of features as small as possible. Apply the k-NN, MLP, NB and J4.8 algorithms in the data mining process and compare the classification results. In so doing, the PCA-GA [10] mechanism is validated as an efficient data reduction method.

THE PCA-GA MECHANISM

The PCA-GA algorithm is a combination of two algorithms, PCA, for data preprocessing and reduction and the GA for feature subset selection method, which makes the whole process a hybrid data mining mechanism. The PCA mechanism is a very useful data dimensionality reduction technique, reducing the number of variables to a few interpretable linear combinations of the data. PCA maps the rows and columns of a given matrix into two or three dimensional points to reveal the structure of dataset. The original data are projected into smaller space. Thus data reduction is performed. The data can be represented by a collection of n points in the z-dimensional space, where each axis corresponds to a measured variable. From this space, a line Y1 can be searched such that the dispersion of n points when projected unto this line is a maximum. The derived variable is denoted by the equation in (1):

$$Y_1 = e_1x_1 + e_2x_2 + \ldots e_px_p \qquad (1)$$

Where, e_i are coefficients satisfying the condition in (2):

$$\sum_{j=1}^{z} e_{i^2} = 1 \qquad (2)$$

After obtaining Y1, the (z-1) – dimensional subspace orthogonal to Y1 is considered and line Y2 is found in this subspace such that the dispersion of points when projected onto this line is also maximum, and is perpendicular to Y1 such that the dispersion of points when they are onto this line is the maximum. Having obtained Y2, a line in the (z-2)-dimensional subspace is considered, which is orthogonal to both Y1 and Y2, such that dispersion of points when projected onto this line is as large as possible. The process can be continued until z mutually orthogonal lines are determined. Each of these lines now defines a derived variable shown in equation (3):

$$Y_i = e_{1i}X_1 + e_{2i}X_2 + e_{3i}X_3 + \ldots + e_{ni}X_i \qquad (3)$$

where the constants ei_j are determined by the requirement that the variance of Yi is a maximum, subject to the constraint of orthogonality as well as in (4) :

$$\sum_{k=1}^{p} e_{ik^2} = 1 \qquad (4)$$

Thus, the Yi obtained in (3) are called principal components of the system. The process produces a list of linear vectors in (5) called principal components.

$$\begin{aligned} Y_1 &= e_{11}X_1 + e_{12}X_2 + \ldots + e_{1p}X_p \\ Y_2 &= e_{21}X_1 + e_{22}X_2 + \ldots + e_{2p}X_p \\ &\ldots. \\ Y_p &= e_{p1}X_1 + e_{p2}X_2 + \ldots + e_{pp}X_p \end{aligned} \qquad (5)$$

Each of the principal components can be thought of as a linear regression predicting Yi in (3) from X_1, X_2, …, X_p. There is no intercept, but e_{i1}, e_{i2}, …, e_{ip} can be viewed as regression coefficients. The first principal component is the linear combination of X variables that has maximum variance among the linear combinations, accounting for as much variation in the data as possible. The remaining principal components, accounts for as much of the remaining variation as possible, thus the principal components are uncorrelated with each other.

GA Process

Genetic algorithms are search algorithms based on natural genetics. It is an iterative process that operates on a population or a set of candidate solutions, in this case, the principal components generated by the PCA mechanism. Each solution is obtained by means of encoding/decoding mechanism, which enables representing the solution. GA is considered as a function optimizer and performs efficient by searching the best representative sets from candidate sets of solutions (principal components). The interest is in the minimization of a set of variables that can represent a dataset with maximum results. Genetic algorithms consist of three essential elements: a coding of the optimization problem, a mutation operator and crossover. The coding of the optimization problem produces the required discretization of the variable values and makes their simple management in a population of search points possible. A binary coding is ideal because in this way the mutation and crossover operators are simple to implement. Thus, the values of the individuals P1…Pn can be encoded with the binary fixed-point coding in (6).

$$\begin{aligned} P_1 &= b_5b_4b_3b_2b_1b_0 \\ &\ldots\ldots. \\ P_n &= b_5b_4b_3b_2b_1b_0 \end{aligned} \qquad (6)$$

The crossover operator, control the recombination of the individuals in order to generate a new, better population of individuals at each iteration step. Before recombining, the individuals must be evaluated by a fitness function (7) for all data structures in the population. The fitness value is then used as the basis for selection in the crossover or mating.

$$\text{Fitness} = \text{countone}(Pn) \qquad (7)$$

A typical reproduction operator is crossover (8). Before the crossover, two individuals P1 and P2 are selected as “parents”, based on their fitness value. Selection is based on tournament using their fitness. Individuals with higher fitness value, wins the tournament and

is chosen to mate. The offspring C1 and C2 are formed so that the left side comes from one parent and the right side from the other. This produces an interchange of the information stored in each parent. The whole process is reminiscent of genetic exchange in living organisms.

$$C1 = Mask1 \,\&\, P1 + Mask2 \,\&\, P2 \quad (8)$$
$$C2 = Mask2 \,\&\, P1 + Mask1 \,\&\, P2$$

Where :

P1 , P2 – parents chromosomes
C1, C2 - children chromosomes
Mask1, Mask2 – bit masks (Mask2 = NOT(Mask1))

A favorable interchange can produce an offspring with better genes. When the individuals P1 = $b_5b_4b_3b_2b_1b_0$ is recombined with the number P2 = $a_5a_4a_3a_2a_1a_0$. The new individual is then:

$$Cn = b_9b_8 \cdots b_ia_{i-1} \cdots a_0. \quad (9)$$

Crossover can be interpreted as a variation of optimization. The mutation operator is the simplest. In binary strings, a mutation corresponds to a bit flip. A mutation of the ith bit of the string Cn = $b_5b_4b_3b_2b_1b_0$ produces a change. Thus a new individual is generated and the fitness is again evaluated.

DATA MINING CLASSIFICATION TECHNIQUES

The book in [11], identifies, presents and describes different data mining classification techniques [12]. Classification [13] is a form of data analysis that can be used to construct a model, which can be used in the future to predict the class label of new datasets. It is a two step process, first is the learning step where the classification algorithm builds the classifier by analyzing a training set made up of database tuples and their associated class labels, using a mapping function in the form of classification rules. In the second step, the accuracy of the classifier is predicted.

Some of the most popular and common classification algorithms are adopted and presented herein, based on their capabilities simplicity and robustness. The k-NN and Naïve Bayes were chosen based on the study in [14], which proves to perform excellent using the WEKA [15] data mining tool, likewise the J4.8 and MLP were used for their exemplary performance in classification problems in different datasets [16].

k-Nearest Neighbor (k-NN)

k-NN is a nearest neighbor algorithm that classifies entities taking a class of the closest associated vectors in the training set via distance metrics. The principle behind this method is to find predefined numbers of training samples closest in the distance to the new point and predict the label from these.

Naïve Bayes

Based on the Bayes rule of conditional probability, it uses all of the attributes contained in the data, and analyses them individually as though they are equally important and independent of each other. It considers each of the attributes separately when classifying a new instance. It assumes that one attribute works independently of the other attributes contained by the sample.

J4.8

A popular tree based machine learner, the J4.8 decision trees algorithm is an open source Java implementation of the C4.5 [17]. It grows a tree and uses divide-and-conquer algorithm. It is a predictive machine-learning model that decides the target value (dependent variable) of a new sample based on various attribute values of the available data. To classify a new item, it creates a decision tree based on the attribute values of the training data. When it encounters a set of items in a training set, it identifies the attribute that discriminates. It uses information gain to tell most about the data instances so that it can classify them the best.

Multi Layer Perceptron (MLP)

MLP is a feed forward artificial neural network model that maps sets of input data onto a set of appropriate outputs. It consists of multiple layers of nodes with each layer fully connected to the next one. Each node is a neuron with a nonlinear activation function. It uses a learning technique called back propagation for training the network.

MATERIALS AND METHODS

The soybean dataset in [18], was used in the experiment. The data mining software used in the experiment is the WEKA version 3.6.10, which contained the implementations of the classification algorithms presented. A computer with two (2) Gigabytes of memory, with a 32 bit 2.80 Ghz processor, and a proprietary 32 bit Operating System was utilized. The default settings in the data mining software and in the configurations of the algorithms were used.

The dataset was cleaned, encoded and saved as attribute relation file format (arff) file using a text editor, the dataset were loaded in WEKA, the PCA was applied as a data preprocessing method to transform and simplify the dataset into smaller representative sets called principal components. The GA was then applied to the PCA transformed dataset that resulted to an optimized dataset. Subsequently, each of the machine learning algorithms in WEKA, the J4.8, Naïve Bayes, MLP and k-NN were then applied to the resulting PCA-GA reduced datasets and results were recorded and compared accordingly.

Classification accuracy was validated using 10-fold cross validation. This validation method is a standard method to estimate classification accuracy over unseen data.

RESULTS AND DISCUSSION

This section presents and discusses the results of the experiment after applying the PCA-GA mechanism used in the study. There are two parts; first, the outcome of applying the PCA-GA mechanism that was used in generating the visualization model of the reduced dataset. Second the comparison of classification results of classifiers between the original and PCA-GA reduced dataset.

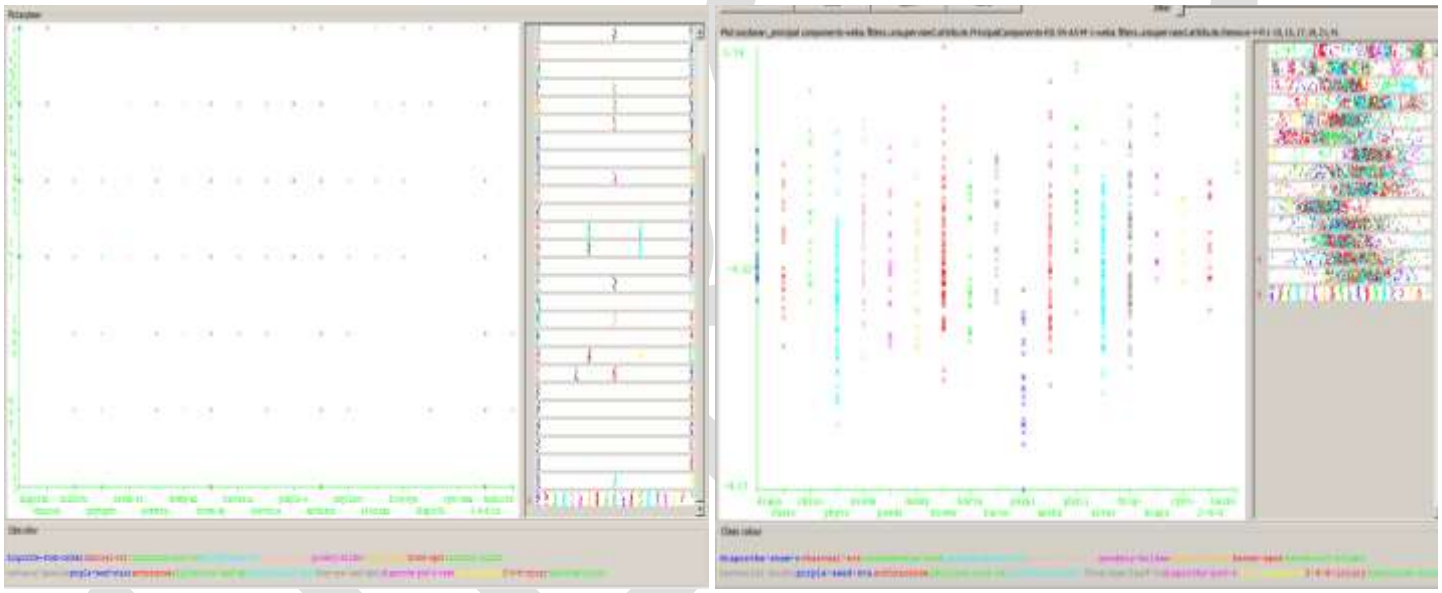

(a) *(b)*

Figure 1. Visualization of the Soybean Disease (a) original dataset, (b) PCA-GA reduced dataset

The soybean dataset originally has thirty six (36) attributes. As can be seen in Figure 1b, after applying the PCA-GA mechanism to the soybean dataset, resulted to fifteen (15) feature sets. This reduced dataset is now considered the smaller representative soybean dataset.

As can be observed, the resulting feature sets in Figure 1b are simplified in structure compared to the original dataset in Figure 1a. The reduced dataset is the optimized smaller representative dataset of the original, thru the optimization technique of GA. The presented visualization in Figure 1b, confirms the PCA-GA efficiency as a dimensionality reduction method, this implies that extracting knowledge from this smaller and optimized dataset is more accurate, efficient and faster. Based on analysis of Figure 1b, the features sets are combinations of the original attributes, that resulted in process of pre-processing through the PCA-GA mechanism. Further the figure shows a distinct variation of the feature sets, classifying the different soybean disease.

Classifier	Original Dataset		PCA-GA Reduced Dataset	
	Accuracy	Time	Accuracy	Time
k-NN	91.22%	0.00 sec	99.85%	0.00 sec
J4.8	91.51%	0.02 sec	98.68%	0.01 sec
Naïve Bayes	92.97%	0.01 sec	94.44%	0.00 sec
MLP	93.41%	112.0 sec	98.83%	18.20 sec

Table 1. Classification Rates of Soybean Dataset When Applied with Different Classifiers

Table 1 shows the comparison of classification rates of various classifiers over the original and PCA-GA reduced soybean dataset. It can be seen that the classification rates between the original and reduced dataset, have noticeable improvements in the J4.8, Naïve Bayes, k-NN and MLP classifiers. Among the classification algorithms tested, the fastest was the k-NN classifier and a significant improvement on accuracy can be observed. Interesting to note also is the speed of the MLP, which is significantly faster on the PCA-GA reduced dataset, the accuracy also significantly increased. Although the MLP improved on its processing time on the reduced dataset, it can be seen that its processing time took longer compared to the other classifiers

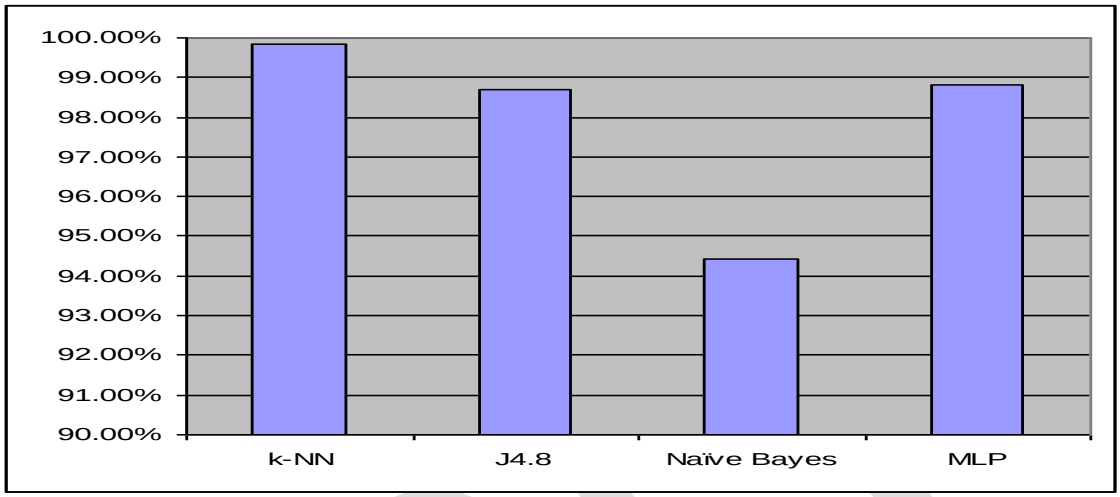

Figure 2. Comparison of Accuracy Rates of the PCA-GA Reduced Dataset When Applied with Different Classifiers

In comparing the classifiers accuracy rates on the PCA-GA reduced dataset, it can be seen in Figure 2, that the k-NN classifier is the most accurate. Naïve Bayes is the least accurate among the classifiers, with MLP and J4.8 are as nearly accurate as the k-NN. Generally, the results presented imply that the PCA-GA method significantly improves classification rates, over the soybean disease dataset with the PCA-GA dimensionality reduction method.

ACKNOWLEDGMENT

The researcher would like to extend his gratitude to the Tarlac College of Agriculture for the support of this study.

SUMMARY AND CONCLUSION

Presented in this study, is the PCA-GA hybrid data reduction method and comparison of classification rates of various data mining classification techniques over the soybean dataset. The k-NN, J4.8. Naïve Bayes ad MLP classifiers were applied to the resulting PCA-GA reduced datasets. Based on the results, the PCA-GA mechanism reduced the original dataset into smaller representative datasets. Visualization model was generated based on the result of the data reduction mechanism based on PCA-GA to present a clearer view of its potential as a hybrid method. Results also show that classification accuracy and processing speed improved for all of the classifiers.

The implementation of the algorithm based on PCA as a preprocessing technique and GA as a feature subset selector is efficient in reducing the dimensionality of the soybean dataset. Results imply that all classifiers can be implemented and are efficient in classifying soybean disease using the PCA-GA pre processing mechanism. Classification speed is further improved for all the classifiers used. On the other hand, results of comparison between the classifiers accuracy rates show that the k-NN is the most accurate and the least accurate is the Naïve Bayes. Generally, using the PCA-GA data reduction technique proves to have significant results in characterizing soybean disease using the presented data mining classification techniques. Thus, simplifies the process of extracting knowledge, discovering patterns and relationships and the interpretation of soybean disease.

REFERENCES:

[1] Arora, Rohit and Suman Suman. "Comparative analysis of classification algorithms on different datasets using WEKA." International Journal of Computer Applications Vol 54, No 13, pp. 21-25, 2012

[2] Raymer, Michael L., William F. Punch, Erik D. Goodman, Leslie Kuhn, and Anil K. Jain. "Dimensionality reduction using genetic algorithms." Evolutionary Computation, IEEE Transactions Vol 4, No 2, pp. 164-171, 2000.

[3] Qu, Guangzhi, Salim Hariri, and Mazin Yousif. "A new dependency and correlation analysis for features." Knowledge and Data Engineering, IEEE Transactions Vol 17, No. 9, pp. 1199-1207, 2005.
[4] Janecek, Andreas, Wilfried N. Gansterer, Michael Demel, and Gerhard Ecker. "On the relationship between feature selection and classification accuracy". Journal of Machine Learning Research-Proceedings Track 4, Antwerp, Belgium, pp. 90-105, 2008.
[5] Gerardo, Bobby D., Jaewan Lee, Inho Ra, and Sangyong Byun. "Association rule discovery in data mining by implementing principal component analysis." In Artificial Intelligence and Simulation, pp. 50-60. Springer Berlin Heidelberg, 2005.
[6] Diepeveen, D. & Armstrong, L. "Identifying key crop performance traits using data mining". IAALD AFITA WCCA2008, World Conference on Agricultural Information and IT, 1-21, 2008
[7] Burges, Christopher JC. "Dimension reduction: A guided tour, Machine Learning". Foundations and Trends in Machine Learning, Vol. 2, No. 4, pp. 275-365, 2009.
[8] Yang, Jihoon, and Vasant Honavar. "Feature subset selection using a genetic algorithm." In Feature extraction, construction and selection, pp. 117-136. Springer US, 1998.
[9] Goldberg, David E., and John H. Holland. "Genetic algorithms and machine learning." Machine learning Vol 3, No. 2 pp. 95-99, 1988.
[10] Cruz, Geraldin B. Dela, Bobby D. Gerardo, and Bartolome T. Tanguilig III. "An Improved Data Mining Mechanism Based on PCA-GA for Agricultural Crops Characterization." International Journal of Computer and Communication Engineering Vol 3, No. 3, pp. 221-225, 2014
[11] Han, Jiawei, Micheline Kamber. Data Mining: Concepts and Techniques, 2nd Edition, Morgan Kaufmann, pp 285-289, 2006
[12] Phyu, Thair Nu. "Survey of classification techniques in data mining." In *Proceedings of the International MultiConference of Engineers and Computer Scientists*, vol. 1, pp. 18-20. 2009.
[13] Kotsiantis, Sotiris B., I. Zaharakis, and P. Pintelas.. "Supervised Machine Learning : A review of Classification Techniques". Informatica 31, pp 246-268, 2007
[14] Wahbeh, A. H., Q. A. Al-Radaideh, M. N. Al-Kabi, and E. M. Al-Shawakfa. "A comparison study between Data Mining Tools over some classification methods. IJACSA, Special Issue on Artificial Intelligence." *SAI Publisher* Vol 2, No 8 (): 18-26, 2010.
[15] Hall, Mark, Eibe Frank, Geoffrey Holmes, Bernhard Pfahringer, Peter Reutemann, and Ian H. Witten. "The WEKA data mining software: an update." *ACM SIGKDD explorations newsletter* Vol 11, No. 1, pp. 10-18, 2009.
[16] Beniwal, Sunita, and Jitender Arora. "Classification and feature selection techniques in data mining." *International Journal of Engineering Research & Technology (IJERT)* Vol 1, No. 6, 2012.
[17] Quinlan, J. Ross. C4. 5: Programs for Machine Learning, Vol.1. Morgan Kaufmann. 1993
[18] Bache, Kevin, and Moshe Lichman. "UCI machine learning repository, 2013." *URL http://archive. ics. uci. edu/ml* (1990): 92.

International Journal of Engineering Research and General Science Volume 3, Issue 5, September-October, 2015
ISSN 2091-2730

Strength of Sway Frame Infilled with Cement Stabilized Laterite Block

M.E. Ephraim[1], L.N. Uzoewulu[2] and T.C. Nwofor[3]

[1, 2] Department of Civil Engineering, Rivers State University of Science and Technology, Port Harcourt, Rivers State, Nigeria

[3]Department of Civil Engineering, University of Port Harcourt, Rivers State, Nigeria

ABSTRACT- The experimental results of the strength and failure mechanism of sway frames with cement stabilized laterite block infill are presented in this study. The engineering properties of cement stabilized laterite block produced from local laterite from Rumueme, Port Harcourt, Nigeria and cement content of zero, two, four, six and eight percent are first investigated to produce blocks at optimum moisture content and then testing for strength property carried out. It was established that four percent cement stabilized laterite block, compacted at its optimum moisture content and dry density produced the best combination of physical and mechanical properties as the tensile, shear and boned strengths for the four percent cement stabilized laterite blocks meet the minimum Code specifications for sandcrete and brick blocks. This agrees with the findings of Nigerian Building and Road Research Institute (NBRRI), from a similar experiment conducted in Kano State, Nigeria. The strength of 1.13N/mm^2 achieved at 28days is higher than the Nigerian Industrial Standard (NIS) specification of IN/mm^2 for cement stabilized laterite block. The strength and failure mechanism of a one-quarter scale model reinforced concrete frame infilled with four percent cement stabilized laterite block followed the trend established for sandcrete and brick infills with the sway resistance capacity of the frame increasing by about 300%. The experimental collapse load of the frame agrees with the theoretical collapse load to about 1%. From the foregoing a wider application of cement stabilized laterite block as infill will lead to cost effective housing delivery as laterite is very available and relatively cheap.

1.0 INTRODUCTION

The need for decent, functional and affordable housing for the citizenry has formed the thrust of government policies since the 1970s. However, the issue of high cost of basic building materials and hence affordability of housing by the masses still remains topical. In an attempt to address this problem, the federal Government of Nigeria through the Nigerian Building and Road Research Institute (NBRRI) has embarked on the research, development and application of Cement Stabilized Laterite Blocks (CSLB) for affordable housing. In driving the research and development of cement stabilized laterite blocks, NBRRI embarked on collaborative research with the Ahmadu Bello University Zaria, Nigeria, using the black cotton soils of Kano. On the basis of the studies, it was established that the optimum cement content, satisfying standards for strength, durability and economy of CSLB was put averagely at four percent [1]. The compressive strength values obtained in these tests ranged from 1.50-1.68 N/mm^2. It is obvious that the optimum cement will depend on the type of larterite, varying from higher values for more sandy to lower values for the clayey lateritic soils. In view of the above, NBRRI has recommended that the required cement for local laterites should be determined from laboratory tests on trial mixes before production of CSLB. Secondly, CSLB is basically used as walling units and therefore may function as infill for structural frame. Although structural frames are generally designed to resist all lateral loads ignoring the contribution of infill, structural cracks are frequently observed on walls of buildings [2], [3]. The fact is that some loads are transferred to the infill, which must therefore, have some capacity to absorb the induced stresses and deformations [4], [5], [6]. The situation throws the second challenge, namely the need to

investigate the structural load carrying capacity and failure mechanism of CSLB inflled frames. In this regard, technical literature reveals a dire paucity in available research studies.

2.0 THEORETICAL AND CONCEPTUAL FRAMEWORK OF STUDY

The study basically based on structural modeling which is an important tool in the analysis, design, and testing of prototype structures. Experiments are carried out on the model that is a reduced scale semblance of the prototype from where the behavior of the prototype is predicted. The theory of dimensional analysis that involves similitude requirements is employed in the sizing and experimentation of the model to predict the prototype behavior.

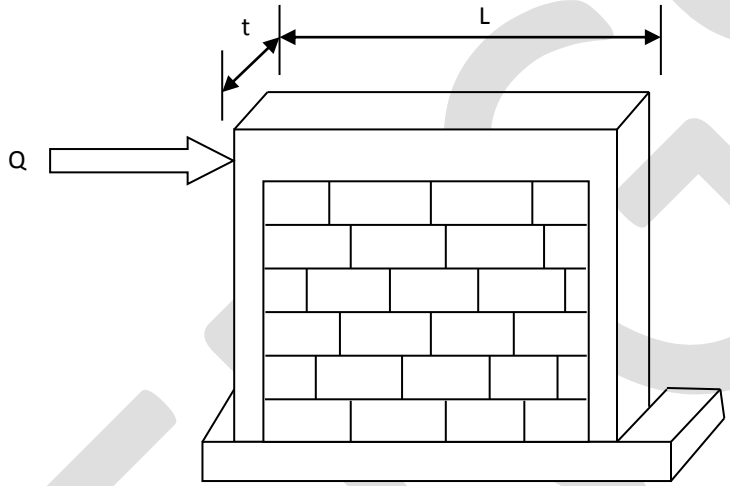

Figure 1: Infilled Frame Model

Considering the infilled frame structure in Figure 1, the following steps are considered to stimulate the physical parameters of the model.

i. The diagonal tensile stress σ of the CSLB infill wall depends on the loading Q, span L, the thickness t and the modulus of elasticity E and may he represented im as;

$$\theta(\sigma, Q, I, t, E) = 0 \quad (1)$$

ii. Taking, the modulus E and span L as dimensionally independent variables [7], [8], the above equation can he expressed as

$$G(\sigma/E, Q/EL^2, t/L) = 0 \quad (2)$$

where

$\sigma = \theta (Q/EL^2, t/L)$ (3)

Hence

$(Q/EL^2)_P = (Q/EL^2)m$

$Q_p = Qm\ S_E\ S^2_{L,}$ Where $S_E = 1$.

iii. For the same material in model and prototype, the scale factor for material $S_E = 1$, and the prototype load $Q_P = Q_M\ S_L{}^2$. Where S_L is the linear scale factor.

Therefore the failure load of the prototype can be computed by multiplying that of the model by the square of the linear factor, and based on material scale factor, the model material is the same as the prototype material hence the stress is the same in model and prototype. The success of this theory reduces cost of experimentation, enhances safety and ease with which the behavior of large prototype structures are analyzed and predicted.

3.0 EXPERIMENTAL PROCEDURE

The method of research was based on structural modeling and experimental test in the laboratory. The determination of basic properties of local laterite produced is done in accordance with BS 1377, 1995- Method of Test for Civil Engineering Soils and BS 3921, (1995) and Method of Test for clay bricks and blocks, [9], [10].

The structural modeling of a previously designed frame was achieved on the assumption of a uniform scale factor for materials (laterite, cement, water, sand) and a linear scale factor of 1:4 was adopted for determination of deflections and dimensions.

3.1 Materials

The basic materials used for this study were as follows; water, local laterite from Rumueme borrow pit in Rivers State Nigeria, cement, and sand. They are described briefly in the sub-headings below.

3.1.1 Equipment

These include wooden mold conforming to 1/4 scale model dimensions of 75x37.5x37.5mm, equivalent to the prototype dimensions of 300x150x150mm, hydraulic jack, strain and dial gages, and proving ring.

3.1.2 Water

Water conforming to BS 3148 (1995); obtained from the university water supply network was used for the experiment.

3.1.3 Laterite

The laterite was obtained from a borrow pit located between Agip and Ada George Roads at Reumueme in Port Harcourt. Laterite for the construction of Ada George Road was obtained from this borrow pit. The preparation of the laterite was in accordance with BS 1377 (1995) with respect to sampling the optimum moisture content (OMC), the maximum dry density (MDD), sieve analysis, and index properties determination.

3.1.4 Cement

Portland cement complying with BS 12 (1995) obtained from Eastern Bulkcem Limited, was used in the experiment.

3.1.5 Aggregate

Aggregate conforming to fine gravel on the particle size curve was used in the production of concrete. The aggregate conformed to BS 882 (1995).

3.2 Laterite Block Production

Production of model blocks was by ramming into a wooden mold with internal dimensions 75x37.5x37.5 mm and pressing down to ensure no voids or honeycomb on block when extruded. Curing was in accordance with BS.3578. (1995). The freshly molded block were cured for 7days by covering with polythene sheets to prevent any loss of water. After 7days, the polythene sheet covering was removed. The strength of the blocks was tested at 7,14 and 28 days. The water absorption test was done at 28days for each sample at ½ hour, 1hour, 2hours and 24hours in accordance with BS 3921

3.3 Construction of Model Frame and Test Setup

The model frame was constructed after analysis of a prototype frame to determine the size of reinforcement and load capacity. Basically the prototype column section was controlled by the prototype block size of 300 x 150x150 mm. The details are set out below in Tables 1.

Table 1: Prototype and Model Frame Dimensions

Member	Prototype (mm)	1/4 Model (mm)
Frame (Full Size)	3000x3000	750x750
Column Section	150x150	37.x37.5
Beam Section	300x150	75x37.5
Block Section	300x150x150	75x37.5x37.5
Mortar thickness	12	3
Reinforcement	Y 12	Y3 (BRC wire)
Stirrup	R6	R1.5 (binding wire)
Binding wire	R1.5	R0.375 (fly screen wire)
Aggregate	12(1/2")	3 (1/8")
Foundation Depth	900 x 600	225x150

Four different models were constructed at the premises of the structural engineering laboratory, Rivers State University of science and Technology Port Harcourt, Rivers State, Nigeria. Each frame foundation was made very rigid to avoid over turning effect during testing. The frame starter reinforcement was fixed and cast in-situ with the foundation. The entire foundation was covered and flushed with the ground level and compacted to represent true site situation. The experiment was carried out in dry season when the ground was dry and strong enough to resist the racky load.. The frames were loaded using a hydraulic jack as shown in Figure 2. The laboratory stanchions provided the reactant action for the jack. The strain gages tagged GI, G2,G3 and G4 are 100mm gages. Gages G1 and G3 measured strain on the compression diagonal while G5 and G4 measured strain on the tension diagonal. The dial gage, G5 measured displacement in the sway direction. The hydraulic jack connected to the proving ring assembly, exerted horizontal force on the frame. The load was applied in steps of 0.50KN and maintained for 5 minutes to allow for stabilization of the frame under the load and observation of cracks which may develop. The load at which crack appeared on the infill was recorded as the collapse load.

3.4 Loading Scheme

The horizontal sway load capacity of the prototype and model frame was calculated as 23.81KN and 1.48KN respectively and the loading scheme for the frame was carried out in accordance with BS 5628: part: 1995. The load values were read on the proving ring. The readings of strain gages G1, G2, G3,G4 and G5 were recorded at each loading cycle, until the infill frame showed cracks on the infill panel. The load at which the cracks appeared on the infill was recorded as the maximum load capacity of the frame. The strain gages G1, G2, G3 and G4 recorded internal strains on the infill, while dial gage G5 recorded the horizontal away of the frame. The frame deflection, stress/strain profiles were plotted to show the infill behavior during loading up to failure.

4.0 RESULTS AND DISCUSSION

This chapter presents the result obtained in the experimental investigation conducted in this study. The results are analyzed with the Table and graphs provided. The discussion of the results is done with comparison with the code provisions and the result of similar researches conducted by researchers in other locations. The graph of deflections and stress- strain behavior of the infill frame are shown, and deflection values calculated. Model horizontal load was applied to the frames and deflections/strains induced on the frames were measured. The mode of failure of each frame was noted and photographed. The average resistance of the infill in the three frames with infill was used in calculating the stresses on captured as would be seen in the figures below.

4.1 Failure Mechanism of the Frames

The failure mechanisms of the frames are shown in the figures below. Figure 2 shows the collapsed mechanisms of the rigid frame (MF0) with hinge formation on the joint of the columns, while figure 3 to 5 shows the collapse mechanisms of infilled frames MFI, MF2, and MF3, respectively with the crack formations at critical sections

Figure 2: Failure Mode of MF0 Frame

Figure 3: Failure Mode of MF1 Frame

Figure 4: Failure Mode of MF2 Frame

Figure 5: Failure Mode of MF3 Frame

The failure of the rigid frame was observed to be by formation of hinges at the upper and lower portions of the two columns, wile the failure of the infill frame was by formation of diagonal cracks starting from the load application point running parallel to the loading diagonal. The crack width ranged between 2 and 3mm. Separation of infill panel from the column near the application of the load as well as, separation of the infill panel from the ground beam was also observed. There were also micro cracks initiating from point of application of the load mainly due to corner crushing mode of the infilled frame. Generally, it was observed that the infill increased the resistance of the frame as would be seen from the readings and the reduced and corresponding calculation from the proving ring and dial gauge.

4.2 Critical Loads on Model Frame.

The critical loads are the loads at which first cracks are initiated on the frames without further increase on the proving ring readings. These loads are shown on the Table 2 below. These loads are used to predict the prototype sway load for the infilled frame.

Table 2: Critical Sway Loads

Frame type	Height (mm)	Span (mm)	Infill Type	Load (kN)
MF0	"	750	"	750
MF1	"	"	CSLB infill	5.00
MF2	"	"	"	3.50
MF3	"	"	"	4.50

From the foregoing the critical load on the prototype model can be predicted as follows:

Critical load on frame MF0 load through experimental modeling = 1.5KN

Predicted load from analysis =1.49KN

Accuracy of predication = 1.5/1.49 = 1.0067

Critical prototype Load, $= 1.5S^2$ (from similitude requirement) $= 1.5x4^2 = 24kN$

It is possible to determine the prototype infill frame sway loads based on the model result by applying the scale factor as also seen in Table 2.

4.3 Deflection of Infilled Frame Model

The deflection of the frames was monitored by dial gage seen in the test set-up in the sway direction. Generally it was observed that the introduction of the cement stabilized Laterite Block with acted as an infill panel reduced the horizontal defection of the frame by 67% as can be seen in the comparison with the load-displacement profile of the rigid frame model

tagged MF0. The MF0 model which is without infill, was swayed through 18.5mm before collapse by a horizontal load of 1.5kN, as recorded by the dial gage. The infilled frame models tagged MF1, MF2 and MF3 were displaced through, 11.6mm 3.6mm and 3.08mm respectively by horizontal load of 4.4, 3.5 and 5kN acting on the frame respectively. The load-displacement diagram is shown in Figure 6 where it is clearly seen that the introduction of infill reduced the sway of the frames at increased load before collapse by stiffening the frame.

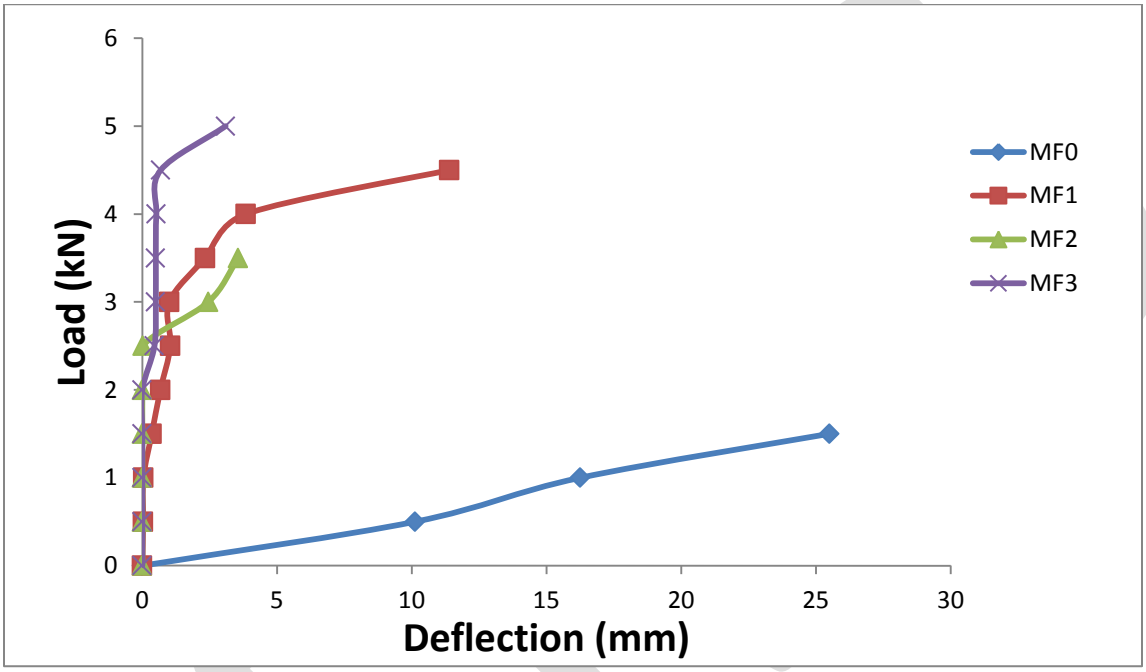

Figure 6: Load-Displacement Profile for Structural Models MF0, MF1, MF2 and MF3

4.4 Streets-Strain Characteristics of Infilled Frame Model

The estimation of the linear strain in the infill was monitored at increased load and measured as points G1, G2, G3, and G4, using strain gages and the values recorded. Diagonal cracks and separation of infill from the frames through a length of about 600mm on each frame were observed, as well as separation from the foundation through the entire length of 750mm as shown in Figure 2 to 5. This could be attributed to the frames bearing pressure on the infill while being acted upon by the external horizontal load and the foundation providing the counter thrust to the horizontal force. The end action was that frame and infill were crushed under the two opposing force leading to the collapse of the frame and infill. Strain gages G1 G3 measured strain in same direction but opposite to strain gages G2, G4 which were placed on the other side of the infill panel measuring strain in same direction. The net strain is given by [19] as G0 = G1 + G2 – G3+ G4 with the stress-strain profile given in Figure 7.

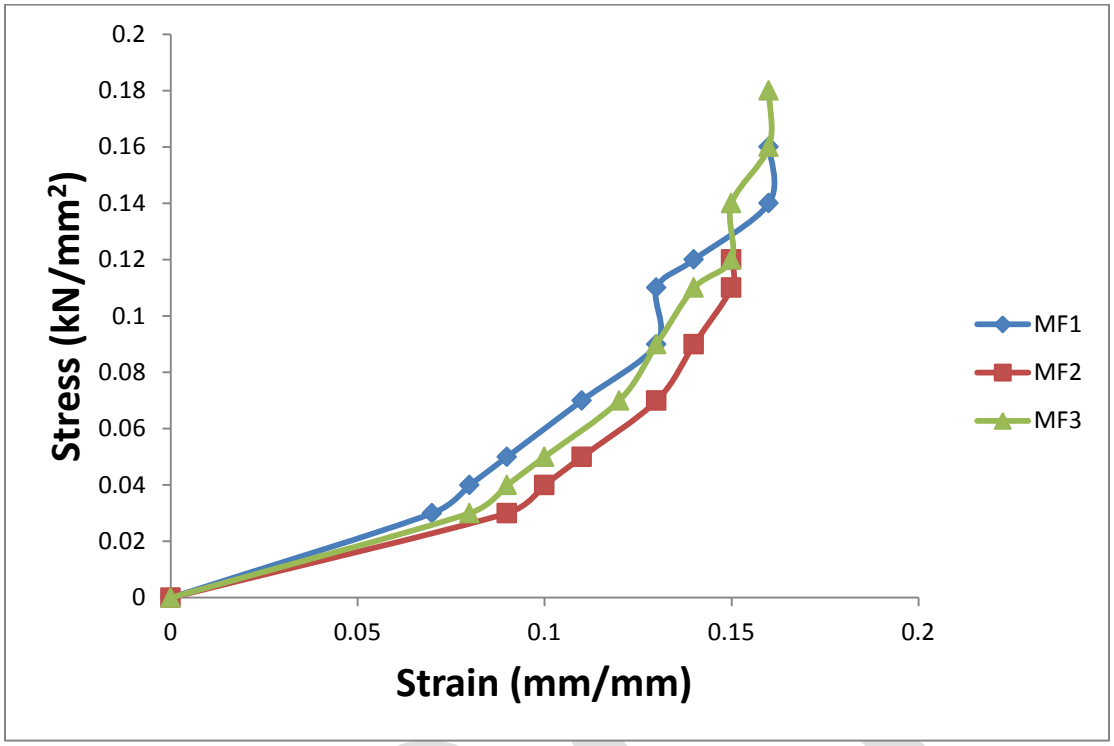

Figure 7: Stress-Strain Profile of Infilled Frame Models, MFI, MF2, MF3

Crack formation on the infill was visible and it is attributed to the limit of shell buckling, which is the point at which failure of the interior web of the infill starts [8],[11]. This behavior is attributed to the failure of each member of the composite even though it still contributes to the overall resistance of the composite frame till collapse mechanisms, thus confirming that the high in-plane rigidity of the masonry wall significantly stiffens the otherwise relatively flexible frame, while the ductile frame contains the brittle masonry after cracking, up to critical sway load. The tensile stress which corresponds to the maximum tensile strain [12], is obtained as 0.09N/mm and it compares favorably with the codes specification [9], [10] for sandcete blocks and clay bricks.

5.0 CONCLUSION

This study the strength of sway frame using cement stabilized literite block unit as structural infill has been presented. From the analysis of the results obtained in the study, the following conclusions are arrived at.

1. Four percent Cement Stabilized Leterite Blocks, produced at optimum moisture content and maximum dry density presents the best combination of physical and mechanical properties. The strength of 1.13 N/mm^2 achieved in

28days is within the Nigerian Industrial Standards (NIS) specification for cement stabilized laterite blocks. This also confirms the applicability of four percent cement content recommended by NBRRI to Niger Delta laterite soil.

2. The strength and failure mechanism of a ¼ scale model reinforced concrete frame, with the four percent CSLB as infill, followed the trend established for sandcrete and burnt brick block infills and the sway resistance capacity increased from 1.5kN to 4.5kN, suggesting an average of 300%

3. The experimental failure load compares favorably with the theoretical failure load from the model collapse load.

4. The tensile, shear and bond stresses for the CSLB are within the code specification for infill material. The values obtained for four percent cement stabilized infill constitute respectively, 0.09N/mm^2, 0.22N/mm^2 and 0.21Nmm^2.

5. The CSLB is cost effective and competitive over sandcrete and burnt brick in terms of strength; thus a wider use of CSLB as infill will lead to cost effective housing delivery in the country.

5.1 RECOMMENDATIONS

1. The CSLB from Rumueme laterite is recommended for the state mass housing project.

2. The effort of Nigerian Building and Road Research Institute should cover the entire nation by collaborating with all the universities in research on the local laterite, to establish the economic cement mix for production of cement stabilized laterite block for the locality in order to help local people in housing.

3. Further research on the carrying capacity of CSLB infill and resistance to both racky and gravity loads is recommended.

REFERENCES:

1) Nigerian Building and Road Research Institute (NBRRI) (1988). *Ten years of Building and Road Research pp13-30.*

2) Riddington J.R. (1994). Composite behavior of walls interacting with flexural members. *Ph.D, Thesis,* University of Southampton.

3) Stafford, S. B. (1974). The composite behavior of infilled frames. *Symposium on tall buildings*, University of Southampton.

4) Weeks, G.A. and Mainstone, R.J. (1970). Influence of a builging frame on racking stiffness and strengths of brick wall. *Second International Brick Masonry Conference,* Stoke on Trent, pp. 165-171.

5) Nwofor, T.C.(2012). Shear resistance of reinforced concrete infilled frames. *International Journal of Applied Science and Technology*, 2(5), 148-163.

6) Nwofor, T.C. and Chinwah, J.G. (2012). Finite Element Modeling of Shear Strength of Infilled Frames with openings. International Journal of Engineering and Technology, 2(6), 992- 1001.

7) Ephraim, M.E. (1999). Modeling techniques and instrumentation in laboratories. *Unpublished lecture note*, University of Science and technology port Harcourt Nigerian, pp.2-19

8) Sabnis, G.M., Harris, H.G., White, R.N., and Saeed Mirza, M. (1983). *Structural Modelling and Experimental Techniques.* Prentice-Hall, Inc., Englewood Cliffs, N.J. 07632, USA

9) *BS 3921 (1995). Method Of Test Of Soil for Civil Engineering purposes,* British Standard Institution London, pp.5-39

10) *BS 1377 (1995). Clay Bricks and Blocks, British Standard* Instauration. London

11) Nwofor, T.C. (2012). Numerical micro-modeling of masonry infilled frames. Archives of Applied Science Research, 4(2), 764-771.

12) Hetenyi, M. "Beams On Elastic Foundations". *Scientific Journal service*, University of Michigan Studies, Vo1. XVI. 1946

International Journal of Engineering Research and General Science Volume 3, Issue 5, September-October, 2015
ISSN 2091-2730

Texture Filter based Medical Images Segmentation for Cancer Disease

Dr. Sana'a khudayer Jadwa

Computer Unit, College of Medicine

Al-Nahrain University

Baghdad- Iraq

E-mail: sanaakhudayer@yahoo.com

Abstract— Medical Image processing is one of the most challenging topics in research field. In medical field, CT (Computed Tomography) scan imaging and MRI (magnetic resonance imaging) are the most important for image based visual diagnostics, but applying segmentation to these images is very tedious and requires an adjusting approach. The main objective of medical image segmentation is to extract and characterize anatomical structures with respect to some input features or expert knowledge. In this paper we have formulated a simple, general, fast, and user-friendly approach to the problem of medical image segmentation based on texture filter. In this method, the experimental results show that the segmentation results are visually satisfactory of medical image texture segmentation.

Keywords— Medical image processing, image texture, image segmentation, texture analysis**,** medical imaging, , Medical image Analysis ,texture filter.

1. INTRODUCTION

Medical imaging application plays an indispensable role by automating or facilitating the delineation of anatomical structures. Medical image segmentation is a challenging task due to the various characteristics of the images, which leads to the complexity of segmentation. [1]. In computer vision, Image segmentation is known as a process of partitioning an image into several segments also known as super pixels. The important goal of image segmentation is to simplify or change the representation of an image into form that is more meaningful and is easy for analysis [2]. Segmentation is an important process in the analysis of MR (Medical Resonance) Images for medical diagnosis. It divides the MR image into different types of classes and groups the homogeneous pixels into clusters. This is used in medical diagnosis in many ways, detecting brain tumor, tissue analysis, bone fractures and similar problems [3]. Segmentation of medical images involves three main image-related problems. The image may contain noise that can alter the intensity of a pixel such that its classification becomes uncertain. Also, the images can exhibit intensity nonuniformity where the intensity level of a tissue class varies gradually over the extent of the image. Third, the images have finite pixel size are subject to partial volume averaging where individual pixel volumes contain a mixture of tissue classes so that the intensity of a pixel in the image may not be consistent with any single tissue class[4].An image texture can be defined as the local spatial variations in pixel intensities and orientation. In order to recognize objects and scenes in computer vision, it is essential to be able to partition an image into meaningful regions with respect to texture characteristics. Texture segmentation has a wide range of applications like content based image retrieval, medical diagnosis, analysis of satellite or aerial images, surface defect detection and terrain classification for mobile robot navigation[5]. This paper produce texture segmentation method for medical images. The organization of the rest of this paper is as follows. Section 2 highlights the related works. Section 3 introduces image texture analysis . Section 4 describes the proposed method. Section 5 present the experimental results and section 6 concludes the paper.

2. RELATED WORKS

Medical image segmentation is a challenging task due to the various characteristics of the images, which leads to the complexity of segmentation **Eldman and Maria** [6] introduced an automatic method of medical image segmentation used in the study of the Central Nervous System (CNS) by multilevel thresholding based on histogram difference. **V. Grau*, A. U. J. Mewes** [7] Presented a method to combine the watershed transform and atlas registration, through the use of markers. This new algorithm applied to two challenging

applications: knee cartilage and gray matter/white matter segmentation in MR images. Numerical validation of the results is provided, demonstrating the strength of the algorithm for medical image segmentation. **Ch.Hima Bindu,QISCET, Ongole** [8] Employed an optimized Otsu method based on improved thresholding algorithm for medical image segmentation ,the experimental results show that the new optimized method dramatically reduces the operating time and increases the separability factor in medical image segmentation while ensures the final image segmentation quality. **Seongjai Kim and Hyeona Lim** [9] proposed the background subtraction (MBS) in order to minimize difficulties arising in the application of segmentation methods to medical imagery. **Ebrahim and Dehmeshki**[10]developed a method that requires the definition of a speed function that controls curve evolution. The image intensity gradient and the curvature are utilized together to determine the speed and direction of the propagation. Although level set methods are highly effective in segmenting image, but. they are sometimes unable to exactly detect objects in images with low-contrast boundaries. In this method hybrid speed functions are used for an implicit active contour (level set) method which is capable of segmenting images with low-contrast boundaries.

3. IMAGE TEXTURE ANALYSIS

The regular repetition of an element or pattern on a surface it is called as texture. It is used to identify different textured and non-textured regions in an image, to classify/segment different texture regions in an image, to extract boundaries between major texture regions ,figure(1) illustrate three examples of image texture[11]:

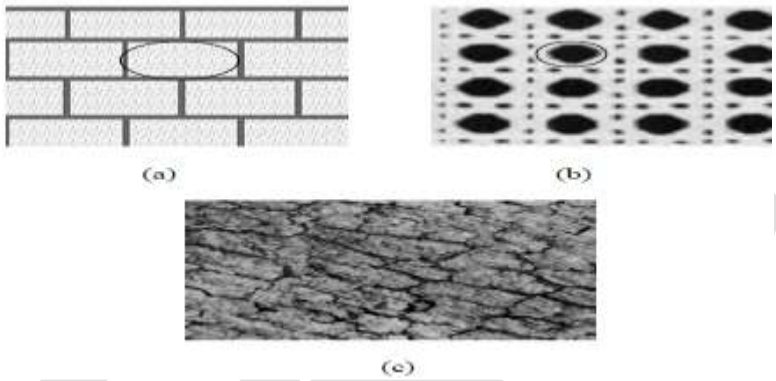

Figure(1): Different examples of image texture

Texture is a difficult concept to represent, the identification of specific textures in an image is achieved primarily by modeling texture as a two-dimensional gray level variation. The relative brightness of pairs of pixels is computed such that degree of contrast, regularity, coarseness and directionality[11]. Texture analysis refers to the characterization of regions in an image by their texture content. Texture analysis attempts to quantify intuitive qualities described by terms such as rough, silky, or bumpy in the context of an image. In this case, the roughness or bumpiness refers to variations in the brightness values or gray levels[12]. Texture analysis of an image gives distributed arrangements of the intensity of the pixel in an image[13].An image texture can be defined as the local spatial variations in pixel intensities and orientation. In order to recognize objects and scenes in computer vision, it is essential to be able to partition an image into meaningful regions with respect to texture characteristics[14].Texture analysis is used in a variety of applications, including remote sensing, automated inspection, and medical image processing. Texture analysis can be used to find the texture boundaries, called texture segmentation[12]. All texture functions operate in a similar way. They define a neighborhood around the pixel of interest calculate the statistic for that neighborhood and then use the computed statistic value as the value of the pixel of interest in the output image. The example that shown in Figure(2) illustrates how the range filtering function operates on a simple matrix. In this example, the value of element B (2, 4) is calculated from A (2, 4). Range filtering function use m by n pixels, in this example 3 × 3, neighborhood around the pixels[12].

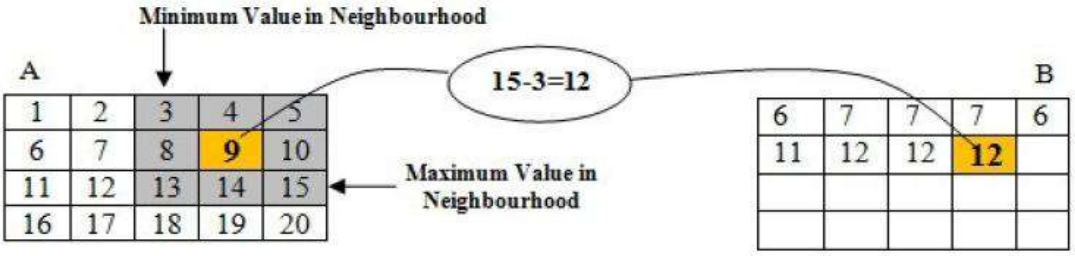

Figure(2): Range filtering function

4. PROPOSED METHOD

In this paper the texture segmentation for medical image based on applying a range filter is proposed. At first the color image is read from a database that contain a collection of medical images, then these images are converted to grayscale image, later the range filter is applied in order to extract the texture content of medical image. The texture segmentation process diagram is illustrated in figure(3) as shown below:

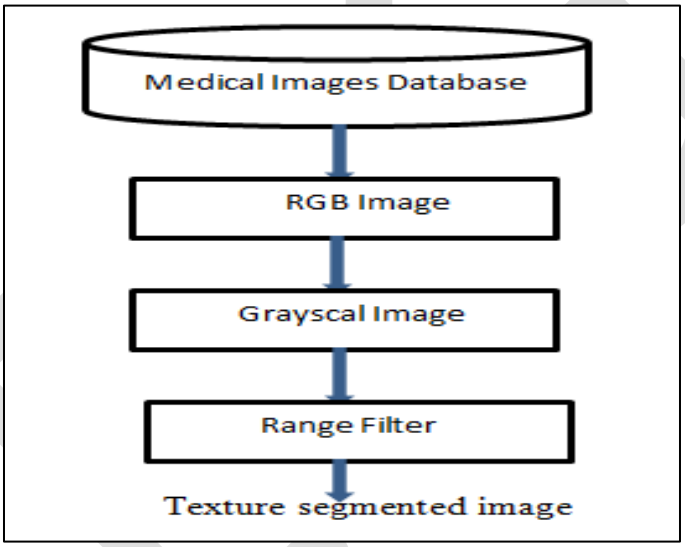

Figure(3): Block diagram for texture image segmentation

4.1 IMAGE DATABASE

The starting point of this work was the creation of a database with six medical images modalities having different sizes that is collect from the web. The database consist of three groups : brain cancer , kidney cancer and stomach cancer images. Figure (4) show the database images.

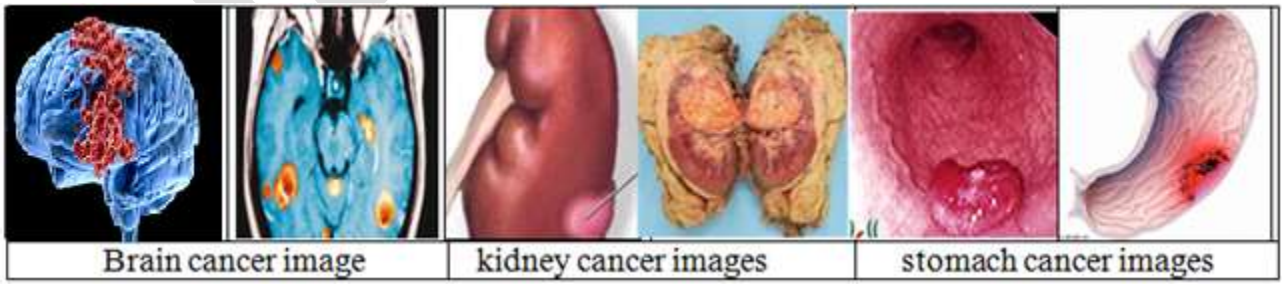

Figure(4): Different medical images

4.2 RGB IMAGE CONVERSION

The colored medical image is converted to gray scale image by converts RGB values to grayscale values by forming a weighted sum of the R, G, and B components using equation(1):

$$y = 0.2989 * R + 0.5870 * G + 0.1140 * B \quad \text{.....(1)}$$

4.3 RANGE FILTERING

Filtering is perhaps the most fundamental operation of image processing. The term filtering can be defined as the value of the filtered image at a given location. It is a function of the values of the input image in a small neighborhood of the same location. Filter operators can be used to sharpen or blur images, to selectively suppress image noise, to detect and enhance edges, or to alter the contrast of the image. The filters use the local statistical variations in an image to reveal the edges and its histogram [15].

5. EXPERIMENTAL RESULTS

The proposed algorithm is applied on the medical images of cancer disease, at first the color image is reading from the database then it converted to grayscale as shown in figure(5):

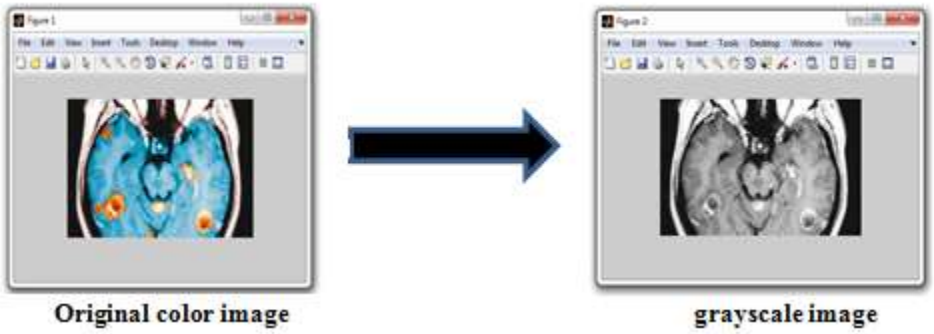

Figure (5): Colored Image conversion.

Then the range filter is applied on grayscale image to obtain the texture segmented medical image as show in figure (6):

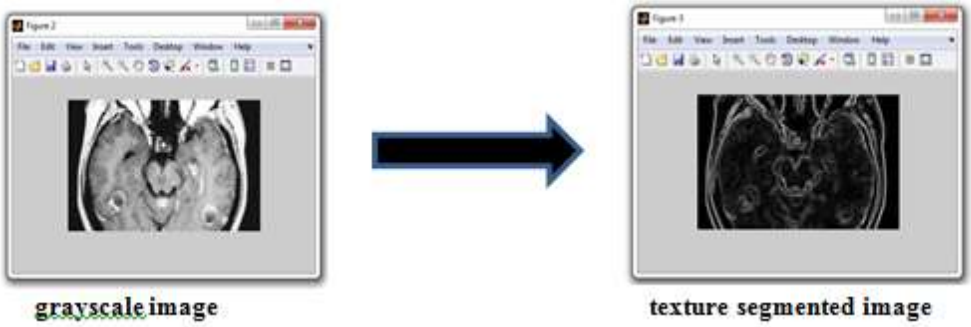

Figure (6): Texture segmented medical image

The same steps applied for the rest image given the result as shown in figure (7):

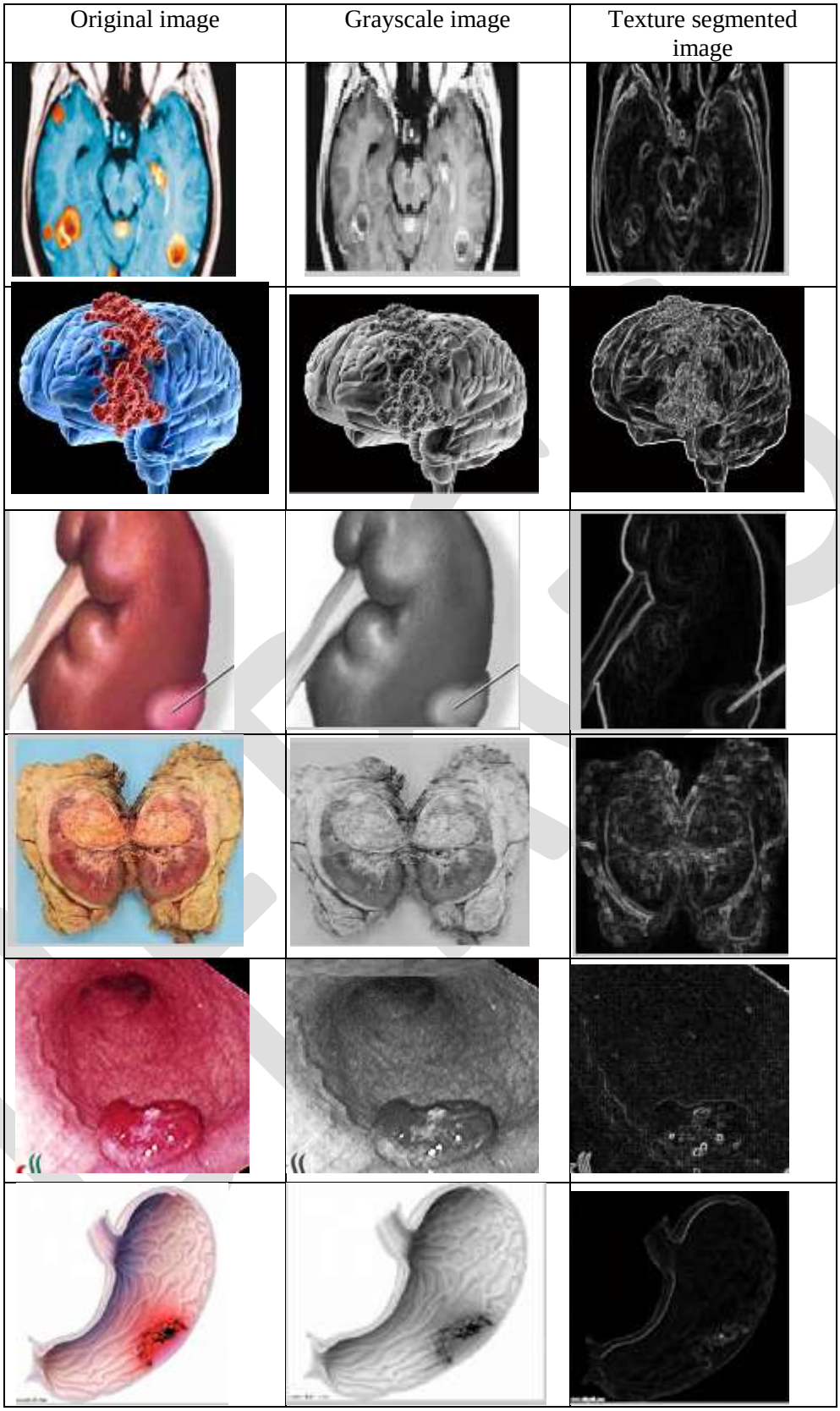

Figure(7): Results of texture segmented for medical images

6. CONCLUSION

In this paper we have considered the method of texture filter for an effective segmentation of medical images. The method uses the range filter to achieve robust and accurate segmentation results which are visually satisfactory. The whole process is autonomous and requires no supervision, which is one of the advantages of the proposed method. The method guarantees best segmentation of textures in poor-quality images also. The resulting figure show the efficiency, simplicity and robustness of medical image texture segmentation.

7. REFERENCES

[1] Ch. Hima Bindu1 and K. Satya Prasad2," An Efficient Medical Image Segmentation Using Conventional OTSU Method", International Journal of Advanced Science and Technology Vol. 38, January, 2012.

[2] Dilpreet Kaur and Yadwinder Kaur," Intelligent Medical Image Segmentation Using FCM, GA and PSO", International Journal of Computer Science and Information Technologies,Vol. 5 (5), 2014.

[3] R. Venkateswaran1and S. Muthukumar," Genetic Approach on Medical Image Segmentation by Generalized Spatial Fuzzy C- Means Algorithm", IEEE International Conference on Computational Intelligence and Computing Research,2010.

[4] Daniel J. Withy and Zoltan J.Koles,"A Review of Medical Image Segmentation: Methods and Available Software", International Journal of Bioelectromagnetism Vol. 10,No.3, pp125-148. 2008.

[5] Saka.Kezia, Dr.I.Santi Prabha and Dr.V.VijayaKumar," A New Texture Segmentation Approach for Medical Images", International Journal of Scientific & Engineering Research Volume 4, Issue 1, ISSN 2229-5518 , January-2013.

[6] Eldman de Oliveira Nunes and Maria Gabriela Pérez," Medical Image Segmentation by Multilevel Thresholding Based on Histogram Difference", 17th International Conference on Systems, Signals and Image Processing, 2010.

[7] V. Grau*, A. U. J. Mewes, M. Alcañiz, Kikinis, and S. K. Warfield " Improved Watershed Transform for Medical Image SEGMENTATION USING PRIOR INFORMATION", IEEE TRANSACTIONS ON MEDICAL IMAGING, VOL. 23, NO. 4, APRIL 2004 .

[8] Ch.Hima Bindu,QISCET, Ongole," AN IMPROVED MEDICAL IMAGE SEGMENTATION ALGORITHM USING OTSU METHOD", International Journal of Recent Trends in Engineering, Vol 2, No. 3, November 2009.

[9] Seongjai Kim and Hyeona Lim" Method of Background Subtraction for Medical Image Segmentation", The work is supported in part by NSF grants DMS- 0312223 & DMS-0609815, 2005.

[10] Ebrahim doost, Y.; Dehmeshki, J. ; Ellis, T.S. and Firooz bakht, M,".Medical Image Segmentation Using Active Contours and a Level Set Model: Application to Pulmonary Embolism (PE) Segmentation", IEEE Fourth International Conference on Digital Society, 269-273, Feb. 2010.

[11] Vaijinath V. Bhosle and Vrushsen P. Pawar " Texture Segmentation: Different Methods",International Journal of Soft computing and Engineering (IJSCE) ISSN: 2231-2307, Volume-3, Issue-5, November 2013 .

[12] Matheel Emaduldeen Abdulmnim," Segmenting the Dermatological Diseases Images by Developing the Range Operator", Iraqi Journal of Science, Vol 55, No.3B, pp:1376-1382, 2014.

[13] Asheesh Kumar, Apurva Mohan Gupta, Naresh Rameshrao Pimplikar and Natarajn P," TEXTURE SEGMENTATION IN MEDICAL IMAGING FOR RED SPOT BLOTCHES ANALYSIS IN HUMAN BODY",International Journal of Advanced Research in Computer and Communication Engineering ,Vol. 3, Issue 3, March 2014.

[14] Saka.Kezia, Dr.I.Santi Prabha and Dr.V.VijayaKumar," A New Texture Segmentation Approach for Medical Images", International Journal of Scientific & Engineering Research Volume 4, Issue 1, January-2013.

[15] Amir Rajaei, LalithaRangarajan and ElhamDallalzadeh," MEDICAL IMAGE TEXTURE SEGMENTATION USINGRANGE FILTER", Computer Science & Information Technology,2009.

Pixel Based Image Fusion Using Fast Discrete Curvlet Transform With Graphical User Interaction

P.Vijaya, P. Murali Krishna

M.Tech, LITAM, Dhulipalla, Guntur(d.t), Andhra Pradesh, India. pratti.vijaya@gmail.com

Asst. Professor, LITAM, Dhulipalla, Guntur(d.t), Andhra Pradesh, India.

Abstract: Image fusion is very important technique used to extract the useful information from several images into a single image. Image fusion is a sequel to data fusion. The basic limitation of the wavelet fusion algorithm is in fusion of curved shapes and this can be accurated by the application of the Curvelet transform(FDCT),would result in the better fusion efficiency. Image fusion algorithms can be categorized into different levels: pixel, feature, and decision levels. Pixel level fusion works directly on the pixels of source images while feature level fusion algorithms operate on features extracted from the source images. The proposed image fusion algorithm is implemented for fusion of medical images. In medical imaging, MRI and CT images are of main concern for diagnosis of brain, chest and spines related diseases. This process can be implemented through graphical user inter-action. The results are analyzed and tested using GUI.

Keywords: Pixel Based, GUI, MRI and CT Images, FDCT,fusion,wavelet.

I.INTRODUCTION

Image fusion can be traced back to the mid-eighties. Multi sensor data fusion has become a discipline which demands more general formal solutions to a number of application cases. Several situations in image processing require both high spatial and high spectral information in a single image. This is important in remote sensing. However, the instruments are not capable of providing such information either by design or because of observational constraints. One possible solution for this is data fusion.

Image fusion has become a common term used within medical diagnostics and treatment. The term is used when multiple images of a patient are registered and overlaid or merged to provide additional information. Fused images may be created from multiple images from the same imaging modality,[4] or by combining information from multiple modalities,[5] such as magnetic resonance image (MRI), computed tomography (CT), positron emission tomography (PET), and single photon emission computed tomography (SPECT). In radiology and radiation oncology, these images serve different purposes. For example, CT images are used more often to ascertain differences in tissue density while MRI images are typically used to diagnose brain tumors.

For accurate diagnoses, radiologists must integrate information from multiple image formats. Fused, anatomically consistent images are especially beneficial in diagnosing and treating cancer. With the advent of these new technologies, radiation oncologists can take full advantage of intensity modulated radiation therapy (IMRT). Being able to overlay diagnostic images onto radiation planning images results in more accurate IMRT target tumor volumes.

Often the ideal fused image is not known or is very difficult to construct. This makes it impossible to compare fused images to a gold standard. In applications where the fused images are for human observation, the performance of fusion algorithms can be measured in terms of improvement in user performance in tasks like detection, recognition, tracking, or classification.

II.RELATED WORK

A.EXISTING METHOD

DISCRETE WAVELET TRANSFORM

A discrete wavelet transform (DWT) is any wavelet transform for which the wavelets are discretely sampled. As with other wavelet transforms, a key advantage it has over Fourier transforms is temporal resolution: it captures both frequency and location information (location in time).

Calculating wavelet coefficients at every possible scale is a fair amount of work, and it generates an awful lot of data. If the scales and positions are chosen based on powers of two , the so called dynamic scales and positions then calculating wavelet coefficients are efficient and just as accurate. This is obtained from discrete wavelet transform (DWT).

Wavelet Toolbox provides functions for the dyadic-scale analysis of signals and images. Obtain both decimated and non decimated wavelet transforms of signals and images including the dual-tree complex and double-density wavelet transform. Fuse

images based on their wavelet decompositions. Explore the multi scale correlation structure of multiple signals using wavelet multi signal analysis. Use a lifting scheme to implement 1-D and 2-D wavelet transforms.

B.CURVELET TRANSFORM

The Curvelet transform (CVT) is a multi-scale transform proposed by Candes and Donoho and is derived from the Ridgelet transform. The Curvelet transform is suited for objects which are smooth away from discontinuities across curves. Fourier Transform does not handle point's discontinuities well because a discontinuity point affects all the Fourier Coefficients in the domain. Moreover, Wavelet transform handles point discontinuities well and doesn't handle curve discontinuities well.

Curvelet transform handles curve discontinuities well as they are designed to handle curves using only a small number of coefficients. Curvelet transform has several applications in various areas such as image denoising, image fusion, Seismic exploration,Turbulence analysis in fluid mechanics and so on.

Fast Discrete Curvelet Transform

Fast discrete curvelet transform based on wrapping is a multi-scale pyramid consisting of different orientations and positions in frequency domain. It uses advantages of Fast Fourier transform (FFT) in special spectral domain Discrete Wavelet Transform (DWT) is the most useful transform successfully applied in image fusion field.

It preserves time and frequency details of the image. In discrete wavelet transform image data are discrete and the spatial and spectral resolution is dependent on the frequency. Show the output using graphical user interface tool for the application. UIs created using MATLAB® tools can also perform any type of computation, read and write data files, communicate with other UIs, and display data as tables or as plots.

III.IMPLEMENTATION WORK

C.IMAGE FUSION

Here fusion of these two images plays a very important role which combines both CT and MRI images into a single fused image which contains accurate information about bones as well as soft tissue details. Thus, the fusion of these two images of same organ provides very useful information about that organ which helps physicians for better diagnosis.

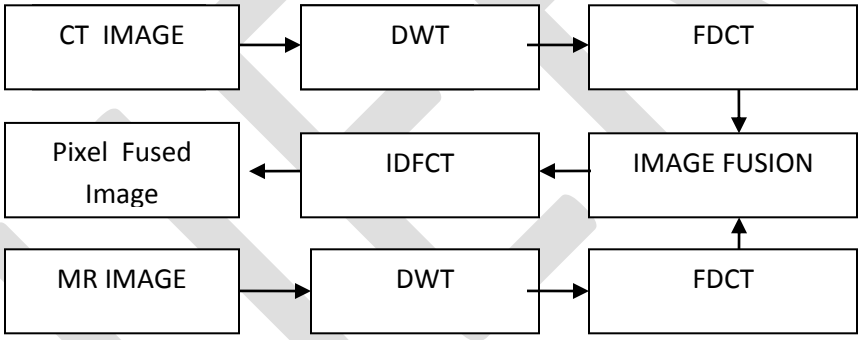

Fig 1: Pixel based image fusion technique

LEVELS OF FUSION:

Analogous to other forms of information fusion, image fusion is usually performed at one of the three different processing levels: signal, feature and decision .

Signal level(pixel-level) image fusion:

It is also known as **pixel-level image fusion**, represents fusion at the lowest level, where a number of raw input image signals are combined to produce a single fused image signal.

Object level image fusion:

It is also called feature level image fusion, fuses feature and object labels and property descriptor information that have already been fusion of probabilistic decision information obtained by local decision makers operating on the results of feature level processing on image data produced from individual sensors extracted from individual input images

The highest level, decision or symbol level image fusion:

It represents fusion of probabilistic decision information obtained by the local decision makers operating on the results of feature level processing on image data produced from the individual sensors.

PROPOSED IMAGE FUSION ALGORITHM :

The steps involved in proposed algorithm can be summarized as follows:
1. Read the MRI as image1 [M1, N1] and CT as image2 [M2, N2] which is to be fused.
2. Resample and register both these images, so that wavelet coefficients of similar component will stay in the same magnitude.
3. Apply 2D-discrete wavelet transform to these images which decompose it into four sub-bands (LL, LH, HL and HH). These four sub-bands are sensitive to low frequency approximate component and three high frequency detailed components.
4. The wavelet coefficients from both the input images are obtained which gives high spatial resolution and high spectral quality contents from input images.
5. Further Fast discrete curvelet transform using frequency wrapping is applied to obtain curvelet coefficients.
6. The steps for FDCT using frequency wrapping algorithm are explained as follows-

- Apply 2D FFT transform to both input images and obtain fourier samples of both images as I1[n1,n2] and I2[n1,n2] where $-n/2 < n1,n2 < n/2$.

The obtained frequency samples of both images are periodized.

- For each scale j and angle a the periodization of widowed data is done which form the product for input image I1[n1,n2] as K1[n1,n2]= Uj,a[n1,n2] I1[n1,n2] (1)
  And input image I2[n1,n2] as K2[n1,n2]= Uj,a[n1,n2] I2[n1,n2] (2)
- The obtained windowed data, wrappedK1[n1,n2]and K2[n1,n2] around the origin to restrict the rectangular window length L1,j and L2,j near the origin. The product obtained is

$$I1j,a[n1,n2] = W(Uj,a\ I1)[n1,n2] \quad (3)$$
$$I2j,a[n1,n2] = W(Uj,a\ I2)[n1,n2] \quad (4)$$

Where the range for n1, n2 is $0<n1<L1,j$, $0<n2<L2, j$ (for $-\pi/4< \theta< \pi/4$).
Thus, the wrapping transformation is nothing but a simple re-indexing of the data.

- Apply the inverse 2D FFT to each I1j,a and I2j,a.
- The curvelet coefficients I1j,a and I2j,a of both the input images are obtained which contains high directionality.
- These coefficients are fused using maximum selection rule.
- For Maximum selection rule, fusion is done by taking the maximum valued pixels from I1[n1,n2] andI2[n1,n2] both sub images of input images.
  Imax = max (I1 [n1, n2], I2 [n1, n2]) (5) Fused coefficients are obtained.

7. The fused image is obtained by applying inverse fast discrete curvelet transform on fused coefficients.
8. The final fused image is reconstructed by applying inverse discrete wavelet transform to fused image.
9. The final fused image can be represented by following equation:

$$I[n1,n2]=W1(\Psi(W(I1[n1,n2])),W(I2[n1,n2))) \quad (6)$$

10. performance analysis is done by using 3 quality metrics parameters as Entropy, RMSE, PSNR.

D.GRAPHICAL USER INTERFACE:

A user interface (UI) is a graphical display in one or more windows containing controls, called *components*, that enable a user to perform interactive tasks. The user does not have to create a script or type commands at the command line to accomplish the tasks.

Designing the visual composition and temporal behavior of a GUI is an important part of software application programming in the area of human-computer interaction. Its goal is to enhance the efficiency and ease of use for the underlying logical design of a stored program, a design discipline known as usability. Methods of user-centered design are used to ensure that the visual language introduced in the design is well tailored to the tasks.

The visible graphical interface features of an application are sometimes referred to as "chrome" or "GUI" (Goo-ee). Typically, the user interacts with information by manipulating visual widgets that allow for interactions appropriate to the kind of data they hold.

IV.RESULT ANALYSIS

The output of this project is graphically shown in below figures. It contains pixel based fused image as output image.Here CT and MR images are input images. Then wavelet transform and DFCT are applied to inputs, the resultant corresponding images are shown. The resultant pixel based fused images are shown in graphical user interface window as well.

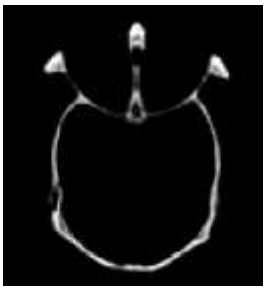

Fig 2: CT IMAGE

fig 3: DWT IMAGE OF CT

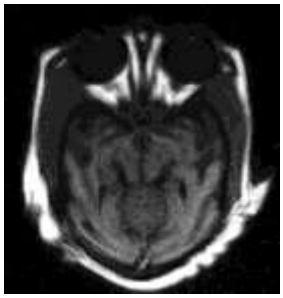

Fig 4:MR IMAGE

fig 5: DWT IMAGE OF MR

Fig 6:OUTPUT OF IDFCT

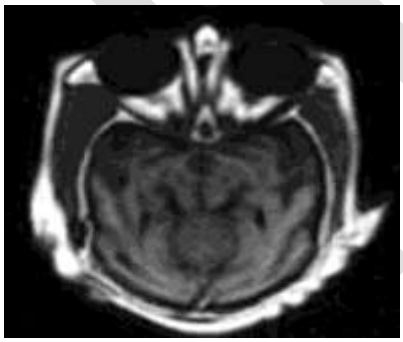

Fig 7:OUTPUT OF IDWT- PIXEL BASED FUSED IMAGE

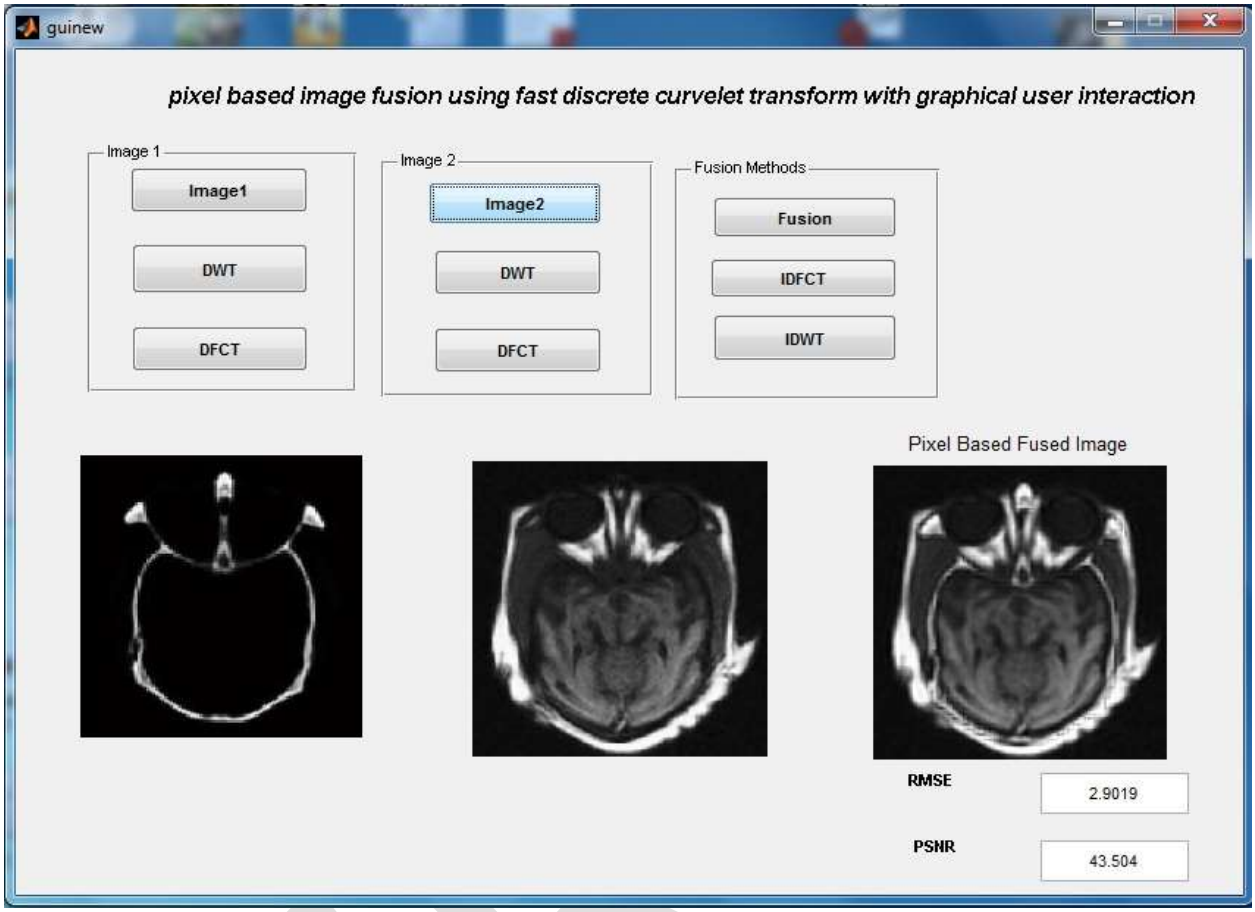

Fig 8: GUI window for pixel based fused image output

V.CONCLUSION

We envisage the design and deployment of more a real-time pixel based fused image which can analyze their own performance and feed back this information to adapt their behavior and to improve the quality of the fused images they produce. Graphical user interaction will help the detection of the object image easily and accurately and it gives the better FDCT images, IDFT and fused images. there is huge scope for research and development in the graphical user interaction with human. The results are implemented and tested successfully.

REFERENCES:

[1] Image Fusion Based on Wavelet Transforms Laxman Tawade1, Abida Bapu Aboobacker2 and Firdos Ghante1 International Journal of Bio-Science and Bio-Technology Vol.6, No.3 (2014), pp.149-162

[2] multilevel image fusion algorithm with comparative analysis of wavelet and curvelet transform by Anup Yadav1, Mrs. Usha M V2 (International Journal For Technological Research In Engineering Volume 1, Issue 10, June-2014

[3] K . Kannan & S. Arumuga Perumal "Optimal Decomposition Level of DiscreteWavelet Transform for Pixel based Fusion of Multi-focused Images" in International Conference on Computational Intelligence and Multimedia Applications 2007, pp. 315- 316

[4] A Survey on Image fusion Techniques used to Improve Image Quality by Sunil Kumar Panjeta1 and Deepak Sharma2 International Journal of Applied Engineering Research, ISSN 0973-4562 Vol.7 No.11 (2012)

[5] Smt. G. Mamatha, L. Gayatri,'an image fusion using wavelet and curvelet transforms', in Global Journal of Advanced EngineeringTechnologies,Vol1,Issue-2,2012,ISSN:2277-6370.

[6] Anjali A. Pure, Neelesh Gupta, Meha Shrivastava, 'An Overview of Different Image Fusion Methods for Medical Applications', Any additional comments: Paper Published in IJSER Volume 4, Issue7, July 2013 Edition (ISSN 2229-5518).

[7] S.Vasuki, S. Gandhimathi, S. Manika VInodhini,' Comparative Analysis of Wavelets for Fusion Application', IJCA, 2012.

[8] Emmanuel Cand`es, Laurent Demanet, David Donoho and Lexing Ying; Fast Discrete Curvelet Transforms, Applied and Computational Mathematics, Caltech Pasadena 2006.
[9] Jianwei Ma and Gerlind Plonka, The Curvelet Transform, IEEE SIGNAL PROCESSING MAGAZINE[118] MARCH 2010
[10] Gang Hong, Yun Zhang, 'The effect of different types of wavelets on image fusion.
[11] E. J. Candes, D.L.Donoho Curvelets: A Surprisingly Effective Nonadaptive Representation forObjects with Edges.
[12] M. Sifuzzaman M.R. Islam, M. Z. Ali, Application Of Wavelet and its Advantages Compared to Fourier Transform, Journal of Physical Science,Vol.13,2009,121-134,ISSN:0972-8791.
[13] Y. Kiran Kumar, Comparison of Fusion Techniques Applied to preclinical images: Fast Discrete Curvelet Transform using Wrapping Technique & Wavelet Transform, JATIT2009
[14] Pao-Yen Lin, An introduction wavelet transforms.
[15] Rafael C. Gonzalez and Richard E. Woods, Digital image Processing, Third Edition.

International Journal of Engineering Research and General Science Volume 3, Issue 5, September-October, 2015
ISSN 2091-2730

An Approach for Detection of the Components in Brain MRI Using Vector Quantization and Morphological Operations based Segmentation

Sneha Anna John, Cinly Thomas

P.G Scholar, Dept of CSE, BMCE, Kollam, Kerala, India

vachisneha1991@gmail.com,9567969780

Abstract— Image segmentation is a technique in image processing where an image is divided into meaningful structures to simplify its representation. Vector quantization helps to map the continuous pixel of input space to discrete pixels in the output image. Here the advantage is to minimize the information loss. The approach in this paper focuses on the spatial as well as the gray level value of the image to effectively derive beneficiary result. The detection of the important components in brain MRI image has become a challenging task in terms of the performance of different existing algorithms. Here the proposed method involves preprocessing of the brain image with tumor, vector quantization, adaptive binarization, application of morphological operations. The calculation of the tumor area is done using the proposed algorithm and manually using active contour method where the accuracy of the proposed method is calculated. In this paper the method extracts the main components of the brain with tumor which includes the skull, the tumor, the gray matter and the white matter. The method could easily extract the tumor of any size from a brain image with tumor having more accuracy than any other existing methods.

Keywords— Image segmentation, Vector Quantization, Adaptive binarization, Morphological operations, MRI images, Contour method, preprocessing.

1. INTRODUCTION

Image segmentation being a part of image processing can be viewed as the technique where the image can be clustered based on the intensity value of pixels [1], similarity of data points [2] etc. The segments obtained after segmentation are meaningful pieces which have similarity in features and properties. Image segmentation plays a crucial role in numerous biomedical imaging applications, clinical operations etc. for diagnosing various diseases using scientific data. High computational complexity is required in this stream where substantial amount of time is needed which limits the capability. Researches that has focused on parallel processing models supports biomedical image segmentation. The special case of biomedical image segmentation is object categorization where spectral clustering is focused on.

In the case of enormous amount of data, space is becoming more enough of consideration. So, inorder to store the information about images it requires image compression technique incorporated with the image segmentation. Vector Quantization (VQ) is a technique of image compression used in accordance with image segmentation where continuous input space is projected on a discrete output space while the information loss will be minimized [3]. Vector quantization has been formed as an efficient encoding technique because it's an infeasible ability for exploiting relationship between the pixels [4]. VQ have mainly four stages namely training set selection, vector formation, codebook generation and quantization [5].

Medical imaging can be viewed as the technical approach for studying the interior especially the tissue wise analysis of the important parts of human body. Other human body structures are made known to experts using medical imaging technology. Medical imaging modal quality as in MRI, CT scan etc. mostly depend on the computer digital image which helps the experts to analyze inner portion of the body parts [6][7].

All parts of the body especially the important parts such as the heart, lungs, kidney etc. are controlled by the brain cells. Hence brain is a vital organ of human body [8] [9]. Brain is the most anterior part of the central nervous system where tumor is an intracranial solid neoplasm. Tumor is actually caused due to abnormal and uncontrollable cell division in brain. Abnormalities causing to the brain which are deadly and intractable diseases named as brain tumor. MRI scan can be used to obtain the images of the brain.

2. RELATED WORKS

Many methods have been proposed for human brain MRI image segmentation. The brain tumors along with various parts of the brain are extracted by considering tumor pixel's centroid from other components of the brain. In [10], two unsupervised methods are proposed for MRI segmentation based on SOM neural network referred as HFS_SOM (Histogram Fast Segmentation Self Organizing Map) and EGS_SOM (Entropy-Gradient Segmentation Self Organizing Map). The HFS_SOM extracts the information from volume image histogram where as in EGS_SOM first and second order statistics are extracted as the feature data. In [11], GHSOM (Growing Hierarchical Self Organizing Map) and multi objective-based feature selection methods where several SOM layers of variable sizes are used to choose the training data. In [12], Wells, Grimson et.al proposed an Expectation Maximization (EM) algorithm to estimate the bias field for correcting the MRI image with intensity inhomogeneity. The Fig 1: represents the brain with tumor and brain without tumor.

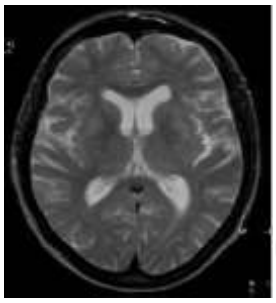
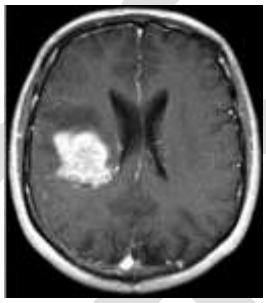

Brain with tumor Brain without tumor

Fig 1: Brain with tumor and without tumor

In [6], a segmentation algorithm is used for brain MRI images using K-means clustering algorithm followed by morphological filtering which avoids the non-clustered regions that can be formed after segmentation of the brain MRI image for detection of tumor location. In [7], the brain image is processed, filtered, skull stripped and segmented. These steps are followed by morphological operation of erosion algorithm to detect the tumor. Then the tumor area is calculated and tumor location is exactly identified.

3. PROPOSED WORK

Several techniques are done in a sequential manner for detecting the tumor. In biopsy process, pathologist takes a specimen of brain cells or brain tumor of the affected human to find the presence of abnormalities from normal human brain. If abnormality is found, it will be referred to an expert doctor. When doctors go for surgery they must know the exact location of tumor.

The paper presents the method based on the location arrangement of each brain component tissue from center of the exact MRI brain image i.e. the spatial arrangement of the brain tissues. Important parts of the brain such as the skull, the grey matter and white matter along with the tumor possess different properties. The Fig 2: represents the flowchart for the proposed algorithm.

The brain MRI images that are undergone a deep biopsy analysis will be given to this computer aided adaptive system for further segmentation. For biopsy a sample tissue of brain that seems to be abnormal will be suggested for test. This is conducted to confirm whether the abnormality is a lesion or a tumor or a mass. The input image will be preprocessed where the halftone image will be converted into grayscale image. After converting to grayscale image the darkest portion will appear in black shade due to total absence of transmitted or reflected light. The lightest portion will appear in white shade due to presence of transmitted or reflected light at all visible wavelengths. The gray scaled image is then vector quantized. In this step a training sequence is chosen as per the [x,y] coordinates of the image pixels. Generate the initial codebook of required size. Compute the transpose of the matrices generated in codebook. Take the mean of the transpose matrix. Compute the transpose of mean matrix. Then codevectors are generated for codebook which is utilized for final step of quantization.

Next step is to binarization of the image. An adaptive binarization technique is used where the vector quantized image is converted to binary image. This step facilitates to compensate the degradation of image causing due to uneven illumination, image contrast variation, smear etc. Then calculate the center of the image to find nearest component that can be recognized as tumor component and demark it. A set of morphological operations are applied on various brain parts based on shape. In morphological operation the value of pixels in the input and output images are compared to get the exact shapes of required parts. Similarly extract

the tumor component, gray matter and white matter and demark it. Then calculate the tumor area according to the proposed system and using manual segmentation. Then compare the obtained values to determine the accuracy.

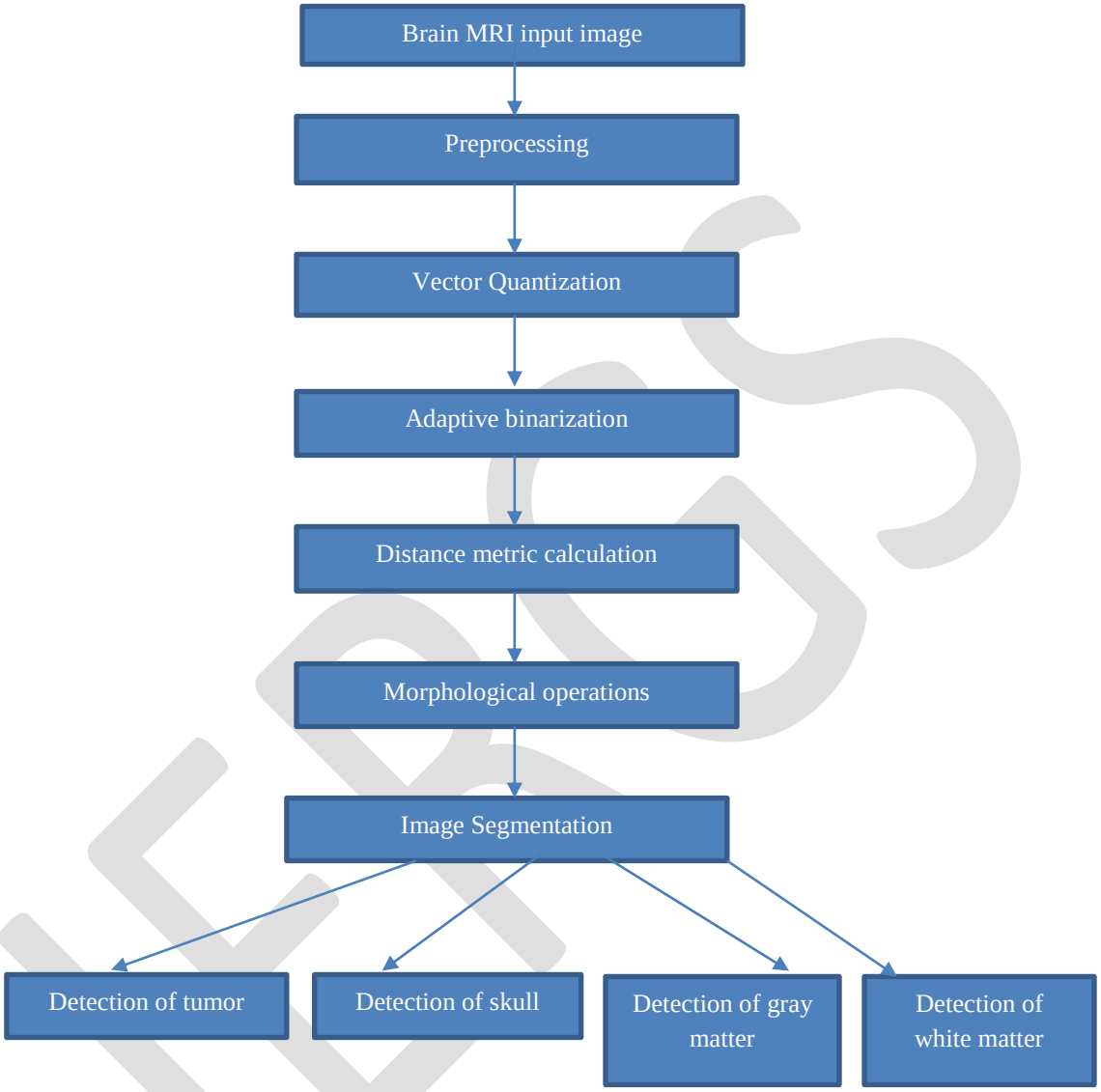

Fig 2: The proposed solution

4. EXPERIMENTAL RESULTS

In this section human brain MRI images obtained from the database are used to demonstrate the effectiveness of the proposed segmentation method. The MRI image can be segmented into tumor component, skull component, gray matter and white matter. The segmented components can be demarked using various morphological operations. It is observable from the experimental result that the proposed work outperforms the existing manual segmentation results.

The Table 1: represents the output of the proposed work. Here the first row represents brain with tumor, second row represents tumor component of the brain image, third row represents skull components of the brain image, fourth row represents the gray matter of the brain image and the last row represents the white matter of the brain image.

Table 1: Experimental results

Brain Images		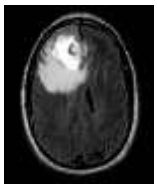		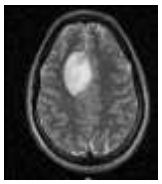	
Tumor			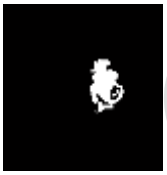	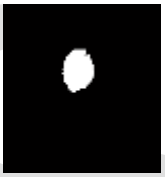	
Skull		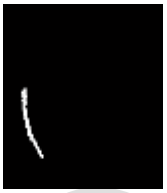			
Gray matter					
White matter					

5. SUMMARY AND FURTHER DISCUSSIONS

The segmentation of the brain MRI image into different components is given as the steps for identifying different components in brain. It will be beneficiary in planning for the surgical and treatment of brain tumor. The proposed system helps in the identification of tumor from other important brain components. It's a computer-aided system for segmentation of brain components that helps to differentiate the tumor part from other brain tissues. The experimental results evaluated according proposed algorithm and manual segmentation method proves that proposed algorithm provides more accurate result than manual segmentation.

REFERENCES:

[1] Gonzalez RC, Woods R E, "Digital image processing", Reading (MA)7 Addison-Wesley; 1992.

[2] Sourav Paul , Mousumi Gupta, "Image Segmentation By Self Organizing Map With Mahalanobis Distance", International Journal of Emerging Technology and Advanced Engineering, Vol 3, Issue 2, February 2013,pg. 288

[3] K. Makhoul, S. Roucos, H. Gish, "Vector quantization is speech coding", Proceedings IEEE, vol. 73, n.11, November 2005.

[4] Nasser. N. Nasrabadi, and Yushu Feng, "A multilayer addresses Vector Quantization technique Transactions on Circuits and Systems", Vol.37, No.7, July 1990.

[5] Mukesh Mittal, Ruchika Lamba, "Image Compression Using Vector Quantization Algorithms: A Review", Vol 3, Issue 6, June 2013 ISSN: 2277 128X IJAR in Computer Science and Software Engineering.

[6] Rohini Paul Joseph, C. Senthil Singh, M.Manikandan, "Brain Tumor MRI Image Segmentation And Detection In Image Processing", IJRET eISSN: 2319-1163 | pISSN: 2321-7308.

[7] Pratibha Sharma, Manoj Diwakar, Sangam Choudhary, "Application of Edge Detection for Brain Tumor Detection", International Journal of Computer Applications, Vol.58, No.16, pg 21-25, 2012.

[8] Swe Zin Oo, Aung Soe Khaing, "Brain Tumor Detection and Segmentation Using Watershed Segmentation and Morphological Operation" , IJRET, eISSN: 2319-1163 | pISSN: 2321-7308.

[9] Pratik P. Singhai, Siddharth A. Ladhake, "Brain Tumor Detection using Marker Based Watershed Segmentation from Digital MR Images", IJITEE, ISSN: 2278-3075, Volume-2, Issue-5, April 2013.

[10] A.Ortiz, J.M.Gorriz, J.Ramirez, D.Salas-Gonzalez, J.M.Llamas-Elvira, "Two fully- unsupervised methods for MR brain image segmentation using SOM- based strategies", Appl.SoftComput.13 (2013)2668–2682.

[11] A.Ortiz, J.M.Gorriz, J.Ramirez, D.Salas-Gonzalez, "Improving MRI segmentation with probabilistic GHSOM and multiobjective optimization, Neurocomputing" 114(2013)118–131.

[12] W.M.Wells, W.E.L.Grimson, R.Kikinis, F.A.Jolesz, "Adaptive segmentation of MRI data", IEEE Trans. Med. Imaging 15(1996)429–442.

[13] Rajesh C. Patil, Dr. A. S. Bhalchandra, "Brain Tumor Extraction from MRI Images Using MATLAB", International Journal of Electronics, Communication & Soft Computing Science and Engineering, ISSN: 2277-9477, Volume 2, Issue 1

[14] Z. Lin, J. Jin and H. Talbot, "Unseeded region growing for 3D image segmentation," ACM International Conference Proceeding Series, Vol. 9, pp. 31-37, 2000.

International Journal of Engineering Research and General Science Volume 3, Issue 5, September-October, 2015
ISSN 2091-2730

Analysis of Plain Circular Journal Bearing lubricated with Micropolar Fluid

Pallavi Jagdale,

[#]Mechanical Engineering Department, DYPIET, Pimpri
[1]pallavi.jadhav293@gmail.com
+91 8308833952

Dr. L.G.Navale
Mechanical Engineering Department, DYPIET, Pimpri
[2]lgnavale2006@yahoo.co.in

Abstract— The research area of hydrodynamic lubrication is widely diversified. The literature includes the analysis and various optimized technique of determination of static and dynamic characteristics of plain circular bearing. However these studies were unable to describe the simultaneous effect of both micropolar fluid parameters and eccentricity ratio on bearing characteristics. In the present study combined effect of micropolar parameters and eccentricity ratios are considered with wide range of variation on the bearing performance characteristics. For linear studies critical mass of journal is determined by Routh-Hurwitz stability criteria. Comparative analysis on critical values of journal mass required for both linear and nonlinear studies is carried out. Also the stability of these bearing are analyzed at various operating conditions.

Keywords— Journal Bearing, Hydrodynamic Lubrication, static characteristics, Dynamic characteristics, eccentricity, eccentricity ratio, comparative analysis.

INTRODUCTION

As per the history a theory of hydrodynamics in lubrication was introduced by Reynolds in 1886. Many numbers of researcher performed analytical and practical studies over hydrodynamic lubrication and put very important concepts and theories. Analysis of literature showed that the research area of hydrodynamic lubrication is widely diversified. The literature includes the analysis and various optimized technique of determination of static and dynamic characteristics of plain circular bearing.

The bearings have been in use for centuries but the recent developments in science and technology demands critical designs of bearings with high precision and optimized performance for the most adverse working conditions. The rapid developments in the fields of rocketry and missile technology, cryogenics, aeronautics and space engineering, nuclear engineering, electronics, computer sciences and technologies, bio-medical engineering and a lot more fields in science and technology make the aspects of designing bearings more and more challenging and innovative. Moreover, the mode, time and place of operations demand exploration of new materials, lubricants and even lubrication theories and technologies.

I. MATHEMATICAL ANALYSIS

BASIC ASSUMPTIONS

The basic assumptions in micropolar lubrication to a journal bearing include the usual lubrication assumptions in deriving Reynold's equation and the assumptions to generalize the micropolar effects.

(i) The Flow is Incompressible and steady, i.e. ρ= constant and $\partial p/\partial t = 0$.

(ii) The flow is laminar i.e. free of vortices and turbulence.

(iii) Body forces and body couples are negligible, i.e. FB=0 and CB=0.

(iv) The variation of pressure across the film $\partial p/\partial y$ is negligibly small.

(v) The film is very thin in comparison to the length and the span of the bearing. Thus, the curvature effect of the fluid film may be ignored and the rotational velocities may be replaced by the translator velocities.

(vi) No slip occurs at the bearing surfaces.

(vii) Bearing surface are smooth, non-porous and rigid i.e. no effects of surface roughness or porosity and the surface can withstand infinite pressure and stress theoretically without having any deformation.

(viii) No fluid flow exists across the fluid film i.e. the lubrication characteristics are independent of y-direction.

(ix) The micropolar properties are also independent of y-direction. The velocity vector, the microrotational velocity vector and the fluid film pressure are given as:

V= [Vx (x,y,z), Vy (x,y,z),Vz (x,y,z)]

υ= [$\upsilon 1$ (x,y,z) ,$\upsilon 2$ (x,y,z),$\upsilon 3$ (x,y,z)]

p=p (x,y,z)

Principle of Conservation of Mass

$\partial\rho/\partial t+\nabla$ (ρV) =0 (1)

Principle of Conservation of Linear Momentum

$(\lambda+2\mu)\nabla(\nabla.V)-[(2\mu+\mathcal{X})/2]\nabla*(\nabla*V)+\mathcal{X}\nabla*\upsilon-\nabla.\pi+FB=\rho*DV/Dt$ (2)

Principle of Conservation of Angular Momentum $(\alpha+\beta+\gamma)\nabla(\nabla.\upsilon)-\gamma\nabla*(\nabla*\upsilon)+\mathcal{X}\nabla*V-2\mathcal{X}\upsilon+CB=\rho jD\upsilon/Dt$ (3)

Where, ρ is the mass density, V is the velocity vector, υ is the micro-rotational velocity vector. π is the thermodynamic pressure and is to be replaced by the hydrodynamic film pressure, p, since, $\pi=-[\partial E/\partial\rho^{-1}]=p$. Where E is the internal energy and p is to be determined by the boundary conditions. λ and μ are the familiar viscosity coefficients of the classical fluid mechanics, while α,β and γ are the new viscosity coefficients derived as the combinational effects of the gyroviscosities for the micropolar fluid as defined by ERINGEN. $\mathcal{X}$ is also a new viscosity coefficient for micropolar fluid, termed as spin viscosity, which establishes the link between velocity vector and the microrotational velocity vector. *FB* is the body force per unit mass, *CB* is the body couple per unit mass and j is the microinertia constant. D/Dt represents the material derivative. The constitutive equations of micropolar are

$tk1=(-\pi+\lambda Vr,)1+(\mu-1/2*\mathcal{X})(Vk,1+V1,k)+\mathcal{X}(V1,k+\eta k1r*\upsilon r)$ (4)

$mk1=\alpha\upsilon r,1+\beta\upsilon k,1+\gamma\upsilon 1,k$ (5)

Where, $tk1$ and $mk1$ are the stress tensor and the couple stress tensor respectively. $\eta k1r$ is an permutation tensor. $\delta k1$ is Kronekar delta. The index following a prime represents the partial derivative to spatial variable $\mathcal{X}k$.

Note that for α=β= γ=$\mathcal{X}$=0 and for negligible body couple per unit mass equation (3) yields υ=0 and so, equation (2) reduces to the classical Navier-Stokes equation. For $\mathcal{X}$=0 the velocity vector and the microrotational velocity vector are uncoupled and the global motion of the fluid becomes free of the microrotation and their effects.

The theoretical prediction of hydrodynamic pressures in the bearing is obtained by the solution of modified Reynolds equation satisfying the appropriate boundary conditions. The steady state and dynamic pressure profile is obtained by finite difference technique.

II. SOLUTION PROCEDURE

Journal bearing systems are analyzed by linear and nonlinear study with the help of MATLAB software incorporation of PDE toolbox. The analysis is carried out by linear and nonlinear study of journal bearing system. These studies are carried out for circular bearing geometries.

Operating conditions of journal bearing system can be varied by combination of characteristic length of the micropolar lubricant ($\overline{l_m}$), Coupling number (N), and eccentricity ratio. Hence with the help of these programs one can obtain results over wide range. Hence it becomes necessary to execute a program at each operating condition separately.

Solution procedure for linear analysis of a plain circular journal bearing with micropolar fluid

1. Acquire input parameters such as attitude angle (ϕ) = 60o, the initial guess for fluid film extent are specified by considering circular coordinate axis X originating from line of centers and Y axis along bearing width. Hence For present finite width bearing Xmax=180o, Xmin=0o, Ymax= 2 (since $\beta = 2$) and Ymin= 0. Characteristic length of the micropolar lubricant. ($\overline{l_m}$), Coupling number (N) and eccentricity ratio ($\bar{\varepsilon}$) specifies the various operating conditions and it acts as variable.
2. Journal centres are located as ($\overline{X_j}$, $\overline{Y_j}$) using Cartesian co-ordinate system originated at geometric centre of bearing.
3. In order to get the solution of PDE finite difference method is employed in practice hence fluid film domain is discretized into optimum mesh size.
4. Fluid film thickness is determined at centroid of each elemental area by using thickness equation.
5. Modified Reynolds equation is solved by using PDE toolbox.
6. The pressure distribution over fluid film thickness is calculated.
7. On the basis of pressure distribution pressure gradient $\left(\frac{dp}{dx}\right)$ is determined along X axis between a mid-node on trailing edge and nearest node. If the pressure gradient $\left(\frac{dp}{dx}\right)$ becomes 'negative' i.e., termination of positive fluid pressure zone and negative pressure start buildings onwards.
8. Bearing load components along horizontal and vertical directions are calculated.
9. In the present case bearing is subjected pure radial this condition is satisfied when bearing load ratio (fx/fy) tends to zero. Here bearing load ratio less than 0.001 is considered as bearing subjected to pure radial load. This load ratio can be reduced to desired value by adjusting the attitude angle in iterations. In each iteration attitude angle is modified by 10^o.
10. Once the attitude angle and trailing edge determined the equilibrium position of journal is located.
11. Bearing load calculated in step (8) are considered as static equilibrium forces.
12. For new displaced position of journal again instantaneous bearing load components are calculated followed by steps (4) to (6).
13. On the basis of Routh- Hurwitz stability criteria critical mass is calculated using equation.

Other dynamic characteristics such as whirl frequency and threshold speed ratios are calculated

IV ANALYSIS RESULTS

1 STATIC CHARACTERISTIC

1.1. LOAD CARRYING CAPACITY

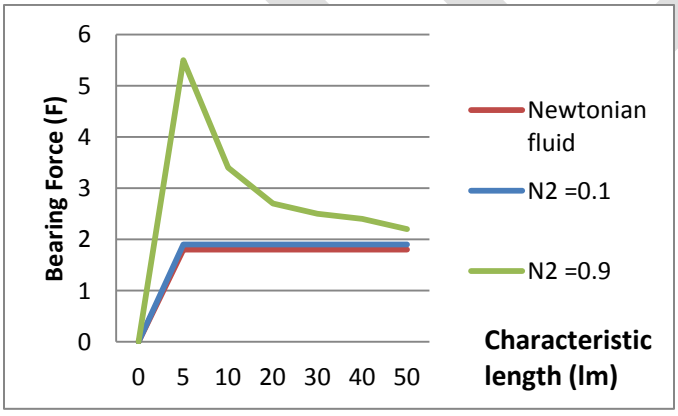

Fig.1 Variation of Bearing force as a function of non-dimensional Characteristic length (lm) at ϵ=0.3

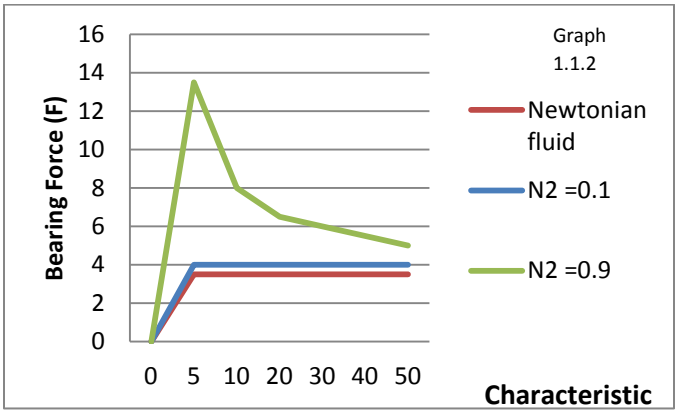

Fig.2 Variation of Bearing force as a function of non-dimensional Characteristic length (lm) at ϵ=0.5

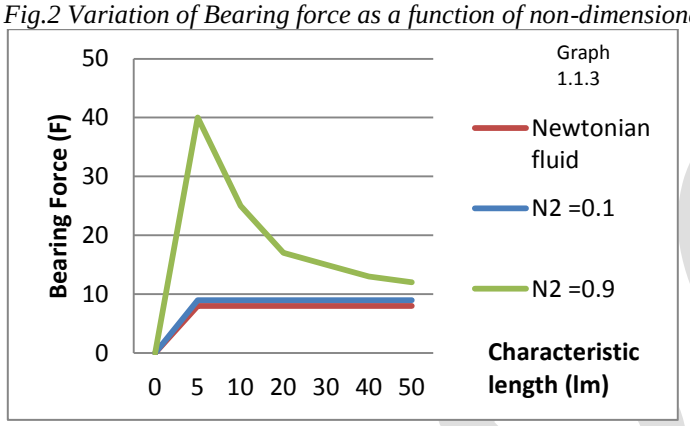

Fig.3 Variation of Bearing force as a function of non-dimensional Characteristic length (lm) at ϵ=0.7

The load carrying capacity reduces as coupling number reduces and approaches to Newtonian fluid for $N2 \rightarrow 0$. It shows that for high coupling number and low characteristic length a plain circular journal bearing lubricated with micropolar fluid provides maximum load carrying capacity as compared to the Newtonian fluid.

It can be seen that for a particular value of *lm* and *N2*, the load carrying capacity increases for micropolar fluid as well as for Newtonian fluid with increase in eccentricity ratio. It is also been observed that the load carrying capacity is higher i.e. 4-5 times as the eccentricity ratio changes from 0.3 to 0.7 for a distinct value of *lm* and *N2***.** The figures depict that the load capacity at any eccentricity ratio is much higher at lower value of *lm* and approaches to Newtonian fluid as $lm \rightarrow \infty$.or $N2 \rightarrow 0$

1.2 ATTITUDE ANGLE (Φ)

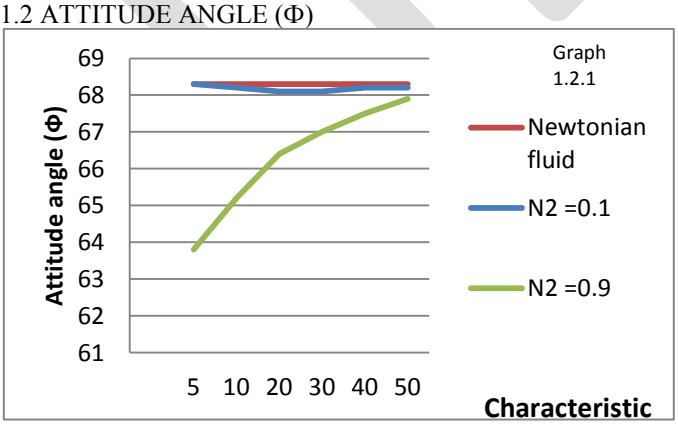

Fig.4 Variation of Attitude angle (ϕ) as a function of non-dimensional Characteristic length (lm) at ϵ=0.3

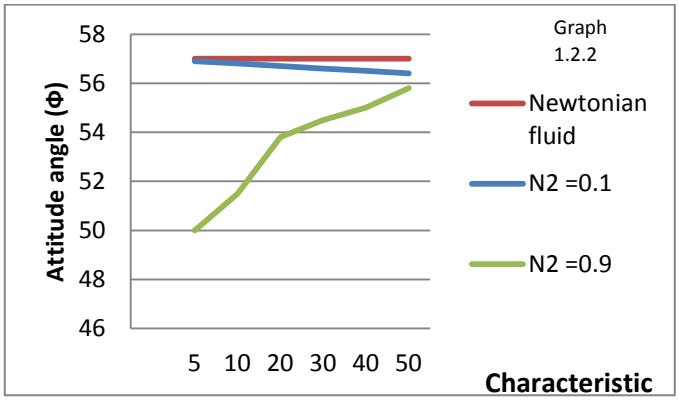

Fig.5 Variation of Attitude angle (ϕ) as a function of non-dimensional Characteristic length (lm) at ϵ=0.5

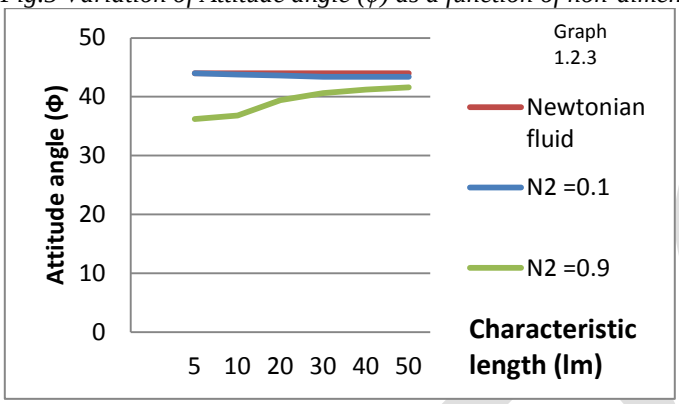

Fig.6 Variation of Attitude angle (ϕ) as a function of non-dimensional Characteristic length (lm) at ϵ=0.7

The attitude angle reduces as coupling number increases and approaches to Newtonian fluid for $N2 \rightarrow 0$. It shows that for high coupling number and low characteristic length a plain circular journal bearing lubricated with micropolar fluid provide low attitude angle as compared to the Newtonian fluid.

It can be seen that for a particular value of lm and N2, the attitude angle decreases for micropolar fluid as well as for Newtonian fluid with increase in eccentricity

2. DYNAMIC CHARACTERISTICS

2.1 CRITICAL MASS PARAMETER (*Mc*)

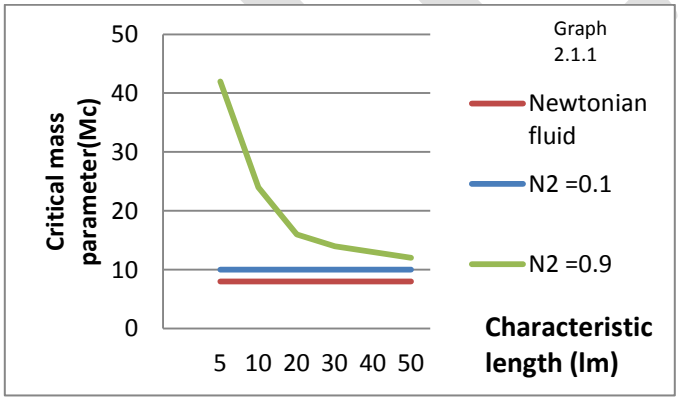

Fig. 7 Variation of Critical Mass (Mc) as a function of non-dimensional Characteristic length (lm) at ϵ=0.3

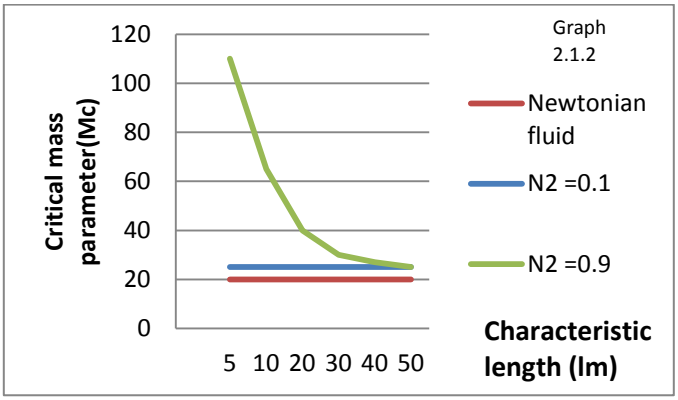

Fig. 8 Variation of Critical Mass (Mc) as a function of non-dimensional Characteristic length (lm) at ϵ=0.5

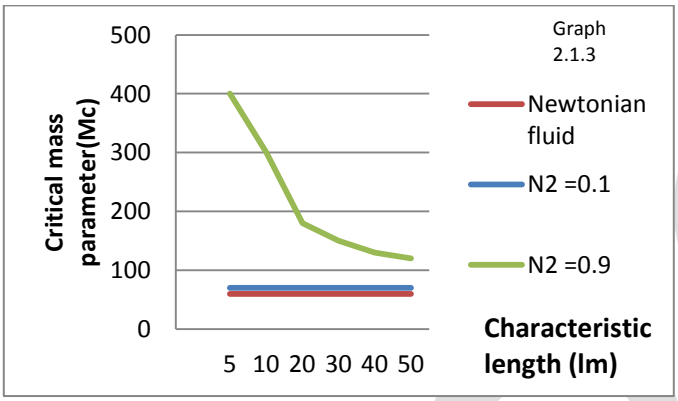

Fig. 9 Variation of Critical Mass (Mc) as a function of non-dimensional Characteristic length (lm) at ϵ=0.7

The critical mass parameter increases as *N* is increased. It also has been found that when $N2 \rightarrow 0$ for any value of *lm*, micropolar fluid approaches to Newtonian fluid. It can be observed from figure that critical mass decreases as increasing *lm* and approaches to Newtonian fluid as *lm* grows indefinitely

2.2 WHIRL FREQUENCY RATIO

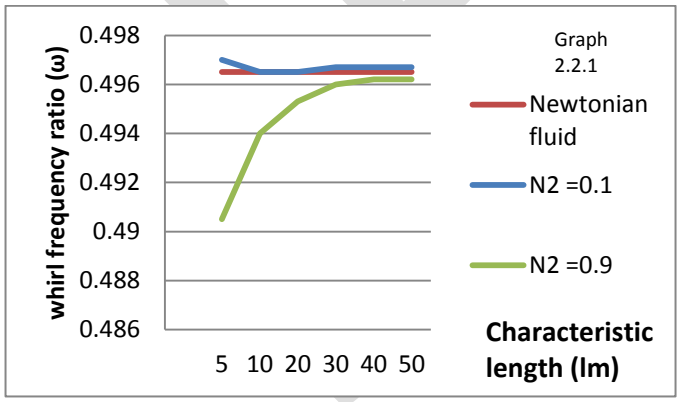

Fig.10 Variation of Whirl frequency ratio (ω) as a function of non-dimensional Characteristic length (lm) at ϵ=0.3

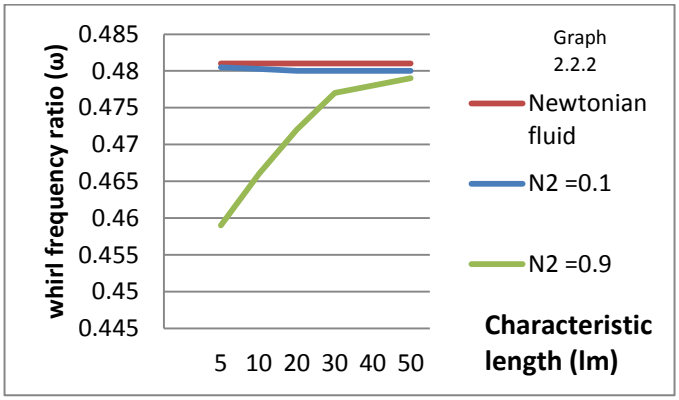

Fig. 11 Variation of Whirl frequency ratio (ω) as a function of non-dimensional Characteristic length (lm) at ϵ=0.5

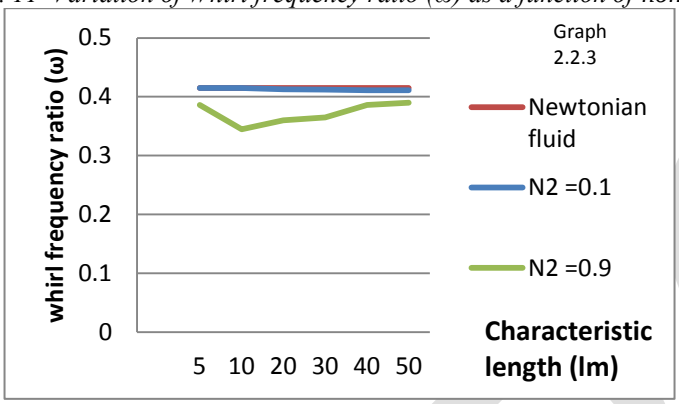

Fig. 12 Variation of Whirl frequency ratio (ω) as a function of non-dimensional Characteristic length (lm) at ϵ=0.7

It observed that for a particular value of coupling number, whirl frequency ratio firstly decreases than increases with increase in *lm*. It clearly shows that there is a decrement in the whirl frequency ratio at small values of *lm*.

It can be seen that for a particular value of *lm* and *N2*, whirl frequency ratio decreases for micropolar fluid as well as for Newtonian fluid with increase in eccentricity ratio.

2.3 THREESHOLD SPEED

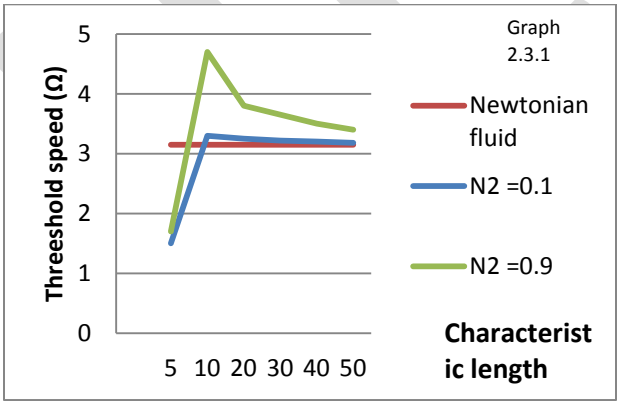

Fig. 13 Variation of Threshold Speed (Ω) as a function of non-dimensional Characteristic length (lm) at ϵ=0.3

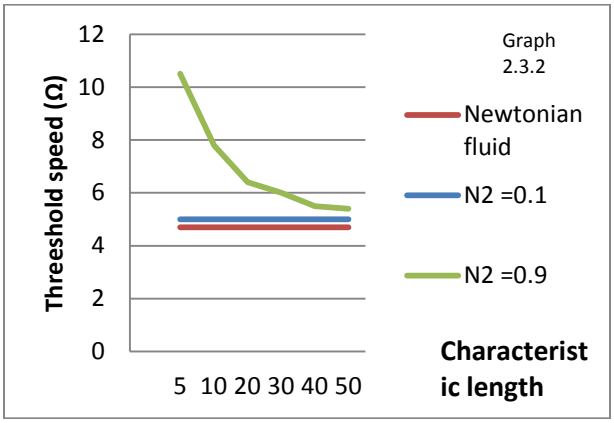

Fig. 14 Variation of Threshold Speed (Ω) as a function of non-dimensional Characteristic length (lm) at ϵ=0.5

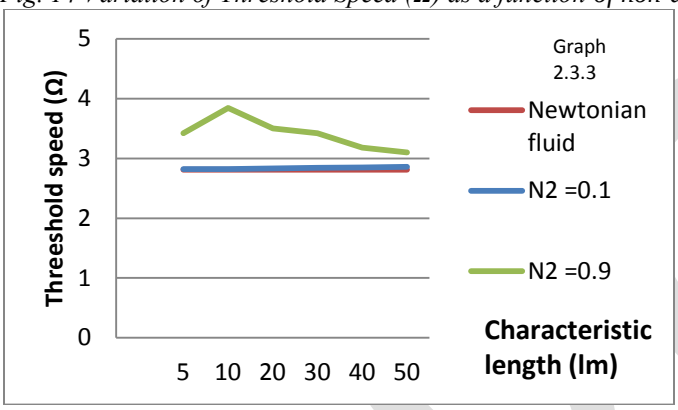

Fig. 15 Variation of Threshold Speed (Ω) as a function of non-dimensional Characteristic length (lm) at ϵ=0.7

we can see that as the coupling number decreases threshold speed decreases. It observed that for a particular value of coupling number, threshold speed increases with increase in *lm*. It clearly shows that there is an augmentation in the threshold speed at small values of lm. Curves illustrate that when lm increases or N2 decreases, the value of threshold speed approaches to that of the Newtonian value.

2.3 STIFFNESS COEFFICIENT

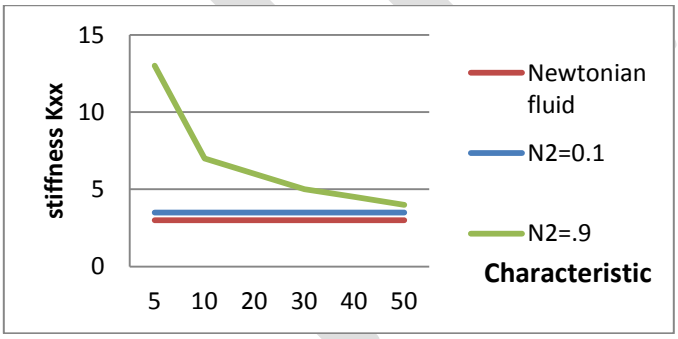

Fig.16 Variation of Stiffness (Kxx) as a function of non-dimensional Characteristic length (lm) at ϵ =0.3

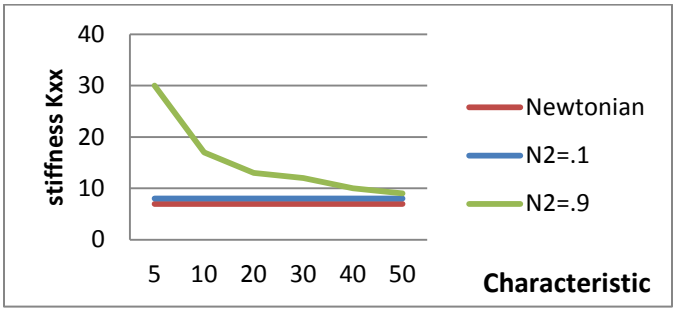

Fig.17 Variation of Stiffness (Kxx) as a function of non-dimensional Characteristic length (lm) at ϵ =0.5

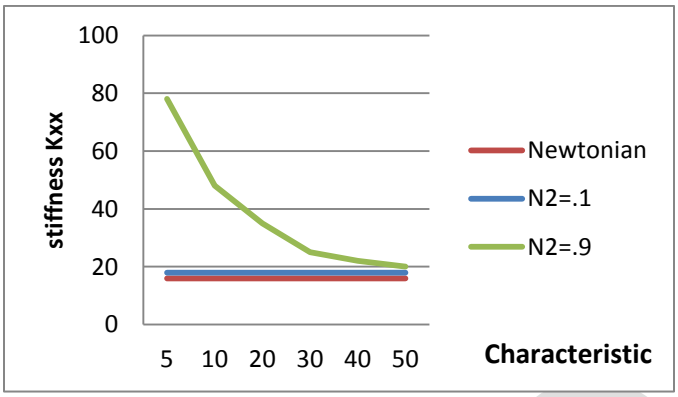

Fig.18 Variation of Stiffness (Kxx) as a function of non-dimensional Characteristic length (lm) at ϵ =0.7

Figs. shows the variation of the non- dimensional components of stiffness coefficients as function of lm for any coupling number, keeping eccentricity ratio and L/R constant at 0.3 and 2 respectively. It can be observed from the figures that at any value of lm, the direct stiffness coefficient Kxx increases with increase in coupling number. For any value of coupling number, Kxx decreases with lm and approaches to Newtonian fluid as lm becomes infinitely large.

ACKNOWLEDGMENT

I am very thankful to my guide Dr. L.G.Navale, and also Head of Department Dr. Dhande, for their valuable guidance throughout my project work.

CONCLUSION

Important conclusion can be made about the use of micropolar fluid in plain circular and elliptical bearing are as follows:

1. It has been observe that load carrying capacity of both the journal bearing with micropolar lubricant at a particular eccentricity ratio increases when compared with that of bearing with Newtonian fluid.

2. The micropolar fluid approaches to Newtonian fluid as characteristic length of the micropolar fluid grows indefinitely or coupling number tends to zero.

3. The critical mass and threshold speed for bearings under micropolar fluid is increases for high coupling number and decreases when characteristic length decreases. Hence, stability of a bearing increases at high coupling number and low characteristic length.

4. The analysis predicts a lower value of critical mass for Newtonian than micropolar fluid.

REFERENCES:

[1] Matthew Cha, Evgeny Kuzetsov, Sergei Glavatshih, “A comparative linear and nonlinear dynamic analysis of compliant cylindrical journal bearings”, Machanism and Machine theory, Feb 2013.

[2] Qiu Zu-gan, Lu Zhang-ji, "Lubrication Theory for Micropolar fluids and its application to a Journal bearing with finite length" Applied Mathematics and Mechanics, vol 8,no.7, July 1987.

[3] D.Sfyris, A Chasalevris, "An exact analytical solution of the Reynolds equation for the finite journal bearing lubrication", Tribology International, May 2012.

[4] Tarun Kumar Bera, "Analysis of Steady-State Characteristics of Rough Hydrodynamic Journal Bearing Lubricated with Micro-Polar Fluids", Birbhum Institute of engineering & Technology, Suri, Birbhum, India.

[5] Steve Pickering, "Tribology of Journal Bearing Subjected to Boundary and Mixed Lubrication", Mechanics of Contact and Lubrication, Northeastern University, 2011

[6] R. Sinhasan, K.C. Goyal, "Transient response of a circular journal bearing lubricated with non-newtonian lubricants, Wear, 156, 1992

[7] Eringen, "Theory of Micropolar Fluids", School of Aeronautics, Astronautics and Engineering Sciences Purdue University Lafayette, Indiana, July 1965.

[8] B.Chetti, "Micropolar Fluids Effects on the Dynamic Characteristics of Four-lobe Journal Bearing", World Academy of Science, Engineering and Technology, Vol;5 2011.

[9] N.P.Mehta, S.S. Rattan, Rajiv Verma, "Stability Analysis of Two Lobe Hydrodynamic Journal Bearing with Couple stress Lubricant", ARPN Journal of Engineering and Applied Science, Jan 2010.

[10] Malcolm E. Leader, "Understanding Journal Bearings", Applied Machinary Dynamics Co.

[11] Jaw-Ren Lin, " Linear stability analysis of rotor-bearing system: couple stress fluid model", Computers and structures, Aug 2000

International Journal of Engineering Research and General Science Volume 3, Issue 5, September-October, 2015
ISSN 2091-2730

Security Profiles for Smart Phones

Pritam R. Tarle, Dr. A. P. Khedkar

Savitribai Phule Pune University, India

prits.tarle@gmail.com, anagha_p2@yahoo.com

Abstract: Increased smart phone usage has raised issues of their security and privacy. This work proposed a system based on mode-of-uses separation in smart phones to provide security profiles for it. This is a software application developed android smart phone that allows user to define and implement security profiles. It provides applications separation and data separation. Profiles are not hardcoded or predefined rather user can define security profiles. Switching between profiles is automatic based on context detection. Rules based security is provided to restrict access to device resource like Bluetooth, Wi-Fi, mobile data, NFC etc. So, other users are restricted from using smartphone resources. Experiments are conducted to observe energy overhead for designed application and to calculate time required for switching of security profiles. Result shows that security profile application does not cause any noticeable overhead.

Keyword*:* Android, Access control, Context, Security, Virtualization

I. INTRODUCTION

Smart phones are playing vital role in our regular life. In the corporate world, smart phones are becoming famous these days. From smart phone user does different functions anywhere anytime with device's high storage and computing speed. Many companies use mobile versions of desktop applications to improve employee productivity by allowing access to company services with smart phones. Many companies are trying the BYOD (Bring Your Own Device) concept. For this, employees connect their personal smart phones to their work place. In such situations, many times, employee has to give his personal phone to other employees for the sake of work and one's personal device gets handled by others. In such cases, no one can guarantee safety of personal data on the device. On the contrary, outside workplace, if any one handles employee's smartphone, company's data stored on that smartphone comes under risk. This may lead to risk of company's confidential data leakages, data losses and data theft etc. Hence securing use of the smart phone and data access control according to different reasons of smartphone use is of the key importance.

Taking security risks related to smart phones into consideration, there is should be some effective and easy to use solution making the use of smart phones secure, as far as the hastily increasing utilization of these devices is considered. Multiple techniques are suggested for securing the data stored on the smart phones. Some of them are android extensions i.e. making change in the android OS. While in some other solutions, mobile virtualization technique is applied. This paper tells about details of implementation of a solution developed for smartphone security using security profiles.

II. RELATED WORK

Many risks associated with smart phones security are identified. Some solutions are suggested and still the experiments are going on. This chapter shows some of the previous research work on smart phone security. Security related techniques for smartphones are mainly divided into following parts as android security extension and mobile virtualizations. Russello, Conti presented a system which consists of security profiles on smartphone. They developed a system called MOSES [1] which separates data and applications in different security profiles. But it does not restrict resource access on device for resources like Bluetooth, Wi-Fi, NFC etc.

A. Android Security Extension

Many solutions have been developed which are android security extensions. CRêPE is a context related policy enforcement system [2]. M. Conti, Crispo developed a fine grained context related policy enforcement. With this user can create policies that automatically control the granting of the permissions during runtime. Context-related access control is not new, but this work used this concept in smart phone environment.

YAASE (Yet Another Android Security Extension) is a very flexible and very powerful privacy enforcement framework [3] transparent to the applications in Android environments. Russello, Crispo have developed an Android security extension by modifying

Android framework, libraries. They implemented a security system for protecting user from various malicious applications. But this system is the modifications of an Android operating system itself. All above solutions are nothing but Android security system extensions i.e. modification of framework of Android OS. Hence, removing these systems will not just as simple as removal of the application and may result in the non working android system.

Flexible data driven security for Android [4] is developed that includes data-driven usage control, and generalization of access controls to the time after data accessed. Feth, Pretschner suggested flexible data driven security for Android. Security policy enforcements are based on event and actions. Policies are built on temporal, spatial, cardinality conditions. But this system assumes non rooted, vulnerability free mobile device. Both assumptions are fairly questionable. The reason for this is that, rooting an android phone is simple even for the unexperienced users and vulnerability reports are pretty frequent.

Other research by Kodeswarn and Nandkumar presented system based on run time information flow control to secure enterprise data on the smart phone [5]. Their privacy policies are based on permissible information flow during different context on phone. But policy conflicts increase with increase in the number of policies.

FlaskDroid [6], is other approach that developed diverse security and privacy policies with flexible and fine grained mandatory access control on Android framework platform. This architecture gives mandatory access control over Android middleware and kernel layers simultaneously. But more flexible policies are required to address attacks.

If a security technique has multiple security policies then, it is necessary to identify the best suitable security policy that should be implemented in a particular scenario. To identify best suitable security policy from multiple policies, optimization technique such as conventional genetic algorithm (GA) [7] can be used. Further GA with novel operators viz. Basic and advanced twin operator can be used for efficiently optimizing the security profiles for accessing mobile applications [8].

B. Mobile Virtualizations

Virtualization gives environments that are partitioned, and indistinguishable from "bare" hardware, from operating system point of view. With the rise of smart phone performance capabilities, virtualization porting to mobile platform became actual. There are some approaches to port Linux hypervisors to the ARM architecture. Xen described design of Xen on ARM, which is a secure system virtualization of ARM [9]. Researchers developed system virtualization for ARM based mobile phones using Xen hypervisor. They isolated secure guest Linux virtual machine from non-secure ones which are executing under Xen hypervisor on ARM. But the system has low performance.

However, all virtual machines are just ported to mobile platforms while being premeditated for PC, they share low performances. Considering android OS security [10], which explained complexity of security of Android and security enforcement and research on security assessment of Android framework for mobile devices [11], researchers identified high risk threats to the framework and suggested some security solutions for mitigating them.

III. SYSTEM ARCHITECTURE

Proposed application which consists of security profiles for smart phones provides security and space isolation based on modes of uses separation on smart phone. Security profiles are nothing but separate compartments which consists of different applications that are assigned to those profiles by user as per his needs. This work also defines rules based security to restrict access to device resource like Bluetooth, Wi-Fi, mobile data, NFC (Near Field Communication) etc. In this work:

- Proposed system separates modes of smartphone use in terms of security profiles.
- Security profile (SP) determines when data can be accessed and what applications can be executed within a profile.
- Within particular SP, only applications assigned to that SP are allowed to execute; this provides application separation.
- Policies are comprised of rules based security. Using rules defined for each SP, access of device resources is controlled for that SP.
- These profiles are associated with a set of contexts which determines the activation of profile.
- Contexts definitions include the use of information like time.
- Profiles can applied any time by the user. Graphical user interface will be provided for this.
  Security profile switching can be manual or automatic as required by user. Automatic switching between the security profiles is possible using context detector system.

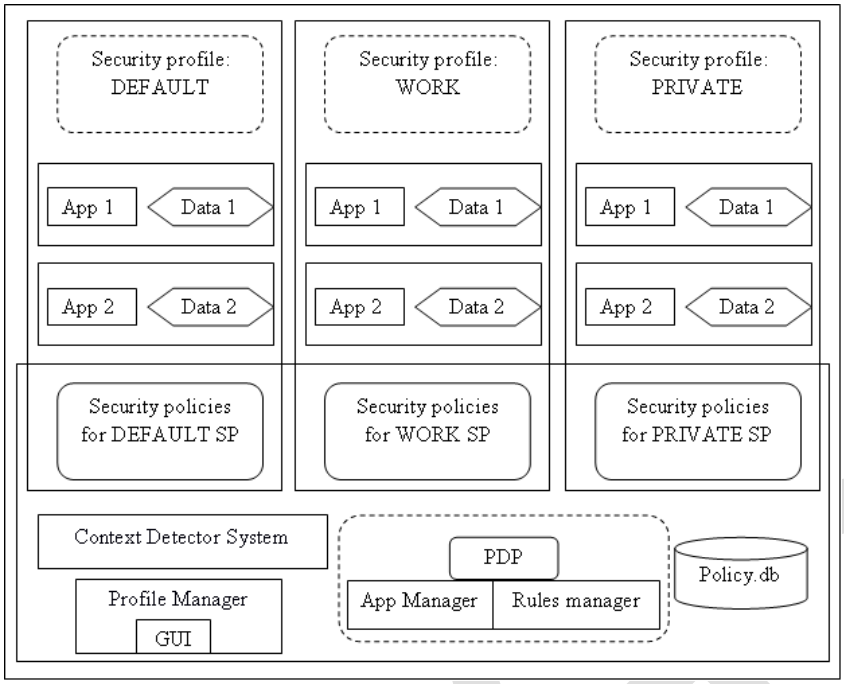

Fig. 1 Proposed Architecture

The Fig.1 summarizes the architecture for the proposed system which describes inter-related functionalities of components of system.

IV. IMPLEMENTATION DETAILS

Proposed system consists of the components presented in above figure. Security profile will be associated with a set of security policies defined for that particular SP. These policies control the access to applications and data and these are user-defined policies that restrict the flow of information between different profiles. Only those applications are assigned to a SP that are required to execute within that SP. And resource access for SPs is controlled by defining rules for them. Policy.db is a database of policies defined for different SPs of this security profiles application.

A. Context Detector System

Main feature of proposed system is automatic switching between security profiles based on current context that is detected by context detector system. Context detector system is responsible for detection or monitoring of activation and deactivation of defined contexts. On the detection of such event, context detector system sends a notification about this to the security profile manager.

Context is any information that can be obtained by a smartphone and that can be used to characterize the state of smartphone. And a context definition is a Boolean expression defined using any information obtained from smartphones sensors (e.g. clock : time). When context definition evaluates to be true, SP associated with that context is activated. The context_id parameter is a context identifier. Functions onTrue(context_id), onFalse(context_id) correspond to activation, deactivation of context respectively.

B. Security Profile Manager

The security profile manager has information that is linking a security profile with context. The security profile manager responsible for activation and deactivation of security profiles. The security profile manager uses following logic. If a new activated context points to the active security profile then that notification is ignored. In other cases, a security profile switch should be performed. That is the currently running security profile has to deactivate and the new security profile is active. When a security profile switch performed, security profile manager sets a command to policy decision point (PDP). To manage the SPs in user's device, GUI is provided.

C. PDP

PDP stands for Policy Decision Point. It is a fundamental point for security checks for the active SP to regulate access to resources. PDP hand over the policy check information to these managers: App manager and Rules manager.
App manager: It is responsible for deciding which apps are allowed to be executed within a security profile.
Rule manager: It is taking care of managing the rules for resource access control.

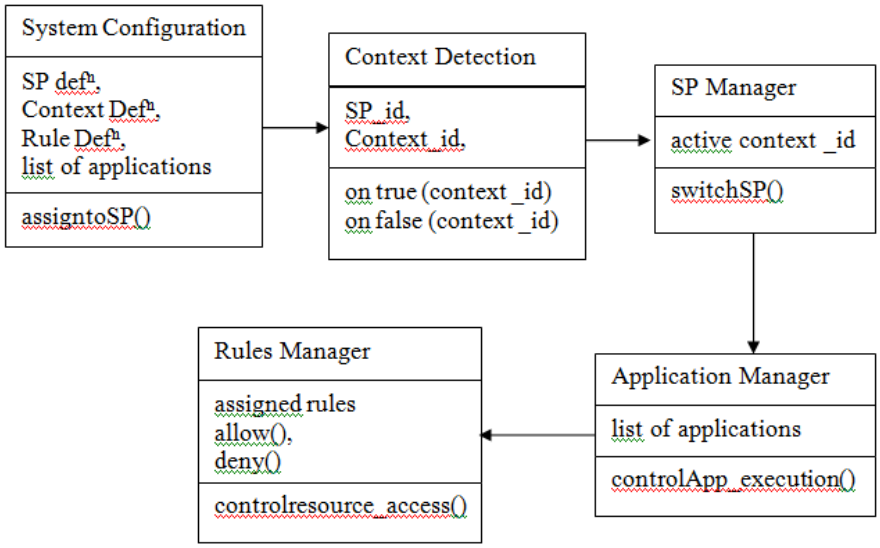

Fig. 2 Class Diagram

Class diagram shows a set of classes and their relations. Functional requirements of a system are explored using class diagram. Fig 2 shows the class diagram for proposed system.

D. Application Separation

Each SP is allocated with list of applications which are allowed to run when that profile is active. Each application during its installation receives its UID. System uses these identifiers to manage what applications can activate for every SP. During SP switching, it selects from the database, the list of applications, which are approved in activated profile. When a new SP is activated, only allowed applications for this profile will be displayed.

When new profile is activated, it may deny execution of some applications that are allowed in the previous profile. If these applications are running while the profile switch, then it is necessary to stop processes as they are no longer allowed in new security profile after the profile switch.

E. Rule Operation

Smartphones have multiple facilities like Wi-Fi, Bluetooth, mobile data etc. Access to these resources will be given to different SPs as per user's requirement. Particular SP may be restricted from accessing these resources. This type of resource access can be controlled by defining rules. Rules defined for SPs will be applied to respective security profiles as and when needed. The rules that can be assigned to SPs are: allow, deny. If rule assigned to a SP is allow, then access to the mobile resources will be permitted. And, if rule assigned to a SP is deny, then access to the mobile resources will be restricted. In this way, user can constrain unwanted use of device resources by other people by assigning rules to SPs.

V. RESULTS

Proposed system is tested taking into account various parameters like number of applications per security profile, time required to switch between security profiles, battery overhead etc. Fig. 3 and Fig. 4 show results of testing of proposed system with respect to parameters listed above.

For measuring energy overhead produced by the designed security profile application, following experiment is performed. The battery of the device is charged fully. Then, the designed application which consists of security profiles is run and for every ten

minutes, level of battery of device is measured. Three sets of this experiment are performed and average of readings is calculated. From these readings, graph for energy overhead is drawn.

Result shows that continuous running of designed application for about one hour, percentage energy overhead is about 4 percent for this application. Figure 3 shows that energy overhead is minor for designed application when compared with stock android.

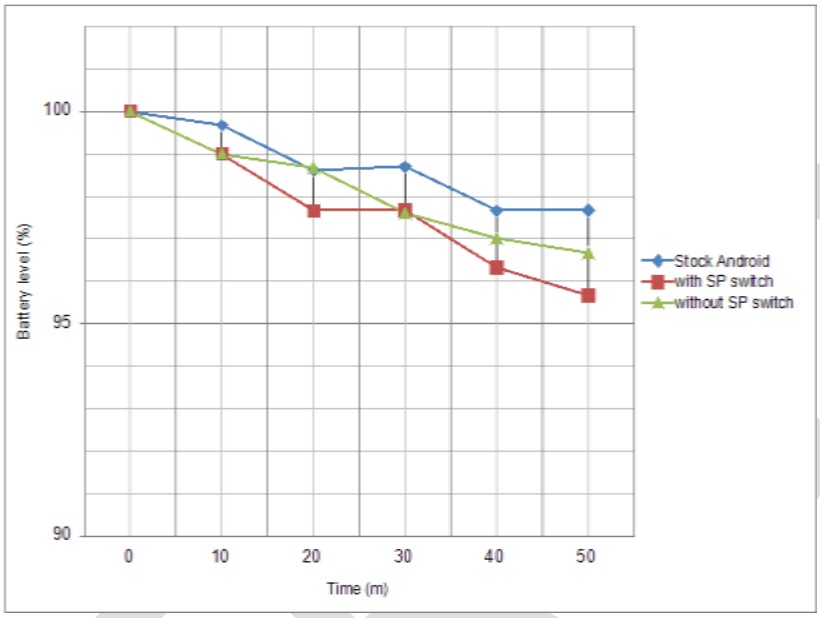

Fig. 3 Energy Overhead

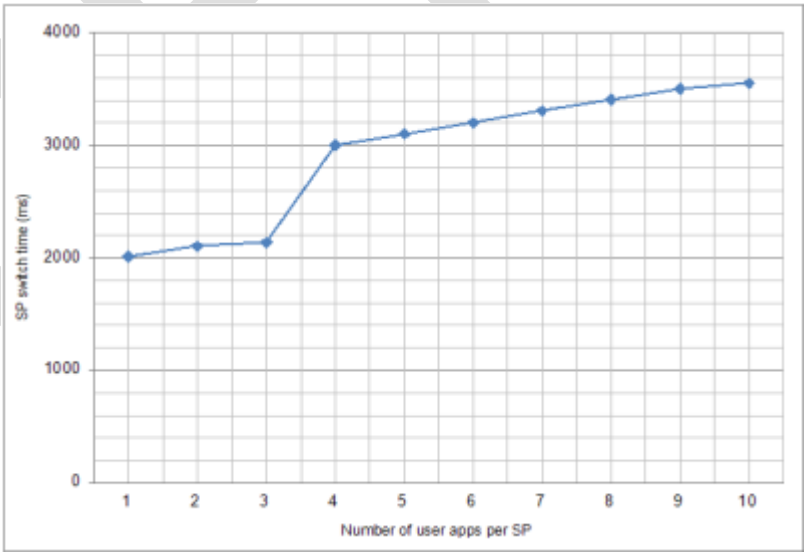

Fig. 4 Time for SP switch as a function of number of applications per SP

Here, results of the experiment measuring the time required to switch between SPs, are presented. To search the dependency between time and number of applications, the number of applications varied from 0 to 10. Three sets of this experiment are performed

and average of readings is calculated. From these readings, graph for time for SP switch is drawn. It is observed that switching time required by SP increases with increase in number of applications. It is approximately 2000 ms for 1 application to approximately 3550 ms for 10 applications per security profile. Figure 4 shows that switching time required by SP increases with increase in number of applications but this increase is very minor as this time is in msec. Hence results show that energy overhead and SP switching time, both are very less.

CONCLUSION AND FUTURE SCOPE

Smart phone security application based on separation of modes of smart phone use is developed to provide security profiles for it. Study of literature related to mobile phone security has shown drawbacks of some previous security solutions like hardcoded environments, modifications of android systems itself. Proposed system overcomes these drawbacks by providing user specified environments, application base security with data and resource access control for different kind of uses.

The application which consists of security profiles for android smart phones can have future scope in some areas. Net banking and online shopping on smart phones is one these areas. Providing such application which consists of security profiles for smart phones will make net banking and online shopping on smart phone safe, preventing misuse of personal banking information and loss. Also, child lock system can be developed using these security profiles. Also, security profiles can be developed for any type of smart phone with any type of operating system in future.

REFERENCES:

[1] M. Conti, B. Crispo, E. Fernandes, and Y. Zhauniarovich, "CR^ ePE: A System for Enforcing Fine-Grained Context-Related Policies on Android," IEEE Trans. Information Forensics and Security, vol. 7, no. 5, pp. 1426-1438, Oct. 2012.

[2] G. Russello, B. Crispo, E. Fernandes, and Y. Zhauniarovich, "YAASE: Yet Another Android Security Extension," Proc. IEEE Third Int'l Conf. Social Computing and Privacy, Security, Risk and Trust (SocialCom/PASSAT), pp. 1033-1040, 2011.

[3] D. Feth and A. Pretschner, "Flexible Data-Driven Security for Android," Proc. IEEE Sixth Int'l Conf. Software Security and Reliability (SERE '12), pp. 41-50, 2012.

[4] P.B. Kodeswaran, V. Nandakumar, S. Kapoor, P. Kamaraju, A. Joshi, and S. Mukherjea, "Securing Enterprise Data on Smartphones Using Run Time Information Flow Control," Proc. IEEE 13th Int'l Conf. Mobile Data Management (MDM '12), pp. 300-305, 2012.

[5] S. Bugiel, S. Heuser, and A.-R. Sadeghi, "Flexible and Fine- Grained Mandatory Access Control on Android for Diverse Security and Privacy Policies," Proc. 22nd USENIX Conf. Security (Security'13), 2013.

[6] J.-Y. Hwang, S.-B. Suh, S.-K. Heo, C.-J. Park, J.-M. Ryu, S.-Y. Park, and C.-R. Kim, "Xen on ARM: System Virtualization Using Xen Hypervisor for ARM-Based Secure Mobile Phones," Proc. IEEE Fifth Consumer Comm. and Networking Conf. (CCNC '08), pp. 257- 261, 2008.

[7] Anagha Parag Khedkar and Subbaraman Shaila, "Effect of Advanced Twin Operator on the performance of Genetic Algorithm", International Journal of Engineering Research and Technology, vol. 3, pp. 721-731, 2010.

[8] Anagha Parag Khedkar and Subbaraman Shaila, "The Novel Approach of Adaptive Twin Probability for Genetic Algorithm", International Journal of Advanced Studies in Computers, Science and Engineering, vol. 2, special issue 2, pp. 31-37, Sept. 2013.

[9] W. Enck, M. Ongtang, and P. McDaniel, "Understanding Android Security," IEEE Security and Privacy, vol. 7, no. 1, pp. 50-57, Jan. / Feb. 2009.

[10] A. Shabtai, Y. Fledel, U. Kanonov, Y. Elovici, S. Dolev, and C. Glezer, "Google Android: A Comprehensive Security Assessment," IEEE Security and Privacy, vol. 8, no. 2, pp. 35-44, Mar./Apr. 2010.

[11] E. Yuan and J. Tong, "Attributed Based Access Control (ABAC) for Web Services," Proc. IEEE Int'l Conf. Web Services (ICWS '05), pp. 561-569, 2005.

[12] (2014) Fixmo SafeZone: Corporate Data Protection, http://fixmo.com/products/safezon.

International Journal of Engineering Research and General Science Volume 3, Issue 5, September-October, 2015
ISSN 2091-2730

BOUNDS ON NON-SYMMETRIC DIVERGENCE

R. N. SARASWAT
Department of Mathematics and Statistics, Manipal University, Jaipur,
INDIA-303007, E-mail: sarswatrn@gmail.com

Abstract: Inequalities are playing a fundamental role in the area of Information Theory and Statistics. Large numbers of Mathematicians like as Taneja , Pranesh Kumar Dragomir etc. have been studied application of Inequalities in different branches of the pure and applied mathematics, physics, computer science etc. In this research article, we shall consider inequalities among information divergence measure and Hellinger discrimination. We shall propose a new non-symmetric information divergence measure and bounds of new information divergence measure are also considered in this research article.

Keywords: - Csiszar's f-divergence measure, Hellinger Discrimination, Bhattacharya divergence measure, relative information of type's, information inequalities, Kullback-Leibler divergence measure and numerical illustrations etc.

1. INTRODUCTION

Let

$$\Gamma_n = \left\{ P = (p_1, p_2, ...p_n) \middle| p_i \geq 0, \sum_{i=1}^{n} p_i = 1 \right\}, n \geq 2 \tag{1.1}$$

be the set of all complete finite discrete probability distributions. There are many information and divergence measures exists in the literature on information theory. Csiszar [2] & [3] introduced a generalized measure of information using f-divergence measure is given by

$$I_f(P,Q) = \sum_{i=1}^{n} q_i f\left(\frac{p_i}{q_i}\right) \tag{1.2}$$

where $f : \mathbf{R}_+ \to \mathbf{R}_+$ is a convex function and $P, Q \in \Gamma_n$.

Here we list some existing divergence measures which are in the category of f-divergence measures, together with the suitable generating function f.

- **Hellinger Discrimination** [4]:-

$$h(P,Q)=\left[1-B(P,Q)\right]=\frac{1}{2}\sum_{i=1}^{n}\left(\sqrt{p_i}-\sqrt{q_i}\right)^2 \qquad (1.3)$$

where $B(P,Q)=\sum_{i=1}^{n}\sqrt{p_i q_i}$ is known as Bhattacharya divergence measure [1]

- **Relative information of type s** [8]

The following measures and particular cases are introduced [8]

$$\Phi_s(P,Q)=\begin{cases} {}^2K_s(P,Q)=\left[s(s-1)\right]^{-1}\left[\sum_{i=1}^{n}p_i^s q_i^{1-s}-1\right], s\neq 0,1 \\ D(Q,P)=\sum_{i=1}^{n}q_i\log\left(\frac{q_i}{p_i}\right), \qquad s=0 \\ D(P,Q)=\sum_{i=1}^{n}p_i\log\left(\frac{p_i}{q_i}\right), \qquad s=1 \end{cases} \qquad (1.4)$$

In whole paper, in the section 2, we have introduced information inequalities. New non-symmetric information divergence measure has discussed in section 3. Bounds of new non symmetric divergence measure have also studied in section 4.

2. NEW INFORMATION INEQUALITY

The following propositions are one of the results of the theorem is give in [8] and similar line to [5], [6] & [7] and proposition 2.2 is the particular case for $s=1/2$ of proposition 2.1.

Proposition 2.1:- Let $f:(0,\infty)\to\mathbf{R}$ be a mapping which is normalized i.e. $f(1)=0$ and satisfies the assumptions.

(i) f is twice differentiable on (r, R) .where $0\le r\le 1\le R\le\infty$

(ii) there exist the real Constants m , M such that $m<M$

$$m\le t^{2-s}f''(t)\le M,\ \forall t\in(r,R), s\in\mathbf{R} \qquad (2.1)$$

If $P,Q\in\Gamma_n$ are discrete probability distributions satisfying assumption

$$0<r\le\frac{p_i}{q_i}\le R<\infty,\ \forall i\in\{1,2,3,.....n\} \qquad (2.2)$$

then we have the inequality

$$m\ \Phi_s(P,Q)\le I_f(P,Q)\le M\ \Phi_s(P,Q) \qquad (2.3)$$

Where $\Phi_s(P,Q)$ is given by (1.2), for $s=1/2$ respectively.

Proposition 2.2:- Let $f:(0,\infty)\to\mathbf{R}$ is normalized i.e. $f(1)=0$ and satisfies the assumptions.

(i) f is twice differentiable on (r, R) .where $0\le r\le 1\le R\le\infty$

(ii) There exist Constant m, M such that $m<M$

$$m\le t^{3/2}f''(t)\le M,\forall t\in(r,R) \tag{2.4}$$

If $P,Q\in\Gamma_n$ are discrete probability distributions satisfying assumption

$$0<r\le\frac{p_i}{q_i}\le R<\infty,\ \forall i\in\{1,2,3,.....n\}$$

Then we have the inequality

$$4m\ h(P,Q)\le I_f(P,Q)\le 4M\ h(P,Q) \tag{2.5}$$

In view of proposition (4.1) we states the following results

3. INFORMATION DIVERGENCE MEASURE

In this section we introduce a new information divergence measure which is the category of Csiszar's f-divergence measure. Let us consider the function $f:(0,\infty)\to\mathbf{R}$

$$f(t)=\frac{(t^2-1)^2}{t},\quad f'(t)=\frac{3t^4-2t^2-1}{t^2},\ f''(t)=\frac{6t^4+2}{t^3}>0,\forall t>0 \tag{3.1}$$

Hence function f (t) is convex from equation 3.1 and figure 3.1, f (1) =0 i.e. normalized.

Applying Csiszar's f-divergence properties on (1.2), then we get

$$I_f(P,Q)=\sum_{i=1}^{n}\frac{(p_i^2-q_i^2)^2}{q_i^2p_i}=4\sum_{i=1}^{n}\left(1\Big/\frac{2p_iq_i}{p_i+q_i}\right)\frac{(p_i+q_i)}{2}\frac{(p_i-q_i)^2}{q_i}=N(P,Q) \tag{3.2}$$

Where " $N(P,Q)$ " is made up the combination of Harmonic, Arithmetic and χ^2 -divergence measure. Above new information divergence measure are represented in the figure 3.1. It is clear that from the figure 3.1 and 3.2 the convex function $f(t)$ gives a steeper slope. Further $f(1)=0$, so that $N(P,P)=0$ and the convexity of the function $f(t)$ ensure that the measure (3.2) is non-negative.

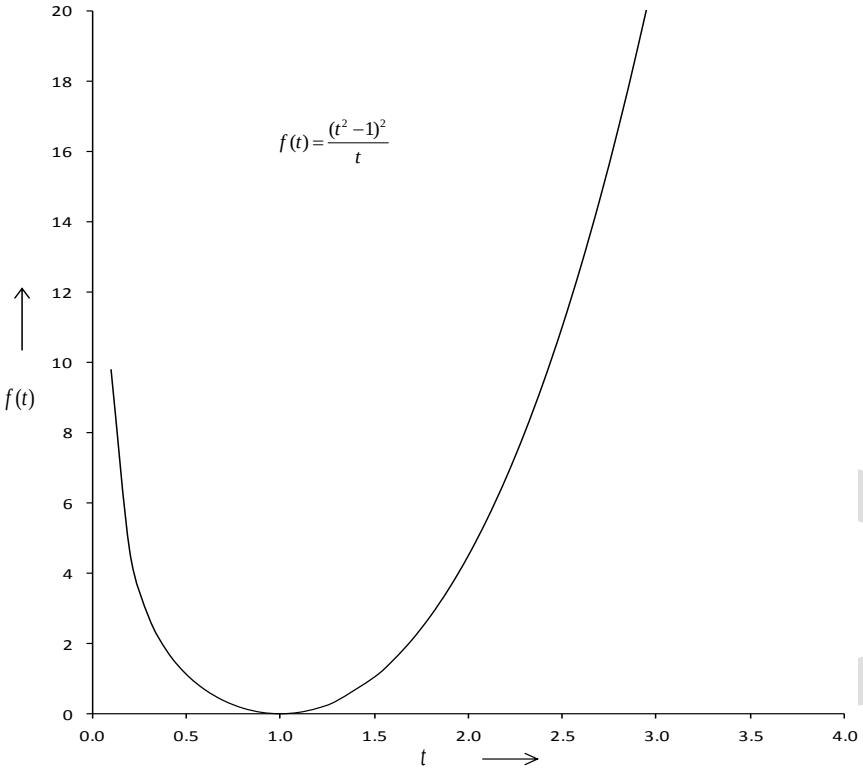

Figure 3.1

Figure 3.1 represent convexity of new non symmetric information divergence measure

In following section we shall consider some results using proposition (2.1) and the measure $N(P,Q)$ given in equation (3.2) which results are similar line to [4], [6] & [7].

4. RESULTS

In this section we shall consider the bounds of new information divergence measure in terms of Hellinger discrimination.

Result: 4.1: - Let $P,Q\in\Gamma_n$ and $s=1/2$ .Let there exists r, R such that r < R and $0<r\le\frac{p_i}{q_i}\le R<\infty\ \forall\ i\in\{1,2,3,.....n\}$

(i) If $0<r<0.67$

$$23.4\,h(P,Q)\le N(P,Q)\le 4\max\left\{\frac{6r^4+2}{r^{3/2}},\frac{6R^4+2}{R^{3/2}}\right\}h(P,Q) \qquad (4.1)$$

(ii) If $0.67<r<\infty$

$$\frac{3r^4+1}{r^{3/2}}h(P,Q)\le\frac{1}{8}N(P,Q)\le\frac{3R^4+1}{R^{3/2}}h(P,Q) \qquad (4.2)$$

Proof:-

From equations (3.1), (3.2) & (2.4), we get

$$g(t) = t^{3/2} f''(t) = \frac{6t^4 + 2}{t^{3/2}} > 0, \forall t > 0$$

$$g(t) = 6t^{5/2} + \frac{2}{t^{3/2}} > 0, \forall t > 0,$$

$$g'(t) = 15t^{3/2} - \frac{3}{t^{5/2}} = 0$$

$$g''(t) = \frac{45}{2} t^{1/2} + \frac{15}{2} t^{-7/2}$$

$$g'(t) = 15t^{3/2} - \frac{3}{t^{5/2}} = 0 \Rightarrow t^4 - \frac{1}{5} = 0 \Rightarrow t = \left(\frac{1}{5}\right)^{1/4} = 0.67$$

It is clear that g (t) is monotonic decreasing on [0, .67) and monotonic increasing on $[0.67, \infty)$.

Also function g has minimum realized at $t_0 = 0.67$

$$g''(t) = \frac{45}{2}(.67)^{1/2} + \frac{15}{2}(.67)^{-3/2} \text{ (Positive)}$$

and

$$\inf_{t \in (0,\infty)} g(t) = g(.67) = 6(.67)^{5/2} + \frac{2}{(.67)^{3/2}} = 2.20 + 3.7 = 5.9$$

We have two cases:

(i) If $0 < r < 0.67$ then

$$\text{m} = \inf_{t \in (r.R)} g(t) = g(.67) = 6(.67)^{5/2} + \frac{2}{(.67)^{3/2}} = 5.85 \qquad (4.3)$$

$$\text{M} = \sup_{t \in (r,R)} g(t) = \max\{g(r), g(R)\} = \max\left\{\frac{6r^4 + 2}{r^{3/2}}, \frac{6R^4 + 2}{R^{3/2}}\right\} \qquad (4.4)$$

(ii) If $0.67 < r < \infty$

$$m = \inf_{t \in (r,R)} g(t) = \frac{6r^4 + 2}{r^{3/2}} \quad M = \sup_{t \in (r,R)} g(t) = \frac{6R^4 + 2}{R^{3/2}} \qquad (4.5)$$

Equation (2.4) of proposition (2.2) using equation (3.2), (4.3), (4.4) & (4.5) gives the results (4.1) & (4.2).

5. NUMERICAL STUDY

Example 5.1

Let P be the binomial probability distribution for the random valuable X with parameter (n=8 p=0.5) and Q its approximated normal probability distribution. The following table have also discussed [8].

Table 5.1 Binomial Probability Distribution (n=8 p=0.5)

x	0	1	2	3	4	5
p (x)	0.004	0.031	0.109	0.219	0.274	0.219
q (x)	0.005	0.030	0.104	0.220	0.282	0.220
p(x)/q(x)	0.774	1.042	1.0503	0.997	0.968	0.997

It is noted that $r = 0.77$ and $R = 1.05$. Here we shall discuss the numerical bounds of new information divergence measure in terms of Hellinger discrimination. From equation (4.1) and (4.2) and using the table of Binomial distribution where R and r are the lower and upper bounds then we get

(i) If $0 < r < .67$.

$$23.4\,h(P,Q) \le N(P,Q) \le 4\max\left\{\frac{6r^4+2}{r^{3/2}}, \frac{6R^4+2}{R^{3/2}}\right\} h(P,Q)$$

$$23.4\,h(P,Q) \le N(P,Q) \le 4\max\left\{\frac{4.155355391}{(.774179933)^{3/2}} = .681181532, \frac{9.302210714}{1.076437122} = 8.4166591\right\} h(P,Q)$$

$$23.4\,h(P,Q) \le N(P,Q) \le 4 \times 8.4166591\, h(P,Q)$$

$$23.4\,h(P,Q) \le N(P,Q) \le 34.5666636\; h(P,Q)$$

(ii) If $.67 < r < \infty$

$$\frac{3r^4+1}{r^{3/2}} h(P,Q) \le \frac{1}{8} N(P,Q) \le \frac{3R^4+1}{R^{3/2}} h(P,Q)$$

$$0.681181532\, h(P,Q) \le \frac{1}{8} N(P,Q) \le 34.5666636\; h(P,Q)$$

REFERENCES:

[1] A. Bhattacharya., "Some analogues to amount of information and their uses in statistical estimation, Sankhya" 8(1946) 1-14.

[2] I. Csiszar "Information-type measures of difference of probability functions and indirect observations". studia Sci. Math.hunger.2(1961). 299-318.

[3] I. Csiszar "Information measure: A critical servey" Trans.7th prague conf. on info. Th.Statist. Decius. Funct, Random Processes and 8th European meeting of statist Volume B. Acadmia Prague, 1978, PP-73-86.

[4] E. Hellinger, "Neue Begrundung der Theorie der quadratischen Formen Von unendlichen vielen veranderlichen", J. Rein. Aug. Math, 136(1909), 210-271.

[5] K. C. Jain and Ram Naresh Saraswat , "Some bounds of Csiszar's f-divergence measure in terms of the well-known divergence measures of Information Theory" International Journal of Mathematical Sciences and Engineering Applications 5(5), (2011), pp. 1-11.

[6] K. C. Jain and Ram Naresh Saraswat "Inequalities among well-known divergence measures and triangular discrimination", International Journal of Computational and Applied Mathematics**,** 4(3) (2012), pp. 215-224.

[7] K. C. Jain and Ram Naresh Saraswat "Some bounds of information divergence measure in term of Relative arithmetic-geometric divergence measure" International Journal of Applied Mathematics and Statistics, 32(2) (2013), pp. 48-58.

[8] Pranesh Kumar and Andrew Johnson, "On a symmetric divergence measure and information inequalities" Journal of inequalities in pure and applied mathematics, 6(3) (2005) 149-160.

[9] Ram Naresh Saraswat "Some Generalized Information Inequalities", International Journal on Information Theory, 4(2) 2015, pp-31-40

[10] Ram Naresh Saraswat "A non-symmetric divergence and Kullback-Leibler divergence measure" International Journal of Current Research, 7(6) (2015), pp.16789-16794

[11] Taneja I. J. and Pranesh Kumar, "Relative Information of type's, Csiszar f-divergence and information inequalities", Information Sciences, 166(1-4) (2004), 105-125.

[12] Taneja I.J., "New Developments in generalized information measures", Chapter in: Advances in imaging and Electron Physics, Ed. P. W. Hawkes 91 (1995), 37-135

International Journal of Engineering Research and General Science Volume 3, Issue 5, September-October, 2015
ISSN 2091-2730

REMEDIAL MEASURES AND IMPROVEMENTS TO RAMOOHALLI JUNCTION, A CASE STUDY

KAMALAKARA.G.K ABHISH M.S

Assistant Professor, Dept of Civil Engineering, Rajarajeshwari College of Engineering, Bangalore -560074. India
Email: kamal.cvkamal018@gmail.com

Abstract: An accident black spot is a term used in road safety management to denote a place where road traffic accidents have historically been concentrated. It may have occurred for a variety of reasons, such as a sharp drop or corner in a straight road, so oncoming traffic is concealed, a hidden junction on a fast road, poor or concealed warning signs at cross-roads. Transportation contributes to the economic, industrial, social and cultural development of any country. Transportation by road is the only mode which could give maximum service to one and all. Due to the increase in population, number of vehicles is increasing day by day which leads to the increase in road network. It has been estimated that over 35,000 persons die and over 12 to 15 million persons are injured every single year in road accidents throughout the world. The present work intended to analyze a black spot (accident prone location) Ramoohalli junction in BANGALORE city. The causes of accidents are studied and suggested different remedial measures to reduce number of accidents.

Keywords: Traffic count, black spots, prioritization, signal timings, accidents, junction

1. Introduction:

Accidents, tragically, are not often due to ignorance, but are due to carelessness, thoughtlessness and over confidence. William Haddon1 has pointed out that road Accidents were associated with numerous problems each of which needed to be addressed separately. Human, vehicle and environmental factors play roles before, during and after a trauma event. Accidents, therefore, can be studied in terms of agent, host and environmental factors and epidemiologically classified into time, place and person distribution. This paper lays emphasis on accident studies on Ramoohalli Junction in Bangalore city. It is a major urban arterial junction with shoulder and side drains. The open side drains exist for some part of the study stretch. For the purpose of the study, a Junction Traffic Accident (JTA) was defined as accident, which took place on the road between two or more objects, one of which must be any kind of a moving vehicle.

1.1 Literature Review:

In literature there is no universally accepted definition of a black spot. According to The Bureau of Transport and Regional Economics of Australia (2001) locations are in general classified as black spots after an assessment of the level of risk and the likelihood of a crash occurring at each location. At certain sites, the level of risk will be higher than the general level of risk in surrounding areas. Crashes will tend to be concentrated at these relatively high-risk locations. Locations that have an abnormally high number of crashes are described as crash concentrated, high hazard, hazardous, hot spot or black spot sites. Sites with potentially hazardous features are sometimes described as grey spots.

In general, the number of crashes is affected by three factors:-

- The road environment
- The condition of vehicles using the road system
- The skills, concentration and physical state of road users.

The demands of the road environment vary due to factors such as traffic flow rates, geometric features of the road and type of road. Drivers normally adapt their performance level to the demands of the road system. A crash occurs when the driver's performance level is insufficient to meet the performance demands of the road environment. Most of the time, driver capabilities exceed performance demands. Black spots are points of peak performance demand. Engineering improvements in the road network lower performance demands on the driver. This increases the safety margin between the driver's performance level and the performance demands of the road environment, and reduces the probability of a crash.

2.0 Accident Scenario in Bangalore

Central Road Research Institute (CRRI) Study report, (2008) reveals that the accident record of the country is among the worst in the world. Road accidents have registered a sharp increase recently following rapid growth in vehicle ownership, construction of high speed roads and expressways. Accident rates could go up further unless both traffic rules and road safety measures are enforced strictly. A review on the road crash analysis world over implies that the human factor attributes to the majority of accidents. A similar instance has been observed in India as well as in Bangalore. In Bangalore about 47% of road users killed are pedestrians & 40% are two-wheeler users. In additions to this annually more than Rs 1550 crores are paid as compensation to the victims & their dependents. Overall Bangalore's accident statistics is presented in the Table 1.

Table No .1 BANGALORE ACCIDENT DATA

YEAR	FATAL	KILLED	NON FATAL	INJURED	TOTAL
2002	783	820	9073	7577	9856
2003	843	883	9662	7980	10505
2004	875	903	8226	6921	9101
2005	796	836	6782	5899	7578
2006	880	915	6681	6048	7561
2007	957	981	7469	6591	8426
2008	864	892	6908	6150	7772
2009	737	761	6138	5668	6875
2010	816	858	5667	5343	6483
2011	727	757	5297	4976	6024

Figure: 1 ACCIDENT DATA

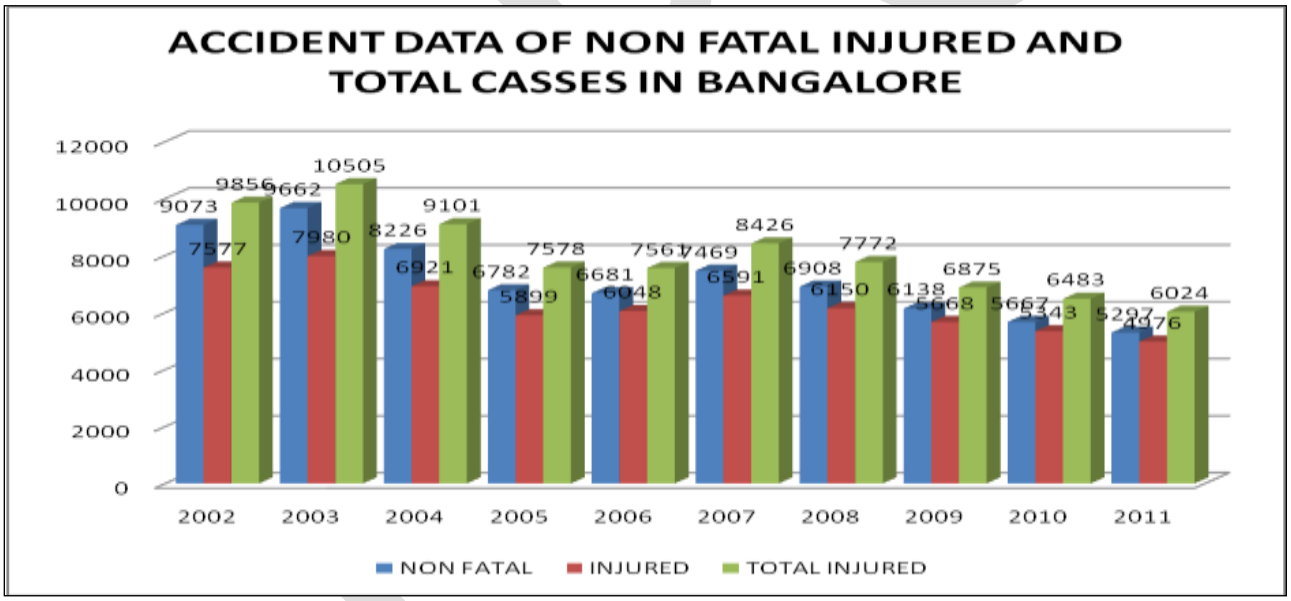

Fig:1 Accident data in bangalore

2.1 Motorization in Bangalore

The conversion of Bangalore from being once a "Garden City" to present "Black City" has been rapid. Bangalore has grown exponentially in the past two decades. The Booming Software, Biotech and manufacturing industries have magnified the requirements of basic and service employments, which generated and magnified urban sprawl into problematic proportions. Improvement in the quality of life along with substandard public transportation has resulted in spiraling growth of private automobiles. The resultant offshoot of such a high automobile growth along with supply intensive actions of the government is accidents. The Motorization index calculated by the author (vehicles for 1000 persons) best describes the high intensity of vehicular growth, which projects that nearly

every 3rd person owns a private vehicle. Motorization index has nearly doubled within a decade. This calculation is highly conservative since it does not consider high intensity of migration of persons with their vehicles from other parts of state to Bangalore. The high intensity of vehicular growth can be known from the simple area analysis. Karnataka State has 1,91,791 sq.kms of area whereas capital Bangalore as per revised Estimates have 561 sq.kms of developed area, which works out to 0.29% of state area. Nearly 39-40% of vehicles registered in Karnataka state belong to Bangalore. Such a massive number of vehicles occupy 4.8% of total road length available in Karnataka. Availability of such a massive number of vehicles results in violation of individual spaces thus contributing to accidents.

3.0 Present Investigation

In the present study Ramoohalli Junction is considered. The detail of accident in the junction is taken from nearest Traffic Police Station and 24 hours classified volume count survey was conducted at the junction. The details of accident and classified traffic volume count were given in Table No.2.

Table No.2 Accident data at Ramoohalli Junction

Year	Ramoohalli Junction				
	Fatal	Killed	Non Fatal	Injured	Total cases
2004	42	43	480	351	**522**
2005	43	44	348	279	**391**
2006	39	39	339	265	**378**
2007	34	35	460	372	**494**
2008	46	46	317	292	**416**
2009	29	29	302	256	**339**
2010	23	23	266	219	**289**
2011	27	28	230	198	**257**
2012	39	41	228	227	**267**

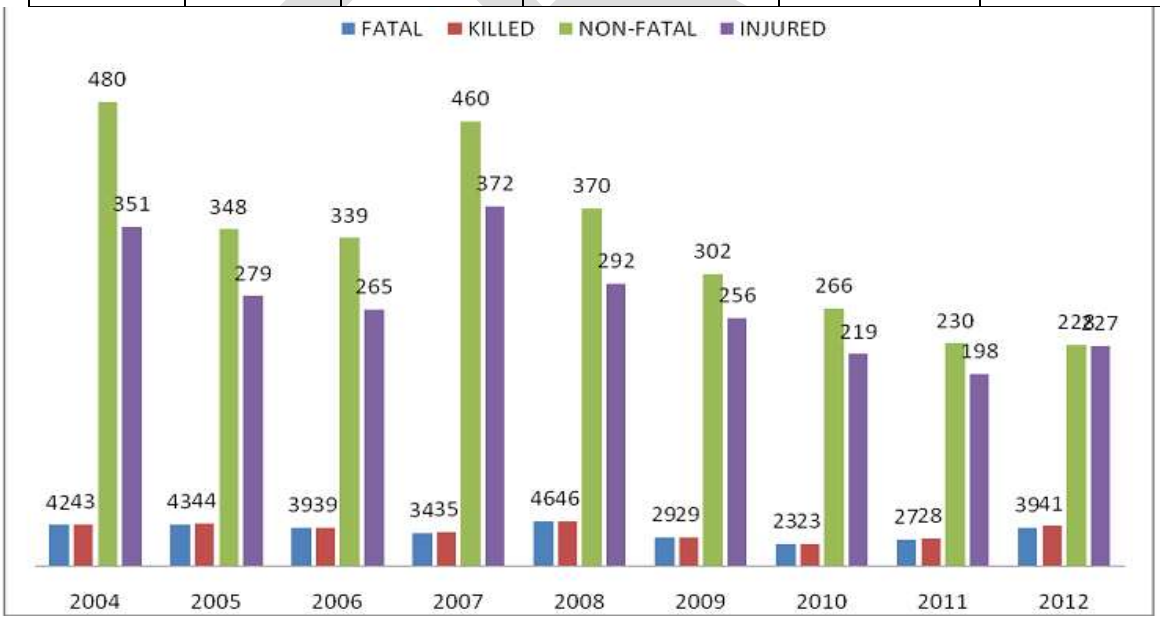

Fig:2 Accident data at Ramoohalli junction

Table No.3 Classified volume Count Data at Ramoohalli Junction

DIRECTION TOWARDS	TOTAL CVPD
Ramoohalli	**10981**
Kengeri	**24281**
Bidadi	**19331**

SIGNAL TIMINGS OF THE AFOREMENTIONED JUNCTIONS

SIGNAL TIMINGS OF RAMOOHALLI JUNCTION

1. Towards ramohalli = 60 secs
2. Towards kengeri=90 secs
3. Bidadi =90 secs

4. Discussions

From the accident scenario of India , we observed that Karnataka stands at the fifth position out of 27 states and 50% fatalities will occur in five major states within India (AP,TN,UP,KA, MH)

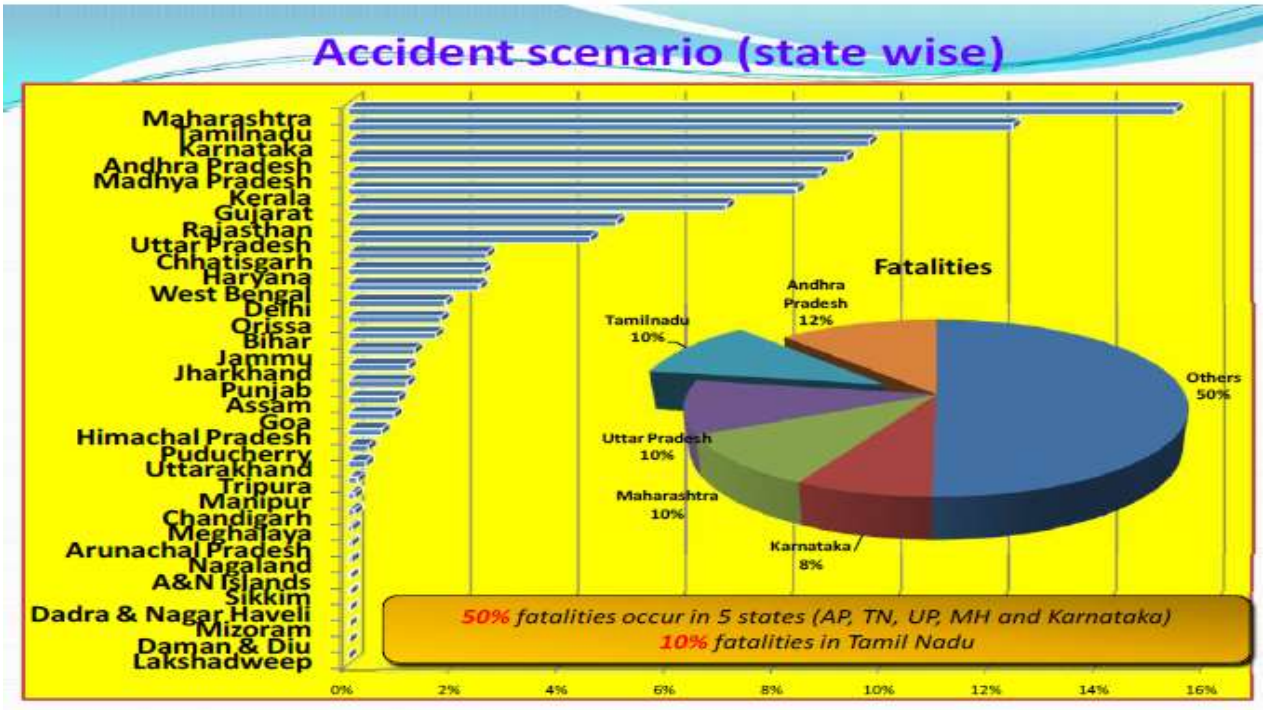

From the studies it has been observed that 65% of the accidents are alone due to human behavior and 24% of the accidents is due to the human and the road interface and 2% is due to road alone.

5. Remedial Measures:

The remedial measures suggested for Improvements of Ramoohalli junction are

1. Pedestrian green time required for major and minor roads are based on walking speed which is equal to 1.2 m/s and initial walking time of 7 sec. This is the minimum green time required on major and minor roads for vehicular traffic.
2. From the accident data, it has been witnessed that 48% of the accidents were occurring at day time and 52% of accidents are occurring at night time out of which 18% amounts at locations without street light and along the mid block. Hence street lights are essential.

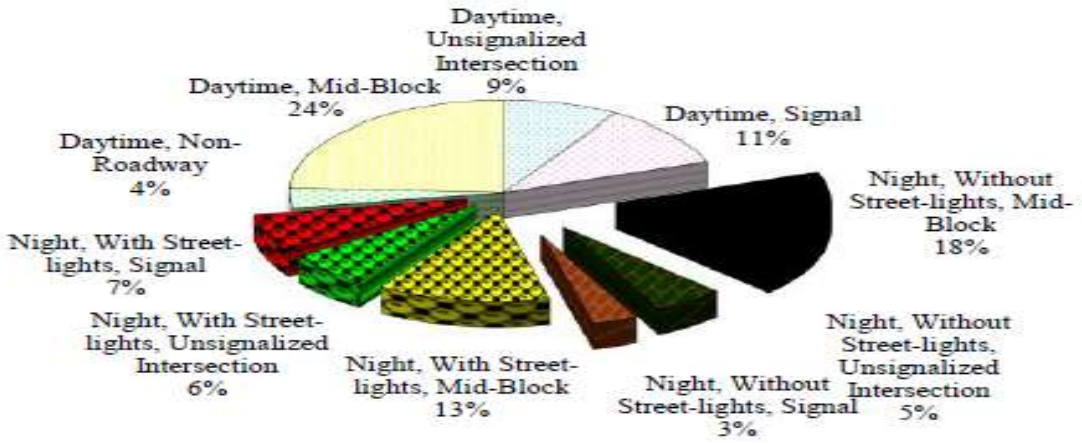

1. Provision of Road humps before the pedestrian signals.
2. Provision of Road Humps in the stretches before Intersection or Junction point.
3. Installation of proper sign posts aside the roads.
4. Improving the sight distance at the intersection by increasing the set back distances in the junctions.
5. Increasing the signal timings by twice to avoid the accumulation of vehicles to reduce the jam lengths.
6. Increasing the signal rest timings by twice to avoid accidents.
7. Repairs of cracked surface and filling up of pot holes to reduce the accidents.
8. Installation of cat eyes and road reflectors in the junctions and also near the road humps

REFERENCES:

[1] G D Jacobs and I.A. Sayer "Road accidents in developing Countries- urban problems and remedial measures" TRRL Supplementary report 839.

[2] M N Shreehari and Ms. Ashwini: Scientific Analysis of Accidents and Mitigative measures-A case study for Bangalore-India, 26 April 2013 National Conference Proceedings Race 2013, Belgaum.

[3] B. Srinivas Rao and E. Madhu "Accidental study on National Highway – 5 between Anakapalli to Vishakpatnam" Proceedings of the Eastern Asia Society for Transportation Studies, Vol. 5, pp. 1973 - 1988, 2005.

[4] K. R. Shanmugam: Valuations of Life and Injury Risks- Empirical Evidence from India- Environmental and Resource Economics **16:** 379–389, 2000.

[5] Mishaps HC suggests change in compensation pattern: Times of India-Bangalore edition, 13 Sep 2001

Mahesh Chand: Accident Scenario in Metropolitan Cities of India- published in Urban Transport journal-September2002

International Journal of Engineering Research and General Science Volume 3, Issue 5, September-October, 2015
ISSN 2091-2730

COST COMPARISON OF INDUSTRIAL STEEL BUILDING WITH STEEL PLATE SHEAR WALL BY CONSIDERING I-SECTION & CONCRETE FILLED SECTION AS COLUMN SECTIONS

Prof.S.D.Ambadkar, Ph.D. Scholar, P.R.M.I.T&R, Badnera-Amravati - 444701.

e-mail : ambadkarswati@gmail.com,

Dr.P.S.Pajgade, Professor, Dept. Of Civil Engg. P.R.M.I.T&R, Badnera-Amravati - 444701.

e-mail: ppajgade@gmail.com

Abstract-Behavior of structure during earthquake motion depends on distribution of weight, stiffness and strength in both horizontal and vertical planes of building. To reduce the effect of earthquake elements steel plate shear walls are used in the building. These can be used for improving seismic response of buildings. The main role of steel shear wall is to collect lateral forces of earthquake in a building and transfer those forces to the foundation. The web plates in steel shear walls are categorized according to their ability to resist buckling. The web plates can be sufficiently stiffened to preclude buckling and allow the full shear strength of the web to be reached. Shear walls are the walls like vertically aligned structural components which are subjected to lateral loads in their plane. These have proved to be very effective for lateral load resistance particularly in the medium to high-rise buildings. These depending upon the material of construction they may be classified as the RCC and steel shear walls. Steel structures are generally lighter than masonry or RC structures. Lower weight translates to lower seismic forces. Steel structures typically show good ductility, even when they are not specifically designed or detailed for seismic resistance. The beams, columns and the plate together act as the vertical plate girder. The columns act as the flanges, the plate as the web and the beams as the horizontal stiffeners of the plate girder. In present study Steel Industrial building with shear wall is analysed & design on STAAD-PRO. Two types of column sections are used i.e. I-section & Concrete filled section. Cost comparison is done for both the cases & compared with Steel Industrial building with & without shear wall.

Key Words : Steel shear wall , Ductility, Seismic Resistance, Shear strength, Plate Girder, I-Section, Concrete filled section

General

Earthquakes are natural phenomena, which cause the ground to shake. Due to earthquake the structure on the ground gets damage or collapse. Earthquake resistant design of structure is a continuing area of research since the earthquake engineering has started not only in India but also in other developed countries. The structure is still damaged due to some or the other reason during earthquakes.

Shear walls are vertical elements of the horizontal force resisting system. Steel shear wall is a lateral load resisting system consisting of vertical steel plate in-fills connected to the surrounding beams and columns and installed in one or more bays along the full height of the structure to form a cantilever wall. The steel plate shear walls are mainly used in multistoried building in the foreign countries such as America, Japan, Canada etc.

Steel structures have historically performed well in earthquakes, and little loss of life can be attributed to collapse of steel buildings in earthquakes. Many of the highly destructive earthquakes around the world have occurred in areas where there are very few steel structures. Thus, the exposure of steel structures to strong earthquakes has been perhaps somewhat less than other types of construction.

Steel Plate Shear Walls have been used in United States since 1970's. In the early period of development of the steel plate shear walls, they were used for seismic retrofit of low and medium-rise existing hospitals and other structures. These initial shear walls were designed with relatively closely spaced horizontal and vertical stiffeners. In a 51-story high-rise building in San Francisco steel shear walls are used as the primary lateral load resisting system.

Now a days the vital properties of steel are made use of in these lateral load resisting systems in the form of steel shear walls. In general the steel plate shear wall system consists of a steel plate welded or bolted to the surrounding beams and columns on all sides.

Behaviour & mechanism of shear resistance of steel plate shear wall.

Its behavior is analogous to a vertical "**Plate Girder**". In this columns acts as a flanges, beams as stiffeners & steel plate as a web.

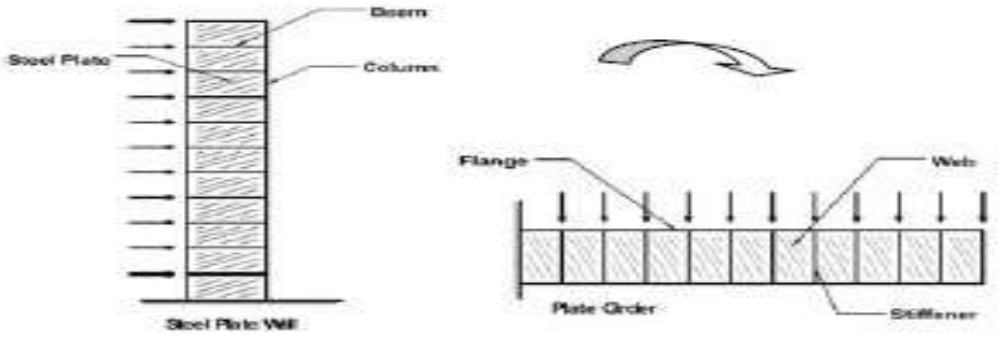

Figure : Steel Plates Shear Wall and Plate Girder Analogy

Basic Types of Shear Walls.

Un-stiffened steel plate shear walls

These are latest and more preferred as compared to the other types. These consist of a thin steel plate welded or bolted to the surrounding beams and the columns. There are no stiffeners on the steel plate. This makes it relatively more economical and easy for fitting and handling. Being thin, it buckles at a relatively small lateral force. But after that it shows full strength as well as stiffness.

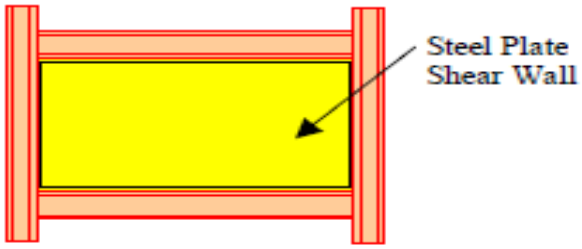

1. Steel Plate Shear Wall
(Unstiffened)

Stiffened steel plate shear walls

These consist of a relatively thick steel plate connected to the beams and columns on its periphery. The plate is stiffened by the horizontal and vertical stiffeners running over it. Thus the plate has got relatively higher strength and stiffness before buckling. The buckling is the criteria used for the design of this shear wall. The cost of fabrication of the stiffeners and the extra material cost increases the overall cost of the shear wall. The tension field stresses do not develop in this case. The yielding of plate occurs before the buckling. stiffeners on the steel plate. This makes it relatively more economical and easy for fitting and handling. Being thin, it buckles at a relatively small lateral force. But after that it shows full strength as well as stiffness.

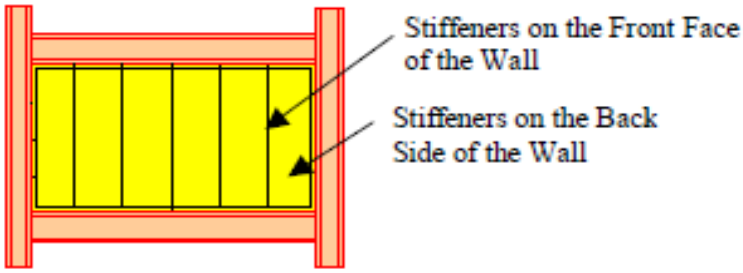

2. Steel Plate Shear Wall
(stiffened)

Table : Difference between RCC and steel shear walls

	RCC Shear Wall	**Steel Shear Wall (SPSW)**
Thickness	About 200 mm	About 6,8,10,12 mm
Material	Stiff, brittle	Flexible , ductile
Mechanism of shear resistance	Direct (through internal shear and bending stresses)	Indirect (through diagonal tension)
Internal resistance force	Shear and bending stress	Diagonal tension forces

Advantages of steel plate shear wall (SPSW)

1. Steel shear wall is very efficient and economical lateral load resisting systems.
2. The steel shear wall system has relatively high initial stiffness, thus very effective in limiting the drift.
3. Compared to reinforced concrete shear walls, the steel shear wall is much lighter which can result in less weight to be carried by the columns and foundations as well as less seismic load due to reduced mass of the structure.
4. By using shop-welded, field-bolted steel shear walls, one can speed-up the erection process and reduce the cost of construction, field inspection and quality control resulting in making these systems even more efficient.
5. Due to relatively small thickness of steel plate shear walls compared to reinforced concrete shear walls, from architectural point of view, steel plate shear walls occupy much less space than the equivalent reinforced concrete shear walls. In high-rises, if reinforced concrete shear walls are used, the walls in lower floors become very thick and occupy large area of the floor plan.
6. Compared to reinforced concrete shear walls, steel plate shear walls can be much easier and faster to construct when they are used in seismic retrofit of existing building.
7. Steel plate shear wall systems that can be constructed with shop welded-field bolted elements can make the steel plate shear walls more efficient than the traditional systems. These systems can also be very practical and efficient for cold regions where concrete construction may not be economical under very low temperatures.

Design of Steel Building With Steel Plate Shear Wall

The mechanism of shear resistance and its behavior of steel plate shear walls is quite different from that of the RCC shear walls. This is because of the fact that the SPSW system consists of not only the steel plate but along with that the columns and the beams to which steel plate is connected. So the beams and columns affect the overall behavior of the SPSW and vice versa. Steel

plate shear wall is modeled as strip model. Hence to find out the effect of the steel plate shear walls on the steel Industrial building (G+3) with I-section & Concrete filled section as column sections present study is done.

Steel Industrial Building without Steel Plate Shear Wall (SPSW) with I-section as Columns-

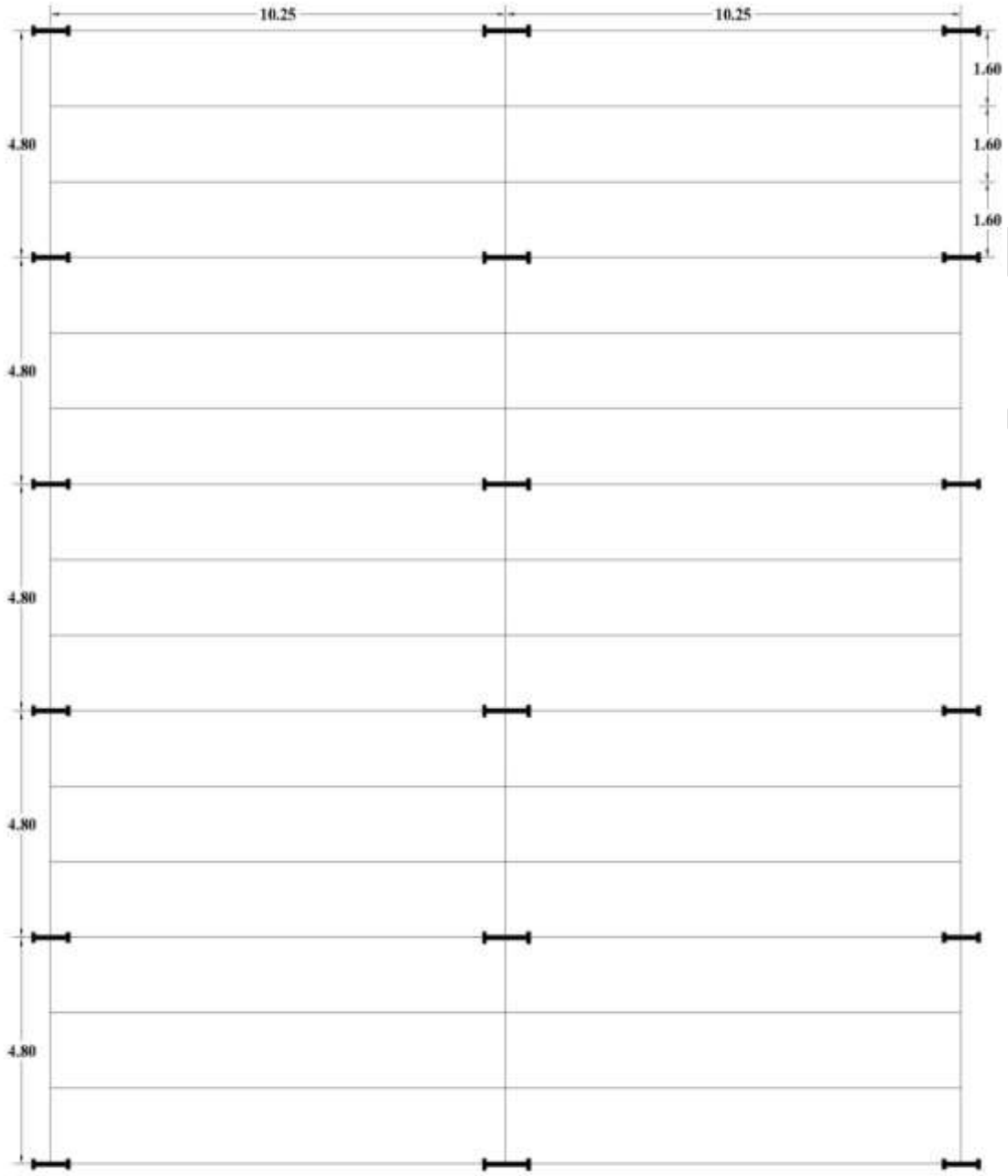

Fig: Plan of Steel Industrial Building without SPSW by using I- section as column

Steel Industrial Building with Steel Plate Shear Wall with Concrete filled section as Column

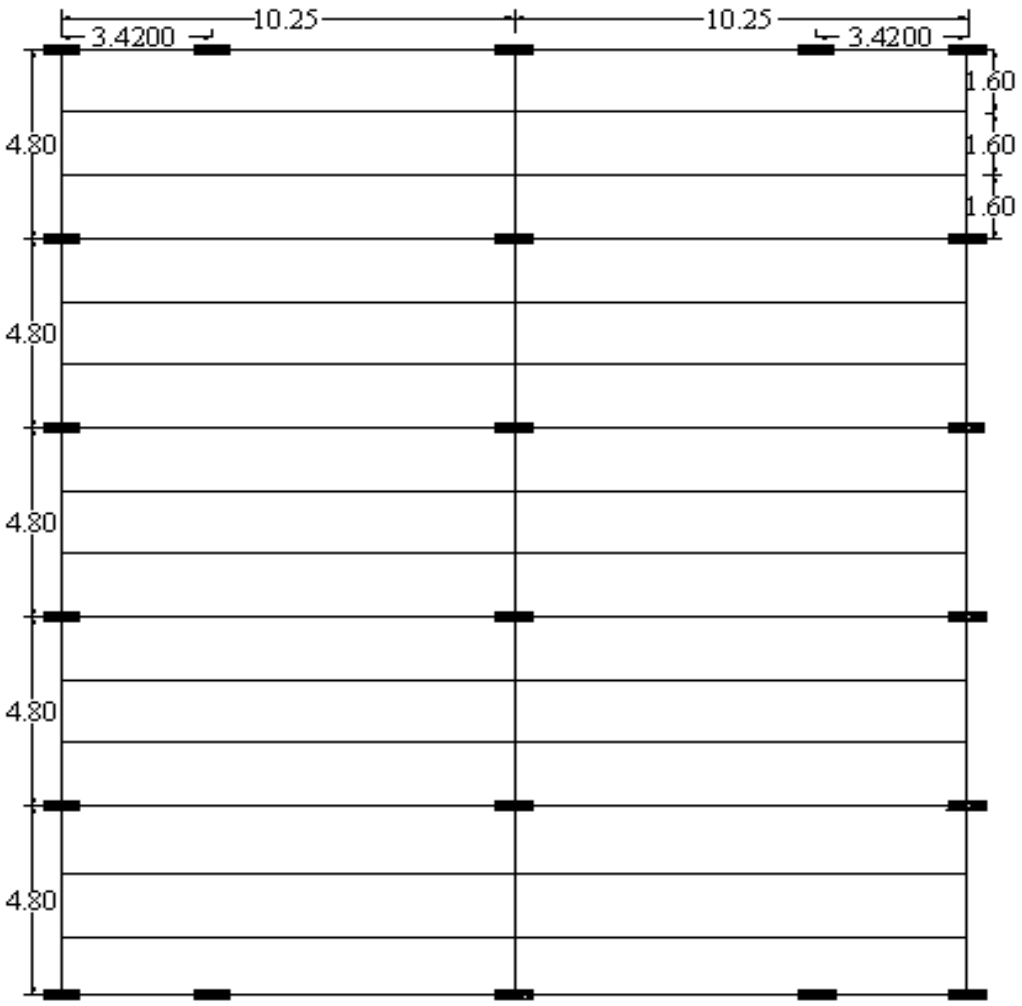

Plan of steel Industrial Building with Steel Plate Shear wall
(By using Concrete filled section as column)

Typical C/S of Column

Fig.: Plan & C/S of Column of Steel Industrial Building with SPSW by using Concrete filled section as column

Steel Industrial Building with Steel Plate Shear Wall with Concrete filled section as Column with Stiffeners

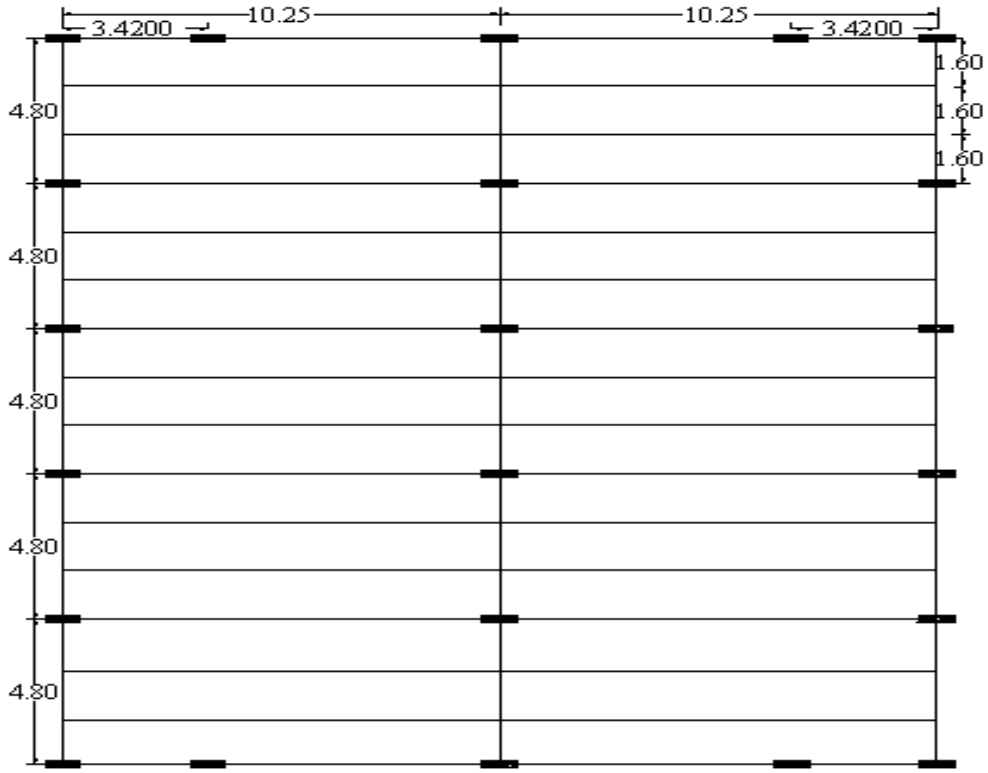

Plan of steel Industrial Building with Steel Plate Shear wall
(By using Concrete filled section as column)

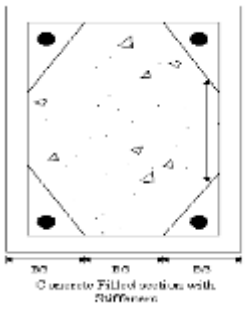

C/S of Column

Fig.: Plan & C/S of Column of Steel Industrial Building with SPSW by using Concrete filled section as column with stiffeners

Table : Cost comparison with & without SPSW

Sr.No.	Type of Steel Building	Cost with SPSW	Cost without SPSW
1.	SPSW with I-section as columns	Rs.1,30,12,800/-	Rs. 1,32,28,000/-
2.	SPSW with Concrete filled section as column	Rs.1,21,52,291/-	Rs. 1,29,47,894/-

3.	SPSW with Concrete filled with stiffeners section as column	Rs.1,17,90,939/-	---

Conclusion –

1. The provision of SPSW is found out to be more economical in Steel Industrial Building with I-section as column.
2. The sizes of inner columns is found out to be smaller in case of steel Industrial building with SPSW than steel industrial building without SPSW by using I-section as column.
3. Cost of steel building with Concrete filled section as column is coming out to be less as compare to Cost of steel building with I-section as column.
4. Steel building with SPSW with Concrete filled section as column is found to be economical compare to Steel building with SPSW with I-section as column.
5. Steel building with SPSW with Concrete filled section as column is found to be economical compare to Steel building without SPSW.
6. Provision of shear wall can reduce the cost of cladding or wall.
7. The steel building with SPSW with concrete filled column with stiffener is found to be economical than steel building with SPSW with concrete filled column without stiffener.
8. Encased I-section is found out to be economical than Concrete filled section with stiffener for medium rise structure. If it is applied for high rise structure reverse may be the case.
9. Because of provision of stiffener, elongated section can be used. Stiffener provides the lateral support.
10. The elastic local buckling of a steel plate can be avoided through an appropriate longitudinal spacing of stiffeners.
11. The steel building with SPSW with concrete filled column with stiffener is found to be economical than steel building with SPSW with I-section as column.

REFERENCES:

1. Mizuo Inukai [1], Kazuya Noguchi[2], Masaomi Teshigawara[3], and Hiroto Kato[4] "*Seismic performance of composite columns using core steel under varying axial load*," 13th World Conference on Earthquake Engineering, Vancouver, B.C., Canada, August 1-6, 2004, Paper No. 598.
2. R.S. Londhe and A.P. Chavan "*Behaviour of building frames with steel plate shear walls"*, Asian Journal of Civil Engineering (building and housing) vol. 11, no. 1 (2010) pages 95-102.
3. Yan Xiao[1], Wenhui HE[2], Xiaoyong Mao[3], Kang-kyu Choi [4] and Pingsheng Zhu[5] "*Confinement design of CFT columns for*

improved seismic performance" PP.217-226.

4. Charles W Roeder[1] And Shosuke Morino[2] "*Research on "CFT column systems*" 12th World Conference on Earthquake Engineering 2000., Paper No.2618. PP.1-8.
5. C. S. Huang[1]; Y.-K. Yeh[2]; G.-Y. Liu[3]; H.-T. Hu[4]; K. C. Tsai[5]; Y. T. Weng[6]; S. H. Wang[7]; and M.-H. Wu[8] "*Axial load behavior of stiffened concrete-filled steel columns"* Journal of Structural engineering / September 2002 .pp. 1222-1230.
6. Jian Cai, Zhen-Qiang He "*Axial load behavior of square CFT stub column with binding bars*" Department of Civil Engineering, South China University of Technology, Guangzhou 510641, China Journal of Constructional Steel Research 62 (2006) 472–483.
7. "Steel Design Guide, Steel plate shear wall" American Institute of Steel Construction (AISC).
8. Engineering, Vancouver, B.C.., Canada, August 1-6, 2004, Paper no. 507. PP 1-15.
9. Sherif EL-Tawil,[1] Associate Member, ASCE, and Gregory G. Deierlein,[2] Member, "*Strength and ductility of concrete encased composite columns"* ASCE Journal of Structural Engineering September 1999. PP.1009-1019.
10. Oreste S. Bursi1, Stefano Caramelli2, Giovanni Fabbrocino3, Artur V. Pinto4, Walter Salvatore5, Fabiottaucer6, Robert Tremblay7 and Riccardo Zandonini8, "*Pseudo-dynamic testing of a 3D full-scale high ductile steel-concrete composite MR frame structure at Elsa*" 13th world conference on Earthquake.
11. IS11384(1985) , "*Code of Practice for Design of Composite Structure*," Bureau of Indian Standards (BIS), New Delhi.
12. IS 800:2007, Code of practice for general construction in steel, Bureau of Indian Standards, New Delhi.

International Journal of Engineering Research and General Science Volume 3, Issue 5, September-October, 2015
ISSN 2091-2730

Adsorption of Copper and Lead ions from aqueous solutions using Nickel oxide nanostructure

Y.V.S. SAI KRISHNA & R.RAVICHANDRA BABU*
Department of chemistry, Institute of science, Gitam University
Visakhapatnam, 530045, Andhra Pradesh, India.
Email:rrcbabu7@yahoo.in,contact no: +919490798683

Abstract- Nickel oxide (NiO) has been synthesized by novel simple method using solution combustion technique employing glycine as a fuel .The synthesized NiO nanostructure is characterized for Surface area by BET analyzer. The ability of NiO nanostructures as adsorbent was investigated for adsorptive removal of Cu (II) and Pb (II) ions from aqueous solutions. Various physical & chemical parameters such as p^H, initial metal ion concentration, adsorbent dosage and equilibrium contact time were studied. The optimum solution P^H for adsorption of Pb (II) and Cu (II) ions in aqueous solutions were at 9.0 and 7.0 respectively and the optimum contact time was found to be 30 min. The adsorption isotherms were obtained using concentrations of the metal ions ranging from 0.1 to 1.0 mg/l. This study revealed that NiO nano structure is an effective adsorbent for removal of Cu (II) and Pb (II) ions from aqueous solutions.

Key words: Solution combustion, Nickel oxide nano structure, Heavy metals, Adsorption studies, Optimum solution, BET Analyzer, Adsorption Isotherm

1. Introduction:

Because access to safe drinking water is the key to protect public health, clean water has become a basic need of all properly functioning societies[1]. Despite their presence at low concentration ranges, environmental pollutants possess serious threats to freshwater supply, living organisms, and public health[2].Contamination of water with toxic metal ions (Hg(II), Pb(II), Cr(III), Cr(VI), Ni(II), Co(II), Cu(II), Cd(II),) etc becoming a severe environmental and public health problem. In order to achieve environmental detoxification, various techniques like adsorption, precipitation, ion exchange, reverse osmosis, electrochemical treatments, membrane filtration, evaporation, flotation, oxidation and biosorption processes are extensively used.[3,4,5].Among these, adsorption is a conventional but efficient technique to remove toxic metal ions and bacterial pathogens from water. Activated carbon, processing high BET surface areas, was adopted as an adsorbent to remove the heavy metals and better adsorption efficiency was achieved[6].Removal of heavy metals from industrial waste water streams has been studied by adsorption phenomenon due to the high threat of such pollutants to public health and environment[7,8].The adsorption process is arguably one of the more popular methods for the removal of heavy-metal ions because of its simplicity, convenience, and high removal efficiency[9].Development of novel and cost-effective nanomaterials for environmental remediation, pollution detection and other applications has attracted considerable attention. Recent advances suggest that many of the issues involving water quality could be resolved or greatly ameliorated using nanoparticles, nanofiltration or other products resulting from the development of nanotechnology [10, 11].

Nanoparticles exhibit good adsorption efficiency especially due to higher surface area and greater active sites for interaction with metallic species[12,13]. Furthermore, adsorbents with specific functional groups have been developed to improve the adsorption capacity[14].Recently, application of nanoparticles for the removal of pollutants has come up as an interesting area of research. The unique properties of nanosorbents are providing unprecedented opportunities for the removal of metals in highly efficient and cost-effective approaches, and various nanoparticles and dendrimers have been exploited for this purpose[15,16].Nanoscale metal oxides potentially offer a more cost efficient water treatment and remediation technology due to their size and adsorption efficiency[17,18].

We here in the present study able to synthesize nickel oxide using solution combustion technique by employing glycine as a fuel. Subsequently the synthesized metal oxide used for adsorption studies for the removal of metals like Lead and Copper.

2.Experimental

2.1Material and Methods

All chemicals used in this study were of analytical grade. Nickel nitrate and glycine were obtained from Merck ,India. The NiO nanostructure was prepared using Nickel nitrate by solution combustion process with glycine employed as a fuel. Specific amount of Nickel nitrate and glycine were dissolved in Millipore water and kept for stirring for 30 min. The solution was then transferred in to a porcelain crucible and kept on hot plate until syrupy state attained. The contents were heated in a muffle furnace at 500^{o}Cfor 3 hr.The crystal water was gradually vaporized during heating and when a crucible temperature was reached, a great deal of foams produced and spark appeared at one corner which spread through the mass, yielding a black voluminous and fluffy product in the container. The product was carefully grinded by using mortar. A fine black colored Nickel Oxide was obtained.

The surface area of the particles was measured by a Brunauer, Emmett, and Teller (BET) surface area analyzer (Nova 1200e) for nitrogen adsorption. The BET method was carried out under relatively high vacuum and measured primarily the external area of the particles and aggregates.

2.2 Adsorption Studies*:*

Nanoparticles formed by metal or metal oxides are inorganic nanomaterials, which are used broadly to remove heavy metal ions in wastewater treatment. Nanosized metal oxides provide high surface area and specific affinity. Besides, metal oxides possess minimal environmental impact and low solubility and no secondary pollution have been adopted as sorbents to remove heavy metals.

Adsorption studies were performed by batch process by taking 0.35 gm of synthesized NiO in a 100 ml clean and dried stoppered bottle. Known concentration of Lead (II) and Copper (II) solution was added in the same stoppered flask. The flask was placed on a mechanical shaker (180 rpm rate) and agitated for a time period of 35 min.. The solution was then filtered using what man filter paper no. 41 and the aliquot is used for metal ion concentration determination using Atomic Absorption Spectroscopy.
In order to obtain the optimal conditions for Pb(II) and Cu(II) removal by NiO nanoparticles, the effect of various parameters such as adsorbent mass, contact time, pH, and initial concentration of metal ions were investigated. The surface area of the freeze-dried NiO particles measured using the Brunauer, Emmett, Teller (BET) method and was found to be 71.985 m2 /g.

3.Results and Discussion

3.1 Effect of pH:

The adsorption experiments were carried out in a series of 250 ml Erlenmeyer flasks containing 0.35 g synthesized NiO with different concentration of Lead (II) and Copper (II) ions at serial pH conditions (3 to 10). The prepared samples were stirred in mechanical shaker for different time intervals. Then solid/liquid phases were separated by filtration. The concentration of the Lead (II) and Copper (II) ions before and after adsorption was determined using Atomic Absorption mass spectrometry (Agilent 240 AA). The recovery efficiency at different pH conditions was shown in the Fig.1 & Fig.2.

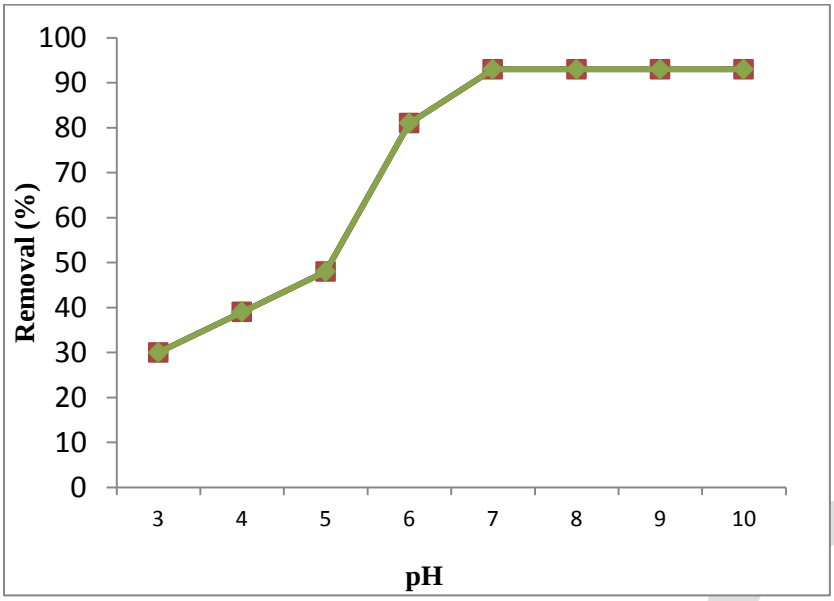

Fig.1-Adsorption percentage of copper at p^H=7.0

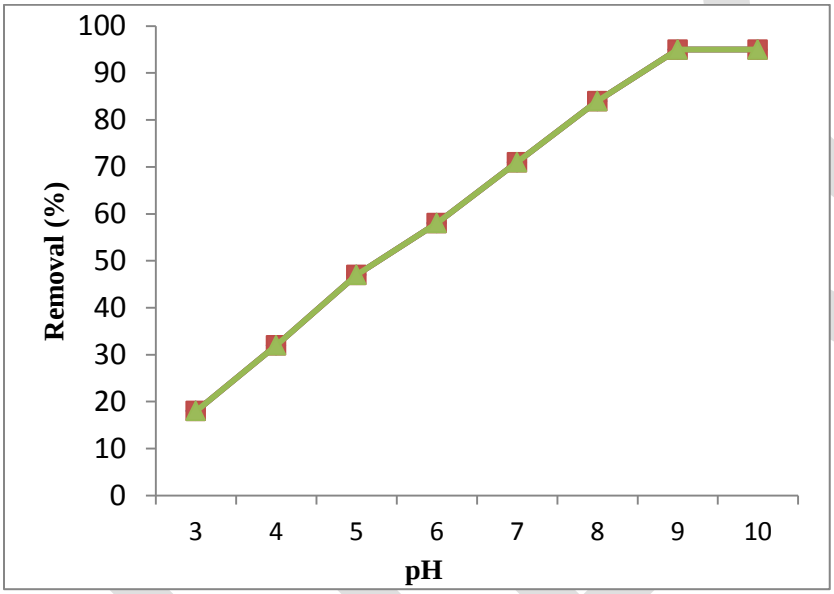

Fig.2-Adsorption percentage of Lead at p^H=9.0

3.2 Effect of Addition of Oxide:

Adsorbent dosage is an important parameter because it determines the capacity of an adsorbent for a given initial concentration of the adsorbate. The effect of adsorbent dosage was studied on Lead (II) and Copper (II) from aqueous solutions by varying the amount of NiO ranging from 0.1 g to 0.5 g , while keeping other parameters constant.(pH, agitation speed, temperature, initial Lead and Copper ion concentrations and contact time). Adsorbent dosage of 0.35g is found to be optimum for effective removal of Copper (II) and Lead (II) represented graphically as shown in Fig.3 & Fig.4.

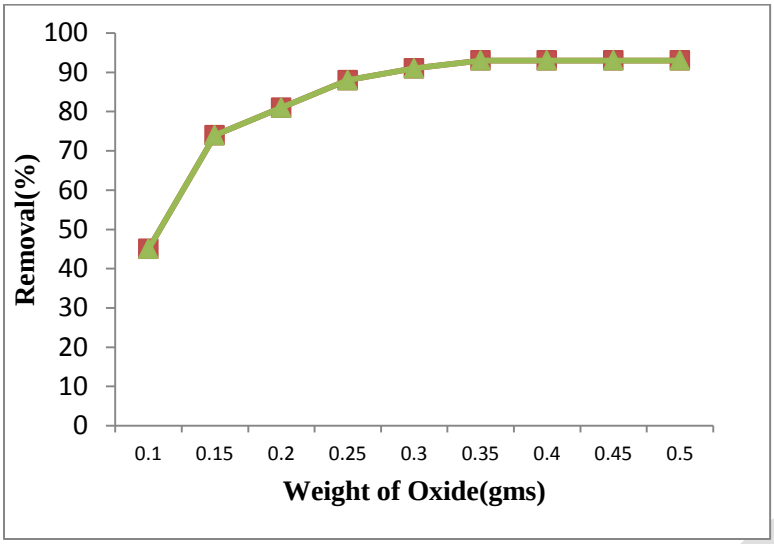

Fig.3-Percentage of copper ions removal at different adsorbate concentration.

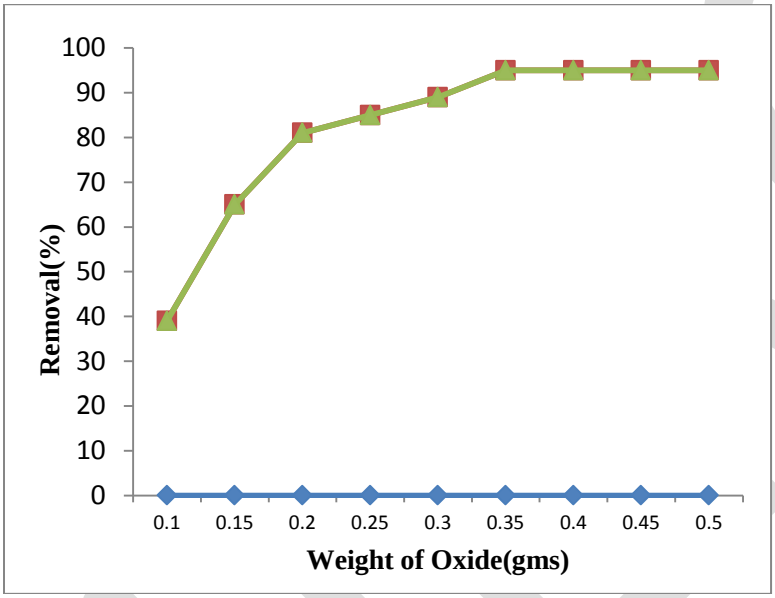

Fig.4-Percentage of lead ions removal at different adsorbate concentration

3.3 Effect of Stirring time:

The effect of time on the removal efficiency of Copper (II) and Lead (II) were also studied at fixed adsorbent dosage of 0.35g at a pH of 7 for Copper(II) and at a pH of 9 for Lead(II)ions at different time intervals starting from 20, 40, 60, 80, &100 min and the results are shown graphically in Fig.5& Fig.6. It has been established that optimum time required to attain the equilibrium between the Copper (II) and lead (II) ions adsorbed on NiO particles was in between 35-40 min.

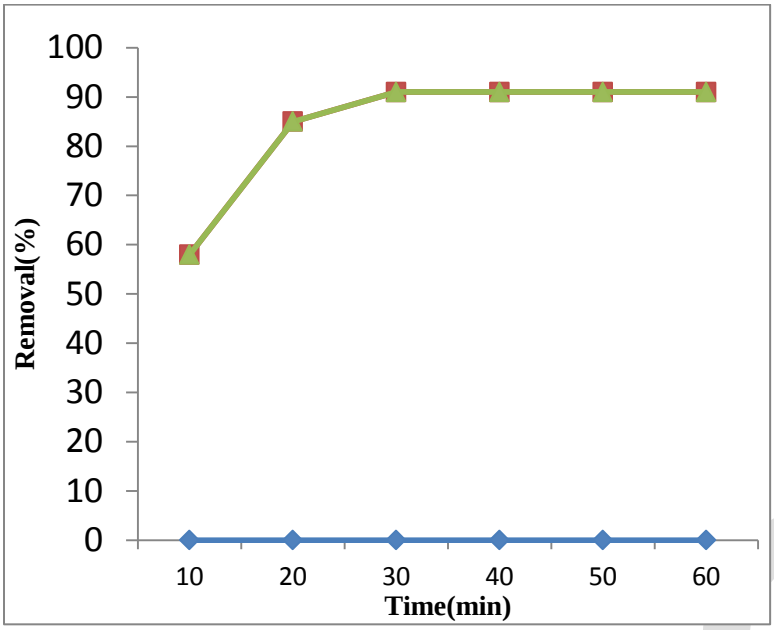

Fig.5-Adsorption capacity of Copper at different time intervals

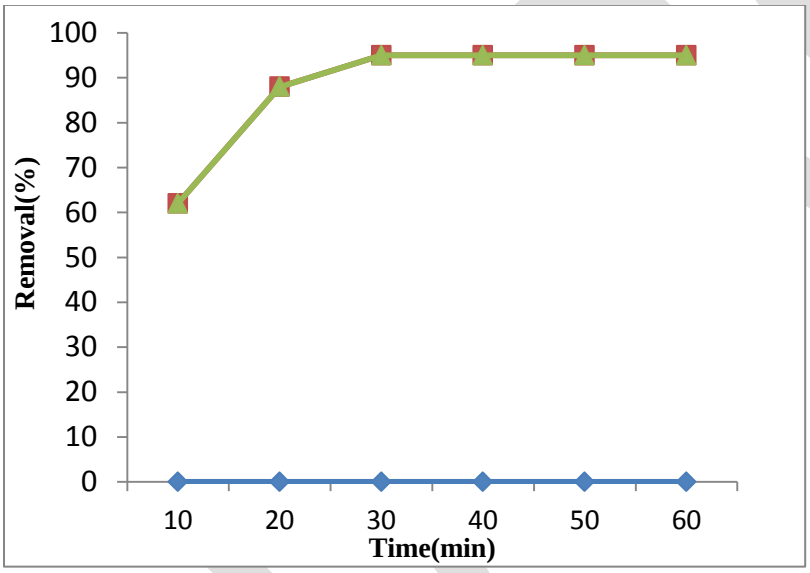

Fig.6-Adsorption capacity of Lead at different time intervals

4.Adsorption isotherm:

Adsorption isotherm is important to describe how solutes interact with the sorbent. Developing an appropriate isotherm model for adsorption is essential to the design and optimization of adsorption processes. The more common models used to investigate the adsorption isotherm are Langmuir and Freundlich equations The equilibrium adsorption isotherms are important in determining the adsorption capacity of metal ions and diagnose the nature of adsorption onto the NiO nanostructures.

The equilibrium adsorption capacity of adsorbent was calculated by the following equation

$$q_e=V\ (C_0-C_e)/W$$

Where qe is the equilibrium adsorption capacity of adsorbent in mg metal/g adsorbent, C_0 is the initial concentration of the metal ions in mg/l, Ce is the equilibrium concentration of metal ions in mg/l, V is the volume of metal ions solution in L, and W is the weight of the adsorbent in g.The experimental results of this study are fitted with Langmuir& Fruendlish models shown in Fig.7 to Fig.10

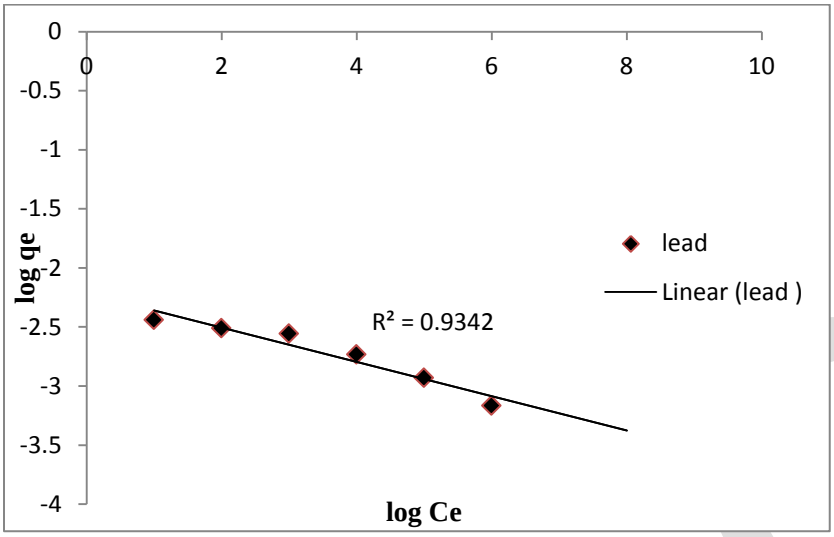

Fig.7-Freundlish isotherm for adsorption of Pb onto NiO nano powder

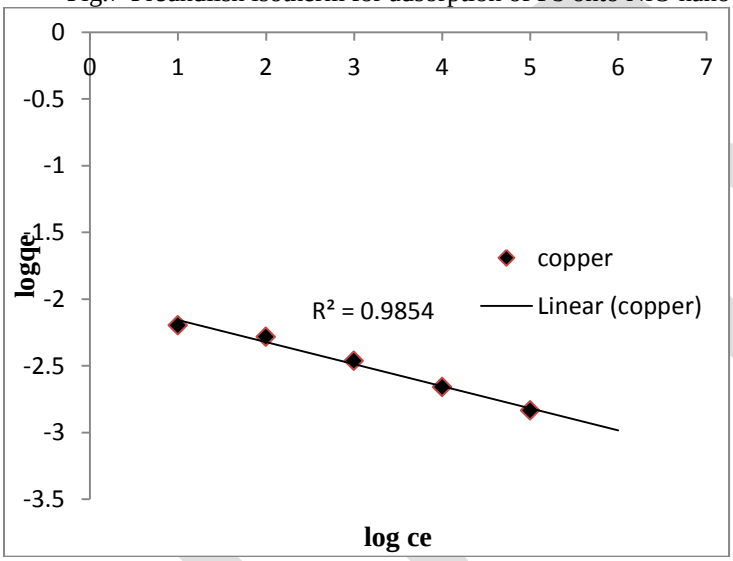

Fig.8-Freundlish isotherm for adsorption of Cu onto NiO nano powder

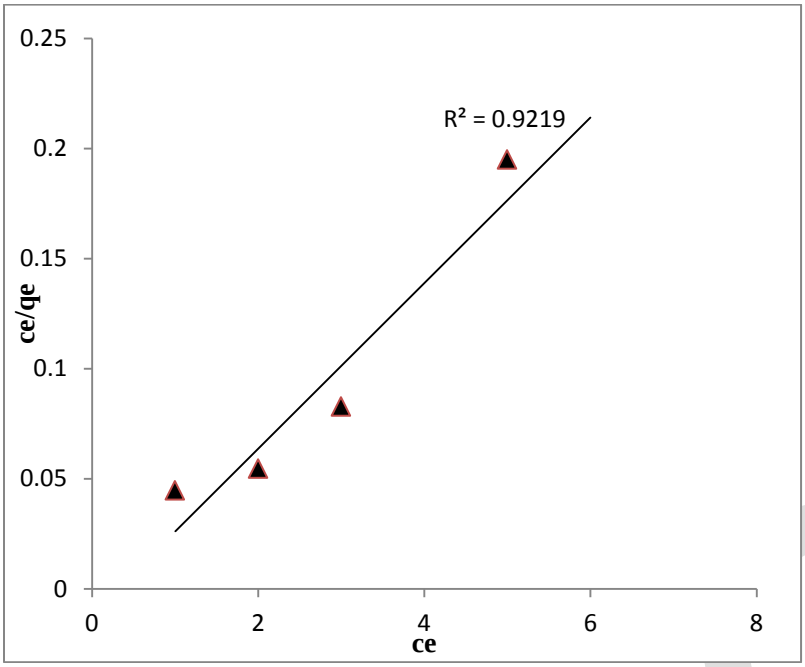

Fig.9-Langmuir isotherm for adsorption of Cu onto NiO nano powder

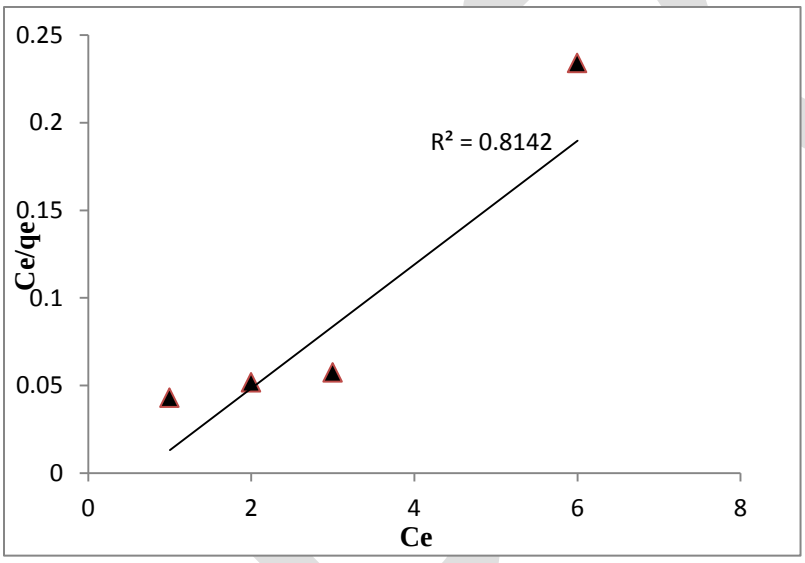

Fig.10- Langmuir isotherm for adsorption of Pb onto NiO nano powder

Acknowledgement:

Generous funding from the University Grants Commission (UGC),New Delhi ,Government of India in the form of Major Research Project(Project file no: F.No.42-327/2013(SR) is gratefully acknowledged.

Conclusions

NiO nanostructure has been synthesized using solution combustion method employing glycine as a fuel. The produced Nickel oxide was characterized by BET and the surface area was found to be 71.985 m2 /g. In this study, batch adsorption experiments for the removal of Pb (II) and Cu (II) ions from aqueous solutions have been carried out using the synthesized nano nanostructure as adsorbent. The adsorption characteristics have been examined at different pH values, contact time, adsorbent dosage and initial metal ion concentrations. The obtained results can be summarized as follows:

- The surface area of the freeze-dried NiO particles measured using the BET method and was found to be 71.985 m2 /g.
- The pH experiment result showed that the removal of Pb increased significantly as the pH increased from 3.0 to 9.0. While the removal of Cu increased significantly as the pH increased from 2.0 to 7.0
- The optimum contact time for adsorption of the heavy metals was considered to be 35 min.
- The adsorption experimental results of these heavy metals are in a good correspondence with the Langmuir and Freundlich isotherms.
- The produced metal oxide was found to be potential adsorbent for the removal of Pb and Cu from aqueous solution.

REFERENCES:

1 World Health Organization, Guidelines for Drinking-water Quality, 3rd Edition, Incorporating the first and second addenda, Vol. 1, Recommendations, Geneva, Switzerland. Retrieved from http://www.who.int/water_sanitation_health/dwq/ fulltext.pdf, (2008).

2 P.L Brezonik., and W.A Arnold., Environmental Science and Technology 46 (2012) pp 5650-5657

3 S. Chen, Y.Zou., Z. Yan, W.Shen, S.Shi., X.Zhang. and .H.Wang, 161 (2009) Journal of Hazardous Materials pp 1355-1359

4 Y.Chen, B. Pan,H. Li, W. Zhang., L Lv. and L Wu., 44 (2010) Environmental Science and Technology pp 3508-3513

5 V.Ivanov., J.H Tay., S.T.L Tay. and H.L Jiang., 50 (2004) Water Science and Technology pp147-154

6 D.C Sharma. and C.F Forster.,(1996) Water SA, 22 pp153-160

7 V.K Gupta., M.Gupta. and S.Sharma. , 35 (2001)Water Research, pp 1125-1134

8 J.T. PollardS., G.D Fowler, C.J Sollars and R.Perry. 11 (1992)" Science of the Total Environment, pp 631-641

9 M.Luisa Cervera, M. Carmen Arnaldela M.Guardia. 375 (2003) Anal Bioanal Chem pp 820-825

10 J.Schulte and J.Dutta, 6 (2005) Science and Technology of Advanced Materials pp 219-220

11 M.Auffan, H.J.Shipley,S.Yean,A.T.Kan, M.Tomson. J.Rose. and J.Y.Bottero. 17 (2007) Environmental Nanotechnology pp 359-362

12 K.E Engates, H.J Shipley 18 (2010) Environ Sci Pollution Res pp 386-395

13 W.Zhang 5 (2003) J Nanoparticle Res pp 323-332

14 A.R.Turker. 35 (2007) Clean-Soil Air Water pp 548-557

15 A.Afkhami, R.Moosavi. 174 (2010) J Hazard Mater pp 398-403

16 M.Jiang, Q.Wang, X Jin, Z.Chen. 332 (2009) J Hazard Mater pp 332-339

17 W. Yantasee, C.LWarner., T. Sangvanich., R.S Addleman, T.G Carter, R.J Wiacek,G.E Fryxell, C.Timchalk. WarnerM.G , 41 (2007) Environmental Science and Technology pp 5114-5119

18 C.A Martinson, Reddy K 336 (2009) J Colloid Interface Sci pp 406-411

International Journal of Engineering Research and General Science Volume 3, Issue 5, September-October, 2015
ISSN 2091-2730

Texture Filter based Medical Images Segmentation for Cancer Disease

Dr. Sana'a khudayer Jadwa

Computer Unit, College of Medicine

Al-Nahrain University

Baghdad- Iraq

E-mail: sanaakhudayer@yahoo.com

Abstract— Medical Image processing is one of the most challenging topics in research field. In medical field, CT (Computed Tomography) scan imaging and MRI (magnetic resonance imaging) are the most important for image based visual diagnostics, but applying segmentation to these images is very tedious and requires an adjusting approach. The main objective of medical image segmentation is to extract and characterize anatomical structures with respect to some input features or expert knowledge. In this paper we have formulated a simple, general, fast, and user-friendly approach to the problem of medical image segmentation based on texture filter. In this method, the experimental results show that the segmentation results are visually satisfactory of medical image texture segmentation.

Keywords— Medical image processing, image texture, image segmentation, texture analysis**,** medical imaging, , Medical image Analysis ,texture filter.

1. INTRODUCTION

Medical imaging application plays an indispensable role by automating or facilitating the delineation of anatomical structures. Medical image segmentation is a challenging task due to the various characteristics of the images, which leads to the complexity of segmentation. [1]. In computer vision, Image segmentation is known as a process of partitioning an image into several segments also known as super pixels. The important goal of image segmentation is to simplify or change the representation of an image into form that is more meaningful and is easy for analysis [2]. Segmentation is an important process in the analysis of MR (Medical Resonance) Images for medical diagnosis. It divides the MR image into different types of classes and groups the homogeneous pixels into clusters. This is used in medical diagnosis in many ways, detecting brain tumor, tissue analysis, bone fractures and similar problems [3]. Segmentation of medical images involves three main image-related problems. The image may contain noise that can alter the intensity of a pixel such that its classification becomes uncertain. Also, the images can exhibit intensity nonuniformity where the intensity level of a tissue class varies gradually over the extent of the image. Third, the images have finite pixel size are subject to partial volume averaging where individual pixel volumes contain a mixture of tissue classes so that the intensity of a pixel in the image may not be consistent with any single tissue class[4].An image texture can be defined as the local spatial variations in pixel intensities and orientation. In order to recognize objects and scenes in computer vision, it is essential to be able to partition an image into meaningful regions with respect to texture characteristics. Texture segmentation has a wide range of applications like content based image retrieval, medical diagnosis, analysis of satellite or aerial images, surface defect detection and terrain classification for mobile robot navigation[5]. This paper produce texture segmentation method for medical images. The organization of the rest of this paper is as follows. Section 2 highlights the related works. Section 3 introduces image texture analysis . Section 4 describes the proposed method. Section 5 present the experimental results and section 6 concludes the paper.

2. RELATED WORKS

Medical image segmentation is a challenging task due to the various characteristics of the images, which leads to the complexity of segmentation **Eldman and Maria** [6] introduced an automatic method of medical image segmentation used in the study of the Central Nervous System (CNS) by multilevel thresholding based on histogram difference. **V. Grau*, A. U. J. Mewes** [7] Presented a method to combine the watershed transform and atlas registration, through the use of markers. This new algorithm applied to two challenging

applications: knee cartilage and gray matter/white matter segmentation in MR images. Numerical validation of the results is provided, demonstrating the strength of the algorithm for medical image segmentation. **Ch.Hima Bindu,QISCET, Ongole** [8] Employed an optimized Otsu method based on improved thresholding algorithm for medical image segmentation ,the experimental results show that the new optimized method dramatically reduces the operating time and increases the separability factor in medical image segmentation while ensures the final image segmentation quality. **Seongjai Kim and Hyeona Lim** [9] proposed the background subtraction (MBS) in order to minimize difficulties arising in the application of segmentation methods to medical imagery. **Ebrahim and Dehmeshki**[10]developed a method that requires the definition of a speed function that controls curve evolution. The image intensity gradient and the curvature are utilized together to determine the speed and direction of the propagation. Although level set methods are highly effective in segmenting image, but. they are sometimes unable to exactly detect objects in images with low-contrast boundaries. In this method hybrid speed functions are used for an implicit active contour (level set) method which is capable of segmenting images with low-contrast boundaries.

3. IMAGE TEXTURE ANALYSIS

The regular repetition of an element or pattern on a surface it is called as texture. It is used to identify different textured and non-textured regions in an image, to classify/segment different texture regions in an image, to extract boundaries between major texture regions ,figure(1) illustrate three examples of image texture[11]:

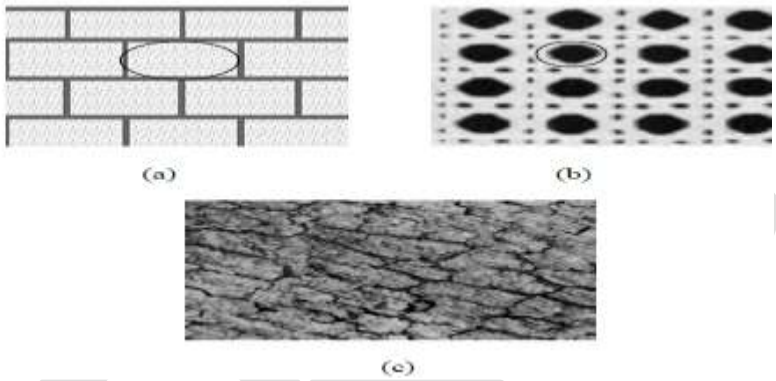

Figure(1): Different examples of image texture

Texture is a difficult concept to represent, the identification of specific textures in an image is achieved primarily by modeling texture as a two-dimensional gray level variation. The relative brightness of pairs of pixels is computed such that degree of contrast, regularity, coarseness and directionality[11]. Texture analysis refers to the characterization of regions in an image by their texture content. Texture analysis attempts to quantify intuitive qualities described by terms such as rough, silky, or bumpy in the context of an image. In this case, the roughness or bumpiness refers to variations in the brightness values or gray levels[12]. Texture analysis of an image gives distributed arrangements of the intensity of the pixel in an image[13].An image texture can be defined as the local spatial variations in pixel intensities and orientation. In order to recognize objects and scenes in computer vision, it is essential to be able to partition an image into meaningful regions with respect to texture characteristics[14].Texture analysis is used in a variety of applications, including remote sensing, automated inspection, and medical image processing. Texture analysis can be used to find the texture boundaries, called texture segmentation[12]. All texture functions operate in a similar way. They define a neighborhood around the pixel of interest calculate the statistic for that neighborhood and then use the computed statistic value as the value of the pixel of interest in the output image. The example that shown in Figure(2) illustrates how the range filtering function operates on a simple matrix. In this example, the value of element B (2, 4) is calculated from A (2, 4). Range filtering function use m by n pixels, in this example 3 × 3, neighborhood around the pixels[12].

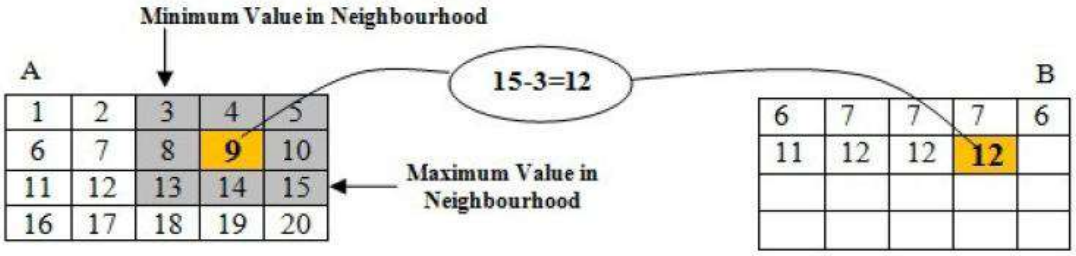

Figure(2): Range filtering function

4. PROPOSED METHOD

In this paper the texture segmentation for medical image based on applying a range filter is proposed. At first the color image is read from a database that contain a collection of medical images, then these images are converted to grayscale image, later the range filter is applied in order to extract the texture content of medical image. The texture segmentation process diagram is illustrated in figure(3) as shown below:

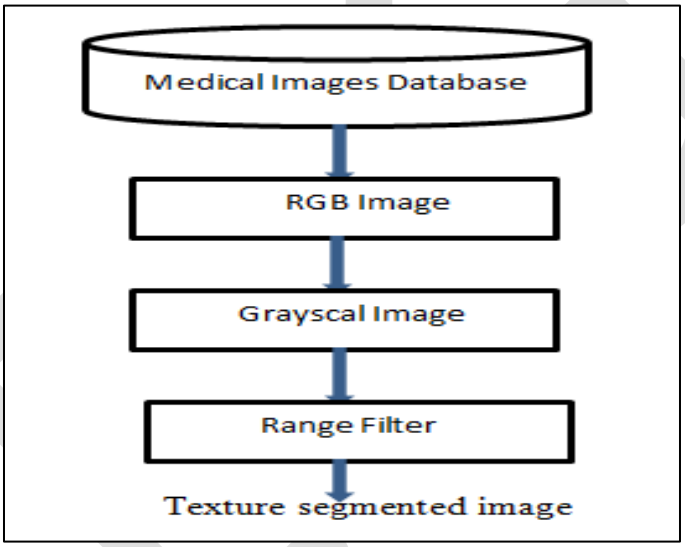

Figure(3): Block diagram for texture image segmentation

4.1 IMAGE DATABASE

The starting point of this work was the creation of a database with six medical images modalities having different sizes that is collect from the web. The database consist of three groups : brain cancer , kidney cancer and stomach cancer images. Figure (4) show the database images.

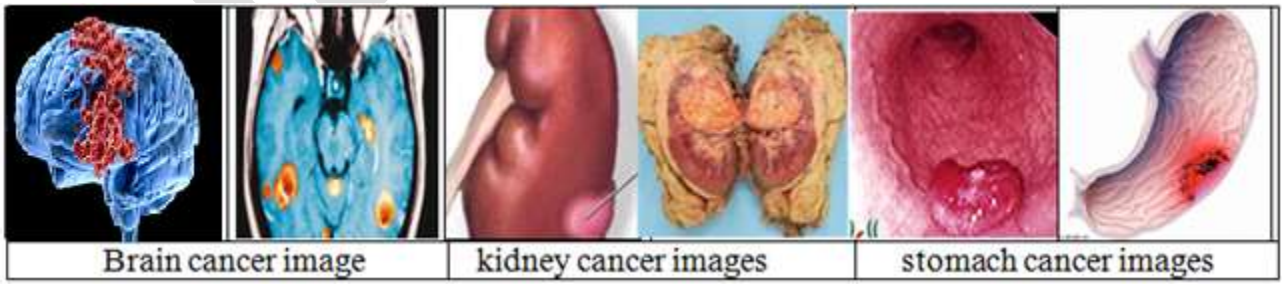

Figure(4): Different medical images

4.2 RGB IMAGE CONVERSION

The colored medical image is converted to gray scale image by converts RGB values to grayscale values by forming a weighted sum of the R, G, and B components using equation(1):

$$y = 0.2989 * R + 0.5870 * G + 0.1140 * B \quad \text{.....(1)}$$

4.3 RANGE FILTERING

Filtering is perhaps the most fundamental operation of image processing. The term filtering can be defined as the value of the filtered image at a given location. It is a function of the values of the input image in a small neighborhood of the same location. Filter operators can be used to sharpen or blur images, to selectively suppress image noise, to detect and enhance edges, or to alter the contrast of the image. The filters use the local statistical variations in an image to reveal the edges and its histogram [15].

5. EXPERIMENTAL RESULTS

The proposed algorithm is applied on the medical images of cancer disease, at first the color image is reading from the database then it converted to grayscale as shown in figure(5):

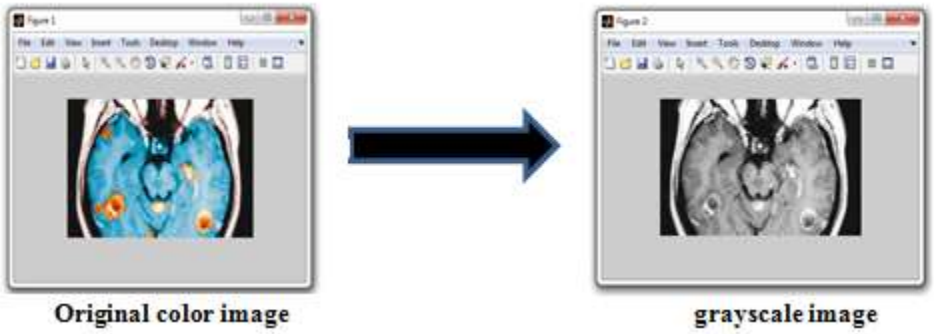

Figure (5): Colored Image conversion.

Then the range filter is applied on grayscale image to obtain the texture segmented medical image as show in figure (6):

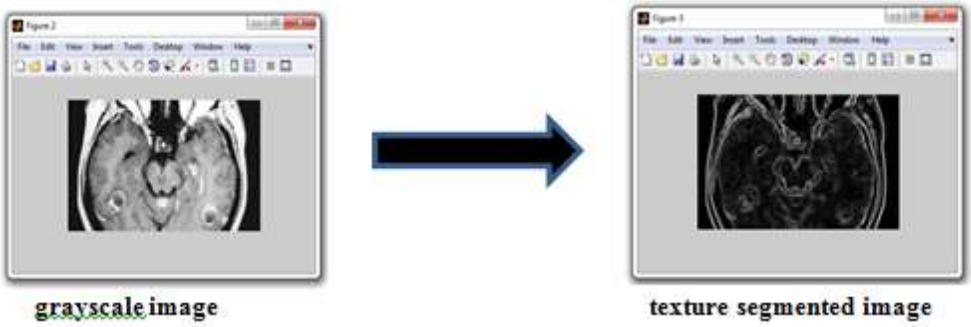

Figure (6): Texture segmented medical image

The same steps applied for the rest image given the result as shown in figure (7):

Original image	Grayscale image	Texture segmented

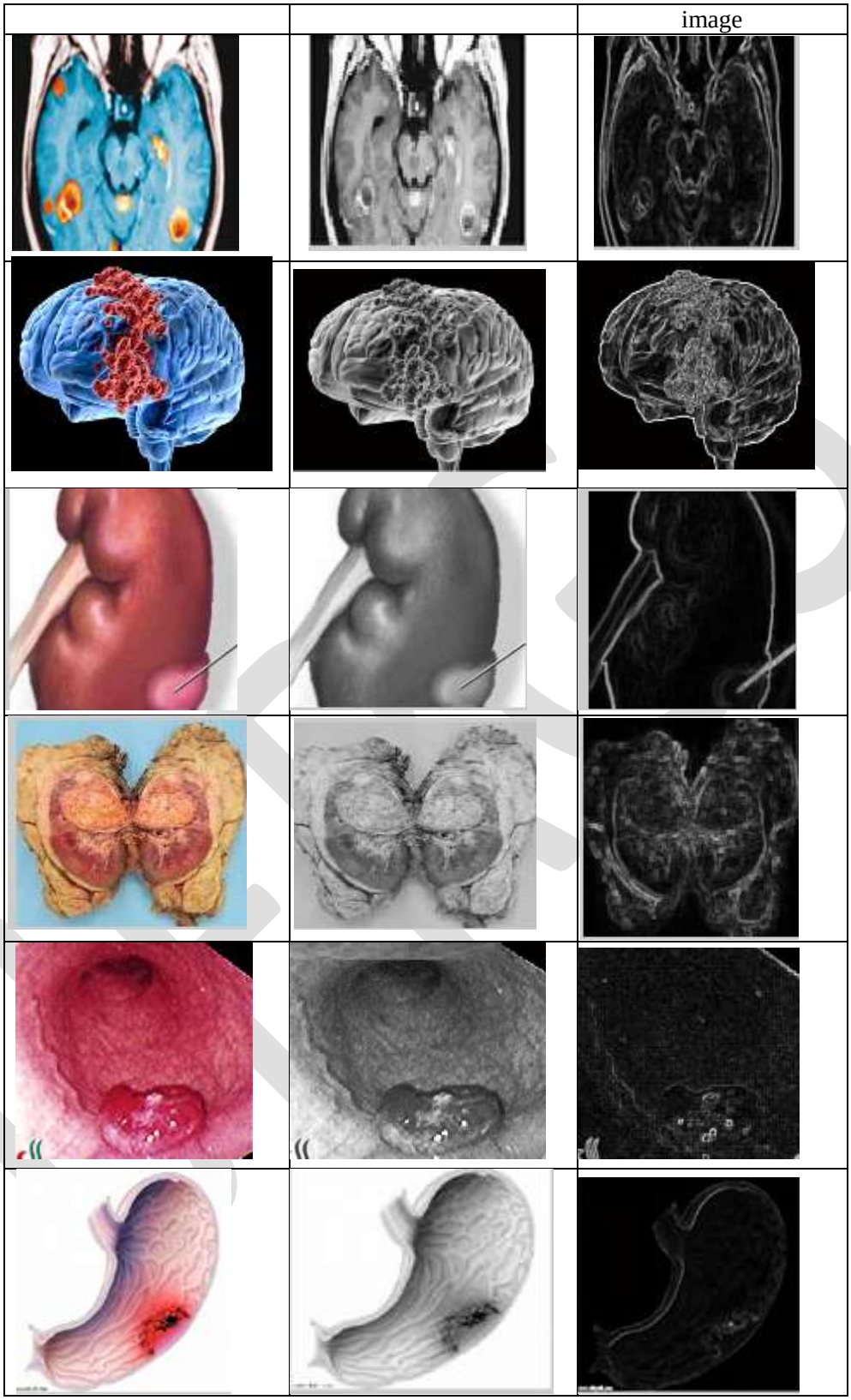

Figure(7): Results of texture segmented for medical images

6. CONCLUSION

In this paper we have considered the method of texture filter for an effective segmentation of medical images. The method uses the range filter to achieve robust and accurate segmentation results which are visually satisfactory. The whole process is autonomous and requires no supervision, which is one of the advantages of the proposed method. The method guarantees best segmentation of textures in poor-quality images also. The resulting figure show the efficiency, simplicity and robustness of medical image texture segmentation.

7. REFERENCES

[1] Ch. Hima Bindu1 and K. Satya Prasad2," An Efficient Medical Image Segmentation Using Conventional OTSU Method", International Journal of Advanced Science and Technology Vol. 38, January, 2012.

[2] Dilpreet Kaur and Yadwinder Kaur," Intelligent Medical Image Segmentation Using FCM, GA and PSO", International Journal of Computer Science and Information Technologies,Vol. 5 (5), 2014.

[3] R. Venkateswaran1and S. Muthukumar," Genetic Approach on Medical Image Segmentation by Generalized Spatial Fuzzy C- Means Algorithm", IEEE International Conference on Computational Intelligence and Computing Research,2010.

[4] Daniel J. Withy and Zoltan J.Koles,"A Review of Medical Image Segmentation: Methods and Available Software", International Journal of Bioelectromagnetism Vol. 10,No.3, pp125-148. 2008.

[5] Saka.Kezia, Dr.I.Santi Prabha and Dr.V.VijayaKumar," A New Texture Segmentation Approach for Medical Images", International Journal of Scientific & Engineering Research Volume 4, Issue 1, ISSN 2229-5518 , January-2013.

[6] Eldman de Oliveira Nunes and Maria Gabriela Pérez," Medical Image Segmentation by Multilevel Thresholding Based on Histogram Difference", 17th International Conference on Systems, Signals and Image Processing, 2010.

[7] V. Grau*, A. U. J. Mewes, M. Alcañiz, Kikinis, and S. K. Warfield " Improved Watershed Transform for Medical Image SEGMENTATION USING PRIOR INFORMATION", IEEE TRANSACTIONS ON MEDICAL IMAGING, VOL. 23, NO. 4, APRIL 2004 .

[8] Ch.Hima Bindu,QISCET, Ongole," AN IMPROVED MEDICAL IMAGE SEGMENTATION ALGORITHM USING OTSU METHOD", International Journal of Recent Trends in Engineering, Vol 2, No. 3, November 2009.

[9] Seongjai Kim and Hyeona Lim" Method of Background Subtraction for Medical Image Segmentation", The work is supported in part by NSF grants DMS- 0312223 & DMS-0609815, 2005.

[10] Ebrahim doost, Y.; Dehmeshki, J. ; Ellis, T.S. and Firooz bakht, M,".Medical Image Segmentation Using Active Contours and a Level Set Model: Application to Pulmonary Embolism (PE) Segmentation", IEEE Fourth International Conference on Digital Society, 269-273, Feb. 2010.

[11] Vaijinath V. Bhosle and Vrushsen P. Pawar " Texture Segmentation: Different Methods",International Journal of Soft computing and Engineering (IJSCE) ISSN: 2231-2307, Volume-3, Issue-5, November 2013 .

[12] Matheel Emaduldeen Abdulmnim," Segmenting the Dermatological Diseases Images by Developing the Range Operator", Iraqi Journal of Science, Vol 55, No.3B, pp:1376-1382, 2014.

[13] Asheesh Kumar, Apurva Mohan Gupta, Naresh Rameshrao Pimplikar and Natarajn P," TEXTURE SEGMENTATION IN MEDICAL IMAGING FOR RED SPOT BLOTCHES ANALYSIS IN HUMAN BODY",International Journal of Advanced Research in Computer and Communication Engineering ,Vol. 3, Issue 3, March 2014.

[14] Saka.Kezia, Dr.I.Santi Prabha and Dr.V.VijayaKumar," A New Texture Segmentation Approach for Medical Images", International Journal of Scientific & Engineering Research Volume 4, Issue 1, January-2013.

[15] Amir Rajaei, LalithaRangarajan and ElhamDallalzadeh," MEDICAL IMAGE TEXTURE SEGMENTATION USINGRANGE FILTER", Computer Science & Information Technology,2009.

International Journal of Engineering Research and General Science Volume 3, Issue 5, September-October, 2015
ISSN 2091-2730

Rainwater Harvesting – Technique to overcome the overall domestic water scarcity of Delhi

Ayush Srivastava[1], Shashi Shekhar Singh[2], Kanupriya Srivastava[3]

MVN University, Palwal, Haryana[1][2], Madan Mohan Malaviya University of Technology, Gorakhpur, U.P.[3]

ayush.srivastava@mvn.edu.in, +918221067344[1], shashishekhar.singh@mvn.edu.in

Abstract— The necessity of useable water in India has put forth, the realization, that the water scarcity can be overcome by adapting ancient technology based reservoirs. It also comprises of natural water storage facilities. In order to reduce over-draft, conserve surface runoff and increase available ground water supplies, storage of water in reservoirs along with suitable recharge techniques has to be adapted. Recharge may be incidental, when it is a by-product of normal land and water utilization measures; and planned when the work is carried out with the sole objective of augmenting ground water storage to improve water availability or water quality, reduce impact of floods or preventing/stopping sea water intrusion. In order to increase the ground water availability, rainwater from rooftops would serve the best option that is easily available and can be conveniently adapted.

Keywords— Rainwater Harvesting, Overhead tank, Underground tank, Limestone, Ground water table, Ground tank, Open land rainwater harvesting

INTRODUCTION

Water harvesting process has been in use and demand since ancient period. Plenty of open lands were available for these purposes during that time. However, in the present day scenario, there is scarcity of available free space in most towns and cities. Hence rainwater harvesting is the easiest and cost-effective process to overcome the scarcity of drinking and/or useable water. An arbitrary roof slab of dimensions $20m \times 15m$ along with the climatic conditions of Delhi has been chosen for this case study.

CASE-STUDY

A. Rooftop rainwater harvesting

Process of harvesting the rainwater, i.e., collecting at the time of rain, storing and using in its original form or after its filtration is called rainwater harvesting. If the catchment area is the roof of the house then it's called rooftop rain water harvesting. Due to depletion of underground water table, people face scarcity of water (even drinking water) in their day-to-day lives. The rainfall pattern is also unreliable in most of the regions. Increasing pollution in present world increases the difficulty to achieve pure form of water. Water bodies are getting drier due to global warming. Without any continuous input in form of materials, cleaning of apparatus, or any form of filtration equipment, we can overcome this difficulty by using rainwater harvesting technique.

B. Open-land Rainwater Harvesting

In those regions where construction is not done i.e. open space area, most part of the rainwater gets wasted in the form of runoff and evaporation. To deal with this situation, designing of rainwater harvesting in such areas should be in such a way that losses are minimized effectively. For this issue the agricultural lands (as agricultural lands serve to be majority of such open-land areas) should be leveled in such a way that all the rainwater would flow through the desired route and it would collect in a tank or would be flown into a bore-well.

C. Rainfall Data

As we are considering the overall land space of Delhi, that includes occupied as well as non occupied zones, a catchment area of dimensions $20m \times 15m$ has been arbitrarily taken for our case study. We have also considered the climatic conditions of Delhi which has an annual rainfall of about 0.715m. In our project we would collect the rain water in the catchment area mentioned above.

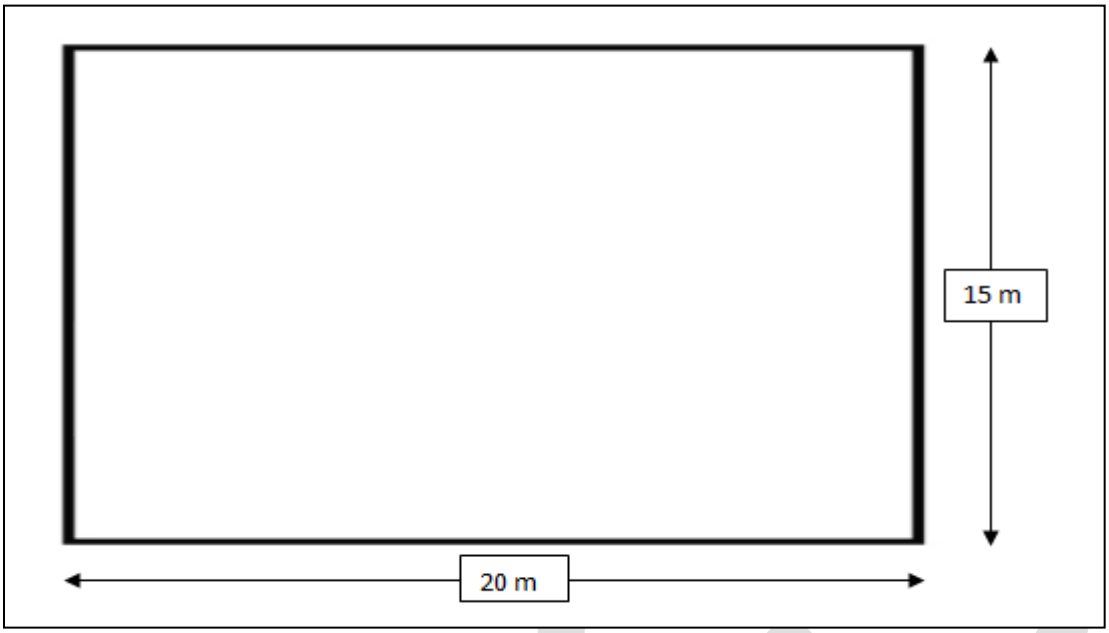

Fig. 1. Plan of Roof Slab

Table – 1
Temperature and rainfall variation of Delhi throughout the year

Rainfall Data Of Delhi			
Month	Mean monthly temperature (max.) (°C)	Mean monthly temperature (min.) (°C)	Mean monthly rainfall (mm.)
January	21	7	25
February	24	10	22
March	30	15	17
April	36	21	7
May	41	27	8
June	40	29	65
July	35	27	211
August	34	26	173
September	34	25	150
October	35	19	31
November	29	12	1
December	23	8	5
Total annual rainfall			**715**

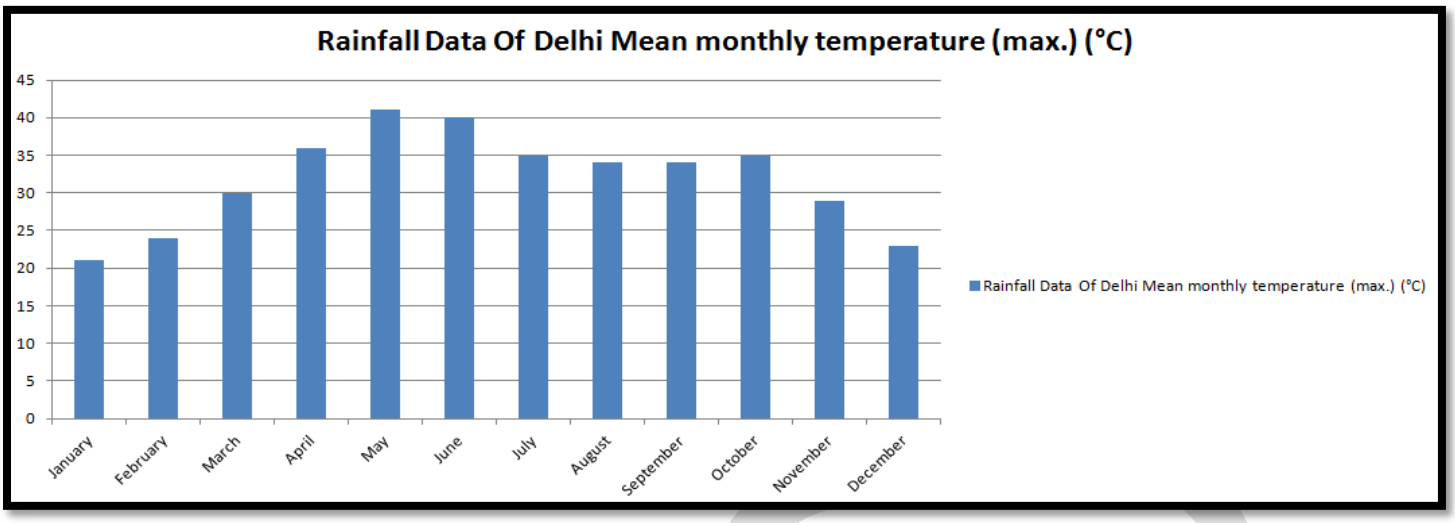

Fig. 2. Temperature (mean maximum) variation in Delhi

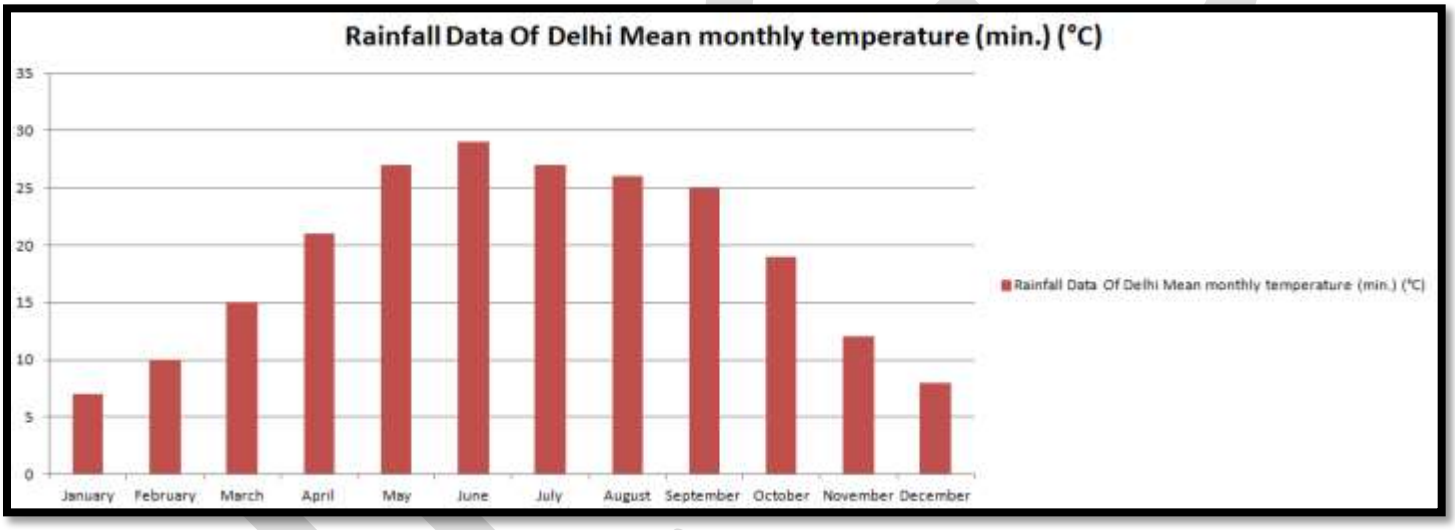

Fig. 3. Temperature (mean minimum) variation in Delhi

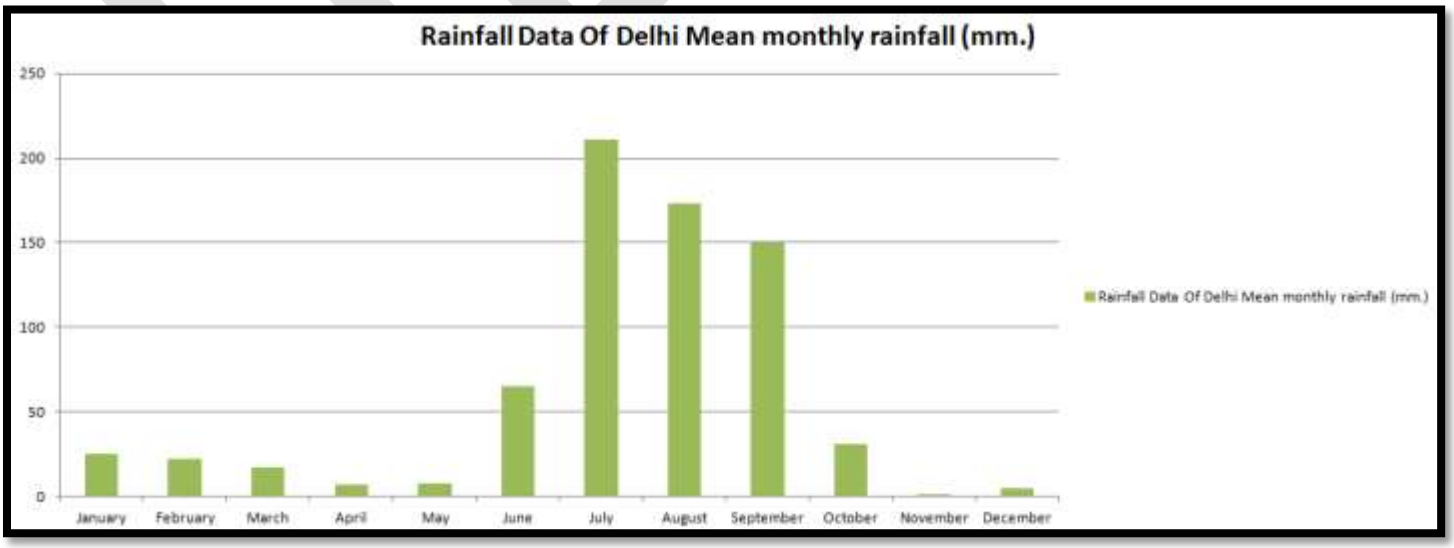

Fig. 4. Mean Monthly Rainfall variation pattern of Delhi

D. Calculations

1. As per the catchment area chosen, the calculation of the amount of water which can be harvested in an year is shown below:

   Length of the roof = 20m
   Breadth of the roof = 15m
   Height of rainfall = 0.715m

$$Water\ that\ can\ be\ harvested\ =\ length\ of\ roof\ \times breadth\ of\ roof\ \times height\ of\ rainfall \times water\ density$$
$$= 20m\ \times 15m\ \times 0.715m\ \times 1000lit/m^3$$
$$= 2{,}14{,}500litre$$

2. Total area of Delhi = 1,483 km^2
   Population projection as in 2021 = 2,20,00,000
   Population density = 14,834 persons/km^2 = 0.0148 persons/m^2
   Total Population as per the chosen catchment area = $20m \times 15m \times 0.0148persons/m^2$
   $= 4.4\ persons$
   Water demand per capita per day = 135liters
   Water demand for the chosen catchment area per day $= 135liters \times 4.4 = 594litres$
   Hence we have taken Average daily use as 600litres
3. Average domestic use of water (demand) per family per year in Delhi (as per observations)

$$Average\ daily\ use\ = 600litre$$
$$Yearly\ usage\ = \frac{600litre}{day} \times 365days\ = 2{,}19{,}000litres$$

4. Losses:
   We assume an average loss of 20% of total water available from the catchment area that includes evaporation and transmission losses. Calculations are shown below:

$$Losses\ = 20\%\ of\ 2{,}14{,}500litres$$
$$= 42{,}900litres$$

5. Final available water

$$Harvested\ water = water\ that\ can\ be\ harvested - losses$$
$$Harvested\ water = 2{,}14{,}500 - 42{,}900 = 1{,}71{,}600litres$$

On comparison of above data it is found that over 78% of the total domestic demand of water in Delhi can be fulfilled just by rainwater harvesting in accordance with the population projection as in the year 2021. The present population density of Delhi is 0.013 persons/m^2. According to present data (2015) the total water demand of Delhi is 1,92,172.50 liters/year for the chosen catchment area. It can also be seen that over 89% of the present water demand of Delhi can be fulfilled by rainwater harvesting.

E. Project Set-up

For Delhi, either of the following three techniques can be adapted as per the requirements and availability of resources.

1. Directly pumping the harvested water to the overhead tank installed at the top of the building in residencial area.

Block diagram of the complete set-up of direct pumping system is shown in Fig. 5.

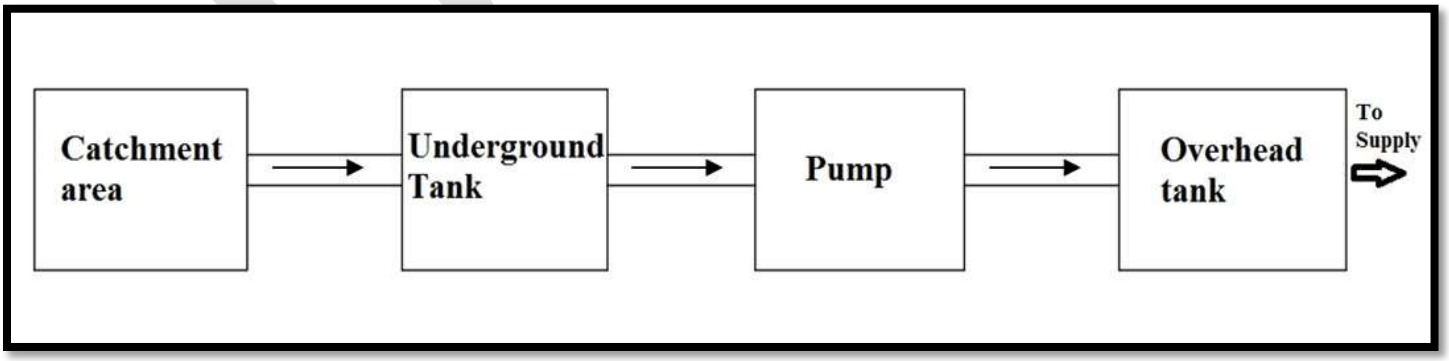

Fig. 5. Block diagram of set-up of RH (pumping method)

Roof serves to be the catchment area where inlet to this area is direct rainfall. Water from catchment area is passed in the underground water tank where the process of filtration takes place. After filtration, water is pumped to the overhead water tank from where it is

supplied for domestic use. A part of water is allowed to percolate into the water table in many cases. A dual mode set-up can be made in the region with heavy rainfall where domestic use as well as percolation both are permitted.

A typical layout of the underground water tank for this method is shown in Fig. 6.

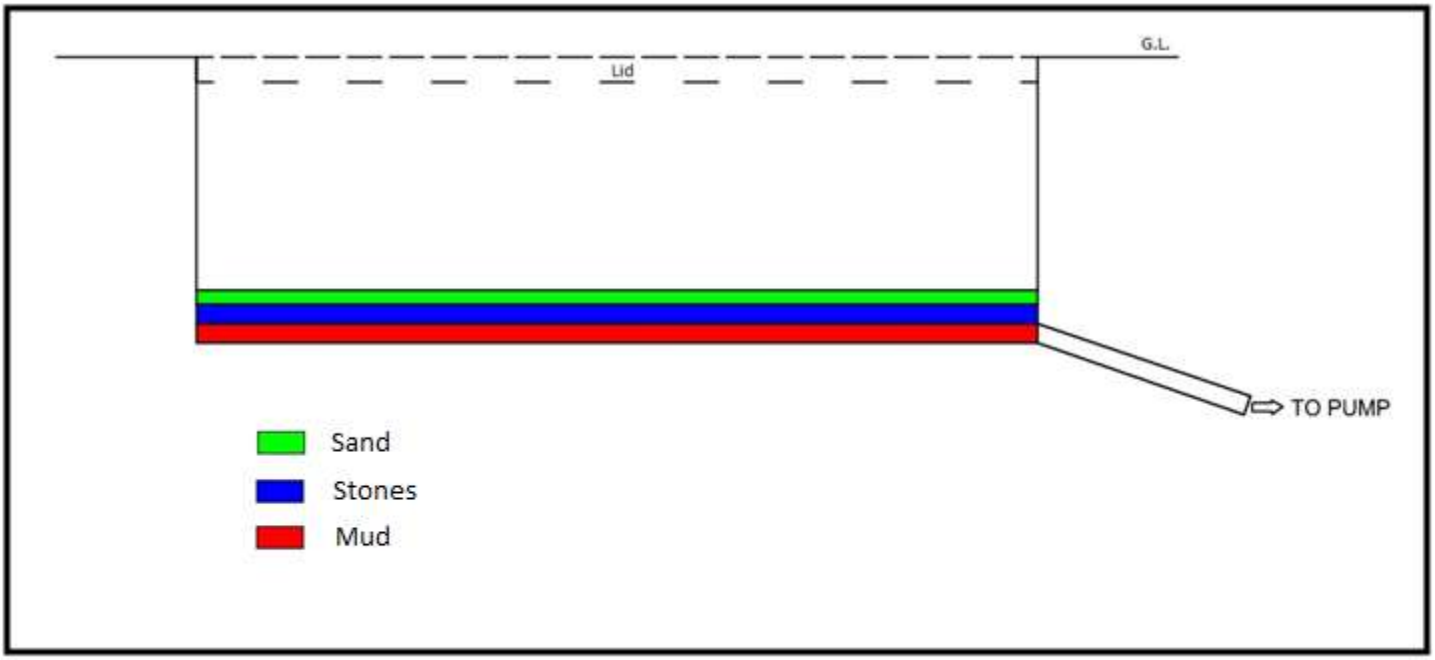

Fig. 6. Typical layout of the underground water tank for RH (pumping method)

If the harvested water contains excess of impurities (synthetic), limestone can be added alongwith stones in the same layer. The layers in the tank are arranged in such a way that it removes the solid wastes from the input water and adds the required minerals to it by natural process as limestone and mud are the best forms of natural water purifiers in themselves.

2. Boring of the harvested water to the underground water table in open land spaces.

Block diagram of the complete set-up of direct boring system is shown in Fig. 7.

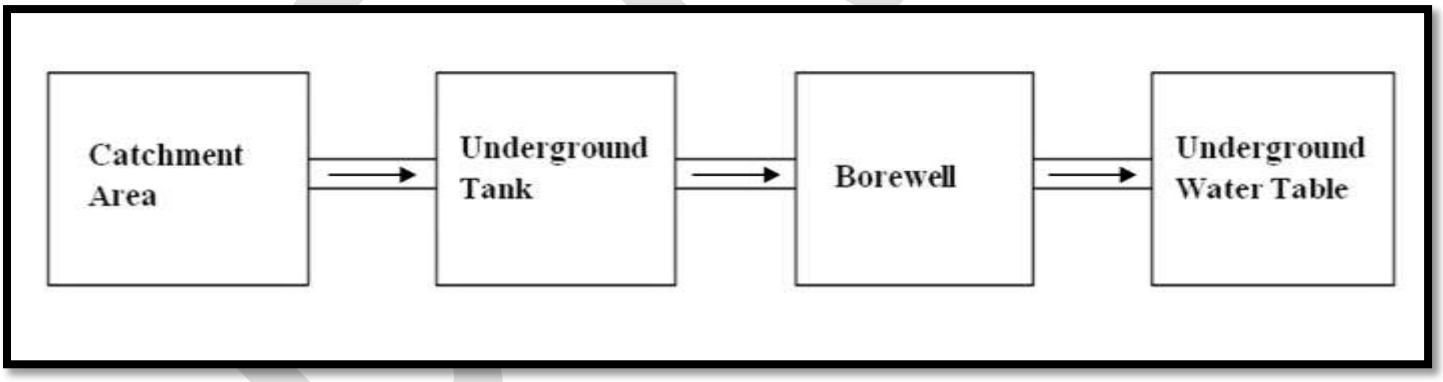

Fig. 7. Block diagram of set-up of RH (boring method)

In this case the harvested water is made to go to the underground water table by installing a bore in the underground tank. This method can be adopted in open land spaces, where instantaneous use of harvested water is not possible. Hence this portion of harvested water serves in increasing the water table.

A typical layout of the underground water tank for this method is shown in Fig. 8.

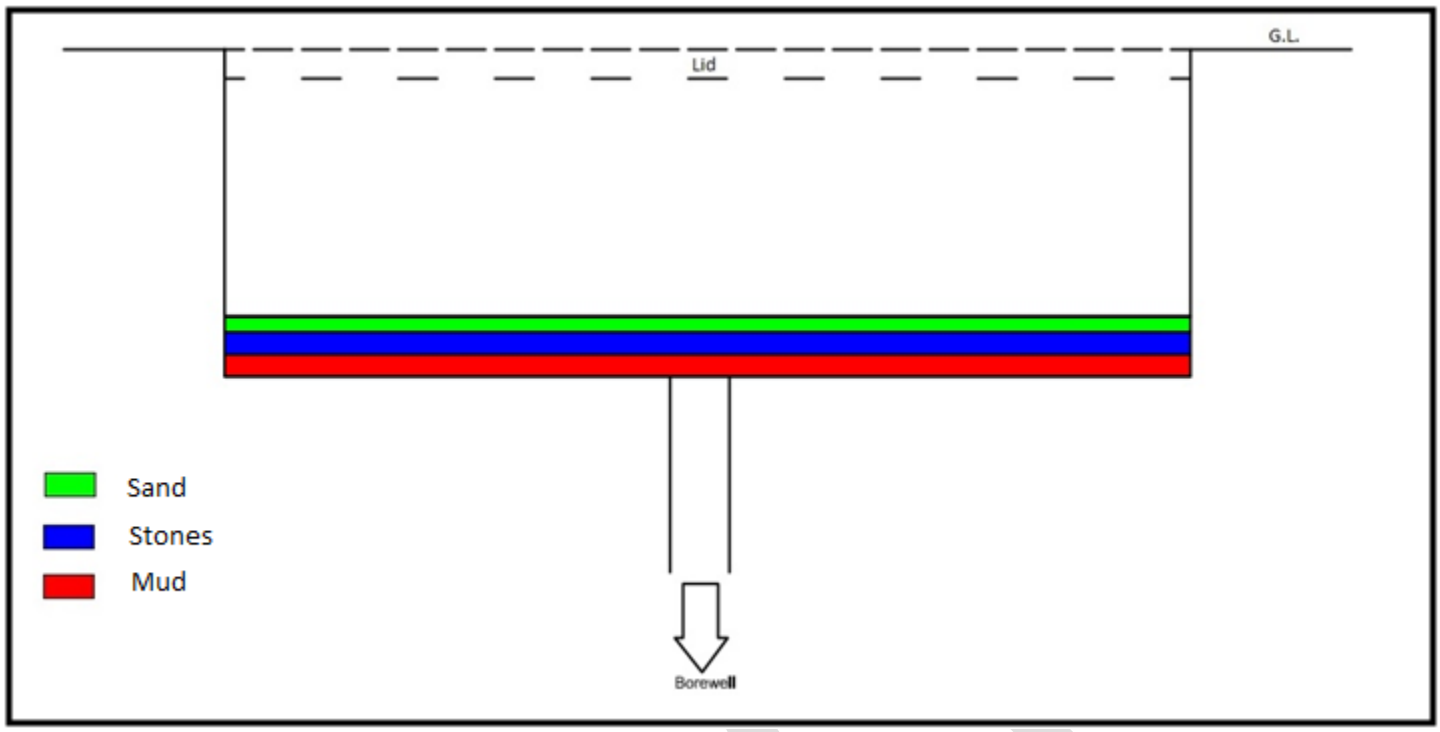

Fig. 8. Typical layout of the underground water tank for RH (boring method)

3. Combined use of pumping and boring systems.

Block diagram of the complete set-up of combined pumping and boring systems is shown in Fig. 9.

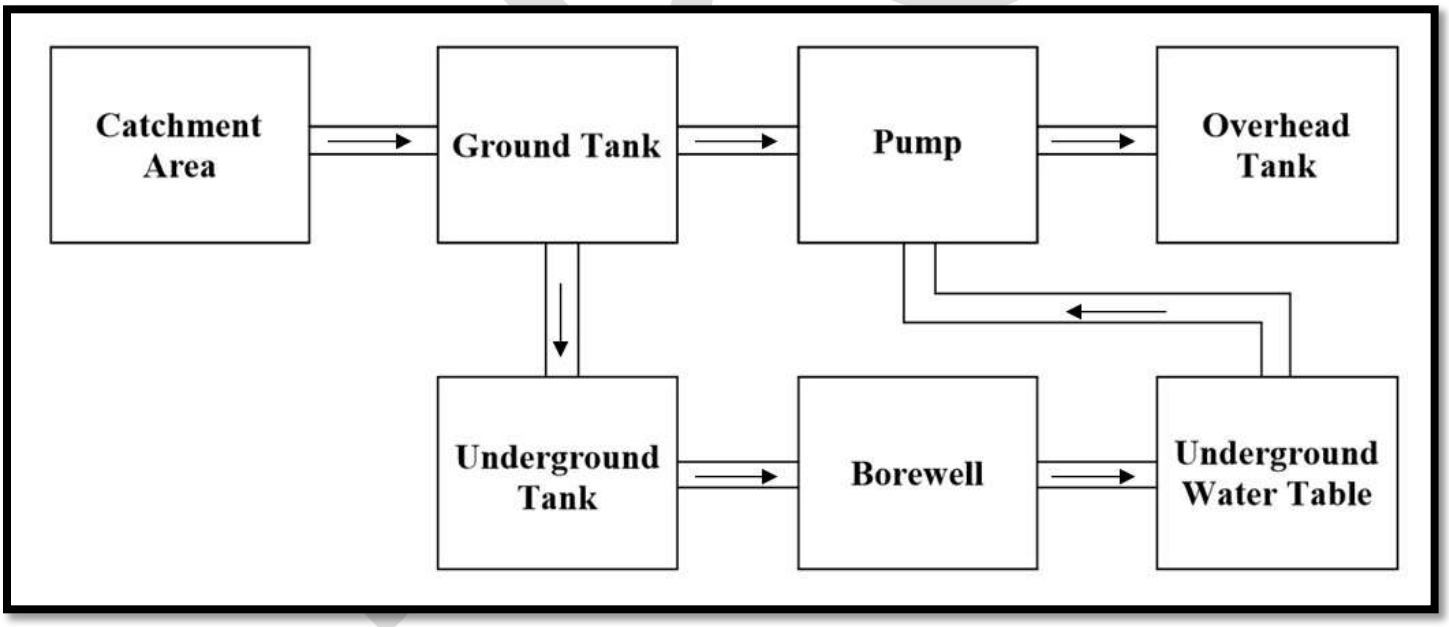

Fig. 9. Block diagram of set-up of RH (combined pumping and boring method)

In this case the water harvested from the catchment area is collected in the ground tank. From the ground tank, it would be pumped to the overhead water tank and can directly be given as supply. It would be designed in such a way that after a certain level, the water would overflow and go to the underground water tank from where it would be passed into the underground water table. This can be used in places where population density is comparitively lower or in a single or two storied building where consumption of water is comparitively less. This in turn increases the level of water in underground water table which can be withdrawn as per necesity or at the time when there is minimum rainfall.

A typical layout of the underground water tank for this method is shown in Fig. 10.

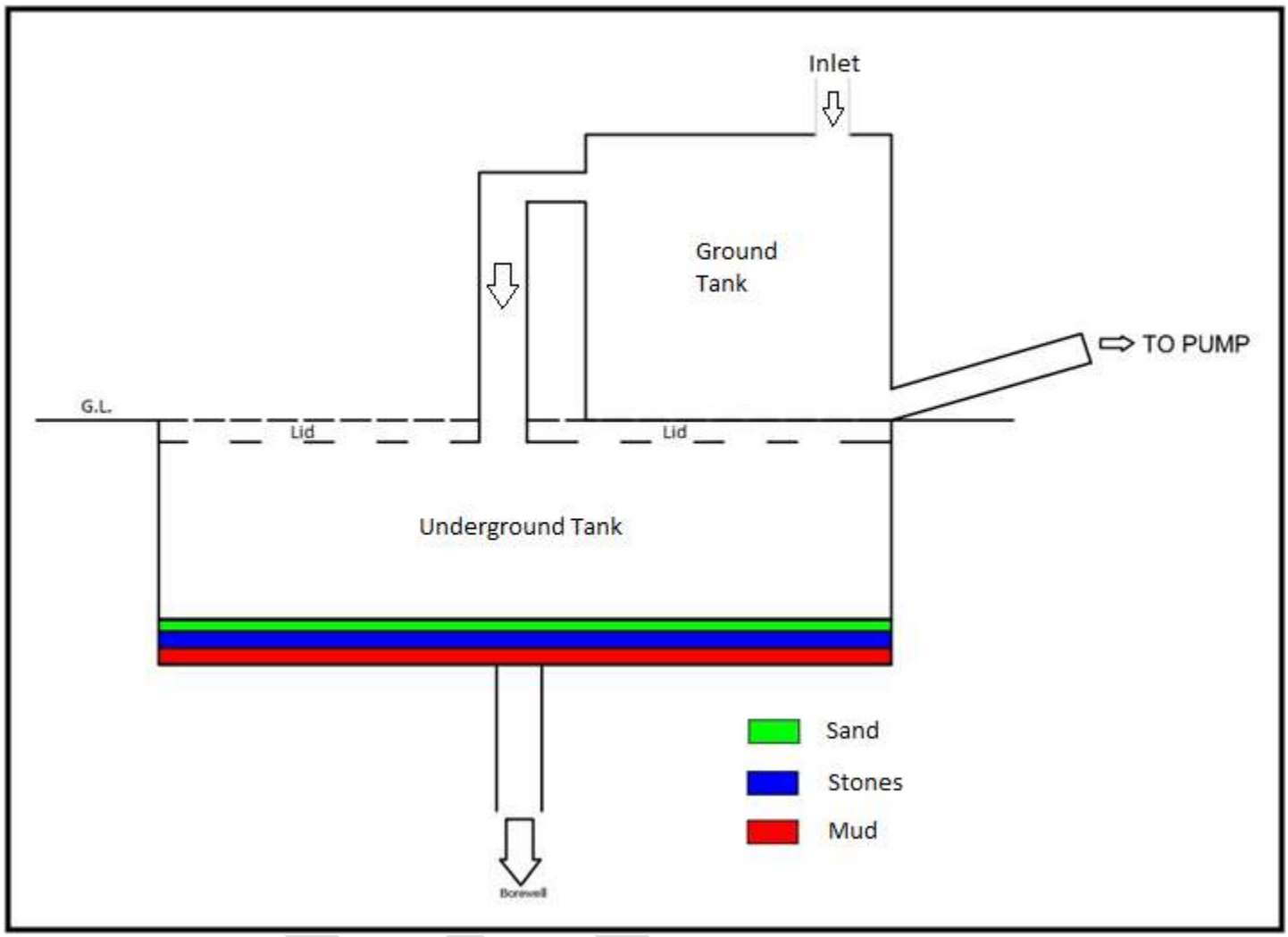

Fig. 10. Typical layout of the underground water tank for RH (combined pumping and boring method)

CONCLUSION

About 80-90% of the water demand can be fulfilled by harvesting the rainwater. This can be achieved when rainfalls on rooftops, as well as open land spaces, both are harvested. The materials used in the underground water tank are to purify the collected water before use or before boring it into the ground. If the harvested water is found to be synthetic, limestone can be introduced along with stones in the middle layer. Limestone acts as the best natural purifier of water. The walls of the tank made up of stone and lime would be preferred to that made by cement concrete.

REFERENCES

[1] C.P. Kumar "Fresh Water Resources: A Perspective", Thesis presented in National Institute of Hydrology Roorkee (Uttaranchal), July, 2003.
[2] http://nidm.gov.in/pdf/dp/Delhi.pdf for climatic data and population data of Delhi.
[3] https://www.youtube.com/watch?v=4BOOill-Jxo speech by Late Sh. Rajiv Dixit.
[4] http://www.researchgate.net/publication/276461005
[5] Anil Agarwal, Sunita Narain and Indira Khurana, "Making water everybody's business: practice and policy of water harvesting", Centre for Science and Environment, New Delhi, April 2001.
[6] E M Tideman , "Watershed management, guidelines for Indian Conditions", Omega Scientific Publications, New Delhi, April, 2000.
[7] A Vaidyanathan, "Water Resources Management Institutions and Irrigation Development in India", Oxford University Press, New Delhi, December, 1999.
[8] Bhatta, Bal Ram. S R Chalise, A K Myint and P N Sharma, "Recent Concepts, Knowledge practices, and New Skills in

Participatory Integrated Watershed Management. - Trainers resource book", International Centre for Integrated Mountain Development (ICIMOD), PWMTA, Food and Agriculture Organisation (FAO) (UN) & Department of Soil Conservation and Watershed Management, Nepal, June, 1999.

[9] Er. Kollegal K.Meghashyam, "Rain Water Harvesting - A New Concept to Utilize Rainwater and Secure the Future", ISBN: 9788181940360.

[10] Kenneth N. Brooks, Peter F. Ffolliott and Joseph A. Magner, "Hydrology and the Management of Watersheds", Wiley-Blackwell (An Imprint of John Wiley & Sons Ltd), New Delhi, 2012.

[11] **Beheim**, E., **Rajwar**, G.S., **Haigh**, M. and **Krecek**, J., "Integrated Watershed Management", ISBN 978-90-481-3769-5, Springer, 2010.

[12] Kashifa Iqbal, Ayush Srivastava and Shashi Shekhar Singh, "Rooftop Rainwater Harvesting – Cost Effective Technique to Overcome the Overall Water Scarcity of an Area", IJSTE - International Journal of Science Technology & Engineering, Volume 1,Issue 10, April 2015, ISSN (online): 2349-784X.

International Journal of Engineering Research and General Science Volume 3, Issue 5, September-October, 2015
ISSN 2091-2730

DESIGN AND OPTIMIZATION OF BOLTED JOINT SUBJECTED TO SHEAR AND BENDING LOAD

Khemchand M. Kapgate
Mechanical Engineering Department
K.D.K.C.E.
Nagpur, India
khemskapgatek2@gmail.com

Dr. C. C. Handa
Professor
Mechanical Engineering Department
K.D.K.C.E. Nagpur, India
chandrahashanda@rediffmail.com

V. D. Dhopte
Assistant Professor
Mechanical Engineering Department
K.D.K.C.E Nagpur, India.
vikrantdhopte@gmail.com

ABSTRACT

In this project a bolted joint, loaded by forces in it is studied. Finite Elements simulations are turned on ANSYS software in order to verify and validate results issued from analytical model. 3D FE simulations are used to show limits of application of developed model and also to study the ultimate stability of bolted joint under loading. APDL programming approach will be used for design optimization Due to flange opening, bending has been noticed in the bolt. Hence the bolts/studs should be designed to withstand against preload, internal pressure load and bending moment. Due to existence of Preload, internal pressure and bending moment at a time, the bolt behaviour is nonlinear which cannot not be evaluated by simple mathematical formulas. 3-Dimensional finite element analysis approach is only the technique which shows some satisfactory result.

Keywords :- Bolt, FEM, Pre-Load, Shear Load, Bending load

1.0 INTRODUCTION

Bolted joints are one of the most common elements in construction and machine design. They consist of fasteners that capture and join other parts, and are secured with the mating of screw threads. There are two main types of bolted joint designs: tension joints and shear joints.

In the tension joint, the bolt and clamped components of the joint are designed to transfer the external tension load through the joint by way of the clamped components through the design of a proper balance of joint and bolt stiffness. The joint should be designed such that the clamp load is never overcome by the external tension forces acting to separate the joint (and therefore the joined parts see no relative motion).

The second type of bolted joint transfers the applied load in shear on the bolt shank and relies on the shear strength of the bolt. Tension loads on such a joint are only incidental. A preload is still applied but is not as critical as in the case where loads are transmitted through the joint in tension. Other such shear joints do not employ a preload on the bolt as they allow rotation of the joint about the bolt, but use other methods of maintaining bolt/joint integrity. This may include clevis linkages, joints that can move, and joints that rely on a locking mechanism (like lock washers, thread adhesives, and lock nuts).

Typically, a bolt is tensioned (preloaded) by the application of a torque to either the bolt head or the nut. The preload developed in a bolt is due to the applied torque and is a function of the bolt diameter, length, the geometry of the threads and the coefficients of friction that exist in the threads and under the bolt head or nut. The stiffness of the components clamped by the bolt has no relation to the preload that is developed by the torque. The relative stiffness of the bolt and the clamped joint components do, however, determine the fraction of the external tension load that the bolt will carry and that in turn determines preload needed to prevent joint separation and by that means to reduce the range of stress the bolt experiences as the tension load is repeatedly applied. This determines the durability of the bolt when subjected to repeated tension loads. Maintaining a sufficient joint preload also prevents relative slippage of the joint components that would produce fretting wear that could result in a fatigue failure of those parts when subjected to in-plane shearing forces.

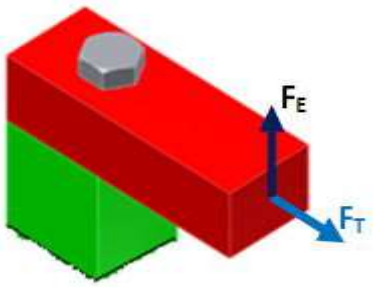

Bolt model with loads

A stacked heat exchanger is a piece of equipment built for efficient heat transfer from one medium to another. The media may be separated by a solid wall to prevent mixing or they may be in direct contact. They are widely used in space heating, refrigeration, air conditioning, power stations, chemical plants, petrochemical plants, petroleum refineries, natural-gas processing, and sewage treatment. The classic example of a heat exchanger is found in an internal combustion engine in which a circulating fluid known as engine coolant flows through radiator coils and air flows past the coils, which cools the coolant and heats the incoming air.

Double pipe heat exchangers are the simplest exchangers used in industries. On one hand, these heat exchangers are cheap for both design and maintenance, making them a good choice for small industries. On the other hand, their low efficiency coupled with the high space occupied in large scales, has led modern industries to use more efficient heat exchangers like shell and tube or plate. However, since double pipe heat exchangers are simple, they are used to teach heat exchanger design basics to students as the fundamental rules for all heat exchangers are the same. To start the design of a double pipe heat exchanger, the first step is to calculate the heat duty of the heat exchanger. It must be noted that for easier design, it's better to ignore heat loss to the environment for initial design.

Stacked Heat Exchanger

Literature review

Nomesh Kumar, P.V.G. Brahamanandam and B.V. Papa Rao "3-D Finite Element Analysis of Bolted Flange Joint of Pressure Vessel"

In this paper it was found that, the stresses in the bolts of the bolted flange joint of the pressure vessel so that bolts/studs should not be failed during proof pressure test. Bolted flange joints perform a very important structural role in the closure of flanges in a pressure vessel. It has two important functions: (a). to maintain the structural integrity of the joint itself, and (b). to prevent the leakage through the gasket preloaded by bolts. The preload on the bolts is extremely important for the successful performance of the joint. The preload must be sufficiently large to seat the gasket and at the same time not excessive enough to crush it. The flange stiffness in conjunction with the bolt preload provides the necessary surface and the compressive force to prevent the leakage of the gases contained in the pressure vessel. The gas pressure tends to reduce the bolt preload, which reduces gasket compression and tends to separate the flange faces. Due to flange opening , bending has been noticed in the bolt. Hence the bolts/studs should be designed to withstand against preload, internal pressure load and bending moment. Due to existence of Preload, internal pressure and bending moment at a time, the bolt behaviour is nonlinear which cannot not be evaluated by simple mathematical formulas. 3-Dimensional finite element analysis approach is only the technique which shows some satisfactory result.

Gowri Srinivasan & Terry F. Lehnhoff "Bolt Head Fillet Stress Concentration Factor Cylindrical Pressure Vessels"

In this paper it is found that, linear three-dimensional finite element analysis (FEA) was performed on bolted pressure vessel joints to determine maximum stresses and stress concentration factors in the bolt head fillet as a result of the prying action. The three-dimensional finite element models consisted of a segment of the flanges containing one bolt, using cyclic symmetry boundary conditions. The maximum stress in the bolt as well as the stress concentration factors in the bolt head fillet increase with an increase in bolt circle diameter for a given outer flange dimension. Keeping the bolt circle diameter constant, bolt stress and stress concentration factors inthe bolt head fillet decrease with increase in outer flange diameter. The maximum stresses in the bolt were also calculated according to the American Society of Mechanical Engineers (ASME) Boiler and Pressure Vessel Code and the Verein Deutscher Ingenieur (VDI) guidelines and compared to the results observed through finite element analysis. The stresses obtained through FEA were larger than those predicted by the ASME and VDI methods by a factor that ranged between 2.96 to 3.41 (ASME) and 2.76 to 3.63 (VDI).

S.H. Ju , C.Y. Fan, & G.H. Wub "3-dimensional finite elements of steel bolted connections"

In this paper it was found that, the three-dimensional (3D) elasto-plastic finite element method is used to study the structural behaviour of the butt-type steel bolted joint. The numerical results are compared with AISC specification data. The similarity was found to be satisfactory despite the complication of stress and strain fields during the loading stages. When the steel reaches the nonlinear behaviour, the bolt nominal forces obtained from the finite element analyses are almost linearly proportional to the bolt number arranged in the connection. Moreover, the bolt failure is marginally dependent on the plate thickness that dominates the magnitude of the bending effect. For the cracked plate in a bolted-joint structure, the relationship between KI and the applied load is near linear, in which the nonlinear part is only about one tenth of the total relationship. This means that the linear elastic fracture mechanics can still be applied to the bolted joint problem for the major part of the loading, even through this problem reveals highly nonlinear structural behaviour.

Iuliana PISCAN, Nicolae PREDINCEA & Nicolae POP "FINITE ELEMENT ANALYSIS OF BOLTED JOINT"

In this paper it was found that, this paper presents a theoretical model and a simulation analysis of bolted joint deformations. The bolt pretension force, friction coefficient and contact stiffness factor are considered as parameters which are influencing the joint deformation. The bolted joint is modelled using CATIA software and imported in ANSYS WORKBENCH. The finite element analysis procedure required in ANSYS WORKBENCH simulation is presented as a predefined process to obtain accurate results.

Ali Najafi, Mohit Garg and Frank Abdi "Failure Analysis of Composite Bolted Joints in Tension"

In this paper it is found that, the failure of preloaded cross-ply laminated composite has been studied through finite element simulation embedded in Progressive Failure Analysis (PFA). Two modelling strategies including low- and high-fidelity models have been considered for this investigation. The high-fidelity FE model consists of fixture components (bolts and washers). It has been shown that both low- and high-fidelity FE models are capable of predicting the experimentally observed failure modes of bolted joints that depends on the geometric parameters with reasonable accuracy. Two catastrophic failure loads, net-tension and shear out can be predicted using both low- and high-fidelity model while the failure load of bearing mode can only be predicted via high-fidelity model that considers the applied preload of the bolt. However, the overall stiffness in the actual experiment is lower than that of predicted via finite element simulation.

CONVENTIONAL DESIGN

Bolt Pretension

Bolt pretension, also called preload or prestress, comes from the installation torque T you apply when you install the bolt. The inclined plane of the bolt thread helix converts torque to bolt pretension. Bolt preload is computed as follows.

$P_i = T/(K\ D)$ (Eq. 1)

Where,

P_i =bolt preload (called F_i in Shigley).

T=bolt installation torque.

K = torque coefficient.

D = bolt nominal shank diameter (i.e., bolt nominal size).

Torque coefficient K is a function of thread geometry, thread coefficient of friction μ_t, and collar coefficient of friction μ_c. Look up K for your specific thread interface and collar (bolt head or nut annulus) interface materials, surface condition, and lubricant (if any). ("Torque specs for screws," Shigley, and various other sources discuss various K value estimates.) If you cannot find or obtain K from credible references or sources for your specific interfaces, then you would need to research to try to find the coefficients of friction for your specific interfaces, then calculate K yourself using one of the following two formulas listed below (Shigley, *Mechanical Engineering Design*, 5 ed., McGraw-Hill, 1989, p. 346, Eq. 8-19, and MIL-HDBK-60, 1990, Sect. 100.5.1, p. 26, Eq. 100.5.1, respectively), the latter being far simpler.

$$K = \{[(0.5\, d_p)(\tan\lambda + \mu_t \sec\beta)/(1 - \mu_t \tan\lambda \sec\beta)] + [0.625\mu_c\, D]\}/D \quad \text{(Eq. 2)}$$

$$K = \{[0.5\, p/\pi] + [0.5\, \mu_t\, (D - 0.75\, p \sin\alpha)/\sin\alpha] + [0.625\, \mu_c\, D]\}/D \quad \text{(Eq. 3)}$$

Where,
D = bolt nominal shank diameter.
p = thread pitch (bolt longitudinal distance per thread).
α= thread profile angle = 60° (for M, MJ, UN, UNR, and UNJ thread profiles).
β = thread profile half angle = 60°/2 = 30°.
tan λ = thread helix angle tan = $p/(\pi\, d_p)$.
d_p = bolt pitch diameter.
μ_t = thread coefficient of friction.
μ_c = collar coefficient of friction.
D and *p* can be obtained from bolt tables such as Standard Metric and USA Bolt Shank Dimensions.

The three terms in Eq. 3 are axial load component (coefficient) of torque resistance due to (1) thread helix inclined plane normal force, (2) thread helix inclined plane tangential (thread friction) force, and (3) bolt head or nut washer face friction force, respectively.

However, whether you look up K in references or calculate it yourself, the engineer must understand that using theoretical equations and typical values for K and coefficients of friction merely gives a preload *estimate*. Coefficient of friction data in published tables vary widely, are often tenuous, and are often not specific to your specific interface combinations and lubricants. Such things as unacknowledged surface condition variations and *ignored dirt* in the internal thread can skew the results and produce a false indication of preload.

The engineer and technician must understand that published K values apply to perfectly clean interfaces and lubricants (if any). If, for example, the threads of a steel, zinc-plated, K = 0.22, "dry" installation fastener were not clean, this might cause K to increase to a value of 0.32 or even higher. One should also note that published K values are intended to be used when applying the torque to the nut. The K values will change in relation to fastener length and assembly running torque if the torque is being read from the bolt head.

One should measure the nut or assembly "running" torque with an accurate, small-scale torque wrench. ("Running" torque, also called prevailing torque, is defined as the torque when all threads are fully engaged, fastener is in motion, and washer face has not yet made contact.) The only torque that generates bolt preload is the torque you apply *above* running torque.

A few more things to be aware of are as follows. Bolt proof strength S_p is the maximum tensile stress the bolt material can withstand without encountering permanent deformation. Published bolt yield strengths are determined at room temperature. Heat will lower the yield strength (and proof strength) of a fastener. Especially in critical situations, you should never reuse a fastener unless you are certain the fastener has never been yielded.

Bolt Preload Measurement

If a more accurate answer for bolt preload is needed than discussed above, the specific combination and lubricant would have to be *measured* instead of calculated. Measurement methods are generally involved, time-consuming, and expensive, and are beyond the scope of this article. But perhaps one of the simplest and least expensive methods, to test specific combinations and lubricants, is to measure the installed fastener with a micrometer, if possible, and compute torque coefficient K as follows, per Shigley, op. cit., p. 345, para. 2.

$$K = T\, L/(E\, A\, \text{delta}\, D) \quad \text{(Eq. 4)}$$

Where,
T = bolt installation torque, L = bolt grip length, E = bolt modulus of elasticity, A = bolt cross-sectional area, D = bolt nominal shank diameter, and delta = measured bolt elongation in units of length.

FASTENER MODELING

A fastener is modeled by CBAR or CBEAM elements [2] with corresponding PBAR or PBEAM cards for properties definition. For the CBAR or CBEAM elements connectivity, a separate set of grid points coincidental with corresponding plate grid points (Figure 3) is created. This set also includes grid points located on intersection of the fastener axis and outer surfaces of the first and last connected plates.

All CBAR or CBEAM elements representing the same fastener reference the same PBAR or PBEAM card [2] with following properties:

· MID to reference the fastener material properties.

· Fastener cross-sectional area

$$A = \frac{\pi {d_f}^2}{4}$$

where d_f- fastener diameter.

· Moments of inertia of the fastener cross section

$$l_1 = l_2 = \frac{\pi {d_f}^4}{64}$$

Torsional constant

$$J = \frac{\pi {d_f}^4}{32}$$

Area factors for shear of circular section

$$K_1 = K_2 = 0.9$$

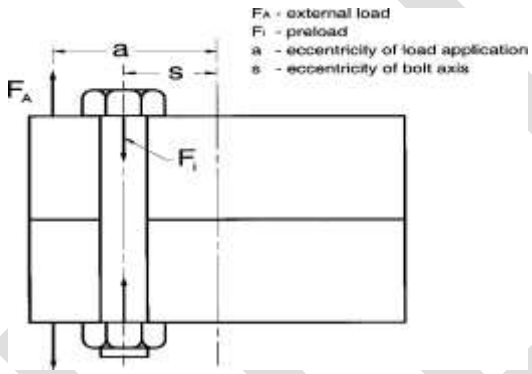

Conventional Bolt

DESIGN DATA

Table 1 Reference Drawings

SR NO.	Description	Drawing NO.
1	HES-R0353AB-E-001-RCModel _GA_Dwg	SDM-235ES-103R1/SDM-235ES-204-R1
2	HES-R0353ABE004RCModel _Nozzle_dwg	SDM-235ES-103R1/SDM-235ES-204-R1
3	HES-R0353ABE005RCModel _Saddle_Dwg	SDM-235ES-103R1/SDM-235ES-204-R1

Table 2 Reference Codes

Sr No.	Description
1	ASME Boiler and Pressure Vessel Code, SectionVIII, Div. 1, Ed. 2013, ADD 2011
2	ASME Boiler and Pressure Vessel Code, SectionVIII, Div. 2, Ed. 2013, ADD 2011
3	ASME Boiler and Pressure Vessel Code, Section II, PartD, Ed. 2013, ADD 2011

Table 3 Design Parameters

COMPONENT CRITERIA	UNIT	CHANNEL SIDE	SHELL SIDE
Design Pressure	Mpa	1.65	5.66
Pretension	N	672475.000	49934.516
No of Bolts		16	8
Load on each Bolt	N	42029.6875	6241.8145
Design Temperature	^{0}c	279	313
Operating Pressure	Mpa	1.509	5.188
Fluid Handled		Hydrocarbons, H2	Hydrocarbons, H2

Table 4 Material Properties

Material Properties has been taken from ASME Sec II Part D.

Component	Material	Design Temp.	Modulus of Elasticity (1)	Allowable Design Stress at Design Temp. (2)
		° C	N/mm^2	N/mm^2
Channel Shell	SA 387 Gr11	313	185698.96	148
Channel Flange & Cover	SA 516 Gr 70	313	185698.96	-
Tubesheet (Equivalent Solid Tubesheet)	SA 336 Gr F12	313	E*=55516	-
Main Shell Head	SA516 Gr70	279	185268.27	137
Main Shell Flange	SA 266 Gr2N	279	185268.27	-
Channel Side Nozzle Flanges	SA182 Gr F12, Cl2	313	185268.27	111
Channel Side Nozzle Neck	SA336 gr F12	313	185268.27	132
Shell Side Nozzles Flanges	SA105 N	279	186412.3	132
Shell Side Nozzle Neck	SA 106 GrB	279	186412.3	118
Saddles & Wrapper plate	SA516 Gr 70	279	186412.3	137

CAD MODELLING (SIMULATION)

MESHING

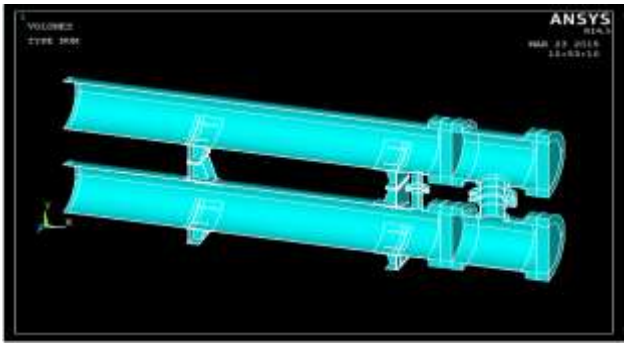

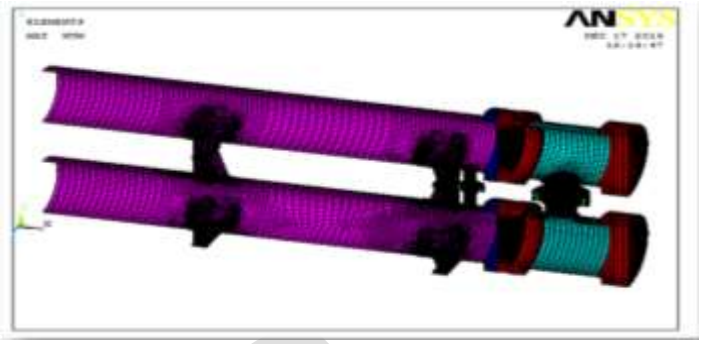

CONTACT AND PRETENSION MODELLING

STEP 1) The first phase is modeling the joint using CAD software. The model geometry was generated using ANSYS software and then opened as a neutral file in ANSYS APDL. Due to symmetry conditions the model is sectioned. Geometric details, such as chamfers, radii of connection have only a local influence on behaviour of the structure therefore those are neglected. In this analysis we neglect the bolt thread and surface roughness.

STEP 2) Next, the prepared geometric structure is reproduced by finite elements. The finite elements are connected by nodes that make up the complete finite element mesh. Each element type contains information on its degree-of-freedom set (e.g. translational, rotational, and thermal), its material properties and its spatial orientation (3D-element types). The mesh was controlled in order to obtain a fine and good quality mapped mesh. The assembly had 574086 nodes and 115534 elements.

STEP 3) In order to solve the resulting system equation, boundary and loaded conditions are specified to make the equation solvable. In our model, the interconnecting nozzle (i.e. N5 nozzle and N6 nozzle) with attached bolts axial load were applied. The pretension in the bolt was generated at the mid plane of the bolt using the pretension element PRETS179, which is contained in the ANSYS v14.5 element library. These elements allow direct specification of the pretension in bolt. For specifying the bolt pretension a local coordinate system was defined, with the Y axes along the bolt length. After the bolt pretension, an external load was applied to the bolted joint.

STEP 4) The last phase is interpreting the results. For contact analysis ANSYS supports three contact models: node to node, node to surface and surface to surface. In this case a surface to surface model was created and contacts elements were used. ANSYS provides several element types to include surface-to-surface contact and frictional sliding. One of these elements is the 3D 8-node surface-to-surface contact element CONTAC174. Contacts elements use a target surface and a contact surface to form a contact pair. According to stiffness behaviour the parts can be rigid or flexible. Our model is defined as flexible one.

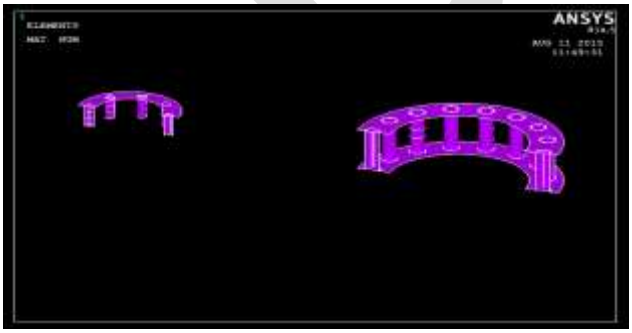

FIG 1. Contacts and Pretension

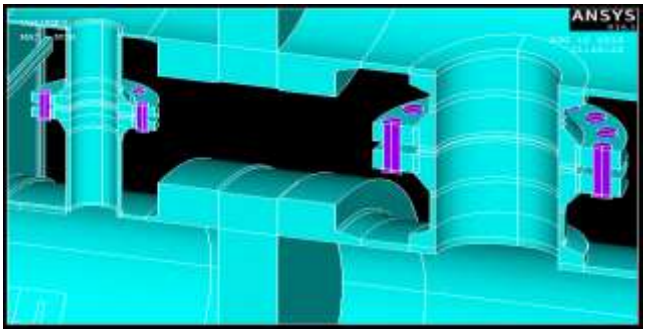

FIG 2. Bolt and Nozzle

BEAM AND PRETENSION MODELLING

STEP 1) to STEP 3) As per the previous technique i.e. contact and pretension the pretension is applied on bolt is as same as STEP 1) to STEP 3), but only difference is that the bolt is not designed but a beam element is introduced and line representing bolt is meshed and in the middle of its node pretension is applied.

STEP 4) The last phase is interpreting the results. A coupling is generated in the flange of the bolt. The top and bottom nodes of flange with centre node are selected where the bolt is to be situated. Then coupling force/moment is generated on top and bottom nodes of flange by selecting middle/master node and coupling is designed.

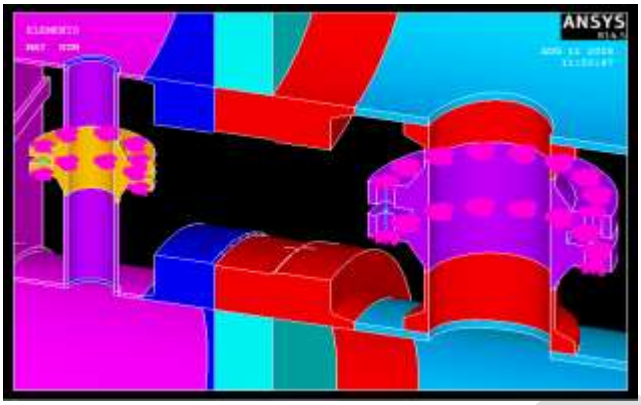

FIG 3. Beam and Nozzle

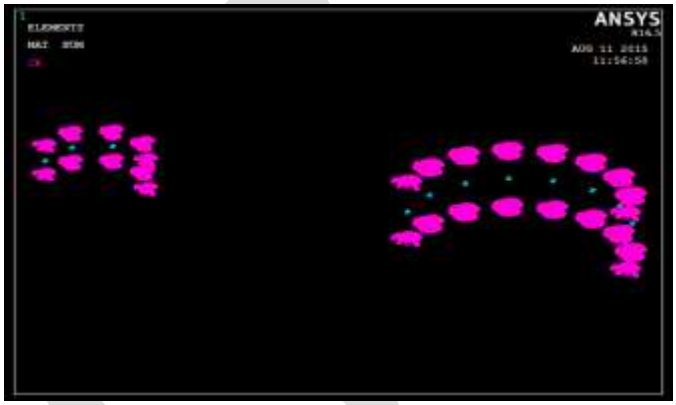

FIG 4. Coupled and Pretension nodes

OPTIMIZATION

Bolt size and the number of bolts are the most important parameters to consider when optimizing bolted joints. Because bolts come in discrete sizes (e.g. M4, M5, M6, etc. for metric bolts) there is only one optimum combination of bolt size and bolt number which will maximize the efficiency of joint under a given load. A procedure aimed at selecting optimum combinations of bolt size and bolt number has been implemented through ANSYS software.

CONCLUSION

The various parameters for design of bolt i.e. pretension, pressure, bolt geometry, deformation, sliding behaviour, friction, contact stiffness, analysis approach has been studied for modeling bolt which is used in stacked heat exchanger.

REFERENCES:

[1] Nomesh Kumar, P.V.G. Brahamanandam and B.V. Papa Rao, "3-D Finite Element Analysis of Bolted Flange Joint of Pressure Vessel" MIT International Journal of Mechanical Engineering, Vol. 1, No. 1, Jan 2011, pp. 35-40.

[2] Gowri Srinivasan and Terry F. Lehnhoff, "Bolt Head Fillet Stress Concentration actors in Cylindrical Pressure Vessels" Journal of Pressure Vessel Technology, Vol. 123, AUGUST 2001, pp.381-386.

[3] S.H. Ju, C.Y. Fan and G.H. Wub, "Three-dimensional finite elements of steel bolted connections" Engineering Structures, Vol. 26, (2004), pp. 403–413.

[4] Iuliana Piscan, Nicolae Predincea, Nicolae Pop, "Finite Element Analysis of Bolted Joints", Proceedings in Manufacturing Systems, Vol. 5, No. 3, 2010, pp. 167-172.

[5] Ali Najafi, Mohit Garg, frank Abdi, "Failure Analysis of composite Bolted Joints in Tension," 50th AIAA/ASME/ASCE Structures, Structural Dynamics and material Conference, 4-7 May 2009, Palm Springs, California. AIAA 2009-2505.

[6] ZHANG Yongjie and SUN Qin, "Joint Stiffness Analysis of Sheared Bolt with Preload", Second International Conference on Intelligent Computation Technology and Automation, 2009, pp. 345-348.

[7] M.P. Cavatorta, D.S. Paolino, L. Peroni and M. Rodino, "A finite element simulation and experimental validation of a composite bolted joint loaded in bending and torsion", Composites, Part A, Vol. 38, 2007, pp. 1251–1261.

[8] Qiwei Guo, Guoli Zhang and Jialu Li, "Process parameters design of a three-dimensional and five-directional braided composite joint based on finite element analysis", Materials and Design, Vol. 46, 2013, pp. 291–300.

[9] Ryosuke Matsuzaki, Motoko Shibata and Akira Todoroki, "Improving performance of GFRP/aluminum single lap joints using bolted/co-cured hybrid method", Composites, Part A, Vol. 39, 2008, pp. 154–163.

[10] Ivana Ilić, Zlatko Petrovic, Mirko Maksimović, Slobodan Stupar and Dragi Stamenković, "Computation Method in Failure Analysis of Mechanically Fastened Joints at Layered Composites", Journal of Mechanical Engineering, Vol. 58, No. 9, 2012, pp. 553-559.

[11] Osman Hag-Elsafi, Sreenivas Alampalli and FrankOwens "Computer aided implementation of a new procedure for design of end-plates and base-plates for traffic support structures", Engineering Structures, Vol. 23, 2001, pp. 1503–1511

[12] Alain Prenleloup, Thomas Gmü, John Botsis, Konstantin O. Papailiou, Kurt Obrist "Stress and failure analysis of crimped metal–composite joints used in electrical insulators subjected to bending", Science direct, Composites: Part A, Vol. 40, 2009, pp. 644–652.

[13] Olanrewaju Aluko "An Analytical Method for Failure Prediction of Composite Pinned Joints", Proceedings of the World Congress on Engineering, Vol III, July 6 - 8, 2011, London, U.K., pp. 978-988.

[14] Lin Liua, Boqin Gub "Analytical Method of Gasket Stress on Bolted Flanged Connections in Consideration of External Bending Moments and Elements Creep", International Conference on Measuring Technology and Mechatronics Automation, IEEE, 2009, pp. 750-754.

[15] Amit P. Wankhade, Kiran K. Jadhao "Design and Analysis of Bolted Joint in Composite Laminated", International Journal Of Modern Engineering Research (IJMER), Vol. 4, Iss. 3, Mar. 2014, pp. 20-24.

[16] Liu Longquan, Zhang Junqi, Chen Kunkun and Wang Hai "Combined and interactive effects of interference fit and preloads on composite joints", Chinese Journal of Aeronautics, Vol. 27(3), 2014, pp. 716–729.

[17] J. E. Jam, N. O. Ghaziani "Numerical and experimental investigation of bolted joints", International Journal of Engineering, Science and Technology Vol. 3, No. 8, 2011, pp. 285-296.

[18] JIANG An-long, YANG Zhao "Research on Shear Model of Ring Joint Bolts in Stragger- Jointed Segmental Linings", International Conference On Computer Design And Appliations, Vol. 3, IEEE, 2010, pp. 190-193.

[19] John Butterworth "Ductile concentrically braced frames using slotted bolted joint", SESOC Journal, Vol. 13, No. 1,April 2000, pp. 39-48.

[20] Simon Šilih, Miroslav Premrov, Stojan Kravanja "Optimum design of plane timber trusses considering joint flexibility", Engineering Structures, Science Direct, Vol. 27, 2005, pp. 145–154.

[21] B. D. Shiwalkar, Design of Machine Elements, Denett Publication, Third Edition, Jun 2009, Reprint Jun 2011

International Journal of Engineering Research and General Science Volume 3, Issue 5, September-October, 2015
ISSN 2091-2730

Waste Rubber Bitumen Modifier

Abir Roy and Guided by Asst.Prof. Avinesh Kumar

Department of Civil Engineering, Mewar University

abirroy14@gmail.com

Cont no.:- 8003653844

Abstract— A lot of research has been conducted to find alternative material in pavement construction that acts as additive or modifier which could improve the performance of its properties. Bitumen is sensitive to temperature and rate of loading. Thus, bitumen modification has become trigger factors to improve the hot mix asphalt (HMA) properties. This dissertation presents a study of laboratory evaluation on the performance of hot mix asphalt (HMA) using rubber waste as an additive. In this study, rubber waste is referred as a free fine rubber particle made by size reduction from byproduct of rubber tire making industry.

The tests conducted were bitumen ductility, softening point and Marshall Mix design test. In this study, an attempt was made to evaluate the relationships between Ductility, Softening Point of the bitumen with the amount of rubber waste in bitumen. Meanwhile, Marshall Test was done to evaluate the suitability of rubber waste as bitumen modifier. After, conducting these tests on various sample of bitumen this was found that the property of bitumen varies consecutively with the application of rubber on the bitumen.

Keywords— Bitumen, Hot Mix Asphalt (HMA), Rubber Waste, Ductility Test, Softening Point Test, Marshall Mix Design, Marshall Test, Bitumen Modification, Asphalt Concrete (AC).

INTRODUCTION

Conventional bituminous materials performed their function satisfactorily in most of the pavements. However, existing highway systems have been dealing with increased traffic volume, higher axle load and tire pressure and extreme environmental impacts. The situation is evident for the last three decades, that the pavement has been facing more demands than before resulting in the need for an enhancement in the properties of bituminous materials.

The study conducts focus on the application of rubber waste as modifier in bitumen and asphaltic concrete. Therefore, the laboratory test is concentrates on bitumen tests and Marshall. In order to investigate the effects of rubber waste on HMA properties, the scope of the study was included preparation of Marshall samples with bitumen grade of 40/50 bitumen content without additive were 4%, 4.5%, 5.0%, 5.5% and 6.0% as control samples. The Marshall Test was conducted to determine optimum bitumen content and properties.

Besides that, content of rubber waste used were 4%, 8%, 12% and 16% of the optimum bitumen content weight into the mixture. The optimum waste content will be determined using Marshall Method. The result on the density, stability, flow, voids in total mix, voids filled bitumen and stiffness from the modified sample and control sample were compared and analyze.

This study is conduct to study the effect used of waste material in bituminous mixture. Rubber waste product used to improve the bitumen used in mixture and increase the strength of the pavement due to its rubbery characteristic. Besides that, the performance of the bituminous mixture need to improved due to the changes in the weather and increased in traffic loading.

Waste product is cheaper and can be obtained directly from the factory where these waste products are not reused by the factory. In directly, it will minimize construction cost. Reused waste product can ideally reduced pollution problem due to disposal aspect. The commercial value of waste material will increase if it was found suitable to be used in highway construction.

MATERIALS

Aggregate, Bitumen Grade 40/50, Waste Rubber Tyres.

METHODOLOGY

In order to evaluate the quality of rubber waste on road asphalt, laboratory experiments have to be done to identify the performance of the modified asphalt with rubber waste compared to the unmodified asphalt. All the laboratory experiment is based on the standard specification on ASTM and AASHTO.

The objective of Marshall Mix Design (ASTM D 1559) is to determine the optimum aggregate and bitumen mixture to ensure the mixture is durable, stable, sufficient void ratio, flexural, economic and quality.

Testing on bitumen have to be carried out is Ductility Test and Softening Point Test in order to ensure it performs well on the specification. Both tests were carried out to test whether the modified binder was appropriate. Ductility Test is the consistency test to determine the material stiffness meanwhile Softening Point Test is the consistency test to determine the temperature where the phase change occur in bitumen.

This study used the Marshall method, and the type of mixes that was designed is DBM. Contents of elastomeric base waste used in the mixes were 4%, 8%, 12% and 16% from the optimum bitumen content used in DBM. Minimum three specimens for each of the mix were prepared the optimum waste content.

EXPERIMENTAL WORK AND ANALYSIS

Through the laboratory work has been conducted, the result and data can be used to determine the properties of HMA. Data analysis was done according to Marshall Test and all result should be compared. The comparison of HMA properties were observed in terms of density, stability, flow, stiffness, VTM, VMA and VFB. This is to ensure that suitability of the industrial waste used as a modifier to conventional bitumen.

SIEVE ANALYSIS AND AGGREGATE DISTRIBUTION

All aggregates were sieved to sizes as stated according to specification. Hot mix asphalt mixture specifications require aggregate particles to be within a certain range of sizes and for each size of particle to be present in a certain proportion. In this study, DBM was used and the calculation was based on the median between upper and lower limit of the gradation. Table 1 shows the result of sieve analysis calculation for DBM Marshall Sample.

Table 1:- Sieve Analysis

Sieve size	Wt. Of aggregate retained (kg)	% wt. Retained	Cumulative % Retained	% wt. of aggregate passing
24 mm	0	0	0	100
20 mm	0.482	9.64	9.64	90.36
16 mm	0.521	10.42	20.06	79.94
12 mm	0.437	8.74	28.80	71.20
10 mm	0.624	12.48	41.28	58.72
6.3 mm	0.598	11.96	53.24	46.76
2.36 mm	0.360	7.20	60.44	39.56
1.18 mm	0.648	12.96	73.40	26.60
425 µm	0.297	5.94	79.34	20.66
150 µm	0.348	6.96	86.30	13.70
75 µm	0.291	5.82	92.12	7.88
Filler	0.394	7.88	100	0

SPECIFIC GRAVITY AND WATER ABSORPTION OF AGGREGATE

As the sample for testing specific gravity of aggregate is based on DBM, the coarse sizes are in the range of 5 - 20mm. Table 2 shows the full result of the specific gravity and water absorption of coarse aggregate.

Table 2:- Specific Gravity and Water Absorption of Coarse aggregate

Coarse Aggregate	Label	Sample 1	Sample 2
Weight of Oven Dry Aggregate (gm)	A	628.0	587.0
Weight of Saturated Surface Dry Aggregate (gm)	B	637.0	602.0
Weight of Aggregate in Water (gm)	C	404.0	384.0
Apparent Specific Gravity, (SG)	SG = A / (B – C)	2.70	2.69
Average	2.695		
Water Absorption (%)	(B – A) / A * 100	1.4	2.6
Average	2		

The specific gravity testing for fine aggregate also utilizes the gradation of DBM. The sizes of aggregates tested ranges from 0.075mm to 2.36mm. The full results of the test conducted are shown in Table 3.

Table 3:- Specific Gravity and Water Absorption of Fine aggregate

Fine Aggregate	Label	Sample 1	Sample 2
Pycnometer Weight + Water (gm)	A	838.8	828.8
Pycnometer Weight + Water + Aggregate (gm)	B	1121.0	1133.3
Weight of Oven Dry Material (gm)	C	492.8	491.6
Weight of Saturated Surface Dry Aggregate (gm)	D	500	500
Apparent Specific Gravity (SG)	SG = C / (A + D – B)	2.268	2.515
Average	2.392		
Water Absorption (%)	(D – C) / C * 100	1.46	1.71
Average	1.585		

SOFTENING POINT TEST

Softening Point Tests were done for normal bitumen and modified bitumen with 4%, 8%, 12% and 16% of rubber waste content. The result was shown in Table 4. From the plotted graph, the softening point for normal bitumen was 83.5°C.

The relationship between the rubber waste added and the softening point of the bitumen are almost linear as shown in Graph 1. Softening Point increased with the increased amount of the waste added. This showed that, the bitumen become less susceptible to

temperature changes as content of rubber waste increased.

Table 4:- Softening Point

Rubber Content (% by Weight of Optimum Bitumen Content)	Reading(^{0}C)		SP(^{0}C)
	Ball A	Ball B	
0	72	75	73.5
4	80	79	79.5
8	85	87	86
12	102	110	106
16	130	126	128

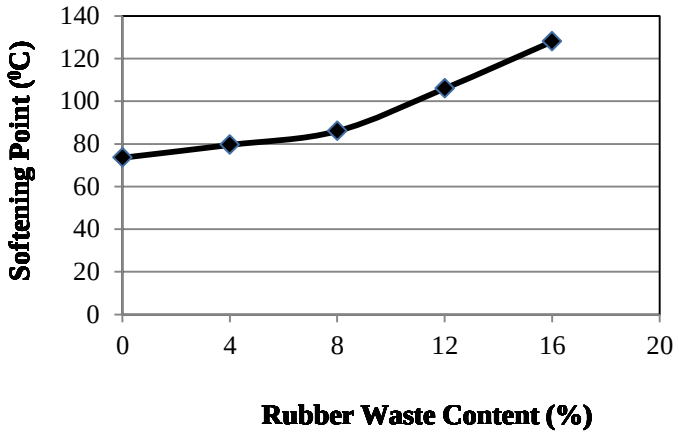

Graph 1:- Softening Point versus Rubber Waste Content

BITUMEN DUCTILITY TEST

Ductility test were done for normal bitumen and modified bitumen with 4%, 8%, 12%, and 16% of rubber waste content. The result was shown in Table 5. The ductility value decrease as the rubber content increase as shown in Graph 2. The result shows that the rubber waste added will harden the bitumen. The bitumen becomes more viscous and harder, which would be useful to obtain stiffer bitumen asphalt.

Table 5:- Ductility Test

(%) Rubber Waste	Sample Reading (cm)			Average
	Reading 1	Reading 2	Reading 3	
0	25	24	27	25
4	21	23	23	22
8	18	19	20	19
12	14	16	17	16
16	13	15	16	15

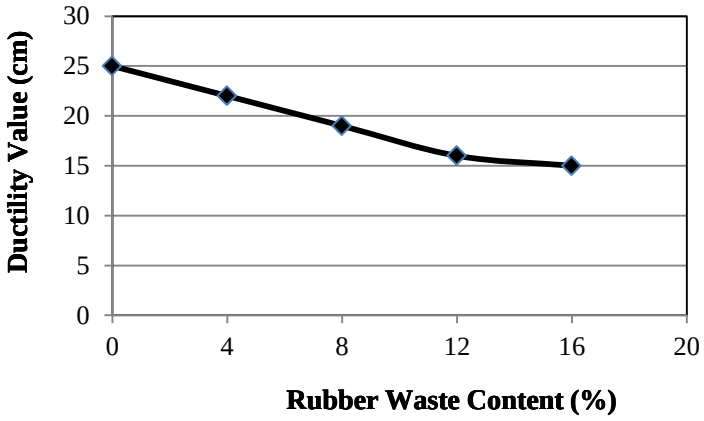

Graph 2:- Ductility Value versus Rubber Waste Content

MARSHALL TEST ANALYSIS

OPTIMUM BITUMEN CONTENT

Optimum bitumen content for AC was determined by using bitumen content of 4%, 4.5%, 5%, 5.5% and 6% according to the specification. Data obtained were analysis using Marshall Properties. The result of Marshall Test for AC was shown in Table 6.

Table 6:- Marshall Test Result

Bitumen Content (%)	Unit Weight (Kg/cm^3)	Stability (Kg)	Flow (mm)	VTM (%)	VMA (%)	VFB (%)	Stiffness (Kg/mm)
4	2.279	1123.1	2.11	12.6	21.45	41.26	532.27
4.5	2.26	1130.22	2.70	12.21	22.04	44.6	418.6
5	2.211	1202	3.14	10.33	20.965	50.728	382.80
5.5	2.202	1281.55	3.98	10.65	22.246	52.126	322
6	2.182	935.69	5.09	9.924	22.404	55.70	183.83

From the Table 6 it is clear that the specimen which has 5.5% bitumen content have maximum stability. So, we used 5.5% bitumen content as optimum bitumen content.

RUBBER WASTE ADDED IN AC MIXTURE

After control sample and optimum bitumen content were obtained, Marshall Test with modified bitumen was conducted. The rubber waste content used in the AC mixtures were 4%, 8%, 12% and 16% by the weight of OBC. Table 7 shows the test result obtained for various content of waste added.

Table 7:- Marshall Test Result for Modified Bitumen Mixture

Rubber Waste Content (%)	Unit Weight (Kg/cm^3)	Stability (Kg)	Flow (mm)	VTM (%)	VMA (%)	VFB (%)	Stiffness (Kg/mm)
4	2.2503	2031	2.7	12.29	23.603	47.93	752.22
8	2.2347	2042.67	2.1	11.01	21.757	49.396	972.70
12	2.2482	1712.33	2.823	11.242	21.614	47.987	606.564
16	2.263	1405	3.28	11.533	21.531	46.4354	428.354

DENSITY ANALYSIS

Specific gravity of cooled compacted sample was determined according ASTM D 2762 after being cooled at room temperature. Graph 3 shows the density versus bitumen content for modified bitumen. The graph shows that the maximum density for modified bitumen was when rubber waste added at 12% and 16%. The graph pattern shows that the density value increase as the rubber waste content added increasing.

The rubber has higher value of density as compare to the normal bitumen. So, when the percentage of rubber is increase the density increase. The effectiveness of compaction reduced due to the addition of rubber waste into bitumen, the area for bitumen coating become increased since the optimum bitumen content was reduced by increased the percentage of rubber waste amount added into the mixture as replacement.

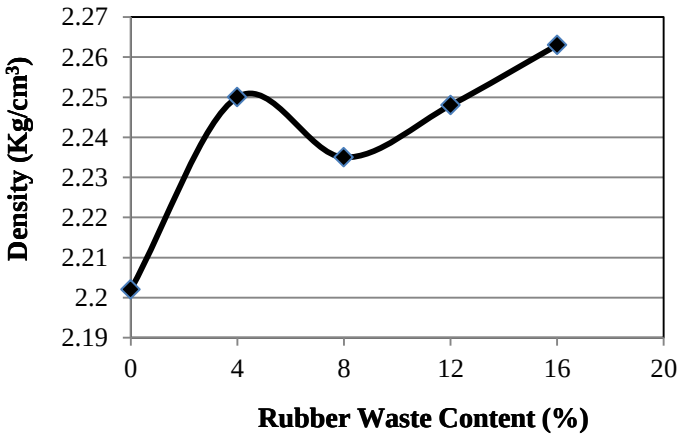

Graph 3:- Effect of Rubber Waste on Mixture Density

STABILITY ANALYSIS

Graph 4 shows the relationship between stability and waste content. The graph shows that the stability value decreases gradually with increasing the percentage of rubber waste content added. As we know, the stability of mixtures depends on bitumen cohesion. Cohesion results from the bonding ability of bitumen and the cohesion increase with increasing bitumen content. However if the stability is too high, it will causes significance effect on mixture. Excess bitumen will cause instability problem. Too high stability value produces a pavement mixture that is too stiff and less durable.

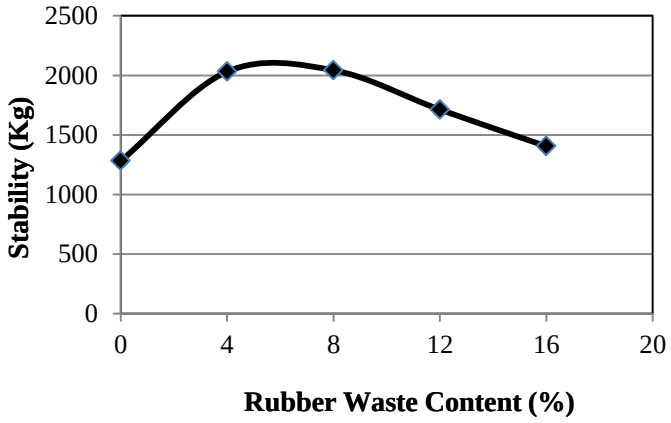

Graph 4:- Effect of Rubber Waste on Mixture Stability

FLOW ANALYSIS

Graph 5 shows the relationship between flow and rubber waste content. Flow was related to the flexibility of the mix. High value of flow shows high flexibility.

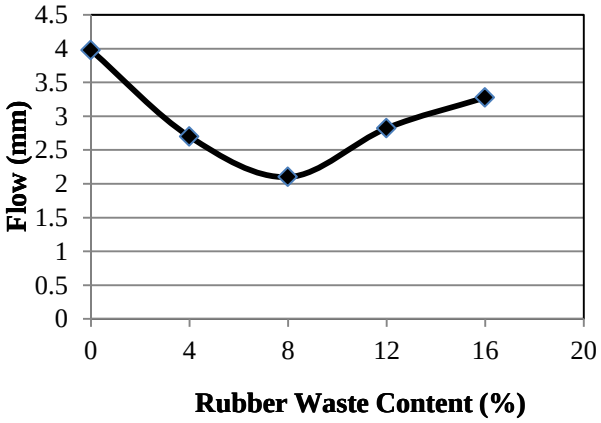

Graph 5:- Effect of Rubber Waste on Mixture Flow

VOIDS IN TOTAL MIX ANALYSIS

From the Marshall test that has been done, the trend of the voids in total mix obtained was decreased until a minimum value is reached and increased after that. The voids in total mix were highly related to the compaction has been done. Graph 6 shows that the samples were under compacted. Higher compaction will caused the small particles filled between aggregate and reduce the voids in the mix. When the waste was added, the waste was not fully melted and under compaction caused by the particles not proper filled between aggregate and increased the voids. When the waste content added above 12%, the waste was not fully melted because of the bitumen content was reduced.

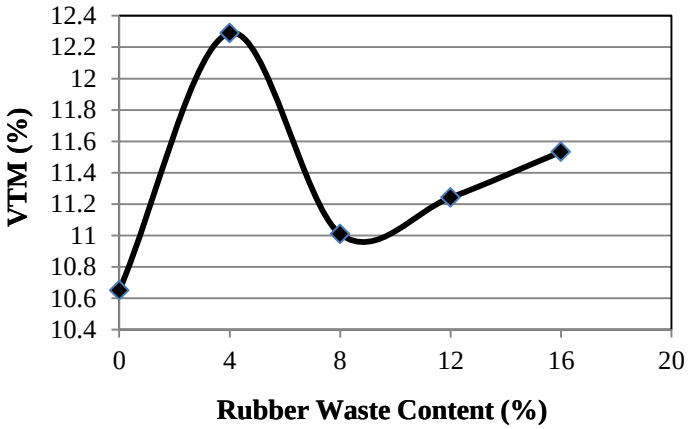

Graph 6:- Effect of Rubber Waste on Mixture VTM

VOIDS IN MINERAL AGGREGATE ANALYSIS

Voids in mineral aggregate are a part of the voids in total mix. Voids in mineral aggregate are the voids which are present in the aggregate mix and which is not filled by the bitumen filler. Graph 7 shows the graph of the voids in mineral aggregate are greatly affected by proportion of waste rubber added.

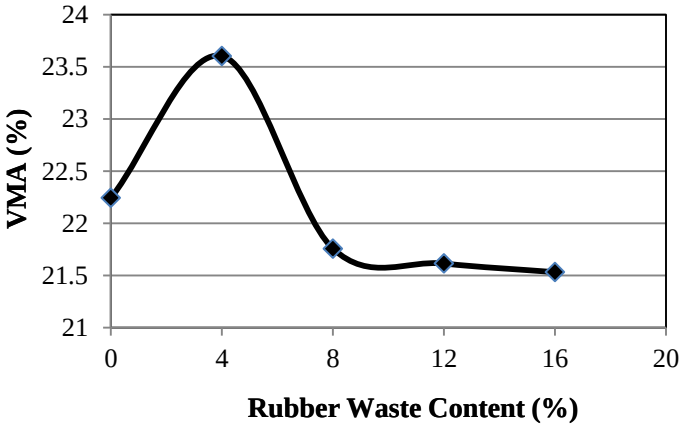

Graph 7:- Effect of Rubber Waste on Mixture VMA

VOIDS FILLED WITH BITUMEN ANALYSIS

Voids filled with bitumen are related to the voids in total mix and density and Graph 8 shows the graph of VFB versus modified bitumen using rubber waste from the test has been done. The percent of air voids filled with bitumen was decreased. Due to the addition of rubber waste into bitumen, the bitumen content become decreased and caused the bitumen not properly filled the voids and affected the bonding between aggregate. This will make the pavement mixture easy to allow air and water permeates. If the bitumen content exceeds the optimum value, it will produce the mix that prone to bleed. The highest voids filled bitumen was 49.396% at 8% waste added.

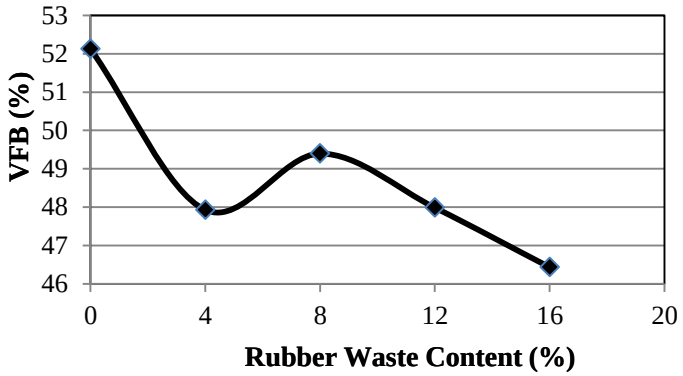

Graph 8:- Effect of Rubber Waste on Mixture VFB

STIFFNESS ANALYSIS

Stiffness of the mixture is important to limit the occurrence of rutting. Higher stiffness value shows that the mixture can take the load without changing in shape. Graph 9 shows the graph of stiffness versus modified bitumen. The stiffness value decreases with increasing percent of rubber waste added. This mean, in term of rut resistance, the asphaltic concrete with higher percent of rubber waste will has deeper rut depth.

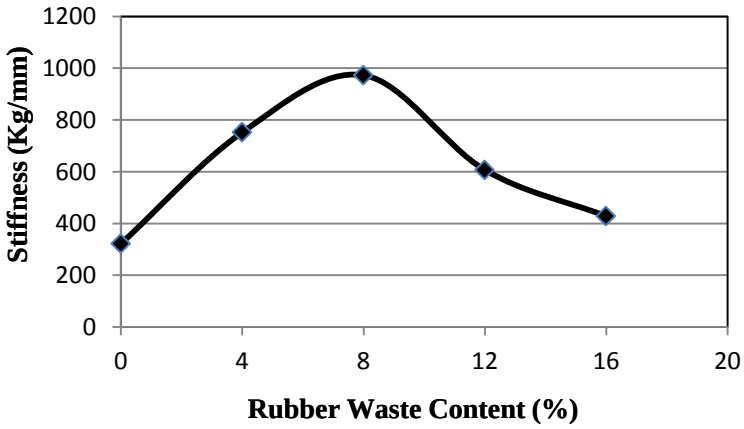

Graph 9:- Effect of Rubber Waste on Stiffness

CONCLUSION

From the comparison shown in Table 8, there are some parameters of the sample with rubber waste added that meet the specification which are stability and stiffness. The optimum waste content is 8%.

Table 8:- Comparison of Marshall Parameter between Control Sample and Modified Sample

Marshall Properties	Control Sample	Rubber Waste Content			
		4%	8%	12%	16%
Stability	1281.55	2031	2042.67	1712.33	1405
Flow	3.98	2.7	2.1	2.823	3.277
Density	2.202	2.25	2.235	2.248	2.263
VTM	10.65	12.29	11.01	11.242	11.533
VMA	22.246	23.603	21.757	21.614	21.531
VFB	52.126	47.93	49.396	47.987	46.4354
Stiffness	322	752.22	972.70	606.564	428.354

The stability of the samples was decreased with the increasing of waste content. The percentage of VTM of modified mix is higher than normal mix. The density of the mix was increase with the increase of rubber waste content. The optimum value of voids filled bitumen was 49.396% at the waste content of 8%. When the waste was added more than 12%, it caused the flow to increase. Rubber waste is suitable to be used as bitumen modifier in order to improve the bitumen properties with the right amount of replacement. Replacement rubber waste as bitumen modifier in the asphaltic concrete mixture increase the adhesion between the aggregate particles, durability and possibility to minimize the deformation of road wearing course.

REFERENCES:

1. Charles J. Glover, Richard R. Davison and Jerry A. Bullin (2000). "A Comprehensive Laboratory and Field Study of High-Cure Crumb-Rubber Modified Asphalt Material, Report – 1460-1". Texas Department of Transportation Research: Research and Technology Implementation Office.
2. Mark S. Buncher (1995). "Evaluating the Effects of the Wet and Dry Processes for Including Crumb Rubber Modifier in Hot Mix Asphalt". National Centre for Asphalt Technology Auburn University, Alabama.
3. Szabolcs Biro and Bence Fazekas (2005). "Asphalt rubber versus other modified bitumen". Bitumen Engineering Angyal u. 19, Budapest, 1094, Hungary.
4. Mohamed Sulyman, Maciej Sienkiewicz, and Jozef Haponiuk (2014). "Asphalt Pavement Material Improvement". International Journal of Environmental Science and Development, Vol. 5.
5. Andreas Meling Kjosavik (2013). "Determining the Rheological Properties of Neat and Rubber Modified Soft Bitumen". Norwegian University of Science and Technology Department of Civil and Transport Engineering.
6. Francisco Javier López-Moro, María Candelas Moro, Francisco Hernández-Olivares (2013). "Microscopic analysis of the interaction between crumb rubber and bitumen in asphalt mixtures using the dry process". Construction and Building Materials 48.
7. Farag Khodary Moalla Hamed (2010). "Evaluation of Fatigue Resistance for Modified Asphalt Concrete Mixtures Based on Dissipated Energy Concept". Department of Civil Engineering and Geodesy Technische Universität Darmstadt.
8. Mujibur Rahman (2004). "Characterisation of Dry Process Crumb Rubber Modified Asphalt Mixtures". University of Nottingham School of Civil Engineering.
9. D. Vasavi Swetha and Dr. K. Durga Rani (2014). "Effect of Natural Rubber on the Properties of Bitumen and Bituminous Mix". International Journal of Civil Engineering and Technology, Volume – 5, pp. 09-21.
10. Miss. Mane Priyanka Arun, Mr. Petkar Deepak Ganesh and Mr. Bhosale S.M (2013). "Laboratory Evaluation of Usage of Waste Tyre Rubber in Bituminous Concrete". International Journal of Scientific and Research Publications, Volume 3, ISSN 2250-3153.
11. Soon-Jae Lee, Serji N. Amirkhanian and Khaldoun Shatanawi (2006). "Effect of Crumb Rubber on the Aging of Asphalt Binders". Department of Civil Engineering, Clemson University, USA.
12. Mohamed O Sulyman, Maciej Sienkiewicz and Jozef Haponiuk (2013). "New Study on Improved Performance of Paving Asphalts by Crumb Rubber and Polyethylene Modification". Department of Polymer Technology, Chemical Faculty, Gdansk University of Technology, Poland.
13. G.N. Narule, Ajit Mendgule and Ganesh Borude (2013). "An Experimental Study of Flexible Pavement by Using Crumb Rubber as Binding Material". International Journal of Pure and Applied Research in Engineering and Technology, Volume – 1: 141-149.
14. Douglas D. Carlson (1999). "Asphalt-Rubber an Anchor to Crumb Rubber Markets". International Rubber Forum Veracruz, Mexico.
15. Carl Christian Thodesen & Inge Hoff (2012). "Effect of crumb rubber modification on binder-aggregate coating". Norwegian University of Technology and Science: Civil Engineering Department, Lerkendalsbygget 2-051.
16. Ye. Tileuberdi, Ye.K. Ongarbaev and Z.A. Mansurov (2013). "Physical and Mechanical Characteristics of Rubber-Bitumen Compounds". Chemical and Materials Engineering 1(4): 105-110.
17. Shirish N. Nemade and Prashant V. Thorat (2013). "Utilization of Polymer Waste for Modification of Bitumen in Road Construction". Sci. Revs. Chem. Commun.: 3(4), 198-213, ISSN 2277-2669.
18. Mohammed Sadeque1* and K A Patil (2014). "An Experimental Study on Effect of Waste Tyre Rubber on 60/70 Grade

Bitumen". International Journal of Structural and Civil Engineering Research, Volume – 3, ISSN: 2319-6009.

19. Niraj D. Baraiya (2013). "Use of Waste Rubber Tyres in Construction of Bituminous Road". International Journal of Application or Innovation in Engineering & Management, Volume – 2: ISSN 2319 – 4847.
20. K. Rajesh Kumar, Dr. N. Mahendran (2014). "Experimental Studies on Modified Bituminous Mixes Using Waste HDPE and Crump Rubber". International Journal of Emerging Technology and Advanced Engineering, Volume – 4: ISSN 2250-2459.
21. Bala Raju Teppala, Prof. C.B. Mishra and Alok Sinha (2014). "Experimental Assessment of Properties of Crumb Rubber Modified Bitumen Mix (CRMB 55) With and Without Application of Nanotechnology Additive". International Journal of Innovative Research in Science, Engineering and Technology, Volume – 3: ISSN 2319-8753.
22. Nabin Rana Magar (2014). "A Study on the Performance of Crumb Rubber Modified Bitumen by Varying the Sizes of Crumb Rubber". International Journal of Engineering Trends and Technology, Volume – 14: ISSN 2231-5381.
23. Saeed Ghaffarpour Jahromi, Ali khodaii (2008). "Empirical Model for Determining Rutting Parameter in Rubber Modified Bitumen". International Journal of Civil Engineering, Volume – 6.
24. Adil Al Tamimi and Isam A. H. Al Zubaidy (2014). "Evaluation of Sustainable Asphalt Mixture". Study of Civil Engineering and Architecture (SCEA), Volume – 3.
25. Afifa Rahman, Syed Ashik Ali and Sajal Kumar Adhikary (2012). "Effect of Fillers on Bituminous Paving Mixes". Journal of Engineering Science, Volume – 3.
26. John B. Johnston and Gayle King (2008). "Using Polymer Modified Asphalt Emulsions in Surface Treatments". A Federal Lands Highway Interim Report.
27. Ramez A. Al-Mansob, Amiruddin Ismail and Aows N. Alduri (2014). "Physical and rheological properties of epoxidized natural rubber modified bitumens". Construction and Building Materials 63 242-248.
28. Mohammed H. Al-maamori and Muntadher Mohammed Hussen (2014). "Use of Crumb Rubber as a Way to Improve Performance Grade for Asphalt Cement". Academic Research International, Volume – 5, ISSN: 2223-9944.
29. M. A. Shafii, M. Y. Abdul Rahman and J. Ahmad (2011). "Polymer Modified Asphalt Emulsion". International Journal of Civil & Environmental Engineering, Volume – 6.
30. Nopparat Vichitcholchai, Jaratsri Panmai and Nuchanat Na-Ranong (2012). "Modification of Asphalt Cement by Natural Rubber for Pavement Construction". Rubber Thai Journal, Volume - 1: 32-39.
31. Saad Abdulqader Ali, Ismail bin Yusof and Madi Hermadi (2013). "Pavement Performance with Carbon Black and Natural Rubber". International Journal of Engineering and Advanced Technology, Volume – 2, ISSN: 2249 – 8958.
32. Taher M.A. Al-ani (2009). "Modification of Asphalt Mixture Performance by Rubber-Silicone Additive". Anbar Journal of Engineering Sciences, Volume – 2.
33. Nrachai Tuntiworawit (2005). "The Modification of Asphalt with Natural Rubber Latex". Proceedings of the Eastern Asia Society for Transportation Studies, Volume – 5, pp. 679 – 694.

International Journal of Engineering Research and General Science Volume 3, Issue 5, September-October, 2015
ISSN 2091-2730

Chaotic Time Series Prediction using Correlation Dimension and Adaptive Neuro-Fuzzy Inference System

Pravin Kshirsagar
Department of Electronics Engineering
S.B.Jain Institute of Technology, Management and Research
Nagpur, Maharashtra, India
pravinrk88@yahoo.com

Dr. Sudhir G. Akojwar
Department of Electronics Engineering
Rajiv Gandhi College of Engineering, Research & Technology Chandrapur, Maharashtra, India
sudhirakojwar@rediffmail.com

Abstract — Nonlinear dynamic signal processing is attracting several researchers owing to its complex behavior which may be deterministic at macro level and may be in order but unruly behavior with respect to time is difficult to understand and interpret. EEG signals fall under such categories. Prediction of seizure in EEG is a challenging task. For this several prediction methodologies have been in use from time to time. But the complexity of signals which differ from person to person makes it complicated. . Keeping this view in mind, we propose to have better prediction of chaotic time series through this paper. Though there have been several attempts in the past, our research is related to use of ANFIS for chaotic time series prediction. Correlation dimension are the factors based on which convergent or divergent or chaotic nature of signal is predicted. In this paper we use correlation dimension for feature extraction providing to ANFIS model for giving précised result.

KEYWORDS - EEG SIGNALS, CORRELATION DIMENSION,ANFIS

INTRODUCTION

EEG signal is a spontaneous bioelectricity activity that is produced by the central nervous system. It includes abundant information about the state and change of the neural system; therefore it is widely used in clinic and neural-electricity physiological research.

An electroencephalograph is a record of the electrical activity generated by a large number of neurons in the brain. It is recorded using surface electrodes attached to the scalp or subdural or in the cerebral cortex. The amplitude of a human surface EEG signal is in the range of 10 to 100 μV. The frequency range of the EEG has a fuzzy lower and upper limit, but the most important frequencies from the physiological viewpoint lie in the range of 0.1 to 30 Hz. The standard EEG clinical bands are the delta (0.1 to 3.5 Hz), theta (4 to 7.5 Hz), alpha (8 to 13 Hz), and beta (14 to 30 Hz) bands. EEG signal analysis is helpful in various clinical applications including predicting epileptic seizures, classifying sleep stages, measuring depth of anesthesia, detection and monitoring of brain injury, and detecting abnormal brain states. Visual analysis of EEG signals in the time domain is an empirical science and requires a considerable amount of clinical and neurological knowledge. Many brain abnormalities are diagnosed by a doctor or an electroencephalographer after visual inspection of brain rhythms in the EEG signals. However, long-term monitoring and visual interpretation is very subjective and does not lend itself to statistical analysis. Therefore, alternative methods have been used to quantify information carried by an EEG signals.

Predicting future behavior of chaotic time series is a challenging area in nonlinear prediction. The prediction accuracy of chaotic time series is extremely dependent on the model and learning algorithm. In addition, the generalization property of the proposed models trained by limited observations is of great importance.

In the past decades, neural networks and related neuro fuzzy models as general function approximations have been the subjects of interest due to their many practical applications in modeling complex phenomena but when the number of observations for training is limited they can neither reconstruct the dynamics nor can learn the shape of attractor.

They may present the most accurate one step ahead predictions, but in larger prediction horizon their performance dramatically falls down. The uncertainty of EEG has repelled human to make efforts for determining predicted EEG signals before time so that feature critical condition of patient will be tackled and managed prior to any vast spread demolition. If we predict real time EEG signals which will help to save the life of patient.

In recent years, many modeling has gained significant importance through Artificial Intelligence (AI) techniques for their ability to learn hidden patterns from historical data and predict highly non-linear systems. The hybrid Adaptive Neuro-Fuzzy Inference System (ANFIS) and Artificial Neural Network (ANN) are commonly used AI techniques which have been applied in variety of domains for such modeling.

Various feature extraction method such as correlation dimension, lyapunov exponent are the factors based on which convergent or divergent or chaotic nature of signal is predicted. This can be suitably applied to a neuro-fuzzy or simply an ANN system application in real time databases such as solar energy production and relative data are pre-processed using Fuzzy Logic techniques.

This paper aims at neuro fuzzy approach to the modeling on EEG signals data in which presence of chaos if any. The paper also throws light over the ANFIS model with feature extracting techniques through which analysis of real time prediction can be done effectively.

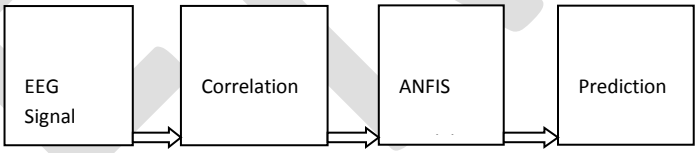

Figure 1.block diagram of system

Figure 1 shows the block diagram of the system.It consist large number of EEG signals which extracted its feature by Correlation Dimension,ANFIS model used for prediction of the neurological disorder from predicted output.

CORRELATION DIMENSION

Using the Grassberger-Procaccia (1983a, 1983b) algorithm to determine the correlation dimension D2, one defines the correlation integral:

$$C(r) = \lim_{n\to\infty} \frac{1}{N^2} \sum_{i\neq j} \theta(r - |\overrightarrow{v_m}(t_i) - \overrightarrow{v_m}(\overrightarrow{t_j})|)$$

where, $\theta(x) = 1$ if $x \geq 0$,θ (x) = 0 if x < 0, and N is the number of points in the time series. Cm(r) measures the fraction of pairs of points in space that are closer than r. If the system is chaotic one has that for sufficiently large m, m>m*, the correlation integral takes the following scaling form, independent of m,

$$C(r) \approx r^{D_2}$$

with the exponent giving the correlation dimension D2 of the attractor corresponding to the measured signal. Hence D2 can be obtained from the slope of In C(r) vs In r. The quantity m* is the minimal embedding dimension as it is the lowest integer dimension containing the whole attractor; m* gives information on the number of independent variables governing the dynamics of the system.

$$\mathrm{d} = \lim_{\mathrm{r}\to 0,\mathrm{n}\to\infty} \frac{\log \mathrm{Cm(r)}}{\log \mathrm{r}}$$

Plotting log Cm(r) against log r yields a curved line that can usually be subdivided into three parts: (i) the depopulation range (an irregular pattern) for small values of log r , (ii) the scaling range (a linear part) for intermediate values of log r , (iii) the saturation range (slope approaches zero) for large values of log r . The correlation exponent value is estimated from the slope of the scaling range. It must be noted that the exact delineation of the scaling region can be difficult and often requires visual inspection. Moreover, the scaling region becomes smaller and smaller with increasing of m , and eventually vanishes for large m (e.g. Ding et al., 1993; Husain and Siva Kumar, 2006). Hence the estimation of the correlation exponent partly is an empirical exercise. The correlation exponent is identified from the scaling range of log Cm(r) against log r plot for different embedding dimensions. Then the values of the embedding dimension m are plotted versus the correlation exponent d(m) . The estimated CD value typically increases with m and reaches a plateau on which the dimension estimate is relatively constant for a range of large enough m . This saturation value is the estimated CD of the analyzed signal, while the embedding dimension corresponding to the plateau onset is sufficient to estimate the dimension of the attractor. That is to say, the nearest integer above the CD provides the minimum dimension of the phase space essential to embed the attractor, while the value of the embedding dimension at which the saturation of the correlation exponent occurs provides an upper bound on the dimension of the phase space sufficient to describe the motion of the attractor (Fraedrich, 1986). If there is no plateau in the $d(m)$ curve, it indicates that the data could be stochastic in nature or severely affected by noise. In that case the CD value cannot be estimated. Therefore, the CD method is able to distinguish chaotic motion from a simple system and stochastic motion (Theiler, 1986).

For sufficiently large number of observations and the embedding dimension obtain above equation, from above equation we calculate CD of EEG signals.

ADAPTIVE NEURO FUZZY INFERENCE SYSTEM

ANFIS topology and the learning method that used for this Neuro-fuzzy network are presented. Both neural network and fuzzy logic are model-free estimators and share the mutual ability to deal with uncertainties and noise. The ANFIS combines two approaches: neural networks and fuzzy systems. If both these two intelligent approaches are combined,

good reasoning will be achieved in quality and quantity. In other words, both fuzzy reasoning and network calculation will be available simultaneously. The ANFIS is composed of two parts. The first is the antecedent part and the second is the conclusion part, which are connected to each other with the fuzzy rules base in network form. As shown in this figure, it is a five layer network that can be described as a multi-layered neural network.

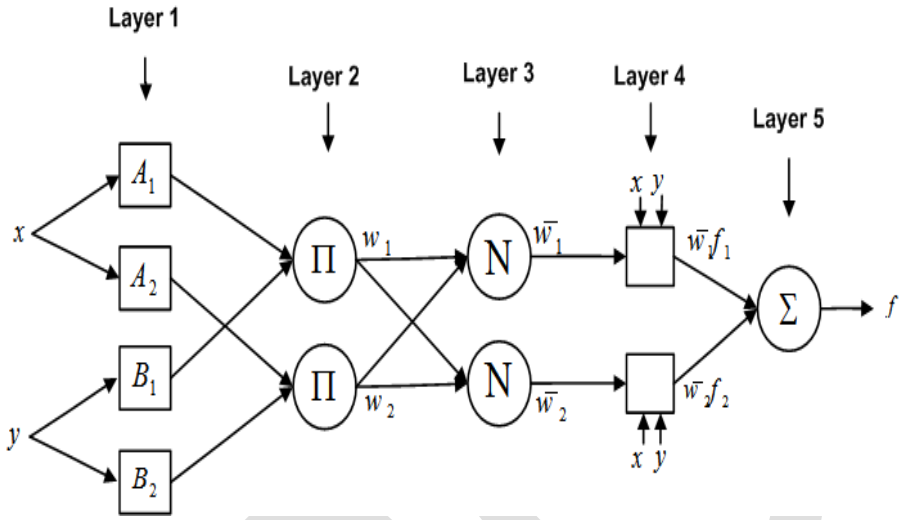

Figure 2. Basic structure of ANFIS

Each layer involves several nodes described by node function. The output signals from nodes in the previous layers will be accepted as the input signals in the present layer. After manipulation by the node function in the present layer will be served as input signals for the next layer. Here square nodes, named adaptive nodes, are adopted to represent that the parameter sets in these nodes are adjustable. Whereas, circle nodes, named fixed nodes, are adopted to represent that the parameter sets are fixed in the system. For simplicity to explain the procedure of the ANFIS, we consider two inputs *x*, *y* and one output *f* in the fuzzy inference system. And one degree of Sugeno's function is adopted to depict the fuzzy rule. Hence, the rule base will contain two fuzzy *if–then* rules as shown in rule 1 and rule 2 equations:

Rule 1: if x is $A1$ and y is $B1$ then $f = p1x + q1y + r1$.
Rule 2: if x is $A2$ and y is $B2$ then $f = p2x + q2y + r2$.

The terms p,q,r denote parameters of the output function whereas A,B are membership functions for inputs x,y respectively. The then-part of the rule is defined as consequent and the if-part of the rule is represented as premise. As shown in Fig.2 there are five layers in ANFIS architecture. Each layers functionality is illustrated below.

Layer 1**:** Every node i in this layer is a square node with node function as:

$$O_{1,i} = \mu_{A_i}(x) \qquad for\ i = 1,2$$

$$O_{1,i} = \mu_{B_{i-2}}(y) \qquad for\ i = 3,4`$$

Where x is the input to node i, and i A (or B_{i-2}) is a linguistic label (such as "small" or "large") associated with this node. In other words, 0l,i is the membership grade of a fuzzy set A and it specifies the degree to which the given input x satisfies the quantifier A. The membership function for A can be any appropriate membership function, such as the Triangular or Gaussian. When the parameters of membership function changes, chosen membership function varies accordingly, thus exhibiting various forms of membership functions for a fuzzy set A . Parameters in this layer are referred to as "premise parameters".

Layer 2**:** Every node in this layer is a fixed node labeled as, whose output is the product of all incoming signals:

$$O_{2,i} = w_i = \mu_{A_i}(x)\mu_{B_i}(y), \quad i = 1,2$$

Each node output represents the firing strength of a fuzzy rule.

Layer 3**:** Every node in this layer is a fixed node labeled N. The i th node calculates the ratio of the rule's firing strength to the sum of all rules' firing strengths:

$$O_{3,i} = \overline{w}_i = \frac{w_i}{w_1 + w_2}$$

Outputs of this layer are called "normalized firing strengths".

Layer 4**:** Every node i in this layer is an adaptive node with a node function as:

$$O_{4,i} = \overline{w_i} f_i = \overline{w_i}(p_i x + q_i y + r_i)$$

Where *wi* is a normalized firing strength from layer 3 and (p_i, q_i, r_i) is the parameter set of this node. Parameters in this layer are referred to as "consequent parameters".

Layer 5**:** The single node in this layer is a fixed node labeled Σ that computes the overall output as the summation of all incoming signals:

$$O_{5,i} = \sum_i \overline{w_i} f_i = \frac{\sum_i w_i f_i}{\sum_i w_i}$$

This then is how, typically, the input vector is fed through the network layer by layer. We now consider how the ANFIS learns the premise and consequent parameters for the membership functions and the rules.

ANFIS has high ability of approximation that will depend on the resolution of the input space partitioning, which is determined by the number of MFs in the antecedent part for each input. In this paper, the MFs are used as Gaussian MF that *m* represents the center and □□determines the width of the MF respectively.

RESULTS

The correlation dimension of EEG signals of 2000 data packets each is calculated. In which enormous information of patients, it helps to analysis the data of patients. The output of correlation dimension is shown below.

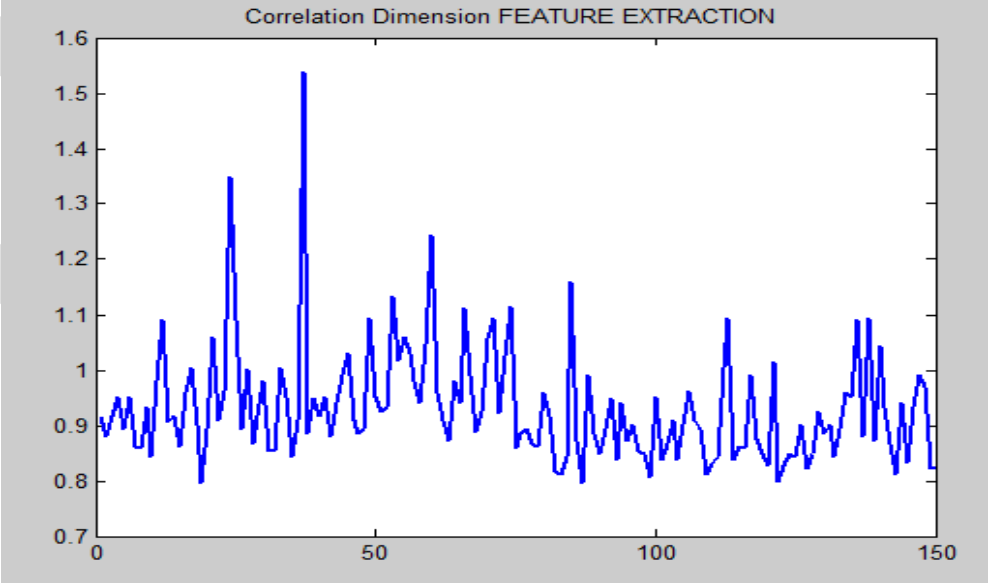

Figure 3. Output of correlation dimension

The figure 3 shows waveform contains the plot of all the features extracted from the EEG signals. Correlation dimension of EEG signals is then trained by anfis model for precise output.

The results obtained by the ANFIS model for EEG signals prediction was noted. After the model was trained using initial data set for 30 epochs, it was tested by using a random input.

The ANFIS is then training the data for 50% input data and checking data for rest of 50% data. The model was then tested over another time slot of the same time series. The results were obtained as shown below.

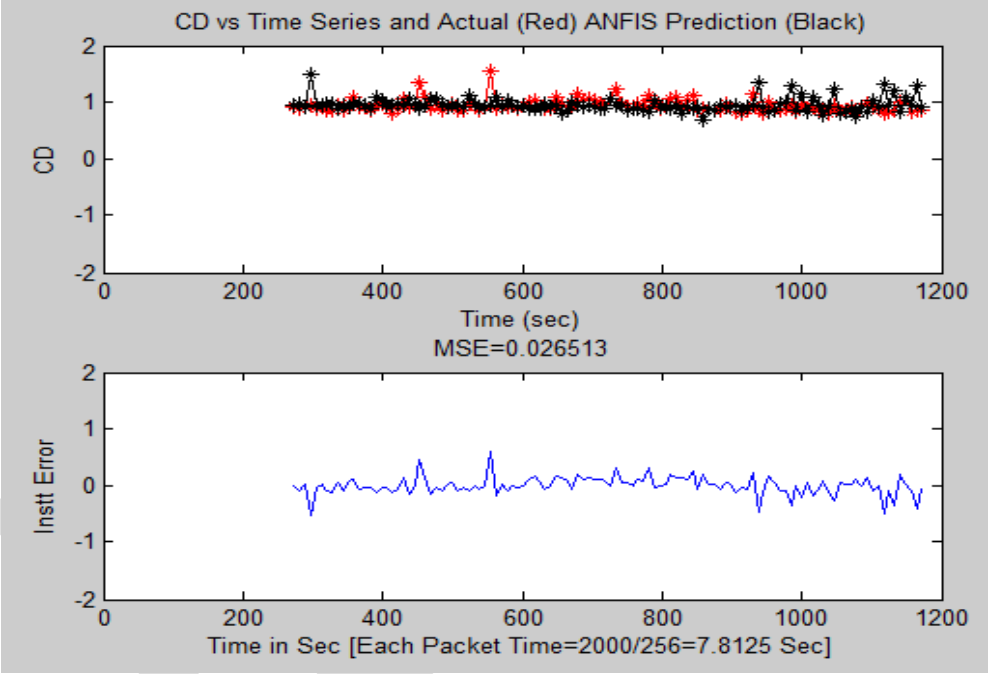

Figure 4. Prediction errors on testing ANFIS for chaotic time Series

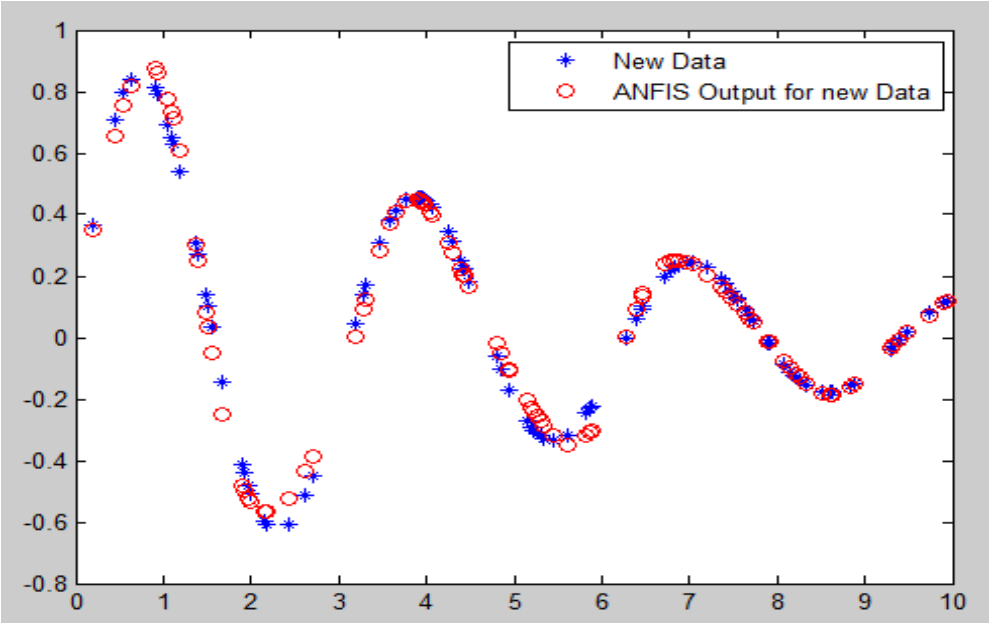

Figure 5. ANFIS Prediction

Fig. 4 shows ANFIS predicted output in which actual signals in red and predicted output in black and error calculate between actual and predicted output.

Thus the root mean square error (RMSE) in the above case was 0.0265 which is acceptable. RMSE in any case is calculated by,

$$RMSE = \sqrt{\frac{1}{n}\sum_{i=1}^{n}(Y\_predicted_i - Y\_actual_i)^2}$$

CONCLUSON

Prediction of seizure in EEG is a challenging task. For this several prediction methodologies have been in use from time to time. But the complexity of signals which differ from person to person makes it complicated. This work is helps to overcome this problem and also work will to explore the prediction potential of chaos for seizure prediction. This work tries to build the bridge between the real time data and the future prediction in presence of chaos. The predicted data results indicate that the ANFIS module itself into any data set in any chaotic conditions and enormous latent on the EEG signal prediction in future helps to save life of patient.

REFERENCES:

1. Faure P, Korn H: Is there chaos in the brain? I. "Concepts of nonlinear dynamics and methods of investigation". Life Sciences324:773-793.(2001)
2. Qiao Meiying, MA Xiaoping, "A new method on Solving Correlation Dimension of chaotic time series". 10th world congress on intelligent and automation,china,2012

3. Alexey Mekler:" Calculation of EEG correlation dimension: Large massifs of experimental data",USA,2008,154-160
4. Jirina,M :"Correlation Dimension-Based classifier" cybernetics Prague, IEEE Trans., 2014
5. Rabbi, A., Aarabi, A. ; Fazel-Rezai, R. ;"Fuzzy rule-based seizure prediction based on correlation dimension changes in intracranial EEG";IEEE,2009
6. Ahmed F. Rabbi, Leila Azinfar, "Seizure Prediction Using Adaptive Neuro-Fuzzy Inference System",IEEE conference. japan,2-7 july 2013
7. Maysam Behmanesh, Majid Mohammadi, Vahid Sattari Naeini." Chaotic Time Series Prediction using Improved ANFIS with Imperialist Competitive Learning Algorithm",International Journal of Soft Computing and Engineering (IJSCE),vol. 4,2014
8. Jignesh Patel, Dr.Falguni Parekh "Forecasting Rainfall Using Adaptive Neuro-Fuzzy Inference System (ANFIS)", IJAIEM,voiume 3,2014
9. Ali Yadollahpour, Mustafa jalilifar" Seizure Prediction Methods: A Review of the Current Predicting Techniques",Biomedical and Pharmacology Journal,2014
10. L.D. Iasemidis, et al., Adaptive epileptic seizure prediction system, IEEE Trans. Biomed. Eng. 50 -55,2003
11. J. S. R. Jang, "ANFIS: Adaptive-Network-based Fuzzy Inference Systems," IEEE.Transactions on Systems, Man, and Cybernetics, Vol. 23, No. 3, pp. 665–685, 1993.

C. H. Chen, C. J. Lin, and C. T. Lin, "An efficient quantum neuro-fuzzy classifier based on fuzzy entropy and compensatory operation," Soft Computing, vol. 12, no. 6, pp.567-583, 2008.

12. M.S.K. A wan and M.M. Awais "Predicting weather events using fuzzy rule based system" Applied Soft Computing II (2011) 56-63 in 2009.
    A. Gholipour, C. Lucas, B. N. Araabi, M. Mirmomeni, and M. Shafiee, "Extracting the main patterns of natural time series for long-term neuro fuzzy prediction," Neural Computing and Applications, doi: 10.1007/s00521-006-0062-x, Aug. 2006
13. Sharma A, Wilson, S.B. and Roy.R, EEG classification for estimating anesthetic depth during halothane anesthesia. *Int. Proc.14th Annual International Conference. IEEE, Newyork,*: pp 2409 -2410, 1992.
14. Guler, E.D. Ubeyli, Application of adaptive neuro-fuzzy inference system for detection of electrocardiographic changes in patients with partial epilepsy using feature extraction, Expert Syst. Appl. 27 ,323–330,2004.
15. J.S.R. Jang, ANFIS: adaptive network based fuzzy inference system, IEEE Trans. Syst., Man Cybern. 23 (3), 665–683,1993
16. M. Sugeno, T. Yasukawa, A fuzzy-logic based approach to qualitative modeling, IEEE Trans. Fuzzy Syst. 1 (1) pp7–31, 1993.
17. Song-Sen Yang and Jing Xu and Guang-Zhu Yao, "Concrete strength evaluation based on fuzzy neural networks", IEEE Xplore, Volume 6, pages:3344-3347, 24 January 2005
18. H. Tamura, K. Tanno, H. Tanaka, C. Vairappan, and Z. Tang. 2008. "Recurrent type ANFIS using local search technique for time series prediction". IEEE Asia Pacific Conf. Circuits Syst. 380–383.

International Journal of Engineering Research and General Science Volume 3, Issue 5, September-October, 2015
ISSN 2091-2730

Application of Data Mining Techniques in Health Fraud Detection

Rekha Pal and Saurabh Pal
VBS Purvanchal University
Jaunpur, U.P., India
E-mail: drsaurabhpal@yahoo.co.in

ABSTRACT- Health smart card is like ATM card which provide cash benefits to patient through insurance company for hospital and medical benefits without expending money from the patient at the time of need. But now-a-days, fraud is done using the health smart card as few patients does not know the real cost of the treatment, so doctor take more payment and benefits through health smart card and generate fraud cash benefits. In this paper we proposed health fraud detection using different data mining techniques with the help of ID3, J48, Naïve Bayes. We have presented better accurate data by classifying all observations of fraud.

Keywords
Fraud detection; Classification: ID3, J48 and Naive Bayes; BPL.

1. INTRODUCTION

Fraud will always be a problem for many insurance companies. Data mining techniques can minimize some of these losses by making use of the collections of customer data, particularly in insurance, credit card, and telecommunications companies
Health care fraud, based on the definition of the NHCAA (National Health Care Anti-fraud Association), is an intentional deception or misrepresentation made by a person or an entity, with the knowledge that the deception could result in some kinds of unauthorized benefits to that person or entity.
In recent years, systems for processing electronic claims have been increasingly implemented to automatically perform audits and reviews of claims data. These systems are designed for identifying areas requiring special attention such as erroneous or incomplete data input, duplicate claims, and medically non-covered services. Although these systems may be used to detect certain types of fraud, their fraud detection capabilities are usually limited since the detection mainly relies on pre-defined simple rules specified by domain experts.
In order to assure the batter operation of a health care insurance system, fraud detection mechanisms are imperative, but highly specialized domain knowledge is required. Furthermore, well-designed detection policies, able to adapt to new trends acting simultaneously as prevention measures, have to be considered. Data mining which is part of an iterative process called knowledge discovery in databases (KDD) [9] [10] can assist to extract this knowledge automatically. It has allowed better direction and use of health care fraud detection and investigative resources by recognizing and quantifying the underlying attributes of fraudulent claims, fraudulent providers, and fraudulent beneficiaries [11]. Automatic fraud detection helps to reduce the manual parts of a fraud screening/checking process becoming one of the most established industry/government data mining applications [7].
A health smart card is a type of plastic card that contains an embedded computer chip–either a memory or microprocessor type–that stores and transacts data. This data is usually associated with either value or information, or both and is stored and processed within the card's chip. The card data is transacted via a card reader that is part of a computing system. Systems that are enhanced with smart cards are in use today throughout several key applications, including healthcare, banking, entertainment, and transportation. All patients do not know about all facility of his card and cost of treatment, so some doctor easily take financial benefit of the health smart card easily and make fraud with patients. Every "below poverty line" (BPL) family holding a yellow ration card pays 30 registration fee to get a biometric-enabled smart card containing their fingerprints and photographs. This enables them to receive inpatient medical care of up to 30,000 per family per year in any of the empanelled hospitals.

2. DATA MINING

Data mining is a term from computer science. Sometimes it is also called knowledge discovery in databases (KDD). Data mining is about finding new information in a lot of data. The information obtained from data mining is hopefully both new and useful. In many cases, data is stored so it can be used later. The data is saved with a goal. Saving information makes a lot of data. The data is usually saved in a database. Finding new information that can also be useful from data is called data mining.

DIFFERENT TYPES OF DATA MINING TECHNIQUES

There are lots of different types of data mining techniques for getting new information.

DECISION TREES

A decision tree is a classifier expressed as a recursive partition of the instance space. The decision tree consists of nodes that form a rooted tree, meaning it is a directed tree with a node called "root" that has no incoming edge. All other nodes have exactly one incoming edge. A node with outgoing edges is called an internal or test node. All other nodes are called leaves (also known as terminal or decision nodes). In a decision tree, each internal node splits the instance space into two or more sub-spaces according to a certain discrete function of the input attributes value. In the simplest and most frequent case, each test considers a single attribute, such

that the instance space is partitioned according to the attribute's value. In the case of numeric attributes, the condition refers to a range .Each leaf is assigned to one class representing the most appropriate target value. Alternatively, the leaf may hold a probability vector indicating the probability of the target attribute having a certain value. Instances are classified by navigating them from the root of the tree down to a leaf, according to the outcome of the tests along the path describes a decision tree that reasons. Decision tree algorithms ID3, J48 and NB Tree can be applied on large amount of data and valuable predictions can be produced. These predictions evaluate future behavior of problem. Decision tree are preferred because they can evaluate information more accurately than other methods. These three algorithms shows the probability of input attributes respectively.

ID3 decision tree algorithm introduced in 1986 by Quinlan Ross [1]. It is based on Hunts algorithm. The tree is constructed in two phases. The two phases are tree building and pruning. ID3 uses information gain measure to choose the splitting attribute. It only accepts categorical attributes in building a tree model. It does not give accurate result when there is noise. To remove the noise pre-processing technique has to be used. To build decision tree, information gain is calculated for each and every attribute and select the attribute with the highest information gain to designate as a root node. Label the attribute as a root node and the possible values of the attribute are represented as arcs. Then all possible outcome instances are tested to check whether they are falling under the same class or not. If all the instances are falling under the same class, the node is represented with single class name, otherwise choose the splitting attribute to classify the instances. Continuous attributes can be handled using the ID3 algorithm by discretizing or directly, by considering the values to find the best split point by taking a threshold on the attribute values. ID3 does not support pruning.

Decision trees and decision rules introduced by Apte and Weiss [2] On attribute values in decision tree generation introduced by Fayyad [3].

J48 classification by decision tree induction decision tree-leaf nodes represent class labels or class distribution

1. A flow-chart-like tree structure internal node denotes a test.
2. On an attribute branch represents an outcome of the test.
3. Decision tree generation consists of two phase's tree.
4. Construction at start, selected attributes tree pruning.
5. Identify and remove branches that reflect noise or outliers.

The Naïve Bayes [4] Classifier technique is particularly suited when the dimensionality of the inputs is high. Despisimplicity, Naive Bayes can often outperform more sophisticated classification methods. Naïve Bayes model identifies the characteristics of dropout students. It shows the probability of each input attribute for the predictable state. A Naive Bayesian classifier is a simple probabilistic classifier based on applying Bayesian theorem (from Bayesian statistics) with strong (naive) independence assumptions. By the use of Bayesian theorem we can write.

$$P(c_i \mid x) = \frac{P(x \mid c_i)P(c_i)}{P(x)}$$

We preferred Naive Bayes implementation because: Simple and trained on whole (weighted) training data

- Over-fitting (small subsets of training data) protection.
- Claim that boosting "never over-fits" could not be maintained.
- Complex resulting classifier can be determined reliably from limited amount of Data.

Naive Bayesian tree consists of [5] classification and decision tree learning. An NB Tree classification sorts to a leaf and then assigns a class label by applying a Naïve Bayes on that leaf. The steps of NB Tree algorithm are:

(a) At each leaf node of a tree, a Naive Bayes is applied.

(b) By using Naive Bayes for each leaf node, the instances are classified.

(c) As the tree grows, for each leaf a Naive Bayes is constructed

The Weka workbench contains a collection of visualization tools and algorithms for data analysis and predictive modeling, together with graphical user interfaces for easy access to this functionality. It is portable and platform independent because it is fully implemented in the Java programming language and thus runs on almost any modern computing platform. Weka has several standard data mining tasks, data preprocessing, clustering, classification, association. The easiest way to do this is simply to download the template, and replace the content with your own material.

3. RELATED WORK-

Al Lin and Yes [6] discussed that the following practices is helpful to adjust the accuracy and coverage ratio of the model, which include the removal of unnecessary data, making data more representative and the preprocessing of missing data.

(a) Removal of unnecessary data: The pattern of question inquiry or thinking can be changed so as to remove needless samples. For example, compared with all applicants or people with or without payment, the relative minority can be removed preferentially when the model is constructed.

(b) Data representative: Where appropriate, advanced data processing methods can be added (such as existing data generated from some statistics) to reinforce the rationality of data interpretation and summarization and to make the data abundant.

(c) Processing of data missing: The missing of some data in the database will bring about difficulties in analyzing. Although some methods can be adopted to supplement the data, the data are not all real and may be inaccurate at times. Therefore, sometimes rules for removing or methods and principles for supplement the missing data can be thought about.

Ashathna and Madan [7] discussed that educational data mining is an area full of opportunities where one can know how to improve student success and institute effectiveness and make it efficient. It is a systematic process which offers firms ability to discover hidden patterns so that all the problems coming forward can be solved and customized and proper decision making can be done. It is concerned with determining the pattern from the hidden information so that the different student's behavior can be identified and according to those necessary steps can be taken and we can know the faculty feedback so as to perform any changes in the work structure or working schedule.

Derrig[8] discussed that measurement, detection, and deterrence of fraud are advanced through statistical models, intelligent technologies are applied to informative databases to provide for efficient claim sorts, and strategic analysis is applied to property-liability and health insurance situations.

Phua, Lee, Smith and Gayler [9] discussed that fraud and corruption in health care industry can be grouped in illicit activities associated to affiliates, medical professionals, staff and manager, and suppliers. Although fraud may not necessarily lead to direct legal consequences, it can become a critical problem for the business if it is very prevalent and if the prevention procedures are not failsafe.

Sokol, Garcia, Rodriguez, West and Ohnson [10] discussed that knowledge discovery in databases (KDD) can assist to extract this knowledge automatically. It has allowed better direction and use of health care fraud detection and investigative resources by recognizing and quantifying the underlying attributes of fraudulent claims, fraudulent providers, and fraudulent beneficiaries.

Pflaum and Rivers [11] discussed that in several countries fraudulent and abusive behavior in health insurance is a major problem. Fraud in medical insurance covers a wide range of activities in terms of cost and sophistication.

Yang , Hwang and Opit [12][13] discussed that health insurance systems are either sponsored by governments or managed by the private sector, to share the health care costs in those countries.

Major and Riedinger [14] discussed that a set of behavioral rules based on heuristics and machine learning are used for performing and scanning a large population of health insurance claims in search of likely fraud.

keuchi, Williams, and Milne [15] discussed that in an on-line discounting learning algorithm to indicate whether a case has a high possibility of being a statistical outlier in data mining applications such as fraud detection is used for identifying meaningful rare cases in health insurance pathology data from Australia's Health Insurance Commission (HIC).

Tennyson and Salsas [16] discussed that in automobile insurance fraud prevention studies case, it results distinguish between two kinds of results, suspected fraud cases and reasonable. Prediction method use Logistic Regression.

In Bureau of National Health insurance [17] discussed that data mining is a process, one of the procedures of knowledge discovery, to discover useful models in the data probably to be used in the future, which have never been seen previously and are easily to be understood.

Weisberg and Derrig [18] discussed that to use these characteristics in the development of insurance fraud reasoning system. These characteristics will be reviewed with an experienced expert assess of the rules of the medical insurance fraud prevention knowledge, for comparison. The medical insurance fraud characteristics include: Damage level insufficient information, suspected diagnosis of proof, insured low willingness to cooperate and Cause of the accident unreasonable.

Becker, Kessler and McClellan [19] discussed that identify the effects of fraud control expenditures and hospital and patient characteristics on up coding, treatment intensity and health outcomes in the Medicare and Medicaid programs.

Cox [20] discussed that applied a fraud detection system based on fuzzy logic for analyzing health care provider claims.

Yadav and Pal [21] conducted a study using classification tree to predict student academic performance using students' gender, admission type, previous schools marks, medium of teaching, location of living, accommodation type, father's qualification, mother's qualification, father's occupation, mother's occupation, family annual income and so on. In their study, they achieved around 62.22%, 62.22% and 67.77% overall prediction accuracy using ID3, CART and C4.5 decision tree algorithms respectively.

In another study Yadav et al. [22] used students' attendance, class test grade, seminar and assignment marks, lab works to predict students' performance at the end of the semester with the help of three decision tree algorithms ID3, CART and C4.5. In their study they achieved 52.08%, 56.25% and 45.83% classification accuracy respectively.

Pal and Pal [23] conducted study on the student performance based by selecting 200 students from BCA course. By means of ID3, c4.5 and Bagging they find that SSG, HSG, Focc, Fqual and FAIn were highly correlated with the student academic performance.

Vikas Chaurasia et al. [24] used CART (Classification and Regression Tree), ID3 (Iterative Dichotomized 3) and decision table (DT) to predict the survivability for Heart Diseases patients.

Bhardwaj and Pal [25] conducted study on the student performance based by selecting 300 students from 5 different degree college conducting BCA (Bachelor of Computer Application) course of Dr. R. M. L. Awadh University, Faizabad, India. By means of Bayesian classification method on 17 attributes, it was found that the factors like students' grade in senior secondary exam, living location, medium of teaching, mother's qualification, students other habit, family annual income and student's family status were highly correlated with the student academic performance.

In this paper we proposed health smart card fraud detection different data mining techniques with weka tool we have presented better accurate data by classifying all observations of fraud.

4. METHODOLOGY

4.1 Data Preparation

A medical post-operative claim charges through smart card payment involves the participation of patient admitted in a Heart care hospital. Claim accepted and investigated by ICICI Lombard and oriental insurance company. A BPL card holder patient admitted in Heart care hospital for heart treatment purpose her Guardian made payment charge by doctor through BPL card the charged claim for payment by hospital authority is 10,000. But the actual amount is only 7,000. The fraud conducted by beneficiary hospital authority is approximately 3,000. Now for performing classification of BPL using several standard data mining tasks, data preprocessing, clustering, classification, association and tasks are needed to be done. The database is designed in MS-Excel and MS word 2010 database management system to store the collected data. The data is formed according to the required format and structures. Further, the data is. converted to ARFF (Attribute Relation File Format) format to process in WEKA. An ARFF file is an ASCII text file that describes a list of instances sharing a set of attributes. ARFF files were developed by the Machine Learning Project at the department of computer science of the university of Waikato for use with the Weka machine learning software which give the solutions by algorithms tools.

4.2 Data selection and transformation

The variables used in the computational technique to identify the fraud claim or none fraud auto motive in insurance claims.The Kappa statistic (or value) is a metric that compares an observed accuracy with an expected accuracy (random chance).The kappa statistic is used not only to evaluate a single classifier, but also to evaluate classifiers amongst themselves computation of observed accuracy and expected accuracy is integral to comprehension of the kappa statistic, and is most use of easily illustrated through a confusion matrix.

TABLE 1.The variables used in the computational technique.

PROPERTY	DESCRIPTION	
Source	Heart care hospital	
Claim type	Post-operative claim charges through smart card payment	
Sample size	61 Total:2 fraud and 59 LGT examine by ICICI Lombard and oriental insurance company.	
Dependable variable		
Fraud(0)	Claim not accepted	
Lgt(1)	Claim accepted	
Explanatory variable	Value	Description
Is	{0-fraud}	Not accepted claim of smart card by investigated surveyor of ICICI Lombard insurance company.
	{1-legle}	Accepted claim of smart card by investigator surveyor of ICICI Lombard insurance company.
Date gap	{0-zeroday,1-threedays,2-sixdays,3-ninedays,4-twalvedays}	Time difference (in day) between insurance claim and the policy report being filled.
Bnp	{0-new policy not found,1-new policy found}	BNP indicates Boolean value for new policy yes (1) or (0).
Clmamt	{0-five thousands,1-ten thousands,2-fifteen thousands,3-twenty thousands,4-twenty five thousands}	Claim amount as a static value.
Fyrs	{0-Year,1-Oneyear,2->Oneyear,3-=Twoyears,4->Two years}	Financial year in which complained.
Clms	{0-Zero,1-One,2-Two,4-Four}	Total number of claims the claimant has filled with in insurance company.

The variables used in the computational technique to identify the fraud claim or none fraud auto motive in insurance claims.The Kappa statistic (or value) is a metric that compares an observed accuracy with an expected accuracy (random chance).The kappa statistic is used not only to evaluate a single classifier, but also to evaluate classifiers amongst themselves computation of observed accuracy and expected accuracy is integral to comprehension of the kappa statistic, and is most use of easily illustrated through a confusion matrix.

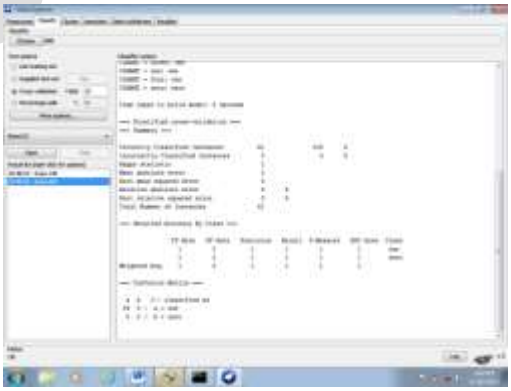

Figure.1. Instances classified by J48.

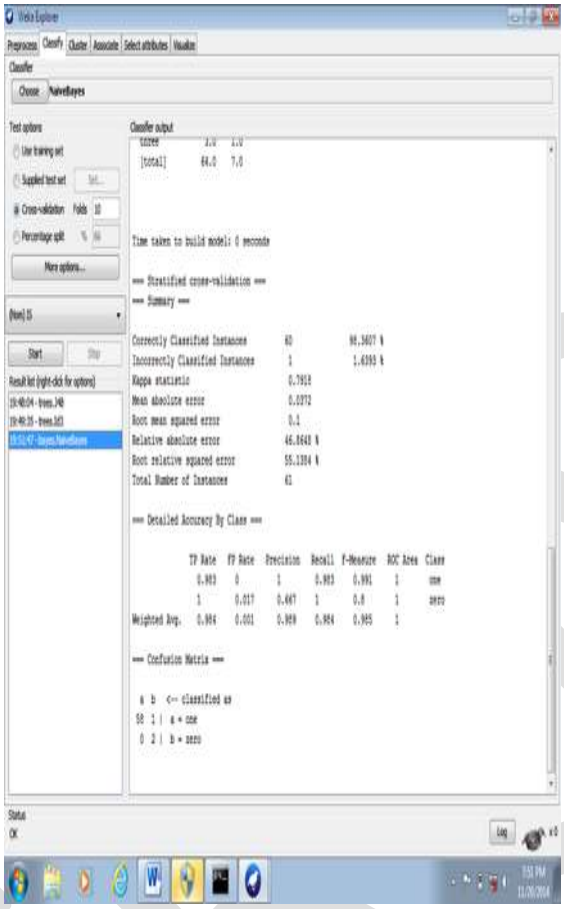

Figure-2. Instances classified by ID3.

Figure -3. Instances classified by NAÏVE BAYES

General, Positive = identified and negative = rejected. Therefore:

- True positive = correctly identified
- False positive = incorrectly identified
- True negative = correctly rejected
- False negative = incorrectly rejected

A confusion matrix, also known as a contingency table or an error matrix is a specific table layout that allows visualization of the performance of an algorithm, typically a supervised learning one (in unsupervised learning it is usually called a matching matrix). Each column of the matrix represents the instances in a predicted class, while each row represents the instances in an actual class.

4.3 Implementation of Data Mining

The paper presents an approach to classifying health smart card in order to predict their amount based on features extracted from logged data in a hospital. They design, implement, and evaluate a series of pattern classifiers and compare performance of an online patient's dataset. Classifiers were used to declare surety of health card holder. They used the J48, ID3 and Naïve Bayes algorithms to improve the prediction accuracy. This method is of considerable usefulness in identifying patient in very large real data set and allow investigator to provide appropriate investigate in a timely manner.

4.4 Results and Discussion

The proposed techniques which are include in WEKA tool, Decision Tree and Bayes techniques. Data mining tools are software components. The proposed tool that will be applied is WEKA software tool because it is support several standard data mining tasks. WEKA is a collection of machine learning algorithms for solving real-world data mining problems. It is written in Java and runs on almost any platform. The proposed technique that will be applied in this paper is Decision Tree (J48, ID3 and NAÏVE BAYES) because it is powerful classification algorithms. From the table-2. it is clear that ID3 Kappa static value observed give the greater value compare to J48 and NB algorithms and ID3 give the less error compare to J48 and NB algorithms.ID3 take 0.2sec in process completion but J48 and NB take 0 sec.

Table -2 Evaluation on test split

		J48	ID3	NAÏVE BAYES
TP rate	LGT	1	1	0.98
	FRAUD	0	1	1
	WEIGHTED	0.96	1	0.98
FP rate	LGT	1	0	0
	FRAUD	0	0	0.02
	WEIGHTED	0.96	0	0
PRECISION	LGT	0.96	1	1
	FRAUD	0	1	0.67
	WEIGHTED	0.94	1	0.99
RECALL	LGT	1	1	0.98
	FRAUD	0	1	1
	WEIGHTED	0.97	1	0.98
F-MEASURE	LGT	0.98	1	0.99
	FRAUD	0	1	0.8
	WEIGHTED	0.95	1	0.99
ROC	LGT	0.09	1	1
	FRAUD	0.09	1	1
	WEIGHTED	0.09	1	1

Table-3. Detailed Accuracy by Class

Detailed	J48	ID3	Naïve Bayes
Correctly classified Instances	59	61	60
Incorrectly classified instances	2	0	1
Kappa static	0	1	0.79
Mean absolute error	0.06	0	0.04
Root mean squared error	0.18	0	0.1
Relative absolute error	80.71 %	0%	46.86 %
Root relative square error	99.67 %	0%	55.13 %
Time taken (Second)	0	0.02	0
Total number of instances	61	61	61

From table 3 it is clear that ID3 give more correctly classified compare to J48 and NB algorithms and ID3 provide greater value of weighted avg. compare to J48 and NB algorithms.

Table-4. Confusion Matrix

Confusion Matrix(J48)	Confusion Matrix(ID3)	Confusion Matrix(Naïve Bayes)
59 0 | a = one	59 0 | a = one	58 1 | a = one
2 0 | b = zero	0 2| b = zero	0 2 | b = zero

Each column of the matrix represents the instances in a predicted class, while each row represents the instances in an actual class. In table4.confusion matrix J48 shows 59 correctly classified and 2 none correctly classified another side 0 none correctly classified and 0 correctly classified arise. Confusion matrix In ID3 represents 59 correctly classified and 0 none correctly classified another side 0 none correctly classified and 2 correctly classified. In NB 58 correctly classified 0 none correctly classified another side 1 none correctly classified and 2 correctly classified. It is clear from analysis correctly classified in ID3 is total instances 61 is greater value compare to other J48 and NB algorithms.

5. CONCLUSION

In WEKA, all data is considered as instances attributes in the data. For easier analysis and evaluation, simulation results are partitioned into several sub items. In the first part, correctly and incorrectly classified instances will be partitioned in numeric and percentage value, and subsequently, Kappa statistics, mean absolute error and root mean squared error will be at a numeric value only. ID3 time taken to build model: 0.02 seconds and test mode: 10-fold cross-validation .Here weka computes all required parameters on given instances with the classifiers' respective accuracy and prediction rate. Based on table2 we can clearly see that the highest accuracy of ID3 is 100% and the lowest accuracy of J48 is 96.7213% so decision tree ID3 is the best in the three respective algorithms as it is more accurate.

REFERENCES:

[1] J. R. Quinlan, C4.5: Programs for machine learning, Morgan Kaufmann, San Francisco, 1993. .

[2] C. Apte and S. Weiss. Data mining with decision trees And decision rules. Future Generation Computer Systems, 13,1997.

[3] U. M. Fayyad. Branching on attribute values in decision tree generation. In Proc. 1994 AAAI Conf.Pages601-606, AAAI Press, 1994.

[4] Harry Zhang "The Optimality of Naive Bayes". FLAIRS2004 conference.

[5] Yumin Zhao, Zhendong Niu_ and Xueping Peng, "Research on Data Mining Technologies for Complicated Attributes Relationship in Digital Library Collections" "Applied Mathematics and Information Sciences, An International Journal", Appl. Math. Inf. Sci. 8, No. 3, 1173-1178 (2014).

[6] Kuo-Chung Lin, Ching-Long Yeh "Use of Data Mining Techniques to Detect Medical Fraud in Health Insurance" International Journal Of Engineering and Technology Innovation, vo no. , 201, pp. 126-137

accepted 26 February 2012.

[7] Anansha Asthana, Komal R. Madan, "Educational Data Mining" in National Student Conference on Advances in Electrical and Informatio Communication Technology"AEICT-2014.

[8] Derrig R. A., "Insurance fraud," Journal of Risk and Insurance, vol. 69.3, pp. 271-287, 2002.

[9] Phua, Lee, Smith, and Gayler, "A comprehensive survey of data mining-based fraud detection research", Artificial Intelligenc Review, submitted, 2005.

[10] Sokol, Garcia, Rodriguez, West and Johnson, "Using data mining to find fraud in HCFA health care claims,"Top Health Information Management, vol. 22, no. 1, pp. 1-13, 2001.

[11] Pflaum and J. S. Rivers, "Employer strategies to combat health care plan fraud," Benefits quarterly, vol. 7, no. 1, pp. 6-14, 1991.

[12] W. S. Yang and S. Y. Hwang, "A process-mining framework for the detection of healthcare fraud and abuse," Expert Systems with Application Article in Press, corrected proof, 2005.

[13] L. J. Opit, "The cost of health care and health insurance in Australia: Some problems associated with the fee for-service," Soc. Sci. Med.vol. 18, no. 11, 967–972, 1984.

[14] J. Major, and D. Riedinger, "EFD: A hybrid knowledge/statistical based system for the detection of fraud," Journal of Risk and Insurance 69(3), pp. 309-324, 2002.

[15] K. Yamanishi, J. Takeuchi, G. Williams, and P. Milne, "On-line Unsupervised outlier detection using finite mixtures with discounting learning algorithms," In Data Mining and Knowledge Discovery vol. 8, pp. 275–300, 2004.

[16] Sharon Tennyson and Pau Salsas, "Patterns of Auditing in Markets with Fraud: Some Empirical Results from Automobile Insurance," Working Paper, 2000.

[17] Bureau of National Health insurance, Codes and scopes of classifications of diseases, National association of insurance commissioners,2014.

[18] Weisberg, H.I. and Derrig, R.A., "AIB Claim Screening Experiment Final Report," Insurance Bureau of Massachusetts, 1998.

[19] D. Becker, D. Kessler and M. McClellan, "Detect in Medicare abuse," Journal of Health Economics, vol. 24, pp. 189–210, 2002.

[20] E. Cox, "A fuzzy system for detecting anomalous behaviors in healthcare provider claims, Goonatilake, S. and Treleaven, P (eds.Intelligent Systems for Financial and Business, pp. 111-134.John Wiley and Sons Ltd., 1995.

[21] S. K. Yadav, Pal., S. 2012. Data Mining: A Prediction for Performance Improvement of Engineering Students using Classification, World of Computer Science and Information Technology (WCSIT), 2(2), 51-56.

[22] S. K. Yadav, B. K. Bharadwaj & Pal, S. 2011. Data Mining Applications: A comparative study for predicting students' performance, International journal of Innovative Technology and Creative Engineering (IJITCE), 1(12).

[23] A. K. Pal, and S. Pal, "Analysis and Mining of Educational Data for Predicting the Performance of Students", (IJECCE) International Journal of Electronics Communication and Computer Engineering, Vol. 4, Issue 5, pp. 1560-1565, ISSN:2278-4209, 2013.

[24] V. Chauraisa and S. Pal, "Early Prediction of Heart Diseases Using Data Mining Techniques", Carib.j.SciTech,,Vol.1, pp. 208-217, 2013.

[25] B.K. Bharadwaj and S. Pal. "Data Mining: A prediction for performance improvement using classification", International Journal of Computer Science and Information Security (IJCSIS), Vol. 9, No. 4, pp. 136-140, 2011.

International Journal of Engineering Research and General Science Volume 3, Issue 5, September-October, 2015
ISSN 2091-2730

Utilizing a Resistance Compression Network for a High Efficiency Resonant dc/dc Converter

D.srinivasulu[1], k.Babu[2]

PG Student [PE&ED], Dept. of EEE, SISTK, nivas.seenureddy52@gmail.com, Andhra Pradesh India[1]

Assistant professor, Dept. of EEE, SISTK, hasini.babu@gmail.com , Andhra Pradesh, India[2]

Abstract— This paper presents a new topology for a high efficiency dc/dc resonant power converter that utilizes a resistance compression network to provide instantaneous zero voltage switching and near zero current switching across a wide range of input voltage, output voltage and power levels. The resistance compression network (RCN) maintains desired current waveforms over a wide range of voltage operating conditions. The use of on/off control in conjunction with narrowband frequency control enables high efficiency to be maintained across a wide range of power levels. The converter performance provides galvanic isolation and enables large (greater than 1:10) voltage adaptation ratios, making the system suitable for large step-up conversion in applications such as distributed photovoltaic converters..

Index Terms- dc/dc converter, resonant converter, on-off control, high efficiency power converter, resistance compression network

1. Introduction

High-voltage-gain dc/dc converters are found in a variety of applications. For example, to connect photovoltaic panels to the grid, interface circuitry is needed. Some architecture for this purpose incorporates dc/dc converters to boost voltage of individual photovoltaic panels to a high dc-link voltage, with follow-on electronics for converting dc to ac (e.g., [1], [4]). The step-up dc/dc converter is a critical part of this system, and must operate efficiently for a large voltage step-up and for a wide voltage range (e.g., at the converter input and/or output depending upon the system). Furthermore, to be compact it must operate at high switching frequencies. In conventional hard-switched power converters, the overlap of current and voltage is large during switching, resulting in significant power loss, especially at high frequencies. Soft switched resonant converter topologies providing zero voltage switching (ZVS) or zero current switching (ZCS) can greatly reduce loss at the switching transitions, enabling high efficiency at high frequencies. Unfortunately, while many soft-switched resonant designs achieve excellent performance for nominal operating conditions, performance can degrade quickly with variation in input and output voltages and power levels.

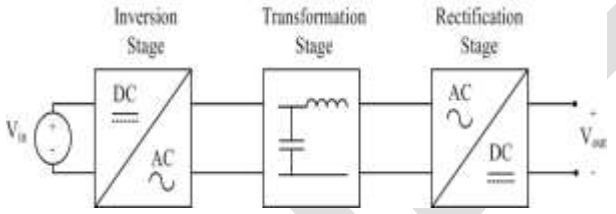

Fig. 1 Architecture of proposed dc/dc converter

This paper introduces a new high efficiency resonant dc/dc converter topology, the Resistance Compression Network (RCN) converter, which seeks to overcome the abovementioned challenges. This converter operates with simultaneous zero voltage switching (ZVS) and near zero current switching (ZCS) across a wide range of input voltage, output voltage and power levels, resulting in low switching losses.

II. RCN CONVERTER TOPOLOGY AND CONTROL

The dc/dc converter proposed here consists of an inversion stage, a transformation stage and a rectification stage, as shown in Fig. 1. The inversion and rectification stages use standard designs. However, the transformation stage and the control of the converter

are new. The topology of the proposed Resistance Compression Network (RCN) converter is shown in Fig. 2. The converter as shown is designed to step-up voltage. The transformation stage consists of a matching network, a transformer, and a resistance compression network (RCN). The Fig. 1: Architecture of proposed dc/dc converter. Matching network composed of Lrp and Crp acts as a filter and provides a voltage gain, hence reducing the transformer turns ratio requirement. One issue with high-turns-ratio step-up transformers that exists in many topologies is that the parasitic leakage inductance of the transformer can undesirably ring with its secondary side winding capacitance at the switching transitions. This creates large ringing in the current and voltage waveforms, and high-frequency losses. The matching network also eliminates this ringing by absorbing the transformer parasitic. The 1:N transformer provides additional voltage gain and isolation. The resistance compression network (composed of Ls and Cs) is a special single input, multi-output matching network that provides desirable impedance control characteristics. The RCN technique was originally proposed and applied for radio-frequency (RF) applications, such as very-high-frequency dc/dc converter systems and RF power amplifiers; here we exploit if for high efficiency power conversion. The function of the RCN is to automatically regulate the converter operating power and waveforms in a desirable manner as the input and output voltages vary. As applied here, the RCN also includes a series resonant tank (composed of Lr and Cr). Its purpose is to provide additional filtering.

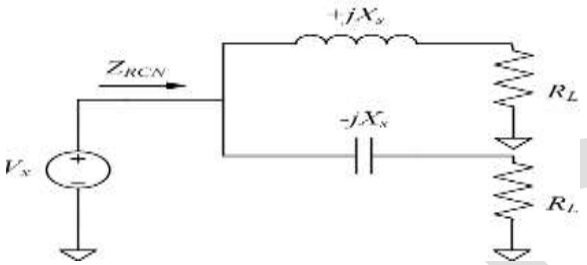

Fig. 2:Fundamental frequency model of the resistance compression network (RCN) and the rectifiers.

The inverter stage is simply a full-bridge inverter (composed of switches S1 - S4). A full-bridge is used instead of a half-bridge to reduce the voltage gain requirement from the matching network and the transformer. The rectification stage is composed of two half bridge rectifiers. The capacitors Cin and Cout are for input and output filtering, respectively, and the two capacitors marked as CDC are for dc blocking purposes.

III.ANALYSIS AND DESIGN METHODOLOGY

Using fundamental frequency analysis, at the switching frequency the half-bridge rectifiers can be modeled as resistors,. The effective resistance of these rectifiers is given by:

$$RL = 4V^2out / \pi^2 Pout; \quad (1)$$

Where Vout is the converter output voltage and Pout is the switching-cycle-average output power. As shown in Fig. 2, one of the branches of the RCN comprises a blocking capacitor CDC and an RCN inductor Ls. The other branch comprises a series LC tank tuned to be net capacitive at the switching frequency (net equivalent capacitance Cs). This branch may be modeled as a series resonant tank (with components Lr and Cr) tuned to the switching frequency for filtering, in series with an additional RCN capacitance Cs. Since the series LC tank appears as a short circuit at the switching frequency, it is treated as such in Fig. 2 and in the following analysis. Hence, at the switching frequency the input impedance of the RCN looks purely resistive and is given by:

$$ZRCN = X^2s + R^2 L /2RL \quad (2)$$

where Xs is the magnitude of impedance of the RCN elements (Ls and Cs) at the switching frequency. The use of the resistance compression network reduces the change in impedance seen by the inverter as the effective rectifier resistance (RL) changes due to variations in output voltage and output power

IV. PROTOTYPE CONVERTER DESIGN

A prototype of the RCN dc/dc converter of Fig. 6 has been designed and built. The designed dc/dc converter is meant for large-step-up applications such as the two-stage photovoltaic-to-grid conversion system shown in Fig. 7. The RCN dc/dc converter can be used to convert the low (widely varying) output voltage of a photovoltaic panel into a high dc link voltage, for example. The design specifications for this prototype are given in Table I. The converter is required to operate over an input voltage range of 25-40 V, an output voltage range of 250-400 V and over a wide output power range of 20-200 W. The switching frequency of the converter was selected as 500 kHz. This frequency minimized the total losses in the magnetic (assuming 3F3 magnetic material and RM cores) and the transistors as shown in Fig. 8. Given that the architecture provides relatively low transistor switching losses, selection of a different magnetic material could enable significantly higher frequencies to be utilized.

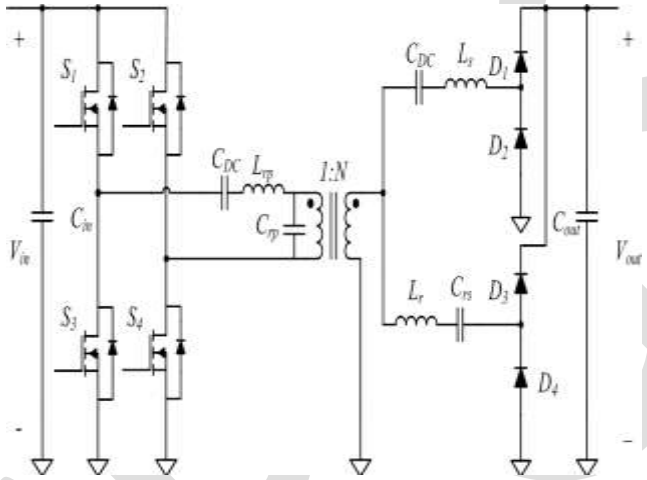

Fig. 5 Implementation of the proposed Resistance Compression Network (RCN) dc/dc converter

For the transformation stage, the reactive elements values were chosen considering the trade-offs between the losses in the parasitic of the transformer, the matching network and the RCN. If the total gain provided by the transformer and matching network is increased, the magnitude of impedance of the RCN also has to be increased. This helps in reducing the increase in output power at higher output voltages, which in turn helps maintain high efficiencies at the higher output voltages. If more gain is provided by the matching network the value of the matching network inductance increases, and thus the matching network loss also increases. However, this results in a decrease in the required gain of the transformer which can result in a decrease in transformer loss

A trade-off of the losses in the transformer and matching network was considered to determine the value of the gain of these elements. For the matching network, an achievable inductor Q was selected, and the results of [17] were used to compute the loss of the matching network for a range of matching network gain values. Each matching network gain results in a specified transformer gain. A computer search routine was then used to identify the best transformer design for each specified gain. Transformers were designed by searching fully across a set of specified cores and wire/foil configurations to minimize transformer loss (the code provided in, which uses the power loss equations given in the appendix, was used estimate these losses). The split of gains (between matching network and transformer) and the transformer design leading to the lowest total computed loss were then selected. For available cores and wires, the transformer turns ratio (N) was chosen to be 6 and the gain of the matching network (G) was chosen to be 1.67, for a total gain of approximately 10. It is noted that more sophisticated optimizations could yield better results. This could include fully optimizing the design of the matching network inductor as part of the search to co-optimize the transformer/matching-network system (e.g., to maximize the achievable overall efficiency in a given volume). Likewise, introduction of more sophisticated loss models could be expected to provide refined results. Nevertheless, the method utilized is efficient and yields good results.

V. SIMULATION RESULTS

The prototype RCN dc/dc converter has been tested using a dc power supply and a resistive load. The tests were carried out with different input voltages (in the 25-40 V range) and different output voltages (in the 250-400 V range). Figure 11 shows current and voltage waveforms for the converter over two switching periods, when operated at an input voltage of 25 V. In particular, it shows the current through the inductor of the matching network, which is also the output current the inverter, the gate drive voltages of the inverter switches S1 and S3, and the drain-source voltage of the switch S3.

As expected, the current through the inductor of the matching network is approximately sinusoidal. Also, the switches achieve zero-voltage switching (ZVS) and near-zero-current switching (ZCS), as can be seen from Fig. 12. Even with the slight distortion in currents that occur owing to limited tank Q, ZVS and near ZCS are still achieved as predicted with sinusoidal approximations. This owes in part to the fact that even with moderate damping of the resonant oscillation owing to the rectifier network, the current waveform still tends towards zero (at a reduced slope) for the next switching transition. Figure 12(a) shows a zoomed in view of the turnoff transition of switch S3. The current through switch S3 at turn-off is small compared to both the peak and average of the current it carries (turn-off current is 15.7% of peak current and 27.5% of average current). Figure 12(b) shows the turn-on transition of switch S3. Notice that the switch turns

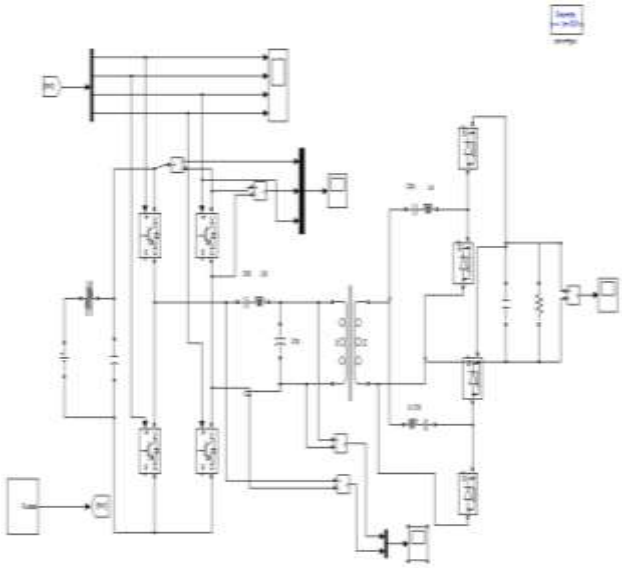

Fig 6 simulation circuit of resonant dc/dc converter

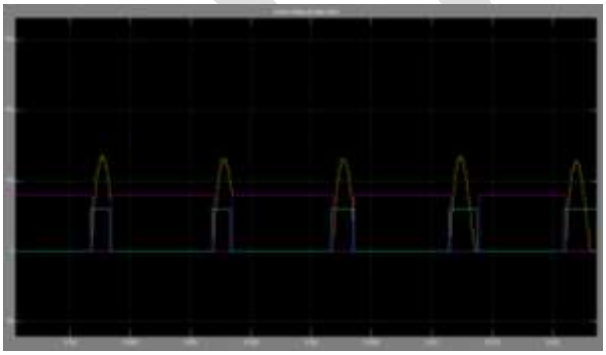

Fig 7 simulation waveforms of voltage and pulse

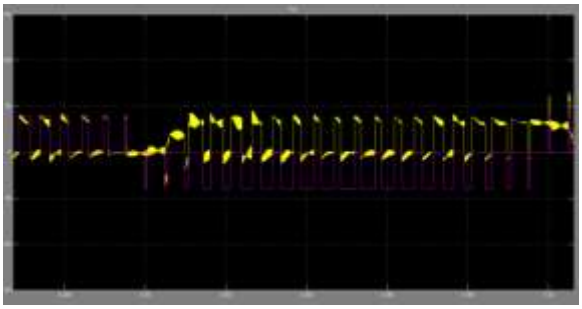

Fig 8 simulation wave form of input voltage

VI. CONCLUSION

This paper presents a new resonant dc/dc converter topology that uses a resistance compression network and a combination of on/off control and narrowband frequency control. The converter implementation provides galvanic isolation and enables large (greater than 1:10) voltage conversion ratios. The proposed converter achieves very high efficiency by maintaining ZVS and near ZCS over a wide input voltage, output voltage and power range.

REFERENCES:

[1] S. M. Chen, T. J. Liang, L. S. Yang, and J. F. Chen, "A Cascaded High Step-up dc/dc Converter with Single Switch for Microsource Applications," IEEE Transactions on Power Electronics, vol. 26, no. 4, pp. 11461153, Apr. 2011.

[2] S. V. Araujo, R. P.Torrico-Bascope and G. V. Torrico-Bascope, "Highly Efficient High Step-Up Converter for Fuel-Cell Power Processing Based on Three-State Commutation Cell," IEEE Transactions Industrial Electronics, vol. 57, no. 6, pp.1987-1997,

[3] Q. Zhao and F. C. Lee, "High-efficiency, high step-up dcdc converters," IEEE Transactions on Power Electronics, vol. 18, no. 1, pp. 6573, Jan. 2003.

[4] B. York, W. Yu, J. S. Lai, "An Integrated Boost Resonant Converter for Photovoltaic Applications," IEEE Transactions on Power Electronics , vol.28, no.3, pp.1199-1207, Mar. 2013

International Journal of Engineering Research and General Science Volume 3, Issue 5, September-October, 2015
ISSN 2091-2730

Effect of TiO_2 nanoparticles on Mechanical Properties of Epoxy-Resin System

N.Annlin Bezy*, A.Lesly Fathima*
Research Department of Physics
*Holy Cross College (Autonomous), Nagercoil, TamilNadu
Email: annlinphysics@gmail.com

Abstract— Nanocomposites are new materials made with fillers having nanosize. The purpose of this study is to analyse the mechanical properties of epoxy resin with titanium dioxide nanoparticles. In this present work, titanium dioxide nanoparticle is prepared by sol gel method, using Titanium tetra isopropoxide and acetic acid. The synthesized Titanium dioxide nanoparticles are characterized by XRD and the grain size in nanoscale is conformed. The sheets of neat epoxy resin and epoxy with addition of TiO_2 are primed by solution casting method. Mechanical studies of developed polymer sheets reveal much variation by incorporation of TiO_2. This is probably due to different dispersion of nanoparticles in epoxy resin.

Keywords— TTIP, Sol Gel method, Titanium dioxide, Solution Casting method, Epoxy, Nanocomposite

INTRODUCTION

In material research, the combination of an organic phase (generally polymers) with inorganic particles has drawn considerable attention since last decades. Nano sized particles allow to improve the mechanical properties of polymer. Mechanical properties like, yield stress, tensile strength and Young's modulus generally suffer a huge increase when compared to pure polymers [1]. Nanosized TiO_2 is of particular interest in nanocomposites, because of their specifically size-related properties, non-toxicity, low cost and long term stability [2].

The effective reinforcement by TiO_2 nanoparticle of epoxy resins favoured in aerospace and other industries. Depending on the dispersion and particles surface, several interfaces can be observed, which can result in special properties. Thus to attain maximum performance from the TiO_2 nanoparticles, uniform dispersion within the matrix must be ensured [3]. The intent of this study is to understand the influence of TiO_2 filler weight percentage on mechanical properties of epoxy incorporated TiO_2 nanoparticles.

MATERIALS AND METHODS

Synthesis of TiO_2 nanoparticles

TiO_2 nanoparticle was prepared by a simple Sol gel method. Titanium Tetra Isopropoxide (TTIP) and Acetic acid were used as the precursors. 1M of TTIP was added to 4M of acetic acid and this mixture was stirred for 1 hour in magnetic stirrer. To this mixture double distilled water was added dropwise. While the addition of double distilled water this mixture transformed to white gel. After aging of 24 hours, the gel was dried in an oven 200°C for 30 minutes. The solid crystals formed were powdered using agate mortor. To induce transition from amorphous to anatase phase, this powder was annealed to the temperature 600°C in muffle furnace. After calcinations the sample was finely powdered and was used for characterization [4].

Synthesis of pure epoxy and epoxy-TiO_2 nanocomposites

In this study ARALDITE Epoxy resin (DBF 103) and hardener (HY- 951) were used to form pure epoxy and epoxy-TiO_2 nanocomposites for different TiO_2weight percentage (1wt %, 3wt %, 5wt %, 7wt %).

Preparation of pure epoxy sheet

Epoxy resin of 60gm and hardener of 6gm were poured separately in two beakers. To remove the air bubbles, both were need to be ultrasonicated for 30 minutes. After the completion of this process, the hardener was added to the epoxy resin and it was mixed by hand stirring. Finally it was ultrasonicated to remove air bubbles generated during the mixing process. After degassing, the mixture

was poured into the metal mould. The metal mould was kept undisturbed for 1 hour at room temperature. Finally the sample was cured by keeping the mould in an oven at 100°C for 2hours. Thus neat epoxy sheet was obtained.

Preparation of epoxy-TiO_2 nanocomposite

The TiO_2 fillers (nano) of 1 weight percentage were dispersed into 60gm of epoxy resin, and both were mixed by a high speed mechanical stirrer (at 600 rpm) for 12 hours. It was then ultrasonicated to remove the air bubbles. After the completion of the degassing process, the 6gm of hardener was added slowly into epoxy-filler with hand stirring. The mixture was again ultrasonicated for 5 minutes to remove gas bubbles generated during the mixing process. After degassing, the mixture was poured into the metal mould. Then the sample was cured by keeping the metal mould in an oven at 100°C for 2 hour. The same procedure was repeated for 3wt%, 5wt%, and 7wt%.

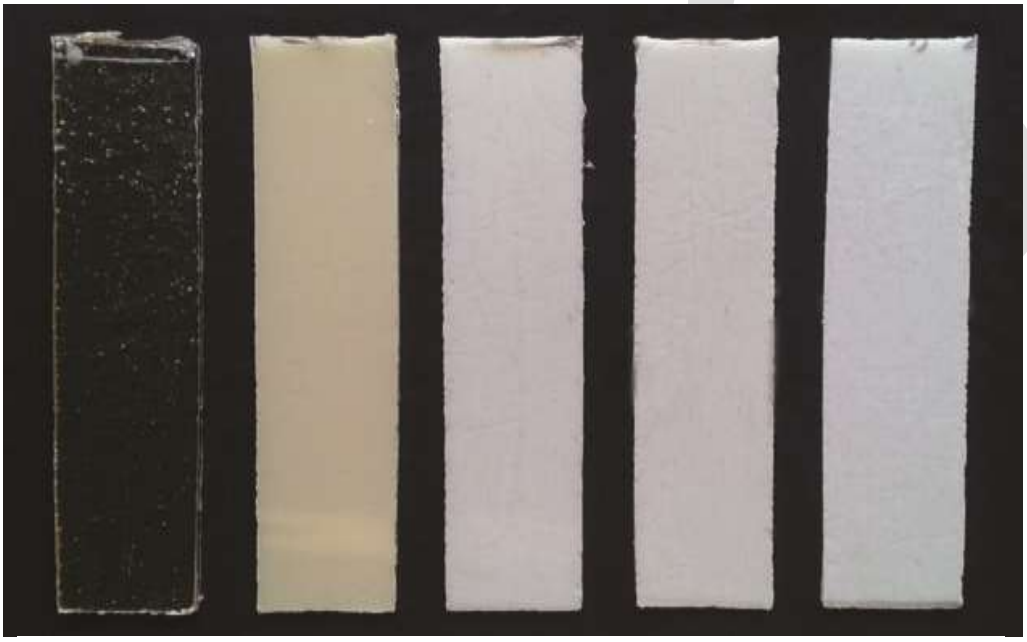

Fig-1 : Photograph of synthesized polymer sheets

CHARACTERIZATIONS AND RESULT

X Ray Diffraction

Powder XRD is used for crystal phase identification and estimation of the crystallite size for synthesized TiO_2 nanoparticle. X-ray diffraction is performed using the XPERT-PROdiffractometer system (PW 3050) with automatic data acquisition using CuKα radiation (λ = 1.54060Å) working at 40 kV/30 mA. The crystallite size D is calculated from XRD data using De-bye Scherrer's formula

$$D = K\lambda/\beta cos\theta$$

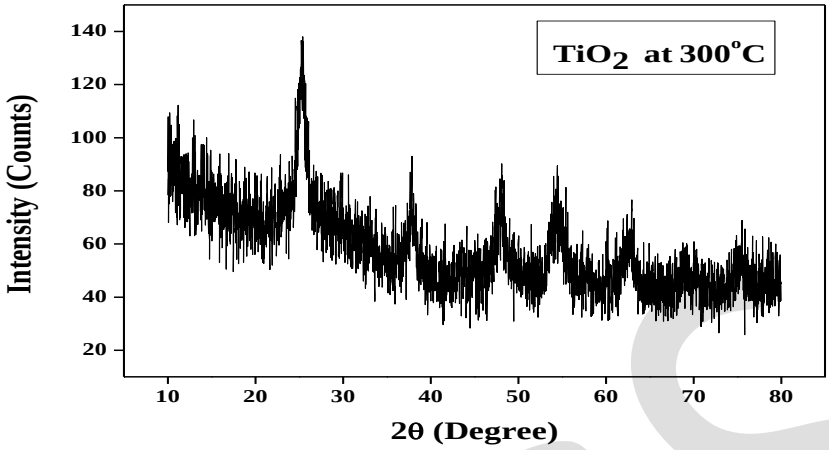

Fig-2: XRD pattern of TiO_2 nanoparticles calcined at 300°C

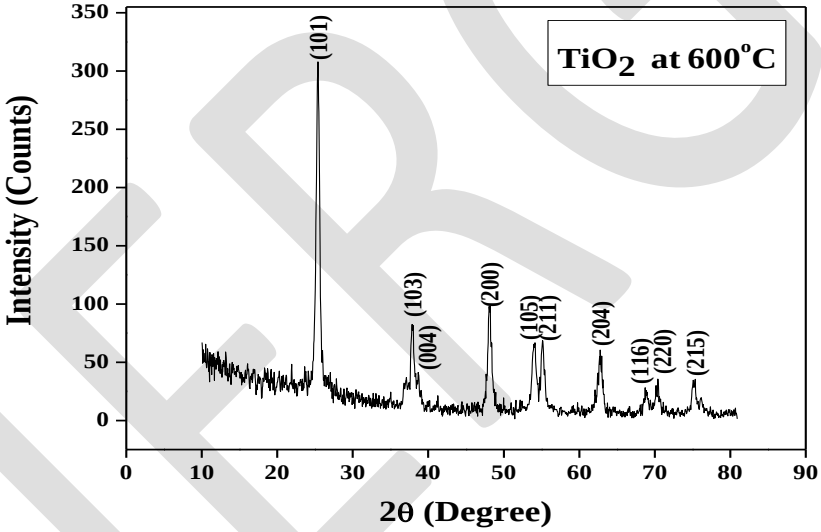

Fig-3: XRD pattern of TiO_2 nanoparticles calcined at 600°C

The above two XRD patterns illustrate that TiO_2 calcined at 300°C is in amorphous structure and annealed at 600°C be in crystalline structure. It concludes that with the increase of temperature to 600°C the TiO_2 synthesized by sol gel method acquired enhanced structure. The XRD data of TiO_2 nanoparticles calcined at 600°C is given in table 1.

Table-1 : XRD data of TiO_2 calcined at 600°C

Angle 2θ (Degree)	Intensity (%)	d- Spacing	hkl
25.357	100.00	3.50961	101
36.93	4.85	2.43224	103
37.90	24.41	2.37220	104
48.10	32.31	1.89025	200
53.97	21.82	1.69755	105
55.12	21.49	1.66489	211
62.69	16.95	1.48078	204
68.81	5.97	1.36319	116
70.27	7.74	1.33845	220
75.17	10.07	1.26293	215

The XRD of TiO_2 nanoparticles calcined at 600°C are found to exhibit ten diffraction peaks and of that, (101) reflection plane is very predominant. The crystallite size of TiO_2 is calculated by De-Bye Scherrer formula. The crystallite size of synthesized TiO_2 is found to be 15.98nm and this confirms that the prepared TiO_2 particle is in nanoscale. The X-ray diffraction spectra confirm that the pure TiO_2 nanopowder is in anatase crystalline phase.

Mechanical Properties

The mechanical properties such as tensile strength, elongation at break, flexural strength, modulus, impact strength are measured using a dynamic mechanical analyzer. Tensile test, Flexural strength and Impact test of developed sheets are performed using mechanical analyzer in tensile mode in accordance with the ASTM D-3039 test standard, Flexural mode with ASTM D-790 test standard, Izod impact mode with ASTM D-256 test standard respectively. Before testing, the rectangular samples of fixed size are cut out from sheet using a clean razor blade and the upper side of cut sample for tensile test is polished to make flat surface. And the edges of the sample are polished by sand paper of a mesh of 1200.

Tensile Test

A tensile test measures the resistance of a material to a static or slowly applied force. A machined specimen is placed in the testing machine and load is applied. A strain gage or extensometer is used to measure elongation. The stress obtained at the highest applied force is the Tensile Strength. The Yield Strength is the stress at which a prescribed amount of plastic deformation (commonly 0.2%) is produced. Elongation describes the extent to which the specimen stretched before fracture. Here, tensile test for all samples are carried out on tensile tester as per ATSM D 3039 standard with different load cells. ASTM D3039 is a testing specification that determines the in-plane tensile properties of polymer matrix composite materials reinforced by high-modulus fibres.

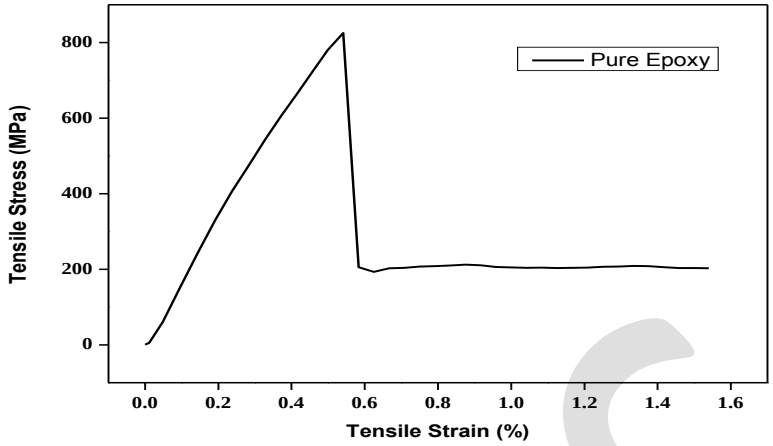

Fig-4 : Stress Vs Strain graph of pure epoxy

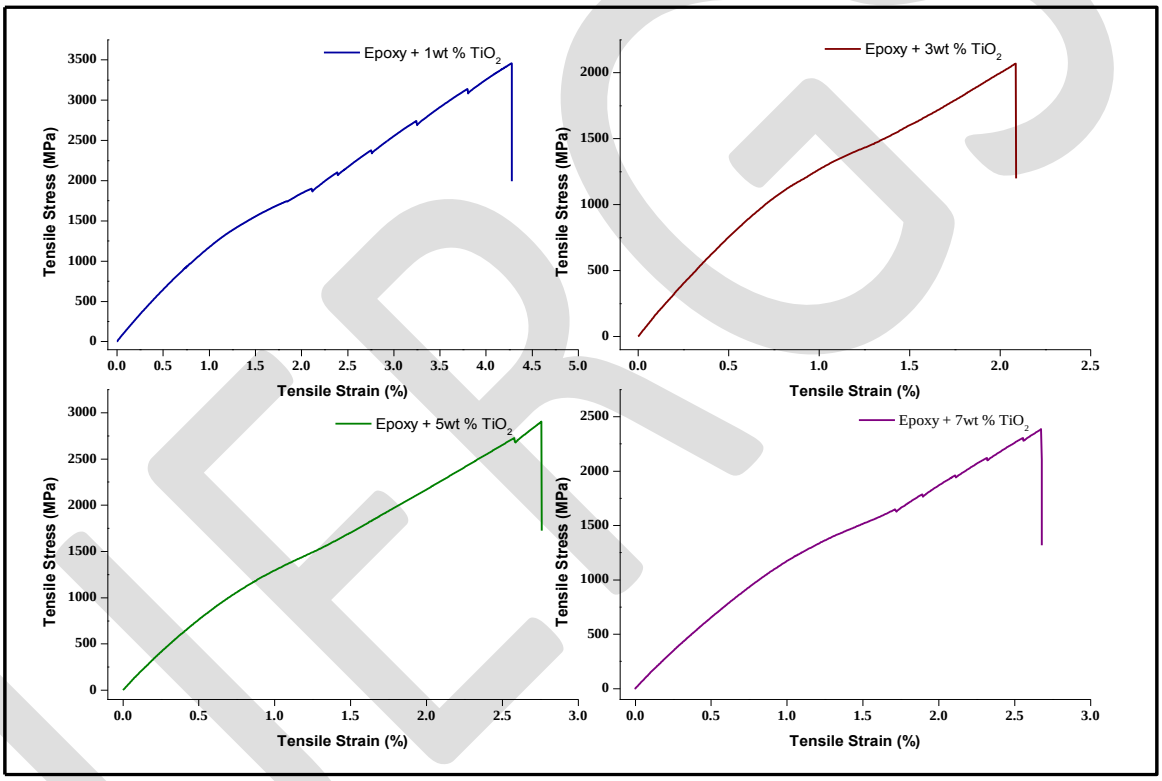

Fig-5: Tensile stress Vs strain graph of TiO_2 modified epoxy

Tensile modulus is calculated using the formula

$$\text{Tensile Modulus} = \frac{\text{Tensile Stress}}{\text{Tensile Strain}}$$

$$= \frac{\text{Difference in load (N)}}{\text{Difference in extension (mm)}}$$

$$= \frac{\Delta P}{\Delta \delta}$$

Table-2 : Tensile Properties

Sample	Maximum Load (N)	Yield Strength (MPa)	Elongation at break (%)	Ultimate Tensile strength (MPa)	Break Strength (MPa)	Maximum Modulus (GPa)
Pure Epoxy	825.09	4.10	1.4582	8.48838	2.0123	1.9335 (1.5-3.6)[6]
Epoxy + 1wt % TiO_2	3,455.8	10.3417	2.8498	35.35057	20.0886	1.6584
Epoxy + 3wt % TiO_2	2,068.7	7.6536	1.3916	21.32218	12.1967	1.8048
Epoxy + 5wt % TiO_2	2,901.6	5.9775	1.8388	28.82103	17.4269	1.9069
Epoxy + 7wt % TiO_2	2,384.7	6.5103	1.7832	24.31754	13.1352	1.7630

Stress - strain curves of pure epoxy, 1wt% 2wt% and 3wt% of TiO_2 – epoxy is shown in figure 4 and 5.

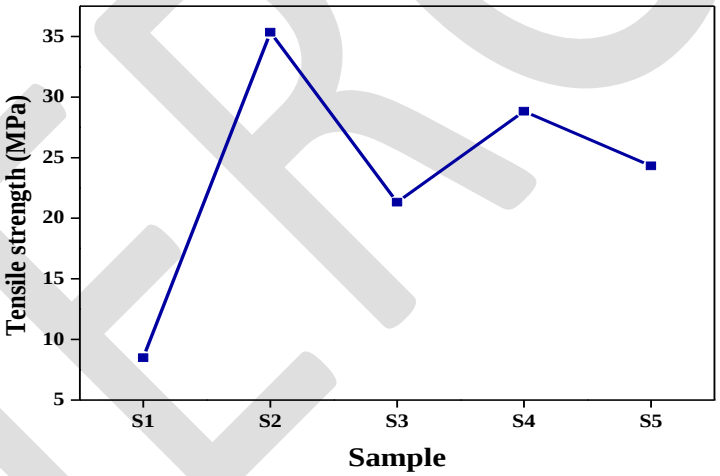

Fig-6 : Variation of Tensile Strength

The tensile strength Vs sample graph is shown figure 6. Table 2 of tensile properties shows that the modified epoxy with 1wt % TiO_2 can withstands the load by 3,455.87N and this has maximum tensile strength. It is due to high dispersion of nanoparticles with epoxy and amine hardner. The higher (3wt %, 5wt % and 7wt %) percentage loading of TiO_2 nanoparticles shows the inferior properties compared to the 1wt% loading of TiO_2 nanoparticles but still they are higher than the pure epoxy polymer. The reason for this is explained as particle loading increases the resulting composites will begin to see more and more particle-to-particle interaction rather than the intended particle-to-polymer interaction. Particle to- particle interaction will lead to agglomerated particles and reduced mechanical properties [7]. This is reflects in the maximum load applied for the study. The modulus value of nanocomposite sample increases with the weight percent of TiO_2, but at 7wt % TiO_2 it decreases due to higher occurrence of agglomeration under gravitational interaction between TiO_2 nanoparticles. On the other hand the low value of tensile strength is due to the formation of chain entanglement in matrix system [5].

Flexural Test

Flexure test measures the force required to bend a specimen under 3 point loading condition. Flexural modulus is a measure of stiffness or rigidity and is calculated by dividing the change in stress by the change in strain at the beginning of the test. In this study the flexural test is carried with standard procedures of ASTM D - 790. ASTM D 790 is a method of measuring the flexural properties of a plastic by setting a test bar across two supports and pushing down in the middle until it breaks or bends a specified distance. The obtained flexural properties of samples are tabulated below in table 3.

Table-3 : Flexural Properties

Sample	Ultimate Flexural strength (MPa)	Maximum Flexural Modulus (GPa)
Pure Epoxy	95.13	2.6262 (2.19)[7]
Epoxy + 1wt % TiO_2	80.67	2.8726
Epoxy + 3wt % TiO_2	57.84	2.8877
Epoxy + 5wt % TiO_2	53.06	3.3819
Epoxy + 7wt % TiO_2	78.21	3.2190

The result in table shows that there is a gradual increase in the flexural modulus and decrease in flexural strength.

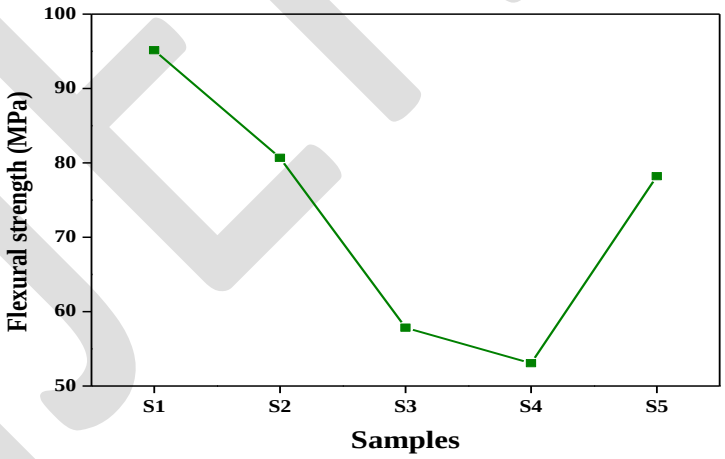

Fig-7 : Variation of flexural strength

The figure 7 is the graph of flexural strength Vs sample. For pure epoxy the flexural modulus has low value 2.6262GPa. The flexural modulus is high with 3.3819GPa for 5wt % TiO_2 added epoxy. TiO_2 7wt % incorporated epoxy has maximum flexural strength comparing with other modified epoxy, may be due to the plasticizing behaviour of TiO_2 into epoxy [6].Thus there is a vast increment in modulus value and shrink in flexural strength with addition of TiO_2 to 5wt %. Decrease flexural strength begin, where increasing the addition of filler lead to increasing the constrained between polymer chains, decreasing the length of chains over certain critical length. This lead to decreasing flexural strength which is depend on chain length, but flexural strength still higher for neat epoxy resin because of van der waals bond which is weak bond but with huge numbers [8].

Izod Impact test

Impact test is a measure of the resistance of material when an impact loading is applied. For this effort, Impact strength is determined from Izod impact strength test. It is performed by the procedures of ASTM D 256 standard. It is used for the determination of the resistance of plastics to "standardized" pendulum-type hammers, mounted in "standardized" machines, in breaking standard specimens with one pendulum swing. The standard test for this method requires specimens made with a milled notch. The acquired impact values are noted below in table 4.

Table-4 : Impact Strength

Sample	Impact Strength kJ/m^2
Pure Epoxy	6.0
Epoxy + 1wt % TiO_2	2.0
Epoxy + 3wt % TiO_2	7.9
Epoxy + 5wt % TiO_2	6.86
Epoxy + 7wt % TiO_2	8.34

Fig-8 : Impact strength of various samples

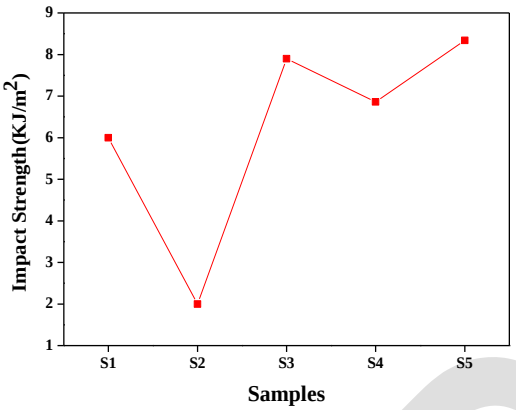

The graph for Impact strength Vs samples is shown in figure 8. Impact strength graph specifies that for pure epoxy the strength is high. When epoxy is modified by TiO_2 nanoparticle of different weight percentage the impact value significantly increases with improvement in TiO_2 mass. The 7wt % TiO_2 added epoxy has high impact strength, shows mechanically it has high strength.

CONCLUSION

In this study the TiO_2 nanoparticles were prepared by sol gel method, and annealed at 300°C and 600°C for 1 h. The structure of the prepared nanopowders has been analyzed by X-ray diffraction technique. TiO_2 synthesized at 600°C shows anatase phase. The polymer samples were prepared by solution casting method. The pure epoxy, epoxy + 1wt % TiO_2, epoxy + 3wt % TiO_2, epoxy + 5wt % TiO_2 and epoxy + 7wt % TiO_2 were the developed composites. The effect of particle dispersion situation on the mechanical properties of nanocomposites has been studied. Tensile strength of epoxy with 1wt % TiO_2 nanoparticle has maximum attainment. The flexural strength of pure epoxy and 7wt % TiO_2 added epoxy has enhanced value because of plasticizing behaviour of TiO_2 into epoxy respectively. The impact strength of 1wt % incorporated epoxy is found to be very low and it increases by increasing the amount of TiO_2. Finally, mechanical studies showed that epoxy with the addition of TiO_2 nanoparticles have certain influence on the mechanical properties.

REFERENCES:

[1] M. Oliveira and A. V. Machado, "Preparation of polymer-based nanocomposites by different routes", In Xiaoing Wang (Ed.) – Nanocomposites: Synthesis, Characterization and Applications. NOVA Publishers p.73-94 ISBN: 978-1-62948-227-9, 2013.

[2] F.T.Mohammed Noori, H.J.Kbashi, N.A.Ali, E.A.Al-ajaj, and H.I.Jaffer, "Effect of Nanocomposites TiO_2 addition on the Dielectric Properties of Epoxy resin", Iraqi Journal of Physics, Vol. 7, No.8, pp 1 – 5, 2009.

[3] Merad. L, Benyousef. B, Abadie. M. J. M, Charles. J. P, "Characterization and mechanical properties of epoxy resin reinforced with TiO_2 nanoparticles", Journal of Engineering and Applied Sciences, Vol. 6, Issue 3, pp 205-209, 2011.

[4] R. D. Kale and Chet Ram Meena, Pelagia Research Library, Advances in Applied Science Research, Vol. 3, Issue 5, pp 3073-3080, 2012.

[5] Anand Kumar Gupta, V. R. Balakrishnan and S. K. Tiwary, "Synthesis of in situ generated ZnO incorporated PI high temperature resistive NC films: FTIR, AFM, XRD, Microhardness and Micromechanical study", International Journal Polymer Technology, Vol. 1, No.2-3, pp 181-188, 2009.

[6] "Materials Handbook", Francois Cardarelli, Springer Publications, 2007.

[7] "Advances in Nanocomposites - Synthesis, Characterization and Industrial Applications"- Polymer Nanocomposite Materials for Structural Applications, Vijaya Rangari, DOI: 10.5772/15615, 2008.

[8] Ikram A. Al-Ajaj, Muhannad M. Abd and Harith I. Jaffer, "Mechanical Properties of Micro and Nano TiO_2/Epoxy Composites", International Journal of Mining, Metallurgy & Mechanical Engineering (IJMMME) Volume 1, Issue 2; ISSN 2320–4060, 2013.

[9] Bu-Ahn Kim and Chang-Kwon Moon, "Study on the Mechanical and Thermal Properties of Tio_2/Epoxy Resin Nanocomposites", International Journal of Ocean System Engineering 3(2), Page 102-109, 2013.

[10] William Gacitua. E, Aldo Ballerini. A, Jinwen Zhang, "Polymer nanocomposites: synthetic and natural filler - A review", Maderas. Ciencia technological, Vol. 7, Issue 3, pp 159-178, ISSN 0717-3644, 2005.

[11] Th. V. Kosmidou, A. S. Vatalis, C. G. Delides, E. Logakis, P. Pissis, G. C. Papanicolaou, "Structural, mechanical and electrical characterization of epoxy-amine/carbon black nanocomposites", eXPRESS Polymer Letters Vol.2, No.5 pp364 –372, 2008.

[12] "A text book of Polymers (Processing and Applications)" – (Volume II), Dr.Bhatnagar. M. S, S. Chand & Company Ltd, 2008.

International Journal of Engineering Research and General Science Volume 3, Issue 5, September-October, 2015
ISSN 2091-2730

Time to Amplitude Converter for Phase Shift Detection

Divya Chacko[1], Mrs. Kanchan Chavan[2]
ME student[1], Assistant Professor[2], Department of Instrumentation, Vivekanand Education Society's Institute of Technology (VESIT)
Mumbai University, Mumbai,divyachacko86@gmail.com, Mob: +91-9029470487

Abstract—Time measurement has significant importance in modern science and in its various fields of applications like low and high energy nuclear physics, solid state applications, high energy particle and neutron physics etc. The objective of this paper is to design and develop a Time to Amplitude Converter (TAC) for detecting the Phase Shifts that occur due to time delays, generally in the range of microseconds. Phase Shift can happen due to various complex loads. Therefore, Phase Shifts needs to be measured with high resolution. Phase Shifts are measured in degree or time units. This paper describes the design considerations to be taken into account for selection of components such as integrator, comparator, and ADC that constitutes a TAC circuitry to achieve the desired high speed resolution.

Keywords—Time to Amplitude Converter, Phase Shift, Zero Crossing Detector, Propagation Delay, Integrator, Aperture Delay, ADC, Aperture Jitter

INTRODUCTION

Phase Shift is the difference between two signal waves having the same frequency and referenced to the same point in time. Phase Shift is introduced by complex loads like inductive load or capacitive load or both. [15] Due to Phase Shift, the output signal comes delayed at exit end. In electrical circuit, Phase Shift causes apparent power to increase over the real power making the load to draw more power and thus increases losses. So compensation has to be done to remove the problems caused by Phase Shift.

Of the many techniques, those have been developed for time measurement, conventional method is to measure the time digitally using a counter with a known frequency. But the usage of high frequency crystals can cause noise which disturbs analog circuits. One of the most widely used method in nuclear instrumentation is based on Time to Amplitude conversion (TAC), in which, single channel or multichannel time analysis is used to measure through events that are automatically classified in a built-in time-sorter. A TAC converts the measurement time interval first to a corresponding analogue voltage, which can then be digitized with an analogue-to-digital converter (ADC). [12]

Here, the Phase Shift measurement circuitry has been divided into two parts:
1. Conversion of Time difference to corresponding Analog voltage
2. Analog voltage is converted to Digital by using ADC

The first section comprises of comparators and Integrator which converts the phase shift into corresponding Analog voltage.The second section comprises of ADC unit where signals need to be processed so that the information that they contain can be analysed and displayed

TAC STRUCTURE & DESIGN

The operating principle of Time to Amplitude Converter (TAC) is as follows: a conversion capacitor is charged by a constant current starting from the rising edge of a START signal until the rising edge of a subsequent STOP signal. This way the voltage across the capacitor increases linearly with time and is proportional to the time interval between start and stop signals. The Time-to-Amplitude Converter (TAC) produces an output pulse with amplitude proportional to the Phase Shift between input "START" and "STOP" pulses. [7]

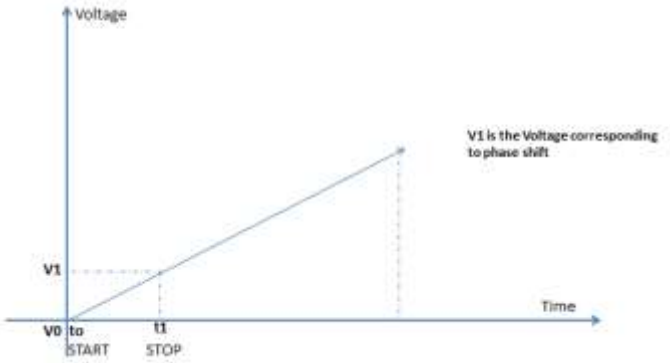

Fig 1.Working Principle of TAC

1.1 Block Diagram

The whole structure of the designed TAC is reported in Fig.1. Each module for Phase Shift measurement consists of two channels. Each channel consists of zero crossing detector (ZCD) and Analog to Digital converter (ADC).The integrator which acts as a time reference is common to all channels. The first channel is taken as reference. The input to each ZCD is a sine wave with Phase Shift arriving the channel at time t_0, t_1 respectively. The output of zero crossing detector in first channel initiates integrator to start a ramp which acts as a START input of TAC and terminate the ramp at a time as per the requirement of user who decides the maximum Phase Shift to be measured. The output of integrator is given as input to all ADCs. The start of conversion for ADCs which acts as a STOP signal of TAC is generated by ZCDs in respective channels. The ADC output is further given to micro controller for processing and output code which represents the Phase Shift is finally displayed on personal computer (PC).

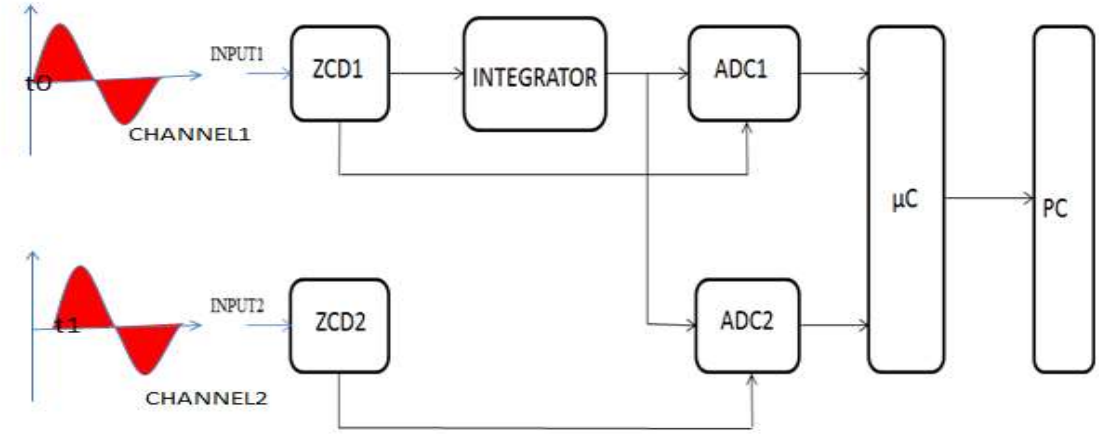

Fig 1.Structure of TAC

1.1.1 Integrator

The integrator acts as a time reference and is common to all channels. The integrator generates a ramp whenever a zero crossover is detected from the reference channel. Selecting the proper OPAMP for this application appears to be very important to avoid nonlinearity of ramp for better performance of the system. The important parameters we have to take into consideration are:

(1) ***Slew rate*** - This represents the maximum rate of change of an OPAMP's output voltage with time. The limitation of output change with time results from internal or external frequency compensation capacitors slowing things down, which in turn results in delayed output changes with input changes. Limitations in slew rate capability can give rise to non-linear effects in electronic amplifiers. Slew rate is usually expressed in units of V/µs. The slew rate of OPAMP has to be very high for this particular application.[11]

(2) ***Input bias current*** – An OPAMP has infinite input resistance and therefore no input current. But in reality, however, small currents typically within Nano amperes to Pico amperes may be drawn by the inputs. The average of the currents entering

into the inverting and noninverting terminals of an OPAMP is referred to as input bias current .it has to be very low for getting expected performances.[11]

(3) Input offset voltage –In theory output voltage of an OPAMP should be zero when both inputs are zero. In reality, however a circuit imbalance within the internal circuitry can result in an output voltage. The input offset voltage is the voltage that must be applied between the input terminals of an OPAMP to nullify the output. The OPAMP chosen to work as an integrator should be of low input offset voltage.

1.1.2 Comparator

The comparator used in the system acts as a zero crossing detector. Zero crossing is the point of choice for measuring phase and frequency [3].The reference is usually easy to establish and the signals amplitude rate of change is maximum at signal zero. In alternating current, the zero-crossing is the instantaneous point at which there is no voltage present. A Zero Crossing Detector detects the transition of a signal waveform from positive and negative, ideally providing a narrow pulse that coincides exactly with the zero voltage condition. The zero crossing detector circuit is an important application of the op-amp comparator circuit. It can also be called as the sine to square wave converter. Anyone of the inverting or non-inverting comparators can be used as a zero-crossing detector. The only change to be brought in is the reference voltage with which the input voltage is to be compared, must be made. Selecting the proper comparator for the particular application appears to be difficult task, considering the thousands of comparators available currently on the market. The selection of comparator is based on following parameters:

(1) Response Time – It is the measure of how quickly a comparator changes output based on an input change. The response time is also referred as propagation delay in data sheets. The response time of the comparator should be very high to get desired response from the system.

(2) Hysteresis – Hysteresis is used to prevent noise from generating multiple zero crossings during the time that the measured signal is very close to zero. Inherently, the signal to noise ratio is the lowest at a zero crossing thus requiring large hysteresis voltages when high noise levels are expected.

(3) TTL compatible output –The output from comparator has to be TTL compatible to make it compatible with other system components especially ADC where output of ZCD is given to start of conversion pin of ADC.

1.1.3 Analog to Digital Converter

Selecting the proper ADC for a particular application appears to be a formidable task, considering the thousands of converters currently on the market. There are various factors to be considered for selecting ADC. These are listed as follows:

(1) Resolution-It is the smallest change in the digital output that can be detected corresponding to a change in analog input. Higher the ADC resolution, better the time resolution for microseconds measurement. It is important to always design a system to allow for more bits than initially required. If an application calls for 12 bits of accuracy, choose a 16-bit converter.

(2) ADC Architecture Selecting the right ADC architecture is important as it decides the performance and successful implementation of the system to a great extent. Following are a few most widely used ADC architectures:

Sigma Delta -For a wide variety of industrial measurement applications, the sigma-delta ADC is ideal; it is available in resolutions from 12 bits to 24 bits. Sigma-delta ADCs are suitable for a wide variety of sensor-conditioning, energy-monitoring, and motor-control applications.[9]

Dual slope - This architecture is eliminates the power line noise of 50Hz / 60Hz and conversion time which is quite large.

Flash – It is very fast: only 1 clock cycle per conversion. High complexity due to presence of 2^{B-1} comparators. Generally flash ADCs have a maximum resolution of 10 bits which is low. Our objective is to design a high resolution ADC. Flash ADCs are most commonly used in applications where only low resolutions are required. One of the key advantages of the Flash topology is that it has a potential latency of only one clock cycle – that is the digital output is available within one clock cycle.[2]

Successive Approximation (SAR) – Successive approximation is the architecture of choice for nearly all multiplexed data acquisition systems, as well as many instrumentation applications. The SAR ADC is relatively easy to use, has no pipeline delay, and is available with resolutions to 18 bits and sampling rates up to 3 MSPS.The algorithm used in Successive Approximation is based on a binary search algorithm, and thus is more component efficient than Flash ADCs which use a brute force approach to perform data conversion. In a SAR ADC the analog input is sampled by a sample-and-hold circuit which operates at the effective Nyquist sampling rate of the

ADC, f_s. The significant advantage of the SAR ADC is that it uses only a few analog components (notably only a single comparator) to implement N-bit data conversion, resulting in a compact area and simple design. The SAR ADC allows for a significant reduction in the number of analog components it comes at the cost of restricting the maximum sampling rate to only a fraction of the maximum speed available by a given technology. SAR ADCs have traditionally been restricted to low to medium speed, and medium to high accuracy applications.[10][1]

***Pipelined* ADC-** Pipelined ADCs are available today with resolutions of up to 14 bits and sampling rates over 100 MHz. They are ideal for many applications that require not only high sampling rates but high signal-to-noise ratio (SNR) and spurious-free dynamic range (SFDR).[1]

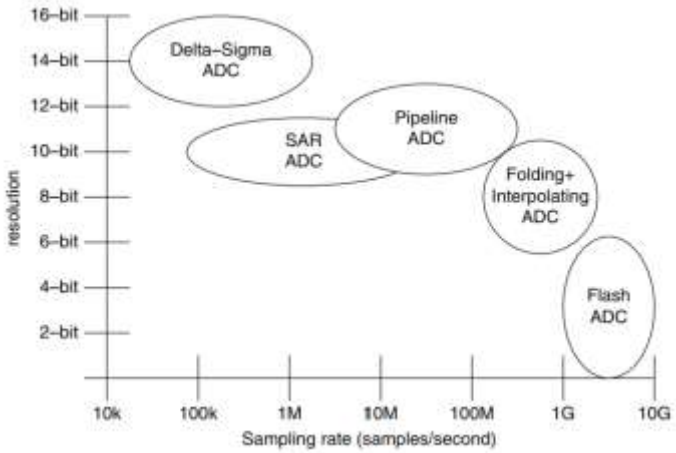

Fig 2.Comparison of ADC Architecture

1.1.4 Non-linearity

Non-linearity in the ADC may cause the actual curve to deviate slightly from the perfect curve. There are two major types of non-linearity that degrade the performance of ADC. They are differential non-linearity (DNL) and integral non-linearity (INL).[8]

***(1) Differential non-linearity (DNL)* –** Differential non-linearity (DNL) is defined as the maximum and minimum difference in the step width between actual transfer function and the perfect transfer function. Non-linearity produces quantization steps with varying widths, some narrower and some wider as shown in Fig 3.

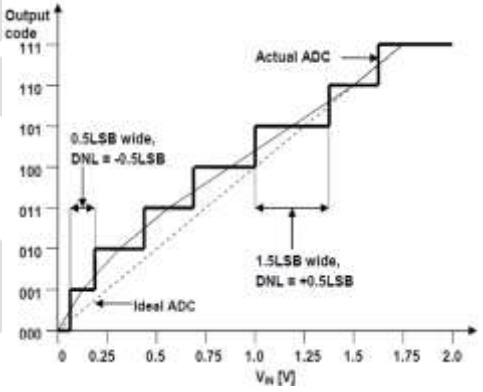

Fig 3.Plot showing the DNL

For the case of ideal ADC, the step width should be 1LSB. But an ADC with DNL shows step widths which are not exactly 1LSB. In Figure3, in a maximum case the width of the step with output value 101 is 1.5LSB which should be 1LSB. So the DNL in this case would be +0.5LSB.Whereas in a minimum case, the width of the step with output value 001 is only 0.5LSB which is 0.5LSB less than the expected width. So the DNL now would be 0.5LSB.

(2) Integral non-linearity (INL) **–** Integral non-linearity (INL) is defined as the maximum vertical difference between the actual and the ideal curve. It indicates the amount of deviation of the actual curve from the ideal transfer curve. INL can be interpreted as a sum of DNLs. For example several consecutive negative DNLs raise the actual curve above the ideal curve as shown in Figure 3 and the INL in this case would be positive. Negative INLs indicate that the actual curve is below the ideal curve. This means that the distribution of the DNLs determines the integral linearity of the ADC.

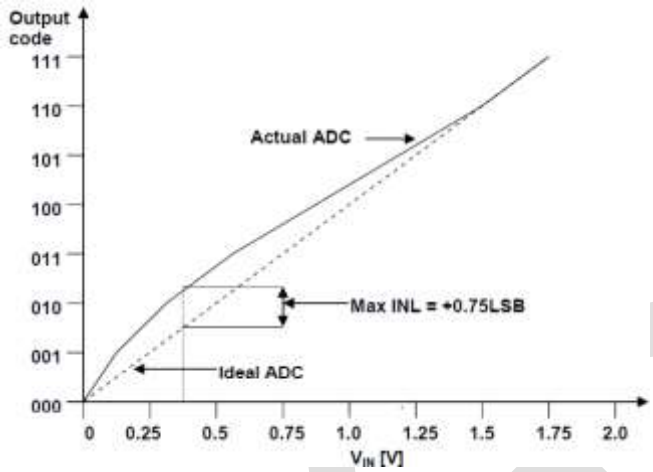

Fig 4.Plot showing the INL

The INL can be measured by connecting the midpoints of all output steps of actual ADC and finding the maximum deviation from the ideal curve in terms of LSBs. From the Figure 4, we can note that the maximum INL is +0.75LSB.

1.1.5 ADC timings

Basically an ADC takes some time for sampling and holding and for conversion.

Sample and hold time-Usually after giving a trigger to an ADC to start a conversion, it take some time (in clock cycles) to charge the internal capacitor to a stable value so that the conversion result is accurate. This time is called as sample time. After the sampling time, the number of clock cycles it takes to convert the charge or the voltage across the internal sampling capacitor into corresponding digital code is called the hold time.

Conversion time-Conversion time is the combination of the sampling time and the hold time, usually represented in number of clock cycles. The conversion time is the main parameter in deciding the speed of the ADC.

Acquisition Time-Acquisition time is the time required to charge and discharge the holding capacitor on the front end of an ADC.It is the maximum time required to acquire a new input voltage once a sample command has been given. (Hold to sample time) This parameter becomes crucial when the time difference between the inputs arriving at the same channel is extremely small.

Aperture Delay-Aperture delay is the measure of the acquisition performance. It is the time between the rising edge of the Convert input and when the input signal is held for a conversion.

Aperture Jitter-Aperture Jitter is the variation in aperture delay from sample to sample. Aperture jitter shows up as input noise. It results from the noise superimposed from the hold command and causes corresponding voltage error. It is usually measured in rms.

TAC CHARACTERISTICS

The characteristic of TAC depends on the components involved in the operation. The characteristics of the TAC described as follows:

(1) Linearity-The property of linearity depend on the ramp produced by integrator is very important. Ramp generated has to be linear to enable proper time to amplitude conversion. Any change in the slope of ramp will lead to errors in the output voltage which represents Phase Shift. Linearity depends on current (I) flowing through integrator current (I) flowing through integrator where

$$I = I_{leakage} + I_{s/wleakage} + I_{bias}$$

$I_{leakage}$ = Leakage current of capacitor

$I_{s/wleakage}$ = Leakage current of switch
I_{bias} = Input bias current of OPAMP

(2) Time Resolution- The time resolution is the ability to distinguish between two time intervals with even the smallest change in the input time that can be reflected at the output voltage. The time resolution of system depends on ADC and range of time measurement. Hence, the TAC output range shall be compatible with ADC voltage range.

TIMING DIAGRAM

The Fig 5 shows the main TAC signals. The TAC is a START-STOP type.

- By the arrival of the new START signal from ZCD of reference channel starts a ramp in integrator and the ramp output voltage is fixed at 5V.
- After the arrival of a start signal, any STOP signal from the ZCD of any of the four channel during which a output voltage corresponding to phase shift is obtained.
- When the rising edge of the STOP signal from ZCD reaches into ADC's start of conversion pin (soc), ADC acquire the instant voltage from the linearly rising ramp which represents the Phase Shift and is displayed on Personal Computer(PC)
- The conversion capacitor is discharged after a defined interval and the converter returns to the initial conditions, so that a new start signal can be accepted.

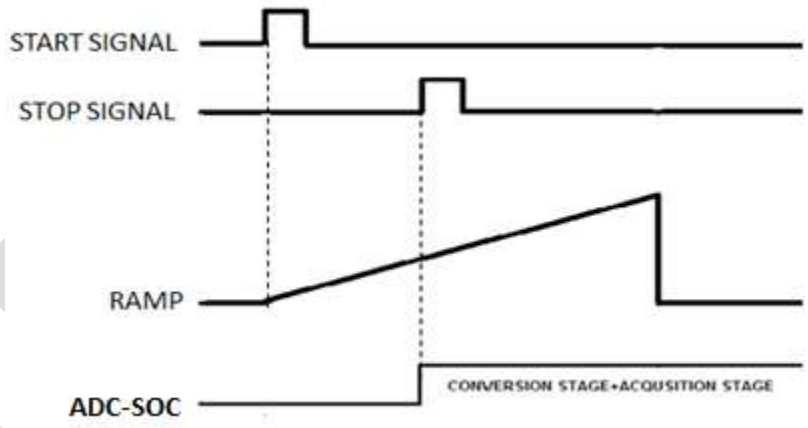

Fig 5.Timing Diagram of main TAC signals

EXPERIMENTAL RESULTS

The designed converter has been experimentally characterized and the performance has been evaluated. The Fig 7&8 shows the output of individual circuits of the designed TAC. The integrator output is a linear ramp whose maximum voltage is 5V for duration of 8.6μs.The ZCD output shows the fast response of the comparator. The proper selection of components leads to the satisfactory response. The following table shows the set voltage value, calculated ADC count, and the obtained ADC count, the voltage obtained by scaling ADC count, and Percentage error of reading.

Fig.6 Experimental setup

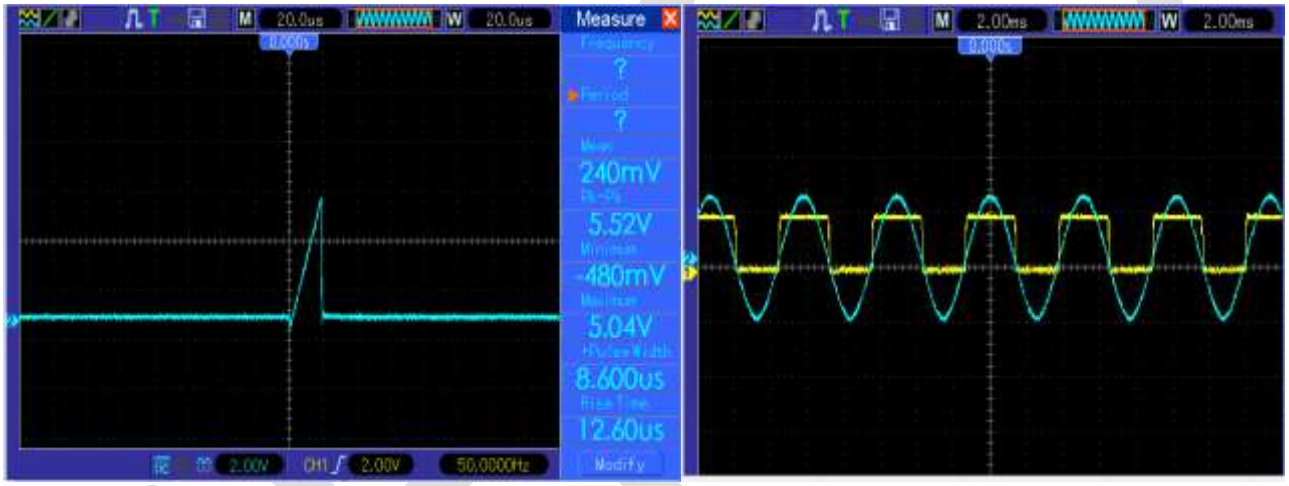

Fig.7Observed output for Integrator and ZCD

Sr.No	Set value	Calculated count	Obtained count	Obtained voltage	% Error reading
	V			V	%
1	0.50492	6616	6616	0.5094	0.004
2	1.4999	19654	19655	1.49998	-0.005
3	2.0001	26208	26211	2.0003	-0.01
4	2.5	32759	32762	2.50025	-0.011
5	3.0001	39312	39316	3.00042	-0.011
6	3.5008	45873	45876	3.50113	-0.009
7	4	52414	52416	4.00015	-0.004
8	4.504	59018	59005	4.503	0.022
9	4.9954	65448	65452	4.99501	-0.022

Fig.8 Observed output of ADC

ACKNOWLEDGEMENT

I Divya Chacko, would like to express my special thanks of gratitude to my guides Dr. P.P. Vaidya and Mrs. Kanchan Chavan (Co-Author) for sharing their pearls of knowledge and wisdom and giving me a golden opportunity to do this wonderful project, as well as our principal Dr. Mrs. J. M Nair for her encouragement. I would also like to thank my family and friends for extending their generous support in the course of work.

CONCLUSION

The results obtained from this high resolution system have very low percentage error. The designed circuit is implemented successfully for measurement of voltages (microvolts) in high resolution. The selected components like OPAMP, comparator and ADC are made to achieve expected output. The chosen ADC is capable to capture instantaneous data with a high resolution of 16 bits. TAC designed in this project is a measure of the distribution of time intervals between starts and stop pulses and is often referred to as "time range".

REFERENCES:

[1]Which ADC Architecture Is Right for Your Application? By Walt Kester
http://www.analog.com/library/analogDialogue/archives/39-06/architecture.pdf.

[2] Walt Kester, "MT020-ADC Architectures I- Flash convertor", Analog Devices,
http://www.analog.com/media/en/trainingseminars/
tutorials/MT-020.pdf

[3] R.W. Wall, Senior Member," Simple Methods for Detecting Zero Crossing",IEEE,Revised: February 3, 2012

[4] Matteo Crotti,Ivan Rech, Member, IEEE, and Massimo Ghioni, Senior Member, IEEE,Four Channel, 40 ps Resolution," Fully Integrated Time-to-Amplitude Converter for Time-Resolved Photon Counting", IEEE JOURNAL OF SOLID-STATE CIRCUITS, VOL. 47,NO. 3, MARCH 2012

[5] M.Ciobanu a,b, A.Schuttaufa, E.Cordierb, N.Herrmannb, K.D.Hildenbranda, Y.J.Kima, Y.Leifelsa, M.Kisa, P.Koczona, X.Lopeza, M.Petrovicic, X.Zhanga"A Front End Electronic card using a high gain and high bandwidth preamplifier with a fast discriminator for time of flight measurements",2006 IEEE Nuclear Science Symposium Conference Record.

[6] ORTEC ,"Time-to-Amplitude Converters and Time Calibrator."

[7] F. ESFANDI, M. SHAHRIARI, F. ABBASI DAVANI AND A. SHARGHI IDO,"Research Note" "DESIGN AND CONSTRUCTION OF A HIGH PRECISION TAC", Iranian Journal of Science and Technology, Transaction A, Vol. 33, No. A2,Printed in the Islamic Republic of Iran, 2009, Shiraz University

[8] Atmel AVR127: Understanding ADC Parameters, APPLICATION NOTE

[9] Walt Kester, "MT020-ADC Architectures III- Sigma Delta ADC", Analog Devices,
http://www.analog.com/media/en/trainingseminars/tutorials/MT-022.pdf.

[10] Walt Kester, "MT020-ADC Architectures II- Successive Approximation ADCs", Analog Devices,
http://www.analog.com/media/en/training-seminars/tutorials/MT-021.pdf

[11] "Practical Electronics For Inventors" by Paul Scherz

[12] "Time to Amplitude Converter"Wikipedia, https://de.wikipedia.org/wiki/Time_to_Amplitude_Converter

[13] Walt Kester, "MT-007 Aperture Time, Aperture Jitter, Aperture Delay Time — Removing the Confusion?", Analog Devices,
http://www.analog.com/media/en/training-seminars/tutorials/MT-007.pdf ,pg3

[14] Knoll, G. F. (2000). Radiation Detection and Measurement. John Wiley & Sons, 230-231

[15] "Phase Shift"https://en.wikipedia.org/wiki/Phase_(waves)

International Journal of Engineering Research and General Science Volume 3, Issue 5, September-October, 2015
ISSN 2091-2730

A Flipped Classroom Approach to Teaching Engineering C Programming

Megha Garg
Assistant Professor, JECRC University, Jaipur
M.Tech,CSE(I.I.T. Kharagpur)
Communication Address: 106-65, Vijay Path,Mansarovar,Jaipur,Rajasthan-302020
meghagarg.1990@gmail.com, megha.garg@jecrcu.edu.in
Contact: 8233095306

Abstract— Flipped classrooms reverse the role of traditional teaching where in students gain exposure through learning material like videos, power point presentations and notes outside classroom and the class time is utilised for problem solving and discussions in order to master the concepts. Flipped classrooms encourage students to learn at their own pace releasing frustrations and undue burden on students to pace up. Those students who have to miss some classes do not lose the course content. It provides opportunity for active interactions among students outside class via an online course website, facilitates social learning and is successful in providing timely, accurate feedback required by instructor to keep track of class progress and render required help to students. The intellectually drilled-down personalised feedback reports of tests helps in identification of the weaker areas or concepts misunderstood during the course of learning. The timely help to combat weaker areas accelerates the pace of learning and is not possible in traditional learning with large students in a classroom. Individual student difficulties are easily traced by the teacher using Outcome Based Education (OBE) reports generated by online OBE softwares.

The online course 'Programming in C' taught using flipped classroom platform Inpods registers the students and divides them into pod groups for group assignments. Short videos of 15 minutes each containing one topic of a chapter were developed to maintain attention level in students, keeping the mind the short attention span of 21st millennia students. The created assignments were meticulously designed to test students on their level of understanding concepts. Timely accurate personalised reports paved an easier way for re-teaching .The student feedbacks aided in improving the course delivery material . Difficulties of the students in programming were handled efficiently by knowing weak-spots well on time and learning pace of C programming in students clearly enhanced using flipped classrooms.

Keywords Flipped classroom, Outcome Based Education(OBE), Feedback, Learning, Teaching, programming, re-teaching

INTRODUCTION

Flipped Classroom is a blended instructional strategy in which the instructional content is delivered to students at home in the form of online videos, presentations via a software portal named as Virtual classroom wherein all students are enrolled and instructor presents material and the class time is utilised for problem solving and doubt clearing of students.

Flipped Classroom is a newer and well –known established strategy. Woodland Park High School chemistry teachers Jonathan Bergmann and Aaron Sams are considered as driving forces in flipped teaching at the high school level. In 2007, they recorded their lectures and posted them online in order to accommodate students who missed their classes[1]. In 2011 educators in Michigan's Clintondale High School flipped every classroom After 20 weeks, students in the flipped classroom were outperforming students in the traditional classrooms. Further, no students in the flipped classrooms scored lower than a C+. [1]The upcoming of Khan Academy brought flipped classroom into limelight.[2]

The flipped classroom encompasses some approaches, including active and collaborative learning, problem-based learning and project-based learning [3].Flipped classrooms give students a chance to learn at their own pace and time. The students can watch online videos distraction free and open up new discussion on doubtful topic leading to active discussions amongst peers.

A flipped classroom approach to teaching engineering C Programming course taught in the 1st year , first semester of a typical undergraduate engineering education is explained. When a programming C course was earlier taught to students, it was observed that they focus more on copying content rather than understanding the fundamental concepts. Eventually, the weak foundations in programming continued next year to C++ and also hampered their coding skills in third year for Java and fourth year in Advanced Java. To combat this weak progress in C programming, the flipped classroom was created using Inpods as a platform for data.

METHODOLOGY

While working on Project GENTLE (**G**lobal **E**ducation **N**etwork for **T**eaching and **L**earning **E**ngineering) in collaboration with IUCEE and inpods , online videos of 15 minutes each were made for each concept in a chapter. The videos were made of shorter duration because the attention span of 21st millennia students is very limited and to make them focus for more than 10 minutes continuously is a challenge. Pertaining to created videos, 2 MCQs of 10 questions each and a few descriptive, long answer assignments were developed to test the grasp of student on that concept taught via video. The MCQs were automatically evaluated after students attempts and scores are displayed to him, along with correct answers .While working with descriptive assignments, the instructors checks the answers manually and scores are uploaded on student portal. The information panel was used to convey important information to students such as quiz time, syllabus.

The students were enrolled in Inpods using their email ids and divided into small pod groups for doing project discussion or group discussions. After the enrolments, students were asked to come prepared by listening and watching videos from home before each lecture. The students were tracked as to videos were watched or not by inpods software available to instructor. The assignments were solved by the students in class and doubts were discussed.

The active discussions were monitored by the instructor and relevant answers were provided for their doubts to keep the motivation level high.The topics in which majority of class had scored less marks in online tests was re-taught and a re-exam was prepared to retest their understanding of the concerned topic.

RESULTS

The flipped classroom approach was liked by the students as well as the instructor. It proved out to be successful in increasing the confidence and improving coding skills better as compared to the previous batch that solely learnt through traditional classroom approach. It was found that students who regularly watched lessons and solved MCQs scored far better than students who just relied on classroom delivery. Since the assignments had a deadline, the students became more professional and false excuses were not able to delay assignment submission.

Individual tracking of participation and personalised reports [Fig1] provided by Inpods paved a way to drill down progress of students individually and collectively. It made it a lot easier to identify the misconceptions among students of a particular topic because most of students attempted its MCQs wrong. The instructor got to know at a early stage where re-teaching was required. And re-teaching helped the students understand difficult concepts easily.

This technique proved advantageous mostly to average students who could re-watch the videos again till they could absorb the information presented. Also, the students could see each others answers via discussions and learn by it without any hesitation.

The various group discussions and survey proved advantageous as they inculcated a sense of social participation among students as well as helped the instructor to re-design the course and customise it as per needs of students .This will add as an asset to the forthcoming semester students.

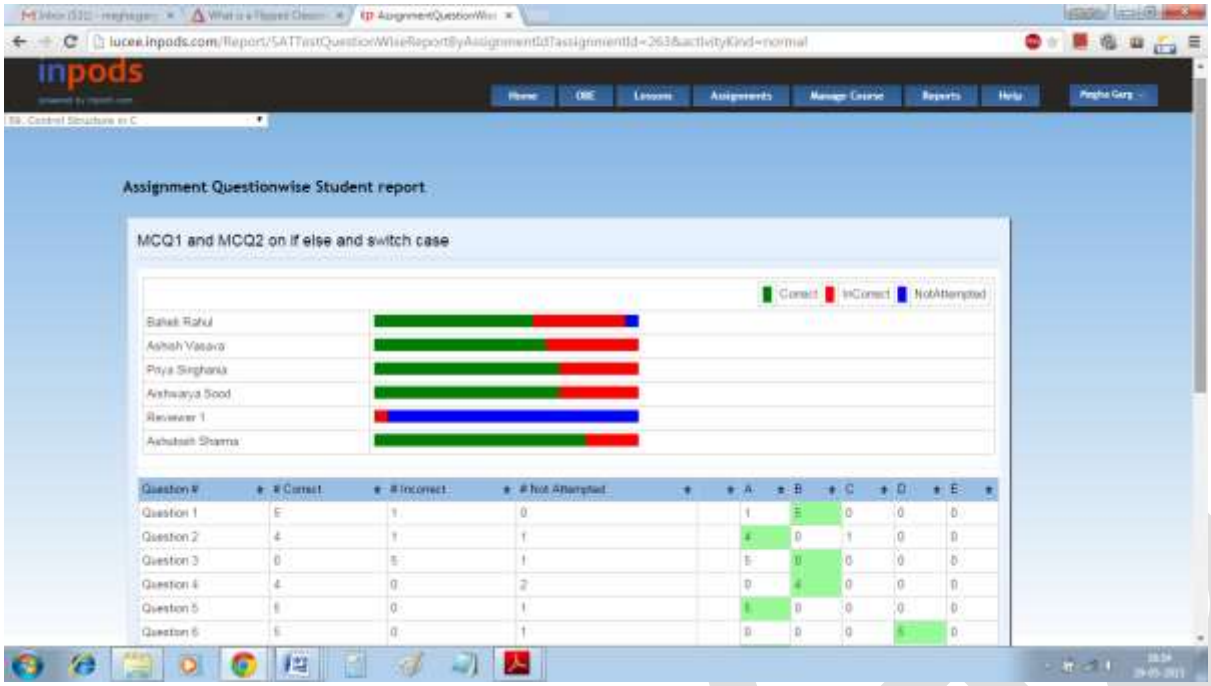

Fig 1: Assignment Report of Students on If-else and Switch Case.

The result of this batch had higher grades as compared to a batch taught with tradition classroom. The students learnt coding skills better, had greater interest to learn programming and understanding fundamentals of programming,making it easier to cope up with future requirements of coding in course taught during higher undergraduate years.

The work done for development of this online flipped classroom course proved inspiring and the university will now be hosting 6 new online flipped courses in the upcoming semester for each branch of engineering.

CHALLENGES

Although flipped classrooms had many advantages, the conduction had its own challenges. The creation of online videos and assignments was very time-consuming and an additional to manual notes preparation done for other batch taught via traditional classroom approach. Sometimes the students had internet accessibility issues, so the concepts had to be taught in classroom ignoring the available online content. A few students had to be motivated a lot to keep watching and working as flipped classroom relies on student a lot. There was no mechanism to test the home-works given were done individually without cheating.

ACKNOWLEDGMENT

I express my sincere gratitude towards IUCEE for helping me learn flipped classroom technique and my parents, Vinod Kumar Garg and Sudha Garg for their undivided support.

CONCLUSION

Flipped Classroom are an innovative pedagogical tool that are an aid to teaching and provide outcome based education, easily tracked by continuous student assessment reports. The online environment eases the social interaction amongst students. The weak spots of students are identified and worked well on time.

RECOMMENDATION

The use of flipped classroom online course in Programming in C using Inpods went successful, was cost-effective, with least technological requirements and is recommended for use by universities having adequate internet access. The flipped course was successful in clearing basic concepts, keeping students motivated and self-driven during course. Also,the course feedback helps in improving the quality of instructional material and students learn better at their own pace.

REFERENCES:

[1]http://en.wikipedia.org/wiki/Flipped_classroom

[2] The Flipped Classroom–Advantages and Challenges, Shi-Chun DU1,a, Ze-Tian FU2,b, Yi WANG3,c,* , International Conference on Economic Management and Trade Cooperation (EMTC 2014)

[3] M. Prince, Does active learning work? a review of the research, J. of Eng. Educ. 93 (2004) 223-231.

International Journal of Engineering Research and General Science Volume 3, Issue 5, September-October, 2015
ISSN 2091-2730

A Review: Varying bit rate data transmission for long haul system in optical communication

Mandeep kaur[1] Atul mahajan[2]

[1]M-Tech Scholar, Department of Electronics & Communication Engineering
ACET, Amritsar, India Email:deepboparai23@gmail.com
[2]Associate professor, Department of Electronics & Communication Engineering
ACET, Amritsar, India

Abstract: Now a day as per requirement of user we require that high data rate along with good quality of service, this requirement can be full fill by using optical fiber communication, but still telecommunication expanding day by day so that we need more good quality factor per bit rate. by increasing the demand of telecommunication we need more bandwidth. We expanding bandwidth day by different method but this not effective method for full fill requirement. in this review paper use single frequency and single bandwidth and vary the bit rate then at what rate quality factor vary and at what level we get good quality factor. By this we can use different bit rate at single bandwidth and by this our bandwidth spectrum get enhanced for telecommunication.
Keyword: optical fiber, telecommunication, spectrum,quality factor, bandwidth, dispersion, bit rate.

I.INTRODUCTION

With the rapid development of the following generation of optical fiber transmission, optical fiber transmission system and its wave length optical fiber transmission system and its wavelength division multiplexing system has now been the focus of research. to be able to enhance the ability of the machine and diminish the degradation of performance would will be brought on by the increased loss of transmission [1].by varying the bit rate per-channel according to demand of telecommunication we want high spectral efficiency[2].

II.OPTICAL COMMUNICATION SYSTEM REVIEW:

An optical communication link is really a means for transmitting data from one place to another using the light source. A simple Optical Communication Systems was made of a transmitter produces the light signal, a visual fiber channel which carries the light and a visual receiver which receives the light signal transmitted for retrieving the information. The device could has additional components such as fiber amplifiers for regenerating the optical power or dispersion compensators for counteracting the consequences of dispersion. The difficulties of the implementation of the optical systems vary from noncomplex (i.e., local area network) to extremely complex and costly (i.e., long term telephone or cable TV network) [3]. The notion of utilizing a glass fiber to transmit information light over long distances was initially introduced by Kao and Hockman in 1966[4].This was realized when low-loss glass optical fibers were first fabricated by Arriving 1970 almost at once, room temperature operating semiconductor diode lasers were produced by Bell Labs [5]. The mixture of a concise optical transmission medium and a miniature diode laser produced a series of revolutions in fiber optical communication technology. This technology was adapted by the telecommunication industry starting in the 1970s. At present optical fiber communication systems are widely applied in different types of systems, such as long term telephone network, Cable or Community Antenna television (CATV) networks, broadband Internet services etc., due to the ever-increasing demand for higher data rates in the transmission of multimedia services like voice, image, video, etc. The maturing of fiber optic technology and communication networks have been gradually updated with the seek out more advance techniques to take full advantageous asset of the transmission potential of a fiber link. Techniques like Dense Wavelength Division Multiplexing (DWDM), optical amplifiers, optical switchers, management of dispersion, and optical burst switching etc. enable us to load more transmission traffic onto an individual glass fiber [6]. However, the pursuing for speed and bandwidth never stopped. Theoretically an individual mode fiber features a potential bandwidth of nearly 50 Tbps. With optical fiber networks we were able to achieve link capacities of the order of 1000s of Gbps [4]. The Dispersion limits the utmost transmission data rate and maximal distances of which electronic repeaters should be positioned along optical link [1]. In the Single-Mode Fiber (SMF) the dominant linear impairments are Group-Velocity Dispersion (GVD) i.e., different frequencies travel at different speeds and Polarization-Mode Dispersion (PMD) i.e., different polarizations arrive at the receiver with various delays. The after effect of chromatic dispersion becomes more and more critical at high data rate transmission, since the linear dispersion tolerance decreases with the square of the bit rate [7].at high data rate dispersion should be compensate by suitable method so that people get good results.

III.DISPERSION COMPENSATION TECHNIQUES

A SMF features a potential bandwidth of nearly 50 Tbps; with optical fiber networks we could achieve link capacities of the order of 1000s of Gbps [4]. Dispersion limits the most transmission rate and maximal distances at which electronic repeaters should be positioned over the optical link [1]. In the SMF fiber the dominant linear impairments are GVD and PMD. The effect of chromatic dispersion becomes more and more critical at high data rate transmission because the linear dispersion tolerance decreases with the square of the bit rate [8]. It's been observed that dispersion of a standard single mode fiber is lowest at 1300 nm, whereas it's minimum attenuation at 1550 nm. But at 1500 nm wave length the dispersion is higher. The usage of dispersion shifted and dispersion flattened fibbers are a number of the common solutions for compensation [7] There are several different ways that can be utilized to compensate for dispersion, including DCF , chirped Bragg gratings , all-pass optical filters and optical phase conjugation [3]. These

methods restore the signal such that it may be received in a standard receiver. An alternate method would be to detect the dispersed signal and perform the dispersion compensation electrically[2].

IV.THEORY

To upgrade the existing optical network by varying the bit rate we want that system should have the exact same amplifier spacing as existing system[2]. Fiber input power is fixed due to the non linear optical effects in the transmission fibre.if we vary the bit rate at that time the interaction between self-phase modulation and group velocity dispersion cause severe wave form distortion in the transmission. For over come these non linear impairments we've several techniques that individuals found in telecommunication for long run system we want the defining the allowable fiber input power in transmission link[3].if we put frequency and bandwidth non variable and we change the data rate differently than we get many quality factor for the reason that case bandwidth spectrum get enhanced. in this way our telecommunication demand should be full fill. In one single channel optical communication system for lower channel power, the most transmission length is set by the accumulated amplifier noise in the system, and for higher channel power, the system behaviour is limited through the non linear effects in the fibre such as for instance spm. Althrough dispersion compensation at the end of each fiber span can correct for the waveform distortion. [12]

The schematic of the optical communication system simulation setup is shown

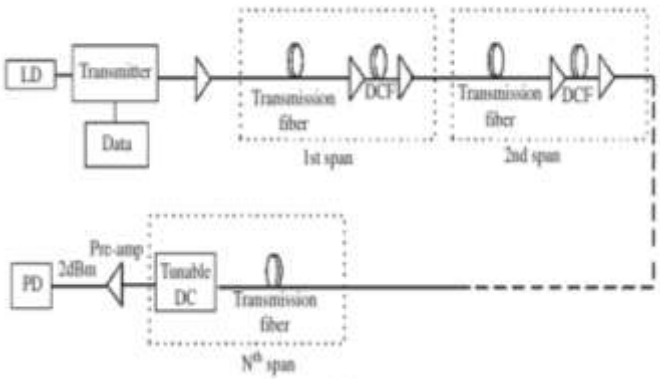

Fig.1. optical communication system setup[2]

V.ADVANTAGES OF OPTICAL FIBER IN TELECOMMUNICATION:

1.**Immunity to Electromagnetic Interference** Although fiber optics can solve data communications problems, they are not required everywhere. Most computer data explains ordinary wires. Most data is sent over short distances at low speed. In ordinary environments, it's not practical to use fiber optics to transmit data between personal computers and printers as it's too costly. Electromagnetic Interference is just a common kind of noise that originates with one of many basic properties of electromagnetism. Magnetic field lines generate an electrical current while they cut across conductors. The flow of electrons in a conductor generates a magnetic field that changes with the existing flow. Electromagnetic Interference does occur in coaxial cables, since current does cut throughout the conductor. Fiber optics are immune to this EMI since signals are transmitted as light as opposed to current. Thus, they are able to carry signals through places where EMI would block transmission.[9,10,]

2. **Data Security**

Magnetic fields and current induction work in two ways. They don't just generate noise in signal carrying conductors; additionally they let the data on the conductor to be leaked out. Fluctuations in the induced magnetic field outside a conductor carry exactly the same information as the existing passing through the conductor. Shielding the wire, as in coaxial cables can reduce the problem, but sometimes shielding can allow enough signal leak to permit tapping, which is exactly what we wouldn't want. You can find no radiated magnetic fields around optical fibers; the electromagnetic fields are confined within the fiber. That makes it impossible to tap the signal being transmitted via a fiber without cutting into the fiber. Since fiber optics do not radiate electromagnetic energy, emissions can't be intercepted and physically tapping the fiber takes great skill to accomplish undetected. Thus, the fiber is the absolute most secure medium available for carrying sensitive data. 3. **Eliminating Spark Hazards**

Sometimes, transmitting signals electrically can be extremely dangerous. Most electric potentials create small sparks. The sparks ordinarily pose no danger, but can be really bad in a chemical plant or oil refinery where the air is contaminated with potentially explosive vapours. One tiny spark can cause a big explosion. potential spark hazards seriously hinder data and communication such facilities. Fiber optic cables do not produce sparks since they cannot carry current.

4. **Ease Of Installation**

Increasing transmission capacity of wire cables generally makes them thicker and more rigid. Such thick cables can be difficult to put in in existing buildings where they need to proceed through walls and cable ducts. Fiber cables are easier to put in being that they are smaller and more flexible. They could also run along exactly the same routes as electric cables without picking right up excessive noise.

5. **High Bandwidth**

Over Long Distances Fiber optics have a big capacity to carry top speed signals over longer distances without repeaters than other forms of cables. [9,10,]

VI.PROBLEMS WITH FIBER OPTICS

1**.System Reconfiguration**

Although fiber optics are renowned for his or her efficiencies and plenty of advantages, there are a few drawbacks in them and one of them is system reconfiguration. Converting existing hardware and software for the utilization of fiber optics does take plenty of time and money which also reduces the turnover for just about any profit making firm in the market. Sometimes it may be far more convenient to transmit top speed computer data serially (one bit after another) than sending several bits at a time in parallel over separate wires. This changeover requires modification in both hardware and software.

2. **Limitations in Local Area Networks**

In Local Area Networks, fiber optics is not used as widely as you might expect. One reason is the implementation requires lot of changes in current networks and systems. This involves plenty of time and effort that your management is not ready to sacrifice.

3. **Economic Evaluation**

The major practical problem with fiber optics is that it always costs more than ordinary wires. All costs elements associated with economic evaluation may be grouped into two main classes; which are investment costs and operation costs. [9,10]

VII.APPLICATION OF OPTICAL FIBER IN TELECOMMUNICATION

- Low signal loss and high bandwidth.
- Small size and banding radius.
- Non conductive, non radiative, non inductive.
- Light weight. [10,11]

VIII.CONCLUSION :

We conclude that for good quality factor needs non linear distortion compensating technique are required without these techniques we does not able get better result and if we vary the bit rate at single frequency and bandwidth in that case our bandwidth spectrum get enhanced. it give better result for telecommunication.

REFERENCES:

[1] Aihan yin, Libi, Xinliang zhang “analysis of modulation format in the 40 gbits/s optical communication sysytem” optic 121 (2010) 1550-1557

[2] Anu sheetal, Ajay k. Shrama, R.S. kaler “impact of optical modulation format on SPM-limited fiber transmission in 10 and 40 gb/s optimum dispersion-managed lightwave system ” optik 121 (2010) 246-252.

[3] R.K.sethi, Dr. Aditya goel “ performance analysis of optical communication system using OFDM by employing QPSK modulation” international journal on recent and innovation trends in computing and communication.

[4] K. C. Kao and G. A. Hockman, “Dielectric Fiber Surface Waveguides for Optical Frequencies," Proc. IEE, Vol. 133, pp. 1151-1158.

[5] C. Lin, “Optical Fiber Transmission Technology - Handbook of Microwave and Optical Components”, Ed. K. Chang, John Wiley, 1991.

[6] Bo huang,Yi An ,Nan Chi, Meng Xiong, Haiyan ou,Wen Liu, Christrophe peucheret “combining DPSK and duobinary for the downstram in 40-Gb/s long –reach WDM-PONs ”optical fiber technology 19 (2013) 179-184.

[7] Neeru Malhotra , Manoj kumar “ investigation on PMD-induced penalties in 40 Gbps optical transmission link” optik 121 (2010) 286-290.

[8] K.K.gan, B.abi, W. Fernando, H.P. kagan ,R.D. kass, A. Law, M.R.M. lebbai, F.Rizatdinova, P.L. skubic, D.S.smith “ radiation-hard/ high speed data transmission using optical links”nuclear instruments and methods in physis research A.

[9] Arun gangwar, Bhawana sharma “optical fiber : the new era of high speed communication (technology ,advantages and future aspect)” internatonal journal of enginnering research and development.

[10] Francis idachaba Dika v ike, orovwode hope “ future trends in fibre optics communiction” proceding of the world congress on engineering 2014 vol 1

[11] Joseba zubia , Jon arrue “plastic optical fibers an introduction to their tehnology processes and application ” optical fiber technology 7,101-190(2001).

[12] Erwan pincemin , Julie karakai,Yann Loussouarn, Hubert poignant, Christophe betoule, Gillles theouenon,Raphael Le Bidan “ challenges of 40/100 gbps and higher rate deployments over long haul transport networks” optical fiber tehnology 17(2011) 335-362

International Journal of Engineering Research and General Science Volume 3, Issue 5, September-October, 2015
ISSN 2091-2730

Carbon Sequestration using Multiphase Pump

Mainak Mukherjee[1], Surajit Mondal[2] , Amit K Choudhury[3]

[1]M.Tech Energy Systems, University of Petroleum & Energy Studies, Dehradun .India

[2]Research Scholar, University of Petroleum & Energy Studies, Dehradun .India

[3]M.E Power Systems, IIEST ,Shibpur Kolkata.India

Abstract: Carbon dioxide is a harmful gas and is leading us to a globally warmer environment. This deciphered the concept of capturing carbon dioxide from air and storing it in places which would not be vulnerable and out of reach from reentering the atmosphere. Carbon sequestration is a highly challenging technology and is therefore quite limited in its application till date. Though there are several practical applications that have been structured out and is very well used. Coming across from capturing and then storing, the process involves a huge implementation of technology. Storing the captured carbon dioxide into exhausted oil and gas beds under sea is supposedly the best option till date. Transferring down the carbon dioxide is usually mapped by using booster pumps. As an alternative multiphase pumps can also be utilized owing to its versatile features.

Keywords: Carbon Sequestration, Carbon Capture, Multi-phase Pumping, Geological Sequestration, Carbon Emission, Global Warming.

1. Introduction:

Carbon negative is a phrase that is used to describe any activity that involves in mitigating carbon dioxide from the atmosphere. Carbon footprint can never be reduced zero or negative. Technically it is utmost challenging and would require extensive research to finally establish a system. In India unfortunately carbon capture and sequestration has not marched out of the laboratory scale yet, since the major hindrances being economic policies and unavailability of geological sequestration sites. Out of the existing beds, in states of India like Assam, where oil reserves are competitive, flushing captured carbon dioxide may lead to geological degradation owing to its geographical features.

Talking about the global carbon emissions from fossil fuel combustion and from industrial processes, there has always been an upscale trajectory. The top 3 emitting regions in 2013, together accounting for more than half (55%) of global carbon dioxide emission are China (10.3 billion tons CO2 or 29%), the United States (5.3 billion tons CO2 or 15%) and the European Union (EU28) (3.7 billion tons CO2 or 11%).

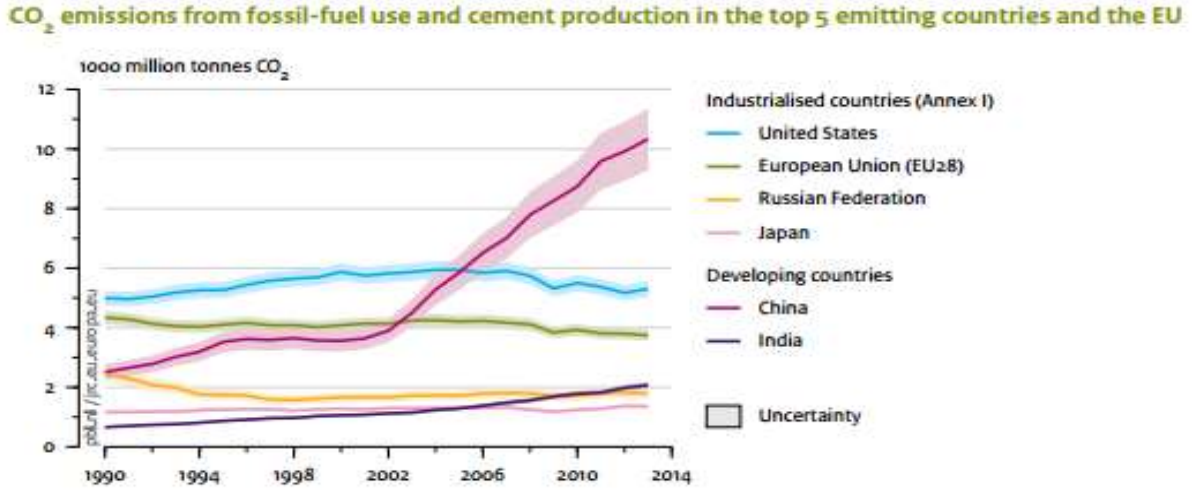

Fig: 1

2. Country wise emission data:

COUNTRY	2010-14, CO2 Emissions MT/Capita
UAE	19.9
USA	17.6
AUSTRALIA	16.9
UK	7.9
CHINA	6.2
FRANCE	5.6
INDIA	1.7

Table: 1

Carbon dioxide emission is accelerating at an enormous rate and to combat this there are various mitigation and adaptation initiatives that are being taken in every country.

Every year countries submit their INDC reports wherein they specify their commitments towards climate change initiatives, this year already 14 countries have committed to their INDC commitments.

3. The Overall Process:

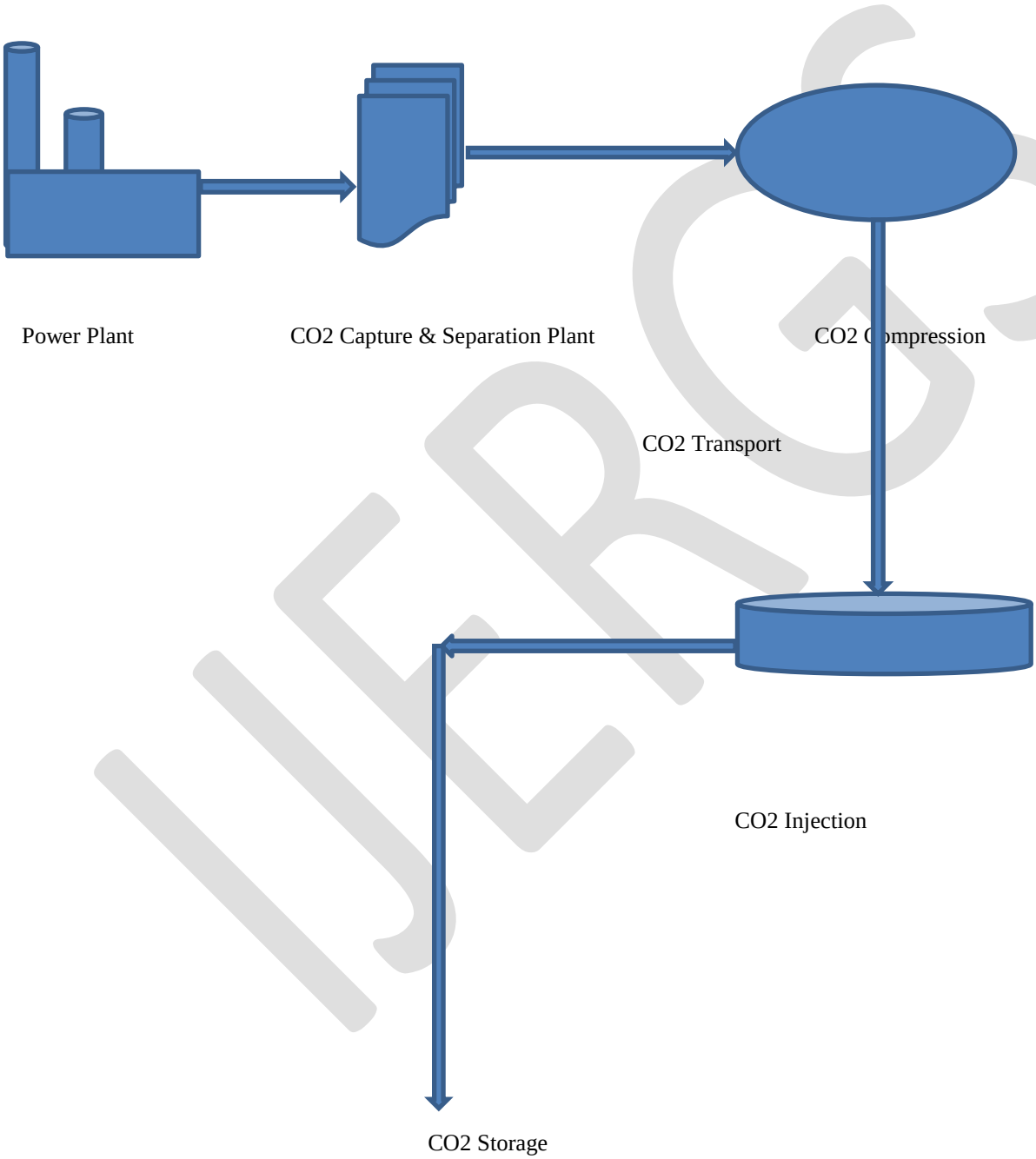

Figure: 2

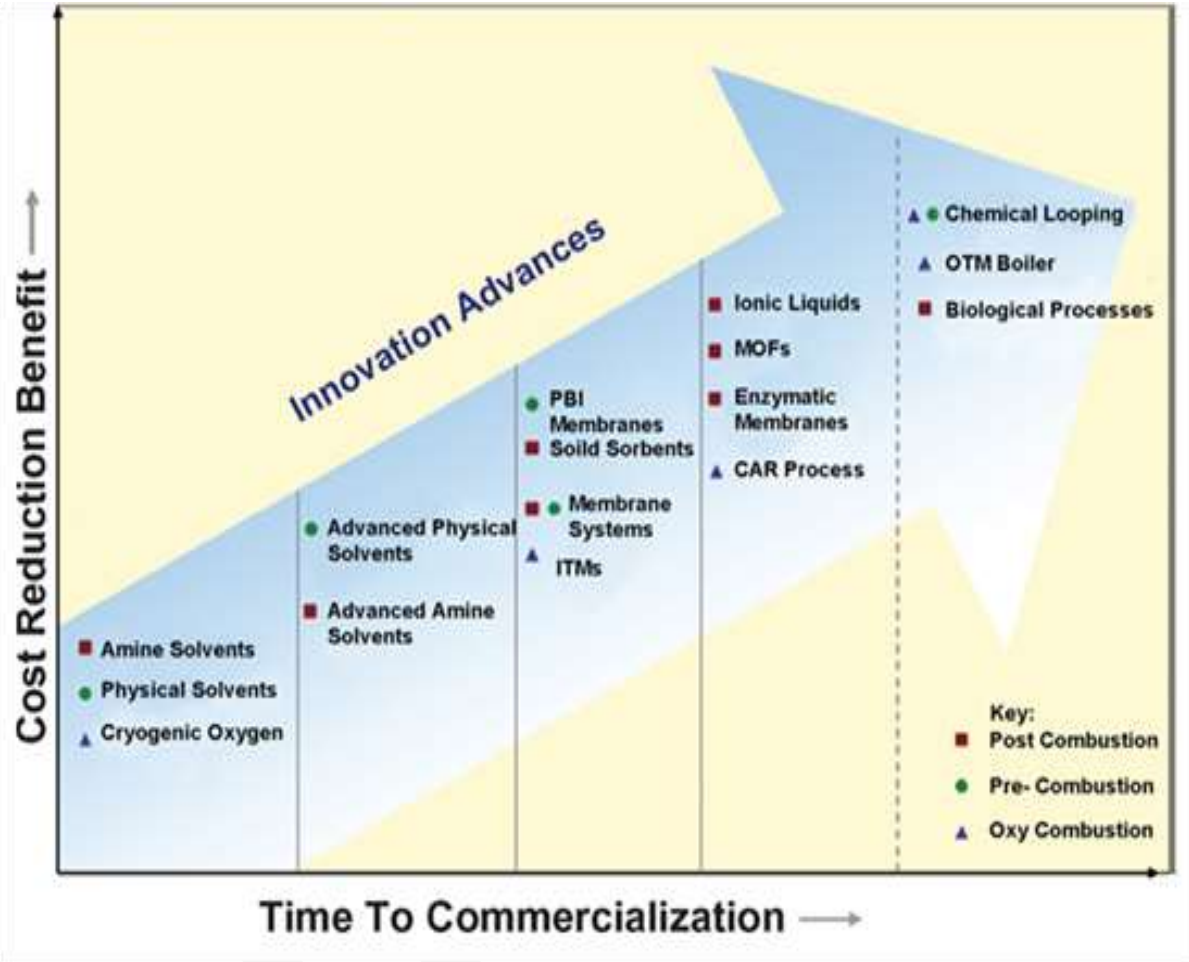

Figure: 3

4. Current Status Worldwide:

With the advent of carbon sequestration technology implementation widely in countries like US, Canada, United Kingdom, a large number of CCS projects are identified studying their feasibility. Few of the potential areas are japan, China, and Australia.

Globally, there are 13 large-scale Carbon Capture and Sequestration projects in operation, with a further nine under construction. The total CO_2 capture capacity of these 22 projects is around 40 million tons annually provision of 56 projects are identified.

Figure: 4

5. Challenges in the existing Booster Pumps for sequestration:

A booster pump is a machine that increase the pressure of a fluid, generally a liquid. It is very similar to a gas compressor, but generally a simpler mechanism which often has only a single stage of compression, which is used to increase pressure of an already pressurized gas. Multi stage boosters are also operational. Boosters may be used for increasing gas pressure, transferring high pressure gas, charging gas cylinders and scavenging

Booster pumps are equipped with limited production and flow ability. There are chances of aberrant flow into wells. Naturally booster pumps present onshore and topside are designed to work in a limited working region with specific differential pressure and flow rate. It is only possible to maintain it once in 2 or 3 years. Auxiliary equipment's like separators, compressor, flow lines maintaining is difficult and requires the process to go under stagnancy, one of the biggest limitations being its inability to handle both liquid and gas.

Hence the above cited limitations increases not only the technical complexity but also digs deep into the economic aspects of carrying out the operation as a whole.

6. Prescribed Alternative:

As a suggestive measure, an alternative can be the Implementation of twin screw multiphase pump.

Twin screw multiphase pump is a positive displacement pump. Positive-displacement pumps operate by forcing a fixed volume of fluid from the inlet pressure section of the pump into the discharge zone of the pump. These pumps generally tend to be larger than equal-capacity dynamic pumps. They provide a fixed displacement per revolution and, within mechanical limitations, infinite pressure to move fluids. Twin screw multiphase pump has the possibility to vary the pump speed between approximately 30 and 130 percent of the design speed

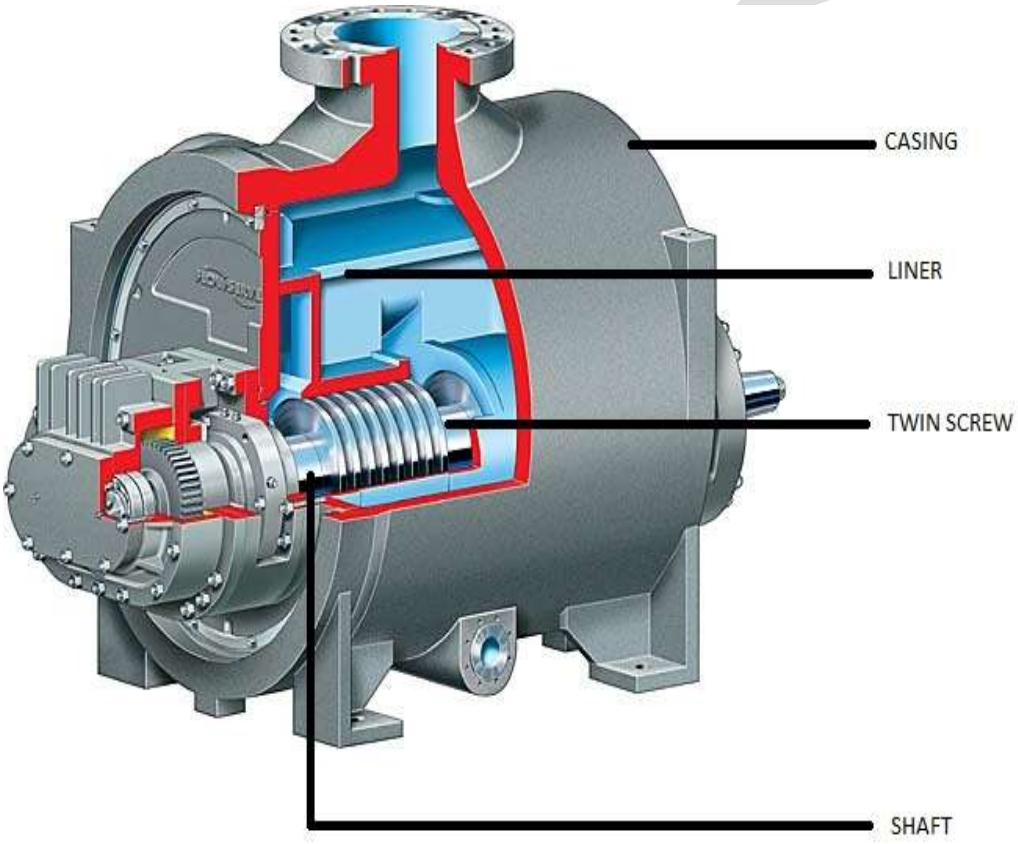

Figure: 5

7. Operating Parameters:

- Flows up to 2258 m3/h
- Pressure up to 1100 bar ; custom designs for higher pressures
- Temperatures to 450°C (842°F)
- Viscosities to 8000 Centipoise
- Gas volume fractions from 0% to 100%

8. Features:

- They can handle considerably high flow rates and pressures at a high gas volume fraction
- The selection of the wetted construction materials must follow the current NACE requirements, which it does.
- They can be found on well head platforms offshore, on onshore field far away from the production facilities or subsea.

9. Comparative Analysis:

TWIN SCREW MULTIPHASE PUMP	BOOSTER PUMP
Capacity : Flow rate ranging from 2000-2500 m^3/ hr	Capacity : Flow rate ranging from 300-1800m^3/ hr
Temperature : Hadalpelagic region is ranged -20 to 450 degree	Temperature : Hadalpelagic region is ranged -15 to 370 degree
Pressure : Up to 1100bar	Pressure : Up to 750 bar
Energy consumed : 44%	Energy consumed : 37%
Lesser Environmental Impact : Around 11%	Comparatively Higher Environmental Impact : 18%

Table: 2

Advantages of Twin Screw Multiphase pumping over Booster pump in sequestration process:

- Accelerates and increases the flow ability
- Stabilizes flow in wells that cannot naturally produce to remote facilities
- Extends subsea tieback distance
- Reduces well intervention cost
- Reduces subsea development cost
- Operates in an environment friendly way

- Permits flow in a harsh environment
- Eliminates offshore flaring and saves the relevant costs
- Reduces backpressure at wellhead

10. Conclusion:

It is extremely crucial to mitigate carbon emissions and hence technologies like carbon capture should be highly encouraged. Usage of Multiphase pumps in sequestration operations has the ability to show greater flexibility than existing booster pumps if incorporated. Climate change and environmental change are crying havoc owing to capricious changes in biosphere, hence needs stern measures of control.

REFERENCES:

1. World Bank
2. Sulzer , Flowserve , Fedco
3. Global CCS Institute
4. PBL Netherlands Environmental Assessment Agency
5. www.Carbonbrief.org
6. www.Spe.org
7. www.Sequestration.mit.edu
8. Center of Negative Carbon emissions- ASU
9. "Multiphase Pumping" – Hans Juergenschoener
10. National Association of Corrosion Engineers –NACE
11. NEERI
12. Leistritz
13. DS Goldberg, T Takahashi "Carbon Dioxide Sequestration in Deep Sea Basalt" , **PNAS**
14. DF Dal Porto , LA Larson " Multiphase Pump field trails " **, SPE**
15. ML Goulden, JW Munger "Measurement of carbon sequestration " **Global Change Biology**

International Journal of Engineering Research and General Science Volume 3, Issue 5, September-October, 2015
ISSN 2091-2730

Review on Mechanical Properties of Sisal and Banana Reinforced Composites

L Laxmana Naik[1, 2], K Gopalakrishna[2], B Yogesha[1]

[1] Department of Mechanical Engineering, Malnad College of Engineering, Hassan, Karnataka, India.

[2] Centre for Emerging Technologies, Jain University, Bangalore, Karnataka, India.

lln@mcehassan.ac.in and +919448438358

Abstract—This review article concerning about natural fibers like sisal and banana fiber reinforced polymers, it gives possible applications in the material group. This paper is a review of the chemical and mechanical properties of natural fibers like sisal and banana reinforced polymer composites. Natural fibers are rich in cellulose and they are cheap and easily renewable source of fibers with the potential for polymer reinforcement. Natural fibers are emerging as low cost, lightweight and apparently environmentally superior alternatives to glass fibers in composites. In most of the cases, the specific properties of the natural fiber composites were found to compare favorably with those of glass.

Keywords— Sisal, Banana, Polymers, Chemical properties Mechanical properties.

INTRODUCTION

Natural fibers are increasingly gaining attention as their application is diversified into engineering end uses such as building materials [1] and structural parts for motor vehicles where light weight is required. Low cost and less tool wear during processing are among the known advantages of plant fibers, and ease of recycling makes them environmentally friendly [2, 3]. The low density of natural fibers is very beneficial in the automotive industry. A study has been carried out which, shows that when 30% of glass fibers is substituted with 65% of hemp fibers, the net energy saving of 50,000 MJ (3 tons of emission) can be achieved [4]. Natural fiber offers many technical and ecological benefits for its use in reinforcing composites. Many types of natural fibers have been investigated for use in plastics including jute, straw, Flax, hemp, wood, sugarcane, bamboo, grass , kenaf, sisal, coir, rice husks, wheat, barley, oats, kapok, mulberry, banana fiber, raphia, pineapple leaf fiber and papyrus etc. and the matrix material used for reinforcing the fibers are classified as thermosets, thermoplastics and elastomers[5]. While, natural fibers traditionally have been used to fill and reinforce thermosets, natural fiber reinforced thermoplastics, especially polypropylene composites, has attracted greater attention due to their added advantage of recyclability. Natural fiber composites are also claimed to offer environmental advantages such as reduced dependence on non-renewable energy/material sources, lower pollutant emissions, lower greenhouse gas emissions, enhanced energy recovery, and end of life biodegradability of components [6]. In general, plant based fibers are lignocellulose in nature composed of cellulose, hemicellulose and lignin eg. Jute, coir, sisal, cotton etc., whereas animal based fibers are composed of proteins e.g. silk and wool [7, 8]. Natural fibers are low-cost fibers, highly available and renewable, with low density and high specific properties as well as they are biodegradable and less abrasive to expensive molds and mixing equipment. However, their potential use as reinforcement is greatly reduced because of their incompatibility with the hydrophobic polymer matrix, their poor resistance to moisture and their tendency to form aggregate during processing. The mechanical properties of natural fiber composites are much lower than those of the synthetic fiber composites. To produce the reactive hydroxyl groups and the rough surface for adhesion with polymeric materials, plant fibers need to undergo physical and/or chemical treatment to modify the surface and structure. Though the synthetic fibers have very good mechanical properties, their disadvantage is difficult recycling. Another advantage of synthetic fiber is their moisture repellency, whereas poor resistance to moisture absorption has made the use of natural fiber reinforced composites less attractive. In this paper, a review of the Physical and Mechanical Properties of natural fibers like sisal and banana reinforced polymer composites are carried out.

PROPERTIES OF SISAL/BANANA REINFORCED POLYMER COMPOSITES

Natural fibers are chemically treated to remove lignin, pectin, waxy substances, and natural oils covering the external surface of the fiber cell wall. This reveals the fibrils, and gives a rough surface topography to the fiber. Sodium hydroxide (NaOH) is the most commonly used chemical for bleaching and/or cleaning the surface of plant fibers. It also changes the fine structure of the native cellulose I to cellulose II by a process known as alkalization [9-12].

SISAL FIBER

Sisal fibers are extracted from Sisal plant by water retting process. The major portion of the fiber contains cellulose that is about 60% and some percentage of lignin. This plant grows enormously in the western hemisphere, Africa and Asia. The plant contains fleshy leaves usually long and narrow, which grow out from a central bud. Usually leaves are 1-2m long, 10-15cm wide and about 6mm thick at the center. The fibers are embedded longitudinally in the leaves and are most abundant near the leaf surfaces. Table 1 shows chemical properties of sisal fiber.

Table.1 Chemical properties of Sisal fibers [13-17].

Property	Value
Cellulose (%)	**66-78**
Hemi-cellulose (%)	**10-14**
Lignin (%)	**10-14**
Pectin (%)	**10**
Moisture content (%)	**10-22**
Microfibrillar angle	**11**
Lumen size (mm)	**5**

BANANA FIBER

Mature banana pseudo-stem was obtained from the farm, and was cut to a length of 50cm sliced longitudinally into four pieces and each was totally submerged in water for 15 days, after which the stems were removed from the water and were loosened by swishing back and forth in a pool of tap water. They were subsequently sun dried for eight hours and further loosened by manual combing. The extracted fibers were then treated with 5% sodium hydroxide (NaOH) solution for four (4) hours, under total immersion conditions to avoid oxidation of the fiber, after which it was washed in overflowing tap water until neutral pH is attained [16]. The treated fibers were then dried in an oven for 24 hours at 105oC to remove free water, and were subsequently cut into lengths of 5, 10, 15, 20 and 25mm and stored separately in an air tight container. The properties of the banana fiber used in this study are given in Table 2.

Table.2 Chemical properties of Bananafibers [13-17].

Property	Value
Cellulose (%)	**62 – 64**
Hemi-cellulose (%)	**19 [15]**
Lignin (%)	**5**
Pectin (%)	**3-5**
Moisture content (%)	**10 – 11.5**
Microfibrillar angle	**20**
Lumen size (mm)	**11**

MECHANICAL PROPERTIES OF SISAL AND BANANA REINFORCED POLYMER COMPOSITES

Natural fibers also have non-uniformity and variety of dimensions, even between individual plants in the same cultivation. To generate fibers suitable for specific end products, the various types of raw material are separated. Bast or stem fibers, for example, are mainly used in the textile or rope industries because of the length of the fibers. Bast straw is not separated into single fibers but into fiber bundles, which may contain thousands of single fibers. In contrast, wood is usually separated into single fibers or very small fiber

bundles suiting the particular needs of the pulp, paper or board industries. Thus, there are a great number of challenges for selecting fibers in different dimensions and properties. Natural polymer composites are more environmental friendly compared to polymer composites with synthetic fibers reinforced. Advantages of natural fibers ones plastic reinforcement are due to its low density, renewability, biodegradability, non-toxicity, good insulation property and machine wear. Natural fiber contains high hydroxyl content of cellulose that makes it susceptible to water absorption affecting the mechanical properties of materials. The mechanical properties of a composite depend on the nature of the resin, fiber, resin-fiber adhesion, cross-linking agents and not the least on the method of the processing. Therefore, any improvement in the property is evaluated and compared to that of the polymer matrix, undergoing the same process. The fibers are impregnated by the liquid resin usually at room temperature and then treated with some cross-linking agent for hardening. Usually with an increase in the fiber content in the composition, the tensile and flexural property gradually improves. Beyond certain limit of the fiber content, however, depending on the method of processing, the adhesion between the resin and the fiber decreases, resulting in the decrease in the strength of final products. Epoxy resin has excellent adhesion to a large number of materials and could be further strengthened with the addition of fiber. Table.3 shows Mechanical properties of Sisal and Banana fibers.

Table.3 Mechanical properties of Sisal and Banana fibers [18-21].

Fiber	**Sisal**	**Banana**
Density (g/cm3)	**1.41**	**1.35**
Elongation at break (%)	**6–7**	**5–6**
Tensile strength (MPa)	**350 ± 7**	**550 ± 6.7**
Youngs modulus (GPa)	**12.8**	**20**
Flexural strength (Mpa)	**29.28-62.50**	**57.33**
Flexural modulus	**1.29-3.16**	**8.9**
Impact strength (KJ/m2)	**8.36**	**13.25**

CONCLUSION

The use of Natural fiber as reinforcement of polymer based composites was reviewed from the viewpoints position and future expectations of natural bio-fibers, construction and properties of natural fibers, fiber surface modifications, and physical and mechanical characteristics of natural fiber based polymer composites. Natural fibers have well prospective as reinforcements in polymers (thermoplastics, thermosets and elastomers) composites. Due to the high specific properties and low density of natural fibers, composites based on these fibers may have very good implications in industry. Moreover, reduced abrasion and consequent reduction of re-tooling makes these composites one of the most effective alternatives. The natural fibers as a source of raw material in polymer industry not only provides a renewable resource, but can also produce a source of economic development for rural areas. From the above discussions, it is quite evident that newer composites using abundantly available natural fibers are on the horizon, this brings new trends in composite materials. Thus it can be concluded that with methodical and constant research there will be a good possibility and better expectations for natural fiber polymer composites in the future.

REFERENCES:

[1] White, N. M.; Ansell, M. P. J.M.Sci 1985, 18, 1549.
[2] Maguno, A. 2nd International wood and natural fiber composites symposium, Kassel, Germany, 29-1, June 28–29, 1999.
[3] Al-Qureshi, H. A.2nd International wood and natural fiber composites symposium, Kassel, Germany, 32-1, June 28–29, 1999.
[4] Faruk, Omar, Andrzej K. Bledzki, Hans-Peter Fink, and Mohini Sain. "Bio composites Reinforced with Natural Fibers: 2000–2010." Progress in Polymer Science (0). doi: 10.1016/j.progpolymsci.2012.04.003.
[5] Dr. Navdeep Malhotra, Khalid Sheikh and Dr. SonaRaniA "Review On Mechanical Characterization Ofnatural Fiber Reinforced Polymer Composites" Journal of Engineering Research and Studies E-ISSN0976-7916.
[6] Mohanty AK, Drazl LT, Misra M. Engineered natural fiber reinforced polypropylene composites: influence of surface modifications and novel powder impregnation processing. J AdhesSciTechnol 2002; 16(8):999–1015.
[7] Abu BakarHariharan , Abdul Khalil HPS (2005) Lignocellulose- based hybrid bilayer laminate composite: part 1–studies on tensile and impact behavior of oil palm fiber-glass fiber-reinforced epoxy resin. J Compos Mater 39(8):663–684.

[8] Panthapulakkal S, Sain M (2007) Injection-molded short hemp fiber/glass fiber-reinforced polypropylene hybrid composites-mechanical, water absorption and thermal properties. J ApplPolymSci 103:2432–2441.
[9] Shenouda, S. G. In Applied Fiber Science; Happey, F., Ed.; Academic Press: London, 1979, vol. 3, Chap. 7.
[10] Zeronian, S. H. In Cellulose Chemistry and Its Applications; Nevell, T. P.; Zeronian, S. H. Eds.; Ellis Horwood: Chichester, 1985, p. 159.
[11] Atkins, E. In Applied Fiber Science; Happey, F., Ed.; Academic Press: London, 1979, vol. 3, chap. 8.
[12] Nguyen, T.; Zavarin, E.; Barrall, E. M., II. J MacromolSci Rev MacromolChem 1981, C20.
[13] M. Sumaila, I. Amber, M. Bawa "Effect Of Fiber Length On The Physical And Mechanicalproperties Of Random Oreinted, Nonwoven Short Banana (Musa Balbisiana) Fiber /Epoxy Composite" ISSN.2186-2476, VOL.2,March 2013.
[14] SatishPujari, A. Ramakrishna and M. Suresh Kumar "Comparison of Jute and Banana Fiber Composites: A Review". International Journal of Current Engineering and Technology E-ISSN 2277 – 4106, P-ISSN 2347 – 5161.
[15] Venkateshwaran, N., Elayaperumal, A. &Sathiya, G. K. (2012). Prediction of tensileproperties of hybrid-natural fiber composites Composites: Part B, 43:793–796.
[16] Ajayi, J. O., Bello, K. A. & Yusuf, S. D. (2000). Influence of Retting media on thePhysical Properties of BastFibers, J. Chemical Society of Nigeria, 25: 112-5.
[17] Mukherjee KG, Satyanarayana KG. Structure and properties of some vegetable fibers. J Mater Sci 1984;19:3925–34.
[18] Maries Idicula , S.K. Malhotra , Kuruvilla Joseph , Sabu Thomas Dynamic mechanical analysis of randomly oriented intimately mixed short banana/sisal hybrid fiber reinforced polyester composites Composites Science and Technology 65 (2005) 1077–1087.
[19] Maleque M.A., Belal F.Y. and Sapuan S.M., Mechanical properties study of pseudo-stem banana fiber reinforced epoxy composite, Arab. J. Sc. Eng., 32(2B), 359-364 (2007).
[20] Leandro Jose da Silva, Tulio Hallak Panzera, Vania Regina Velloso, Andre Luis Christoforo, Fabrizio Scarpa (2012) Hybrid polymeric composites reinforced with sisal fibers and silica microparticles. Composites: Part B 43, pp.3436–3444.
[21] Olusegun David Samuel, Stephen Agbo, Timothy Adesoye Adekanye (2012) Assessing Mechanical Properties of Natural Fiber Reinforced Composites for Engineering Applications. Journal of Minerals and Materials Characterization and Engineering, 11, pp.780-784.
[22] Sanjay M R, Arpitha G R, B Yogesha, Study on Mechanical Properties of Natural - Glass Fibre Reinforced Polymer Hybrid Composites: A Review, Materials Today: Proceedings, Volume 2, Issues 4-5, 2015, pp: 2959-2967.

International Journal of Engineering Research and General Science Volume 3, Issue 5, September-October, 2015
ISSN 2091-2730

A COMPARATIVE STUDY OF DIFFERENT NOISE FILTERING TECHNIQUES IN DIGITAL IMAGES

Sanjib Das[1], Jonti Saikia[2], Soumita Das[3] and Nural Goni[4]

[1]Deptt. of IT & Mathematics,ICFAI University Nagaland, Dimapur, 797112, India, dassanjib1990@gmail.com

[2]Service Engineer, Indian export & import office, Shillong- 793003, Meghalaya, India, jontiroads14@gmail.com

[3]Department of IT, School of Technology, NEHU, Shillong-22, Meghalaya, India, wingsoffire72@gmail.com

[4]Department of IT, School of Technology, NEHU, Shillong-22, Meghalaya, India, nuralgoni@gmail.com

Abstract:

Although various solutions are available for de-noising them, a detail study of the research is required in order to design a filter which will fulfil the desire aspects along with handling most of the image filtering issues. In this paper we want to present some of the most commonly used noise filtering techniques namely: Median filter, Gaussian filter, Kuan filter, Morphological filter, Homomorphic Filter, Bilateral Filter and wavelet filter. Median filter is used for reducing the amount of intensity variation from one pixel to another pixel. Gaussian filter is a smoothing filter in the 2D convolution operation that is used to remove noise and blur from image. Kuan filtering technique transforms multiplicative noise model into additive noise model. Morphological filter is defined as increasing idempotent operators and their laws of composition are proved. Homomorphic Filter normalizes the brightness across an image and increases contrast. Bilateral Filter is a non-linear edge preserving and noise reducing smoothing filter for images. Wavelet transform can be applied to image de-noising and it has been extremely successful. Salt and pepper noise, Speckle noise and Gaussian noise are introduced to clean images and filtered using the filtering techniques mentioned above. The performance of the filtering techniques is evaluated based on signal to noise ratio. It is found that Wavelet based filter gives the best result amongst the chosen filtering techniques.

Keywords: Median Filter, Gaussian filter, Wiener Filter, Kuan filter, Wavelet transform, Bilateral filtering, Morphological Filtering, Homomorphic Filtering.

1. Introduction

1.1 Image processing:

Digital Image Processing is a component of digital signal processing .The area of digital image processing refers to dealing with digital images by means of a digital computer. Digital image processing is the process of enhancing samples of image which may or may not degraded by noise and other distortion.

There are some fundamental steps of image processing:

a. **Image Acquisition**: This is the first step or process of the fundamental steps of digital image processing. Image acquisition could be as simple as being given an image that is already in digital form. Generally, the image acquisition stage involves pre-processing, such as scaling etc.
b. **Image Enhancement**: Image enhancement is among the simplest and most appealing areas of digital image processing. Basically, the idea behind enhancement techniques is to bring out detail that is obscured, or simply to highlight certain features of interest in an image. Such as, changing brightness and contrast etc.
c. **Image Restoration**: Image restoration is an area that also deals with improving the appearance of an image. However, unlike enhancement, which is subjective, image restoration is objective, in the sense that restoration techniques tend to be based on mathematical or probabilistic models of image degradation.
d. **Morphological Processing**: Morphological processing deals with tools for extracting image components that are useful in the representation and description of shape.
e. **Segmentation**: Segmentation procedures partition an image into its constituent parts or objects.
f. **Object recognition**: Recognition is the process that assigns a label, such as, vehicle to an object based on its descriptors.
g. **Representation and Description**: Representation and description almost always follow the output of a segmentation stage, which usually is raw pixel data, constituting either the boundary of a region or all the points in the region itself. Choosing a representation is only part of the solution for transforming raw data into a form suitable for subsequent computer processing. Description deals with extracting attributes that result in some quantitative information of interest or are basic for differentiating one class of objects from another.
h. **Knowledge Base**: Knowledge may be as simple as detailing regions of an image where the information of interest is known to be located, thus limiting the search that has to be conducted in seeking that information.

1.2 Types of digital images:

a. **Binary**: In binary image the value of each pixel is either black or white. The image have only two possible values for each pixel either 0 or 1, we need one bit per pixel.
b. **Grayscale**: In grayscale image each pixel is shade of gray, which have value normally 0 [black] to 255 [white]. This means that each pixel in this image can be shown by eight bits that is exactly of one byte.
c. **True Color or RGB**: Each pixel in the RGB image has a particular color; that color in the image is described by the quantity of red, green and blue value in image. If each of the components has a range from 0255, this means that this gives a total of 2563 different possible colors values.

1.3 Noise in Images

Noise in image, is any degradation in an image signal, caused by external disturbance while an image is being sent from one place to another place via satellite, wireless and network cable.

Types of Image Noise:

a. **Salt and pepper noise**: It known as shot noise, impulse noise or Spike noise. Its appearance is randomly scattered white or black or both pixel over the image.
b. **Gaussian Noise**: Gaussian noise is caused by random fluctuations in the signal; it's modelled by random values added to an image. This noise has a probability density function [pdf] of the normal distribution. It is also known as Gaussian distribution.
c. **Speckle noise**: It can be modelled by random values multiplied by pixel values of an image.

2. Filtering Techniques

2.1 Median Filter:

2.1.1 Introduction:

Each imaging system suffers with a common problem of "Noise". Unwanted data which may reduce the contrast deteriorating the shape or size of objects in the image and blurring of edges or dilution of _ne details in the image may be term as noise [9].it may be due to one or more of the following reasons:

- Shortcomings of image acquisition devices
- Image developing mechanism
- Due to environment
- Physical nature of the system

Mathematically there are two basic models of Noise; additive and multiplicative. Additive noise is systematic in nature and can be easily modelled and hence removed or reduced easily [10]. Whereas multiplicative noise is image dependent, complex to model and hence difficult to reduce. When multiplicative noise caused by the de-phased echoes from the scattering appears, it is called Speckle Noise. Although it appears as noise but it contains useful information because it is due to surroundings of the target. Speckle may appear distinct in different imaging systems but it is always manifested in a granular pattern due to image formation under coherent waves.

2.1.2 Basic principle of median filter:

First we need to understand what a median filter is and what it does. In many different kinds of digital image processing, the basic operation is as follows:

At each pixel in a digital image we place a neighbourhood around that point, analyze the values of all the pixels in the neighbourhood according to some algorithm, and then replace the original pixel's value with one based on the analysis performed on the pixels in the neighbourhood [11]. The neighbourhood then moves successively over every pixel in the image, repeating the process.

The median filter is a sliding-window spatial filter. The median filter is normally used to reduce noise in an image, somewhat like the mean filter. However, it often does a better job than the mean filter of preserving useful detail in the image. This class of filter belongs to the class of edge preserving smoothing filters which are non-linear filters. This means that for two images A(x) and B(x)

$$median[A(X) + B(X)]\ 6 = median[A(X)] + median[B(X)] \quad (2.1)$$

These filters smooth the data while keeping the small and sharp details.

The median is just the middle value of all the values of the pixels in the neighbourhood. Note that this is not the same as the average (or mean); instead, the median has half the values in the neighbourhood larger and half smaller. The median is a stronger "central indicator" than the average. In particular, the median is hardly affected by a small number of discrepant values among the pixels in the neighbourhood. Consequently, median filtering is very effective at removing various kinds of noise. But it is special for "Salt and pepper noise" [12].

Like the mean filter, the median filter considers each pixel in the image in turn and looks at its nearby neighbours to decide whether or not it is representative of its surroundings. Instead of simply replacing the pixel value

with the mean of neighbouring pixel values, it replaces it with the median of those values. The median is calculated by first sorting all the pixel values from the surrounding neighbourhood into numerical order and then replacing the pixel being considered with the middle pixel value. (If the neighbourhood under consideration contains an even number of pixels, the average of the two middle pixel values is used). A template of size 3x3, 5x5, 7x7, etc is applies to each pixel. The values within this template are sorted and the middle of the sorted list is used to replace the templates central pixel. Figure 2.1illustrates an example of median filtering.

2.1.3 Advantages of Median filter:

- No need to generate new pixel value.
- Easy to implement.
- Since the median is less sensitive than the mean to extreme values (outliers), those extreme values are more effectively removed.

2.1.4 Disadvantages of median filter:

- Median filter is not good for all types of noise, it is very good only for removing salt and Pepper noise.

2.2 Gaussian filter:

Gaussian filtering is used to blur images and remove noise and detail. In one dimension, the Gaussian function is:

$$G(x) = \frac{1}{\sqrt{2\pi\sigma^2}} e^{\frac{-x^2}{2\sigma^2}} \quad (2.2)$$

Where σ is the standard deviation of the distribution The distribution is assumed to have a mean of 0.The Standard deviation of the Gaussian function plays an important role in its behaviour. The values located between +/- σ account for 68 % of the set, while two standard deviations from the mean account for 95 % and three standard deviations account for 99.7 %. This is very important when designing a Gaussian kernel of fixed length [8].

In probabilistic terms, it describes 100% of the possible values of any given space when varying from negative to positive values Gauss function is never equal to zero. It is a symmetric function.

2.2.1 Application of Gaussian filter:

- It defines a probability distribution for noise or data.
- It is used in mathematics.
- It is a smoothing operator.

2.2.2 Algorithm of Gaussian Filter:

- The filter can be understood as taking a pixel as the average value of its surrounding pixels. From value perspective, it's a smoothing. On graphic, it's a blur effect. The centre point will lose its detail. If the value range is very large, the blur effect is very strong.
- Normal distribution is an acceptable weight distribution model. On graphic, normal distribution is a Bell-shaped curve, the closer to the centre, the bigger the value.
- The normal distribution above is one dimensional, the graph is two dimensional. We need two dimensional normal distribution. The density function of normal distribution is called Gaussian function.
- To calculate the weight matrix, we need to set the value of σ
- With weight matrix, we can calculate the value of Gaussian Blur.
- If a point is at the border, there are not enough points, we need to copy all the existing points to respective places to form a new matrix [7].

2.2.3 Advantages of Gaussian filter

- Gaussian smoothing is very effective for removing Gaussian noise
- The weights give higher significance to pixels near the edge.
- Computationally efficient.
- Rotationally symmetric.

2.2.4 Disadvantages of Gaussian filter

- It takes much time.
- It reduces details.

2.3 Wiener Filter:

The Wiener filter purpose is to reduce the amount of noise present in a signal by comparison with an estimation of the desired noiseless signal. It is based on a statistical approach [2].

Typical filters are designed for a desired frequency response. The Wiener filter approaches filtering from a different angle. One is assumed to have knowledge of the spectral properties of the original signal and the noise, and one seeks the LTI filter whose output would come as close to the original signal as possible. Wiener filters are characterized by the following:

- Assumption: signal and (additive) noise are stationary linear stochastic processes with known spectral characteristics or known auto-correlation and cross-correlation.
- Requirement: the filter must be physically realizable, i.e. causal (this requirement can be dropped, resulting in a non-causal solution).
- Performance criteria: minimum mean-square error.

A useful approach to this filter-optimization problem is to minimize the mean-square value of the error signal that is defined as the difference between some desired response and the actual filter output. For stationary inputs, reduce the amount of noise present in a signal by comparison with an estimation of the desired noiseless signal [1].

The final details of the filter specification, however, depend on two other choices that have to be made:

- Whether the impulse response of the filter has finite or infinite duration.
- The type of statistical criterion used for the optimization.

1.3.1 Applications of Wiener Filter:

Wiener filters play a central role in a wide range of applications such as linear prediction, echo cancellation, signal restoration, channel equalization and system identification [1].

1.3.2 Steepest descent search algorithm for finding the Wiener FIR optimal filter:

Given the autocorrelation matrix

$$\mathbf{R = E[x\,(n)\,xt\,(n)]} \qquad \textbf{(2.3)}$$

The cross-correlation vector

$$\mathbf{p(n) = Eu(n)d(n)} \qquad \textbf{(2.4)}$$

Initialize the algorithm with an arbitrary parameter vector w(0). Iterate for
n = 0, 1, 2, 3. . . . . n_{max}

$$\mathbf{w(n + 1) = w(n) + \mu[P — Rw(n)]} \qquad \textbf{(2.5)}$$

Stop iterations if

$$\mathbf{— P – Rw\,(n) — !\varepsilon}$$

1.3.3 Advantage of Wiener filter:

- Here we can use a large window to smooth the speckle noise.
- We can use a small window to avoid blurring edges such as field boundaries.

1.3.4 Disadvantage of Wiener Filter:

- It is difficult to estimate the power spectra.
- It is very difficult to obtain a perfect restoration for the random nature of the noise.
- Wiener filters are comparatively slow to apply since they require working in the frequency domain.

1.4 Kuan Filtering:

Speckle is the result of the diffuse scattering, which occurs when a sound wave (RF sound or Ultrasound) pulse randomly interferes with the small particles or objects on a scale comparable to the sound wavelength. Speckle is an inherent property of SAR and Ultrasound images, and is modelled as spatial correlated multiplicative noise. In most cases, it is considered a contaminating factor that severely degrades image quality. Medical imaging like Ultrasound is very popular due to its low cost, least harmful to human body, real time view and small size. But this imaging has major disadvantage of having Speckle [13].Synthetic Aperture Radar (SAR) is an active sensor that uses microwave signals for transmission and it detects the wave that is reflected back by the objects. SAR is widely used for obtaining high resolution images of the earth. It is used in the fields of remote sensing, oceanography, geology, ecology etc. Pixels in the image represent the back scattered radiation from an area in the imaged scene. Brighter areas are produced by stronger radar responses and darker areas are from weaker radar responses. Consider an original image Y corrupted by the Multiplicative noise. The resultant distorted image X, may be written as:

$$\mathbf{X(i, j) = h(i, j) \_ Y\,(i, j);} \qquad \textbf{(2.6)}$$

Where Y (i, j) is Original image, h(i, j) is noise and X(i, j) is resultant noisy image.

1.4.1 Basic principle of Kuan filter:

Kuan Filtering technique transforms multiplicative noise model into additive noise model. Let us denote L the filter window cantered at pixel coordinates (x,y), CL the centre pixel in L, and W a weighting function. The gray level of the Kuan filtered pixel f at position (x,y) is given by:

$$\mathbf{f(x; y) = \mu_L + W(CL — \mu_L)} \qquad \textbf{(2.7)}$$

Where μ_L is the local mean within the filter window L. The weighting function in a Kuan filter is defined as [14].

$$W = \frac{1 - \frac{c_u^2}{c_i^2}}{1 + c_u^2}; \quad (2.8)$$

Where $C_i = \frac{\sigma_L}{\mu_L}$, σ_L the standard deviation in L, and $Cu = \frac{1}{\sqrt{NLOOK}}$

The NLOOK parameter effectively controls the amount of smoothing applied to the image by varying the noise variation coefficient Cu. Theoretically, the value of NLOOK should be the Effective Number of Looks (ENL) of the image. It should be close to the actual number of looks of the noisy image, but may be different if the image has undergone re sampling. A smaller NLOOK value leads to more smoothing and a larger NLOOK value preserves more image features (e.g. edges). The user may experimentally adjust the NLOOK value so as to control the effect of the filter [15]. The ENL can be estimated from a uniform image region A by:

$$ENL = \left(\frac{\mu_A}{\sigma_A}\right)^2 \quad (2.9)$$

Where μ_A and σ_A are the mean and standard deviation of A, respectively.

1.4.2 Advantages of Kuan filter:

- It does not make an approximation on the noise variance within the filter window.
- Kuan filter simply models the multiplicative model of speckle into an additive linear form.

1.4.3 Disadvantage of Kuan filter:

- It relies on the Effective Number of Looks (ENL) from a SAR image to determine a different weighting function W.

1.5 Wavelet transform for de-noising:

The application of the wavelet transform to image de-noising has been extremely successful. Nowadays, it has been used in image processing, data compression, and signal processing. Here we will discuss how thresholding is applied to de-noise an image in wavelet domain. In conventional Fourier transform, we use sinusoids for basic functions. It can only provide the frequency information. Temporal information is lost in this transformation process. In some applications, we need to know the frequency and temporal information at the same time, such as a musical score, we want to know not only the notes (frequencies) we want to play but also when to play them. Unlike conventional Fourier transform, wavelet transforms are based on small waves, called wavelets. It can be shown that we can both have frequency and temporal information by this kind of transform using wavelets. Moreover, images are basically matrices. For this reason, image processing can be regarded as matrix processing. Due to the fact that human vision is much more sensitive to small variations in color or brightness, that is, human vision is more sensitive to low frequency signals. Therefore, high frequency components in images can be compressed without distortion. Wavelet transform is one of a best tool for us to determine where the low frequency area and high frequency area is .When we look at some images, generally we see many regions (objects) that are formed by similar texture. If the objects are small in size, we normally examine them at high resolutions. Contrary we examine big objects at low resolutions. This is the fundamental motivation for multi-resolution processing [19].

We can create a multi resolution pyramid of images at each level, we just store the differences (residuals) between the image at that level and the predicted image from the next level we can reconstruct the image by just adding up all the residuals.

1.5.1 Wavelet transform:

Wavelets are families of functions $\psi_{s,t}(x)$ generated from a single base wavelet $\psi(x)$ by dilations and translations

$$\psi_{s,t}(x) = \frac{1}{\sqrt{s}}\psi\left(\frac{x-t}{s}\right) \qquad s \neq 0 \quad (....1) \quad (2.10)$$

Where s is the dilation (scale) parameter and t is the translation parameter. Wavelets must have mean zero, and the useful ones have localized support in both spatial and Fourier domains. There are orthogonal and non-orthogonal wavelet sets that span $L^2(R)$.It is very close to the derivative of a Gaussian function. The set of $\psi_{m,n}(x)$ spans $L^2(R)$ when $s = 2^n$; t = n.

$$\psi_{m,n}(x) = 2^{\frac{-m}{2}}\psi(2^{-m}(x - n)) \quad (....2) \quad (2.11)$$

Where m is the scale index (m = 0,1,2,. . .), and n is the translation (spatial) index (n = . . . , -2, -1,0, 1,2,. . .). The discrete wavelet transform W(m, n) of a 1-D function f(x) is defined as the projection of the function onto the wavelet set $\psi_{m,n}(x)$.

$$W(m, n) = \int_{-\infty}^{\infty} f(x)\psi_{m,n}(x)dx \quad (....3) \quad (2.12)$$

Since the set of $\psi_{m,n}(x)$ spans the space containing *f(x)*, the reconstruction of function *f(x)* from its wavelet transform *W(m, n)* is possible. The wavelet coefficients measure how closely correlated the wavelet is with each section of the signal [1].

$$F(x) = \sum_m \sum_n \psi'_{m,n}(x)W(m, n) \quad (....4) \quad (2.13)$$

Where $\psi'_{m,n}(x)$ is the normalized dual basis of $\psi_{m,n}(x)$ for the wavelet expansion we use here $\psi' \approx \psi$. The wavelet transform ***W(m, n)*** gives a scale-space decomposition of signals and, with simple modifications, images. It decomposes the signal into different resolution scales, with m indexing the scale and n indexing position in the

original signal space. In practice, we are concerned with a finite length, discrete (sampled), 1-D data set *f(k); k = 1, 2, ...N* and we need appropriate discrete and finite versions of the calculations involved in the wavelet decomposition [9]. In particular, there is a fixed limit to the resolution and, therefore, a lower bound on the scale index m, which we may take as m = 1 without loss of generality. It is useful to model this resolution limit by representing the data *f(k)* as samples of a smoothed, or low-passed, version of a continuous signal.

$$\boldsymbol{f(k) = \int_{-\infty}^{\infty} f(x)\emptyset'(x-k)} \qquad \textbf{(....5) (2.14)}$$

With respect to a smoothing or scaling function a. Based on this representation of the data, one may compute the wavelet coefficients in (3) by means of a purely discrete algorithm, as detailed in [9]. Beyond these considerations, there is also an effective upper limit on the scale m imposed by the finite length of the signal. Consequently, the non-orthogonal, discrete, dyadic wavelet coefficients *W(m, n)* are computed on a 2-D space of m = 1, 2, ..., M-1 and n = 1, 2, ..., N where M = $\log_2 N$ with the remaining information contained in the coarse scale averages

$$\boldsymbol{S(M,n) = 2^{-M}\int_{-\infty}^{\infty} f(x)\emptyset\left(2^{-M}(x-n)\right)dx} \qquad \textbf{(2.15)}$$

This information determines the signal *f(x):*

$$\boldsymbol{f(x) = \sum_{m=1}^{M-1}\sum_{n=1}^{N} \Psi'_{m,n}(x)W(m,n) + \sum_{n=1}^{N}\emptyset\left(2^{-M}(x-n)\right)S(M,n)} \qquad \textbf{(....6) (2.16)}$$

The M.N coefficients obviously form an over complete representation of the signal. For a data set of N = 256 points, M is equal to 8, i.e., there are eight wavelet scales. At each scale, there are 256 data points corresponding to the signal detail projected at that scale [16].

1.5.2 Wavelet based image compression by decomposition:

- The wavelet transforms decomposes an image into a set of different resolution sub images corresponding to the various frequency bands.
- The analysis filter consists of high pass filter and low pass filter.
- The low pass filter (average operation) extracts the coarse information.
- While High pass filter (differencing operation) extracts detail information [21].

1.5.3 The noise reduction based on wavelet analysis:

One of the important applications of wavelet analysis is for noise reduction. Wavelet transform provides a powerful tool for the solution to this problem, with its good time-frequency localized character [18]. At present, the basic methods of wavelet noise reduction are:

- Using wavelet transform modulus maxima: according to signal and noise on different scales of modulus maxima of different propagation characteristics, select signal modulus maxima in all wavelet transform modulus maxima, remove the modulus maxima of the noise, then reconstruct signal with the remaining wavelet transform modulus maxima. This method can retain the singular point information of signal effectively while reducing the noise.
- Based on the correlation of wavelet coefficients of each scale: there is correlation among the wavelet coefficients of each scale, and the correlations between the signal and the noise of each scale is different. The correlation of the signal wavelet transform of each scale is obvious, while that of the noise wavelet transform is not obvious. Retain the wavelet transform coefficient in the large scale and high correlation coefficient in the small scale, leave the weak correlation coefficient, and then reconstruct the signal. This method can acquire the steady noise reduction effect.
- Using the nonlinear wavelet transform threshold method: it is generally thought that after the wavelet transform, the relatively large amplitude wavelet coefficients is mainly the signal, while the relatively small amplitude wavelet coefficients is mainly the noise. Noise reduction with threshold is to decompose noisy signal, retain the wavelet coefficients greater than the proper threshold set in advance and adjust the wavelet coefficients less than the proper threshold to zero. Finally, reconstruct the signal with the treated wavelet coefficients. This method can restrain the white noise of the signal completely [22].

1.5.4 Wavelet Threshold Decreasing noise method:

The model of a one-dimensional noisy signal can be noted down as Eq. (3).

$$\boldsymbol{s(t) = f(t) + \sigma e(t)} \qquad \textbf{(....7) (2.17)}$$

Where *f(t)* is the useful signal, *e(t)*noise, *σ*-noise level and *s(t)*the signal under consideration. In most cases it suggested that the function *e(t)* is described by the white (Gaussian) noise model, which meets the condition *N(0,1*) and the noise level for one. In actual project, information about the noise is contained in the high frequency spectral region of the signal, while the useful information is contained in the low frequency one or some of the stable one. Therefore, the signal noise reduction process can be handled as follows: first make the signal wavelet decomposition, such as carrying out three-tier decomposition and the process of decomposition. Noise is usually part of the cd1, cd2, cd3. We can treat the wavelet coefficients with the threshold, and then reconstruct the signal to meet the purpose of the noise reduction. Because the threshold method can get the approximate optimal estimation of original signal, calculate speedily and adapt widely, it is one of the most widely used wavelet decreasing-noise method. Threshold decreasing-noise method is applied mainly to the signal mixed with white noise; using threshold decreasing-noise method has the advantage of almost completely restraining the noise and well as reserving the peak point reecting the characteristics of the original signal. Soft threshold decreasing-noise method can even make the decreasing- noise signal the

approximate optimal estimation of original signal and the estimated signal and the original signal are at least the same smooth without additional oscillation [17].

Generally, the wavelet threshold decreasing noise method of signal can be divided into the following three steps:

- Wavelet decomposition of signal. Choose a wavelet and determine the level N of wavelet decomposition, then according to the corresponding wavelet, from the noisy signal, obtain the high frequency coefficients decomposed in each order.
- Threshold quantification of the high frequency coefficients of wavelet decomposition. Quantify the threshold of the high frequency coefficients in the corresponding order after 1- N order scale decomposition, to get a new high frequency coefficient of wavelet.
- Wavelet reconstruction. According to the N-order low-frequency coefficients got from wavelet decomposition and the high-frequency 1 – N order coefficients after threshold processing, synthesis and reconstruct the signal with wavelet to get the noised signal.

In these three steps, the key is how to choose the threshold and how to quantify the threshold, to a certain degree, it relates to the quality of the noise reduction of signal.

At present, there are a variety of threshold selection methods: VisuShrink, RiskShrink, Sure- Shrink, WaveJSShrink and so on. One of the most common method is VisuShrink, which introduces the overall unified threshold $\lambda=\sigma\sqrt{2logN}$, where σ is the standard deviation of the noise signal, N is the signal length.

Choose a threshold to quantify the each high frequency coefficient of wavelet decomposition. Make *cd(j)* as the original high-frequency coefficient of decomposition scale, and as the threshold quantified high-frequency coefficient. During the threshold quantification of wavelet decomposition in the high frequency coefficients, threshold function embodies the different treatment strategies and quantitative methods to the high-frequency coefficients module exceeded or below the threshold [20].

Define:

$$\boldsymbol{cd(j)} = \begin{cases} \boldsymbol{cd(j)}, & |\boldsymbol{cd(j)}| \geq \boldsymbol{\lambda(j)} \\ \boldsymbol{0}, & |\boldsymbol{cd}\,(\boldsymbol{j})| \leq \ | \leq \boldsymbol{\lambda(j)} \end{cases} \qquad \textbf{(....8)} \quad \textbf{(2.18)}$$

as hard threshold quantification method;

Define:

$$\boldsymbol{cd(j)} = \begin{cases} \boldsymbol{sign}\big(\boldsymbol{cd(j)}\big), & (|\boldsymbol{cd(j)}| - \boldsymbol{\lambda(j)}), \ |\boldsymbol{cd(j)}| \geq \boldsymbol{\lambda(j)} \\ \boldsymbol{0}, & |\boldsymbol{cd}\,(\boldsymbol{j})| \leq \ | \leq \boldsymbol{\lambda(j)} \end{cases} \qquad \textbf{(....9)} \quad \textbf{(2.19)}$$

as soft threshold quantification method.

1.5.5 Main algorithm for Wavelet Threshold Noise Reduction:

There are generally three approaches to threshold with the wavelet analysis:

- The default threshold decreasing-noise. This method uses function dencmp to generate the default threshold of signal, then use function wdencmp for the noise reduction.
- Given threshold decreasing-noise. In actual decreasing-noise process, the threshold can be usually obtained through experience formula, and the credibility of such threshold is higher than that of the default threshold. Function wthresh is available when conducting threshold quantification processing.
- Mandatory decreasing-noise. Adjust all of the high-frequency coefficients of the wavelet decomposition to zero, which means removing all of the high-frequency part, and then reconstruct the signal with wavelet. This method is relatively simple and decreasing-noise signal is smooth, but it easily loses the useful components of the signal.

1.5.6 Comparison of hard and soft thresholding:

- It is known that soft thresholding provides smoother results in comparison with the hard thresholding.
- More visually pleasant images, because it is continuous.
- Hard threshold, however, provides better edge preservation in comparison with the soft one.
- Sometimes it might be good to apply the soft threshold to few detail levels, and the hard to the rest.

1.6 Bilateral filtering:

The idea underlying bilateral filtering is to do in the range of an image what traditional filters do in its domain. Two pixels can be close to one another, that is, occupy nearby spatial location, or they can be similar to one another, that is, have nearby values, possibly in a perceptually meaningful fashion. Closeness refers to vicinity in the domain, similarity to vicinity in the range. Traditional filtering is domain filtering, and enforces closeness by weighing pixel values with coefficients that fall of with distance. Similarly, we define range filtering, which averages image values with weights that decay with dissimilarity. Range filters are nonlinear because their weights depend on image intensity or colour. Computationally, they are no more complex than standard non-separable filters. Most importantly, they preserve edges.

Spatial locality is still an essential notion [24]. In fact, we show that range filtering by itself merely distorts an image's colour map. We then combine range and domain filtering, and show that the combination is much more interesting. We denote the combined filtering as bilateral filtering. Since bilateral filters assume an explicit notion of distance in the domain and in the range of the image function, they can be applied to any function for which these two distances can be defined. In particular, bilateral filters can be applied to colour images just as easily as they are applied to black-and-white ones.

1.6.1 Image Smoothing with Gaussian Convolution:

Blurring is perhaps the simplest way to smooth an image; each output image pixel value is a weighted sum of its neighbours in the input image. The core component is the convolution by a kernel which is the basic operation in linear shift-invariant image filtering. At each output pixel position it estimates the local average of intensities, and corresponds to low-pass filtering. An image filtered by Gaussian Convolution is given by:

$$\boldsymbol{GC}[\boldsymbol{I}]_{\boldsymbol{p}} = \sum_{\boldsymbol{q}\in\boldsymbol{s}} \boldsymbol{G}_{\boldsymbol{\sigma}}(\|\boldsymbol{p}-\boldsymbol{q}\|)\boldsymbol{I}_{\boldsymbol{q}} \quad \textbf{(1)} \quad \textbf{(2.20)}$$

Where G_σ denotes the 2D Gaussian kernel.

$$\boldsymbol{G}_{\boldsymbol{\sigma}}(\boldsymbol{x}) = \frac{\boldsymbol{1}}{\boldsymbol{2\pi\sigma^2}}\boldsymbol{exp}(\frac{\boldsymbol{-x^2}}{\boldsymbol{2\sigma^2}}) \quad \textbf{(2)} \quad \textbf{(2.21)}$$

Gaussian filtering is a weighted average of the intensity of the adjacent positions with a weight decreasing with the spatial distance to the centre position p. The weight for pixel q is defined by the Gaussian $G_\sigma(\| p-q\|)$, where σ is a parameter defining the neighbourhood size. The strength of this influence depends only on the spatial distance between the pixels and not their values. For instance, a bright pixel has a strong influence over an adjacent dark pixel although these two pixel values are quite different. As a result, image edges are blurred because pixels across discontinuities are averaged together.

1.6.2 Edge-preserving Filtering with the Bilateral Filter:

The bilateral filter is also defined as a weighted average of nearby pixels, in a manner very similar to Gaussian convolution. The difference is that the bilateral filter takes into account the difference in value with the neighbours to preserve edges while smoothing. The key idea of the bilateral filter is that for a pixel to influence another pixel, it should not only occupy a nearby location but also have a similar value. The bilateral filter, denoted by *BF [ ]*, is

$$\boldsymbol{BF}[\boldsymbol{I}]_{\boldsymbol{p}} = \frac{\boldsymbol{1}}{\boldsymbol{W_p}}\sum_{\boldsymbol{q}\in\boldsymbol{s}} \boldsymbol{G}_{\boldsymbol{\sigma_s}}(\|\boldsymbol{p}-\boldsymbol{q}\|)\boldsymbol{G}_{\boldsymbol{\sigma_s}}(\mid \boldsymbol{I_p}-\boldsymbol{I_q}\mid)\boldsymbol{I_q} \quad \textbf{(3)} \quad \textbf{(2.22)}$$

Where normalization factor W_p ensures pixel weights sum to 1.0:

$$\boldsymbol{W_p} = \sum_{\boldsymbol{q}\in\boldsymbol{s}} \boldsymbol{G}_{\boldsymbol{\sigma_s}}(\|\boldsymbol{p}-\boldsymbol{q}\|)\boldsymbol{G}_{\boldsymbol{\sigma_s}}(\mid \boldsymbol{I_p}-\boldsymbol{I_q}\mid) \quad \textbf{(4)} \quad \textbf{(2.23)}$$

Parameters σ_s and σ_r will specify the amount of filtering for the image I. Equation (3) is a normalized weighted average where $\boldsymbol{G}_{\boldsymbol{\sigma_s}}$ is a spatial Gaussian weighting that decreases the influence of distant pixels, σ_r is a range Gaussian that decreases the influence of pixels q when their intensity values differ from I_p.

1.6.3 Parameters:

The bilateral filter is controlled by two parameters: σ_s and σ_r .

- As the range parameter σ_r increases, the bilateral filter gradually approximates Gaussian convolution more closely because the range Gaussian $\boldsymbol{G}_{\boldsymbol{\sigma_s}}$ widens and flattens, i.e., is nearly constant over the intensity interval of the image.
- Increasing the spatial parameter σ_s smooth's larger features.

An important characteristic of bilateral filtering is that the weights are multiplied: if either of the weights is close to zero, no smoothing.

Iterations: The bilateral filter can be iterated. This leads to results that are almost piece-wise constant. Although this yields smoother images, the effect is different from increasing the spatial and range parameters. Increasing the spatial parameters σ_s has a limited effect unless the range parameter σ_r is also increased. Although a large σ_r also produces smooth outputs, it tends to blur the edges whereas iterating preserves the strong edges.

Separation: The bilateral filter can split an image into two parts: the filtered image and its 'residual' image. The filtered image holds only the large-scale features, as the bilateral filter smoothed away local variations without affecting strong edges. The residual image, made by subtracting the filtered image from the original, holds only the image portions that the filter removed. Depending on the settings and the application, this removed small-scale component can be interpreted as noise or texture [22].

1.7 Morphological Filtering:

1.7.1 Mathematical Morphology:

Mathematical morphology mostly deals with the mathematical theory of describing shapes using sets. In image processing, mathematical morphology is used to investigate the interaction between an image and a certain chosen structuring element using the basic operations of erosion and dilation. Mathematical morphology stands somewhat

apart from traditional linear image processing, since the basic operations of morphology are non-linear in nature, and thus make use of a totally different type of algebra than the linear algebra [27].

1.7.2 Morphology and Sets:

Morphology is formulated in terms of set theory. Sets represent objects in image. Morphological processing is constructed with operations on sets of pixels. Basically it is constructed for binary images. The set of all white pixels in a binary image is a complete morphological description of an image [5]. In binary images, the sets are members of the 2D integer space Z2, where each element of a set is a tuple (2D vector) whose coordinates are the (x,y) coordinates of a white (or black) pixel in the image. The same can be extended for grey-scale images. Gray-scale images can be represented as sets, whose components are in Z3: two components are coordinates of a pixel and the third its discrete intensity value.

Morphological operations for binary images provide a basic techniques and those operations for gray scale images requires more sophisticated mathematical concepts for extracting image components that are useful in the representation and description of region shape, such as boundaries, skeletons, etc [28].

1.7.3 Structuring Elements:

The structuring elements are small set of sub images used to probe an analyzed image for properties of interest. The structuring element has both a shape and an origin.

Depending on shape, structuring element can take additional parameters. There are two types of structuring element, i) Flat Structuring Element, ii) Non-at Structuring Element. Basically, Flat structuring element are used for two dimensional image and Non at structuring element for three-dimensional object, the parameter added for Non-at i.e. height. The structuring element like: Disk, Diamond, Arbitrary shape, Pair, Periodic line, Rectangle, Line, Disk and Octagon are belongs to at structuring element, whereas Arbitrary and Ball are the non-at Structuring element [29].

1.7.4 Morphological processing operations:

More formal descriptions and examples of how basic morphological operations works are given below:

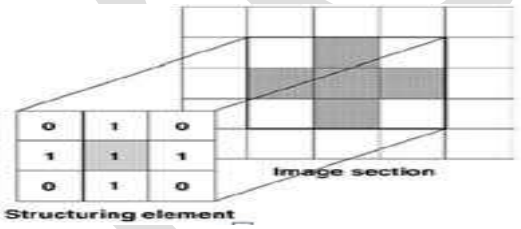

Figure: Example of a structuring element

1.7.5 Erosion and dilation:

Dilation grows or enlarges objects in a binary image. The manner and extend of this growth image is controlled by the structuring element.

$$\boldsymbol{X \oplus B = \{P \in Z^2 \mid P = x + b, x \in X, b \in B\}} \quad \textbf{(2.24)}$$

This equation is based on reflecting B about its origin and shifting this reflection by z. The dilation of X by B then is the set of all displacements z, such that and X overlap by at least one element.

However, the preceding equations are more intuitive when viewing the structural element as a convolution mask. Dilation is based on set operations and therefore is a nonlinear operation, while the convolution is linear.

The disadvantage of dilation operation is that during the time of removing the noisy pixels inside the foreground or object region, the boundary of the object region also gets increased.

Erosion shrinks or removes objects in a binary image. With X and B as sets, the erosion of X by B is defined as

$$\boldsymbol{X \ominus B = \{P \in Z^2 \mid P + b \in X \forall b \in B\}} \quad \textbf{(2.25)}$$

Where P is the Translation member.

The erosion of X by B is the set of all points z such that B, translated by z, is contained in X, where set B is a structuring element.

In image processing applications, dilation and erosion are used most often in various combinations. An image undergoes a series of dilations and/or erosions using the same or different structuring elements.

1.7.6 Opening and Closing:

Opening generally smoothes the contour of an object and eliminate thin protrusions. The opening of a set X by structuring element B is defined as:

$$X \bullet B = (X \ominus B) \oplus B \quad (2.26)$$

Therefore, the opening X by B is the erosion of X by B, followed by a dilation of the result by B.

Closing also tends to smooth sections of contours but fusing narrow breaks and long, thin gulfs and eliminating small holes and filling gaps in the contour. The closing of a set X by structuring element B is defined as:

$$X \bullet B = (X \oplus B) \ominus B \quad (2.27)$$

Therefore, the closing X by B is the dilation of X by B, followed by an erosion of the result by B.

1.7.7 Hit or Miss Transform:

The **hit or miss transformation** is useful to match specified configurations of pixels in an image, such as isolated foreground pixels, or pixels that are endpoints of line segments.

One of the important applications of this operation is used in forensics. Employment of fingerprints as evidence of crime has been one of the most important utilities in forensics since 19th century. Where there are no witness to a certain crime, finger prints can be very useful in determining the offenders. In most cases, they are incomplete and degraded. The individual features that uniquely identify a fingerprint are called minutiae. Thus, the basic ridge pattern together with the minutiae and their location on the finger print pattern uniquely identify a fingerprint. The Morphological Image Processing enhances the degraded noisy and / or incomplete latent fingerprints.

In physics and related fields, computer techniques routinely enhance images of experiments in areas such as high-energy plasmas and electron microscopy. Similarly successful applications of image processing concepts can be found in astronomy, biology, nuclear medicine, law enforcement, and defence.

1.7.8 Applications of Gray scale morphology:

Gray morphological operations are used generally to extract the edge of the image for the conditions, the multi-level geodetic expansion to expand to fill the target area, through which the algorithm can improve the detection of image accuracy, enhanced noise immunity, effectively identify the target and also to efficiently reduce the number of skeleton points and the entropy of morphological decomposition.

- Blood vessel edge enhancement and reconnection.
- Geographic pattern recognition for a satellite remote sensing image.
- Recognition and classification of vehicle on the traffic road in the hi-resolution satellite image.
- Solution to problem of luminal contour detection in intravascular ultrasound images.
- A robust vision system for vehicle license plate recognition Industrial parts recognition and inspection by image morphology.
- Multiresolutional texture analysis based on morphological techniques.
- Image matching using morphological operations.
- Extraction of grid patterns on stamped metal sheets.
- Application of Morphological Operations in Human Brain CT Image with SVM.
- Morphological detection based on size and contrast criteria application to cells detection.

1.8 Homomorphic Filtering:

1.8.1 Introduction:

If the image model is based on illumination-reflectance, then frequency domain procedures are not as easy to perform. The main reason is that illumination and reflectance components of the model are not separable. To be able to improve appearance of an image by simultaneous brightness range compression and contrast enhancement it is necessary to separate the two components [32]. As you recall, an image can be modelled mathematically in terms of illumination and reflectance as follow:

$$F(x.y) = I(x,y) * R(x,y) \quad (2.28)$$

Where $*$ is the multiplicative noise High Pass is one such technique for removing the multiplicative noise. Before applying high pass filtering we generally take the logarithmic values of the both the sides. i.e.

$$ln(F(x;\ y)) = ln(I(x;\ y) * R(x;\ y)) \quad (2.29)$$

Now we very well know from the logarithmic properties that if we take log of both the sides then we can express log(intensity) as the sum of log(illumination) and log(reflectance) i.e.

$$ln(F(x;\ y)) = ln(I(x;\ y)) + ln(R(x;\ y)) \quad (2.30)$$

The Fourier transformed signal is processed by means of a filter function H(u,v) and the resulting function is inverse Fourier transformed. Finally, inverse exponential operation yields an enhanced image. This enhancement approach is termed as homomorphic filtering [33].

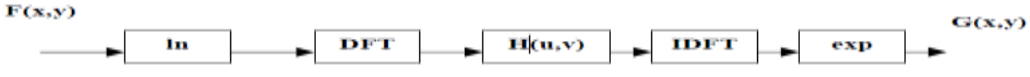

Figure: Operation of Homomorphic filtering

1.8.2 Operation steps of Homomorphic filtering:

Following are the steps for Homomorphic filtering:

- We will first convert the image to float.
- Convert the image next to the log domain
- Apply the High pass filtering in either the spatial domain or the frequency domain
- Apply inverse filter and retain the real part of the result
- Apply the exponential function to invert the log transform
- See the homomorphic filtered image using ifftshow() function

2. Conclusion

In practical applications, the original noise-free image is not available and only the noisy version exists. We have presented a comparative study between Median Filter, Kuan filter, Wiener filter, Gaussian filter, Wavelet Threshold filter, Bilateral filter, Morphological filter, Homomorphic filter, Gaussian noise, Speckle noise. All these filtering techniques performance can be evaluated on the basis of SNR. Through which we will be able to get our best image filtering techniques.

In future work we are planning to evaluate the performance of all the filtering techniques using Signal Noise Ratio and planning to implement soft computing based noise filter for digital images and comparatively evaluate the performance with the filtering techniques mentioned in this paper.

REFERENCES:

[1] Darcy Tsai, \Graduate Institute of Electronics Engineering,Nation Taiwan University,Taipei,Taiwan,ROC,Wiener Filters\.
[2] O. Laligant , GARCIA Frederic,\Wiener filtering Image Analysis\.
[3] C. M. Leung and W.-S. Lu,\Image restoration by two-dimensional recursive regularization filters\ in Proc. Canadian Conf on Electrical and Computer Engineering, vol. I, pp. MA3.6.1-MA3.6.4, Toronto, Ont.,Sept. 1992
[4] Prof. William H. Press Spring Term,\Wiener Filtering (and some Wavelets)\, 2008 ,The University of Texas at Austin
[5] R. L. Lagendijk and J. Biemond, \Iterative Identification and Restoration of Images\, Norwell, MA:KluweP- Academic Publishers, 1991.
[6] S. Haykin, \Adaptive Filter Theory\, Prentice Hall 2002.
[7] Gernot Ho_man,\Gaussian Filtering\,December 20,2002.
[8] The university of auckland,new zealand,\Gaussian Filtering\,2010.
[9] Venkata Rukmini . Ch, MR. M. D. Singh, \Filter Selection for Speckle Noise Reduction\,JUNE 2008.
[10] Rafael C. Gonzalez, Richard E. Woods,\Digital Image Processing\, 2nd ed, 2002. Prentice Hall, Upper Saddle River, NJ.
[11] Rafael C. Gonzalez and Richard E. Woods, \Digital Image Processing\, 2001, pp.220 - 243.
[12] J. Chen, A. K. Jain, \A Structural Approach to Identify Defects on Textural Images\, Proceedings of the IEEE International Conference on Systems, Man, and Cybernetics, pp. 29-32, 1988.
[13] Kiyo Tomiyas, \Computer Simulation of Speckle in a Synthetic Aperture Radar Image Pixel\, IEEE TRANSACTIONS ON GEOSCIENCE AND REMOTE SENSING, 1983.
[14] D. T. Kuan, \Adaptive Noise Smoothing Filter for Images with Signal Dependent Noise\, IEEE Transactions on Pattern Analysis and Machine Intelligence, Vol. PAMI-7, No. 2, pp 165-177, 1985.
[15] Adib Akl, Kamal Tabbara, Charles Yaacoub,\EDGE-BASED SUBOP-TIMAL KUAN FILTERING FOR SPECKLE NOISE REDUCTION\,1986.
[16] Yansun Xu, John B. Weaver, Dennis M. Healy, Jr., and Jian Lu, \Wavelet Transform Domain Filters: A Spatially Selective Noise Filtra-tion Technique\, IEEE TRANSACTIONS ON IMAGE PROCESSING, VOL. 3, NO. 6, NOVEMBER 1994.
[17] S. Grace Chang, Student Member, IEEE, Bin Yu, Senior Member, IEEE, and Martin Vetterli, Fellow, IEEE \Adaptive Wavelet Thresholding for Image De-noising and Compression\,IEEE TRANSACTIONS ON IMAGE PROCESSING, VOL. 9, NO. 9, SEPTEMBER 2000. [18] Aleksandra Pizurica, Wilfried Philips and Marc Acheroy, \A Versa-tile Wavelet Domain Noise Filtration Technique for Medical Imaging\,IEEE TRANSACTIONS ON MEDICAL IMAGING, VOL. 22, NO.3, MARCH 2003.
[18] Pao-Yen Lin, \An Introduction to Wavelet Transform\, Graduate Institute of Communication Engineering National Taiwan University, Taipei,Taiwan, ROC.
[19] [20] Shi Zhong,Dept. of ECE, Univ. of Texas at Austin Dept. Of ECE, Vladimir Cherkassky,Univ. of Minnesota szhong @ece.utexas.edu cherkass @ece.umn.edu\Image De-noising using Wavelet Thresholding and Model Selection\.
[20] 1P. Raviraj and 2M.Y. Sanavullah,\The Modi_ed 2D-Haar Wavelet Transformation in Image Compression\.
[21] Sylvain Paris, Pierre Kornprobst, Jack Tumblin and Fredo Du-rand,\Bilateral Filtering: Theory and Applications\, Computer Graph- ics and VisionVol. 4, No. 1 (2008) 173,2009 S. Paris, P. Kornprobst, J. Tumblin andF. Durand.
[22] Sylvain Paris, Pierre Kornprobst, Jack Tumblin and Fredo Du-rand,\Bilateral Filtering: Theory and Applications\, Computer Graph- ics and VisionVol. 4, No. 1 (2008) 173,2009 S. Paris, P. Kornprobst, J.Tumblin and F. Durand.

[23] Ming Zhang and Bahadir K. Gunturk,\Multiresolution Bilateral Filter-ing for Image De-noising\,IEEE TRANSACTIONS ON IMAGE PRO-ESSING, VOL. 17, NO. 12, DECEMBER 2008.
[24] C. Tomasi,R. Manduchi,\Bilateral Filtering for Gray and Color Images\
[25] T. Boult, R. A. Melter, E Skorina, and I. Stojmenovic. G-neighbors. Proc. SPIE Con on Vision Geometry II, 96-109.1993.
[26] Athanasios Papoulis. Probability, random variables, and stochastic processes. McGraw-Hill, New York, 1991.
[27] Mugdha A. Rane, \Fast Morphological Image Processing on GPU using CUDA\.
[28] Gleb V. Tcheslavski, \Morphological Image Processing:Gray -scale morphology\.
[29] V. Danell, Matthew J. Thurley, \Fast Morphological Image Processing Open Source Extensions with CUDA\, IEEE Journal of Signal Processing, Vol. X, 2012.
[30] J. Gil and R. Kimmel, \E_cient dilation, erosion, opening and closing algorithms\, Pattern Analysis and machine Intelligence, vol. 24, no. 12, pp. 1606-1617, dec. 2002.
[31] E. R. Dougherty and R.A. Lotufo, \hands on Morphological Image Processing\. SPIE - The International Society for Optical Engineering, 3002,vol. tt59.
[32] Nithya Sundaram, \HOMOMORPHIC PROCESSING AND ITS APPLICATION TO IMAGE ENHANCEMENT\.
[33] Dr.Rashi Agarwal,UIET,CSJM University, \Kanpur Homomorphic Filtering in Fourier Domain\.

International Journal of Engineering Research and General Science Volume 3, Issue 5, September-October, 2015
ISSN 2091-2730

Numerical Simulation of Gas Turbine Can Combustor Engine

CH UMAMAHESHWAR PRAVEEN[1*], A HEMANTH KUMAR YADAV[2]

1. Engineer, CDG BOEING Company, Chennai, India.
2. B.Tech Aeronautical Engineer 2012 passout, Bharat Institute of Engineering and Technology, Hyderabad, India.

*email: chpraveen52@gmail.com, *Ph: +91-09677143692

Abstract— In the Gas Turbine combustion system, the flow into combustor play one of the key roles in controlling pressure loss, air flow distribution around the combustor liner, and the attendant effects on performance, durability, and stability. This paper produces design methodology and describes a computational fluid dynamics (CFD) simulation of the flow in the can combustor. The main aim is to study and examine the performance influence of turbulence models, combustion models and rate mechanism on the prediction of the chemical species concentration and temperature fields which are useful to design the combustor within design limits. Numerical simulations are performed to analyze the combustion behavior in three-dimensional combustor model by solving swirl flow field inside pre-mixer, reacting flow field inside the liner, to understand the combustion phenomena and resultant emissions.

Keywords— Gas Turbine Engines, Combustion Chamber, Combustion Aerodynamics, Stoichiometric ratio, Combustion Models, Turbulence Models, NO_X formation, Non-Premixed Combustion, Combustion Chemistry.

INTRODUCTION

The development of the gas turbine engine as an aircraft power plant has been so rapid that it is difficult to appreciate that prior to the 1950s very few people had heard of this method of aircraft propulsion. The possibility of using a reaction jet had interested aircraft designers for a long time, but initially the low speeds of early aircraft and the unsuitably of a piston engine for producing the large high velocity airflow necessary for the 'jet' presented many obstacles. The mechanical arrangement of the gas turbine engine is simple, for it consists of only two main rotating parts, a compressor and a turbine and one or a number of combustion chambers. This simplicity, however, does not apply to all aspects of the engine. They result from the high operating temperatures of the combustion chamber and turbine, the effects of varying flows across the compressor and turbine blades, and the design of the exhaust system through which the gases are ejected to form the propulsive jet. The combustion chamber has the difficult task of burning large quantities of fuel, supplied through the fuel spray nozzles, with extensive volumes of air, supplied by the compressor and releasing the heat in such a manner that the air is expanded and accelerated to give a smooth stream of uniformly heated gas at all conditions required by the turbine. This task must be accomplished with the minimum loss in pressure and with the maximum heat release for the limited space available. The amount of fuel added to the air will depend upon the temperature rise required. However, the maximum temperature is limited to within the range of 850 to 1700 deg. C. by the materials from which the turbine blades and nozzles are made. The air has already been heated to between 200 and 550 deg. C. by the work done during compression, giving a temperature rise requirement of 650 to 1250 deg. C. from the combustion process. Since the gas temperature required at the turbine varies with engine thrust, and in the case of the turbo-propeller engine upon the power required, the combustion chamber must also be capable of maintaining stable and efficient combustion over a wide range of engine operating conditions. Efficient combustion has become increasingly important because of the rapid rise in commercial aircraft traffic and the consequent increase in atmospheric pollution, which is seen by the general public as exhaust smoke.

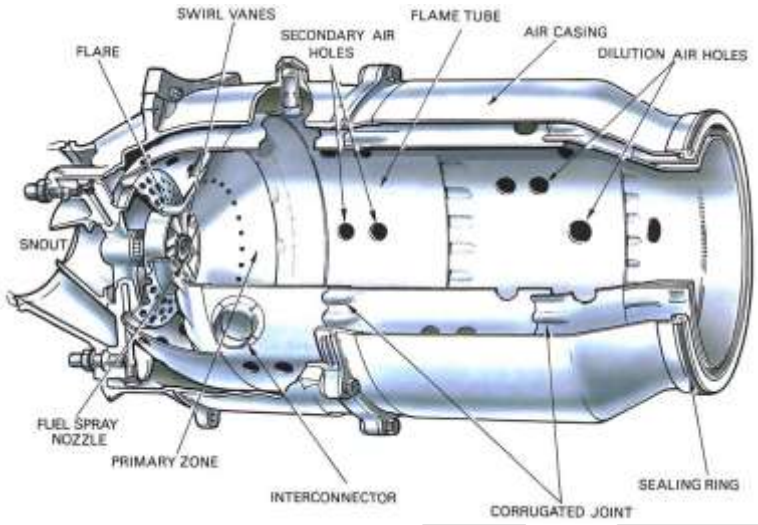

Figure 1: Can combustor

The study of air-fuel ratio, swirler angle at air inlet, axial position of holes is changed to investigate the effects of parameters on combustion chamber performance and emissions. The outcome of results will help in finding the correct geometry for a particular operation.

DESIGN OF COMBUSTOR

Combustor sizing refers to the definition of the reference area (or diameter) to provide sufficient stability without incurring excessive pressure losses. All operating points (i.e., idle, full power) are considered and the smallest size that provides stability over the entire range of operation is chosen. For simplicity, the static conditions are assumed equal to those at stagnation for both temperature and pressure. This is a reasonable assumption since the Mach number everywhere is below 0.25. For a Mach number of 0.25, the static pressure and temperature deviate from stagnation by only 4 percent and 1 percent, respectively.

Design point of view for reference:

Maximum Inlet temperature 480K, mass flow rate 1.3 kg/s with pressure 3.6 bar.

Thus, for each point the following conditions are known:

- The air flow rate, m_3
- The inlet temperature, T_3
- The outlet temperature, T_4
- The inlet pressure, P_3

And from the ideal gas law, we know the inlet density,

$$\rho_3 = \frac{P3}{Ra * T3}$$

Where Ra is the ideal gas constant for air.

The casing size for most combustors is dictated by the overall pressure loss ΔP_{3-4}.

The cross-sectional area of the casing, A_{ref}, is determined from

$$A_{ref} = \left[\frac{Ra}{2}\left(m3 * \frac{T3^{0.5}}{P3}\right)^2 * \left(\frac{\Delta P3-4}{P3}\right)^{-1}\right]\text{^}0.5$$

Suitable values for $\Delta P_{3-4}/P3$ and $\Delta P_{3-4}/q_{ref}$ are chosen by the designer based on
The casing diameter for a can may then be derived from geometry.

$$D_{ref} = \sqrt{(4/\pi)Aref + 2t\ liner}$$

The liner diameter must be chosen carefully. It would appear desirable to select the largest diameter possible and reduce the velocity of the flow within the liner. This increases the residence time in the combustor and promotes stability. However, for any given casing area, increasing the liner diameter results in a reduction of the annulus flow area A_{an}. The smaller area results in higher annulus velocities that decrease the static pressure in the annulus. Therefore, a larger liner diameter is undesirable since a high static pressure drop across the liner admission holes is necessary to provide adequate penetration of the jets. Sawyer (1985) provided a general rule of thumb for selecting the liner diameter of conventional combustors. The author stated that the liner cross-sectional area should be kept within 60-72 percent of the casing area for conventional combustors. A value of 70 percent is chosen and hence, the liner cross-sectional area is

$$A_{liner} = 0.7*A_{ref}$$

The diameter of the liner is

$$D_{liner} = \sqrt{(4/\pi) * Aliner}$$

and the annulus cross-sectional flow area is

$$A_{an} = [D^2ref - (D_{liner} + 2t_{liner})^2] * \frac{\pi}{4}$$

The liner diameter of the contracted section is

$$Dliner,2 = \sqrt{0.7 * Dliner}$$

and the length of the contraction is

$$L_2 = \frac{Dliner - Dliner,2}{2\tan\theta}$$

The wall angle contract is chosen to be 30 degree

To maintain a constant annulus area, the casing diameter shall be

$$Dref,2 = \sqrt{(Dliner, 2 + 2tliner + (4/\pi) * Aan)\text{^}2}$$

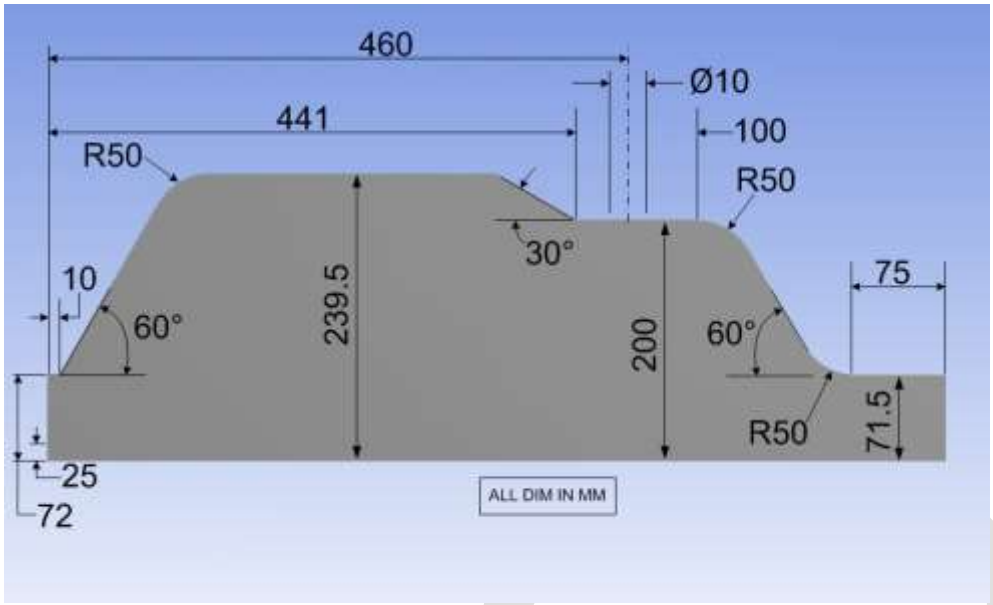

Figure 2: Combustor Dimensions

Can Combustor diameter is 479 mm in the Y direction outlet diameter of combustor is 143 mm, Area of air Inlet is 0.0142922 mm^2, Area of Fuel Inlet is 0.0159984 mm^2 (for 5 holes), where diameter of each fuel Inlet hole will be 6.25 mm. Swirler length and diameter has to match to diameter of air inlet, where swirler angle blade geometry considered as 45^0

MODELLING, MESHING AND BOUNDARY CONDITIONS

EDDY DISSIPATION COMBUSTION MODEL

In Eddy Dissipation Combustion chemical reaction takes place very fast in molecular level relative to transport processes to the flow. When reactants mix at lower molecule level, instantaneously form products. The model assumes reaction rate is directly proportional to time required to mix reactant. In case of turbulent flow reaction rate is directly proportional to Kinetic Energy and Kinetic dissipation. In this model mixing rate is dominated by eddy properties.

MESHING

The partial differential equations which give solutions for fluid flow and heat transfer is not simple. To achieve solution domains are splitted into subdomains. The governing equations are then discretized and solved inside each subdomain. For this thesis work mesh adaption has done with tetrahedral and prism elements at boundary layer. The mesh generated automatically with 431389 elements and 88982 nodes.

BOUNDARY CONDITIONS

Boundary condition can be varying for air inlet and fuel inlet, since the relation depends upon the Air-fuel mixture ratio. The boundary conditions for air inlet are: mass flow rate is 0.2636 kg/s, total Inlet temperature of 300 K, component as oxygen with flow normal to the direction, low turbulence intensity and eddy viscous ratio. The boundary conditions for fuel inlet are: CH_4 mass fraction as 1, mass flow rate for fuel is 0.00352 kg/s, Total Inlet Temperature 300K with flow normal to the direction, medium intensity and Eddy viscosity ratio. The boundary condition of the outlet of combustion is defined by zero pressure value. Heat transfer will set to adiabatic with no slip wall condition. The finite volume Eddy dissipation combustion model is used with total energy heat transfer, thermal radiation set to P1, turbulence model with k-epsilon.

RESULTS

COMBUSTOR OUTLET TEMPERATURE

The contour of predicted gas temperature for the methane combustion is 1271 K which shows effective combustion between air and methane fuel mixture. The theoretical temperature flame produced from natural gas or methane fuel with atmospheric conditions (1bar, 200C) is 1950K with fast combustion rate.

The maximum outlet temperature can be finding out by using technical formula:

$(M_a * Cp * Tair) + (M_f * H_f) = (M_a + M_f) * C_{pg} * T\ exit$

Where

M_a = Mass of air Inlet

M_f = Mass of fuel Inlet

Tair = Temperature of air inlet

H_f = Calorific value of methane fuel

C_{pg} = Const. pressure of gas

(0.2636*1005*300) + (0.00352*55000) = 0.26712*1.182* T exit

Total Temperature at Exit = 864.9 K (Manually)

Total Temperature at Exit = 949.6 K (Software)

Since software calculation is approximate to manual calculation. The both values reached nearby condition.

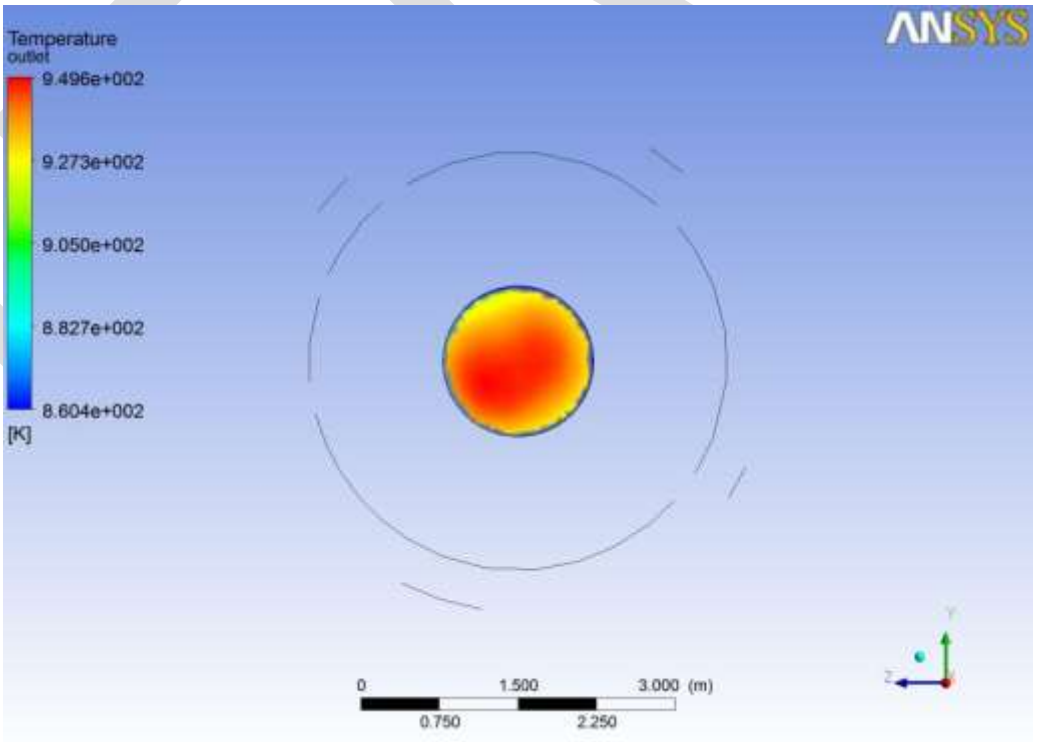

Figure 3: Temperature profile on outlet

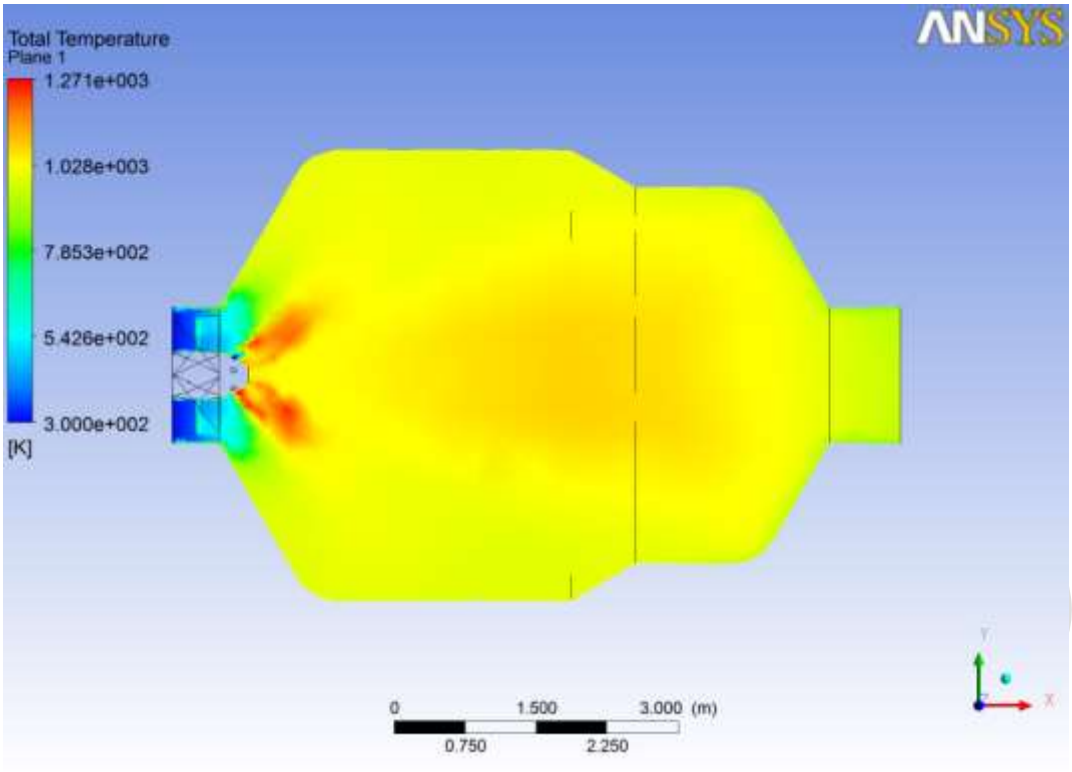

Figure 4: Temperature plane on longitudinal plane

PATTERN FACTOR

Modelling of the jets issuing from liner holes is essential to their design. Modelling of the jet trajectory is essential to ensure that good mixing and a suitable exit pattern factor are provided. Temperature variance should be linearly increased in radial direction. The pattern factor is defined as (Lefebvre, 1999)

$$\text{Pattern factor} = \frac{\text{Max}\,record\ Exhaust\ Temperature - Mean\ Exhaust\ Temperature}{Mean\ Exhaust\ Temperature - Inlet\ air\ Temperature}$$

$$= \frac{949.60 - 935.663}{935.663 - 300}$$

$$= 0.02$$

Holdeman et al. (1987) and Holdeman (1993) provided empirical correlations for the determination of the jet centreline trajectory, jet temperature profile, and the jet width for confined ducts with single-sided and opposed rows of jets. These models correspond well with experimental and numerical data. Much of the work on single and multiple jets in a confined cross flow has been summarized by Lefebvre (1999). Pattern factor should be less than 0.3 as per design standards. The result of pattern factor lies within the design limit.

PRESSURE LOSS FACTOR

The difference in total pressure between the inlet and outlet of the combustor, called the overall total pressure loss together with the reference velocity head determine the size of the combustor. The quantity is of great importance to combustor design and are generally quoted pressure loss factor. The Pressure loss should not be greater than 8% including factor concerns which results in lack of Performance for jet Engine.

$$\text{Pressure loss percentage} = \frac{Total\ air\ pressure\ Inlet - Total\ air\ pressure\ Outlet}{Total\ air\ Pressure\ Inlet} * 100$$

Pressure loss Percentage = $\frac{102105.314-101690.475}{102105.314} * 100$

= 0.4% Pressure loss

As we used the angle of swirler as 45^{o} the zone covered by the primary air inlet of combustion chamber is more also a recirculation zone is ahead of swirler which helps in efficient combustion. The sudden rise in temperature observed near the tip of the injector indicates the generation of shocks which help in superior air-fuel mixing. Superior air-fuel mixing resulting in better quality of combustion and thus better performance. As predicted, the results obtained from this study show an enhanced air-fuel mixing and a proper combustion which can be attributed to the geometry of the ramp injector considered in this study & shows the turbulent intensity is high in the immediate vicinity of the ramp injector indicating a superior air-fuel mixing.

A very high turbulent intensity indicates a superior air-fuel mixing. The high value of mass fraction of NO formed indicates an efficient combustion process. The peak gas temperature is located in the primary zone where combustion of mixture air and methane takes place. The fuel from 5 injectors is first mixed in the swirling air before burning in the primary reaction zone. The gas temperature decreases after the primary zone. In case there will be dilution holes are provided at dilution zone, to reduce the temperature this can be done when the temperature inside the combustor is high. The air required from dilution zone is get from compressor.

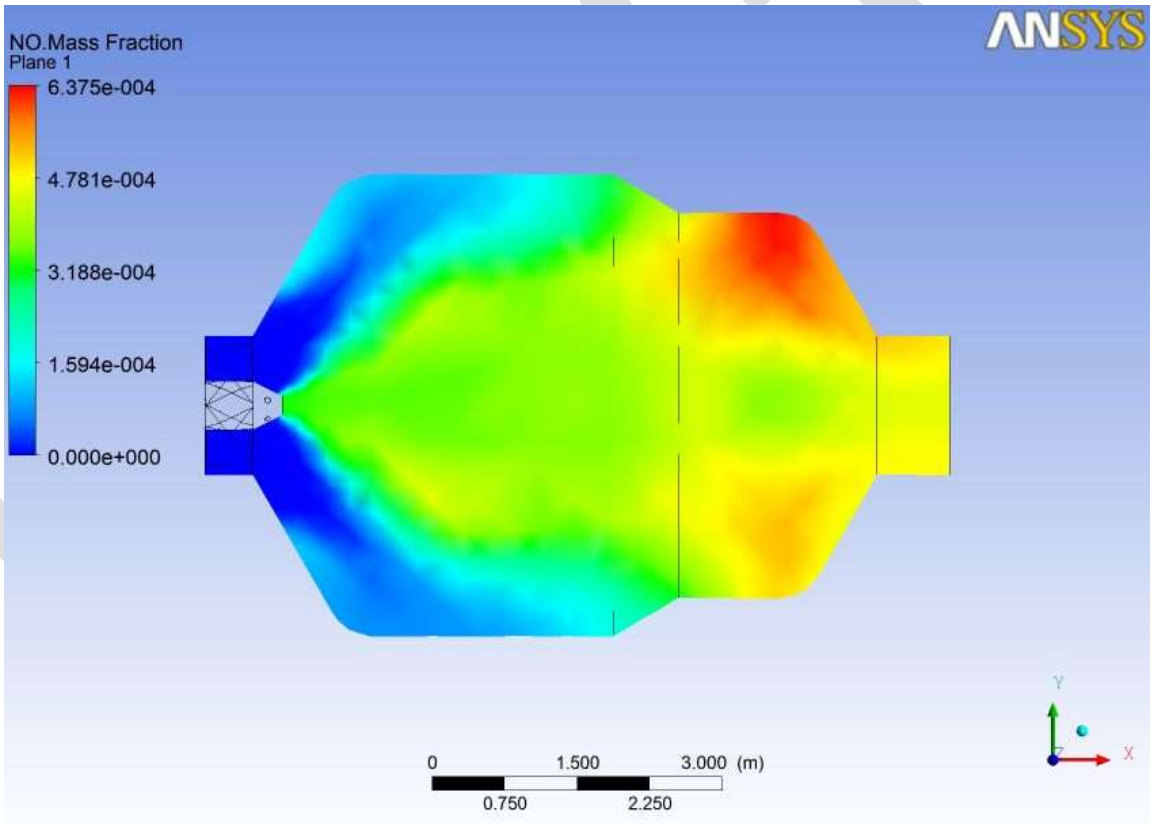

Figure 5: NO Mass fraction.

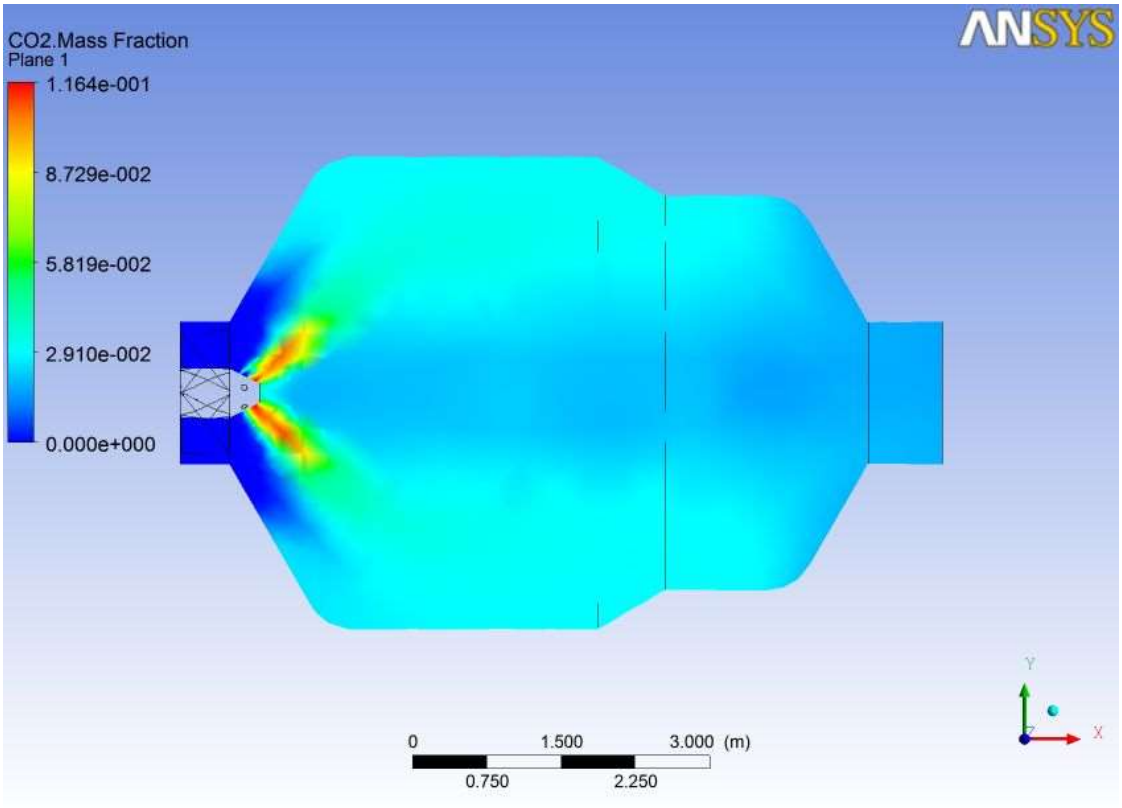

Figure 6:CO_2 Mass Fraction

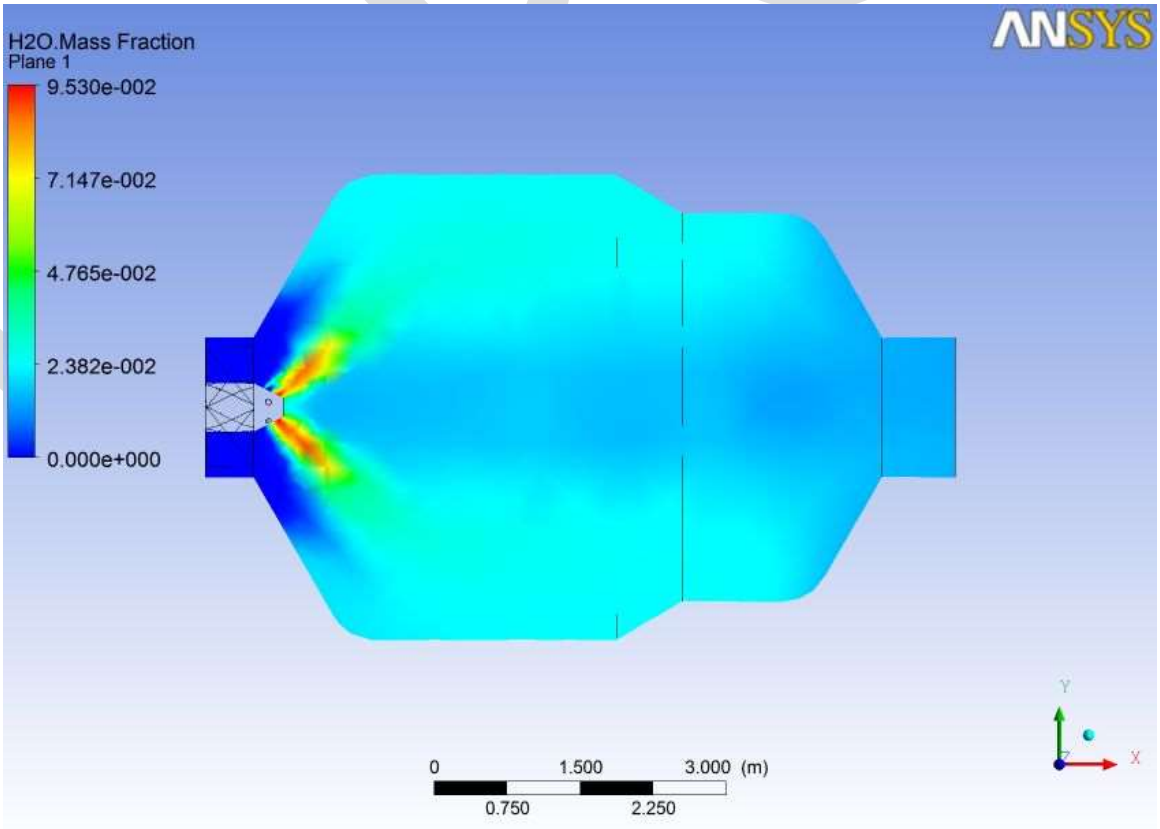

Figure 7:H_2O Mass Fraction

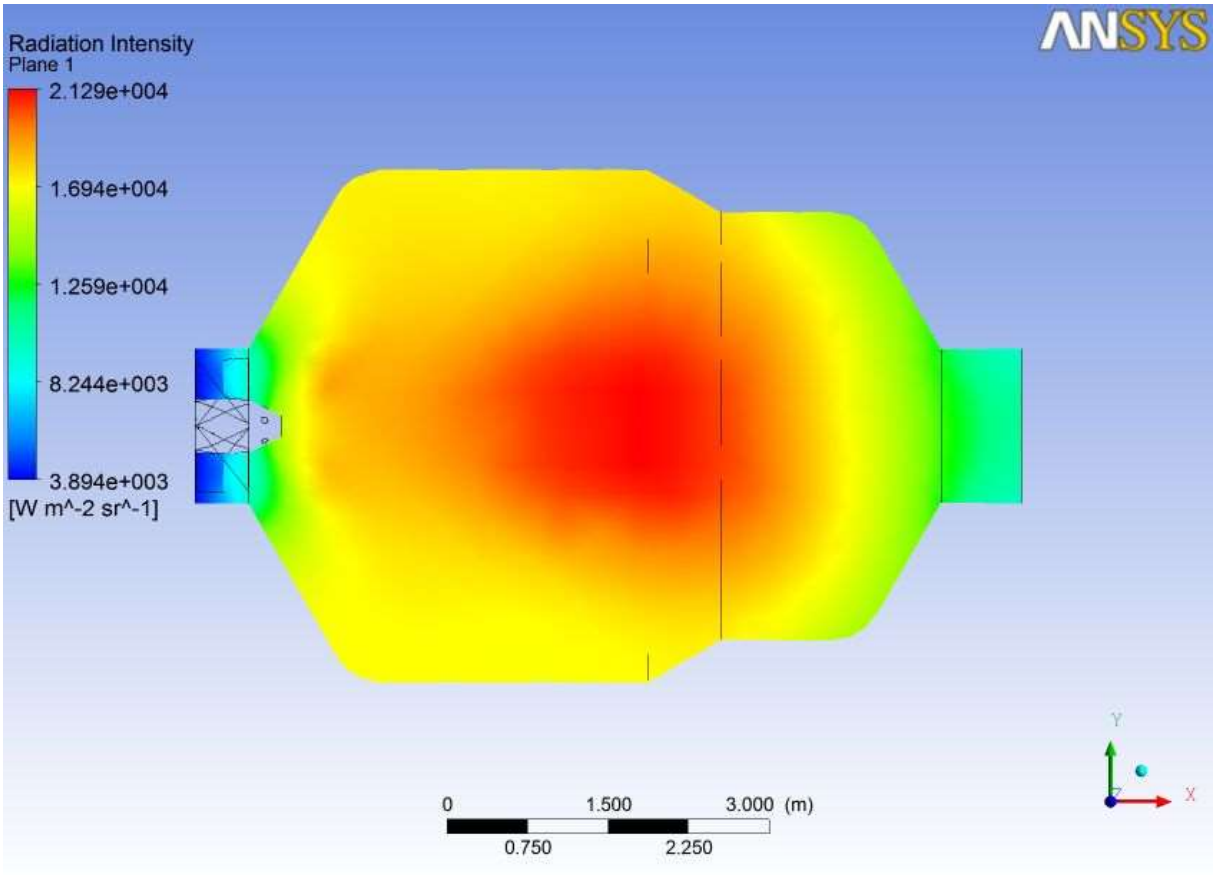

Figure 8: Radiation Intensity

Total mass of the reactants equals the total mass of the products leading to the insight that the relations among quantities of reactants and products typically form a ratio of positive integers. This means that if the amounts of the separate reactants are known, then the amount of the product can be calculated.

$$CH_4 + 2\ O_2 \rightarrow CO_2 + 2\ H_2O$$

CONCLUSION

Analysis on Can Combustors shows following results which are in design limits thereby Air-fuel ratio 75 was acceptable.

For Methane as fuel and with initial atmospheric conditions, the flame temperature produced by flame with fast combustion was reached to 1271K which shows effective combustion.

1. Temperature profile at outlet of combustor shows radially increased, which states there will be less thermal stresses on the turbine blades which are located next to the combustor.

2. Outlet Temperature of the can combustor result is approximate equivalent to manual calculations, since the software calculation done by Finite Volume Method which is apprx. to manual calculation method.

3. Pressure Loss factor determines the efficiency in combustion. Pressure loss factor should be minimum as possible, there by more pressurized gas will exists it can be determined from inlet and outlet pressures. In the model there is low pressure loss which shows effective pressure in the gas at the exit of the combustor.

REFERENCES:

[1] An Improved Method for Accurate prediction of Mass Flows Through Combustor Liner Holes – by Adkins, RC &Gueroui D

[2] Principles of Combustion New York: Jon Wiley & Sons, Kuo, K.K. 1986.

[3] Fuel Effects on Gas Turbine Combustion - Ignition, Stability, and Combustion Efficiency, Lefebvre, A.H. 1985

[4] Y.T. Yu, M.F. Lau, "A comparison of MC/DC, MUMCUT and several other coverage criteria for logical decisions", Journal of Systems and Software, 2005, in press.

[5] Spector, A. Z. 1989. Achieving application requirements.In Distributed Systems, S. Mullende.

[6] Holdeman, J.D. 1993. Mixing of Multiple Jets with a Confined Subsonic Crossflow. Progress in Energy and Combustion Science

International Journal of Engineering Research and General Science Volume 3, Issue 5, September-October, 2015
ISSN 2091-2730

Efficient Document Retrieval using Content and Querying Value based on Annotation with Proximity Ranking

[1]Ms. Sonal Kutade, [2]Prof. Poonam Dhamal

[1] ME Student, Department of Computer Engg, G.H. Raisoni College of Engineering and Management, Savitribai Phule Pune University, Pune.

[2]Assistant Professor, Department of Information Technology, G.H. Raisoni College of Engineering and Management, Savitribai Phule Pune University, Pune.

sonal.kutade@gmail.com

Abstract— Always it is hard to discover the relevant information in unstructured text documents. The structured information remains buried in unstructured text. Annotations in the form of Attribute name-value pairs are more expressive for retrieval of such documents. This system proposes a novel, different, alternative approach for document retrieval which includes annotations identification and also extends the existing system using fuzzy search with proximity ranking. This system identifies the values of structured attributes by reading, analyzing and parsing the uploaded documents. Searching process will make use of fuzzy search with proximity ranking for searching the user interested documents only. Thus this system proposes an approach for efficient document retrieval using effective methods.

Keywords— Document retrieval, instant-fuzzy search, proximity ranking, document annotation, OpenNLP, content, querying value, natural language processing.

INTRODUCTION

There are many application areas where users create and share their information; for instance, online job portal websites, news blogs, disaster management networks, scientific networks, social networking groups. Usually such data exists in unstructured text format. It also contains structured information but it remains buried in the presence of unstructured text. Current tools of information sharing allow the users for documents sharing and annotating/tag them in the ad hoc way, like the software of content management (e.g. MS Share-Point). Likewise, Google Base allows the users to define the attributes for their objects or choose from the predefined templates. This process of annotation can facilitate later information discovery. Various annotation systems allow only the "untyped" keyword annotation: e.g., a user may annotate a resume using a tag such as "Profile Computer Engineer"

Annotation strategies which use "attribute name-value" pairs are usually more expressive, because they contain more information than the untyped approaches. The above information can entered as (Profile, Computer Engineer) in such case. Existing system facilitates the structured metadata generation by identifying the documents which are likely to contain user interested information and this information is subsequently used for querying of the database. It uses CADS which stands for Collaborative Adaptive Data Sharing platform and which is used as an "annotate-as-you-create" infrastructure for facilitating the fielded data annotation. And later document owner modifies them by adding more annotation fields i.e. attributes. So here it requires more efforts of document owner which become time consuming process. Another limitations of existing system are no use of any searching and ranking technique.

So we propose an alternative, different and innovative approach which facilitates the identification of structured "attribute values". Later these values will be subsequently useful at the time of querying the database. It also uses Instant-fuzzy search with proximity ranking for searching the user interested documents only. The resultant documents will be ranked using keyword weightage.

The main Objectives of this system are to save the time by minimizing the user efforts in filling the information, to identify the attribute values i.e. content for attributes names when such information actually exists in document instead of prompting users to fill it, and to retrieve only the documents of user interest.

RELATED WORK

This system presented an annotation approach [1] which facilitates the structured metadata generation using CADS. It is done by identifying the documents that are likely to contain needed information and later this information will be useful for database querying. They presented the algorithms to identify the structured attributes which are likely to appear in the document, by utilizing both the content of text and query workload. The idea behind this approach is that humans are more expected to add the metadata during time of creation, if prompted by some interface or/and that it is much easier for the algorithms and/or humans to identify the metadata when such kind of information is actually existing in document, instead of fill up forms by naively prompting users with information which is not present in the document.

*CADS***:** This paper [1] proposed CADS system, which is used as a Collaborative Adaptive Data Sharing platform, and is a data sharing platform where the integration and annotation take place at the time of data insertion i.e. production and querying i.e. consumption actions. A main goal of CADS [3] is to influence the information demand for creation of adaptive insertion and query forms.

Instant Search: The integration of proximity information in instant fuzzy search for achieving the better complexities is explained in [2]. Many recent studies focused on the instant search. The studies in [6] proposed query and indexing techniques to support the instant search. Li et al. [8] studied the instant search on relational data which is modeled as a graph.
*Fuzzy Search***:** Fuzzy search studies can be categorized into two categories, first gram-based and second are trie- based approaches. In former approach, the data sub-strings are used for matching the fuzzy string. In second class approaches keywords are indexed as the trie, they depend on a traversal on the trie to determine the similar keywords [7]. This trie based approach is specially suitable for instant and fuzzy search [7] since every query is a prefix and trie supports efficient incremental computation.
Proximity Ranking: The Recent studies show that the term proximity is highly correlated with relevancy of document, and proximity-aware ranking increases the top results precision significantly. And, there are only few studies which increase proximity-aware searching query efficiency using techniques of early-termination [4], [5]. The techniques which are discussed in [4], [5] generate an additional inverted index for each term pair, which results in a large space. [5] studied only the problem for queries with two-keywords.

IMPLEMENTATION

A. Proposed System Architecture:

This system will use OpenNLP for stopword removal, checking of identification of attribute values. As shown in fig 1, here we have dataset of newsgroups containing thousands of documents. The Structured attribute names are stored in the database. The user can search by using either content i.e. attribute name of document or query containing attribute name and value. As user enters the query, the attribute name and value will be separated and identified by Preprocessing (OpenNLP). Then analysis and parsing of text file will be done using parser.. It will read, analyze & parse the whole document. At the other side these attribute names and values of content and queries i.e annotations will be useful to user for querying the database. At another side user will enter his query and finally he will get the resultant documents that are searched and ranked using instant fuzzy search and ranked with ranking based on calculation of keyword weightage (1) in documents. So user will receive only documents of his interest. In this way, this system is trying to prioritize document annotations that are many times used by users that are querying. After searching the documents, we can download required document and can view the annotations as per query in respective documents. And another main advantage of this system is that the resultant documents will be searched using fuzzy search and ranked using advanced technique of modified proximity ranking. The natural language processing tasks of OpenNLP are as shown in figure 2.

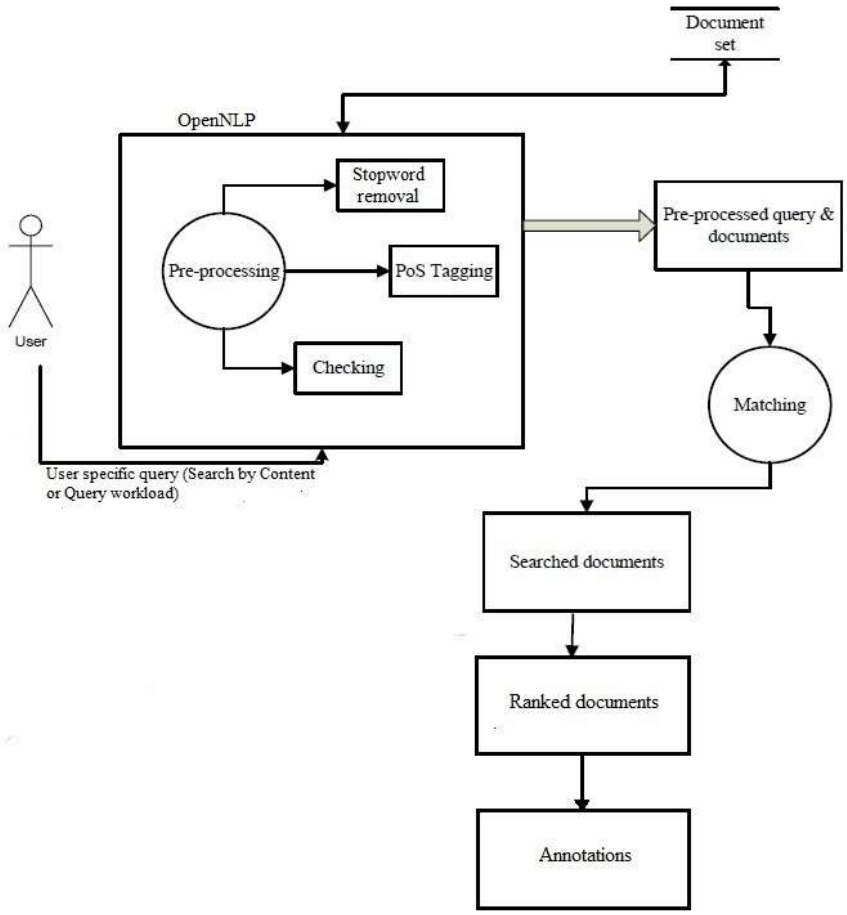

Fig. 1. Proposed System architecture

B. OpenNLP:

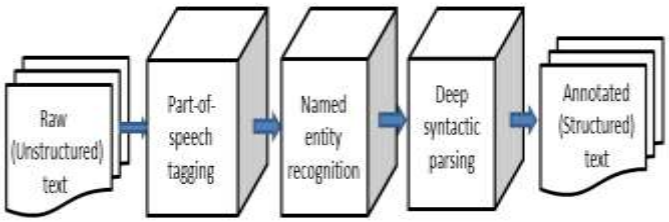

Fig. 2. OpenNLP tasks

The Apache OpenNLP library is a machine learning based toolkit for text processing of text of the natural language. It supports most of the tasks of NLP, like tokenization, sentence segmentation, named entity recognition, part-of-speech tagging, as well as parsing, chunking, and coreference resolution. These tasks are required to build more latest and advanced services of text processing. Text annotation usually involves these tasks at different linguistic levels. These tasks are done with right combinations of Open NLP tools. Splitter determines the sentences. It can find that a punctuation character marks the sentence end or not. Tokenizer segments the input character sequence into tokens such as words, punctuations and numbers.

POS tagger does the identification of the part of speech is done such as a noun, verbs, adverb for each word of sentence helps in analyzing role of each rule in sentences. So here "tag" method is used for tagger class of Open NLP. Example: Input – Tokens and Output – tag to each token. OpenNLP POS Tagger uses a probability model for predicting the right pos tag from tag set. A token can have many POS tags which depends on token and context.

Some tag set examples – DT:- singular determiner/ quantifier (e.g.that), NN:- singular noun / mass noun, IN :- preposition, NNS:- plural noun, VBZ:- verb, etc.

Instant search: It is referred as an emerging information-access model. Based on a partial query typed by user, it returns the answers instantly to user. E.g., Internet Movie Database has a search interface which offers the instant results to the users while they type their queries. When the user types "maha", the system returns answers such as "mahadiscom", "mahanews", "maharashtra times". Most of the users prefer to see search results instantly and they formulate their queries accordingly instead of being left in dark awaiting hitting the search button. This new technique helps users for discovering their answers with fewer efforts.

Fuzzy Search: Many of the users normally make typing mistakes in the search queries. The reasons for the same can be lack of caution, small keyboards of mobile, limited knowledge about data. So in this case, we cannot determine relevant answers. This problem can be solved by supporting the fuzzy search, in that we determine answers with keywords which are similar to query keywords. Combination of instant search and fuzzy search can provide better search experiences, particularly for the users of mobile-phone, who frequently having problem of "fat fingers" i.e., each keystroke is error prone and is time consuming.

Proximity ranking: Proximity ranking looks for document where two or more independent occurrences of matching terms are within a specified distance, where the distance is equal to the number of in-between words/characters. Here ranking will use the function for ranking which can be called as modified proximity ranking function which is defined in mathematical model.

C. Mathematical Model

Let S be the system which contains inputs, functions, and outputs.

S = {I, F, O} where

1)I = {I1, I2, I3. . . In}

Where, `I' is the set of documents that user wants to upload in

text, pdf, word format and there can be multiple files uploaded on server by multiple users or dataset of documents.

2) F = {F1, F2}

Here, two functions are defined which forms the system where

F1= Identification, separation of attribute values from attribute names and their insertion in csv file.

F2= Instant-fuzzy search with proximity ranking

3) O = {O1, O2, O3. . . O}

Where, `O' is the set of outputs which contain:

O= Set of resulted documents

- Ranking function:

Ranking will use following function to rank the resultant documents:

For each document d,

$$W=\sum_1^n i \qquad (1)$$

Where,

1) W = Weightage of query keywords in documents

2} i = weightage of each word in the document
=1/total no. of words in the document

3) n = total no. of query keywords

D. Algorithms

Algorithms used for fuzzy searching and ranking relevant documents:

Inputs: Documents in dataset D,

Query entered by user Q.

Output: Ranked relevant documents list

Let n be the total no. of documents in dataset.

I. When user enters a valid query,

1. for i =1 to n

2. Read document content

3. Compare query keyword with content of document

4. If (70% word match found)

Display the document

5. Else

Ignore and Go to next document.

II. Ranking function:

Finally, the valid segmentations are ranked using (1).

RESULTS

We test the system using the dataset of newsgroups containing thousands of documents. The system is built using ASP.NET using C# and MS SQL Server 2008. The maximum size of document is 32kb. Following graphs show result of searching of system annotated documents and ranking of them.

Figure 3 shows the graph of time taken for searching thousand no. of documents using content based search, query based search and their ranking.

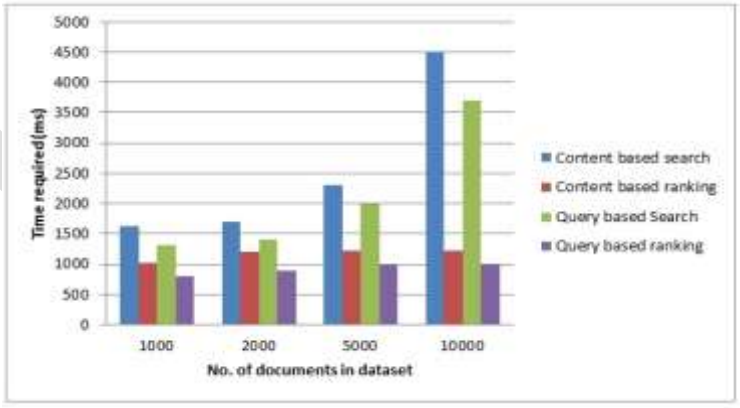

Fig. 3. Graph of time taken for searching/ranking relevant documents Vs total no. of documents

Figure 4 shows the graph of total no. of documents found by searching whole documents using content based search, query based search and more specific query based search.

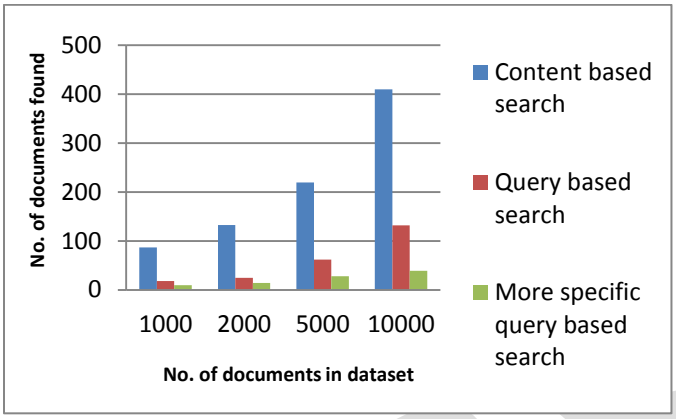

Fig. 4. Graph of total no. of documents Vs no. of documents found

After searching the documents, we can download required document and can view the annotations as per query in respective documents as shown in figure below.

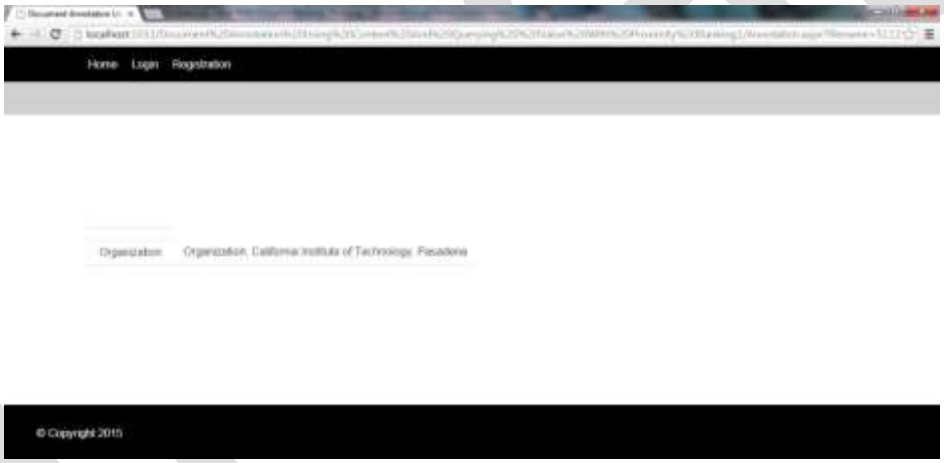

Fig 5. Annotation in required searched document

CONCLUSION AND FUTURE SCOPE

This paper proposes a new approach for efficient document retrieval including smart annotation, searching & ranking techniques. The system tries to satisfy querying needs of user efficiently. This system gives different ways for searching: the values of Content and Query. Using these techniques, we can increase chances of documents visibility up to maximum percent. Also using the fuzzy search and proximity ranking will achieve efficient time and space complexities and improve the overall performance of system. Users will get less and distinct results of documents. The text mining will be highly boosted due to this system.

Query based searching can be said as the future in information retrieval. Documents with complicated formats like can also be used in future. Document clustering can also be used in future. This system can surely give a huge boost in text mining and can be thought of as a changing trend.

ACKNOWLEDGEMENT

This is to acknowledge and thank all the individuals who played defining role in shaping this paper. Without their constant support, guidance and assistance this paper would not have been completed. Without their Coordination, guidance and reviewing this task could not be completed alone.

I avail this opportunity to express my deep sense of gratitude and whole hearted thanks to my guide Prof. Poonam Dhamal for giving her valuable guidance, inspiration and encouragement to embark this paper.

I would personally like to thank all staff members and my friends for their support.

REFERENCES:

1. Vagelis Hristidis, Eduardo J. Ruiz, Panagiotis G. Ipeirotis, , "Facilitating Document Annotation Using Content and Querying Value", volume 6, no 2, IEEE 2014
2. Chen Li , Cetindil, I., Taewoo Kim , Esmaelnezhad, "Efficient instant fuzzy search with proximity ranking", Data Engineering (ICDE), 30th International Conference ,IEEE 2014
3. V. Hristidis, E. Ruiz, " CADS: A Collaborative Adaptive Data Sharing Platform", SCIS, International University, Florida, 2009

A. Broschart, R. Schenkel, , S. Won Hwang, G. Weikum, M. Theobald, "Efficient text proximity search," SPIRE, 2007.

4. H. Yan, J. Wen, S. Shi, F. Zhang, T. Suel,, "Efficient term proximity search with the term-pair indexes,"CIKM, 2010, pp. 1229-1238.
5. H. Bast, , A. Chitea, F. Suchanek,Weber, "Ester : efficient search on text,entities, and relations," SIGIR, 2007.

B. Li, J. Feng, G Li, S. Ji, "Efficient interactive fuzzy keyword search," WWW, 2009.

C. Li, G. Li, J. Feng S. Ji, "Efficient type-ahead search on the relational data: a tastier approach" , SIGMOD, 2009.

6. Sonal Kutade, Poonam Dhamal, "Efficient Document Retrieval using Annotation, Searching and Ranking", IJCA, (0975 – 8887) Vol 108, No. 5, December 2014
7. Harshal J. Jain, M. S. Bewoor, S. H. Patil, "Context Sensitive Text Summarization Using K Means Clustering Algorithm", International Journal of Soft Computing and Engineering (IJSCE) ISSN: 2231-2307, Volume-2, Issue-2, May 2012
8. Md. Abu Nisar Masud, Md. Munasir Mamun, "A General Approach to Natural Language Generation" In Proceeding of IEEE, INMIC, 2003.
9. Yiyao Lu, Hai He, Hongkun Zhao, Weiyi Meng, "Annotating Search Results from Web Databases", IEEE Transactions On Knowledge And Data Engineering, Vol. 25, No. 3 YEAR 2013.
10. Akshay Shingote Nikhil Vispute Priyanka Dhikale," Facilitating Document Annotation Using Content & Querying Value", International Journal of Computer Trends and Technology (IJCTT) – volume 9 number 4– Mar 2014
11. M. J. Cafarella, J. Madhavan, and A. Halevy, "Web-scale extraction of structured data," SIGMOD *Rec.*, vol. 37, pp. 55–61, March 2009.
12. M. Hadjieleftheriou and C. Li, "Efficient approximate search on string collections," PVLDB, vol. 2, no. 2, pp. 1660–1661, 2009.
13. D. Xin, K. Chakrabarti, V. Ganti, S. Chaudhuri, "An efficient filter for approximate membership checking," SIGMOD Conf pp.805–818, 2008.

International Journal of Engineering Research and General Science Volume 3, Issue 5, September-October, 2015
ISSN 2091-2730

A Fuzzy based Two Warehouse Inventory model for deteriorating items with Cubic Demand and different fuzzy cost parameters

Parag Dutta, Purabi Deb Choudhury

Department of Mathematics, Assam University, Silchar; Email: parag0611@gmail.com and Mobile: +918876833192

Abstract— This paper deals with a fuzzy based two warehouse inventory model for decaying items in which demand is taken to be cubic function of time, holding cost, ordering cost, backorder costs which are fuzzy in nature. Shortages are allowed in the owned warehouse. Due to lack of historical data and information the probability of certain new products are not known and in that case to remove certain uncertainty fuzzy concept is used. In this context we have used triangular fuzzy numbers to represent the fuzzy parameters. Finally the model is solved mathematically and profit maximization technique is used to illustrate the system using Signed Distance method.

Keywords— Inventory, Own warehouse, Rented warehouse, Cubic demand, Fuzzy model, Signed distance method, Triangular fuzzy number, Holding cost.

INTRODUCTION

An inventory system deals with the decision that minimizes the net cost of the system and maximizes the net profit of the system. In the present competitive business world many of the inventory models are formulated with the unrealistic assumption that all produced items are of good quality. But it is impossible for the production company to produce all the good quality products as there always remains some defective items .In an inventory model the cost parameters such as holding cost, ordering cost, purchase cost, demand etc are known and have definite value without ambiguity. Some of the business fit such conditions , but in most of the cases due to the changing market scenario the parameters are imprecise. This uncertainty concept can be defined as fuzziness or vagueness. The authority have to decide how much and when to order or manufacture so that the profit should be maximum and total cost associated with the inventory system should be minimum. Also in reality there are so many physical goods which deteriorate during the stock in periods due to different factors like dryness, damage, spoilage and vaporization. Deterioration means worsening of products. It is a natural phenomenon in our daily life. Products like vegetables, milk, domestic goods, fashion goods; electronic components etc are deteriorating items. So this deteriorating must be considered to formulate an inventory model.

During the last few decades Inventory models have been widely applied in the competitive business world. Ghare and Schrader(1963) developed for the first time an inventory model for deteriorating items. Convert and Philip(1973) extended their work. Hartely (1976) first proposed a problem in his book "Operations Research – A Managerial Emphasis". In the formulation, the transportation cost for transferring the items from *RW* to *OW* was not considered. After Hartely (1976), Sarma (1983) extended the model under the assumption that stocks of *RW* are transferred from *RW* to *OW* in a bulk release fashion with fixed transportation cost per unit. Dave (1988) discussed the two-warehouse inventory models for finite and infinite rate of replenishment rectifying the errors of the model developed by Sarma (1983) and gave analytical solution of each model. Further, Goswami and Chaudhuri (1992) developed the models with and without shortages for linearly time dependent demand. In their formulation, stocks of *RW* are transferred to *OW* in equal time interval. Correcting and modifying the assumptions of Goswami and Chaudhuri (1992), Bhunia and Maiti (1994) discussed the same model and graphically presented the sensitivity analyses on the optimal average cost and the cycle length for the variations on the location and shape parameters of demand. The same type of model was developed by, Kar et al. (2001), Zhou and Yang (2003) and Mondal et al. (2007) for different types of demand. Donaldson (1977) developed an optimal algorithm for solving classical no shortage inventory model. Sarma (1987) developed a two-warehouse inventory model with infinite replenishment and completely backlogged shortages. Dave (1989) proposed a deterministic lot size inventory model with shortages and a linear trend in demand. Goswami and Chaudhuri (1991) discussed different types of inventory models with linear trend in demand. Pakkala and Achary (1992) then extended Sarma's (1987) model for finite replenishment rate. All the models in Sarma (1987) and Pakkala and Achary (1992) were developed for prescribed scheduling period (cycle length), uniform demand and stocks of *RW* transferred to *OW* in continuous release fashion ignoring the transportation cost for this purpose. Benkherouf (1997) presented a two-warehouse model for

deteriorating items with the general form of time dependent demand under continuous release fashion. Bhunia and Maiti (1997) discussed the same type of problem considering linearly (increasing) time dependent demand with completely backlogged shortages. This model was developed for infinite time horizon with the repetition of entire cycle with the changed value of the location parameter of the time dependent demand. Recently, very few researchers developed this type of model considering finite time horizon. All these models mentioned earlier were discussed only for non-deteriorating items. Lee and Ma (2000) developed a no-shortage inventory model for perishable items with free form of time dependent demand and fixed planning horizon. In their model, some cycles are of single warehouse system and the remaining is of two-warehouse system. Kar et al. (2001) discussed two storage inventory problems for non-perishable items with linear trend in demand over a fixed planning horizon considering lot-size dependent replenishment cost (ordering cost). On the other hand, considering two-storage facilities, Yang (2004) developed two inventory models for deteriorating items with uniform demand rate and completely backlogged shortages under inflation. Recently, Yang (2006) extended the models introduced in Yang (2004) by incorporating the partially backlogged shortages. In the year 2007, Chung and Huang (2007) proposed two-warehouse inventory model for deteriorating items. Deb Choudhury.P and Dutta.P developed a two warehouse inventory model considering demand as cubic function of time. However, all these models were developed based on an impractical assumption that the rented warehouse has unlimited capacity.

The concept of fuzzy logic was first proposed by Zadeh(1965) .Bellam and Zadeh(1970) discussed the difference between randomness and fuzziness . Silver and Peterson(1985) developed decision systems for inventory management and production planning. Zimmermann(1985) gave a review on applications of fuzzy set theory. Park (1987) discussed the EOQ model in which trapezoidal fuzzy numbers are used. Yao and Lee(1999) presented a fuzzy inventory model with and without backorder for fuzzy order quantity with trapezoidal fuzzy number.

A deterministic inventory model for deteriorating items with two warehouses is developed. Inventory cost in rented warehouse is higher than that of own warehouse. Demand is taken cubic (time dependent) in nature. Holding costs, ordering cost and backorder cost are considered as fuzzy numbers. The triangular fuzzy numbers are used to represent the fuzzy parameters. The total profit of the system is obtained with the help of Sign distance defuzzification method.

PRELIMINARIES:

FUZZY SET

A fuzzy set $\check{A}$ in a universe of discourse X is defined as the set of pairs $\widetilde{A} = \{(x, \mu_{\check{A}}(x)): x \in X\}$, where $\mu_{\check{A}}(x)$:X→ [0,1] is a mapping and $\mu_{\check{A}}(x)$ is called membership function of $\widetilde{A}$ or grade of membership of x in $\widetilde{A}$.

CONVEX FUZZY SET

A fuzzy set $\widetilde{A}$ in a universe of discourse is called convex if for all

$x_1, x_2 \in X, \mu_{\check{A}}(\delta x_1 + (1-\delta)x_2 \geq \min\{\mu_{\check{A}}(x_1), \mu_{\check{A}}(x_2)\}, where\ \delta \in [0,1]$.

NORMAL FUZZY SET

A fuzzy set $\check{A}$ is called normal fuzzy set if there exists at least one $x \in X$ such that $\mu_{\check{A}}(x_1) = 1$.

FUZZY NUMBER

A fuzzy number is a special case of a fuzzy set. Different definitions and properties of fuzzy numbers are encountered in the literature .But it actually represents the notation of a set of real numbers ‘closer to a’ where ‘a’ is the number being fuzzified. A fuzzy number is a fuzzy set which is both convex and normal.

TRIANGULAR FUZZY NUMBER (TFN)

A triangular fuzzy number $\check{A}$ is represented by the triplet (a_1, a_2, a_3) and is defined by its continuous membership function where $\mu_{\check{A}}(x)$:X→ [0,1] is given by

$$\mu_{\check{A}}(x) = f(x) = \begin{cases} \dfrac{x - a_1}{a_2 - a_1} & \text{if } a_1 \le x \le a_2 \\ 1 & \text{if } x = a_2 \\ \dfrac{a_3 - x}{a_3 - a_2} & \text{if } a_2 \le x \le a_3 \\ 0 & \text{otherwise} \end{cases},$$

ASSUMPTIONS & NOTATIONS

The following assumptions and notations have been used in developing the model:

1. Replenishment rate is infinite and lead time is constant.
2. Holding cost, demand both depends on time.
3. Shortages are allowed and unsatisfied demand in backlogged at a rate **A+Bx**, where A is constant, B is backlogging parameter (positive) and x is the waiting time.
4. Inventory cost in rented warehouse is higher than that of own warehouse.
5. Demand is assumed as, $D = a + bt + ct^2 + dt^3, where\ a, b, c, d > 0$
6. Holding cost in own warehouse assumed is h_o

   Holding cost in rented warehouse assumed is h_r . These parameters are fuzzy in nature.

7. C_s =fuzzy backlogging cost per unit per unit time
8. R =opportunity cost per unit
9. T =The length of the replenishment cycle
10. t_1 =time at which the inventory level falls to zero in RW
11. t_2 =time at which the inventory level falls to zero in OW
12. RW : Rented warehouse
13. OW : Own warehouse
14. α : deterioration rate in OW
15. β : deterioration rate in RW, $0 \le \alpha, \beta < 1$
16. $I_1(t)$: Inventory level in RW at time t
17. $I_2(t)$: Inventory level in OW at time t
18. $I_3(t)$: The level of negative inventory at time t.
19. C : The purchase cost per unit.
20. P : Fuzzy Ordering cost.
21. q : capacity of own warehouse
22. p : selling price per unit, where p>C
23. Q : The ordering quantity
24. S : The maximum inventory level per cycle.

THE MATHEMATICAL MODEL

The model begins at time t=0.Initially the business community purchases a certain amount of item from market. From which certain amount is used to meet up the backorder quantities in previous cycle and 'q' units of products are kept in OW and the remaining amount in RW. During the time interval $0 \le t \le t_1$ the inventory level in RW decreases due to both demand and deterioration and becomes zero at t=t_1.But in OW the inventory level q decreases during $0 \le t \le t_1$,due to deterioration only and during $t_1 \le t \le t_2$ due to both demand and deterioration. At time $t = t_2$, the inventory level in OW reaches to zero. Then shortages are allowed to occur during $t_2 \le t \le T$ .Our objective is to find the maximum total average profit by considering all the relevant costs per unit time of the inventory system.

The inventory levels in RW and OW are given by the following differential equations

$$\frac{dI_1}{dt}+\beta I_1 = -(a+bt+ct^2+dt^3) \quad , 0\le t\le t_1. \qquad \text{..... (1)}$$

With the condition $I_1(t) = 0$, at $t=t_1$

And $$\frac{dI_2}{dt}+\alpha I_2=0 \quad , 0\le t\le t_1. \qquad \text{..... (2)}$$

With the condition $I_2(0) = q$

The solution of (1) and (2) are,

$$I_1 = -[a+b\,(t_1-\tfrac{1}{\beta})+c\,(t_1^2-\tfrac{4t_1}{\beta}+\tfrac{6}{\beta^2})+d\,(t_1^3-\tfrac{9t_1^2}{\beta}+\tfrac{36t_1}{\beta^2}-\tfrac{60}{\beta^3})]\,e^{\beta(t_1-t)}+[a+b\,(t-\tfrac{1}{\beta})+c\,(t^2-\tfrac{4t}{\beta}+\tfrac{6}{\beta^2})+d\,(t^3-\tfrac{9t^2}{\beta}+\tfrac{36t}{\beta^2}-\tfrac{60}{\beta^3})] \qquad \text{..... (3)}$$

$$I_2 = qe^{-\alpha t} \qquad \text{..... (4)}$$

Again during the time $t_1 \le t \le t_2$, the inventory level in OW decreases due to both demand and deterioration.

The differential equation involved here is:-

$$\frac{dI_2}{dt}+\alpha I_2 = -(a+bt+ct^2+dt^3) \quad , t_1\le t\le t_2$$

With the condition $I_2(t) = 0$, at $t=t_2$

Therefore,

$$I_2 = -[a+b\,(t_2-\tfrac{1}{\alpha})+c\,(t_2^2-\tfrac{4t_2}{\alpha}+\tfrac{6}{\alpha^2})+d\,(t_2^3-\tfrac{9t_2^2}{\alpha}+\tfrac{36t_2}{\alpha^2}-\tfrac{60}{\alpha^3})]\,e^{\alpha(t_2-t)}+[a+b\,(t-\tfrac{1}{\alpha})+c\,(t^2-\tfrac{4t}{\alpha}+\tfrac{6}{\alpha^2})+d\,(t^3-\tfrac{9t^2}{\alpha}+\tfrac{36t}{\alpha^2}-\tfrac{60}{\alpha^3})] \qquad \text{..... (5)}$$

From (4) and (5) and due to the continuity at $t= t_1$ is,

$$I_2(t_1) = qe^{-\alpha t_1}$$

$$\Longrightarrow -[a+b\,(t_2-\tfrac{1}{\alpha})+c\,(t_2^2-\tfrac{4t_2}{\alpha}+\tfrac{6}{\alpha^2})+d\,(t_2^3-\tfrac{9t_2^2}{\alpha}+\tfrac{36t_2}{\alpha^2}-\tfrac{60}{\alpha^3})]\,e^{\alpha(t_2-t_1)}+[a+b\,(t_1-\tfrac{1}{\alpha})+c\,(t_1^2-\tfrac{4t_1}{\alpha}+\tfrac{6}{\alpha^2})+d\,(t_1^3-\tfrac{9t_1^2}{\alpha}+\tfrac{36t_1}{\alpha^2}-\tfrac{60}{\alpha^3})] = qe^{-\alpha t_1}$$

$\Longrightarrow q= (e^{\alpha t_1} - e^{\alpha t_2}) [a+b (t_1- t_2) +c (t_1^2- t_2^2 - \frac{4t_1}{\alpha} + \frac{4t_2}{\alpha}) +d (t_1^3- t_2^3+ \frac{9}{\alpha}(t_2^2- t_1^2) + \frac{36}{\alpha^2}(t_1- t_2)]$

$\Longrightarrow e^{\alpha t_1} - e^{\alpha t_2}= \frac{q}{[a+b (t_1- t_2) +c (t_1^2- t_2^2 - \frac{4t_1}{\alpha} + \frac{4t_2}{\alpha}) +d (t_1^3- t_2^3+ \frac{9}{\alpha}(t_2^2- t_1^2) + \frac{36}{\alpha^2}(t_1- t_2)]}$

$\Longrightarrow e^{\alpha t_2}=e^{\alpha t_1} - \frac{q}{[a+b (t_1- t_2) +c (t_1^2- t_2^2 - \frac{4t_1}{\alpha} + \frac{4t_2}{\alpha}) +d (t_1^3- t_2^3+ \frac{9}{\alpha}(t_2^2- t_1^2) + \frac{36}{\alpha^2}(t_1- t_2)]}$

$\Longrightarrow t_2= \frac{\ln (e^{\alpha t_1} - \frac{q}{[a+b (t_1- t_2) +c (t_1^2- t_2^2 - \frac{4t_1}{\alpha} + \frac{4t_2}{\alpha}) +d (t_1^3- t_2^3+ \frac{9}{\alpha}(t_2^2- t_1^2) + \frac{36}{\alpha^2}(t_1- t_2)]})}{\alpha}$ ..... (6)

Again during, $t_2 \leq t \leq T$, shortage occurs, so inventory level is backlogged follows the differential equation

$\frac{dI_3}{dt} = -(a+bt+ct^2+dt^3) (A+Bt)$, $t_1 \leq t \leq T$..... (7)

With the condition $I_3 (t) = 0$, at $t=t_2$

Therefore,

$I_3=Aa (t_2-t)+(\frac{aB}{2} + \frac{Ab}{2}) (t_2^2- t^2) +(\frac{Ac}{3} + \frac{Bb}{3}) (t_2^3- t^3) + (\frac{Bc}{4}+\frac{dA}{4}) (t_2^4- t^4) + \frac{Bd}{5}(t_2^5- t^5)$ .....(8)

The order quantity about replenishment cycle is given as,

$Q = I_1 (0) + I_2 (0) - I_3 (T)$

$=-[a+b (t_1- \frac{1}{\beta}) +c (t_1^2 - \frac{4t_1}{\beta} + \frac{6}{\beta^2}) +d (t_1^3- \frac{9t_1^2}{\beta} +\frac{36t_1}{\beta^2} -\frac{60}{\beta^3})] e^{\beta t_1} +[a - \frac{b}{\beta} + \frac{6c}{\beta^2} - \frac{60d}{\beta^3}] +q -[Aa (t_2-T)+(\frac{aB}{2} + \frac{Ab}{2}) (t_2^2- T^2) +(\frac{Ac}{3} + \frac{Bb}{3}) (t_2^3- T^3) + (\frac{Bc}{4}+\frac{dA}{4}) (t_2^4- T^4) + \frac{Bd}{5}(t_2^5- T^5)]$..... (9)

The maximum inventory level per cycle is,

$S = I_1 (0) + I_2 (0)$

$= -[a+b (t_1- \frac{1}{\beta}) +c (t_1^2 - \frac{4t_1}{\beta} + \frac{6}{\beta^2}) +d (t_1^3- \frac{9t_1^2}{\beta} +\frac{36t_1}{\beta^2} -\frac{60}{\beta^3})] e^{\beta t_1} +[a - \frac{b}{\beta} + \frac{6c}{\beta^2} - \frac{60d}{\beta^3}] +q$ ..... (10)

Holding cost per cycle in RW,

$C_{H1} = \int_0^{t_1} h_r I_1 dt$

$= h_r\{[a + b \left(t_1 - \frac{1}{\beta}\right) + c \left(t_1^2 - \frac{4t_1}{\beta} + \frac{6}{\beta 2}\right) + d \left(t_1^3 - \frac{9t_1^2}{\beta} + \frac{36t_1}{\beta 2} - \frac{60}{\beta 3}\right)][\frac{1}{\beta} - \frac{e^{\beta t_1}}{\beta}] +(a - \frac{b}{\beta} - \frac{60d}{\beta^3} +\frac{6c}{\beta^2})t_1 + (b- \frac{4c}{\beta} +\frac{36d}{\beta^2}) \frac{t_1^2}{2} + (c- \frac{9d}{\beta}) \frac{t_1^3}{3} + d \frac{t_1^4}{4} \}$.....(11)

Holding cost per cycle in OW,

$C_{H2} = \int_0^{t_1} h_o I_2 dt + \int_{t_1}^{t_2} h_o I_2 dt$

$$=-\frac{h_o q e^{-\alpha t_1}}{\alpha}+h_o\{[a+b\left(t_1-\frac{1}{\beta}\right)+c\left(t_1^2-\frac{4t_1}{\beta}+\frac{6}{\beta 2}\right)+d\left(t_1^3-\frac{9t_1^2}{\beta}+\frac{36t_1}{\beta 2}-\frac{60}{\beta 3}\right)][\frac{1}{\beta}-\frac{e^{\beta(t_2-t_1)}}{\beta}]+(a-\frac{b}{\alpha}-\frac{60d}{\alpha^3}+\frac{6c}{\alpha^2})(t_2-t_1)+(b-\frac{4c}{\beta}+\frac{36d}{\beta^2})(\frac{t_2^2}{2}-\frac{t_1^2}{2})+(c-\frac{9d}{\beta})(\frac{t_2^3}{3}-\frac{t_1^3}{3})+d(\frac{t_2^4}{4}-\frac{t_1^4}{4})\}$$ .....(12)

Total holding cost, $C_H = C_{H_1}+C_{H_2}$ ..... (13)

Ordering cost =P

Backlogging cost per cycle, SC= $-C_s\int_{t_2}^{T}(A+Bt)dt$

$$=-C_s[(T-t_2)\,A+B\,(\frac{T^2-{t_2}^2}{2})]$$ ..... (14)

Opportunity cost, OC = $R\,(T-t_2)[1-A-\frac{B}{2}(T+t_2)]$ ..... (15)

Purchase cost per cycle, PC =CQ..... (16)

Sales revenue per cycle,

SR = $p\,[\int_0^{t_2}(a+bt+ct^2+dt^3)dt+\int_{t_2}^{T}(a+bt+ct^2+dt^3)\,(A+Bt)\mathrm{d}t]$

$$=p(at_2+b\frac{t_2^2}{2}+c\frac{t_2^3}{3}+d\frac{t_2^4}{4})+p[Aa(T-t_2)+(aB+bA)(\frac{T^2}{2}-\frac{{t_2}^2}{2})+(bB+Ac)(\frac{T^3}{3}-\frac{{t_2}^3}{3})+(Bc+Ad)(\frac{T^4}{4}-\frac{{t_2}^4}{4})+Bd(\frac{T^5}{5}-\frac{{t_2}^5}{5})]$$ .....(17)

Total profit per unit is,

X = $\frac{1}{T}$ [SR-Ordering cost- C_H-OC-SC-PC]

$$=\frac{1}{T}\{p(at_2+b\frac{t_2^2}{2}+c\frac{t_2^3}{3}+d\frac{t_2^4}{4})+p[Aa(T-t_2)+(aB+bA)(\frac{T^2}{2}-\frac{{t_2}^2}{2})+(bB+Ac)(\frac{T^3}{3}-\frac{{t_2}^3}{3})+(Bc+Ad)(\frac{T^4}{4}-\frac{{t_2}^4}{4})+Bd(\frac{T^5}{5}-\frac{{t_2}^5}{5})]-P-h_r\{[a+b\left(t_1-\frac{1}{\beta}\right)+c\left(t_1^2-\frac{4t_1}{\beta}+\frac{6}{\beta 2}\right)+d\left(t_1^3-\frac{9t_1^2}{\beta}+\frac{36t_1}{\beta 2}-\frac{60}{\beta 3}\right)][\frac{1}{\beta}-\frac{e^{\beta t_1}}{\beta}]+(a-\frac{b}{\beta}-\frac{60d}{\beta^3}+\frac{6c}{\beta^2})t_1+(b-\frac{4c}{\beta}+\frac{36d}{\beta^2})\frac{t_1^2}{2}+(c-\frac{9d}{\beta})\frac{t_1^3}{3}+d\frac{t_1^4}{4}\}-\frac{h_o q e^{-\alpha t_1}}{\alpha}+h_o\{[a+b\left(t_1-\frac{1}{\beta}\right)+c\left(t_1^2-\frac{4t_1}{\beta}+\frac{6}{\beta 2}\right)+d\left(t_1^3-\frac{9t_1^2}{\beta}+\frac{36t_1}{\beta 2}-\frac{60}{\beta 3}\right)][\frac{1}{\beta}-\frac{e^{\beta(t_2-t_1)}}{\beta}]+(a-\frac{b}{\alpha}-\frac{60d}{\alpha^3}+\frac{6c}{\alpha^2})(t_2-t_1)+(b-\frac{4c}{\beta}+\frac{36d}{\beta^2})(\frac{t_2^2}{2}-\frac{t_1^2}{2})+(c-\frac{9d}{\beta})(\frac{t_2^3}{3}-\frac{t_1^3}{3})+d(\frac{t_2^4}{4}-\frac{t_1^4}{4})\}+C_s[(T-t_2)A+B(\frac{T^2-{t_2}^2}{2})]-R(T-t_2)[1-A-\frac{B}{2}(T+t_2)]-C[-\{a+b\,(t_1-\frac{1}{\beta})+c\,(t_1^2-\frac{4t_1}{\beta}+\frac{6}{\beta^2})+d(t_1^3-\frac{9t_1^2}{\beta}+\frac{36t_1}{\beta^2}-\frac{60}{\beta^3})\}e^{\beta t_1}+[a-\frac{b}{\beta}+\frac{6c}{\beta^2}-\frac{60d}{\beta^3}]]-Cq-C[Aa(t_2-T)+\frac{aB}{2}({t_2}^2-T^2)+\frac{Ab}{2}({t_2}^2-T^2)+\frac{Bb}{3}({t_2}^3-T^3)+\frac{Ac}{3}({t_2}^3-T^3)+\frac{Bc}{4}({t_2}^4-T^4)+\frac{dA}{4}({t_2}^4-T^4)+\frac{Bd}{5}({t_2}^5-T^5)]$$ .....(18)

Now, the total profit of the system is maximum if it satisfies

$\frac{\partial X}{\partial t_2}=0$, $\frac{\partial X}{\partial T}=0$; $\frac{\partial^2 X}{\partial {t_2}^2}>0$, $\frac{\partial^2 X}{\partial T^2}>0$

$$\frac{\partial^2 X}{\partial {t_2}^2}\frac{\partial^2 X}{\partial T^2}-(\frac{\partial^2 X}{\partial t_2 \partial T})^2<0$$

FUZZY MODEL

In the above model we have developed a crisp model in which holding costs in RW and OW are fuzzy in nature along with ordering cost and backorder cost. We have considered these cost parameters as triangular fuzzy numbers and then defuzzified by the method of Signed distance defuzzification method.

SIGNED DISTANCE METHOD

Here holding costs, ordering cost, backorder cost are considered as triangular fuzzy number. Suppose the following numbers

(i) $h_r \in [h_r - \Delta_1, h_r + \Delta_2], 0 < \Delta_1 < h_r, 0 < \Delta_1\Delta_2$
(ii) $h_o \in [h_o - \Delta_3, h_o + \Delta_4], 0 < \Delta_3 < h_o, 0 < \Delta_3\Delta_4$
(iii) $P \in [P - \Delta_5, P + \Delta_6], 0 < \Delta_5 < P, 0 < \Delta_5\Delta_6$
(iv) $C_s \in [C_s - \Delta_7, C_s + \Delta_8], 0 < \Delta_7 < C_s, 0 < \Delta_7\Delta_8$

The signed distance method of the above fuzzy numbers are as

(i) $d(\widetilde{h_r}, 0) = h_r + \frac{1}{4}(\Delta_2 - \Delta_1)$
(ii) $d(\widetilde{h_o}, 0) = h_o + \frac{1}{4}(\Delta_4 - \Delta_3)$
(iii) $d(\check{P}, 0) = P + \frac{1}{4}(\Delta_6 - \Delta_5)$
(iv) $d(\check{C_s}, 0) = C_s + \frac{1}{4}(\Delta_8 - \Delta_7)$

Now, $\check{X} = (X_1, X_2, X_3)$

$X_1 = \frac{1}{T}$ { p($at_2 + b\frac{t_2^2}{2} + c\frac{t_2^3}{3} + d\frac{t_2^4}{4}$) +p[Aa(T-$t_2$)+(aB+bA)($\frac{T^2}{2} - \frac{t_2^2}{2}$)+(bB+Ac)($\frac{T^3}{3} - \frac{t_2^3}{3}$) +(Bc+Ad)($\frac{T^4}{4} - \frac{t_2^4}{4}$)+ Bd($\frac{T^5}{5} - \frac{t_2^5}{5}$)] –(P−$\Delta_5$) − ($h_r - \Delta_1$){[a + b $\left(t_1 - \frac{1}{\beta}\right)$ + c $\left(t_1^2 - \frac{4t_1}{\beta} + \frac{6}{\beta 2}\right)$ + d $\left(t_1^3 - \frac{9t_1^2}{\beta} + \frac{36t_1}{\beta 2} - \frac{60}{\beta 3}\right)$][$\frac{1}{\beta} - \frac{e^{\beta t_1}}{\beta}$] +($a - \frac{b}{\beta} - \frac{60d}{\beta^3} + \frac{6c}{\beta^2}$)$t_1$ + (b-$\frac{4c}{\beta} + \frac{36d}{\beta^2}$)$\frac{t_1^2}{2}$ +(c−$\frac{9d}{\beta}$)$\frac{t_1^3}{3} + d\frac{t_1^4}{4}$ }−$\frac{(h_o - \Delta_3)qe^{-\alpha t_1}}{\alpha}$ + ($h_o - \Delta_3$){[a + b $\left(t_1 - \frac{1}{\beta}\right)$ + c $\left(t_1^2 - \frac{4t_1}{\beta} + \frac{6}{\beta 2}\right)$ + d $\left(t_1^3 - \frac{9t_1^2}{\beta} + \frac{36t_1}{\beta 2} - \frac{60}{\beta 3}\right)$][$\frac{1}{\beta} - \frac{e^{\beta(t_2 - t_1)}}{\beta}$] +($a - \frac{b}{\alpha} - \frac{60d}{\alpha^3} + \frac{6c}{\alpha^2}$)($t_2 - t_1$) + (b-$\frac{4c}{\beta} + \frac{36d}{\beta^2}$) ($\frac{t_2^2}{2} - \frac{t_1^2}{2}$)+ (c-$\frac{9d}{\beta}$) ($\frac{t_2^3}{3} - \frac{t_1^3}{3}$) + $d(\frac{t_2^4}{4} - \frac{t_1^4}{4})$}+($C_s - \Delta_7$)[($T - t_2$)A+B($\frac{T^2 - t_2^2}{2}$)]− R($T - t_2$)[$1 - A - \frac{B}{2}(T + t_2)$]-C[-{a+b ($t_1$-$\frac{1}{\beta}$) +c ($t_1^2$-$\frac{4t_1}{\beta} + \frac{6}{\beta^2}$)+d($t_1^3$-$\frac{9t_1^2}{\beta} + \frac{36t_1}{\beta^2} - \frac{60}{\beta^3}$)} $e^{\beta t_1}$+[a -$\frac{b}{\beta} + \frac{6c}{\beta^2} - \frac{60d}{\beta^3}$]] −Cq –C[Aa($t_2$-T)+ $\frac{aB}{2}$(t_2^2-T^2)+ $\frac{Ab}{2}$(t_2^2-T^2)+ $\frac{Bb}{3}$(t_2^3- T^3)+ $\frac{Ac}{3}$(t_2^3- T^3)+ $\frac{Bc}{4}$(t_2^4- T^4)+ $\frac{dA}{4}$(t_2^4- T^4)+ $\frac{Bd}{5}$(t_2^5- T^5)]}

$X_2 = X$

$$X_3=\frac{1}{T}\{p(at_2+b\frac{t_2^2}{2}+c\frac{t_2^3}{3}+d\frac{t_2^4}{4})+p[Aa(T-t_2)+(aB+bA)(\frac{T^2}{2}-\frac{t_2^2}{2})+(bB+Ac)(\frac{T^3}{3}-\frac{t_2^3}{3})+(Bc+Ad)(\frac{T^4}{4}-\frac{t_2^4}{4})+Bd(\frac{T^5}{5}-\frac{t_2^5}{5})]-(P+\Delta_6)-(h_r+\Delta_2)\{[a+b\left(t_1-\frac{1}{\beta}\right)+c\left(t_1^2-\frac{4t_1}{\beta}+\frac{6}{\beta 2}\right)+d\left(t_1^3-\frac{9t_1^2}{\beta}+\frac{36t_1}{\beta 2}-\frac{60}{\beta 3}\right)][\frac{1}{\beta}-\frac{e^{\beta t_1}}{\beta}]+(a-\frac{b}{\beta}-\frac{60d}{\beta^3}+\frac{6c}{\beta^2})t_1+(b-\frac{4c}{\beta}+\frac{36d}{\beta^2})\frac{t_1^2}{2}+(c-\frac{9d}{\beta})\frac{t_1^3}{3}+d\frac{t_1^4}{4}\}-\frac{(h_o+\Delta_4)qe^{-\alpha t_1}}{\alpha}+(h_o+\Delta_4)\{[a+b\left(t_1-\frac{1}{\beta}\right)+c\left(t_1^2-\frac{4t_1}{\beta}+\frac{6}{\beta 2}\right)+d\left(t_1^3-\frac{9t_1^2}{\beta}+\frac{36t_1}{\beta 2}-\frac{60}{\beta 3}\right)][\frac{1}{\beta}-\frac{e^{\beta(t_2-t_1)}}{\beta}]+(a-\frac{b}{\alpha}-\frac{60d}{\alpha^3}+\frac{6c}{\alpha^2})(t_2-t_1)+(b-\frac{4c}{\beta}+\frac{36d}{\beta^2})(\frac{t_2^2}{2}-\frac{t_1^2}{2})+(c-\frac{9d}{\beta})(\frac{t_2^3}{3}-\frac{t_1^3}{3})+d(\frac{t_2^4}{4}-\frac{t_1^4}{4})\}+(C_s+\Delta_8)[(T-t_2)A+B(\frac{T^2-t_2^2}{2})]-R(T-t_2)[1-A-\frac{B}{2}(T+t_2)]-C[-\{a+b(t_1-\frac{1}{\beta})+c(t_1^2-\frac{4t_1}{\beta}+\frac{6}{\beta^2})+d(t_1^3-\frac{9t_1^2}{\beta}+\frac{36t_1}{\beta^2}-\frac{60}{\beta^3})\}e^{\beta t_1}+[a-\frac{b}{\beta}+\frac{6c}{\beta^2}-\frac{60d}{\beta^3}]]-Cq-C[Aa(t_2-T)+\frac{aB}{2}(t_2^2-T^2)+\frac{Ab}{2}(t_2^2-T^2)+\frac{Bb}{3}(t_2^3-T^3)+\frac{Ac}{3}(t_2^3-T^3)+\frac{Bc}{4}(t_2^4-T^4)+\frac{dA}{4}(t_2^4-T^4)+\frac{Bd}{5}(t_2^5-T^5)]\}.....(19)$$

Total profit per unit time by signed distance method is as follows,

$$d(\check{X})=X+\frac{1}{T}\{p(at_2+b\frac{t_2^2}{2}+c\frac{t_2^3}{3}+d\frac{t_2^4}{4})+p[Aa(T-t_2)+(aB+bA)(\frac{T^2}{2}-\frac{t_2^2}{2})+(bB+Ac)(\frac{T^3}{3}-\frac{t_2^3}{3})+(Bc+Ad)(\frac{T^4}{4}-\frac{t_2^4}{4})+Bd(\frac{T^5}{5}-\frac{t_2^5}{5})]-(\frac{\Delta_6-\Delta_7}{4})-(\frac{\Delta_2-\Delta_1}{4})\{[a+b\left(t_1-\frac{1}{\beta}\right)+c\left(t_1^2-\frac{4t_1}{\beta}+\frac{6}{\beta 2}\right)+d\left(t_1^3-\frac{9t_1^2}{\beta}+\frac{36t_1}{\beta 2}-\frac{60}{\beta 3}\right)][\frac{1}{\beta}-\frac{e^{\beta t_1}}{\beta}]+(a-\frac{b}{\beta}-\frac{60d}{\beta^3}+\frac{6c}{\beta^2})t_1+(b-\frac{4c}{\beta}+\frac{36d}{\beta^2})\frac{t_1^2}{2}+(c-\frac{9d}{\beta})\frac{t_1^3}{3}+d\frac{t_1^4}{4}\}-\frac{(\Delta_4-\Delta_3)qe^{-\alpha t_1}}{4\alpha}+(\frac{\Delta_4-\Delta_3}{4})\{[a+b\left(t_1-\frac{1}{\beta}\right)+c\left(t_1^2-\frac{4t_1}{\beta}+\frac{6}{\beta 2}\right)+d\left(t_1^3-\frac{9t_1^2}{\beta}+\frac{36t_1}{\beta 2}-\frac{60}{\beta 3}\right)][\frac{1}{\beta}-\frac{e^{\beta(t_2-t_1)}}{\beta}]+(a-\frac{b}{\alpha}-\frac{60d}{\alpha^3}+\frac{6c}{\alpha^2})(t_2-t_1)+(b-\frac{4c}{\beta}+\frac{36d}{\beta^2})(\frac{t_2^2}{2}-\frac{t_1^2}{2})+(c-\frac{9d}{\beta})(\frac{t_2^3}{3}-\frac{t_1^3}{3})+d(\frac{t_2^4}{4}-\frac{t_1^4}{4})\}+(\Delta_8-\Delta_7)/4[(T-t_2)A+B(\frac{T^2-t_2^2}{2})]-R(T-t_2)[1-A-\frac{B}{2}(T+t_2)]-C[-\{a+b(t_1-\frac{1}{\beta})+c(t_1^2-\frac{4t_1}{\beta}+\frac{6}{\beta^2})+d(t_1^3-\frac{9t_1^2}{\beta}+\frac{36t_1}{\beta^2}-\frac{60}{\beta^3})\}e^{\beta t_1}+[a-\frac{b}{\beta}+\frac{6c}{\beta^2}-\frac{60d}{\beta^3}]]-Cq-C[Aa(t_2-T)+\frac{aB}{2}(t_2^2-T^2)+\frac{Ab}{2}(t_2^2-T^2)+\frac{Bb}{3}(t_2^3-T^3)+\frac{Ac}{3}(t_2^3-T^3)+\frac{Bc}{4}(t_2^4-T^4)+\frac{dA}{4}(t_2^4-T^4)+\frac{Bd}{5}(t_2^5-T^5)]\}$$

.....(20)

Hence it is possible to get the optimum solution for any particular situation with the help of the above equation (20). Also numerical solution can be obtained with suitable software.

CONCLUSION

In real life, uncertainty plays an important role in formulating a decision making problem of any industry or business company. Due to this uncertainty several parameters may be imprecise. To deal with such problem fuzzy logic is used. In this paper, a two warehouse Fuzzy inventory model is developed considering demand as cubic function of time t, different cost parameters are considered to be fuzzy in nature. Here triangular fuzzy number is used to depict the cost parameters. The deterioration factor is also taken in to consideration here as almost all the products will undergo decay in the course of time due different factors and different preserving facilities in both the warehouses. Also it is assumed that preserving facility of RW is better than in OW. With the help of our formulated system any numerical illustration can be studied with suitable values.

REFERENCES:

[1] Aggarwal, S.P. and Jaggi, C.K. (1995), Ordering policies of deteriorating items under permissible delay in payments, Journal of Operational Research Society (J.O.R.S), 46,658-662.

[2] Benkherouf, L A. (1997), A deterministic order level inventory model for deteriorating items with two storage facilities, International Journal of Production Economics, 48, 167-175.

[3] Balkhi,Z.T. and Benkherouf, L. (2004),On an inventory model for deteriorating items with stock dependent and time varying demand rates, Computers & Operations Research,31,223-240.

[4] Bhunia, A. K. and Maiti M. (1994), A two-warehouse inventory model for a linear trend in demand, Opsearch, 31, 318-329.

[5] Bhunia, A. K. and Mait, M. (1997b), A two warehouses inventory model for deteriorating items with linear trend in demand and shortages, Journal of Operational Research Society, 49, 287-292.

[6] Bellman, E, and Zadeh, L.A (1970).Decesion making in a fuzzy environment.Management Science17 (4):B141-B164

[7] Covert,R.P and Philip,G.P(1973), "An EOQ model for items with Weibull distribution deterioration",AIIE Trans,5(4),323-329

[8] Deb Choudhury.P and Dutta.P(2015), "A Two Warehouse Inventory Model for Deteriorating Items with Cubic Demand, Quadratic Holding Cost and Variable Backlogging Rate", IJAENT,Volume-2 Issue-10, September 2015

[9] Dave, U. (1988), On the EOQ models with two levels of storage, Opsearch, 25.

[10] Donaldson W.A. (1977), Inventory replenishment policy for a linear trend in demand-an analytical solution, Operational Research Quarterly, 28,663-670.

[11] Ghare, P.M and Schrader,G.P (1963) "A model for exponentially decaying inventory", Journal of Industrial Engineering(J.I.E),14,228-243

[12] Goswami, A. and Chaudhuri, K. S. (1992), An economic order quantity model for items with two levels of storage for a linear trend in demand, Journal of Operational Research Society, .43, 157-167.

[13] Haringa.M.A (1995), Effects of inflation and time-value of money of an inventory model on an inventory model with time-dependent demand rate and shortages, E.J.O.R, 81(3), 512-520.

[14] Hartely, R. V. (1976), Operations Research-a managerial emphasis, Goodyear publishing Company, 315-317.

[15] Kar, S., Bhunia, A. K. and Maiti, M. (2001), Deterministic inventory model with two levels of storage, a linear trend in demand and a fixed time horizon, Computers and Operations Research, 28 , 1315-1331.

[16] Lee, C. C. and Ma, C. Y. (2000), Optimal inventory policy for deteriorating items with two warehouse and time dependent demands, Production Planning And Control, 7, 689-696.

[17] Mondal, M and Maiti, M.(1999),Inventory of damageable items with variable replenishment rate, stock-dependent demand and some units in hand, Applied Mathematical Modelling,23(1999),pp.799-807.

[18] Mondal, B., Bhunia, A.K. and Maiti, M. (2007), A model on two storage inventory system under stock dependent selling rate incorporating marketing decisions and transportation cost with optimalrelease rule, Tamsui Oxford Journal of Mathematical Sciences, vol-23(3), 243-267.

[19] Mahapatra, N.K. and Maiti, M. (2005), Multi objective inventory models of multi items with quality and stock dependent demand and stochastic deterioration, Advanced Modelling and Optimization.7, 1, 69-84.

[20] Pakkala, T.P.M. and Achary, K.K. (1992), A deterministic inventory model for deteriorating items with two warehouse and finite replenishment rate, European Journal of Operational Research,57, 71-76.

[21] Panda, S, Saha, S. and Basu,M.(2007),An EOQ model with generalized ramp-type demand and Weibull distribution deterioration, Asia Pacific Journal of Operational Research, 24(1),1-17.

[22] Park, K.S (1987) Fuzzy set theoretic interpretation of economic order quantity, IEEE Transactions on systems, Man and Cybernetics,17(6), 1082-1084.

[23] Sana, S, and Chaudhuri, K.S (2008), A deterministic EOQ model with delays in payments and price-discounts offer, E.J.O.R, 184,504-533.

[24] Sharma, K. V. S. (1983), A deterministic inventory model with two levels of storage and anoptimum release rule, Opsearch, 29, 175-180.

[25] Sharma, K. V. S. (1987), A deterministic order-level inventory model for deteriorating items with Two storage facilities, European Journal of Operational Research, 29, 70-72.

[26] Wu, K.S, Ouyang, L.Y.and Yang, C.T. (2006), An optimal Replenishment policy for non-instantaneous deteriorating items with stock dependent demand and partial backlogging, I.J.P.E, 101-369-384.

[27] Yadav.A.S and Swami.A. (2013),A two-warehouse inventory model for decaying items with exponential demand and variable holding cost, IJIES.

[28] Yadav .R.K and Vats .A.K. (2014), A deteriorating inventory model for quadratic demand and constant holding cost with partial backlogging and inflation, IOSR.

[29] Yang, H.L (2004). Two-warehouse inventory models for deteriorating items with shortages under inflation, European Journal of Operational Research, 157, 344-356.

[30] Yang, H.L (2006). Two-warehouse partial backlogging inventory models for deteriorating items under inflation, International Journal of Production Economics, 103, 362-370.

[31] Yao J.S and Lee H.M,(1999) Fuzzy inventory with or without backorder for fuzzy order quantity with trapezoidal fuzzy number. Fuzzy sets and Systems,105,311-337.

[32] Y.W.Zhou(2003).A multi-warehouse Inventory model for items with time –varying demand and shortages. Computers and operation Research,vol 30,no 14,pp 2115-2134.

[33] Zadeh,L.A(1965).Fuzzy sets,Information and control,8,338-353.

[34] Zimmermann, H.J (1991).Fuzzy set theory and its applications ,Kluwer Academic Press: Dordrecht.

[35] Zhou, Y.W. and Yang, S.L. (2003), A two-warehouse inventory model for items with stock-level-dependent demand rate, International Journal of Production Economics, 95, 215-228

International Journal of Engineering Research and General Science Volume 3, Issue 5, September-October, 2015
ISSN 2091-2730

Scheduling of Dynamically Generated Tasks to find Energy Efficient Clock-cycle in CPU

Mrs. Bhuvaneshwari S Patil[1], Sheta Vipul B[2]

[1]Asst.Professor, Dept. of Computer Science and Engineering , NMIT, Bangalore, bsp14052001@gmail.com

[2]PG Student, Dept. of Computer Science and Engineering ,NMIT,Bangalore,vipul.sheta@gmail.com

Abstract— In computing field, central processing unit (CPU) plays role of running the jobs. The aim of CPU is to handle the jobs with respect to the scheduling methods of operating system. Jobs are being generated and executed which also allow preemption during running. Different numbers of scheduling methods already exist and many are in progress. In usual scheduling, there are chances of jobs not done, so completion of given set of jobs on time basis has created. Some techniques are used to find total possible jobs done along with its utilization. Concept used is smallest period and fastest deadline and some variation to complete the set of jobs. One of the concepts of green computing is to minimum power usage in CPU with keeping the clock cycle fixed .Energy usage is critical part of any computer systems. This can be used in any devices which run through battery e.g. mobile, laptops, embedded system, servers, etc. with respect to this project which will be mostly used for servers, where jobs are never ending. At operating system position, scheduling has being executed at different clock cycle and calculated energy used during their run time. Hence comparisons are made and analysis is done to find the energy efficient clock cycle with respect to fixed set continuous amount of jobs. The analysis involves the approximately constant time which is important criteria. Conclusion is derived which says "What Megahertz (MHz) of the CPU will perform jobs and save energy efficiently?"

Keywords—Scheduling ,CPU utilization,clock-cycle,preemptions,deadline,jobs,rate,monotonic,frequency,energy.

INTRODUCTION

Power consumption is important issue in battery held computing devices as it has limited energy. Using devices with full power and 100 percent CPU power will result in excessive heat and high electricity cost and even lifetime of that device decreases. Then again to cool those devices extra energy is used. This all leads to waste of resource. Thus question of reliability arises. In software side, the best way is to use different scheduling techniques and to choose the best according to device in which the software is going to be used. It's the combination of hardware and software, which plays far better role, rather than going alone. As per research much of energy is used by CPU rather than all other hardware like screen, cooling fan, speaker, etc. because workload is on CPU only. Because in nature, energy is limited and the usage in limited battery devices should be researched and response of all jobs should be done carefully. One method which is most common is dynamic voltage scaling is already playing important role. But here static clock-cycle and dynamic is task that is running. Here change in frequency at various times is done but kept constant till the jobs are completed.

GOALS

1. Find usage and availability of jobs.

Here, consideration of utilization factor of jobs is done which is from 0 to 100. With respect to this factor, possibility of jobs that would occur at various level of utilization needs to be count. This count is done in parallel with respect to all scheduling algorithm. The number will be displayed at each level of usage which shows amount of jobs that can be run and its value decreases as usage increases.

2. Fixing the clock-cycle and count the time.

With the help of a tool, clock-cycle values are being kept constant for entire period of execution. It is also being cross verified with the help of another tool before and after the execution of program. Time is being calculated through by default function in ubuntu. The consideration of user time is done because this is actual time taken by execution of process. The real and system time is not useful in the consideration. Hence they are ignored.

3. Count the energy used.

Energy calculation is based on amount of energy before execution of process minus amount of energy after execution. The result is termed as energy count for that specific process. Energy count also includes energy consumption of various hardware components but solution for that is also provided.

4. Compare the time and energy for respective clock-cycle.

This is analysis part which is being done by setting the frequency fixed and calculates energy and time factor for entire period of execution. Multiple times such value is counted in order to find energy efficient clock-cycle.

SURVEY

Energy is defined as multiplication of power and time at any instant [1].

$$E = P * t \quad \text{----------(1)}$$

E=energy consumption during execution.

P=power consumption

t = total time taken for execution

Depending upon task running or not, we have two types:

1 Dynamic: when CPU have task inside and power are used.

2. Static: when CPU don't have task, still power is being used.

Static scaling using rate monotonic and earliest deadline first gives better output and even all deadline are achieved [5].

Hard real time scheduling: It can be done in offline way to find worst case execution time (WCET) in task [6]. This method is definitely going to complete all jobs before their individual deadline.

Power can be estimated with respect to various simulations of jobs. Fixing the CPU clock-cycle values lead to more saving of energy. Balancing both factor that is of timeliness and energy is also important. Hence the system with variation of voltage levels is used to make experiment. For implementing these, set of task for execution is used but without pre-emption [8]. Starting with low energy earliest deadline first, check out initially with lowest frequency in order to check whether jobs are completed within time. Now, comparison can be made for power used with respect to utilization of task which proves earliest deadline first (EDF) consumes high but utilization is also high. Thus allowing pre-emption during runtime will lead to energy saving [8].

Basic requirements in Scheduling

1] Types of scheduling.
2] Types of jobs handling.
3] Allowable conditions.
4] Methodology with respect to hardware

1] Types of scheduling:

First come first served [FCFS]: It simply queues processes in the order that they arrive in the ready queue. It can give lower throughput because longer task can hold CPU for long time. This further leads to long waiting time and arrival time.

Earliest deadline first [EDF]:It is a dynamic scheduling algorithm used in real-time operating systems to place processes in a priority queue. Whenever a scheduling occurs, the queue finds for the process closest to its deadline, which will be the next to be scheduled for execution. In this algorithm, one can use the gap of time between consecutive jobs and within a single job. Within that loose timing, if it is used it will result in great difference in actual consumption of voltage in CPU [3].In [5] importance is given to deadline, the reason is real time task, if task is not completed as per time, the output is declared as wrong or unwanted.

Shortest remaining time job first : Here, the scheduler arranges processes with the shortest estimated execution time remaining to be next in the queue. This requires estimations about the time required for a process to complete. If a shorter process arrives during another process execution, the currently running process may be interrupted, dividing that process into two separate computing blocks The same rate monotonic based method with a difference can be used to minimize the energy for periodic jobs. It is applicable on jobs which are real time hard [4]. Along with this, three approaches can be combined. One is for each job, providing individual speed. Achieving the task allocation done perfectly is second. Third is main that is rate monotonic statically.

Fixed priority pre-emptive scheduling [FPPS]: Here, assignment of fixed priority rank to every process is done, and the scheduler arranges the processes in the ready queue as per their priority. Lower-priority processes get interrupted by new higher-priority processes.

Round-robin [RR]: The scheduler assigns a fix value time unit per process, and cycles continuously through them. It involves extensive overhead, more with a small time unit. As they have to repeat multiple times during cycle. Throughput here is shorter jobs are completed faster than in FIFO and longer processes are completed faster than in shortest job first. It has better average response time and waiting time depends on number of processes.

Specified level of assumptions: Here, whenever higher prior jobs enter, the smaller jobs have being given a threshold value for assumptions. Thus jobs can disable assumptions up to some level. So every job has a combination of priority assigned to them and addition to them this threshold value. Pre-emption is taking place with the condition that higher task has passed that value of threshold of executing job. Each jobs have their own priority, once they come into CPU for execution their priority is valued to their threshold. Hence non pre-emptive jobs can be controlled at much higher level. So, higher prior task can be held for some threshold period prescribed before start of execution [2]. It shows the advantage of decrease in overhead during execution.

Similar time for assumptions: In this algorithm, similar amount of time is provided to each jobs addition to their execution of period. This slot of time is equal among all set of jobs. Pre-emption is only allowed after that additional amount of time gets over for the smaller priority task. So this gives more time to low priority jobs.

Static assumptions: Here, whenever the jobs are running the pre-emption is not allowed at first. For introducing pre-emption some points are fixed at some locations before hand, so only at that points pre-emption is allowed, so set of jobs are divided into slots in a way that such slot do not allow pre-emption. If higher prior jobs occur during this slot, they have to wait till the slot is over or the fixed point comes. So here jobs need to give slot at some point.

2] Types of jobs handling:

There are devices which are not fully utilized and most of the time they are idle but the power utilization is constant throughout, thus need is to minimize it [1].

Periodic task is one that repeats itself after a certain fixed period interval. The precise time instants at which periodic tasks recur are usually limited by clock interrupts. For this reason, periodic tasks are sometimes called to as clock-driven tasks. The fixed time interval after which a task repeats is called the period of the task.

An aperiodic task can arise at random instants. However, in case of an aperiodic task, the minimum gap between two consecutive instances can be 0. That is, two or more instances of an aperiodic task might occur at the same time instant. Also, the deadline for aperiodic tasks is expressed as either an average value or is expressed statistically. Aperiodic tasks are soft real-time tasks.

3]Allowable conditions:

1. Whether to consider pre-emption or not?

When higher priority jobs arrive, the lower priority is stopped and higher is executed and rest of them are run at later.

2. Whether to migrate the running job or not?

It checks whether jobs can be changed during runtime from one processor to another.

3. Whether job can run on different processor simultaneously?

4] Methodology with respect to hardware:

DVFS method of reduction of energy can be used in many aspects. The real time of jobs cannot be counted because their execution takes separate path every time in inter task. In intra task the same job is being run, while change in frequency is done to minimize the time gap. During run time there is need of scaling up or down of voltage .Finding that point scaling point is aim to save energy [3].

Hardware and Software Interfaces

This project work is dependent on both hardware and software. The system should be run on battery operated laptop or notebook because that only will count total energy used. With different amount of processor power and ram power, the value of each scheduling and energy may vary. Rest all of above mentioned software should be installed without error.

Modules

1>header files: two header files are created for giving commonness of project parameters.

2>rest of main c program files are created.

3>on output side, we will check creation of pre-emption taking place in both of main algorithm.

4>second output generate total possibility of jobs created and usage.

5>analysis shows time factor and energy consumption during runtime of each output.

Diagrams

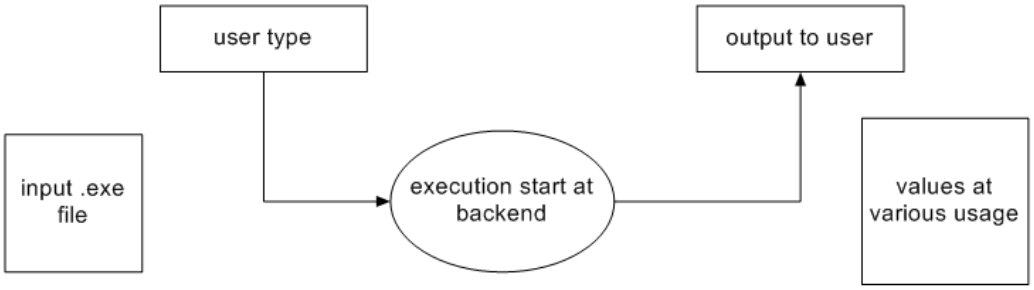

Fig:1 Dfd diagram level 0 for scheduling

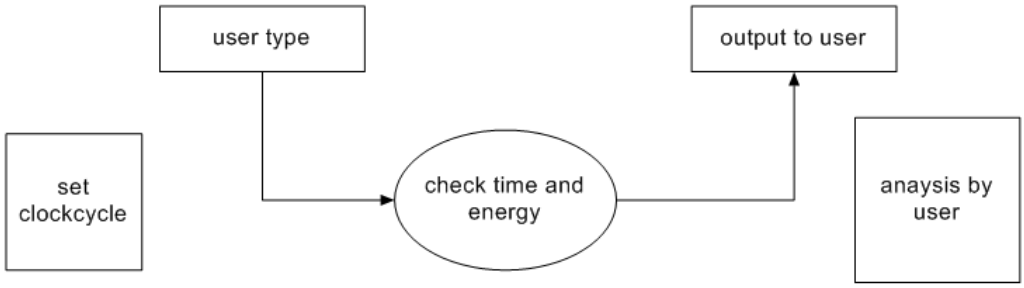

Fig:2 Dfd diagram level 1 for scheduling

Flow chart

Chart description: It is started with setting the clockcyle static for next process execution and checking the current energy level of the battery. In terminal, should be open and write the execution input. Here in this case it is .exe file. Now the process has started and various figures will start flowing on screen. The output will be time taken for execution and job possibility for all scheduling methods with respect to its usage. As soon as the execution is over, the energy is checked. On basis of it the analysis is done which contains counting of energy used.

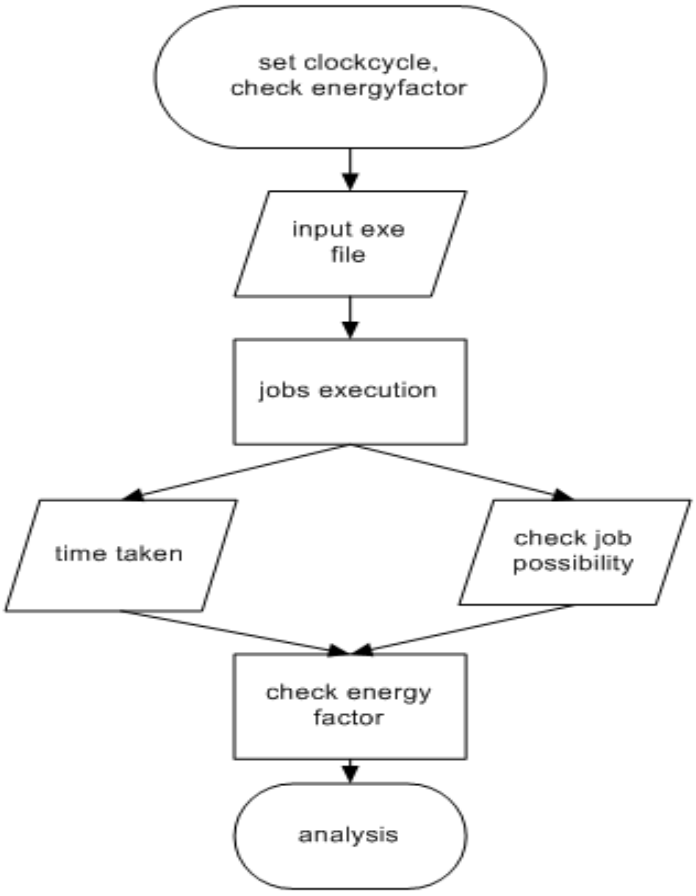

Fig:3 Flow chart for checking job possibility ratio

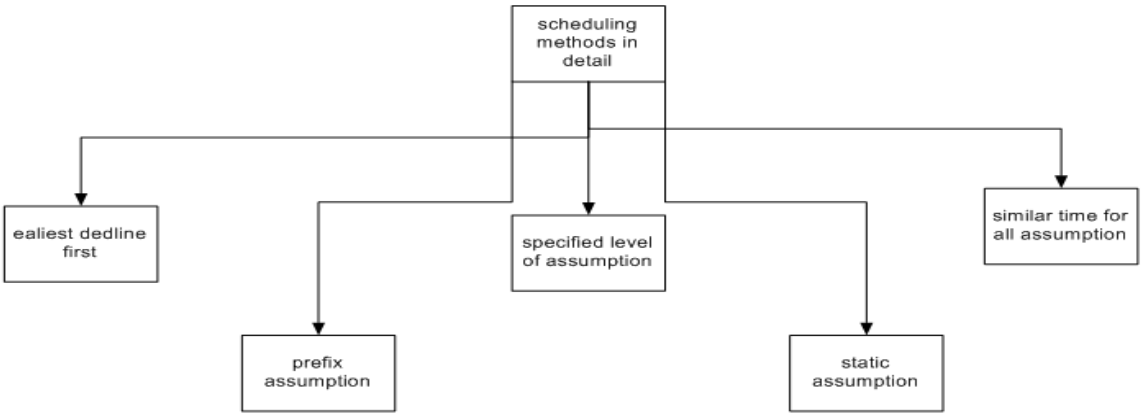

Fig:4 Block diagram for all scheduling techniques

Those are earliest deadline first which depends on deadline of the jobs, prefix assumption which depends on the period of completion of jobs, specified level of assumptions where at multiple level in execution the pre-emption is kept constant, static assumption where fixing the assumption is done and kept constant, similar time for all where each incoming jobs are given additional time of similar slot in order such that when some higher prior task is approaching it has to wait for that extra time.

PARAMETERS

1. Entire usage: the parameter is limited to proportion from zero to one hundred.
2. Cost: cost of assumption during the execution.
3. Task: total number of task.
4. States: all states in queue that is waiting, ready, current.
5. Prior: giving priority to job starting from zero.
6. Specifying level of assumption.
7. Worst case execution time.
8. Period of execution.
9. Deadline of jobs.
10. Arrival time of next job.

11 Remaining time of execution.

12. Allowance of pre-emption time.
13. Virtual time for job to be completed.
14. Similar time for all.
15. Static points for assumptions.

ALGORITHMS

Period and deadline based algorithm:

Steps:

1> Checking for possibility of process when pre-emption is allowed.
When the job is going to execute, the check is made for feasibility. So job can be said valid only if response time is before deadline period, if valid then job is counted in further step, else ignore.

2> Checking for possibility of complete set.
These check whether the entire set of jobs is feasible or not under pre-emptive conditions.

3> Counting of pre-emption done during execution time for rate monotonic.
It checks for virtual time is less than the execution time which is prescribed.

4> Insertion of process keeping factor deadline as main.
For EDF scheduling insertion of one by one task will take place under queue which is ready.

5> Keeping variable zero again.
Setting the variables pre-emption, virtual time of current job and last job has to reset to zero.

6> Entering the new upcoming process in pending line.
New job entering the execution needs to be in queue which is pending and also verifying that enqueue is ready.

7> Comparing the priority of current process and new coming process.

Comparison helps to decide for the pre-emption occur, if priority of new job is high than pre-emption will take place else will be ignored. Then the function puts the upper limit to algorithm. Again the check is made for possibility.

8> Getting response time and then checking for possibility of complete sets.

First the busy period of task is calculated and job is started. Response time of set is calculated in rate monotonic scheduling. Now the possibility of set is found with respect to rate monotonic.

Static assumption algorithm:

Steps:

1> Compute the function for float case.

The function is created to for calculating limit of task number which will be used in floating case. The limit is upper bound.

2> Calculating function by removing maximum chunk of task.

The new function is calculated referring to upper bound by removing the maximum chunk found in task.

3> Find active period of task.

The task remains busy for sum amount of time, that period is called active state. So for each task, the period is calculated as per their job number.

4> Find beta variable for non-float case.

Every task has to its blocking tolerance value, so it has to be found by keeping beta variable. For beta value equal to bound function along with the ending time.

5> Calculate chunk size of task.

Calculation of slot size is done for algorithm based on integer and possibility is checked. Also calculation of the floating value of chunk is done. Check for number of pre-emption taking place.

6> Check possibility of task.

For task with higher priority, the need of finding jobs is not required; requirement is chunk value and its block tolerance. Find worst case response time of job in order to predict possibility.

Specific level of assumption algorithm:

Steps:

1>Compare two task running and ready.

Initially, every job has increased its range to threshold described and thus pre- emption has its value higher than normal. Comparison is based on priority of current running job and upcoming new job.

2>Schedule the set.

The job set is scheduled again on basis of new threshold value, as increment is done to each job.

3>Block the low priority task

The task is blocked on basis of tolerance which occurred because of low priority task.

4>Calculate busy period.

It includes initial value of task starting with zero and new length of the task. If new length is bigger than the length is replaced with new length.

5>Start the jobs.

Job starting time is noted and loop is initiated to consecutive next jobs and finds lower bound of job.

6>Find worst case execution time (WCRT).

This step needs to check whether the job will complete in limited possible time, if not than job cannot be included.

7>Check the possibility.

Giving the least or lowest pre-emption threshold value and provide highest value to task in order to reduce the pre-emption.

RESULTS

Deadline and rate based algorithm preemption output.

USAGE	EDF	RM
50	9632	9794
55	11572	11789
60	13453	13726
65	15521	15880
70	17821	18277
75	19957	20527
80	22862	23526
85	26345	27078
90	30978	31802
95	36083	37356

Table1: total takeover of jobs vs. usage

These values changes with respect to type of processor. But the EDF will always has less number than rate monotonic (ratmo).

column	description
2	jobs with deadline based algorithm
3	static assumption with floating values
4	specified level of assumption
5	prefix assumption
6	similar time for all
7	static assumption with integer values

Table 2: Description details of table3

Scheduling of six algorithm ratio output

TOT USAGE	FASTDF	FIXFLPR	PREMTH	FIPRS	NONPRER	FIXFLPRINT
60	5000	5000	5000	5000	4356	5000
63	5000	5000	5000	5000	4261	5000
66	5000	5000	5000	5000	4088	5000
69	5000	5000	5000	5000	3887	5000
72	5000	5000	5000	4998	3617	5000
75	5000	5000	5000	4993	3303	5000
78	5000	4999	4996	4956	2837	4999
81	5000	4981	4958	4821	2260	4981
84	5000	4927	4803	4436	1427	4927
87	4997	4688	4315	3696	754	4688
90	4996	4008	3157	2353	247	4009
93	4977	2524	1516	1032	26	2524
96	4903	661	200	126	0	663
99	4234	3	1	1	0	3

Table 3: shows total usage of jobs vs. ratio of total possible job

Energy count

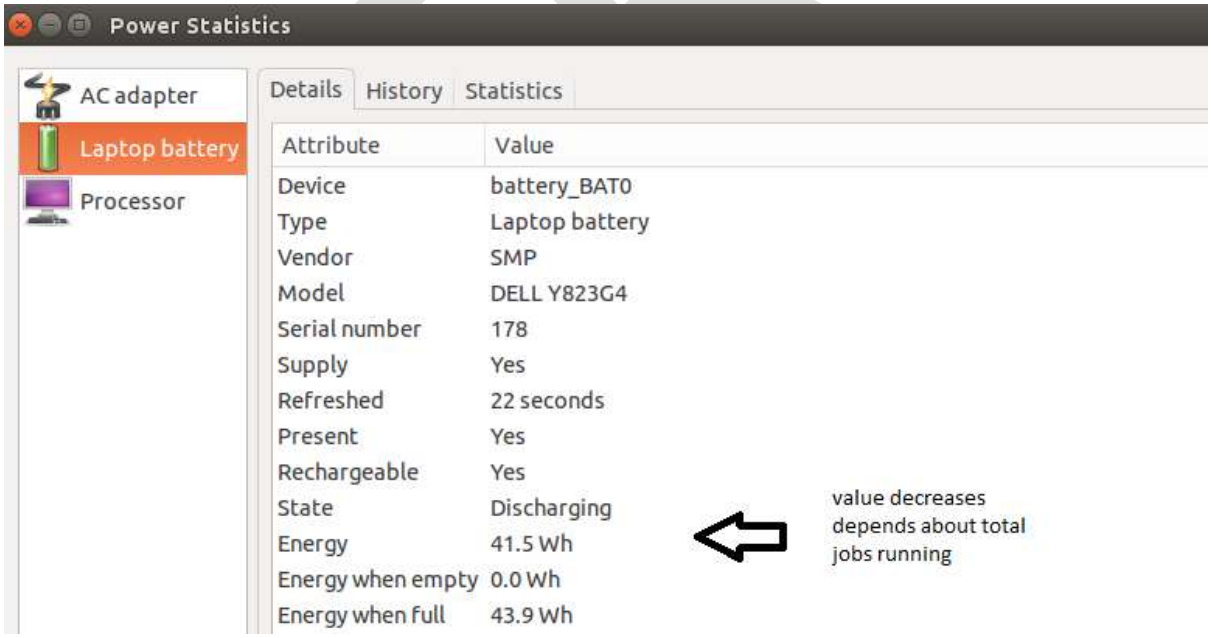

Here in above figure, energy is **41.5Wh** .That value decreases as usage is done by complete system hardware and jobs going on through some amount of time. Now say for e.g. while running the system constant for 2167 and do not work than also the system will be power drain in 1 hour 32 minutes approx.

But the same condition for 1000 MHz, duration longs with 2 hours 40 minutes. The difference can be seen in values itself. So this project analysis tells which frequency is optimum of all four frequencies which will satisfy both our situation of energy saving and good scheduling with good number of pre-emption.

The factor considering is both above stated, along with it is time factor. The frequency 1334 MHz here plays great role in completion of jobs and time factor. This is based on analysis.

Analysis

Frequency (MHz)→		1000		**1334**		1667		2167	
User time	Energy (W h)	23m 16.808s	5.8	**17m 29.844s**	**6.2**	15m 15.776s	6.3	10m 44.548s	7.2
		23m 25.611s	5.7	**17m 21.645s**	**6.1**	15m 23.568s	6.4	10m 48.680s	7.4
		23m 11.332s	5.7	**17m 36.237s**	**6.0**	15m 21.322s	6.4	10m 29.988s	7.3
		23m 9.221s	5.8	**17m 26.788s**	**6.1**	15m 29.462s	6.2	10m 32.365s	7.2

Table 4:Analysis for time taken and energy used for result two methods

Frequency(MHz)→		1000		**1334**		1667		2167	
User time	Energy(W h)	1m5.639s	0.4	**49.252s**	**0.3**	39.276s	0.4	30.232s	0.4
		1m5.532s	0.5	**49.332s**	**0.3**	39.332s	0.4	30.240s	0.4
		1m5.588s	0.4	**49.388s**	**0.3**	39.348s	0.4	30.226s	0.5
		1m5.488s	0.4	**49.364s**	**0.3**	39.326s	0.3	30.261s	0.5
		1m5.511s	0.4	**49.259s**	**0.3**	39.330s	0.4	30.278s	0.5
		1m5.610s	0.4	**49.271s**	**0.3**	39.359s	0.4	30.271s	0.4
		1m5.618s	0.5	**49.322s**	**0.4**	39.298s	0.4	30.220s	0.4

Table 5: Analysis for time taken and energy used for all scheduling methods

Here, the **1334 MHz** is best at long time execution of program. Differentiation with energy factor 6.2 of 1334 MHz and 6.3 of 1667 MHz. In general, as all other component is also working other than CPU, those parts also draining energy in equal quantity for longer time. So for first frequency the parts take more energy than the second frequency. The reason is longer time is taken by the first one.

The following example proves the point.

The overall components energy usage other than CPU is 1Wh per second. So for time 15 seconds, it will be 15Wh. For 30 seconds it will be 30Wh. So its components energy level is higher, while CPU energy level is gradually increasing at its own rate.

ACKNOWLEDGMENT

I extend my complete credit to my project guide, Mrs. Bhuvaneshvari S Patil, Asst. Professor ,Dept of CSE (PG), for helping me throughout the project work. She provided me with complete direction regarding the project and supported during entire period for completion of my project.I thank the complete teaching and non-teaching staff for their support and help.

CONCLUSION

The scheduling methods described here can be used in real time processing. The new methods described can be applied to set of jobs and can be executed for successfully completion of jobs efficiently. These methods as explained can run on CPU where there is continuous amount of jobs coming over time. The frequency which came as output can be considered more energy and time efficient. Even though basic method based on deadline and period are mostly used by making changes and updating, the new methods described can also be used to get better output and make flow of process in best possible manner. Finally it will ensure long lifetime in battery operated laptops or devices and decrease the consumption of energy in alternate current running devices. So the advantage of this work is great amount of energy savings in devices which have a varied range of frequency. Long time availability of device, so more work can be done for same amount of energy.

REFERENCES:

1] Power Aware Scheduling Algorithm for Real-Time Tasks over Multi-Processors, Muhammad Zakaiya, Uzma and Ayaz Ali Khan, Middle-East Journal of Scientific Research 15 (1),Islamabad, 2013.

2] Scheduling Fixed-Priority Tasks with Pre-emption Threshold, Yun Wang, Manas Saksena, RTCSA-IEEE, Hongkong, 1999.

3] Improving Energy-Efficient Real-Time Scheduling by Exploiting Code Instrumen- tation, Thorsten Zitterell and Christoph Scholl, Preprint from Proceedings of International Workshop on Real Time Software(RTS), Wisla, Poland, October 2008.

4] Energy-Aware Task Allocation for Rate Monotonic Scheduling, Tarek A. AlEnawy and Hakan Aydin, Real Time and Embedded Technology and Applications Symposium, 11th IEEE , 2005.

5] Power-Aware Scheduling in Embedded Systems: Adaptation of SDVS Scheduling
using Deadline Overrun Detection, Jonas Höglund, Stefan Olofsson, Magnus Persson, Johan Fredriksson, Detlef Scholle. Enea AB, Kista, First International Workshop on Energy Aware Design and Analysis of Cyber Physical Systems , Sweden, 2010.

6] Dynamic and Aggressive Scheduling Techniques for Power-Aware Real-Time
Systems, Hakan Aydin, Rami Melhem, Daniel Mosse, Pedro Mejıa-Alvarez, Real-Time Systems Symposium,(RTSS) Proceedings. 22nd IEEE, 2001.

7] Algorithms for Energy Saving. Susanne AlbersS, H. Alt, and S. Naher (Eds.) Festschrift Mehlhorn, LNCS 5760, Springer, 2009.

8] Experiences in Implementing an Energy-Driven Task Scheduler in RT-Linux, Vishnu Swaminathan, Charles B. Schweizer, Krishnendu Chakrabarty and Amil A. Patel, Proceedings of the Eighth IEEE Real-Time and Embedded Technology and Applications Symposium,2002.
9] Software or Hardware: The Future of Green Enterprise Computing, Maria Kazandjieva, Brandon Heller, Omprakash Gnawali, Wanja Hofer, Philip Levis, Christos Kozyrakis. Stanford university edu, California, 2011-12.

10] Fundamentals of Power-Aware Scheduling, Xiaobo Sharon Hu1 and Gang Quan2, J. Henkel and S.Parameswaran (eds.), Designing Embedded Processors A Low Power Perspective, Netherlands, 2007.

11] https://wiki.archlinux.org/index.php/CPU_frequency_scaling

12] http://www.makeuseof.com/tag/control-power-usage-gnome-power-statistics-linux/

13] Power-Aware Scheduling for Periodic Real-Time Tasks, Hakan Aydin, Daniel Mosse, Pedro Mejia-Alvarez, IEEE transactions on computers, 2004.

14] An Efficient Power-Aware Scheduling Algorithm in Real Time System, Hyekseong Kweon, Younggu Do, Jaejeong Lee, Byoungchul Ahn, PACRIM IEEE,2007.

15] Frequency-Utilization Based Power-Aware Schedule Policy for Real-Time Multi-cores System, Lin Zhou, Lei Yu, IEEE International Conference on Green Computing and Communications and IEEE Internet of Things and IEEE Cyber, Physical and Social Computing, 2013

International Journal of Engineering Research and General Science Volume 3, Issue 5, September-October, 2015
ISSN 2091-2730

BARGE TRAIN FOR CARGO TRANSPORTATION IN NW-1: A NEW CONCEPT IN INDIAN INLAND SHIPPING

Gautham Krishnan C.G,

BTech- NAVAL ARCHITECTURE & SHIPBUILDING

Dept. of Ship Technology, Cochin University of Science & Technology

GAUTHI.SHIPTECH36@GMAIL.COM

Abstract— With an ever-increasing pace in urbanization & trade dynamics, cities & towns are prone to traffic-crunches & shooting pollution levels. It is a good time to switch to the inland waterways as India possesses an enriching source of water resources being surrounded by seas in three sides with inlets to various rivers, lakes & inland waters. This paper brings out the development of barge trains, that can transport cargo to industries & floating markets, and are designed to ensure economic, efficient, reliable, less emissive & hassle-free transportation

Keywords— Inland Waterways, Naval Architecture, Stability, Metacentric Height, Resistance, Froude's number

INTRODUCTION

Water transport has forever been a reliable and economical mode of transporting goods and people for civilizations across the world. Inland Water Transport includes natural modes as navigable rivers, lakes and artificial modes such as man-made canals. India has an extensive network of inland waterways ranging from rivers to creeks. Freight transportation by waterways is highly under-utilised in India compared to other large countries and geographic areas like the Americas, China and the European Union. Just to quote figures of comparison: -

*In Europe, more than 37 000 kms of waterways connect hundreds of cities and industrial regions. Inland waterway transport is the perfect mode for all kind of goods. Success stories from all over Europe prove the advantages of transporting goods on Europe's integrated network of rivers and canals

*The percentage of freight moved by India is merely 0.1% as against 21% for USA

These figures quote the under-utilisation of Inland Water transport in India and the problem is not in terms of the navigable length which comes to almost 14500 km of which over 9500 km in the form of rivers and canals are navigable. Water-borne tourism is popular in many parts of India already; it is only cargo transportation that has to pick up steadily.

The Indian Inland waterways constitute of 5 National Waterways: -

1. **National Waterway-1**: - The Ganga – Bhagirathi – Hooghly river system between Haldia & Allahabad (1620 kms) was declared as National Waterway 1(NW-1) during October 1986

2. **National Waterway-2:** - The river Brahmaputra having a length of 891 km between Bangladesh border to Sadiya in Assam was declared as National Waterway 2 (NW-2) on 1st September, 1988

3. **National Waterway 3**: - This Waterway based in Kerala constitute the West Coast canal from Kollam to Kottapuram, the Udyogamandal and Champakkara canals

4. **National Waterway-4**: - This waterway declared as NW-4 runs from Kakinada to Pondicherry.

5. **National Waterway-5**: - It is slated to run from Paradip to Haldia

6. The Barak River in Assam is touted to be National Waterway-6

In addition to this are state developed riverine systems, canals & backwaters.

II. BARGES

A barge is a flat-bottomed vessel, built mainly for river and canal transport of cargo Some barges are not self-propelled and need to be towed or pushed by towboats. Barges are used today for low-value bulk items, as the cost of hauling goods by barge is very low. These were the predominant and most effective means of Inland Cargo Transport in under-developed regions of the World before the advent of the highways and the railways that came with industrial development.. On the Mississippi riverine system today, including that of other sheltered waterways, industrial barge trafficking in bulk raw materials such as coal, coke, timber, iron ore and other minerals is extremely common. In the developed world use of huge **cargo barges** that connect in groups and trains-of-barges in ways that allow cargo volumes and weights which if used effectively can revolutionise the transportation sector.

III. ADVANTAGE INLAND

Cheaper capital cost

The extensive length of Indian waterways is a gift of nature, much like nature having already done the initial engineering work for 5,700 km of waterways. Therefore, there is potential for cheaper capital costs. the government estimates that capital cost of developing inland waterways is about 5-10% of the cost of developing an equivalent 4-lane expressway or railway.

Cheaper maintenance cost

Waterways are generally cheaper to maintain except for those subject to heavy siltation which requires large scale maintenance dredging. Again based on government figures, maintenance costs are potentially of the order of 20% of that of road.

Greater fuel efficiency

The same studies show that inland waterways transport (IWT) also has the potential to be very fuel-efficient. it is estimated that one litre of fuel can move 24 ton-km of freight by road, 85 ton-km by rail and 105 ton-km by inland water transport. IWT has the potential to be a very cost-efficient transport mode. It is estimated that every shift of one billion ton-km to inland waterways will reduce transport fuel costs by $5 million and overall transport costs by $9 million. It can be best used to transport heavy loads and oversized cargo.

Carrying capacity

Inland vessels offer an enormous carrying capacity per transport unit. one motorized cargo vessel with a load of 2,000 tons carries as much cargo as 50 railway cars at 40 tons each or 80 trucks at 25 tons each. combined with comparably low transport costs, inland vessels show an excellent cost-benefit-ratio

Safety

Inland navigation has an exemplary safety record. there is a very low probability of accidents, and should an accident happen, the costs of that accident are low in economic and human terms. barges will lead the way for safe transport, especially for dangerous cargoes, as they come with extremely high standards of inspection, training and licensing. the presence of a regulator such as a classification society gives an extra niche to safety.

IV. BARGE-TRAIN CONCEPT

The barge train concept consists of a group or fleet of barges interconnected together by couplings and towed by a couple of tugs in the popular push-pull method so that the system looks similar to a freight train and can manoeuvre well even in twisted and rough waterways, enabling extensive cargo transfer. Individual barges have self-sustaining buoyancy.

The concept of Marine trains is rare but not unheard of. Similar trains are operational in the Rhine and in parts of US. Current R&D work in this area focuses on designing very-large marine trains called sea snakes for trans-ocean cargo transportation.

4.1 NEED OF BARGE-TRAINS IN INDIA

In the context of Inland Water Transport, barge trains are an ideal choice or could be labelled as the next-gen cargo carriers, for their efficiency, versatility, reliability, ability to carry & handle cargo of different types at the same time & low risk of loss of cargo as they are stored in watertight barge-bogies so that they can withstand sinking. They also result in fewer emissions, are eco-friendly, can escape traffic and more fuel savings, i.e. reduced fuel bills. The barges could be unloaded safely at the location by use of derricks or cranes and the cargo will be sealed by a watertight hatch. Also with increasing congestion in Roadways and increased railway freight rates, Inland Waterways can be utilised really well, and particularly in areas where large amount of cargo can be transferred feasibly, subject to the route and economic constraints, Barge Trains can create wonders in the transportation sector.

V. NAVAL ARCHITECTURAL PART

Since this is a concept design, or the first of this kind and there are no parent ships in Indian Inland Waters of this kind the detailed design is not dealt with. The initial design features are decided based on operating conditions, owner's requirements, and economics.

5.1 CONCEPT DESIGN

The barge train consists of a series of barges three-to-five in number, their hulls designed to offer as low a resistance as possible, & such that they can handle different types of cargo at one time say coal, grain, fruits at the same time within the constraints posed by freeboard, stability etc.

ROUTE SELECTION & SUMMARY:

The Ganga – Bhagirathi – Hooghly river system between Haldia & Allahabad is chosen. IWAI (Inland water Authority of India) is carrying out various developmental works on the waterway for improvement of its navigability as laid down in the IWAI Act, 1985 (82 of 1985). NW-1 comprises the following stretches:

Stretch I: - Haldia to Farakka- 560 km

Stretch II: - Farakka to Patna- 460 km

Stretch III: - Patna to Allahabad- 600 km

Total length of waterway: 1620 km

The waterway is being used by tourism vessels, Over Dimensional Cargo (ODC) Carriers, IWAI vessels etc. Approximately 10 Thermal/Super Thermal Power Stations including that of NTPC's are located in the region. The power plant of NTPC requires Coal for Operation and the required amount is estimated to be as much as 3 million tons per year. The power plant situated in the vicinity of Farakka relies mainly on coal imports from Australia and many other ways, which are recessive. This implies the Haldia-Farakka stretch of NW-1 as the region of operation, where the Least Available Depth (LAD) [which is a major factor in the design of the vessel] is 2.5-3.0 m.

FIG-1: LOCK GATE ON THE FARAKKA

Route: Haldia-Farakka (NW-I)

Radius of Action: 560 km

Service Speed: 9 Knots

5.2 PUSH-PULL MECHANISM

The barges are to be towed by tugs in the push-pull method i.e. one tug is set to pull the barge-train, the other will act behind & push the barge-train the dual-action can improve efficiency of the system and impart desired speed. This also reduces effort in steering; fuel consumption too could be reduced to the order of 15-20% or more. The system is to be streamlined as much as possible to reduce drag or resistance.

5.3 BARGE DIMENSION FIXING

ROUTE CONSTRAINTS	
Maximum Draft: -	4.00 m
Least Available depth: -	2.50-3.00 m
Air Draft (Max): -	9.00 m
Lock Gates: -	Yes at Farakka
Breadth Span: -	16.00 m

The presence of a lock gate restricts the convenient manoeuvrable length to 90 m, but the presence of the push pull mechanism and the flexibility of the Barge train will allow a total length of approximately 150 m, because it's easily manoeuvrable.

Maximum Barge Dimensions:-

Length: 22 m

Breadth: 12 m

Depth: - 4 m

Draught: 2.5 m

The Barges in the middle are practically rectangular in nature, The Barges at the either ends will be designed with swim-ends, for hydrodynamic purposes, and will be coupled to the towboats. Block Coefficient: 0.9, considering all the barges together as a single entity.

Max No: of Barges: 4 (With a check on restrictions in manoeuvrability)

Total Volume displaced: 1585 t (approximately)

Using Bari & Chowdury's Equation for Computing Steel Mass: -

Steel Weight = 0.0011*(LOA)^a1 * (B)^The Steel Mass Per Barge is 45.71 Ton, based on the Steel mass calculation formulae, the total steel weight comes to 183T, for the 4 barges plus this the total outfit weight and crew cum stores comes to 50 T, thus the steel weight may come to close to 233 T.

Payload/ (Cargo Capacity): - 1350 T

Note: The payload of only the barges are considered here as the tugs are to direct the barge train.

Joining Mechanism: - Use of a coupler and seal arrangement which is hydraulic, this will be rigid and can be used to detach manually on unloading.

MAXIMUM TUG DIMENSIONS

Length:	18 m
Breadth:	4.0 m (max)
Depth:	4.0 m (max)
Maximum Speed:	9 knots

Propulsor: - Thruster Propeller, as this will aid in manoeuvring but no ducts are used, as the presence of fishing grounds pose a risk of the nets getting entangled in it.

The Breadth to draught ratio of 6.4 ensures good intact stability. The Barges will be fitted with a bulwark as a practise for most Inland Vessels, and to counter the highest waves in the region.

Preliminary Stability Calculations: -

The indicator of stability is the Initial Metacentric height (GM), which if positive indicates good intact stability. It is calculated from the Simpson's Formula (SNAME-1957)

$$B = \sqrt{\left(KM - T\frac{5C_{WP} - 2C_B}{6C_{wp}}\right)\frac{T}{m}}$$

$$\Rightarrow KM = B^2\frac{m}{T} + T\frac{5C_{WP} - 2C_B}{6C_{wp}}$$

Where B and T are the breadth & draughts of the vessel, C_B is the block coefficient and C_{WP} is the waterplane area coefficient. (m=0.0948), from which we get, KM= 11.025 m and GM= KM-KG, where KG is the height of the Centre of Gravity from the Baseline (which is the keel), since the barges are rectangular their weights and that of the loaded cargo will mostly act at 0.5D from the baseline, though it will be a little higher for the end barges and the tugs due to the shape of the hull. Even if we were to safely assume that the Vertical centre of Gravity for the train as a whole is at 0.6 times the depth, considering the bulwark and coupling etc. i.e.

KG= 2.4 m, **GM= 8.625 m,** which indicates the vessel is extremely stable

Rough Resistance Calculations:

Resistance is the force offered by water which opposes the forward motion of the ship. The main components of the resistance are the frictional component and the wave-making component. The Barge Train as a single unit represents as a unit similar to an ultra-slender ship, with extremely high L/B Ratios, (here approximately 10.33). The high L/B Ratio and the lower Froude's number (on account of high Length) indicates that wave making resistance is negligible which is an advantage offered by the design.

Coefficient of Frictional Resistance $C_f = 0.075/ (\log (\text{Reynolds's number}) - 2)^2$

= 0.0016787, in addition to this there will be a component of resistance (added) due to the separation/ at the junction of the barges which is taken as 20% of the frictional Resistance, for safety thus $C_f = 0.0020144$, after accounting for appendage and air resistances which is taken as 5% of the above, **C_t = 0.002115**

Wetted Surface Area(S): We compute the Wetted Surface Areas of the tugs through Mumford's formulae: -

$S= (1.7\ LT+ LBC_B)* 2=$ **239.40 square. metres**

The Wetted Surface of the Barges was computed as: - (Since they will be practically rectangular and a Shape allowance of 0.98 is given considering the swum ends)

S= 2LT+ LB. = **1521 square. metres**

Total Wetted Surface Area = **1760 square. metres**

Velocity (V) =9.00 knots

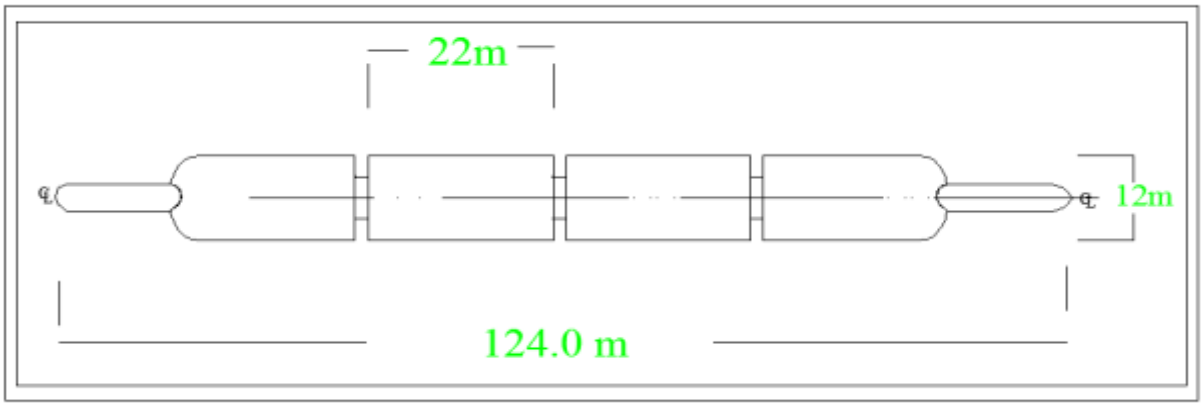

FIG 2: TOP VIEW/ PLAN OF THE BARGE TRAIN, (SWIM ENDS FOR THE END BOGIES

Using the relation: - **Rtotal**= Ct*0.5*S*V*V =**39.90 kN approx.**

Power required= Rtotal *V = **184.72 kW** (These are the power requirements for normal operations against resistance, however during Manoeuvring; the power requirement will be more).

After manoeuvring requirements, Power required is **240 kW** (1.3 times the power for countering resistance). Quoting a Q.P.C of 0.5 and a shaft transmission efficiency of 0.97, (as the propellers are thrusters) The Brake Horsepower P_D comes to 495 kW. Considering this plus the electrical power required the total Installed Capacity or the Indicated power of the engine will come to 600kW. (max.) , this will be shared by the engines on the towboats. Also, Ample Ballast is to be provided when some bogies are partially loaded and others full

ACKNOWLEDGMENT

I thank Prof. Dileep Krishnan and Prof Dr. K Sivaprasad, who taught me the fascinating subject of Naval Architecture and encouraging innovations in this arena as I commence my career as a Naval Architectural Engineer.

CONCLUSION

The design parameters of the barge-train accounting the route-considerations, dimensions and the approximate power required are computed and presented based on calculations and by including design margins for assumptions where there is no apt availability for data. However, the detailed design involving structural analysis and fabrication is not presented as it's still under the research scanner for production & route studies are going on. However, owing to the advantages it vests and the returns and savings both on economic & environmental front, that includes lesser emissions, lesser operating cost, less vibration & noise (much lower than that caused by individual propelled barges), lesser number of trips. and the degree of safety offered, this concept will no doubt revolutionise the Indian transportation sector, through proper implementation.

REFERENCES:

[1] "The SES Sea-Train", Bob-Scher, SNAME SD-5 Panel / International Hydrofoil Society Alion Science & Technology, 24-Febraury-2011.
[2] " Principles of Naval Architecture- PNA", Lewis E.U, Third Edition, Volume-II, Resistance and Propulsion, SNAME, 1988
[3] ""Study On Development of Inland Water Transportation: India", Department of Ship Technology, Class-NK Report, 18- November 2012.
[4] "Bari and Chowdury- Steel Weight Estimation", International Journal for Shipbuilding Progress
[5] "Development of Barge Trains for Less Emissive Hassle free transportation in Indian Inland Waters", C.G Gautham Krishnan, Manu Shankar, September 2013
[6] "The Water-Snake Concept", Student presentation at Institution of Naval Architects (INA)-Kochi Chapter Conference on Student Innovations in Naval Architecture, January 18,2015 by C.G Gautham Krishnan, Manu Shankar

International Journal of Engineering Research and General Science Volume 3, Issue 5, September-October, 2015
ISSN 2091-2730

FORECASTING TELECOMMUNICATIONS DATA WITH AUTOREGRESSIVE INTEGRATED MOVING AVERAGE MODELS

Nilesh Subhash nalawade[a], Mrs. Meenakshi Pawar[b]

[a]SVERI's College of Engineering, Pandharpur.
nileshsubhash15@gmail.com

Abstract— The ability to perform forecasting calculations is an important thing for forecasting practitioners as it helps them in planning and determining their networks. Accurate forecasting helps forecasting practitioners to provide guidance to business peoples to take important decisions about their business in advance. The International Telecommunication Union (ITU) Recommendation E.507 explains about many techniques for evaluating the forecasting models and choice of the model. But, it does not provide any guidance to select which models are more proper for forecasting the telecommunications series. This paper deals with Autoregressive Integrated Moving Average model for forecasting telecommunication data. Evaluation metrics such as Sum of Squared Regression, Root Mean Square Error, Mean Absolute Deviation, Mean Absolute Percentage Error and Maximum Absolute Error shows that the ARIMA models provides good forecasting performance. Abstract must be of Time New Roman Front of size 10 and must be justified alignment.

Keywords— Telecommunication forecasting; ITU Recommendations; ARIMA model; Time series; M-3 Competition data; autocorrelation; Future trend estimation.

INTRODUCTION

In the growing telecommunications industry the ability to determine the future trends is an important endeavor [12]. The boundaries of the telecommunication industries are increasing very fast and the competition among the industries is also growing as well. Telecommunications companies are in need to develop new strategies to face challenges in providing the best communication services. Many industries depend on data monitoring to improve their business by analyzing the future trends and marketing value for their products. Data forecasting has a major role in network traffic management, optimizing infrastructures and in planning process. [1, 4].

The forecasting ability of a time series data is an important thing for the forecasting practitioners. The forecasters can determine the outcome of any event with the priori knowledge about the event. While forecasting telecommunication data, many errors occurs and it motivates to find a better forecasting approach which minimizes the forecasting errors. If a time series data is not forecasted accurately, then reducing the forecasting error will be ineffective. So, it is necessary to find new ways to minimize the effects of poor forecasts [2]. The forecastability of a time series depends on the regularity of the data. If the time series is less regular, then achieving good level of forecasting accuracy is very difficult [3, 9-11, 17].

There are several techniques for forecasting such as Random walk (simple forecasting method), exponential smoothing methods such as simple exponential smoothing (SES), Holt, Holt-winters, Robust trend etc. In the random walk model, the value of the variable follows a random step for each time interval. It assumes that the current observation is only important and the previous observations provide no information [15]. Simple exponential smoothing is a suitable method for forecasting seasonal data. But it is not a suitable method when there is a trend [16]. Holt method is an extended form of simple exponential smoothing method and it allows forecasting data with trends. It can be improved to deal with both trend and seasonal variations. Holt-winter method overcomes Holt method by considering the seasonal variations [18]. Robust trend methods are suitable for forecasting univariate time series data in the presence of outliers. When using this method, incorrect labeling of samples as outliers may occur.

In this paper, ARIMA model for forecasting telecommunication data is proposed. M3-Copetitive data is used here and the performance is measured in terms of Sum of Squared Regression (SSR), Root Mean Square Error (RMSE), Mean Absolute Deviation (MAD), Mean Absolute Percentage Error (MAPE), Maximum Absolute Error (MAE). The paper is structured as follows. Section 2 describes the M3-Competition telecommunication data. Section 3 describes about the ARIMA based forecast model. Section 4 evaluates forecasting performance. Forecast results are given in section 5 and section 6 concludes the paper.

M3-Competition Data

As the forecasting availability is growing up, there is a need for analyzing the adequacy of forecasting methods. Makridakis and Hibon developed the M-Competition which is considered to be one of the important researches in this field [5, 13]. Data used here are obtained from the Institute of Forecasters. The last edition (M3) is referred to year 2000 and it includes 3003 time series classified in to various types such as micro (828), industry (519), macro (731), finance (308), demographic (413) and other (204) and the different time intervals between the successive observations are gives by yearly, quarterly, monthly and of unknown periodicity('others').

Minimum number of observations is required for each type of data to ensure that enough data can develop an appropriate forecasting model. This minimum was set as 14 observations for yearly series, 16 for quarterly, 48 for monthly and 60 for 'other' series. Table 1 show the classification of the 3003 series according to the two major grouping discussed above. The table shows the number of time series based on both time interval and domain.

Table 1 The classification of the 3003 time series used in the M3-Competition

Time interval between successive observations	Types of time series data						
	Micro	Industry	Macro	Finance	Demographic	Other	Total
Yearly	146	102	83	58	245	11	645
Quarterly	204	83	336	76	57		756
Monthly	474	334	312	145	111	52	1428
Other	4			29		141	174
Total	828	519	731	308	413	204	3003

ARIMA-based forecast model

Box and Jenkins introduced the Autoregressive integrated moving average (ARIMA) model. It is used as one of the popular method for forecasting data [6, 14]. The ARIMA model is used for time series forecasting where the future value of a variable is a linear function of past observations and random errors and is expressed as,

$$y_t = \theta_0 + \phi_1 y_{t-1} + \phi_2 y_{t-2} + \cdots + \phi_p y_{t-p} + \varepsilon_t - \theta_1 \varepsilon_{t-1} - \theta_2 \varepsilon_{t-2} - \cdots - \theta_q \varepsilon_{t-q}$$

Where, y_t is the actual value and ε_t is the random error at time t, and ϕ_i (i = 1, 2, . . . , p) and θ_j (j= 0, 1, 2, . . . , q) are model parameters. Integers, p and q are the order of the model. The random errors, ε_t are assumed to be independent and identically distributed with a zero mean a constant variance of σ^2. ARIMA model involves the following three iterative steps [7].

(i) Model Identification: ARIMA model has the assumption that the time series is stationary. So, data transformation is done to produce a stationary time series. For stationary time series, the mean and autocorrelation structure are constant over time. So, differentiation and power transformation are needed to change the time series to be stationary. To identify the appropriate model form, autocorrelation and partial autocorrelation are calculated from the data and it is compared to the theoretical autocorrelation and partial autocorrelation for the various ARIMA models. Steps (ii) and (iii) will determine whether the model is appropriate [8].

(ii) Parameter Estimation: Parameters in ARIMA model is estimated using the nonlinear least square procedure.

(iii) Diagnostic Checking: Several diagnostic statistics and plots such as Histogram, normal probability plot and time sequence plot are used to check the fitness of the model estimated in step (i). Chi-square test can be used to test the model adequacy.

Once a satisfactory model is obtained, the selected model will be used for forecasting.

Evaluation metrics

Forecast accuracy is measured using Sum of Squared Regression (SSR), Root Mean Square Error (RMSE), Mean Absolute Deviation (MAD), Mean Absolute Percentage Error (MAPE), Maximum Absolute Error (MAE).

(i) SSR: The Sum of Squares Regression (SSR) is the sum of the squared differences between the prediction for each observation and the population mean.

$$SSR = \sum_{l=1}^{L} y - \bar{y}$$

(ii) MSE: Mean Square Error (MSE) averages the squared prediction error at the same prediction horizon. A derivation of MSE is Root mean Square Error (RMSE).

$$MSE(i) = \frac{1}{L}\sum_{l=1}^{L}\Delta^{l}(i)^{2}$$

(iii) MAD: Mean Absolute Deviation from the sample median (MAD) is the resistant estimator of the dispersion /spread of the prediction error. It is intented to be used when the error plots do not resemble those of a normal distribution.

$$AD(i) = \frac{1}{n}\sum_{l=1}^{L}\left|\Delta^{l}(i)\right| - M$$

where, $M = \underset{l}{median}\left(\Delta^{l}(i)\right)$ and median is the $\frac{n+1}{2}th$ order statistic.

(iv) MAPE: Mean Absolute Percentage Error (MAPE) averages the absolute percentage errors in the predictions of multiple UUTd at the same prediction horizon. Instead of the mean, median can be used to campute Median absolute percentage error (MdAPE) in a similar fashion.

$$MAPE(i) = \frac{1}{L}\sum_{l=1}^{L}\left|\frac{100\Delta^{l}(i)}{r_{\bullet}^{l}(i)}\right|$$

v) MAE : Mean Absolute Error (MAE) averages the absolute prediction error for multiple UUTs at the same prediction horizon. Using median instead of mean gives absolute error (MdAE).

$$MAE(i) = \frac{1}{L}\sum_{l=1}^{L}\left|\Delta^{l}(i)\right|$$

Results and discussion

This section presents the performance evaluation of the ARIMA model in M3C data. The ARIMA is implemented using Matlab 8.2.0.701 (R2013b) with a system configuration of 2GB RAM Intel processor and 32 bit OS. To determine the forecasting ability of the ARIMA model, it is applied to the yearly, quarterly, monthly and 'other' data. The Graphical User Interface (GUI) for the ARIMA model for forecasting telecommunication data is shown in figure 1.

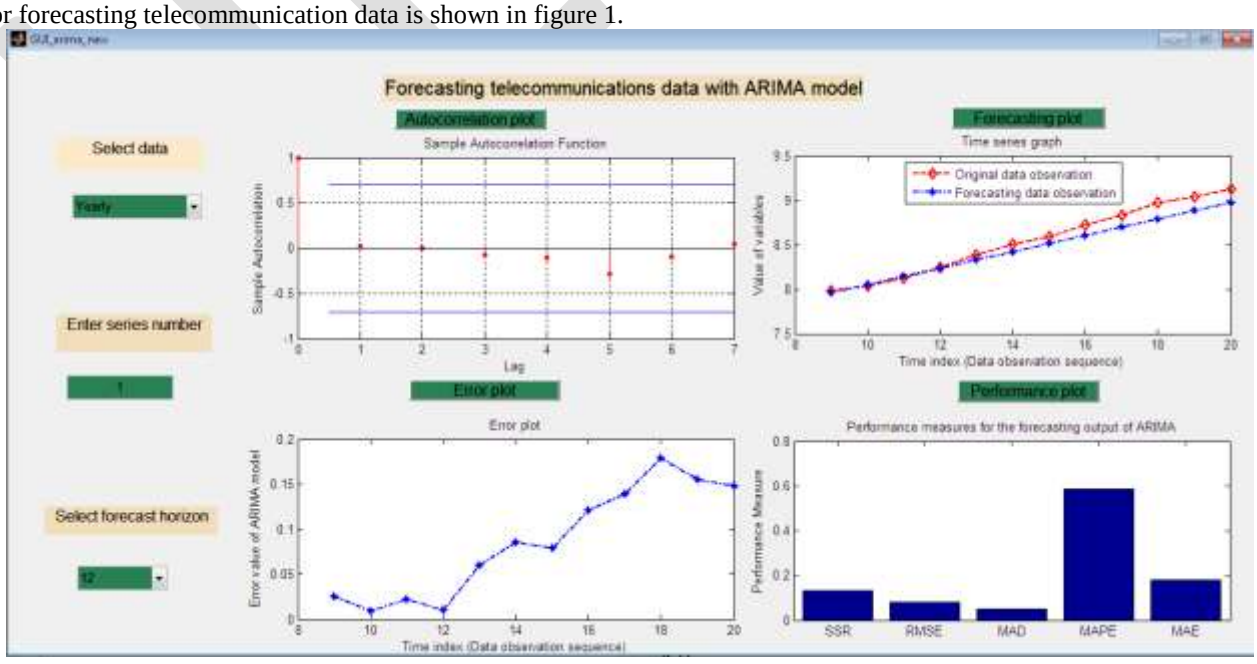

Figure 1. GUI

The autocorrelation plots are used in the model identification stage of the ARIMA time series models. Autocorrelation plots are used to check the randomness in a data set. To find the randomness, the autocorrelations for data values at varying time lags are computed. If the autocorrelation is near to zero for all the time-lag separations, then the data is random. If the autocorrelations are not zero, then the data is not random. Partial autocorrelation are used to find the order of the autoregressive model. The sample autocorrelation plots are given in figure 2. Table 2 shows the statistics of ARIMA (1,0,0) Model extracted from the input data.

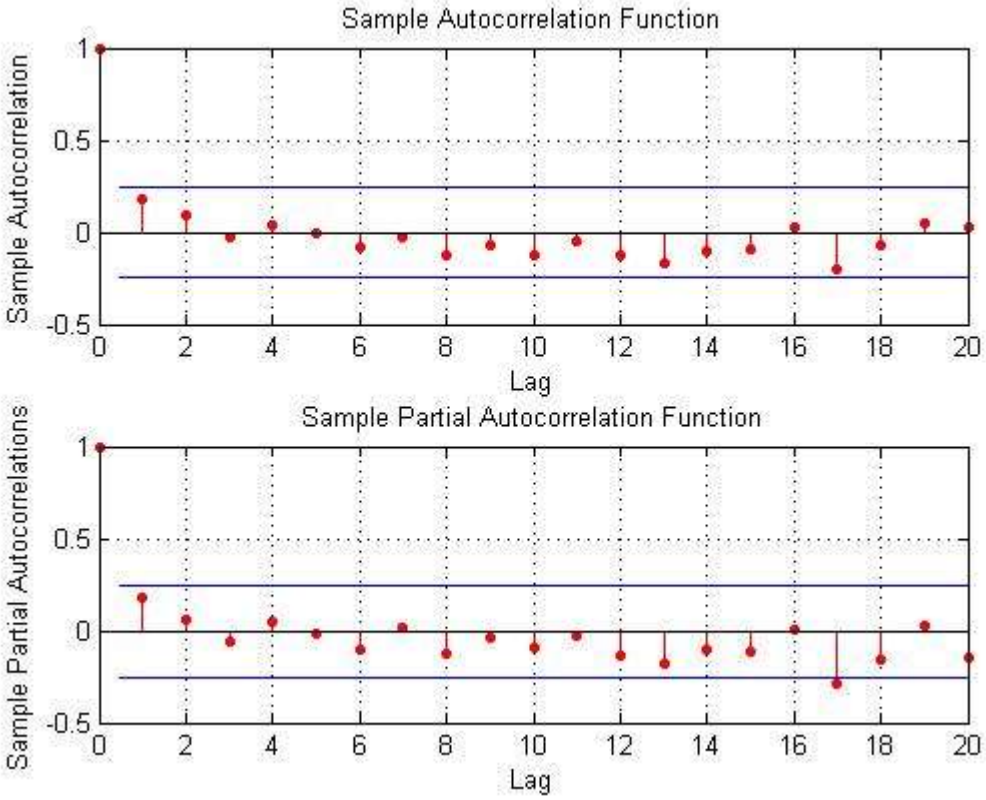

Figure 2. Autocorrelation plot

Table 2. ARIMA(1,0,0) Model

ARIMA(1,0,0) Model:			
Conditional Probability Distribution: Gaussian			
Parameter	Value	Standard Error	t-Statistic
Constant	-0.019818	0.0500035	-0.396333
AR{1}	1	0.00605097	165.263
Variance	0.000294433	3.70139e-05	7.95465

The time-series graph illustrates the data points at successive time intervals. The time is measured on the horizontal axis and the variable is measured on the vertical axis. The time series graph for the comparison between the original data observed and the observed forecasting data and respective performance measure for the yearly data, quarterly data, monthly data and 'other' data are shown in figure 3, 4, 5 and 6 respectively.

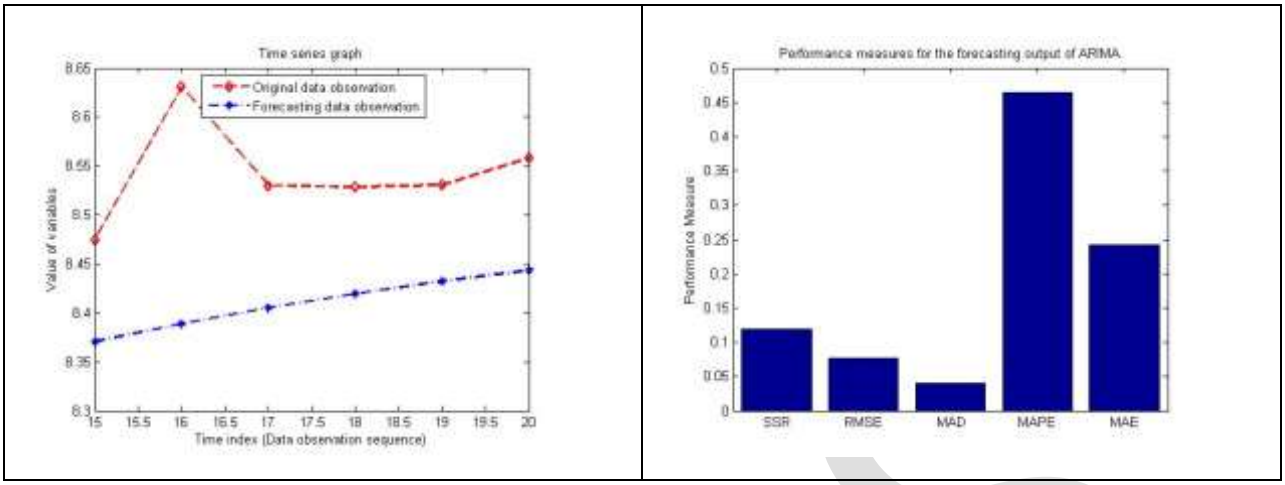

Figure 3. Yearly data

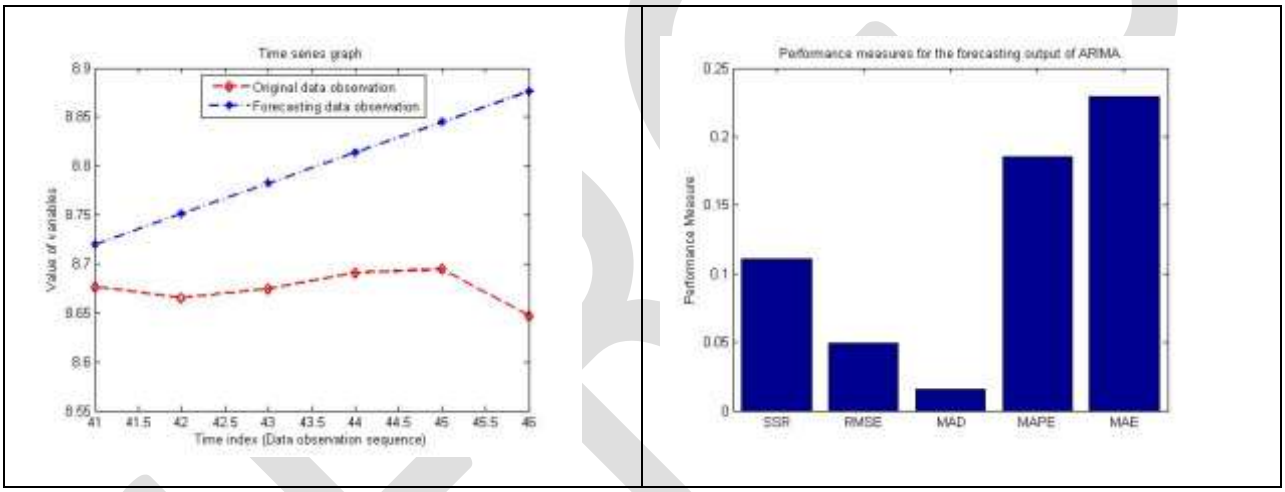

Figure 4. Quarterly data

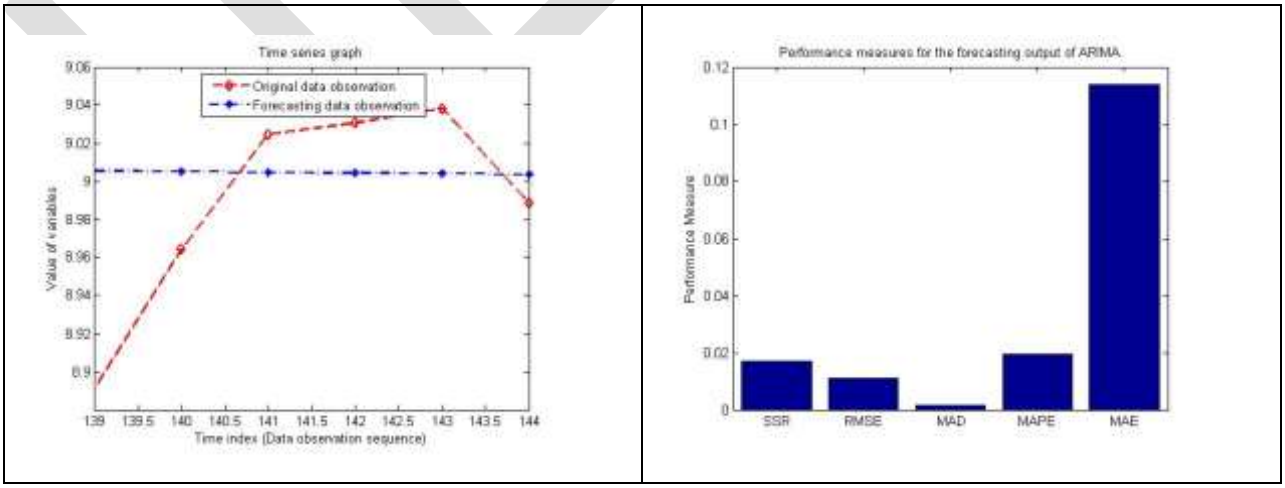

Figure 5. Monthly data

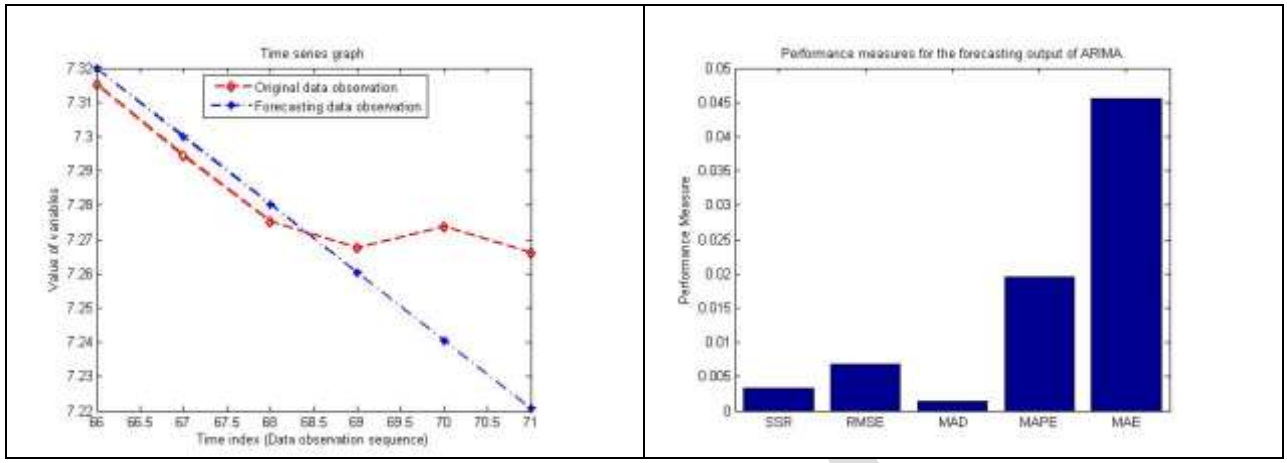

Figure 6. 'Other' data

6. Conclusion

In this study, we have applied the ARIMA model to the M3-competition data set of 3003 time series to determine its forecasting ability. It is observed that the ARIMA model provides better forecasting even when little detail about the data is available. The forecasting accuracy of the ARIMA model is measured using parameters such as SSR, RMSE, MAD, MAPE, and MAE for the yearly, quarterly monthly and 'other' data and it is compared with the results given in [19] using MAPE. It showed that the performance of ARIMA model is better than the other models. We therefore conclude that the ARIMA model is the better forecasting method for telecommunication data.

REFERENCES:

[1] Boylan, J.E. Towards a more precise definition of forecastability. Foresight: the International Journal of Applied Forecasting 2009, 34–40.
[2] Kolassa, S. How to assess forecastability. Foresight: the International Journal of Applied Forecasting 2009, 41–45.
[3] Tashman, L.J. Special feature on forecastability: Preview. Foresight: the International Journal of Applied Forecasting 2009, 23.
[4] Gary Madden, Joachim Tan, "Forecasting telecommunications data with linear models", Telecommunications Policy, vol. 31, pp. 31–44, 2007.
[5] Makridakis, S. and Hibon, M. (2000): "The M-3 Competition: results, conclusions and implications", International Journal of Forecasting, 16, pp. 451-476.
[6] P. F. Pai and C. S. Lin, "A hybrid ARIMA and support vector machines model in stock price forecasting," Omega, vol. 33, no. 6, pp. 497–505, 2005.
[7] G. P. Zhang, "Time series forecasting using a hybrid ARIMA and neural network model," Neurocomputing, vol. 50, pp. 159–175, 2003.
[8] J. E. Hanke and D. W. Wichern, Business Forecasting, Prentice Hall, Englewood Cliffs, NJ, USA, 2009
[9] Armstrong, J., & Collopy, F. (1992). Error measures for generalizing about forecast methods: Empirical comparisons. International Journal of Forecasting, 8, 69–80.
[10] Fildes, R. (1992). The evaluation of extrapolative forecasting methods. International Journal of Forecasting, 8, 81–98.
[11] Fildes, R., Hibon, M., Makridakis, S., & Meade, N. (1998). Generalising about univariate forecasting methods: Further empirical evidence. International Journal of Forecasting, 14, 339–358.
[12] Grubesic, T., & Murray, A. (2005). Geographies of imperfection in telecommunication analysis. Telecommunications Policy, 29, 69–94.
[13] Makridakis, S., Chatfield, C., Hibon, M., Lawrence, M., Mills, T., Ord, K., et al. (1993). The M-2 competition: A real-time judgmentally based forecasting study. International Journal of Forecasting, 9, 5–23.
[14] Parzen, E. (1982). ARARMA models for time series analysis and forecasting. Journal of Forecasting, 1, 67–82.
[15] Simmons, L. F. (1986). M-Competition — A closer look at Naıve2 and median APE: a note. International Journal of Forecasting 4, 457–460.
[16] Gardner, E., 2006. Exponential smoothing: The state of the artpart ii. International Journal of Forecasting 22, 637–666.
[17] Kotsialos, A., Papageorgiou, M., Poulimenos, A., 2005. Long-term sales forecasting using Holt-Winters and neural network methods. Journal of Forecasting 24, 353–368.
[18] Fildes, R. & Petropoulos F. (2013). An evaluation of simple forecasting model selection rules (LUMS Working Paper 2013:2). Lancaster University: The Department of Management Science.
[19] Makridakis, S., & Hibon, M. (2000).The M-3 competition: results, conclusion and implications. International Journal of

Forecasting, 16, 451-476

International Journal of Engineering Research and General Science Volume 3, Issue 5, September-October, 2015
ISSN 2091-2730

A REVIEW ON IMPLEMENTATION OF ENTREPRENEURSHIP EDUCATION-Rise of Entrepreneurs

SREE HARSHA BHARADWAJ HOTUR
B.E, M.Tech (student)
Mysore
hasrshabharadwaj123@gmail.com
Contact Info. +91- 90086 64600

Abstract-The scope of this study is mainly focussed on the implementation of the entrepreneurship as a part of curriculum at every schools of under-graduation in order to gain as much as profit to the nation and for self-employment. It has become a major need in the present scenario. India is one of the developing countries among the world which also has high level of unemployment and greatly women and rural areas. Entrepreneurship facilitates the rate of development of a country by increasing the rate of growth in GDP (gross domestic product) of a country. It helps in increasing the productivity and continued innovation in techno – managerial practices. Entrepreneurship brings an improving in international competitiveness. It also brings out a major impact on the economic diversification and the optimum usage of the local resources which finally adds to pride of the nation. The research study will reveal the facts which are important to develop entrepreneurship as a career option among every school of under-graduation in current scenario section below.

Keywords- entrepreneurship, unemployment, techno managerial, GDP

I. INTRODUCTION

Though the entrepreneurship word is not a new to the present world as it has evolved around 1700 A.D when the term was used for architects and contractor of public works. There are so many institutes and organizations which are involved in entrepreneurship development activities and there are people who join these programmes as a stepping stone to become entrepreneur. The entrepreneurship is a very old concept according to which anyone who runs business is called an entrepreneur. The word "entrepreneur" is derived from the French verb "enterprendre" [1]. It means "to undertake". The Frenchmen who organized and led military expeditions were referred to as "entrepreneurs". The entrepreneur is the aggressive catalyst for change in the world of business. But there's one problem: The start-up world is cluttered with "wantrapreneurs" who fail to recognize that success demands a tenacity, resiliency and energy unlike any traditional job short of combat infantry soldier or SWAT team member.

II. CURRENT SCENARIO

Entrepreneurship and business are rarely accorded a serious place in discussions around drivers of economic development. A cursory look at the numbers makes this seem very surprising. China has pulled approximately 600 million people out of absolute poverty since Deng Xiaoping unleashed market reforms in the late 1970s. Never in human history have so many people been pulled out of grinding poverty is such a short span of time. Similarly, South Korea has gone from a per-capita income of $291 in 1970 to $20,000 today. Even reform laggards like India have managed to pull a couple of hundred million people out of grinding poverty since economic reforms were initiated. Across the world, we find countries that created an entrepreneurship and business friendly environment were successful in reducing poverty drastically. There are three kinds of entrepreneurs: The entrepreneur selling tea at a road side stall in India, owners of small and medium enterprises (SMEs), and the Steve Jobs/Bill Gates type of entrepreneur who builds massive businesses, creates enormous shareholder wealth and employs thousands of people. Any well-functioning society will try to eliminate the first kind and create an environment that fosters the other two, mostly because the first is survival disguised -- and often misdiagnosed -- as entrepreneurship. Governments remain a major stumbling block to entrepreneurship. A cursory look at the World Bank's ease of doing business index reveals that some of the poorest countries in the world are also some of the most business unfriendly countries, while some of the richest rate as business friendly.

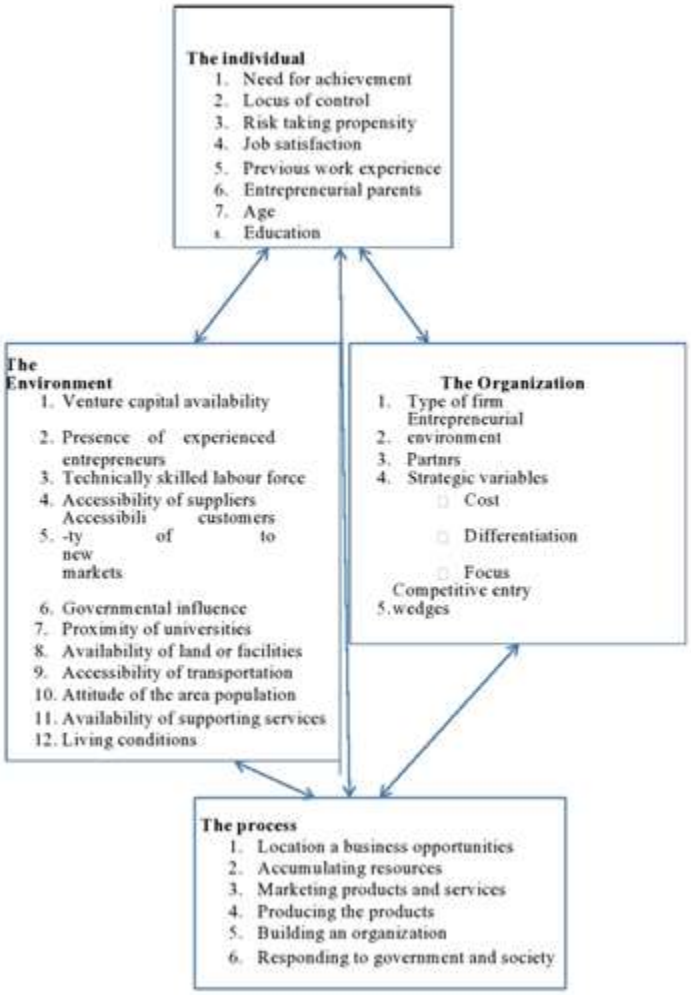

fig1: Variables in New Venture Creation [2]

The typical variables which play a major role in creating a new venture are depicted in the above fig 1. Examples of these hurdles include exit and entry barriers for entrepreneurs, and onerous labour laws. Early stage entrepreneurs in developing countries have very hard time raising money of any sort. The problem is exacerbated in non-tech industries, and in early rounds of financing. Even in countries like India with a reasonably good venture capital environment, the scarcity of early stage capital remains a major roadblock. Entrepreneurs, even half-successful ones, have a very hard time accessing distant (most likely high-margin) markets. Early-stage entrepreneurs in developing countries lack access to the best technologies, best practices and knowledge networks. Finally, entrepreneurial ventures have a hard time attracting high quality talent, across the board.

In the next couple of decades, two sets of transformations will most likely occur. Developing countries need to, and most likely will, understand the importance of business and entrepreneurship to their continued development. Improved rankings in the ease of doing business index will become a key international metric to aim for. Moreover, subsequent wealth creation will obviate the need for hand outs from developed countries.

At the same time, business friendliness in developing countries opens new markets for western business and capital, especially at a time when their domestic markets are not in great shape. Helping these countries deal with the barriers mentioned above can be very profitable for western countries; provision of capital is a great example.

At the same time, the aid establishment can continue to play an influential role if it changes gears from being primarily a source of hand-outs, to helping developing countries build strong institutions that will assist them in overcoming barriers and creating an entrepreneur-friendly environment. Africa also leads the world in the number of women starting businesses, with almost equal levels of male and female entrepreneurs. In fact, in countries like Ghana, Nigeria and Zambia the women outnumber the men. Overall, the continent has a much higher proportion of female entrepreneurs compared to other regions, with Nigeria and Zambia (both 40.7%) coming on top and countries like the United States (10.4%), the UK (5.5%), Norway (3.6%) and France (3.1%) lagging far behind. Today, Japan has one of the lowest levels of entrepreneurship in the developed world. The country has long lacked venture capitalists

who tend to invest in start-ups elsewhere in the world. And approaching banks for financing help is a big challenge for entrepreneurs. But some young Japanese are now beginning to challenge this and stet up businesses on their own. Stanford University, one of the world's great institutions for turning hi-tech ideas into huge businesses, is going to start teaching in London from the autumn. The Californian University, where Google began as a PhD project, is going to offer its "Stanford Ignite" entrepreneurship course in London for the first time from September. Universities around the world have been experimenting in ways to teach students beyond their own campuses. There have been much-hyped attempts to provide courses online, in the wave of massive open online courses, or so-called Moocs. 'Growing hub'- The research showed that there was a 4% rise in the number of enterprises in Scotland in 2014, compared with the previous year, making the country home to 157,000 enterprises. Most parts across the UK reported growth in this area, with London leading the way with 401,000 enterprises. The Barclays and BGF Entrepreneurs Index said there was a 5.7% increase in high-growth businesses settling in Scotland in the year to March 2014.

III. LITERATURE REVIEW

Teresa Paiva, Pedro Tadeu [3] presented the tendencies of entrepreneurship education and explores the main discussions on how it can be developed based in a more urgent need of creativity integration on educational curriculum and pedagogies, particularly as a way of reaching innovation and applied ideas to the economic context. So the link between creativity and entrepreneurship is made through knowledge. The Problem based learning methodology give also a boost to this knowledge and creativity integration by integrating them in a real life context and directing them to an innovative solution

The influence of entrepreneurial education in the propensity for entrepreneurship, as referenced in this work, has already been widely exploited. However, Teresa Tiago, Sandra Faria, João Pedro Couto, Flávio Tiago[4] analysed with respect to the North American context where there remains a gap with respect to empirical evidence of the determinants of this tendency. Paper aimed to bridge this gap by presenting empirical evidence from four European countries, culturally and geographically distinct and differentiated educational projects.

Giulia Faggio, Olmo Silva[5] This paper shows a positive and significant correlation between the incidence of self-employment and business creation as measured by gross and net firm creation rates in urban TTWAs. Similarly, it finds a positive and significant correlation between self-employment and innovation in urban areas. However, none of these results were holding for rural TTWAs, where we find that self-employment does not ‘line up’ with firm creation or innovation. The paper also carried implications for public policies that promote self-employment with the aim of stimulating business creation and innovation, and narrowing gaps in economic performance between dynamic and lagging regions.

Anca Otilia Dodescu, Ioana Crina Pop-Cohu, Lavinia Florentina Chiril [6] a quantitative research was undertaken which led to the following conclusions regarding the potential of practice and internship stages in entrepreneurial skills empowering and encouraging entrepreneurship of students in Economics:

• 60.98% of young people believe that they have entrepreneurial skills which they have acquired through practice/internship stages activity undertaken within a specialized company, through direct contact with experts in the field;

• 76.74% of young people who said they would initiate or consider initiating a business consider practice /internship stage as the most relevant experience for the implementation of this plan, because even if they have acquired some necessary skills within specialized courses, through practice they took contact with the labor market, with the requirements on the labor market and with the way in which a business is managed and implemented.

Maria Paristiowati, Riskiono Slamet, Rizqi Sebastian[7] made a research which was conducted at SMAN 39 Jakarta with the students grade XI as a sample, which concluded that the improvement of the ability of the student's cooperation and communication happened through the implementation of chemo-entrepreneurship (CEP) learning approach.

Cosmin Mihai Nacu a, Silvia Avasilcăi [8] the research focused on successful business idea in technological entrepreneurship, using a number of factors. The first category of factors of influence used was represented by the personal and professional characteristics of a young (potential) entrepreneur. This category included the following factors: vision, creativity, industry knowledge, perseverance and determination, charisma and persuasion, positive thinking, passion for your own business, trust in people and attitude. The second category of factors of influence that was used is the environment inside and outside the business, this category of factors of influence being composed of natural geographical environment, demographic environment, legal environment, economic environment and

political environment. The third category of factors that influence the success of a business idea is composed of temporal resources, physical resources (ex. machines, equipment, etc.), informational resources, financial resources and human resources. Based on these factors it has been created a mathematical model that aims to determine the success of a business idea of technological entrepreneurship.
The limitations of this research are providing only the equation for the nature of assumption of how it can be a business idea, from the young (potential) entrepreneur point of view. The smallest is the standard deviation, the accurate is the result.

Olcay b [9] focussed on strategic intentions of universities on acting as entrepreneurs and teaching entrepreneurship which is important for understanding the orientation of universities about expanding their roles in economic growth and development. This paper analysed the strategies and organizations of public universities in Turkey for contributing to the expansion of entrepreneurship in the country. The vast majority of the public universities in Turkey does not emphasize entrepreneurship in their strategic statements; Entrepreneurship education has received higher (but still not sufficient) attention in strategies, hence public Universities in Turkey has a higher intention of teaching entrepreneurship rather than acting as entrepreneurs.

Sorina Moica, Teodor Socaciua, Elena R a [10] -This paper worked to provide a new technological innovation model for the Central Region Romania in order to improve the level of regional innovation. Research, development and innovation can be a key point of recovery from the crisis and building a sustainable economy, connected to the real priorities of the country. The model innovation system for economic development such as individuals and society that are the heart model as an engine of the whole system. Basic processes of innovation are formed in three stages: assimilation and application of knowledge, dissemination and knowledge transfer, knowledge generation which is explained in this article.

Hesham A. E. Magd, Mark P. McCoya[11] suggested the benefits that SMEs provide and how their success or failure should be defined. Paper was focussed on the Oman as a case study. It provided motivational factors for starting up a business and the barriers that potential entrepreneurs can face. Finally, current initiatives in the Sultanate a were examined in addition to recommendations relating to how Oman can facilitate an environment conducive to entrepreneurial activity

Mery Citra Sondari[12] provides the explanation on graduate unemployment phenomenon in Indonesia and its relationship to entrepreneurship and also conceptual framework to examine the antecedent of entrepreneurial career intention that will lead to the understanding of the role of entrepreneurship education. This case study was performed with respect to the Indonesia which can be co related with the present status of the India.

IV. CONCLUSION

Many research finding and literature review has suggested that entrepreneurship education is important in order to emerge the intention of the student to start the business. This article has explained the role of entrepreneurship education in creating entrepreneurial intention among student conceptually. Following with the factual things revealed in the current scenario section and case studies performed presented in the literature survey proves that the art of entrepreneurship should be cultivated at the basic stage of education which finally proves promising for the growth of entire nation by increasing employment, productivity, making relations with foreign countries, lessening the import, improvement in techno – managerial practices and finally increasing GDP of the country.

REFERENCES:

[1] Robert C. Ronstadt, “For a compilation of definitions,Entrepreneurship” (Dover, MA: Lord Publishing, 1984),p.28; Howard H. Stevenson and David E. Gumpert, "The Heart of Entrepreneurship," Harvard Business Review (March/April 1985):p.85-94; and J. Barton Cunningham and Joe Lischeron, "Defining Entrepreneurship:' Journal of Small Business Management (January 1991): p.45-61.
[2] Source: William B. Gartner, ―A Conceptual Framework for Describing the Phenomenon of New Venture Creation‖, Academy of Management Review (October 1985): 702.
[3] Teresa Paiva, Pedro Tadeu (2015), ”An approach project to develop entrepreneurship in primary schools”, Procedia - Social and Behavioral Sciences no. 174, pp 1908 – 1915.
[4] Tiago Teresa, Sandra Fariaa, Joao Pedro Coutoa, Flávio Tiagoa (2015), ”Fostering innovation by promoting entrepreneurship: from education to intention”, International Conference on Strategic Innovative Marketing, IC-SIM 2014, September 1-4, 2014, Madrid, Spain, Procedia - Social and Behavioural Sciences no. 175 pp 154 – 161.

[5] Faggio Giulia, Olmo Silva (2014). "Self-employment and entrepreneurship in urban and rural labour markets", Journal of Urban Economics no. 84 pp 67–85.

[6] Anca Otilia Dodescua, Ioana Crina Pop-Cohua, Lavinia Florentina Chiril (2014), " Do practice stages encourage students in Economics to practice entrepreneurship? Practeam project" Emerging Markets Queries in Finance and Business, no. 15 pp. 1083 – 1090.

[7] Paristiowati Maria, Riskiono Slameta, Rizqi Sebastiana (2014), " Chemo-entrepreneurship: learning approach for improving student's cooperation and communication(Case Study at Secondary School, Jakarta)" Procedia - Social and Behavioral Sciences no. 174 pp 1723 – 1730.

[8] Cosmin Mihai Nacu a, Silvia Avasilcăi (2014), " Environmental factors influencing technological entrepreneurship: research framework and results", 2nd World Conference on Business, Economics and Management – WCBEM 2013, Procedia - Social and Behavioural Sciences no. 109 pp 1309 – 1315.

[9] Olcay (2012), "Entrepreneurship Intentions of Public Universities in Turkey: Going Beyond Education and Research?" 8th International Strategic Management Conference, Procedia - Social and Behavioral Sciences no.58 pp 953 – 963.

[10] Moica Sorina, Teodor Socaciua, Elena R, " Model innovation system for economical development using entrepreneurship education" , Emerging Markets Queries in Finance and Business, Procedia Economics and Finance no.3 pp521 – 526

[11] Hesham A. E. Magd, Mark P. McCoya (2014), "Entrepreneurship in Oman: Paving the Way for a sustainable Future" Procedia Economics and Finance no. 15 pp 1632 – 1640

[12] Sondari Mery Citra(2013), "Is Entrepreneurship Education Really Needed ? : Examining the Antecedent of Entrepreneurial Career Intention (2014)", The 5th Indonesia International Conference on Innovation, Entrepreneurship, and Small Business (IICIES 2013), Procedia - Social and Behavioral Sciences no. 115 pp 44 – 53

International Journal of Engineering Research and General Science Volume 3, Issue 5, September-October, 2015
ISSN 2091-2730

STATIC AND DYNAMIC ANALYSIS OF RC BRIDGE

Simulation

Prof. Dr. D. N. Shinde (Guide) [1], Mr. Mahesh D. Patil (Student)[2]

Civil department P.V.P.I.T. Budhgaon/Shivaji University, India

Email : mdpatson@gmail.com M.- 959509003

Abstract-While designing any structure, now days the seismic performance of structure is very much important. The basic aim of this dissertation is to analyze the RCC, bridge, statically and dynamically. The performance of bridge is studied with and without application of isolation system. This includes the study of rigid bridge, base isolated bridge, and bridge with bearings between girder and top of pier. The effect of seismic force on these bridge model is carefully studied by applying the seismic force. Depending on behavior of these models the actual seismic demand of bridge is determined and also the importance of isolation system is taken into consideration. The attempts are done to reduce the seismic effect thereby introducing the isolation. The isolations are of various type, here elastomeric bearing and led rubber isolator is used. Also, the comparison of isolated and un isolated bridge structure is carried out. The analysis is mainly consists of response spectrum analysis, time history analysis, eigen value analysis, moving load analysis, and non linear push over analysis etc.

Keyword- Rigid bridge structure , isolated bridge structure , elastomeric bearing and rubber pad.

Introduction- The three span continuous bridge is taken under study. The span of bridge is kept 28m with lane width of 8m. The girder is of rectangular shape having size of 0.53m wide and 0.3m deep along longitudinal direction. The diaphragm is provided only at the ends having size 0.23m wide and 0.4m deep. There are no any intermediate diaphragms. Two types of vehicles i.e. 70R and class A type are run for 8m width of width as per IRC-6-2000. The end pier is solid rectangular type of 0.4m wide and 0.3m depth ant that of mid pier cap is also solid rectangular type of size 0.8m wide by 0.3m deep. The piers are solid octagonal of 1m width. The footing is rigid one. There are two types of isolators are used namely elastomeric bearing and lead rubber bearing. The design of these isolator is based on vertical load coming from sub structure and super structure.

There are three types of model are studied, those are described as follows.

Model No. I In the Model I, the total structure is monolithic. No any isolation or isolator is provided. The model is fixed at the base and also at the foundation.

Model No. II In the model II, the elastomeric bearings are provided between pier and deck slab. The bridge model is fixed at the base (Foundation).

Model No. III In case of model III, the base isolation is provided at the foundation. Base isolation is Lead Rubber Type. The pier and deck slab are kept fixed.

The static and dynamic analysis of these three models is carried out. The results are compared and best performance bridge model are taken into consideration. In all the three models the physical properties like deck, pier, I-girder, span, width, loading, etc are remain same. The results of respective models are as follows. The figure **5.6** shows the three dimensional view of model

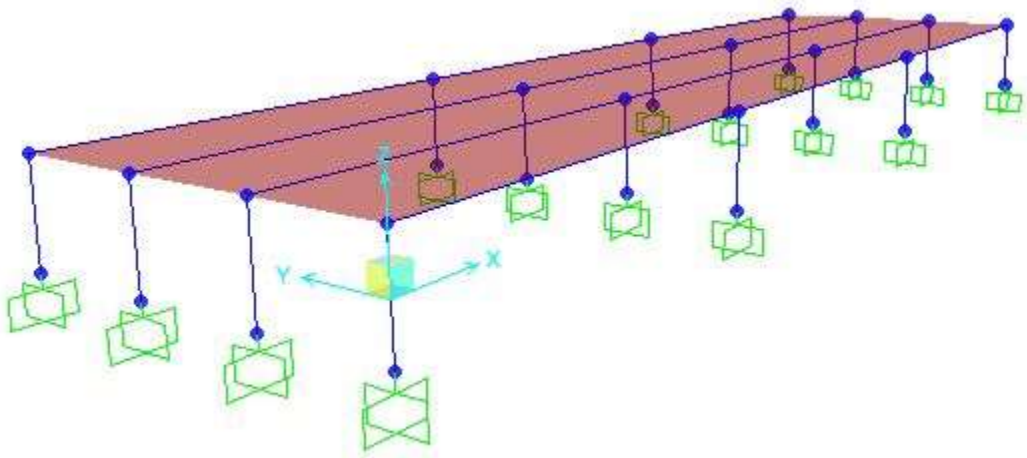

Fig. 8.1 Three-dimensional View of Bridge

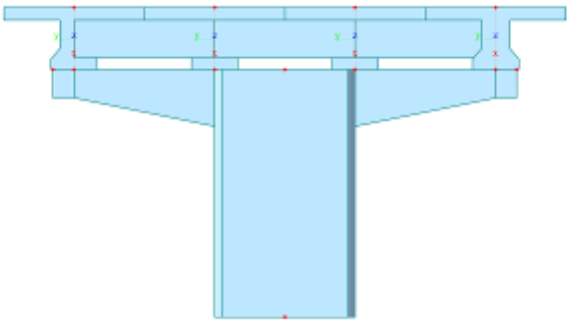

Fig. 8.2 Side View of Bridge Structure

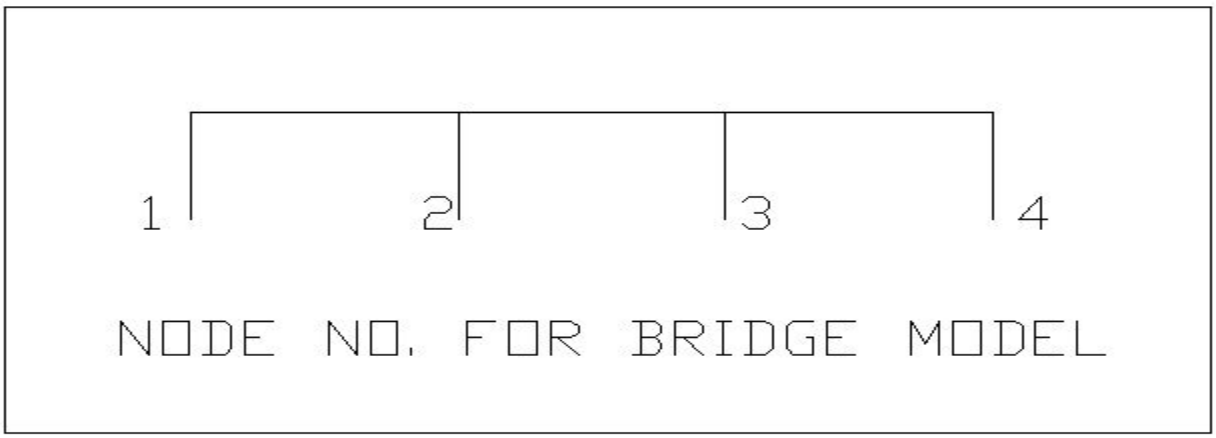

Fig. 8.3 Node No. for Bridge model

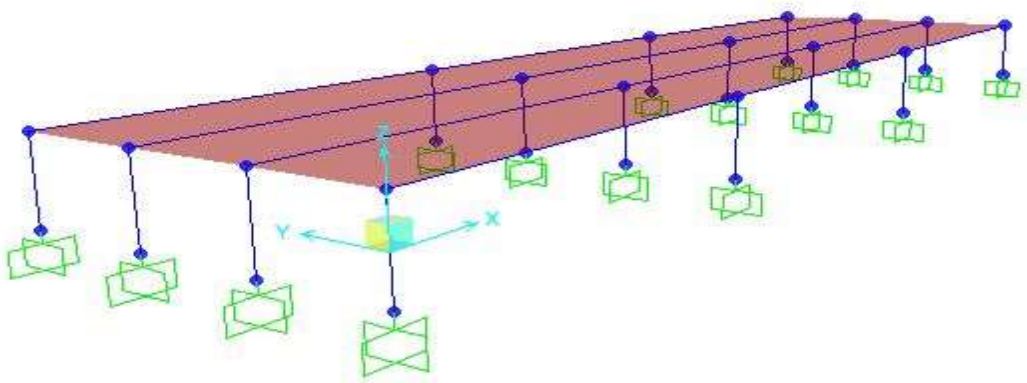

Fig. 8.4 Three-dimensional View of model – I

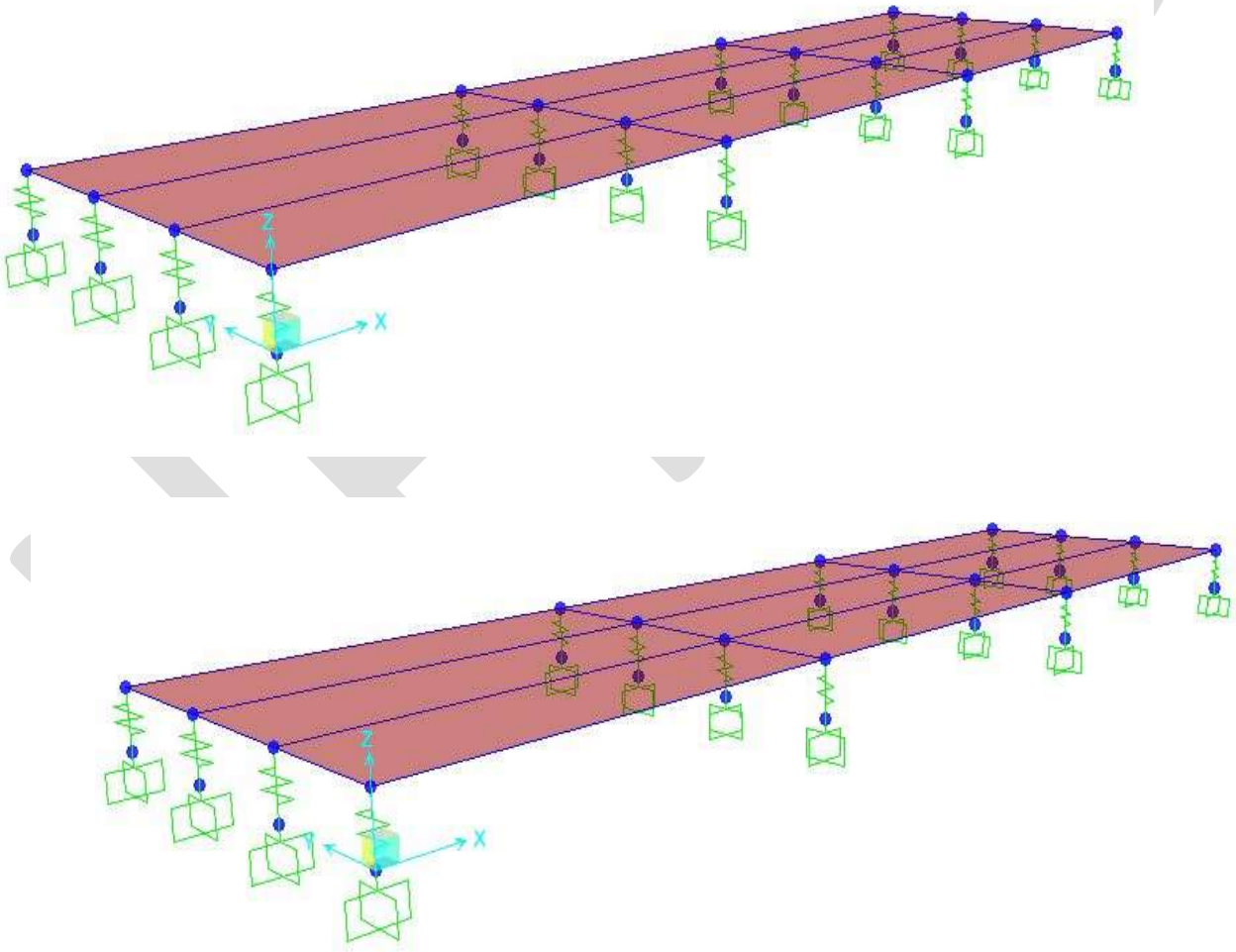

Fig. 8.5 Three-dimensional View of model – II

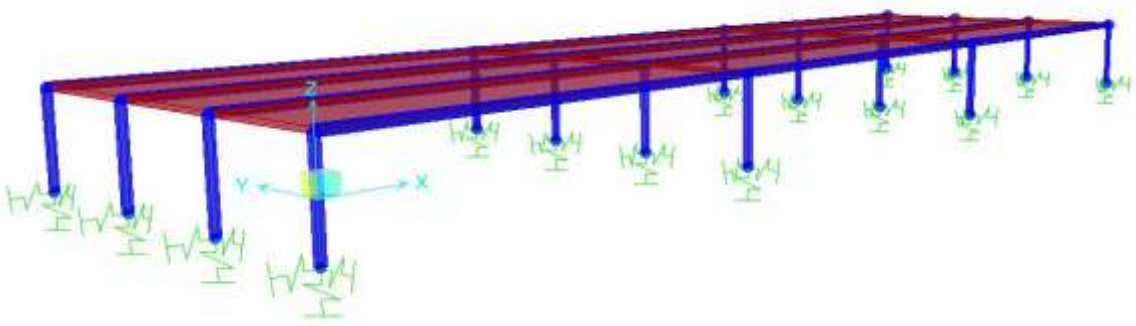

Fig. 8.5 Three-dimensional View of model – III**Results and Discussion**

1. Reactions:

Table 1.1 Support Reaction of Model No. I

Node	**FX (tonf)**	**FY (tonf)**	**FZ (tonf)**	**MX (tonf*m)**	**MY (tonf*m)**	**MZ (tonf*m)**
1	65.91	0.31	205.96	67.52	43.80	0.82
2	34.58	0.44	253.04	69.19	27.95	0.85
3	49.45	0.39	264.61	69.52	44.80	0.84
4	57.68	0.27	273.80	64.12	50.72	0.76

Table 1.2 Support Reaction of Model No. II

Node	**FX (tonf)**	**FY (tonf)**	**FZ (tonf)**	**MX (tonf*m)**	**MY (tonf*m)**	**MZ (tonf*m)**
1	65.91	0.31	205.96	58.48	34.19	0.66
2	34.58	0.44	253.04	61.12	16.20	0.68
3	49.45	0.39	264.61	61.19	27.23	0.70
4	57.68	0.27	273.80	53.11	31.81	0.59

Table 1.3 Support Reaction of Model No. III

Node	**FX (tonf)**	**FY (tonf)**	**FZ (tonf)**	**MX (tonf*m)**	**MY (tonf*m)**	**MZ (tonf*m)**
1	65.91	0.31	205.96	60.61	38.32	0.68
2	34.58	0.44	253.04	65.38	19.18	0.70
3	49.45	0.39	264.61	65.45	30.38	0.72
4	57.68	0.27	273.80	58.30	35.21	0.62

2. Beam stresses

Table 2.1 Beam Member Stresses of Model No. I

Elem	**Axial (tonf/m^2)**	**Shear-y (tonf/m^2)**	**Bending(+y) (tonf/m^2)**	**Bending(-y) (tonf/m^2)**
1	1.21E-08	1.74E-06	2.05E-05	1.51E-05
2	1.01E-06	1.80E-06	2.71E-06	2.93E-05
3	1.38E-07	1.72E-06	2.08E-05	2.79E-05
4	1.43E-07	1.82E-06	2.67E-05	2.78E-05

Table 2.2 Beam Member Stresses of Model No. II

Elem	**Axial (tonf/m^2)**	**Shear-y (tonf/m^2)**	**Bending(+y) (tonf/m^2)**	**Bending(-y) (tonf/m^2)**
1	1.18E-08	1.33E-06	2.01E-05	1.48E-05
2	0.87E-06	1.55E-06	2.53E-05	2.68E-05
3	1.13E-07	1.56E-06	1.97E-05	2.57E-05
4	1.24E-07	1.69E-06	2.35E-05	2.50E-05

Table 2.3 Beam Member Stresses of Model No. III

Elem	**Axial (tonf/m^2)**	**Shear-y (tonf/m^2)**	**Bending(+y) (tonf/m^2)**	**Bending(-y) (tonf/m^2)**
1	1.20E-08	1.65E-06	2.03E-05	1.50E-05
2	0.93E-06	1.68E-06	2.61E-05	2.87E-05
3	1.23E-07	1.66E-06	2.05E-05	2.61E-05
4	1.35E-06	1.78E-06	2.49E-05	2.63E-05

3. Time period & frequencies

Table 3.1 Modal period & frequencies of Model No.I

Mode No.	Frequency		Period
	(rad/sec)	(cycle/sec)	(sec)
1	21.844511	3.476662	0.287632
2	22.711735	3.614685	0.276649
3	25.86059	4.115841	0.242964
4	27.144447	4.320173	0.231472
5	27.636088	4.39842	0.227354
6	31.064328	4.944041	0.202264

Table 3.2 Modal period & frequencies of Model No.II

Mode No.	Frequency		Period
	(rad/sec)	(cycle/sec)	(sec)
1	12.191533	1.940343	0.515373
2	12.845544	2.044432	0.489133
3	15.24686	2.426613	0412097
4	15.503384	2.46744	0.405278
5	19.194798	3.054947	0.327338
6	21.55689	3.430886	0.29147

Table 3.3 Modal period & frequencies of Model No.III

Mode No.	Frequency		Period
	(rad/sec)	(cycle/sec)	(sec)
1	2.532597	0.24392	4.099697
2	3.9439466	0.627698	1.593122
3	12.120785	1.929083	0518381
4	16.675773	2.654032	0.376785
5	21.276782	3.386305	0.295307
6	21.734488	3.459151	0.289088

4. Nodal Inertia Force

Table 4.1 Inertia Force of Model No.I

Mode No.	Node No.	FX (tonf)	FY (tonf)	FZ (tonf)
1	1	0	0	-0.0094
1	2	0	0	-0.0096
1	3	0	0	-0.0096
1	4	0	0	-0.0094

Table 4.2 Inertia Force of Model No.II

Mode No.	Node No.	FX (tonf)	FY (tonf)	FZ (tonf)
1	1	-0.0013	0.0015	0.0334
1	2	0.0017	0.0015	0.0308
1	3	-0.0003	0.0036	0.1341
1	4	-0.0004	0.0037	0.1324

Table 4.3 Inertia Force of Model No.III

Mode No.	Node No.	FX (tonf)	FY (tonf)	FZ (tonf)
1	1	0	0.1935	0.1327
1	2	0	0.1966	0.045
1	3	0	0.1935	-0.1327
1	4	0	0.1967	-0.045

5. Push Over Analysis:

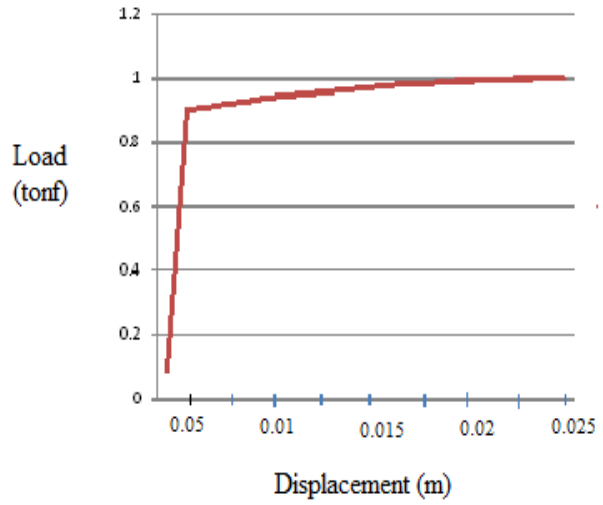

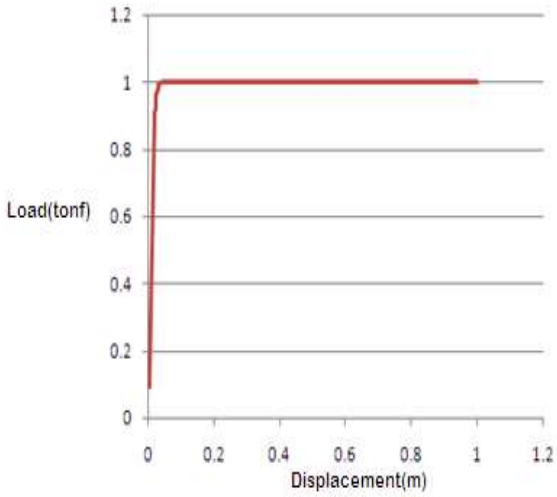

Graph.1 Load vs Displacement of Model I **Graph.2** Load vs Displacement of Model II

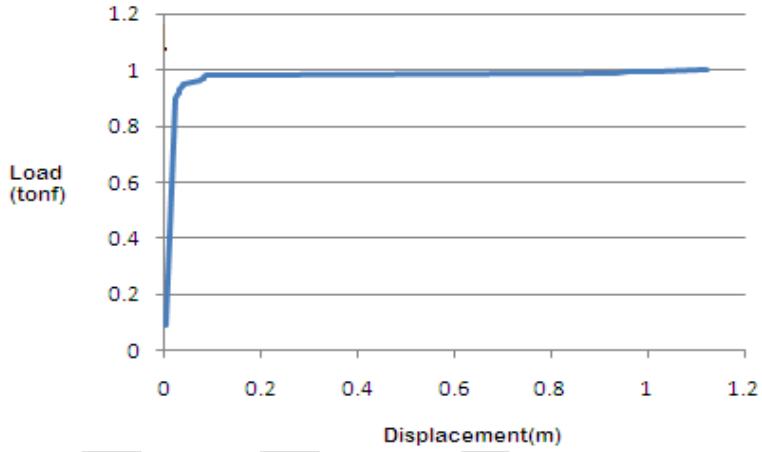

Graph.3 Load vs Displacement of Model III

6. Time History Analysis

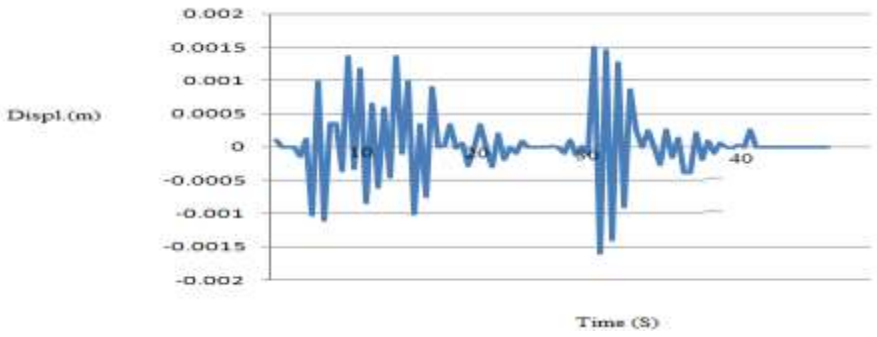

Graph 4. Time History Analysis of Model No. I

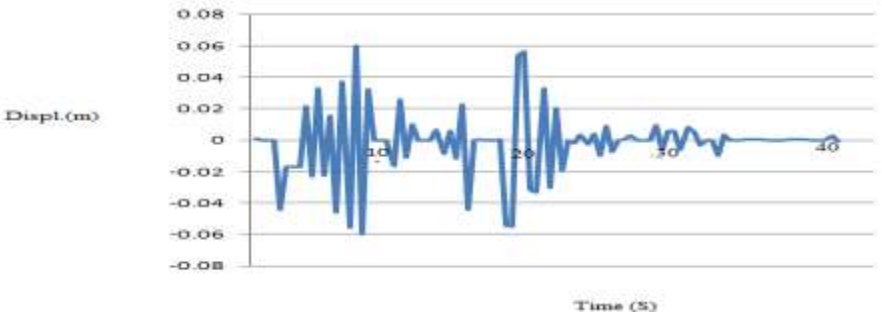

Graph 5. Time History Analysis of Model No. II

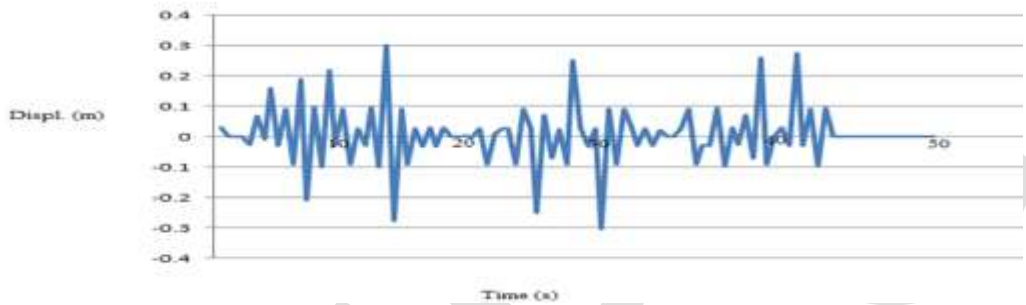

Graph 6. Time History Analysis of Model No. III

CONCLUSION

As stated earlier there are three types of model having same physical properties are taken into consideration those models are rigid type (Model No.I), isolated bridge i.e. bearing between girder and pier(Model II), base isolated bridge i.e. isolation at the foundation (Model III) are analyze and their seismic performance are studied. The results are compared and best model are find out for best performance during earthquake. The following conclusions are drawn.

1. Study of virtual model developed in the software gives results such as modal period (table- 3.1, 3.2, 3.3) , frequencies(table- 3.1, 3.2, 3.3) , moments(table- 1.1, 1.2, 1.3); beam stresses (table- 2.1, 2.2, 2.3) were minimum in model II as compared with model I and III.

2. The period of model I is very less. This is because of more rigidity. Though this period is not worst but this amount of period is not enough in moderate or heavy earthquakes in region IV or V. These periods are increased by application of elastomeric bearing. The

max period for model 3 is very high which is suitable only during high magnitude of earthquakes. Also the installation of base isolation is very costly hence it is rarely used. Hence model II is best suited. (table- 3.1, 3.2, 3.3)

3. During an Earthquake the inertia force is generated and it is transmitted to the foundation of bridge which leads to its collapse. Thus direct transmition of inertia force to the foundation must be avoided and this can be achieved by the application of isolation system. the result shows that in case of model-I the inertia forces are only in z- direction which is directly transmitted to foundation but in case of model-II this inertia force is contributed by various bridge units in x,y,z direction which not even possible in model-III . Hence model II is feasible. (table- 4.1, 4.2, 4.3)

4. By providing isolation system in the form of elastomeric bearing at the top of pier below the deck of bridge, time period will increase, frequency will decrease, moments will get minimum and the inertia force also will get transferred in three directions. The beam member stresses will also reduces. (table- 3.1, 3.2, 3.3) (table- 3.1, 3.2, 3.3) (table- 1.1, 1.2, 1.3)

5. The period of model III is very high which is best only during high magnitude of earthquake, but the installation of base isolation is very costly. Hence seldom used. In case of model II the time period as compare to that of model III is less, but it is enough for region IV or V and it is not as costly as in case of model III. In case of model II max displacement is about 60 mm which is well enough for bridge structure for its best performance during earthquake. But in case of model-III, the displacement is about 300 mm which is very high and as stated earlier the base isolation system is best only for high intensity of earthquake. (graph 4, 5, 6)

6. In case of unisolated bridge structure,

- Time period is less, frequency is high.
- Beam stresses are high.
- Inertia forces are transmitted only in z-direction.
- Displacement is less but flexibility is also very less which is not required for bridge structure.
- Moments are high.

In case of isolated bridge structure

- Time period is more, frequency is less.
- Beam stresses are low.
- Inertia forces are transmitted in all 3 directions.
- Displacements are more than that in case of unisolated structure but are well within the limits and also the structure is flexible.
- Moments are low.

REFERENCES:

01. Billings, L. J. (1993). “Finite element modeling of elastomeric seismic isolation bearings.” Ph.D. Dissertation, University of California, Irvine, California.

02. Chaudhary, M.T.A., Abe, M. and Fujino, Y. (2001b).“Performance evaluation of base isolated Yama-age bridge with high damping rubber bearings using recorded seismic data.” *Engineering Structures*, 23(8), 902-910.

03. Chaudhary, M. T. A., Abe, M. and Fujino, Y. (2002a). “Investigation of atypical seismic response of a base-isolated bridge.” *Engineering Structures*, 24(7), 945-953.

04. Chopra Anil K. “Dynamic of Structures”-Theory and Application to Earthquake Engineering

05. Chung C. Fu and Hamed Alayed, “Seismic Analysis of Bridges using Displacement Based Approach”, (University of Maryland).

06. Crouse, C. B., Hushmand, B. and Martin, G. R. (1987). “Dynamic soil structure interaction of a single-span bridge.” *Earthquake Engineering & Structural Dynamics,* l5(6), 7ll-729.

07. Dendrou, B., Werner, S. and Toridis, T. (1984). “Three-dimensional response of a concrete bridge system to traveling seismic waves.” *Computers and Structures,* 20(1- 3), 593-6.

08. E.L. Wilson, A. Der Kiureghian and E.P. Bayo, (1981). A replacement for the SRSS method in seismic analysis, J. Earthq. Eng. d Str-uct. Dyn. 9, 187-194

9. Ghobarah AA, Tso WK. 1974 “Seismic analysis of skewed highway bridges with intermediate supports”. Earthquake Engng Struct Dynam 235–48.

10. Imbsen and 3. Penzien R.A, (1986). “Evaluation of energy-absorption characteristics of highway bridges under seismic conditions”, Volume 1, Report UCB/EERC-84/17-VOL-1, Univ. of California, Berkeley, CA,

11. IRC6:2000, Standard Specifications and Code of Practice for Road Bridges (Section-II) Loads and Stresses (Fourth Revision).

12. K. Toki, (1980). “Nonlinear response of continuous bridge subjected to traveling seismic wave”, Proceedings of the Fh World Conf. Earthq. Eng., Istanbul, Turkey, pp. 467-474,

13. L.F. Greimann, P.S. Yang and A.M. Wolde-Tinsae, (1986). “ Nonlinear analysis of integral abutment bridges”, J. Struct. Eng., ASCE 112, 2263-2280

14. M.A. Ahmed, (1991). “Three dimensional nonlinear inelastic seismic analysis of highway overcrossing”, Ph.D. Thesis, Univ. of Pittsburgh, Pittsburgh, PA,

15. Maragakis E. 1984.” A model for the rigid body motions of skew bridges. PhD thesis, California Institute of Technology”, Pasadena, CA,

16. Mark Yashinsky and M.J. Karshinas, “Fundamentals of Seismic Protection for Bridges” EERI Publication, 2003, MNO-9.

17. Matthies H. and Strang G,(1979)” The solution of nonlinear finite element equations”, ***J. Num. Meth.*** Eng. 14, 1613-1626 .

18. N.M. Newmark, (1959). ”A method of computation for structural dynamics”, J. Eng. Me&., ASCE 85, 67-94

20. Razaqpur A.G. and Nofal M, (1990). Analytical modeling of nonlinear behavior of composite bridges, *J. Struct.* Eng., ASCE 116, 1715-1733

21. Seismic design guidelines for highway bridges, Report ATC-6, Applied Technical Council of California (ATC), (1981).

22. Wai-Fan Chen and Lian Duon, (2000). "Bridge Engineering (Seismic Design)" Eds., CRC Press, Boca Raton, FL,

23. Wakefield RR, Nazmy AS, Billington DP. (1991) " Analysis of seismic failure in skew RC bridge". Struct Engng;117(3):972–86.

24. W.S. Tseng and J. Penzien, (1975). "Seismic analysis of long multiple-span highway bridges", J. ***Earthq. Eng. & Strct. Dyn.*** 4 (l), 3-24

25. Y. Chen, (1992). "Effects of seismic ground motion on bridge analysis and design", Proceedings oj the ASME PVP Conf., (Edited by A.C. Singhal et al.), Volume 227, pp. 2%40, ASME, New York,

26. Yochia Chen, (1992) "Non Linear Seismic Analysis of Bridges: Practical Approach and Comparative Study", (The Pennsylvania State University).

27.https://www.google.co.in/search?q=static+and+dyanamic+analysis+of+rc+bridge+structure+image&tbm=isch&tbo=ojhbswgan

International Journal of Engineering Research and General Science Volume 3, Issue 5, September-October, 2015
ISSN 2091-2730

A Review: Sparse Web Graph Compression using Eulerian Data Structure and its Optimization

Ankita Singh

UPTU University, ankjai121292@gmail.com

Abstract— The purpose of this paper is to review the sparse web graph compression technique using Eulerian data structure and optimization of the designing of compressed scheme based on careful application. Web graphs form the foundation of social networks but their storage is a big challenge due to their large size. Compression techniques are proposed in the recent time in which queries can be carried out without decompressing the graph. This paper reviews graph compression using Eulerian data structure and multiposition linearization which is capable of solving in and out query and hence exclude the need of storing transpose of Web graph for in-neighbor query determination. Some optimization approaches are also proposed which depends on compression ratio and k- factor.

Keywords— Graph, compression, optimization, sparse, query, application, Eulerian data

INTRODUCTION

The World Wide Web has become the focus of research in the recent times. Social networks, network consisting of individuals or organization as nodes, are an important part of World Wide Web. In social networks, nodes are connected by one or more type of interdependency such as friendship and kinship. Compression of networks, using Eulerian data structure and multiposition linearization, such that neighbor queries can be carried out on the same graph without decompressing the graph or storing its transpose. Various factors such as optimal value of k and compression ratio are to be analyzed.

NOTIONS

1. Network-: A network is modeled as directed graph G = (V, E) where V is a set of vertices and E ⊆ V × V is a set of edges. We also refer to V by V(G) and E by E(G). For an edge e= (u,v), we refer to u as the source of e and v as the destination of e.(u,v) ≠e(v,u).
2. Undirected Graph-: For an undirected graph G, we can obtain the directed version G of G by placing two directed edges (u,v) and (v,u) in Gd for each undirected edge {u, v) in G.
3. Transpose-: For a graph G, the transpose of G, is denoted by GT, is a graph such that V(GT) = V(G) and (u,v) belongs to E(GT) if and only if (v, u) belongs to E(G).
4. Reciprocal-: In a graph G, an edge (u,v) belongs to E is called reciprocal if (v,u) belongs to E as well. In such a case, u and v are immediately connected in both directions. Let Fre(G) be the fraction of reciprocal edges in E(G), i.e.,
5. In- Neighbor Query-: For a vertex u belongs to V(G) v2 belongs to V(G) is an in-neighbor of u if (v2, u) belongs to E(G).
6. Out- Neighbor Query-: For a vertex u belongs to V(G) v2 belongs to V(G) is an out neighbor of u if (u, v1) belongs to E(G).

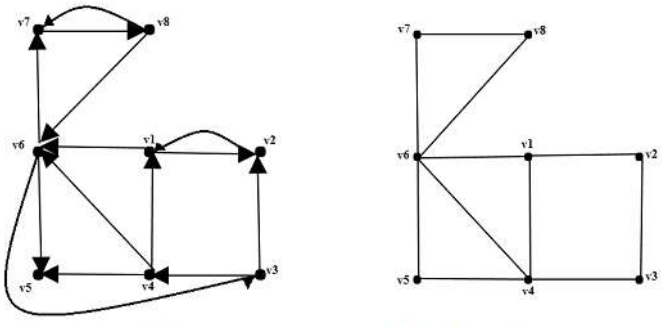

Figure 1: A directed graph G and its underlying undirected graph G'

FORMULATION OF PROBLEM AND ITS SOLUTION

A directed network model is given and its MP1 linearization is required. For a sequence S, the S-distance between u and v, denoted by S-dist(u,v), is the minimum norm-1 distance among all pairs of appearances of u and v. An Mpk linearization of a Graph G is a sequence S of vertices of the graph with possible replication, such that S covers G and for all (u, v) belongs to E(G), S- dist(u,v)<= k. The length of an Mpk linearization is equa to length of S. Eulerian Data Structure stores MPk linearization L of G using an array of same length as L. Two piece of information are kept. First, local information of two bits specifying if edges (V(i-1), v(i) and (V(i), V(i-1)) belongs to E(G) respectively. Second, a pointer to the next appearance of v(i). If this is the last appearance of v(i), then the pointer points to the first appearance of the vertex.

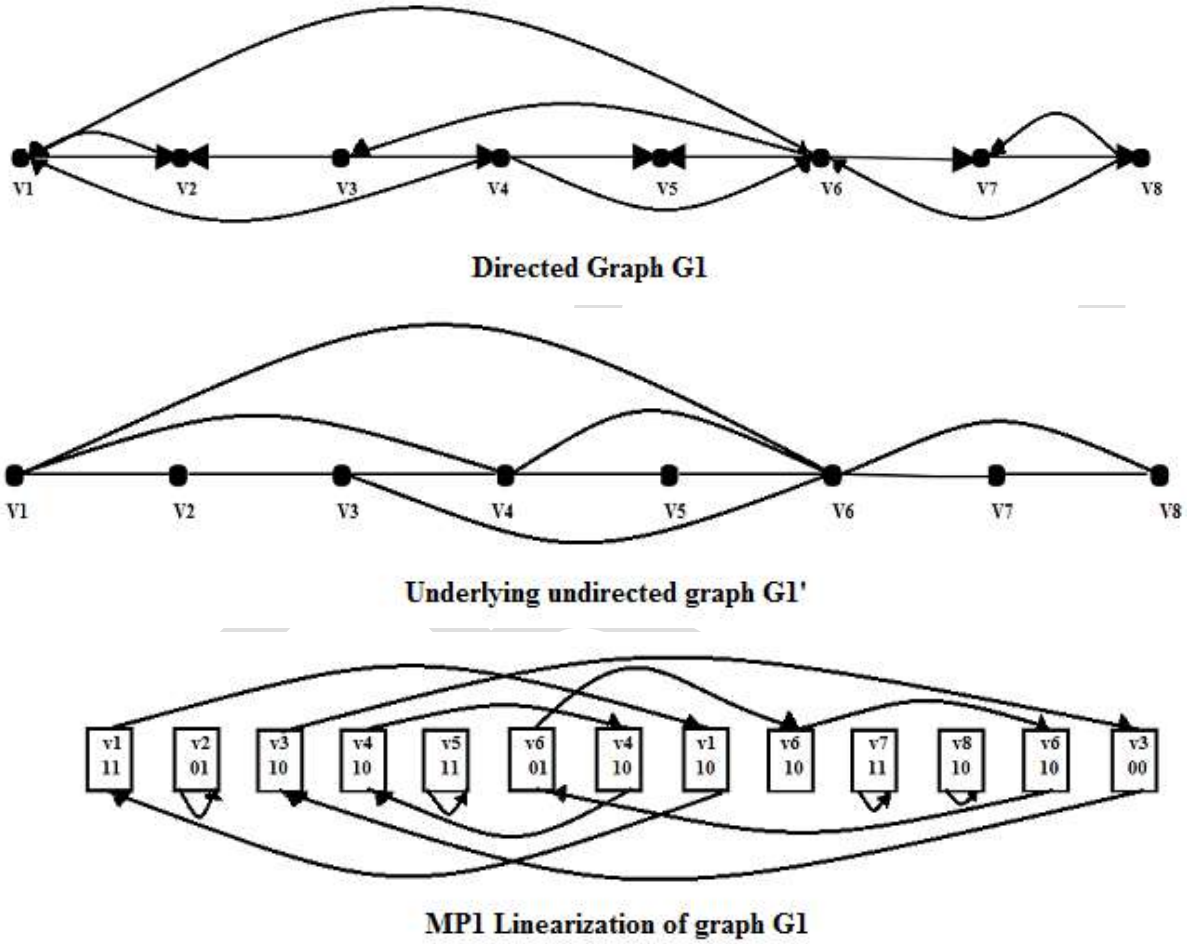

Figure 2: MP1 linearization of the graph G presented in Figure 1

The Eulerian data structure of the above shown graph G1 using an MP1 linearization is illustrated. Here we show the pointers by arcs. Since the length of the linearization is 18, we need log2(13) = 4 bits to encode each pointer. Therefore, for each position we need 4+2(local information) bits. In total we need 13×(4+2)=78 bits, which make a compression rate of 78/13 ≈ 6 bits per edge. As the value of k is increased from 1 to 2 there is a significant decrease in required bits per edge is seen. But after a certain value inefficiency in compression rate is noticed.

MP1 linearization algorithm-:Both graph G and its transpose is required to be stored in order to answer neighborhood queries such as in and out neighbor queries but Eulerian data structure stores MP1 linearization L of G.

- Start from an odd degree node, if there is no such node, start from an arbitrary node.
- Choose an edge whose deletion does not disconnect the graph, unless there is no such choice left.
- Move across the edge and remove it.
- Keep removing edges until getting to a node that does not have any remaining edge to choose.
- If the graph is not empty go to step 1.

This algorithm partitions the edges to exactly Nodd/2 edge-disjoint paths, where Nodd is the number of vertices with odd degree (assuming Nodd>0). It can be implemented in O(|E|).

OPTIMIZATION

A greedy approach for Mpk linearization is used, since it gives the optimized version.

MPk linearization greedy algorithm [10]:

- Start with a random vertex.
- At each step, add to the list the vertex having the largest number of edges with the last k nodes in the list.
- Remove these edges from the graph
- Iterate until no edge is left.
- If none of the last k vertices in the list have a neighbor, and graph is not empty go to step 1.

This requires 2k bits to encode the local information for each position. Having a fixed k all the time is not a good idea since the rear part of the linearization may have very few new edges to encode.

To be adaptive, a relaxed version of the linearization notion is used. For start, a relatively large value of k is taken. Average local density is considered for the graph node positions. If it drops down below a predefined density threshold DT, k is to be reduced by multiplying it to another predefined factor known as reducing factor RF. As the edges are removed, graph become sparse, now the value of k can be decreased so that local information in Euler data structure decreases.

Peter-hamster dataset is used for testing our algorithm for different k values. That graph was having around 22,900 edges with 2400 vertices. and Fre(G) = 0.55 For different k values we obtain different compression ratios.

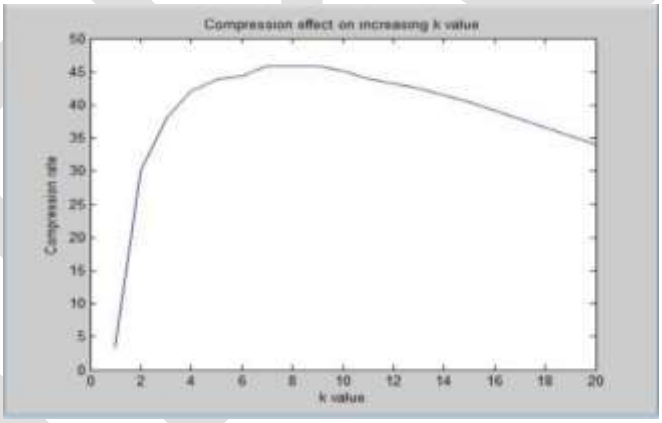

Figure 3: Relation between Compression rate and k value for Peter-hamster dataset

Here we can see as we increase the value of k compression ratio increases but after a certain value it start decreasing. Here maximum compression in on k=8 around 46.2% without using heuristic.

Name	Description	V(G)	E(G)	Fre(G)
Peter-hamster	Social network datasets of peter-hamster	2422	22962	0.55

Figure 4: Details of Peter-hamster dataset

For a large sparse graph where each vertex has the same out degree, and their destinations are picked randomly, increasing k would not influence the length of the linearization significantly. However, for a large random dense graph G where the existence of an edge from every node to another is independently determined by a probability of 50%, increasing k up to |V (G)|, the number of vertices, is actually beneficial.

While considering different datasets k = 5 to 10 proved to be a good value.

APPLICATION

Neighborhood queries are most essential operations on any network. Various other operations can be built using neighborhood queries. One such operation is outlier detection. Outlier detection is the observation of the deviation from a set measurement such that a suspicion is aroused that it does not fit into a certain criteria. A technique for outlier detection is, by using k-nearest neighbor graph. Moreover, an effective way for a k-nearest neighbor graph to be built for a large sparse network is, by using the Eulerian data structure and multiposition linearization. Another operation is community finding, where nodes belonging to similar profiles are clustered. This technique is useful for various other operations as well such as pattern mining.

CONCLUSION

The web graph compression using Eulerian data structure is an efficient way to compress the graph network which can be queried without decompressing the graph. There are various factors affecting the efficiency of this technique, such as value of k, compression ratio and structure of graph. It is observed that $5 \leq k \leq 10$, provides a good range for efficient compression.

REFERENCES:

[1] Hossein Maserrat and Jian Pei, In ACM-KDD Cup: 2010, "Neighbor Query Friendly Compression of Social Networks".
[2] Jérôme Kunegis, "KONECT - the Koblenz Network Collection". Online konect.uni-koblenz.de, 2013.
[3] P. Boldi, M. Santini, and S. Vigna. Permuting web graphs, Berlin, Heidelberg, 2009, In Proceedings of the 6th International Workshop on Algorithms and Models for the Web-Graph (WAW'09).
[4] M. Adler and M. Mitzenmacher, In Data compression conference: 2001, "Towards compressing web graphs".
[5] K. H. Randall et al., In DCC :2002, "The link database: Fast access to graphs of the web".
[6] P. Boldi and S. Vigna, WWW :2004, "The web-graph framework I: compression techniques".
[7]] P. Boldi and S. Vigna, In Data Compression Conference :2004, "The web- graph framework II: Codes for the world-wide web".
[8] G. Buehrer and K. Chellapilla. In WSDM :2008, "A scalable pattern mining approach to web graph compression with communities".
[9] Fang Zhou, In Data compression conference :2009, "Graph Compression".
[10] F. Chierichetti et al. , ACM-KDD Cup, 2009, "On compressing social networks",
[11] Torsten Suel and Jun Yuan, In proc. IEEE Data Compresson Conference 2001, "Compressing the Graph structure of the Web".
[12] Susana Ladra González, In Tesis Doctoral, "Algorithms and compressed data structures for information retrieval".
[13] Sriram Raghavan and Hector Garcia-Molin, In Proc. Of the IEEE Intl. Conference on Data Engineering, 2003. "Representing Web graphs".
[14] John M. Kleinberg, In journal of the ACM, 46(5):604-632, September 1999, " Authoritative sources in hyperlinked environment".

International Journal of Engineering Research and General Science Volume 3, Issue 5, September-October, 2015
ISSN 2091-2730

DWT-SVD Based Highly Secure Image Data Hiding System with AES Encryption

Madhvi Dhankar, Jigyasha Soni

M.Tech. Digital Electronics
Rungta College of Engineering and Technology, Bhilai, Chhattisgarh, India
madhvi.dhankar@gmail.com
Contact no. - +919827580063

Abstract — In the past few years,a serious problem about unauthorized and illegal access of secure contents or data, along with manipulation of multimedia files over internet or wireless channels has been strongly noticed. This leads to a serious requirement of a robust technique that can hide the secure data with high security efficiency and also have robustness against the various attacks often occurred after transmission of data in the wireless channels or internet. With the advancement in digital information exchange in the form of image and videos this field has become highly insecure. Most of the time a secure image which has to be transmit securely is first embedded on a cover image and then the cover image will be then transmitted instead of original secure image. This process is known as invisible watermarking or also known as image data hiding. This is the most important and crucial process for transmitting a secure image over open communication channel. Lots of techniques have been developed in past years to achieve high security and robustness against the various attacks. This paper proposed a novel technique for highly secure image data transmission based on discrete wavelet transform (DWT) and Singular value decomposition (SVD) based image data hiding along with advance encryption standard (AES) to enhance the security level. Particularly DWT and SVD based image data embedding over cover image is proposed to achieve higher robustness against various attacks, while AES ensures higher efficiency of transmission security. This hybrid technique leads to optimize both the fundamentally conflicting requirements. To present complete data security efficiency of the proposed technique various parameters like, peak signal to noise ratio (PSNR), mean square error (MSE), embedding rate (ER) and bit error rate (BER) have been employed.

Keywords— Image data security, image embedding, discrete wavelet transform (DWT), singular value decomposition (SVD), advance encryption standard (AES), peak signal to noise ratio (PSNR), mean square error (MSE), embedding rate (ER) and bit error rate (BER).

INTRODUCTION

In the recent few years, there is a serious problem about unauthorized and illegal access and manipulation of multimedia files over internet. Especially the case is more critical in the sense of image and video content privacy. Therefore a need for a robust method in order to protect the copy rights of media especially images and videos has become an essential constraint during the communication of secure images and videos over open communication channel. Invisible digital watermarking provides copyright protection of data by hiding the secure data inside a cover image or video. It is also done by embedding additional information called digital signature or watermark into the digital contents such that it can be detected, extracted later to make an assertion about the multimedia data. For image watermarking, the algorithms can be categorized into one of the two domains: spatial domain or transform domain [1,2]. In Spatial domain the data is embedded directly by modifying pixel values of the host or cover image, while transform domain schemes embed data by modifying transform domain coefficients [1,2]. Algorithms used for special domain are less robust for various attacks as the changes are made at Least Significant Substitution (LSB) of original data. While in the transform domain the watermark is embedded by changing the magnitude of coefficients in a transform domain with the help of discrete cosine transform, discrete wavelet transform (DWT), and singular value decomposition (SVD) techniques [3,5]. This provide most robust algorithm for many common attacks [7]. This paper proposed a novel technique for highly secure image data transmission based on discrete wavelet transform (DWT) and Singular value decomposition (SVD) based image data hiding along with advance encryption standard (AES) to enhance the security level. Particularly DWT and SVD based image data embedding over cover image is proposed to achieve higher robustness against various attacks, while AES ensures higher efficiency of transmission security. This hybrid technique leads to optimize both the fundamentally conflicting requirements. To present complete data security efficiency of the proposed technique various parameters like, peak signal to noise ratio (PSNR), mean square error (MSE), embedding rate (ER) and bit error rate (BER) have been employed.

Foundations of DWT, SVD and AES

1. Discrete Wavelet Transform (DWT)

Wavelets are functions defined over a finite interval and have an average value equal to zero. The wavelet transform represents any arbitrary function (t) as a superposition of a set of basis function. These basis functions or baby wavelets are obtained from a single prototype wavelet called the mother wavelet. Basis functions include scaling function and wavelet function. The image is first divided into blocks and each block is then passed through the two filters: scaling filter (basically a low pass filter) and wavelet filter (basically a high pass filter). Four sub images are formed after doing the first level of decomposition namely LL, LH, HL, and HH coefficients [8-10].

At level 1: Image is decomposed into four sub bands: LL, LH, HL, and HH where LL denotes the coarse level coefficient which is the low frequency part of the image. LH, HL, and HH denote the finest scale wavelet coefficient. The LL sub band can be decomposed further to obtain higher level of decomposition. This decomposition can continues until the desired level of decomposition is achieved for the application. The secure image can also be embedded in the remaining three sub bands to maintain the quality of image as the LL sub band is more sensitive to human eye.

2. Singular Value Decomposition (SVD)

An image can be represented as a matrix of positive scalar values. Formally, SVD for any image say A of size $m \times m$ is a factorization of the form given by $A = U * S * V^T$, Where U and V are orthogonal matrices in which columns of U are left singular vectors and columns of V are right singular vectors of image A. S is a diagonal matrix of singular values in decreasing order. The basic idea behind SVD technique of watermarking is to find SVD of image and the altering the singular value to embed the watermark. In Digital watermarking schemes, SVD is used due to its main properties:

- A small agitation added in the image, does not cause large variation in its singular values.
- The singular value represents intrinsic algebraic image properties [4].

3. Advance Encryption Standard (AES)

The AES algorithm is a symmetric-key cipher, in which both the sender and the receiver use a single key for encryption and decryption. The data block length is fixed to be 128 bits, while the key length can be 128, 192, or 256 bits, respectively. In addition, the AES algorithm is an iterative algorithm. Each iteration can be called a round, and the total number of rounds is 10, 12, or 14, when the key length is 128, 192, or 256 bits, respectively. The 128-bit data block is divided into 16 bytes. These bytes are mapped to a 4×4 array called the State, and all the internal operations of the AES algorithm are performed on the State. Each round in AES, except the final round, consists of four transformations: Sub-Bytes, Shift-Rows, Mix- Columns, and Add-Round-Key. The final round does not have the Mix-Columns transformation. The decryption flow is simply the reverse of the encryption flow and each operation is the inverse of the corresponding one in the encryption process [11].

The initial step of AES is to convert the input plaintext matrix into state matrix. State matrix is obtained calculating hexadecimal value of input matrix which is given as input to the forthcoming steps of encryption. The plaintext matrix is rearranged into state matrix and iteratively loops the state through 4 steps: Addroundkey, Subbytes, Shiftrows, and Mixcolumns. The Addroundkey block performs bitwise xor of the state matrix and the round key matrix. The Subbytes block applies the S-box to one or more input bytes of input matrix. It performs the substitution function in which each byte of input matrix is replaced by the corresponding value in Sbox. The block shiftrows cyclically permutes (shifts) the rows of state matrix to the left. It takes the output matrix from subbytes step, cyclically shift the rows and give its output to next step. Polynomial matrices are used in the mixcolumns function, both matrices have the size of 4 × 4 and every row is a cyclic permutation (right shift) of the previous row. The mixcolumns transformation computes the new state matrix S0 by left multiplying the current state matrix S by the polynomial matrix P. The input parameters for encryption process are: the substitution table S-box, the key schedule w, and the polynomial matrix. The flowchart for AES encryption process is shown in Figure (1), figure (2) shows flow chart representation of AES decryption process.

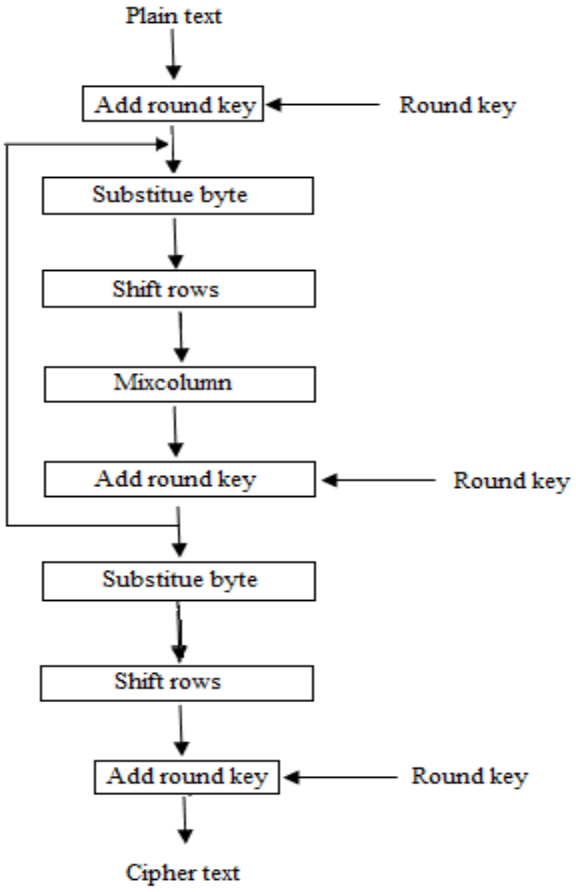

Figure (1). AES Encryption

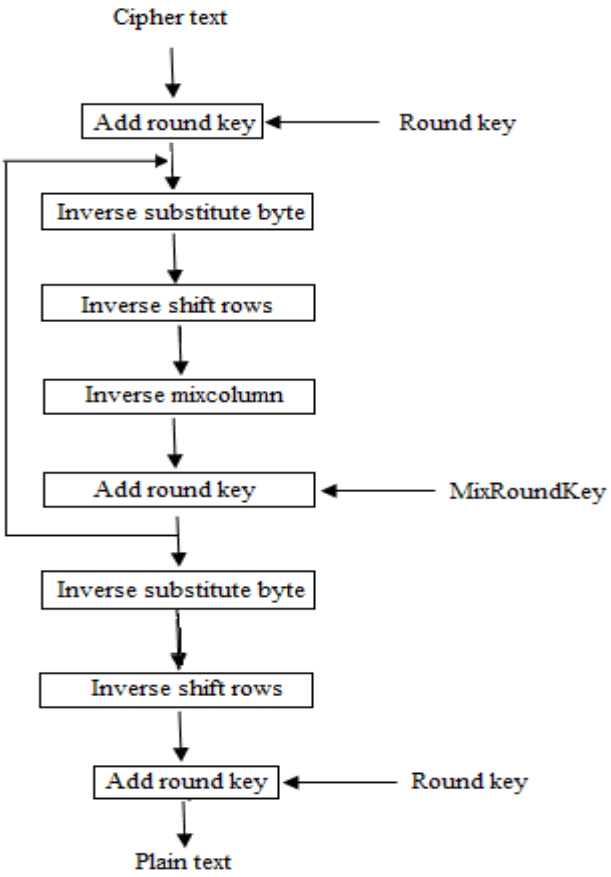

Figure (2). AES Decryption

PROPOSED DWT-SVD BASED HIGHLY SECURE IMAGE DATA HIDING SYSTEM WITH AES ENCRYPTION

Any data hiding algorithm basically consists two sections, first one is the secure data hiding and next one is the extraction of secured data from the embedded cover image. This section briefly describes the proposed DWT-SVD based image data hiding system with AES encryption technique.

1. Proposed Secure Image Data Embedding

The main steps of proposed secure image data embedding process are as follows:

i. Apply three level Haar DWT to decompose the cover or host image A in to four sub bands (i.e.,$LL3$, $LH3$, $HL3$,$andHH3$).

ii. Apply SVD to $HL3$ sub band of cover image i.e.,

$$A_C = U_C * S_C * V_C^T \quad \ldots(1)$$

Where $A_C = HL3$ sub band of cover image DWT decomposition.

iii. Apply three level Haar DWT to decompose the secure image SI, (which is to be embed on the cover image) into four sub bands (i.e.,$LL3$, $LH3$, $HL3$,$andHH3$).

iv. Apply SVD to$HL3$ sub band of the secure image i.e.,

$$A_{SI} = U_{SI} * S_{SI} * V_{SI}^T \quad \ldots(2)$$

Where $A_{SI} = HL3$ sub band of secure image DWT decomposition.

v. Modify the singular value of A_C by embedding singular value of A_{SI} such that

$$S_{CSI} = S_C + \alpha S_{SI} \quad \ldots(3)$$

Where S_{ISI} is modified singular matrix of A_C, and αdenotes the scaling factor which is used to control the strength of watermark signal

vi. Next apply SVD to this modified singular matrix S_{ISI} i.e.,

$$S_{CSI} = U_{S_{CSI}} * S_{S_{CSI}} * V_{S_{CSI}}^{T} \quad \ldots(4)$$

vii. Now obtain the modified DWT coefficients for cover image , i.e.,

$$A_{CSI} = U_C * S_{S_{CSI}} * V_C^{T} \quad \ldots(5)$$

viii. Obtain the Embedded image A_E by applying inverse DWT using one modified A_{CSI} component and other non-modified DWT coefficients of cover image.

ix. Now finally apply AES encryption to enhance security of this embedded image A_E.

2. **Proposed Secure Image Data Extraction Process**

i. First apply AES decryption to obtain the embedded image A_E.

ii. Apply three level haar DWT to decompose the embedded image A_E in to four sub bands (i.e., $LL3, HL3, and HH3$).

iii. Apply SVD to $HL3$ sub band i.e.,

$$A_{CSI} = U_{CSI} * S_{CSI} * V_{CSI}^{T} \quad \ldots(6)$$

iv. Where $A_{CSI} = HL3$ of the decrypted and three level DWT decomposed embedded image A_E.

v. Compute $S_{SI}* = (S_{CSI} - S_C)/\alpha$, where $S_{SI}*$, is singular matrix of extracted Secured image.

vi. Apply SVD to $S_{SI}*$ i.e.,

$$S_{SI}* = U_{S_{SI}*} * S_{S_{SI}*} * V_{S_{SI}*}^{T} \quad \ldots(7)$$

vii. Now Compute extracted secured image $SI*$ as,

$$SI* = U_{SI} * S_{S_{SI}*} * V_{SI}^{T} \quad \ldots(8)$$

Finally the complete block diagram representation of the proposed image data hiding and extraction systems are shown in figure (3) and figure (4).

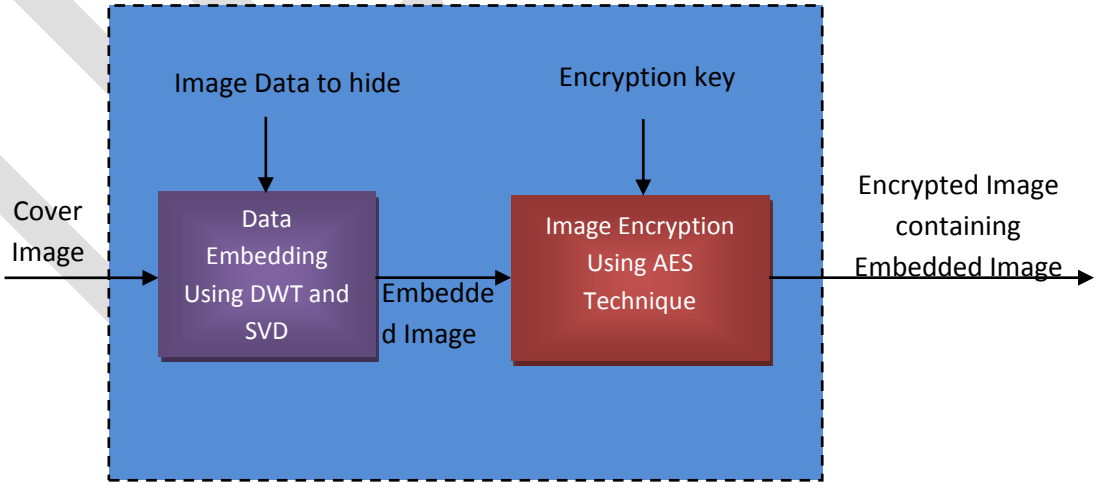

FIGURE (3) PROPOSED SECURE IMAGE DATA HIDING SYSTEM

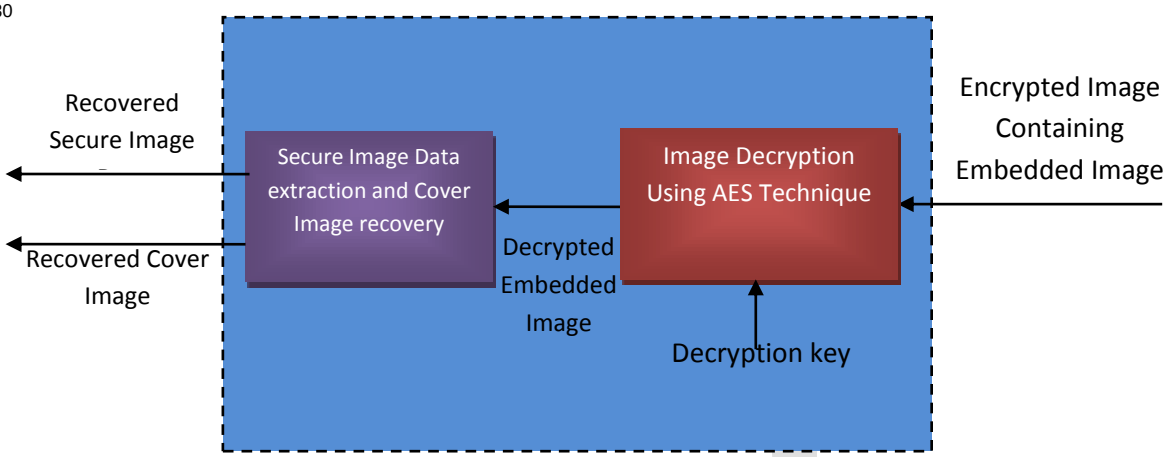

FIGURE (4) PROPOSED SECURE IMAGE DATA EXTRACTION SYSTEM

PERFORMANCE EVALUATION OF PROPOSED SYSTEM

To demonstrate the efficiency of proposed approach, five different standard gray level image all of size 512 × 512 (Shown in Fig.5) have been used as the cover image and the gray level image "RCET.jpg" of size 64 × 64 (Shown in Fig.6)has been used as the secure image. To present complete data security efficiency of the proposed technique various parameters like, peak signal to noise ratio (PSNR), mean square error (MSE), embedding rate (ER) and bit error rate (BER) have been employed.

As discussed in previous section, the image data embedding capability of the proposed system highly depends on the scaling factor α, hence in this paper, we will present the image data hiding efficiency of the proposed system with variable scaling factor α. Consequently table-1 shows the visual quality assessment of the proposed system with different values of the α, while for this visual quality assessment "Lena.png" image has been considered as cover image. Table -2 shows the statistical performance parameters obtained after the performance evaluation of proposed system with "Lena.png" as a cover image. On the same manner table-3 to table-5 gives the statistical performance parameters obtained after the performance evaluation of proposed system with "Barbara.png", "Baboon.jpg" and "Peppers.jpg" as a cover image respectively.

(a) Lena.png (b) Barbara.png (c) Baboon.jpg (d) Peppers.jpg

Figure (5). Four standard test cover images used for performance evaluation

Figure (6). "Rungta.jpg" Used as Secure image

Table 1. Performance evaluation of proposed image data hiding system with first test cover image "Lena.png".

Scaling Factor (α)	Cover Image	Embedded Image	Secure Image (Rungta.jpg)	Extracted Secure Image
.2				
.4				
.6				
.8				
1				

Table 2. Statistical Performance parameters obtained after performance evaluation of proposed image data hiding system with first test cover image "Lena.png".

Scaling Factor	**Cover Image**	**Secure Image (Rungta.jpg)**	**PSNR (in db)**	**MSE**	**Embedding Rate (ER)**	**Bit-error Rate (BER)**
0.2	Lena.png	Rungta.jpg	69.140	0.008	0.908	0.012
0.4			62.814	0.034	0.908	0.037
0.6			53.834	0.269	0.908	0.092
0.8			49.608	0.712	0.908	0.170
1			46.516	1.450	0.908	0.242

Table 3, Statistical parameters obtained after performance evaluation of proposed image data hiding system with second test cover image "Barbara.png".

Scaling Factor	Cover Image	Secure Image (Rungta.jpg)	PSNR (in db)	MSE	Embedding Rate (ER)	Bit-error Rate (BER)
0.2	Barbara.png	Rungta.jpg	69.161	0.008	0.908	0.011
0.4			81.244	0.000	0.908	0.001
0.6			61.785	0.043	0.908	0.025
0.8			54.873	0.212	0.908	0.058
1			50.396	0.594	0.908	0.120

Table 4, Statistical parameters obtained after performance evaluation of proposed image data hiding system with third test cover image "Baboon.jpg".

Scaling Factor	Cover Image	Secure Image (Rungta.jpg)	PSNR (in db)	MSE	Embedding Rate (ER)	Bit-error Rate (BER)
0.2	Baboon.jpg	Rungta.jpg	71.127	0.005	0.908	0.007
0.4			82.493	0.000	0.908	0.000
0.6			72.798	0.003	0.908	0.006
0.8			61.957	0.041	0.908	0.044
1			56.493	0.146	0.908	0.081

Table 5, Statistical parameters obtained after performance evaluation of proposed image data hiding system with third test cover image "Baboon.jpg".

Scaling Factor	Cover Image	Secure Image (Rungta.jpg)	PSNR (in db)	MSE	Embedding Rate (ER)	Bit-error Rate (BER)
0.2	Peppers.jpg	Rungta.jpg	64.078	0.025	0.908	0.036
0.4			53.580	0.285	0.908	0.178
0.6			49.034	0.812	0.908	0.261
0.8			45.694	1.753	0.908	0.305
1			43.376	2.989	0.908	0.346

From the visual inspection of the results obtained as shown in table-1, of proposed image data hiding and extraction system, it is clearly observable that, the proposed system provides a very good secure image quality after extraction from proposed system. This high quality secure image extraction capability is also subjectively reflected by table 2. Furthermore the same system has also been tested with three different test cover images. With the deep assessment of results obtained for other test images, the proposed system is found efficient for image data hiding and quality extraction with all the test cover images.
In addition to this as discussed, the efficiency of the proposed system depends on the scaling factor, so a good analytical exploration of its dependency has been also presented for all the test cover images.

CONCLUSION

This paper proposed a novel technique for highly secure image data transmission using discrete wavelet transform (DWT) and Singular value decomposition (SVD) based image data hiding along with advance encryption standard (AES) to enhance the security level. Particularly AES technique ensures higher efficiency of transmission security. This hybrid technique leads to optimize both the fundamentally conflicting requirements. To present complete data security efficiency of the proposed technique various parameters like, peak signal to noise ratio (PSNR), mean square error (MSE), embedding rate (ER) and bit error rate (BER) have been employed. A complete visual and subjective analysis have been included in this paper to present high image data embedding and extraction efficiency of proposed system. After successful implementation of proposed system in MATLAB 2012(b) software platform, the proposed system is tested for four test cover images with the variable scaling factor scenario. For all the variations in scaling factor the

proposed system provides very high efficiency. In terms of resultant parameters obtained after testing, the proposed system leads maximum PSNR and minimum MSE as compare to state of art techniques and hence prove higher efficiency of proposed system.

REFERENCES:

[1] P. Ramana Reddy, Dr. Munaga.V .N. K.prasad, Dr. D. Sreenivasa Rao, ―Robust Digital Watermarking of Images using Wavelets.‖ International Journal of Computer and Electrical Engineering, Vol. 1, No. 2, June 2009.

[2] J. Sang and M. S. Alam, ―Fragility and robustness of binary-phase-only filter-based fragile/semifragile digital image watermarking,‖ IEEE Trans. Instrum. Meas., vol. 57, no. 3, pp. 595–606, Mar. 2008.

[3] R. Liu and T. Tan, ―An SVD-based watermarking scheme for protecting rightful ownership,‖ IEEE Trans. Multimedia, vol. 4, no. 1, pp. 121–128, Mar. 2002.

[4] H.-T. Wu and Y.-M. Cheung, ―Reversible watermarking by modulation and security enhancement,‖ IEEE Trans. Instrum. Meas., vol. 59, no. 1, pp. 221–228, Jan. 2010.

[5] A. Nikolaidis and I. Pitas, ―Asymptotically optimal detection for additive watermarking in the DCT and DWT domains,‖ IEEE Trans. Image Process., vol. 12, no. 5, pp. 563–571, May 2003.

[6] V. Aslantas, L. A. Dogȼan, and S. Ozturk, ―DWT-SVD based image watermarking using particle swarm optimizer,‖ in Proc. IEEE Int. Conf. Multimedia Expo, Hannover, Germany, 2008, pp. 241–244.

[7] Chih-Chin Lai, and Cheng-Chih Tsai,‖ Digital Image Watermarking Using Discrete Wavelet Transform and Singular Value Decomposition,‖ IEEE Transactions on Instrumentation and Measurement., vol. 59, no. 11, pp. 3060-3063, Nov. 2010.

[8] Thakur, V. S., Thakur K. (2014). "Design and Implementation of a Highly Efficient Gray Image Compression Codec Using Fuzzy Based Soft Hybrid JPEG Standard". International Conference on Electronic Systems, Signal Processing and Computing Technologies (ICESC), pp.484,489, 9-11 Jan 2014.

[9] Thakur, V. S., Dewangan, N. K. and Thakur, K. (2014). "A Highly Efficient Gray Image Compression Codec Using Neuro Fuzzy Based Soft Hybrid JPEG Standard". Proceedings of Second International Conference, Emerging Research in Computing, Information, Communication and Applications (ERCICA), vol. 1, pp. 625-631, 9-11 Jan 2014.

[10] Thakur, V. S., Gupta, S. and Thakur, K. (2015). "Optimum Global Thresholding Based Variable Block Size DCT Coding For Efficient Image Compression". Biomedical & Pharmacology Journal, vol. 8(1), pp. 453-468, 2015.

[11] JebaNegaCheltha, C.; Velayutham, R , "A novel error-tolerant method in AES for satellite images" ,Emerging Trends in Electrical and Computer Technology (ICETECT), 2011.

[12] G. Bhatnagar and B. Raman, ―A new robust reference watermarking scheme based on DWT-SVD,‖Comput. Standards Interfaces, vol. 31, no. 5, pp. 1002–1013, Sep. 2009.

[13] E. Ganic and A. M. Eskicioglu, ―Robust DWT-SVD domain image watermarking: Embedding data in all frequencies,‖ in Proc. Workshop Multimedia Security, Magdeburg, Germany, 2004, pp. 166–174.

[14] Q. Li, C. Yuan, and Y.-Z. Zhong, ―Adaptive DWT-SVD domain image watermarking using human visual model,‖ in Proc. 9thInt. Conf. Adv. Commun. Technol., Gangwon-Do, South Korea, 2007, pp. 1947–1951.

[15] S. Mallat, ―The theory for multiresolution signal decomposition: The wavelet representation,‖ IEEE Trans. Pattern Anal. Mach. Intell., vol. 11, no. 7, pp. 654–693, Jul. 1989.

International Journal of Engineering Research and General Science Volume 3, Issue 5, September-October, 2015
ISSN 2091-2730

A Novel High Efficiency High Step-up Interleaved Converter with Voltage Multiplier Circuit for a PV System

D.Byragi Naidu[1], D.Vijaya kumar[2], Bibhuti bhusan rath[3]

[1]*P.G student, Dept. of EEE, AITAM Engineering College, AP, India, duppatlaeee@gmail.com*

Abstract- A high step-up converter is proposed for a photovoltaic system. A voltage multiplier used here provides high voltage gain without extreme duty cycle. The voltage multiplier is composed of a conventional boost converter and coupled inductors. An extra conventional boost converter is integrated into the first phase to achieve a considerably higher voltage conversion ratio. The two-phase configuration not only reduces the current stress through each power switch, but also constrains the input current ripple, which decreases the conduction losses of metal–oxide–semiconductor field-effect transistors (MOSFETs). It also functions as a clamp circuit which alleviates the voltage spikes across the power switches. So, the low-voltage-rated MOSFETs can be adopted for reductions of conduction losses and cost. Efficiency improves because the energy stored in leakage inductances is recycled to the output terminal.

Keywords- Boost–Fly back converter, High step-up, photovoltaic system, Voltage multiplier module.

I. INTRODUCTION

Renewable sources of energy are increasingly valued worldwide because of energy shortage and environmental contamination. Renewable energy systems generate low voltage output and thus, high step-up dc/dc converters are widely employed in many renewable energy applications, including fuel cells, wind power, and photovoltaic systems are expected to pay an important role in future energy production. Such system transform light energy into electrical energy, and convert low voltage into high voltage via a step-up converter, which can convert energy into electricity using a grid-by-grid inverter or store energy into a battery set. Figure 1 shows a typical photovoltaic system that consists of a solar module, a high step up converter, a charge-discharge controller, a battery set, and an inverter.

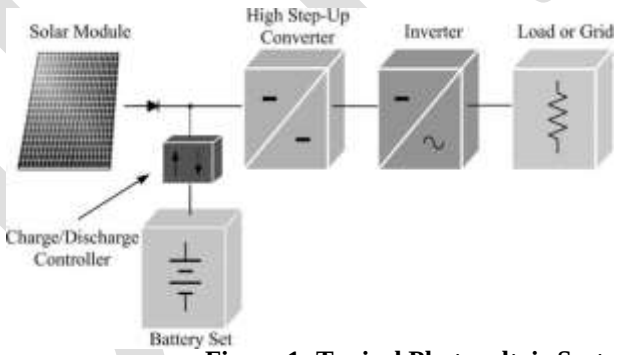

Figure 1: Typical Photovoltaic System

Conventional step-up converters, such as the boost converter and flyback converter, cannot achieve a high step-up conversion with high efficiency because of the resistances of elements or leakage inductance. Thus, a modified boost-flyback converter was proposed. Modifying a boost-fly back converter, shown in Figure 2(a) is one of the simple approaches step-up gain and the gain is realized via a coupled inductor. The performance of the converter is similar to an active-clamped flyback converter; thus, the leakage energy is recovered to the output terminal. An interleaved boost converter with a voltage-lift capacitor shown in Figure 2(b) is highly similar to the conventional interleaved type. It obtains extra voltage gain through the voltage-lift capacitor, and reduces the input current ripple, which is suitable for power factor correction (PFC) and high-power applications.

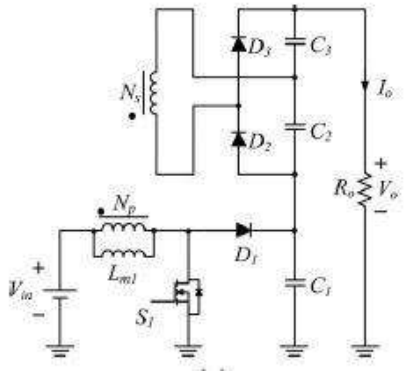

Figure 2(a): Modified Boost Flyback Converter

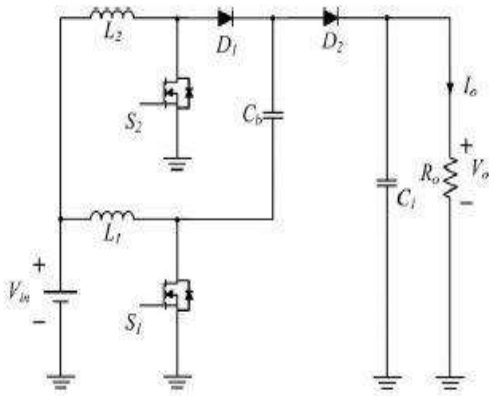

Figure 2(b): Interleaved Boost Converter with a Voltage-lift Capacitor Structure

II. PROPOSED TOPOLOGY

In this paper, an asymmetrical interleaved high step-up converter that combines the advantages of the aforementioned converters is proposed, which combined the advantages of both. In the voltage multiplier module of the proposed converter, the turns ratio of coupled inductors can be designed to extend voltage gain, and a voltage-lift capacitor offers an extra voltage conversion ratio. The advantages of the proposed converter are as follows:

1) The converter is characterized by a low input current ripple and low conduction losses, making it suitable for high power applications;
2) The converter achieves the high step-up voltage gain that renewable energy systems require;
3) Leakage energy is recycled and sent to the output terminal, and alleviates large voltage spikes on the main switch;
4) The main switch voltage stress of the converter is substantially lower than of the output voltage.
5) Low cost and high efficiency are achieved.

A. Circuit Description

The proposed high step-up converter with voltage multiplier module is shown in Figure 3(a). A conventional boost converter and two coupled inductors are located in the voltage multiplier module, which is stacked on a boost converter to form an asymmetrical interleaved structure. Primary windings of the coupled inductors with N_p turns are employed to decrease input current ripple, and secondary windings of the coupled inductors with N_s turns are connected in series to extend voltage gain. The turns ratios of the coupled inductors are the same. The coupling references of the inductors are denoted by "." and "∗".

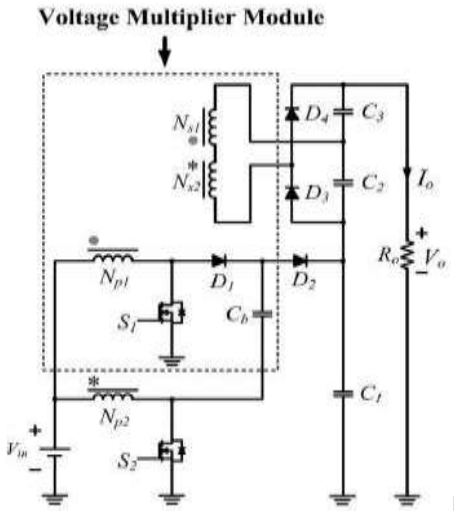

Figure 3(a): Proposed High Step-up Converter with a Voltage Multiplier Module

The equivalent circuit of the proposed converter is shown in Figure 3(b), where L_{m1} and L_{m2} are the magnetizing inductors, $L_{k1}$and L_{k2} represent the leakage inductors, S_1 and S_2 denote the power switches, C_b is the voltage-lift capacitor, and n is defined as a turns ratio N_s/N_p.

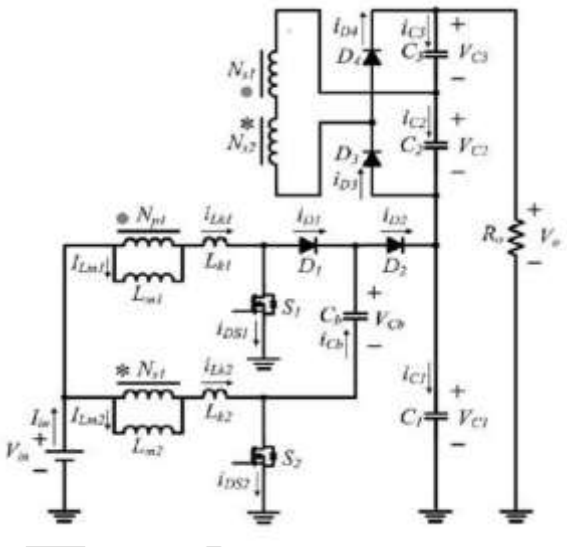

Figure 3(b): Equivalent Circuit

III. MODAL ANALYSIS

The proposed converter operates in continuous conduction mode (CCM), and the duty cycles of the power switches during steady operation are interleaved with a 180^o phase shift and the duty cycles are greater than 0.5. The key steady waveforms in one switching period of the proposed converter contain six modes.

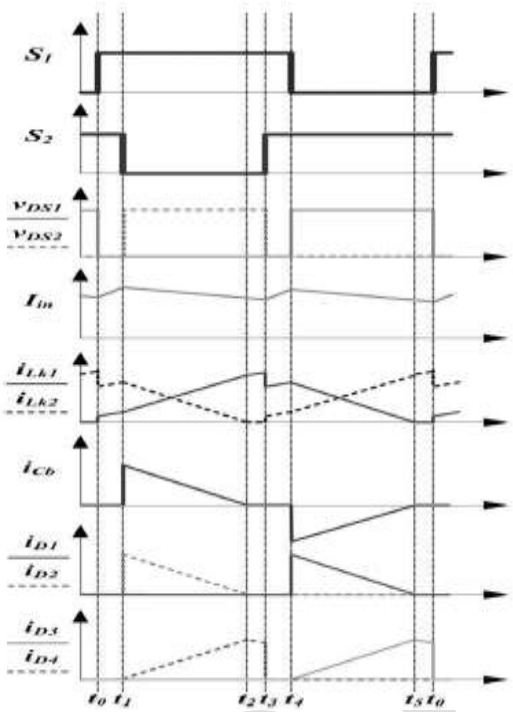

Figure 4: Steady Waveforms of the Proposed Converter

Mode 1[t_0, t_1]: At $t = t_0$, the power switches S_1 and S_2 are both turned ON. All of the diodes are reverse-biased. Magnetizing inductors L_{m1} and L_{m2} as well as leakage inductors $L_{k1}$and L_{k2} are linearly charged by the input voltage source V_{in}.

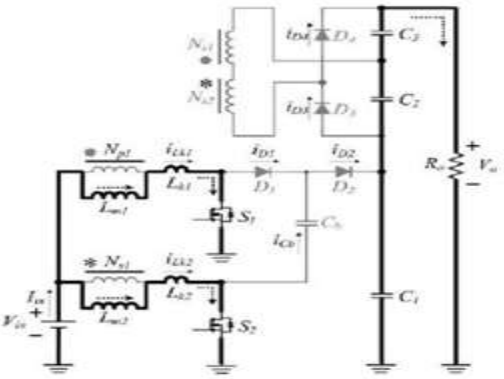

Figure 5(a): Mode 1

Mode 2[t_1, t_2]: At $t = t_1$, the power switches S_2 is switched OFF, thereby turned ON diodes D_2 and D_4. The energy that magnetizing inductor L_{m2} has stored is transferred to the secondary side charging the output filter capacitor C_3. The input voltage source, magnetizing inductor L_{m2}, leakage inductor L_{k2}, and voltage-lift capacitor C_b release energy to the output filter capacitor C_1 via diode D_2, thereby extending the voltage on C_1.

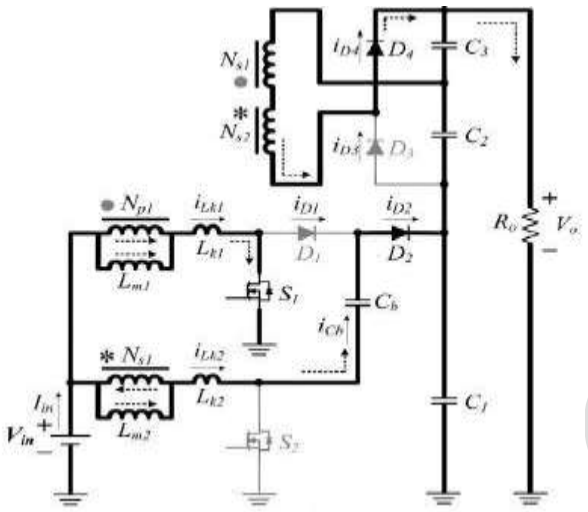

Figure 5(b): Mode 2

Mode 3[t_2, t_3]: At $t = t_2$, diode D_2 automatically switches OFF because the total energy of leakage inductor L_{k2} has been completely released to the output filter capacitor C_1. Magnetizing inductor L_{m2} transfers energy to the secondary side charging the output filter capacitor C_3 via diode D_4 until t_3.

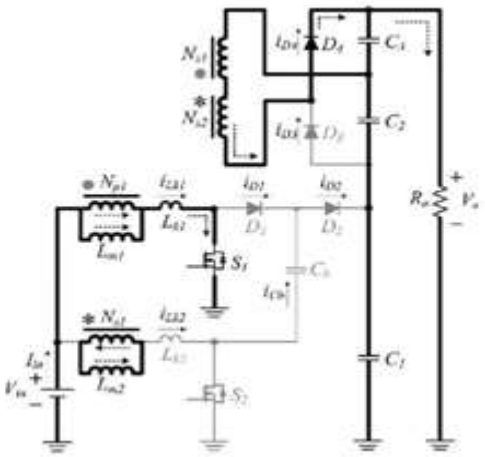

Figure 5(c): Mode 3

Mode 4[t_3, t_4]: At $t = t_3$, the power switch S_2 is switched ON and all the diodes are turned OFF. The operating states of modes 1 and 4 are similar.

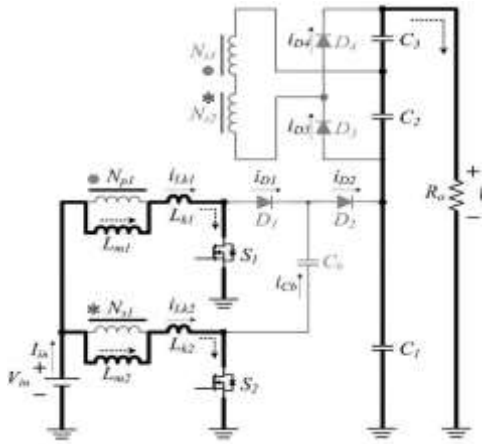

Figure 5(d): Mode 4

Mode 5[t_4, t_5]: At $t = t_4$, the power switch S_1 is switched OFF which turns ON diodes D_1 and D_3. The energy stored in magnetizing inductor $L_{m1}$is transferred to secondary side charging the output filter capacitor C_2. The input voltage source and magnetizing inductor L_{m1} release energy to voltage-lift capacitor C_b via diode D_1, which stores extra energy in C_b.

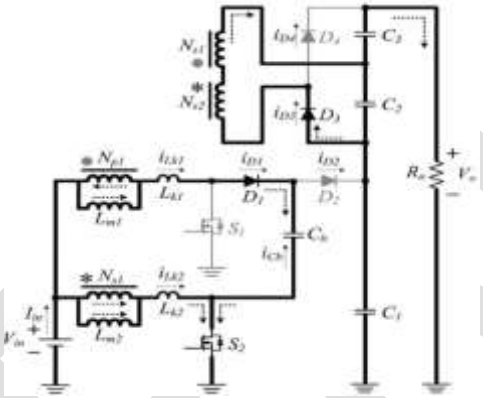

Figure 5(e): Mode 5

Mode 6[t_5, t_0]: At $t = t_5$, diode D_1 is automatically turned OFF because the total energy of leakage inductor L_{k1} has been completely released to voltage-lift capacitor C_b. Magnetizing inductor L_{m1} transfers energy to the secondary side charging the output filter capacitor C_2 via diode D_3 until t_0.

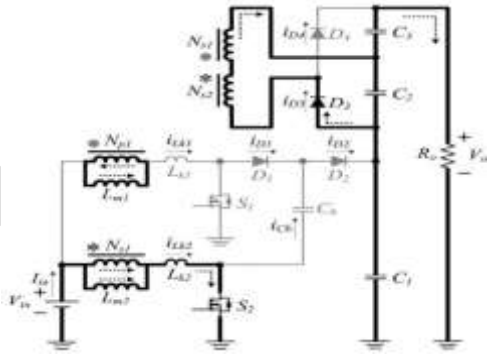

Figure 5(f): Mode 6

IV. STEADY STATE ANALYSIS

The transient characteristics of circuitry are disregarded to simplify the circuit performance analysis of the proposed converter in CCM, and some formulated assumptions are as follows:

1) All of the components in the proposed converter are ideal;
2) Leakage inductors $L_{k1}$and L_{k2} are neglected.
3) Voltage V_{cb}, V_{c1}, V_{c2}, and V_{c3} are considered to be constant because of infinitely large capacitance.

A. Voltage Gain

The first-phase converter can be regarded as a conventional boost converter, thus voltage V_{cb} can be derived from:

$V_{cb} = V_{in}\frac{1}{1-D}$ ------ (1)

When switch S_1 is turned ON and switch S_2 is turned OFF, voltage V_{C1} can be derived from:

$\mathrm{V_{C1}} = \frac{1}{1-\mathrm{D}}\mathrm{V_{in}} + \mathrm{V_{cb}} = \frac{2}{1-\mathrm{D}}\mathrm{V_{in}}$ -------- (2)

The output filter capacitors C_2 and C_3 are charged by energy transformation from the primary side. When S_2 is in turn-on state and S_1 is in turn-off state, V_{C2} is equal to induced voltage of N_{s1} plus induced voltage of N_{s2}, and when S_1 is in turn-on state and S_2 is in turn-off state, V_{C3} is also equal to induced voltage of N_{s1} plus induced voltage of N_{s2}. Thus, voltages V_{c2} and V_{c3} can be derived from

$\mathrm{V_{c2}} = \mathrm{V_{c3}} = \mathrm{nV_{in}}\left(1 + \frac{\mathrm{D}}{1-\mathrm{D}}\right) = \frac{\mathrm{n}}{1-\mathrm{D}}\mathrm{V_{in}}$ --------- (3)

The output voltage can be derived from:

$\mathrm{V_o} = \mathrm{V_{c1}} + \mathrm{V_{c2}} + \mathrm{V_{c3}} = \frac{2\mathrm{n}+2}{1-\mathrm{D}}\mathrm{V_{in}}$ ------- (4)

The voltage gain of the proposed converter is

$\frac{\mathrm{V_o}}{\mathrm{V_{in}}} = \frac{2\mathrm{n}+2}{1-\mathrm{D}}$ --------- (5)

Above equation confirms that the proposed converter has a high step-up voltage gain without an extreme duty cycle.

B. Voltage Stresses on Semi Conductor Components

The voltage ripples on the capacitors are ignored to simplify the voltage stress analyses of the components of the proposed converter.

The voltage stresses on power switches S_1 and S_2 are derived from:

$\mathrm{V_{s1}} = \mathrm{V_{s2}} = \frac{1}{1-\mathrm{D}}\mathrm{V_{in}}$ --------- (6)

The voltage stresses on power switches S_1 and S_2 related to the output voltage V_o and the turns ratio n can be expressed as:

$\mathrm{V_{s1}} = \mathrm{V_{s2}} = \mathrm{V_o} - \frac{2\mathrm{n}+1}{1-\mathrm{D}}\mathrm{V_{in}}$ ---------- (7)

The voltage stresses on the power switches account for half of output voltage V_o, even if turns ratio n is 0. The voltage stress on D_1 is equal to V_{C1}, and the voltage stress on diode D_2 is voltage $V_{C1} - V_{cb}$. These voltage stresses can be derived from:

$\mathrm{V_{D1}} = \mathrm{V_{C1}} = \frac{2}{1-\mathrm{D}}\mathrm{V_{in}}$ ---------- (8)

$\mathrm{V_{D2}} = \mathrm{V_{C1}} - \mathrm{V_{cb}} = \frac{1}{1-\mathrm{D}}\mathrm{V_{in}}$ ---------- (9)

The voltage stressed on the diodes D_1 and D_2 and D_3 and D_4 related to the output voltage V_o and the turns ratio n can be expressed as:

$\mathrm{V_{D1}} = \mathrm{V_o} - \frac{2\mathrm{n}}{1-\mathrm{D}}\mathrm{V_{in}}$ --------- (10)

$\mathrm{V_{D2}} = \mathrm{V_o V_{in}} = \frac{2}{1-\mathrm{D}}$ -------- (11)

$\mathrm{V_{D3}} = \mathrm{V_{D4}} = \mathrm{V_o} - \frac{2}{1-\mathrm{D}}\mathrm{V_{in}}$ ---------- (12)

V. MATLAB SIMULATION DIAGRAM

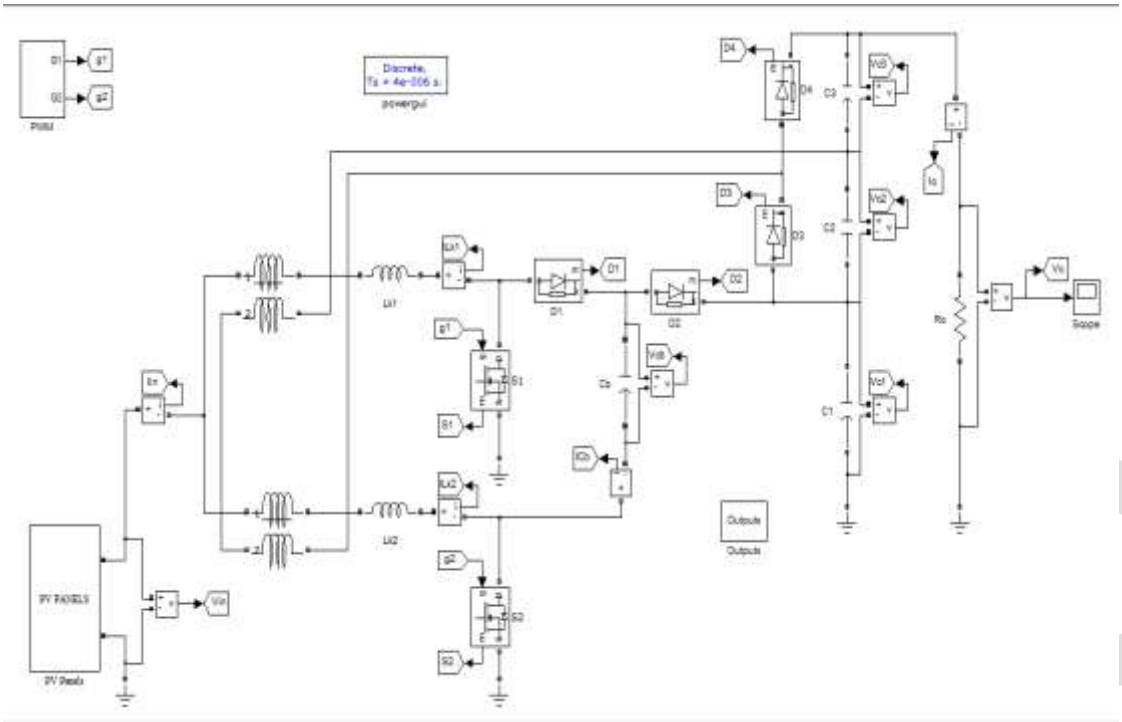

Figure 6: Simulation Diagram

VI. MEASURED WAVEFORMS

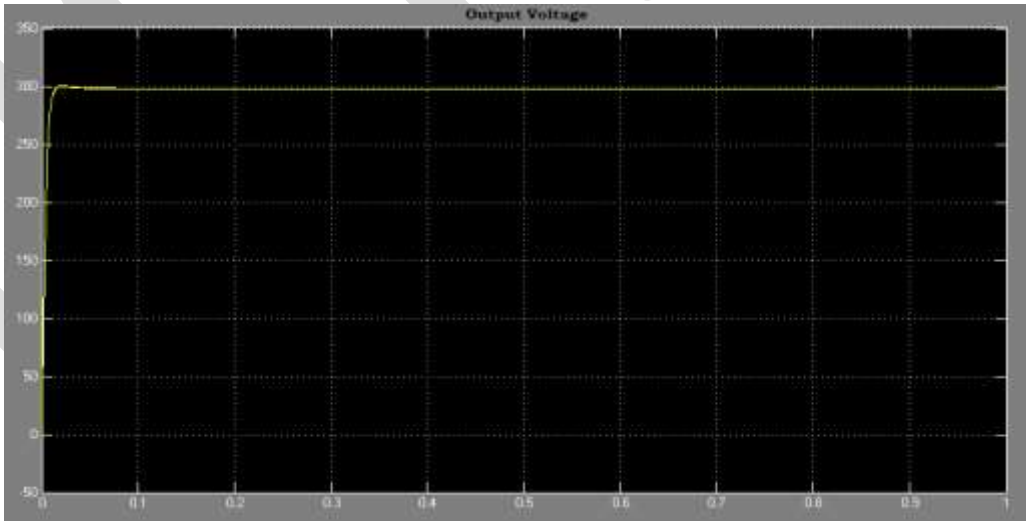

Figure 7(a): output voltage

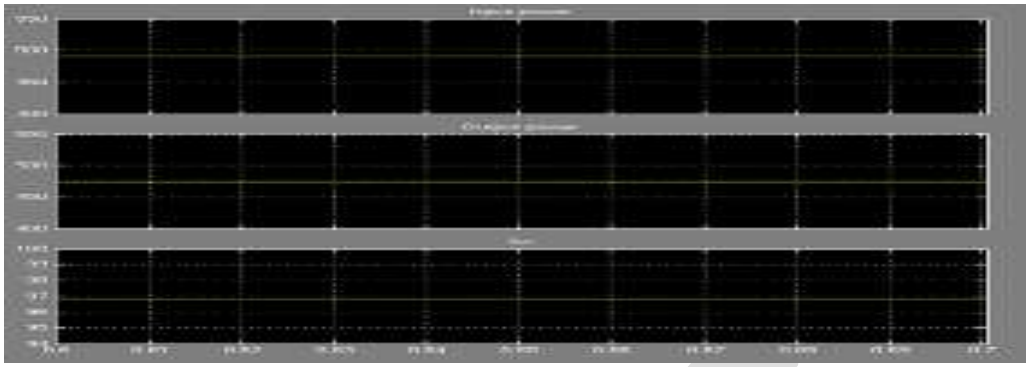

Figure 7(b): input and output power and efficiency

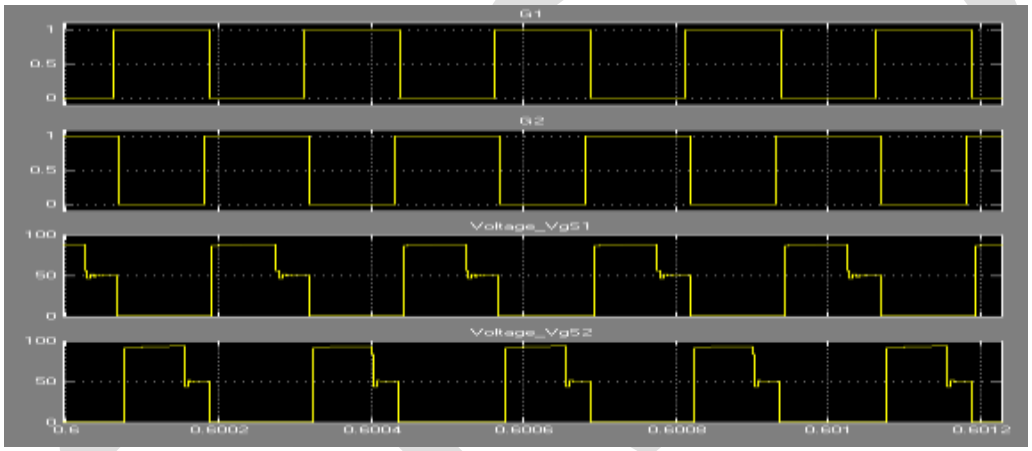

Figure 7(c): Measured $V_{g1} and V_{g2}$ waveforms

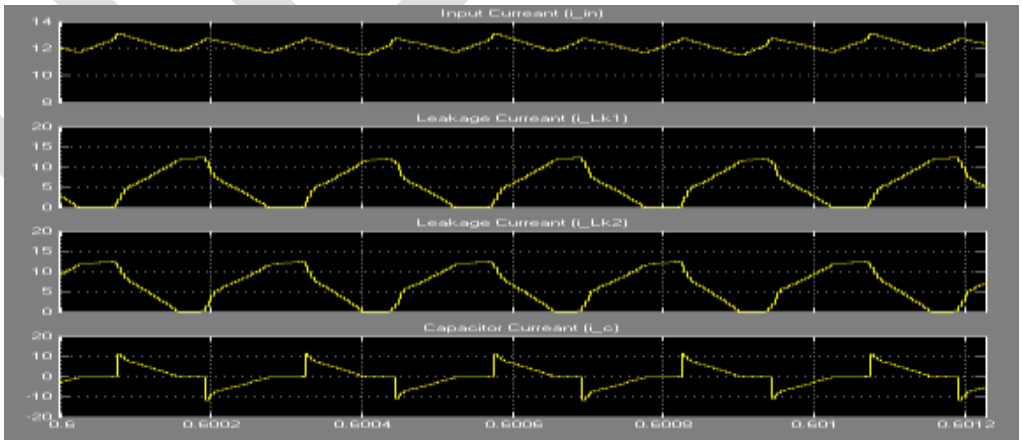

Figure 7(d): measured current wave forms

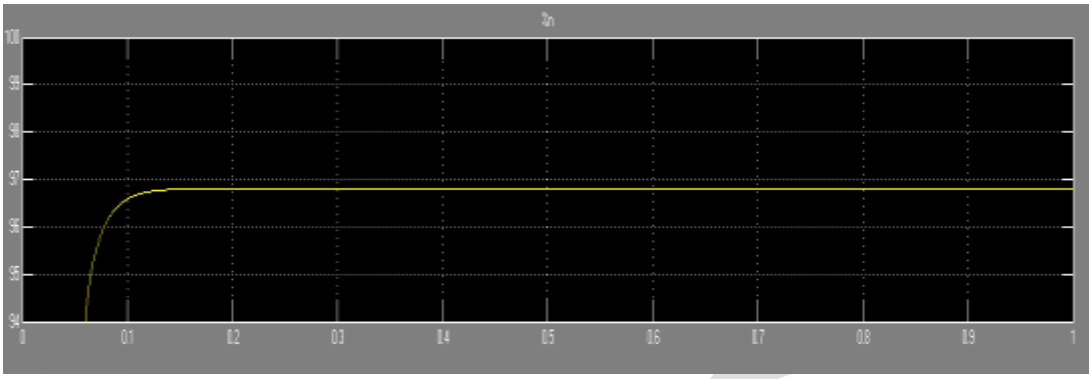

Figure 7(e): Measured output efficiency

VII. PROPOSED CONCEPT

The proposed high step-up interleaved converter with a voltage multiplier module is shown in Figure 2. The voltage multiplier module is composed of two coupled inductors and two switched capacitors and is inserted between a conventional interleaved boost converter to form a modified boost-flyback-forward interleaved structure. When the switches turn off by turn, the phase whose switch is in OFF state performs as a flyback converter, and the other phase whose switch is in ON state performs as a forward converter.

Primary windings of the coupled inductors with N_p turns are employed to decrease input current ripple, and secondary windings of the coupled inductors with N_s turns are connected in series to extend voltage gain. The turn ratios of the coupled inductors are the same. The coupling references of the inductors are denoted by "." and "∗".

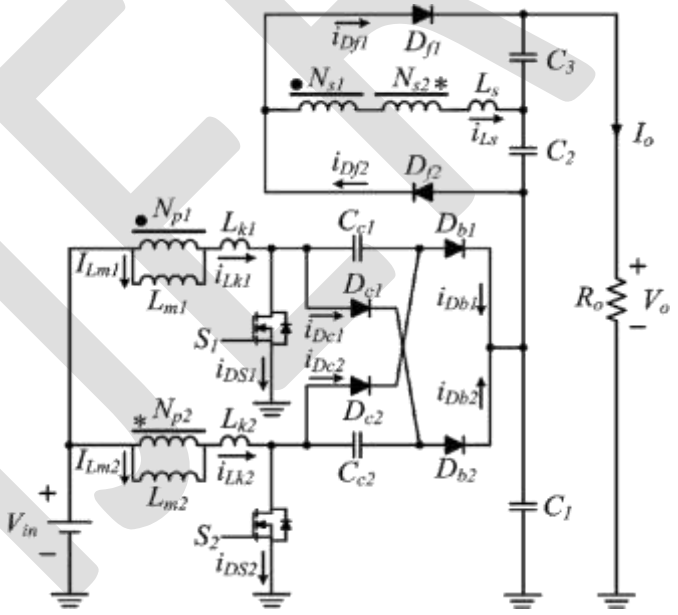

Figure 8: Equivalent Circuit of the Proposed Converter

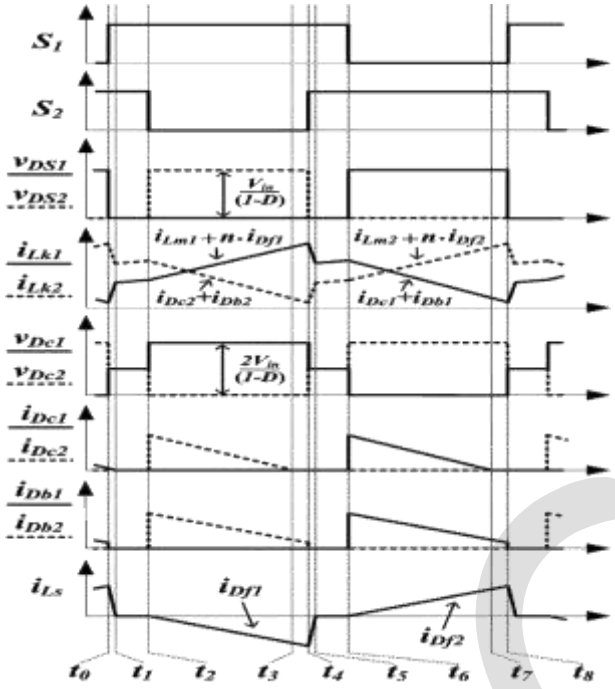

Figure 9: Steady Waveform of the Proposed Converter in CCM

VIII. PROPOSED STEADY-STATE ANALYSIS

The transient characteristics of circuitry are disregarded to simplify the circuit performance analysis of the proposed converter in CCM, and some formulated assumptions are as follows:

1) All of the components in the proposed converter are ideal.
2) Leakage inductors L_{k1},L_{k2}, and L_s are neglected.
3) Voltages on all capacitors are considered to be constant because of infinitely large capacitance.
4) Due to the completely symmetrical interleaved structure, the related components are defined as the corresponding symbols such as D_{c1} and D_{c2} defined as DC.

A. Step-up Gain

The voltage on clamp capacitor C_C can be regarded as an output voltage of the boost converter; thus, voltage V_{Cc} can be derived from the equation.

$$V_{cc} = \frac{1}{1-D} V_{in} \text{---------- (1)}$$

When one of the switches turns off, voltage V_{C1} can obtain a double output voltage of the boost converter derived from the equation.

$$V_{c1} = \frac{1}{1-D} V_{in} + V_{cc} = \frac{2}{1-D} V_{in} \text{ ---------- (2)}$$

The output filter capacitors C_2 and C_3 are charged by energy transformation from the primary side. When S_2 is in ON state and S_1 is in OFF state, V_{C2} is equal to the sum of the induced voltage of N_{S1} and the induced voltage of N_{S2}, and when S_1 is in ON state and S_2 is in OFF state, $V_{C3}$is also equal to the sum of the induced voltage of $N_{S1}$and the induced voltage of N_{S2}. Thus, voltages V_{C2} and V_{C3} can be derived from:

$$V_{c2} = V_{c3} = nV_{in}\left(1 + \frac{D}{1-D}\right) = \frac{n}{1-D} V_{in} \text{ ---------- (3)}$$

The output voltage can be derived from:

$$V_o = V_{c1} + V_{c2} + V_{c3} = \frac{2n+2}{1-D} V_{in} \text{ ---------- (4)}$$

In addition, the voltage gain of the proposed converter is

$$\frac{V_o}{V_{in}} = \frac{2n+2}{1-D} \text{ ---------- (5)}$$

B. *Voltage Stresses on Semi Conductor Components*

Voltage ripple on capacitor was ignored to simplify the voltage stress analysis of the components of the proposed converter. The voltage stress on power switch S was clamped and derived from

$$V_{s1} = V_{s2} = \frac{2}{1-D} V_{in} = \frac{1}{2n+2} V_o \text{ ---------- (6)}$$

The voltage stress can be derived from

$$V_{dc1} = V_{dc2} = \frac{2}{1-D} V_{in} = \frac{1}{n+1} V_o \text{ ---------- (7)}$$

IX. DESIGN AND EXPERIMENT OF PROPOSED CONVERTER

A 0.5 kW prototype of the proposed high step-up converter is tested. The electrical specifications are $V_{in} = 40\ V$, $V_o = 300\ V$ and $f_s = 40\ kHz$.The major components have been chosen as follows: Magnetizing inductors L_{m1} and $L_{m2} = 133\mu H$; turn ratio $n = 1$; power switches S_1 and S_2 are IRFP4227; diodes D_{c1} and D_{c2} are BYQ28E-200; diodes $D_{b1,}D_{b2,}$ D_{f1} and D_{f2} are FCF06A-40;capacitors C_{c1}, C_{c2}, C_2 and $C_3 = 220\mu F$; and $C_1 = 470Mf$.

Design Parameters

PARAMETER	**VALUE**
Input Voltage	40 V DC
Output Voltage	380 V DC
Switching Frequency	40 KHz
Magnetizing Inductors (L_{m1} & L_{m2})	133 μH
Capacitors (C_{c1}, C_{c2}, C_2 & C_3)	220 μF
Capacitor (C_1)	470 μF
Output Power	500 W

The design consideration of the proposed converter includes component selection and coupled inductor design, which are based on the analysis present in the previous section. In the proposed converter, the values of primary leakage inductor of coupled inductors set as close as possible for current sharing performance and the leakage inductors L_{k1} and L_{k2} are 1.6 μH. Due to the performance of high step-up gain, the turn ratio n can be set as one for the prototype circuit with 40 V input voltage and 380 V output voltage to reduce cost, volume and conduction loss of winding. Thus, copper resistance which affect efficiency much can be decreased.

X. MATLAB SIMULATION DIAGRAM

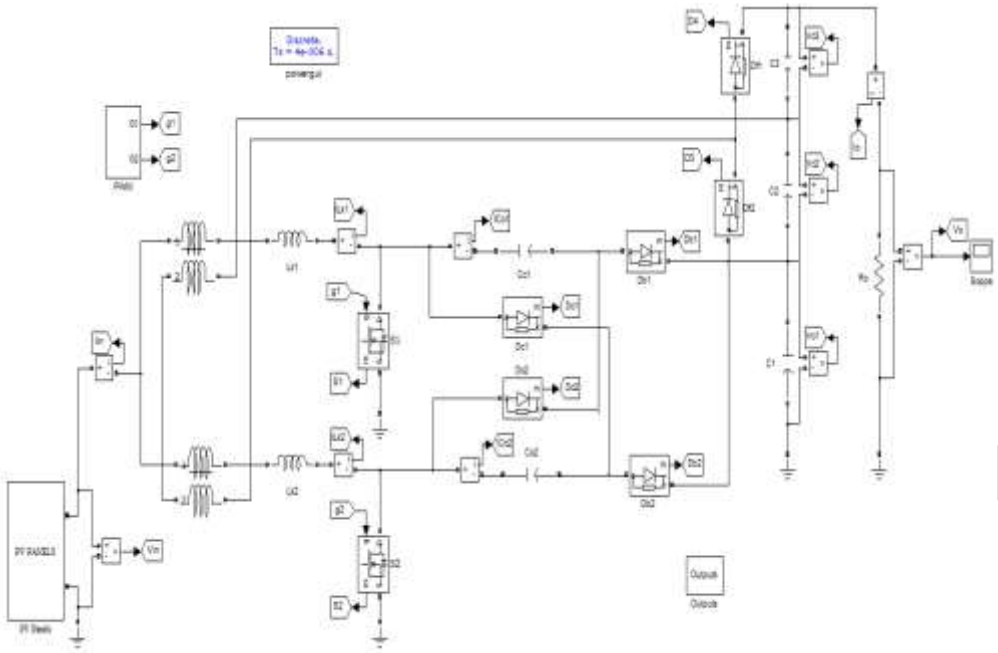

Figure 10: Simulation diagram

XI. MEASURED WAVEFORMS

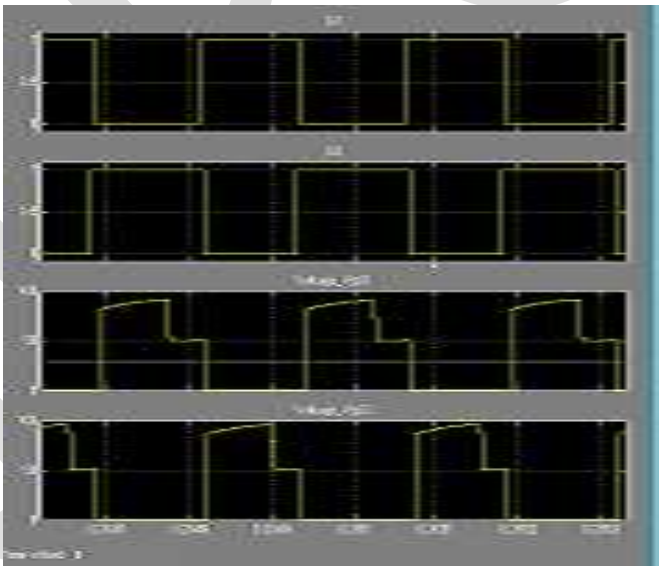

Figure 11(a): gate pulse and $V_{gs1} and V_{gs2}$ measured wave forms

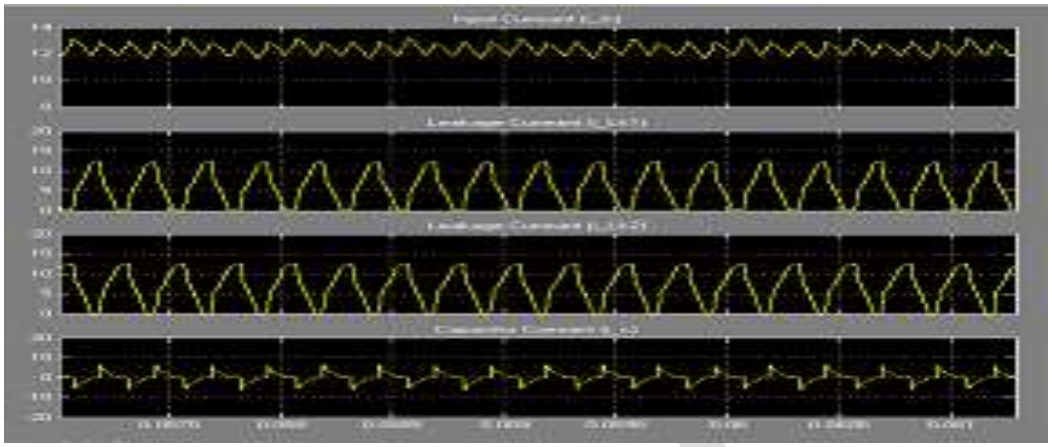

Figure 11(b): Measured current wave forms

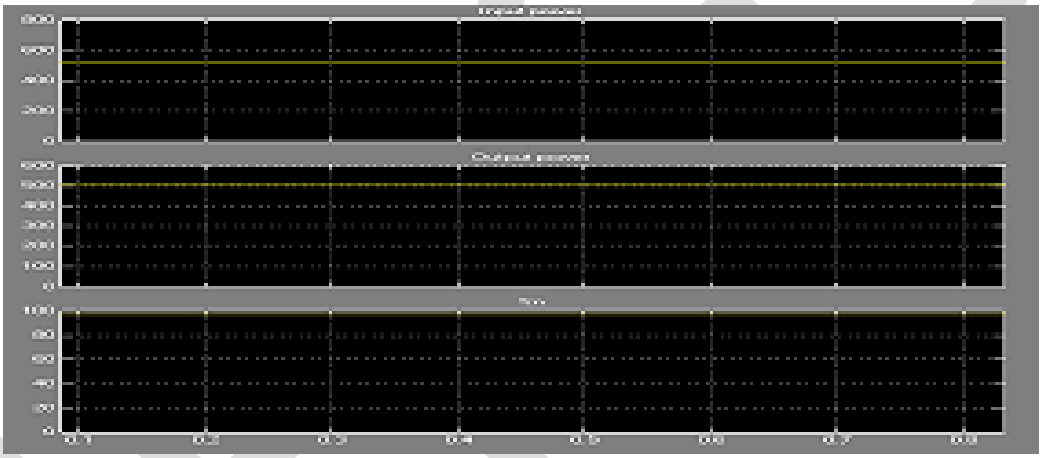

Figure 11(c): input and output power and efficiency waveforms

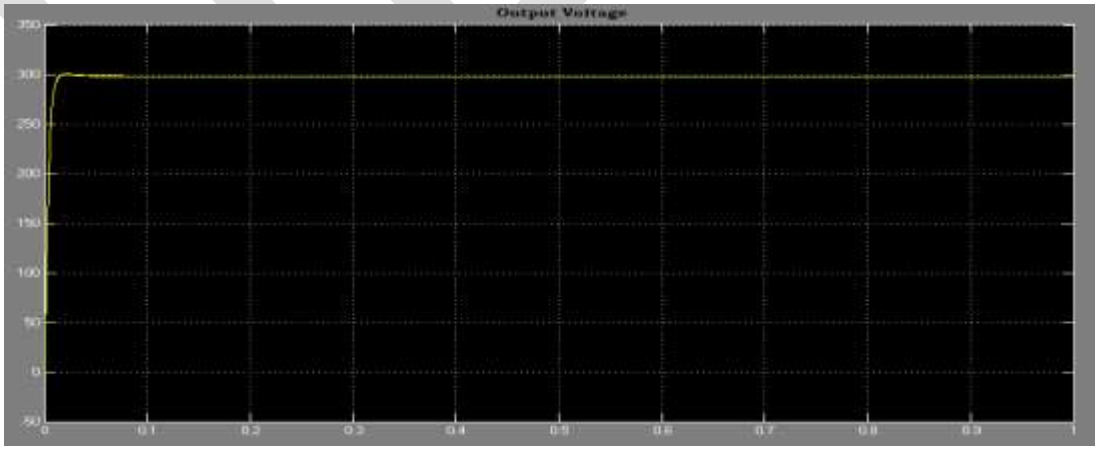

Figure 11(d): Measured output voltage

XII. CONCLUSION

This paper has presented the theoretical analysis of steady state, related consideration, simulation results for the proposed converter. The proposed converter has successfully implemented an efficient high step-up conversion through the voltage multiplier module. The interleaved structure reduces the input current ripple and distributes the current through each component. In addition, the lossless passive clamp function recycles the leakage energy and constrains a large voltage spike across the power switch. Meanwhile, the voltage stress on the power switch is restricted and much lower than the output voltage (300 V). Furthermore, the full-load efficiency is 96.4% at $P_o = 500\ W$, and the highest efficiency is 97.7%.Thus, the proposed converter is suitable for high-power or renewable energy applications that need high step-up conversion.

REFERENCES:

[1] C. Evangelista, P. Puleston, F. Valenciaga, and L.M. Fridman, "Lyapunov designed super-twisting sliding mode control for wind energy conversion optimization," IEEE Trans. Ind. Electron., vol. 60, no. 2, pp. 538–545, Feb. 2013.
[2] T. Kefalas and A. Kladas, "Analysis of transformers working under heavily saturated conditions in grid-connected renewable energy systems,"IEEE Trans. Ind. Electron., vol. 59, no. 5, pp. 2342–2350, May 2012.
[3] Y. Xiong, X. Cheng, Z. J. Shen, C. Mi, H. Wu, and V. K. Garg, "Prognostic and warning system for power-electronic modules in electric, hybridelectric, and fuel-cell vehicles," IEEE Trans. Ind. Electron., vol. 55, no. 6,pp. 2268–2276, Jun. 2008.
[4] A. K. Rathore, A. K. S. Bhat, and R. Oruganti, "Analysis, design and experimental results of wide range ZVS active-clamped L–L type currentfedDC/DC converter for fuel cells to utility interface," IEEE Trans. Ind.Electron., vol. 59, no. 1, pp. 473–485, Jan. 2012.
[5] C. T. Pan and C. M. Lai, "A high-efficiency high step-up converter withlow switch voltage stress for fuel-cell system applications," IEEE Trans.Ind. Electron., vol. 57, no. 6, pp. 1998–2006, Jun. 2010.
[6] R. J.Wai and R. Y. Duan, "High step-up converter with coupled-inductor," IEEE Trans. Power Electron., vol. 20, no. 5, pp. 1025–1035, Sep. 2005.
[7] S. K. Changchien, T. J. Liang, J. F. Chen, and L. S. Yang, "Novel highstep-up DC–DC converter for fuel cell energy conversion system," IEEETrans. Ind. Electron., vol. 57, No. 6, pp. 2007–2017, Jun. 2010.
[8] Y. P. Hsieh, J. F. Chen, T. J. Liang, and L. S. Yang, "Novel high step-up DC–DC converter with coupled-inductor and switched-capacitor techniques for a sustainable energy system," IEEE Trans. Power Electron.,vol. 26, no. 12, pp. 3481–3490, Dec. 2011.
[9] C. Hua, J. Lin, and C. Shen, "Implementation of a DSP-controlled photovoltaic system with peak power tracking," *IEEE Trans. Ind. Electron.*, vol. 45, no. 1, pp. 99–107, Feb. 1998.
[10] J. M. Carrasco, L. G. Franquelo, J. T. Bialasiewicz, E. Galvan, R. C. P. Guisado, M. A. M Prats, J. I. Leon, and N. Moreno-Alfonso, "Power-electronic systems for the grid integration of renewable energy sources: A survey," *IEEE Trans. Ind. Electron.*, vol. 53, no. 4, pp. 10021016, Jun. 2006.
[11] J. T. Bialasiewicz, "Renewable energy systems with photovoltaic powergenerators: Operation and modeling," *IEEE Trans. Ind. Electron.*, vol. 55,no. 7, pp. 2752–2758, Jul. 2008.
[12] F. S. Pai, "An improved utility interface for micro-turbine generation systemwith stand-alone operation capabilities," *IEEE Trans. Ind. Electron.*,vol. 53, no. 5, pp. 1529–1537, Oct. 2006.

International Journal of Engineering Research and General Science Volume 3, Issue 5, September-October, 2015
ISSN 2091-2730

STUDY OF EFFECT OF BRACING ON CRITICAL STOREY OF HIGH RISE FRAME STRUCTURE

Lekhraj Pandit[1],R. R. Shinde[2]
[1]P.G. Student, [2]Assistant Professor, lekhraj.p009@gmail.com ,+917276646045
Civil Engineering Department, Late G.N. Sapkal College of Engineering, Maharashtra, India

Abstract— A Bracing is a system that is provided to minimize the lateral deflection of the structure. The use of braced frames has become more popular in high rise structure and also in seismic design of structure. So this thesis aims to investigate the performance of steel bracing steel structure. In this project a steel building model is taken, this model is compared in different aspects such as axial force and bending moment in column and story displacement. Using different sections as bracing at critical storey Among these numbers of trials which type of bracing at critical section is more suitable from the observed results would be selected for the structure
Keywords— Bracing system, concentric and eccentric bracing, lateral storey displacement, Column forces, column moment.

INTRODUCTION

ABraced Frame is designed primarily to resist wind and earthquake forces in a structural system. These braced frames are made of steel members. Steel braced frame is the structural systems used to resist lateral loads in the multistoried buildings. Lateral loads are often resisted by using braced frame but they can interfere with some architectural components. The steel braces are usually placed in vertically aligned spans lateral loading. The main aim of study has been to identify the type of bracing which causes minimum storey displacement such contributes to greater lateral stiffness to the structure. This system allows a great increase of stiffness with a small amount of added weight, and thus it is very effective for the existing structure in which the poor lateral stiffness is the main problem.

METHODOLOGY

This study involves linear analysis of steel building.by using e-tab software. Structural steel of grade Fe 345 and Fe 250 Mpa

MODEL DESCRIPTION

A 15m x 20m plan area is selected for the study same model for different configurations are prepared for different Pattern and Sections of bracing.
Table 1:

Name of parameter	Value	Unit
Number of stories	11	NOS
Storey height	3.5	M
Total height of the structure(above GL)	38.5	M
Length in long direction	20	M
Length in short direction	15	M
Thickness of Deck	200	MM
Dead Load (1) Wall	12.6	KN/M
(2) Floor finish	2	KN/M²
Live load	5	KN/M²

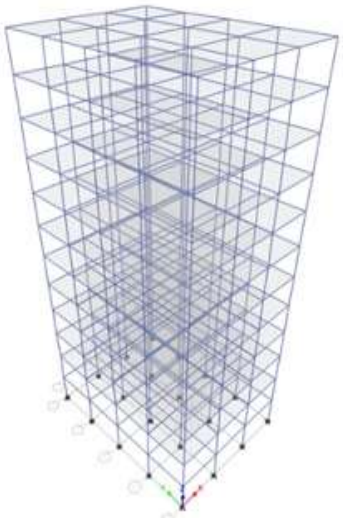

Figure 1:3D view of building

Figure 2:Plan

MODEL DESCRIPTION

Model 1: Normal building.

Model 2: Building with unidirectional bracing (ISA 130X130X15).

Model 3: Building with X bracing (ISA 150X150X15).

Model 4: Building with unidirectional bracing 2 ISA placed back to back (2ISA 65X65X65)

Model 5: Building with unidirectional Bracing ISMB 225.

Model 6: Building with V bracing (ISA 110X110X12).

Model 7: Building with bracing at corner (ISA 90X90X10).

Model 8: Building with unidirectional eccentricity (2ISA 65X65X6 back to back).

Model 9: Building with 1000 mm eccentricity at top (2ISA 65X65X6 back to back).

Model 10: Building with V bracing with both side eccentricity (2ISA 65X65X6 back to back).

Table 2: PROPERTIES of channel section place back to back (Fe 345 Mpa)

	Depth(mm)	**Flange width(mm)**	**Thickness of flange (mm)**	**Thickness Of Web (mm)**	**Back to back Distance (mm)**
Bottom 3 storey	400	150	20	18	215
Middle 4 storey	300	100	20	18	165
Above 4 storey	225	50	12	10	120
Beam	ISMB 350	140	14.2	10.1	

Table 3: PROPERTIES of channel section place back to back (Fe 250 Mpa)

	Depth (mm)	**Flange width (mm)**	**Thickness of flange (mm)**	**Thickness Of Web (mm)**	**Back to back Distance (mm)**
Bottom 3 storey	550	200	30	25	260
Middle 4 storey	350	125	18	15	200
Above 4 storey	27	75	12	10	160

Beam	ISHB 300	250	10.6	7.6	

RESULTS AND DISCUSSION.

Table 4: REDUCTION in Lateral Deflection in %(of all models compare with most efficient section –M8)

ECTIONS	**Fe 345**		**Fe 250**	
	X %	Y %	X %	Y %
M2	0.3	0.4	29.55	30.29
M3	1.29	1.37	30.73	31.69
M4	1.52	1.54	31.68	32.45
M5	0.3	0.4	29.31	30.29
M6	1.82	1.94	31.78	32.7
M7	4.1	4.69	35.93	36.12
M9	10.85	13	13.12	14.07
M10	6.45	5.65	34.75	35.36

1. AXIAL FORCE

Table 5: PERCENTAGE increased/decreased in Axial forces in column C1 at 8th storey (critical storey) comparison of Fe250 with Fe345

SECTIONS	**Percentage increased/decreased**
M2	4.11
M3	-5.36
M4	-2.60
M5	5.75
M6	25.82
M7	6.63
M8	-3.61
M9	10.23
M10	2.48

Table 6: PERCENTAGE increased/decreased in Axial forces in column C9 at 8th storey (critical storey)comparison of Fe250 with Fe345

SECTIONS	**Percentage increased/decreased**
M2	2.80
M3	6.88
M4	5.69
M5	8.58
M6	7.90
M7	6.29
M8	3.23
M9	-2.04
M10	-4.33

Table 7: PERCENTAGE increased/decreased in Axial forces in column C10 at 8th storey (critical storey)comparison of Fe250 with Fe345

SECTIONS	**Percentage increased/decreased**
M2	7.00
M3	-13.32
M4	9.33
M5	9.07
M6	15.00
M7	14.52

M8	11.14
M9	10.05
M10	11.00

2. BENDING MOMENTS

Table 8: PERCENTAGE increased in bending moments in column C1 8th storey (critical storey) COMPARISON of Fe250 with Fe345

SECTIONS	Percentage increased
M2	57.89
M3	40.35
M4	40.35
M5	52.13
M6	26.32
M7	20.80
M8	48.87
M9	28.07
M10	24.06

Table 9: PERCENTAGE increased in bending moments in column C9 8th storey (critical storey) COMPARISON of Fe250 with Fe345

SECTIONS	Percentage increased
M2	117.13
M3	108.51
M4	114.98
M5	93.43
M6	120.37
M7	117.13
M8	111.21
M9	115.52
M10	139.22

Table 10: PERCENTAGE increased in bending moments in column C10 8th storey (critical storey)comparison of Fe250 with Fe345

SECTIONS	Percentage increased
M2	114.44
M3	101.07
M4	93.05
M5	127.27
M6	97.33
M7	134.22
M8	82.35
M9	97.33
M10	98.40

Table 11: QUANTITY of Steel Required For Various Types Of Sections Used In Bracings at critical storey

Bracings	**Quantity Of Steel Used For Bracing**
Sections	**Total Weight In Kg**
Unidirectional Bracing (ISA 130x130x15) =190 M	5491
X Bracing (ISA 150x150x15) =380 M	12768
Unidirectional Bracing 2isa Place Back To Back (65x65x6) =380 M	2926
Unidirectional Bracing ISMB 225 =380 M	5928
V Bracing (ISA 110x110x12) =270 M	5292
Bracing At Corner (ISA 90x90x10) =255 M	3417
Unidirectional Eccentricity (2isa 65x65x6)=330 M	2541
Building With 1000 Mm Eccentricity At Top (2isa Back To Back 65x65x6) =472 M	3635
Building With V Bracing With Both Side Eccentricity (2isa Back To Back 65x65x6) =452 M	3480

DISCUSSION

1. LATERAL DISPLACEMENT-

After observing the storey displacement results from analysis it has been found that lateral storey displacement in longer direction is greatly reduced by the bracing system.. It has also been noted that eccentric. bracing reduces storey displacement considerably. Therefore it can be said that eccentric bracing provides greater lateral stiffness to the steel structure than concentric bracing. Maximum reduction in deflection in x direction is 10.85% , 35.93% and in y direction 13% , 36.12% for Fe 345 and Fe 250 respectively.

2. BENDING MOMENT

it has been observed that value of bending moment in column C1 (exterior) is more than value of bending moments in column C9 and C10 (interior columns).at critical storey.

CONCLUSIONS

- Steel Bracing is one of the advantageous concepts to be used in a high rise structure to reduce lateral displacement and also to strengthen damage structure.
- Lateral storey displacements are greatly reduced by the use of eccentric bracing, as compared toconcentric bracing system.
- Comparing the weight of bracing for critical storey, Buildingwithunidirectional eccentricity (M-8 2ISA 65X65X6) provides most economical solution as compare with other sections used in bracings.(Ref table no 4.36)
- If we compare Fe 250 and Fe 345 then it shows saving of 1000kg for Fe 345 grade.
- At critical storey there is reduction in bending moments for interior column(C9 C10) but not much variations find out in exterior column.(C1)
- For control of Lateral displacement the eccentric bracing is found most suitable one under the present study.

REFERENCES

[1] ZasiahTafheem, ShovonaKhusru “Structural behavior of steel building with concentric and eccentric bracing: A comparative study” Volume 4, No 1, 2013 ISSN 0976 – 4399

[2] D.C. Rai, S.C. Goel “Seismic evaluation and upgrading of chevron braced frames” Journal of Constructional Steel Research 59 (2003) 971–994

[3] Di Sarno,A.S. Elnashai “Bracing systems for seismic retrofitting of steel frames” Journal of Constructional Steel Research 65 (2009) 452–465

[4] Egor P Popov & Michael D. EngelhardtJinkoo Kim and Junhee Park “Seismic behavior factors of buckling-restrained braced frames” Structural Engineering and MechanicsVolume 33, Issue ,3, 2009, pp.261-284

[5] Mohsen Tehranizade, TourajTaghikhani, Mahdi Kioumarsi, Leila Hajnajafi “Comparative Study on Seismic Behavior of SCBF with Comparative Study on Seismic Behavior of SCBF with EBF” Systems 2007 AEES Conference.

[6] O.S. Bursia, b K.H. Gerstleb, A. Sigfusdottirb, J.L. Ziturb “Behavior and analysis of bracing connections for steel frames” Journal of Constructional Steel Research Volume 30, Issue 1, 1994, Pages 39–60

[7] Feng Fu “Response of a multi-storey steel composite building with concentric bracing under consecutive column removal scenarios” journal of Constructional Steel Research 70 (2012) 115–126

[8] G. Federico, R.B. Fleischman, K.M. Ward “Buckling control of cast modular ductile bracing system for seismic-resistant steel frames” Journal of Constructional Steel Research 71 (2012) 74–82

[9] Jesumi, M.G. Rajendran “ Bracing System for Steel Towers” ISSN: 2248-9622 Vol. 3, Issue 2, March -April 2013, pp.729-732

[10] M.A. Youssef, H. Ghaffarzadeh, M. Nehdi "Seismic performance of RC frames with concentric internal steel bracing" Engineering Structures 29 (2007) 1561–1568

[11] AdilEmreOzel, Esra Mete Guneyisi"Effects of eccentric steel bracing systems on seismic fragility curves of mid-rise R/C buildings: A case study"Structural Safety 33 (2011) 82 – 95

[12] Massumi, M. Absalan "Interaction between bracing system and moment resisting frame in braced RC frames" archives of civil and mechanical engineering 13 (2013) 260 – 268

[13] Hendramawat A Safarizki, S.A. Kristiawan and A. Basuki "Evaluation of the Use of Steel Bracing to Improve Seismic Performance of Reinforced Concrete Building"Procedia Engineering 54 (2013) 447 – 456

International Journal of Engineering Research and General Science Volume 3, Issue 5, September-October, 2015
ISSN 2091-2730

A Review to handle Sustainability problems in Software

Razia Falik
Department of Computer Science,
University of Agriculture, Faisalabad, Pakistan

Abstract- One of the major challenge of our society was to achieve sustainability development. Sustainability contains three factor: social, environmental and economics sustainability. For individuals, sustainability was the ability to undergo and the probable for long lasting maintenance. So there was a need to develop a sustainable software with a liable feeding of resources. In software development process, a pattern was a written document that provides a general solution to a design problem that occurs repeatedly in many projects. Requirement engineering was considered one of the most important phases in the development life cycle. Requirement engineering was the crucial activity which can affect the entire life cycle of software development process. The main objective of the requirements elicitation phase was to collect requirements from different views such as requirements from the business, requirements from the customer side, requirements from the user side, and requirements from the security point of view. This research will explore to handle the sustainability problem in design, a new software pattern based on singleton and service locator design pattern will be defined. This research will also focus on requirement engineering techniques that will be affective to overcome these problems. These techniques will be focus groups, interviews and ethnography for eliciting the requirements.

Key Words: Sustainability, Software, Design Patterns

INTRODUCTION

For solving the usually taking place software design problems in software engineering, design pattern was a suitable tool. It was not the easy task to search an appropriate design pattern for solving software design Problem for inexperience developers, therefore it was required to search a design pattern. At present, to regain design Patten, there are several proposed tools for research. Inappropriately, there was a keyword search problem for theses research tools. This problem was solved by using the acquaintance experience. To solve this problem CBR was most suitable model. Furthermore, to refine problem, FCA was useful for maintaining indexes, thus both CBR and FCA will be used consecutively [7].

In the process of software development, Requirement elicitation and analysis are the most important phase. Requirement engineering (RE) includes numerous activies which are requirements elicitation, analysis, negotiation, specification and validation. Frequent studies have shown the importance of requirements engineering process for successful software projects. There was a clear relationship among requirement gathering and analysis and software quality (Tahir and Ahmad, 2010).

For the solution of commonly occurred software problems, design patterns are the best solution that are used by the software developers. These are offered at the domain independent level. In this fashion, consequently design patterns are applicable through several domains and at the multiple domains of the construct. However, there was a difficulty to adopt the design patterns due to generic nature so it was not always easy that how these can be made functional in that domain. In their research, they discourse this problem by concentrating on an approach that was to gather requirements that was specific to that domain [4].

Sustainability was very important for software engineers due to two reasons. One was the need to learn and teach in exact domain that how we can use the resources in an efficient manner. And the other was want to take an advantage of developing markets to attract industrial investors and partners for research collaborations. Therefore, we contend that in software engineering, sustainability was an important future topic. Sustainability was the capability and prospective for long lasting preservation **[9].**

This research provided a new design pattern that has been based on singleton and service locator design pattern methodology so that to solve the problems in designing the software. This research has focused on requirement engineering techniques that will be affective to overcome these problems. These techniques could be focus groups, interviews and ethnography for eliciting the requirements.

REVIEW OF LITERATURE

[2]mentioned that from several years the typical process for requirements gathering has not been changed for large projects. Functional requirements for the software process can be defined by analysts and software developers. When the requirements are gathered in the natural language so there can be misunderstanding between requirements and the first release of the software. So there are different non-functional requirements that can be defined by different software developers at different spaces of the world.

[13] stated that the software development that was considered debauched and precise, Software design patterns are good proposals. They are defined in terms of interfaces and classes, promising an anticipated functionality. It was necessary to implement a software design pattern at correct pattern level. Conventional testing does not expose mistakes from the desired pattern. The proposed solution was to measure the software design pattern behaviors by verification at run-time that ensure that they meet the specified standards.

[5] mentioned that sustainability was the major issue in software engineering field. They also stated that requirements engineers must add sustainability for achieving quality requirements checklist. It requires the same importance as the other quality requirements. Sustainability was becoming more important in the software projects. So it was necessary to use the tool in the requirements process to achieve sustainability. An environment specialist must cooperate with requirement engineers who will help to mitigate the environmental threats.

[6] said that one of the main reasons of the software project failure was incomplete and incorrect requirements so in the software development process, requirements engineering was considered the most important activity and software project success depend on it. One of the main intentions of requirement engineering process was to describe requirements that exactly meet user's need. Software Many researchers and practitioners highlighted the need for choosing the appropriate techniques and models during the software process. For effective requirements analysis, it was essential to apply the proper technique for a given problem. On the base of project characteristics, it was also necessary to use blend of RE techniques. Advantage of using theses blend of techniques was that other techniques can be used with a special technique that was used for problem solving. By doing this high quality requirements will be achieved in software developments.

[14] mentioned that when errors are detected at the implementation or testing phases, it was extremely difficult and expensive to remove them, so requirements engineering phases are time costing. In the past two decades, several problems are found in order to gather requirements in software engineering situations so experts have discovered a large number of substitute approaches such as interviews, group-meetings, goals, questionnaires, viewpoints, aspects and scenarios. Requirements engineering was basically an interdisciplinary issue that are large number of contextual, Social, Psychological, human, economic, political, functional and educational factors that may generally employ more or less impacts on the requirements elicitation and management processes. Project managers and requirements analysts face some common problems during requirements engineering activities in the software development phase.

[10] mentioned that by using agents, any task or sub task can be carried out, so the goal of each agent was obviously placed in any software application. They define that an agent was a portion of code that achieve a definite goal; whether this goal was a single task or collection of tasks. Requirements engineering was the field of software engineering in which the software to be developed achieved the desired objectives for a particular software. RE was animportant phase within software engineering, meanwhile success of software systems can be measured by satisfying their requirements. Most of the present software engineering approaches have

focused on the design of the software system and them payed less consideration to requirements engineering that was the major cause of software failure.

[12] stated RE was the key factor that measures the importance of product. A well-defined requirement elicitation reduces the time and cost of development and increases the quality of the software system. Therefore, todegree and additionally identify the current methods and difficulties that are challenged by the software developers, it was most significant to design well-defined RE methods. So it was considered a positive thing for software developers to define good requirements engineering.

[1] stated that RE was the process of gathering, analyzing, trimming, documenting, and authenticating the needs, and requirements of the stakeholders for the desired system. They also stated that improper RE can lead to system failure, by using appropriate RE approach, software quality can be improved. There are some features of ES that are same as in the requirements of basic projects that are application domain, types of requirements engineers, resources of information, involment of users and requirements possessions. In this research, their main goal was to enhance the quality of ES by offering appropriate RE approaches that are used in the development process of ES. The use of these appropriate approaches can reduce the cost, time and scope and avoid the effort to rework in the development process of ES.

[4] discussed that from software architectural design patterns, domain specific software architectures can be build. For building the software that uses the specific domain from architectural patterns was the main purpose of this research. By taking the advantage of software design patterns, this methodology increases the quality of DRE software architecture. To plot a design pattern by using a single domain specific feature and to discourse a wide variety of architectures, this approach was a flexible. Moreover, the engineers' time was saved by using executable design pattern templates when building software architectures, for performing design time validation on the software architecture produced they also provide the foundation using this approach.

[8] stated that in the software development process, requirements engineering was the most important phase. Its objective was to gather quality requirements from numerous stakeholders by using suitable approaches. It's one of the objective was to gather quality requirements from numerous sources for the whole software development process. Requirement analysis was achieved by information and system developers in the early stage before the designing, development and delivery process irrespective of the technique that was used. Contextual inquiry was one of the most beneficial approach for information requirements analysis which was established in the Digital Equipment Cooperation as a research technique that was used to gather and examine the user requirements for design of the product in detail.

[9] mentioned that they presented a concept sustainability intosoftwareengineering. In the typical quality characteristic, Sustainability was one of the importantquality attribute as identical to correctness and efficiency. They said that there are two reasons why sustainability was important for software engineering educators: First, need to teach and learn how we can use the resources in an efficient manner in a specific domain. Second, need to attract the students, industrial investors and partners to work collaboratively. Therefore we can say that sustainability was an important topic in the field of software engineering.

[15] mentioned that for designing object oriented systems, use of design patters was best practice. Many experienced developers used design patters for their design problem and consider it as a solution of the problem. Many developers focuses on the identification and documentation of patterns instead of their experiences about using the patterns because design patters are generated from the experiences of the software developers. Design patterns provide a good tool to develop design for specific problem, so it was essential for design pattern to be used by unexperienced developers.

[11] stated that software systems have the sound effects on our environment and its sustainability that we need to talk. We estimate that there are two basic motives in the process of dominant software's development Firstly was that when we take sustainability in the process of software develop, there must be an intelligent blockade that was overwhelmed that was a difficult task. Secondly, this difficulty can increase the cost of the software development process, particularly when we want to hire experts for the

measurement of sustainability. For inspiring software developers to measuring sustainability, we proposed a pattern for the requirements that are to be sustainable. These patterns offer direction to measure the requirements for achieving sustainability. These requirements consists material on the conditions in which we should use these patterns taking as a preliminary edge for the development of sustainable requirements and it also contains data that was required to development of these requirements.

[3] mentioned that many organizations faced problems for achieving sustainability in their business. Although, these companies need extra energy to incorporate sustainability factor in their industry. Because in the process of old business and also in the old software development processes finding sustainability factor was a difficult task. In the traditional business processes, there was a no clear definition of sustainability. Because it was not considered sustainability an important factor in all the phases of software life cycle. So, if we want to consider sustainability a most important factor we have to understand sustainability in the software development process.

REFERENCES:

[1] Ang, J.K., Leong, S. B., Lee, C. F. and Yusof, U.K. 2011. Requirement Engineering Techniques inDeveloping Expert Systems. *IEEE sunoisium on Computers &Informatics*(ISCI),1(1):640-645.

[2] Berenbach, B and M. Gall. 2006. Toward a Unified Model for Requirements Engineering. *IEEE International Conference on Global Software Engineering* (ICGSE'06),1(1):237-238.

[3] Betz, S and T. Caporale. 2014 Sustainable Software System Engineering. *IEEE Fourth International Conference on Big Data and Cloud Computing*,1(1):612-619.

[4] Fant, J. S., 2011. Building Domain specific Software Architectures from Software Architectural Design Patterns.*Proceeding of the 33rd International Conference on Computers & Informatics(ICSE)*, 1(1):1152-1154.

[5] Mahaux, M., P. Heymans and G. Saval. 2011. Discovering Sustainability Requirements: An Experience Report. *In 17th International Working Conference on Requirements Engineering: Foundation for Software Quality*,6606(1):19-33.

[6]Mishra, D., A. Mishra and A. Yazici. 2008. Successful Requirement Elicitation by Combining Requirement Engineering Techniques. *In proceeding of the First International Conference on the application of Digital Information and Web Technologies*,1(1):258-263.

[7] Muangon,W and S. Intakosum . 2009. Adaptation of Design Pattern Retrieval Using CBR and FCA. *IEEE Fourth International Conference on Computer Sciences and Convergence Information Technology*,1(1):1196-1200.

[8] Pandey, D. ,U.Suman and K. A. Ramani, 2011. An Approach to Information Requirement Engineering. *IEEE International Conference on Information Science and Application (ICISA)*,1(1):1-4.

[9] Penzenstadler, B and A.Fleichmann. 2011. Teach Sustainability in Software Engineering?.*In 24th IEEE-CS Conference on Software Engineering Education and Training (CSEET)*,1(1):454-458.

[10] Ranganathan, P and K. Magel. 2010. Understanding Requirement Engineering (REQ) from a Software Agent Modeling Perspective. *IEEE International Conference on Software Engineering and Service Science (ICSESS)*,1(1):83-85.

[11] Roher, K and D. Richardson. 2013. Sustainability Requirement Patterns. *IEEE third International Workshop on Requirement Patterns (RePa)*,1(1):8-11.

[12] Tahir, A and R. Ahmad. 2010. Requirement Engineering Practices – an Empirical Study. *IEEE International Conference on Computational Intelligence and Software Engineering (CiSE)*,1(1):1-5.

[13] Teplitsky, M and I. Exman. 2006. Measuring Behavioral Software Design Patterns. *IEEE 24th Convention of Electrical and Electronics Engineers*,1(1):8-11.

[14] Yang, Y., F. Xia., W. Zhang., X. Xiao., Y. Li and X. Li. 2008. TowardsSemanticRequirement Engineering. *IEEE International Workshop on Semantic Computing and Systems*,1(1):67-71.

[15] Zhang, C and D. Budgen. 2012. What Do You Know about the Efectiveness of Software Design Patterns?. *IEEE Transactions on Software Engineering*,38(5):1213-1231

International Journal of Engineering Research and General Science Volume 3, Issue 5, September-October, 2015
ISSN 2091-2730

Security in Cloud Computing using Hybrid of Algorithms

Jasleen Kaur[1], Dr. Sushil Garg[2]
[1]Student,M.tech(CSE),RIMT,Mandi Gobindgarh,Punjab
E-mail: jasudhingra@gmail.com
Contact No.: 9914341118
[2]Principal, ,RIMT,Mandi Gobindgarh,Punjab

Abstract-Cloud is a metaphor for network that provides its services such as dynamic resource pools, high availability and virtualization using Internet know as Cloud Computing. Cloud Computing provides resources to the users over internet as per their demand. Service on demand is an important feature of cloud computing as it enables the user to pay for the required resources only. There are many Cloud Service Providers (CSP) such as Google, Microsoft, IBM, Oracle Corporation, Amazon Web Services, etc. which provide cloud services to users. Since cloud computing involves sending data over internet, security breach needs to be monitored and controlled. So, this paper introduces a new hybrid algorithm which is blend of two cryptographic algorithms: public key cryptography and secret key cryptography. This new algorithm is hybrid of RSA as Digital Signature and Blowfish Algorithm and will provide security to the data while being uploaded or downloaded from cloud.

Keywords- Cloud Computing, Security, Deployment Models, Service Models, Security, RSA as Digital Signature, Blowfish Algorithm

1 INTRODUCTION

Cloud Computing is internet based technology which has evolved in the field of IT over the past few years. Cloud computing makes the transfer or storage of bulk data easy to be transferred and maintained for usage. Organizations need not buy special hardware for deploying different applications since cloud computing provides with pay-as-you-go pricing basis which means that all the resources like firewall, server, database and so on that are required by an organization for the deployment of an application may be leased out by some other organization which deals in providing those resources. The latter organizations are known as cloud vendors. Hence leasing out of resources does not levy high cost on the users and at the same time it gives business to other people as well. So, cloud computing is fast becoming popular in the field of IT and is gaining attention of various organizations.

Some of the famous cloud providers are:

A. Google: Google provides internet services for storing and accessing the data as and when required. It provides various services such as mailing, storing of various documents, translation, sharing of documents to selected users, etc. The most commonly used service of Google is Google Drive which is used for sharing of personal data through internet.

B. Microsoft: Microsoft provides internet services for file sharing and storing through its office applications. Microsoft Cloud storage patents are Microsoft Azure and OneDrive for storing enormous data and then accessing it from any location.

C. Salesforce.com: Salesforce provides online services for sales, support and businesses through remote access from any location and at any time.

Figure: Cloud Computing

1.1 Cloud Computing Service Models

a.) Infrastructure as a Service (IaaS):

IaaS is the last layer of the cloud computing stack and this layer provides the consumers with various facilities like that of storage, processors, servers, networking and other hardware facilities and as well as some software facilities like virtualization and file system . This layer controls and manages various operations required by the consumer. It allows the consumers to equip resources as per their demand. It allows the users to deploy their applications or software services effectively and they may access resources with all their rights. In IaaS, an organization leases out its resources to the consumer and the consumer pays back on per-use basis.

b.) Platform as a Service (PaaS):

PaaS is the layer that lies above the IaaS in the stack. It deals with providing development as well as deployment options to the consumers. It basically provides an environment for developing the application with some built-in tools which have some pre-defined functions which help the user to build the application as per requirement. Also, once the application is developed, it may be deployed within the same environment. But, the application so developed becomes environment specific and cannot be run on any other vendor's environment. It also supports the feature of renting of resources and the consumers have to pay on per-use basis.

c.) Software as a Service (SaaS) :

SaaS is the topmost layer in the stack and lies above the PaaS layer. It provides deployment of the end product or software or some web application on the IaaS and PaaS services and provides access to different consumers through some network, probably Internet nowadays. The services of this layer are perceived and manipulated by the consumers. The consumers access these services through Internet once the software has been deployed. The license to these services may be subscription based or usage based. The consumer may extend the services (subscription as well as scalability) based on the demand.

1.2 Deployment models

There are different deployment models in cloud computing. These are:

a.) Private Cloud: Private Cloud is the one in which cloud infrastructure is established within the organization and provides limited access to the users. Since, only privileged users can access the resources on the cloud, it is considered as most secure of all other deployment models. It is deployed where the number of users accessing the information is small.

b.) Public Cloud: Public Cloud is the one in which cloud infrastructure is shared among different organizations. The public cloud is managed by some third party who lease out the resources to the organizations as per their demand. Hence, the public cloud supports the feature pay-as-you-go pricing. Public clouds are vulnerable to data tampering as there are multiple organizations accessing the applications on sharing basis and hence, it may give easy access to some intruder.

c.) Hybrid Cloud: Hybrid Cloud is the combination of different clouds. As it is the combination of models, it offers the advantages of multiple deployment models. It provides ability to maintain the cloud as recovery of data is easy in this cloud. It provides more flexibility.

d.) Community Cloud: Community Cloud is the one in which the cloud infrastructure is shared between different organizations with same interests or concerns. The organizations having same requirements (like security, policy, etc.) agree to share the resources from the same party or cloud vendor. Hence, community cloud is basically a public cloud with enhanced security and privacy just like that in private cloud. The infrastructure may be maintained within the organization or outside the organization.

2 LITERATURE SURVEY

A.) Sanjoli and Jasmeet [7], "Cloud data security using authentication and encryption technique", state that cloud computing is an internet based technology that will provide everything as service on demand . This paper proposes blend of two cryptographic algorithms, EAP-CHAP(Extensible Authentication Protocol- Challenge Handshake Authentication Protocol) and Rijndael Encryption Algorithm. EAP is used to provide authenticated access to the cloud environment. CHAP, a method of EAP, is implemented for authentication purpose. This is then followed by encryption using Rijndael Encryption Algorithm. The complete methodology involves few steps. In the first step, Cloud Service Provider (CSP) receives an authentication request from the user. In the second step, CSP sends acknowledgement after verifying the user identity using EAP-CHAP. In the third step, once the user is authenticated, the user encrypts the data using Rijndael Encryption Algorithm and uploads the encrypted data on to the server of CSP. The data is saved in encrypted form on to the server. Hence, when the user receives any encrypted data from CSP, it can be decrypted using same key same as that used for encryption. In this paper, client side security has been focused and encryption is in the hands of user for providing better security.

B.) Shirole and Sanjay[6], "Data Confidentiality in Cloud Computing with Blowfish Algorithm", propose a system that uses encryption technique to provide reliable and easy way to secure data for resolving security challenges. Scheduler performs encryption on plain data into cipher data followed by uploading of ciphered data on the cloud. When the data is to be retrieved from the cloud, it is obtained in plain data format and is stored on the system. This preserves data internally. And hence, this builds a relationship of cooperation between
operator and service provider. This model uses OTP(One-Time Password) for authentication purpose and Blowfish algorithm for encryption purpose.

C.) Garima and Naveen [5], "Triple Security of Data in Cloud Computing", state that cloud computing is a networking model which is connected to a number of servers and is based on client server architecture providing various facilities due to its flexible infrastructure. According to this paper, since cloud computing is internet based technology, so, security stands as a major concern and introduce a mechanism to protect the data in the cloud using combination of two cryptographic algorithms and steganography. This paper proposes blend of two cryptographic algorithms viz.a.viz., DSA(Digital Signature Algorithm) and AES(Advanced Encryption Standard) and Steganography. DSA is used for authentication purpose, AES is used for encrypting the data and Steganography is used for further encryption. The working involves signing of the data in the first step. The signature is generated by first applying a hash function on the data and this gives compact form of data which is called message digest. The message digest is then signed using sender's private key. Once the message is signed, the data is encrypted along with the signature using AES. Once encryption is completed using AES algorithm, the data is further encrypted using steganography. Steganography hides message along with another media which does attract the attention of the intruder and hence the data is protected. This complete mechanism is implemented on ASP.NET Platform and ensures to achieve authenticity, data integrity and security of data in the cloud. This paper concludes that time complexity of the complete mechanism is high since it is one by one process.

D.) Parsi and Sudha[4], "Data Security in Cloud Computing using RSA Algorithm", state that cloud computing is an emerging technology and is fast becoming the hottest area of research. Cloud computing is effective in reducing the costs and provides on demand services to the users. Since cloud computing is based on the concept of open environment, security stands as a hindrance to the deployment of cloud environments. To provide data security in cloud environment, RSA algorithm has been implemented to provide the same. RSA stands for Ron Rivest, Adi Shamir and Len Adleman. RSA is public key cryptography. In the proposed system, RSA is used for encryption as well as decryption of data. The process involves that the data is encrypted and then uploaded onto the cloud. For decryption of data, data required is downloaded from the cloud, cloud provider authenticates the user and then the data is decrypted. RSA is used to provide authenticated access to intended user only and hence makes the system secure. The working of RSA consists of two keys: public key and private key. Public key is distributed and shared with others while the private key is only available with the original data owner. Thus, Cloud Service Provider(CSP) perform the encryption and decryption is performed by the consumer or cloud user. Hence, once the data is encrypted using public key, private key must be known in order to decrypt the data. RSA algorithm has three steps: Key Generation, Encryption and Decryption. Key generation
is done between CSP and user and then encryption and decryption are performed further. The proposed system provides authenticated access and prevents any intruder access. Hence, the system is made secure.

3 PROPOSED WORK

The proposed work is based on blending two popular encryption algorithms viz.a.viz., RSA as Digital Signature and Blowfish algorithm.
RSA was introduced by Ron Rivert,Adi Shamir and Leonard Adleman in 1977. RSA has been named using initials of their names.
RSA is public key cryptography. RSA as Digital Signature is used for authentication and non-repudiation purpose. It makes sure that the message is received from the desired sender. For signing the document or message, two keys are required: public key and private key. The private key, as the name suggests, is not shared with anyone and hence is used for signing the document. The public key is known to all and is used to authenticate the sender. The working of RSA as Digital Signature has following steps:
a.) Firstly, a hash function is framed to create the message digest.
b.) For encryption, the private key generated using RSA algorithm is used to sign the document.
c.) For decryption, the public key generated using RSA algorithm is used to verify the document.

Once the document is signed, then further the encryption is performed by Blowfish algorithm in order to make a secure system.

Blowfish algorithm is a very popular and fast secret key cryptography. It was introduced by Bruce Schneier in 1993. The encryption/decryption process of this algorithm is complex and cannot be broken by any intruder. So, it will make the system secure. Blowfish consists of a 64-bit block size and a variable key length which varies from 32 bits up to 448 bit. The process is a 16-round Feistel cipher and large key-dependent S-boxes are used. The working includes of following steps:

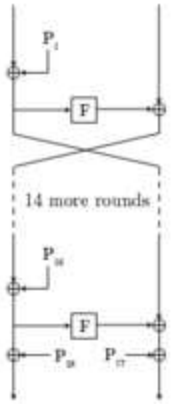

The Feistel structure of Blowfish

a.) The diagram above is pictorial representation of Blowfish. Each row represents 32 bits.

b.) The algorithm uses two subkey arrays: the 18-entry P-array and four 256-entry S-boxes.

c.) The S-boxes take 8-bit input and give 32-bit output.

d.) In every round, an entry from P-array is taken, and after the final round, each half of the data block is XORed with one of the two remaining unused P-entries.

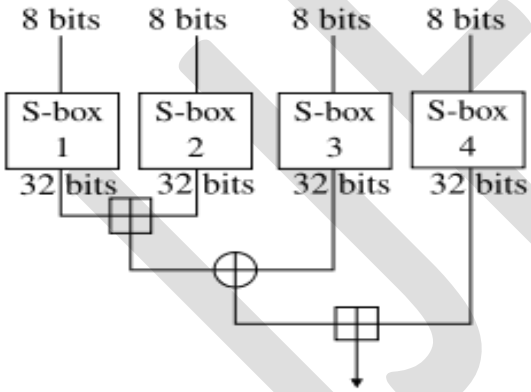

e.) The diagram above shows Blowfish's F-function.

- Firstly, the input is split into four eight-bit quarters
- these quarters are then input to the S-boxes
- The outputs are added modulo 2^{32} and XORed and a final output of 32-bit are obtained.

f.) Decryption is performed using the steps, except that P1, P2,..., P18 are used in reverse order.

4 WORKING OF PROPOSED ALGORITHM

The Proposed Algorithm consists of hybridization of two algorithms: RSA as Digital Signature and Blowfish Algorithm. Digital Signature will provide authentication and non-repudiation to the data while Blowfish will be used for encryption/decryption. Once the document is signed and encrypted using the hybrid algorithm, it will be uploaded onto the cloud provided by Cloud Service Providers (CSP). For decryption, document will be downloaded and then decrypted after authentication using public key.

Step1. RSA Key Generation Algorithm

Public key and private key will be generated using RSA algorithm.

The steps for RSA algorithm are:

a.) Choose two distinct large random prime numbers p and q.
b.) Find n = pxq, where n is the
modulus for public and private keys.
c.) Find the totient: $\phi(n) = (p-1)(q-1)$.
d.) Choose an integer e such that $1< e < \phi(n)$, and e and $\phi(n)$ have no factors other
than 1 , where e is declared as the public
key exponent.
e.) Find d to satisfy the congruence
relation $d \times e = 1$ modulus $\phi(n)$; d is the private key exponent.
f.) The public key is (n, e) and the private
key is (n, d). All the values d, p, q and
phi must be kept secret.

Step2. Digital Signature

a.) Before signing the document, the sender creates a message digest using a hash function.
b.) Message digest is basically a crushed form of entire message and so any hash function may be used for creating the message digest.
c.) Once the message digest M, is created it may be used for signing the document using private key.
d.) The private key(n,d) is used to sign the document using $S=M^d \bmod n$.
e.) After the document is signed, the document is further encrypted.

Step3. Encryption

a.) Once the document is signed, it is ready to be encrypted.
b.) For encryption, Blowfish algorithm is used.
c.) It has 16 round Fiestel structure and key dependent S-boxes.
d.) Basic operation performed in this algorithm is XOR logic function.
e.) XOR operation is performed on the output of each row.
f.) After 16 rounds of XOR operation, the encryption process is complete.

Step4. Decryption

a.) The decryption process is achieved using reverse of Blowfish algorithm.
b.) This process gives the message digest generated during digital signing of the document.

Step5. Verifying the Sender

a.) The receiver verifies the sender by using the public key of the sender.
b.) Receiver uses sender's public key (n, e) to compute integer $V=S^e \bmod n$.
c.) Receiver extracts the message digest from the integer V.
d.) Then, receiver independently computes the message digest of the information that has been signed.
e.) If both message digests are identical, the sender is valid.

5CONCLUSION

Cloud computing is fast becoming popular in IT field and is being adopted by every organization in order to keep their data all at one place. So, keeping the data secure is an important aspect of cloud computing. The new hybrid algorithm will provide security of data. RSA as Digital Signature will provide authenticity and non-repudiation to the data while Blowfish algorithm will provide security as it will encrypt the data. Also, the chances of breach in this hybrid algorithm will be quite less as the encryption process of Blowfish

algorithm is complex and cannot be broken easily and RSA as Digital Signature will make sure that the data is from a valid sender only. So, the hybrid algorithm aims at securing the very sensitive data of every organization that will be uploaded onto the cloud.

REFERENCES:

[1] http://en.wikipedia.org/wiki/Category:Cloud_computing_providers
[2] http://www.cloudcomputingchina.cn/Article/luilan/200909/306.html
[3] http://searchcloudcomputing.techtarget.com/sDefinition/0, sid201_gci1287881,00.html
[4] Kalpana, Parsi, and Sudha Singaraju. "Data security in cloud computing using RSA algorithm." *IJRCCT* 1.4 (2012): 143-146.
[5] Saini, Garima, and Naveen Sharma. "Triple Security of Data in Cloud Computing." *International Journal of Computer Science & Information Technologies* 5.4 (2014).
[6] Subhash, Shirole Bajirao. "Data Confidentiality in Cloud Computing with Blowfish Algorithm."*International Journal of Emerging Trends in Science and Technology* 1.01 (2014).
[7] Singla, Jasmeet Singh. "Cloud data security using authentication and encryption technique." *Global Journal of Computer Science and Technology* 13.3 (2013).
[8] Naik, Uma, and V. C. Kotak. "Security Issues with Implementation of RSA and Proposed Dual Security Algorithm for Cloud Computing."
[9] Somani, Uma, Kanika Lakhani, and Manish Mundra. "Implementing digital signature with RSA encryption algorithm to enhance the Data Security of cloud in Cloud Computing." *Parallel Distributed and Grid Computing (PDGC), 2010 1st International Conference on*. IEEE, 2010.
[10] Hashizume, Keiko, et al. "An analysis of security issues for cloud computing." *Journal of Internet Services and Applications* 4.1 (2013): 1-13.
[11] Rani, Sunita, and Ambrish Gangal. "Cloud security with encryption using hybrid algorithm and secured endpoints." *International journal of computer science and information technologies* 3.3 (2012): 4302- 4304.
[12] Saravanan, N., et al. "An implementation of RSA algorithm in google cloud using cloud SQL." *Research Journal of Applied Sciences, Engineering and Technology* 4.19 (2012): 3574-3579.
[13] http://cloudcomputingcafe.com/
[14] Devi, G., and M. Pramod Kumar. "Cloud Computing: A CRM Service Based on a Separate Encryption and Decryption using Blowfish algorithm." *International Journal Of Computer Trends And Technology* 3.4 (2012): 592-596.
[15] Kaur, Randeep, and Supriya Kinger. "Analysis of Security Algorithms in Cloud Computing."
[16] Thakur, Jawahar, and Nagesh Kumar. "DES, AES and Blowfish: Symmetric key cryptography algorithms simulation based performance analysis." *International journal of emerging technology and advanced engineering* 1.2 (2011): 6-12.
[17] Kumar, K. Vijay, Dr N. Chandra Sekhar Reddy, and B. Srinivas Reddy. "Preserving Data Privacy, Security Models and Cryptographic Algorithms in Cloud Computing." *International Journal of Computer Engineering and Applications* 7.1 (2015).
[18] Kaur, Jasleen, et al. "SURVEY PAPER ON SECURITY IN CLOUD COMPUTING." (2015)

International Journal of Engineering Research and General Science Volume 3, Issue 5, September-October, 2015
ISSN 2091-2730

Weight-Based-Approach for Searching File Using File Attributes in Forensic

MAHENDRA SHIVAJI PANDIT , IRFAN SIDDAVATAM

K.J. SOMAIYA COLLEGE OF ENGINEERING, MUMBAI, EMAIL ID - MECOMP2012@GMAIL. COM
K.J. Somaiya College of engineering, Mumbai, email id - irfansiddavatam@somaiya.edu

Abstract— The main goal of digital forensics is the extraction of suspected files from the target devices that can be defined as digital evidence. The digital world is developing at a very fast pace. The size of hard disks made available to the users is also increasing rapidly. The volume of data or the number of files that can be stored is also increasing. To find a particular file the investigators rely on filters and traces. The traceability process has become a key or an important element of the digital investigation process, as it is capable to map the events of an incident from difference sources in obtaining evidence of an incident to be used for other auxiliary investigation aspects. Filter are used by the investigator to remove unwanted data and get the required files. But the traceability and filter have not been explored to its limits. Because of these, little manipulation in the data on the digital device makes the use of specific trace or filter useless. These work like a loophole, which can be used by criminals to divert the investigation away from evidence. The loophole can be made less harmful by creating a priority based investigation using traces and filters. Priority is given to files which may be or may not be evidence, by assigning them the weight on the basis of the results of traces and filters. By assigning the weight, all files will be taken into consideration and files can be arranged based on the weight. So with weight-based-priority in use, the little or more manipulation to data will be taken into consideration.

Keywords— Digital Forensic, traceability, filters, weight , priority, data analysis, file search, attributes.

INTRODUCTION

Computers and other digital devices are becoming ubiquitous in our modern society. It was inevitable that they would begin to feature as heavily in crime and law. Since the late 1970s the amount of crime involving computers has been growing very quickly, creating a need for constantly developing forensic tools and practices. Almost 99 percent of criminals leave evidence which could be captured and analyzed through proper computer forensic procedure. At one end as the technology is getting advanced, the space of the digital devices are increasing rapidly. The global data supply reached 2.8 zettabytes (ZB) in 2012 - or 2.8 trillion GB - but just 0.5% of this is used for analysis, according to the Digital Universe Study. Volumes of data are projected to reach 40ZB by 2020, or 5,247 GB per person, with emerging economies accounting for an increasingly large proportion of the world's total[1]. Thus the data to be analyzed becomes huge and a challenge for the forensic investigator to perform the forensic investigation in time. One of the important factor in analyzing the data is traceability.

Whenever any operation is done on a device, it makes a lot of entries for security and auditing purpose. These entries are often called as traces. With the help of these traces, it will be known what should be traced and what location and what data. This process is known as traceability. Traceability is the means to identify and follow real or imaginary objects through a process chain. It gives the opportunity to back-track a chain of events, or to predict process outcomes given in the origin of an object. In digital forensic investigation process, tracing is described as a process of finding or discovering the origin or cause of certain scenario. The tracing activities are able to discover the traces left in digital devices. In the computer crime perspective, trace can be found in any digital devices. These traces consist of activities such as login and logout of the system, visit of pages, accesses documents, create items and affiliation groups found in records of data [2].

BACKGROUND

Digital forensic have solved many crimes committed with the help of computers where evidence may reside on a computer. From its start in 1970 till today, the field of digital forensic have came a long way and have made many developments. Digital forensic started in early 1970. At that time forensic techniques were developed primarily for data recovery. By the late 1980s utilities were being widely advertised that could perform a variety of data recovering, including "Unformat, Undelete, Diagnose & Remedy. In these early days forensics was largely performed by computer professionals who worked with law enforcement. The years from 1999

to 2007 were a kind of "Golden Age" for digital forensics. During this time digital forensics became a kind of magic window that could see into the past (through the recovery of residual data that was thought to have been deleted) and into the criminal mind (through the recovery of email and instant messages). The Golden Age was also marked by a rapid growth in digital forensics research and professionalization. Universities around the world started offering courses in digital forensic[3]. On the other hand many companies developed software's specialized for forensic investigation. Open source platform also contributed towards the development of digital forensic.

A. Size of digital devices - A problem

Today much of the last decade's progress is quickly becoming irrelevant. Digital Forensics is facing a crisis. Hard-won capabilities are in jeopardy of being diminished or even lost as the result of advances and fundamental changes in the computer industry:[4]

- The growing size of storage devices means that there is frequently insufficient time to create a forensic image of a subject device, or to process all of the data once it is found.
- The increasing prevalence of embedded flash storage and the proliferation of hardware interfaces means that storage devices can no longer be readily removed or imaged.
- The proliferation of operating systems and file formats is dramatically increasing the requirements and complexity of data exploitation tools and the cost of tool development.
- Whereas cases were previously limited to the analysis of a single device, increasingly cases require the analysis of multiple devices followed by the correlation of the found evidence.

The vast size of today's storage devices means that time honored and court-approved techniques for conducting investigations are becoming slower and more expensive. External hard disks of any size starting from 1tb are easily available in market at reasonable prices. This rapid increase in size is becoming a challenge for forensic investigators.

B. Working of search filter

Filters have always been of great help to the investigators in getting the particular file from many files on device. The filter works in very simple way. The following figure explains the use of filter.

In the diagram, the rectangle represents the digital device space and the circle represents the result of filter. It can be clearly seen how some specified data is separated from all the data using the filter. More than one filter can be used to get more specific files[5].

Figure - Use of filter

The figure below, explains the working of use of more than one filter. In the Diagram, 3 filters are being used. Lets represent the result of filter 1 as 'A', result of filter 2 as 'B' and result of filter 3 as 'C'. Let the final output of all 3 filters be 'O'. So 'O' can be written as-

$$O = A \cap \mathbf{B} \cap C$$

The black color represents the final output.

Figure - Use of more than one filter(3)

TRACES AND FILTERS

Most important factor in retrieving the evidence are the traces or filters. So traces and filters play very important role in getting the evidence or the hint for evidence

A trace is any entry that the operating system makes on the device when a certain operation is executed. The operating system maintains many such traces when working. Some of the trace points are listed below.

1. Recent files
2. Prefetch files
3. Jumplist
4. Lnk files
5. Event log
6. System log
7. MFT
8. Memory dump
9. Registry
10. Previous version

Filters are the nothing but the user specified conditions. The filters can be the metadata or contents of the file. The investigator uses the filters to filter out the excess data and get the data that may be the evidence. For example - Type Filter, if we give .pdf as type filter then outcome will be only .pdf file and all other file types will be not considered.

EXPLORING FILTERS

With the current working of filters, result only contains the files that satisfy all filters. If any changes is made to the data, then the files affected by the change may or may not be the be the part of the results. In such case, the evidence itself may not be taken into consideration.

Implementing weight-based-priority can handle such changes effectively. Let's see how the weight-based-priority helps. Let's use simple weight system given below -

Weight(File) = No_Of_Filters_Satisfied(File)

According to above equation, weight of a file will be equal to number of filters satisfied by the file. So, files in red colored area will have weight 3, files in blue colored area will have weight 2, files in orange colored area will have weight 1 and files in white colored area will have weight 0. Files can be then giving priority based on this weights. There are two cases :

Some investigator would like to have the traditional way of working with filters. For them , the files of importance will be the files which satisfy the condition below -

Weight(File) = No_Of_Filters_Satisfied(File)

= Total_No_Of_Filters

This files would have the highest weight and based on priority will be placed at the top of all files. So the traditional way of working with filters have changed but still the investigator can get the result of filters as if it were working in traditional way.

Other files with less weight will follow high priority files. The question is why this files are important. consider files whose weight will be equal to -

Weight(File) = Total_No_Of_Filters - 1

Example - Name, Author, Type, CreationTime, AccessTime, ModifyTime are the filters used by investigator for analysis. Suppose the suspect have renamed the file . So with traditional way of filters, all the filters will not be satisfied and the file will not be shown in results. With weight based priority, the file will be placed immediately following the top priority files(if any). The file which was changed by the suspect is also shown in results. Similarly if suspect changes the extension of file, the file will still be shown in results based on its priority.

Taking into consideration traditional search, the result of applying filters would be -

$O = A \cap B \cap C$

If any changes are made to the data, then the evidence may or may not be shown in the results. This would make things more difficult.

While on the other hand, the weight-based- priority approach will take whole space into consideration. The files can be arranged by weight to get most important files on top.

$O = A \cup B \cup C \cup U$

[Note: U represents whole device space.]

EXPLORING TRACES FOR SEARCHING

A trace is nothing but a entry of certain operation being executed on the OS. The trace when followed leads to certain file on the digital device. There are two possibilities - either the file may be present or file may not be present there. In current scenario, the trace that leads to a file that is not present in its location is ignored.

There are many possibilities of why the file may not be present at its location. For example - file may have been deleted, file may have been renamed, file may have been moved to some other location and so on. Instead of Ignoring such traces, it is possible to use the result of the traces in further exploring the devices. The next important point to consider is , they are many types of traces written on the devices. Each trace leads to certain file or location. Each type of trace is evaluated independently of other type of trace. Instead of evaluating each trace independently, the results of one trace can be used further with the results of other traces. This process if continued will build up a relationship among the traces. This in turn will lead to pointing out to the evidence with higher possibilities. The following figure shows how the traces can be used in exploring the data:

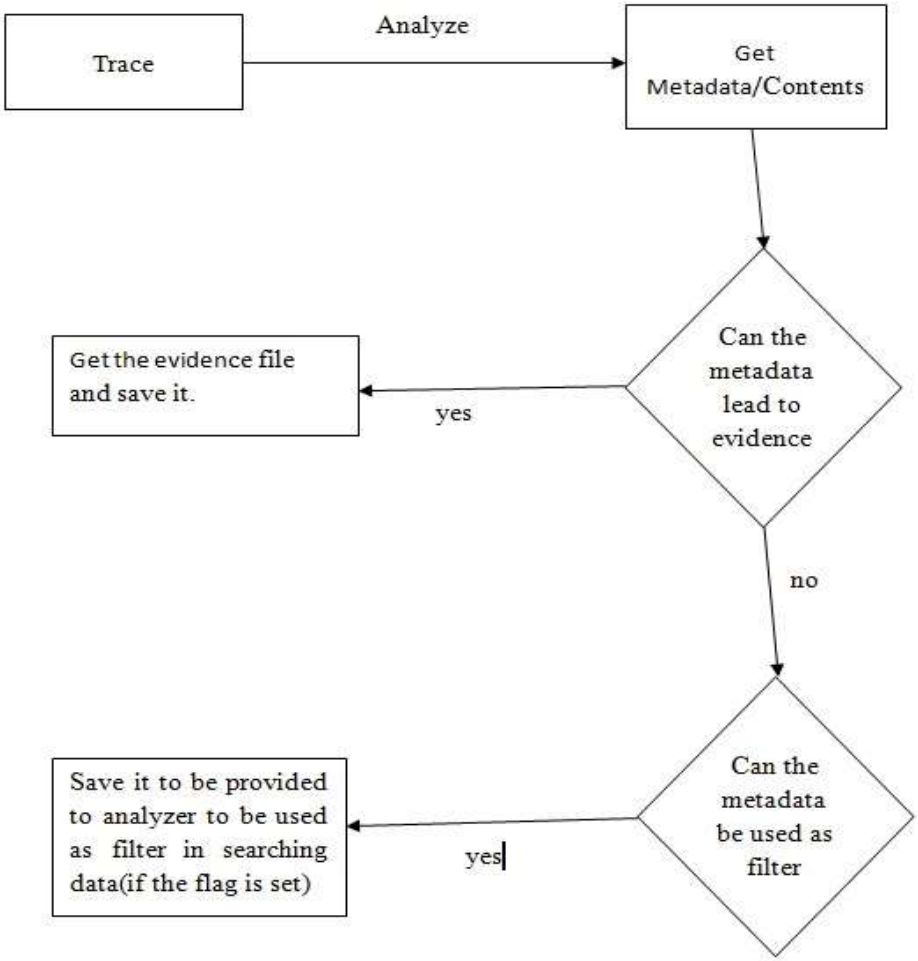

Figure - Use of traces to get metadata

Steps:

1. Get the trace.
2. Analyze the trace.
3. If it's associated file/location is present save the file as evidence.
4. If the file is not present, the metadata recovered from the trace will be provided to search filter.
5. Are there any more traces left. If yes, get the next trace and go to step 2.
6. Follow this process until all traces have been analyzed.

IMPLEMENTATION DETAILS

A. System details

- System Type - 64 bits
- OS - Windows 7 Ultimate (Service pack 1)
- Hard disk size - 500 GB
- Ram - 6 GB
- Processor - Intel(R) Core(TM) i3-2348M @ 2.30 GHz 2.30 GHz

B. File System Details

- File System type - NTFS
- Number of drives - 7

Table - File System Information

Volume	Letter	Total size	Files	Dir
1	H:	97.3	15755	2252
2	I:	48.8	21713	4764
3	C:	48.8GB	182993	81872
4	D:	71.6	19952	2681
5	E:	25.9	17855	18066
6	F:	73.9	62033	20996
7	G:	98.8	7097	2694

C. Program implementation

3 Modules were written to implement the Weight-Based-Approach for file search. One third party software was also used to assist in collecting the information. The software's used is - Log Parser 2.2 provide by Microsoft. The three module programmed for the implementation of Weight-Based-Approach for file search are -

1. FS_collector.bat - This module is designed to collect all file system information on hard disk. This module uses the Log Parser 2.2 tool to collect information.
2. Analyze.py - This module is designed to analyze the information collected by FS_collector.bat . This module is a command line script. It provides different options to take input from user.

Table - Options for analyze module

-h		Show this help message and exit
-f	FILE_NAME	File name to be searched
-e	EXTENSION	The Extension of file to be searched
-m	MODIFICATION_TIME	Provide the range of time of file modification
-a	ACCESS_TIME	Provide the range of time of file access time
-c	CREATION_TIME	Provide the Range of time of file creation (from-to)
-s	FILE_SIZE	Size of file
-p	FILE_PATH	Path of file
-w	MINIMUM_WEIGHT	Minimum weight of file to be satisfied
-t		Use the traditional way of search filter

3. Get_file.py - This module is used to get the results or search within the results created by Analyze.py module.

The 3 module were run on the system(details are provide above) and the results were as follows. First the FS_collector was run. The FS_collector gathered file name, Size, Path, creation time, last access time, modification time of all the files present on the disk. This module created 7 files corresponding to 7 drives. Each file contained all the files information and its attributes contained in that drive. Secondly the Analyze.py was executed. If analyze.py is executed without any arguments then it will analyze all the seven files created by the FS_collector and give weight zero to all files and store the result in on file. This scenario is never used. It is used only when its needed to check the maximum amount of time that the program will take to analyze the files. The graph below represents the amount of time needed to collect and analyze the files.

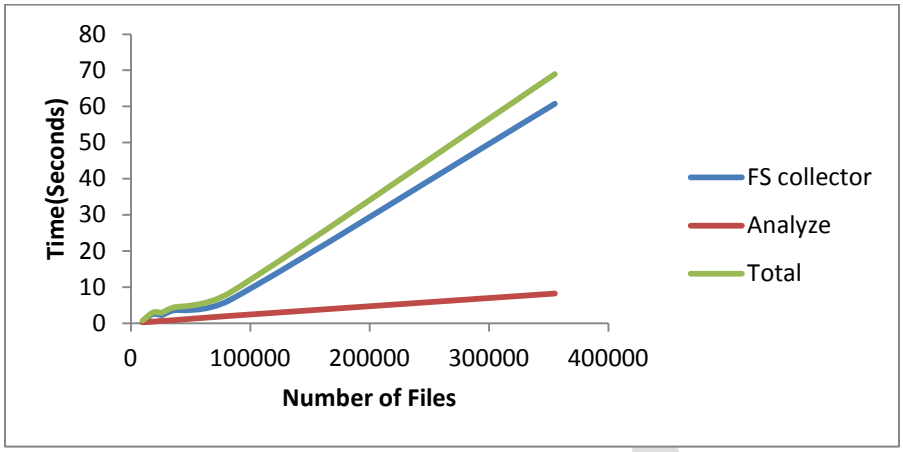

Figure - Time required to collect and analyze

The main module to understand weight-based-system is Analyze module. This module actually analyzes the data collected by FS_collector to perform weight-based searching. This searching can be done in 3 ways.

1. The Traditional way - In this case, the files are searched in traditional way i.e. the result of search will include only those file that satisfies the filters given. That means -

weight(file) = Number of Filters.

2. Weight-Based-Approach where weight is not given - In this case analysis to find a file is done on the basis weight-based-approach but weight is not assigned. So automatically weight is assigned a value of zero. The result will show all the files and their associated weight. That means -

weight(file) = Number of Filters Satisfied >= 0

3. Weight-Based-Approach where weight is given(W) - In this case, weight is given and it is some positive integer. The file are analyzed and only those results are stored where weight of file is greater than the weight given(W). That means -

weight(file) = Number of Filters satisfied >= W

Few commands were run randomly to check the results. In all cases the files to be searched were found(that existed on disk). The only difference was seen in the execution time taken by them. The graph below represents the time taken by them .

Table - Time taken when different number of filters are provided

No. of filters	Time -t	Time Weight Based
1	8.9466	14.4066
2	9.2586	15.6936
3	9.6408	14.235
4	10.1556	15.3406
5	10.8186	15.7638
6	11.817	19.4064
7	12.1602	31.8162

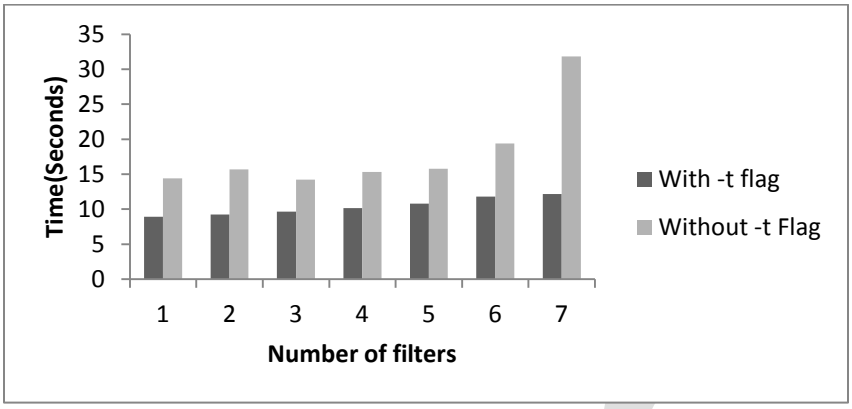

Figure - Time taken by different number of filter

With -t flag means traditional way and without -t flat means weight-based-approach where weight was not provided.

D. How weight based approach is different

In traditional search, if the file is not found then it becomes little more difficult to find the file. Sometimes the investigators have to apply different approaches(hash calculation and matching , content matching etc) to all the files. This process is time consuming and requires resources. In most of cases if the metadata of file is changed, then it becomes a hectic job to find the file with traditional search.

With weight based approach, it will be little easy for searching the file even if the metadata of file is changed. The following command was executed to find a file named gui.py.

analyze.py -e py -s 10-100000 -a 2015-201508 -m 2015-20150825 -c 2015-201508 -f gui -p d:\

The results of this command(given by get_file.py) were as follows -

- Number of files satisfying 0 filters - 127096
- Number of files satisfying 1 filters - 253756
- Number of files satisfying 2 filters - 57238
- Number of files satisfying 3 filters - 22802
- Number of files satisfying 4 filters - 4846
- Number of files satisfying 5 filters - 1662
- Number of files satisfying 6 filters - 1
- Number of files satisfying 7 filters - 0

The following graph represents the results -

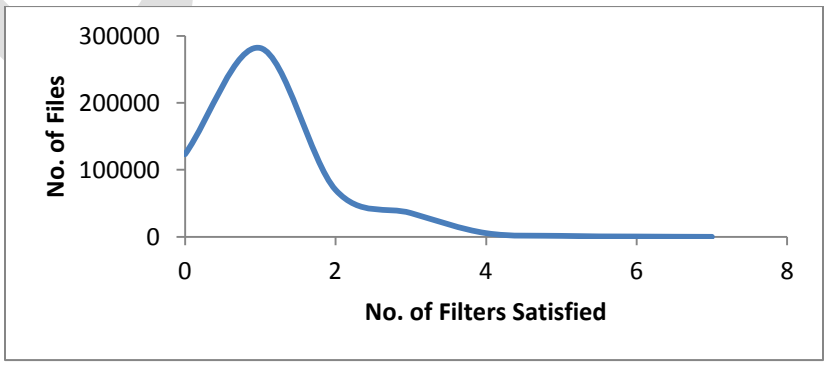

Figure - Number of files VS Number of filters satisfied

From the above graph and reading, it can be concluded that for all non-zero positive number, more the number of filters satisfied less the number files. As the number of filters being satisfied decreases, the number of files increases. In the example the file was present and it satisfied all the filters and so was easily found. Suppose one of the property of gui.py was changed. So if the same command was executed this time, it's obvious this time the file satisfying 7 filters will be zero and files satisfying 6 filters will increase by 1. Now instead of doing different function(hash matching, content matching etc) on all files(nearly half million on this system), this functions can be done on the 505 files instead (i.e. files satisfying 6 filters).Same will be the case when 2 or more properties are changed. In this way the probability of finding the file as soon as possible increases. This would reduce time and make less use of resources.

E. Use of traces

The traces can be further used to get more accurate data about the files. This information can be further used to provide filters to analyze.py module more accurately and precisely. In our project, prefetch files were used. From prefetch files , information like when was the particular application last time opened. Analyze.py takes the MAC time as a range rather than a specific date and time. So the timestamp recovered from prefetch will be used as a upper end limit while providing the date and time range for analyze.py module.

When information recovered from traces are used as filters to search a file, the number of files satisfying higher number of filters will decrease and the number of files satisfying less number of filters will increase. This also increases the probability of getting the file faster. For example - if from .lnk files we get the file path. But if the file is renamed or moved to other folder or deleted then the .lnk file will not be able to trace the file and so the trace becomes useless. But the .lnk files have ceratin metadata like the path. So if we use the path found in .lnk file to provide the filter then it may or may not help us to get more accurate results.

Let's take the same example executed above in section D. But this time the path will be set to the path extracted from .lnk file

analyze.py -e py -s 10-100000 -a 2015-201508 -m 2015-20150825 -c 2015-201508 -f gui -p E:\PROJECT\implementation

The results of the command(given by get_file.py) are as follows -

- Number of files satisfying 0 filters - 127014
- Number of files satisfying 1 filters - 241227
- Number of files satisfying 2 filters - 56340
- Number of files satisfying 3 filters - 35725
- Number of files satisfying 4 filters - 5393
- Number of files satisfying 5 filters - 1700
- Number of files satisfying 6 filters - 1
- Number of files satisfying 7 filters - 1

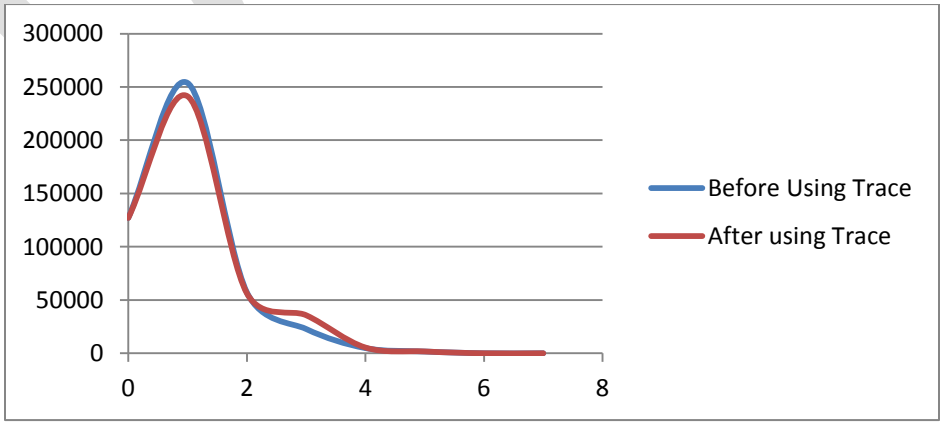

Figure - Difference in result after using .lnk trace

This is the general behaviour of how the number of files and number of filters satisfied will be affected when filter are used from data extracted from traces.

There are other traces that can be used to extract more information . This information can then be used to more precisely provide filters.[6]

1. Registry - List of executed commands, search keywords, last accessed folder, recently executed files and application usage
2. Web Browser File - Visited URL/time, downloaded files, search keywords
3. Specific Document File - Encrypted files, file name and files with modified extension
4. $MFT file : file and directory names, file extension, creation time, modification time, access time, file size, and file location and its possessor.

More the number of traces used as filters, more precise will be results.

CONCLUSION

The use of traces and filters in forensic investigation for analysis and getting evidence have always been very important. Little changes to data associated with traces and filters can get the evidence away from investigation prompting the investigator to use more complex investigation process. But using the weight based approach to get the evidence by use of traces and filter can help the investigator in getting the all the data on their priority basis. Even if the evidence file is changed, weight-based-approach will help in placing it among the results(which would not be placed among results using traditional working) based on changes made to file and the weight assigned to it during process of analysis.

REFERENCES:

1. TheGuarding Newspaper [Online] Available : http://www.theguardian.com/news/datablog/2012/dec/19/bigdatastudydigitaluniverseglobalvolume
2. Siti Rahayu Selamat, Robiah Yusof, Shahrin Sahib, Nor Hafeizah Hassan, Mohd Faizal Abdollah, Zaheera Zainal Abidin "Traceability in Digital Forensic Investigation Process" published in 2011.
3. Shelton Donald E. " The 'CSI Effect': does it really exist? " March 2008; http://www.ojp.usdoj.gov/nij/journals/259/csieffect.htm.
4. Simson L. Garfinkel "Digital forensics research: The next 10 years" published in 2010.
5. Mahendra S. Pandit " Weight-Based-Priority Approach for Analyzing Data Using Traces and Filters " - (IJCSIT) International Journal of Computer Science and Information Technologies, Vol. 6 (3) , 2015, 2537-2540
6. SeungBong Lee, Jewan Bang, KyungSoo Lim_, Jongsung Kim, and Sangjin Lee "A Stepwise Methodology for Tracing Computer Usage" in 2009.
7. Joshua I. James and Pavel Gladyshev, "Challenges with Automation in Digital Forensic Investigations" published in 2013.
8. Brian Carrier "Open Source Digital Forensics Tools: The Legal Argument" published in October 2002
9. Brian D. Carrier Eugene H. Spafford, "Automated Digital Evidence Target Definition Using Outlier Analysis and Existing Evidence" published in 2005.
10. Xiyan Zhao ; Key Lab. of Intell. Comput. & Novel Software Technol., Tianjin, China ; Yukun Li ; Jingyu Liu ; Yingyuan Xiao "Searching Desktop Files Based on Synonym Relationship" , Published in: Web Information System and Application Conference (WISA), 2013 10th.
11. Pavel Dmitriev , Pavel Serdyukov ,Sergey Chernov "Enterprise and Desktop Search" published in http://www.wwwconference.org/ in 2010.
12. Chang-Tien Lu ; Virginia Polytech. Inst. & State Univ., Blacksburg ; Shukla, M. ; Subramanya, S.H. ; Yamin Wu "Performance Evaluation of Desktop Search Engines" Published in Information Reuse and Integration, 2007. IRI 2007. IEEE International Conference
13. Cole, B. "Search engines tackle the desktop" Published in Computer (Volume:38 , Issue: 3) IEEE Paper.
14. Gaugaz J. ;Costache, S. ; Chirita, P.-A. ; Firan, C.S. ; Nejdl, W."Activity Based Links as a Ranking Factor in Semantic Desktop Search" Published in Web Conference, 2008. LA-WEB '08., Latin American

International Journal of Engineering Research and General Science Volume 3, Issue 5, September-October, 2015
ISSN 2091-2730

Apportioning the Secondary Particles in Atmospheric PM_{10} in a Residential Area

Sheo Prasad Shukla
Professor, Civil Engineering, Institute of Engineering & Technology, Lucknow 226 021, India
E-mail: sps.iet@gmail.com, Contact No.: +91 9415190054

Abstract- Quality (characteristics) and quantity (concentrations) of atmospheric particles are critical in neutralizing the atmospheric acidity and aiding to formation of secondary particles. To examine the formation of secondary particles, an integrated approach involving seasonal measurements and characterization of particulate matter (PM) is adopted. 109 PM_{10} samples were collected at Kidwai Nagar during 2000-2001 in a three season study. The concentration of metals and water-soluble ions in collected samples were determined for source apportionment estimations. Soil-road dust (26-36%) and inorganic secondary particles (4-11%) were two important PM_{10} sources. It was found that role of ammonia was crucial in formation of secondary particles.

Keywords: apportionment analysis, particulate matter, secondary particles, residential area, seasonal variation, factor analysis, ambient air sampling

INTRODUCTION

India has set a target of 215 804 MW power generation capacity by March 2012 from the present level of 100 010 MW [1]. Thermal power generation will be the main contributor to the overall power generation (approximately 68%). The new power plants and other industries will add to the existing emissions of SO_2, NO_x and PM significantly. The growth situation warrants a closer examination of the impacts of emission of SO_2, NO_x, PM and their interactions. SO_2 and NO_x are not only primary pollutants but also contribute to the formation of secondary particles in the atmosphere. Indian atmospheric conditions pose certain challenges in adopting or using the information from other sources or internationally published literature on formation of secondary particles. First, significant photochemical activities at high temperature and the second, high PM_{10} (particle size less than or equal to 10µm) levels around 350 µg m^{-3} make modeling and source apportionment of secondary particles difficult.

The winter levels of PM were found to be less than those in summer at each of the seven sampling locations in Delhi during the year 1990 [2]. A five-year long study (1981-85) by the Central Pollution Control Board (CPCB) at Agra concludes that PM levels were significantly less (270 µg m^{-3} 5-year average) in winter months compared to summer months (400 µg m^{-3} 5-year average). The anthropogenic emission of PM are likely to be the same throughout the year; therefore, the variation in PM levels could be due to seasonal variation in emissions from natural sources (such as soil dust) in the atmosphere caused by variable atmospheric conditions and/ or photochemistry responsible for formation of secondary particles. Seasonal variation in temperature, humidity, wind speed, mixing height, soil moisture content, emission of ammonia etc. affects the atmospheric chemistry and particle generation (from soil)/ formation. Hence, to understand the issue of secondary particle formation and source apportionment analysis, seasonal variation of PM concentration, their characterization, and their sources have to be studied together [3], [4], [5].

The objective of present study was to understand atmospheric PM sources in a residential area for which a study was designed and completed from June 2000 to December 2001 at Kidwai Nagar (KN) in Kanpur City (longitude 88°22'E and latitude 26°26'N). Finally, the sources contributing to the PM_{10} levels have been quantitatively apportioned and subsequently the role of NH_3, SO_2 and NO_x in formation of PM_{10} has been examined. Factor analysis-multiple regression (FA-MR) technique [6], a receptor model, was employed to source apportionment.

Experimental

Description of study area

Predominant land use pattern of study area, Kidwai Nagar in Kanpur City (Fig. 1) is residential. Kanpur City experiences three dominant seasons each year: winter (November-February), summer (March–June), and monsoon (July–October). Within 1 km radius of the study area there are markets and sizeable traffic. The study area lies about 200 m away from a National Highway (connecting

New Delhi) and experiences traffic load from heavy duty diesel vehicles (such as trucks), two stroke vehicles and diesel driven three wheelers (Vikram tempos) throughout the day.

Sampling and quality control

PM_{10} measurements were carried at a height of about 10 m (above the ground), at the roof of a house in Kidwai Nagar during the study period. The frequency of sampling was two 24-h (6 am - 6 am) samples per week in accordance with National Air Quality Monitoring Program in the country. The collected PM_{10} was analyzed quantitatively as well as qualitatively (details in Table 1). Weighing of filter papers was done in humidity-controlled room using 440 Mettler Balance with sensitivity 0.00001 g and filters were conditioned in desiccators for 24 hours before and after the sampling. High volume sampler (model: APM 450, Envirotech, New Delhi) was used for sampling PM_{10} on Whatman GF/A 8″×10″ size filter paper at a flow rate of 1 $m^3 min^{-1}$ [7]. During the sampling period, meteorological parameters were recorded using wind monitor (model: WM251, Envirotech, New Delhi).

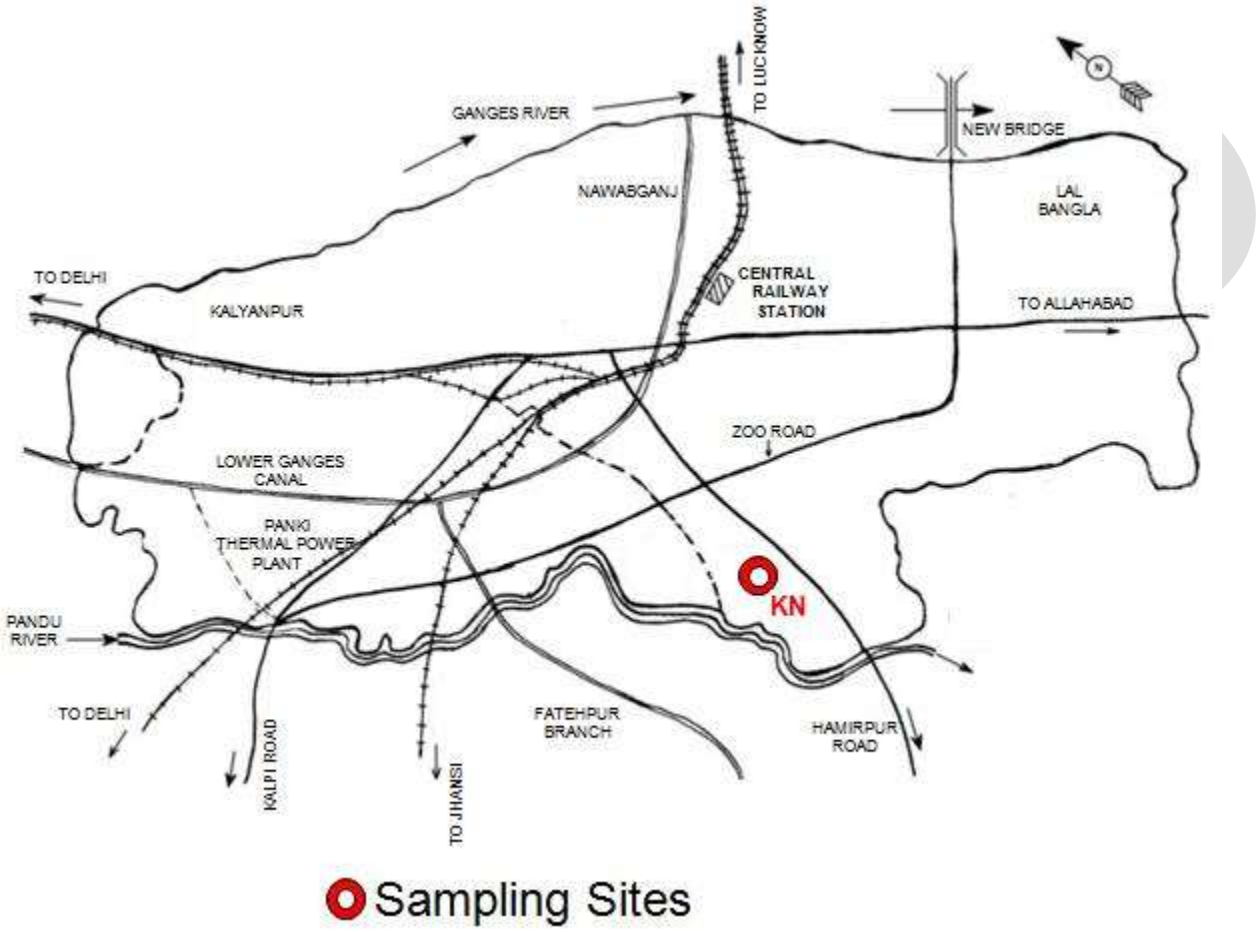

Fig. 1. Map showing location of sampling site

Table 1. Details of PM_{10} sampling

Sampling Seasons	***Sampling Months***	***Number of Samples***
Summer	June, 2000 March-June, 2001	32

Monsoon	July-October, 2000 July-October, 2001	38
Winter	November, 2000-February, 2001 November-December, 2001	39

Estimation of heavy metals and water soluble ions

Half of the filter paper was used for metal (Al, As, Ba, Ca, Fe, K, Mg, Mn and Pb) analysis and remaining half of the filter paper was used for analysis of water-soluble ions. The extraction and analysis of metals was carried out as per the USEPA method [8] using atomic absorption spectrophotometer (AAS) (Model Varian SpectrAA 220FS and GBC Avanta, Australia). The water-soluble cation NH_4^+ and anions F^-, Cl^-, NO_3^- and SO_4^{2-} were analyzed by ion chromatograph (IC) (model: Metrohm 761 compact) following the prescribed extraction procedure [9].

Source apportionment analysis

A multivariate analysis technique, FA-MR which does not require a priori information on source composition [10] is used in this study. [6] have also used one such technique of FA, principal component analysis (PCA), successfully for source apportionment of PM at traffic junctions in Mumbai and the same has been used in this study. A detailed description of the FA-MR can be seen in [11]. Varimax rotated PCA, to apportion sources of PM_{10}, has been conducted using a conventional R analysis of elemental correlations about their means using a statistical software package, SYSTAT. On the basis of measured variables of data set for each season, PC loadings and scores are determined. However, the 'absolute zero' PC scores (APCS) have subsequently been estimated for each PC by subtracting the PC score of an extra 'observation' (wherein concentrations of all the variables are assumed as zero) from PC scores of each observation [11]. Regressing observed PM_{10} concentration on APCS gave regression coefficients, which convert the APCS into PM_{10} source mass contributions for each observation. Mathematically for j^{th} observation,

$$[PM]_j = C_0 + \sum_{i=1}^{n} C_i [APCS]_j$$

where, n = number of PCs

j = 1, 2,….., m.

m = number of observations

C_0 = constant

C_i = regression coefficient

Product of corresponding $APCS_i$ for observation j and estimated regression coefficient (C_i) will give the contribution of i^{th} source in PM_{10}.

RESULTS AND DISCUSSION

24-h average PM_{10} concentrations in ambient air measured at the sampling site are presented in Fig. 2. PM_{10} levels show significant seasonal variations, lowest concentration in monsoon and higher variability in summer. Seasonal variability in chemical composition of PM_{10} from one season to another can be observed from Table 2. Similar observations have been reported by [12] for other parts of Kanpur city. Levels of soil-derived elements (Ca, Al and Mg) are highest in summer due to dry soil, which gets airborne due to high speed winds. Indicators of secondary particles (SO_4^{2-} and NO_3^-) have shown marked variation in winter as compared to other seasons. The variation in quantity and chemical species concentration of PM_{10} will impact the neutralization of acid (gas phase) present in atmosphere to form secondary particles.

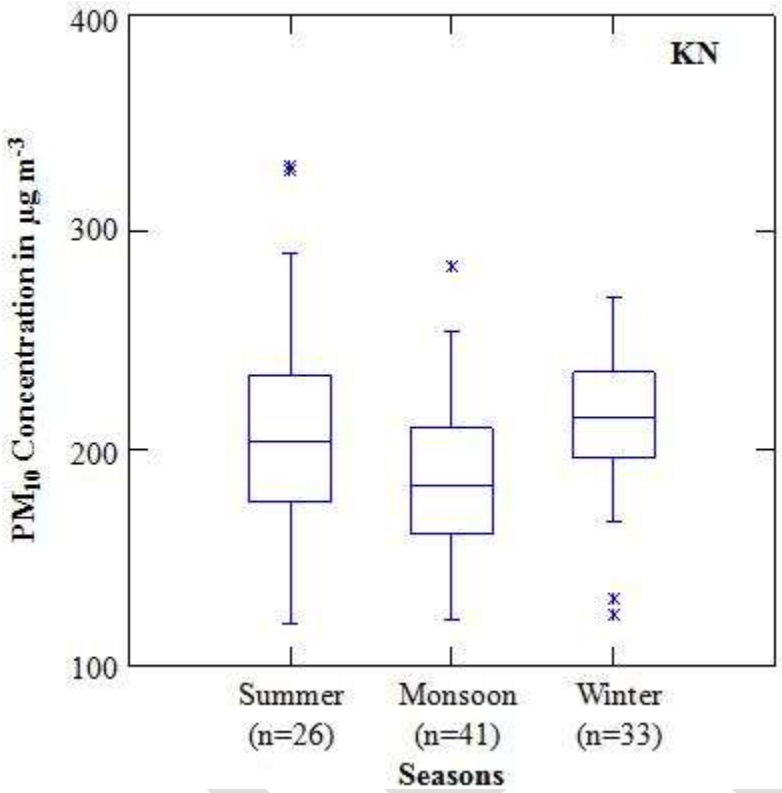

Fig. 2. 24-h average ambient air PM_{10} concentrations

Table 2. Mean ambient air (24-h) PM_{10} concentrations of various species

Species	***Summer (n=32)***	***Monsoon (n=38)***	***Winter (n=39)***
	(µg m^{-3})		
Al	26.65±16.17	10.92±4.11	8.74±2.16
As	0.16±0.13	0.04±0.02	0.12±0.07
Ba	7.40±6.62	2.03±1.17	10.67±6.33
Ca	35.76±18.84	11.80±6.11	17.12±3.61
Fe	0.46±0.26	2.19±0.85	0.88±0.24

K	5.97±7.79	2.16±2.03	4.79±2.24
Mg	4.36±2.13	6.65±3.63	2.58±0.56
Mn	0.11±0.07	0.07±0.04	0.07±0.03
Pb	0.23±0.16	0.16±0.08	0.25±0.15
NH_4^+	1.62±2.46	5.40±3.49	4.29±2.83
F^-	0.22±0.15	0.17±0.12	0.16±0.08
Cl^-	1.88±2.03	1.50±1.53	2.20±1.29
NO_3^-	7.11±9.45	18.12±10.62	14.72±8.61
SO_4^{2-}	11.24±7.21	10.74±5.01	8.97±4.11

Identification of sources contributing towards PM_{10}

Seasonal PM_{10} data were analyzed to get information of seasonal dominant contributing sources. Results of PCA along with corresponding sources are presented in Tables 3, 4 and 5 for summer, monsoon and winter seasons respectively. Based on strong loadings of various variables in factors, the sources have been identified. [13] classified the factor (PC) loadings as 'strong', 'moderate', and 'weak' corresponding to absolute loading values of >0.75, 0.75–0.50 and 0.50–0.30. Strong loading of crustal elements in all seasons can be identified as originating from crustal contribution which can be identified to soil dust emission.

Table 3. Varimax rotated PC matrix for PM_{10} during summer

Species	***Identified Emission Sources***		
	Soil & Road Dust	***Secondary Particles***	***Vehicular Emission and Biomass Burning***
Al	**0.83**	0.16	0.40
As	**0.89**	-0.04	-0.17
Ba	0.09	-0.01	**0.95**
Ca	**0.90**	0.32	0.16
Fe	**0.80**	0.48	0.01
K	0.11	-0.03	**0.74**
Mg	**0.72**	0.54	0.21
Mn	0.30	**0.79**	0.05
Pb	0.13	**0.79**	0.13
NH_4^+	0.34	**0.74**	-0.22

F^-	0.49	0.50	0.06
Cl^-	-0.13	0.64	0.45
NO_3^-	0.16	**0.81**	-0.10
SO_4^{2-}	0.53	**0.75**	-0.13
Eigenvalue	4.24	4.33	2.01
% variance	30.30	30.89	14.34
Cumulative % variance	30.30	61.19	75.54

Table 4. Varimax rotated PC matrix for PM_{10} during monsoon

Species	***Identified Emission Sources***		
	Soil & Road Dust	***Secondary Particles***	***Vehicular Emission and Biomass Burning***
Al	**0.91**	0.22	0.28
As	0.64	0.07	-0.61
Ba	0.21	0.20	**0.71**
Ca	**0.92**	0.26	0.14
Fe	**0.87**	0.28	0.29
K	0.25	-0.07	**0.74**
Mg	**0.87**	0.41	0.15
Mn	0.67	0.62	-0.02
Pb	**0.82**	0.36	0.06
NH_4^+	0.33	**0.83**	0.24
F^-	0.11	**0.75**	-0.09
Cl^-	0.21	0.6	-0.28
NO_3^-	0.33	**0.83**	0.24
SO_4^{2-}	0.33	**0.84**	0.23
Eigenvalue	5.22	4.03	1.87
% variance	37.30	28.78	13.38
Cumulative % variance	37.30	66.08	79.45

Table 5. Varimax rotated PC matrix for PM_{10} during winter

Species	***Identified Emission Sources***		
	Soil & Road Dust	***Secondary Particles***	***Vehicular Emission and Biomass Burning***
Al	**0.71**	0.30	0.49
As	0.30	0.43	0.23
Ba	0.38	-0.05	0.69
Ca	**0.86**	0.26	0.26
Fe	**0.70**	0.50	0.34
K	0.34	0.06	**0.76**
Mg	**0.77**	0.27	0.40
Mn	**0.70**	0.49	0.28
Pb	0.07	0.62	0.36
NH_4^+	0.27	**0.93**	0.01
F^-	**0.73**	0.04	-0.04
Cl^-	-0.17	0.57	0.65
NO_3^-	0.27	**0.93**	0.01
SO_4^{2-}	0.27	**0.93**	0.00
Eigenvalue	3.96	4.24	2.31
% variance	28.26	30.31	16.48
Cumulative % variance	28.26	58.57	75.05

In the receptor domain first factor having strong loading of crustal source consists of (i) natural windblown dust in ambient aerosol and (ii) dust present on the road/ road shoulders kept in suspension by vehicular movement. Hence, this source has been identified as 'soil and road dust'. Major portion of the percentage variance (28.3% to 30.3%) is explained by soil and road dust. The second factor explained 28.8% to 30.9% variance with high loading of NH_4^+, NO_3^- & SO_4^{2-} (secondary fine particles produced from gas to particle conversion of NH_3, NO_x & SO_2) and hence this source can be identified as the 'secondary particles'. The factor strongly loaded with Ba can be identified with vehicular emissions. Factor strongly loaded with K can be traced as a complex mixture of biomass burning.
Total variance explained by various sources contributing towards PM_{10} concentrations is about 76% (during summer), 79% (during monsoon), and 75% (during winter). Soil and road dust and secondary particles are invariably present in all seasons as major sources contributing to PM_{10} and large chunk of the percentage variance (61%, 66%, and 59% during summer, monsoon and winter seasons respectively) is being explained by these two sources. Other sources (such as vehicular emission, biomass burning) are also contributing to PM_{10}, but in small proportions. This source identification is compatible with general land use pattern of the sampling site.

Quantification of sources contributing towards PM_{10}

To apportion the PM_{10} concentrations for each observation, APCS were regressed against the observed PM_{10} concentrations and the following seasonal models were obtained:

Summer season: $PM_{10} = 119+43*APCS1+22*APCS2+9*APCS3$

Monsoon season: $PM_{10} = 88+40*APCS1+13*APCS2+9*APCS3$

Winter season: $PM_{10} = 176+6*APCS1+7*APCS2+20*APCS3$

Contribution of each source (factor) in individual PM_{10} observations has been estimated from above models (Fig. 3). Local soil & road dust (26% to 36%) and secondary particles (4% to 11%) are the key sources in all three seasons. The study by [6] in Mumbai, India for source apportionment of PM was conducted for traffic intersection. Their study indicated major contribution of 33-41% from road dust or soil followed by contribution from vehicles and marine aerosols. The plots of estimated PM_{10} concentration against observed PM_{10} levels (Fig. 4) signify that estimated and observed data compare well ($R^2 > 0.89$).

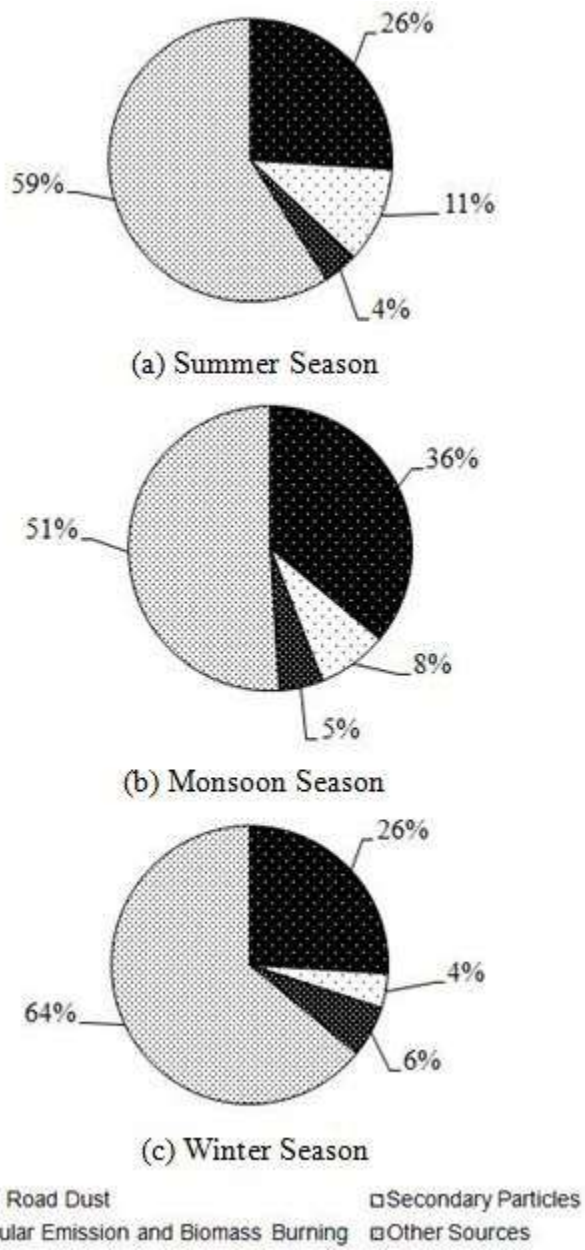

Fig. 3. Percentage contribution of different sources towards PM_{10} levels

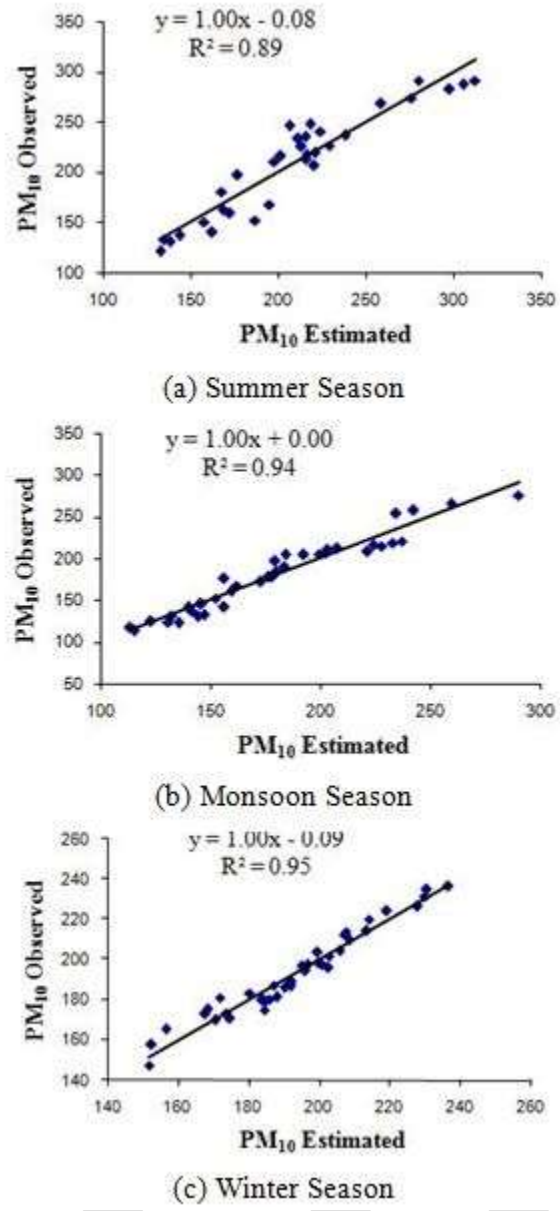

Fig. 4. PM_{10} observed vs. PM_{10} estimated (in µg m^{-3})

Formation of secondary particles like NH_4^+, SO_4^{2-} and NO_3^- depends not only on the concentration of precursor primary pollutants (NH_3, SO_2 and NO_X) but also on temperature and relative humidity. In the present study, winter-time NO_3^- is higher than summer-time levels (Table 2). [14] have also reported lower summer time concentration of NO_3^- (as compared to winter) since particulate NH_4NO_3 will be volatile at high temperatures and low relative humidity in summer. This implies that formation of inorganic secondary particulate in winter will be higher. SO_4^{2-} concentrations will be higher in summer due to increased rate of photochemical activity and high OH· concentration [14]. In the present study also levels of SO_4^{2-} are higher in summer (Table 2). [6] could not resolve the contribution of secondary particles as that will require measurements of water soluble ions like NH_4^+, NO_3^- and SO_4^{2-} in atmospheric particles. In the present study, focus is to understand the formation of secondary particles and their quantitative contribution to ambient levels of PM_{10}. NH_4^+ ion is correlated strongly with both SO_4^{2-} and NO_3^- in all seasons and through FA-MR analysis, group of these ions is identified as one of the main components (of PM_{10}) in all seasons. [15] emphasized the vital role of NH_3 in neutralizing acidic substances (such as H_2SO_4, HNO_3), mostly as a sole neutralizer of acidic species, leading to formation of secondary particles. It is also reported that available NH_3 will be first taken up by H_2SO_4 and then the remaining NH_3 will be available to react with HNO_3 to produce NH_4NO_3.

Although NH_3 was not measured in the present study, the concentration of NH_3 observed at Indian Institute of Technology Kanpur by [16] as 19.09±5.70 μg m^{-3} during winter and 18.69±6.0 μg m^{-3} during summer can be taken. The correlation between NH_4^+ and SO_4^{2-} and NH_4^+ and NO_3^- was in the range 0.56-0.79 in winter (day and night) 0.75-0.88 (summer night); no correlation was found in summer day time. This study once again signifies the formation of secondary particles and vital role played by NH_3. It may, therefore, be concluded that NH_3 is playing a significant role in formation of secondary particles that has been seen through air quality sampling, source apportionment studies and also through the atmospheric chemistry. Findings are similar to those observed by [17].

CONCLUSIONS

To apportion the sources of PM_{10} at a residential area in Kanpur City, source apportionment technique, FA–MR was applied. Two important PM_{10} sources are soil & road dust (26-36%) and inorganic secondary particles like $(NH_4)_2SO_4$ and NH_4NO_3 (4-11%). Ambient NH_3 has been found dominating primary pollutant responsible for secondary particle formation and its role is very important in overall atmospheric chemistry of particulate formation.

REFERENCES:

[1] Abbi Y.P. (2001), Thermal power generation: Key issues in India. *TERI Newswire*, **7**, 1-15.
[2] Sharma M., McBean E.A., Ghosh U. (1995), Prediction of atmospheric sulfate deposition at sensitive receptors in Northern India, *Atmospheric Environment*, **29**, 2157-2162.
[3] Shukla, S.P. and Sharma, M. (2008). Source apportionment of atmospheric PM_{10} in Kanpur, India. *Environmental Engineering Science*, 25 (6), 849-861.
[4] Shukla, S.P. and Sharma, M. (2010a). Neutralization of rainwater acidity at Kanpur, India. *Tellus*, 62B, 172-180.
[5] Shukla, S.P. and Sharma, M. (2010b). Seasonal variation of PM_{10} in an Industrial Area. *Indian Journal of Environmental Protection*, 30(7), 581-586.
[6] Kumar A.V., Patil R.S., Nambi K.S.V. (2001), Source apportionment of suspended particulate matter at two traffic junctions in Mumbai, India, *Atmospheric Environment*, **35**, 4245-4251.
[7] Shukla S.P. (2007), *Investigations into neutralization of atmospheric acidity through characterization of rainwater and particulate matter*, Ph.D. Thesis, Department of Civil Engineering, Indian Institute of Technology, Kanpur.
[8] USEPA (1999), Compendium of Methods for the Determination of Inorganic Compounds in Ambient Air, Office of Research and Development, EPA/625/R-96/010a, U.S. Environmental Protection Agency, Washington, DC 20460, 1-18.
[9] Lodge J.P. (1989), *Methods of Air Sampling and Analysis*, Lewis publishers, USA.
[10] Henry R.C., Lewis C.W., Hopke P.K., Williamson H.J. (1984), Review of receptor model fundamentals, *Atmospheric Environment*, **8**, 1507-1515.
[11] Thurston G.D., Spengler J.D. (1985), A quantitative assessment of source contributions to inhalable particulate matter pollution in metropolitan Boston, *Atmospheric Environment*, **19**, 9-25.
[12] Shukla, S.P., Sharma, M. and Singh, N.B. (2010). Air quality survey of Kanpur City. *Indian Surveyor*, 64(1), 74-80.
[13] Liu C.W., Lin K.H., Kuo Y.M. (2003), Application of factor analysis in the assessment of groundwater quality in a blackfoot disease area in Taiwan, *Science of Total Environment*, **313**, 77–89.
[14] Utsunomiya A., Shinzi W. (1996), Temperature and humidity dependence on aerosol composition in northern Kyushu, Japan, *Atmospheric Environment*, **30**, 2379-2386.
[15] Seinfeld J.H., Pandis S.N. (1998), *Atmospheric chemistry and physics, from air pollution to climate change*, John Wiley, New York.
[16] Kishore, S. (2005), *Investigation into seasonal and diurnal formation of atmospheric nitrate*, M. Tech. Thesis, Department of Civil Engineering, Indian Institute of Technology, Kanpur.
[17] Shukla, S.P. (2010). Characterization of atmospheric PM_{10} of a Commercial Area in Kanpur City. *Journal of Environmental Research and Development*, 4(3), 770-779

International Journal of Engineering Research and General Science Volume 3, Issue 5, September-October, 2015
ISSN 2091-2730

Mind Mapping Vs traditional: A comparison of two instructional methods to teach Theories of Growth and Development of children among B.Sc(N) III year students

T. Mary Minolin
Assistant Professor, Saveetha College Of Nursing, Saveetha University, Chennai.

Abstract: Mind maps comprise a network of connected and related concepts. However, in mind mapping, any idea can be connected to any other. Free-form, spontaneous thinking is required when creating a mind map,and the aim of mind mapping is to find creative associations between ideas. Pictures and structured diagrams are thought to be more comprehensible than just words, and a clearer way to illustrate understanding of complex topics. **Objective**: To determine the effectiveness among two instructional methods namely Mind Mapping and traditional method. **Statistical Methods used:** Quasi experimental Post tests only Design was used. **Result:** The purpose of this study was to compare the effectiveness of Mind mapping and traditional method of instruction on the knowledge on Theories of Growth and development of children. . The results indicated that knowledge on growth and development of children in Group I is effective than the traditional group of students in Group II.

Key Words: Mind mapping v/s Traditional method, Theories of Growth & Development of children,

Introduction

- Mind maps comprise a network of connected and related concepts. However, in mind mapping, any idea can be connected to any other. Free-form, spontaneous thinking is required when creating a mind map, and the aim of mind mapping is to find creative associations between ideas. Thus mind maps are principally association maps. Formal mind mapping techniques arguably began with (Buzan1974)Mind mapping allows students to imagine and explore associations between concepts. The over-riding aim of all mapping techniques is similar. If students can represent or manipulate a complex set of relationships in a diagram, they are more likely to understand those relationships, remember them, and be able to analyze their component parts. This, in turn, promotes ‘‘deep’’ and not ‘‘surface’’ approaches to learning (Biggs1987)
- In recent years, academics and educators have begun to use software maps for a number of education-related purposes. Typically, the tools are used to help impart critical and analytical skills to students, to enable students to see relationships between concepts, and also as a method of assessment. The common feature of all these tools is the use of diagrammatic relationships of various kinds in preference to written or verbal descriptions. Pictures and structured diagrams are thought to be more comprehensible than just words, and a clearer way to illustrate understanding of complex topics.

Need for the study:

- Mind Maps have proved to be a simple but vital aid to learning, and have had amazing success in classrooms all over the world. Pupils and students of all ages, helping them understand course material, boost memory and recall, generate ideas, assist as a revision aid and help structure coursework .There has been significant research into the benefits Mind Mapping can bring to the education system, and why they offer such an essential tool for teaching and learning.
- Mind mapping (or ‘‘idea’’ mapping) has been defined as ‘visual, non-linear
- Representations of ideas and their relationships’ (Biktimirov and Milson(2006)
- In the former hypothesis, representations are encoded as separate intact units; in the latter, visual representations are synchronously organized and processed simultaneously and verbal representations are hierarchically organized and serially processed (Vekiri2002). In simple terms, processing information verbally as well as pictorially helps learning by virtue of using more than one modality.
- **Boyson** (2009)the use of Mind Maps in teaching and learning was examined in three different ways:
- Using Mind Maps as a note making tool in developing the teacher’s own subject knowledge.
- Using Mind Maps to present information to students in lessons.
- Introducing Mind Mapping as a note making format for students.

- From the perspective of the teacher, using Mind Mapping for planning brought about increased understanding of module objective, helped in identifying a logical teaching route and increased recall of the subject matter. The results of the student survey revealed.
- More than 80% of students agreed that Mind Mapping might help them to remember information.72% of students agreed that Mind Mapping helped them to know how each topic fits into a subject. More than 68% said they would use Mind Mapping for revision. More than 75% of respondents said they would like to use Mind Maps in other subjects.
- Research into children from the age of 9-12 years examined the difference in the children's recall of a set of words when the Mind Map technique was used in comparison to a list technique Preliminary results revealed that the children's
- Memory of words increases in both groups but this increase is significantly higher in the Mind Map group with improvements in memory of up to 32%providing evidence supporting the notion that using Mind Maps improves recall of words more effectively than using lists.

Objective

To determine the effectiveness among two instructional methods namely Mind Mapping and traditional method

Hypothesis

There is a difference between Mind mapping and traditional method of instruction on the knowledge on Theories of Growth and development of children

Assumption

Traditional method is widely used teaching method in Schools and Colleges

Research Design

Quantitative approach – Quasi experimental Post test only Design

Samples	Manipulation	Post test
Group I (R)	X1	O1
Group II (R)	X2	O2

Group I –Mind mapping
Group II – Traditional
X1 – Lecture by using black board &OHP on Theories of Growth and Development of children
X2 – Lecture by using black board &Mind mapping chart on Theories of Growth and Development of children
O1 – Post test
O2 – post test

Setting

The study was conducted in Saveetha College of Nursing, Saveetha University.

Population

All B.Sc (Nursing) II year students

Sample

B.Sc(Nursing) II Year students of Saveetha College of Nursing, Saveetha University

Sample Size

The sample size consists of 15 in each group

Sampling Technique

Random sampling technique by lottery method

Criteria for Selection of sample

Inclusion Criteria

B.Sc(N) III year students who are studying in Saveetha College of Nursing

Students who are willing to participate in the study

Exclusion Criteria

Students who were absent on the day of data collection

Data Collection Procedure

Group I

Lesson plan was prepared on Theories of Growth and Development of children and the lesson was taken by lecture method using black board and Mind mapping for 45 minutes. Students clarified their doubts.

Group II

Lesson plan was prepared on Theories of Growth and Development of children and the lesson was taken by lecture method using black board and OHP for 45 minutes. Students clarified their doubts.

Post Test

Knowledge was assessed using Structured Multiple Choice Questionnaire for both the groups on the same day and time by 2 different faculties for 10 minutes.

Statistical Methods used

Descriptive Statistics

Mean and Standard Deviation.

Inferential Statistics

Student 't' test to compare the knowledge on Theories of growth and Development of children.

Results:

Group		**N**	**Mean**	**SD**	**Standard Error Mean**	**Standard Error difference**	**Independent t test (2- tailed)**
Knowledge	**Web based**	15	8.4	1.183	0.306	0.644	3.104 P<0.01 S
	Traditional	15	6.4	2.197	0.567		

This table shows the effectiveness and compares the traditional and Mind mapping approached in teaching of Theories of Growth and Development of children. Knowledge on Theories of Growth and Development of children among students in Mind mapping group is effective in the mean score of 8.4 with 1.183 standard deviation and the standard error mean was 0.306 than that of students in the traditional group. Student t test also revealed that there is a significant difference between the traditional and Mind mapping teaching at the level of P<0.01.

Discussion

The purpose of this study was to compare the effectiveness of Mind mapping and traditional method of instruction on the knowledge on Theories of Growth and development of children. Lesson plan was prepared on Theories of Growth and Development of children and the lesson was taken by lecture method using black board and Mind mapping for Group I. Lesson plan was prepared on Theories of Growth and Development of children and the lesson was taken by lecture method using black board and OHP for Group II. The main difference between the two instructional methods was that students in the Mind Mapping group were more effective than the students in the traditional group who received the same information with traditional instruction. The results indicated that knowledge on growth and development of children in Group I is effective than the traditional group of students in Group II. Student's participation in Mind Mapping helped them to acquire meaningful learning in knowledge. This helped them to understand and whole-brain thinking of students.

Conclusion

I concluded that 'Mind Maps provide an effective study technique when applied to students' and are likely to 'encourage a deeper level of processing' for better memory formation. The increased use of Mind Maps within nursing curricula should therefore be welcomed. On a cautionary note, it is recommended that consideration is given towards ways of improving motivation amongst users before Mind Maps are generally adopted as a study technique. The author suggest that effective training is provided so that students are enthusiastic about adopting this approach in preference to other traditional study techniques.

REFERENCES:

1. Textbook of Pediatric Nursing, ed. 4, by Dorothy R. Marlow, R.N., Ed.D. Philadelphia/London/Toronto: W.B. Saunders Co., 1973, 776 pp.
2. "Mind Map noun - definition in the British English Dictionary & Thesaurus - Cambridge Dictionaries Online". Dictionary.cambridge.org. Retrieved 2013-07-10.
3. "Who invented mind mapping". Mind-mapping.org. Retrieved 2013-07-10.
4. "Roots of visual mapping - The mind-mapping.org Blog". Mind-mapping.org. 2004-05-23. Retrieved 2013-07-10.
5. Buzan, Tony 1974. Use your head. London: BBC Books.
6. Buzan claims mind mapping his invention in interview. *Knowledge Board* retrieved Jan. 2010.
7. 'Mind maps as active learning tools', by Willis, CL. Journal of computing sciences in colleges. ISSN: 1937-4771. 2006. Volume: 21 Issue: 4
8. 'Introduction to the applications of mind mapping in medicine', by José M Guerrero, Pilar Ramos. ISBN 978-1502580245
9. Beel, Jöran; Gipp, Bela; Stiller, Jan-Olaf (2009). "Proceedings of the 5th International Conference on Collaborative Computing: Networking, Applications and Worksharing (CollaborateCom'09)". Washington: IEEE. -->|chapter= ignored (help)
10. {G}lennis {E}dge {C}unningham (2005). *Mindmapping: Its Effects on Student Achievement in High School Biology* (Ph.D.). The University of Texas at Austin.
11. {B}rian {H}olland, {L}ynda {H}olland, {J}enny {D}avies (2004). "An investigation into the concept of mind mapping and the use of mind mapping software to support and improve student academic performance".
12. D'Antoni, A.V., Zipp, G.P. (2006). "Applications of the Mind Map Learning Technique in Chiropractic Education: A Pilot Study and Literature".
13. Farrand, P.; Hussain, F.; Hennessy, E. (2002). "The efficacy of the mind map study technique". *Medical Education***36** (5): 426–431. doi:10.1046/j.1365-2923.2002.01205.x. PMID 12028392. Retrieved 2009-02-16.
14. {N}esbit, {J}.{C}., {A}desope, {O}.{O}. (2006). "Learning with concept and knowledge maps: A meta-analysis". *Review of Educational Research* (Sage Publications) **76** (3): 413. doi:10.3102/00346543076003413.
15. {J}oeran {B}eel, {S}tefan {L}anger (2011). "An Exploratory Analysis of Mind Maps". *Proceedings of the 11th ACM Symposium on Document Engineering (DocEng'11)*(PDF). ACM. Retrieved 1 November 2013.
16. {C}laudine {B}rucks, {C}hristoph {S}chommer (2008). "Assembling Actor-based Mind-Maps from Text Stream". *CoRR*. abs/0810.4616.
17. Rothenberger, T, Oez, S, Tahirovic, E, Schommer, Christoph (2008). "Figuring out Actors in Text Streams: Using Collocations to establish Incremental Mind-maps". *arXiv preprint arXiv:0803.2856*.
18. {R}obert {P}lotkin (1009). "Software tool for creating outlines and mind maps that generates subtopics automatically". *USPTO Application: 20090119584*.
19. {M}ahler, {T}., {W}eber, {M}. (2009). "Dimian-Direct Manipulation and Interaction in Pen Based Mind Mapping". *Proceedings of the 17th World Congress on Ergonomics, IEA 2009*.
20. {S}hih, {P}.{C}., {N}guyen, {D}.{H}., {H}irano, {S}.{H}. and {R}edmiles, {D}.{F}., {H}ayes, {G}.{R}. (2009). "Groupmind: supporting idea generation through a collaborative mind-mapping tool". pp. 139–148.
21. Santos, Devin (15 February 2013). "Top 10 Totally Free Mind Mapping Software Tools". IMDevin. Retrieved 10 July 2013.
22. Farrand, Paul; Hussain, Fearzana and Hennessy, Enid (May 2002). "The efficacy of the 'mind map' study technique". *Medical Education***36** (5): 426–431. doi:10.1046/j.1365-2923.2002.01205.x. PMID 12028392

International Journal of Engineering Research and General Science Volume 3, Issue 5, September-October, 2015
ISSN 2091-2730

Role of Bio-Tribolgy in Medical Insertion

SYED HASAN MEHDI[1], Dr. ZAHIR HASAN[2]
1. Franchise Partner of
IACT Global Education Pvt. Ltd. Noida.
At Lucknow Territory, INDIA
Email: syed_005.m@rediffmail.com , +91-9651217514

2. Department of Mechanical Engg.,
Faculty of Engineering,
Jazan University, Jazan, KSA.
Email: zahir.hasan09@gmail.com

Abstract: Tribology is the study of rubbing, friction and wear. When it applied to biological entities then Bio-Tribology came into consideration. The principle of Tribological study and understanding is not just constrained for solving Mechanical Engineering problems. In fact, effective solutions of friction, wear and lubrication related problems can be entertain by Bio-Tribology in human daily life. Bio-Tribology has a critical role in medical processes like medical insertion. This paper describes the role of Bio-Tribology in medical insertion especially in urinary catheterization, which is an essential process in medical field. Catheterization causes rubbing action which causes friction as patient discomfort. Lubrication plays an important and vital role in the operation of any machine/ device. Therefore the role of lubrication for human body can be explained under the environment of Bio-Tribology.

Keywords: Bio-Tribolgy, Medical Insertion, Catheter, Lubrication, Lubricating Layer, Human Comfort.

Introduction:

Word Tribology came from Greek word "Tribos" means Rubbing. Tribology is the study about wear, friction and lubrication [1]. Bio-Tribology is the science of Tribology applied to biological entities. In human being Tribology considered with interacting surfaces. Bone joints are the major area of Bio-Tribology, which is an articulating bearing with one end of a bone rubbing against another [2].

Table. 1 Classifications of representative Bio-Tribology research and associated research focuses [2].

Classification Type	Major Investigations
Joint Tribology	Hip Joint, Knee Joint, Articular Cartilage, Joint Fluid, Implant Interfaces, etc.
Skin Tribology	Skin Care, Synthetic Skin, Skin in contact with articles (such as tactile texture, shaving devices, shoes, socks) for daily use, Various Medical as well as Sport Devices, Medical and Cosmetic Treatment, Skin Friction and Grip of Objects, Skin Irritation and Discomfort, etc.
Oral Tribology	Natural Teeth, Tongue, Saliva, Implant Teeth, Toothpaste, Swallow, etc.
Tribology of the Other Human Bodies or Tissues	Hairs, Bone, Cells, Contact Lenses, Capillary Blood Flow, etc
Medical devices	Scalpel, Operation Forceps, **Urinary Catheters**, Gastroscope, Artificial Cardiovascular System, Medical Gloves, etc.

Others instances of Bio-Tribology are:

- Wear of dentures
- Friction of skin and garments affecting comfort
- Tribology of contact lens with eye tissue
- Blinking of an eye
- Fetus moving in a womb

In medical field there are various processes by which medical professionals insert a device (tube, valve, cardiac or urinary catheter etc.) to human body. Catheters are generally used by medical professionals by inserting a tube into body cavity, to allow drainage [3]. Friction is the definite outcome by medical insertion and causes patients discomfort. Lubrication is most important agent/ tool for minimizing rubbing action and reducing patient discomfort.

A urinary catheter is a thin, clean hollow tube which is usually made of soft plastic or rubber. Urinary catheterisation is the insertion of a catheter (tube) into the bladder via urethra. Urinary catheterization used for urinary retention (urinary failure, inability to urinate). It reduces the risk of infection and kidney damage by ensuring the bladder is emptied adequately, continuously or at regular intervals.

Friction and Lubrication:

Friction is the force that acts at the surface of two articulating solid bodies so as to resist sliding on one other. Simply it is the resistance to motion of surfaces in relative motion, this force which tends to prevent one surface sliding over another [4]. Lubrication may be defined as any means capable of controlling friction and wear of interacting surfaces in relative motion under load [5]. Lubrication has been applied to solve friction problems far longer [4].

There are various lubrication mechanisms, which have developed to control friction. Some time friction is helpful and necessary. But in some areas it causes trouble and uncomfortable, especially in medical insertion. Without proper lubrication some of the medical insertion cannot be possible. Appropriate lubrication is recommended in medical insertion for reducing the risk of trauma, minimizes discomfort and friction which in turn may reduce infection.

Role of Bio-Tribology in Medical Insertion:

Medical device industry has influenced by Bio-Tribology due to its importance and challenges. Bio-Tribology focuses on friction, wear and lubrication in biological system. Lubrication is the reduction in friction through a third body that separates two solid surfaces in relative motion. In biological system interactions between medical devices and soft surfaces of living being are still a challenging area. Lubricity has a critical role in the functionality and safety of these devices [6].

The essential roles of Tribology are controlling friction, reducing wear and improving lubrication. Similarly Bio-Tribology focuses on minimizing friction and better lubrication for living being. Obviously, in this regard, Bio-Tribology is much better able to fulfil the demands of human comfort. Human comfort is the most important parameter of any society.

The major area of Bio-Tribology is related to lubrication. Therefore, Bio-Tribology may be thought, as the study of biological lubrication processes, for example, lubrication in urinary catheterization. Urethra is the most sensitive area of human body. It is very difficult to insert a rubber tube into the body through urethra, it causes discomfort, burning sensation and pain. Catheterization is not easy for patients especially in male. Fiction during insertion and removal of the catheter must be controlled by proper lubrication to avoid tissue damage and enable the device to be inserted smoothly into the proper location. Catheters are widely used by medical professionals to allow drainage, administration of fluids or gases. For reducing patients discomfort lubricants are placed between tube and the internal walls of urethra.

Before catheterization medical professional provides lubrication for entire length of urethra. Urethra has a tubular shape and a layer of lubrication should be build up around the walls of urethra. Catheter moves to bladder with guiding of lubricating layer. But in general cases this lubricating layer dropped by catheter insertion and tube come up to direct contact with urethra walls. When catheter touches urethra walls then friction arises and it causes more discomfort to patients. If there can be a proper technique to build-up a lubricating layer and it does not destroyed by catheter insertion then there will be less friction between urethra walls and catheter.

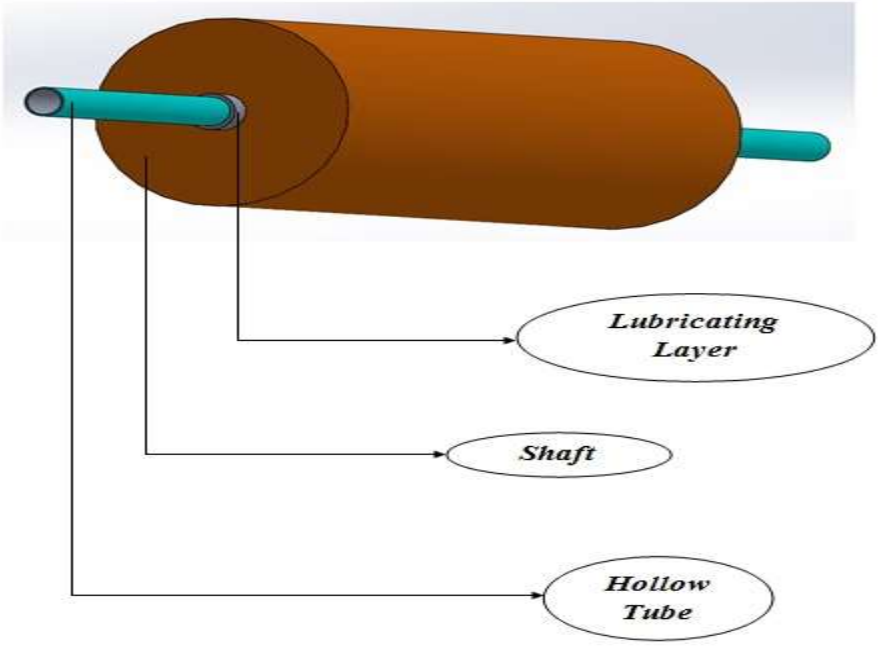

Figure 1

Figure 1 is the representation of urethra and catheter insertion simulation design, with the help of SolidWorks designing software in enlarges view, in which urethra as a shaft and a hollow tube as catheter. As shown in figure a lubricating layer between inner walls of the shaft and hollow tube reduces friction and prevents direct contact of tube with shaft. If lubricating layer does not destroyed until catheter reaches to bladder then high level of comfort can be achieved.

Thus the role of Bio-Tribology in medical insertion is important and it is beneficiary for living creatures or in simple language of engineering, Bio-Tribology is the integration of human comfort level.

Conclusion:

Bio-Tribology is the study of rubbing in which friction and wear are in critical role. Rubbing always causes friction. In medical insertion especially in urinary catheterization friction is directly proportional to discomfort (more friction more discomfort). This discomfort can be overcome by the Lubrication. Lubrication plays an important and vital role in urinary catheterization. Without proper lubrication urinary catheterization will be more difficult for health care professionals and discomfort for patients.

Discussion was made about the selection of different types of lubricants for human ease but still there is a scope for the selection of healthier technique which can be more comfortable and favourable for living being. If health care professionals concentrate on Bio-Tribology, then they can reduce friction during rubbing action of medical insertion especially in urinary catheterization. Friction during rubbing action depends on the sliding surface. In urinary catheterization there is a lubricating layer between tube and urethra wall, but in general cases it has destroyed and dropped by the tube movement. If tube does not touch the urethra walls and slide with lubricating layer then role of lubrication will be fulfil in catheterization.

Due to very small diameter of urethra it is not easy to catheter movement without patient discomfort. It is not possible to fully disappearance of patients discomfort but it can be minimized by a temporary lubricating layer.

Bio-Tribology will continue to make possible progress in the quality of life, which will be great challenge and understanding for Bio-Tribologist.

REFERENCES:

[1]. Ramanpreet Singh, M Sreedhar, Bio-Tribology and its Applications In Medical Sciences - A Review, International Journal of Mechanical Engineering and Robotics Research, Vol.-3 No.3, July 2014,

[2]. Z.R. Zhou, Z.M. Jin, Biotribology: Recent progresses and future perspectives, ScienceDirect Biosurface and BioTribology 1 (2015) pp. 3-24

[3]. Zhongmin JIN, Duncan DOWSON, Bio-friction, Fiction; Vol-1 Number2, TSINGHUA University Press, Springer 2013, pp. 107

[4]. Peter J. Blau, Friction Science and Technology: From Concept to Applications, ii Edition, Society of Tribologist and Lubrication Engineers, CRC Press. pp 1-9.

[5]. Stephen M. Hsu, Richard S. Gates, Boundary Lubrication and Boundary Lubricating Films 2001 (http://www.ewp.rpi.edu/hartford/~ernesto/S2015/FWLM/OtherSuppMtls/Hsu-Gates2001-BoundaryLubrications.pdf)

[6]. Gang Pu, Ryan Farel, June Li, Dehua Yang — Ebatco, Eden Prairie, MN, Lubricity and Durability Evaluation of Medical Device Surfaces sur fact in biomaterials vol-20, issue 1 winter pp. 7, 2015.

International Journal of Engineering Research and General Science Volume 3, Issue 5, September-October, 2015
ISSN 2091-2730

Controlled Switching of High Voltage SF6 Circuit breaker

Rade Prashant Vasant, Prof. Harpreet Singh

M. Tech (Power System) I.E.T. Alwar, prashant.rade@yahoo.com

Abstract— In controlled switching technology, an effective way to reduce transients produced by switching action, equipment failure preventions, and to inhance power quality, that is, already defined controlled strategies are to close and/or open each independent circuit breaker pole. Controlled switching of high voltage AC gas circuit breaker (GCB) and explains the controlled switching methods that are existing now a days is presented in this paper. Also the paper discusses the merits of controlled switching technology with an application. The accurate prediction of the operating time, subject to the various affecting parameters at that instant. Consistency of CB open and closing time is decides the success of CSS and reliability of CSW device to operate in high voltage environment system. The work presented in the paper focuses on suitability check of the circuit breaker for controlled switching application from mechanical scatter point of view and finds the mechanical scatter window. The allowed circuit breaker scatter for various controlled switching application is discussed in the paper.

Keywords— Gas Circuit Breaker, transients, mechanical scatter, suitability for controlled switching

INTRODUCTION

Energy is one of the major inputs for the economic development of any country. In the case of the developing countries, the energy sector assumes a critical importance in view of the ever increasing energy needs. This is the reason electrical power system network is expanding day by day to serve the increasing energy demand of the nation. Electrical power system comprises of generation, transmission and distribution of electrical energy. Power system should meet following fundamental requirements, System must be able to meet the continually changing load demand of active and reactive power Quality of power supply should meet certain standards in terms of constant frequency, constant voltage and reliability.Generator, power transformer, circuit breaker, surge arrestors, current transformers and voltage transformers are the vital power system equipments. A circuit breaker is protective switching device and hence, it plays a very important role in the power system at the time of abnormal conditions. Circuit breaker is required for the normal switching operation as well. In the EHV and UHV transmission system SF6 gas circuit breakers are used. To maintain the adequate reactive power for voltage control, frequent switching of capacitors and reactors is required through circuit breaker. These are the two applications where transient conditions can occur frequently, which results into electrical and mechanical stresses and sometimes may lead to equipment failure. High current transients associated with uncontrolled energization of capacitors can cause voltage sags, swells on the primary system, which may create problems with power system equipment and customer processes.

Any electrical circuit has got resistance, inductance and capacitance parameters. Under steady state condition the energy stored in inductances and capacitances is being transferred cyclically between the L and C of the circuit. When there is sudden change in circuit conditions *i.e.* switching, redistribution of the energy takes place to meet new condition. This period of redistribution of energy is nothing but the transient. Transients are associated with the excessive currents or voltages. Though the transient period is very short, the circuit components get overstressed during this period and it can lead to an equipment failure, protection mal operation, plant shut down *etc.* Following are the alternatives for mitigation of electrical transients [4].

Modification of the primary system to reduce the transients eliminating the transients requires that the source of switching transients be addressed. Conventional solutions include. Closing resistors on EHV circuit breakers to control the voltage transient associated with energizing (particularly re–closing) long lines. Circuit breaker pre-insertion resistors for reactor and capacitor switching. Circuit breaker opening resistors for shunt reactor switching. Selecting a specific type of circuit breaker. Surge arresters for limiting the voltage transients.

In principle, all primary side solutions incur significant costs and may reduce the overall primary system reliability. The design and mounting arrangements of these systems is very complicated. With the use of pre insertion resistors and reactors, initial transients and bypass transients has to be faced by the power system. Strengthen the primary system to withstand the transients withstanding the imposed stresses requires that system components susceptible to damage or mal operation be configured for greater strength. The

conventional approach is to design the system components, such as capacitor banks, transformers, and circuit breakers, to withstand the voltage and current transients associated with frequent occurrence of worst case switching phenomena.This is a new method which is becoming popular day by day for the switching transient mitigation. Controlled switching is nothing but switching the load at the optimum point on voltage or current wave so that the transients will be minimum possible. This method Controlled switching has become an economical substitute for a closing resistor and is commonly used to reduce switching surges. The number of installations using controlled switching has increased rapidly due to satisfactory service performance since the late 1990s. Currently, it is often specified for shunt capacitor and shunt reactor banks because it can provide several economic benefits such as elimination of closing resistors and extension of a maintenance interval for nozzle and contact. It also provides various technical benefits such as improved power quality and suppression of transients in transmission and distribution systems. The aim of point on wave switching is to minimize switching transients, over voltages and current surges, thereby reducing the stress on equipment insulation. Controlled switching is the economical method as compared to other conventional methods discussed above. The installation part of controlled switching system is not so complicated as compared to pre-insertion resistors, pre insertion reactors, surge arrestors *etc.* Controlled switching system comprises of circuit breaker, controller and other auxiliary components like sensors, cables *etc.* The circuit breaker is one of the vital equipment responsible for the success of controlled switching success. The circuit breaker behaviour in all respect should be known thoroughly, and then only one can feed the information in the controller.

LITERATURE REVIEW

A paper on "Controlled Switching of HVAC Circuit Breakers: Application Examples and Benefits" by Dan Goldsworthy and Tom Roseburg have detected and investigated Controlled switching technology that is predefined controlled strategies for closing and/or opening each independent circuit breaker pole, is an effective way to reduce switching transients, prevent equipment failures, and improve power quality. The paper presents a tutorial on controlled switching of high voltage ac (HVAC) circuit breakers and describes the controlled switching theory and technology that is in use today. The paper discusses the benefits of controlled switching and shares one utility's applications and experiences with the controlled switching of shunt capacitors, shunt reactors, transformers using modern protective relays and control devices. The paper also discusses how to select the optimum controlled switching times to reduce switching transients**.** [1].

A paper on "Identification of Capacitor Switching Transients With Consideration of Uncertain System and Component Parameters" by H. Y. Zhu and Chen, this paper described and improved methods for identifying the capacitor switching transient. Capacitor switching transient is one of the most commonly countered power quality distributions. Measuring and identifying these transient remains challenge as the characteristics depend on the system parameter. systematic approach to design and automated system for identifying capacitor switching transients also capable of identifying transients caused by switching of both isolated and back to back capacitors. The proposed method combines the techniques of wavelet transform, rank correlation and fuzzy logic to account for the uncertainties [2].

John Brunke and Klaus Frohlich, suggested a "Method for Potentially Eliminate Inrush Current Transient By Effectively Transformer Controlled Switching". This paper explored the theoretical consideration of core flux transient Transformer inrush currents are high magnitude, harmonic rich currents generated when transformer cores are driven into saturation during energization. These currents have undesirable effects, including potential damage or loss of life to the transformer, protective relay misoperation, andreduced power quality on the system. Controlled transformer switching can potentially eliminate these transients if residual core and core flux transients are taken into account in the closing algorithm. Based on these studies algorithms were developed which allow controlled energization of most transformers without inrush current and concluded it is possible to use residual flux measurements and controlled closing to eliminate transformer inrush transient [3].

"Overall Benefits of Controlled Switching" by Victor F. Hermosillo, proposed a general overview of the benefits offered by the use controlled switching of switchgear HV and EHV electric power system was presented. The benefits of applying controlled switching are technical and economical. Technical benefits include the reduction of the severity of switching transients and their effect on equipment and system life cycle and performance. Economic benefit assessment may be qualitative or quantitative. Controlled switching offers an effective means of transient controlled and an attractive alternative to others traditional means of achieving this purposed. It may be applied as the sole solution or may be combined with other means, such as surge arrestors, to increase reliability [4].

Michel Stanek and his colleagues, studied Experience with "Improving power quality by controlled switching". The practical examples presented in this paper demonstrate the effectiveness of controlled switching as a means to reduce the effects switching

operation in various applications, for energization of capacitor banks, reactor and transformer. Switching operations in power networks are a common cause of transient disturbances. Depending on the network configuration and the characteristics of the switching condition, these transients can cause undesirable effects, not only on the switched load, but also on the entire network. As a consequence, the power supply can be drastically affected, as for example by nuisance protection operation due to high inrush currents, or under voltage due to transformer energization. Such disturbances can in turn provoke interruption of power supply to certain loads or parts of the network. Also, sensitive industrial processes can be severely impacted even if no power supply interruption occurs. Therefore, it is desirable to eliminate these potentially dangerous switching transients as far as possible [5].

Controlled switching technology is predefine methodology an effective way to reduce switching transients, prevent equipment failures, and improves power quality. Applications and benefits of CSW for capacitor, inductor and transformer switching investigated. But for this purpose, GCB is also plays an important role to successful operation of CSW device. Hence it is necessary to check the consistency of GCB for CSW application. Consistency is related with the mechanical scatter of circuit breaker. Consistency and mechanical scatter of CB operating time are the main problems to affect the successful operation of Cntrolled switching [5].

CONTROLLED SWITCHING METHODOLOGY

Controlled switching is a method for eliminating harmful transients by time instant controlled switching operation. Making and breaking commands to the circuit breaker are delayed in such a way that making or contact separation will occur at the optimum time instant related to the phase angle. By means of CSW it can be possible both energizing and de-energizing operations can be controlled with regard to the point on wave, and no harmful transients will be generated. This is a new method which is becoming popular day by day for the electrical transient minimisation. Controlled switching is nothing but switching the load at the optimum point on voltage or current wave so that the transients will be minimum possible.

PRINCIPLE OF CONTROLLED SWITCHING

Controlled switching is a technique that uses an intelligent electronic device, *i.e.* a modern numerical relay or a controller as shown in the figure 3.2, to control the timing of closing and opening of independent pole breakers with respect to the phase angle of an electrical reference voltage or current. The desired accuracy and repeatability of current conduction at a specific point on the waveform is ±1 msec. or less, and requires that the CB be constructed so that it provides this consistency under all operating and ambient conditions. Alternatively, the controller issuing the breaker close commands for the point on wave operations must be able to measure the operational variables such as CD control voltage, ambient temperature, and idle time, and remove the effect of these variations by compensating the breaker control Signal timing.

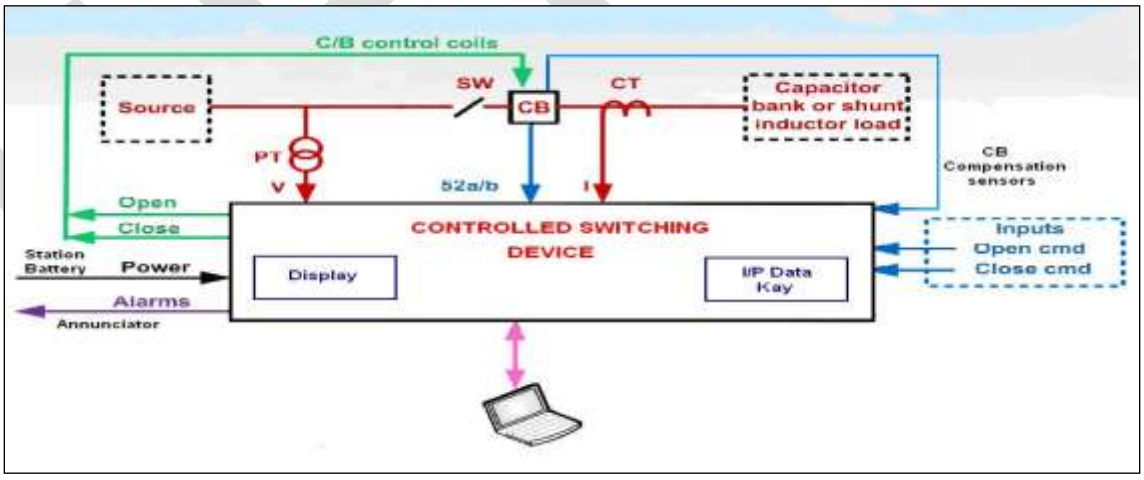

Fig. 1. Block diagram of controlled switching

CONTROLLED CLOSING

Controlled closing refers to controlling the point of conduction of each pole of the breaker with respect to the phase angle of the voltage. Breakers used in these applications must be constructed to provide the consistency to successfully repeat the controlled closing operations. The controller monitors the source voltage for a controlled closing operation. The closing command is issued

randomly with respect to the phase angle of the reference signal at some instant, as shown in Figure 3.3 [1]. The example sequence shown in Figure 3.3 relates to closing of capacitive load, where the optimum closing instant is at a voltage zero assuming that the prestrike time is less than one half cycle. The controller delays the randomly received closing command by some time, Total time, which is the sum of mechanical closing time (Tc) of the circuit breaker and an intentional synchronizing time delay (waiting time interval).

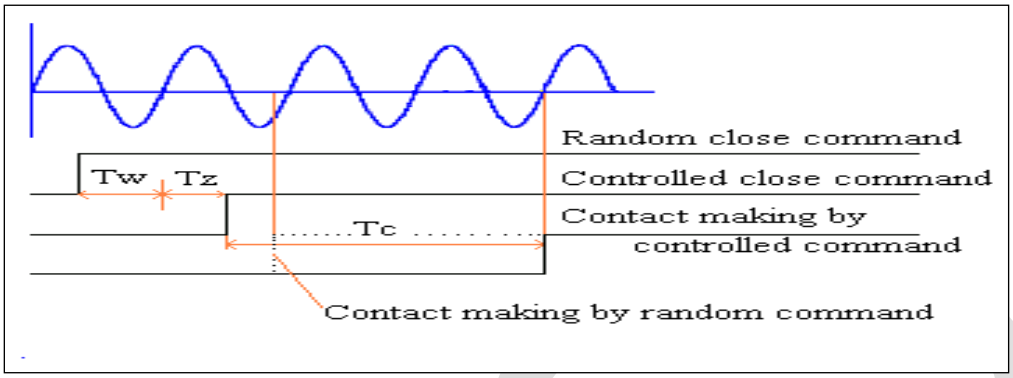

Fig 2. Controlled closing sequence

Total time = Tw + Tz +Tc

Where,

Tw = Total wait time

Tz = time with respect to relevant zero crossing

Tc = Total closing time of circuit breaker

The controller introduces delay with respect to a relevant zero crossing that is calculated by assuming circuit breaker closing time. The current starts to flow at time and the corresponding interval, is defined with respect to the following zero crossing. The closing time is the time from circuit breaker closing coil energisation to when the mechanical contacts touch.

The controller takes into account variations of circuit breaker operating times and prestrike characteristics as required by specific applications. Operating times and their dependency on environmental and operating conditions as well as the prestrike behavior are particular to every type of circuit breaker.

CONTROLLED OPENING

Controlled opening refers to controlling the contact separation of each circuit breaker pole with respect to the phase angle of the current. Controlling the point of contact separation determines the arcing time of the contacts to help prevent breaker and circuit switcher failures and to minimize stress and disturbances to the power system. The implementation of controlled opening is approximately the same regardless of the equipment being switched. The control is straightforward once timing data for a breaker is available, particularly the time from energizing the trip coil to contact separation. Although controlled opening is best done using the current through the breaker, the bus voltage can be used if the voltage current phase relationship is always known, such as for shunt reactor and shunt capacitor switching. The breaker is controlled so that its contacts will part just after a current zero. As the contacts continue to open they draw out an arc that will extinguish less than a half cycle later at the next current zero. When the arc does extinguish, the contacts have been separated as far apart as practical, which provides the maximum dielectric strength available for the circumstances. This gives the breaker its best chance of successfully withstanding the recovery voltage and not having a re-ignition or a re-strike. Re-ignition is a dielectric breakdown that reestablishes current within 90 electrical degrees of interruption. Re-strike is a dielectric breakdown after 90 degrees. Figure 3.4 shows the timing sequence for controlled opening [1]. The control command is issued randomly with respect to the phase angle of the reference signal at an instant. The randomly received opening command is delayed by the controller by some time, Total time, which is the sum of mechanical opening time of circuit breaker and an intentional

synchronizing time delay (waiting time), synchronizing time is calculated with respect to a relevant zero crossing which is a function of the opening time (Tz) and waiting time (Tw), The mechanical opening time, is the time interval from energization of the breaker trip coil to the start of breaker contact separation, shown in Fig

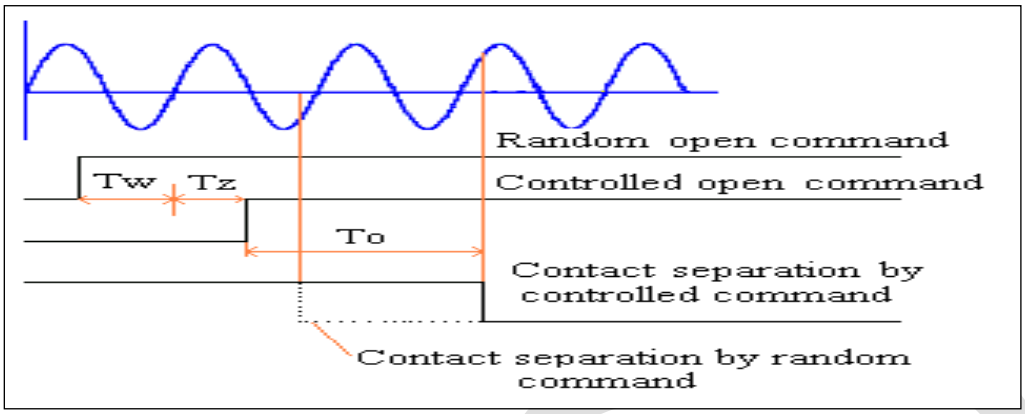

Fig.3. Controlled opening sequence

Ttotal = Tw + Tz + To

Where,

Tw = total wait time

Tz = Calculated time with respect to a relevant zero crossing which is a function of the opening time.

To = Mechanical opening time of contacts of circuit breaker

CONTROLLED SWITCHING UNIT

The purpose of the Circuit Breaker Synchronous Control (Controller unit) system is to provide controlled (synchronous) switching commands to the open and close coils of the circuit breaker. Successful controlled switching reduces the mechanical and electromagnetic stresses endured during normal switching operations by reducing the inrush currents upon closing and re-ignition currents during opening. A further benefit is that the insertion resistors, as commonly found in air blast breakers, can be done away with as well as their costly recurring maintenance requirements. Given the well documented effect of fluctuations in operating variables (temperature, pressure, auxiliary voltage *etc.*) on the operating time of the breaker, compensation is built into the calculation algorithm, ensuring optimum performance over a wide range. Due to differences in operating times between phases, Controller unit is designed to compute and send phase segregated switching commands to the breaker. Monitoring of inrush and re-ignition currents confirms successful synchronous switching of the breaker. The operating principles use the zero crossings of a sinusoidal signal; a voltage signal will be used as reference prior to closing and a current or voltage signal can be used prior to opening. When the breaker characteristics are identical for each phase, then a constant time delay (T/6) exists between synchronous commands in each phase, for example in the "A,C,B" sequence (1/3 of a cycle overall). For ungrounded capacitor bank switching, simultaneous switching of the two leading phases is followed by a quarter cycle delay in the switching of the third phase.

As soon as a close command is received, Controller unit is blocked and a time delay is initiated, awaiting the first zero crossing of voltage. Should no zero crossing be detected within the preset time delay, synchronous switching is aborted and a 3-phase random close is executed. Should a zero crossing occur within the preset delay and no further failures are detected, synchronous close commands to each phase are issued after the computed time delays. The computed time delays are measured from the reference zero crossing and compensated for variable effects and variations in the breaker characteristics of each phase. Sequencing of individual phase is monitored to insure proper sequencing at the breaker coils.

Sequencing of individual phase commands is monitored. Output control circuits are monitored for timing analysis, if a sequence error is detected, synchronous control is aborted and a 3-phase random control switching is executed. The functional design of the open operation is the same as that for close with the variation that a current or a voltage zero crossing can be used as the reference signal and that re-ignition currents are monitored

Technical Specifications of CB Controller unit

CB Controller unit is designed to meet the requirements of **SF6** based Circuit Breakers for EHV applications and has the followings technical and functional specifications.

- *Mechanical scatter*

It is a random statistical variation of the mechanical operating time of a circuit breaker excluding the influence of external variables and the effect of long term wear and/or drift. Circuit breaker main contacts and auxiliary contacts which are used for position feedback in a controlled switching system should be tested to prove their accuracy and repeatability. Auxiliary contact repeatability plays a very vital role in success of control switching system. When the breaker is connected to line the auxiliary contact should act as a replica of main contact to give circuit breaker operating time information to the controller. It has two type mechanical scatter closing and opening mechanical scatter It is a random statistical variation of the opening time of a circuit breaker excluding the influence of external variables and the effect of long term wear and/or drift. Closing mechanical scatter.

SYSTEM MODIFICATION

One of the challenges in controlled switching application lies in the accurate prediction of the operating time, subject to the various affecting parameters at that instant. The success of controlled switching system depends on the consistency of circuit breaker operating time and reliability of controller to operate in high voltage environment and other is to know, whether the circuit breaker is suitable for the required controlled making application or not. If the circuit breaker is not suitable for the same then, one can change the conditions like closing velocity, SF6 gas pressure, Mechanical play in the joints and check that whether it can become suitable or not. Then the change in condition can be implemented in the actual circuit breaker. For this purpose I developed a circuit breaker suitability check flow chart.

FLOW CHART FOR SUITABILITY CHECK OF GCB FOR CONTROLLED SWITCHING APPLICATION

A simple Flow chart is developed for suitability check of circuit breaker to controlled switching as shown in the figure 4.2. Find mechanical scatter and if it is more than 0.5 then it needs some modifications in the breaker to minimize the scatter

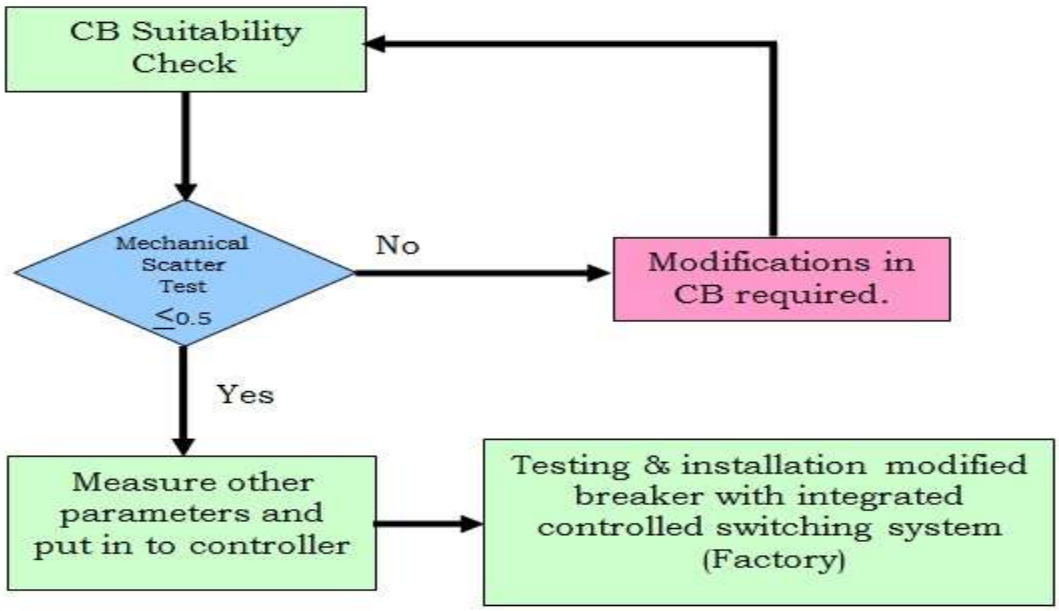

After modification again find mechanical scatter of CB operating time. When it is less than 0.5 then goes for next parameter measurement which is required and put all these parameters in to the controller setting with help of HMI.

- *EXPERIMENTAL ARRANGEMENT*

Testing arrangement for suitability check of breaker controlled switching *i.e.* speed time measurement of circuit breaker arrangement shown in the figure 4.3, for this arrangement needs circuit breaker, speed time measurement instrument, power supply, mechanism rotary transducer and spare wires for connection. Connect the required apparatus to the CB as shown in the figure 4.3. CB operating command is send to CB with help of speed time measuring instrument and display the results in the form of graphical representation as shown in the figure 4.4 and 4.5

- *SPEED TIME MEASUREMENT INSTRUMENT*

This instrument is digital software based instrument manufacture by Scope Electrical Instruments Ltd. It use to raise the closing and open command to circuit breaker and displays the closing and opening speed, Main and auxiliary contact opening and closing timing, Travel of mechanism movements.

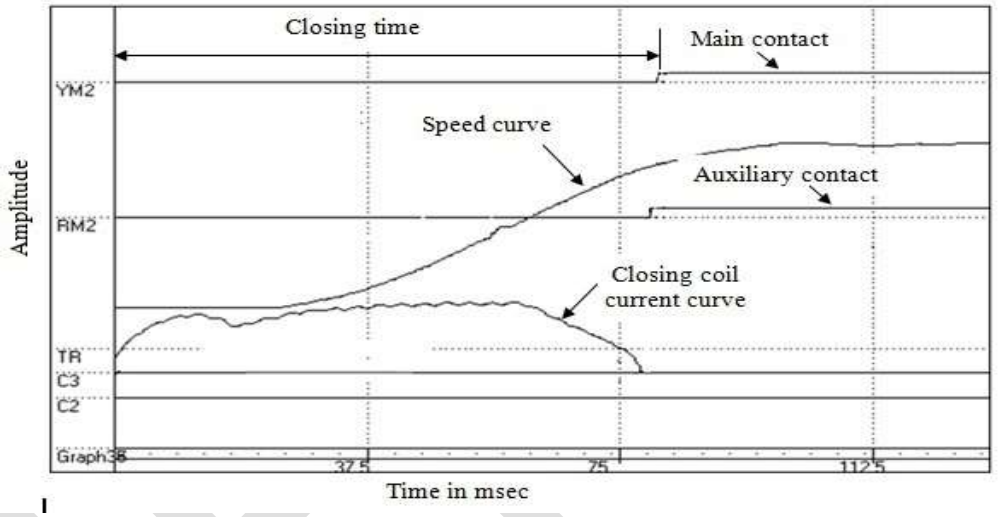

Graph.1. Speed time graph for closing

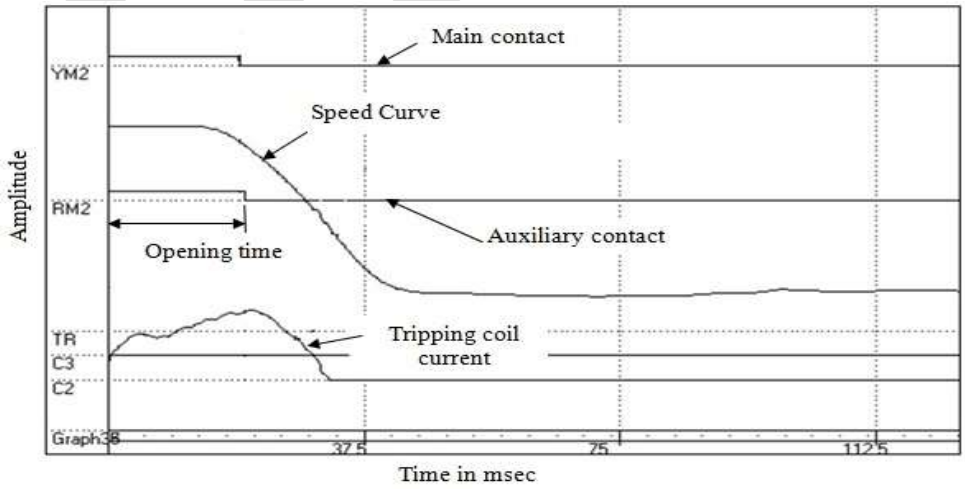

Graph 2. Speed time graph for opening

INITIAL MECHANICAL SCATTER MEASUREMENT

Initial 50 operations are carried out on circuit breaker (table 4.2) and calculate the mechanical scatter (table 4.3). It is found that mechanical scatter is 1.1 at closing time of circuit breaker as shown in the observations table 4.3.

From the table 4.3 it is cleared that the mechanical scatter is stay in the circuit breaker. The value of scatter should be kept as low as possible to avoid the high inrush current. From the performed some simulations on MATLAB software at 1msec. scatter (graph 4.4), inrush current increased 55.17%. To eliminate this it is necessary to make some modifications in the CB as per flow chart (figure 4.2).

Table 1. Scatter of initial operating time of CB

Max closing time	80	79.8
Min closing time	77.8	77.6
Max-Min	2.2	2.2
Scatter	1.1	1.1

Max opening time	22.4	22.4
Min opening time	22	22
Max-Min	0.4	0.4
Scatter	0.2	0.2

CB DEVELOPMENTS AND MODIFICATIONS

Scatter found 1.1 msec. in the initial closing operations and 0.2 msec. scatter in the opening operations from the table of breaker. Opening scatter within the limit hence it is not necessary to make modifications in the opening scatter side but regarding other side scatter is beyond the limit hence to make some modifications in the closing side with help of flowchart shown in the fig

Auxiliary switch is the replica of the main contact of the breaker as shown in the fig. Some mechanical play observed in the auxiliary switch during the operation of circuit breaker because of this scatter increases. Mechanical play observed in the adjusting rod which is connected between mechanism shaft and auxiliary rotating shaft as shown in fig. to avoid this mechanical play new ball and bearing arrangement as shown in fig and performed operations.

Closing speed of breaker is depends on closing spring by varying the load of spring and load of spring is increased by compressing spring as shown in the fig. Speed increases with increasing the load and load increase with compression of the spring hence closing speed is directly proportional to compression of spring. To increase speed such way that the optimum scatter produced for this purpose some operations are taken on breaker at different speed and note down closing time as shown in the table.

VERIFICATION OF GCB USING CONTROLLED SWITCHING UNIT

The aim of point on wave switching is to minimize switching transients, over voltages and current surges, thereby reducing the stress on equipment insulation. To achieve this, it requires a control device which receives a random command for circuit breaker operation, and synchronizes it with a reference waveform, such that the circuit breaker operates at a given point on wave (POW).

EXPERIMENTAL TEST SETUP

The experimental test setup to measure and verify whether the GCB is suitable controlled switching or not and also find error from the expected target on point on wave during closing and opening operation of circuit breaker with controlled switching unit. This test setup consists of voltage and current source for inject current and voltage in to circuit breaker and control voltage for breaker operation and controlled switching device and Sf6 gas circuit breaker.

RESULTS

CAPACITOR SWITCHING

Verification of CSW device and GCB is a no load test *i.e.* no capacitor is used to connect to the system and not apply rated voltage (420kV). Single phase 100V voltage is applied to the GCB through voltage current source. Connect Controlled switching device as shown in the fig. and connect laptop to the CSW device for observing the switching characteristic. After connecting all devices and

setting of Controlled switching device at capacitor load, raise the closing command to the GCB. Observed the switching characteristics on laptop as shown in the graph 3. and calculate target error.

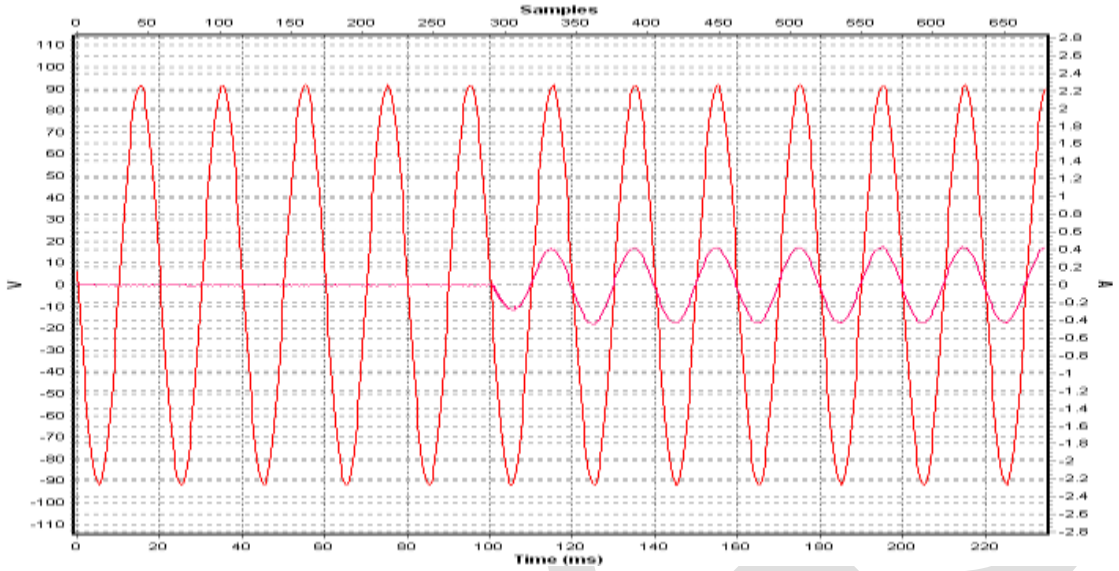

Graph 3. Capacitor switching characteristic with controlled device

Target for capacitor switching = Voltage zero point.

Error from target of above graph = Zero msec.

- *INDUCTOR SWITCHING*

Similarly as mentioned in the 4.6.2 section only change is set the CSW device at inductive load instead of capacitor load. Observed the switching characteristics on laptop as shown in the graph 4. and calculate target error.

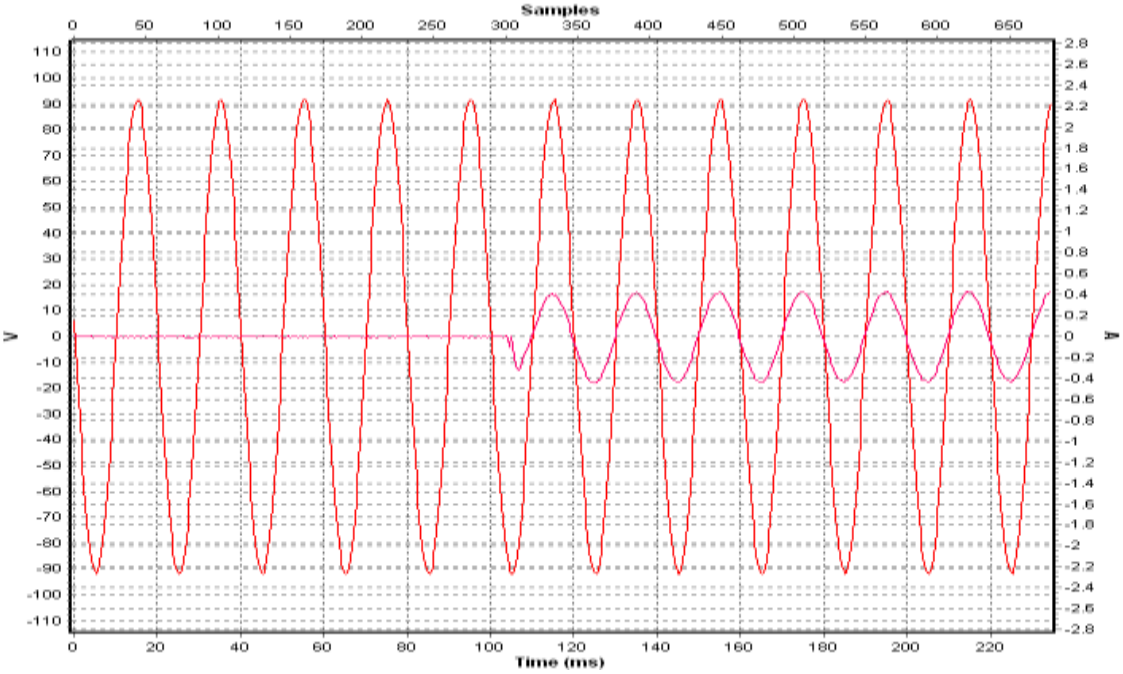

Graph. 4. Inductor switching with controlled device

- Target for inductor switching = Voltage peak point.
  Error from target of above graph = 0.13 msec.

ADVANTAGES

- System and equipment transient reduction.
- Power quality improvement.
- Circuit breaker contact burn reduction.
- Circuit breaker enhanced performance during current interruption in the dielectric region.
- Avoidance of nuisance relay operations.
- Avoidance of re-ignition and re-strike region

CONCLUSION

Controlled switching is feasible with reasonable economical effort. It is capable of very precise breaker timing control for switching a wide variety of reactive power system loads and improves power quality also prevents switchgear and other system components from severe stresses. Effectiveness of controlled switching depends on several factors, the most important of which is the circuit breaker operating time consistency. Breakers with a deviation in operating times (*i.e.* statistical scatter of main and auxiliary contact) of less than ±0.5 ms are best suited for controlled switching applications. Accurate circuit breaker characteristics establishment for all parameters which affect operating time is also one of the important factor for the success of controlled switching system.Some modifications and test should be required to high voltage breaker suitable for controlled switching. 420kV gas circuit breaker is modified and tested and it is conclude that controlled switching error has been found ± 0.5ms for opening and closing. Experimentation is carried out for the spring-spring type circuit breakers. The mechanical scatter found is in the range of ± 0.5 ms. This can be acceptable for the total allowed making window of ± 1 ms.

REFERENCES:

[1]. Dan Goldsworthy and Tom Roseburg, "Controlled Switching of HVAC Circuit Breakers: Application Examples and Benefits", 978-1-4244-1949-4/08, IEEE, Published, 2008, Bonneville Power Administration Demetrios Tziouvaras and Jeff Pope, Schweitzer Engineering Laboratories.

[2]. H. Y. Zhu and Chen, "Identification of Capacitor switching transients with consideration of uncertain system and component Parameters", 0885-8977, IEEE, 2007.

[3] John H. Brunke, khlaus J. Frohlich, "Elimination of transformer inrush currents by controlled switching" , IEEE, 2008.

[4]. Victor F. Hermosillo "Overall benefits of controlled switching", WG 13.07, CIGRE, 2007.

[5]. Michel Stanek , "Experiences with improving power quality by controlled switching", WG A3.07, CIGRE, May - 2003.

[6] S. A. Boggs and his colleagues, "Disconnect switch induced transients and trapped charge in gas-insulated substations". 1982, IEEE.

[7] U. Riechert, C. Neumann, H. Hama, S. Okabe, U. Schichler, H. Ito, E. Zaima "Very fast transient over voltages in gas-insulated UHV" CIGRE, 2012

[8] H. Ito, H. Tsutada, H. Wilson, "Factory and field verification test of controlled switching system", CIGRE, 2007

[9] P. Rajpal, A .P. Pandharkar, N. Rao, S.Shete, S.S. Kale and S.B.Potnis, "Controlled switching of high voltage circuit breaker", CIGRE, 2011.

[10] Satendra bhola, Arthur Manolosa and Robert lees, "Control Philosophy of Capacitor Banks In Transend Network", CIGRE. 2007

[11]. CGRE working group, "Controlled switching of HVAC circuit breakers - Planning, Specification and Testing Of Controlled Switching Systems'', 13-00(WG07) IWD 31, 2007

International Journal of Engineering Research and General Science Volume 3, Issue 5, September-October, 2015
ISSN 2091-2730

Fluoride induced water pollution issue and its health efficacy in India- A review

Sanghratna S. Waghmare, Tanvir Arfin

Senior Scientist, Environmental Materials Division, National Environmental Engineering Research Institute (CSIR), Nehru Marg, Nagpur-440020, India, ss_waghmare@neeri.res.in; Tel: + 917122247828

Scientist, Environmental Materials Division, National Environmental Engineering Research Institute (CSIR), Nehru Marg, Nagpur-440020, India, t_arfin@neeri.res.in; Tel: + 917122247828

Abstract— Fluoride is an ordinary constituent of characteristics in water samples. Its concentration, however, different fundamentally relying upon the water source. Fluoride is deductively demonstrated to counteract tooth decay and to help in accomplishing and keeping up great oral wellbeing. Water fluoridation is a safe and practical general wellbeing measure that is prescribed by more than 90 medical, dental, and health organizations at the national and worldwide level. The fluoride deliberate of groundwater at Kommala zone of Warangal district uncovered that around 85.83% specimens are discovered surpassing allowable breaking point Dental fluorosis is more inclined in the youngsters upto the age of 8-10 of fluoride influenced ranges where fluoride concentration is more than passable cutoff of 1.5 mg/l. The local government likewise has a key part to play in guaranteeing that people have admittance to fluoridated water wherever they live and empowering districts over the territory to have the capacity to convey it by sponsoring expenses where important. In the present review, the indian situation and wellbeing issue have been progressed for further view.

Keywords— Defluoridation; Health issue, indian scenario, skeletal fluorosis, dental fluorosis

INTRODUCTION

Water is the elixir of life for their survivals, well-creatures, societal up- liftmen and manageable development [1]. The water covers very nearly 71 percent of surface of the earth approximately 1,39,500,000 sq. miles. The water availability on earth covering is extensively characterized into surface water and sub-surface or ground water. The significant wellspring of water are surface water while ground water contributes just 0.6 % rate of them. However, the greater part of the creating nations like India rely on upon ground water to fulfill their every day necessities beginning from drinking to agricultural purposes. The ground water was the most secure wellspring of drinking water accesible on the globe previously. Presently, this ground water sources are not safe and get badly polluted due to human interferences such as urbanization, industrialization as well as dissolution and mixing of chemical elements from natural mineral resources available in the earth itself. Fluoride is one of the chemical pollutants available in water that comes into water by dissolution of fluoride containing rocks by their weathering and leaching or discharge by agricultural and industrial activities during manufacturing glass, electronics, steel, aluminium, bricks, tiles, ceramics, pesticide and fertilizer [2].

The presence of fluoride in groundwater for drinking purposes may be beneficial or detrimental depends on its concentration and amount indigested. The drinking water having lower concentration of fluoride in the range of 0.4 to 1.0 mg/l beneficial to promote calcification of dental enamel and protects teeth against tooth decay, while excessive level of fluoride causes multiple health problems ranging from mild dental fluorosis to crippling skeletal fluorosis [3]. According to the World Health Organization (WHO) [4], the maximum acceptable concentration of fluoride is 1.5 mg/l, while India's permissible limit of fluoride in drinking water is 1 mg/l [5]. Keeping in view of climatic condition of hot humid region, the US Public Health Service reduces the permissible limit of fluoride from 1.7 to 0.8 mg/l with increases of the average maximum daily air temperature [6]. High F intake has been suspected being involved in a range of adverse health problems in addition to fluorosis, including cancer, impaired kidney function, digestive and nervous disorders, reduced immunity, Alzheimer's disease, nausea, adverse pregnancy outcomes, respiratory problems, lesions of the endocrine glands, thyroid, liver and other organs [7,8].

INDIAN SCENARIO

In India, the fluorosis is broad, concentrated and disturbing throughout the nations since out of 85 million tons of fluoride deposited on earth's shell; 12 millions are found in India [9]. The fluoride was initially identified in mid 1930 at four states including Andhra Pradesh, Tamil Nadu, Uttar Pradesh and Panjab. In 1986, fluorosis was established in 13 states under innovation mission on drinking water. In 1990-1992, two additional states Kerala and Jammu and Kashmir have likewise been distinguished as fluoride inclined states. In 2002, it was secured 17 states, at present, In India, more than 6 million individuals are truly influenced by fluorosis and

another 62 million individuals are at the danger. Fluorosis issue was predominant in 20 out of the 35 states of India, 70-100% districts are influenced in Andhra Pradesh, Gujarat and Rajasthan, 40-70% districts are influenced in Bihar, National Capital Territory of Delhi, Haryana, Jharkhand, Karnataka, Maharashtra, Madhya Pradesh, Odisha, Tamil Nadu and Uttar Pradesh, 10-40% districts are affected in Assam, Jammu & Kashmir, Kerala, Chhattisgarh and West Bengal. While the endemicity for whatever remains of the states are not known. For the most part influenced states because of fluorosis are Rajasthan, Andhra Pradesh, Gujrat, Karnataka, Odisha, Panjab, Haryana, Delhi, Madhya Pradesh, Tamil Nadu and Uttar Pradesh. In Rajasthan, 24 out of 32 districts have been influenced with fluorosis and 15 million of the population are at danger [10,11].

In the examination of groundwater study of Todaraisingh area of Tonk district of Rajasthan, 65.63 percent of samples were crossing the admissible furthest reaches of W.H.O. for drinking water [12]. The middle and eastern parts of the Hanumangarh, a northern most district of Rajasthan can be filed as high hazard area of skeletal fluorosis because moderately high concentration of fluoride (3-4 mg/l) in groundwater [13]. The fluoride concentration of groundwater of four blocks in Ajmer district of Rajasthan changed from 0.24 to 17.60 mg/l with 66 % samples in overabundance of passable utmost of 1.5mg/l bringing on dental and skeletal fluorosis [14,15]. The ten tribal villages of Abu road of Rajasthan were likewise crossing as far as possible [16]. In Andhra Pradesh, 16 out of 23 districts are influenced by fluoride. The fluoride studied of groundwater at Kommala area of Warangal district uncovered that around 85.83% specimens are discovered surpassing admissible utmost [17].

The ground water samples of Nalgonda district of Andhra Pradesh had fluoride concentration upto 8.8 mg/l and around 30% of wells had fluoride concentration over as far as possible [18]. The studied demonstrated that fluoride concentration of distinctive parts of Talupula area of Anantapur district (Andhara Pradesh) reaches between 0.78 to 6.10 mg/l. The general population of this area suffered from dental fluorosis and mild skeletal fluorosis [19]. In Gujrat around 18 districts are confronting fluoride threat. Mehsana, Patna and Banaskantha districts are most fluoride affected districts apart from Amreli, Ahmedabad, Sabarkantha and Baroda. The people of these areas are suffering from dental and skeletal fluorosis [20].

In Karnataka states, fluorosis are spreading in 18 to 20 districts including Bagalkot, Bangalore, Bellary, Belgaum, Bidar, Bijapur, Chamarajnagar, Chikmanglur, Chitradurga, Devangere, Dharwar, Gadag, Gulbarga, Haveri, Kolar, Koppala, Mandya, Mysore, Raichur and Turnkur. The Southern part of Karnataka, covering districts of Gulbarga (2.60 – 7.40 mg/l), Raichur (2.02 – 5.15 mg/l), Bellary (0.80 – 7.40 mg/l), Chitradurga and Tumkur (0.97 – 2.60 mg/l) and Kolar (1.55 – 2.60 mg/l) are epidemic in fluorosis [21].

In Orissa, around 18 districts are influenced by fluorosis. The drinking water quality in numerous villages of Angul, Khurda, Puri, Nayagarh, Boudh, Kandhamal, Bolangir,Nuapada and Balasore districts are contaminated with huge amount of fluoride. The circumstance is additionally distrubing in Balsingh-Singhpur in Khurda district, Karlakote in Nuapada district, Gohiriapadar in Kalahandi District, Krushakpalli in Bargarh district and Balgopalpur Industrial Estate in Balasore districts .

According to CPCB, Kolkata, the fluoride contaminated water established in 57% of tube wells and 67% of dug wells; 10% of these assets had fluoride more than 1.0 mg/l. The fluoride concentration of lake water varies from 0.47 to 3.70 mg/l. The people of Balsingh and Singhpur in Khurda district were completely suffered from fluorosis; over 200 persons have died of fluorosis in last 16 years. The fluoride level was happened in village tube well was 3.18 mg/l while it was as high as 7.10 mg/l and 10.55 mg/l in the open wells and lakes [22].

The groundwater of South – Western districts of Punjab had fluoride concentration of 0.28 to 14.04 mg/l. The people of arid region of Punjab have suffering from dental fluorosis and in addition constant sicknesses like cancer [23]. The districts of Haryana having fluoride concentration more than 6.0 mg/l includes Sonepat, Faridabad, Bhiwani and Fatehabad while districts such as Jind, Hisar, Sirsa, Rohatak, Rewari, Panipat and Mahendragarh having more than 3.0 mg/l. Ambala and Yamunanagar are safe from problem of fluorosis [24]. The fluoride concentration of groundwater in various villages of Gurgaon district of Haryana varied from 0.02 – 6.4 mg/l [25]. The Mega city of Delhi is endemic for fluorosis with 32 ppm of fluoride concentration. Around 50% of the groundwater in Delhi surpasses the most extreme passable point of confinement of fluoride in drinking water.

As indicated by Source Economic Survey of Delhi (2007-08) [26], the fluoride concentrations in distinctive locations in Delhi are Mohammadpur (2.50 mg/l), Shahbad (7.36 mg/l), JJ Colony (6.67 mg/l), Narela (4.87 mg/l), Okhla village (3.00 mg/l), Rohini (4.35 mg/l), Najafgarh (8.70 mg/l), Suraj Park (4.23 mg/l), Sabzi Mandi (1.30 mg/l), Green Park (19.33 mg/l), Hari Nagar (Asharam) (1.50 mg/l), Jangpura (2.44 mg/l), Lodhi Road (4.00 mg/l) and Srinivaspuri (1.38 mg/l). According to Water Aid India 2005 [27], around 4018 villages with 7746 sources in 22 districts have fluoride contamination in water. In Tamil Nadu, totally 214 blocks in 23 districts having fluoride issue. The most influenced districts because of fluorosis are Dindigul, Theni, Virudhunagar and Kanyakumari. Some areas in Tiruvarur, Kancheepuram, Ramnathapuram and western part of Vellore are likewise influenced by fluoride [28].

The dental fluorosis was found in 10 villages of Anthoor block and Nilakkotai block of Dindigul Anna District because of fluoride had found in the range of 1 to 3 ppm whereas skeletal fluorosis was predominant in four villages of Ayodhyapatnam block of Salem District with fluoride extent changed from 3.8 to 8.0 ppm [29,30]. The fluoride accessibility investigation of 61 villages of

Ottapidaram block of Tamilnadu having 81.97% samples crossing the reasonable furthest reaches of 1.5 mg/l. The fluoride concentration in drinking water varies 0.936 to 4.34 mg/l in the study area [31].

The districts of Uttar Pradesh having fluoride concentration more than reasonable point of confinement incorporates Agra, Aligarh, Etah, Firozabad, Jaunpur, Kannuaj, Mahamaya Nagar, Mainpuri, Mathura and Mau. The fluoride concentration in groundwater of three blocks namely Naujhil, Mat and Raya of Mat Tahsil of Mathura district differed from 0.1 to 2.5 mg/l [32] while groundwater samples of Tanda taluka of Rampur district shifted from 0.46 to 4.36 mg/l [33]. Table 1, and 2 demonstrates the state-wise presence of fluoride concentration in ground water of India, and Fluoride in ground water in India for most recent fifteen years (2000-2015).

Table 1: Indian scenario of Fluoride Endemicity

State	Total Districts	Endemic Districts	Fluoride Level
Andhra Pradesh	23	16 (69.57%)	**0.4 - 29.0 mg/L**
Gujarat	19	18 (94.74%)	1.5 - 18.0 mg/L
Rajasthan	32	32 (100.0%)	0.10 - 10.0 mg/L
Karnataka	27	18 (66.66%)	0.2 - 7.79 mg/L
Orissa	32	18 (56.25%)	0.6 - 9.2 mg/L
Punjab	17	14 (82.35%)	0.4 - 42.0 mg/L
Maharashtra	32	10 (31.25%)	0.11 - 10.00 mg/L
Madhya Pradesh	48	16 (35.55%)	1.5 - 4.20 mg/L
Haryana	19	12 (63.16%)	0.2 - 48.32 mg/L
Bihar	41	06 (14.63%)	0.2 - 8.32 mg/L
Tamil Nadu	29	08 (27.59%)	0.1 - 7.0 mg/L
Uttar Pradesh	83	18 (21.69%)	0.2 - 25.0 mg/L
West Bengal	18	04 (22.22%)	1.1 - 14.47 mg/L
Kerala	14	03 (21.43%)	**0.2 - 5.40 mg/L**
Assam	23	02 (08.69%)	1.6 - 23.4 mg/L
Delhi	09	04 (44.44%)	0.2 - 32.0 mg/L
Jammu & Kashmir	14	01(07.14%)	0.5 -4.21 mg/L
Jharkhand	-	-	0.5 - 14.32 mg/L
Chhattisgarh	-	-	-
Uttaranchal	-	-	-

Table 2: Fluoride in groundwater in India (2000-2015)

Location	Fluoride concentration	Reference
Rohtas, Bihar	0.1-2.5 mg/l	Ray et. al. (2000) [33]
Nayagarh district, Orissa	0.16-10.1 mg/l	Kundu et. al. (2001) [34]
Rajgarh Tehsil, Churu district, Rajasthan	0.1 -14.0 mg/l	Murlidharan et. al. (2002) [35]
Delhi	0.11-32.5 mg/l	Susheela et. al. (2003) [36]
Guwahati, Assam	0.18-6.88 mg/l	Das et. al. (2003) [37]
Five villages of Haryana	0.3 – 6.9 mg/l	Meenakshi et. al. (2004) [38]
Seventeen villages of Tehsil Sanganer, District Jaipur, Rajasthan	2.17 – 10.14 mg/l	Sharma et. al. (2005) [39]
Tanda taluka of Rampur district	0.46-4.36 mg/l	Shinde & Shinde (2006) [32]
Andhra Pradesh	0.38-4.0 mg/l	Sreedevi et. al. (2006) [40]
Birbhum , West Bengal	0.006-1.95 mg/l	Gupta et. al. (2006) [41]
Yavatmal district, Maharashtra	0.30-13.41 mg/l	Madhnure et. al. (2007) [42]
Palghat district, Kerala	1.51-5.75 mg/l	Shaji et. al. (2007) [43]

Rajasthan	1.0-5.2 mg/l	Choubisa (2007) [44]
Ajmer district, Rajasthan	0.24-17.60 mg/l	Sharma (2007) [14]
Orissa	0.47-10.55 mg/l	Mahapatra (2007) [22]
Ottapidaram block of Tamil Nadu	0.936-4.34 mg/l	Mishra & Mishra (2007) [31]
North Rajasthan	3.0 – 4.0 mg/l	Suthar et. al. (2008) [13]
Kadayam block of Tirunelveli district	0.73 – 3.02 mg/l	Alagumuthu & Rajan (2008) [45]
Nine blocks of Kanyakumari district, Tamil Nadu	1.5-1.7 mg/l	Baskaradoss et al. (2008) [46]
Sonbhadra, Uttar Pradesh	0.48-6.7 mg/l	Raju et. al. (2009) [47]
Visakhapatnam, Andhra Pradesh	1.15-1.28 mg/l	Rao et. al. (2009) [48]
Hirakud, Orissa	0.5-0.60 mg/l	Mishra et. al. (2009) [49]
Nilakottai block of Dindigul district in Tamil Nadu	0.49-3.12 mg/l	Viswanathan et. al. (2009) [29]
Ajmer, Rajasthan	0.20-17.607 mg/l	Vikas et. al. (2009) [50]
Todaraisingh area of Tonk district, Rajasthan	3.0-4.0 mg/l	Yadav & Khan (2010) [12]
Around Tanda taluka of Rampur district, Uttar Pradesh	1.0-2.5 mg/l	Yadav & Kumar (2010) [32]
Villages of Modasa taluka, Sabarkantha district, North Gujrat	1.0-3.0 mg/l	Dave et. al. (2010) [51]
Ottapidaram block Tamilnadu	0.936 – 4.34 mg/l	Veeraputhiran & Alagumuthu (2010) [52]
Sonitpur District, Assam	0.17 – 5.602 mg/l	Joydev Datta et.al. (2010) [53]
Guntur district, Andhra Pradesh	0.3 – 1.8 mg/l	Subba Rao (2010) [54]
Malpura Tehsil, Tonk, Rajasthan, India	0.08 – 11.30 mg/l	Tailor & Chandel (2010) [55]
Erode district, Tamilnadu	0.5 – 8.2 mg/l	Karthikeyan et.al. (2010) [56]
Wailpalli watershed,Nalgonda district Andhra Pradesh	0.97- 5.83 mg/l	Reddy et.al (2010) [57]
Parts of Nalgonda district, Andhra Pradesh	0.1 – 8.8 mg/l	Brindha et.al. (2011) [58]
Nawa tehsil of Nagaur district, Rajastan	1.10-14.62 mg/l	Gautam et. al. (2011) [59]
Talupula , Andhra Pradesh	0.78 – 6.10 mg/l	Arveti et.al. (2011) [60]
Rameswaram Area Tamilnadu, Southern India	1.5-2.5 mg/l	Sivasankar & Ramachandramoorthy. (2011) [61]
Deoli Tehsil (Tonk District) Rajasthan	0.3-9.6 mg/l	Meena et.al. (2011) [62]
Agra district, Uttar Pradesh	0.1-14.8 mg/l	Sharma et. al. (2011) [63]
Mettur taluk of Salem District, Tamilnadu	0.1-2.8 mg/l (pre-monsoon) 0.4-4.0 mg/l (Post-monsoon)	Srinivasamoorthy et.al. (2012) [64]
Kommala area in Warangal district, Andhra Pradesh	1.1-5.8 mg/l	Veerati Radhika and Praveen (2012) [65]
Dungarpur district of Rajasthan	1.5-4.4 mg/l	Choubisa (2012) [66]
Rural habitations of central Rajasthan	>1.5 – 5.91mg/l	Hussain et.al. (2012) [67]
Mudhol Taluk , Karnataka	0.06-0.573 mg/l	Pol et.al. (2012) [68]
Patripal panchayat of Balasore , Odisha	0.6 – 5.83 mg/l	Das et.al. (2012) [69]
Karera block in Shivpuri district, Madhya Pradesh	1.65 – 3.91 mg/l	Saksena & Narwaria (2012) [70]
Mathura district, Uttar Pradesh	3.4 – 4.6 mg/l	Rawat et.al. (2012) [71]
Anantapur District, Andhra Pradesh	1.8 – 5.2 mg/l	Sunitha et.al. (2012) [72]
Kadiri,Mudigubba & Nallamada mandals of Anantapur District, Andhra	0.1 – 7.0 mg/l	Reddy (2013) [73]

Pradesh		
South and Western Parts of Punjab	0.28-14.04 mg/l	Singh et. al. (2013) [23]
Bassi tehsil of district Jaipur, Rajasthan	0.1-12.5 mg/l	Saxena & Saxena (2013) [74]
Angul district of Orissa	0.2-2.4 mg/l	Reza & Singh (2013) [75]
Didwana block of Nagaur district, Central Rajasthan	0.5-8.5 mg/l	Arif et. al. (2013) [76]
Nilakottai block, Dindigul district, Tamil Nadu	1.5-3.0 mg/l	Amalraj and Pius (2013) [77]
Mysore district, Karnataka	0.25-3.0 mg/l	Mamatha et. al. (2013) [78]
Villages of Jind District, Haryana	0.2-2.0 mg/l	Singh et.al. (2013) [79]
Dindigul town, Tamilnadu	2.47 – 5.26 mg/l	Mohamed & Zahir Hussain (2013) [80]
Central Rajasthan	0.5 – 5.8 mg/l	Hussain et.al. (2013) [81]
Faridabad , Haryana	1.0 – 40 mg/l	Garg & Singh; (2013) [82]
Chittoor District	0.2-2.75 mg/l	Lakshmi (2013) [83]
Vinukonda Mandal of Guntur District, Andhra Pradesh	3.28-4.27 mg/l	Suneetha et. al. (2014-15) [84]
East coastal region from Rameshwaram to Thiruvanmiyur, Tamil Nadu	0.02-1.54 mg/l	Umari & Ramu (2014) [85]
Some villages of West Bengal	1.08-1.75 mg/l	Datta et. al. (2014) [86]
Haryana	3.0-6.0 mg/l	Gupta & Mishra (2014) [24]
Devli Tehsil of Tonk district, Rajasthan	0.2-15.8 mg/l	Agarwal & Chauhan (2014) [87]
Rajasthan	1.0-6.0 mg/l	Jain & Singh (2014) [88]
Gaya district, Bihar	0.6-2.5 mg/l	Ranjan & Yasmin (2015) [89]
Palamu and Garhwa, Jharkhand	0.14-6.98 mg/l	Kumari et. al. (2015) [90]
Kalwakurthyarea, Mahabubnagar District, Telengana	0.16-3.4 mg/l	Ravikanth et. al. (2015) [91]
Five blocks of Kishanganj district, Bihar	0.61-3.74 mg/l	Kumar & Kumar (2015) [92]

HEALTH EFFECTS OF FLUORIDE

The vicinity of fluoride in the drinking water may be useful or perilous to every single leaving creatures, animals and plants relying upon its concentration, amount of indigestion and time of exposure. The fluoride is an essential for human body for the improvement of teeth by hardening the enamel, security against tooth decay and densification of bones when present in allowable farthest point (0.4 – 1.0 mg/l) [93] yet unnecessary intake of fluoride reasons dental fluorosis, skeletal and non-skeletal fluorosis and different issue. The fluoride is more attracted towards calcium because of its most electronegative nature.

Henceforth impact of fluoride on teeth and bone are more critical because of vicinity of calcium and deposited as calcium fluorapatite crystals prompting the formative adjustments. Tooth enamel is made chiefly out of crystalline hydroxyapatite. The ingestion of fluoride containing water prompts the fuse of fluoride ion into the apatite crystal lattice of calciferous tissue enamel its development. The hydroxyl ion gets substituted by fluoride ion since fluorapatite is more steady than hydroxyapatite. In this manner, a lot of fluoride gets bound in these tissues and just a little amount is discharged through sweat, pee and stool.

The strength of fluorosis is not just reliant on the fluoride content in water, additionally relies on upon other source, physical activity and dietary habits. The different types of fluorosis emerging because of intemerate intake of fluoride are indicated in Table 3.

Table 3 – Biological Effects by fluoride [94]

Concentration of Fluoride	Medium	Effects
0.002	Air	Injury to vegetation

< 1.0	Water	Dental carrier reduce
1.0 – 3.0	Water	Dental fluorosis (discoloration, mottling and pitting of teeth
3.0 – 4.0	Water	Stiffened and brittle bones and joints
4.0 – 6.0 and above	Water	Deformities in knee and hip bones and finally paralysis making the person unable to walk or stand in the straight posture, Crippling Fluorosis
500	Food and Water	Thyroid changes
100	Food and Water	Growth retardation
120	Food and Water	Kidney changes

DENTAL FLUOROSIS

Dental fluorosis is more inclined in the youngsters upto the age of 8-10 of fluoride influenced areas where fluoride concentration is more than admissible farthest point of 1.5 mg/l. Because of intemperate fluoride intake, enamel loses its radiance. The gentle type of dental fluorosis is described by white, opaque areas on the tooth surface while in extreme structure yellowish brown to black stains and severe pitting of teeth are showed up. The grown-ups are likewise get influenced by dental fluorosis however the harm appearance are not visible when contrasted with milk teeth. Table 4 demonstrates the predominance of dental fluorosis.

Table 4 : Prevalence (%) of dental fluorosis in different parts of India by age groups

State/Area	Age group (Years)	Prevalence (%)	Author
Alapuzzha, Kerala	10-17	35.6	Gopalakrishnan et.al. (1999) [95]
Assam	All ages	31.3	Chakraborti et. al. (2000) [96]
Davangere region of South India	12-15	16 – 100	Acharya et. al. (2005) [97]
Raigad, Maharashtra	0-23	91.7	Bawaskar and Bawaskar (2006) [98]
Villages of North-Western district, Tamil Nadu	5-14	42.0	Kumar et. al. (2007) [99]
Cuddalore, TN	5-12	31.4	Savannah et.al. (2008) [100]
Palamau Jharkhand	children	83.2	Srikanth et. al. (2008) [101]
Kanyakumari, Tamil Nadu	11-15	15.8	Baskaradoss et. al. (2008) [46]
Jhajjar, Haryana	7-15	30-94.9	Yadav et. al. (2009) [102]
Kaiwara, Chintamani Taluka, hickballapur district	Adults	24.0	Isaac et. al. (2009) [103]
Nalgonda, Andha Pradesh	Adults	30.6	Nirgude et al. (2010) [104]
Durg, Chattisgarh	Adults	8.2	Pandey (2010) [105]
Dungarpur, Udaipur	All ages	39.2-72.1	Choubisa et. al.

(Rajasthan)			(2010) [106]
Birbhum, West Bengal	Adults	61-66.7	Majumdhar (2011) [107]
Punjab	5-60	91.1	Shashi and Bhardwaj (2011) [108]
Raigarh, Chhattisgarh	Adults	8.0	Beg et. al. (2011) [109]
Kanyakumari district	All ages	17.32	Subramanian (2011) [110]
Panyam, Andhra Pradesh	13-15	41.0	Anuradha et. al. (2011) [111]
Uttar Pradesh	All ages	28.6	Srivastava et. al. (2011) [112]
Kareka, Shivpuri Madhya Pradesh	13-50	86.8	Saksena and Narwaria (2012) [70]
Cherapally, Nalgonda district	Adults (41-60)	28.0	Kiran & Vijaya (2012) [113]
Dausa district, Rajasthan	All ages	25.0	Yadav et. al. (2012) [114]
Nalgonda, A.P	12-15	71.5	Shekar et. al. (2012) [115]
Vadodara, Gujarat	Adults	39.2 - 59.3	Kotecha et al. (2012) [116]
Mundaragi, Gadag district, Karnataka	Adults	29.25	Shivayogimath et. al. (2012) [117]
Birdhum, West Bengal	All ages	61.0-66.70	Majumdar (2012) [118]
Sardar Teshil, Udaipur, Rajasthan	6-12	69.84	Sarvaiya et. al. (2012) [119]
Doda district, Jammu and Kasmir	All ages	76.77	Arya et. al. (2013) [120]
Chandrapur, Maharashtra	5-14	80.0	Ragini et. al. (2013) [121]
Sriperumbudur taluka, Kachipurum, Tamil Nadu	12	60.60	Prabhu et. al. (2013) [122]
Chittor district	7-9	2-12	Lakshmi (2013) [83]
Jaipur, Rajasthan	5-16	34.50	Gupta et. al. (2013) [123]
Purulia district, West Bengal	Adults	18.26	Mujumdar & Sundarraj (2013) [124]
Chhatisgarh	All ages	21.40	Gitte et. al. (2014) [125]
Ananthapuram	7-15	33.80	Rani & Kusuma (2014) [126]
Bommireddy palli & Kasipuram, Prakasam District, Andha Pradesh	Adults	70.5 & 59.0	Basha & Rao (2014) [127]
Salem district, Tamil Nadu	11-17	30.80	Ramesh et. al. (2014) [128]
Nalgonda district	12-15	76.80	Sukhabogi et. al.

			(2014) [129]
Himachal Praesh - Northern hilly state	5,9,12	41.0	Chauhan et. al. (2015) [130]
Kishanganj, Bihar	Adults	53.60	Kumar and Kumar (2015) [92]

SKELETAL FLUOROSIS

The skeletal fluorosis in intense to endless structure has happened because of draw out intake of fluoride contaminated water with concentration more than 3 – 6 mg/l. The disabling skeletal fluorosis may happen in individuals who have ingested 10 to 20 mg of fluoride for every day more than 10 to 20 years. India and China has been great extent influenced by disabling skeletal fluorosis, 2.7 million individuals were influenced in China and 6 million individuals have been suffered from skeletal fluorosis in India. The significant source of fluoride bringing about skeletal fluorosis originates from ground water, blazing of coal and different industrial activities. It influences the people as well as creatures encouraged with fluoride rich water and fodder. Skeletal fluoride spread among youngsters and grown-ups with same side-reactions. Additionally harmed the foetus – if mother devoured fluorinated water and foods amid pregnancy or breast feeding, newborn child mortality because of calcification of blood vessels can likewise happens.

Fluoride for the most part gets kept in the joints of neck, pelvic and shoulder bones and makes it hard to move or walk. The side effects of skeletal fluorosis are like spondylitis or arthritis. Early indications incorporates sporadic pain, burning like sensation, pricking and tingling in the limbs, muscle weakness, chronic fatigue, abnormal calcium deposits in bones and ligaments. The propelled stage is osteoporosis in long bones and bony outgrowths may happen. Vertebrae may combine and inevitably the casualty may be disabled. It may even prompt an uncommon bone cancer; osteosarcoma and lastly spine, significant joints, muscles and nervous system get harmed [94,131]. Table 5 demonstrates the commonness of skeletal fluorosis.

Table 5: Prevalence (%) of skeletal fluorosis in different parts of India by age group

State/Area	Age group (Years)	Prevalence (%)	Author
Assam	Adults	1.74	Chakraborti et al. (2000) [96]
Mundagari taluk Dharwad district, Karnataka	All Ages	5.45	Bharati & Rao (2003) [132]
Bihar, India	1-5	20.0	Khandare et al. (2005) [133]
Villages of North-Western district, Tamil Nadu	5-14	42.0 – 53.0	Kumar et. al. (2007) [99]
Palamau, Jharkhand	Adults	47.4	Srikanth et al. (2008) [101]
Central Rajasthan	Above 21	28.33	Hussain et. al. (2010) [134]
Nalgonda, Andhra Pradesh	All ages	24.9	Nirgude et al. (2010) [104]
Durg, Chattisgarh	Adults	6.3- 38.1	Pandey (2010) [105]
Dungarpur and Udaipur Rajasthan	All ages	12-27.6	Choubisa et al. (2010) [106]
Birbhum, West Bengal	Adults	4.8-23.8	Majumdhar (2011) [107]
Uttar Pradesh	All ages	14.2	Srivastava et al. (2011) [112]
Kareka, Shivpuri	13-50	39.2	Saksena and Narwaria

Madhya Pradesh			(2012) [70]
Cherapally, Nalgonda district	Adults (41-60)	21.0	Kiran & Vijaya (2012) [113]
Villages of Chandrapur district, Maharashtra	All ages	31.15	Dhawas et. al. (2013) [135]
Villages of Kankar district, Chhattisgarh	All ages	6.0	Gitte et. al. (2014) [125]
Nelakondapally Mandal of Khammam district, Andhra Pradesh	6-54	13.70	Shanti et. al. (2014) [136]
Kishanganj, Bihar	Adults	11.20	Kumar and Kumar (2015) [92]

NON-SKELETAL FLUOROSIS/OTHERS PROBLEMS

Aside from dental and skeletal fluorosis, other wellbeing's issues happen because of wxorbitant utilization of fluorides from different sources is muscle fibre degeneration, low haemoglobin levels, disfigurements in RBCs, unreasonable thirst, migraine, skin rashes, nervousness, neurological sign, depression, gastrointestinal issues, urinary tract failing, nausea, abdominal pain, tingling sensation in fingers and toes, reduced immunity, repeated abortions or still births, male sterility, and so on. Fluoride additionally influences or changes the functional mechanism of liver, kidney, digestive system, respiratory and excretory system, central nervous system, reproductive system and destruction of around 60 enzymes.

The protestations with the G-l system in endemic ranges are presently settled as ahead of schedule cauting indications of fluoride poisonous quality. Fluoride is known not with hydrochloric acid of the stomach and is changed over to hydrofluoric acid. Hydrofluoric Acid is exceptionally destructive and henceforth the stomach and intestinal lining (mucosa) is annihilated with loss of microvilli [136,137].

It is presently realized that when fluoride is ingested, it will likewise gather on the erythrocyte membrane, which thus looses calcium content. This change causes development of echinocytes. The life span of these echinocytes is not exactly the typical life span of RBC, and subsequently early demolition of the RBCs as echinocytes reasons iron deficiency [138].

Fluoride in abundance anyplace in an biological community has been indicated to have conceivably unsafe impacts on the body systems. Each of the three parts of bone and teeth that is collagen, proteoglycans and calcium are unfavorably influenced by ingestion of high amount of fluoride for delayed span [139,140]. The net consequence of this prompts corruption of collagen and ground substance in bones and teeth and along theses lines prompts side of fluorosis like, delayed eruption of teeth, dental fluorosis, clinical fluorosis, premature aging and so on [141].

In view of the adjustments in ground substance because of high fluoride intake, elevated content of glycosaminoglycans (Mucopolysaccharides - synonymous with the term "Seromucoid" utilized by Winzler) [142] in bone and its reflection in serum is appearance is serum is considered as a file to evaluate fluoride harmfulness and fluorosis at ahead of schedule stages [139,143].

Conclusions

The nature of drinking water is critical for open security and the personal satisfaction [144,145]. The tainting of drinking water with fluoride ions is a genuine wellbeing issue, particularly in parched and semi-dry zones where geography gives wellsprings of fluoride ions. India is drastically concerned by fluorosis. In Gujrat around 18 districts are confronting fluoride threat. Mehsana, Patna and Banaskantha districts are most fluoride influenced districts separated from Amreli, Ahmedabad, Sabarkantha and Baroda. The populance of these areas are experiencing dental and skeletal fluorosis. Fluoride in overabundance anyplace in a biological system has been demonstrated to have possibly unsafe consequences for the body systems. A lot of fluoride gets bound in these tissues and just a little sum is discharge through sweat, pee and stool.

REFERENCES:

[1] Waghmare S.S, Arfin, T, Manwar N, Lataye D.H, Labhsetwar N, and Rayalu S, "Preparation and characterization of polyalthia longifolia based alumina as a novel adsorbent for removing fluoride from drinking water", Asian J. Adv. Basic Sci. 4, 12, 2015.

[2] Ma W, Fei-Qun, Ya, Han M, and Wang R, "Characteristics of equilibrium, kinetics studies for adsorption of fluoride on magnetic-chitosan particle", J. Hazard. Mater. 143, 296, 2007.

[3] Fawell J, Bailey K, Chilton E, Dahi E, Fewtrell L and Magara Y, "Fluoride in Drinking Water", World Health Organization, IWA Publishing, UK, 2006.

[4] World Health Organisation, Guidelines for Drinking-water Quality, Volume 2. Health Criteria and Other Supporting Information, second ed., World Health Organisation, Geneva, 1996.

[5] Bureau of Indian Standard – Drinking water specification BIS 10500, 1991.

[6] U.S. Public Health Service, US Public Health Service Drinking Water Standards, US Government Printing Office, Department of Health Education and Welfare, Washington DC, 1962.

[7] Kumar E, Bhatnagar A, Minkyu J, Jung W, Lee S, Kim S, Lee G, Song H, Choi J, Yang J and Jeon B, " Defluoridation from aqueous solutions by granular ferric hydroxide (GFH)", Water Res. 43, 490, 2009.

[8] Meenakshi R.C, Maheshwari, "Fluoride in drinking water and its removal"J. Hazard Mater. B 137, 456, 2006.

[9] UNICEF , State of the art report on the extent of fluoride in drinking water and the resulting endemicity in India., Report by Fluorosis Research & Rural Development Foundation for UNICEF, New Delhi. 1999

[10] Naklak B, Husain I, and Husain J, "Community perception in adaptation of technical and traditional fluoride mitigation practices", Indian water week 2012- Water, Energy and Food Security: Call for solution, New Delhi, 10-14 April 2012.

[11] Hussain J, Sharma KC, and Hussain I, "Fluoride in drinking water in Rajasthan and its ill effects on human health", J. Tissue Res, 4, 263, 2004.

[12] Yadav AK, and Khan P, "Fluoride and fluorosis status in groundwater of Todaraisingh area of district Tonk (Rajasthan, India) – A case study", Int. J. Environ. Pharm Res, 1, 6, 2010.

[13] Suthar S, Garg VK, Jangir S, Kaur S, Goswami N, and Singh S, "Fluoride contamination in drinking water in rural habitations of Northern Rajasthan, India", Environ Monit Assess. 145, 1, 2008.

[14] Sharma P, "Groundwater quality in some villages of Rajasthan (India) – focused on fluoride", J. Environ Res Dev. 1, 383, 2007.

[15] Vikas C, Kushwaha RK, and Pandit MK, "Hydrochemical status of groundwater in district Ajmer (NW India) with reference to fluoride distribution", J. Geological Soc. India, 73, 773, 2009.

[16] Chouhan HS, and Sharma A, "Indentification and removal of fluoride in water from tribal areas of Abu road", Int. J. Green Herbal Chem. 3, 124, 2014.

[17] Radhika V, and Praveen GV, "Determination of fluoride status in groundwater of Kommala area of district Warangal (Andhra Pradesh, India) – a case study", Adv. Applied Sci. Res. 3, 2523, 2012.

[18] Brindha K, Rajesh R, Murugan R, and Elango L, "Fluoride contamination in groundwater in parts of Nalgonda district, Andhra Pradesh, India", Environ Monit Assess. 172, 481, 2011.

[19] Arveti N, Sarma MRS, Aitkenhead-Peterson JA, and Sunil K, "Fluoride incidence in groundwater – a case study from Talupula, Andhra Pradesh, India", Environ Monit Assess. 172, 427, 2011.

[20] Sharma S, Ramani J, Bhalodia J, and Thakkar K, "Fluoride and fluorosis in context to Gujrat state of India – a review", Res. J. Pharm. Bio. Chem. 85-94.

[21] Latha SS, Ambika SR, and Prasad SJ, " Fluoride contamination status of groundwater in Karnataka", Current Sci. 76, 730, 1999.

[22] Mahapatra MK, Fluoride Menace in Orissa, RCDC Centre for Water for Life, 2007.

[23] Singh K, Hundal HS, and Singh D, "Groundwater quality assessment of arid regions of Punjab, India with special reference to fluoride", J. Agr. Sci. Appl., 2, 1, 2013.

[24] Gupta R, and Misra AK, "Groundwater fluoride in Haryana state: A review on the status and its mitigation", Study Civil Engg. and Arch. 3, 24, 2014, 24.

[25] Manjit B. , and Sharma JK, "Assessment of quality of ground water in some villages of Gurgaon district, Haryana (India) – focus on fluoride", Int. J. Innov. Res. Sci. Engg. Tech. 3, 11441, 2014.

[26] Source Economic Survey of Delhi (2007-08).

[27] Water Aid India 2005 (Water and Sanitation in Madhya Pradesh – A Profile of the State, Institutions and Policy Environment)

[28] Kulasekaran A, and Balakrishnan P, "Status of fluoride in ground water in Tamilnadu", TWAD Board, 2002.

[29] Viswanathan G, Jaswanth A, Gopalkrishnan S, and Ilango SS, "Mapping of fluoride endemic areas and assessment of fluoride exposure", Sci. Total Environ. 407, 1579, 2009.

[30] Veeraputhiran V, and Alagumuthu G, "A report on fluoride distribution in drinking water", Int. J. Environ. Sci. 1, 558, 2010.

[31] Misra AK, and Mishra A, "Study of quaternary aquifers in Ganga Plain, India – focus on groundwater salinity, fluoride and fluorosis", J. Hazard. Mater. 144, 438, 2007.

[32] Yadav SS, and Kumar R, "Assessment of groundwater pollution due to fluoride content and water quality in and around Tanda Taluka of Rampur district, Uttar Pradesh, India", J. Chem. Pharm. Res. 2, 564, 2010.
[33] Ray D, Rao RR, Bhoi AV, Biswas AK, Ganguly AK, and Sanya PI, "Physico-chemical quality of drinking water in Rohtas district of Bihar", Environ Monit Assess. 61, 387, 2000.
[34] Kundu, N, Panigrahi, MK, Tripathy S, Munshi S, Powell MA, and Hart BR, "Geochemical appraisal of fluoride contamination of groundwater in the Nayagarh District of Orissa, India", Environ Geology 41, 451, 2001.
[35] Muralidharan D, Nair AP, and Sathyanarayana U, "Fluoride in shallow aquifers in Rajgarh Tehsil of Churu District, Rajasthan – an arid environment", Current Sci. 83, 699, 2002.
[36] Susheela AK (2003). A Treatise on Fluorosis. 2nd edition, Fluoride, 36(3).
[37] Das B, Jitu T, Surashree S, Biren G, Robin KD, Himangshu BD, and Subhash CD, "Fluoride and other inorganic constituents in groundwater of Guwahati, Assam, India"Current Sci. 85, 657, 2003.
[38] Meenakshi, Garg VK, Kavita, Renuka, Malik A, "Groundwater quality in some villages of Haryana, India: focus on fluoride and fluorosis", J. Hazard. Mater. 106, 85, 2004.
[39] Sharma, JD, Sharma MK, Jain P, and Sohu D, "Quality Status of Potable Water of Tehsil-Sanganer, District-Jaipur, Rajasthan", Asian J. Exp. Sci. 19, 113, 2005.
[40] Sreedevi PD, Ahmed S, Made B, Ledoux E, and Gandolfi JM, "Association of hydro-geological factors in temporal variations of fluoride concentration in a crystalline aquifer in India", Environ. Geology, 50,1, 2006.
[41] Gupta S, Banerjee S, Saha R, Datta JK, and Mondal N, "Fluoride geochemistry of groundwater in Nalhati-1 block of the Birbhum district, West Bengal, India", . Fluoride 39, 318, 2006.
[42] Madhnure P, Sirsikar DY, Tiwari AN, Ranjan B, and Malpe DB, (2007). "Occurrence of fluoride in the ground waters of Pandharkawada area, Yavatmal district, Maharashtra, India", Current Sci. 92, 675, 2007.
[43] Shaji E, Bindu JV, and Thambi DS, "High fluoride in ground-water of Palghat District, Kerala" Current Sci. 92, 240, 2007.
[44] Choubisa SL, "Fluoridated ground water and its toxic effects on domesticated animals residing in rural tribal areas of Rajasthan, India", Int. J. Environ. Studies. 64,151, 2007.
[45] Alagumuthu G, and Rajan M, "Monitoring of fluoride concentration in groundwater of Kadayam block of Tirunelveli District, India : Correlation with physic chemical parameters", Rasayan J.Chem. 1, 757, 2008.
[46] Baskaradoss JK, Clement RB, and Narayanan A,"Prevalence of dental fluorosis and associated risk factors in 11–15 year old school children of Kanyakumari District, Tamilnadu, India: A cross sectional survey", Indian J Dent Res, 19, 297, 2008.
[47] Raju N, Dey S, and Das K, "Fluoride contamination in Groundwaters of Sonbhadra District, Uttar Pradesh, India", Current Sci. 96, 979, 2009.
[48] Rao S, "Fluoride in groundwater, Varaha River Basin, Visakhapatnam District, Andhra Pradesh, India", Environ Monit Assess. 152, 47, 2009.
[49] Mishra PC, Meher K, Bhosagar D, and Pradhan K,"Fluoride distribution in different environmental segments at Hirakud Orissa (India)", African J. Environ Sci Tech. 3, 260, 2009.
[50] Vikas C, Kushwana RK, and Pandit MK, "Hydrochemical status of groundwater in District Ajmer (NW India) with reference to fluoride distribution", J Geol Soc Ind. 73, 773, 2009
[51] Dave RS, Acharya DG, Vediya SD, and Machhar MT, "Status of fluoride in ground water of several villages of Modasa Taluka, North Gujarat for drinking purpose", Der Pharma Chemica, 2, 237, 2010.
[52] VeeraputhiranV, and Alagumuthu G, "A report on fluoride distribution in drinking water", Int. J Environ Sci. 1, 558, 2010.
[53] Dutta J, Nath M, Chetia M, and Misra AK, "Monitoring of Fluoride concentration in groundwater of small tea gardens in Sonitpur District, Assam,India: correlation with physic-chemical parameters", Int J Chem Tech Res. 2, 1199, 2010.
[54] Subba RN, "Groundwater quality : focus on fluoride concentration in rural parts of Guntur district, Andhra Pradesh, India", Hydrogeological Sci J. 48, 835, 2010.
[55] Tailor GS, and Chandel CPS, "To Assess the Quality of Ground water in Malpura Tehsil (Tonk, Rajasthan, India) with emphasis to Fluoride Concentration", Nat. Sci. 8, 20, 2010.
[56] Karthikeyan K, Nanthakumar K, Velmurugan P, Tamilarasi S, and Lakshmanaperumalsamy P, "Prevalence of certain inorganic constituents in groundwater samples of Erode district Tamilnadu, India, with special emphasis on fluoride , fluorosis and its remedial measures", Environ Monit Assess. 160,141, 2010.
[57] Reddy AGS, Reddy DV, Rao PN, and Prasad KM,"Hydrogeochemical characterization of fluoride rich groundwater of Wailpalli watershed, Nalgonda District, Andhra Pradesh, India", Environ Monit Assess. 171, 561, 2010.
[58] Brindha K, Rajesh R, Murugan R, and Elango L,"Fluoride contamination in groundwater in parts of Nalgonda District, Andhra Pradesh India", Environ Monit Assess. 172, 481, 2011.
[59] Gautam R, Bhardwaj N, and Saini Y,"Study of fluoride content in groundwater of Nawa Tehsil in Nagaur, Rajasthan", J Environ Bio. 32, 85, 2011.
[60] Nagaraju A,"Fluoride incidence in groundwater: a case study from Talupula, Andhra Pradesh, India", Environ Monit Assess . 172, 427, 2011.
[61] Sivasankar V, and Ramachandramoorthy T, "Fluoride in groundwater and Dental Fluorosis in Rameswaram area, Tamilnadu, Southern India", J. Environ Anal Toxicol. 1, 110, 2011.

[62] Meena KS, Gunsaria RK, Meena K, Kumar N, Meena PL, and Meena RR, "Fluoride contaminated ground water and its implications on human health in Deoli Tehsil (Tonk District) in Rajasthan", J Chem Bio Phy Sci. Sec B, 1, 275, 2011.
[63] Sharma BS, Agrawal J, and Gupta AK, "Emerging Challenge:Fluoride Contamination in Groundwater in Agra District, Uttar Pradesh", Asian J Exp Biol Sci. 2, 131, 2011.
[64] Srinivasamoorthy K, Vijayaraghavan K, Vasanthavigar M, Sarma S, Chidambaram S, Anandhan P, and Manivannan R, "Assessment of groundwater quality with special emphasis on fluoride contamination in crystalline bed rock aquifer of Mettur region, Tamilnadu,India" Arab J. Geosci. 5, 83, 2012.
[65] Veerati R, and Praveen GV, "Determination of fluoride status in groundwater of Kommala area of District Warangal, Andhra Pradesh, India. : A case study", Adv Appl Sci Res. 3, 2523, 2012.
[66] Choubisa SL,"Fluoride in drinking water and its toxicosis in tribes of Rajasthan", Proceedings of the National academy of sciences, India Sec B: Bio. Sci. 82, 325, 2012.
[67] Hussain I, Arif M, and Hussain J, "Fluoride contamination in drinking water in rural habitations of Central Rajasthan, India", Environ Monit Assess . 184, 5151, 2012.
[68] Pol PD, Sangannavr MC, and Yadawe MS, "Fluoride contamination status of groundwater in mudhol taluk, Karnataka, India: Correlation of Fluoride with other physic-chemical parameters, Rasayan J Chem. 5, 186, 2012.
[69] Das KK, Panigrahi T, and Panda RB, "Occurrence of fluoride in groundwater of Patripal Panchayat in Balasore District, Odisha, India", J Environ. 01, 33, 2012.
[70] Saksena DN, and Narwaria YS, "Incidence of fluoride in groundwater and its potential health effects in ten villages of Karera block in Shivpuri District, Madhya Pradesh, India", Int J Environ Sci. 3, 1141, 2012.
[71] Rawat KS, Mishra AK, and Sehgal VK, "Identification of geospatial variability of fluoride contamination in groundwater of Mathura District, Uttar Pradesh", J Appl Nat Sci. 4, 117, 2012.
[72] Sunitha V, Muralidhara RB, and Ramakrishna RM, "Variation of fluoride and correlation with alkalinity in groundwater of shallow and deep aquifers – A case study in and around Anantapur district, Andhra Pradesh", Int J Appl Sci Eng Res. 1, 569, 2012.
[73] Reddy BM, Sunitha V, and Reddy MR, "Fluoride and Nitrate geochemistry of Groundwater from Kadiri, Mudigubba, and Nallamada Mandals of Anantapur District, Andhra Pradesh, India", J Agr Eng Biotech. 1, 37, 2013.
[74] Saxena S, and Saxena U, 2013, : Study of Fluoride contamination status of groundwater in Bassi Tehsil of district Jaipur, Rajasthan, India", Int J Environ Sci. 3, 2251, 2013.
[75] Reza R, and Singh G, "Groundwater quality status with respect to fluoride contamination in industrial area of angul district orissa India", Ind J Sci Res Tech. 1, 54, 2013.
[76] Arif M, Husain I, Hussain J, and Kumar S, "Assessment of fluoride level in groundwater and prevalence of dental fluorosis in Didwana block of Nagaur district, central Rajasthan, India" Int J Occup Environ Med. 4, 178, 2013.
[77] Amalraj A, and Pius A, "Health risk from fluoride exposure of a population in selected areas of Tamil Nadu South India", Food Science and Human Wellness 2, 75, 2013.
[78] Mamatha SV, and Haware DJ, "Document on Fluoride Accumulation in Ground and Surface Water of Mysore, Karnataka, India," Current World Environ. 8, 259, 2013.
[79] Singh A, Laura JS, and Rana A, "Fluoride distribution in groundwater and prevalence of Dental fluorosis among school children in villages of Jind District, Haryana (India)", Int J Current Res. 5, 998, 2013.
[80] Mohamed HM, and Zahir HA, "Study of groundwater quality at Dindigul Town, Tamilnadu, India", Int Res J Environ Sci. 2, 68, 2013.
[81] Hussain J, Husain I, and Arif M, "Fluoride contamination in groundwater of Central Rajasthan, India and its toxicity in rural habitants", Toxicol Environ Chem. 95, 1048, 2013.
[82] Garg K, and Singh B, "Fluoride signatures in groundwater and dental fluorosis in permanent teeth of school children in rural areas of Haryana state, India", Int J Occup Environ Med. 4, 107, 2013.
[83] Lakshi V, "Dental Fluorosis Prevalence among Children in Endemic Fluoride Areas of Chittoor District", Int J Sci Res. 2, 109, 2013.
[84] Suneetha M, Sundar BS, and Ravindhranath K,"Ground Water Quality Status with Respect to Fluoride Contamination in Vinukonda Mandal, Guntur District, Andhra Pradesh, India and Defluoridation with Activated Carbons", Int J Chem Tech Res. 7, 93, 2014-15
[85] Umarani P, and Ramu A, "Fluoride Contamination Status of Groundwater in East Coastal Area In Tamilnadu, India", Int J Innovative Res Sci Engg Tech. 3, 10045, 2014.
[86] Datta AS, Chakrabortty A, De Dalal SS, and Lahiri SC,"Fluoride contamination of underwater in west bengal, india", Res Report Fluoride. 47, 241, 2014.
[87] Agarwal R, and Chauhan SS, "The status of groundwater fluoride in rajasthan: A case study of devil tehsil, Tonk district", Int J Geology Earth Environ Sci. 4, 133, 2014.
[88] Jain A, Singh SK, "Prevalence of Fluoride in Ground Water in Rajasthan State: Extent, Contamination Levels And Mitigation",Open J Water Pollution Treat. 1, 50, 2014.
[89] Ranjan S, and Yasmin S,"Assessment of Fluoride Intake Through Food Chain and Mapping of Endemic Areas of Gaya District, Bihar, India", Bull Environ Contam Toxicol. 94, 220, 2015.

[90] Kumari N, Pathak G, and Singh TB,"The overall assessment of quality and quantity of drinking water with focus on fluoride in the areas of extreme western parts of Jharkhand", Int J Environ Sci. 5, 814, 2015.
[91] Ravikanth P, Sundaraiah R, and Sateesh P, "Fluoride and Nitrate Contamination in the Groundwater of Kalwakurthy Area, Mahabubnagar District, Telangana State, India", Indian J Applied Res. 5, 469, 2015.
[92] Kumar A, and Kumar V, "Fluoride Contamination in Drinking Water and its Impact on Human Health of Kishanganj, Bihar, India", Res J Chem Sci. 5, 76, 2015.
[93] Mohapatra M, Anand S, Mishra BK, Giles DE, and Singh P, "Review of fluoride removal from drinking water", J Environ Manag. 91, 67, 2009.
[94] Meenakshi , Maheshwari RC, "Fluoride in drinking water and its removal", J Hazard Mater B 137, 456, 2006.
[95] Gopalakrishnan P, Vasan RS, Sarma PS, Ravindrannair KS, and Thankappan KR, "Prevalence of dental fluorosis and associated risk factors in Alappuzha district, Kerala", National Med J Ind. 12, 99, 1999.
[96] Chakraborti D, Chanda CR, Samanta G, Chowdhury UK, Mukherjee SC, Pal AB, Sharma B, Mahanta KJ, Ahmed HA, and Singh B, " Fluorosis in Assam, India", Current Sci. 78, 1421, 2000.
[97] Acharya S, "Dental caries, its surface susceptibility and dental fluorosis in South India", Int Dent J. 55, 359, 2005.
[98] Bawaskar HS, and Bawaskar PH, "Endemic fluorosis in an isolated village in western Maharashtra,India", Trop Doct. 36, 221, 2006.
[99] Kumar RH, Khandare AL, brahman GNV, Venkiah K, Reddy CG, and Sivakumar B, "Assessment of Current Status of Fluorosis in North-Western Districts of Tamil Nadu Using Community Index for Dental Fluorosis", J. Hum Ecol. 21, 27, 2007.
[100] Saravanan S, Kalyani C, Vijayarani M, Jayakodi P, Felix A, Nagarajan S, Arunmozhi P, and Krishnan V, "Prevalence of Dental Fluorosis Among Primary School Children in Rural Areas of Chidambaram Taluk, Cuddalore District, Tamil Nadu, India", Indian J Community Med. 33, 146, 2008.
[101] Srikanth R, Chandra TR, and Kumar BR, "Endemic fluorosis in five villages of the Palamau district, Jharkhnd , India", Res. Report Fluoride. 41, 206, 2008.
[102] Yadav JP, Lata S, Kataria S.K, and Kumar S, "Fluoride distribution in groundwater and survey of dental fluorosis among school children in the villages of the Jhajjar District of Haryana, India", Environ Geochem Health. 31, 431, 2009.
[103] Isaac A, Cre WDS, Somanna SN, Mysorekar V, Narayana K, and Srikantaiah P, "Prevalence and manifestations of water-born fluorosis among schoolchildren in Kaiwara village of India: a preliminary study", Asian Biomed. 3, 563, 2009.
[104] Nirgude AS, Saiprasad GS, Naik PR, and Mohanty S, "An Epidemiological Study on Fluorosis in an Urban Slum Area of Nalgonda, Andhra Pradesh, India", Indian J Public Health. 54, 194, 2010.
[105] Pandey A, "Prevalence of fluorosis in an endemic village in central India", Trop Doct. 40, 217, 2010.
[106] Choubisa SL, Choubisa L, and Choubisa D, "Osteo-dental fluorosis in relation to age and sex in tribal districts of Rajasthan, India", J Environ Sci Eng. 52, 199, 2010.
[107] Majumdar KK,"Health Impact of Supplying Safe Drinking Water Containing Fluoride Below Permissible Level on Flourosis Patients in a Fluoride-endemic Rural Area of West Bengal", Indian Journal of Public Health. 55, 303, 2011.
[108] Shashi A, and Bhardwaj M, "Prevalence of dental fluorosis in endemic fluoride areas of Punjab, India", Biosci Biotech Res Comm. 4, 155, 2011.
[109] Beg MK, Srivastav SK, Carranza EJM, and de Smeth JB, "High fluoride incidence in groundwater and its potential health effects in partsof Raigarh District, Chhattisgarh, India", Current Sci. 100, 750, 2011.
[110] Subramanian A, "Epidemiology Study of Dental Fluorosis in Rural Population of Kanyakumari District", J Bio Agr Healthcare. 1, 1, 2011.
[111] Anuradha B, Laxmi GS, Sudhakar P, Malik V, Reddy KA, Reddy SN, and Prasanna AL, "Prevalence of dental caries among 13 and 15-year-old school children in an endemic fluorosis area: a cross-sectional study", J Contemp Dent Pract. 12, 447, 2011.
[112] Srivastava AK, Singh A, Yadav S, and Mathur A, "Endemic Dental and Skeletal Fluorosis: Effects of High Ground Water Fluoride in some North Indian Villages", Int J Oral Maxillofacial Pathology. 2, 7, 2011.
[113] Ravi KE, and Vijaya K, "A Study of Dental Fluorosis among high school children in a rural area of Nalgonda District, Andhra Pradesh", IJRRMS. 2, 29, 2012.
[114] Yadav RK, Gautam R, Saini Y, and Singh A, "Endemic Dental Fluorosis and Associated Risk Factors in Dausa District, Rajasthan (India)", World Applied Sci J 16, 30, 2012.
[115] Shekar C, Cheluvaiah MB, and Namile D, "Prevalence of Dental Caries and Dental Fluorosis among 12 and 15 Years Old School Children in Relation to Fluoride Concentration in Drinking Water in an Endemic Fluoride Belt of Andhra Pradesh", Indian J Public Health. 56, 122, 2012.
[116] Kotecha PV, Patel SV, Bhalani KD, Shah D, Shan VS, and Mehta KG, "Prevalence of dental fluorosis & dental caries in association with high levels of drinking water fluoride content in a district of Gujarat, India", Indian J Med Res 135, 837, 2012.
[117] Shivayogimath CB, Hiremath MN, and Shivalingappa SN, "Prevalence of dental Fluorosis among residents of nine villages in and around mundaragi of Gadag district in Karnataka, India", Elixir Pollution 50, 10410, 2012.

[118] Majumdar KK, "Health Impact of Supplying Safe Drinking Water Containing Fluoride Below Permissible Level on Flourosis Patients in a Fluoride-endemic Rural Area of West Bengal", Indian Journal of Public Health. 55, 303, 2011.
[119] Sarvaiya BU, Bhayya D, Arora R, and Mehta DN, "Prevalence of dental fluorosis in relation with different fluoride levels in drinking water among school going children in Sarada tehsil of Udaipur district, Rajasthan", J Ind Soc Pedodontics Preventive Dentistry. 30, 317, 2012.
[120] Arya S, Gazal S, and Raina AK, "Prevalence and severity of dental fluorosis in some endemically afflicted villages of district Doda, Jammu and Kashmir, India", J Appl Nat Sci. 5, 406, 2013.
[121] Ragini M, Varsha D, Jaya K, and Rashmi U, "Fluoride distribution in drinking water and dental fluorosis in children residing in Chandrapur District of Maharashtra", Int J Life Sci. 1, 202, 2013.
[122] Prabu, John J, and Sarvanan S, "Impact of Dental Caries and Dental Fluorosis on the Quality of Life of 12- year old Children in Tamil Nadu, India", Chettinad Health City Medical J. 2, 74, 2013.
[123] Rashmi G, Akhil S, Kusum G, Afifa Z, and Monohar RK, "Dental Fluorosis Status in School Children of Jaipur (Raj) India", IOSR J Dental Med Sci. 8, 51, 2013.
[124] Majumdar KK, and Sundarraj SN, "Health Impact of Supplying Safe Drinking Water on Patients Having Various Clinical Manifestations of Fluorosis in an Endemic Village of West Bengal", Journal of Family Medicine and Primary Care. 2, 74, 2013.
[125] Vilasrao GS, Kamble KM, and Sabat RN,"Child Fluorosis in Chhattisgarh, India: A Community-based Survey", Indian Pediatrics. 51, 903, 2014.
[126] Rani KS, and Kusuma DL, " High fluoride levels in drinking water: A major detrimental factor affecting health and nutritional status among select age groups of children in ananthapuram district, Int J Nutrition Agr Res. 1, 43, 2014.
[127] Basha SK, and Rao KJ, "Endemic Survey of Fluorosis in Prakasam District area: A report", IJPLCP. 5, 3305, 2014.
[128] Ramesh M, Shankar R, Krishnan R, Mlathi N, and Aruna RM, "Prevalence of dental fluorosis in the district of Salem, Tamil Nadu, South India: A pilot study", J Orofacial Sci. 6, 37, 2014.
[129] Sukhabogi JR, Parthasarathi P, Anjum S, Shekar BRC, Padma CM, and Rani AS, Dental Fluorosis and Dental Caries Prevalence among 12 and 15-Year-Old School Children in Nalgonda District, Andhra Pradesh, India", Annals Medical Health Sci Res. 4, 245, 2014.
[130] Chauhan D, Chauhan T, Sachdev V, and Kirtaniya BC, "A study of prevalence and severity of dental fluorosis among school children in a Northern hilly state of India", SRM J Res Dental Sci. 3, 170, 2012.
[131] Khandare HW,"Fluoride contaminated water and its implications on human health – a review", Int J Chem Tech Res. 5, 502, 2013.
[132] Bharati P, and Rao M, "Epidemiology of Fluorosis in Dharwad District, Karnataka", J. Hum. Ecol. 14, 37, 2003.
[133] Khandare AL, Harikumar R, and Sivakumar B, "Severe Bone Deformities in Young Children From Vitamin D Deficiency and Fluorosis in Bihar-India", Calcif Tissue Int. 76, 412, 2005.
[134] Hussain J, Hussain I, and Sharma KC,"Fluoride and health hazards: community perception in a fluorotic area of central Rajasthan (India): an arid environment", Environ Monit Assess. 162,1 2010.
[135] Sonal D, Varsha D, Jaya K, and Rashmi U, "An epidemiological study of skeletal fluorosis in some villages of chandrapur distric, Maharashtra, India", J Environ Res Dev. 7, 1679, 2013.
[136] Shanthi M, Reddy BV, Venkataraman V, Gowrisankar S, Reddy BVT, and Chennupati S, "Relationship Between Drinking Water Fluoride Levels, Dental Fluorosis, Dental Caries and Associated Risk Factors in 9-12 Years Old School Children of Nelakondapally Mandal of Khammam District, Andhra Pradesh, India: A Cross-sectional Survey", J Int Oral Health. 6, 106, 2014.
[137] Gupta IP, Das TK, Susheela AK, Dasarathy S, and Tandon RK, "Fluoride as a possible etiological factor in non-ulcer dyspepsia", J. Gastroenterol. Hepatol. 7, 355, 1992.
[138] Siddiqui AH, "Fluorosis in areas of India with a high natural content of water fluoride. Fluorides and human health". WHO Monograph No. 59, 284, 1970.
[139] Jha M, Shusheela AK, Krishna N, Rajyalaxmi K, and Venkiah K, "Excessive ingestion of fluoride and the significance of sialic acid: glucosaminoglycans in the serum of rabbit and human subjects", Clinical toxicol. 19, 1023, 1983.
[140] Rao RL, "Recent advances in research on fluoride toxicity and fluorosis. ICMR bulletin, 3, 1, 1979.
[141] Waddington RJ, Embery G, Hall RC, "The influence of fluoride on proteoglycan structure using a rat odontoblast in vitro system", Calcif-Tissue-Int. 52, 392, 1993.
[142] Mayes PA, Carbohydrates of physiologic significance. In: Harper,s Biochemistry, eds. Murray RK, Granner DK, Mayes PA and Rodwell VW. 25th edn, Appleton & Lange. Stamford, Connecticut, 2000 ; pp 149 –159.
[143] Shusheela AK, and Jha M, "Fluoride ingestion and its influence on glucosaminoglycans in cancellous and cortical bones – A structural and biochemical study", Fluoride 15, 191, 1982.
[144] Waghmare SS, and Arfin T," Fluoride removal from water by calcium materials: a state-of-the-art review", Int J Innovative Res Sci Eng Technol.4, 8090, 2015.
[145] Waghmare SS, and Arfin T, "Fluoride removal from water by mixed metal oxide adsorbent materials: a state-of-the-art review", Int J Eng Sci Res Technol. 4, 519, 2015.

International Journal of Engineering Research and General Science Volume 3, Issue 5, September-October, 2015
ISSN 2091-2730

Malware in Beautiful Three Dimensional (3D) visual Models - Analysis

PRIYANKA BHATI [1] K.V.V. PRASAD [2] ANISETTI ANIL [3]

prriyanka00@gmail.com kvvp.knl@gmail.com anisetti0101@gmail.com

Digital Forensic Analyst POLICE INSPECTOR Director,

eSF Labs,Hyderabad SATCOMBAT-OCTOPUS-AP eSF Labs Ltd, Hyderabad

Hyderabad- INDIA

Abstract: As the more number of users are connected to the internet the computer users are targeted by the various potential malwares. The number of malware increasing day by day had become a serious threat. The malware that has irritative and destructive functionality has become wild now days. As everyone use internet and downloading is common need for user. Unfortunately, the smart (3D) Three Dimensional visual model images are freely available in the archives of the websites. Some of the specified models which are very much useful for the defense organizations to design their security posts, navigate through high resolution 3D world environment created by fusing the 3D model images which can be useful to present the information in a realistic view to the senior management. Once the 3D images which binds with malware are downloaded and executed the malware will takes the advantage and infects the target machines and makes the network machines infected and spread through the removable media. Whenever the user restarts the infected system then it displays the black screen only. One of the leading GIS & Remote sensing organizations while inducting training to the Government Police Officers [2] who is working in the SATCOMBAT Computer Forensic Division faces this type of malware infection in their network. The GIS maps and Terra Explorer software intuitively placed on the Digital globe for terrain 3D analysis exclusively for Military defense critical infrastructures, Law enforcement Agencies were frequent access to the Geo spatial files.

This paper includes the analysis of malware and its spreading mechanism. Behavior analysis shows the functionality of the malware. In summary, the analysis reveals the malicious intention of malware author

Keywords -Dynamic Analysis, Military Defence, Malware, Virus in folders, Malware Behavior, Performance, Security, 3D Models, Malware in Digital Globe, Malware in three Dimensional Models ,Malware threat in GIS Software

INTRODUCTION

Malware attack is one of the most terrible and major security threats facing the Internet today. Normal users are unaware of these kinds of threats. One of the reasons is the rising popularity of the downloading. Malware can be downloaded unintentionally from internet presuming that these are genuine files. In this paper we analyze the malware downloaded from the archives of the 3D visualization model images.

Malware is a growing area of expertise and need skill set to analyze in virtual environment to meet the latest challenges.

Malware Analysis is the study of a malware by dissecting its different components and studies its behavior on the host computer's operating system. Malware analysis techniques are being followed, which can be either static or dynamic. The malware analysis techniques help the analysts to understand the risks and intention associated with a malicious code sample. The malware name is

system3_.exe and it contains the folder icon. In windows operating system by default the extension of files are not visible, so it fools the user in believing that it is a folder but actually it is a executable file.

2. ANALYSIS

There are different methodologies used in malware analysis. We used static and dynamic analysis of malware. Analyzing malicious software without executing it is called static analysis.

The malware download with Three Dimensional (3D) visual model images named as *system3_.exe*. Start with unique fingerprinting of malware.

The MD5 hash of system3_.exe is ***2EEE4E87DC250DDA8064C 22E0F3A8498***. It contains the folder icon as resources as shown in figure. It displays all icons stored as resources.

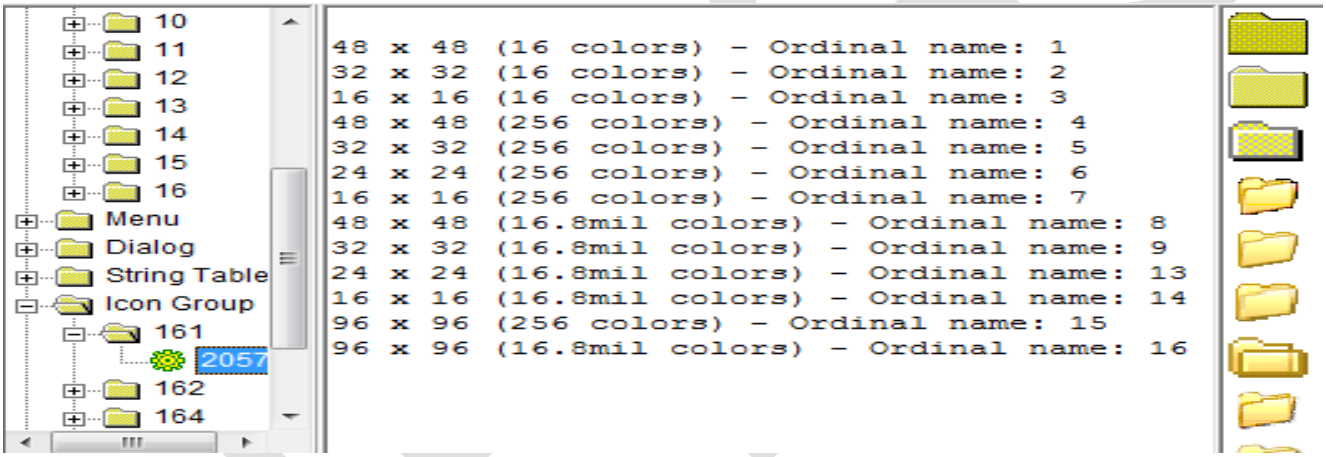

Fig. 1. Resource section

We run the system3_.exe within a controlled environment and monitoring its action in order to analyze the malicious behavior is called dynamic analysis. In this analysis, VMware is used as a secure environment to perform dynamic analysis.

3. BEHAVIOR OF MALWARE

This malware has the functionality of virus and creates its copy into system32 and temp folder in below mention path:

3.1 File Created:

C:\Documents and Settings\ESF10\LocalSettings \Te mp\00066237_Rar\system3_.exe

C:\WINDOWS\system32\system3_.exe

C:\WINDOWS\system32\autorun.inf

C:\ljbl.pif

C:\autorun.inf
C:\WINDOWS\Tasks\At1.job
It creates schedule job to execute itself everyday at 9:00 am.

3.2 Spreading Mechanism:

Malware search for any drive and copy itself into that drive. So if you connect any removable media into infected system it makes copies into USB. Afterwards, when you attach the same pen drive in another system it autoruns the virus and infects the system. The NewFolder.exe is a copy of system3_.exe binary as their hash value is same.

3.3 Files Created via USB infection:

[Any Drive]:\ autorun.inf

[Any Drive]:\ New Folder.exe

[Any Drive]:\ iblx.exe (random name)

[Any Drive]:\ New system3_.exe

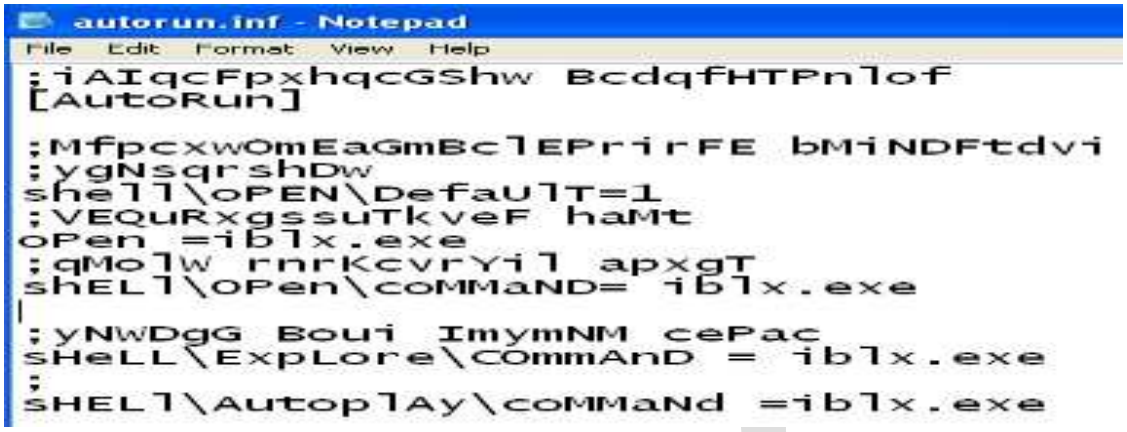

Fig. 2. Autorun file that automatically execute virus

REGISTRY MODIFICATION

Persistent mechanism

Most of the malware use various locations in registry to remain persistent on the systems. Persistent means malware will execute at every reboot. It creates two registry keys to remain persistence.

HKLM\SOFTWARE\Microsoft\Windows NT\CurrentVersion\Winlogon\Shell: explorer.exe system3_.exe

HKCU\Software\Microsoft\Windows\CurrentVersion\Run\Yahoo Messengger: C:\WINDOWS\system32\system3_.exe

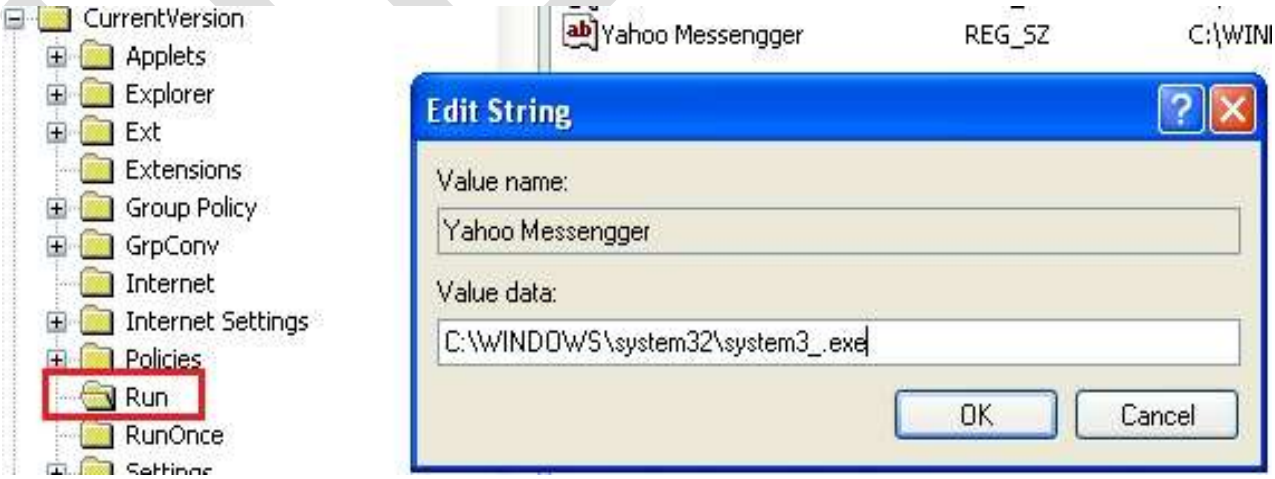

Fig. 3. Malware create registry key to autostart

4.2 Modified Registry Value:

The below registry entries confirm that the malware disables the Firewall notification message, Antivirus disable notification message and Window update disable notification message.

Path:

HKLM\SOFTWARE\Microsoft\Cryptography\RNG\Seed: Random data

HKLM\SOFTWARE\Microsoft\Security Center\AntiVirusDisableNotify: 0x00000001

HKLM\SOFTWARE\Microsoft\Security Center\FirewallDisableNotify: 0x00000001

HKLM\SOFTWARE\Microsoft\Security Center\UpdatesDisableNotify: 0x00000001

HKLM\SOFTWARE\Microsoft\Security Center\AntiVirusOverride: 0x00000001

HKLM\SOFTWARE\Microsoft\Security Center\FirewallOverride: 0x00000001

4.3 Internet Explorer modification:

It also modifies the default page, default search, search page and start page of internet explorer browser shown in below registry keys:

HKLM\SOFTWARE\Microsoft\Internet Explorer\Main\Default_Page_URL: "http://www.mydreamworld.50webs.com"

HKLM\SOFTWARE\Microsoft\Internet Explorer\Main\Default_Search_URL: "http://www.mydreamworld.50webs.com"

HKLM\SOFTWARE\Microsoft\Internet Explorer\Main\Search Page: "http://www.mydreamworld.50webs.com"

HKLM\SOFTWARE\Microsoft\Internet Explorer\Main\Start Page: "http://www.mydreamworld.50webs.com"

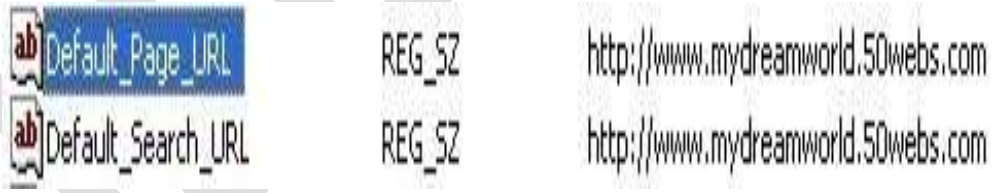

Fig. 4. Internet Explorer modification

4.4 Random registry values added:

Malware created 916 random registry values. It contains the random value & data. Here, below list & figure displays only few of registry values.

HKU\S-1-5-21-583907252-162531612-682003330-1003\Software\Aipwr\E1_0: 0x62E483CA

HKU\S-1-5-21-583907252-162531612-682003330-1003\Software\Aipwr\E2_0: 0x00001DE2

HKU\S-1-5-21-583907252-162531612-682003330-1003\Software\Aipwr\1207202201\826692421: 0x0000009E

HKU\S-1-5-21-583907252-162531612-682003330-1003\Software\Aipwr\1207202201\1653384842: 0x00000000

a1_0	REG_DWORD	0x62e483ca (1659143114)
a1_1	REG_DWORD	0xc9d4153c (3386119484)
a1_10	REG_DWORD	0xe471f503 (3832673539)
a1_100	REG_DWORD	0xed754da9 (3983887785)
a1_101	REG_DWORD	0x5f67f313 (1600647955)
a1_102	REG_DWORD	0x4a9db7fb (1251850235)
a1_103	REG_DWORD	0x658ff958 (1703934296)
a1_104	REG_DWORD	0x60faddb1 (1627053489)
a1_105	REG_DWORD	0x01365f94 (20340628)

Fig. 5. Random registry value

5. NETWORKING ACTIVITY

Malware tries to communicate with many websites. Below screenshot displays the DNS request send by the malware. Most of these URL are randomly generated by malware except those two underlined URL that is ***Ilo.brenz.pl*** and ***ant.trenz.pl.*** These two URL is malicious URL and might install another malware into the system.

Domain Requested	
ccbixb.com	www.balu011.0catch.com
ilo.brenz.pl	www.balu011.0catch.com
fzuyxv.com	h1.ripway.com
ekrzei.com	www.balu012.0catch.com
ant.trenz.pl	www.balu012.0catch.com
yzhowh.com	h1.ripway.com
aybxbp.com	ant.trenz.pl
giiyqp.com	www.balu013.0catch.com
broekhuisjuweliers.nl	www.balu013.0catch.com
btech.ac.th	h1.ripway.com
ilo.brenz.pl	www.balu014.0catch.com
btr.gen.tr	www.balu014.0catch.com
burakasansor.com	h1.ripway.com

Fig. 6. DNS request send by malware

After all these infection, commonly user get irritated and restart the system. So, when system reboots this malware displays only black screen. It also kills the process of task manager, registry editor, System Configuration, cmd and explorer.exe.

The 3D visualization models looks like this and it is the burden of the user for any damage caused by these models.

Fig. 7. 3D model images

6. CONCLUSION

In this research paper we have shown that the 3D model images downloaded from internet is not always safe enough as it brings malware with them. Malicious *System_3.exe* tricks the user by using folder icon resource. This virus creates entry in autoruns location and makes its copy in drives. In that drives it replicates inside different folder with the same name of folder with extension .exe. It also modifies the default page, default search, search page and start page of internet explorer browser by making changes in different registry location. The system3.exe virus spreads through removable devices and sends DNS request to ***Ilo.brenz.pl*** and ***ant.trenz.pl.***

7. ACKNOWLEDGMENTS

Special thanks to M/s e-Security Forensics Labs pvt. Ltd Hyderabad and M/s RSI Softech Pvt Ltd,Hyderabad for giving us the time to work on this project and permission to present our results. This analysis will give alert to all the Revenue, Military Defense and Civil engineering designers on security precautions

REFERENCES:

1. Google Scholars
2. www.bing.com
3. www.google.com
4. Various research articles

International Journal of Engineering Research and General Science Volume 3, Issue 5, September-October, 2015
ISSN 2091-2730

Resolving Security Issues in the Virtual Machine File System

Achal Sancheti
Master of Science in Information Systems,
Northeastern University
achalsancheti@gmail.com

Abstract - Security is an evolving domain of computer security, network security, cloud security and, more broadly, information security. It refers to a broad set of policies, technologies, and controls deployed to protect data, applications, and the associated infrastructure of the system. The physical machines are logically divided into virtual machines and virtual machines are rapidly replacing physical machine infrastructures for their abilities to emulate hardware environments, share hardware resources, and utilize a variety of operating systems. Its security becomes more important. This paper focuses on the security issues that are still to be overcome in Virtual Machine File System and Network File System.

Keywords – Virtualisation, Security, integrity, cloud computing, virtual machine, VMFS, hyper jacking.

1. Introduction

Organisations today are increasingly looking towards cloud computing as a new revolutionary technology promising to cut the cost of development and maintenance and still achieve highly reliable and elastic services. [1]

Virtualisation: Virtualisation means to hide the physical characteristics of the computing resources. The virtual machines can be created by VMware. VMware enables users to set up one or more virtual machines on a single physical machine, and use them simultaneously along with the actual machine.

The term virtualization has become somewhat of a buzzword, and as a result the term is now associated with a number of computing technologies including the following:

Storage virtualization: The amalgamation of multiple network storage devices into what appears to be a single storage unit.

Server virtualization: The partitioning a physical server into smaller virtual servers.

Operating system-level virtualization: A type of server virtualization technology which works at the operating system (kernel) layer.

Network virtualization: Using network resources through a logical segmentation of a single physical network.

Application virtualization: Application virtualization is layered on top of other virtualization technologies, such as storage virtualization or machine virtualization to allow computing resources to be distributed dynamically in real time. [2] There are different types of files like text file (.doc, .pdf), log file, bios file, image file, etc but here the security issue of virtual machine file system (vmfs) and network file system (nfs) is the primary concern.

VMFS: VMware Virtual Machine File System (VMware VMFS) is a virtual machine file system used in VMware ESX Server software to store files in a virtualized environment. VMWare VMFS was designed to store files, images and screen shots within a virtual machine. Multiple virtual machines can share a single virtual machine file system. Its storage capacity can be increased by spanning multiple VMFS. This file system is not mandatory and is therefore not installed with every virtual machine

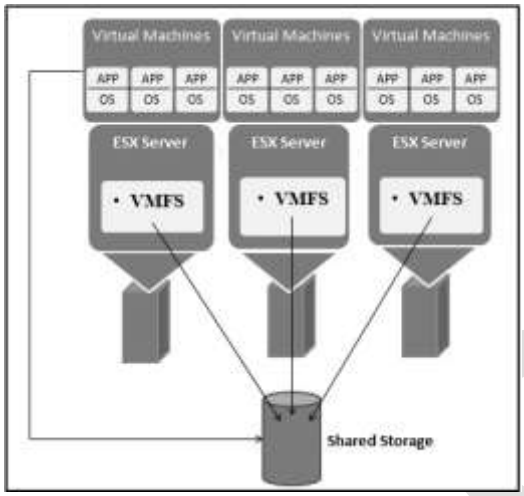

Figure1.1: Architecture of VMFS

VMware VMFS manages the creation, allocation and management of virtualized storage for all the different sets of virtual machines and servers created using VMware's set of tools and technologies. VMware VMFS is also known as VMFS vStorage.

The following are the **key features** of VMFS:

- It simplifies the storage issues of virtual machines as multiple virtual machines installed over different ESX servers can share a single shared storage area.
- Multiple instances of an ESX server run simultaneously and share VMFS.
- VMFS strongly supports the distributed infrastructure of virtualization by using various VMware services. [3]

2. Problem Domain

Cloud is totally depending on virtualisation of computing devices, network, applications and storage devices. Cloud services should ensure data integrity and provide trust to the user privacy. Data or file integrity means the accuracy and consistency of the data /file without being any alteration of those data/files. Security is the protection of systems and the data that they store or access. System security is the application of operating, technical, and management techniques and principles to the security aspects of a system throughout its life to reduce threats and vulnerabilities to the most practical level through the most effective use of available resources.

Figure 2.1 Factors of cloud security

Like physical machines, VMs are vulnerable to theft and denial of service attacks. The contents of the virtual disk for each virtual machine are usually stored as a file, which can be run by hypervisors on other machines, allowing attackers to copy the virtual disk and gain unrestricted access to the digital contents of the virtual machine. Virtual machines are inherently not physical, which means their theft can take place without physical theft of the host machine.

The second danger of virtual disks is that the attacker could corrupt or externally modify the file while the VM is offline. This means the integrity of an offline VM may be compromised if the host is not securely protected. [4]

The problems with the existing system are:

- Integrity of the system
- Hyper jacking

2.1 Hyper jacking

Hyper jacking is an attack which takes control over the Hypervisor that creates the virtual environment within a VM Host. It is a critical threat to the security of every virtualized environment. Hyper jacking involves installing a rogue hypervisor that can take complete control of a server. Gaining control of the hypervisor the attacker can control everything running on the machine and may spoil the integrity of the system. [5]

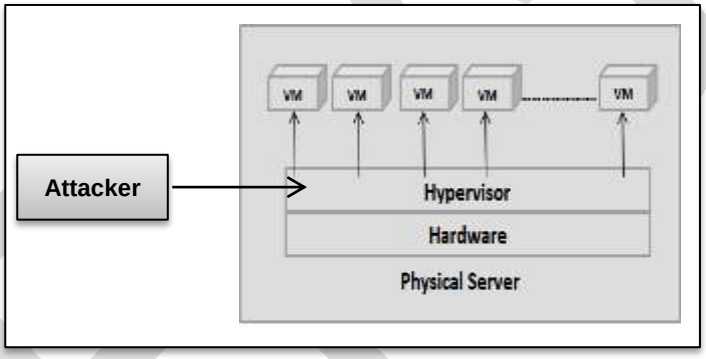

Figure 2.1.1 Process of hyperjaking

3. Proposed Solution: Flow Chart

Today security risks to cloud computing are active, including privacy, trust, data location, security policy and security threats and attacks. The virtual files on these virtual storages are prone to these risks. In order to deal with them, many security features are present which provide Data Integrity, Non-Repudiation, Encryption but somewhere lacks to provide higher levels of Authentication and Confidentiality. Finally, a multi-layered architecture is being proposed to assist the users for their satisfaction when choosing cloud delivery services.

Majority of cloud service providers store customers' data on large data centres. Although cloud service providers say that data stored is secure and safe in the cloud, customers' data may be damaged during transition operations from or to the cloud storage provider. In fact, when multiple clients use cloud storage or when multiple devices are synchronized by one user, data corruption may happen.

All data on the network need to be secured. [6]

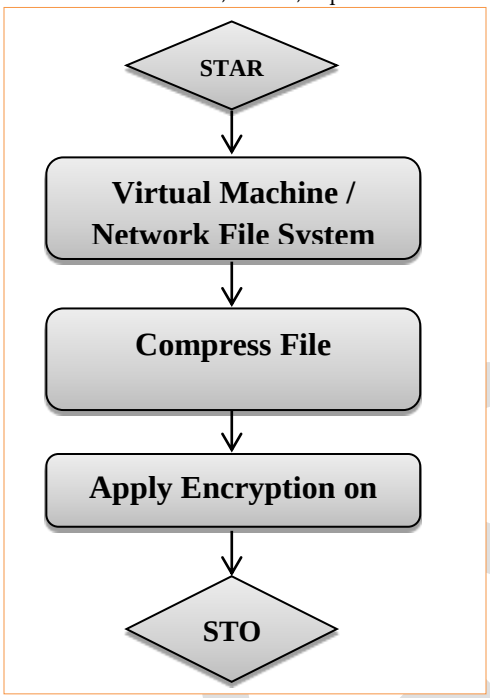

Figure 3.1: Flow of System

Let the file in the VMFS and NFS format has been saved by the registered organization on the cloud box. The authorized user may have only access to these files of the particular organisation. It is dependent on the user whether to encrypt these file and then save or save only in compressed format. The encrypted file may be decrypted by only the user who is authorized to access these files. In this way, this flow continues to provide a secured environment in cloud and to maintain the file integrity.

4. Application Domain

VMware, VCloud, Networking and Security Edge deliver an operationally efficient, simple and cost-effective security services gateway to secure the perimeter of virtual data centre.
The solution's virtual security appliance delivers gateway services such as firewall/NAT, load balancer, VPN and DHCP and is fully integrated with VMware.

- Easily support multi-tenant IT environments.
- Safely share network resources by creating logical security zones that provide complete network isolation for virtual systems.
- Enable role-based access control and separation of duties as part of a unified framework for managing virtualization security. [7]

5. Conclusion

Security includes the integrity and confidentiality. Integrity is a concept of consistency of actions, values, methods, measures, principles, expectations, and outcomes. The proposed algorithm will prove to be beneficial in the context of resolving the security related issues in the system. This system is expected to be secured. Integrity of data and files will be maintained of the system.

REFERENCES:

1. 'About file integrity in cloud computing' at "http://www.academia.edu/1475574/Ensuring_Data_Integrity_in_Cloud_Computing_-_EICA272" accessed on 06/04/2015.
2. 'Virtualization' at "www.webopedia.com/TERM/V/virtualization.html" accessed on 24/03/2015.
3. 'Virtual machine file system' at "www.techopedia.com/definition/16827/vmware-virtual-machine-file-system-vmwarevmfs" accessed at 24/03/2015.

4. 'Attacks on Virtual machine' available at "http://www.cse.wustl.edu/~jain/cse571-09/ftp/vmsec/index.html" accessed on 17/08/14.
5. 'Hyperjacking' at "itsecurity.telelink.com/hyperjacking/" accessed on 24/03/2015
6. 'Security in cloud computing' available at "http://cloudtweaks.com/2014/07/computing-security-network-application-levels/" accessed on 18/08/14.
7. 'Application of cloud security' available at "http://www.vmware.com/cloud-security-compliance/cloud-security#sthash.ZlPNsEsd.dpuf" accessed on 20/08/14

International Journal of Engineering Research and General Science Volume 3, Issue 5, September-October, 2015
ISSN 2091-2730

Dynamics and Regulatory Control of Biodiesel Purity from a Reactive Distillation Process

Saidat Olanipekun GIWA[1], Abel Adekanmi ADEYI[2], Abdulwahab GIWA[3]

[1]Chemical Engineering Department, Faculty of Engineering and Engineering Technology, Abubakar Tafawa Balewa University, Tafawa Balewa Way, 740004, Bauchi, Bauchi State, Nigeria

[2,3]Chemical and Petroleum Engineering Department, College of Engineering, Afe Babalola University, KM. 8.5, Afe Babalola Way, 360231, Ado-Ekiti, Ekiti State, Nigeria

Emails: [1]sogiwa@atbu.edu.ng; [2]abeladeyi@abuad.edu.ng; [3]agiwa@abuad.edu.ng

Abstract – The open loop and disturbance rejection (regulatory) closed loop dynamic simulation of a reactive distillation process used for the production of biodiesel, details of which are given in the work of Giwa *et al.* (2015a), have been carried out in this work. The first-order-plus-dead-time transfer function model of the system used was developed with the aid of System Identification Toolbox of MATLAB. The input and output variables of the process were the reboiler duty of the column and the mole fraction of biodiesel obtained from the bottom section of the column, respectively while the disturbance variable was the reflux ratio. Both the open loop and the closed loop simulations of the system were achieved from the Simulink model of the system developed and run via written *m-file* codes. The results obtained from the open loop dynamic simulation of the process revealed that the disturbance variable had effects on the output (biodiesel mole fraction obtained from the bottom section) of the process because the steps applied to it made the output not to be at the desired set point. Furthermore, the application of P, PI and PID controllers tuned with Cohen-Coon and Ziegler-Nichols techniques showed that the process could be made to behave in a desired manner. However, the response given by the simulation of the system with P-only controller was found not to settle at the desired set-point value, while the simulations with PI and PID were able to bring the output to the desired reference value. Moreover, the performance of PID controller tuned with Cohen-Coon technique was found to be the best among the ones considered for this case of regulatory control of the process because its IAE and ISE were obtained to be the lowest. This finding was observed to be in contrary to that of Giwa *et al.* (2015b) who obtained that the best controller for biodiesel production using reactive distillation process was PID controller tuned with Ziegler-Nichols. However, it was discovered that their own work considered set-point tracking only but not disturbance rejection. This has, therefore, shown that a particular controller type may not be able to handle both set-point tracking and disturbance rejection in a best way in all cases.

Keywords: Biodiesel, reactive distillation, System Identification Toolbox, MATLAB, disturbance rejection control.

INTRODUCTION

Biodiesel is an alternative fuel that is currently receiving attention owing to the limited availability of conventional petroleum diesel and, also, due to environmental concerns. This material can be used to replace petroleum diesel without any modification because of their similar properties (Simasatitkul *et al.*, 2011; Giwa *et al.*, 2014; Giwa *et al.*, 2015a). Furthermore, it has a number of advantages as it can be derived from a renewable domestic resource. In addition, it reduces emission of carbon dioxide apart from being nontoxic and biodegradable (Wang *et al.*, 2004; Jaya and Ethirajulu, 2011; Giwa *et al.*, 2014; Giwa *et al.*, 2015a).

Biodiesel can be obtained in high purity by carrying out an esterification reaction of a fatty acid and an alcohol via a reactive distillation process (Giwa *et al.*, 2014). The use of reactive distillation process is preferred for the production of biodiesel in order to overcome the problems associated with the use of conventional batch reactor, which include low conversion, heavy capital investments and high energy costs (Kusmiyati and Sugiharto, 2010; Giwa *et al.*, 2014; Giwa *et al.*, 2015a; Giwa *et al.*, 2015b).

Generally, reactive distillation is defined as a process that combines both separation and chemical reaction in a single unit (Giwa and Giwa, 2012). It is found to be more advantageous than a conventional process having reaction and separation sections separately (Al-Arfaj and Luyben, 2002a; Giwa and Karacan, 2012b; Giwa, 2013a; Giwa and Karacan, 2012d; Giwa and Karacan, 2012e; Giwa and Karacan, 2012f; Giwa and Karacan, 2012g; Giwa, 2012; Giwa and Giwa, 2013a; Giwa, 2013a; Giwa *et al.*, 2013; Giwa and Giwa, 2013b; Giwa, 2014). It has been used in a small number of industrial applications for many years, but the last decade has shown an increase in both its research and applications (Al-Arfaj and Luyben, 2002b; Giwa *et al.*, 2015a). In reactive distillation, the temperature levels for both reaction and vapour-liquid equilibrium must overlap (Al-Arfaj and Luyben, 2002a; Giwa *et al.*, 2015a). By carrying out chemical reaction and separation in one process, the operating and investment costs can be minimized. Some additional benefits offered by reactive distillation technology include: (i) increased yield, because of overcoming chemical and thermodynamic equilibrium limitations, (ii) improved selectivity via suppression of side reactions (Giwa and Karacan, 2012c), (iii) reduced energy consumption, due to effective utilization of reaction heat, in the case of exothermic reactions, (iv) avoidance of hot spots by simultaneous liquid evaporation, (v) ability to separate close boiling components (Prakash et al., 2011; Giwa *et al.*, 2015a) and (vi) ability to avoid azeotropes (Giwa and Karacan, 2012a). Due to these advantages and with growing process understanding, the chemical process industry has developed an increasing number of processes based on reactive distillation (Bock *et al.*, 1997; Giwa *et al.*, 2015a). However, this process is not extensively used in industry because it is perceived that understanding its dynamics will be problematic and that its operation and control are more difficult than those of the conventional systems.

In order to address those issues concerning the dynamics and control of the process, different investigations have been carried out on it by some researchers. For instance, Sneesby *et al.* (1997) carried out the dynamic simulation and control of reactive distillation process used for ethyl *tert*-butyl ether synthesis. They presented recommendations for the control of the reactive column of this type such as the need for early addressing of the control issues in the design process. Bock *et al.* (1997) developed a structure for the control of a reactive column with recovery by analysing the steady state and dynamic sensitivity of the column with respect to possible disturbances and manipulated variables. Sneesby *et al.* (1999) worked on an ethyl tert-butyl ether reactive distillation column as a case study to demonstrate how a two-point control configuration recognizing the importance of both composition and conversion could be developed and implemented for a reactive distillation process. Kumar and Daoutidis (1999) investigated the dynamic behaviour and control of a reactive distillation column used for the production of ethylene glycol. They derived a detailed tray-by-tray model that explicitly included the vapour-phase balances. Also developed in their work was a nonlinear controller that yielded good performance with stability in the high-purity region. The superior performance of the developed controller over linear PI controllers was demonstrated in the work through simulations. Monroy-Loperena *et al.* (2000) studied the control problem of an ethylene glycol reactive distillation column in order to regulate the ethylene glycol composition in the product by manipulating the reboiler boil-up ratio. A new idea for robust stabilization based on an analysis of the underlying input/output bifurcation diagram and on modelling error compensation techniques was proposed in the work. Al-Arfaj and Luyben (2000) studied the closed loop control of a reactive distillation column with two products and discovered that single end temperature control could be used to keep both products at or above specified purity values, even in the presence of large disturbances, because the reaction zone holdup was sufficiently large. Vora and Daoutidis (2001) studied the dynamics and control of an ethyl acetate reactive distillation process and designed model-based linear and nonlinear state feedback controllers along with classical single-input single-output (SISO) proportional-integral (PI) controllers. The superior performance of the nonlinear controller over both the linear and the classical PI controllers was demonstrated in the work. Grüner *et al.* (2003) carried out the simulation of an industrial reactive distillation column unto which asymptotically exact input/output-linearization was applied and discovered that, in comparison with a well-tuned linear controller, it showed a superior performance with respect to set-point changes and disturbances, even in the presence of unknown input delays. Khaledi and Young (2005) studied the nonlinearity of a reactive distillation column producing ethyl *tert*-butyl ether and developed a 2 x 2 unconstrained model predictive control scheme for product purity and reactant conversion control using the process dynamics approximated by a first-order-plus-dead-time model as an estimate of the process model of the controller. They found from the study carried out that the controller was very efficient for disturbance rejection and set-point tracking. Völker *et al.* (2007) designed a multivariable controller for a medium-scale semi-batch reactive distillation column and demonstrated that the controller performed well for large set-point changes and in the face of disturbances. Furthermore, Giwa and Karacan (2012a) used two black-box models (AutoRegressive with eXogenous Inputs (ARX) and AutoRegressive Moving Average with eXogenous Inputs (ARMAX) models) they developed using experimental data to study the dynamics of a reactive distillation column used for ethyl acetate production, and discovered that the performance of ARMAX model was better because of its higher calculated fit value. They also found that ARX model was faster in getting to steady state upon the application of a step input to the two models. However, the models developed in their work were not utilized to study the control of the process. Giwa and Karacan (2012c) developed dynamic models for a reactive packed distillation starting from first principles and solved them (the developed models) with the aid of MATLAB. The comparisons made between the experimental and the theoretical results obtained revealed that there were good agreements between them because the calculated percentage residuals were small. Also, the models they developed were not used for the control of the column in the work. Giwa and Karacan (2012d) studied the application of decouplers in the design of model predictive controllers for a reactive distillation process used for the production of ethyl acetate. In the work, top segment temperature, reaction segment temperature and bottom segment temperature were taken as the controlled variables while reflux ratio, feed ratio and reboiler duty were the manipulated variables of the control system. The results obtained from the work showed that the performance of neural network decoupling model predictive controller (NNDMPC) was better than that of transfer function decoupling model predictive controller (TFDMPC) as the integral squared error values calculated for the top segment and the reaction segment temperatures from the control simulation carried out with NNDMPC were found to be less than those of the TFDMPC. Moreover, Giwa and Karacan (2012e) applied decoupling proportional-integral-derivative control to a reactive distillation column for set-point tracking and disturbance rejection using tuning parameters calculated with Ziegler-Nichols and Cohen-Coon techniques, and the results obtained from the simulations of the work showed that decoupling PID control with Cohen-Coon tuning technique was better than that of Ziegler-Nichols, for the process considered in the work. Giwa *et al.* (2015b) studied the dynamics and set-point tracking control of a reactive distillation process used for biodiesel production by taking the biodiesel purity obtained from the bottom section of the column as the controlled variable, the reboiler duty as the manipulated variable and considering Cohen-Coon and Ziegler-Nichols tuning techniques. From the comparisons made among the controllers considered by them, they were able to discover that the best one for the system was PID controller tuned with Ziegler-Nichols method because its integral absolute error (IAE) and integral squared error (ISE) were found to be the lowest.

It can be seen from the literature review carried out that the dynamics and control of a reactive distillation process for biodiesel production has been carried out, but the control there was a servo (set-point tracking) type. It is important that the behaviour of the system to the presence of a disturbance be known so as to know how it should be handled in that case because, even, when trying to make a system to follow a particular set point, any disturbance can set into it anytime. Therefore, this work was carried out to study

the dynamics and perform regulatory (disturbance rejection) control of a reactive distillation process used for the production of biodiesel from an esterification reaction.

METHODOLOGY

Transfer Function Modelling of the Process

The process model used in this work was formulated by adding the transfer function relation between the output variable (reflux ratio) and the disturbance variable developed using the data generated from the prototype plant setup with the aid of Aspen HYSYS and reported in detail in the work of Giwa *et al.* (2015a). The process model formulation was done with the aid of the System Identification Toolbox contained in MATLAB (MathWorks, 2015). The type of the transfer function model of the disturbance relation was also chosen to be the same as that of the main process transfer function, that is, first-order-plus-dead-time, and this made the model of the process to be as shown in Equation (1).

$$x_{biod}(s) = \frac{K_p e^{(-T_{dp}s)}}{\tau_p s + 1} Q(s) + \frac{K_d e^{(-T_{dd}s)}}{\tau_d s + 1} R(s) \quad (1)$$

Simulink Modelling and Open Loop Simulation of the Process

After obtaining the transfer function of the process, as given in Equation (1), it was thereafter modelled in Simulink, also contained in MATLAB, by combining the different appropriate blocks required, and the developed Simulink model for the open loop case of the system is as shown in Figure 1. Furthermore, the open loop dynamics of the process was studied by applying step changes to the disturbance variable of the developed model, while keeping the main input variable of the process at its steady state value, and running it using the codes written in *m-file* of MATLAB.

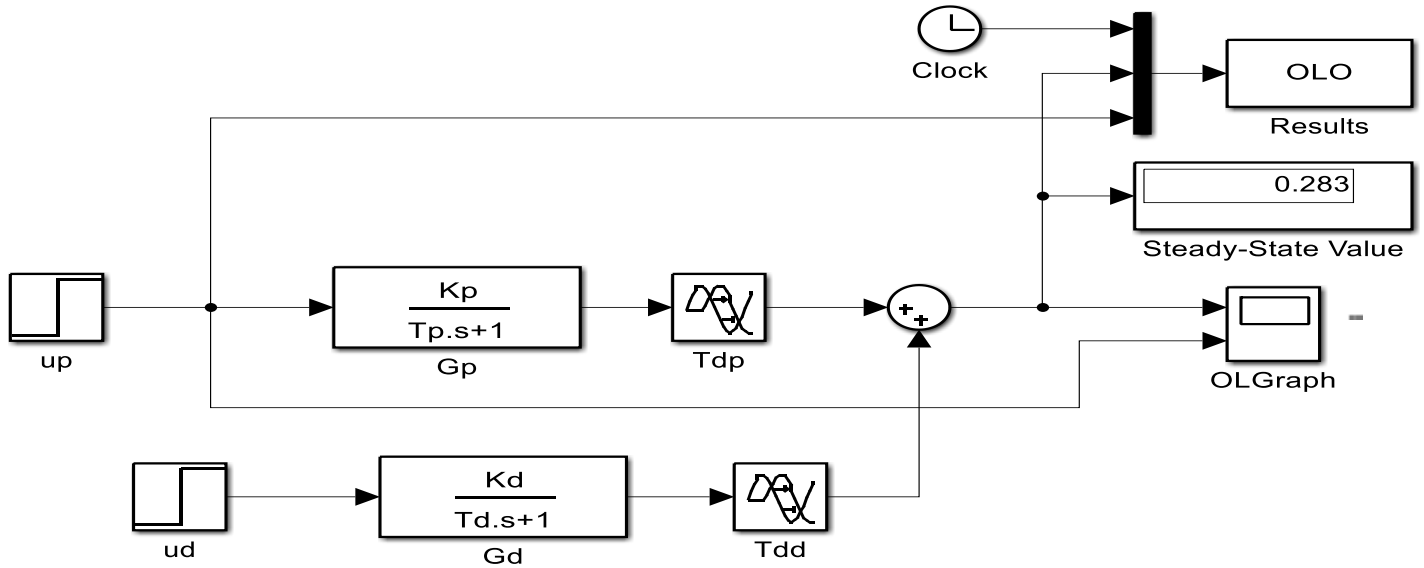

Figure 1. Open loop model of the process

Simulink Modelling and Closed Loop Simulation of the Process

After developing the model of the process and studying its open loop behaviours, its closed loop simulations were also carried out using the closed loop models, shown in Figures 2 – 4, developed with the aid of Simulink for P-only, PI and PID controllers, respectively. The developed closed loop models of the process were simulated for regulatory (disturbance rejection) with the controllers (P-only, PI and PID) tuned with both Cohen-Coon and Ziegler-Nichols techniques by applying a unit step change to the steady state value of the disturbance variable. The controlled, manipulated and disturbance variables of the closed loop models were biodiesel bottom mole fraction, reboiler duty and reflux ratio, respectively.

The calculations of the values for the tuning parameters of the controllers, using Cohen-Coon and Ziegler-Nichols tuning techniques, were carried out by taking the transfer function of the controllers to be as shown in Equation (2) and applying the expressions given in Table 1.

$$G_c(s) = K_c\left(1 + \frac{1}{\tau_I s} + \tau_D s\right) \tag{2}$$

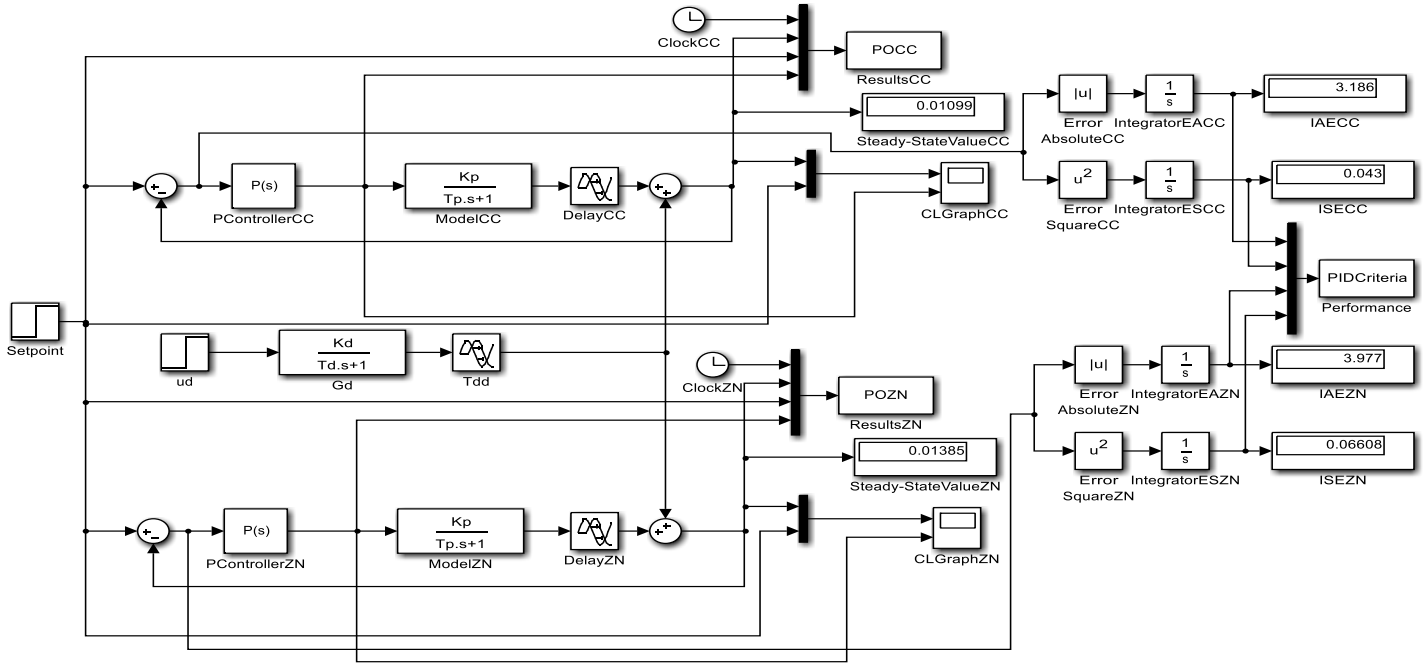

Figure 2. Closed loop model of the process with P-only controllers tuned with Cohen-Coon and Ziegler-Nichols techniques

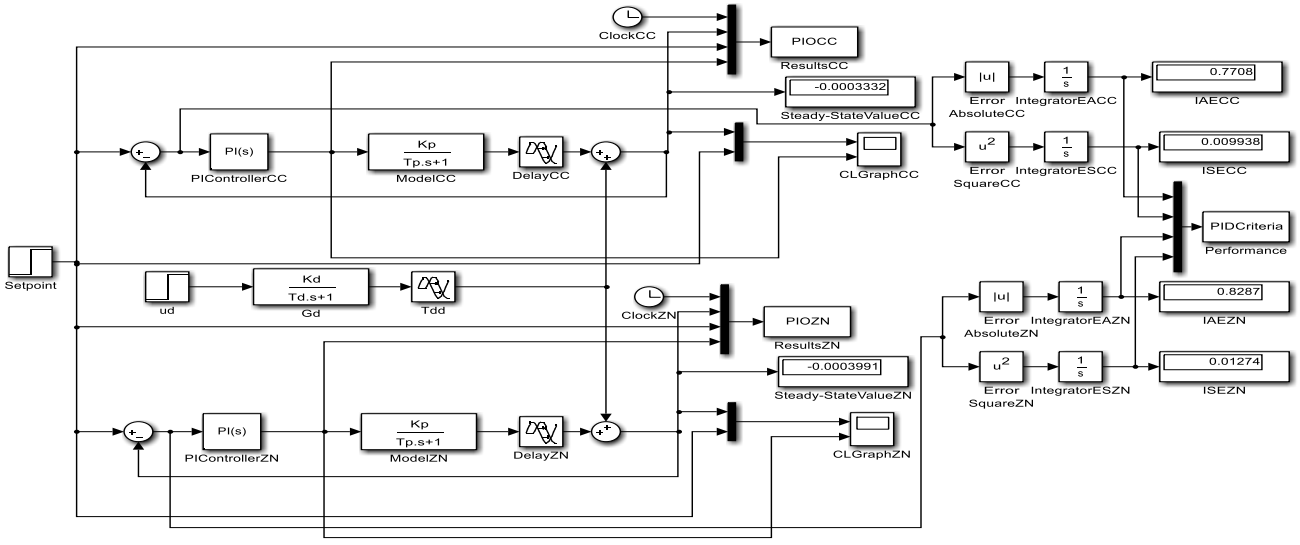

Figure 3. Closed loop model of the process with PI controllers tuned with Cohen-Coon and Ziegler-Nichols techniques

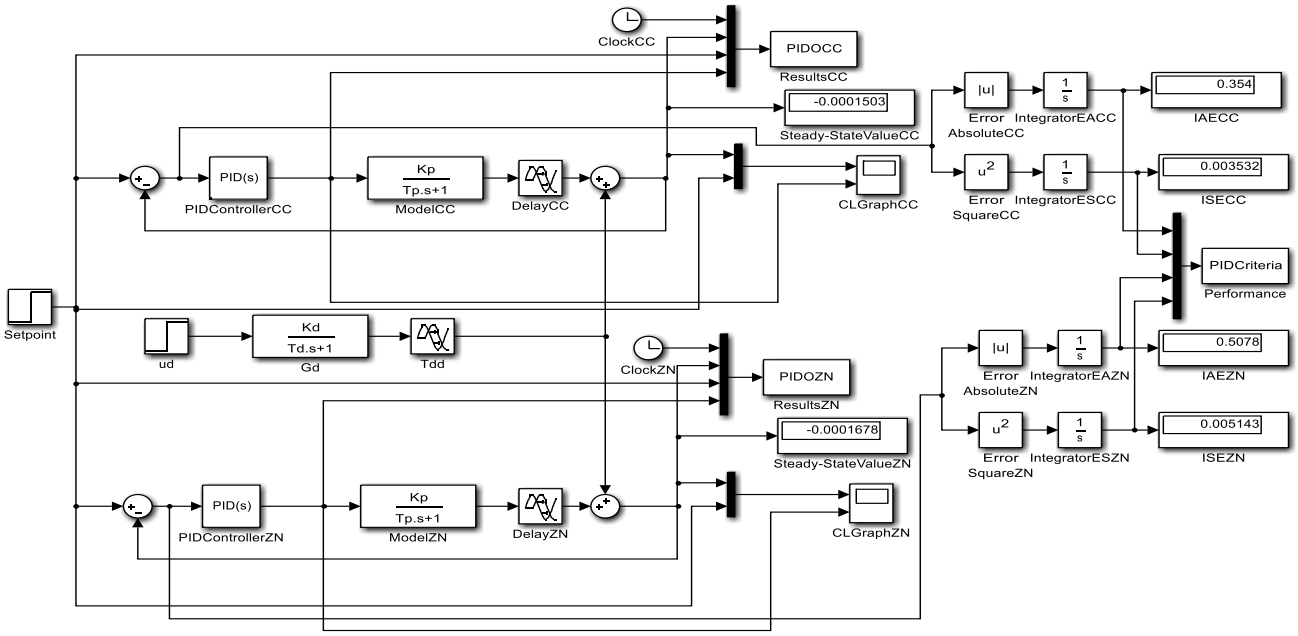

Figure 4. Closed-loop model of the process with PID controllers tuned with Cohen-Coon and Ziegler-Nichols techniques

Table 1: Cohen-Coon and Ziegler-Nichols tuning parameter expressions

Type of Control	Cohen-Coon Tuning Technique	Ziegler-Nichols Tuning Technique
Proportional (P)	$K_c = \frac{1}{K_p}\frac{\tau}{T_d}\left(1+\frac{T_d}{3\tau}\right)$	$K_c = \frac{K_u}{2}$
Proportional-Integral (PI)	$K_c = \frac{1}{K_p}\frac{\tau}{T_d}\left(0.9+\frac{T_d}{12\tau}\right)$	$K_c = \frac{K_u}{2.2}$
	$\tau_I = T_d\,\frac{30+3T_d/\tau}{9+20T_d/\tau}$	$\tau_I = \frac{P_u}{1.2}$
Proportional-Integral-Derivative (PID)	$K_c = \frac{1}{K_p}\frac{\tau}{T_d}\left(\frac{4}{3}+\frac{T_d}{4\tau}\right)$	$K_c = \frac{K_u}{1.7}$
	$\tau_I = T_d\,\frac{32+6T_d/\tau}{13+8T_d/\tau}$	$\tau_I = \frac{P_u}{2}$
	$\tau_D = T_d\,\frac{4}{11+2T_d/\tau}$	$\tau_D = \frac{P_u}{8}$

Source: Stephanopoulos, 1984

RESULT AND DISCUSSION

The resulting model obtained for the process after the incorporation of the disturbance transfer function model term was as given in Equation (3),

$$x_{biod}(s) = \frac{0.3382e^{(-8.999s)}}{248.43s+1} Q(s) + \frac{0.283e^{(-1.993s)}}{151.87s+1} R(s) \quad (3)$$

From Equation (3), it was observed that all the parameters (static gain, time constant and dead time) of the disturbance transfer model were, in magnitude, less than those of the main process transfer function model of the process. The lower time constant of the disturbance model was found to be an indication of the fact that the disturbance would respond faster than the main process if the same unit step change is applied to the two of them.

Shown in Figures 5 – 7 are the open-loop responses of the process to 1, 2, and 3 step unit(s) change in the reflux ratio, which was the disturbance variable of the process. As can be seen from the figure, the process was able to respond to the changes in the reflux ratio, but not as desired. Normally, it was expected of the output of the system to remain at zero, which was its set point in this case, even, in the presence of any disturbance. However, the observations made from the results (Figures 5 – 7) indicated that the simulation of the model with the applied step input changes were correct, as can be noticed from the magnitudes of the output variable (biodiesel mole fraction) of the three simulations carried out.

As such, it was clear from the deductions made from the figures that the process had to be controlled so as to keep its output at its desired set point (in this case of regulatory control, zero).

Based on this, the results obtained from the control of the process carried out with a unit step change in the disturbance variable using proportional (P), proportional-integral (PI) and proportional-integral-derivative (PID) controllers were as given in Figure 8 – 10. In each of the figures, the closed-loop dynamic responses of the process to a unit step change in the disturbance variable obtained using the three controller types tuned with Cohen-Coon and Ziegler-Nichols techniques are shown.

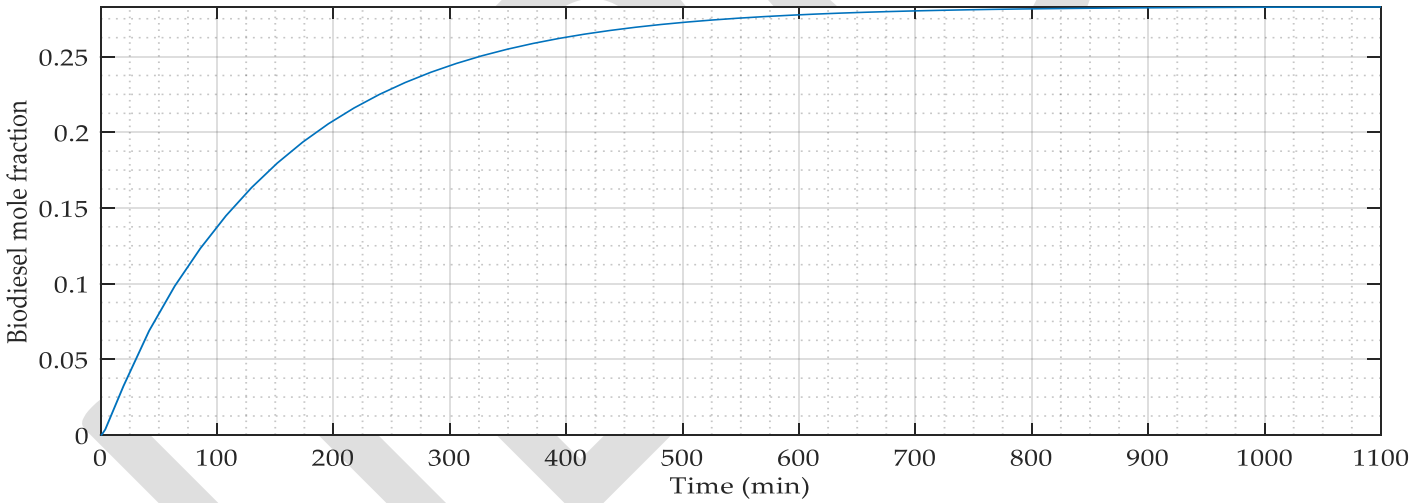

Figure 5. Open loop response of the process to 1 unit step change in the reflux ratio of the process

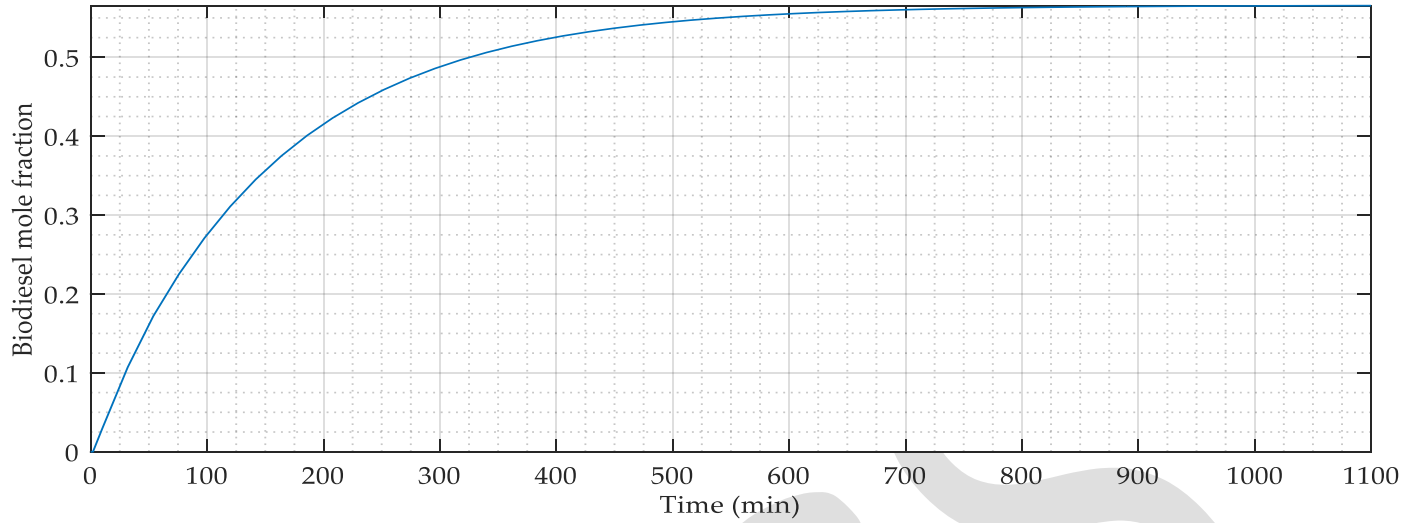

Figure 6. Open loop response of the process to 2 units step change in the reflux ratio of the process

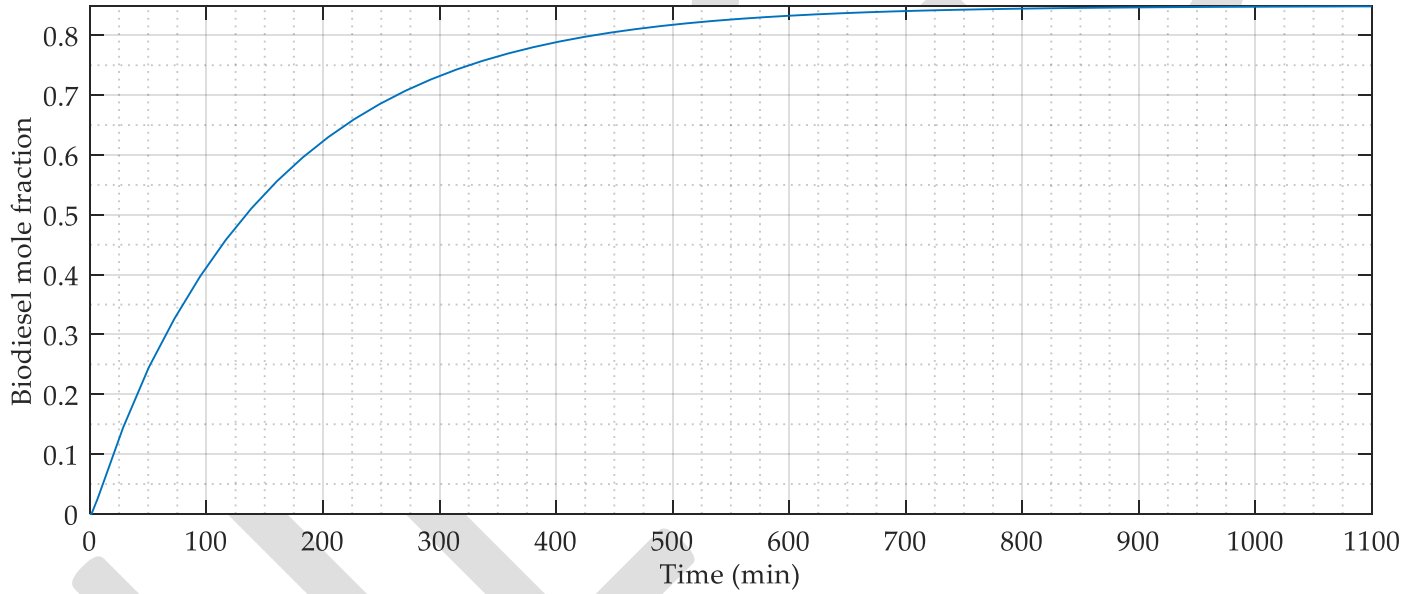

Figure 7. Open loop response of the process to 3 units step change in the reflux ratio of the process

From Figure 8, it was clear that the performance of P-only controller was not good for the process because it was not able to make the system settle at the desired set point at the end of the simulation time of 450 min chosen. Looking at the results, there seemed to be offsets associated with the responses of the P-only controllers tuned with Cohen-Coon and Ziegler-Nichols techniques, but the response of the Cohen-Coon tuning technique was found to be closer to the desired set-point of the system than that of the Ziegler-Nichols. From the responses given in Figure 8, it was very obvious that the performance of Cohen-Coon was better than that of Ziegler-Nichols for this case of the P-only controller in handling this process of biodiesel production for the regulatory control.

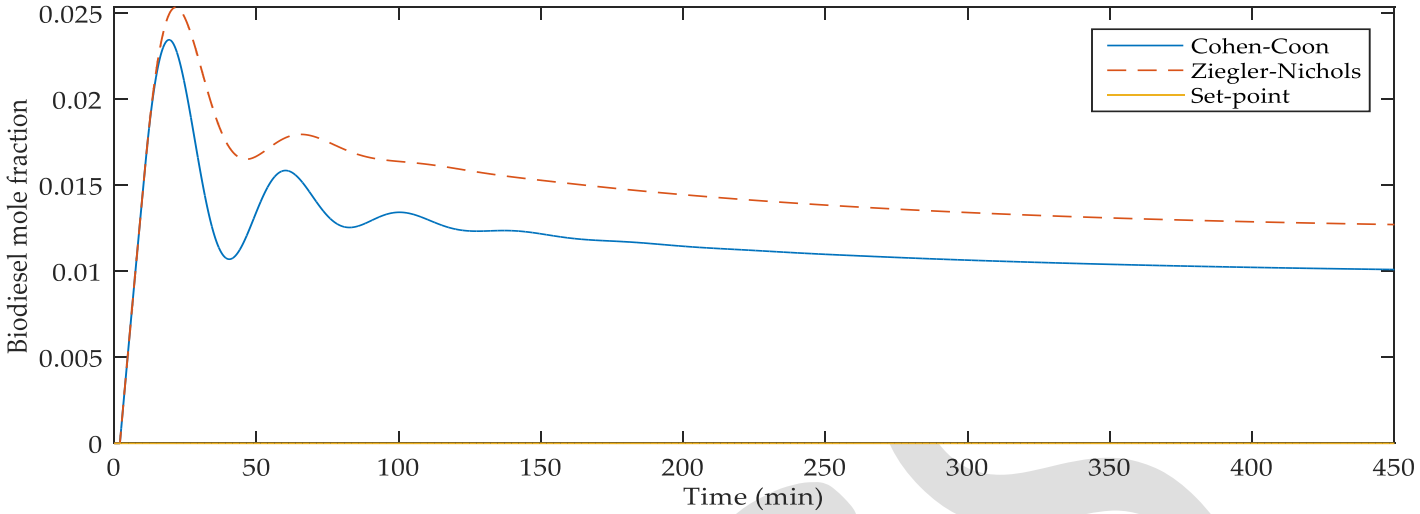

Figure 8. Closed loop responses of P-only controlled process

Shown in Figure 9 are the closed loop dynamic responses of the system obtained when Cohen-Coon and Ziegler-Nichols tuned PI controllers were used to control it. From the figure, it was seen that the performances of the two controllers (PI controller tuned with Cohen-Coon and Ziegler-Nichols techniques) were better than those of the P-only controllers considered before. Moreover, it was also noticed that even though the overshoot of the PI controller tuned with Ziegler-Nichols method was higher than that of the one tuned with Cohen-Coon technique, its number of oscillations was found to be lesser and decay faster. All in all, the responses of both of them were found to get stabilized at the desired set point within the simulation time of 450 min considered.

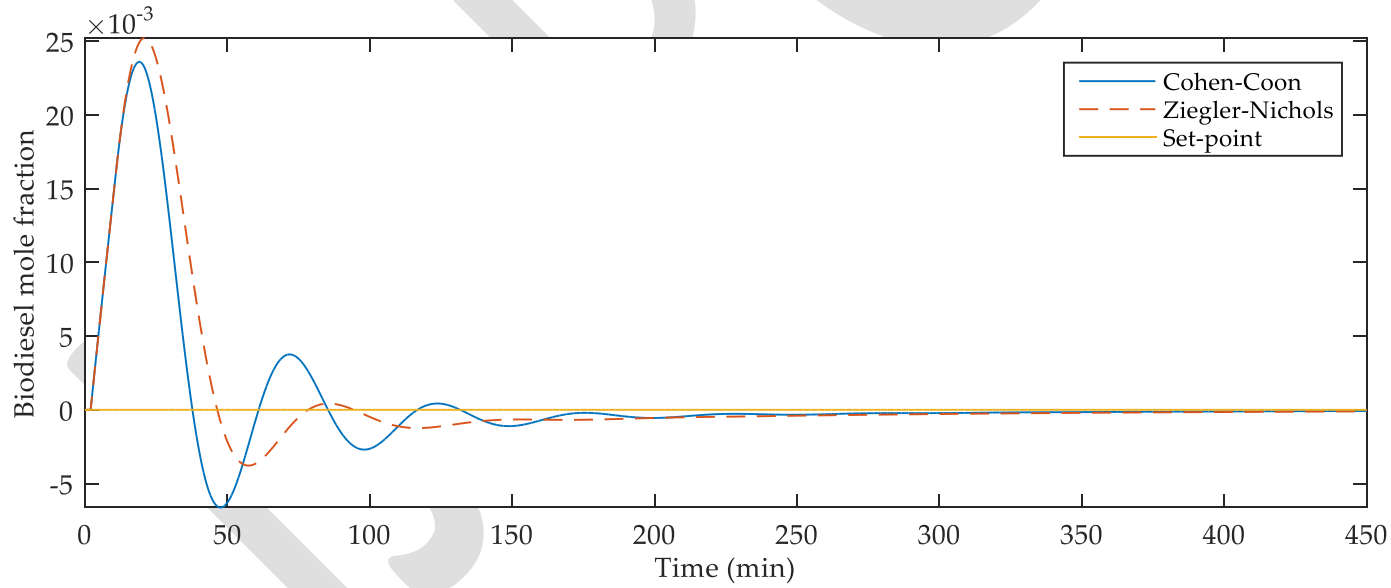

Figure 9. Closed loop responses of PI controlled process

Although the performances of the Cohen-Coon and Ziegler-Nichols tuned PI controllers were found to be better than those of the P-only controllers and satisfactory, it was still deemed necessary to get the responses of the system when controlled with Cohen-Coon and Ziegler-Nichols tuned PID controllers, and given in Figure 10 are the responses obtained.

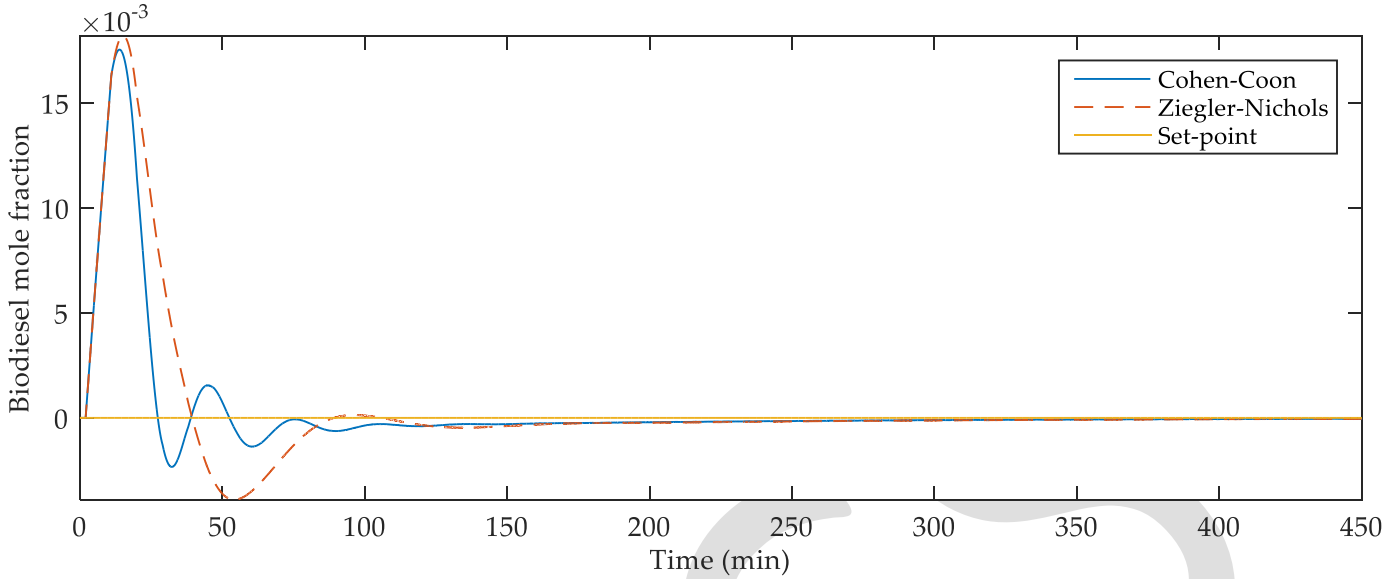

Figure 10. Closed loop responses of PID controlled process

From the figure (Figure 10), it was seen that the response with the higher overshoot was the one obtained from the simulation carried out using PID controller tuned with Ziegler-Nichols technique, just as it was obtained in the case of the PI controller investigated earlier, but its magnitude was found to be less than that given by the PI controller tuned with the same technique (Ziegler-Nichols). Also noticed from the results given in Figure 10 was that less oscillations were found to occur with the use of PID controllers.

In order to get a clearer picture on the performances of the controllers considered, their performance criteria values were calculated, and given in Table 2 are the results obtained from the estimation of the integral absolute error (IAE) and the integral squared error (ISE) of the controllers (P, PI and PID) tuned with Cohen-Coon and Ziegler-Nichols techniques.

Table 2. Performance criteria values of the controllers

Controller	Cohen-Coon Tuning Technique		Ziegler-Nichols Tuning Technique	
	IAE	ISE	IAE	ISE
P	5.28	0.06	6.61	0.10
PI	0.80	0.01	0.87	0.01
PID	0.37	0.00	0.53	0.01

From the results given in Table 2, for this case of disturbance rejection (regulatory) control study of the reactive distillation process, the performances of the controllers tuned with Cohen-Coon technique were discovered to be better than those of the ones tuned with Ziegler-Nichols technique because most of their corresponding IAEs and ISEs were found to be lower.

CONCLUSION

The results obtained from the open loop dynamic simulation of the reactive distillation process used for biodiesel production have shown that the disturbance variable had effects on the output of the process because the steps applied to it made the output not to be at the desired set point. Furthermore, the application of P, PI and PID controllers tuned with Cohen-Coon and Ziegler-Nichols techniques revealed that the process could be made to behave as desired. However, the response given by the simulation of the system with P-only controller was found not to settle at the desired set-point value, while the simulations with PI and PID were able to bring the output to the desired reference value within the time considered. Moreover, the performance of the PID controller tuned with Cohen-Coon technique was found to be the best among the ones studied for this case of the regulatory control of biodiesel production using reactive distillation because its IAE and ISE were found to be the lowest. This finding was, actually, found to be in contrary to that of Giwa *et al.* (2015b) who obtained that the best controller for the biodiesel production system was PID controller tuned with Ziegler-

Nichols. However, their own work considered set-point tracking only. This has, therefore, shown that a particular controller type may not be able to handle both set-point tracking and disturbance rejection best in all cases.

NOMENCLATURE

τ_D	Derivative time of the controller (min)
τ_d	Time constant of the disturbance process model (min)
τ_I	Integral time of the controller (min)
τ_p	Time constant of the main process model (min)
$G_c(s)$	Controller transfer function
$G_p(s)$	Process transfer function
IAE	Integral Absolute Error
ISE	Integral Squared Error
K_c	Proportional gain of the controller
K_d	Static gain of the disturbance process model
K_p	Static gain of the main process model
K_u	Ultimate gain
NNDMPC	Neural Network Decoupling Model Predictive Controller
P	Proportional
PI	Proportional-Integral
PID	Proportional-Integral-Derivative
P_u	Ultimate period (min/cycle)
Q	Reboiler duty (kJ/s)
R	Reflux ratio
SISO	Single-input single-output
T_{dd}	Dead time of the disturbance process model (min)
T_{dp}	Dead time of the main process model (min)
TFDMPC	Transfer Function Decoupling Model Predictive Controller
x_{biod}	Bottom biodiesel mole fraction

REFERENCES:

1) Al-Arfaj M.A. and Luyben W.L. (2002a). Design and Control of an Olefin Metathesis Reactive Distillation Column. Chemical Engineering Science. 57, 715-733.
2) Al-Arfaj M.A. and Luyben W.L. (2002b). Comparative Control Study of Ideal and Methyl Acetate Reactive Distillation. Chemical Engineering Science. 57, 5039-5050.
3) Al-Arfaj, M.A. and Luyben, W.L. (2000). Comparison of Alternative Control Structures for an Ideal Two-Product Reactive Distillation Column. Industrial and Engineering Chemistry Research, 39, 3298-3307.
4) Bock, H., Wozny, G. and Gutsche, B. (1997). Design and Control of a Reaction Distillation Column Including the Recovery System. Chemical Engineering and Processing, 36, 101- 09.
5) Giwa, A. (2012). Steady-State Modeling of n-Butyl Acetate Transesterification Process Using Aspen PLUS: Conventional versus Integrated. ARPN Journal of Engineering and Applied Sciences, 7(12), 1555-1564.
6) Giwa, A. (2013a). Sensitivity Analysis of ETBE Production Process Using Aspen PLUS. International Journal of Advanced Scientific and Technical Research. 3(1), 293-303.
7) Giwa, A. (2014). Solving the Dynamic Models of Reactive Packed Distillation Process Using Difference Formula Approaches. ARPN Journal of Engineering and Applied Sciences, 9(2), 98-108.
8) Giwa, A. and Giwa, S.O. (2012). Optimization of Transesterification Reaction Integrated Distillation Column Using Design Expert and Excel Solver. International Journal of Advanced Scientific and Technical Research. 2(6): 423-435.
9) Giwa, A. and Giwa, S.O. (2013a). Isopropyl Myristate Production Process Optimization Using Response Surface Methodology and MATLAB. Journal of Engineering Research & Technology, 2(1), 853-862.
10) Giwa, A. and Giwa, S.O. (2013b). Estimating the Optimum Operating Parameters of Olefin Metathesis Reactive Distillation Process. ARPN Journal of Engineering and Applied Sciences, 8(8), 614-624.
11) Giwa, A. and Karacan, S. (2012a). Modeling and Simulation of a Reactive Packed Distillation Column Using Delayed Neural Networks, Chaotic Modeling and Simulation, 2(1), 101-108.

12) Giwa, A. and Karacan, S. (2012b). Black-Box Modelling of Ethyl Acetate Reactive Packed Distillation Column, AU Journal of Technology, 15(3), 172-178.
13) Giwa, A. and Karacan, S. (2012c). Development of Dynamic Models for a Reactive Packed Distillation Column. International Journal of Engineering, 6(3), 118-128.
14) Giwa, A. and Karacan, S. (2012d). Decoupling Model Predictive Control of a Reactive Packed Distillation Column. Journal of Advances in Science and Technology, 4(6), 39-51.
15) Giwa, A. and Karacan, S. (2012e). Decoupling PID Control of a Reactive Packed Distillation Column. Journal of Engineering Research & Technology, 1(6), 1924-1933.
16) Giwa, A. and Karacan, S. (2012f). Nonlinear Black-Box Modeling of a Reactive Distillation Process, International Journal of Engineering Research & Technology, 1(7), 548-557.
17) Giwa, A. and Karacan, S. (2012g). Decoupling Control of a Reactive Distillation Process Using Tyreus-Luyben Technique. ARPN Journal of Engineering and Applied Sciences, 7(10), 1263-1272.
18) Giwa, A., Bello, A. and Giwa, S. O. (2014). Performance Analyses of Fatty Acids in Reactive Distillation Process for Biodiesel Production. International Journal of Scientific & Engineering Research, 5(12), 529-540.
19) Giwa, A., Bello, A. and Giwa, S. O. (2015a). Artificial Neural Network Modeling of a Reactive Distillation Process for Biodiesel Production. International Journal of Scientific & Engineering Research, 6(1), 1175- 1191.
20) Giwa, A., Giwa, S.O. and Adeyi, A.A. (2015b). Dynamics and Servo Control of Biodiesel Purity from a Reactive Distillation Process. International Journal of Scientific & Engineering Research, 6(8), 146-156.
21) Giwa, A., Giwa, S.O., Bayram, İ., and Karacan, S. (2013). Simulations and Economic Analyses of Ethyl Acetate Productions by Conventional and Reactive Distillation Processes Using Aspen Plus. Journal of Engineering Research & Technology, 2(8), 594-605.
22) Grüner, S., Mohl, K.D., Kienle, A., Gilles, E.D. Fernholz, G. and Friedrich, M. (2003). Nonlinear Control of a Reactive Distillation Column. Control Engineering Practice, 11, 915-925.
23) Jaya, N. and Ethirajulu, E. (2011). Kinetic Modeling of Transesterification Reaction for Biodiesel Production Using Heterogeneous Catalyst. International Journal of Engineering Science and Technology, 3(4), 3463-3466.
24) Khaledi, R. and Young, B.R. (2005). Modeling and Model Predictive Control of Composition and Conversion in an ETBE Reactive Distillation Column. Industrial and Engineering Chemistry Research, 44, 3134-3145.
25) Kumar, A. and Daoutidis, P. (1999). Modeling, Analysis and Control of Ethylene Glycol Reactive Distillation Column. AIChE Journal, 45, 51-68.
26) Kusmiyati, K. and Sugiharto, A. (2010). Production of Biodiesel from Oleic Acid and Methanol by Reactive Distillation. Bulletin of Chemical Reaction Engineering & Catalysis, 5(1), 1-6.
27) MathWorks. (2015). MATLAB, The Language of Technical Computing. The MathWorks, Inc., Natick.
28) Monroy-Loperena, R., Perez-Cisneros, E. and Alvarez-Ramirez, J. (2000). A Robust PI Control Configuration for a High-Purity Ethylene Glycol Reactive Distillation Column. Chemical Engineering Science, 55, 4925-4937.
29) Prakash K.J.J, Patle D.S. and Jana A.K. (2011). Neuro-Estimator Based GMC Control of a Batch Reactive Distillation. ISA Transactions. 50, 357-363.
30) Simasatitkul, L., Siricharnsakunchai, P., Patcharavorachot, Y., Assabumrungrat, S., and Arpornwichanop, A. (2011). Reactive Distillation for Biodiesel Production from Soybean Oil. Korean J. Chem. Eng., 28(3), 649-655.
31) Sneesby, M.G., Tade, M.O. and Smith, T.N. (1999). Two-Point Control of a Reactive Distillation Column for Composition and Conversion. Journal of Process Control, 9, 19-31.
32) Sneesby, M.G., Tade, M.O., Datta, R. and Smith, T.N. (1997). ETBE Synthesis via Reactive Distillation. 2. Dynamic Simulation and Control Aspects. Industrial and Engineering Chemistry Research, 36, 1870-1881.
33) Stephanopoulos, G. (1984). Chemical Process Control: An Introduction to Theory and Practice. PTR Prentice Hall, New Jersey.
34) Völker, M., Sonntag, C. and Engell, S. (2007). Control of Integrated Processes: A Case Study on Reactive Distillation in a Medium-Scale Pilot Plant. Control Engineering Practice, 15, 863-881.
35) Vora, N. and Daoutidis, P. (2001). Dynamics and Control of an Ethyl Acetate Reactive Distillation Column. Industrial and Engineering Chemistry Research, 40, 833-849.
36) Wang, S., Ma, X., Gong, J., Yang, X., Guo, H., and Xu, G. (2004). Transesterification of dimethyl oxalate with phenol under SnO_2/SiO_2 catalysts, Industrial and Engineering Chemistry Research, 43, 4027-4030.

International Journal of Engineering Research and General Science Volume 3, Issue 5, September-October, 2015
ISSN 2091-2730

Hiding The Results of Medical Test in Medical Digital Image

Orooba Ismaeel Ibraheem Al-Farraji

Orooba1@gmail.com

Abstract— Digital image steganography has been proposed as a method to enhance medical data security . confidentiality and integrity . Medical image steganography requires extreme care when embedding additional data within the medical images because the additional information must not affect the image quality. Many of the exploration systems used for medical diagnosis are based on the medical study images.

Keywords— medical Image, results of medical tests, steganography, text in Image steganography , Information Hiding

INTRODUCTION

Steganography is an art and science of invisible communication [10].In recent years image steganography has become an important research area in data security , confidentiality and image integrity. Medical image steganography requires extreme care when embedding additional data within the medical images because the additional information must not affect the image quality.

Medical images are stored for different purposes such as diagnosis , long time storage and research .

In the medical field the importance of the medical data security has been emphasized , especially with respect to the information referring to the patients (personal data, studies and diagnosis) [1]. On other hand the amount of digital medical images transmitted over the internet has increased rapidly , on the other hand the necessity of fast and secure diagnosis is important in the medical field ,i.e telemedicine, making steganography the answer to more secure image transmission . For applications that with images , the steganography aim is to embed invisible message in an image.

USES OF STEGANOGRAPHY

Steganography can be used anytime you want to hide data. There are many reasons to hide data but they all boil down to the desire to prevent unauthorized persons from becoming aware of existence of message. In the business world Steganography can be used to hide a secret chemical formula or plans for a new invention. Steganography can also be used for corporate espionage by sending out trade secrets without anyone at the company being any the wiser. Steganography can also be used in the non-commercial sector to hide information that someone wants to keep private. Spies have used it since the time to pass messages undetected [1].

The healthcare industry and especially medical imaging systems may benefit from information hiding techniques the use standards such as DICOM (digital imaging and communication in medicine) which separates image data from the caption, such as the name of the picture is lost, thus, embedding the name of the patient in the image could be a useful safety measure [5].

DIGITAL MEDICAL IMAGE

A digital image is a two dimensional function, f, that takes an input two spatial coordinates x and y and returns a value f(x,y). The value f(x,y) is a gray level of the image at that point. The gray level is also called the intensity.

Digital images are a discretized partition of the spatial images into small cells which are referred to as pixels - picture elements.

Medical imaging is a field where researchers develop tools and technology to acquire, manipulate and archive digital images which are used by the medical profession to provide better care to the patients.

THE NEW PROPOSED SYSTEM

The new proposed system take as input the embedded-object which in our case file of text and the cover object which is either a 256 color-image or gray scale image (size 640 x 480).

We use in our case an 8-bit image and since 8-bit image and since 8-bit values can only have a maximum of 256 colors the image must be chosen much more carefully.

BACKGROUND

Steganographic software is new and very effective. Such software enables information to be hidden in image, sound and apparently "blank" media.

In the computer, an image is an array of numbers that represent light intensities at various points in the image. A common size is 640 by 480 and 256 colors (or 8 bits per pixel). Such an image could contain about 300 kilobits of data [3].

There are usually two types of files used when embedding data into an image. The innocent looking image which will hold the hidden information a "container." A "message" is the information to be hidden. A message may be plain-text, cipher text, other images or any thing that can be embedded in the least significant bits (LSB) of an image.

For example: Suppose we have a 24-bit image 1024 x 768 (this is a common resolution for satellite images, electronic astral photography and other high resolution graphics). This may produce a file over 2 megabytes in size (1024x768x24/8 =2,359,296 bytes). All color variations are derived from three primary colors, Red, Green and Blue. Each primary color is represented by 1 byte (8 bits). 24-bit images use 3 bytes per pixel. If information is stored in the least significant bit (LSB) of each byte, 3 bits can be a stored in each pixel. The "container" image will look identical to the human eye, even if viewing the picture side by side with the original. Unfortunately, 24-bit images are uncommon (with exception of the formats mentioned earlier) and quite large. They would draw attention to themselves when being transmitted across a network. Compression would be beneficial if not necessary to transmit such a file. But file compression may interfere with the storage of information.

THE NEW PROJECT OPERATION

The embedding process of new system has many operations:

Select cover image, by taking the medical image for specific patient stored previously.

Input the results of medical tests to be hidden that can be done by open new file and entered directly or by select a previous stored file.

Open –cover (bmp file) and split the body to blocks , we split the body in order to obtain small number of position to be easy in hide.

Find the position where to hide the bytes of the text in the blocks of image (cover) and store the block numbers and the number of position in file to use later.

Substitute the character in the position get from the search program, in fact the substitution it merely locate the position that hide in it.

Hide position will hide the block numbers where the character was hidden.

Combine the blocks into a one file and then combine the header and the body file into a file to perform the stego-object (bmp file).

The new proposed system has a key which is used to extract the embedding image from stego –image. , the key is the size of text file and number of position we began hide in it the second key is transferred separately.

In figure (1) shows the flowchart of system.

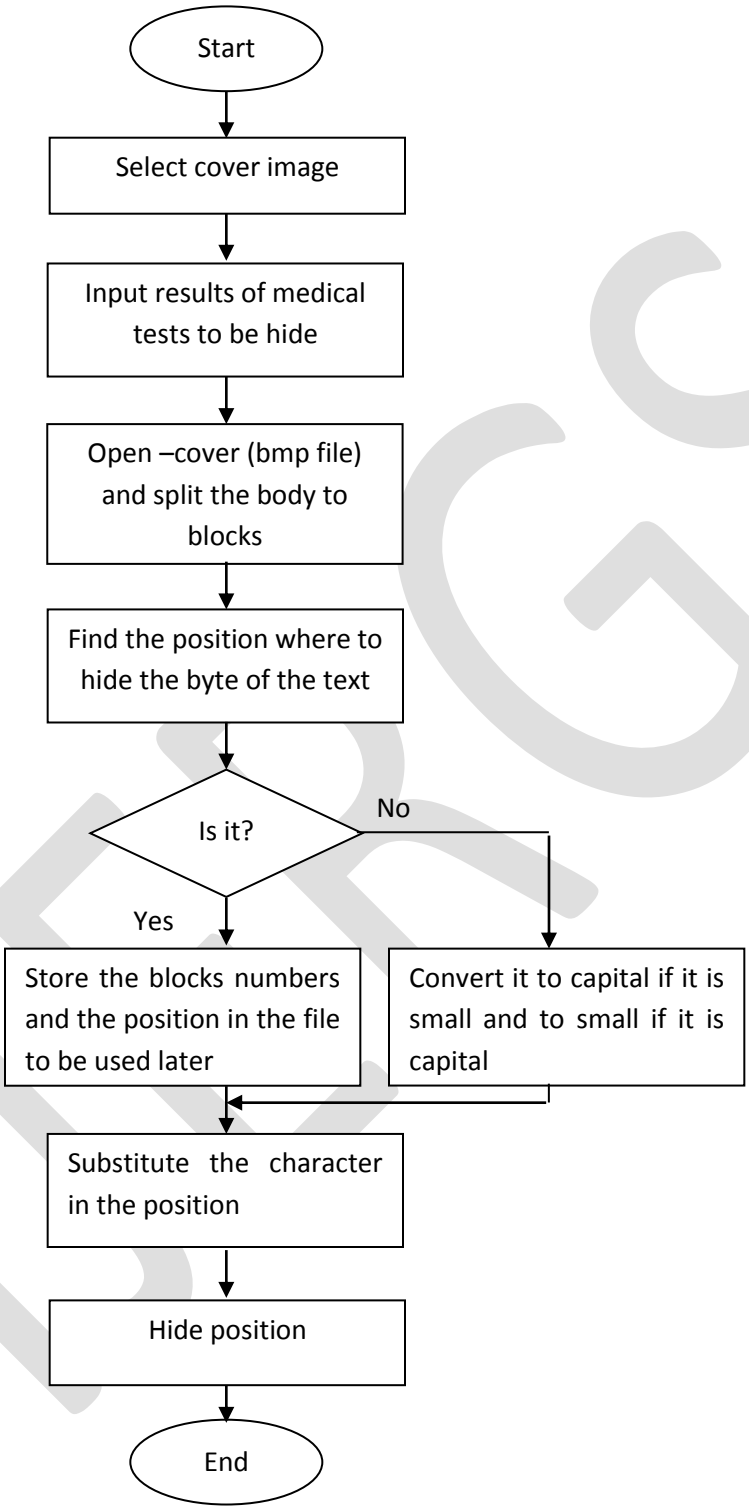

Figure (1) Flowchart of the system

The following steps describe the algorithm:

Step1- Open Cover (the bmp-file) Operation

This operation will open the bmp file and save header in a file and save the palette value of body in another file.

Step2- Split the body of the image file operation

This operation will split the body image in equal blocks to use these blocks in hide medical tests, we split the body in order to obtain small number of position to be easy in hide.

Step3- Find the position operation this operation is done by read a block from block image file and test if block is suitable to hide a byte from text file or not. The testing is done by compare the value of the palette with ASCII value of character. Then we find the position that we hide the character and save the block number and position in a file.

Step4- Substitute the character operation this operation is done by read character from text file and locate the position was to hide the character in the block. Replace the character in specific position and hide the position of the replaced character in the first row and last row of the block.

To find the coordinates (i.e., row and column number) of position we apply the following equations:

R= pos div 20 ……1

R: row

Pos: position in array

The equation for the column position is:

C= pos mod 20 ……..2

C: column

We substitute the row value that is calculated, from equation 1 into the current block that we search on it. We substitute it into first row (in LSB). While for the column value that is calculated from equation 2, we substitute it into last row of the current search block .we substitute it into LSB, in this operation the substitute of character don't change any thing in the pixel because the value of pixel in the palette equal to ASCII value of character, only change the places in the picture that we substitute the position of character in it. This change is unnoticeable because the number of position is small and substitute in LSB.

7 EXTRACTING THE EMBEDDING TEXT

Extracting the text is done by using the key stored into first block position that contains the key which is the length of the text that is hidden in the image.

Later get the row position from the first row and convert the binary value to a decimal value and in the same way we position by applying the following equation

Pos =(r+1) * 20- (20-c)

Get the character value from the specific position.

The following steps describe the algorithm:

Step1- Open the bmp file by reading the header and getting the body of the file

Step2- Split the file into blocks

Step3- by using the key get the first block that contains the first byte of the text.

Step4- Read the second byte of the key (which is the length of the text that is hidden in the image)

- For I= 1 to the length of the message do

Step5- Find the position of the embedded character from the first and the last row of the block.

Get the row position from the first row.

Convert the binary value to a decimal value.

Get the column position from the last row

Convert the binary value to a decimal value, get the position by applying the following equation:

Pos =(r+1) * 20- (20-c)

Get the character value from specific position.

Step6- From the current block find the position of the next block.

The number of the block is hidden in the first row (the second half) and the second half of the last row.

Step7- The end

EXPERIMENTAL RESULTS

The proposed system has been built using Borland C++ and can run on Pentium I computer and above, the setting of screen must be 800 X 600.

The results of the proposed system has been illustrated in the following

EXAMPLE

The medical test results size 110 character with space is:

RBC = 0-I/HPF , Pus cell= I-3/HPF , Casts=Nil ,Crystals= Amorph.ueate(+) Ca.oxalate(Few), Epi.Cell: Few, Other: Mucus(+)

And the gray scale image 640X 480 pixels so as mentioned previously shown in figure (2).

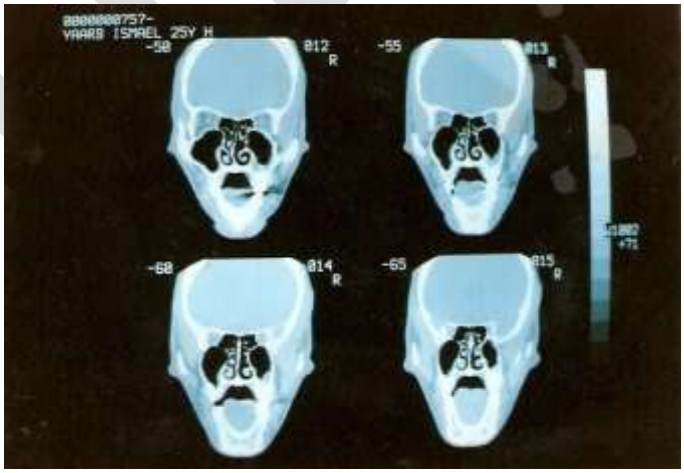

Figure (2): CT-scan Image (before Steganography)

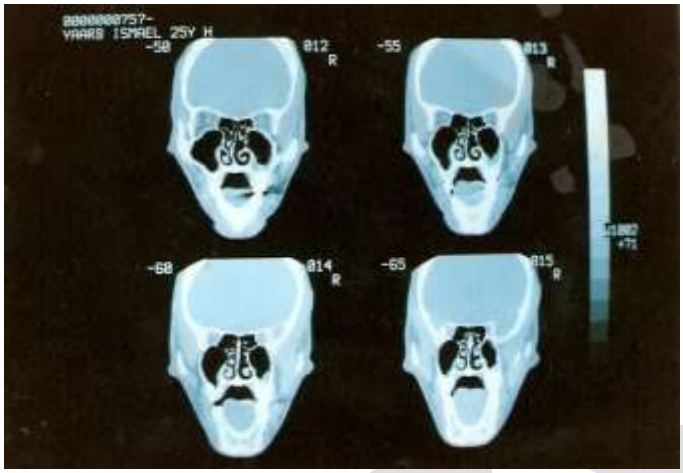

Figure (3): CT-scan Image (After Steganography)

Experimental Results And Performance Analysis

Use PSNR Function to Test the results

Signal to Noise Ratio (PSNR) is generally used to analyze quality of image, sound and video files in dB (decibels). PSNR calculation of two images, one original and an altered image, describes how far two images are equal. Figure 5 shows the famous formula.

MSE: Mean-Square error.
x: width of image.
y: height.
x*y: number of pixels (or quantities).

This function displays the PSNR (peak signal-to-noise ratio) between two images. The answer is in decibels (dB).

PSNR is very common in image processing. A sample use is in the comparison between an original image and a coded/decoded image. Typical quoted PSNR figures are in the range +25 to +35dB.

The syntax for this file is PSNR(A,B), where A and B are MATLAB Intensity Images, with matrix-elements in the interval [0,1]

$$PSNR(dB) = 10 * \log(\frac{255^2}{MSE})$$

$$MSE = \sum_{i=1}^{x}\sum_{j=1}^{y}\frac{\left(\left|A_{ij} - B_{ij}\right|\right)^2}{x * y}$$

.**PSNR formula**.

In watermarking. We asked each one of them of she/he could tell a watermarked image if they are presented with a pair of same size images printed on a piece of paper, one watermarked and the other not. None could tell the watermarked image from the non-watermarked image.

In order to observe the image quality of watermarked image objectively, the PSNR (Peak Signal to Noise Ratio) value of the image is calculated using the equation 3 and if the PSNR value is greater than 35dB, the watermarked image is within acceptable degradation levels.

PSNR =10×lg((2*n* −1)2 /*MSE*) (3)

Where *n* means the number of bits per sample value, the *MSE* represents mean square error between the host image and the watermarked image.

By using Matlab we input figure(2) and figure(3) to function PSNR the results equal 28.722 db and this value acceptable.

CONCLUSIONS

The proposed system proved to be a good system used to hide a text in medical digital image by compare value of palette with ASCII of character and if equal we hide position un another Place .

- In the proposed system transfer the medical image with The Results of Medical Test in high security

- The proposed system proved to be easy to use and efficient in terms security and hide every things about the patients.

- the proposed connect the computer science with medicine by useful a way and help in transfer medical information among the doctors in different country .

REFERENCES:

[1] G. Coatrieux et al. "Relevance of watermarking in Medical imaging " In IEEE embs Information Technology Applications in Biomedicine , Arlington, USA. 2000, pp. 250-255.

[2] Mike cry " Font color Steganography" , May ,11,2009

[3] Francesco Queirolo "steganography in Images", final communications Report, visited on : 26-2-2002, http://google.yahoo.com/bin/

[4] Johnson, Neil F., Duric, Zoron, Jajodia, "Information Hiding steganogarphy and watermarking- Attacks and Countermeasures" , Kluwer Academic Publishers., 2001

[5] Johnson, N.A., "Steganography", visited on: 2-2-2002. http://www.jjtc.com/stegdoc/indexz.html

[6] Johnson, N. F. "steganograhpy " , visited on: 18-2-2002. http://www.jjtc.com/stegdoc/sec313.html

[7] Katzenbeisser S. and petitcolas F., "Information Hiding Techniques for . steganograhpy and Digital Watermarking ",Artech House, USA 2000.

[8] Stevens, Roger T. "Graphics Programming in C",BPB Publications, 1993.

[9] Rodriguez-Colin Raul, Feregrino-Uribe Claudia, Trinidad-blas Gershom de J. "Data Hiding Scheme for Medical Images", Luis Enrique Erro No. 1 Sta . Maria Tonantzintla, Puebla, Mexico C. P. 72840 , 2008

[10] Shuliang Sun[1,2], "A New Information Hiding Method Based on Improved BPCS Steganography" , Volume 2015 , Article ID 698492, 7 pages , 2015

International Journal of Engineering Research and General Science Volume 3, Issue 5, September-October, 2015
ISSN 2091-2730

EFFECT OF WATER TEMPERATURES ON THE COMPRESSIVE STRENGTH, SLUMP AND SETTING TIME OF CONCRETE

UMEONYIAGU IKECHUKWU ETIENNE

Dept. of Civil Engineering,

Chukwuemeka Odumegwu Ojukwu University,

P.M.B.02, Uli.

umeonyiaguikechukwu@yahoo.com

ABSTRACT- This research conducted in Eastern Nigeria was aimed at determining the effects of mixing-water temperature on the compressive strength, workability and setting time of concrete. The river sand used was from River Otamiri and granite stones from Abakaliki were used as the coarse aggregates. These materials were prepared based on BS 812: 1987, BS410:1986 and BS 1881:1983. The temperatures of the water used were variously: – 5^0C, 10^0 C, 15^0C, 28^0C, 35^0C, 45^0C, 50^0C, 60^0C, 70^0C, 75^0C, 90^0C and 100^0C. The mix ratio of 1:2:4 with water –cement ratio of 0.58 by weight of concrete was used. It was found that the compressive strengths were increasing as the age increased. This increase reached a peak of 33.65Mpa at 50^0C after which the strength declined gradually to as low as 1.97Mpa at a water temperature of 100^0C. In terms of workability, the workability of the concrete increased as the temperature of the mixing-water increased, getting to a high of 175mm slump at 100^0C and became constant for temperatures between 28^0C – 50^0C. For setting time, the setting time of the paste increased with the rise in temperature of the mixing water. The study has revealed that water temperature has a significant influence on the strength, workability and setting time of concrete. Also, it was shown that the optimal temperature to achieve a high strength at 28 days was 50^0C.

Keywords: compressive strength, setting time, workability, aggregates, mixing water, temperature,slump.

1.0 INTRODUCTION

Concrete is defined as a material used in building construction, consisting of a hard, chemically inert particulate substance known as aggregate (usually made from different types of sand and gravels), that is bonded together by cement and water [1][2]. The first concrete was made by a British engineer, John Smeaton by adding pebbles as a coarse aggregate and mixing powdered brick into the cement. Many factors such as aggregate properties, weather conditions, and water purity level and water temperature affect the strength development of concrete [3][4]. To a large extent, the durability of concrete depends on the type of aggregate used. Aggregates can be either fine or coarse [5][6]. Water being an essential component in concrete mix has a direct influence on the strength, workability, durability and performance of concrete. A mechanical property of aggregates is water absorption [7] [8].

2. MATERIALS AND METHOD

2.1 MATERIALS

The coarse aggregate used was granite of 19mm size. It was sourced from Abakaliki, Eastern Nigeria. The fine aggregate was fine river sand from Otamiri River, also in Eastern Nigeria. The cement used was ordinary Portland cement.

2.2 METHODS

2.2.1 PREPARATIONS, CURING AND TESTING OF CONCRETE CUBE SAMPLES

The concrete mix ratio used was 1:2:4 with a water-cement ratio of 0.58. The water used in preparing the experimental samples satisfied the conditions prescribed in BS 3148 [9]. The water used in the experiment was either heated with a boiling ring or refrigerated to the required temperature. The required concrete specimens were made in threes in accordance with the method specified in BS 1881: 108 [10]. These specimens were cured for 3, 7, 14 and 28 days in accordance with BS 1881: Part 111 [11]. The testing of the cubes was done in accordance with BS 1881: Part 116 [12] using the compressive testing machine.

2.2.2 SLUMP TEST OF THE FRESH CONCRETE

The slump apparatus was a mould of 1.18mm thick galvanized metal in the form of frustrum of a cone with the base 200mm in diameter. The top was 100mm in diameter and the height 300mm. The taping end was a hemisphere 16mm in diameter.

2.2.3 SETTING TIME OF CEMENT PASTE

The setting time of the concrete was conducted using Vicat apparatus. The cement used for the test was mixed with water of 5, 10, 15, 28, 35, 50, 60, 70, 90 and 100^0C. The paste was then placed under a penetrometer and a stop watch was used to time the penetration of the pin.

3. RESULTS AND DISCUSSION

3.1 COMPRESSIVE STRENGTH TESTS

Figure 1 shows the graph of the compressive strength in Mpa against temperature (Celsius) from Day 1 to Day 28. At the control temperature (28.7 ^{0}C), the compressive strength ranged from 16.37 Mpa to 29.45 Mpa. At 5 degree Celsius, the compressive strength ranged from 11.47 Mpa at Day 1 to 26.65 Mpa at Day 28. At 10 degree Celsius, the compressive strength ranged from 14.07 Mpa at Day 1 to 28.12 Mpa at Day 28. At 15 degree Celsius, the compressive strength ranged from 14.66 Mpa at Day 1 to 28.22 Mpa at Day 28. At 35 degree Celsius, the compressive strength ranged from 7.75 Mpa at Day 1 to 30.38 Mpa at Day 28. At 45 degree Celsius, the compressive strength ranged from 10.08 Mpa at Day 1 to 34.19 Mpa at Day 28. At 50 degree Celsius, the compressive strength ranged from 8.41 Mpa at Day 1 to 33.90 Mpa at Day 28. At 60 degree Celsius, the compressive strength ranged from 5.58 Mpa at Day 1 to

22.78 Mpa at Day 28. At 70 degree Celsius, the compressive strength ranged from 5.15 Mpa at Day 1 to 20.62 Mpa at Day 28. At 75 degree Celsius, the compressive strength ranged from 4.13 Mpa at Day 1 to 18.57 Mpa at Day 28. At 90 degree Celsius, the compressive strength ranged from 3.09 Mpa at Day 1 to 10.64 Mpa at Day 28. At 100 degree Celsius, the compressive strength ranged from 2.05 Mpa at Day 1 to 8.20 Mpa at Day 28.

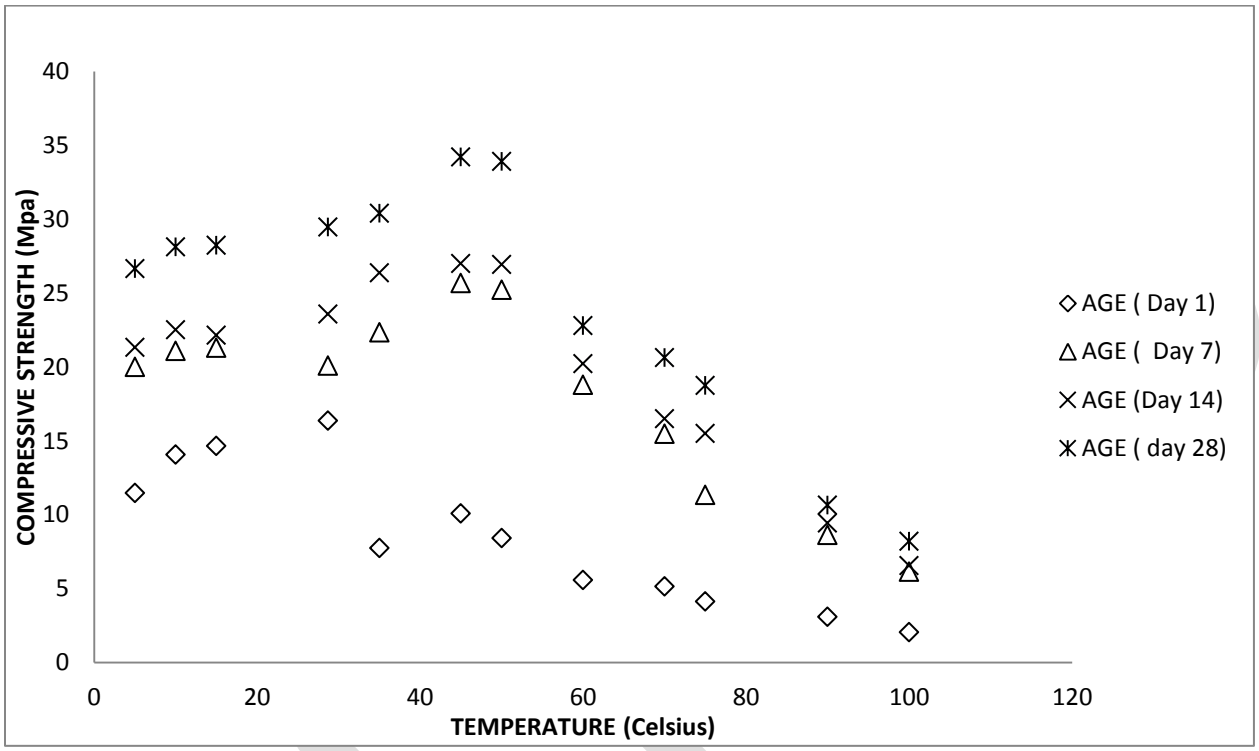

Figure 1 Graph of Compressive strength (Mpa) versus concrete mix – water temperatures (Degree Celsius)

3.2 SLUMP TESTS

Figure 2 shows the graph of slump (mm) at various water temperatures. The slump increased from 5mm at 5^0C to 175mm at 100^0C. In effect, the slump increased progressively as the water temperature increased.

3.3 SETTING TIME

Figure 3 shows the initial setting and the final setting time of cement paste at various water temperatures. The setting time of the cement paste increased as the water temperature increased.

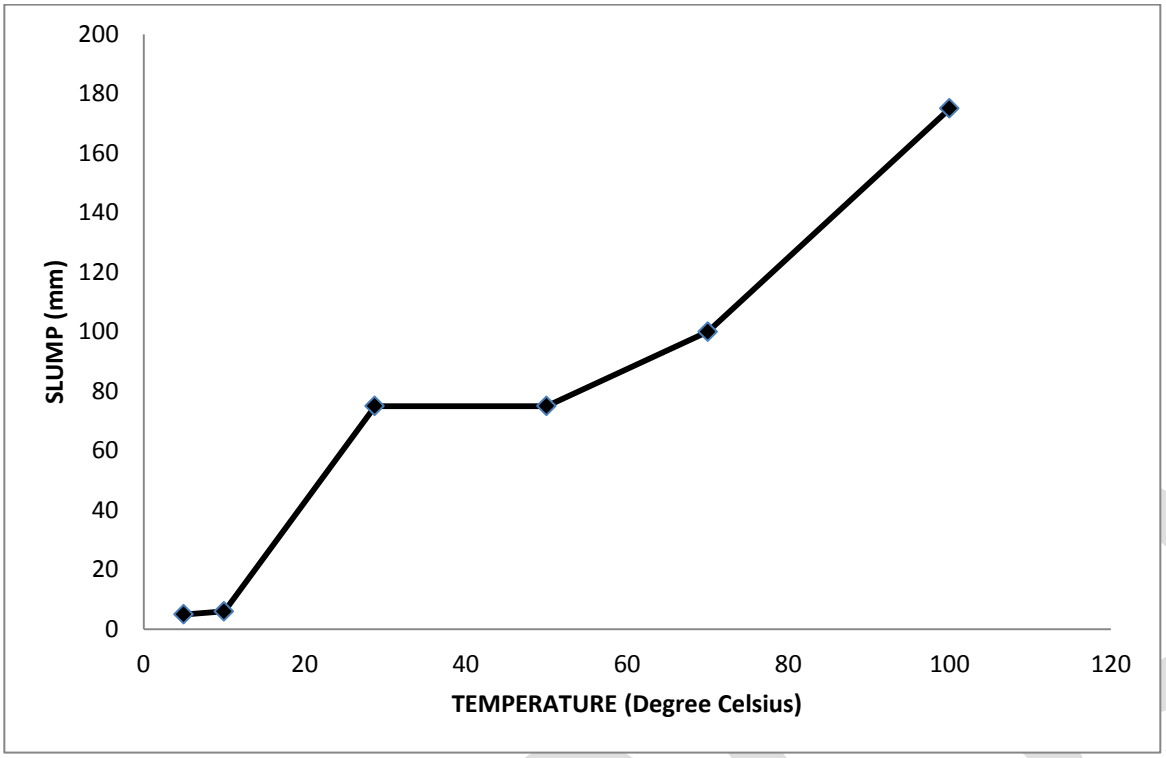

Figure 2 Graph of Slump (mm) versus concrete mix – water temperatures (Degree Celsius)

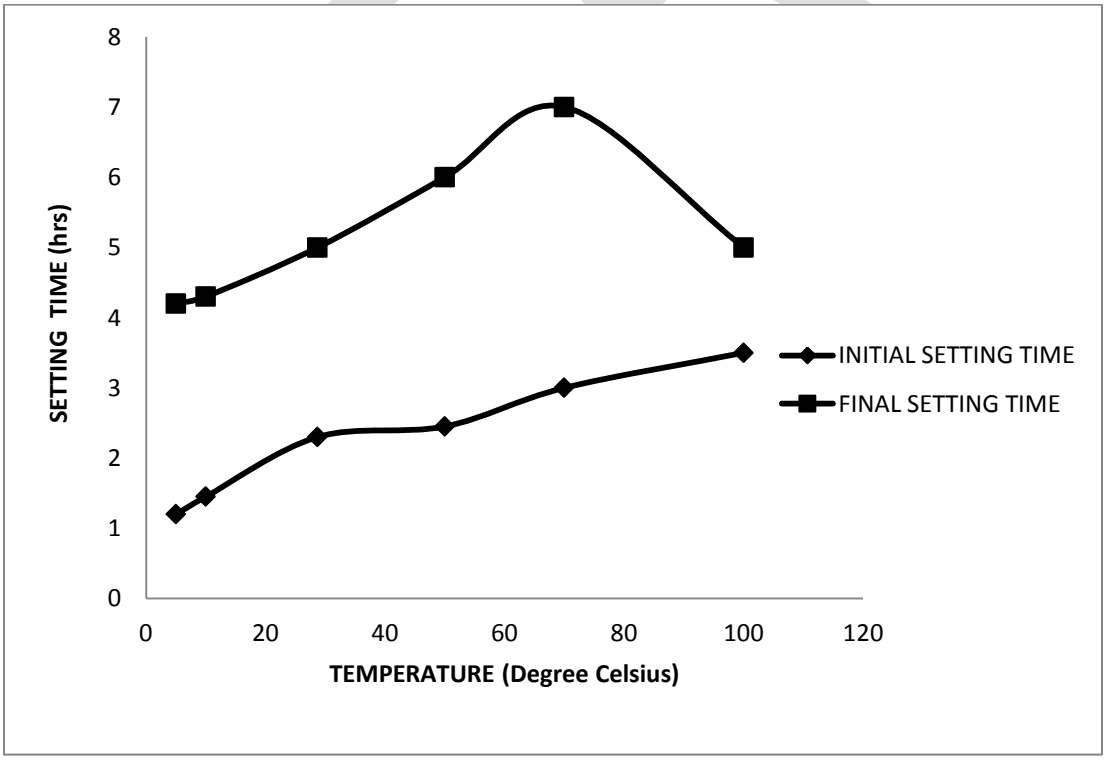

Figure3 Graph of Setting time (hrs) versus Water temperature (Degree Celsius)

4. CONCLUSIONS AND RECOMMENDATION

From the studies, the effect of water temperature, the effect of water temperature on the compressive strength and setting time of concrete was significant. It was found that the compressive strength increased with increase in mixing water temperature. Also, it was observed that the compressive strength for each age was a maximum at 50^0C. At above 50^0C water temperature, the compressive strength started declining. The maximum compressive strength was 33.65 Mpa at the age of 28 days. The workability of the concrete increased as the temperature of the mixing water increased getting to a high of 175mm slump at 100^0C. The setting time of concrete increased with rise in the temperature of the mixing water. This showed that water temperature had a significant influence on the strength, workability and setting time of concrete.

REFERENCES:

[1] Neville, A. M., *Properties of Concrete, Third Edition,* Pearson Education, Delhi, India, 2003, pp.268-358.

[2] Jackson, N and Dhir, R.K.,Civil Engineering Material, Macmillian ELBS, Hampshire RG21 2XS, England, 1988, pp. 10 – 32.

[3] Munoz, J.F., Tejedor, I., Anderson, M.A., and Cramer, S.M. *Effect Of Coarse Aggregate Clay-Coating On Concrete Performance*, Innovative Pavement Research Foundation, Report, 2005, p. 35.

[4] Verbeck, G.J., and Helmuth, R.A., Structures and Physical Properties of Cement Paste, Proc. 5th Int. Symp. on the Chemistry of Cement, Tokyo, 1968, pp. 1 – 32.

[5] Kaplan, M. F., Flexural and Compressive Strength of Concrete as Affected by the Properties of Coarse Aggregates, J. Amer. Concr. Inst.,55, 1959, pp. 1193 -1208.

[6] BS 882 *Specification for aggregates from natural sources for concrete.* British Standards Institution Publication, London, 1992, pp.2 – 6.

[7] ASTM. Standard C125 *Standard Terminology Relating To Concrete And Concrete Aggregates,* American Society for Testing and Materials Publication, New York, 2003, pp.10 – 12.

[8] Eurolightcon *Mechanical Properties of Lightweight Aggregate Concrete*, BE 96, 2000, pp.23.

[9] BS 3148 *Tests for water for making concrete.* British Standards Institution Publication, London, 1980, pp. 1 – 8.

[10] British Standard 1881: Part 108 *Method for making test cubes from fresh concrete.* British Standards Institution Publication, London, 1983,pp. 1 -4.

[11] British Standard 1881: Part 111 *Method of normal curing of test specimens (20 ^{o}C).* British Standards Institution Publication, London, 1983, pp. 1 -5.

[12] British Standard 1881: Part 116 *Method for determination of compressive strength.* British Standards Institution Publication, London, 1983, pp. 20 -30

International Journal of Engineering Research and General Science Volume 3, Issue 5, September-October, 2015
ISSN 2091-2730

A Survey on Coverage Problem in Wireless Ad Hoc and Sensor Networks

Er. Madhusmita Balabantaray, Er. Jyoti Prakash Swain,Dr.Madhumita Dash

1. Asst. Professor, 2.Lecturer, 3.Professor, Orissa Engineering College, Bhubaneswar, India

Email- madhusmita.sundaray@gmail.com,Contact no-9777615966

Abstract— A wireless sensor network (WSN) is composed of a group of small power-constrained nodes with functions of sensing and communication, which can be scattered over a vast region for the purpose of detecting or monitoring some special events.Today One of the fundamental issues in sensor networks is the *coverage* problem, which reflects how well a sensor network is monitored or tracked by sensors. In this paper, we formulate this problem as a decision problem, whose goal is to determine whether every point in the service area of the sensor network is covered by at least *k* sensors, where *k* is a given parameter. The sensing ranges of sensors can

be unit disks or non-unit disks. We present polynomial-time algorithms, in terms of the number of sensors, that can be easily translated to distributed protocols. The result is a generalization of some earlier results where only $k = 1$ is assumed. Applications of the result include determining insufficiently covered areas in a sensor network, enhancing fault-tolerant capability in hostile regions, and conserving energies of redundant sensors in a randomly deployed network. Our solutions can be easily translated to distributed protocols to solve the coverage

Keywords—Ad hoc network, Computer geometry, Coverage problem, Deployment, Ubiquitous Computing, wireless network, Sensor network

1.INTRODUCTION

The advancing in the sensor technology, micro-electromechanical systems, modern networking and wireless communications technology has greatly promoted the emergence and development of modern WSNs (Pottie, 1998; Stankovic, 2008).

For rapid progress of wireless communication and embedded micro-sensing MEMS technologies has made *wireless sensor networks* possible. Such environments may have many inexpensive wireless nodes, each capable of collecting, storing, and processing environmental information, and communicating with neighboring nodes. In the past, sensors are connected by wire lines. Today, this environment is combined with the novel *ad hoc* networking technology to facilitate inter-sensor communication [13,17]. The flexibility of installing and configuring a sensor network is thus greatly improved. Recently, a lot of research activities have been dedicated to sensor networks, including design issues related to the physical and media access layers [15,22,24] and routing and transport protocols [3,5,7]. Localization and positioning applications of wireless sensor networks are discussed in [2,4,11,14,19].

Since sensors may be spread in an arbitrary manner, one of the fundamental issues in a wireless sensor network is the *coverage problem*. In general, this reflects how well an area is monitored or tracked by sensors. In the literature, this problem has been formulated in various ways. For example, the *Art Gallery Problem* is to determine the number of observers necessary to cover an art gallery (i.e., the service area of the sensor network) such that every point in the art gallery is monitored by at least one observer. This problem can be solved optimally in a 2D plane, but is shown to be NP-hard when extended to a 3D space [12]. Reference [8] proposes polynomial time algorithms to find the *maximal breach path* and the *maximal support path* that are least and best monitored in the sensor network. How to find the *minimal and maximal exposure path* that takes the duration that an object is monitored by sensors is addressed in [9,20]. Localized exposure-based . coverage and location discovery algorithms are proposed in[10].

On the other hand, some works are targeted at particular applications, but the central idea is still related to the coverage issue. For example, sensors' on-duty time should be properly scheduled to conserve energy. Since sensors may be arbitrarily deployed, if some nodes share the common sensing region and task, then we can turn off some of them to conserve energy and thus extend the lifetime of the network. This is feasible if turning off some nodes still provide the same "coverage" (i.e., the provided coverage is not affected). Slijepcevic and Potkonjak [16] proposes a heuristic to select mutually exclusive sets of sensor nodes such that each set of sensors can provide a complete coverage of the monitored area. Also targeted at turning off some redundant nodes, Ye et al. [23] proposes a probe-based *density control* algorithm to put some nodes in a sensor-dense area to a doze mode to ensure a long lived, robust sensing coverage. A coverage-preserving node scheduling scheme is presented in [18] to determine when a node can be turned off and when it should be rescheduled to become active again. In this work, we consider a more general sensor coverage problem: given a set of sensors deployed in a target area, we want to determine if the area is sufficiently *k-covered*, in the sense that every point in the target area is covered by at least k sensors, where k is a given parameter. As a result, the aforementioned works [18,23] can be regarded as a special case of this problem with $k = 1$. Applications requiring $k > 1$may occur in situations where a stronger environmental monitoring capability is desired, such as military applications. It also happens when multiple sensors are required to detect an event. For example, the triangulation-based positioning protocols [13,14,19] require at least three sensors (i.e., $k \geq 3$) at any moment to monitor a moving object. Enforcing $k \geq 2$ is also desirable for fault-tolerant purpose. The work [21] also considers the same coverage problem combined with the communication connectivity issue. However, it incurs higher computational complexity to determine a network's coverage level as compared to the solution proposed in this paper. The *arrangement* issue [1,6], which is widely studied in combinatorial and computational geometry, also considers how a finite collection of geometric objects decomposes a space into connected elements. However, to construct arrangements, only *centralized* algorithms are proposed in the literature, whilst what we need for a wireless sensor network is a distributed solution. The solutions proposed in this paper can be easily translated to distributed protocols where each sensor only needs to collect local information to make its decision. In this paper, we propose a novel solution to determine whether a sensor network is *k*-covered. The sensing range of each sensor can be a unit disk or a non-unit disk. Rather than determining the coverage of each location, our approach tries to look at how the perimeter of each sensor's sensing range is covered, thus leading to an efficient polynomialtime algorithm. Note that this step can be executed by each sensor based on location information of its neighbors. This can lead to an efficient distributed solution. As long as the perimeters of sensors are sufficiently covered, the whole area is sufficiently covered. The *k*-coverage problem can be further extended to solve several application-domain problems. In Section 5, we discuss how to use our results for discovering insufficiently covered areas, conserving energy, and supporting hot spots. At the end, we also show how to extend our results to situations where sensors' sensing regions are irregular. This paper is organized as follows. Section 2 formally defines the coverage problems. Our solutions are presented in Section 3. Section 4 presents our simulation results and demonstrates a tool that we implemented to solve the *k*coverage problem. Section 5 further discusses several possible extensions and applications of the proposed solutions. Section 6 draws our conclusions.

2. PROBLEM STATEMENT

We are given a set of sensors, $S = \{s1, s2, \ldots, sn\}$, in a two dimensional area A. Each sensor si , $i = 1, \ldots, n$, is located at coordinate (xi , yi) inside A and has a sensing range of ri , i.e, it can monitor any point that is within a distance of ri from si .

DEFINITION 1. A location in A is said to be *covered* by si if it is within si 's sensing range. A location in A is said to be *j-covered* if it is within at least j sensors' sensing ranges.

DEFINITION 2. A *sub-region* in A is a set of points who are covered by the same set of sensors. We consider two versions of the coverage problem as follows.

DEFINITION 3. Given a natural number *k*, the *k-Non-unit-disk Coverage (k-NC) Problem* is a decision problem whose goal is to determine whether all points in *A* are *k*-covered or not.

DEFINITION 4. Given a natural number *k*, the *k-Unit-disk Coverage (k-UC) Problem* is a decision problem whose goal is to determine whether all points in *A* are *k*-covered or not, subject to the constraint that $r1 = r2 = \cdots = rn$.

Figure 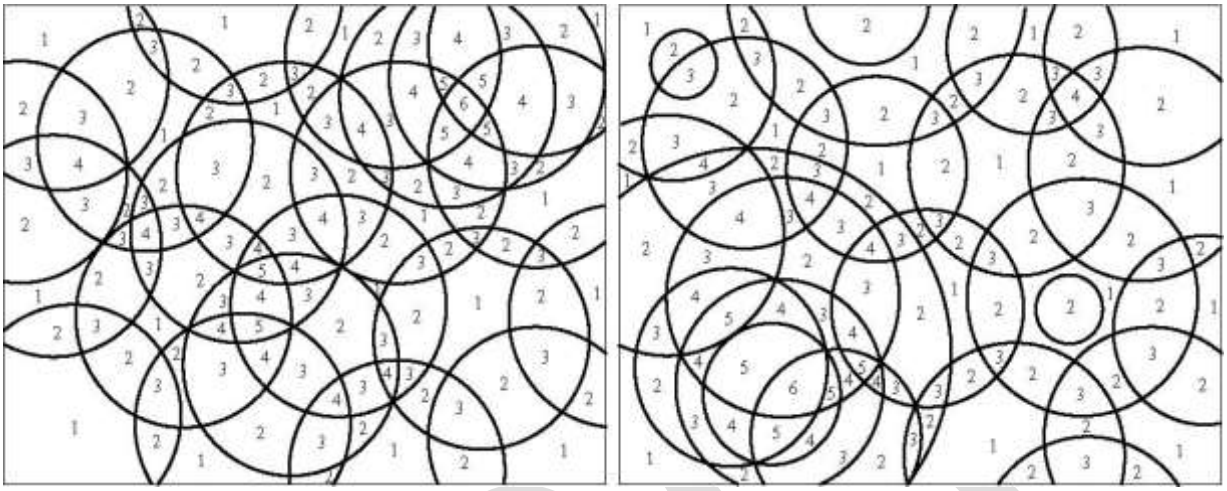

(a) *(b)*

Figure 1. Examples of the coverage problem: (a) the sensing ranges are unit disks, and (b) the sensing ranges are non-unit disks. The number in each sub-region is its coverage.

3. THE PROBLEM SOLUTIONS

At the first glance, the coverage problem seems to be very difficult. One naive solution is to find out all sub-regions divided by the sensing boundaries of all *n* sensors (i.e., *n* circles), and then check if each sub-region is *k*-covered or not, as shown in figure 1. Managing all sub-regions could be a difficult and computationally expensive job in geometry. There may exit as many as $O(n2)$ sub-regions divided by the circles. Also, it may be difficult to calculate these sub-regions.

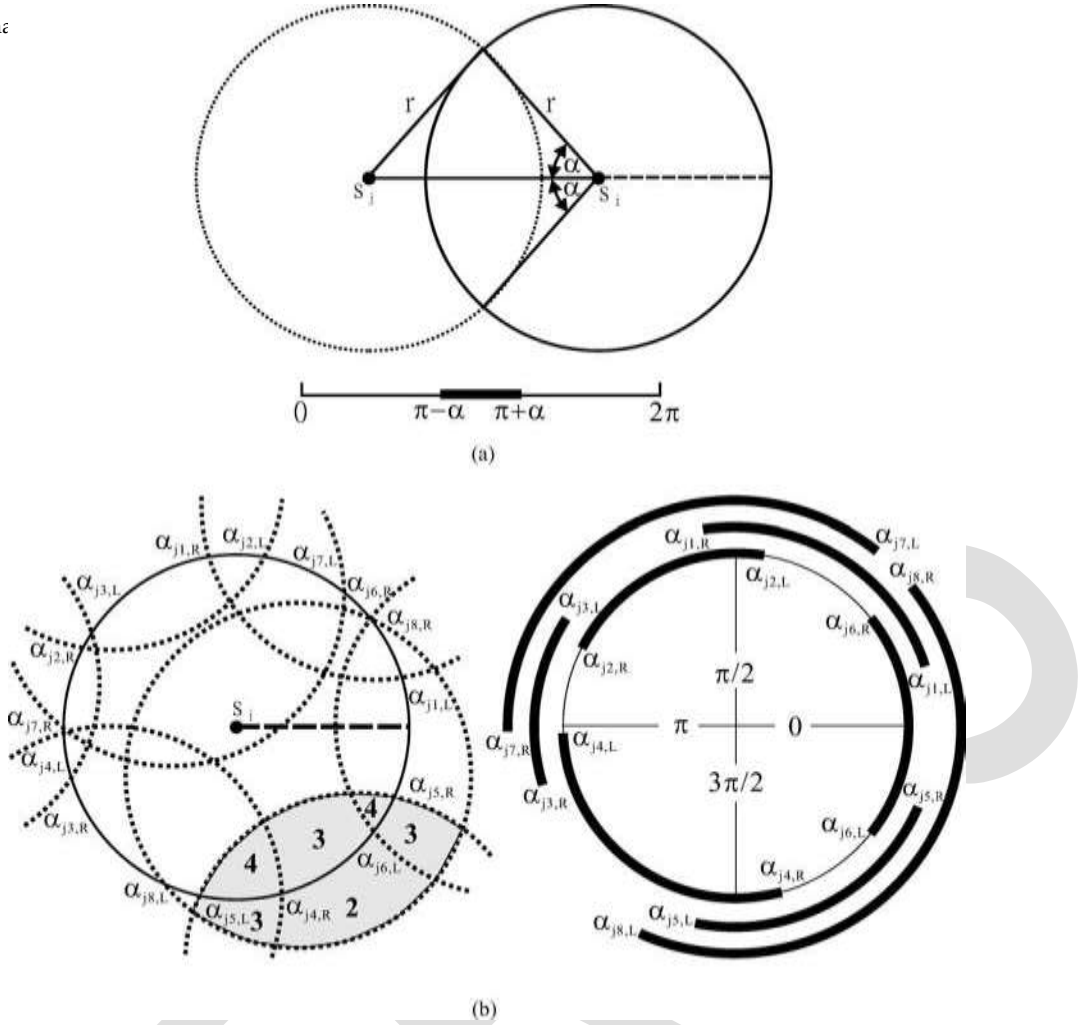

Figure 2. Determining: (a) the segment of *si* 's perimeter covered by *s j* , and (b) the perimeter-coverage of *si* 's perimeter.

3.1. THE K-UC PROBLEM

In the section, we propose a solution to the *k*-UC problem, which has a cost of *O*(*nd* log *d*), where *d* is the maximum number of sensors whose sensing ranges may intersect a sensor's sensing range. Instead of determining the coverage of each sub-region, our approach tries to look at how the perimeter of each sensor's sensing range is covered. Specifically, our algorithm tries to determine whether the perimeter of a sensor under consideration is sufficiently covered. By collecting this information from all sensors, a correct answer can be obtained.

DEFINITION 5. Consider any two sensors *si* and *s j*. A point on the perimeter of *si* is *perimeter-covered by* ***s j*** if this point is within the sensing range of ***s j* .**

DEFINITION 6. Consider any sensor *si*. We say that *si* is *k-perimeter-covered* if all points on the perimeter of *si* are perimeter-covered by at least *k* sensors other than *si* itself. Similarly, a segment of *si* 's perimeter is *k-perimeter-covered* if all points on the segment are perimeter-covered by at least *k* sensors other than *si* itself.

Below, we propose an $O(d \log d)$ algorithm to determine whether a sensor is k-perimeter-covered or not. Consider two sensors si and $s\,j$ located in positions $(xi\ ,\ yi\ )$ and $(x\,j\ ,\ yj\ )$, respectively. Denote by $d(si\ ,\ s\,j\ ) = \_|xi - x\,j\ |2 + |yi - yj\ |2$ the distance between si and $s\,j$. If $d(si\ ,\ s\,j\ ) > 2r$, then $s\,j$ does not contribute any coverage to si 's perimeter. Otherwise, the range of perimeter of si covered by $s\,j$ can be calculated as follows (refer to the illustration in figure 2(a)). Without loss of generality, let $s\,j$ be resident on the west of si (i.e., $yi = yj$ and $xi > x\,j$). The angle α = arcos ($d(si\ ,s\,j\ )\ 2r$). So the arch of si falling in the angle $[\pi - \alpha,\ \pi + \alpha]$ is perimeter-covered by $s\,j$.

The algorithm to determine the perimeter coverage of si works as follows.

1. For each sensor $s\,j$ such that $d(si\ ,\ s\,j\ ) \leq 2r$, determine the angle of $s\_i\ s$ arch, denoted by $[\alpha j,L,\ \alpha j,R]$, that is perimeter covered by $s\,j$.

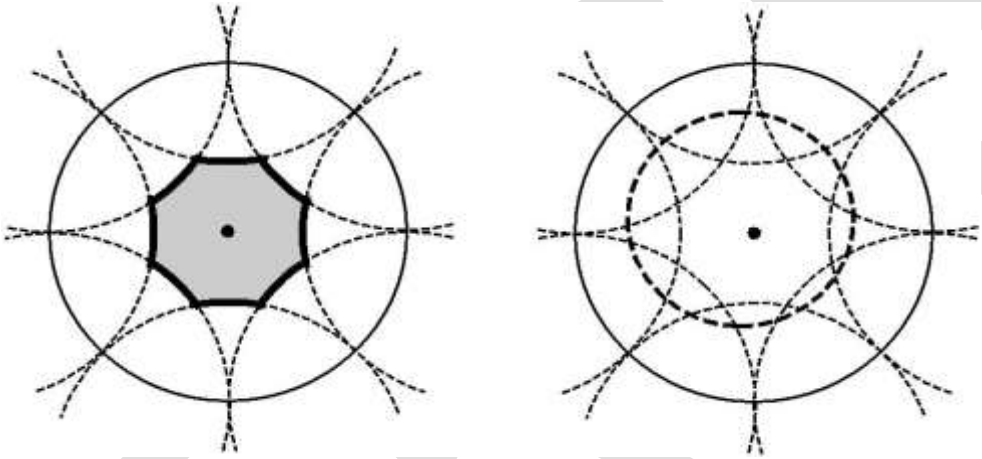

(a) (b)

Figure 3. Some examples to utilize the result in Theorem 1.

2. For each neighboring sensor $s\,j$ of si such that $d(si\ ,\ s\,j\ ) < 2r$, place the points $\alpha j,\ L$ and $\alpha j,\ R$ on the line segment $[0,\ 2\pi]$, and then sort all these points in an ascending order into a list L. Also, properly mark each point as a left or right boundary of a coverage range, as shown in figure 2(b).

3. (Sketched) Traverse the line segment $[0,\ 2\pi]$ by visiting each element in the sorted list L from left to right and determine the perimeter-coverage of si .

The above algorithm can determine the coverage of each sensor's perimeter efficiently. Below, we relate the perimeter coverage property of sensors to the coverage property of the network area.

LEMMA 1. Suppose that no two sensors are located in the same location. Consider any segment of a sensor si that divides two sub-regions in the network area A. If this segment is k-perimeter-covered, the sub-region that is outside si 's sensing range is k-covered and the sub-region that is inside si 's sensing range is $(k + 1)$-covered. *Proof*. The proof is directly from Definition 6. Since the segment is

k-perimeter-covered, the sub-region outside *si* 's sensing range is also *k*-covered due to the continuity of the sub-region. The sub-region inside *si* 's sensing range is (*k* + 1)-covered because it is also covered by *si* .

An example is demonstrated in figure 2(b). The gray areas in figure 2(b) illustrate how the above lemma works .

THEOREM 1. Suppose that no two sensors are located in the same location. The whole network area *A* is *k*-covered if each sensor in the network is *k*-perimeter-covered.

Proof. For the "if" part, observe that each sub-region inside *A* is bounded by at least one segment of a sensor *si* 's perimeter. Since *si* is *k*-perimeter-covered, by Lemma 1, this sub-region is either *k*-covered or (*k* + 1)-covered, which proves the "if" part.

For the "only if" part, it is clear by definition that for any segment of a sensor *si* 's perimeter that divides two sub regions,

both these sub-regions are at least *k*-covered. Further, observe that the sub-region that is inside *si* 's sensing range must be covered by one more sensor, *si* , and is thus at least (*k* + 1)-covered. So excluding *si* itself, this segment is perimeter-covered by at least *k* sensors other than *si* itself, which proves the "only if" part. Note that Theorem 1 is true when *all* sensors are claimed to be *k*-perimeter-covered. When a specific sensor *si* is *k*-perimeter-covered, it only guarantees that each point right outside *si* 's perimeter is *k*-covered, and each point right inside *si* 's perimeter is (*k* + 1)-covered. However, it does not guarantee that *all* points inside *si* 's perimeter is

(*k* + 1)-covered. An example is shown in figure 3. In figure 3(a), sensor *si* is 2-perimeter-covered since each segment of its perimeter is

covered by two sensors. This only implies the coverage levels of the points nearby the perimeter of *si* . The gray area, which is outside the coverage of *si* 's neighboring sensors, is only 1-covered. In fact, the segments that bound the gray area are only 1-perimeter-covered. If we add another sensor to cover these segments (shown in thick dotted line) as shown in figure 3(b), then *si* 's sensing region will be 2-covered.

Below, we comment on several special cases which we leave unaddressed on purpose for simplicity in the above discussion. When two sensors *si* and *s j* fall in exactly the same location, Lemma 1 will not work because for any segment of *si* and *s j* that divides two sub-regions in the network area, a point right inside *si* 's and *s j* 's sensing ranges and a point right outside their sensing ranges will differ in their coverage levels by two, making Lemma 1 incorrect (refer to the illustration in figure 4(a)). Other than this case, all neighboring sub-regions in the network will differ in their coverage levels by exactly one. Since in most applications we are interested in areas that are insufficiently covered, one simple remedy to this problem is to just ignore one of the sensors if both sensors fall in exactly the same location. Another solution is to first run our algorithm by ignoring one sensor, and then increase the coverage levels of the sub-regions falling in the ignored sensor's range by one afterward. The other boundary case is that some sensors' sensing ranges may exceed the network area *A*. In this case, we can simply assign the segments falling outside

A as∞-perimeter-covered, as shown in figure 4(b).

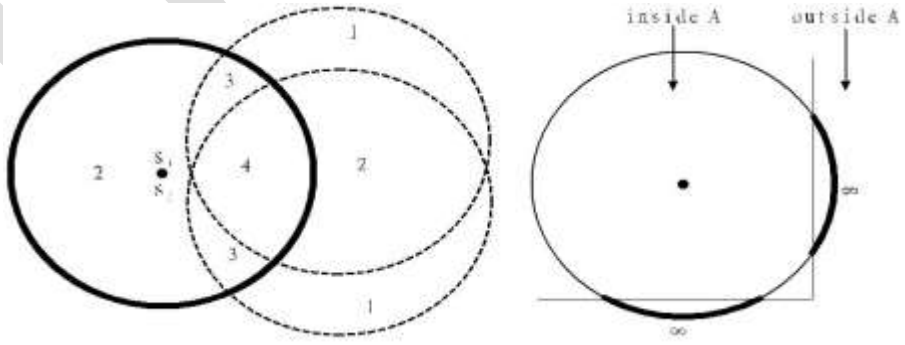

Figure 4. Some special cases: (a) two sensors falling in the same location (the number in each sub-region is its level of coverage), and (b) the sensing range of a sensor exceeding the network area *A*.

3.2. THE K-NC PROBLEM

For the non-unit-disk coverage problem, sensors' sensing ranges could be different. However, most of the results derived above remain the same. Below, we summarize how the *k*-NC problem is solved. First, we need to define that how the perimeter of a sensor's sensing range is covered by other sensors. Consider two sensors *si* and *s j* located in positions (*xi* , *yi*) and (*x j* , *yj*) with sensing ranges *ri* and *r j* , respectively. Again, without loss of generality, let *s j* be resident on the west of *si*. We address how *si* is perimeter-covered by *s j* . There are two cases to be considered..

Case 1. Sensor *s j* is outside the sensing range of *si* , i.e. ,$d(si , s j) > ri$.

(i) If $r j < d(si , s j)-ri$, then *si* is not perimeter-covered by *s j* .

(ii) If $d(si , s j)-ri \le r j \le d(si , s j)+ri$, then the arch of *si* falling in the angle $[\pi -\alpha, \pi +\alpha]$ is perimeter-covered

by *s j* , where α can be derived from the formula:$r2j= r\,2i + d(si , s j)2 - 2ri \cdot d(si , s j) \cdot \cos(\alpha)$. (1)

(iii) If $r j > d(si , s j)+ri$, then the whole range $[0, 2\pi]$ of *si* is perimeter-covered by *s j* .

Case 2. Sensor *s j* is inside the sensing range of *si*, i.e., $d(si , s j) \le ri$.

(i) If $r j < ri - d(si , s j)$, then *si* is not perimeter-covered by*s j* .

(ii) If $ri - d(si , s j) \le r j \le ri + d(si , s j)$, then the arch of *si* falling in the angle $[\pi - \alpha, \pi + \alpha]$ is perimeter-covered

by *s j* , where α is as defined in equation (1).

(iii) If $r j > d(si , s j)+ri$, then the whole range $[0, 2\pi]$ of *si* is perimeter-covered by *s j* .

The above cases are illustrated in figure 5. Based on such classification, the same algorithm to determine the perimeter coverage of a sensor can be used. Lemma 1 and Theorem 1still hold true (observe that in the corresponding proofs, we do not use any property about the absolute sensing ranges of sensors).

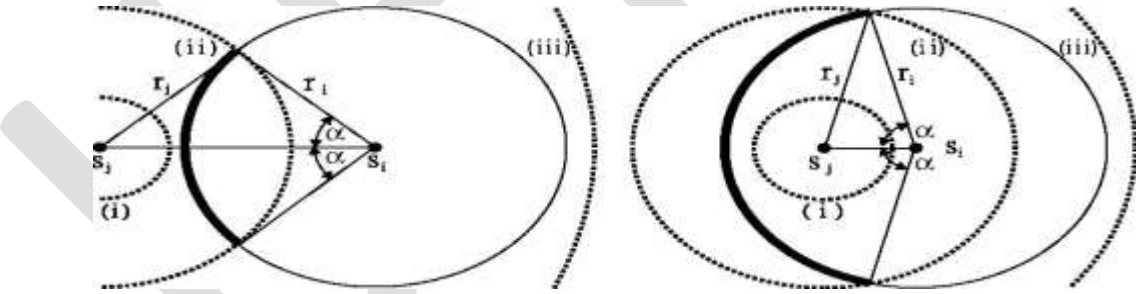

Figure 5. The coverage relation of two sensors with different sensing ranges: (a) *sj* not in the range of *si* , and (b) *sj* in the range of *si* .

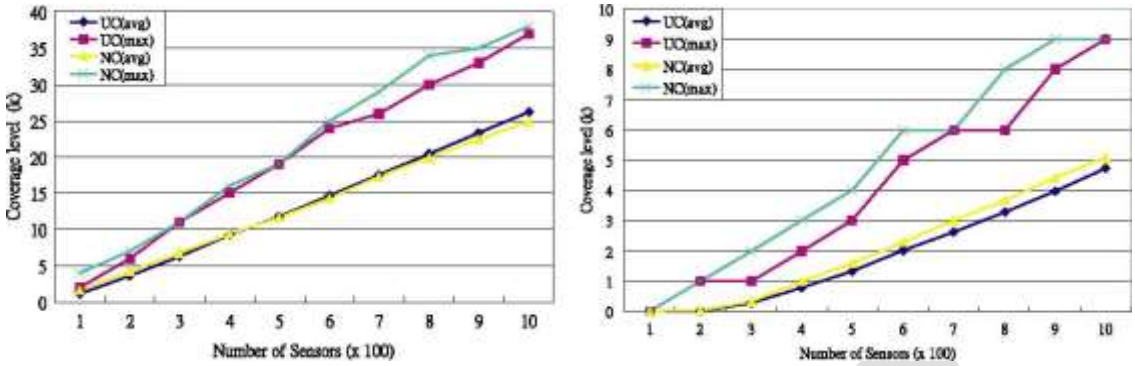

Figure 6. Number of sensors v.s. coverage level for sensor fields of sizes: (a) 500 × 500, and (b) 1000 × 1000.

3.3. COMPLEXITY ANALYSIS

Consider the algorithm in Section 3.1. Let d be the maximum number of sensors that are neighboring to a sensor ($d \leq n$). The complexities of steps 1 and 2 are $O(d)$ and $O(d \log d)$,respectively. The last step 3, though sketched, can be easily implemented as follows. Whenever an element $\alpha j,L$ is traversed, the level of perimeter-coverage should be increased by one. Whenever an element $\alpha j, R$ is traversed, the level of perimeter-coverage should be decreased by one. Since the sorted list L will divide the line segment $[0, 2\pi]$ into as many as $2d + 1$ segments, the complexity of step 3 is $O(d)$. So the complexity to determine a sensor's perimeter coverage is $O(d \log d)$. The overall complexity for the k-UC problem is thus $O(nd \log d)$. The k-NC problem can also be solved with complexity $O(nd \log d)$, except that the neighbors of a sensor need to be redefined. The work [21] also proposes a solution to determine the coverage level of a sensor network. It looks at how intersection points between sensors' sensing ranges are covered. Since there are as many as $O(n^2)$ intersection points in the network and the calculation of the coverage level of each intersection point takes time $O(n)$, the overall complexity is $O(n^3)$.

4. SIMULATION RESULTS AND A SENSOR COVERAGE TOOLKIT

We have developed a simulator and implemented a toolkit based on the proposed algorithms. Square sensor fields are simulated with randomly placed nodes. There are two settings of sensing ranges: unit-disc sensing range and non-unit disc sensing range. All results presented below are from the average of at least 1000 runs.

First, we investigate the level of coverage (i.e., k) that can be achieved by using different numbers of sensors. Sensor fields of sizes 500×500 and 1000×1000 are simulated with 100–1000 nodes. The unit-disc sensing range is 100 units and the non-unit-disc sensing range falling uniformly between 50–150 units. Both the average and the maximum levels of coverage are evaluated. The results are in figure 6. As can be seen, the average value of k grows about linearly as the number of sensors increases. Next, we investigate the level of coverage that can be achieved by setting different sensing ranges of sensors. Sensor fields of sizes 500×500 and 1000×1000 are simulated with 500 nodes. For the unit-disc case, the sensing range is fixed from 50 to 150 units. For the non-unit-disc case, we first pick an average sensing range avg, and the sensors' sensing ranges are uniformly distributed between $avg - 50$ and $avg + 50$.The results are in figure 7. The average value of k grows as the average sensing range of sensors increases.

We have also implemented a toolkit based on the proposed algorithms to determine the coverage level of a given sensing field. Figure 8 shows the user interface of the toolkit. In the drawing area, one can easily deploy sensors by pointing out their locations and dragging their sensing ranges. By clicking on the "Deploy" button, the deployment of sensors will be fed into our program. There are three major functions of this toolkit, as described below.

1. *COMPUTE THE LEVEL OF COVERAGE*: By clicking on the "Compute Coverage" button and then the "Display Coverage"

button, the system will calculate and return the current coverage level of the whole area, as illustrated

in figure 9(a).

2. *COLOR THE DRAWING AREA*: By clicking on the "Paint the drawing area" button, the drawing area will be colored based on each region's coverage level. The coloring speed can also be modified, which will reflect on the coloring quality. An example is shown in figure 9(b).

3. *DISPLAY INSUFFICIENTLY COVERED SEGMENTS:* One can first select the desired value of *k* followed by clicking on the "Commit" button to feed *k* into the system. Clicking on the "Get Low Coverage Segments" button will generate an output file which contains all segments that are insufficiently *k*-perimeter-covered, as shown in the figure 10. Each line in the file is a segment of one sensor's perimeter that is insufficiently covered. Fields in a line include: sensor ID, location, sensing range, starting and ending angles of the corresponding segment, and the levels of coverage inside and outside this segment. This toolkit is publicly downloadable from http://hscc.csie.nctu.edu.tw/download/coverage.zip.

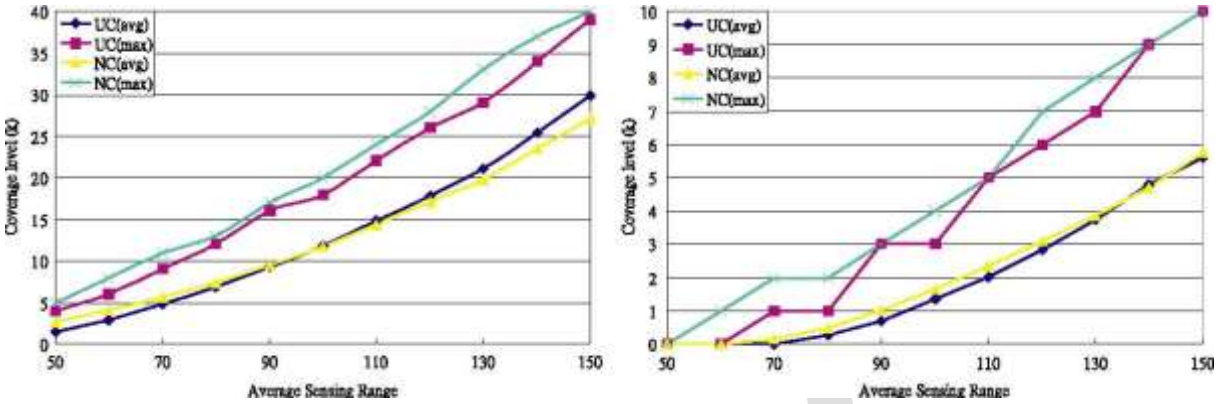

Figure 7. Sensing range v.s. coverage level for sensor fields of sizes: (a) 500 × 500, and (b) 1000 × 1000.

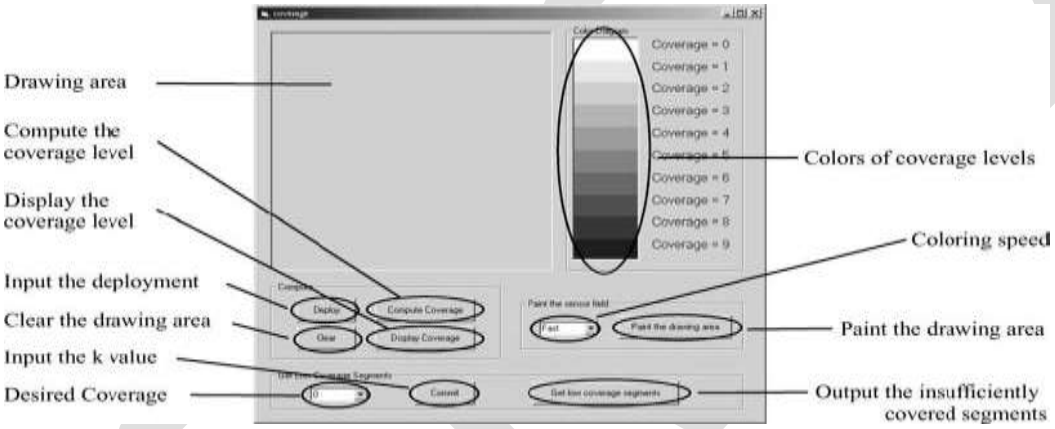

Figure 8. Functional descriptions of the toolkit.

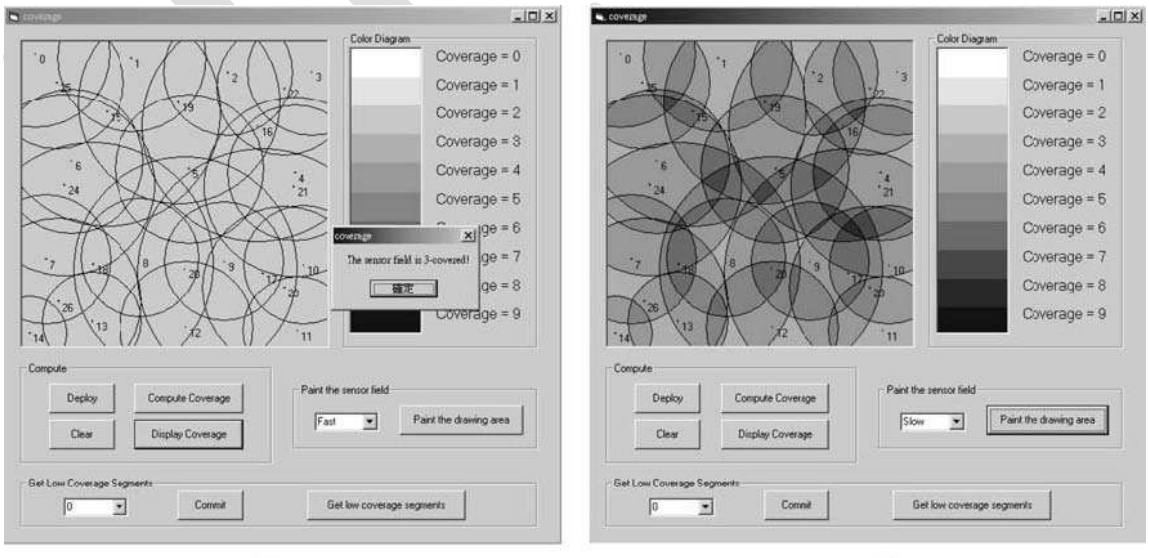

Figure 9. Execution results of the toolkit: (a) coverage level, and (b) painting results.

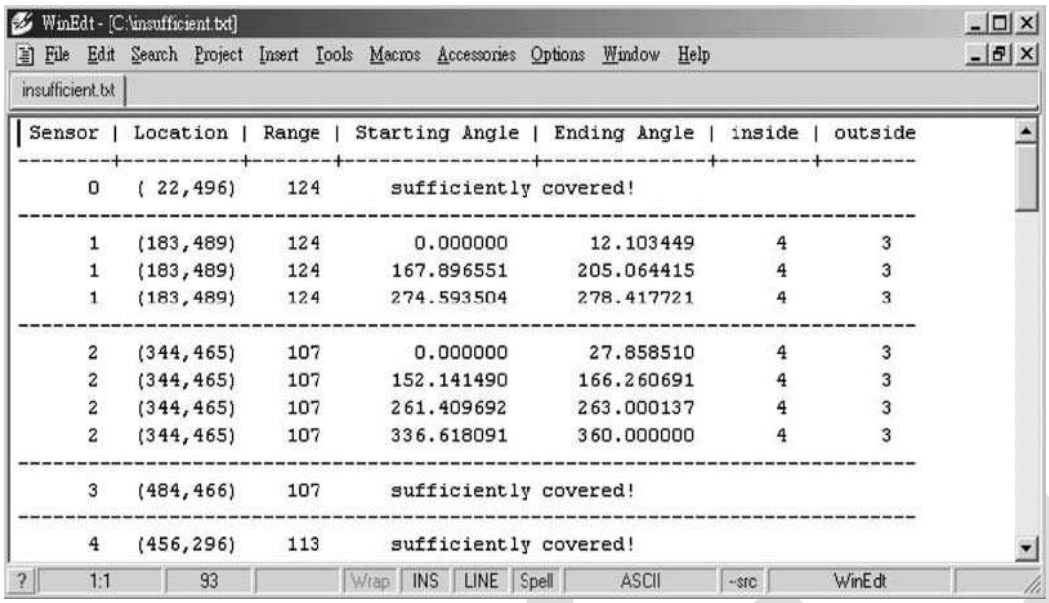

Figure 10. Insufficiently 4-perimeter-covered segments for the example in figure 9.

5. APPLICATIONS AND EXTENSIONS OF THE COVERAGE PROBLEM

The sensor coverage problem, although modeled as a decision problem, can be extended further in several ways for many interesting applications. The proposed results can also be extended for more realistic situations. In the following, we suggest several applications of the coverage problem and possible extensions of our results.

5.1. DISCOVERING INSUFFICIENTLY COVERED REGIONS

For a sensor network, one basic question is whether the network area is fully covered. Our modeling of the *k*-UC and *k*-NC problems can solve the sensor coverage problem in a more general sense by determining if the network area is *k*-covered or not. A larger *k* can support a more fine-grained sensibility. For example, if $k = 1$, we can only detect in which sensor an event has happened. Using a larger *k*, the location of the event can be reduced to a certain intersection of at least *k* sensors. Thus, the location of the event can be more precisely defined. This would support more fine-grained location-based services. To determine which areas are insufficiently covered, we assume that there is a central controller in the sensor network. The central controller can broadcast the desired value of *k* to all sensors. Each sensor can then communicate with its neighboring sensors and then determine which segments of its perimeter are less than *k*-perimeter-covered. The results (i.e., insufficiently covered segments) are then sent back to the central controller. By putting all segments together, the central controller can precisely determine which areas are less than *k*-covered. Note that since Theorem 1 provides a necessary and sufficient condition to determine if an area in the network is *k*-covered, false detection would not happen.

Further actions can then be taken if certain areas are insufficiently covered. For example, the central controller can dispatch more sensors to these regions. An optimization problem is: how can we patch these insufficiently covered areas with the least number of extra sensors. This is still an open question and deserves further investigation.

5.2. POWER SAVING IN SENSOR NETWORKS

Contrary to the insufficient coverage issue, a sensor network may be overly covered by too many sensors in certain areas. For example, as suggested in [18], if there are more sensors than necessary, we may turn off some redundant nodes to save energy. These sensors may be turned on later when other sensors run out of energy. Tian and Georganas [18] proposes a node-scheduling scheme to guarantee that the level of coverage of the network area after turning off some redundant sensors remains the same.

Based on our result, we can solve a more general problem as follows. First, those sensor nodes who can be turned off, called *candidates*, need to be identified. A sensor *si* is a candidate if all of its neighbors are still *k*-perimeter-covered after *si* is removed. To do so, *si* can communicate with each of its neighbors and ask them to reevaluate their perimeter coverage by skipping *si*. If the responses from all its neighbors are positive, *si* is a candidate. After determining the candidates, each sensor can compete to enter the doze mode by running a scheduling scheme, such as that in [18], to decide how long it can go to sleep. However, [18] only considers a special case of our results with $k = 1$

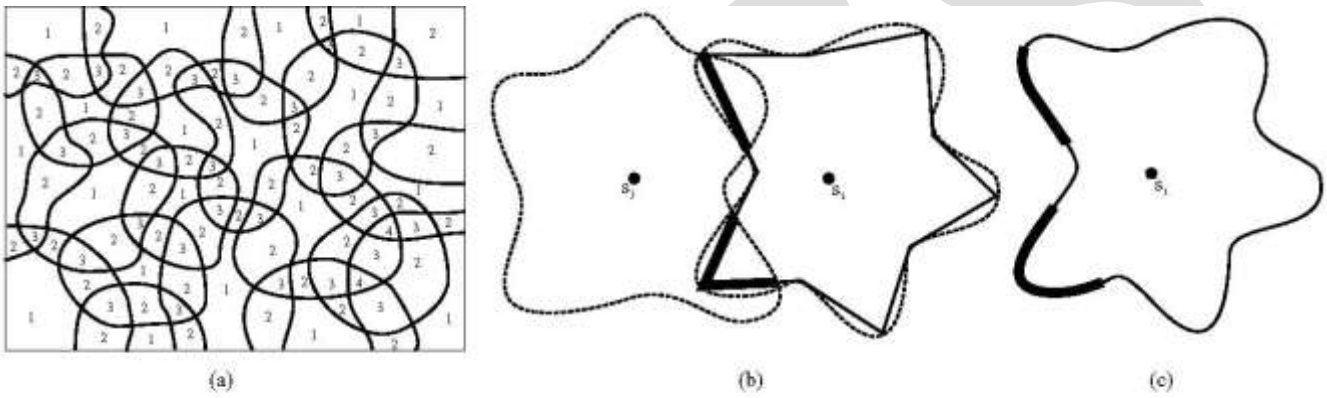

Figure 11. The coverage problem with irregular sensing regions: (a) coverage levels of irregular sub-regions, (b) polygon approximation of sensor s_i's sensing region, and (c) covered segments of s_i.

5.3. HOT SPOTS

It is possible that some areas in the network are more important than other areas and need to be covered by more sensors. Those important regions are called *hot spots*. Our solutions can be directly applied to check whether a hot spot area is *k*-covered or not. Given a hot spot, only those sensors whose perimeters are within or have crossings with the hot spot need to be checked. So the central controller can issue a request by identifying the hot spot. Each sensor that is within the hot spot or has crossings with the hot spot needs to reevaluate the coverage of its perimeter segment that is within the hot spot. The results in Lemma 1 and Theorem 1 are directly applicable. So a hot spot is *k*-covered if and only if all perimeter segments within this hot spot are *k*-perimeter-covered. Note that a hotspot can be defined in other shapes too.

5.4. EXTENSION TO IRREGULAR SENSING REGIONS

The sensing region of a sensor is not necessarily a circle. In most cases, it is location-dependent and likely irregular.1 Fortunately, our results can be directly applied to irregular sensing regions without problem, assuming that each sensor's sensing region can be precisely defined. Observe that the sensing regions of sensors still divide the network area into sub-regions. Through Lemma 1, we can translate perimeter-covered property of sensors to area-covered property of the network. Then by Theorem 1, we can decide whether the network is *k*-covered. figure 11(a) shows an example.

Given two sensors' sensing regions that are irregular, it remains a problem how to determine the intersections of their perimeters. One possibility is to conduct polygon approximation. The idea is illustrated in figure 11(b), which can give the perimeter coverage in figure 11(c).

6. CONCLUSION

In this paper, we have proposed solutions to two versions of the coverage problem, namely *k*-UC and *k*-NC, in a wireless sensor network. We model the coverage problem as a decision problem, whose goal is to determine whether each location of the target sensing area is sufficiently covered or not. Rather than determining the level of coverage of each location, our solutions are based on checking the perimeter of each sensor's sensing range. Although the problem seems to be very difficult at the first glance, our scheme can give an exact answer in $O(nd \log d)$ time. With the proposed techniques, we also discuss several applications (such as discovering insufficiently covered regions and saving energies) and extensions (such as scenarios with hot spots and irregular sensing ranges) of our results. A software tool that implements the proposed algorithms is available on the web (http://hscc.csie.nctu.edu.tw/download/coverage.zip) for free Download

REFERENCES:

[1] P.K. Agarwal and M. Sharir, Arrangements and their applications. in: *Handbook of Computational Geometry*, eds. J.-R. Sack and J. Urrutia,(Elsevier, North-Holland, New York, 2000) pp. 49–119.

[2] P. Bahl and V.N. Padmanabhan, RADAR: an in-building RF-based user location and tracking system, in: *IEEE INFOCOM* (2000) pp. 775–784

[3] D. Braginsky and D. Estrin, Rumor routing algorithm for sensor networks, in: *ACM Int'l Workshop on Wireless Sensor Networks and Applications (WSNA)* (2002).

[4] N. Bulusu, J. Heidemann and D. Estrin, GPS-less low cost outdoor localization for very small devices, IEEE Personal Commun. 7(5) (2000)28–34.

[5] D. Ganesan, R. Govindan, S. Shenker and D. Estrin, Highly resilient, energy efficient multipath routing in wireless sensor networks, ACM Mobile Comput. and Commun. Review 5(4) (2001) 11–25.

[6] D. Halperin, Arrangements, in: *Handbook of Discrete and Computational Geometry*, eds. J.E. Goodman and J. O'Rourke, chapter 21, (CRC Press LLC, Boca Raton, FL, 1997) pp. 389–412.

[7] W.R. Heinzelman, A. Chandrakasan and H. Balakrishnan, Energyefficient communication protocols for wireless microsensor networks, in: *Hawaii Int'l Conf. on Systems Science (HICSS)* (2000).

[8] S. Meguerdichian, F. Koushanfar, M. Potkonjak and M.B. Srivastava, Coverage problems in wireless ad-hoc sensor networks. in: *IEEE INFOCOM* (2001) pp. 1380–1387.

[9] S. Meguerdichian, F. Koushanfar, G. Qu and M. Potkonjak, Exposure in wireless ad-hoc sensor networks, in: *ACM Int'l Conf. on Mobile Computing and Networking (MobiCom)* (2001) pp. 139–150

[10] S. Meguerdichian, S. Slijepcevic, V. Karayan and M. Potkonjak, Localized algorithms in wireless ad-hoc networks: location discovery and sensor exposure, in: *ACM Int'l Symp. on Mobile Ad Hoc Networking and Computing (MobiHOC)* (2001) pp. 106–116.

[11] D. Nicules and B. Nath, Ad-hoc positioning system (APS) using AoA, in: *IEEE INFOCOM* (2003).

[12] J. O'Rourke, Computational geometry column 15, Int'l Journal of Computational Geometry and Applications 2(2) (1992) 215–217.

[13] G.J. Pottie and W.J. Kaiser, Wireless integrated network sensors, Commun.ACM 43(5) (2000) 51–58.

[14] A. Savvides, C.-C. Han and M.B. Strivastava, Dynamic fine-grained localization in ad-hoc networks of sensors, in: *ACM Int'l Conf. on Mobile Computing and Networking (MobiCom)* (2001) pp. 166–179.

[15] E. Shih, S.-H. Cho, N. Ickes, R. Min, A. Sinha, A. Wang and A. Chandrakasan. Physical layer driven protocol and algorithm design for energy-efficient wireless sensor networks, in: *ACM Int'l Conf. on Mobile Computing and Networking (MobiCom)* (2001) pp. 272–287.

[16] S. Slijepcevic and M. Potkonjak, Power efficient organization of wireless sensor networks, in: *IEEE Int'l Conf. on communications (ICC)* (2001) pp. 472–476.

[17] K. Sohrabi, J. Gao, V. Ailawadhi and G.J. Pottie, Protocols for selforganization of a wireless sensor network, IEEE Personal Commun.7(5) (2000) 16–27.

[18] D. Tian and N.D. Georganas, A coverage-preserving node scheduling scheme for large wireless sensor networks, in: *ACM Int'l Workshop onWireless Sensor Networks and Applications (WSNA)* (2002).

[19] Y.-C. Tseng, S.-P. Kuo, H.-W. Lee and C.-F. Huang, Location tracking in a wireless sensor network by mobile agents and its data fusion strategies, in: *Int'l Workshop on Information Processing in Sensor Networks (IPSN)* (2003).

[20] G. Veltri, Q. Huang, G. Qu and M. Potkonjak, Minimal and maximal exposure path algorithms for wireless embedded sensor networks. in:*ACM Int'l Conf. on Embedded Networked Sensor Systems (SenSys)*(2003) pp. 40–50.

[21] X. Wang, G. Xing, Y. Zhang, C. Lu, R. Pless and C. Gill, Coverage and connectivity configuration in wireless sensor networks. in: *ACM Int'l Conf. on Embedded Networked Sensor Systems (SenSys)* 2003 pp. 28–39.

[22] A. Woo and D. E. Culler, A transmission control scheme for media access in sensor networks, in: *ACM Int'l Conf. on Mobile Computing and Networking (MobiCom)* (2001) pp. 221–235.

[23] F. Ye, G. Zhong, S. Lu and L. Zhang, PEAS: a robust energy conserving protocol for long-lived sensor networks, in: *Int'l Conf. on Distributed Computing Systems (ICDCS)* (2003).

[24] W. Ye, J. Heidemann and D. Estrin, An energy-efficient MAC protocol for wireless sensor networks, in: *IEEE INFOCOM* (2002) pp. 1567–1576.

[25] Ankita Joshi, Lakshmi Priya M, "A Survey of Hierarchical Routing Protocols in Wireless Sensor Network" MES Journal of Technology and Management May 17, 2011

International Journal of Engineering Research and General Science Volume 3, Issue 5, September-October, 2015
ISSN 2091-2730

Performance Analysis and Feasibility Study of Solar-Wind-Diesel Hybrid Power System in Rural Areas of Bangladesh

Mahabub Hasan*‡, Oishe Binty Momin*

*Department of Electrical and Electronic Engineering, Ahsanullah University of Science and Technology, Bangladesh

‡ Corresponding Author; Mahabub Hasan, mahabubaust64@gmail.com, +8801839841274

Abstract— Continuous usage conventional resources to meet the growing demand of electricity have resulted in increased energy crisis and the pollutants created from the burning of the conventional resources cause respiratory illnesses and death in humans and destroy fragile ecosystems. These are some prominent reasons that make renewable energy extremely important for the future of our society as they are more reliable, effective, sustainable and pollution-free power supply source. The first initiative that is needed to design a hybrid power generation system (HPGS) is the feasibility study. The goal of this paper is to evaluate the performance and study the feasibility of a solar-wind-diesel hybrid energy system through computer simulation studies to achieve an efficient and cost competitive system. The feasibility study mainly focuses on the technical and economic analysis of the components of the hybrid power generation system. Considering the Net Present Cost (NPC), Cost of Energy (COE) and Renewable fraction (RF), the prospects of solar and wind energy was evaluated with the help of the Hybrid Optimization Model for Electric Renewable (HOMER). From the study, it can be interpreted that the solar-wind-diesel system consumes less fuel than the diesel generator which is run by only diesel. As a result, the total net present cost of solar-wind-diesel system is less than the diesel generator. The study found a wind-pv-diesel hybrid power system with 65% renewable energy penetration (41% wind and 24% solar PV) to be the feasible system with the cost of energy of 0.822US$/kWh. The hybrid system will reduce CO2 emission by 60% in the local atmosphere compared to electricity draw from the national grid.

Keywords— Hybrid Renewable Energy System, PV, Wind, Feasibility study, Performance analysis, HOMER.

1. INTRODUCTION

Energy is essential to our society not only to ensure our quality of life but also for our economy. The demand of electrical energy has developed largely across the whole world; in every country, in every society we live. This demand has been stimulated by the relative ease with which electricity can be generated, distributed, and utilized, and by the great variety of its applications. Now, the controversial question is whether the consumption of electricity should be allowed to grow in an uncontrolled manner where the demand is increasing day by day. In that situation, the world's electricity generation capacity surely has to keep pace with the increasing demand of electric energy. Presently, almost all the electricity generation takes place at a central power station where coal, gas, fossil fuels and nuclear materials are used as the primary fuel source. But if we keep depending on these conventional sources for energy generation or further development, then definitely we have to face problems in the future as they are finite sources. In the geographically suitable areas, Hydro-power generation is inadequate. In additional, the reserves of coal may be plentiful at present, but they are being used continuously and if this continues, the day is not far away when there will be insufficient amounts of coal and these resources are not even renewable. The possible hazards of nuclear power have been much publicized, particularly those concerning the storage and military use of nuclear waste material [1]. It is high time to think about the alternatives, and renewable energy can be the best alternative of these fossil fuels. Renewable energy is the cleanest and infinite sources of energy, which is more sustainable and has a much lower environmental impact that the conventional sources of energy [2].

Bangladesh is a small developing country endowed with plentiful natural resources. Currently, electricity produced from both renewable energy and energy sources is being used by 70% of total populations [3]. The installed electricity generation capacity in

Bangladesh is about 11532 MW in June, 2015 [4]. Bangladesh is one of those countries which have lower per capita energy consumption (321 kWh) in the world [5]. The major and most available energy source in Bangladesh is natural gas, which is greatly used in most of the power generation unit. About 62.26% % (6809 MW) energy comes from natural gas, followed by HFO (21.04 %, 2301 MW), HSD (8.2 %, 897 MW), hydro (2.1 %, 230 MW) and Coal (1.83 %, 200 MW) [6]. But the country lags behind than its expected production capacity and meets the demand of its population because of the limitation of resources, weak policies, inefficient power plants and high system losses [7]. Adequate power generation capacity is the main enforcement of social and economic development of a country. But it's a matter of sorrow that most of the rural households in Bangladesh are divested from steady electricity supply as the national grid is incapacitated to meet the energy demand of vast populations. So, increasing the power generation is the only accession for the overall development of the country. And this can only be done by fuel diversification. At present, more than 1% share is added by the renewable energy to the total power generation of Bangladesh. According to the anticipation of the Renewable Energy Policy, Bangladesh has to achieve 5% of total energy production by 2015 and 10% by 2020 from renewable energy for overall development [8]. And to achieve this target local energy resources such as Micro, Hydro, Wind, PV etc. through the stand alone hybrid system can be ensconced in the remote areas of Bangladesh. Renewable energies which are plenty in our country like solar, wind can be installed as a self-contained energy system. A diesel generator can be used as a backup of a solar-wind-diesel hybrid system due to unavailability of sunlight during the night and wind speed fluctuation during day time so that the supply of electricity remains uninterrupted.

In Bangladesh, renewable energy has a prosperous future. The simple generation structure and availability make the Hybrid renewable energy systems (HRES) more captivating and popular in the power generation sector in Bangladesh HRES combines renewable energy sources like solar, wind, and others to deliver useful energy. A combined system of various renewable energy sources can be a good example of the energy system in case of balance, reliability and stability. The balanced system can provide substantial outputs from sources with a minimized dependency of the output upon seasonal changes and by this way utilization of the different renewable sources of energy can be optimized [9]. A dramatic decrease in the cost and investment of energy storage can be done if multiple energy storage devices with complementary performance characteristics are used [10] together, but the main problem with these types of system is to maintain the continuity and reliability. The storage systems are costly and usually they are large in size. So, cost-effective size of the storage system is required and to reduce these requirements Hybrid Power system can be used [11].

The purpose of the paper is to evaluate the performance and feasibility of PV-wind-diesel hybrid system in rural areas of Bangladesh through computer simulation using the Hybrid Optimization Model for Electric Renewable (HOMER) software. Besides, the study estimates the amount of CO_2 emission and helps in reducing CO_2 emission to atmosphere.

The following is the arrangements of this paper. Section 2 illustrates a brief description of solar and wind energy resources at different locations in Bangladesh. Section 3 presents information about hybrid systems. The system descriptions including the electric load demand profile of the selected location and details about simulation software HOMER are presented in section 4. Section 5 delineates the results and discussions and at the end section 6 concludes.

2. RENEWABLE ENERGY RESOURCES IN BANGLADESH

The electricity that is gained from the conversion of sunlight is known as Solar Power; the conversion can be done by either directly using photovoltaic (PV), or indirectly using concentrated solar power (CSP). By using the photovoltaic effect electric current can be transmuted from light in the Photovoltaic [12]. Bangladesh is a small country of 147,500 km2 area with nearly 162 million populations. It is situated between 20.34° and 26.38° north latitude and 88.01° and 92.41° east longitude, which is very much convenient for the production of solar energy. And for the wind energy we can mention the 724 km long coastline and a number of small islands namely Saint Martin, Kutubdia, Swandip and Hatia in the Bay of Bengal of Bangladesh.

2.1. Solar Energy Resources

Solar Energy can be a great source of electricity by which power crisis can be overcome. On a horizon plane the average annual power density of solar radiation is 100-300 W/m^2. To initiate an average power output of 100 MW, which is about 10% of a large coal or nuclear power plant, a solar PV efficiency of 10% and an area of 3-10 km2 are required [13]. For

the limitlessness and pollution free quality energy conversion technologies can be installed near consumers. It will also reduce the total production cost. An unused land or rooftops can be used for the installation of solar energy technologies. About 4670 km2 household roof area is available in Bangladesh [14] which are 3.2% of total land area of the country. In Dhaka city, there are 7.86% of rooftop areas that can be used for solar PV electricity generation [15].

The total the potential of grid-connected solar PV in Bangladesh is about 50,174 MW. This number is obtained by calculating the annual mean value of solar radiation (200 W/m2) and a 10% efficiency of the solar PV system [16]. Table 1 shows the average daily solar radiation at different locations in Bangladesh.

Table 1. Monthly global solar radiation at different cities of Bangladesh (in kWh/m^2/day) [17]

Month	Dhaka	Rajshahi	Sylhet	Bogra	Barishal	Jessor
January	4.03	3.96	4.00	4.01	4.17	4.25
February	4.78	4.47	4.63	4.69	4.81	4.85
March	5.33	5.88	5.20	5.68	5.30	4.50
April	5.71	6.24	5.24	5.87	5.94	6.23
May	5.71	6.17	5.37	6.02	5.75	6.09
June	4.80	5.25	4.53	5.26	4.39	5.12
July	4.41	4.79	4.14	4.34	4.20	4.81
August	4.82	5.16	4.56	4.84	4.42	4.93
September	4.41	4.96	4.07	4.67	4.48	4.57
October	4.61	4.88	4.61	4.65	4.71	4.68
November	4.27	4.42	4.32	4.35	4.35	4.24
December	3.92	3.82	3.85	3.87	3.95	3.97
Average	4.73	5.00	4.54	4.85	4.71	4.85

From table 1, we can see that about 4.64 kWh/m^2 solar radiations per day is being received in Bangladesh and it is a very good number for generating electricity. If we account an average standard 50 WP solar panel per household, then the total capacity stands to 200 MW (200 MWp) [18].

2.2. Wind Energy Resources

Wind power is the kinetic energy of wind, which is generated from air using wind turbines to make electrical power, windmills for mechanical power, wind pumps for water pumping or drainage, or sails to propel ships [19]. Bangladesh has 724 km long coast line and a number of small islands namely Saint Martin, Kutubdia, Swandip and Hatia in the Bay of Bengal of Bangladesh. After passing a long distance over the water surface the strong south-westerly monsoon wind which has come from Indian Ocean enters Asia over the coastal area of Bangladesh. With a monthly average speed 3 m/s to 6 m/s these winds flow all over Bangladesh from March to September [20]. This wind is more boosted when it enters the V- shaped coastal region of the country. In consonance with preliminary studies, (from meteorological department, BCAS, LGED, and BUET) during the monsoon and around one to two months before and after the monsoon (7 months, March to September), there is available winds in Bangladesh. The wind remains either too high or either too low during October to February in Bangladesh. The peak wind speed occurs during the months of June and July [21].

The study done by the Bangladesh Center of the Advance Studies (BCAS) project in collaboration with the Local Government Engineering Department (LGED) and the UK's Energy Technology Support Unit (ETSU) showed that the average annual wind speed measured in the seven coastal stations ranged from 2.94 m/s to 4.52 m/s which is shown in Table 2.

Table 2. Monthly average wind speeds at 25 meter height at seven coastal stations measured by WEST [22].

Year	Month	Monthly average wind speed (m/s) at the monitoring stations stated Kuakata						
		Patnga			Noakhali	Char Fasion		
	June	8.75						
	July	5.87	5.42	5.77				
	August	5.32	5.33	4.9	4.7	5.2	5.7	
2009	September	3.36	3.69	3.46	2.94	3.34	3.77	3.58
	October	3.2	3.74	3.3	2.83	3.7	2.18	3.98
	November	2.61	2.93	2.29	1.91		1.98	3.23
	December	2.97	1.78	1.44	1.35	3.09	3.35	3.38
	January	3.25	2.33	1.99	1.31	2.8	3.18	3.67
	February	3.13	1.99	1.9	1.9	2.69	3.37	3.29
	March	2.88	2.42	2.26	2.38	3.54	4.84	3.53
	April	4.96	1.84	1.65	2.25	3.29	4.93	3.1
2010	May	5.83	3.97	3.09	3.99	4.81	6.28	4.89
	June	5.67	4.64	3.26	5	5.76	7.31	5.9
	July	5.13	4.8	4.33	4.92	5.22	7.34	6.17
	August		4.31	4.03	3.85	5.17		5.34
	September		2.96	1.83	2.77	3.08		3.97
Annual Average		3.95	3.34	2.94	2.96	4.07	4.52	4.21

3. Hybrid System

The main obstacle of the renewable energy such as solar and wind energy is these changes randomly and for that reason these are less reliable. Again, if we think of a stand-alone energy production system with PV modules or wind turbine, it will cost a lot in case of technical solution. For this solution, a large surface is compulsory. In winter, the solar potential remains low and in that case, the consumers can be supplied with energy through a large storage capacity. From the above discussion, we can see a lot of disadvantages if a stand-alone energy production system is used. But if a combined system of solar and wind resources is used so that they can complement each other by means of daily and seasonal variations [23]. As the Hybrid systems involve several generation methods, it provides a high level of energy security. Usually, the Hybrid systems incorporate a storage system (battery & fuel cell) or small fossil-fueled generator to ensure maximum supply reliability & security. Due to the regional conditions, the system costs might slightly reduce [24].

Wind turbines & Solar panels are the noteworthy renewable energy devices that are frequently used in hybrid power systems. In villages, various hybrid power systems can be found which differ in size. There is the small size of hybrid power systems which covers small household systems (100 Wh/day) and again, there is the largest size of hybrid power systems which covers a whole area (10 MWh/day). Micro grids and Mini grids are the two types of village scale hybrid power system. Wind, PV, Batteries and conventional generator are the essentials of Micro-Grid (100 kWh/day) power system and the generator is for providing DC power. Same components but larger in size is used for the Mini-Grid power systems (700 kWh/day). The various combinations of the hybrid system are PV-Wind, PV-Fuel cell, PV-Wind–Fuel cell, PV-Wind-Battery etc. Hybrid system provides certain advantages such as lower energy cost, high reliability, low maintenance, flexibility, longer equipment life and utility grade potential, which are unavailable in a single resource energy system [25]. Figure 1 shows the general block diagram of a hybrid power system:

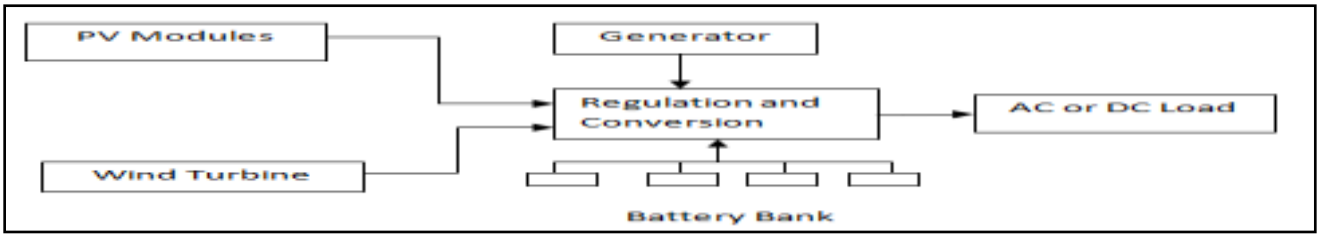

Fig. 1. General block diagram of a Hybrid Power System

4. System Design and Simulation

A solar-wind-diesel hybrid system is one of the projects that are focused for the feasibility study in Bangladesh. Hybrid Optimization Model for Electrical Renewable (HOMER) software has been used for the Hybrid Energy System design and simulation. The design and simulation procedure is described below:

4.1. System Description

A solar-wind-diesel hybrid system is used to provide power supply in remote areas, which are far from the public power grid or rural areas in Bangladesh. The system consists of a PV Panel, wind turbine, diesel generator, battery and converter. The system comprises two buses; AC and DC bus. The DC power produced from PV arrays and the fuel cell is converted into AC power, and then fed to the AC bus. The AC power generated from the wind turbines is directly fed to the AC Bus. Excess power goes to the battery bank and is utilized by the fuel cell in case of unavailability of power from wind or PV sources. Figure 2 shows the design of the system:

Fig. 2. Configuration of the proposed hybrid system

4.2. System Sizing

The equipments that we used in our simulator are wind turbine (10kW), PV array (20kW), battery (360 Ah) and DC/AC converter (20kW). A diesel back-up system (15 kW) is considered for reliable supply of electricity. The HOMER software is used to determine the best optimal sizing and pre-feasibility study of the system. The HOMER determines the optimal system based on input assumptions. The detailed descriptions of the loads and key assumptions about the price of different components of the hybrid system are given below.

4.2.1 AC Load Data

The seasonal load profile of the hypothetical community situated in the rural or remote areas in Bangladesh is presented in figure 3. The energy consumption by a hypothetical community on the proposed site is 219.92 kWh/day with 25.64 kW peak demand and the load factor is 0.36.

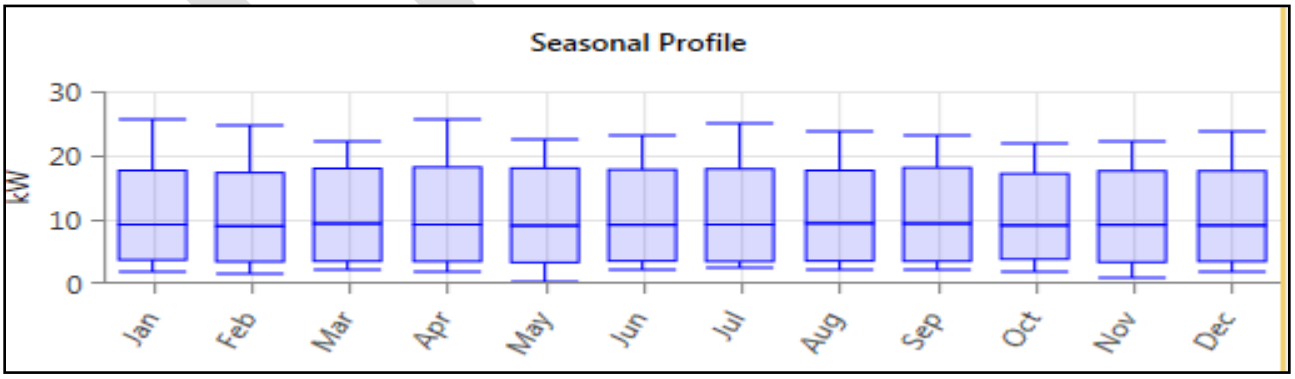

Fig. 3. Seasonal load profile

4.2.2. Wind Turbine

Norvento nED 100 wind turbine has been used in this system. The rated capacity of the turbine is 10kW and it provides AC power. The Cost of one unit is considered to be capital cost and is estimated as $5000. The replacement cost is estimated at $4000 and annual operation and maintenance cost is estimated at $50 and the lifetime of the turbine is taken to be 15 years. The power curve of the wind turbine is shown in fig. 4.

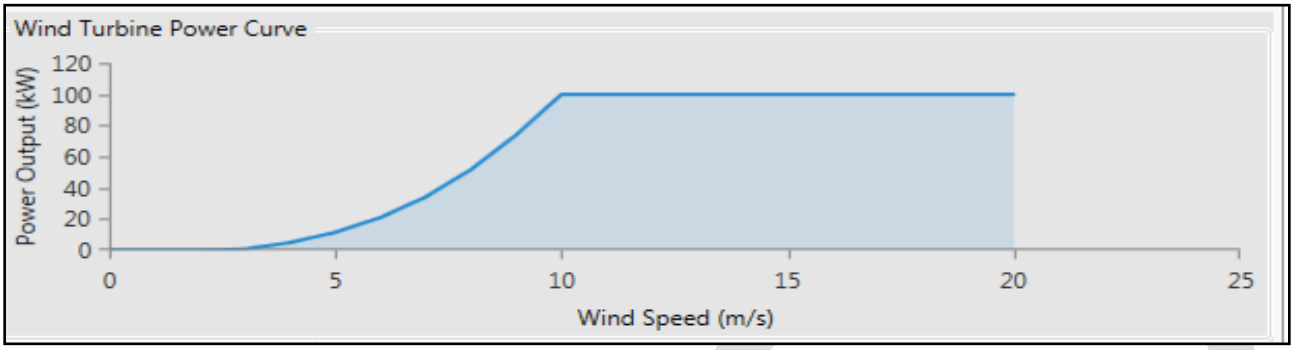

Fig. 4. Wind turbine power curve

4.2.3. Photovoltaic Array

The sun rays are absorbed by the solar panels and in turns solar panels convert them into electricity. A 20kW solar energy system's installation, replacement costs and operation-maintenance cost are taken approximate as $5000 and $2500 and $3 respectively. The expected lifetime of a solar panel is 20 years.

4.2.4. Diesel Generator

The 15 kW diesel generator capital cost, replacement cost, operation-maintenance cost are $8000, $6000, $0.7 respectively. Diesel generator's lifetime is defined in operating hour and that is 15000 hours. Diesel price at the site is $0.6 per liter.

4.2.5. Battery

Trojan L16P type batteries have been used in this system whose nominal voltage, nominal capacity and lifetime throughout are 6V, 360Ah and 2.16kWh respectively. The one battery initial capital cost, replacement cost, and maintenance and operation cost are about $225, $200 and $1 respectively.

4.2.6. Power Converter

The flow of energy between the AC and the DC bus is maintained by a converter and its capacity is 20kW. The initial capital cost and replacement cost and operation-maintenance cost is $400, $250 and 1 respectively. The converter is assumed to be replaced after 20 years.

4.3. Simulation Procedure

The simulation of the hybrid power system is carried out in HOMER software. The Hybrid Optimization Model for Electric Renewable (HOMER) is a software tool that simulates and optimizes an electric power system which is the combination of conventional generators, cogeneration, wind turbines, solar photovoltaic, hydropower, batteries, fuel cells, hydropower, biomass and other inputs [26]. It performs detailed chronological simulations at an hourly level. That detail is necessary to realistically model intermittent renewable power sources, such as wind and solar. Using site-specific information about loads, resources, technology costs and performance, HOMER simulates all possible permutations of the system and then ranks the results, clearly showing the optimal, least-cost configuration. In addition, its sensitivity analyses demonstrate the results of changes to and uncertainty in the input parameters [27].

HOMER provides an important overview that compares the operating expenses of the system and feasibility of different configurations so that the designers or users can be aware of the potential impact of the uncertain factors. This overview is also very much helpful when more specialized software is used to model technical performance as the users know the uncertain factors. Its sensitivity analysis allows the users to understand how a hybrid renewable system works [28].

Its overall features can be classified into three steps [29]:

- Simulation – Estimate the cost and determine the feasibility of a system design over the 8760 hours in a year
- Optimization – Simulate each system configuration and display list of systems sorted by net present cost (NPC)
- Sensitivity Analysis – Perform an optimization for each sensitivity variable.

5. RESULT AND DISCUSSION

HOMER is mainly responsible for the elimination of all infeasible systems and thus it presents the results in ascending order of net present cost (NPC). Different hybrid options were analyzed to get an optimized hybrid system. Optimization analysis of the HOMER shows that the most least lowest cost and the optimal combination of energy system components is the combination of the 15 kW diesel generator, 20 kW solar PV array, 10 KW wind turbine, 140 L16P Battery and a 20 KW converter. Figure 5 shows the simulation result of HOMER.

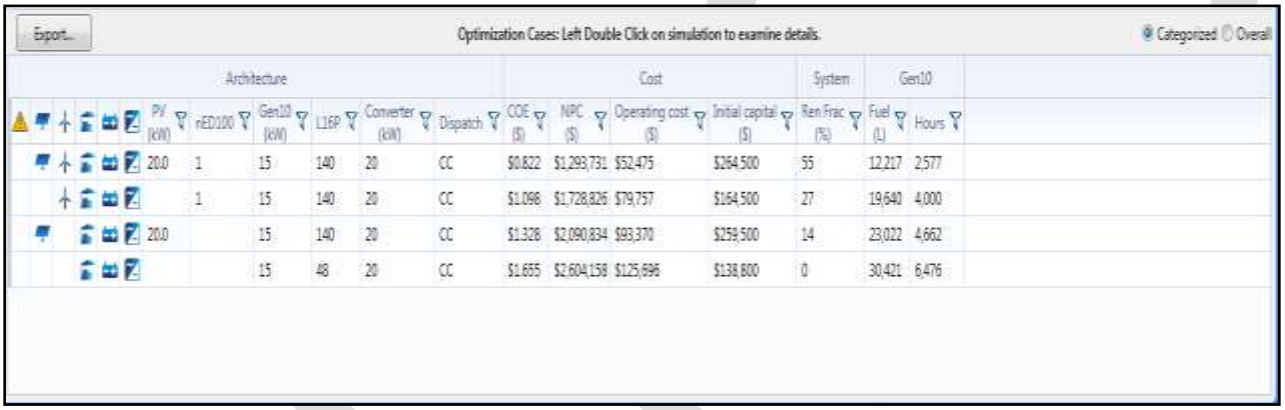

Fig. 5. Simulation Result from HOMER

The electricity production, economic costs and environmental characteristics of each system has been provisioned from the simulation result of HOMER.

5.1. Energy Yield Analysis

Calculating wind power = 41% and solar power = 24% in total 65%; the energy requirement of the village was met by the renewable energy by the proposed wind-pv-diesel hybrid system incorporated with the existing diesel only power system.) In Figure 6 the energy contribution by wind, solar pv system and the existing generator is manifested. As seen from this fig. 6, 35% of the energy is supplied by the diesel generator and the remaining 65% by the wind and solar pv system. In terms of excess energy, which is 11.5% or 12,193 kWh/yr is most favorable for the proposed 65% wind and solar pv hybrid power penetration system.

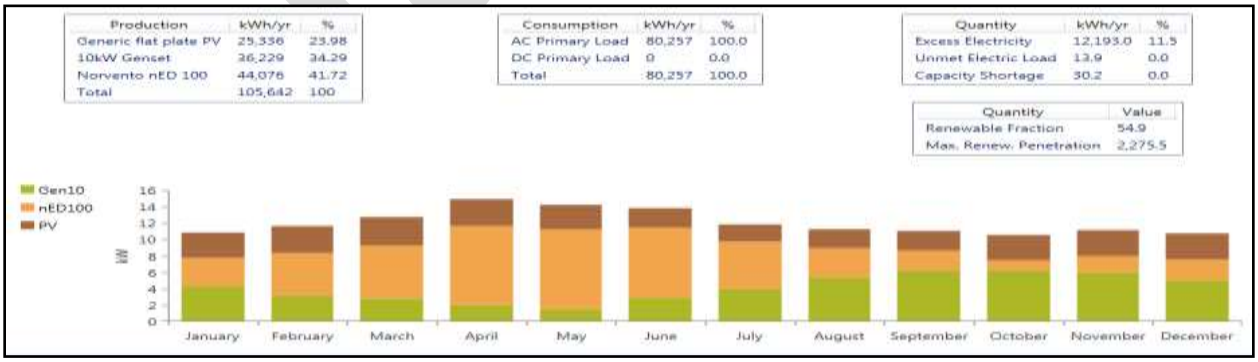

Fig. 6. Annual energy production from the optimized hybrid system

From the above graph, it is esteemed that power contribution of pv systems to the hybrid power system remains almost same with slight variation in peak and base value in the month of November and December. In figure 6, it is seen that wind power varied between a maximum in April and a minimum in October. And the power generated by the generator is maximum in September and minimum in May.

5.2. Economical analysis

In fig. 7, the total cost of the hybrid power systems is shown. Here, the wind turbine, pv panel, generator, batteries and a power converter are the components which costs are taken in account of during counting the total cost.

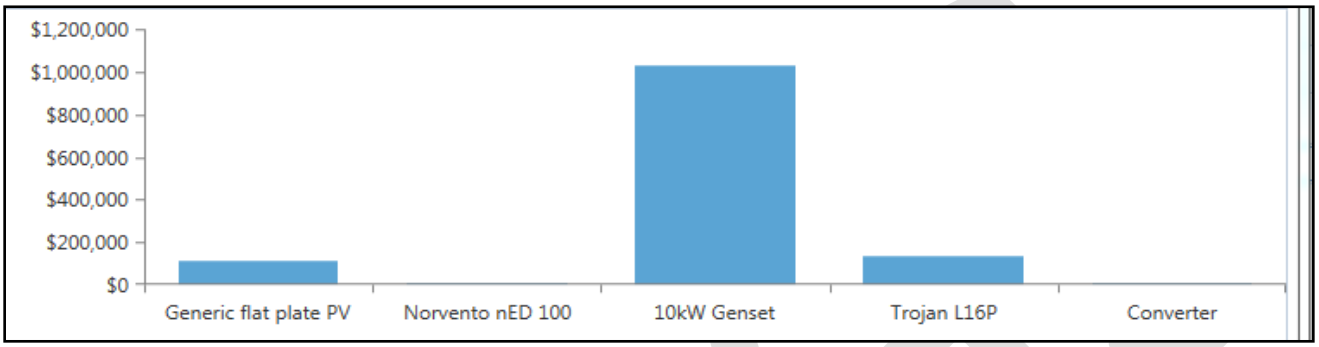

Fig. 7. Cash flow summary of various components of the hybrid power system

In fig. 8, the breakdown of capital, replacement, O & M, fuel and salvage costs of wind-pv-diesel power system are given. From the fig. 8, it can be clearly seen that for diesel generator the net present cost (NPC) is highest. The capital cost of the proposed hybrid power system was estimated as $2,64,500 with replacement, O & M, and fuel cost of $4,22,380, $5,36,011, and $1,43,768 respectively.

Component	Capital ($)	Replacement	O&M ($)	Fuel ($)	Salvage ($)	Total ($)
Generic flat plate PV	$100,000.00	$33,908.00	$1,176.80	$0.00	($23,078.00)	$112,007.00
Norvento nED 100	$5,000.00	$2,989.20	$980.68	$0.00	($820.56)	$8,149.40
10kW Genset	$120,000.00	$273,556.00	$530,715.00	$143,768.00	($39,048.00)	$1,028,991.00
Trojan L16P	$31,500.00	$108,536.00	$2,745.90	$0.00	($7,673.70)	$135,108.00
Converter	$8,000.00	$3,390.80	$392.27	$0.00	($2,307.80)	$9,475.30
System	$264,500.00	$422,380.00	$536,011.00	$143,768.00	($72,929.00)	$1,293,730.00

Fig. 8. Summary of various costs related to the wind-pv-diesel hybrid power system

The comparison of an optimized hybrid system with PV-wind-Diesel generator-battery has been done with PV-diesel generator-battery, wind-diesel generator-battery and diesel generator-battery is given in table 3.

Table 3. The comparisons among the optimized hybrid options

Options	Initial Cost (USD)	Operating Cost (USD/Year)	Total NPC (USD)	COE (USD/KWh)
PV-Wind-Diesel Generator-Battery	264,500	52,475	1,293,731	0.822
Wind-Diesel Generator-Battery	164,500	79,757	1,728,826	1.098
PV-Diesel Generator-Battery	259,500	93,370	2,090,834	1.328
Diesel Generator-Battery	138,800	125,696	2,604,158	1.655

From the table 3, it can be perceived that the optimized PV-wind-diesel generator-battery system has the lowest NPC (1,293,731 USD) with a COE of 0.822 USD/kW. It is mentionable that the system reduces the NPC about 62% and 34% compared with PV-diesel generator-battery and wind-diesel generator-battery respectively. The source of revenue is only the selling of electricity.

In a brief, it is noticed that though the diesel only system had the least initial capital cost, but the total net production cost for the whole project goes high at the end for this type of system. On the other hand, though the initial capital cost is high in the hybrid system topologies but the total net production cost for the whole project goes low at the end for this type of system.

5.3. Green house gas (GHG) emissions

This system emits 32,171 kg of CO_2, 79.41 kg of CO, 8.80 kg of UHC, 5.99 kg of Particulate Matter, 64.60 kg of SO_2, and 708.57 kg of NO**x** annually into the atmosphere as shown in table 4.

Table 4. Comparisons of simulation results of Pollutant Emissions

Pollutant (kg yr^{-1})	Emissions (kg yr^{-1})	
	Diesel Only System	Solar-Wind-Diesel System
Carbon Dioxide	80,109.00	32,171.00
Carbon Monoxide	197.74	79.41
Unburned Hydrocarbons	21.90	8.80
Particulate matter	14.91	5.99
Sulfur Dioxide	160.87	64.60
Nitrogen Oxides	1,764.40	708.57

In table 4, it is noticed that if renewable energy is used as a power generation system, then 60% decrease of pollutant can be rendered. The reduction in the quantity of different air pollutants for 65% renewable penetration compared to that diesel only are thus: 47,938 kg of CO_2, 118.33 kg of CO, 13.1 kg of UHC, 8.92 kg of PM, 96.27 kg of SO_2, and 1055.83 kg of NO**x** where the diesel only system generates 80,109 kg of CO_2, 197.74 kg of CO, 21.90 kg of UHC, 14.91 kg of PM, 160.87 kg of SO_2, and 1,764.40 kg tones of NO**x.**

5.4. Socio-economic Benefits

The study evaluates the performance of the hybrid system which is a combined system of 3 independent and globally tested and proven technologies (PV, wind and diesel). This combined hybrid system is designed in such a way so that by this system a good symmetry between environmental benefits and socio-economic development can be maintained in a convenient way. Deploying the hybrid system will not only provide electricity to the rural and remote areas of Bangladesh but also it will become a stimulant for the effective contribution in the social life. The benefits of this hybrid project are discussed below.

- The proposed PV-wind-diesel Hybrid power plant can be a secured and imperishable source of power generation and can be a better alternative in the rural and remote areas where there is an irregular supply of electricity.
- The implementation of the project will minimize the GHG Emission, resulting in a net reduction of the GHGs, thus bringing a local as well as a global carbon benefit.
- The successful implementation and operation of the hybrid system will lead to further future propagation and also scale-up of the system to larger capacities. This system can be the substitute of conventional grid where old diesel units are being used presently to produce unreliable and high emission.
- A number of households, who is currently meeting their lighting needs with kerosene, will switch over the electricity soon and this will definitely contribute to reduce fire-hazards.
- Being a small central rural power plant, the direct employment generation will be limited only to a few plant operators and maintenance personnel, including a Plant In-Charge. However, due to the enhancement of quality of life and facilitation of economic activities, the indirect employment generation will increase small rural incomes through handicrafts, weaving and other production activities.

6. CONCLUSION

Extensive and wide ranging change may occur in both the social and economic lives of people in rural and economic areas of Bangladesh by the adaptation of the hybrid system as there is an acute crisis of reliable supply of electricity. Various energy sources (wind, solar, and diesel generator) and storage systems (batteries) have been considered to evaluate the features of the hybrid system. NREL's optimization tool HOMER was used in identifying probable hybrid configurations and their feasibility. From this study, it is seen that a developing a stand-alone hybrid power system is more cost effective, reliable and suitable for rural applications than running stand-alone diesel generator. It is clearly perceived from the study that the optimized wind-PV-diesel hybrid system is more cost effective in terms of Net Present Cost (NPC) and the Cost of Energy (COE) compared to PV-diesel and wind-diesel system. Besides that, renewable energy offers a smart, affordable climate solution which will definitely make an impact in the future in both nationally and internationally. The annual emission of the system can be illustrated by the hybrid system which is environment benevolent in nature and another advantage of this system is it is very swift in power generation and response. It is also adapted for its effectiveness, reliability and durability. For effective and continuous power supply, the diesel generator will incorporate with the other technology to provide the required power in the absence of wind and sunlight. This proposed model of wind and solar hybrid system can be a role model of energy generation in the rural electrification. However, more experiments can be done to analysis the potential and effectiveness, advantages and disadvantages of the hybrid system so that it can bring a remarkable change in energy production of our country.

REFERENCES:

[1] Sandeep kumar , Vijay garg, "HYBRID SYSTEM OF PV SOLAR / WIND & FUEL CELL". IJAREEIE Vol. 2, Issue 8, pp. 3666-3679, August 2013.
[2] Duffe J.A, Beckman W. A.," Solar Engineering of Thermal Processes", New York: John Willey and Sons, 1980.
[3] Power cell Bangladesh. Bangladesh's Power Sector at a Glance (June 2015) from http://www.powercell.gov.bd/index.php?page_id=267
[4] Bangladesh Power Development Board (BPDB). Retrieved June, 2015 from http://www.bpdb.gov.bd/bpdb/
[5] Electricity sector in Bangladesh from http://en.wikipedia.org/wiki/Electricity_sector_in_Bangladesh
[6] Bangladesh Power Development Board (BPDB). Power Generation Units (Fuel Type Wise). Retrieved July, 2015 from http://www.bpdb.gov.bd/bpdb/index.php?option=com_content&view=article&id=150&Itemid=16
[7] A, Doraswami, "National energy policy for Bangladesh". Energy for Sustainable Development, vol. 2, no.2, pp. 5-8, 1996.
[8] Bangladesh Power Development Board (BPDB). Development of Renewable Energy Technologies by BPDB from http://www.bpdb.gov.bd/bpdb/index.php?option=com_content&view=article&id=26&Itemid=24
[9] J.J. Ding, J.S. Buckeridge, "Design considerations for a sustainable hybrid renewable energy system". IPENZ Transactions, vol. 27, no. 1, pp. 1-5, 2000.
[10] S.R. Vosen, J.O. Keller, "Hybrid energy storage systems for stand-alone electric power systems: optimization of system performance and cost through control strategies". International Journal of Hydrogen Energy, vol 24, Issue 12, pp. 1139-1156, December 1999.
[11] Molla Shahadat Hossain Lipu, Md. Shazib Uddin, Muhammad Ahad Rahman Miah, "A Feasibility Study of Solar-Wind-Diesel Hybrid System in Rural and Remote Areas of Bangladesh". IJRER, vol.3, no.4, pp. 892-900, 2013.
[12] Solar Power. Retrieved 27 July, 2015 from http://en.wikipedia.org/wiki/Solar_power
[13] B. Van der Zwaan & A. Rabl, "Prospects for PV: a learning curve analysis". Solar Energy, vol. 74, pp.19-31, 2003.
[14] Ariful Islam, Kazi Tanvir Ahmed, Sreebash Chandra Debnath, "Ensuring Food Security and Power Crisis Solution in Bangladesh through Renewable Sources". European Researcher, DOI:10.13187/issn.2219-8229, vol. 65, no. 12-2, pp. 2892-2905, 2013.
[15] M.H. Kabir, W. Endlicher, & J. Jagermeyr. "Calculation of bright roof-tops for solar PV applications in Dhaka Megacity", Bangladesh. Renewable Energy, vol.35, pp. 1760-1764, 2010.
[16] A.H. Mondal and M. Denich, "Assessment of renewable energy resources potential for electricity generation in Bangladesh", Renewable and Sustainable Energy Reviews, vol.12, pp. 2401-2413, 2010.
[17] Mazharul Islam,"Assessment of Renewable Energy Resources of Bangladesh", version 1. Retrieved 28 July, 2015 from http://www.geni.org/globalenergy/library/energytrends/currentusage/renewable/wind/global-wind-resources/bangladesh/bangladesh.pdf

[18] H.J. Khan, A.J. Huque, S. Khatun and M.A Mannan. Commercialization of solar home systems: market assessment survey in Bangladesh, Solar photovoltaic systems in Bangladesh: experience and opportunities. Dhaka, Bangladesh: The University Press Limited, pp. 95-102, 2005.

[19] National Center of Renewable Energy. Retrieved 28 July, 2015 from http://usncre.org/wind

[20] A.N. M. Mominul Islam Mukut, Md. Quamrul Islam, Muhammad Mahbubul Alam, "ESTIMATION OF WIND ENERGY POTENTIAL IN COASTAL AREAS OF BANGLADESH BY USING WEIBULL DISTRIBUTION", 4th BSME-ASME International Conference on Thermal Engineering, Dhaka, Pp. 725: 727-729 December, 2008.

[21] A.N. M. Mominul Islam Mukut, Md. Quamrul Islam and Muhammad Mahbubul Alam, "ANALYSIS OF WIND CHARACTERISTICS IN COASTAL AREAS OF BANGLADESH". Journal of Mechanical Engineering, vol. ME39, no. 1, pp. 45-49, June 2008.

[22] M.A.H. Mondal, "Technical and socio-economic aspects of selected village based solar home systems in Gazipur District, Bangladesh", Sustainable energy systems and management (SESAM). Flensburg, Germany: University of Flensburg; 2005.

[23] Mustafa Engin, "Sizing and Simulation of PV-Wind Hybrid Power System". International Journal of Photoenergy, Article ID 217526, vol 2013, pp. 1-10.

[24] Hybrid power From Wikipedia. https://en.wikipedia.org/wiki/Hybrid_power

[25] M.M Hoque, I.K.A Bhuiyan, Rajib Ahmed, A.A .Farooque & S.K Aditya, " Design, Analysis and Performance Study of a Hybrid PV-Diesel-Wind System for a Village Gopal Nagar in Comilla". Global Journal of Science Frontier Research Physics and Space Sciences, Vol. 12, Issue 5, pp. 12-17, Version 1, 2012.

[26] **HOMER: Hybrid Optimization Modeling Software. Retrieved 25 July, 2015 from** http://gcmd.gsfc.nasa.gov/KeywordSearch/Metadata.do?Portal=GCMD&MetadataType=1&MetadataView=Full&KeywordPath=&EntryId=HOMER

[27] Microgrid News by Homer Energy from http://microgridnews.com/about-us/

[28] Anchal Paliya, Manish Khemariya, Naveen Aasati," OPTIMIZATION OF HYBRID SYSTEM USING HOMER". IJATER Volume 4, Issue 4, pp. 56-59, July 2014.

[29] HOMER The Micropower Optimization Model. Ppt by National Renewable Energy Laboratory from http://files.harc.edu/Documents/EBS/CEDP/HOMER.pdf

International Journal of Engineering Research and General Science Volume 3, Issue 5, September-October, 2015
ISSN 2091-2730

DESIGN AND PERFORMANCE ANALYSIS ON PISTON RING

PARTHIBAN S[1], ARSHAD MOHAMED GANI P[2], VASUDEVAN R[3], NAVEEN KUMAR C[4]

[1, 3, 4] U.G. SCHOLAR, DEPARTMENT OF MECHANICAL ENGINEERING, DHAANISH AHMED COLLEGE OF ENGINEERING, CHENNAI, TAMILNADU ,INDIA.

[2] ASST. PROFESSOR, DEPARTMENT OF MECHANICAL ENGINEERING, DHAANISH AHMED COLLEGE OF ENGINEERING, CHENNAI, TAMILNADU ,INDIA.

EMAIL: MNCGANI@GMAIL.COM

ABSTRACT- The main objective of this work is to study the wear characteristics that govern on the piston ring pack inside the piston assembly of an engine. Among several methods, most profitable method is to provide a coating layer on the piston ring pack. Since, ring seal is essential to the performance of the engine, it is must be a perfect seal between the ring pack and cylinder wall. In this phase, existing material of the piston ring material were considered and studied, a model corresponding to its dimensions were prepared and analysis were done on them in static conditions. Also, Mathematical calculations were performed in designing the ring pack for modelling. The study on coating materials were made and suitable materials were chosen for coating.

KEYWORDS: Piston Ring design, Nano Coating, Thermal Analysis, Static analysis, High Speed Steel, Silicon di Oxide, Calcium stabilized Zirconium oxide,

1. INTRODUCTION

Nano technology is an engineering functional system at the molecular scale. It involves the creation and/or manipulation of materials at the nanometer (nm) scale either by scaling up from single groups of atoms or by refining or reducing bulk materials. A nanometer is 1 x 10^{-9} m or one millionth of a millimeter. To give a sense of this scale, a human hair is of the order of 10,000 to 50,000 nm. Two main approaches are used in Nano technology. In the "bottom-up" approach, materials and devices are built from molecular components which assemble themselves chemically by principles of molecular recognition. In the "top-down" approach, Nano objects are constructed from larger entities without atomic level control.

2. NANO COATING

Nano coating is a surface modification technique to create the Nano layer on the surface to improve the physical and mechanical performances.

- Increase the hardness.
- Superior wear resistance.
- Oxidation resistance
- Friction resistances

This coating is widely used for cutting and forming tools, bearings, I.C engine components, seals, valves, glass etc.Nano-layered multilayer coatings have periodic structures of layer with proper control of the layers composition and structure. Chemical vapor deposition (CVD) was the first technology used, which advanced from single layer to current multilayer types combining, TiC, TiN, TiCN and Al_2O_3. The coatings with very low electronic conductance, such as SiO_2 TiO_2, non-conducting coatings Al_2O_3 or mix-oxides coating of TiO2, SiO2, and Al_2O_3 have been reported as the wear protections in the literatures.

3. PISTON RING

The function of a piston ring is to seal off the combustion pressure, to distribute and control the oil to transfer heat, and to stabilize the piston. The piston is designed for thermal expansion, with a desired gap between the piston surface and linear wall.

The piston rings have three types:

- Top Compression ring
- 2nd Compression ring

Oil Scratch ring

Top and 2nd compression rings seal the combustion chamber perfectly to avoid the escape of combustible rich mixture from the chamber. Oil ring helps in removing the lubricant oil from the surface of the cylinder wall and reduces the combustion of lubricant oil.

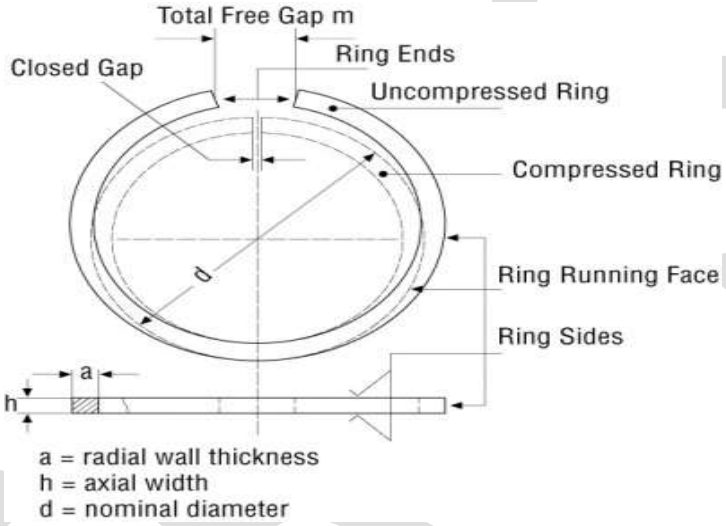

FIGURE 3.1 NOMENCLATURE OF PISTON RING

4. MATERIALS AND COATING METHOD

4.1 HIGH SPEED STEEL (HSS OR HS)

HSS is a subset of tool steels, commonly used in tool bits and cutting tools. This property allows HSS to cut faster than high carbon steel. To increase the life of high speed steel, tools are sometimes coated. Most coatings generally increase a tool's hardness and/or lubricity. The coating also helps to decrease the temperature associated with the cutting process and increase the life of the tool.

Table 4.1- Composition of AISI440C Steel

Grade440C		
Ingredients	Min.	Max.
Carbon	0.95	1.20
Manganese	-	1.00
Silicon	-	1.00
Phosphorus	-	0.040
Sulphur	-	0.030

Chromium	16.00	18.00
Molybdenum	-	0.75
Iron	Balance	

4.2 SILICON DI-OXIDE (SiO_2)

Silicon dioxide, also known as Silica is natural compound of oxide of silicon. Silicon dioxide has many advantageous properties such as Low electrical conductor and thermal insulator.

4.3 CALCIUM STABILIZED ZIRCONIUM OXIDE (CSZ)

Zirconium oxide is one of the sub products of zirconium. It is in white color and it is a crystalline oxide of zirconium. Zirconium oxides were known for their thermal stability and high wear resistance.

4.4 DIAMOND LIKE CARBON (DLC)

Diamond like carbon (DLC) is a class of amorphous carbon material which displays some similar properties of diamond. DLC is usually applied as coatings to other materials such as steels, brass, copper etc .DLC exists in three forms:

- Amorphous
- Crystalline
- Monolithic

5. MODELLING AND MESHING

5.1 DESIGN CONSIDERATIONS FOR PISTON RING

Design considerations for designing the piston ring were:

- Must form a perfect seal with cylinder wall
- Must maintain constant blow-by and lock the chamber pressure
- Addition in weight of piston rings was acceptable.
- Ring pack must be rigid to withstand thermal and shock loads.
- Oil ring must remove excess lubricant from the cylinder wall.
- Rings must also act as a fin structure to remove heat from the engine chamber.
- It must have resistance over heat and pressure.

6. PROCEDURE FOR PISTON RING DESIGN

6.1 CALCULATING MAXIMUM PRESSURE

Considering Mechanical efficiency = 0.8

Brake Power BP = $(T*2*\pi* N)/60$

Indicated Power, IP = Brake Power/Mechanical efficiency

= $(P*\pi*D^2*L*N)/2$

Where,

P - Maximum Pressure in N/mm^2

N - Engine Speed in rpm

D - Cylinder bore in mm

L - Length of stroke in mm

6.2 RADIAL THICKNESS OF THE RING

$T_1 = D\sqrt{((3*P_w)/S_t)}$

Where,

P_w = Wall pressure on the ring

= 0.025 N/mm^2 to 0.042 N/mm^2

S_t = Tensile stress of the steel ring

= 745 N/mm^2

6.3 AXIAL THICKNESS OF THE RING

T_2 = $0.7*T_1$ TO T_1

Where,

T_1 = Radial thickness of ring in mm

6.4 ANGLE OF CIRCUMFERENCIAL GAP

Circumferential gap, C = $0.02*(\pi*D)$

Angle of circumferential gap, θ = $(C/R)*(180°/\pi)$

Where,

C = Circumferential gap in mm

R = Radius of the ring in mm

7. GEOMETRY MODEL

From the above calculations, dimensions of the piston ring were designed using any modelling software such as CATIA V5. In this design, we have considered the cross section of top compression ring as rectangular one with dimensions of 3.5mm*2.5mm. As far the oil ring is considered, cross section is considered to be a C-Section. Here, we have considered the thickness of oil ring is much greater than the compression ring. When coating is provided, the sealing is considered to be a perfect one with reduced blow-by gas escape and better lubrication under dry conditions.

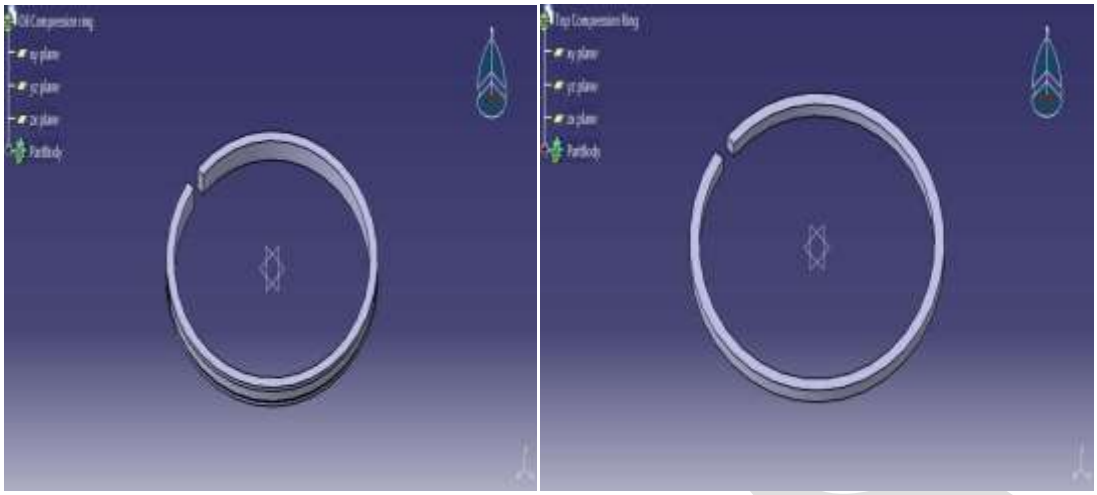

FIGURE 7.1 GEOMETRY MODEL OF PISTON RING PACK

7.1 MESHING

After the model is created according to the dimensions, we import the geometry file using ANSYS V12. In this analysis, we have achieved fine number of meshing constraints, with values up to 45970 numbers of nodes.

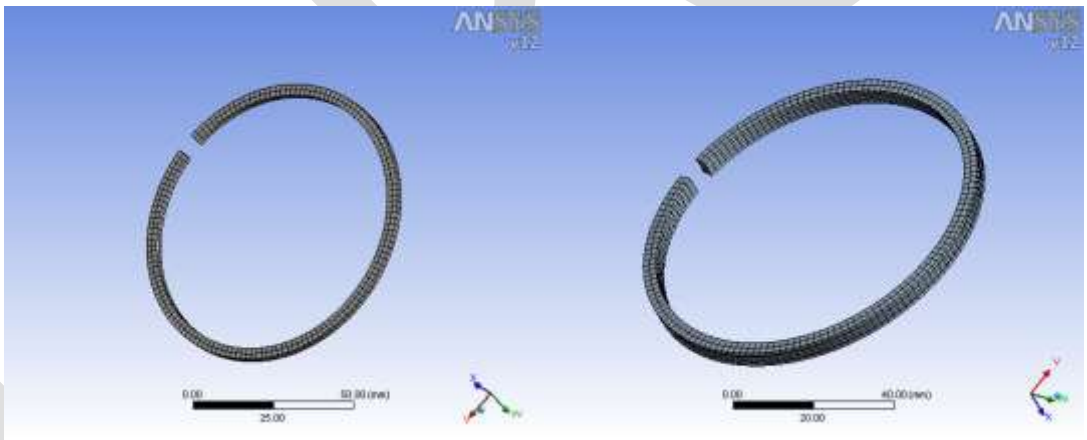

FIGURE 7.2 MESHED MODEL OF PISTON RING PACK

8. COMPUTATIONAL ANALYSIS

8.1 STATIC ANALYSIS

Static analysis calculates the effects of steady loading conditions on a structure, while ignoring inertia and damping effects, such as those caused by time varying loads.

Typical structural quantities are:

1. Total Deformation
2. Equivalent Stress
3. Equivalent Strain

8.2 BOUNDARY CONDITIONS

The maximum pressure of about **14.95 MPa** is applied on the top surface of the ring structure. Both the coated and uncoated structures were recommended to use constant pressure for this analysis.

8.3 TOTAL DEFORMATION

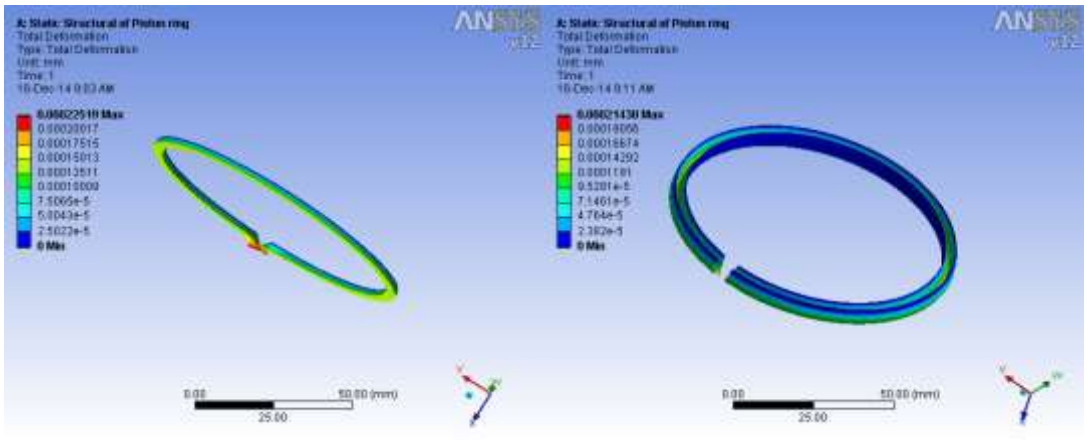

FIGURE 8.1 TOTAL DEFORMATION OF UNCOATED PISTON RINGS

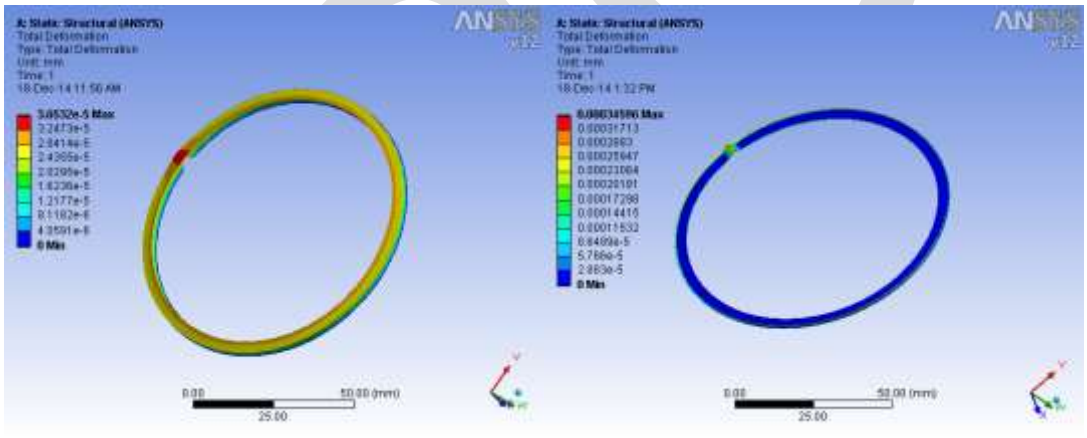

FIGURE 8.2 TOTAL DEFORMATION OF COATED PISTON RINGS

8.4 EQUIVALENT STRAIN

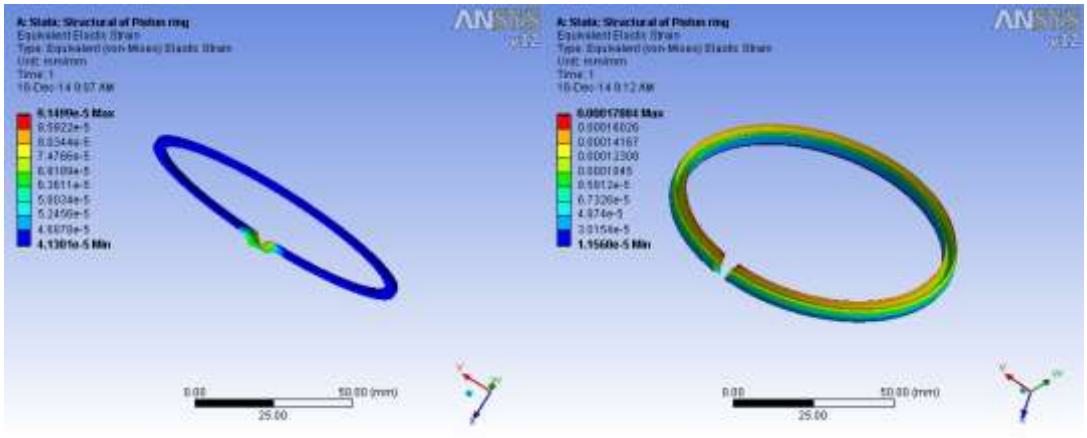

FIGURE 8.3 STRAIN IN UNCOATED PISTON RINGS

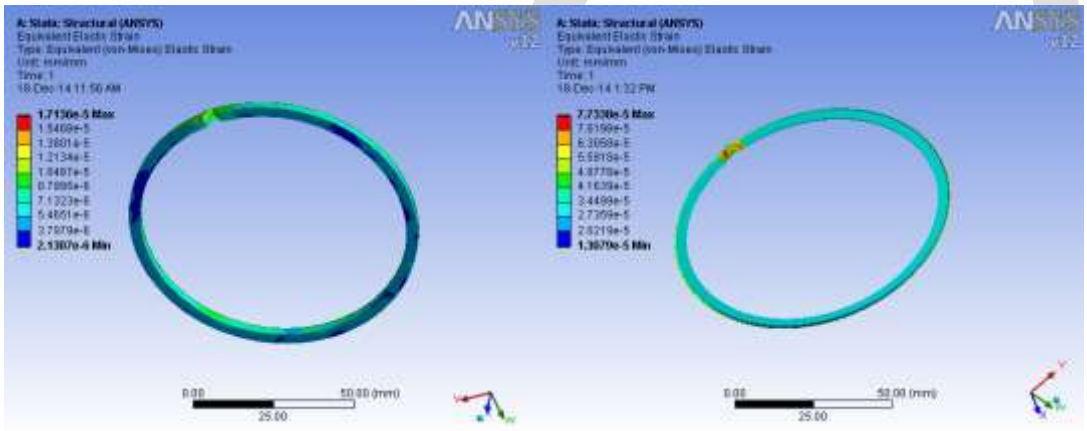

FIGURE 8.4 STRAIN IN COATED PISTON RINGS

8.5 EQUIVALENT STRESS

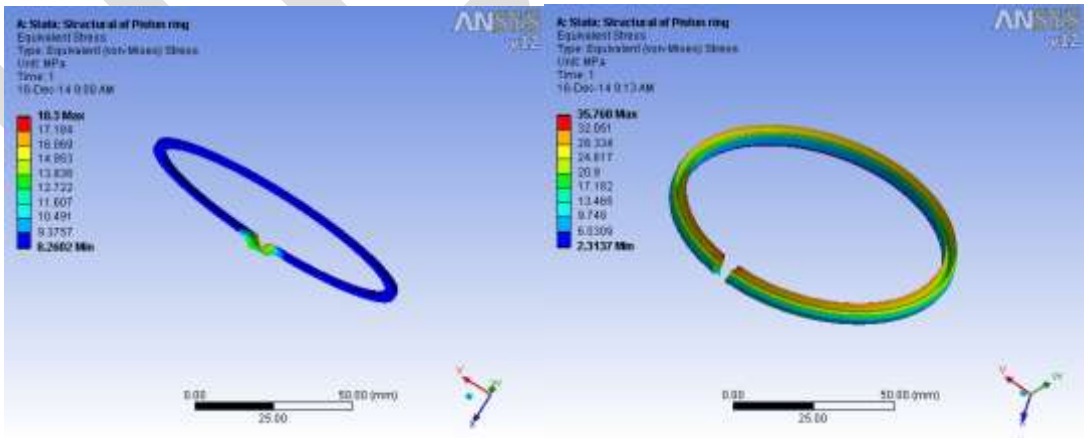

FIGURE 8.5 STRESS ACTING ON UNCOATED PISTON RING

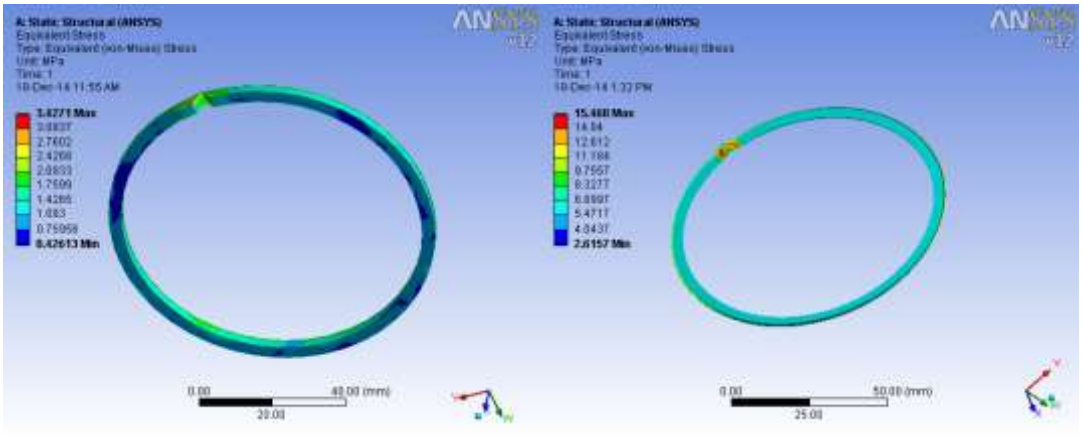

FIGURE 8.5 STRESS ACTING ON COATED PISTON RINGS

8.6 THERMAL ANALYSIS

A thermal analysis calculates the temperature distribution and related thermal quantities in a system or component. Typical thermal quantities are:

1. The temperature distributions.
2. Thermal fluxes
3. Thermal error.

8.7 BOUNDARY CONDITIONS

Engine temperature of 1100°C is produced on the rings as convection heat transfer and thermal coefficient were given for all the sides of the ring. The results obtained by this analysis were shown below.

8.8 TEMPURATURE DISTRIBUTION

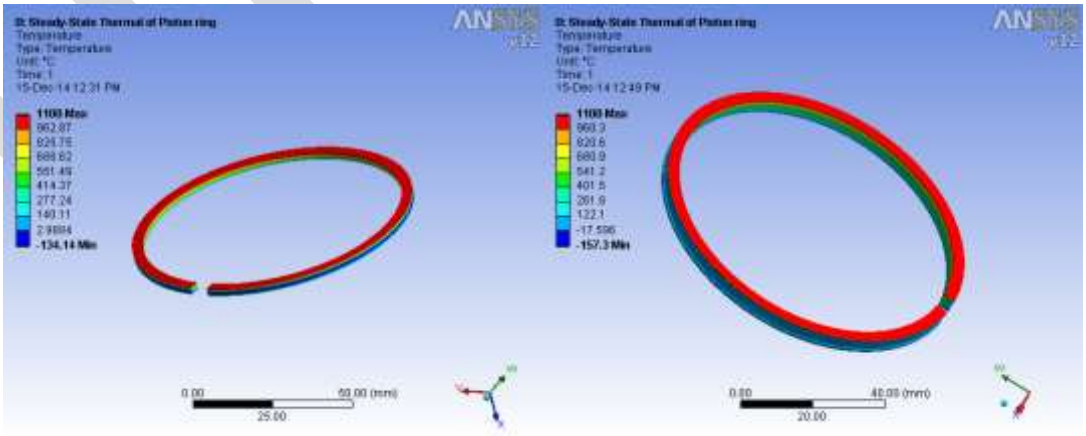

FIGURE 8.6 TEMPURATURE DISTRIBUTION OF UNCOATED RINGS

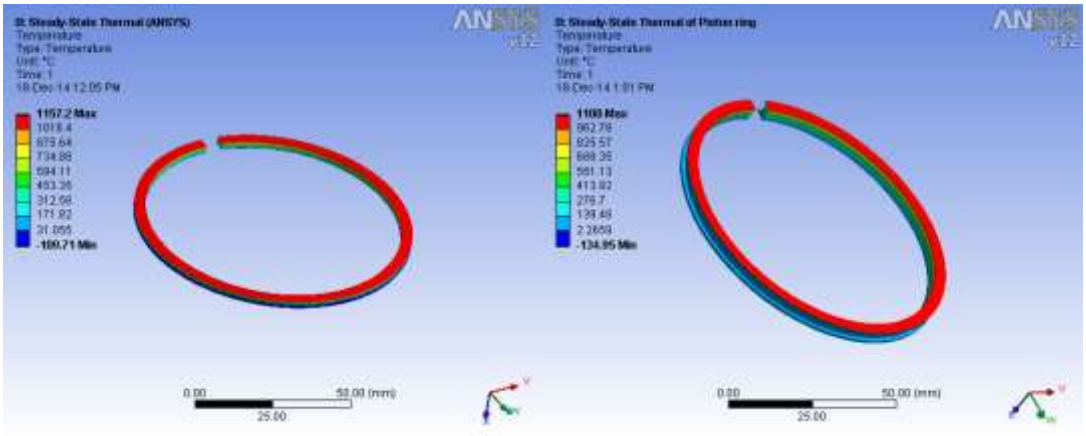

FIGURE 8.6 TEMPURATURE DISTRIBUTION OF COATED PISTON RINGS

8.9 TOTAL HEAT FLUX

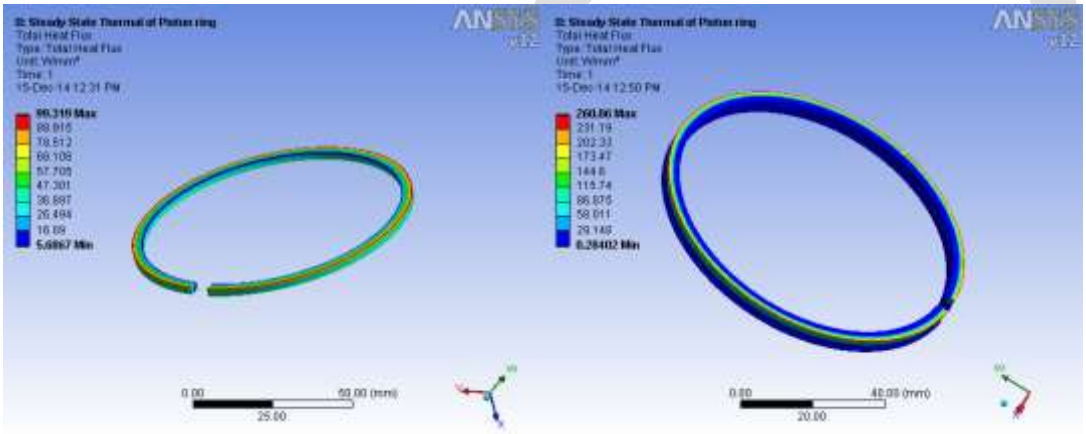

FIGURE 8.7 TOTAL HEAT FLUX DISTRIBUTION ON UNCOATED PISTON RINGS

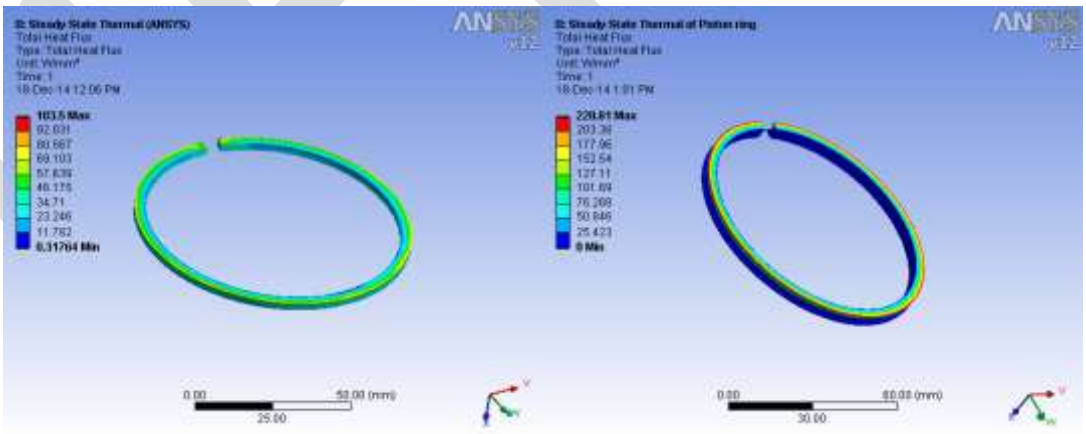

FIGURE 8.8 TOTAL HEAT FLUX DISTRIBUTION ON COATED PISTON RINGS

9. MODAL ANALYSIS

This analysis is used to determine the vibration characteristics (natural frequencies and modal shapes) of a structure during the design stage itself.

1. Total Deformation

9.1 Boundary Conditions

The Boundary conditions given for the Thermal Analysis of the Piston are as follows:

- Friction less support for the inner and outer sides of the ring pack in order to study the mode of frequency generated during this analysis

TOTAL DEFORMATION

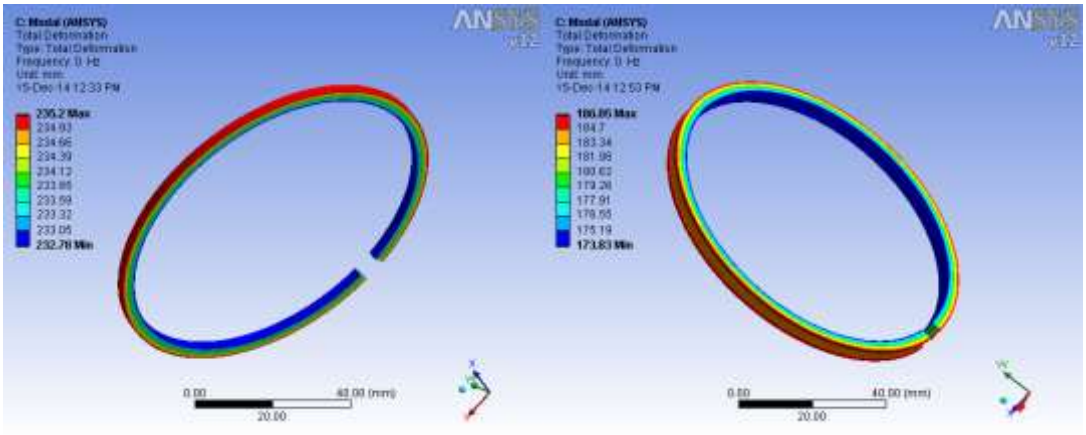

FIGURE 8.9 TOTAL DEFORMATION IN UNCOATED PISTON RINGS

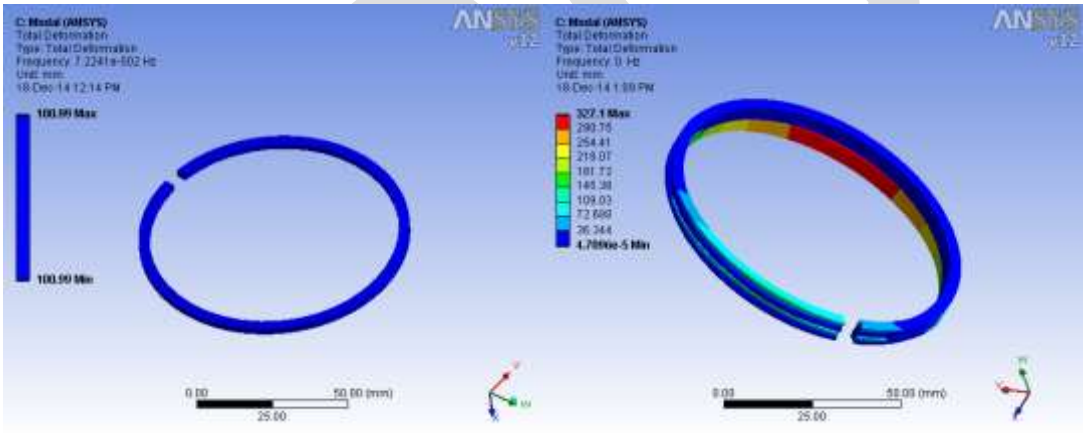

FIGURE 8.10 TOTAL DEFORMATION IN COATED PISTON RINGS

10. COMPARISON OF RESULTS

Based on the pressure load, friction less support, convection are applied on the piston after applying thermal loads, the Von Mises stresses, deformation, on mises strain, vibration and displacement values are calculated and compare between the results of uncoated and coated piston ring pack. The graphs plotted below contain the values obtained from the analysis. Plotting makes us easy to understand and prioritize the requirement.

STATIC STRUCTURAL ANALYSIS

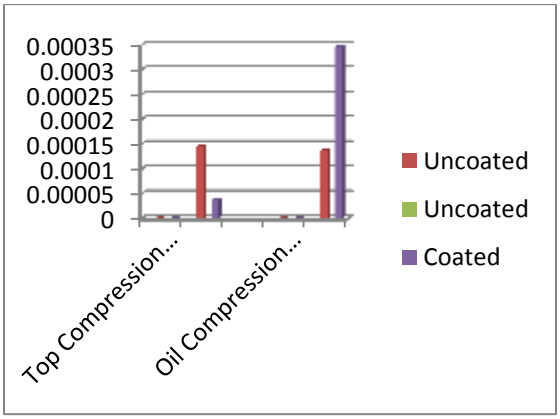

FIGURE 10.1 DEFORMATION IN THE COATED AND UNCOATED RING PACKS

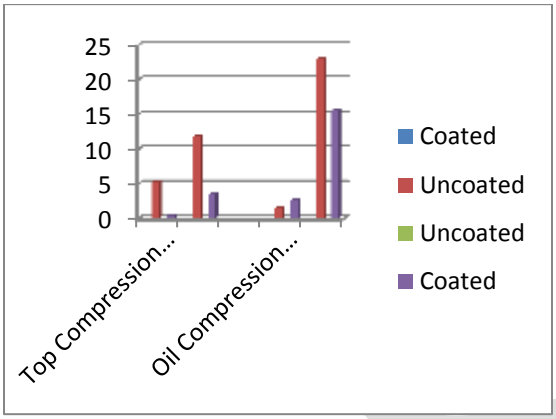

FIGURE 10.2 STRESS DISTRIBUTIONS IN UNCOATED AND COATED RING PACKS

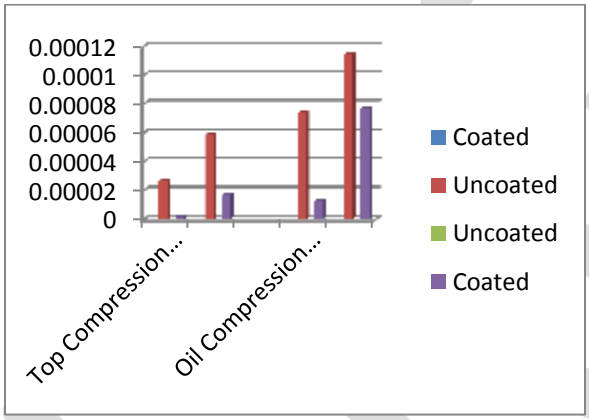

FIGURE 10.3 STRAIN CONCENTRATION IN UNCOATED AND COATED RING PACKS

THERMAL ANALYSIS

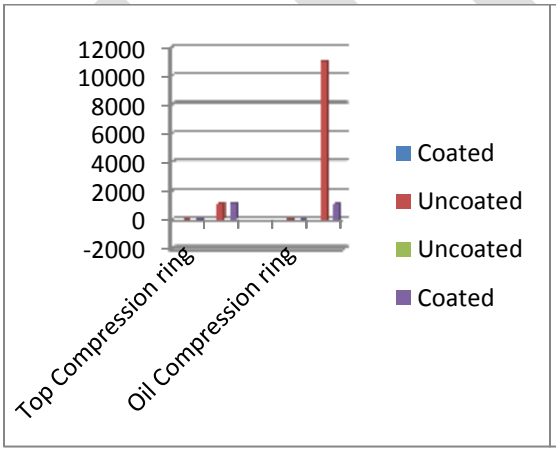

FIGURE 10.4 TEMPURATURE DISTRIBUTIONS IN UNCOATED AND COATED RING PACKS

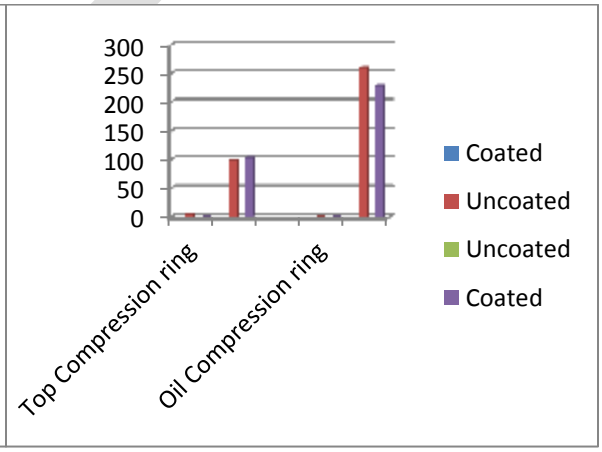

FIGURE 10.5 TOTAL HEAT FLUX PRODUCED ON UNCOATED AND COATED RING PACKS

MODAL ANALYSIS

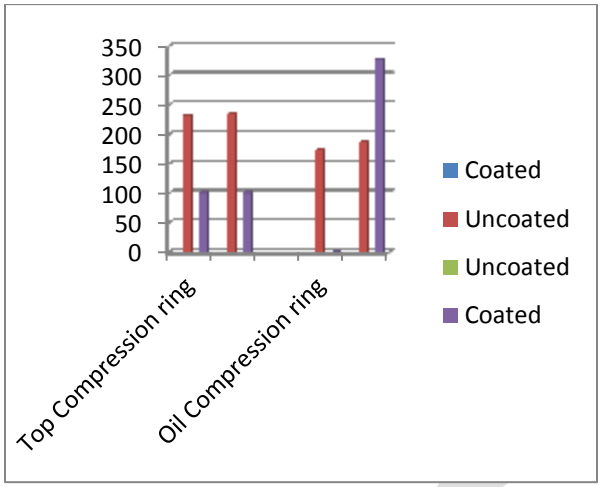

FIGURE 10.6 DEFORMATION PRODUCED ON UNCOATED AND COATED RING PACKS

11. CONCLUSION

From the above analysis and plotted graphs, we can achieve some results based on it. Some are:

- It is observed that maximum deformation occurs on the top face and sides of the piston rings. This is due to scuffing and wear losses that occur during running conditions.
- Tempurature distribution in the piston ring shows that maximum tempurature occur on the face towards the chamber and next tempurature occur on the sides which are in contact with cylinder wall.

Thus, high refractoriness and high lubricancy is nessasary for the coating which we are about to be prepared on it. Multilayer coating consisting Calcia-Partially Stabilized Zirconia, Magnesia-Partially Stabilized Zirconia, Silicon Dioxide, Diamond like carbon which sounds to be effective under such extreme conditions.

REFERENCES:

[1] Ajayi N, C.Lorenzo-Martin,R.A.Erck,G.R.Fenske," Analytical predictive modeling of scuffing initiation in metallic materials in sliding contact",journal of wear 301(2013)57-61.

[2] David Pech, Norbert Schupp, Philippe Steyera, Theo Hack, Yves Gachonc, Christophe Héau, Anne-Sophie Loir , Juan Carlos Sánchez-López," Duplex SiCN/DLC coating as a solution to improve fretting—Corrosion resistance of steel",journalofWear 266 (2009) 832–838.

[3] Dong-Wook Kim, Kyung-Woong Kim," Effects of sliding velocity and normal load on friction and wear characteristics of multi-layered diamond-like carbon (DLC) coating prepared by reactive sputtering",journal of Wear 297 (2013) 722–730.

[4] Eugenia L. Dalibon ,RaúlCharadia , Amado Cabo , Vladimir Trava-Airoldi , Sonia P. Brühl," Evaluation of the mechanical behaviour of a DLC film on plasma nitrided AISI 420 with different surface finishing",journal of Surface & Coatings Technology 235 (2013) 735–740.

[5] Eugenia L. Dalibon , Vladimir Trava-Airoldi , Lânia A. Pereira , Amado Cabo , Sonia P. Brühl," Wear resistance of nitrided and DLC coated PH stainless steel",journal of Surface & Coatings Technology(2013).

[6] T. Fu , Z.F. Zhou , Y.M. Zhou , X.D. Zhu , Q.F. Zeng , C.P. Wang , K.Y. Li , J. Lu ," Mechanical properties of DLC coating sputter deposited on surface nanocrystallized 304 stainless steel",journal of Surface & Coatings Technology 207 (2012) 555–564.

[7] M. Hassana, A. Qayyumb, S. Ahmadb, S. Mahmoodc, M. Shafiqa, M. Zakaullaha,P. Leec, R.S. Rawatc," DLC coating on stainless steel by pulsed methane discharge inrepetitive plasma focus",journal of Applied Surface Science 303 (2014) 187–195.

[8] JussiOksanen , TimoJ.Hakala , SannaTervakangas , PetriLaakso , LauriKilpi , Helena Ronkainen , JariKoskinen," Tribological properties of laser-textured and ta-C coated surfaces with burnished WS2 at elevated temperatures",journal of TribologyInternational70(2014)94–103.

[9] Liu Hongxi , Jiang Yehua , Zhou Rong , Tang Baoyin," Wear behaviour and rolling contact fatigue life of Ti/TiN/DLC multilayer films fabricated on bearing steel by PIIID",journal of Vacuum 86 (2012) 848-853.

[10] Masahiro Suzuki, ToshiyukiSaito , AkihiroTanaka ," Tribological properties of DLC films against different steels", Wear304(2013)83–87.

[11] Robert Sherman," Auger analysis of a calcium partially stabilized zirconia",journal of Materials Science Letters August 1984, Volume 3, Issue 8, pp 711-714.

[12] Sresomroeng .B, V. Premanond , P. Kaewtatip , A. Khantachawana , N. Koga , S. Watanabe ," Anti-adhesion performance of various nitride and DLC films against high strength steel in metal forming operation",journal of Diamond & Related Materials 19 (2010) 833–836.

International Journal of Engineering Research and General Science Volume 3, Issue 5, September-October, 2015
ISSN 2091-2730

Study of the mechanical behavior of high performance polypropylene yarn for geotextile application

Dr. S. B. Chaudhari and S. A. Agrawal

Department of Textile Engineering, Faculty of Technology & Engineering,

The M. S. University of Baroda, Vadodara, Gujarat, India.

Email: s.b.chaudhari-ted@msubaroda.ac.in, sweetyagrawal88@yahoo.com

Abstract –The textiles used in geotechnical application require long-term durability and high strength under tough conditions. The selected high tenacity polypropylene yarn was studied for its characteristics regarding geotextile application. The tensile strength found in the range of high tenacity and the stress relaxation increased with increase in load applied, these properties were studied under the Lloyd universal strength tester. Polypropylene has found more stable in primary creep and secondary creep behavior, was studied to see the deformation under constant load. The torsional rigidity was tested on torsional pendulum and found increased with increase in tension applied, which is an indication of maintaining constant tension during twisting process.

Keywords –Polypropylene yarn, tensile strength, creep properties, stress relaxation, torsional rigidity, primary creep, secondary creep

INTRODUCTION

Polypropylene and polyester fibers are still the most commonly used raw material for production of geofabrics in international market [1]. The deformation behavior under load with time called as creep behavior of these yarns adds to its usability for geotextiles. It has been stated that for a fabric to be dimensionally stable, it has not only to be stiff, low stretch and shrinkage, but it should have good recovery properties [2]. Polypropylene fibers are of advantage for their inertness, low gravity, low cost and ease of processability [3]. It has excellent mechanical properties, chemical and fungal resistance [4-6]. Polypropylene has found its applications related to filtration, separation, reinforcement and drainage [7, 8]. PP being chemically inert doesn't lose its strength when buried under the soil for geotechnical applications. The mechanical durability of the fabrics is of prime concern in a reinforcing geotextiles and tensile creep data provides a good index of its durability [9, 10].

When a plastic material is subjected to a constant load, it deforms continuously. The initial strain is roughly predicted by its stress-strain modulus. The material will continue to deform slowly with time indefinitely or until rupture or yielding causes failure. The primary region is the early stage of loading when the creep rate decreases rapidly with time. Then it reaches a steady state which is called the secondary creep stage followed by a rapid increase (tertiary stage) and fracture. This phenomenon of deformation under load with time is called creep [11]. Stress relaxation is a gradual decrease in stress with time under a constant deformation or strain. This behavior of polymer is studied by applying a constant deformation to the specimen and measuring the stress required to maintain that strain as a function of time. The torsional rigidity is a measure of the initial resistance of fibres to twist. This affects the behavior of fibre during twisting process. In this paper, the high tenacity polypropylene yarn characteristics have been studied for geotextile application such as tensile strength, creep behavior, stress relaxation and torsional rigidity.

MATERIAL & METHOD

Materials

Polypropylene multifilament 867.89 Denier yarn with 155 filaments having tenacity of 6.49 g/den was used in the present study.

Methods

Polypropylene multifilament conditioned for 24 hours at standard atmosphere for tropical regions, 65% ± 2% relative humidity and 27°C ± 2°C temperature before testing [12]. Denier was measured by BISFA method [13]. Tenacity and breaking extension were tested on Lloyd tensile tester as per ASTM Standards D 2256-02 [14]. Five samples of 5 cm gauge length with five different loads were used to study the creep behavior of polypropylene filament. The extension at various time intervals was measured.

For Stress Relaxation specimen of gauge length 200 mm was mounted on a board on LIoyd tensile tester and applied load equivalent to 10%, 20% and 30% of breaking load. Time taken for load relaxation at all the three stages was measured. Torsional rigidity was measured on torsion pendulum instrument as shown in figure 1 [15]. Fiber was hanged on the stand with dead weight and a small deflection of $\theta<40$ was given to the end of pendulum and the average time period for oscillation was measured. The moment of inertia is calculated as per equation 1. Four pendulums of different lengths were used. The length, weight and moment of inertia for the four torsion pendulums are tabulated in Table 1. On the basis of the time period measured, the torsional rigidity and modulus of rigidity were calculated as per equation 2 and 3.

Table 1 Parameters for the torsional pendulums

Pendulum No.	**Weight (gm)**	**Length (cm)**	**Radius (mm)**	**Moment of Inertia (I)**
I1	0.4193	1.05	2.13	0.51338
I2	0.8196	2.1	2.13	1.2294
I3	1.22351	3.05	2.14	2.349
I4	1.58379	3.95	2.15	3.8895

$$Moment\ of\ Inertia\ (I) = m\left[\left(\frac{R^2}{4}\right) + \left(\frac{l^2}{12}\right)\right] \quad \ldots\ldots Equation\ 1$$

$$Torsional\ Rigidity\ (\tau) = \frac{8\pi^3 IL}{T^2} \quad \ldots\ldots Equation\ 2$$

$$Modulus\ of\ Rigidity\ (G) = \frac{\tau}{S^3\varepsilon} \quad \ldots\ldots Equation\ 3$$

Where, m= Mass of rod, l= length of rod, R= Radius of rod, L= Free length of fiber, T=Period of oscillation in sec, S= Area of cross section of fiber, ε =Shape factor.

Figure 1 Torsional pendulum

RESULTS AND DISCUSSION

Tensile Behavior

The physical and mechanical properties of the polypropylene filament yarn are summarized in Table 2. The tensile behavior of the yarn is shown in figure 2. The result is showing that the polypropylene yarn is of high tenacity. The curve's initial part is a straight line and hence it can be inferred that crystalline structure of pp is contributing towards the tensile property of fiber.

Table 2 Physical and Mechanical parameters of the polypropylene filament tested.

Physical Parameters		**Mechanical parameters**		
Denier	**No. of filaments**	**Tenacity (gpd)**	**Elongation at break (%)**	**Initial modulus (gpd)**
867.89	155	6.49	21.95	33.33

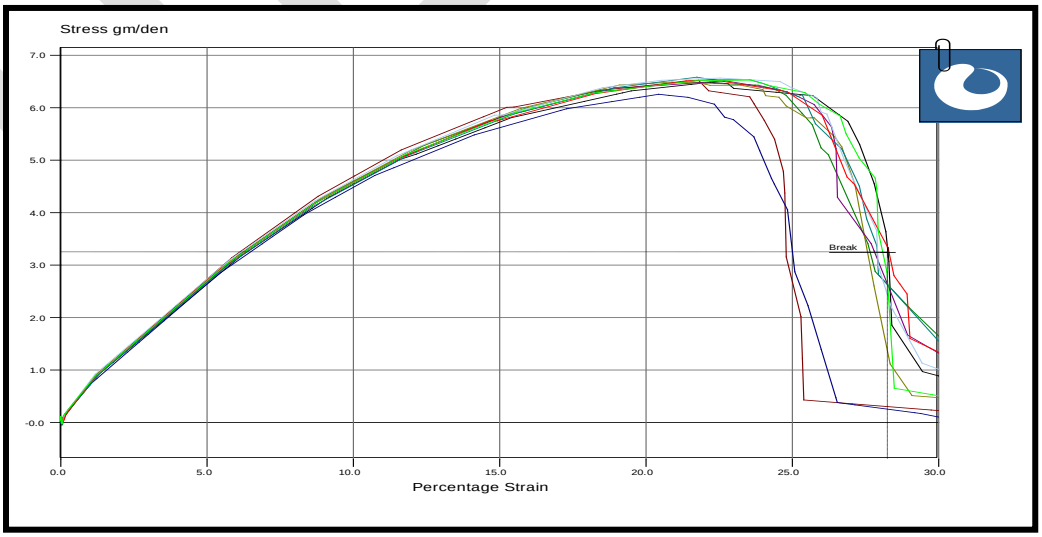

Figure 2 Mechanical behavior of high tenacity polypropylene filament

Normally the stress or tenacity is used to compare the strengths of different polymers. However, from reinforcing point of view, initial modulus which indicates the initial resistance to extension of a polymer is of greater significance. When a polymer has resistance to stretching, it will have high Modulus indicating fiber's inextensibility and stiffness (3). Higher tenacity and higher Elongation are the pre-requisites for a good quality geotextiles, where this fibre is showing the similar properties as per the requirements.

Creep Behavior

The creep behavior of polypropylene yarn is shown in Table 3. For 2, 3, 4 gm load, it has shown no change in primary creep and then it increases. The secondary creep i.e. permanent deformation initially increases and then has shown constant creep at higher load. The instantaneous recovery should be equal to instantaneous extension which was not found, this may be due to the samples were kept under tension for a long time between 30 to 60 minutes.

Table 3 Creep behavior of Polypropylene yarn

Sample No	Gauge Length (cm)	Load (gm)	Instantaneous Extension (cm)	Total Creep (cm)	Instantaneous Contraction (cm)	Primary creep (cm)	Secondary creep (cm)
1	5	1	0.17	0.43	0.33	0.02	0.26
2	5	2	0.25	0.4	0.28	0.05	0.3
3	5	3	0.35	0.25	0.1	0.05	0.43
4	5	4	0.35	0.35	0.1	0.05	0.5
5	5	5	0.35	0.4	0.05	0.1	0.5

Stress Relaxation

Stress relaxation behavior of the polypropylene yarn is shown in table 4. The study of stress relaxation behavior of polypropylene yarn is showing 40% relaxation in load at 10% of maximum breaking load. But at 20% and 30% of maximum breaking load it shows only 2.7% and 8.6% additional stress relaxation as compare to 10% specimen.

Table 4 Stress Relaxation behavior of polypropylene yarn

Sr. no	Load applied (gm)	Extension (mm)	Time (min)	Load relaxation (%)
1	560.00	2.5	40	40
2	1110	6.6	60	41.09
3	1699.7	8.33	50	43.45

Torsional Behavior

The torsional rigidity of polypropylene fibre found increased with increase in tension upto 1.22 gms and then decreases with further increased tension i.e. 1.58 gms as shown in table 5. Overall the tension applied is high as compare to Meredith [16], therefore it may be affecting the configuration of the fibre and possibly producing a comparatively large change in measured torsional rigidity. From this change in torsional rigidity it can be said that the spinning tension during staple yarn spinning of polypropylene should be maintained constant to have the advantage of consistent torsional rigidity. This will help in maintaining yarn twist per unit length constant. Similarly, this factor will also affect the twisting process of filament yarn.

Table 5 Torsional property of polypropylene yarn.

Sr. No.	**Inertia bar**	**Length of Fibre (cm)**	**Period (sec)**	**Torsional rigidity dyn.cm^2 (τ)**	**modulus of rigidity in dyn/cm^2 (G)**
1	I1	4	40	0.03	$4.40*10^3$
2	I1	6	40	0.48	$7.04*10^4$
3	I2	4	120	1.94	$2.84*10^5$
4	I2	6	120	1.53	$2.22*10^5$
5	I3	4	120	2.3	$3.37*10^5$
6	I3	6	180	2.4	$3.5*10^5$
7	I4	4	240	1.5	$2.2*10^5$
8	I4	6	260	2	$2.93*10^5$
				τ=1.52	**G=$2.23*10^5$**

The effect of change in length of fibre on torsional rigidity is not showing any change in trend. The Torsional rigidity and modulus of rigidity is found low as compare to the Morton and Permanyer findings. Lower rigidity requires lower twist multiplier (TM) to be put for same count of yarn. Overall the torsional rigidity of polypropylene is less as compare to other fibres [16]; this may be because of presence of the small methane group present in the propylene monomer as compare to other textile polymers.

CONCLUSION

The yarn selected was of heavy denier high modulus and tenacity. The primary creep is found almost constant, similar trend is observed at high load incase of secondary creep. This high tenacity and creep makes the yarn suitable for geotextile application. Stress relaxation is found increasing with increase in load applied. The torsional rigidity has increased with increase in tension which is an indication of maintaining constant tension during twisting process.

REFERENCES:

1) Jagielski, K., "Geotextile market report – an industry evolving", Geotechnical fabrics report No.7 (5), 1989, pp. 45-47.
2) Gerald, W. Davis, "Durability and Ageing of Geosynthetics", Proceeding of a seminar Philadelphia, U.S.A., Published by Elsevier Applied Science, New York, 1989, pp 65-81.
3) Anon, "Geotextiles take to the track in USA", Textile Month, pp 13.

4) Kannan, V., "Polypropylene based geosynthetic", Proceeding of National level One week up gradation program on geosynthetic, Anchor Institute, May 2010.
5) Bhattacharya, S.S., and Chaudhari, S.B., Study on structural and thermal properties of polypropylene silica nanocomposite filaments, International Journal of Textile and Fashion Technology, Vol 5, No 1, 2015, pp 15-22.
6) Shaikh, T.N., Chaudhari, S.B., Patel, B.H., and Patel, M., Study of conductivity behavior of nano copper loaded nonwoven polypropylene based textile electrode for ECG, International Journal of Emerging Science and Engineering, Vol 3, No 4, 2015, pp 11-14.
7) Chaudhari, S.B., Shaikh, T.N., Patel, B.H., and Pandey, P., Engineering polypropylene TiO2 nanocomposite filament to improve UV resistance, International Journal of advances in management, technology & engineering science, Vol 4, No 1, 2014, pp 22-25.
8) Chaudhari, S.B., Shaikh, T.N., Patel, B.H., and Pandey, P., Influence on thermal and dyeing characteristics of polypropylene filament on reinforcing TiO2 nanoparticles, International conference on Application of nano-materials in textile, 23-25 April 2015, pp 110-116.
9) Banerjee, P. K., Gupta, K. K., & et al, Publication of two week course on Testing and Evaluation of Geotextiles, IIT Delhi, Dec 1991.
10) Bhattacharya, S.S., and Chaudhari, S.B., Effect of addition of silica nanoparticles on mechanical properties of polypropylene filament, International conference on Application of nano-materials in textile, 23-25 April 2015, pp 64-70.
11) http://www.me.umn.edu/labs/composites visited on 25/07/2014.
12) Booth, J.E., "Principles of Textile testing, Third edition, CBS publishers & distributors, New Delhi, 1996, pp 101.
13) R & D Centre Calico Mills. "Standard for flat and textured polyester filament yarns", Synthetic Fibers, 1984, pp. 24-27,
14) ASTM Standards D 2256-02, "Standard test method for tensile properties of yarns by single-strand method". 2002.
15) R. Meredith, "The Torsional Rigidity of Textile Fibers",Textile Institute, Vol.45, No. 7, 1954, pp 489-503.
16) W. E. Morton and J.W.S. Hearl, "Physical properties of textile fibres" Fourth edition, Woodhead publishing limited, Cambridge, England, 2008, pp 437.

International Journal of Engineering Research and General Science Volume 3, Issue 5, September-October, 2015
ISSN 2091-2730

Comparison of Wind Turbine Driven PMSG Fed Wind Energy Conversion Systems Using Reactive Power Controlled Two Level Inverter

Anjali R D, Sheenu. P

PG Scholar, EEE Dept
Mar Baselios College Of Engineering and Technology
Trivandrum, Kerala, India
anjaliavani14@gmail.com

Abstract— Wind energy conversion systems are now seeking great importance today. Replacing Fixed speed wind turbine system with variable speed turbine system improves the performance. To extract and deliver maximum power from wind energy systems, power electronic devices are using. To reduce the harmonics due to the switching action , reactive power control algorithm is used in this work. To maintain the dc link voltage, a rectifier is used. The whole system is simulated for wind energy conversion systems using reactive power controlled Two level inverter with controlled and uncontrolled rectifiers.

Keywords— Wind energy conversion system, Permanent Magnet Synchronous Generator, Pitch angle control, diode rectifier, DC link Voltage, Sine PWM, Two level inverter, Reactive Power control, Total Harmonic Distortion.

INTRODUCTION

Throughout the world, in last three to four decades the generation of electricity using renewable sources has created great interest. Solar and Wind are the main sources that we can use. The advantages of this sources are they are pollution free, environmental friendly and sustainable. Using this sources we can meet the energy deficiency present over the world. There are countries , where there is no continuous power is not present . So in such places, the utilization of such natural sources are very useful.

Wind is such a natural source to replace the conventional sources. There are many areas over the world , where there is a large availability of wind. In those places wind energy conversion system (WECS) can be taken as a energy production system to support the grid. For a WECS it is very critical to select the generators and to design the wind turbine and converter control algorithms. The wind turbine system design should be done for maximum power tracking. There are mainly two types of wind turbine systems. One is fixed speed wind turbine (FSIG) system and other is variable speed wind turbine systems (VSIG) [1,2].

The turbine converts the kinetic energy present in wind to mechanical energy and the mechanical energy is to be converted to electrical energy by means of a generator. The fixed speed wind turbine uses SCIG and WRIG. They always produces a electrical power with a fixed frequency corresponding to its synchronous speed. The rotor always runs at a constant speed for all wind speed. The fixed speed wind turbine can never achieve or operate at peak efficiency across a range of wind speeds. Also the FSIG needs to draw a small amount of current for its excitation , from grid. That will introduce reactive power consumption. Due to above drawbacks VSIG are preferring in most cases. VSIG are mainly permanent magnet synchronous generator (PMSG), Doubly fed induction generator(DFIG). Among PMSG and DFIG , PMSG is preferred due to its small size ,presence of permanent magnet rotor, and absence of excitation [3].

The electrical power produced from PMSG is having variable frequency, since the wind speed is varying. So in order to convert this variable frequency power to a constant frequency power the system uses power electronic interfaces. The power electronic interface is a AC/DC/AC converter. The AC-DC conversion can be done by using a diode rectifier or a controlled rectifier. If the rectifier is controlled one, it is easy to maintain constant DC link voltage. The DC-AC conversion is offered by inverters, mainly two level inverters. There may be switching actions and due to that harmonics content may present there. The harmonic content leads to reactive power consumption. So in order to overcome the reactive power consumption control algorithms uses. Here in this work a reactive power control algorithm is proposed [4,5].

PROPOSED SYSTEM

The proposed WECS is shown in fig 1. The wind turbine converts kinetic energy to mechanical energy and the PMSG converts the mechanical energy to electrical energy. Pitch angle provided in the system is for tracking maximum power. The two mass driven train act as a mean to overcome the vibrations present in shaft of a wind turbine. The entire system is studied by using a diode rectifier and a controlled rectifier. The diode rectifier present will convert the AC power into DC power. The electrical power generated will be a

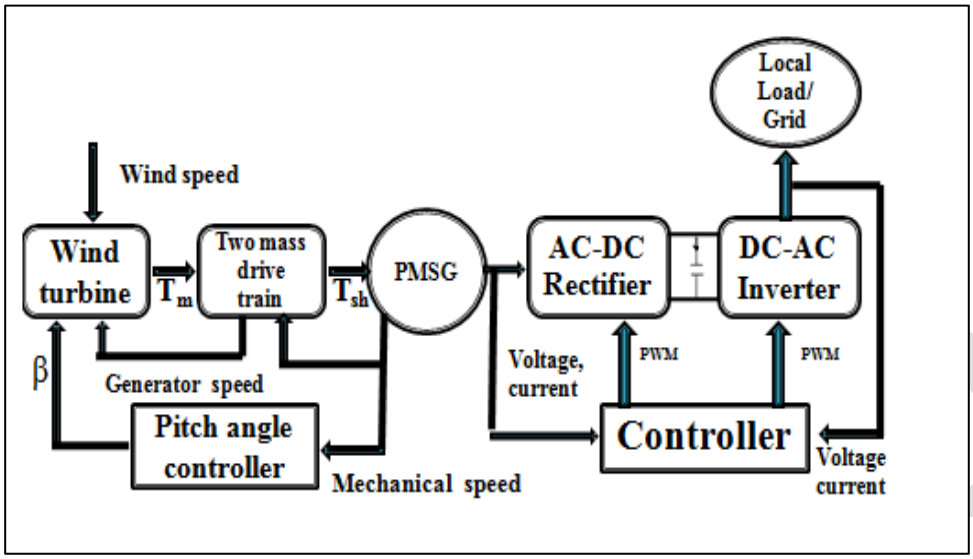

Fig. 1 proposed wind energy conversion system

variable frequency one. That is o be converted in to constant grid frequency supply by using the power electronic interface. The controllable inverter helps in converting the DC power to an AC power with grid frequency and magnitude.

WIND TURBINE DRIVEN PMSG MODELING

The modeling of wind turbine is the most important part for a WECS. The turbine modeling should be done to capture maximum kinetic energy from the wind with less cost. The mathematical expressions for the modeling of wind turbine systems are given below.

The expression of the mechanical torque developed by a wind turbine *Tm* is given by the following [4, 6]:

$$T_m = \frac{1}{2}\rho\pi {R_t}^2 C_p(\lambda,\beta)\frac{v^3}{\Omega_r} \quad (1)$$

Such that:

$$\lambda = \frac{R_t\Omega_r}{v} \quad (2)$$

In order to simulate the wind generation system, expression of *Cp (λ , β)* has been considered , such that; [4]

$$C_P = [0.5 - 0.00167(\beta - 2)]\sin\left(\frac{\pi(\lambda+0.1)}{12-0.3(\beta-2)}\right) - 0.00184\,(\beta-2)(\lambda-3) \quad (3)$$

The conversion of wind energy into mechanical energy over the rotor of a wind turbine is influenced by various forces acting on the blades and on the tower of the wind turbine. So this may change the pitch angle. According to bets concept maximum power can be captured when coefficient of performance value is maximum. Which is maximum when pitch angle is zero. So inoder to keep the pitch angle zero for all wind speed a pitch angle controller is also provided. There may be vibrations in the mechanical torque produced from the turbine due to sudden variation of wind speed. So that should be avoided by using a two mass drive train. The modeling equation for the drive train are given below.

The equation of the torque for drive train is given by

$$H_g\frac{d\omega_g}{dt} = T_e + \frac{T_m}{n} \quad (4)$$

Since the wind turbine shaft and generator are coupled together via a gearbox, the wind turbine shaft system should not be considered stiff.

$$H_m.\frac{d\omega_m}{dt} = T_\omega - T_m \quad (5)$$

The mechanical torque *Tm* can be modeled with the following equation.

$$T_m = K\frac{\theta}{n} + D\frac{\omega_g - \omega_m}{n} \quad (6)$$

$$\frac{d\theta}{dt} = \omega_g - \omega_m \quad (7)$$

where n is the gear ratio, θ is the angle between the turbine rotor and the generator rotor, ω m , ω g , H m and H g are the turbine and generator rotor speed and inertia constant, respectively .K and D are the drive train stiffness and damping constants, Tω is the torque provided by the wind and T e is the electromagnetic torque.

The modeling of PMSG system is also important for a WECS. The mathematical modeling equations based on d-q reference frame are given below [7,8].

$$\begin{bmatrix} V_d \\ V_q \end{bmatrix} = \begin{bmatrix} r_s & 0 \\ 0 & r_s \end{bmatrix}\begin{bmatrix} i_d \\ i_q \end{bmatrix} + \frac{d}{dt}\begin{bmatrix} \varphi_d \\ \varphi_q \end{bmatrix} + \omega_r \begin{bmatrix} 0 & -1 \\ 1 & 0 \end{bmatrix}\begin{bmatrix} \varphi_d \\ \varphi_q \end{bmatrix} \quad (8)$$

For a sinusoidal distribution of the back e.m.f, the flux and current phases are linked by the following expressions:

$$\varphi_d = L_d i_d + \varphi_r \quad (9)$$

$$\varphi_q = L_q i_q$$

where φ_r is the rotor flux.

Substituting equation (5) on equation (4), we obtain the following system via *Laplace* transformation

$$\begin{cases} v_d = (r_s + L_d\rho)i_d - e_d \\ v_q = (e_s + L_q\rho)i_q + e_q \end{cases} \quad (10)$$

Such that the direct and the quadrature back e.m.f components are expressed as:

$$\begin{cases} e_d = \omega_r L_q i_q \\ e_q = \omega_r L_d i_d + \omega_r \varphi_r \end{cases} \quad (11)$$

The stator active and reactive powers of the PMSG Machine are given by the equations (8):

$$\begin{cases} P_s = \frac{3}{2}(v_d i_d + v_q i_q) \\ Q_s = \frac{3}{2}(v_q i_d - v_d i_q) \end{cases} \quad (12)$$

Under generator operation, the mechanical equation is expressed as follows:

$$T_m - T_{em} = J\frac{d\Omega_r}{dt} + K_f\Omega_r \quad (13)$$

The electromagnetic torque can be expressed ,in (d, q frame)as follows:

$$T_{em} = \frac{3}{2}n_p(\varphi_r - (L_q - L_d)i_d)i_q \quad (14)$$

REACTIVE POWER CONTROL ALGORITHM

Presence of power electronic devices and non linear components draw reactive power from the grid. This will reduce the active power produced and will affect the power quality of the system. In order t reduce the reactive power consumption d-q axis control can be done. The reactive power controlled inverter control algorithm presented here is used to increase the efficiency of wind energy conversion system by reducing the reactive power present in the system. The control algorithm also helps in interfacing the variable power produced from the PMSG driven wind energy conversion system to a grid supply. The control method used here is to produce a reference signal for pulse production which is meant to reduce the reactive power consumption and THD. There is an abc-dq transformation for the easier control of dc link voltage and reactive power control. [9-14] .

WECS using uncontrolled rectifier and reactive power controlled Two level inverter

The WECS using uncontrolled rectifier and controlled two level inverter is shown in Fig. 2. Here the uncontrolled rectifier will introduces a large amount of harmonic content in the switching system and since there is no control DC link voltage cant be maintained to constant. The wind turbine system is a variable speed one. So the variation in speed will also be there in the dc link voltage and obviously in the inverter output also. Since we are using a reactive power control in the inverter side, the control will reduce the reactive power control and THD component not the voltage amplitude.

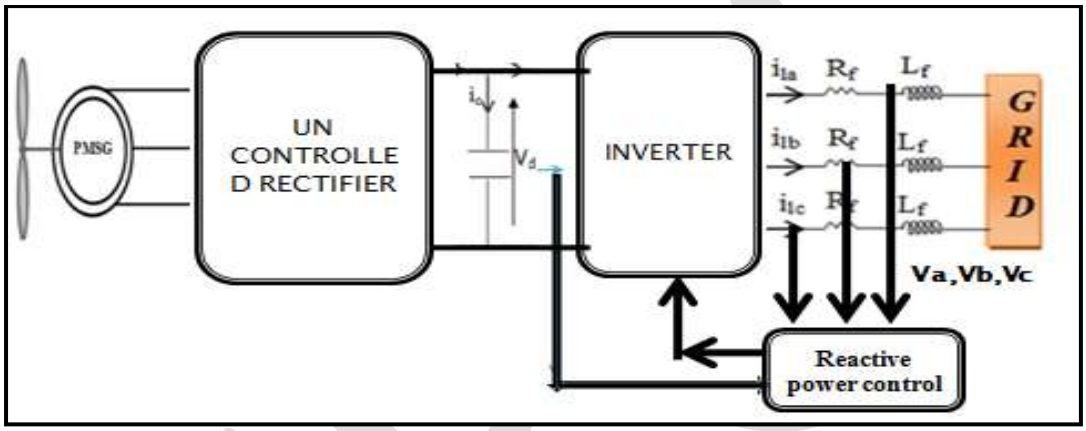

Fig. 2 WECS using uncontrolled rectifier and two level inverter

WECS using controlled rectifier and reactive power controlled Two level inverter

The WECS using controlled rectifier and controlled two level inverter is shown in Fig. 3, which is having controlled rectifier to control the dc link voltage. The control of dc link voltage is done by controlling the speed and torque of the PMSG. The current controller and voltage controller provided in the rectifier controller will helps to maintain the torque and speed of PMSG. So there will not be any vibrations in the output of PMSG and will get a constant DC link voltage. By using reactive power controlled two level inverter a constant 415V, 50Hz supply with less THD can be obtained.

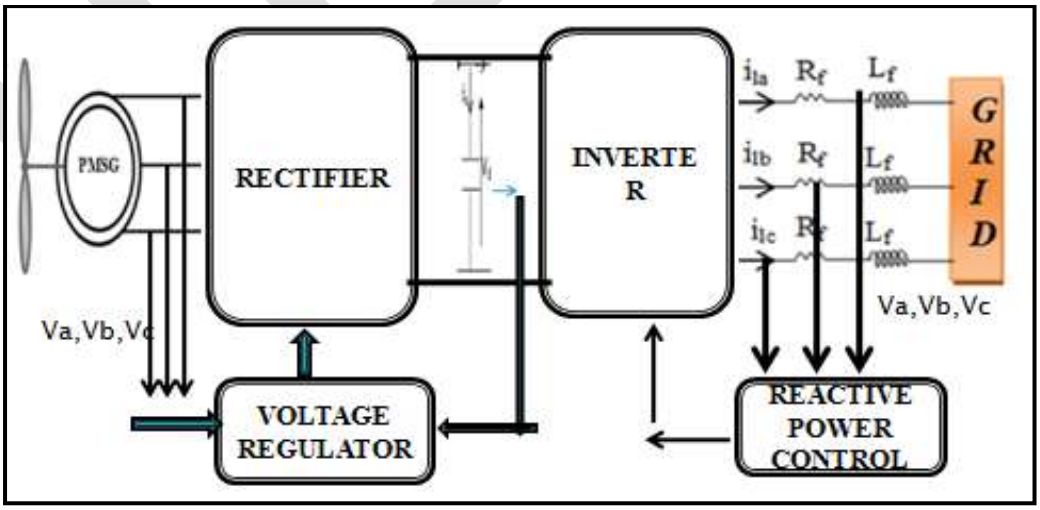

Fig. 3 WECS using controlled rectifier and two level inverter

RESULTS OBTAINED

The simulation study of the WECS using the controlled and uncontrolled rectifiers are done by choosing the following parameters. A four pole PMSG machine is used for the study. The parameters are given in table 1.

Table XII Parameters for both the wind turbine and PMSG

Parameters of machine		Parameters of turbine	
PARAMETER	VALUE	PARAMETER	VALUE
P_r, rated power	2.00 KW	Air density	1.08 kg/m^3
L_d L_q	0.01 H	A, area swept by blades	31.98 m^2
R_r , rotor resistance R_s, stator resistance	0.425 ohm	V, base wind speed	12 m/s
Pole pairs	4	C_{pmax}	0.48
Voltage constant	300 V_{pp}/rpm	Lambda	8.1
Torque constant Inertia constant Viscous	2.48 Nm/A 0.01197 kgm^2 0.001189 N.m.s	Pitch angle , β	0

The wind turbine and PMSG modeled using above equations are shown in fig 4 and fig 5.

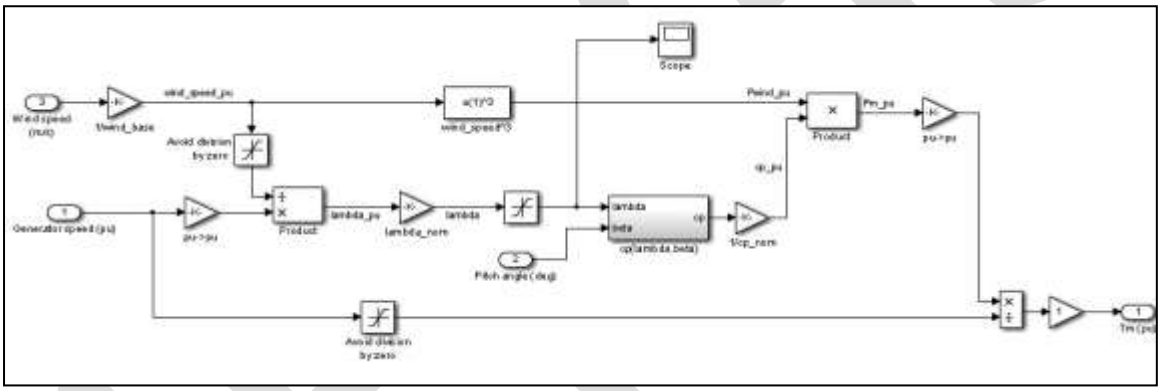

Fig. 4 Model For Wind Turbine System

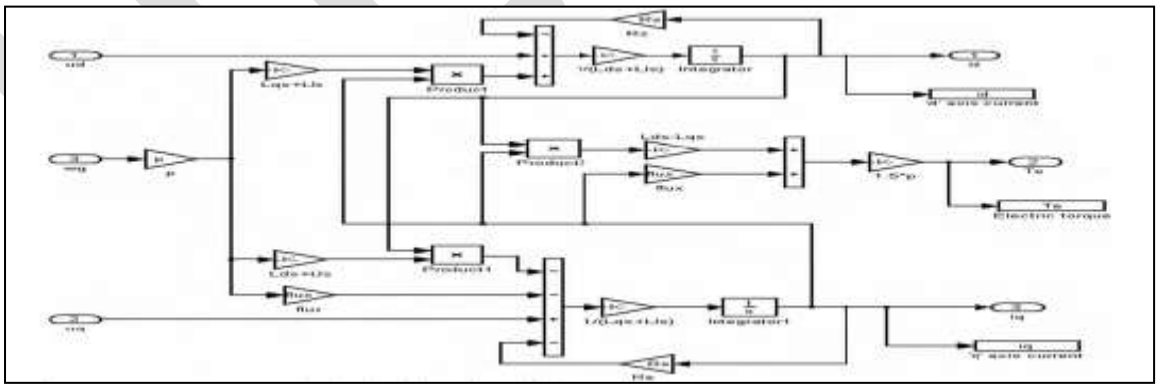

Fig. 5 Model For PMSG System

The simulation waveforms for wind velocity, torque produced from wind turbine system (T_m) and torque given to PMSG after two mass drive train (T_{sh}) are shown in below Fig. 6 . It is clear that the sudden torque variations in the input side of a PMSG affects its performance.

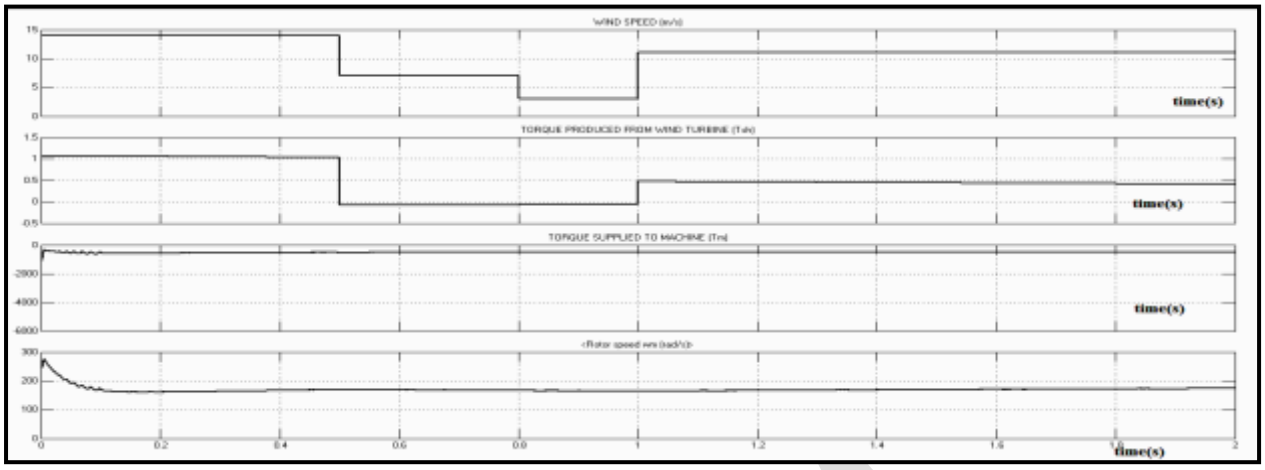

Fig. 6 Wind speed, Shaft torque, machine torque and rotor speed

The WECS using uncontrolled rectifier MATLAB model is shown in fig. 7.

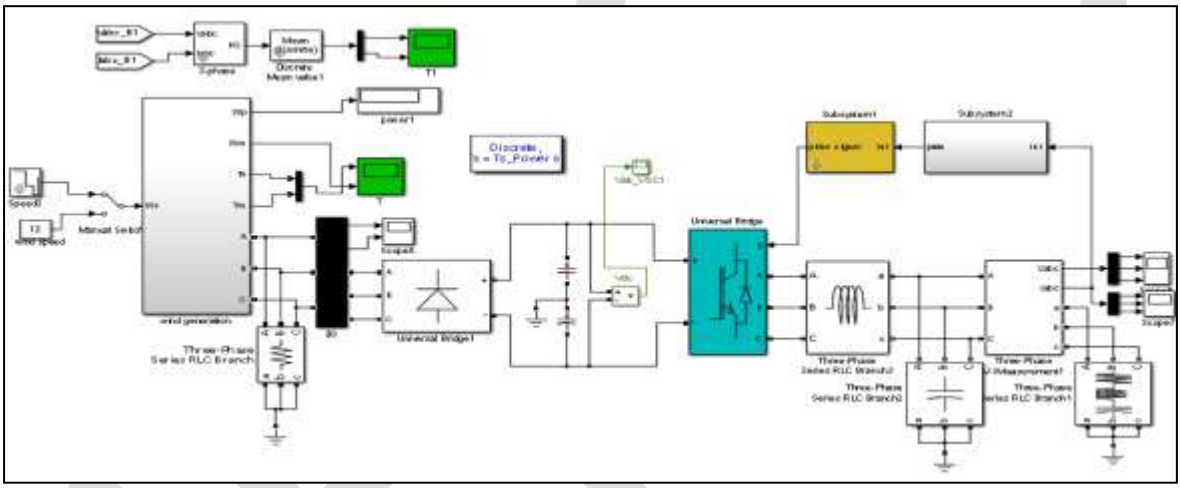

Fig. 7 Simulink model of WECS using uncontrolled rectifier and five level inverter

The generated voltage and current wave forms from PMSG of a WECS using uncontrolled rectifier is shown in Fig. 8. The DC link voltages using an uncontrolled rectifier with variations are shown in Fig. 9.

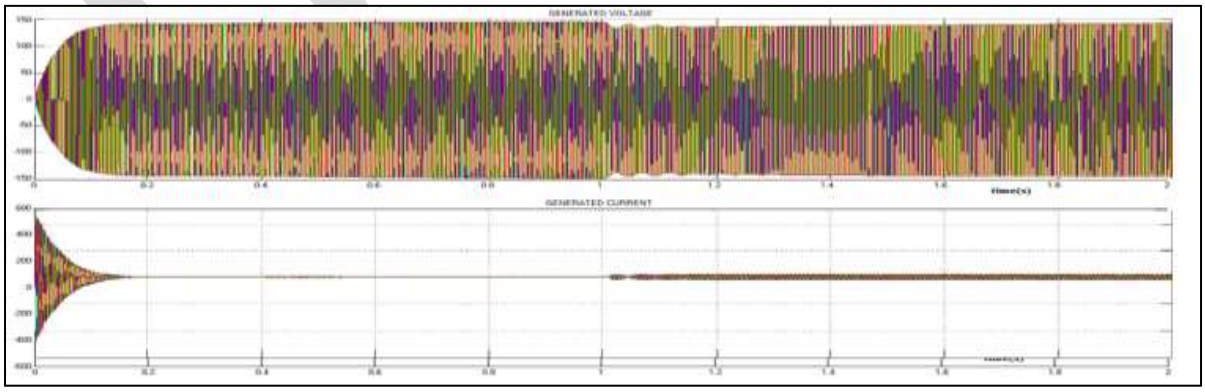

Fig. 8 Generated voltage and current from PMSG

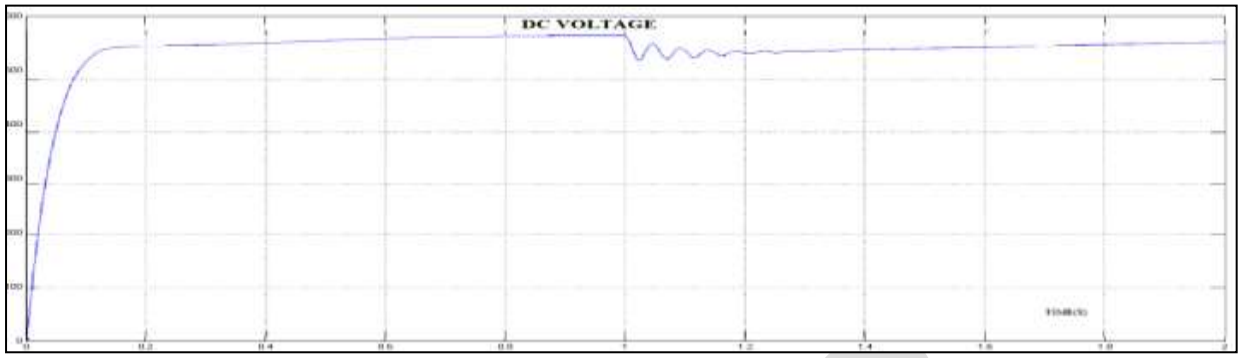

Fig. 9 Dc link voltage

The output voltage and current obtained from the Two level inverter using reactive power control is shown in Fig.10.

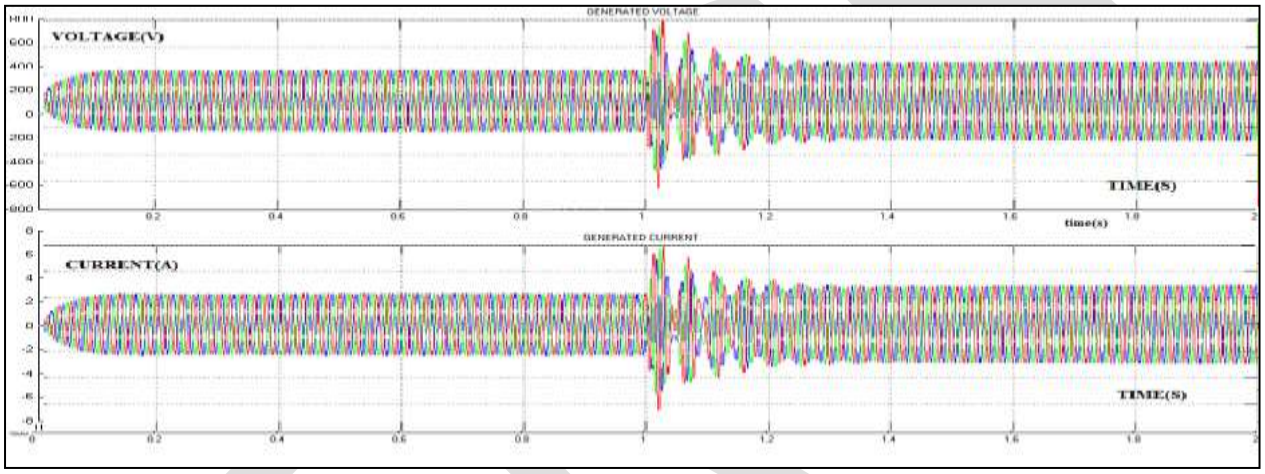

Fig. 10 Three phase output voltage and current from inverter

The WECS using controlled rectifier MATLAB model is shown in fig. 11. Here the vector control provided on the rectifier side will maintain a constant dc link voltage.

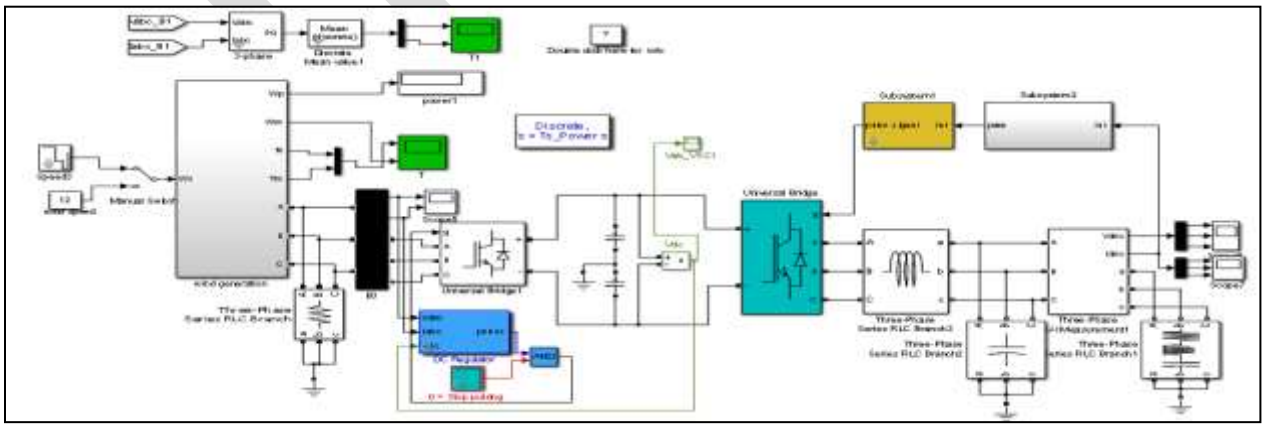

Fig. 11 Simulink model of WECS using uncontrolled rectifier and Two level inverter

The generated voltage and current wave forms from PMSG of a WECS using controlled rectifier is shown in Fig. 12. The DC link voltages using an controlled rectifier without variations are shown in Fig. 13. Where there is a small dip only in dc link voltage at 1 s due sudden high variation.

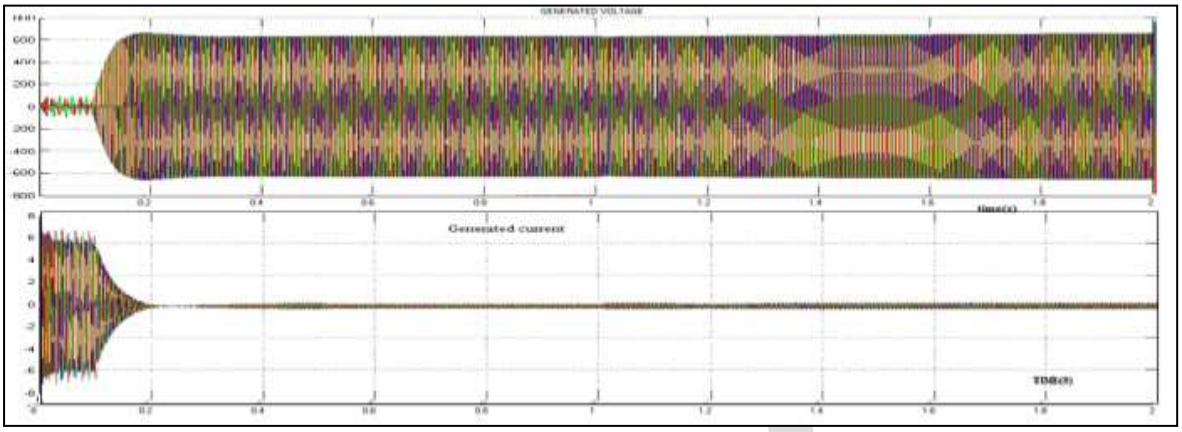

Fig. 12 Generated voltage and current from PMSG

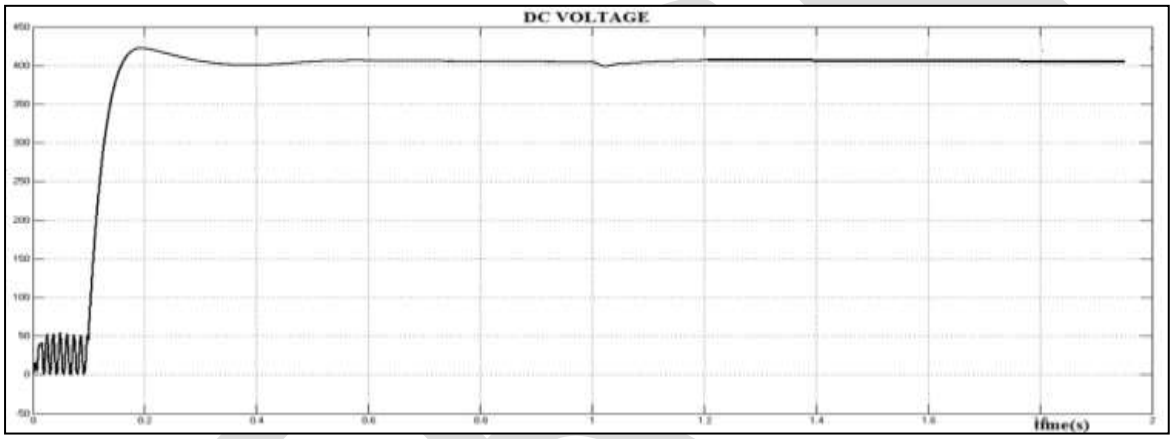

Fig. 13 Dc link voltage

The output voltage and current obtained from the Two level inverter using reactive power control is shown in Fig.14

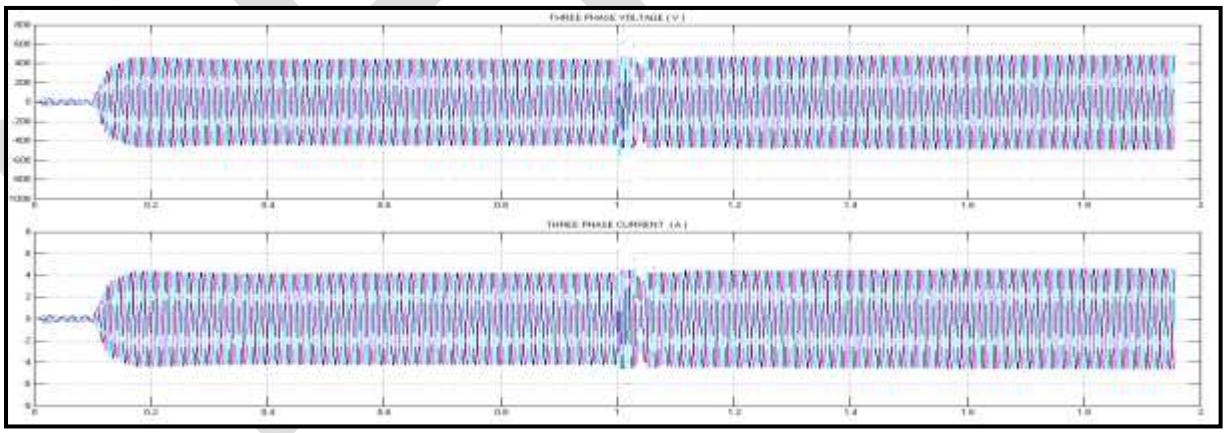

Fig. 14 Three phase output voltage and current from inverter

The THD analysis of both the system with controlled and uncontrolled rectifier system with Two level inverter is given below. It is clear from the analysis that using a controlled rectifier and a reactive power controlled inverter the reactive power consumption and THD can be reduced

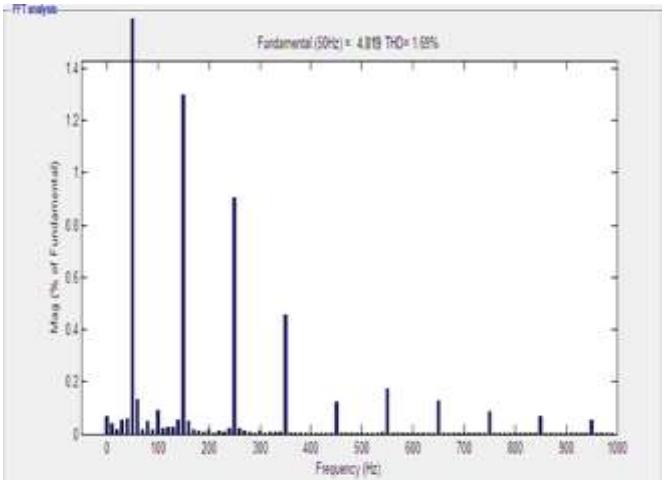

Fig. 15 THD of WECS with uncontrolled rectifier

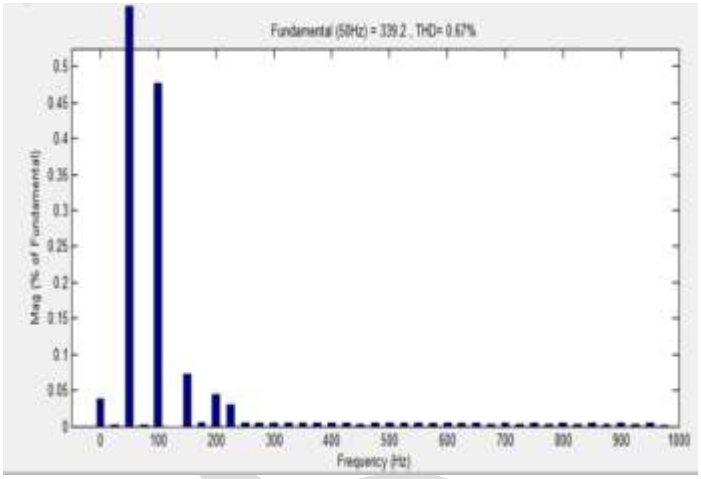

Fig. 16 THD of WECS with uncontrolled rectifier

CONCLUSION

In this paper a wind energy conversion system with two level inverter using controlled and uncontrolled rectifier systems has been introduced. Model has been implemented using MATLAB/Simulink software. The control provided on the rectifier side and reactive power control on inverter side improves the system performance. The THD level and reactive power consuming for a local load were studied for both the systems. By using a two level inverter and a controlled rectifier in a WEC system it is noted that the THD value and the reactive power consumptions are reduced than a system with two level inverter and uncontrolled rectifier. The THD values are lower than the IEEE standards also. This system provides a smooth grid interacting supply.

REFERENCES:

[1] M. P. Papadopoulos, S. A. Papathanassiou, N. G. Boulaxis, and S. T. Tentzerakis, "Voltage quality change by grid-connected wind turbines," in European Wind Energy Conference,Nice, France, 1999, pp. 783 -785.

[2] Anaya-Lara O., Jenkins N., Ekanayake J., Cartwright P., & Hughes M., "Electricity Generation from Wind Energy," In Wind Energy Generation: Modeling and Control, First ed. John Wiley & Sons, Ltd, pp. 1-18. ,2009

[3] Johnson G.L, "Wind Turbine Power, Energy, and Torque," In Wind Energy System, Electrical Edition ed. Prentice-Hall Englewood Cliffs (NJ), pp.4-1-4-54 ,2006

[4] E. Muljadi and C.P. Butterfield, "Pitch-Controlled Variable-Speed Wind Turbine Generation", IEEE Transactions on Industry Applications, Vol.37, No.1, pp: 240-246, January/February 2001.

[5] T. Senjyu, N. Nakasone, A. Yona, S. A. Yousuf, T. Funabashi, and H. Sekine, "Operation Strategies for Stability of Gearless Wind Power Generation Systems," Proceedings of IEEE/PES General Meeting 2008 (GM 2008), CD-ROM, pp. 1-7, 20-24 July 2008, Pittsburgh, USA.

[6] S.M.B. Wilmshurst, "Control strategy for Wind Turbines", Wind Energy, Vol. 12, No. 4, pp: 236-250, 1988. Leon M. Tolbert, Fang Zheng Peng and Thomas G. Habetler," Multilevel PWM Methods at Low Modulation Indices," IEEE Transactions on Power Electronics, Vol.15, No. 4, July 2000

[7] Y. Chen, P. Pillay, A. Khan, "PM Wind Generator Comparison of Different Topologies", Industry Applications Conference, 39th IAS Annual Meeting, Conference Record of the 2004 IEEE, Vol.3, pp: 1405-1412, October 2004.

[8] P. Pillay, R. Krishnan, "Modeling, Simulation, and Analysis of Permanent-Magnet Motor Drives. I. The Permanent-Magnet Synchronous Motor Drive", IEEE Transactions Industry Applications, Vol.25, No.2, pp: 265-273, March/April 1989.

[9] L.P. Colas, F. Francois, B. Yongdong Li, "A Modified Vector Control Strategy for DFIG Based Wind Turbinesto Ride-Through Voltage Dips", Power Electronics and Applications, EPE'09, pp: 1-10, September 2009.

[10] Karim A. and Sam Ri, "A New Approach for Maximum Power Extraction from Wind Turbine Driven by Doubly Fed Induction Generator Based on Sliding Mode Control", Energy Management, Vol 1, No 2, 2012.

[11] Emna Mahersi , Adel Khedher, M.Faouzi Mimouni The Wind energy Conversion System Using PMSG Controlled by Vector Control and SMC Strategies international journal of renewable energy research et al., vol.3, no.1, 2013

[12] Djellad, P.O. Logerais, A. Omeiri, O. Riou, J.F. Durastanti, A. Khelf 2013, Modeling of Wind Energy Conversion System and Power Quality Analysis IEEE Transactions on power electronics, 23, (3) 1254-1417

[13] Li S.H., Haskew T.A., Swatloski R.P., &Gathings W. 2012. Optimal and Direct-Current Vector Control of Direct-Driven PMSG Wind Turbines. IEEE Transactions on power electronics, 27, (5) 2325-2337

[14] Bharanikumar R., Yazhini A.C., & Kumar A.N. 2010. Modeling and Simulation of Wind Turbine Driven Permanent Magnet Generator with New MPPT. Asian Power Elevtronics Journal, Vol. 4, (2) 52-58

International Journal of Engineering Research and General Science Volume 3, Issue 5, September-October, 2015
ISSN 2091-2730

THE USE OF ARTIFICIAL NEURAL NETWORK FOR CATEGORIZATION AND INDICATION OF WEATHER FORECASTING DATASET WITH DYNAMIC LIBRARY

Pankaj G Devikar[1], Prof. Pankaj Sahu[2]

M.Tech Scholar[1], Asst. Professor[2]

GGITS, Jabalpur, India[1,2]

Pankaj.devikar@gmail.com and +918600144181

Abstract— Collection of data related to weather parameter such as temperature, precipitation, pressure, wind speed and direction, dew point and rainfall. This process of collection of data is called as weather prediction. For safety of life and property it is essential to indicate the changes. Categorization and indication of weather predicts the state and changes in weather for future time. Weather forecasting can be done by analyzing data and collecting it for present state of atmosphere. To map input and output relations neural network technique is used. Collected data is used for prediction by training neural network which will provide future prediction of data. This can be done by using BPP (back propagation algorithm). The variation in one parameter will reflect the changes in other parameters will be discussed in this paper. The biggest advantage of the back propagation neural network is that it will give large class of function and it is efficient for numerical differentiation.

Keywords— weather prediction, Categorization, Weather forecasting, neural network, future prediction, back propagation algorithm, numerical differentiation.

INTRODUCTION

Weather is condition of air on earth at a different place and time. It is the application of science and technology which helps to predict the state of the atmosphere in future time for a particular location. It is important due to its effectiveness. It is done by collecting quantitative data of the atmosphere. The changing nature of the atmosphere will have arises the need of computational power required to solve the formal equations describing the atmospheric conditions in the systems. Two methods are used for weather forecasting

1. The empirical approach and
2. The dynamical approach.

The first approach is based on the occurrence of analogs and is often referred by meteorologists as analog forecasting. This approach is very useful to predict weather if recorded data's are plentiful.

The second approach is based on equations and forward simulations of the atmosphere and is often referred to the computer model. The dynamic approach is only used to model large-scale weather phenomena and may not forecast short-term weather efficiently. Most of the weather systems use a combination of both empirical and dynamical techniques. Artificial Neural Network (ANN) provides a methodology for solving many types of nonlinear problems that are difficult to be solved by traditional methods.

Future weather can be predicted by ANN technique. This technique trains the data with past experience and future data can be predicted.

RELATED WORK

Classification and Prediction of Future Weather by Using Back Propagation Algorithm-An Approach proposed by Sanjay D. Sawaitul, Prof. K. P. Wagh, Dr. P. N. Chatur. [1]

This paper gives a rough step by step description of procedure for the classification and prediction of weather forecasting. The designing phase of "Classification and Prediction of Future Weather by using Back Propagation Algorithm" technique is described.

Temperature Prediction System Using Back propagation Neural Network: An Approch proposed by Parag. P. Kadu, Prof. K. P. Wagh, Dr. P. N. Chatur. [2]

In this model, it explains back propagation neural network which is used for temperature forecasting. The technical milestones, that have been achieved by the researchers in this field has been reviewed and presented in this paper.

An Artificial Neural Network Model for Rainfall Forecasting in Bangkok, Thailand was developed by N. Q. Hung, M. S. Babel, S. Weesakul, and N. K. Tripathi. [3]

This model was predicted the rainfall and management of flood like situation before 6 hours. This was used in Bangkok for rainfall prediction and managing the passing of flood water. This model predicts rainfall only but can't predict the temperature, humidity.

TOOLS AND TECHNIQUES

Back Propagation Method – Back propagation was created by generalizing widrow Hoff learning rule to multiple layer network and nonlinear differentiable transfer function. Input vectors and corresponding target vectors are used to train a network until it can approximate a function, associate input vectors with specific output vectors. Back propagation algorithm consists of two paths; forward path and backward path. Forward path contain a feed forward network, initializing weight, simulation and training the network. Feed forward network often have one or more hidden layers of sigmoid neurons followed by output layer. The back propagation is a multilayer supervised learning and error is propagated back through earlier layer of network.

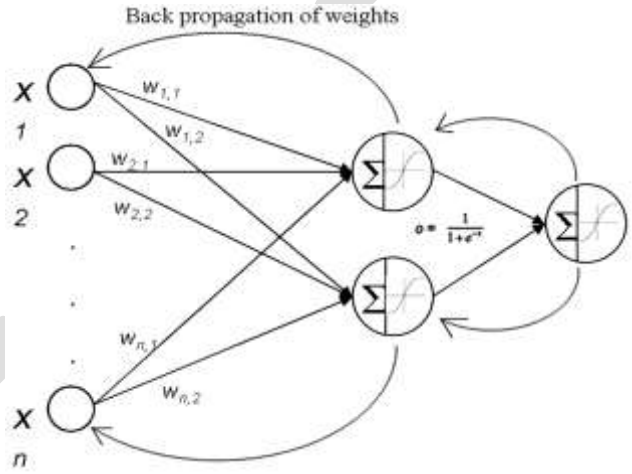

Fig : Back Propagation Algorithm

Data Mining – Today's manufacturing, engineering, business and computing process in public and private organization are generating massive amount of data. This explosive growth of data has outpaced the ability to interpret and digest the data. Therefore, data mining tool for automated data analysis and knowledge discovery are needed. There are many software tools implementing data mining and knowledge discovery techniques that are designed to work efficiently over large amount of data and carry out simple analysis to uncover relationships in data. The users may then perform further investigation and data analysis to confirm or better understand the relationship. Extraction of required data from resulting data has been done by quantitative analysis in order to prevent interface of one parameter with another.

Artificial Neural Network – A neural network is a powerful data modeling tool that is able to capture and represent complex input/output relationships. The motivation for the development of neural network technology stemmed from the desire to implement an artificial system that could perform intelligent tasks similar to those performed by the human brain. Neural network resemble the human brain in the following two ways:

- A neural network acquires knowledge through learning.
- Neural network knowledge is stored within interneuron connection strengths known as synaptic weights.

DESIGN AND IMPLEMENTATION

Phases in Back Propagation Technique – There are two basic phases of Back propagation learning algorithm i.e. propagation phase and weight update phase along wise.

Phase 1: Propagation – Each Propagation involves the following steps

1. The input of the training pattern of Forward propagation is provided by the NN in order to get the output activations of the propagation.

2. The target of the training pattern of Back propagation of the output activations propagation through the neural network is to generate important deltas belonging to all the output and hidden neurons in the systems.

Phase 2: Weight update – For each weight-synapse

1. Multiply its input activation and output delta to get the gradient of the weight.

2. Bring the weight in the direction of the gradient by adding a ratio of it from the weight.

The speed and quality of learning has a major impact by that ratio. This is called the rate of learning. The sign of the gradient of a weight shows the increasing error area in the system. Thus the weight must necessarily be updated in the direction opposite of the system. Neural networks have a remarkable ability to derive and extract meaning rules and trend from complicated, noisy and imprecise data.

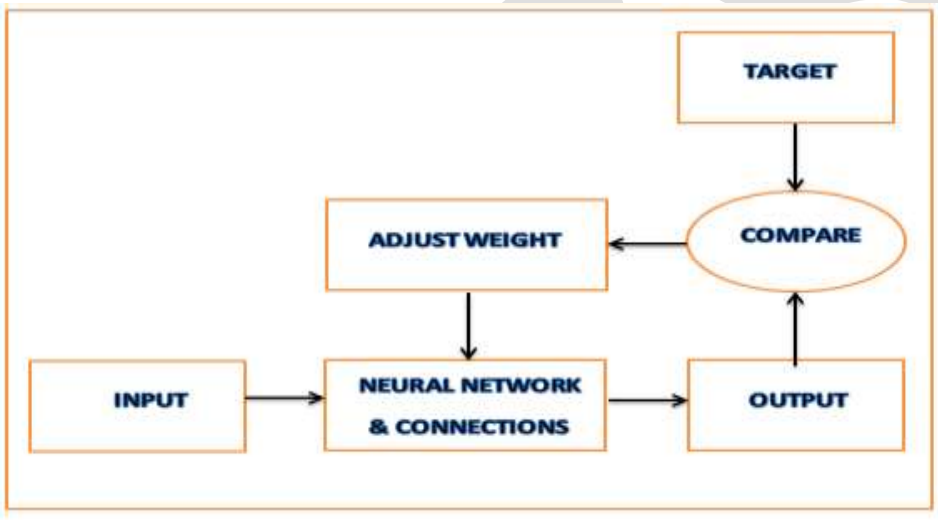

Fig : Neural Network Block Diagram

Operations to be Performed –

- **Data Collection**
- **Pre-processing**
- **Data Transfer**
- **Data Mining**
- **Prediction of Future Weather Using ANN by Back Propagation Algorithm**
- **Classification**

Architecture for the Design of Project

The input layer sends some data to the hidden layer and the hidden layer sends the processed data to the output layer. The input may be the collection of data i.e. temperature, humidity, rain and wind recorded by the different sensors and stored in the form of Excel sheet. This technique is also known as Multilayer Perceptron.

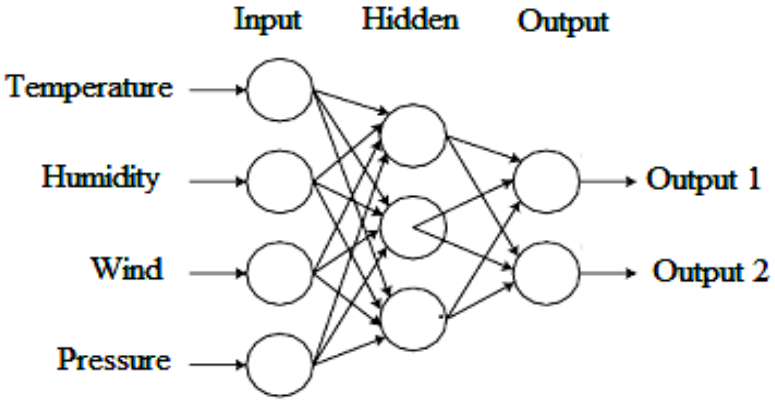

Fig : Architecture of Design

.

Flowchart –

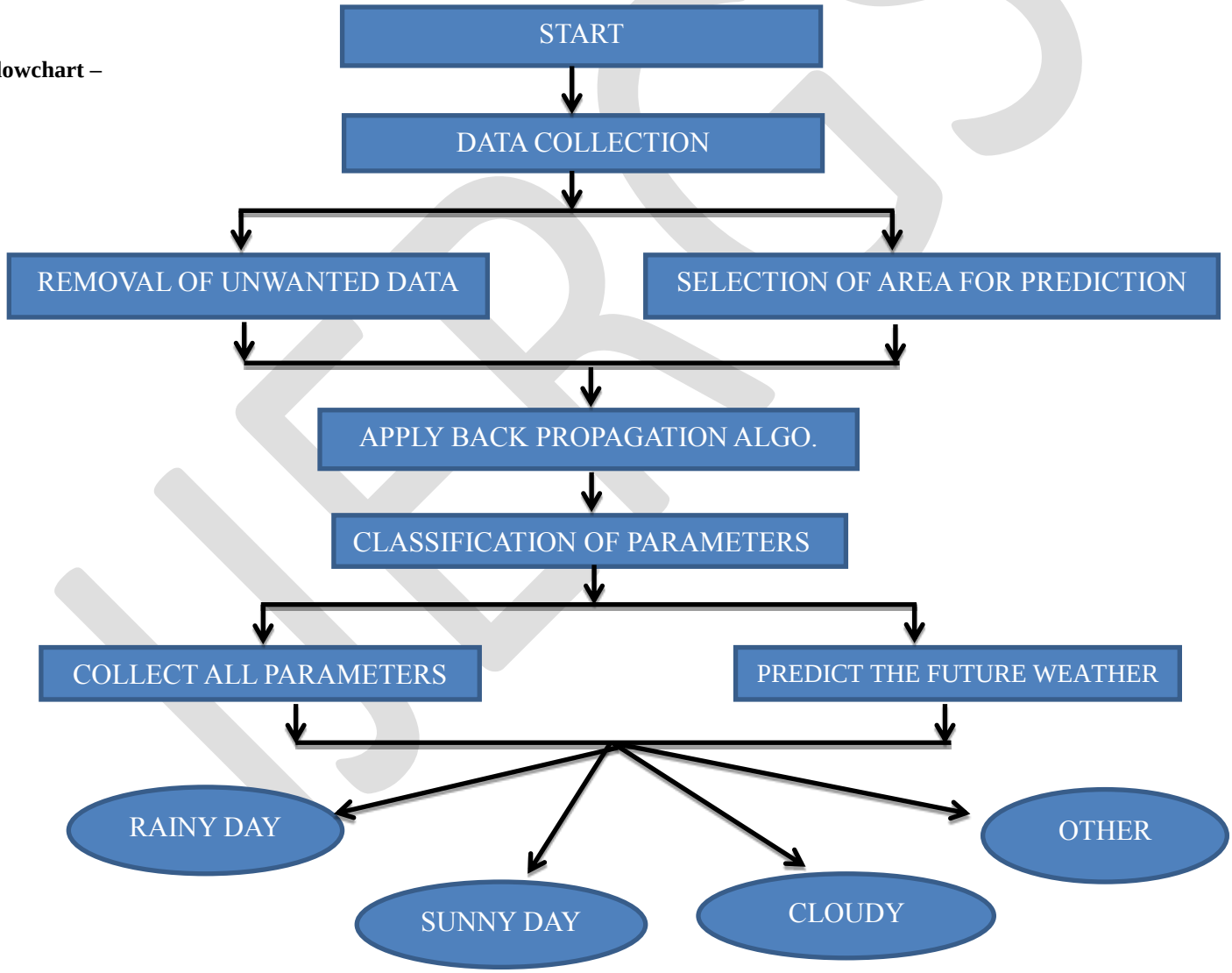

In the above data flow diagram, the data is collected with the help of different sensors and the recorded data is sent to the PC and this data is stored in the form of data sheets and are represented in the form of graphs and charts. The unwanted data are removed and the data for the particular area is sent to the statistical software for the further process. This selection of data is done by the Data Miner software. In Artificial Neural Network the Back propagation Algorithm is implemented and the variations in parameters are observed.

According to these variations the logic in Back propagation will be developed and the change in other parameters with respect to one parameter will be predicted. The back propagation algorithm consists of two paths; forward path and backward path.

Project GUI –

Fig : Project GUI

This project GUI is having five buttons as Weather, Image, Graph, Clear and Close. Weather button will show the dialog box showing the weather of that particular date. Image button will show the result in pictorial form. Graph button will show the output in the form of graph. Clear button will clear all the text box recordings of weather forecasting parameters shown in project GUI. Close button will exit from the application. The Pop up window displaying the output will vary with respect to the combination of weather parameters retrieved in the project GUI from the database on that particular date.

RESULTS AND DISCUSSIONS

When the parameters are loaded on GUI, user has to click on weather button to see the weather condition of that day. The entries in project GUI is loaded by accessing the data from database. GUI acts as a frontend for "The Use of Artificial Neural Network for Categorization and Indication of Weather Forecasting Dataset with Dynamic Library" software designed in MATLAB.

In the below graph, rainfall is plotted with respect to time. In the same manner, graph for temperature, humidity, dew point and other weather parameters can also be plotted. The result is shown and calculated by back propagation algorithm.

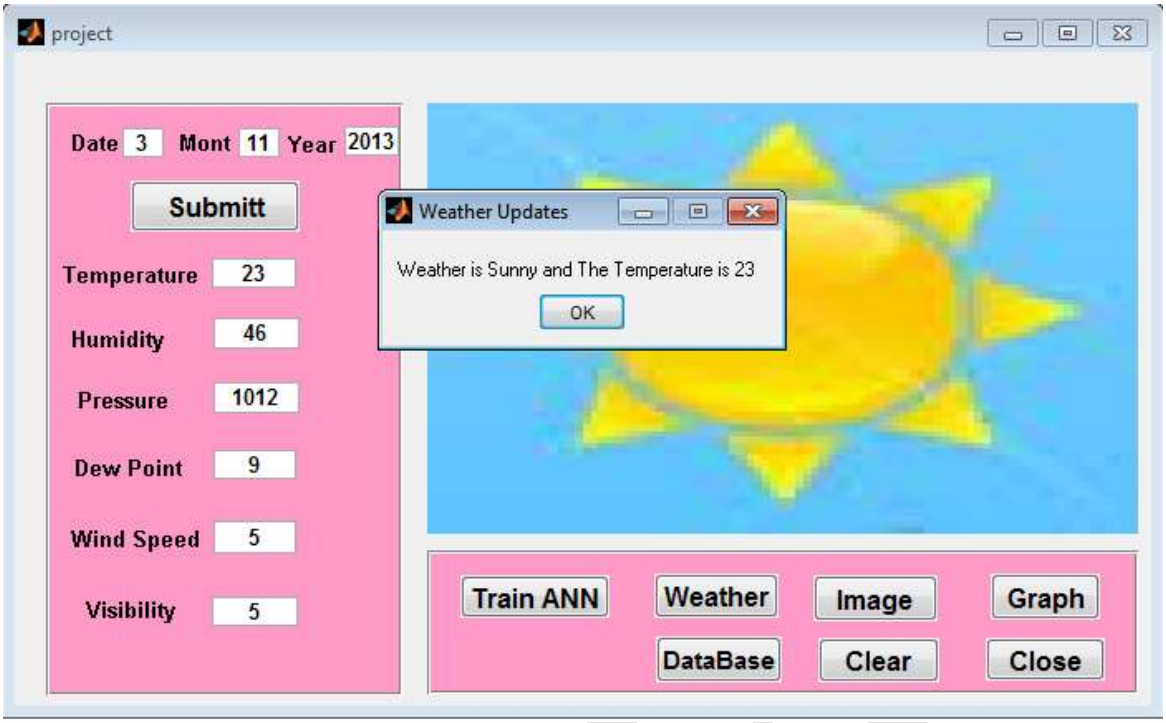

Fig : Weather Form

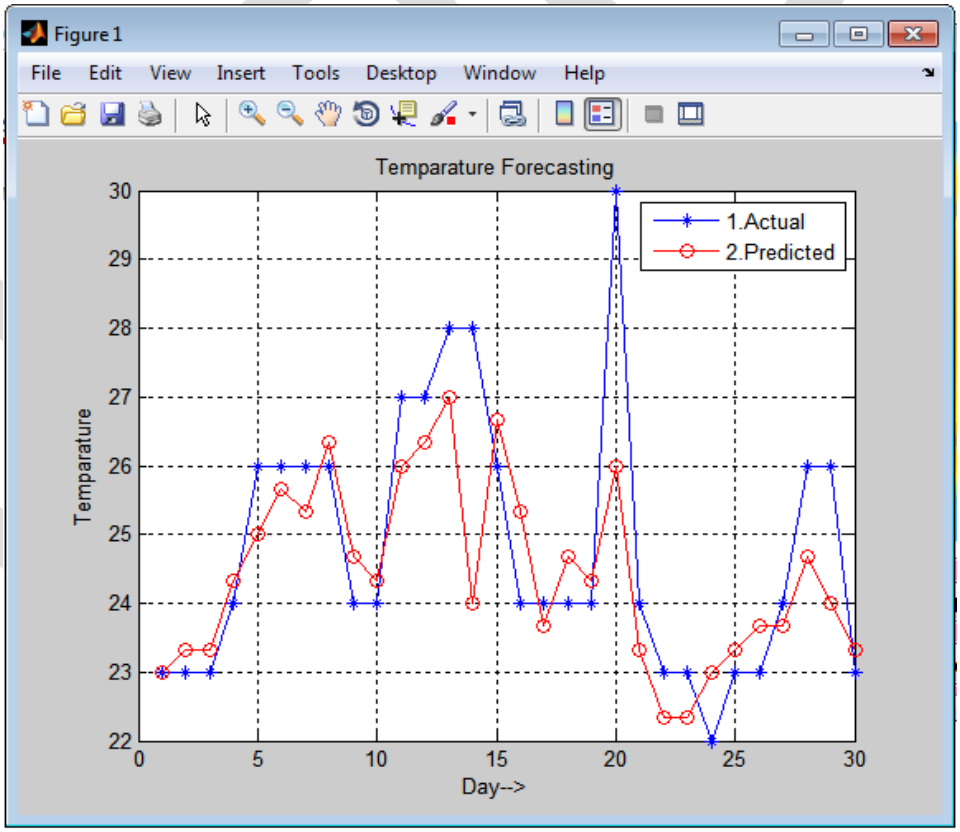

Fig : Graph

CONCLUSION

The main objective is to detect the variation in weather after some period of time or the effect on other parameters of weather with respect to any one parameter. The main aim of the project is to provide the information of future weather after some period of time by changing some parameters, or probability of what will be the effect on other parameters if there is change in one of them. To prevent from adverse effect of climatic change or to provide information about weather and its variation, this project and back propagation algorithm is used.

It also concludes that the Back propagation Algorithm can also be applied on the weather forecasting data. The results suggest that this Neural Network could be an important tool for weather forecasting. Neural Networks are capable of modeling a weather forecast system. Statistical indicators chosen are capable of extracting the trends, which can be considered as features for developing the models. Statistical indicators except coefficients of skewness and kurtosis are found suitable to extract the hidden patterns present in whether data. The Neural Network signal processing approach for weather forecasting is capable of yielding good results and can be considered as an alternative to traditional meteorological approaches.

REFERENCES:

[1] Sanjay D. Sawaitul, Prof. K. P. Wagh, Dr. P. N. Chatur "Classification and Prediction of Future Weather by using Back Propagation Algorithm-An Approach" International Journal of Emerging Technology and Advanced Engineering (ISSN 2250-2459, Volume 2, Issue 1, January 2012).

[2] Parag.P.Kadu, Prof. K. P. Wagh, Dr. P. N. Chatur "Temperature Prediction System Using Back propagation Neural Network : An Approch" International Journal of Computer Science & Communication Networks,Vol 2(1), 61-64 (ISSN 2249-5789).

[3] N. Q. Hung, M. S. Babel, S. Weesakul, and N. K. Tripathi "An artificial neural network model for rainfall forecasting in Bangkok, Thailand" Hydrol. Earth Syst. Sci., 13, 1413–1425, 2009.

[4] Dr. S. Santhosh Baboo and I.Kadar Shereef "An Efficient Weather Forecasting System using Artificial Neural Network" International Journal of Environmental Science and Development Vol. 1, No. 4, October 2010 ISSN: 2010-0264

[5] Sharma A., "A Weather Forecasting System using concept of Soft Computing: A new approach", PG Research Group SATI, Vidisha (M.P.), India, IEEE 2006.

[6] Ch.Jyosthna Devi, B.Syam Prasad Reddy, K.Vagdhan Kumar, B.Musala Reddy, N.Raja Nayak. "ANN Approach for Weather Prediction using Back Propagation" International Journal of Engineering Trends and Technology- Volume3Issue1- 2012.

[7] [10] Pielke R.A., "A comprehensive meterological modeling system RAMS," Meteorology and Atmosphe-ric Physics, Springer-Verlag Vol. 49, 69-91p, 1992.

[8] Siddiqui Khalid J. and Nugen Steve M., "Knowledge Based System for Weather Information Processing and Forecasting", Department of computer science, SUNY at Fredonia, NY 14063, IEEE 1966.

[9] www.wunderground.com

[10] www.wikipedia.com

[11] Neural network, fuzzy logic and genetic algorithm: synthesis and application by Rajasekaran S. and Pai G. A. vijayalakshmi

International Journal of Engineering Research and General Science Volume 3, Issue 5, September-October, 2015
ISSN 2091-2730

Analysis of steel structure against Progressive collapse

Prof.G.N.Narule[1], Mr.A.V.Mendgule[2]

VPCOE Baramati,

gnnarule@gmail.com[1] , mendguleajit@gmail.com[2]

9922458871[1], 9960869551[2]

Abstract— A building undergoes progressive collapse when a primary structural element fails, resulting in the failure damage is disproportionate to the original cause, so the term disproportionate collapse is also used to describe this collapse type. Progressive collapse can be triggered by manmade, natural, intentional, or unintentional causes. Explosion, fires, earthquakes creates large amounts of stresses and the failure of supporting structural members can lead to a progressive collapse failure. Progressive collapse is a complicated dynamic process where the collapsing system redistributes the loads in order to prevent the loss of critical structural members. For this reason beams, columns, and frame connections must be designed in a way to handle the potential redistribution of large loads. This research provides insight into the structural configuration to achieve a demand to capacity ratio of appropriate quantity and prevent collapse in the event of a single column loss. Several relationships developed between various analysis procedure against shear forces. Ultimately, all this information can be used in design codes where there are currently very limited or no specific rules or guidelines.

Keywords— Progressive collapse, Demand capacity ratio, Base shear, GSA(General Service Administration), Dead load, Live load, Dynamic analysis.

INTRODUCTION

The progressive collapse of building structures is initiated when one or more vertical load carrying members (typically columns) are removed. Once a column is removed due to a vehicle impact, fire, earthquake or any other man-made or natural hazards, the building's weight (gravity load) transfers to neighboring columns in the structure. If these columns are not properly designed to resist and redistribute the additional gravity load that part of the structure fails. The vertical load carrying elements of the structure continue to fail until the additional loading is stabilized. As a result, a substantial part of the structure may collapse, causing greater damage to the structure than the initial impact. In the United States and other Western nations, progressive collapse is a relatively rare event. But after the remarkable partial collapse of the Ronan Point apartment tower in 1968 initiated an intellectual discussion among the engineering community on the possible ways to design buildings against such catastrophic progressive types of failure. While there have been several notable building collapses with similar characteristics in the years since Ronan Point, the debate considerably intensified after the World Trade Center disaster on 11 September 2011.

Buildings are vulnerable to progressive collapse if one or more columns are lost due to extreme loadings; which underlines the importance of establishing the likelihood of progressive collapse of structures in order to avoid catastrophic events. Published design guidelines and codes are now available to design engineers for mitigating progressive collapse or minimizing the damages caused by progressive collapse of a structure. Sasani and Kropelnicki (2008) made a 3/8 model of a building was produced and tested and compared with a detailed finite element model of the structure. Many different details were analyzed to determine the adequacy of the structure. The finite element model (FEM) was compared to a demand capacity ratio (DCR) method and determined that the DCR method is overly conservative. Giriunas (2009) did a study involving the comparison of real building behavior to that of a computer model he developed on the computer program SAP2000. Giriunas placed strain gauges throughout various places in the structure to gather physical data of the building's response to the loss of a sequential set of columns. While his experiment dealt with a steel framed structure, the information provided by his study gives great insight into the steps used to gather experimental data and how to use it to determine the credibility and accuracy of a specific analysis method. This paper presents important specification of GSA guidelines for progressive collapse analysis. Linear static, linear dynamic methods have been followed for progressive collapse analysis.

GSA GUIDELINES

The Progressive Collapse Analysis and Design Guidelines for New Federal Office Building and Major Modernization Projects" is developed by the United State General Service Administration to evaluate the potential of progressive collapse for new and existing reinforced concrete as well as steel framed building. The guidelines are based on alternative load path method and removal of vertical load carrying member.

ANALYSIS OF LOADING

For progressive collapse analysis, the following load combination shall be applied after the removal of load carrying member:

For liner static analysis: 2 (D.L. + 0.25 L.L.)

For linear dynamic analysis: (D.L. + 0.25 L.L.)

Where:

D.L. = Dead Load and L.L. = Live Load In static analysisload case, dynamic amplification factor 2 is provided.

CALCULATION OF DEMAND CAPACITY RATIO (DCR)

In order to determine the susceptibility of the building to progressive collapse, Demand Capacity Ratio should be calculated based on the following equation:

$$DCR=Q_{UD}/Q_{CE} \quad \ldots.(1)$$

In which:

Q_{UD}= Acting force (Demand) determined or computed in element or connection/joint.

Q_{CE}= Probable ultimate capacity (Capacity) of the component and/or connection/joint.

Referring to DCR criteria defined through static as well as dynamic approach, different elements in the structures and connections with quantities value less than 1.5 or 2 are considered not collapsed as follows:

- DCR < 2.0: for regular structural configuration
- DCR < 1.5: for irregular structural configuration
- Cases which have been chosen for this study have regular structural configuration as well as irregular structural configuration.

CONSIDERATION FOR COLUMNS REMOVING FOR PROGRESSIVE COLLAPSE ANALYSIS

To calculate DCR according to GSA guidelines, structures should be analyzed as below

Exterior consideration:(a) Analyzing the sudden removal of a column in one floor above the ground (1st story) which is located at or near the middle of the short side of the building.(b) Analyzing the sudden removal of a column in one floor above the ground (1st story) which is located at or near the middle of the long side of the building.(c) Analyzing the sudden removal of a column between the ground floor and the floor above the ground level (1st story) which is located at the corner of the building.

Interior consideration: (a) Analyzing for the loss of a column that extend from the floor of the underground parking area or uncontrolled public ground floor area to the next floor.

ANALYSIS OF STEEL STRUCTURE

The building considered for the study is a G+15 steel moment frame structure, four bays in longitudinal direction and three in transverse direction. The longitudinal direction spacing is 3m and transverse direction is column spacing is 4m.Floor to floor height is 3m and plinth height is 2m.Also vertical irregularity is provided to same structure for analysis purpose.

LOADINGS

Dead load includes self weight of structure. It is automatically generated by the software based on element volume and material. Thickness of slab is considered 125mm. For seismic loading, the building is located in zone IV with importance factor 1, soil type 2 and response reduction factor 3.

COLUMN AND BEAM SCHEDULED

Beam: ISMB 600.

Column: ISMB 600.

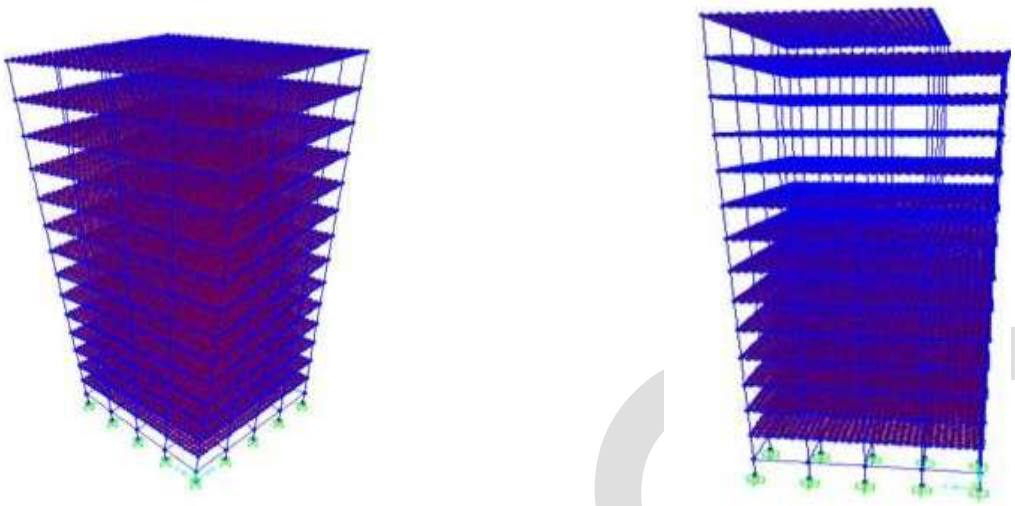

Fig.1. Elevation of regular and irregular building.

ANALYSIS OF REGULAR BUILDING

ANALYSIS OF REGULAR BUILDING WITH CENTRAL COLUMN OF LONGITUDINAL DIRECTION REMOVE.

A graph is plotted taking analysis methods as abscissa and base shear as ordinate for central column removed of longitudinal direction as shown fig.2.

From the fig.2 it can be seen that base shear for linear static analysis is larger than linear dynamic as well as non linear dynamic analysis. Base shear increases in linear static analysis by 6% than non linear dynamic analysis.

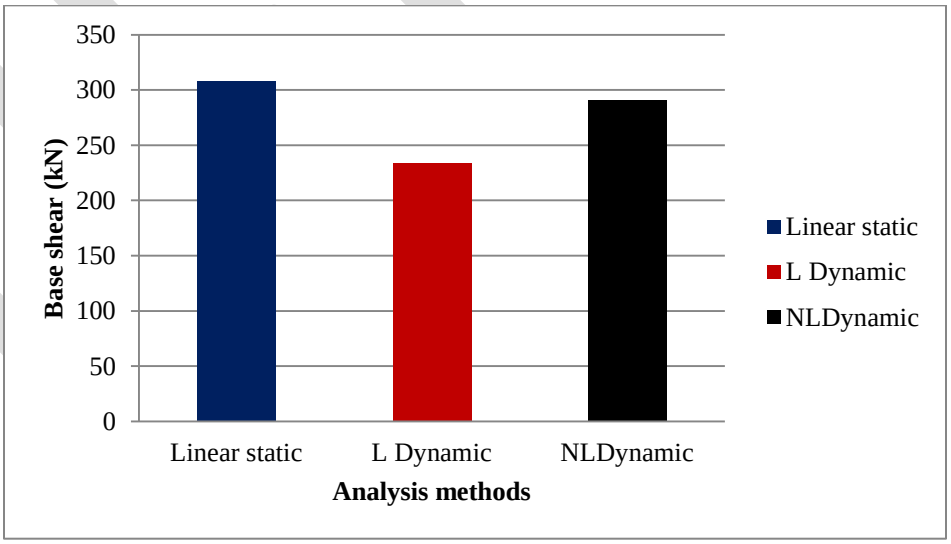

Fig.2 Base shear.

ANALYSIS OF REGULAR BUILDING WITH CENTRAL COLUMN OF TRANSVERSE DIRECTION REMOVE.

From the fig.3 it can be seen that base shear for non linear dynamic analysis is larger than linear static as well as linear dynamic analysis. Base shear increases in non linear dynamic analysis by 51.15 times than linear dynamic analysis.

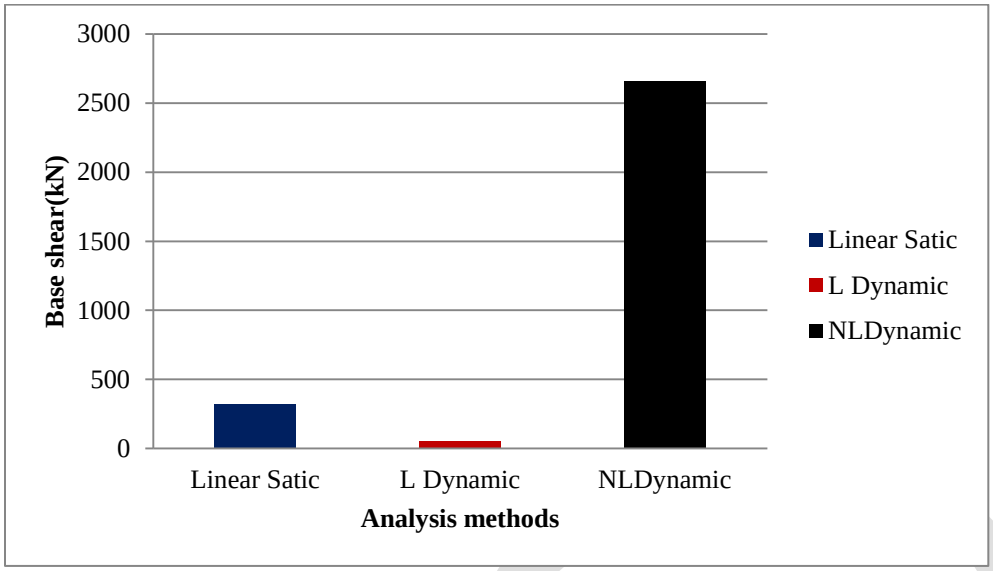

Fig.3 Base shear.

ANALYSIS OF REGULAR BUILDING WITH CORNER COLUMN REMOVE.

From the fig.4 it can be seen that base shear for linear static analysis is larger than linear dynamic as well as non linear dynamic analysis. Base shear increases in linear static analysis by 34.78% than linear dynamic analysis.

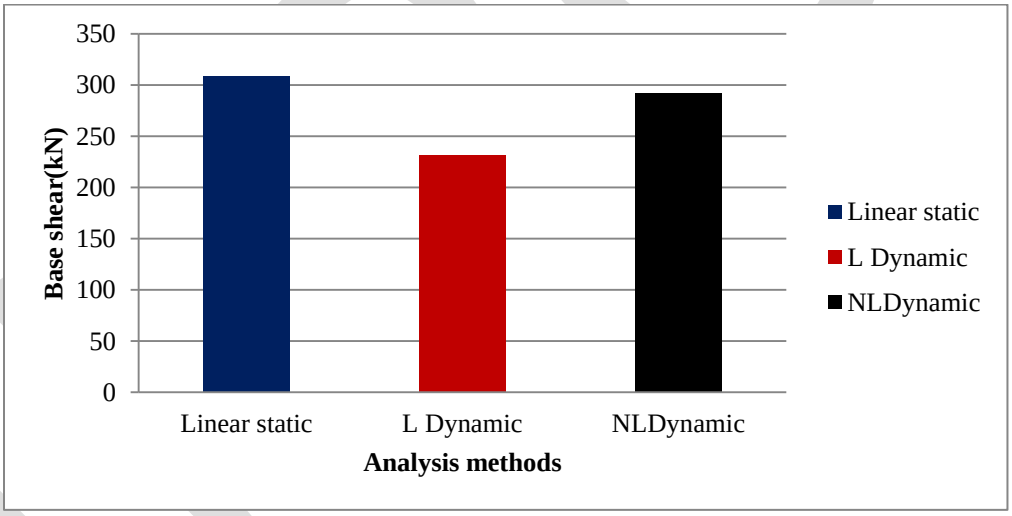

Fig.4 Base shear.

ANALYSIS OF IRREGULAR BUILDING

ANALYSIS OF REGULAR BUILDING WITH CENTRAL COLUMN OF LONGITUDINAL DIRECTION REMOVE.

From the fig.5.it can be seen that base shear for non linear dynamic analysis is larger than linear static as well as linear dynamic analysis. Base shear increases in non linear dynamic analysis by 2.8 times than linear dynamic analysis.

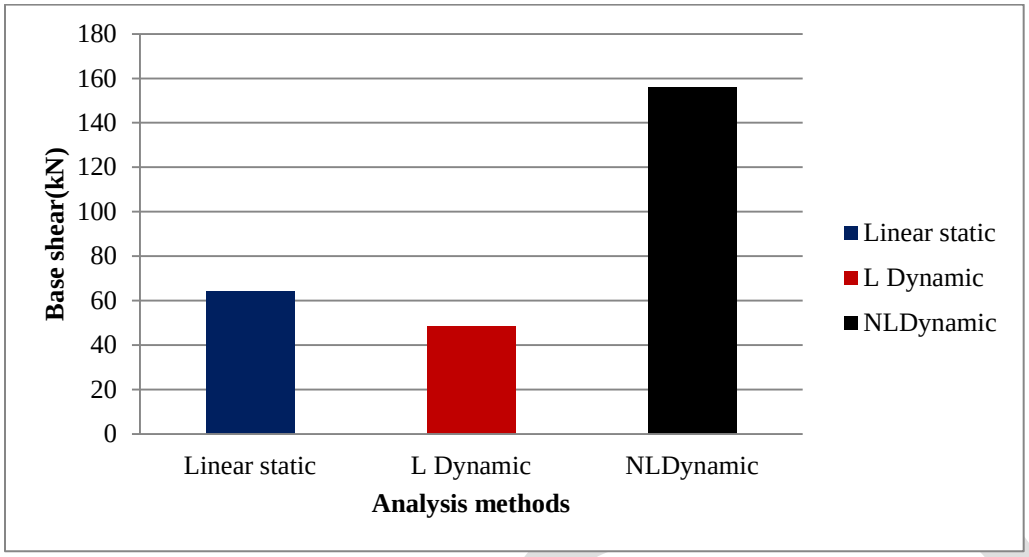

Fig.5 Base shear.

ANALYSIS OF IRREGULAR BUILDING WITH CENTRAL COLUMN OF TRANSVERSE DIRECTION REMOVE.

From the fig.6 it can be seen that base shear for linear static analysis is larger than linear dynamic as well as non linear dynamic analysis. Base shear increases in linear static analysis by 50% than linear dynamic analysis.

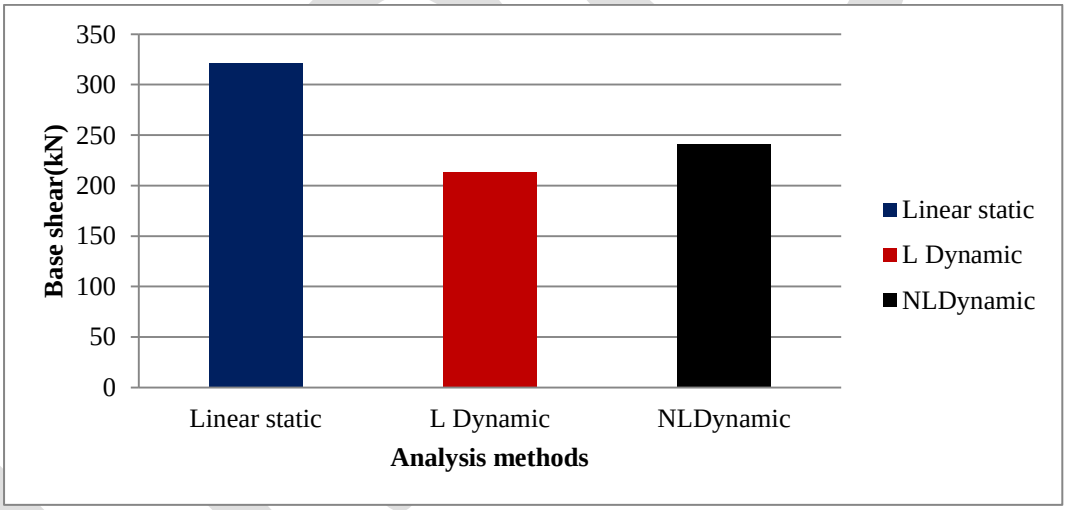

Fig.6 Base shear.

ANALYSIS OF IRREGULAR BUILDING WITH CORNER COLUMN REMOVE.

From the fig.7 it can be seen that base shear for linear static analysis is larger than linear dynamic as well as non linear dynamic analysis. Base shear increases in linear static analysis by 26% than linear dynamic analysis.

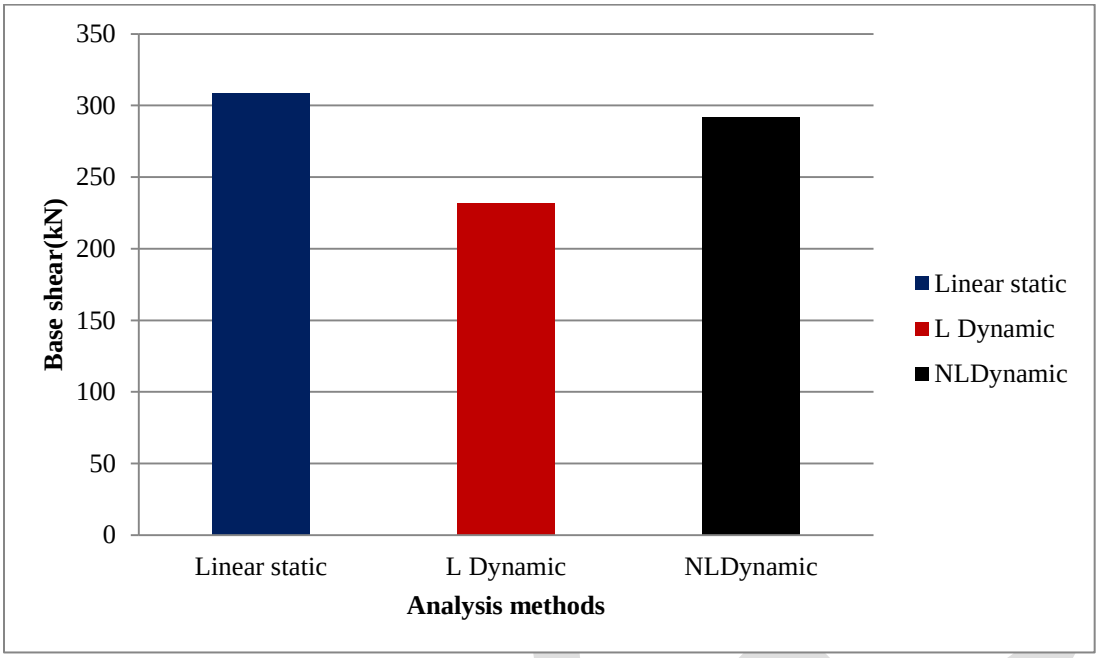

Fig.7 Base shear.

CONCLUSION

1) The variation in the linear static analysis and non linear static analysis seemed to be only 6% in whole structure.
2) The variation in the linear dynamic analysis and non linear dynamic analysis is seemed to be 20% for middle column of longitudinal direction is get removed in whole structure.
3) The variation in the linear dynamic analysis and non linear dynamic analysis is seemed to be 23% for middle column of transverse direction is get removed in whole structure.
4) The variation in the linear dynamic analysis and non linear dynamic analysis is seemed to be 20% for corner column is get removed in whole structure.
5) From above point it can be concluded that to obtain the better result along with linear dynamic analysis procedure, non linear dynamic analysis procedure should also be carried out.
6) Maximum base shear is obtained 2650Kn in regular structure when transverse direction middle column is removed where as in irregular structure when corner column is removed base shear is 330Kn.
7) For regular structure base shear is maximum when transverse direction middle column is removed. So, it can be concluded that regular steel structure is most vulnerable to progressive collapse when transverse direction middle column is get removed.
8) For irregular structure base shear values is maximum when transverse direction middle column is removed. So, it can be concluded that irregular steel structure is most vulnerable to progressive collapse when transverse direction middle column of building is get removed.

REFERENCES:

[1] B. R. Ellingwood and D. O. Dusenberry., "Building design for abnormal loads and progressive collapse", Computer-Aided Civil and Infrastructure Engineering, Vol.20 (3),pp 194–205, 2005.

[2] U. Starossek and M. Haberland, "Measures of structural robustness - requirements and applications", ASCE SEI 2008 Structures Congress Crossing Borders, Vancouver, Canada, 2008.

[3] Robert Smilowitz and Weidlinger Associates, "Analytical Tools for Progressive Collapse Analysis", pp.5-6.

[4] B. R. Ellingwood, "Mitigating risk from abnormal loads and progressive collapse", Journal of Performance of Constructed Facilities, Vol.20 (4),pp 315-323,2006.

[5] E. Agnew and S. Marjanishvili, "Dynamic analysis procedures for progressive collapse", Structure magazine (www.structuremag.org), pp 24–27, Apr 2006.

[6] S.Kokot and G.Solomos, "Progressive collapse risk analysis: literature survey, relevant construction standards and guidelines" European Laboratory for Structural Assessment, pp 55-59,November 2012.

[7] Hayes Jr., J. R., Woodson, S. C., Pekelnicky, R. G., Poland, C. D., Corley, W. G., and Sozen, M.2005. "Can strengthening for earthquake improve blast and progressive collapse resistance?", Journal of Structural Engineering, Vol.131, (8): 1157-1177.

[8] Pekau, O. A., and Cui, Y. 2006, "Progressive collapse simulation of precast panel shear walls during earthquakes", Computers and Structures, Vol. 84, (5-6): 400-412.

[9] Rushi Patel, "Progressive collapse analysis of steel structure", ICU Structural Engineering Jan.2014.

[10] GSA, the U.S. General Services Administration. (2003), Progressive collapse analysis and design guidelines for new federal office buildings and major modernization projects.

[11] Applied Technology Council 40 (ATC40), "Seismic evaluation and retrofit of concrete buildings", Vol.1 and 2, Applied Technology Council, Redwood City, CA, USA, Report No. SSC 96-01, 1996.

[12] FEMA 356, "Prestandard and commentary for the seismic rehabilitation of buildings",American society of civil engineers, Reston, Virginia, Nov.2000.

[13] SAP2000 V14.2.4, "Integrated finite element analysis and design of structures basic analysis reference manual", Berkeley, CA, USA: Computers and structures INC, Aug. 2010.

[14] Nair, R. S., Preventing Disproportionate Collapse. Journal of Performance of Constructed Facilities ASCE, 20 (4), 2006, pp. 309-314.

[15] Luccioni, B.M., Ambrosini, R.D., Danesi, R.F. (2003). "Analysis of building collapse under blast loads." Engineering Structures 26 (2004) 63-71.

[16] Karim, Mohammed R.; Michelle S. Hoo Fatt "Impact of the Boeing 767 Aircraft into the World Trade Center",(October 2005, pp.28-63).

[17] Hiroshi Akiyama,"Collapse Modes of Structures under Strong Motion of Earthquake" Annals of GeophysicsVol.45, December 2002, pp16-19.

International Journal of Engineering Research and General Science Volume 3, Issue 5, September-October, 2015
ISSN 2091-2730

SWOT-Based Learning Management System Performance Analysis in FEU Institute of Technology

Dr. Ace C. Lagman, Amy Lyn M. Maddalora, Josephine T. Casin
FEU Institute of Technology
09173402584

Abstract- The application of technology has dramatically changed the delivery of education. E-learning is the integration of technology in education that covers a variety of activities to support the teaching and learning practice. This paper examines the Learning Management System issues related to the implementation of the E-learning facility in FEU Institute of Technology. The researchers conducted SWOT analysis based on the response of faculty and students through questionnaire. The result of the responses is analyzed to measure the effectiveness of the e-learning facility by being able to trace the strengths, and to find new opportunities in implementing the e-learning facility in FEU Institute of Technology, which will contribute to the improvement of teaching and learning practice. This paper also includes the tools awareness survey to identify web technologies that can be used as e-learning tools in higher education.

Keywords— e-learning, learning management system, swot analysis, analytics, performance, assessment, technology, webapplication

INTRODUCTION

Technology is rapidly changing that can be seen as supporting modernization, economic growth and lifestyle improvement. The application of technology has dramatically changed business organizations and the delivery of education. Online-learning appears to be a classic disruptive innovation with the potential not just to improve the current model of education delivery, but to transform it (Staker, 2011). This integration of technology in education is called e-learning. JISC (2014) defined e-learning as learning facilitated and supported through the use of information and communications technology. It can cover a spectrum of activities from use of technology to support learning as part of a blended approach (a combination of traditional and e-learning approaches), to learning that is delivered entirely online.

The implementation of e-learning can be an additional avenue and medium for knowledge exchange that supports teaching and learning practice. There are related critical factors to assess the readiness of higher educational institution in implementing e-learning such as technological bandwidth, which is considered as one of the barriers. Suhail (2014) found out that low internet speed, inadequate telecommunication infrastructure, high cost of bandwidth, non-existent or inadequate bandwidth management policies and accessibility were the technological related challenges faced by the organizations seeking to implement e-learning solutions in their systems. Therefore, information technology resources must be provided adequately to academic staff and students to aid the demands of developing online resources available and accessible on and off campus. Furthermore, strategic planning and implementation must be made by managers to drive e-learning to the mainstream of educational practice. However, any strategy that gives technology an independent role as problem solver is doomed to fail (Lundvall, 2004). From an educational view point, Collis (1996) states that it is not technology but instructional implementation of the technology that determines the defects on learning.

The pedagogical and socio-economic forces that have driven the higher learning institutions to adopt and incorporate ICTs in teaching and learning include greater information access; greater communication; synchronous and asynchronous learning; increased cooperation and collaboration, cost-effectiveness and pedagogical improvement. However, ICTs have not permeated to a great extent in many higher learning institutions in most developing countries due to many socio-economic and technological circumstances (Sife et al, 2007). Clearly, though, for technology-enhanced assessment to be effective, pedagogically sound developments need to be supported by robust and appropriate technology, within a supportive institutional or departmental context (Gray, 2014).

This paper aims to conduct SWOT analysis to measure the effectiveness of the e-learning facility of FEU Institute of Technology that will help the institution analyze the needs for their e-learning initiatives, and in turn will be instrumental in developing their e-learning strategies. Through this comprehensive implementation assessment process, the institution can establish its e-learning goals. This paper also includes the tools awareness survey to identify web technologies that can be used as e-learning tools in higher education.

Statement of the problem

The study sought to answer to the following questions:

1. What is the descriptive analytics of the assessment of the e-learning facility of FEU Institute of Technology as perceived by faculty and students?
2. What are the strengths and weaknesses of the implemented e-learning facility of FEU Institute of Technology?
3. What opportunities and threats can be drawn from the assessment of the e-learning faculty?
4. What web technologies can be used as e-learning tools in higher education?
5. How effective is the implementation of e-learning based from faculty and students' assessment?
6. What recommendations may be drawn from the findings of the study?

Objectives of the Study

1. To describe the assessment of the e-learning facility of FEU Institute of Technology as perceived by faculty and students
2. To determine the strengths and weaknesses of the implemented e-learning facility of FEU Institute of Technology
3. To find out opportunities and possible threats which can be drawn from the assessment of the e-learning facility
4. To identify web technologies that can be used as e-learning tools in higher education
5. To determine how effective the implementation of e-learning based from faculty and students' assessment
6. To formulate recommendations on the e-learning implementation

Scope and Limitations of the Study

The e-learning facility currently used by FEU institute of technology has been assessed using SWOT-based analysis. The SWOT-based consists of the strength, weakness, opportunities and threats. The respondents were divided into two groups namely faculty and students from the Information Technology Education Department. The sets of questions were provided as an assessment tool to determine e-learning effectiveness.

SPSS (Statistical Package for the Social Sciences) statistical package was used to analyze the data and describe the results of the e- learning assessments. The research was delimited to e-learning users within the two years of e-learning implementation.

1.4 Significance of the Study

The findings of this study is expected to be of great value to the following groups:

FEU Institute of Technology Administrators. The study could serve as basis for defining and maintaining quality control standards for implementing the e-learning facility.

Faculty researchers. This study will serve as reference and guide to other faculty members who will undertake parallel research study.

Methodology

This chapter presents the research design, specifically, the method and techniques, the respondents of the study, the instrument of the study, and the data processing and statistical treatment that will be applied in the study.

Methods and Techniques Used

The study will make use of the descriptive analysis. Descriptive analysis attempts to describe, explain and interpret conditions of the present i.e. "what is'. The purpose of a descriptive analysis is to examine a phenomenon that is occurring at a specific place(s) and time. This method will be used to determine the frequency of the indicators provided by the researchers.

In this study, FEU Institute of Technology e-learning facility will be assessed through a set of questionnaires. The questionnaires were drawn from the paper of Raga et al (2014). Documentary analysis will be used extensively in gathering data and information from sets of respondents which include faculty and students.

Population and Sample of the Study

The study will be using purposive sampling technique. Purposive sampling is a form of non-probability sampling in which decisions concerning the individuals to be included in the sample are taken by the researcher, based upon a variety of criteria which may include specialist knowledge of the research issue, or capacity and willingness to participate in the research. Some types of research design necessitate researchers taking a decision about the individual participants who would be most likely to contribute appropriate data, both in terms of relevance and depth.

The respondents of the study consists of 5 faculty members and 77 students who used the e-learning facility in two years of its implementation.

Data Processing and Statistical Treatment

The data to be analyzed came from sets of answers in the lists of indicators in the questionnaire provided. SPSS that will be used in the study will make every effort to make the software easy to use. This prevents the researcher for making mistakes or even forgetting something. It begins by defining a set of variables and enters the data for the variable to create member of cases. After the data is entered into SPSS, the cases will be all defined by value stored in the variables. The following statistical tools will be utilized in reporting the findings of the study.

Mean. As defined by Barnes (2000), the mean is the most common measurement of average. It is the point which balances all values on either side. It is preferred as the measure of central tendency when the distribution is symmetrical. When the mean is computed from a grouped data, the accuracy of the result may be affected by the loss of the true identity of the original numbers.

Percentage. To find out what part of the population was represented out of one hundred equal parts, the percentage method is used.

To measure the level of assessments of students and faculty to e-learning facility, likert scale was used

Table 1 *Likert scale*

Range	Interpretation
4.51 – 5.00	Strongly Agree
3.51 – 4.50	Agree
2.51 – 3.50	Neutral
1.51 – 2.50	Disagree
1.00 – 1.50	Strongly Disagree

Results and Discussion

1. The descriptive analytics of the assessment of the e-learning facility of FEU Institute of Technology as perceived by faculty and students.

Table 2 *Students' perception in e-learning*

Indicators	**Mean**	**Interpretation**
1. The e-learning system in your institution helps to support and improve communication between faculty and students.	3.77	Agree
2. The e-learning system in your institution helps to minimize the academic workload of faculty.	3.95	Agree
3. The e-learning system in your institution helps to enhance the knowledge and understanding that students gain from lectures, tutorials, and practicals.	3.77	Agree
4. The e-learning system in your institution helps to make administering tests and quizzes easier for the faculty and students.	4.00	Agree
5. The e-learning system in your institution enables students to learn at a place and time of their choosing.	3.83	Agree
6. The e-learning system allows the faculty to track the performance of students and provides students with the ability to track their own performance.	3.73	Agree
7. The faculty spend sufficient amount of time in supporting the students' exploration of topics posted in the e-learning system.	3.49	Neutral
8. The students are sufficiently motivated in using the e-learning system.	3.42	Neutral
9. The e-learning system can only be utilized by qualified faculty.	3.62	Agree
10. The IT setup and network connectivity is sufficient to provide every faculty and student easy access to the e-learning system.	3.47	Neutral
11. The e-learning system can only be utilized by technology-savvy students.	3.36	Neutral

12. The e-learning system enables students to access educational materials in a variety of learning elements and media format (e.g., HTML content, videos, audio recordings, text files, presentations, FAQs, etc).	3.57	Agree
13. The e-learning system makes it easier for faculty to track the-learning progress of individual students.	3.56	Agree
14. The e-learning system helps to provide students with opportunities to exchange ideas with each other and even learn from their mistakes and experiences.	3.48	Neutral
15. The materials provided in the e-learning system provides students the opportunity to study part-time and make-up for lost lessons in case they incur absences in classroom sessions.	3.66	Agree
16. The e-learning system enables students to cover more-learning materials per course.	3.73	Agree
17. Sufficient measures have been taken to prevent students from hacking the course materials or cheating by sharing assignments and online tests answers.	3.62	Agree
18. Students learn much faster with the help of the e-learning system than in the traditional faculty-led lectures.	3.49	Neutral
19. The e-learning system, as a learning environment, prohibits students from developing their social skills.	3.57	Agree
20. Faculty are unable to deliver courses and manage student effectively through the e-learning system.	3.52	Agree
21. The high cost of development prohibits the e-learning system to be developed to its full potential.	3.58	Agree
Average Mean	**3.63**	**Agree**

Table 3 *Faculty perception in e-learning*

Indicators	**Mean**	**Interpretation**
1. The e-learning system in your institution helps to support and improve communication between faculty and students.	3.80	Agree
2. The e-learning system in your institution helps to minimize the academic workload of faculty.	3.20	Neutral
3. The e-learning system in your institution helps to enhance the knowledge and understanding that students gain from lectures, tutorials, and practicals.	3.40	Neutral
4. The e-learning system in your institution helps to make administering tests and quizzes easier for the faculty and students.	3.20	Neutral
5. The e-learning system in your institution enables students to learn at a place and time of their choosing.	3.60	Agree

6. The e-learning system allows the faculty to track the performance of students and provides students with the ability to track their own performance.	3.00	Neutral
7. The faculty spend sufficient amount of time in supporting the students' exploration of topics posted in the e-learning system.	2.80	Neutral
8. The students are sufficiently motivated in using the e-learning system.	3.00	Neutral
9. The e-learning system can only be utilized by qualified faculty.	3.40	Neutral
10. The IT setup and network connectivity is sufficient to provide every faculty and student easy access to the e-learning system.	2.60	Neutral
11. The e-learning system can only be utilized by technology-savvy students.	3.40	Neutral
12. The e-learning system enables students to access educational materials in a variety of learning elements and media format (e.g., HTML content, videos, audio recordings, text files, presentations, FAQs, etc).	3.20	Neutral
13. The e-learning system makes it easier for faculty to track the-learning progress of individual students.	2.80	Neutral
14. The e-learning system helps to provide students with opportunities to exchange ideas with each other and even learn from their mistakes and experiences.	2.40	Disagree
15. The materials provided in the e-learning system provides students the opportunity to study part-time and make-up for lost lessons in case they incur absences in classroom sessions.	3.60	Agree
16. The e-learning system enables students to cover more-learning materials per course.	3.40	Neutral
17. Sufficient measures have been taken to prevent students from hacking the course materials or cheating by sharing assignments and online tests answers.	2.40	Disagree
18. Students learn much faster with the help of the e-learning system than in the traditional faculty-led lectures.	2.60	Neutral
19. The e-learning system, as a learning environment, prohibits students from developing their social skills.	3.20	Neutral
20. Faculty are unable to deliver courses and manage student effectively through the e-learning system.	3.20	Neutral
21. The high cost of development prohibits the e-learning system to be developed to its full potential.	3.00	Neutral
Average Mean	**3.10**	**Neutral**

Table 4 *Faculty and students' perception in e-learning*

Indicators	Mean	Interpretation
1. The e-learning system in your institution helps to support and improve communication between faculty and students.	3.77	Agree
2. The e-learning system in your institution helps to minimize the academic workload of faculty.	3.90	Agree
3. The e-learning system in your institution helps to enhance the knowledge and understanding that students gain from lectures, tutorials, and practicals.	3.74	Agree
4. The e-learning system in your institution helps to make administering tests and quizzes easier for the faculty and students.	3.95	Agree
5. The e-learning system in your institution enables students to learn at a place and time of their choosing.	3.82	Agree
6. The e-learning system allows the faculty to track the performance of students and provides students with the ability to track their own performance.	3.68	Agree
7. The faculty spend sufficient amount of time in supporting the students' exploration of topics posted in the e-learning system.	3.45	Neutral
8. The students are sufficiently motivated in using the e-learning system.	3.39	Neutral
9. The e-learning system can only be utilized by qualified faculty.	3.61	Agree
10. The IT setup and network connectivity is sufficient to provide every faculty and student easy access to the e-learning system.	3.41	Neutral
11. The e-learning system can only be utilized by technology-savvy students.	3.37	Neutral
12. The e-learning system enables students to access educational materials in a variety of learning elements and media format (e.g., HTML content, videos, audio recordings, text files, presentations, FAQs, etc).	3.55	Agree
13. The e-learning system makes it easier for faculty to track the-learning progress of individual students.	3.51	Agree
14. The e-learning system helps to provide students with opportunities to exchange ideas with each other and even learn from their mistakes and experiences.	3.41	Neutral
15. The materials provided in the e-learning system provides students the opportunity to study part-time and make-up for lost lessons in case they incur absences in classroom sessions.	3.66	Agree
16. The e-learning system enables students to cover more-learning materials per course.	3.71	Agree
17. Sufficient measures have been taken to prevent students from hacking the course materials or cheating by sharing assignments and online tests	3.55	Agree

answers.		
18. Students learn much faster with the help of the e-learning system than in the traditional faculty-led lectures.	3.44	Neutral
19. The e-learning system, as a learning environment, prohibits students from developing their social skills.	3.55	Agree
20. Faculty are unable to deliver courses and manage student effectively through the e-learning system.	3.50	Neutral
21. The high cost of development prohibits the e-learning system to be developed to its full potential.	3.55	Agree
Average Mean	**3.60**	**Agree**

2. The strengths and weakness of the implemented e-learning facility of FEU Institute of Technology

Based on the results of the analysis, the following are the perceived strengths of the e-learning facility:

- It helps to minimize the workload of faculty, as it facilitates tracking of students' performance and learning progress, as well as making easier the administration of class activities such as exams and quizzes.
- It helps enhance the knowledge and understanding of students from the varied activities and learning materials that can be accessed.
- It helps to support and improve communication between faculty and students.
- The materials provided in the e-learning system gives students the opportunity to study part-time and make-up for lost lessons in case they incur absences in classroom sessions, thus enabling the students to learn at their choice of place and time.
- As a security measure, sufficient actions have been taken to prevent students from hacking the course materials or cheating by sharing assignments and online tests answers. Further, the facility can only be utilized by qualified faculty.

Based on the results of the analysis, the following are the perceived weaknesses of the E-learning facility;

- The faculty spend insufficient amount of time in supporting the students' exploration of topics posted in the e-learning system as the e-learning facility is designed to be utilized by technology-savvy students.
- The students are insufficiently motivated in using the e-learning system. They learn faster with the traditional faculty-led lectures than with the help of the e-learning facility.
- There is no provision for students to exchange ideas with each other and even learn from their mistakes and experiences.
- The IT setup and network connectivity is insufficient to provide every faculty and student easy access to the e-learning system.

3. Opportunities and threats drawn from the assessment of the e-learning facility.

Based from the strengths, the following are the perceived opportunities of the e-learning facility.

- Since the faculty can track the students' performance, badges may be issued to motivate the students to perform better in class. Faculty will be able to perform other academic-related activities.
- Students can track their academic performance, thus the initiative on their part to pursue better grades.
- Mining of students' data could be a potential in determining the characteristics of students who passed and failed the subjects, thus interventions could be done so that passing rate will be increased.
- Other forms of media could be used to improve teaching and learning activities.
- Social media tools which include forums, chat, personal messages can be beneficial in improving communication between faculty and students.
- The e-learning facility encourages students to self-paced learning.
- No authorized users can penetrate the e-learning facility based on the security measures implemented by the institution.

Based from the weaknesses, the following are the perceived threats of the e-learning facility.

- Familiarity of the e-learning facility and resources could cause intimidation to technically inexperienced students.
- The full potential of the e-learning facility is not yet maximized which causes students not to embrace the e-learning technology.
- Interaction among students is prevented due to restrictions settings, thus exchange of ideas is limited.
- The e-learning infrastructure is not sufficient to support the performance of the e-learning facility, especially when it comes to concurrency of users.

4. Web technologies that can be used as e-learning tools in higher education

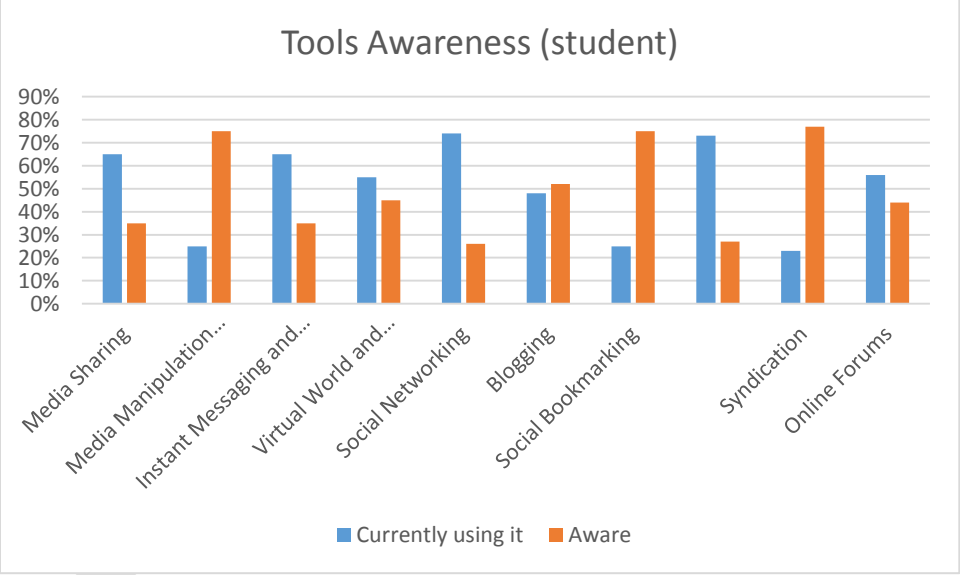

Figure 1 Tools Awareness (student)

Figure 1 shows that 65%-74% of the students are currently using social networking media, media sharing, instant messaging and chat, and wikis and collaborative editing tools. However, 75%-77% are aware of media manipulation and mashups, social bookmarking, and syndication.

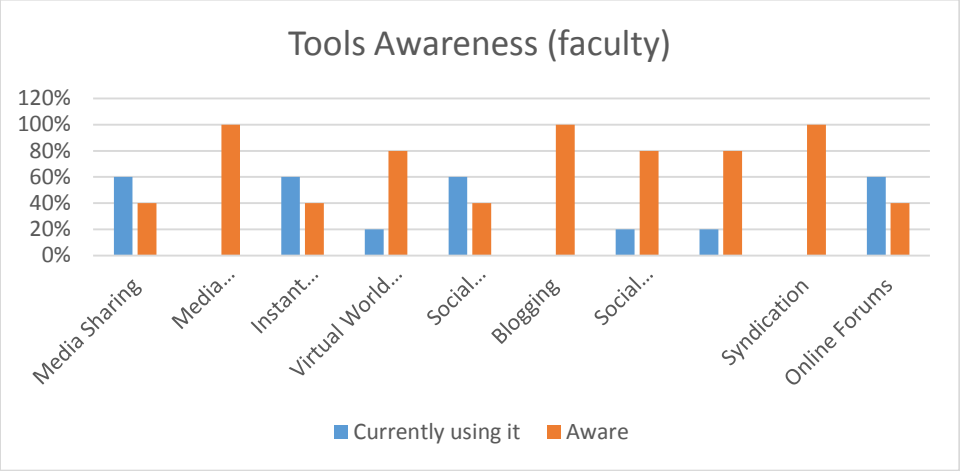

Figure 2 Tools Awareness (faculty)

Figure 1 shows that 60% of the faculty are currently using media sharing, instant messaging and chat, social networking media, and online forums. However, 80%-100% are aware of media manipulation and mashups, virtual world and online games, blogging, wikis and collaborative editing tools, and syndication.

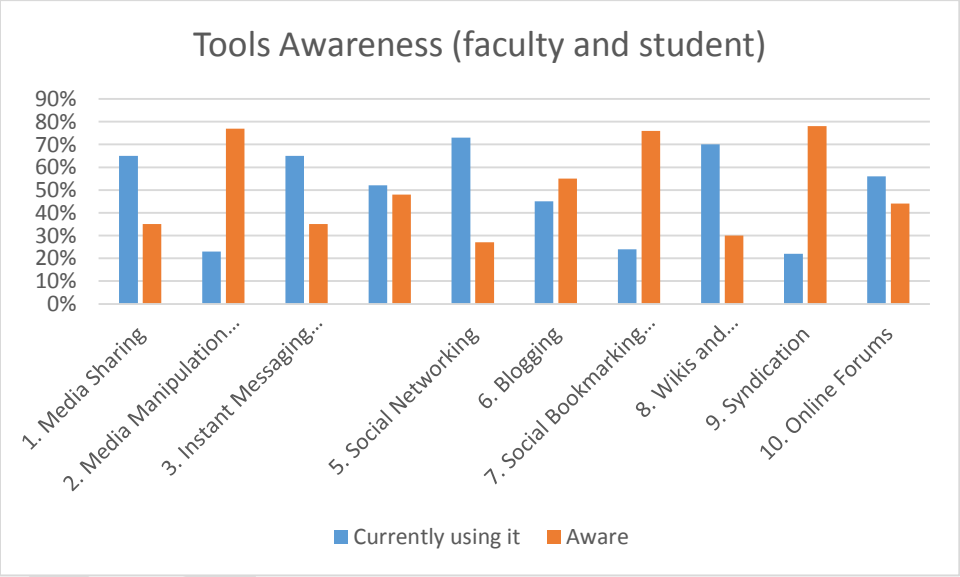

Figure 3 Tools Awareness (faculty and student)

Figure 3 shows that 65%-73% of both the faculty and students are currently using media sharing, instant messaging and chat, social networking media, and wikis and collaborative editing tools. However, 76%-78% are aware of media manipulation and mashups, social bookmarking, and syndication.

5. The effectiveness of the implementation of e-learning based from faculty and students assessment.

In terms of student assessment on e-learning implementation, Table 2 shows that the student assessment recorded an arithmetic mean of 3.63 with an interpretation result as "Agree" or effective in the usage of e-learning facility.

In terms of faculty assessment on e-learning implementation, Table 3 shows that the faculty assessment recorded an arithmetic mean of 3.10 with an interpretation result as "Neutral" as moderately effective in the usage of e-learning facility.

In totality, the assessment of e-learning facility both from students and faculty as shown in Table 4, gained an arithmetic mean of 3.60 with an interpretation of "Agree" or effective in the usage of e-learning facility.

ACKNOWLEDGMENT

If acknowledgement is there wishing thanks to the people who helped in work than it must come before the conclusion and must be same as other section like introduction and other sub section.

CONCLUSION

The application of technology has dramatically changed the delivery of education. E-learning is the integration of technology in education that covers a variety of activities to support the teaching and learning practice. For the past two years of e-learning implementation in FEU Institute of Technology, the teaching and learning practice has improved through various web technologies. However, limited features of the e-learning facility had been utilized due to some restriction settings. Implementing some other features needs proper orientation to students who are technically inexperienced to motivate the students to embrace e-learning technology. The e-learning infrastructure, such as the server specifications and network connection, should be given importance to effectively support the performance of the e-learning facility.

Web technologies like media sharing, instant messaging and chat, social bookmarking, and syndication can be integrated as e-learning tools in higher education.

In general, the implementation of e-learning facility in FEU Institute of Technology is effective in the improvement of teaching and learning practice.

REFERENCES:

[1]Collis, Betty. (1996). "Tele-learning in a digital world: the future of distance learning." Boston: International Thompson Computer Press.

[2]Haynes, M. and others. 2003. eLearning – A tutor guide. Middlesex University Press.

[3]Janossy, J. (2008). Proposed Model for Evaluating C/LMS Faculty Usage in Higher Education Institutions. "Immersed In Learning" 13th Annual Instructional Technology Conference. Murfreesboro: Middle Tennessee State University

[4]JISC (2014). JISC Digital Media, August 8, 2010. Retrieved from http://www.jiscdigitalmedia.ac.uk/guide/introduction-to-elearning.

[5]Lundvall, A. et al (2003). "Why the new economy is a learning economy," vol. 2003 (117).

[6]Machado, Carlos (2006). "Developing an e-readiness model for higher education institutions: results of a focus group study," Blackwell Publishing, UK and USA.

[7]Raga, R. Jr., et al (2014). "Perceptions and Utilization of a Blended Learning Implementation: An Analysis from Two Perspectives." 2nd International Conference on Open Distance E-Learning retrieved from http://www.icodel.org/home/ICODEL%202014%20CONCURRENT%20SESSIONS.pdf.

[8]Sheard, J., Ceddia, J., Hurst, J. & Tuovinen, J. (2003), 'Inferring student learning behaviour from website interactions: A usage analysis', Education and Information Technologies 8(3), 245–266.

[9]Silber, H.K. (2007). A Principle-Based Model of Instructional Design: A new way of thinking about and teaching ID. Educational Technology, 47(5), 5-19.

[10]Sife, A. S., Lwoga, E. T. and Saga Sokoine, C. (2007). "New technologies for teaching and learning: Challenges for higher learning institutions in developing countries," University of Agriculture, Tanzania.

[11]Staker, Heather (2011). "The Rise of K–12 Blended Learning Profiles of emerging models," Innosight Institute.

[12]Suhail, Nazir Ahmad (2014). "E-Readiness Assessment Model for Low Bandwidth Environment," School of Computer Science and Information Technology, Kampala University. ACSIJ Advances in Computer Science: an International Journal, Vol. 3, Issue 4, No.10, July 2014

International Journal of Engineering Research and General Science Volume 3, Issue 5, September-October, 2015
ISSN 2091-2730

COMPARATIVE STUDY ON GFRP JACKETED RC COLUMNS AND CFRP JACKETED RC COLUMNS OF DIFFERENT SHAPES

Jijin V.[1], Preetha Prabhakaran[2]

[1] M.Tech Scholar, Dept of Civil Engg., SNGCE, Kerala, India
[2] Assoc. Professor, Dept of Civil Engg., SNGCE, Kerala, India
[1]jijinv4u@gmail.com, 09497689780

Abstract— Column jacketing with FRP sheets plays an important role in enhancing the performance of RC column. FRP is an Advanced Composite Material (ACM) that is relatively new material to civil engineering. It holds a better choice than reinforcing steel in certain applications. In order to attain large deformation before failure occurs and to enhance an adequate load resistance capacity, RC columns has to be laterally jacketed. Jacketing RC column with FRP improves column performance not only by carrying some fraction of axial load applied to it but also by providing lateral confining pressure to the column externally. In this work a comparative study on GFRP jacketed RC columns and CFRP jacketed RC columns of different shapes having same cross-sectional area were analysed. Buckling analysis on RC columns of circular, rectangular and square cross-sectional shapes has been done in ANSYS 15. FRP Jacketing increases the load carrying capacity of all RC columns. CFRP Jacketed RC columns shows a better load carrying capacity than GFRP Jacketed RC Columns when both axial and eccentric loadings were applied in circular, rectangular and square cross-sectional shapes**.**

Keywords— Column Jacketing, Rectangular, Square, Circular, Crossesctional Shapes, Repair and Rehabilitaion, Buckling Analysis, Ultimate Load Carrying Capacity etc.

1.INTRODUCTION

Concrete deterioration is one of the issue affecting most structures. Problems associated with the deterioration of RC structures are usually due to corrosion of the reinforcing steel and spalling of the concrete. Most of the structures are designed for gravity loading as per IS 456:2000. During a severe earthquake, the structure is likely to undergo inelastic deformation and has to depend on ductility and energy absorption capacity to avoid collapse. Such buildings designed for gravity loading need to be strengthened to increase strength, stiffness and ductility. Thus, retrofitting measures must be taken to maintain the integrity of the structure.

In recent years, For strengthening and rehabilitation of existing structures Fiber Reinforced Polymer (FRP) composites have their advantage over traditional materials. The advantages such as corrosion resistance, light weight, high-strength to weight ratio, and high efficiency in construction encourage civil engineers to use this material. Effective lateral confinement is provided by FRP jackets to the concrete columns that can improve their compressive strength and ultimate axial strain. Retrofitting with FRP materials provides successful solutions for strengthening, repairing, adding ductility, rapid execution, long-term durability, and consequently lower life-cycle costs. R.Kumutha reported that GFRP jacketing in RC column resulted in enhancing the compressive strength and ductility [1].

The Glass Fiber Reinforced Polymer (GFRP) jacketed RC column performed much better than steel reinforced column. GFRP has significantly increased the strength and ductility of concrete by creating a perfect adhesive bond in between concrete and the jacketing material [8].

Fig.1.1.Jacketing of GFRP sheets around column

Carbon Fiber Reinforced Polymer (CFRP) is a very light, strong composite material used in the past two decades for structural engineering purposes. The most popular use of CFRP is retrofitting, where the load capacity of structures, is increased through CFRP wraps[3]. External confinement of concrete columns by means of jacketing high-strength fiber composites around the perimeter of the column enhances their strength and ductility.

Fig.1.2.Jacketing of CFRP sheets around column

2.SCOPE

The scope of work includes comparison of the effectiveness of external Glass Fiber Reinforced Polymer (GFRP) and Carbon Fiber Reinforced Polymer (CFRP) strengthening on behaviour of circular, rectangular and square. RC columns to upgrade existing concrete structures. From past studies, most of the works were carried out for circular column jacketing. Only few studies were conducted for rectangular and square column jacketing. However, the majority of columns in buildings are rectangular columns. Hence their strength and retrofitting must be given more attention to maintain the integrity of building structures. The use of externally jacketed FRP composite for strengthening and rehabilitation can be an economical alternative for restoring or upgrading the overall performance of existing concrete columns.

3.OBJECTIVES

1. To determine the effect of cross-sectional shape in RC columns.
2. To investigate the number of FRP layers: Models with zero, one, and two layers of FRP.
3. To study the performance of column under axial and eccentric compression loadings.
4. To find out the parameter i.e. ultimate failure load of the columns using Finite Element software.
5. Comparison of results will be done from GFRP jacketed RC Columns and CFRP jacketed RC Columns.

4. METHODOLOGY

- Preparation of Literature Review.
- Validation of Finite Element software.
- Finite element modelling will be done in ANSYS 15.
- Analysis of the structure using FE Software.
- Interpretation of results.

5. VALIDATION

A finite element model of RC control column and FRP confined RC column of circular, square and rectangular cross-sectional shapes was developed and validated by existing experimental results in journal [1] and [2].

Table.5.1.Validation Model Details

Column c/s Shape	Breadth (mm)	Depth (mm)	Height (mm)	Main Bars	Lateral Ties
Circular	Diameter 150 mm		600	6# 12 mmØ	8 mmØ @ 190 mm c/c
Square	125	125	750	4# 10 mmØ	6 mmØ @ 125 mm c/c
Rectangular	112	140	750	4# 10 mmØ	6 mmØ @ 125 mm c/c

The validation results are shown in **Table.5.2**.

Table.5.2.Validation of Results

Column Designation	Ultimate Failure load	Deformation (Experiment)	Deformation (ANSYS 15)	Error (%)
0 Square	766.3 kN	1.18 mm	1.25 mm	5.9
1 Square	786 kN	1.2 mm	1.27 mm	5.8
0 Rectangular	750 kN	1.21 mm	1.22 mm	0.82
1 Rectangular	772 kN	1.34 mm	1.24 mm	7.4
0 Circular	509 kN	4.5 mm	4.26 mm	5.33
1 Circular	876 kN	7.9 mm	7.3 mm	7.5

6. PRESENT STUDY

6.1 RC COLUMNS

Circular, square, and rectangular columns having approximately same cross-sectional area and 3m height were modelled. Design details of RC column are presented in **Table.6.1**. Reinforcement detailing are shown in **Fig.6.1**.

Table.6.1.Design details of RC columns.

Column c/s Shape	b (mm)	d (mm)	h (mm)	Main Bars	Lateral Ties
Square	150	150	3000	4# 8 mmØ	6 mmØ @ 100 mm c/c
Rctngulr	110	210	3000	4# 8 mmØ	6 mmØ @ 100 mm c/c
Circular	Diameter 170mm		3000	4# 8 mmØ	6 mmØ @ 100 mm c/c

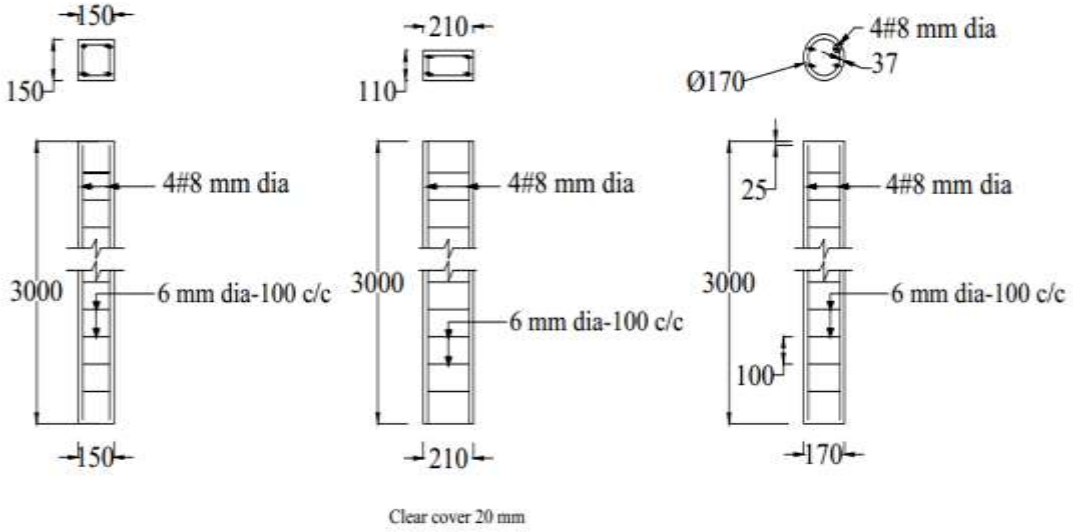

Fig.6.1.Reinforcement details of square, rectangular and circular columns.

6.2 FINITE ELEMENT MATERIAL MODELS

6.2.1 Concrete

M25 mix concrete having modulus of elasticity (E) = 25000 N/mm^2 is used to model the RC columns. The Poisson's ratio (ν) = 0.15 was taken.

6.2.2 Reinforcement

Fe415 steel was used in reinforcement steel bars having modulus of elasticity (E) = 200000 N/mm^2 is used to model the RC columns. The poisson's ratio (ν) = 0.2 was taken.

6.2.3 FRP Sheet

The properties of GFRP sheet and CFRP sheet are presented in **Table.6.2**.

Table.6.2.Properties of GFRP sheet [1] and CFRP sheet [14]

FRP Sheets	Modulus of Elasticity (E)	Poison's ratio (ν)	Thickness of Sheet	Ultimate Tensile Strength	Shear Modulus (G)
GFRP	10500 MPa	0.26	1.1 mm	3400 MPa	1520 MPa
CFRP	230000 MPa	0.22	1.1 mm	3500 MPa	3270 MPa

6.3 FE MODEL

Finite Element modelling has been done in ANSYS 15. All control RC columns and FRP jacketed RC columns were modelled. Following figures shows the geometry and meshed model of all columns.

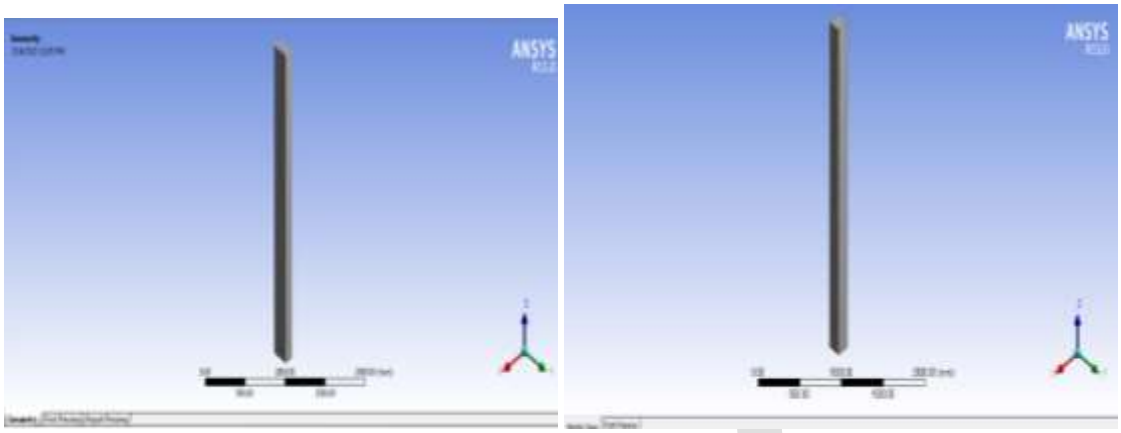

Fig.6.2.Geometry of Rectangular control and FRP jacketed RC column.

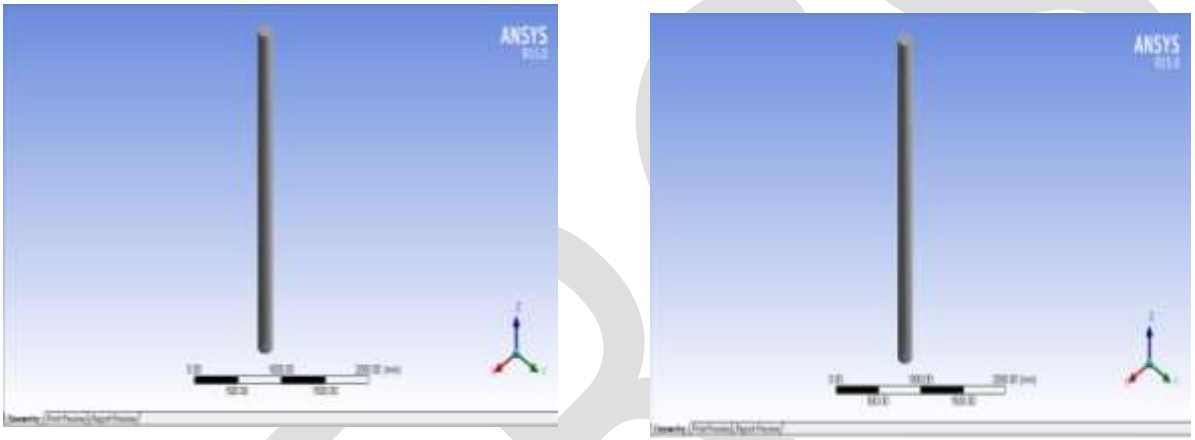

Fig.6.3.Geometry of Circular control and FRP jacketed RC column.

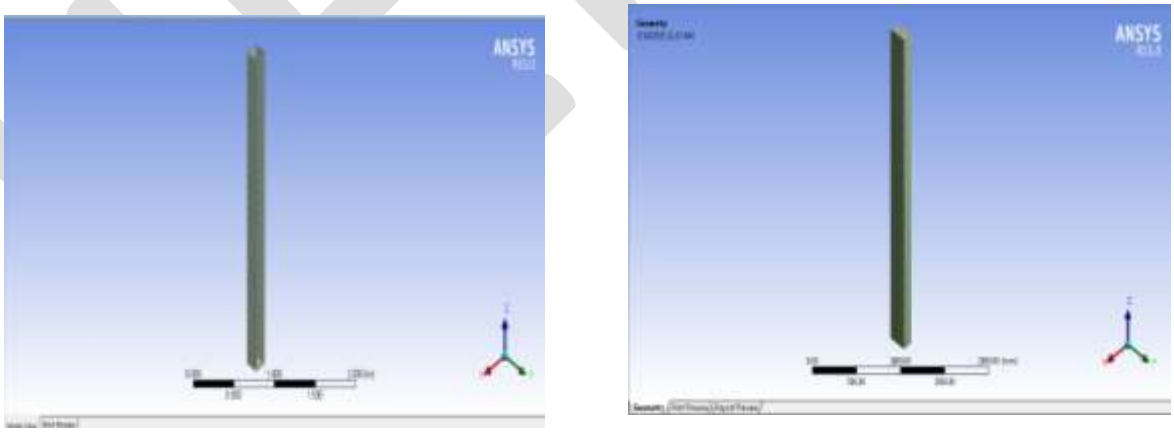

Fig.6.3.Geometry of Square control and FRP jacketed RC column.

6.4 BOUNDARY CONDITION

Fig.6.4. shows the boundary condition with loading for RC control and FRP jacketed columns. All columns were fixed at one end and free at other end.

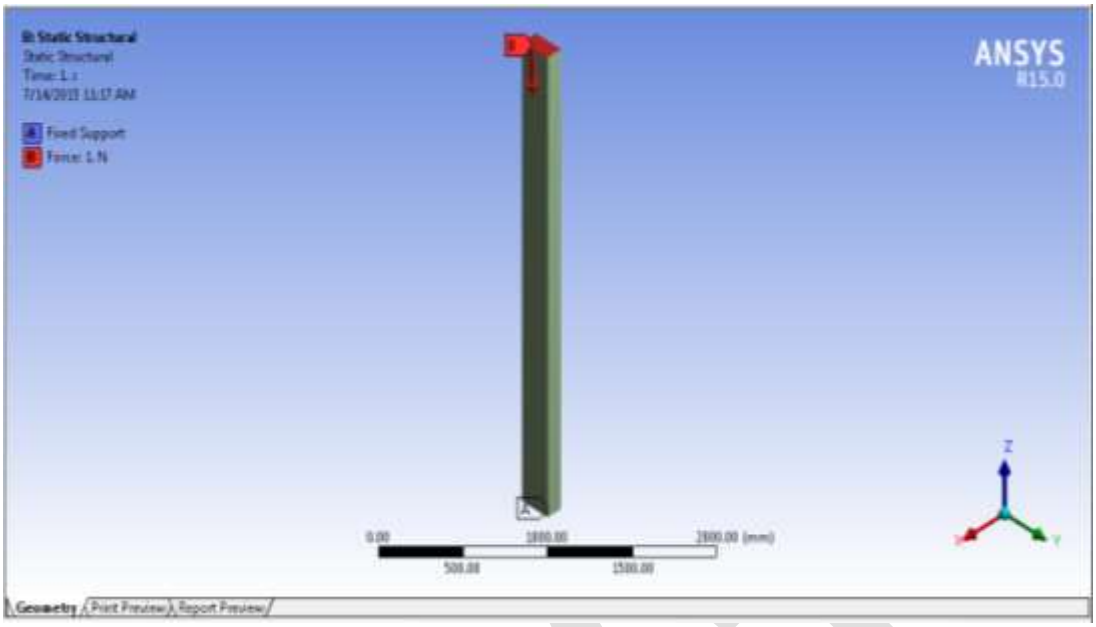

Fig.6.4.Boundary condition with loading for control and FRP jacketed RC columns.

6.5 LOADING CONDITION

6.5.1 RC Column subjected to Axial Loading

If the load on a column is applied along the center of gravity of cross section, it is called an axial load or it can be force applied along the lengthwise centerline of column. Axial force can be compressive or tensile force on the member.

6.5.2 RC Column subjected to Eccentric Loading

Columns are basically vertical compression members that transfer axial loads to the foundations. Although the main function of the column is to transfer axial loads, most of the time, columns are subjected to moments as well. This may be due to accidental eccentricity arising from minor misalignment during construction, or due to reduction of the column size in multi-storey buildings. This may also occur due to lateral drift, even in cases when the columns are not part of the structural system resisting horizontal forces.

In this study RC control columns and FRP jacketed RC columns are analyzed for 25 mm eccentric loading The performance of the columns were evaluated by analyzing their load carrying capacity.

7. RESULTS AND DISCUSSION

7.1 RC COLUMNS SUBJECTED TO AXIAL LOADING

Buckling analysis has been carried out on all control columns to find out the ultimate load carrying capacity.

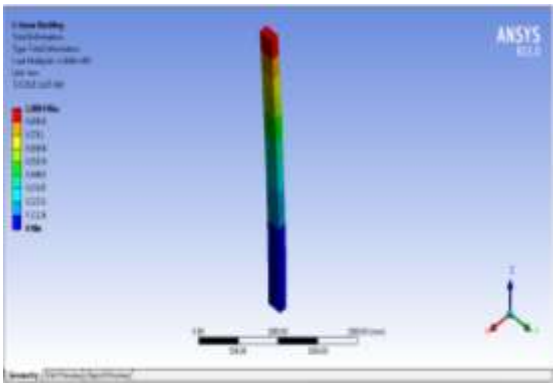

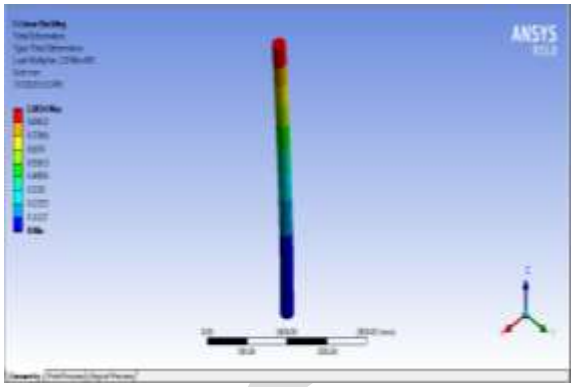

Fig.7.1.Rectangular and circular RC column subjected to Axial Loading.

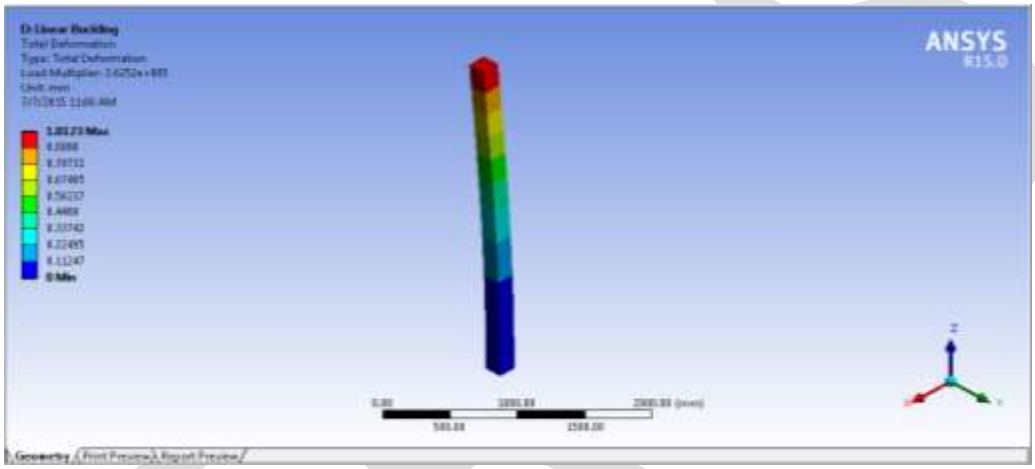

Fig.7.2.Square RC column subjected to Axial Loading.

Long columns can be analysed with Euler column formula

$$F = \frac{n \pi r^2 E I}{L^2}$$

Where

F = allowable load

n = factor accounting for the end conditions

E = modulus of elasticity

L = length of column

I = Moment of inertia

Comparison of the critical value of controlled column from ANSYS with Eulers equation has been represented in the **Table.7.1** below.

Table.7.1.Comparison of Results with Eulers equation.

Column Types	Critical Load ANSYS 15 (kN)	Allowable Load (Eulers Equation) (kN)	% Variation
Rectangular	149.09	159.64	7.07
Circular	257.48	280.9	8.90
Square	262.52	285.14	8.61

Hence the load carrying capacity of controlled RC columns increases in the order of square, circular and rectangular.

7.1.1 GFRP Jacketed RC Column subjected to Axial Loading

GFRP jacketed RC columns of rectangular, square, and circular cross-section were axially loaded to find out the ultimate load carrying capacity.

Fig.7.3.One and two layers GFRP jacketed rectangular RC column subjected to axial loading

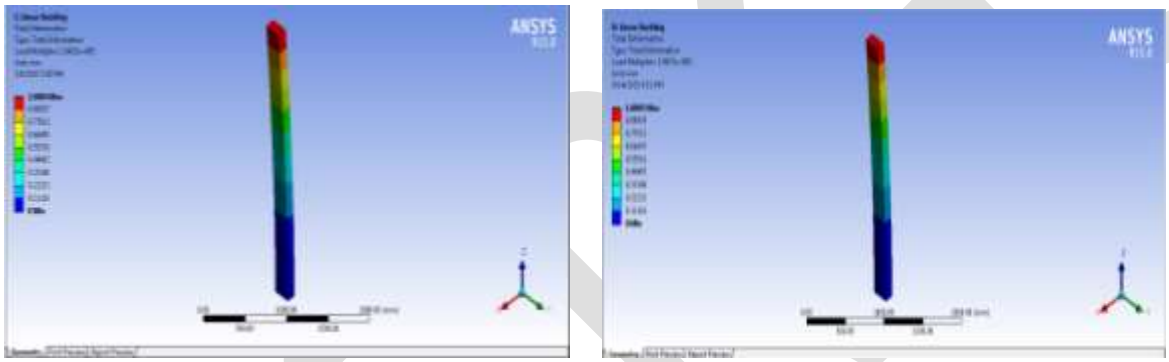

Fig.7.4.One layer and two layers GFRP jacketed circular RC column subjected to axial loading

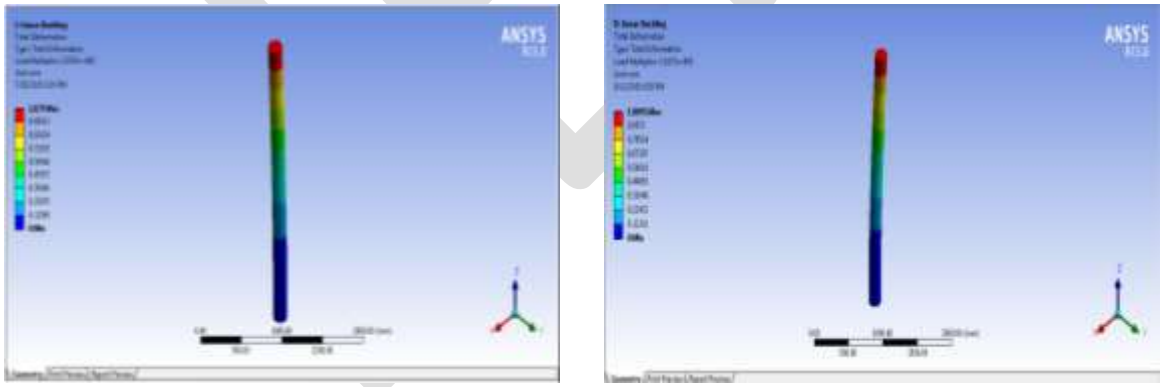

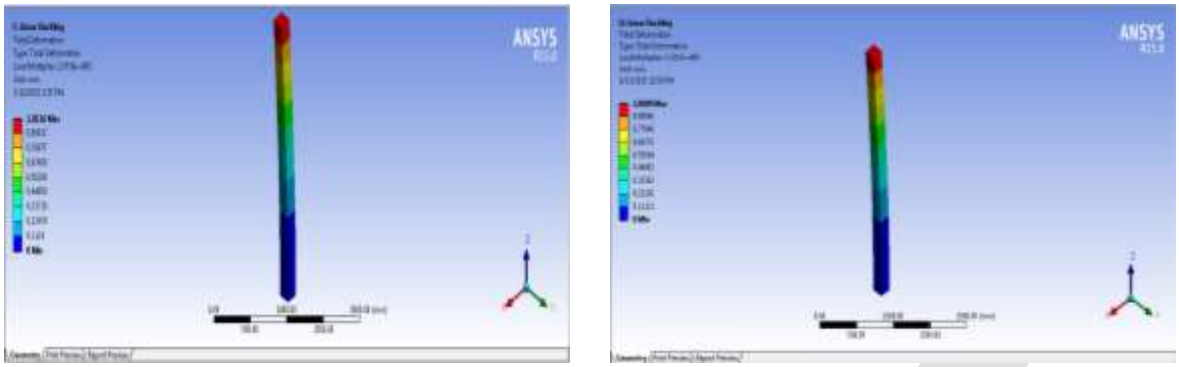

Fig.7.5.One layer and two layers GFRP jacketed square RC column subjected to axial loading.

From the above results we can conclude that GFRP jacketing increases the load carrying capacity of all columns of different cross-sectional shapes. Load carrying capacity increases when two layer GFRP jacketing is provided compared to one layer GFRP jacketing. Hence the load carrying capacity of one and two layer GFRP jacketed RC columns increases in the order of square, circular and rectangular. Load increment of one layer GFRP jacketing increases in the order of rectangular, square and circular.

7.1.3 CFRP Jacketed RC Column subjected to Axial Loading

CFRP jacketed RC columns of rectangular, square, and circular crossection was axially loaded to find out the ultimate load carrying capacity.

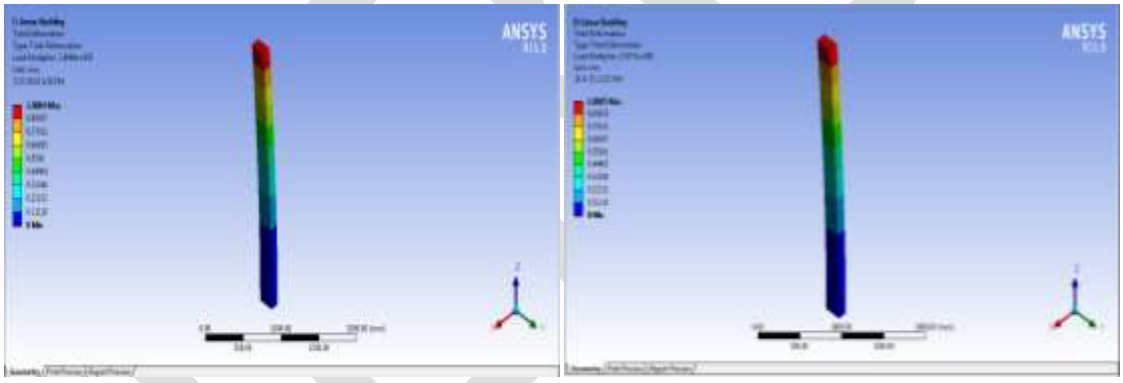

Fig.7.6.One and two layers CFRP jacketed rectangular RC column subjected to axial loading.

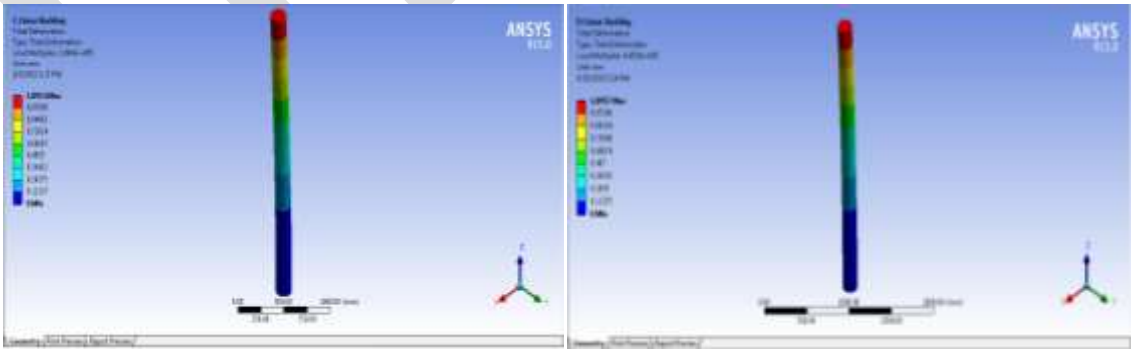

Fig.7.7.One and two layers CFRP jacketed circular RC column subjected to axial loading.

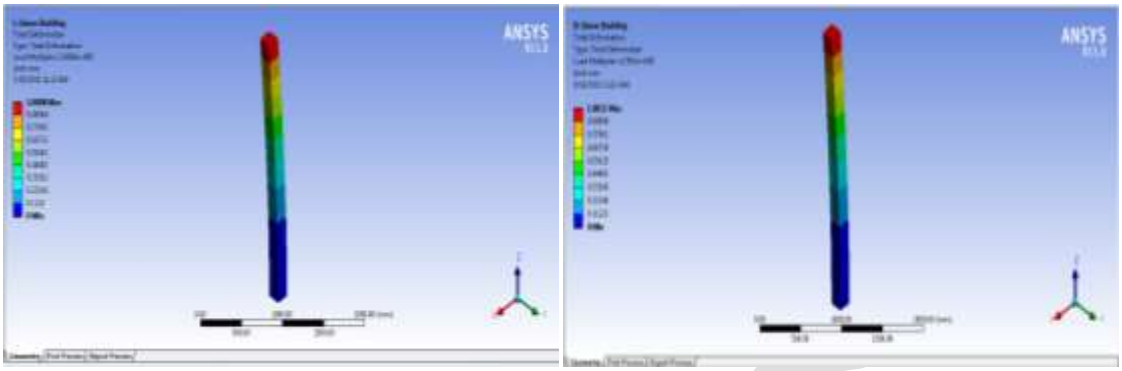

Fig.7.8.One and two layers CFRP jacketed square RC column subjected to axial loading.

From the above results we can conclude that CFRP jacketing also increases the load carrying capacity of all columns of different cross-sectional shapes. Load carrying capacity increases when two layer CFRP jacketing is provided compared to one layer CFRP jacketing. Hence the load carrying capacity of one and two layer CFRP jacketed RC columns increases in the order of square, circular and rectangular. Load increment of one layer CFRP jacketing increases in the order of rectangular, square and circular.

FRP jacketing increases the load carrying capacity of all RC columns subjected to axial loading. The percentage increase in load carrying capacity is shown in **Table 7.2**.

Table.7.2. Percentage increase in load carrying capacity of columns under axial loading.

Column c/s Shape	Jacketing Provided	No. of Layers of FRP Jacketing	Ultimate Load Carrying Capacity (kN)	% Increase in Load Carrying Capacity
Rectangular	Control	-	140.94	-
	GFRP	1	164.23	16.52
		2	199.27	41.38
	CFRP	1	249.49	54.49
		2	293.73	77.01
Circular	Control	-	257.48	-
	GFRP	1	287.87	11.80
		2	318.57	23.72
	CFRP	1	399.98	55.34
		2	445.38	72.97
Square	Control	-	262.52	-
	GFRP	1	297.36	13.27
		2	333.17	26.91
	CFRP	1	369.08	40.59
		2	479.52	82.66

7.2. RC COLUMN SUBJECTED TO ECCENTRIC LOADING

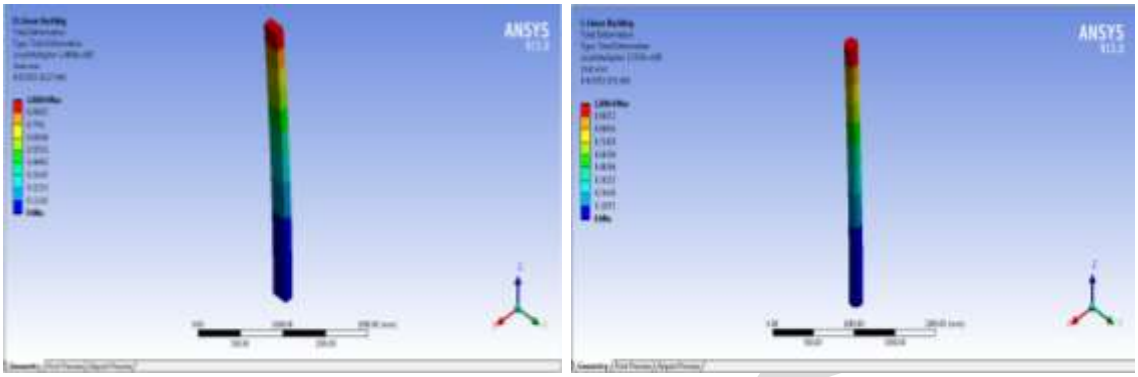

Fig.7.9.Rectangular and circular RC column subjected to eccentric loading.

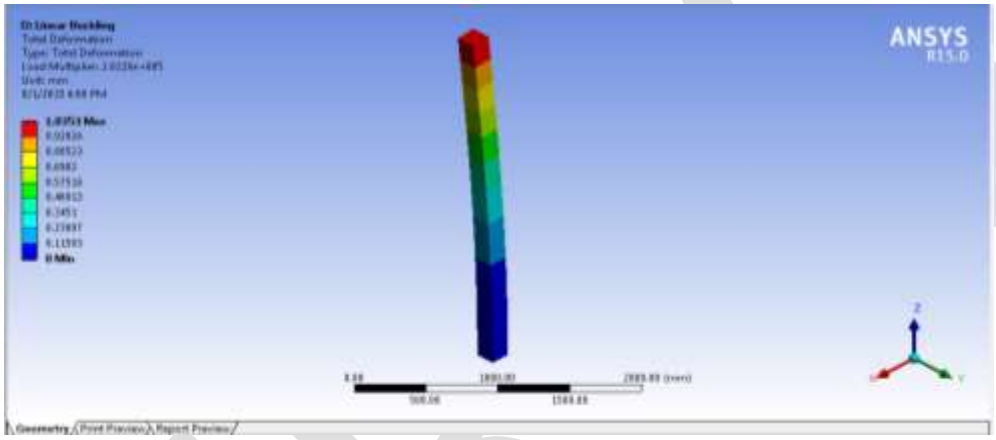

Fig.7.10.Square RC column subjected to eccentric loading.

Eccentric loading decreases the load carrying capacity compared to axial loading in all RC columns of different cross-sectional shapes and the load carrying capacity of RC columns in eccentric loading increases in the order of square, circular and rectangular.

7.2.1 GFRP Jacketed RC Column subjected to Eccentric Loading

GFRP jacketed RC columns of rectangular, square, and circular cross-section was eccentrically loaded to find out the ultimate load carrying capacity

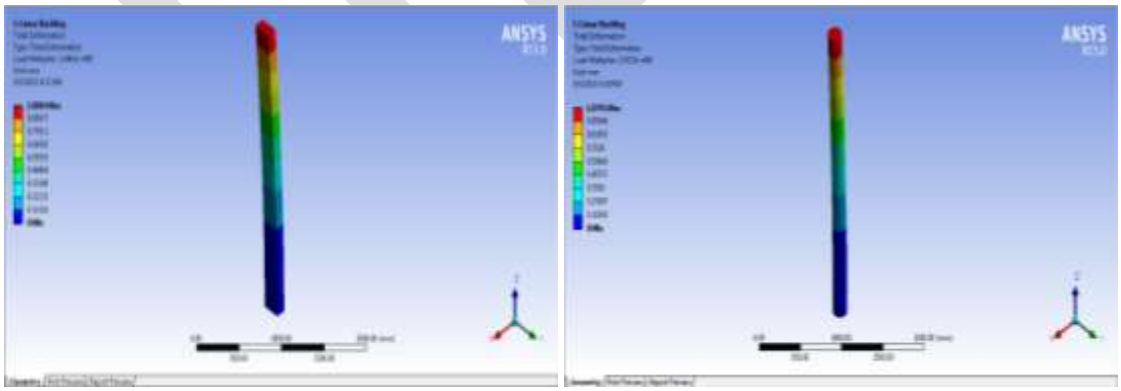

Fig.7.11.GFRP jacketed rectangular and circular RC column subjected to eccentric loading.

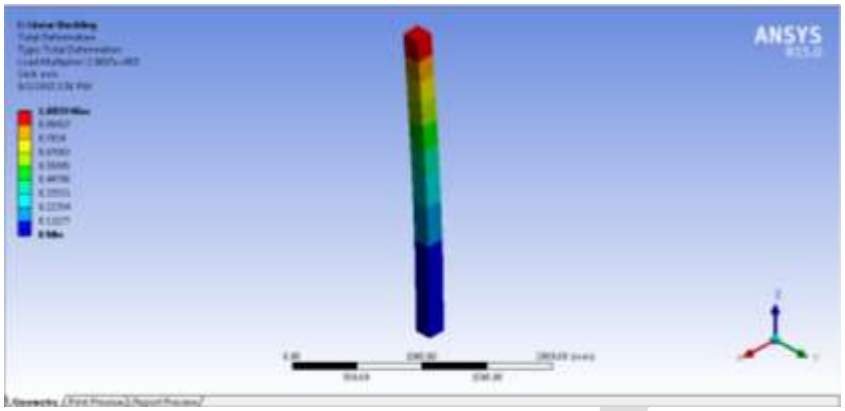

Fig.7.12.GFRP jacketed square RC column subjected to eccentric loading.

From the above results we can conclude that GFRP jacketing increases the load carrying capacity of all columns subjected to eccentric loading of different cross-sectional shapes. Hence the load carrying capacity of GFRP jacketed RC columns increases in the order of square, circular and rectangular.

7.2.3 CFRP Jacketed RC Column subjected to Eccentric Loading

CFRP jacketed RC columns of rectangular, square, and circular cross-section was eccentrically loaded to find out the ultimate load carrying capacity.

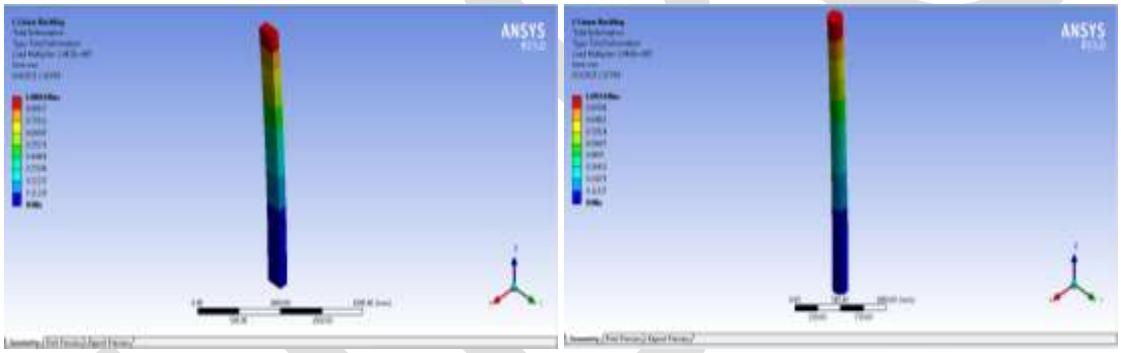

Fig.7.13.CFRP jacketed rectangular and circular RC column subjected to eccentric loading.

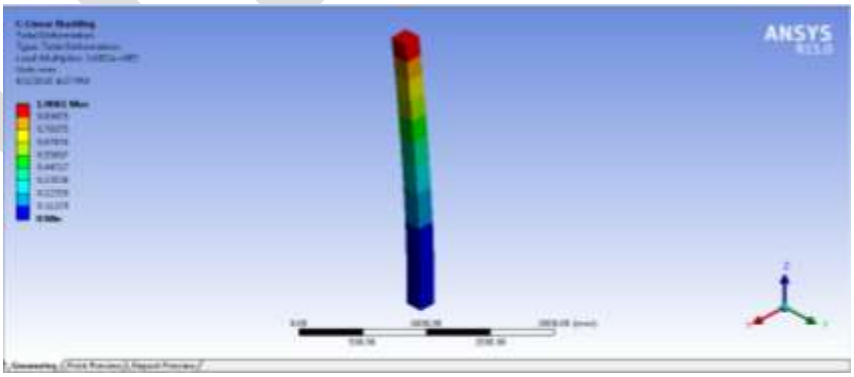

Fig.7.14.CFRP jacketed square RC column subjected to eccentric loading.

From the above results we can conclude that CFRP jacketing also increases the load carrying capacity of all columns subjected to eccentric loading of different cross-sectional shapes. Hence the load carrying capacity of CFRP jacketed RC columns increases in the order of square, circular and rectangular.

FRP jacketing increases the load carrying capacity of all RC columns subjected to eccentric loading. The load carrying capacity of RC column subjected to eccentric loading is less than column subjected to axial loading. The percentage increase in load carrying capacity is shown in **Table 7.3**.

Table.7.3. Percentage increase in load carrying capacity of columns under eccentric loading.

Column c/s Shape	Jacketing Provided	Ultimate Load Carrying Capacity (kN)	% Increase in Load Carrying Capacity
Rectangular	Control	140.88	-
	GFRP	164.63	16.85
	CFRP	249.25	76.92
Circular	Control	257.65	-
	GFRP	287.23	11.48
	CFRP	399.43	54.91
Square	Control	262.26	-
	GFRP	296.97	13.23
	CFRP	368.52	40.51

ACKNOWLEDGEMENTS

The authors would like to thank the Civil Engineering Department of Sree Narayana Gurukulam College of Engineering for giving them the opportunity to conduct and complete the work.

8. CONCLUSION

- Load carrying capacity of control RC columns increases in the order of square, circular, rectangular.
- GFRP and CFRP jacketing enhances the axial load carrying capacity by providing additional confinement without increasing the column size.
- Effective confinement with GFRP and CFRP jacketing resulted in improving the compressive strength. GFRP and CFRP jacketing for square columns produced progressive increase in axial load carrying capacity followed by circular and rectangular columns.
- From this study it can be concluded that the eccentricity in loading reduces the load carrying capacity and performance of RC columns.
- RC column jacketing with FRP sheets also increases the load carrying capacity when subjected to eccentric loading.
- CFRP jacketing is found to be more effective than GFRP in case of both axial and eccentric loading.
- CFRP jacketed rectangular RC column provides higher increment in load carrying capacity followed by circular and square RC column compared to GFRP jacketing in axial and eccentric loading.
- Thus, it can be recommended from the study that FRP jacketing is a very good alternative for strengthening of existing square, circular and rectangular RC column and it helps in economical construction by concrete reduction in designing new RC columns.

REFERENCES:

[1]. R. Kumutha, R. Vaidyanathan, M.S. Palanichamy., (2007), " Behaviour of reinforced concrete rectangular columns strengthened using GFRP, Cement & Concrete Composites 29, 609–615.

[2]. Atri Dave, Poojan Nagar, Jay Parmar (2014), "Comparative study of GFRP laminated RC column using Experimental results and ISIS-canada", International Journal of Research in Engineering and Technology, 700 – 704.

[3]. A. Belouar, A. Laraba, R. Benzaid, and N. Chikh (2013), "Structural Performance of Square Concrete Columns Jacketed with CFRP Sheets", Procedia Engineering 54 ,232 - 240

[4]. K. P. Jaya, Jessy Mathai, (2012), "Strengthening of RC Column using GFRP and CFRP", Journal of Materials in Civil Engineering, ASCE. 334-342.

[5]. Khaled Abdelrahman, and Raafat El-Hacha, M. (2012), "Behavior of Large-Scale Concrete Columns Jacketed with CFRP and SFRP Sheets", J. Compos.Constr.16,430-439.

[6]. Ida Bagus Rai Widiarsa, and Muhammad N.S. Hadi (2013), "Performance of CFRP Jacketed Square Reinforced Concrete Columns Subjected to Eccentric Loading", Procedia Engineering 54, 365 – 376.

[7]. Mohamed H. Harajli., (2006), " Axial stress–strain relationship for FRP confined circular and rectangularconcrete columns ", Cement & Concrete Composites 28, 938–948.

[8]. Rahul Raval , Urmil Dave (2013), "Behavior of GFRP jacketed RC Columns of different shapes", Procedia Engineering 51 ,240 – 249.

[9]. Ashraf Mohamed Mahmoud., (2012), " Strengthening of concrete beams having shear zone openings using orthotropic CFRP modeling", Ain Shams Engineering Journal, 177–190.

[10]. Amir Fam, Bart Flisak and Sami Rizkalla., (2005). " Experimental and Analytical Modelling of Concrete-Filled FRP Tubes Subjected to Combined Bending and Axial Loads", Journal of Structural Engineering , 583-599.

[11]. Chris P. Pantelides, Zihan Yan, Lawrence D. Reaveley, (2014), " Shape Modification of Rectangular columns confined with FRP composites ", International Journal of Civil and Structural Engineering, 1, 3, 449-457.

[12]. Kinjal V Ranolia , B K Thakkar, J D Rathod (2013), "Effect of Different Patterns and Cracking in FRP Jacketing on Compressive Strength of Confined Concrete", Procedia Engineering 51 , 169 – 175.

[13]. Ahmed Shaban Abdel-Hay (2013) "Partial strengthening of R.C square column using CFRP", Production and hosting by Elsevier B.V. on behalf of Housing and Building National Research Center, pp.279-286.

[14]. G. P. Lignola, A. Prota ,G. Manfredi and E. Cosenza (2007), "Experimental Performance of RC Hollow Columns Confined with CFRP", Journal of Composites for Construction , 42-49.

International Journal of Engineering Research and General Science Volume 3, Issue 5, September-October, 2015
ISSN 2091-2730

One Time Password Generation for Multifactor Authentication using Graphical Password

Nilesh B. Khankari[1], Prof. G.V. Kale[2]

[1,2]Department of Computer Engineering, Pune Institute of Computer Technology,

Pune, India

[1]nilesh111khankari@gmail.com, [2]gilkale@gmail.com

Abstract— Single factor authentication such as password authentication is no longer considered as secure in the Internet world. There is a rapid growth in demand for strong authentication on the highly critical web-based applications. A higher level security mechanism is needed to access the financial and banking applications. Existing system provides authentication mechanism based on the static password, personal identification number (PIN) etc. These methods are vulnerable against eavesdropping and replay attack. In this work, a two factor authentication scheme is proposed for user authentication. The presented scheme generates dynamic password for two factor authentication. This scheme will provide user assurance of authentication and will improve authentication level. The proposed scheme provides strong protection against cryptanalysis.

Keywords— Security and protection, Authentication, Graphical Password.

INTRODUCTION

Authentication is process in which right user will be given access to resource. During authentication only authorize user will get access to resources. There are various types of methods available for authentication. Multifactor authentication uses the combination of more than one technique for authentication. More than one form of authentication used in multifactor authentication that's why multifactor authentication. Multifactor authentication provides extra layer of authentication which minimizes risk in risk based authentication.

In today's world to access critical resources authentication is required. To secure our critical resources more secure authentication is necessary. Authentication is process in which authorized user (i.e user which has rights to access particular resource) will be given access to resource. During authentication only authorize user will get access to resources. For example user who needs to perform internet banking operations is required to provide authentication details to access his internet banking account.

In this paper, we analyzed current existing authentication schemes, proposed an effective dynamic user authentication scheme. The proposed system generates dynamic password using seed factors which are associated to graphical password and random string. Thus using this proposed scheme identity and access manager system will be secured from Brute-force attack, especially Perfect-Man-In-The-Middle attack.

RELATED WORK

There are various types of techniques established for authentication. Most widely used and traditional authentication technique is alphanumeric password. This password consists of secret series of characters. The user id and password act as user identification and authentication to access required resources. This technique secures resources but it has many disadvantages .In this technique user picks password which is easily guessed and vulnerable to shoulder surfing. When user selects difficult to guess text password then it is hard for user to remember password and thus compel the users to write them down, which impairs their secrecy. Also dictionary attack, brute force attack, spyware is possible in this method. Password can also be system generated but these passwords are difficult to remember.

To overcome the problems related to traditional text password method some researchers developed authentication methods that uses pictures as password. [2], proposed recognition based a graphical password mechanism. In this user is asked to select certain no of images from given set of images as a password. Later, for authentication user has to select previously selected images. Graphical passwords are more difficult to break using the traditional attack methods such as brute force search, dictionary attack, or spyware.

Another way for authentication is biometric based authentication. Biometric based authentication uses certain physiological or behavioral characteristics which are unique for each person [3].

Luigi Catuogno and Clemente Galdi proposed a PIN-based mechanism is presented that uses a secret sequence of objects to analyze security vs. usability. This work does not consider the use of contextual information to influence the generation of the challenge [4]. Jakobsson M., et.al introduced the notion of implicit authentication that consists in authenticating users based on behavioral patterns [5]. Xuguang Ren, Xin-Wen Wu proposed generation of dynamic OTP. They have considered user's password, the authenticating time, as well as a unique property that the user possesses at the moment of authentication (for example, the MAC address of the machine that the user uses for authentication) to generate OTP. This system effectively protects user's account against various attacks such as phishing attack, reply attack, and perfect-man-in-the-middle attack [6]. Hayashi E., et.al present a framework is presented that combines passive factors (e.g. location) and active factors (e.g. tokens) in a probabilistic model for selecting an authentication scheme that satisfies security requirements; however, it does not consider client device constraints [7]. Huiyi L. and Yuegong Z proposed scheme which uses two one-way hash functions, one is a hash chain-which is the core of the authentication scheme, and the other is used to secure the hash chain for information transmission between the user and server. This scheme provides functions of bidirectional identity authentication and presents higher security and lower computational cost [8]. Yair H., et.al proposed context-aware multi-factor authentication scheme based on a Dynamic PIN. The scheme presented in this paper produces a graphical challenge for this authors considered context, client device constraints, and risk associated [9]. Jeonil Kang, et.al in this paper, a two-factor face authentication scheme using matrix transformations and a user password is suggested [10]. Soon-Nyean Cheong, et.al presented a secure two-factor authentication NFC smartphone access control system using digital key and the proposed Encrypted Steganography Graphical Password [11].

MATHEMATICAL MODEL

Let S be a system such that S ={s, e, X, Y, C, R, f, $f_{friend,}$| Φ}
Where, s is the start state.
e is end state.
X is Input of the system.
Y is output of the system.
f is set of functions in the system.
$f_{friend,}$ is set of friend function used in system.
Φ is constrains to the system.

C= (I_1, I_2…I_n) be a set of n image objects.
Where I_i is image object which can be icon, animal picture etc.

R = (r_1, r_2…r_n) be the vector of seeds.
Where r_i is seed factor related to each image object I_i.

X = {Pass}
Pass is the password entered by user. Pass⊂ C

Y = {DynPass}
DynPass is dynamic password generated by system.

f_{friend} = {S(X), Rand}

S is Rijndael substitution box function which takes 2byte number(X) as input and generates 1byte number.

Rand is function used to generate random number or string.

f = {Challenge(C), V (Pass), G (UserPassword, RS)}

Challenge function will generate image challenge for user for authentication. Input for this function is C i.e. set of image objects. Output of this function will be ChallengeImages.

ChallengeImages=Union(SecretImages,NonSecretImages) with cardinality |q+p|

|SecretImages|=q, |NonSecretImages|=p

V is validation function which validates user.
SecretImages is set of images selected as a password when user registered as a new user.
If Pass = SecretImages then user is validated. If user is authorized user then it generates UserPassword.
UserPassword is 2 bytes long number, that is, each hexadecimal digit hex_i is a nibble (half byte).

$$\text{UserPassword}=\text{XOR}\ (r_1,r_2,r_3,\ldots..r_{|\text{secretImages}|})$$
$$= hex_1 hex_2 hex_3 hex_4$$

G is dynamic password generation function. This function takes UserPassword and RS as input.
RS is random generated 8 byte string.
$RS = RB_0RB_1RB_2\ldots RB_7$ where RB_i is a byte.
So output of function G is DynPass.
DynPass = $byte_1 byte_2 byte_3 byte_4$.

This password is generated using S-Box function S(X). Each $byte_i$ digit is computed from 4 substitutions between UserPassword (2 bytes long) and 2 bytes of RS and 4 iterations through the s-box S(X) then after XOR operation will be performed on results of 4 iterations. Fig. 1 shows the sequence of iterations and substitutions to produce $byte_1$. In the diagram each arrow indicates one iteration through S(X). During each iteration, S(X) takes as input one byte consisting of two nibbles: a hexadecimal digit of UserPassword and a nibble of RB_i; and outputs a new byte, hereafter S_i. The following are the 4 iterations performed to generate $byte_1$.

$$S(hex_1, RB^H_0)=S_1$$
$$S(hex_2, RB^L_0)=S_2$$
$$S(hex_3, RB^H_1)=S_3$$
$$S(hex_4, RB^L_1)=S_4$$

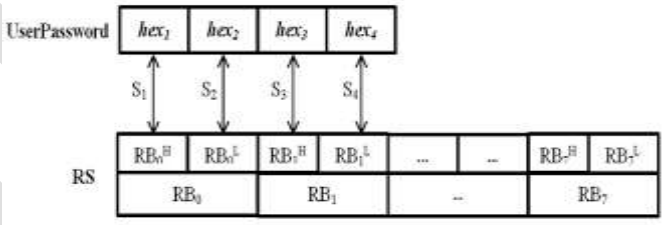

Fig.1 Chain of iterations to generate $byte_1$

$$(S_1 \text{ XOR } S_1 \text{ XOR } S_1 \text{ XOR } S_1) = byte_1$$

PROPOSED SYSTEM

As per survey, current existing systems have problems and don't give more randomness. So I have proposed a new multifactor authentication method which has more randomness.

Proposed system has 2 phases: 1. Registration and 2. Login.

1. Registration :

1.1 Registering the Image-Based Password(s). The user is presented with image objects C. A randomly generated number is linked with each image object I_i. Let $R = (r_1, r_2 \ldots r_n)$ be the vector of seeds. Length of each r_i is 2 bytes and represented as 4 hexadecimal digits. User has to select number of images as a password from given images.

2. Image Challenge and Dynamic Password Generation:

Steps:

i. The server generates a random string (RS) and the graphical challenge. The RS is used as part of the dynamic password generation algorithm. The challenge is constructed by combining secret and non-secret images.
ii. The user is asked to recognize the secret images.
iii. The crypto-function is then used to generate the dynamic password.
iv. The client device sends the dynamic password to the server for validation.

2.1 Generation of RS and Image Challenge:

- Random Strings: RS is pseudo-randomly generated string of 8 bytes.
  $RS = RB_0RB_1RB_2 \ldots RB_7$ where RB_i is a byte.

- Image Challenge:
  This step will generate image challenge for user for authorization. Challenge function will generate image challenge.

2.2 User Response to Challenge:

- User responds to the challenge by selecting secret images.
- Algorithm selects random number linked with secret images and performs XOR operation on them to generate UserPassword.

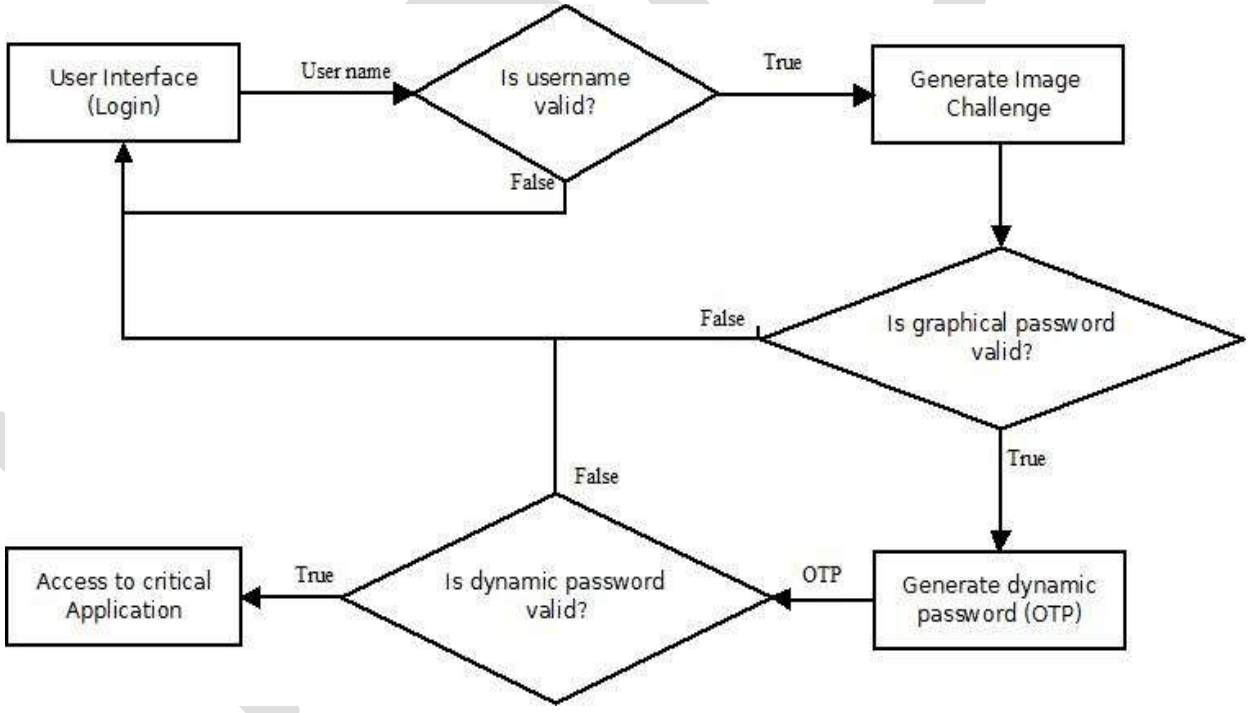

Fig.2 System flow

2.3 Generation of Dynamic Password:

A Substitution Box (S-Box) is a component used in cryptosystems to perform substitutions in a way that relations between output and input bits are highly non-linear. This protects against cryptanalysis. An S-Box designed to be resistant to linear and differential cryptanalysis is the Rijndael S-Box. Function G will generate dynamic password.

RESULTS AND ANALYSIS

Fig.3 shows image challenge generated for user authorization In proposed system images are recognized in random order (not sequentially). Numbers of possible combinations are $! / (n - q)! q!$.

Fig.3 Image challenge

In proposed system user has to recognize 5 icons from 25 provided icons. So p=5, q=20 and n=25 i.e. 53130 combinations are possible. UserPassword is generated after valid graphical password is entered. UserPassword is number generated by performing XOR operation 5 random numbers which are linked with 5 secret images. Suppose this 5 random numbers are 21546, 31289, 12678, 30876, 20369 on this 5 numbers XOR operation will be performed and this will generate number 10100010011000 which is in binary format. As mention in mathematical model generated number after performing XOR operation on 5 random numbers and RS are inputs to function G. Function G will generate dynamic password.

CONCLUSION

Here, we have analyzed the disadvantages of existing authentication schemes, proposed an effective dynamic user authentication scheme. The proposed system integrates the security techniques Image Based Password Authentication and one time password based on Image Based Password. The proposed system generates dynamic password (OTP) using seed factors which are associated to graphical password and random string. Thus using this proposed scheme critical application will be secured from Replay attack, Dictionary attack, Brute-force attack, especially Perfect-Man-In-The-Middle attack. Using proposed dynamic password generation scheme there is improvement in user assurance of authentication.

REFERENCES:

[1] X. Suo, Y. Zhu, and G. S. Owen, "Graphical passwords: A survey," Computer Security Applications Conference, 21st Annual. IEEE, pp. 10-19, 2005.

[2] R. Dhamija and A. Perrig, "Deja Vu: A User Study Using Images for Authentication," Proceedings of 9th USENIX Security Symposium, 2000.

[3] Wayman, J., Jain, A. K., Maltoni, D., & Maio, D. (Eds.). (2004). Biometric systems: Technology, design and performance evaluation. New York: Springer.

[4] Luigi Catuogno, Clemente Galdi,"A Graphical PIN Authentication Mechanism with Applications to Smart Cards and Low-Cost Devices", Information Security Theory and Practices. Smart Devices, Convergence and Next Generation Networks, LNCS, vol. 5019, pp. 16–35, 2008.

[5] Jakobsson M., Shi E., Golle P., Chow R.," Implicit authentication for mobile devices", Proceedings of the 4th USENIX Conference on Hot Topics in Security, p. 9. USENIX Association, 2009.

[6] Xuguang Ren, Xin-Wen Wu, "A Novel Dynamic User Authentication Scheme", International Symposium on Communications and Information Technologies, pp. 713-717, 2012.

[7] Hayashi E., Das S., Amini S., Hong J., Oakley, "CASA: context-aware scalable au-thentication", Proceedings of the Ninth Symposium on Usable Privacy and Security, pp. 1–10. ACM, Newcastle 2013.

[8] Huiyi L., Yuegong Z., "An Improved One-time Password Authentication Scheme", Proceedings of ICCT, pp 1-5, 2013.

[9] Yair H. Diaz-Tellez, Eliane L. Bodanese, Theo Dimitrakos, Michael Turner, "Context-Aware Multifactor Authentication Based on Dynamic Pin", IFIP Advances in Information and Communication Technology, Volume 428, pp 330-338,2014.

[10] Kang, J., Nyang, D., Lee, K., "Two-factor face authentication using matrix permutation transformation and a user password", Information Science. 269, pp. 1–20, 2014.

[11] Cheong, Soon-Nyean, Huo-Chong Ling, Pei-Lee The, "Secure Encrypted Steganography Graphical Password Scheme for Near Field Communication smartphone access control system", Expert Systems with Applications 41.7, pp. 3561-3568, 2014.

[12] Khankari, Nilesh, and Geetanjali Kale, "Survey on One Time Password", International Journal of Computer Engineering and Applications, Volume 9, Issue 3, March 15

International Journal of Engineering Research and General Science Volume 3, Issue 5, September-October, 2015
ISSN 2091-2730

In vitro anti-cancer activity of ethanolic extract of curcumin longa (turmeric) in HEp-2 cell lines

Pragya Srivastava[1], Ayush Srivastava[2]

G.C.R.G. Memorial Trust Group Institution, Lucknow, U.P.[1], MVN University, Palwal, Haryana[2]

pragyasrivastava851@gmail.com[1], ayush.srivastava@mvn.edu.in, +918221067344[2]

Abstract— Curcumin, an active constituent of Curcuma longa, is responsible for the anticarcinogenic activities which are mediated through multiple mechanisms. The cytotoxicity tests were performed in this experiment which defines the upper limit of the extract concentration, which can be used in subsequent anticancer studies. In vitro cytotoxic activity of turmeric extracts against Hep2 cancer cell lines were evaluated in this experiment. Hep2 cells were treated with different concentration of plant extracts and morphological changes were observed under inverted microscope. First, the cell viability check was done with the trypan blue and then different concentrations of turmeric extracts were treated with MTT (3 4, 5dimethylthiazolyl2)2,5diphenyltetrazoliumbromide) and NRU (Neutral Red Uptake). The test sample showing cytotoxicity of more than 97% at 1000µg/ml, were considered to be less active at minimum concentration. At last DNA fragmentation method was used to determine the induction of apoptosis inside the cell.

Keywords— MTT (3 4, 5dimethylthiazolyl2)2,5diphenyltetrazoliumbromide), NRU (Neutral Red Uptake), Anti-cancer activity, Curcumin longa, apoptosis, ethanolic extracts, cytotoxicity

INTRODUCTION

Cancer is a leading cause of death worldwide and had accounted for 7.9 million deaths (approximately 13% of all deaths) in 2007. Most drugs currently available for the treatment of cancer have limited potential, because they are highly toxic, inefficient in treating cancer, or highly expensive. Treatments without these disadvantages are needed. Hence, the identification and synthesis of novel, efficient and less toxic anticancer agents remains an important and challenging task for the cancer treatment. Use of plant extracts as medicine for cancer treatment is certainly the effective method and dozens of plant based products have been reported for cancer treatment progress. Plant based products such as curcumin occupied significant role against cancer, microbial infections and other inflammatory diseases. Due to its wide range of biological and pharmacological effects and lack of toxicity, curcumin was selected for this study. Curcumin is a naturally occurring yellow pigment isolated from the rhizome of the perennial herb Curcuma longa which has been cultivated for centuries in several Asian countries.

Curcumin is known for its antioxidant, anti-inflammatory, anti-fatigue, antiparasitic, antiallergic, anti-microbial, anti-mutagenic and anticancer properties. It exhibits wide therapeutic potential due to the multi-targeting nature against variety of different cancers including leukemia, gastrointestinal cancers, genitourinary cancers, breast cancer, etc. Curcumin has been shown to suppress transformation, proliferation, and metastasis of tumors. It also inhibits proliferation of cancer cells by arresting them in various phases of the cell cycle and by inducing apoptosis. It is obvious that curcumin's multitargeting ability may be the key to its therapeutic potential against cancer. An ethanolic extract of turmeric, as well as an ointment containing curcumin, is reported to produce remarkable symptomatic relief in patients with external cancerous lesions. It is now proved that the antioxidants present in turmeric neutralize carcinogenic free radicals.

Curcuminoids possess anti-carcinogenic property due to their oxygen radical-scavenging property. In a comparative study of curcuminoids for their free radical-scavenging activity, turmeric is found to be the most potent free radical scavenger, followed by dimethoxycurcumin and bis-demethoxy curcumin. Acetyl curcumin was found inactive. Reports showed the use of turmeric preparations in the treatment of cancer. In the course of a search for antitumor agents, the extract of turmeric was found to be effective in inducing apoptosis or programmed cell death (PCD) in human myeloid leukemia cells (HL - 60). Curcuminoids protect the normal human keratinocytes from hypoxanthine/xanthine oxidase injury. Further, they proposed that since curcuminoids synergistically

inhibited nitrobluetetrazolium reduction, a decrease in superoxide radical formation, leading to lower levels of cytotoxic hydrogen peroxide, might explain the protective effect.

REVIEW OF LITERATURE

Cancer is the uncontrolled cell proliferation and production of a growing mass cell. Cancer cells can break away and spread to other body parts, particularly in the blood stream and lymphatic system, causing metastatis. Over the years, different approaches have been employed and are still in use, individually or in combination, in the treatment of cancer. These include chemotherapy, radiotherapy, surgery and immunotherapy. Plants have a long history of use in the treatment of cancer and the interest in nature as a source of potential chemotherapeutic agent continues. The present day research and development tailored towards the discovery of new anti proliferative agents from natural products has been buoyed by improvement in science and technology of anticancer drug discovery. Cancer initiation has been produced by oxidative stress and chronic inflammation. Inflammation acts a key regulator in promotion of these initiated cells, possibly by providing them with proliferating signals and by preventing apoptosis. The role of inflammation in tumor induction and subsequent malignant progression has been investigated. Inflammatory response produces cytokines which act as growth and/or angiogenic factors leading transformed cells to proliferate and undergo promotion.

Turmeric (Curcuma longa) is extensively used as a spice, food preservative and coloring material in India, China and South East Asia. It has been used in traditional medicine as a household remedy for various diseases, including cough, diabetic wounds hepatic disorders. Curcumin (diferuloylmethane), the main yellow bioactive component of turmeric has been shown to have a wide spectrum of biological actions and isolated from the rhizome of the plant Curcuma longa. These include its anti-inflammatory, antioxidant, anticarcinogenic, anticoagulant, antifertility, antidiabetic, antibacterial, antifungal, antiprotozoal, antiviral, antifibrotic, antivenom, antiulcer, hypotensive and hypocholesteremic activities. Its anticancer effect is mainly mediated through induction of apoptosis. Safety evaluation studies indicate that curcumin is well tolerated at a very high dose without any toxic effects. Thus, curcumin has the potential for the development of modern medicine for the treatment of various diseases. Curcumin longa, botanically related to ginger (Zingiberaceae family), is a perennial plant having a short stem with large oblong leaves and bears ovate, pyriform or oblong rhizomes, which are often branched and brownish-yellow in color. Curcumin (diferuloylmethane) (3–4%) is responsible for the yellow color.

It exhibits wide therapeutic potential due to the multi-targeting nature against variety of different cancers including leukemia, gastrointestinal cancers, genitourinary cancers, breast cancer, etc. Curcumin has been shown to suppress transformation, proliferation, and metastasis of tumors. It also inhibits proliferation of cancer cells by arresting them in various phases of the cell cycle and by inducing apoptosis. It is obvious that curcumin's multitargeting ability may be the key to its therapeutic potential against cancer. Curcumin induced apoptosis mainly involves the mitochondria-mediated pathway in various cancer cells. Curcumin causes Hep2 cells to develop characteristic features of cell shrinking, rounding and partial detachment, thus demonstrating the lobulated appearance of apoptotic cells. Curcumin was found to inhibit the generation of ROS including superoxide dismutase and hydrogen peroxide in peritoneal macrophages. It inhibits lipo-polysaccharide and interferon-γ-induced production of nitric oxide in macrophages and inhibition of inducible nitric oxide synthase gene expression in isolated BALB/c mouse peritoneal macrophages. Curcumin prevents phosphorylation and degradation of inhibitor κ B α, thereby blocking NF-κB activation which down regulates iNOS gene transcription. Deregulatory imbalances between adaptive and innate immunity results in chronic inflammation, is associated with epithelial tumorigenesis, through the NF-κB activation. Curcumin was found to inhibit cell proliferation and cytokine production by inhibiting NF- κB target genes involved in this mitogen induction of Tcell proliferation, interleukin and nitric oxide generation. Reduction induced over expression of cytokines, such as IL-10, IL-6, and IL-18, is accompanied by NF-κB induction which is controlled by and inhibited by curcumin. Curcumin has been demonstrated to increase expression of conjugation enzymes (phase II). These have been shown to suppress ROS-mediated NF-κB, AP-1 and mitogen activated protein kinases (MAPK) activation.

For the last few decades, extensive work has been done to establish the biological activities and pharmacological actions of turmeric and its extracts. Curcumin was first isolated in 1815 and its chemical structure was determined by Roughley and Whiting in 1973. It has a melting point at 176–177° C; forms a reddish-brown salt with alkali and is soluble in ethanol, alkali, ketone, acetic acid and chloroform. Turmeric was already proved beneficial in various types of cancers like duodenal tumors, tongue carcinoma, colon cancer, human breast cancer cells in-vitro, mammary tumor in vivo.

Fig. 1. Curcumin longa

Curcumin has been shown to promote apoptosis in certain cancer cell lines and to inhibit telomerase activity, an important factor in tumorigenesis. One possible mechanism for the induction of tumor cell death is through the generation of reactive oxygen intermediates. Although curcumin is the acknowledged active principal in turmeric, the oleoresin of turmeric (after extraction of curcumin) also was found to have anti mutagenic properties, thought to be mediated through its antioxidant action.

The anti-inflammatory properties of curcumin are thought to be due in part to suppression of prostaglandin synthesis. Prostaglandin synthesis from arachidonic acid is catalyzed by two isoenzymes: COX-1 and COX-2, both found in colon tumors of rodents and humans. Goel et al found that curcumin significantly inhibited expression of COX-2 in human colon cancer cell and in COX-2 non-expressing cell lines, without altering the expression of COX-1. This is an important benefit of curcumins since chronic use of nonsteroidal anti-inflammatory drugs (NSAIDs) and non-specific inhibition of COX-1 lead to undesirable gastrointestinal and renal side effects. Curcumin also was shown by Mahady et al to inhibit the growth of Helicobacterpylori, a group carcinogen, as a possible explaining mechanism for its role in prevention of gastric and colon cancers in rodents. Animal studies involving rats and mice, as well as in vitro studies utilizing human cell lines, have demonstrated curcumin's ability to inhibit carcinogenesis at three stages: tumor promotion, angiogenesis, and tumor growth. In two studies of colon and prostate cancer, curcumin inhibited cell proliferation and tumor growth. Turmeric and curcumin are also capable of suppressing the activity of several common mutagens and carcinogens in a variety of cell types in both in vitro and in vivo studies. The anticarcinogenic effects of turmeric and curcumin are due to direct antioxidant and free-radical scavenging effects, as well as their ability to indirectly increase glutathione levels, thereby aiding in hepatic detoxification of mutagens and carcinogens, and inhibiting nitrosamine formation

CELL LINE AND ITS ROLE IN SCREENING

Hep2 cell line is the required cell line and it was: Originated from tumors produced in irradiated-cortisonised weanling rats after injecting with epidermoid carcinoma tissue from the larynx of a 56 year old male. This cell line was found to be indistinguishable from HeLa by STR PCR DNA profiling. Therefore, the cell line should be considered as derived from HeLa. HeLa contaminant; adherent; Cells contain human papilloma virus. The cells are positive for keratin by immunoperoxidase staining. The base medium for this cell line is ATCC-formulated Eagle's Minimum Essential Medium (EMEM).

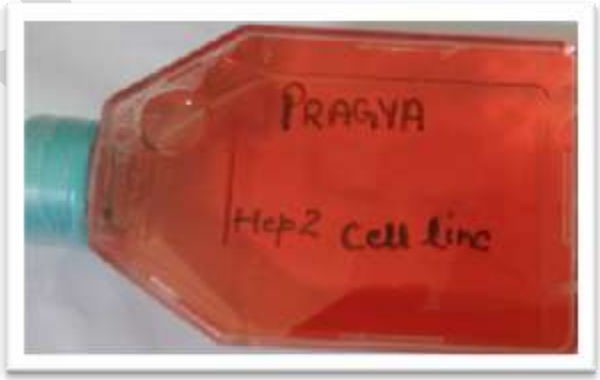

Fig. 2. Cultured hep2 cell line

The purpose of this study was to evaluate, in vitro the efficacy of turmeric extract as anti cancer agent in hep2 cell line. Most drugs currently available for the treatment of cancer have limited potential, because they are highly toxic1, inefficient in treating cancer, or highly expensive. Treatments without these disadvantages are needed.

Hence, the identification and synthesis of novel, efficient and less toxic anticancer agents remains an important and challenging task for the cancer treatment. Use of plant extracts as medicine for cancer treatment is certainly the effective method and dozens of plant based products have been reported for cancer treatment progress.

Since the plant based products have the natural multi-targeting ability as well as inexpensive and is safe as compared to synthetic agents. Among them, plant based products such as curcumin occupied significant role against cancer, microbial infections and other inflammatory diseases.

MATERIALS AND METHODS

F. Plant Extraction

Curcuma longa plant rhizome collected from Biotech Park Lucknow, dried at room temperature were grind and powdered. The plant material 6g was loaded in the inert tube of soxhlet apparatus and then filtered into round bottom flask containing 200ml acetone. The solvent were boiled gently over a water bath using the adjustable rheostat. The extraction was continues for 8 hours and solvent was removed at the reduced pressure with the help of vacuum pump distillation.

G. Chemicals

Trypan blue, Ladder

Trypsin

Eagle's Minimum Essential Media

DMSO

1% Glacial Acetic Acid

MTT (3 4, 5 dimethylthiazolyl2)2,5diphenyltetrazoliumbromide)

NRU (Neutral Red Uptake)

Isopropanol

Lysis Buffer

40% ethanol

RNAase

Proteinase

Sodium acetate

TE buffer

EtBr

H. Cell Culture

Cell culture media are complex mixtures of salts, carbohydrates, vitamins, amino acids, metabolic precursor, growth factors, hormones and trace elements. The requirement for these components varies among cell lines, and these differences are partly responsible for the extensive number of medium formulations. Carbohydrates are supplied primarily in the form of glucose. In some instances, glucose is replaced with galactose to decrease lactic acid build-up, as galactose is metabolized at a slower rate. Other carbon sources include amino acids and pyruvate.

In addition to nutrients, the medium helps maintain the pH and osmolality in a culture system. The pH is maintained by one or more buffering system; CO2/Sodium bicarbonate, phosphate and HEPES are the most common.

Eagle's Minimum Essential Medium (EMEM) was among the first widely used media was formulated by Harry Eagle from his earlier and simpler basal medium there have numerous variations on EMEM formula for different applications. EMEM contains balanced salt solution, non essential amino acids, and sodium pyruvate.

I. Passaging

To culture our cell lines the trypsinization process will be done first and or EMEM media will be added. After the centrifugation the supernatant will be discarded and in the pellet again the complete media will be added and two other flask will be prepared process is called subculturing.

J. Cell viability count

It is a blue colour dye which is used in the haemocytometer to estimate the cell viability. To estimate the cell viability first we mix the cell suspension and the trypan blue dye then load the mixture into the haemocytometer and estimate the viability the cell into the inverted microscope.Case-Study.

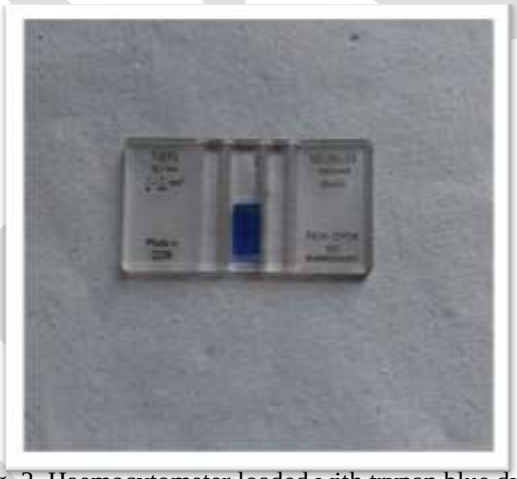

Fig. 3. Haemocytometer loaded with trypan blue dye

K. MTT Assay

Measurement of cell viability and proliferation forms the basis for numerous in vitro assays of a cell population's response to external factors. The reduction of tetrazolium salts is now widely accepted as a reliable way to examine cell proliferation. The yellow tetrazolium MTT (3 4, 5 dimethylthiazolyl2)2,5diphenyltetrazoliumbromide) is reduced by metabolically active cells, in part by the action of dehydrogenase enzymes, to generate reducing equivalents such as NADH and NADPH. The resulting Intracellular purple formazan can be solubilized and quantified by spectrophotometric means. The MTT Cell Proliferation Assay measures the cell proliferation rate and conversely, when metabolic events lead to apoptosis or necrosis, the reduction in cell viability.

L. Treatment schedule

In my experiment there are six treatment groups first one is control group in which 40% ethanol is added, second one is T1 group in which 20mg/ml concentration of turmeric extract will be added, third one is T2 group in which 2mg/ml concentration of turmeric

extract will be added, fourth group is T3 group in which 0.2 mg/ml concentration of turmeric extract will be added, fifth group is T4 group in which 0.02mg/ml concentration of turmeric extract will be added and last group is positive control group in 2µl paclitaxin will be added which is a anticancer drug.

Fig. 4. Stock solution for the treatment

M. Procedure of MTT Assay:

100µl cell suspension will be added into 96 well plates and leave it for one day. When the cell will grow properly the new media will be added and the treatment will be given to the cell lines. After 20 hours the MTT will be added and leave it for 2 h. After 2 h the yellow color MTT becomes blue in color then the whole media will be taken out properly without damaging the present cells into the well plate and then 100 µl DMSO will be added. Mix the DMSO and cells properly and take the reading into the ELISA reader.

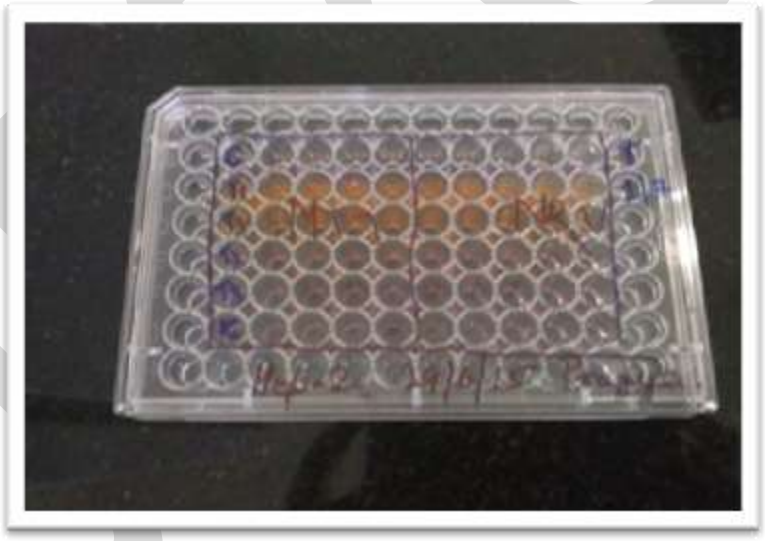

Fig. 5. 96 Well plate after the treatment of MTT

N. NRU ASSAY

The neutral red uptake assay provides a quantitative estimation of the number of viable cells in a culture. It is one of the most used cytotoxicity tests with many biomedical and environmental applications. It is based on the ability of viable cells to incorporate and bind the supra vital dye neutral red in the lysosomes. Most primary cells and cell lines from diverse origin may be successfully used. Cytotoxicity is expressed as a concentration dependent reduction of the uptake of NR after chemical exposure, thus providing a sensitive, integrated signal of both cell integrity and growth inhibition.

Cells are seeded in 96-well tissue culture plates and are treated for the appropriate period. The plates are then incubated for 2 h with a medium containing neutral red. The cells are subsequently washed, the using a spectrophotometer.

O. Treatment schedule

The same treatment is given to the NRU also which will be described above in MTT ASSAY.

P. Procedure used for NRU ASSAY

100µL cell suspension will be added into the 96 well plate and leave it for overnight. Next day fresh media will be added and the treatment will be given as described above and leave it for 20 hours. Then the NR will be added and leave it for 4 hours and then the whole medium will be taken out properly without disturbing the cell lines and then 100µl, 1% Glacial Acetic Acid in 40% acidified alcoh ol and reading will be taken into the ELISA reader.

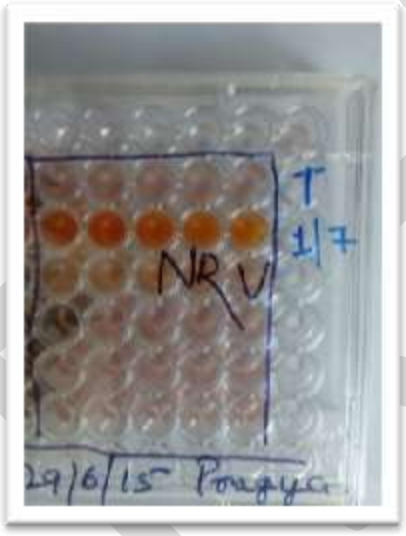

Fig. 6. 96 Well plate after the treatment of NRU

Fig. 7. While recording the absorbance into the ELISA reader

Q. DNA Fragmentation Assay

It is the separation or breaking of DNA into pieces. It can be done intentionally by laboratory personell or by cells. DNA fragmentation was first documentated by Williamson in 1970 when he observed discrete oligomeric fragments occurring during cell death in primary neonatal liver cultures. He described the cytoplasmic DNA isolated from mouse liver cells after culture as

characterized by DNA fragments with a molecular weight consisting of multiples of 135 Kda. This finding was consistent with the hypothesis that these DNA fragments were a specific degradation product of nuclear DNA.

R. Treatment schedule

In this experiment there were 5 treatment groups, first one is control in which 40% ethanol will be added, second one is turmeric extract at the concentration of 20 mg/ml, third one is 10 times less than the T1 i.e. 20 mg/ml and the fourth one is ten times more less than the T2 i.e. 2 mg/ml and the last one is at the concentration of 0.2 mg/ml.

S. Procedure used for the DNA fragmentation

The precultured cells were first trypsinized then plated into the 6 well plate (1.5 ml/well) and leave it for overnight. Next day media will be changed and the treatment will be provided as discussed above and leave it for 24 h. Then the media will be discarded and 200 µl lysis buffer will be added for the cell scrapping and washing and collect it into the 5 different eppendrofs, then RNAase will be added (2µl) and incubate it for 1h after the time duration Proteinase (2µl) will be added and again incubate it for 1h. After all this treatment centrifuge the sample at 10,000 rpm for 10 min. Then take the supernatant and add sodium acetate (50µl) and Isopropanol (200µl). Now the strands of DNA will be isolated again centrifuge it, now discard the supernatant and add 70% ethanol Again centrifuge it discard the supernatant and dry pellet, then add t he TE buffer and take the re ading into the nano drop.

Fig. 8. 6 Well plate after the treatment

Fig. 9. Eppendrofs containing lysis buffer

T. Agarose gel electrophoresis

First 30mg agarose was dissolved in 30ml distilled water and 75µl TE buffer. Boil the solution until it became transparent then add0.5µl and pour 15ml agarose into the casting tray. After 15-20 min place you're casting tray into the electrophoresis unit and load your sample into the wells. When then gel will run take the reading into gel documentation system.

	Conc.(ng/µl)	sample volume for400ng DNA	Amount of loading Dye	Amount to loaded into gel
C	87.2	4.6	0.458716	5.0
T1	40.9	9.8	0.977995	10.8
T2	33.7	11.9	1.186944	13.1
T3	23.8	16.8	1.680672	18.5
T4	90.9	4.4	0.440044	4.8

Fig. 10. Reading of sample loaded in gel electrophoresis

Fig. 11. Gel casting

Fig. 12. Gel electrophoresis unit

RESULTS

A. For cell viability count

100% viability was found

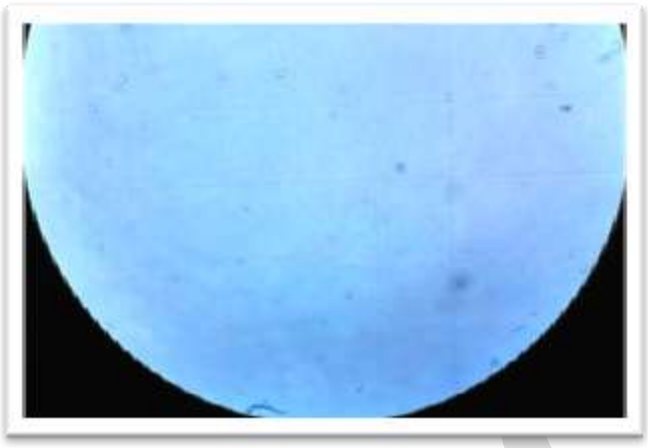

Fig. 13. Cells under the inverted microscope

B. MTT Assay

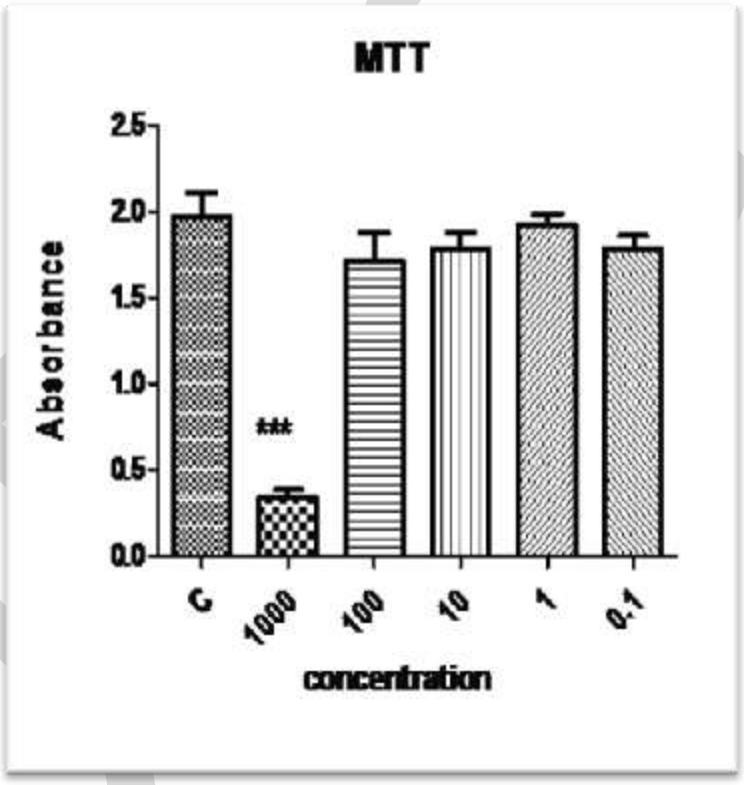

Fig. 14. Graph Showing MTT result

Extract of turmeric was treated with MTT at different concentration and maximum significant death was found at 1000µg/ml as compared to low concentration. Very less amount of viable cells were detected at this concentration which shows the maximum inhibition concentration. While decreasing the concentration of curcumin to and the viability of the cell showing negligible amount of cell death and minimum lethal dose.

C. NRU Assay

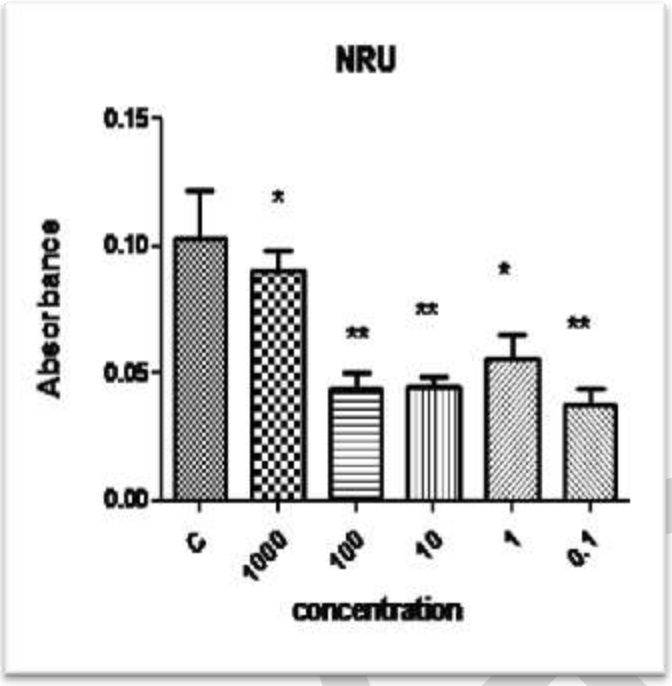

Fig. 15. Graph showing NRU result

Extract of turmeric when treated with NRU then significant death of cells was observed at low concentrations also.

D. DNA Fragmentation assay

Fig. 16. While taking the reading into the nanodrop spectrophotometer

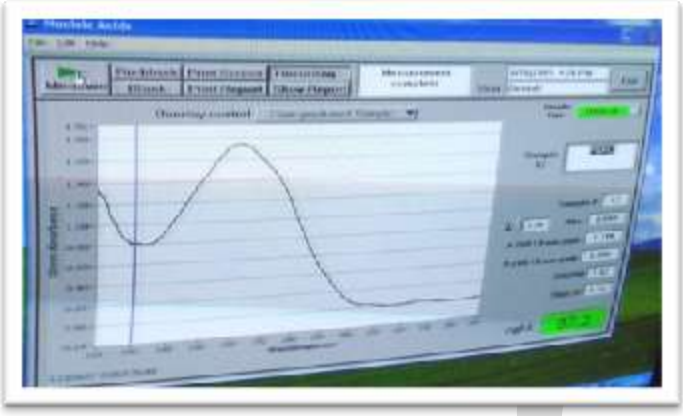

Fig. 17. Nano drop reading for control

Control contains the pure DNA there is no contamination of the RNAase and Proteinase because the 260/280 ratio is 1.82

E. Nano drop reading

Table 1. Data of DNA samples in Nano drop spectrophotometer

concentration	ABSORBANCE	260nm	280nm	260/280nm	260/230nm
C	0.808	1.744	0.956	1.82	2.16
T1	0.394	0.818	0.448	1.82	2.08
T2	0.332	0.674	0.366	1.84	2.03
T3	0.251	0.476	0.285	1.67	1.90
T4	0.201	0.344	0.199	1.62	1.80

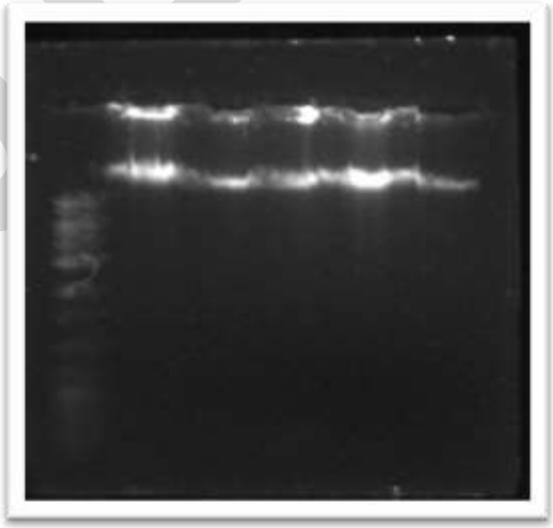

Fig. 18. DNA bands of gel documentation

DISCUSSION

Previous studies has indicated that the turmeric has the ability to induce the apoptosis in very cancerous cell lines like HL-60, HELA etc. Curcumin is the principal component present in turmeric which posses the anticarcinogenic property. The cytotoxicity study was carried out with the Hep2 cell lines at different concentrations which indicated that it inhibits the cell growth at 1 mg/ml. Furthermore, DNA fragmentation assay also indicated the fragmentation of DNA at the same dose.

CONCLUSION

Based on the reported results, it may be concluded that pure curcumin and the crude ethanolic extract have great potential in the prevention and cure of cancer. At higher dose of curcumin on cancerous cell line apoptosis has been started inside the cells and the maximum reduction of growth shows. We therefore conclude that plant extracts showed selective in-vitro cytotoxicity against Hep2 cancer cell lines and plants were found to be highly effective against various cancerous cells. However, there is further in-vivo studies are also needed to ensure the anti-tumorogenic property of turmeric in cancerous cell line.

REFERENCES:

[1] Ayyadurai, N., Valarmathy, N., Kannan, S. & Jansirani, D. Evaluation of cytotoxic properties of Curcuma longa and Tagetes erecta on cancer cell line (Hep2). 7, 736–739 (2013).

[2] Hare, B. et al. The domestication hypothesis for dogs' skills with human communication: a response to Udell et al. (2008) and Wynne et al. (2008). Anim. Behav. 79, (2010).

[3] Shay, J. W. et al. Telomerase and cancer. Hum. Mol. Genet. 10, 677–85 (2001).

[4] Ramachandran, C., Fonseca, H. B., Jhabvala, P., Escalon, E. A. & Melnick, S. J. Curcumin inhibits telomerase activity through human telomerase reverse transcritpase in MCF-7 breast cancer cell line. Cancer Lett. 184, 1–6 (2002).

[5] Wootton, J. T., Parker, M. S. & Power, M. E. Wooton et al. 1996.pdf. Science 273, 1558–1561 (1996).

[6] Ruby, A. J., Kuttan, G., Babu, K. D., Rajasekharan, K. N. & Kuttan, R. Anti-tumour and antioxidant activity of natural curcuminoids. Cancer Lett. 94, 79–83 (1995).

[7] Use, T. M. Anticancer Potential of Turmeric. 2, (2003).

[8] Jangle, S. N. A a o c. 2, (2010).

[9] Agarwal, N., Majee, C. & Chakraborthy, G. S. Natural herbs as anticancer drugs. Int. J. PharmTech Res. 4, 1142–1153 (2012).

[10] Steffi, P. F. & Srinivasan, M. CURCUMIN , A POTENT ANTICARCINOGENIC POLYPHENOL – A REVIEW. 7, 1–8 (2014).

[11] Chattopadhyay, I., Biswas, K., Bandyopadhyay, U. & Banerjee, R. K. Turmeric and curcumin : Biological actions and medicinal applications. 87, (2004).

[12] Kuttan, R., Bhanumathy, P., Nirmala, K. & George, M. C. Potential anticancer activity of turmeric (Curcuma longa). Cancer Lett 29, 197–202 (1985).

[13] Goel, A., Boland, C. R. & Chauhan, D. P. Specific inhibition of cyclooxygenase-2 (COX-2) expression by dietary curcumin in HT-29 human colon cancer cells. Cancer Letters 172, 111–118 (2001).

[14] Kuttan, R., Bhanumathy, P., Nirmala, K. & George, M. C. Potential anticancer activity of turmeric (Curcuma longa). Cancer Lett. 29, 197–202 (1985).

[15] Yang, W. L. & Frucht, H. Activation of the PPAR pathway induces apoptosis and COX-2 inhibition in HT-29 human colon cancer cells. Carcinogenesis 22, 1379–1383 (2001).

[16] Mohiuddin, E., Asif, M. & Sciences, A. CURCUMA LONGA AND CURCUMIN : A REVIEW ARTICLE. 55, 65–70 (2010).

[17] Bar-Sela, G., Epelbaum, R. & Schaffer, M. Curcumin as an anti-cancer agent: review of the gap between basic and clinical applications. Curr. Med. Chem. 17, 190–197 (2010).

[18] Type, A. & Collection, C. MTT Cell Proliferation Assay Instruction Guide. 6597, 1–6

[19] Repetto, G. et al. Neutral red uptake assay for the estimation of cell viability / cytotoxicity . Neutral red uptake assay for the estimation of cell viability / cytotoxicity. (2008). doi:10.1038/nprot.2008.75

[20] Shrishail, D., K, H. H., Ravichandra, H., Tulsianand, G. & Shruthi, S. D. TURMERIC : NATURE ' S PRECIOUS MEDICINE. 6, (2013).

International Journal of Engineering Research and General Science Volume 3, Issue 5, September-October, 2015
ISSN 2091-2730

A Novel ROM based DDFS Architecture for Portable and Wide band Communication

Parameshwara M. C[*] and Srinivasaiah H. C[+]

*Assistant Professor, Department of E & CE, Vemana Institute of Technology, VTU, Bangalore-34, Karnataka, India.

*Email:pmcvit@gmail.com, Phone: +919620902171

[+]Professor, Department of TCE, Dayananda Sagar College of Engineering, VTU, Bangalore-78, Karnataka, India.

[+]Email:hcsrinivas@gmail.com

Abstract— In this paper we propose a novel architecture for 'Read Only Memory (ROM)' based 'Direct Digital Frequency Synthesizer (DDFS)' based on simple sine trigonometric approximation formula. In this proposed architecture, to synthesize the sine wave from 0 to π/2 we use the sine samples from 0 to π/4 and the cosine samples from 0 to π/4, a digital multiplier, and a scaling block. Further the quarter wave symmetry of the sine wave is explored to derive the remaining samples that are required to synthesize the sine wave from π/2 to 2π. In the proposed DDFS architecture the sine and cosine samples are stored in two separate ROMs this saves the ROM area about 14.6 % than the traditional ROM based DDFS where the single ROM is used to store the sine samples from 0 to π/2. Further at every input clock cycle one sample from each ROM is read and multiplied to generate the first quadrant sine samples corresponding to an angle [0, π/2) with magnitude being mapped to [0, 0.5) this results in doubling the frequency of the output signal with the magnitude being halved. Further the halved magnitude of the output sine wave can be restored to full scale [0, 1) by using a scaling factor of '2' (or multiplied by 2). To verify and validate our proposed novel concept we have designed and simulated an 11-bit DDFS using MATLAB-Simulink tool. The calculated SFDR for the plotted frequency spectrum of the designed 11-bit DDFS is -66 db.

Keywords— Direct Digital Frequency Synthesizer, DDFS, Frequency synthesizer, sine ROM, cosine ROM, sine -approximation, SFDR.

1. INTRODUCTION

The tremendous growth in modern wireless communications [1] and the rapid advancements in semiconductor IC technologies [2] have made direct digital frequency synthesizers (DDFSs) as an inevitable choice for frequency synthesis. The traditional communication systems are augmented with analog phase locked loop frequency synthesizers (PLLs) because of their high output frequency capabilities and high spectral purity. In spite of these advantages the analog PLLs suffer from various issues like long frequency tuning time, high phase noise, closed loop stability issues and also bulky when implemented [5-20]. On the other hand the DDFSs offer many promising advantages viz. fine frequency steps in sub-hertz range, fast frequency switching times, smooth frequency transitions, ease of fabrication, low cost, and low power. Thus these advantages of DDFSs have made them an indispensable integral part of modern high speed digital communication systems. The simplified block diagram of standard DDFS is shown in Fig.1. This block diagram has been derived from Joseph Tierney et al. [3]. The DDFS shown in Fig.1 has an 'L' bit phase accumulator, a phase to sine amplitude mapper (or converter), a linear digital to analog converter (DAC), and a low pass filter.

Further depending on how the 'M' bit phase accumulator output is mapped onto corresponding sine amplitude of 'K' bits, the traditional DDFS are classified into two types, viz. digital recursion and direct computation based DDFSs. The digital recursion based DDFS such as CORDIC based DDFS suffer from phase noise issues. On the other hand the direct computation based DDFSs are less sensitive to phase noise where the sine samples are directly computed and stored in ROM look-up table. The stored samples are used to synthesize the digital sine wave. The sine samples can be directly computed by using the following equation [3].

$$exp\left[j\left(\frac{2\pi}{N}\right)[nk+C]\right] = cos\left(\left(\frac{2\pi}{N}\right)[nk+C]\right) + j\,sin\left(\left(\frac{2\pi}{N}\right)[nk+C]\right).$$

Where 'k' is the frequency index, 'n' is the time index, 'N' is a design parameter, and 'C' is a constant. The direct computation based

standard DDFS architectures are further classified into three main types viz. ROM, ROM less, and sine computation based architectures.

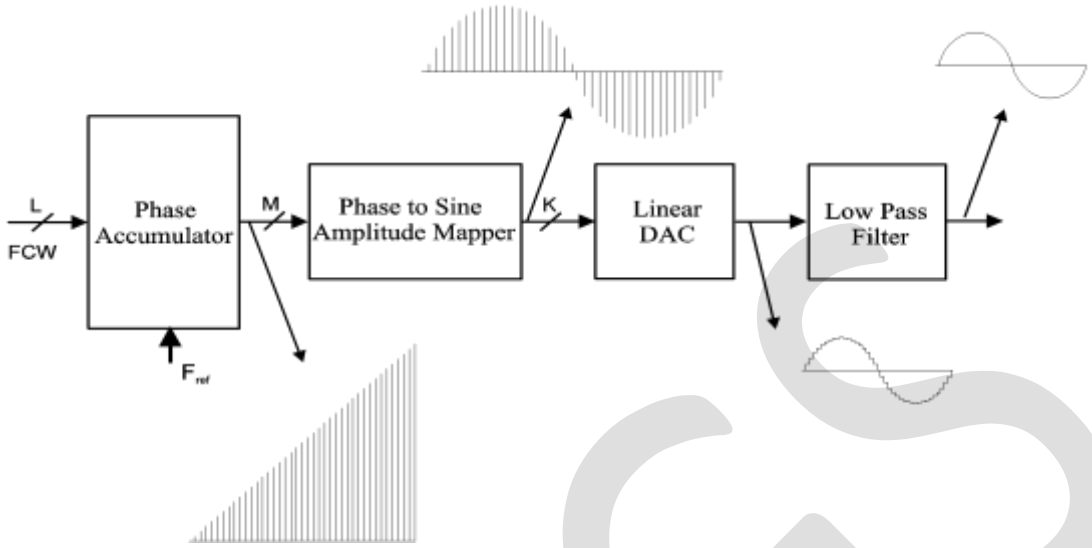

Fig. 1. Simplified block diagram of direct computation based standard DDFS [3].

In the aforementioned classification the ROM less and the sine computation based architectures are more complex and tedious in terms of hardware design and implementation. Whereas the ROM based DDFS architectures are simple in terms of hardware and hence easy to design and implement. The critical block in ROM based architectures is the ROM block that store the sine samples required to synthesize the sine output. The two parameters that affect the performance of ROM based DDFS are the size of ROM look up table and the ROM word access time. The size of the ROM look up table can be decided based on the number of words that are required to store and number of binary bits that are needed to represent each ROM word. The ROM size doubles for every 1-bit increase in input address word. The ROM word access time is the important parameter that decides the maximum frequency of operation of the ROM based DDFS. The ROM word access time is exponentially proportional to the size of the ROM. Thus it is very important to reduce the size of the ROM and hence to minimize the ROM word access time to improve the overall performance of the DDFS. In the till date literature, there are several state-of-the art ROM compression algorithms listed and are available to optimize the size of the ROM such algorithms are [5-18]:

- ROM compression using phase truncation
- Sine-phase difference
- Coarse-Fine ROM using Hutchinson algorithm
- Coarse-Fine ROM using Sunderland algorithm
- Coarse-Fine ROM using Nicholas algorithm
- Double Trigonometric approximation
- Quad line approximation
- Langlois's technique
- Liao's technique
- Parabolic approximation
- Quantization and Error ROM techniques

In this paper we propose a novel architecture for ROM based DDFS using simple trigonometric approximation. The proposed architecture uses two sub ROMs namely sine-ROM (ROM-1) and cosine-ROM (ROM-2), a multiplier, and a scaling block. In this architecture the ROM-1 stores the sine samples only from 0 to $\pi/4$ and ROM-2 stores the cosine samples only from 0 to $\pi/4$, thus saving about 14.6 % overall size of the ROM as compared to conventional ROM based architectures. The ROM word access time is also reduced which ultimately enhances the speed of the DDFS.

Rest of this paper is organized as follows: Section-2 presents the conventional ROM based DDFS architecture and its salient features. Section-3 describes about the concept of the proposed architecture of the DDFS. Section-4 discusses the MATLAB-simulink based implementation of the proposed architecture with 11 bit DDFS as a case study. Finally conclusions are drawn in section -5.

2. CONVENTIONAL ROM BASED DDFS ARCHITECTURE

The block diagram of conventional ROM based DDFS [5] is as shown in the Fig. 2. The block diagram consists of an 'M' bit phase accumulator, a π/2 sine ROM look-up table, an 'M-2' bit phase complementor, and an 'N-1' bit sine amplitude complementor. The DDFS has two inputs viz. an 'L' bit frequency control word (FCW) and a reference clock (F_{ref}). The phase accumulator accumulates an 'L' bit FCW on every cycle of F_{ref} and overflows after $2^L - 1$ clock cycles. Thus the phase accumulator generates $2^L - 1$ sine ROM addresses for each overflow and generates maximum number of addresses when FCW=1. For example if L =32 bit and FCW=1 then the phase accumulator generates 2^{32}-1 ROM word addresses. Further corresponding to $2^L - 1$ address locations we need to store the sine samples in the π/2 sine ROM and considering again the aforementioned example with L=32 bit and FCW =1, we need to store about 2^{32}-1 sine samples which is ~4 billion words. Thus, it is highly impractical to store all the words because the ROM size becomes very huge. Further the larger ROM size leads to higher power dissipation and longer word access time and hence not suitable for portable and wideband applications, where power, speed, and bandwidth (BW) are more critical. Thus one has to reduce the ROM size to fit DDFS in the aforementioned applications. There are many state-of-the art ROM compression techniques that are available to reduce the size of the ROM look up table. The Foremost technique is the phase truncation where the LSBs of the phase accumulator output are truncated to reduce the number of phase addresses required to scan the ROM, this introduces an error called 'phase truncation error'. Thus to reduce the size of the ROM look-up table phase truncation is inevitable.

In the Fig. 2 at the output of the phase accumulator 'M' most significant bits (MSBs) would be retained after the phase truncation of appropriate number of least significant bits (LSBs). Thus the phase accumulator is now required to address 2^M address locations instead of original $2^L - 1$ address locations, this greatly reduces the size of ROM look-up table at the cost of phase truncation error. Further the first two MSBs (M1 and M2) out of M bits are used to explore quarter wave symmetry of the sine wave by controlling the phase and sine amplitude complement blocks. The second MSB M2 is used to control phase complement, M2 = '0' implies phase increment and M2 = '1' implies phase decrement. The first MSB M1 is used to control sine amplitude complement, M1= '0' implies sine amplitude increment or decrement in the first half cycle of the sine wave and M1= '1' implies second half cycle of the sine wave. The M-2 output bits of the phase complementor are used to generate address locations for the π/2 sine ROM, thus the maximum number of address locations that are generated corresponding to FCW=1 is 2^{M-2}-1 and hence sine ROM needs to be stored only 2^{M-2}-1 words instead of $2^L - 1$. The 'N-1' number of bits is used to represent each word in π/2 sine ROM. Thus the total size of the π/2 sine ROM is given by $(2^{M-2}-1) \times (N - 1)$ bits. Thus the DDFS finally synthesizes an 'N" bit sine wave at its output and the frequency of the synthesized output signal is given by

$$F_{out} = FCW \times F_{res}$$

Where F_{res} is the frequency resolution and is give by

$$F_{res} = \frac{F_{ref}}{2^L}$$

Since the DDFS is basically a sampled system and hence the minimum frequency at which DDFS operates is dictated by Nyquist theorem. Thus the minimum frequency ($F_{ref} = F_{min}$) of the input clock signal that is required to operate DDFS should be at least equal to twice the maximum frequency of the DDFS output signal. However this is just a theoretical limit but in practice for all practical purposes the limitation on input reference clock is given by [4].

$$F_{ref} = F_{min} \geq 2.5 \times max(F_{out})$$

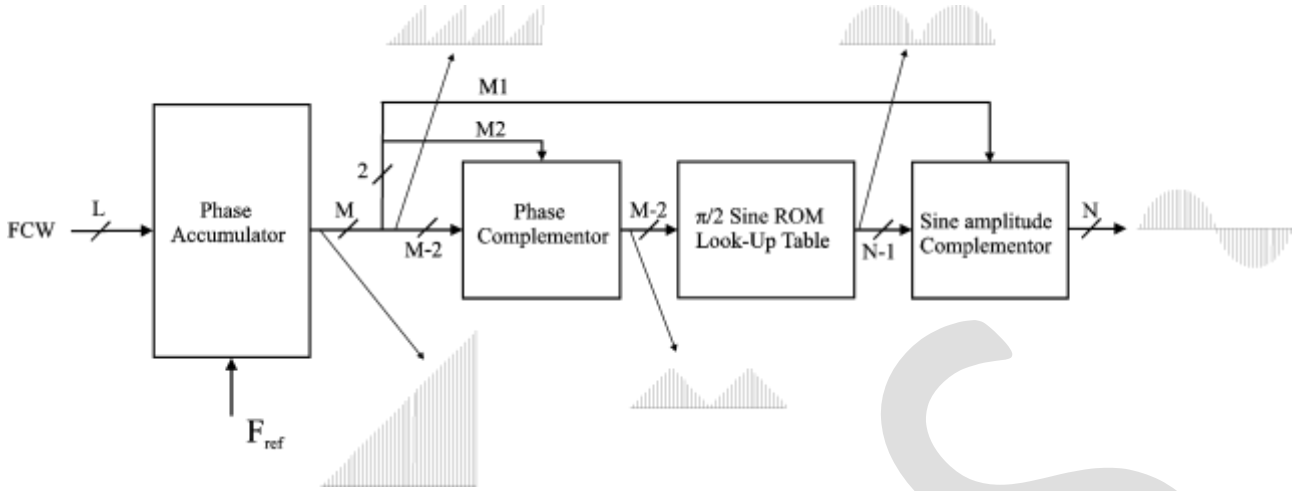

Fig. 2. Simplified block diagram of the conventional ROM based DDFS using sine quarter wave symmetry [5].

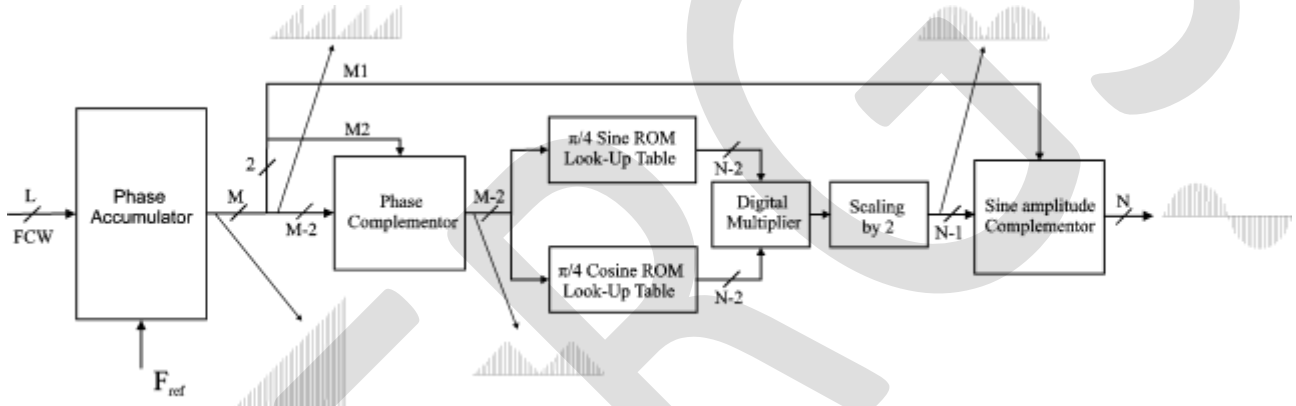

Fig. 3. Block diagram of proposed novel ROM based DDFS using sine quarter wave symmetry.

3. PROPOSED NOVEL ROM BASED DDFS ARCHITECTURE

The block diagram of the proposed novel architecture of ROM based DDFS is as shown in Fig. 3. This block diagram is derived based on sine trigonometric formula. Let us consider the sine angle summation formula, that is

$$sin(A + B) = \sin A \cos B + \cos A \sin B$$

Where 'A' and 'B' are two angles and suppose if $A = B$ then,

$$sin(A + A) = \sin A \cos A + \sin A \cos A$$

$$sin(2A) = 2 \sin A \cos A$$

Thus by using the above concept we can express $sin\left(\frac{\pi}{2}x\right)$ that is used to derive the samples to store in a π/2 sine ROM look-up table as

$$sin\left(\frac{\pi}{2}x\right) = 2\, sin\left(\frac{\pi}{4}x\right) cos\left(\frac{\pi}{4}x\right)$$

where 'x' is the phase value in the range [0, 1). Thus, we can express a π/2 sine ROM look-up table into a π/4 sine sub ROM look-up table and a π/4 cosine sub ROM look-up table.

The block diagram of proposed ROM based DDFS architecture derived based on the above concept is shown in the Fig. 3. The Fig. 3 consists of an 'M' bit phase accumulator, a phase complementor, a sine amplitude complementor, a π/4 sine sub ROM, a π/4 cosine sub ROM, a digital multiplier, and a scaling block. The M-2 bits of the phase accumulator are used to address two sub ROM blocks.

Each sub ROM stores $2^{M-2} \times N$-2 bits. The output of two sub ROM blocks are applied to the digital multiplier and subsequently scaled up by a factor 2 in order to map the amplitude of the samples corresponding to an angle between [0 $\pi/2$). At the output of scaling block N-1 bits should be retained and remaining bits would be truncated. Finally with N-1 bits along with the first MSB M1 are used to synthesize the N –bit sine wave. The main advantages of this architecture can be explained below:

- The ROM size is reduced as compared to conventional DDFS architecture, for example if M=10 and N=8, then conventional DDFS ROM requires to store $(2^{M-2}-1) \times (N-1) = (2^8-1) \times 7 = 1785$ bits, where as the proposed DDFS ROM stores $(2^{M-3}-1) \times (N-2) \times 2 = (2^7-1) \times 6 \times 2 = 1524$ bits. Thus we can save about 14.6 % overall ROM area as compared to the conventional method.
- The ROM word access time is reduced due to reduction in number of words and word size. This reduction in ROM word access time is achieved at the cost of an extra multiplier and scaling block.
- The extra multiplier delay is not that much significant compared to ROM word access delay. Suppose if multiplier delay is comparable with the delay of total ROM word access time, then the delay can be reduced by using pipelining or any other speed optimization techniques, whereas ROM operation cannot be pipelined and hence reducing the total ROM word access time at the cost of an extra multiplier does not have much impact on overall performance of the DDFS system.
- The ROM word access speed is two times faster than the conventional ROM based DDFS; this is because at every clock we read two words, one from $\pi/4$ sine sub ROM look-up table and one from $\pi/4$ cosine sub ROM look-up table. This doubles the BW of the DDFS system.
- There is a wide scope for further ROM size reduction using state-of-the art ROM compression techniques as listed in section-1.
- The proposed architecture can be modified as multiplier free by replacing multiplier using shift and add techniques.
- Considering all those above merits the proposed architecture is a best candidature for the applications such as portable and wide band communication systems where power and bandwidth are critical.

4. DESIGN AND SIMULATION OF AN 11-BIT DDFS BASED ON NOVEL ARCHITECTURE

To verify the feasibility of the proposed ROM based DDFS architecture, we have designed an 11-bit DDFS with L=16-bits, M=12-bits, and N=11-bits using MATLAB-simulink tool version R2012a. The Fig. 4 shows the design and implementation of an 11-bit DDFS. Fig.4 (a) is a 12-bit phase accumulator, where the unsigned 16-bit integer FCW value is stored in a register and is accumulated at every reference clock cycle. Further the output of 16-bit phase accumulator is converted into 16-bit binary using integer to binary conversion block and this output of the phase accumulator is represented by port '1' (output1) and is applied as an input to the Fig. 4 (b) represented by port '1' (input1). Fig. 4 (b) is the phase complementor sub system, the main functionality of this sub system is to control phase increment or phase decrement. This sub system consists of a demux block, a complementor block composing a set of XOR gates, and a mux block. The function of the demux block is to truncate 4-LSBs of 16-bit unsigned binary number that is received at its input (input1) and then output the remaining 12 MSBs. Out of the 12 MSBs the first two MSBs referred as 'M11' and 'M10' respectively are used to control the phase increment or decrement and to generate positive or negative sine half cycles. The remaining 10 bits (12MSBs-2 MSBs) viz. M9, M8, ……., M0 are applied to 10 XOR logic gates and each of these 10 bits should be applied at the second input of each respective XOR gate. Whereas the first input of each 10 XOR gates should be connected to the MSB 'M10'. The M10 is used to control phase increment or decrement, the M10 = '0' indicates phase increment and M10 = '1' indicates phase decrement. The outputs of 10 XOR gates are applied as an input to the mux. The mux block combines 10 XOR gates output into a single bus wide 10 bits. The output of this mux block indicated by port '2' (output2) is applied as an input (input2) to the sub system shown in Fig. 4 (c).

The Fig. 4 (c), is a phase to amplitude converter sub system, this sub system consists of binary to integer conversion block, sine and cosine look-up tables, a multiplier, a scaling block, and an integer to binary converter block. The functionality of this sub system is explained as follows: the 10 bit binary phase signal that is received at port 2 (input2) is first converted into unsigned 10 bit integer and is then used to address the two sub ROM look up tables viz. sine ROM and cosine ROM look up tables. Where, the sine ROM look up table stores the sine samples from 0 to $\pi/4$ and cosine ROM stores the samples from 0 to $\pi/4$. At each reference cycle one sample from each look-up table is read and applied to a multiplier block. The multiplier block multiplies the samples received from the look-up tables and then outputs the sine samples corresponding an angle [0, $\pi/2$). Further the output of the multiplier is scaled up by factor '2' in order to map the amplitude of the sine samples corresponding to an amplitude in the range [0, 1). The sine samples so obtained are in the range [0, 1) are first converted into integer values and subsequently converted from integer to 10 bit binary signal. This binary signal is available at the port '3' (output3).

The Fig. 4 (d) is the sine complementor block and is used to generate the positive or negative half cycle of the sine wave that is to be synthesized. This block consists of demux, a set of XOR logic gates, and a mux block. The working operation of this block is similar to the Fig .4 (b). Here the signal to be complemented is sine amplitude and the signal that is used to control this complementary operation is the very first MSB of the phase accumulator truncated output that is 'M11'. The M11 = '0' implies the positive half cycle

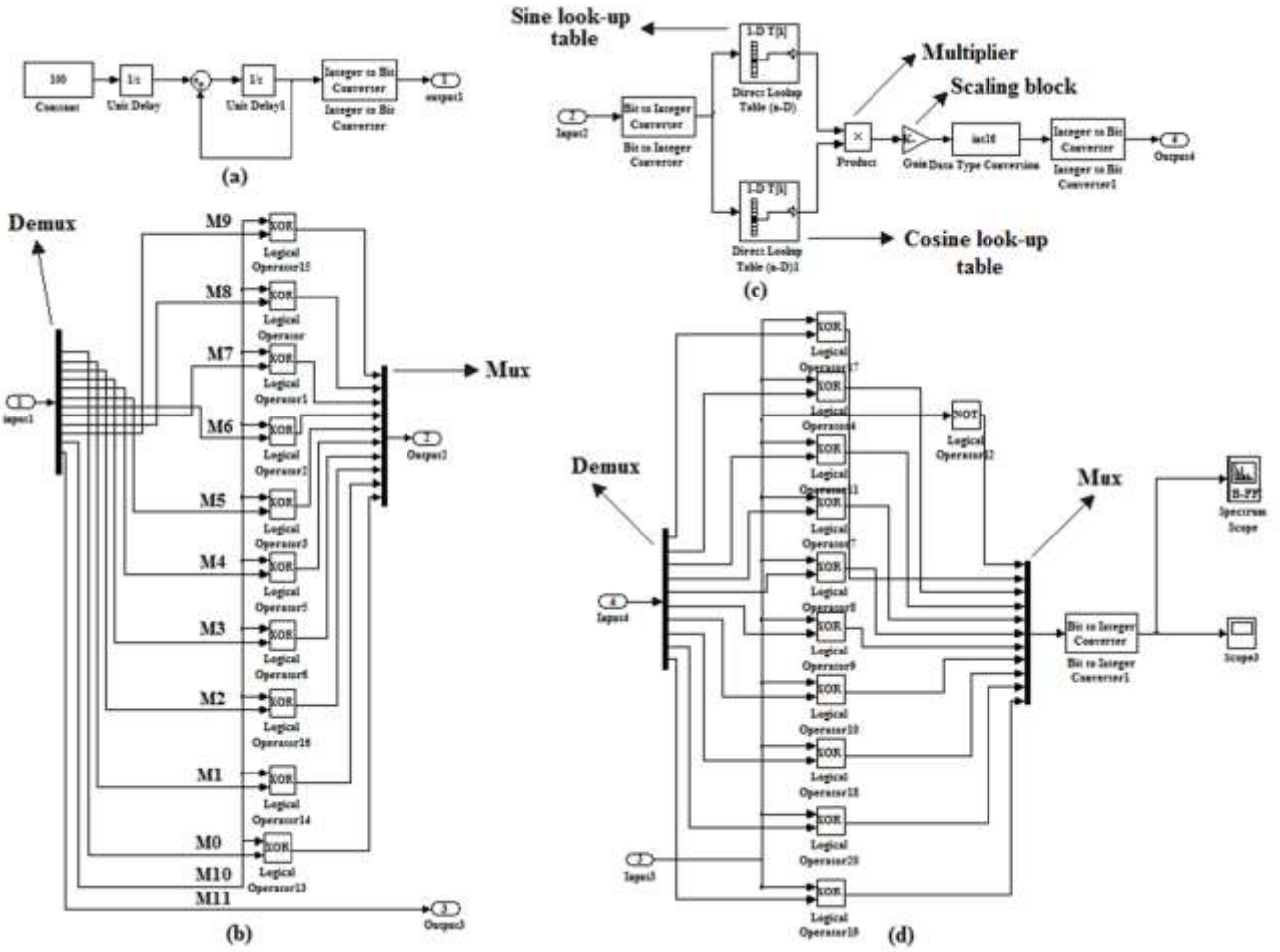

Fig. 4. An 11-bit DDFS designed and implemented in MATLAB-Simulink tool: (a) Phase accumulator (b) Phase complementor (c) Phase to sine converter (d) Sine amplitude complementor.

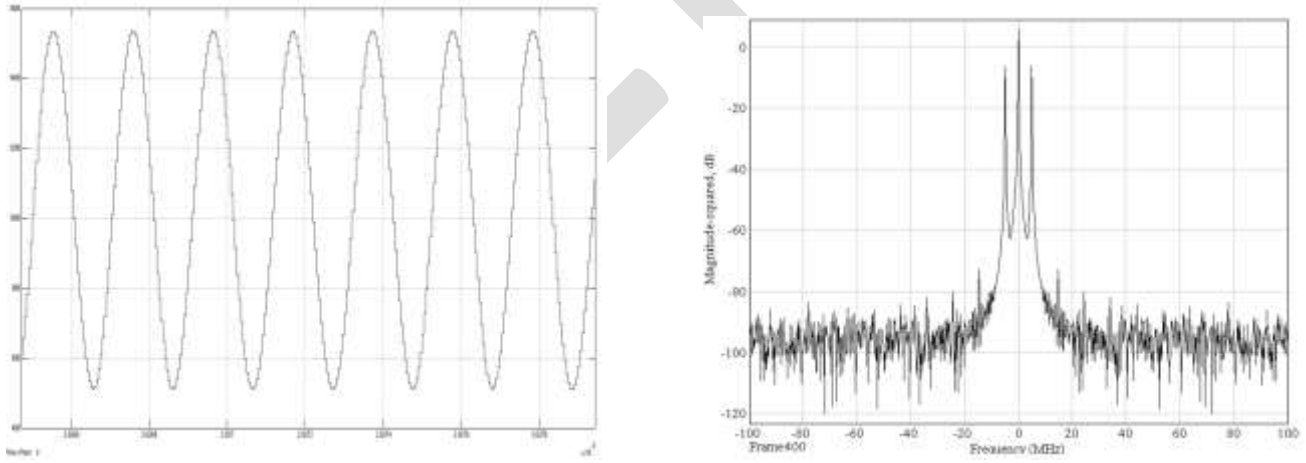

(a) (b)

Fig. 5. Simulation results of 11-bit DDFS for FCW =100: (a) Synthesized sine wave (b) Frequency spectrum of the synthesized sine wave .

of sine wave and M11 = '1' implies negative half cycle of the sine wave that is to be synthesized.

The design is simulated with FCW =100 and Fref = 200 MHz and the simulated results shows that the sine wave that is synthesized is having an output signal frequency of 4.88 MHz and measured SFDR indicates a spectral purity of -66 db. The synthesized sine wave and its frequency spectrum plot are shown in the Fig. 5 (a) and Fig. 5 (b) respectively. Further the ROM size and the ROM

compression ratio that is achieved using the proposed technique with some of the standard compression technique are compared and the results are tabulated in Table-1. For L=16, M=12, and N=11 The proposed architecture achieves the total ROM size of 9216 bits and compression ratio of 78.22 with respect to uncompressed memory without phase truncation.

ACKNOWLEDGMENT

Authors acknowledge management, Vemana Institute of Technology and Dayananda Sagar Group of Institutions (DSI), Bangalore for all their support in pursuing this research in the Research centre, Department of Telecommunication Engineering, Dayananda Sagar College of Engineering, Bangalore, VTU, Karnataka, India.

5. CONCLUSION

In this paper we have proposed a novel architecture for the ROM based DDFS. The proposed DDFS architecture uses two sub ROMs instead of a single ROM. The two sub ROMS are used to store samples of sine and cosine functions corresponding to an angle $[0, \pi/4)$. The remaining samples corresponding to an angle $[\pi/4, \pi/2)$ can be derived using a digital multiplier and a scaling block. Thus by storing the samples in two separate sub ROMs corresponding to angle $[0, \pi/4)$ the proposed architecture reduces the ROM area about 14.6 % compared to the conventional ROM based architecture. Also the proposed architecture generates two cycles of the output signal for each overflow of the phase accumulator corresponding to two samples that are read at every reference clock cycle. This doubles the BW of the DDFS. Further an 11-bit DDFS based on the proposed architecture was designed and simulated using MATLAB-Simulink tool. Also the DDFS synthesizes an 11-bit sine wave with an output signal frequency of 4.88 MHz with a spectral purity of -66 db corresponding to FCW=100. Considering also these merits the proposed architecture can be considered as good candidature for the portable and wideband applications. Also there is a wide scope for further reduction of two sub-ROM sizes by using the state-of-the art compression techniques.

TABLE -1
COMPARISON OF ROM SIZE AND ROM COMPRESSION RATIOS OF PROPOSED ARCHITECTURE WITH THE STANDARD TECHNIQUES FOR L=16-BITS, M=12-BITS, AND N=11-BITS

ROM compression technique used	Total number of ROM bits required	Total compression ratio achieved	Additional hardware required
Uncompressed memory without phase truncation	$2^{16}\times11=720896$	1:1	-
Compressed memory with phase truncation	$2^{12}\times11=45056$	16:1	-
Compressed memory with phase truncation and sine quarter wave symmetry (CM-PTQS)	$2^{10}\times10=10240$	70.4:1	-
Sine phase difference using CM-PTQS	$2^{10}\times8=8192$	88:1	1-adder
Double trigonometric approximation using CM-PTQS	$2^{10}\times7=7168$	100.57:1	1-adder , 1-complementor
Quad line technique using CM-PTQS	$2^{10}\times6=6144$	117.33:1	2-adders, 1-complementor, 1-mux
Proposed technique using CM-PTQS	$2^{9}\times9\times2=9216$	78.22:1	1-multiplier, 1-scaling block

REFERENCES:

[1] F. Akyildiz, David M. Gutierrez-Estevez, and Elias Chavarria Reyes, "The evolution to 4G cellular systems: LTE-Advanced," Elsevier Journal of Physical Communication, pp. 217-244, 2010.
[2] 2013PIDS_Summary.pdf, available at http://www.itrs.net/ITRS.
[3] J. Tierney, C. Rader, and B. Gold, "A Digital Frequency Synthesizer,'' IEEE Trans. Audio Electro acoustics, vol. AU-19, no. **1,** pp. 48-56, Mar 1971.
[4] Emanuele Lopelli, Johan D. van der Tang, and Arthur H. M. van Roermund, "Minimum Power-Consumption Estimation in ROM-Based DDFS for Frequency-Hopping Ultralow-Power Transmitters," IEEE Transactions on circuits and systems—I: Regular Papers, Vol. 56, No. 1, January 2009.
[5] Byung-Do Yang, Jang-Hong Choi, Seon-Ho Han, Lee-Sup Kim, and Hyun-Kyu Yu, "An 800 MHz Low-Power Direct Digital Frequency Synthesizer With an On-Chip D/A Converter*",* IEEE Journal of solid-state circuits, Vol. 39, no. 5, pp. 761-774, May 2005.
[6] H. T. Nicholas, III, H. Samueli, and B. Kim, "The optimization of direct digital frequency synthesizer performance in the presence of finite word length effects," in Proc. 42nd Annual Frequency Control Symposium USER-ACOM, pp. 357–363, May 1988.
[7] H. T. Nicholas, III, and H. Samueli, "An analysis of the output spectrum of direct digital frequency synthesizers in the presence of phase accumulator truncation," in Proc. 41st Annual. Frequency Control Symposium.USERACOM, pp. 495–502, May 1987.
[8] A. Yamagishi, M. Ishikawa, T. Tsukahara, and S. Date, "A 2-V, 2-GHz low-power direct digital frequency synthesizer chip-set for wireless communication," IEEE J. Solid-State Circuits, vol. 33, pp. 210–217, Feb. 1998.
[9] J. M. P. Langlois and D. Al-Khalili, "ROM size reduction with low processing cost for direct digital frequency synthesis," in Proc. IEEE Pacific Rim Conf. Communications, Computers and Signal Processing, pp. 287–290, Aug. 2001.
[10] B.-D. Yang and L.-S. Kim, "A direct digital frequency synthesizer using a new ROM compression method," in Proc. Eur. Solid-State Circuits Conf., pp. 288–291, 2001.
[11] A. M. Sodagar and G. R. Lahiji, "Mapping from phase to sine-amplitude in direct digital frequency synthesizers using parabolic approximation," IEEE Trans. Circuits Syst. II, vol. 47, pp. 1452–1457, Dec. 2000.
[12] S. Liao and L.-G. Chen, "A low-power low-voltage direct digital frequency synthesizer," in Proc. Int. Symposium. VLSI Technology, Systems, and Applications, pp. 265–269, June 1997.
[13] H. T. Nicholas III and H. Samueli, "A 150-MHz direct digital frequency synthesizer in 1.25µm CMOS with 90-dBc spurious performance," IEEE J. Solid-State Circuits, vol. 26, pp. 1959-1969, Dec. 1991.
[14] Loke Kun Tan, and Henry Samueli, "A 200MHz Quadrature Digital Synthesizer/Mixer in 0.8µm CMOS," IEEE Journal of Solid State Circuits, Vol. 30, No. 3, pp. 193-200, March 1995.
[15] D. A. Sunderland, R. A. Strauch, S. S. Wharfield, H. T. Peterson, and C. R. Cole, "CMOS/SOS frequency synthesizer LSI circuit for spread spectrum communications," IEEE JSSC, pp. 497-505, Aug. 1984.
[16] J. Vankka, "Methods of Mapping from Phase to Sine Amplitude in Direct Digital Synthesis", IEEE Tr. On ultrasonics, ferroelectrics, and frequency control, Mar. 1997, pp. 526-534.
[17] B.H. Hutchison, Jr., Frequency Synthesis and Applications, IEEE Press, 1975.
[18] Bar-Giora Goldberg, "Digital frequency synthesis demystified," LLH Technology Publishing, 1999.
[19] Bennet C. Wong, and Henry Samueli, "A 200MHz All-Digital QAM Modulator and Demodulator in 1.2µm CMOS for Digital Radio Applications," IEEE Journal of Solid State Circuits, vol. 26, no 12, pp. 1970-1979, Dec. 1991.
[20] F. P. Chan, M. P. Quirk, and R. F. Jurgens, "High-Speed Digital Baseband Mixer," TDA Progress Report 42-81, Communication System Research Section, January-March, pp. 63-80, 1985.

International Journal of Engineering Research and General Science Volume 3, Issue 5, September-October, 2015
ISSN 2091-2730

STUDY ON BUCKLING EFFECT OF CUTOUTS ON THE OPTIMIZED FIBRE ORIENTATED LAMINATED COMPOSITE PLATE

Anu George[1], S. Usha[2]

[1] M. Tech Scholar, Civil Department, SNG College of Engineering, Kerala, India
[2] Professor, Civil Department, SNG College of Engineering, Kerala, India
[1]anugeorge023@gmail.com, 09539258170

Abstract- Laminate composite materials are composite materials in which layers of different properties are bonded together to act as an integral part. In structures, cutouts provided in laminated composite plate show reduction in strength, stiffness and inertia. Laminated composite plates have wide application in the aerospace, automotive, marine and civil areas. Cutouts are necessary to serve the purpose of weight reduction, venting and attachments to other units for the cable to pass through are so on. This paper compares the critical buckling load of the laminated composite plate with and without cutout by changing the fibre orientation by experimental and numerical methods. Glass/epoxy laminated composite plate was used here. Laminated composite plate with circular cutout shows a decrease in buckling load than plates without cutout. Also the buckling load decreases with increase in fibre angles. The maximum buckling load combination was obtained with fibre orientation 45/-45/45/-45/45/-45/45/-45 with circular cutout.

Key Words- Buckling Analysis, Circular, Cutouts, Finite Element Method, Glass Fibre, Hardener, Laminated Composite Plate, Resin

1. INTRODUCTION

A lamina is fibre reinforced composite, prepared from fibres and matrix (sometimes woven fabric may also used for making lamina). Laminae having varying fibre orientations are bonded together to form an integral structural component, which is known as laminate. A lamina is considered to be homogenous at macroscopic level. It has three planes of symmetry and hence termed as orthotropic. The laminates may be symmetric or anti-symmetric or unsymmetric. The mechanical performance of laminated composite plates are highly dependent on the degree of orthotrophy of individual layers, the low ratio of transverse shear modulus to in-plane modulus and the stacking sequence of laminates. Lamination is used to bond the best aspects of the adjoining layers and bonding material to develop a more useful material.

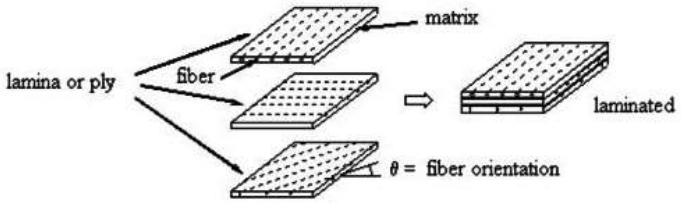

Fig -1: Laminated Composite Plate

Glass-reinforced plastic is a composite material made of epoxy resin matrix reinforced by fine fibers made of E glass. GRP is a lightweight, strong material with very many uses, including boats, automobiles, water tanks, roofing, pipes and cladding. Moreover, by placing multiple fiber layers on top of other, with each fiber layer oriented (stacked) in different preferred directions, the strength and stiffness parameters of the entire material can be enhanced in an efficient manner.

The mechanical behaviour of laminated composite plates are strongly dependent on the degree of orthotrophy of individual layers, the low ratio of transverse modulus of rigidity to the in-plane modulus of elasticity and the stacking sequence of laminates. Lamination helps to combine the better aspects of the combining layers and bonding material in order to achieve a useful composite material. Fiber- reinforced composites are extensively used in the form of relatively thin plate, and they have consequently higher load carrying capability against buckling.

2. SCOPE

Laminated composite plates have wide application in the aerospace, automotive, marine and civil areas. In structures, laminated composite plate consists of cutout which reduces their strength, stiffness and inertia. Cutouts are necessary to serve the purpose of weight reduction, inspection, venting and attachment to other units for the cable to pass through are so on. Cutouts are required for ventilation as well. Hence the effects of cutout in laminated composite plate are to be investigated.

3. OBJECTIVES

- To determine the critical buckling load of laminated composite plate without cutout and with circular cutout by changing the five fibre orientation by experimental and numerical methods.
- To optimize the fibre orientation by performing the buckling analysis using numerical methods.

4. EXPERIMENTAL PROGRAM

4.1 MATERIALS

The materials used for making the laminated composite plate are:

4.1.1 Glass Fibre

The bidirectional glass fibre woven roving of 360 GSM with 0.3 mm thickness was used for the experimental work.

4.1.2 Epoxy Resin

Araldite LY 556 was used as epoxy resin which is medium viscosity, unmodified liquid epoxy resin based on Bisphenol-A.

4.1.3 Hardener

Low viscosity, unmodified, aliphatic polyamine hardener, Aradur HY 951 was used for the experiment which has excellent water resistance property.

4.1.4 Polyvinyl Alcohol

Polyvinyl Alcohol act as a releasing agent applied by means of spray gun.

4.2. MIXING RATIO

Araldite LY 556 and Aradur 951 were mixed well before applying into laminated composite plate. Resin and hardener should be mixed uniformly until a homogenous mixture is formed. It provides a low viscosity, solvent free room temperature curing laminating system. By varying the contents of hardener from 10 to 12 parts, the reactivity of the system can be adapted to suit the processing and curing conditions.

Table -1: Properties of the Mix

Viscosity	at 25^0C	1700 mPa.s
	at 40^0C	650 mPa.s
Useable Life Gel Time	upto 1500 mPa.s	10 minutes
	at 25^0C	120-180 minutes
	at 40^0C	30 minutes

4.3 PREPARATION OF LAMINATED COMPOSITE SPECIMEN

The laminated composite plate specimens used in this research were made from 0/90 woven glass fiber with epoxy matrix. Hand layup technique was used for fabrication of plates. The percentage of glass fiber and mixture of epoxy resin and hardener had taken as 1:1 in weight for fabrication of the plates. A rigid platform made of iron was selected to make a flat surface. A milosh sheet was placed on the rigid platform. Then polyvinyl alcohol i.e releasing agent was applied on the milosh sheet by using the sprayer. After applying that, gel coat (mixture of epoxy resin and hardener) was spread to provide a smooth surface and to avoid the direct exposure of the fibre to environment. Glass fibres from the rovings were placed on the top of the gel coat and again gel coat was applied. The entrapped air was removed by using the steel rollers. The process was continued as above before the gel coat had fully hardened. After the completion of all layers, again a milosh sheet was placed on the top of the gel coat by applying poly vinyl alcohol. A heavy metal rigid platform was placed over it. Then the whole mould was kept at the compression moulding machine for 20 minutes. The temperature was kept at 80^0C. After 20 minutes, switch off the machine and kept the specimen for 4 hours. After 48 hours of curing, cut the specimen in the desired size by water jet cutting with and without cutout for the experimental study.

Fig -2: Pouring of Epoxy Resin

Fig -3: Removal of Entrapped Air by Rollers

Fig -4: Temperature Setting in Machine

Fig -5: Prepared Plate without Cutout

Fig -6: Prepared Plate with Cutout

A total of seven types of laminated composite plate with and without circular cutout of different fibre orientation were prepared for the experimental study.

1. Laminated composite plate 0/90/0/90/0/90/0/90 orientation without cutout (LCPWOC 1)
2. Laminated composite plate 45/-45/45/-45/45/-45/45/-45 orientation without cutout (LCPWOC 2)
3. Laminated composite plate 0/90/0/90/0/90/0/90 orientation with cutout (LCPWC 1)
4. Laminated composite plate 45/-45/45/-45/45/-45/45/-45 orientation with cutout (LCPWC 2)
5. Laminated composite plate 0/90/45/-45/45/-45/0/90 orientation with cutout (LCPWC 3)
6. Laminated composite plate 0/90/60/30/60/30/0/90 orientation with cutout (LCPWC 4)
7. Laminated composite plate 60/30/60/30/0/90/0/90 orientation with cutout (LCPWC 5)

4.4 TEST PROCEDURE

The specimens were tested in an axial compression testing machine having a capacity of 100 kN. The specimen was placed vertically and clamped at top and bottom ends. The other two ends were kept as free. All specimens were loaded slowly until buckling. For axial loading, the plate specimen was placed between the two machine heads, of which the lower head was permanently fixed and the upper head was moving during the test with the help of hydraulic cylinder. The plate was loaded at the rate of 2 mm/min. As the load starts increasing, the dial gauge needle also moves and at a particular point, there was a sudden movement of the needle. The load at this point was the buckling load of the specimen. The testing machine was connected to the computer to obtain the load displacement curve and the critical buckling load. The initial part of the curve was linear, the point where the curve deviates from its linearity was taken as the critical buckling load.

4.5 EXPERIMENTAL RESULTS

The buckling load and load versus displacement curve of the maximum buckling load with circular cutout specimen obtained from the experiment is shown in figure 7.

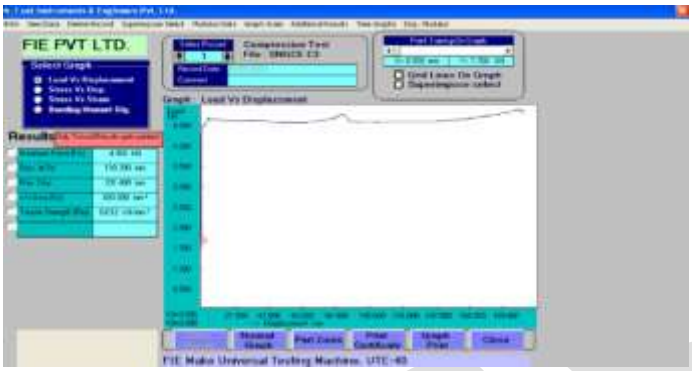

Fig -7: Load Displacement Curve of LCPWC 2

5. FINITE ELEMENT ANALYSIS

Finite element analysis of the above seven different plates were done using the software 'ANSYS 14.5 APDL' also.

Table -2: Element Type and Material Properties

Material No:	Element Type	Material Property
1	Shell 281	Density = 1.2 g/cm^3
		Youngs modulus E = 10 GPa
		Poisons ratio = 0.12

'Shell 281' element was used to model the laminated composite plate. This is an eight- node linear shell element having six degrees of freedom at each node. Those are translation in x, y, z direction and rotation about x, y, z axis. It was used in cases for linear, large rotation, and/or large strain nonlinear applications.

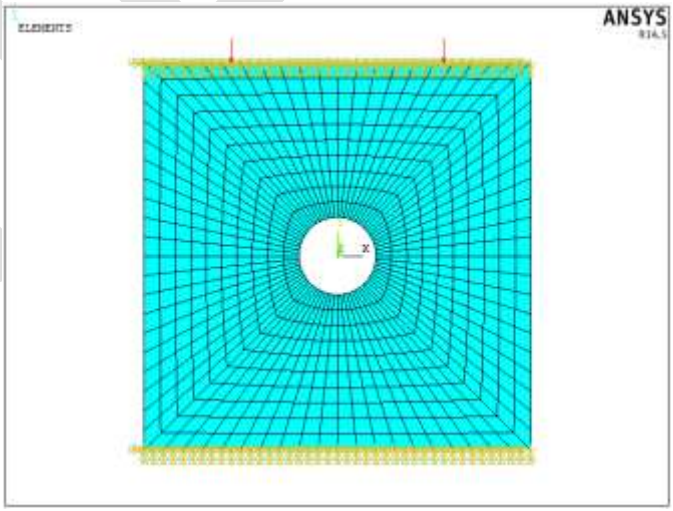

Fig -8: Boundary Condition of Plate with Circular Cutout

5.1 FINITE ELEMENT RESULTS

The plate specimens were modelled in ANSYS software. Analysis of plates was done to obtain critical buckling load.

Table -3: Results obtained from ANSYS 14.5

ID No. of Plate Specimen	Buckling Load (kN)
LCPWOC 1	5.8
LCPWOC 2	6.1
LCPWC 1	4.9
LCPWC 2	4.8
LCPWC 3	4.68
LCPWC 4	4.482
LCPWC 5	4.68

6. RESULTS AND DISCUSSION

Results obtained from software were compared with the experimental results for the seven laminated plate specimens. The results showed satisfactory convergence.

Table -4: Comparison between Experimental Value and Software Value

ID No. of Plates	Buckling Load		Percentage Variation
	Experimental Value	Software Value	
LCPWOC 1	6.4	5.8	9.375
LCPWOC 2	6.6	6.1	9.09
LCPWC 1	4.78	4.9	2.44
LCPWC 2	4.9	4.8	2.04
LCPWC 3	4.62	4.68	1.28
LCPWC 4	4.7	4.482	4.63
LCPWC 5	4.7	4.68	1.5

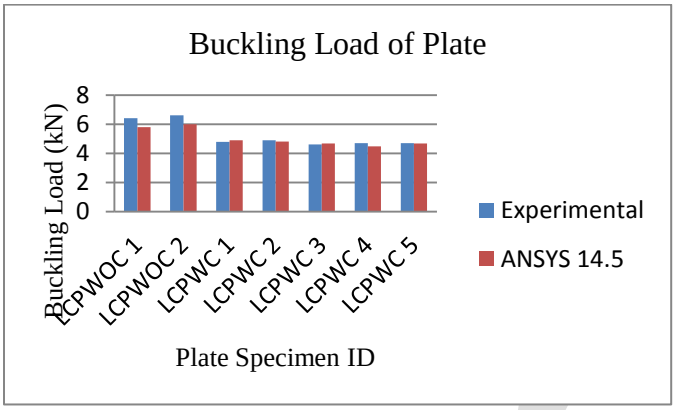

Chart -1: Comparison of Buckling Load

The maximum buckling load capacities was obtained with LCPWC 2 (fibre orientation 45/-45/45/-45/45/-45/45/-45 with circular cutout). The percentage reduction due to the circular cutout at centre was 25 % compared to laminate without cutout.

7. ACKNOWLEDGEMENT

The authors would like to thank the Composite Technology Centre, Aerospace Engineering Department, IIT Madras for giving them the opportunity to conduct and complete the experimental work.

8. CONCLUSIONS

Experimental results on laminated composite plate of size 250 mm x 250 mm x 1.6 mm with different seven cases were compared with results obtained in the buckling analysis in ANSYS 14.5 software. The results are summarized as below:

- Laminated plates with cutout shows a decrease in buckling load carrying capacity compared to plate without cutout.
- The maximum buckling load depends on fibre orientation of the different layers used. It is observed that the laminated composite plate with fibre orientation 45/-45/45/-45/45/-45/45/-45 shows the maximum buckling load.
- The percentage reduction in buckling load carrying capacity was observed as 25% for LCPWC 2 compared with LCPWOC.

REFERENCES:

1. M Mohan Kumar, Colins V Jacob , Lakshminarayana N , Puneeth BM , M Nagabhushana, “Buckling Analysis of Woven Glass Epoxy Laminated Composite Plate”, American Journal of Engineering Research (AJER), e-ISSN : 2320-0847 p-ISSN: 2320-0936 Volume-02, Issue-07, pp-33-40, 2013

2. Pandey M D, “Effect of Fiber Waviness on Buckling Strength of Composite Plate”, Journal of Engineering Mechanics, (1999), pp. 1173-1179

3. K.Vasantha Kumar , Dr.P.Ram Reddy , Dr.D.V.Ravi Shankar, “Effect of Angle Ply Orientation On Tensile Properties Of Bi Directional Woven Fabric Glass Epoxy Composite Laminate”, International Journal of Computational Engineering, Issn 2250-3005, Researc,Vol, 03, Issue, 10, October, 2013

4. Shukla K.K, Kreuzer E, Sateesh Kumar K.V, Nath Y, “Buckling of Laminated Composite Rectangular Plate, Journal of Aerospace Engineering”, pp. 215-223, October 2005

5. Sandeep M.B , D.Choudhary , Md. Nizamuddin Inamdar , Md. Qalequr Rahaman, “Experimental Study Of Effect of Fiber Orientation on the Flexural Strength of Glass/Epoxy Composite material”, International Journal of Research in Engineering and Technology eISSN: 2319-1163, p ISSN: 2321-7308, Volume: 03 Issue: 09, September, 2014

6. Liecheng Sun, Issam E Harik, "Buckling of Stiffened Antisymmetric Laminated Plates", Journal of Engineering Mechanis(ASCE), pp.1110-1123, August, 2013

7. Adnan Naji Jameel, Dr. Louay Sabah Yousaf, "Buckling Analysis of Stiffened and Unstifffened Laminated Composite Plates", Journal of Engineering, (August 2014)No.8, Vol.20

8. Basharia A.A. Yousef, Mohamed H. Elsheikh, Mohd F. M. Sabri, Hakim S. S. Aljibori, Suhana M. Said, "Effect of Buckling on Glass Fiber/Epoxy Plate", International Journal of Engineering Research and Development e-ISSN: 2278-067X, p-ISSN : 2278-800X,Volume 5, Issue 5, PP. 60-68, December, 2012

9. Nagendra Singh Gaira, Nagengra Kumar Maurya, Rakesh Kumar Yadav, "Linear Buckling Analysis of Laminated Composite Plate, International Journal of Engineering Science and Technology", ISSN: 2250–3676 Vol. 2, Issue 4, pp. 886-891, July-August, 2014

10. K.Mallikarjuna Reddy, B.Sidda Reddy, R.Madhu Kumar, "Buckling Anlysis of Laminated Composite Plates Using Finite Element Method ", International Journal of Engineering Sciences and Research Technology, ISSN: 2277-9655, 3281-3286, November, 2013

11. Zhang Y.X. and Yang C.H., "Recent developments in finite element analysis for laminated composite plates", (2009), Composite Structures 88, Science Direct, pp. 147-157

12. Amit Kumar Tanwer, "Mechanical Properties Testing of Uni-directional and Bi-directional Glass Fibre Reinforced Epoxy Based Composites", International Journal of Research in Advent Technology, Vol.2, No.11, E-ISSN: 2321-9637, November 2014

13. Sidda Reddy B, "Vibration Analysis Of Laminated Composite Plates Using Design Of Experiments Approach", International Journal of Scientific Engineering and Technology, Vol.2, Issue No.1, pp. 40-49, 2013

14. Junaid Kameran Ahmed, "Static and Dynamic Analysis of Composite Laminated Plate", International Journal of Innovative Technology and Exploring Engineering, Vol.3, Issue 6, 2013

International Journal of Engineering Research and General Science Volume 3, Issue 5, September-October, 2015
ISSN 2091-2730

Experimental Study and Parameter Optimization of Turning Operation of Aluminium Alloy-2014

Arjun Pridhvijit[1], Dr. Binu C Yeldose[2]
[1]PG Scholar, Department of Mechanical Engineering, MA college of Engineering Kothamangalam, Kerala, India.
[2]Professor, Department of Mechanical Engineering, MA college of Engineering Kothamangalam, Kerala, India.

Email: arjunpjit@gmail.com,+91-9895146500

Abstract— In this study an experimental investigation of cutting parameters (cutting speed, feed rate and depth of cut) in turning operation of Aluminium alloy-2014 was done and influence of cutting parameters on surface roughness was studied. The machining was performed using two different tools such as carbide tool and TiN coated carbide tool. Taguchi method is used to find optimum result. Orthogonal array, signal to noise ratio and ANOVA is used to study the performance characteristic in turning operation. The result shows that better surface finish is achieve at low feed rate (0.05mm/rev), high cutting speed (314m/min) and at high depth of cut. Experimental data collected are tested with regression model and ANN technique, and a comparison study of model has been done.

Keywords— Surface Roughness, Aluminium Alloy -2014, Taguchi, Signal to Noise Ratio, ANOVA, Regression, ANN

INTRODUCTION

Nowadays the manufacturing industries are continuously challenged for achieving higher productivity and high quality products in order to remain competitive. The desired shape, size and finished, ferrous and non-ferrous materials are conventionally produced through turning. Turning is an important and widely used machining processes in engineering industries. Aluminium alloy-2014 has wide use of application especially in light aircraft which is used in landing gear struct. Due to low surface finish of the struct high friction is produced in the movement of struct. The parameters that we are dealing with in the roughness measurement area are very small which fall in the range of micrometers. But this value will affect several functional attributes of parts, such as friction, wear and tear, heat transmission, ability if distributing and holding a lubricant. The objective of this study is to find optimal solution which will give better surface finish and create a predictive model which will predict the result under any contrition within the cutting range.

LITERATURE SURVEY

Literature survey is done to explore the various process parameters of turning operation and their effect on various output responses and a thorough study of taguchi's optimization and ANOVA have been conducted to optimize the process parameters of this study [1-7]. The concept of prediction of results using regression model and ANN were also conducted [8-13].

3. EXPERIMENTAL SETUP AND DESIGN

All the machining processes were done with a "GALAXY MIDASC" Computer Numerical Control (CNC) turning machine with programme controller "FANUC" having 10 KW power and revolving capability of 40-4000 rev/min. For removing the buildup edge formation on the tool rake face kerosene is used as coolant, which is pumped into the work piece and tool tip interface.

3.1 Workpiece

The Aluminium alloy 2014 rod with 40mm diameter and 70 mm length is used as work piece for the study. Identification number is marked on the flat surface of the work piece from 1 to 9 which is shown in the figure no 1.

Figure No 1 Workpiece

3.2 Cutting tools

To improve the surface finish a comparison study of two tools has been conducted. Tools used for turning operation are CNMG 120404 Aluminium grade which is an uncoated carbide tool insert and YBC151 grade description: MT-TiCN + Al2O3 + TiN coated carbide insert are used. The special multi-layer coating of YBC151 offers superb wear resistance and smooth surface finish.

3.3 Output Response

Surface roughness is considered as performance characteristic that is to be evaluated. Surface roughness of work piece is measured after machining each piece with different tool using portable surface roughness tester of "MITUTOYO".

3.4 Design of Experiments

In this work, the optimum conditions for surface roughness in turning operation of Aluminium alloy-2014 is obtained by using Taguchi robust design . L9 (3^3) orthogonal array is used to conduct the experiment.

3.4.1 Selection of control factors and levels

Based on Carmita Camposeco (2014) and Ghorbani Siamak (2013), tool manufacturer recommendations and machine range, feasible range of cutting parameters for a given cutting tool–workpiece system were selected which is shown on the table 1.

Table 1 Process parameters and their levels used for experiment

Parameters	Units	Levels and values		
		1	2	3
Cutting speed	m/min	150	232	314
Feed	mm/rev	0.05	0.10	0.15
Depth of cut	mm	0.1	0.3	0.5

3.4.2 Selection of orthogonal array

The L9 orthogonal array with all values selected for the experimental run is shown in table 2. There are 9 parameter combinations that need to be tested. Each parameter combination is tested for three replications for effective error reduction and for accurate S/N ratio.

Table 2 Experimental Design

Experiment	Speed(m/min)	Feed rate (mm/rev)	Depth of Cut(mm)
1	150	0.05	0.1
2	150	0.1	0.3
3	150	0.15	0.5
4	232	0.05	0.3
5	232	0.1	0.5
6	232	0.15	0.1
7	314	0.05	0.5
8	314	0.1	0.1
9	314	0.15	0.3

4. RESULTS AND DISCUSSION

After conducting the experiment the result obtained for surface roughness for tools CNMG 120404 and YBC 151 is shown on the table 3. Better surface finish is achieved for YBC 151 insert which is coated with titanium nitride.

Table 3 Experimental result obtained

Speed (m/min)	Feed rate (mm/rev)	Depth of cut (mm)	**$Ra_{CNMG\ 120404}$**	**Ra_{YBC151}**
150	0.05	0.1	0.423	0.377
150	0.1	0.3	1.031	0.468
150	0.15	0.5	1.72	0.603
232	0.05	0.3	0.381	0.311
232	0.1	0.5	1.001	0.402
232	0.15	0.1	1.499	0.606
314	0.05	0.5	0.366	0.24
314	0.1	0.1	0.642	0.44

314	0.15	0.3	1.305	0.52

In the experiment, the desired characteristic for surface roughness is lower the better. The equation to find the S/N ratio for this characteristic is given below.

$S/Ns = -10\log_{10}[\text{Mean of sum of squares of measured data}]$ (1)

$= -10\log_{10}[(\sum y^2)/n]$

Where n is the number of measurements in a trial and y is the measured value in a trial. The S/N ratio obtained for CNMG cutting tool is shown in the table 4

Table 4 S/N ratio for surface roughness

Speed (m/min)	Feed rate (mm/rev)	Depth of cut (mm)	S\N Ra (CNMG)
150	0.05	0.1	7.473192652
150	0.1	0.3	-0.265173306
150	0.15	0.5	-4.710568938
232	0.05	0.3	8.381500486
232	0.1	0.5	-0.00868155
232	0.15	0.1	-3.516032657
314	0.05	0.5	8.730378292
314	0.1	0.1	3.849299439
314	0.15	0.3	-2.312210233

The main effect values are plotted in Figure no 2 for the cutting speed, feed rate and depth of cut respectively. The main effects plot shows the influence of each level of factors and the SN ratio with maximum value is taken as the optimum values of surface roughness.

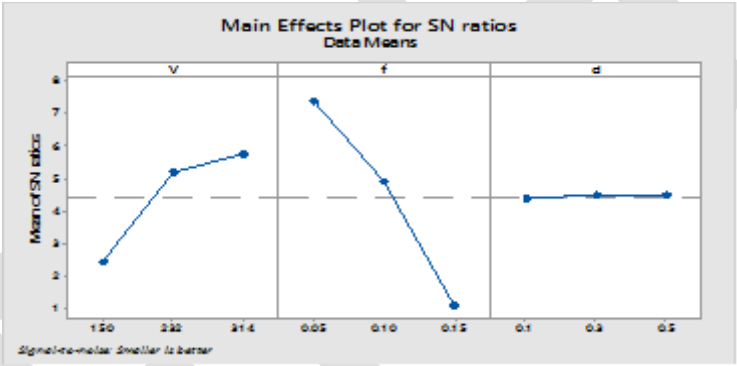

Figure no 2 Signal to noise ratio

The plot shows that as the feed rate and cutting speed increases surface roughness decreases. Depth of cut changes is negligible compared to other two factors.

Table 5 Response Table for Surface Roughness S/N Ratios

Symbol	Process Parameters	Surface roughness CNMG 120404				rank	optimum
		Mean S/N ratio			max-min		
		Level-1	Level-2	Level-3			
V	Speed	2.42792	5.19316	5.72255	3.2946320	2	314
f	Feed rate	7.36420	4.90301	1.07641	6.2877856	1	0.05
d	Depth of cut	4.37925	4.47010	4.49427	0.1150106	3	0.5

Based on the analysis of S/N ratio, shown on the table 5 response table of Signal to Noise ratios for surface roughness the optimal machining performance for the surface roughness is obtained at a cutting speed of 314 m/min (level 3), feed rate of 0.05mm/rev (level 1) and depth of cut of 0.5(level 2). In the analysis, feed rate is shown as the most influencing parameter followed by cutting speed and depth of cut.

Table 6 Analysis of variance

Source	DF	Adj SS	Adj MS	F- value	P-value	% contribution
V	2	0.10624	0.053122	35.62	0.027	24.05
f	2	0.33180	0.165902	111.24	0.009	75.11

d	2	0.00368	0.001842	1.23	0.447	0.83
error	2	0.00298	0.001491			
Total	8	0.44471				

Based on the ANOVA results in Table 6, the percentage contribution of various factors to surface roughness is identified. Here, feed rate is the most influencing factor followed by cutting speed. The percentage contribution of feed rate is 75.11%, this is because as it is well known that for a given tool nose radius, the theoretical surface roughness ($Ra=f^2/(32\times r)$) is mainly a function of the feed rate for cutting speed and depth of cut is 24.05% and 0.83% respectively. Also the probability level of depth of cut is much more than α (0.05) which indicates that depth of cut has least contribution towards surface roughness.
The optimal combination is cutting speed = 314 m/min, feed rate = 0.05 mm/rev, depth of cut =0.5mm
The S/N ratio obtained for cutting tool YBC 150 is shown on the table 7.

Table 7 Signal to Noise Ratio for Surface Roughness

Speed (m/min)	Feed rate (mm/rev)	Depth of cut (mm)	S\N Ra (TiN)
150	0.05	0.1	8.995432939
150	0.1	0.3	7.958800173
150	0.15	0.5	5.161218445
232	0.05	0.3	10.99501783
232	0.1	0.5	8.825828589
232	0.15	0.1	3.87640052
314	0.05	0.5	12.39577517
314	0.1	0.1	9.243618099
314	0.15	0.3	6.87803596

The main effect values are plotted in Figure no 3 for the cutting speed, feed rate and depth of cut respectively. The main effects plot shows the influence of each level of factors and the SN ratio with maximum value is taken as the optimum values of surface roughness. The plot shows that as the feed rate decreases surface roughness decreases. As cutting speed and depth of cut increased surface roughness decreased.

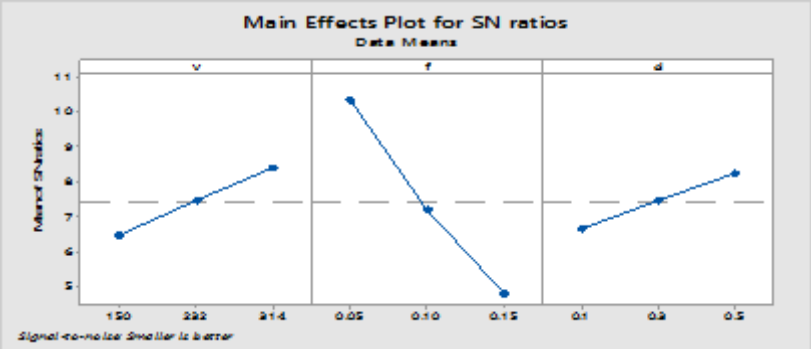

Figure no 3 S/N ratio obtained

Table 8 Response Table for Surface Roughness S/N Ratios

Symbols	Process Parameters	Surface roughness YBC 150 Mean S/N ratio			max-min		
		Level-1	Level-2	Level-3		rank	optimum
V	Speed	7.37181	7.899082	9.50581	2.133992555	2	314
f	Feed rate	10.7954	8.676082	5.305218	5.490190338	1	0.05
d	Depth of cut	7.3718	8.610618	8.794274	1.422456881	3	0.5

Based on the analysis of S/N ratio, shown on the response table 8 of Signal to Noise ratios for surface roughness the optimal machining performance for the surface roughness is obtained at a cutting speed of 314 m/min (level 3), feed rate of 0.05mm/rev (level 1) and depth of cut of 0.5(level3). In the analysis, feed rate is shown as the most influencing parameter followed by cutting speed and depth of cut. Based on the ANOVA results in Table 9, the percentage contribution of various factors to surface roughness is identified.

Table 9 Analysis of variance

Source	DF	Adj SS	Adj MS	F- value	P-value	% contribution
v	2	0.01025	0.00512	19.03	0.050	8.33
f	2	0.10701	0.05350	198.57	0.005	87.17
d	2	0.00555	0.00277	10.30	0.088	4.5
Error	2	0.00053	0.00026			
Total	8	0.12335				

Here, feed rate is the most influencing factor followed by cutting speed. The percentage contribution of feed rate is 87.17%, for depth of cut and cutting speed is 8.33% and 4.5% respectively. Also the probability level of depth of cut is much more than α (0.05) which indicates that depth of cut has least contribution towards surface roughness. The optimal combination is cutting speed = 314 m/min, feed rate = 0.05 mm/rev, depth of cut =0.5mm.

4.1 Regression Equation

The relationship between the factors and the performance measures were modeled by quadratic regression. The roughness Ra model is given below. Its coefficient of determination (R^2) is 98.9%.

Ra = 0.3394- 0.000271v+1.764f- 0.106d + 0.0000001 v*v + 5.20 f*f + 0.225 d*d - 0.00114 v*f - 0.000813 v*d

4.2 Verification of surface roughness through comparison test

The experimental data has been tested with the regression model and created ANN model. Model has been constructed with back-propagation algorithm with input parameters of depth of cut, cutting speed and feed rate. Output parameter is surface finish of the machined component.

Table 10 Validation of result for surface roughness

Speed	Feed rate	Depth of cut	Experimental value	Regression value	Predicted value from ANN
150	0.05	0.1	0.377	0.340	0.3916
150	0.1	0.3	0.468	0.451	0.4659
150	0.15	0.5	0.603	0.596	0.601
232	0.05	0.3	0.311	0.296	0.3165

Table 11 Validation of results of surface roughness obtained using ANN

Reading no:	Surface roughness (Ra) in experimental value (µm)	Predicted value (µm)	Error microns(µm)	Percentage error
1	0.377	0.3916	-0.0146	3.87267905
2	0.468	0.4659	0.0021	0.448717949
3	0.603	0.601	0.002	0.331674959
4	0.311	0.3165	-0.0055	1.76848875

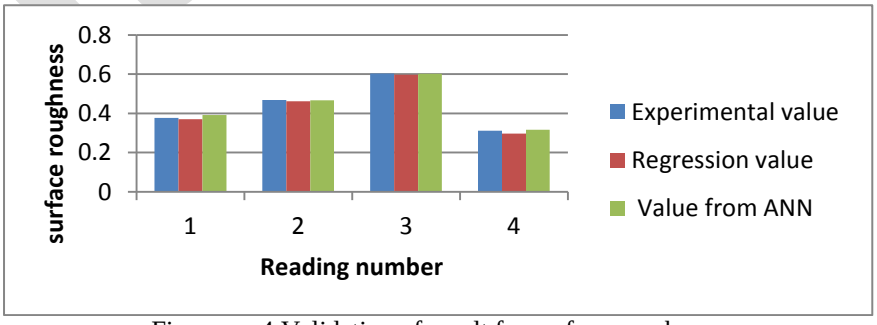

Figure no 4 Validation of result for surface roughness

After completing the experiment ANN has been used to predicted the behavior of the system within the operating range which is shown in the table 10. Average error for ANN is conducted which is given as 1.6% which is shown on the table 11. ANN model has been tested using training data and graph where plotted shown on the figure no 4. ANN is suitable tool to predict the surface roughness. From the table it shows that minimum percentage error was 0.33 and maximum of 3.87. This is a reasonable one and give ANN shows a satisfactory predicted value for surface roughness (Lin, 2003).

ACKNOWLEDGMENT

The authors gratefully acknowledge the technical support and guidance provided by the PSG College Of Engineering,Coimbatore.

CONCLUSION

In this study the effect of process parameters on surface roughness during the turning operation of Aluminium alloy-2014 under wet condition. Using signal to noise (S/N) ratio and ANOVA results the significance of cutting parameters was determined to get better surface roughness. The experimental results revealed that YBC 150 shows better surface finish compared to CNMG 120404, because Ti carbide reduces the tendency of chips to weld to the tool, decrease wear of the tool by diffusion and increase its hot hardness. Minimum Ra value obtained from the YBC 150 insert is 0.24µm and that from CNMG 120404 insert is 0.366 µm. From ANOVA it is revealed that the feed rate provides main contribution and influences most significantly on the surface roughness, and the effect of depth of cut and effect of speed provide less contribution to the surface roughness. Good surface roughness can be achieved when cutting speed and depth of cut are set nearer to their high level of the experimental range and feed rate is at low level of the experimental range. The optimized control factors settings for Ra are: V_3 (cutting speed 314 m/min), f_1 (feed rate 0.05 mm/rev), d_3 (depth of cut 0.5 mm).The results of ANN model shows close matching between the model output and the directly measured surface roughness.

REFERENCES:

[1] Axir M.H, O.M. Othman, A.M. Abodiena, Study on the inner surface finishing of aluminum alloy 2014 by ball burnishing process", Journal of materials processing technology 2 0 2 , (2008) , 435–442.
[2] CarmitaCamposeco-Negrete, "Optimization of cutting parameters using Response Surface Method for minimizing energy consumption and maximizing cutting quality in turning of AISI 6061 T6 aluminum", Journal of Cleaner Production (2014) 1-9.
[3] Chattopadhyay A.K, P. Roy, S.K. Sarangi, A. Ghosh, "Machinability study of pure aluminium and Al–12% Si alloys against uncoated and coated carbide inserts" Int. Journal of Refractory Metals & Hard Materials 27 (2009) 535–544
[4] Lalwani D.I, N.K. Mehta, P.K. Jain, "Experimental investigations of cutting parameters influence on cutting forces and surface roughness in finish hard turning of MDN250 steel", Journal of Materials Processing Technology 206 (2008) 167–179
[5] Mehmet Turker ,Ibrahim Ciftci , UlviSeker " Evaluation of tool wear when machining SiCp-reinforced Al-2014 alloy matrix composites" Materials and Design 25 (2004) 251–255
[6] Ning Fang & P. SrinivasaPai& S. Mosquea "The effect of built-up edge on the cutting vibrations in machining 2024-T351 aluminum alloy" Int J AdvManufTechnol (2010) 49:63–71
[7] Rubio E.M , A.M. Camacho, J.M. Sanchez-Sola , M. Marcos "Surface roughness of AA7050 alloy turned bars Analysis of the influence of the length of machining" Journal of Materials Processing Technology 162–163 (2005) 682–689
[8] Hamdi Aouici, Mohamed Athmane Yallese, Kamel Chaoui , Tarek Mabrouki, Jean-Francois Rigal, "Analysis of surface roughness and cutting force components in hard turning with CBN tool: Prediction model and cutting conditions optimization"Measurement 45 (2012) 344–353
[9] Lin J.T, D. Bhattacharyya, V. Kecman, "Multiple regression and neural networks analyses in composites machining" Composites Science and Technology 63 (2003) 539–548
[10] Franci Cus, Uros Zuperl "Approach to optimization of cutting conditions by using artificial neural networks" Journal of Materials Processing Technology 173 (2006) 281–290
[11] Mehmet Cunkas, Ilhan Asilturk "Modeling and prediction of surface roughness in turning operations using artificial neural network and multiple regression method" Expert Systems with Applications 38 (2011) 5826–5832
[12] Muthukrishnan N, J. Paulo Davim "Optimization of machining parameters of Al/SiC-MMC with ANOVA and ANN analysis" journal of materials processing technology 2 0 9 (2 0 0 9) 225–232
[13] Ravinder Kumar , Santram Chauhan "Study on surface roughness measurement for turning of Al 7075/10/SiCp and Al 7075 hybrid composites by using response surface methodology (RSM) and artificial neural networking (ANN)" Measurement 65 (2015) 166–180.

International Journal of Engineering Research and General Science Volume 3, Issue 5, September-October, 2015
ISSN 2091-2730

FPGA BASED DIGITAL BEAM FORMING FOR PHASED ARRAY RADAR

YOGESH P SAJJAN[1], KRISHNA R[2], SHAHUL H[3]
[1]Research Scholar (MTech), Department of ECE, Bangalore Institute of Technology, Bengaluru, India
[2]Assistant Professor, Department of ECE, Bangalore Institute of Technology, Bengaluru, India
[3]Sci/Eng.-SD, RDA, ISTRAC, ISRO, Bengaluru, India
Email: *yogeshpsajjan@gmail.com*

Abstract— with the widespread use of digital techniques in modern communication systems, Digital Beam Forming (DBF) technique can be used for radar transmitter Beam Steering. Beam forming is a signal processing technique used for directional signal transmission or reception in antenna arrays and is achieved by controlling the phase and amplitude of each antenna element. The functions of a Timing Signal Generator (TSG) of a radar system is been implemented using VHDL programming and targeting it on to a FPGA. TSG works directly under the control of Radar Controller (RC) implemented using MATLAB and interfaced through Ethernet. Multiple DDS chips is used to generate multichannel radar waveforms and FPGA is used to send data and control signals to these DDS chips via SPI to achieve DBF. DDS (Direct Digital Synthesis) is a digitally controlled method of generating signals whose frequency, phase and amplitude are controlled by the respective description words.

A sixteen channel direct-digital waveform synthesizer has been developed to enable Digital Beam Steering of the transmitting side for a 4x4 array Patch Antenna. Each antenna element has separate beam forming exciter. The RC communicates to the TSG unit implemented in FPGA and sends commands to TSG. Through the RC GUI, the control parameters like frequency and phase shift values are sent to the TSG. Based on the control signals, data has to be sent to internal registers of each DDS. Xilinx FPGA is used to program sixteen AD9957 DDS and output of FPGA and DDS devices are analyzed.

Keywords — Radar Controller, FPGA, dsPIC Microcontroller, Direct Digital Synthesizer, Digital Beam Forming, Frequency Tuning Word, Phase Offset Word.

1. INTRODUCTION

Phased arrays have been used widely in both civilian and military applications. In civilian applications, they can be found in areas such as air traffic control, smart antennas and satellite communications. As for the military applications, phased arrays have been used in areas such as radar, communications, electronic warfare (EW) and missile guidance. Currently, phased array systems play an important role in defining the type of radar and communications system that will be installed on the next generation military platforms.

An approach in the design of a phased array antenna is to use digital beam forming. Digital beam forming consists of the spatial filtering of a signal where the phase shifting, amplitude scaling, and adding are implemented digitally. The idea is to use a computational and programmable environment which processes a signal in the digital domain to control the progressive phase shift between each antenna element in the array. Digital beam forming has many of the advantages a digital computational environment has over its analog counterpart. In most cases, less power is needed to perform the beam steering of the phased array antenna. Another advantage is the reduction of variations associated with time, temperature, and other environmental changes found in analog devices. The phased array antenna will still contain analog components such as Low Noise Amplifiers (LNAs) and Power Amplifiers (PA) found in the RF stages, but the number of analog components in general can be greatly reduced for large antenna arrays. Digital beam formers can accomplish minimization of side-lobe levels, interference canceling and multiple beam operation without changing the physical architecture of the phased array antenna. Every mode of operation of the digital beam former is created and controlled by means of code written on a programmable device of the digital beam former.

The advances in digital circuit technology made possible and feasible the idea of implementing the beam forming networks through digital signal processing. Digital Beam forming (DBF) offers advantages in terms of power consumption, flexibility, and accuracy. In general, digital systems tend to consume less power. Phased array antenna designs based on DBF implementation are currently being devised for radar applications.

1.1 RADAR WAVEFORM GENERATOR

Generally for any equipment, it is important to readily produce and control accurate waveforms of different frequencies. Some of the examples include agile frequency sources with low spurious signal content and less phase noise for communications, which will be used for industrial and biomedical applications. For those applications, we should be capable of generating an adjustable waveform cost effectively and conveniently which is a key design consideration. Several approaches are available for generating the signal but among those Direct Digital Synthesis (DDS) is most flexible one because DDS is a digital method to generate arbitrary waveforms with control of Frequency, Phase and Amplitude. [3]

2. PROPOSED SYSTEM ARCHITECTURE

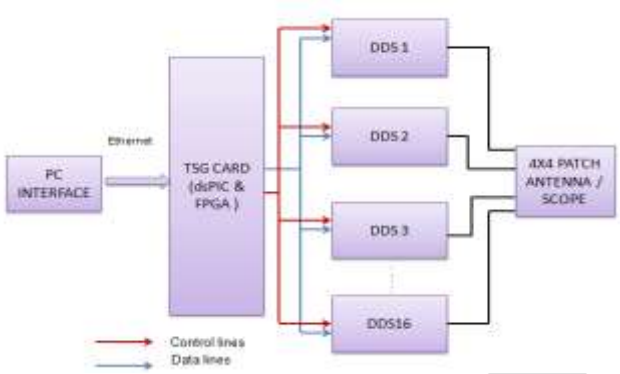

Figure 1.1 Proposed System Block Diagram

PC INTERFACE:- A Graphical User Interface, for inputs from the user. Calculations are done based on input and data frame to be forwarded to TSG is generated and sent via Ethernet.

TSG CARD:- mainly has a Xilinx FPGA, Microcontroller and buffers. The data is accepted by dsPIC and sent to FPGA for data processing. The data and control signal is sent to DDS from FPGA.

DDS BOARD:- DBF is accomplished in DDS board. 16 DDS are used to produce sine waves to 16 channel inputs with needed Phase, Frequency and amplitude, fed to 4x4 patch antenna.

2.1 SYSTEM SPECIFICATIONS

	PARAMETERS	SPECIFICATIONS
1	Output frequency	30MHz – 50MHz
2	Frequency tuning resolution	0.5Hz
3	Output waveform shape	Sine wave
4	No of channels	16
5	Input Clock	10MHz
6	Phase Tuning	0 to 360 degree, 0.05 degree steps

3. DDS TECHNOLOGY

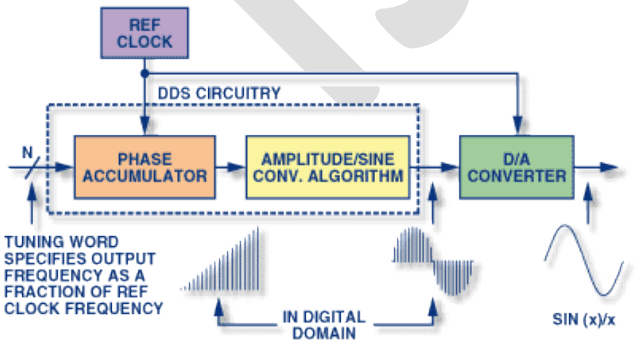

Figure 3.1: DDS Architecture

Direct digital synthesis (DDS) is a method of generating an analog waveform such as sine wave by using time varying signal in digital form. Then using digital to analog converter we can generate an analog signal. It has an ability to control and generate a signal with accurate signal parameters with low cost and low power consumption. DDS principle of operation can be easily understood by the Fig.3.1. Phase accumulator will take the Frequency Tuning Word (FTW) as input and converts into angular phase and then it is converted into the sine wave amplitudes by Amplitude/Sine Conversion Algorithm and then it is converted to analog sine wave output by D/A converter. The output frequency mainly depends on the reference-clock frequency

and tuning word. Phase accumulator is used to compute the phase (angle) address for the sine look up table, which gives the digital value of amplitude corresponding to that phase angle. The DAC will convert that digital value into corresponding analog current or voltage. To generate sine wave of fixed frequency a constant value is added to phase accumulator. If tuning word is large, the phase accumulator will step through the look up table quickly. If it is small the phase accumulator will take more steps thus generating a slower waveform.

4. IMPLEMENTATION

Figure 4.1 GUI for PC Interface

A GUI is developed in MATLAB to provide inputs. Code to calculate the Frequency Tuning Word (FTW) and Phase Offset Word (POW) is written using the required formulae. A XML is created with required parameters and their values. The data from the XML is taken to create a data frame which is sent to TSG Block via Ethernet.

The dsPIC is programmed, to receive the data frame via Ethernet from the PC INTERFACE. The Data frame is processed and sent to FPGA using SPI. Programming FPGA is done in Xilinx ISE, using VHDL code to receive data from microcontroller, store the data in a memory array. DDS Registers' initialization values are also stored in other memory arrays. According to configuration signal, FPGA will send the corresponding control signals and data to all 16 channel DDS.

In the DDS Board, for the implementation of 16 channels Phased Array Radar, 16 DDS are used. Synchronization of 16 DDS is achieved by considering one DDS chip to be Master and its SYNC_OUT signal is distributed to all the 16 DDS chips at SYNC_IN input, thus they will operate synchronously to the single internal clock.

The DDS chips are operated in the Single Tone Mode and sine wave is selected as the output waveform of the DDS.

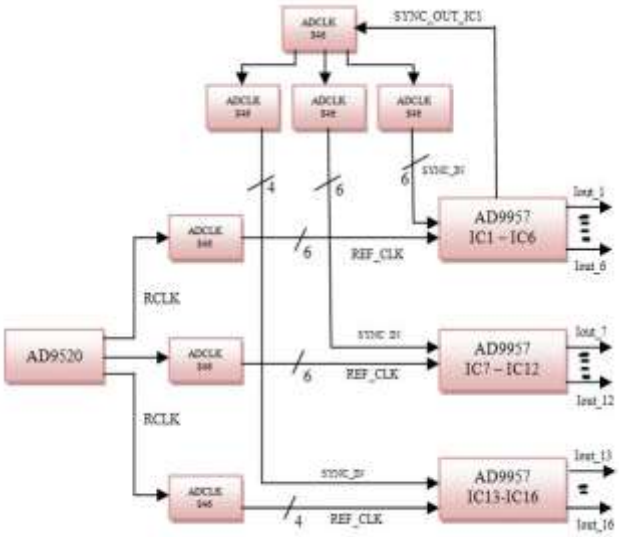

Figure 4.2 DDS Board Block Diagram

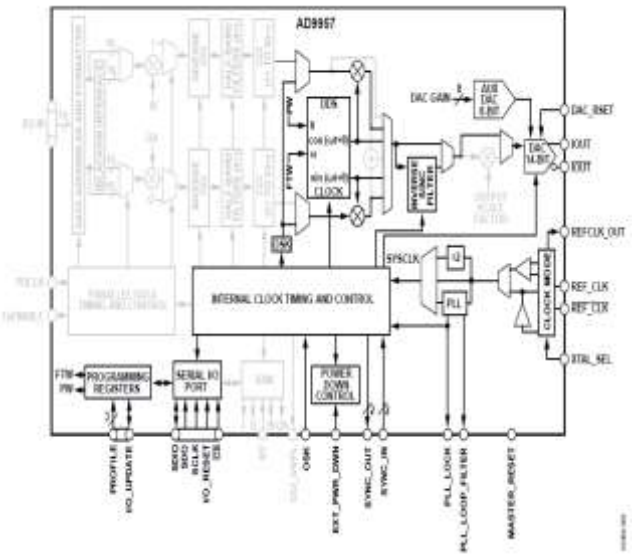

Figure 4.3 Single Tone Mode of AD9957 (From Analog Devices)

FPGA sends control signals to these DDS chips via SPI. FPGA is connected to PC through SPI. The DDS chips have some common control lines, and some that are individual per channel. Sysclk and sclk signal are provided from FPGA and are

distributed to all DDS chips using AD9520 and ADCLK846. An external clock of 10 MHz is provided from an external source which is fed to the AD 9520 clock divider.

5. EXPERIMENTAL RESULTS

The Device Utilization Summary obtained in Xilinx ISE after the synthesis of the VHDL code is given below,

Device Utilization Summary			
Logic Utilization	**Used**	**Available**	**Utilization**
Number of Slice Flip Flops	1,295	9,312	13%
Number of 4 input LUTs	945	9,312	10%
Number of occupied Slices	1,084	4,656	23%
Number of Slices containing only related logic	1,084	1,084	100%
Number of Slices containing unrelated logic	0	1,084	0%
Total Number of 4 input LUTs	1,016	9,312	10%
Number used as logic	945		
Number used as a route-thru	71		
Number of bonded IOBs	37	232	15%
Number of RAMB16s	2	20	10%
Number of BUFGMUXs	3	24	12%
Number of DCMs	1	4	25%

Figure 5.1Device Utilization Summary

The On-chip power is analyzed using Xilinx XPower Analyzer, and the values obtained are shown below,

Table 13 On-chip Power Values

On-Chip	Clocks	Signals	DCMs	IO	Leakage	Total
Power(W)	0.037	0.014	0.019	0.127	0.085	0.283

The FPGA outputs are connected to a digital Oscilloscope and the CRO screen shots are shown below,

The signal channels are:- Channel 3 – 100 MHz System Clock, Channel 1 – IO_Update, Channel 2 – IO_Reset, Channel 0 – 12.5 MHz sclk for Data transfer, Channel 4 – Master_Reset, Channel 5 – Profile, Channel 6 to 14 – DDS1 to DDS9

When the Master_Reset and IO_Reset are low, Data Transmission starts and the data is forwarded with the rising edge of sclk. The IO_Update signal becomes high when the transmission is complete and then the sclk is halted.

Figure 5.2 Outputs generated for Initialization of DDS Registers

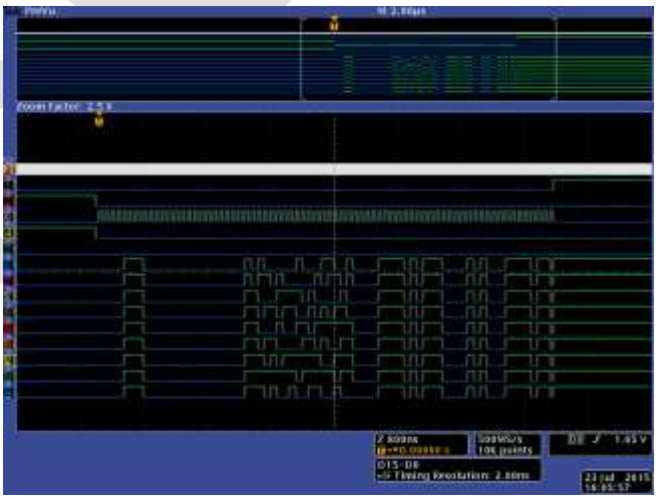

Figure 5.3 Outputs generated for Configuration of DDS Profile Register

DDS Board Simulation Outputs obtained in Simulink is shown below,

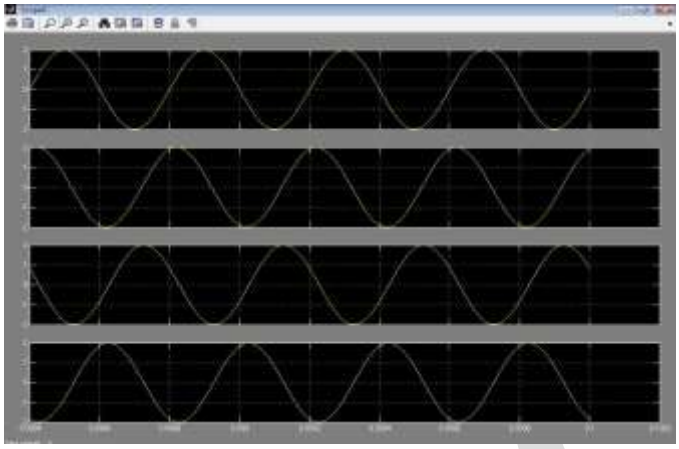

Figure 5.4 Phase Shifted Sine Waveforms of different DDS w.r.t 1st DDS Sine Wave as Reference

ACKNOWLEDGMENT

I'm indebted to Supreme Almighty for his beloved blessings on me with his grace. I would like to thank Mr. K V Prasad, Mr. VijayaPrakash from BIT, Mr. Pradeep Kumar, Mr. Arjun S, Mr. Chinni P and Mr. Shivakumara Swamy from ISTRAC for their Valuable Guidance and support for the work. I would mention my sincere and heartfelt gratitude to my Parents and all my Family members for their wholehearted constant support. I would also thank all the persons who have directly and indirectly supported me in this work.

CONCLUSION

In this work, we propose a method to achieve Digital Beam Forming in Transmitter section of 16 channel Phased Array Radar using Direct Digital Synthesizer chips to generate a multi channel VHF radar frequencies. Timing Signal Generator and Configuration Card was designed and developed as an intermediate device between PC and DDS board, which based on control signals, performs the data handling and forwards the required data to DDS, for the operation of MPAR. With the idea of implementing an advanced technology, design of DDS based RF waveform generator is demonstrated using the XILINX FPGA and dsPIC33F Micro Controller that results in a more stable and durable RF signal generator. The 16 channel DDS board is been simulated. The design has fine tunable resolution, sub-degree phase tuning capability, extremely fast hopping speed, fast settling & switching time and low spurious noise. Thus the DDS based DBF developed has enormous potential to be used for Multifunctional Phased Array Radar(MPAR), launch vehicles traffic controller, climate monitoring and in providing wind velocity data for aircrafts.

REFERENCES:

[1] Anudeepa S. Kholapure, Dr. Arvind Agarwal, ― Design of a Timing Signal generator for RADAR using FPGA ‖, Institute of Communications and Navigation, VOL. 19, NO. 2, 2009

[2] B.Suresh, M.V.Srikanth, ― Radar waveform generator based on DDS, International journal for advanced research in computer and communication engineering, September 2013

[3] Lathasree.G, Pradeep Kumar, - DDS technique based RF-excited card, International Journal combined research and development, October 2013

[4] Sanjay M Trivedi1, B. S. Raman, - FPGA based control signal generator for pulsed radar, Proc. IEEE, vol. 95, no. 7, pp. 1430-1469, September 2012.

[5] P Srinivasulu, P. Kamaraj, ― Control system for VHF phased array radar, Tech. Rep. GDD-05-04, NSF, 2005

[6] Henrik Ohlsson, Lars Wanhammar, ― Implementation of a digital beam former in an FPGA using distributed arithmetic, SE 581 83,

2010.

[7] Dr.A.Jhansi rani,Dr.A.Jaya Lakshmi, - Phased Array Antenna & Beam forming Subsystems in Phased Array Radar

[8] Okorogu V.N, Nwalozie G.C, Okoli K.C, Okoye E.D, - Design and Simulation of a Low Cost Digital Beamforming (DBF) Receiver for Wireless Communication

[9] Dr.Jeffrey S.Herd, ― Multifunction phased array radar panel, ACM/ Springer Wireless Networks, vol. 18, no. 2, pp. 215-226, February 2011.

[10] H. Aliakbarian, V. Volski , ― Analogue versus digital for baseband beam steerable array used for LEO satellite application, Stellanbosch University, February 2011.

[11] Wenfeng Dong; Quan Liu; Shirui Peng; Haihong Li "Design and realization of arbitrary radar waveform generator based on DDS technology", Radar Handbook Edition 3, Publication Year: 2010,

[12] Chao Huang, Li-xiang Ren, Er-ke Mao, "A Systematic Frequency Planning Method in Direct Digital Synthesizer Design",

International Conference on Wireless Communication, 2009

International Journal of Engineering Research and General Science Volume 3, Issue 5, September-October, 2015
ISSN 2091-2730

Review-Paramatreic investigation of electrospun nanofiber

[a]Sachin Chavan [b] Nand Jee Kanu

[a b] *Research Scholar Bharati Vidyapeeth University College of Engineering, Pune-Satara Road ,Pune410043,India*

Email-sschavan@bvucoep.edu.in,sachin_72887@rediffmail.com,Contact-9271635407

Abstract- Nanotechnology has brought revolutionary change the field of advances materials and their properties. The electrospinning process offers a potential enabling breakthrough to remove the barriers by dramatically reducing fiber diameters, resulting in vast improvements in fiber mechanical properties. To start with this process we should be familiar with the parameter with are contributing to get optimum diameter. For the new research here we have reviewed data for various parameters such as viscosity, molecular weight, ionic salt, voltage, distance between spinneret and collector, flow rate and concentration.

Keywords*:Nanotechnology*,electrospining,process parameters and diameter

1.Introduction

Drawing, Template Synthesis, Phase Separation and Self assembly are the methods useful for developing 1-D nano structures but these methods have limitations of scalability. In contrast, Electrospinning is a simple and versatile process to generate uniform diameter fibers in random, as well as aligned fashion from wide variety of polymer, ceramic or composite solutions in cost effective manner. Low cost, scalability for mass manufacture, several areas of applications, wide variety of materials are the parameters that make electrospinning very popular process among research community associated with One Dimensional (1-D) nanostructures. Thus, the electrospinning process seems to be the only method which can be further developed for mass production of one-by-one continuous nanofibers from various polymers[17].

There are fundamental four components associated with the electrospinning process viz. spinneret, voltage supply, and collector and dispensing pump as seen in the schematic of Figure 1. There are basically three parts 1) A high voltage supplier, 2) A capillary tube with a pipette or needle of small diameter, and 3) Metal collecting screen. One electrode is placed into the polymer solution/melt and the other attached to the metal collector. The electric field produces surface tension on the polymer, which induces a charge on the surface of the polymer. Further with increasing the electric field, a critical value is attained at which the repulsive electrostatic force overcomes the surface tension and the charged jet of the fluid is ejected in form of polymer nanofibers. Also, for the quality and variety of nanofibers produced by electrospinning, certainly cost associated is very-very low. Figure 1.a is schematic for aligned and Figure 1.b for random fibers.

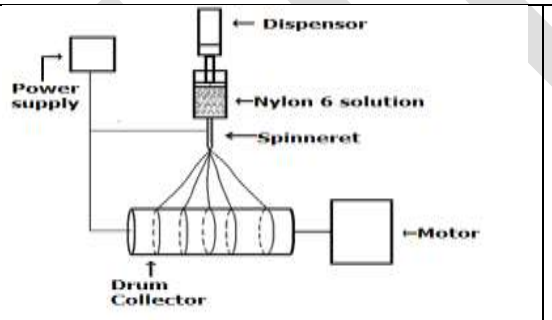

Fig 1.a)Schematic of Electrospinning Setup for Aligned Fiber Deposition[19]

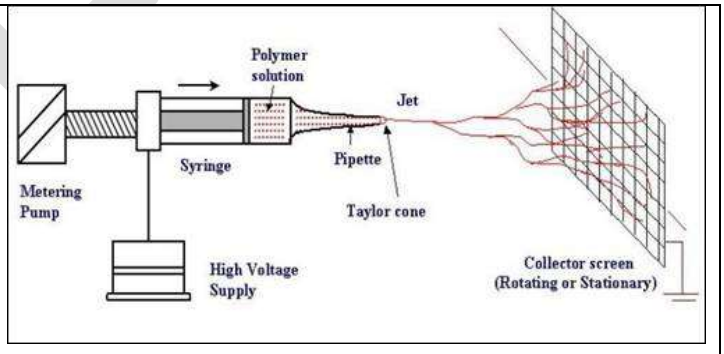

Fig 1.b) Schematic of Electrospinning Setup for Random Fiber Deposition[19]

To get uniform fibers and minimum diameter depends on main three controlling parameters i.e solution, process and ambient parameters as shown in the table 1.1

Table 1.1. Electrospinning Parameters and Fiber Characteristics [18]

Controllable Parameters	Fiber Characteristics
A) Solution Parameters: Viscosity, Concentration Conductivity, Surface tension, Elasticity, Molecular weight	A) Structure: Diameter, Solid, hollow, ribbon, Surface roughness, with beads or pores
B) Process Parameters: Rate of dispensing, Potential difference, Distance between spinneret and grounded collector	B) Alignment: Random Non-woven, Aligned or Unidirectional
C) Ambient Conditions: Temperature, Humidity, Velocity of Air	C) Properties: Modulus, Shear strength, Glass transition temperature, Surface to weight ratio, Refractive Index etc.

Review of Solution parameters –Viscosity,Concentration ,Molecular weight and Process Parameters: Rate of dispensing, Potential difference, Distance between spinneret and grounded collector is done as follow

1.1. Effect of viscosity [independent parameter]:

SOLUTIONS	RESULTS	REFERENCES
Aluminium Borate nanofibers. Solution: Polyvinyl Alcohol [PVA] &Aluminium Acetate stabilized with Boric Acid.	1. Beads formed at low viscosity. 2. To obtain smooth fibers viscosity is increased. 3. For spinnability, viscosity must be neither very high nor very low. 4. Viscosity does not change with time [indicating stability of solution]. 5. Viscosity increases with increasing concentration of solute. 6. Thin fibers formed at 6% concentration of solute, whereas large diameter fibers formed at 10% concentration of solute. 7. Low spinnabiliity at 6% concentration of solute whereas high spinnability at 10% concentration of solute.	1
Nylon 6 [15%-25%]; Solvent: Formic Acid [96.7%]	1. If viscosity increases then diameter increases. 2. If concentration increases then viscosity increases. 3. More concentration and more viscosity and lowering surface tension favor the uniform fibers. 4. If viscosity is increased along with surface tension then diameter increases.	2
Polyurethene Polymer Solution [in various concentration of salt]; Solvent: Dimethylformamide	1. If viscosity increases then length of jet increases. 2. If concentration of salts increases then viscosity first increases and then decreases. Here fiber diameter decreases but after adding more salts fiber diameter increases.	5
Nylon 6,6, PA 6,6; Solvent: Formic Acid. Nylon 4,6, PA 4,6; Solvent: Formic Acid. Polyurethanes PU; Solvent: Dimethylformamide Polycarbonate PC;	1. At viscosity above 20 poises, electospinning was prohibited. 2. At viscosity less than 1 poise droplets formed. 3. Polymer concentration is proportional to solution viscosity. 4. Large diameters fibers being observed at higher viscosity.	6

Solvent: Dimethylformamide		
Tetra Ethyl Orthosilicate [TEOS] nanofiber using electrospinning.	1. At higher viscosity lower beads formed and vice versa. 2. Diameter increases as viscosity increases and vice versa. 3. If viscosity increases then there is good surface quality. 4. If viscosity increases than porosity increases.	7
Curcumin [1%], Geletin [1.5%]; Solvent: Formic Acid [96.7%]	1. The paper indirectly suggests that with increase in viscosity, polymeric concentration increases & hence fiber diameter increases. 2. Viscosity plays major role in determining fibers diameters/jet radius.	10
Polyacrylates Solution PA	1. The paper shows that with increase in viscosity fiber diameter increases.	11

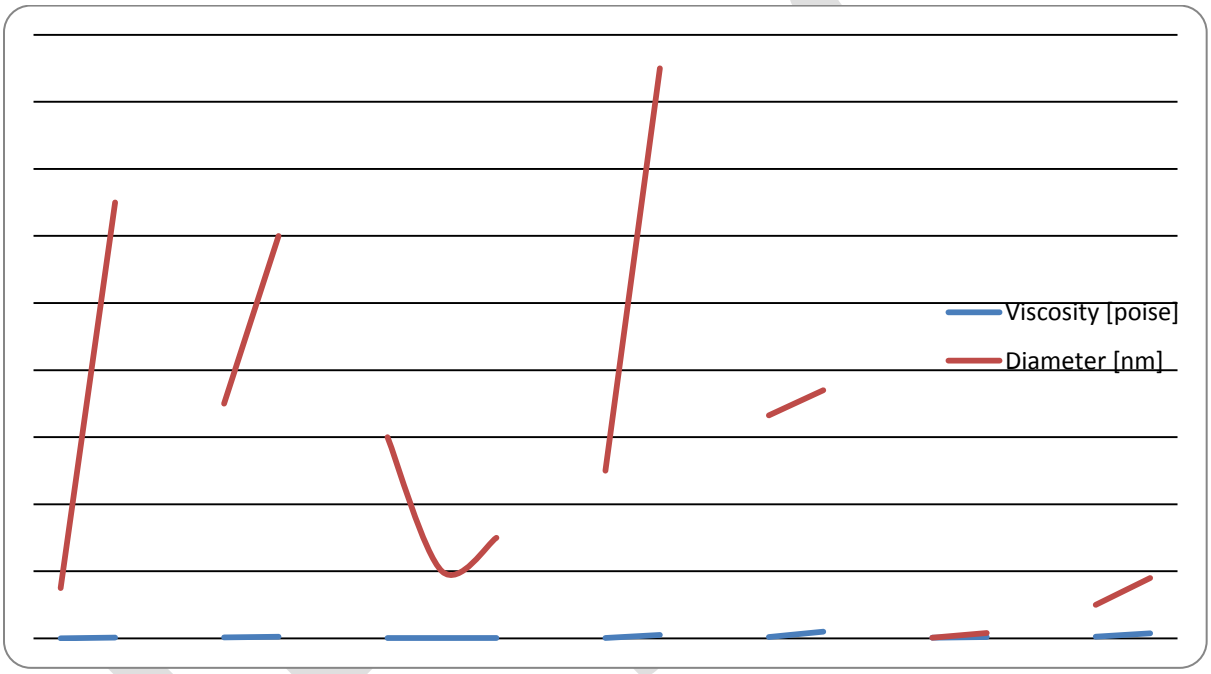

Inference

- As viscosity increases beads are reduced.
- Higher the viscosity higher the diameter.
- For spinnability, viscosity must be neither very high nor very low.

1.3. Effect of Molecular Weight (Solution parameter)

SOLUTIONS	RESULTS	REFERENCES
Biopolymers: Chitosan; Solvent: AcOH, TFA Chitin; Solvent: HFIP	The paper reveals the mystery on molecular weight as, with increase in molecular weight, fiber diameter increases.	3
Tetra Ethyl Orthosilicate [TEOS] nanofiber using electrospinning.	1. At higher molecular weight there are less beads formation. 2. Good surface quality at higher molecular	7

	weight. 3. Diameter increases with increasing molecular weight.	
PMMA [Polymethyl Methacrylate]; Solvents: Toluene, Dichloromethane, Tetrahydrofuran,1,1,1,3,3,3-Hexafluoro-2 Propanol [HFIP], Acetone, Chloroform, 2,2,2-Trifluoroethanol [TFE]	The paper states that the different morphologies of nanofibers were not due to solvents abilities to dissolve solute [PMMA] but rather due to other properties such as boiling points, molecular weight and molecular structure of the solvent.	8
Polyacrylates Solution PA	1. Fiber diameter is constant at high and low molecular weight. 2. The elecrospunnanofiber diameter depend mainly on the polymer and its molecular weight	11

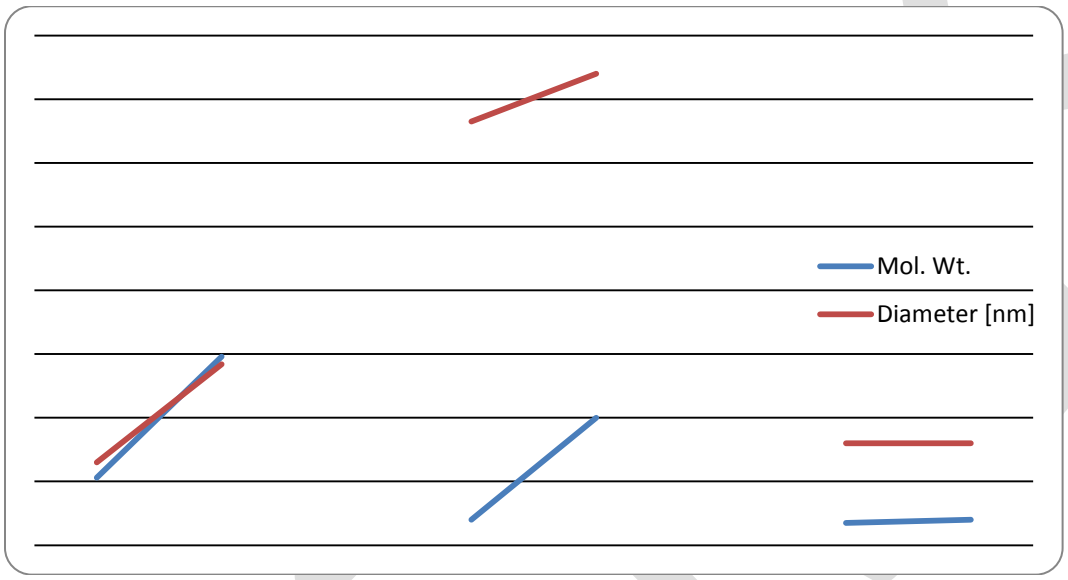

Inference

- At higher molecular weight there are less beads formation.
- Diameter increases with increasing molecular weight.

1.3. Effect of Ionic Salt (Solution Parameter)

Polyurethene Polymer Solution [in various concentration of salt]; Solvent: Dimethylformamide	1. Fiber diameter decreases with salt but after adding more salt fiber diameter increases. 2. Fiber diameter decreases with conductivity. 3. Jet length of polymer solution on drum is decreased with increasing conductivity. 4. Length of jet decreases with increasing the percentage of salt in the polymer solution. 5. With increase in concentration of salt conductivity increases and surface tension increases.	5
Tetra Ethyl Orthosilicate [TEOS] nanofiber using electrospinning.	1. Addition of ionic salt reduces beads. 2. Addition of ionic salt gives uniform diameter and reducing diameter of nanofibers. 3. Addition of salt increases surface quality, and reduced diameter has more enhanced mechanical properties.	7
Polyacrylates Solution PA	The paper suggests that with increase in amount of ionic salt fiber diameter increases.	11

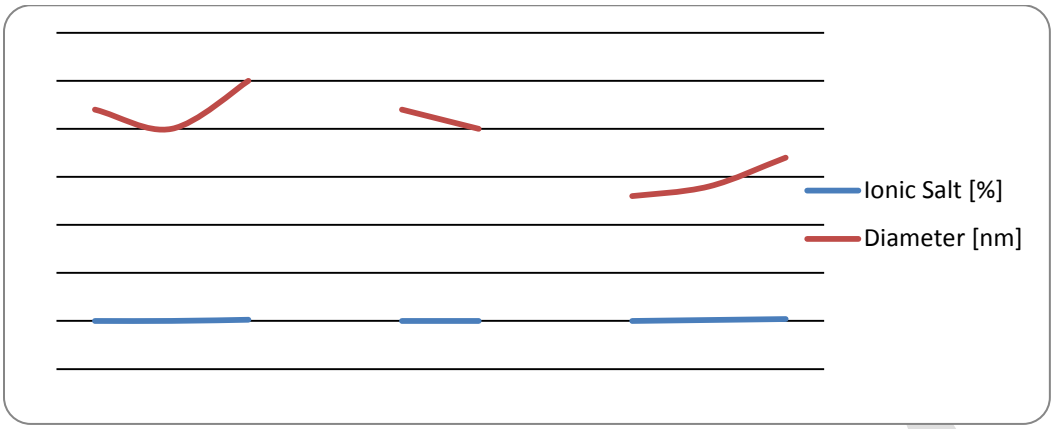

Inference

- Addition of ionic salt reduces beads.
- Addition of ionic salt gives uniform diameter and reducing diameter of nanofibers.

1.4. Effect of Voltage ([Process parameter)

SOLUTIONS	RESULTS	REFERENCES
Aluminium Borate nanofibers. Solution: Polyvinyl Alcohol [PVA] &Aluminium Acetate stabilized with Boric Acid.	High voltage i.e. greater stretching of solution due to greater columbic forces and thus reducing the fiber diameter.	1
Nylon 6 [15%-25%]; Solvent: Formic Acid [96.7%]	1. More voltage results in thin diameter. 2. Increase in voltage favours fiber diameter.	2
Biopolymers: Chitosan; Solvent: AcOH, TFA Chitin; Solvent: HFIP	1. The electrospinning process is initiated at a point at which the electrostatic force in a solution overcomes the surface tension of the solution. 2. Increasing voltage results in higher stretching and thus finer fibers as well as higher extrusion of polymer from the needle that could cause thicker fiber formation. 3. The effect of decreasing distance is almost same as that of increasing voltage.	3
Solution of PCL [Mn=80000] & the Solvent N,N-Dimethylformamide [DMF] & Methylene Chloride [MC].	1. Whipping is the main reason for the decreasing the fiber diameter, as the voltage increase, diameter decreases.	4
Nylon 6,6, PA 6,6; Solvent: Formic Acid. Nylon 4,6, PA 4,6; Solvent: Formic Acid. Polyurethanes PU; Solvent: Dimethylformamide Polycarbonate PC; Solvent: Dimethylformamide	1. Smooth fiber at low voltage. 2. Rough fiber at high voltage. 3. Higher applied electric voltage ejects more fluid in a jet. 4. Higher fiber diameter at more electric voltage.	6
Tetra Ethyl Orthosilicate [TEOS] nanofiber using electrospinning.	1. If electric field increases then beads formation increases. 2. Diameter increases when electric field	7

	increases. 3. Lower electric field results in good surface quality.	
Tetra Ethyl Orthosilicate [TEOS] nanofibers; Solution: Gel process is adapted to get the required TEOS solution.	1. Less diameter at high voltage. 2. TEOS fiber with minimum diameter are produced with two extreme values of voltage and distance between spinneret and ground collector.	9
Curcumin [1%], Geletin [1.5%]; Solvent: Formic Acid [96.7%]	1. More electric potential/electric potential base is responsible for increase in fiber diameter. 2. Electric field has moderate effect on jet radius.	10
Polyacrylates Solution PA	With increase in voltage, fiber diameter first increases, then decreases and again increases.	11

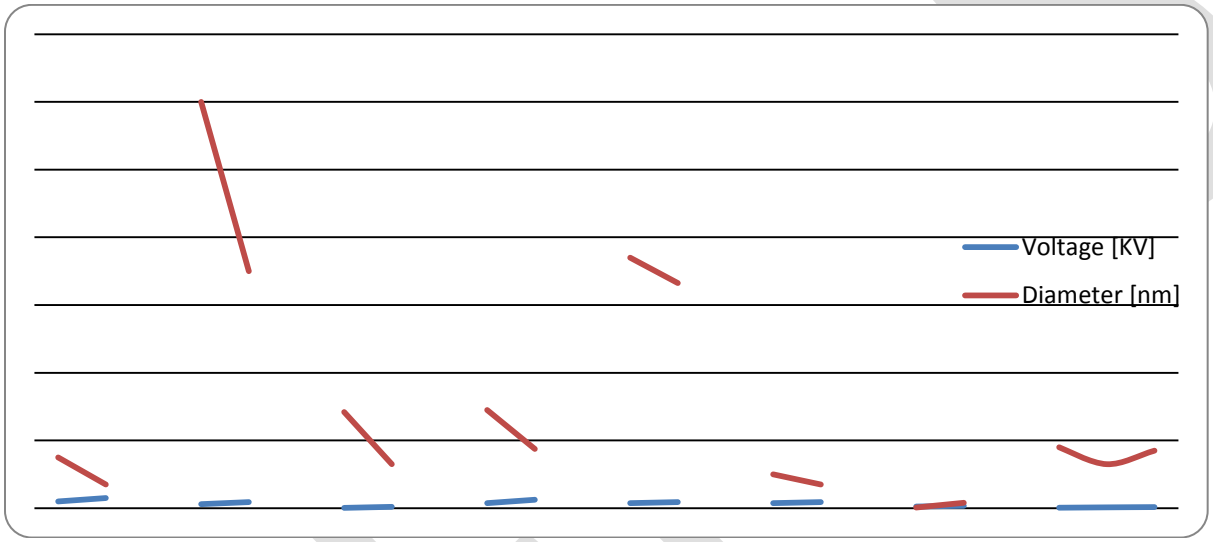

Inference

- Higher the voltage lower is the diameter.

1.5. Effect of Distance (Process Parameter)

SOLUTIONS	RESULTS	REFERENCES
Aluminium Borate nanofibers. Solution: Polyvinyl Alcohol [PVA] &Aluminium Acetate stabilized with Boric Acid.	Distance between tip and drum must be more for thin fibers.	1
Solvent: Formic Acid [96.7%]	More distance is responsible for thin nano fibers.	2
Biopolymers: Chitosan; Solvent: AcOH, TFA Chitin; Solvent: HFIP	1. Distance has direct influence on jet flight and electric field strength. 2. Decrease in distance shortens flight times and solvent evaporation time and increases the electric field strength which results in more bead formation.	3
Solution of PCL [Mn=80000] & the Solvent N,N-Dimethylformamide [DMF] & Methylene Chloride [MC].	With increase in voltage, and then increase in flow rate and keeping distance constant i.e. 15 cm for same experiment time, it has been observed that ultimately fiber diameter increases.	4
Tetra Ethyl Orthosilicate [TEOS]	With increase in distance there is increase in	7

nanofiber using electrospinning.	diameter.	
Tetra Ethyl Orthosilicate [TEOS] nanofibers; Solution: Gel process is adapted to get the required TEOS solution.	1. With increase in distance diameter reduces. 2. TEOS fibers with minimum diameter are produced with 02 extreme values and distance between spinneret and ground collector.	9
Curcumin [1%], Geletin [1.5%]; Solvent: Formic Acid [96.7%]	1. With increase in distance, jet radius decreases. 2. With increase in collector distance, radius of fiber decreases.	10
Polyacrylates Solution PA	With distance fiber diameter increases first, then decreases and finally increases.	11

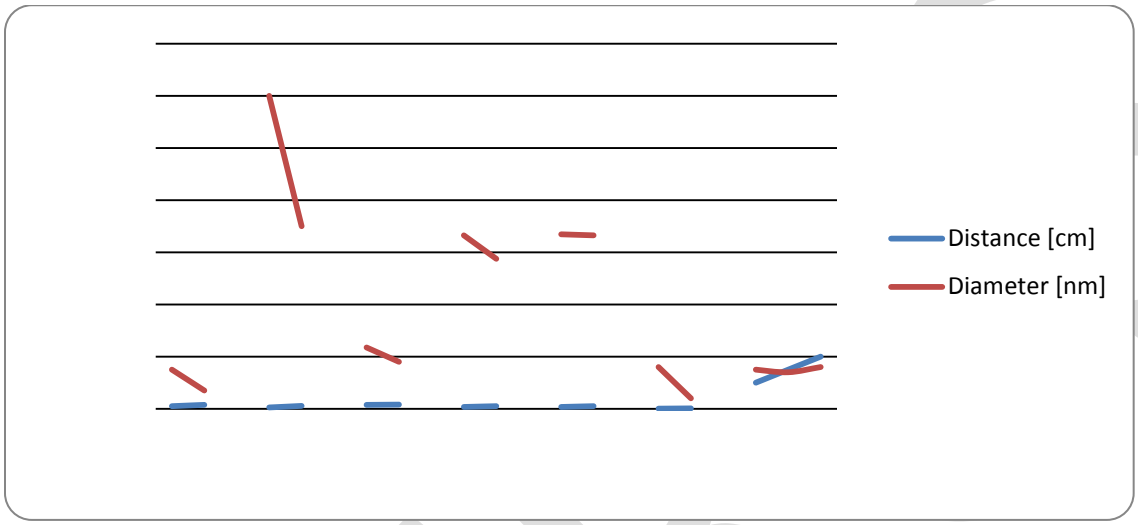

Inference
As distance increases diameter reduces.

1.6. Effect of Flow Rate(Process Parameter)

SOLUTIONS	RESULTS	REFERENCES
Aluminium Borate nanofibers. Solution: Polyvinyl Alcohol [PVA] &Aluminium Acetate stabilized with Boric Acid.	When feed rate increases then diameter increases.	1
Solvent: Formic Acid [96.7%]	More flow rate means more diameters.	2
Biopolymers: Chitosan; Solvent: AcOH, TFA Chitin; Solvent: HFIP	1. Increase in flow rate increases fiber diameter and bead size. 2. Smaller diameter of tip reduces clogging as well as the no. of beads which leads to less exposure of the solution to the atmosphere.	3
Solution of PCL [Mn=80000] & the Solvent N,N-Dimethylformamide [DMF] & Methylene Chloride [MC].	1. With increase in voltage, and increase in flow rate and keeping distance constant i.e. 15 cm, then height of Taylor-Cone [pixel points] decreases and thus fiber diameter decreases.	4
Tetra Ethyl Orthosilicate [TEOS] nanofiber using electrospinning.	1. As feed rate increases then beads increases. 2. Larger diameter forms at higher feed rate. 3. As feed rate increases surface quality decreases.	7

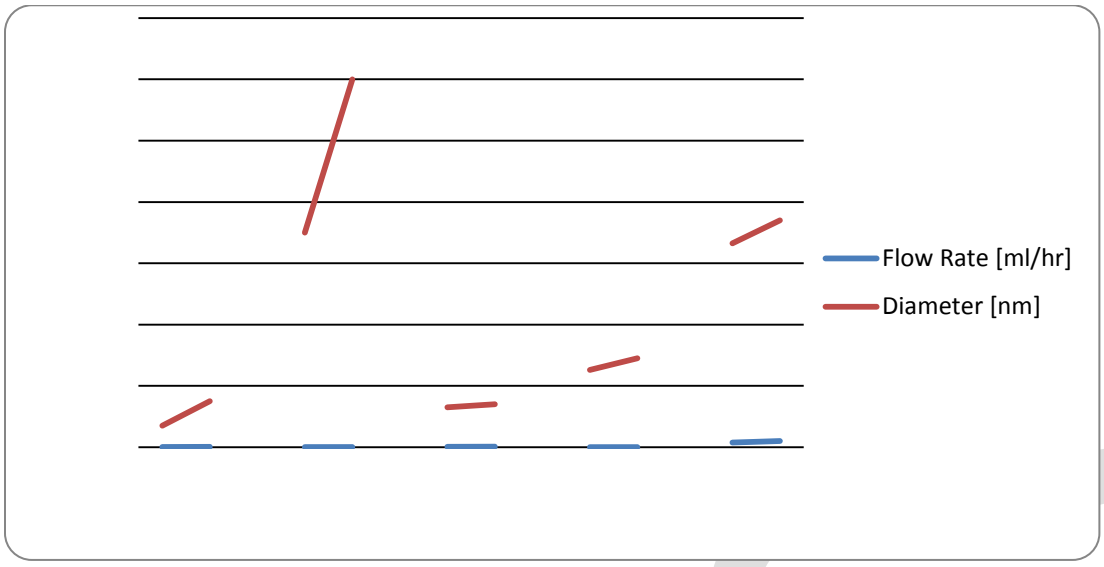

Inference
As flow rate increases diameter increases.
As flow rate increases beads increases.

1.7. Effect of Concentration (Solution parameters)

SOLUTIONS	RESULTS	REFRENCES
Aluminium Borate nanofibers. Solution: Polyvinyl Alcohol [PVA] &Aluminium Acetate stabilized with Boric Acid.	1. At 6% concentration of solute, thin fibers form at low viscosity whereas at 10% concentration of solute, large diameter of fibers form at high viscosity. 2. Finally increase in concentration, increases viscosity until smooth fibers obtained. 3. For spinnability, concentration must be neither very high nor very low. 4. At 6%, low spinnability and at 10%, high spinnability.	1
Solvent: Formic Acid [96.7%]	1. Concentration increases then viscosity increases. 2. Furthermore concentration and more viscosity and lowering surface tension favours the uniform fibers. 3. Beads disappear when concentration increases.	2
Biopolymers: Chitosan; Solvent: AcOH, TFA Chitin; Solvent: HFIP	1. Determines the resistance of polymer solution against stretching and fiber forming in electrospinning technique. 2. Decreasing the concentration increase the diameter of electrospun fibers.	3
Polyurethene Polymer Solution [in various concentration of salt]; Solvent: Dimethylformamide	1. With increase in concentration of salts, fiber diameter is decreased and after adding more salts, fiber diameter is increased. 2. Length of jet decreases with increasing the	5

	percentage concentration of salt in the polymer solution. 3. With increase in concentration of salts, viscosity increases and so length of jet increases [by using polyvinyl alcohol].	
Nylon 6,6, PA 6,6; Solvent: Formic Acid. Nylon 4,6, PA 4,6; Solvent: Formic Acid. Polyurethanes PU; Solvent: Dimethylformamide Polycarbonate PC; Solvent: Dimethylformamide	1. Higher polymeric concentration means large diameter. 2. Fiber diameter depends primarily on jet size as well as on polymer content in the jet.	6
Tetra Ethyl Orthosilicate [TEOS] nanofiber using electrospinning.	1. Higher concentration results in less beads formation. 2. Diameter as per power law relationship with exponent of about 0.5 and 0.3. 3. Good surface quality can be obtained at higher concentration.	7
Curcumin [1%], Geletin [1.5%]; Solvent: Formic Acid [96.7%]	1. With increase in polymer concentration/polymer concentration base, fiber diameter increases. 2. Polymer concentration has moderate effect on jet radius.	10
Polyacrylates Solution PA	1. With increase in salt content [which leads to increase in viscosity finally], and ultimately fiber diameter increases. 2. The fiber diameter of the electrospun web depend mainly on the polymer and its molecular weight.	11

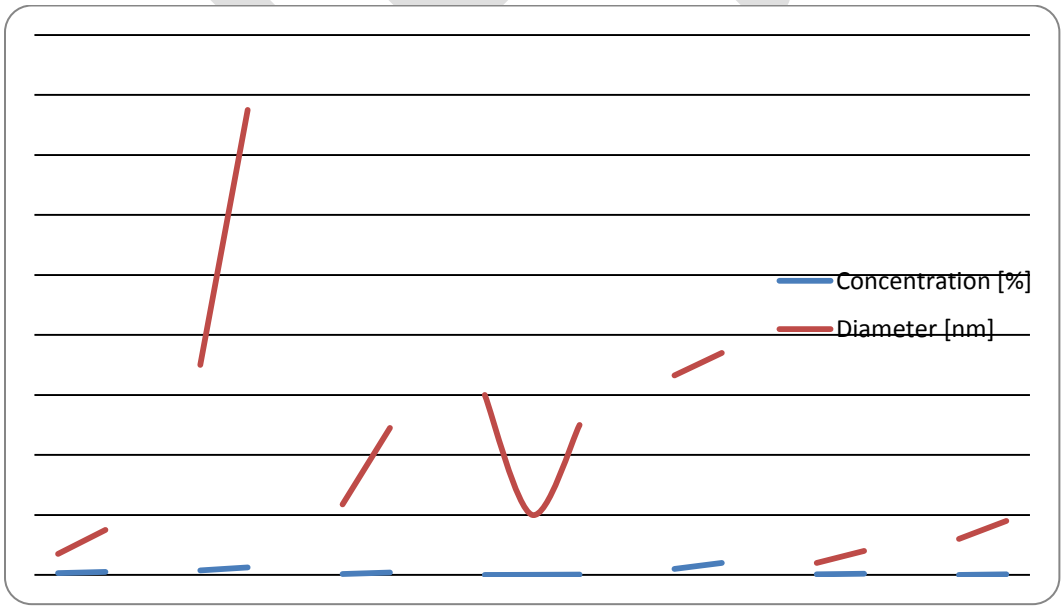

Inferenece

- Concentration increases then diameter increases
- Concentration increases then viscosity increases.
- Beads disappear when concentration increases.

Conclusion.

1. Electrospinning is one of the best methods for spinning the polymer nanofibers .
2. Higher the viscosity higher the diameter.
3. For spinnability, viscosity must be neither very high nor very low.
4. Diameter increases with increasing molecular weight.
5. Addition of ionic salt gives uniform diameter and reducing diameter of nanofibers.
6. Higher the voltage lower is the diameter.
7. As distance increases diameter reduces.
8. As flow rate increases diameter increases.
9. Concentration increases then diameter increases
10. Concentration increases then viscosity increases.

REFERENCES:

1.Mehtap Ozdemir, ErdalCelik, UmitCocen, Effect of Viscosity on the Production of Alumina Borate Nanofibers Via Electrospinning, Original Scientific Article, VDK 6203:66,017,ISSN 1580-2949, MTAEC9, 47(6)735(2013).
2. Mohammad Chowdhary and George Stylios, Effect of Experimental Parameters on the Morphology of Electrospun Nylon 6 fibers, International Journal of Basic & Applied Sciences IJBAS-IJENS VOL: 10 NO: 06.
3. MasoumehValizadeh, SeyedAbdolkarimHosseiniRavandiAndSeeramRamakrishna, Recent Advances in Electrospinning of some selected Biopolymers, Journal of Textiles and Polymers, Vol-1, No.2, June 2013.
4. Yuanyuan Liu, Changjuan Jing, Dali Liu, Qingxi Hu, Research on high quality NanofiberElectrospinning Manufacturing System: Detecting Method of Taylor-Cone And Fiber Diameter control strategy, PrzegladElektrotechniczny (Electrical Review), ISSN 0033-2097, R88 NR96/2012.
5. FatmaYEVER, BaturalpYELEINKAYA, OldrichJIRSAK, New Measurement Methods for studying of Mechanism of roller Electrospinning , Nanocon 2013, 16.-18.10.2013, Brno, Czech Republic, Eu.
6. Zheng-Ming Huang, Y-Z. Zheng, M.Kotaji, S.Ramakrishna, A Review on Polymer Nanofibers by Electrospinning and their applications in Nanocomposites, Elsevier, Composite Science & Technology 63(2003)2223-2253.
7. Dr.S.M.Shendokar, Mr.S.S.Chavan, Mr.P.V.Londhe, Assesment of ElectrospunNanofiber properties in Two Phase Composites, Nancon 2010.
8. Yong-Fang Qian, Yan Su, Xiao-Qiang Li, Hong-Sheng Wavg And Chuang-Long He, Electrospinning of Polymethyl Methacrylate Nanofibers in different Solvents, Iranian Polymer Journal 19(2), 2010, 123-129.
9. Sachin S. Chavan, Mukesh K. Sinha, P.V.Londhe, Synthesis & Characterization of Composite Nanofibers with VARTM and Electropinning Process, Applied Scence Innovations Pvt. Ltd., India, Carbon-Sci. Tech 5/3(2013)289-295.
10. C.J. Thompson,G.G.Chase, A.L.YarinYarin, D.H.Renekar, Effects of Parameters on Nanofiber diameter determined from Electrospinning Model, Elsevier, Science Direct, Polymer 48(2007)6913-6922.
11. Ruotsalainen.T., Turker J., Heikkila. P., Ruokolainen J., Nykanan A., Laitinen T., Torkkeli M; Serimaa R, Ten Brinke G, Harlin A, Ikkala O., Towards Internal Structuring: ElectrospunNanofibers by Self-Assembly of Polymeric Comb-Shaped Supramolecules, Advanced Materials, 17(8)2005, 1048-1052.
12. Ristolainen N. Heikkila P., Harlin A., Seppala J., Polyvinyl Alcohol & Polyamide-66 Nanocomposites Prepared By Electrospinning, Macromolecular Materials & Engineering, 291(2)2006,114-122.
13. Heikkila P., Sipila A., Peltola M., Taipale A., Harlin A., ElectrospunPA Coating on Textile Surfaces, Textile Research Journal, 77(11)2007, 864-870.
14. Heikkila P., Uusimaki J., Soderlund L., Kettunen L. Harlin A., Exploitation of Electric Field in Controlling of Nanofiber Spinning Process, Polymer Engineering & Science, 47(12)2007, 2065-2074.
15. Heikkila P., Taipale A., LehtimakiM.Harlin A., Electrospinning of Polyamides with different Chain Composites for Filtration Application, Polymer Engineering & Science, 48(6)2008, 1168-1176.
16. Heikkila P., Harlin A., Parametric Study Of Electrospinning Of Polyamide-6, European Polymer Journal, accepted 23 June 2006, Doi: 10.1016/j.eurpolym.2008.06.03R.
17. Zheng-Ming HuangY.-Z. Zhang, M. Kotaki, S. Ramakrishna "A review on polymer nanofibers by electrospinning and their pplications in nanocomposites" Composites Science and Technology 63 (2003) 2223–2253
18. Doshi J., Reneker D.H, "Electrospinning process and applications of electrospun fibers," *Journal of Electrostatics*, Vol. 35, (1995), Pg. 151-160

19.Bergshoef MM, Vancso GJ. Transparent nanocomposites with ultrathin, electrospun Nylon-4,6 fiber reinforcement. Adv Material Science 1999;11(16):1362–5

International Journal of Engineering Research and General Science Volume 3, Issue 5, September-October, 2015
ISSN 2091-2730

Design and Analysis of Low Noise Amplifier for 2.47GHz, build for Wireless LAN and WI-FI (802.11G Protocol)

Author – 1) Mr. Mayur K..Mohod (M.E. EXTC)

mayurmohod29@gmail.com

Mb No-9503764268

Abstract- The LNA function, play an important role in the receiver designs. Its main function is to amplify extremely low signals without adding noise, thus preserving the required Signal-to-Noise Ratio (SNR) of the system at extremely low power levels.

Amplification is one of the most basic and prevalent RF circuit functions in modern RF and microwave systems. Microwave transistor amplifiers are rugged, low cost, and reliable and can easily be integrated in both hybrid and monolithic integrated circuitry. To amplify the received signal in a RF system, a low noise amplifier (LNA) is required. The goal of this is to design an LNA with lowest noise figure possible, with gain as high as possible for the given FET and information. An amplifier is designed for the purpose on increasing level of voltage, current or power. The amount of this increase is known as gain on amplifier.

First stage of a receiver is typically a low noise amplifier (LNA), whose main function is to provide enough gain to overcome the noise of subsequent stages. Aside from providing this gain while adding as little noise as possible, an LNA should accommodate large signal without distortion and frequently must also prevent specific impedance, such as 50Ω, to the input source. CMOS amplifier will implement in 90 nm CMOS technology using ADS tool operating on wireless and Wi-fi Application. This ADS tool gives the advantages in the designing of LNA.

Keywords- LNA, SNR, RF, FET, CMOS, VLSI, BJT, ADS.

INTRODUCTION-

The LNA is the first block in most receiver front ends. Its job is to amplify the signal while introducing a minimum amount of noise to the signal. Gain can be provided by a single transistor. Since a transistor has three terminals, one terminal should be ac grounded, one serves as the input, and one is the output. There are three possibilities, as shown in Figure 6.1. Each one of the basic amplifiers has many common uses and each is particularly suited to some tasks and not to others. The common-emitter amplifier is most often used as a driver for an LNA. The common-collector, with high input impedance and low output impedance, makes an excellent buffer between stages or before the output driver. The common-base is often used as a cascade in combination with the common-emitter to form an LNA stage with gain to high frequency, as will be shown. The loads shown in the diagrams can be made either with resistors for broadband operation, or with tuned resonators for narrow-band operation. In this chapter, LNAs with resistors will be discussed first, followed by a discussion of narrowband LNAs. Also, refinements such as

2. Objective:-

The objective here is to develop **Low Noise Amplifier** with desired specifications. In the following project we have tried to explain how we designed an amplifier at 2.45 GHz for W-LAN application.To achieve LNA with improved gain with the help of CMOS Technology by using single stage n-MOS amplifier .Evaluation of noise figure, gain, input and output reflection coefficient. Design and simulation of RF circuit in Advanced Design Tools(ADS). We used “ADVANCED DESIGN SYSTEM 2009” for simulation

purpose. It is user friendly tool and easy to understand. ADS is ***the "Hi-Frequency &Hi-Speed" platform for IC, Package and Board Co-Design.***

3. Literature review:-

- One of the important implementation of Design and noise optimization for a RF low noise amplifier by Ravinder Kumar, Manish Kumar , and Viranjay M. Srivastava in this, they proposed Amplifier is a non-linear characteristics device and causes two main problems one is blocking and other is inter-modulation

- Wenjian Chen, Tins Copani, Hugh J. Barnaby, SayfeKiaeiIn the context of A 0.13 um CMOS ultra-low power front-end receiver for wireless sensor networks they proposed feedback techniques to reduce the current consumption while optimizing the input matching and noise performance.

- Another importantperformance of the forward-biased RF LNA with deep n-well n-MOS transistor given byS.F. WAN Muhamad Hatta, N. Soin in this they proposedThe common gate transformer feedback transconductance boosting is used to minimized the current consumption then gain is doubled due to the sum of n-mos and p-mos transcondctances. The main function of LNA is mutually dependent on a set of design parameter values. LNA design with deep n-well into a fully integrated LNA with forward biasing exhibits better power gain & noise-figure performance.

4. Research methodology to be employed:-

STEP 1:- Selection of MOS Transistor

This is the first and the most important step while designing an on chip LOW NOISE AMPLIFIER. The selection of MOS depends on its mobility, so we have selected an enhancement type of n-MOS transistor. The three important parameters in the transistor are V_{ds}, V_{gs} and I_{ds}.Values of V_{ds} and V_{gs} are predetermined. We have to obtain the desired value of Ids which is dependent on W/L ratio of MOS transistor. Since we are using 0.09µm technology, our device length is fixed at 0.09 micrometer. The only parameter on which the Ids depends is "width" of the device.

$$\mathbf{I_{ds} = [\frac{\mu n * cox}{2}]*[\frac{W}{L}]*(V_{gs}-V_t)^2}$$

Values of μ_n and C_{ox} are dependent on fabrication process. Since we are using 0.09µm technology C_{ox} = 8.42 fF. For simulation purpose we are using BSIM 3 model, hence the device width is reduced by 20% to 30% of the calculated width.

STEP 2:- DC Simulation

Biasing in electronics is the method of establishing predetermined voltages or currents at various points of an electronic circuit to set an appropriate operating point. The operating point of a device, also known as bias point, quiescent point, or Q-point, is the steady-state operating condition of an active device (a transistor or vacuum tube) with no input signal applied.

The importance of DC simulation is to determine the quiescent point of the device MOS. The DC Simulation controller calculates the DC operating characteristics of a design under test (DUT). Fundamental to all RF/Analog simulations, DC analysis is used on all

RF/Analog designs. It performs a topology check and an analysis of the DC operating point, including the circuit's power consumption. The simulator computes the response of a circuit to a particular stimulus by formulating a system of circuit equations and then solving them numerically. The DC simulation accomplishes this analysis as follows:

- Solves a system of nonlinear ordinary differential equations (ODEs)
- Solves for an equilibrium point
- All time-derivatives are constant (zero)
- System of nonlinear algebraic equations

You can also set up the DC simulation to sweep one or more parameters, enabling you to perform tasks such as verifying model parameters by comparing the simulated DC transfer characteristics (I-V curves) of the model with actual measurements. We are using a fixed biasing scheme for DC biasing. In self bias and voltage divider bias, resistors are involved, which increase the size and parasitic effect of device. So we are using self bias to optimize the devise.

STEP 3:- Feedback Network Design

Feedback can be either negative or positive. In amplifier design, negative feedback is applied to effect the following properties.

- Desensitize the gain
- Reduce non-linear distortion
- Reduce the effect of noise
- Control the input and output impedance

STEP 4:- S Parameter Analysis

The fact that the average analog engineer is unfamiliar with these concepts (and has probably never used a program like Genesis before), is not a good reason not to learn and use these techniques. It is quite certain that these tools are very useful even if you are designing low frequency circuits. A few of the many reasons this statement is made are:

1) The transistors you use don't know that they are supposed to work only at audio frequencies. They are perfectly happy to oscillate at many GHz if allowed.

2) Genesis (and other programs like it) contains modules that enable you to do EM modeling of things like circuit boards. This can be quite useful in making your circuit EMI hardened (a bane of many analog circuits).

3) These tools provide new insights into analog design broadening your knowledge and capabilities; insights that may help keep you ahead of your competitors. So while understanding s-parameters and having access to tools like Genesis is critical for the RF and high frequency, wide bandwidth analog designer, they are extremely useful for the low frequency analog designer as well.

Scattering parameters are all about power; both reflected and incident in a linear two port system. It assumes that the system must be treated like a transmission line system; lumped elements no longer adequately describe the system. For the following analysis, refer to Figure6.10.

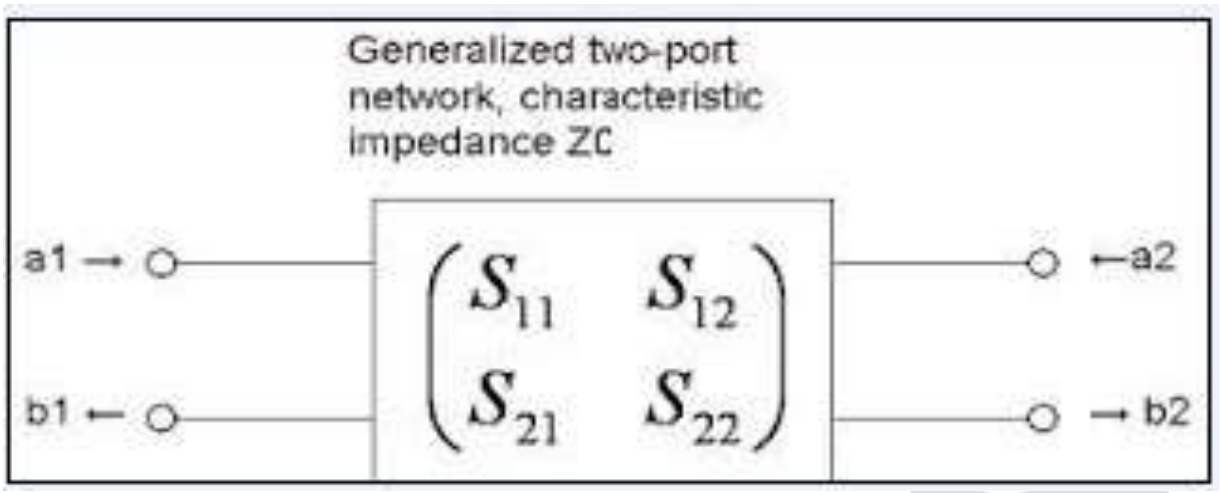

Figure: S Parameter Two Port Model

The s-parameter definition is:

$b_1 = a_1 s_{11} + a_2 s_{12}$

$b_1 = a_1 s_{21} + a_2 s_{22}$

where,

$|a_1|^2$ = Power incident on the input of the network.

= Power available from source impedance Z_0.

$|a_2|^2$ = Power incident on the output of the network. = Power reflected from the load

$|b_1|^2$ = Power reflected from input port of network.

$|b_2|^2$ = Power reflected from the output port of the network.

= Power incident on the load.

= Power that would be delivered to a Z_0 load.

And

$$|S11| = \frac{Power\ reflected\ from\ the\ network\ input}{\text{Power incident on the network input}}$$

$$|S22| = \frac{Power\ reflected\ from\ the\ network\ output}{\text{Power incident on the network output}}$$

$$|S21| = \frac{Power\ delivered\ to\ a\ Zo\ load}{\text{Power available from Zo source}}$$

= Transducer power gain with both load and source having impedance as Zo.

$$|S12| = Reverse\ Transducer\ power\ gain\ with\ Zo\ \ load\ and\ source$$

STEP 5:- Noise Figure Analysis

Besides stability and gain, another important design consideration for a microwave amplifier is its noise figure. In receiver applications, it is often required to have a preamplifier with as low a noise figure as possible, as the first stage of a receiver front end has the dominant effect on the noise performance of the overall system. The noise figure parameter, N, are given where, the quantities F_{min}, Γ_{opt} and R_N are the characteristics of the transistor being used and are called the noise parameters of the device.

STEP 6:- Impedance Matching

The impedance matching network is lossless and is placed between the input source and the device. The need for matching network arises because amplifiers, in order to deliver maximum power to a load, or to perform in a certain desired way must be properly terminated at both the input and the output ports. The impedance matching networks can be either designed mathematically or graphically with the aid of Smith Chart. Several types of matching networks are available, but the one used in this design is open single stubs whose length is found by matching done using smith chart manual.

It is necessary to match this impedance to the impedance of the source driving the circuit. The output impedance must be similarly matched. It is very common to use reactive components to achieve this impedance transformation, because they do not absorb any power or add noise. Thus, series or parallel inductance or capacitance can be added to the circuit to provide an impedance transformation. Series components will move the impedance along a constant resistance circle on the Smith chart.

STEP 7:- Power Analysis

a) Third-Order Intercept Point

One of the most common ways to test the linearity of a circuit is to apply two signals at the input, having equal amplitude and offset by some frequency, and plot fundamental output and inter-modulation output power as a function of input power as shown in Figure 5.7. From the plot, the *third-order intercept point* (IP3) is determined. The third-order intercept point is a theoretical point where the amplitudes of the intermodulation tones at $2V_1 - V_2$ and $2V_2 - V_1$ are equal to the amplitudes of the fundamental tones at V_1 and V_2. From table 5.1, if $V_1 = V_2 = V_i$, then the fundamental is given by

$F_{und} = k_1 V_i((9/4)k_3 v^3_i)$

The linear component of the above equation can be given by

$F_{und} = k_1 V_i$

can be compared to the third-order inter modulation term given by

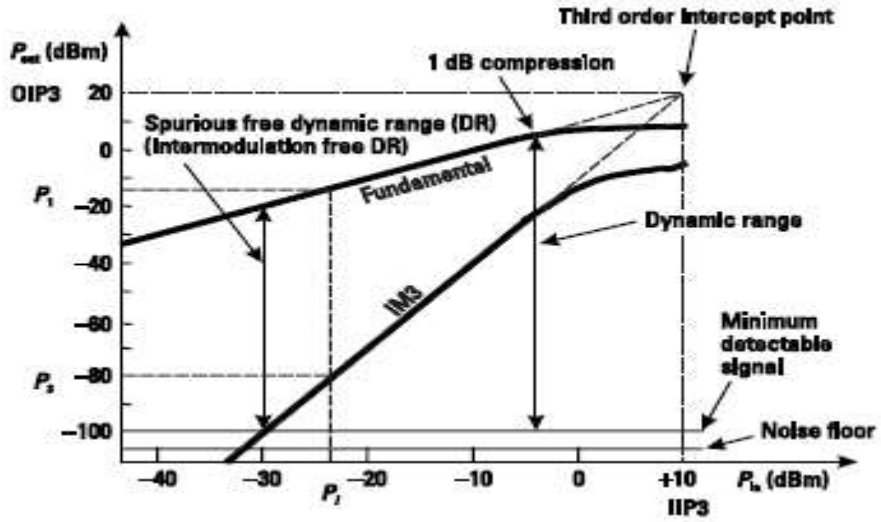

Figure 5.7: Plot of input output power of fundamental and IM3 versus input power.

5. Expected Outcome and Future Work:-

In this project the Low Noise Amplifier will be design in ADS and will meet the following specification

1. Frequency : 2.47GHz
2. Gain : 14.0dB
3. Noise Figure : 0.5dB
4. IRL and ORL less than -12 db
5. DC Current=1 mA

6. ACKNOWLEDGMENTS

We take this opportunity to express our deep sense of gratitude and while hearted thanks to my project guide **Prof.V.B.Padole** for his invaluable guidance, inspiration and encouragement. It is because of them that we could synchronize our efforts.

We also express our sincere thanks to our Department for her tremendous support, encouragement and invaluable guidance throughout completion of my work.

We shall be failing in our duties until and unless we express our sincere thanks to all the members and our friends who have directly or indirectly contributed of my work.

7. CONCLUSION

In this way I have design Low noise amplifier for IEEE 802.11 protocol by using Advance digital design system. ADS platform easy for implementation and working with, so it is most joyful and tough work to design LNA wth improved parameter as already present in the market. Also this improved LNA also helpful for society and technical aspirant to study ADS and LNA in details.

REFERENCES:

[1] AminaMsolliNasri, AbdelhamidHelali, HassenMaaref , Faculty of Sciences of Monastir , Tunisia "Ultra low power Low Noise Amplifier design for 2.4GHz application".

[2] Jing Li, Runbo Ma, Liping Han, Rongcao Yang, and Wenmei Zhang college of physics and electronics shanxi university "A co-design study of Low Noise Amplifier and Band-Pass filter. 2012 IEEE.

[3] Ravinder Kumar, Munish Kumar, and Viranja"Design and noise optimization for a RF low noise amplifier,"vol 3.

[4] S.F. WAN MuhamadHatta, N. Soin, "Performance of the forward-biased RF LNA with deep n-well n-MOS transistor," Proc. Of IEEE Int. Conf. OnSemiconductor Electronics, Malaysia, Nov.2008.

[5] Viranja M. Srivastava,K. S.Yadav, and G. Singh "Design and performance analysis of cylindrical surrounding double-gate MOSFET for RF switch," Oct.2011

[6] CMOS Ultra-Low Power Front-End Receiver for Wireless SensorNetworks"; IEEE Radio Frequency Integrated Circuits (RFIC)Symposium, 2007.

[7] Morici, A.; Rodriguez, S.; Rusu, A.; Ismail, M.; Turchetti, C., "A3.6mW 90 nm CMOS 2.4 GHz receiver front-end design for IEEE802.15.4 WSNs", International Symposium on Signals, Circuits andSystems, 2009.

[8] Sasilatha, T.; Raja, J.,"A 1V, 2.4 GHz low power CMOS receiverfront end for wireless micro sensor nodes", International ConferenceonCommunications, Signals and Coding, 2008.

[9] Chihoon Choi; Joonwoo Choi; Ilku Nam, "A low noise and highlylinear 2.4-GHz RF front-end circuit for wireless sensor networks",IEEE 9th International Conference on ASIC (ASICON), 2011.

[10] Narendra,K.; M,S,Bhat., "Design of CMOS RF Receiver Front-endfor IEEE 802.11b ", International Conference on Electronic Design,2008.

[11] Datta, S.; Dutta, A. ; Datta, K.; Bhattacharyya, T.K.,"Pseudo Concurrent Quad-Band LNA Operating in 900 MHz/1.8 GHz and 900MHz/2.4 GHz Bands for Multi-Standard Wireless Receiver," IEEE24th International

[12] CihanKarakuzu. "Fuzzy logic based smart traffic light simulator design and hardware implementation". Kocaeli University, Engineering Faculty, Electronics & Tell. Eng. Department, 41070 VezirogluYerleskesi, Izmit-Kocaeli, Turkey.

International Journal of Engineering Research and General Science Volume 3, Issue 5, September-October, 2015
ISSN 2091-2730

Seismic Evaluation of Retrofitted Reinforced Concrete Framed Buildings

Sachin Dattatrya Aherkar, Giridhar Narule

ME Civil (Structure) Second Year Student
VPCOE, Baramati – 413133
sachin.aherkar96@gmail.com

Abstract— Many existing buildings lack the seismic strength and detailing requirements of IS: 1893-2002 and IS: 13920-1993, because either they were designed for only gravity loads or built prior to the implementation of these codes. Hence it is required to assess the performance level of such buildings for safety of the structure during earthquake. In present study three buildings 8, 12 and 16 storied are considered. They are designed for only gravity loads according to IS: 456-2000 without ductile detailing. Seismic evaluation of these buildings is carried out with nonlinear static pushover analysis using SAP2000 software. Performance points and performance levels of these buildings are determined by capacity spectrum methods. All three buildings are found in life safety to collapse prevention (LS-CP) range for design basis earthquake condition. Then various retrofitting schemes viz. steel X braces, infill walls, and shear wall are employed for strengthening of these buildings, performance level requirement of operational to immediate occupancy (B-IO) under design basis earthquake is aimed at. Idealized force-displacement capacity curve is implemented to evaluate various seismic parameters from pushover curve which is based on the method recommended by FEMA 356. The results are compared based on performance point, hinge formation pattern, yield strength and lateral stiffness. The results show that there is no unique solution and several different strengthening schemes can be provided to give adequate performance. Most increase in the lateral strength and stiffness is related to using infill wall and shear wall.

Keywords— Performance point, FEMA 356, SAP2000, Lateral stiffness, steel X braces, infill walls, and shear wall.

INTRODUCTION

Evaluation of building is required at two stages (a) before retrofitting, to identify the weakness of the building to be strengthened, and (b) after retrofitting, to estimate the adequacy and effectiveness of retrofit. Evaluation is complex process, which has to take not only the design of building but also the deterioration of the material and damage caused to the building, if any. The difficulties faced in the seismic evaluation of the building are threefold. There is no reliable method to estimate the in-situ strength of the material in components of the building. Analytical method to model the behavior of the building during earthquake is either unreliable or too complex to handle with the generally available tools. The third difficulty is the unavailability of reliable estimate of earthquake parameters, to which the buildings expected to be subjected during its residual life. Hence the engineering tools needs to be sharpened for evaluating structures performance under the action of earthquake forces. The aim of the seismic evaluation is to assess the seismic capacity of earthquake vulnerable buildings or earthquake damage buildings for the future use. The evaluation may also prove helpful for degree of intervention required in seismically deficient structures [5].

Need: The Bhuj earthquake of 26 January, 2001 in Gujarat, India caused the major destruction of medium-rise and high-rise buildings. After this earthquake, many questions arose about our professional practices, building by-laws, construction materials, and education for civil engineers and architects. In addition to this current Indian codes do not address the evaluation of seismic resistance of existing building stock, which may not have been designed for earthquake forces. Seismic deficiencies should first be identified through a seismic evaluation of the structure. The selection of an appropriate intervention technique based on the structural type and its deficiencies is the most important step in retrofitting. Seismic evaluation consists of gathering as built information and obtaining the results of a structural analysis based on collected data. The prestandard and commentary for the seismic rehabilitation of buildings ATC40 and FEMA356 provides guidance for evaluating the seismic performance of existing structures and determining the necessary retrofitting methods to achieve the performance objectives. In light of these facts, it is necessary to seismically evaluate the buildings with the present knowledge to avoid the major destruction during the earthquakes in future. The buildings found to be seismically deficient should be retrofitted/ strengthened.

Scope: The scope of present study aims at evaluation of RC buildings designed as per IS: 456-2000. Total three gravity designed buildings 8, 12 and 16 storied having symmetrical plan and identical floors located in zone V are designed using SAP2000. Designed buildings are evaluated using nonlinear static pushover analysis in X and Y directions. For pushover analysis guidelines laid by

ATC40 and FEMA356 are followed. Based on performance objective operational (B) to immediate occupancy (IO) performance level is targeted at. Performance point is found out by using capacity spectrum method. Since above all three buildings failed to give desired target performance level that is operational (B) to immediate occupancy (IO), hence buildings need to be retrofitted.

Steel X braces, infill wall and shear wall are employed as the retrofitting strategies for all three buildings. Retrofitting schemes are placed at exterior bays only. Modeling of shear wall and infill wall is done by wide column analogy and single compressive strut respectively. Then from pushover curve idealized curve is drawn as per FEMA356 recommendation to extract seismic parameters.

The results of analysis are compared in terms of seismic parameters such as performance levels, hinge formation pattern, yield strength and lateral stiffness. The effectiveness of retrofitting schemes on above parameters is studied.

METHODOLOGY

In the present work 8, 12 and 16 storied gravity designed reinforced concrete buildings are considered for study. For all three buildings, the following data is used including the loadings as per relevant IS code.

1. The buildings are situated in zone V.
2. The buildings have ordinary moment resisting frame.
3. The plan area of all three buildings is 25 x 20 m.
4. It consists of 5 bays of 5 m each in X-direction and 5 bays of 4 m each in Y-direction.
5. Plinth height above GL is 0.55 m. Depth of foundation is 0.65 m below GL.
6. Height of each typical storey is 3.1 m.
7. Slab thickness is 150 mm.
8. External wall thickness is 230 mm and internal wall thickness is 150 mm. Parapet height is 1.5 m.
9. Grade of concrete is M 20.
10. Grade of steel is Fe 415.
11. Imposed load on floor is 3 kN/m^2 and imposed load on roof is 1.5 kN/m^2.
12. Floor finishes is 1 kN/m^2 and roof treatment is 1.5 kN/m^2.
13. Density of concrete is 25 $kN/m^3$and density of masonry wall is 20 kN/m^3.

The plan of buildings is shown in figure 1 and 3-D view of 8, 12, and 16 storied buildings are shown in figure 2 (a), (b) and (c) respectively and Table 1 shows the geometrical properties of buildings.

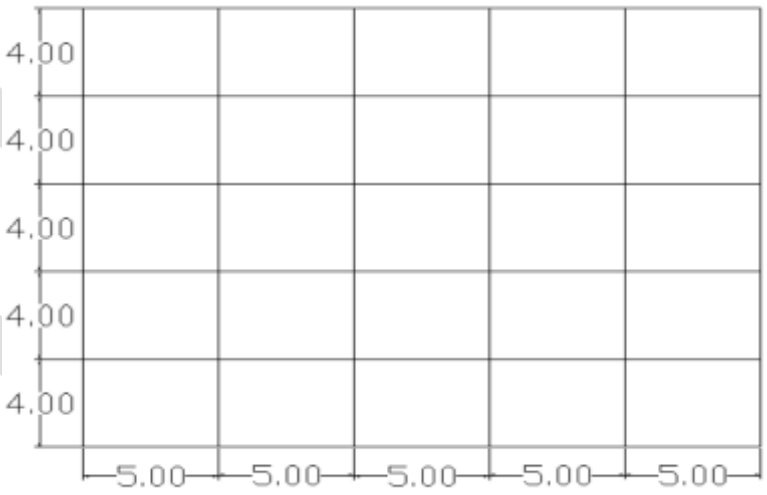

Figure 1 Plan

Note - All dimensions are in m.

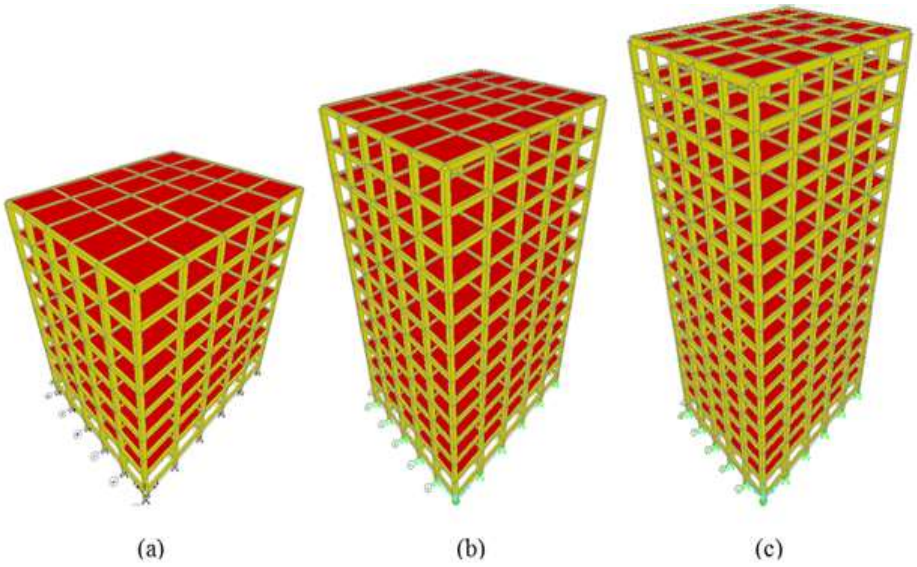

Figure 2 3D view of (a) 8 storied (b) 12 storied (c) 16 storied buildings.

Table 1 Geometrical properties of buildings

Building	Beam sizes in mm.		Column sizes in mm	
	External	Internal	External	Internal
8 storied	300x500	300x600	300x600	500x600
12 storied	300x600	300x700	500x700	700x700
16 storied	300x700	300x800	600x700	800x800

The main objective of performance based earthquake engineering of buildings is to avoid total catastrophic damage and to restrict the structural damages caused to the performance limit of the buildings. This paper deals with evaluation of the real strength of the structure and to check its performance level. For this purpose static pushover analysis is used.

RETROFITTING OF REINFORCED CONCRETE BUILDING

The most important step in the retrofitting process of a building is to create an appropriate model that will adequately represent its stiffness, mass distribution and energy dissipation so that its response to earthquake could be predicted with sufficient accuracy. After going through the extensive literature study and in order to investigate effect of steel X bracing, infill wall and shear wall as a retrofitting scheme on seismic performance of buildings it is very imperative to design and model them very precisely. This section deals with design and modeling methods adopted for above mentioned retrofitting schemes, also describes various properties considered for accurate modeling.

1 Design and modeling of steel X bracings

The steel X braces are designed to resist the base shear for DBE level earthquake according to IS: 1893 (part 1) as a first trial, and then trial and error method was adopted to bring the structural performance level within B-IO range. The braces are assigned at exterior bays only as shown in figure 3 (a), (b) and (c) for 8, 12 and 16 storied buildings respectively. Brace members are selected as round hollow section with modulus of elasticity E = 200,000 MPa and f_y = 350 MPa. Braces are modeled as truss element having pin joints at both the ends. Auto steel-axial hinges are applied at both ends of the bracings.

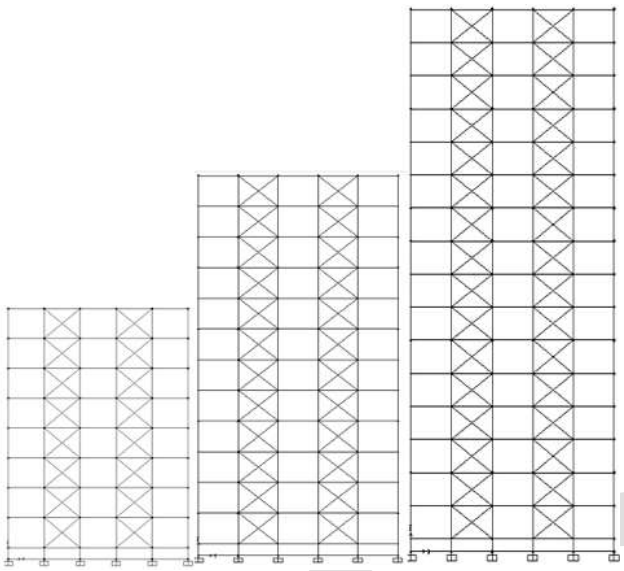

(a) (b) (c)

Figure 3 Arrangement of steel X braces

2 Design and modeling of infill wall

Significant experimental and analytical research is reported in the literature since last five decades, which attempts to understand the behavior of infilled frames. Different types of analytical models based on the physical understanding of the overall behavior of an infill panels were developed over the years to mimic the behavior of infilled frames. The available infill analytical models can be broadly categorized as i) macro model and ii) micro models. Thus RC frames with unreinforced masonry walls can be modeled as equivalent braced frames with infill walls replaced by equivalent diagonal strut which can be used in rigorous nonlinear pushover analysis. Arrangement of infill wall (a) plan (b) elevation (c) 3-D view as shown in figure 4.

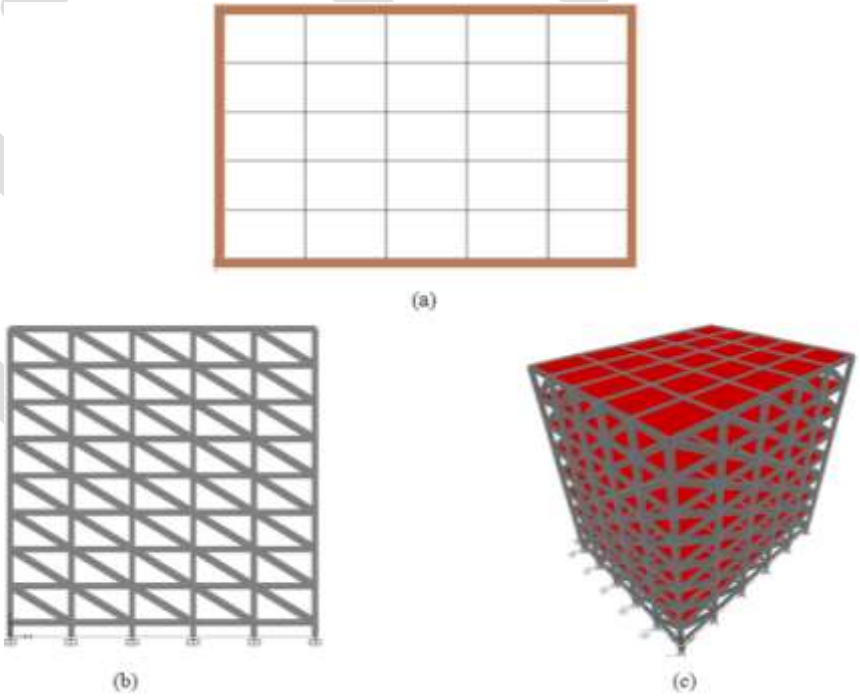

Figure 4 Arrangement of infill wall (a) plan (b) elevation (c) 3-D view

3 Modeling of shear wall

Buildings that incorporate concrete shear wall as structural elements to resist both vertical and lateral loads are common place. The calculation of stresses and deflection in a simple shear wall requires only simple bending theory. In this project work shear wall is modeled by using equivalent frame method also referred as wide column analogy. In equivalent frame method, which is also known as wide column analogy, each shear wall is replaced by an idealized frame structure consisting of a column and rigid beams located at floor levels. The column is placed at the wall's centroidal axis and assigned to have the wall's inertia and axial area. In this method, the axial area and inertia values of rigid arms are assigned very large values compared to other frame elements. Due to its simplicity, the equivalent frame method is especially popular in design offices for the analysis of multistorey shear wall-frame structures. Modeling of shear wall by wide column analogy as shown in figure 5.

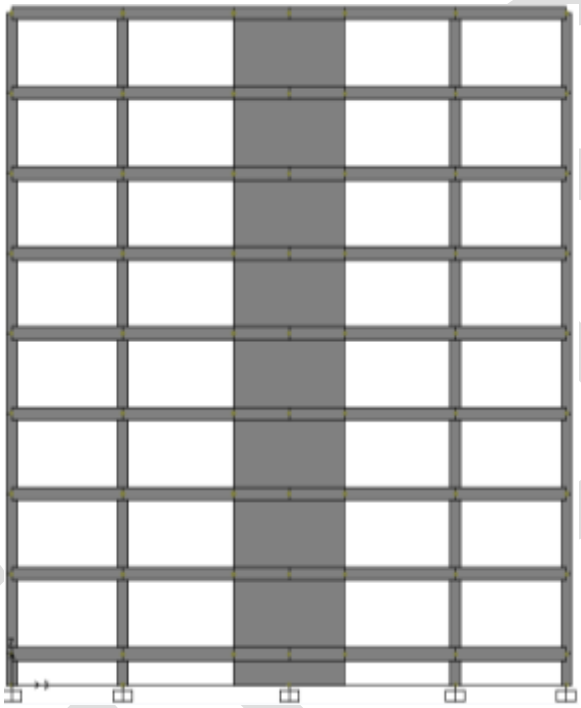

Figure 5 Modeling of shear wall by wide column analogy

PUSHOVER ANALYSIS PROCEDURE

The ATC 40 [1] provides detailed guidelines about how to perform a nonlinear static pushover analysis. The following procedure is based on the ATC 40 procedure.

• Form the analytical model of the nonlinear structure.

• Set the performance criteria, like drift at specific floor levels, limiting plastic hinge rotation at specific plastic hinge points, etc.

• Apply the gravity load and analyze for the internal forces.

• Assign the equivalent static seismic lateral load to the structure incrementally.

• Select a control point to see the displacement.

• Apply the lateral load gradually using incremental iteration procedure.

• Draw the "Base Shear vs. Controlled Displacement" curve, which is called "pushover curve".

• Convert the pushover curve to the Acceleration- Displacement Response-Spectra (ADRS) format.

• Obtain the equivalent damping based on the expected performance level. Get the design Response Spectra for different levels of damping and adjust the spectra for the nonlinearity based on the damping in the Capacity Spectrum.

• The capacity spectrum and the design response spectra can be plotted together when they are expressed in the ADRS format.

• The intersection of the capacity spectrum and the response spectra defines the performance level.

In SAP2000, a frame element is modeled as a line element having linearly elastic properties and nonlinear force-displacement characteristics of individual frame elements are modeled as hinges represented by a series of straight line segments. A generalized force-displacement characteristic of a non-degrading frame element (or hinge properties) in SAP2000 is shown in figure 6.

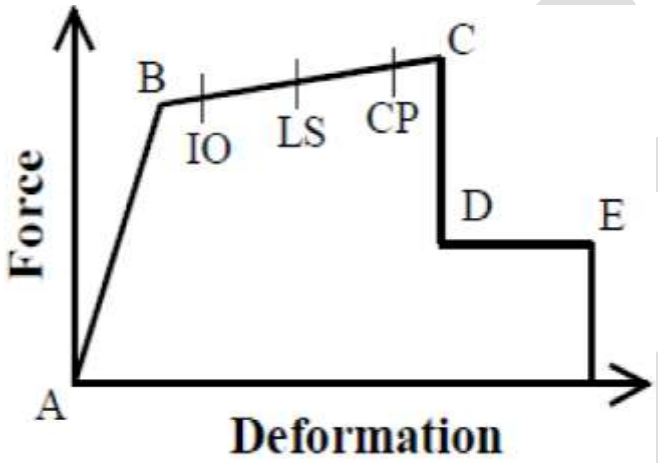

Figure 1 Generalized force-displacement characteristic [2]

Point A corresponds to unloaded condition and point B represents yielding of the element. The ordinate at C corresponds to nominal strength and abscissa at C corresponds to the deformation at which significant strength degradation begins. The drop from C to D represents the initial failure of the element and resistance to lateral loads beyond point C is usually unreliable. The residual resistance from D to E allows the frame elements to sustain gravity loads. Beyond point E, the maximum deformation capacity, gravity load can no longer be sustained. Hinges can be assigned at any number of locations (potential yielding points) along the span of the frame element as well as element ends. Uncoupled moment (M2 and M3), torsion (T), axial force (P) and shear (V2 and V3) force displacement relations can be defined. As the column axial load changes under lateral loading, there is also a coupled P-M2-M3 (PMM) hinge which yields based on the interaction of axial force and bending moments at the hinge location. Also, more than one type of hinge can be assigned at the same location of a frame element. There are three types of hinge properties in SAP2000. They are default hinge properties, user-defined hinge properties and generated hinge properties. Only default hinge properties and user-defined hinge properties can be assigned to frame elements.

RESULT AND DISSCUSSION

All three buildings 8, 12 and 16 storied gravity designed buildings attained the performance level of Life Safety (LS) - Collapse Prevention (CP) as discussed in chapter 4. The significant improvement in the seismic performance of gravity designed buildings is observed when retrofitting schemes are used as shown in table no. 2, however all strengthening schemes are able to provide the same performance level. The result of nonlinear static pushover analysis shows that building retrofitted with steel X braces, infill wall and shear wall provided targeted performance level of operational (B)-immediate occupancy (IO).

In this section, some important seismic parameters and hinge formation patterns are discussed. In addition to this comparison of performance points and capacity curves are as shown in table 2 and figure 7 to figure 12 is carried out.

Table 2 Improvement in seismic parameters

Parameters	8 storied building					
	X bracing		Infill wall		Shear wall	
	X	Y	X	Y	X	Y
Ratio of initial stiffness	2.09	1.30	3.059	1.94	3.76	2.53
Increase in yield strength	3390	2475	4300	2950	4080	3965
	12 storied building					
Ratio of initial stiffness	1.07	1.26	1.68363	1.71	1.70	1.78
Increase in yield strength	4968	3831	5145	4556	5895	6221
	16 storied building					
Ratio of initial stiffness	1.09	1.13	1.35	1.43	1.73	1.57
Increase in yield strength	4328	4938	5848	5266	7308	6578

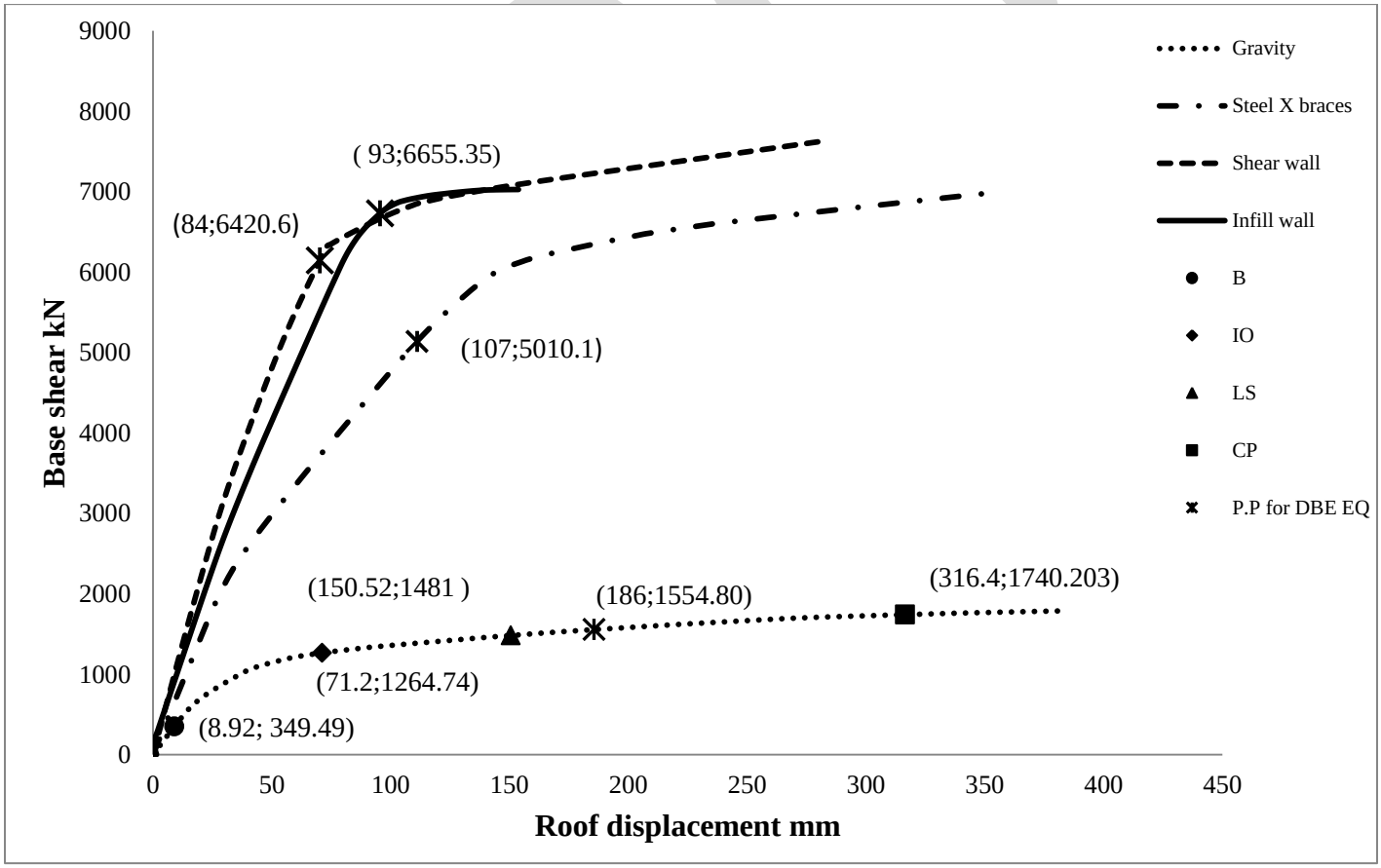

Figure 7 Comparison of various retrofitting schemes for 8 storied building in X direction

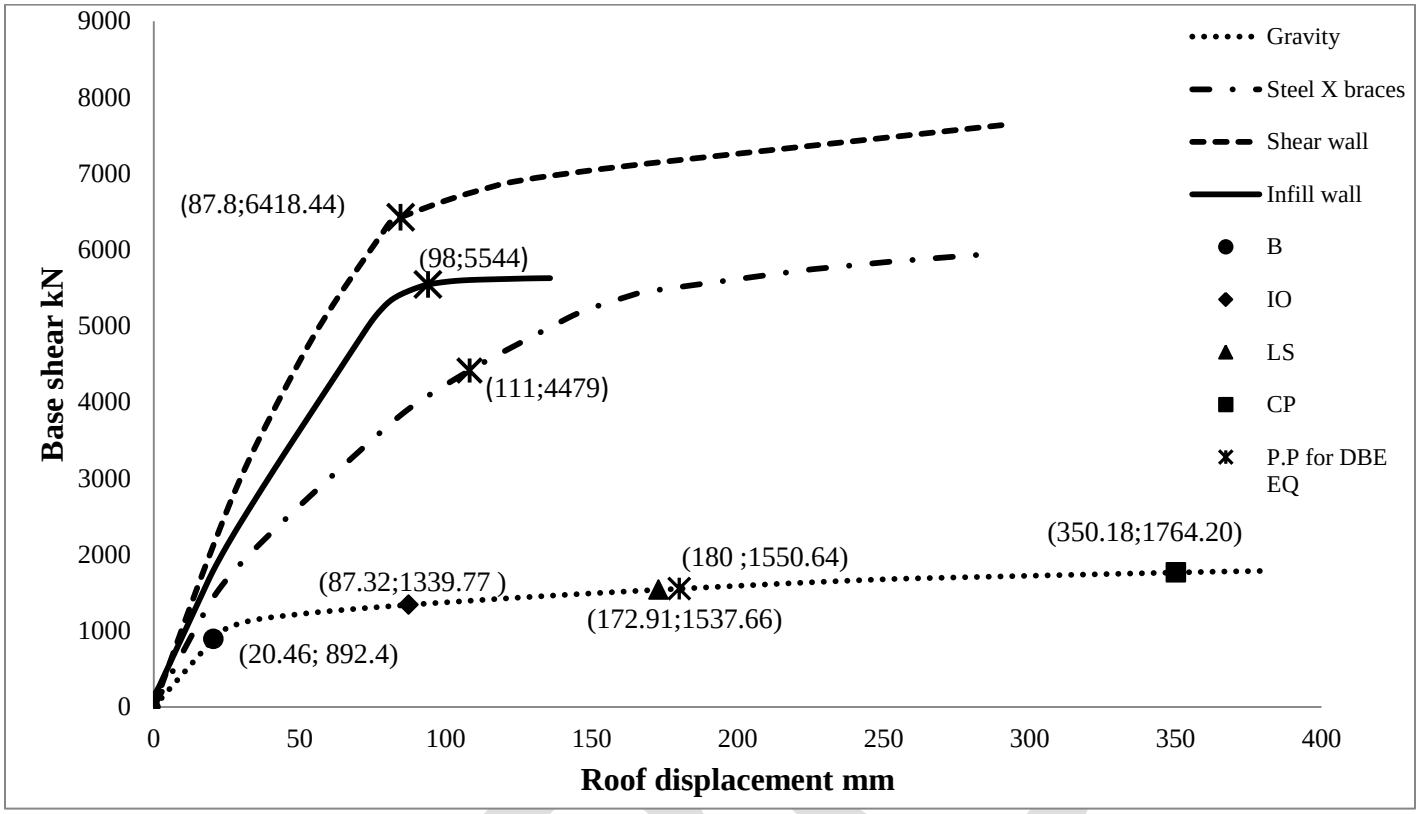

Figure 8 Comparison of various retrofitting schemes for 8 storied building in Y direction

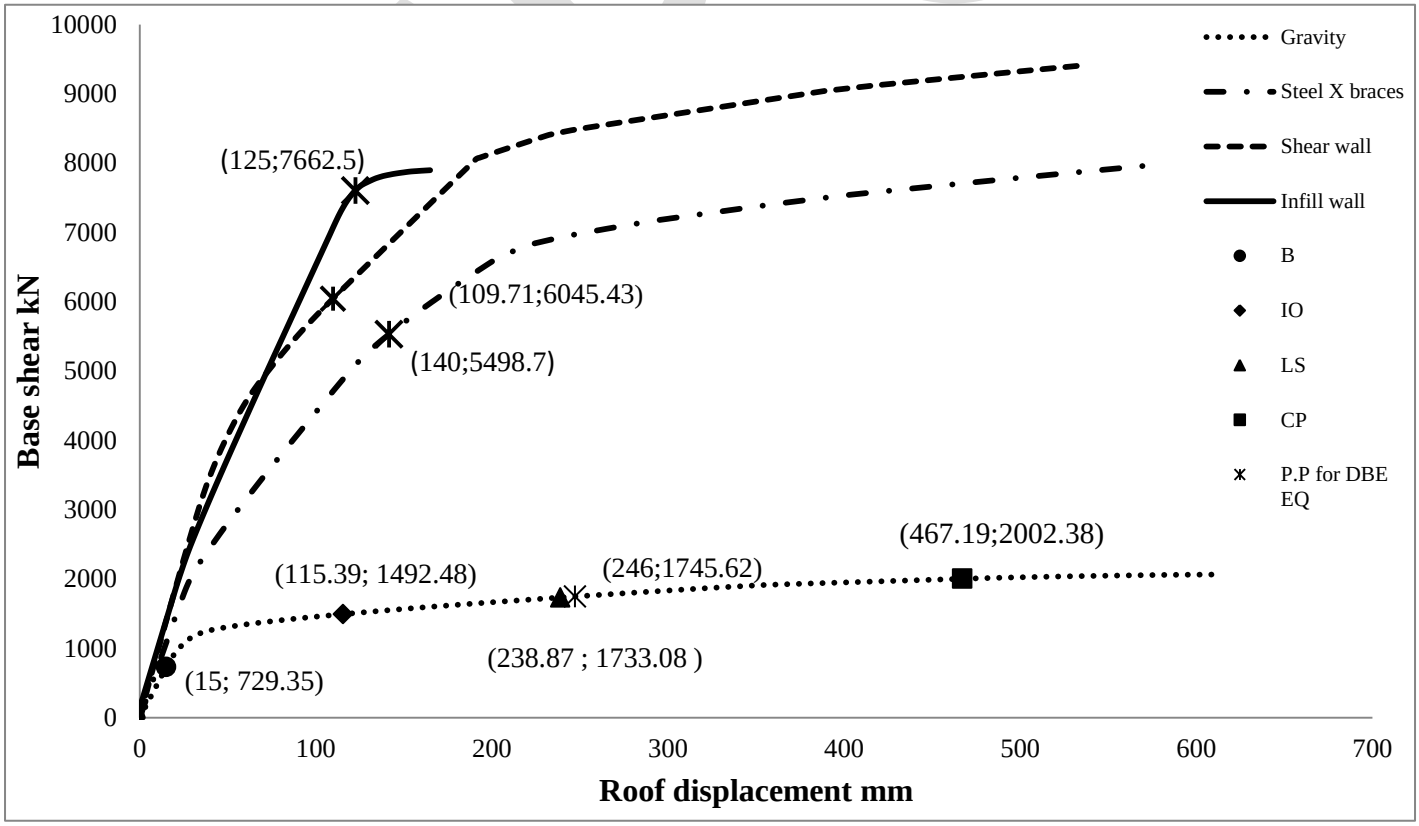

Figure 9 Comparison of various retrofitting schemes for 12 storied building in X direction

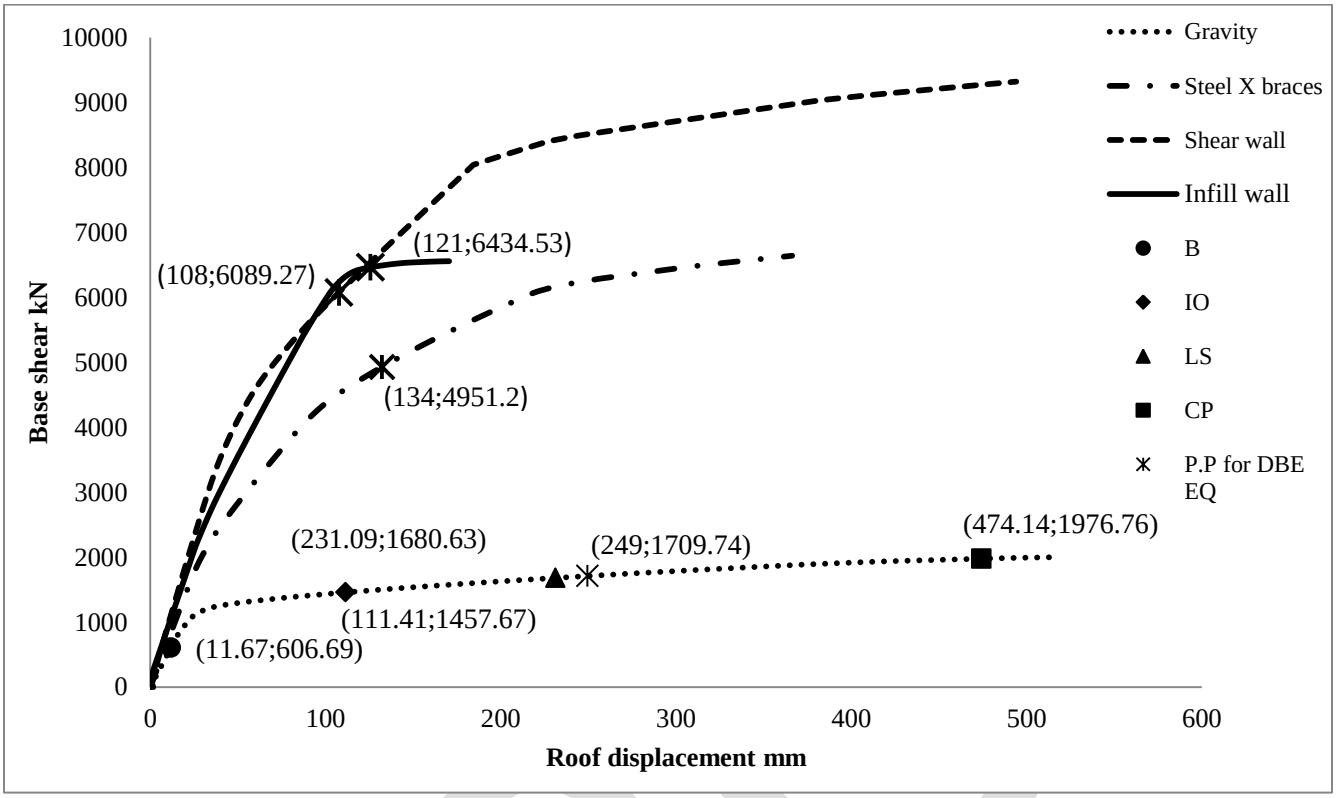

Figure 10 Comparison of various retrofitting schemes for 12 storied building in Y direction

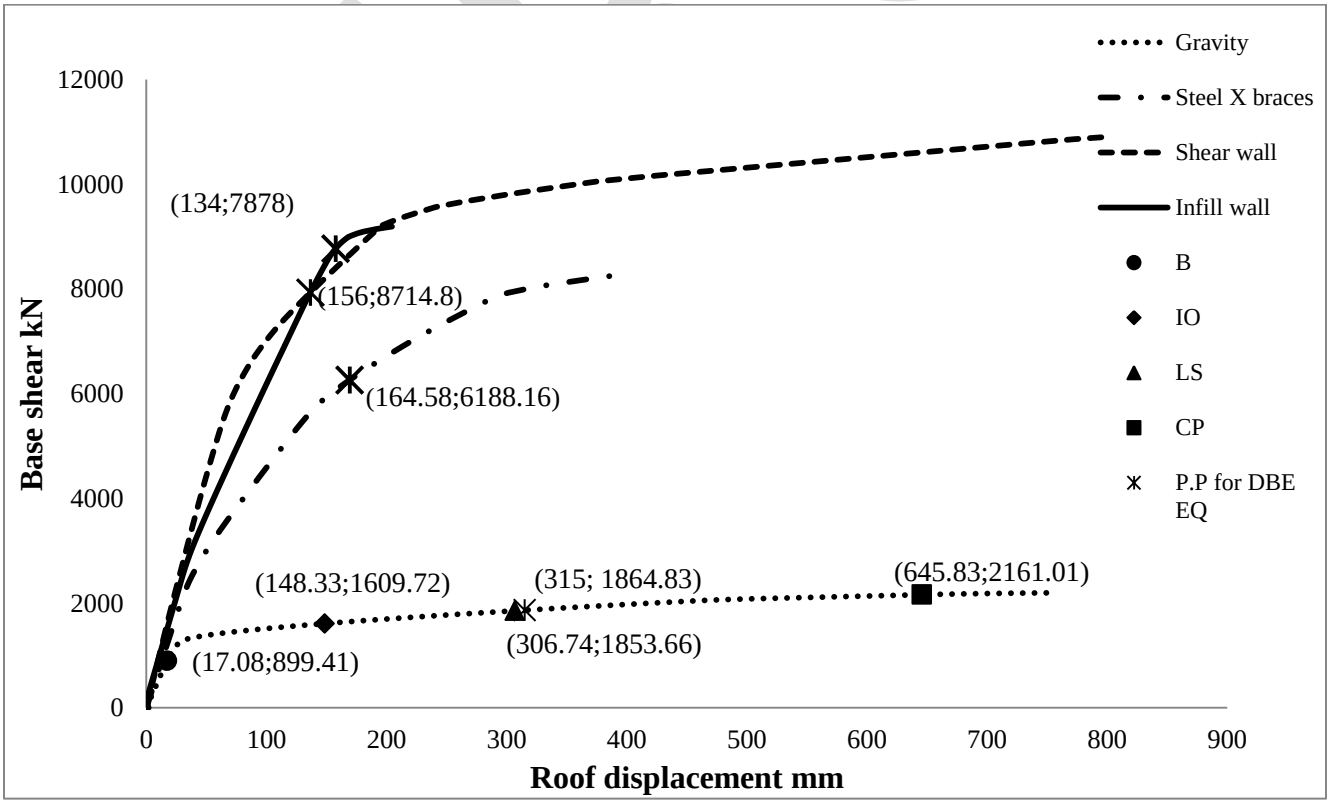

Figure 11 Comparison of various retrofitting schemes for 16 storied building in X direction

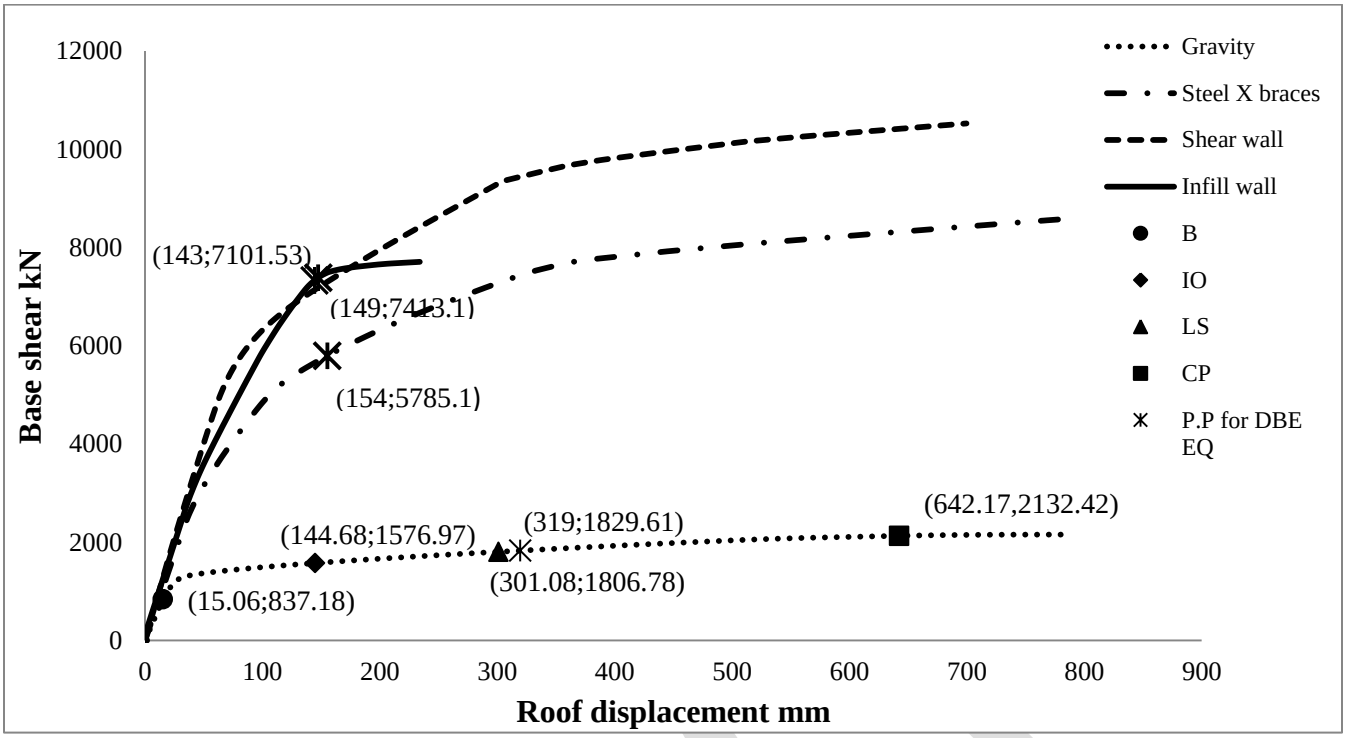

Figure 12 Comparison of various retrofitting schemes for 16 storied building in Y direction

Performance points and capacity curves for various retrofitting schemes are shown in the table no. 2 and figure 7 to figure 12 respectively. The resulting capacity curves for three retrofitting schemes shows improvement in performance levels. The buildings which were initially at LS-CP level, after retrofitting they are at O-IO level. For gravity designed buildings value of base shear and roof displacement goes on increasing as number of storeys increases. Also the base shear and roof displacement is maximum in X direction as compare to Y direction. The comparison between capacity curves shows that when the building is retrofitted with steel X bracings its roof displacement is more than any other retrofitting scheme employed. Steel X brace produces more ductility than other two retrofitting schemes. Buildings retrofitted at external bays with infills produces maximum base shear at performance point. On the other hand the building yields less roof displacement when it is retrofitted with shear walls. The base shear capacity of buildings retrofitted with shear wall is comparatively higher than other schemes.

CONCLUSION

Assessment of the performance levels of gravity designed buildings shows that these buildings are seismically deficient. As a result different strengthening schemes are used to improve performance of deficient buildings; all these different retrofitting strategies are aimed at providing B-IO performance level for DBE condition. Based on results following conclusions are drawn:

- Buildings designed as per IS: 456-2000 is seismically deficient. These buildings are unable to produce sufficient lateral load resisting capacity during an earthquake to avoid sever damages. Moreover, performance of analyzed buildings is at life safety (LS) to collapse prevention (CP) level.
- The study of hinge formation patterns shows that most of the hinges are formed in beams and very few in columns. The LS-CP hinges are formed at middle storeys only, whereas IO-LS hinges are formed at upper and lower storeys.
- It is observed that as building height increases value of base shear and roof displacement also increases. The value of base shear at performance point is maximum for 16 storied building and it is 1.19 times and 1.06 times more than 8 and 12 storied building in X direction. Whereas in Y direction it is 1.80 times and 1.07 times more than 8 and 12 storied buildings base shear values at performance point.

Assessment of the performance levels of gravity designed buildings shows that these buildings are seismically deficient. As a result different strengthening schemes are used to improve performance of deficient buildings; all these different retrofitting strategies are aimed at providing B-IO performance level for DBE condition. Based on results following conclusions are drawn:

- Comparison between three strengthening strategies shows that most increase in effective lateral stiffness at yield point is maximum when building is retrofitted with shear wall.
- For 8 storied building lateral stiffness is increased by 3.48 times, 1.79 times and 1.22 times in X direction whereas in Y direction it is increased by 2.37 times, 1.94 times and 1.32 times when retrofitted with shear wall over gravity building, steel X braced building and infill building respectively.
- For 12 storied building lateral stiffness is increased by 1.70 times, 1.58 time and 1.01 times in X direction whereas in Y direction it is increased by 1.78 times, 1.40 times and 1.04 times when retrofitted with shear wall over gravity building, steel X braced building and infill building respectively.
- For 16 storied building lateral stiffness is increased by 1.73 times, 1.59 time and 1.27 times in X direction whereas in Y direction it is increased by 1.57 times, 1.39 times and 1.09 times when retrofitted with shear wall over gravity building, steel X braced building and infill building respectively.
- Maximum base shear carrying capacity is noted in case of infill wall at performance point. It is because of infill wall increase stiffness of the building more than other two retrofitting schemes and hence attracts more lateral loads.
- At performance point maximum roof displacement is observed in case of steel X braces. This is because steel itself more ductile material than concrete also steel braces contributes negligible mass and stiffness to the original mass and stiffness of the structure.

A number of different strengthening systems can be adopted to improve the seismic performance of deficient buildings. The performance of particular retrofitting strategies depends upon the structural properties of original deficient building. In this case shear wall placed in outer bay improved the performance to desired level.

REFERENCES:

[1] Applied Technology Council 40 (ATC40), "Seismic evaluation and retrofit of concrete buildings", Vol.1 and 2, Applied Technology Council, Redwood City, CA, USA, Report No. SSC 96-01, 1996.

[2] FEMA 356, "Prestandard and commentary for the seismic rehabilitation of buildings", American society of civil engineers, Reston, Virginia, Nov.2000.

[3] SAP2000 V14.2.4, "Integrated finite element analysis and design of structures basic analysis reference manual", Berkeley, CA, USA: Computers and structures INC, Aug. 2010.

[4] Jain Sudhir K, "Indian earthquake: an overview", Indian concrete journal, pp.555-561, 1998.

[5] Agarwal Pankaj and Shrikhande Manish, "Earthquake resistance design of structures", PHI learning private limited, pp.524-555, 2006.

[6] Krawinkler H. and Seneviratna, "Pros and cons of a pushover analysis of seismic performance evaluation", Engineering Structures, vol.20, pp.452- 464, 1998.

[7] Davis Robin, Krishna Praseetha, Menon Devdas, A. Meher Prasad, "Effect of infill stiffness on seismic performance of multi-storey RC framed buildings in India", World Conference on Earthquake Engineering, Vancouver, B.C., Canada, Paper No. 1198,2004.

[8] Murty C. V. R. and Jain Sudhir K., "Beneficial influence of masonry infill walls on seismic performance of RC frame buildings", 12th World Conference on Earthquake Engineering, Paper no.1790, 2000.

[9] Girgin Konuralp and Darilmaz Kutlu, "Seismic Response of Infilled Framed Buildings Using Pushover Analysis", ARI The Bulletin of the Istanbul Technical University Vol. 54, No. 5.

[10] Anshuman S., Dipendu Bhunia, Bhavin Ramjiyani, "Solution of Shear Wall Location in Multistorey Building", International journal of civil and structural engineering, Vol. 2, No 2, 2011Research article ISSN 0976 – 4399.pp493-506,2011.

[11] Mattacchione Angelo, "Equivalent frame method applied to concrete shearwalls", ACI Concrete International, pp.65-72, 1991.

[12] Kaltakci M.Y.,Arslan M.H., and Yavuz G., "Effect of external and internal shearwall location on strengthening weak RC frames", *Scientia irianca, pp.312-323, 2010.*

[13] IS 1893 (Part 1):2002 Criteria for earthquake resistant design of structures (Fifth Revision) Indian standards, New Delhi.

International Journal of Engineering Research and General Science Volume 3, Issue 5, September-October, 2015
ISSN 2091-2730

Multiterm Keyword Searching For Key Value Based NoSQL System

Pallavi Mahajan[1], Arati Deshpande[2]

Department of Computer Engineering,
PICT, Pune, Maharashtra, India.
Pallavinarkhede88@gmail.com[1], ardeshpande@pict.edu[2].

Abstract— Today, the enterprise landscape faces large amount of data. The information gathered from these data sources are useful for improving on product and services delivery. However, it is challenging to perform searching activities on these data sources because of its unstructured nature Due to unstructured nature of these data, NoSQL storage has been adapted by many enterprises because it provides better storage facility. NoSQL storage can store schema oriented, semi structured, schema less data and its document append storage has received high attention because it provides the flexibility to store JSON based data. However to provide effective indexing and searching on these data is a challenging task. This work discuss concept of multiterm inverted index which is used with index pruning algorithm. The multiterm inverted indexing reduces the overhead for intersecting the inverted lists of keys in multi-term queries, by storing combinations of terms as keys in the index.

Keywords— Data mining, inverted indexing, NoSQL system, multikeyword searching, ranking, key-value store, index pruning.

I. INTRODUCTION

The concept of Index has been devised in order to enable flexible use of recorded data and make these large data sets easily accessible. One of the main design concepts to allow access to data in multiple ways is using Indexing. There are some indexing techniques available but the most widely used indexing technique is inverted indexing. Inverted index is an index data structure that maps a number or word to its location in database or in document or a set of documents. The purpose of inverted index is to provide full text searches. There are two main types of inverted index. First, A Record Level Inverted Index (or inverted file index or inverted list) contains the list of documents that contains the word. Second type is a word level inverted index (inverted list or full inverted index) contains the position of each word within document. Almost all of the large scale text retrieval systems make use of compressed inverted list indexes, which are considered the most useful indexing technique for very large collections. here are two ways to create inverted index that are on single term and on multiple terms.

The inverted index on multiple terms performs faster than single term. However the data being generated nowadays have no schema and has no particular structure. The data comes in several formats such as multimedia data, files, but the RDBMS systems are designed to store schema-based data in certain predefined format and do not support these types of data. Thus, the NoSQL storage has been proposed to support both large amount of data and data in unstructured formats. Multimodal databases, graph databases, object databases, are the different types of NoSQL storages. In this work, we shall focus on the document-append style NoSQL storage (mongoDB) for storing the documents. This style of storage supports structured, semi-structured, and unstructured data. The NoSQL system implements key-to-value map in their core featuring like hash table which uses PUT/GET /DELETE methods for inserting, accessing and updating data. As the NoSQL supports large amount of data, the problem however that is, we are faced with the challenge of performing data mining tasks from such storage facilities.

There are various solutions existing that perform searching only with single term inverted index which does not scale very well on large databases. Since multi-term queries represents the majority of user queries, to support this various approaches that utilizes multi-term inverted index are proposed in previous work which consider all the n terms and in that case the number of possible term combinations are in O(n) which is the worst case. To select the meaningful subsets of terms is one of the main considerations of the proposed system. The two main contributions of the paper are 1) Selection of meaningful terms for combination. 2) Use of index pruning algorithm to minimize the scale of the term set index. The remainder of this paper is organized as follows: section II discusses related work. In section III the design of the system is presented. Section IV shows the half experimental results and the paper is concluded in section V

II. RELATED WORK

There has been significant amount of work done on indexing with distributed environment (peer to peer networks) in which several different ways to organize a text index (inverted index) are mentioned such as local index, global index and hybrid index. The traditional solutions based on relational database systems, are limited to key based queries. i.e. queries where data object can be retrieved using primary key. The use of inverted index has a long history in information retrieval. Their use in computer vision was pioneered by Sivic and Zisserman. The inverted index data structure is central component of search engine. Basically An inverted file is the sorted list (or index) of keywords (attributes), with each keyword having links to the documents containing that keyword.

A lot of work has been done on peer to peer search engine using inverted index which are in distributed manner using single keyword and multiterm keyword search. P. Reynolds [5], proposed efficient peer to peer keyword search in which he designed fully distributed search system using inverted index with keywords evenly distributed among available servers. This work describes the design of distributed inverted index including three techniques: bloom filters, caches, incremental results which minimize the bandwidth during keyword searches. Bloom filters are useful for eliminating the need to send entire document match list among servers. Caching reduces the frequency with which servers must transfer the Bloom filters. Incremental results allow search operations to halt after finding a fixed number of results, which reduces the cost of searching.

The use of bloom filter is an effective way to reduce the communication cost but simply using the bloom filter to minimize the false positive rate raise the high traffic cost [9]. Here they address the problem of optimizing the settings of a BF and show, through mathematical proof, that the optimal setting of BF in terms of traffic cost is determined by the statistical information of the involved inverted lists, not the minimized false positive rate as claimed by previous studies. The advantage of this design is it significantly reduces the search traffic and latency of the existing approaches.

In [8], the general keyword index and search scheme for structured p2p networks is proposed to avoid several problems such as unbalanced load, fault tolerance, storage redundancy that are in peer to peer network. This paper presents general keyword index and search scheme for structured peer to peer network. In this paper a general keyword index and search scheme for DHT network is proposed where each object is map to an r-bit vector according to its keyword set and view this r-bit vector as points in an r-dimensional hypercube. This hypercube index technique is efficient when more keywords are given. This hypercube index technique provides the facility of ranking and query expansion.

The index scheme proposed in above paper is decomposable that means instead of using single large hypercube to index objects, the entire keyword set is divided into smaller subsets and on that small subsets the hypercube is used. While some approaches [4] used discriminative keys for indexing and retrieving, in which the keywords that are appear in most of documents are marked as discriminative keys, and the keywords having low discriminative power are marked as non discriminative keys.

To reduce the number of generated keys proximity filtering method is used. In this contribution a novel indexing/retrieval model that achieve high performance, cost efficient retrieval by indexing with highly discriminative keys (HDKs) stored in a distributed global index maintained in a structured P2P network. HDKs correspond to carefully selected terms and term sets appearing in a small number of collection documents. The results shown in this paper despite increased indexing costs, the total traffic generated with the HDK approach is significantly smaller than the one obtained with distributed single-term indexing strategies.

The existing techniques for keyword search in structured peer-to peer (P2P) networks support only to single- keyword or exact match lookups. In multiple-keyword search, the query contains more than one word and in storage the multiple terms are associated with data item which contain that word. The search result for a query should include all the words contained in query. Traditional DHT-based approaches performed the multikeyword searching by storing a data item or its index multiple times, that is one keyword is stored against its associated document. A query is processed by searching each of the query keywords once. Therefore, the storage cost and search cost are both linear with the number of keywords.

In [3], a hybrid structured network called Mkey is proposed to address this problem. Its backbone is a structured network in which the data store in the form of clusters. At the time of inserting a data item, multiple copies of the data and its index are stored in a few different clusters. When user enters the query, the query is also mapped to multiple clusters, and the searching is performed within these clusters. After searching the union of all the search results is returned to users as the final result. In [10], a more efficient index

structure, the Generalized Inverted Index (Ginix) is proposed in which consecutive IDs in inverted lists are merges into intervals to save storage space. Along with this index structure, more efficient algorithms can be implemented to perform basic keyword search operations such as the union and the intersection operations. A keyword search using Ginix can be more efficient than traditional inverted indices. The results shows that Ginix requires less storage space as well as it also improves the keyword search performance, compared with traditional inverted indexes.

In [11] extension of the Generalized Inverted Index (GINIX) is presented. Ginix merges the consecutive IDs in inverted lists into interval lists and it reduces the size of the inverted index. The new index structure is called Extended Inverted Index (XINIX) which extends the structure of Ginix. The primary objective of Xinix is to minimize the storage cost. Xinix not only reduces the storage cost, but also increase the search performance, compared with traditional inverted indexes.

All the work mentioned above is for distributed environment but as the amount of unstructured data has growing day by day, there is a need to propose the effective approach to search over this unstructured approach. In [2], Multiterm keyword searching is performed in NoSQL system in which to perform the multiterm keyword search inverted index is created on set of combination of terms, the creation of the combination of terms is a crucial part. As each document contains thousand of keywords making the combinations of all these terms is very difficult task. To address this issue selection of more representative keyword is one of the considerations of this work.

III. SYSTEM DESIGN

This section introduces the design overview and then discusses the Multiterm indexing scheme with proposed pruning method.

A. System outline

The system involves three modules: data preprocessing module, construction of inverted index module and query processing (fig.1). Every document in document collection goes through some preprocessing steps like tokenization, stemming, normalization, stop word removing etc. are applied on each document which gives list of tokens. Before indexing the terms the TF (Term Frequency which denotes the frequency of term within the document) and IDF (Inverse Document Frequency which denoted number of documents containing the term) of each term is calculated. The values of TF and IDF are used to calculate the weight of terms. To calculate the similarity between document and term set and to rank the results vector space model is used. After calculating the similarity between set of combination of terms and documents and the top term set-document pairs are stored in the index. In order to reduce documents and the top term set- document pairs are stored in the index. In order to reduce the size of index pruning method is used which inserts the meaningful and top term set-document pairs in the index.

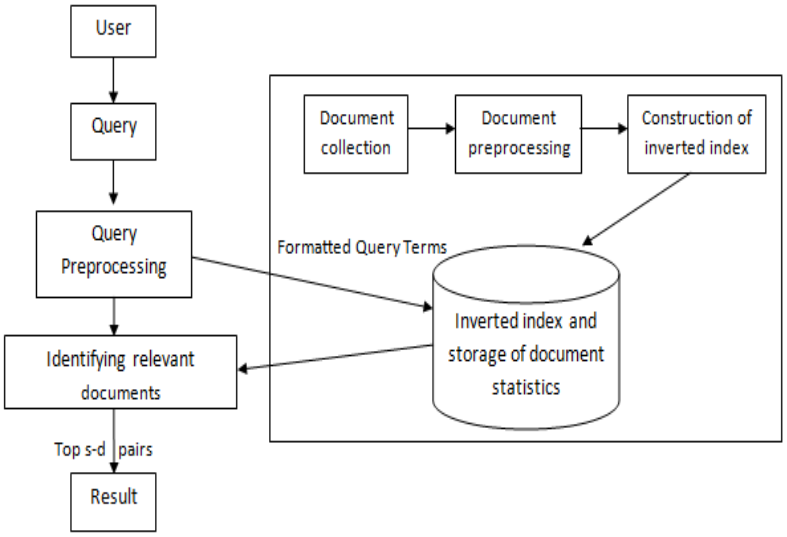

Fig. 1: Creation of Inverted Index

B. Multiterm indexing

The entire document collection goes through various data preprocessing function which gives list of terms. Now with the list of terms and the list of documents, the inverted index can map the term set to the list of document. In a given document there are n distinct terms and hence the set of all possible combined terms has 2^n element which is the worst case hence the pruning method is proposed to address this issue. To select the meaningful terms the concept of TF $\times$ IDF is used by using which the weight of each term is calculated and only top w_{max} terms are selected for the combination.

$w_{max} = \lambda\, n \log n$…… (1)

Where n is the number of documents and λ is the pruning parameter used to set pruning scale. The basic strategy of the pruning method is to index the short term combinations only ($S_{max} = 3$) as the long term combinations have little opportunity to be queried. With ($S_{max} = 3$) the index for n-term document can be significantly reduced. To calculate the Similarities between term set and documents the vector space model is used.

$Sim_{(s,d)} = \frac{\sum w_{s,t} \times w_{d,t}}{\sqrt{s} \times \sqrt{d}}$ ….. (2)

In above equation d is document and we compute the relevance of each document with term set s by cosine similarity: where $\omega_{s,t}$ and $\omega_{d,t}$ represents the weight of term t in s and d respectively.

$\omega = TF \times IDF$ ……... (3)

To calculate the weight of term $TF \times IDF$ scheme is used. TF denotes the term frequency of the term associated with the document.

$TF = 1 + \log(f_{d,t})$……. (4)

Here $f_{d,t}$ is number of times the term present in document d. IDF denotes the inverse document frequency of the term.

$IDF = (1 + \frac{N}{f_t})$…… (5)

Here, N denotes the total number of documents in collection and f_t is the number of document that contains the term t.

C. Steps in Index Pruning

1) For each document in collection perform document preprocessing.
2) Compute w_t i.e. weight of each term associated with the document using $TF \times IDF$.
3) Compute w_{max} using (1) and based on weight select only top w_{max} terms for indexing.
4) Similarly, for $S_{max} = 2$ repeat step 3.
5) For $S_{max} = 3$ check if the combination has frequent subsets or not, if yes then create an index on the set, otherwise keep the subsets in index as it is.

IV. EXPERIMENTAL SETUP AND RESULTS

An implementation is carried out with the help of JAVA Eclipse IDE, and NoSQL database The experiment is carried out using Reuters dataset which was originally collected and labeled by Carnegie Group, Inc. and Reuters, Ltd. The dataset is converted into mongodb dataset which contains document id, category, tokens. All data set was preprocessed with various document preprocessing operations to reduce the number of words.

Fig 2 plots average precision over recall level and reflects the search behavior. The results show that MTKS has better precision at almost all given recall levels than STKS. Fig. 3 shows the precision of top k that is top ranked documents returned by MTKS and STKS

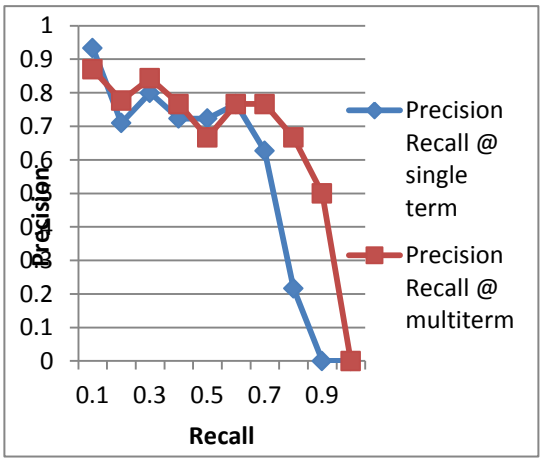

Fig. 2: Precision recall curve

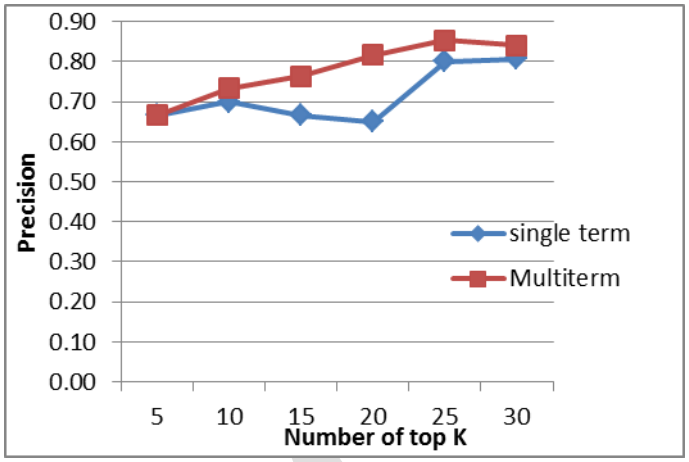

Fig. 3: Precision @ top k documents

V. CONCLUSION

The NoSQL systems are more and more deployed as a backend for various applications nowadays which support both Semi structured and unstructured data. The keyword based search based on single term inverted index performs poorly on such type of data. Therefore in above work the inverted indexing technique has been discussed to perform multiterm keyword search over the unstructured data. The effective index pruning method is used to reduce the index size in which the more representative keywords are selected to create term set with the aim that to provide efficient result to the user.

REFERENCES:

[1] H. Chen et al., TSS: Efficient Term Set Search in Large Peer-to- Peer Textual Collections, IEEE Trans. Computers, vol. 59, no. 7, 2010, pp. 969-980.
[2] C. Wetch, Anwitaman Data, Multiterm Keyword Search In NoSQL System,IEEE Internet Computing, 2011.
[3] Xing Jin, W.-P. Ken, Yiu S.-H., Supporting Multiple-Keyword Search in A Hybrid Structured Peer-to-Peer Network, Gary Chan Department of Computer Science The Hong Kong University of Science and Technology Clear Water Bay, Kowloon, Hong Kong
[4] I. Podnar et al., Scalable Peer-to-Peer Web Retrieval with Highly Discriminative Keys, Proc. Intl Conf. Data Eng. (ICDE 07), IEEE Press, 2007, pp. 1096-1105.
[5] P. Reynolds and A. Vahdat, Efficient Peer-to-Peer Keyword Searching, Proc. Middleware, Springer, 2003, pp. 21-40.
[6] J. Zhang, T. suel, Efficient Query Evaluation on Large Textual Collection in a Peer to Peer Environment, CIS dept. polytechnic university Brooklyn, NY 11201.
[7] H. Chen et al., Efficient Multi-Keyword Search Over P2P Web,Proc. Conf. World Wide Web (WWW), ACM Press, 2008, pp. 989-998.
[8] Yuh-Jeer Joung, L. Yang, C. Fang, Keyword Search In DHT Based Peer To Peer Networks IEEE conference 2007
[9] Hanhua Chen, Hai Jin, Lei Chen, Optimizing Bloom Filter Settings in Peer-to-Peer Multi keyword Searching, Liu, Senior Member, IEEE, and Lionel M. Ni, Fellow, IEEE.
[10] Hao Wu, Guoliang Li, and Lizhu Zhou, Ginix: Generalized Inverted Index for Keyword Search IEEE Transactions on Knowledge And Data Mining Vol:8 No:1 Year 2013.
[11] Uniform access to NoSQL system paolo atzeni, Francesca bugiotti, luca rossi.
[12] D. Li, J. Cao, X. Lu, and K. Chen, Efficient Range Query Processing in Peer-to-Peer Systems, IEEE Trans. Knowledge and Data Eng., vol. 21, no. 1, pp. 78-91, Jan. 2009.
[13] O.D. Gnawali, A Keyword-Set Search System for Peer-to-Peer Networks, Masters thesis, MIT, 2002.
[14] J. Lu and J. Callan, Content-Based Retrieval in Hybrid Peer-to-Peer Networks, Proc. Intl Conf. Information and Knowledge Management (CIKM), 2003.
[15] I. H. Witten, A. Moffat, and T. C. Bell, Managing gigabytes: Compressing and indexing documents and images, Morgan Kaufmann Publishing: San Francisco, May 1999, PP. 36-56.
[16] E.-J. Goh, Secure indexes, Cryptology ePrint Archive, Report 2003/216, 2003.
[17] P. S. Mahajan, A. R. Deshpande, Review on Multiterm Inverted Index, CIIT 2015, in press.

[18] J. Lu and J. Callan, Content -Based Retrieval in Hybrid Peer-to-Peer Networks, Proc. Intl Conf. Information and Knowledge Management (CIKM), 2003.

International Journal of Engineering Research and General Science Volume 3, Issue 5, September-October, 2015
ISSN 2091-2730

Radar Clutter, its avoidance and rejection Methods

Shaik Mohammad Khaja[1], Dr.V.K.Suman[2], Dr. Syed Azeemuddin[3]

[1]Research Scholar, Shri Venkateshwara University, Gajraula, Dist. Amroha, U.P. India
smkhaja@gmail.com, Ph. +91-9030715498
[2]Professor & Dean, IIMT, Meerut, U.P.India
suman.glbitm@yahoo.co.in, Ph. +91-8791223770
[3]Assistant Professor, IIITHyderabad, Hyderabad, A.P. India

Abstract: Radar clutter may be defined as unwanted signals in a search Radar. Different types of clutters, their identification, avoidance and various types of techniques are illustrated in this paper. Clutter rejection, various radars used for this purpose, and the applications of such radars are discussed in this paper. Illustrative samples have also been discussed for emulators

Keywords— Radar, ATC, TSC, RAGCLEM, ARI, ARPA, UWB, DAR

I INTRODUCTION:

Radar returns are produced from nearly all surfaces when illuminated by radar. Therefore, in competition with the return from an aircraft, there are many sources of unwanted signals. Unwanted signals in a Search Radar are generally described as noise and clutter. Clutter is the term used and includes ground returns, sea returns, weather, buildings, birds and insects. The definition of clutter depends on the function of the Radar. For Instance, weather is not clutter in a weather detecting radar.

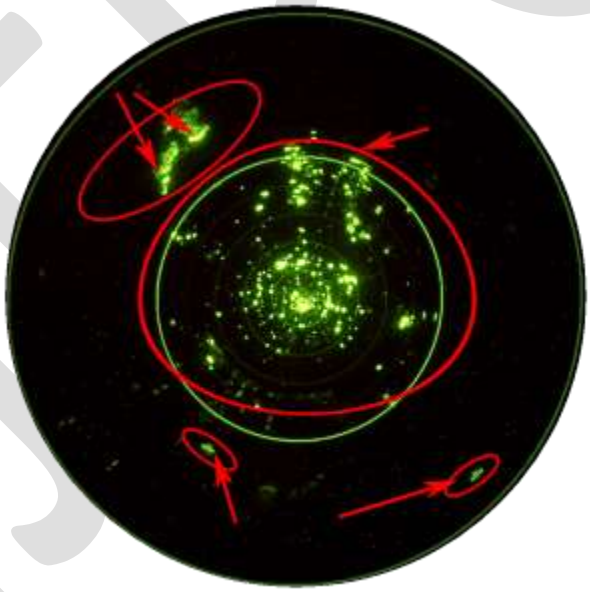

PPI screen of an ATC Radar with targets

II.TYPES OF CLUTTER: Clutter can be fluctuating or non-fluctuating. Ground clutter is generally non-fluctuating in nature because the physical features are normally static. On the other hand, weather clutter is mobile under the influence of wind and is generally considered fluctuating in nature. Clutter can be defined as homogeneous if the density of all the returns is uniform. Most of the surface and volume clutter are analyzed on this basis, however, in practice, this simplification does not hold good in all cases. Non-homogeneous clutter is non-uniform clutter where the amplitude of the clutter varies significantly from cell to cell. Typically non-homogeneous clutter is generated by tall buildings in built up areas.

The basic types of clutter can be summarized as follows:

Surface Clutter: Ground or sea returns are typical surface clutter. Returns from geographical land masses are generally stationary; however, the effect of wind on trees etc… means that the target can introduce a Doppler shift to the radar return. This Doppler shift is an important method of removing unwanted signals in the signal processing part of a radar system. Clutter returned from the sea generally also has movement associated with the waves. Doppler shift can be calculated by $\Delta\lambda/\lambda_0 = V/C$, where

$\Delta\lambda$ is the shift in wavelength.

λ_0 is the wavelength of source not moving/ stationary source.

V is velocity of source-line of site

C is speed of light.

Doppler shift can be either Red-shift (a shift of frequency to a lower wavelength, away from the observer) or Blue-shift (a shift of frequency to a higher wavelength, towards the observer). The power received from the clutter is given by

$$C= P_tGA_e\sigma_c/[(4\Pi)^2R^4]$$

Where P_t is the transmitter power

G is gain of Antenna

A_e is antenna effective aperture

R is Range

σ_c is clutter cross-section.

Volume Clutter: weather or chaff are typical volume clutter. In the air, the most significant problem is weather clutter. This can be produced from rain or snow and can have a significant Doppler content.

Point Clutter: Birds, windmills and individual tall buildings are typical point clutter and re not extended in nature. Moving point clutter is sometimes described as angels. Birds and insects produce clutter, which can be very difficult to remove because the characteristics are very much like aircraft.

Sea-Clutter: Sea Clutter are disturbing radar-echoes of sea wave crests. This clutter gets also a Doppler-speed by the wind. This means, the scenario, moves away i.e. changes with time, while for ground clutter, it stays the same. Therefore, in practice, Sea-Clutter is very difficult to control without some loss in detection. Sea-Clutter can be seen here in the below picture, the wind comes from about 3100(NO) or from the opposite direction. (Unfortunately, whether the Doppler frequency is positive or negative cannot be recognized on the PPI-Scope. But this region, in which the radial speed of the waves is very small, is cleaned by the MTI system very clearly.

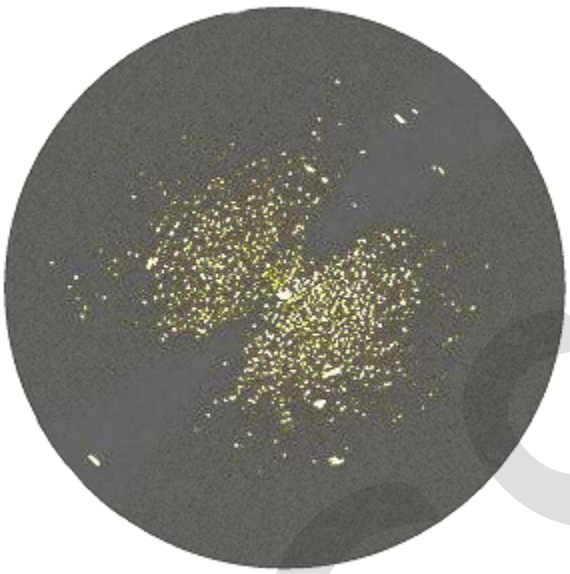

SEA-CLUTTER ON A PPI-SCOPE

III DETECTION AND REDUCTION MECHANISMS: Airborne maritime surveillance radars must detect small targets against a background of sea clutter whilst maintaining surveillance over a large area of sea. This task is very demanding and requires the radar to dynamically adapt to the local environment in order to obtain the best possible detection sensitivity. An aircraft flying at, say 3000 ft would be able to observe an area of sea of about 49,000 km, with a range to the horizon of about 124 km. Over this area, the clutter characteristics observed the radar will be continuously changing as a function of range and look direction. These characteristics will vary in a manner dependent on the prevailing conditions, the radar characteristics and the viewing geometry. In practice, the radar must cope with a very wide dynamic range of signal amplitude, with amplitude statistics varying from those of thermal noise to very spiky sea clutter and land. Continuous adaptation to this environment is required as a function of range and bearing. The dynamic behaviour of the radar as it adapts in this way is often a much more relevant measure of performance than more traditional static measures such as detection range.
Methods used to adapt to the environment are surveyed in this paper, together with indications of how their dynamic behavior can influence performance.

With the advent of a new airborne radar signal processing technology entitled, "space-time adaptive processing (stap)," previous testing methods have proven inadequate. stap algorithms minimize the amount of interference competing with the desired signal. the algorithms are complex and their reaction to an actual in the air scenario difficult to predict via analysis and simulation. the desired test is to evaluate the performance on the ground in a controlled environment prior to installation and test in the air. the problem is that although jamming signals can be relatively easily generated, ground clutter, which depends on the aircraft speed, antenna beam width and antenna look-angle is difficult to represent realistically. Technology service corporation (TSC) has developed a realistic radar ground clutter emulator (ragclem) which can be used to test stap processors.

The problem of clutter rejection when processing down-looking Doppler radar returns from a low altitude airborne platform is a paramount problem. With radar as a remote sensor for detecting and predicting wind shear in the vicinity of an urban airport, dynamic range requirements can exceed 50 dB because of high clutter to signal ratios. This presentation describes signal processing considerations in the presence of distributed and/or discrete clutter interference. Previous analyses have considered conventional range cell processing of radar returns from a rigidly mounted radar platform using either the Fourier or the pulse-pair method to estimate average wind speed and wind speed variation within a cell. Clutter rejection has been based largely upon analyzing a particular environment in the vicinity of the radar and employing a variety of techniques to reduce interference effects including notch filtering, Fourier domain line editing, and use of clutter maps. For the airborne environment the clutter characteristics may be somewhat different. Conventional clutter rejection methods may have to be changed and new methods will probably be required to provide useful signal to noise ratios. Various considerations are described. A major thrust has been to evaluate the effect of clutter rejection filtering upon the ability to derive useful information from the post-filter radar data. This analysis software is briefly described. Finally, some ideas for future analysis are considered including the use of adaptive filtering for clutter rejection and the estimation of

wind speed spatial gradient directly from radar returns as a means of reducing the effects of clutter on the determination of a wind shear hazard.

The ARI Radar/ARPA simulator is a complete simulation solution meeting the requirements for simulators as per regulation I/12 of STCW 2010 and incorporates all the required features pursuant to MSC Res. 64(67) and MSC Res. A. 823(19) and is a complete emulation of shipboard Radar/ARPA equipment. The Radar Simulator can be used to conduct the IMO Model course 1.07 and has been type approved by the DGS, Government of India for that purpose. It may be used to conduct Radar/ARPA courses for navigators at both operational and management levels.

IV SPECIAL SIMULATOR APPLICATIONS: The simulator emulates a variety of the functionalities found in modern marine radar and provides control over traffic density, waterways, sea state and weather conditions. The ARI Radar/ARPA simulator is an extremely efficient and cost-effective solution which can be used in standalone mode for self-teaching, or in networked mode along with an Instructor console. The advanced mathematical design of this simulator enables replication of wide variety of control to provide training in a highly realistic environment. Features available include:

1. Environment Effects like wind, current and waves
2. True and Relative Motion Displays
3. X-Band or S-Band
4. Pulse Length
5. Clutter Suppression
6. Ground or Sea Stabilized
7. Course Up, North Up, Head Up Display
8. Range Rings On/Off
9. Gain Control
10. Brilliance
11. EBL/VRMs
12. Trial Manoeuver
13. Roll and Pitch Effects
14. Set and Drift Effects
15. Parallel Indexing
16. Target Acquisition; auto or manual
17. Target Tracking; saves up to 50 targets in memory
18. Target Data Display
19. CPA/TCPA Limit Setting
20. True and Relative Vectors
21. Guard Zones
22. Visual and Audio Alarms
23. Realistic Interference: Starring, Spoking, Multiple Echoes, Side Lobe Effect, Blind Sector, Shadow Sector
24. Performance Monitor
25. RAMARK and RACONS
26. SART activated by Instructor

The **W1905 Radar Model Library** saves development time and verification expense in R&D for radar system architects, algorithm developers, and system verifiers.

The library provides approximately 90 highly-parameterized simulation blocks and several dozen ready-made reference designs for creating working radar system scenarios, including radar processing blocks, environmental effects items such as clutter, targets, and even hardware measurements. Instead of modeling an entire scenario from primitive function calls for each object, simply connect realistic reference designs with RF models and test equipment to study and verify radar system architectures. The W1905 library can

be applied to a wide range of radar technologies, making it a useful algorithmic reference for both commercial and military applications.

The W1905 library recently added 3D inertial modeling "layers" above the baseband radar signal processing references (see Figure 4 below). They account for the 3-D positions, velocities, rotations, and beam forming directions of each transmitter, receiver and target, allowing modelers to create and script meaningful airborne, ship borne and multi-static scenarios or environments.

Radar Technologies

(a) ultra-wideband (UWB) radars, and wideband receivers

(b) phased array and digital array radars (DAR), with dynamic coordinates, attitude, and beam forming weights

(c) synthetic aperture radars (SAR) and beam forming for raster imaging and mapping

(d) stepped-frequency radars (SFR) for ground- and wall-penetrating applications

(e) frequency modulated continuous-wave (FMCW) radars for automotive applications

(f) MIMO radars for increased range resolution and robustness

(g) Multi-static radars with multiple TX and RX locations, which can be in motion (vehicle/ship/air/space-borne)

(h) signal generation for embedded simulators and test & measurement applications

(i) Pulsed and pulsed-Doppler (PD) radar architectures for telemetry and EW applications

The W1905 block set and its example workspaces serve as algorithmic and architectural reference designs to verify radar performance under different signal conditions. These can include target and RCS scenarios, clutter conditions, jammers and environmental interferers, and more. By accounting for a diverse set of environmental effects, while maintaining an open modeling environment (.m, C++, VHDL, test equipment), the Radar system designer can explore architectures with high confidence in early R&D, without requiring expensive outdoor range testing or hardware simulators.

V SYSTEM VUE'S ALGORITHM MODELS: SystemVue connects baseband algorithm modelers with a variety of other domains. SystemVue can also be used to create reference signals for download to test equipment, as well as post-process signals captured from test equipment, to create virtual verification systems at low cost.

SystemVue's W1905 radar library helps model the signal processing algorithms as well as the radar environment, and connects to UWB test equipment, such as the new Keysight M8190A AWG, M9703A digitizer, and Keysight's 90000-series oscilloscopes as shown in the figure below.

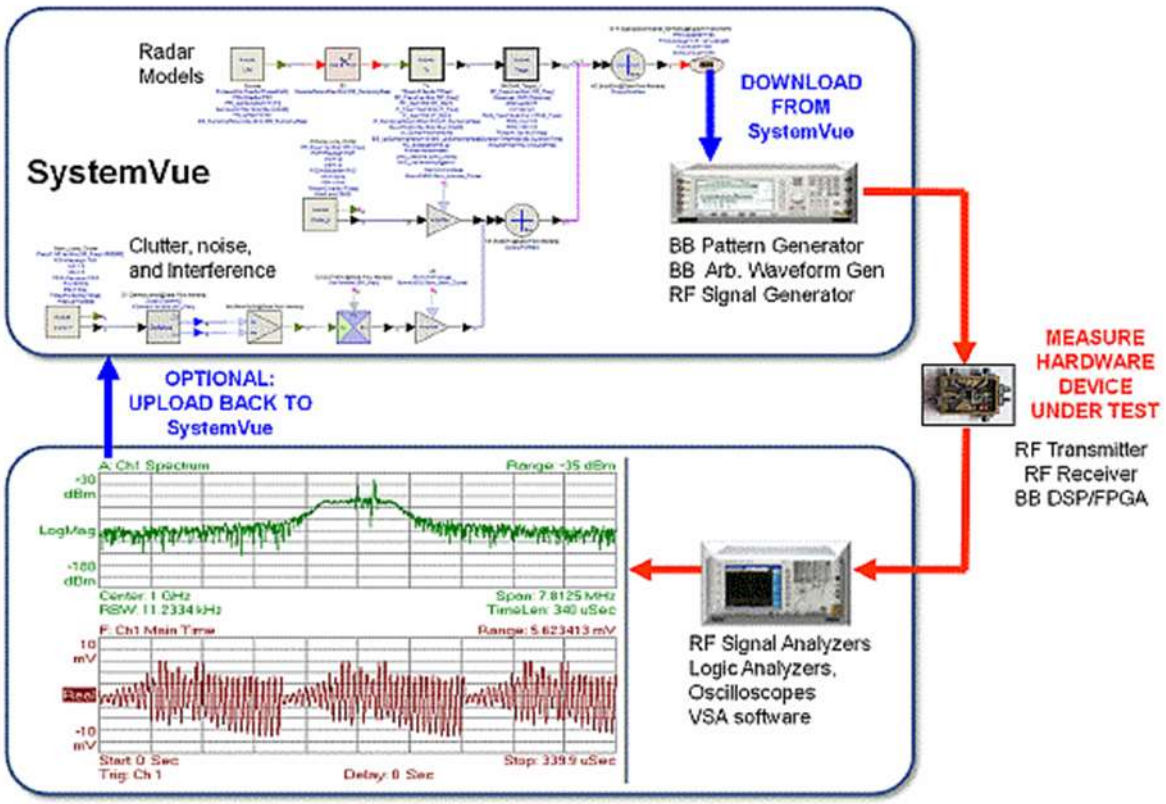

Recent Upgrades (as of SystemVue 2013.08 SP1)

a. Now provides an inertial coordinate framework for modeling moving platforms, targets, clutter, and including the effect of dynamic RCS and beam forming patterns in 3-dimensions. This allows easier creation of multi-static airborne and ship-borne scenarios.

b. New blocks and examples for MIMO Radar, Phased Array Radar with dynamic beam forming, Stepped-Frequency Radar (SFR), Synthetic Aperture Radar (SAR), Automotive Radar, electronic warfare (EW) and electronic counter measures (ECM)

c. New and updated models for user-defined antenna patterns and scanning, clutter models, moving targets, polarization, time-gating, pulse compression, CFAR, Direction of Arrival, MUSIC, SPIRIT and other algorithms

d. External scriptability and control of the SystemVue platform, allowing integration with other application providers, such as terrain map databases and structured verification suites

Updated instrument drivers for Keysight's family of wideband arbitrary waveform generators (AWG), such as M8190A. SystemVue also includes a new waveform utility called "Waveform Sequence Composer". Sources can also now include jitter and programmable pulse offsets.

Applications:

a. Create proposals and assess feasibility quickly

b. Accurate radar system architecture and scenario analysis
   1. Include realistic RF effects, clutter, fading, and directly-measured waveforms
   2. Leverage your existing math, HDL, and C++ algorithms
   3. Continue into hardware test using the same SystemVue environment and IP
   4. Multi-Emitter Environment Test Signals

c. Algorithmic reference & test vector generation for baseband DSP hardware design

d. Precisely-degraded BB/RF signal generation for receiver testing
    1. Reduce the need for expensive chambers, hardware emulators, faders, and field testing in the early phases of design
    2. Reduce NRE and scripting with regression suites of simulated scenarios
    3. Save time by verifying algorithms prior to targeted FPGA/ASIC implementation

e. Minimize project costs with easily reconfigured Keysight simulation tools and test equipment

VI CONCLUSION: Thus we can use various methods like ARPA, Systemvue's simulation techniques for detection and reduction of radar clutter in almost all the applications.

REFERENCES:

[1] Radar Handbook, second edition, M. Skolnik, McGraw-Hill, 1990.
[2] LI Ming, LIN Yu-mei, Ruan Feng "A Simple Simulation Method of Ground Clutter for Airborne Pulse DopplerRadar"IEEE Trans 2006.
[3] Mike Peardon, "A beginner's guide to programming GPUs with CUDA" School of Mathematics Trinity College,Dublin April 24, 2009.
[4]McMillan, R.W.; Kohlberg, H., "A probabilistic model of the radar signal-to-clutter and noise ratio for Weibull-distributed clutter," *Radar Conference, 2010 IEEE* , vol., no., pp.882,886, 10-14 May 2010
[5]Gregers-Hansen, V.; Mital, R., "An Improved Empirical Model for Radar Sea Clutter Reflectivity," *Aerospace and Electronic Systems, IEEE Transactions on*, vol.48, no.4, pp.3512-3524, October 2012
[6] Pola, M.; Bezousek, P.; Pidanic, J., "Model comparison of bistatic radar clutter," *Microwave Techniques (COMITE), 2013l Conference on*, vol., no., pp.182- 185,17-18April,2013.
[7] http://www.nvidia.com/object/cudalearn products.html.
[8]http://en.wikipedia.org/w/index.php?title=Graphics_processing_unit&oldid=575413080

International Journal of Engineering Research and General Science Volume 3, Issue 5, September-October, 2015
ISSN 2091-2730

Medical Image Watermarking using CGR

Vani Shaji[1] and Vani. V. Prakash[2]

PG Scholar, Department of Computer Science, India,vani.shaji00@gmail.com, No:+918943003247

Abstract— Chaos Game Representation (CGR) is used to produce unique images from symbolic sequences, which can serve as signature images of the sequence. In this paper, we pose and answer an interesting question- can we use CGR as a substitution of hashing in medical images? We show that it is possible to generate CGR for medical images as well as can be used to verify the integrity of the image. We go on to show that we can watermark the image using CGR to further verify the confidentiality and authenticity of the medical image.

***Keywords*—** CGR; Watermarking; Compression; Embedding; Extraction; DWT; Authentication.

INTRODUCTION

Medical imaging is the technique of creating visual representations of the interior of a body for clinical analysis and medical intervention. Medical imaging seeks to reveal internal structures hidden by the skin and bones, as well as to diagnose and treat disease. Safety and confidentiality is required for medical images, because critical judgment is done on medical images, which leads to the proper treatment. Privacy protection of medical images has always been an important issue. Medical image communications require a very high level of security for maintaining their communication secrecy. Constant efforts are being made to provide security to ensure (i) medical image transmission cannot be accessed by unauthorized users (confidentiality), (ii) images are not modified during transmission (integrity), and (iii) images have originated from the correct sources to the claimed receivers (authentication) [1]. One effective tool for providing image authentication and source information is digital watermarking. Watermarking, however, is a copyright protection method includes the embedding and extraction process [2]. Extraction process deals with the extraction of secret message or watermark, which is embedded in the medical image. If failure occurs in extraction process the physician would come to know that there has been some kind of tampering with that image, and he would take precaution of not making diagnosis based on that image. However, if the extraction process extracts the correct watermark, physician can continue with diagnosis.

Watermarking is the technique which amends the image information invisibly to implant the watermark. Digital watermarking also has proved to be beneficial in medical imaging. The main role of watermarking in medical imaging is to act as an interface to enhance the protection of its contents, without degrading the quality of data [3]. Its role also extended to the traceability from the origin to the destination. Watermark enhances the security of the image, as it is expected to be a part of the image and at the same time is invisible.

Watermarking techniques can be generally classified into two categories, reversible and irreversible [4]. The main idea behind reversible watermarking is to avoid irreversible distortion in original image , by formulating techniques that can extract the original image exactly. Medical image watermarking is one of the most important fields that need such techniques where distortion may cause misdiagnosis. The reversibly watermarked image is not at all distortion free, but that distorted image is used as a carrier for data to be embedded. and not for diagnosis. The losslessly recovered image is the final one used for diagnosis. Although reversible schemes seem to be adequate for medical images, it must meet all the requirements of image watermarking : imperceptibility, integrity control and authentication. From the literature, the purposes of medical image watermarking are classified into two categories [4]:

1. Tamper detection and authentication
2. Electronic Patient Records (EPR) data hiding.

Tamper detection watermarks are able to locate the regions or pixels of the image where tampering was performed. Authentication watermarks are used to identify the source of the image. EPR data hiding techniques give more importance in hiding high payload data in the images keeping the imperceptibility very high [4]. Depending on the purpose of the watermarking a proper watermarking technique is used accordingly.

In this paper, a new approach for securing medical images and detecting tampering is proposed. Given a medical image, an algorithm named Chaos Game is implemented to generate a unique signature image named Chaos Game Representation images (CGR images). The following section of the paper are organized as follows: The related research works are summarized in Section 2 and 3 describes the proposed CGR method and proposed medical image watermarking technique is described in Section 4. The results and analysis is given in Section 5 and section 6 concludes the paper.

RELATED WORK

Many watermarking schemes were proposed for medical images. Those techniques can be spatial domain techniques, frequency domain techniques, or a combination of the two domains. A security technique based on watermarking and encryption for DICOM is proposed by Mohamed M. AbdEldayem et al. [3] where the original image can be recovered completely. In this paper, a R-S vector is created which is then compressed. A hash value of the image is determined using MD5 hash function. This MD5 hash value along with the compressed R–S vector of the original image are concatenated, and then they are encrypted using AES encryption technique. This watermark is then embedded into the original image. During the extraction process, the exact reverse of the embedding process is performed and the original image is retrieved. Then the hash value of the extracted original image is calculated and is compared with the previous hash value. If they are equal, the image is authenticated, and it has right integrity, else the image is discarded because its integrity is broken. Extended Huffman algorithm is used to decompress the decrypted R–S Vector. The performance of the proposed technique is measured using the performance parameters: Signal to Noise Ratio (SNR), Mean Square Error (MSE), and Bit Error Rate (BER). The experiment results shows that the proposed technique is totally revertible and the original images can be retrieved at the receiver side without any distortion.

Another lossless watermarking scheme for DICOM images is proposed by Osamah M. et al. [4]. This paper is based on a fragile scheme combining two reversible techniques. These techniques are based on difference expansion and protecting the region of interest (ROI) with tamper detection and recovery capability. Here two watermarks are produced where the 1st watermark, which consists of patient's data and the hash message of ROI is embedded into ROI. As a result, an embedding map is produced which will be used to extract the 1st watermark. The map is then combined with recovery information to become a part of the 2nd watermark. This watermark is embedded into RONI. The experiment result shows that the watermarked images have good visual quality in terms of PSNR, with high embedding capacity.

Many works can be seen on investigation into use of CGRs as unique signature images for genomes and also other bio-sequences. The initial proposal of CGR for DNA sequences is made by H. Joel Jeffrey in the paper named Chaos game representation of gene structure in 1990 [5]. In this paper, chaotic dynamic concept is being applied which produces an image of a gene sequence displaying both local and global patterns. This image is named as attractor. Since the DNA sequence is represented using four letters 'a', 'g', 'c', 't', here a square is drawn labeling the four corners with these letters. Then applying the chaos game algorithm , the CGR is generated for the sequence. Each point in the CGR corresponds to exactly one subsequence. This shows a one-to-one correspondence between the subsequences of a gene and points of the CGR. The CGR method thus provides a graphic way of displaying the composition of a sequence.

Another paper named CGR based DNA sequence compression method [6], an efficient way of compressing DNA sequences is proposed where the CGR is used to compress the DNA sequence. This DNA sequence is later reconstructed from the CGR; given the coordinates of the final point in the CGR image. The algorithm is based on trace-back of nucleotides from final CGR coordinates, thereby tracing back the whole genomic sequences and regenerating the complete sequence from the last coordinate. This paper claims that the sequence can be compressed successfully but with a limitation of resolution of the CGR coordinate.

CHAOS GAME REPRESENTATION (CGR)

The 'chaotic dynamical systems' or simply 'chaos' is the field of study in mathematics that studies the behavior of dynamical systems that are highly sensitive to initial conditions—a response popularly referred to as the butterfly effect. Small differences in initial conditions may yield widely diverging outcomes for such dynamical systems. The Chaos Theory is stated as "When the present determines the future, but the approximate present does not approximately determine the future". Chaotic systems are predictable for a while and then 'appear' to become random.

The Chaos Game is an algorithm which allows one to produce pictures of fractal structures [5]. In simplest form, it proceeds as follows [5]:

1. Locate three dots or vertices on a piece of paper. They can be anywhere, as long as they are not all on a line.

2. Label one vertex with the numerals 1 and 2, one of the others with the numerals 3 and 4, and the third with the numerals 5 and 6.

3. Pick a point anywhere on the paper, and mark it. This is the initial point.

4. Roll a 6-sided die. Since in Step 2 the vertices were labeled, the number that comes up on the die is a label on a vertex. Thus, the number rolled on the die picks out a vertex. On the paper, place a mark half way between the previous point and the indicated vertex.

5. Continue to roll the die, on each roll marking the paper at the point halfway between the previous point and the indicated vertex. The result is shown in figure 1.

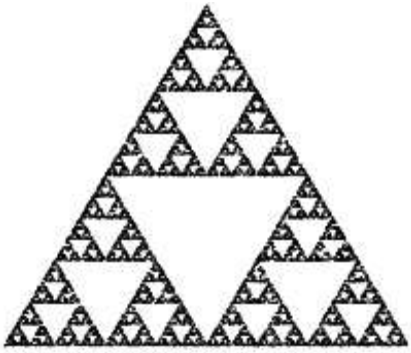

Fig 1: Sierpinski triangle-The Result of the Chaos Game on Three Points.

This original CGR algorithm is later used to produce pictures revealing patterns in DNA sequences [6]. Even though the technique is first proposed for DNA sequence, it is now being used for sequence of arbitrary symbols. Basically, the whole set of frequencies of the words found in a given genomic sequence can be displayed in the form of a single image in which each pixel is associated with a specific word [8]. CGR acts as a means to visualize the non-randomness of genomic sequence by using the concept of chaotic dynamical systems. Since a genetic sequence can be treated formally as a string composed from the four letters 'a', 'c', 'g', and 't', a square is drawn with each of the four corners of the square labeled as 'a', 'c', 'g', or 't' [5]. For plotting a given sequence, it is started from the centre of the square. A nucleotide is represented as one point in the square [6]. The first point plotted halfway between the centre of the square and the corner corresponding to the first nucleotide of the sequence and successive points plotted halfway between the previous point and the corner corresponding to the base of each successive sequence site.

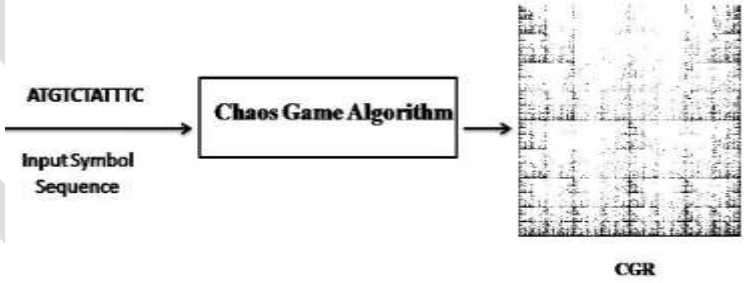

Fig 2: Chaos Game Representation process.

In this paper, we use this algorithm to generate CGR for medical images which may act as the unique signature image for the corresponding medical image. Consider a binary sequence 11100101001010110101001 01.... To derive a Chaos Game Representation of this sequence, a square is first drawn to any desired scale and corners marked 00,01,10 and 11. Here the sequence is taken as two-digit pattern. For plotting a given sequence, we start from the centre of the square [6]. The first point is plotted halfway between the centre of the square, and the corner corresponding to the first number of the sequence, and successive points are plotted halfway between the previous point, and the corner corresponding to the base of each successive numbers. Fig 3 shows all segments in a CGR square.

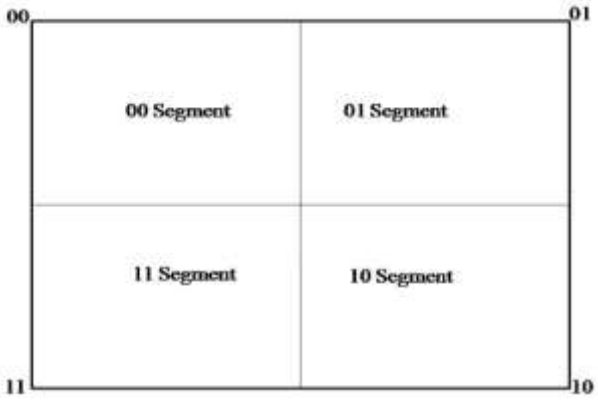

Fig 3: Segments in a CGR Square

The general steps for plotting a given sequence are concluded below [6].

1. Select the first number from the given sequence.
2. Calculate the midpoint between the centre and the corner corresponding to the first number (xN, yN). Let the midpoint be (xi, yi). Let (xc, yc) be the co-ordinates of the midpoint of the square. Then
   xi = (xc+ xN)/2 and yi= (yc+ yN)/2

3. Do the following steps until all the numbers are processed: Read the next number in the sequence. Calculate the midpoint between the current point (xi, yi) and the corner corresponding to the newly read number:
   xi+1 = (xi+ xN)/2 and yi+1 = (yi+ yN)/2.

We will demonstrate this basic idea with a toy example. Let us plot the sequence 11011010 into the CGR square. Points are marked within the square corresponding to the bases in the sequence, as follows:

1) Plot the first point X1, halfway between the center of the square X0, and the 11 corner.
2) The next point X2 is plotted halfway between X1 and the 01 corner.
3) The next point X3 is plotted halfway between X2 and the 10 corner.
4) The next point X4 is plotted halfway between X3 and the 10 corner.

The final CGR is given in Fig. 4.

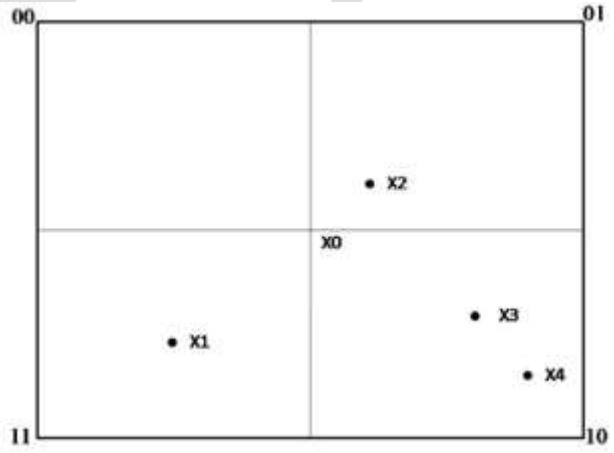

Fig 4. Plot of CGR points for the sequence "11011010"

A CGR has many interesting properties. Every binary-sequence has a unique CGR [7]. In fact every number in a sequence will have a corresponding unique point in the CGR. Every point on the CGR is a representation of all the numbers in the sequence up to that point. Each sub-square in a CGR has a special significance. If we divide the CGR into four quadrants, then the top right corner will

contain points representing sub-sequences that end with 01, as a midpoint between any other point in the square and the 01-corner has to fall in this quadrant.

PROPOSED SCHEME

In the proposed scheme, the medical image integrity for medical images based on reversible watermarking is proposed. Here, the concept of CGR is being implemented in medical images especially on X-ray images. For any given medical image, the CGR is generated and this CGR is watermarked into the corresponding medical image itself [3]. Later on, during transmission the watermarked image is being transmitted and at the receiver site, the watermark and the original image is extracted. From the original image, the CGR is again generated and is compared with the watermarked CGR. If they are equal, then the image is not modified and is validated, otherwise the two CGRs are different, therefore the image was modified [3], and it is no longer authenticated. Here, the DWT watermarking technique is used to watermark the image. The watermark embedding and extraction process are shown.

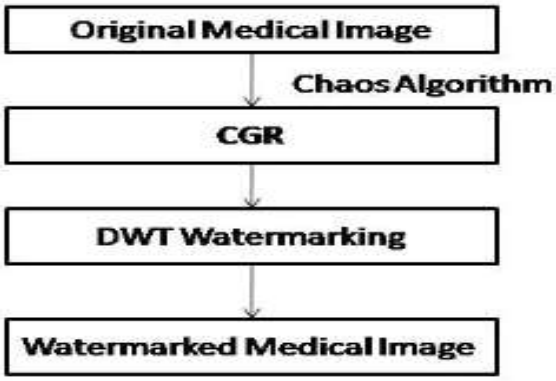

Fig 5. Proposed Scheme- Embedding Process

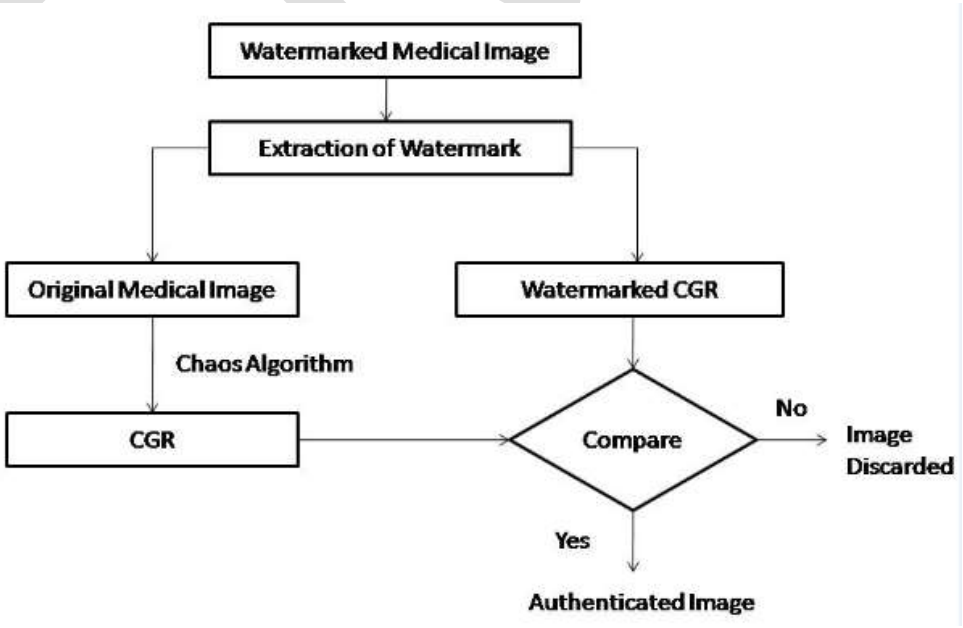

Fig 6. Proposed Scheme- Extraction Process

RESULTS AND ANALYSIS

The proposed CGR-based medical image watermarking algorithm has been applied against different type of medical image such as, CT scan, MRI, X-Ray and Ultrasound. We have tested the system over different size of medical images like 320 X 256, 384 X 384, and 512 X 512. The CGRs, are then embedded as the watermark into the original medical image. The extracted CGR and the computed CGR are compared at the receiver side using the statistical measures MSE, RMS, PSNR and correlation coefficient.

CONCLUSION

In this paper, a unique way of securing medical images using CGR is proposed. This technique provides image integrity service as the CGR involves treating an image as an abstract string of numbers. Here, the CGR algorithm has been used as a substitution of hashing algorithm. The generated CGR i watermarked into the medical image using DWT watermarking algorithm. Since DWT is a reversible watermarking method, the original medical image can be retrieved at the receiver side without any distortion.

As a future work, the proposed technique can practically be included within the medical information systems to provide medical image integrity, system authentication and confidentiality. Other revertible watermarking methods can be proposed to increase the amount of embedded data.

REFERENCES:

[1] Mingyan Lia , Radha Poovendran, "Protecting patient privacy against unauthorized release of medical images in a group communication environment" Department of Electrical Engineering, University of Washington, Seattle, WA 98195, USA

[2] Sonika C. Rathi1 and Vandana S., "Medical Images Authentication Through Watermarkingp Reserving Roi" Health Informatics - An International Journal (HIIJ) Vol.1, No.1, August 2012.

[3] Mohamed M. Abd-Eldayem “A proposed security technique based on watermarking and encryption for digital imaging nd communications in medicine ,” Department of Information Technology , Faculty of Computers and Informatics, Cairy University, Egypt

[4] Osamah M. Al-Qershi, Khoo Bee Ee , "Authentication and Data Hiding Using a Reversible ROI-based Watermarking Scheme for DICOM Images " Proceedings Of World Academy Of Science, Engineering And Technology Volume 38 February 2009 Issn: 2070-3740.

[5] H. Joel Jeffrey "Chaos game representation of gene structure", Nucleic Acids Research , Vol. 18, No. 8, 1990.

[6] Arun K. S* , Achuthsankar S. Nair, Oommen V. Oommen "A Novel DNA Sequence Compression Method Based on Chaos Game Representation." International Journal for Computational Biology (IJCB) Vol.2, No.1, 2013, Page: 01-11 ISSN: 2278-8115

[7] Manju Susan Thomas "Investigation of Distance Measure in Proteins usi ng Chaos Game Representation", Centre of Bioinformatics, University of Kerala, March 2005.

[8] Patrick J. Deschavanne,* Alain Giron et al., " Genomic Signature: Characterization and Classification of Species Assessed by Chaos Game Representation of Sequences ", *Laboratoire de Mutage´ne`se, Institut Jacques Monod, Paris, France.

[9] Nyeem Hussain, (2013) "Utilizing Least Signi cant Bit-Planes of RONI Pixels for Medical Image Watermarking," Proceedings of Digital Image Computing Techniques and Applications,.

[10] Arun K. S, Achuthsankar S. Nair and Oommen V. Oommen, (2013) " A Novel DNA Sequence Compression Method Based on Chaos Game Representation," International Journal for Computational Biology.

[11] Vrinda V. Nair, Karthika Vijayan, Deepa P. Gopinath and Achuthsankar S. Nair, (2010) "ANN based Genome Classi er using Frequency Chaos Game Representation," IACSIT International Journal of Engineering and Technology.

[12] Hill KA, Schisler NJ and Singh SM, (1993) "Chaos Game Representation of Coding Regions of Human Globin Genes and Alcohol Dehydrogenase Genes of Phylogenetically Divergent Species," Journal of Molecular Evolution.

[13] Goldman N, (1993) "Nucleotide, Dinucleotide and Trinucleotide Frequencies Explain Patterns Observed in Chaos Game Representations of DNA Sequences," Nucleic Acids.

[14] Oliver JL, Bernaola-Galvan P, Guerrero G, and Roman-Roldan R, (1993) "Entropic Pro les of DNA Sequences through Chaos Game Derived images," Journal Of Theoritical Biology.

[15] Basu S, Pam A, Dutta C and Das J, (1997), "Chaos Game Representation of Proteins," Journal of Molecular Graph Model.

.

International Journal of Engineering Research and General Science Volume 3, Issue 5, September-October, 2015
ISSN 2091-2730

Automatic MA detection method for Diabetic Retinopathy

Hajare K.R. , Patil S.N.

Department of Electronics engineering, PVPIT, BUDHGAON, INDIA,

komal.hajare5@gmail.com ,9130014643

Department of Electronics engineering, PVPIT, BUDHGAON, INDIA, sanjaypatil70@gmail.com

Abstract— We have evaluated our approach for micro aneurysm detection in an online competition, where this algorithm is currently ranked as first, and also on two other databases. Since micro aneurysm detection is decisive in diabetic retinopathy (DR) grading. Grading performance of computer aided DR screening system highly depends on MA detection. In this paper we propose a MA detector that provides remarkable results from both aspect. The earlier systems used manual methods for detecting microanuersym that caused increase in obtaining wrong results. so an ensemble based system is being used which contains a combination of pre-processing and candidate extractors.

Keywords—Diabetic retinopathy (DR) grading, ensembles based systems, micro aneurysm (MA) detection.ROC (retinopathy online challenge), hemorrhages, candidate extractor , machine learning .

I. Introduction

Diabetes is disease that affect blood vessels thought the body especially on kidneys & eyes. Along with diabetes, high blood sugar level in long periods can affect small vessels in the retina. Diabetic retinopathy (DR) is complicated eye dieses which is cause blindness for human being.

MA is early sign of DR. so detection of MA is essential in an efficient screening process. MA is nothing but small circular spot on the surface of retina. MA is near thin vessel but they cannot actually lies on the vessels. DR can be prevented by earlier detection of MA & slows down progression of MA. Therefore regular eye checkup & timely treatment is needed. But due to the higher medical cost makes regular check up costly. To fill this gap development of low cost & versatile MA detection technique is needed. We develop MA detector & DR Grading which give better result.

II. Bakground information

Anatomy of human eye:

The anatomy of the human eye consists of different cellular structures which are responsible to maintain proper functioning of our vision system. Light entering the eye passes through the anterior and posterior regions before it is processed in the visual cortex. The anterior region which consists of cornea, iris, pupil, and lens mainly serves as a pre-processing step to control the amount of entering light and converges it on the retina. The posterior region contains retina

which is a multi-layered sensory tissue made of millions of photo-receptors to capture incoming light. The central area within retina is called the macula which consists of the central fovea, rich in cones, and a peripheral area, rich in rods. Cones are highly color sensitive photo-receptors and are mainly responsible for day vision. On the other hand rods are highly sensitive to contrast variations and active during night vision or dark light condition.

Dibetic retinopathy:

These dieses originate from diabetic mellitus. It causes progressive damage to the retina. The light sensitive lining at back of eye. It is serious complication of diabetes. DR damages to the tiny blood vessels that nourishes to the retina. They leak blood & other fluid that cause swelling of retinal tissue & clouding of vision. Some time patients can only differentiate between dark & light part of the image. It affects to the both eyes. There are 5 stages of progression of DR. (1) No apparent retinopathy -no abnormalities. (2) Mild non-proliferative DR- the presence of dot & blot hemorrhages & micro aneurysms (MA) in the retina. Presence of MA only. (3) Moderate non proliferative DR- In this stage some of blood vessel in retina actually blocked. It decreases the supply of nutrients & oxygen to certain areas of retina. (4) Sever non-proliferative DR- as more blood vessel become blocked retina is not getting properly nourishments. (5) Proliferative DR – the retina grows abnormal blood vessel which are fragile & tends to break easily leading & profound vision loss.

(a) Normal Vision.

(b) Vision with Diabetic Retinopathy.

Figure 2: Normal Human Vision vs. Vision affected by Diabetic Retinopathy

III. Present theories

An approach to improve micro aneurysm detection in digital color funds images. Instead of following the standard process which considers preprocessing, candidate extraction and classification, we propose a novel approach that combines several preprocessing methods and candidate extractors before the classification step. We ensure high flexibility by using a modular model and a simulated annealing-based search algorithm to find the optimal combination. Our experimental results show that the proposed method outperforms the current state-of-the-art individual micro aneurysms candidate extractors

Automated detection of lesions in retinal images can assist in early diagnosis and screening of a common disease: m. We propose a new constraint for optic disk detection where we first detect the major blood vessels first and use the intersection of these to find the approximate location of the optic disk. This is further localized using color properties. We also show that many of the features such as the blood vessels, exudates and micro aneurysms and hemorrhages can be detected quite accurately using different morphological operations applied appropriately. These compare very favorably with existing systems and promise real deployment of these systems.

A new algorithm is proposed for removing large objects from digital images. This paper presents a novel and efficient algorithm that combines the advantages of these two approaches. We first note that exemplar-based texture synthesis contains the essential process required to replicate both texture and structure; the success of structure propagation, however, is highly dependent on the order in which the filling proceeds. We propose a best-first algorithm in which the confidence in the synthesized pixel values is propagated in a manner similar to the propagation of information in inpainting. The actual color values are computed using exemplar-based synthesis. Computational efficiency is achieved by a block based sampling process

We present an approach to improve micro aneurysm detection in digital color fundus images. Instead of following the standard process which considers preprocessing, candidate extraction and classification, we propose a novel approach that combines several preprocessing methods and candidate extractors before the classification step. We ensure high flexibility by using a modular model and a simulated annealing-based search algorithm to find the optimal combination.

IV. Preprocessing methods

The pre-processing method is been selected so that from the noisy images is been removed so that the MA detection is done easily.The best methods is been selected from image processing so that the image obtained will have all the characteristics needed to detect diabetic retinopathy. These pre-processing method used can be modified for future purpose

Walter -Klein Contrast Enhancement

This method is used to improve the contrast by using the gray level transformation which is been applied to the retinal image that is been used as input image.

Contrast Limited Adaptive Histogram Equalization

The popular technique that is been used in image processing because it increases the clarity of the salient part of the image making it visible and clear.The borders between the image is been eliminated by using bilinear interpolation.

Vessel Removal and Extrapolation

The unwanted vessels is been removed from the input image and extrapolation method is been done to fill the holes that has been created during the in painting algorithm used. thus this makes the image more clear to detect the MA.

Illumination Equalization

This method is used to eliminate the uneven illuminations of the fundus image that is obtained after the extrapolation. Illumination Equalized image

No Pre-processing

Without doing the pre-processing method directly the candidate extraction method is been done.

V. Candidate extraction

Candidate extraction is the process that is to spot the characteristics of the MA image obtained after the pre-processing method. For future enhancement of the system, the new candidate extractors methods can be used.

Walter et al

This method used is to find small dark patterns on the green channel by using grayscale diameter closing.

Spencer et al

The retinal image extracts a vascular map and top-hat transformation is done .The final image obtained is then bilinear zed

Circular-Hough Transformation

This technique is used for extraction of circular objects from the image.

Zhang et al

This method is used to constructs maximal correlation response for the input image. the methods like vessel detection is done to reduce the number of candidates and to determine the size of the image.

Lazar et al

Cross-sectional profiles of pixel wise are used to construct multidirectional height map and this map set the height values that describes the distinction of the pixel that is used in the surrounding image.

VI. Ensemble creation

We provide an ensemble creation framework to select the best combination. In our framework, an ensemble E is a set of (preprocessing method, candidate extractor) pairs. The meaning this pair is that first we apply preprocessing method to the input image & then candidate extractor. Collect candidate whose Euclidian distance d is smaller than predefined constant r ∈ R from where HE is set of candidate & c is individual candidate.

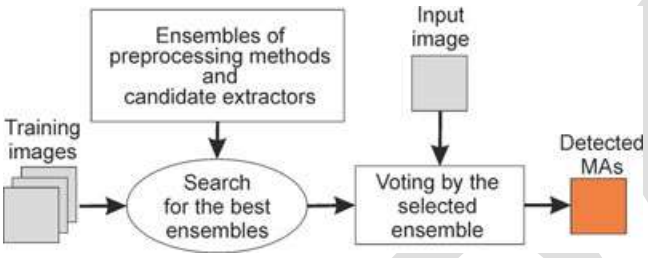

Figure 4 : Flow chart of the ensemble-based framework.

Centroid calculate by using HE & IC. Ensemble creation is process where all ensemble E from ensemble pool E is evaluated & best performing one Ebest ∈ E. select that one to find E, output candidate set HE must be compared to ground truth in the following way: for c ∈ HE there exist a point ground truth , whose Euclidian distance d from c is smaller than a predefined constant r ∈ R , the c is considered true positive otherwise c is false positive. While each ground is truth point is false negative. That does not have a a close candidate from HE .If M=N preprocessing methods and candidate extractor, then we have 25pair with 225 number os possible combination to form ENSEMBLE .It is very resource demanding. we use search algorithm : To evaluate such condition. Large number of combination. So we used stimulate annealing as search algorithm :

Algorithm 1: Selection of the optimal combination of preprocessing methods and candidate extractors.

1. $\mathcal{E} \leftarrow P(PP_i \times CE_j)$, $i = 1, \ldots, M$, $j = 1, \ldots, N$
2. $CPM_{best} \leftarrow 0$
3. $E_{best} \leftarrow NULL$
4. **for all** $E \in \mathcal{E}$ **do**
5. $\quad H_E \leftarrow \emptyset$
6. $\quad$ **for all** $p \in E$ **do**
7. $\quad\quad$ **for all** MA candidate c detected by p **do**
8. $\quad\quad\quad I_c \leftarrow \{c' | c'$ is a MA candidate found by a $p' \in E$, with $p \neq p'$ and $d(c, c') < r\} \cup \{c\}$
9. $\quad\quad\quad confidence(c) = \frac{|I_c|}{|E|}$,
10. $\quad\quad\quad H_E \leftarrow H_E \cup centroid(I_c)$
11. $\quad\quad$ **end for**
12. $\quad$ **end for**
13. $\quad$ **if** $CPM(H_E) > CPM_{best}$ **then**
14. $\quad\quad CPM_{best} \leftarrow CPM(H_E)$
15. $\quad\quad E_{best} \leftarrow E$
16. $\quad$ **end if**
17. **end for**
18. **return** E_{best}

Figure 5: algorithm to find final ensemble to find the final ensemble

VII. Implementation

It is proposed to develop new & effective detection technique of MA which use set of different algorithms for candidate extractors & pre-processing methods (pair). The corresponding energy function value is computed on the union of the candidate sets belonging to the pairs in the collection. The candidates of this collection are compared to a set of micro aneurysm centroids (ground truth) selected manually by clinical experts. If the Euclidean distance of the centroid of a candidate and a manually selected MA is smaller than a given threshold, then it is regarded as a true positive (TP), otherwise it is a false positive (FP).If an ensemble E contains more (preprocessing method, candidate extractor) pairs, their outputs are determined in the following way: Take 10 training images which are already disease affected images. Then we use the selected preprocessing methods, which we consider to be applied before executing MA candidate extraction. There may be 5 methods present in preprocessing method. Candidate extraction is present next to preprocessing method. Similar to preprocessing there are 5 techniques are present in Candidate extractors. For a single image, 25 combinations are available. Since there are 5 methods available in both preprocessing and candidate extraction, for each method in preprocessing there are 5 candidate extraction methods are processed. Likewise it repeated for 5 methods in preprocessing. So there are 25 methods are proceeded for a single image. Then we should have to calculate the entropy for all 25 results. Then after calculating the entropy for the 25 methods, we can predict the best technique or method, considering whose entropy is highest. For ex., if third method's entropy is highest means we determine that third one is the best technique. Likewise, we should calculate for a set of 10 training images, by following the procedure mentioned above we can determine best techniques for 10 images. After analyzing the best techniques whose entropies are highest for 10 images, mentioned above, we can see that third technique is repeated many times than other. So we can conclude that the third technique is the best technique.

VIII. Result

The above paper is study paper so result is as per previous paper. The practically results are obtain after completion of project. In this section, we present our experimental results for both

MA detection

The corresponding energy function value is computed on the union of the candidate sets belonging to the pairs in the collection. The candidates of this collection are compared to a set of micro aneurysm centroids (ground truth) selected manually by clinical experts. If the Euclidean distance of the centroid of a candidate and a manually selected MA is smaller than a given threshold, then it is regarded as a true positive (TP), otherwise it is a false positive (FP). After applying preprocessing methods & candidate extraction methods, in this paper we propose the approach for MA detection.

DR grading:

In DR grading, measure the performance of proposed system. Measure the specificity accuracy sensitivity of total image and false positive image. We have also evaluated our ensemble-based approach to see its grading performance to recognize DR. For this aim, we determined the image-level classification rate of the ensemble on the Messidor1 dataset containing images. That is, the presence of any MA means that the image contains signs of DR, while the absence of MAs indicates a healthy case. In other words, a pure yes/no decision of the system has been tested. In this grading we also calculate eccentricity, major axis ,minor axis, area of the MA. And finally detected MA and stage of MA on the no. MA detected.

CONCLUSION

In this paper, we have proposed an ensemble-based MA detector that has proved its high efficiency in an open online challenge with its first position. Our novel framework relies on a set of $\langle$ preprocessing method, candidate extractor $\rangle$ pairs, from which a search algorithm selects an optimal combination. Since our approach is modular, we can expect further improvements by adding more preprocessing methods and candidate extractors. However, a proper screening system should contain other components, which is expected to increase the performance of this approach, as well.

REFERENCES:

[1] B. Antal and A. Hajdu, "Improving micro aneurysm detection using an optimally selected subset of candidate extractors and preprocessing methods," Pattern Recog., vol. 45, no. 1, pp. 264–270, 2012

[2] S. Ravishankar, A. Jain, and A. Mittal, "Automated feature extraction for early detection of diabetic retinndus images," in Proc.IEEE Conf. Comput. Vision Pattern Recog., 2009, pp. 210–217.

[3] A. Criminisi, P. Perez, and K. Toyama, "Object removal by Exemplarbased inpainting," in Proc. IEEE Conf. Comput. Vision Pattern Recog., vol. 2, 2003, pp. II-721–II-728

[4] V. Kalesnykiene , J. -k. Kamarainen , R. Voutilainen , J. Pietilä , H. Kälviäinen , H. Uusitalo "The DIARETDB1 diabetic retinopathy database and evaluation protocol"- 2005

[5] D. P. Chakraborty , "The DIARETDB1 diabetic retinopathy database and evaluation protocol"- 2010

[6] Bálint Antal, András Hajdu "Improving Micro aneurysm Detection Using an Optimally Selected Subset of Candidate Extractors and Preprocessing Methods" – 2012

International Journal of Engineering Research and General Science Volume 3, Issue 5, September-October, 2015
ISSN 2091-2730

Recovery of Nutrients from Dairy Wastewater by Struvite Crystallization

Amit Krishan[1], Ankita Srivastava[2]

[1]Assistant Professor, Department of Civil Engineering,

G. L. Bajaj Institute of Technology & Management, Greater Noida-201308 (UP), India

[2]Assistant Professor, Department of Civil Engineering,

Accurate Institute of Management & Technology, Greater Noida-201308 (UP), India

E-mail: krishan001amit@gmail.com,

Contact Number: +91-8595010856

Abstract— Discharge of untreated nutrient rich dairy industry wastewater is a problematic issue, which may cause pollution and eutrophication of receiving water. The recovery of nutrients using a chemical precipitation and crystallization technique will provide value added product struvite (MgNH4PO4.6H2O), known as magnesium ammonium phosphate hexahydrate, a slow releasing fertilizer from dairy wastewater. 20 liters capacity Struvite Fed Batch Reactor was designed to perform the experiment. In this study the characteristic of dairy wastewater was analyzed to assess the recovery potential of method and percentage of reduction in pollutant concentration. The concentration of total solid, total dissolved solids, total hardness and magnesium hardness were increased after the treatment but the concentration of calcium hardness was decreased. It was observed that the efficiency of BOD, COD, Phosphate and Ammonia removal was 66%, 87%, 93 % and 89% respectively. Application of struvite precipitation method will save the nutrients and reduce environmental pollution.

Keywords — Dairy wastewater, nutrient, struvite, precipitation, crystallization, crystal, recovery

1. INTRODUCTION

A great increase in the number of industries in India has led to the production of a large volume of complex wastes. Numerous works have been carried out on the assessment of freshwater pollution by the discharge of effluent from the industries [1]. Dairy industry is noted as one of the significant contributor to water pollution. The generation of wastewater due to washing of equipment, milk spillage, other milk products waste, wash-down of yard area contains urine and manure, detergents, spilled milk. Dairy waste is basically biodegradable, produces an undesirable odour and contains an appreciable quantity of oil and can have adverse effect on environment due to high Biochemical Oxygen Demand (BOD), Chemical Oxygen Demand (COD), Total Suspended Solids (TSS) and nutrients such as phosphorus and nitrogen.

The key source of nitrogen in milk or milk products is in the form of casein and whey proteins. Typically, milk with 3.7% fat would contain about 3.15% protein and about 295 mg/l of non-protein nitrogen [2]. Fresh raw milk would normally contain about 3-8 mg/l of ammonia nitrogen and no measurable nitrate [3]. It was reported that typical wastewater from dairy processing plants contains 15-180 mg of nitrogen/l with an average of 76 mg/l [4]. Raw wastewater from dairy facilities has a typical BOD of 2,500 mg/l. At a nitrogen concentration of 50 mg/l, the BOD to N ratio would be 50:1.The most common forms of nitrogen in wastewater are ammonia (NH_3), ammonium ion (NH_4^+), nitrite (NO_2^-), nitrate (NO_3^-) and organic nitrogen. Phosphorus in wastewater is in one of three forms as phosphate (also called orthophosphate) polyphosphate, or organically bound phosphorus. One of the major problems caused by discharging biochemically treated wastewater effluents into lakes and streams is the eutrophication of these waters. This eutrophication is generally attributed to the discharge of fertilizing elements such as phosphorus and nitrogen. The impacts of excess nutrients on water quality have been well documented [5, 6, 7, 8]. The removal of phosphorus and nitrogen from dairy industry effluents appears to be a practical way of limiting algal blooms in the receiving waters. The removal of these elements by biochemical or chemical means appears to be feasible. Various laboratory and field studies have shown that the biochemical wastewater treatment processes can be modified such that significant removal of nitrogen and/or phosphorus can be attained [9, 10].

In recent years, struvite has emerged as the most promising compound for recovery of nutrient (especially nitrogen and phosphorous) from wastewater plants. Struvite ($MgNH_4PO_4.6H_2O$) is a white crystalline substance consisting of magnesium, ammonium and phosphorus in equal molar concentration. It is a valuable slow-release fertilizer, the production of which could offset much of the cost of chemical treatment [11]. The basic chemical reaction to form struvite has been expressed as equation $Mg_2^+ + NH_4^+ + PO_4^{3-} + 6H_2O \rightarrow MgNH_4PO_4.6H_2O$ with $pK_s = 12.6$ at 25^oC [12, 13]. The precipitation of struvite is affected by several factors, namely the pH, the chemical composition of the wastewater (degree of saturation with respect to magnesium, ammonium and phosphate; presence of other ions, such as, calcium, ionic strength of the solution), and the temperature of the solution [14, 15]. Numerous literature reports show the recovery of nutrients from wastewaters in the form of struvite through anaerobic digestion [16, 17, 18, 19, 20].

The objective of this study is the recovery of nutrients based on the precipitation ability of struvite. In this study, the precipitation of struvite is investigated with the purpose to reduce harmful effects on the environment and retrieve nutrients.

2. MATERIALS AND METHODS

2.1 Characteristics of Dairy Wastewater

The concentrations of important constituent in a dairy wastewater sample are shown in Table 1.

Table 1—Characteristics of dairy wastewater

Constituent	Concentration
pH	6.035 ± 0.065
Ammonia	69.96 ± 1.16 mg/l
Phosphate	45.05 ± 0.45 mg/l
TDS	756.5 ± 35.5 mg/l
Total Solids	938 ± 60 mg/l
BOD	216.17 ± 4.17 mg/l
COD	890 ± 14 mg/l
Total Hardness	501.5 ± 13.5 mg/l as CaCO3
Calcium Hardness	348 ± 10mg/l as CaCO3
Magnesium Hardness	156.5 ± 16.5 mg/l as CaCO3

2.2 Design of Fed Batch Reactor

A Struvite Fed Batch Reactor was designed with a capacity of 20 liters. The shape of reactor was cylindrical with conical base. It was divided into two distinct parts; the upper part which was rectangular cuboids and the lower part of reactor was rectangular pyramid. The pyramidal part of reactor act as settling zone. The bottom of the reactor contains tap for removal of sludge, crystals and wastewater. A submersible pump was provided for proper mixing of wastewater, $MgCl_2.6H_2O$ solution and NaOH solution in the reactor. The schematic sketch of Struvite Fed Batch Reactor is shown in Figure 1.

Design criteria for holding tank

Diameter of reactor = 260 mm

Height of cylindrical part of reactor = 350 mm

Height of conical part of reactor = 100 mm

HRT of holding tank = 24 hr

2.3 Crystallization of struvite from Dairy Wastewater

Struvite crystallization from dairy wastewater using the Struvite Fed-Batch Reactor was performed in Chemistry Laboratory, Department of Chemistry, SRM University. About 12 batches of experiments were performed during February and March 2011.

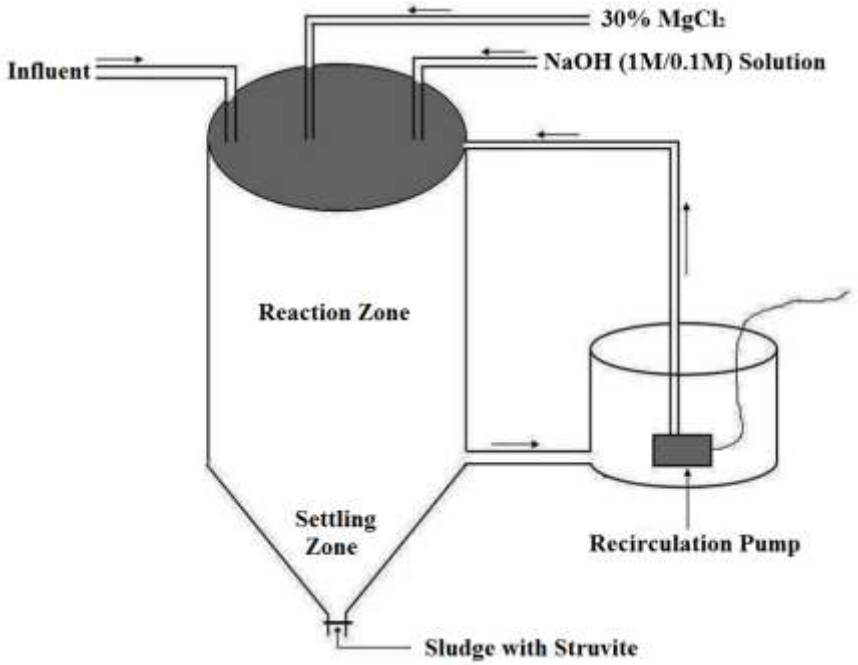

Figure 1. Schematic sketch of Struvite Fed Batch Reactor

The Struvite Fed Batch Reactor was cleaned with diluted HCl solution and washed with deionized water. The reactor was allowed for drying at room temperature (25°C). After cleaning the reactor, it was filled with 14 liters of dairy wastewater. The pH of dairy wastewater was increased with the help of NaOH solution, till solution attains its investigated pH. Two litres of 30% magnesium chloride solution was added into reactor at the rate of 7.5 ml/minute. The rate of magnesium chloride mixing may be varied according to the concentration of PO_4^+ and NH_4^+ in the sample. Then solution was seeded with 1 g of previously generated pure struvite as parent crystal. The mixing of solution was done by submersible pump till whole solution of magnesium chloride was finally added into the dairy wastewater and precipitate was formed at very low rate. The HRT of reactor was maintained about 5 hours. After 5 hours addition of NaOH and magnesium chloride solution was stopped and whole solution was kept for 24 hours for formation of precipitate in the reactor bottom. The precipitate was filtered by Whatman filter paper No. 42 and filtrate was kept in desiccator for drying with interfering air for 12 hours. Finally, filtrate was air dried at room temperature. The struvite cluster aggregate on parent seed material and grow with sludge which was finally separated by hand picking or by sieving with less than 45-63µm ASTM standard sieves. Sludge was sieved by this sieve resulting in the struvite crystals.

2.4 Sampling and Pre-treatment of Wastewater

Two wastewater samples were collected for analysis in each set of experiment, one sample from reactor input and another after the precipitation of struvite at reactor output. The samples were taken in plastic cane of 1 liter capacity labeled and stored in cool place (at 4^0C). All experimental analysis was done by using of standard guideline prescribed in 17^{th} and 21^{st} edition of APHA. Adequate amount of wastewater samples were taken for pre-treatment and mixed with the help of submersible pump for 10 minutes. The supernatant was used as sample for the analysis.

3. RESULTS AND DISCUSSION

3.1 Impact of pH on the struvite precipitation

pH plays a vital role in struvite precipitation. The experiment was to identify the optimum pH for struvite formation. The pH of dairy wastewater was found in the range of 6.035 ± 0.065 which was increased up to the pH 9.2 with the help of NaOH solution. After that, 30% magnesium chloride solution was mixed with wastewater and it was observed that when the precipitation started, the pH of the solution decreases in the range of 8.74 - 8.98 from its original pH 9.2. The optimum pH range for struvite formation is 8.5 - 9.5 [21, 22].The impact of precipitation on the pH was shown in Figure 2.

3.2 Impact of Struvite Precipitation on the Ammonia and Phosphate concentration

Initially the concentration of ammonia and phosphate in the dairy wastewater was found in the range of 69.96 ± 1.16 mg/l and 45.05 ± 0.45 mg/l respectively, but after the precipitation of struvite it was observed that their concentration decline sharply in the range of 4.6 ± 0.5 mg/l and 4.76 ± 0.4 mg/l. About 89% ammonia and 93% of phosphate was recovered in the form of various compounds along with struvite. The impact of struvite precipitation on the concentration of ammonia and phosphate is shown in Figure 3 and 4.

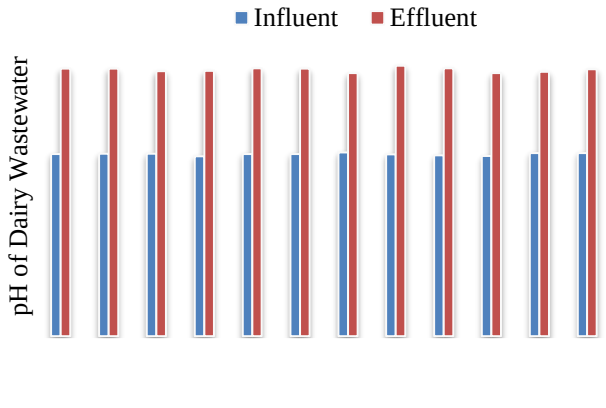

Figure 2.Impact of struvite precipitation on the pH of dairy wastewater.

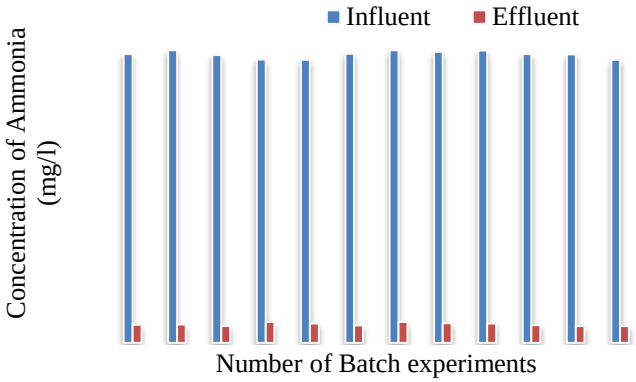

Figure 3.Impact of struvite precipitation on the concentration of ammonia of dairy wastewater

Metal salt precipitation is the most common approach for recovering nutrient from wastewater, which makes the precipitate unrecoverable for possible industrial processing into fertilizer [23, 24]. Nutrient recovery is possible, using existing technologies without metal salt precipitation from municipal wastewater [25, 26, 27, 28, 29]. It is economically feasible to recover 10%–80% of the nutrient flowing into wastewater treatment.

Recovering NH_4^+ is not only to recover the nutrients for agriculture purposes by forming the fertilizer as struvite but also to reduce the emission of greenhouse gases into the atmosphere significantly. Ammonia emission eventually contributes to atmospheric N input into natural or near natural ecosystems, not only promoting eutrophication but also causing N_2O emissions, thus being an indirect greenhouse Ammonia is not considered a direct greenhouse gas because of its short lifetime in the atmosphere. It is postulated, that 1% of emitted NH_3-N is converted to N_2O-N, and therefore it is possible to integrate NH_3 losses into Global warming potential [30]. Hence, the retrieval of NH_4^+ in this study by forming the chemical precipitation can recover a significant amount NH_4^+ and limit the amount of greenhouse gases.

3.3 Impact of Struvite Precipitation on Solids

In dairy wastewater, the concentration of TDS and TS was found in the range of 756.5 ± 35.5 mg/l and 938 ± 60 mg/l respectively. After the addition of NaOH and 30% magnesium chloride solution, it was observed that the concentration of TDS of the wastewater was sharply increased in the range of 1814 ± 30 mg/l which result in increase of TS in the range of 1872.5 ± 34.5 mg/l. This shows that there was no 100% recovery of magnesium chloride. The maximum amount of magnesium was still in the solution and it affects the treatment facility of wastewater. The amount of TDS and TS was found within the permissible limit after the completion of treatment. The impact of precipitation on the TDS and TS of dairy wastewater is shown in the Figure 5 and 6.

3.4 Impact of struvite precipitation on the BOD and COD concentration

The BOD and COD of the dairy wastewater were found in the range of 216.17 ± 4.17 mg/l and 890 ± 14 mg/l respectively which was decreased sharply in the range of 72.13 ± 3.46 mg/l and 112 ± 8 mg/l, after the struvite precipitation. The dairy wastewater itself contains large numbers of microorganisms. They started consuming organic matter of the wastewater as food materials. Therefore a sharp decline was observed in BOD and COD concentration. As a result of decomposition the organically bound phosphate and ammonia was released in the solution and they were ready to participate in struvite precipitation. The impact of struvite precipitation on the BOD and COD concentration has been shown in Figure 7 and 8. On an average around 66% of BOD and 87% of COD was removed by this experiment.

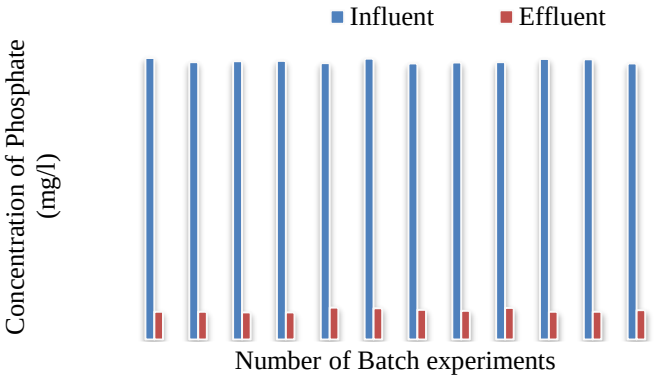

Figure 4. Impact of struvite precipitation on the concentration of phosphate of dairy wastewater

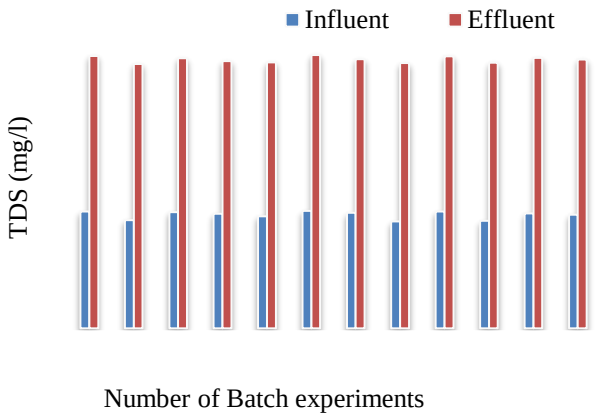

Figure 5.Impact of struvite precipitation on the concentration of TDS of dairy wastewater

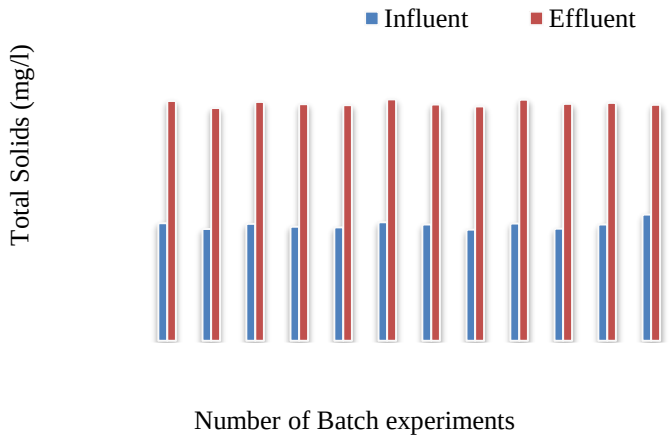

Figure 6.Impact of struvite precipitation on the concentration of TS of dairy wastewater

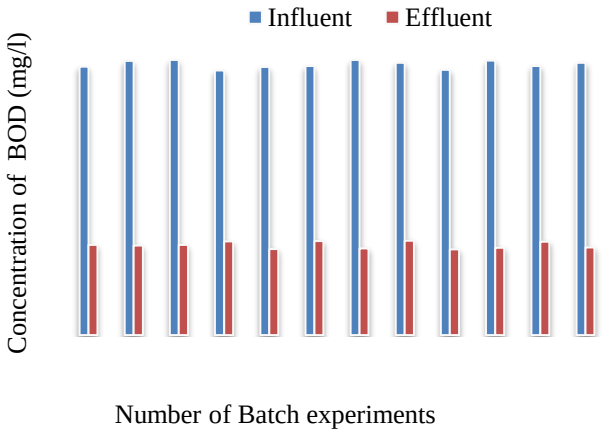

Figure 7. Impact of struvite precipitation on the concentration of BOD of dairy wastewater.

3.5 Impact of Struvite Precipitation on the Hardness

The total hardness of the dairy wastewater was found in the range of 501.5 ± 13.5 mg/l as $CaCO_3$. After the struvite precipitation, the concentration of total hardness sharply increased. The total hardness was high because magnesium was supplied from outside in the solution for struvite precipitation. There was no 100% recovery that's why maximum amount of magnesium was remaining in the solution and increases total hardness of the solution. It was lowered down in the further treatment of wastewater in different treatments units. The impact of struvite precipitation is shown in Figure 9. After the experiments the concentration of total hardness was found in the range of 1506 ± 26 mg/l as $CaCO_3$.

The calcium hardness and magnesium hardness of the dairy wastewater was found in the range of 348 ± 10 and 156.5 ± 16.5 mg/l as $CaCO_3$ respectively. After the precipitation of struvite, the concentration of calcium hardness decreased due to the precipitation of calcium phosphates has been observed in addition to or instead of struvite [31, 32]. Calcium is a common interfering ion to struvite formation in dairy manure [33]. But the concentration of magnesium hardness was sharply increased because magnesium was supplied from outside in the solution for struvite precipitation and there was no 100% recovery that's why maximum amount of magnesium was remaining in the solution. The impact of struvite precipitation is shown in Figure 10 and 11. After the experiments the concentration of calcium hardness and magnesium hardness was found in the range of 116 ± 8 and 1391.5 ± 31.5 mg/l as $CaCO_3$ respectively.

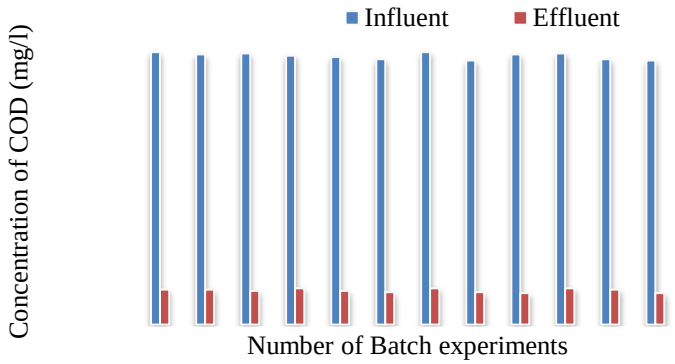

Figure 8. Impact of struvite precipitation on the concentration of COD of dairy wastewater

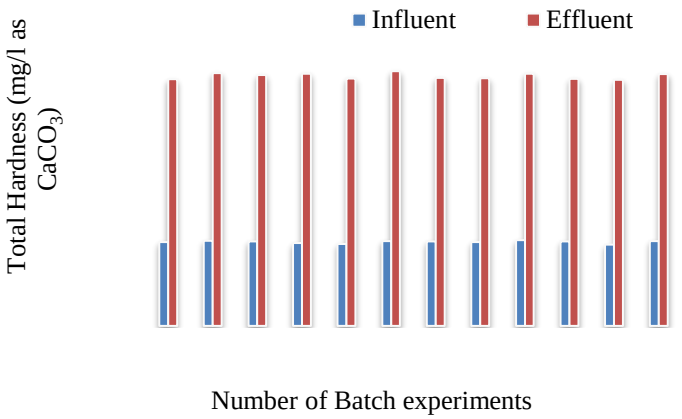

Figure 9. Impact of struvite precipitation on the concentration of Total Hardness of dairy wastewater

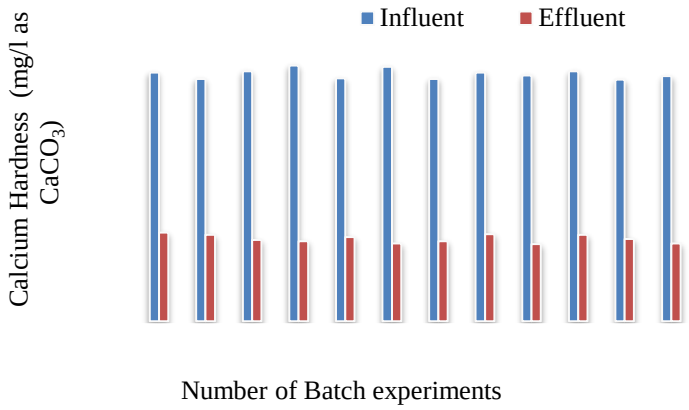

Figure 10. Impact of struvite precipitation on the concentration of Calcium Hardness of dairy wastewater

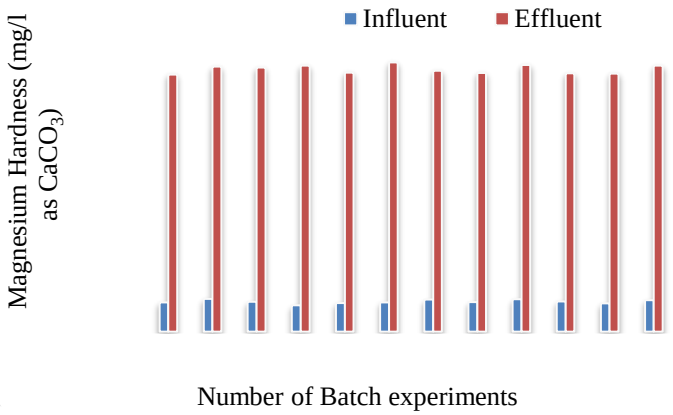

Figure 11. Impact of struvite precipitation on the concentration of Magnesium Hardness of dairy wastewater

4. CONCLUSION

In this study, struvite precipitation is used to recover nutrients from dairy wastewater. 20 liters capacity Struvite Fed Batch Reactor was designed to perform the experiment. Based on the preliminary experimental observations the conclusions drawn are:

The characteristic of dairy wastewater was analyzed to assess the recovery potential of method and percentage of reduction in pollutant concentration. The concentration of total solid and total dissolved solids were increased after the treatment and it was found in the range of 1784- 1844 and 1838- 1907 mg/l respectively.

As the result of experiments the concentration of total hardness and magnesium hardness was increased and it was found in the range of 1480-1532 and 1360-1423 mg $CaCO_3$/l respectively but calcium hardness was decreased and it was found in the range of 108- 124 mg $CaCO_3$/l.

It was observed that the efficiency of BOD, COD, Phosphate and Ammonia removal was 66%, 87%, 93% and 89% respectively. Application of struvite precipitation method will save the nutrients and reduce environmental pollution.

REFERENCES:

[1] Rama, Rao S.V., Singh, V.P. and Mall, L.P., Biological methods for monitoring water pollution level. Studies at Ujjain In B Gopal and J.S. Singh edited. Glimpses of ecology, 1978, 341-348.

[2] Ballou, L.U., Pasquini, M., Bremel, R.D., Everson, T. and Sommer, D., Factors affecting herd milk composition and milk plasmin at four levels of somatic cell counts. J. Dairy Sci., 1995, 78, 2186-2195.

[3] Harper, W. F. and Blaisdell, J. L., State of the art of dairy food plant wastes and waste treatment. Proceedings of the Second National Symposium on Food Processing Wastes, Denver (Colorado), USA, March, 1971, 23–26.
[4] Soederhjelm, P. and Lindqvist, B., The ammonia content of milk as an indicator of its biological deterioration or ageing. Milchwissenschaft, 1980, 35, 541-543.
[5] Daniel, T. C., Sharpley, A. N., Edwards, D. R., Wedepohl, R. and Lemunyon, J. L., Minimizing surface water eutrophication from agriculture by phosphorus management. J. Soil Water Conserv. Suppl., 1994, 49, 30-38.
[6] Correll, D. L., The role of phosphorus in the eutrophication of receiving waters: A review. J. Environ. Qual., 1998, 27, 261-266.
[7] Sims, J. T., Simard, R. R. and Joern., B. C., P losses in agricultural drainage: Historical perspective and current research. J. Environ. Qual., 1998, 27, 277-293.
[8] Edwards, A. C., Twist, H. and Codd, G. A., Assessing the impact of terrestrially derived phosphorus on flowing water systems. J. Environ. Qual., 2000, 29, 117-124.
[9] Sawyer, C. N., Biological engineering in sewage treatment, sewage Wks J. 16, 1944, 925-935.
[10] Ludzack, F. J. and Ettinger, M. B., Controlling operation to minimize activated sludge effluent nitrogen. Wat. Poll. Contr. Fed., 1962, 34, 920-931.
[11] Liao, P. H., Gao, Y. and Lo, K. V., Chemical precipitation of phosphate and ammonia from swine wastewater. Biomass and Bioenergy, 1993, 4(5), 365-371.
[12] Siegrist, H., 1996. Nitrogen removal from digester supernatant comparison of chemical and biological methods. Water Science and Technology, 1996, 34, 399-406.
[13] Tunay, O., Kabdasli, I., Orhon, D. and Kolcak, S., Ammonia removal by magnesium ammonium phosphate precipitation in industrial wastewater. Water Science and Technology, 1997, 36, 225-228.
[14] Battistoni, P., Fava, G., Pavan, P., Musacco, A. and Cecchi, F., Phosphate removal in anaerobic liquors by struvite crystallization without addition of chemicals: preliminary results. Water Resources, 1997, 31, 2925-2929.
[15] Stratful, I., Scrimshaw, M. D. and Lester, J. N., Conditions influencing the precipitation of magnesium ammonium phosphate. Water Resources, 2001, 35, 4191-4199.
[16] Doyle, J. D. and Parsons, S.A., Struvite formation, control and recovery. Water Resources, 2002, 36, 3925-3940.
[17] Battistoni, P., Pavan, P., Prisciandaro, M. and Cecchi, F., Struvite crystallization: A feasible and reliable way to fix phosphorus in anaerobic supernatant. Water Research, 2000, 34, 3033-3041.
[18] Nelson, N. O., Mikkelsen, R. L. and Hesterberg, D. L., Struvite precipitation in anaerobic swine lagoon liquid: Effect of pH and Mg:P ratio and determination of rate constant. Bioresource Technology, 2003, 89, 229-236.
[19] Demirer, S. U., Demirer, G. N. and Chen, S., Ammonia removal from anaerobic digested diary manure by struvite precipitation. Process Biochem., 2005, 40, 3667-3674.
[20] Ali, M.I., Struvite crystallization in fed-batch pilot scale and description of solution chemistry of struvite. Chemical Engineering Research and Design, 2007, 85(A3), 344-356.
[21] Demirer, S.U. and Othman, M., Removal of ammonia and phosphate from supernatant of anaerobically digested waste activated sludge by chemical precipitation. Bioresource Technology, 2009, 100, 3236-3244.
[22] Booker, N. A., Priestley, A. J. and Fraser, I. H., Struvite formation in wastewater treatment plants: opportunities for nutrient recovery. Environmental Technology, 1999, 20, 777-782.
[23] Buchanan, J. R., Mote, C. R. and Robinson, R. B., Struvite control by chemical treatment. Transactions of the American Society of Agricultural Engineers, 1994, 37, 1301-1308.
[24] Donnert, D. and Salecker, M., Elimination of phosphorus from waste water by crystallization. Environ. Technol., 1999b, 20, 735-742.
[25] Donnert, D. and Salecker, M., Elimination of phosphorus from municipal and industrial waste water. Water Sci. Technol., 1999b, 40, 195-202.
[26] Stratful, I., Brett, S., Scrimshaw, M.B. and Lester, J.N., Biological phosphorus removal, its role in phosphorus recycling. Environ. Technol., 1999, 20, 681-695.
[27] Driver, J., Lijmbach, D. and Steen, I., Why recover phosphorus for recycling, and how? Env. Tech., 1999, 20, 651-662.
[28] Durrant, A. E., Scrimshaw, M. D., Stratful, I. and Lester, J.N., Review of the feasibility of recovering phosphate from wastewater for use as a raw material by phosphate industry. Environ. Technol., 1999, 20(7), 749-758
[29] Strickland, J., Perspectives for phosphorus recovery offered by enhanced biological P removal. Environmental Technology, 1999, 20(7), 721-725.
[30] Woods, N.C., Sock, S.M. and Daigger, G.T., Phosphorus recovery technology modeling and feasibility evaluation for municipal wastewater treatment plants. Environmental Technology, 1999, 20(7), 663-679.
[31] Wulf, S., Maeting, M., Bergmann, S. and Clemens, J., Simultaneous measurement of NH3, N2O and CH4 to assess efficiency of trace gas emission abatement after slurry application. Phyton (Horn, Austria), 2001, 41(3), 131–142.
[32] Harris W. G., Wilkie A. C., Cao X.., Sirengo R., 2008. Bench-Scale Recovery of Phosphorus from Flushed Dairy Manure Wastewater. Bioresour. Technol., 99 (8), 3036–3043.
[33] Zeng, L. and Li, X., Nutrient Removal from Anaerobically Digested Cattle Manure by Struvite Precipitation. J. Environ. Eng. Sci., 2006, 5(4), 285–294.

International Journal of Engineering Research and General Science Volume 3, Issue 5, September-October, 2015
ISSN 2091-2730

Analyzing Criminal Behavior

POOJA SINGHAL[1], AMAN SINGHAL[2]

M.TECH[1] (Computer science & engineering) Uttarakhand Technical University, poojasinghalrose@gmail.com, +919997161387

B.TECH[2] (Computer science & engineering), Dr. B. R. Ambedkar National Institute of Technology, Jalandhar
aman.nitj321@gmail.com, +918971177466

Abstract— Criminal behavior is an important area of research to prevent crime. For the study large amount of data is required to arrive at some conclusive results. This paper deals with new ideas of data analysis of such huge volume of data. The data here is first filtered to retain only the useful data and then analysis is done. Genetic algorithm with fuzzy logic has been used to determine soft and hardcore criminals and possibility of a soft-core criminal turning into a hardcore criminal by considering parameters like background, education, modus operandi, number of cases, weapon used [1-3].

Keywords— Criminal, Criminal behaviors, Data mining, Soft core criminal, Hard core criminal, Genetic algorithm, Fuzzy logic

INTRODUCTION

It is always a challenge to design an algorithm to run smoothly on large amount of data. Criminal database is one such example as crime rate is growing day by day and new methods are being adopted by the criminals to commit crimes; it is difficult to analyze the data and do predictions. To accomplish our task we applied data mining techniques with genetic algorithm to filter out and retain just the required data [4] [5]. Certain attributes of the Criminals like background, education, modus operandi etc. were considered to arrive at the conclusion whether a soft-core criminal would convert into a hardcore criminal [6] [7].

Soft core criminal, for the study, is one who commits a soft-crime like robbery; pick pocketing etc. a hard core criminal [8] is one who commits heinous crime like murderer, rape.

The analysis the criminal data we considering here different attributes take one by one to detect the similar pattern between them in criminal, age of criminal in which they doing a crime, gender of the criminal, current location of the criminal to do a crime, Education of the criminal, Modus-operandi of the criminal, Which weapon used to commit the crime, number of cases they have charged to the criminal, Reasons to commit a crime these are the attribute consider to get the similar pattern between the criminal [9].

Crime is major problem for everyone. Crime analysis is a way in which we analyze what are the factors to come to do a crime so today crime database available in vast amount in the database we have necessary to extract only knowledge able data from criminal data base for this Data mining techniques have greater advantage in this fields [10].

Crime analysis need data mining technique, this is an iterative process of extracting knowledge hidden from large volumes of raw data [11] [12].

Data mining involves the use of sophisticated data analysis tools to discover formerly undiscovered, valid patterns and relationships in large data sets. Therefore, data mining contain of more than collecting and managing data, it also includes analysis and prediction. The main advantage to use data mining with crime analysis is: too much data but too small knowledgeable, and a need to extract useful information from the data and to interpret the data. [13]

1. THE PROPOSAL OF CRIME ANALYSIS

To present the proposal of criminal data here we consider the large amount of data taken from internet to analyses the seminal pattern between the criminal and get result that the soft core criminal can become a hard core criminal in future. [14]

General Algorithm of Proposal Model

Input : Raw of crime data from internet [15] [16].

Output: a model design in which you put the detail of soft core criminal and get result it might possible he become a hard criminal in future.

These are steps to taken account consider the proposal:-

1. **Understanding the crime domain**, this taken the related to the prior knowledge and goals of the crime detection and prediction [15] [16].

2. **Extracting the target dataset,** here in this we consider the following attribute so that consider these attribute detect the similar pattern using genetic algorithm they are the age of criminal to commit crime, the modus operandi to commit crime, education of criminal, reason to crime, the weapon used to commit a crime [16].

3.Collect attribute values of criminal database, we consider here are name of criminal, age, location, education, gender, modus-oprandi, reason for crime, weapon used, and number of cases of criminal [14].

4. **Store the data**; we store each attribute value in database so that we have the large database of criminal with useful database value use in this proposed system.

5. Further divide the attribute in category, in this we further divide the each attribute in different category so that divide the criminals category soft core and hardcore take one by one we have get the data they are[16]:

Criminal Name: define each criminal name

Age: divide the age further three categories
1. Age below 18
2. Age between 18 to 60
3. Age above 60

Criminal education: education of criminal divide in six categories
1. Illiterate: no study
2. Primary: up to fifth
3. Secondary: up to tenth
4. Senior secondary: up to twelfths
5. Graduate : up to graduate
6. Masters: above graduate

Number of cases: here in this we divide the cases that are against the criminal in court divide in four parts
1. One case: only one case
2. 2-3 case: between 2-3 cases
3. 3-5: case: between 3-5 cases
4. >5 case: greater than cases 5

Weapon used: this define the weapon used when he done a crime this divide in four categories
1. Gun
2. Bomb
3. Knife
4. Fire

6. Count the categories of each attribute: in this we fetch the data from data base to calculate each category this gives the maximum criminal lie in which category by the help of data mining we analyses the data

7. Analyzing the data: we design the attribute and get each category value now use these value we divide the criminal in four categories they are:

1. Soft core criminal
2. Soft core criminal moving towards hard core

3. Hard core criminal
4. Completely hard core criminal

8. Compare the new criminal data with data analysis: compare the data with data analysis and divide the criminal in which category he belongs to

9. Check criminal can become hardcore: enter the details of any criminal compare the details of it to the analysis data and get result in which category the criminal it was.

10. End

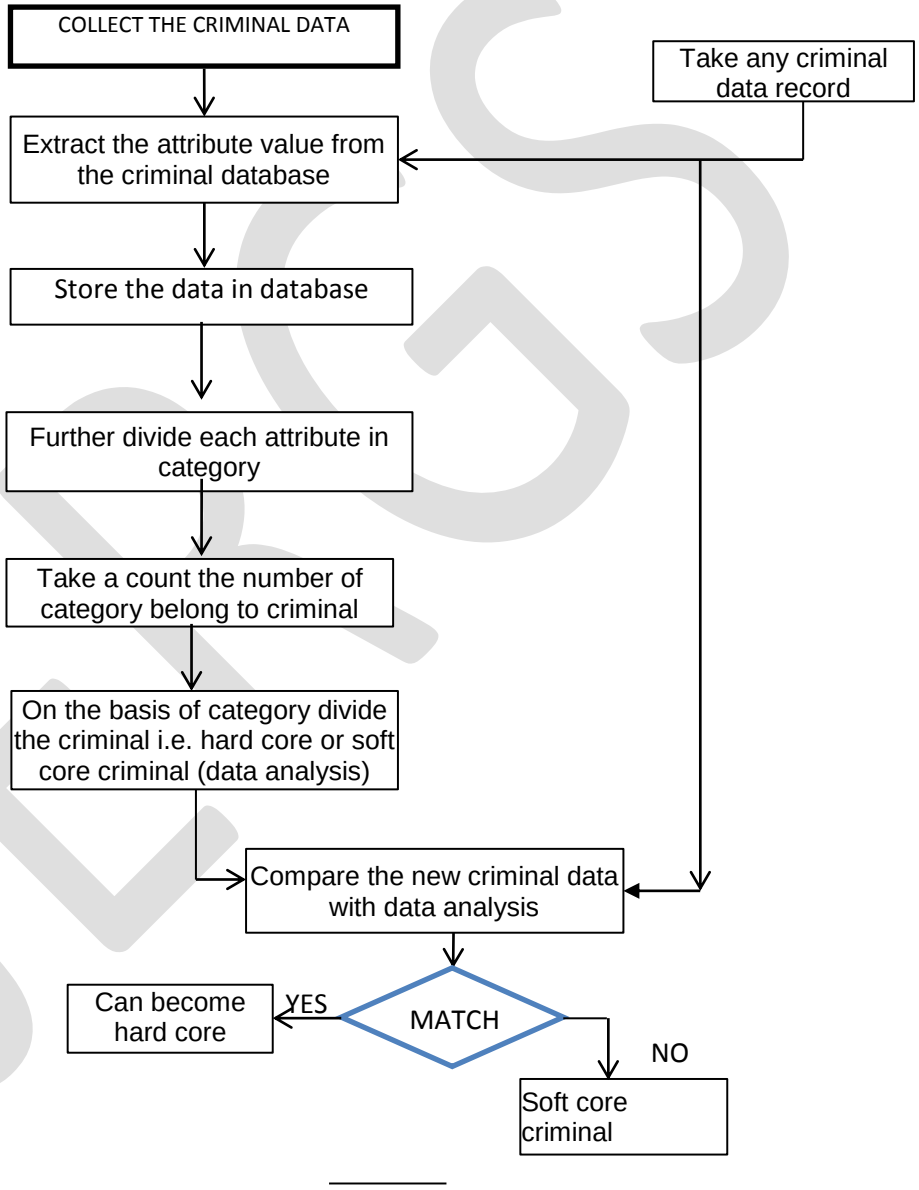

Figure 1: Proposed model of analyzing criminal behaviour

2. METHODS

Analysis of criminal Behavior we collected the large amount of data from internet and collected the different attribute to analyses the data analyses the each attribute and get results the following process occur step by step as below [16]:

2.1 Model Requirements

As input into the criminal data we considering the different variables the algorithm variables are ctr,ctr2 used for increment value hcocre1(i), hcocre2(i), hcocre3(i), hcocre4(i) data store the data

1. **//Algorithm to analyses data**
2. Import data from database
3. **//Detect Frequency of weapons used for crime**
4. for i ←1 to max
5. if weapon ← 'gun'
6. ctr← increment by
7. otherwise if weapon ← 'bomb'
8. ctr2 ← increment by one
9. otherwise repeated for all the expected weapons
10. end if
11. end for
12. **//Calculate severity of criminal based on number of cases**
13. for I ← 1to max
14. if no of crime ← 1
15. hcocre1(i).data ← store data
16. otherwise if no of crime ← between2 and 3
17. hcocre2(i).data ← store data
18. otherwise if no of crime ← between 4 and 5
19. hcocre3(i).data ← store data
20. otherwise if no of crime ← greater than 5
21. hcocre4(i).data ← store data
22. end if
23. end for
24. **// Calculate education level of the criminals**
25. for I ← 1to max
26. if education ← 'illitrate'
27. ill ← increment by one
28. otherwise calculate for other criminals
29. **// Detect pattern of criminal movement using genetic algorithm**
30. /* based on traveller example matlab */
31. locations ← read from database
32. distances ←$\sqrt{(x1-x2)^2+(y1-y2)\text{^}2}$
33. FitnessFcn←criminal_fitness(x,distances)
34. /* pass calculated parameters to genetic algorithm to get future value*/
35. [x,fval]←ga(FitnessFcn,crimes,[],[],[],[],[],[],[],options)
36. **// Fuzzy Rule Set**
37. **// Calculate Probability of Softcore Criminal converting into type of criminal**
38. Step1. Compare result with
39. for I ← 1 to l
40. if education ← same as of type one criminal
41. if modus operandi ← same as of type one criminal
42. if weapon used ← same as of type one criminal
43. prob← type1 criminal
44. end if
45. end if

46. end if
47. if education ← same as of type two criminal
48. if modus operandi ← same as of type two criminal
49. if weapon used ← same as of type two criminal
50. prob← type2 criminal
51. end if
52. end if
53. end if
54. end for
55. if education ← same as of type three criminal
56. if modus operandi ← same as of type three criminal
57. if weapon used ← same as of type three criminal
58. prob← type3 criminal
59. end if
60. end if
61. end if
62. if education ← same as of type four criminal
63. if modus operandi ← same as of type four criminal
64. if weapon used ← same as of type four criminal
65. prob← type4 criminal
66. end if
67. end if
68. end if

Result:

69. Type1 → soft core criminal
70. Type2 → soft core criminal moving towards hard core
71. Type3 → hard core criminal
72. Type4 → completely hard core criminal

2.2. Collecting the database

Collected the data of criminals we consider here the following attribute from the large amount of raw data of criminal: Name, Age, Location, Education, Modus operandi, No. of cases, Reason to crime.

- Criminal Name: name of the criminal
- Age: age of individual Criminal
- Crime Address: location of the crime
- Criminal Education: status of the criminal.
- Criminal Modus operandi: plan to do a crime.
- Criminal Weapon used: with the help of done a crime
- Criminal Cases: number of crime done by criminal
- Crime reason: understanding towards the crime

Collected the data criminal from the internet this is an raw data contain the detail of each criminal from that raw data we get the attribute values form that data store our data base which was contain the 50 records of data of criminal the data firstly store in the database using workbench then we fetch data in mat file and store in the mat file.

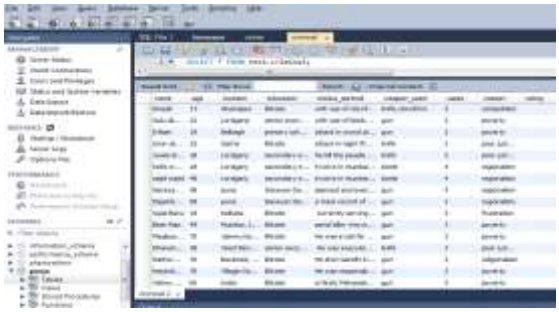

Fig 2.2(a): Database of Criminal data store in work bench consider here attribute values of criminal data

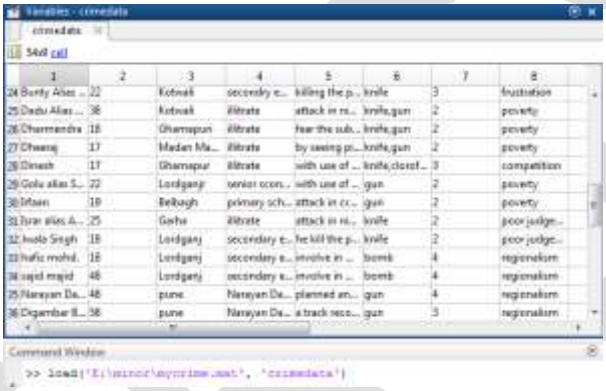

Fig 2.2(b): Store criminal data in mat file

Fig 2.2(b) represent the mat file of the load database of criminal data. The data of criminal is large consider only the attribute values of the data. we used workbench to store data so the futher analysis done. The data collected is current data of the criminals which are collected from different genuine websites and police record data.

2.3 Generating Data

Here we analysis the data of criminals we have collected all the required attributes of the criminal store all the attributes in the database now consider each attribute one by one we analyses that data and then we have detect a single pattern to analyses the whole data.

we use different attributes to analyses the data when we analyses each attribute after that we come end result by comparing each attribute of criminal in our result we find out that the soft core criminal can become a hard core criminal.

3. EXPERIMENTAL EVALUATION

In this we have considered attribute one by one and come in to the result. We have get result using the bar graph and pie chart the result we found get detail in brief and compare to other the result here further divides the each attribute in category.

3.1 Weapon used by criminal

Weapon used is an attribute of criminal data which was further divide in the category analyses each category and get the result the number of criminal belong to that category there are the following categories divide the weapon used:

1. Gun
2. Bomb
3. Knife
4. Fire

In fig. 3 we analyses the weapon used by the criminal by the help of pie chart and bar chart we easily show that our estimate data in the form of graphical interface.

Here we count the number of counts the which weapon used the criminal more with the use of looping on the basis we plot a pie chart and graph to show the result maximum number criminal used which weapon to done crime

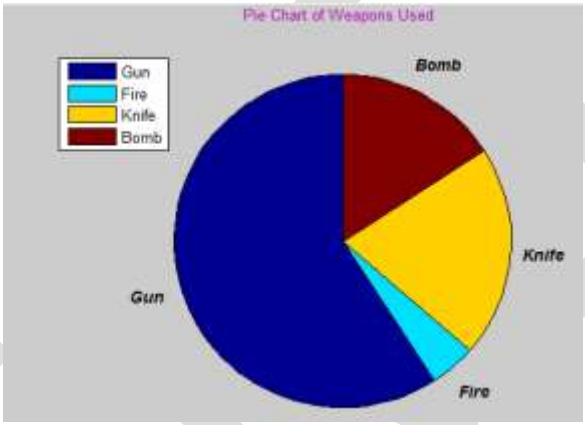

Fig: 3.1(a): Analysis which weapon used by the criminal through pie chart

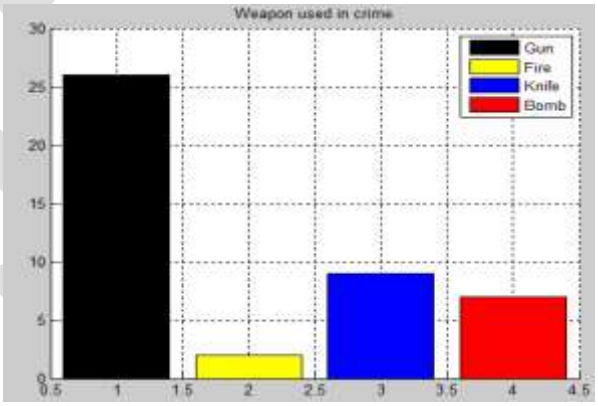

Fig: 3.1(b) Calculate the number of which weapon used by criminal

On the basis of pie chart or bar graph result we get the result the number criminal which weapon used more to done a crime we draw a table for above result

Table 14: Analysis of weapon used by criminal

Weapon used by criminal	Calculate the number of weapon used by the criminal
GUN	28
BOMB	8
KNIFE	10
FIRE	4

The steps used to determine the data are the following:-

- Import data from database
- Divide the weapon data in different category i.e. gun, bomb, knife, fire.
- Calculate the each weapon used by different criminal
- Increment the number weapon used
- Design a bar graph to represent the maximum number of which weapon used

We get the estimate from the graph and table that from the record of database get the details of the criminal and get the estimate results that which weapons priority order.

3.2 Number of cases by criminal

In this we analysis the data of criminal in which the number of cases in criminal mean the number of case are occur to criminal to done crime if it is done one crime there is one case more than one crime the no. of crime he done he no. of cases occur.

In fig. 3.2 cases are analyses of the criminal cases means how many crime done by criminals if criminals done a one crime so we consider him in case1 else so on if the no. of cases maximum of the criminal it means it done that no. of crimes. So we have divide the no. of cases in 4 parts they are:-

- One case: only single crime done by criminal
- 2-3 cases: between 2- 3 crime done by criminal
- 3-5 cases: between 3- 4 crime done by criminal
- >5 cases: Greater than five crimes done by criminal

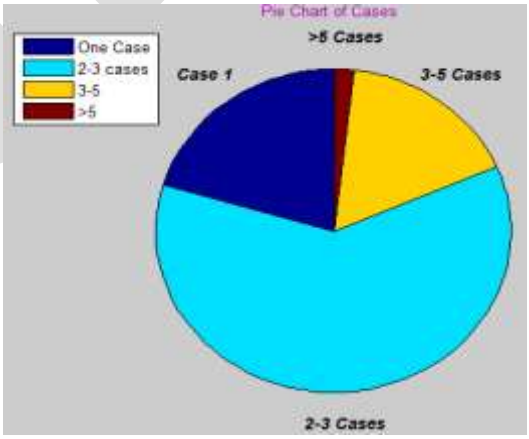

Fig: 3.2(a): Analysis number of cases done by criminal through pie chart

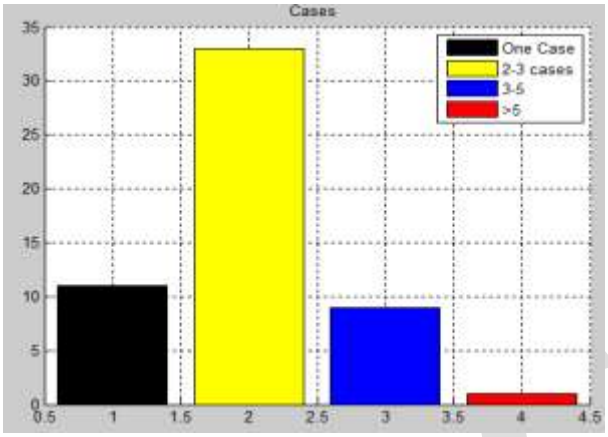

Fig: 3.2(b) Calculate number of cases done by criminal represent through bar graph

Through the bases of data of criminal we estimate the result in the form of table that the no. of crimes or cases occur in the criminal are done.

Table 2: Analysis of number of cases of the criminal

Divide the No. of cases of criminal	**Cases done by the criminal**
ONE CASE	10
2-3 CASE	30
3-5 CASE	9
>5 CASE	1

The steps used to determine the data are the following:-

- Import data from database
- Divide the number of cases in different category i.e. case one, case between 2-3, case between 3-5, above 5 cases.
- Calculate the each no of crime or cases done by criminal
- Increment the number of cases of the criminal

We get the estimate results by the analysis of number of cases done by the criminal further use the results of criminal and this data helps found results

3.3 Analysis education of the criminal

we have analyses the Education background of the criminals this data help us to define our end result so criminal education is important because it define which background criminals belong in fig: 3.3 we divide the education in different category calculate the number of criminal belong to the which category so we define education in different categories they have seven categories they are:-

- Illiterate: criminals not study
- Primary: criminals study up to primary classes

- Secondary: criminals study up to 10^{th} class
- Senior secondary: criminals study up to 12^{th} class
- Graduate: criminals study up to Graduate
- Masters: criminals study up to masters

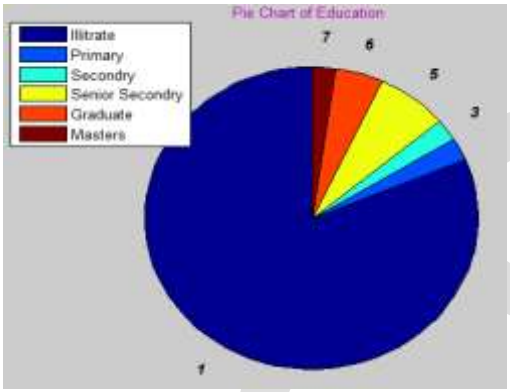

Fig: 3.3: Analysis education of criminal through pie chart

By get the result of the criminal education data we estimate the result to draw the maximum criminal what their education background if they do a crime so by seeing the result we draw a table with the respective results.

Table 3: Analysis of education of the criminal

Education of Criminal	Number of Education
ILLITRATE	35
PRIMARY	2
SECONDARY	2
SENIOR SECONDARY	1
GRADUATE	7
MASTERS	3

The steps used to determine the data are the following:-

- Import data from database
- Divide the education data in different category i.e. illiterate, primary, secondary, senior secondary, graduate, and masters.
- Calculate the each criminal education background
- Increment the number of education mostly criminal done
- Design a pie chart to represent the education of the criminals

We get estimate result in table 3 that mostly criminals are illiterate this data help in further proceeds to get the end results

3.4 Detect pattern of criminal movement using genetic algorithm

In this we get criminal location what was there next location of crime we have data collected of criminal what his exact location and the distance in which he do a crime.

let us take an example a person p he wants to make an p name in the world so he start to make line first then completes the p when he make a line he used 10 gap then we get idea the next target also lie within 10 meter gap for this we collected a large data of criminal location where he do a crime with the help of genetic algorithm we plot a graph of similar pattern.

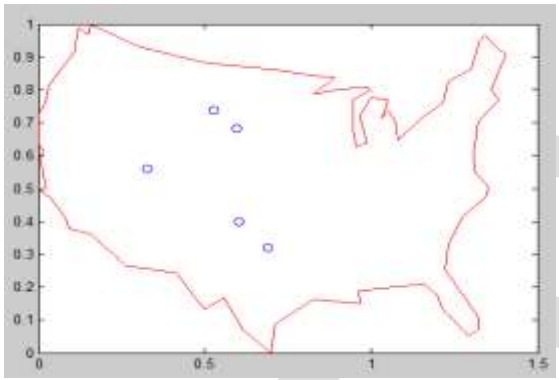

Fig: 3.4(a): shows position of crime done by criminal

In this graph we get the position of criminal in that country and these are the position of one criminal who do a crime based on these location.

Now we have join these location and get the distance between them in what distance he make a next target.

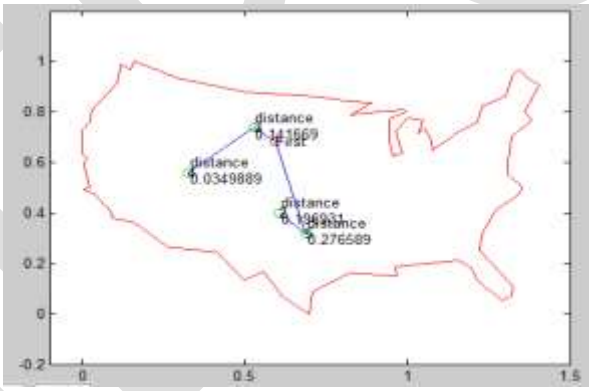

Fig: 3.4(b): Connect all the position of crime which was done by the criminal

Here we connect all the connectors in which criminal done crime now using the genetic method which find the similar pattern between the graph we get the net position where he done a crime

The steps used to determine the data are the following:-

- Import data from database
- The data contain the location of crime where a single person done a crime in different location
- We get the points which shows on graph which shows different places where he done a crime
- In the next graph we calculate the distance between them and also connect the points in graph
- By using this data and the genetic algorithm we draw a graph which shows the next position where he might done a crime

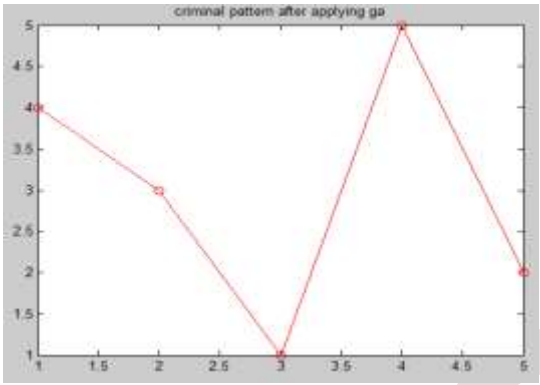

Fig: 3.4(c): This graph shows the next position of crime location of criminal

4. RESULT

We have analysis all the attributes one by one now we consider all the attributes apply the algorithm and find the result that the can a soft core criminal become a hard core criminal in future so we apply the algorithm and get four results that what is the possibility of soft core criminal become a which type of hard core criminal in future their four types are:-

Type1 → soft core criminal
Type2 → soft core criminal moving towards hard core
Type3 → hard core criminal
Type4 → completely hard core criminal

Certain steps are taken to get the result of Calculate Probability of Soft core criminal converting into type of criminal steps are:-

1. Import all the data analysis done is prior
2. We have calculate the data that maximum criminal belongs to which category
3. Here we not compare only with one category butt all the category
4. If no match with the analysis data or less attribute match called soft core criminal
5. If 2-3 data of attribute are match with data analysis attribute of criminal called soft core criminal moving towards hard core
6. If 3-4 attribute match called hard core criminal might be in future
7. If all the data match it is an completely hard core criminal might be in future

For this we design a model in which read data button read data from database which already store in matlab in mat files then we have proposed model which we discuss prior then we have a button of new criminal data in this we enter the detail of new criminal.

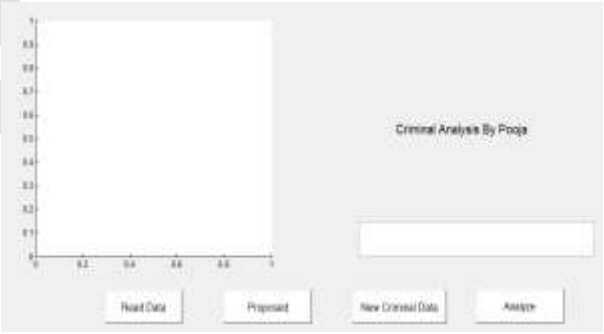

Fig: 4: Represent the model of analyzing criminal behavior

Now by click the button of new data we have another window open in which we enter the detail of the criminal which shows which type of criminal it was in future

4.1 Enter the detail of new criminal data record 1

We enter the detail of new criminal and analyses that in future it will become a hard core or it remain soft core criminal we enter the detail of one criminal enter only the attribute value of criminal than save the value in mat file.

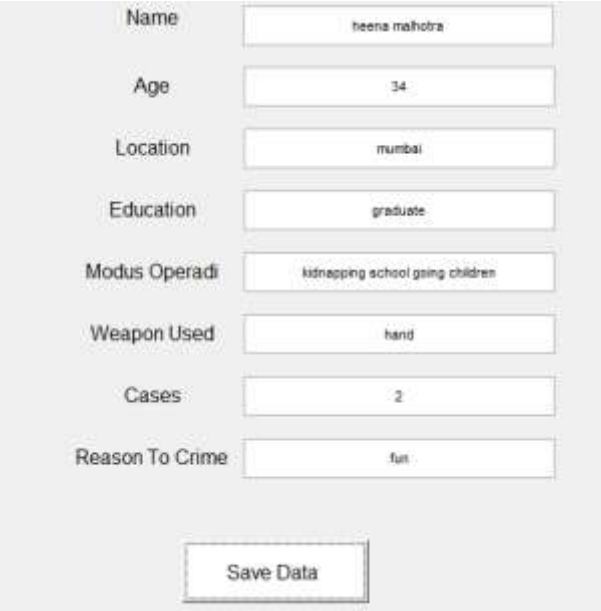

Fig 4.1(a): Enter the detail of new criminal data record1

We have enter the new criminal data of record 1 and save file in mat file for further analysis of data.

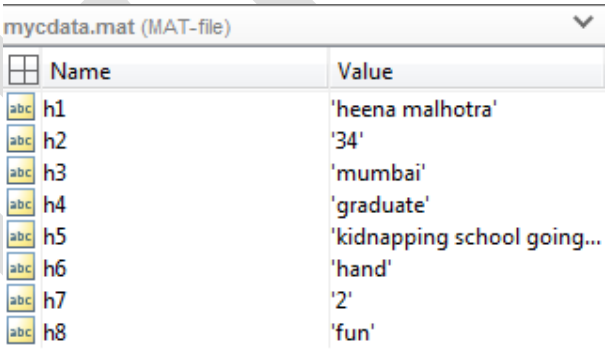

Fig 4.1(b): Save the detail of new criminal data record1in mat file

4.1.1 Analyze the record 1 new criminal data

Now by click the button of analyze we get the result whether it is hard core criminal or soft core criminal.

Fig: 4.1.1(a): Analysis of record 1 data of new criminal

We get here we see this data are shows that this criminal are little chances to become a hard core criminal we have the statement this is a command prompt.

Fig: 4.1.1(b): Analysis of record 1 data of new criminal in Command Prompt

4.2 Enter the detail of new criminal data record 2

We enter the detail of new criminal and analyses that in future it will become a hard core or it remain soft core criminal we enter the detail of one criminal enter only the attribute value of criminal than save the value in mat file.

Fig 4.2(a): Enter the detail of new criminal data record2

We have enter the new criminal data of record 2 and save file in mat file for further analysis of data.

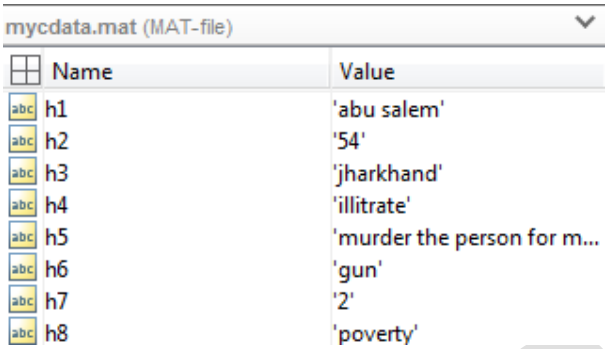

Fig 4.2(b): Save the detail of new criminal data record 2 in mat file

4.2.1 Analyze the record 2 new criminal data

Now by click the button of analyze we get the result whether it is hard core criminal or soft core criminal

Fig: 4.2.1(b): Analysis of record 2 data of new criminal

We get here we see this data are shows that this criminal are greater chances to become a hard core criminal we have the statement this is a command prompt.

Fig: 4.1.1(b): Analysis of record 2 data of new criminal in Command Prompt

4.3 Compare the data of record 1 and record 2

Here we have two record i.e. record 1 which is record of the criminal there is less chances he became a hard core criminal and we have record 2 criminal which has more chances become a hard core criminal we get the result by analyzing the criminal behavior that maximum attribute matches with the data analysis it shows it has more chances to become a hard core criminal

Fig: 4.3(b): Compare record 1 and record 2 data

CONCLUSION

This research explores a new method to understand and analyze behavior of criminals. Several data of criminals was collected from genuine sources; the data was stored in graph database for its effective analysis. Sub graph of criminal database was used to reduced data so as to achieve efficient results; optimization is performed in the behavior analysis. We have achieved greater accuracy using fuzzy logic for comparison of new criminal data with the stored data. Thus the objective of the dissertation is achieved and the criminal behavior is analyzed.

In future the analysis can be done adding more parameters like behavior and handwriting patters.

REFERENCES:

[1] VandeMoere, A., "Time-varying data visualization using information flockingBoids", In IEEE Symposium on Information Visualization 2004 (Austin, TX: IEEE), pp. 97-104
[2] Nath S. V., "Crime Pattern Detection Using Data Mining", Proceedings of the 2006 IEEE/WIC/ACM international conference on Web Intelligence and Intelligent Agent Technology , 41- 44, 2006
[3] Yan J. , Liu N., Yang Q., Zhang B., Cheng Q., Chen Z., "Mining Adaptive Ratio Rules from Distributed Data Sources", Data Mining and Knowledge Discovery, 12, 249–273, 2006, 2005 Springer Science+Business Media, Inc. Manufactured in the United States. [IVSL]
[4] E.S. McCord, G.H. Ratcliffe, R.M. Garcia, and R.B. Taylor,"Nonresidential crime attractors and generators elevate perceived crime and incivilities," Journal of Research in Crime and Delinquency, vol.44(3), pp. 295-320, 2007
[5] E.S. McCord, and G.H. Ratcliffe, "A micro-spatial analsysis of the demographic and criminogenic environment of drug markets in Philadelphia," Austrian and New Zealand Journal of Criminology, vol.40(1), pp. 43-63, 2007
[6] R.K. Rai, M. Balmer, M. Rieser, V.S. Vaze, S. Schonfelder and K.W. Axhausen, "Capturing human activity spaces-new geometries," Transportation Research Record, vol. 2021, pp. 7080, 2007
[7] Natalia Iwanski, Richard Frank, VahidDabbaghian, Andrew Reid and Patricia Brantingham, "Analyzing an Offender's Journey to Crime: A Criminal Movement Model (CriMM)", 978-0-7695-4406-9/11 $26.00 © 2011 IEEE DOI 10.1109/EISIC.2011.13
[8] S.D. Johnson and K.J. Bowers, "Permeability and burglary risk: are culde- sacs safer?" Journal of Quantitative Criminology, vol. 26 pp. 89-111, 2010
[9] R. Frank, V. Dabbaghian, S.K. Singh, A.A. Reid, J. Cinnamon and P.L. Brantingham, "Power of criminal attractors: modeling the pull of activity nodes," Journal of Artificial Societies and Simulation, vol 14(1), p.6, 2011
[10] Malathi. A and. Baboo S. S., "Enhanced Algorithms to Identify Change in Crime Patterns", International Journal of Combinatorial Optimization Problems and Informatics, Vol. 2, No.3, Sep-Dec, 2011, pp. 32-38, ISSN: 2007-1558
[11] Malathi. A and. Baboo S. S., "Enhanced Algorithms to Identify Change in Crime Patterns", International Journal of Combinatorial Optimization Problems and Informatics, Vol. 2, No.3, Sep-Dec, 2011, pp. 32-38, ISSN: 2007-1558
[12] Malathi. A , Baboo S. S. and Anbarasi A., " An intelligent Analysis of a City Crime Data Using Data Mining", 2011 International Conference on Information and Electronics Engineering, IPCSIT vol.6 (2011) © (2011) IACSIT Press, Singapore
[13] Sathyaraj S. R., Thangavelu A., Balasubramanian S., Sridhar R., Chandran M. and Prashanthi M. D., "Clustered Spatial Association Rule To Explore Large Volumes Of Georeferenced Crime To Crime Data", 3rd International Conference On Cartography And Gis 15-20 June, 2010, Nessebar, Bulgaria
[14] Chen N. and Wang Y., "Prediction of Series Criminals: An Approach Based on Modeling", 2010 International Conference on Computational and Information Sciences
[15] Yu C.H., Ward M. W., Morabito M., and Ding W., "Crime Forecasting Using Data Mining Techniques", 2011 11th IEEE International Conference on Data Mining Workshops
[16] Emad K. Jabar, Soukaena H. Hashem, and Enas M. Hessian, "Propose Data Mining AR-GA Model to Advance Crime analysis", IOSR Journal of Computer Engineering (IOSR-JCE) e-ISSN: 2278-0661, p- ISSN: 2278-8727Volume 14, Issue 5 (Sep. - Oct. 2013), PP 38-45 www.iosrjournals.org

International Journal of Engineering Research and General Science Volume 3, Issue 5, September-October, 2015
ISSN 2091-2730

Seismic Evaluation and Retrofitting of Existing Reinforced Concrete Water Tank Staging System

Mr.V.D.Salunkhe[1],Assistant Prof.Y.P.Pawar[2]

[1]PG student SKN college of engineering korti,pandharpur,Maharashtra,India.

Email :- Vikasvpcoe45@gmail.com

[2]Assistant Professor Of Civil EngineeringDepartment,SKN sinhgad college of engineering Korti,Pandharpur, Maharashtra,IndiaYashwant3153@gmail.com

Department of civil engineering,SKNCOE,Korti

Abstract - The Indian standard "Criteria for Earthquake Resistant Design of Structures: IS 1893:2002" has been revised.The seismic zone factors have been changed. Response spectra are now specified for 03 types of founding soil strata & a response reduction factor has been introduced. E Elevated water tanks are vulnerable to earthquakes, owing to large mass concentrated at the top of relatively slender supporting systems. Existing elevated water tanks in India designed using IS 1893:1984 needs to be checked for safety as per revised code (IS 1893-2002) by carrying out static analysis. It is observed that the structure is unsafe due to under estimation of seismic load as per old code provisions. Retrofit measures such as additional structural elements and passive devices like viscous and friction dampers are modelled and structure analysed again to check for compliance with the revised code.

Keywords: Seismic zone factors, Water tank, Dynamic properties, NDT test, Retrofit, Static Analysis by SAP.

INTRODUCTION

The basic design procedure for new structures consist of selection of an appropriate level of lateral forces for design purpose & then providing a complete appropriately detailed lateral force resisting system to carry these forces from mass level to foundation. Deformations are checked as secondary issue & except for the design of flexible structures they are not likely to control the design. seismic evaluation of existing tank – A higher degree of damage in a elevated tank is expected during an earthquake if the seismic resistance of elevated tank is inadequate. Hence a detail seismic evaluation of existing elevated tank needs to be performed to determine the nature and extent of deficiencies, which can cause poor performance in future earthquake.

Deformation control is the secondary consideration is design of many new structures to code of life safety requirements because the modern materials and ductile detailing practices specified by current codes allow new structures to experience large deformation while expressing limited damage. older structures however do not have advantage of this inherent ductility. therefore control of deformation become and extremely important issue in design of seismic retrofit.

Seismic evaluation of existing structure

A higher degree of damage in a elevated tank is expected during an earthquake if the seismic resistance of the elevated tank is an inadequate. Hence a detailed seismic evaluation of existing elevated tank needs to be performed to determine the nature and extent of deficiencies, which can cause poor performance in future earthquakes . this evaluation also helps to decide weather structural modifications are required at few location in the structure for deficient components only or interventions are needed structural level so that global behaviour is improved and thus seismic demands on components are reduced the decision to strengthen it before an earthquake occurs depends on the tanks seismic resistance. the seismic evaluation procedure gives a measure of the seismic resistance

of the structure . the seismic performance of the structure may not be improved by retrofitting or rehabilitation unless the structural engineer selects an appropriate intervention technique based on seismic evaluation of structure. Hence to select appropriate retrofitting method, an accurate evaluation of the seismic performance and the condition of an existing structure is necessary. based on this evaluation ,engineer can choose the most effective retrofit among the various intervention technique and optimize the improvement in seismic performance foe an existing structure. seismic evaluation consists of gathering as –built information and obtaining the results of a structural analysis based on collected data as built information refers to the configuration of the structural system ,as well as the type, detailing , material strength and condition of the structural elements .

Summary of Previous Research

Ramaiah & Gupta [6]

Investigated the factors such as size of columns, braces, number of panels. With the increase in size of bracing rods, the period was found to decrease, while lateral force & seismic coefficient increased**.**

Shepherd [8]

As per IS 1893-1984,an elevated water tank may be modelled by a single degree of freedom system. However research indicate that the single degree of freedom idealization is approximate only for closed tank ,which are completely filled with liquid. Shepherd Presented the two-mass idealization of elevated water tanks.

Jain & Sameer[9]

Proposed approximate methods to estimate lateral stiffness of tank staging.

Ingle[18]

Suggested an approximate method to estimate lateral stiffness & fundamental time period for tank structures with rectangular configuration of columns & braces in plan. It has also proposed an equation for the lateral stiffness of the staging of the overhead water tank.

Srisanthi[15]

Carried out analysis of braced steel frame with friction damper using FE software. It has concluded that increasing the size of dampers will cause reduction in the response & deflection in the structure. It has also concluded that load carrying capacity of the steel frame with friction damper was 20% more than that of the frame without a damper **.**

S.C.Datta,jain and Murty CVR[12]

The companion paper [Dutta SC, Jain SK, Murty CVR. Assessing the seismic torsional vulnerability of elevated tanks with RC frame-typestaging. Soil Dynamics and Earthquake Engineering 2000;19(3):183–97] shows that many of the currently designed reinforced concrete elevated water tanks supported on frame-type stagings have the ratio of torsional and lateral natural periods, t , in the critical range of 0.7– 1.25. This may amplify the effect of small accidental eccentricity and cause large torsional vibration during translational ground shaking in earthquakes [Dutta SC. Torsional behaviour of elevated water tanks with reinforced concrete frame-type stagings during earthquakes

It is seen in the companion paper [1] that elevated water tanks supported on reinforced concrete frame-type stagings having all the columns resting on the perimeter of a circle (shown in Fig. 1 of the companion paper [1] and referred as *basic configuration* in the rest of this paper) may often have
their natural period ratio t (ratio of torsional and lateral natural periods) in the range 0:7 , t , 1:25: This tuning of torsional and lateral natural periods makes them prone to severe amplified torsional vibration during earthquake, arising out of any small accidental eccentricity (e.g. Refs. [2,3]).

Staging with radial beams

Addition of the radial beams to the basic staging configuration (Fig. 1a) provides increased lateral stiffness with no change in the torsional stiffness. Therefore, the natural period ratio (t) is increased. Addition of the radial beams may also be a feasible solution for seismic strengthening of the existing elevated water tanks.

. Lateral stiffness

. Due to bending deformation of staging members

The derivation of the stiffness is carried out as in the case of basic configuration in the companion paper [1]. The entire staging is modelled as a single equivalent column attached with a single equivalent rotational spring at each beam level. The moment of inertia of equivalent column is equal to the sum of moment of inertia of all the columns. The equivalent rotational spring at each beam level accounts for the rotational spring action provided by both the circumferential as well as radial beams at that level. To account for the additional effect of radial beams, *k*st and *k*sb in Eq. (3) of the companion paper [1], for basic configuration, are replaced by *k*st 1 *k*srt and *k*sb 1 *k*srb; respectively. Here, *k*st and *k*sb are the sum of rotational stiffness parameters of circumferential beams at top and bottom joints of a panel, respectively, in the direction of lateral force, as defined and derived in Eq. (4) of the companion paper [1]. Similarly, *k*srt and *k*srb are the sum of rotational stiffness parameters in the direction of lateral force of all radial beams at all the top and bottom joints, respectively, of the panel considered. Assuming that all the radial beams have their points of inflection at the centre of the staging circle, ***k*srt =*k*srt = *k*srb= .X*N*=c*i*.1*k*brt= .*XN i*.1*k*brb = . *E*b*I*br/2*R*sX=*N*c*i*.=1cos2 b*i* . *E*b*I*br*N*c/4*R*s

where *k*brt and *k*brb are the rotational stiffness parameters of Individual radial beams at top and bottom joints of the panel, respectively

*K*p.lateral. =12*EcIcNch*3/1 1g*K*r1 1 0:5d0sin.p*N*c.

. Torsional stiffness

The addition of radial beams does not change torsional stiffness of the staging. The torsional stiffness of the panel is same as that for the basic configuration given by Eq. (10) of the companion paper [1]

METHODOLOGY

The elevated Water Tank (WT) consists of tank supported by staging system composed of columns, braces and foundations. Only R.C.C. WTs have been considered. The criteria for a seismic design of structures are given in IS 1893-2002 part 1 [3] and the explanatory code [4]. Elevated WTs have generally performed well in a seismic zones. However large number of tank collapses have been observed during earthquakes from as early as the 1906 San Francisco Earthquake to the 2001 Bhuj Earthquake[5]. The seismic zone maps have been recently revised. The new zone map has only four seismic zones – 11, 111, 1V and V instead of the five zones in the earlier

version.

1. Assessment of safety of existing R.C. water tanks (designed using IS 1893:1984) under revised provisions of is 1893:2002.
2. To check the efficiency of additional structural members as retrofit scheme.
3. To find suitability of appropriate retrofitting Technique

ACKNOWLEDGMENT

I would like to sincere thanks to my guide Assistant Prof. Pawar Y.P. for support and guidance they have provided to us enduring patience, motivation & valuable time. He gave me to be a gradually appreciated when he holding responsibility as assistant professor in civil Engineering department.

I also grateful to Prof. Pise Head Of Department of civil Engineering Department For providing all necessary facility.

I extend sincere thanks to Principal Dr. K. J. Karande for his guidance & inspiration. I express deep sense of gratitude to all staff member for their co-operation. I finally sincere thanks to all those who directly Or indirectly help me

Summary and Conclusions :

1.This paper investigated the factors such as size of column, braces, number of panels. with increase in size of bracing the period found to decrease while seismic coefficient increased.

2. This paper describe suitable retrofitting technique for Elevated Reinforced concrete water tank. And torsional vulnerability is explained.

3. The work presented in this paper can be particularly useful for seismic retrofitting of the existing tank stagings. Existing tank stagings with basic configuration can be conveniently modified into one of the alternate configuration, particularly those with radial beams only, and with diagonal braces.

REFERENCES:

[1]. IS 805 – 1968 Code of Practice for use of Steel in Gravity Water Tanks, Bureau of Indian Standards, New Delhi.

[2]. IS 800 – 2000 Code of Practice for Structural Use of Steel, Bureau of Indian Standards, New Delhi.

[3]. IS 1893(Part 1) 2002 Criteria for Earthquake resistant design of structures, Bureau of Indian Standards, New Delhi.

[4]. SP 22 (S&T) – 1982 Explanatory handbook on codes for Earthquake Engineering, Bureau of Indian Standards, New Delhi.

[5]. Paul, D.K., 2002, Building Damage during Earthquakes, Short Term Training Programme on Design and Construction of Earthquake Resistant Structures, Bangalore, pp.11-32, August.108 *ICCBT 2008 - C - (09) - pp99-108*

[6]. Ramaiah, B.K. and D.S.R. Gupta, 1966, Factors affecting seismic design of water towers, Journal of the Structural Division, Proceedings of ASCE, 92, 13-29.

[7]. IS 1893 1984 Criteria for Earthquake resistant design of structures, Bureau of Indian Standards, New Delhi.

[8]. Shepherd, R., 1972, The two-mass representation of a water tower structure, Journal of Sound and Vibration, 23, 391-396.

[9]. Jain, S.K.and Sameer,U.S., 1992, Approximate methods for determination of time period of water tank stagings, The Indian Concrete Journal, 691-698.

[10]. Fischer, F.D. and R.Seeber, 1988, Dynamic response of vertically excited liquid storage tanks considering liquid-soil interaction, Earthquake Engineering and Structural Dynamics, 16, 329-342**.**

[11]. Velestos, A.S. and Y.Tung, 1990, Soil Structure interaction effects for laterally excitedliquid storage tanks, Earthquake Engineering and Structural Dynamics, 19, 473-496.

[12]. Dutta SC, Jain SK, and CVR Murthy, 2000a, Assessing the seismic torsional vulnerability of elevated tanks with RC frame type staging, Soil Dynamics and Earthquake Engineering, Elsevier Science, 19, 183-197

International Journal of Engineering Research and General Science Volume 3, Issue 5, September-October, 2015
ISSN 2091-2730

PERFORMANCE ANALYSIS OF PaaS CLOUD COMPUTING SYSTEM

Akmal Basha[1] Krishna Sagar[2]

[1]PG Student,Department of Computer Science and Engineering, Madanapalle Institute of Technology & Science, India.

[2]Associate Professor,Department of Computer Science and Engineering, Madanapalle Institute of Technology & Science, India.

Abstract: Cloud computing is business infrastructure paradigm that promising to remove the need for organizations to keep up an exclusive computing hardware. Cloud computing provides to users with various capabilities to store and process the data in third-party data centers. Cloud computing maximizes the effectiveness of shared resources. During the use of time sharing and virtualization cloud address with the particular set of material resources in a large scaled user's base with different needs. In this paper computing the performance of Platform-as-a-Service (PaaS) model and integrating the mechanisms to capture the virtual machine migrations. We study the cloud services on different large applications. In this paper we are presenting the performance of Platform-as-a-Service (PaaS) by using systematic model to perform end-to-end analysis of a cloud service. The systematic model designed by using scheduling algorithm i.e., Adaptive First Come First Serve under different job sizes. The performance is analyzed by using performance metrics such as consumption, availability, response time, waiting time. The cloud performance metrics depends upon the behavior of the cloud data center.

Keywords: Virtualization, Platform-as-a-Service (PaaS), Adaptive First Come First Serve.

1. INTRODUCTION

The cloud computing is a condition of information technology communications throughout the internet. I.e. the provision of mutual resources, services, software and application in excess of the internet to convene the flexible insist of the client with bare lowest amount exertion or communication with the service providers.

1.1 Types of cloud computing services

1.1.1 SaaS

Software as a service (SaaS) provides application to the users by means of a cloud communications or policy, relatively than provided that cloud features themselves i.e., application, software or correspondences are intended for clients deliver over the web. SaaS is not essential for the customers to have a substantial replica of the S/W installed on a personal computers, laptops or whichever other client devices. SaaS can be treated it as application or service cloud. Frequently, this can be a type of usual applications S/W methodology presented in cloud.

Ex: Google maps, Google search, Sales force CRM.

1.1.2 PaaS

Platform as a service (PaaS) is the combination of services and tools intended to create code and deployment of application in excess of the web rapid and proficient for the customers. The customers doesn't have access to the fundamental cloud communications together through system, servers, OS, or storage space, but has manage above the deploy tool/service and possibly arrangement settings for the application launching environments. It can be provide a group of developer's surroundings though a client can utilize to construct their application having not any hint concerning what is going away on under the services. PaaS is a platform anywhere application can be residential, experienced and use.

Ex: Google Drive, Microsoft windows XP, Java.

1.1.3 IaaS

Infrastructure as a service (IaaS) is the substantial layers that are created by the H/W resources which are required to hold the cloud services organism provide, and characteristically include server, storage, OS and system mechanism. Thus it can be hardware and software that power the cloud. Here the client doesn't have access to the fundamental cloud communications but has control in excess of OS, storage space, and deploy applications and possibly restricted manage in excess of selected network mechanism.

Ex: Amazon, Microsoft windows azure SQL.

1.2 Cloud Usage Models (Cloud Deployment model)

Cloud computing is also can be categorized into 4 main groups depends on procedure or exploitation: Private cloud, Public cloud, Community cloud and Hybrid cloud.

1.2.1 Personal (Private) Clouds

Personal (Private) Clouds are characteristically own or lease by the particular association or individuals. It might be manage and operate by the association or a group of them, and it might exist off or on property.

Ex: Flip kart

1.2.2 Community (domain-specific) Clouds

The clouds are maintained for precise necessities by a group of organization. It is compute resource provide more the internet for constrained utilize by an exact community of users as of organization that have common attention. Frequently the user's are a grouping of community with a general environment or by means of mutual concern surrounded by the community or the public. Community clouds are a go between among public and private clouds. It might be manage and operate by 1 or more organizations in the exact community or various combinations of them and it might be present off or on property.

1.2.3 Public (General) Clouds

The clouds provides services to the more number of the populate. It is the mainly recognizable and fashionable form of cloud. Here in the general cloud, computing resources are animatedly arranged over the internet. They survive on the premise of the cloud providers. It might be own, manage, and operate by businesses, academics or public organizations or some combination of them.

Ex: Google apps, Windows Azure, Amazon.

1.2.4 Hybrid (Mixed) Clouds

A mixed cloud is essentially a arrangement of two or more clouds. It is a combination of public and private cloud infrastructure meant at achieve ultimate cost diminution all the way through outsourcing whereas maintain the preferred stage of organization. Based on ELC Technologies 2010,mixed cloud model are probable to materialize as the mainly general structure of cloud in the expectations as they make available subscribes better option and opportunity to access explicit services contained by the same cloud exclusive of the require to control to an completely dissimilar contributor, if business wants modify. Hybrid clouds characteristically also engage an elasticity which service is hosted in the clouds.

2. PROPOSED WORK

Platform-as-a-Service (PaaS) user segment and infrastructure management users will be different from each other and their interest would be on the business aspects. PaaS user segment covers the key SDLC cycles and the deployment management rather than the infrastructure level details. we are presenting the performance of Platform-as-a-Service (PaaS) by using systematic model to perform end-to-end analysis of a cloud service. The systematic model designed by using scheduling algorithm i.e., adaptive first come first serve under different job sizes. The cloud performance metrics depends upon the behavior of the cloud data center.

The following figure1 depicts that job requests are placed in the queue and the queue has a finite size F. If the queue reaches its maximum limit is reached extra requests are rejected. The system queue follows FCFS scheduling policy. If the resource is available then job is accepted and mapped to the corresponding Virtual Machine. Assume the instantiation time is omitted and the service time is exponentially distributed with its mean. The system considers virtual machine under two different conditions such as insufficiency and overload. In the overload condition waited jobs are placed in dispatcher virtual machine. Dispatcher virtual machine used in particular situations by the system and the public cloud systems offers the resources through a paying and sharing model. If the virtual machine is idle then there is no waiting job.

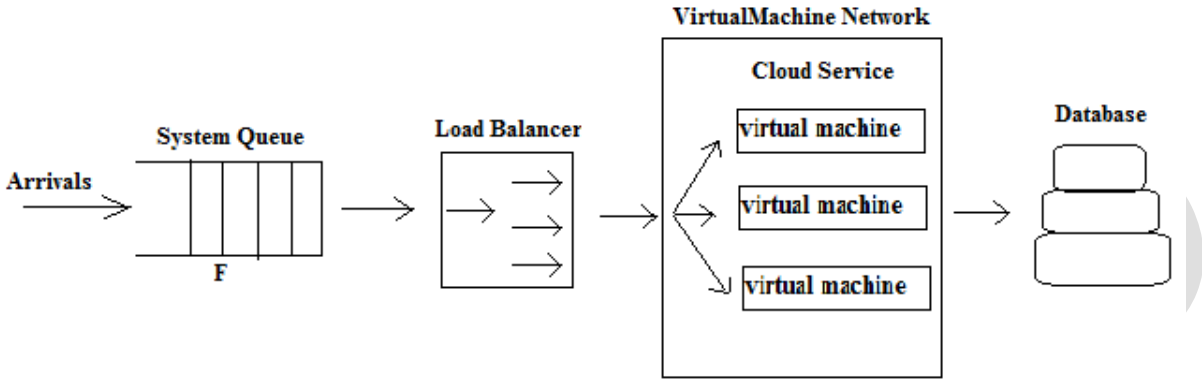

Figure 1: PaaS Performance Systematic Model

Algorithm:

Step 1: Arrival job requests are placed in queue in First Come First Serve manner

Step 2: If the Virtual Machine index is 0 then the Virtual Machines are in available state.

Step 3: If the virtual machines are available then Data center (DC) receives a new request.

Step 4: Data Center queries for next allocation.

Step 5: The Virtual Machines were parsed by Data Center Controller to get next available Virtual Machine

If (resource is available) {

// found

Returns the Virtual Machine id to Data Center Step2 continues}

Else { // resource is not available

Virtual Machine index initialized to zero. }

Step 6: When the Virtual Machine finishes the processing client request and the Data Center receives acknowledgement and it notices the load balancer of the Virtual Machine for de-allocation.

Step 7: The Load Balancer updates the status of Virtual Machine whether it is available or not.

Step 8: Continue from Step2.

3. STEADY STATE ANALYSIS

In steady state analysis the particular state of the proposed model is represented by using systematic model. System performance metrics are used to characterize the behavior of provider and user. Those metrics helps the system designer to manage the cloud data center. The performance of Platform-as-a-Service (PaaS) model is analyzed by using the metrics such as consumption, availability, service time, responsiveness.

3.1 Performance Metrics

3.1.1 CONSUMPTION OR UTILIZATION:

Utilization can be calculated by considering actual work and total hours. Actual work can be considered as number of resources utilized in steady state. The actual work can be indicated as 'Aw' and Total Hours can be indicated as 'T'. If the number of jobs will increase in queue the utilization of a data centre will be increased. The utilization factor can be computed as:

Utilization = Aw/ T (in hours).

3.1.2 AVAILABILITY:

If the system is able to accept a request then the system is available. Availability can be shown by using Boolean values 0 and 1.If the requested job is available the Virtual Machine index will be pointed to 1 otherwise it will be 0.

3.1.3 RESPONSE TIME:

It is the steady state probability within a given time deadline that the system is to accepting a request. Throughput indicates the number of transactions per second an application can handle, the amount of transactions produced over time during a test.

Response time (RT) is computed by service time (ST) and the wait time (WT). Service time (ST) is the time to do the work and waiting time (WT) is the time you waited for the turn to be serviced. Response time (RT) can be computed as:

$$R_T = W_T + S_T$$

$$W_T = N_{JS} / A_{JA}$$

W_T -Wait Time

N_{JS} - Average number of jobs in the system

A_{JA} - Average rate of jobs arrival

3.2 Performance Analysis:

The result will be analyzed by considering the number of jobs in queue and time needed to complete the jobs. If the arrival of jobs in queue increased then the response time of the system will be increased. If the jobs in queue will increase then the utilization of cloud datacenter will be increased as shown in figure 2. As shown in figure 3 when the congestion is increased the throughput increases linearly and finally reaches a throughput plateau. After this point as if the load is increased the throughput remains saturated at this level. The response time starts increasing non-linearly with increase in load and low at low traffic levels and continues to increase up to maximum of system resources like the memory and CPU. Throughput measures the amount of work performed by Application Server and defined as the

number of requests processed per minute per server instance. The response time is includes the factors such as bandwidth, number of users, number and type of requests submitted. If the load increases the response time for a request also increases

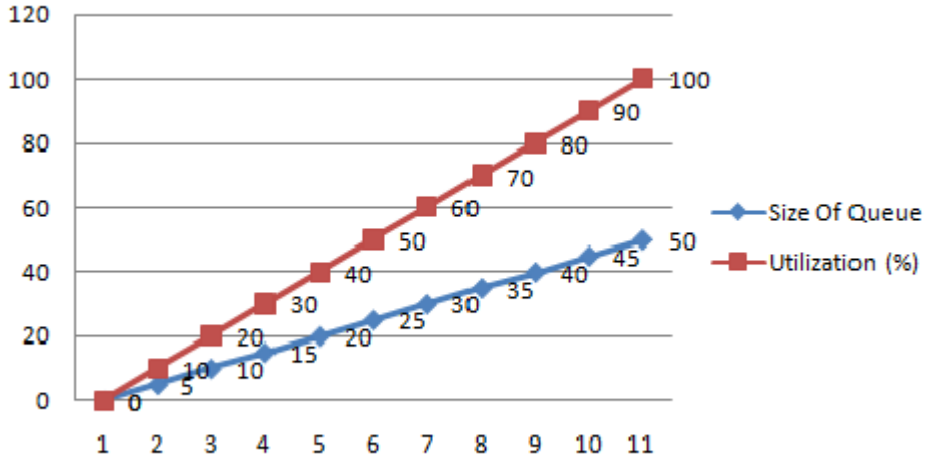

Figure 2: Size vs Utilization

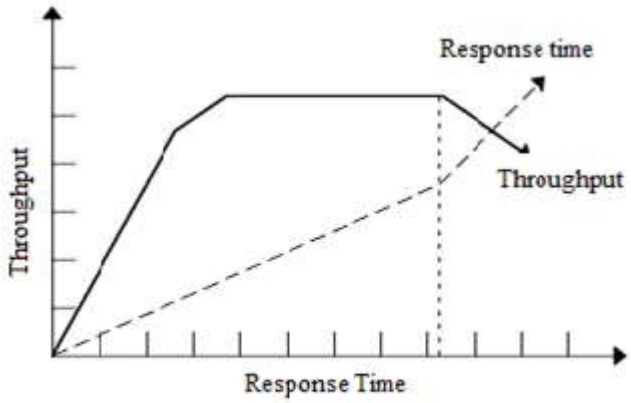

Figure 3:Throughput vs Response Time

4. CONCLUSION:

The cloud computing is internet based computing in which resources are provided to users based on Adaptive FCFS (First Come First Serve) manner. In this paper we have presented the performance of PaaS (platform-as-a-service) model by using performance metrics and integrating the mechanisms to capture the virtual machine migrations. Metrics are the important elements for evaluating the quality for enabling the identification of a good Cloud Computing. In this paper we have presented the data center utilization and response time at different workloads. The cloud performance metrics depends upon the behavior of the cloud data center.

REFERENCES:

1. R. Buyya et al., "Cloud computing and emerging it platforms: Vision, hype, and reality for delivering computing as the 5th utility," Future Gener. Comput. Syst., vol. 25, pp. 599–616, June 2009.
2. X. Meng et al., "Efficient resource provisioning in compute clouds via vm multiplexing," in Proceedings of the 7th international conference on Autonomic computing, ser. ICAC '10. New York, NY, USA: ACM, 2010, pp. 11–20.
3. H. Liu et al., "Live virtual machine migration via asynchronous replication and state synchronization," Parallel and

Distributed Systems, IEEE Transactions on, vol. 22, no. 12, pp. 1986 –1999, dec. 2011.

4. B. Rochwerger et al., "Reservoir - when one cloud is not enough," Computer, vol. 44, no. 3, pp. 44 –51, march 2011.
5. R. Buyya, R. Ranjan, and R. Calheiros, "Modeling and simulation of scalable cloud computing environments and the cloudsim toolkit: Challenges and opportunities," in High Performance Computing Simulation, 2009. HPCS '09. International Conference on, june 2009, pp. 1 –11.
6. "Cloud computing for enterprise architechtures" By Zaigham Mahmood, Richard Hill.
7. A. Iosup, N. Yigitbasi, and D. Epema, "On the performance variability of production cloud services," in Cluster, Cloud and Grid Computing (CCGrid), 2011 11th IEEE/ACM International Symposium on, may 2011, pp. 104 –113.
8. V. Stantchev, "Performance evaluation of cloud computing offerings," in Advanced Engineering Computing and Applications in Sciences, 2009. ADVCOMP '09. Third International Conference on, oct. 2009, pp. 187 –192.
9. S. Ostermann et al., "A Performance Analysis of EC2 Cloud Computing Services for Scientific Computing," in Cloud Computing, ser. Lecture Notes of the Institute for Computer Sciences, Social Informatics and Telecommunications Engineering. Springe Berlin Heidelberg, 2010, vol. 34, ch. 9, pp. 115–131.
10. H. Khazaei, J. Misic, and V. Misic, "Performance analysis of cloud computing centers using m/g/m/m+r queuing systems," Parallel and Distributed Systems, IEEE Transactions on, vol. 23, no. 5, pp. 936 –943, may 2012.
11. M. Armbrust et al., "A View of Cloud Computing," Comm. ACM, vol.53,pp.50-58,Apr.2010.
12. Dario Bruneo.. "A Stochastic Model to Investigate Data Center Performance and QoS in IaaS Cloud Computing Systems" IEEE TRANSACTIONS ON PARALLEL AND DISTRIBUTED SYSTEMS,VOL. 25, NO. 3, MARCH 2014

International Journal of Engineering Research and General Science Volume 3, Issue 5, September-October, 2015
ISSN 2091-2730

EFFICIENT ERROR CORRECTING MECHANISM FOR MEMORIES USED IN RADIATED ENVIRONMENT

Sanilkumar N S[1], Aby Thomas[2]
1.PG Scholar, Department of Electronics and communication Engineering, MACE. Kothamangalam, Kerala, India.
2. Asst.Professor, Department of Electronics and communication Engineering, MACE. Kothamangalam, Kerala, India.

Email: sanilkns@gmail.com,+91-8891769105

Abstract— Nowadays, memories we use are cheap, easily available in market, compact, have high programmability and available on various ranges of size and type. But the dis-advantage with these memories is that whenever there is a radiation strike on sensitive part of memory circuit, the data stored in the memory will be corrupted. These types of errors are common in radiation-prone environment like space, aircrafts, radiation research laboratories, power plants, mines etc. One of the remedies for this is to use error correction codes. Different error correction codes are available, from simple to complex. As the complexity increases efficiency also increases. Radiation will effect closer memory locations mainly as they are adjacent to each other. SEC-DAED code provides single error correction and double adjacent error detection, but cannot do anything about triple error detection. Codes like SEC-DED-TAED will also provide triple error detection but there is no provision for double error correction. This project compare different error correction codes and develop a new method which will provide single and double adjacent error correction which is occurring most time and also provide double non adjacent and triple adjacent error detection. The coding is done using VHDL in Xilinx 14.5 and simulations were obtained using ISim simulator. The project was implemented on Spartan3 XC3s200 FPGA platform.

Keywords—- single event effect(SEE), multiple cell upset(MCU), single error correction –double adjacent error detection (SEC-DAED),single error correction –double error –detection (SEC-DED-TAED),), Orthogonal Latin Square Codes(OLS).

1. INTRODUCTION

Reconfigurable SRAM based FPGA's are widely used in many applications due to their high programmability, high density, availability in market and cost effectiveness. Despite of these advantages they are limited use in space or air craft, because of their high susceptibility to noise or radiation; when a high energized particles striking on sensitive part of circuit there will be errors on data, which stored in that memory. If it affect only a single bit it known as single bit upset(SBU) and if it is affect more than one bits it known as multiple cell upset(MCU). Now a day's technology is scale down day by day so the radiation induced soft errors will effect more than one memory location. Normally use "error correcting" to solve these errors. Error correction codes from simple hamming codes to most complex BCH and Euclidian codes. In any error correcting codes generally encode the data when it is writing to the memory and decode when it is reading. So the encoding and decoding latency will affect the memory access time. So keep reducing the encoding and decoding latency. Single error correction codes has low latency, but if a double error occur it will miss correct; silent data corruption occurring. The radiation induced soft errors will effect closer memory locations. In many case they are adjacent to each other. This is because errors are created along the path through which it passing. This is shown in figure1.

This project make comparative study of different type of error correcting mechanism and from that produce an efficient error correcting mechanism. By this method correct all single errors, double adjacent errors and detect all non-adjacent double errors, triple adjacent errors. Different error correcting codes comparing here are single error correction-double adjacent error detection (SEC-DAED), single error correction-double error detection-triple adjacent error detection (SEC-DED-TAED), single error correction-double adjacent error correction (SEC-DAEC), single error correction-double adjacent error correction-non adjacent double error detection using OLS (SEC-DAEC-DED-OLS), and error correction using Decimal Matrix Code. Rest of this paper organized as follows. Chapter 2 analyse different error correcting codes. Chapter 3 presents proposed error correcting mechanism. Chapter 4 is the simulation results. Chapter 5 is the conclusion.

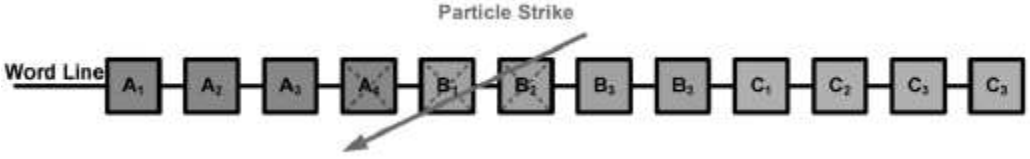

Fig 1: radiation particle strike.

2. ANALYSIS OF DIFFERENT ERROR CORRECTION MECHANISMS

The strategy using in error correcting mechanism is that encoding the data when it is writing to the memory and decoding when it is reading.

In the encoding section, from the given data bits creating extra bits, known as parity bits. If the number of information is 'k' produce 'r' number of extra bits so the total code length will be 'n'.

$$n=k + r$$

In decoding section, from the given code (n), produce another set of values known as "syndrome". Based on the syndrome determine whether there is an error or not. If the syndrome is zero there is no error else there is an error in the data. Form code word, parity bits are extracting and gives the data output. All the encoding and decoding process is based on some matrices.

Different error correcting codes comparing here are single error correction-double adjacent error detection (SEC-DAED), single error correction-double error detection-triple adjacent error detection (SEC-DED-TAED), single error correction-double adjacent error correction (SEC-DAEC), single error correction-double adjacent error correction-non adjacent double error detection using OLS (SEC-DAEC-DED-OLS), and error correction using Decimal Matrix Code.

Table 1 : Comparison table of different error correcting mechanisms.

Methods	Redundant bits	specification
Sec- daed	5	•Single error correction •Double adjacent error detection
Sec-ded-taed	6	•Single error correction •Double error detection •Triple adjacent error detection
Sec-daec	6	•Single error correction •Double adjacent error correction •Miss correct if non adjacent errors present
DMC	18	•Correction up to 5 bits •Miss correction if redundant bits have error
OLS	12	•Single error correction •Double adjacent error correction •Non adjacent double error detection •Error in redundant bit cannot correct

3. PROPOSED ERROR CORRECTION MECHANISM

The proposed mechanism is based on, SEC-DED-TAED based on hamming and OLS code. So there are two encoding modules are needed. One for hamming code and other for OLS. In the hamming encoder if we have 16 number of information data after encoding there available 22 bit of data. And this encoding based parity check matrix. And this matrix is derived from a large matrix with dimension 31 row and 26. From this matrix columns are selected with the following weight order (odd odd even odd odd even . . . and so on). . The matrix is given by:

1 0 1 **0** 1 1 **0** 1 0 1 0 1 **0** 1 0 1 0 0 1 0 1 **0**

0 1 0 **0** 1 0 **0** 1 0 0 1 0 **0** 1 0 0 1 0 0 1 0 **0**

0 0 1 **1** 1 0 **0** 0 1 1 1 0 **0** 0 1 1 1 0 0 0 1 **0**

0 0 0 **0** 0 1 **1** 1 1 1 1 0 **0** 0 0 0 0 1 1 1 1 **0**

0 0 0 **0** 0 0 **0** 0 0 0 0 1 **1** 1 1 1 1 1 1 1 1 **0**

Fig 2: matrix for sec-ded-taed code for 16 bit data word

By looking matrix, the bold columns represent parity bits and other for data bits. For find parity p1, take the first row and it is clear that positions 16,15,14,13,11,9,8,6,3,1 has value'1' so take data positions 16,15,14,13,11,9,8,6,3,1 then XOR it's values. Similarly for p2, take second row and so on. By doing this, getting 5 numbers of parity and for the last parity xor all data and newly produced parity. So total 6 parity and 16 number data so the total code length will be 22. And code word arranged in the order of parity check matrix.

$$H = \begin{bmatrix} M_1 \\ M_2 \\ M_3 \\ M_4 \end{bmatrix} I_{4m}$$

Fig 3: H-matrix representation of OLS code.

M_1

1	1	1	1	0	0	0	0	0	0	0	0	0	0	0	0	1	0	0	0	0	0	0	0	0	0	0	0	0	0	0	0
0	0	0	0	1	1	1	1	0	0	0	0	0	0	0	0	0	1	0	0	0	0	0	0	0	0	0	0	0	0	0	0
0	0	0	0	0	0	0	0	1	1	1	1	0	0	0	0	0	0	1	0	0	0	0	0	0	0	0	0	0	0	0	0
0	0	0	0	0	0	0	0	0	0	0	0	1	1	1	1	0	0	0	1	0	0	0	0	0	0	0	0	0	0	0	0

M_2

1	0	0	0	1	0	0	0	1	0	0	0	1	0	0	0	0	0	0	0	1	0	0	0	0	0	0	0	0	0	0	0
0	1	0	0	0	1	0	0	0	1	0	0	0	1	0	0	0	0	0	0	0	1	0	0	0	0	0	0	0	0	0	0
0	0	1	0	0	0	1	0	0	0	1	0	0	0	1	0	0	0	0	0	0	0	1	0	0	0	0	0	0	0	0	0
0	0	0	1	0	0	0	1	0	0	0	1	0	0	0	1	0	0	0	0	0	0	0	1	0	0	0	0	0	0	0	0

M_3

1	0	0	0	0	1	0	0	0	0	1	0	0	0	0	1	0	0	0	0	0	0	0	0	1	0	0	0	0	0	0	0
0	1	0	0	1	0	0	0	0	0	0	1	0	0	1	0	0	0	0	0	0	0	0	0	0	1	0	0	0	0	0	0
0	0	1	0	0	0	0	1	1	0	0	0	0	1	0	0	0	0	0	0	0	0	0	0	0	0	1	0	0	0	0	0
0	0	0	1	0	0	1	0	0	1	0	0	1	0	0	0	0	0	0	0	0	0	0	0	0	0	0	1	0	0	0	0

M_4

1	0	0	0	0	0	1	0	0	0	0	1	0	1	0	0	0	0	0	0	0	0	0	0	0	0	0	1	0	0	0	0
0	1	0	0	0	0	0	1	0	0	1	0	1	0	0	0	0	0	0	0	0	0	0	0	0	0	0	0	1	0	0	0
0	0	1	0	1	0	0	0	0	1	0	0	0	0	0	1	0	0	0	0	0	0	0	0	0	0	0	0	0	1	0	0
0	0	0	1	0	1	0	0	1	0	0	0	0	0	1	0	0	0	0	0	0	0	0	0	0	0	0	0	0	0	1	0

Fig 4: H-matrix for OLS code.

In the case of OLS code, It has k number of data bits, where k=m2. And have 2tm extra bits. Number of errors correcting here are 'm'. OLS codes has simple and faster decoding section, it is because of decoding is based on OS-MLD. Decoding in OS-MLD based on simply taking majority value on set of recalculated syndrome values. The errors are calculated based on parity check matrix that is syndrome value is obtaining by multiplying stored code word with this parity check matrix. Parity check matrix is derived from traditional OLS matrix which given below given in fig 3.

The first k columns represent data bits and next r column for parity bits. From matrix I4m is the identity matrix of size 4m and M1, M2, M3, M4 are matrices with size m × m2. When we take only the M1 matrix its adjacent columns are sharing one, it must avoid in this proposed mechanism so avoid that matrix (M1) and also make interleave and re-arrange the matrix to avoid this type of sharing. Otherwise when there is an error in the adjacent data bits which correspond to the column values which sharing the one value will shows miss correction. The matrix reduced matrix is given below:

p_7	p_9	p_1	p_5	p_4	p_{11}	p_{12}	p_8	p_{10}	p_6	p_2	p_3
1 0 0 0 0 1 0 0 1 0 0 0 0 0 0 0 1 0 0 0 0 0 0 0 1 0 0 0
0 0 1 0 0 0 0 0 0 0 1 0 0 0 0 0 0 0 1 0 0 1 0 0 0 1 0 0
0 0 0 0 1 0 0 0 0 0 0 0 1 0 0 0 0 0 0 0 1 0 0 1 0 0 1 0
0 0 0 0 0 0 1 0 0 1 0 0 0 0 1 0 0 0 0 0 0 0 1 0 0 0 0 1
1 0 0 0 0 0 0 1 0 0 1 0 0 0 0 0 0 0 0 0 1 0 0 0 0 0 0 1
0 0 1 0 0 0 0 0 1 0 0 0 0 0 0 0 0 0 0 1 0 0 1 0 0 0 1 0
0 1 0 0 1 0 0 0 0 0 0 0 0 0 1 0 1 0 0 0 0 0 0 0 0 1 0 0
0 0 0 0 0 0 1 0 0 0 0 0 1 0 0 1 0 0 1 0 0 0 0 0 1 0 0 0
1 0 0 1 0 0 0 0 0 0 0 0 1 0 0 0 0 0 0 0 0 0 1 0 0 1 0 0
0 0 1 0 0 0 0 0 0 0 0 0 0 0 1 0 0 1 0 0 1 0 0 0 1 0 0 0
0 0 0 0 1 0 0 0 1 0 0 1 0 0 0 0 0 0 1 0 0 0 0 0 0 0 0 1
0 0 0 0 0 0 1 0 0 0 1 0 0 1 0 0 1 0 0 0 0 0 0 0 0 1 0

Fig.5. Reduced parity check matrix H after the removal of M1 with the proposed bit placement.

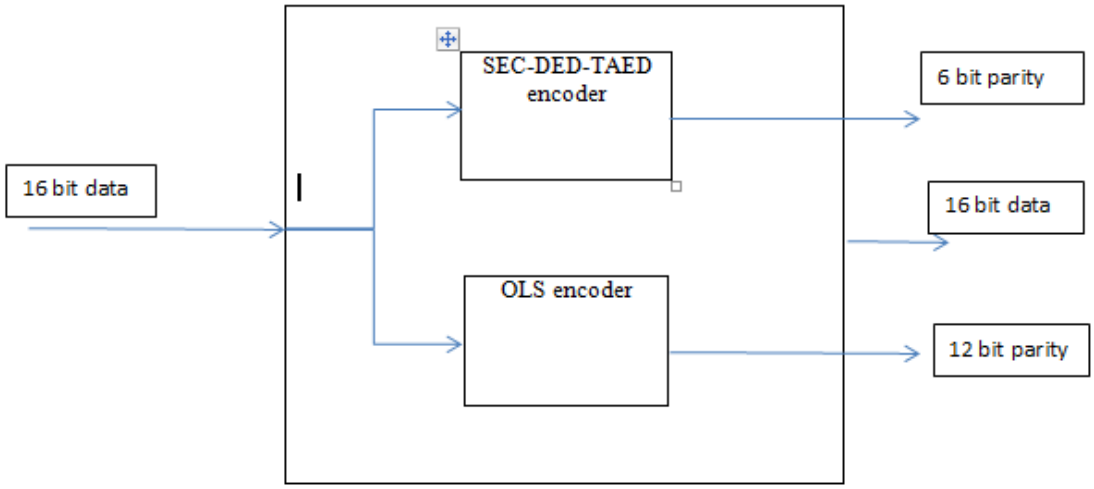

Fig 6: proposed encoder module

And the encoding is same is that of previous type, here only matrix is changed. So after encoding using OLS code there are 28 number of code word for a 16 number of data bits. So after complete encoding mechanisms of two different method there total 18 bits of parity and 16 number data and total 34 number of code word. The code word is arranged in the order given below:

P1 P2 D16 P3 D15 D14 P4 D13 D12 D11 D10 D9 P5 D8 D7 D6 D5 D4 D3 D2 D1 P6 P1 P2 P3 P4 P5 P6 P7 P8 P9 P10 P11 P12

First 22 bit contains original data bits and 6 parity of SEC-DED-TAED. Next 12 bits are parity of OLS codes. The block diagram of encoder for the proposed system is given in fig 6:

In the decoding module also there are two types of decoder sections are need one for hamming and other for OLS. And in the decoding section data and parity are extracting and corresponding parity and data is passing to its corresponding decoder modules. In the case of hamming decoder, there is a parity check matrix available, “AND” the code word with each row of matrix then ”XOR” so getting a 6 bit syndrome value. To check the triple error there is one more value is need, this done by “XOR” all the code word. So after decoding there are a 6 bit syndrome and single bit parity value is available, based on these values error is determine. If syndrome is 000000 and parity is 0 then no error. If syndrome is not equal to 000000 and parity is 0 then double error. If syndrome is equal to 000000 and parity is 1 then error in last parity. If syndrome is correspond to any column value and parity is 1 then single error in data bit. If syndrome is correspond to any other value and parity is 1 then triple error in data bit.

In the case of OLS code, there is also a parity check matrix available. So based on this matrix find out the syndrome value, here syndrome is 16 bit. Based on this syndrome error is determine. Error correction based on the figure 7.

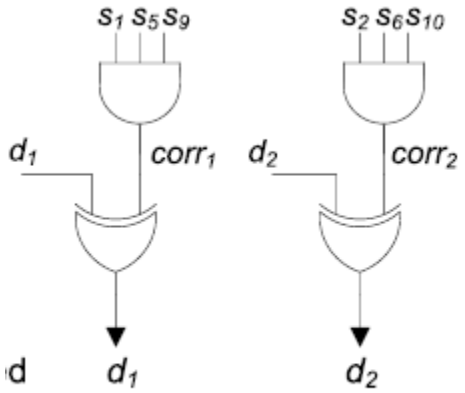

Fig 7: Illustration of the decoder for data bits 1 and 2.

Diagram show error correcting circuit for the first two data bits, where s_i is the corresponding syndrome value of data. There is also a provision to detect the double non adjacent error, which is based on figure 8.

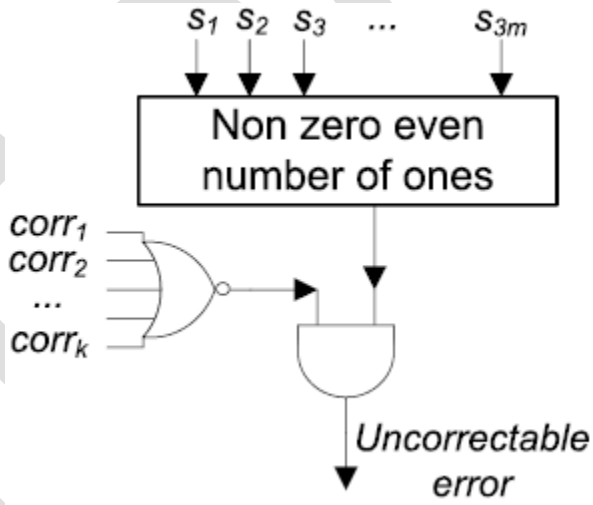

Fig.8. Detection of double un correctable errors in the proposed scheme.

It is based on the fact that when there is a double error, the syndrome value is become even value. If there is a double adjacent error is it can correct using previous diagram but when there is non-adjacent error is present it cannot correct. So if there is a nonadjacent double error is present, it indicated as un correctable error.

The out puts of hamming code are 16 bit data, single_error1 for single error, double-error1 for double error, taed1 for triple adjacent error and parity_error1 for last parity. The out puts of OLS code are 16 bit data and "ue" for indicating un correctable errors. The proposed error correcting mechanism is based on the proper selection from these out puts.

The selection is based on the following strategy:

If there is no errors indicating in both mechanism, then there is no error happened to data then select output from any mechanism. If there is only a single error in SEC-DED-TAED code and no error for OLS code, it is corresponds to a parity error in SEC-DED-TAED code and no error to the data, it can be corrected by either method. So take output from any mechanism and tagged it as no error. If there is a double error occurs in SEC-DED-TAED code and no error to OLS code, then it is a double error for parity only in the SEC-

DED-TAED code. So select the outputs of OLS code. If there is double error in SEC-DED-TAED code and un correctable error in OLS code it correspond to a non-adjacent error. It cannot be corrected it only detect. If there is triple adjacent error in SEC-DED-TAED code and un correctable error in OLS code it correspond to a adjacent triple error. It cannot be corrected it only detect. The block diagram for the decoder of proposed mechanism is given below

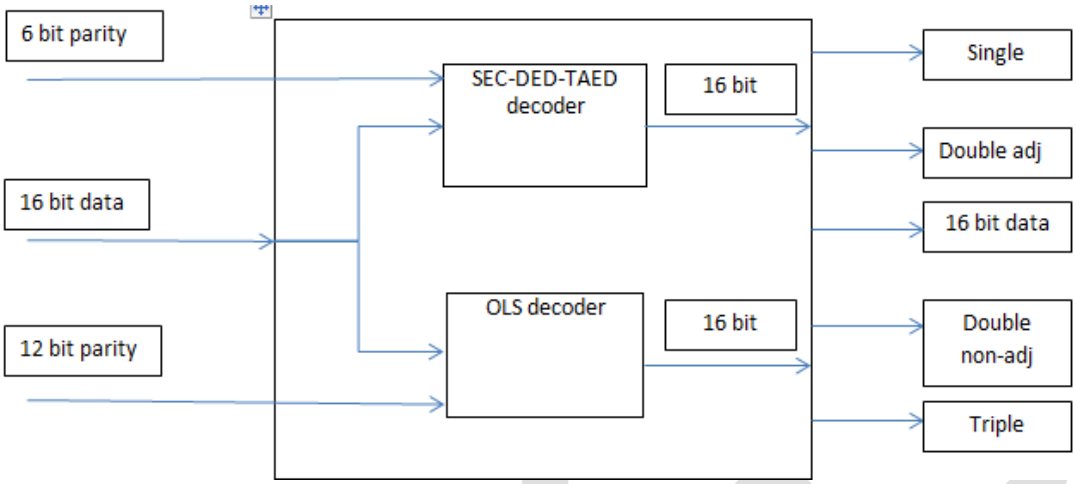

Fig 9: proposed decoder module

4. SIMULATION RESULTS

If there are 16 number of data after encoding there 34 number of code words. Result of encoder module given below:

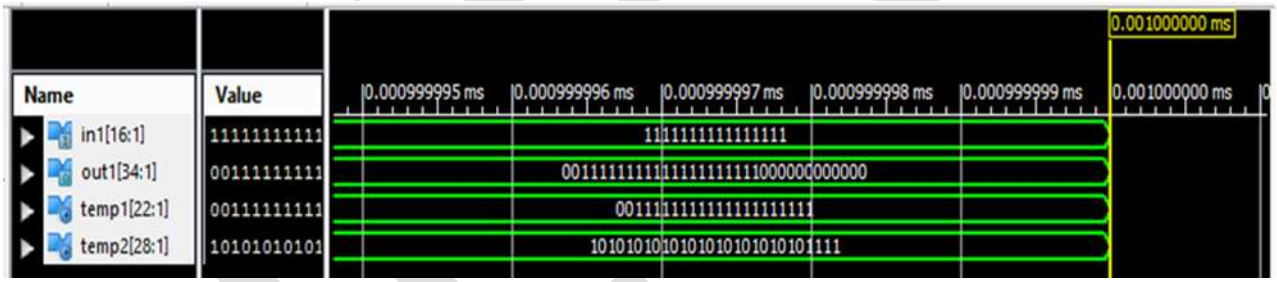

Fig.10. Result of encoder

If there is a single error, error in the third position of code word, correct the value and extract the data bits from code word and error indicators points to zero

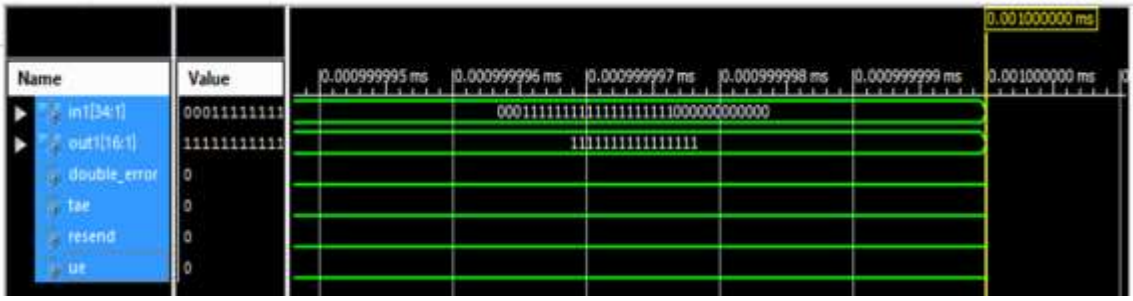

Fig.11. Result of decoder with single error

If there is a double adjacent error, error in fifth and sixth position of code word, correct the value and extract the data bits from code word and error indicators points to zero

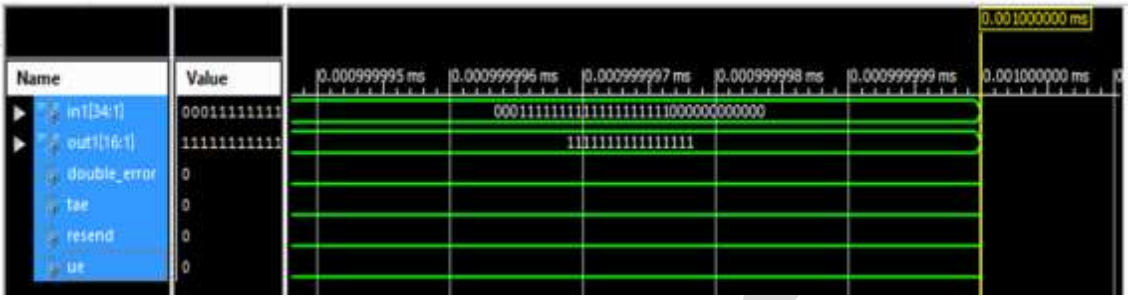

Fig.12. Result of decoder with double adjacent error

If there is a non-adjacent double error, error in third and nineteenth position of code word, cannot correct the its value and extracted the data bits from code word are un known but error indicators, that double-error and ue is points to one. Also there is an indicator that is resend, it is also high.

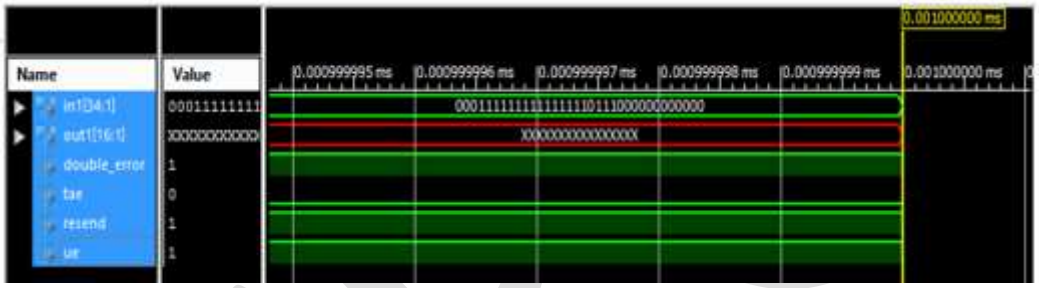

Fig.13. Result of decoder with double non-adjacent error

If there is an adjacent triple error, error in eighteenth, nineteenth and twentieth position of code word, cannot correct its value and extracted the data bits from code word are un known but error indicators, that is tae and ue points to one. Also there is an indicator that is resend, it is also high.

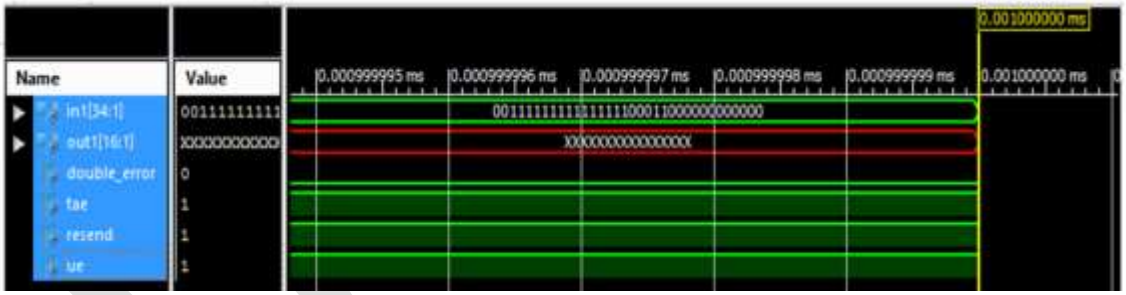

Fig.14. Result of decoder with triple adjacent error

5. CONCLUSION

There are different error correcting mechanisms are available, by compare and analyses them properly it is understand that each has its own advantages and limitation. The proposed mechanism which derived from the existing codes, single error correction-double error-detection –triple-adjacent error detection using hamming code and single error correction-double error detection –double adjacent error correction Codes Derived From Orthogonal Latin Square Codes will provide single and double adjacent error correction and double nonadjacent and triple error detection. These all combination is not provided any other codes. But here the number of parity bits increased compare to others so this code will use precision is greater than cost. The code is implemented in Spartan 3 FPGA trainer board. This project provides correction up to 2 errors that is single and adjacent double errors are corrected. And detection up to 3 errors that is detecting double non adjacent errors and triple adjacent errors. Radiation will affect closed memory locations mainly they are adjacent locations. So there is higher chance to occur double adjacent errors, triple adjacent errors etc. But this project provides correction up to double adjacent errors so the future works are to correct triple errors.

REFERENCES:

[1] S. Satoh, Y. Tosaka, and S. A. Wender, "Geometric effect of multiple-bit soft errors induced by cosmic ray neutrons on DRAM's," IEEE Electron Device Lett., vol. 21, no. 6, pp. 310–312, Jun. 2000.
[2] R. W. Hamming, "Error detecting and error correcting codes," Bell Syst.Tech. J., vol. 26, no. 2, pp. 147–160, Apr. 1950.
[3] R. C. Baumann, "Radiation-induced soft errors in advanced semiconductor technologies," IEEE Trans. Device Mater. Rel., vol. 5, no. 3, pp. 305–316, Sep. 2005.
[4] C. Argyrides and D. K. Pradhan, "Improved decoding algorithm for high reliable reed muller coding," in Proc. IEEE Int. Syst. On Chip Conf., Sep. 2007, pp. 95–98.
[5] C. L. Chen and M. Y. Hsiao, "Error-correcting codes for semiconductor memory applications: A state-of-the-art review," IBM J. Res. Develop.,vol. 28, no. 2, pp. 124–134, Mar. 1984.
[6] H. Lin, F. Yeh, I. Chen, and S. Kuo, "An efficient perfect algorithm for memory repair problems," in Proc. 19th IEEE Int. Symp. Defect Fault Toler. VLSI Syst., Oct. 10–13, 2004, pp. 306–313.
[7] S. Liu, P. Reviriego, and J. A. Maestro, "Efficient majority logic fault detection with difference-set codes for memory applications," IEEE Trans. Very Large Scale Integr. (VLSI) Syst., vol. 20, no. 1, pp. 148–156, Jan. 2012.
[8] P. Reviriego, M. Flanagan, and J. A. Maestro, "A (64,45) triple error correction code for memory applications," IEEE Trans. Device Mater. Rel., vol. 12, no. 1, pp. 101–106, Mar. 2012.
[9] E. Ibe, H. Taniguchi, Y. Yahagi, K. Shimbo, and T. Toba, "Impact of scaling on neutron-induced soft error in SRAMs from a 250 nm to a 22 nm design rule," IEEE Trans. Electron Devices, vol. 57, no. 7, pp. 1527–1538, Jul. 2010.
[10] C. Argyrides, D. K. Pradhan, and T. Kocak, "Matrix codes for reliable and cost efficient memory chips," IEEE Trans. Very Large Scale Integr. (VLSI) Syst., vol. 19, no. 3, pp. 420–428, Mar. 2011.
[11] M. Richter, K. Oberlaender, and M. Goessel, "New linear SEC-DED codes with reduced triple bit error miscorrection probability," in Proc. 14th IEEE IOLTS, Jul. 2008, pp. 37–42.
[12] C. A. Argyrides, P. Reviriego, D. K. Pradhan, and J. A. Maestro, "Matrix-based codes for adjacent error correction," IEEE Trans. Nucl. Sci., vol. 57, no. 4, pp. 2106–2111, Aug. 2010

International Journal of Engineering Research and General Science Volume 3, Issue 5, September-October, 2015
ISSN 2091-2730

Blind JPEG Steganalysis using Statistical Moment and Second Order Statistics

[1]Mrs. Swagota Bera, [2]Dr. Monisha Sharma

[1]Associate Professor, Dept. of Electronics & Tele. SSIET, Durg, India

[2]Professor, Dept. of Electronics & Tele. SSCET, Bhilai, India

Abstract - A blind steganalysis technique is developed to attack the JPEG steganographic schemes using DCT and optimized quantization. The proposed method exploits the correlations between block-DCT coefficients in both intra-block and inter-block sense and the Characteristic function of the test image is selected as features. The features are extracted from the BDCT JPEG 2-array. Support Vector Machine with cross-validation is implemented for the classification.The proposed scheme gives improved outcome in attacking Outguess, F5 and Jsteg stego images.

Key words: Steganography, Steganalysis, Cover image, Stego image, cover Image, Attack, Least Significant Bit (LSB), DCT,DWT

I.Introduction

Steganography is the science for secret data concealing. If the data hiding is done after applying DCT and quantization to the image pixel, comes under the transform domain steganography. Since JPEG (Joint Photographic Expert Group) format is the most dominant image format for image storage and exchange at this time, the JPEG steganography is attracting attention of the researcher .Several steganographic in transform domain for JPEG images has been developed. In this paper we focus on attacking three well known and most advanced steganographic methods, i.e., Outguess [1], F5 [2] and Jsteg [11]. Jsteg[11] is JPEG hiding technique in which the zero and one coefficient is not used for hiding. OutGuess [1] is a universal steganographic scheme that embeds hidden information into the redundant bits of data sources. It preserves the global histogram of BDCT. It adjust untouched coefficient to preserve the histogram. F5[2] works on JPEG by modifying the block-DCT coefficients to embed messages. This technique is based on straddling and matrix coding.Straddling scatter the message as uniformly distribution and matrix coding improves embedding efficiency. In reverse process detection of hidden data is known as steganalysis. Various approaches are discussed by the different researchers in the area of steganalysis. Broadly, there are two approaches to the problem of steganalysis, and one is to come up with a steganalysis method specific to a particular steganographic algorithm known as embedding algorithm based steganalysis techniques. The other technique is more general class of steganalysis techniques pioneered independently can be designed to work with any steganographic embedding algorithm, even an unknown algorithm. Such techniques have been called universal steganalysis techniques or blind steganalysis techniques.

Features of typical natural images which can get violated when an image undergoes some embedding process .Hence, designing a feature classification based universal steganalysis technique consists of tackling two independent problems. The first is to find and calculate features which are able to capture statistical changes introduced in the image after the embedding process. The second is coming up with a strong classification algorithm which is able to maximize the distinction captured by the features and achieve high classification accuracy. Prediction accuracy can be interpreted as the ability of the measure to detect the presence of a hidden message with minimum error on average. Similarly, prediction monotonicity signifies that the features should ideally be monotonic in their relationship to the embedded message size. This image features should be independent on the type and variety of images supplied to it .Embedding techniques affect different aspects of images.

Farid[3] proposed a universal steganalyzer based on image's high order statistics .Quadrature mirror filters are used to decompose the image into wavelet subbands and then the high order statistics are calculated for each high frequency subband. The second set of statistics is calculated for the errors in an optimal linear predictor of the coefficient magnitude.

In [6], Shi et al presented a universal steganalysis system. The statistical moments of characteristic functions of the image, its prediction-error image, and their discrete wavelet transform (DWT) subbands are selected as features. All of the low-low wavelet subbands are also used in their system. This steganalyzer can provide a better performance than [3] in general.

In [4], Fridrich has proposed a set of distinguishing features from the BDCT domain and spatial domain aiming at detecting information embedded in JPEG images.The statistics of the original image are estimated by decompressing the JPEG image followed by cropping the four rows and four columns on the boundary, and then recompressing the cropped image to JPEG format using the original quantization table. Designed specifically for detecting JPEG steganography. This scheme performs better than [3,5] in attacking JPEG steganography .

In [7], a new scheme is proposed, in which the inter-pixel and intra-pixel dependencies are used and a Markov chain model is adopted . The empirical transition matrix of a given test image is formed. The average transition probability matrix is calculated for the horizontal, vertical, main diagonal and minor diagonal difference JPEG 2-array[4].

The proposed technique is an improved steganalysis scheme to effectively attack the advanced JPEG steganographic methods. In our scheme, the correlations between block-DCT coefficients in inter-block sense and the statistical moments of characteristic functions of the test image is selected as features. The embedding process often decreases the dependencies of the intra and inter pixel values exiting in original cover data to some extent. These changes are captured by comparing these statistical parameters. The first and second order statistical parameters and statistical moment parameter is used as features which is calculated from JPEG 2-array. Finally we evaluate the proposed features with support vector machines (SVM) as classifier by conducting experiments over a diverse data set of 4000 JPEG images. The superior results have demonstrated the effectiveness of our proposed scheme.

The rest of this paper is organized as follows. Section II discusses the proposed scheme for feature generation. Classification performance results are presented in Section III and conclusions are drawn in Section IV.

II. Proposed Scheme for Feature Generation

Steganographic embedding causes disturbance on the smoothness, regularity, continuity, consistency and periodicity and therefore correlation among the cover image pixels get distorted. There exist inter and intra block correlation among the image pixel which maintain the above features of the image. Any statistical parameter which includes these relationship may become a good tool for the detection purpose.

First Order Features

The statistical features are calculated from the DCT coefficient .The simplest first order statistic of DCT coefficients is the histogram. Suppose , $d_k(i, j)$ is the DCT coefficient array with quantized value . Q(i, j), i, j = 1,…,8, k = 1, …, B represents the quantized value of the JPEG file .The symbol $d_k(i, j)$ denotes the (i, j)-th quantized DCT coefficient in the k-th block (there are total of B blocks). The global histogram of all 64k DCT coefficients will be denoted as H_r, where r = L, …, R, L = $\min_{k,i,j} d_k(i, j)$ and R = $\max_{k,i,j} d_k(i, j)$. Many of the steganographic programs preserves the global histogram but fails to preserve the histogram of the individual DCT modes.Thus, we add individual histograms for low frequency DCT modes to our set of functionals. For a fixed DCT mode (i, j), let

h_r^{ij} , r =L, …, R, denote the individual histogram of values $d_k(i, j)$, k = 1, …, B. We only use Histograms of low frequency DCT coefficients because histograms of coefficients from medium and higher frequencies are usually statistically unimportant due to the small number of non-zero coefficients. For a fixed coefficient value d, the dual histogram is an 8×8 matrix g_{ij}^d where δ(u,v)=1 if u=v and 0 otherwise. In words , g_{ij}^d is the number of how many times the value d occurs as the (i, j)-th DCT coefficient over all B blocks in the JPEG image. The dual histogram captures how a given coefficient value d is distributed among different DCT modes[4].

$$g_{ij}^d = \sum_{k=1}^{B} \delta\big(d, d_k(i,j)\big) \qquad (1)$$

Second Order Features

The natural images can exhibit higher-order correlations over distances larger than 8 pixels, individual DCT modes from neighboring blocks are not independent. Thus, the features that capture inter-block dependencies can be violated by the various steganographic algorithms. Let I_r and I_c denote the vectors of block indices while scanning the image "by rows" and "by columns", respectively. The first functional capturing inter-block de-pendency is the "variation" V defined as

$$V = \frac{\sum_{i,j=1}^{8}\sum_{k=1}^{|I_r|-1}\left|d_{I_{r(k)}}(i,j) - d_{I_{r(k+1)}}(i,j)\right| + \sum_{i,j=1}^{8}\sum_{k=1}^{|I_c|-1}\left|d_{I_{c(k)}}(i,j) - d_{I_{c(k+1)}}(i,j)\right|}{|I_r| + |I_c|} \qquad (2)$$

Most steganographic techniques in some sense add entropy to the array of quantized DCT coefficients and thus are more likely to increase the variation V than decrease. Embedding changes are also likely to increase the discontinuities along the 8×8 block boundaries. In fact, this property has proved very useful in steganalysis in the past . Thus, we include two blockiness measures B_α, α = 1, 2, to our set of functionals. The blockiness is calculated from the decompressed JPEG image and thus represents an "integral measure" of inter-block dependency over all DCT modes over the whole image:

$$B_\alpha = \frac{\sum_{i=1}^{[(M-1)/8]}\sum_{j=1}^{N}\left|x_{8i,j} - x_{8i+1,j}\right|^\alpha + \sum_{j=1}^{[(N-1)/8]}\sum_{i=1}^{M}\left|x_{i,8j} - x_{i,8j+1}\right|^\alpha}{N[(M-1)/8] + M[(N-1)/8]} \qquad (3)$$

In the expression above, M and N are image dimensions and x_{ij} are grayscale values of the decompressed JPEG image[4].

Statistical Moment Feature

The histogram of an image is essentially the probability mass function (pmf) of the image . Multiplying each component of the

pmf by a correspondingly shifted unit impulse results in the probability density function (pdf). The pf pdf is exchangeable. Thus, the pdf can be thought as the normalized version of a histogram. The characteristic function (CF) is the Fourier transform of the pdf .The statistical moment get varies for different JPEG 2-array coeffiecient . This property is desirable for steganalysis. The statistical moments of the CFs of an image is defined as follows.

$$\mathrm{Mn} = \frac{\sum_{j=1}^{\binom{N}{2}} f_j^n\,|H(f_i)|}{\sum_{j=1}^{\binom{N}{2}} |H(f_i)|} \qquad (4)$$

where *H(fi)* is the characteristic function component at frequency *fi*, *N* is the total number of points in the horizontal axis of the histogram. Note that we have purposely excluded the zero frequency component of the CF, i.e., *H(f0)*, from calculating the moments because it represents only the summation of all components in the discrete histogram. For an image, it is the total number of pixels. For a JPEG 2-array, it is the total number of the coefficients[6] .

III. Experiments

Image set

An image set consisting of 4000 JPEG images with quality factors ranging of 90 is used in our experimental work. Each image was cropped (central portion) to the dimension of either 640 X 480. Some sample images are given in Fig.(1).

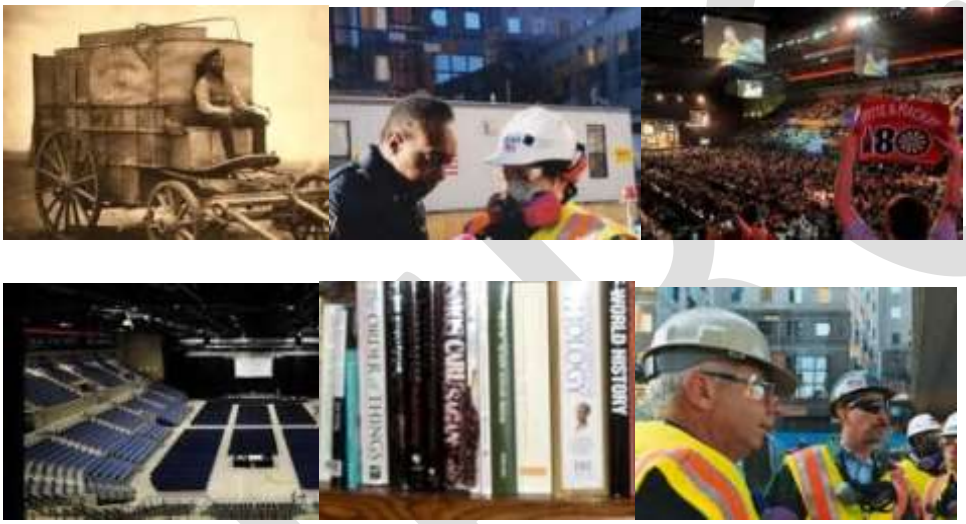

Fig.(1) Some Sample Images used in this Experimental Work

Stego images generation

On the basis of above approaches the steganalysis algorithm is designed using the MATLAB software and implemented to the stego image database , where database includes few different images of different size and formats encoded with JPEG Steganography technique Outguess, F5 and Jsteg of different capacities 0.05 , 0.1, 0.2 bpnc are used[1,2,11].

Experimental results for first and second order statistics

The images from the database has been used for both training and testing of the SVM classifier. The cross-validation technique is used in which 90 % of the data is used for training and rest 10 % is used for testing purpose. All the images in the dataset becomes the training and testing data simultaneously. Fridrich's first and second order[4] , shi's statistical moment[6] and proposed steganalyzer is

implemented for the detection of Jsteg[11], F5[2] and outguess[1] on randomly used 100 images .The classification result is shown in the Table 1. for the proposed scheme and the obtained result is compared with the existing one in Table 2.

Table 1. Performance of the SVM classifier for the proposed one where bpnc stand for bit per non zero coefficient, Sen. stands for sensitivity, Pre. stands for precision, Accu. stands for accuracy, Speci. stands for specifity and Detec. Relia. Stands for detection reliability.

Hiding Method	Bpnc.	Sen.	Pre.	Accu.	Speci.	Detec. Relia.
Outguess	0.05	0.657	0.442	65.5629	0.66	0.014
	0.1	0.656	0.444	65.667	0.66	0.02
	0.2	0.663	0.455	66.333	0.67	0.02
F5	0.05	0.666	0.443	66.5541	0.67	0
	0.1	0.669	0.447	66.8896	0.67	0
	0.2	0.679	0.783	67.893	0.68	0.02
Jsteg	0.05	0.661	0.456	66.1017	0.67	0.024
	0.1	0.674	0.459	67.4497	0.68	0.004
	0.2	0.695	0.483	69.5205	0.70	0

Table 2. Comparision of the Accuracy of the proposed detection technique with the reference. where bpnc stand for bit per non zero coefficient

Hiding Method	bpnc	Fridrich's	Shie et al's	Proposed
Outguess	0.05	64.90	58.00	65.5629
	0.1	65.33	58.61	65.667
	0.2	65.67	60.00	66.333
F5	0.05	66.81	57.19	66.5541

	0.1	66.89	57.43	66.8896
	0.2	67.56	66.89	67.893
Jsteg	0.05	63.73	60.00	66.1017
	0.1	63.76	60.07	67.4497
	0.2	65.75	62.67	69.5205

IV. Discussion and Conclusions

(1) In [6] the statistical moment of the test image and their wavelet subbands are used as features and in [4] the first order and second order statistical parameters are calculated from the JPEG-2 array of the test image. Since JPEG which use DCT and quantization is widely used for the data restoration and its transmission, so in the proposed scheme the statistical moment is calculated form the JPEG-2 array of the image.For the feature extraction the MATLAB software.

(2) The obtained features are used for the SVM classification with the help of weka data mining software. The cross-validation is selected for the better result.

(3) For developing Jsteg [11] stego image set , the optimized quantization table is used on the Block DCT coefficient for the implementation of conventional jsteg.

(4) For F5, Jsteg and Ouguess hiding technique , the detection accuracy is higher than [6] but slightly higher than [4].

(5) Among all the four the value is high for Jsteg[11] for the proposed one since it is an conventional one which does not restore the global histogram , but other two outguess[1] and F5[2] have the global restoration property.

REFERENCES:

[1] http://www.outguess.org/

[2] http://wwwrn.inf.tu-dresden.de/~westfeld/f5.html.

[3] Siwei Lyu "Detecting Hidden Messages using Higher-Order Statistics nd Support Vector Machines" Information Hiding, Springer,

Pg. No. 340–354, 2003.

[4] Jessica Fridrich "Feature Based Steganalysis for JPEG Images and its Implications For Future Design of Steganographic Schemes"

Information Hiding, Springer, Pg. No. 67–81, 2005.

[5] Farid . Hany. and Siwei Lyu " Steganalysis using Higher Order Image Statistics" IEEE Trasactions on Information Forensics and

Security. Vol. No.1, Issue No.1, Pg. No. 111–119, 2006.

[6] Chunhua Chen, Yun Q. Shi , Wen Chen and Guorong Xuan "Statistical Moments Based Universal Steganalysis using Jpeg 2-D Array

and 2-D Characteristic Function" IEEE international conference on image processing, Pg. No.105-108, 2006.

[7] Yun Q. Shi, Chunhua Chen and Wen Chen " A Markov Process Based Approach to Effective Attacking JPEG Steganography"

Lecture Notes in Computer Science , Information Hiding, Springer, pg. No. 249–264, 2007.

[8] Dongdong Fu, Yun Q. Shi, Dekun Zou and Guorong Xuan " JPEG Steganalysis using Empirical Transition Matrix in Block DCT

Domain" IEEE Workshop on Multimedia Signal Processing, Pg. No. 310–313, 2007.

[9] Chunhua Chen and Yun Q. Shi "JPEG Image Steganalysis Utilizing Both Intrablock and Interblock Correlations" IEEE International

Symposium on in Circuits and Systems, Pg. No. 3029- 3032, 2008.

[10] Mahendra Kumar "Steganography and Steganalysis of Joint Picture Expert Group (JPEG) Images " Ph.D. Thesis, University of

Florida, 2011.

[11] Swagota Bera and Monisha Sharm"Frequency Domain Steganography System using Modified Quantization Table" International

Journal of Advanced and Innovative Research,Vol. No.1, Issue No.1, Pg. No. 193-196, 2012.

[12] Swagota Bera and Monisha Sharma " Development and Analysis of Stego Image Using Discrete Wavelet Transform" International Journal of Science & Research ,Vol. No.2, Issue No.1, Pg. No. 142-148, 2013

International Journal of Engineering Research and General Science Volume 3, Issue 5, September-October, 2015
ISSN 2091-2730

Neural Network Based Model for Forecasting Reservoir Storage for Hydropower Dam Operation

Taofeeq Sholagberu ABDULKADIR[1*], Adebayo Wahab SALAMI[2], Bolaji Fatai SULE[3] - Josiah A ADEYEMO[4] -

[1, 2] Department of Civil Engineering, University of Ilorin, Ilorin, Nigeria
[3]National Centre for Hydropower Research and Development, University of Ilorin, Nigeria
[4]Department of Civil Engineering and Surveying, Durban University of Technology, Durban, South Africa

[1*] Corresponding author: abdulkadir.ts@unilorin.edu.ng
[2]salami_wahab@unilorin.edu.ng, [3] bolajifsule@yahoo.com, [4] josiaha@dut.ac.za,

Key words: Neural Network, Forecasting, Reservoir operation, reservoir storage, hydrological variables.

Abstract- Reservoirs are constructed to accommodate unregulated excess random water flows in the periods of high flows for use in low-flow periods. In most cases, these reservoirs are meant to perform multiple objectives. As a result of high variability of annual rainfall and conflicting demand for water resources, the study of reservoir operation requires accurate forecasting of available water in the reservoir, which helps in planning and management of multi-objective reservoirs. This paper therefore, presents the operation of hydropower reservoirs in Nigeria by forecasting their future storage using Neural Network (NN) model. The networks were created and trained with monthly historical data such as reservoir inflow, turbine releases, reservoir storage and evaporation losses for Jebba, Kainji and Shiroro hydropower dams. The trained networks yielded 95% & 97% of goodness of fit respectively for training and testing of data at Jebba, 69% &75% at Kainji and 98% & 97% at Shiroro. The correlation coefficients between the forecast and observed reservoir storage of 0.64, 0.79 and 0.84 were obtained for Jebba, Kainji and Shiroro reservoirs respectively. The values of correlation coefficient suggested that the model fairly fit the variables and can subsequently be used for prediction of reservoir storage for operational performance.

1. Introduction

Reservoirs are built to accommodate unregulated excess random flows. This excess water is stored in reservoir in the periods of high inflows for use in low-flow periods. In the storage process, unregulated inflows are transformed by the reservoir into three kinds of outflows as highlighted by Campos (2010): the yield or regulated outflows, to supply societal water demand; evaporation losses from the reservoir surface; and the spillage. At the planning stage of a dam development, optimization modeling is very important in determining the optimum size of the reservoir. This procedure is called the operation study of a dam. The variables required for this study are inflow, evaporation losses and the amount of water planned to be taken from the reservoir (demand or release). This demand may be used for domestic, industrial, irrigation or hydropower generation purposes. This implies that improvement in reservoir operation can lead to large benefits (Bosona and Gebresenbet, 2010). Different operational models have been developed and applied to evaluate alternative plans for solving water management problems. The selection of an appropriate model for the derivation of reservoir operating guide curves is difficult and there is need for further improvement (Jothiprakash and Ganesan, 2006). The choice of techniques usually depends on the reservoir specific system characteristics, data availability, the objectives specified and the constraints imposed (Bosona and Gebresenbet, 2010). Salami and Sule (2012) developed optimal water management model for hydropower (HP) system on River Niger in Nigeria. The analysis found that an optimal energy of 5995.60 GWH can be generated, which is about 41% higher than the average energy generation of 4261.12 GWH obtained from the historical records at the power plants. The study also found that flood wall with the crown level at 76.50m above mean sea level (a.m.s.l) would be sufficient to prevent flooding downstream of Jebba dam. Abdulkadir *et al.* (2013) modeled reservoir variables of two hydropower dams along the River Niger (Kainji and Jebba dams) in Nigeria for energy generation using multilayer perceptron neural network. The reservoir variables considered were inflow, storage, reservoir elevation, turbine release, net generating head, plant use coefficient, tail race level and evaporation losses. It was found that the networks are reliable for modeling energy generation as a function of reservoir variables for future energy prediction.

The operation of the three major HP reservoirs namely Jebba, Kainji and Shiroro in Nigeria was studied by forecasting their future storage from historical data of reservoir inflow, outflow (release) and the evaporation loses. The multi-objective nature of these reservoirs anchored majorly on the volume of water (reservoir storage) present at a particular period of time (Abdulkadir *et al.*, 2012a), hence through the adequate forecasting, the following can be achieved;

- Optimization of reservoir volume for abstracting sufficient amount of water for hydropower generation, domestic and industrial water uses, irrigation, etc
- Control of flood of the downstream reaches of the three hydropower dams that might affect infrastructural developments and agricultural activities.
- Evaluation of reservoir capacities of three hydropower dams.

Recently, data driven models are emerging. The data serve as source of information for the development of model and to build rules to simulate the operation of hydrological systems. Thus, artificial intelligence tools such as genetic algorithms, artificial neural network and fuzzy logic are increasingly used as soft computing techniques to solve modelling issues. The main advantage of these techniques lies in handling noisy data, addressing non-linear and dynamic systems (Swingler, 1996). These tools are equally useful when it is difficult to explain the physical relationships that exist within the data as well as the ability to self-train (Ogwueleka and Ogwueleka, 2009; Cigizoglu and Kilinc, 2005). Of recent, there is a significant advancement in the application of Artificial Neural Network (ANN) in modelling, especially in the field of hydrology and hydraulic engineering (Abdulkadir *et al.,* 2013). In this study, the goal is to develop an ANN model to predict the future reservoir storage for the three hydropower dams in Nigeria.

2 Materials and Method

2.1 Description of Study Area

River Niger is the third longest river in Africa after the Nile and Congo/Zaire Rivers. It has a total length of about 4200 km with a theoretical area of about 2 million sq km. This area has reduced to an active catchment area of just about 1,500,000 sq km thus excluding Algeria which is among the 10 countries covered by the Niger River basin. Other countries are Benin, Burkina Faso, Cameroon, Chad, Guinea, Ivory Coast, Mali, Niger and Nigeria. It includes two deltas: an inland delta in central Mali and a coastal delta along the Gulf of Guinea. The coastal delta is the largest in Africa, spanning nearly 190 km (120 mi). Niger River is usually subdivided into upper, the middle and the lower Niger, along with its tributaries forms the most important water resources of the Sahel region of West Africa. A series of dams have been constructed in the Niger basin for irrigation, domestic and industrial water supply and hydroelectric power generation. Notable among these dams especially in lower Niger are the Kainji and Jebba while Shiroro HP dam is located along River Kaduna which is one of the tributaries of River Niger. The study area is however restricted to the Jebba, Kainji and Shiroro hydropower dams in which Jebba dam is located about 100km downstream of Kainji and on latitude $9^{0}06^{1}$N and longitude $4^{0}50^{1}$E. Shiroro dam on latitude $9^{0}58^{1}$N and longitude $6^{0}5^{1}$E located along River Kaduna originated from North West of Jos and flow through Kaduna and Shiroro George and discharged into River Niger. Fig. 1.1 is the map of Nigeria showing hydrological areas with hydropower location outlined while Fig. 1.2 shows location of the three Hydropower dams with floodplain hatched. The important characteristics for the three reservoirs are presented in Tab. 1. The flow of River Niger downstream of Jebba Dam is governed by the operations of the Kanji and Jebba hydroelectric schemes and runoff from the catchments (Sule *et al.,* 2009). Reservoir releases from Kainji HP dam constitute the major inflow into Jebba HP dam since it lies directly under it.

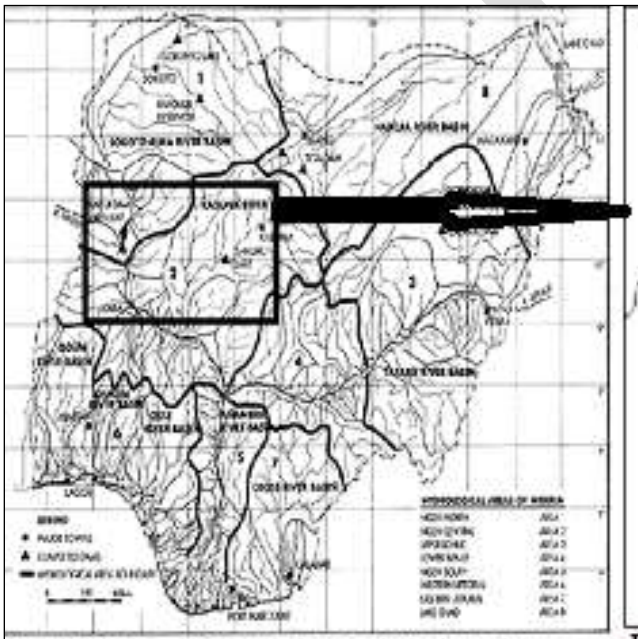

Figure 1.1 Map of Nigeria showing hydrological areas with hydropower location outlined

Figure 1.2 Location of the three hydropower dams with flood plain hatched

Tab. 1: *Basic Data of the Hydropower Reservoirs in Nigeria*

Parameters	Kainji	Jebba	Shiroro
First year of operation	1968	1984	1990
Installed capacity (MW)	760	560	600
Design power plant factor	0.86	0.70	0.8
No. of generators	8	6	4

Reservoir surface area (km^2)	1,250	270	312
Reservoir flood storage capacity (Mm^3)	15,000	4,000	7,000
Reservoir flood level (m)	143.50	103.55	385.00
Maximum operating reservoir elevation (m.a.s.l)	141.83	103.00	382.00
Minimum operating reservoir elevation (m.a.s.l)	132.00	99.00	342.00
Maximum storage (Mm^3)(active storage capacity)	12,000	3,880	6,500

Source: Power Holding Company of Nigeria (PHCN), 2012

2.2 Artificial Neural Network

Artificial neural networks (ANN) are black box models used for forecasting and estimating purposes in many different areas of the science and engineering (Abdulkadir *et al.*, 2013). ANN in the context of statistical analysis is an alternative to or in addition to multiple regressions which is an information processing paradigm that is inspired by the way biological nervous systems, such as the brain, process information (Andy *et al.*, 2004; Hung *et al.*, 2008; Abdulkadir *et al.*, 2012b). The key element of this paradigm is the novel structure of the information processing system. Its computing system composed of a large number of highly interconnected processing elements (neurons) working together to solve a specific problem. ANNs, like people, learn by example (Juan and Julian, 2006). An ANN model is designed for specific applications which include data classification through a learning process, extracting patterns and detecting trends that are too complex to be noticed and deriving meanings from complicated or imprecise data. Learning in biological systems involves adjustment to the synaptic connections that exist between the neurons (Richard, 1987). The same occurs in ANN in which neurons (units) receive inputs from single or multiple sources and produces output in accordance with a predetermined nonlinear function called activation function. A neural network model is created by interconnecting many of these neurons in a known configuration. Haykin (1994) identified the following areas of application of ANN model; pattern matching (adaptive learning), optimization, data compression, self-organization and function optimization. There have been a number of reported hydrological and hydraulic studies in which ANN model have been used to address. Dogan *et al.* (2009) applied ANN for forecasting of daily stream-flow, Modarres (2008) used ANN to model rainfall-runoff process and rainfall forecasting model was done using ANN by Kin *et al.* (2009) and Abdulkadir *et al.* (2012b). Omid and saeed (2005) also worked on evaluation of ANN in optimization models of hydropower reservoir operation.

The three essential features of a neural network are network topology, the computational functions of its elements and the training of the network. Network topology is the number and organization of the computing units, the type of connections between neurons and the direction of flow of information in the network. The number of nodes in the input layer is the number of independent variables while that of output nodes corresponds to the number of variables to be predicted. A simple ANN model is characterized by a network of three layers of processing units: p-input nodes, q-hidden nodes and r-Output nodes which are connected to one and other as shown in Fig. 2.

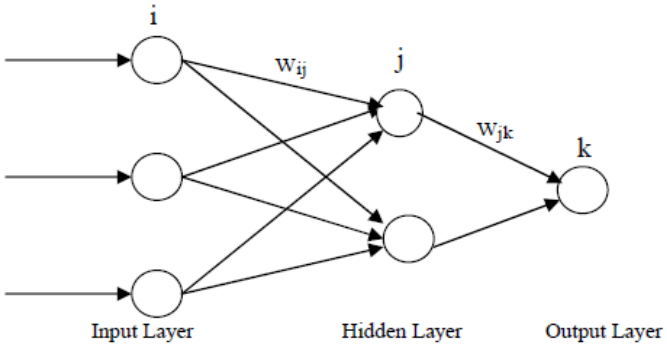

Fig. 2: *Typical Neural Network Computational Structure*

The number of hidden layers and nodes used within the hidden layer vary according to the complexity of the task the network must perform. Kristen and Lee (2003) observed that there is no rigorous rule that determine the optimum configuration of a neural network to solve a specific problem. The computational function is another feature of the neural network which consists of the operations of the individual neurons and the way they are connected. The first layer ***i***, (independent variables) that receives input information, is called an input layer. The last layer ***k***, (dependent variables) which produces output information, is called an output layer. There exists between the output and input layers the hidden layer ***j***. There can be one or more hidden layers with many nodes. Information is transmitted through the connections between nodes in different layers with the aid of connection weights w_{ij} and w_{jk}. Somvanshi *et al.* (2006) recommended the use of one hidden layer in preliminary studies. Having more than one hidden layers will definitely increase the number of parameters to be estimated. This may slow down the training process without reasonably improving the efficiency of the network.

Various ANN models approaches have been proposed for modeling since its inception. Multilayer perceptron (MLP) otherwise known as feed forward back propagation (FFBP), radial basis function (RBF), time-delay neural network (TDNN) and partial

recurrent neural network (PRNN). The first two are the most widely used model. MLP maintains high level of research interest due to its ability to map any function to arbitrary degree of accuracy (Modarres, 2008) and amount to 80% of practical applications in field of engineering and science (Kin *et al.*, 2009). It is composed of multiple simple processing nodes, or neurons, assembled in several different layers. Each node computes a linear combination of weighted inputs (including a bias terms) from the links feeding into it (Ricardo and Jean, 1999). The summed value (net input) is transformed using a non-linear function called log-sigmold function as shown in Equation 1. This function maps any input to a finite output range usually between 0 and 1 or -1 and 1. Then, the output obtained serves as an input to other nodes. In modeling of hydrological variables, a set of variables is divided into three prior to the model building: the training, testing and validation sets. A set is used for training and the other is used to evaluate the accuracy of the model derived from the training set. In validation phase, the model output is compared with the actual output using statistical measurements such as root-mean-square error (RMSE), mean square error (MSE), Mean Absolute Percent Error (MAPE) and the coefficient of correlation (CORR) to examine the model performance (Somvanshi *et al.*, 2006; Khaing and Thinn, 2008; Hung *et al.*, 2008; Karim, 2009).

$$\boldsymbol{y_{i=}} \frac{\mathbf{1}}{\mathbf{1+}\, \boldsymbol{e^{-x_i}}} \qquad (1)$$

Where y_i = model output, x_i = model input, e = exponential function

2.3 ANN training algorithms

The training of the network is aimed at determining the main control parameters of ANN called weights. The processes of estimating these parameters are known as training where optimal connection weights are determined by minimizing an objective function (Somvanshi *et al.*, 2006). There are basically two types of training mechanisms: supervised and unsupervised training. A supervised training algorithm also known as back propagation training algorithms requires an external teacher to guide the training process. The goal of supervised training is to minimize the error at the output layer by searching for a set of connection strengths that cause the ANN to produce outputs that are equal to or closer to the targets (Shiru and McCann, 2011 and Karim, 2009). A supervised training mechanism is normally adopted in most of the engineering applications. An unsupervised training algorithm called self-organizing neural network is used when the training set lacks target output values (Shiru and McCann, 2011). The most famous self-organizing neural network is the Kohonen's Self-Organizing Map (SOM) classifier, which divides the input-output space into a desired number of classes (Karim, 2009). In supervised training, the network compares the generated values with the target values. The error resulting from the comparison is propagated backward through the network, and the weights are adjusted to minimize this error. The procedure continues until network generates value of error closer to the validation value. Thus, the performance criterion is the minimization of square error and this is expressed in Equation 2.

$$\boldsymbol{error} = \sum_{\boldsymbol{p,i}} (\boldsymbol{t_{ip}} - \boldsymbol{y_{ip}})^{\mathbf{2}} \qquad (2)$$

Where i indexes unit of output, p indexes the input – output pairs to be learned. t_{ip} = desired output, y_{ip} = learned (network) output.

The standard training algorithm used in most hydrological applications is the back-propagation algorithm (Abdulkadir *et al.*, 2012a). The full mathematical derivation of this can be found in several neural networks textbooks. The main steps involved in the training are as illustrated below:

(i) initialize network weight value, usually using small numbers obtained from random number generator;
(ii) carry out forward propagation of the first input vector through the whole network. i.e. input signals multiplied by corresponding synaptic weights and then summed at each node. This is further transformed by an activation function in Equation 1 and sent to the output node;
(iii) compute the error by comparing the model output with the target (observed) data;
(iv) back-propagate the error information through the network;
(v) update the weights and
(vi) repeat the previous steps for several iterations until the error is within an acceptable range.

2.4 Statistical Analysis of hydropower Reservoir Variables

Total monthly HP reservoir inflow (Mm^3), turbine release (Mm^3), evaporation losses (Mm^3) and storage (Mm^3) data were obtained from PHCN for a period twenty nine years (1984–2012) for Jebba reservoir, forty three years (1970-2012) for Kainji reservoir and twenty three years (1990– 2012) for Shiroro reservoir. The number of total monthly data for each of the variables for Jebba, Kainji and Shiroro HP reservoirs are 348, 516 and 276 respectively. Summary of the statistical analysis of the data such as mean, median, standard deviation, minimum, maximum and skewness is presented in Tab. 2.

Tab. 2: *Statistical Analysis of the HP Reservoir Variables*

Reservoir Inflow (Mm^3)			Turbine Release (Mm^3)			Evaporation Loss (Mm^3)			Reservoir Storage (Mm^3)		
Jebba	Kainji	Shiroro	Jebba	Kainji	Shiroro	Jebba	Kainji	Shiroro	Jebba	Kainji	Shiroro

Mean	2711.1	2504.4	289.9	2612.6	1882.0	274.1	18.7	141.5	374.9	3604.4	8063.3	11.2
Min	1012.4	24.4	9.9	956.5	513.9	20.8	10.0	26.8	355.3	2774.0	1579.0	3.0
Max	9738.7	7944.5	1752.5	8680.7	3871.2	792.5	30.0	297.3	423.8	3911.0	12173.0	25.2
St dev	1330.7	1887.8	364.6	1001.3	580.1	111.9	5.0	65.8	14.2	167.7	2881.7	5.3
Skew	2.6	0.3	1.5	2.0	0.4	0.7	0.6	0.3	1.9	-0.6	-0.2	0.4

2.5 Application of NN Model to HP Reservoir Variables

Series of computer programs have been written by many researchers to ease the applicability of ANN in modeling. Some are Neuro-solution, Alyuda Forecaster XL, EasyNN Plus, NueNet Plus, MATLAB toolbox, SPSS, etc. In applying ANN model, the first step is the preparation of the training and testing. Having known the inter-dependence of the parameters, then, the structure of an ANN model will be constructed. This defines the number of hidden layers and neurons in each layer and selection of transformation function's type. The historic storage volume of reservoir is a discrete variable (i.e. decision variable) and inflow, evaporation losses and the optimum release of the reservoir are state variables and formed the input data of the model.

The HP reservoir data for each of the stations were partitioned into three (3) sets: training, validation and testing set. The training set was used to train the network whereas the validation set was used to monitor or test the network performance at regular stages during the training. The training stopped when the errors on the validation set reached the minimum. Finally, the performance of the network was evaluated on the test data set which had not been involved in the training process. In this study, the neural network was trained in Alyuda forecaster XL with 342, 510 and 270 data of each of inflow, turbine release, and evaporation losses respectively for Jebba, Kainji and Shiroro reservoirs being the independent parameters (as input layers) and reservoir storage were used, being the dependent variable (as output layer). The weights of input layer and hidden layer node are automatically adjusted by checking the training and testing stage performances of neural networks. The coefficient of correlation and the mean square error are the performance criterion for the testing stage. In testing the performance of these models after the training, set of six (6) data of reservoir inflow, turbine release and evaporation losses for each of the locations that were not involved in the training of the network were used to forecast the future reservoir storage. The network's forecasted result for reservoir storage values were then compared with the measured storage values that were not involved at all in the training and the result is presented in Tab. 3.

Tab. 3: *Comparison of ANN Forecasted with Measured Reservoir Storage (Mm^3)*

S/No	Actual reservoir storage			ANN forecasted reservoir storage			Absolute Error			% Error		
	Jebba	Kainji	Shiroro	Jebba	Kainji	Shiroro	Jebba	Kainji	Shiroro	Jebba	Kainji	Shiroro
1	3418	4986.4	355.4	3500.6	5187.9	339.5	82.6	201.5	15.9	2.4	4	4.49
2	3623	4251.2	416	3610.4	4395.9	399.9	12.6	144.7	16.1	0.4	3.4	3.88
3	3585	6951.6	378.6	3651.3	7398.4	398.6	66.3	446.8	-20.0	1.9	6.4	-5.28
4	3266	8342.8	381.8	3357.5	8747.8	357.6	91.5	405	24.2	2.8	4.9	6.35
5	3615	8628.6	381.8	3577.5	9089.8	366.3	37.5	461.2	15.5	1	5.3	4.06
6	3653	9854.1	379.5	3714	10446.1	369.4	61	592	10.1	1.6	6	2.66

The relationship between the ANN forecasted and actual reservoir storage for Jebba, Kainji and Shiroro reservoirs for all the data involved in the training exercise are presented in Fig. 3, 4 and 5 respectively.

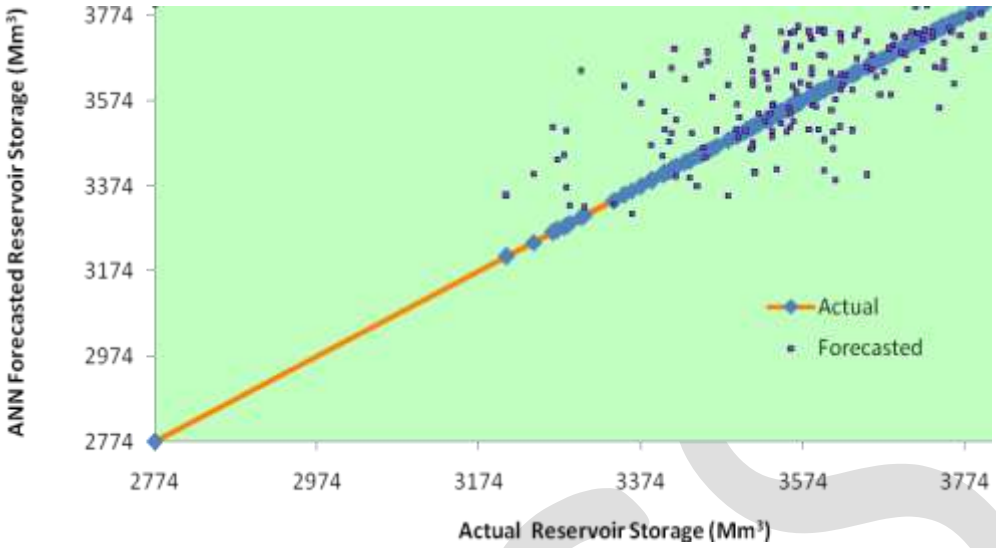

Fig. 3: *ANN Forecasted and Actual Reservoir Storage for Jebba HP dam*

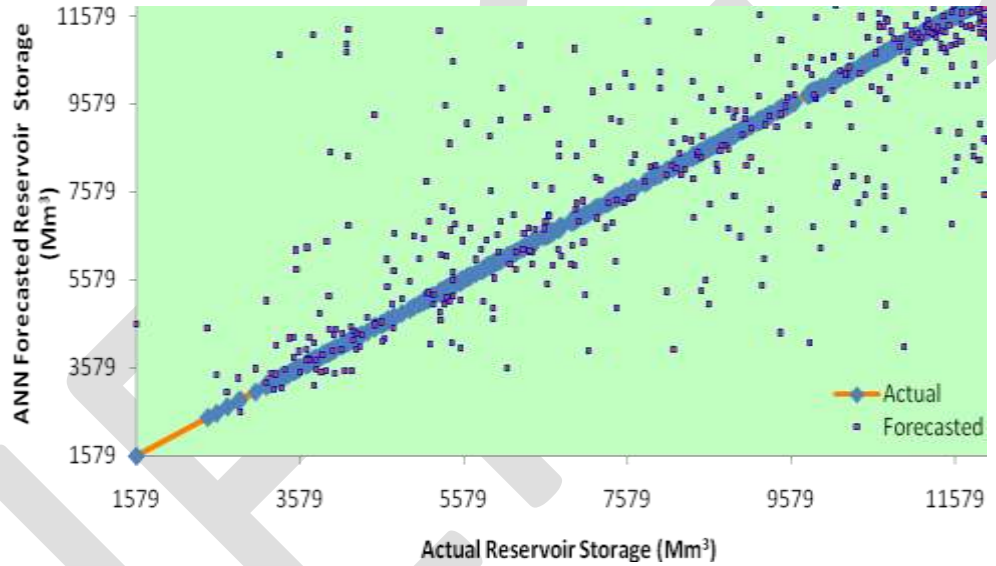

Fig. 4: *ANN Forecast and Actual Reservoir Storage for Kainji HP dam*

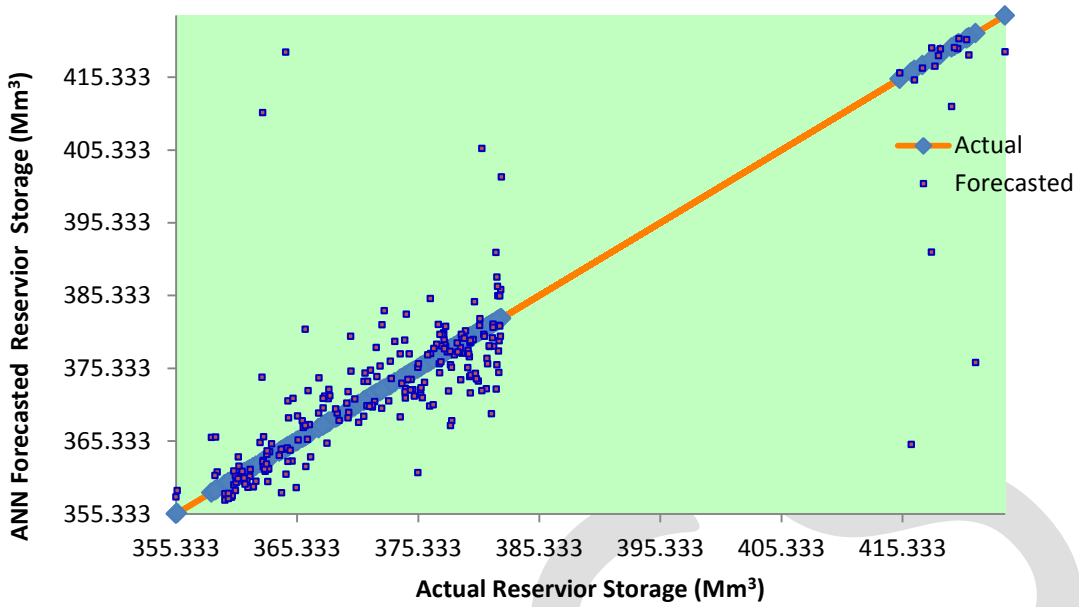

Fig. 5: *ANN Forecast and Actual Reservoir Storage for Shiroro HP dam*

3. Results and Discussion

The historical monthly data such as inflow, turbine releases, evaporation loss and reservoir storage at Jebba, Kainji and Shiroro hydropower reservoirs were statistically analyzed. Statistical parameters such as mean, median, standard deviation, minimum, maximum and skewness were estimated for each variable as presented in Tab. 2. Application of NN model to Jebba hydropower reservoir inflow, turbine releases, evaporation losses and storage generated a network structure (Number of neurons in input, hidden and output layers) of 3:15:1. This topology having one hidden layer with 15 neurons produced 95% and 97% of good forecast of reservoir storage in the training and testing set respectively. Also the ANN model for Kainji reservoir generated a network structure of 3:22:1 with 69% and 75% of good forecast in the training and testing set respectively, while for Shiroro reservoir network structure was 3:11:1 with 98% and 97% of good forecast for training and testing set respectively. The correlation coefficients (CORR) between the forecast and observed storage obtained for Jebba, Kainji and Shiroro HP reservoirs were 0.64, 0.79 and 0.84 respectively. The percentage errors of estimate between ANN forecasted and actual reservoir storage data not used in the training exercise showed that the forecasts done were closer with a maximum error of 2.8% for Jebba, 6.4% for Kainji and Shiroro HP reservoirs. Literatures had shown that CORR and MAPE are some of the tools to examine the model performance (Somvanshi *et al.*, 2006; Khaing and Thinn, 2008; Hung *et al.*, 2008; Karim, 2009; Abdulkadir *et al*, 2012a,b). The closeness of the values of CORR to one and MAPE to zero, the better the results. This showed that the networks are fit to be used for subsequent prediction of reservoir storage.

4. Conclusion and Recommendation

Operation of Jebba, Kainji and Shiroro hydropower reservoirs by forecasting their respective future storages would assists in planning and optimum management of multi-objective uses of the reservoirs. Having predicted future storage values, an operating policy can be formulated as regards to the quantity of water that will be available for domestic and industrial uses, irrigation and hydropower generation. Neural network analysis during training yielded 95%, 69% and 98% of good forecasts for Jebba, Kainji and Shiroro HP reservoirs, while during testing it yielded 97%, 75% and 97% respectively. Also, the respective correlation coefficient between forecast and observed storage are 0.64, 0.79 and 0.84. This showed that the networks are reliable for forecasting. It can therefore be concluded that forecasting using ANN is very versatile tool in reservoir management modeling.

It is recommended that other NN modeling approaches be employed and further studies are required to forecast the discharge/release from the HP reservoirs in order to model the flood regime and consequently control the effect on infrastructural developments and agricultural activities in the downstream reaches of the three hydropower reservoirs.

REFERENCES:

Abdulkadir, T. S. - Sule, B. F. - Salami, A. W. (2012a) *Application of Artificial Neural Network Model to the Management of Hydropower Reservoirs along River Niger, Nigeria.* Annals of Faculty Engineering, Hunedoara–International Journal of Engineering, Tome X –FASCICULE 1(ISSN 1584-2673), pp. 419-424. Available online at http://annals.fih.upt.ro/pdf-full/2012/ANNALS-201.

Abdulkadir, T. S. - Salami, A. W. - Kareem, A. G. (2012b) *Artificial Neural Network Modeling of Rainfall in Ilorin, Kwara State, Nigeria.* USEP, Journal of Research Information in Civil Engineering, Vol. 9 No 1, pp. 108–120. Available online at http://www.useprice.webs.com

Abdulkadir, T. S. - Salami, A. W. - Anwar, A. R. - Kareem, A. G. (2013) *Modeling of Hydropower Reservoir Variables for Energy Generation: Neural Network Approach.* Ethiopian Journal of Environmental Studies and Management Vol. 6, pp. 310 – 316. Available online at http://dx.doi.org/10.4314/ejesm.v6i3.12

Andy P. D. - Peter, L. M. - Goethals, W. G. - Niels, D. P. (2004) *Optimization of Artificial Neural Network Model Design for Prediction of Macro-invertebrates in the Zwalm River Basin.* Ecological Modelling (174), pp. 161–173.

Bosona, T. G. - Gebresenbet, G. (2010) *Modelling Hydropower Plant System to Improve its Reservoir Operation.* International Journal of Water Resources and Environmental Engineering
Vol. 2(4), pp. 87-94, http://www.academicjournals.org/IJWREE.

Campos, J. N. B. (2010) *Modelling the Yield–Evaporation–Spill in the Reservoir Storage Process: The Regulation Triangle Diagram.* Water Resource Manage 24, pp. 3487–3511.

Cigizoglu, K. - Kilinc, I. (2005) *Reservoir Management Using Artificial Neural Network*. 14th Reg. Directorate of DSI, Turkey.

Dogan, E. - Isik, S. - Toluk, T. - Sandalci, M. (2009) *Daily Stream-flow Forecasting Using Artificial Neural Networks*. Journal of River Basin Flood Management, pp. 448 – 459

Haykin, S. (1994) *Neural Networks: A comprehensive Foundation*. Macmillan College Publishing Company, Inc., New York, USA

Hung, N. Q. - Babel, M. S. - Weesakul, S. - Tripathi, N. K. (2008) *An Artificial Neural Network Model for Rainfall Forecasting in Bangkok, Thailand.* Hydrol. Earth Syst. Sci. Discuss., 5, pp. 183 –218

Jothiprakash, V. - Ganesan, S. (2006) *Single Reservoir Operating Policies Using Genetic Algorithm*. Water Resources Management, 20: pp. 917- 929.

Juan, R. R. - Julian, D. (2006) *Artificial Neural Network in Real-Life Applications*. Idea Group Publishing, Singapore.

Karim, S. (2009) *Rainfall-Runoff Prediction Based on Artificial Neural Network (A Case Study: Jarahi Watershed).* American-Eurasian J. Agric. & Environ. Sci., 5 (6), pp. 856-865.

Khaing, W. M. - Thinn T. N. (2008) *Optimum Neural Network Architecture for Precipitation Prediction of Myanmar*. World Academy of Science, Engineering and Technology, 48, pp. 130 – 134

Kin, C. L. - James - E. B. - Ashish, S. (2009) *An Application of Neural Networks for Rainfall Forecasting.* Mathematical and Computer Modeling, 33, pp. 883 - 699.

Kristen B. D.- Lee, W. L. (2003) *Artificial Neural Networks for the Management Researcher: The State of the Art*. Department of Organizational Leadership and Strategy, Marriott School of Management Brigham Young University Provo, UT 84602.

Modarres, R. (2008) *Multi-Criteria Validation of Artificial Neural Network Rainfall-Runoff Modelling*. Journal Hydrology and Earth System Sciences Discussion, 5, pp. 3449–3477.

Ogwueleka, T. C. - Ogwueleka, F. N. (2009) *Estimating the Heat Value of Municipal Solid Waste Using Neural Network*. USEP-Journal of Research Information in Civil Engineering, Vol. 6, No. 2, pp. 1 – 12.

Omid, B. H. - Saeed A. M., (2005) *Evaluation of Artificial Neural Networks in Optimization Models of Hydropower Reservoir Operation.* 9th International Water Technology Conference, Sharm El-Sheikh, Egypt, pp. 985-998.

Ricardo, M. T. - Jean, P. P. (1999) *Simulation of Daily Temperature for Climate Change Scenarios Over Portugal: A Neural Network Model Approach*. Climate Research, Vol. 13: pp. 45-59.

Richard P. L. (1987) *An Introduction to Computing with Neural Nets.* IEEE ASSP Magazine.

Salami, A. W. - Sule, B. F. (2012) *Optimal Water Management Modeling for Hydropower System on River Niger in Nigeria.* International Journal of Engineering. FASCICULE 1(ISSN 1584-2665) Annals of Faculty of Engineering Hunedoara. Tome X. 185-192.

Shiru, S. Q. - McCann, C. (2011) *Finite Design of Solar-Chimney System by Artificial Neural Network.* USEP. Journal of Research Information in Civil Engineering, Vol. 8 No 1, pp. 40 – 55.

Somvanshi, V. K. - Pandey, O. P. - Agrawal, P. K. - Kalanker, N. V. - Prakash, M. R. - Ramesh, C. (2006) *Modelling and Prediction of Rainfall Using Artificial Neural Network and ARIMA Techniques.* J. Ind. Geophys. Union, Vol. 10, No. 2, pp. 141-151.

Sule, B. F. - Salami, A. W. - Okeola, O. G. (2009) *Operational Impact of Hydropower Generation and Highlights on Preventive Measures in Lowland Area of River Niger, Nigeria*. International Electronic Engineering Mathematical Society IEEMS, Volume (7), pp. 109-126.

Swingler, K. (1996) *Applying Neural Networks: A Practical Guide.* Academic Press, London UK, pp. 21 – 39.

International Journal of Engineering Research and General Science Volume 3, Issue 5, September-October, 2015
ISSN 2091-2730

Sum-to-Modified Booth (S-MB) Recoding Schemes using 4:2 compressors

Naveen Kumar N M, Associate Prof. Aby Thomas

naveenmenon666@gmail.com, +91 9567567737

Abstract— Complex arithmetic operations are widely used in Digital Signal Processing (DSP) applications. In this work, we focus on optimizing the design of the fused Add-Multiply (FAM) operator for increasing performance. We investigate techniques to implement the direct recoding of the sum of two numbers in its Modified Booth (MB) form using 4:2 compressors. Introduction of a structured and efficient recoding technique and exploring three different schemes by incorporating them in FAM designs. Comparing to the existing recoding schemes, the proposed technique yields considerable reductions in terms of critical delay, hardware complexity and power consumption of the FAM unit.

Keywords— Booth Algorithm – Modified Booth Encoder – S-MB recoder – Sign Extension Algorithm – Fused Add-Multiply unit – Signed Half Adder and Full Adder - Compressors.

INTRODUCTION

Modern consumer electronics make extensive use of Digital Signal Processing (DSP) providing custom accelerators for the domains of multimedia, communications etc. Typical DSP applications carry out a large number of arithmetic operations as their implementation is based on computationally intensive kernels, such as Fast Fourier Transform (FFT), Finite Impulse Response (FIR) filters etc. As expected, the performance of DSP systems is inherently affected by decisions on their design regarding the allocation and the architecture of arithmetic units. Recent research activities in the field of arithmetic optimization have shown that the design of arithmetic components combining operations which share data, can lead to significant performance improvements. Based on the observation than the addition can often be subsequent to a multiplication, the Multiply Accumulator (MAC) and Multiply-Add (MAD) units were introduced leading to more efficient implementations of DSP algorithms compared to the conventional ones, which use only primitive resources.

Several architectures have been proposed to optimize the performance of the MAC operation. As noted, MAC components increase the flexibility of DSP data path Synthesis as a large set of arithmetic operations can be efficiently mapped onto them. Except the MAC/MAD operations, many DSP applications are based on Add-Multiply (AM) operations. The straightforward design of the AM unit, by first allocating an adder and then driving its output to the input of a multiplier, increases significantly both area and critical path delay of the circuit. Targeting an optimized design of AM operators, fusion techniques are employed based on the direct recoding of the sum of two numbers (equivalently a number in carry-save representation) in its Modified Booth (MB) form. Thus, the carry-propagate (or carry-look-ahead) adder of the conventional AM design is eliminated resulting in considerable gains of performance.

Another Research paper presented a signed-bit MB recoder which transforms redundant binary inputs to their MB recoding form. A special expansion of the preprocessing step of the recoder is needed in order to handle operands in Carry-save representation. In a paper, the author proposes a two-stage recoder which converts a number in carry-save form to its MB representation. The first stage transforms the carry-save form of the input number into signed-digit form which is then recoded in the second stage so that it matches the form that the MB digits Request. Recently, this technique has been used for the design of high performance Flexible coprocessor architectures targeting the computationally intensive DSP Applications. A present optimized design of previous paper which results in Improvements in both area and critical path.

More specifically, we propose a new recoding technique which decreases the critical path delay and reduces area and power consumption. The proposed *S-MB* algorithm is structured, simple and can be easily modified using compressor circuits in order to be applied either in signed (in 2's complement representation) or unsigned numbers, which comprise of odd or even number of bits. We explore three alternative schemes of the proposed *S-MB* approach using conventional and signed-bit Full Adders (FAs) and Half Adders (HAs) as building blocks. We evaluated the performance of the proposed *S-MB* technique by comparing its three different schemes with the state-of the- art recoding techniques.

BOOTH ALGORITHM

Booth multiplication algorithm or Booth algorithm was named after the inventor Andrew Donald Booth. It can be defined as an algorithm or method of multiplying binary numbers in two's complement notation. It is a simple method to multiply binary

numbers in which multiplication is performed with repeated addition operations by following the booth algorithm. Again this booth algorithm for multiplication operation is further modified and hence, named as modified booth algorithm.

MODIFIED BOOTH ENCODER

This modified booth multiplier is used to perform high-speed multiplications using modified booth algorithm. This modified booth multiplier's computation time and the logarithm of the word length of operands are proportional to each other. We can reduce half the number of partial product. Radix-4 booth algorithm used here increases the speed of multiplier and reduces the area of multiplier circuit. In this algorithm, every second column is taken and multiplied by 0 or +1 or +2 or -1 or -2 instead of multiplying with 0 or 1 after shifting and adding of every column of the booth multiplier. Thus, half of the partial product can be reduced using this booth algorithm. Based on the multiplier bits, the process of encoding the multiplicand is performed by radix-4 booth encoder. The overlapping is used for comparing three bits at a time. This grouping is started from least significant bit (LSB), in which only two bits of the booth multiplier are used by the first block and a zero is assumed as third bit as shown in the FIG

Booth recoding table for radix-4

Multiplier Bits Block			Recoded 1-bit pair		2 bit booth	
i+1	i	i-1	i+1	i	Multiplier Value	Partial Product
0	0	0	0	0	0	Mx0
0	0	1	0	1	1	Mx1
0	1	0	1	-1	1	Mx1
0	1	0	1	0	2	Mx2
1	0	0	-1	0	-2	Mx-2
1	0	1	-1	1	-1	Mx-1
1	1	0	0	-1	-1	Mx-1
1	1	0	0	0	0	Mx0

TABLE 1.**Booth Recoding Table for Radix-4**

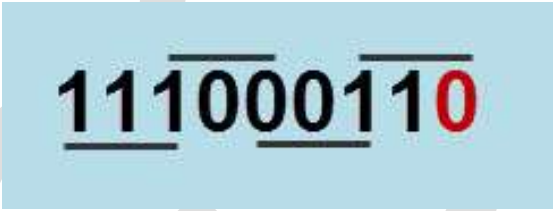

FIG 1.**Bit Pairing as per Booth Recoding**

FUSED AM IMPLEMENTATION

The main focus is on AM units which implement the operation Z=X (A+B). The conventional design of the AM operator requires that its inputs and are first driven to an adder and then the input X and the sum Y=A+B are driven to a multiplier in order to get Z. The drawback of using an adder is that it inserts a significant delay in the critical path of the AM. As there are carry signals to be propagated inside the adder, the critical path depends on the bit-width of the inputs. In order to decrease this delay, a Carry-Look-Ahead (CLA) adder can be used which, however, increases the area occupation and power dissipation. An optimized design of the AM operator is based on the fusion of the adder and the MB encoding unit into a single data path block by direct recoding of the sum Y=A+B to its MB representation. The fused Add-Multiply (FAM) component contains only one adder at the end (final adder of the parallel multiplier). As a result, significant area savings are observed and the critical path delay of the recoding process is reduced and decoupled from the bit-width of its inputs. In this work, we present a new technique for direct recoding of two numbers in the MB representation of their sum.

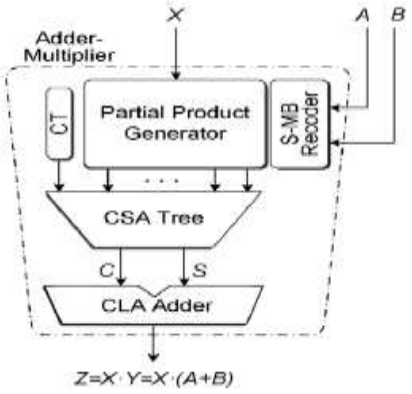

FIG 2. Fused AM scheme

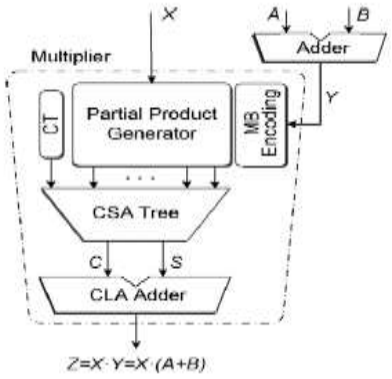

FIG 3. Conventional scheme

Consider multiplication of 2's compliment numbers X and Y with each number consisting of n=2k bits for even number of digits and n=2k+1 for odd number of digits. The multiplicand Y can be represented in Modified Booth form as follows:

$$Y = \langle y_{n-1} y_{n-2} \cdots y_1 y_0 \rangle_{2's} = -y_{2k-1} \cdot 2^{2k-1} + \sum_{i=0}^{2k-2} y_i \cdot 2^i$$

$$= \langle \mathbf{y}_{k-1}^{MB} \mathbf{y}_{k-2}^{MB} \cdots \mathbf{y}_1^{MB} \mathbf{y}_0^{MB} \rangle_{MB} = \sum_{j=0}^{k-1} \mathbf{y}_j^{MB} \cdot 2^{2j}$$

Where, $\mathbf{y}_j^{MB} = -2y_{2j+1} + y_{2j} + y_{2j-1}$.

$$y_{-1} = 0$$

$$\mathbf{y}_j^{MB} \in \{-2, -1, 0, +1, +2\}, 0 \le j \le k-1$$

Each digit is represented by three bits named ‘s’, ‘one’ and ‘two’. The sign bit ‘s’ shows whether the digit is negative or positive. Signal ‘one’ shows if the absolute value of the digit is equal to 1 or not. Signal ‘two’ shows if the absolute value of the digit is equal to 2 or not. Using these three digits, we can calculate as follows,

$$\mathbf{y}_j^{MB} = (-1)^{s_j} \cdot [one_j + 2 \cdot two_j].$$

$$one_j = y_{2j-1} \oplus y_{2j}$$

$$two_j = (y_{2j+1} \oplus y_{2j}) \cdot \overline{one_j}$$

$$s_j = y_{2j+1}$$

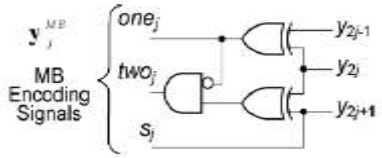

(a) Boolean equations

FIG 4. Gate level schematic

If we take the partial product as -2y, -y, 0, y, 2y then, we have to modify the general partial product generator. Now, every partial product point consists of two inputs (consecutive bits) from multiplicand and, based on the requirement, the output will be generated and its complements also generated in case if required.

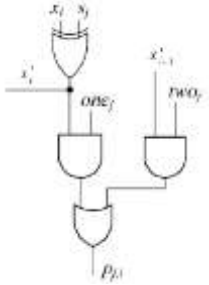

FIG 5.Generation of i-th bit of the partial product PP_j

The generation of i-th bit for the partial product generation is based on the logical expression:

$$p_{j,i} = ((x_i \oplus s_j) \wedge one_j) \vee ((x_{i-1} \oplus s_j) \wedge two_j)$$

Generation of the partial product is given by the equation:

$$PP_j = X \cdot \mathbf{y}_j^{MB} = \overline{p}_{j,n} 2^n + \sum_{i=0}^{n-1} p_{j,i} \cdot 2^i$$

After the partial products are generated, they are added, properly weighted, through a Wallace carry-save adder tree along with the correction term which is given by the equation:

$$Z = X \cdot Y = CT + \sum_{j=0}^{k-1} PP_j \cdot 2^{2j}$$

Correction term is found out by equation:

$$CT = CT(low) + CT(high) = \\ = \sum_{j=0}^{k-1} c_{\text{in},j} \cdot 2^{2j} + 2^n \left(1 + \sum_{j=0}^{k-1} 2^{2j+1}\right)$$

Where, $c_{\text{in},j} = (one_j \vee two_j) \wedge s_j$

Finally, the carry-save output of the Wallace CSA tree is leaded to a fast Carry Look Ahead (CLA) adder to form the final result as Z=X*Y.

SUM TO MODIFIED BOOTH RECODING TECHNIQUE

In *S-MB* recoding technique, we recode the sum of two consecutive bits of the input A with two consecutive bits of B to form one MB digit. As observed, three bits are included in forming a MB digit. The most significant of them is negatively weighted while the two least significant of them have positive weight. Consequently, in order to transform the two aforementioned pairs of bits in MB form we need to use signed-bit arithmetic. For this purpose, we develop a set of bit-level signed Half Adders (HA) and Full Adders (FA) considering their inputs and outputs to be signed. In sum to modified booth recoding technique, we use signed half adders (HA* and HA**) and signed full adders (FA* and FA**)

HA** $c = \overline{p} \wedge q$, $s = p \oplus q$ FA** $c_o = ((p \vee q) \wedge \overline{c_i}) \vee (p \wedge q)$, $s = p \oplus q \oplus c_i$

HA* $c = p \vee q$, $s = p \oplus q$ FA* $c_o = ((p \vee \overline{q}) \wedge c_i) \vee (p \wedge \overline{q})$, $s = p \oplus q \oplus c_i$

S-MB1 recoding scheme for even numbers of bits and odd number of bits are done using the following diagram:

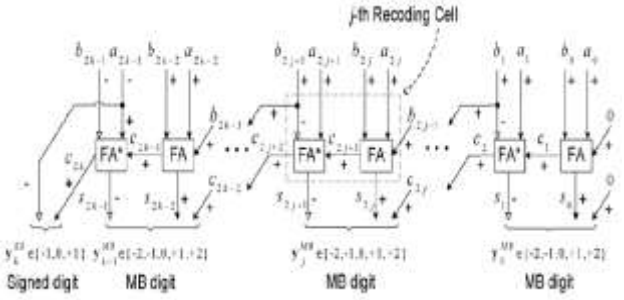

FIG 6.

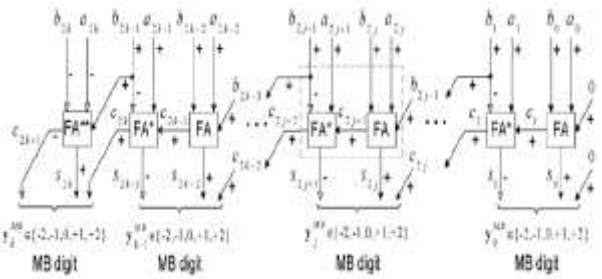

FIG 7.

S-MB2 recoding scheme for even numbers of bits and odd number of bits are done using the following diagram:

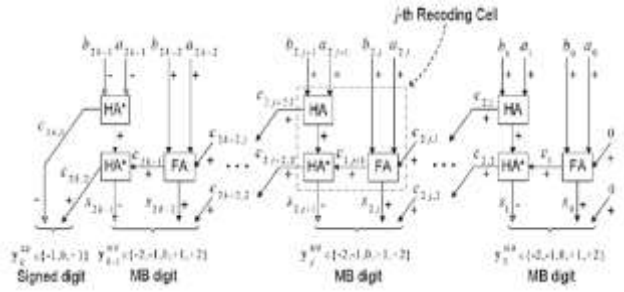

FIG 8.

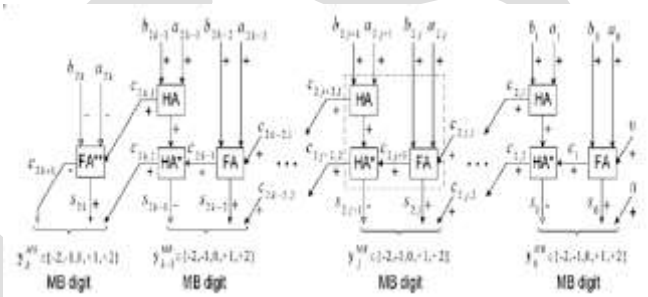

FIG 9.

S-MB3 recoding scheme for even numbers of bits and odd number of bits are done using the following diagram:

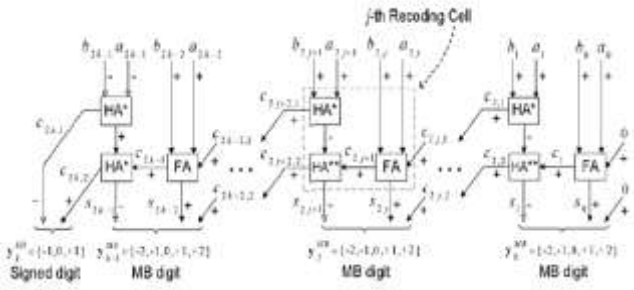

FIG 10.

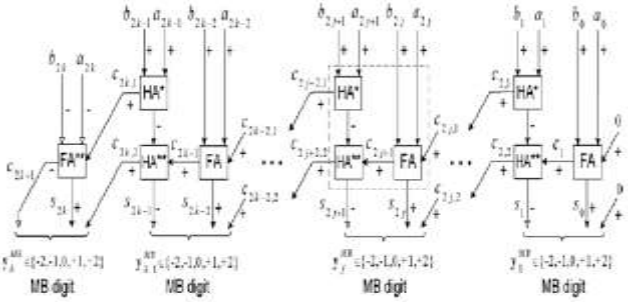

FIG 11.

4:2 COMPRESSORS

A 4-2 compressor consists of five inputs and three outputs. It is called compressor, since it compress four partial products into two. This can be implemented with two stages of full adders (FA) connected in series. By using compressors in the circuit, produced considerable reduction in area as well as delay.

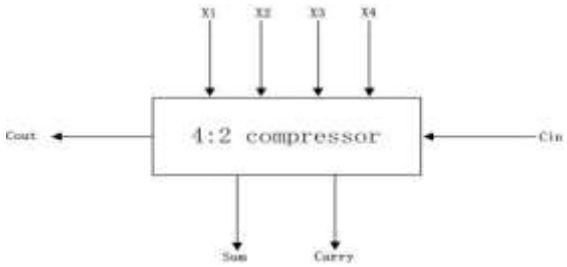

FIG 12.

SIMULATION RESULTS

Z = X (A + B)

Here, N = 8 (Even no: of bits)

A = 9 (“00001001”) , B = 11 (“00001011”) , X = 5 (“00000101”)

Z = 5 (9+11) = 5 (20) = 100 (“01100100”)

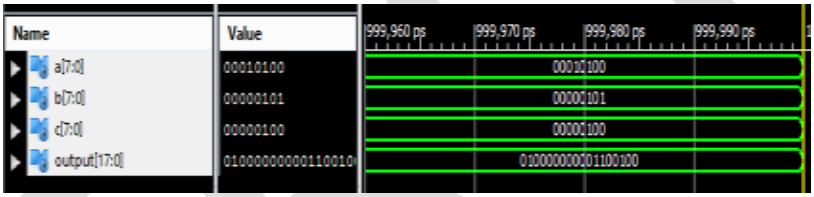

No: of slices – 4% (86 out of 1920) Delay – 25.253 ns

FIG 13. Simulation results for modified SMB1 even no: of bits

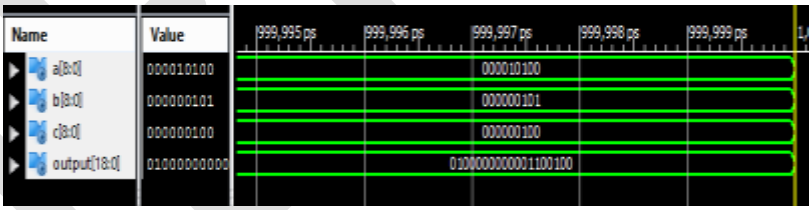

No: of slices – 5% (110 out of 1920) Delay – 31.822 ns

FIG 14. Simulation results for modified SMB1 odd no: of bits

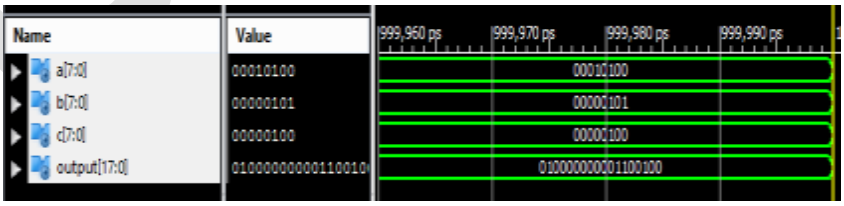

No: of slices – 4% (85 out of 1920) Delay – 25.331 ns

FIG 15. Simulation results for modified SMB2 even no: of bits

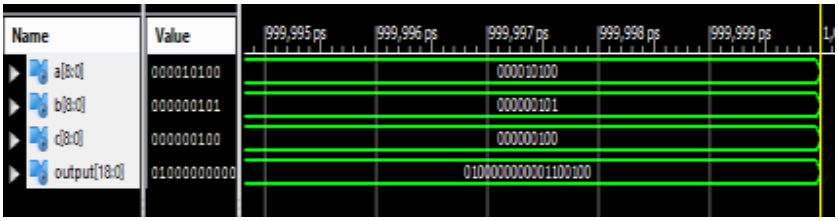

No: of slices – 5% (110 out of 1920) Delay – 32.064 ns

FIG 16. Simulation results for modified SMB2 odd no: of bits

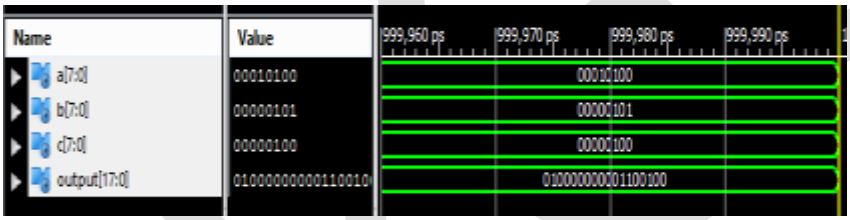

No: of slices – 4% (82 out of 1920) Delay – 25.318 ns

FIG 17. Simulation results for modified SMB3 even no: of bits

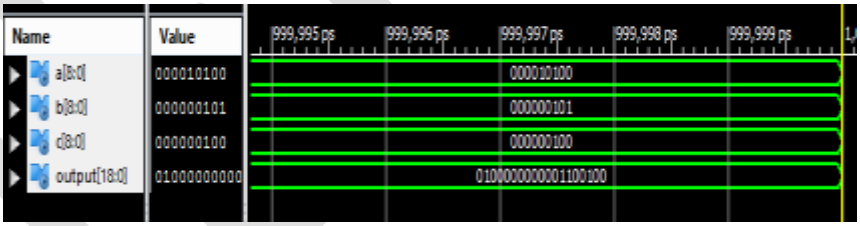

No: of slices – 5% (107 out of 1920) Delay – 31.921 ns

FIG 26. Simulation results for modified SMB3 odd no: of bits

CONCLUSION

The modified S-MB recoding schemes focuses on optimizing the design of the Fused-Add Multiply (FAM) operator. Also, proposing a structured technique for the direct recoding of the sum of two numbers to its MB form. Explore alternative designs of the proposed *S-MB* recoder and compare them to the existing ones. The proposed recoding schemes, when they are incorporated in FAM designs, yield considerable performance improvements in comparison with the most efficient recoding schemes found in literature. Sum to modified booth recoding scheme (S-MB1) for optimizing fused add-multiply unit has been presented. Proposed scheme allows considerable improvement in performance.S-MB1 scheme, when incorporated with FAM designs decreases critical path delay as well as area consumption compared to conventional recoding schemes used.

REFERENCES:

[1] C. N. Lyu and D. W. Matula, "Redundant binary Booth recoding," in*Proc. 12th Symp. Comput. Arithmetic*, 1995, pp. 50–57.

[2] W.C. Yeh, "Arithmetic Module Design and its Application to FFT," Ph.D. dissertation, Dept. Electron. Eng., National Chiao-Tung University, Chiao-Tung, 2001.

[3] M. Daumas and D. W. Matula, "A Booth multiplier accepting both a redundant or a non redundant input with no additional delay," in *Proc. IEEE Int. Conf. on Application-Specific Syst., Architectures, and Processors*, 2000, pp. 205–214.

[4] R. Zimmermann and D. Q. Tran, "Optimized synthesis of sum-of-products," in *Proc. Asilomar Conf. Signals, Syst. Comput.*, Pacific Grove, Washington, DC, 2003, pp. 867–872.

[5] K. Tsoumanis, S. Xydis, C. Efstathiou, N. moschopoulus and K. Pekmestzi, " An Optimized Modified Booth Recoder for Efficient Design of the Add-Multiply Unit" , in *Archemidis III: Funding of Research Groupsin TEI*, Athens, 2014

International Journal of Engineering Research and General Science Volume 3, Issue 5, September-October, 2015
ISSN 2091-2730

PREAPARATION OF BIODIESEL FROM NON EDIBLE ANIMAL FAT

Mr. Roshan R. More, Prof. C.B Kothare, Prof. K. S. Raizada
M-Tech 2nd year (Heat Power),
SSPACE Wardha,
roshansingmore@gmail.com,
Mob- 8983211748

Abstract— Energy crises, resulted into studies of various non-traditional bio-oriented fuels, biodiesel can be used as additives for diesel engine. Researches on ethanol show better replacement of diesel without any modification of engine to some extent for ethanol. Further advancement in technology explored the chances of ethanol as alternative fuel for diesel engine. It is seen that the addition of biodiesel is valuable to remove diesel-ethanol phase separation which validated the use of its blends on the diesel engine .In this study, biodiesel which is defined as a fuel comprised of mono-alkyl esters of long-chain fatty acids has produced from animal fat oil by transesterification process and its different properties are calculated and studied and also compared with the properties of diesel and ethanol. Blends of biodiesel, ethanol and diesel are made on the percentage of volume basis. In these blends, biodiesel used 5-15%, ethanol 15-30% and remaining was the percentage of diesel.

Keywords—Biodiesel, Animal fat, Transesterification, Diesel, Blends.

1) INTRODUCTION:

Diesel fuel has limited resources which available for us upto 2098. The combustion of diesel fuels causes environmental problems and human health problems, emission like CO_2, NOx, CO product which caused for global warming. As the diesel price increasing and resources decreasing, it required some attention to find other alternative fuel that cheaper and renewable. Research on reducing emissions resulted from diesel engines and studies on decrease fuel consumption are being founded worldwide. There are many works on reliable researching and implementations and useful results are came to exist. Research and developing alternative diesel engine fuel is one of these studies. The alternative diesel fuels must be technically acceptable, economically competitive, environmentally acceptable and easily available. Continuing depletion of the reserves of non-renewable petroleum, price volatility, feedstock availability concerns have caused an intensified search for alternative sources of energy. Biodiesel derived from biological sources, among them lipid materials such as fats and oils have received increasing attention. [1]

Researches on biodiesel derived from vegetable oils and animal fat are being used as alternate fuels to petroleum based diesel fuel. It has been concluded by many studies that as an alternative fuel biodiesel reduce the emissions of carbon monoxide (CO), hydrocarbon (HC), sulphur dioxide (SO2), but NOx to increase in the exhaust compared with diesel fuel. Biodiesel has higher cetane number than diesel fuel, contains high oxygen by weight, non-toxic, biodegradable is its attractive properties. Although biodiesel has many advantages, higher cetane number, more calorific value etc. [2]

2) LITERATURE REVIEW:

P. Shreenivas et.al [3], has investigated method of producing biodiesel from castor oil (treated with mineral turpentine oil) by transesterification of the crude oil with methanol in the presence of NaOH as catalyst. This paper mainly involves “Esterification”. Factors effecting the biodiesel production (reaction temperature, reaction rate & catalyst) are analyzed. The esterification procedure converts castor oil to its methyl esters. Important fuel properties of methyl esters of biodiesel produced from castor oil like viscosity, flash point, fire point, calorific value etc., was found out and compared to the properties of Indian standard biodiesel. This paper study supports the production of biodiesel from castor oil as a viable alternative to the diesel fuel.

Gerhard Knotheet.al. [4], 2010 described the preparation of biodiesel from mutton fat. The use of MgO impregnated with KOH as heterogeneous catalyst for the esterification of mutton fat with methanol has been evaluated. In this process >98% conversion of fats into biodiesel in 20 minutes is become possible. At 0.02% weight of moisture and free fatty acid 0.002% with methanol completely converted into biodiesel but additional 1% weight of moisture result in soap formation. MgO-KOH-20 (MgO with 20% KOH) catalyst found to tolerate additional 1% of water in the fat.

Shaoyang Liu et.al [5], 2010 Paper described efficient biodiesel production from beef tallow was achieved with radio frequency (RF) heating. A viscosity of biodiesel products from beef tallow was 5.23±0.01 mm^2 s^{-1}, meeting the specification in ASTM D6751. RF heating has a higher energy dissipating rate than conventional heating. There are several obstacles, e.g. high viscosity, incomplete combustion and carbon build up, preventing vegetable oil and animal fat to be directly used in modern diesel engine. Among them, high viscosity may be the most important one. The viscosity will remarkably decrease after the conversion from oil/fat into biodiesel.

Cengiz Oner et.al. [6], 2009 had describes biodiesel production from inedible animal tallow and its usability was investigated as pure biodiesel and its blends with petro diesel fuel in a diesel engine. Due to lower heating value of biodiesel, the addition of biodiesel to diesel fuel decreases the thermal efficiency of engine and increase specific fuel consumption. However, the effective engine power was comparable to diesel fuel. B100 were reduced emissions of CO, NOx, SO_2 and smoke opacity around 15%, 38.5%, 72.7% and 56.8%, respectively. For B20, lowest CO, NOx emissions and the highest exhaust temperature were obtained among all other fuels. The reduction in exhaust emission made tallow methyl ester and its blends, especially B20 a suitable alternative fuel for diesel engine and thus could help in controlling air pollution.

Dhiraj darunde et.al. [7], Oct. 2012, has discuses fuel production, fuel properties, environmental effects including exhaust emissions and co-products. This also describes the use of glycerol which is the by-product in esterification process along with biodiesel. The impact of blending of biodiesel with ethanol and diesel on the diesel engine has described. Mainly animal fats and vegetable oils are used for the production of biodiesel. Several types of fuels can be derived from triacylglycerol-containing feedstock. Biodiesel which is defined as the mono-alkyl esters of vegetable oils or animal fats. Biodiesel is produced by transesterifying the oil or fat with an alcohol (methanol/ethanol) under mild conditions in the presence of a base catalyst.

3) EXPERIMENTAL PROCEDURE:

This chapter describes system development with the help of used material and instrument for experiment. Also, the methodology used for standardization of transesterification process for animal fat oil. It studies characteristic fuel properties and experimental procedure adopted to evaluate performance of biodiesel-diesel-ethanol (BDE) (5-15%v/v+85-55%v/v+15-30%v/v) with comparison of diesel fuel on the diesel engine. Tests were performed at the I.C Engine laboratory of PRMIT & R, Badnera. The laboratory consists of engine test rig coupled with rope brake dynamometer, smoke meter. Exhaust temperature was measured with the help of thermocouple.

Animal fat is one of the main feedstock for the production of biodiesel. About one-third of the fats and oils produced in the United States are from animal fats. This includes beef tallow, pork lard, and chicken fat. Animal fats are attractive feed stocks for biodiesel because their cost is substantially lower than the cost of vegetable oil. This is partly because the market for animal fat is much more limited than the market for vegetable oil, since much of the animal fat produced in the U.S. is not considered edible by humans

Figure 3.1: Heating animal fat

There are various methods to produce biodiesel; transesterification is the method that we have used for the production of biodiesel from animal fat oil. Fatty acid methyl ester of animal fats as biodiesel fuel was prepared by base-catalyzed transesterification of tallow with Methanol in the presence of kOH as base-catalyst. The properties of tallow methyl ester, diesel fuel, ethanol and its blends were determined at Chemistry Department of Dhamangaon Engineering college, Dhamangaon Rly, Amrawati, Maharashtra, India. The petroleum diesel fuel was purchased from a local commercial supplier (Indian Oil fuelling station, located near badnera, Amrawati, Maharashtra). Animal fats was purchased from city meat market, Amrawati. Methanol (99.9% pure) was purchased from Shreeganesh Chemicals, Rajkamal squre, Amrawati. Pottasium hydroxide (kOH) with purity of 98%, provided from Chemistry Department of Dhamangaon Engineering college, Dhamangaon Rly, Amrawati, Maharashtra, India. The transesterification reaction conditions used in this study were as described by [8,9]

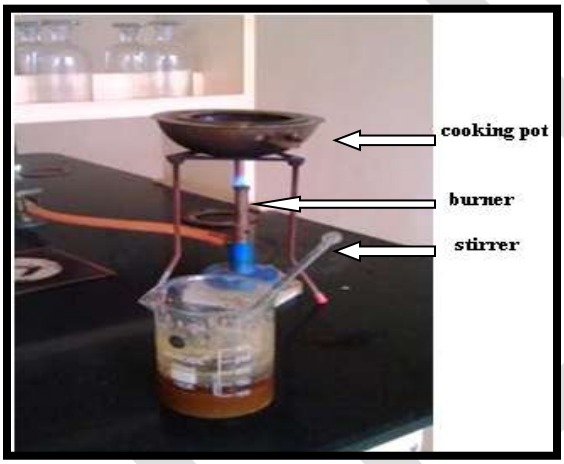

Figure3.2:- Tranesterification of biodiesel

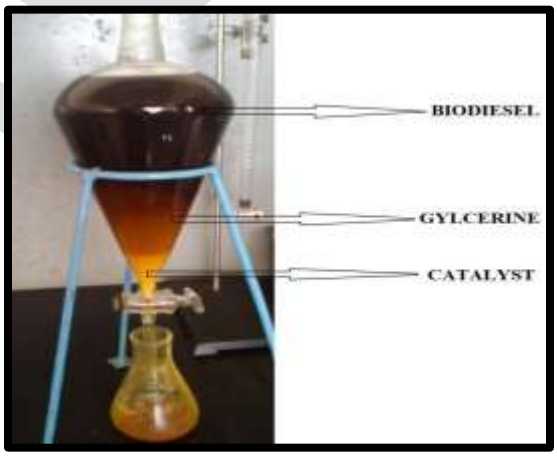

figure3.3:- Separating biodiesel and byproduct

Before transesterification, animal fats was heated at 105-110oC for 1hour and then strained the sediment out of the fat with cloth filter. Impurities and bubbles formed on surface of tallow were picked during heating process. After this process, the weight of tallow reduced about 5% to 6%. A sample of 400g of animal fat oil was placed in a 1000 ml flat-bottom flask equipped with a stirrer-heater and thermometer. This oil was heated to 60 ‘C slowly. In another beaker, 89.3g of methanol (6:1 molar ratio ethanol /fat oil) was mixed with 2g of KOH (0.5% by weight assuming 98% pure KOH), until all of the KOH was dissolved in methanol. This mixture was then added to the melted fat, stirred and further heated to 60 ^{0}C, for about 15 to 20 minutes. The mixture is allowed to cool to room temperature for 12 hour, and the ester and glycerol layers were separated in a separator funnel. We have produced biodiesel about 2 liters as per the requirement. [10,11]

4) PROPERTIES OF BIODIESEL:-

Table 3.4, Shows the fuel properties of the blends at different ratios of diesel, biodiesel and ethanol. It can be observed that the density of the blends decreased with an increasing of the percentage of ethanol in the blends. This is attributed to the fact that ethanol has lower density and as such will lower the density of the mixture. But, when the percentage of biodiesel was increased, the density increased, which is due to the fact that biodiesel has a higher density than the other two components. Normally, it is recognized that higher density leads to higher flow resistance of fuel oil, resulting in higher viscosity. This finding suggests that the higher viscosity can lead to inferior fuel injection.

Table 4.1: Properties of diesel, ethanol and biodiesel:

Properties	**Diesel**	**Ethanol**	**Biodiesel**
Density(kg/m^3) 15^{o}C	833.9	716.8	880
Viscosity (CSt) at 40^{o}c	3.67	1.4	14.3
Calorific value (kj/kg)	42,800	29,700	39242.03
Cetane number	47	8	69.52
Flash point, ^{0}C	58	13	52

Heat of combustion is one of the most important fuel properties. The heat of combustion of BDE blends decreased, when greater amounts of ethanol and biodiesel were added, which is due to the lower heating value of biodiesel and ethanol. Lower heating value of a fuel has a direct influence on the power output of an engine. Fuel was prepared by mixing considered volume.

Table 4.2: Composition of the Test Fuel:

Diesel	Biodiesel	Ethanol
80%	5%	15%
75%	10%	15%
70%	15%	15%
75%	5%	20%
70%	10%	20%
65%	15%	20%
65%	5%	30%
60%	10%	30%
55%	15%	30%
95%	5%	0%
90%	10%	0%
85%	15%	0%

5) CONCLUSION:

An experimental study was carried out to investigate the performance characteristics of animal fat biodiesel (5%, 10%, 15% volume) and its blends with ethanol (15%, 20%, 30%volume) and diesel (95%, 90%, 85%, 80%, 75%, 70%, 65%, 60%, 55% volume) in diesel engine and the results were compared with diesel fuel. Based on the experimental results, the following conclusions can be drawn:-

- The calorific value of animal fat biodiesel (39242.03 Kj/Kg) is found to be lower than that of diesel (42800 Kj/kg).
- Cetane number of animal fat biodiesel is 69.52 which are greater than diesel (47).
- Viscosity and density of BDE blends are found to be very close to that of diesel.
- BDE blends can be used without any engine modifications in a direct injection diesel engine. It was also observed that the addition of biodiesel to the diesel fuel decreases the thermal efficiency of engine and increases the specific fuel consumption. This is due to the lower calorific value of biodiesel compared to diesel fuel.

REFERENCES:

[1] Jon H. Van Gerpen "Biodiesel an Alternative Fuel for Compression Ignition Engines" Published by the American Society of Agricultural and Biological Engineers 2950 Niles Road, St. Joseph, MI 49085-9659 USA.

[2] Ayhan Demirbas "Biodiesel production from vegetable oils via catalytic and non-catalytic supercritical methanol transesterification methods" Progress in Energy and Combustion Science 31 (2005) 466–487.

[3] P. Shreenivas, Venkata Ramesh Mamilla, K .Chandra Sekhar "Development of Biodiesel from Castor Oil" International Journal of Energy Science.

[4] Gerhard Knothe "Designer Biodiesel: Optimizing Fatty Ester Composition to Improve Fuel Properties "Energy & Fuels 2008, 22, 1358–1364

[5] Shaoyang Liu, Yifen Wang, Jun-Hyun Oh, Josh L. Herring, "Fast biodiesel production from beef tallow with radio frequency heating", Renewable Energy 36, 2011, pp.1003-1007.

[6] Cengiz Oner, Sehmus Altun, "Biodiesel production from inedible animal tallow and an experimental investigation of its use as alternative fuel in a DI diesel engine", Applied Energy 86, 2009, pp.2114-2120.

[7] D. S. Darunde and Prof M. M. Deshmukh, "Biodiesel Production From Animal Fats And Its Impact On The Diesel Engine With Ethanol-Diesel Blends: A Review ",International Journal of Emerging Technology and Advanced Engineering (IJETAE) ,ISSN 2250–2459, Volume 2, Issue 10, October 2012.

[8] A P Pathre, H S Farkade, "Performance of Alcohol gasoline blends in SI engine on the basis of Oxygen Percentage", International conference on Advances in Engineering & Management, Royal Institute of Technology and science, Hyderabad, 28&29 Feb2012.

[9] Ayhan Demirbas "Biodiesel production from vegetable oils via catalytic and non-catalytic supercritical methanol transesterification methods" Progress in Energy and Combustion Science 31 (2005) 466–487.

[10] Daming Huang, Haining Zhou, Lin Lin, "Biodiesel: an Alternative to Conventional Fuel", Energy Procedia 16, 2012, pp.1874-1885.

[11] S. Jaichandar1 and K. Anna malai "The Status of Biodiesel as an Alternative Fuel for Diesel Engine an Overview" Journal of Sustainable Energy & Environment 2 (2011) 71-75.

[12] Farooq Anwar, Umer Rashid, Muhammad Ashraf , Muhammad Nadeem "Okra (Hibiscus esculentus) seed oil for biodiesel production" Applied Energy 87 (2010) 779–785.

[13] A.S. Ramadhas, S. Jayaraj, C. Muraleedharan "Use of vegetable oils as I.C. engine fuels—A review" Renewable Energy 29 (2004) 727–742.

[14] Javier Dufour and Diego Iribarren "Life cycle assessment of biodiesel production from free fatty acid-rich wastes "Renewable Energy 38 (2012) 155-162.

[15] Metin Guru, AtillaKoca, Ozer Can, Can Cinar, FatihSahin, "Biodiesel production from waste chicken fat based sources and evaluation with Mg based additive in a diesel engine", Renewable Energy 35, 2010, pp.637-343.

International Journal of Engineering Research and General Science Volume 3, Issue 5, September-October, 2015
ISSN 2091-2730

Plant secondary metabolites: a review

Ruby Tiwari, C.S.Rana
Department of Biotechnology, IMS Engineering College, Ghaziabad, U.P., India
rubytiwari_lucknow@yahoo.com
Mob.-09451218865

Abstract- Plants are important source for the discovery of new products of medicinal value for drug development and plants secondary metabolites are unique sources for pharmaceuticals food additives, flavors and others industrial values. Commercial importance of these secondary metabolites has resulted in a great interest in its production and in exploring possibilities of enhancing its production by means of tissue culture technology in the recent years. Plants cell culture technologies were introduced at the end of 1960's as a possible tool for both studying and producing plant secondary metabolites. The focus of the present review is the application of tissue culture technology for the production of some others important plant secondary metabolites. The present communication deals the brief introduction, classification, recent improvements of production, anti microbial properties and importance of plant secondary metabolites.

Keywords: Metabolites; plant secondary metabolites; pharmaceuticals; recent improvements; microbial properties; drug development; tissue culture.

INTRODUCTION

Metabolites are the intermediates and products of metabolism. The term *metabolite* is usually restricted to small molecules. Metabolites have various functions, including fuel, structure, signaling, stimulatory and inhibitory effects on enzymes, catalytic activity of their own (usually as a cofactor to an enzyme), defense, and interactions with other organisms. Plant produce a vast and diverse assortment of organic compounds the great majority of which do not appear to participate directly in growth and development. These substances, traditionally referred to as secondary metabolites, often are differentially distributed among limited taxonomic groups within the plant kingdom**.** The evolving commercial importance of secondary metabolites has in recent years resulted in a great interest particularly in the possibility of altering the production of bioactive plant metabolites by means of tissue culture technology[1]**.** Plant cell and tissue culture technologies can be established routinely under sterile conditions from explants, such as leaves, stems, roots, and meristems for both the ways for multiplication and extraction of secondary metabolites. *In-Vitro* production of secondary metabolite in plant cell suspension cultures has been reported from commercial medicinal plants[1]**.**

Plant secondary metabolites are unique sources for pharmaceuticals, food additives, flavors, and other industrial materials[1] and the use of plant cell cultures has overcome several inconveniences for the production of these secondary metabolites. Organized cultures, and especially root cultures, can make a significant contribution in the production of secondary metabolites**.** Secondary metabolites are described as an organic compounds which were not directly involved in the normal growth, development, or reproduction of an organism[2]. These metabolites are those metabolites which are often produced in a phase of subsequent to growth, have no function in growth (although they may have survival function), are produced by certain restricted taxonomic groups of microorganisms, have unusual chemicals structures, and are often formed as mixtures of closely related members of a chemical family.

Unlike primary metabolites, absence of secondary metabolites does not result in immediate death, but rather in long-term impairment of the organism's survivability, fecundity, or aesthetics, or perhaps in no significant change at all. These are often restricted to a narrow set of species within a phylogenetic group[3]. And these are also play an important role in plant defense against herbivory[4] and other interspecies defenses[5]. Humans use secondary metabolites as medicines, flavorings, and recreational drugs in the recent past.

Srivastava et al. (2007) also added that use differentiated cultures instead of cell suspension cultures have focused on transformed (hairy) roots[6]. Smetanska (2008) has summarized the process for obtaining the secondary metabolites from plant cell cultures is represented as a multi-stage strategy, and each link should be described according to specifications of cell cultures or products[7]. For the establishing of high-producing and fast-growing cell lines, the parent plants should be selected. The expression of synthetic pathways can be influenced by environmental conditions, the supply of precursors, and the application of elicitors, and it can be altered by special treatments such as biotransformation and immobilization.

Kossel was the first to define these metabolites as opposed to primary ones. It has been clearly demonstrated that secondary products play a major role in the adaptation of plants to their environment (Kossel et al., 1981). Due to antibiotic, antifungal, and antiviral, activities have been recorded to ability to protect plants from pathogens[8].

CLASSIFICATION

Secondary metabolites can be classified on the basis of chemical structure (for example, having rings, containing a sugar), composition (containing nitrogen or not), their solubility in various solvents, or the pathway by which they are synthesized (e.g., phenylpropanoid, which produces tannins). And usually classified according to their biosynthetic pathways[9]. Three large molecule families are generally considered: Phenolics, Terpenes and Steroids, and Alkaloids, Flavanoids[10].Some of them can have severe consequences.

Alkaloids

Alkaloids are originally defined as pharmacologically active, nitrogen-containing basic compounds of plant origin. And they can block ion channels, inhibit enzymes, or interfere with neurotransmission, producing hallucinations, loss of coordination, convulsions, vomiting, and death.

Phenolics

Phenolics interfere with digestion, slow growth, block enzyme activity and cell division, or just taste awful[11].

Terpenes

Terpenes are among the most widespread chemically diverse groups of natural products. Terpenes are a unique group of hydrocarbon-based natural products whose structures may be derived from isoprene. Terpenes are classified by the number of 5-carbon units. The function of terpenes in plants is generally considered to be both ecological and physiological: Allelophathy, Insecticidal, Insect pollinators, Plant hormone (Abscisic acid, gibberlellin).

Flavonoids

With more than 4500 different representatives known thus far, the flavanoids constitute an enormous class of phenolic natural products. Present in most plant tissues, often in vacuoles, flavonoids can occur as monomers, dimmers and higher oligomers. Flavonoids comprise a diverse set of compounds and perform a wide range of functions. Specific flavonoids can also function to protect plants against UV-B irradiation. The flavonoids consist of various groups of plant metabolites which include chalcones, aurones, flavanones, isoflavonoids, flavones, flavonols, leucoanthocyanidins, catechins, and anthocyanins.

Coumarins and Stilbenes

Coumarins belong to a widespread family of plant metabolites called the benzopyranones, with more than 1500 representative in more than 800 species. In plants these compounds can occur in seed coats, fruits, flowers, roots, leaves, stems, although in general the greatest concentration are found in fruits and flowers. Their roles in plants appear to be mainly defense-related, given their antimicrobial antifectant, UV-screening and germination inhibitor properties. Stilbenes are present in bryophytes, pteridophyte, gymnosperms and angiosperms, with more than 300 different stilbenoids known today. The stilbenes play important roles in plants, particularly in heartwood protection and also have significance in pharmacology and human health.

Due to their large biological activities, plant secondary metabolites have been used for centuries in traditional medicine. Nowadays, they correspond to valuable compounds such as pharmaceutics, cosmetics, fine chemicals, or more recently nutraceutics. Recent surveys have established that in western countries, where chemistry is the backbone of the pharmaceutical industry, 25% of the molecules used are of natural plant origin[12].

PRODUCTION OF SECONDARY METABOLITES AND RECENT IMPROVEMENTS OF PRODUCTION PROCESS

Plant secondary metabolites are unique resources for pharmaceuticals, food additives, and fine chemicals. They also provide original materials used in other areas. Besides direct extraction from plants, and chemical synthesis to provide those compounds or derivatives with similar uses, plant cell culture has been developed as a promising alternative for producing metabolites that are difficult to be obtained by chemical synthesis or plant extraction. However, in spite of decades of efforts, production of plant secondary metabolites by plant cell culture technology is still facing many biological and biotechnological limitations. One of the major obstacles is the low yield of plant secondary metabolites in plant cell cultures. Since the major roles of plant secondary metabolites are to protect plants from attack by insect, herbivores and pathogens, or to survive other biotic and a biotic stresses, some strategies for culture production of the metabolites based on this principle have been developed to improve the yield of such plant secondary metabolites and they include treatment with various elicitors, signal compounds, and a biotic stresses[13-18].

Many such treatments indeed effectively promote the production of a wide range of plant secondary metabolites, both in vivo and *in-Vitro*. However, the productivity is still rarely competitive for industrial application[19].

A recent work for improving production of plant secondary metabolites was mainly focused on the following aspects: 1) manipulation of plant cell cultures to improve productivity of target compounds, through improving chemical processing and bioreactor performance or employing elicitors, a biotic stresses, and other approaches, regardless of their mechanisms[20]; 2) studying signal transduction pathways underlying various effective strategies leading to biosynthesis of target secondary metabolites; 3) studying transcription factors and their regulation mechanisms, including genetic manipulation of regulator genes to improve production of target secondary metabolites[21]; 4) cloning of secondary metabolite biosynthetic genes, and genetic modification of key genes to engineer the metabolic flux to target compounds[22]; 5) studying metabolic flux and profiling metabolic intermediates to understand whole pathways and overall regulation of target compound accumulation[23]; and 6) studying gene transcripts for plant secondary metabolism by profiling and analyzing global gene expression under different conditions to understand the regulation of plant secondary metabolism in a whole sense[24].

Plant cell culture are able to produce secondary metabolites came quite late in the history of *in-Vitro* techniques. It had been considered for a long time that undifferentiated cells, such as callus or cell suspension cultures were not able to produce secondary compounds, unlike differentiated cells or specialized organs[25]. Zenk and co-workers experimentally demonstrated that this theory was wrong, as they could observe dedifferentiated cell culture of *Morinda citrifolia* yielding 2.5 g of anthraquinones per litre of medium[26].This finding opened the door to a large community of vitro culturists who extensively studied the possible use of plant cultures for the production of secondary compounds of industrial interest[27] and the possible use of plant cell cultures for the specific biotransformation of natural compounds has been demonstrated[28-31].

The major advantages of cell culture system over the conventional cultivation of whole plants are: (1) Useful compounds can be produced under controlled conditions independent of climatic changes or soil conditions; (2) Cultured cells would be free of microbes and insects; (3) The cells of any plants, tropical or alpine, could easily be multiplied to yield their specific metabolites; (4) Automated control of cell growth and rational regulation of metabolite processes would reduce of labor costs and improve productivity; (5) Organic substances are extractable from callus cultures. Due to these advantages, research in the area of tissue culture technology for production of plant chemicals has bloomed beyond expectations.

Transgenic hairy root cultures also have revolutionized the role of plant tissue culture in secondary metabolite production. They are unique in their genetic and biosynthetic stability, faster in growth, and more easily maintained. Using this methodology a wide range of chemical compounds has been synthesized[32, 33]. Advances in tissue culture, combined with improvement in genetic engineering, specifically transformation technology, have opened new avenues for high volume production of pharmaceuticals, nutraceuticals, and other beneficial substances[34]. Recent advances in the molecular biology, enzymology, and fermentation technology of plant cell cultures suggest that these systems will become an important viable source for the secondary metabolites.

Large-scale plant tissue culture is found to be an attractive alternative approach to traditional methods of plantation as it offers a controlled supply of biochemical's independent of plant availability[35]. Kieran et al. (1997) detailed the impact of specific engineering-related factors on cell suspension cultures[36]. Current developments in tissue culture technology indicate that transcription factors are efficient new molecular tools for plant metabolic engineering to increase the production of valuable compounds [37].The main research programs for the production of secondary metabolites from plant cell cultures are represented in fig.1.

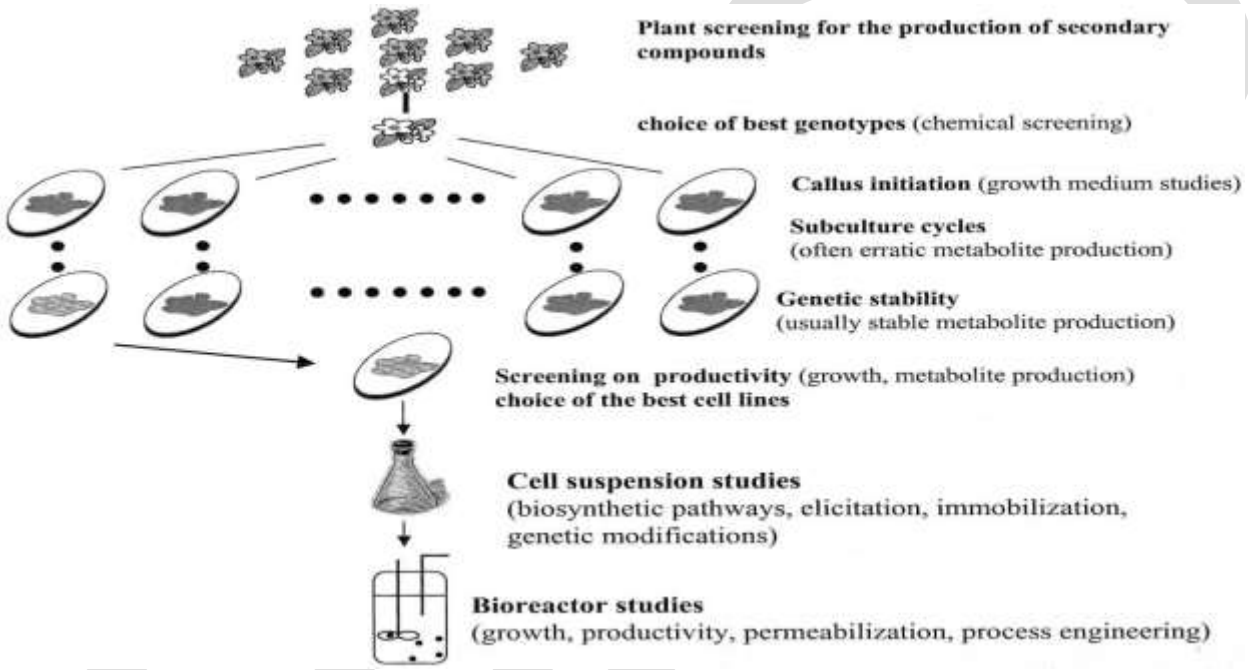

Fig.1-Guidelines for the production of secondary metabolites from plants cell.

Once interesting compounds are identified from plant extracts, the first part of the work consists in collecting the largest genetic pool of plant individuals that produce the corresponding substances. This work allows the screening of hyper-producing plants that present the most valuable secondary metabolites. However, a major characteristic of secondary compounds is that their synthesis is highly inducible. After choosing the most promising individual plants, begins the real work of *in-Vitro* cultures with callus initiation. This work consists mainly in determining the medium that will be best adapted for cultivation. And when calli are obtained, it is well known that they can undergo somaclonal variation[38], usually during several subculture cycles. This is a critical period where, due to this vitro-variation, secondary metabolite production is often variable from one subculture cycle to another. When genetic stability is reached, it is necessary to screen the different callus lines according to their aptitudes to provide an efficient metabolite production. Hence, each callus must be assessed separately for its growth speed as well as intracellular and extracellular metabolite concentrations. This allows an evaluation of the productivity of each cell line so that only the best ones will be taken to cell suspensions and reactor studies. When growth stops, carbon is no longer needed in large quantities for primary metabolism and

secondary compounds are more actively synthesized. Bioreactor studies represent the final step that leads to a possible commercial production of secondary metabolites from plant cell cultures. This is an important phase as numerous problems arise when scaling up the work realized on Erlenmeyer flasks. After successful optimization of the biomass production in a bioreactor, plant cell cultures must undergo well-adapted processes to achieve a good production of secondary metabolites.

ANTIMICROBIAL PROPERTIES OF PLANT SECONDARY METABOLITES

Plants produce a huge variety of secondary compounds as natural protection against microbial and insect attack. Some of these compounds are also toxic to animals, but others may not be toxic. Indeed, many of these compounds have been used in the form of whole plants or plant extracts for food or medical applications in man. The potential of essential oils and saponins as beneficial feed additives in ruminant production will be used here as an illustration of the potential benefits of plant compounds[39].

Essential Oil and its effects

Essential oils are steam-volatile or organic-solvent extracts of plants used traditionally by man for many centuries for the pleasant odour of the essence, its flavor or its antiseptic and/or preservative properties. Recently, for example, useful effects of essential oils have been demonstrated against pathogenic bacteria. Oils from *Cinnamomum osmophloeum* have been shown to possess antibacterial activity against Escherichia coli, *Enterococcus faecalis*, Staphylococcus aureas (including the clinicallyproblematic methicillin-resistant S. aureus), Salmonella sp. and Vibrio parahemolyticus; cinnamaldehyde is the main antibacterial component of the mixture[40]. E. coli O157:H7 is inhibited by oregano oil[41], peppermint oil[42], and essential oils from other herbs[43]. Helicobacter pylori are highly sensitive to spearmint oil[44]. Essential oils are potent against a wide range of oral bacteria[45], and they are used widely in antiseptic mouthwashes.

With this range of antimicrobial activity, it was considered logical to evaluate essential oils for possible beneficial selective effects against rumen micro-organisms. Essential oils were examined many years ago in rumen bacteria in relation to their contribution to poor palatability in some plant species[46]. Oh et al. (1967) have demonstrated that individual oils have different effects on mixed rumen bacteria. Monoterpene hydrocarbons are less toxic and sometimes stimulatory to microbial activity compared with the corresponding oxygenated compounds, the monoterpene alcohols and aldehydes[47]. R.J.Wallace (2004), stated that essential oils are not necessarily toxic to rumen bacteria, and their effects may be expected to persist[48].

Saponins and effects of saponins in ruminants

Saponins, like essential oils, cover a wide variety of chemical compounds and, also like essential oils, man has made use of their properties for centuries[49]. The word ‘saponin’ is derived from the Latin word sapo (soap) and traditionally saponin-containing plants have been utilized for washing. Chemically, saponins are high-molecular-weight glycosides in which sugars are linked to a triterpene or steroidal aglycone moiety[49].

Van Nevel & Demeyer (1990) have found no indication of any toxic effects or effects of sarsaponin on microbial growth or protein breakdown *in-Vitro*. In contrast, Lu et al. (1987) have reported that Lucerne (Medicago sativa) saponins appear to suppress fermentation in continuous culture[50].There are many consequences for the fermentation, and consequently for nutrition, that result from the removal of protozoa[51]. A meta-analysis has recently demonstrated that the benefits of defaunation outweigh any disadvantages[52]. Antiprotozoal agents, such as surface-active agents, that have been investigated in attempts to apply defaunation at the farm level have been hampered by problems with toxicity, either to other rumen micro-organisms[53-56] or to the host[57]. Lipids are toxic to protozoa[58-60], and also to fiber digestion[61]. Thus, there has been, until now, no reliable safe on-farm method available for suppressing rumen protozoa[62].

IMPORTANCE AND NATURAL FUNCTIONS OF SECONDARY METABOLITES

SECONDARY METABOLITES, WHICH ARE A CHARACTERISTIC FEATURE OF PLANTS, ARE ESPECIALLY IMPORTANT AND CAN PROTECT PLANTS AGAINST A WIDE VARIETY OF MICROORGANISMS (VIRUSES, BACTERIA, FUNGI) AND HERBIVORES (ARTHROPODS, VERTEBRATES). AS IS THE SITUATION WITH ALL DEFENSE SYSTEMS OF PLANTS AND ANIMALS, A FEW SPECIALIZED PATHOGENS HAVE EVOLVED IN PLANTS AND HAVE OVERCOME THE CHEMICAL DEFENSE BARRIER[63].

SECONDARY METABOLITES, INCLUDING ANTIBIOTICS, ARE PRODUCED IN NATURE AND SERVE SURVIVAL FUNCTIONS FOR THE ORGANISMS PRODUCING THEM. SECONDARY METABOLITES SERVE: (I) AS COMPETITIVE WEAPONS USED AGAINST OTHER BACTERIA, FUNGI, AMOEBAE, PLANTS, INSECTS, AND LARGE ANIMALS; (II) AS METAL TRANSPORTING AGENTS; (III) AS AGENTS OF SYMBIOSIS BETWEEN MICROBES AND PLANTS, NEMATODES, INSECTS, AND HIGHER ANIMALS; (IV) AS SEXUAL HORMONES; AND (V) AS DIFFERENTIATION EFFECTORS. ALTHOUGH ANTIBIOTICS ARE NOT OBLIGATORY FOR SPORULATION, SOME SECONDARY METABOLITES (INCLUDING ANTIBIOTICS) STIMULATE SPORE FORMATION AND INHIBIT OR STIMULATE GERMINATION. FORMATION OF SECONDARY METABOLITES AND SPORES ARE REGULATED BY SIMILAR FACTORS. THUS THE SECONDARY METABOLITE CAN: (I) SLOW DOWN GERMINATION OF SPORES UNTIL A LESS COMPETITIVE ENVIRONMENT AND MORE FAVORABLE CONDITIONS FOR GROWTH EXIST; (II) PROTECT THE DORMANT OR INITIATED SPORE FROM CONSUMPTION BY AMOEBAE; OR (III) CLEANSE THE IMMEDIATE ENVIRONMENT OF COMPETING MICROORGANISMS DURING GERMINATION[64].

CONCLUSION

Secondary metabolites are the useful natural products that are synthesized through secondary metabolism in the plants. The production of some secondary metabolites is linked to the induction of morphological differentiation and it appears that as the cells undergo morphological differentiation and maturation during plant growth. It is observed that *in-Vitro* production of secondary metabolites is much higher from differented tissues when compared to non-differentiated or less –differentiated tissues. There are lots of advantages of these metabolites like there is recovery of the products will be easy and plant cultures are particularly useful in case of plants which are difficult or expensive and selection of cell lines for high yield of secondary metabolites will be easy. Many other examples could be presented with plant metabolic engineering as this research area is developing actively. Metabolic engineering is probably a large step forward but playing on the genes will not solve all the problems that have prevented the development of commercial success in the field of plant secondary metabolites. And Advances in plant cell cultures could provide new means for the cost-effective, commercial production of even rare or exotic plants, their cells, and the chemicals that they will produce. Knowledge of the biosynthetic pathways of desired compounds in plants as well as of cultures is often still rudimentary, and strategies are consequently needed to develop information based on a cellular and molecular level. Because of the complex and incompletely understood nature of plant cells *in-Vitro* cultures, case-by-case studies have been used to explain the problems occurring in the production of secondary metabolites from cultured plant cells. Advance research has succeeded in producing a wide range of valuable secondary phytochemical in unorganized callus or suspension cultures till to date; in other cases production requires more differentiated micro plant or organ cultures[65].

DUE TO THESE ADVANCES, RESEARCH IN THE AREA OF TISSUE CULTURE TECHNOLOGY FOR PRODUCTION OF PLANT CHEMICALS HAS BLOOMED BEYOND EXPECTATIONS[66]. THE MAJOR ADVANTAGES OF A CELL CULTURE SYSTEM OVER THE CONVENTIONAL CULTIVATION OF WHOLE PLANTS ARE AS FOLLOWS:

- Useful compounds can be produced under controlled conditions independent of climatic, environmental changes or soil conditions due to over pollution.
- Cultured cells would be free of microbes and insects.
- The cells of any plants, tropical or alpine, could easily be multiplied to yield their specific metabolites.

- Automated control of cell growth and rational regulation of metabolite processes would reduce labor costs and improve productivity.
- Organic substances are extractable from callus cultures.

Acknowledgments: Author is grateful to the head, Department of Biotechnology, IMS Engineering College Ghaziabad, UP for providing facilities & library consultation. And very special thanks to Mr. Satyendra Kumar Principle research Scientist, Dabur India Limited, Ghaziabad; who is the real source of inspiration and motivation for author during her research work.

REFERENCES:

[1] Jian Zhaoa,T, Lawrence C. Davisb and Robert Verpoortec "Elicitor signal transduction leading to production of plant secondary metabolites" Biotechnology Advances, 283–333, 23 (2005)

[2] Fraenkel, and Gottfried S. "The raison d'Etre of secondary plant substances" *Science* 129 (3361) 1466 470. doi:10.1126/science,129.3361,1466, PMID 13658975(May1959)

[3] "Chemical plants". Retrieved 2008-12-19.

[4] Stamp, and Nancy "Out of the quagmire of plant defense hypotheses".*The Quarterly Review of Biology* 78 (1): 23 55 ,doi:10.1086/367580, PMID 12661508, (March 2003)

[5] Samuni-Blank, M., Izhaki, I., Dearing, MD., Gerchman, Y., Trabelcy, B., Lotan, A., Karasov, WH., Arad, Z. "Intraspecific Directed Deterrence by the Mustard Oil Bomb in a Desert Plant" *Current* 22 (13): 1218–1220, doi:10.1016/j.cub.2012.04.051, (2012)

[6] Srivastava S[1], Srivastava AK., "Hairy root culture for mass-production of high-value secondary metabolites" Crit Rev Biotechnol, 27(1):29-43. 2007 Jan-Mar

[7] Smetanska I[1]. "Production of secondary metabolites using plant cell cultures" Adv Biochem Eng Biotechnol. 2008; 111:187-228. doi: 10.1007/10_2008_103.

[8] A. Kossel "Uber die chemische Zusammensetzung der Zelle" Archiv fur Physiologie(1891)181-186

[9] J.B.Harborne , N.J.Walton,D.E.Brown "Classes and functions of secondary products in chemicals from Plants, Perspectives on Secondary plant products" Imperial college press,pp.1-25, 1996

[10] F. Bourgaud, A. Gravot, S. Milesi, E. Gontier "Production of plant secondary metabolites: a historical perspective" Volume 161, Issue 5, Pages 839–851, October 2001

[11] Biology Encyclopedia

[12] G.F.Payne, V.Bringi, C.Prince, M.L.Shuler "The quest for commercial production of chemicals from plant cell culture in:G.F.Payne,V.Bringi,C.Prince,M.L.Shuler(Eds.), Plant cell and Tissue Culture in Liquid Systems" Hanser, pp.1-10, 1991

[13] Yukimune Y, Tabata H, Higashi Y, Hara Y "Methyl jasmonate-induced overproduction of paclitaxel and baccatin III in Taxus cell suspension cultures" Nature Biotechnol, 14:1129– 32, 1996

[14] Zhao J, Zhu WH, Hu Q, He XW "Improved indole alkaloid production in Catharanthus roseus suspension cell cultures by various chemicals" Biotechnol Lett 2000, 22:1221– 6.

[15] Zhao J, Fujita K, Yamada J, Sakai K "Improved beta-thujaplicin production in Cupressus lusitanica suspension cultures by fungal elicitor and methyl jasmonate" Appl Microbiol Biotechnol, 55:301– 5, 2001a

[16] Zhao J, Hu Q, Guo YQ, Zhu WH. "Elicitor-induced indole alkaloid biosynthesis in Catharanthus roseus cell cultures is related to Ca2+-influx and the oxidative burst" Plant Sci,161:423 – 31, 2001b

[17] Zhao J, Hu Q, Zhu WH. "Enhanced catharanthine production in Catharanthus roseus cell cultures by combined elicitor treatment in shake flasks and bioreactors" Enzyme Microb Technol, 28:673– 81, 2001c

[18] Zhang C, Yan Q, Cheuk W, Wu J. "Enhancement of tanshinone production in Salvia miltiorrhiza hairy root culture by Ag+ elicitation and nutrient feeding" Planta Med, 70:147– 51, 2004

[19] Jian Zhaoa,T, Lawrence C. Davisb, Robert Verpoortec "Elicitor signal transduction leading to production of plant secondary metabolites" Biotechnology Advances 283–333, 23 (2005)

[20] Zhong JJ. "Biochemical engineering of the production of plant-specific secondary metabolites by cell cultures" Adv Biochem Eng Biotechnol,72:1– 26, 2001

[21] Memelink J, Kijne JW, van der Heijden R, Verpoorte R. "Genetic modification of plant secondary metabolite pathways using transcriptional regulators" Adv Biochem Eng Biotechnol, 72:103– 25, 2001

[22] Verpoorte R, Memelink J. "Engineering secondary metabolite production in plants" Curr Opin Biotechnol, 13:181– 7, 2002

[23] Sumner LW, Mendes P, and Dixon RA "Plant metabolomics: large-scale phytochemistry in the functional genomics era" Phytochem, 62:817– 36, 2003

[24] Goossens A, Hakkinen ST, Laakso I, Seppanen-Laakso T, Biondi S, De Sutter V, et al. "A functional genomics approach toward the understanding of secondary metabolism in plant cells" Proc Natl Acad Sci U S A,100:8595– 600, 2003

[25] A.D.Krikorian,F.C.Steward "Biochemical differentiation:the biosynthetic potentialities of growing and quiescent tissue" in:F.C. Steward(Ed.),Plant Physiology, A Treatise,Academic,Press, pp.227-326. 1969

[26] M.H.Zenk, "Chasing the enzymes of secondary metabolism: plant cultures as a pot of gold" Phytochemistry 3861-3863, 30 (1991)

[27] F. Bourgaud', A. Gravot, S. Milesi, E. Gontier "Production of plant secondary metabolites: a historical perspective" Volume 161, Issue 5, Pages 839–851, October 2001

[28] Cheetham, P.S.J "Biotransformations: new routes to food ingredients" Chem Ind., pp. 265-268, 1995

[29] Scragg, A.H. "The production of aromas by plant cell cultures" *In* T. Schepier (ed.), Adv Biochem. Eng. Biotechnol. Vol. 55. Berlin: Springer-Verlag, pp. 239-263,1997

[30] Krings, U. and R.G. Berger "Biotechnological production of flavours and fragrances" Appl. Microb. Biotechnol,49:1-8,1998

[31] Ravishankar, G.A. and S. Ramachandra Rao "Biotechnological production of phyto-pharmaceuticals" J. Biochem. Mol. Biol. Biophys ,4: 73-102, 2000

[32] Shanks, J.V. and J. Morgan "Plant hairy root culture" Curr. Opin. Biotechnol, 10: 151-155, 1999

[33] Giri, A. and M.L. Narasu "Transgenic hairy roots: recent trends and applications" Biotechnol. Adv., 18: 1-22, 2000

[34] Hansen, G. and M.S. Wright "Recent advances in the transformation of plants" Trends Plant Sci., 4: 226-231, 1999

[35] Sajc, L., D. Grubisic, and G. Vunjak-Novakovic "Bioreactors for plant engineering: an outlook for further research" Biochem. Eng. J., 4: 89-99,2000

[36] Kieran, P.M., P.F. MacLoughlin, and D.M. Malone "Plant cell suspension cultures: some engineering considerations" J. Biotechnol, 59: 39-52, 1997

[37] Gantet, P. and J. Memelink "Transcription factors: tools to engineer the production of pharmacologically active plant metabolites" Trends Pharmacol. Sci., 23: 563-569, 2002

[38] P.J. Larkin, W.R. Scowcroft :Somaclonal variation — A novel source of variability from cell cultures for plant improvement" Theoretical and Applied Genetics 197–214, 60 (1981)

[39] R. John Wallace "Antimicrobial properties of plant secondary metabolites" Proceedings of the Nutrition Society, 63, 621–629, (2004)

[40] Chang ST, Chen PF & Chang SC "Antibacterial activity of leaf essential oils and their constituents from Cinnamomum osmophloeum" Journal of Ethnopharmacology 77, 123–127, (2001)

[41] Elgayyar M, Draughon FA, Golden DA & Mount JR "Antimicrobial activity of essential oils from plants against selected pathogenic and saprophytic microorganisms" Journal of Food Protection 64, 1019–1024, (2001)

[42] Imai H, Osawa K, Yasuda H, Hamashima H, Arai T and Sasatsu M "Inhibition by the essential oils of peppermint and spearmint of the growth of pathogenic bacteria" Microbios 106, Suppl. 1, 31–39, (2001)

[43] Marino M, Bersani C & Comi G "Impedance measurements to study the antimicrobial activity of essential oils from Lamiaceae and Compositae" International Journal of Food Microbiology 67, 187–195, (2001)

[44] Imai H, Osawa K, Yasuda H, Hamashima H, Arai T & Sasatsu M "Inhibition by the essential oils of peppermint and spearmint of the growth of pathogenic bacteria" Microbios 106, Suppl. 1, 31–39, (2001)

[45] Shapiro S, Meier A & Guggenheim B "The antimicrobial activity of essential oils and essential oil components towards oral bacteria" Oral Microbiology and Immunology 9, 202–208, (1994)

[46] Oh HK, Jones MB & Longhurst WM "Comparison of rumen microbial inhibition resulting from various essential oils isolated from relatively unpalatable plant species" Applied Microbiology 16, 39–44, (1968)

[47] Oh HK, Sakai T, Jones MB and Longhurst WM "Effect of various essential oils isolated from Douglas fir needles upon sheep and deer rumen microbial activity" Applied Microbiology 15, 777–784, (1967)

[48] R. John Wallace "Antimicrobial properties of plant secondary metabolites" Proceedings of the Nutrition Society, 63, 621–629,(2004)

[49] Hostettmann K & Marston "A Saponins" Cambridge: Cambridge University Press(1995)

[50] Lu CD, Tsai LS, Schaefer DM & Jorgensen NA "Alteration of fermentation in continuous culture of mixed rumen bacteria" Journal of Dairy Science 70, 799–805, (1987)

[51] Williams AG & Coleman GS "The Rumen Protozoa" New York: Springer Verlag New York Inc. (1992)

[52] Euge`ne M, Archime`de H & Sauvant D "Quantitative metaanalysis on the effects of defaunation of the rumen on growth, intake and digestion in ruminants" Livestock Production Science 85, 81–97,(2004)

[53] Orpin CG "Studies on the defaunation of the ovine rumen using dioctyl sodium sulfosuccinate" Journal of Applied Bacteriology 43, 309–318, (1977)

[54] Bird SH & Leng RA "The effect of defaunation of the rumen on the growth of cattle on low-protein high-energy diets" British Journal of Nutrition 40, 163–167,(1978)

[55] Bird SH, Hill MK & Leng RA "The effect of defaunation of the rumen on the growth of lambs on low-protein high energy diets" British Journal of Nutrition 42, 81–87, (1979)

[56] Eadie JM & Shand WJ "The effect of synperonic NP9 upon ciliate free and faunated sheep" Proceedings of the Nutrition Society 40, 113A, (1981)

[57] Lovelock LKA, Buchanan-Smith JG and Forsberg CW "Difficulties in defaunation of the ovine rumen" Canadian Journal of Animal Science 62, 299–303, (1982)

[58] Newbold CJ & Chamberlain DG "Lipids as rumen defaunating agents" Proceedings of the Nutrition Society 47, 154A, (1988)

[59] Matsumoto M, Kobayashi T, Takenaka A and Itabashi H "Defaunation effects of medium-chain fatty acids and their derivatives on goat rumen protozoa" Journal of General Microbiology37, 439–445, (1991)

[60] Machmuller A, Osowski DA, Wanner M and Kreuzer M "Potential of various fatty feeds to reduce methane release from rumen fermentation *in-Vitro* (Rusitec)" Animal Feed Science and Technology 71, 117–130, (1998)

[61] Broudiscou L, Sylvie P & Poncet C "Effect of linseed oil supplementation on feed degradation and microbial synthesis in the rumen of ciliate free and refaunated sheep" Animal Feed Science and Technology 49, 189–202, (1994)

[62] R. John Wallace "Antimicrobial properties of plant secondary metabolites" Proceedings of the Nutrition Society 63, 621–629,(2004)

[63] M. Wink "Plant breeding: importance of plant secondary metabolites for protection against pathogens and herbivores", Volume 75, Issue 2, pp 225-233 ,January 1988

[64] Demain AL[1], Fang A. "The natural functions of secondary metabolites" Adv Biochem Eng Biotechnol. ; 69:1-39, 2000

[65] Davioud E, Kan C, Hamon J, Tempe J and Husson HP "Production of indole alkaloids by *in-Vitro* root cultures from Catharanthus trichophyllus" Phytochemistry, 28:2675–80, 1989

[66] Md. Sarfaraj Hussain, Sheeba Fareed, Saba Ansari, Md. Akhlaquer Rahman, Iffat Zareen Ahmad,[1] and Mohd. Saeed[1,] "Current approaches toward production of secondary plant metabolites" J Pharm Bioallied Sci. Jan-Mar; 4(1): 10–20, 2012

International Journal of Engineering Research and General Science Volume 3, Issue 5, September-October, 2015
ISSN 2091-2730

Voice Recognition based Home Automation System for Paralyzed People – A Review

Mukesh Kumar [1], Shimi S.L [2].

[1]M.E. Student, Electrical Engineering Department, NITTTR, Chandigarh

[2]Assistant Professor, Electrical Engineering Department, NITTTR, Chandigarh

[1] mukesh.elect@nitttrchd.ac.in, [2] shimi.reji@gmail.com

Abstract— This paper presents the review on different voice recognition based home automation technologies for the paralyzed and elderly people. Elderly people and people suffering from paralysis require third person assistance most of the time. The home automation systems are gaining popularity now a day due to their wide operation capability. Some use these home automation system seeking luxury while for the disabled people it provides a great assistance. With voice as interacting medium to control devices it becomes more user friendly and easy to operate the system rather than using some remote controller which requires physical movement which the disabled person may find uncomfortable. The voice recognition based home automation system for paralyzed and elderly people are mainly focus on controlling the electrical appliances in the home like switching the fan on or off, turning a.c on or off etc. The other voice recognition based automation system which aids the disabled people is voice automated wheel chair. There has not been any voice automated control for the bed elevation positioning by which disabled people can adjust the elevation angle of bed according to their need and comfort. From above perspective, this paper attempts to present review of existing home automation system for the paralyzed people, deliberations on pros and cons, and a proposal for voice recognition based home automation system which can control the home appliances and can actuates the bed elevation according to the disabled person need and comfort.

Keywords— Home automation system, Paralyzed people, Voice recognition, Electrical Appliances.

.

INTRODUCTION

People with severe speech and motor impairment due to cerebral palsy are great difficult to move independently and also cannot control home electric devices and need third person's assistance. Table 1 shows the statistical data of the number of people suffering from paralysis in different countries. This data shows that every 1 in 100 people is living with paralysis. The home automation system has much to offer these people. Interfaces based on gestures or voices have been widely used for home automation. However, gesture recognition is difficult or impossible for people suffering from severe motor impairments, such as paraplegia and tremors. The speech integrated home automation systems provides an alternative to the above problem.

Table 1Populations of People Suffering from Paralysis in Different Countries

Country	Extrapolated Prevalence	Population
United states of America	2,642,898	293,655,405
Canada	292,570	32,507,874
United Kingdom	542,436	60,270,708
India	9,585,635	1,065,070,607
Germany	741,821	82,424,609
Italy	522,517	58,057,477
China	11,689,628	1,298,847,624

The wireless home automation system [1] built to control lights and other electrical appliances at home or office using voice commands and touch screen responses. The system is mainly developed for the disabled people. The voice recognition application is implemented using the Microsoft speech API running on windows operating system. Since the control action is taking place wirelessly the system eliminates the complexity arises due to the wires. The speech recognition accuracy of the system is very high about 90-95%.

The system allows the disable and elderly people to control the home appliances [2] using the voice commands wirelessly. The speech recognition application is implemented using the LabVIEW software. The speech recognition accuracy of the system is more than 90%. The Zigbee module is used to control appliances wirelessly [1] [2]. The use of PC makes system more expensive [1] [2].
An Intelligent Home Navigation System (IHNS) which comprises of a wheelchair, voice module and navigation module [3]. The wheel chair automatically navigates to the different locations according to the voice commands received with the help of predefined routes of house. The wheel chair is also comprises of a obstacle avoidance feature. The voice recognition is done through the SR-07 speech recognition module which eliminates the need of PC.

The system has been developed to provide support and assistance to the disabled or elderly people at home [4]. The user can control the home appliances by voice or through the graphical user interface developed on the android platform. The android operating phone captures the voice and process the voice. The processed data is sent to the Arduino using Bluetooth and accordingly the devices are controlled. The use of Bluetooth limits the range of operation up to 20 meters.

The DSP processor is used for the voice recognition process [5]. The digital signal processor processes the voice and control the appliance accordingly. The voice recognition algorithm is written in the c language. The Zigbee module is used to control devices wirelessly. The various home appliances are controlled with the help of microcontroller and relay driver circuit.

The voice recognition based industrial automation system is developed [6] so that the disabled people can use the system for automation of industrial loads using their voice commands and thereby find jobs in industries. The voice recognition is performed using the HM2007 voice recognition module. The system has 95% of voice recognition accuracy for the person uses his own profile and the accuracy is 80% when person uses other person profile.

The voice recognition module V3 is used to recognize the voice commands [7]. It can store 80 commands in its library of 1500ms each. Only seven commands are effective at a time. The voice recognition module V3 replaces other commercially available modules due to its economical price. The home automation system is developed using this module to control the various home appliances like cooler, Air conditioner etc. The voice recognition module has an accuracy of 99% under ideal conditions.

PROPOSED SYSTEM

Fig 1 shows the block diagram of the proposed system. The voice command is by the user through the microphone. The microphone is connected to the voice recognition module where the voice commands are compared with the previously stored samples. If the voice command is recognized the Ardunio controller will actuate the corresponding load with the help of the relay driver circuit. The bed elevation control circuit comprises of a motor and motorized jack to lift the bed up or lower the bed down as shown in Fig 2.

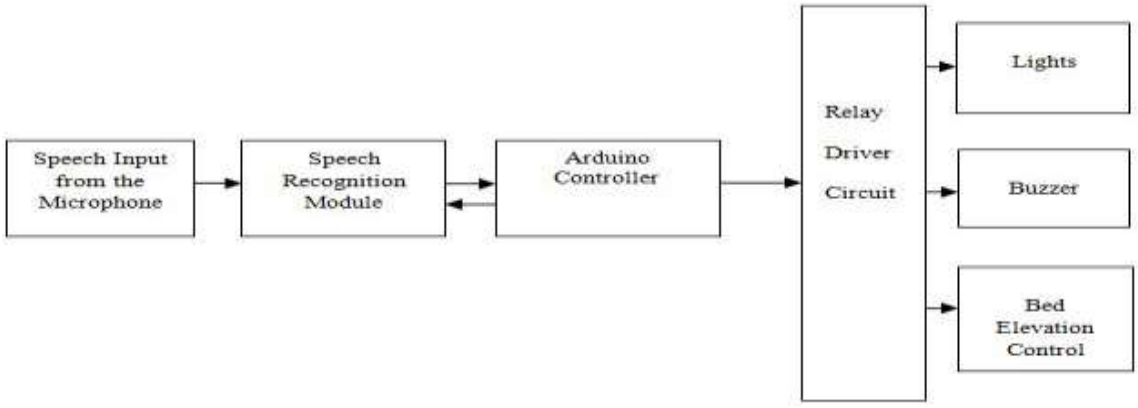

Fig.1 Block Diagram of Proposed System

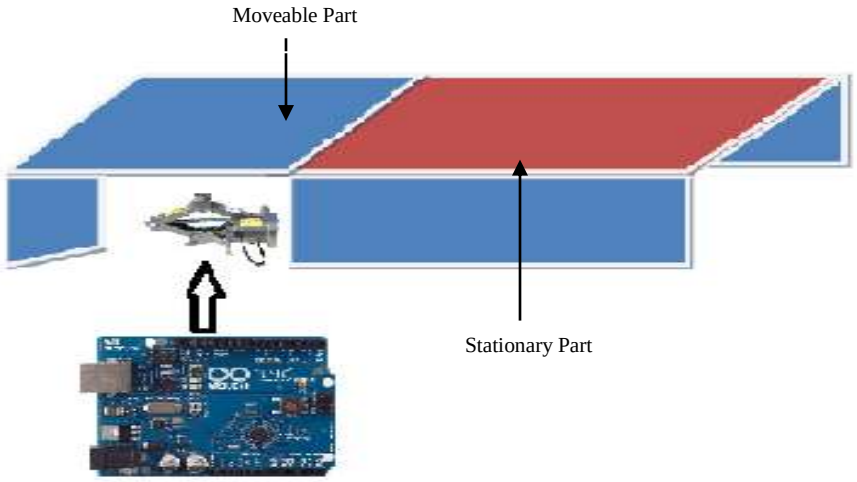

Fig.2 Motorized Jack Positioning to Lift the Bed Up or Lower it Down

The motorized jack is fitted beneath the moveable part of the bed. The Arduino controller actuates the relays which further make the motor to move in clockwise and anti clock wise direction due to which jack opens up or closes in vertical direction which in turn lifts the bed up or down. The programming of the voice recognition module and controlling section will be done in Arduino IDE.

CONCLUSION

This paper reviews the home automation system based on the voice recognition for the paralyzed people or elderly people, and since there has not been any voice recognition based home automation system which actuates the bed elevation according to the user voice commands, a new system is proposed. Hence this paper proposes the implementation of an efficient and robust voice recognition based home automation system for the paralyzed people which can change the state of home appliances on or off and adjust the bed elevation to different angles according to the person voice commands.

REFERENCES:

[1] T.Kirankumar and B. Bhavani "A Sustainable Automated System for Elderly People Using Voice Recognition and Touch Screen Technology", International Journal of Science and Research (IJSR), Vol. 2, pp. 265-267, August 2013.
[2] Arthi.J.E and M.Jagadeeswari "Control of Electrical Appliances through Voice Commands", IOSR Journal of Electrical and Electronics Engineering, Vol. 9, pp. 13-18, February 2014.
[3] Rajesh Khanna Megalingam, Ramesh Nammily Nair, and Sai Manoj Prakhya "Automated Voice based Home Navigation System for the Elderly and the Physically Challenged", International Conference on Advanced Communication Technology, Seoul, pp. 603-608, February 2011.
[4] Norhafizah bt Aripin and M. B. Othman "Voice Control of Home Appliances using Android" , International Conference on Electric Power, Electronic, Communication, Control, And Informatic Systems, Malang ,pp. 142-146, August 2014.
[5] Parameshachari B D, Sawan Kumar Gopy, Gooneshwaree Hurry and Tulsirai T. Gopaul."A Study on Smart Home Control System through Speech", International Journal of Computer Applications, Vol. 69,pp. 30-39, May 2013.
[6] A.K.Gnanasekar, and P.Jayavelu "Voice Based Wireless Industrial Automation with Enhanced Feedback System", Proceedings of the International. Conference on Advances in Computer, Electronics and Electrical Engineering, pp. 51-55, 2012.
[7] Gayatri R.Shinde, Jyoti N.Borole and Kantilal P. Rane "Voice and Non Voice Control Based Wireless Home Automation System", International Journal of Innovative Research in Science, Engineering and Technology, Vol. 4, pp. 5064-5067, July 2015.
[8] Manisha Bansode, Shivani Jadhav and Anjali Kashyap "Voice Recognition and Voice Navigation for Blind using GPS", International Journal of Innovative Research in Electrical, Electronics, Instrumentation and Control Engineering, Vol. 3, pp. 91-94, April 2015

International Journal of Engineering Research and General Science Volume 3, Issue 5, September-October, 2015
ISSN 2091-2730

OVERVIEW OF GRAIN DRYING AND STORAGE PROBLEMS IN INDIA

Javed Ali*, Aaushi Sharma and Poonam Rani
College Of Technology, G. B. Pant University of Agriculture & Technology,
Pantnagar, India
*Email: javedali28@gmail.com

Abstract- India produces about 150 million tons of food grains per year and production is rising due to higher cropping intensities and the introduction of high-yielding varieties. However, annual post production losses are 10%, which means that about 15 million tons of food grains are lost during harvesting, threshing, and storage. So these losses can be minimized by a drying operation that can preserve grain. In India, 70% of the grain stored is sun dried which is not a best method to drying crops. Farmers use sun drying due to the non-availability of dryers within their reach; high initial capital investment required. So my main concern is to provide farmers a modern drying-cum-storage complex for drying crops and their proper storage. An awareness of availability of dryers and of their use and advantages in drying food grain for better storage and marketing is lacking among crop growers. This paper describes the use of various types of dryers in the Indian food industry and the efforts of research and development organizations to devise dryers suitable for individuals or small groups in the rural population. And what can be done to minimize the losses of food grain with the help of various scientific drying method or different scientific storage structures.

Keywords: Food grain; Drying; Storage; Dryers; Food safety; India.

Introduction

India produces about 150 million tonnes of food grains per year. The major components of production are 47 million tonnes of wheat, 64 million tonnes of rice, and 13 million tonnes of pulses (Anon. 1987). Due to technological advances in agriculture and the introduction of high-yielding varieties, this may increase. From this production, an average 10% is lost during postharvest operations between the field and the consumers. This means that about 15 million tonnes of food grain, valued at about $A240 million (Indian Rupees 2400 million) goes to waste. The major share of the loss occurs during storage of surplus stock. Among the various causes of losses, the most important one is improper drying before storage. The preservation of agricultural produce by drying is a long-established technique. Sun drying in the open, on mud-plastered or concrete floors, is the conventional method of drying grain and also cash crops like chilies, and plantation and horticultural crops. The drying time required in the open sun for these crops ranges from 5 to 45 days depending upon the crop to be dried. Unfavorable weather conditions are likely to occur during the drying period and degradation in quality of the final produce therefore becomes unavoidable. Annual postproduction losses by crop in India, expressed as a percentage of total production, are estimated to be as follows: wheat, 8%; paddy, 11%; pulses, 9.5%; and all food grains, 9.3%.

It is well-known that deterioration in quality caused by improper drying cannot be eliminated until improved drying systems based on mechanical dryers have been adopted. However, for many reasons, these systems have not been adopted. The main reason that is encountered is a lack of organizational or government incentive to the farmer to deliver a quality product that might command a premium price. This results in not only a negative attitude, but also leads to the overall quality of the product gathered at market points being alarmingly poor.

A second important reason for not using dryers is their high initial costs. Most of the commercially available dryers are designed to suit the needs of the processing industry and their output capacity is therefore far above the needs of individuals, or even of farmer groups.An awareness of availability of dryers and of their use and advantages in drying food grain for better storage and marketing is lacking among crop growersThis paper describes the use of various types of dryers in the Indian food industry and the efforts of research and development organizations to devise dryers suitable for individuals or small groups in the rural population. However, even with properly dried grain, scientific storage remains important and recent advances in developing various storage structures are also described.

DRYING

Drying is one of the most practical methods for primary preservation. A corollary to the hypothesis is that system dryers offer an advantage over the traditional drying practices under certain conditions. The agricultural commodities that are traditionally dried are

paddy, maize, groundnuts, soybeans, coffee berries, some fruits (e.g. mangoes and longan), spices (e.g. chill), garlic, onions), fish, meat, chipped root crops (e.g. cassava and sweet potato), and coconut meat (cope). Direct sun drying or free/natural convection drying over a fire is the traditional practice.

Methods of grain drying

Generally speaking, grain drying can be classified into sun drying and mechanical drying.

India is a large agricultural country at a low level of agricultural mechanisation. particular, mechanical grain drying capacity cannot keep pace with the increase in grain production. At present, only about 30% of wet grain in state depots is mechanically dried; the rest has to be sun dried. All grain retained at farm level for consumption by farmers is sun dried.

Sun Drying

As is well known, sun drying has greater requirements of labour and space, especially in the case of large-scale and centralized treatment Although labour is relatively cheap in India, the cost of commercial-scale sun drying is still very high.In addition, sun drying depends very much on the weather, and takes more time. If there are long spells of bad weather, there is a high risk of grain losses. Also, the handling losses during sun drying are not insubstantial. However, sun drying does have some advantages. There appears to be no appreciable reduction in grain quality associated with the process, and grain can be kept fresh, of good colour, and free of contaminants.There are many ways of sun drying in India. The most popular method is to spread wet grain on the ground, turning it from time to time to remove extra moisture.

In the north-east, farmers usually put maize cobs into hubs. Moisture is removed by natural aeration during storage. Farmers also take measures before maize is harvested. When it is in its waxy ripening stage, farmers tear the husks off the cobs for sun drying while on the stalk. This method not only removes moisture but also promotes maturity, thus increasing yield. Under the climatic conditions of the north-east, it takes about 10 days to reduce maize moisture by 4%.Clearly, the main disadvantages of sun drying are that it is more labour intensive and takes longer. Some local governments give farmers incentives to encourage sun drying at farm level so as to solve the problem of insufficient capacity in state depots. This has not been successful to date.

Mechanical Drying

A mechanical way to remove the water from wet grains by blowing (heated) air through the grain. This drying is done until the grain has the desired moisture content.

Mechanical drying has some advantages over sun drying:

- Better control over the temperature and moisture content
- Drying can be done day or night
- Less labor (especially if mixing is mechanical e.g. re-circulating dryers)
- Mechanical drying will lead to more even drying of grain and higher milling yield and head rice recovery.

Since rice quality is becoming more important to rice consumers, medium-sized grain dryers have become a common sight throughout Asia. For production of premium quality rice or seed, mechanical drying with heated air dryers is highly recommended.

Commercial use of dryers

Dryers are used extensively in grain processing industries such as rice milling, pulse milling, and oil extraction. Here the need for dryers has been realised not only for proper storage of stock but also for timeliness of subsequent operations where wetting of grain and redrying are involved.

In the case of the rice milling industry, parboiling of rice is a common practice. The population of the coastal belt of the country consumes parboiled rice and about 70% of production is processed in this manner. The paddy is soaked in water for variable lengths of time depending on the process used and is then steaming.

Dryers are also used in the pulse milling industry. Here both LSU-type and flat-bed perforated-floor dryers are wed, ranging in capacity from 1-4 t/h. There are about 4000 pulse mills in India having an average processing capacity of 10-20 t/day. Dryers are required in industry for the following reasons:

- to dry the stock purchased from market before storing it; and
- to dry the grain which has become wet during processing.

Use of dryers at farmer level or in community drying systems

About 70% of total grain production in India is retained at farmer level: only 30% is sold on the open market. This means that a sizeable quantity of about 105 million tonnes is kept by farmers. The losses here, though perhaps not felt by individuals, on a collective basis have a substantial impact on the country. It is therefore essential that drying technology be disseminated to this group which is a major custodian of the nation's grain.To promote the use of dryers in rural areas, the concept of a community drying-cum-storage system was put forward by T.P. Ojha in 1984. He suggested that changes in ecological balances and the introduction of high-yielding varieties of field crops necessitated the use of mechanical dryers and other devices to protect the food grains from spoilage due to untimely rains.

If rain-soaked food grains are not dried properly, farmers have to sell their excess stocks at low prices to meet urgent financial needs. A community drying-cum-storage centre would therefore serve them well by way of protecting the grain from spoilage and also by advancing temporary loans on their grain deposits. As soon as grain prices stabilise, stocks can be sold and payments can be made to the farmers after deducting dues such as rental and service charges, loans paid, and interest on advances. Such a system would no doubt benefit farmers. They would not be required to make forced sales of their produce and, as a result, storage losses would be minimised.

For such complexes, selection of a dryer of the correct design is very important. The largecapacity dryers used in grain-processing industries are not economical or feasible for most farmer groups. In India, the average village has a population of about 1000 and the small amount of surplus grain available for drying at this level suits dryers of 2-4 t/day capacity operating for 60 days per year. In India, many research organizations have developed, or are currently developing dryers for village groups, but so far with little success. The main considerations for selection of a grain dryer suited to this level are:

- The dryer should be of a size that matches the amount of grain available in a village or a cluster of villages;
- The dryer's cost should be within the reach of users;
- It must be simple in construction and operation and easily understandable to users;
- The dryer should be simple in design so that it is easy for local artisans to repair, and
- The dryer should be suitable for drying a range of crops.

Grain dryers suitable for rural level use

Some important grain dryers developed at different R&D institutions and agricultural universities are described in the following sections.

Small-Capacity, Continuous Grain Dryer

The dryer developed at G.B. Pant University of Agricultural and Technology, Pantnagar, is a continuous type consisting of a frame, grain column, plenum chamber, feed hopper, discharge hopper, heating unit, and blower (Fig. 2). The grain column consists of two vertical columns sandwiched between two vertical screens. Each screen wall consists of an expanded metal netting and wire mesh

screen on the inner and outer sides. The plenum chamber has been provided between the two grain columns in order to distribute the air uniformly and at right angles to the direction of grain movement. A centrifugal blower forces the air at 37 m3/min airflow against 2.5 cm of Hg. The air is heated from 40°C to 70°C by 20 kW electric heaters. The dryer has capacities of 0.8 t/h for wheat, 0.8 Ah for paddy, 0.96 t/h for maize, and 0.8 t/h for red gram. The cost of the dryer, excluding the heater and fan, is about $A330 (Indian Rupees 3300), based on 1982 estimates, and the cost of drying is around $A0.50/t (Singh et al. 1982).

Cup and Cone Dryer for Paddy Drying

A somewhat different design of dryer has been tested at the Paddy Processing Research Centre (PPRC) at Thiruwarur in India. It consists (Fig. 3) of five cups each having a diameter of 1070 mm and a slope of 52°. Each cup and cone is made of mild steel rod and wire mesh. A hot-air duct of 300 mm diameter passes through the centre of the dryer from the top; the bottom end of the duct is closed.

Individual cups and cones are mounted one above the other by means of bolts and nuts. Paddy passes through the inner surfaces of the cups and exteriors of the cones. To divert the flow of paddy from the outer surfaces of the cones to the inner surfaces of the cups, cylindrical retainers of mild steel sheet are provided. A two-way valve is provided just beneath the bottom of the dryer. A slide is provided at the junction of the two-way valve and the bottom of the cup. This is kept completely open during recirculation and bagging. The hot air generated in a husk-fired furnace passes through a vertical duct and enters the paddy column by means of a central duct having perforations at points covered by cones and the top portion. A circulation rate of 3.5 to 4.5 tonnes per hour is maintained while drying.

Trials conducted during high humidity weather indicated that 950 kg of parboiled paddy of 30% m.c. can be dried to 14% in 2 hours at a drying temperature of 120°c and an airflow rate of 127.5 m^3/min. The drying cost is calculated at $A2.10(Rs 21.33)/t (Pillaiyar et al. 1982).

Community Grain Dryer

The dryer developed at the Central Rice Research Institute (CRRI), Cuttack, is useful for village communities or small-scale rice millers (Fig. 5). It consists of a drying chamber, a husk-fired furnace (inclined grate 0.5 m² at 45° inclination, horizontal revolving grate 0.15 m², and fluted roller-type husk feeding mechanism), solar collector (flat plate, black painted galvanised iron corrugated sheet with 23° slope towards south, 43.5 m² surface area provided with 40 mm thick insulation of paddy straw and tar-felt sheet combination), blower {backward curved fan operated by a 5 hp motor with airflow capacity of 160 m³/min at 25 mm water gauge static pressure), and a bucket elevator (2 t/h capacity operated by a 0.5 hp electric motor). Generally, it takes 6.5 hours to dry 1 t of paddy from 24% to 1496 m.c. The cost of the dryer is estimated at $A5000 and the cost of drying $A10.6/t (Kachru et al. 1986).

Solar cum Husk-Fired Paddy Dryer

This dryer has been developed at the Indian Institute of Technology (IIT.), Kharagpur (Fig. 6). The system consists of an unglazed flatplate collector which houses an inclined-type husk-fired grated furnace, a 3 hp electric blower and a batch-type dryer. Dampers are provided to put either the collector or the furnace into operation, depending on weather conditions. The absorber surface is a corrugated galvanised iron sheet coated with ordinary blackboard paint. A false roof of bamboo functions as an insulator. Two sides are closed to form channels for airflow. The blower assembly forces the heated air to pass it onto a batch dryer. The capacity of the dryer is I t/day. The cost of the dryer has been estimated at $A2000 and drying cost at $A8.8 /t (Kachru et al. 1986).

Storage Structures at Farmer Level

The major construction materials for storage structures in rural areas are mud, bamboo, stones, and plant materials. They are neither rodent-proof, nor secure from fungal and insect attack. On average, out of a total 6% loss of food grain in such storage structures, about half is due to rodents, and half to insects and fungi. Some of the major considerations in building a storage structure to minimise losses are:

- the structure should be elevated and away from moist places in the house;
- as far as possible, the structure should be airtight, even at loading and unloading ports;
- rodent-proof materials should be used for construction of rural storages;
- the area surrounding the structure should be clean to minimise insect breeding; and
- the structure should be plastered with an impervious clay layer to avoid termite attack, or attack by other insects.

Various research and development organizations in India have identified some proven, age-old structures from certain areas of the country and based on these, some improvised storage structures have also been developed and recommended for use at farmer level.

For scientific storage, drying of food grains to a safe moisture level is a top priority. In India there are about 35 000 dryers in the rice and pulse milling industry, but all of them are used to process the grain. The use of dryers to dry surplus grain kept for storage is not common. The main reasons for this are a lack of awareness among the rural populations, high capital cost, and no incentive given for farmers to produce properly dried grain. An immediate answer to this problem would therefore be to develop and select a proper size of dryer which is simple in construction and operation, and lower in cost.

Setting up a community drying-cum-storage complex as suggested by Ojha (1984) has great potential as it will help to reduce losses and to provide a better return for the grower. The types of dryers suitable for this level are identified and described. They need to be popularised among potential users. Storage of grain in India is done at many levels. The major production is stored at farmer level and the root cause of massive storage loss lies here. The suitable low-cost structures developed have been identified.

Conclusions

India produces about 150 million tonnes of food grains per year. Production has been steadily increasing due to advancement in production technology, but losses have remained static at 10%. This means that the loss of food grains is also increasing with the increase in food production. The main reason for this is improper storage, and an average of 6% out of a total 10% loss takes place during storage of food grains. The various are described in this paper by which we can minimise the loss of food grains.

On-farm storage is also important as it stores the surplus for a short duration and appropriate structures are explained with design features and construction procedures. Large-scale structures like silos and organizationally maintained structures are also explained. The use of dryers and scientific storage practices, if followed, can reduce the loss by about 6% and this will save Rs 13 500 million ($A1350 million) every year, and make available an additional 9 million tonnes of grain to feed the people.

REFERENCES:

Anonymous 1987. India 1986, a reference manual. Allied Publishers. 772 p.

Birewar, B.R. 1985. Recent development in storage structures. In: Storage of agricultural durables and semi-perishables. CIAE, Bhopal, 90-93.

Chouksey, R.G. 1985. Bag and bulk storage of food grains at farmers level. In: Storage of agricultural durables and semi-perishables. CIAE, Bhopal, 5556.

Ojha, T.P. 1985. Problems and prospects of community type drying-cum-storage complexes in rural areas. In: Storage of agricultural durables and semi-perishables. CIAE, Bhopal, 1-6.

CHIEF."Grain conditioning, storage, aeration guide". IRRI, Safe storage condition for grain.

North Dakota State University, Cooperative Extension Service, 1974, Grain Drying on the Farm.
Pillaiyar, P., Yusuff, K.M., Narayanswamy, R.V., Venkatesan, V., and Ramachandran, K. 1981. Drying parboiled paddy with cup and cone dryer. Journal of Agricultural Engineering, 18, 122-126

International Journal of Engineering Research and General Science Volume 3, Issue 5, September-October, 2015
ISSN 2091-2730

LOCATION BASED QUERY ON LOCATION SERVER FOR PRIVACY EFFICIENCY

Mr. Naveen Kumar.Chundy
Computer Science and Engineering
BVSR Engineering College
Chimakurthy A.P. India
naveenchundy@gmail.com

Mrs. K.Suma Anusha M.Tech
Asst.Professor Dept.of CSE
BVSR Engineering College
Chimakurthy A.P. India
Kondaveeti.suma@gmail.com

Abstract— In this paper we present a solution to one of the location-based query problems. This problem is defined as follows: (i) a user wants to query a database of location data, known as Points Of Interest (POIs), and does not want to reveal his/her location to the server due to privacy concerns; (ii) the owner of the location data, that is, the location server, does not want to simply distribute its data to all users. The location server desires to have some control over its data, since the data is its asset. We propose a major enhancement upon previous solutions by introducing a two stage approach, where the first step is based on Oblivious Transfer and the second step is based on Private Information Retrieval, to achieve a secure solution for both parties. The solution we present is efficient and practical in many scenarios. We implement our solution on a desktop machine and a mobile device to assess the efficiency of our protocol. We also introduce a security model and analyse the security in the context of our protocol. Finally, we highlight a security weakness of our previous work and present a solution to overcome it.

Keywords—componentdata mining,computing,users,mobile service providers,Location Server,civil laibility,Black mail,Free storage

1. Introduction

What is Data Mining?

Structure of Data Mining

Generally, data mining (sometimes called data or knowledge discovery) is the process of analyzing data from different perspectives and summarizing it into useful information - information that can be used to increase revenue, cuts costs, or both. Data mining software is one of a number of analytical tools for analyzing data. It allows users to analyze data from many different dimensions or angles, categorize it, and summarize the relationships identified. Technically, data mining is the process of finding correlations or patterns among dozens of fields in large relational databases.

How Data Mining Works?

While large-scale information technology has been evolving separate transaction and analytical systems, data mining provides the link between the two. Data mining software analyzes relationships and patterns in stored transaction data based on open-ended user queries. Several types of analytical software are available: statistical, machine learning, and neural networks. **Generally, any of four types of relationships are sought:**

- **Classes**: Stored data is used to locate data in predetermined groups. For example, a restaurant chain could mine customer purchase data to determine when customers visit and what they typically order. This information could be used to increase traffic by having daily specials.

- **Clusters**: Data items are grouped according to logical relationships or consumer preferences. For example, data can be mined to identify market segments or consumer affinities.

- **Associations**: Data can be mined to identify associations. The beer-diaper example is an example of associative mining.

- **Sequential Patterns**: Data is mined to anticipate behavior patterns and trends. For example, an outdoor equipment retailer could predict the likelihood of a backpack being purchased based on a consumer's purchase of sleeping bags and hiking shoes.

Data mining consists of five major elements:

1) Extract, transform, and load transaction data onto the data warehouse system.
2) Store and manage the data in a multidimensional database system.
3) Provide data access to business analysts and information technology professionals.
4) Analyze the data by application software.
5) Present the data in a useful format, such as a graph or table.

Different levels of analysis are available:

- **Artificial Neural Networks**: Non-linear predictive models that learn through training and resemble biological neural networks in structure.

- **Genetic Algorithms**: Optimization techniques that use process such as genetic combination, mutation, and natural selection in a design based on the concepts of natural evolution.

- **Decision Trees**: Tree-shaped structures that represent sets of decisions. These decisions generate rules for the classification of a dataset. Specific decision tree methods include Classification and Regression Trees (CART) and Chi Square Automatic Interaction Detection (CHAID). CART and CHAID are decision tree techniques used for classification of a dataset. They provide a set of rules that you can apply to a new (unclassified) dataset to predict which records will have a given outcome. CART segments a dataset by creating 2-way splits while CHAID segments using chi square tests to create multi-way splits. CART typically requires less data preparation than CHAID.

- **Nearest Neighbor Method**: A technique that classifies each record in a dataset based on a combination of the classes of the *k* record(s) most similar to it in a historical dataset (where *k*=1). Sometimes called the *k*-nearest neighbor technique.

- **Rule Induction**: The extraction of useful if-then rules from data based on statistical significance.

- **Data Visualization**: The visual interpretation of complex relationships in multidimensional data. Graphics tools are used to illustrate data relationships.

Characteristics of Data Mining:

- **Large Quantities of Data**: The volume of data so great it has to be analyzed by automated techniques e.g. satellite information, credit card transactions etc.
- **Noisy, Incomplete Data**: Imprecise data is the characteristic of all data collection.
- **Complex Data Structure**: conventional statistical analysis not possible
- **Heterogeneous Data Stored In Legacy Systems**

Benefits of Data Mining:

1) It's one of the most effective services that are available today. With the help of data mining, one can discover precious information about the customers and their behavior for a specific set of products and evaluate and analyze, store, mine and load data related to them
2) An analytical CRM model and strategic business related decisions can be made with the help of data mining as it helps in providing a complete synopsis of customers
3) An endless number of organizations have installed data mining projects and it has helped them see their own companies make an unprecedented improvement in their marketing strategies (Campaigns)
4) Data mining is generally used by organizations with a solid customer focus. For its flexible nature as far as applicability is concerned is being used vehemently in applications to foresee crucial data including industry analysis and consumer buying behaviors
5) Fast paced and prompt access to data along with economic processing techniques have made data mining one of the most suitable services that a company seek.

Advantages of data mining:

1. *Marketing / Retail:*

Data mining helps marketing companies build models based on historical data to predict who will respond to the new marketing campaigns such as direct mail, online marketing campaign…etc. Through the results, marketers will have appropriate approach to sell profitable products to targeted customers.

Data mining brings a lot of benefits to retail companies in the same way as marketing. Through market basket analysis, a store can have an appropriate production arrangement in a way that customers can buy frequent buying products together with pleasant. In addition, it also helps the retail companies offer certain discounts for particular products that will attract more customers.

2. *Finance / Banking*

Data mining gives financial institutions information about loan information and credit reporting. By building a model from historical customer's data, the bank and financial institution can determine good and bad loans. In addition, data mining helps banks detect fraudulent credit card transactions to protect credit card's owner.

3. *Manufacturing*

By applying data mining in operational engineering data, manufacturers can detect faulty equipments and determine optimal control parameters. For example semi-conductor manufacturers has a challenge that even the conditions of manufacturing environments at different wafer production plants are similar, the quality of wafer are lot the same and some for unknown reasons even has defects. Data mining has been applying to determine the ranges of control parameters that lead to the production of golden wafer. Then those optimal control parameters are used to manufacture wafers with desired quality.

4. *Governments*

Data mining helps government agency by digging and analyzing records of financial transaction to build patterns that can detect money laundering or criminal activities.

5. Law enforcement:

Data mining can aid law enforcers in identifying criminal suspects as well as apprehending these criminals by examining trends in location, crime type, habit, and other patterns of behaviours.

6. Researchers:

Data mining can assist researchers by speeding up their data analyzing process; thus, allowing those more time to work on other projects.

What is Secure Computing?

Computer security (Also known as cyber security or IT Security) is information security as applied to computers and networks. The field covers all the processes and mechanisms by which computer-based equipment, information and services are protected from unintended or unauthorized access, change or destruction. Computer security also includes protection from unplanned events and natural disasters. Otherwise, in the computer industry, the term security -- or the phrase computer security -- refers to techniques for ensuring that data stored in a computer cannot be read or compromised by any individuals without authorization. Most computer security measures involve data encryption and passwords. Data encryption is the translation of data into a form that is unintelligible without a deciphering mechanism. A password is a secret word or phrase that gives a user access to a particular program or system.

Diagram clearly explain the about the secure computing

Working conditions and basic needs in the secure computing:

If you don't take basic steps to protect your work computer, you put it and all the information on it at risk. You can potentially compromise the operation of other computers on your organization's network, or even the functioning of the network as a whole.

1. Physical security:

Technical measures like login passwords, anti-virus are essential. (More about those below) However, a secure physical space is the first and more important line of defense.

Is the place you keep your workplace computer secure enough to prevent theft or access to it while you are away? While the Security Department provides coverage across the Medical center, it only takes seconds to steal a computer, particularly a portable device like a laptop or a PDA. A computer should be secured like any other valuable possession when you are not present.

Human threats are not the only concern. Computers can be compromised by environmental mishaps (e.g., water, coffee) or physical trauma. Make sure the physical location of your computer takes account of those risks as well.

2. Access passwords:

The University's networks and shared information systems are protected in part by login credentials (user-IDs and passwords). Access passwords are also an essential protection for personal computers in most circumstances. Offices are usually open and shared spaces, so physical access to computers cannot be completely controlled.

To protect your computer, you should consider setting passwords for particularly sensitive applications resident on the computer (e.g., data analysis software), if the software provides that capability.

3. Prying eye protection:

Because we deal with all facets of clinical, research, educational and administrative data here on the medical campus, it is important to do everything possible to minimize exposure of data to unauthorized individuals.

4. Anti-virus software:

Up-to-date, properly configured anti-virus software is essential. While we have server-side anti-virus software on our network computers, you still need it on the client side (your computer).

5. Firewalls:

Anti-virus products inspect files on your computer and in email. Firewall software and hardware monitor communications between your computer and the outside world. That is essential for any networked computer.

6. Software updates:

It is critical to keep software up to date, especially the operating system, anti-virus and anti-spyware, email and browser software. The newest versions will contain fixes for discovered vulnerabilities.

Almost all anti-virus have automatic update features (including SAV). Keeping the "signatures" (digital patterns) of malicious software detectors up-to-date is essential for these products to be effective.

7. Keep secure backups:

Even if you take all these security steps, bad things can still happen. Be prepared for the worst by making backup copies of critical data, and keeping those backup copies in a separate, secure location. For example, use supplemental hard drives, CDs/DVDs, or flash drives to store critical, hard-to-replace data.

8. **Report problems:**

If you believe that your computer or any data on it has been compromised, your should make a information security incident report. That is required by University policy for all data on our systems, and legally required for health, education, financial and any other kind of record containing identifiable personal information.

Benefits of secure computing:

- **Protect yourself - Civil liability**:
  You may be held legally liable to compensate a third party should they experience financial damage or distress as a result of their personal data being stolen from you or leaked by you.
- **Protect your credibility - Compliance**:
  You may require compliancy with the Data Protection Act, the FSA, SOX or other regulatory standards. Each of these bodies stipulates that certain measures be taken to protect the data on your network.
- **Protect your reputation – Spam:**
  A common use for infected systems is to join them to a bot net (a collection of infected machines which takes orders from a command server) and use them to send out spam. This spam can be traced back to you, your server could be blacklisted and you could be unable to send email.
- **Protect your income - Competitive advantage:**
  There are a number of "hackers-for-hire" advertising their services on the internet selling their skills in breaking into company's servers to steal client databases, proprietary software, merger and acquisition information, personnel detail set al.
- **Protect your business – Blackmail**:
  A seldom-reported source of income for "hackers" is to· break into your server, change all your passwords and lock you out of it. The password is then sold back to you. Note: the "hackers" may implant a backdoor program on your server so that they can repeat the exercise at will.
- **Protect your investment - Free storage:**
  Your server's hard drive space is used (or sold on) to house the hacker's video clips, music collections, pirated software or worse. Your server or computer then becomes continuously slow and your internet connection speeds deteriorate due to the number of people connecting to your server in order to download the offered wares.

2. System Analysis

Existing system:

The Location Server (LS), which offers some LBS, spends its resources to compile information about various interesting POIs. Hence, it is expected that the LS would not disclose any information without fees. Therefore the LBS has to ensure that LS's data is not accessed by any unauthorized user. During the process of transmission the users should not be allowed to discover any information for which they have not paid. It is thus crucial that solutions be devised that address the privacy of the users issuing queries, but also prevent users from accessing content to which they do not have authorization.

Disadvantages of existing system:

- Among many challenging barriers to the wide deployment of such application, privacy assurance is a major issue
- The user can get answers to various location based queries,

Proposed system:

- In this paper, we propose a novel protocol for location based queries that has major performance improvements with respect to the approach by Ghinita at el. And. Like such protocol, our protocol is organized according to two stages. In the first stage, the user privately determines his/her location within a public grid, using oblivious transfer. This data contains both the ID and associated symmetric key for the block of data in the private grid. In the second stage, the user executes a communicational efficient PIR, to retrieve the appropriate block in the private grid. This block is decrypted using the symmetric key obtained in the previous stage.
- Our protocol thus provides protection for both the user and the server. The user is protected because the server is unable to determine his/her location. Similarly, the server's data is protected since a malicious user can only decrypt the block of data obtained by PIR with the encryption key acquired in the previous stage. In other words, users cannot gain any more data than what they have paid for. We remark that this paper is an enhancement of a previous work.

Advantages of proposed system:

- ✓ Redesigned the key structure.
- ✓ Added a formal security model.

Implemented the solution on both a mobile device and desktop machine. □□□□□□□□□□□□□ □□□ □□□

3. Implementation

MODULES:

1. Users
2. Mobile Service Provider
3. Location Server

Modules Description:

Users:

The users in our model use some location-based service provided by the location server LS. For example, what is he nearest ATM or restaurant? The purpose of the mobile service provider SP is to establish and maintain the communication between the location server and the user. The location server LS owns a set of POI records ri for $1 \leq ri \leq \rho$. Each record describes a POI, giving GPS coordinates to its location (xgps,ygps), and a description or name about what is at the location.

Mobile Service Provider:

We reasonably assume that the mobile service provider SP is a passive entity and is not allowed to collude with the LS. We make this assumption because the SP can determine the whereabouts of a mobile device, which, if allowed to collude with the LS, completely subverts any method for privacy. There is simply no technological method for preventing this attack. As a consequence of this assumption, the user is able to either use GPS (Global Positioning System) or the mobile service provider to acquire his/her coordinates.

Location Server:

We are assuming that the mobile service provider SP is trusted to maintain the connection, we consider only two possible adversaries. Each and every one for individual communication direction. We consider the case in which the user is the adversary and tries to obtain more than he/she is allowed. Next we consider the case in which the location server LS is the adversary, and tries to uniquely associate a user with a grid coordinate.

4. Conclusion

In this paper we have presented a location based query solution that employs two protocols that enables a user to privately determine and acquire location data. The first step is for a user to privately determine his/her location using oblivious transfer on a public grid. The second step involves a private information retrieval interaction that retrieves the record with high communication efficiency. We analysed the performance of our protocol and found it to be both computationally and communication ally more efficient than the solution by Ghinita *et al.*, which is the most recent solution. We implemented a software prototype using a desktop machine and a mobile device. The software prototype demonstrates that our protocol is within practical limits.

Future work will involve testing the protocol on many different mobile devices. The mobile result we provide may be different than other mobile devices and software environments. Also, we need to reduce the overhead of the primality test used in the private information retrieval based protocol. Additionally, the problem concerning the LS supplying misleading data to the client is also interesting. Privacy preserving reputation techniques seem a suitable approach to address such problem. Once suitable strong solutions exist for the general case, they can be easily integrated into our approach.

REFERENCES:

[1] G. Ghinita, P. Kalnis, A. Khoshgozaran, C. Shahabi, and K.-L. Tan,"Private queries in location based services: anonymizers are not necessary," in Proc. 2008 ACM SIGMOD Int. Conf. Management of Data, New York, NY, USA, 2008, pp. 121–132, ser. SIGMOD'08, ACM.

[2] E. H. Moore, "On certain crinkly curves," Trans. Amer. Math. Soc., vol. 1, pp. 72–90, Jan. 1900.

[3] H. Sagan, Space-Filling Curves. New York, NY, USA: Springer- Verlag, 1994.

[4] M. Naor and B. Pinkas, "Oblivious transfer with adaptive queries," Proc. CRYPTO'99, 1999, vol. 1666, pp. 791 - 791.

[5] M. Bellare and S. Micali, "Non-interactive oblivious transfer and applications," Proc. CRYPTO'89. 1990, pp. 547 - 557.

[6] M. Mokbel, "Towards privacy-aware location-based database servers," in Proc. 22nd Int. Conf. Data Engineering Workshops, 2006, pp. 93–102.

[7] P. Kalnis, G. Ghinita, K. Mouratidis, and D. Papadias, "Preventing location- based identity inference in anonymous spatial queries," IEEE Trans. Knowl. Data Eng., vol. 19, no. 12, pp. 1719–1733, Dec. 2007.

[8] A.-A. Hossain, A. Hossain, H.-K. Yoo, and J.-W. Chang, "H-star: Hilbert-order based star network expansion cloaking algorithm in road networks," in Proc. IEEE 14th Int. Conf. Computational Science and Engineering (CSE), Aug. 2011, pp. 81–88.

[9] T. ElGamal, "A public key cryptosystem and a signature scheme based on discrete logarithms," *IEEE Trans. Inform. Theory*, vol. 31, no. 4, pp. 469–472, Jul. 1985.

[10] B. Gedik and L. Liu, "Location privacy in mobile systems: A personalizedanonymization model," in *Proc. ICDCS*, Columbus, OH, USA, 2005, pp. 620–629.

[11] C. Gentry and Z. Ramzan, "Single-database private information retrieval with constant communication rate," in *Proc. ICALP*, L. Caires, G. Italiano, L. Monteiro, C. Palamidessi, and M. Yung, Eds., Lisbon, Portugal, 2005, pp. 803–815, LNCS 3580.

[12] Marco Gruteser and Dirk Grunwald. Anonymous usage of locationbased services through spatial and temporal cloaking. In Proceedings of the 1st international conference on Mobile systems, applications and services, MobiSys '03, pages 31–42, New York, NY, USA, 2003. ACM.

[13] Ling Liu Bugra Gedik. A customizable k-anonymity model for protecting location privacy. Technical Report GIT-CERCS-04-15, Georgia Institute of Technology, April 2004. [14] Chi-Yin Chow, Mohamed F. Mokbel, and Xuan Liu. A peer-to-peer spatial cloaking algorithm for anonymous location-based service. In Proceedings of the 14th annual ACM international symposium on Advances in geographic information systems, GIS '06, pages 171–178, New York, NY, USA, 2006. ACM.

[15] Reza Shokri, Julien Freudiger, Murtuza Jadliwala, and Jean-Pierre Hubaux. A distortion-based metric for location privacy. In Proceedings of the 8th ACM workshop on Privacy in the electronic society, WPES '09, pages 21–30, New York, NY, USA, 2009. ACM

International Journal of Engineering Research and General Science Volume 3, Issue 5, September-October, 2015
ISSN 2091-2730

Instant fuzzy search with proximity

Bhagyashri G. Patil, Sushilkumar N. Holambe

Perusing M.E. at Dr. B. A. M. U., Aurangabad

Perusing Ph.D. at Dr. B. A. M. U., Aurangabad

E-MAIL:BHAGYAPATIL11@GMAIL.COM, E-MAIL:SNHOLAMBE@YAHOO.COM

Abstract— In the present data warehousing environment schemes face lots and lots of issues to fetch out the resources with the help of referential or relational keyword terminologies. So the system requires some kind of advanced data manipulating schemes to extending the keyword search paradigm to relational data has been an active area of research within the database and information retrieval (IR) community. Instant search is important information retrieval technology for finding search results instantly as user query words. In instant fuzzy search it improves the searching results by comparing answers similar to typed query keywords. In this paper, we are using posstagger, soundex and wordnet for computing better results. All the existing systems contains basic solution is to compute all the answers and rank them but cannot meet the high speed requirements. All the existing systems contain basic solution for computing answers as user typing keywords, the previously searched results are not considered. So in this paper technique is proposed to use previously searched results.

Keywords- Auto complete, index, top-k, keyword search, edit distance, posstager, soundex

I. INTRODUCTION

As an emerging technology instant search returns answers to queries immediately based o user typed in. User many times makes search same queries. In this phase we cannot find correct answers as searched previously. In this case, by using fussy search technique user can find answers efficiently and correct [2]. Main computational challenge in this search technique is to achieve high speed requirement. As humans don't feel delay, from user typing queries character by character to the time result should be shown on device that full time is of 100 milliseconds. In instant search every query keystroke invokes question so it needs best speed to achieve high question turn over [3]. A Part-Of-Speech Tagger (POS Tagger) is a piece of software that reads text in some language and assigns parts of speech to each word (and other tokens), such as noun, verb, adjective, etc. Generally computational applications use more fine-grained POS tags like 'noun-plural'.

In auto completion system suggests many possible suggestions to user [4], [5]. Early termination techniques are used to minimize the number of possible results. Proximity ranking improve the results significantly [9], [10], [11], [6], [7], [8] .Our study shows to compute answers efficiently base on proximity of phrases.

Ranking

Here for this technique ranking is performed based on the relevancy of phrases into the records and frequencies and multiple co-occurrences of keyword in records. In [1] focus on the phrase matching in ranking operation. Basically three index structures are used inverted index forward index and tries [12]. Tries are used to show the keyword terms in dictionary D. In inverted leaf nodes are these dictionary terms. And forward index is for showing integers of each term of each record. These indexes are used for keyword matching a prefix condition.

Top-k answering

There are various methods to take top k answers first is computing all answers , which is useful for all types of ranking functions but it doesn't support when more matching keywords found . Second method is using early termination, which maintains heap for each keyword and it's monotonic. Third method is of using term pair in which is useful for only one or two keyword search.

II. PROPOSED WORK

A. Phrase indexing

To make early termination we must consider the records which match the query phrases, we have to access that records first. for example for query q=⟨xml data⟩, we have to access record containing the phrase "xml data" before the record containing "xml " and "data " separately. Index all available phrases based on mysql indexing strategy. In which B-tree indexing technique is used.

B. Finding valid phrases

In this section we compute the valid phrases based on post tagger technique. In which we are taking those phrases which consists noun and adjectives in typed queries. Most often user types or search name and previously cached valid phrases. Ontology based technique is used such as for finding semantic search soundx ad word net are used. Receiving a list of valid phrases, the Query Plan Builder computes the valid segmentations. The basic segmentation is the one where each keyword is treated as a phrase. Each generated segmentation corresponds to a way of accessing the indexes to compute its answers. The Query Plan Builder needs to rank these segmentations to decide the final query plan, which is an order of segmentations to be executed.

C. Top-k Query

The ranking needs to guarantee that the answers to a high-rank segmentation are more relevant than the answers to a low-rank segmentation. There are different methods to rank segmentation. Our segmentation ranking relies on a segmentation comparator to decide the final order of the segmentations. This comparator compares two segmentations at a time based on the following features and decides which segmentation has a higher ranking; the comparator ranks the segmentation that has the smaller minimum edit distance summation higher. If two segmentations have the same total minimum edit distance, then it ranks the segmentation with fewer segments higher.

D. Segmentation

Next step is to generate efficient segmentations, and that segmentation is nothing but phrase. User computed a query plan based on valid segmentations, and ran the segmentations one by one until top-k answers were computed. The database of segments and may be applied to an arbitrary text, preferably query, for splitting it into segments according to a segmentation procedure. The procedure matches all possible subsequences of the given tokenized query segmentation it is meant to segment the input query into segments, typically natural language phrases, so that the performance of relevance ranking in search is increased. For example query q=⟨"xml query processing"⟩, efficient segmentation is "xml | query| processing". If more phrases in the query then there more segmentations. In previous example "xml query" is valid phrase and "xml query | processing" is possible efficient segmentation. Many combinations of valid phrases are takes place if we consider more than three keywords or phrases from all valid segmentations the user typed keywords are searched. As shown in table 1, all possible efficient segmentations.

E. Ranking

These segmentations must be rank in order to get appropriate ranked results. Ranking is based upon the number of keywords in the segmentation and average nearest edit distance of valid phrases.

Table 1: three segmentations for query q=⟨"xml query processing"⟩.

1	"xml query processing"
2	"xml query |processing"
3	"xml | query | processing"

In this technique we calculate average distance of two or three keywords present in one record, according to those results are computed. At the time of ranking soundx is used for calculating semantic search of keywords. Word net library is used for semantic search which takes semantic keywords from database.

III. CONCLUSION

In this paper, we study, how efficiently integrate proximity information to ranking to compute relevant top –k answers. We use technique to find important phrases by avoiding considering large space overhead. And next is to compute and rank segmentations

including all indexed phrases. This technique is useful for 2-keywod or 3-keyword and more than 3-keyword search which is common. We concluded that computing all answers for all queries gives good performance and satisfy high speed requirement demand of instant search.

REFERENCES:

[1] Inci Cetindil, Iamshid Esmaelnezhad, Taewoo Kim, and Chen Li, "Efficient instant fuzzy search with proximity raking," in ICDE, 2014.
[2] Centennial, J. Esmaelnezhad, C. Li, and D. Newman, "Analysis of instant search query logs," In WebDB, 2012,pp.7-12.
[3] R. B. Miller, "Response time in man-computer conversational transactions," in Proceedings of the December 9-11, 1968, fall joint computer conference, part I, ser. AFIPS '68 (fall, part I). New York, NY, USA: ACM, 1968, pp. 267–277.
[4] K. Grabski and T. Scheffer, "Sentence completion," in SIGIR, 2004, pp.433-439.
[5] A. Nandi and H.V. Jagadish, "Effective phrase prediction," in VLDB, 2007, pp.219-230.
[6] R. Schenkel, A. Broschart, S. wonHwang, M. Theobald, and G. Weikum, "Efficient text proximity search," in SPIRE, 2007, pp. 287-299.
[7] H. Yan, S. Shi, F. Zhang, T. Suel, and R. Wen, "Efficient term proximity search with term pair indexes," in CIKM, 2010,pp. 1229-1238.
[8] M. Zhu, S. Shi, F. Zhang, T. Suel, and R. Wen, "Can phrase indexing helps to non-phrase queries?, "in CIKM, 2010, pp. 1229-1238.
[9] R. Fagin, A. Lotem, and M. Naor, "Optimal aggregation algorithm for middleware," in PODS, 2001.
[10] F. Zhang, H. Yan, S. Shi, and R. Wen, "revisiting globally sorted indexes for efficient document retrieval," in WSDM, 2010, pp. 371-380.
[11] M. Persin, J. Zobel, R. Sacks-Davis, "Filtered document retrieval with frequency-sorted indexes," JASIS, val. 47, no. 10, pp. 749-764, 1996.
[12] S. Ji, G. Li, C. Li, and J. Feng, "efficient interactive fuzzy keyword search," in WWW, 2009, pp.371-380

International Journal of Engineering Research and General Science Volume 3, Issue 5, September-October, 2015
ISSN 2091-2730

Language Processing for MT: Need, Problems and Approaches

Ruchika Sinhal[1], Kapil Gupta[2]

[1]Dept of CSE, DMIETR, Sawangi(M), Wardha
ruchisinhal04@gmail.com
[2]Dept of CSE, DMIETR, Sawangi(M), Wardha
kaps04gupta@gmail.com

Abstract— Over the past years there is continuous involvement in field of Machine Learning. There are different applications which help common man to tackle with different languages all over the world. The demand for language translation has greatly increased in recent times due to increasing cross-regional communication and the need for information exchange. Most material needs to be translated, including scientific and technical documentation, instruction manuals, legal documents, textbooks, publicity leaflets, newspaper reports etc. Some of this work is challenging and difficult but mostly it is tedious and repetitive and requires consistency and accuracy. It is becoming difficult for professional translators to meet the increasing demands of translation. In such a situation the machine translation can be used as a substitute. Then also there are many challenges faced in this filed and building the applications. The paper gives the brief description about the concept in machine translation, the challenges involved and our way of solving the problem.

Keywords— Machine translation, Need, Problems in Translation, Types of MT Systems, Approaches in MT

INTRODUCTION

The language, which human beings speak, is termed as natural language. The natural language is used by every common man. People use natural language for communication. Natural language processing includes refining, modifying and translating i.e. operating on the natural languages.

Divergence is one of the main problems in any NLP system, which proves the need of research in NLP domain. The divergence is defined as difference between language, or the form of text in which the language is present. In India itself, there are more than 438 languages spoken [1]. The most ancient of all languages is Sanskrit. Many people do not understand Sanskrit but they can if the text is translated into their national language or languages they are familiar with. Therefore, for understanding and making communication easy, there is a basic need of translation tools. The translation can be done by humans; so why there is a need of machine translation? The need of MT is described in following points:

a) Too much to be translated

The first reason is that the "world of text" is huge. There are many large documents to be translated and it is not possible for a human to translate gigabytes of data in a short time. To reduce the human efforts and to give the results quickly the machine translators are used which can translate the text from one language to another by just one click.

b) Boring for human translators

A second reason is that the all technical materials are too boring for human translators to translate as humans do not like to translate them continuously. Hence they look for help from computers.

c) Major requirement that terminology used consistently

As far as large corporations are concerned, there is the major requirement that terminology is used consistently, the terms to be translated in the same way every time. Computers are consistent, but human translators tend to seek variety; they do not like to repeat the same translation and this is not good for technical translation.

d) Increase speed and throughput

The use of computer-based translation tools can increase the volume and speed of translation throughput, and organizations like to have translations immediately.

e) Top quality translation not always needed

The fifth reason is that, top quality human translation is not always needed. Computers do not produce good translations. The fact is that there are many different circumstances in which top quality translation is not essential, and in this case, automatic translation can be used widely.

History of Machine Translation

W. John Hutchins, 1986 explained vast history of machine translation [2-4]. Many people are under the impression that MT is something quite new. MT has a long history – almost since before electronic digital computers existed. In 1947 when the first non-military computers have been developed, the idea of using a computer to translate has been proposed. In July 1949 Warren Weaver [5] (a director at the Rockefeller Foundation, New York) proposed method, which introduced Americans to the idea of using computers for translation. From this time on, the idea spread quickly, and in fact machine translation became the first non-numerical application of computers. The first conference on MT was held in 1952 [6]. Just two years later, there has been the first demonstration of a translation system in January 1954 [7]. Unfortunately this demonstration has been the wrong kind of attention as many readers thought that machine translation has been just around the corner and that not only would translators be out of a job but everybody would be able to translate everything and anything at the touch of a button. However, it has been not too long before the first systems have been in operation, even though the quality of their output has been quite poor. In 1959 a system has been installed by IBM at the Foreign Technology Division of the US Air Force [8], and in 1963 and 1964 Georgetown University, one of the largest research projects at the time, installed systems at Euratom and at the US Atomic Energy Agency**.** But in 1966 there appeared a rather damning report for MT from a committee set up by most of the major sponsors of MT research in the United States. The committee found that the results being produced have been just too poor to justify the continuation of governmental support and recommended the end of MT research in the USA altogether. The committee advocated the development of computer aids for translators. Consequently, most of the US projects – the main ones in the world at that time – came to an end. The Russians also started to do MT research in the mid 1950's. Russians concluded that if the Americans were not going to do MT any more than they would not either, because their computers have not been as powerful as the American ones. However, MT did continue in fact, and in 1970 the Systran system has been installed at the US Air Force (replacing the old IBM system). The Systran system for Russian to English translation continues in use to this day [9]. The year 1976 is one of the turning points for MT. In this year, the Météo system for translating weather forecasts has been installed in Canada and became the first general public use of a MT system [10]. The European Commission decided to purchase the Systran system. The Systran has been producing poor quality output, therefore committee decided to support the development of system better than systran, and began the Eurotra project– which did not produce a system in the end During the 1970's other systems began to be installed in large corporations [11]. In 1981, came the first translation software for the newly introduced personal computers, and gradually MT came into more widespread use [12]. In the 1980's there had been a revival of research, Japanese companies began the production of commercial systems, and computerized translation aids became more familiar to professional translators. Then in 1990, the first translator workstations came to the market [13]. In the last decade MT has become an online service on the Internet [14-15].

The term machine translation (MT) is translation of one language to another. The ideal aim of machine translation system is to produce the best possible translation without human assistance. Basically every machine translation system requires automated programs for translation, dictionaries and grammars to support translation [16].

Machine Translation systems are needed to translate literary works from any language into native languages. The literary work is fed to the MT system and translation is done. Such MT systems can break the language barriers by making available work rich sources of literature available to people across the world.

MT also overcomes the technological barriers. Most of the information available is in English which is understood by only 3% of the population [17]. This has led to digital divide in which only small section of society can understand the content presented in digital format. MT can help in this regard to overcome the digital divide.

Problems in Machine Translation

There are several structural and stylistic differences among languages, which make automatic translation a difficult task. Some of these issues are as follows:

Word Order

Word order in languages differs. Some classification can be done by naming the typical order of subject (S), verb (V) and object (O) in a sentence [18]. Some languages have word orders as SOV. The target language may have a different word order. In such cases, word to word translation is difficult [19]. For example, English language has SVO and Hindi language has SOV sentence structure.

Word Sense

The same word may have different senses when being translated to another language. The selection of right word specific to the context is important [19].

Pronoun Resolution
The problem of not resolving the pronominal references is important for machine translation. Unresolved references can lead to incorrect translation [19].

Idioms
An idiomatic expression may convey a different meaning, that what is evident from the words in sentence. For example, an idiom in English language 'No brick in their walls', would not convey the intend meaning when translated into Hindi language [19].

Ambiguity
In computational linguistics, Word Sense disambiguation (WSD) is an open problem of natural language processing, which governs the process of identifying which sense of a word (i.e. meaning) is used in a sentence, when the word has multiple meanings [19].

Types of MT systems

The following are four types of Machine Translation (MT) systems:

MT for Watcher (MT-W)
MT for watchers is intended for readers who wanted to gain access to some information written in foreign language who are also prepared to accept possible bad 'rough' translation rather than nothing. This has been the type of MT envisaged by the pioneers. This came in with the need to translate military technological documents [20].

MT for revisers (MT-R)
MT for revisers aims at producing raw translation automatically with a quality comparable to that of the first drafts produced by human. The translation output can be considered only as brush-up so that the professional translator can be freed from that boring and time consuming task [20].

MT for translators (MT-T)
MT for translator's aims at helping human translators do their job by providing on-line dictionaries, thesaurus and translation memory. This type of machine translation system is usually incorporated into the translation work stations and the PC based translation tools [20].

MT for Authors (MT-A)
MT for authors aims at authors wanting to have their texts translated into one or several languages and accepting to write under control of the system or to help the system disambiguate the utterance so that satisfactory translation can be obtained without any revision [20].

MT Approaches

Machine Translation is an attempt to automate, all or part of the process of translating one human language to another. The translation requires some knowledge of source and target languages and its way of interpretation to carry out the translation work. The MT systems can broadly be categorized on the basis of knowledge type, representation and interpretation of translation tools.

The categories of MT systems are described in the next three sections. Since our research focuses on EBMT, this model is described in more detail [16].

Knowledge Based MT

"The term knowledge based MT describe a system, displaying extensive semantic and pragmatic knowledge of domain, including an ability to reason to some limited extent, about concepts in the domain."

The basic aim of KBMT is to obtain high quality output in a specific domain with no post-editing work. The KBMT systems are generally domain specific, especially a domain that is less ambiguous, like technical documents. The reason for KBMT to be domain specific is that representing complete knowledge of the whole world is very difficult. The domain model is used to represent the meaning of the source language text.

The basic components of a KBMT system are:-

1. Ontology of the domain, which serves as an intermediate representation during translation. Ontology usually includes the set of distinct objects resulting from an analysis of a domain.
2. Source language lexicon and grammar for the analysis.
3. Target language lexicon and grammar for the generation.
4. The mapping rules between the intermediate and source/target language.

For example, the KANT system developed by CMT at Carnegie Mellon University is a practical translation system for technical documentation from English to Japanese, French and German [15].

Statistical MT

The researchers in the field of speech recognition first outlined the idea of statistical approach in machine translation. SMT is based on statistics derived from corpora of naturally occurring language, not with pre-fabricated examples. The view of the statistical approach is that every sentence in one language is a possible translation of any sentence of other language. The statistical model tries to find the sentence *S* in the source language for which the machine translator has produced a sentence *T* in the target language. This is based on the *Bayesian* or *Noisy channel* model used in speech recognition.

The model works with the intuition that the translated sentence has been passed through a noisy channel, which distorted the source sentence to the translated sentence. To recover the original source sentence we need to calculate the following –

1. The probability of getting the original sentence *S* in the source language.
2. The probability of getting the translated sentence *T* in the target language.

These are known as *Language model* and *Translation model* respectively. We assign to every pair of sentence (S, T) a joint probability, which is the product of the probability Pr(S) computed by the language model and the conditional probability Pr(T/S) computed by translation model. We choose that sentence in the source language for which the probability Pr(S/T) is maximum. Using Bayes theorem, we can write

$$\Pr(S/T) = \big(Pr(S) * Pr(T/S)\big)/Pr(T)$$

where S = Source Text, T = Target Text, Pr (S/T) = probability that the decoder will produce S when presented with T, Pr(S) = probability that S would be produced in the source language, Pr(T/S) = probability that the translator will produce T when presented with S, and Pr(T) = probability that T would be Target language, but, here Pr(T) does not change for each S as we are looking for most-likely S for the same translation T.

In order to get the most-likely translation, we need to maximize *Pr(S)*P(T/S).* Thus, the formula to find the most likely translation *T* for a given sentence *S* is as follows –

$$Pr(S/T) = agrmax(\Pr(S) * Pr(T/S))$$

The statistical system computes the language model probabilities (the probability of a word given, all the words preceding it in a sentence), the translation probabilities (the probability of the translation being produced) and uses a search method to find the greatest value (agrmax) for the product of these two probabilities thus giving the most probable translation.

Rule Based MT

A rule based machine translation system consists of collection of rules called grammar rules, lexicon and software programs to process the grammar rules [21]. The collection of rules in RBMT is extensible and maintainable. Rule based approach is the first strategy ever developed in the field of machine translation. Rules are written with linguistic knowledge gathered from linguists. Rules play major role in various stages of translation as, syntactic processing, semantic interpretation, and contextual processing of language.

Tree structure is used to represent the structure of the sentence. A typical English sentence consists of two major parts: noun phrase (NP) and verb phrase (VP) [22]. These two parts can be further divided as per the structure of the sentence. 'Rewrite rules' are used to

describe what tree structures are allowable for a given sentence. Only the sentences with right structure lead to correct translation. Following is the example of rules representing a simple grammar:

S → NP VP

VP → V NP

NP → Name

NP → ART N

where S stands for sentence, V for verb, N for noun and ART for article. A grammar can derive a sentence if there is a sequence of rules to rewrite the start symbol, S, into a sentence.

Logical form is commonly used in semantic interpretation. For example the sentence, Joe has been happy, can be written in logical form as:

$$(\langle PAST\ HAPPY \rangle\ (NAME\ j1\ "Joe"))$$

where PAST stands for past tense. Semantic interpretation is a compositional process in which interpretations can be built incrementally from the interpretations of subphrases. Lexicon plays a major role in semantic interpretation. Grammar rules are used to compute the logical form of the given sentence. Consider the grammar rule given below.

$$(S\ SEM\ (?\ semvp\ ?\ semnp)) \rightarrow\ (NP\ SEM?\ semnp)\ (VP\ SEM?\ semvp)$$

where SEM stands for semantic feature. The rule above states that a sentence consists of a noun phrase and verb phrase.

Example Based MT

EBMT is a corpus based machine translation, which requires parallel-aligned three machine-readable corpora. Here, the already translated example serves as knowledge to the system. This approach derives the information from the corpora for analysis, transfer and generation of translation. These systems take the source text and find the most analogous examples from the source examples in the corpora. The next step is to retrieve corresponding translations. And the final step is to recombine the retrieved translations into the final translation.

EBMT is best suited for sub-language phenomena like – phrasal verbs; weather forecasting, technical manuals, air travel queries, appointment scheduling, etc. Since, building a generalized corpus is a difficult task, the translation work requires annotated corpus, and annotating the corpus in general is a very complicated task.

Nagao (1984) has been the first to introduce the idea of translation by analogy and claimed that the linguistic data are more reliable than linguistic theories [23]. In EBMT, instead of using explicit mapping rules for translating sentences from one language to another, the translation process is basically a procedure for matching the input sentence against the stored translated examples. Figure 2.1 shows the architecture of a pure EBMT [24].

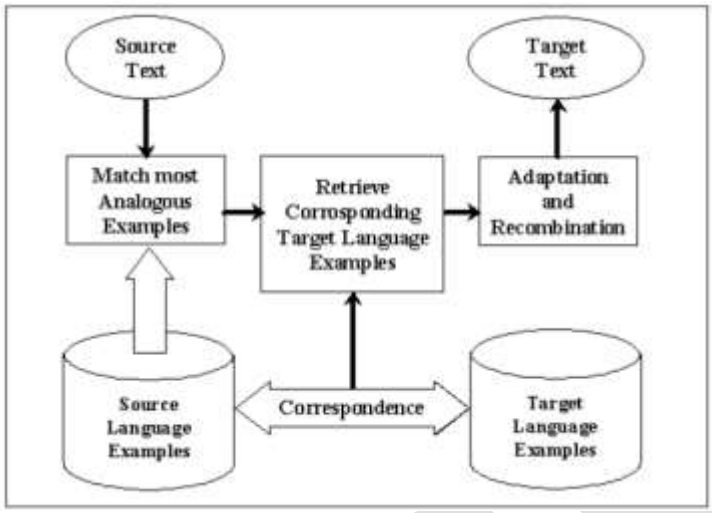

Fig. 1 EBMT Architecture

The basic tasks of an EBMT system are –
- Building Parallel Corpora
- Matching and Retrieval
- Adaptation and Recombination

The knowledge base, *parallel aligned corpora* consist of two sections, one for the source language examples and the other for the target language examples. Each example in the source section has one to one mapping in the target language section. The corpus may be annotated in accordance with the domain. The annotation may be semantic (like name, place and organization) or syntactic (like noun, verb, preposition) or both. For example, in the case of phrasal verb as the sub-language the annotations could be subject, object, preposition and indirect object governed by the preposition.

In the matching and retrieving phase, the input text is parsed into segments of certain granularity. Each segment of the input text is matched with the segments from the source section of the corpora at the same level of granularity. The matching process may be syntactic or semantic level or both, depending upon the domain. On syntactic level, matching can be done by the structural matching of the phrase or the sentence. In semantic matching, the semantic distance is found out between the phrases and the words. The semantic distance can be calculated by using a hierarchy of terms and concepts, as in WordNet. The corresponding translated segments of the target language are retrieved from the second section of the corpora.

In the final phase of translation, the retrieved target segments are adapted and recombined to obtain the translation. The final phase identifies the discrepancy between the retrieved target segments with the input sentences' tense, voice, gender, etc. The divergence is removed from the retrieved segments by adapting the segments according to the input sentence's features.

Let us consider the following sentences –
- [Input sentence] John brought a watch.
- [Retrieved - English] He is buying a book.
- [Retrieved - Hindi] vaHa eka kitaba kharida raha he

The aligned chunks are –
- [He] → [vaha]
- [is buying] → [kharida raha he]
- [a] → [eka]
- [book] → [kitaba]

The adapted chunks are –
- [vaha] → [jana]
- [kharida raha he] → [kharida]
- [kitaba] → [gaghi]

The adapted segments are recombined according to sentence structure of the source and target language. For example, in the case of English to Hindi, structural transfer can be done on the basis of Subject-Verb-Object to Subject-Object-Verb rule.

CONCLUSION

The paper thus discusses the concept of machine translation. The history of machine translation with its boons. Machine translation is a vast field. The different types of approaches are present in which research and work is being performed. Example Based Machine Translation is the main approach in project so it is explained briefly. The main challenge of divergence is phased in translation.

REFERENCES:

[1] The Economist online, "Speaking in tongues-Language diversity around the world", 15 Feb, 2012, http://www.economist.com/blogs/graphicdetail/2012/02/daily-chart-9?fsrc=gn_ep
[2] Hutchins W. John and Harold L. Somers, (1992). An Introduction to Machine Translation. *London: Academic Press.*
[3] D. Arnold, L. Balkan, S. Meijer, L.L. Humphreys, L. Sadler: *Machine Translation: an Introductory Guide*. Blackwells-NCC, London, Great Britain, 1994.
[4] Hutchins 95 J. Hutchins: Reflections on the history and present state of machine translation. In Proc. of *Machine Translation Summit V*, pp. 89–96, Luxembourg, July 1995.
[5] W.Weaver. Translation. In W.N. Locke, A.D. Booth, editors, *Machine Translation of Languages: fourteen essays*, pp. 15–23. MIT Press, Cambridge, MA, 1955.
[6] John Hutchins, *Milestones in machine translation No.4: The first machine translation conference*, June 1952 Language Today, no. 13, October 1998, pp.12-13 http://www.hutchinsweb.me.uk/Milestones-4.pdf
[7] The first public demonstration of machine translation: The Georgetown-IBM system, 7th January 1954, http://www.hutchinsweb.me.uk/GU-IBM-2005.pdf
[8] Masterman, Margaret and Kay, Martin, "Operational system (IBM-USAF Translator Mark I), at Foreign Technology Division, USAF, in 1959", www.hutchinsweb.me.uk/sources/Russian-IBM-1959.doc
[9] Systran, [Online]. Available: http://www.hutchinsweb.me.uk/IntroMT-10.pdf
[10] The EUROTRA project, http://www-sk.let.uu.nl/stt/eurotra.html
[11] J. Chandioux, A. Grimaila: Specialized machine translation. *In 2nd Conf. of the Association for Machine Translation in the Americas (AMTA 96)*, pp. 206–212, Montreal, Canada, Oct. 1996.
[12] "Machine Translation", http://en.wikipedia.org/wiki/Machine_translation
[13] John Hutchins, "The origins of the translator's workstation", Machine Translation, vol.13, no.4 (1998), p. 287-307
[14] Hutchins and Lovtsky, *in press.*
[15] Hutchins, J. 1986. Machine Translation: Past, Present, Future, Ellis Horwood/Wiley, Chichester/New York.
[16] Sergei Nirenburg and Yorick Wilks, Machine Translation
[17] D. D. Rao, "Machine Translation A Gentle Introduction", RESONANCE, July 1998.
[18] "Statistical machine translation", http://en.wikipedia.org/wiki/Statistical_machine_translation
[19] S.K. Dwivedi and P. P. Sukadeve, "Machine Translation System Indian Perspectives", *Proceeding of Journal of Computer Science Vol. 6* No. 10. pp 1082-1087, May 2010.
[20] "Machine Translation –A Rosetta stone for the 21th century?", http://www.ida.liu.se/~729G11/projekt/studentpapper-10/maria-hedblom.pdf
[21] "Rule-based machine translation", http://en.wikipedia.org/wiki/Rule_based_machine_translation
[22] Robin, "Machine Translation-Natural Language Processing-Rule based machine translation",http://language.worldofcomputing.net/category/machine-translation/page/2
[23] Makoto Nagao, A Framework of A Mechanical Translation between Japanese and English by Analogy Principle, *In Artificial and Human Intelligence* 1984, http://www.mt-archive.info/Nagao-1984.pdf
[24] Indranil Saha et.al. (2004). Example-Based Technique for Disambiguating Phrasal Verbs in English to Hindi Translation. Technical Report KBCS Division CDAC Mumbai.

International Journal of Engineering Research and General Science Volume 3, Issue 5, September-October, 2015
ISSN 2091-2730

Analysis of Milk Adulteration Using MID-IR Spectroscopy – A Review

Kunal Kishor [1], Ritula Thakur [2].

[1]M.E. Student, Electrical Engineering Department, NITTTR, Chandigarh

[2]Assistant Professor, Electrical Engineering Department, NITTTR, Chandigarh

[1] kunal.elect@nitttrchd.ac.in, [2] ritula.thakur@gmail.com

Abstract — This paper presents the review on different types of milk adulteration based upon conventional method. A straight forward and quick strategy for measurement of milk adulteration has been developed using mid-infrared (MIR) spectrometers. Milk samples was purchased from local supermarkets and spiked with tap water, hydrogen peroxide, glucose, urea and formaldehyde in different concentrations in milk. Spectral data was collected using mid-infrared (MIR) spectrometers. Partial least-square regression (PLSR) has been used to estimate adulteration level and results indicated high coefficients of determination (R^2) and standard error of predication (SEP). The use of Fourier transform infrared (FTIR) spectroscopy coupled with chemo metric techniques to differentiate of milk adulteration. These results proved that FTIR spectroscopy in combination with multivariate calibration can be used for the detection of milk adulteration. The proposed technique is quick, non-dangerous, straightforward and simple to utilize.

Keywords — Adulteration, Multivariate analysis, MIR spectroscopy, PLS, Chemo metric.

.

INTRODUCTION

Milk is commonly consumed by people of all age groups. Also, India is the largest producer and consumer of milk. According to a recent report, India is likely to produce 140.6 million tonnes of milk in 2014 and the demand is set to rise to 150 million tonnes of milk. To meet the growing demand, milk and its products have been adulterated to decrease the quality and increase the quantity for economic value. The normal adulterants found in milk are urea, starch/blotching paper, glucose/sugar, harsh pop, refined vegetable oil (modest cooking oil), white paint and basic cleanser or cleanser. These not only reduce the nutritious value of the beverage but also danger to health.

Table 1Comparison of various methods

S. No.	Methods	Advantages	Disadvantages
1	Liquid Chromatography Method	High accuracy, high precision, good linearity, Low uncertainty.	Not portable and expensive.
2	Chemical method	No calibration required.	Human contact with harmful reactants. Wastage of chemicals in testing.
3	Piezoelectric crystal method	Low cost, high DC output voltage when compared to other methods.	Sensitive to stray gases present in the sample.
4	Teflon temperature sensing method	Selective absorption of Ammonia.	Output signal needs to be amplified as it is very low.
5	Electrolytic Capacitance Method	High sensitivity and good reproducibility.	Calibration errors involved.

Milk gives fundamental supplements like (starch, fat, protein, minerals and vitamins) of incredible nutritious importance for people, Generally during childhood. Presently the days event of milk adulteration is a major issue in the dairy industry and has been causing concerns among costumers and food manufacturers. Milk is the seven most basic focuses for defilement by and large refined by the expansion of water, whey, sodium hydroxide and urea.

The use of FT-MIR spectroscopy coupled to chemo metric methods, adopting the specificity of the IR signals for identifying chemical components and the minimal sample preparation needed for the measurements. The instrumental design of FT-MIR spectrometers coupled with chemo metrics methods have also been described and this enable trace level detection and satisfactory analysis. Fourier Transformed Infrared spectroscopy (FT-MIR) has been applied to determine compositional differences between samples on the basis of vibration of various chemical groups at specific wavelengths in the mid infrared region of the spectrum from 400 to 4000 cm^{-1}. Chemo metric methods, especially partial least squares regression (PLS) is among the most commonly used multivariate calibration. The ultimate aim of this paper was to investigate the potential of PLS method coupled with FT-MIR spectroscopy technique, as an alternative analytical tool for non-destructive and fast quantitative determination of added glucose, formaldehyde, hydrogen peroxide and urea in milk.

PROPOSED WORK

Fig. 1 shows the functional block diagram of the proposed work. It consists of light source, interferometer and detector. The sample was placed between interferometer and detector. Ceramic is used to produce infrared light source which fall on the sample, produces corresponding interferrogram in the detector. This interferrogram obtained from the spectroscopy was Fourier transformed and the resultant spectrum was analyzed using chemo metric Technique.

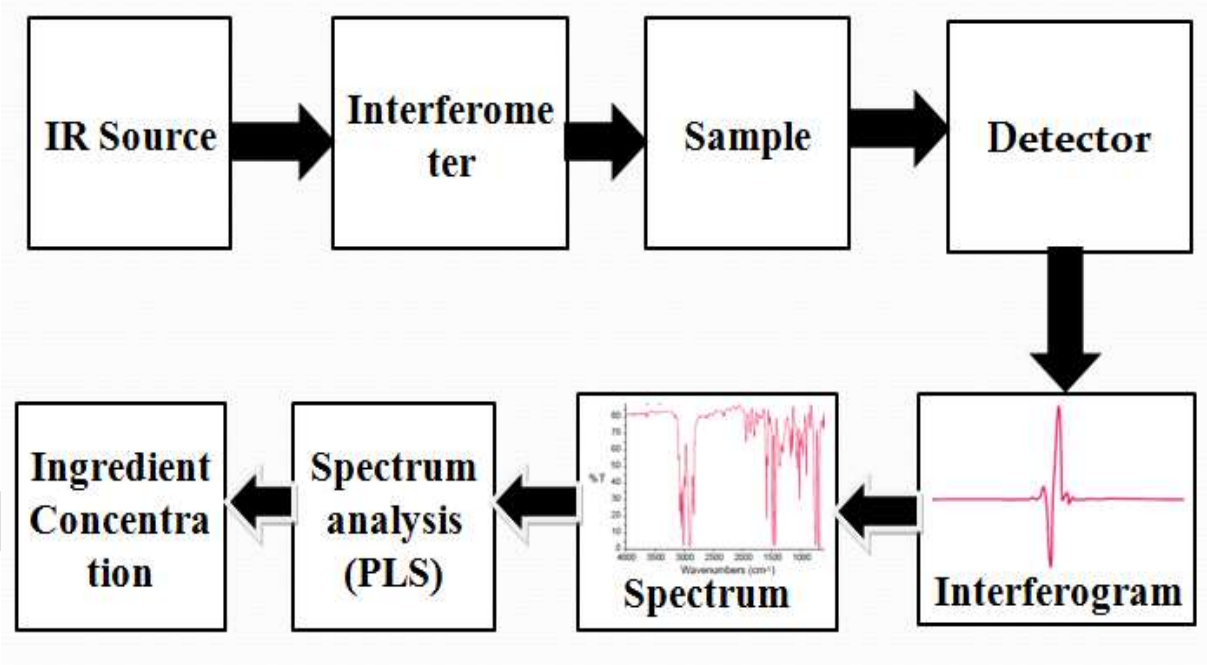

Fig.1 Block Diagram of Proposed Work

CONCLUSION

This paper reviews the milk adulteration based on MID-IR Spectroscopy. The aim of the present work is to be developed a new application of the analytical method association as a rapid, inexpensive and non-destructive authenticity measuring tool useful to determine the adulteration in milk. The results demonstrate a better prediction ability of the PLS technique to determine glucose, formaldehyde, hydrogen peroxide and urea in milk samples. By the use of ATR mid infrared Fourier transform spectroscopy it has been possible to successfully identified the content of adulterant in milk samples.

REFERENCES:

[1] Poliana M Filho, Mustajab P. and Khan I., "Application of hand-held and portable Infrared spectrometers in bovine milk analysis", Journal of Agricultural and Food Chemistry, Vol. 61, pp. 1205-1211, January 2013.

[2] Albanell E. Rohman, Caceres P., Caja G., Molina E. and Gargouri A., "Determination of Fat Protein and total solids in Ovine milk by Near-Infrared Spectroscopy", Journal of Association of Official Analytical Chemists (AOAC), Vol. 12 pp.753–758, December 1999.

[3] Ramadan Omar Ahmed, Arora S, Sharma V, Raj D, Ram M, Kishore K., "Authentication analysis of butter from beef fat using Fourier Transform Infrared (FTIR) Spectroscopy Coupled with Chemo metrics", International Food Research Journal, Vol. 20, pp. 1383-1388, December 2012.

[4] R.J. Yang, R. Liu, and K.X. Xu, "Evaluation of Raw Milk for Common Commercial Additives and Heat Treatments", International Journal of Food Safety, Vol. 15, pp. 7-10, February 2011.

[5] S Rehman, Borin A., M. F. Ferrao, C. Mello, D. A. Maretto and R. J. Poppi," Application of 2D Correlation Infrared Spectroscopy to Identification of Adulterated Milk using NPLS-DA Method", Third International Conference on Instrumentation, Measurement, Computer, Communication and Control, Vol. 28, pp. 259-263, May 2011.

[6] M. M. Chakrabarty, C. Bandyopadhyay, D. Bhattacharyya and A. K. Gayen, "Detection of Adulteration, Chemical Composition and Hygienic Status of milk supplied to various canteens of Educational Institutes and public places in Faisalabad", The Journal of Animal and Plant Sciences, Vol. 23, pp. 119-124, November 2013.

[7] M Bellal Hossain, John-hyeon Chang, Jungil Park, Youngmi Pak, and James Jungho Pak, "Fitting Improvement using a New Electrical Circuit Model for Electrode Electroyte InterfaceFitting", 3rd International IEEE Conference Neural Engineering, Kohala Coast, Hawaii, Vol. 1, pp. 2-7, May 2007.

[8] M Nielen, H.J. Biggadike, I. Ohnstad, R.A. Laven, and J.E. Hillerton, "Physiochemical Charateristics of Various Raw Milk Samples in aSelected Dairy Plant of Bangladesh", International Journal of Engineering and Applied Sciences, Vol. 03, pp. 2305-8269, January 2013.

[9] Peter Zachar, Enne G., Elez D., Fondrini F., Bonizzi I., Feligini M., Aleandri R., "Design and Construction of a System for Measuring the Concentration of Water in Milk", Journal of Dairy Science, Vol. 75, pp. 606-614, July 2002.

[10] Pallavi Gupta, Arora S., Sharma V., Raj D., Ram M., "Status of Milk Adulteration in Some States of North India", Indian Journal Dairy Sci., Vol. 57, pp. 65-66, April 2004.

International Journal of Engineering Research and General Science Volume 3, Issue 5, September-October, 2015
ISSN 2091-2730

DESIGN AND ANALYSIS OF REINFORCED COMPOSITE MATRIX DISC BRAKE

Vishal asokan[1], Arshad Mohammed Gani P[2], Vimal M[3], Mohammed nooh muballigh A[4],
Muthu mohammed inzamam bari M[5]
U.G. scholar, Department of Mechanical Engineering,
Dhaanish Ahmed College of Engineering[1,3,4,5].
Assistant Professor, Department of Mechanical Engineering,
Dhaanish Ahmed College of Engineering[2].
E-mail: mncgani@gmail.com

ABSTRACT: Each single system has been studied and developed in order to meet safety requirement. Instead of having air bag, good suspension systems, good handling and safe cornering, there is one most critical system in the vehicle which is brake systems. Without brake system in the vehicle will put a passenger in unsafe position. Therefore, it is must for all vehicles to have proper brake system. In this paper carbon ceramic matrix disc brake material and steel material use for calculating normal force, shear force and braking torque. And also calculating the brake distance of disc brake. The standard disc brake (Four) wheelers model using in Ansys and done the Static Structural analysis also calculate the deflection of the brake model. This is important to understand action force and friction force on the disc brake new material, how disc brake works more efficiently, which can help to reduce the accident that may happen in each day.

Keywords— *Disc Brake ,Static analysis, silicon –carbide, disc caliper, stainless steel.*

1. INTRODUCTION

Brakes are most important safety parts in the vehicles. Brakes function to slow and stop the rotation of the wheel. To stop the wheel, braking pads are forced mechanically against the rotor disc on both surfaces. The increases in travelling speeds as well as the growing weights of cars have made these improvements essential. An effective braking system is needed to accomplish this task with challenging term where material need to be lighter than before and performance of the brakes must be improved. Today's cars often use a combination of disc brakes and drum brakes. However, the effectiveness of braking system depends on the design itself and also the right selection of material. System that follow with some improvements. In order to understand the behaviors of braking system, there are three functions that must be complied for all the time

a) The braking system must be decelerate a vehicle in a controlled and repeatable fashion and when appropriate cause the vehicle to stop.

b) The braking should permit the vehicle to maintain a constant speed when traveling downhill.

c) The braking system must hold the vehicle stationary when on the flat or on a gradient.

2. STATEMENT OF PROBLEM

Brakes is such a crucial system in stopping the vehicle on all moving stages including braking during high speed, sharp cornering, traffic jam and downhill. All of those braking moments give a different value of temperature distribution and thermal stress.

This project concerns of the temperature distribution and constraint of the disc brake rotor. Most of the passenger cars today have disc brake rotors that are made of grey cast iron (Mackin, 2002). Grey cast iron is chosen for its relatively high thermal conductivity, high thermal diffusivity and low cost (Mackin, 2002). In this project, the author will investigate on the thermal issues of normal passenger vehicle disc brake rotor, High temperature during braking will caused to:

- Brake fade
- Premature wear
- Brake fluid vaporization
- Bearing failure
- Thermal cracks
- Thermally-excited vibration

Due to the application of brakes on the car disk brake rotor, heat generation takes place due to friction and this thermal flux has to be conducted and dispersed across the disk rotor cross section. The condition of braking is very much severe and thus the thermal analysis has to be carried out. The thermal loading as well as structure is axis-symmetric. Hence axis-symmetric analysis can be performed, but in this study we performed 3-D analysis, which is an exact representation for this thermal analysis.

3. BRAKE SYSTEMS

3. 1 PARTS OF DISC BRAKE

3. 1. 1 DISC CALIPERS

There are two types of disc calipers where further classified as floating and fixed caliper shows a type of floating caliper. This type of brake uses only a single piston to squeeze the brake pad against the rotor (BOSCH, 1992). The reactive force shifts the caliper housing and presses opposite side of braking pad against rotor. Referring to Figure the brake fluid pushes the piston when the brake is applied to the left of the piston and immediately pushes the inner pads and presses it against the rotor disc, the sliding caliper housing reacts by shifting towards right pushing the left pad against the disc. Floating Caliper Design (Source: BOSCH Automobile Handbook, 1992) Other type of disc calipers is a fixed caliper shows a type of fixed caliper. In these types of brakes, the caliper body is fixed and uses two or more pistons on each side of the rotor. The pistons are located in each half section of the fixed caliper.

3. 1. 2 BRAKE PADS

Brake pads consist of steel carrier which the pad are bonded to the steel carrier. According to (Gerschler, 1980), organically bonded pads consist of metallic, ceramic or organic friction materials in a bonded mass such as rubber or synthetic resin. The bonded friction materials can withstand temperatures up to 750°c, with short term peaks-up to 950'~ where the friction coefficient is between 0.25 and 0.5. There is an advantage of brake pads, where most of them are poor to thermal conductivity which protects the hydraulic actuating elements from overheating.

3. 1. 3 BRAKE DISC / DISC BRAKE ROTOR

The heat generated on the surfaces of disc brake rotor when brake applied. Materials of disc brake rotor usually are made from cast iron, spheroidal- graphite cast iron or cast steel. It is chosen as a rotor material due to low cost of material and performs high thermal resistance. This type of material normally suit to normal passenger vehicle but not for high performance car. Once brake pads contacts to rotating rotor, there will be huge amount of heat generated to stop or slow down the vehicle. The rotor temperature can exceed 350° for normal cars and 1500° for race cars (Halderman, 1992).

3. 1. 4 BRAKE PADS:

Brake pads consist of steel carrier which the pad are bonded to the steel carrier. According to (Gerschler, 1980), organically bonded pads consist of metallic, ceramic or organic friction materials in a bonded mass such as rubber or synthetic resin. The bonded friction materials can withstand temperatures up to 750°c, with short term peaks-up to 950'~ where the friction coefficient is between 0.25 and 0.5. There is an advantage of brake pads, where most of them are poor to thermal conductivity which protects the hydraulic actuating elements from overheating.

4. MATERIAL PROPERTIES, CONSIDERATIONS AND CALCULATIONS

Table 4. 1 MATERIAL PROPERTIES OF THE DISC:

Material Properties	*Silicon Carbide- Reinforced Carbon Composite matrix*	*Stainless Steel*
young's Modulus	250 GPa	193 GPa
Density	1.8 g/cm^3	7750 Kg/m^3
Poisson's Ratio	0.32	0.31
Ultimate Tensile Strength	185 MPa	580 MPa
Bulk Modulus	250 GPa	151 GPa
Shear Modulus	220 GPa	81 GPa
Compressive Strength	3000 MPa	250 MPa

5. CALCULATIONS:

5. 1 DIMENSIONS OF THE DISC PLATE:

Assumptions made for proceeding with the calculations:

Brake disc diameter	:	355 mm
Contact area diameter (Inner)	:	340 mm
Contact area diameter (Outer)	:	190 mm
Pressure applied on the disc during braking	:	P_{max}

Axle diameter	:	85 mm
Hole diameter for bolting	:	20 mm
Disc thickness	:	33 mm
Caliper pad thickness	:	12 mm
Coefficient between disc and pad (Dry friction coefficient, **μ**)	:	0.5
Vehicle Curb Weight	:	20000 N
Axle weight distribution ratio (γ)	:	0.3
Initial velocity	:	112.5 m/s
Final velocity	:	0 m/s
Percentage of kinetic energy absorbed by the disc	:	0.9

Vehicle load on the disc (F_V) = Total load of the vehicle * Axle weight ratio

= 20000 N * 0.3

= 6000 N

Area of contact (A) = Area of segment from Outer radius – Area of segment from Inner radius

= 17463.931-1042.13 mm^2

= 16421.801 mm^2

P_{max} = Force on the disc/ Area of the contact

(1.5*20000)/A

= 1.82632 N/mm^2

i) *Tangential Load acting on the disc due to brake pressure:*

Normal load on the disc (F_N) = (P_{max}/2) * Area of the brake pad

= (1.82632/2)* 16421.801

= 14995.7318 N

Tangential Load (F_T) = Normal load * Coefficient of friction

= 14995.7318 * 0.5

= 7497.8659 N

Total load on disc while braking (F_S) = $F_N + F_T + F_V$

= 14995.7318+7497.8659+ 6000

= 28493.5977 N

ii) *Brake torque acting on the disc brake*:

Brake torque on the disc = Total load on the disc * Radius of the rotor disc

= (28493.5977 N) * 0.1675 N-m

= 4772.6776 N-m

iii) *Braking distance:*

Distance covered by the

Vehicle during braking = x

Work done during braking = Total load on the disc * Braking distance

.... (Eq.1)

Kinetic energy released

During braking = (mass of the vehicle *Velocity of the vehicle^2) / 2

…. (Eq.2)

Since,

Work done during braking = Kinetic energy released during braking

$F_S * x$ = $(mv^2) / 2$

28493.5977 N * x = $(20000 * [(\pi*355*4000)/60]^2) / 2$

Braking distance of the vehicle (x) = 31.5 m

6. MODELLING OF COMPOSITE BRAKE DISC

6. 1 GENERAL MODELING PROCESS FOR EACH PART

- Plan the part
- Create the base feature
- Create the remaining features
- Analyze the part

- Modify the features as necessary
- Assembly modelling

Assemblies can be created from parts, either combined individually or grouped in subassemblies. The CATIA V5 builds these individual parts and sub assemblies into an assembly in a hierarchical manner according to relationships defined cy constrains.

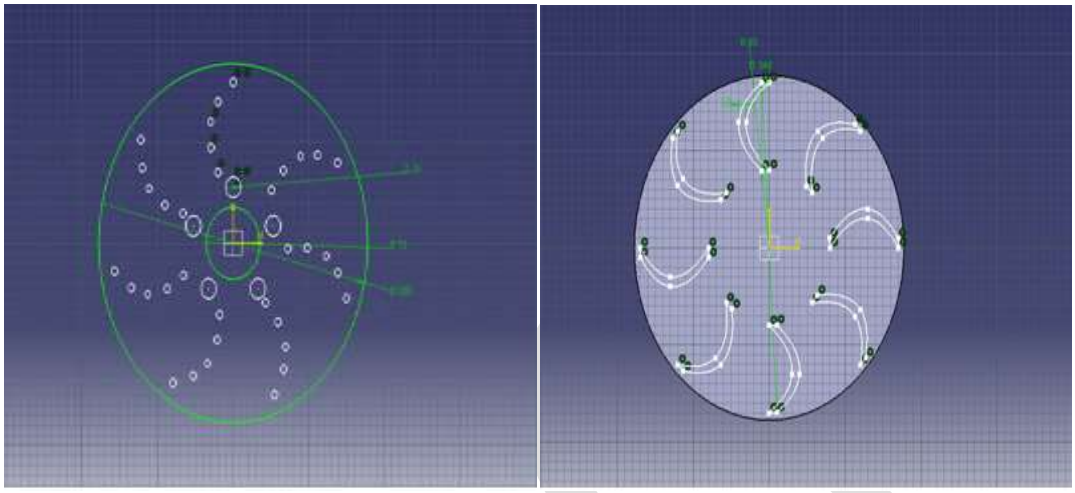

Fig 6.1 2-D View Of Disc Rotor(Composite And Solid Rotor) And 2-D View Of Disc Rotor (Vented Rotor)

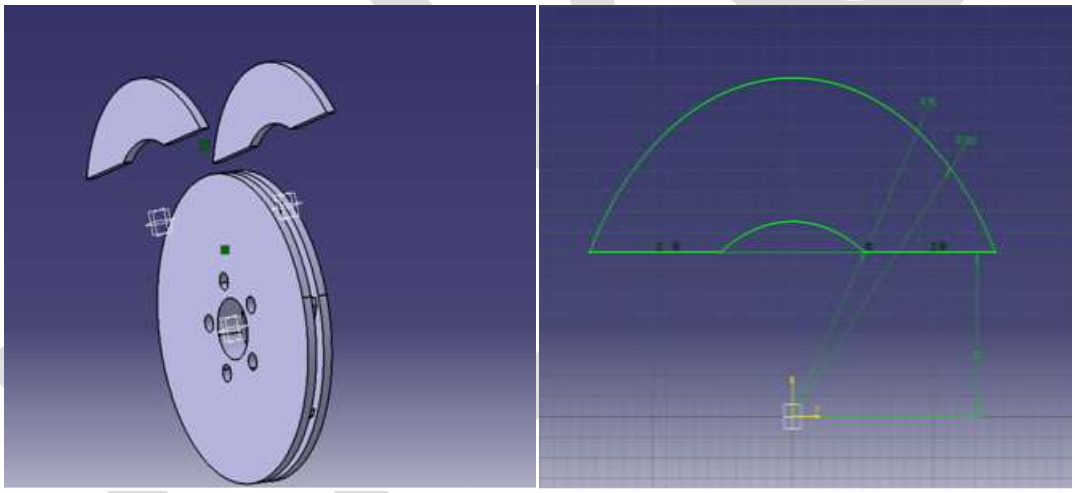

Fig 6.2 Exploded View Of Rotor Disc Assembly And 2-Dimensional View Of Friction Pad

7. ANALYSIS OF COMPOSITE BRAKE DISC

7.1.1 STRUCTURAL STATIC ANALYSIS:

A static analysis calculates the effects of steady loading conditions on a structure, while ignoring inertia and damping effects such as those caused by time varying loads. A static analysis can, however include steady inertia loads (such as gravity and rotational velocity), and time varying loads that can be approximated as static equivalent loads (such as static equivalent wind and seismic loads.

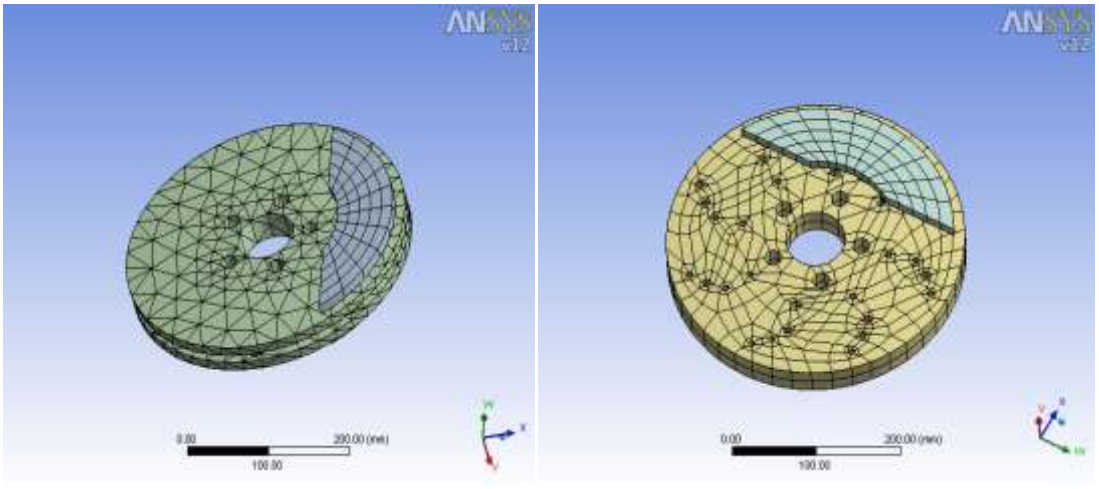

Fig 7.1 Meshed Model Of The Vented Disc Rotor And Meshed Model Of Solid Disc Rotor

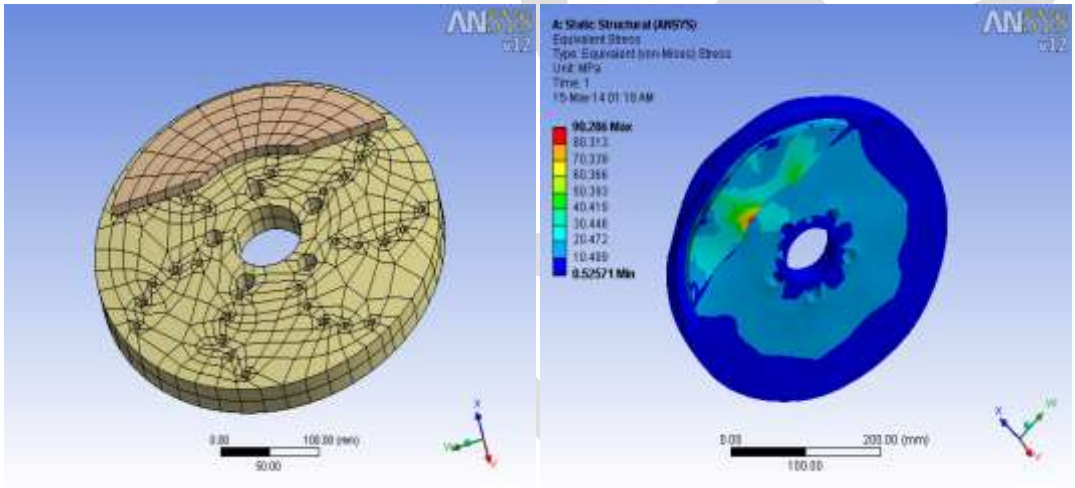

Fig 7.2 Meshed Model Of Composite Disc Rotor And Equivalent Sress Vented Disc Rotor

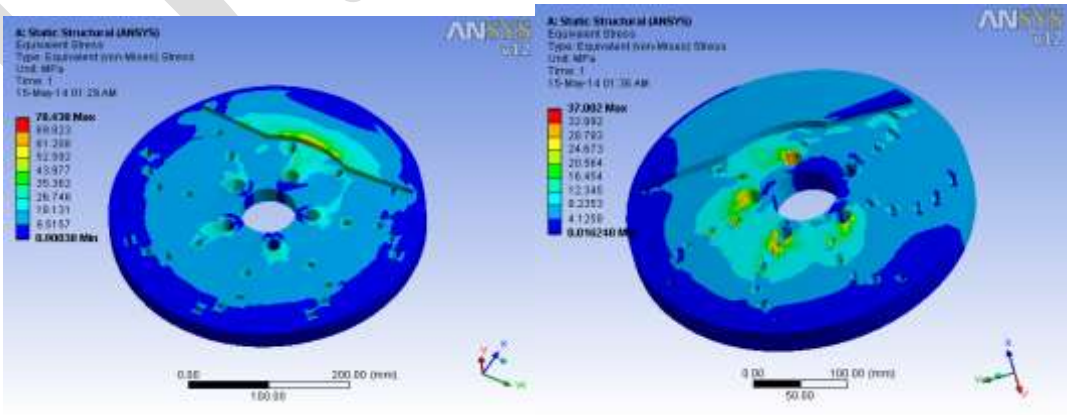

Fig 7.3 Equivalent Stress- Solid Disc Rotor And Equivalent Strain-Vented Disc Rotor

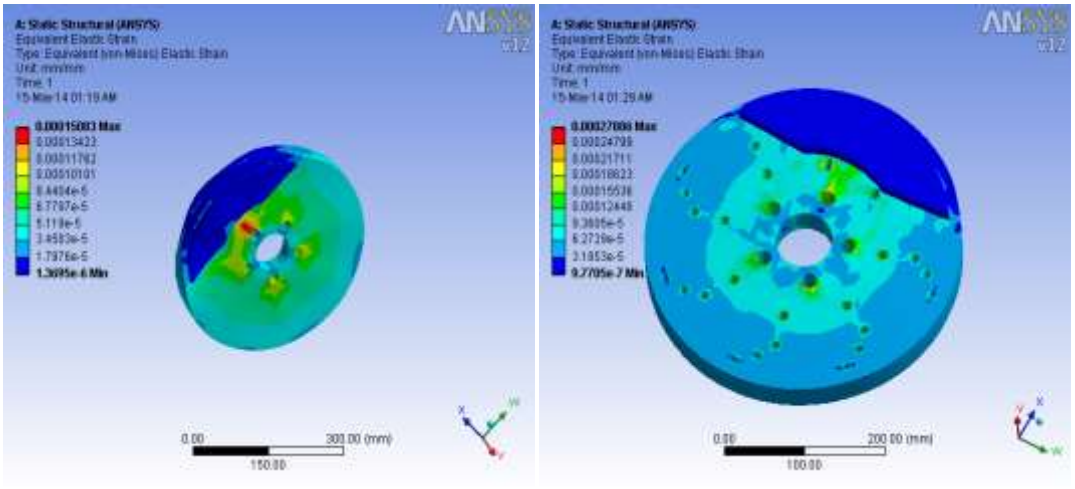

Fig 7.4 Equivalent Strain-Vented Disc Rotor And Equivalent Strain-Solid Disc Rotor

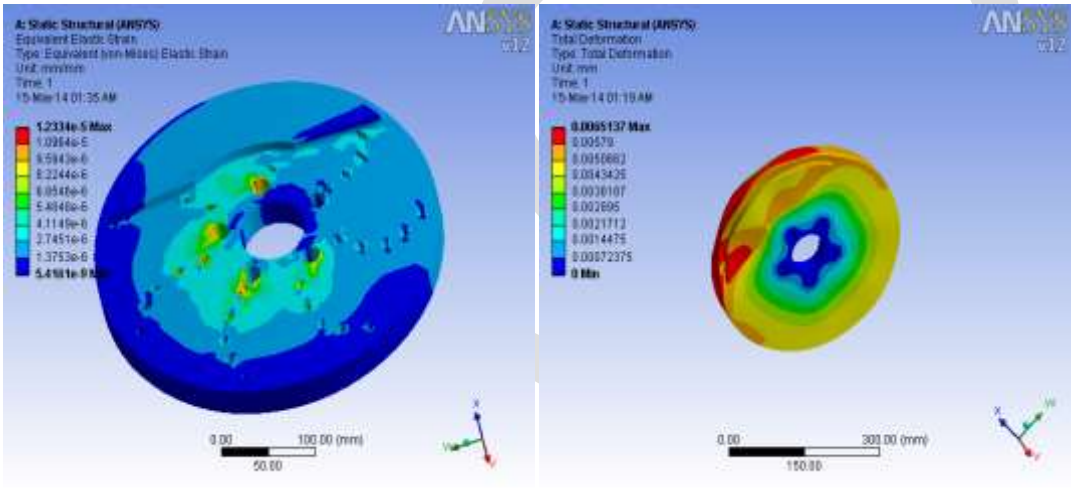

Fig 7.5 Equivalent Strain- Composite Disc Rotor And Total Deformation- Vented Disc Rotor

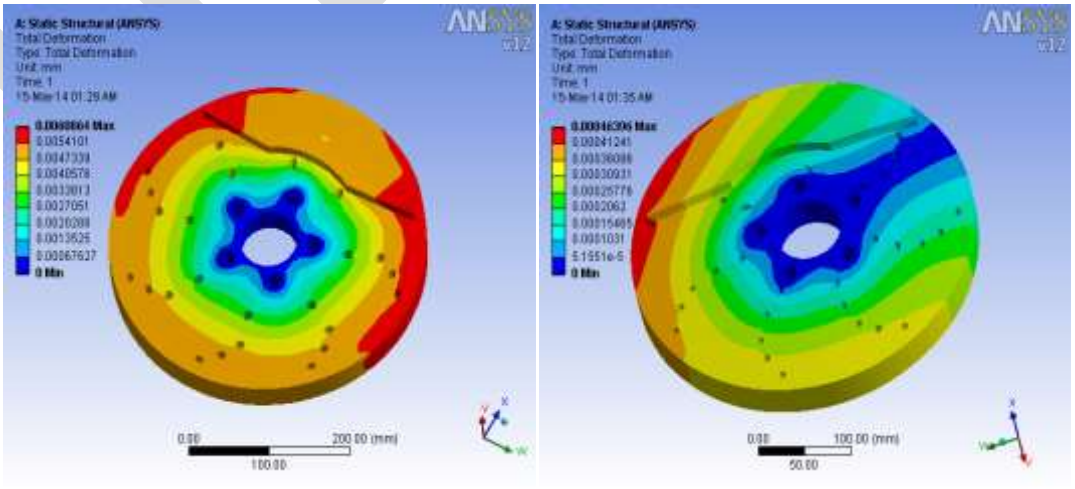

Fig 7.6 Equivalent Strain- Solid Disc Rotor And Equivalent Strain- Composite Disc Rotor

10. CONCLUSION

From the results obtained above, we can come to the conclusion that:

- Practical use of C-SiC composite material produces much effective braking compared to steel disc brakes.
- Deformation in steel is much higher than composite, which implies the deformation resistance of the composite structure than the steel material.
- Stress accumulated on the composite is much less, which proves the wear resistance, rigid & stable braking during high speeds.

REFERENCES:

1. Swapnil R. Abhang, D.P.Bhaskar, "Design and Analysis of Disc Brake" International Journal of Engineering Trends and Technology (IJETT) – Volume 8 Number 4- Feb 2014
2. Manjunath T V, Dr Suresh P M, "Structural and Thermal Analysis of rotor disc in Disc Brakes", IJIRSET ISSN No: 2319-8753, December 2013
3. B.Brown, "Performance enhancement to a brake caliper design" Masters of Science Thesis, Wichita State University, 2003
4. Halderman J.D "Automotive Brake Systems", Prentice Hall, Inc, NJ, USA, 1996 Kubota Masahiro, Hamabe Tsutomu, Nakazono Yasunori, Fukuda Masayuki, Doi Kazuhiro,"Development of a lightweight brake disc rotor: a design approach for Achieving an optimum thermal,vibration and weight balance", Nissan Motor Co., Ltd, Japan, 2000
5. Grieve, D. G., Barton, D. C., Crolla, D. A., and Buckingham, J. T., "Design of a Light weight automotive brake disc using finite element Techniques", University of Leeds, November 1997
6. Jancirani, J., Chandrasekaran, S. and Tamilporai, P., "Design and heat transfer Analysis of automotive disc brakes", ASME Summer heat transfer Conference, Las Vegas, Nevada, July 2003
7. Miha Pevec[a],Grega Oder[a],Iztok Potrč[a],Matjaž Šraml[b] , "Elevated temperature low cycle fatigue of grey cast iron used for automotive brake discs" 13 April 2014.
8. Peter Andersson, Björn Hemmin Determination of wear volumes by chromatic confocal measurements during twin-disc tests with cast iron and steelOriginal . 15 September 2015.
9. Blaž Šamec, Iztok Potrč, Matjaž Šram "low cycle fatique of modular cast iron used for railway brake disc". Engineering failure analysis, volume 18 issue September 6 2011.
10. A.A Yevtushenko, P. Grzes :" 3D fea model of frictional heating and wear with a mutual influence of sliding velocity and temperature in a disc brake.

International Journal of Engineering Research and General Science Volume 3, Issue 5, September-October, 2015
ISSN 2091-2730

TECHNO ECONOMICAL USE OF QUARTZITE ROCK DUST AND EFFECT OF GLASS FIBERS IN RIGID PAVEMENTS

Ramarao Chimata[1], Venkateswara rao.J[2]

[1] Post Graduate Student, Civil Engineering Department, GMRIT, Rajam, AP,India

[2] Associate Professor, Civil Engineering Department, GMRIT, Rajam, AP,India

[1] Chimata.ramarao7@gmail.com

[2]Venkateswararao.j@gmrit.org

ABSTRACT- In this experimental study sand is replaced by quartzite rock dust from available sources. Quartzite rock dust replacement up to 40% by weight of cement in steps of 10% increments and 0.2% glass fibers by weight of cement was also included for further enhancing flexural strength of concrete. Thickness of pavement was evaluated with required parameters as per IRC-58:2002.From the results it was found that the pavement thickness can be reduced up to 19.04%.

Key Words: Quartzite rock dust, Glass fibers, Flexural strength, Pavement thickness

1. INTRODUCTION

In the recent past good attempts have been made for the successful utilization of various industrial by products (such as fly ash, silica fume, rice husk ash, foundry waste, slag, limestone powder) in concrete. In addition to this, an alternative source for the potential replacement of natural aggregates in concrete has gained good attention. As a result reasonable studies have been conducted to find the suitability of quartzite rock dust in conventional concrete to overcome the stress and demand for river fine aggregate and cement in construction of roads and other works.

2. LITERATURE

In previous investigations researchers used foundry sand, ceramic dust;,fly ash, hypo-sludge, waste plastic and quarry dust were used as alternative materials for sand. Past experimental studies have revealed that use of glass fibers significantly enhances flexural strength of concrete, which in turn reduces the thickness of pavement. Venkata Sairam Kumar,N.B.PandurangaRao,Krishna Sai.M.L.N;et al [1] have investigated on partial replacement of cement with quarry dust for studying mechanical properties of concrete. In this experimental work, the percentages of quarry dust used as a partial replacement of cement in concrete was 0, 10%, 15%, 20%, 25%, 30%, 35%, and 40% for M20, M30, M40 grade concrete. They have concluded from the experimental studies that 25% of partial replacement of cement with quarry dust improved hardened concrete properties**. Nagesh Tatoba Suryawanshi Samitinjay S Bansode Dr Pravin D Nemade et al [2]** have been carried out experiments on fly ash to replace some part of cement and sand to the extent of 10-30 percent and 5-15 percent respectively. Because of the use of fly ash, rigid pavement behaves as a semi rigid pavement causing substantial reduction in cost of construction. If the fly ash is utilized on large scale for road construction. **K Vamshi krishna1 J Venkateswara Rao et al [3]** have been studied the influence of glass fibers on the mechanical properties of the M20 grade concrete. Glass fibers of 0.1%, 0.2%, and 0.3% by weight of cement are added to the mix. It is found that 0.2% fibers by weight of cement is the optimum dosage. Using the flexural strength values at 0.2% fiber content, pavement thickness is evaluated as per IRC : 58, it is observed that there is a reduction in the pavement thickness by 25.8%.**K vamshi krishna1 J Venkateswara Rao et al [4]** have done experimental investigation on mechanical properties of M20 grade concrete by incorporating polyester fibers in the mix. Polyester fibers of 0.1%,0.2%,0.3%,0.4% by weight of cement are added to the mix. It is observed that 0.3% fibers by weight of cement is the optimum dosage. It is found that with 0.3% fiber content results in 20% reduction of pavement thickness. In this

experimental study cement is replaced by quartzite rock dust up to40% and 0.2% Glass fibers by weight of cement were also included. Thickness of pavement is evaluated with parameters by IRC-58:2002.

3. MATERIALS & MIX DESIGN

3.1 Materials

Ordinary Portland cement (OPC) of grade 43 with a specific gravity of 3.12, quartzite rock dust is taken from locally available sources, aggregate with a maximum size of 20mm down size with a specific gravity of 2.78 was used. Various physical properties of coarse aggregates are given in Table.1.Locally available sand with a specific gravity of 2.71 was used as fine aggregate. The glass fibers of 6 mm length and diameter of 0.012mm are used in the present study. A water reducing admixture, rheo build 920kk is used in concrete. Its density and pH are 1.19 and >6 respectively.

Material property	Water absorption	Aggregate Impact	Aggregate Crushing	Flakiness Index	Elongation Index
Percentage by weight	0.5%	26%	29%	9%	12%

3.2Mix Design

Samples are prepared for M-40 grade. For the design of mix IS: 10262-2009 recommendations are adopted. Mix proportions of M-40 are given in the following table.1.

Material	Cement	Sand	Coarse aggregate	W/C Ratio	Admixture
Weight	440.52kg/m^3	563.5kg/m^3	1135kg/m^3	0.38	2.07it

Table 1.Mix Proportions

3.3 Specimens Preparation

In a mixer quartzite dust and cement are mixed thoroughly in required proportions until uniform color was achieved. Next, sand and coarse aggregates are added and mixed thoroughly again for 2 to 3 minutes. Glass fibers respective quantity of fibers are added and mixed for 1 to 2 minutes. The mix was then transferred in to cubes (150mm x 150mm x 150mm) and prisms (100mm x100mm x 500mm). During transferring the mix was compacted in three layers. Mix was then compacted on vibrator to expel the air.

3.4 Test Setup

The specimens were tested for 7 and 28 day compressive strength. The specimens were subjected to a compressive force at the rate of 5 KN/sec until they failure occurs. The mean value of the compressive strengths of three test cubes in a series is reported as compressive strength of a particular mix. For finding the flexural strength of prisms IS: 516-1959 guide lines are followed.

Fig4.1.Cube Testing

Fig 4.2.Prisims Testing

4. RESULTS AND DISCUSSIONS

4.1 Compressive Strength Test

Compressive strength values of cube specimens were at 7&28 days testing given in below graph. From the figure 4.3 it was observed that rate of increment in compressive strength of the Quartzite rock dust concrete is 9.04% and 8.94% at age of 7&28 days respectively compared to conventional concrete. From the graph it was clear that there is an improvement in compressive strength of the Quartzite rock dust with glass fibers is 14.59% and 14.67% at age of 7&28 days respectively compared to quartzite rock dust concrete. It is evident that from results compressive strength of Quartzite rock dust concrete with glass fiber increases to 24.95% and 24.93% at age of 7&28 days respectively compared to Quartzite rock dust concrete.

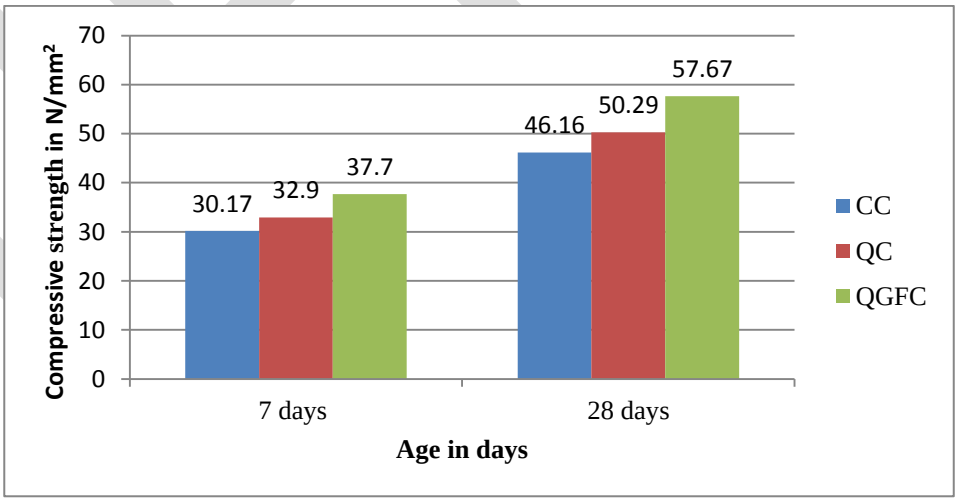

Fig 4.3 Compressive strength of CC,QC & QGFC at 7&28 days

4.2 Flexural Strength Test

Flexural strength of beam specimens are tested on UTM at 7&28 days .results are given below

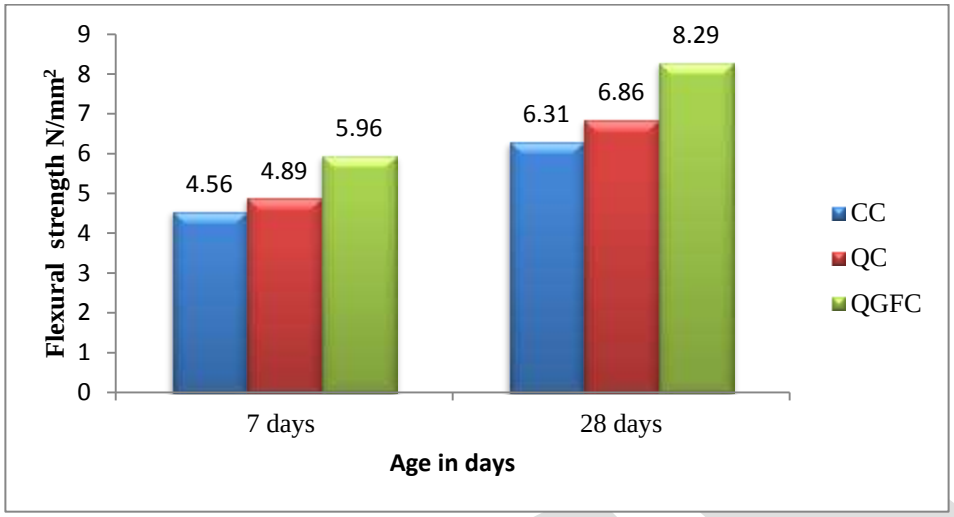

Fig 4.4 Flexural strength values of different mixes at 7&28 days

From the figure 4.4 it was observed that rate of increment in flexural strength of the Quartzite rock dust concrete is 7.23% and 8.71% at age of 7&28 days respectively compared to conventional concrete. From the graph it was clear that there was an improvement in flexural strength of the Quartzite rock dust with glass fibers was 21.88% and 20.84% at age of 7&28 days respectively compared to quartzite rock dust concrete. It was evident that from results flexural strength of Quartzite rock dust concrete with glass fiber increases to 30.7% and 31.38% at age of 7&28 days respectively compared to Conventional concrete.

5. PAVEMENT SLAB DESIGN AND ANALYSIS

Pavement slab was designed as per IRC 58:2002. The flexural strength is directly taken from the beam flexural test. The axial load spectrum is taken from IRC: 58-2002 and other data used in this design are given below. A cement concrete pavement was to be designed for a two lane two-way National Highway. The total two-way traffic is 7842 commercial vehicles per day at the end of the construction period.

The design parameters are

Effective modulus of subgrade reaction of the DLC sub-base	=	8 kg/cm^3
Elastic modulus of concrete	=	3×10^5kg/ cm^2
Poisson's ratio	=	0.15
Coefficient of thermal expansion of concrete	=	$10\times10^{-6}/^0$C
Tyre pressure	=	8 kg/cm^2
Rate of traffic increase	=	0.075
Spacing of contrction joints	=	4.5 m
Width of slab	=	3.5 m
Design life	=	30 years
Present traffic	=	7842 cvpd

Single Axles		Tandem Axles	
Load in tones	Expected repetitions	Load in tones	Expected repetitions
20	644496	36	322248
18	1353442	32	193348
16	3158032	28	580046
14	7218361	24	1417892
12	10183045	20	7282810
10	10311945	16	94909649
Less than 10	14178924	Less than 16	4640375

Table 2 Expected repetitions for single and tandem axles

Taking the above design parameters and expected repetition values into considerations and design the slab thickness according to IRC-58:2002 for conventional, quartzite with and without glass fiber concretes.

Grade of concrete(M_{40})	Flexural strength ($Kg/cm^{2)}$	Slab thickness (cm)	Fatigue life consumed	Corner stress (Kg/cm^2)
CC	61.9	25	0.56	23.8
QC	71.9	24	0.52	26.95
QGFC	88.04	21	0.43	32.65

Table 3 Slab thickness design

6. Cost Comparison of Pavements

A cement concrete pavement was to be laid with 25cm,24cm and 21cm thick slabs for CC,QC and QGFC respectively . Quantity and cost of each material for that stretch is calculated and compared for conventional concrete and quartzite dust with and without glass fiber concrete in this section. In this analysis cost was estimated for 1m length and 3.5m width of pavement.

S.no.	Material	Rate per kg in Rs.
1	Cement	6.11
2	Fine aggregate	0.46
3	Coarse aggregate (20mm)	0.88
4	Coarse aggregate (10mm)	0.63
5	Super plasticizer	60
6	Fibers(glass)	150
7	Quartzite rock dust	0.13

Table 4 Cost of each material

Pavement type	Thickness (cm)	Cost (rupees)
CC	25	3714.46
QC	24	2852.74
QGFC	212	2576.50

Table 5 Cost analysis of CC,QC&QGFC pavements

From the above results we can save 1137.96 /- Rs per 1m length by using combination of glass fiber and quartzite dust. The construction cost of the pavement was reduced by 44.17% by using combination of glass fiber and quartzite rock dust.

7. CONCLUSIONS

1. Optimum dosage of replacement of cement by quartzite rock dust was 30%.
2. Rate of increment in flexural strength of the Quartzite rock dust concrete is 8.71% at age of 28 days compared to conventional concrete.
3. About 20.84% of increment in flexural strength was found by using quartzite rock dust with glass fibers at age of 28 days compared to quartzite rock dust concrete.
4. Glass fibers addition to quartzite rock dust concrete enhances its compressive strength by 31.38%.
5. Thickness of pavement is reduced up to 19.04% by replacement of cement with quartzite rock dust and addition of glass fibers in concrete.
6. Construction cost of the pavement is reduced up to 44.17%, by partial replacement of cement with quartzite rock dust and inclusion of glass fibers in concrete.

REFERENCES

1. G.Balamurugan, Dr.P.Perumal, Use of quarry dust to replace sand in concrete an experimental study, International journal of scientific and research publications, Volume 3, Issue 12, December 2013 1 ISSN 2250-3153.
2. Dipan Patel, Use of steel fiber in rigid pavement, International global research analysis, volume2,Issue6, june-2013,ISSN:2277-8160.
3. Venkata Sairam Kumar N, Dr. B. Panduranga Rao, Krishna Sai M.L.N, Experimental study on partial replacement o f cement with quarry dust, International journal of advanced engineering research and studies e-ISSN2249–8974.
4. Vipul D. Prajapati, Nilay Joshi, Prof. Jayeshkumar Pitroda, Techno- economical study of rigid pavement by using the used foundry sand, International journal of engineering trends and technology (IJETT) - Volume4Issue5- May 2013.
5. K. VamsiKrishna , J.Venkateswara Rao, Effect of glass fibers in rigid pavement, International journal of scientific research and education ,Volum2,Issue9,Pages 1797-1804,September-2014, ISSN (e): 2321-7545.
6. Rajarajeshwari B Vibhuti, Radhakrishna, Aravind N, Mechanical properties of hybrid fiber reinforcedconcrete for pavements, International journal of research in engineering and technology eISSN: 2319-1163 | pISSN: 2321-7308.
7. Bahoria B.V, Parbat D.K. and Naganaik P.B, Replacement of natural sand in concrete by waste products: a state of art journal of environmental research and development, Vol. 7 No. 4A, April-June 2013.
8. K. Vamshikrishna , J.Venkateswara Rao, Experimental study on behavior of fiber reinforced concrete for rigid pavements ,IOSR Journal of Mechanical and Civil Engineering (IOSR-JMCE), Volume 11, Issue 4 Ver. VII (Jul- Aug. 2014), PP 49-53 , e-ISSN: 2278-1684,p-ISSN: 2320-334X.

9. Pooja Shrivastavaa, Dr.Y.p. Joshi, Innovative use of waste steel scrap in rigid pavements, Civil and environmental research, ISSN 2224-5790 (Paper) ISSN 2225-0514 (Online) ,Vol.6, No.7, 2014.
10. Chandana Sukesh, Katakam Bala Krishna, P.Sri Lakshmi Sai Teja, S.Kanakambara Rao, Partial replacement of sand with quarry dust in concrete, International journal of innovative technology and exploring engineering (IJITEE) ISSN: 2278-3075, Volume-2, Issue-6, May 2013.
11. Electricwala Fatima, Ankit Jhamb, Rakesh Kumar, Ceramic dust as construction material in rigid pavement, American journal of civil engineering and architecture, 2013, Vol. 1, No. 5, 112-116.
12. GATESI JEAN DE DIEU, Prof. M.H.Lunagaria , A review of use steel slag in concrete mixes for rigid pavement, International journal of advance engineering and research development, e-ISSN(O): 2348-4470 p-ISSN(P): 2348-6406 Volume 2,Issue 3, March -2015.
13. Mr.Nagesh Tatoba Suryawanshi , Mr. Samitinjay S. Bansode, Dr. Pravin D. Nemade, Use of eco-friendly material like fly ash in rigid pavement construction & it's cost benefit analysis , International journal of emerging technology and advanced engineering, Volume 2, Issue 12, December 2012.
14. Jayeshkumar Pitroda, Dr. L. B. Zala, Dr F. S. Umrigar, Hypo sludge management: opportunities for developing low cost concrete with glass fibers, global research analysis, e-ISSN(O): 2277-8170 Volume 1,Issue 7, Dec -2012.
15. Rama Mohan Rao. P,Sudarsana Rao.H , Sekar.S.K, Effect of glass fibers on fly ash based concrete, international journal of civil and structural engineering , ISSN 0976 – 4399, Volume 1, No 3, 2010.
16. IRC-58:2002

International Journal of Engineering Research and General Science Volume 3, Issue 5, September-October, 2015
ISSN 2091-2730

A Coupled Microstripline Directional Coupler Simulated Using CST-MWS

Prachi Choubey, Vandana Roy

Electronics and Communication Department, Gyan Ganga Institute of Technology & Sciences, Jabalpur, India

prachoubey88@gmail.com

Abstract— Directional Coupler (DC) is a passive device which is primarily employed for monitoring purposes. It is also used in wide range of applications such as antenna feeds, balanced mixers, modulators, phase shifters, as power combiners, as reflectometers. The paper discusses the designing issues of a coupled line-microstripline directional coupler and designs a directional coupler yielding directivity of ~21 dB for the frequency 505.8 MHz. The effects of strip thickness, and substrate thickness have been studied while optimizing the design parameters in order to enhance the directivity of the coupler.

Keywords— Directional Coupler, Microstripline, 505.8MHz, CST-MWS, Coupled Lines, RF designing, Coupled lines

INTRODUCTION

Directional Coupler (DC) is essentially a four port device whose function is to tap a small portion of incident power and use it according to the application. The proportion of the amount of power extracted to incident power depends upon a factor called coupling ratio.

A directional coupler can be configured with the help of lumped elements and transmission lines. But its waveguide and coaxial versions are discussed more often. These variants are very large in size, costly to construct, and introducing changes in design of these at higher frequencies is difficult. A microstripline coupled directional coupler is made by sandwiching a dielectric slab between a conducting ground plate on one side and two conducting strips on other side. The coupling action takes place by virtue of electromagnetic interaction between the two strips placed in proximity to each other for a particular distance called coupling length. Because of these interactions coupled microstrip supports two modes of propagation viz. even mode and odd mode [2]. The configuration enjoys all the pros associated with microstripline structure and gets hampered by its cons as well. The structure enables the directional coupler to be easily integrated with other devices and allows easy troubleshooting. But because of inhomogenity of the medium, the phase velocities of the two modes differ and degrade the performance of directional coupler.

Along with coupling, characterization of devices like directional coupler is done with respect to few more parameters like isolation of undesired port; directivity, which is the difference between coupling and isolation; reflection, measure of amount of incident power reflected from input port itself; insertion loss, the measure of loss incurred when device is inserted in a transmission path. Mathematically, the ratios viz. Directivity, Coupling, Isolation can be expressed as follows (Figure 1) [11]:

$$\text{Coupling} = 10 \text{ Log } \frac{\text{Pi}}{\text{Pf}} \text{ decibels}$$

$$\text{Directivity} = 10 \text{ Log } \frac{\text{Pf}}{\text{Pb}} \text{ decibels}$$

$$\text{Isolation} = 10 \text{ Log } \frac{\text{Pi}}{\text{Pb}} \text{ decibels= Coupling (in dB) +Directivity (in dB)}$$

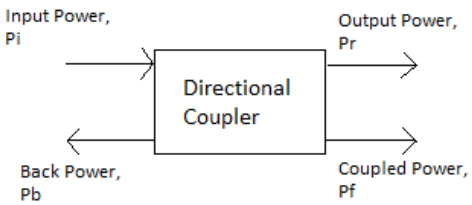

Figure 1. 4-Port Directional Coupler

Extensive research has been conducted on the design of microstrip directional couplers due to their widespread application. Akhtarzad et. al. reports design equations for the coupled microstripline in the paper [4]. Krisching and Jasen [5] also presents closed form expressions that can be implemented with the help of computers. J. H. Hinton [3] reports updated wheelers formula to yield more accurate results for wide range of width of striplines to height of substrate ratio. Erogulu [6] incorporates modifications introduced by Hinton in the design equations reported by Akhtarzad. Gupta et al [2] have given detailed analysis of microstripline structure. T. Vijayan [8] formulates the modified equations to design a directional coupler for the frequency 300 MHz using IE3D, a planar electromagnetic simulation tool.

MICROWAVE STUDIO (MWS), a Computer Simulation Technology **(**CST) software tool is used for three dimensional electromagnetic simulation of high frequency devices for antennas, filters and couplers etc.. Features like easy-to-use interface, parameterization and optimization capabilities, including post-processing options to increase the speed of development process.

The paper studies the considerations involved in designing a directional coupler and designs a directional coupler utilizing the various features of CST-MWS.

DESIGN EQUATIONS:

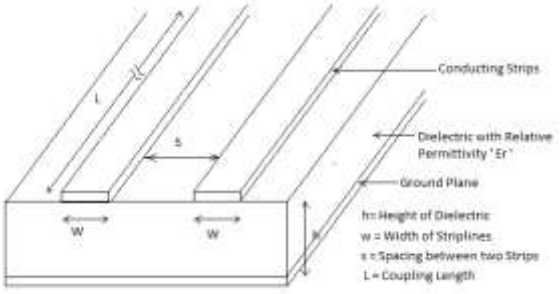

Figure 2. Schematic of Coupled microstripline directional coupler

The figure 2 introduces the various design parameters related to microstripline structure. It also shows their symbols which have been used in the text. Microstripline consists of a metallic ground plane and two strips of width 'w', separated laterally by's'. A dielectric substrate of height 'h' and relative permittivity 'Er' is sandwiched between ground and strips.

The design procedure adopted in this paper implements closed formulas given in [2, 4] which give a complete design of symmetrical two-line microstrip directional couplers, for MHz frequency range.

The coupling ratio of a directional coupler is usually given in terms of decibel. To convert it into its antilogrithmic form following equation can be used.

$$c = 10^{\frac{-Cr}{20}}$$

Where,

Cr = coupling ratio in dB

c = coupling ratio

The above ratio is then used to determine even mode and odd mode impedances Zoo and Zoe. These relations have been derived from the relation of Cr: [6, 7, 9]

$$Z_{oo} = Z_o \sqrt{\frac{1-c}{1+c}}$$

$$Z_{oo} = Z_o\sqrt{\frac{1+c}{1-c}}$$

Where,

Z_o = Characteristic Impedance in Ohms

Z_{oo} = Odd mode characteristic impedance in Ohms

Z_{oe} = Even mode characteristic impedance in Ohms

Halves of the above derived odd and even mode impedances give their counterparts for single microstriplines as: [6, 7, 9, 12]

$$Z_{oso} = \frac{Z_{oo}}{2}$$

$$Z_{ose} = \frac{Z_{oe}}{2}$$

The ratio of width of strips to height of substrate for single line is given by [1, 2]:

$$\frac{w}{h} = \begin{cases} \frac{8e^A}{e^{2A}-2}, & for\ \left(\frac{w}{h}\right) < 2 \\ \frac{2}{\pi}\left[B - 1 - ln(2B-1) + \frac{Er-1}{Er+1}(0.23 + \frac{0.11}{Er})\right], & for\ \left(\frac{w}{h}\right) < 2 \end{cases}$$

Where,

$$A = \frac{Z_O}{60}\sqrt{\frac{Er+1}{2}} + \frac{Er-1}{Er+1}(0.23 + \frac{0.11}{Er})$$

$$B = \frac{377}{2Z_o\sqrt{Er}}$$

To determine even and odd mode single line w/h ratios Zo is replaced by Zoso and Zose in equation for single line w/h ratio. That is:

$$\frac{w}{h_{se}} = \frac{w}{h}\Big|_{Z=Zose}$$

$$\frac{w}{h_{so}} = \frac{w}{h}\Big|_{Z=Zoso}$$

Where,

$\frac{w}{h_{se}}$ = Even mode w/ h ratio for single line

$\frac{w}{h_{so}}$ = Odd mode w/h ratio for single line

Now, the above calculated even and odd mode single line w/h ratios are used to find out spacing between lines ‘ s’ as [4,9]:

$$\frac{s}{h}=\frac{2}{\pi}\cosh^{-1}\left[\frac{\cosh((\frac{\pi}{2})(\frac{w}{h})_{se})+\cosh((\frac{\pi}{2})(\frac{w}{h})_{so})-2}{\cosh((\frac{\pi}{2})(\frac{w}{h})_{so})-\cosh((\frac{\pi}{2})(\frac{w}{h})_{se})}\right]$$

As already stated the strips are placed parallel to each other for a particular distance called coupling length 'L'. This factor plays a major role in Directional couplers performance. For better coupling, L should be in accordance with the operating frequency so that it gives maximum coupling at desired frequency. For a quarter wave coupler the relation [9,6] used for L is:

$$L=\frac{\lambda}{4}=\frac{3\times10^{8}(m/sec)}{4\times f(MHz)\times\sqrt{Eff}}$$

It is clear from the above relation that to determine the coupling length, effective permittivity is needed which, for coupled microstriplines structure, is derived in terms of even-odd mode capacitances as [9]:

$$\sqrt{Eff}=\frac{c\times C_e\times Z_{oe}+c\times C_o\times Z_{oo}}{2}$$

Where [2, 9, 6,7],

$$C_e=C_p+C_f+C'f$$

Where,

C_e = Even mode capacitance

C_p = Parallel plate capacitance

$= E_r E_0 \frac{w}{h}$

C_f = Fringe capacitance

$= \frac{1}{2}\left(\frac{\sqrt{Ef}}{cZ_o}-C_p\right)$

Where,

The effective dielectric constant for single line directional coupler is given by [2]:

$$Ef=\frac{Er+1}{2}+\frac{Er-1}{2}F(W/h)$$

Where,

$$F\left(\frac{W}{h}\right) = \begin{cases} \frac{1}{\sqrt{1+12h/w}} + 0.04(1-w/h)^2 & \left(\frac{w}{h} \le 1\right) \\ \frac{1}{\sqrt{(1+12h/W)}} & \left(\frac{w}{h} \ge 1\right) \end{cases}$$

Now,

$$C_f' = \frac{C_f}{1 + A(h/s)tanh(8s/h)} \sqrt{\frac{E_r}{E_{ff}}}$$

Where,

$$A = exp(-0.1exp(2.333-2.53w/h))$$

C_p is the parallel plate capacitance between the strip and the ground plane. Fringe capacitance depends on single microstrip geometry and parallel plate capacitance. $C_f^{'}$ corresponds to the effect of second line on single line fringe capacitance.

Also, the odd mode capacitance (C_O) is sum of four capacitances [2, 9, 6,7]:

$$C_O = C_p + C_f + C_{ga} + C_{gd}$$

Where,

$$C_{ga} = E_0 \frac{K(k^{'})}{K(k)}$$

Where,

$$k = \frac{s/h}{s/h + 2w/h},$$

$$k^{'} = \sqrt{1-k^2},$$

$$\frac{K(k^{'})}{K(k)} = \begin{cases} \frac{1}{\pi} \ln\left(2\frac{1+\sqrt{k^{'}}}{1-\sqrt{k}}\right), & for\ 0 =< k^2 =< 0.5 \\ \frac{\pi}{\ln(2(1+\sqrt{k})/(1-\sqrt{k}))}, & for\ 0.5 =< k^2 =< 1 \end{cases}$$

$$C_{gd} = \frac{E_0 E_r}{\pi} \ln\left\{\coth\left(\frac{\pi}{4}\frac{s}{h}\right)\right\} + 0.65C_f\left(\frac{0.02}{s/h}\sqrt{E_r} + 1 - E^{-2}{}_r\right)$$

C_{ga} is the capacitance through air gap. Its value is obtained from capacitance of a slot line of width 'w' with air as dielectric. K (k) and K (k`) represents elliptic function and its complement. C_{gd} is capacitance due to air dielectric interface. The first term corresponds to coupled stripline and next to it stands the relation for the coupled microstrip.

SIMULATION & RESULTS:

From the above described design equations it is clear that before starting with designing process, the designer should assign initial values to few factors like height of subsrate, thickness of metal strips, thickness of ground plane, operating frequency, coupling ,

permittivity of substrate used, and characteristic impedance. Since, usually type of substrate, characteristic impedance, coupling, operating frequency are system defined constraints, therefore the designer has only height of substrate and thickness of strips and ground plane in its hands, for any kind of manipulation.

The substrate here was Teflon whose permittivity is 2.1. The characteristic impedance was taken to be 50 ohms which is a very general value. Rests of the parameters were chosen arbitrarily.

The design created in CST-MWS is shown in Figure 3.

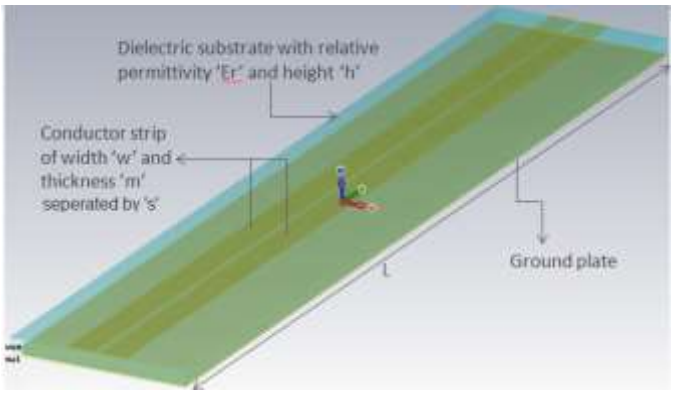

Figure 3. 3-D View of Directional Coupler in CST-MWS Design Environment

The design was created in CST-MWS design environment, implementing the equations using its wide parameterization capabilities. The results obtained after running transient solver are shown in the plot in figure 4**.** From the plot it is clear that the insertion loss is -1.17 dB, isolation is -19.769 dB, coupling is 11.27 dB, and directivity is 13.79 dB. Here the input port was numbered port 1, isolated port was port 2, output port was port 3, and coupled port was port 4

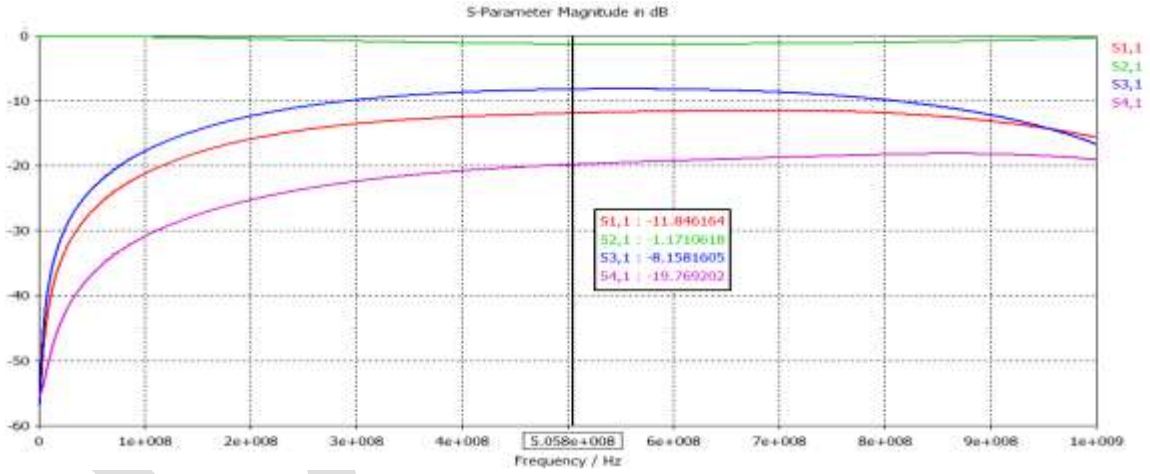

Figure 4. 1-D Plot showing S Parameters in dB

The aim was to design a 20 dB coupler but the results show that the design gave coupling of -8.15 dB and 11.61 dB directivity. Therefore, to improve directivity and achieve required coupling, further optimizations of the geometrical design parameters were done. The value of coupling came out to be -12.14 dB and directivity improved to 20.967 dB. The reflection and isolation obtained were -20.98 dB and -33.107 dB respectively. The S-Parameters chart in decibel form and the derived design parameters are shown in the figure 5 and table 1 respectively.

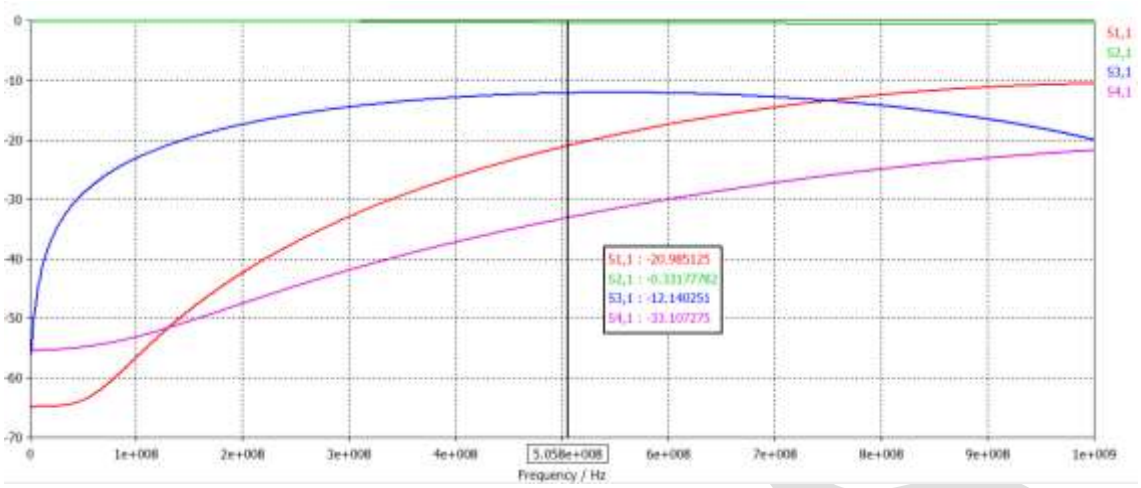

Figure 5. 1-D Plot showing final values of S Parameters in dB

The final values of parameters after optimizations, along with their symbols and description, as well as units considered, are given in table 1.

Table 1. Values of parameters

S.No.	Parameter	Description	Value
1.	Zo	Characteristic impedance of ports	50ohms
2.	Er	Relative permittivity of substrate	2.1
3.	f	Operating frequency	505.8 MHz
4.	s/h	Spacing to height of substrate ratio	0.27
5.	m	Thickness of conductor	0.2 mm
6.	Cr	Coupling ratio in dB	20 dB
7.	w/h	Width to height of substrate ratio	1.13

Now, while optimization the variations in directivity and other characterization parameters were studied with respect to changes in m and h. The associated observation tables are as follows:

Effect of strip thickness:

The values of characterization parameters of directional coupler with respect to change in strip thickness is given in table 2.

Table 2. Observation table for Strip thickness (in mm) and Directivity, coupling, isolation, reflection, insertion loss (in dB)

m(mm)	Directivity (dB)	Coupling (dB)	Isolation (dB)	Insertion loss (dB)	Reflection (dB)
0.4	-9.637	-7.365	-17	-1.56	-10.64
0.3	-10.19	-7.412	-17.6	-1.373	-11.76
0.2	-9.94	-7.449	-17.39	-1.492	-10.821
0.16	-17.04	-11.558	-28.606	-0.398	-19.47

0.15	-17.10	-11.577	-28.681	-0.395	-19.548

The best directivity and coupling, though not equal to the design value, was obtained for m= 0.15 mm therefore this value was selected.

Effect of substrate height:

After varying m, h was also varied and Directivity, coupling, isolation, reflection, insertion loss were recorded in the table 3:

Table 3. Observation table for Substrate Height (in mm) and Directivity, coupling, isolation, reflection, insertion loss (in dB).

h(mm)	Directivity (dB)	Coupling (dB)	Isolation (dB)	Insertion loss (dB)	Reflection (dB)
5	-20.566	-12.148	-32.714	-0.333	-20.923
4.5	-20.993	-12.143	-33.136	-0.331	-21.019
4.22	-21.005	-12.140	-33.145	-0.332	-20.989
4	-20.795	-12.057	-32.852	-0.337	-20.847
3	-19.506	-11.984	-31.49	-0.344	-20.619
2	-17.706	-11.663	-29.369	-0.381	-19.857

The most optimum value of h was chosen to be 4.5 mm because at this value insertion loss was the least though the difference between that obtained at 4mm, 4.5 mm and 4 mm is very minimal.

ACKNOWLEDGEMENTS

The authors would like to thank Mr. Manjeet Ahlawat, Scientific Officer/D, & Mr. R. S. Shinde, Scientific Officer/ H^+, Head, Accelerator Magnet Technology Division, Raja Ramanna Centre for Advanced Technology, India, for their motivation, guidance and support throughout the observation process carried out at Raja Ramanna Centre for Advanced Technology, India.

CONCLUSION & FUTURE SCOPE

The designed directional coupler gives a coupling of -12.14 dB, improved directivity of -20.967 dB, -20.98 dB reflection and isolation of -33.107 dB, for the frequency of 505.8 MHz. Also effect of changes in parameters like substrate height and strip thickness was observed. It was observed that the as the strip thickness is reduced and substrate height is increased, the directivity improves.

The next attempt of the author is to study the power handling capacity of the device. There are certain modifications discussed by various researchers [3, 8, and 6]. The author is attempting to implement them to achieve better coupling and directivity with reasonable values of other characterization parameters. The directivity is a factor which is very important for applications requiring accurate impedance matching. But it is equally difficult get a satisfactory value for it. Therefore, further modifications like using dielectric overlay techniques and adding delays, could be done to improve the directivity.

REFERENCES:

[1] Pozar, David M., “Microwave engineering”, second edition, Wiley, New York 1998.
[2] Gupta, K.C., Garg, Ramesh , Bahal, I.J., “Microstriplines and slot line”, Artech house EDHAM, Mass. 1979
[3] Hinton, J.H., "On Design of Coupled Microstrip Lines (Letters)," Microwave Theory and Techniques, IEEE Transactions *on* , vol.28, no.3, pp.272,272, Mar 1980
[4] Akhtarzad, S.; Rowbotham, T.R.; Johns, Peter B., "The Design of Coupled Microstrip Lines," Microwave Theory and Techniques, IEEE Transactions on , vol.23, no.6, pp.486,492, Jun 1975

[5] Kirschning, M.; Jansen, R.H., "Accurate Wide-Range Design Equations for the Frequency-Dependent Characteristic of Parallel Coupled Microstrip Lines," Microwave Theory and Techniques, IEEE Transactions on , vol.32, no.1, pp.83,90, Jan 1984.
[6] Erogulu, Abdullah "RF Circuit Design Techniques for MF-UHF Applications", CRC press, ©2013 by Taylor & Frances group.
[7] Matzner, Dr. Haim , L., Shimshon, "Basic RF Technic and Laboratory Manual", April 2002
[8] T., Vijayan, "Performance of Microstrip Directional Coupler Using Synthesis Technique", IJAREEIE, Vol. 2, Issue 3, March 2013.
[9] http://kilyos.ee.bilkent.edu.tr/~microwave/programs/magnetic/dcoupler/theory.html
[10] Gardiol, Fred "E. Microstrip circuits", Wiley, New York 1994.
[11] Kulkarni, M., "Microwave and radar engineering", Umesh Publications, 2002
[12] S. Maheswari and T. Jayanthy," Microstrip Coupler with High Isolation", International Journal of Electronics and Communication Engineering, Volume 7, Number 2 (2014), pp. 105-110

International Journal of Engineering Research and General Science Volume 3, Issue 5, September-October, 2015
ISSN 2091-2730

HARDWARE IMPLEMENTATION OF RC4 WITH TWO BYTES PER CLOCK CYCLE THROUGHPUT

Asha Krishna U K
Dept. of Electronics and Communication Engineering
MACE, Kothamangalam, Ernakulum.
Email:ashaushakrishna@gmail.com,+91-7356681700

Abstract- RC4 is very widely used as encryption algorithm in practical software applications. It comes under the category software stream ciphers since they are best suited in software platform. In this work, the study of RC4 stream ciphers in hardware platform is done. Basic RC4 output is improved to 2 RC4 key stream bytes per clock cycle, by merging the ideas of two technics. The technics involved in this are hardware pipelining and loop unrolling. All three of the proposed methods are designed in VHDL description, synthesized with Xilinx ISE Design Suit 14.1 and implemented in Spartan 5 FPGA trainer board.
Keywords- Loop unrolling, hardware pipelining, encryption, stream ciphers,RC4 keystream, throughput, pipelined-A, cipher.

1. INTRODUCTION

Encryption is the technology used to transmit data securely through a medium where third parties are present. So it enables secret communication. In encryption data to be send is converted to apparent nonsense in the transmission end using a secret key. This nonsense information (converted data or converted plain text) is send over the transmission medium to the receiver side. Any third person who receives this data can't understand any useful information from this cipher text. But the desired recipient have the key that used in encryption. The receiver can read the plain text using the same key and algorithm. A cipher is the sequence of steps that follows for performing encryption. If a cipher algorithm is using same key for encryption and decryption then such cipher is called symmetric cipher. RC4 is a symmetric key cipher.

Before RC4, the stream cipher technology was focused around linear feedback shift registers. The analysis of their security was an attractive topic because the device was very easy to study from a mathematical point of view.

In 1987, RC4 was developed by Ron Rivest. RC4, due to its byte operation is friendlier than linear feedback shift registers. Simplicity, compact implementation and reduced error prone are the reasons behind the popularity of RC4 stream ciphers. Despite of much research and many attacks, it's still secure enough for many applications.

In this paper, several hardware implementation aspects of RC4 is studied with respect to its efficiency. The paper presents three designing methods which is very fast to produce RC4 key stream.

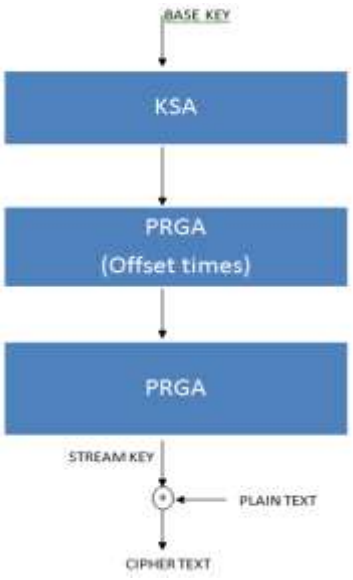

Fig.1. flow chart of RC4algorithm

2. BASIC FRAME WORK OF RC4 STREAM CIPHER

One can say RC4 as a finite state machine which have a finite number of internal states. Internal states will change according to a function of current state. The output stream is completely determined by the internal states of RC4. At first, the internal states are loaded with some initial values. are changed randomly according to some initial values. "key" is the input to the cipher. It can be variable in size. The state change of the finite state machine is completely depends on this input "key".

The complete RC4 stream cipher has 2 basic parts. First part is key scheduling algorithm. In short we can call it as KSA. It is this part where we give input. The input is a "key " which uses to randomize the internal states of RC4. Second part is called pseudo random generation algorithm (PRGA). It produces the output stream of the cipher, as a function of the internal states, after been shuffled by both KSA and PRGA.

Key scheduling algorithm is also called as key stream generation algorithm. It is Initialization:

for i = 0 to 255 do

S[i] = i

K [i] = KEY [i mod keylength]

Initial permutation

j = 0

for i = 0 to 255 do

$j = [j + S[i] + K[i]]$ *mod 256*

Swap $[S[i], S[j]]$

In this, i and j are two word sized registers. They are used to hold the index. KEY is the input to the KSA and is a variable. Here t is a register. We store the repeated KEY in it. Key length is the length of the KEY. S[] is called as substitution-box or S-box or simply S. it is basically an array of 256 words for 8-bit RC4 stream cipher. In initialization process the S-box contains 0 to 255 in its 9 to 256 locations. This is the initial state in the state machine. Then, according to the values in the word registers, i and j, the S-box values get permuted. The word register j is calculated with t-register which is a function of input KEY. So the S-box permutation is related to the input KEY. So we can say that the output of the KSA is the shuffled internal states of the S-box according to the KEY.

Pseudo random generation algorithm (PRGA) is

i=j=0

while (true) do

i=(i+1) mod 256

$j = [j + S[i]]$ *mod 256*

Swap $[S[i], S[j]]$

Temp = $S[S[i] + S[j]]$*mod 256*

Output = S [temp]

In PRGA the input is the random internal states . And in PRGA the S-box is again permuted to increase the randomness. And then output is generated. Output is a function of arithmetic addition of repeatedly permuted internal states.

All the addition in the algorithm is modulo-256 addition for the 8_bit RC4.

The output is then XOR-ed with the plain text(byte per byte) to form the encrypted text or cipher text at the sender. In the receiving side, the receiver will also have the information about the KEY. The sender and the receiver have the same KEY, because the RC4 is a symmetric stream cipher. Using the key the receiver will also generate the permuted internal states and the output stream. The cipher text which is received will XOR-ed with the output stream (byte per byte) to get back the plain text.

- RC4 generate a stream of output and each output byte is used to XOR-ed with consecutive bytes of plaintext.
- The paper proposes three methods to improve the efficiency of rc4 in terms of throughput.
- Design 1 can produce one byte per clock cycle. Loop unrolling is the technique we used in this.
- Design 2 can produce two bytes per clock cycles.
- Loop unrolling and hardware pipelining is the technique we used in METHOD 2.
- Design 3 is also produce two bytes per clock cycles. But it can release 32 bit or 64 bit per each iterations of PRGA.

3. DESIGN 1: ONE BYTE PER CLOCK CYCLE

We can see that two consecutive cycle's output bytes of RC4 can formed together for two consecutive plain-text bytes when the algorithm is analyzed in detail.

The first loop of PRGA algorithm is

$i1 = i0 + 1$

$j1 = [j0 + S0[i1]]$

$Swap\ [S0[i1], S0[j1]]$

$Z1 = S1[S0[i1], S0[j1]]$

The second loop of PRGA algorithm is

$i2 = i1 + 1 = i0 + 2$

$j2 = j1 + S1[\ i2\ ]$

$= j0 + S1[\ i2\ ] + S0\ [\ i1\ ]$

$Swap\ [S1[i2], S1[j2]]$

$Z2 = S2\ [S1[i2], S1[j2]]$

Here Z is the output formed after EACH iteration and Z1 is the first output, Z2 is the second output, and so on. Likewise S0 is the initial S-box or non-permuted internal states. S1 is formed after one permutation and so on.

From the first and second loops of PRGA, we can see that i1 is formed from i0 and i2 is formed from i1 by increment i0 by 1. But in detailed analysis we can see that i2 can calculated from i0 by incrementing it by 2. Likewise j1 value is calculating from j0 and S0, and j2 is calculated by j1 and S1. But j2 can also calculated by j0 and S0. So from this analysis, we can come to the conclusion that i1, i2, j1 and j2 can calculate with the same set of input. So they can calculate in a single clock cycle. i1 and j1 is needed for the first output Z1 and i2 and j2 is needed for the second output Z2. So actually we can calculate Z1 and Z2 in a single clock cycle. So we can calculate two consecutive outputs in a single clock cycles.

3.1 Designing components

The S-box keeps the internal states of the cipher. It is eight bit register that used for holding each internal state and there are 256 such registers in total to form the whole S-box. Each state is accessed through a 256 to 1 multiplexer and the output of the multiplexer is set by the inputs i1, i2, j1 and j2.

The overall design can be divided into four separate parts. One part is to calculate i1 and i2. Only clock is needed for the first design with a initial state. For second design j0, i1 and i2 are the inputs. Third design is for swapping the S-box. The locations to be swapped is determined by the I and j values. Forming the output stream is the final design step.

3.1.1.First step of design1 : Design for calculating i1 and i2.

For formation of i1 and i2, two synchronous 8 bit counters is used and each bit is formed by a flip-flop. We can say that i1, i3, i5 etc. will be odd numbers where as i2, i4, i6 etc. will be even numbers. So we can say that, for i1 the least significant bit will always be a one. And for i2 the least significant bit will always be a zero. So actually a seven bit counter is only needed and the least significant flip-flop does not need a clock. It always carries a constant value, 0 for i2 and 1 for i1.

Initial value of i-counter is set differently for i1 and i2. It is 00000001 for i1 and 00000010 for i2. Calculation of i1 and i2 serves for first two rounds of KSA as well as PRGA.

Thereafter for every other clock pulse which gets for i1 and i2 the output is produced.

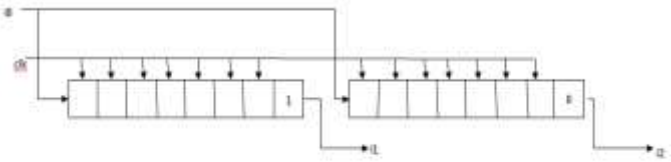

Fig.2. diagram of i1 and i2

i value is used to calculate the j value. Both are word sized registers used to provide the addresses from where values needed to be shuffled. The circuit diagram for i1 and i2 is there in fig.1.

3.1.2 Second step of design 1 : Design for calculating j1 and j2

Like I, j1 and j2 can also calculated simultaneously. The input to j-design is i1 , i2 and j0. j0 is the initial value for the j1 and j2. J0 is the initial state and it is same for both j1 and j2.

The two computed j-values are stored in two 8 bit registers. One component of circuit is 2-input adder which can construct by carry look ahead adder. Carry input is not needed and we can set it to one always. And only sum output I needed as output. Carry output can be set to 0 always or can avoid calculating carry which is a better method.

For calculating j, along with j0, s0 is also needed. S0 is the S-box which contains initial permutation. That means the 0^{th} register of total 256 contain a 0, 1^{st} register contain 1, 2^{nd} register contain 2,…254^{th} register contain 254 and 255^{th} register contain 255. We always want S-box values of the location specified by i-values. So for accessing S-box a 256 to 1 multiplexer is used. Two such multiplexer is needed because i1 and i2 is simultaneously access S-box to calculate j1 and j2 simultaneously.

There two cases to calculate j2

$j2 = j0 + S0[i1] + S1 [i2]$

It can analyze in more detail like

if i2 ≠ j1 then

j2 = j0 + S0[i1] + S1 [i2]

if i2 = j1 then

j2 = j0 + S0[i1] + S1 [i1]

So for checking whether i2 equal to j1 or not, a comparator is used. A 8-bit comparator is used to compare and it will produce a single bit output according to the values. According to the comparator output j2 select its inputs. Actually both j2 is produced with two separate three input adder and produces both 8-bit outputs. We need to perform modulo-256 addition. So there is no need for a carry out in this. Both possible j2 values are giving as inputs of a 2-input multiplexer. The control input of the multiplexer is the output from the comparator

For designing the three input adder, denote the k-th bit of the j0, S [i1], S1 [i2] (either S0 [i2] or S0 [i1])by a_k, b_k, C_k . K can take any value from 0 to 7.from these input we can calculate 2 nine bit values, R and C.

$R_k = XOR (a_k, b_k, c_k)$ for k = 0 to 7

$R_8 = 0$

$C_0 = 0$
$C_k = abk-1 + bck-1 + ack-1$ for k = 0 to 7

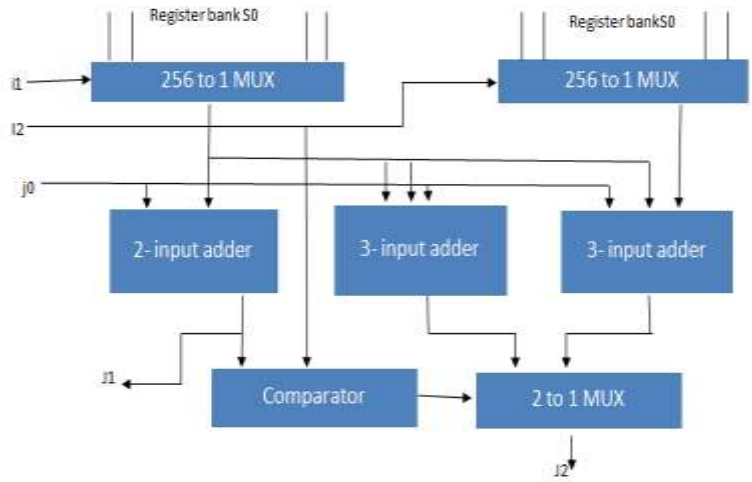

Fig.3. diagram to calculate j1 and j2

Even though the addition contains two 9 bit values, we can simply add them together to form a nice bit value. We need to perform a modulo-256 addition. We need to take out only two 8 bit values from the circuit by discarding the 8th bit.then the two bytes are added together for the desired output.this two input addition can done by the parallel adder we constructed for calculating j1. Fig.3. shows the circuit diagram for calculating j1 and j2.

3.1.3 Second step of design 1: permutation of the S-box

S-box contains 256 eight bit values. Initial state of the S-box is containing a certain internal state. These internal state values are permuted according to i1, i2, j1 and j2. J1 and j2 index is random. The values containing in the random address locations are shuffled according to the i1, i2, j1, and j2. Which two address locations will be shuffled is determined by some conditions. Conditions are checked by comparators. Total three comparators are needed. Since the three conditions are checked to make decisions about the locations to be shuffled.

Here S0 is used to find out S1 and S1 is used to find out S2. But we know i2 and j2 also with i1 and i2. So we can calculate S2 directly from S0 without calculating S1.

The conditions to be checked and the corresponding swap operation is specified in the table.1

Data to be stored in S-box is taken from any of the four 8 to 1 multiplexer. And the output line of the multiplexer is controlled by three comparator. Each checks one condition from the total 3 conditions. The 8 to one multiplexer contains 3 control lines. It forms by combining the outputs from all three comparator.

It is better to construct the 256 eight bit registers using master slave JK-flip-flop because it will help to save data simultaneously.

Conditions and corresponding shuffles of S- box are

i2 ≠ j1 and j2 ≠ i1 and j2 ≠ j1

S0[i1] → S0[j1]

S0[j1] → S0[i1]

S0[i2] → S0[j2]

S0[j2] → S0[i2]

i2 ≠ j1 and j2 ≠ i1 and j2 = j1

S0[i1] → S0[i2]

S0[i2] → S0[j1] =S0[j2]

S0[j1] → S0[i1]

i2 ≠ j1 and j2 = i1 and j2 ≠ j1

S0[i1] → S0[j1]

S0[i2] → S0[i1] = S0[j2]

S0[j1] → S0[i2]

i2 ≠ j1 and j2 = i1 and j2 = j1

S0[i1] → S0[i2]

S0[i2] → S0[i1] = S0[j1] = S0[j2]

i2 = j1 and j2 ≠ i1 and j2 ≠ j1

S0[i1] → S0[j2]

S0[j2] → S0[j1] = S0[i2]

S0[j1] → S0[i1]

i2 = j1 and j2 ≠ i1 and j2 = j1

S0[i1] → S0[j1] =S0[i2] = S0[j2]

S0[j1] → S0[i1]

i2 = j1 and j2 = i1 and j2 ≠ j1

No permutation.

No data transfer is shuffling.

i2 = j1 and j2 = i1 and j2 = j1

It is an impossible condition, because i1 will never be equal to i2

3.1.4 Fourth step of the design: design for calculatingZ1 and Z2.

Like all other designs Z can also make use of loop unrolling. So we can find out Z1 and Z2 in a single clock cycle. For finding them we need S0, S2, i1, i2, j1, j2. Those values are available.

Z1 is selected from the internal states of the S-box after permutation. The factors deciding which internal state will come to the Z1 is the internal states of identity permuted internal states selected using the word registers j1 and i1.

if S0[j1] + S0[i1] = j2 then

Z1 = S2 [i2]

if S0[j1] + S0[i1] = i2 then

Z1 = S2 [j2]

if S0[j1] + S0[i1] ≠ j2 ≠ i2 then

Z1 = S2 [S0[j1] + S0[i1]]

S0 [j1] and S0 [i1] will added first to check the conditions. They are compared with word registersi2 and j2. We can give adder inputs to a 4 to 1 multiplexer. And comparator outputs to its control inputs. According to the address specified in the output of multiplexer, the data is taken out from the register bank. It can do by a 256 to 1 decoder. The control line of the decoder is given from the output of the multiplexer.

Z2 = S2 $\left[S2[i2] + S2[j2]\right]$= S2 $\left[S1[i2] + S1[j2]\right]$

3.2 The complete circuit

Fig.4. shows the complete design. It includes all 4 design components. First circuit works in the trailing edge of first clock cycle. In the next cycle circuit 2 produces outputs and the output latches releases values of circuit 2 and circuit 1 to the input of circuit 3.

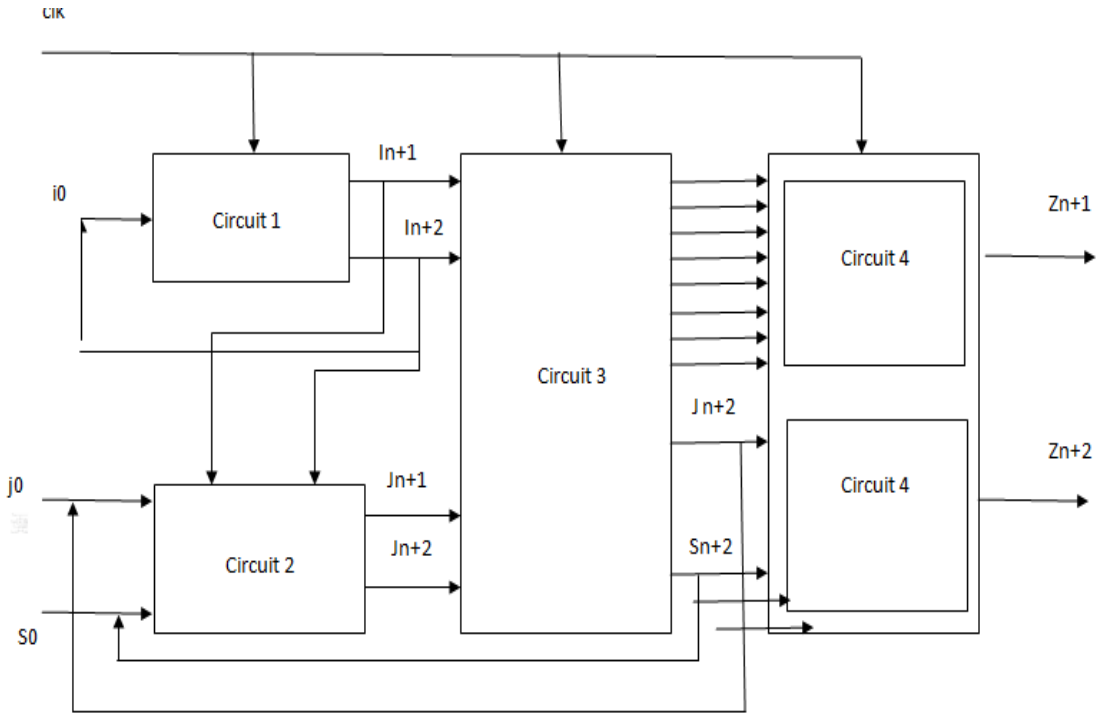

Fig.4. complete design

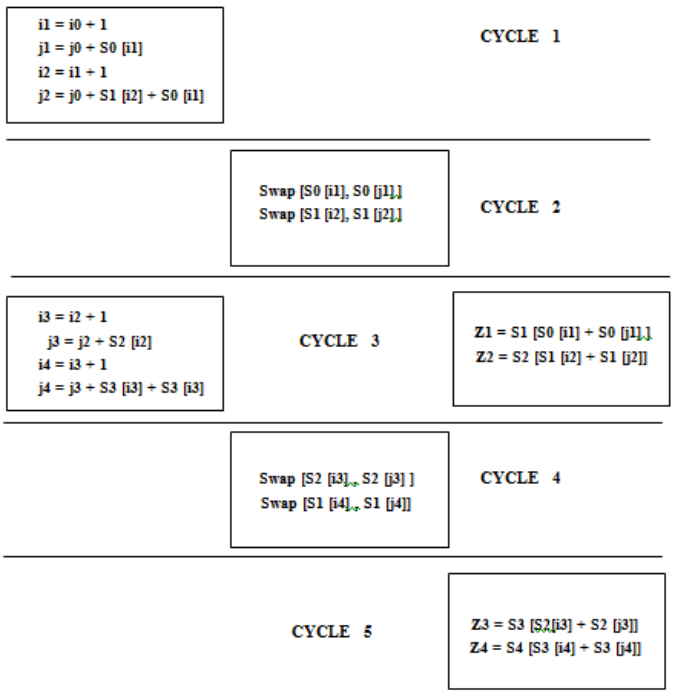

Fig.5. pipelining structure in first design

The combinational circuit in the circuit 3 works in 2nd cycle. The latch in the output of the circuit 3 activates. And in the next cycle, circuit 4 get activates and two consecutive outputs will get in 3rd clock cycle.

Along with the hardware unrolling we can see a pipeline structure in design 1. First and second circuit works together in a single cycle. Swapping done in next cycle. And outputs calculated in next half cycle. But first cycle can repeat in third One, so after

the initial delay of two half cycle we can see that our circuit is producing two outputs in alternating clock cycles. That makes it a output per cycle architecture. Figure 6 shows the diagram of the architecture.

4. DESIGN 2: TWO BYTE PER CLOCK CYCLE

Along with the concept of loop unrolling there is a technique called hardware pipelining.

In pipelining concept, in 1st cycle, calculation of i and j along with swapping is done. But index of only first loop can find. So in 1st cycle i1, j1 and S1 can find. In second cycle output byte is calculated. Only Z1 can find out. But during the 2nd cycle itself we can calculate i2, j2, and S2. By doing so we could find out next output, Z2 in 3rd cycle. That means it also provide one byte per clock cycle with an initial delay of one cycle.Fig.6.shows the structure of pipelined-architecture.

We already saw the concept of loop unrolling. It can provide two outputs in one cycle. In detail view of two concepts:

Loop unrolling steps are

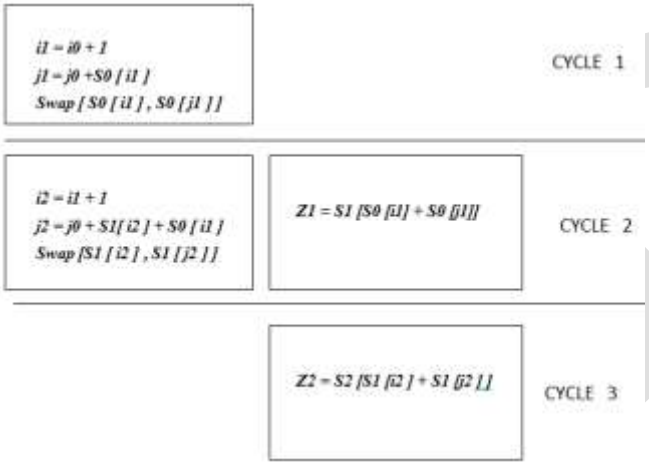

Fig.6. pipelined-A architecture

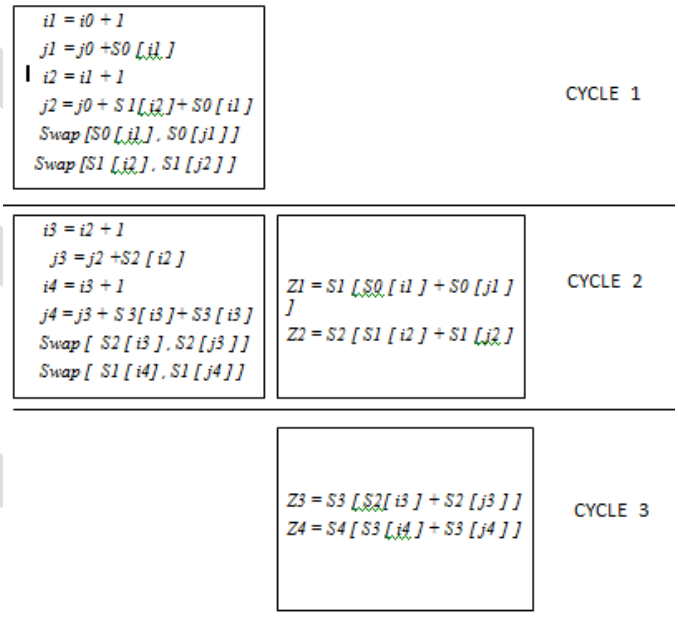

Fig.7. pipeline structure for design 2

- Calculating two consecutive values of word registers i s and j.
- Finding consecutive permutations by swapping.
- Read two consecutive output bytes Z1 and Z2 simultaneously.

Pipelined-A architecture steps are

- Calculating value of word registers i and j. then perform swap operation of internal states.
- Read output corresponding to the first step.

So the advantage of loop unrolling is that it provides two outputs in a single clock cycle. But the problem is it gets us output only in alternate clock cycles. While pipelined-A gives output in all clock cycle. But it can only give away one output per clock cycle.

So if we could combine the two concepts of loop unrolling and pipelined-A then we can produce two outputs in every single clock cycle. Pipeline structure of this concept is given in the figure 6.

Consecutive loops for KSA are

- First loop of algorithm

  $i1 = i0 + 1$

  $j1 = j0 + S0[i1] + KEY[i1]$

  $Swap\ [S0[i1], S0[j1]]$

- Second loop of algorithm

  $i2 = i1 + 1 = i0 + 2$

  $j2 = j1 + S1[i2] + KEY[i2]$

  $= j0 + S0[i1] + S1[i2] + KEY[i2]$

  $Swap\ [S1[i2], S1[j2]]$

The double swap operation starts in the first stage in this design. So we need to use pipelined registers to maintain read and write. After the swap operation Z values are reading from the internal states. Two outputs are getting from a clock cycle because of loop unrolling. The shared structure is shown in figure.8.

5. DESIGN 4: TWO 16 BIT OUTPUT PER CLOCK CYCLES

The proposed structure enables us to release 16 bits or 32 bits, in each iterations of PRGA loop. Even though the architecture keeps S-box size smaller than 2^{32} or 2^{16} . So from this we can see that output stream is increased without taking too much area. Here the size of i or j is not increasing considerably. N is the size of the counters and the S_box states. And M is the output word size.

PRGA algorithm for 8-bit word registers and S-box and 16 bit output.

$i = 0$

$j = 0$

while (true)

$i = [i + 1] \bmod 2^8$

$j = [j + S[i]] \bmod 2^8$

$k = k + S[j]] \bmod 2^{16}$

$output = [S[[S[i] + S[J]] \bmod 2^8] + k] \bmod 2^{16}$

By incorporating loop unrolling to it we can calculate 2 outputs simultaneously. So we could get two 16 bit output in a single clock cycle. Due to pipelining we will get two outputs in all clock cycles.

Algorithm which gives two output in one clock cycle.

- First loop of algorithm

$i0 = 0$

$j0 = 0$

while (true)

$i1 = [\, i0 + 1 \,] \bmod 2^8$

$j1 = \left[j0 + S0[i1]\right] \bmod 2^8$

$k1 = \left[k1 + S0[j1]\right] \bmod 2^{16}$

$$Z1 = \left[S1\left[\left[S0[i1] + S0[j1]\right] \bmod 256\right] + k1\right] \bmod 2^{16}$$

- Second loop of algorithm

$i2 = [\, i1 + 1 \,] \bmod 2^8$

$= [\, i0 + 1 \,] \bmod 2^8$

$j2 = [j0 + S0[i1] + S1[i2]] \bmod 2^8$

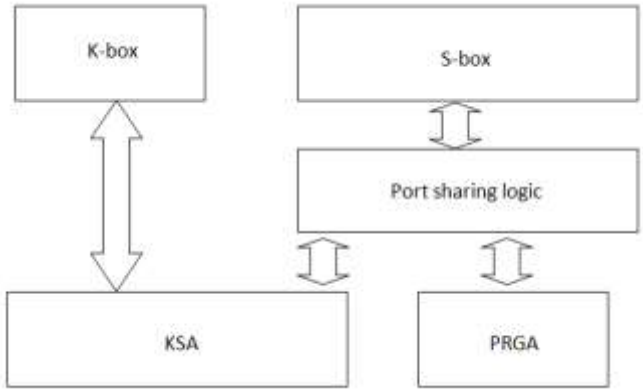

fig.8. shared access of PRGA and KSA.

$k2 = k2 + S[\, j2 \,]\,] \bmod 2^{16}$

$= k2 + S[[j0 + S1[i2] + S0\,[\, i1 \,]] \bmod 2^8]\,] \bmod 2^{16}$

$$Z2 = \left[S2\left[\left[S1[i2] + S1[j2]\right] \bmod 256\right] + k2\right] \bmod 2^{16}$$

However now the contents of array S does not undergo complete permutation. In RC4 , swapping is done to update output in a random manner. In this approach we use modulo 2^{16} integer addition. We update the output by replacing the internal state by a random number. The most important fact is that the size of the array is a very small fraction of the all possible numbers in the Z.

The main difference is the presence of k , a third variable. k, along with i and j. the k has two significant.

- It masks the output so that it does not simply represent value stored in the array.
- It ensure that the new value in the update step

6. CONCLUSION

RC4 is a very popular stream cipher which is very popular in the domain of cryptography. It is a software cipher. This paper is based on its hardware implementation. RC4 and three methods to improve its throughput with respect to clock cycle is done. In first design one byte per clock cycle and in second design two byte per clock cycle is obtained. In third design output stream of rather large size can be get. The size of the array is a very small fraction of all the possible numbers in the output. This variation is done without complicating or enlarging the size of the design. The four algorithm designs are coded in VHDL description, simulated with Xilinx ISE Design Suit 14.1 and was implemented in Spartan 5 FPGA trainer board.

REFERENCES:

1. Chang N. Zhang and Qian Yu, "an rc4 based light weight secure protocol for sensor networks" Department of Computer Science, University of Regina3737 Wascana Parkway, Regina, SK S4S 0A2 Canada {zhang, yu209}@cs.uregina.ca
2. Souradyuti Paul and Bart Preneel, "A New Weakness in the RC4 KeystreamGenerator and an Approach to Improve theSecurity of the Cipher?".
3. Matthew E. McKague," Design and Analysis of RC4-like StreamCiphers".
4. Guang Gong, Kishan Chand Gupta, Martin Hell and Yassir Nawaz,"Towards a General RC4-like KeystreamGenerator".
5. Ilya Mironov," (Not So) Random Shu_es of RC4".
6. Lae Lae Khine," A New Variant of RC4 Stream Cipher".
7. Sourav Sen Gupta, Anupam Chattopadhyay," High-Performance Hardware Implementation for RC4 Stream Cipher". ieee transactions on computers, vol. 62, no. 4, april 2013
8. Rick Wash ,"Lecture Notes on Stream Ciphers and RC4", ieee transactions on computers, vol. 62, no. 4, april 2013
9. Scott fluhrer, Sdi Shamir , "Weaknesses of key sheduling algorithm of rc4, ".
10. Machalis Galanis,paris Kitsos,giorgos Kostopoulos,Nickolas Sklavos,and Costas Goutis ,"Comparison of haedware implementation of sream ciphers",
11. Panu hamalainen,Marko Hannikainen, Jukka Saaarineen, Timo Hamaalaineen, "Hardware implementation of improved WEP and RC$ encryption algorithms for wireless terminals".
12. Ilya Mironov, "(Not So) Random shuffles of RC4".

International Journal of Engineering Research and General Science Volume 3, Issue 5, September-October, 2015
ISSN 2091-2730

RECONSTRUCTION OF 3D MODEL FROM 2D SURVEILLANCE IMAGES

Noel Vincent[1], Shiny Mathew[1], Shilu Mathew[2] and Ishtiaq Qadri[3]*

[1]Department of multimedia technology, Karunya University, Coimbatore, India

[2]Center of Excellence in Genomic Medicine, King Abdul Aziz University, Jeddah, Saudi Arabia

[4]King Fahad Medical Research Center, King Abdul Aziz University, Jeddah, Saudi Arabia

*Corresponding author
E-mail: ishtiaq80262@yahoo.com

***Abstract* —** This paper presents a comprehensive scheme for 3D modeling of objects from series of images that perform multi-view calibration and dense 3D point cloud computation. The proposed methodology is induced by 3D model construction which involves Image matching that finds common local sub-image between two pictures ,on which Structure from Motion (SFM) estimates the relative camera position from anchor points computed in the previous step and Multiple View Stereovision (MVS) which calculates a dense representation of the 3D model (Dense point cloud). The position of a camera can also be computed from correspondences between 3D points and corresponding projections in the image plane such that the Pi configuration minimizes the re-projection errors between the rays passing through optical camera center to 3D points and the 2d image plane coordinates. The modern techniques of SFM and Image Based modeling have provided simple and accurate automation to record and construct 3 dimensional data.

Index Terms—3d model, Photographs, Three-dimensional, 3D Reconstruction, Image matching.

I.INTRODUCTION

Getting three dimensional (3D) models of scenes from pictures has been an enduring exploration theme in photogrammetric and in computer vision. Numerous applications exist, for example, laser (ground), Lidar (Aerial), organized light etc. But they have their own advantages and disadvantages [1, 2]. The advancement of computers is such that today even personal computers can show complex 3D models. Computer recreations are situated in 3D universes and the utilization of 3D models and situations is not currently a typical practice in the Internet. But there are difficulties in generating such 3D models is the when we take into consideration of the cost.

3D recreation has been an enduring examination enthusiasm for some scientists and researchers. Distinctive systems have been proposed with variable camera situating approaches based upon their application.

In this paper we propose a 3D innovation in picture coordinating which has been setup with novel building design in putting the camera position for observation in a successful way to catch most extreme extent with least turn. The goal is to make a 3D model from image sequence by a surveillance camera for modeling an ordinary object or by using the new architecture in setting up the camera position to reconstruct a 3D model for the use of surveillance. This paper proposes a methodology of 3D reconstruction of scenes on surveillance using image acquisition and processing the images through Patch Multi View Stereo for effective results. The methodology is applicable for indoor and outdoor surveillance.

II. RELATED WORKS

The 3D model development or remaking of a scene caught from distinctive perspectives by the arrangement of 2D pictures is a noteworthy issue being considered for quite a long time in the region of computer vision. There are a vast number of problems already published on addressing them. Here some of the problems 1) the amount of input; 2) the complexity of the information given; 3) the representation of the output and 4) 3d model construction of a human model [3].

The quantity of inputs given will give a related yield. The multi-view camera adjustment remains a testing undertaking. This multi-view adjustment is critical since it is the person who focus the scene's exactness development and the nature of the 3D dense model.

Late research gave a proficient item, for example, ARC 3D [4] and 123D catch [5] display however the issue is that they utilize the cloud as capacity and computational stage, so the pictures are figured and all the control is not given to the client. In any case, some are free, yet at the same time they utilize cloud for calculation.

Since the developing of OpenSource structure has begun to perform multi-view alignment and dense 3D point cloud calculation [6]. Here the paper proposes a new camera positioning architecture and also a free developing software to make a 3D digital model in ease. The only problem is that of the computational speed, which depends on the user's computer. The processing is fast for small scenes or small images, but computation takes time for large scenes or large images [7] [8].

III.METHODOLOGY

IV. 3D from Images

Building a 3D model from pictures comprises in recoup 3D camera positions identified with pictures and 3D positions of specific substance of the pictures. It is finished by distinguishing comparative substance between N views and tackles 3D geometry issues [9]. Client info comprises of a picture gathering and camera parameters. The processed yield is an arrangement of 3D camera positions and 3D point in a thick cloud [10]. 3D points Fig. 1.

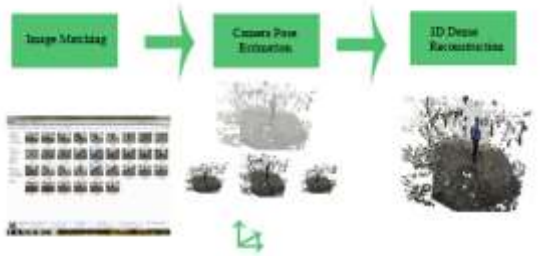

Fig. 1: Structure from Motion/Image-Based Modeling's standard work process.

3D from pictures is a dynamic exploration space that depends on Computer Vision and all the more particularly, Image recovery/coordinating, Structure from Motion (SFM) and Multiple View Stereovision (MVS) [11].

• Picture coordinating discovers normal neighborhood sub-picture between two photos [14].

• Structure from Motion appraises the relative camera position from stay focuses figured at the past step [18].

• Multiple View Stereovisions appraise a dense representation of the 3D model (Dense point cloud).

B. Proposed Architecture Camera Positioning

To make a 3D model of an object for surveillance, image acquisition is performed by a camera which is setup and the images are taken. The new camera architecture involves in placing three cameras exactly 120 degree apart from each other, where each camera can rotate from 0 degree to 60 degree to left taking five images and again to the right using 60 degrees taking five images and these images are sent for processing.

The same process is followed by other cameras, thus sequentially taking the series of image covering most of the area of interest for surveillance 3D modelling.Fig.2.

Fig. 2. Proposed Architecture Camera Positioning

C. Camera Pose Estimation

The camera posture estimation finds the camera positions by taking care of the relative estimation issues [13]. The posture estimation by assessing an inflexible to movement between the cameras a turn R and an interpretation T. Fig.3. If the object is not exactly aligned or very far away from the camera which has been placed the images being captured won't be producing the exact 3D model. The images won't be of exact focus hence the image feature extraction won't be possible.

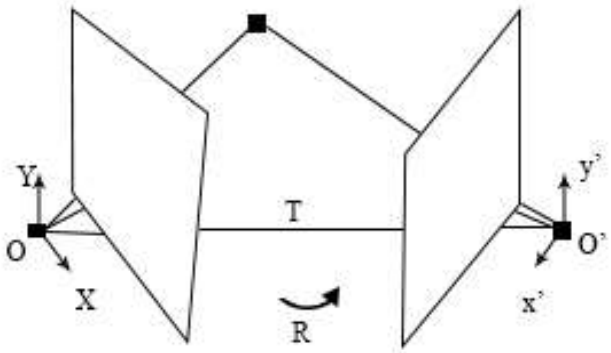

Fig.3. Camera Position Estimation

D. Feature Detection

The feature detection is done by the SFM (Structure from motion) from each and every images which has been given as an input. For every image I and next image J, F (I) is the image feature of the first image I.

For each feature $f_i \in F(I)$ and each corresponding feature $f_i' \in F(J)$ gets the nearest neighbor $f_{nn} \in F(J)$ by

$$f_{nn} = \arg\min_{f' \in F(J)} ||f\hat{i} = f'_i||_2$$

D. Image Matching

Picture coordinating recognizes the pictures that can be utilized to figure the relative introduction of the cameras and in this way to ascertain the pictures' geometry. This procedure of picture coordinating is done in 3 stages:

1. Register the substance on every picture (Feature and Descriptor calculation, for case SIFT) [12],

2. Discovering the matches between two photos (locate the closest descriptor in the other picture of the sets),

3. Checking the geometry of the similar matches.

When the picture coordinating is done between the conceivable pictures the geometric chart is assembled.Fig.4.

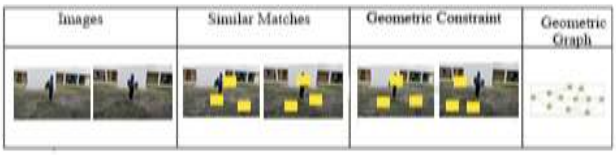

Fig 4: Three steps of Image Matching and final geometric graph

The position of a camera can likewise be figured from correspondences between 3D focuses and comparing projections in the picture plane [15]. This 3D-2D correspondence issue is known as Resection Fig.5. It comprises in assessing Pi (revolution, interpretation) with imperative geometry. It finds the Pi arrangement that minimizes the re-projection slips between the beams going through camera focus to 3D focuses and the 2D picture plane directions [21]. Once the cameras are connected with the Essential network then the 3D focuses are constructed.

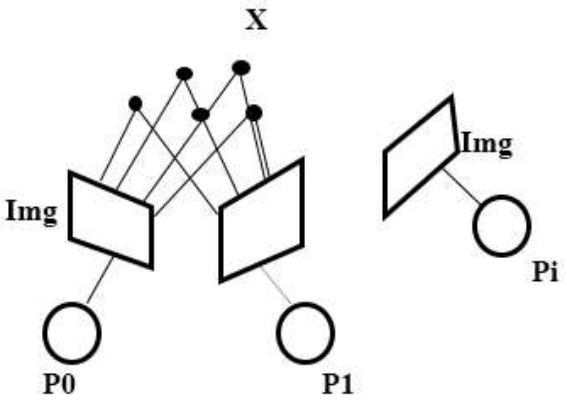

Fig.5. 2D- 3D Resection

Fig.6. Image Acquisition

E Multiple View Stereovision

Multiple View Stereovision (MVS) is the system for mapping picture pixel to 3D focuses to point cloud. The dense representation can be a dense point cloud or a dense mesh. Then it determines a 3D position for each corresponding pixel of the image series. MVS utilizes numerous pictures to diminish lapses and aides in achieving an exact model in co connection with pictures gave. One of the techniques utilized is the Patch methodology called PMVS (Patch Multi View Stereo) [20]. It is taking into account a seed developing method, which discovers relating patches in the middle of pictures and grows the district by an iterative extension and separating strides to uproot terrible correspondences. This methodology finds extra correspondences that were rejected or not found at the picture coordinating procedure. The vacant 3D territories relate to ineffectively textured picture.

V.RESULTS AND EXPERIMENTAL ANALYSIS

The experiment was carried out by placing the camera as said above and series of images where taken and was inputted for making the 3D model. The images retrieved are put into a folder and the program is run for making the 3D model from the 2D images. Fig.6.

The user has the option to select the image quality this is done because of the low computing power of the user's personal computer. The feature extraction is done and which is saved in a dataset and which will be used for the 3D dense reconstruction of the image.

The image set is loaded to convert the 2D images for image matching to find the similar matches among the series of images by removing the resection among images due to distortion due to movement of camera. Image of the tool box used is given below. Fig.7.

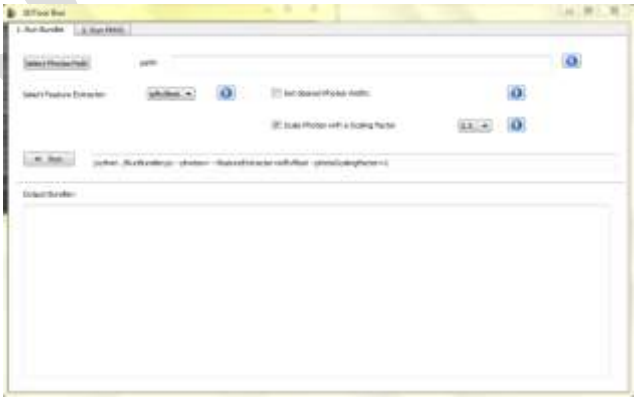

Fig.7. Toolbox

After the image extraction the PMVS (Patch Multi-view stereo) is done with the SIFT algorithm for reconstruction from the image feature stored. The user has the option to select the number of cluster from the images and the model is created in a ply format by a dense cloud formation which can be viewed in a Mesh lab. The missing pixels will be present that will be in a formation of hole. The working is show in the below image. Fig.8.

The output produced is better and not of high precision but in a satisfactory level, the computation time takes time based on the user's personal computer based on the ram. The output below in Fig.9 was done in a System having Windows 7 as Os having a 4GB Ram and 1GB Graphics Card, the computation time took around 1 hour for the given output and 5 minutes for smaller objects. E.g. Box. Fig.10.

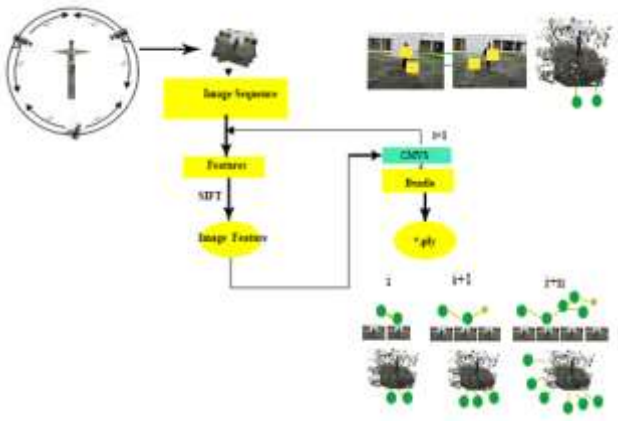

Fig.8. Workflow

Fig.9 3D dense model of a Person

Fig.10. 3D dense model of Box

V. PERFORMANCE METRICS

The performance of the system implemented is shown is graph. In which the first graph Fig.11. Shows the performance of the system with time vs. images.

Fig.11. Time Vs Images

The second graph Fig.12. Shows the comparison between other existing systems and the newly proposed system.

Fig.12. Existing system Vs Proposed System

The Third and final graph Fig.13. Shows the time with respected to the graphics processor used in making different model or scenes.

Fig.13 Time Vs Graphics Processor

V. CONCLUSION

This is an easy to use application to perform 3D computerized duplicates of the picture arrangement. A low-cost, which opens a direct access to a solution for Image –Based Modeling to anyone who has a digital camera. A SIFT algorithm is the only drawback since it uses a feature descriptor. The SFM is a fast and simple with an easy data processing which is able to satisfy the needs of a project. The 3D reconstruction from images has become a lot easier, in which the user can use it will full efficiency. The only

drawback is the time required for processing but that depends on the user having a higher computing power, at a mostly a higher Ram around 16GB with a 4GB graphics card can make a far more difference in computing.

REFERENCES:

[1] Richard A. Vincent the Sanborn Map Company Michael Ecker Light Detection and Ranging (LiDAR) Technology Evaluation

[2] Daniel Huber and Burcu Akinci Using Laser Scanners for Modeling and Analysis in Architecture, Engineering, and Construction

[3] Pierre Moulon Alessandro Bezzi A free solution for Three-Dimensional Documentation

[4] David Tingdahl and Luc Van Gool, "A Public System for Image Based 3D Model Generation", Computer Vision/Computer Graphics Collaboration Techniques 5th International Conference, MIRAGE 2011

[5] Erickson, M., Bauer, J., and Hayes, W., "The Accuracy of Photo-Based Three-Dimensional Scanning for Collision Reconstruction Using 123D Catch," SAE technical Paper 2013-01-0784, 2013, doi:10.4271/2013-01-0784

[6] Constructing 3D human model from front and side images Yueh-Ling Lin, Mao-Jiun J. Wang

[7] S. Agarwal - N. Snavely - I. Simon - S. M. Seitz - R. Szeliski, Building Rome in a day, in ICCV 2009, 72-79.

[8] H. Bay – A. Ess - T. Tuytelaars – L. Van Gool, SURF: Speeded Up Robust Features, in CVIU 2008, 346-359

[9] A. Bezzi – L. Bezzi – D. Francisci – R. Gietl, L'utilizzo di voxel in campo archeologico, in Geomatic Workbooks,6, 2006.

[10] J. -M. Frahm – P. Georgel - D. Gallup – T. Johnson – R. Raguram – C. Wu – Y.-H. Jen – E. Dunn - B. Clipp - S. Lazebnik, Building Rome on a Cloudless Day, in ECCV 2010, 368-381.

[11] Y. Furukawa – B. Curless – S. M. Seitz – R. Szeliski. Towards Internet-scale multi-view stereo, in CVPR 2010, 1434-1441.

[12] D. G. Lowe, Distinctive image features from scale-invariant keypoints, in IJCV 2004, 91-110.

[13] D. Nister, An Efficient Solution to the Five-Point Relative Pose Problem, in IEEE Trans. Pattern Anal. Mach. Intell. 2004, 756-777.

[14] N. Snavely – S. M. Seitz – R. Szeliski. Modeling the World from Internet Photo Collections, in IJCV 2008, 189- 210.

[15] Bae, S.-H., Balakrishnan, R., And Singh, K. 2008. ILoveSketch:As-natural-as-possible sketching system for creating 3D curve models. In Proceedings of the ACM symposium on User.interface software and technology (UIST), 151–160.

[16] AUTODESK, 2009. Maya. http://www.autodesk.com/maya.

[17] A Rayleigh reconstruction/interpolation algorithm for 3D ultrasound Jo~ao M. Sanches , Jorge S. Marques

[18] Reconstruction of 3D human body pose from stereo image sequences based on top-down learning

[19] A neural network for recovering 3D shape from erroneous and few depth maps of shaded images Mohamad Ivan Fanany , Itsuo Kumazawa

[20] A Flexible And Automatic 3d Reconstruction Method

Shunyi Zhenga , Zongqian Zhana, Zuxun Zhanga

[21] Xiao, J., Baker, S., Matthews, I., Kanade, T.: Real-Time Combined 2D+3D Active Appearance Models. In: CVPR, IEEE. (2004) 535-542

[22]Jiang, H.:3D Human Pose Reconstruction Using Millions of ICPR,IEEE. (2010) 1674-1677

International Journal of Engineering Research and General Science Volume 3, Issue 5, September-October, 2015
ISSN 2091-2730

Hybrid Medical Image Compression Method Using SPIHT Algorithm and Haar Wavelet Transform

Ashmika Tiwari[1], Mr. Chandrashekhar Kamargaonkar [2], Dr.Monisha Sharma[3]
[1]M.E. Scholar, Department of Electronics & Telecommunication Engineering,

Shri Shankaracharya Technical Campus (SSTC), SSGI (FET), Junwani Bhilai C.G.

[1]ashmika.mini@rediffmail.com, phone no.-9584372427

Abstract— CT or MRI Medical imaging produces digital form of human body pictures. There exists a need for compression of these images for storage and communication purposes. Current compression schemes provide a very high compression rate with a considerable loss of quality. In medicine, it is necessary to have high image quality in region of interest, i.e. diagnostically important regions. So, ROI part can be compressed with the help of the Lossless compression whereas Non Region of interest part can be compressed with help of Lossy compression as it is of lesser importance for diagnosis. In this paper Region of interest part is extracted with the help of thresholding method of segmentation and compressed with the help of SPIHT Algorithm thus producing a good quality image. And NROI part is compressed with the help of Haar wavelet transform.Our algorithm provides better PSNR values for medical images.

Keywords— SPIHT(Set Partitioning In Hierarchical Tree),Haar wavelet transform, Binary Thresholding, median filter, PSNR(Peak signal to noise ratio), ROI, NROI

INTRODUCTION

Image compression based on region of interest has been one of the hot issues in the field of image compression and coding. However, there is not a fixed model for region of interest automatic detected. In order to reduce storage spaces and transmission times of infrared target image data, a coding way is proposed for ROI automatic detected of image based on the region growing segmentation algorithm. In order to improve efficiency for transferring image data in real time, a coding-crossed algorithm for ROI automatic detected of infrared target image is studied as same time as it is realized on the frame of SPIHT Algorithm. An experimental study is also conducted that is proved the method of detecting automatically and compression algorithm based on region of interest automatic detected is reliable and effective, significant in applications. Non region of interest part is of lesser importance as it is the background part which is not much helpful in diagnosis of the disease. So, using the lossy method of compression for compressing the background part will make the compression more easier and will also not effect the issue of diagnosing the disease.

Currently, many applications want a representation of the image with minimal storage. Most images contain duplicate data. There are two duplicated parts of data in the image. The first is the existence of a pixel that has the same intensity as its neighboring pixels. These duplicated pixels waste more storage space. The second is that the image contains many repeated sections (regions). These identical sections do not need to be encoded many times to avoid redundancies and, therefore, we need an image compression to minimize the memory requirement in representing a digital image. The general principle used in the process of image compression is to reduce duplication of data within the image so that the memory needed to represent the image is smaller than the original image.

The block diagram of the proposed methodology is shown below in figure 1.

The methodology consist of following parts:-

1. Filtering
2. Segmentation of ROI and NROI
3. ROI compression using SPIHT Algorithm
4. NROI compression using Haar wavelet transform

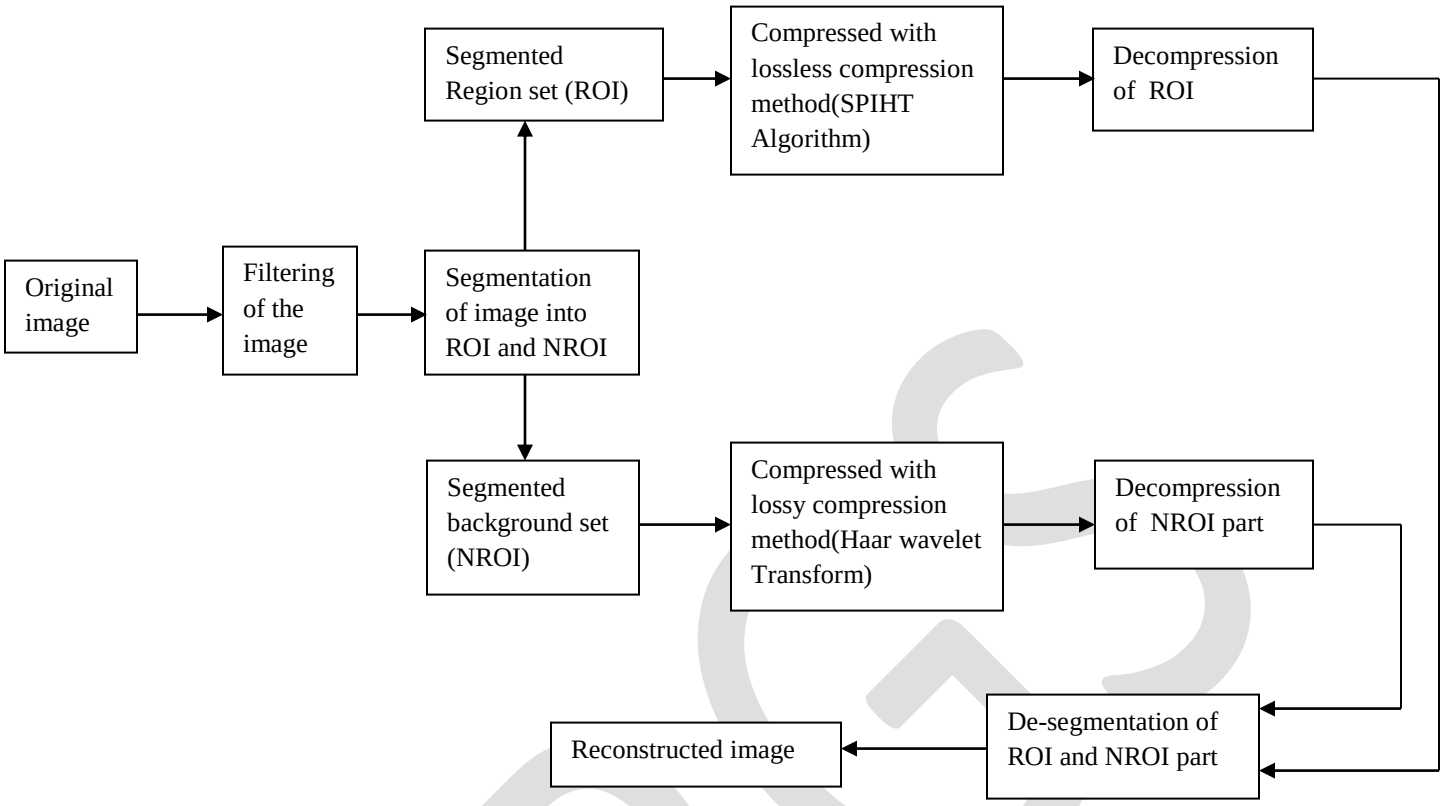

FIGURE 1: BLOCK DIAGRAM OF METHODOLOGY

METHODOLOGY

1.FILTERING

In image processing, it is often desirable to be able to perform some kind of noise reduction on an image so that image could be clearly visible. In this methodology median filter is used.

The median filter is a non linear digital filtering technique, often used to remove noise. Such noise reduction is a typical pre-processing step to improve the results of later processing (for example, edge detection on an image). Median filtering is very widely used in digital image processing because, under certain conditions, it preserves edges while removing noise

The main idea of the median filter is to run through the signal entry by entry, replacing each entry with the median of neighboring entries. The pattern of neighbors is called the "window", which slides, entry by entry, over the entire signal .For 2D (or higher-dimensional) signals such as images , more complex window patterns are possible (such as "box" or "cross" patterns). In this methodology a *brain tumor* image is considered as shown below:-

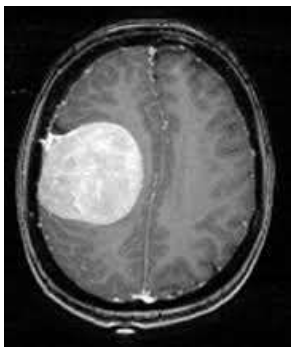

Figure 2: Brain Image with Tumor

Noise in the form of salt & pepper noise is added. It is filtered with the help of median filter and output is shown below:-

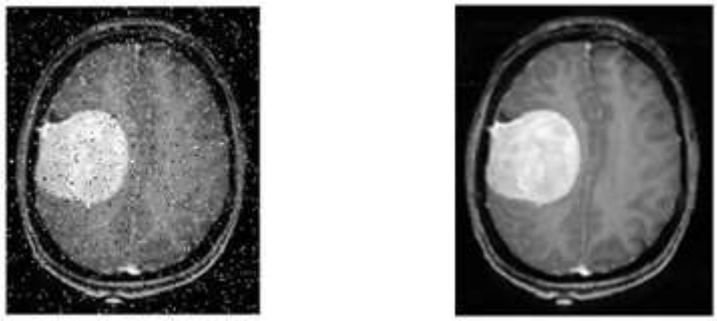

(a) (b)

Figure 3: (a) Brain image with salt and pepper noise (b) Filtered image(PSNR-37.8858 dB)

2. SEGMENTATION OF ROI AND NROI

In the proposed methodology Binary thresholding method is used for segmenting the image into ROI and NROI part.

Image thresholding is a simple, yet effective, way of partitioning an image into a foreground and background. This image analysis technique is a type of image segmentation that isolates objects by converting grayscale images into binary images. Image thresholding [6] is most effective in images with high levels of contrast. The simplest thresholding methods replace each pixel in an image with a black pixel if the image intensity is less than some fixed constant T (that is), or a white pixel if the image intensity is greater than that constant.

In this method the ROI part is the tumor part in the brain having the intensity greater than the background part so tumor part is separated from the original brain image and further compressed for transmission.

The segmentation of ROI and NROI part is shown below:

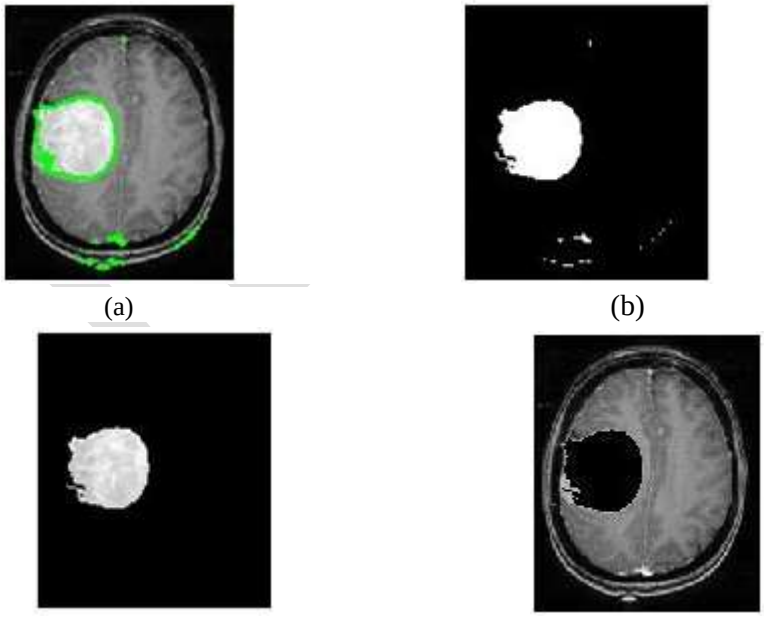

(a) (b)

(c) (d)

Figure 4: (a) Outlined tumor part in the Brain image (b) Binary image obtained after thresholding, threshold value(T=190) (c) Tumor part (ROI) (d) Background part after removal of the tumor(NROI)

3. SPIHT ALGORITHM

SPIHT (Set Partition in Hierarchical Trees) [5] is one of the most advanced schemes, even outperforming the state-of-the art JPEG 2000 in some situations. The basic principle is the same; a progressive coding is applied, processing the image respectively to a lowering threshold. The difference is in the concept of zero trees (spatial orientation trees in SPIHT). There is a coefficient at the highest level of the transform in a particular sub band which considered insignificant against a particular threshold; it is very probable that its descendants in lower levels will be insignificant too. Therefore we can code quite a large group of coefficients with one symbol. A spatial orientation tree is defined in a pyramid constructed with recursive four sub bands splitting.

Normally most of an images energy is concentrated in the low frequency components Consequently the variance decreases as we move from the highest to the lowest levels of the sub band pyramid Furthermore it has been observed that there is a spatial self similarity between sub bands and the coefficients are expected to be better magnitude ordered if we move downward in the pyramid following the same spatial orientation [1].

.

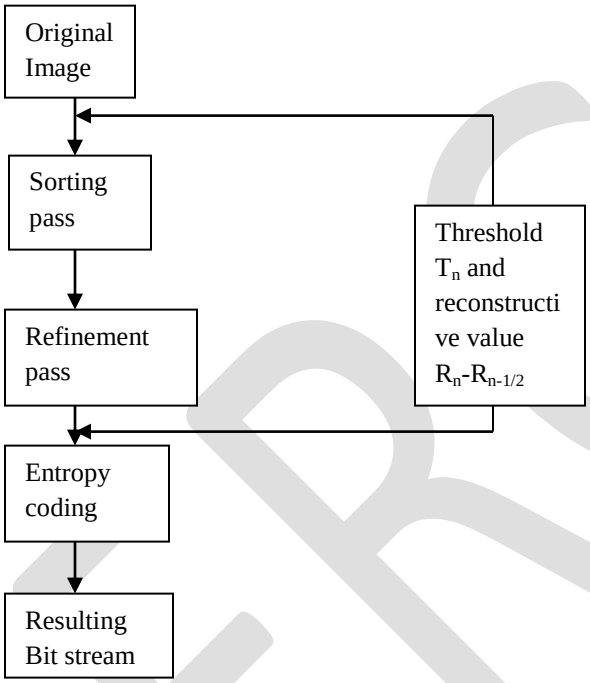

Figure 5: Flowchart of SPIHT

In the proposed methodology the Brain tumor image is then separated into ROI and NROI part. The ROI part is compressed with help of SPIHT Algorithm and then reconstructed at receiver end. The PSNR of reconstructed image is calculated and shown below:-

(a) (b)

Figure 7:(a) ROI uncompressed part before applying SPIHT Algorithm (b) Reconstructed image of the tumor of the brain with PSNR=69.7988 dB for bpp=1.00

4. HAAR WAVELET TRANSFORM

Haar wavelet compression is an efficient way to perform both lossless and lossy image compression. It relies on averaging and differencing values in an image matrix to produce a matrix which is sparse or nearly sparse. A sparse matrix is a matrix in which a large portion of its entries are 0. A sparse matrix can be stored in an efficient manner, leading to smaller file sizes. In these notes we will concentrate on grayscale images; however, rgb images can be handled by compressing each of the color layers separately. The

basic method is to start with an image A, which can be regarded as an m × n matrix with values 0 to 255. In Matlab, this would be a matrix with unsigned 8-bit integer values. We then subdivide this image into 8 × 8 blocks, padding as necessary. It is these 8 × 8 blocks that we work with.

In the proposed methodology the separated NROI part is compressed with the help of the Haar wavelet transform and then reconstructed at the receiver end. The PSNR of reconstructed image is calculated and shown below:-

(a) (b)

Figure 8:NROI uncompressed part before applying Haar Wavelet Transform (b) Reconstructed image of the background of the brain with PSNR=44.74 dB for bpp=1.00

CONCLUSION

At the final stage of the algorithm we have combined the background part and region of interest part and calculated the PSNR value. Table-1 illustrates compressed image quality with different bit rate values (number of bits per pixel).We have varied the bits per pixel from 0.25-2.00 Bpp and PSNR is calculated. We have compared our algorithm with SPIHT method of compression and we have found that our algorithm is better. From Table-1 it is evident that for higher bit rate higher PSNR is obtained and our algorithm shows better PSNR output than SPIHT. Hence we have obtained a satisfactory result and in future we would try to compress colored image.

Table 1: PSNR Calculation

S.No.	BPP(Bits per Pixel)	SPIHT(ROI) and HAAR (NROI)	SPIHT
1	0.25	37.4182	19.9700
2	0.50	39.9725	25.2000
3	0.75	41.4570	30.3384
4	1.00	41.8750	34.8400
5	1.25	41.9874	36.2500
6	1.50	42.0072	38.8800
7	1.75	42.0109	40.0100
8	2.00	42.0153	41.1850

REFERENCES:

[1] Md. Ahasan Kabir, M. A. Masud Khan, Md. Tajul Islam, Md. Liton Hossain, Abu Farzan Mitul Image Compression Using Lifting Based Wavelet Transform Coupled With SPIHT Algorithm Informatics, Electronics & Vision (ICIEV), 2013 International Conference on 17-18 May 2013 at Dhaka

[2] Jia ZhiGang Guo XiaoDong Li LinSheng, A Fast Image Compression Algorithm Based on SPIHT, Industrial Electronics and Applications, 2009. ICIEA 2009. 4th IEEE Conference on 25-27 May at Xi'an.

[3] T.P. Fowdur D. Indoonundon K.M.S. Soyjaudah ,An Unequal Error Protection Scheme for SPIHT Image Transmission with Prioritised Retransmissions and De-noising**,** AFRICON, 2013, 9-12 Sept. 2013 at Pointe-Aux-Piments.

[4] Sure. Srikanth, Sukadev Meher, Compression Efficiency for Combining Different Embedded Image Compression Techniques with Huffman Encoding International conference on Communication and Signal Processing, April 3-5, 2013, India,IEEE

[5] Amir Said, William A Pearlman, A New Fast and Efficient Image Codec Based on Set Partitioning in Hierarchical Trees IEEE Transactions on Circuits and Systems for Video Technology Vol6 June 1996

[6] Rajesh C. Patil, Dr. A. S. Bhalchandra, Brain Tumour Extraction from MRI Images Using MATLAB International Journal of Electronics, Communication & Soft Computing Science and Engineering,ISSN: 2277-9477, Volume 2, Issue 1

[7] P. Vasanthi Kumari, Dr.K.Thanushkodi ,A Secure Fast 2D - Discrete Fractional Fourier Transform Based Medical Image Compression Using Hybrid Encoding Technique**,** International Conference on Current Trends in Engineering and Technology, ICCTET'13 1© *IEEE 2013*

[8] LiBin meng qingang ,An Improved SPIHT Wavelet Transform in the Underwater Acoustic Image Compression, 2013 2nd International Conference on Measurement, Information and Control,978-1-4799-1392-3/13 IEEE

[9] C. Rengarajaswamy, S.Imaculate Rosaline ,SPIHT Compression on Encrypted Images Proceedings of 2013 IEEE Conference on Information and Communication Technologies (ICT 2013).

[10] Salija.P , Manimekalai.M.A.P, N.A Vasanthi, PhD. ROI and Seam-SPIHT based Efficient Image Compression for Mobile Multimedia and Medical Applications, International Journal of Computer Applications (0975 – 8887) Volume 64– No.12, February 2013.

[11] Papitha, G. Merlin Nancy and D. Nedumaran, *Member*, *IEEE*, Compression Techniques on MR Image – A Comparative Study, International conference on Communication and Signal Processing, April 3-5, 2013, India.

[12] U.S.Ragupathy,D.Baskar,A.Tamilarasi New Method of Image Compression Using Multiwavelets and Set Partitioning Algorithm, 2008 IEEE Region 10 Colloquium and the Third International Conference on Industrial and Information Systems, Kharagpur, INDIA December 8 -10, 2008

International Journal of Engineering Research and General Science Volume 3, Issue 5, September-October, 2015
ISSN 2091-2730

MEDICAL DECISION SUPPORT SYSTEM FOR TYPHOID DIAGNOSIS

Shiny Mathew[1], Noel Vincent[1], Shilu Mathew[2] and Ishtiaq Qadri[3]*

[1]Department of multimedia technology, Karunya University, Coimbatore, India

[2]Center of Excellence in Genomic Medicine, King Abdul Aziz University, Jeddah, Saudi Arabia

[4]King Fahad Medical Research Center, King Abdul Aziz University, Jeddah, Saudi Arabia

*Corresponding author
Tel.:+966549574512; fax: +966549574512

E-mail: ishtiaq80262@yahoo.com

Abstract- This paper defines an intelligent decision support system for diagnostics for typhoid fever. Typhoid fever has numerous variables involved in identification of the disease. These variable are transformed into membership functions and passed onto the Fuzzy Logic System. The fuzzy logic System consists of the following stages fuzzification which converts the crisp data into variable data, Hidden layers which performs logical functions and using firing rules from the fuzzy data, lastly the defuzzification stage involves in transforming the fuzzy data into crisp data for analysis and identification of the disease.This decision support system works parallel with the centralized server for easy utilization of the application in different units.

Keywords: Diagnostic, Typhoid fever, Fuzzification

Introduction

Typhoid Fever (TF) remains a major public health quandary in developing countries. Despite the availability of a few medications throughout the years for the treatment of TF there has dependably had Intolerable horribleness and mortality in developing countries nations. There are several variables involved in TF analysis and management, making it complex to make a diagnosis.

Expert System (ES) is PC based choice apparatus that uses actualities and standards to take care of reasoning so as to test genuine issues and taking into account the information procured from one or more human master in an individual field. An expert system is a computer system that emulates the decision-making ability of a human expert with intelligent user interactive interfaces [1].

Fluffy Logic (FL) has been perceived as a noteworthy delicate figuring device that is utilized to speak to the learning of a specialist in a computer is like human master. The execution of ESs is finished by widely utilizing FL as a part of the field of solution because of its capacity in taking care of the imprecision and vulnerability innate in therapeutic records. Fuzzy expert framework coordinates segments of FL which manages steady, precise, and convenient results [2].

The enrollment capacities are one of the key components of fuzzy frameworks as it quantitatively characterizes the phonetic marks or the variables included in the diagnostics for typhoid malady, by which frameworks generally set aside more time to outline and tune to adjust new circumstances or cases. Since neural system has the accompanying abilities: self-learning, self-tuning, and can be utilized to naturally produce enrollment capacities for fuzzy frameworks [3][4].

We propose a WBDSS driven by a Neuro-fluffy methodology for the finding and administration of TF in light of the standards and practices of restorative analysis. The framework was produced with the point of giving a choice bolster stage to medicinal professionals, TF scientists, and human services suppliers in creating nations of the world.

Methodology

- Fuzzification

The fuzzification procedure includes the change of crude info variables (estimations of signs, side effects, and research facility tests) by the use of given function:

- Hidden Layer -1(μ)

  In this equation, ' μ x' is the membership of the crisp input 'x' to the triangular fuzzy set 'A', 'ac' is the base of the triangle, and 'b' is its midpoint

  $$\mu_x(A) = \Delta(x; a, b, c)$$

- Hidden Layer -2

  AND operation is performed here

- Hidden Layer -3

  The method, by which firing strengths (FS) of a particular rule has been computed. In this equation, ' μ_{x1}, μ_{x2}, …, μ_{xn} ' are the membership values of the crisp inputs to the triangular fuzzy sets 'A1, A2,. . ., An'.

  $$\mathrm{FS} = \min(\mu_{x1}(A1), \mu_{x2}(A2), \ldots \mu_{xn}(An)$$

- Defuzzification

The defuzzification procedure deciphers the derivation's yield motor into fresh values which is for the most part needed by medicinal specialists for legitimate investigation and translation utilizes the Centroid of Area (CoA) system for its defuzzification.

$$O_f = \frac{\sum_{i=1}^{p} \mathrm{FA}_j \times cn_i}{\sum_{j=1}^{p} \mathrm{FA}_j}$$

- BPNN

The error could be further minimized using BPNN by iteratively updating the weight vectors. The training is said to be completed when the minimum MSE value is obtained

Results and Discussion

Architecture: Proposed system with performance metrics

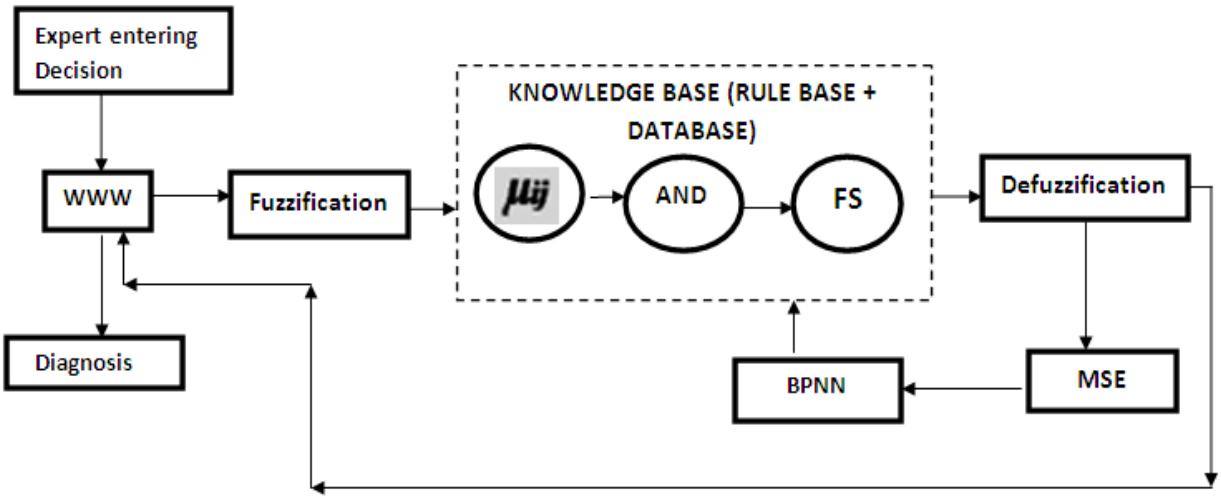

The building design includes interface by means of which the restorative master gives qualities speaking to signs, side effects, and research facility examinations of a specific patient amid the determination process. The www segment makes it feasible for the proposed framework to be gotten to remotely from any piece of the world. The KB is comprised of the Database and Rule Base (RB). The database stores quiet bio-information, innate information, force of signs, indications, lab examination results, restorative

conclusion result, and therapeutic master's points of interest while the RB is made out of an arrangement of IF-THEN proclamations that speaks to the learning utilized by medicinal specialists when diagnosing TF patients.

Inputs and the yield are discretionarily appointed class marks – 'mild ('m')', 'moderate ('M')', and 'severe ('s')' with some numeric range.

The input is passed on to the fuzzification unit i.e., calculation of membership values using TMFD (Triangular membership function distribution) in the first layer. The AND operations are performed in the second layer. The FS (firing strength) has to be computed in the third layer according to the production rules defined by the domain experts.

The predicted output is then compared with the target output for each case and Mean Squared Error (MSE) is then computed. Finally, weights are updated during back propagating with the error and the training is said to be completed when the minimum MSE value is obtained.

Performance metrics

To measure the performance of this Web based neuro fuzzy medical decision support system we use its sensitivity (Sn),specificity (Sp), precision (Pr), and average accuracy (Acc). All values are expressed in %.

$$S_n = \frac{tp}{p} \times 100$$

$$S_p = \frac{tn}{n} \times 100$$

$$P_r = \frac{tp}{tp + fp} \times 100$$

$$A_{cc} = \left[S_n \times \frac{p}{N} + S_p \times \frac{N}{N+P} \right] \times 100$$

In these equations 'p' and 'n' denote total positive and negative cases; 'tp' and 'np' are true and false positive cases and 'N' is the total number of cases.

We propose an online choice emotionally supportive network for the determination of TF. The framework is driven by neuro fuzzy procedure and has the capacity to keep running on the Internet. The framework can be utilized by therapeutic specialists and prepared medicinal services work force to give an exact and auspicious analysis of TF paying little mind to the restorative's area faculty. The framework will help supplement the deficient quantities of medicinal specialists in creating nations and in the end diminish the

tremendous expense connected with patient conclusion. Since the KB of the proposed framework is unified, it has the ability of lodging gigantic measure of data from which valuable learning and examples that could help choice making can be mined.

REFERENCES:

1. A neuro-fuzzy approach for the diagnosis of depression ,Subhagata Chattopadhyay,Elsevier, 2014

2. A web based decision support system driven by fuzzy logic for the diagnosis of typhoid fever ,O.W. Samuel , M.O. Omisore, B.A. Ojokoh, Elsevier,2013

3. Implementing Decision Tree Fuzzy Rules in Clinical Decision Support System after Comparing with Fuzzy based and Neural Network based systems, Dr. Anooj P.K ,IEEE ,2013

4. Diagnosis Support System based on clinical guidelines: comparison between Case-Based Fuzzy Cognitive Maps and Bayesian Networks, Nassim Douali, Huszka Csabab, Jos De Roob, Elpiniki Papageorgiouc,Marie-Christine Jaulent,Elsevier ,2014

International Journal of Engineering Research and General Science Volume 3, Issue 5, September-October, 2015
ISSN 2091-2730

A Passive Traffic Pattern Discovery Attack to reveal Anonymity of MANET Communication

Gayatri K.A., Aravind S.

Sree Buddha College of Engineering for Women, gaya3.rajasekharan@gmail.com

Abstract— Communication anonymity includes sender anonymity, recipient anonymity and channel anonymity. To break the anonymity in communication traffic analysis is performed. Traffic detection in MANETs is difficult compared to traditional wired infrastructure due to the mobility of the nodes and the lack of a fixed infrastructure. Passive statistical analysis utilize the statistical properties of the captured traffic to reveal the identity of the sender, recipient and the end-to-end link. We analyze Statistical Traffic Pattern Discovery System(STARS) with empirical results.

Keywords— - Anonymity, fpr, fnr, MANET, passive analysis, RREQ, RREP

INTRODUCTION

Secure communication should be built with the pillars of confidentiality, integrity and availability . For applications which require an additional layer of confidentiality (eg; military applications) , the communication should be untraceable or anonymous. Communication anonymity includes sender anonymity, recipient anonymity and link anonymity. The anonymity in communication is defined as an important security property by G.Danezis in [3]. Mobile Adhoc Networks(MANETs) are a set of nodes that form a network dynamically so that any node can join or leave the network any time. The typical features of MANET adhoc nature, ease of deployment, lightweight, high mobility etc. makes it suitable for implementing sensitive communication applications.

Various techniques are used to enhance the anonymity of MANET communication. Anonymous networking techniques like data encryption, encryption of packet headers at different layers using different encryptions function help to protect the traffic content .Using multiplexed traffic and introducing dummy packets or dummy delay provide difficulty for the attacker to analyze the traffic. Anonymous routing protocols hide node identities, relationship between nodes(source/ destination/ neighbouring/ forwarding node) and other routing information using techniques like dynamic pseudonyms, mixing, per-hop encryption,or timing perturberation etc. ANODR(ANonymous On Demand Routing), MASK and SDAR are examples of routing protocols which provide identity-free and on-demand routing, help to protect the anonymity in a mobile environment. Onion-routing, mix-net and DC-net are examples of anonymous communication systems.

Statistical traffic analysis attack discovers the sensitive information by evaluating the statistical characteristics of the captured raw traffic. Predecessor attack and statistical disclosure attacks are examples. But these attacks are suitable for static wired networks. In the case of infrastructure-less MANETS, traffic analysis is difficult because of the three adherent features of MANETS-the broadcasting nature, the adhoc nature and the mobile nature. STARS[1] proposed by Yang Qin et al. is a typical example of such a statistical traffic pattern analysis attack, designed for MANETs. The analysis takes into consideration the broadcasting nature, the adhoc nature and the mobility of the nodes, which are the three special characteristics of MANETs. The communication between the adversary sensors takes place through a separate channel. Thus the signal detection occurs passively, without intervening the actual channel. The adversaries can locate the signal source according to some properties and that they can trace the mobility of the nodes. Traffic matrices are constructed and probability distribution of source, destination and end-to-end links is derived using a heuristic approach. In order to speculate the actual traffic patterns from the probability distributions, the system performance is evaluated in terms of false positive rate (fpr) and false negative rate (fnr).

Extending the work in STARS, the scope of the work includes performance analysis of STARS in terms of average delay, packet drop and packet throughput Simulations were done using NS-2 platform and the result was analyzed. The rest of the paper is organized as follows: Section II describes the related work in the area; section III describes the system architecture; section IV describes the experiments and section V is the conclusion.

RELATED WORKS

The Dining Cyptographer's Network(DC-Net) by Chaum in [1] is one of the early approaches in preserving anonymity of communication. Here one participant among a group of communicating nodes broadcasts a message. The sender encrypts the message and since it is received by all the nodes in the network, recipient anonymity is maintained. Chaum in [5] introduced the concept of Mix-Node, a node is capable of re-arranging the messages that comes in a random order so that it is impossible to correlate between the input and output messages of the node. A network with all the participants are mix-nodes is called a Mix-Network or simply mix-net.

ANODR (ANonymous On Demand Routing) was devised by Kong et al. in [6]. ANODR is a hybrid protocol which uses identity-free routing and on-demand routing as the design principles. The on-demand approach ensures that anonymous routes are set up in real-time as needed, which limits the chance of traffic analyzing to a time-critical control window. Instead of using node identities, ANODR uses one-time cryptographic trap doors to hide node identities, which satisfies the identity-free criterion. MASK[7] is an anonymous on-demand routing protocol, which can accomplish both MAC-layer and network-layer communications without disclosing real IDs of the participating nodes under a rather strong adversary model. MASK offers the anonymity of senders, receivers, and sender-receiver relationships in addition to node unlocatability and untrackability and end-to-end flow untraceability. But MASK is vulnerable to denial-of service attack. It can provide security only against external adversaries. Once becoming internal adversary by compromising certain nodes, it is easy to launch an attack. In [8], Boukerche et al. describes a protocol named SDAR (Secure Distributed Anonymous Routing Protocol) for Wireless and Mobile Ad Hoc Networks. The protocol encrypts routing packet header and abstains from using unreliable intermediate node for preserving anonymity of the established route. The entire process is divided into the path discovery phase, the path reverse phase and the data transfer phase. During the path discovery phase, distributed information gathering about intermediate nodes that can be used along with the anonymous path takes place. Path reverse phase consists of conveying this information to the source node. During the data transfer phase, official data exchange takes place. SDAR provides prevention against active attacks and passive attacks that exploit path discovery path reverse messages. Reed et al. in [9] describes Onion Routing which is an infrastructure to protect anonymity in public networks. An onion is a multi-layered data structure that encapsulates the route of the anonymous connection starting from the onion router for the exit funnel and working backward to the onion router at the entry funnel. The system provides anonymity against eavesdropping and traffic analysis attacks. The authors themselves are stating that 'the implementation of a secure design can be insecure'. Traffic analysis becomes easy if part of the onion network is taken down.

A comprehensive listing of various attacks against mix-nets is provided by Raymond in [10]. In a brute force attack, the attacker follows every possible paths that the message could have taken. The attacker can create a list of possible adversaries and if the network is not well designed, he can easily track the sender and the receiver. The node flushing attack,if the nodes have to wait until they have t messages, before flushing,the attacker can send t-1 messages and easily associate messages leaving the node with those having entered. The route timing information is exploited in timing attacks,i.e., if different routes take different amount of time, the messages in the incoming and outgoing sets of a network can be correlated. Contextual attacks are targeted against real-time interactive communications. In communication pattern attack, the attacker observes the communication pattern over a period of time , making use of the fact that the communicating participants do not talk at the same time. An adversary can count the unusual number of packets sent from a participant and devise a packet counting attack. In intersection attack, attacker having information about what users are active at any given time can, through repeated observations, determine what users communicate with each other. Sender-receiver matching information can be gained by exploiting the fact that user behavior depends on the message received. The nodes not expecting to receive this message will react differently with respect to the nodes expecting the message. In a sting attack, the recipient tries to find the sender's identity and in a "send n' seek" attack, the sender tries to find the recipient's identity.

Distinguished from the above mentioned attacks, the statistical traffic analysis intends to break the anonymity by analyzing the statistical characteristics of the traffic. The predecessor attack and statistical disclosure attack are examples. Reiter and Rubin first described the predecessor attack in [11]. In this attack, the attacker tracks an identifiable stream of communications over a number of rounds. In each round, the attacker simply logs any node that sends a message that is part of the tracked stream. The attack does not always require analysis of the timing or size of packets (although that can speed up the attack), but instead exploits the process of path initialization. The statistical disclosure attack was described in [12] by G.Danezis. The attacker can identify all possible recipients of a message initiated by a particular sender node under this type of attack. This is possible if the attacker has information about the recipient anonymity set, the batch size of the mix and the probability distribution used by all other senders to select their recipients for each round of mixing and the number of observation. An evidence-based statistical traffic analysis was proposed in [2] by D.Huang.

In evidence based statistical traffic analysis each data packets are captured which are considered as evidence that support a point to point transmission between sender and receiver. In this analysis first create a sequence of point-to-point matrices, and then using that matrices derive end-to-end relations between the communication paths. This method fails when deriving the multi-hop traffic from the one hop evidences. This approach does not provide any method to detect the actual source and destination. It utilizes a nave accumulative traffic ratio to detect the multi hop communication which leads a lot of inaccuracies in the derived probability distributions.

STARS(Statistical Traffic Pattern Discovery System) was proposed by Yang Qin et al. in [4]. The analysis takes into consideration the broadcasting nature, the adhoc nature and the mobility of the nodes, which are the three special characteristics of MANETs. The attack model assumes the adversaries as passive signal detectors,who are connected through an additional channel which is different from the one used by the target MANET,the adversaries can locate the signal source according to some properties and that they can trace the mobility of the nodes. The source/destination probability distribution and the end-to-end link probability distribution are derived. A sequence of point-to-point traffic matrices are constructed from which end-to-end traffic matrices are derived in the first step. During the second step, a heuristic approach is used to identify the actual source/destination and then correlate the source node with the corresponding destination.

THE PASSIVE TRAFFIC DISCOVERY SYSTEM

Assumptions about the Network

The attacker nodes in a passive traffic analysis system do not directly involve in the communication that is flowing through the network. Their goal is to detect the traffic and to figure out the source, destination and link. These nodes make use of wireless location tracking techniques to find out the source of the detected signal. This demands that the targeted network should have limited node density, otherwise the source could not be correctly located from the set of close nodes. A separate channel is used by the adversary nodes for their communication. Encrypted packets having unique size are send by all the noble nodes through the channel so that the attacker cannot decrypt the content nor determine the source with the size of the packet. The mobility of the nodes is traced by the attacker using sensors. The system uses AODV routing protocol with random way-point mobility model. The physical/ MAC layer is controlled by IEEE 802.11(a/b/g) protocol. Every mobile node in the adhoc network maintains a routing table which has information about the next hop router to a destination node. A particular source node, in the absence of a valid, next hop path to the destination, initiates a Route Request Procedure. Since the message is broadcast over the network, the nodes having valid route replies with a Route Reply (RREP) message.

System Model

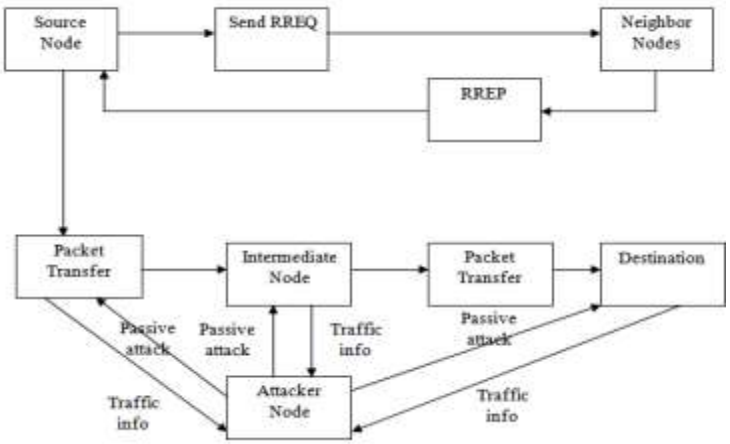

Fig.1 System Model

When the source node wishes to communicate with another, it broadcast an RREQ message in the network. When the RREP message is received from the neighboring nodes, the source node selects the path with minimum number of hops to the destination. The source node begins to send packets to the destination through intermediate nodes. The attacker nodes are deployed in a distributed manner in

the network. If an attacker node is present around an intermediate node through which the packet passes, then the attacker can detect the signal and use STARS to find out the source, destination and routing path. The probabilistic approach used in STARS, after constructing a sequence of traffic matrices yields more or less a complete attacking system. Now we analyze the system in terms of empirical parameters.

EXPERIMENTS

Experiments were done using NS-2 simulation tool with tcl coding in the front-end and C++ coding in the back end. The scope of the work is limited to finding the source probability distribution based on STARS and then evaluating the system performance in terms of average delay, packet drop and packet throughput .

Demonstration

We create a network consisting of a set of mobile nodes, deployed in 800 x 800 m^2 area. The number of nodes and the number of sources among them can be fixed by the user. One of the nodes is kept as the sink node and we consider that there are multiple source nodes. Fig.2 demonstrate the source probability distribution. The nodes having maximum probability are considered to be the source of the traffic. From the probability distribution, the nodes 5,18,24 and 26 have the highest probability to be the source node.

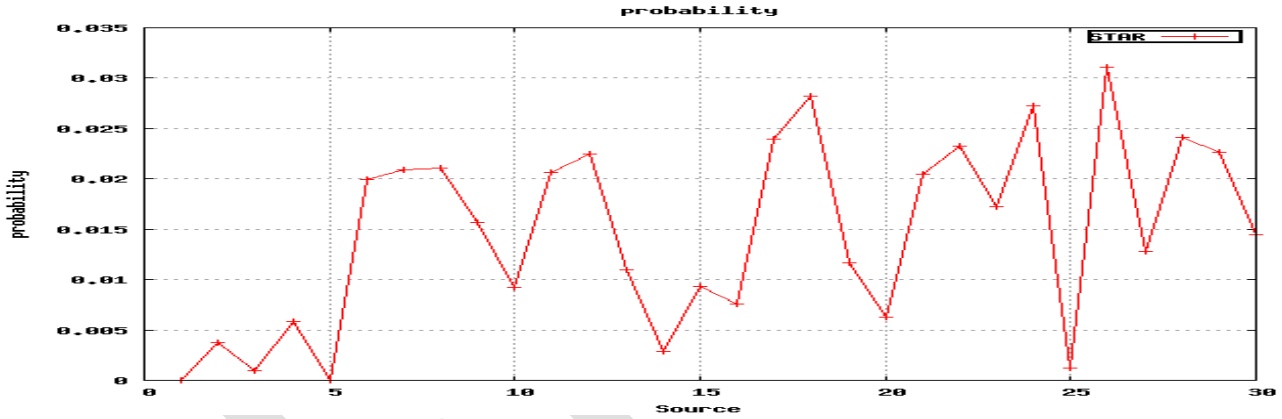

Fig.2 Source Probability Distribution

Performance evaluation

Once we execute the script, the output values are stored on to trace files. The values read from the trace file are used to plot the graph. We first analyze the system in terms of average delay in the network. Average delay is calculated as the ratio of total delay in the network to the number of packets. The graph is plotted against the number of nodes. This is depicted in Fig. 3. From the figure, it is clear that the delay increases with the node density. Fig.4 demonstrates the packet drop in the network. The packet drop retains a small value until there are about 35 nodes in the network. Thereafter the drop increases abruptly. The packet throughput of the network is depicted in Fig.5 . The throughput increases linearly until the number of nodes reaches 45, thereafter it decreases abruptly. From the performance evaluation, it is clear that when the STARS attack pattern achieves good performance when the number of nodes is limited to about 45. The system shows good performance in terms of average delay, drop and throughput until the number of nodes reaches 45.

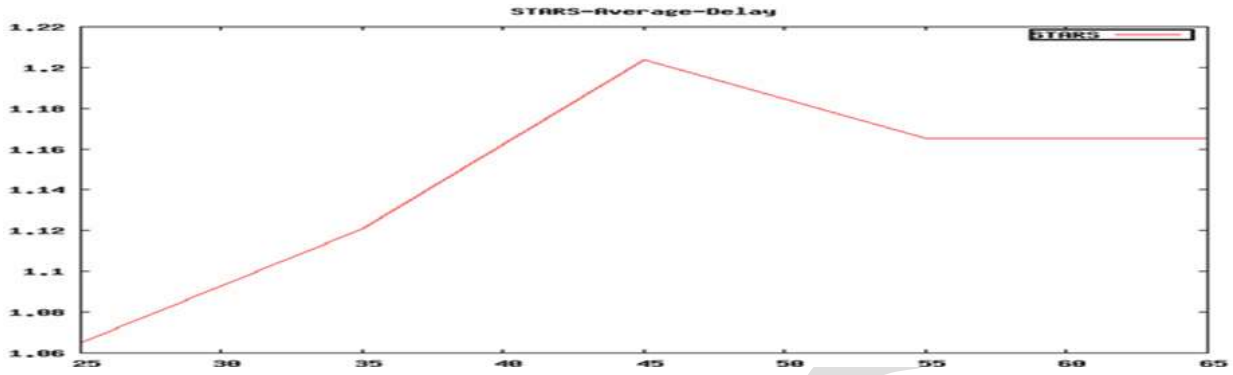

Fig.3 Average delay versus number of nodes

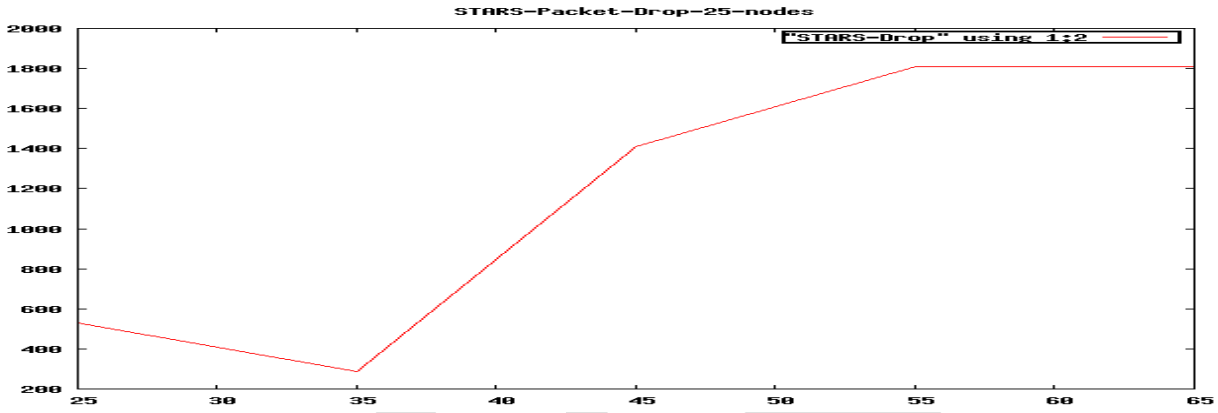

Fig.4 Packet drop versus number of nodes

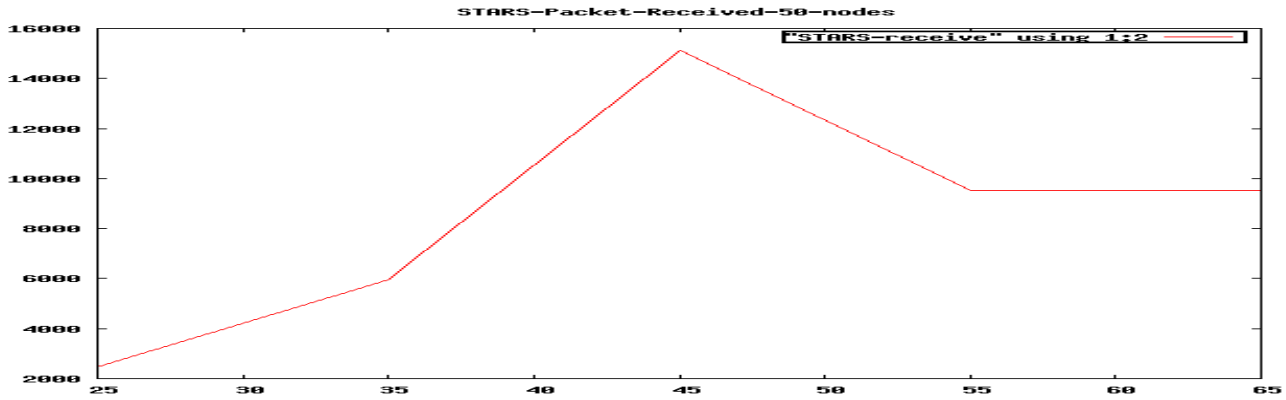

Fig.5 Packet throughput versus number of nodes

CONCLUSION

STARS attack model was analyzed in terms empirical parameters against the number of nodes in the network. From the study, it is revealed that STARS is able to find out the source of a traffic flow accurately. The system shows good performance when the number of nodes in the network is limited. But there are certain limitations of the system. Some of the routing nodes can be incorrectly determined to be the source node. Also the assumption about the adversary nodes having a global view of the network is difficult to implement as it requires deployment of large number of sensor nodes . The future work includes designing a complete attacking system addressing the above requirements.

REFERENCES:

[1] D. Chaum,The Dining Cryptographers Problem: Unconditional Sender and Recipient Untraceability, J. Cryptology, vol. 1, no. 1,pp. 65-75, 1988.

[2] D. Huang,Unlinkability Measure for IEEE 802.11 Based MANETs,IEEE Trans.Wireless Comm., vol. 7, no. 3, pp. 1025-1034, Mar. 2008

[3] G. Danezis, "Better Anonymous Communications," PhD thesis, University of Cambridge, January 2004.

[4] Yang Qin, Dijiang Huang and Bing Li, STARS: A Statistical Traffic Pattern Discovery System for MANETs, IEEE Trans. on Dependable and Secure Computing , vol. 11,no. 2,March/April 2014.

[5] D. Chaum,Untraceable Electronic Mail, Return Addresses, and Digital Pseudonyms, Comm. ACM, vol. 24, no. 2, pp. 84-88, 1981.

[6] J. Kong, X. Hong, and M. Gerla,An Identity-Free and On-Demand RoutingScheme against Anonymity Threats in Mobile Ad Hoc Networks, IEEE Trans. Mobile Computing, vol. 6, no. 8,pp. 888-902, Aug. 2007.

[7] Y. Zhang, W. Liu, W. Lou, and Y. Fang,MASK: Anonymous On-Demand Routing in Mobile Ad Hoc Networks,IEEE Trans.Wireless Comm., vol. 5, no. 9, pp. 2376-2385, Sept. 2006.

[8] A. Boukerche, K. El-Khatib, L. Xu, and L. Korba,SDAR: A Secure Distributed Anonymous Routing Protocol for Wireless and Mobile Ad Hoc Networks,Proc. IEEE 29th Ann. Intl Conf. Local Computer Networks (LCN 04), pp. 618-624, 2004.

[9] M. Reed, P. Syverson, and D. Goldschlag,Anonymous Connections and Onion Routing,IEEE J. Selected Areas in Comm., vol. 16,no. 4, pp. 482-494, May 2002

[10] J. Raymond,Traffic Analysis: Protocols, Attacks, Design Issues,and Open Problems, Proc. Intl Workshop Designing Privacy Enhancing Technologies: Design Issues in Anonymity and Unobservability, pp. 10-29, 2001

[11] M. Reiter and A. Rubin,Crowds: Anonymity for Web Transactions, ACM Trans.Information and System Security, vol. 1, no. 1,pp. 66-92, 1998

[12] G. Danezis,Statistical Disclosure Attacks: Traffic Confirmation in Open Environments,Proc. Security and Privacy in the Age of Uncertainty (SEC 03), vol.122, pp. 421-426, 2003

International Journal of Engineering Research and General Science Volume 3, Issue 5, September-October, 2015
ISSN 2091-2730

RESOLUTION ENHANCEMENT OF COMPRESSED SATELLITE IMAGES USING DISCRETE WAVELET TRANSFORM

POOJA PRASENAN, M-Tech(AECS),Lecturer, KUFOS
Kerala, India
poojaprasenan@gmail.com

Abstract- A new method based on compressive sensing and resolution enhancement is proposed in this paper.This method initially compresses the satellite image and then increases its resolution using DWT.Initially the satellite image is compressed,so it eliminates the requirement of taking all the samples. The main purpose of this technique is that it eliminates the Nyquist criteria, that is, sampling frequency must be greater Compressive Sensing technique and it gives the best results in signal compression as it increases the PSNR and visual quality of the satellite images as compared to existing techniques,then to this image again DWT is applied, in order to obtain sub-band images after whichbicubic interpolation of the high-frequency sub-band images is done and the input image along with the interpolated compressed image is combined using IDWT. In order to achieve a sharper image.The proposed technique has been tested on various images. The quantitative PSNR (i.e peak signal-to-noise ratio) and visual results shows the superiority of the proposed technique based on DWT(discrete wavelet transform)**.** The proposed technique is better compared with the state-of-art techniques.

KEYWORDS: *Discrete Wavelet Transform (DWT),satellite-image-resolution enhance-ement**,** Compressive sensing, run length encoding, interpolation.*

1.INTRODUCTION

Compressive sensing (CS) technique addresses the issue of compressing the signal.Lossless satellite image compression is required (or desired) in applications where the pictures are subject to further processing, intensive editing or repeated compression/decompression. Thus, medical imaging, satellite imaging, image archival systems, precious art works to be preserved, and remotely sensed satellite images, are all candidates for lossless compression. For some satellite images there are always issues of compression, and the compressive sensing is found to be a better technique that works in a manner such that it first acquires samples less than signal dimensionality and reconstructs the same signal, here wavelet transform is applied along with compressive sensing on images.

In this paper Compressive sensing is performed at the transmitter end. And then the satellite image is passed through a Gaussian channel and is received at the receiver end where resolution enhancement is performed.Resolution has been frequently referred as an important aspect of an image. Images are being processed in order to obtain more enhanced resolution. One of the commonly used techniques for image resolution enhancement is Interpolation. Image resolution enhancement in the wavelet domain is a relatively new research topic and recently many algorithms have been proposed. The proposed technique has been compared with conventional image resolution enhancement techniques and has been found to be a better technique. Resolution enhancement is performed at the receiver end. Thus my paper is based on compressing the satellite image at transmitter end so that the satellite image is easily send through gaussian channel at a faster rate and then enhancing the resolution of the image at receiver to obtain super resolution image.

2.ResolutionEnhancement OfCompressed ImagesUsing Discrete Wavelet Transform

My paper proposes a new technique which generates sharper and highly detailed super resolved satellite images from compressed images at the receiver end. The proposed technique uses discrete wavelet transform(DWT) to compress an image. This compression is performedat the transmitted end.This produces as many coeffients as there are pixels in an image.These coefficients can then be compressedmore easily because the information is statistically concentrated in just a few coefficients. This principle is called transform coding.After that the coefficients are quantized and the quantized values are entropy encoded or run length encoded.Here I have used Huffman coding for encoding purpose.Thus this produces a compressed image which is then passed through the channel,where Gaussian noise is added to the image,this completes the transmission part in the proposed method. After this the satellite image is received at the receiving end of the channel,where it is decompressed and its resolution is enhanced and after that inverse DWT is applied. The proposed technique has been compared with conventional satellite image resolution enhancementation techniques.The main loss in any satellite image occurs in its edges (i.e. high-frequency components), which is due to the smoothing caused by interpolation. Hence, in order to increase the quality of the super resolved satellite image, preserving the edges is essential. In this paper DWT has been employed in order to preserve high-frequency components of the satellite image. Compression uses the requirement of taking all the samples at acquisition. The main purpose of this technique is that it eliminates the Nyquist criteria,that means sampling frequency must be greater than two times the maximum original signal frequency.

Using compressive sensing one can recover certain signals or images from far fewer samples than traditionally required. On encoding side it requires two properties of a signal: sparsity and incoherence. First, any signal is converted into dimension Nx1 vector, with the help of sensing matrix of dimension MxN. It extracts required coefficients and hence gives resultant Mx1 matrix which is also called M measurements which are non-adaptive. On decoding side we know that measurements M < N, so it requires convex optimization to solve this problem. Apart from this, greedy algorithms and basis pursuit are also helpful. Convex optimization provides solution to undetermined linear systems without knowing nature of undergoing parameters through the systems. L0, L1, L2 minimizations are used for reconstruction but L1 provides best reconstruction for more sparse signals Compressive Sensing technique gives the best results in signal acquisition as well as in signal compression. In my paper, as the number of measurements are increased, it increases the PSNR and visual quality of the images, with decrease RMSE as compared to existing techniques like JPEG and JPEG2000, as in these calculations has been applied on all the pixels of image and that is not required in our technique.

2.1 Proposed technique

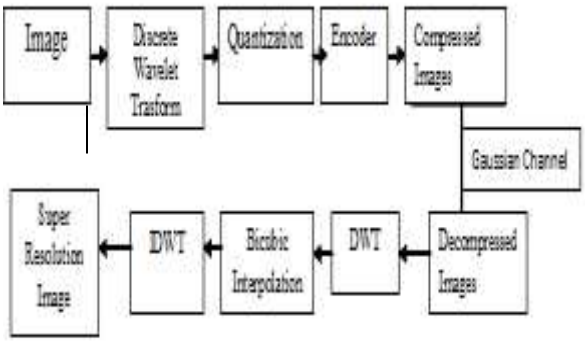

Fig1.Block diagram for Resolution Enhan-cement of Compressed Images

2.2 Block Diagram Explanation

DWT is used to compress and decompress the satellite images. Here to the satellite image initially DWT is applied and then it is quantized and passed through the encoder after which the satellite image is compressed and then passed through the channel,where Gaussian noise is added to it. Then at the receiver end when the satellite image is decompressed some of the information will be lost,so in order to improve the quality of satellite image DWT is again applied where the satellite images are divided into sfour sub-bands and this sub-bands are then bicubically interpolated. After this the input satellite image is also interpolated with half the interpolation factor α. Now, the two interpolated up-scaled images are generated. Finally by interpolating the input image by α/2 and the high-frequency sub-band images by α and then to this IDWT is applied,then the output image will contain sharper edges than the interpolated satellite image obtained by interpolation of the input satellite image directly.This is due to the fact that the interpolation of the isolated high frequency components in the high frequency sub-band images will preserve more high-frequency components after the interpolation of the respective sub-bands separately than interpolating the input satellite image directly. Thus the proposed technique interpolates not only the decompressed satellite image but also the high frequency sub-band images obtained through the DWT process. The final high-resolution output image is generated by using the IDWT of the interpolated images and the input satellite image. The visual and the peak signal-to-noise ratio (PSNR) results, show that the proposed technique outperforms the conventional method. And thus a super resoluted satellite image from a compressed image is obtainted.

3.PROJECT OUTCOME

The final result of my project is the visual analysis of an satellite image in which initially a satellite image is given as input which is 550 Kb and first it is compressed and the size is reduced to 120 kb to pass it through a Gaussian channel effectively. In the channel Gaussian noise is added and at the receiver end of the channel all the noise is removed to obtain the denoised image. And finally to this satellite image an DWT based enhancement technique is applied to obtain a high resolution satellite image. .

Fig 2: Graphic User Interface

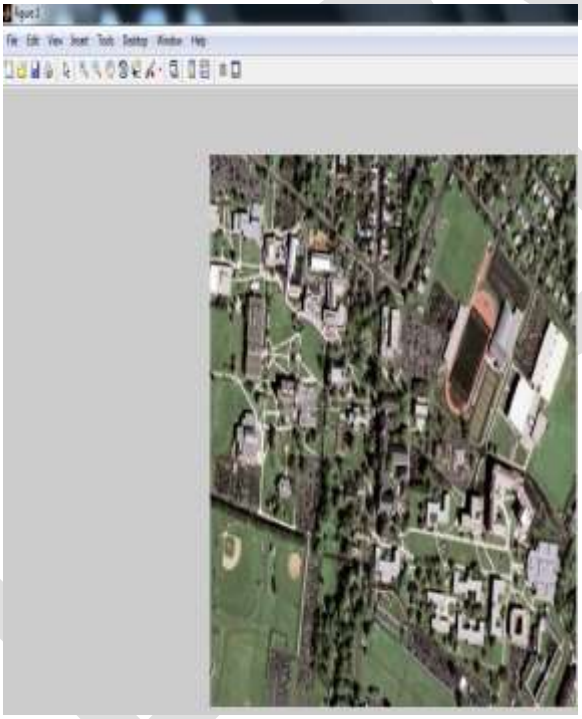

Fig 2(a)

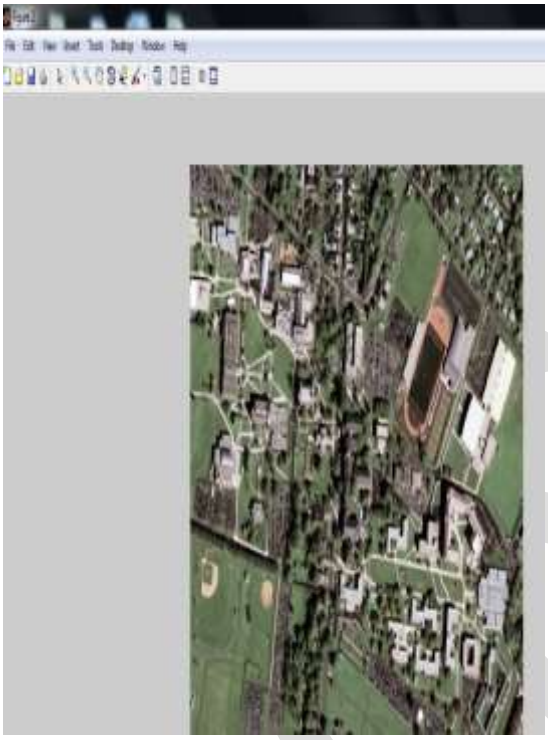

Fig.2(b)

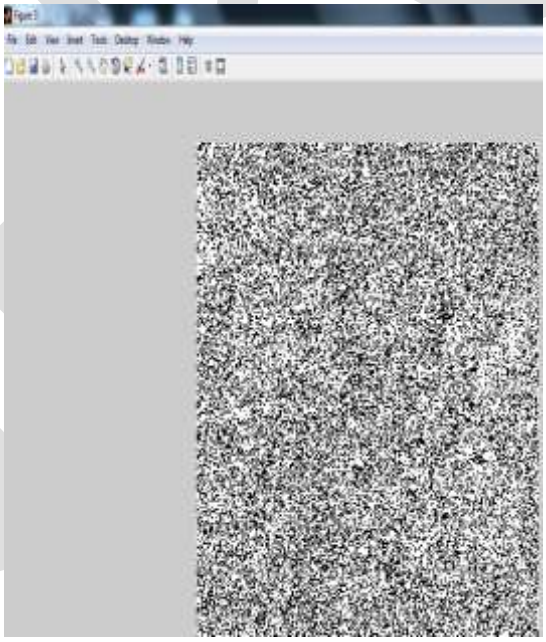

Fig.2(c)

Fig.2(d)

Fig.2(e)

Fig2:Project Outcome, (a)Input Image, (b)Compressed Iimage, (c)Transmitted Image, (d)Received Image, (e)High Resolution Image.

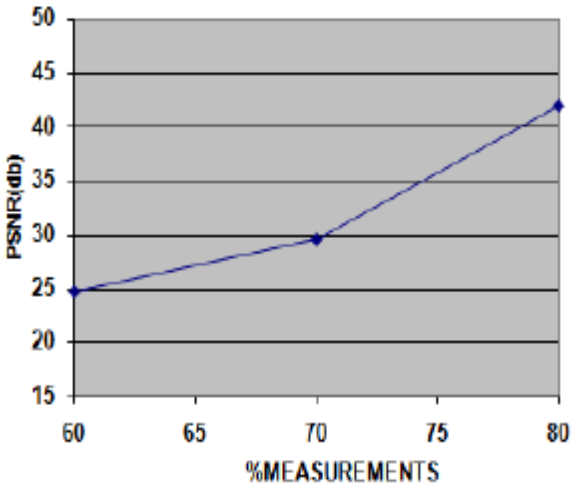

Fig 3:Graph of PSNR using conventional method for Compressive Sensing

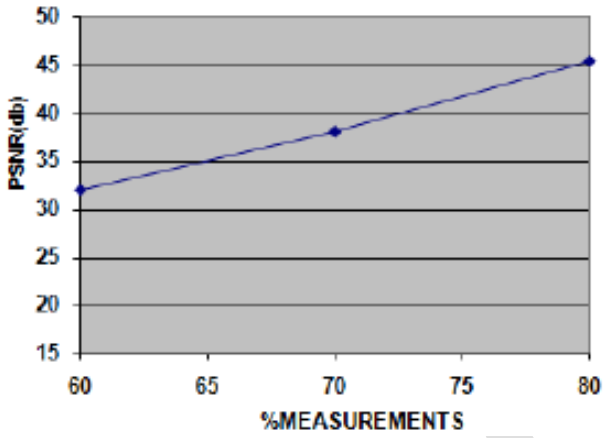

Fig 4: Graph of PSNR using proposed method for Compressive Sensing

Calculation of PSNR: PSNR is most commonly used to measure the quality of reconstruction of lossy compression (e.g., for image compression). The signal in this case is the original data, and the noise is the error introduced by compression.
PSNR = $10 \log_{10} (255^2/\text{MSE})$
Where, MSE is mean square error.

PSNR(db)			
Method/Image	Lena Image	Satellite Image	Other color Image
Fourier Transform	19.89	18.27	18.37
DCT	21.66	23.44	18.09
CWT	18.11	26.1	18.36
Proposed Method	22.02	28.97	18.58

Table 1: PSNR Measurements for different Images

4.APPLICATIONS

1.Research purpose: The proposed technique is used to analyze the whether conditions, along with the presence of fog and also one can find the presence of any type of foreign body in the space by analyzing the high resolution image obtained at the output.

2. It can be applied for both color images and black and white images. That is by programming accordingly this method can be applied for grey images and also for color images.

5.CONCLUSION

A new method based on Compressive sensing and resolution enhancement technique of satellite image is proposed. This method initially compresses the satellite image and then increases its resolution is enhanced using DWT. First the satellite image is compressed. So it eliminates the requirement of taking all the samples. The main purpose of this technique is that it eliminates the Nyquist criteria, that is, sampling frequency must be greater Compressive Sensing technique and it gives the best results in signal

compression as it increases the PSNR and visual quality of the images as compared to existing techniques, this satellite image is then made to be passed through the Gaussian channel and at the receiver end this satellite image is decompressed & to this satellite image again DWT is applied, in order to obtain sub-band images after which bicubic interpolation of the high-frequency sub-band satellite images is done and the input satellite image along with the interpolated compressed satellite image is combined using IDWT. The proposed technique is better compared with the state-of-art image techniques in visual basis.

6.FUTURE SCOPE

My paper involves a method of compressing the satellite image by using compressive sensing which uses discrete wavelet transform and then it is passed to the channel. After retrieving the image from channel the resolution of image is increased by using discrete wavelet transform. As compression and resolution enhancement are the emerging fields in image processing thus in future instead of using DWT another emerging transform called SWT(stationary wavelet transform) can be used to improve the compression and resolution of the satellite image visually and also it may improve the PSNR values.

REFERENCES:

[1] **Chintan.K Modi, Falgun N Thakkar, Mayur M Sevak, Rahul K Kher**, "CT Image Compression using Compressive Sensing and Wavelet Transform", 2012 International Conference on Communication Systems and Network Technologies.

[2] **D. Donoho, Yakov Tsaig**, "Fast Solution of L1-Norm Minimization Problems When the Solution May Be Sparse", IEEE Transaction on information theory, VOL. 54, NO. 11, November 2008.

[3]**E.Candes, M.Wakin**, "An introduction to Compressive Sampling",IEEE signal processing magazine, 1053-5888, 2008 IEEE, March 2008.

[4]**Hasan Demirel, Gholamreza Anbarjafari** 2011 IEEE Transactions on Geoscience and Remote Sensing," in Proc. ICIP , Oct. 7–10, 2011, vol. 3,pp. 864–867.

[5]**G. Anbarjafari and H. Demirel,** " Image super resolution based on interpo-lation of wavelet domain high frequency subbands and the spatial domain input image," *ETRI J.*, vol. 32, no. 3, pp. 390394,Jun. 2010.

[6] **Hui Hui Bai, Anhong Wang, Meng Meng Zhang**, "Compressive Sensing For DCT image", 978-0-7695-4202-7/10,IEEE 2010.

[7] **Li Fan, Yudong Zhang, Zhenyu Zhou, David P. Semanek, Lenan Wu**, "An Improved Image Fusion Algorithm Based On Wavelet Decomposition" ,Journal of Convergence Information Technology Volume 5, Number 10.December 2010.

[8] **V. K. Bairagi, A. M, Sapkal**, "Selection of wavelets for medical Image Compression" International Conference on Advances in Computing, Control, and Telecommunication Technologies 978-0-7695-3915-7/09, 2009 IEEE.

[9] **Y. Rener, J. Wei, and C. Ken**, "Down sample-based multiple description coding and post-processing of decoding," in Proc. 27th CCC , Jul. 1–18,2008, pp. 253–256.

[10] **C. B. Atkins, C. A. Bouman, and J. P. Allebach**, "Optimal images caling using pixel classification," in *Proc. Int. Conf. Image Process.*,Oct. 7–10, 2001, vol. 3, pp. 864–867.

[11] **A. Temizel and T. Vlachos**, "Wavelet domain image resolution enhancement using cycle-spinning," *Electron. Lett.*, vol. 41, no. 3, pp.
119–121, Feb. 3, 2005.

[12] **A. Temizel and T. Vlachos**, "Image resolution upscaling in the wavelet domain using directional cycle spinning," *J. Electron. Imag.*, vol. 14,
no. 4, 2005.

International Journal of Engineering Research and General Science Volume 3, Issue 5, September-October, 2015
ISSN 2091-2730

Space Elevators: A Feasible Solution for Sending People and Goods into Space More Cost Effectively

Rupesh Aggarwal[1], Pavleen Singh Bali[2], Pranay Kami[3], A.K. Raghav[4]

[1]Teaching Assistant, Department of Aerospace Engg. Amity University Gurgaon, Haryana, India

[2]Research Associate, Department of E & C Engg. Amity University Gurgaon, Haryana, India

[3]UG, Department of Aerospace Engg., Amity University Gurgaon, Haryana, India

[4]M.Tech. IISc Bangalore, Phd. IIT Delhi, Director- IR&D, Amity University Haryana, India

Abstract— The Present study focuses on the fascinating concept of Space Elevators. Object of this study is to get introduced with every aspect in Designing, Working & Construction of Space Elevators. It's a concept in which tether is used to uplift any type of cargo or personnel from Earth surface to an orbit in space. Such invention not only becomes the new path for heavy loads to get into space but also becomes a cheap one. Also from the top of it, loads can be launch in any desired direction. By this not only the cost of the launch through rocket gets reduced but also the personnel handling this launch i.e. reduction of human error too. Perfect suitable material for such operation is Carbon Nano-tube which hundred times stronger and ten times lighter then Steel. In coming 50 years, it might be possible that many space elevators are ready to launch the spacecraft in space. Its application is not just only limited to the launching but also it can help in carrying heavy payloads to International Space Stations. It simply can give access to space for scientific, commercial & military purposes.

Keywords— Space Elevators, Space-Towers, Geostationary Orbit, Space Cables, Tethers, Carbon Nano-tube, floating platforms.

INTRODUCTION

A concept which can make possible the fantasy of physical connection between Earth and Space. In Space it can be go high from LEO (Low Earth Orbit) to GEO (Geostationary Orbit), approximately ~ 100 to 23,000 miles. The most general description can be Space Elevator is a long tower attached with one end to earth and other long high in space. The concept first came from an inventive Russian in 1960.[1] Many science fictions even kept the insights of Space Elevators also. Its Intended use is literally a transportation of Payloads, personnel, power, etc. from earth surface to space. A recent patent filed by a Canadian company on the same concept in which a 12.4 miles long tower from the earth used to launch the spacecraft in space. Space Elevators can directly provide access to astronauts, which can help in mining asteroids, placing a satellite into an orbit. Through the introduction of this concept attaining the escape velocity by spacecraft to get to the orbit will not be a problem anymore. This concept reduce a major stage of getting into space i.e. launching through Rockets, which not only reduce the cost of the mission but also protect the environment from the harmful gases thrown out of exhaust nozzle of rockets. Sending things into space from the earth's surface is extremely expensive. Chemical rockets are complicated and dangerous as well as expensive to build and launch. Space elevators have shown the possibility of a simpler, safer and cheaper alternative. This is the main argument for developing an elevator that will take things from the earth's surface into orbit. So far technological and logistical roadblocks have been holding the concept of a space elevator from becoming a reality. The technology of carbon nanotubes is a ways away from becoming the 60,000 km tether for the elevator.[2] Finding the funding and manpower for building such a massive structure in itself will prove to be a logistical marvel in itself. If the understanding and utilization of carbon nanotube technology does not improve, and the needs for massive funding, manpower, and engineering genius are not met, there will be no space elevator.

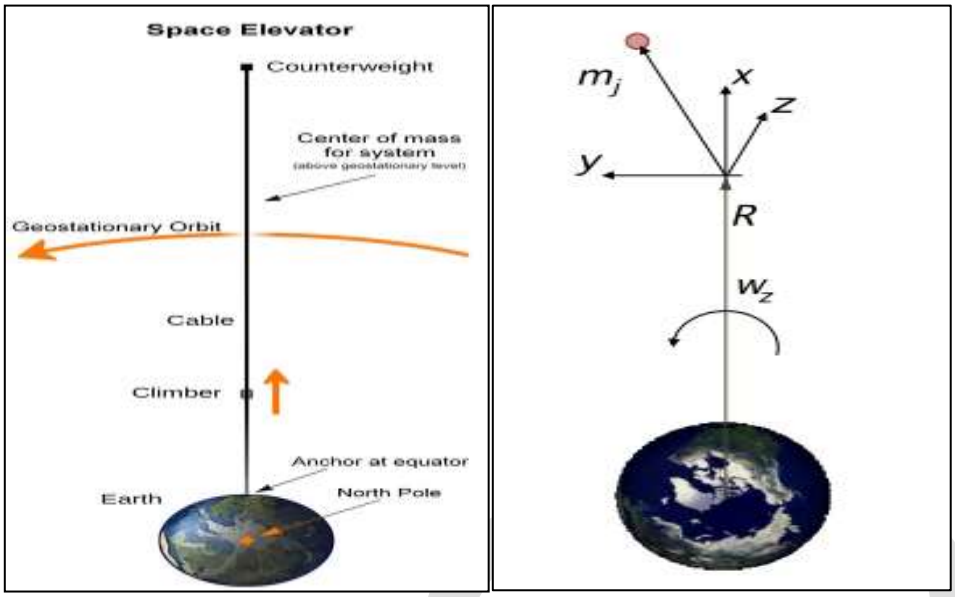

Fig 1: Space Elevator Methodology

Propellants used in rocket can cause the depletion of Ozone layer or can cause acid rain or can cause smoke-trails all over the sky. Space Elevators can directly be link to the International Space Station (ISS) or any other Space Station floating in the orbit, it helps astronauts in their researches. They don't have to depend or wait for the space organization to sanction a new rocket launch just for bringing some samples back. Surface labs can be directly connected to the labs setup in space. Another application of this concept in future is that, it can be direct link from the settlement in Space to the Earth surface.

BASIC CONCEPT

Main Principle behind the Space Elevator is the centrifugal force of earth's rotation. As it rotates, centrifugal force tends to align the cable/tower in a stretched manner. Basic Components that every design includes Base Station, Cable, Climbers, Counterweight.

1. ***Base Station:*** Generally Base Station categorize as Mobile or Stationary. Mobile are large ocean based vessels which maneuver in order to avoid high winds & Storms. Stationary Stations would normally be located in high altitude locations, like top of mountains or high towers which generally reduce the length of the cable.
2. ***Cable:*** CNTs are the strong candidates as a material for cable. The required strength of the cable will vary with its length. The cable should be made of a material with large tensile strength/mass ratio.
3. ***Climbers:*** Climbers are generally Elevators which climbs the cable. On elevator design, with cables as planner ribbons, most of the time rollers are being used to hold the cable with friction. Elevators must be placed on optimum time for minimizing cable stress & Oscillations and also to maximize the payload. Though often lighter climber being used so that several climbers climb at same time which not only increase the payload capacity but also lowers the stress acting due to extreme payload on the cables as well as climbers.

Apparently there are two major factors which affects the physics of Space Elevators:

1. ***Apparent Gravitational Field:*** Along with the rotation of the Earth, the space elevator cable rotates. Objects attached to cable will experience upward centrifugal force which opposes the downward gravitational force at that point. The actual downward gravity minus the upward centrifugal force gives the apparent gravitational field.
2. ***Cable Section:*** The cable material includes its design must be strong enough from the strength point of view so that it can support 23,000 miles itself. By designing any cable larger in cross-sectional area at top compared to the bottom, it can hold up longer length of itself. Due to this another important design factor in addition to the material is how the cross-sectional area tapers down from the maximum altitude to minimum at the surface. To maximize strength/weight ratio of the cable, the

cross-sectional area will needs to be designed in such a manner that at any given point, it is directly proportional to the force it has to withstand.

DEVELOPMENTS & BACKGROUND REVIEW

There has been lots of studies and theoretical researches done on Space Elevators. They were focused on its physics and some components like its optimal design.[3][4][5] But because of unavailability of proper material, this concept has been discarded. Then Carbon Nano-tubes (CNT) were discovered in 1991, which is hundred times more strong then steel and ten times lighter.[6] In CNT, atoms are structured in a particular pattern, same as of Geodesic domes. Moreover it is a very long chain of carbon atoms only. They are strong per kilogram than any other kind of material by a factor of 40, which means a fiber of CNT with a diameter of 1/8 inches could support a load of 45 tons.

Later in 1975, Pearson Physical base for designing & construction of Space Elevators. With Clarke, he stated that tower should be fabricated in both direction of Earth to Geostationary Orbit to maintain the gravitational balance of Structure. With the help of force derivatives, he calculated the tower must be minimum of 89,478 miles in order to be balanced state with Surface gravity, Earth's radius, Net weight of zero & period of rotation. He then proposed an exponent, area taper for the structure of 0.776r/h where r be radius of earth and h be characteristic height to which a uniform diameter of tower could built in 1g field. Proper materials can be classified from below relation:

$$h = \sigma/\rho g$$

Where, σ: Max material stress

g: Surface Gravity.

Graphite Crystals based Elevator is proposed by Pearson with σ of 46.5 GPa & density, ρ of 2200 kgm^{-3} which yield a solution with characteristic height, $h = 2150$ km & taper ratio of 10 without any kind of safety factor is applied. He stated that such structure would have certainly significant utility, like ascending payloads can be injected into space orbits directly without use of rockets. However, from construction point of view, still requirement of innovation in material as well as in space manufacture systems, programs, etc. and also there be requiring minimum of 24,000 spacecraft flights which is modified only for working in geostationary orbit.

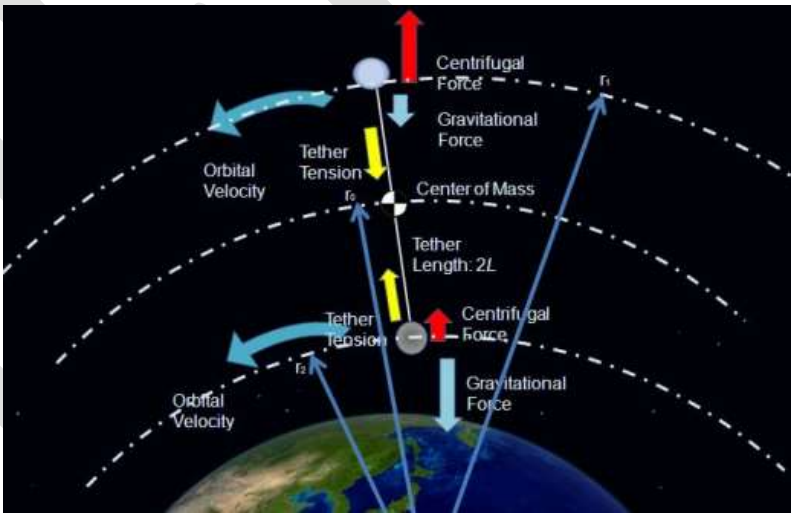

Fig 2: Orbital layering

In 1978, Arthur C. Clarke in his novel, *The Fountains of Paradise*, proposed that a space elevator can be constructed using a counter-balanced mass system and a cable. For Earth's spin rate and gravity such proposal requires cable of at least 23,000 miles long & a counter-balanced mass similar to mass of small asteroid. Later then such system could be constructed through launching cable in space or manufacturing it on site. Though there be some technological obstacles that must be overcome, including the manufacturing of cable with suitable strength or on-site construction. These obstacles have not been realized until Clarke proposed this concept.

In 1985, Lofstrom proposed *launch loop*, which is a 2000 km long cable structure fixed at both ends and at every 80 km vertically along its length.[7]

Later again in 2000, Edwards proposed a ribbon composed structure comprising 1.5 μm ribbons each with mass 5000 kg.[8] According to Edward, ribbon comprising CNT with tensile strength of 130 GPa requires 4 Titan IV/Centaur launches to deliver ribbons to GEO. These ribbon would be capable of holding a climbing payload of 528 kg with a safety margin of 2. After such 250 assents, the cable become capable of raising a 13,000 kg payload in every 5 days. This concept approach is quite better than other known. However, from his study Edwards found many challenges that one might face while engineering this design.

In 2000, Boyd & Thomas also proposed a design for space elevators in which a cable system is capable of transporting the payloads between orbital locations.[9] Basically in their design, payload moves between locations located at fixed orbital distance from the earth. Since the device is not attached to earth so there must be secondary means to attach the payload initially to the elevator.

Such studies keeps on going concluding all structures rely on innovation & development of materials to construct towers/cables of greatest strength. The best known is still CNT, but in 2006, Pugno argues that even presence of microscale defect alone will prevent the fabrication of cable with sufficient strength only if theoretical strength limit can be estimated in a microscopic cable.[10] He concludes that if elevator built based on today's design then it will break.

APPLICATIONS

A space elevator would be cheaper than using chemical rockets. To build the first space elevator it is projected to cost around 6- 12 billion dollars.[11] The cost of building any additional elevators is said to cost around 2 billion dollars each because the materials to build them could be sent up on the first elevator. In comparison the Saturn V rocket alone cost 6.5 billion dollars during its operation between 1964 and 1973. Also space elevators would be completely reusable. Once the elevator was built it would go until a part was broken or worn out. There would be no need to have expensive booster stages that would be dropped back down to earth and destroyed once used up. Once the space elevator was built it would be much cheaper to use continually without much maintenance.

The most expensive part of any space mission using chemical rockets is getting to Low Earth Orbit. This is because of the earth gravity and atmosphere. Because the fuel for chemical rockets weighs so much itself they have to carry a tremendous amount of fuel to be able to lift a relatively small payload into Low Earth Orbit. Also the whole time the rocket is also fighting air resistance until it leaves the atmosphere, which takes more fuel, which reduces payload and increases cost per kilogram of the payload. The Saturn V rocket, one of the most powerful rockets ever launched carried a payload of around 119,00kg into Low Earth Orbit and cost 1.1 billion dollars per launch, which comes out to around 8403 dollars per kilogram. The cost of sending a kilogram of payload into Low Earth orbit on a space elevator would be around $220 per kilogram. It is said that a space elevator could carry payloads of 11,193kg per climber and that up to eight climbers could be sent up the tether at once.[12]

Many times payloads need to be sent into what is called a geosynchronous orbit or a geostationary orbit. A geostationary orbit allows a satellite to follow a single point of the earth surface for its entire orbit. A geosynchronous orbit allows a satellite to oscillate from north south in a figure eight pattern over a specific area of the earth's surface. For instance satellites used for satellite TV need to have an orbit that allows them to send information to its consumers where they live. To achieve a Geosynchronous a transfer orbit is required to gain the additional altitude needed. This in turn takes much more fuel that reduces the overall payload by a third, and makes the cost per kilogram much higher. A space elevator would eliminate the fuel costs for getting a payload for this type of mission into Low Earth Orbit. Since there is no gravity and no air resistance in space cheaper more efficient types of rockets could be used to bring satellites into geostationary or geosynchronous orbits. Electrical and nuclear rockets that have extremely high specific impulses that do not weigh very much could be sent up on the elevator and used to put satellites into these orbits.

A space elevator could be much safer in some ways than using chemical rockets. The climbers would use power beamed from the ground instead of highly volatile chemicals. There would be none of the dangers that you have when you are using chemical rocket fuel. There would be no fuel that needed to be kept in a liquid state. You would not have to build a massive flame trench or have people standing three miles away to watch it lift off. There could be safety mechanisms that would grab onto the tether if something went wrong with the elevators propulsion system. When something goes wrong with a chemical rocket during lift off the payload is usually ejected or destroyed.

CONCLUSION & FUTURE SCOPE

Space elevators are not yet a feasible solution for sending people and goods into space. There are too many technological and engineering roadblocks. The challenges of building such a thing are far beyond anything that has been attempted before. The anchor for the elevator would be one of the most massive structures ever built and it would most likely has to be a ship that could move the entire elevator from the sea. A way to collect a giant asteroid and a way to attach this giant asteroid to the end of the tether needs to become a real life possibility for the elevators counterweight. The technology for wireless energy transfer needs to be greatly improved if the space elevator has any hope of being a more efficient way of getting things to space.

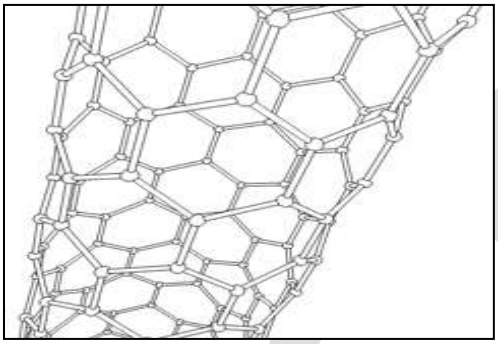

Fig3: Carbon Nano-Tube Structure

The technology for the carbon nanotube tether is far from being ready. Carbon nanotubes need to be made 66,000 km long and on a literally astronomical scale. Once this is accomplished a way to make this nanotube tether withstand the harsh weather and temperatures of the earth atmosphere as well as intense vibrations, radiation, satellites, meteoroids, and micrometeoroids would need to be found. The climber must endure these challenges as well but it must also be able to keep human passengers safe from them. The elevator must protect humans from intense radiation and the vacuum of space along with the challenges of the earth's atmosphere for days on end. These challenges are too much for the technology that we have at hand at this point in time. As Dr. Bryan E. Laubscher said, "As soon as we can build it, we should build it". But as of now a space elevator is not a feasible solution for sending things into space because we haven't built one yet. Therefore Space Elevators are only a sufficient but not a necessary condition for the viability of the space elevator as a practical transport system.

REFERENCES:

[1] Artsutanov, Y. 1960. V Kosmos na Elektrovoze, Komsomolskaya Pravda, (contents described in Lvov 1967 *Science* 158:946).

[2] Edwards B.C., The Space Elevator. Study conducted for NASA under NIAC program.

[3] Clarke, A.C. 1979. The Space Elevator: 'Thought Experiment', or Key to the Universe. *Adv. Earth Oriented Appl. Science Techn.* 1:39.

[4] Isaacs, J.D., Vine, A.C., Bradner, H., and Bachus, G.E. 1966. Satellite Elongation into a true 'Sky-Hook'. *Science* 151:682.

[5] Pearson, J. 1975. The Orbital tower: a spacecraft launcher using the Earth's rotational energy. *Acta Astronautica* 2:785.

[6] Iijima, S. 1991. *Nature* 354:56. *The Infrared and Electro-Optical Systems Handbook: Atmospheric Propogation of Radiation*, Vol. 2. 1993. Editor:Fredrick G. Smith. Bellingham Washington: SPIE Optical Engineering Press. 228.

[7] Lofstrom K. H., The Launch Loop: A low cost earth-to-high-orbit launch system, AIAA-85-1368, 21st joint propulsion conference, 1985.

[8] Edwards B. C., Design and deployment of a space elevator, *Acta Astronautica*, 2,785-799, 2000.

[9] Boyd R. R. and D. D. Thomas, Space Elevator, US Patent 6491258, Filing date: Dec 6, 2000, Issue date: Dec 10, 2002, (Assignee: Lockheed Martin Corporation).

[10] Pugno N., On the strength of the carbon nanotube-based space elevator cable: from nanomechanics to megamechanics, *J. Phys.: Condens. Matter*, 18, S1971-S1990, 2006.

[11] Chang, Kenneth. "Not Science Fiction: An Elevator to Space - New York Times." The New York Times - Breaking News, World News & Multimedia. Web. 21 Nov. 2011.

[12] Quine B.M., Seth R.K., Zhu Z.H., A free standing elevator structure: a practical alternative to the space tether

International Journal of Engineering Research and General Science Volume 3, Issue 5, September-October, 2015
ISSN 2091-2730

PARAMETRIC ANALYSIS OF INDUSTRIAL COLD DRAWING PROCESS

Praveen Kumar Loharkar

SVKM's NMIMS MPSTME Shirpur Campus Dhule 425405 India,ploharkar@gmail.com

Abstract— Seamless tube cold drawing is one of the most important bulk deformation processes as the products manufactured through this process are utilized in various engineering sectors like automobile manufacturing, mining industry, pipelines, boiler manufacturing etc. Therefore, it becomes quite significant to establish optimum values of parameters associated with the process and use the existing computational facilities to develop a simulation environment for the cold drawing process itself. This paper is an effort to demonstrate the use of finite element method to analyse cold drawing process and to determine the effect of the process by variation of the parameters like die entry angle and cross-section reduction on the industrial cold drawn seamless tube.

Keywords — Seamless tube, Cold drawing, bulk deformation process, finite element method, die entry angle, cross section reduction.

INTRODUCTION

Cold drawn seamless tubes of alloy steels have wide area of applications. They are used in automobile industry, mining industry, boiler manufacturing etc. Cold drawing process adds value to the product as it not only improves the surface finish and geometrical tolerances but it also enhances the mechanical properties.

Cold drawing process have been analyzed earlier through different analytical methods like slab method, upper bound method or slip line theory [1]. With the development in computational capabilities, Finite element analysis has started playing a major role in enabling industries towards new product development. Ironically, still there are many industries which still have not utilized the full potential of these advancements and therefore are lagging behind at the development and innovation index.

An attempt is made to carry out parametric study of the cold drawing process using finite element analysis by considering industrial data.

COLD DRAWING PROCESS

Cold drawing is essentially a bulk deformation process, that is, it involves plastic deformation to achieve the desired shape and size [2]. It can be classified under two categories. In the first category of the process, wire or rod is given the shape and the cross-sectional dimensions of the drawing die. While in the latter case, the outside is formed by the drawing die and the inner side is formed by a plug or a rod using the combination of tensile and compressive forces. This work is concerned with the tube drawing process.

FINITE ELEMENT ANALYSIS

The finite element analysis is carried out on an axisymmetric model of seamless tube in the ABAQUS Software. The dimension of the hollow tube on which the drawing simulation was carried is 110x9.50. The Final tube size was determined for different cross-section reductions, viz. 0.2, 0.3, 0.4 by keeping the inner diameter constant at 91 mm.

The finite element analysis was performed by choosing the drawing conditions based on full factorial design of experiments (D.O.E.). In this design, two factors, namely, die entry angle (20^o, 24^o, 30^o) and cross section reduction (20%,30%,40%) with three levels are used. As far as friction condition is concerned, the value of coefficient of friction was kept as 0.05 which resembles the actual drawing friction scenario [3].The drawing speed is kept constant at 400 mm/s.

1. Assigning Material Property

The material chosen for the analysis is STR 525, which is an alloy steel, used specially for making hydraulic cylinders. The composition of the alloy steel is close to ST 52 which is a standard alloy steel. For checking the actual composition of the material, an instrument called X-Met was used. Young's modulus and density values were chosen from standard data available for the alloy steel.

2. Mesh Generation and Other Computation Parameters

The finite elements used for meshing tube are 4 noded-2D axisymmetric elements with reduced integration points (CAX4R).Deformation was initiated with the provision of down-ward motion of the hollow. Adaptive remeshing facility given by the software has been used to repair the meshes during deformation. Adaptive remeshing is an excellent feature that makes the analysis more realistic thereby increasing the reliability of the solution obtained. Mass scaling was done with a factor of 1600 to speed up the analysis. Two steps were used for the simulation. The first step, initial, which is a default step, was used to define the boundary conditions, while the next step, tube drawing, was used to establish the contact between hollow (tube at inlet), tools and to initiate material deformation.

SIMULATION RESULTS AND ANALYSIS

Model was validated by comparing the strains developed in actual drawing practice to the strains developed in the finite element model after drawing simulation. Then simulation was carried out for other combination of parameters and results were obtained as discussed below.

1. Die Entry Angle and Equivalent Plastic Strain Distribution

On observing the diagrams (Fig.4.1 a, Fig. 4.1 b, Fig. 4.1 c) of the equivalent plastic strain (P.E.E.Q) for different die angles, that is 20^0, 24^0, 30^0, it was found that the strain values increase in accordance to the angle values (although there is not much difference). P.E.E.Q in case of die entry angle 20^0 is around 0.3238 in the steady state condition at step time 0.45. But the same value for die entry angles 24^0 and 30^0 is 0.3812 and 0.4074 respectively.

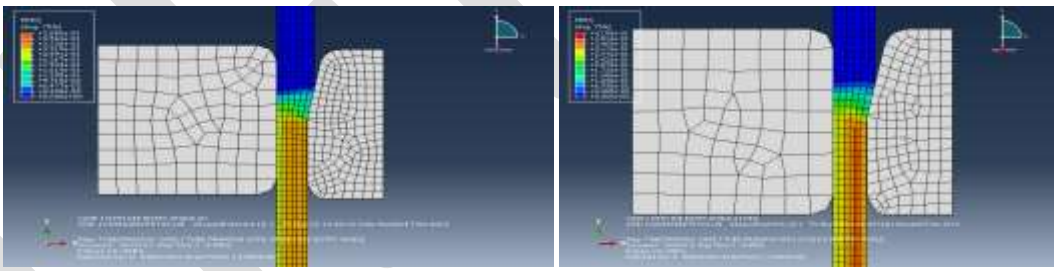

(a) P.E.E.Q. for r=0.2, 2α=20^0, **(b) P.E.E.Q. for r=0.2, 2α=24^0**

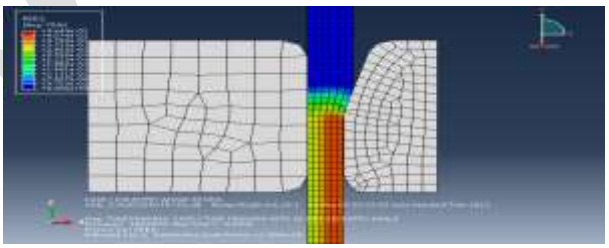

(c) P.E.E.Q. for r=0.2, 2α=30^0

Fig. 4.1 Effect of Die Entry Angle on Equivalent Plastic Strain

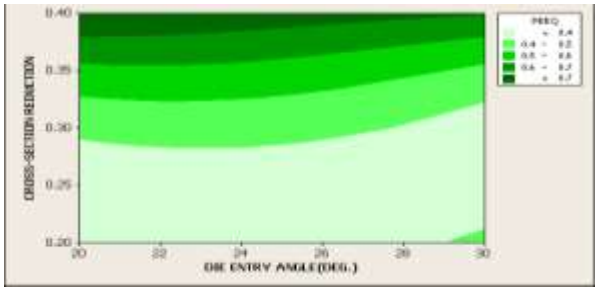

Fig. 4.2 Effect of Die Entry Angle and Cross-section reduction on Equivalent Plastic Strain

2. Die Entry Angle and von-Mises Stress Distribution

As can be seen in the Fig.4.3, when the initial contact is established, stresses are induced in other regions of hollow that are still not in the deformation zone. Although the maximum stress at deformation doesn't vary but it can be clearly seen that in the drawing region, increase in the die entry angle results in an increase in the von-Mises stress (compare Fig. 4.3 a, Fig. 4.3 b, Fig. 4.3 c). The effect of variation of die entry angle and cross-section reduction on von Mises stress is shown in Fig. 4.4. As is seen in the contour diagram, increase in values of both the parameters lead to increase in von-Mises stress.

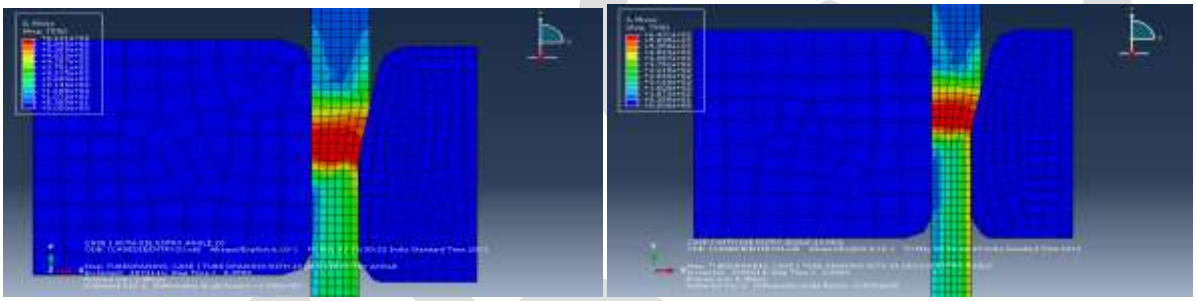

(a) von- Mises Stress Distribution for r=0.2, 2α=20^0, (b) von- Mises Stress Distribution for r=0.2, 2α=24^0

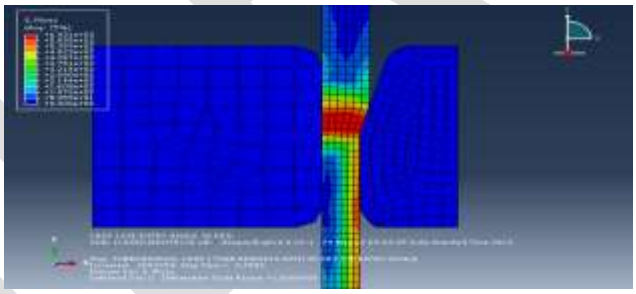

(c) von- Mises Stress Distribution for r=0.2, 2α=30^0

Fig. 4.3 Effect of Die Entry Angle on von-Mises Stresses

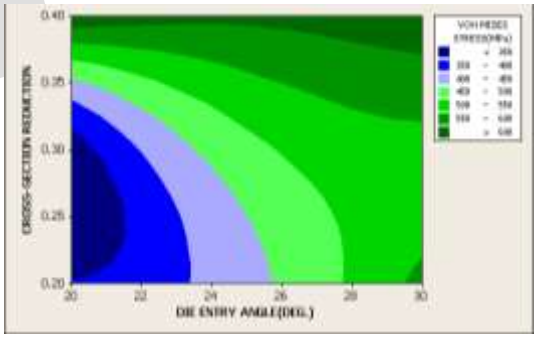

Fig. 4.4 Von-mises stress v/s Cross-section Reduction and Die Entry Angle

3. Cross-Section Reduction and Equivalent Plastic Strain Distribution

The cross-section reduction, naturally affects the strain component in any metal forming process significantly. When we see the diagrams (Fig. 4.5 a, Fig. 4.5 b, Fig. 4.5 c) for equivalent plastic strain with varying cross-section reduction it is evident that as the reduction in cross-section is increased the strain is also increased. For cross-section reduction 0.2, under steady state conditions at step time 0.45, P.E.E.Q. is 0.3238 which rises to 0.3753 and 0.5285 for cross section reductions 0.3 and 0.4 respectively.

4. Cross-Section Reduction and von-Mises Stress Distribution

Diagrams show that von-Mises stress increases with the increase in the area reduction (compare Fig. 4.6 a, Fig. 4.6 b, Fig. 4.6 c).This is primarily due to the increase in reaction forces as load required to carry out high reduction is greater which induces higher stresses in the material.

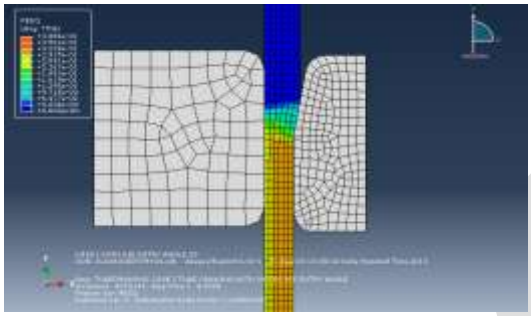

(a) P.E.E.Q. for r=0.2, $2\alpha=20^0$,

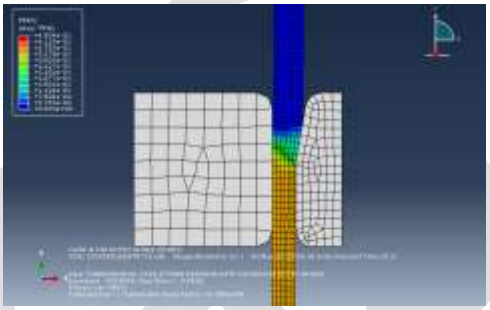

(b) P.E.E.Q. for r=0.3, $2\alpha=20^0$

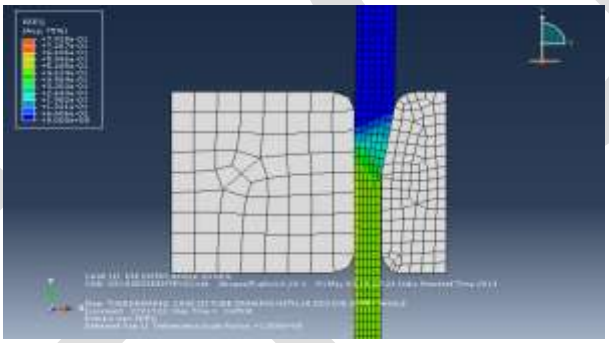

(c) P.E.E.Q. for r=0.4, $2\alpha=20^0$

Fig. 4.5 Effect of Cross-section Reduction on Equivalent Plastic Strain

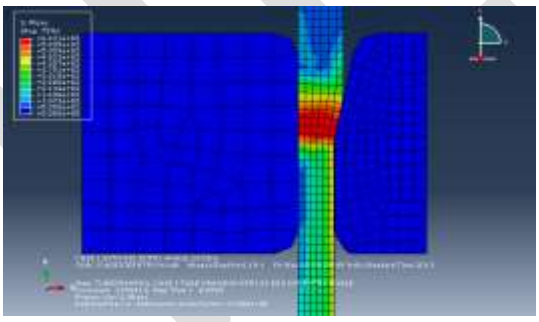

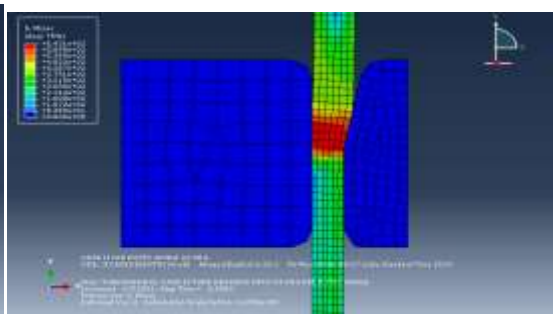

(a) von-Mises Stress Distribution for r=0.2, $2\alpha=24^0$, (b) von-Mises Stress Distribution for r=0.3, $2\alpha=24^0$

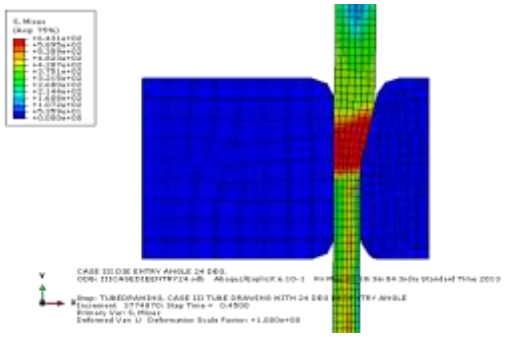

(c) von-Mises Stress Distribution for r=0.4, $2\alpha=24^0$

Fig. 4.6 Effect of Cross-section Reduction on von-Mises stress

CONCLUSION

The Finite element analysis of seamless tube cold drawing process is done using industrial data. Based on the results obtained through this effort following conclusions were drawn. Stress distribution patterns were observed in the parts of tube even before coming in contact with the die, it suggests that elastic deformation of the tube material starts well before it enters into the deformation zone.

- It was observed that cross-section reduction has significant effect on equivalent plastic strain, von-Mises stresses and axial stresses. They all increase with the increase in the cross-section reduction value. Cross-section reduction upto 0.3 maintains the flow stresses at lower side and hence most preferred zone of metal working.
- Die entry angle is a crucial parameter in the drawing process. It was found that beyond 24 degrees, the value of flow stresses follow the rising pattern with the increase in the die entry angle. Consequently, the load on drawing mechanism increases.
- It is also found that maximum equivalent plastic strain existed in subsurface region for smaller values of cross-section reduction and die entry angle. The plastic deformation is much more uniform at higher die entry angles and higher cross-section reduction.

REFERENCES:

[1] Kumar, Praveen, and Geeta Agnihotri. "Cold Drawing Process–A Review." metal forming 3.3 (2013).
[2] Groover, M. P. Fundamentals of Modern Manufacturing. John Wiley & Sons (2010).
[3] Neves, F. O, S. T. Button, C. Caminaga and F. C. Gentile Numerical and Experimental Analysis of Tube Drawing with Fixed Plug. J. of the Braz. Soc. of Mech. Sci. & Eng., Vol. XXVII, No. 4/426-431(2005)..

International Journal of Engineering Research and General Science Volume 3, Issue 5, September-October, 2015
ISSN 2091-2730

Inertial Pen Based Alphabet Recognition using KNN Classifier

Shaikh J.K.

D.Y.Patil College of Engineering, subhedarjj@gmail.com, gulshanashaikh@yahoo.com

Abstract— In today's electronics world human machine interface is important part. Pen with inbuilt inertial sensors devices capture human handwriting or drawing motions in real-time and use the sensor data for recognition. An inertial sensor based Inertial pen consist of an inertial sensor MPU 9150(accelerometer gyroscope and magnetometer), microcontroller, and a wireless transmission module, for sensing and collecting movement data for writing alphabet. The sensor data is received and processed for alphabets, recognition. The recognition algorithm composes of the steps of sensor data acquisition, signal pre-processing, feature generation, feature selection, and classification. KNN Classifiers for classification among 26 capital alphabets classes is built. The project aims at to validate the effectiveness of the inertial pen based motion data acquisition and recognition of class of test sample from among 26 classes. The recognition accuracy achieved is 82%. The recognition accuracy of 93 % is achieved for recognition of four gestures.

Keywords— inertial Pen, KNN classifiers, MPU9150, alphabet recognition, feature generation, Statistical features, Confusing classes.

INTRODUCTION

Touchscreen and keyboard are the most commonly used devices for alphanumeric entry. As the size of the electronics gadget is reducing, size of the keypad is also becoming small. Touchscreen entry of alphanumeric character is tedious as the size of the alphabet/number on the touchscreen is less than the tip of the finger, so requires very attentive and precise handling. Also text entry using keys which has size smaller than fingertip is time consuming and requires great attention for accuracy. So text entry by touchscreen or keyboard using for continuously reducing electronic gadget is tedious. As an effective alternative for text entry researchers have focused on inertial sensor based human machine text interface.

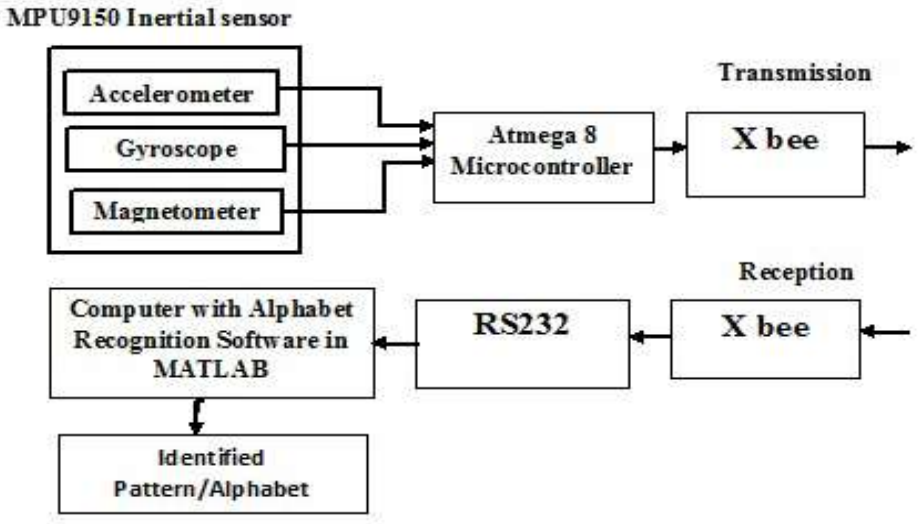

Figure 2: Block diagram of alphabet recognition system

RELATED WORK

More work is done for human machine interface using gestures. Machine is trained to recognize few gestures which are used to give command i.e. to control the machine. Accuracy obtained in gesture recognition (up to 7 gestures) is 99.99% by using one inertial sensor accelerometer and pattern recognition techniques.

Different types of input or sensing devices were used by researchers. Body-worn sensors, camera, combination of head mounted camera and accelerometers worn at the wrist [2], data glove [1], hand held pen like device equipped with inertial sensors. Different combinations of the inertial sensors were used. Single triaxial accelerometer [3], two dual-axis accelerometers mounted on pen [4], combination of accelerometer and gyroscope inbuilt with smartphone [5], accelerometer gyroscope and magnetometer [6]. Inertial sensor based input devices gives the convenience like writing with pen, as size of inertial sensor with processing is reduced to few tens of millimeter.

The motion data obtained from inertial signal is processed for recognition using pattern recognition or classifier technics. The most successful techniques for pattern recognition are dynamic time wrapping and trajectory recognition algorithm. For online digit recognition [7], digits written with accelerometer based pen are recognized using dynamic time wrapping algorithm. In this after pre-processing of the sensor signal the test signal sequence in time domain is directly compared with reliable training template of each class. Euclidean distance of each class template and test sequence was calculated, then the pattern with the minimum distance is selected as the class of test sequence. User dependent recognition rate obtained was 90.6% and user independent recognition obtained was 84%. Digit (0-9) and eight hand gesture recognition [3] using trajectory recognition algorithm gave good recognition rate of 98% and 98.75% respectively. Trajectory recognition algorithm consists of signal preprocessing, feature generation, feature selection (with KBCS (kernel-based class separability) and LDA (linear discriminate analysis)) and PNN classifier.

In majority of research work on character or gesture recognition classification among less number (maximum 10) of classes was carried out.

In this paper recognition of 26 capital letter is implemented using inertial pen with 9 degree of freedom and KNN classifier. The hand movement and hence the inertial sensor data for writing letters like 'D' and 'P' or 'C' and 'U' has a great similarity. So it is challenging to implement the character recognition for 26 alphabets which consists of many such confusing classes. Hence to improve recognition rate KNN classifier is used on large feature dimension vector (9X6=54).

Character Recognition System

In this project, we have designed an inertial signal acquisition device called inertial Pen." This inertial pen consists of a tri-axial accelerometer a tri-axial gyroscope, a tri-axial magnetometer and microcontroller. The microcontroller is connected to computer via RF transmitter.

The major components of the hardware implemented includes, the MPU-9150 as inertial sensor, ATmega8 a low-power CMOS 8-bit microcontroller and X-bee. In MPU9150 multiple sensors are integrated into one small package. It h combine an accelerometer/gyro with a Hall-sensor magnetometer and a Digital Motion Processor (DMP) hardware accelerator engine into one 4 mm x 4 mm package. It is the smallest 9-axis freedom sensor.

The MPU-9150 has three 16-bit analog-to-digital converters (ADCs) for digitizing the gyroscope outputs, three 16-bit ADCs for digitizing the accelerometer outputs and three 13-bit ADCs for digitizing the magnetometer outputs. The MPU-9150 communicates to the system processor i.e. ATmega8 microcontroller using an I^2C serial interface which operates at 400 kHz.

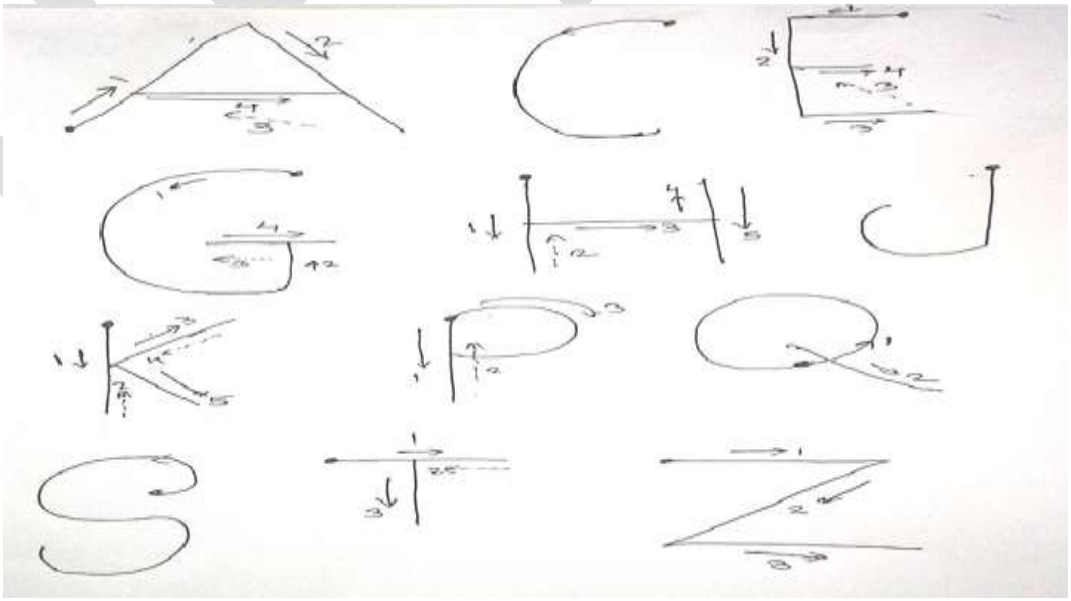

Figure 3: The trajectories of few alphabets

When the user draws some pattern on the paper or makes some gestures in 3-D space by using the Inertial pen, the inertial pen acquires the inertial signals produced. The accelerometer, gyroscope, and magnetometer are used to detect accelerations, angular velocities, and magnetic signals generated by hand movements. The microcontroller collects the digital accelerations, angular velocities, and magnetic signals, and transmits the inertial signals for further signal processing and analysis.
The trajectories of few alphabets is shown in the figure [2].

This transmitted data is nothing but the X, Y and Z directional acceleration, angular and positional data. Thus, there is a set of 9 values transmitted by the inertial pen hardware to the PC at every instant.

Flow of software development is as shown in fig [3]. A signal processing and software system built using MATLAB R2013a.
Software developed can be divided into following parts

1) Preparing database for both training and testing stages.
2) Training stage.
3) Testing stage both offline and real time.

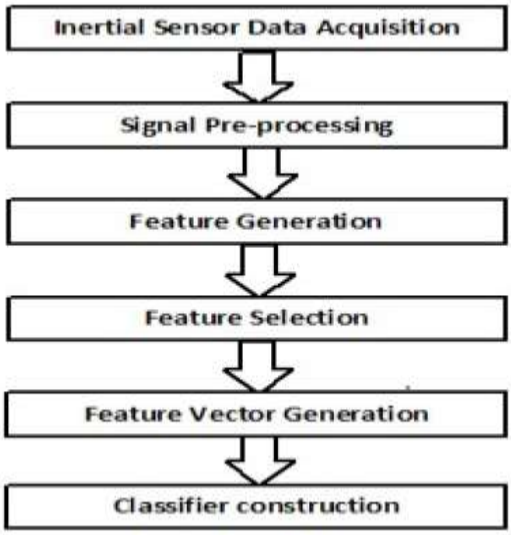

Figure 4: Flow of Software Development

Software development start with inertial signal acquisition for training stage, which is used to prepare database. The database of 26 Capital alphabet is prepared. Each letter is written 10 times so there are 10 samples of each alphabet. So 26X 10 =260 samples are obtained. The data from sensor is transmitted and received by using X bee .The data from serial port is read and saved in a text files. To prevent the movement data other than the movement of inertial pen for writing letter, the inertial pen is held in a constant reference position(vertical)for certain time say 5 seconds before starting to write the letter. A letter is written in fixed time frame of 25 sec. If letter is written in less than 25 sec again the pen is held in reference position for rest of the time within 25 sec. The next step is to generate the feature vector template of all classes. It includes reprocessing of signal and feature generation. The preprocessing of the signal is done to reduce the amount of data to be processed. It is done by filtering, and confining the data values within a range (normalization to remove an outlier i.e. An extreme value that differs greatly from other values.) . The processed and unprocessed inertial sensor signal is as shown in figure [4] .Then the following statistical features are extracted.

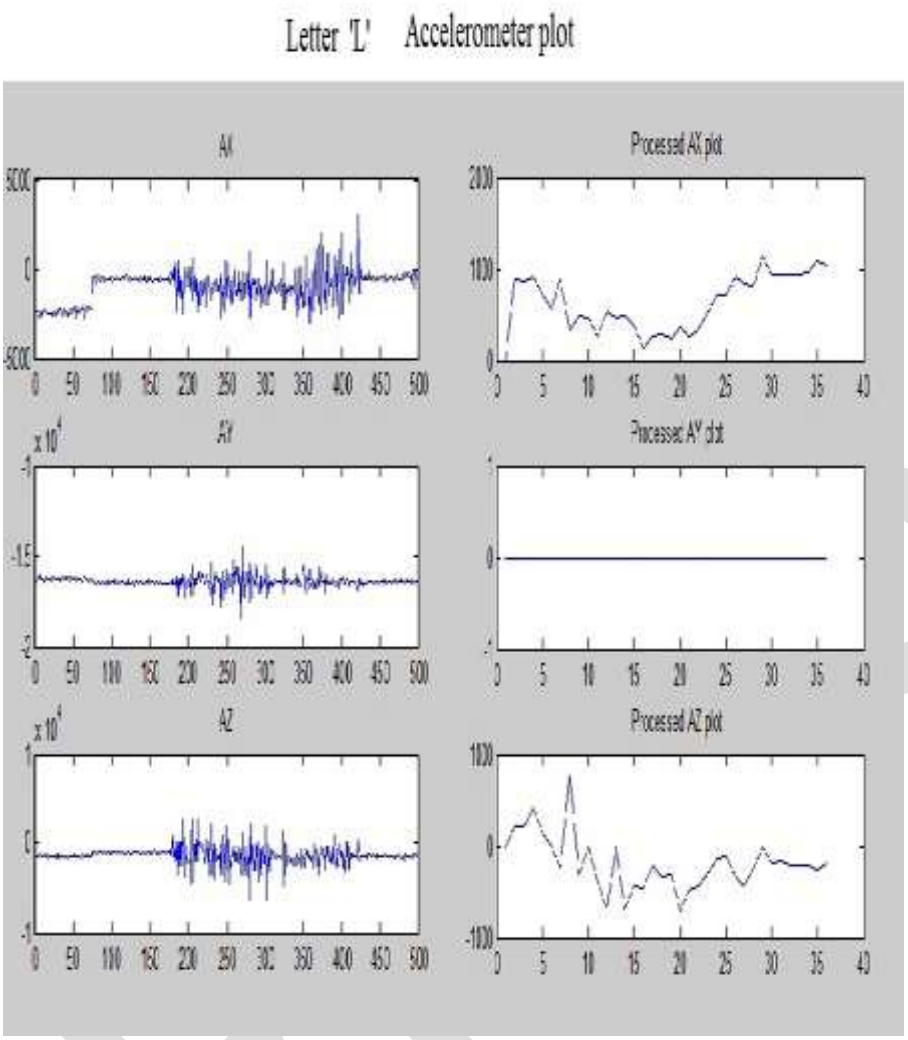

Figure 4: unprocessed and preprocessed accelerometer signal of letter 'L'

Statistical features describe the amount of variability or spread in a set of data. The most common measures of variability are the range, the interquartile range (IQR), variance, and standard deviation .The features generated are Mean, Variance, Mean absolute deviation, standard deviation, interquartile range, range, number of zero crossing and RMS. A feature vector containing the values of these features for each letter is formed and stored in a array as template classes.

During testing stage the processes of test signal acquisition pre-processing and feature vector generation is similar to training stage. The feature vector of test signal and feature vector array of all classes are passed to classifier function for recognition. Since the recognition is be achieved from among comparatively large number (26) of confusing classes KNN classifier is used.

The implemented system is tested using five sets of test sample, i.e. each letter is written five times. Each time the result is recorded. The results obtained are given in Table [1].

$$\text{Percentage Recognition} = \frac{R \times 100}{130}$$

$$R = 107$$

$$\text{Percentage Recognition} = \frac{107 \times 100}{130}$$

$$= 82\%$$

The same system when used for recognition of four gesture gave 93 % recognition rate.

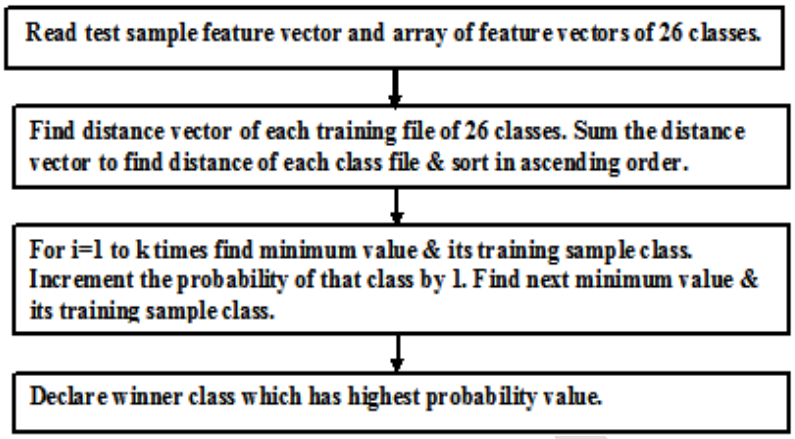

Figure 5: Implementation of KNN classifier

Table 15: Recognition table for 5 test samples

Alphabet	Test Sample 1	Test Sample 2	Test Sample 3	Test Sample 4	Test Sample 5	NO.Of Correct Recog-nition
A	√	√	√	E	F	3
B	U	X	√	√	√	3
C	U	U	√	√	√	3
D	√	√	√	√	√	5
E	√	D	√	√	√	4
F	√	√	√	√	G	4
G	√	√	√	√	√	5
H	√	√	√	√	√	5
I	√	√	√	√	√	5
J	√	√	√	√	√	5
K	√	√	√	√	√	5
L	√	√	J	J	√	3
M	√	√	J	J	√	3
N	√	√	√	H	√	4
O	√	√	√	√	√	5
P	√	D	√	D	√	3
Q	√	√	√	√	A	4
R	√	H	√	√	√	4
S	√	√	√	√	√	5
T	√	√	E	√	√	4
U	√	√	√	√	√	5
V	W	√	√	M	√	3
W	H	√	√	√	√	4
X	√	√	B	√	√	4
Y	√	P	√	√	√	4
Z	√	√	√	√	√	5
Total no of correct recognition out of 130(26×5)						107

Conclusion:

I implemented inertial pen which consists of sensor MPU 9150 to collect motion data while writing alphabets. The sensor is selected as it consists of accelerometer, gyroscope and magnetometer and is of very small in size. Alphabet recognition is very challenging as there is great similarity between various characters, contains angular movements, straight line movement and also number of characters to be recognized are also large(classification in 26 classes). After signal preprocessing 8 statistical features are extracted. Alphabet recognition is accomplished in two stages, First is training stage and second is testing stage. Each of 26 alphabet is written 10 times i.e.it gives 10 samples for each letter. Out of 10 samples for of each alphabet 5 samples are used as training samples. Remaining 10 samples are used for testing. During training stage, feature vector is generated for each of 5 training samples of 26 alphabets is generated. Recognition accuracy is calculated for two classifiers, Simple PNN classifiers and KNN classifiers. KNN classifier gave better recognition accuracy (82%) for 26 characters. Recognition accuracy highly depends upon,

1. Consistency in writing style and speed
2. No of training samples.

REFERENCES:

[1] Christoph Amma, Dirk Gehrig, Tania Schultz. Airwriting Recognition using Wearable Motion Sensors. ACM 978-1-60558-825-4/10/04, Augmented Human Conference April 2-3, 2010, Megève, France.

[2] H. Brashear, T. Starner, P. Lukowicz, and H. Junker.Using multiple sensors for mobile sign language recognition. *Seventh IEEE* International Symposium on Wearable Computers, 2003. Proceedings. Pages 45–52, 2003.

[3] Jeen-Shing Wang, and Fang-Chen Chuang. An Accelerometer-Based Digital Pen with a Trajectory Recognition Algorithm For Handwritten Digit and Gesture Recognition. IEEE Transactions on Industrial Electronics, Vol. 59, No. 7, July 2012.

[4] B. Milner, "Probabilistic neural networks," in Proc. Inst. Elect. Eng.—Colloq. Doc. Image Process. Multimedia, 1999, pp. 5/1–5/6.

[5] Thomas Deselaers, Daniel Keysers, Jan Hosang, and Henry A. Rowley. GyroPen: Gyroscopes for Pen-Input with Mobile Phones. IEEE Transactions on Human-Machine Systems.

[6] Yu-Liang Hsu, Cheng-Ling Chu, Yi-Ju Tsai, and Jeen-Shing Wang, An Inertial Pen with Dynamic Time Warping Recognizer for Handwriting and Gesture Recognition. IEEE Sensors Journal 2014.

[7] Jeen-Shing Wang, Yu-Liang Hsu, Cheng-Ling Chu. Online Handwriting Recognition Using an Accelerometer-Based Pen Device. 2nd International Conference on Advances in Computer Science and Engineering (CSE 2013).

[8] Ruize Xu, Shengli Zhou, and Wen J. Li. MEMS Accelerometer Based Nonspecific-User Hand Gesture Recognition. IEEE Sensors Journal, Vol. 12, No. 5, May 2012.

[9] J. S. Wang, Y. L. Hsu, and J. N. Liu, "An inertial measurement- unit-based pen with a trajectory reconstruction algorithm and its applications". IEEE Trans. Industrial Electronics, vol. 57, no. 10, pp. 3508-3521, 2010.

[10] Ramzi A., Zahary A, "Online Arabic handwritten character recognition using online-o_ine feature extraction and Back-propagation neural network. Publication Year: 2014, Page(s): 350 - 355, IEEE Conference Publications.

[11] Davide Figo Pedro C. Diniz Diogo R. Ferreira Joao M. P. Cardoso, "Preprocessing Techniques for Context Recog-nition from Accelerometer Data", Personal and Ubiquitous Computing, vol.14, no.7, pp.645662, 2010.

[12] Jong K. Oh, Sung-Jung Cho, Won-Chul Bang, Wook Chang, Eunseok Choi, Jing Yang, Joonkee Cho, Dong Yoon Kim , "Inertial Sensor Based Recognition of 3-D Character Gestures with an Ensemble of Classi_ers, Proceedings of the 9th Intl Workshop on Frontiers in Handwriting Recognition (IWFHR-9 2004) 0-7695-2187-8/04 2004 IEEE

International Journal of Engineering Research and General Science Volume 3, Issue 5, September-October, 2015
ISSN 2091-2730

Nanoparticles concentration and environmental effects on cogeneration system in cement industry

Ali Amer A. Hadi

Department of Materials Engineering. Faculty of Engineering

University of Kufa, 21- Kufa-Najaf, Iraq

Abstract- Cement production considers one of the most intensiveenergy consumingand largest carbon emitting industrial sectorsaccording to very high temperature required to produce cement clinker. This paperhighlights the importance of the waste heat recovery in the clinker cooler of cement industry via indirect approach to reheat the working fluid of cogeneration cycle. Diverse base fluids with Al_2O_3nanoparticlesas a working fluid were used in a closed recoverycycle.The effect of inlet working fluid temperatureand volume fraction of nanoparticles on the energy saving, emission reductions and cost saving werestudied.It was found that the utilization of Al_2O_3-engine oil as a working fluid for a closed recovery cycle gave the best indication as a comparison with Al_2O_3-water and Al_2O_3-ethylene glycol. As well as, it was found that the energy saving, emissions reduction and cost saving increase as a result of increasing in nanoparticles concentration and inlet working fluid temperature.

Keywords: Energy saving; Al_2O_3 nanoparticles; cogeneration system; cement industry.

Nomenclature	
Cp	Specific heat at constant pressure, kJ/kg K
CS	Cost savings, USD/yr
E	Energy, kJ
EC	Energy cost, USD
EF	Emission factor, tCO_2/MWh
ER	Emission reduction, tCO_2/year
ES	Energy saving kW
FP	Feed pump
G	Generator
$\dot{m}$	Mass flow rate, kg/s
Q	Heat transfer. KJ
ST	Steam turbine
T	Temperature. K
$\dot{V}$	Volume flow rate, m^3/s
WHRSG	Waste heat recovery steam generator
Greek symbols	
φ	Volume fraction
Subscripts	
ca	Cooling air

cc	Cooled clinker
ch	Hot clinker
conv.	Heat losses due to convection
ha	Hot air (Exhaust)
in	Input
nf	Nanofluid
rad.	Heat losses due to radiation
s	Solid particles
sa	Secondary air
ta	Tertiary air
out	Output

1. Introduction

Energy conservation has come to the forefront as a key priority for the well-being of the global economy and is expected to remain so in the foreseeable future. The most effectual approach to reduce the demand of energy is to use energy more competently [1].The current global energy consumption is between 4 and 5 GJ per tonne of cement. The industry has turned to progressively developing technologies for efficient energy use to improve its profitability and competitiveness [2].A considerable number of studies have focused on energy use and analysis in the cement industry. Madlool*et al*. [3] reported that the cement industry consumed about 12% and 15% of total energy in Malaysia and Iran respectively. Doheim*et al*. [4] examined the consumption of thermal energy, losses and the potential of heat saving. Engin*et al*. [5] focused on the energy audit of rotary kiln system and discussed the probable approaches of heat recovery from some major sources of heat loss. Kabir*et al*. [6] evaluated the consumption of thermal energy for the dry process.Khurana*et al*. [7] presented thermodynamic analysis and cogeneration for a cement plant. Rasul*et al*. [2] evaluated the thermal performance and investigated the opportunities of energy conservation in Indonesia.

In the grate cooler, almost 70 % of the clinker released heat can be recovered through its recirculation as secondary air to the kiln. While the tertiary air and vent air at 300^{o}C and 275^{o}C, respectively, are filtered in the hot electrostatic precipitators (ESP) in addition to releasing both of them to the atmosphere without being used [8]. From the pre-heater and grate cooler exit gases, approximately 40% of the total heat input is expelled as waste heat. The heat lost from grate cooler exit gases is about 334.72 to 543.92 kJ/ kg clinker at a temperature range of 200 to 300^{o}C. These waste heats can be used in diverse applications such as to dry raw materials and preheat the air required for the coal combustion and cogeneration [9].Madlool*et al.* [10] investigated the waste heat recovery in cement industry g a by studying case study in addition to estimate the energy saving.

Saneipoor*et al*. [11] examined the performance of a new Marnoch Heat Engine (MHE) which was used to recover the waste heat from a typical cement plant. Sogut*et al*. [12] studied the heat recovery from rotary kiln for a cement plant in Turkey. Caputo *et al*. [13] evolved a mathematical model for heat exchange sizing and estimation of performance to recover the waste heat from the

external surfaces of rotating kilns. Wang *et al*. [14] examined the performances of cogeneration power plants using four kinds of cycles for a cement plant.

The most effective ways to increase the energy efficiency and reduce CO_2 emissions are a consequence of improving the cement production process. However, the consumption of energy and the emissions of CO_2 can also be reduced by improving the operation of available cement plants. The training of the plant operator plays an essential role in this respect [11, 15].

The majority of the studies about waste heat recovery are limited to the rejected gases from pre-heating and clinker cooling systems. There is a need forintensive research to reduce the losses caused byradiationand convectionin the clinker cooler. Recovering these losses can contribute to increasing the efficiency of the clinker cooler.

However, far too little attention has been paid to the losses due to radiation and convection in the grate cooler. This paper attempts to show that the waste heat lost through radiation and convection in the grate cooler can be recovered via an indirect approach. In this work, different working fluids were used in another cycle to recover waste heat and then to heat the working fluid of the cogeneration cycle. The comparison was carried out at different volume fraction of nanoparticles and inlet temperature of working fluid of closed recovery cycle for the same conditions of waste heat.

2. Energy analysis of a grate cooler

The conventional industrial process energy analysis is based on the first law of thermodynamics. This analysis involves a simple energy accounting, by quantifying the input and output energy to and from the clinker cooler. Fig. 1 shows the input energy which consists of energy of hot clinker and energy of cooled air, whereas, the output energy represents the energies of cool clinker, secondary air, tertiary air and hot air.

In order to thermodynamically analyze the cooler system, the following assumptions were made to simplify the analysis:

- Steady state working conditions.
- Leakage of cold air into the system is negligible.
- Clinker compositions do not change.
- Changes of kinetic and potential energy for input and output materials are negligible.
- Grate work in addition to energy losses which take place in the connections of pipeline among units are ignored.
- Assuming all gas streams are ideal gases.

For a general steady state, the equation of mass balance is applied as shown belowin the rate form [17]. The following balance equations are also applied [18]:

$$\sum \dot{m}_{in} = \sum \dot{m}_{out} \quad (1)$$

The energy balance in general form:

$$\sum \dot{E}_{in} = \sum \dot{E}_{out} \quad (2)$$

Heat input into the clinker cooler:

$$\dot{Q}_{in} = \dot{Q}_{ch} + \dot{Q}_{ca} \quad (3)$$

Heat output from the clinker cooler:

$$\dot{Q}_{out} = \dot{Q}_{sa} + \dot{Q}_{ta} + \dot{Q}_{cc} + \dot{Q}_{ha} \quad (4)$$

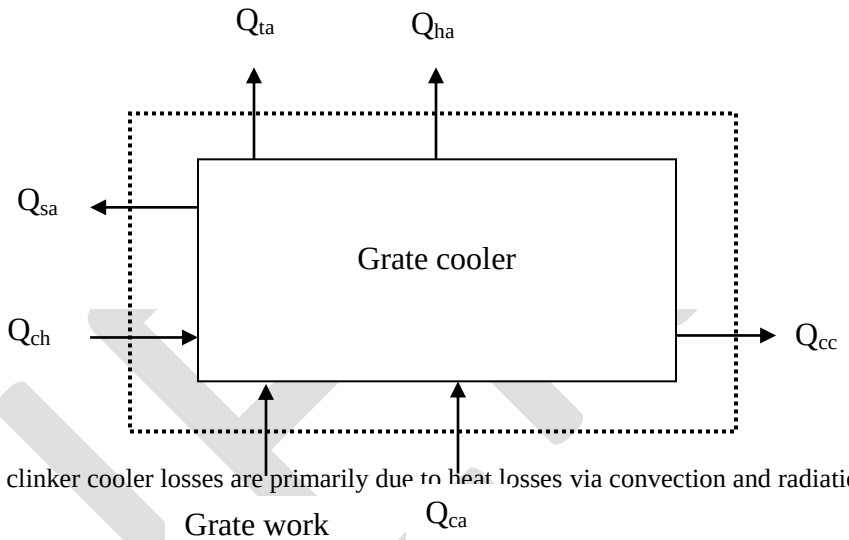

The unaccountable clinker cooler losses are primarily due to heat losses via convection and radiation heat transfers.

3. Nanofluid as a working fluid for a closed recovery cycle

Over thepast few decades, many attempts by scientists and engineers have been made to develop fluids which can offer better performance of cooling or heating for a variety of thermal systems, compared to fluids of conventional heat transfer. Nanofluidswere engineered by dispersing solid particles of nanometer-size in fluids of conventional heat transfer such as water, engine oil and ethylene glycol. The enhancement of the fluids heat transfer capability with suspended nanoparticles makes fluid use in convection loops and thermosyphons an interesting option, leading to better performance of the system and resulting in improvement of energy efficiency [19].

The heat exchanger is a general apparatus for process heating in the industry. It is used to transfer thermal energy between two or more media at different levels of heat capacity. It is widely applied to power engineering, chemical industries, petroleum refineries,

food industries etc[20].Mapa and Sana [21] demonstrated heat transfer using nanofluids in a mini heat exchanger. Vijjha and Das [22] presented measurements of specific heat for three nanofluids containing particles of zinc oxide, aluminum oxide, and silicon dioxide.

The process ofnanofluid production may be accomplished in either a one-step or two-step method. Both methods are sophisticated andrequireadvanced equipment.In fact,the high cost ofnanofluidsis an obstacle toits utilizationin the industry. While the physical analysis does not entail losses in the closed cycle, they are bound to be present in a real setting. The quantity of nanofluids used in this work was chosen to suffice the needs of a closed recovery cycle for a year.

4. 1 Equation of specific heat and density for nanofluids.

According to the dispersion of solid particles in a liquid, the specific heat and density equations for the two-phase mixture are a function of the particle concentration [23].

$$Cp_{nf} = (1-\varphi)Cp_{bf} + \varphi Cp_s \quad (5)$$

$$\rho_{nf} = (1-\varphi)\rho_{bf} + \varphi\rho_s \quad (6)$$

Table 1 presents the thermophysical properties of differenttypes of working fluids which were used in a closed cycle to recover the heat losses.

Table 1.Specific heat of base fluid and nanoparticles of closed recovery cycle.

Working fluid	Specific heat, Cp (J/kg.K)	Density, ρ (kg/m^3)	Refrence
Water	4190	1000	[24]
Engine oil	1910	884	
Ethylene glycol	2415	1114	[25]
Al_2O_3	775	3970	

5. Utilizing radiation and convection losses to heat the working fluid of cogeneration cycle indirectly

The unaccounted loss is a fairly high value of 324.21 kJ/kg clinker, mostly caused due to the convection and radiation losses from the uninsulated cooler [2]. The constraints of the cement quality and the corresponding effects on secondary and tertiary air impede the recovery of these losses. After the author's personal consultation with experts in the industry, it was discovered that the

abovementioned constraints can be overcome by passing a nanofluid inside the pipe which traverses compartments 3 to 8 of a grate cooler as shown in Fig. 2. This pipe will act as a heat exchanger with a grate cooler and absorb a portion of the heat losses. If 50% of the heat loss is attributed to radiation and convection heat losses and half of this proportion may be recovered, the temperature of thenanofluid will increase by 80% with the pipe technique.

The heat exchange capacity of the pipe withnanofluids that functions as a heat exchangeris based on the measured temperatures of the inlet and outlet, the mass flow rate and the specific heat of nanofluid and can be expressed as follows [26]:

$$Q_{rad.+conv.} = \dot{m}_{nf}\, Cp_{nf} (T_{out_{nf}} - T_{in_{nf}}) \quad (7)$$

The working fluid is directed to the heat exchanger to exchange heat with water, which enters the cogeneration cycle as shown in Fig. 2.

The source of waste heat in the cement plant comprises of the exhaust gases from suspension pre-heater (SP) and the discharge hot air from the clinker cooler. For cogeneration power plant, these two sources which have different temperature levels may be used either separately or in combination. The hot air temperature from the cooler discharge is 220^{o}C and the temperature of exhaust gases from the suspension pre-heater is 325^{o}C. These waste heats can generate steam if directed to WHRSG. The steam generated would be used to power a steam turbine driven electric generator.

The sensible and latent heat of exhaust gases and hot air that are recovered substitute the purchased energy in a cement production plant and thus make it more efficient.The energy saving with respect to the net output power which is generated by the steam turbine can be estimated according to the following equation:

ES = Net output power × Working hours (8)

As a result, a reduction in emissions from the fuels used by the cogeneration power plant is made possible.

The emission reductionthat brings about energy savings can be expressed by the following equation [28]:

$$ER = ES \times EF \quad (9)$$

where EF is the *electricity emission factor*, which for Iraq can be taken as 0.744 tCO2/MWh[27].

With reduced energy consumption comes reduced cost. The average of the unit price of electricity is 0.07 USD/kWh [5]. The predictable cost savings can be estimated as follows:

$$CS = ES \times EC \quad (10)$$

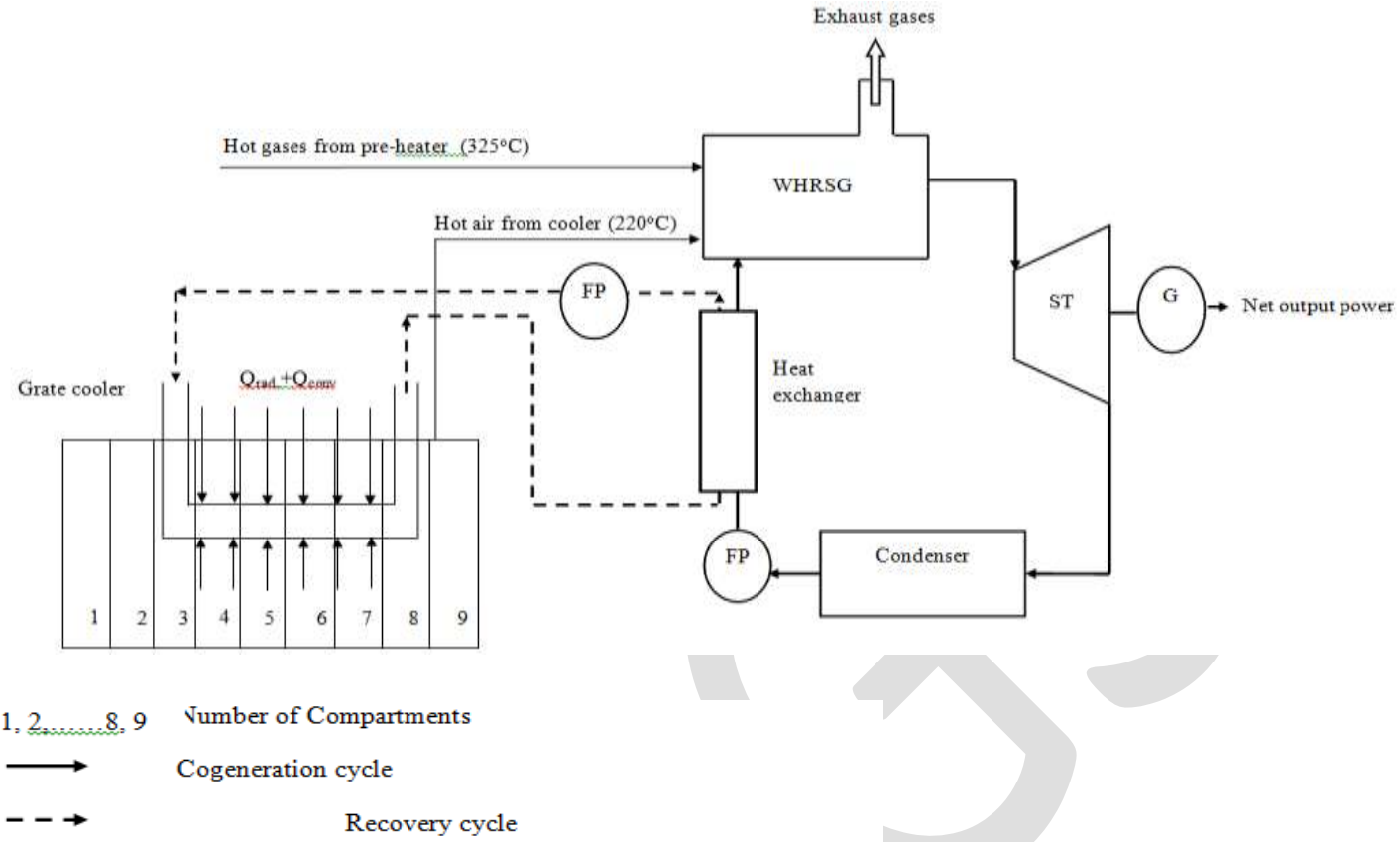

Fig. 2.Schematic of cogeneration cycle with recovery cycle.

6. Results and discussion

6.1 Energy savings

For a closed recovery cycle, the heat capacity of nanofluids should be minimized to get maximum heat transfer. A maximum possible temperature difference of nanofluids is needed to increase the temperature of the working fluid for the cogeneration cycle. Al_2O_3-engine oil has the smallest heat capacity among nanofluids, which enables maximum heat transfer and thus increases themean temperature of heat addition in the cogeneration cycle. Consequently, a high net output power is obtained which contributes significantly to energy savings.Increasing nanoparticles concentration will lead to increase the rate of heat exchange between the nanofluid of closed recovery cycle and the working fluid of steam generation cycle. And this will be affected in more energy saving as shown in Fig. 3.

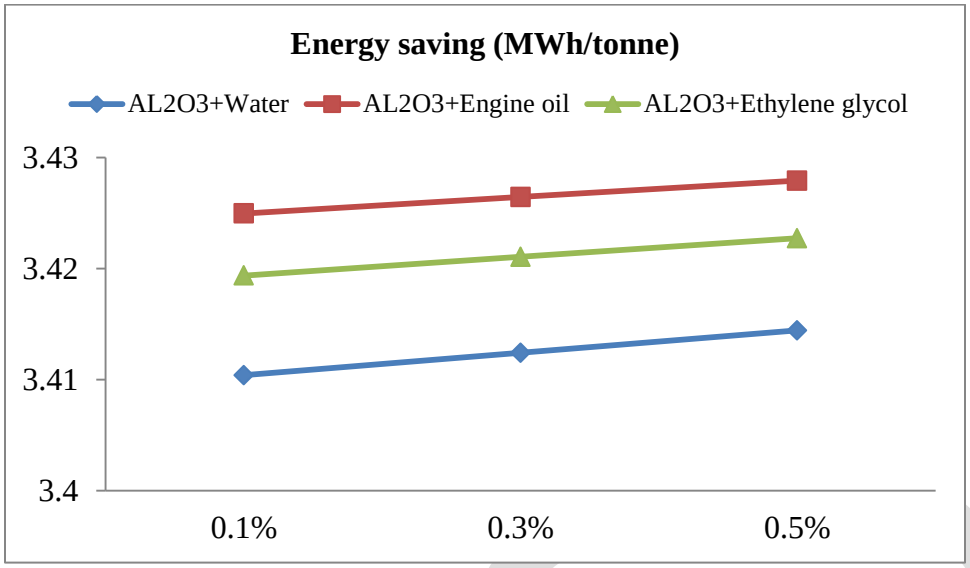

Fig. 3. Effect of nanoparticlesconcentration in closed recovery cycle on the energy saving.

Increase of inlet temperature of working fluid of closed recovery cycle increases the maximum heat transfer and leads to high outlet temperature of the nanofluid in a closed recovery cycle. Al_2O_3-engine oil as a working fluid in the closed recovery cycle causes the highest energy saving due to its low heat capacity. Fig. 4 shows the effect of inlet temperature on energy savings. On the other hand, Al_2O_3-water has the highest heat capacity and therefore the lowest improvement in energy savings, which increase with rising inlet temperature.

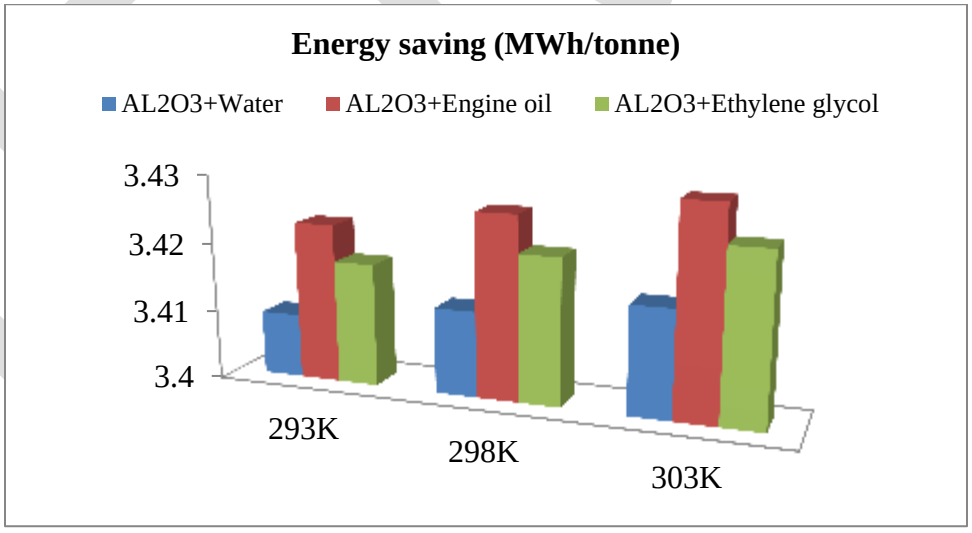

Fig. 4. Effect of inlet nanofluids temperatures in closed recovery cycle on the energy saving.

6.2 Emission reductions

The emissions reduction is estimated by using eq. (9). The emissions reduction increases in direct proportion to the energy savings.In Fig. 5, Al_2O_3-engine oil as a working fluid caused

the highest emission reductions of CO_2 as a result of highest energy saving when it was utilized in a closed recovery cycle.

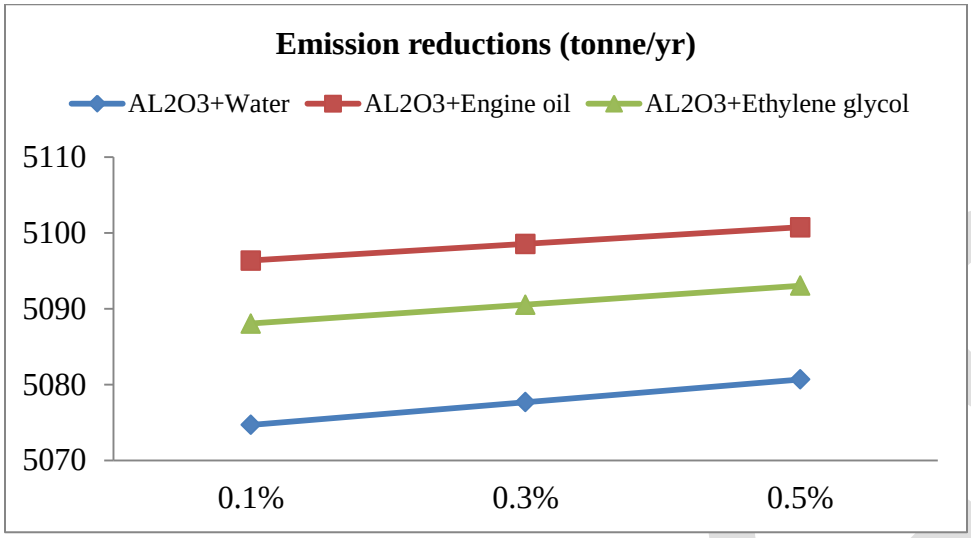

Fig. 5. Effect of different volume fraction of nanofluids in closed recovery cycle on emissions reduction.

As shown in Fig. 6, an increase of inlet temperature of the nanofluid increases the emissions reduction. Increasing of emissions reduction behaves the same with respect to energy savings as the increase of inlet temperature of nanofluids in a closed recovery cycle. Al_2O_3-engine oilin a closed recovery cycle causes the highest emissions reduction of $CO_2$and emissions reduction increases with increase of inlet temperature.

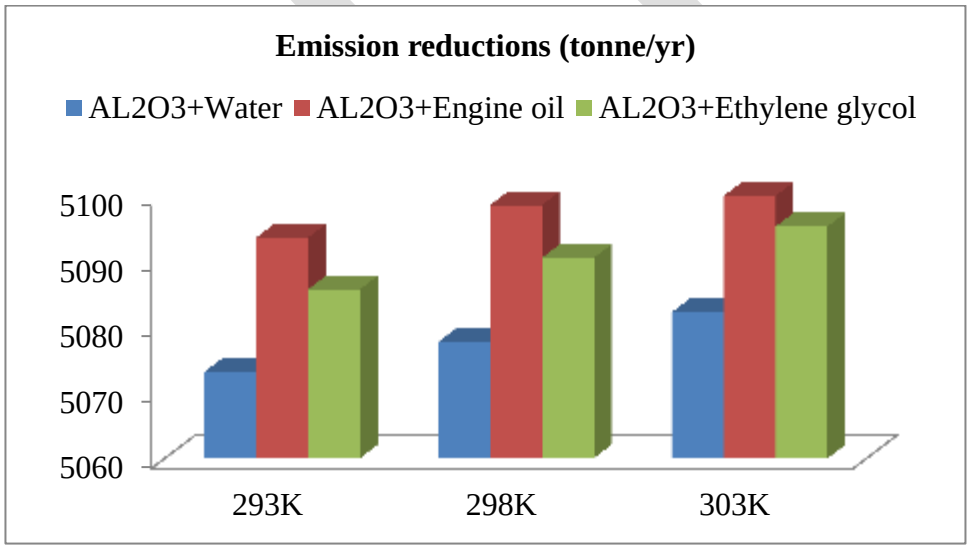

Fig. 6. Inlet temperature effect of nanfluids in closed recovery cycle on the emissions reduction.

6.3 Cost saving

Eq. (10) can be used to estimate the cost saving. Fig. 7 presented the cost saving by using the nanofluid in a closed recovery cycle. It was noticed that use of Al_2O_3-water leads to the lowest cost saving, due the low heat capacity allowing only low energy saving. As noticed in eq.(10), the cost saving can be determined according to the amount of energy saving and the energy cost.

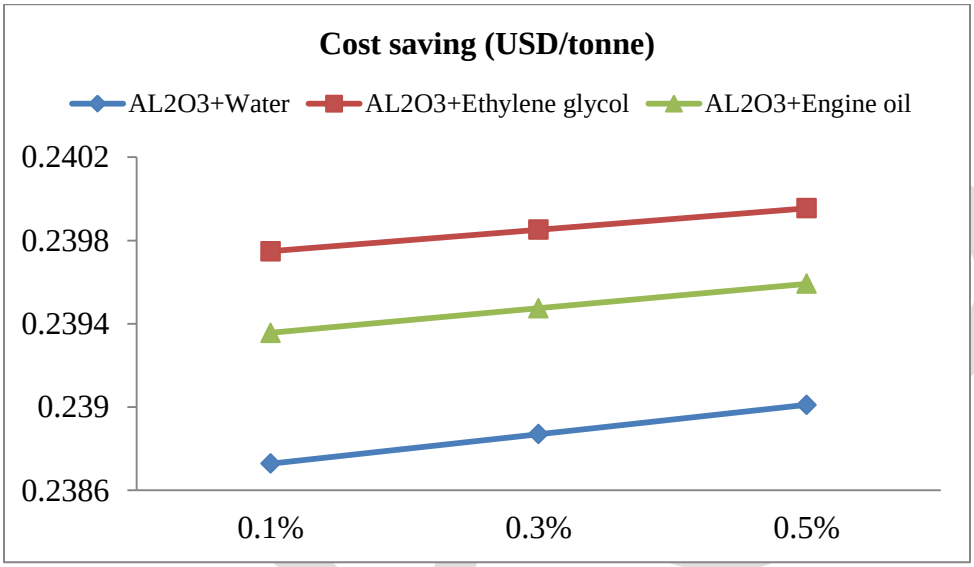

Fig. 7 Influence of nanofluids concentration in closed recovery cycle on the cost saving.

Fig. 8 shows the effect of changing the inlet temperature of nanofluid on the cost saving as a result of using cogeneration system in conjunctionwith closed recovery cycle. It was found that the increase of inlet temperature for Al_2O_3-engine oil provides the highest value of cost saving. The highest cost saving follows the highest energy saving. It increases with increase of inlet temperature of nanofluids in a closed recovery cycle.

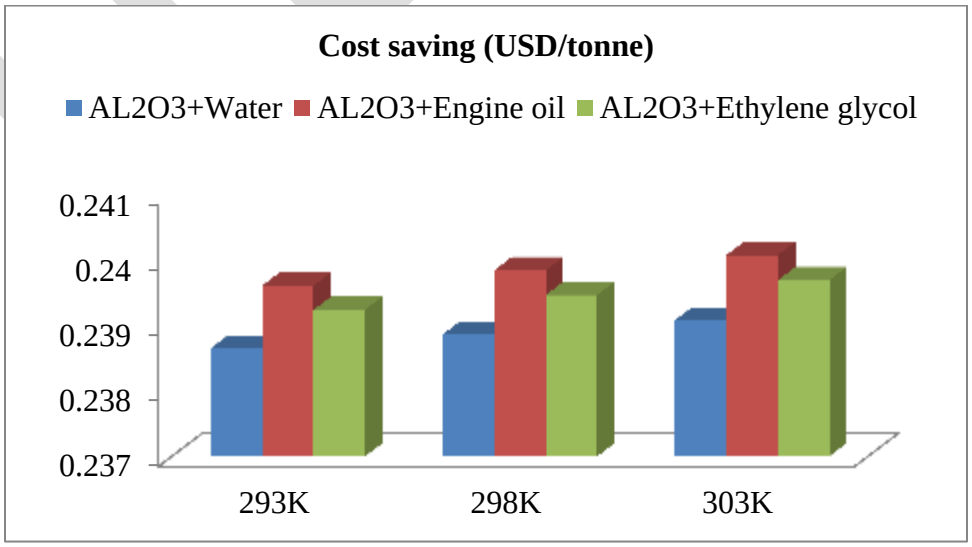

Fig. 8. Cost saving improvement as a result of different inlet temperature of nanfluids in closed recovery cycle.

7. Conclusions

The following conclusions are drawn from this work:

1. Low specific heat capacity produces high heat transfer between working fluids.
2. Al_2O_3-engine oil gives the highest values of energy saving, cost saving and emissions reduction compared to Al_2O_3-ethylene glycol and Al_2O_3-water.
3. Al_2O_3-water is the lowest in efficiency among the tested nanofluids.
4. Increase of working fluid inlet temperature and volume fraction of nanofluids in a closed recovery cycle causes an increase in energy saving, cost saving and emissions reduction for each type of nanofluid.

Acknowledgement

The author would like to acknowledge the financial support from the University of Kufa.

REFERENCES:

1. Saidur, R., Hasanuzzaman, M., Sattar, M.A., Masjuki, H.H., IrfanAnjum, M. and Mohiuddin, A.K.M. (2007) An analysis of energy use, energy intensity and emissions at the industrial sector of Malaysia. *International Journal of Mechanical and Materials Engineering*, 2: 84 - 92.
2. Rasul, M.G., Widianto, W. and Mohanty, B. (2005) Assessment of the thermal performance and energy conservation opportunities of a cement industry in Indonesia. *Applied Thermal Engineering*, 25**:** 2950–2965.
3. Madlool, N.A., Saidur, R., Hossain, M.S. and Rahim,N.A.(2011) A critical review on energy use and savings in the cement industries.*Renewable and Sustainable Energy Reviews*, 15: 2042–2060.
4. Doheim, M.A., Sayed, S.A. andHamed, O.A. (1987) Analysis of waste heat and its recovery in a cement industry. *Heat Recovery Systems and CHP*, 7**:** 441-444.
5. Engin, T. and Ari, V. (2005) Energy auditing and recovery for dry type cement rotary kiln systems: A case study. *Energy Conv. Manage*., 46**:** 551-562.
6. Kabir, G., Abubakara, AL. and EL-Nafatya, U.A. (2010) Energy audit and conservation opportunities for pyroprocessing unit of a typical dry process cement plant. *Energy*, 35: 1273-1243.
7. Khurana, S., Banerjee, R. and Gaitonde,U. (2002) Energy balance and cogeneration for cement plant.*Applied Thermal Engineering*, 22: 485-494.
8. Citrin, D. ORMAT® Energy Converters Proven Power from Cement Plant Waste Heat.Available at: http://www.ormat.com/research/papers/test.

9. Cogeneration of Power Utilising Waste Heat in Cement Manufacture: Technological Perspectives. Available at: http://www.energymanagertraining.com/Journal/24032006/CogenerationofPowerUtilisingWasteHeatinCementManufacture.pdf.

10. N.A. Madlool, R. Saidur, N.A. Rahim. (2012) Investigation of waste heat recovery in cement industry: A case study. IACSIT International Journal of Engineering and Technology,4: 665-667.

11. Saneipoor, P., Naterer, G.F. andDincer, I. (2011) Heat recovery from a cement plant with a Marnoch Heat Engine. *Applied Thermal Engineering*, 31**:**1734-1743.

12. Sogut, Z., Oktay, Z. andKarakoç, H. (2010) Mathematical modeling of heat recovery from a rotary kiln. *Applied Thermal Engineering*, 30**:**817-825.

13. Antonio C. Caputo, Pacifico M. Pelagagge and Paolo Salini (2011) Performance modeling of radiant heat recovery exchangers for rotary kilns. *Applied Thermal Engineering*, 31**:**2578-2589.

14. Jiangfeng Wang, yipingdai and Lin Gao. (2009) Exergy analyses and parametric optimizations for different cogeneration power plants in cement industry. *Applied Energy*, 86: 941–948.

15. Akimasa, Y., Katsushi, T., Tadashi, M. and Makoto, Y. (2001). Cement process modeling using process simulator. *Cement manufacturing technology*, 39–44.

16. UNEP. Thermal Energy Equipment: Waste Heat Recovery. Available at: http://www.google.com.my/url?sa=t&rct=j&q=waste%20heat%20is%20heat%20generated%20in%20a%20process%20by%20way%20of%20fuel%20combustion%20or%20chemical%20reaction%2C&source=web&cd=1&sqi=2&ved=0CCIQFjAA&url=http%3A%2F%2Fwww.retscreen.net%2Ffichier.php%2F937%2FChapter-Waste%2520Heat%2520Recovery.pdf&ei=obZVT9THJNGIrAf_-JChBw&usg=AFQjCNHUAlL7Xn9CYJgETobvFml7HQq8wA.

17. Sogut, M. Z., Oktay, Z. andHepbasli, A. (2009) Energetic and exergetic assessment of a trass mill process in a cement plant *energy Conv. Manage.*, 50**:** 2316-2323.

18. Bejan, A. (1988) Advanced engineering thermodynamics. New York: Wiley.

19. Shijo Thomas and ChoondalBalakrishnaPanickerSobhan (2011) A review of experimental investigations on thermal phenomena in nanofluids. *Nanoscale Research Letters*, 6:377.

20. Hasanuzzaman, M., Saidur, R. and Rahim, N.A. (2011) effectiveness enchancement of heat exchanger by using nanofluids. IEEE First Conference on Clean Energy and Technology CET.

21. Mapa, L.B. and Sana Mazhar (2005) Heat transfer in mini heat exchanger using nanofluids. American Society for Engineering Education – Northern Illinois University, DeKalb, Illinois.2005 IL/IN Sectional Conference.

22. Ravikanth S. Vajjha and Debendra K. Das, (2008) Measurements of Specific Heat and Density ofAI2O3 Nanofluid.Proceedings of the International Workshop on Mesoscopic, Nanoscopic and Macroscopic Materials. Available at: http://proceedings.aip.org/resource/2/apcpcs/1063/1/361_1?isAuthorized=no.

23. Pak, B.C. and Cho, Y.I. (1998) Hydrodynamic and heat transfer study of dispersed fluids with submicron metallic oxide particles. *Experimental Heat Transfer*, 11: 151-170.

24. Bai, M., Xu, Z. and Lv, I. (2008) Application of Nanofluids in Engine Cooling System. *SAE International*. Available at: http://papers.sae.org/2008-01-1821.

25. SohelMurshed, S.M. (2012) Simultaneous Measurement of Thermal Conductivity, Thermal Diffusivity, and Specific Heat of Nanofluids. *Heat Transfer Engineering*, 33:722–731.

26. MasoudHaghshenasFard , Mohammad Reza Talaieb and Somaye Nasr (2011) Numerical and experimental investigation of heat transfer of Zno/water nanofluid in the concentric tube and plate heat exchangers.*Thermal science*, 15: 183-194.

27. WISIONS. Sustainable Energy Project Support (SEPS). Available at: http://www.wisions.net/files/downloads/Baseline_Calculation_2011.pdf.

28. Galitsky, C., Worrell, E. (2008) Energy Efficiency Improvement and Cost Saving Opportunities for the Vehicle Assembly Industry, LBNL-50939-Revision.

International Journal of Engineering Research and General Science Volume 3, Issue 5, September-October, 2015
ISSN 2091-2730

Dynamics and Tyreus-Luyben Tuned Control of a Fatty Acid Methyl Ester Reactive Distillation Process

Abdulwahab GIWA[1], Saidat Olanipekun GIWA[2]

[1]Chemical and Petroleum Engineering Department, College of Engineering, Afe Babalola University, KM. 8.5, Afe Babalola Way, 360231, Ado-Ekiti, Ekiti State, Nigeria

[2]Chemical Engineering Department, Faculty of Engineering and Engineering Technology, Abubakar Tafawa Balewa University, Tafawa Balewa Way, 740004, Bauchi, Bauchi State, Nigeria

Emails: [1]agiwa@abuad.edu.ng, [2]sogiwa@atbu.edu.ng

Abstract – This research work has been carried out to apply Tyreus-Luyben technique in tuning proportional-integral (PI) and proportional-integral-derivative (PID) controllers to the control of a reactive distillation process used for the production of methyl palmitate, a fatty acid methyl ester, from the esterification reaction between palmitic acid and methanol. The model used to represent the process was obtained from the work of Giwa *et al.* (2015c), and its open loop dynamics was first studied before carrying out its closed loop simulations with the aid of the model of the process developed in Simulink that was run via MATLAB *mfile*. The results obtained from the open loop dynamic simulation of the process revealed that the developed Simulink model of the process was correct because the responses were discovered to compare very well with those obtained in the work of Giwa *et al.* (2015b and c). The results of the servo closed loop simulation carried out using the Tyreus-Luyben tuned PI and PID controllers showed that the system was able to get stabilized within the simulation time considered for the two control systems. However, the performance of the PID controller was found to be better because its estimated integral absolute error and integral squared error were lower. Furthermore, when the system was simulated for regulatory problem, the responses given by the two control systems were found to be very satisfactory. Moreover, from the values obtained when the integral absolute error and the integral squared error of the controllers were calculated for the regulatory problem, the PID controlled system was found to be better for this process. The comparison of the results obtained in the servo control of this work with that of Giwa *et al.* (2015b) revealed that Tyreus-Luyben tuning technique was the best for estimating the parameters for PI and PID controllers for the process considered because the number of oscillations observed in this case was found to be low. Also, the comparison made between the results of the regulatory control of this work to that of Giwa *et al.* (2015c) showed that the tuning technique (Tyreus-Luyben) investigated in this work was able to make the system maintain the desired state with lesser oscillations.

Keywords: Fatty acid methyl ester, reactive distillation, MATLAB/Simulink, servo control, regulatory control.

INTRODUCTION

Owing to the limited availability of conventional petroleum diesel and, also, as a result of environmental concerns, fatty acid methyl ester, otherwise known as biodiesel, which is an alternative fuel, is currently receiving attention in both academic and industrial research. This material can be used to replace petroleum diesel without any modification because their properties are similar (Simasatitkul *et al*., 2011; Giwa *et al.*, 2014; Giwa *et al.*, 2015a; Giwa *et al.*, 2015c). A number of advantages are associated with this fuel as it can be derived from a renewable domestic resource as well as its reducing emission of carbon dioxide. Apart from that, it is nontoxic and biodegradable (Wang *et al.*, 2004; Jaya and Ethirajulu, 2011; Giwa *et al.*, 2014; Giwa *et al.*, 2015a; Giwa *et al.*, 2015c).

One of the ways of obtaining fatty acid methyl ester, especially in high purity, is through an esterification reaction of a fatty acid and an alcohol in a reactive distillation column (Giwa *et al.*, 2014; Giwa *et al.*, 2015c). Actually, the use of reactive distillation process is preferred for the production of fatty acid methyl ester so as to overcome the problems associated with the use of conventional batch reactor such as low conversion, heavy capital investments and high energy costs (Kusmiyati and Sugiharto, 2010; Giwa *et al.*, 2014; Giwa *et al.*, 2015a; Giwa *et al.*, 2015b; Giwa *et al.*, 2015c).

Reactive distillation is known to be a process that combines both separation and chemical reaction in a single unit (Giwa and Giwa, 2012; Giwa *et al.*, 2015c). It is more advantageous than a conventional process with separate reaction and separation sections (Al-Arfaj and Luyben, 2002a; Giwa and Karacan, 2012b; Giwa and Karacan, 2012d; Giwa and Karacan, 2012e; Giwa and Karacan, 2012f; Giwa and Karacan, 2012g; Giwa, 2012; Giwa and Giwa, 2013a; Giwa, 2013a; Giwa *et al.*, 2013; Giwa and Giwa, 2013b; Giwa, 2014). A small number of industrial applications have witnessed the application of this process for many years, but the last decade has shown an increase in both its research and applications (Al-Arfaj and Luyben, 2002b; Giwa *et al.*, 2015a).

Furthermore, the operating and investment costs of a plant can be minimized by carrying out chemical reaction and separation in one process. Also, increased yield, because of its overcoming chemical and thermodynamic equilibrium limitations, improved selectivity via suppression of side reactions (Giwa and Karacan, 2012c), reduced energy consumption, due to effective utilization of reaction heat, in the case of exothermic reactions, avoidance of hot spots by simultaneous liquid evaporation, ability to separate close boiling components (Prakash *et al.*, 2011; Giwa *et al.*, 2015a) and ability to avoid azeotropes (Giwa and Karacan, 2012a) are some other benefits resulting from the application of reactive distillation technology. As a result of these advantages and with growing process understanding, an increasing number of processes based on reactive distillation have been developed by chemical process industries

(Bock *et al.*, 1997; Giwa *et al.*, 2015a), but it is not extensively used because of the perception that its operation, dynamics and control are difficult to handle.

In an attempt to address those issues raised about the dynamics and control of the process, different researches have been carried out on the subject matter. To start with, Sneesby *et al.* (1997) worked on the dynamic simulation and control of reactive distillation process that was used for ethyl *tert*-butyl ether synthesis and presented some recommendations required for the control of the reactive distillation column studied. The recommendations included the need for early addressing of the control issues in the design process. Bock *et al.* (1997) developed a structure for the control of a reactive column with recovery by analysing the steady state and dynamic sensitivity of the column with respect to possible disturbance and manipulated variables. Sneesby *et al.* (1999) used an ethyl *tert*-butyl ether reactive distillation column to demonstrate how a two-point control configuration recognizing the importance of both composition and conversion could be developed and implemented for a reactive distillation process. Kumar and Daoutidis (1999) studied the dynamic behaviour and control of a reactive distillation column used for the production of ethylene glycol. A detailed tray-by-tray model that explicitly included the vapour-phase balances was derived in their work. Also developed in the work was a nonlinear controller that yielded good performance with stability in the high-purity region; through simulations carried out, the superior performance of the developed controller over linear PI controllers was demonstrated. In order to regulate ethylene glycol composition in the product, Monroy-Loperena *et al.* (2000) studied the control problem of a reactive distillation column taking the reboiler boil-up ratio as the manipulated variable. In their work, a new idea for robust stabilization based on an analysis of the underlying input/output bifurcation diagram and on modelling error compensation techniques was proposed. Al-Arfaj and Luyben (2000) worked on the closed loop control of a reactive distillation column and discovered that, even in the presence of large disturbances, single end temperature control could be used to keep the products at or above the specified purity values provided that the reaction zone holdup was sufficiently large. Vora and Daoutidis (2001) studied the dynamics and control of an ethyl acetate reactive distillation process and designed model-based linear and nonlinear state feedback controllers with classical single-input single-output (SISO) proportional-integral (PI) controllers. They demonstrated the superior performance of the nonlinear controller over both the linear and the classical PI controllers in the work. Grüner *et al.* (2003) carried out the simulation of an industrial reactive distillation column unto which asymptotically exact input/output-linearization was applied and discovered that the designed controller in the work showed a superior performance with respect to set-point changes and disturbances, in comparison to a well-tuned linear controller, even in the presence of unknown input delays. Khaledi and Young (2005) studied the nonlinearity of a reactive distillation column used for the production of ethyl *tert*-butyl ether and developed a 2 x 2 unconstrained model predictive control scheme for product purity and reactant conversion control using a first-order-plus-dead-time model estimated as the process model of the controller. They found from the study carried out that the controller was very efficient for disturbance rejection and set-point tracking. Völker *et al.* (2007) designed a multivariable controller for a medium-scale semi-batch reactive distillation column and demonstrated that the controller performed well for large set-point changes and in the face of disturbances. Also, Giwa and Karacan (2012a) used AutoRegressive with eXogenous Inputs (ARX) and AutoRegressive Moving Average with eXogenous Inputs (ARMAX) models they developed from some generated experimental data to study the dynamics of an ethyl acetate reactive distillation column. They discovered from the work carried out that the performance of the ARMAX model was better because it had higher calculated fit value. It was also discovered from the studies of the work that the ARX model was faster in getting to steady state upon the application of a step input to the two models. However, the models they developed were not utilized to study the control of the process. Giwa and Karacan (2012c) started from first principles and developed dynamic models for a reactive packed distillation column. They solved the developed models with the aid of MATLAB and compared the experimental and the theoretical results obtained. It was revealed from their results that there were good agreements between them (the experimental and the theoretical results) because the calculated percentage residuals were small. Similarly, the models they developed were not used for the control of the column in the work. Giwa and Karacan (2012d) studied the application of decouplers in the design of model predictive controllers for a reactive distillation process used for ethyl acetate production by taking the top segment temperature, the reaction segment temperature and the bottom segment temperature as the controlled variables while the reflux ratio, the feed ratio and the reboiler duty of the process were the manipulated variables of the control system. The results they obtained from the work showed that neural network decoupling model predictive controller (NNDMPC) was able to perform better than that transfer function decoupling model predictive controller (TFDMPC) because the calculated integral squared error values for the top segment and the reaction segment temperatures obtained from the control simulation carried out with the NNDMPC were found to be less than those of the TFDMPC. Moreover, Giwa and Karacan (2012e) applied decoupling proportional-integral-derivative control to a reactive distillation column for set-point tracking and disturbance rejection using tuning parameters calculated with Ziegler-Nichols and Cohen-Coon techniques. The results obtained from the simulations of the work revealed that, for the process considered in the work, decoupling PID control with Cohen-Coon tuning technique was better than that of Ziegler-Nichols. Giwa *et al.* (2015b) studied the dynamics and, also, performed the set-point tracking control of a reactive distillation process used for biodiesel production taking the biodiesel purity obtained from the bottom section of the column as the controlled variable and the reboiler duty as the manipulated variable. They used Cohen-Coon and Ziegler-Nichols tuning techniques to calculate the controller parameters, and from the comparisons made among the controllers considered, it was discovered that the best one for the system was PID controller tuned with Ziegler-Nichols method because its calculated integral absolute error (IAE) and integral squared error (ISE) were the lowest. Giwa *et al.*, 2015c also carried out the control of a reactive distillation process used for biodiesel production from an esterification reaction between palmitic acid and methanol for regulatory

problem using P, PI and PID controllers tuned with Ziegler-Nichols and Cohen-Coon techniques and discovered that the best controller for the disturbance rejection control of this process was PID controller tuned with Cohen-Coon technique.

As can be seen from the literature review carried out, most of the researches carried out on the control of reactive distillation process for biodiesel (fatty acid methyl ester) production has been based on using Ziegler-Nichols and Cohen-Coon methods as the tuning techniques. It was, therefore, deemed necessary to investigate how the process would behave to a controller tuned with another technique. As a result of that, this work has been carried out to apply Tyreus-Luyben tuning technique to proportional-integral (PI) and proportional-integral-derivative (PID) controllers used for the control of a reactive distillation process producing palmitic acid methyl ester (fatty acid methyl ester).

METHODOLOGY

Process Modelling

The model used in this work to study the dynamics and the control of the palmitic acid methyl ester (methyl palmitate) reactive distillation process was a transfer function obtained from the work of Giwa *et al.* (2015c), and it is given in Equation (1).

$$x_{fame}(s) = \frac{0.3382e^{(-8.999s)}}{248.43s+1} Q(s) + \frac{0.283e^{(-1.993s)}}{151.87s+1} R(s) \quad (1)$$

The input variable of the model was taken as the reboiler duty while the reflux ration was chosen as the disturbance variable, and the output variable was the mole fraction of palmitic acid methyl ester obtained from the bottom section of the reactive distillation column used.

Open Loop Simulation

To carry out the open loop simulation of the process, the transfer function model taken from the work of Giwa *et al.* (2015c) was first represented as a Simulink (MathWorks, 2015) model of the process as shown in Figure 1. The process Simulink model composed of two parts, viz. the main fatty acid methyl ester reactive distillation system and the disturbance system, as can be seen from the Figure 1. As can be seen from the figure, the blocks (transfer function and delay Simulink blocks) for the two parts of the model have been inserted inside a subsystem of the Simulink to make the appearance of the model look tidy.

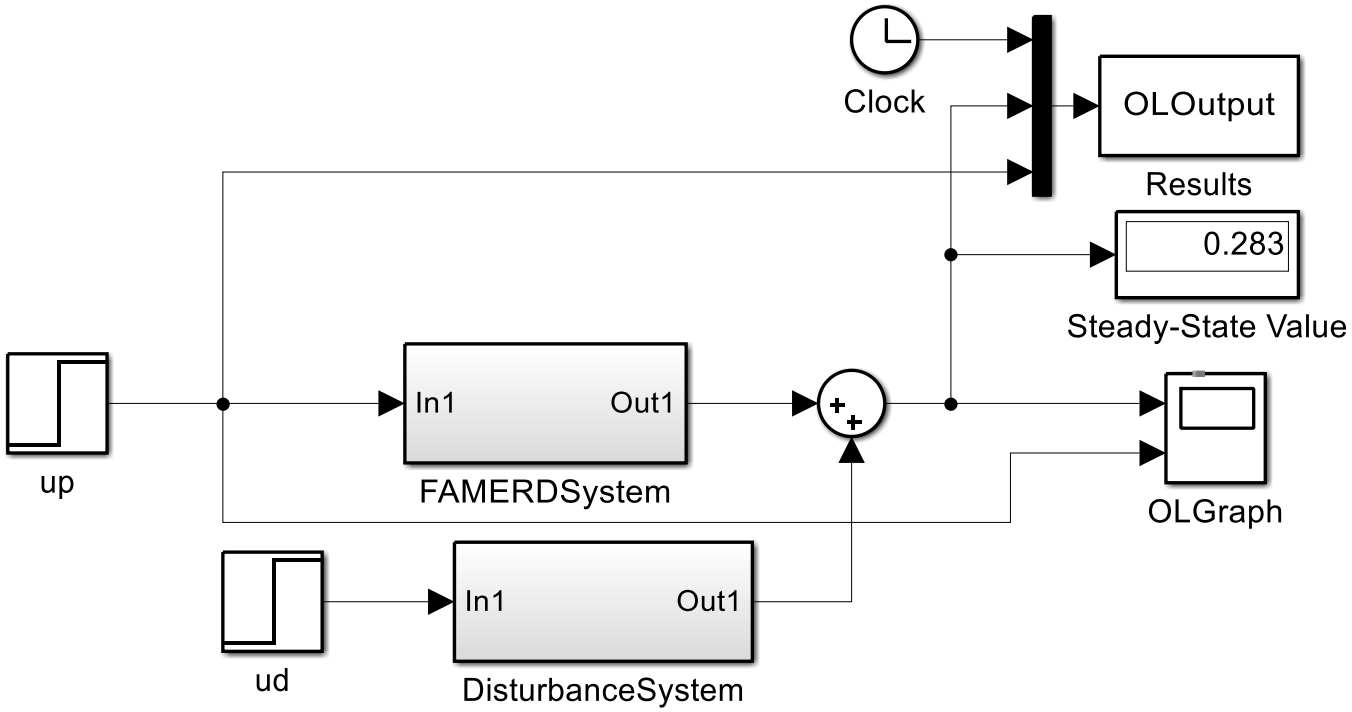

Figure 1. Open loop Simulink model of the palmitic acid methyl ester reactive distillation process

After the Simulink modelling of the process, it was run by applying steps to both the input and the disturbance variables of the process via codes written in *m-file* of MATLAB.

Closed Loop Simulation

Upon the completion of the open loop simulation of the process, its closed loop dynamics were also investigated by simulating the closed loop dynamic model developed, also, with the aid of Simulink and shown in Figures 2 and 3, respectively, for PI and PID controllers tuned with Tyreus-Luyben technique. The closed loop models of the process developed were simulated for both servo (set-point tracking) and regulatory (disturbance rejection) with the controllers (PI and PID) by applying step changes to the steady state value of the output (controlled) and the disturbance variables, accordingly. For the control system of this work, as mentioned earlier, the controlled, the manipulated and disturbance variables of the process were selected to be the palmitic acid methyl ester bottom mole fraction, the reboiler duty and the reflux ratio, respectively.

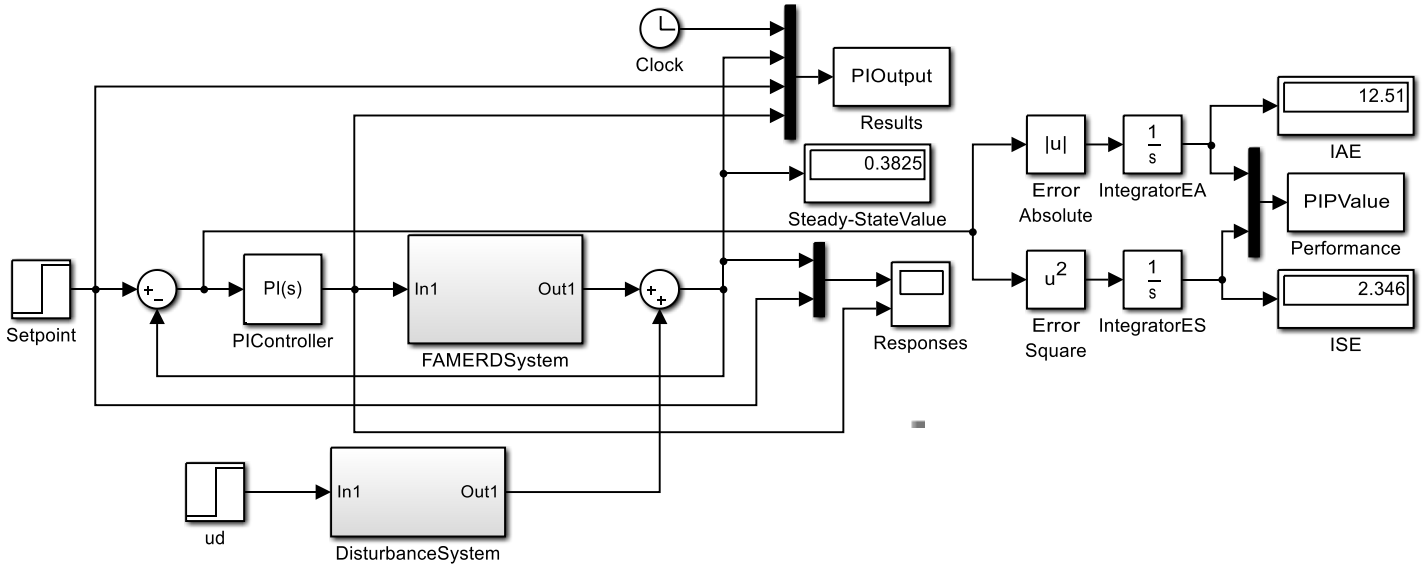

Figure 2. Closed loop Simulink model of the process with PI controller tuned with Tyreus-Luyben technique

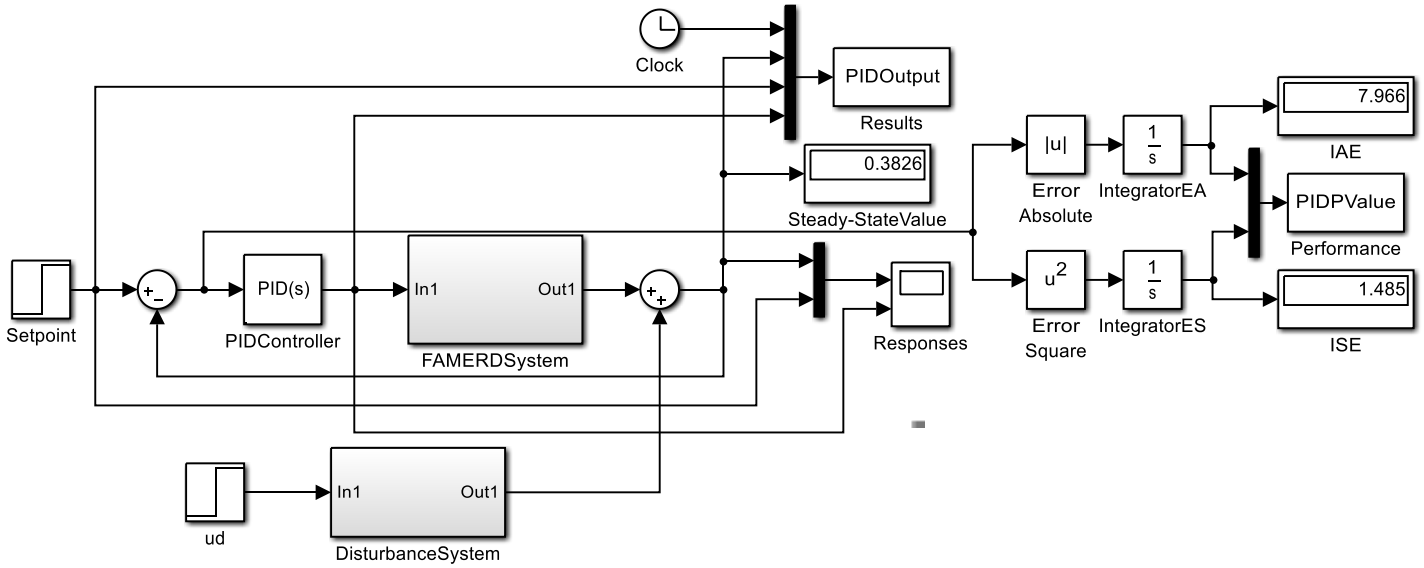

Figure 3. Closed-loop Simulink model of the process with PID controller tuned with Tyreus-Luyben technique

In order to use the expressions of the Tyreus-Luyben tuning technique (shown in Table 1) to calculate the required parameters of the controllers, their (the controller's) transfer function was taken to be as given in Equation (2).

$$G_c(s) = K_c\left(1 + \frac{1}{\tau_I s} + \tau_D s\right) \tag{2}$$

Table 1: Tyreus-Luyben tuning parameter expressions

Parameter	Proportional-Integral (PI)	Proportional-Integral-Derivative (PID)
K_c	$0.31K_u$	$0.45K_u$
τ_I	$2.2P_u$	$2.2P_u$
τ_D	0	$\frac{P_u}{6.3}$

Source: Seborg *et al.* (2004)

RESULT AND DISCUSSION

Shown in Figure 4 is the closed loop dynamic response of the fatty acid methyl ester reactive distillation process studied in this work to a unit step change in the reboiler duty, which was the input variable, of the process. As can be seen from the figure, even though the time was a little bit long, the system was able to get to a steady state value that was found to compare very well with the one obtained in the work of Giwa *et al.* (2015b). That was an indication that the open loop Simulink model of the reactive distillation process developed in this work was very correct.

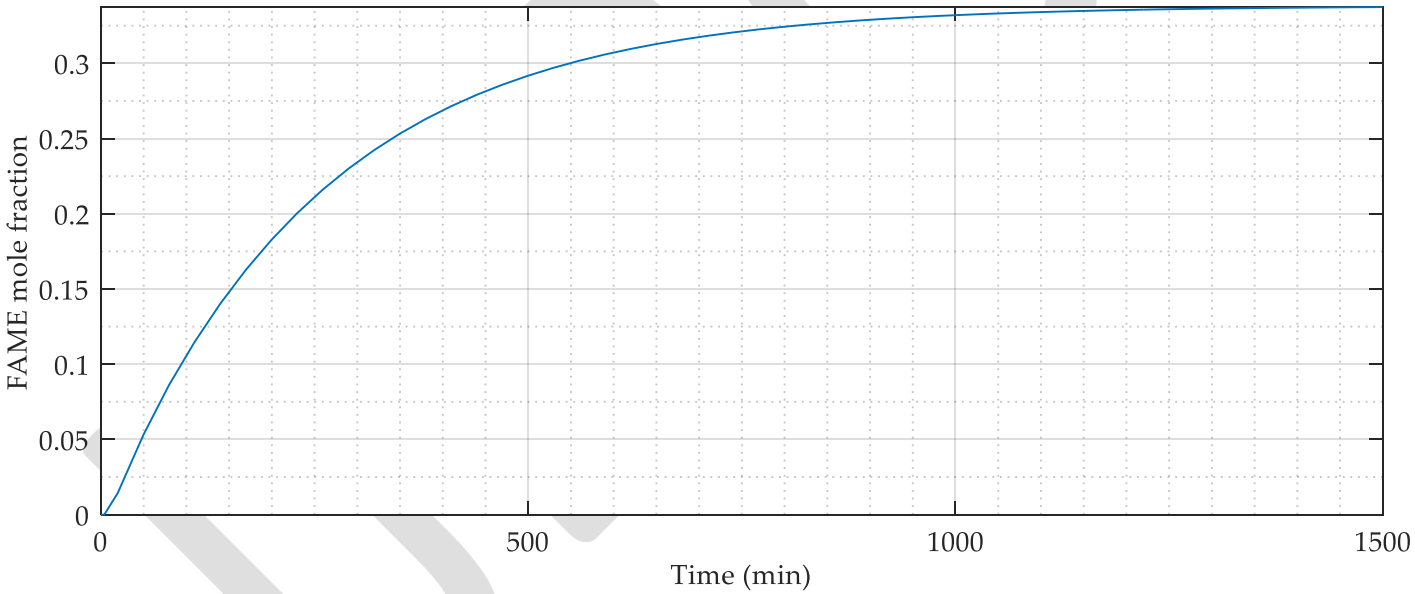

Figure 4. Open loop response of the process to 1 unit step change in the reboiler duty of the process

After carrying out the open loop simulation, Tyreus-Luyben tuning technique was used to obtain the tuning parameters of the controller for set point tracking, and the results obtained from the control of the process accomplished by applying a step change of 0.1 to the steady-state value of the mole fraction of palmitic acid methyl ester, which was the controlled variable of the closed loop system, were as given in Figures 5 and 6.

Figure 5 shows the response of the system to a 0.1 step change in the set point when it was controlled with a PI controller. From the figure, it was discovered that the system was able to attain its desired steady state within 300 min of the simulation time used. Comparing the response obtained in this work for the PI controller tuned with Tyreus-Luyben to that tuned with Ziegler-Nichols and Cohen-Coon techniques (see Giwa *et al.*, 2015b), it was found that the response obtained in this work for the control was less oscillatory. In addition, the time required by the system to get to a value higher than that of the open loop simulation has been found to reduce, meaning that the control carried out on the process with the PI controller tuned with Tyreus-Luyben technique was effective.

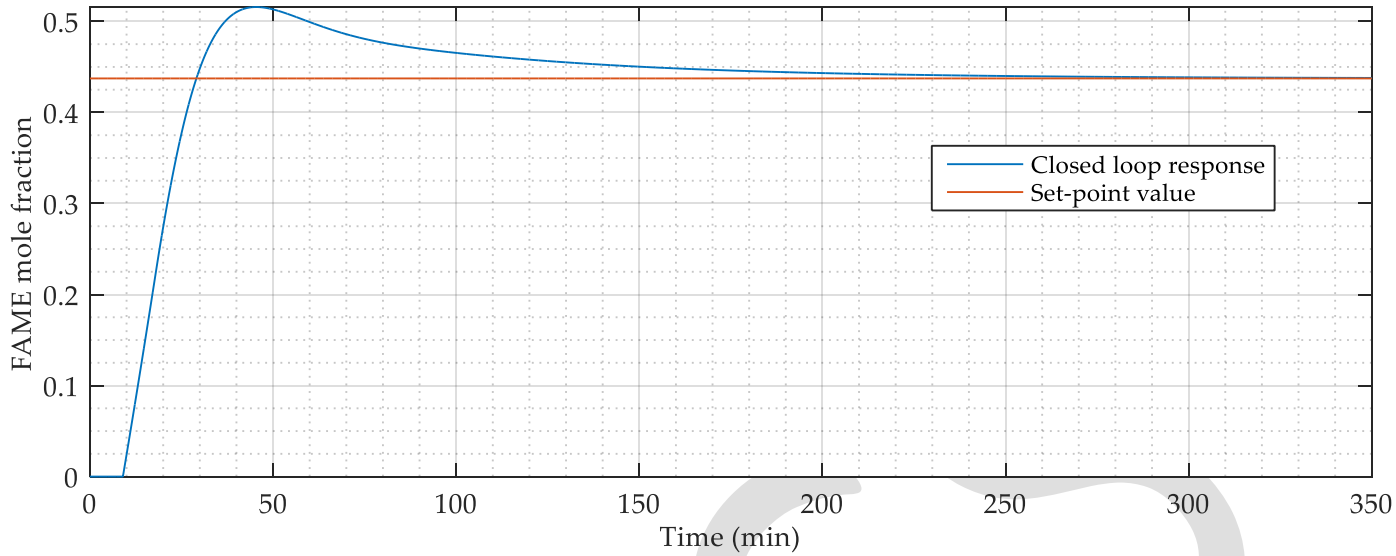

Figure 5. Closed loop response of Tyreus-Luyben tuned PI controlled process to a 0.1 step change in the controlled variable

Shown in Figure 6 is the dynamic response of the closed loop system to a step change of 0.1 in the set point of the output variable controlled with PID controller tuned with Tyreus-Luyben technique. According to the figure, the response of the PID controlled system tuned with Tyreus-Luyben technique was also found to get to its desired set point within 300 min, but it was found to be more oscillatory than that of the PI controller system tuned with the same technique. This observation can be clearly seen by comparing Figures 5 and 6.

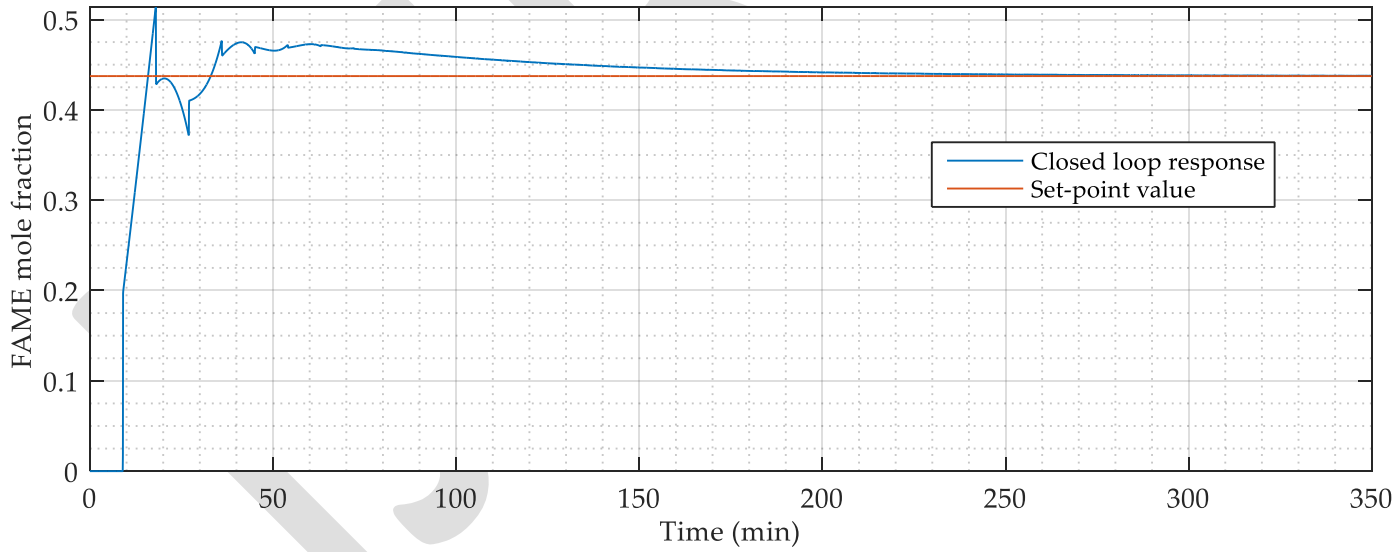

Figure 6. Closed loop response of Tyreus-Luyben tuned PID controlled process to a 0.1 step change in the controlled variable

Table 2. Performance values of PI and PID controllers tuned with Tyreus-Luyben technique for servo problem

Controller	IAE	ISE
PI	13.28	3.09
PID	8.36	1.94

In order to be able to compare the two controllers, their performance values were calculated. The performance criteria used in this work were integral absolute error (IAE) and integral squared error (ISE) and their calculated values for the controllers considered are given in Table 2. Comparing the two (PI and PID) controllers based on the values of the performance criteria given in Table 2, it was

discovered numerically that the PID controller tuned with Tyreus-Luyben technique was better than the PI controller in controlling the process because its IAE and ISE were lesser.

Also considered in this work was the behaviour of the system with the controllers tuned with Tyreus-Luyben technique after a unit step change was applied to the reflux ratio (disturbance variable) of the process; that is, the disturbance rejection control. However, before doing that, the open loop simulation involving a unit step change in the disturbance variable (reflux ratio) of the process was first carried out.

Shown in Figure 7 is the open loop dynamic response given by the system when a unit step change was applied to the reflux ratio. The response obtained was observed to compare very well with that obtained in the work of Giwa *et al.* (2015c), and this was found to be another indication of the fact that the developed Simulink model of the process was a good representation of the palmitic acid methyl ester reactive distillation system and that the disturbance variable was actually having effects on the system because the response was, then, supposed to be zero, but was not.

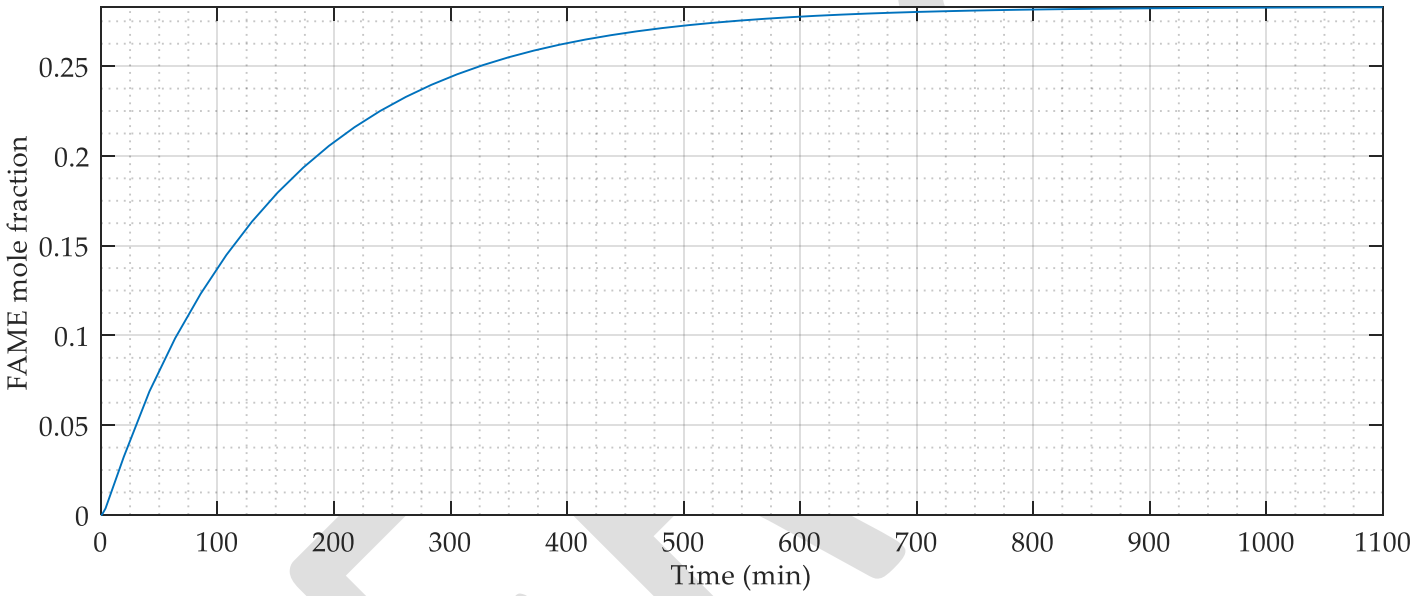

Figure 7. Open loop response of the process to 1 unit step change in the reflux ratio of the process

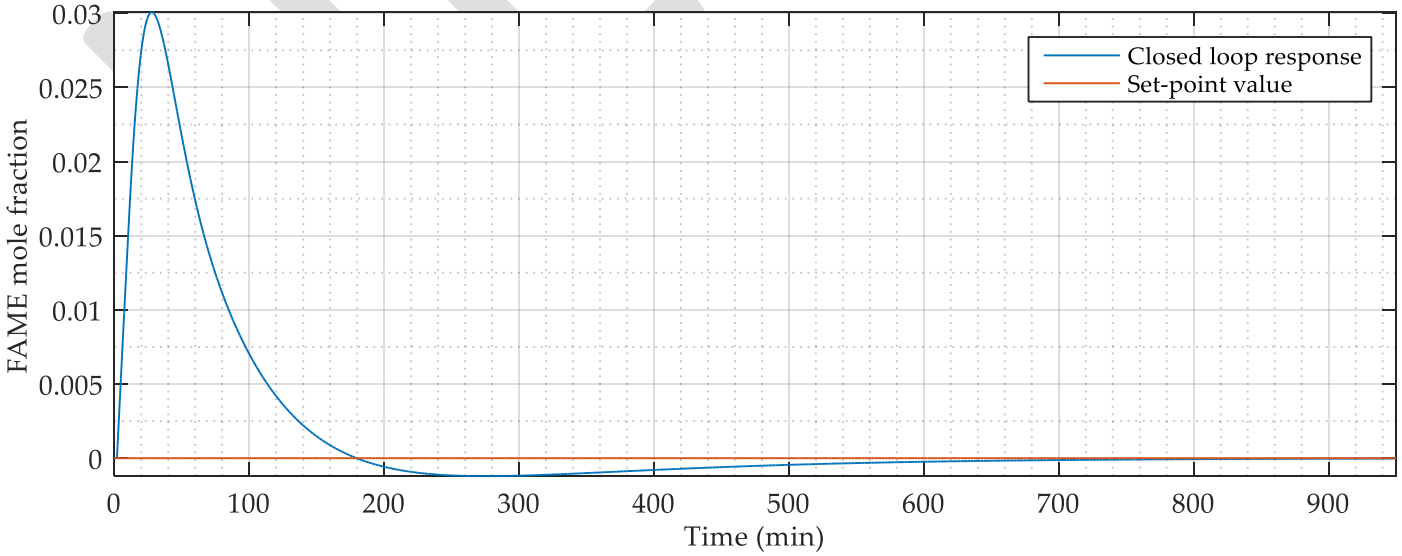

Figure 8. Closed loop response of Tyreus-Luyben tuned PI controlled process

Consequently, Tyreus-Luyben tuning technique was applied to obtain the controller parameters used with the control system to maintain the response of the controlled variable at the desired value (in this case of the regulatory control, zero). Given in Figures 8 and 9 are the responses obtained from that.

As can be seen from Figure 8, which is showing the dynamic response of the system to a Tyreus-Luyben tuned PI controller, the response was able to get settled with very few oscillations at the desired set point. In fact, the oscillations found in this response obtained with the Tyreus-Luyben tuned PI controller were found to be less than that given by the same PI controller tuned with Ziegler-Nichols and Cohen-Coon methods, as can be seen in the work of Giwa *et al.* (2015c). It should be recalled that similar observations were made in the case of the servo control of the system. This is, actually, showing the superiority of Tyreus-Luyben tuning technique over Ziegler-Nichols and Cohen-Coon techniques, at least, for this reactive distillation process studied.

Moreover, Figure 9 shows the response of the process when it was controlled using a PID controller that was tuned with Tyreus-Luyben technique. From the figure, it was discovered that the number of oscillations displayed by the closed loop system of the palmitic acid methyl ester reactive distillation process was not up to that of the ones given by a similar (PID) controlled system tuned with Ziegler-Nichols and Cohen-Coon techniques (cf. Giwa *et al.*, 2015c).

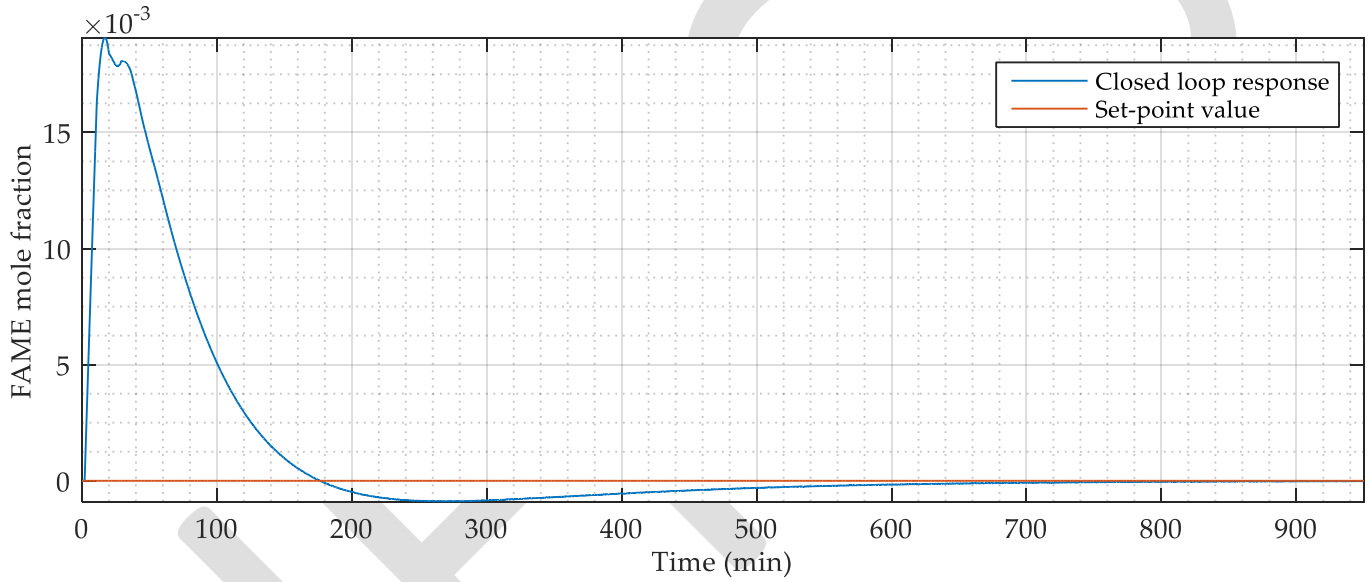

Figure 9. Closed loop response of Tyreus-Luyben tuned PID controlled process

Table 3. Performance criteria values of PI and PID controllers tuned with Tyreus-Luyben technique for regulatory control

Controller	IAE	ISE
PI	2.30	0.04
PID	1.60	0.02

The two controllers tuned with Tyreus-Luyben technique that were considered in this work for regulatory problem were also compared by estimating their IAEs and ISEs, and the results obtained were as given in Table 3. Looking at the values of the IAEs and ISEs given in the table, it was found that the performance of the PID controller tuned with Tyreus-Luyben technique was better than that of the PI controller tuned with the same technique because it had lower IAE and ISE values, and the lower the values of the IAE and ISE of a controller, the better the performance of that controller.

CONCLUSION

From the results given by the open loop dynamic simulation of the reactive distillation process used for the production of palmitic acid methyl ester, it was revealed that the developed model of the process was correct because the responses compared very well with those

obtained in the work of Giwa *et al.* (2015b and c). The results of the servo closed loop simulation carried out with the Tyreus-Luyben tuned PI and PID controllers showed that the system was able to get stabilized at the desired set point within 300 min of the simulation time considered with the two controllers. However, the performance of the PID controller was found to be better because its estimated integral absolute error and integral squared error were lower. Furthermore, when the system was simulated for regulatory problem, the responses given by the two control systems were found to be very satisfactory. In addition, from the values obtained when the integral absolute error and the integral squared error were calculated, the performance of the PID controlled system was found to be better. The comparison of the results obtained in the servo control of this work with that of Giwa *et al.* (2015b) revealed that Tyreus-Luyben technique was the best in tuning the controllers for the process because the number of oscillations observed in this case was found to be low. Also, comparing the results of the regulatory control with that of Giwa *et al.* (2015c), it was discovered that the tuning technique (Tyreus-Luyben) investigated in this work was able to make the system remain at the desired steady state with fewer oscillations.

NOMENCLATURE

τ_D	Derivative time of the controller (min)
τ_d	Time constant of the disturbance process model (min)
τ_I	Integral time of the controller (min)
τ_p	Time constant of the main process model (min)
$G_c(s)$	Controller transfer function
$G_p(s)$	Process transfer function
IAE	Integral Absolute Error
ISE	Integral Squared Error
K_c	Proportional gain of the controller
K_d	Static gain of the disturbance process model
K_p	Static gain of the main process model
K_u	Ultimate gain
NNDMPC	Neural Network Decoupling Model Predictive Controller
P	Proportional
PI	Proportional-Integral
PID	Proportional-Integral-Derivative
P_u	Ultimate period (min/cycle)
Q	Reboiler duty (kJ/s)
R	Reflux ratio
SISO	Single-input single-output
T_{dd}	Dead time of the disturbance process model (min)
T_{dp}	Dead time of the main process model (min)
TFDMPC	Transfer Function Decoupling Model Predictive Controller
x_{fame}	Bottom fatty acid methyl ester mole fraction

REFERENCES:

1) Al-Arfaj M.A. and Luyben W.L. (2002a). Design and Control of an Olefin Metathesis Reactive Distillation Column. Chemical Engineering Science. 57, 715-733.
2) Al-Arfaj M.A. and Luyben W.L. (2002b). Comparative Control Study of Ideal and Methyl Acetate Reactive Distillation. Chemical Engineering Science. 57, 5039-5050.
3) Al-Arfaj, M.A. and Luyben, W.L. (2000). Comparison of Alternative Control Structures for an Ideal Two-Product Reactive Distillation Column. Industrial and Engineering Chemistry Research, 39, 3298-3307.
4) Bock, H., Wozny, G. and Gutsche, B. (1997). Design and Control of a Reaction Distillation Column Including the Recovery System. Chemical Engineering and Processing, 36, 101- 09.
5) Giwa, A. (2012). Steady-State Modeling of n-Butyl Acetate Transesterification Process Using Aspen PLUS: Conventional versus Integrated. ARPN Journal of Engineering and Applied Sciences, 7(12), 1555-1564.
6) Giwa, A. (2013). Sensitivity Analysis of ETBE Production Process Using Aspen PLUS. International Journal of Advanced Scientific and Technical Research. 3(1), 293-303.
7) Giwa, A. (2014). Solving the Dynamic Models of Reactive Packed Distillation Process Using Difference Formula Approaches. ARPN Journal of Engineering and Applied Sciences, 9(2), 98-108.
8) Giwa, A. and Giwa, S.O. (2012). Optimization of Transesterification Reaction Integrated Distillation Column Using Design Expert and Excel Solver. International Journal of Advanced Scientific and Technical Research. 2(6): 423-435.

9) Giwa, A. and Giwa, S.O. (2013a). Isopropyl Myristate Production Process Optimization Using Response Surface Methodology and MATLAB. Journal of Engineering Research & Technology, 2(1), 853-862.
10) Giwa, A. and Giwa, S.O. (2013b). Estimating the Optimum Operating Parameters of Olefin Metathesis Reactive Distillation Process. ARPN Journal of Engineering and Applied Sciences, 8(8), 614-624.
11) Giwa, A. and Karacan, S. (2012a). Modeling and Simulation of a Reactive Packed Distillation Column Using Delayed Neural Networks, Chaotic Modeling and Simulation, 2(1), 101-108.
12) Giwa, A. and Karacan, S. (2012b). Black-Box Modelling of Ethyl Acetate Reactive Packed Distillation Column, AU Journal of Technology, 15(3), 172-178.
13) Giwa, A. and Karacan, S. (2012c). Development of Dynamic Models for a Reactive Packed Distillation Column. International Journal of Engineering, 6(3), 118-128.
14) Giwa, A. and Karacan, S. (2012d). Decoupling Model Predictive Control of a Reactive Packed Distillation Column. Journal of Advances in Science and Technology, 4(6), 39-51.
15) Giwa, A. and Karacan, S. (2012e). Decoupling PID Control of a Reactive Packed Distillation Column. Journal of Engineering Research & Technology, 1(6), 1924-1933.
16) Giwa, A. and Karacan, S. (2012f). Nonlinear Black-Box Modeling of a Reactive Distillation Process, International Journal of Engineering Research & Technology, 1(7), 548-557.
17) Giwa, A. and Karacan, S. (2012g). Decoupling Control of a Reactive Distillation Process Using Tyreus-Luyben Technique. ARPN Journal of Engineering and Applied Sciences, 7(10), 1263-1272.
18) Giwa, A., Bello, A. and Giwa, S. O. (2014). Performance Analyses of Fatty Acids in Reactive Distillation Process for Biodiesel Production. International Journal of Scientific & Engineering Research, 5(12), 529-540.
19) Giwa, A., Bello, A. and Giwa, S. O. (2015a). Artificial Neural Network Modeling of a Reactive Distillation Process for Biodiesel Production. International Journal of Scientific & Engineering Research, 6(1), 1175- 1191.
20) Giwa, A., Giwa, S.O. and Adeyi, A.A. (2015b). Dynamics and Servo Control of Biodiesel Purity from a Reactive Distillation Process. International Journal of Scientific & Engineering Research, 6(8), 146-156.
21) Giwa, A., Giwa, S.O., Bayram, İ., and Karacan, S. (2013). Simulations and Economic Analyses of Ethyl Acetate Productions by Conventional and Reactive Distillation Processes Using Aspen Plus. Journal of Engineering Research & Technology, 2(8), 594-605.
22) Giwa, S.O., Adeyi, A.A. and Giwa, A. (2015c). Dynamics and Regulatory Control of Biodiesel Purity from a Reactive Distillation Process. International Journal of Engineering Research and General Science, 3(5), 371-381.
23) Grüner, S., Mohl, K.D., Kienle, A., Gilles, E.D. Fernholz, G. and Friedrich, M. (2003). Nonlinear Control of a Reactive Distillation Column. Control Engineering Practice, 11, 915-925.
24) Jaya, N. and Ethirajulu, E. (2011). Kinetic Modeling of Transesterification Reaction for Biodiesel Production Using Heterogeneous Catalyst. International Journal of Engineering Science and Technology, 3(4), 3463-3466.
25) Khaledi, R. and Young, B.R. (2005). Modeling and Model Predictive Control of Composition and Conversion in an ETBE Reactive Distillation Column. Industrial and Engineering Chemistry Research, 44, 3134-3145.
26) Kumar, A. and Daoutidis, P. (1999). Modeling, Analysis and Control of Ethylene Glycol Reactive Distillation Column. AIChE Journal, 45, 51-68.
27) Kusmiyati, K. and Sugiharto, A. (2010). Production of Biodiesel from Oleic Acid and Methanol by Reactive Distillation. Bulletin of Chemical Reaction Engineering & Catalysis, 5(1), 1-6.
28) MathWorks. (2015). MATLAB, The Language of Technical Computing. The MathWorks, Inc., Natick.
29) Monroy-Loperena, R., Perez-Cisneros, E. and Alvarez-Ramirez, J. (2000). A Robust PI Control Configuration for a High-Purity Ethylene Glycol Reactive Distillation Column. Chemical Engineering Science, 55, 4925-4937.
30) Prakash K.J.J, Patle D.S. and Jana A.K. (2011). Neuro-Estimator Based GMC Control of a Batch Reactive Distillation. ISA Transactions. 50, 357-363.
31) Seborg D.E., Edgar T.F. and Mellichamp D.A. (2004). Process Dynamics and Control. 2nd Edition, John Wiley and Sons, New Jersey, USA.
32) Simasatitkul, L., Siricharnsakunchai, P., Patcharavorachot, Y., Assabumrungrat, S., and Arpornwichanop, A. (2011). Reactive Distillation for Biodiesel Production from Soybean Oil. Korean J. Chem. Eng., 28(3), 649-655.
33) Sneesby, M.G., Tade, M.O. and Smith, T.N. (1999). Two-Point Control of a Reactive Distillation Column for Composition and Conversion. Journal of Process Control, 9, 19-31.
34) Sneesby, M.G., Tade, M.O., Datta, R. and Smith, T.N. (1997). ETBE Synthesis via Reactive Distillation. 2. Dynamic Simulation and Control Aspects. Industrial and Engineering Chemistry Research, 36, 1870-1881.
35) Völker, M., Sonntag, C. and Engell, S. (2007). Control of Integrated Processes: A Case Study on Reactive Distillation in a Medium-Scale Pilot Plant. Control Engineering Practice, 15, 863-881.
36) Vora, N. and Daoutidis, P. (2001). Dynamics and Control of an Ethyl Acetate Reactive Distillation Column. Industrial and Engineering Chemistry Research, 40, 833-849.
37) Wang, S., Ma, X., Gong, J., Yang, X., Guo, H., and Xu, G. (2004). Transesterification of dimethyl oxalate with phenol under SnO_2/SiO_2 catalysts, Industrial and Engineering Chemistry Research, 43, 4027-4030.

International Journal of Engineering Research and General Science Volume 3, Issue 5, September-October, 2015
ISSN 2091-2730

Power System Stability Improvement Using FACTS Devices

Yugant A. Parate[1] Ankita Y. Pai[2]

[1]Department of Electrical Engineering, Sardar Patel College of Engineering, Mumbai, Maharashtra, India
yugantparate5@gmail.com, +918149477702

[2]Department of Electrical Engineering, Sardar Patel College of Engineering, Mumbai, Maharashtra, India
ankitapai94@gmail.com,+917045336852

Abstract— In the last two decades, power demand has increased substantially while the expansion of power generation and transmission has been severely limited due to limited resources and environmental restrictions. As a consequence, some transmission lines are heavily loaded and the system stability becomes a power transfer-limiting factor. Flexible AC transmission systems (FACTS) controllers have been mainly used for solving various power system steady state control problems. Flexible AC transmission systems or FACTS are devices which allow the flexible and dynamic control of power systems. Enhancement of system stability using FACTS controllers has been investigated. This paper is aimed towards the benefits of utilizing FACTS devices with the purpose of improving the operation of an electrical power system. Performance comparison of different FACTS controllers has been discussed. In addition, some of the utility experience and semiconductor technology development have been reviewed and summarized. Applications of FACTS to power system studies have also been discussed.

Keywords. AC, FACTS, IPFC, PSS, SVC, STATCOM, SSSC, TCSC, TCPS, UPFC.

INTRODUCTION

The FACTS controllers offer a great opportunity to regulate the transmission of alternating current (AC), increasing or diminishing the power flow in specific lines and responding almost instantaneously to the stability problems. The potential of this technology is based on the possibility of controlling the route of the power flow and the ability of connecting networks that are not adequately interconnected, giving the possibility of trading energy between distant agents. Flexible Alternating Current Transmission System (FACTS) is a static equipment used for the AC transmission of electrical energy. It is meant to enhance controllability and increase power transfer capability. It is generally a power electronics based device. The FACTS devices can be divided in three groups, dependent on their switching technology: mechanically switched (such as phase shifting transformers), thyristor switched or fast switched, using IGBTs. While some types of FACTS, such as the phase shifting transformer (PST) and the static VAR compensator (SVC) are already well known and used in power systems, new developments in power electronics and control have extended the application range of FACTS. Furthermore, intermittent renewable energy sources and increasing international power flows provide new applications for FACTS. The additional flexibility and controllability of FACTS allow to mitigate the problems associated with the unreliable of supply issues of renewable. SVCs and STATCOM devices are well suited to provide ancillary services (such as voltage control) to the grid and fault rid through capabilities which standard wind farms cannot provide Furthermore, FACTS reduce oscillations in the grid, which is especially interesting when dealing with the stochastic behavior of renewable.

2. CONTROL OF POWER SYSTEMS

2.1. Generation, Transmission, Distribution

In any power system, the creation, transmission, and utilization of electrical power can be separated into three areas, which traditionally determined the way in which electric utility companies had been organized. These are illustrated in Figure 1 and are:
• Generation
• Transmission
• Distribution

Although power electronic based equipment is prevalent in each of these three areas, such as with static excitation systems for generators and Custom Power equipment in distribution systems [8], the focus of this paper and accompanying presentation is on transmission, i.e, moving the power from where it is generated to where it is utilized.

2.2. Power System Constraints

As noted in the introduction, transmission systems are being pushed closer to their stability and thermal limits while the focus on the quality of power delivered is greater than ever. The limitations of the transmission system can take many forms and may involve power transfer between areas or within a single area or region and may include one or more of the following characteristics:

- Steady-State Power Transfer Limit
- Voltage Stability Limit
- Dynamic Voltage Limit
- Transient Stability Limit
- Power System Oscillation Damping Limit
- Inadvertent Loop Flow Limit
- Thermal Limit
- Short-Circuit Current Limit
- Others

Each transmission bottleneck or regional constraint may have one or more of these system-level problems. The key to solving these problems in the most cost-effective and coordinated manner is by thorough systems engineering analysis.

Each of the above mentioned controllers have impact on voltage, impedance, and/or angle (and power)

- Thyristor Controlled Series Compensator (TCSC)-Controls impedance
- Thyristor Controlled Phase Shifting Transformer (TCPST)-Controls angle
- Super Conducting Magnetic Energy Storage (SMES)-Controls voltage and power

2.4. Benefits of Control of Power Systems

Once power system constraints are identified and through system studies viable solutions options are identified, the benefits of the added power system control must be determined. The following offers a list of such benefits:

- Increased Loading and More Effective Use of Transmission Corridors
- Added Power Flow Control
- Improved Power System Stability
- Increased System Security
- Increased System Reliability
- Added Flexibility in Starting New Generation
- Elimination or Deferral of the Need for New Transmission Lines

2.5. Benefits of utilizing FACTS devices

The benefits of utilizing FACTS devices in electrical transmission systems can be summarized as follows [1]: •Better utilization of existing transmission system assets •Increased transmission system reliability and availability •Increased dynamic and transient grid stability and reduction of loop flows •Increased quality of supply for sensitive industries •Environmental benefits Better utilization of existing transmission system assets

2.6. Classification

There are different classifications for the FACTS devices: Depending on the type of connection to the network FACTS devices can differentiate four categories

- Serial controllers
- Derivation controllers
- Serial to serial controllers
- Serial-derivation controllers

2.3. Controllability of Power Systems

To illustrate that the power system only has certain variables that can be impacted by control, we have considered here the power-angle curve, shown in Figure 2. Although this is a steady-state curve and the implementation of FACTS is primarily for dynamic issues, this illustration demonstrates the point that there are primarily three main variables that can be directly controlled in the power system to impact its performance. These are:

- Voltage

• Angle
• Impedance

Conventional Equipment For Enhancing Power System Control

• Series Capacitor -Controls impedance
• Switched Shut-Capacitor and Reactor - Controls voltage
• Transformer LTC -Controls voltage
• Phase Shifting Transformer -Controls angle
• Synchronous Condenser -Controls voltage
• Special Stability Controls-Focuses on voltage control but often include direct control of power
• Others (When Thermal Limits are Involved) - Can included reconductoring, raising conductors, dynamic line monitoring, adding new lines, etc.

Example of FACTS Controllers for Enhancing Power System Control

• Static Synchronous Compensator (STATCOM)
• Static VAR Compensator (SVC) -Controls voltage
• Unified Power Flow Controller (UPFC)
• Convertible Series Compensator (CSC)
• Inter-phase Power Flow Controller (IPFC)
• Static Synchronous Series Controller (SSSC)

Depending on technological features, the FACTS devices can be divided into two generations
• First generation: used thyristors with ignition controlled by gate (SCR).
• Second generation: semiconductors with ignition and extinction controlled by gate (GTO´s, MCTS, IGBTS, IGCTS, etc.).

These two classifications are independent, existing for example, devices of a group of the first classification that can belong to various groups of the second classification. The main difference between first and second generation devices is the capacity to generate reactive power and to interchange active power. The first generation FACTS devices work like passive elements using impedance or tap changer transformers controlled by thyristors. The second generation FACTS devices work like angle and module controlled voltage sources and without inertia, based in converters, employing electronic tension sources (three-phase inverters, auto-switched voltage sources, synchronous voltage sources, voltage source control) fast proportioned and controllable and static synchronous voltage and current sources.

3. FIRST GENERATION OF FACTS

3.1. Static VAR Compensator (SVC)

A static VAR compensator (or SVC) is an electrical device for providing fast-acting reactive power on high-voltage electricity transmission networks. SVCs are part of the Flexible AC transmission system device family, regulating voltage and stabilising the system. The term "static" refers to the fact that the SVC has no moving parts (other than circuit breakers and disconnects, which do not move under normal SVC operation). Prior to the invention of the SVC, power factor compensation was the preserve of large rotating machines such as synchronous condensers. The SVC is an automated impedance matching device, designed to bring the system closer to unity power factor. If the power system's reactive load is capacitive (leading), the SVC will use reactors (usually in the form of Thyristor-Controlled Reactors) to consume VARs from the system, lowering the system voltage. Under inductive (lagging) conditions, the capacitor banks are automatically switched in, thus providing a higher system voltage. They also may be placed near high and rapidly varying loads, such as arc furnaces, where they can smooth flicker voltage. It is known that the SVCs with an auxiliary injection of a suitable signal can considerably improve the dynamic stability performance of a power system. It is observed that SVC controls can significantly influence nonlinear system behavior especially under high-stress operating conditions and increased SVC gains.

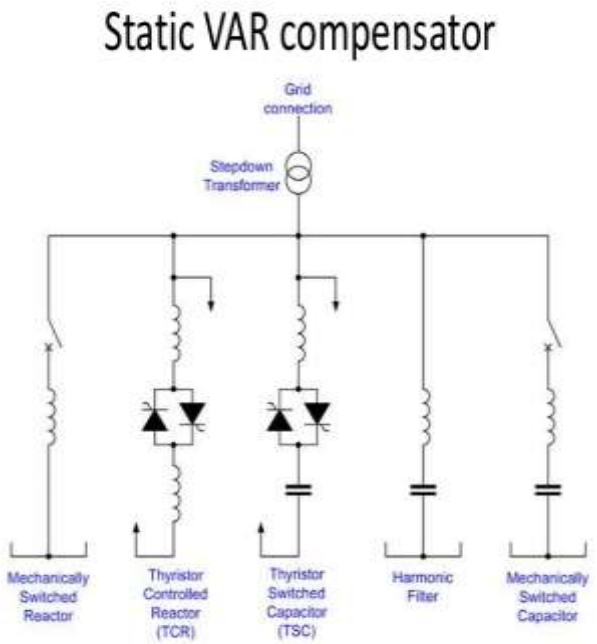

Fig. 1. Static VAR Compensators

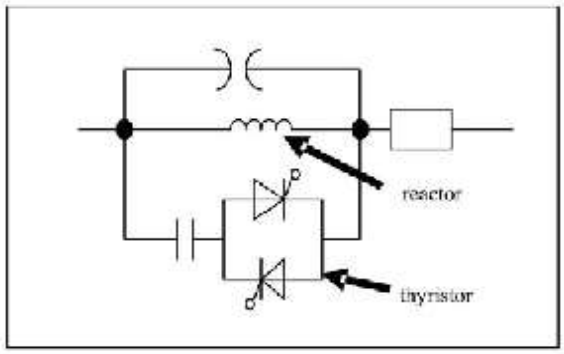

Fig.2. Thyristor-Controlled Series Capacitor

3.2. Thyristor-Controlled Series Capacitor (TCSC)

TCSC controllers use thyristor-controlled reactor (TCR) in parallel with capacitor segments of series capacitor bank. The combination of TCR and capacitor allow the capacitive reactance to be smoothly controlled over a wide range and switched upon command to a condition where the bi-directional thyristor pairs conduct continuously and insert an inductive reactance into the line. TCSC is an effective and economical means of solving problems of transient stability, dynamic stability, steady state stability and voltage stability in long transmission lines. TCSC, the first generation of FACTS, can control the line impedance through the introduction of a thyristor controlled capacitor in series with the transmission line. A TCSC is a series controlled capacitive reactance that can provide continuous control of power on the ac line over a wide range. The functioning of TCSC can be comprehended by analyzing the behavior of a variable inductor connected in series with a fixed capacitor

3.3. Thyristor-Controlled Phase Shifter (TCPS)

In a TCPS control technique the phase shift angle is determined as a nonlinear function of rotor angle and speed. However, in real-life power system with a large number of generators, the rotor angle of a single generator measured with respect to the system reference will not be very meaningful.

4. SECOND GENERATION OF FACTS

4.1. Static Compensator (STATCOM)

The emergence of FACTS devices and in particular GTO thyristor-based STATCOM has enabled such technology to be proposed as serious competitive alternatives to conventional SVC [21] A static synchronous compensator (STATCOM) is a regulating device used on alternating current electricity transmission networks. It is based on a power electronics voltage-source converter and can act as either a source or sink of reactive AC power to an electricity network. If connected to a source of power it can also provide active AC power. It is a member of the FACTS family of devices. Usually a STATCOM is installed to support electricity networks that have a poor power factor and often poor voltage regulation. There are however, other uses, the most common use is for voltage stability. From the power system dynamic stability viewpoint, the STATCOM provides better damping characteristics than the SVC as it is able to transiently exchange active power with the system.

. 4.2. Static Synchronous Series Compensator (SSSC)

This device work the same way as the STATCOM. It has a voltage source converter serially connected to a transmission line through a transformer. It is necessary an energy source to provide a continuous voltage through a condenser and to compensate the losses of the VSC. A SSSC is able to exchange active and reactive power with the transmission system. But if our only aim is to balance the reactive power, the energy source could be quite small. The injected voltage can be controlled in phase and magnitude if we have an energy source that is big enough for the purpose. With reactive power compensation only the voltage is controllable, because the voltage vector forms 90º degrees with the line intensity. In this case the serial injected voltage can delay or advanced the line current. This means that the SSSC can be uniformly controlled in any value, in the VSC working slot.

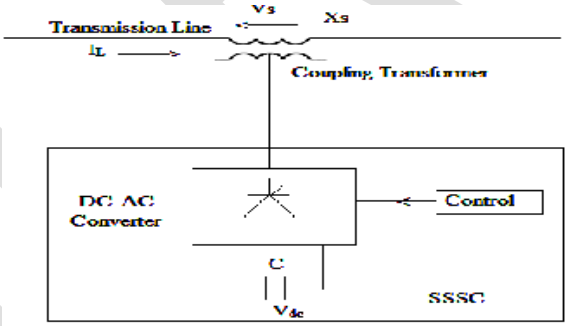

Fig.3. Static synchronous series capacitor

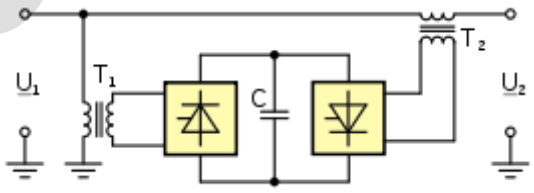

Fig.4.Unified Power Flow Controller

4.3. Unified Power Flow Controller (UPFC)

A unified power flow controller (UPFC) is the most promising device in the FACTS concept. It has the ability to adjust the three control parameters, *i.e.* the bus voltage, transmission line reactance, and phase angle between two buses, either simultaneously or

independently. A UPFC performs this through the control of the in-phase voltage, quadrature voltage, and shunt compensation. The UPFC is the most versatile and complex power electronic equipment that has emerged for the control and optimization of power flow in electrical power transmission systems. It offers major potential advantages for the static and dynamic operation of transmission lines. The UPFC was devised for the real-time control and dynamic compensation of ac transmission systems, providing multifunctional flexibility required to solve many of the problems facing the power industry. Within the framework of traditional power transmission concepts, the UPFC is able to control, simultaneously or selectively, all the parameters affecting power flow in the transmission line. Alternatively, it can independently control both the real and reactive power flow in the line unlike all other controllers.

5. TYPES OF NETWORK CONNECTION

5.1. Serial controllers

.It can consist of a variable impedance as a condenser, coil, etc or a variable electronics based source at a fundamental frequency. The principle of operation of all serial controllers is to inject a serial tension to the line. A variable impedance multiplied by the current that flows through it represents the serial tension. While the tension is in quadrature with the line current the serial controller only consumes reactive power; any other phase angle represents management of active power. A typical controller is Serial Synchronous Static Compensator (SSSC).

5.2. Controllers in derivation.

As it happens with the serial controller, the controller in derivation can consist of a variable impedance, variable source or a combination of both. The operation principle of all controllers in derivation is to inject current to the system in the point of connection. A variable impedance connected to the line tension causes variable current flow, representing an injection of current to the line. While the injected current is in quadrature with the line tension, the controller in derivation only consumes reactive power; any other phase angle represents management of active power. A typical controller is Synchronous Static Compensator (STATCOM)

5.3. Serial-serial Controllers.

This type of controllers can be a combination of coordinated serial controllers in a multiline transmission system. Or can also be an unified controller in which the serial controllers provide serial reactive compensation for each line also transferring active power between lines through the link of power. The active power transmission capacity, that present a unified serial controller or line feed power controller, makes possible the active and reactive power flow balance and makes the use of transmission bigger. In this case, the term "unified" means that the DC terminals of the converters of all the controllers are connected to achieve a transfer of active power between each other. A typical controller is the Interline Power Flow Compensator (IPFC).

5.4. Serial-derivation Controllers

This device can be a combination of serial and derivations controllers separated, coordinately controlled or a unified power flow controller with serial and derivation elements. The principle of operation of the serial-derivation controllers is to inject current to the system through the component in derivation of the controller, and serial tension with the line utilizing the serial component. When the serial and derivation controllers are unified, they can have an exchange of active power between them through their link. A typical controller is Unified Power Flow Controller (UPFC), which incorporating function of a filtering and conditioning becomes a Universal Power Line Conditioner (UPLC).

6. FACTS APPLICATIONS TO STEADY STATE POWER SYSTEM PROBLEMS

For the sake of completeness of this review, a brief overview of the FACTS devices applications to different steady state power system problems is presented in this section. Specifically, applications of FACTS in optimal power flow and deregulated electricity market will be reviewed.

6.1. FACTS Applications to Optimal Power Flow

In the last two decades, researchers developed new algorithms for solving the optimal power flow problem incorporating various FACTS devices [11]. Generally in power flow studies, the thyristor controlled FACTS devices, such as SVC and TCSC, are usually modeled as controllable impedance [4, 9, 10, 12-14]. However, VSC-based FACTS devices, including IPFC and SSSC, shunt devices like STATCOM, and combined devices like UPFC, are more complex and usually modeled as controllable sources [4, 9,13-17, 20]. The Interline Power Flow Controller (IPFC) is one of the voltage source converter (VSC) based FACTS Controllers which can effectively manage the power flow via multi-line Transmission System

7. APPLICATIONS AND TECHNICAL BENEFITS OF FACTS

FACTS The technical benefits of the principal for dynamic applications of FACTS in addressing problems in transient stability, dampening, post contingency voltage control and voltage stability are summarized in Table-1. FACTS devices are required when there is a need to respond to dynamic (fast-changing) network conditions. The conventional solutions are normally less expensive than FACTS devices, but limited in their dynamic behavior. It is the task of the planners to identify the most economical solution. Table 1. Technical benefits of the main FACTS devices

8. CONCLUSION

The essential features of FACTS controllers and their potential to improve system stability is the prime concern for effective & economic operation of the power system. The location and feedback signals used for design of FACTS-based damping controllers were discussed. The coordination problem among different control schemes was also considered. Performance comparison of different FACTS controllers has been reviewed. The likely future direction of FACTS technology, was discussed. In addition, utility experience and major real-world installations and semiconductor technology development have been summarized. A brief review of FACTS applications to optimal power flow and deregulated electricity market has been presented.

REFERENCES:

[1] Y. N. Yu, *Electric Power System Dynamics*. Academic Press, 1983.

[2] P. W. Sauer and M. A. Pai, *Power System Dynamics and Stability*.Prentice Hall, 1998.

[3] J. R. Smith, G. Andersson, and C. W. Taylor, "Annotated Bibliography on Power System Stability Controls: 1986- 1994", *IEEE Trans. on PWRS*, 11(2)(1996), pp. 794–800.

[4] N. G. Hingorani and L. Gyugyi, *Understanding FACTS: Concepts and Technology of Flexible AC Transmission Systems*. New York: IEEE Press, 2000.

[5] N. G. Hingorani, "FACTS-Flexible AC Transmission System", *Proceedings of 5th International Conference on AC and DC Power Transmission-IEE Conference Publication* 345, 1991, pp. 1–7.

[6] N. G. Hingorani, "Flexible AC Transmission", *IEEE Spectrum*, April 1993, pp. 40–45.

[7] N. G. Hingorani, "High Power Electronics and Flexible AC Transmission System", *IEEE Power Engineering Review*, July 1988

[8] R. M. Mathur and R. S. Basati, *Thyristor- Based FACTS Controllers for Electrical Transmission Systems*. IEEE Press Series in Power Engineering, 2002.

International Journal of Engineering Research and General Science Volume 3, Issue 5, September-October, 2015
ISSN 2091-2730

RETRIEVAL OF SEMANTIC VIDEO ACTIONS USING GENETIC ALGORITHM

Adarsh Purohit

Department Of Computer Science

+919407133295, Adarshpurohit@gmail,com

Nisha Bhalse

Department Of Computer Science

Abstract - For the huge amount of complexity and rich information in a video, it is difficult to preview and query a user interest video segmentation. More and more researchers are addressed in segmentation, content summarization, annotation and indexing within the video and then to develop a video retrieval system recently years. Unlike the text retrieval technologies, video and the voice content got less semantic definition. But with the growing network facilities and the mass storage technologies. our study on motion exploration, which is a most consistent feature between every one low-level construction for videos. The motion recovery method proposes in the research existing attempt in motion-based video retrieval. For practical video retrieval system, it should support multimodal and multi feature retrieval using genetic algorithm.

INTRODUCTION

With the development of the information science and
knowledge, and the accessibility of video capturing devices such as digital cameras, mobile telephone with cameras ,the size of digital video assembly is increasing quickly. As necessary technique in video index and search, content base video annotation has been major discover topic in the multimedia research community [1]. Though, nearly all videos have not explanation and manually annotating video is a time-consuming, error prone and individual process. Therefore, automatic or semi-automatic video annotation is the issue of a lot continuing research [2]. Its major aim is to repeatedly annotate video

Using a predefined lexicon to explain the video semantics, which has been predictable as a promising method for bridging the semantic gap among low-level features and high-level semantic concept? Still, real-world function is impossible to be classifying,
Simply to recognition of pre-studied carefully modeled measures. Furthermore, when dealing with
all-purpose video data, often there is no prior information about the types of events in the video succession, their worldly and spatial extent, or their nature (periodic/non-periodic). Among the a variety of types of video-semantic in sequence, actions pose the most challenge in terms of the accuracy that can be achieve in their automatic model and classification. Throughout the earlier decade, there has been important quantity of video annotation and event considerate research in a variety of function domains. The majority of the current approach to video annotation and event detection are collected of important models for precise event types that suit the objective in a exacting domain and increasing technical recognition methods. Hidden Markov Model (HMM) [3], and Dynamic Bayesian Network [4], were planned to incarcerate the spatial and temporal correlation of video events, and then the learnt model are utilize for predefined video event categorization or irregular event detection. Automatic appreciation of video highlights has been the focus of a number of research pains in recent years, however to replica and take out events for semantic classification by low-level video features remains a main challenge. It is though a current subject mostly due to an growing require for automatic classification of precise events in the networked society, at extremely least for examination and perceptual user interfaces. As is plain in numerous supervised learning problems, feature selection is significant. Support vector machine have been revealed to make defectively when there are numerous inappropriate features. Ad boost and SVM are included for feature selection and all together classification. Other researchers have deliberate optimization of support vector machine using genetic algorithms during feature subset and by combine these two used this method for image identification. Setting kernel parameters for a support vector machine in a training process has a comprehensible impact on the accuracy of the final classification. Simultaneous genetic-based optimization of feature subset selection and kernel parameters is presently establishment to be explore in multimedia documents classification. While the exceeding study we optimize one or two factors of using GA, we a different significant factor optimize instance selection. This method we selects an suitable reduce subset of the training sample and only uses the select subset for training. Our objective in this investigate to prevent the distort training of support vector machine by reducing the possibility of selecting noisy training samples as the support vectors, to improve classification accuracy .Our approach is narrative since no preceding study have introduce this simultaneous optimization of the GA in the field of video event classification. An assortment of data obtainable in the image and video format are being make,

stored, transmit, analyze, and access with advance in computer technology and communication network. To devise use of these data, an proficient and effective technique requirements to be developed for the retrieval of multimedia information. amongst the a variety of types of video-semantic information, measures pose the furthermost confront in terms of the accuracy that can be achieve in their automatic model and categorization.

RELATED WORK

Chengde Zhang in at al [1]proposed a novel framework, which determines the statistics and the delivery characteristics of the assembled terms in clustered key frames for web video event classification. They have proposed framework, an adaptive association rule mining technique is first established to address the subjects connected to the noisy data and the infrequent textual information. Subsequent, transitive closure is practical to collection the terms together, while the semantic associations between terms support better bridge the gap between NDKs and the high-level semantic notions.

Mohammad A. Mezher in at al [2]they have proposed genetic folding as an evolutionary algorithm for SVR model selection. In the experimentations, they have found GF was equivalent as operative as predefined models. This method is vigorous to the expletive of the kernel superiority which their assessment might have a suboptimal simplification due to the numerous dataset they have in hand. GF can characterize an NP problem using a unpretentious array of floating number illustration instead of using the tree structure. The proposed algorithm presented for regression problems due to its straightforwardness, ease of implementation, and sturdiness. However, the GF methodology is mostly design to grip kernel selection problems.

Si Xiao Yang in at al[3] they have solve varies problems under consideration., if the rule set is tremendously imbalanced the SVM may consequence in a bad model and the rule correctness may be too low on the underground points with an exact prediction on the mainstream. Subsequent, if we are reluctant to illustration a balanced model and fond of replacement all the patterns, they have should the meaning of accuracy and reliability.

Patharawut Saengsiri in at al[4]thee have declared above, high dimensionality of gene countenance data is stimulating because it is time incontrollable and similarly has high miss classification. Numerous algorithms are not appropriate for large dimensional data. However, they have few methods which work with the filter and wrapper methods together. So, this research suggests evaluation of hybrid feature assortment models on gene expression data. The consequence of the investigate displayed improved performance which concentrated subsets of genes and correspondingly increased accuracy.

Ho Sun Shon in at al[5] compared and assessed the performance, constructing the classifiers using the genes designated by the exceeding technique, and then applying the test data set to them. Also they have assessed the performance of the feature assortment by LASSO regression after applying filter technique. They have used leukemia data as testing data. Also the have tested Bayesian network, naive Bayesian, logistic regression, support vector machine, and random forest as classifiers. Establish the selection collective filter technique with LASSO technique outperforms the current important gene assortment approaches.

Shutao Li in at al [6] in this paper, a feature extraction method based on the discrete wavelet transform (DWT) is proposed. The approximation coefficients of DWT, together with some useful features from the high-frequency coefficients selected by the maximum modulus method, are used as features. The combined coefficients are then forwarded to a SVM classifier. The combined coefficients are then forwarded to a SVM classified.

Prabakaran Subramani In at al[7]In the present paper, the problem of feature selection of microarray gene expression data was considered. We analyzed the wavelet power spectrum of genes and proposed a clustering and feature selection method useful for classification based on haar wavelet power spectrum, it is technique for problem domains like disease classification, gene network identification and personalized drug design.

Yihui Liu in at al [8]In this paper we propose a novel method of feature extraction to characterize the localized features of microarray data. One dimensional multilevel wavelet decomposition is performed on microarray data to extract features and reduce dimensionality. The microarray data is actually composed of four separate exponentials at different times. Localized features occur in the four derivatives

Sun, K. in at al [9] n this paper, we introduce w-support a new measure of item sets in databases with only binary attributes. The basic idea behind w-support is that a frequent item set may not be as important as it appears, because the weights of transactions are different. paper is organized as follows: First, WARM is discussed. Next, we present the evaluation of transactions with HITS, followed by the definition of w-support.

Singh S, In at al [10] This article presents a bibliographic survey over the last 40 years on the research and development and on the procedures for evaluating faults by dissolved gas analysis of power transformers.

Akbari, A In at al[11] in this paper they reprent Condition monitoring and software-based diagnosis tools are central to the implementation of efficient maintenance management strategies for many engineering applications including power transformers.

David Martens in at al [12] in this paper, we propose a new Active Learning-Based Approach (ALBA) to extract comprehensible rules from opaque SVM models. Through rule extraction, some insight is provided into the logics of the SVM model. ALBA extracts rules from the trained SVM model by explicitly making use of key concepts of the SVM, This performance increase, both in terms of predictive accuracy as comprehensibility, is confirmed in our experiments where we apply ALBA on several publicly available data sets.

D. Martens in at al [13] we provide an overview of previous ant-based approaches to the classification task and compare them with state-of-the-art classification techniques, such as C4.5, RIPPER, and support vector machines in a benchmark study. On the other hand, a new ant-based classification technique is proposed, named Ant Miner+. The key differences between the proposed Ant Miner+ and previous Ant Miner versions are the usage of the better performing MAX-MIN ant system, a clearly defined and augmented environment for the ants to walk through, with the inclusion of the class variable to handle multiclass problems.

Chih-Wei Hsu in at all [14] In this paper we give decomposition implementations for two such "all-together" methods. We then compare their performance with three methods based on binary classifications: "one-against-all," "one-against-one," and directed acyclic graph SVM (DAGSVM). Our experiments indicate that the "one-against-one" and DAG methods are more suitable for practical use than the other methods.

PROPOSED METHODOLOGY

Human action recognition in video supervision. in the case of video- supervision attractive events can be precise events such as people inflowing a illegal area, being aggressive or person destructive public assets, and so on. object recognition there is require to cope with the problem of high inconsistency in lighting variation, geometrical alteration, clutter and occlusion. Approach to symbolize domain knowledge and relative information of behavior and actions. In the broadcast information domain numerous events of attention do not occupy people furthermore a number of of them do, but more information can be obtain from connected cues as an example visual cues of smoke and fire, in concert with a detection of a urban prospect can distinguish a riot. as well in the sport domain related information and its temporal development include nearly all of the information, thus no being motion study is frequently performed to detect attractive events. Events might as well narrate to the motion of an object such as a vehicle, in this case we pass on to object motion and vehicle motion actions which are of attention in the broadcast and in the video- supervision domains. actions connecting multiple community or occurrence in longer timeframes can be referred as behavior . Activity examination requires higher level representation frequently build with action detectors and reasoning engines. actions can be distinct behavior as long as there is not extreme inter-person occlusion and therefore a system is capable to analyze every individual motion. In case of attendance of a big quantity of people, the assignment is distinct as crowd analysis people are no further measured as persons but the worldwide motion of a crowd is model. In this case the discovery of irregular events is famous since of its applicability to supervision scenario and because of the inherent impenetrability of exactly important crowd behaviors. Human actions are enormously helpful in important the video semantics in the domains of movies and customer generate satisfied. In both domains the analysis method are comparable and confront happen mostly from the high intra-class variance. suitable information such a static features or scene classifiers might get better event approval performance. Some supportive solution has to be inventive in terms of efficiency and strength in manipulative a content descriptor that represent the semantics of the data item. Great volume: In real life request, the size of video data is enormous still every item is a great deal better than a tuple in a conservative data repository). Dealing with such data items necessitates huge amounts of computational possessions such as storage and data processing power. Novel technique for helpful such large data sets require to be developed to give economic and efficient way in and management. Elevated dimensionality: Video contains a huge quantity of visual, audio and textual information. The connected illustration is high-dimensional in environment. In extreme cases. Intricate inside structure: Video can be treat as a nonlinear work of different kind of information. This might guide to complexity level of video satisfied enormously high. In this case, apply established solutions developed for the extraction of information and classify consequences from structured data is not practicable and stratificatory consequence can not be predictable. Further, it appear that information finding and retrieval in video compilation cannot be just based on the linear concatenation of the incomplete information obtain from every part of the aim object. Therefore, rising multimodal technique to put together dissimilar kinds of information effortlessly is middle of importance for effectual knowledge discovery and information retrieval. chiefly, event detection is an significant problem for mining huge video collection and to the greatest of our information, no existing techniques consider multimodal information combination.

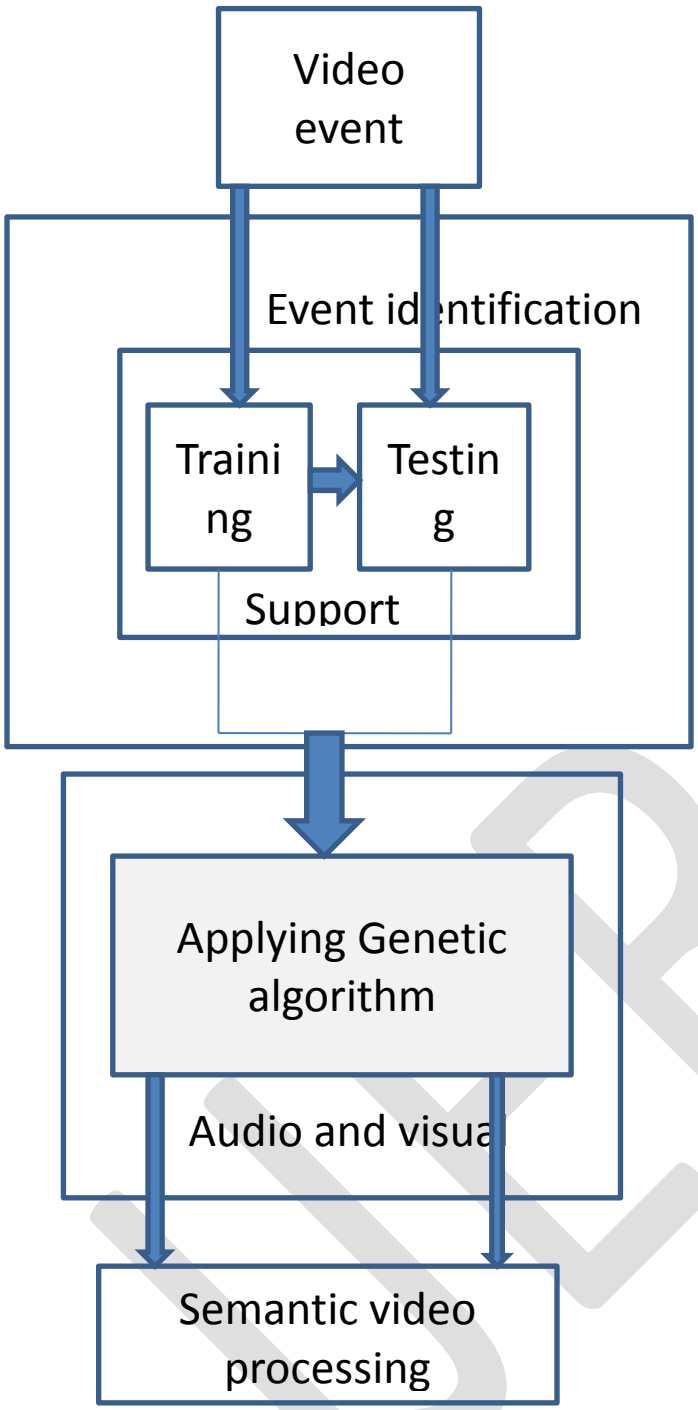

Figure 1: framework for video event classification

One of nearly everyone significant reasons behind the attractiveness of video data are the affluence of its content and its attractiveness. The meaning of information finding over huge video collection is reflective and however to be fully investigated. How to propose and expand the method to make easy effective video information organization is still a difficult task. This work explains a narrative event detection framework to help the process. The essential thought of this move toward is to relate a narrative subspace selection method to make video descriptor via learning process. As a GA, the optimization methods focus on the interclass scope points. These points have added discriminant capability than the inclusive interclass points. Meanwhile, the interrelated technique can preserve the intermodal geometric structure by with linear restoration coefficients. An integrated exchange matrix can be learnt for the raw video data formed by a diversity of modalities. It enables the system further flexible since it can furthermore work well when one or added modalities of the testing sample are not accessible. On the further hand, Kernel variant has been as well proposed to overcome the nonlinear problem and additional improve the facility of basic scheme. The system has been entirely implemented. As shown figure 1 in new estimate based on huge video collections, our method considerably improves the efficiency and effectiveness

over the state of art systems. At the same time, enhanced robustness beside dissimilar kind of noise or distortion is achieved. The present work can be comprehensive in
an only some directions for potential analysis.

Training illustration Generation: One of the most important limitations is that routine of that method largely depends on the limited size of the labeled training data set. The present approach to choose training example is at rest exclusive in terms of human-related cos. To address the difficulty of the limited number of labeled training sample and expensive cost, a probable solution is to use unlabeled data to get more accurate view. Basic idea of the advance is to use existing data to train classifier to label data and label them based on suitable class information. Those classified data can be used as training sample.

• **Analysis of Statistical Evaluation Results:** Since currently evaluation scheme used in this study have been tested based on limited classes of video collections. It would be interesting to apply same techniques to video collections in other domains and make a comprehensive empirical study. The results from such quantitative analysis should be helpful in rounding out our understanding of system behavior and in providing feedback into the Design and tuning of identification systems. System Performance Prediction: A huge number of estimation techniques have been developed to develop performance information concerning effect distribution. It is practicable to apply some of them, such as regression estimators, to evaluate stability estimation over dissimilar collection sizes video. In calculation, other multivariate data analysis method also automated cluster analysis, such as multidimensional scaling and logistic regression, could be helpful for reducing relation data size considerably. Our propose framework is to optimize feature selection, instance selection as well as the SVM kernel parameters simultaneously using GA. To intend to evolve the optimal kernel using the GA itself and we will evaluate the classification performance of the framework using different visual and spatiotemporal feature. Accurate models for video event classification and it is important research issue since they are essential components for effective video indexing and retrieval. To analysis newly kernel-based methods, mainly support vector machines have develop into accepted in multimedia classification tasks. To offer a novel approach to enhance the performance of GA for video events classification based on a search method.

Our process technique: The proposed technique based on the comparative location of the semantic object, according to the principle of comparative motion of objects in the video object study, we work out the distance among a variety of semantic objects exposed in the video, as time goes on, the distance between objects modify, several of the objects fixed relation location in the video, while the relative dislocation among some objects are greater. We form a group of the objects among which comparative displacements small alter in the video. Then, the video can be created on a quantity of semantic object collection. We can set the tone of this group as the environment group and the rest collection as the fore collections, compute the relation displacement between the collections, we can get trajectory of the object in the foreground collections.

A. Semantic object recognition

Semantic video objects recognition is an important step in trajectory detection, follow-up of the semantic object tracking and semantic analysis are based on the semantic object recognition. Semantic object recognition is the key feature extraction of semantic objects, because each type of video object itself contains a consistent structure definition and forms, video object recognition usually requires extraction of the features of a particular structure, then this feature is introduced into the corresponding pattern recognition tasks [4].

Extract a semantic object includes the following three steps:

Video semantic segmentation, the video is divided into a series of semantic fragments, the semantic information of these split fragments stored in the database.

Object recognition, the video frame is divided into several irregularly shaped regions based on texture and contour, video frame image segmentation using the method of extracting contours and gets the edges of region on the frame; every region is seen as a semantic object.

Tagging semantic for the objects and indicating that the meaning of objects. Video object tagging can be defined in two ways: one way is according to the understanding and knowledge of the objects in the feature extraction process, such as extraction of car shape, the face model, cloud, sky and other features; the other algorithms is on a large number of objects through the process of learning the model samples to get the class object features. The first algorithm requires a lot of prior information. It is used into the semantics of a specific video detection, such as sports video, news and video. The second algorithm is suitable for generic video. Learning-based semantic object recognition algorithm, KNN (K-nearest neighbor) algorithm, SVM (support vector machine) algorithm is better [6].

. Semantic object detection and tracking

Object - Location Information Semantic trajectories detection based on the results of the semantic object detection, according to the semantics recognition algorithm described above, the semantic fragment is divided into a series of semantic object,

Conclusion

Our study on motion exploration, which is a most consistent feature between every one low-level construction for videos. The motion recovery method propose in the research existing attempt in motion-based video retrieval. For practical video retrieval system, it must support multimodal and multi feature retrieval. Thus every these work will be extensive to develop retrieval function base on elevated-level semantic query combined with frequent features. From the consequences, it classifies the situation of the object group, and according to the relative dislocation of the object detected management track plane. The algorithm for trajectories finding of affecting semantic objects in video is simple to implement and has superior performance.

REFERENCES:

[1] Chengde Zhang, Xiao Wu, Mei-Ling Shyu, Qiang Peng," Adaptive Association Rule Mining forWeb Video Event Classification" IEEE IRI 2013, August 14-16, 2013, San Francisco, California, USA

[2] Mohammad A. Mezher, Myasam F. Abbod," A New Genetic Folding Algorithm For Regression Problems" 14th International Conference on Modelling and Simulation- 2012.

[3] Si Xiao Yang, Ying Jie Tian, Chun Hua Zhang," Rule Extraction from Support Vector Machines and Its Applications" IEEE/WIC/ACM International Conferences on Web Intelligence and Intelligent Agent Technology- 2011.

[4] Patharawut Saengsiri, Sageemas Na Wichian, Phayung Meesad, Unger Herwig," Comparison of Hybrid Feature Selection Models on Gene Expression Data" Eighth International Conference on ICT and Knowledge Engineering- 78-1-4244-9875-8/10 -2010.

[5] Ho Sun Shon,Kenu Ho Ryu," Feature Selection of Gene Expression Data Using Regression Model" 2010 10th IEEE International Conference on Computer and Information Technology (CIT 2010).

[6] L. Shuto, L. Chen, and T. K. James, "Wavelet-based Feature Extration for microarray Data Classification", International Joint Conference on Neural Networks, pp.5028-5033, 2006.

[7] P. Subramani, R. Sahu, and S. Verma, "Feature selection using Haar wavelet power spectrum", Bioinformatics, Vol.7, No.432(Issue1), 2006.

[8]Yihui Liu, Wavelet feature extraction for high-dimensional microbar ray data, Neurocomputing72 (2009)985–990,on & 2008 ElsevierB.V.Allrightsreserved.

[9] Sun, K. Fengshan Bai, (2008), Mining Weighted Association Rules without Pre-assigned Weights IEEE Transactions on Knowledge and Data Engineering Vol.20,Iss. 4,pp. 489 -495

[10] Singh S, Bandyopadhyay M. Dissolved gas analysis technique for incipient fault diagnosis in power transformers: a bibliographic survey. IEEE Electrical Insulation Magazine 2010; 26(6): 41-46.

[11] Akbari A, Setayeshmehr A, Borsi H, Gockenbach E. Intelligent agent-based system using dissolved gas analysis to detect incipient faults in power transformers. IEEE Electrical Insulation Magazine 2010; 26(6): 27-40

[12] David Martens, Decompositional Rule Extraction from Support Vector Machines by Active Learning, IEEE transaction on knowledge & Data Engineering

[13] D. Martens, M. De Backer, R. Haesen, M. Snoeck, J. Vanthienen, and B. Baesens, "Classification with Ant Colony Optimization," IEEE Trans. Evolutionary Computation, vol. 11, no. 5, pp. 651-665, 2007.

[14] Chih-Wei Hsu and Chih-Jen Lin,, A Comparison of Methods for Multiclass Support Vector Machines,, IEEE TRANSACTIONS ON NEURAL NETWORKS, VOL. 13, NO. 2, MARCH 2002.

[15] CHIH-WEI HSU,CHIH-JEN LIN A Simple Decomposition Method for Support Vector Machines Machine Learning, 46, 291–314, 2002c 2002 Kluwer Academic Publishers. Manufactured in The Netherlands.

[16] V. S. Tseng, M.-H. Wang, and J.-H. Su, "A new method for image classification by using multilevel association rules," in IEEE International Conference on Data Engineering (ICDE05), April 2005, pp. 1180–1188.

[17] C. S. Kanimozhih Selvi and A. Tamilarasi, "Association rule mining with dynamic adaptive support thresholds for associative classification," in IEEE International Conference on Computational Intelligence and Multimedia Applications (ICCIMA07) December 2007, pp.76–80.

[18] P. Vateekul and M.-L. Shyu, "A conflict-based confidence measure for associative classification," in IEEE International Conference on Information Reuse and Integration (IRI08), July 2008, pp. 256–261.

[19] A. F. Smeaton, P. Over, and W. Kraaij, "Evaluation campaigns and TRECVid," in ACM International Workshop on Multimedia Information Retrieval (MIR06) October 2006, pp. 321–33

[20] I. Bouzouitz and S. Elloumi, "Integrated generic association rule based classifier," in IEEE International Conference on Database and Expert Systems Applications(DEXA07) , September 2007, pp. 514–518

International Journal of Engineering Research and General Science Volume 3, Issue 5, September-October, 2015
ISSN 2091-2730

Resource allocation & avoidance dead node occurrence using overlap sensing ratio with dual base station in WSN

Aashish Anand
Bharati Vidyapeeth College Of Engineering, Pune-Satara Road, Pune-411043,
Maharashtra, India
E-Mail: aashishanand92@gmail.com
Ph: 9582834508

Abstract-- In current technology advances have led to the beginning of small, low-power devices that integrate sensors and actuators with limited on-board processing and wireless communication capabilities to a large extent the effectiveness of the wireless sensor networks depends on the coverage provided by the sensor deployment scheme. There are different deployment demands and optimization goals in different environment. In this research paper, first sensor node sense the dead node occurrence zone & then overlap randomly shift the node on target location an overlap sensing ratio has been proposed for the coverage which is divided with dual base station, single base station coverage is fifty percent of the network size which get improving sensing area for maximum distance in WSNs. This method increases the total coverage ratio by overlap sensing after the initial deployment with AWGN channel.

Keywords--- WSNs, Enhance Coverage ratio, sensor nodes, grid, resource allocation, overlap sensing ratio, dual base station, AWGN channel.

I INTRODUCTION

In wireless sensor network assigning few heterogeneous nodes is an effective way to increase network lifetime and reliability. The WSNs is the networks composed of low-cost, low-power, and small-size sensors that have circle sense area and communicate information by multiple node & only provide simple sensing data, such as temperature, humidity, and so not as to meet the necessity of more difficult and accurate data applications. But WSNs is the circulated sensing networks composed of video cameras that have sector sense area and can process, send, and receive more concentrated and complicated video information data by packaging with wireless transceiver and differ from the WSNs due to their characteristic of directivity and turn ability.

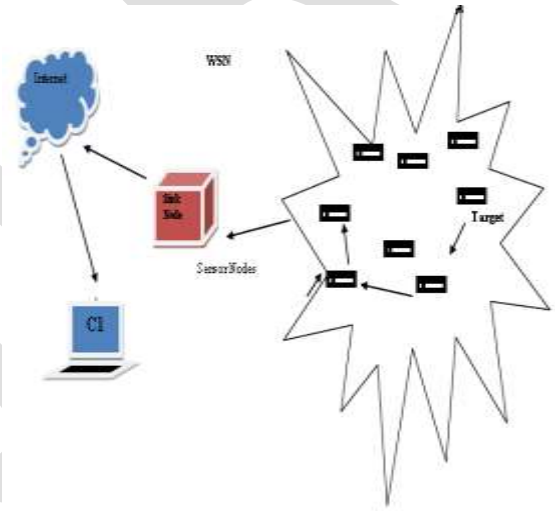

Figure. 1 Wireless Sensor Network with sensor node

ECRM (enhance coverage ratio)

The process of ECRM can be separated into rounds and there are three phases in each round: backbone setup phase, cluster formation phase and steady communication phase. On the first stage, considered only fixed nodes, the communication backbone of network is formed, which should be continued until the first fixed node die, according to ECR protocol. After the backbone setup, Cluster will be formed and the cluster heads on each layer will be selected. On the last stage, data will currents to the base station via the communication link setup by the first two phases. Obviously, the critical phase of ECRM will be implemented in the second phase. In ECRM, cluster heads are in charge of long distance communication and data fusing which are serious energy consumption tasks.

Additive white Gaussian noise (AWGN)

The AWGN is a noise channel. It is a simple model of the imperfections that a communication channel consists of The disturbance caused by the Thermal noise is modeled as Additive White Gaussian Noise.

This noise channel classically is decent for cable and profound space communication but not in experienced communication since of multipath, land obstructive and interfering.

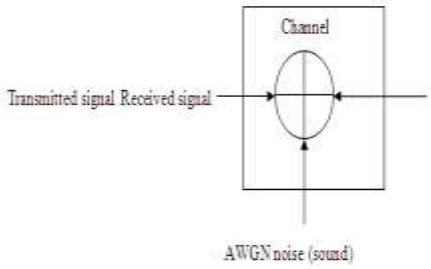

Figure 2: AWGN channel (frequency)

AWGN is used to pretend contextual noise (sound) of channel. In time domain the noise gets added in the transmitted signal so the received signal can be represented as – r (t) = s(t) + n(t) , where s(t) is conveyed signal and n(t) is contextual noise (sound). C AWGN = W log2 (1+P/N0W) bits/Hz

II PROBLEM DEFINITION

Numerous workings have been approved in the field of WSN to remove the redundant data. In our paper [1] it is deliberated that whenever, an event takes place in a detected region it is first of all detected by the hexagonal sensors. Once detecting the event the scalars communicate the information to their respective sensor node. The condition is that the sensor node should lie within the field of view of camera. Then the sensors exchange their reading with each other collaboratively and decide in a distributed manner that who among them are to be actuated. However, the problem is that when the event takes place sensing of event not only occurs within the event region but also up to some extent outside the event region.

III SYSTEM MODEL

Grid points are used in two ways in WSN deployment; either to measure coverage or to determine sensors positions. The grids points can also be used in decide deployment technique. Coverage percentage is ratio of area covered to the area of region of area. A grid-based sensor network as described is to divide the Region of interest (ROI) into grids and the sensors can only be placed at the center of the grid [1],[2].

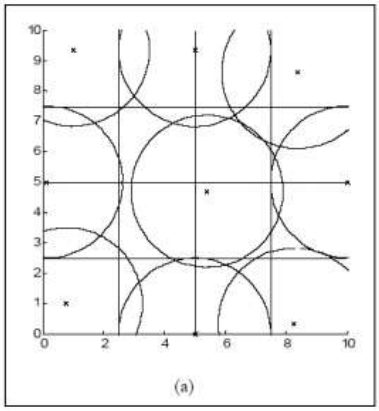

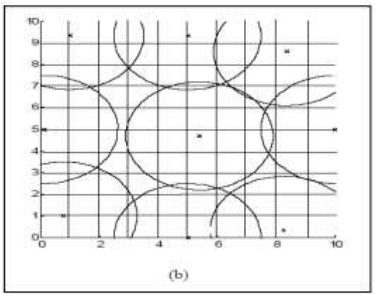

Figure 2: Grid based coverage estimation for 9 sensors

But in a sparse network large grid size is better as it will avoid overlapping of sensors' sensing range therefore ensuring occupied utilization of their sensing abilities. The guaranteed coverage assured by grid based deployment can be cooperated by errors such as misalignment and misplacement. Grid-based sensor networks as described in divide the ROI into square grids and the sensors can only be placed at the center of the square. This results in the bigger the grid size with respect to the sensing range the higher the probability that an object can penetrate the area without detection, provided that the object is traversing along the grid lines [7].

Sensor Deployments A) Sensor Deployments Based on Square:

i) Four sensors at four vertexes of the square (its edge length is equal to r) as illustrated in Fig. 4, four sensors are respectively deployed at four vertexes of the square the length of which edge is equal to the length of the radius r of circle. The efficient coverage area SEACsI is

$$S_{EACsI}=\frac{150}{360}\pi r^2\times 4+\frac{1}{2}r\times r\sin\left(\frac{\pi}{3}\right)\times 4+r\times r$$

$$=\frac{5}{12}\pi r^2\times 4+\frac{1}{2}r^2\times\frac{\sqrt{3}}{2}\times 4+r^2$$

$$=\left(\frac{5\pi}{3}+\sqrt{3}+1\right)r^2$$

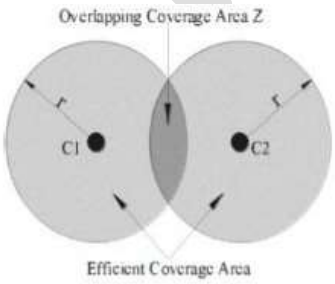

Figure 3: Efficient coverage area

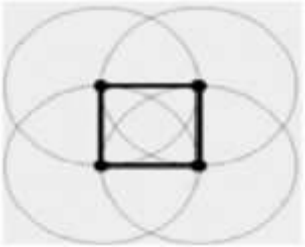

Figure 4: Four sensors at vertexes of square (edge length is r)

The sensor nodes in this technique need to be carefully placed accurately at the selected grid points. This technique promises to provide certain percentage and degree of coverage and also the connectivity. There are three types of grids commonly used in networking; triangular lattice, square grid and hexagonal grid. Triangular lattice is the best among the three kinds of grids as it has the smallest overlapping area hence this grid requires the least number of sensors, square grid provide fairly good performance for any parameters while hexagonal grid is the worst among all since it has the biggest overlapping area .Other than type of grid the size of grid also plays an important role. The size of grid need to be chosen based on how dense the WSN going to be. For a highly dense network small size grids help in reducing coverage nodes thus providing better result.

IV PROPOSED METHOD

ALGORITHM FOR ECOSR

1. Find neighboring sensors nodes in grid ;
2. If dead node occurrences;
3. Shift advance node due to dead node in another grid or area;
4. Set parameter state=1
5. While (overlap==1)
6. Calculate OSR;
7. Node overlap optimal angle according to the rotation angle function;
8. if (network is equilibrium)
9. overlap =0;
10. end
11. end
12. calculate OSR;
13. while(OSR>=predefined threshold)
14. calculate priority;
15. if(priority is highest)
16. state=0;
17. send state information to its neighboring sensors
18. else
19. calculate OSR;
20. end
21. end

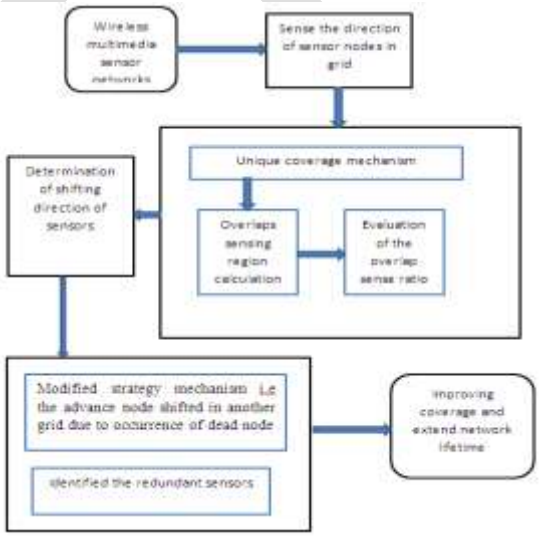

Figure 5: Proposed flow chart

V.RESULT

We evaluate the performance of the Enhance coverage overlap sensing ratio with dual station (ECOSR) algorithm, the Random approach each sensor select its sensing direction randomly.

We also take help of AWGN channel for reduce the noise during sensing ratio & shifting the node on target location without any noise.

Simulation Parameters	Values
Network of field size (area)	**200*200**
Number of sensor nodes (N)	**100**
Number of advanced nodes (an)	**0.2**
Number of normal nodes (nn)	**0.8**
Energy of a normal node (E_0)	**0.5**
Location of the base station	**Centroid**
Sensor network deployment type	**Random**
Simulator software Version	**2012a**
Mobility model	**Random wave-point**
Sensing range	**100**
Grid radius	**3.5**
Fading	**AWGN**

Table 1: Simulation parameter

In figure 1 sensor area predicting for minimum energy node which is executing towards low or dead

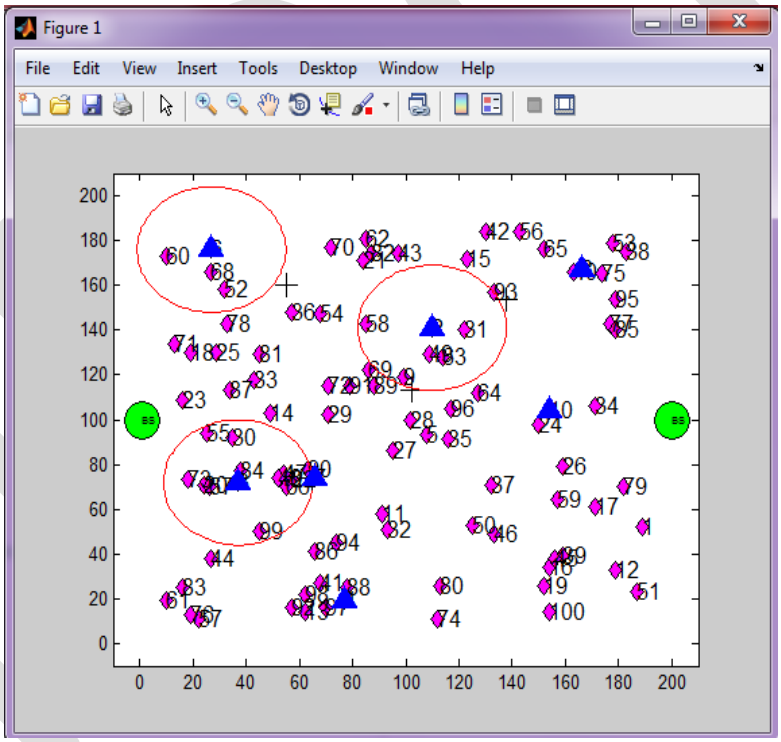

Fig. 1: 100 Nodes with lower energy node sensing in 100 coverage range with dual station

In the below figure 2, higher energy node shifting towards week node into the void grid or single sensor node in a network.

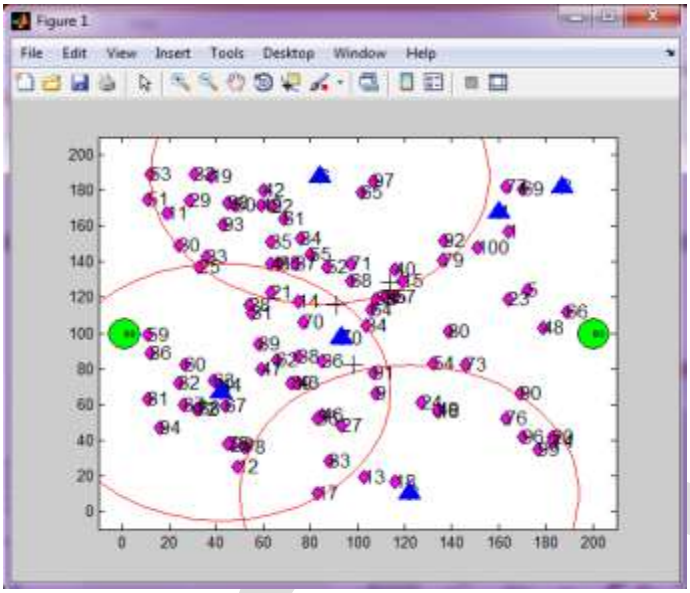

Fig. 2: After shifting the nodes network update the nodes position

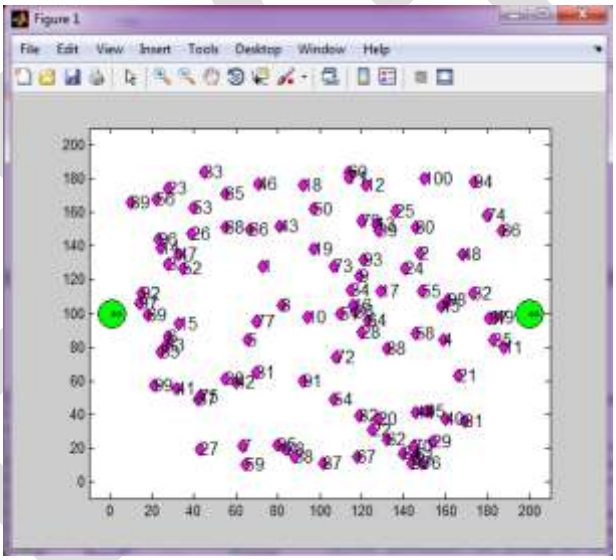

Figure 3: After overlapping lower energy to higher energy node

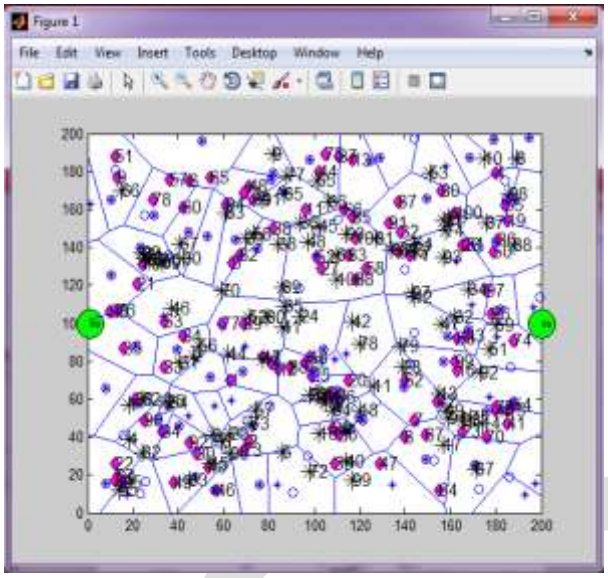

Fig. 4: Updating the node energy in Hexagonal grid for 100 nodes

VI CONCLUSION

In wireless communication systems have enabled the development of low-cost, low-power, multifunctional, tiny sensor nodes that can sense, process, and communicate with one another over random deployment distances. A sensor node by itself has severe resource constraints, including low battery power, limited signal processing, limited computation and communication capabilities, and a small amount of memory. Optimal resource management and assuring reliable QoS (qulity of service) are two of the most fundamental requirements in wireless sensor networks. Sensor deployment strategies play a very important role in providing better QoS, which relates to the issue of how well each point in the sensing field is covered. As we know based on the experimental records, coverage hole problems may exist in the sensor networks if the random deployment strategy is used to deploy the static sensor nodes. In this paper, we have proposed a grid-based with overlap sensing ratio recovery mechanism for wireless sensor networks. The whole network will be divided into grids to ensure the coverage ratio and connectivity.

In future work, the virtual force has been taken into consideration for allocating the mobile nodes to recover the hole grid. The proposed hole recovery mechanism could resolve the hole problem and maintain a high coverage ratio in hybrid wireless sensor networks. Furthermore, it could enhance network performance and prolong the network lifetime.

REFERENCES:

[1] Y. Mohamed and K. Akkaya, "Strategies and techniques for node placement in wireless sensor networks: A survey," *Ad Hoc Networks*, vol. 6, no. 4, pp. 621–655, 2008.

[2] Kansal, W. Kaiser, G. Pottie, M. Srivastava, and G. Sukhatme, "Reconfiguration methods for mobile sensor networks," *ACM Transactions on Sensor Networks*, vol. 3, no. 4, 2007.

[3] M. A. Guvensan and A. G. Yavuz, "On coverage issues in directional sensor networks:A survey," *Elsevier AdHoc Network s* , February 2011.

[4] D. Tao, H. Ma, and L. Liu, "Coverage-enhancing algorithm for directional sensor networks," in *Lecture Notes in Computer Science:Mobile Ad-hoc and Sensor Networks*, vol. 4325, November 2006, pp. 256–267.

[5] J. Zhao and J.-C. Zeng, "An electrostatic field-based coverage-enhancing algorithm for wireless nmultimedia sensor networks," in Proc. of IEEE Intl. Conf. on Wireless Communications, Networking and Mobile *Computing (WiCom'09)*,Beijing, China, September 2009, pp. 1–5.

[6] H. Ma, X. Zhang, and A. Ming, "A coverage-enhancing method for 3d directional sensor networks,"in *Proc. Of IEEE Intl.Conf.on Computer Communications(INFOCOM'09)*,Rio de Janerio, Brazil, April 2009, pp. 2791–2795.

[7] L., Adler, R., Buonadonna, P., Chhabra, J., Flanigan, M., Kushalnagar, N., Nachman, L., and Yarvis, M.: Design and deployment of industrial sensor networks: experiences from a semiconductor plant and the North Sea. In Proceedings of the 3rd international conference on Embedded networked sensor systems . (2014) 64-75

[8] GaoJun Fan and ShiYao, Jin, "Coverage Problem in Wireless Sensor Network: A Survey", Journal of Networks, Vol. 5, No. 9, September 2010.

[9] Jian Chen, Lu Zhang, and YounghongKuo, "Coverage Enhancing Algorithm Based on Overlap-Sense Ratio in Wireless Multimedia Sensor Networks",IEEE SENSORS JOURNAL,vol. 13,no.6,june. 2013.

[10] C.-Y. Chong and S. P. Kumar, "Sensor networks: evolution, opportunities, and challenges," Proceedings of the IEEE, vol. 91, no. 8, pp. 1247–1256, 2003.

[11] W. Dargie and C. Poellabauer, Fundamentals of wireless sensor networks: theory and practice. Wiley. com, 2010.

[12] Elizabeth Basha, Sai Ravela, and Daniela Rus. Model-Based Monitoring for Early Warning Flood Detection. In Proc. of Sensys, 2008.

[13] Jude Allred, Ahmad Bilal Hasan, Saroah Panichsakul, William Pisano, Peter Gray, Jyh Huang, Richard Han, Dale Lawrence, and Kamran Mohseni. SensorFlock: An Airborne Wireless Sensor Network of Micro-Air Vehicles. In Proc. of Sensys, 2007.

[14] M. Cardei, M. Thai, and W. Wu. Energy-efficient Target Coverage in Wireless Sensor Networks. In Proc. of IEEE Infocom, Miami, Forida, USA, March 2005

[15] Younghun Kim, Thomas Schmid, Zainul Charbiwala, Jonathan Friedman, and Mani Srivastava. NAWMS: Nonintrusive Autonomous Water Monitoring System. In Proc. of Sensys, 2008

International Journal of Engineering Research and General Science Volume 3, Issue 5, September-October, 2015
ISSN 2091-2730

Modified bridgeless SEPIC for BLDC motor with ripple free input current

Surumi. S

M.Tech Student of MG University, Kerala, surumi2459@gmail.com

Abstract— A modified version of the bridgeless single-ended primary inductance converter (BL-SEPIC) as preferred to varying the speed of BLDC motor is presented in this paper. The conduction losses and ripple current in the input side of conventional SEPIC converter can be overcome by bridgeless SEPIC converter with auxiliary circuit. The performance of the system was analyzed through a MATLAB/Simulink model during discontinuous inductor current mode (DICM).

Keywords— SEPIC- Single Ended Primary Inductance Converter, PFC- Power Factor Correction

INTRODUCTION

The Brushless DC (BLDC) motor is rapidly gaining popularity by its utilization in various industries, such as appliances, automotive, aerospace, consumer, medical, industrial automation equipment and instrumentation. A BLDC motor is known as a "synchronous" type because the magnetic field generated by the stator and the rotor revolve at the same frequency. One benefit of this arrangement is that BLDC motors do not experience the "slip" typical of induction motors. While the motors can come in one, two, or three phase types. As the name implies, the BLDC motors do not use brushes for commutation; instead they are electronically commuted[3]. BLDC motors have many advantages over brushed DC motors and induction motors, a few of these are,

a. Better speed Vs torque characteristics
b. High dynamic response
c. High efficiency
d. Long operating life
e. Noiseless operation

Fig.1 shows the typical driving circuit for BLDC motor. The input circuit consists of a half wave or full wave bridge rectifier followed by a capacitor capable of maintaining a voltage of approximately the peak voltage of input sine wave until the next peak come along to recharge the capacitor. So the power factor will decrease. In such cases, active or passive power factor correction may be used to counteract the distortion and raise the power factor. Passive PFC uses a capacitive filter at the AC input to correct poor power factor. Passive PFC may be affected when environmental vibration occurs. Passive PFC requires that the AC input voltage be set manually. Passive PFC does not use the full energy potential of the AC line**.**

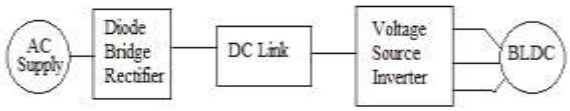

Fig.1 Typical driving circuit for BLDC motor

Many types of active power factor correction circuits are there buck converter, boost converter, buck-boost converter, conventional SEPIC converter, etc. Since, the input current of the PFC buck converter has dead angles during the time intervals when the input voltage is lower than the output voltage, there is a strong trade off between power factor and output voltage selection. On the other

hand, a SEPIC PFC converter can provide a high power factor regardless its output voltage due to its step up/down function. Several bridgeless single-ended primary inductor converters (SEPICs) were proposed. The efficiency of these converters is improved by removing the input bridge diode. However, bulk input inductor or another *LC* filter is required to suppress the input current ripple.

II. PROPOSED CONTROL SCHEME FOR PFC CONVERTER

Fig.2 shows the block diagram of the efficient bridgeless SEPIC converter for BLDC motor with improve power factor. The bridgeless SEPIC PFC converter the component count is reduced and it shows high efficiency due to the absence of the full-bridge diode. However, in this converter, an input inductor with large inductance should be used in order to reduce the input current ripple. In addition, the conduction losses on intrinsic body diodes of the switches are caused by using single pulse width modulation (PWM) gate signal[3].

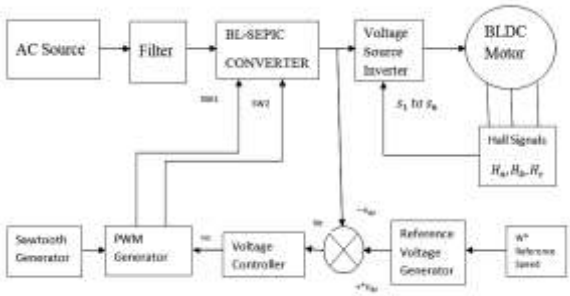

Fig.2 Block diagram of the proposed model

In order to overcome these problems, a bridgeless SEPIC converter with ripple-free input current is proposed in Fig. 3. An auxiliary circuit, which consists of an additional winding of the input inductor, an auxiliary small inductor, and a capacitor, is utilized to reduce the input current ripple. Coupled inductors are often used to reduce current ripple.

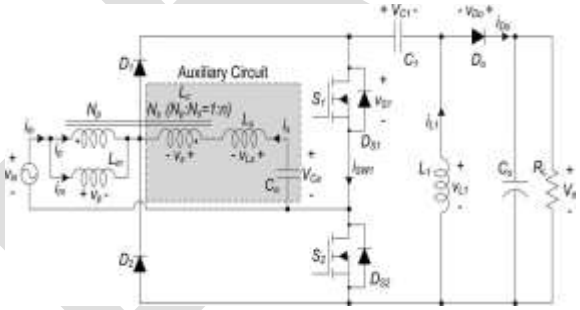

Fig.3 Proposed bridgeless SEPIC converter

A. Modelling of Proposed PFC Converter Based PMBLDCM Drive

The equivalent circuit of brushless dc motor is shown in Fig. 4. It consists of three phase star connected stator winding with phase resistance, inductance and induced back emf. The modelling is based on the following assumptions[4].

(1) Induced currents in the rotor due to stator harmonic fields are neglected.

(2) Iron and stray losses are also neglected.

(3) Damping is provided by the inverter control

Table. 1 switching sequence for 120 degree

Hall sensor position			Conducting Phases			Conducting switches					
A	B	C	A	B	C	S1	S2	S3	S4	S5	S6
1	0	0	+1	0	-1	1	1	0	0	0	0
1	1	0	0	+1	-1	0	1	1	0	0	0
0	1	0	-1	+1	0	0	0	1	1	0	0
0	1	1	-1	0	+1	0	0	0	1	1	0
0	0	1	0	-1	+1	0	0	0	0	1	1
1	0	1	+1	-1	0	1	0	0	0	0	1

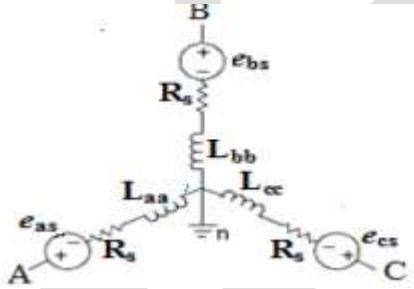

Fig. 4 Equivalent circuit

The system equation is given by,

$$\begin{bmatrix} v_{as} \\ v_{bs} \\ v_{cs} \end{bmatrix} = \begin{bmatrix} R_s & 0 & 0 \\ 0 & R_s & 0 \\ 0 & 0 & R_s \end{bmatrix} \begin{bmatrix} I_{as} \\ I_{bs} \\ I_{cs} \end{bmatrix} + p \begin{bmatrix} L_{aa} & L_{ab} & L_{ac} \\ L_{ba} & L_{bb} & L_{bc} \\ L_{ca} & L_{cb} & L_{cc} \end{bmatrix} \begin{bmatrix} I_{as} \\ I_{bs} \\ I_{cs} \end{bmatrix} + \begin{bmatrix} e_{as} \\ e_{bs} \\ e_{cs} \end{bmatrix}$$

Where, Rs is rotor resistance per phase, p is differential operator and eas, ebs and ecs are the induced emf. The induced emf is given by

$e$as = kbfas(θr)ωr(volt)

Where fas is a unit function generator correspond to the trapezoidal induced emf as a function of rotor electrical position θr. kb is the emf constant and ωr rotor electrical speed.

fas is given by

fas(θr) = (θr) 6/π, 0< θr< π/6

= 1, π/6< θr<5 π/6

= (π -θr) 6/π, 5π/6< θr<7 π/6

= -1, 7π/6< θr<11π/6

= (θr -2π) 6/π, 11π/6< θr<2π

The electromagnetic torque (Te) is developed by the motor is given by

Te = *k*t {fas (θr) ias+fbs (θr) ibs+fcs (θr) ics}

Te =kt ϕasIas

The electromechanical equation with the load is given by

Jpωr+Bωr =(Te-TL)

where J is the moment of inertia, B is the friction coefficient and TL is the load torque

ωr =∫(Te-TL-Bωr)/Jdt

θr =∫ωrdt

B. Analysis of the proposed converter

The circuit diagram of the proposed bridgeless SEPIC with ripple-free input current as shown in fig.3 consists of the auxiliary circuit includes an additional winding *Ns* of the input inductor *Lc* , an auxiliary inductor *Ls* , and a capacitor *Ca* . The coupled inductor *Lc* is modelled as a magnetizing inductance *Lm* and an ideal transformer which has a turn ratio of 1:*n* (*n*=*Ns* /*Np*). The leakage inductance of the coupled inductor *Lc* is included in the auxiliary inductor *Ls*. The capacitance of *Ca* is large enough, so *Ca* can be considered as a voltage source *VCa* during a switching period. Since the average inductor voltage should be zero at a steady state according to the volt-second balance law, the average capacitor voltage *VCa* is equal to the input voltage *v*in during a switching period. Similarly, the average capacitor voltage *VC*1 is equal to *v*in . Diodes *D*1 and *D*2 are the input rectifiers and operate like a conventional SEPIC PFC converter. *D*S1 and*D*S2 are the intrinsic body diodes of the switches S1 and S2.

Fig. 4 shows the operating modes in the positive input voltage. Before *t*0 , the switch S1 and the diode *Do* are turned OFF and the switch S2 is conducting. The input current is the sum of the freewheeling currents *Is*2 and *IL*2[1].

Mode 1 [t0, t1]:

At *t*0, the switch S1 is turned ON and the switch S2 is still conducting. Since the voltage *vp* across *Lm* is *V*in , the magnetizing current *im* increases from its minimum value *Im*2 linearly with a slope of *V*in /*Lm* as follows:

$$i_m(t) = I_{m2} + \frac{V_{\text{in}}}{L_m}(t - t_0). \quad \text{.....(1)}$$

The voltage *vLs* across *Ls* is equal to (1–*n*)*V*in . Therefore,

the current *is* increases from its minimum value –*Is*2 linearly

with a slope of (1–*n*)*V*in /*Ls* as follows:

$$i_s(t) = -I_{s2} + \frac{(1-n)V_{\text{in}}}{L_s}(t - t_0). \quad \text{.....(2)}$$

Since,

$$i_{\text{in}} = i_m + i_p = i_m - ni_s$$

The input current *iin* can be written as follows,

$$i_{\text{in}}(t) = I_{m2} + nI_{s2} + \left(\frac{V_{\text{in}}}{L_m} - \frac{n(1-n)V_{\text{in}}}{L_s}\right)(t - t_0) \quad \text{.....(3)}$$

From (3), the input current ripple can be cancelled out and *i*in can be constant as *Im*2 + *nI*s2 by satisfying the following condition,

Ls = *n* (1 − *n*) *Lm*..... .....(4)

Mode 2 [t1, t2]

At *t*1, the switch S1 is turned OFF and the switch S2 is still conducting. Since the voltage *vp* across *Lm* is $-Vo$, the magnetizing current *im* decreases from its maximum value *Im*1 linearly with a slope of $-Vo$ /L*m* as follows

$$i_m(t) = I_{m1} - \frac{V_o}{L_m}(t - t_1).$$ ……...(5)

The voltage vLs across Ls is −(1 − n)Vo , so that the current is decreases from its maximum value Is1 linearly with a slope of −(1 − n)Vo /Ls as follows

$$i_s(t) = I_{s1} - \frac{(1-n)V_o}{L_s}(t - t_1).$$ …….(6)

From (5) and (6), the input current *i*in can be written as follows,

$$i_{\text{in}}(t) = I_{m1} - nI_{s1} + \left(-\frac{V_o}{L_m} + \frac{n(1-n)V_o}{L_s}\right)(t - t_1).$$

…….(7)

With the ripple-free condition of (4), the input current ripple in this mode can be cancelled out and *i*in can be constant as *Im*1 – *n Is*1.

Mode 3 [t2, t0]

At *t*2, the current *iDo* becomes zero, and the diode *Do* is turned OFF. Since *i*in = *im* − *nis* = −*is* − *iL* 1 in this mode, the input current *i*in is the sum of freewheeling

Currents, *I*s2 and *IL*2 as follows,

*I*in = *Im*2 + *n*Is2 = *I*s2 + *IL*2 ……..…..(8)

Since the average voltage across *Lm* should be zero under a steady state, the time ratio Δ1 is obtained by

$$\Delta_1 = \frac{V_{\text{in}}}{V_o}D$$ ……..…(9)

Where, *D* is the duty cycle. In a switching period *Ts* , the maximum current of each inductor is rewritten as follows,

$$I_{m1} = I_{m2} + \frac{V_o}{L_m}\Delta_1 T_s$$ ……..…..…(10)

$$I_{s1} = -I_{s2} + \frac{(1-n)V_o}{L_s}\Delta_1 T_s$$ .....(11)

$$I_{L1} = -I_{L2} + \frac{V_o}{L_1}\Delta_1 T_s.$$ ……..……(12)

From (8), (9), (11), and (12), the maximum current of the output diode *IDo* can be obtained by,

$$I_{Do} = I_{\text{in}} + I_{s1} + I_{L1} = \left(\frac{1-n}{L_s} + \frac{1}{L_1}\right)V_{\text{in}}DT_s.$$ ……..(13)

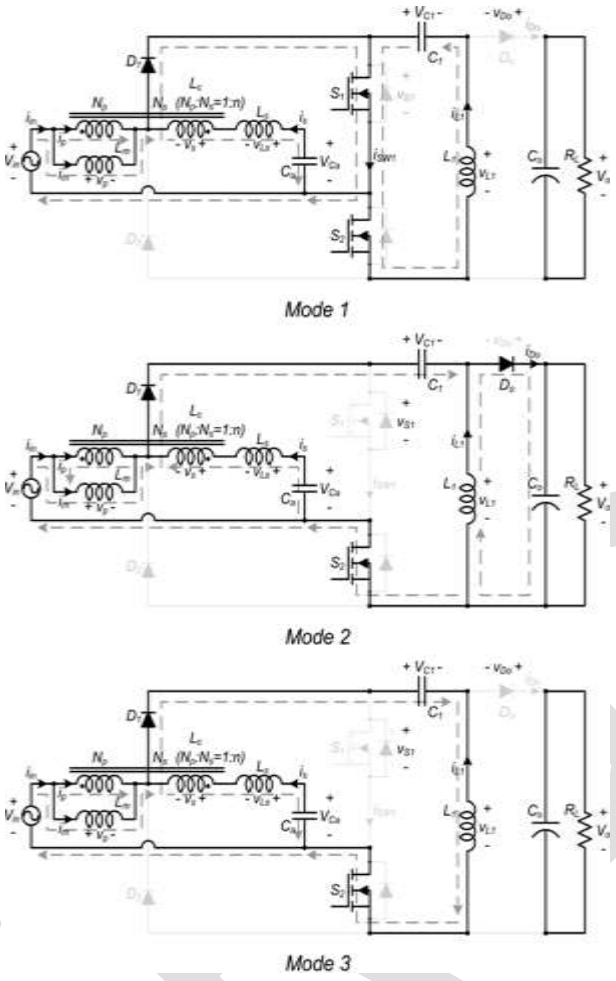

Fig 4. Operating modes

III. SIMULATION MODELS

Simulation model of bridgeless SEPIC converter is implemented in MATLAB/Simulink environment and simulation results are verified. The bridgeless configuration reduces the number of switches leading to better efficiency. Moreover, the conduction losses are reduced and better performance is achieved. The torque ripples are eliminated and the power quality is improved especially the power factor is maintained at unity.

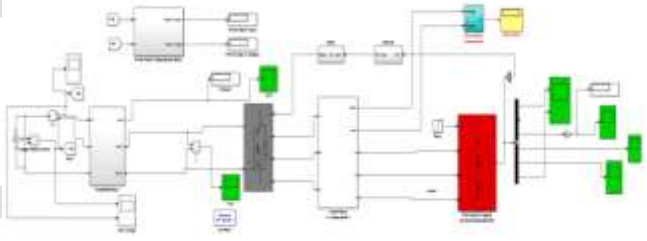

Fig.5 Simulation circuit for BLDC with modified SEPIC converter

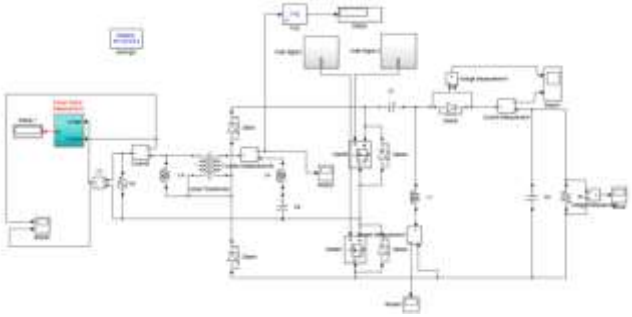

Fig .6 Simulation circuit for SEPIC

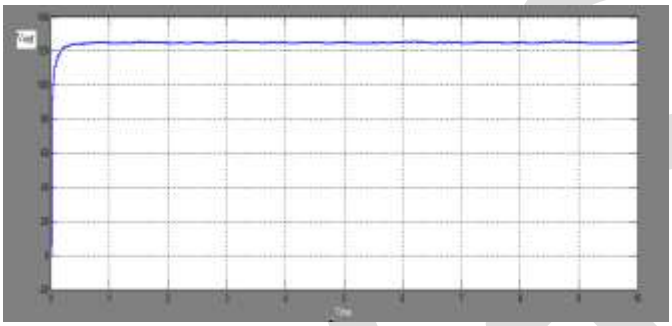

Fig. 7 Simulation result for input of SEPIC converter

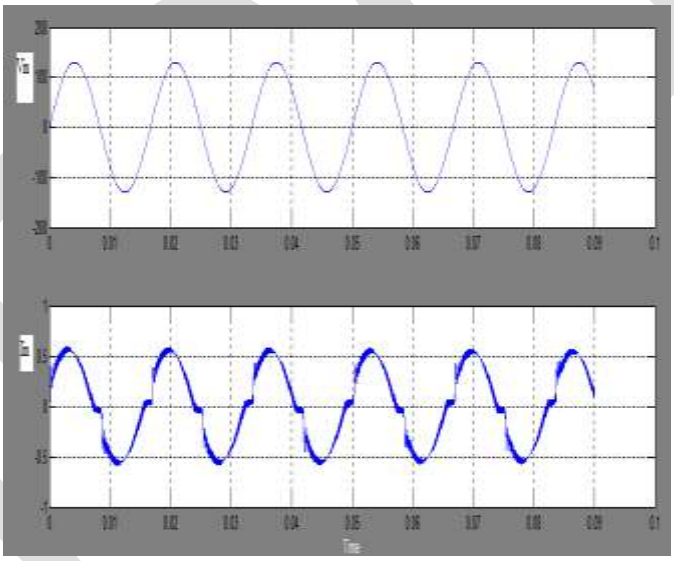

Fig. 8 Simulation result for output of SEPIC converter

IV. CONCLUSION

The conduction losses in the conventional SEPIC converter is high, this can be overcome by bridgeless SEPIC converter. The ripple current in the input side can reduce by bridgeless SEPIC converter. The final efficiency of PMBLDC can increase by using this converter and power factor can also increase.

REFERENCES:

[1] Jae-Won Yang and Hyun-Lark Do, "Bridgeless SEPIC Converter With a Ripple-Free Input Current" *IEEE Trans. On Power Electronics*, Vol. 28, No. 7, July 2013.

[2] L. Huber, Y. Jang, and M. M. Jovanovic, "Performance evaluation of bridgeless PFC boost rectifiers," *IEEE Trans. Power Electron.*, vol. 23, no. 3, pp. 1381–1390, May 2008.

[3] Joseph.S, Ravi.A, Jasper Gnana Chandran, "Efficient Bridgeless SEPIC Converter for BLDC Motor with Improved Power Factor*"* *International Journal of Advanced Research in Electrical, Electronics and Instrumentation Engineering*

[4] S.Assly Steffy, B.Mangaiyarkarasi, S.Sherin Jasper, K.Priyanka, K.Soorya, "Analysis And Simulation Of Speed Control Of PMBLDC motor by PI Controller" *International Journal of Advanced Research in Computer and Communication Engineering Vol. 3, Issue 2, February 2014*

[5] Mr. V. Sarankumar, Mr. M. Murugan, Mr. R. Jeyabharath," Implementation of blsepic converter fed bldc motor drive with power factor rectification" *International Journal of Advanced Research in Computer and Communication Engineering Vol. 3, Issue 2, February 2014*

[6] C.Umayal, D.Saranya Devi, "Modeling and Simulation of PFC SEPIC Converter fed PMBLDC Drive for Mining Application" *International Journal of Advanced Trends in Computer Science and Engineering, Vol.2 , No.2, Pages : 203- 208 (2013).*

[7] Dr.T. Govindaraj1, H.Ashtalakshmi, "simulation of bridgeless sepic Converter with power factor Correction fed dc motor" *international journal of innovative research in electrical, electronics, instrumentation and control engineering Vol. 2, Issue 1, January 2014*

International Journal of Engineering Research and General Science Volume 3, Issue 5, September-October, 2015
ISSN 2091-2730

ENERGY CONSERVATION AT HOCL

Eldhose Joy

P. G Student [Energy Systems], yeldhosejoy@gmail.com, +91-9567876950

Abstract— Nowadays we all are aware that man's urban and modern life style requires huge amount of ever increasing energy. This is the energy required to run manufacturing units, factories, machines, automobiles, homes, etc. in terms of electricity for heating, lighting and many other purposes. As most of this energy comes from non-renewable sources, it is essential to conserve it. Energy conservation refers to efforts made to reduce energy consumption. This project deals with various methods adopted for the conservation of energy at HOCL. This study was conducted in the Cochin unit of HOCL where various energy saving techniques for energy conservation is adopted by the petrochemical industry. And suggestions for implementing new techniques are proposed. They are:
1) Energy efficient lighting involves use of energy efficient tube lights,
2) Variable Frequency Drives, employed for motors with variable load,
3) Trimming of pump impellers,
4) FRP blades for fans.
After implementing the suggested conditions it is anticipated to save 14,50,428 Units of energy annually. This will save ₹ 84,26,987 for the company annually. For implementing the suggested modifications, a capital investment of ₹ 15,76,750 is needed. This amount can be recovered by the company in just 3 months of simple payback period.

Keywords— Affinity Laws, Energy Conservation, Motors, Pumps, Fans, VFD, Pay Back Period.

INTRODUCTION

Energy conserved is energy generated. Energy as we all know is a crucial input in the process of economic, social and industrial development. Energy consumption is increasing at a very fast rate. Though our country has taken rapid strides towards self-reliance on energy over last few years, still on the energy supply side India is facing severe shortage. With growing demand for energy it has become essential to minimise energy losses. Energy conservation should be considered as the wise and efficient use of the available energy for achieving maximum activities with productive work and profitability. Thus conservation does not mean the curtailment in energy use at the expense of industrial and economic growth. It means the efficient utilisation of energy resources ensuring the same level of economic and industrial activity with less energy inputs of energy. Energy efficiency is achieved when energy intensity in a specific product, process or area of production or consumption is reduced without affecting output, consumption or comfort levels.

AREAS OF FOCUS

2.1 Motors

Electric motors in industry constitute the single largest component of the electrical load and account for about 72% of the total electrical energy consumed by the industrial sector. The 3-phase squirrel cage motor is the workhorse of industry; it is rugged and reliable, and is by far the most common motor type used in industry. These motors drive pumps, blowers and fans, compressors, conveyers and production lines.
HOCL has 10 HT motors and about 172 LT motors. The 66 kV supply is stepped down to 6.6 kV and fed to HT motors. The 6.6 kV supply is further stepped down to 433 V and supplied to loads at various locations.

2.1.1 Steps to Improve Electric Motor System Efficiency [4]

i. Use variable Frequency Drives (VFDs) or two-speed motors where appropriate.
ii. Convert delta to star connection for lightly loaded motors.
iii. Install soft start-cum-energy saver for lightly loaded motors.
iv. Avoid frequent rewinding of motors. Greater the number of rewind, lesser the efficiency.
v. Choose energy-efficient motors for new applications. Consider replacement V/s repair for older, inefficient motors.
vi. Match motor operating speeds, and size motors for overall system efficiency.

2.1.2 Present Condition

In HOCL, flameproof squirrel cage induction motors are the most widely used because of their low cost, reliability of operation and ruggedness.

It was found out that many of the maintenance practices are not done regularly and efficiently. A checklist of good maintenance practices to be undertaken in HOCL to ensure reliable and efficient motor operation are suggested.

2.2 Pumps

In the chemical industry, about 26% of all electricity use in motors is for pumps. This equals 16% of the total electrical energy in the chemical industry making pumps the one of the largest electricity users in the chemical industry together with compress air systems and material processing. Pumps are used throughout the industry to generate a pressure and move liquids. Studies have shown that on average in the manufacturing industry, 20% of the energy consumed by these systems could be saved through equipment or control system changes, roughly equally divided between speed reduction or control measures and other system efficiency measures. The potential for the chemical industry is with 21% close to the manufacturing industry average.

2.2.1 Present condition

In HOCL, during the study it was found out that all the pumps and associated motors are oversized. Thus lot of energy is wasted in pump operations. Reasons for oversized pumps are:

- to provide margin for design error
- to provide margin for equipment deterioration
- to provide margin for pump deterioration
- to provide surge capacity
- to provide margin for process upsets/errors
- to provide for process changes

For example, the DM water pump at the Boiler section is not sized optimally. The rating is 150 m^3/h and the actual requirement is between 10-40 m^3/h. The hot oil charge pump is another example for oversized pump. The rating of the pump is 413 m^3/h and the maximum required flow is only 300 m^3/h. The required flow is controlled by using valves and by-passing. By doing so, lots of energy is wasted because the energy consumption by the pump-motor will be the same.

2.3 Fans and Blowers

Fans are used in boilers, furnaces, cooling towers and many other applications. In the chemical industry, 12% of motor related energy use if for fans, corresponding to approximately 8% of the total electricity use in the chemical industry. As in other motor applications, considerable opportunities exist to upgrade the performance and improve the energy efficiency of fan systems. Efficiencies of fan systems vary considerably across impeller types. Overall energy saving potentials in these systems in the Manufacturing industry are estimated at 5.5% and for the chemical industry at 5.9%. However, the cost-effectiveness of energy efficiency opportunities depends strongly on the characteristics of the individual system.

2.3.1 Fan oversizing

Most of the fans are oversized for the particular application, which can result in efficiency losses of 1-5%. However, it may often be more cost-effective to control the speed than to replace the fan system. For example, ID and FD fans at the boiler was oversized to work at the worst condition. VFDs are installed in both fans to control the fan speed and thereby reducing the fan energy consumption.

2.3.2 Variable Frequency Drives (VFDs)

Significant energy savings can be achieved by installing variable frequency drives on fans. Savings may vary between 14 and 49% when retrofitting fans with VFDs [5].

2.3.3 Present Condition

The main fans working in HOCL are at Boiler section (four no.s), Tempered Cooling tower (two no.s), Cooling Towers (five no.s).

i. 55 kW ID fans (two no.s)
ii. 22 kW FD fans (two no.s)
iii. 30 kW Tempered cooling tower fan (two no.s)
iv. 55 kW Cooling tower fans (five no.s)

2.3.3.1 Cooling Tower Fans

Cooling towers are a very important part of many chemical plants. The primary task of a cooling tower is to reject heat into the atmosphere. They represent a relatively inexpensive and dependable means of removing low-grade heat from cooling water. The make-up water source is used to replenish water lost to evaporation. Hot water from heat exchangers is sent to the cooling tower. The water exits the cooling tower and is sent back to the exchangers or to other units for further cooling.

After detailed study, it was inferred that the area which could potentially contribute to considerable energy saving was cooling tower fans. This was mainly because the atmospheric temperature at the company varies with time. There is about $5\text{-}8^0$ C dip in the temperature during late night hours. So, demand for artificial cooling through fans is less because the lower atmospheric temperatures aid for significant natural cooling. Thus the desired temperature can be maintained even at lower fan speeds. Installing VFDs to the fans is the best way to maintain the desired cooling and in turn reducing the energy consumption of the fans. But it need accurate

readings of the temperature variations at day and night. Readings should be taken for many days and different seasons. A detailed VFD run readings also needed to calculate the potential energy savings so that the company can analyse the results and carryout the project.

2.3.3.2 FRP Fan Blades

The fan efficiency in turn is greatly dependent on the profile of the blade. An aerodynamic profile with optimum twist, taper and higher coefficient of lift to coefficient of drop ratio can provide the fan total efficiency as high as 85–92 %. However, this efficiency is drastically affected by the factors such as tip clearance, obstacles to airflow and inlet shape, etc. As the metallic fans are manufactured by adopting either extrusion or casting process it is always difficult to generate the ideal aerodynamic profiles. The FRP blades are normally hand moulded which facilitates the generation of optimum aerodynamic profile to meet specific duty condition more efficiently. Cases reported where replacement of metallic or Glass fibre reinforced plastic fan blades have been replaced by efficient hollow FRP blades, with resultant fan energy savings of the order of 20–30% and with simple payback period of 6 to 7 months. Also, due to lightweight, FRP fans need low starting torque resulting in use of lower HP motors. The lightweight of the fans also increases the life of the gear box, motor and bearing is and allows for easy handling and maintenance [10].

2.4 Power Factor Correction

Power factor correction is an important energy conservation method. HOCL has already installed capacitor banks to improve the power factor. The monthly average power factor is maintained between 0.98 and unity. HOC gets incentive from KSEB for maintaining a good power factor.

2.5 Lighting System

Energy conservation techniques applied to lighting installations can result in significant saving in energy without reducing lighting standards. Although new lighting installations are designed to incorporate energy savings, many existing schemes are lacking in terms of energy efficiency. A lot of opportunities exist to improve lighting standards by using modern equipment and techniques with the added benefit of lower energy consumption. Artificial lighting is provided to permit people to carry out tasks safely and with relative ease where insufficient or no natural lighting is available.

Artificial lighting from electrical sources is provided by three types of lamps: Incandescent lamps, Fluorescent lamps, Discharge lamps.

2.5.1 Present Condition

No. of tubes which glow for 8 hours/day & 25 days/month = 400
No. of tubes which glow all the time = 250
No. of 200 W GLS lamps (12 hours) = 80
No. of 125 W HPMV = 140
No. of 250 W HPMV = 220
No. of 400 W HPMV = 123
HOCL has already implemented many energy conservation measures in lighting system like:
i. Replacement of HPMV lamps with HPSV lamps
ii. Replacement of GLS lamps with LED lamps
iii. Providing Lighting Transformers at MRS, Utility Substation, H_2O_2 Auxiliary Substation and Propylene Recovery Unit.

The identified potential area in lighting system was the replacement of old 40W tube lights with 36W energy efficient tube lights.

2.5.2 Energy Efficient Tube Lights

Energy efficient tube light E+ consumes 36 W compared to a 40 W for a conventional tube light. There would be direct saving of 4 W per tube light. It also gives a lamp output more than 20 % compared to a conventional 40 W tube light. By installing a 36 W tube light in place of 40 W lamps, annual energy saving of 10 % per lamp can be achieved [7].

METHODOLOGY

3.1 Affinity laws

The affinity laws for pumps/fans are used in hydraulics/HVAC to express the relationship between variables involved in pump or fan performance (such as head, flow rate, shaft speed and power). They apply to pumps, fans, and hydraulic turbines. In these rotary implements, the affinity laws apply both to centrifugal and axial flows.

The affinity laws are useful as they follow prediction of the head discharge characteristic of a pump or fan from a known characteristic measured at a different speed or impeller diameter. The only requirement is that the two pumps or fans are dynamically similar, that is the ratios of the fluid forced are the same.

Law 1. With impeller diameter (D) held constant:

Law 1a. Flow is proportional to shaft speed;
$Q1/Q2 = (N1/N2)^1$
Law 1b. Pressure or head is proportional to the square of shaft speed;
$H1/H2 = (N1/N2)^2$
Law 1c. Power is proportional to the cube of shaft speed
$P1/P2 = (N1/N2)^3$

Law 2. With shaft speed (N) held constant:

Law 2a. Flow is proportional to the cube of the impeller diameter:
$Q1/Q2 = (D1/D2)^3$
Law 2b. Pressure or Head is proportional to the square of impeller diameter:
$H1/H2 = (D1/D2)^2$

SUGGESTED MEASURES

4.1 Installation of VFD in Hydrogenation Feed Pump

Rated Power, KW = 45 KW
Rated Voltage, V = 415 V
Rated Current, I = 80 A max
Rated Speed, N = 2960 RPM
Rated Frequency, f = 50 Hz
Power Factor = 0.87
Power Consumption without VFD = 33.5 KW
Avg Motor speed reduction using VFD = 25 %
Power consumed is proportional to cube of speed.
$P \alpha N^3$
Motor speed = 75 % of normal.
Power consumed with VFD= $(0.75)^3$ x 33.5 KW = 14 kW
Annual energy savings= (19.5)×24×330 = 1,54,440 kWh
Avg cost of energy = ₹ 5.81
Annual savings in Energy charges = (33.5-14) x24x330x5.81 = ₹ 8,97,296
Investment cost = ₹ 3.5 lakhs
Simple payback period = 5 months

4.2 Installation of VFD in Oxidiser feed pump.

Rated Power, KW = 75 KW
Rated Voltage, V = 415 V
Rated Current, I = 128 A
Rated Speed, N = 3000 RPM
Rated Frequency, f = 50 Hz
Power Factor = 0.87
Power Consumption without VFD = 55.2 KW
Avg Motor speed reduction using VFD = 25 %
Power consumed is proportional to cube of speed.
$P \alpha N^3$
Avg Motor speed = 75 % of normal.
Avg Power consumed with VFD = $(0.75)^3$ x 55.2 KW = 23.3 kW
Annual Energy savings [(55.2-23.3) x24x330] = 2,52,648 kWh
Average energy cost = ₹ 5.81
Annual savings in Energy charges = ₹ 2,52,648×5.81= ₹ 14,67,885
Investment cost = ₹ 5 Lakhs
Simple Payback period = 5 Months

4.3 Installation of VFD in DM water pump.

Rated Power, KW = 22 KW
Rated Voltage, V = 415 V
Rated Current, I = 41 A
Rated Speed, N = 2920 RPM

Rated Frequency, f = 50 Hz
Power Factor = 0.87
Avg Power Consumption without VFD = 18 kW
Avg Motor speed reduction using VFD = 35 %
Power consumed is proportional to cube of speed.
$P \alpha N^3$
Avg Motor speed = 65 % of normal.
Avg Power consumed with VFD = $(0.65)^3$ x 18 KW
= 5 kW
Annual Energy savings [(18-5) x24x330] = 1,02,960 kWh
Annual savings in Energy charges = ₹ 1,02,960×5.81= ₹ 5,98,198
Investment cost = ₹ 1.5 Lakhs
Simple Payback period = 4 Months

4.4 Replace Aluminium blades with FRP blades in Cooling Tower Fans.

No. of fans = 3 Nos
Rated Power = 55 kW
Rated voltage = 415 V
Rated Current = 96 A
Rated Speed = 1480 RPM
Avg Power consumption with Aluminium blades= 47 kW
Anticipated Energy Savings = 25%
Avg Power consumption with FRP blades = 35.25 kW
Avg Power Savings = 11.75 kW
Annual Energy Savings (11.75×24×330) = 93,060 kWh
Average cost of Energy = ₹ 5.81/kWh
Annual savings in energy charges (93,060×5.81) = ₹ 5,40,679
Annual savings for 3 fans (5,98,198×3) = ₹ 16,22,037
Cost of implementation for 3 FRP blade sets = ₹ 1,80,000×3 = ₹ 5,40,000
Simple Payback period = 4 months

4.5 Impeller Trimming of Hot Oil Charge Pump.

Rated Power, kW = 450 kW
Diameter of impeller, D_1 = 510 mm
Power consumption, P_1 = 200.3 kW
Discharge, Q_1 = 413 m^3/h
Required max flow, Q_2 = 300 m^3/h
By Affinity law,

$$\frac{Q_1}{Q_2} = \left(\frac{D_1}{D_2}\right)^3$$

Diameter of impeller for 300 m^3/h flow, $D_2^3 = D_1^3 \times (Q_2 \div Q_1)$
$= (510)^3 \times (300 \div 413)$, $D_2 = 459$ mm
By Affinity law,

$$\frac{P_1}{P_2} = \left(\frac{D_1}{D_2}\right)^5$$

Power consumption at reduced impeller diameter, $P_2 = P_1 \div (D_1 \div D_2)^5$
$= 200.3 \div (510 \div 459)^5$
= 118.3 kW
Reduction in power consumption = 200.3-118.3= 82 kW
Annual Energy savings (82×24×330) = 6,49,440 kWh
Average energy cost = ₹ 5.81
Annual savings in Energy charges = ₹ 37,73,246
Investment cost = ₹ 7500
Simple Payback Period = 1 day

4.6 Replacement of 40W tube light with Philips (With BEE mark) made Energy Efficient 36W tube lights [7].

No. of tubes to be replaced = 650
Power savings = 4W per Tube
No. of tubes which glow for 8 hrs/day and 25 days/month =400
Annual Energy savings for 400 tubes = (400×4)×(8×25×12)
= 3,840 kWh

No. of tubes which glow all the time = 250
Energy savings for 250 tubes = (250×4)×24×330
= 7,920 kWh
Total annual energy savings = 3,840 + 7,920
= 11,760 kWh
Avg energy cost = ₹ 5.81
Annual savings in Energy charges = 11,760 × 5.81
= ₹ 68,326
Investment cost = ₹ 29,250
Simple Payback period = 6 months

RESULT AND DISCUSSION

We can summarize the results of the energy conservation measures suggested in HOCL as follows:

5.1 Potential Energy Savings in Motors

i. Anticipated annual saving in energy charges after the installation of VFD

a) In Hydrogenation feed water pump = ₹ 8,97,296
b) In Oxidiser feed pump = ₹ 14,67,885
c) In DM water pump = ₹ 5,98,198

ii. Anticipated annual saving in energy charges after installation of FRP blades in CT fans = ₹ 16,22,036
iii. Anticipated annual Saving in energy charges after impeller trimming of Hot oil charge pump = ₹ 37,73,246
Total Potential Energy Savings in Motors = ₹ 83,58,661

5.2 Potential Energy Saving In Lighting

By replacement of 40 W tube light with Philips made 36 W tube light.
Anticipated annual savings in Energy charges = ₹ 68,326
Total Potential Energy Savings in Lighting = ₹ 68,326

5.3 Total Potential Energy savings

Total potential energy savings considering both motors and lighting = ₹ 84,26,987
Total investment needed = ₹ 15,76,750
Simple Payback Period = 3 months

CONCLUSION

This project work discusses about the Energy Conservation measures to be adopted in the petrochemical industry, HOCL, from this we can infer that a large amount of energy can be conserved by adopting conservation measures. Studies were conducted on the Energy Conservation activities implemented in some of the electrical systems at HOCL. Large reduction in energy cost is obtained by implementing the conservation measures.

Implementation of energy conservation activity can result in harmonics in supply but it can be got rid of by making use of proper filters [8]. In spite of these harmonics, energy conservation activities can increase energy saving compared to which effect of harmonics can be neglected.

This project focussed only on the Electrical Department of HOCL. After studying the present condition of the Electrical system, possible conservative measures were identified and suggested. By implementing the suggested measures the company can save 14,50,428 Units of energy annually. This will save ₹ 84,26,987 for the company annually. The capital investment needed was calculated and found out to be ₹ 15,76,750. The company will be able to recover the invested capital by 3 months after implementing the suggested measures. There is more scope of energy conservation in the Mechanical and also in the Electrical department of the company.

Like in those of electrical sector, if sufficient technological innovations are brought about in every sector, a substantial monitory benefits could be achieved. It not only benefit the company but instead becomes an asset to the entire mankind.

REFERENCES:

[1] P.S.Shah, "Energy Efficient Induction Motor", Electrical India, Vol 50, No 11, pp 113-116, 2010.
[2] M. Sidharth Bhatt, "Energy Efficient Pumping Systems for R & AC plants", Electrical India, Vol 52, No 12, pp68-73, 2012.
[3] S.Ponnayira Sundaravel, "Automatic Power Factor Controller", Electrical India, Vol 54, No 1, pp 167-169, 2014.
[4] Vijwajit Nayak & P.K. Pattanaik, "Conservation of Electrical Energy", Electrical India, Vol 49, No 2, pp 30-41, 2009.
[5] Dr. H.V.K.Shetty, "Variable Speed Drives with Electric Motors", Electrical India, Vol 47, No 11, pp 214-220, 2007.
[6] Bureau of Energy Efficiency. Cooling Tower. [Online].
Available:http://www.beeindia.in/energy_managers_auditors/documents/3Ch7.pdf.
[7] Bureau of Energy Efficiency. Tubular Fluorescent Light.Ministry of Power, Government of India. [Online].
Available: http://www.beeindia.com.
[8] Carrier Corporation Syracuse. (2005). Operation and Application of Variable Frequency Drive Technology. [Online].
Available: http://www.dms.hvacpartners.com/docs/1001.pdf
[9] Bureau of Energy Efficiency. Pumps and Pumping System. [Online].
Available:http://www.beeindia.in/energy_managers_auditors/documents/3Ch6.pdf.
[10] Parag Fans and Cooling Systems Ltd. Energy Efficient Axial Flow FRP Fans.[Online].
Available: http://www.paragfans.com.
[11] Douglas Reindl, "Applying Variable Speed Drives in Industrial Refrigeration Systems", IRC.WISC, Vol 4, No 1, 2009.
[12] Zanutto, "Case Studies of VFD Applications", IRC WISC, Vol 2, No 4, 2009.

International Journal of Engineering Research and General Science Volume 3, Issue 5, September-October, 2015
ISSN 2091-2730

Increase of Aluminum Particles in the Environment due to Chemtrails during the period of Autumn 2012 to Summer 2015 within Lahore, Pakistan

[1]Humza Bin Masood, [2]Dr. Seemal Jelani
[1]IESE, National University of Sciences and Engineering, Islamabad, Pakistan, 15-10333@formanite.fccollege.edu.pk
[2]Department of Chemistry, Forman Christian College, Lahore, Pakistan

Abstract— Currently the most prevailing issue of the climate change in the world is geo-engineering and one of the most prevailing issue in this is using of Chemtrails to change the climate. These Chemtrails are left over in the sky with the help of special types of jet planes which use to spray Aluminum, Barium and Strontium is the sky to make a thick parallel lines with the help of condensation due to change of air pressure at the height. These thick parallel lines are the condense layers of Aluminum, Barium and Strontium which use to stop the some rays of sunlight coming to the sky but sadly it also prevents the heat rays to go out of the earth space due to the layers formed. These sprays are causing the increase of Aluminum in the Environment as these particles can move trillions of miles and are causing different problems and diseases like Asthma in our planet earth. The analysis performed helps to know about the increase of these Aluminum particles in our planet and the studies performed shows the problem caused by the spraying to these nano-particles in the Atmosphere.

Keywords— Chemtrails, Aluminum, Water, Atmosphere, Sky, Seasons, Soil

INTRODUCTION

Engineering the climate is the Last and the Scariest option to save planet Earth (US Scientists). Many ways are there to engineering the climate like Artificial Rain, Cloud Seeding, Giant Reflectors, Using Aerosols, Haarp Project, Silver Iodide but Chemtrails is one of the cheapest sources for engineering the climate. In fact it cost thousands of Dollars but relating to other Climate modification techniques it is the one of the cheapest sources [1]. Trillions of Nano-particles of Aluminum, Barium and Strontium are sprayed every day over our heads in our blue sky which seems like white clouds. This is done by special kind of Air Planes which have special types of engine placement by which these air planes can move to several miles in the atmosphere. Then these air planes spray Aluminum, Barium and Strontium in form of Nano-particles. These Nano-particles can move millions of miles in atmosphere (Michel J. Murphy) [2]. When Ever you see jet Chemtrails going over you are going to get Aluminum, Barium, Strontium coming down on you; and what should it be there in the soil? Yes, it should be in the soil, it was there, always was there, well should it be in the rain; absolutely not [3]. These Nano-particles are sprayed and due to change in pressure at higher altitudes they are condensed. These condense particles form a layer and they stop sunlight coming to our planet earth [4]. This causes global dimming (Why in The World are they Spraying?). Global dimming is basically a term refer when the sun rays are not able to get to the earth which may cause problems of plants to grow green. Some of the scientist says that chemtrails are nothing else but the special type of contrails which causes global dimming while those who don't support chemtrails says that this is a war technique which allows to change weather [5].

There is a debate that chemtrails are the military weapons as well as debate that it is tool for many traders to earn money. "The growing evidence repeatedly confirms that aircraft are spraying dirty aerosols to warm the climate in Polar Regions for drilling access by BIG OIL as faux "National Security" [6]. Some Scientists believes that these techniques are also used by great traders to make a loss to other trader and make a profit out of that. Some use to change the weather of the particular area for their trades and many believes that it is use in war as a military weapon. The question that arises here is that is there any need for climate modification in wars and if so how do they help the military forces? Not only the chemtrails but there are many military projects that cause the climate to change and one of those projects is HAARP (High frequency Active Auroral Research Program) but only the one time use of HAARP cost trillions of dollars and relatively Chemtrails are less cheaper but Chemtrails require some hours for weather modification but HAARP can do the same thing within the seconds [7]. These weather modification techniques are very helpful in warfare. These are use to blew snow storms on the enemy. With the help of these snow ball can be upsized easily to the size that it can break glass [8]. It is also used in places where there is soil to cause rain and it cause the soil to be muddy which is a hurdle for an enemy not only this but it also effects their health.

Beside all the facts of climate modification the nano-particles of Aluminum used in this process can travel billions of miles these are causing very harmful diseases (Barb Peterson). The increase in amount of Alzheimer, Asthma, ADD, Allergy and Respiratory Orders is due to Oxides of Aluminum sprayed from chemtrails to modify the temperature of our planet earth. Beside the fact that it causes air pollution it is true that it also causes water pollution and soil pollution. So we are not going to get oxides of aluminum by inhalation through air but also from plants. Aluminum causes defects in Plants [9].

Rose Cairns explains that there is a conspiracy of contrails and chemtrails. Many big mafias who use to make profit of this use to intermix both the terms and say that these use to disappear very soon as there are no chemtrails. Contrails are the lines caused by airplanes when going at high altitude caused under the atmospheric pressure in our blue sky which disappears hardly within 10 seconds but Chemtrails are the aerosol sprays that are used to engineer the climate. This uses to spray the nano-particles of Aluminum, Barium and Strontium in parallel lines and don't disappears within hours [10].

On Daily basis chemtrail jets is been seen in the blue sky of Lahore but public is unaware about is that what is happening. Here the study focuses on the spray of the Aluminum from the chemtrail jets in the sky and as Michael J. Murphy had explained that these nano-particles are travel trillions of miles so the rate is increasing drastically in the environment and are causing many health effects within the living organisms. The rate of Asthma is increasing drastically and now according 334 million patients of asthma around the globe [11]. About 15% of Pakistan's population suffers from asthma which includes 10% children of Pakistan [12] while the annual increase of asthma is 5% [13].

MATERIALS AND METHODS USED

A. STUDY AREA: The study that was analyzed is Lahore city which consists of Sheikhpura district at on the North-West, on the east is India and on the district Kasur and on the North River Ravi flows. The entire city occupies the space of 404 Km^2 [14]. At GPS coordinates it is located at 31.5497°N, 74.3436°E [15].

B. SAMPLING: Samples of Drinking Water, Surface Soil and Air was collected from different places in all the four seasons of these three years. The samples were collected from 5 different places every time. These places consist of Thokar Niaz Baig, Jallo, Kahna, Shadra and Muslim Town. Drinking water samples were collected in the sterilized bottles for Quality Assurance and reduction of error, Surface Soil was collected in sterilized jars and air is sterilized syringes. All the samples were kept air tight to eliminate the external contamination.

C. ANALYSIS: Aluminum Analysis at AAS (Atomic Absorption Spectrometer) was performed. For black samples in each case Distilled H_2O was used after CO_2 bubbling. For Soil, each 10g sample was mixed in 100 ml Distilled H_2O was used after CO_2 bubbling and was stirred for 1 hour each. For Air, each sample was bubbled up to 15 ml in 100ml of CO_2 bubbled distilled H_2O.

D. QUALITY CONTROL AND QUALITY ASSURANCE (QC/QA): For the quality control all the instruments were calibrated on the regular basis. For calibration of measuring instruments CO_2 bubbled distilled H_2O was used as the weight and volume of water is always the same i.e. 1L of water is 1Kg of Water. Weight balance was also calibrated regularly with the help of mercury balance and similarly AAS was also calibrated as per-required standards. Every time strict quality control and strict procedure for calibration was used for the maximum reduction of error.

RESULTS AND DISCUSSIONS

The samples were collected overtime and were coded according to sample type, season, year and site of collection e.g. for Soil Sample collected from Thokar Niaz Biag in Autumn 2012 was coded as SSTNBA2 (SS: Soil Sample, TNB: Thokar Niaz Baig, A: Autumn, 2: 2012).

A. RESULTS FOR AIR SAMPLES: The results of Air Samples overtime are shown as under

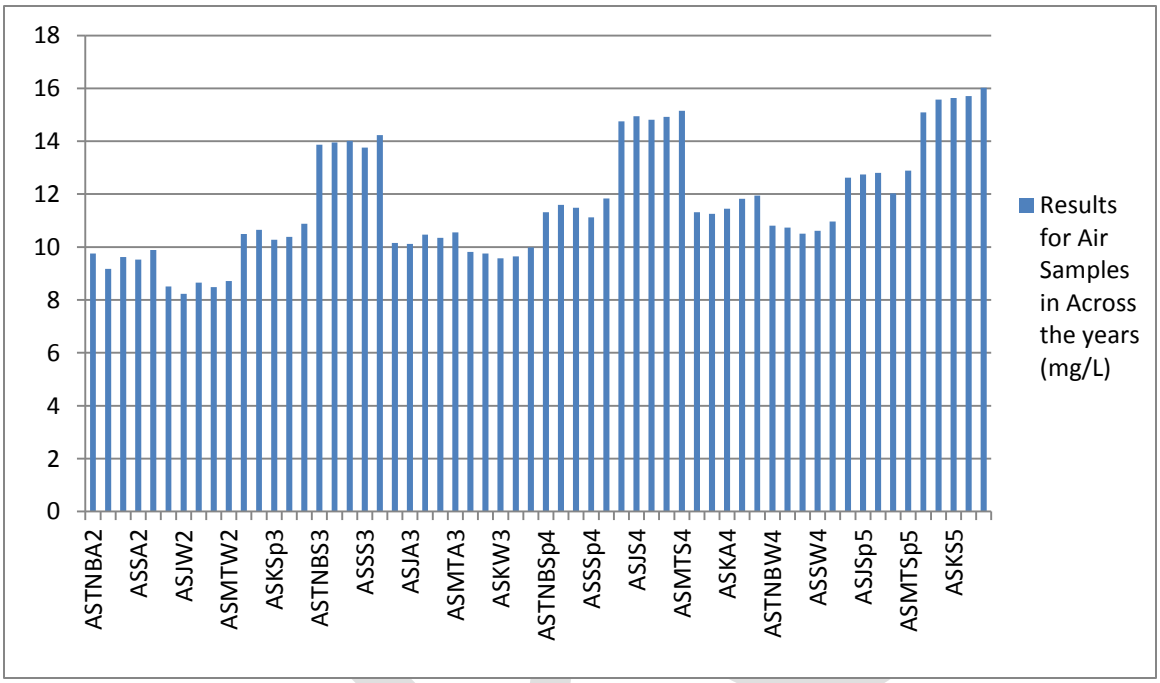

Graph 16: Aluminum Results of Air Samples across the years (mg/L)

The graph above shows the results of Aluminum in Air Samples across the three years. The graph below shows the average Amount of Aluminum detected in the samples across the seasons and years.

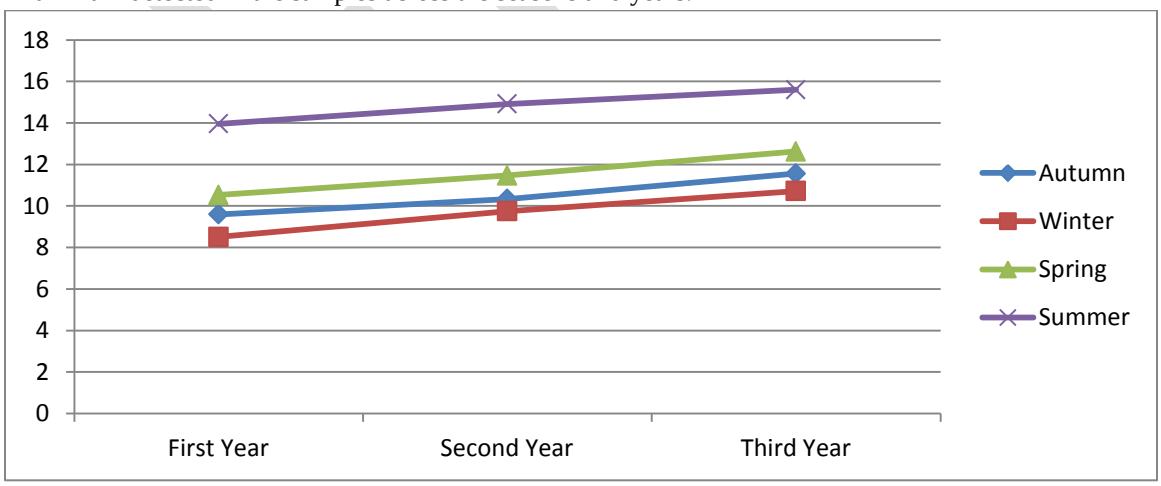

Graph 2: Average Change of Aluminum in Air Samples across the Years (mg/L)

B. RESULTS OF SOIL SAMPLES: The results of soil samples overtime is shown as under.

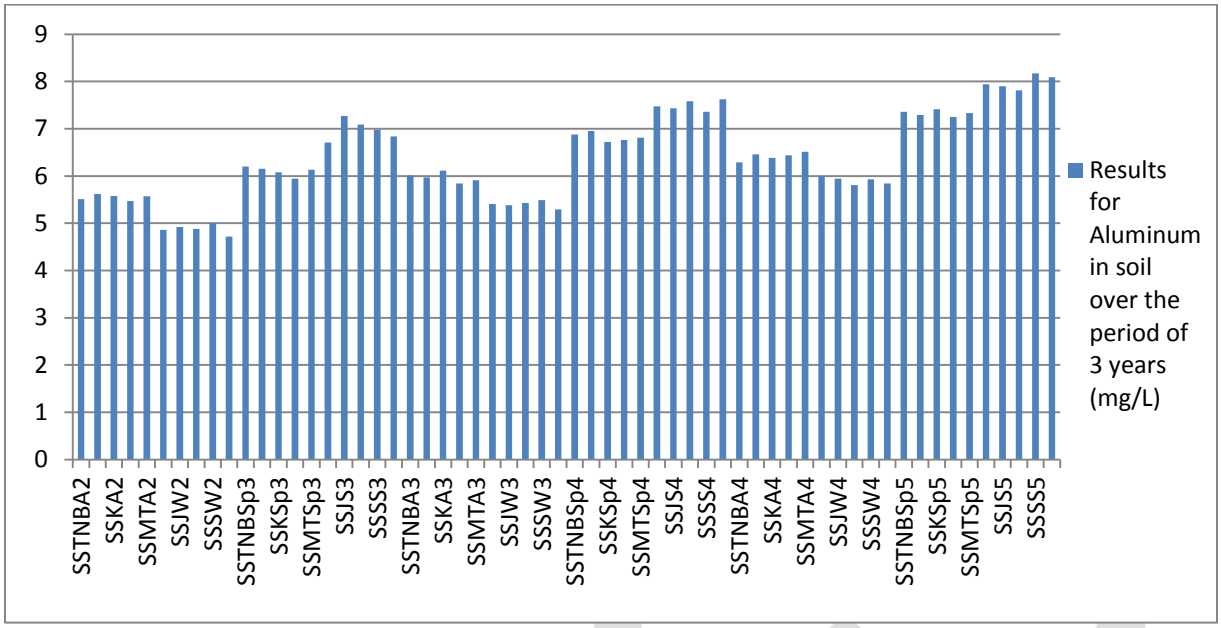

Graph 3: Results for Aluminum in soil over the period of 3 years

The graph above shows the results of Aluminum within the Soil Samples in the time span of three years while the table below shows the average Amount of Aluminum detected in the soil samples across the seasons and years.

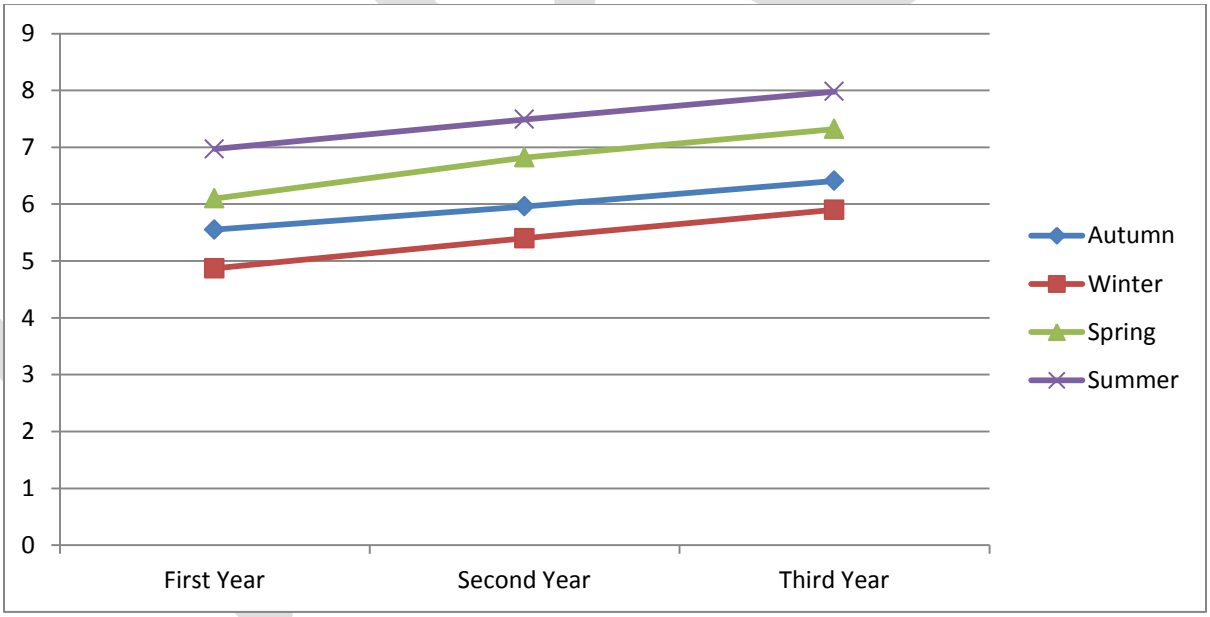

Graph 4: Average Change of Aluminum in Soil Samples across the Years (mg/L)

C. RESULT OF WATER SAMPLE: The aluminum detection results of water samples over the period of three years are given as under.

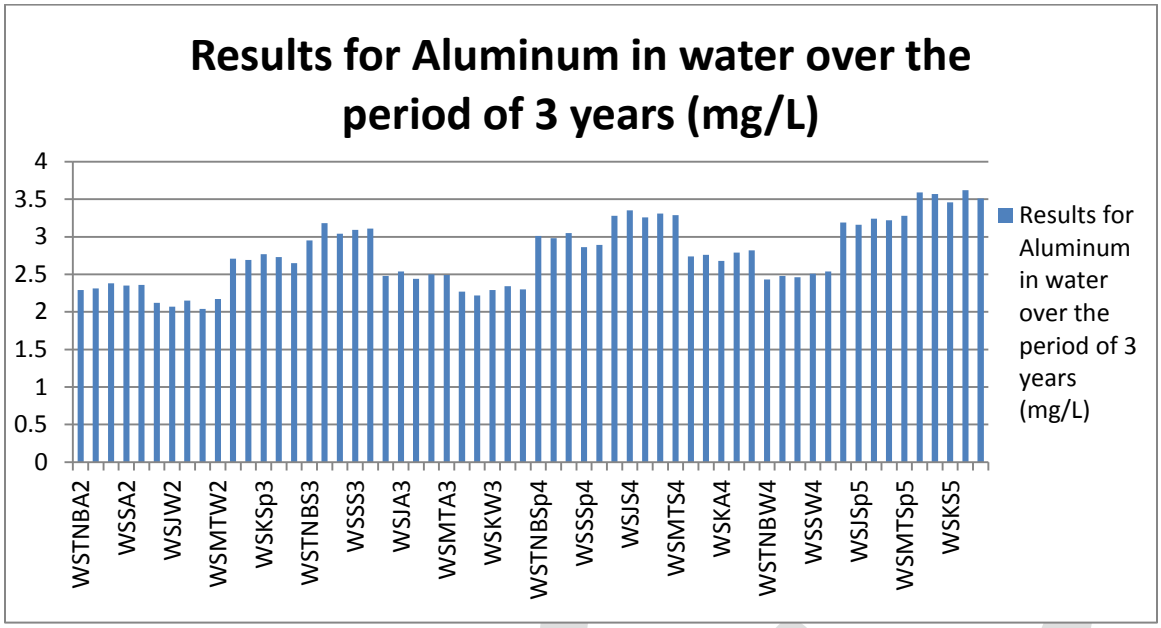

Graph 5: Results for Aluminum in water over the period of 3 years (mg/L)

The Graph Above shows the results of Aluminum in the water collected from different places from Lahore in different seasons over the period of three years. The graph below shows the average change of amount of aluminum in drinking water of Lahore over the period of three years.

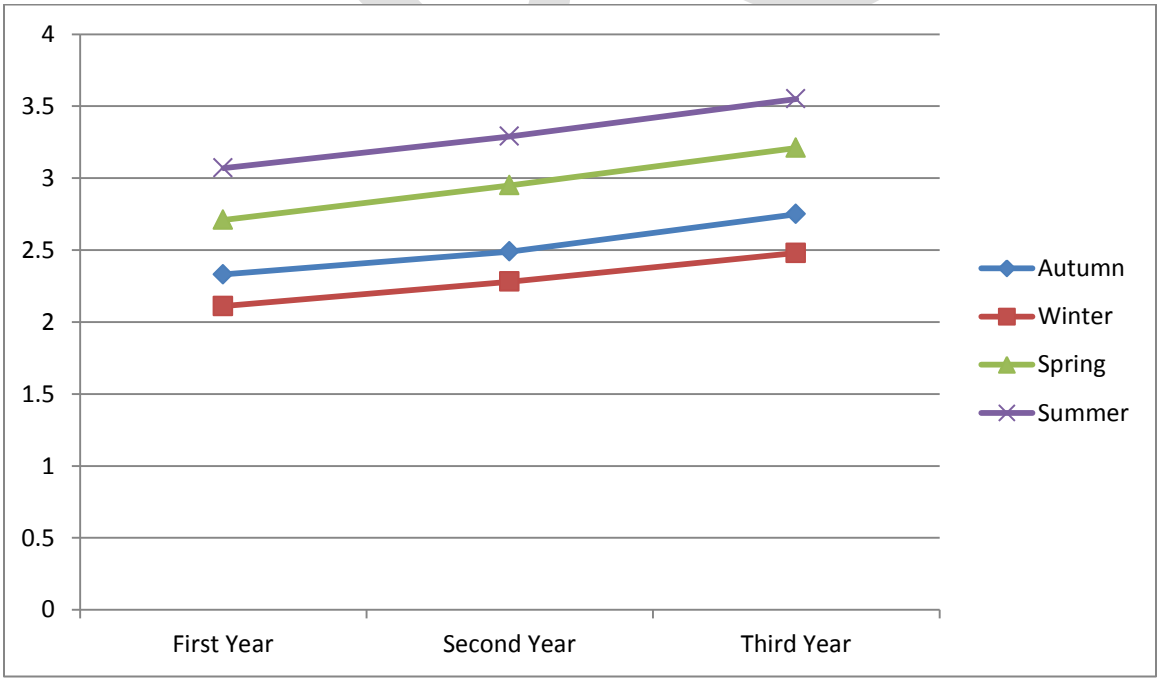

Graph 6: Average Change of Aluminum in Water Samples across the Years (mg/L)

The results above show that the amount of aluminum is increasing every year and have crossed the EPA (Environmental Protection Agency) Quality Assurance Standards of Pakistan.

ACKNOWLEDGMENT

Authors are thankful to Dr. Muddasir Abbas (Ex-Faculty Member, Department of Chemistry, Forman Christian College, Lahore, Pakistan)

and the lab staff of Department of Chemistry, Forman Christian College, Lahore, Pakistan. Authors are also thankful to Dr. Hamid Saeed and Dr. Sohaib Aslam of Environmental Sciences Program, FC College, Lahore, Pakistan for all the possible support in the work carried out.

CONCLUSION

The amount of Asthma is increasing every year due to Chemtrails in Pakistan. On the daily basis jets are been seen in the sky spraying the chemtrails which are increasing drastically and are causing diseases like Asthma, Allergies, Skin Infection, ADD, Autism, etc. As the results shows the regular increase in aluminum in soil, water and air it is recommended that the government and related organizations should take this issue at the international level and stop the spraying of Chemtrails in the sky because these trails don't only effect the atmosphere but its nano-particles can travel trillion of miles effecting our soil, water and air.

REFERENCES:

[1] Ten Technologies to save the planet earth by Chris Goodall; Greystone Books, D&M publisher, Vancouver/Toronto/Berkley
[2] Michel J. Murphy, 2012, Documentary: "Why in the world are they spraying"?
[3] Franchis Mangels, 2012, Documentary: "Why in the world are they spraying"?
[4] Clark S, 2002, "Conspiracy Theories and Conspiracy Theorizing *Philosophy of the Social Sciences" Vol. 32 Page.* 131–150
[5] Vapour Trail; Encyclopedia Brattian.
[6] Chemtrails Planet, May 1st 2014, (www.chemtrailsplanetuk.com)
[7] William Harris, 2010, "Can we control the weather?"
[8] Hamblin JD, 2013, "Arming Mother Nature", Oxford University Press
[9] Barb Peterson, 2012, Documentary: "Why in the world are they spraying"?
[10] Rose Cairns, 2014, "Climates of Suspicion: 'chemtrail' conspiracy narratives and the international politics of geoengineering". Geo-engineering Governance Research.
[11] "Global Asthma Report", 2014 (www.globalasthmareport.com)
[12] "Rising Pollution escalating asthma prevalence in Pakistan", 7th of May, 2015, The News.
[13] Muhammad Qasim, "Two Million Asthma Patients in Pakistan", 1st of May, 2012, The News.
[14] Lahore Data, "Government of Punjab", (http://www.punjab.gov.pk/lahore)
[15] Google Maps

International Journal of Engineering Research and General Science Volume 3, Issue 5, September-October, 2015
ISSN 2091-2730

Efficient Inter-area Power Oscillation Controller for Two Area Four Machine System Using Multiband Power System Stabilizer

Lumesh Kumar Sahu[1], Ankit Dubey[2], Shailesh M. Deshmukh[3]

[1]M. Tech Scholar, EEE Department, DIMAT Raipur,

[2]Assistant Professor, EEE Department, DIMAT Raipur,

[1]Lumeshsahu@gmail.com,09827347726

Abstract— Most of Power systems are steadily increasing with ever higher capacity. All individual systems are interconnected to each other. The Modern power systems have transformed into the system of very large size. With growing generation capacity, different areas in power system are added with very large inertia. As a consequence in large interconnected power systems, low frequency oscillations have large importance. Low frequency oscillations include local area modes and inter-area modes. Inter-area modes of oscillations may be caused by the either high gain exciters or heavy power transfer across weak tie line. The occurrence of the inter-area oscillations depends on various reasons such as weak ties between interconnected areas, voltage level, transmitted power and load. At time, the oscillations may continue to grow causing the instability of the power system. lots of power system stabilizers have been developed by the researchers in the past few years, but the area is still open for the efficient power stabilizer development which can efficiently able to handle the power oscillations without increasing the system controller system complexity. This paper deals with the development and implementation of a multiband power system stabilizer (MB-PSS) for the efficient power oscillation damping in two area four machine transmission system. The implementation of the proposed work is with the Simulink of MATLAB 2012(b). This paper also presents a complete comparative analysis of Inter- area power oscillation damping capabilities of proposed multiband power system stabilizer (MB-PSS) and conventional PID power system stabilizer (PID-PSS). The obtained results shows that the Inter-area power oscillation damping capability of proposed multiband power system stabilizer (MB-PSS) is much higher than the PID-PSS. In addition the damping time required by proposed MB-PSS is 50% less as compare to PID-PSS.

.

Keywords—PID Controller, Power System Stabilizer (PSS), Multi area machine system, Power oscillation Damping, MB-PSS, PID-PSS.

1. INTRODUCTION

Many power systems will complex non-linear systems, that are often subjected to some what low frequency oscillations. The useful application in power system stabilizers to improving stability especially dynamic stability of power systems and damping out the low frequency oscillations due to problems and disturbances has received much attention recently. Power system is a highly nonlinear system and it is very difficult for obtaining correct mathematical model for the system. For adaptive self-tuning and variable structure with artificial neural network based PSS, fuzzy logic based PSS, have been proposed to provide optimum damping to the system oscillations which under wide value of variations in all operating conditions and all system parameters. Oscillation like low frequency oscillation problems that are very difficult to solve because power systems that are very large, complex with geographically distributed. Therefore, it is necessary for utilize most efficient optimization all methods for taking full of advantages in simplifying the problem and their implementation [1-5].

From this view, many succeeded and powerful optimization methods and algorithms have been employed in formulating and solving this problem. These days swarm intelligence has become more and more attractive for the researchers, who work in the relevant research field. It can be classified as one of the branches in evolutionary computing. Swarm intelligence can be defined as a measure for introducing the collective behavior of social insect colonies or other animal groups to develop algorithms or various distributed problem-solving devices. Generally, the algorithms in swarm intelligence are used to solve various optimization problems. Many swarm intelligence algorithms for solving problems of optimization have proposed such as the Cat Swarm Optimization (CSO), the Parallel Cat Swarm Optimization (PCSO), the Artificial Bee Colony (ABC), the Particle Swarm Optimization (PSO), the Fast

Particle Swarm Optimization (FPSO), and the Ant Colony Optimization (ACO). Moreover, several applications of optimization algorithms based on computational intelligence or swarm intelligence one after another [6-9].

Artificial Bee Colony (ABC) algorithm based particular intelligent behavior of the system. In addition, the accuracy and efficiency of ABC are compared with Differential Evolution (DE), PSO and the Evolutionary Algorithm (EA) for numeric problems at multi-dimensions. On observing the operation and structure of the ABC algorithm, we notice that the operation of agent, e.g. the artificial bee, can only move straight to one of sources which are discovered by employed. Nevertheless, this characteristic which may narrow down the zones of which all bees can explore and may that become a drawback of ABC.

This work deals that development and implementation of a multiband power system stabilizer for the efficient power and their oscillation damping in that two area four machine transmission systems.

Aim of this work is to analyze the power stabilization capability of proposed multiband power system stabilizer as compared to conventional PID power system stabilizer for interred power oscillation damping of two areas with four machine transmission line systems.

2. Four Machines Two Area Test System

Here two fully symmetrical areas linked to each other with two tie 230KV lines of 220Km length as shown in given Fig.1. It was specifically designed to study low frequency electromechanical oscillations all in large interconnected power systems. Despite its small size, so here it mimics very closely so the behavior of typical system in actual operation. Each area is has two identical round rotor generators rated 20 KV/900 MVA. The synchronous machines contains identical parameters leaving the inertias which are H = 6.5s in area 1 and H is = 6.175s in area 2. Thermal plants that having identical speed regulators are which further assumed at all locations, in addition to fast static exciter with a 200 gain. The load is represented as constant impedance and spilt between the areas.

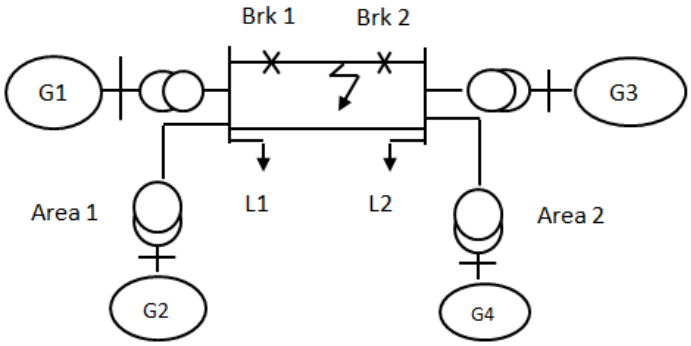

Fig -1: Two Area Four-Machine power system for Stability Analysis

Now the actual simulation model implemented for analysis of the PID-PSS and proposed MB-PSS for Inter-area power oscillation stability is shown in fig.2. Fig.3. Shows the internal structure of area-1 of the implemented power study testing system and fig. 4. Depicts the Internal configurations of Turbine and regular consisting the conventional PID-PSS and proposed MB-PSS.

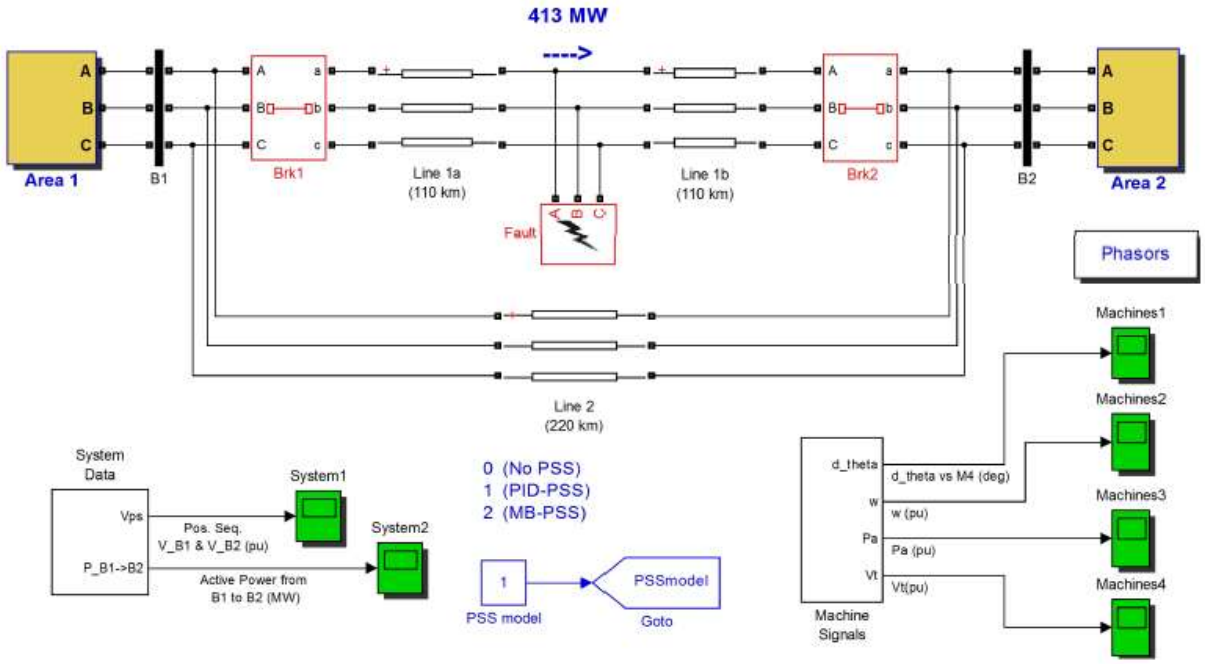

Fig - 2: Actual simulation model implemented with PID-PSS and proposed MB-PSS for Inter-area power oscillation stability Analysis.

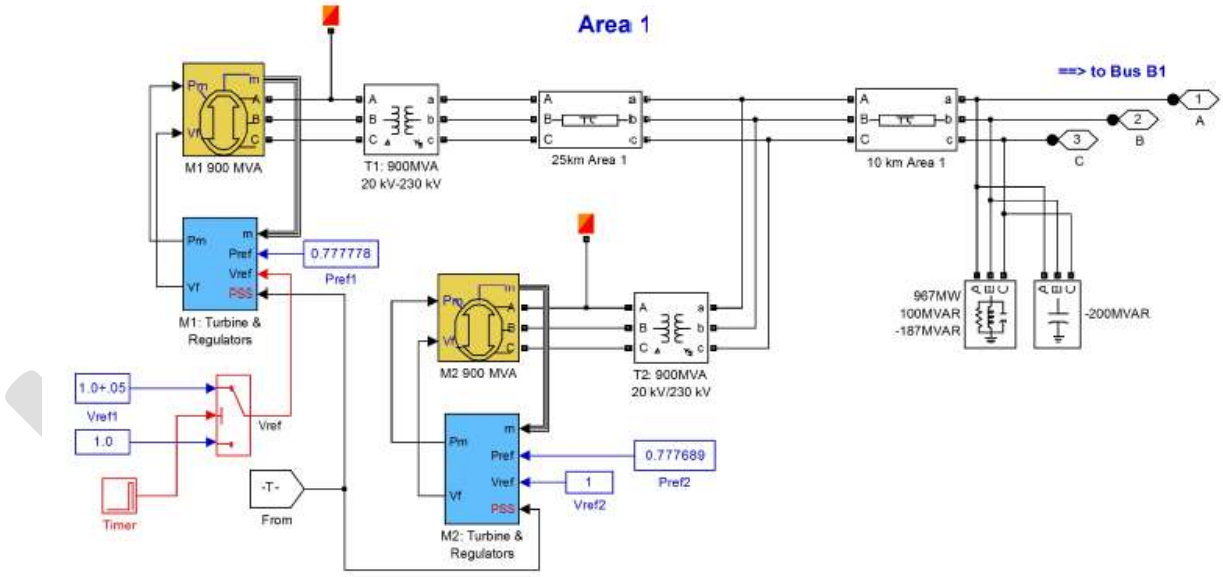

Fig-3: Internal configuration of area 1(subsystem)

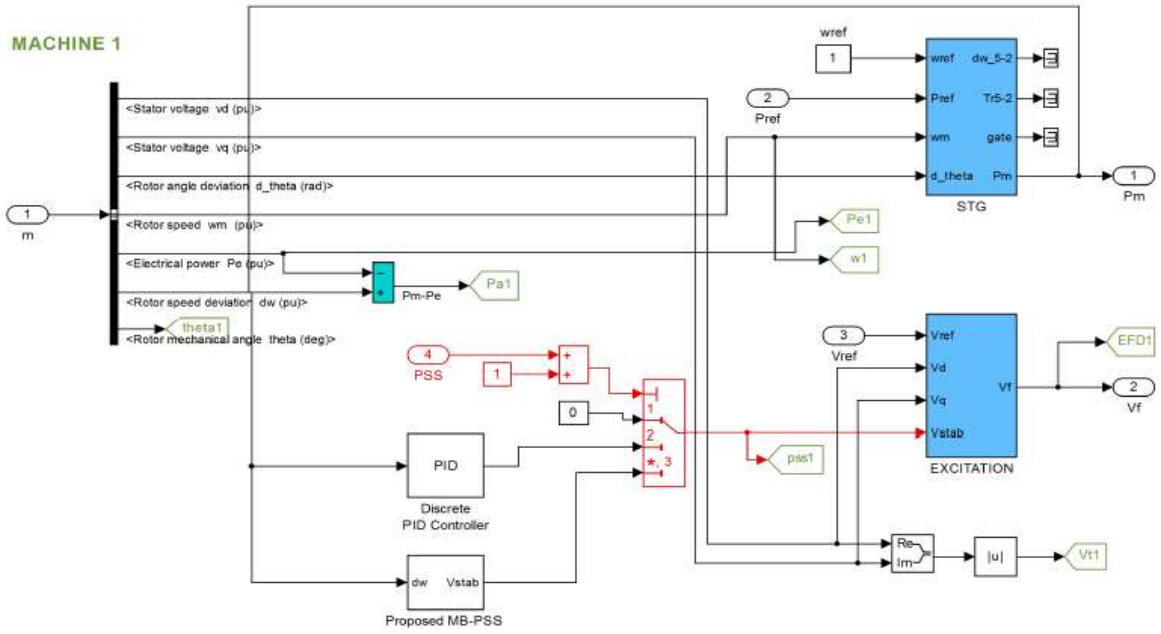

Fig-3: Internal configuration of Turbine and regulator With PID-PSS and proposed MB-PSS.

3. Proposed Multiband power system stabilizer (MBPSS)

The main features of the MB-PSS model (IEEE PSS4B) are given in fig.4 and fig.5. As for conventional PSS, the MB-PSS has three main functions, first , the transducers, another , the lead-lag compensation and the limiters. Two speed deviation transducers are necessary to feed the three band structure used as lead-lag compensation. Four adjustable limiters are given, one for each band and one for total PSS output.

The low band is looking of very slow oscillating phenomena such as common modes resulted on isolated system. Hydro-Quebec system is the best example with its 0.05 Hz global mode. The intermediate band is needed for inter-area modes usually found in the range of 0.2 to 1.0 Hz. The high band is working with local modes, either plant or inter-machines, with a typical frequency range of 0.8 to 4.0 Hz.

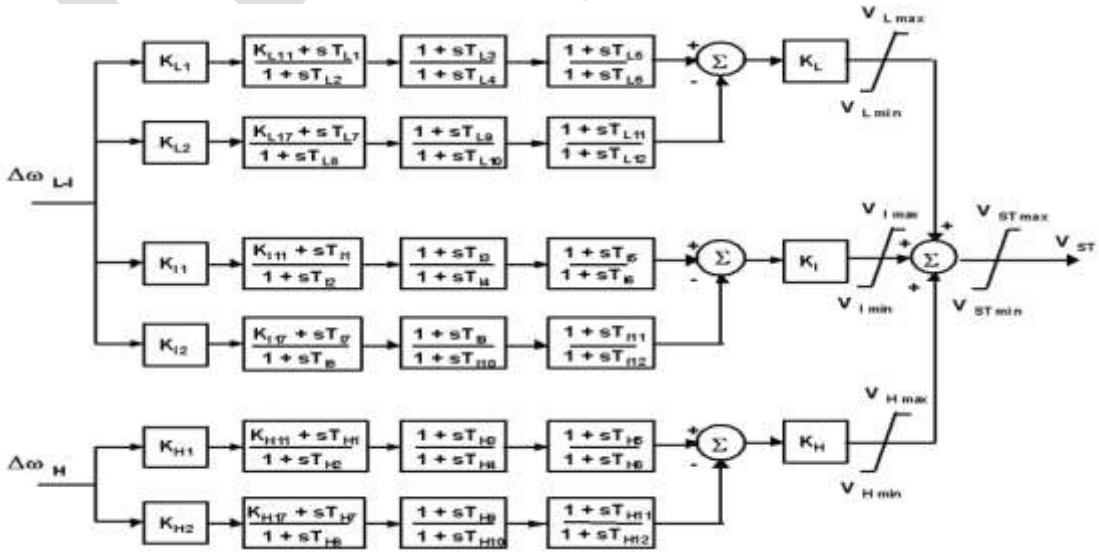

Fig-4: IEEE PSS4B model of the MB-PSS

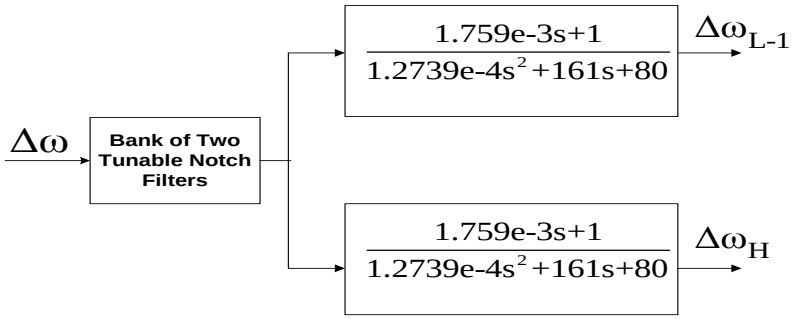

Fig-5: MB-PSS Speed Deviation Transducers

Lead-lag compensation bands are based on differential filters that may be used in several ways. Fig.6 zooms on the high hand to illustrate its characteristics.

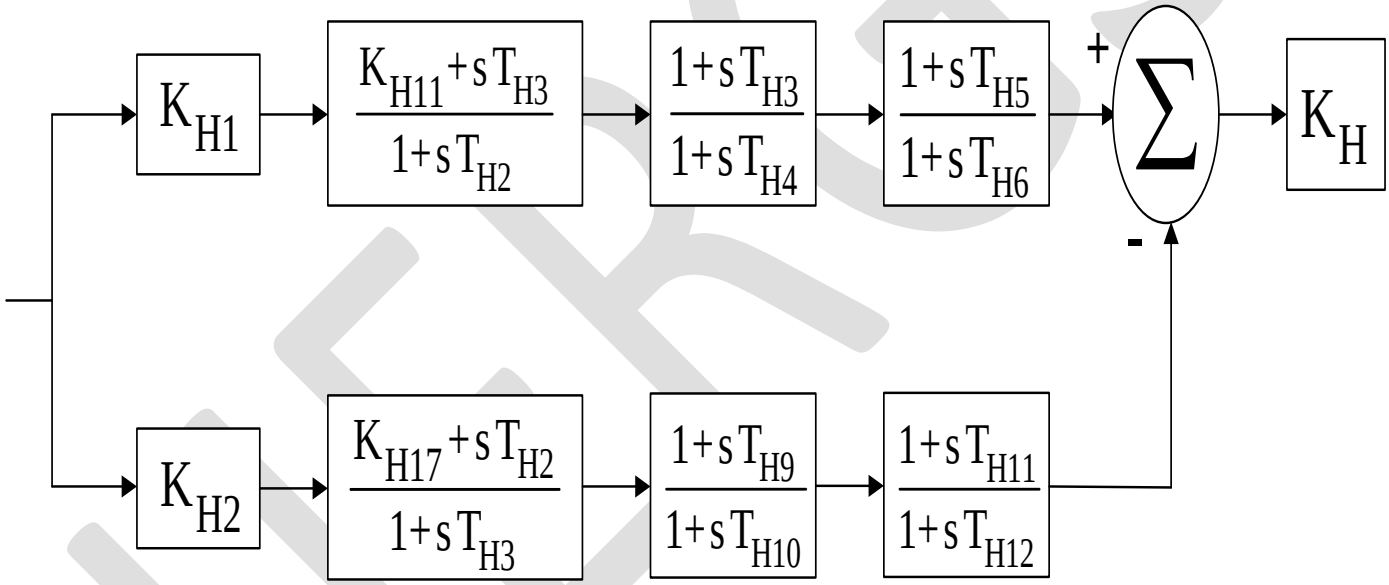

Fig-6: The high band differential filter

4. Simulation Results

The performance of the PID-PSS and proposed MB-PSS was evaluated by applying a large disturbance caused by three-phase fault applied at the middle of one tie line at 0.2 sec. and cleared after 0.133 sec by opening the breakers, with one tie-line the system can reach a stable operating point in steady state. The Parameters of PID-PSS used in test generators are given in Table 1. Each generator parameters are based on data in Table 2.

Table -1: Parameter of PID controller

Parameter	Kp	Kl	Kd
G1	30	10	0.001
G2	10.50	0.67	0.45
G3	10.50	0.67	0.45
G4	10.50	0.67	0.45

Table -2: Parameters of the generator

Parameter	Generator
X_d	1.8
X_d'	0.3
X_d''	0.25
X_q	1.7
X_q'	0.55
X_q''	0.25
X_t	0.2
T_{do}	8
T_{do}'	0.03
T_q	0.4
T_q'	0.05

To investigate the Inter-area power oscillation damping performance of PID-PSS and proposed MB-PSS with two-area four-machine test system, the three phases to ground fault was considered in the simulation studies. A three-phase fault of 0.4sec duration is simulated at line-1. Fig. 7, Shows the performance of test system response of without power system stabilizer (PSS).

To investigate the Inter-area power oscillation damping performance of PID-PSS and proposed MB-PSS with two-area four-machine test system, the three phases to ground fault was considered in the simulation studies. A three-phase fault of 0.4sec duration is simulated at line-1. Fig. 7, Shows the performance of test system response of without power system stabilizer (PSS).

To investigate the Inter-area power oscillation damping performance of PID-PSS and proposed MB-PSS with two-area four-machine test system, the three phases to ground fault was considered in the simulation studies. A three-phase fault of 0.4sec duration is simulated at line-1. Fig. 7, Shows the performance of test system response of without power system stabilizer (PSS).

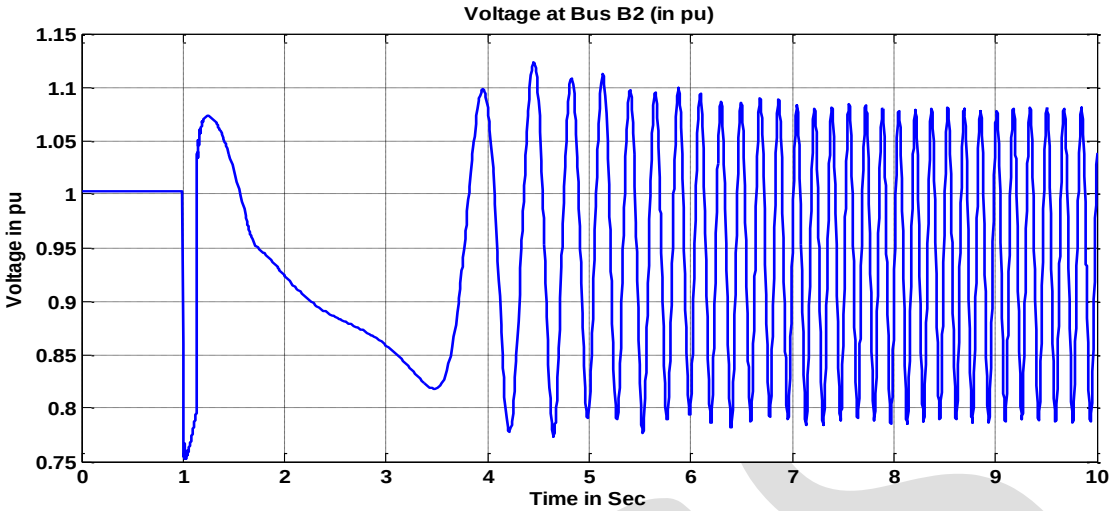

Fig-7(a): Voltage at Bus_1 without PSS.

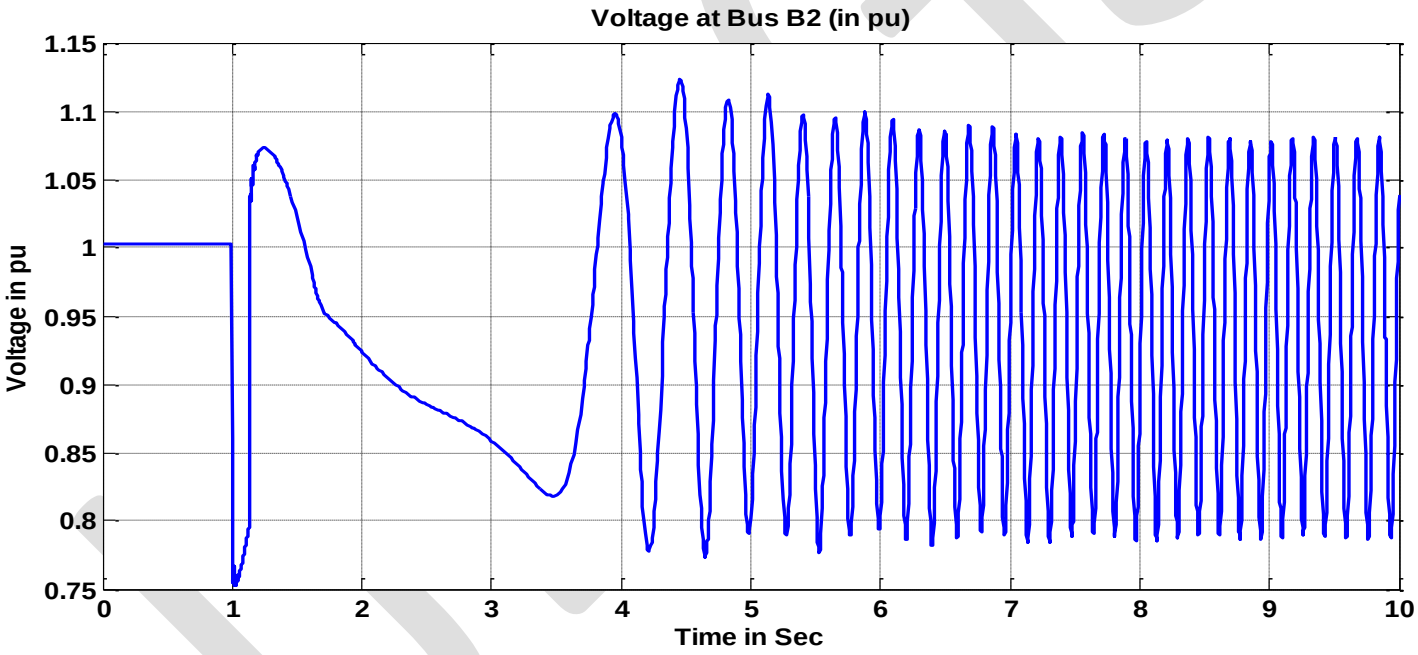

Fig-7(b): Voltage at Bus_2 without PSS.

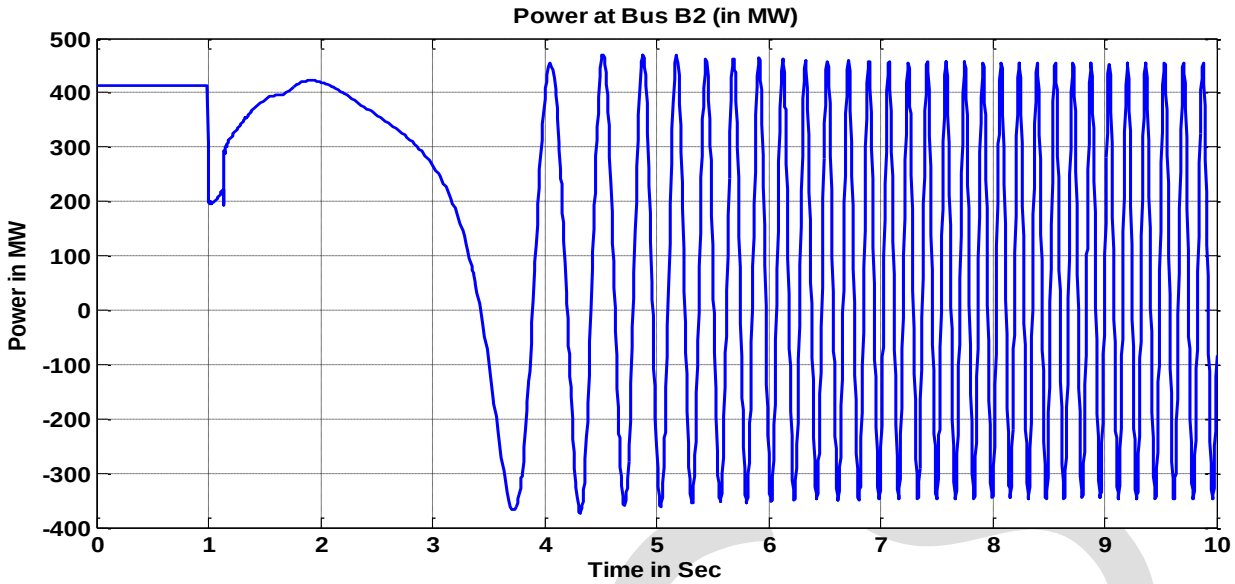

Fig-7(c): Power at Bus_2 without PSS

Now Fig.8. Presents the results of the examined power system with the same three phase fault under PID PSS

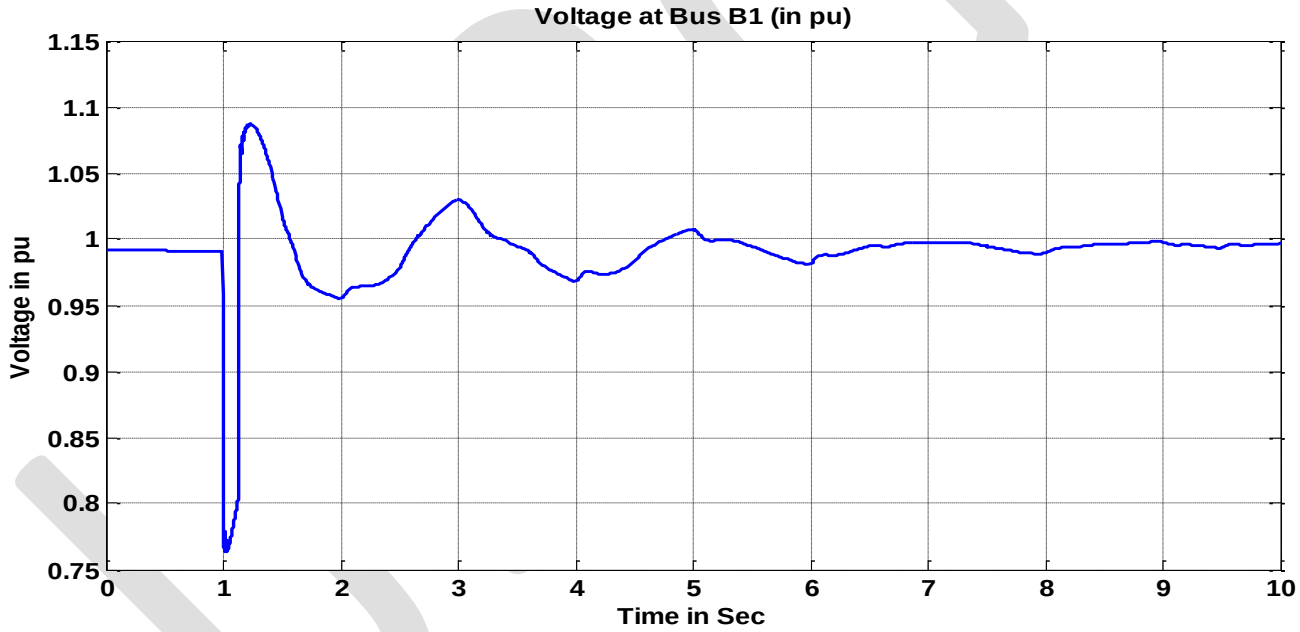

Fig-8(a): Voltage at Bus_1 with PID-PSS.

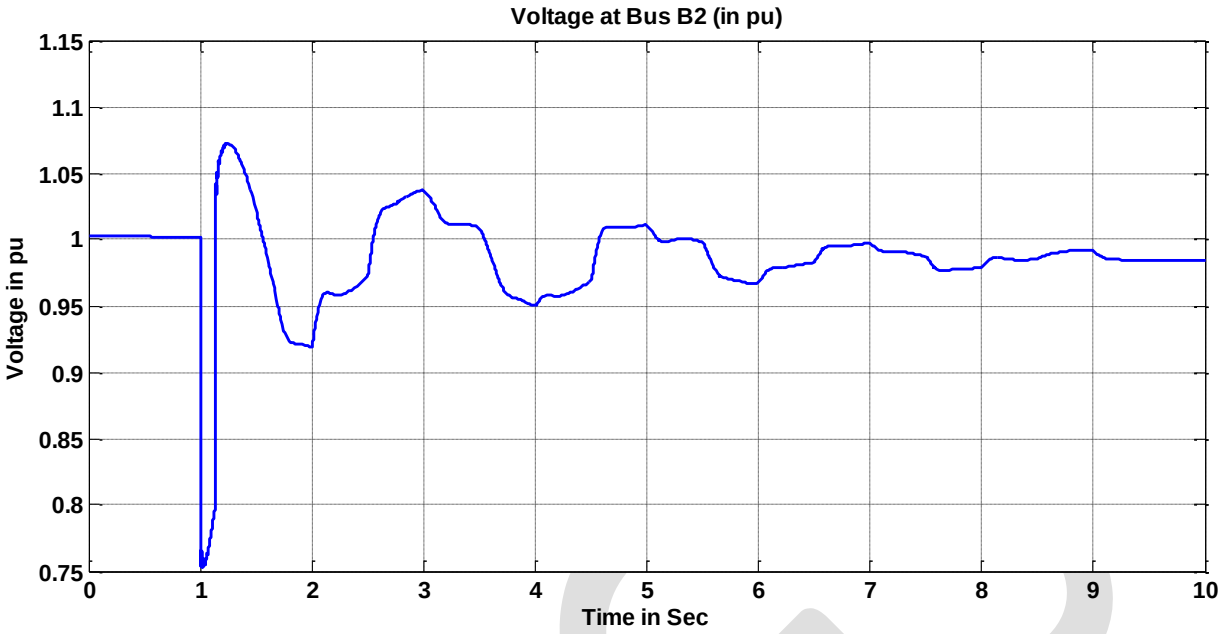

Fig-8(b): Voltage at Bus_2 with PID-PSS.

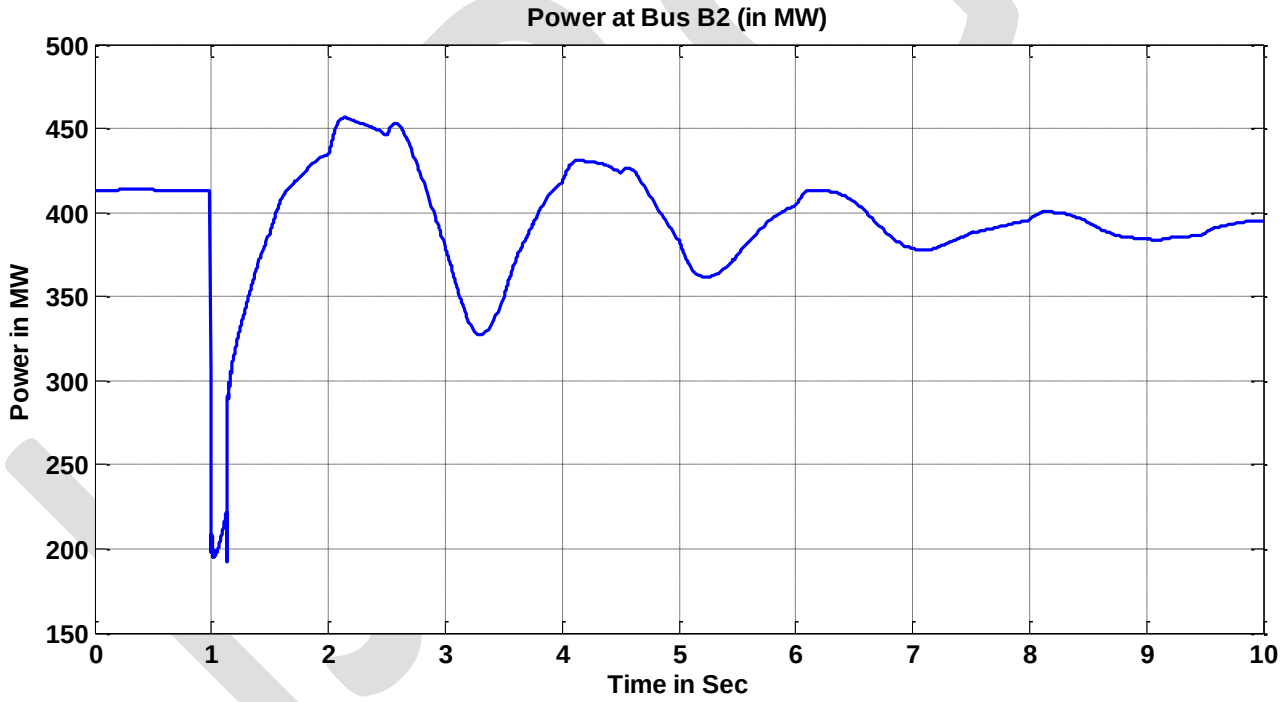

Fig-8(c): Power at Bus_2 with PID-PSS.

Now Fig. 9 presents the results of the examined power system with the same three phase fault under proposed MB-PSS.

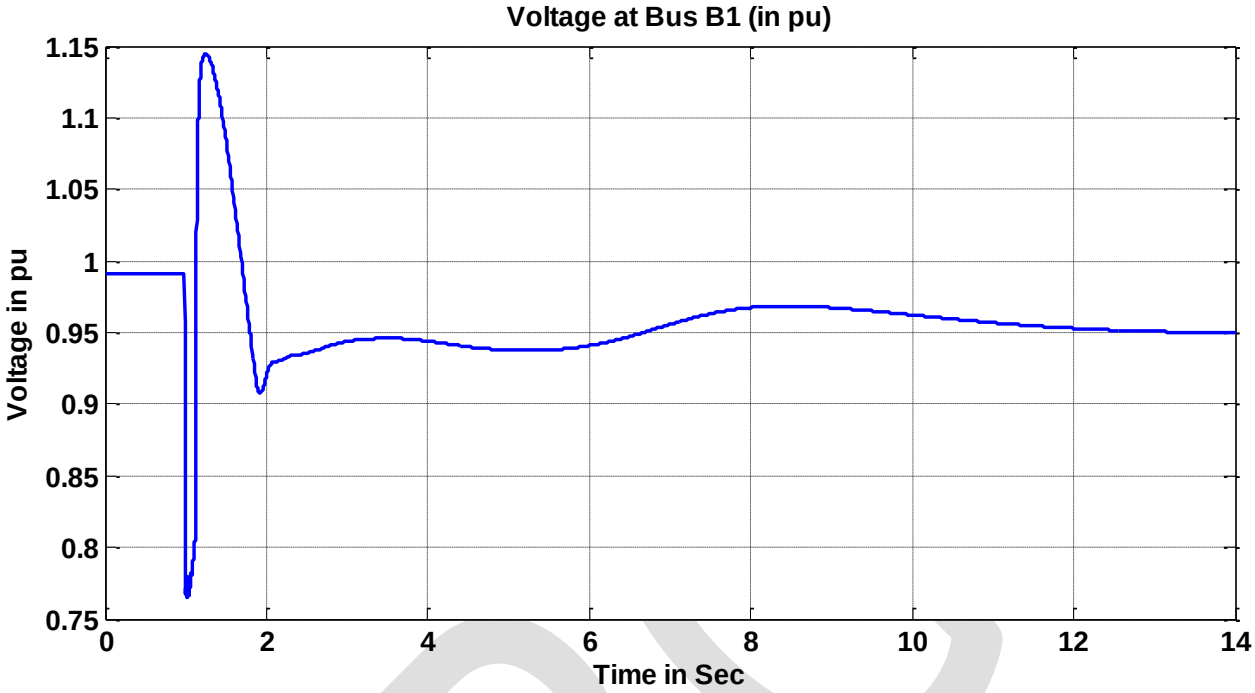

Fig-9(a): Voltage at Bus_1 with proposed MB-PSS.

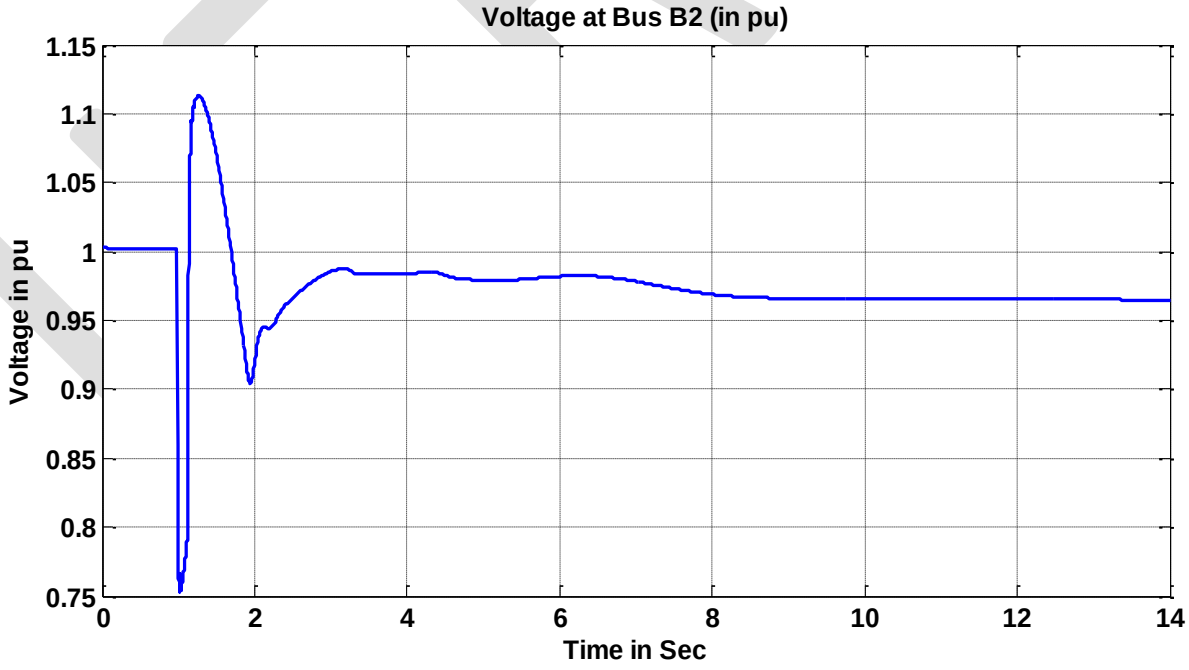

Fig-9(c): Power at Bus_2 with PID-PSS.

Finally fig.10, Shows the comparative Inter-area power oscillation damping performance of test system without power system stabilizer (PSS), with PID-PSS and with proposed MB-PSS.

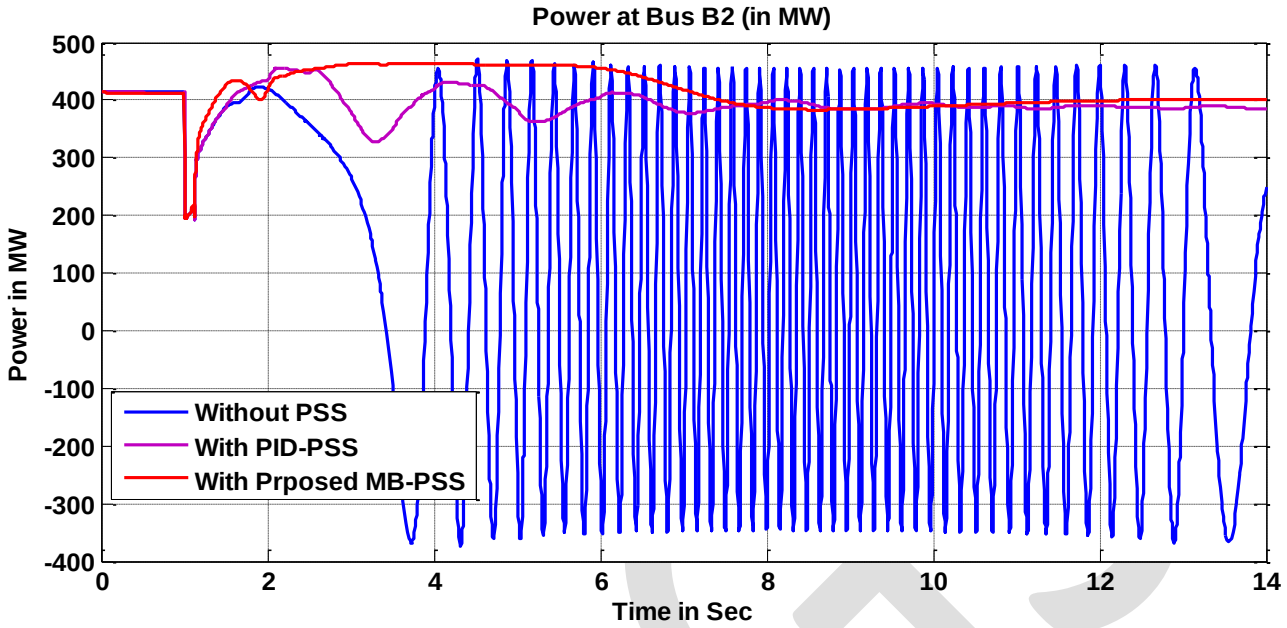

Fig-10: comparative Inter-area power oscillation damping performance.

5. CONCLUSION

Here a complete performance analysis that are two area four machine transmission lines power oscillation damping with which proposed MB-PSS, PID-PSS and without any PSS. After the simulation of this testing system without PSS, it is found that the power transfer between sending and receiving end, Here highly suffers with large oscillation. In addition to this the useful part with this simulation is that the system without PSS is not able to damp the power oscillation that even after 14 sec in this simulation. On the other side with the PID-PSS at the same system response which is quite acceptable, but here the response is still suffering from oscillations and that needs further improvement to all efficiently damp the oscillations. To overcome this problem this paper proposed a novel which multiband power system stabilizer. This result of Inter area power oscillation damping using proposed MB-PSS clearly indicates the high efficiency of proposed and PSS as compare to conventional PID-PSS. In addition with this the results also indicates that, the proposed model of MB-PSS takes only few seconds 10 sec to completely damp the Interarea power oscillations and whereas PID-PSS takes even more like greater than 14 sec to control the power supply oscillations.

REFERENCES:

[1] Junbo Zhang; Chung, C.Y.; Shuqing Zhang; Yingduo Han, "Practical Wide Area Damping Controller Design Based on Ambient Signal Analysis," Power Systems, IEEE Transactions on , vol.28, no.2, pp.1687,1696, May 2013.

[2] Hussein, T.; Shamekh, A., "Direct Adaptive Fuzzy Power System Stabilizer for a Multi-machine System," Computer Modeling and Simulation (UKSim), 2013 UKSim 15th International Conference on , vol., no., pp.33,38, 10-12 April 2013.

[3] Qudaih, Y.S.; Mitani, Yasunori; Mohamed, T.H., "Wide-Area Power System Oscillation Damping Using Robust Control Technique," Power and Energy Engineering Conference (APPEEC), 2012 Asia-Pacific , vol., no., pp.1,4, 27-29 March 2012.

[4] Babaei, E.; Golestaneh, F.; Shafiei, M.; Galvani, S., "Design an optimized power system stabilizer using NSGA-II based on fuzzy logic principle," Electrical and Computer Engineering (CCECE), 2011 24th Canadian Conference on, vol., no., pp.000683, 000686, 8-11 May 2011.

[5] Alsafih, H. A.; Dunn, R. W., "Performance of Wide-Area based Fuzzy Logic Power System Stabilizer," Universities' Power Engineering Conference (UPEC), Proceedings of 2011 46th International, vol., no., pp.1, 6, 5-8 Sept. 2011.

[6] Daryabeigi, E.; Moazzami, M.; Khodabakhshian, A.; Mazidi, M.H., "A new power system stabilizer design by using Smart Bacteria Foraging Algorithm," Electrical and Computer Engineering (CCECE), 2011 24th Canadian Conference on, vol., no., pp.000713, 000716, 8-11 May 2011.

[7] Babaei, E.; Galvani, S.; Ahmadi Jirdehi, M., "Design of robust power system stabilizer based on PSO," Industrial Electronics & Applications, 2009. ISIEA 2009. IEEE Symposium on, vol.1, no., pp.325, 330, 4-6 Oct. 2009.

[8] Babaei, E.; Galvani, S.; Ahmadi Jirdehi, M., "Design of robust power system stabilizer based on PSO," Industrial Electronics & Applications, 2009. ISIEA 2009. IEEE Symposium on, vol.1, no., pp.325, 330, 4-6 Oct. 2009.

[9] Huaren Wu; Qi Wang; Xiaohui Li, "PMU-Based Wide Area Damping Control of Power Systems," Power System Technology and IEEE Power India Conference, 2008. POWERCON 2008. Joint International Conference on, vol., no., pp.1, 4, 12-15 Oct. 2008.

[10] Athanasius, G.X.; Pota, H.R.; Subramanyam, P.V.B.; Ugrinovskii, V., "Robust power system stabilizer design using minimax control approach: Validation using Real-time Digital Simulation," Decision and Control, 2007 46th IEEE Conference on, vol., no., pp.2427, 2432, 12-14 Dec. 2007.

[11] Hunjan, M.; Venayagamoorthy, G.K., "Adaptive Power System Stabilizers Using Artificial Immune System," Artificial Life, 2007. ALIFE '07. IEEE Symposium on, vol., no., pp.440, 447, 1-5 April 2007.

[12] Dobrescu, M.; Kamwa, I., "A new fuzzy logic power system stabilizer performances," Power Systems Conference and Exposition, 2004. IEEE PES, vol., no., pp.1056, 1061 vol.2, 10-13 Oct. 2004.

International Journal of Engineering Research and General Science Volume 3, Issue 5, September-October, 2015
ISSN 2091-2730

Design of a Keypad Operated CNC Drilling Router

Olufemi B. Akinnuli[1], Vincent A. Balogun*[2], Tunde C. Akintayo[1]

[1]Department of Mechanical Engineering, Federal University of Technology, Akure, Nigeria.

[2]Department of Mechanical & Mechatronics Engineering, Afe Babalola University, Ado Ekiti, Nigeria

*Corresponding author: E-mail: balogunav@abuad.edu.ng

Abstract— The CNC router can be adapted for drilling and engraving operations based on the imagination and creative skills of the operator. A CNC router consists of three main parts: a mechanical setup that can move in X, Y and Z directions, a driving circuitry which includes the stepper motor and a software program that controls the operation of the system. Although, CNC router is commonly and commercially available, the emphasis is to increase the understanding and encourage developing countries like Nigeria on the developmental process of the CNC router machine. This work presents the development of a CNC drilling router machine using a keypad with the aid of Autodesk 3D Max and Proteus 8 software. The CNC router has a liquid crystal display (LCD) which is linked to the microcontroller. The program of instructions is written in C program compiler. The column strength of the X, Y, and Z axis of the machine were evaluated to be 508.86N, 1142.5N and 7872.64N respectively while the critical speeds of the various axes were determined to be 3222, 7234.14 and 49847.78 RPM respectively. The forces due to the guide rails were evaluated to be 890 N on both the Y and Z axes. This gave a force moment along these axes to be 400.5 and 10.1 kNmm respectively. The stepper motor utilized for the machine has a 1440 steps/ rev, 500 RPM with 1/8 micro-stepping with a phase current of 3.5A and voltage of 2.45V. It is anticipated that the developed machine is able to drill plastics and soft wood materials. The development strategy will aid the CNC router design concept within the developing economy as Nigeria.

Keywords— CNC router, mechatronics system, machine design, CNC machine, microcontroller, drilling, router development.

INTRODUCTION

Conventional Computer numerically controlled (CNC) machining is a technology which has set the manufacturing industry in an entirely new direction [1]. This has also changed the 'Business as Usual (BAU)' practice adopted through the use of conventional machine tools [2]. A CNC router is a computer controlled shaping machine. The tool paths can be controlled via computer numerical control system. Routing is usually used for high speed cutting, trimming, or shaping, on wood, light metals, plastics and many other materials. Also, a CNC router can perform machining operations (i.e. drilling, milling and cutting, engraving) and thermoforming of plastics by automating the trimming process. Schneider, [3] in 2010 reported that approximately 75% of all metal-cutting process is of the drilling operation. This therefore implies that drilling machines are one of the most commonly used industrial equipment. CNC drilling machine can be classified as CNC Printed Circuit Board (PCB) drill, CNC vertical drill, CNC deep-hole drill, drilling centre and other large CNC drilling machine. CNC machines are generally automated. Automation is the use of control systems and information technologies in order to reducing the need for human intervention. It is implemented with program of instructions combined with the control systems [4].

Machining is one of the most versatile and accurate of all manufacturing processes. This is as a result of its capability to produce a diversity of part geometries and geometric features [5]. Machining is a general term which refers to the selective removal of material from a part or work piece by a wedge shaped tool [6]. More recent advances in machining technology have made it possible to replicate extremely small tolerances on a large scale and exhibit superior finishing characteristics on the machined workpiece material [7]. The geometry of the part is achieved by the linear and rotary combinations of the workpiece and the cutting tool. For example, milling, shaping, planning, and sawing [4]. Due to the

relative cost and versatility, conventional CNC machining is still been adopted to manufacture large quantities of high-quality goods at unprecedented speed [8]. Modern day CNC machine now has new technologies with various milling features and functionalities [9] to ensure optimum performance.

COMPUTER NUMERICAL CONTROL AND COMPUTER NUMERICAL ROUTERS

Numerical control or numerically controlled (NC) machine tools are machines that are automatically operated by commands that are received by their processing units. The Electronic Industry Association (EIA) defined CNC as 'a system in which actions are controlled by the direct insertion of numerical data at some point' [10]. The system must automatically interpret at least some portion of this data. The input signals (NC codes) through the controller are sent to the machine tool for the execution of the required task. However, for an open loop machine tool, the signals from the controller to the machine tool receive no information in return while a closed loop machine tool receives information back due to the feedback mechanism for cutting adjustments. These adjustments help minimize detrimental conditions such as tool deflection or work piece slip.

The 3-axis CNC router is a computer controlled shaping machine. The Numerical codes (g-codes) that relates to the Computer Aided Design CAD of the workpiece is generated and sent to the CNC router so that the part designed with the computer can be replicated. The 3-axis CNC router comprises of the base or table frame, cutting table, x, y and z-axis linear drive system, y-axis gantry, the cutting tool (spindle), CNC controller and computer system. The trend and applications of CNC router are well documented in literature [11]. Onwubolu et. al., [12] developed a PC-based computer numerical control (CNC) drilling machine. The authors adopted a PC as a separate front-end interface for the drilling machine. The system developed and integrated the customized machine control unit, enhanced parallel port communication and neural network based optimizer in order to find the best distance optimized sequence of points to be drilled. Salihmuhsin et al., [13] developed a PCB prototyping system such that it produced a trace line on a PCB board and drilled the holes on both end of the trace line.

STATEMENT OF PROBLEM

In line with the sustainability agenda of United Nation Environment Program, UNEP, operations and processes are to produce more from less materials thereby increasing productivity at zero or near zero waste [14]. Furthermore, the growth of Nigeria manufacturing sector depends largely on its productivity and quality. Productivity level in Nigeria can be enhanced by having good machining processes which is actually the most versatile and accurate manufacturing processes and also having the capability to produce diversity of part geometries and geometric features using machines that can be controlled automatically with the computer. This could improve resource efficiency and sustainable manufacture. It is therefore envisaged that the CNC controlled toolpath be adopted to reduce human interaction in the drilling of holes since it is somewhat difficult to manually ascertain the locations of the holes to be drilled. Also, different size holes require the changing of the drill bit. This process is cumbersome and time consuming for repeated multiple jobs. This could lead to low productivity hence the need to automate the drilling process through the use of a CNC router.

AIM & OBJECTIVES OF THE STUDY

The aim of this research is to design and produce an animated model of a CNC drilling machine router. The specific objectives of this study are to:

- Design a computer numerical control (CNC) drilling machine router operated using a keypad.
- Animation of the computer numerical control (CNC) drilling machine router.
- Development of a piece of software for controlling the direction of the stepper motors.
- Simulation of the machine.

RESEARCH METHOD

The Machine Frame

The mechanical subsystems of the CNC router are those unit components which eventually make up the machine. For example, the mechanical subsystems comprises of the guide rail and bearings, the drive system, and the frame housing structure. Each of these systems has a direct impact on the qualities of a CNC. The materials selection for the mechanical subsystems has a direct impact on performance, precision, repeatability, longevity, and mechanical noise transfer into the parts.

The CNC machine frames (shown in Figure 1) are made of materials that have strength in order to support the weight of the gantry and the cutting head and at the same time withstand forces that could result from the cutting processes. Other design considerations for the machine frame include; the stiffness (to prevent any deflections due to both static forces and dynamic forces resulting from the acceleration of the tool head) and the total weight of the frame (contributes to both the static and the acceleration forces). Williams et al., [15] proposed the use of a range of different materials for the fabrication of the machine frame. This is as result of their exhibition of improved mechanical properties (i.e. modulus of elasticity, yield strength, and density). The ratio of the modulus of elasticity to density was calculated to give an indication of stiffness and the ratio of yield strength to density was found to give a strength value relative to weight [16]. The advantage of building the machine frame with aluminum is the high percentage of the weight-to-strength ratio it exhibits.

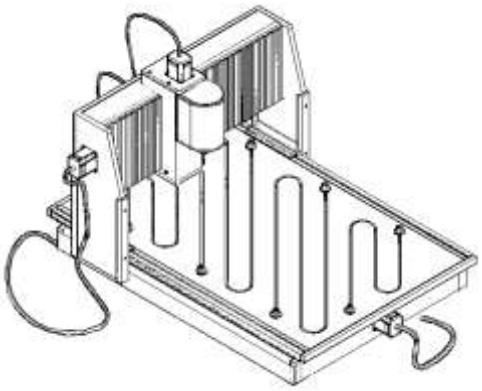

Figure 1: 2D Wireframe drawing of the proposed Router

DRIVE SYSTEM

In achieving the transmission of the rotational motion of the stepper motor to the linear movement of the gantry and the motor of the drill machine, a 0.5'' diameter, 10 threads per turn (TPT) and a 2- start ACME lead screw with an anti-back-lash nut is utilized. The ACME lead screw is selected due to the several advantages it offers. It include no back-driving under load, readily available as standard part, low cost, fine leads, unusual diameters, adaptability of custom designed follower nuts to the lead screw and high loads capabilities. The selected stepper motor has 1440 steps per turn capacity (i.e. $0.25° \; per\ step\ to\ complete\ 1\ revolution$).

$major\ diameter\ of\ screw, D = 0.5$ inches

$number\ of\ threads\ per\ inches\ (TPI) = 10$

$$number\ of\ turns\ per\ inches = \frac{TPI}{no\ of\ starts} = \frac{10}{2} = 5\ turns\ per\ inches$$

$$precision\ or\ steps\ per\ inches = 1440 \times 5 = 7200\ steps\ per\ inches$$

Picth of the leadscrew can be estimated as shown in Equation 1.

$$pitch = \frac{1}{TPI} = \frac{1}{10} = 0.1 \quad (1)$$

Therefore,

$$Lead = pitch \times no\ of\ starts = 0.1 \times 2 = 0.2 \quad (2)$$

$$minor\ diameter, K_s = D - \frac{1.22687}{n}$$

$$K_s = 0.5 - \frac{1.22687}{10}$$

$K_s = 0.377inches \equiv 9.58mm$

$minor\ diameter\ of\ the\ nut\ thread, K_n = D - \frac{1.08253}{n}$

$K_n = 0.5 - \frac{1.08253}{10}$

$K_n = 0.392inches \equiv 9.96mm$

$basic\ pitch\ diameter, D' = D - \frac{0.64954}{n}$

$D' = 0.5 - \frac{0.64954}{10}$

$D' = 0.435inches \equiv 11.05mm$

$Stress\ area, A_s = 0.7854\left\{D + \frac{K_s}{2}\right\}^2$

$A_s = 0.7854\left\{0.435 + \frac{0.377}{2}\right\}^2$

$A_s = 0.1295inches \equiv 3.29mm$

GUIDE RAIL AND BEARINGS

One of the machine's frame subsystems to be considered in the design is the conventional railing system which consists of a linear motion bearing and shaft assembly which would simply allow unrestricted movement along their lengths. For the Y and Z-axis, 2 pieces steel shafts of 16 mm diameter and 400 mm length were assembled with four rubber bushings to aid smooth transition of the motor along the steel shafts. A ball bearing design is incorporated on the X-axis. This is to reduce the rotational friction and to provide radial and axial loads support along the X-axis. It achieves this by using at least two races to contain the balls and transmit the loads through the balls. Because the balls are rolling, they have a much lower coefficient of friction than if two flat surfaces were sliding against each other.

Determining the Column Strength, Critical Speed and Force analysis

For each of the table axis, the column strength and critical speeds under the maximum weight were evaluated and shown in Table 1. Equations 3, 4 and 5 are adopted to evaluate the column strength, critical speed and Bending moment respectively along the X, Y and Z-axis.

The maximum load the lead screw can withstand in compression before failure is the Column strength, any compression load which exceeds this estimated column strength will cause the lead screw to buckle.

$$C_l = \frac{[N \times 14.03 \times 10^6 \times k_s^4]}{L^2} \quad (3)$$

$$C_s = \frac{[N \times 4.76 \times 10^6 \times K_S]}{L^2} \quad (4)$$

Where;

C_l = Column strength, C_s = critical speed, N = *fixity type (fully supported frame type being used in this design) = 1.00*, L= *length of the lead screw* = $23.6\ inches\ or\ 600\ mm$, $k_s = minor\ diameter\ of\ the\ x - axis\ lead\ screw = 0.377\ inches$

Table 1: Column Strength, The Critical Speed and Force analysis

Axis	Column Strength (N)	Critical Speed (RPM)
X	508.86	3222
Y	1142.5	7234.14

Z	7872.64	49847.78

FORCE ANALYSIS

When the machine is in operation, there are certain forces and moments worthy of consideration in the design of the machine in order not to stress the machine beyond what it can actually take for optimum performance.

Y-Axis Gantry Assembly

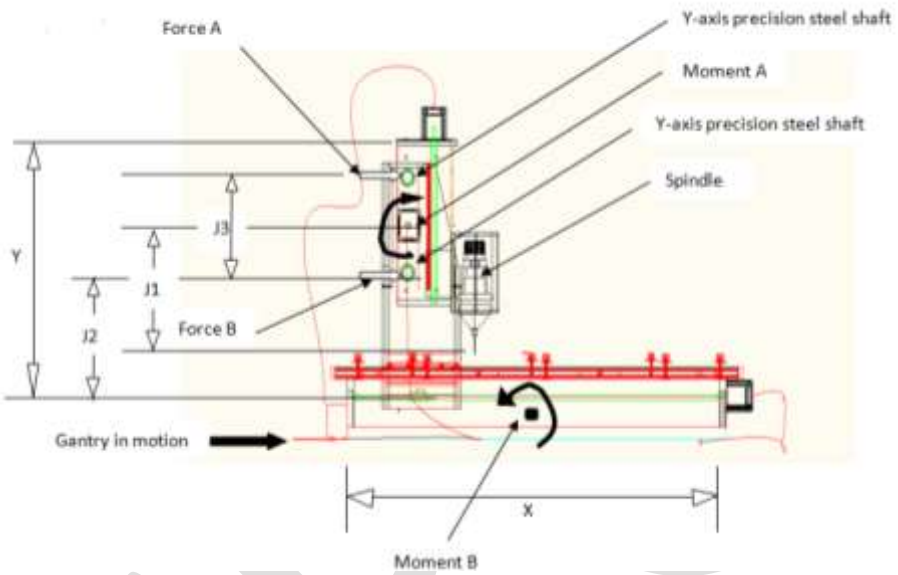

Figure 2: Analysis of the Y-axis assembly Parameters

From Figure 2,

$J1 = distance\ between\ \ cutting\ tool\ and\ center\ between\ the\ two\ \ - axis\ precision\ steel\ shaft = 400mm$

$J2 = distance\ between\ lower\ Y - axis\ precision\ shaft\ and\ bottom\ X - axis\ linear\ precision\ shaft = 450mm$

$J3 = distance\ between\ lower\ and\ upper\ Y - axis\ precision\ steel\ shaft = 300mm$

When the gantry moves by action of the CNC drive system and the spindle cuts, this cutting action opposes the movement of the gantry resulting in a cutting force (www.*cncroutersource.com*).

The cutting force being applied at distance $J1$ results in moment at point A as shown above.

$moment\ A = J1 \times C_f$

$where$:

$J1 = 400mm$

$Maximum\ expected\ cutting\ force, C_f = 150lbs\ or\ 667.5N$

$Moment\ A = \ 667.5\ \times 400 = 267kNmm$

It is to be pointed out that the longer the distance$J1$, the larger will be the moment even if our cutting force remains the same.

The moment A, resulting here results in 2 forces on the Y-axis precision steel shaft. The forces resulting are labeled as force A & B, as shown above.

$Force\ A = Force\ B\ (for\ a\ safe\ operation\ of\ the\ machine)$

$$Force\ A = \frac{momet\ A}{2} \div \left(\frac{1}{2}J3\right)$$

$$Force\ A = \frac{moment\ A}{J3}$$

$where$:

$J3 = 300mm$

$$Force\ A = \frac{267000}{300} = 890N$$

It is noted that as the vertical distance, J3 between the two precision steel shafts increase, the resulting forces A and B reduces.

This aids in reducing the amount of centralized torque which is on the gantry itself.

In finding the second moment B;

$Moment\ B = J2 \times fore\ A$

$where$:

$J2 = 450mm$

$Moment\ B = 450 \times 890 = 400.5kNmm$

This moment B could cause the whole gantry to rock due to the cutting force, hence, we aim at reducing it to barest minimum by reducing J3 so to have equal amount of force on our linear bearings and reduced deformation and chatter of the machine

Forces and Moment on the Z-axis Assembly

While the machine moves in the Z-axis direction to the right, riding on the Y-axis linear bearing rail, the plunge arm is at a maximum Z travel and cutting into a material as it moves from left to right. This cutting action taking place produces a cutting force which opposes the movement of the Z-axis assembly.

This cutting force created causes a moment C as illustrated below:

$Moment\ C = J7 \times cutting\ force$

Taking the thickness of the plunger arm as 15mm

$Moment\ C = 15 \times 667.5 = 10.1kNmm$

This moment C causes a torque on the plunger arm in the opposing direction of the cutting force, which in turn, torques the entire Z-axis assembly. This moment results in resultant forces which are applied to the Z-axis linear bearing rails and even the Z-axis linear bearings themselves.

As J9 increases in length, the resultant forces decreases.

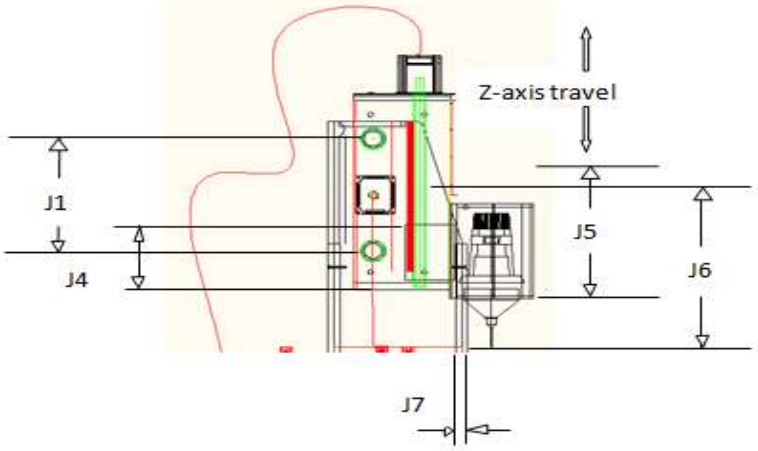

Figure 3: Side view of the Z-axis assembly

From Figures 3 and 4:

J1= *distance between cutting tool and centre between the two Y-axis precision steel shaft*

J4= *vertical distance between the upper and lower sets of the Z-axis linear bearing*

J5= *the length of the spindle attachment plunge arm*

J6= *distance between the cutting force and* $\frac{1}{2}J4$

J7= *thickness of the plunge arm*

J8=$the\ width\ of\ the\ Z-axis\ assembly$

J9=$horizontal\ distance\ between\ the\ Z-axis\ line\ precision\ shaft$

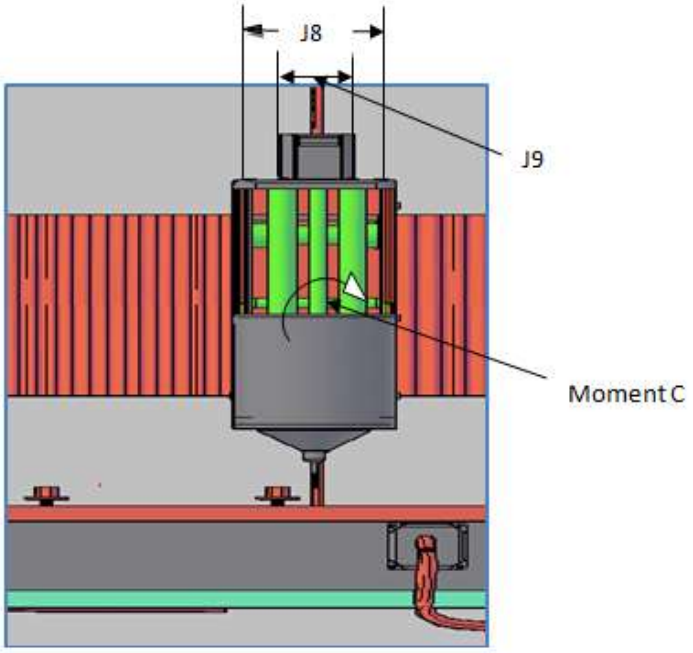

Figure 4: Front view of the machine

Cutting speed, depth of cut, feed rate are collectively known as cutting conditions of a machine. They form the three dimensions of the cutting process.

CALCULATION FOR LEAD SCREW ASSEMBLY VELOCITY (IN IPM)

We need to estimate for the desired velocity at which the lead screw assembly is to move. It is often measured in inches per minute (IPM).

$$RPM = \frac{velocity\ (inch/min)}{lead\ (in/rev)}$$

$$velocity = RPM \times lead$$

Where:

$Lead\ = 0.2$

$RPM\ of\ the\ stepper\ motor = 500\ rpm$

$velocity = 0.2 \times 500 = \ 100\ IPM$

In the X-axis;

With our lead screw being 23.6 inches in length, pitch of 0.1'' and lead of 0.2, 500 RPM motor would give a rapid feed or velocity of 100 inch/minute, or taking 14.16 seconds for the full slide travel.

In the Y- axis;

With our lead screw being 15.75 inches in length, pitch of 0.1'' and lead of 0.2, 500 RPM motor would give a rapid feed or velocity of 100 inch/minute, or taking 9.45 seconds for the full slide travel.

In the Z-axis;

With our lead screw being 15.75 inches in length, pitch of 0.1'' and lead of 0.2, 500 RPM motor would give a rapid feed or velocity of 100 inch/minute, or taking 9.45 seconds for the full slide travel.

Motor step/inch calculation

This is regarded as the number of steps the motor runs in order for the nut to move 1 inch on the lead screw in either axis. The equation for this estimate has put into consideration also the type and size of our lead screw, as well as the micro stepping.

$$steps/inches = \ leadscrew's \frac{rev}{inch} \times \frac{1}{microstep} \times motor's \frac{step}{rev}$$

Where:

The leadscrew's (rev/inch) $=$ 5 rpi

Motor's (step/ rev) $=$ 1440 steps/rev

Motor's microstepping of $1/8$

$$\frac{steps}{inch} = 5 \times \left(\frac{1}{\frac{1}{8}}\right) \times 1440 = \ 57{,}600 \ steps \ per \ inch$$

2.7.1 The motor step per second

This estimate is essential so to specify the clock speed which our computer system must send pulses out so to ensure that the machine moves at a specific speed. If the clock speed is set too low while machine speed is high could have a negative effect on the machine's performance in terms of missed steps or limited speed.

$$\frac{steps}{second} \ Hz = \frac{inch}{minute} \times \frac{step}{inch} \times \frac{1 \ minute}{60 \ seconds}$$

$$\frac{steps}{second} \ in \ Hz = 100 \times 57{,}600 \times \frac{1}{60}$$

$$clock's \ steps \ per \ second = \ 96{,}000Hz = 96kHz$$

THE ELECTRONIC SYSTEM

Stepper motor selection

There are two electromechanical approaches that can be used to drive the mechanical system. There is a servo controlled and the stepper motor drive approach. The servo systems have a basic drive system with feedback, stepper motors have multiple methods in which they can be driven. These techniques can be simple or complicated, and it becomes a question of performance versus cost which determines the type used.

Stepper motors are well known to use between 50 to 100 pole brushless motors. They can accurately move between step positions because of the high number of poles. Stepper motors move incrementally using pulses of current and do not require the use of a closed loop feedback system. The high number of poles of the stepper motor helps it in delivering more torque at lower speeds than of the same size servo motor. Torque reduction of the stepper motor at higher speeds can however be minimized by increasing the driving voltage of the motor. In this project a motor with 1440 steps/ rev, 500 rpm, 1/8 micro-stepping is used to powering the lead screw.

The PIC 18F452 Microcontroller

The CNC controller is well regarded as the brain of a CNC system. The controller completes the all-important link between a computer system and the mechanical components of the developed CNC router machine. The primary task of the CNC controller is to receive conditioned signals from the computer and interpret those signals into various mechanical motions as required through the stepper motor output. The microcontroller consists of a microprocessor, memory, I/O capabilities, and other on-chip resources. The choice of microcontroller is governed by low cost, versatility, ease of programming, and sizes. The PIC microcontroller 18F452 adopted for this work has Liquid Crystal Display LCD that displays the X, Y and Z and spindle speed instructions being sent to the machine. The microcontroller is interfaced with the LCD using the C programming software and the Proteus simulation software.

RESULTS AND DISCUSSIONS

Machine Animation

The 3D animation of the various modes of movement of the machine was carried out. This was achieved with the aid of the Autodesk 3ds max animation software. The design stages of the animation process using the 3ds max software are as shown in Figure 5 for X, Y and Z axes respectively. The maximum machine movements for the simulated router are 600, 400 and 152.4 mm along the X, Y and Z axes respectively.

Figure 5: X, Y and Z- axis movement of the machine

The program of instructions, to interface the stepper motors with the microcontroller was written using the *C* programming language software. The Proteus software was used in the simulation of the machine's component based on the program of instructions encoded using the *C* language. Proteus is a piece of software used in simulation of microprocessors, printed circuit board design and schematic capture. Figure 6 shows the Proteus circuit simulation design.

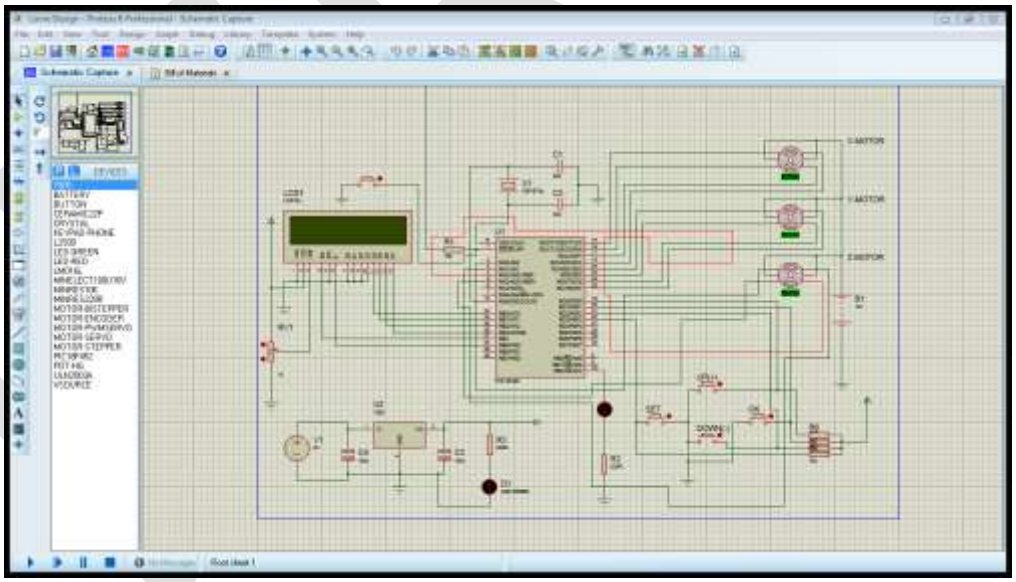

Figure 6: Snap shot of the Circuit Simulation Design using Proteus

The developed CNC router machine integrated with a microcontroller is designed for drilling operations (i.e. reaming, counter boring, countersinking etc). The microcontroller is an integral part of the system (i.e. the brain box for the machine). The programmed microcontroller enabled the CNC router to carry out specific operations. The ease of data input of the software enables the operator to input the coordinates of the axis with the aid of a keypad. Electric signals are sent to the microcontroller as soon as the coordinates are inputted using the keypad. This translates the electric signals to

positional movement along the X, Y and Z axes as the case may be with the aid of the stepper motors. The animation of the working principle of the CNC machine was developed using the Autodesk Inventor package.

CONCLUSIONS AND RECOMMENDATIONS

The development a low cost CNC router machine described in this work, and to be adopted within the small scale industries, would increase the understanding of the machine development and strategy in Nigeria. It is anticipated that the designed CNC drilling router machine could bring about the resource efficiency of the small scale industries if adopted for drilling of holes on wood, light metals and plastics materials. The workability of the developed CNC drilling router machine is also exhibited on the result of the simulation obtained. The CNC router machine designed can be useful to those who are hobbyist and in the small tasks workshops. Further conclusions deduced from this work include:

1. The designed strategy can be adopted to increase the capacity of the CNC router machine. The machine can also be adopted for engraving tasks.
2. If the developed CNC router machine is integrated with a PC based controller (i.e. a PC controlled CNC software installed on it), it will have the capability to design and define the shapes that needs to be cut e.g. circles, rectangles, drill patterns etc.
3. A developed transfer function incorporated into the CNC router machine could aid the control of the spindle mechanisms.

REFERENCES:

[1] Bramble, K. (2007). Engineering design for manufacturing. Engineers edge, Monroe (GA).

[2] Ryan, V. (2009), CNC work- an introduction retrieved from www.technologystudent.com/.../cnc1 May 2013.

[3] Schneider, G. (2002). Cutting Tool Applications. T & P: Tooling and production, 68(4), 14-23.

[4] Groover, M.P. (2010), Fundamentals of Modern Manufacturing, Materials, Processes and System, International Editions, Prentice Hall, pp 50764

[5] Balogun, V. A., Mativenga, P. T., (2014). Impact of un-deformed chip thickness on specific energy in mechanical machining processes, Journal of Cleaner Production 69: 260-268.

[6] Kalpakjian, S., Schmid, S., 2003. Manufacturing Processes for Engineering Materials. Prentice-Hall, Englewood Cliffs, New Jersey.

[7] Erdel, B. (2003), *High-speed machining*, SAE technical paper.

[8] Patrick, C., Charles, C., Wesley, D., and Paul, J. (2011), *CNC Application and Design*, Worcester Polytechnic Institute, Worcester, Massachusetts, United States. pp 1-19

[9] Yash, S. (2012), *History of Milling Machine* retrieved 20th of May 2013

[10] Electronic Industries Association, (1992). ANSI/EIA-494-B-1992, 32 Bit Binary CL (BCL) and 7 Bit ASCII CL (ACL) Exchange Input Format for Numerically Controlled Machines. Washington, D.C.

[11] Chen, Q., Chen, X., (2006). Application and development trend of CNC router. Journal of Harbin Bearing, 1, 024.

[12] Onwubolu, G. C., Aborhey, S., Singh, R., Reddy, H., Prasad, M., Kumar, S., & Singh, S., (2002). Development of a PC-based computer numerical control drilling machine. Proceedings of the Institution of Mechanical Engineers, Part B: Journal of Engineering Manufacture, 216(11), 1509-1515.

[13] Salihmuhsin, M., Baba, S., Yılmaz, A. S., & Sekkeli, M., (2015). Development of a Computer Controlled Automated PCB Machine. APJES III-II14-21, DOI: 10.5505/apjes.2015.83803.

[14] Quental, N., Lourenço, J. M., da Silva, F. N. (2011). Sustainable development policy: goals, targets and political cycles. Sustainable Development, 19(1), 15-29.

[15] Williams, N., Burry, J., Davis, D., Peters, B., de Leon, A. P., & Burry, M. (2015). FabPod: Designing with temporal flexibility & relationships to mass-customization. Automation in Construction, 51, 124-131.

[16] Ashby.,Michael,F.,(2005), Materials Selection in Mechanical Design 3rd edition, Oxford: Elsevier, London, pp.23

International Journal of Engineering Research and General Science Volume 3, Issue 5, September-October, 2015
ISSN 2091-2730

An Active Power Filter for Improving the Power Quality of a Distribution Grid

Anju R K[1], Fossy Mary Chacko[2]

PG Student, Dept. of EEE, Saintgits College of Engineering, Kottayam, Kerala, India[1]

Assistant Professor, Dept. of EEE, Saintgits College of Engineering, Kottayam, Kerala, India[2]

Abstract— The electric power quality has become an important part of the distribution power system .The aim of this paper is to improve the power quality of the distribution grid. Here, an energy storage is integrated into dc-link of the Active Power Filter through a bidirectional dc-dc converter that helps in providing a stiff dc-link voltage. The integration helps in providing active/reactive power support, intermittency smoothing, and harmonic compensation. The design and control of both the dc-ac inverters and the dc-dc converter is also developed.

Keywords—Distributed Energy Resource (DER), Active Power Filter (APF), Power Conditioner (PC), Total Harmonic Distortion (THD), Distribution Grid (DG), Power Quality (PQ), Plug-in Hybrid Electric Vehicle(PHEV)

INTRODUCTION

PQ may be defined as a provision of voltages and a system design so that the user of electric power can utilize electric energy from the distribution system successfully, without interference on interruption [1].Harmonics are the primary cause for the poor power quality of the distribution system. Harmonics are caused by non-linear loads i.e. loads that draw a no sinusoidal current from a sinusoidal voltage source. Some examples of harmonic producing loads are electric arc furnaces, static VAR compensators, inverters, DC converters, switch-mode power supplies, and AC or DC motor drives.

Renewable energy generation is growing fast and ideas such as smart grid are trying to change the role of a consumer from being a passive consumer to an active contributor who can supply stored excess power in various DERs, such as solar, wind and PHEVs back to the distribution grid or the micro-grid. Most of the DERs are intermittent and integrating them with energy storage not only improves the reliability of the DERs but also gives an opportunity to provide additional functionalities such as active and reactive power support and harmonic compensation to distribution grid. Of all the energy storage technologies Ultracapacitors (UCAP) have low energy density and high power density and fast charge/discharge characteristics[3, 5]. Therefore, they are ideally suited for providing support to events on the distribution grid which require high power and low energy for short spans of time. UCAPs also have higher number of charge-discharge cycles and higher terminal voltage per module when compared to batteries which again make them ideal choice for providing grid support for short time. UCAP based energy storage can be integrated into the distribution grid through a bi-directional dc-dc converter and a dc-ac inverter and this integration can be carried out by connecting the dc-ac inverter in shunt as an Active Power Filter (APF) with the grid.

SYSTEM CONFIGURATION

The one-line diagram of the system is shown in Figure 1.The system consists of a UCAP on the input side of the bi-directional dc-dc converter which acts as an interface between the UCAP and the 3-phase grid connected inverter. The major advantage of integrating the UCAP and the APF system is that the system now has the capability to supply and absorb Active Power from the grid [14].A bi-directional dc-dcconverter interface is necessary since the UCAP voltage profile changes as it charges/discharges energy while the inverter dc-link voltage has to stay constant for accurate control of inverter. Therefore, it acts as a boost converter while the UCAP is discharging energy into the grid and as a buck converter while charging the UCAP from the grid.

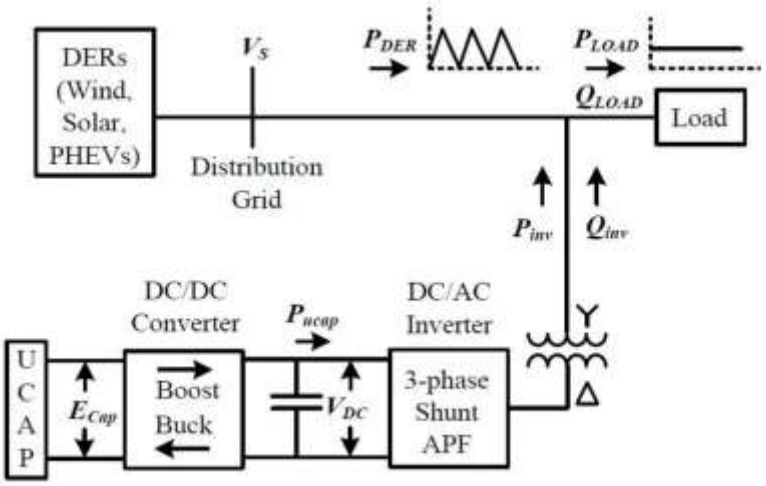

Fig 1. One line diagram of APF with UCAP energy storage

The complete circuit diagram of the shunt APF, and the bidirectional dc-dc converter is shown in Figure 2. The inverter systems consist of IGBT module, its gate-driver, LC filter, and an isolation transformer. The dc-link voltage, V_{dc} is regulated at 260 V for optimum voltage and current compensation of the converter and the line-line voltage, V_{ab} is 208 V.

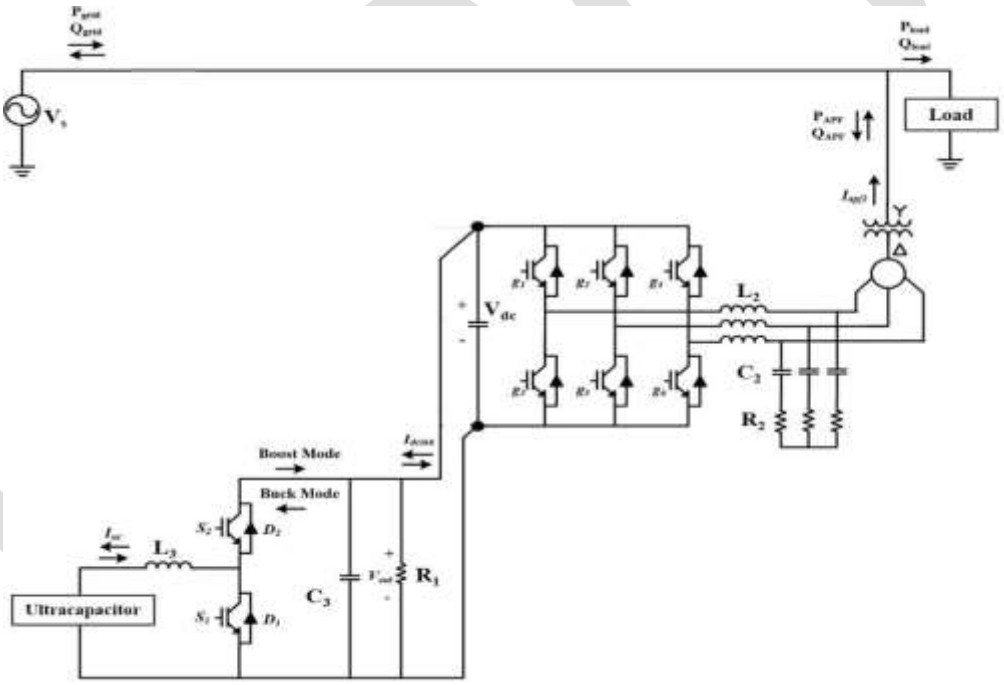

Fig 2. Model of APF with UCAP energy storage

There are various methods to control the 3-phase shunt APF to provide harmonic and reactive power compensation of which the most common approaches are the p-q method and the i_d-i_q method [2, 11] .The i_d-i_q control performs better in non-sinusoidal and unbalanced conditions when compared to the p-q method, while both methods perform in a similar manner in balanced sinusoidal conditions. In this system, the i_d-i_q method is modified to provide active and reactive power compensation such that i_d controls the reactive power and i_q controls the active power. Therefore, based on the references for active and reactive powers P_{ref} and Q_{ref} the reference currents i_{qref} and i_{dref} in d-q domain can be calculated using (2) and (4) where v_q is the system voltage in q-domain.Once the reference currents are calculated they are compared with the actual inverter currents and the error is passed through a PI controller.

$$P_{ref} = -\frac{3}{2}\left(V_q I_{qref} + V_d I_{dref} \right) \quad \textbf{(1)}$$

If V_d=0, then

$$P_{ref} = -\frac{3}{2}\left(V_q I_{qref} \right) \quad \textbf{(2)}$$

$$Q_{ref} = \frac{3}{2}\left(V_d I_{qref} - V_q I_{dref} \right) \quad \textbf{(3)}$$

If V_d=0, then

$$Q_{ref} = -\frac{3}{2}\left(V_q I_{dref} \right) \quad \textbf{(4)}$$

$$\begin{bmatrix} i_{refa} \\ i_{refb} \\ i_{refc} \end{bmatrix} = \begin{bmatrix} 1 & 0 \\ -\frac{1}{2} & \frac{\sqrt{3}}{2} \\ -\frac{1}{2} & -\frac{\sqrt{3}}{2} \end{bmatrix} \begin{bmatrix} \cos\theta & \sin\theta \\ -\sin\theta & \cos\theta \end{bmatrix} \begin{bmatrix} i_{dref} \\ i_{qref} \end{bmatrix} \quad \textbf{(5)}$$

The load currents are tracked upon which Park's transformation is performed to obtain corresponding d-q axes currents. According to i_d-i_q control strategy, only the average value of d-axis component of load current should be drawn from supply. Here the fundamental frequency component of d-q axes currents are separated i.e the oscillating components are filtered out using low-pass filter [10].

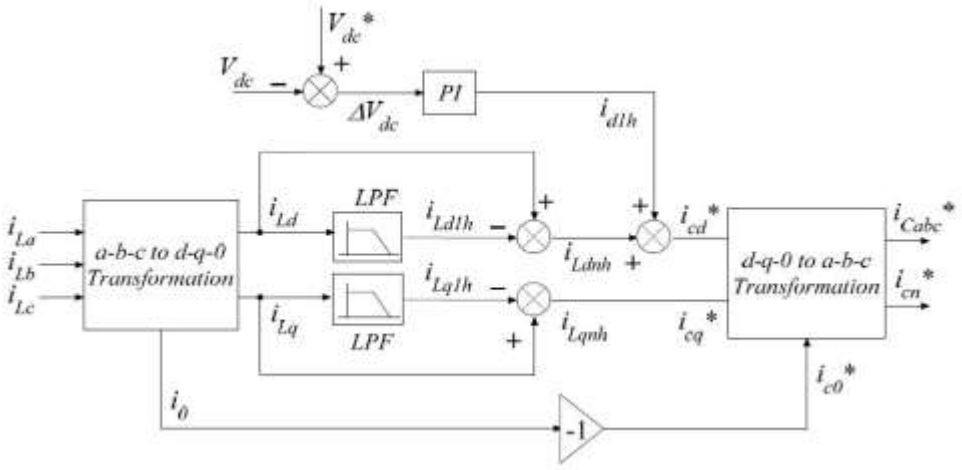

Fig 3. Reference current extraction with i_d-i_q method

These currents are utilized to generate reference filter currents in d-q coordinates, followed by inverse Park transformation giving away the compensation currents [8, 9]. Ultimately, the filter provides necessary compensation for harmonics in the source current, reactive power unbalance and active power support in the system.

BIDIRECTIONAL DC-DC CONVERTER

A bidirectional dc-dc converter [6] is required as an interface between the UCAP and the dc-link, since the UCAP voltage varies with the amount of energy discharged,while the dc-link voltage has to be stiff. The model of the bidirectional dc-dc converter is shown in Figure 4. The dc-dc converter should operate in Discharge mode, while providing active/reactive power support and voltage sag

compensation. The dc-dc converter should also be able to operate in bidirectional mode to be able to charge or absorb additional power from the grid during intermittency smoothing. In this paper, the bidirectional dc-dc converter acts as a boost converter while discharging power from the UCAP and acts as a buck converter while charging the UCAP from the grid.

Average current mode control [4, 13] is used to regulate the output voltage of the bidirectional dc-dc converter in both Buck and Boost modes, while charging and discharging the UCAP bank. While the UCAP-APF system is discharging power, the dc-link voltage V_{out} tends to be less than V_{ref} , which causes the reference current I_{ucref} to be positive, thereby operating the dc-dc converter in Boost mode. Along similar lines, when theUCAP-APF system is absorbing power from the grid, the dc-link voltage V_{out} tends to be greater than V_{ref}, which causes the reference current I_{ucref} to be negative and thereby operating the dc-dc converter in Buck mode. Average current mode control technique was found as the ideal method for UCAP-APF integration as it tends to be more stable when compared with other methods like voltage mode control and peak current mode control [12].This is a major advantage in the present topology, where the stability of the dc-dc converter has to be ensured over a wide operating range and in both Buck and Boost modes ofoperation.

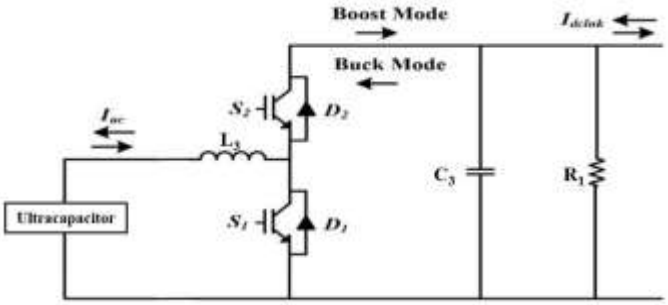

Fig 4. Model of bidirectional dc-dc converter

ULTRACAPACITORS

Ultracapacitors are a new technology that allows storing 20 times more energy than conventional electrolytic capacitors. Ultracapacitors are electrochemical double layer capacitors that have unique characteristics when compared to other energy storage devices. Ultracapacitors (UCAPs) have high energy density and large time constants as well. The benefits of using ultracapacitors are quite extensive. Ultracapacitors have low losses while charging and discharging. They have a very low ESR, allowing them to deliver and absorb very high currents and to be charged very quickly, making them well suited for energy buffer applications [7]. Ultracapacitors are highly efficient components even at very high currents. The characteristics of the UCAP allow it to be charged and discharged at the same rates, something most batteries cannot tolerate. Ultracapacitors have a wide voltage window and can be deeply discharged. The energy storage mechanism of an UCAP is a highly reversible process. The process moves charge and ions only. It does not make or break chemical bonds like batteries; therefore it is capable of millions of cycles with minimal change in performance. It is therefore capable of many years of continuous duty with minimal change in performance. These advantages make ultracapacitors well suited for power quality conditioning applications. Higher order ultracapacitor models are essential for simulation studies in which the timescale of interest is on the order of microseconds. In the current application, the timescale of interest is on the order of minutes; therefore the single RC branch model is sufficient to capture the UCAP behavior of interest.

MODES OF OPERATION

The different modes of operation of the APF are as described below:

1. Active Power Support Mode
2. Reactive Power Support Mode
3. Renewable Intermittency Smoothing Mode
4. Harmonic Compensation

1. Active Power Support Mode

In active power support mode, the APF must provide active power to the grid. Based on the reference value, P_{ref}, the APF supplies the active power. The dc-dc converter will operate in a bidirectional fashion in both Buck and Boost modes to respond to the active

power requests and regulate the dc-link voltage in a stable fashion, while the inverter controller should respond such that the commanded P_{ref} is supplied by the inverter through current control.

2. Renewable Intermittency Smoothing Mode

In Renewable Intermittency Smoothing Mode, the APF must be capable of both supplying and absorbing active power. The dc-dc converter will operate in a bidirectional fashion in both Buck and Boost mode to regulate the dc-link voltage in a stable fashion, while the inverter controller should respond such that the commanded P_{ref} is supplied/absorbed through the inverter current control.

3. Reactive Power Support Mode

In reactive power support mode, the APF must provide reactive power to the grid. In this mode, the APF does not provide any active power to the grid and even the APF losses are supplied by the grid. Based on the reference Q_{ref}, the power conditioner supplies the reactive power.The goal of the dc-dc converter controller is to regulate the dc-link voltage in a stable fashion, while the inverter controller should respond such that the commanded Q_{ref} is supplied by the inverter through current control.

4. Harmonic Compensation

The APF is controlled to eliminate the harmonics caused by non-linear load connected to the network. The controller maintains the THD well within the IEEE-519 standards.

SIMULATIONS AND RESULT

The proposed model is implemented in MATLAB/Simulink. The simulated model is as shown in figure 5. The simulation parameters are as listed in Table I.

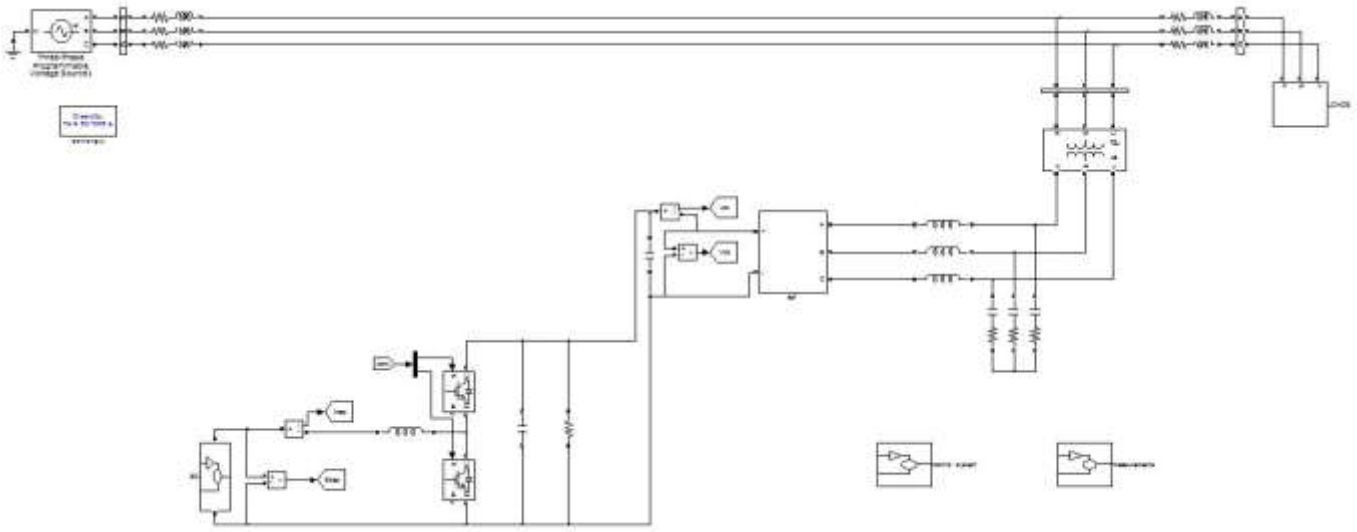

Fig 5. MATLAB/Simulink model of the APF

Table I. Simulation Parameters

Parameter	Values
Source Voltage	0.208kV
Inverter Component	IGBT based
DC Link Voltage	V_{dc}=260 V
DC Link Capacitor	C_{dc}=3500 µF
Load	Three phase non-linear RL load P_{load} = 1000 W Q_{load} = 4.0 kVar

The simulation of the complete system which includes the 3-phase grid tied inverter and the dc-dc converter is performed using

MATLAB. The ability of the system to supply commanded active power is simulated with i_{qref} =-12.0A which translates to P_{ref} of 3054 W. The simulation results are shown in Figure 6(a) and Figure 6(b) where it can be observed that P_{inv} have converged to steady state values closely tracking the commanded P_{ref}.

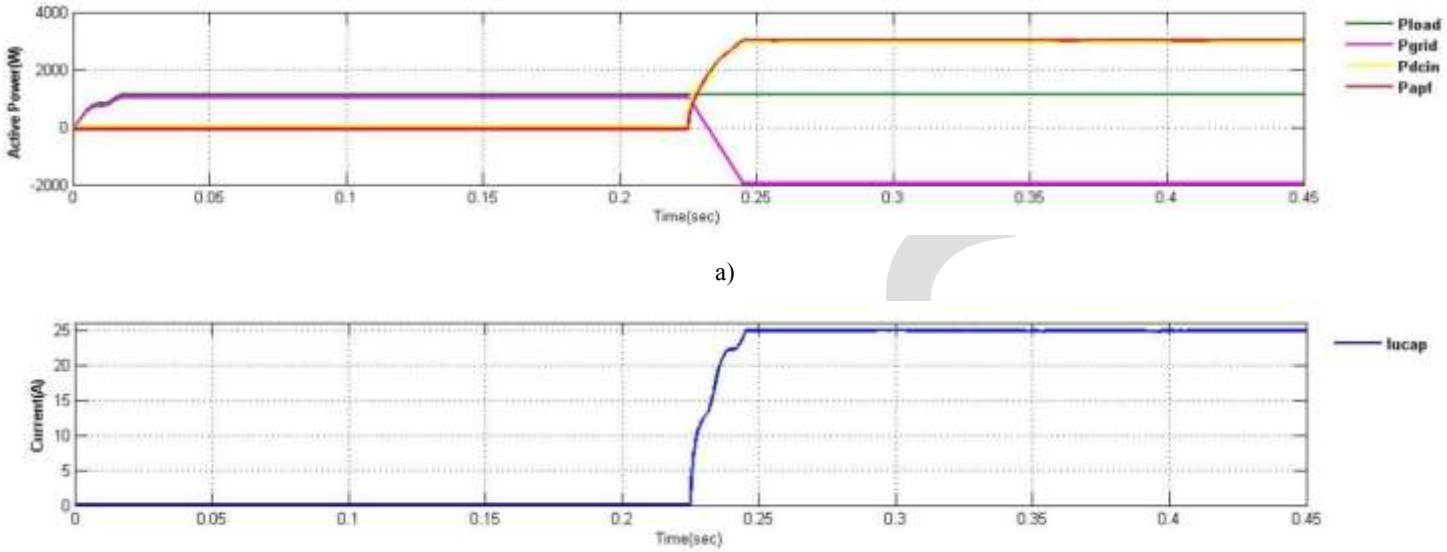

a)

b)

Fig 6. a) Grid, load and inverter active power curves for i_{qref}=-12.0A (active power support) b) UCAP current

The ability of the system to supply the reactive power requirement of the load is simulated with a Q_{ref} of 4000Var. The simulation setup is the same as in the previous case and thesimulation results are shown in Figure 7(a) and Figure 7(b). It can be observed that Q_{inv} have converged to the steady state values closely tracking Q_{ref}.

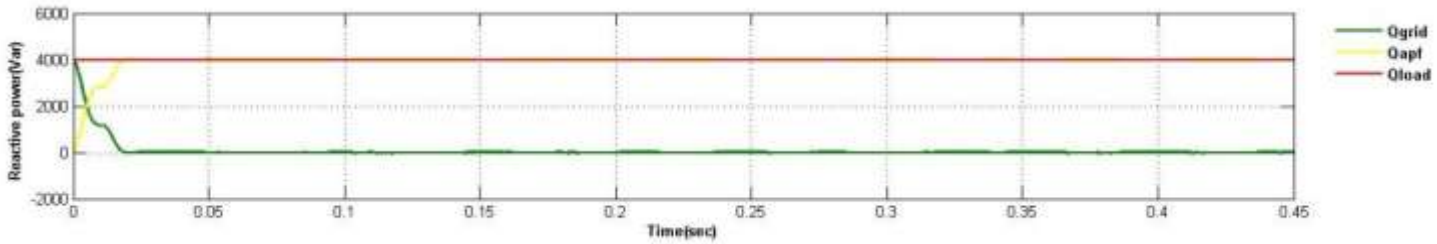

a)

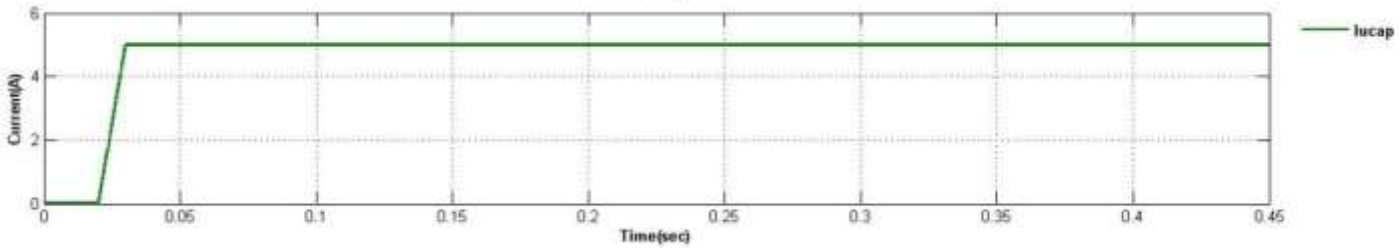

b)

Fig 7. a) Grid, load and inverter reactive power curves (reactive power support)b) UCAP current

The simulation results for the renewable intermittency smoothing applications where the PC must be capable of both supplying and absorbing active power are illustrated. Since the results for the case where the UCAP and the inverter system supply active power to the grid are already presented in Figure 6 so in Figure 8(a) and Figure 8(b) similar results are presented for the case where the UCAP and inverter system absorb active power from the grid which is achieved by commanding a positive i_{qref} of 7A which corresponds to a P_{ref} of -1782W. It can be observed that P_{inv} have converged to steady state values tracking the commanded P_{ref} closely.

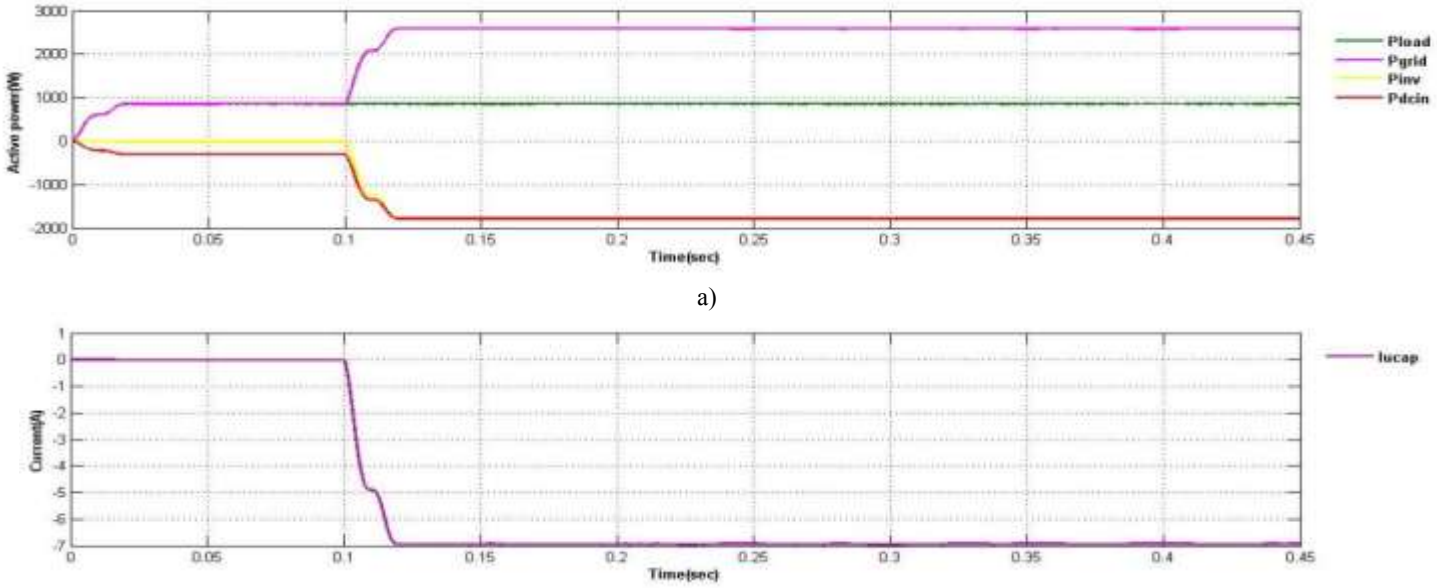

a)

b)

Fig 8. a) Grid, load and inverter active power curves for i_{qref}= 7.0A (renewable intermittency smoothing; absorbing active power) b) UCAP current

The supply current without APFcontains harmonic components. With the insertion of APF the THD of the grid current is reduced from 29.15% to 2.64%. Figure 9(a), Figure 9(b) and Figure 9(c) shows the single phase source current, load current and compensating current. The DC link voltage V_{dc} is as shown in Figure 10 and it can be seen that the voltage is maintained at a constant value of 260V.

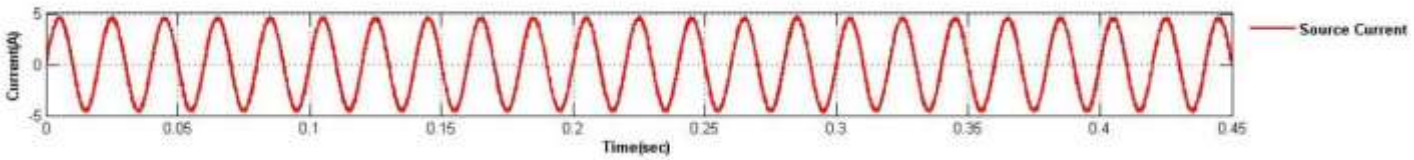

a)

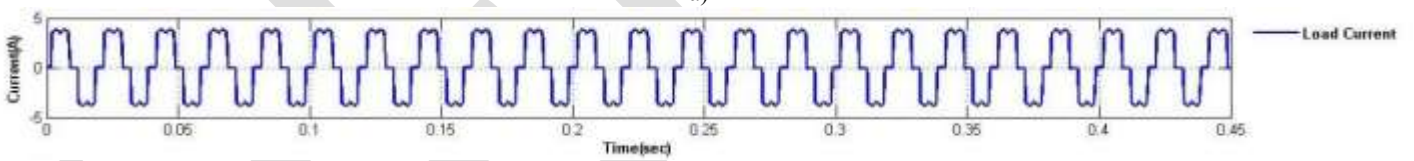

b)

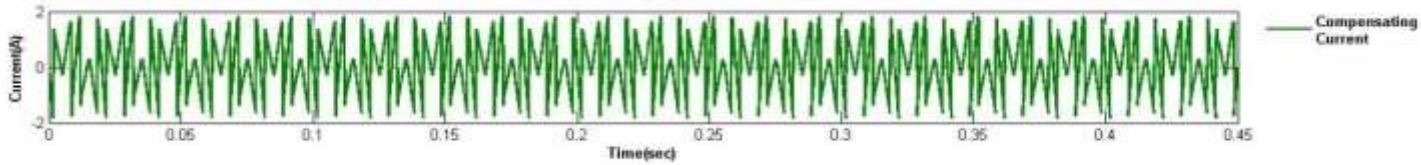

c)

Fig 9. a) Single Phase source current b) Single Phase load current c)Single Phase compensating current

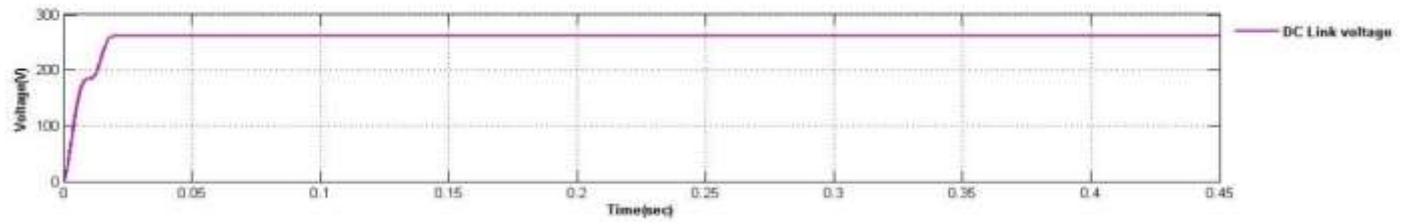

Fig10.DC Link Voltage

Therefore, it is evident from the simulations that the UCAP and APF system can together provide active and reactive power support to the grid. It is also evident that both the dc-dc converter and inverter can operate in a bi-directional fashion which is necessary when the system is used in renewable intermittency smoothing applications. Active power support, reactive power support, renewable intermittency smoothing and harmonic compensation are the primary functionalities the UCAP integrated APF system will be providing to the distribution grid.

CONCLUSION

Renewable intermittency smoothing is one application that requires active power support from energy storage in the seconds to minutes time scale. By incorporating an Active Power Filter with adequate energy storage, the power quality of the distribution grid is improved.In this paper, a power conditioner system to improve the power quality of the distribution grid is presented. With this integration of suitable energy storage the APF will be able to provide active/reactive power support, renewable intermittency smoothing and harmonic compensation to the distribution grid. This cannot be achieved by a conventional APF with dc-link capacitor which does not have active power capability and thus provides additional functionalities on comparing with an UPQC. The proposed APF was simulated with a PI controller.Average current mode control is used to regulate the output voltage of the dc-dc converter due to its inherently stable characteristic. The simulation of the proposed model is carried out using MATLAB.

REFERENCES:

[1] E.F. Fuchs and M.A.S. Masoum, "Power Quality in Electrical Machines and Power Systems", Elsevier, Academic Press, USA, Feb. 2008 (ISBN- 13: 978-0-12-369536-9).
[2] V. Soares, P. Verdelho, and G. D. Marques, "An Instantaneous Active and Reactive current component method for active filters," IEEE Trans. Power Electron., vol. 15, no. 4, pp. 660-669, Jul. 2000.
[3] K. Sahay and B. Dwivedi, "Supercapacitors energy storage system for power quality improvement: An overview," J. Energy Sources, vol. 10 , no. 10, pp. 1-8, 2009.
[4] C. Philip, "Modeling average current mode control [of power convertors]," in Proc. IEEE Applied Power Electronics Conference and Exposition, Feb. 2000, pp. 256-262.
[5] P. F. Ribeiro, B. K. Johnson, M. L. Crow, A. Arsoy, and Y. Liu, "Energy storage systems for advanced power applications," Proc. IEEE, vol. 89 , no. 12, pp. 1744- 1756, Dec. 2001.
[6] ArchanaBhat, "Analysis of Ripple Content in DC-DC Converters",International Journal of Inventive Engineering and Sciences (IJIES) ISSN: 2319–9598, Volume-1, Issue-7, June 2013.
[7] W. Li, G. Joos, and J. Belanger, "Real-time simulation of a wind turbine generator coupled with a battery supercapacitor energy storage system," IEEE Trans. Ind. Electron., vol. 57, no. 4, pp. 1137-1145, Apr. 2010.
[8] S. Bhattacharya, D.M. Divan, T.M. Frank, and B. Banerjee, "Active filter system implementation," IEEE Ind. Appl. Mag., vol. 4, no. 5, pp. 47–63, Sep./Oct. 1998.
[9] Rejil C, Anzari M, Arun Kumar R, "Design and Simulation of Three Phase Shunt Active Power Filter Using SRF Theory",Advance in Electronic and Electric Engineering. ISSN 2231-1297, Volume 3, Number 6 (2013), pp. 651-660.
[10] Chennai Salim, Benchouia Mohamed Toufik, "Intelligent Controllers for Shunt Active Filter to Compensate Current Harmonics Based on SRF and SCR Control Strategies", International Journal on Electrical Engineering and Informatics - Volume 3, Number 3, 2011.
[11] Maria Isabel Milanes Montero, Enrique Romero Cadaval, Fermin Barrero Gonzalez," Comparison of Control Strategies for Shunt Active Power Filters in Three-Phase Four-Wire Systems", IEEE Transactions on Power Electronics, vol. 22, no. 1, January 2007.
[12] K. Wan, J. Liao, and M. Ferdowsi, "Control methods in dc-dc power conversion – a comparative study," in Proc. Power Electronics Specialists Conference, Jun. 2007,pp. 921-926.
[13] K. Wan and M. Ferdowsi, "Projected Cross Point – a new average current-mode control approach," in Proc. IEEE Applied Power Electronics Conference and Exposition, Austin, Texas, Feb. 2008.
[14] Deepak Somayajula, Mariesa L. Crow, "An Integrated Active Power Filter–Ultracapacitor Design to Provide Intermittency Smoothing and Reactive Power Support to the Distribution Grid", IEEETransactions on Sustainable Energy, vol. 5, no. 4, October 2014.

International Journal of Engineering Research and General Science Volume 3, Issue 5, September-October, 2015
ISSN 2091-2730

INNOVATIVE SOLAR DRYERS FOR FRUITS, VEGETABLES, HERBS AND AYURVEDIC MEDICINES DRYING

Taransum Bano, Neeru Goyal, Prashant Kumar Tayal

[1,3]Faculty, Department of Electrical Engineering, LIET, ALWAR (Raj)

[2]Faculty, Department of Electrical Engineering, Govt. Polytechnic College, ALWAR (Raj)

[1]*taransum@yahoo.co.in*
[2]neerugoyal2007@gmail.com
[3]prashanttayal2007@yahoo.co.in
Contact no-8742827250

Abstract: Dehydration of fruits and vegetables is a promising food processing technology that increases shelf life of products for almost a year. It is a value addition process that can save 1/3rd losses of seasonal agro-products. Solar dryers can be used to carry food dehydration without relying on electricity. India is primarily an agriculture-dependent country. However, the pace at which agricultural and economic activities are changing is so fast that traditional methods of working are increasingly being considered out dated. Modernization, with many innovations, is the order of the day, such as progress in the field of information technology, which has gone forward in leaps and bounds. Indian rural economy is also improving at an accelerated rate with each passing day. The pattern of crops is changing fast with the farmers realizing that they cannot survive solely on conventional crops. This awareness is making farmers look towards horticultural crops such as fruits, vegetables spices, etc., which yield high income. In fact, rural women have also turned into successful entrepreneurs by starting cottage industries and microenterprises that fetch attractive returns through DWACRA and other Self Help Groups (SHGs).

Keywords: Solar Dryers, Convectional Crops, Horticultural Crops, Cottage Industries, Food Processing Technology, Agro-Products, Food Dehydration.

INTRODUCTION

Fruits and vegetables are an essential part of human diet providing micronutrients, vitamins, enzymes, and minerals. Most fruits and vegetables have a high moisture content and water activity. This makes them vulnerable to microbial and other spoilages due to biochemical reactions, such as enzymatic activity, respiration, and senescence. Therefore, preventive measures are taken to lower water activity; drying or dehydration is one such method. Drying is a process of removal of water from the food to inhibit biochemical processes and microbial growth. Drying increases
the shelf-life of the product, so that it can be available during off season. Drying can be done at high temperature, such as hot air drying or dielectric heating, at low temperature, such as freeze drying, or at ambient temperature, such as desiccant drying. Nevertheless, it is an energy guzzling process. With the depletion of fossil fuels and hike in energy prices, more and more emphasis is being given to utilize renewable energy sources for drying.

SUN DRYING

Since time immemorial, human beings have been using sun as a source of energy. This is one of the most prevalent and cheap methods practiced by most developing and underdeveloped countries, especially in tropics, where good sunshine hours prevail throughout the year. Food commodities are laid on a platform with intermittent stirring for uniform drying. The sun's heat not only reduces the moisture level as desired, but also kills insects present in the food product. Sun drying has certain limitations as it is dependent on the weather and sunshine hours. During uncertain rain and precipitation, the materials are not dried properly, which causes microbial growth and other qualitative deteriorations. The drying process usually takes a long time, thus causing infestation from insects, birds, and animals. Also, drying requires a large area. Despite these disadvantages, sun drying is still practiced in many parts of the World.

Fig.1 Drying Of Fruits and Vegetables

Solar Dryer

Over the years, the practice of open air drying or sun drying has become limited due to growing concern over quality of the final product. Due to high rise of fuel prices, depletion of fossil fuels, and emergence of modern and efficient but not so economic drying technologies, solar drying systems have made a place for themselves. The final product quality of a solar dried product may not be as good as freeze-dried product, but for the economically and energy deprived farmers and entrepreneurs, solar drying is the best in the business. Solar drying is achieved by direct sun radiation and greenhouse effect. The solar energy received by the drying chamber is dependent on the sunshine hours, climate, weather, atmospheric clearness, and location. According to E V Fodor, on a clear day solar radiation available to any location is dependent on the angle of the sun relative to horizon. Solar energy is free, renewable, abundant, and an environment friendly energy source. This reduces drying time due to effective utilization of solar energy. It maintains the quality of the food products and acts as an ideal substitute for fossil fuel based dryers. The two basic limitations faced by the solar dryers are sunshine hours and weather change. There are two types of solar driers; the Passive Type (natural convection) dryer and the Active Type (forced convection) or Hybrid Solar dryer. As per Ekechukwu, these solar driers may be again sub-grouped under three categories: (*i*) integral type (direct mode), (*ii*) distributed type (indirect type), and (*iii*) mixed mode. In a direct type, solar drying material is placed in a drying chamber having a transparent cover through which solar radiation enters and heats the food materials to be dried. In an indirect mode, solar energy is captured by a solar collector, which in turn heats the air. This heated air is then passed to the drying cabinet/chamber. In mixed mode, solar energy is collected in separate solar collector and heated air is then passed over the drying material. The drying materials absorb the solar energy directly through the transparent cover and walls.

Fig.2 Dried Tomatoes

Fig.3 Dried Bananas

Solar Natural Dryer

These are directly irradiated solar dryers, where the commodities absorb solar energy directly. The dryers are provided with transparent cover, such as glass or polyethylene. The upper layer is heated and dried by direct solar radiation and the subsequent layers are heated through conduction. Polyhouse or greenhouse drying is an example of solar natural dryers. Since the drying process is weather and sunshine hours' dependant, a constant drying temperature cannot be maintained. High outdoor temperature, low humidity, and clear skies are the ideal conditions for solar dryers. The inside air temperature of the polyhouse is about 20–30 °C warmer than the outside air temperature, which makes the drying faster as compared to open sun drying, thus reducing drying time. Pangavhane et al. have designed a solar dryer consisting of a solar air heater and a drying chamber. They observed that the drying time in a solar dryer was four days as compared to seven days in open sun drying and 15 days in shade drying for production of resins from grapes. A solar tunnel dryer designed for drying agricultural crops, by Bala et al., consisted of a transparent plastic covering the flat plate collector. The drying tunnel is connected in a series to supply hot air directly into the drying tunnel using two DC fans operated by a solar module. Bena and Fuller described that biomass-generated energy serves as a backup for such direct convection type natural solar dryers, thus improving the dryer efficiency.

Semi Artificial Solar Dryers

These are direct heated solar convective dryers. In these dryers, air is preheated b solar energy in a collector. The drying system usually consists of a solar collector and a fan for maintaining a specified air flow through the drying space. These driers are cheap to construct and can be employed where the drying material is not sensitive to periodic changes in the drying conditions caused by periodic nature of the solar radiation and changing atmospheric conditions. K Lutz and his co-workers had developed a multipurpose solar tunnel dryer consisting of a fan, solar heater, and tunnel dryer. The use of this dryer had reduced the drying time considerably with better end product quality.

Solar Assisted or Indirect Type Solar Dryer

In this type of dryer, solar energy is used to heat a fluid or sand pebble, which in turn heats the drying air. These usually have auxiliary energy source, such as a thermo-generator fuelled by biomass, natural gas or oil, to be used in situations where solar energy collected is insufficient for drying purpose. Better control of temperature results in a better quality product. The solar dryer developed by El-Sebaii et al. consisted of a flat plate solar air heater connected to a cabinet, acting as a drying chamber. The air heater is designed to insert various storage materials under the absorber plate to improve the drying process. Sand is used as a storage material. Since heat dissipated by sand is gradual, it reduces the drying time by 12 hours and the total drying time can be achieved in eight hours with suitable pre-treatment given to the fruits.

Hybrid Dryer

These dryers are usually direct-type solar dryers, but are backed up by an auxiliary energy source, so that during the less sunshine hours and cloudy weather the energy back-up can be utilized to dry food materials without interruption. This usually results in better product quality. Bhattacharya et al. have developed a hybrid solar dryer using direct solar energy and a heat exchanger. The dryer consists of a solar collector, reflector, heat exchanger cum heat storage unit, and a drying chamber. The drying chamber is placed beneath the collector. The dryer is operated during normal sunny days as a solar dryer and as a hybrid solar dryer during cloudy days. Drying is also carried out at night using stored heat energy, in which it is collected during the day time and with electric heaters located at water tank. The efficiency of the solar dryer is enhanced by recycling about 65 per cent of the drying air in the solar dryer. Under mid-European summer conditions, it can increase the air temperature 30– 40 °C above the ambient temperature.

Fig.4 Solar Biomass Hybrid Drying System

Fig.5 Greenhouse

CONSTRUCTION MATERIALS

For the frame, GI pipes, light-weight aluminum pipes or locally available materials such as bamboo, can be used to erect the structure. The covering material could vary from low thickness cheap polythene sheets, which is susceptible to photovoltaic degradation, erosion and wear, to expensive plastic, glass, and high density polymers that are resistant to photovoltaic degradation. Depending on the strength, the cover may last for one season to life long. Though glasses are durable, but during hailstorms they get damaged, and thus need replacement. While choosing the covering material solar transmittance should also be considered, apart from economics and durability.

MAINTENANCE

Rooftop solar collectors are very popular; they do not need extra space. The collected solar energy supplies heat energy to the drying chamber. Many a times, the collectors are mounted on the roofs which may not be suitably oriented to get maximum benefits from solar radiation. The collectors should be properly designed, considering the geographical location of the place. Proper insulation should be provided to the duct transmitting the hot air. The solar collectors should be cleaned regularly to maintain its efficiency. Maximum solar radiation reaches us during 10 am to 2 pm; hence, the temperature of drying will be more during this period. There will be a temperature variation in the drying environment as well as in the product. To maintain a constant drying air temperature, supplementary heat may be provided.

Advantages of Fruits & Vegetables Solar Dryer:

- Savings in time
- Increased production possible
- Less space requirement for drying
- More hygienic than drying outside in the sun
- Cost Effective
- Negligible maintenance costs
- Free and Clean energy
- Just one time investment, after that the energy is Free!
- Quick Return on Investment (ROI) - just 3 year

RURAL DEVELOPMENT AND WOMEN EMPOWERMENT

The Government of India launched many schemes and projects for creating job opportunities through rural employment guarantee schemes, poverty alleviation programs, 'Bharat Nirmaan', Prime Minister 'Grameen Sadak Yojana', 'Rajeev Yuva Sakthi' programs, etc. These are implemented at the village level by government agencies and NGOs. They consist of small enterprises, SHGs, and infrastructure development in several areas connected to rural development. In rural India, the main occupation of women and youth is based on horticultural operations. The horticulture crops consist of fruits, vegetables, medicinal plants, and other commercial plants, such as spices, etc. In recent times, the area of cultivable land under agriculture and horticulture has enormously increased due to the development of major and minor irrigation projects and modern methods of drip-and-sprinkle irrigation techniques. The volume of production from this sector is growing fast and post-harvest treatment of the product has become an important technology development program for value addition and preservation. Income generation schemes in the horticultural sector are most suitable and appropriate from the view point of stability of rural habitation. The manufacturing and associated commercial activity connected with the horticulture is providing proper solution for income generation and employment creation in the villages. Food processing technology is one of the priority sectors in our country. If this technology can be introduced at micro level in the villages, it would be a boon for rural women and youth.

DEVELOPMENT OF SOLAR FOOD PRODUCTS

In the last few years, intensive R&D work taken place by SEED for processing of fruits, vegetables, spices, herbs, forest product, chemicals, etc., using solar dryers for value addition and long shelf-life on a commercial scale. The dehydration process requires pre-treatments, addition of Class II preservatives
to enhance shelf-life, and fast drying to reduce the moisture levels. This process can be accomplished with zero energy cost, unlike the electrical dryers, in solar powered solar air dryers

CONCLUSION

A solar drying system, particularly for agro-products and marine products, is viable particularly in developing countries where labor costs are low and cost of fossil fuel energy is very high. In the future, larger systems could be designed utilizing solar, thermal, photovoltaic panels combined with wind power. As solar and wind energy is necessarily intermittent, advances in thermal and electrical energy storage is needed to make use of renewable energy viable in drying. To minimize use of oil or gas, biomass can be used for heating in the absence of insulation and wind. Farmers can use the locally available material for construction of solar dryers. The covering material should be carefully chosen.

REFERENCES:

[1] Atungulu G, Nishiyama Y, Koide S (2004). Respiration and climacteric patterns of apples treated with continuous and intermittent direct current electric field. J. Food Eng., 63: 1-8.

[2] Bala BK (1998). Solar drying systems: Simulation and Optimization, Agrotech Publishing Academy, India,

[3] Smitabhindu R, Janjai S, Chankong V (2008) Optimization of a solar assisted drying system for drying bananas. Renew Energy, 33: 1523- 1531.

[4] Bala BK, Janjai S (2009) Solar drying of fruits, vegetables, spices, medicinal plants and fish: Developments and potentials. International Solar Food Processing Conference 2009.

[5] Norton, Brian (2013). Harnessing Solar Heat. Springer. ISBN 978-94-007-7275-5.

[6] Heinz, Gunter and Hautzinger, Peter (2007). "Meat drying". Meat processing technology for small- to medium-scale producers. RAP Publication 2007/20. Bangkok, Thailand: Regional Office for Asia and the Pacific, Food and Agriculture Organization of the United Nations. ISBN 978-974-7946-99-4. Archived from the original on 23 May 2010.

[7] Oyunbayar, N. "Mongolian Food: Meat, milk and Mongolia". Mongoluls.Net. Archived from the original on 5 April 2005.

[8]Shaffer, Marcella (1999). "Solar Food Drying". Backwoods Home Magazine (58). Archived from the original on 16 August 2000.

[9]Trim, D. S. and Curran, C. A. (1983). "Solar dryers". Comparative Study of Solar and Sun Drying of Fish in Ecuator. London: Tropical Products Institute. ISBN 978-0-85954-158-9. Archived from the original on 2 September 2015.

[10]Olokor, Julius Oghenekaro and Omojowo, Funso Samuel (2009). "Adaptation And Improvement Of A Simple Solar Tent Dryer To Enhance Fish Drying" (PDF). Nature and Science **7** (10): 18–24. Archived (PDF) from the original on 2 September 2015.

[11]Fodor, Eben (2006). "Build a Solar Food Dehydrator" (PDF). Mother Earth News **2006** (August/September): 66–70. Archived from the original on 2 September 2015.

[12]Robishaw, Sue (1999). "Drying Food with the Sun". Countryside & Small Stock Journal **1999** (July/August). Archived from the original on 2 September 2015.

[13]Weiss, Werner and Buchinger, Josef (2001). "Solar Drying" (PDF). Austrian Development Cooperation and Institute for Sustainable Technologies (AEE INTEC). Archived (PDF) from the original on 26 May 2012.

[14] Jackson TH, Masry ME (1977). Sun Drying of Fruits and Vegetables in Ethiopia. Food Processing Section (Nazreth), Addis Ababa, Ethiopia, pp. 18-40.

International Journal of Engineering Research and General Science Volume 3, Issue 5, September-October, 2015
ISSN 2091-2730

Fiber Optic Sensor technology for Non-optical parameter measurement

Swapnil R. Chilap [1], Mrs. Kadambari Sharma [2],
[1]M.E.Student, [2]Assistant Professor, Department of Instrumentation Engineering,
Vivekanand Education Society's Institute of Technology,
Mumbai, swapnil.chilap@ves.ac.in, 09821757816.

Abstract— Use of traditional electronic sensors is limited in harsh, electromagnetic and high radio frequency environments which started interest in fiber optical sensing. Fiber optic sensors were developed by combining optoelectronic devices with fiber optic telecommunications systems. Optimization of components, cost reductions and recent researches gives fiber optic sensors with improvement in size, quality and performance. Commonly used fiber optic sensors are Intensity based, phase modulated and wavelength modulated fiber optic sensors. In this paper, an overview of fiber optic sensors, their working principle and non-optical parameter measurement applications are presented.

Keywords— Optical fibers, fiber optic sensors, optical sensing, Extrinsic sensors, Intrinsic sensors, interferometers, light field

INTRODUCTION

In recent years the field of measurement and instrumentation with particular sensor development is rapidly expanding. Growth of optoelectronic and the fiber optic telecommunication industries leads to the development of fiber optic sensors. In fiber optic sensor optical fiber is used in two ways, either it is used to communicate with a sensor device or use fiber as the sensor itself. Now fiber optics is opted in many fields which results into the constant development and mass production of optical fibers and fiber optic sensors. Fiber optic sensors are replacing traditional sensors because of their compact size, better performance and cost reductions.

Fiber optic sensors are capable of measuring a wide range of environmental parameters. The advantages of fiber optic sensors over conventional electronic sensors are as follows:

- Easy implementation.
- Bad conductors of electric current.
- Ability to withstand electromagnetic interference and radio frequency interference.
- Lightweight, Robust, more resistant to harsh environments.
- High sensitivity, Multiplexing capability to form sensing networks.
- Distributed and quasi distributed sensing capability.
- Capability to sense a wide range of environmental parameters [2-8].

Fiber optic sensor:

The general structure of an optical fiber sensor system consists of light source, optical fiber, sensing element i.e. transducer, an optical detector and signal processing electronics (oscilloscope, optical spectrum analyzer etc). Optical signal generated by the light source is passed to the transducer through optical fiber. Environmental parameters sensed by the transducer modulates the optical signal. Modulation can be in the form of intensity, phase, wavelength or polarization state which is detected by an optical detector and passed to the processing electronics for further interpretation. Light source can be LED, LASER or laser diodes etc.

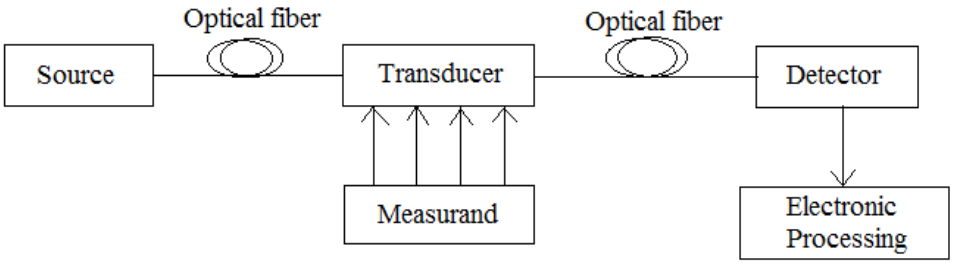

Figure 1 Basic components of fiber optic sensor system

Classification of Fiber optic sensors:

Fiber optic sensors can be classified under three categories:

- The sensing location,
- The operating principle,
- The application.

Depending upon the sensing location, a fiber optic sensor can be classified as extrinsic or intrinsic. In an extrinsic fiber optic sensor (Figure 2), the optical fiber is used to carry light to and from sensing or modulating element. Here optical fiber is used just to carry the optical signal.

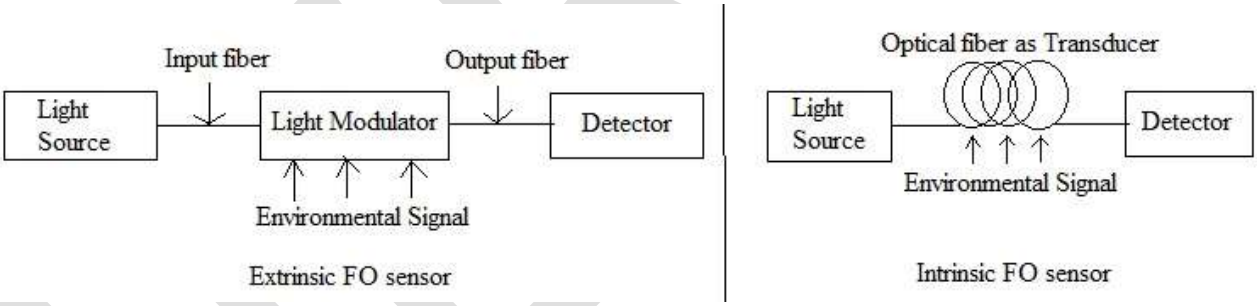

Figure 2 Extrinsic and Intrinsic type of Fiber optic sensors

In an intrinsic fiber optic sensor optical fiber itself acts as a sensor. External perturbations directly act on the fiber which changes the physical properties of the fiber resulting in modulation of the optical properties of the light signal.

Depending upon the operating principle further categories of fiber optic sensors are intensity based, phase modulated, wavelength modulated and polarization modulated fiber optic sensors. External perturbations acting on the optical fiber or the sensing element change the optical properties (intensity, phase, frequency and polarization state) of light signal propagating through the fiber. Therefore, by detecting these properties we can measure the external perturbation.

Based on the application, a fiber optic sensor can be classified as follows:

- Physical sensors: Used to measure physical properties like temperature, stress, etc.
- Chemical sensors: Used for pH measurement, gas analysis, spectroscopic studies, etc.
- Biomedical sensors: Used in bio-medical applications like measurement of blood flow, glucose content etc. [6].

Fiber optic sensor types:

1. Intensity based fiber optic sensors

Signal undergoing some loss is important for Intensity-based fiber optic sensors. These sensors use multimode fibers, as they require more light. A measurand-induced change in the optical intensity can be obtained by micro-bending loss, attenuation, and evanescent fields. The advantages of these sensors are: Easy implementation, low cost, multiplexing capability and real distributed sensing capability [3-6].

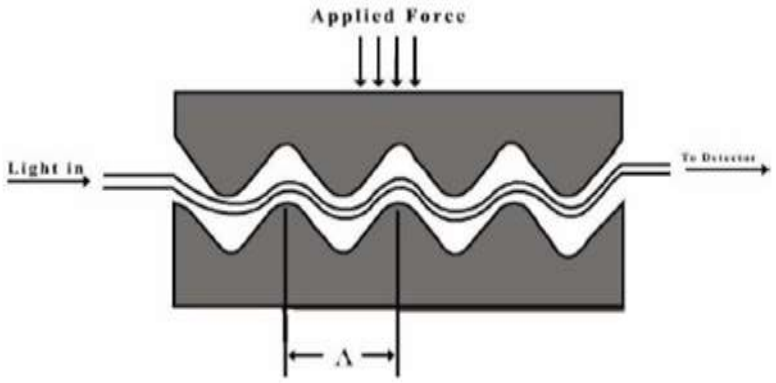

Figure 3 Intensity based Micro-bend sensor

Microbend sensor is one of the intensity-based sensors where mechanical periodic micro bends results in attenuation of the transmitted light. As seen in Figure 3, optical fiber is passed through two grooved plates. In this arrangement, the upper plate can move in response to pressure. When the bend radius of the fiber is more than the critical angle, light starts leaking into the cladding which results in an intensity modulation [6].

2. Wavelength modulated Fiber optic sensors

Changes in the wavelength of light are used for detection in wavelength modulated fiber optic sensors. Examples of wavelength-modulated sensors are Fluorescence sensors, black body sensors, and the Bragg grating sensor.

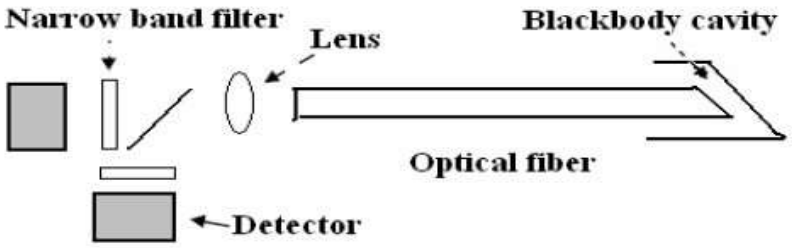

Figure 4. Blackbody Fiber Optic Sensor

The blackbody sensor is the simplest wavelength based fiber optic sensor, as shown in Figure 4[6]. Here, at the end of an optical fiber blackbody cavity is placed. Blackbody cavity starts to glow and act as a light source when its temperature increases. Narrow band filters are combined with detectors to determine the black body curve profile. This type of sensor is used to measure temperature within a few degrees centigrade under intense RF fields.

The Bragg grating sensor is the most widely used wavelength based fiber optic sensor. In a short section of singlemode optical fiber index of refraction of core is periodically changed to form Fiber Bragg gratings (FBGs) which generates a reflection response. In this the measured information is wavelength encoded in the Bragg reflection of the grating. Fiber Bragg grating sensors offer quasi distributed strain measurement and structural health monitoring.

3. Phase modulated Fiber optic sensors

Phase modulated sensors detect changes in the phase of light by using interferometric technique. Here phase of light propagating through the signal fiber is compared with the phase of light in a reference fiber. Mach-Zehnder, Michelson, Fabry-Perot, or Sagnac are some of the interferometric techniques. Interferometric technique is used to convert the phase change of optical signal into the intensity change which is detected by the detector. Phase modulated fiber optic sensors are more sensitive than Intensity based fiber optic sensors. These interferometric fiber optic sensors are constructed using single mode optical fiber. These sensors have applications in the areas like military, scientific research and industries.

4. Polarization modulated Fiber optic sensors

The direction of the electric field defines the polarization state of the light field. Linear, elliptical and circular are the different types of polarization states of the light field. If the direction of the electric field stays in the same line during the propagation of light, then the polarization state is linear and if the direction of electric field gets altered then the polarization state is elliptical.

Stress or strain on optical fiber changes the refractive index of the fiber which induces the phase difference and changes the output polarization state of the light field passing through the fiber. So, external perturbation are sensed by detecting the change in the output polarization state of the light field.

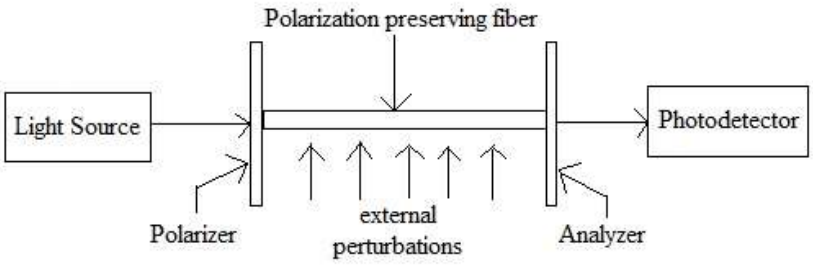

Figure 5 Polarization based Fiber optic sensor

Optical set up for the polarization based fiber optic sensor is as shown in figure 5. The main elements of this sensor are polarizer, polarization preserving fiber and analyser. The polarized light is passed to the sensing element i.e. polarization preserving fiber at specific angle. External perturbation acts on this section where it results into the change of phase difference between two polarization states. The Output polarization state is further analysed and given to the photodetector to detect or measure the external perturbation.

Applications of Fiber optic sensors:

During the late 1970s and early 1980s fiber optic sensors were mainly used for military and aerospace applications only. In 1980s lot of efforts were made for the commercialization of fiber optic sensors with their increasing popularity. In last couple of decades lot of research and development were carried out for precise fiber optic sensors. Now fiber optic sensors have been widely used to monitor a wide range of environmental parameters such as position, vibration, strain, temperature, humidity, viscosity, chemicals, pressure, current, electric field and several other environmental factors [2-6].

Fiber optic sensors are used in:

- Mechanical Measurement such as rotation, acceleration, electric and magnetic field measurement, temperature, pressure, acoustics, vibration, linear and angular position, strain, humidity, viscosity, chemical measurements
- Electrical & Magnetic Measurements
- Chemical & Biological Sensing
- Monitoring the physical health of structures in real time.

- Buildings and Bridges: Concrete monitoring during setting, crack (length, propagation speed) monitoring, spatial displacement measurement, neutral axis evolution, long-term deformation (creep and shrinkage) monitoring, concrete-steel interaction and post-seismic damage evaluation.

- Tunnels: Multipoint optical extensometers, convergence monitoring, shotcrete / prefabricated vaults evaluation, and joints monitoring damage detection.

- Dams: Foundation monitoring, joint expansion monitoring, spatial displacement measurement, leakage monitoring, and distributed temperature monitoring.

- Heritage structures: Displacement monitoring, crack opening analysis, post-seismic damage evaluation, restoration monitoring, and old-new interaction.

- Detection of Leakage in pipelines [7].

Future trends:

Different types of fiber optic sensors were developed and redeveloped with improved size and quality. These advancements and cost reductions gives the promising future to fiber optic sensors. So, the use of fiber optic sensors in various fields along with many niche engineering and biomedical fields will increase with better performance.

Some future trends are as follows:

- For new sensing mechanisms and sensor configurations Special waveguides can be designed.

- Sensor performance, functionality, reliability and capability of harsh environment operation will be improved with improved microfabrication techniques.

- To obtain high density fiber optic sensor networks, advanced signal processing and network technology needs to be designed.

ACKNOWLEDGMENT

We would like to express our special thanks of gratitude to our H.O.D. Dr. P.P. Vaidya and our principal Dr. Mrs. J.M Nair for sharing their pearls of knowledge, wisdom and encouragement. We would also like to thank our family and friends for extending their generous support in the course of work.

CONCLUSION

An overview of fiber optics sensors and their applications has been presented in this paper. Development of high quality fiber optic sensors is possible due to optimizations of components, recent advances and cost reductions. Now fiber optic sensors are replacing traditional electronic sensors, as they are capable of measuring wide range of environmental parameters with better performance. Fiber optic sensors have been successfully applied to many fields such as Military, Medical, Electrical, Civil engineering structures, Gas and Oil industry etc. The future of fiber optic sensors is very promising.

REFERENCES:

[1] "Introduction to Fiber Optics", second Edition, by John Crisp

[2] "Fiber Optic sensors", second edition, by Shizhuo Yin, Paul B. Ruffin, Francis T. S. Yu, CRC Press.

[3] C.R.Batchellor, C.Edge, "Some recent advances in Fibre optic sensors", Electronics & Communication Engineering Journal, Oct 1990.

[4] M. Mahdikhani1 and Z. Bayati, "Application and development of Fiber optic sensors in Civil engineering", The 14th World Conference on Earthquake Engineering, Beijing, China, October 12-17, 2008.

[5] Bahareh Gholamzadeh and Hooman Nabovati, "Fiber Optic Sensors", International Journal of Electrical, Computer, Energetic, Electronic and Communication Engineering Vol:2, No:6, 2008

[6] Fidanboylu K., Efendioglu H.S., "Fibre Optic Sensors & Their Applications", 5th International Advanced Technologies Symposium, Turkey, May 2009.

[7] Shaveta Thakral, Pratima Manhas, "Fibre Optic Sensors Technology & their Applications", International Journal of Electronics & Communication Technology, Vol.2, Issue 2, June 2011.

[8] Venu Gopal, Madhav Annamdas, "Review on Developments in Fibre Optical Sensors & Applications", International Journal of Materials Engineering 2011; 1(1):1-16.

[9] Dhiraj Ahuja and Deepa Parande, "Optical sensors and their applications", Journal of Scientific Research and Reviews Vol.1 (5), pp.060-068, November 2012.

[10] "Optical fiber sensors Guide, Fundamentals and Applications", Micron Optics

[11] "Pipeline Technology Journal", 2013.

[12] Pipe Patrol Technical Bulletin Articles.

[13] "Fiber Dynamics"(online) Available: www.fiberdynamics.com

International Journal of Engineering Research and General Science Volume 3, Issue 5, September-October, 2015
ISSN 2091-2730

An Inventory Model For Deteriorating Items With Two Parameter Weibull Deterioration And Price Dependent Demand

[1]K.Geetha [2]Dr.N.Anusheela

[1]Assistant Professor, Department of Mathematics, Bharathiar University Arts and Science College, Gudalur, The Nilgiris-Tamilnadu.India.Email:geethachandru24@gmail.com, Mobile: +919443093583.

[2]Assistant Professor, Department of Mathematics,
LRG Arts College for Women, Tirupur-Tamilnadu.India. Email:anusheeln@gmail.com

Abstract - This paper presents an inventory model for deteriorating items with price dependent demand. Deterioration rate follows two parameter weibull distribution. Shortages are allowed and are completely backlogged.

Keywords: Deterioration items, holding cost, inventory, price-dependent demand time, shortages, weibull, completely backlogged.

INTRODUCTION:

Deterioration of items in an inventory is a common phenomenon in business situations. This is due to the fact that the items in the inventory become obsolete, devalued, decay or damaged depending on the type of goods. As a consequence of the deterioration shortages may occur. Hence deterioration factor has to be given importance while determining the optimal policy for an inventory model.

Ajanta Roy [1] presented an inventory model for time proportional deterioration rate and demand is function of selling price. The Author discussed the model without shortage and also with shortages in which the shortages are completely backlogged. Mukesh Kumar, Anand Chauhan, Rajat Kumar [9] extended Ajanta Roy models with trade credit. Tripathy C.K and L.M. Pradhan [14] gave a model in which the demand of the product decreases with the increase of time and sale price and deterioration rate follows a three parameter Weibull distribution functions. Tripathy C.K and L.M.Pradhan[15] gave a model in which the demand of the product decreases with the increase of time and sale price and deterioration follows a three parameter weibull distribution. Padmanabhan. G,Prem Vrat[10] formulated an EOQ model perishable items under stock dependent selling rate. Sahoo.N.K.,Sahoo.C.K. & Sahoo.S.K[12] described an inventory model for price dependent demand and time varying holding cost. Vikas Sharma and Rekha Rani Chaudhary [17] explained and inventory model for two parameter Weibull deterioration rate. They found profit for their model. Sanjay JAIN and Mukesh KUMAR [13] explained an inventory model with ramp type demand and three parameter Weibull deterioration rate. The Authors also analyzed and summarized economic order quantity models done by few researchers. There are some products which start deteriorate only after some interval of time. This was explained by taking three parameter Weibull distribution deterioration rate. Anil Kumar Sharma, Manoj Kumar Sharma and Nisha Ramani [3] described an inventory model for two – parameter Weibull distribution deterioration rate and demand rate is power pattern. Manoj Kumar Meher, Gobinda Chandra Panda, Sudhir Kumar Sahu [8] adopted a two – parameter Weibull distribution deterioration to develop an inventory model under permissible delay in payments. Kun – Shan Wu [7] made an attempt in his paper to obtain the optimal ordering quantity of deteriorating items for two – parameter Weibull distribution deterioration under shortages and permissible delay in payments. P.K.Tripathy and S.Pradham [16] also define an inventory model with two – parameter Weibull distribution as demand rate and deterioration rate increases with time. Recently R.Amutha and E.Chandrasekaran [2] developed an inventory model for deteriorating items with three-parameter weibull deterioration and price dependent demand.

In this present paper, we have developed an inventory model for two-parameter Weibull deterioration rate and price dependent demand. Shortages are allowed and are completely backlogged. Holding cost is assumed to be constant. Our aim is to increase the profit.

ASSUMPTIONS AND NOTATIONS

(i) The demand rate is a function of selling price.

(ii) Shortages are allowed and are completely backlogged

(iii) Lead time is zero.

(iv) Replenishment is instantaneous

(v) A is the set up cost

(vi) C is the unit cost of an item

(vii) p is the selling price

(viii) Demand D (t) = f (p) = a-p, where a > p.

(ix) C_2 is the shortage cost per unit time.

(x) $\theta(t) = \alpha\beta t^{\beta-1}$, $0 \le \alpha < 1$, $\beta > 0$ and $-\infty < \gamma < \infty$ is the deterioration rate. At time T_1 the Inventory becomes Zero and shortages start occurring.

(xi) h is the constant holding cost.

(xii) T is the length of the cycle.

MATHEMATICAL FORMULATION AND SOLUTION

Let I (t) be the inventory at time T ($0 \le t \le T$) the differential equation for the instantaneous state over (0,T) are given by

$\frac{dI(t)}{dt} + \alpha\beta t^{\beta-1} I(t) = -(a-p)$ $\quad 0 \le t \le t_1$ (1)

$\frac{dI(t)}{dt} = -(a-p)$ $\quad t_1 \le t \le T$ (2)

Solving equations (1) and (2) with boundary condition $I(t_1)$ we get

$I(t) = -(a-p)[(t-t_1) + \frac{\propto}{\beta+1}[t^{\beta+1} - t_1^{\beta+1}] + \frac{\propto^2}{2(2\beta+1)}[t^{2\beta+1} - t_1^{2\beta+1}]]$ (3)

$I(t) = -(a-p)(t-t_1)$

Shortage cost (4)

$SC = \frac{-C_2}{T}\int_{t_1}^{T} -(a-p)(t-t_1)dt$

$= \frac{C_2}{2T}(a-p)(t-t_1)^2$ (5)

Holding cost

$HC = \frac{h}{T}\int_0^{t_1} I(t)dt$

$= \frac{-h}{T}(a-p)(-\frac{t_1^2}{2} + \frac{\propto}{\beta+1}[\frac{t_1^{\beta+2}}{\beta+2} - t_1^{\beta+2}] + \frac{\propto^2}{2(2\beta+1)}[\frac{t_1^{2\beta+2}}{2\beta+2} - t_1^{2\beta+1}])$ (6)

Stock loss due deterioration

$D = (a-p)\int_0^{t_1} e^{\propto t^\beta} dt - (a-p)\int_0^{t_1} dt$

$= (a-p)[\frac{\propto t_1^{\beta+1}}{\beta+1} + \frac{\propto^2 t_1^{2\beta+1}}{2(2\beta+1)}]$ (7)

Order quality

$Q = D + \int_0^T (a-p)dt$

$= (a-p)\left[\frac{\propto t_1^{\beta+1}}{\beta+1} + \frac{\propto^2 t_1^{2\beta+1}}{2(2\beta+1)} + T\right]$ (8)

Purchase cost $= \frac{CQ}{T}$

$= \frac{(a-p)C}{T}\left[\frac{\propto t_1^{\beta+1}}{\beta+1} + \frac{\propto^2 t_1^{2\beta+1}}{2(2\beta+1)} + T\right]$ (9)

Total profit per unit is = $p(a-p) - \frac{1}{T}$ [OC + SC + HC + PC]

$K(p,T,T_1) = p(a-p) - \frac{1}{T}\left[A + \frac{C_2}{2T}(a-p)(t-t_1)^2 - \frac{h}{T}(a-p)\left(\frac{-t_1^2}{2} + \frac{\propto}{\beta+1}\left[\frac{t_1^{\beta+2}}{\beta+2} - t_1^{\beta+2}\right] + \frac{\propto^2}{2(2\beta+1)}\left[\frac{t_1^{2\beta+2}}{2\beta+2} - t_1^{2\beta+1}\right]\right) + \frac{(a-p)C}{T}\left(\frac{\propto t_1^{\beta+1}}{\beta+1} + \frac{\propto^2 t_1^{2\beta+1}}{2(2\beta+1)} + T\right)$ (10)

Let $t_1 = vT$, $0 < v < 1$

Therefore we have profit function,

$K(p,T) = p(a-p) - \frac{1}{T}\left[A + \frac{C_2}{2}(a-p)(t-vT)^2 - h(a-p)\left(-\frac{(vT)^2}{2} + \frac{\propto}{\beta+1}\left[\frac{(vT)^{\beta+2}}{\beta+2} - (vT)^{\beta+2}\right] + \frac{\propto^2}{2(2\beta+1)}\left[\frac{(vT)^{2\beta+2}}{2\beta+2} - (vT)^{2\beta+2}\right]\right) + c(a-p)\left(\frac{\propto(vT)^{\beta+1}}{\beta+1} + \frac{\propto^2(vT)^{2\beta+1}}{2(2\beta+1)} + vT\right)\right]$ (11)

$\frac{\partial K(p,T)}{\partial T} = \frac{1}{T^2}\left[A + \frac{c_2}{2}(a-p)(t-vT)^2 + h(a-p)\left[\frac{(vT)^2}{2} + \frac{\propto}{\beta+2}(vT)^{\beta+2} + \frac{\propto^2}{2}\frac{(vT)^{2\beta+2}}{2\beta+2}\right]\right.$

$\left. + (a-p)c\left[\frac{\propto(vT)^{\beta+1}}{\beta+1} + \frac{\propto^2(vT)^{2\beta+1}}{2(2\beta+1)} + vT\right]\right] + -\frac{1}{T}\left[c_2(a-p)(vT-t)v + c(a-p)(\alpha v^{\beta+1}T^{\beta}\right.$

$\left. + \frac{\propto^2}{2}v^{2\beta+1}T^{2\beta} + v) + h(a-p)\left(v^2T + \propto T^{\beta+1}v^{\beta+2} + \frac{\propto^2}{2}v^{2\beta+2}T^{2\beta+1}\right)\right]$ (12)

$\frac{\partial K(p,T)}{\partial p} = a - 2p + \frac{c_2}{2T}(t-vT)^2 - \frac{h}{T}\left[\frac{(vT)^2}{2} + \frac{\propto}{\beta+2}(vT)^{\beta+2} + \frac{\propto^2}{2(2\beta+2)}(vT)^{2\beta+2} - \frac{c}{T}\left[\frac{\propto(vT)^{\beta+1}}{\beta+1} + \frac{\propto^2(vT)^{2\beta+1}}{2(2\beta+1)} + vT\right]\right.$ (13)

For the maximization of profit we set

$\frac{\partial K(p,T)}{\partial T} = 0$ and $\frac{\partial K(p,T)}{\partial p} = 0$ provided $\frac{\partial^2 K(p,T)}{\partial T^2} < 0$, $\frac{\partial^2 K(p,T)}{\partial p^2} < 0$ and

$\left(\frac{\partial^2 K(p,T)}{\partial T^2}\right)\left(\frac{\partial^2 K(p,T)}{\partial p^2}\right)\left(\frac{\partial^2 K(p,T)}{\partial T \partial p}\right) > 0$.

CONCLUSION

A deterministic inventory model for deteriorating inventory model with two parameter Weibull distribution deterioration rate has been developed. Demand rate is function of selling price and holding cost is constant occurring shortages and completely backlogged.

REFERENCES:

[1] Ajanta Roy "An inventory model for deteriorating items with price dependent demand and time-varying holding cost." AMO-Advanced Modeling and Optimization, volume 10, November 1, 2008.

[2] Amutha.R, E.Chandrasekaran, "An inventory model for deteriorating items with three parameter weibull deterioration and price dependent demand" International Journal of Engineering Research & Technology Vol.2,Issue -5,May-2013,1931-1935.

[3] Anil Kumar Sharma, ManojKumar Sharma and Nisha Ramani "An Inventory model with Weibull distribution deteriorating power pattern demand with shortages and time dependent holding cost." American Journal of Applied Mathematics and Mathematical Sciences (Open Access Journal Volume 1, Number 1-2 January – December 2012, Pp. 17-22.

[4] Biplab Karmakar and Karabi Dutta Choudhury, "A Review on Inventory Models for Deteriorating Items with Shortages," Assam University Journal of Science& Technology, Physical Sciences and Technology, Vol.6, Number II, 51-59,2010

[5] Ghosh S.K and K.S.Chaudhri, "An order level inventory model for a deteriorating item with Weibull distribution deterioration time – quadratic demand and shortages", Advanced Modeling and Optimization, volume 6, Number 1.

[6] Goyal S.K, B.C.Giri "Recent trends in modeling of deteriorating inventory" European Journal of Operation Research, 134 (2001) 1-16

[7] Kun –Shan Wu "An Ordering Policy for Items with Weibull distribution Deterioration under permissible Delay in Payments." Tamsui Oxford Journal of Mathematical Science 14 (1998) 39-54.

[8] Manoj Kumar Meher , Gobinda Chandra Panda, Sudhir Kumar Sahu," An Inventory Model with Weibull Deterioration Rate under the Delay in Payment in Demand Dec ling Market" Applied Mathematical Sciences,Vol.6, 2012, no.23, 1121 -1133.

[9] Mukesh Kumar, Anand Chauhan, Rajat Kumar "A Deterministic Inventory Model for Deteriorating Items with Price Dependent Demand and Time Varying Holding cost under Trade Credit" International Journal of Soft computing and Engineering (IJSCE) ISSN:2231-2307, Volume-2, Issue-1, March 2012

[10] Padmanabhan.G., Prem Vrat "EOQ models for perishable items under stock dependent selling rate"

[11] Pattnaik.M, "A Note on Non Linear Optimal Inventory Policy Involving Instant Deterioration of Perishable Items with Price Discounts", The Journal of Mathematics and Computer SCienceVol.3, No.2 (2011) 145-155.

[12] Sahoo.N.K, Sahoo .C.K. & Sahoo.S.K. "An Inventory Model for Constant Deteriorating Items with Price Dependent Demand and Time p Varying Holding Cost" International Journal of computer cuience & communication Vol.1, No.1, January –June 2010, pp.267-271

[13] Sanjay JAIN, Mukesh KUMAR "An EOQ Inventory Model for Items with Ramp Type Demand, Three-Parameter Weibull Distribution Deterioration and Starting with Shortage", Yugoslav Journal Of Operations Research Volume 20(201), No. 2, 249-259

[14] Tripathy C.K and L.M. Pradhan, "Optimal Pricing and Ordering Policy for Three Parameter Weibull Deterioration .Int. Journal of math .Analysis, Vol.5,2011,no.6,275-284

[15] Tripathy C.K and L.M. Pradhan An EOQ model for three parameter Weibull deterioration with permissible delay in payments and associated salvage value," International Journal of Industrial Computations3(2012)115-122

[16] TripathyP.K, S.Pradhan, "An Integrated Partial Backlogging Inventory Model having Weibull Demand and Variable Deterioration rate with the Effect of Trade Credit", International Journal of Scientific & Engineering Research Volume 2, Issue 4, April 2011

[17] Vikas Sharma, and Rekha Rani Chaudhary, "An inventory Model for deteriorating items with Weibull Deterioration with Time Dependent Demand and Shortages", Research journal of Management sciences, Vol. 2(3), 28-30, March (2013) ISSN 2319-1171.

International Journal of Engineering Research and General Science Volume 3, Issue 5, September-October, 2015
ISSN 2091-2730

Computational analysis and simulation of thermo-electric power generation from automotive exhaust gas

Jins Jose(P.G student), Prof. Reji Mathews, Ernest Markose Mathew(Associate professor)

Mar Athanasius College of Engineering, Kothamangalam.

Affiliated to Mahatma Gandhi University Kottayam, Keralaand AICTE, India,

Email:jinsjose.tcr@gmail.com, Tele: +919037383920

Abstract—The growing demand for energy, increasing fuel price, and the environmental pollution issues associated with conventional energy generating technologies has increased interest in the use of Thermo electrics, which can directly convert thermal energy into electrical energy. There is a great possibility in utilizing thermoelectric devices for automobile exhaust to electricity conversion.Studies show that significant energy savings can be achieved by recovering even a small portion of this wasted energy. From the energy balance of combustion engine, it is found that approximately 40% of the fuel energy is lost in exhaust gas. Thermoelectricmodulescan operate over a wide range of transient temperature conditions. The electric power is generated as a result of the temperature difference based on the Seebeck effect.Computational fluid dynamics (CFD) is used to simulate the exhaust gas flow within the heat exchanger.The isothermal modeling approach is used in simulation.In this paper, two cases of heat exchangers such as rectangular type and square type were used in exhaust of internal combustion engine (ICE) are modeled numerically to recover the exhaust waste heat. The heat exchangerswere proposed and designed to recover energy from exhaust of apetrol engine. The simulations are done in five engine loads (idling, suburban driving, urban, cruisingand maximum power) and After the analysis, results of irreversibility, recovered heat, surface temperature, pressure drop, average power developed and current developed etc. are compared in different engine loads and speeds. The Rectangular heat exchanger made up of aluminium shows better performance among the two proposed designs. The analysis predicts optimum conditions forthermoelectric leg pairs that maximize the power extracted for any TEG modules, and the change in this optimum conditionmay degrade the system performance.

Keywords—Automotive exhaust, Isothermal approach, Seebeck effect, Thermoelectric , Heat exchangers,Design optimization, Convergence study, Power generation.

INTRODUCTION

In recent years there is a substantial interest in utilizing thermoelectric devices for automobile exhaust to electricity conversion. Studies show that significant energy savings can be achieved by recovering even a small portion of this wasted energy. From the energy balance of combustion engine, it is found that approximately 40% of the fuel energy is lost in exhaust gas and just12 to 25 % of the fuel energy converts to useful work, which results in the energy crisis and environment pollution[1]. Thermoelectric generation (TEG) technology have some distinct advantages such as, they are simple, have no moving parts, highly reliable, zero emission, low noise and are able to operate over a wide range of transient temperature conditions. The electric power is generated as a result of the temperature difference based on the Seebeckeffect[2].Computational fluid dynamics (CFD) is used to simulate the exhaust gas flow within the heat exchanger.The isothermal approach is followed throughout the research, thermal characteristics of heat exchangers with various heat transfer enhancement features are studied, such as; internal structure, material and surface area[3]. With the thermal energy of exhaust gas harvested by thermoelectric modules, a temperature gradient appears on the heat exchanger surface, so as the

interior flow distribution of the heat exchanger.In this paper, two cases of heat exchangers such as rectangular type and square type were used in exhaust of internal combustion engine (ICE) are modeled numerically to recover the exhaust waste heat. The heat exchangers were proposed and designed to recover energy from exhaust of apetrol engine. The simulations are done in five engine loads (idling, suburban driving, urban, cruising and maximum power) and After the analysis, results of irreversibility, recovered heat, surface temperature, pressure drop, average power developed and current developed etc. are compared in different engine loads and speeds. The Rectangular heat exchanger made up of aluminium shows better performance among the two proposed designs. The limiting conditions, for the theoretical power generation used in previous studies are followed in this paper.

MODELLING

The computational fluid dynamics (CFD) is used to simulate the exhaust gas flow within the heat exchanger. The isothermal modelingapproach is followed during simulation[4]. Three dimensional views, wall thickness, internal structure and cross sectional view of the heat exchangers are shown in Fig.1

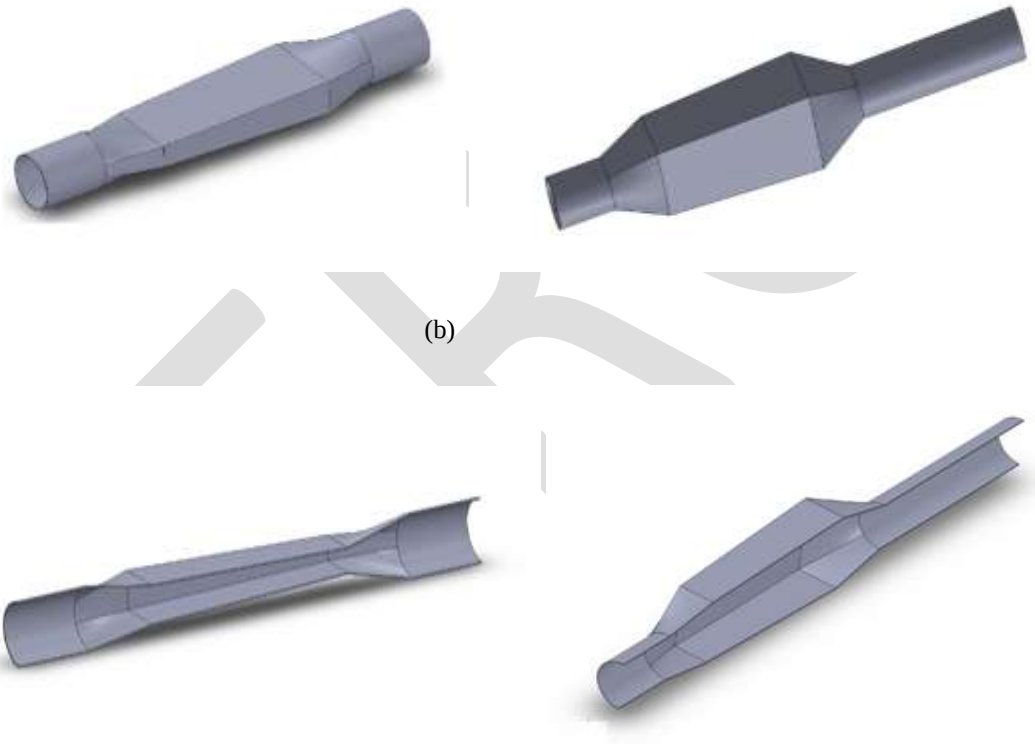

(a) (b)

(c) (d)

Fig.1 (a)three dimensional view of Rectangular heat exchanger (b) three dimensional view of Square heat exchanger (c) sectional view of Rectangular heat exchanger (d)sectional view of Square heat exchanger

The heat exchangers made up of aluminiumhave inlet and outlet manifold diameters as 80mm, the width of the wall at inlet as110mm and at the outlet 130mm. The cross sectional area of the square heat exchanger is 110mm x 110mm. The wall thickness is about 5mm. From inlet of the heat exchanger the cross section is found to be increasing gradually to the outlet, which provides smooth interaction of the exhaust gas with the exchanger walls. This causes the high temperature exhaust gas to diffuse in the entire lateral area rather than concentrating in the central region.

THERMAL SIMULATION

By applying fundamental formula of convective heat transfer Q = h A Δ T, heat convection can be greatly strengthened by the increase of the heat transfer area A. This target can be achieved by providing a sufficient conduction surface. Another approach is to increase the heat transfer coefficient h. According to the fluid dynamics theories, under the condition of Reynolds number Re >104, macro turbulent fluid flow is a significant factor for improving the heat transfer. Moreover, the greater the heat transfer coefficient h, the better the heat transfer quantity[5]. The thermal resistance of turbulent flow of convection mostly exists in the boundary layer. The better the synergy was between the temperature field and velocity field, the better the heat transfer[6].

According to both the theories mentioned above, the strengthening of the heat transfer can be approached by adding turbulence devices or altering the geometry to enhance the fluid disturbance and damage the boundary layer[7]. On the basis of the theories of thermal convection and turbulent flow as mentioned above, the three-dimensional models of heat exchangers such as rectangular type and square type are put forward by providing a new design. Among these internal structure, the geometrical model of the heat exchanger including rectangular internal structure, square internal structure are showed in Fig.1 a,b,c, d. The CFD simulation results including the temperature contour are showed in Fig. 3.a,b andFig. 4.a, b, however, the rectangular-shape design presents a better uniform temperature distribution than the square-shape. Considering the temperature distribution, the heat exchanger with rectangular-shape internal structure is more ideal for TEG.

BOUNDARY CONDITION

Simulation model is assured that the exhaust flow in the heat exchanger is fully turbulent and molecular viscosity can be neglected, so the standard κ–ε model is adopted in the CFD simulation. As Near wall area processing with standard wall function, the natural convection heat transfer coefficient and the environment temperature are set.

The mass flow rates for different conditions are as follows; idling: 1.2 g/sec, Urban: 5.7 g/sec, Suburban: 14.4 g/sec, Cruising: 24.3 g/sec, Maximum power: 80.1 g/sec. The Inlet temperature: 573.15 kand outlet: pressure outlet with gauge pressure 300 kPa.

As for the heat exchanger presenting an approximately axial symmetry in geometry, so the flow, pressure and temperature fields also show axisymmetric characteristics in the absence of ambient winds.

EXHAUST GAS PROPERTIES

The major properties of the exhaust gas at any temperature were shown in table.1[8].

Table.1

Properties	$A + B \times T + C \times T^2 + D \times T^3$			
	A	B	C	D
ρ (kg/m^3)	2.504012288761e + 00	-5.958486188418e - 03	5.578942358587e - 06	-1.772600918994e - 09
$C_{p\ (J/kg\ k)}$	1.015580935928e + 03	-1.512248401853e - 01	4.544870294058e - 04	-1.785063817137e - 07
μ (kg/ms)	1.325186910351e -06	6.740061370040e - 08	-3.749043579926e - 11	1.110074961972e - 14
K(w/mk)	-3.182421851331e - 03	1.185847825677e - 04	-7.706004236629e -08	2.939653967062e - 11

MESH CONVERGENCE

The Fig.2a, b shows the mesh convergence for the rectangular andsquare heat exchanger simulations. The convergence for rectangular heat exchanger was found to be at an element number1067831 corresponding to the centerline temperature of 555k. Similarly for the square heat exchanger, aboutan element number 1075104 and corresponding to the centerline temperature of 544k.

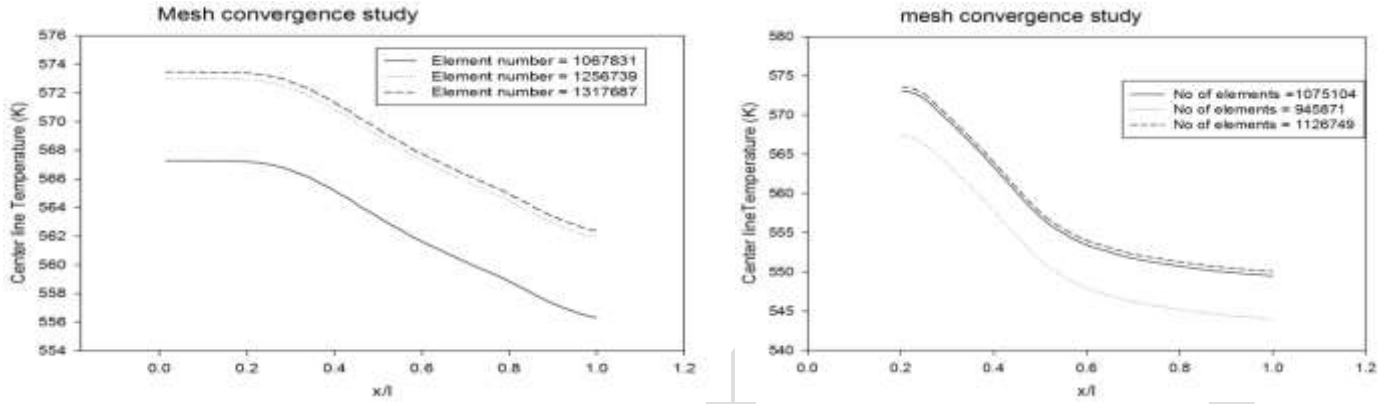

(a) (b)

Fig.2 (a)convergence for Rectangular heat exchanger (b) convergence for square heat exchanger

TEMPERATURE FIELD ON HEAT EXCHANGERS

The temperature field on the heat exchanger plays an important role in thermoelectric energy conversion in three aspects such as: firstly, it determined the available thermoelectric material by maximum continues operating temperature; secondly, it affects the energy conversion efficiency of heat to electricity; thirdly, dominates the thermal stresses in device level and module level. A non uniform thermal stress may cause performance deterioration and permanent damage to the TEG modules[9].

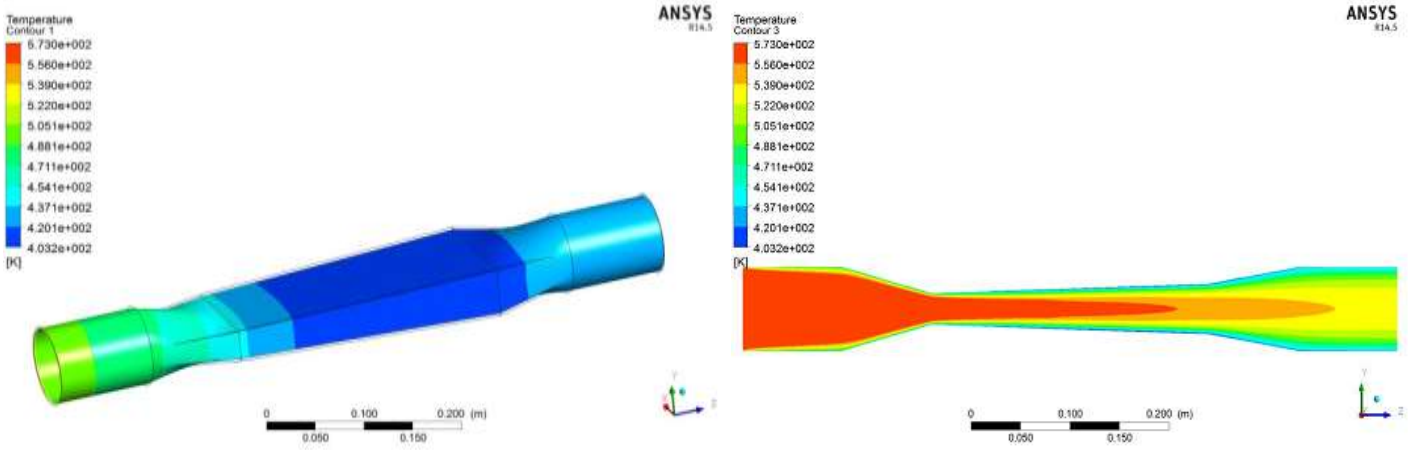

(a) (b)

Fig.3 Temperature field: (a)on rectangular heat exchanger surface (b) Sectional view of Rectangular heat exchanger

The Fig.3. a,b and Fig.4. a,b illustrates the temperature distribution upon the heat exchanger surface. From the simulation it can be clearly seen that(Fig.3. a) the rectangular heat exchanger can give a uniform temperature distribution, closer to the isothermal model approach.

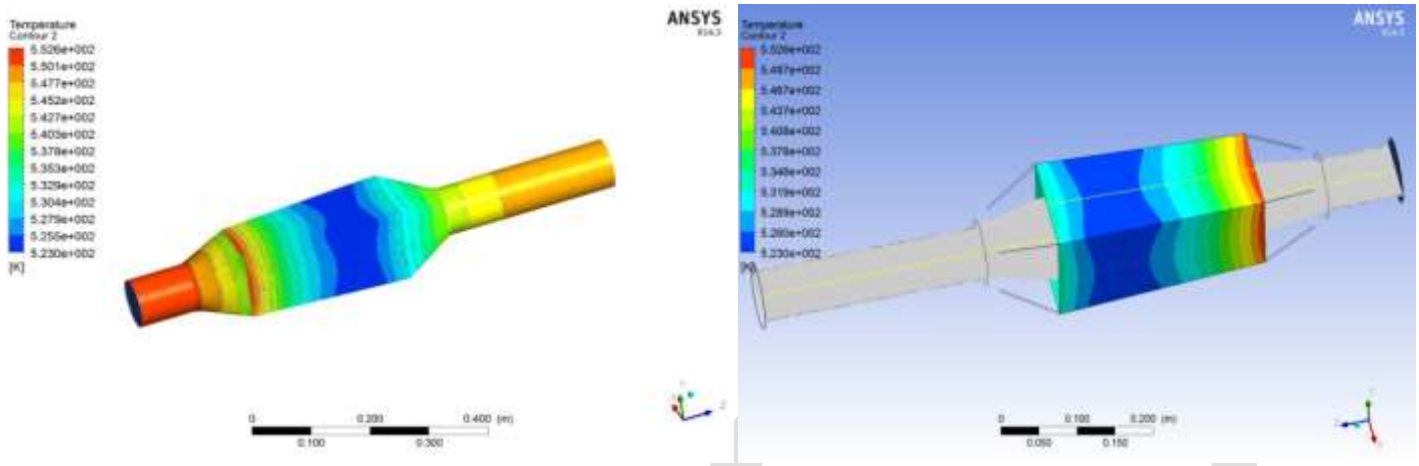

(a) (b)

Fig.4 Temperature field: (a)on square heat exchanger (b) on square heat exchanger surface alone

PRESSURE FIELD ON HEAT EXCHANGERS

The hot exhaust gas flow from engine, when interacts with the walls and transfer energy, experiences drop of pressure. As in the case of an I.C engine system, this drop of pressure is equivalent to the rise of atmospheric pressure and causes a drop in output power[10]. The pressure field in heat exchangers is showed in Fig.5. a, b. The pressure drop is dominant in rectangular heat exchanger than square heat exchanger.

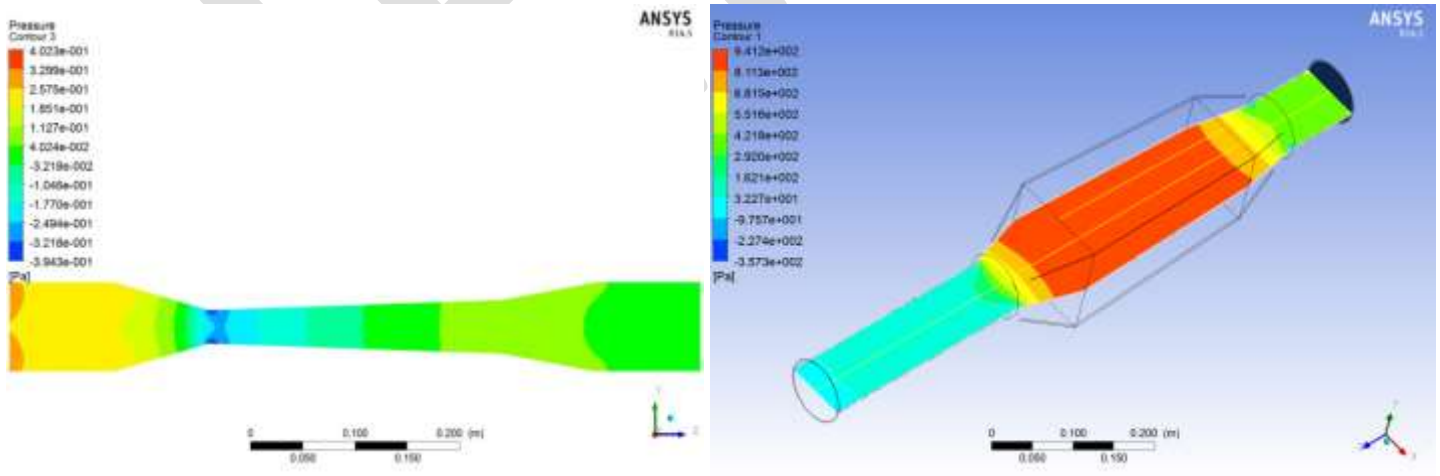

Fig.5 Pressure field: (a)on rectangular heat exchanger (b) on square heat exchanger

THERMAL SIMULATION RESULTS

The simulations are done in five engine loads such as; idling, suburban driving, urban, cruising and maximum power and the results were plotted below. The Fig.6 shows the simulation results for the surface temperatures in different conditions. Fig.6 (a) shows the rectangular heat exchanger surface temperature, which varies from 411k to 442.7k in idling to the range of 550.4k to 563.5k at maximum power. As in the case of square heat exchangerFig.6 (b) the surface temperature varies in the order of 392.7k to 406.4k at idling and from 534.5k to 552.7k at the maximum power.

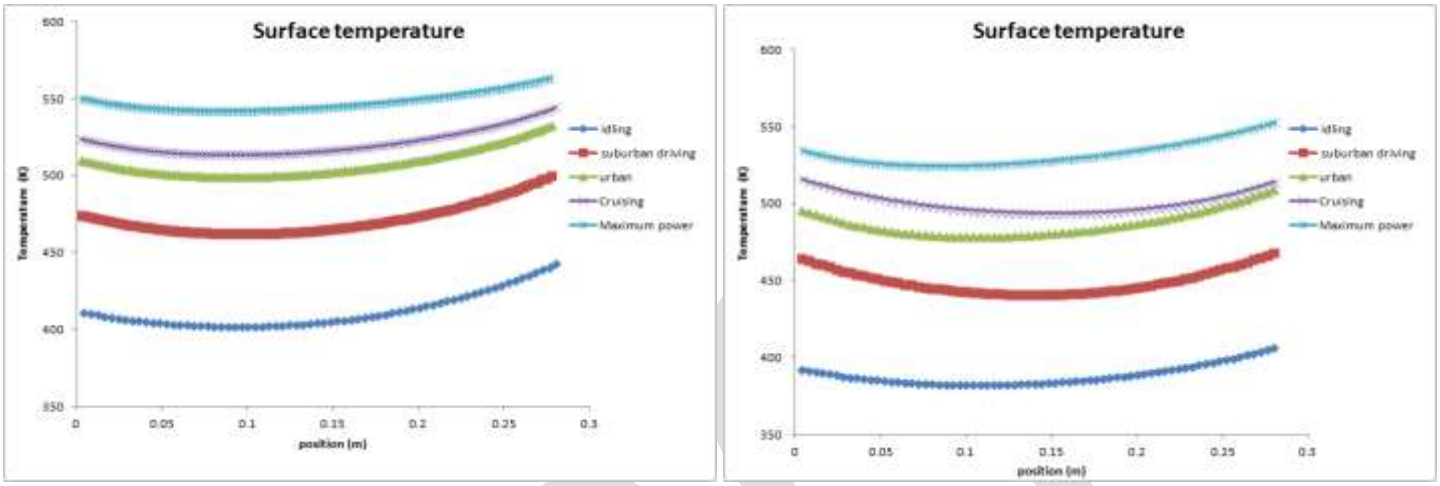

Fig.6 surface temperature: (a)on rectangular heat exchanger (b) on square heat exchanger

Fig.7 shows the variation of centerline velocity in both the heat exchangers under the given conditions. The centerline velocity of the rectangular heat exchangerFig.7 (a) varies from 1.618m/s to 1.029m/s at idling and from 83.7m/s to 55.3m/s at maximum power. The velocity variation in square heat exchanger Fig.7 (b) ranges from 0.936m/s to 1.026m/s at idling and 52.038m/s to 48.85m/s at maximum power.

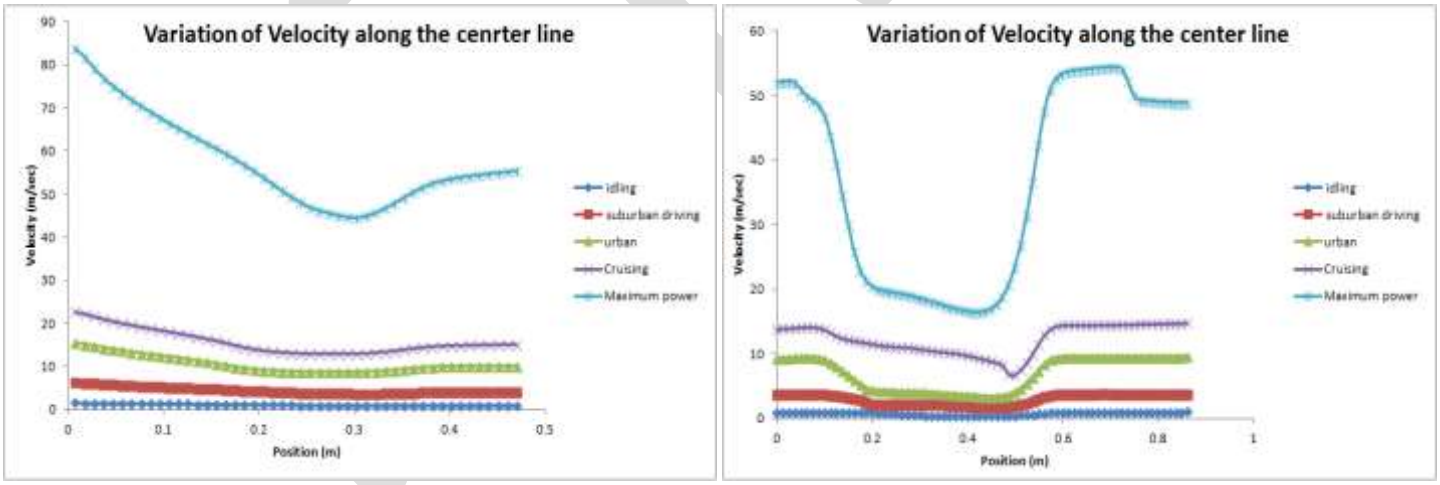

Fig.7 velocity along centerline: (a)rectangular heat exchanger (b) square heat exchanger

The pressure variation of the heat exchangers along the centerline is shown in Fig.8. The pressure variation shows less deviation as in the case of rectangular heat exchanger (Fig.8.a). For the rectangular heat exchanger a maximum deviation occurs during cruising and it varies between 300.04Pa to 299.94Pa. Similarly for the square heat exchanger (Fig.8.b), the pressure variation occurs at cruising and ranges between 300.06Pa to 300Pa.

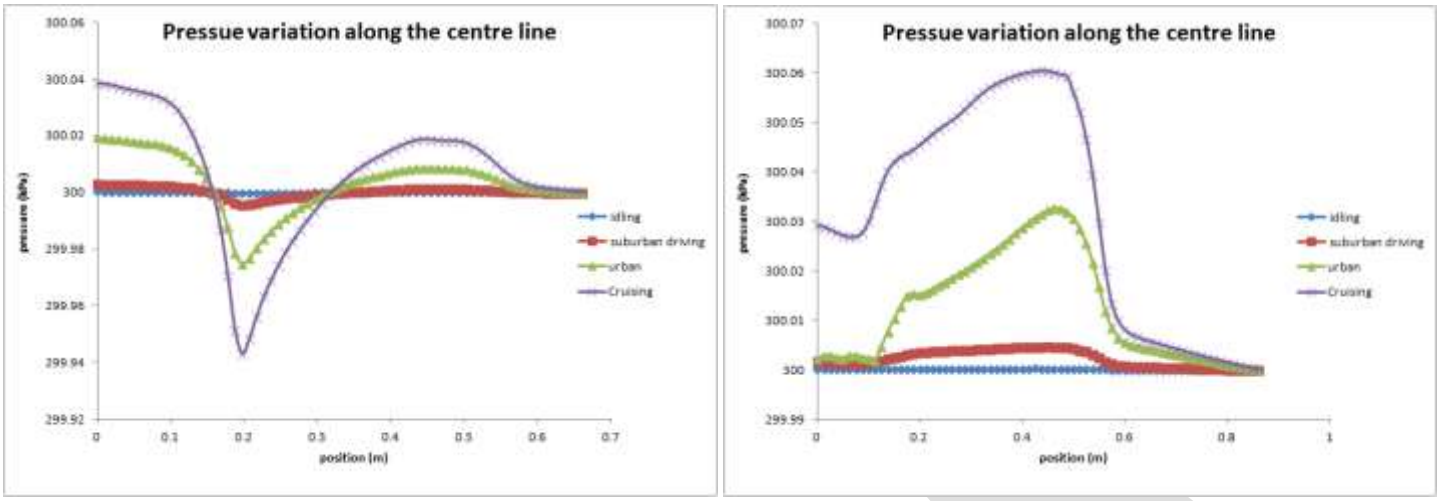

Fig.8 Pressure variation: (a)rectangular heat exchanger (b) square heat exchanger

A clear comparison of the pressure drop as well as heat flux of both the heat exchangers was shown in Fig.9 a, b below. From the chart shown below, it can be seen that the pressure drop was slightly predominant in the case of rectangular heat exchanger especially during the maximum power. But the heat flux available in the rectangular heat exchanger is higher in all conditions.

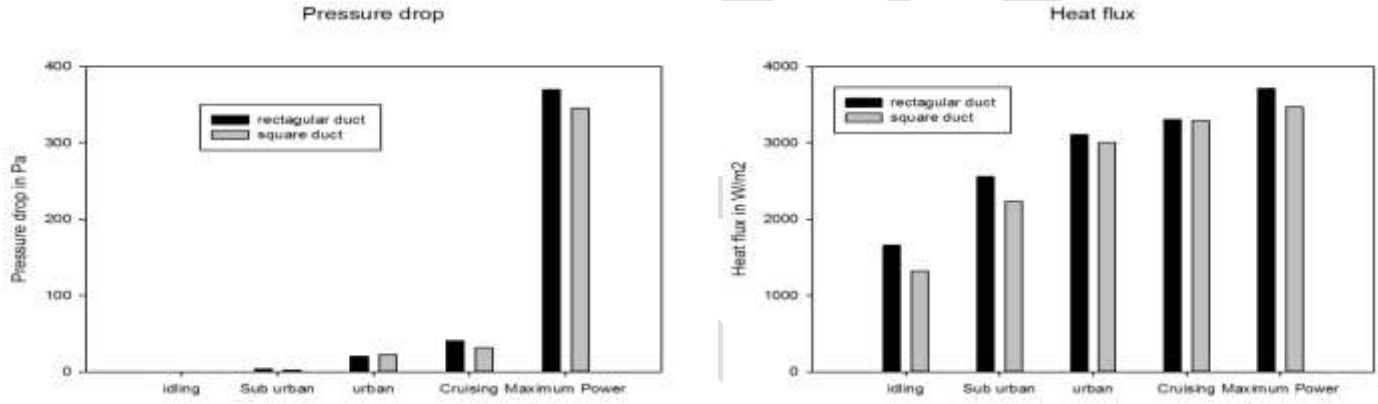

Fig.9 (a)Pressure drop(b) heat flux

From the previous studies and literature conducted on thermoelectric modules, the theoretical limit for the thermoelectric heat exchangers can be calculated. This may help us to predict the available current and power for the proposed design. For this, we need to predict and assign thermoelectric properties for the heat exchanger along with its thermoelectric materials[11]. The assumptions for p-type and n- type materials were shown in Table.2[12]. The total rate of energy transferred to all thermoelectric elementsin the form of heat is shown by equation (1).Thetotal rate of energy transferred from the thermoelectric elementson the coolant side of the system is represented by equation (2). The electrical power (p) generated by the entire system is the difference in the two energy rates as shown in equation (3)[13]. Where,Q_h heat transferred at hot side, Qc Heat transferred to the cold fluid, m mass flow rates, $c_p$specific heat capacity, $T_{h,i}$ temperature at hot side inlet, $T_{h,o}$ temperature at hot side outlet, $T_{c,i}$ temperature at cold side inlet and $T_{c,o}$temperature at cold side outlet.

$$Q_h = (m\, c_p)_h(T_{h,i}–T_{h,o}) \quad (1)$$

$$Qc = (mc_p)_c(T_{c,o}–T_{c,i}) \quad (2)$$

$$P = Q_h–Q_c \quad (3)$$

We then assume that, the length of any leg pair is small comparedwith the totallength of the system, i.e., b/L<<1, whichallows us to view the system as a single continuous module alongwhich the temperatures and current can vary. Consistent with thisapproximation, we define a local current flux (i.e., current perarea), j(x)[14].

$$I = w.\ b.j(x). \quad (4)$$

$$J(x) = \alpha\ (T_1 - T_2) / R\ddot{e}(1+m) \quad (5)$$

$$m = (1+ Z\overline{T})^{0.5} \quad (6)$$

$$Z = \alpha^2 / \ddot{K}\ R\ddot{e} \quad (7)$$

$$\overline{T} = (T_1 + T_2) / 2 \quad (8)$$

Here the current is now interpreted as being continuous.

Where,
I is the current generated, w width of the leg, b breadth of the leg, j(x) is the current flux, αseebeck coefficient, k thermal conductivity, $\overline{T}$ average temperature and R contact resistance of the conductor.

Table.2

Parameters	p type	n type
Seebeck coefficient, α	200 x 10^{-6} v/k	-150 x 10^{-6} v/k
Electrical resistivity, ρ	1.5 x 10^{-3} Ω cm	2.0 x 10^{-3} Ω cm
Thermal conductivity, k	1.1 w/m k	1.3 w/m k
Leg length, l	1mm	1mm
Leg area, A	2.25mm^2	2.25mm^2
Electrical contact resistance, Rc̈	0 Ω m^2	0 Ω m^2

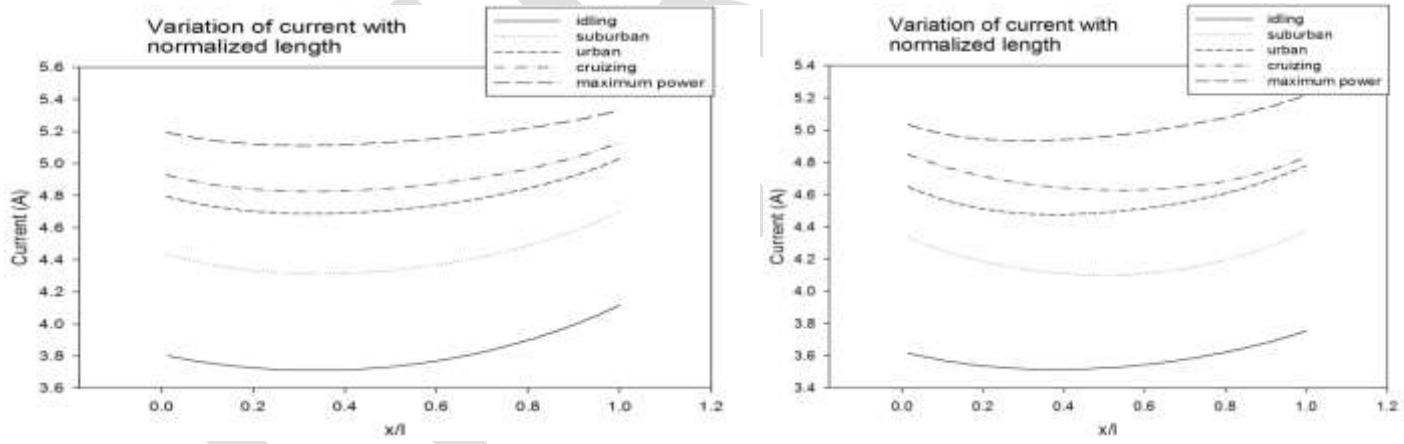

Fig.10 current: (a)rectangular heat exchanger (b) square heat exchanger

The Fig.10.a,b shows the current generated in heat exchangers, at the given set of conditions. It can be seen that maximum current was produced during the maximum power condition. The rectangular heat exchanger can generate more current compared to the square heat exchanger. The current ranges from 3.8A to 5.4A, as in the case of rectangular heat exchanger and from 3.6A to 5.2A in the case of square heat exchanger.

The average power produced by the heat exchangers is shown in Fig.11.a, b below. It can be seen that the rectangular heat exchanger gives better power output and it ranges between 260W to 590W. But in the case of square heat exchanger it ranges between 100W to 270W.

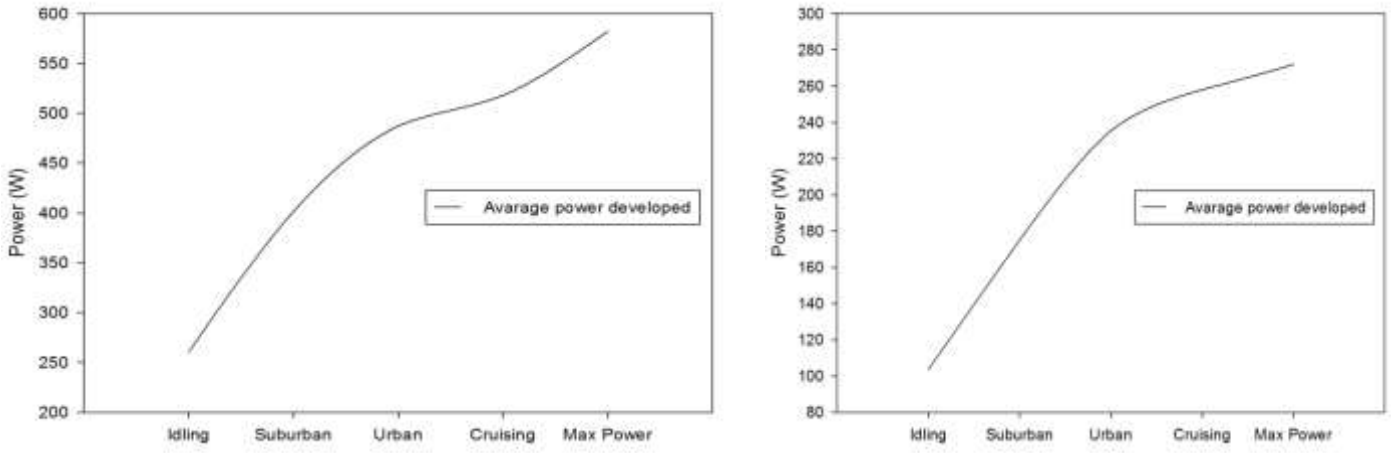

Fig.11 power: (a)rectangular heat exchanger (b) square heat exchanger

ACKNOWLEDGMENT

I acknowledge the support from Dr. Roy N Mathews and Prof. Reji Mathews,Ernest Markose Mathew (Associate professor)Mar Athanasius College of Engineering, Kothamangalam (Affiliated to Mahatma Gandhi University Kottayam, Keralaand AICTE, India,) and Mr.Jinshah B.S (Assistant Professor, U K F College of Engineering, Kollam, Kerala.).

CONCLUSION

In this work, two heat exchangers of rectangular as well as square cross section were analyzed. In which the rectangular heat exchanger shows better surface temperature, an ideal temperature uniformity which improves TEG performance. Also the rectangular heat exchanger shows comparatively less pressure drop as well as better heat flux. Further, an improved current and power generation can be observed in rectangular heat exchanger model.

In future study, the method of simulation modeling with infrared experimental verification needs to be combined with heat transfer theory and material science to serve for further structural design and optimization of thermoelectric modules and TEG, so as to improve the overall exhaust heat utilization and enhance the power generation.

REFERENCES:

[1] JihuiYang and StablerFrancis R. “Automotiveapplicationsofthermoelectricmaterials”.JElectronMater2009;38: 1245–51.
[2] Martinez J G, Vian D, Astrain A, Rodriguez Berrio I. “Optimization of the heat exchangers of a thermoelectric generation system”. J Electron Mater 2010; 39:1463–8.
[3] AstrainD,ViánJG,MartínezA,RodríguezA.“Studyoftheinfluenceofheatexchangers'thermalresistancesonathermoelectricgenerationsystem”. Energy 2010; 35:602–10.
[4] Martinez JG,VianD,AstrainA,RodriguezBerrioI. “Optimizationoftheheatexchangersofathermoelectricgenerationsystem.JElectronMater 2010; 39:1463–8.
[5] C. Q. Sun, W. S. Wang, X. Liu, Y. D. Deng “Simulation and experimental study on thermal optimization of the heat exchanger for automotive exhaust-based thermoelectric generators”, Thermal Engineering 4(2014)85–91.
[6] Guo ZY,TaoWQ,ShahRK. “Thefieldsynergy(coordination)principleanditsapplicationsinenhancingsinglephaseconvectiveheattransfer”.IntJHeat Mass Transf2005; 48(9):1797–807.
[7] YangS.M. “HeatTransferTheory”.Beijing,China:HigherEducation; 2004, p.207–11.

[8] M. Hatami, D.D. Ganji, M. Gorji-Bandpy. "Experimental investigations of diesel exhaust exergy recovery usingdelta winglet vortex generator heat exchanger". International Journal of Thermal Sciences 93 (2015) 52 – 63.

[9] Lu Hongliang,WuTing. "Experimentonthermaluniformityandpressuredropofexhaustheatexchangerforautomotivethermoelectricgenerator". Energy 2013; 54:372–7.

[10] X. Liu, Y.D. Deng, S. Chen, W.S. Wang, Y. Xu, C.Q. Su. "A case study on compatibility of automotive exhaust thermoelectric generation system, catalytic converter and muffler". ThermalEngineering2 (2014)62–66.

[11] YuchaoWanga, ChuanshanDai,Shixue Wang."Theoretical analysis of a thermoelectric generator using exhaust gas of vehicles as heat source". Applied Energy 112 (2013) 1171–1180.

[12] Robert J. Stevens , Steven J. Weinstein b, Karuna S. Koppula."Theoretical limits of thermoelectric power generation from exhaust gases". Applied Energy 133 (2014) 80–88.

[13] Zhou S, Sammakia BG, White B, Borgesen P. "Multiscale modeling ofthermoelectric generators for the optimized conversion performance". Int J Heat Mass Transf 2013; 62:435–44.

[14] Min G, Rowe DM. "Conversion efficiency of thermoelectric combustion systems".Energy Convers, IEEE Trans 2007; 22:528–34.

International Journal of Engineering Research and General Science Volume 3, Issue 5, September-October, 2015
ISSN 2091-2730

Performance Evaluation for Frequent Pattern mining Algorithm

Mr.Rahul Shukla, Prof(Dr.) Anil kumar Solanki

Mewar University,Chittorgarh(India), Rsele2003@gmail.com

Abstract— frequent pattern mining is an essential data mining task, with a goal of discovering knowledge in the form of repeated patterns. Many efficient pattern mining algorithms have been discovered in the last two decades to enhance the performance of Apriori Algorithm, for the purpose of determining the frequent pattern. The main issue for any algorithm is to reduce the Execution time. In this paper we compare the performance of Apriori and ECLAT Algorith on the medical data and find out the interesting pattern in medical data.

Keywords— Apriori, Frequent Patterns, Support , Eclat , Association rule ,confidence, Itemset

introduction

frequent pattern mining has applications ranging from intrusion detection and Market basket analysis, to credit card fraud prevention and drug discovery it is the analysis of dataset to find unsuspected relationship and to summarize the data in new ways that are both understandable and useful. Evolutionary progress in digital data acquisition and storage technology has resulted in huge and voluminous databases. Data is often noisy and incomplete, and therefore it is likely that many interesting patterns will be missed and reliability of detected patterns will be low. This is where, knowledge Discovery in databases (KDD) and Data Mining (DM) helps to extract useful information from raw data. Frequent patterns are those that occur at least a user-given number of times (referred as minimum support threshold) in the dataset. Frequent item sets play an essential role in many data mining tasks that try to find interesting patterns from databases, such as association rules, correlations, sequences, episodes, classifiers, clusters. Frequent pattern mining is one of the most important and well researched techniques of data mining. The mining of association rules is one of the most popular problems. The original motivation for searching association rules came from the need to analyze so called supermarket transaction data, that is, to examine customer behavior in terms of the purchased products. Association rules describe how often items are purchased together. Such rules can be useful for decisions concerning product pricing, promotions, store layout and many others. Being given a set of transactions of the clients, the purpose of the association rules is to find correlations between the sold articles. Knowing the associations between the offered Products and services help those who have to take decisions to implement successful marketing techniques. Based on the obtained results and comparative statistical interpretations, we Issued hypotheses referring to performance, precision and accuracy of the two processes Apriori and Eclat Frequent pattern Approach.

A. Association Rule

Association rule is used to find out the items which are frequently used together. The Presence of one set of items in a Transaction implies other set of items. The terms used in these Rules are

Support*:* The support of an association rule X implies Y is the Percentage of transaction in the database that consists of X U Y.

Confidence: The confidence for an association rule X implies Y is the ratio of the number of transaction that contains X U Y

To the number of transaction that contains X.

Large Item Set: A large item set is an item set whose number of occurrences is above a threshold or support. The task of association rule mining is to find correlation relationships among different data attributes in a large set of data items, and this has gained lot of attention since its introduction. Such relationships observed between data attributes are called association rules. A typical example of association rule mining is the market basket analysis [2].

Limitation of Apriori

One is to find those item sets whose occurrences exceed a predefined Support in the database; those item sets are called frequent Pattern The Apriori Algorithm can be further divided into two sub-part candidate large item sets generation process and frequent item sets generation process. Frequent item set or large item set are those item sets whose support count exceeds the value of support threshold. Due to Number of passes apriori takes the more time. It scan the Database many time for Frequent pattern Discovery.

Apriori Algorithm for Frequent Pattern Mining

It searches for large item sets during its initial database pass and uses its result as the seed for discovering other large datasets during subsequent passes. Rules having a support level above the minimum are called large or frequent item sets and those below are called small item sets. The algorithm is based on the large item set property which states: Any subset of a large item set is large and any subset of frequent item set must be frequent. The first algorithm for mining all frequent item sets and strong Association rules were the AIS algorithm by [3]. Shortly after that, the algorithm was improved and renamed Apriori. Apriori algorithm is, the most classical and important algorithm for mining frequent itemsets.The Apriori algorithm performs a breadth-first search in the search space by generating candidate k+1-itemsets from frequent k item sets. The frequency of an item set is computed by counting its occurrence in each transaction. Apriori is an influential algorithm for mining frequent item sets For Boolean association rules. Since the Algorithm uses prior knowledge of frequent item set it has been given the name Apriori. It is an iterative level wise search Algorithm, where k Item sets are used to explore (k+1)-item sets. First, the set of frequents 1- item sets is found. This set is denoted by L1. L1 is Used to find L2, the set of frequent 2-itemsets, which is used to Find L3 and so on, until no more frequent k-item sets can be found. The finding of each Lk requires one full scan of Database
There are two steps for understanding that how Lk-1 is used to find Lk:-

A. The join step:-

To find Lk, a set of candidate k-item sets is generated by joining Lk-1 with itself. This set of candidates is denoted Ck.

B. The prune step:-

Ck is a superset of Lk, that is, its members may or may not be Frequent, but all of the frequent k-item sets are included in Ck.

A scan of the database to determine the count of each candidate in Ck would result in the determination of Lk.Ck, however, can be huge, and so this could involve heavy computation to reduce the size of Ck.

A scan of the database to determine the count of each candidate in Ck would result in the determination of Lk. Ck,However, can be huge, and so this could involve heavy computation. To reduce the size of Ck , the Apriori property is used as Follows.

i. Any (k-1)-item set that is not frequent cannot be a subset of frequent k-item set.

ii. Hence, if (k-1) subset of a candidate k item set is not in Lk-1 then the candidate cannot be frequent either and so can be removed from C.

Based on the Apriori property that all subsets of a frequent item set must also be frequent, we can determine that four latter Candidates cannot possibly be frequent. How? For example, let's take {I1, I2, I3}. The 2-item subsets of it are {I1, I2}, {I1, I3} & {I2, I3}. Since all 2-item subsets of {I1, I2, I3} are members of L2, We will keep {I1, I2, I3} in C3.

Let's take another example of {I2, I3, I5} which shows how the pruning is performed. The 2-item subsets are {I2, I3}, {I2, I5} & {I3,I5}.

BUT, {I3, I5} is not a member of L2 and hence it is not

Frequent violating Apriori Property. Thus we will have to

Remove {I2, I3, I5} from C3.

Therefore, C3 = {{I1, I2, I3}, {I1, I2, I5}} after checking for

All members of result of Join operation for Pruning.

C.Apriori algorithm pseudo code:

Procedure **Apriori** (T, *minSupport*)

{ //T is the database and *minSupport* is the minimum support

L1= {frequent items};

for (k= 2; Lk-1 !=∅; k++)

{

Ck= candidates generated from Lk-1

for each transaction **t** in database **do**

{

increment the count of all candidates in Ck

that are contained in t

Lk = candidates in Ck with *minSupport*

}//end for each

}//end for

return ;

}

ECLAT Based Approach on Apriori Algorithm

Eclat is a vertical database layout algorithm used for mining frequent itemsets. It is based on depth first search algorithm. In the first step the data is represented in a bit matrix form. If the item is bought in a particular transaction the bit is set to one else to zero. After that a prefix tree needs to be constructed. To find the first item for the prefix tree the algorithm uses the intersection of the first row with all other rows, and to create the second child the intersection of the second row is taken with the rows following it [6]. In the similar way all other items are found and the prefix tree get constructed. Infrequent rows are discarded from further calculations. To mine frequent itemsets the depth first search algorithm is applied to prefix tree with backtracking.. Frequent patterns are stored in a bit matrix structure. Eclat is memory efficient because it uses prefix tree. The algorithm has good scalability due to the compact representation.

EXPERIMENTS

In this section, we evaluate the performance of Apriori and Eclat based Algorithm. To make the evaluation, we check the performance of Apriori and Eclat approach on the different support count and fixed support count with different size of dataset.

A. Dataset

In tune with our application, we have taken a database of Hospital transaction of 633 items. In this analysis process we considered 2000 transactions in Horizontal Transaction format to generate the frequent pattern . In

the horizontal Transaction each Transaction contain the multiple medicine in the single row.The horizontal Transaction view is Given below in Table 1.

TID	Medicine
1	STERILE WATER 5ML,COLISPAS DROP,PERINORM INJ
2	MEROTEC 250 MG INJ
3	kefragard 0.75 inj
4	combiflam tab
5	MONOCEF SB 1GM INJ
6	RANTAC INJ,DISPO VAN 2ML SYREING,DISPO VAN 5ML SYRIENG,DISPO VAN 1 ML SYRIENG,Dany Ing.,DISPO VAN 50ML SYRINGE,AUGPEN-300 INJ
7	RANTAC INJ,PYRIMOL INJ,Dany Ing.,MONOCEF 500 INJ
8	MIKACIN 250 INJ,MONOTAX SB 750 INJ
9	NIZONIDE-O SYP
10	ALLEGRA 120 TAB,CRITUS-XF SYP,SENSICLAV-625 TAB,DOLO-500 TAB

Table-1.

Time Comparison of Apriori and Eclate Algorithm

As a result of the experimental study,revealed the performance of Apriori and Eclat algorithm.The run time is the time to mine the frequent pattern.we have taken transaction 2063 and experiment is applied on 2000 transaction of hospital data with different support count result of time is shown in the figure-1 reveals that outperformance over Eclat Algoruthm.

A. Dataset

In tune with our application, we have taken a database of Hospital transaction of 633 items. In this analysis process we considered 2000 transactions in Horizontal Transaction format to generate the frequent pattern . In the horizontal Transaction each Transaction contain the multiple medicine in the single row.The horizontal Transaction view is Given below in Table 1.

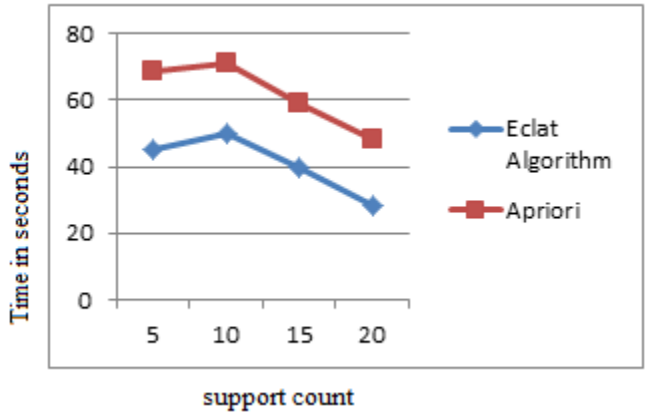

Fig-1:Execution Time Comparison on different support Count

Now The experimental is again applied on different size dataset with fixed support count 10 result of time is shown in the Fig-2 reveals that the Eclat performs better than Apriori

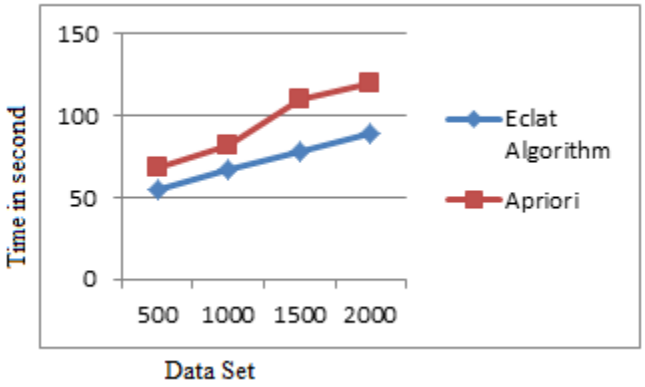

Fig-2:Execution Time comparison on different size of dataset

Conclusion

The association rules play a major role in many data mining applications, trying to find interesting patterns in data bases.Apriori is the simplest algorithm which is used for mining of frequent patterns from the transaction database. The main drawback of Apriori algorithm is that the candidate set generation is costly, especially if a large number of patterns and/or long patterns exist.Apriori algorithm uses large item set property, easy to implement, but it repeatedly scan the database. Apriori takes more time to scan the large Frequent patterns**.** The Eclat approach is used for efficient mining of frequent patterns in large databases. Eclat approach we use the intersection query and it is more efficient than apriori algorithm and also takes lesser time and gives better performance.

REFERENCES:

[1] Rahul Mishra, Abha choubey, Comparative Analysis of Apriori Algorithm and Frequent Pattern Algorithm for Frequent Pattern Mining in Web Log Data, (IJCSIT) International Journal of Computer Science and Information Technologies, Vol. 3 (4) , 2012

[2]Huiping peng “Discovery of Interesting Association Rules on Web Usage

Mini ng" 2010 International Conference.

[3] Agrawal R, Srikant R., "Fast Algorithms for Mining Association Rules",

VLDB. Sep 12-15 1994, Chile, 487-99, pdf, ISBN 1-55860-153-8.

[4] Paresh Tanna, Dr. Yogesh Ghodasara**,** Using Apriori with WEKA for Frequent Pattern Mining, (IJETT) – Volume 12 Number 3 - Jun 2014

[5]Agrawal, R., Imielinski, T., and Swami, A. N. 1993. Mining association rules between sets of items in large databases. In Proceedings of the 1993 ACM SIGMOD International Conference on Management of Data, 207-216

[6] C.Borgelt. "Efficient Implementations of Apriori and Eclat". In Proc. 1st IEEE ICDM Workshop on Frequent Item Set Mining Implementations, CEUR Workshop Proceedings 90, Aachen, Germany 2003.

[7] D.N. Goswami, Anshu Chaturvedi, C.S. Raghuvanshi. Frequent Pattern Mining Using Record Filter Approach. International Journal of Computer Science Issues. 2010; 7(4): 38–43. Available from: ijcsi.org/papers/7-4-7-38-43.pdf

[8] R. Agrawal and R. Srikant. Fast algorithms for mining association rules. IBM Research Report RJ9839, IBM Almaden Research Center, San Jose, California, June 1994.

[9] A. Amir, R. Feldman, and R. Kashi. A new and versatile method for association generation. Information Systems, 2:333–347, 1997.

[10] J. Park, M. Chen and Philip Yu, "*An Effective Hash-Based*

Algorithm for Mining Association Rules", Proceedings of ACM Special Interest Group of Management of Data, ACM SIGMOD'95, 1995.

[11] M. Zaki, S. Parthasarathy, M. Ogihara, and W. Li, "*New Algorithms for Fast Discovery of Association Rules*", Proc. 3rd ACM SIGKDD Int. Conf. on Knowledge Discovery and Data Mining (KDD'97, Newport Beach, CA), 283-296 AAAI Press, Menlo Park, CA, USA 1997

[12] Shruti Aggarwal, Ranveer Kaur, "*Comparative Study of Various Improved Versions of Apriori Algorithm*", International Journal of Engineering Trends and Technology (IJETT) - Volume4 Issue4- April 2013

[13] Adriano Veloso, Matthew Eric Otey, Srinivasan Parthasarathy, Wagner Meira Jr.; Parallel and Distributed Frequent Itemset Mining on Dynamic Datasets; Int'l Conf. on High Performance Computing; 2003.

[14] Haixun Wang, Wei Fan, Philip S. Yu, Jiawei Han; Mining Concept-Drifting Data Streams using Ensemble Classifiers; ACM SIGKDD Int'l Conf. on Knowledge Discovery and Data Mining; August 2003.

[15] Ran Wolff, Assaf Schuster; Association Rule Mining in Peer-to-Peer Systems; IEEE Transactions on Systems, Man and Cybernetics, Part B, Vol. 34, Issue 6; December 2004.

[16] Similarity Search using Concept Graphs, Rakesh Agrawal Sreenivas Gollapudi Anitha Kannan Krishnaram Kenthapadi

International Journal of Engineering Research and General Science Volume 3, Issue 5, September-October, 2015
ISSN 2091-2730

Otsu Segmentation Method for American Sign Language Recognition

Dr. Sana'a khudayer Jadwa

Computer Unit, College of Medicine

Al-Nahrain University

Baghdad- Iraq

E-mail: sanaakhudayer@yahoo.com

Abstract— Sign language recognition is a growing research area in the field of gesture recognition. Research on sign language recognition has been done around the world, using many sign languages. An accurate hand segmentation is the first and important step in sign language recognition systems. This paper proposed Otsu segmentation method that helps to build a better vision based sign language recognition system for its simplicity and efficiency. It is based on thresholding technique. It depends on selecting the optimal threshold value that maximizes the between-class variance of resulting object and background classes. This work is used to segment the signs representing the numbers from one to nine of the American Sign Language (ASL).The Experimental results demonstrate the effectiveness of this proposed method.

Keywords— Sign Language, Image segmentation, American Sign Language, Otsu Segmentation, ASL recognition, Image thresholding, Image processing

1. INTRODUCTION

Sign language (SL) is a visual-gestural language used by deaf and hard-hearing people. They use three dimensional spaces and the hand movements (and other parts of the body) to convey meanings. It has its own vocabulary and syntax which is entirely different from spoken and written languages [1]. Many countries have their own sign languages associated with their own grammars and rules. American Sign Language (ASL), British Sign Language (BSL), French Sign Language (LSF), and Indian Sign Language (ISL) [2]. Sign Language recognition system transfers the communication from human-human to human-computer interaction. The aim of the sign language recognition system is to present an efficient and accurate mechanism to transcribe text or speech, thus the "dialog communication" between the deaf and hearing person will be smooth[3]. Recognition of sign language is one of the major concerns for dump and deaf people. Sign language recognition is a research area involving pattern recognition, computer vision, natural language processing. Sign language recognition is a comprehensive problem because of the complexity of the visual analysis of hand gesture and the highly structured nature of sign language. As well as it is considered as a very important function in many practical communication applications, such as sign language understanding, entertainment, and human computer interaction (HCI) [4]. Hand Segmentation is the part of computer vision based natural human computer interaction. Hand tracking and segmentation are the primary steps for any hand gesture recognition system. Survey and sign language study shows that from various gesture communications modality, the hand gesture is most easy and natural way of communication [5]. An accurate face and hand segmentation is the first and important step in sign language recognition systems. Segmentation and detection of hand and face reduce processing time and increase precision of recognizing postures in sign language recognition systems [1]. Good segmentation process leads to perfect features extraction process and the later play an important role in a successful recognition process [6]. In this paper, an Otsu thresholdindg segmentation method is proposed for ASL gesture recognition. The remainder of this paper is organized as follows. Section 2 highlights the related works. Section 3 introduces American Sign Language concept. Section 4 describes the Otsu Segmentation algorithm. Section 5 presents the proposed method. Section 6 provides the experimental results. Finally, the paper is concluded in section 7.

2.RELATED WORK

Research in sign language recognition started to appear in literature at the beginning of 1990s [7]. **Neha et al.** [8] presented a methodology which recognizes the Indian Sign Language (ISL) and translates into a normal text. Skin color segmentation is performed using k-means clustering method. **Sumaira K. et al.** [9] introduced a fuzzy classifier to recognize Pakistani Sign Language (PSL). Marked color glove has been used to segment hand and then these marks are also used to extract features to be used by the classifier to recognize sign. **Xu Zhang et al**.[10] presented a framework for Chinese Sign Language (CSL)recognition based on the information fusion of a three-axis accelerometer (ACC) and multichannel electromyography (EMG) sensors using the active segments. **Cao Dong, Ming C. Leu**[11] employed a per-pixel classification method that was adapted to segment the hand into parts. The input of this process was the depth image of the hand region, and the output was the classification label of each pixel. **Divya S and Kiruthika** [12] developed a design for a SLR (sign language recognition) system computerizes the work of a sign language translator, the image is segmented using skin colour based on HSV, RGB and YCbCr Colour spaces.

3. AMERICAN SIGN LANGUAGE

ASL is a complete, complex language that employs signs made with the hands and other movements, including facial expressions and postures of the body. It is the first language of many deaf North Americans, and one of several communication options available to deaf people. ASL is said to be the fourth most commonly used language. American Sign Language is a unique system of communication because it is both a visual language and manual language. Instead of expressing himself through sound, a speaker using ASL employs a combination of facial expressions, body language, gestures, palm orientations, and hand shapes.[13] ASL consists of about 6,000 signs for representing the commonly used words, most of signs in ASL could be considered as a combination of 36 basic hand shapes. These 36 hand shapes include most of ASL alphabets and their variations. Therefore, the recognition of ASL alphabets is not only important for spelling a person's name and the words which are not in the ASL vocabulary, but vital for further research on word and sentence recognition[7]. Figure (1) show an example of ASL alphabets:

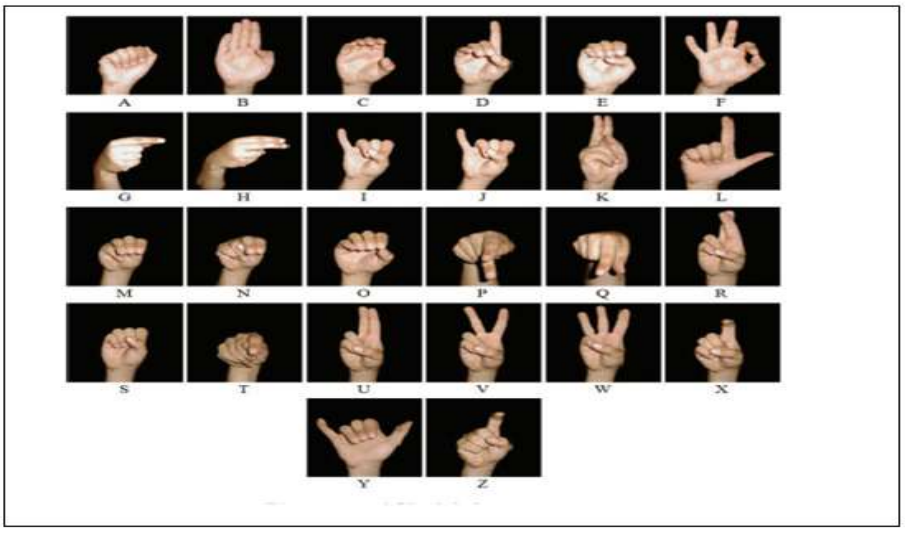

Figure (1): American sign language alphabets.

4. OTSU SEGMENTATION ALGORITHM

Image segmentation is one of the most fundamental and difficult problems in image analysis. Image segmentation is an important part in image processing. In computer vision, image segmentation is the process of partitioning an image into meaningful regions or objects[14]. Among all the segmentation methods, Otsu method is one of the most successful methods for image thresholding because of its simple calculation. Otsu's method [15] is one of the most popular methods for its simplicity and efficiency. It is based in thresholding technique. It depends on selecting the optimal threshold value that maximizes the between-class variance of resulting object and background classes. The search for the optimal threshold done sequentially until finding a value that makes variance between two classes or more maximum[16]. Otsu method is type of global thresholding in which it depend only gray value of the image. Otsu method is global thresholding selection method, which is widely used because it is simple and effective . Otsu is an

automatic threshold selection region based segmentation method .The Otsu method requires computing a gray level histogram before running [14]. Otsu's thresholding method based on a simple idea. Find the threshold that minimizes the weighted within-class variance. This turns out to be the same as maximizing the between-class variance. Assumptions for OTSU's method:

• Histogram (and the image) is bimodal.
• No usage of spatial coherence, nor other notion of object structure.
• Assumes stationary statistics, but can be altered to be locally adaptive.[17]

Suppose the intensity of a gray level image be expressed in L gray levels [1,2,...,L] the number of points with gray level at i is denoted by x_i and the entire number of points can be expressed as $X = x_1 + x_2 + \cdots + x_L$. The histogram of this gray –level image is regarded as a occurrence distribution of probability :

$p(i) = \frac{x_i}{X}$, $x_i \geq 0$, $\sum_{i=1}^{L} x_i = 1$ ……(1)

The image pixels are divided into two parts C0 and C1 , i.e. foreground and background by a threshold t. Where C0 represents pixels within levels [1,2,...,t] , and C 1 denotes pixels within levels [t+1,..., L].The occurrence probabilities of this class and average can be expressed as respectively[16] :

$w_0 = w(t) = \sum_{i=1}^{t} p(i)$ ……..(2)

$w_1 = 1 - w(t) = \sum_{i=t+1}^{L} p(i)$ ……(3)

$\mu_0 = \sum_{i=1}^{t} \frac{i.p(i)}{w_0} = \frac{1}{w(t)} \sum_{i=}^{t} i.p(i)$ ……(4)

$\mu_1 = \sum_{i=t+1}^{L} \frac{i.p(i)}{w_1} = \frac{1}{1-w(t)} \sum_{i=t+1}^{L} i.p(i)$ …… (5)

Total mean can be written as :

$\mu_T = \sum_{i=1}^{L} i.p(i)$ ……..(6)

And then :

$\mu_T = w_0 \mu_0 + w_1 \mu_1$ ……..(7)

Where w_0 and w_1 denote probabilities of foreground part and background part .Besides, μ_0 , μ_1 refer to the mean in gray levels of the foreground of the gray image, the background of the gray image and the entire gray of level image.The between-class variance σ_B^2 of the C0 and C1 is given by :

$\sigma_B^2 = w_0 (\mu_0 - \mu_T)^2 + w_1 (\mu_1 - \mu_T)^2$ .... (8)

The separable degree η of the class, in the discrimination analysis , is

$\eta = \max_{1 \leq t \leq L} \sigma_B^2$ ……(9)

Finally, maximizing σ_B^2 to choose the optimal threshold t^*

$t^* = \arg \max_{1 \leq t \leq L} \sigma_B^2$ …….. (10)

5. PROPOSED METHOD

The proposed method consists of four stages which include reading image from the database that contains some of ASL signs, image resizing, color space conversion, and then applying Otsu algorithm. The general architecture of the proposed Otsu segmentation method is shown below in figure(2):

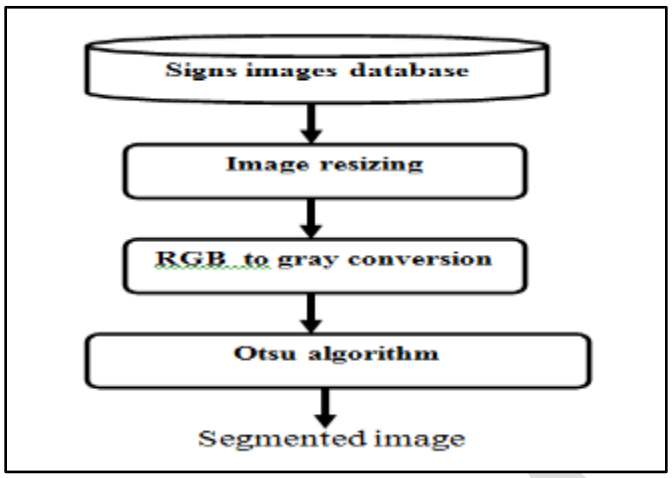

Figure (2): Architecture of the proposed method

5.1 IMAGE DATABASE

In this work, the ASL signs were used for image segmentation purpose. The database consists of nine RGB images for ASL signs that representing the numbers from one to nine which is collect from the web. The images with the same size have the dimensions (320 x320) pixels. Figure (3) show the database images:

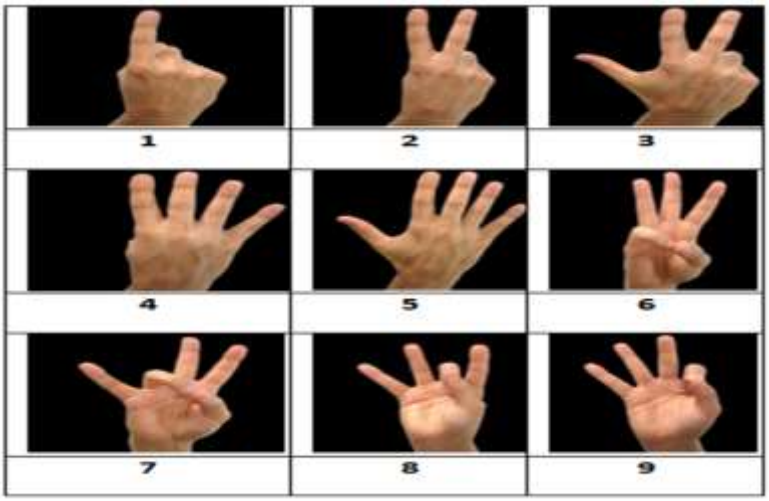

Figure (3): ASL numbers from one to nine.

5.2 IMAGE RESIZING

The input image is first resized into the size of (200 x 200) pixels. Image resizing is done to reduce the processing time by the computer and allowing algorithm for better performance.

5.3 COLOR SPACE CONVERSION

The images are converted to gray scale image thus removing all color
information, leaving only the luminance of each pixel using equation (11). The gray scale image has the gray level intensity ranging from 0 to 255.

$$y = 0.2989 * R + 0.5870 * G + 0.1140 * B \quad \ldots\ldots\ldots\ldots\ldots\ldots(11)$$

5.4 OTSU ALGORITHM

The steps of the OTSU algorithm: For each potential threshold T,

1. Separate the pixels into two clusters according to the threshold.
2. Find the mean of each cluster.
3. Square the difference between the means.
4. Multiply by the number of pixels in one cluster times the number in the other.[18].

6. EXPERIMENTAL RESULTS

The experiments of the proposed Otsu segmentation method are implemented on Intel Core i7-2330M CPU, 2.20 GHz with 2 GB RAM under Matlab environment and a Windows 8 platform. At first the color sign image is reading from the database then it resized .The RGB resizing image is converted to grayscale as shown in figure (4):

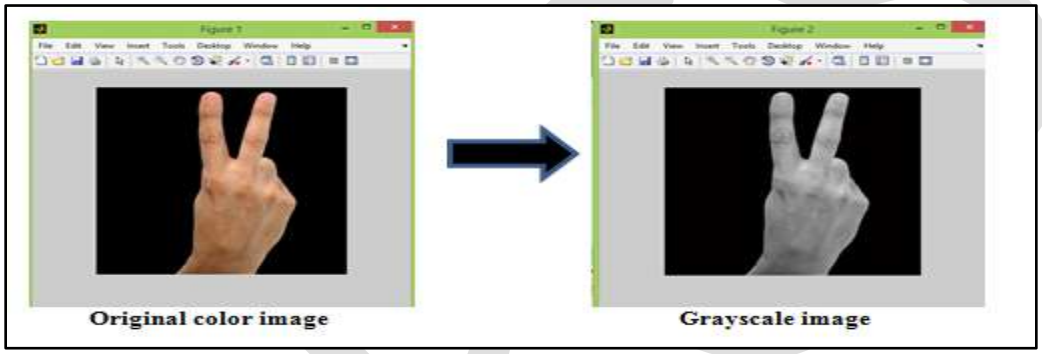

Figure (4): Colored Image conversion.

Then the Otsu segmentation algorithm is applied on grayscale image to obtain the segmented image as show in figure (5):

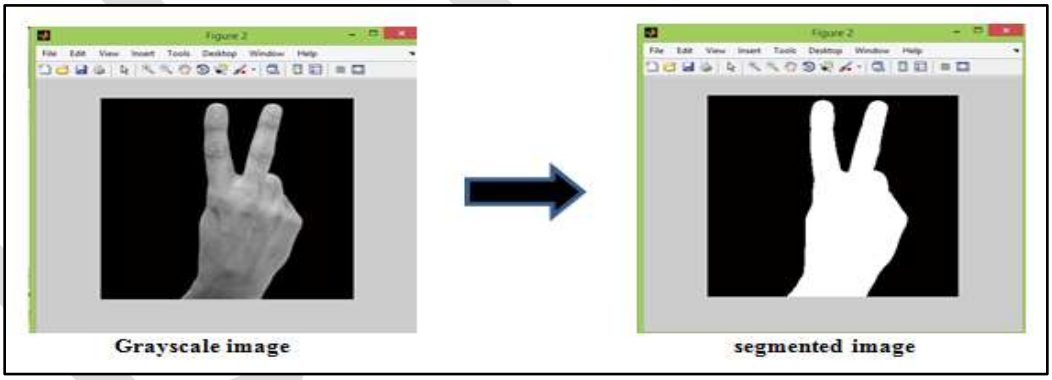

Figure (5): Otsu segmentation algorithm result

The same steps applied for the rest images given the result as shown in figure (6):

Original sign image	Grayscale image	Segmented image

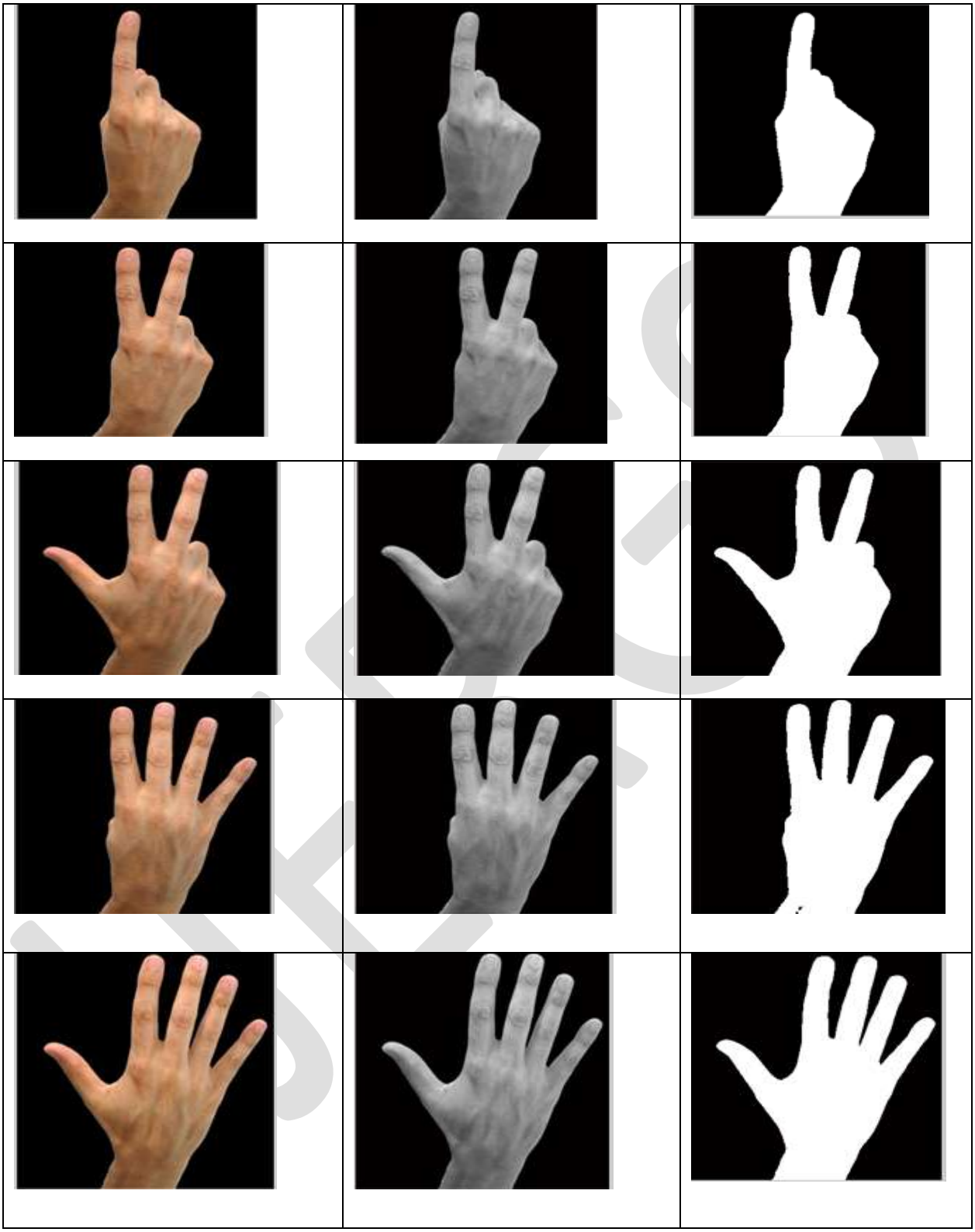

Figure(6): Results of Otsu segmented algorithm for signs numbers from one to five.

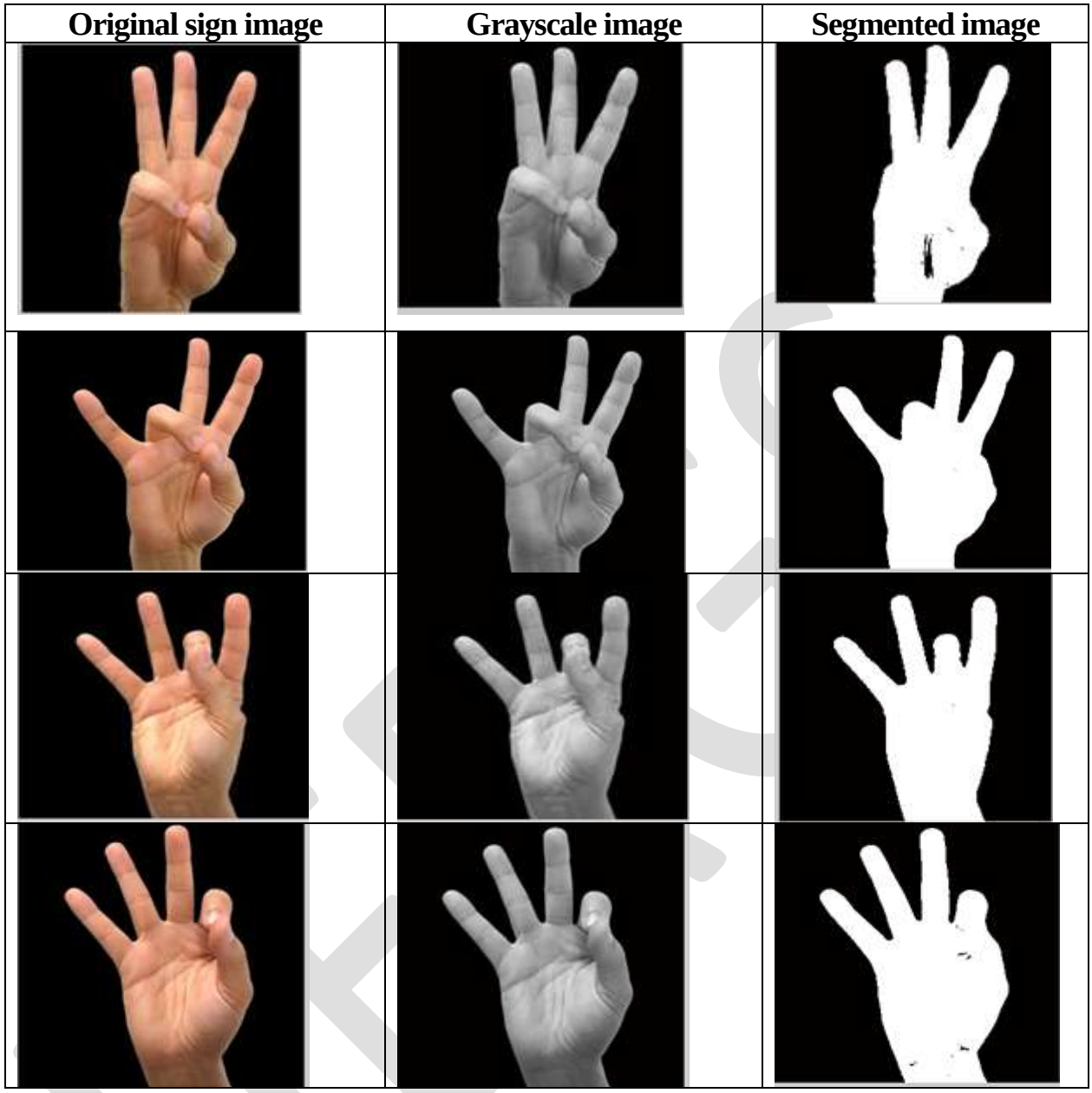

Figure(6): continued -Results of Otsu segmented algorithm for signs numbers from six to nine

7. CONCLUSION

Image segmentation is often used to distinguish the foreground from the background. In this paper, the Otsu thresholding method has been proposed for ASL sign image segmentation. This method is robust, fast and very easy to implement and produces suitable binary images, which can be used in further processing stages such as feature extraction and recognition. The Otsu method is very efficient method to threshold the gray images. The experimental results show that the proposed Otsu threshold method can be obtained easily with a better result of image segmentation.

REFERENCES:

[1] Madhuri Sharma, Ranjna Pal and Ashok Kumar Sahoo, "Indian Sign Language Recognition using Neural Network and KNN Classifiers", ARPN Journal of Engineering and Applied Sciences , vol. 9, No. 8, August 2014.

[2] Rohit Sharma, Yash Nemani, Sumit Kumar, Lalit Kane, Pritee Khanna,Member,IAENG,"Recognition of Single Handed Sign Language Gestures using Contour Tracing Descriptor" , Proceedings of the World Congress on Engineering Vol II, July , 2013.

[3] Neha S. Chourasia, Kanchan Dhote, Supratim Saha , "Analysis on Hand Gesture Spotting using Sign Language through Computer Interfacing", International Journal of Engineering Science and Innovative Technology (IJESIT) Volume 3, Issue 3, May 2014.

[4] Jayashree R. Pansare, Shravan H. Gawande, Maya Ingle ," Real-Time Static Hand Gesture Recognition for American Sign Language (ASL) in Complex Background",Journal of Signal and Information Processing, 2012.

[5] Sunita Patidar, Dr. C.S.Satsangi, "Hand Segmentation and Tracking Technique using Color Models", International Journal of Software & Hardware Research in Engineerin Volume(1)Issue(2),October ,2013.

[6] Neha V. Tavari, Prof. A. V. Deorankar, "Indian Sign Language Recognition based on Histograms of Oriented Gradient", International Journal of Computer Science and Information Technologies, Vol. 5 , 2014.

[7] Honggang Wang, Ming. Leu and Cemil OZ, "American Sign Language Recognition Using Multi-dimensional Hidden Markov Models*", Journal of Information Science and EngineeringG , (2006) .

[8] Neha S. Chourasia, Kanchan Dhote, Supratim Saha ,"Analysis on Hand Gesture Spotting using Sign Language through Computer Interfacing", International Journal of Engineering Science and Innovative Technology (IJESIT) Volume 3, Issue 3, May 2014.

[9] S. Kausar, M. Y. Javed, and S. Sohail, "Recognition of Gestures in Pakistani Sign Language using Fuzzy Classifier," in Proc. the 8th International Conference on Signal Processing, Computational Geometry and Artificial Vision, Greece, 2008.

[10] Xu Zhang, Xiang Chen, Associate Member, IEEE, Yun Li, Vuokko Lantz, Kongqiao Wang, and Jihai Yang, "A Framework for Hand Gesture Recognition Based on Accelerometer and EMG Sensors",IEEE Transactions On Systems, Man, And Cybernetics ,PART A: Systems and Humans, Vol. 41, No. 6, November, 2011.

[11] Cao Dong, Ming C. Leu and Zhaozheng Yin, "American Sign Language Alphabet Recognition Using Microsoft Kinect", IEEE,Computer Vision Foundation , 2015.

[12] Divya S , Kiruthika ,S Nivin Anton A L and Padmavathi S," Segmentation, Tracking And Feature ExtractionFor Indian Sign Language Recognition", International Journal on Computational Sciences & Applications (IJCSA) Vol.4, No.2, April 2014.

[13] Prof.Sayyad T.J. "Recognition of ASL using Hand Gestures", International Journal of Emerging Trends & Technology in Computer Science (IJETTCS), Volume 2, Issue 5, September – October ,2013.

[14] Miss Hetal J. Vala, Prof. Astha Baxi " A Review on Otsu Image Segmentation Algorithm", International Journal of Advanced Research in Computer Engineering & Technology (IJARCET) Volume 2, Issue 2, February 2013.

[15] Otsu N., "A threshold selection method from gray-level histogram," IEEE Trans. On System Man Cybernetics, 1979, Vol. 9, No. 1, pp. 62- 66.

[16] Ali El-Zaart and Ali A.Ghosn, " MRI Images Thresholding For Alzheimer Detection",", International Journal of Computer Science & Information Technology (CS & IT),2013.

[17] D. Palani , K. Venkatalakshmi,E. Venkatraman," Implementation & Comparison Of Different Segmentation Algorithms For Medical Imaging" , International Journal of Innovative Research in Science, Engineering and Technology Volume 3, Special Issue 3, March 2014.

[18] Y.Ramadevi, T.Sridevi, B.Poornima, B.Kalyani, " Segmentation and Object Recognition Using Edge Detection Techniques", International Journal of Computer Science & Information Technology (IJCSIT), Vol 2, No 6, December 2010.

International Journal of Engineering Research and General Science Volume 3, Issue 5, September-October, 2015
ISSN 2091-2730

Criticality Factor of Modules with the Application of Modified Neighborhood Integration Testing and Initiating Build Testing

Dr. Namita Gupta[1], Nitesh Goyal[2]

1 Head of Department, Computer Science Engineering, Maharaja Agrasen Institute of Technology, Rohini, Delhi - 110086, India

2 Student, Computer Science Engineering, Maharaja Agrasen Institute of Technology, Rohini, Delhi - 110086, India

(me.niteshgoyal@gmail.com, +919310345131, +919599944144)

Abstract— Software testing is the process used to measure the quality of developed computer software. It is done to find all the bugs, flaws, broken paths, stray components etc. in a given program or software. The initial step of doing software testing includes testing the most critical module of all, so that main body of software is tested first. In this paper the technique of finding the most critical module of all depending on functional dependency is being discussed with the initiation of build testing.

Keywords— Software Testing, Software Module, Module Criticality, Structural Testing, Integration Testing, Build Testing and Call Graph.

INTRODUCTION

Software testing is an art of finding flaws, bugs and causes of errors in a given software.
The software testing is must as most of the machines work on a computer algorithm and if any bug or flaw occurs in this algorithm the results may be catastrophic. Testing enhances the quality of a given software. Before initiating testing process, several test cases or constraints are defined on the given software, on the basis of which best testing technique is chosen. Without declaring these constraints the tester cannot decide what kind of testing is being needed in a specific software.
The test cases must include the following information:

The Input Information: a) Preconditions, it includes the information of circumstances hold prior to test case execution.
b) The actual inputs identified by some *Testing Method*.

The Output Information: a) Postconditions, it includes information of circumstances that need to be satisfied after the execution, like, number of outputs should be finite.
b) Actual outputs identified by some *Testing Method*.

Different testing techniques are available to generate the test cases based on software code complexity to be tested. Two fundamental approaches used to determine the test cases are – *Functional Testing and Structural Testing.*
*Functional Testing c*onsider software as function which will give an output for some given input or as a software which is generating a set of outputs (range) for set of inputs (domain). In this approach, the code of software is considered as *Black Box* which is generating a set of outputs for the entered input. If the output is not as per the requirements (constraints on software) than it is considered to contain bug(s), which needs to be rectified.
Structural Testing considers the structure/ internal logic of the software to find the bugs. That is why it is also termed as *White Box Testing*. The approach helps to detect defects like linking bugs, missing statements, unused code fragments and many more.

Process of testing starts in parallel to first phase of Software development life cycle (SDLC). Test cases are generated considering the user's requirements collected during requirement gathering phase of SDLC. This is called static testing. Similarly, different testing techniques are available to test the activities performed at design phase. Various black-box and white-box testing techniques are used to test each and every module implemented during the coding phase of SDLC. Then Integration testing is performed to test the interface between the individual modules. *Call Graph based Neighbourhood Integration Testing* is one of the integration testing technique used to detect the interface errors between the modules. In this technique, call graph showing all the modules of software is drawn.
Call Graph is basically a directed graph, which represents the links between modules, that is, it represents the directed link(s) between software modules telling the tester that which module(s) is/are being called by a particular module. The internal structure of the software is clearly represented by a call graph.

For example, here the modules are represented as nodes (numbered from 1 to 11) and the arrows represent the links between the different software modules as per the module calls made by them. The obtained structure forms a *call graph.*

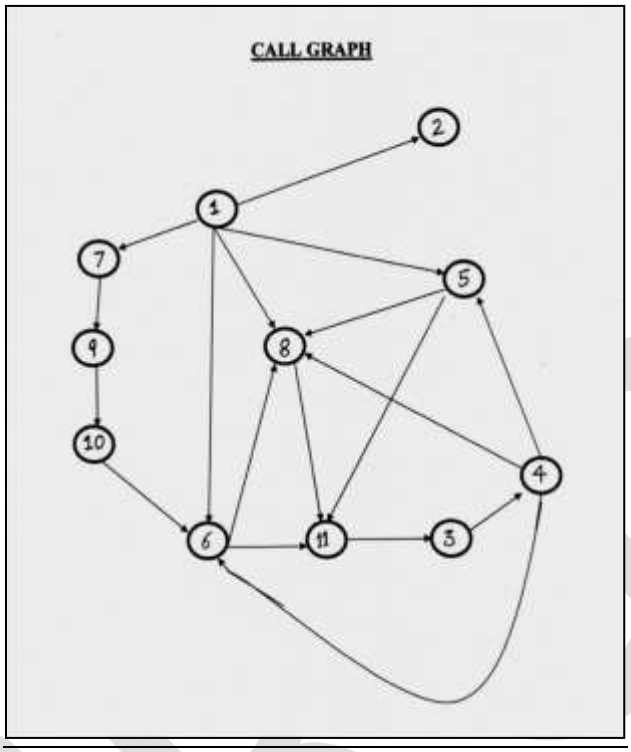

Fig. 1
The call graph of a BANK system.

Neighbourhood Integration Testing considers the neighbour modules of each and every software module represented as nodes in call graph. Topmost module in call graph with zero indegree is termed as root node, all modules having outdegree zero are termed l*eaf nodes*, and the modules being called are termed as *Successors, and* modules calling some other modules are termed *Predecessors.*
The biggest *advantage* of using this technique is that it reduces the number of test cases thus saving testing time.
But, the technique also has some disadvantages mention below:

1. If a node (module) that has been repeated most of the numbers of times and it is found that it has some error in that case the whole process need to be repeated again from the very starting for all the neighbourhoods related to that faulty node (module).
2. The modules are being checked only from its outer cover, but a lot depends on the internal threads also of those individual modules.

To overcome the above two disadvantages of call graph based neighbourhood integration testing, in this paper a new integration testing technique called "*Friend Integration testing*" is proposed. This new technique identifies the friends or (neighbours) of each node of call graph, including the root and the leave nodes and then identifies the most critical nodes to be tested based on the criticality which is discussed in next section.

PROPOSED FRIEND INTEGRATION TESTING TECHNIQUE

Software containing multiple integrated modules interface with each other and exchange necessary information among themselves to accomplish the required functionality as documented in user's specification document.
Due to time constraint, testing each and every module is not possible. Hence build testing is used to test the modules in different builds, each build containing modules of same criticality. Criticality of a module is determined based on its interaction with other modules of the same software. Module with highest indegree and outdegree is the most critical node as any defect in that module has direct impact on its calling and called modules.

Proposed *Friend* technique determines the criticality of each module using the formula given below:

$$C = \frac{Module\ (Successores)}{Graph\ (Successors)} \quad ; such\ that\ 0 \leq C \leq 1$$

Module (Predecessors) = Number of modules calling the i^{th} module
Module (Successors) = Number of modules being called by i^{th} module
Graph (Successors) = ΣModule (Successors), where indegree ≠0

Builds are created based on the following observations:

1. If Criticality Factor (C) of two modules M1 and M2 shows same value, then
   If Module M1 (Predecessor) > Module M2 (Predecessor) then
   Module M1 is considered more critical than module M2.
   Reason - Higher the number of predecessors more the module is being called by other modules. Thus higher the *Criticality Factor.*

2. If M1(Successors) == M2(Successors) and
   M1 (Predecessor) == Module M2 (Predecessor) then
   Compute the path length from root node to M1 and M2 using *Breath First Search (BFS) method.*
   Module with smaller path length is considered more critical.

   Reason –*main()* module is the most critical module of any software and Module near to Main module affects it more as compared to module far from Main module.

3. Modules showing same value of *Criticality Factor (C)* are kept in same build.

4. Module(s) are tested in decreasing order of their criticality factor values.

CASE STUDIES

CASE STUDY 1

Taking in account the example of BANK System.

The *BANK System* represents the minimal features that a bank constitutes. A user can see the bank branch, set up a new account, account number will be generated automatically on which user sets a password, and the deposit or withdrawal of money can be done with user login only. The balance of the account can be seen, every time, after any action on the user account take place.

Modules are:

MODULE NUMBERS	MODULES
1	main() *//Main function*
2	branch() *//Tell branch of bank*
3	get_password() *//Password of specific account.*

4	check_password ()	*//Password verification.*
5	withdraw()	*//Withdraw money from bank*
6	deposit()	*//Deposit money in bank*
7	new_account ()	*//Creating new account.*
8	balance()	*//Display balance of the account*
9	generate_ac_no ()	*//Generating account number for new account.*
10	set_password()	*//Creating new password*
11	ac_no()	*//Taking account number of existing account.*

Table 1
Layout of BANK system.

(The call graph for BANK System is given in Fig 1)

MODULE NUMBERS	MODULE PREDECESSORS	MODULE SUCCESSORS
1	-	2, 5, 6, 7, 8
2	1	-
3	11	4
4	3	5, 6, 8
5	1, 4	8, 11
6	1, 10	8, 11
7	1	9
8	1, 4, 5, 6	11
9	7	10
10	9	6
11	5, 6, 8	3

TABLE 2
Friends of nodes in Bank System

Criticality Factor of modules using the formula —

$$C = \frac{Module\ (Successores)}{Graph\ (Successors)} \quad ; such\ that\ 0 \leq C \leq 1$$

Module (Predecessors) = Number of modules calling the i^{th} module
Module (Successors) = Number of modules being called by i^{th} module
Graph (Successors) = ΣModule (Successors), where indegree ≠0

Using Table 2 Graph (Successors) = **18**.

1. For Module 1(From Table 2)

Module (Successors) = **5** ≡ (2, 5, 6, 7, 8 are the Module Successors)
The Criticality Factor for Module 1 using the above formula is calculated as follows:

$\mathbf{C_1 = \frac{5}{18} = 0.28}$

2. For Module 2(From Table 2)

   Module (Successors) = **0** ≡ (No Module Successors)
   The Criticality Factor for Module 2 using the above formula is calculated as follows:

   $\mathbf{C_2 = \frac{0}{18} = 0}$

3. For Module 3(From Table 2)

   Module (Successors) = **1** ≡ (4 is the Module Successor)
   The Criticality Factor for Module 3 using the above formula is calculated as follows:

   $\mathbf{C_3 = \frac{1}{18} = 0.056}$

4. For Module 4(From Table 2)

   Module (Successors) = **3** ≡ (5, 6, 8 are the Module Successors)
   The Criticality Factor for Module 4 using the above formula is calculated as follows:

   $\mathbf{C_4 = \frac{3}{18} = 0.167}$

5. For Module 5(From Table 2)

   Module (Successors) = **2** ≡ (8, 11 are the Module Successors)
   The Criticality Factor for Module 5 using the above formula is calculated as follows:

   $\mathbf{C_5 = \frac{2}{18} = 0.111}$

6. For Module 6(From Table 2)

   Module (Successors) = **2** ≡ (8, 11 are the Module Successors)
   The Criticality Factor for Module 6 using the above formula is calculated as follows:

   $\mathbf{C_6 = \frac{2}{18} = 0.111}$

7. For Module 7(From Table 2)

   Module (Successors) = **1** ≡ (9 is the Module Successor)
   The Criticality Factor for Module 7 using the above formula is calculated as follows:

   $\mathbf{C_7 = \frac{1}{18} = 0.056}$

8. For Module 8(From Table 2)

   Module (Successors) = **1** ≡ (11 is the Module Successor)
   The Criticality Factor for Module 8 using the above formula is calculated as follows:

   $\mathbf{C_8 = \frac{1}{18} = 0.056}$

9. For Module 9(From Table 2)

   Module (Successors) = **1** ≡ (10 is the Module Successor)

The Criticality Factor for Module 9 using the above formula is calculated as follows:

$$\mathbf{C_9 = \frac{1}{18} = 0.056}$$

10. For Module 10(From Table 2)

Module (Successors) = **1** ≡ (6 is the Module Successor)
The Criticality Factor for Module 10 using the above formula is calculated as follows:

$$\mathbf{C_{10} = \frac{1}{18} = 0.056}$$

11. For Module 11(From Table 2)

Module (Successors) = **1** ≡ (3 is the Module Successor)
The Criticality Factor for Module 11 using the above formula is calculated as follows:

$$\mathbf{C_{11} = \frac{1}{18} = 0.056}$$

The table of Criticality Factor of Modules for BANK System is:

MODULE NUMBERS	CRITICALITY FACTOR
1	0.28
2	0
3	0.056
4	0.167
5	0.111
6	0.111
7	0.056
8	0.056
9	0.056
10	0.056
11	0.056

Table 3
Criticality factor of modules of BANK system using Formula 1

Step 1:

If Criticality Factor (C) of two modules M1 and M2 shows same value, then
If Module M1 (Predecessor) > Module M2 (Predecessor) then
Module M1 is considered more critical than module M2.

The modules (5, 6) and (3, 7, 8, 9, 10, 11) have the same Criticality Factor, based on given rule the criticality of modules is:
N5 = N6
N8 > N11 > (N3 =N7 = N9 = N10)

Step 2:

If M1 (Successors) == M2 (Successors) and
M1 (Predecessor) == Module M2 (Predecessor) then
Compute the path length from root node to M1 and M2 using *Breath First Search (BFS) method.*
Module with smaller path length is considered more critical.

There is ambiguity in modules (5, 6) and (3, 7, 9, 10), following above rule:

By applying BFS the results is:
Path for N5 = **N1 -> N5**
Path for N6 = **N1 -> N6**
Path for N3 = **N1 -> N8 -> N11 ->N3**
Path for N7 = **N1 -> N7**
Path for N9 = **N1 -> N7 -> N9**
Path for N10 = **N1 -> N7 -> N9 -> N10**

From above observation the criticality of modules is:
N5 = N6
N7 > N9 > N10 = N3

Step 3:

Modules showing same value of C are kept in same build.

Distinction in the criticality of modules N3, N10 **and N5, N6** cannot be made, following above rule the criticality of all the modules is:

N1 > N4 > N5 = N6 > N8 > N11 > N7 > N9 > N10 = N3 > N2

Step 4:

Module(s) are tested in decreasing order of their criticality factor values.

Using above rule, the builds are:
Build 1 = N1
Build 2 = N4
Build 3 = N5, N6
Build 4 = N8
Build 5 = N11
Build 6 = N7
Build 7 = N9
Build 8 = N10, N3
Build 9 = N2

Each build will contain more than one modules (in most of the cases) if a more complex software system (containing many modules) is taken into account.
The build testing can now be applied to these builds which tell the tester that the given system can be tested further or not, that is, whether the given system is of any use or not.

CASE STUDY 2

Taking in account the example of User Data Storage Device (UDSD) System

The *User Data Storage Device (UDSD) System* represents the minimal features of user data storage device. User can load new data on storage device, update the existing data (data on storage device), and can directly load the network data (user data taken directly from internet). Using the network data user can access the E-Mails or other relevant data. The user data is automatically processed after every action on the storage media take place. At the end user can exit from the system.

Modules are:

MODULE NUMBERS	MODULES	
1	Main()	//main function
2	Load_user_data()	//loads user data
3	Process()	//processes user data
4	Done()	//display message processing is done
5	Mark_read()	//marks read when data is read by device
6	Get_sms_email()	//takes sms/email from internet()
7	Update_data()	//updates user data
8	Load_network_data()	//load data from the internet
9	Exit()	//exits from program

TABLE 4
Layout of User Data Storage Device (UDSD) System

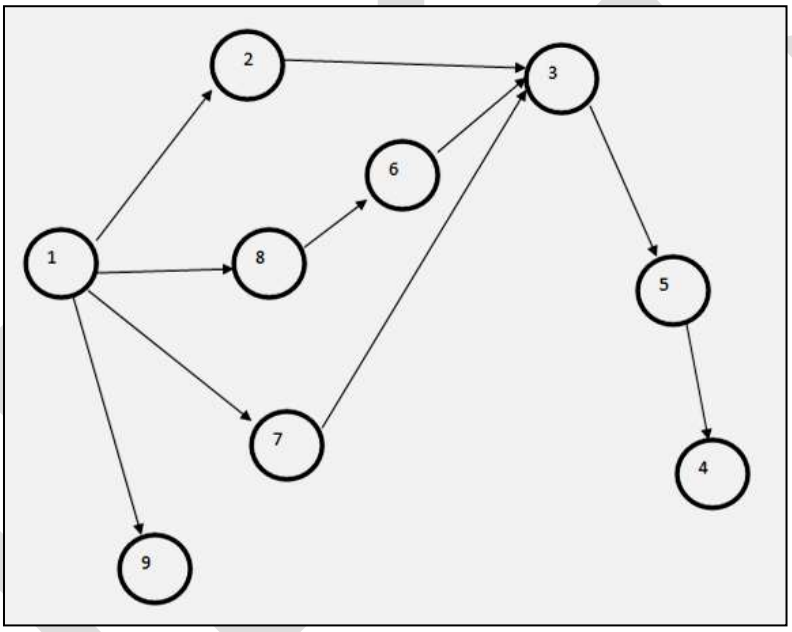

FIG 2
Call graph of User Data Storage Device (UDSD) System

MODULE NUMBERS	MODULE PREDECESSORS	MODULE SUCCESSORS
1	-	2, 7, 8, 9
2	1	3
3	2, 6, 7	5
4	5	-
5	3	4
6	8	3
7	1	3
8	1	6
9	1	-

TABLE 5
Friends of nodes in UDSD System

Criticality Factor of modules using the formula —

$$C = \frac{Module\ (Successores)}{Graph\ (Successors)} \quad ; such\ that\ 0 \leq C \leq 1$$

Module (Predecessors) = Number of modules calling the i^{th} module
Module (Successors) = Number of modules being called by i^{th} module
Graph (Successors) = ΣModule (Successors), where indegree ≠0

Using Table 5, *Graph (Successors)* = **10**
The table of Criticality Factor of Modules for UDSD System is:

MODULE NUMBERS	CRITICALITY FACTOR
1	0.4
2	0.1
3	0.1
4	0
5	0.1
6	0.1
7	0.1
8	0.1
9	0

TABLE 6
Criticality factor of modules of UDSD system using Formula 1

Step 1:

If Criticality Factor (C) of two modules M1 and M2 shows same value, then
If Module M1 (Predecessor) > Module M2 (Predecessor) then
Module M1 is considered more critical than module M2.

The modules (4, 9) and (2, 3, 5, 6, 7, 8) have the same Criticality Factor, based on given rule the criticality of modules is:
N4 = N9
N3 > N5 = N6 = N7 = N8

Step 2:

If M1 (Successors) == M2 (Successors) and
M1 (Predecessor) == Module M2 (Predecessor) then
Compute the path length from root node to M1 and M2 using *Breath First Search (BFS) method.*
Module with smaller path length is considered more critical.

There is ambiguity in modules (4, 9) and (2, 5, 6, 7, 8), following the above rule:
By applying BFS the result is:
Path for N4 = **N1 -> N2 -> N3 -> N5 -> N4**
Path for N9 = **N1 -> N9**
Path for N2 = **N1 -> N2**

Path for N5= **N1 -> N2 -> N3 -> N5**
Path for N6 = **N1 ->N8 -> N6**
Path for N7 = **N1 -> N7**
Path for N8 = **N1 -> N8**

From above observation the criticality of modules is:
N9 > N4
N2 = N7 = N8 > N6 > N5

Step 3:

Modules showing same value of C are kept in same build.

Distinction in the criticality of modules N2**, N7, N8** cannot be made, following above rule the criticality of all the modules is:

N1 > N3 > N2 = N7 =N8 > N6 > N5 > N9 > N4

Step 4:

Module(s) are tested in decreasing order of their criticality factor values.

Using above rule, the builds are:
Build 1 = N1
Build 2 = N3
Build 3 = N2, N7, N8
Build 4 = N6
Build 5 = N5
Build 6 = N9
Build 7 = N4

The build testing can now be applied to these builds which tell the tester that the given system can be tested further or not, that is, whether the given system is of any use or not.

CASE STUDY 3

Taking in account the example of Movie Theatre System

The *Movie Theatre System* represents the minimal features of a movie theatre. User can choose the movie of the choice, can book required number of seats as per the luxury (only if seats are available in asked slot), and can buy food items. The tickets will be printed automatically with a bill signifying total payable amount to user.

Modules are:

MODULE NUMBERS	MODULES	
1	Main()	*//Main function*
2	Movie1()	*//Movie name*
3	Movie2()	*//Movie name*
4	Movie3()	*//Movie name*
5	Movie4()	*//Movie name*
6	Number_of_seats()	*//Number seats chosen*

7	Type_of_seats()	*//Type of seats (diamond, gold, silver, etc.)*
8	Payable_amount()	*//Total payable amount*
9	Food()	*//Food bought*
10	Print_bill()	*//Print bill*
11	Print_ticket()	*//Print movie tickets*

TABLE 7
Layout of Movie Theatre System

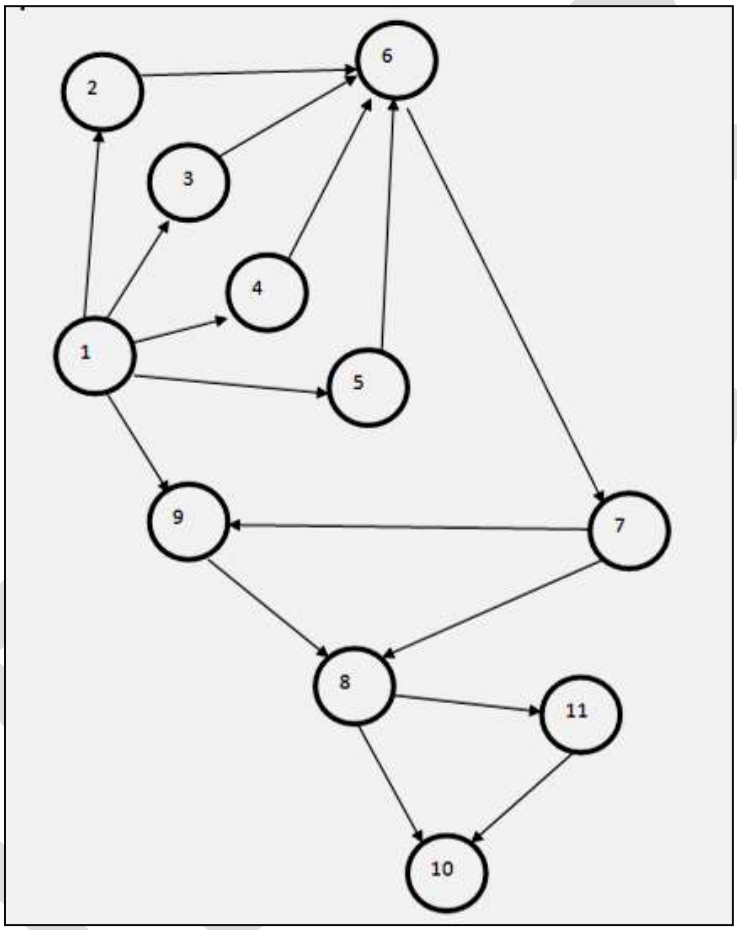

FIG 3
Call graph of User Data Storage Device (UDSD) System

MODULE NUMBERS	MODULE PREDECESSORS	MODULE SUCCESSORS
1	-	2, 3, 4, 5, 9
2	1	6
3	1	6
4	1	6
5	1	6
6	2, 3, 4, 5	7
7	6	8, 9
8	7, 9	10, 11
9	1, 7	8
10	10, 11	-

11	8	10

TABLE 8
Friends of nodes in Movie Theatre System

Criticality Factor of modules using the formula—

$$C = \frac{Module\ (Successores)}{Graph\ (Successors)} \quad ; such\ that\ 0 \leq C \leq 1$$

Module (Predecessors) = Number of modules calling the i^{th} module
Module (Successors) = Number of modules being called by i^{th} module
Graph (Successors) = ΣModule (Successors), where indegree ≠0

Using Table 8, *Graph (Successors)* = **16**
The table of Criticality Factor of Modules for Movie Theatre System is:

MODULE NUMBERS	CRITICALITY FACTOR
1	0.3125
2	0.0625
3	0.0625
4	0.0625
5	0.0625
6	0.0625
7	0.125
8	0.125
9	0.0625
10	0
11	0.0625

TABLE 9
Criticality factor of modules of MOVIE THEATRE system using Formula 1

Step 1:

If Criticality Factor (C) of two modules M1 and M2 shows same value, then
If Module M1 (Predecessor) > Module M2 (Predecessor) then
Module M1 is considered more critical than module M2.

The modules (7, 8) and (2, 3, 4, 5, 6, 9, 11) have the same Criticality Factor, based on given rule the criticality of modules is:
N8 > N7
N6 > N9 > N2 = N3 = N4 = N5 = N11

Step 2:

If M1 (Successors) == M2 (Successors) and
M1 (Predecessor) == Module M2 (Predecessor) then
Compute the path length from root node to M1 and M2 using *Breath First Search (BFS) method.*

Module with smaller path length is considered more critical.

There is ambiguity in modules (2, 3, 4, 5, 11), following the above rule:
By applying BFS the result is:
Path for N2 = **N1 -> N2**
Path for N3 = **N1 -> N3**
Path for N4 = **N1 -> N4**
Path for N5 = **N1 -> N5**
Path for N6 = **N1 -> N9 -> N8 -> N11**

From above observation the criticality of modules is:
N2 = N3 = N4 = N5 > N11

Step 3:

Modules showing same value of C are kept in same build.

Distinction in the criticality of modules N2**, N3, N4, N5**cannot be made, following above rule the criticality of all the modules is:

N1 > N8 > N7 > N6 > N9 > N2 = N3 = N4 = N5 > N11 > N10

Step 4:

Module(s) are tested in decreasing order of their criticality factor values.

Using above rule, the builds are:
Build 1 = N1
Build 2 = N8
Build 3 = N7
Build 4 = N6
Build 5 = N9
Build 6 = N2, N3, N4, N5
Build 7 = N11
Build 8 = N10

The build testing can now be applied to these builds which tell the tester that the given system can be tested further or not, that is, whether the given system is of any use or not.

CASE STUDY 4

Taking in account the example of Simple Automatic Teller Machine (SATM) System, (taken from "Software Testing, A Craftsman's Approach ", Third Edition, by Paul C. Jorgensen ")

The *Simple Automatic Teller Machine (SATM) System* consists most of the features of an ATM. The user can withdraw or deposit money from it only after the PIN verification, can modify the account password, can see the present balance and print a receipt for it. The machine automatically dispenses the money entered by user (only if amount of money in user account is greater than or equal to the entered amount), and the balance is updated automatically depending on the transaction. At the end user can close the present session.

Modules are:

MODULE NUMBER	MODULE SEQUENCE	MODULES
1	1	SATM System
2	1.1	Device Sense and Control
3	1.1.1	Door Sense and Control
4	1.1.1.1	Get Door Status
5	1.1.1.2	Control Door
6	1.1.1.3	Dispense Cash
7	1.1.2	Slot Sense and Control
8	1.1.2.1	Watch Card Slot
9	1.1.2.2	Get Deposit Slot Status
10	1.1.2.3	Control Card Roller
11	1.1.2.4	Control Envelope Roller
12	1.1.2.5	Read Card Strip
13	1.2	Central Bank Communication
14	1.2.1	Get PIN for PAN
15	1.2.2	Get Account Status
16	1.2.3	Post Daily Transactions
17	1.3	Terminal Sense and Control
18	1.3.1	Screen Driver
19	1.3.2	Key Sensor
20	1.4	Manage Session
21	1.4.1	Validate Card
22	1.4.2	Validate Pin
23	1.4.2.1	Get PIN
24	1.4.3	Close Session
25	1.4.3.1	New Transaction Request

26	1.4.3.2	Print Receipt
27	1.4.3.3	Post Transaction Local
28	1.4.4	Manage Transaction
29	1.4.4.1	Get Transaction Type
30	1.4.4.2	Get Account Type
31	1.4.4.3	Report Balance
32	1.4.4.4	Process Deposit
33	1.4.4.5	Process Withdrawal

TABLE 10
Layout of SATM System

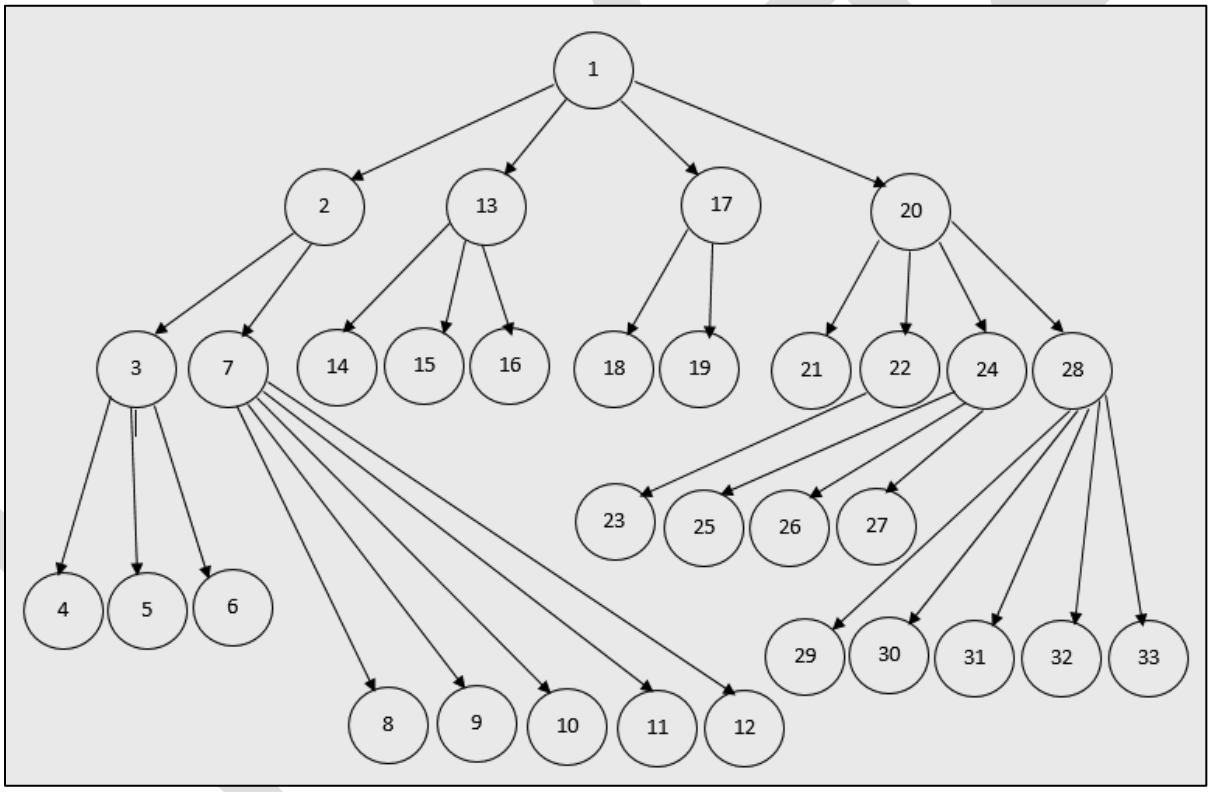

FIG 4
Call graph of User Data Storage Device (UDSD) System

MODULE NUMBERS	MODULE PREDECESSORS	MODULE SUCCESSORS
1	-	2, 13, 17 ,20
2	1	3, 7

3	2	4, 5, 6
4	3	-
5	3	-
6	3	-
7	2	8, 9, 10, 11, 12
8	7	-
9	7	-
10	7	-
11	7	-
12	7	-
13	1	14, 15, 16
14	13	-
15	13	-
16	13	-
17	1	18, 19
18	17	-
19	17	-
20	1	21, 22, 24, 28
21	20	-
22	20	23
23	22	-
24	20	25, 26, 27
25	24	-
26	24	-
27	24	-
28	20	29, 30, 31, 32, 33
29	28	-
30	28	-

31	28	-
32	28	-
33	29	-

TABLE 11
Friends of nodes in SATM System

Criticality Factor of modules using the formula—

$$C = \frac{Module\ (Successores)}{Graph\ (Successors)} \quad ; such\ that\ 0 \leq C \leq 1$$

Module (Predecessors) = Number of modules calling the i^{th} module
Module (Successors) = Number of modules being called by i^{th} module
Graph (Successors) = ΣModule (Successors), where indegree ≠0

Using Table 11, *Graph (Successors)* = **32**
The table of Criticality Factor of Modules for SATM System is:

MODULE NUMBERS	CRITICALITY FACTOR
1	0.125
2	0.062
3	0.093
4	0
5	0
6	0
7	0.156
8	0
9	0
10	0
11	0
12	0
13	0.093
14	0

15	0
16	0
17	0.062
18	0
19	0
20	0.125
21	0
22	0.031
23	0
24	0.093
25	0
26	0
27	0
28	0.156
29	0
30	0
31	0
32	0
33	0

TABLE 12
Criticality factor of modules of SATM System using Formula 1

Step 1:

If Criticality Factor (C) of two modules M1 and M2 shows same value, then
If Module M1 (Predecessor) > Module M2 (Predecessor) then
Module M1 is considered more critical than module M2.

The modules (1, 20), (2, 17), (3, 13, 24), (7, 28) and (4, 5, 6, 8, 9, 10, 11, 12, 14, 15, 16, 18, 19, 21, 23, 25, 26, 27, 29, 30, 31, 32, 33) have the same Criticality Factor, based on given rule the criticality of modules is:
N20 > N1
N2 = N17
N3 = N13 = N24
N7 = N28
N4 = N5 = N6 = N8 = N9 = N10 = N11 = N12 = N14 = N15 = N16 = N18 = N19 = N21 = N23 = N25 = N26 = N27 = N29 = N30 = N31 = N32 = N33

Step 2:

If M1 (Successors) == M2 (Successors) and
M1 (Predecessor) == Module M2 (Predecessor) then
Compute the path length from root node to M1 and M2 using *Breath First Search (BFS) method.*
Module with smaller path length is considered more critical.

There is ambiguity in modules (2, 17), (3, 13, 24), (7, 28) and (4, 5, 6, 8, 9, 10, 11, 12, 14, 15, 16, 18, 19, 21, 23, 25, 26, 27, 29, 30, 31, 32, 33), following the above rule :
By applying BFS the result is:
Path for N2 = **N1 -> N2**
Path for N17 = **N1 -> N17**
Path for N3 = **N1 -> N2 -> N3**
Path for N13 = **N1 -> N13**
Path for N24 = **N1 -> N20 -> N24**
Path for N7 = **N1 -> N2 -> N7**
Path for N28 = **N1 -> N20 -> N28**
Path for N4 = **N1 -> N2 -> N3 -> N4**
Path for N5 = **N1 -> N2 -> N3 -> N5**
Path for N6 = **N1 -> N2 -> N3 -> N6**
Path for N8 = **N1 -> N2 -> N7 -> N8**
Path for N9 = **N1 -> N2 -> N7 -> N9**
Path for N10 = **N1 -> N2 -> N7 -> N10**
Path for N11 = **N1 -> N2 -> N7 -> N11**
Path for N12 = **N1 -> N2 -> N7 -> N12**
Path for N14 = **N1 -> N13 -> N14**
Path for N15 = **N1 -> N13 -> N15**
Path for N16 = **N1 -> N13 -> N16**
Path for N18 = **N1 -> N17 -> N18**
Path for N19 = **N1 -> N17 -> N19**
Path for N14 = **N1 -> N13 -> N14**
Path for N21 = **N1 -> N20 -> N21**
Path for N23 = **N1 -> N20 -> N22 -> N23**
Path for N25 = **N1 -> N20 -> N24 -> N25**
Path for N26 = **N1 -> N20 -> N24 -> N26**
Path for N27 = **N1 -> N20 -> N24 -> N27**
Path for N29 = **N1 -> N20 -> N28 -> N29**
Path for N30 = **N1 -> N20 -> N28 -> N30**
Path for N31 = **N1 -> N20 -> N28 -> N31**
Path for N32 = **N1 -> N20 -> N28 -> N32**
Path for N33 = **N1 -> N20 -> N28 -> N33**

From above observation the criticality of modules is:
N2 = N17
N13 > N3 = N24
N7 = N28
N14 = N15 = N16 = N18 = N19 = N21 > N4 = N5 = N6 = N8 = N9 = N10 = N11 = N12 = N23 = N25 = N26 = N27 = N29 = N30 = N31 = N32 = N33

Step 3:

Modules showing same value of C are kept in same build.

Distinction in the criticality of modules (**N2, N17), (N3, N24), (N7, N28), (N14, N15, N16, N18, N19, N21)** and **(N4, N5, N6, N8, N9, N10, N11, N12, N23, N25, N26, N27, N29, N30, N31, N32, N33)** cannot be made, following above rule the criticality of all the modules is:

N7 = N28 > N20 > N1 > N13 > N3 = N24 > N2 = N17 > N22 > N14 = N15 = N16 = N18 = N19 = N21 > N4 = N5 = N6 = N8 = N9 = N10 = N11 = N12 = N23 = N25 = N26 = N27 = N29 = N30 = N31 = N32 = N33

Step 4:

Module(s) are tested in decreasing order of their criticality factor values.

Using above rule, the builds are:
Build 1 = N7, N28
Build 2 = N20
Build 3 = N1
Build 4 = N13
Build 5 = N3, N24
Build 6 = N2, N17
Build 7 = N22
Build 8 = N14, N15, N16, N18, N19, N21
Build 9 = N4, N5, N6, N8, N9, N10, N11, N12, N23, N25, N26, N27, N29, N30, N31, N32, N33

The build testing can now be applied to these builds which tell the tester that the given system can be tested further or not, that is, whether the given system is of any use or not.

CONCLUSION

The above mentioned method for finding criticality factor of nodes (Software Modules) is very useful whenever it is difficult for the software tester to decide which modules are more critical on the basis of functional dependency of the modules. Using this methodology, tester can even find out the most critical and least critical modules as well.
This method can be vastly used by tester before beginning any test. For initialising the *Build Testing*, which depends on the criticality of different modules of the given system, this technique is very useful as shown in above examples.
It is found that testing the most critical node is always the first priority of every tester and hence this technique is very useful in every aspect.

REFERENCES:

[1] Paul C. Jorgensen, "Software Testing, A Craftsman's Approach ", Third Edition

[2] K. K. Aggarwal, Yogesh Singh, "Software Engineering", Third Edition

[3] Kan S H, Basili V R, Shapiro L N 1994 Software Quality : An overview from the perspective of total quality management

[4] Roge´rio Paulo, "Integration Testing", January 12, 2007

[5] V V S Sarma, D Vijay Rao, "A re-entrant line model for software product testing", 1997

[6] Praveen Ranjan Srivastava, Subrahmanyan Sankaran, Pushkar Pandey, Optimal Software Release Policy Approach Using Test Point Analysis and Module Prioritization, 2013

[7] http://www.cognizant.com/InsightsWhitepapers/Risk%20Based%20Testing.pdf

[8] https://en.wikipedia.org/wiki/Integration_testing

[9] https://en.wikipedia.org/wiki/Build_verification_test

[10] http://www.softwaretestingstuff.com/2008/06/build-verification-testing.html

[11] http://searchsoftwarequality.techtarget.com/definition/build

[12] https://www.google.co.in/url?sa=t&rct=j&q=&esrc=s&source=web&cd=1&cad=rja&uact=8&ved=0CBwQFjAAahUKEwj8w82KqrPIAhULBo4KHba5A98&url=http%3A%2F%2Fwww.istqb.org%2Fdownloads%2Ffinish%2F20%2F212.html&usg=AFQjCNEYHr045l6c8qE44Q66LFmQfhMFiw

International Journal of Engineering Research and General Science Volume 3, Issue 5, September-October, 2015
ISSN 2091-2730

STUDIES ON HYDRODYNAMICS, MIXING TIME AND RESIDENCE TIME DISTRIBUTION BEHAVIOUR OF EXTERNAL LOOP AIRLIFT REACTOR

Velmurugan.S[1], Shajin.M.H[2], Gengadevi.R[**], Deepika.J[**]

[1,2]DEPARTMENT OF PETROLEUM ENGINEERING, JCT COLLEGE OF ENGINEERING AND TECHNOLOGY, PICHANUR, COIMBATORE

** (ASSISTANT PROFFESOR) DEPARTMENT OF PETROLEUM ENGINEERING, JCT COLLEGE OF ENGINEERING AND TECHNOLOGY, PICHANUR, COIMBATORE

Email id: gengachem9@gmail.com

ABSTRACT: Mixing is one of the important unit operations in chemical and allied industries. Airlift reactors are known to be efficient contactors for processes involving gases, liquids and solids. Airlift reactors are mostly used in biological processes, aerobic waste water treatment, fermentation processes. In the present work focused on investigation of hydrodynamics and mixing index behavior (i.e., gas holdup, residence time distribution) in an external-loop airlift reactor and a stimulus-response tracer technique were used in the measurements. The geometry of External loop airlift reactor of column diameter 100mm and height 1000mm. Pressure drop, Gas hold-up, Mixing time, Residence time distribution have been measured for various electrolytes and solvents with various concentrations have been studied. In addition, the effects of superficial gas velocities on the gas holdup and RTD were also investigated. Comparisons made on both electrolytes and solvents by graphically.

Keywords*:* external loop airlift reactor, electrolytes, solvents, gas holdup, pressure drop, mixing time, residence time distribution

INTRODUCTION

The airlift reactor (ALR) is a multiphase reactor which is used in gas–liquid or gas–liquid–solid pneumatic contacting devices that are characterized by fluid circulation. It is also defined as a cyclic pattern through channels built specifically for this purpose.. Recent literature reveals that 80% of losses in process is due to improper mixing. Mixing can be achieved in two ways one with moving parts and another without moving parts. Batch and flow reactors come under the first category. The second category includes bubble column, fluidized bed and air lift reactor. The main difference between ALRs and bubble columns (which are also pneumatically agitated) lies in the type of fluid flow, which depends on the geometry of the system. This class of reactor is very attractive for use in the chemical process industry and biotechnology due to their design flexibility, low power requirement, and less pressure drop with further advantages of good mass and heat transfer. The rate of liquid circulation depends on gas flow rate. Two basic classes of the gas lift are distinguished: (i) the internal-loop gas lift reactor (IL-ALR) and (ii) the external-loop gas lift reactor (EL-ALR). The External loop airlift reactor has greater flexibility (Weiland and Onken, 1981) and its performance could be manipulated better by controlling parameters for the individual sections. EL-ALR is selected in this study. Gas holdup is an important hydrodynamic parameter in the reactor. It affects to mass and heat transfer in the system. Gas holdup measurements usually provide overall average information, i.e.

level measurement, pressure measurement. However, local gas holdup information is important for accuracy design and performance prediction. The residence time distribution (RTD) is one of the most informative characterizations that describe mixing behavior in a reactor. The knowledge of the liquid RTD is important for a number of reasons (Danckwerts, 1953) allowing an accurate kinetic modeling of the system, help reactor design to achieve or preserve a desired flow pattern, and to compare the behavior of real reactors to their ideal models. A stimulus-response tracer technique is a well-established method in investigation of a flow process dynamics and evaluation of residence time distribution (RTD). The principle of a tracer experiment consists of a common impulse-response method: injection of a tracer at the inlet of a system followed by the measurement of some relevant property of the outlet solution (e.g. the solution electrical conductivity) is the most commonly used RTD experiment in loop reactors. Therefore, this work focused on investigation of hydrodynamics and mixing index behavior (i.e., gas holdup, residence time distribution) in an external-loop gas lift reactor and a stimulus-response tracer technique were used in the measurements. In addition, the effects of superficial gas velocities on the gas holdup and RTD studies were also investigated. The main objective of the project is (i) To study the effect of hydrodynamics characteristics of gas and liquid phase in an external loop airlift reactor. (ii)To study mixing time and Residence Time Distribution (RTD) characteristics of external loop airlift reactor. (iii) Model was developed based on the experimental results

2. EXPERIMENTAL SECTION

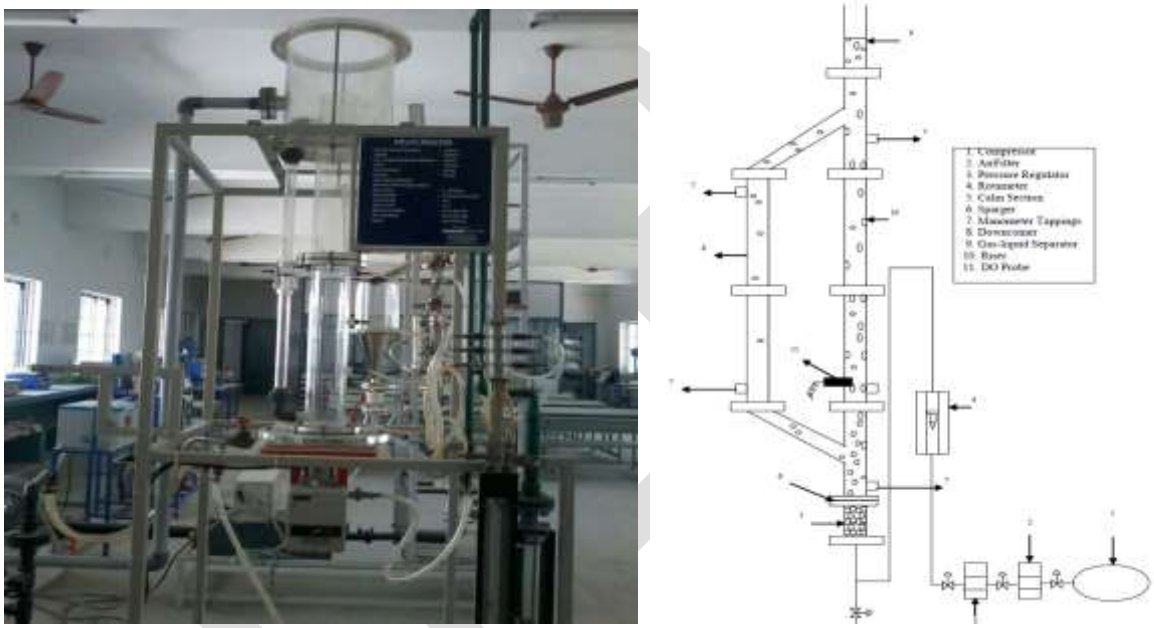

Fig 2.1 External loop airlift reactor

Table 2.1: Physical properties of the materials used

SYSTEM(vol %)	DENSITY(kg/m3)	SURFACE TENSION(x10^3,N/m)
Tap water	998.2	72.8
Nacl(5%)	1018.2	49.32
Nacl(10%)	1021.6	48.37

Acetic acid(5%)	1011.5	24.59
Acetic acid(10%)	1026	22.23
Sucrose(5%)	1014	21.54
Sucrose(10%)	1031	22.11
Methanol(0.25%)	997.7	72.1
Methanol(0.5%)	997.2	71.7
Methanol(0.75%)	996.7	71.6
Ethanol(0.25%)	997.7	71.4
Ethanol(0.5%)	997.2	70.3
Ethanol(0.75%)	996.8	69.3
Propanol(0.25%)	997.7	71.5
Propanol(0.5%)	997.2	69.9
Propanol(0.75%)	996.7	65.1
Benzene (0.25%)	996.5	70.5
Benzene (0.5%)	996.2	69.7
Benzene (0.75%)	995.7	69.3

A schematic of the external loop airlift reactor used in this study is as shown in figure 2.1. It consists of acrylic column and a column diameter of 100mm and height 1000mm with a supporting screen diameter of 0.8mm.The external loop airlift column has perforated plate gas sparger with 243holes of 1mm diameter on a triangular pitch placed at the base of the column. The down-comer and riser are connected via two horizontal acrylic tubes. The gas phase that is the compressed air is injected at the bottom of the column. Water, electrolytes and solvents are used as liquid phase. The experiment was conducted in room temperature. Gas hold-up is one of the important design parameter of airlift reactors. Gas hold-up was measured by level measurements (Expansion volume method).Pressure drop, Gas hold-up, Mixing time, Residence time distribution was measured for various electrolytes and solvents of various concentrations for different superficial gas velocities.

3. RESULTS AND DISCUSSION

3.1 GAS HOLD-UP AND PRESSURE DROP FOR AIR - WATER SYSTEM

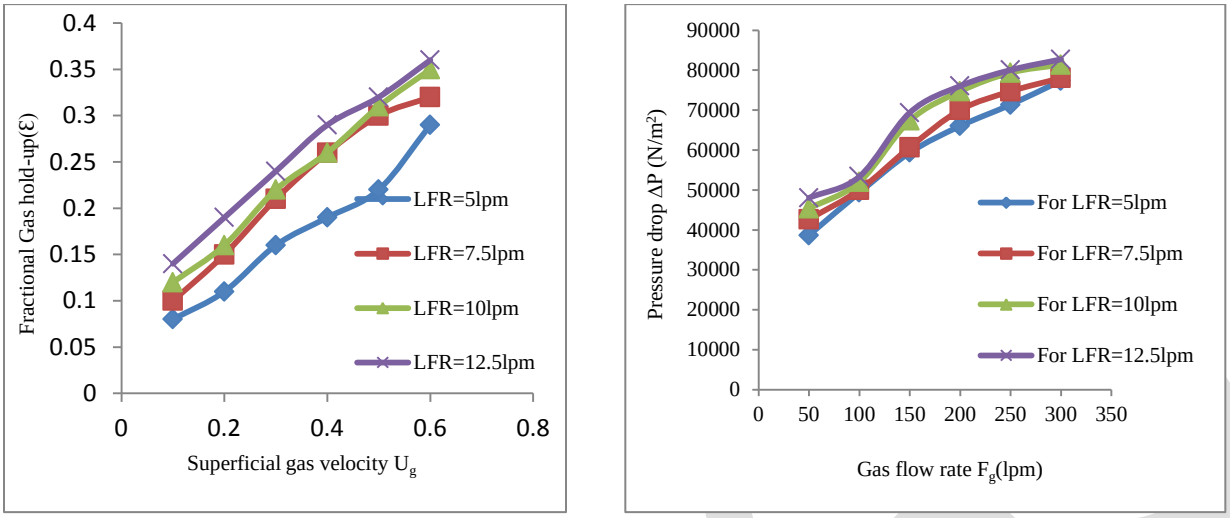

Figure 3.1.1 Effect of superficial gas velocity on Fractional gas hold-up and Gas flow rate on Pressure drop by varying liquid flow rates

From the figure 3.1.1 it can be observed that superficial gas velocity increases the fractional gas hold-up and pressure drop also increases with increasing liquid flow rates from 5 lpm to 12.5 lpm.

3.2GASHOLD-UP FOR ELECTROLYTES AND SOLVENTS BY VARYING LIQUID FLOW RATES:

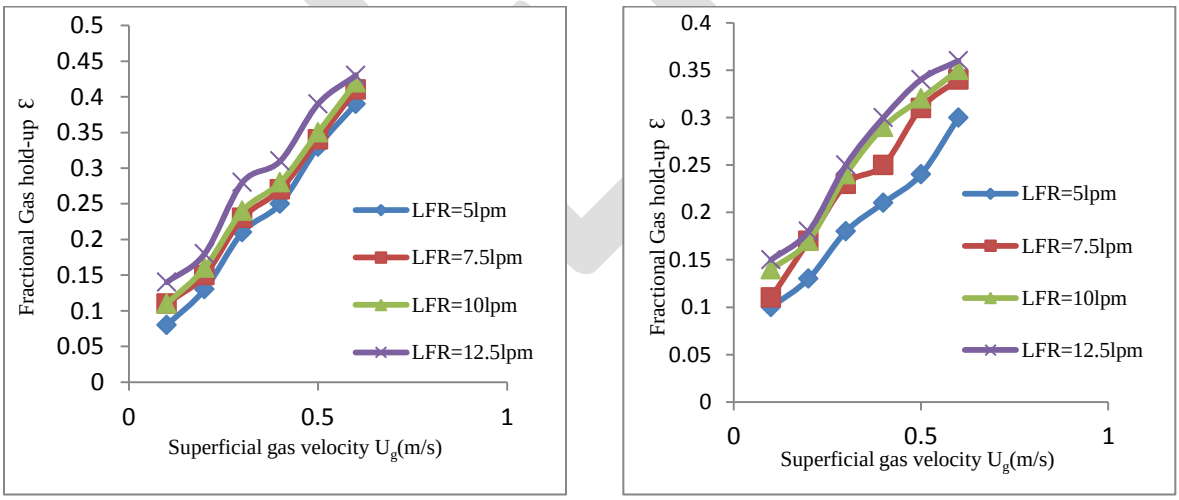

Fig 3.2.1: Effect of superficial gas velocity on Fractional gas hold-up by varying liquid flow rates for 5% Nacl and 0.25% Methanol

From the figure 3.2.1 it was found that the fractional gas hold-up increases with increasing superficial gas velocity and increasing liquid flow rates for both electrolytes and solvents. When we increasing the concentration of electrolytes (acetic acid, sucrose) and solvents (ethanol, propanol and benzene) the same observations are made.

3.3 GASHOLD-UP FOR ELECTROLYTES AND SOLVENTS BY VARYING SOLUTIONS:

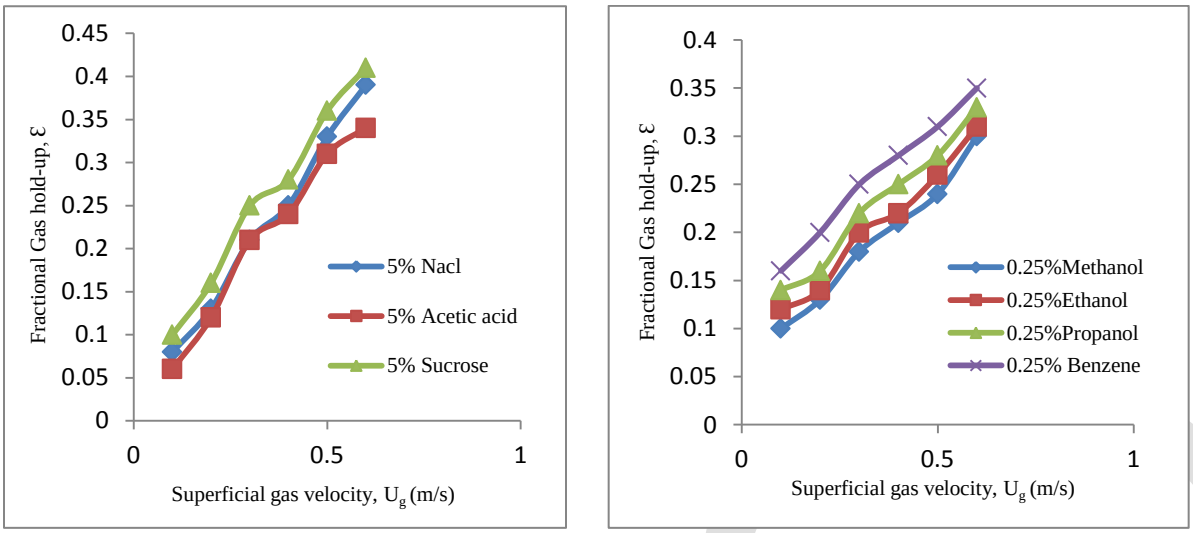

Figure 3.3.1 Effect of superficial gas velocity on fractional gas hold-up by varying electrolytes at constant concentration of 5% and varying solvents at constant concentration 0.25%

From the figure 3.3.1 it can be found that sucrose have higher gas hold-up compared to other electrolytes. Because sucrose has lower surface tension, so it yields higher gas hold-up. From the figure4.3.2it can be observed that the gas hold increases with increasing the concentration of the solvents(0.25%,0.5% and 0.75%) and also increases with increasing the carbon atoms in the alcohol molecules. As the number of carbon atom increases the surface tension reduces it causes to create smaller bubbles. So gas hold-up rises (Propanol with longest carbon chain has the maximum gas hold-up). The gas hold-up increased as: Water < methanol< ethanol< propanol< benzene

3.4 GASHOLD-UP FOR ELECTROLYTES AND SOLVENTS BY VARYING CONCENTRATIONS:

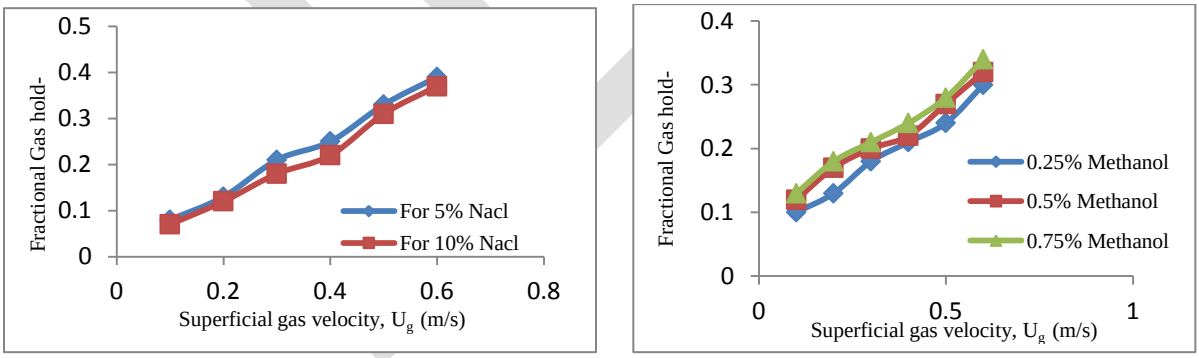

Figure 3.4.1 Effect of superficial gas velocity on fractional gas hold-up by varying concentration of electrolyte (Nacl) and solvent (CH_3OH)

From the figure 3.4.1 it can be seen that gas holdup increases with increasing the superficial gas velocity but decreases with increasing the electrolyte concentration for various liquid flow rates. Low electrolyte concentrations have no noticeable effect on the surface tension of the solution. However the ionic force in the liquid bulk reduces the bubble rise velocity and the bubble coalescence. As a result, the gas hold-up increase. For high electrolyte concentration, the interfacial tension increases, resulting in increased the bubble

size and reduce gas hold-up. And also it can be observed that the gas hold increases with increasing the concentration of the solvents(0.25%,0.5% and 0.75%) When we increasing the concentration of the solvents the surface tension reduces it causes to create smaller bubbles. So gas hold-up rises. The alcohols with concentration of 0.75% have higher gas hold-up compared to those with concentration of 0.5% and 0.25%.

4.1. RTD STUDIES

4.1.1 Air –Water System

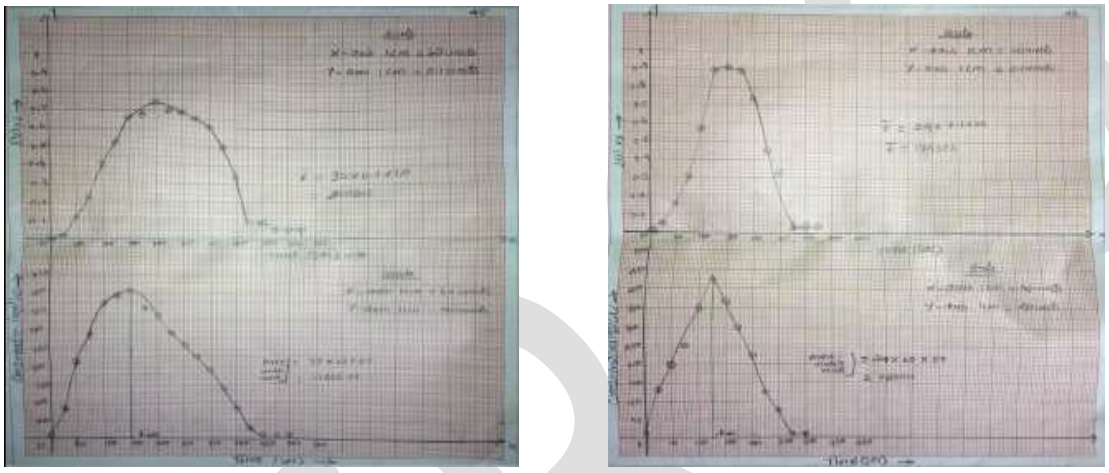

(a) (b)

Fig:4.1 Effect of time on concentration and E(t)*t for Air-Water system at constant (a) gas flow rate =25lpm (b) gas flow rate =50lpm

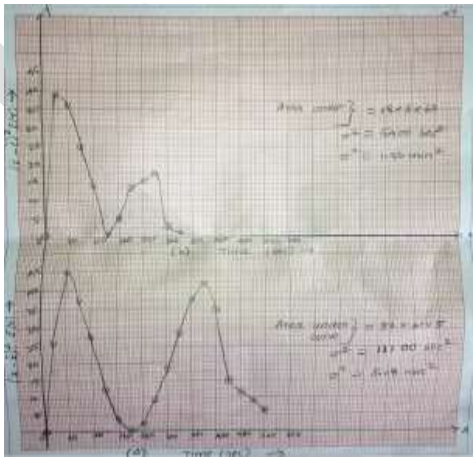

Fig 4.2: Effect of time on variance for air –water system

RTD characteristics of External loop airlift reactor using the stimulus response tracer technique was carried out. Works were carried out at two gas flow rates i.e. 25lpm and 50lpm. The water flow rate is maintained constant as 5lpm. From the results, it was

found that the mean residence time were 210sec and 174sec for 25lpm and 50lpm respectively. It is shown in the figure 4.1(a) and (b). The mixing times were obtained from the c-curve and it is found as 180sec and 150sec for those flow rates. The reduction in the residence time value while increasing the gas flow rate was expected because when the gas flow rate increases, mixing takes place more vigorously and which leads to the early outcome of the fluid.

The RTD kinetic data obtained were applied to the compartment models. This particular mixed flow reactor can be only fit to the tank in series model since the dimensionless parameter (D/uL) obtained nearly to infinity. From the results it was found to be the number of tanks was 4 and 5 for the gas flow rates 25lpm and 50lpm respectively. The reason may be attributed to the decrease in the residence time would leads to the increase in number of tanks.

Table 4.1: Table shows mean residence time and mixing time for solvent and electrolyte

SYSTEM	GAS FLOW RATE lpm	MEAN RESIDENCE TIME(sec)	VARIANCE (min^2)	MIXING TIME (sec)	NO. OF TANKS
Air-water	25	210	3.08	180	4
Air-water	50	174	1.50	150	5
Air –Acetic acid (0.25%)	25	318	4.91	300	5
Air –Acetic acid (0.25%)	50	252	3.08	240	6
Air –Acetic acid (0.5%)	25	372	6.17	360	6
Air –Acetic acid (0.5%)	50	282	3.16	270	7
Air –Methanol (0.25%)	25	228	3.83	150	3
Air –Methanol (0.25%)	50	180	1.83	120	4
Air –Methanol (0.5%)	25	276	4.67	120	4
Air –Methanol (0.5%)	50	198	2.00	120	5

4.1.2 Air – Acetic acid System

In this study, the flow rates are maintained as similar to the air-water system. Experiments are done by varying the acetic acid concentration such as 0.25 vol% and 0.5vol% . From the results of 0.25vol% acetic acid- air system, it was found that the mean residence time were 318sec and 252sec for the case1 and 2 respectively. As similar to the air water system the mixing time were obtained from the C-curve and the values are 300sec and 240sec for those flow rates.

When the concentration of the acetic acid is increase to 0.5vol%, the mean residence time were changed to 372sec and 282 sec for the gas flow rates of 25lpm and 50lpm respectively. Similarly the mixing time were varied as 360sec and 270sec for case 1 and 2 respectively. The reason may be due to the higher viscosity of acetic acid compared to water. since the viscosity and specific gravity of the acetic acid is higher than that of water, the mixing requires more time.

Since the dimensionless parameter obtained for this kinetic data were very high, tank in series model is proposed for the system. For the 0.25vol% acetic acid, it was found to be the number of tanks was 5 and 6 for case1 and 2 respectively. Similarly for the 0.5vol% acetic acid, the number of tanks was found to be 6 and 7 for case1 and 2 respectively.

4.1.3 Air – Methanol System

In this study, the flow rates are maintained as similar to the air – water system. Experiments are done by varying the methanol concentration such as 0.25vol% and 0.5vol%. From the results, of 0.25vol% methanol- air system, it was found that the mean residence time were 228sec and 180sec for the case1 and 2 respectively. As similar to the air water system the mixing time were obtained from the C-curve and the values are 150sec and 120sec for those flow rates.

When the concentration of the methanol is increases to 0.5vol%, the mean residence time were changed to 276sec and 198 sec for the gas flow rates of 25lpm and 50lpm respectively. Similarly the mixing time were varied as 120sec and 120sec for case 1 and 2 respectively. The reason may be due to the lower viscosity of methanol compared to water. since the viscosity and specific gravity of the methanol is lower than that of water, the mixing requires less time.

Since the dimensionless parameter obtained for this kinetic data were very high, tank in series model is proposed for the system. For the 0.25vol% methanol, it was found to be the number of tanks was 3 and 4 for case1 and 2 respectively. Similarly for the 0.5vol% methanol, the number of tanks was found to be 4 and 5 for case1 and 2 respectively.

5. CONCLUSION

- Fractional Gas hold-up increases with increasing the gas flow rates
- Fractional Gas hold-up increases with increasing the concentration of solvents
- Fractional Gas hold-up decreases with increasing the concentration of electrolytes
- Among the solvents and electrolytes studies shows Benzene and Sucrose more fractional gas hold-up
- Pressure drop increases for both electrolytes and solvents when we increasing the concentration as well as gas flow rates
- RTD and mixing time characteristics of External loop airlift reactor was studied and found that experimental data fits well with tank in series model and number of tanks was varies from 4 to 6

REFERENCES:

1. Ali Abdul Rahman-Al Ezzi and Ghazi Faisal Najmuldeen 'The Effects Of Superficial Gas Velocity and Liquid Phase Properties On Gas Holdup and Mass Transfer In An Airlift Reactor" American Journal of Engineering Research, 2, 25-32, 2013.
2. W.A.Al-Masry "Influence of Gas Separator and Scale-up on the hydrodynamics of External Loop Circulating Bubble Columns" Chemical Engineering Research and Design,82(A3), 381-389, 2004.
3. Annie X. Meng, Gordon A.Hill and Ajay K. Dalai "Hydrodynamic Characteristics in an External Loop Airlift Bioreactor Containing a Spinning Sparger and a Packed Bed" Ind. Eng. Chem. Res., 41, 2124-2128, 2002.
4. ChafaaBentifraouine, Catherine Xuereb and Jean-Pierre Riba "Effect of gas Liquid Separator and Liquid Height on the Global Hydrodynamic Parameters of an External Loop Airlift Reactor" Chemical Engineering Journal,66,91-95, 1997.
5. Changqing Cao, Shuqin Dong and QingjieGuo "Experimental and Numerical Simulation for Gas – liquid Phases Flow Structure in an External-Loop Airlift Reactor" Ind. Eng. Chem. Res. , 46, 7317-7327, 2007.
6. Changqing Cao, Shuqin Dong, QijinGeng and QingjieGuo "Hydrodynamics and Axial Dispersion in a Gas-Liquid-Solid EL-ALR with Different Designs" Ind. Eng. Chem. Res., 47, 4008-4017, 2008.
7. Gerald D. Stang, Douglas G. Macdonald and Gordon A. Hill "Mass Transfer and Bioethanol Production in an External-Loop Liquid-Lift Reactor" Ind. Eng. Chem. Res. , 40, 5074-5080, 2001.

8. H.Ghasemi and S.H. Hosseini "Investigation of Hydrodynamics and Transition Regime in an Internal Loop Airlift Reactor Using CFD" Brazilian Journal of Chemical Engineering, 29, 821-833, 2012.
9. T k Ghosh, Debnath Bhattacharyya and Tai-hoon-Kim "Gas Hold-Up Characteristics of an External Loop Air-Lift Contactor" International Journal of Hybrid Technology, 3, 25-32. 2010.
10. Giuseppe Olivieri, Antonio Marzocchella and PieroSalatino "Hydrodynamics and Mass Transfer in a Lab Scale Three-Phase Internal Loop Airlift Reactor" Chemical Engineering Journal, 96, 45-54, 2003.
11. Joanna Karcz, MarcelinaBitenc, MarekDomanski and Lukasz Kacperski "Numerical Study of Hydrodynamics in an External Loop Air-Lift Reactor", 2013.
12. Jordan Hristov "External Loop Aitlift with Magnetically Controlled Liquid Circulation" Powder Technology, 149, 180-194, 2005.
13. Liu Mengxi, Lu Chunxi, Shi Mingxian and GeBaoli, Huang "Hydrodynamics and Mass Transfer in a Modified Three-Phase Airlift Loop Reactor" Petroleum Science, 4, 91-96, 2007.
14. Maria Gavrilescu and Radu Z. Tudose "Mixing Studies in External-Loop Airlift Reactor" Chemical Engineering Journal, 66, 97-104, 1996.
15. MostafaKeshavarzMoraveji "Hydrodynamic Analysis of a Concentric Draft Tube airlift Reactor using Computational Fluid Dynamics" Middle-East Journal of Scientific Research, 12, 1420-1425, 2012.
16. RagupathyPrabhuArunkumar and KaruppanMuthukumar "Phenomenological Simulation Model for the Prediction of Hydrodynamic Parameters of an Internal Loop Airlift reactor" Ind. Eng. Chem. Res. , 49, 4995-5000, 2010.
17. Renzo and Di Felice "Liquid Circulation Rates in Two- and Three-Phase External Airlift Reactors" Chemical Engineering Journal, 109, 49-55, 2005.
18. S.Sarkar, KaustubhaMohanty and B.C. Meikap "Hydrodynamic Modelling of a Novel Multi-Stage Gas-Liquid External Loop Airlift Reactor" Chemical Engineering Journal, 145, 69-77,2008.
19. Tongwang Zhang, Jinfu Wang, Tiefang Wang, Jing Lin and Yong Jin "Effect of Internal on the Hydrodynamics in External-Loop Airlift Reactors" Chemical Engineering and processing, 44, 81-87, 2005.
20. SivakumarVenkatachalam, KannanKandasamy and AkilamudhanPalaniappan "Prediction of Riser Gas Holdup in Three-Phase External Loop Airlift Fludized Bed Reactor" Modern Applied Science, 4, 75-8, 2010 .
21. J.B.Snape, J.Zahradnik, M.Fialova and N.H.Thomas "Liquid-Phase Properties and Sparger Design Effects in an External-Loop Airlift Reactor" Chemical Engineering Science, 50, 3175-3186, 1995

International Journal of Engineering Research and General Science Volume 3, Issue 5, September-October, 2015
ISSN 2091-2730

Efficient Prevention of Vampire Attack in Ad-hoc Wireless Sensor Network

Ms. Raisa I. Mulla[1], Prof. Rahul N. Patil[2]
[1]PG Scholar, Computer Engineering Department, Bharati Vidyapeeth College Of Engineering, Navi-Mumbai, India
[2]Assistant Professor, Computer Engineering Department, Bharati Vidyapeeth College Of Engineering, Navi-Mumbai, India

Email: raisamulla38@gmail.com

Abstract— Ad-hoc low-power wireless networks are the challenging analysis direction in sensing and pervasive computing. Wireless Senor Network (WSN) basically use for security and energy efficiency. Early work on security in this area has been focused on denial of service (DOS) at the routing or medium access control (MAC) levels. Previously, the resource depletion attacks are considered as a routing problem, under this model are classified in to a new group called "Vampire attacks". This difficult work examine thoroughly the identification of resource depletion attacks at the routing protocol layer and in the application layer, which completely disable networks by quickly exhausting nodes' battery power. Vampire attacks are not a protocol specific and they do not rely on design properties but rather exploits properties of protocol classes of routing protocols. Vampire attacks are liable to be influenced or harmed by a particular thing, which are disastrous, hard to find, and are easy to carry out using as few as one malicious insider sending only protocol compliant messages. A single Vampire can increase network-wide energy usage by a factor of O (N), where N in the number of network nodes, happens in worst case. In this work a detection and control strategy is proposed for these vampire attacks, along with a secure packet forwarding mechanism, which will keep safe from harm and danger Ad-hoc wireless nodes from power exhaust due to Vampires at packets forwarding level.

Keywords— Medium Access Control(MAC), Denial of Service(DOS), Routing Protocol, Ad-hoc Wireless Network, Wireless Sensor Network(WNS), Wireless Network Security.

INTRODUCTION

A group of two or more computers are communicate together are known as a network. Basically networks are classified into three different networks Local Area Network (LAN), Wide Area Network (WAN), and Metropolitan Area Network (MAN). Large number of sensor nodes that are deployed in a particular region known as sensor network. To monitor physical and environmental condition such as Temperature, Sound, Pressure, etc and to cooperatively pass their data through the network to a main location is called a Wireless Sensor Network (WSN). Wireless Sensor Network is a distributed network. Basic characteristic of wireless sensor network is a resource constrains.

A wireless ad hoc sensors network spreads a number of sensor nodes across a geographical area. Ad-hoc wireless sensor networks (WSNs) gives honor to be introduce new applications, such as on demand computing power, continuous connectivity, and quickly spread communication for military and responders. Communication among nodes of network without any pre-existing infrastructure is a characteristic of an ad hoc sensor network. WSNs become more excellent to the day to day functioning of people and organizations, availability faults become moderately good, lack of availability can make the difference between business as usual and lost productivity, power outages, environmental disasters, and even lost lives; thus high availability of these networks is a decisive property, and should hold even under malicious conditions. Due to their ad-hoc organization, wireless ad-hoc networks are exposed to

denial of service (DOS) attacks, and a research has been done to enhance survivability. These are secure to attacks on the short-term availability of network, they do not address attacks that affect long-term availability the most permanent denial of service attack is to entirely deplete nodes batteries. This is an instance of a resource depletion attack, with battery power as the resource of interest. In this consider how routing protocols, even those designed to be secure, lack protection from these attacks, since they exhaust the life from networks nodes. These attacks are distinct from denial of services (DOS) , reduction of quality(ROQ), and routing infrastructure attacks as they do not disrupt immediate availability, but rather work over time to entirely disable a network.

Vampire attacks are exploits general properties of protocol classes such as link-state, distance-vector, source routing, and geographic and beacon routing. Neither do these attacks rely on flooding the network with large amounts of data, but rather try to transmit as little data as possible to achieve the largest energy drain, preventing a rate limiting solution. Vampires use protocol-compliant messages, these attacks are much hard to detect and prevent. Each node participates in routing by forwarding data for other nodes, so the determination of which nodes forward data is made dynamically on the basis of network connectivity. Ad-hoc networks not provide support to wired gateway. Flooding for forwarding data use in Ad-hoc network. An Ad-hoc network provide support to any set of networks where all devices have equal status on a network and are free to associate with any other Ad-hoc network device in link range. Ad hoc network refers to a mode of operation of IEEE 802.11 wireless networks and network device's ability to maintain link status information for any number of devices in a hop range. Minimal configuration and quick deployment make ad hoc networks suitable for emergency situations like natural disasters or military conflicts. The presence of dynamic and adaptive routing protocols enables ad hoc networks to be formed quickly.

A mobile ad-hoc network (MANET) is a self-configuring infrastructure less network of mobile devices connected by wireless. Each device in a MANET is free to move independently in any direction, and will therefore change its links to other devices frequently. The basic challenge in building a MANET is equipping each device to continuously maintain the information required to properly route traffic. Different protocols are then evaluated based on measure such as the packet drop rate, the overhead introduced by the routing protocol, end-to-end packet delays, network throughput etc.

Contributions—

The basic three primary contributions make this paper.

a. To evaluate the vulnerabilities of existing routing protocol when done battery depletion attack on routing layer. An existing secure routing protocol such as Ariadne, SAODV, and SEAD are vulnerable to Vampire attack. Existing work on secure routing attempts to ensure that adversaries cannot cause path discovery to return invalid network path, but vampire do not disrupts or alter discovered paths instead using existing valid network paths and protocol compliant messages. Protocols that maximize power efficiency are also inappropriate and cannot optimize battery power usage.
b. Simulation Results of quantifying performance of several representative protocols in the presence of Vampire (Single insider adversaries).
c. Modification of an existing sensor network routing protocol is made to prevent the damage caused by vampire attack during packet forwarding phase.

A. Classification

Denial of service (DOS) Attack is malicious attempt by a single person to cause a victim, site or node to deny service to its' customer. Denial of service is an attack, where a victim can cause multiple of 10 times of the CPU time to transmit a data packet, but whereas honest node uses multiple of 1 time of CPU time to transmit the same data packet. A composing a shortest path from source to destination and transmit data packet to next hop in multi hop routing protocol. Composing and transmitting a malicious message that select the longest path which consumes more energy of the network than if an honest node transmit a message that select the shortest path which consumes less energy of the network is defined as vampire attack. The ratio of network energy used in honest case as well as malicious case can measure strength of attack.

B. Protocols and Assumptions

Effects of vampire attacks on link-state, distance vector, source routing, geographic, beacon routing protocols and logical ID-based sensor network routing protocol proposed by Parno et al. These all protocols are subset of routing solution and also prevent from vampire attack. There are two different routing protocols such as on –demand routing protocol in which topology is discovered during transmission time and static protocol in which topology is discovered during an initial phase. To attack on many honest nodes few vampires are allow sending packet automatically. Adversaries are nothing but a malicious insider and have same resources and level of network access as honest nodes. Adversary corrupts a number of honest nodes after network developed. Honest nodes are safe when vampire sleeps and vulnerable while active.

C. Overview

In this paper, defines a series of increasingly damaging vampire attacks, evaluate vulnerability of several protocols, and suggest how to improve flexibility. In source routing protocol, source suggested path for forwarding packets and show how malicious packet source can specify paths through the network, which are far longer than optimal thus wasting energy at intermediate nodes that forward the packet from source. In routing schemes, each node independently made forwarding decision. In this paper suggest, how directional antenna and wormhole attack can be used to deliver packets to multiple remote network positions, forcing packet processing at nodes that would not normally receive that packet at all and increasing network wide energy expenditure. End of this paper, route and topology discovery phases can target by an adversary at packet forwarding phase.

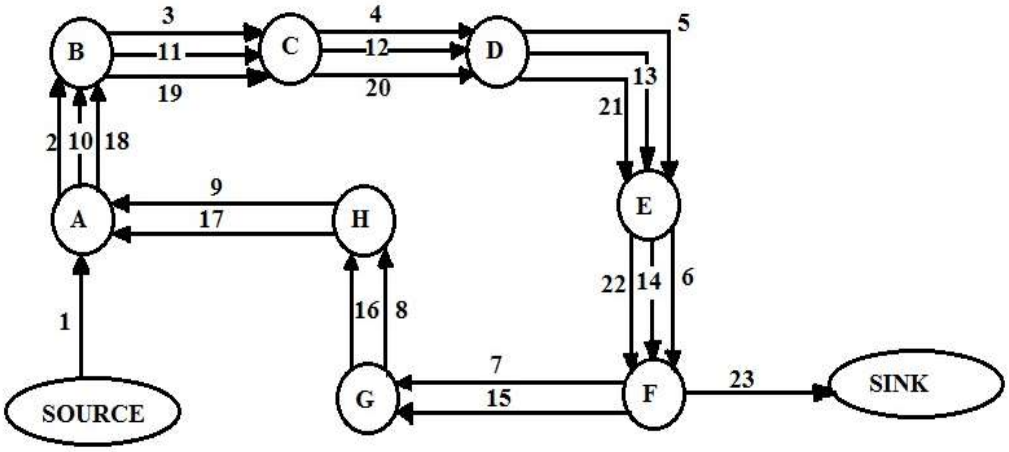

Fig.1. Carousal Attack

CAROUSAL ATTACK:

In this type of attack, adversary constructs routing loops. A malicious node sends a packet with a route composed as a series of loop with the same node appears in the route many times this attack called Carousal attack. It sends packets in circles. In carousal attack, targets source routing protocols by exploiting the limited verification of message headers at forwarding nodes, allowing a single packet to repeatedly traverse the same set of nodes.

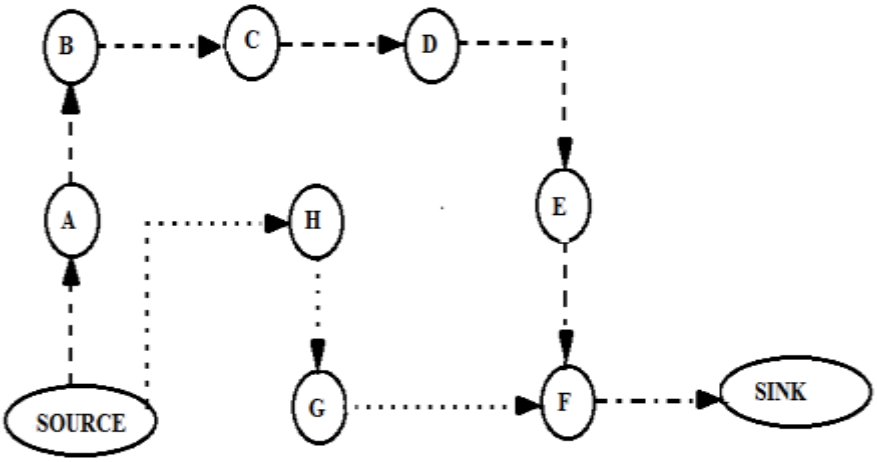

Fig.2. Stretch Attack

STRETCH ATTACK:

In this type of attack, adversary construct artificially long route. If shorter route being available then also a malicious node constructs artificially long routes from the source to destination. A number of nodes that is independent of hop count along the shortest path between the adversary and packet destination which causing packets to be processed and it increases packet path lengths.

SYSTEM METHODOLOGY

The network is collection of many nodes. To detect vampire attack energy based mechanism is implemented. After constructing a network, a malicious message will be send from attacker node to normal node. Normal node consumes more energy than the normal message level so it assumes that node is affected by an attack. If affected node is identified in the network that node eliminated from network. Hence attack node unable to communicate with normal node in the network. Present system uses one way hash chain, which limits packet transmission rate. Malicious nodes are drains their own batteries and reduce energy usage. Present System & All leaf nodes are physical nodes in network and virtual addresses corresponds to their position in the network. Original version is vulnerable to vampire attacks.

CLEAN-SLATE SENSOR NETWORK ROUTING (PLGP):

Developed By Parno,Luk, Gaustad and Perrig (PLGP). PLGP consist of two phases.

Two phases:

a) Topology discovery Phase

b) Packet forwarding phase

a) Topology Discovery Phase: In this network converges to a single group. Virtual address, public key and certificate are knows by each node. Each node has its own group address of size one, with virtual address zero. Groups merge with smallest neighboring group which may be single node. Example, 1) node 0 and group 0 becomes 0.0, 2) node 0 group 1 becomes 1.0 and so further. Every node broadcast certificate of identity including public key.

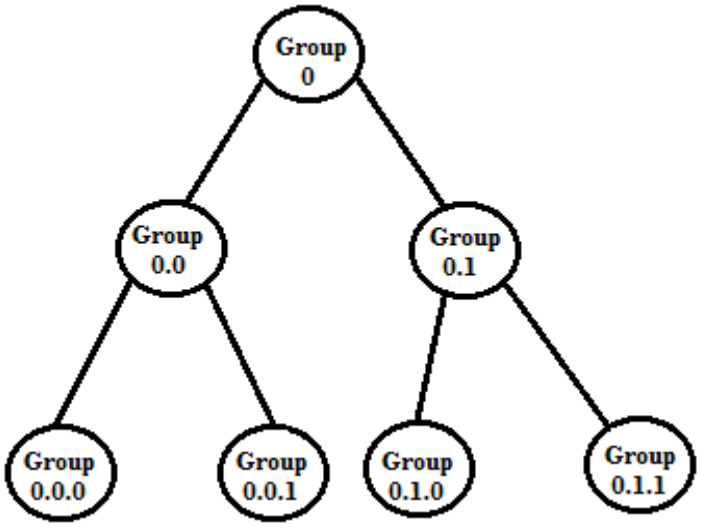

Fig.3. Binary tree of all addresses in the network

b) Packet forwarding phase: In packet forwarding phase, each node independently made all decision. A node when receives a packet determines next hop by finding the most significant bit of its address that differs from the message originators address. Every forwarding event minimize the logical distance to destination.

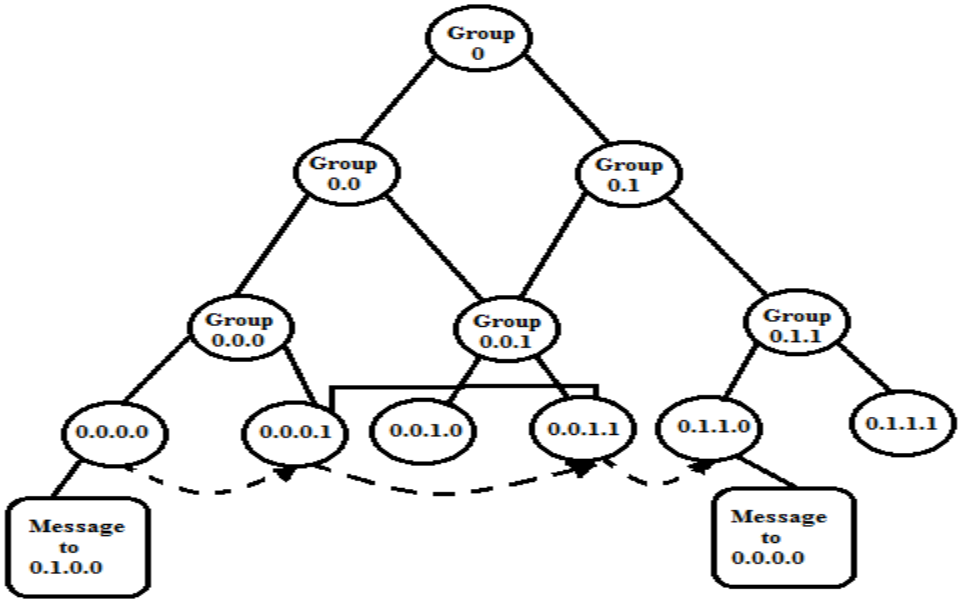

Fig.4. Final address tree for fully-converged 6-node network

PLGP in presence of vampires:

In the worse case, if packet returns to vampire as it can reroute. Theoretical energy increase of O(d) where d is the network diameter and N the number of network nodes. Vampire moves packet away from the destination. But honest node knows only its address and destination address. Honest node may be farther away from the destination than malicious nodes. Forwarding nodes don't know the path of a packet and allowing adversaries to divert packet to any part of the network.

Provable Security against vampire attacks (**No-backtracking property**):

No-backtracking implies vampire resistance. Nodes keep track of route cost. More formally: No-backtracking is satisfied if every packet p traverses the same number of hops whether or not an adversary is present in the network.

PLGP WITH ATTESTATION (PLGP-a) PHASE:

Every PLGP packet has verifiable path history. These signatures form a chain attached to every packet, allowing any node receiving it to validate its path. Every forwarding node verifies the attestation chain to ensure that the packet has never traveled away from its destination in the logical address space. PLGP with attestations (PLGP-a) uses this packet history together with PLGP's tree routing structure so every node can securely verify progress, preventing any significant adversarial influence on the path taken by any packet which traverses at least one honest node. Add a verifiable path history to every PLGP packet.

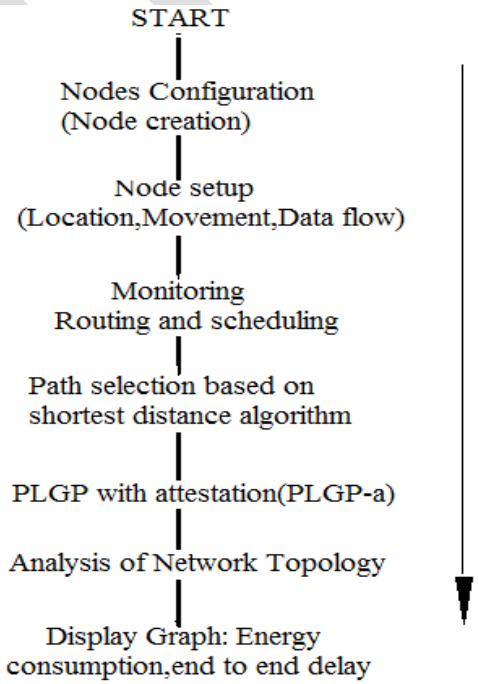

Fig.5. Proposed flow

M-DSDV NETWORK ROUTING

M-DSDV is a modified destination sequence distance vector. It is proactive network routing protocol. Proactive means utilizes more battery power and bandwidth. It helps to protect from Vampire attack during packet forwarding phase. Existing DSDV is designed basically to resolve routing loop problem. M-DSDV consist of both packet forwarding phase as well as topology discovery phase. A proper or legal network node has a unique certificate of membership. A unique certificate of membership includes it's public key and code word. Code word assigned by a trusted offline authority before spread. For transmitting data packets, topology discovery of the neighboring nodes begins.

Each node knows itself only very well. To discover their neighbors, nodes use local broadcasting scheme. In local broadcasting scheme certificate identity verification is done to isolate external unauthorized nodes from the network. If node is honest node, they know it's neighbor node's address and public key.

For example source node S, want to send a data packet to destination D, initially construct and broadcast a route request (RReq) packet consisting of (source address, destination address, sequence number, next hop, metric, index number and time to live) fields. Source address and destination address are internet protocol address, sequence number is used to differentiate new route from stale route, each node maintained next hop and metric are a local counter and each time RReq is broadcasted, index number is initialize to zero is basically used to keep track of the loops the packet has made, and lastly time to live field is used as a clock which increments whenever a RReq packet is sent.

On receipt of RReq, intermediate nodes inspect it to see if it is a duplicate, in which case it is rejected. If not pair is entered into the local history table. The destination address looked up in the routing table, if a fresh route to it is known an RRep a route reply packet is sent back to S. This also creates a backward route towards S. When destination receives RReq, it sends back an RRep packet to the node from which it got the first RReq packet.

The format of the route reply packet includes (Source address, Destination address, Destination sequence, index number, life time). In this source address, destination address and index number are copied from the incoming RReq packet, but the destination sequence number is taken from its counter in memory. The life time field indicates how long the route is valid.

On receipt of RRep, intermediates nodes on the way back, inspect the packet and create a backward route towards destination. Intermediate nodes that got the original RReq packet but were not on the reverse path discard the reverse route table entry when associated timer expires. When the next hop link in the routing table entry breaks, all active neighbors are informed by means of RERR packets which updates the sequence number. RERR packets are also generated when a node X is unable to forward packet P from node S to node D on link (X, Y). Incremented sequence number N is include in RERR. When node S receives the RERR ,it initiates a new route discovery for D using the sequence number that is at least as large as N

In the presence of vampires carousal attack and stretch attack can be prevented by using index number. In carousal attack packet traversed through the shortest path of network. Index number stored on the packet header and index number stored on local routing table of the node. In stretch attack the nodes keep track of route "Metric" and when acknowledgement return back , the route metric value and index number which indicates hop count, can be verified. If the index value > the metric value it concludes stretch attack as occurred. Clean slate sensor routing or PLGP and proposed PLGP-a help to prevent from attack on wireless ad hoc sensor network.

CONCLUSION

Vampire attack has been defined as a class of resource consumption attacks that use routing protocol to completely disable ad hoc wireless sensor networks by exhaust nodes' battery life. Resource consumption attacks are not protocols specific. Network energy

expenditure increased when forwarding phase attack has been proposed. Clean Slate Sensor Network Routing (PLGP) is first routing protocol that reduces damage from Vampire attack by verifying packets consistently make progress towards their destination. M-DSDV routing protocol used in packet forwarding phase, bounds damage from Vampire attacks.

REFERENCES:

[1] Imad Aad, Jean-Pierre Hubaux, and Edward W. Knightly, Denial of service resilience in ad hoc networks, MobiCom, 2004.

[2] David R. Raymond, Randy C. Marchany, Michael I. Brownfield, andScott F. Midkiff, Effects of denial-of-service attacks on wireless sensor network MAC protocols, IEEE Transactions on Vehicular Technology 58 (2009), no. 1.

[3] David R. Raymond and Scott F. Midkiff, Denial-of-service in wireless sensor networks: Attacks and defenses, IEEE Pervasive Computing 7 (2008), no. 1.

[4]] Jing Deng, Richard Han, and Shivakant Mishra, Defending against path based DoS attacks in wireless sensor networks, ACM workshop on security of ad hoc and sensor networks, 2005.

[5] Mina Guirguis, Azer Bestavros, Ibrahim Matta, and Yuting Zhang, Reduction of quality (RoQ) attacks on Internet end-systems, INFOCOM, 2005.

[6] David B. Johnson, David A. Maltz, and Josh Broch, DSR: the dynamic source routing protocol for multihop wireless ad hoc networks, Ad hoc networking, 2001.] Volkan Rodoplu and Teresa H. Meng, Minimum energy mobile wireless networks, IEEE Journal on Selected Areas in Communications 17 (1999), no. 8.

[7] Sheetalkumar Doshi, Shweta Bhandare, and Timothy X. Brown, An on demand minimum energy routing protocol for a wireless ad hoc network, ACM SIGMOBILE Mobile Computing and Communications Review 6 (2002), no. 3.

[8] Yih-Chun Hu, Adrian Perrig, and David B. Johnson, Ariadne: A secure on-demand routing protocol for ad hoc networks, MobiCom, 2002.

[9] Packet leashes: A defense against wormhole attacks in wireless ad hoc networks, INFOCOM, 2003.

[10] Rushing attacks and defense in wireless ad hoc network routing protocols, WiSE, 2003.

[11] Packet leashes: A defense against wormhole attacks in wireless ad hoc networks, INFOCOM, 2003

International Journal of Engineering Research and General Science Volume 3, Issue 5, September-October, 2015
ISSN 2091-2730

CORRECTIONS TO CCW PREDICTIONS FOR THE MOTION OF CYLINDRICAL HYDROMAGNETIC STRONG SHOCK WAVES IN SELF-GRAVITATING AND ROTATING GAS

C.V.SINGH
DEPARTMENT OF PHYSICS
N.R.E.C.COLLEGE ,KHURJA-203131
(Affiliated-CCS UNIV.MEERUT)

ABSTRACT: The effects of overtaking disturbances have been included in CCW[1—3] predictions to improve their accuracy for the motion of diverging cylindrical hydro magnetic shock waves through in an ideal gas under its own gravitating and rotating gas in the presence of constant axial magnetic field .Assuming an initial density distribution $\rho_o = \rho' r^{-w}$,where ρ', is the density at the axis of symmetry and w , is constant, the analytical expression for flow variables representing both the situations via; weak and strong cases of shock have been obtained .Their numerical estimates only at permissible shock front location have been computed with the results describing free propagation.

KEY-WORDS--hydro-magnetic shock waves, $\rho_o = \rho' r^{\pm w,}$ rotating gas, self gravitating gas , shock front , permissible shock front location, alfven speed $\sqrt{\mu H_o^2/\rho_o}$.

1. INTRODUCTION: Study of propagation of hydro-magnetic shock waves has proved its importance in different branches of Science and Technology. In recent past Kumar[4—6]; and Kumar and Prakash[7—8] have assuming initial density distribution $\rho_o = \rho' r^{\pm w}$ have investigated the propagation of hydro magnetic cylindrical shock waves through axial magnetic field for both cases of weak and strong shock using CCW method . J.B. Singh and S.K.Pandey[9] have studied the propagation of magnetogasdynamics cylindrical shock waves in self gravitating and rotating gas on the presence of constant axial magnetic field for both cases of weak and strong shock using CCW method. Assumption of any arbitrary initial density distribution of the form $\rho_o = \rho' r^{\pm w}$ or $\rho_o = \rho' \exp(\pm \lambda r)$ impose restriction values of propagation distance r, which are permitted by the fulfillment of initial entropy distribution condition i.e. $p_o \rho_o^{-\square} = c^*$. Thus such study by CCW method already have two limitations viz. (i)as it takes care of state just behind the shock and (ii) for any arbitrary choice of the initial density distribution ,the computational of numerical estimates of flow variables only at (psfl). Yousaf[10-12] has further ,established the need to including the effect of overtaking disturbances behind the flow on the motion of shock waves, in general, has helped to Rankin interest in problems investigated before to include it to make earlier results reliable ,particularly in absence of purely developed experimental basis. In this paper ,the EOD on motion of diverging cylindrical hydro magnetic shock waves through an ideal gas under its own gravitation and rotation in presence of constant axial magnetic field simultaneously , for both (i) weak and (ii) strong cases of shock ,assuming an initial density decrease of the unperturbed medium as $\rho_o = \rho' r^{-w}$,the modified form of analytical expressions for flow variable have been derived. Their numerical estimates only at permissible shock front location have been computed and compared with results describing free propagation (FP). Correction percentages have also been computed.

2. BASIC EQUATIONS: The equations governing the flow of gas enclosed by the shock front are

$$\frac{\partial u}{\partial t} + u\frac{\partial u}{\partial r} + \frac{1}{\rho}\frac{\partial P}{\partial r} + \frac{\mu}{2\rho}\frac{\partial H^2}{\partial r} + \frac{Gm}{r^2} - \frac{v^2}{r} = 0$$

$$\frac{\partial \rho}{\partial t} + u\frac{\partial \rho}{\partial r} + \rho\left(\frac{\partial u}{\partial r} + \frac{u}{r}\right) = 0$$

$$\frac{\partial P}{\partial t} + u\frac{\partial \rho}{\partial r} - a^2\left(\frac{\partial \rho}{\partial r} + u\frac{\partial \rho}{\partial r}\right) = 0 \qquad (1)$$

$$\frac{\partial m}{\partial r} - 2\pi r\rho = 0$$

$$\left(\frac{\partial}{\partial t} + u\frac{\partial}{\partial r}\right)(vr) = 0$$

$$\frac{\partial H}{\partial t} + u\frac{\partial H}{\partial r} + H\frac{\partial H}{\partial r} + H\frac{u}{r} = 0$$

Where r is the radial coordinate and r, v are the radial and azimuthal components of the particle velocity. P, ρ, H, μ and m denote respectively ,the pressure, the density, the axial magnetic field ,the magnetic permeability of the gas and mass inside the cylinder of unit cross- section of length r

3. BOUNDARY CONDITIONS: The magneto-hydrodynamic shock condition can be written in terms of single parameter $\xi = \rho/\rho_o$ as

$$\rho = \rho_o\xi \ , \ H = H_o\xi \ , \ u = \frac{\xi-1}{\xi}U \qquad (2)$$

$$U^2 = \frac{2\xi}{(\gamma+1)-(\gamma-1)\xi}\left[a_o^2 + \frac{b_o^2}{2}\{(2-\gamma)\xi+\gamma\}\right] \text{ and}$$

$$P = P_o + \frac{2\rho_o(\xi-1)}{(\gamma+1)-(\gamma-1)\xi}\left[a_o^2 + \frac{\gamma-1}{4}b_o^2(\xi-1)^2\right]$$

Where 0 stands for the states immediately ahead of the shock, U is the shock velocity. a_o is the sound speed $\sqrt{\gamma P_o/\rho_o}$ and b_o is the alfven speed $\sqrt{\mu H_o^2/\rho_o}$.

STRONG SHOCK: For the strong shock, ρ/ρ_o is large. Now consider the two cases of weak and strong magnetic field.

Case I : For weak magnetic field $b_o^2 \ll a_o^2$,using this condition the boundary conditions (2) become:

$$\rho = \rho_o\xi \ , \ H = H_o\xi \ , \ u = \frac{\xi-1}{\xi}U$$

$$\frac{P}{P_o} = 1 + \{\chi' a_o^2 + A' b_o^2\}\frac{U^2}{a_o^4} \text{ , where} \qquad (3)$$

$$\chi' = \gamma(\xi-1)/\xi \ , \ A' = \frac{\gamma(\xi-1)}{4\xi}[(\gamma-1)(\xi-1)^2 - 2\{(2-\gamma)\xi+\gamma\}]$$

Case II: For strong magnetic field at $b_o^2 \gg a_o^2$ using this condition, the boundary condition (2) becomes

$$\rho = \rho_o\xi \ , \ H = H_o\xi \ , \ u = \frac{\xi-1}{\xi}U$$

$$\frac{P}{P_o} = 1 + \chi\{b_o^2 + Aa_o^2\}\frac{U^2}{a_o^2 b_o^2} \text{ , where} \qquad (4)$$

$$\chi = \frac{\gamma(\gamma-1)(\xi-1)^3}{2\xi(2-\gamma)(\xi+\gamma)} \ , A = \frac{4}{(\gamma-1)(\xi-1)^2} - \frac{2}{(2-\gamma)\xi+\gamma}$$

4. CHARACTERISTIC EQUATIONS: The characteristic form of the system of equation (1) is easily obtained by forming a linear combination of first and third equation of system of equation (1) an only one direction in (r, t) plane can be written as

$$dP + \mu H dH + \rho c du + \frac{\rho c^2 u dr}{(u+c)r} + \frac{\rho c G m}{(u+c)}\frac{dr}{r^2} - \frac{\rho c v^2}{(u+c)}\frac{dr}{r} = 0 \qquad (5)$$

In order to estimate the strength of overtaking disturbance an independent characteristic is considered .The differential relation valid across C_+ disturbance is written by replacing c by –c in equation (5) we get

$$dP + \mu H dH - \rho c du + \frac{\rho c^2 u dr}{(u-c)r} + \frac{\rho c G m}{(u-c)}\frac{dr}{r^2} + \frac{\rho c v^2}{(u-c)}\frac{dr}{r} = 0 \qquad (6)$$

Where $c^2 = a^2 + b^2 = \frac{\gamma P}{\rho} + \frac{\mu H^2}{\rho}$.

5. ANALYTICAL RELATION FOR FLOW VARIABLES:

The equilibrium state of the gas is assumed to be specified by the condition $\partial/\partial t$ =0 and $H\mathbf{z}_o$ = constant.

(7)

Using (7) the first equation of the system of the equation (1) the equilibrium prevailing condition in front of the shock can be written as

$$\frac{1}{\rho_o}\frac{dP_o}{dr} + \frac{Gm}{r^2} - \frac{V^2}{r} = 0 \qquad (8)$$

Assuming an initial density distribution law as $\rho_o = \rho' r^{-w}$,where ρ' is the density at the axis of symmetry and w is constant.

Using $\rho_o = \rho' r^{-w}$, from the forth equation of the system of equation (1) we get

$$m = 2\pi\rho' r^{2-w}/(2\text{-}w) \qquad (9)$$

From equation (7) and (8) we get

$$\frac{P_o}{P_1} = K + K_1 r^{2-w} + K_2 r^{1-2w} \qquad (10)$$

$$\frac{da_o}{a_o} = \frac{1}{2}\left(\frac{dP_o}{P_o} + w\frac{dr}{r}\right) \qquad (11)$$

Where K′ is constant of integration $\frac{K'}{P^1} = K$, $K_1 = \frac{\Omega_o^2 \rho'}{(2-w)P'}$, $K_2 = \frac{2\pi\gamma}{D(1-2w)(w-2)}$, $v = \Omega_o r$ and

$D = a'^2/G\rho' P'$ is the pressure at the axis and a' is the sound velocity at the axis .

5(a). STRONG SHOCK WITH WEAK MAGNETIC FIELD (SSWMF):

By substituting the shock conditions (3) in to equation (5) and respective values of various quantities, we get

$$\frac{dU^2}{dr} + U^2\left[\frac{M_1}{r} + M_2\beta^2 r^{1-w} + M_3\beta^2 r^{-2w} + M_4\beta^2 r^{3-2w} + M_5\beta^2 r^{2-3w} + M_6\beta^2 r^{1-4w}\right] + M_7 r^{-w}$$

$$+ M_8 r + M_9\beta^2 r^{1-3w} - M_{1o} r^{3-3w} + M_{11}\beta^2 r^{2-2w} = 0 \qquad (12)$$

Where $M = \left[\frac{\chi'}{\gamma} + \frac{\xi'}{2}\sqrt{\frac{\chi'}{\xi}}\right]$, $N = \left[\frac{(\xi-1)}{(\xi-1)+\sqrt{\chi'\xi}} - \frac{w}{\gamma}\right]\frac{\chi'}{m}$, $N_1 = \left[\frac{w}{\gamma} + \frac{N}{M\gamma}\right]\frac{A'\beta^2}{MK}$, $M_1 = N - N_1$

$M_2 = \left[\frac{N}{M} - 2(1-w)\right]\frac{A'K_1}{M\gamma K^2}$, $M_3 = \frac{A'K_2}{M\gamma K^2}\left[(3w-1) + \frac{N}{M}\right]$,

$M_4 = 2A'K_1^2(2-w)/M\gamma K^3$, $M_5 = 6K_1K_2(1-w)/M\gamma K^3$,

$M_6 = 2K_2^2(1-2w)A'/M\gamma K^3$, $M_7 = N_2 - N_3$, $M_8 = N_5 - N_4$,

$M_9 = N_2K_2A'/M\gamma K^2$, $M_{10} = N_4A'/M\gamma K^2$,

$M_{11}= A'(N_2K_1 - N_4K_2)/M\gamma K^2$

$N_2= \frac{2\pi a^2}{D(2-w)M}\left[\frac{\xi\sqrt{\chi'\xi}}{\{(\xi-1)+\sqrt{\chi'\xi}\}} - 1\right]$, $N_3= \beta^2 A'N_2/M\gamma K$,

$N_4= \frac{\Omega^2}{M}\left[\frac{\xi\sqrt{\chi'\xi}}{\{(\xi-1)+\sqrt{\chi'\xi}\}} - 1\right]$, $N_5 = \beta^2 A'N_4/M\gamma K$,

On integration equation (27) we get

$$\frac{U^2}{F_P} = [K_p r^{-M1} - M_{12}r^{1-w} - M_{13}r^{-2} - M_{14}\beta^2 r^{2-3w} + M_{15}\beta^2 r^{4-3w} - M_{16}\beta^2 r^{3-2w} - M_{17}\beta^2 r^{5-3w} - M_{18}\beta^2 r^{4-4w} - M_{19}\beta^2 r^{3-5w} - M_{2o}r^{4-w} + M_{21}\beta^2 r^6 - 2w = 0 \quad (13)$$

Exp.{ β^2($M_{22}r^{2-w} + M_{23}r^{1-2w} + M_{24}r^{4-2w} + M_{25}r^{3-3w} + M_{26}r^{2-4w}$)} where K_p is constant of integration and M_{12}……..M_{26} are other constants.

For the C_- disturbance generated by the shock ,the fluid velocity increment using may be expressed as

$$du_- = \frac{\xi-1}{2\xi}[U(\frac{M_1}{r} + M_2\beta^2 r^{1-w} + M_3\beta^2 r^{-2w} + M_4\beta^2 r^{3-2w} + M_5\beta^2 r^{2-3w} + M_6\beta^2 r^{1-4w})] + \frac{1}{U}(M_7 r^{-w} + M_8 r + M_9\beta^2 r^{1-3w} - M_{1o}r^{3-3w} + M_{11}\beta^2 r^{2-2w})]dr \quad (14)$$

Substituting the shock condition (3) in to equation (6) and using the shock condition (3), we get

$$du_+ = -\frac{\xi-1}{2\xi}[U(\frac{H_1}{r} + H_2\beta^2 r^{1-w} + H_3\beta^2 r^{-2w} + H_4\beta^2 r^{3-2w} + H_5\beta^2 r^{2-3w} + H_6\beta^2 r^{1-4w})] + \frac{1}{U}(H_7 r^{-w} + H_8 r + H_9\beta^2 r^{1-3w} - H_{1o}r^{3-3w} + H_{11}\beta^2 r^{2-2w})]dr \quad (15)$$

Now in presence of both C_+ and C_- disturbances the fluid velocity increment behind the shock will be related as

$$du_- + du_+ = \frac{\xi-1}{\xi}dU \quad (16)$$

using equation (14),(15) and relation(16) we get

$$\frac{dU^2}{dr} + U^2[\frac{S_1}{r} + S_2\beta^2 r^{1-w} + S_3\beta^2 r^{-2w} + S_4\beta^2 r^{3-2w} + S_5\beta^2 r^{2-3w} + S_6\beta^2 r^{1-4w}] + S_7 r^{-w} + S_8 r + S_9\beta^2 r^{1-3w} - S_{1o}r^{3-3w} + S_{11}\beta^2 r^{2-2w} = 0 \quad (17)$$

Where $S_1 = H_1 + M_1$, $S_2 = M_2 + H_2$, $S_3 = M_3 + H_3$, $S_4 = M_4 + H_4$, $S_5 = M_5 + H_5$, $S_6 = M_6 + H_6$, $S_7 = M_7 + H_7$, $S_8 = M_8 + H_8$, $S_9 = M_9 + H_9$, $S_{10} = M_{10} + H_{10}$, $S_{11} = M_{11} + H_{11}$ on integration , we get

$$U^2_{EOD} = [K_p^* r^{-S1} - S_{12}r^{1-w} - S_{13}r^{-2} - S_{14}\beta^2 r^{2-3w} + S_{15}\beta^2 r^{4-3w} - S_{16}\beta^2 r^{3-2w} - S_{17}\beta^2 r^{5-3w} - S_{18}\beta^2 r^{4-4w} - S_{19}\beta^2 r^{3-5w} - S_{2o}r^{4-w} + S_{21}\beta^2 r^6 - 2w]\exp.\{\beta^2(S_{22}r^{2-w} + S_{23}r^{1-2w} + S_{24}r^{4-2w} + S_{25}r^{3-3w} + S_{26}r^{2-4w})\}$$

where K_p^* is constant of integration and S_{12}……..S_{26} are other constants. (18)

5(b). STRONG SHOCK WITH STRONG MAGNETIC FIELD (SSSMF):

By substituting the shock conditions (4) in to equation (5) and respective values of various quantities, we get

$$\frac{dU^2}{dr} + U^2[\frac{B_1}{r} + B_2\beta^{-2}r^{-2w} + B_3\beta^{-2}r^{1-w}] + B_4 r^{-w} + B_5 r - B_6\beta^{-2}r^{1-3w} + B_7\beta^{-2}r^{3-w}$$

$$+B_8\beta^{-2}r^{2-2w}= 0 \qquad (19)$$

Where $B=\left[\frac{\chi}{\gamma}+\frac{\xi-1}{2}\sqrt{\frac{\chi}{\xi}}\right], Z=\left[\frac{\chi(\xi-1)}{B\{(\xi-1)+\sqrt{\chi\xi}\}}-\frac{\chi w}{B\gamma}\right]$, $Z_1=\left[\frac{\chi w}{\gamma B}-Z\right]\frac{\chi A\beta^2 K}{B\gamma}$, $B_1= Z+Z_1$

$$B_2=\frac{A\chi K_2}{B\gamma}\left[(1-3w)+\frac{wX}{\gamma B}-\frac{\chi(\xi-1)}{B\{(\xi-1)+\sqrt{\chi\xi}\}}+\frac{\chi w}{B\gamma}\right], Z_5=\frac{Z_4\chi A\beta^2 K}{B\gamma}$$

$$B_3=\frac{A\chi K_1}{B\gamma}\left[(2-2w)+\frac{wX}{\gamma B}-\frac{\chi(\xi-1)}{B\{(\xi-1)+\sqrt{\chi\xi}\}}+\frac{\chi w}{B\gamma}\right], Z_3=\frac{Z_2\chi A\beta^2 K}{B\gamma}$$

$B_4= Z_2-Z_3$, $B_5= Z_5-Z_4$, $B_6=\frac{Z_2\chi AK_2}{B\gamma}$, $B_7=\frac{Z_4\chi AK_1}{B\gamma}$, $B_8=\frac{\chi A[Z_4K_2-Z_2K_1]}{B\gamma}$

$$Z_2=\frac{2\pi a^2}{D(2-w)B}\left[\frac{\xi\sqrt{\chi\xi}}{\{(\xi-1)+\sqrt{\chi\xi}\}}-1\right], \quad Z_4=\frac{\Omega^2}{B}\left[\frac{\xi\sqrt{\chi\xi}}{\{(\xi-1)+\sqrt{\chi\xi}\}}-1\right]$$

On integration equation(19) ,we get

$$\frac{U^2}{F_P}=[K_s r^{-B1}-B_9r^{1-w}-B_{1o}r^2-B_{11}\beta^{-2}r^{2-3w}-B_{12}\beta^{-2}r^{4-2w}-B_{13}\beta^{-2}r^{3-2w}]$$

$$\exp.\{\ \beta^2(B_{14}r^{1-2w}+B_{15}r^{2-w})\} \qquad (20)$$

where K_s is constant of integration and B_9……B_{15} are other constants.

For the C_- disturbances generated by the shock ,the fluid velocity increment using may be expressed as

$$du_-=-\frac{(\xi-1)}{2\xi}[(\frac{B_1}{r}+B_2\beta^{-2}r^{-2w}+B_3\beta^{-2}r^{1-w})U+\frac{1}{U}+(B_4r^{-w}+B_5r-B_6\beta^{-2}r^{1-3w}$$

$$+B_7\beta^{-2}r^{3-w}+B_8\beta^{-2}r^{2-2w})]dr \qquad (21)$$

Substituted the shock condition(3) in to equation(6) and again using shock condition(3), we get

$$du_+=\frac{(\xi-1)}{2\xi}[(\frac{B_1}{r}+B_2\beta^{-2}r^{-2w}+B_3\beta^{-2}r^{1-w})U+\frac{1}{U}+(B_4r^{-w}+B_5r-B_6\beta^{-2}r^{1-3w}$$

$$+B_7\beta^{-2}r^{3-w}+B_8\beta^{-2}r^{2-2w})]dr \qquad (22)$$

Now in presence of both C_+ and C_- disturbances the fluid velocity increment behind the shock will be related as

$$du_- +du_+ =\frac{\xi-1}{\xi}dU \qquad (23)$$

using equation(21),(22) and (23) we get

$$\frac{dU^2}{dr}+[\frac{h_1}{r}+h_2\beta^{-2}r^{-2w}+h_3\beta^{-2}r^{1-w}]U^2+h_4r^{-w}+h_5r-h_6\beta^{-2}r^{1-3w}+h_7\beta^{-2}r^{3-w}$$

$$+h_8\beta^{-2}r^{2-2w}= 0 \qquad (24)$$

Where $h_1=B_1+L_1$, $h_2=B_2+L_2$, $h_3=B_3+L_3$,$h_4=B_4+L_4$, $h_5=B_5+L_5$,$h_6=B_6+L_6$,$h_7=B_7+L_7$,$h_8=B_8+L_8$

On integration (24) we get

$$U^2_{EOD}=[K_s^* r^{-h1}-h_9r^{1-w}-h_{1o}r^2-h_{11}\beta^{-2}r^{2-3w}+h_{12}\beta^{-2}r^{4-2w}-h_{13}\beta^{-2}r^{3-2w}]$$

$$\exp.\{\ \beta^{-2}(h_{14}r^{1-2w}+h_{15}r^{2-w})\} \qquad (25)$$

where K_s^* is constant of integration and

$h_9=h_4/1+h_1-w$, $h_{10}=h_5/(2+h_1)$, $h_{11}=[h_2h_4/(1-2w)-h_6]/2+h_1-3w$, $h_{12}=[h_3h_5/(2-w)+h_7]/4+h_1-w$

$h_{13}=[h_2h_5/(1-2w)+h_3h_4/(2-w)+h_8]/3+h_1-2w$, $h_{14}=h_2/(2w-1)$, $h_{15}=h_3/(w-2)$

The flow variable expressions F.P. and EOD can be written by substituting (13,20) and (18,25) respectively in (3) and (4) and use for computation.

Permissible Shock Front Location (pslf): The pressure and the density in unperturbed state given by expression (13) and $\rho_o=\rho' r^{-w}$ must fulfill the initial entropy distribution condition i.e. $P_0\rho_o^{\gamma}-c^*$ where C^* is constant, substituting the respective expression for P_0 and ρ_o,we get

$$Kr^{w\gamma}+K_1r^{2-w(1-\gamma)}+K_2r^{1-w(1-\gamma)}-\frac{c^*\rho'^{\gamma}}{p'}=0 \qquad (26)$$

This is an equation in different powers depending upon the value of w and γ of propagation distance r it may have number of roots equal to highest powers of r, in general. The roots have been evaluated by expression (26). Hit and trial method.

Acknowledgment- I am very thankful to my wife smt Hemlata whose encouragement me to publish this research paper

RESULT AND DISCUSSION: Numerical estimates of flow variables for both F.P. and having included the EOD have been computed only at those locations of the shock front which are permitted by the initial entropy distribution condition in the unperturbed state. The results have also shown the comparison with F.P. predictions (a)(i) taking U/a_0=5098543, 6.38539, 6.583945, 6.78935, 7.01525 at r= 0.55, β^2=0.1, 0.15 Ω^2=10, 15 w=1.0, 1.05 γ=1.4, D=0.2, 0.3, 0.4, ξ=1.5 (ii) taking U/a_0=12.5436 at r=0.55, β^2=1.5 , γ=1.4, w=1.0 ,D=0,2 , ξ=3 (iii) taking U/a_0=20.0568 at r=0.55, β^2=1.5, γ=1.4, w=1.0 , D=0,2 ξ=4.5 (iv) taking U/a_0=120.3856 at r=0.55, β^2=1.5, γ=1.4, w=1.0 , D=0,2 ξ=5.9 SSWMF (b)(i) taking U/a_0=7.80538, 9.5869, 9.58685, 9.78345, 9.98523 at r=0.55 β^2=10,15 Ω^2=10,15 w=1.0,1.05 , γ=1.4 , D=0.2,0.3,0.4, ξ=1.5 (ii) taking U/a_0=17.54369 at r=0.55, β^2=15, γ=1.4, w=1.0 D=0,2, ξ=3 (iii) taking U/a_0=35.89546 at r=0.55, β^2=15, γ=1.4, w=1.0 D=0,2, ξ=4.5 (iv) taking U/a_0=140.58395 at r=0.55, β^2=15, γ=1.4, w=1.0 , D=0,2 ξ=5.9 SSSWF, numerical estimates of flow variables have been computed at permissible propagation distance for both F.P. and having included the EOD. It is observed from comparison those numerical values of flow variables, representing free propagation with the present values of flow variables included the EOD that the EOD over all retains the qualitative variation with parameter r, β^2, Ω^2, ξ,w and D unchanged. However,the reverse trend of variation with propagation distance have been observed for (i) the flow variables in the pressure and density (ii) the shock velocity and pressure, SSWMF (iii) the shock strength except(ς=3.0) particle velocity in case of SSSMF as compared to F.P. cases. It is very useful to mention that the present analysis gives description of shock propagation with better degree of accuracy by applying the corrections due to EOD behind the flow. Quantitatively the values of variables have increaced/decreased 1.32% to -0.853%, -0.59% to 1.12% respectively in case of SSWMF and SSSMF.

REFERENCES:

1.Chisnell, R.F. :Proc. R.Soc. London,232 A,350 (1955).

2.Chester,W:Phil.Mag.45,7,1293(1954).

3.Whitham ,G.B:J.Fluid, Mech.,4,337(1958).

4.Kumar.S and Singh C.V.:J.Ultra.Sci.Phy.Sci.16,(1),77,2004.

5.Kumar.S and Saxena, D.K.:Astrophys.space sci.100,65(1984).

6. Kumar.S and Kishor B.:J.P.A.S. 6,156 (2000).

7. Kumar.S andPrakash R.:II. Nuovo Ciminto 77,B,191(1983).

8. Kumar.S and Prakash R : Astrophys.space sci.235 27(1996).

9.Singh JB and Pandey, S.K,: Astrophys.space sci. 141 221 (1988).

10.Yousaf,M : J.Fluid, Mech.,66 577 (1974).

11.Yousaf,M :Phys. Fluid,25 (1), 45,(1982).

12.Yousaf,M : Phys. Fluid,28 1659 (1985).

13.S.Chandrashekhar: Hydrodynamics and hydro magnetic stability clarendon press, oxford (1961)

International Journal of Engineering Research and General Science Volume 3, Issue 5, September-October, 2015
ISSN 2091-2730

Distance Protection and Fault Location for line to ground fault utilising postfault current

Achu S[1], Emil Ninan Skariah[2]

PG Student, Dept. of EEE, SAINTGITS College of Engineering, Kottayam, Kerala, India[1]

Assistant professor, Dept. of EEE, SAINTGITS College of Engineering, Kottayam, Kerala, India[2]

Abstract: In the interconnected transmission networks, the fault current is fed by several sources and its direction depends on the fault place and is not fixed. The need for directional relaying in distribution networks has been raised due to the emergence of distributed generation (DG) units. The application of voltage as a reference quantity for the detection of fault direction is a common practice in transmission lines. Nevertheless, this approach is not applicable in distribution networks due to the absence of potential transformers. So a novel directional relaying scheme is introduced which is able to detect the fault location using only the postfault current. Also an algorithm to calculate distance of fault location during L-G is included in this system.

Keywords: Distributed generation, Fast Fourier Transform, Forward fault, Phase angle, Postfault current, Reverse fault.

INTRODUCTION

When the Electricity Supply Industry (ESI) began its activity the need for electric energy in a place was, in general, satisfied by municipal companies that installed generators located according to the distribution needs. Later on, the increasing electricity demand was satisfied installing huge generation plants, generally near the primary energy sources (e.g. coal mines, rivers, etc.). The great efficiency difference between one big generation plant and a small one, summing up the fact that the reserve margin that had to be taken in the first case was less than if the same power was installed in a distributed way, gave as a result the traditional conception of the Electrical Power Systems (EPS). Today there are technologies that allow generation using relatively small sized plants with respect to conventional generation, and with smaller costs per MW generated. Interconnecting distributed generation (DG) to an existing distribution system provides various benefits to several entities as for example the owner, utility and the final user. DG provides an enhanced power quality, higher reliability of the distribution system and can peak shaves and fill valleys. However, the integration of DG into existing networks has associated several technical, economical and regulatory questions. Penetration of a DG into an existing distribution system has many impacts on the system, with the power system protection being one of the major issues. DG causes the system to lose its radial power flow, besides the increased fault level of the system caused by the interconnection of the DG. Short circuit power of a distribution system changes when its state changes. Short circuit power also changes when some of the generators in the distribution system are disconnected. This may result in elongation of fault clearing time and hence disconnection of equipments in the distribution system or unnecessary operation of protective devices.

In this paper, a new protection philosophy based on postfault current is presented. All schemes present nowadays for detection of power flow direction depends on line voltage. Therefore, their application may be costly in non-radial distribution systems. So a new protection philosophy is required to cope with bi-directional power flows and unwanted tripping. So a new scheme for fault detection based on the postfault current can be considered. By avoiding the use of voltage or pre fault current, we are able to resolve the problems in existing methods. Moreover, the proposed scheme can be used in transmission and distribution networks.

SYSTEM MODEL

A 33-kV system including three buses is considered with the system parameters as given in Table 1. In this system, which is shown in fig 1, source A is an equivalent model of the utility grid. Moreover, source C represents an equivalent model of a microgrid which consists of a collection of DG units. F1 and F2 are faults located at the middle

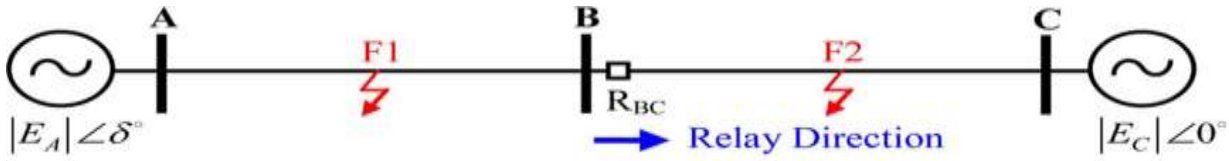

Fig. 1 System Model

of lines AB and BC, respectively. The sampling rate used in the simulation studies is 20samples/cycle. R_{BC} is a relay whose direction of operation is shown in fig 1.

TABLE 1

System Parameters.

PARAMETER	Value	Unit
System voltage	33	kV
System frequency	50	Hz
Length of line AB	10	Km
Length of line BC	12	Km
Positive seq. impedance of the lines	0.106 + j0.115	Ω/km
Zero seq. impedance of the lines	0.502 + j0.321	Ω/km
Positive seq. impedance of the sources	0.038 + j1.86	Ω
Zero seq. impedance of the sources	0.051 + j2.15	Ω

PROPOSED SCHEME

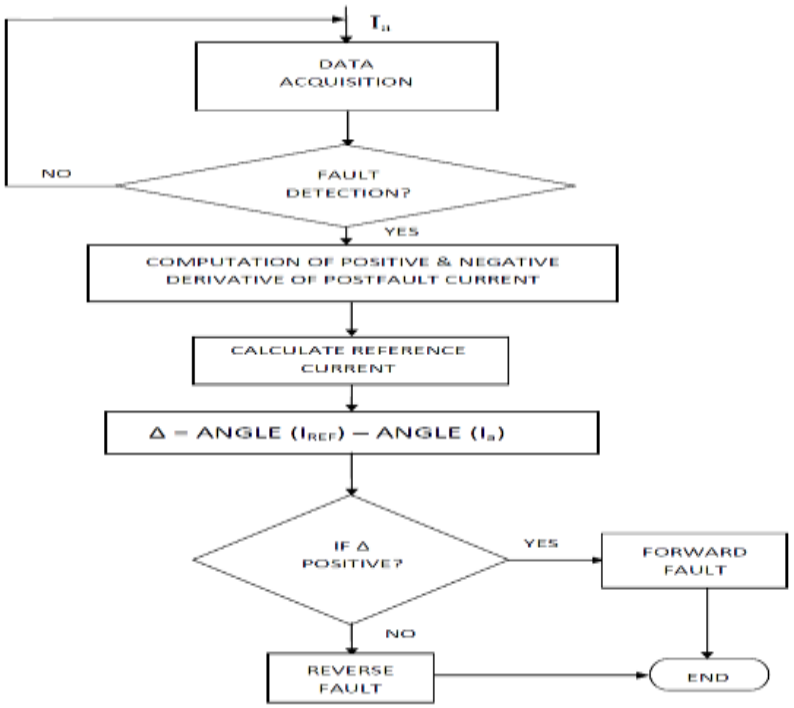

Fig. 2 Flow Chart

In this scheme, the phase current in each phase is obtained using a data acquisition technique. During normal operation this process of data acquisition continues in a regular interval. Whenever a fault occurs, both positive and negative derivative of postfault current are calculated. Also a reference current value is calculated based on the phase values of both forward and reverse currents. The difference between the angles of reference current and postfault current is used for determining the direction of fault current. If this value is positive, the fault is in the forward direction of relay and if the value is negative, the fault is in the reverse direction of the relay. This method for fault direction detection based on postfault current can be used for both bidirectional power flow systems with distributed generations.

ALGORITHM FOR DISTACE CALCULATION

For the case of line to ground fault, input parameters used for fault distance calculation are phase current phasors along with zero sequence impedance of line. Voltage phasor is not used as an input data. Fast Fourier transform (FFT) is used for calculating pre and postfault phasors.Given a phase-to-ground short circuit on the transmission line, the following complex equation is utilized in calculating the fault distance:

$$\bar{V} = [\bar{z}\,\bar{I} + (z_0 - \bar{z})\bar{I_0}]l + 3R\,\bar{J_0}$$

where $\bar{V}$ and $\bar{I}$ are the input voltage and current phasors to the faulted phase relays, $\bar{I_0}$ is the input zero sequence current to faulted phase relays, $\bar{J_0}$ is the zero sequence current at fault location, $\bar{z}$ and z_0 are the positive and the zero sequence line impedances per unit length, l is per unit distance from source to fault and R is the total fault resistance. Zero sequence current at fault location, $\bar{J_0}$ is not measurable, but it can be expressed in terms of the input zero sequence current, $\bar{I_0}$ and parameters from the zero sequence equivalent circuit of the analyzed network. By using the circuit theory, the system model can be replaced with the equivalent star circuit. For the line to ground short circuits, the sequence currents are equal to each other ($\bar{J_0} = \bar{J_d} = \bar{J_1}$).

$$l = \frac{\bar{I_0}\,\overline{Z_{0e}}\,(Z_{i2} + \bar{z}\,D) - \bar{I_\iota}\,\overline{Z_{\iota e}}\,(\overline{Z_{02}} + \bar{z_0}D)}{\bar{I_0}\,\overline{Z_{0e}}\,\bar{z} - \bar{I_\iota}\,\overline{Z_{\iota e}}\,\bar{z_0}}$$

where $\overline{Z_{01}}$ and $\overline{Z_{02}}$ are the impedances of the network equivalent star circuit, $\overline{Z_{\iota 1}}$ and $\overline{Z_{\iota 2}}$ are the negative sequence impedances, $\overline{I_{\iota}}$ is the input negative sequence current to faulted phase relays, D is the line length, $\overline{Z_{0e}} = \overline{Z_{01}} + \overline{Z_{02}} + \bar{z}_0 D$, $\overline{Z_{\iota e}} = \overline{Z_{\iota 1}} + \overline{Z_{\iota 2}} + \bar{z}\, D$.

RESULTS AND DISCUSSION

The results in table 2 shows that the angles of $I_{Postfault}$ and I_{Ref} are varied, based on the change in power flow direction. But the value of $Ø_{\Delta}$ is not affected by change in power flow. For both forward and reverse power flow, $Ø_{\Delta}$ is +1.57rad in forward faults and -1.57rad in reverse faults.

TABLE 2

Effect of Power Flow Direction.

POWER FLOW	FAULT TYPE	FAULT LOCATION	$Ø_1$ (Rad)	$Ø_{ref}$ (Rad)	$Ø_{\Delta}$ (Rad)	FAULT DIRECTION
Forward	Ag	F2	-0.226	1.344	+1.57	Forward
Forward	Ag	F1	1.86	0.29	-1.57	Reverse
Reverse	Ag	F2	-1.23	0.33	+1.57	Forward
Reverse	Ag	F1	2.939	1.369	-1.57	Reverse

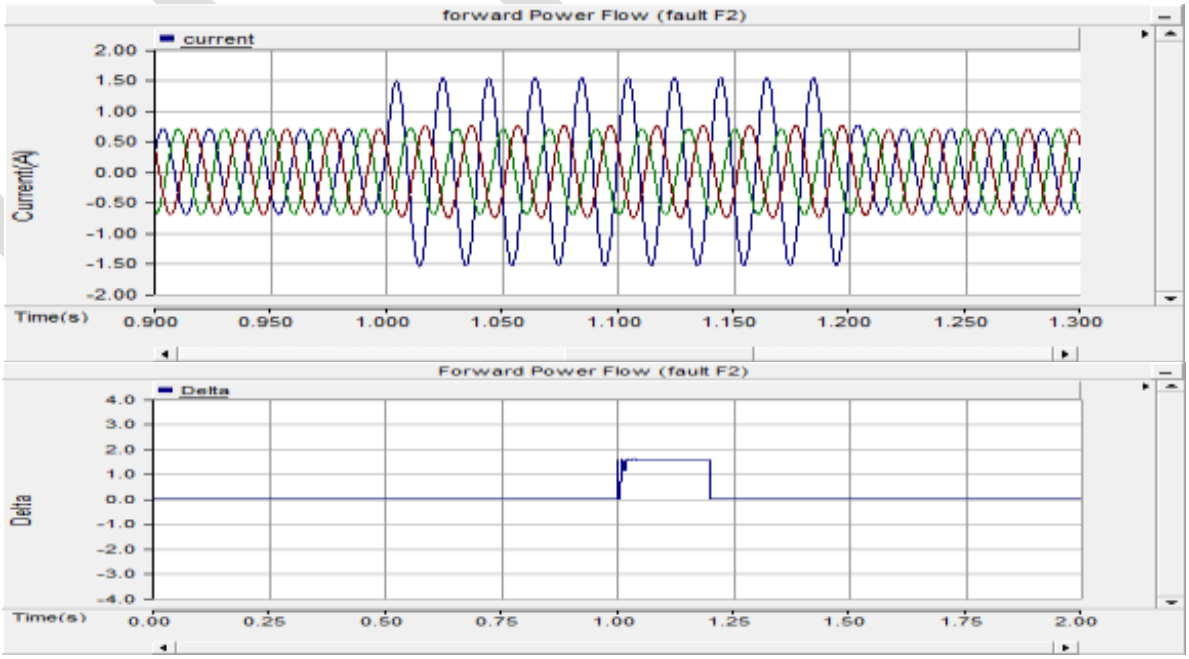

Fig. 3 Change in $Ø_{\Delta}$ and current with forward power flow with L-G fault at F2.

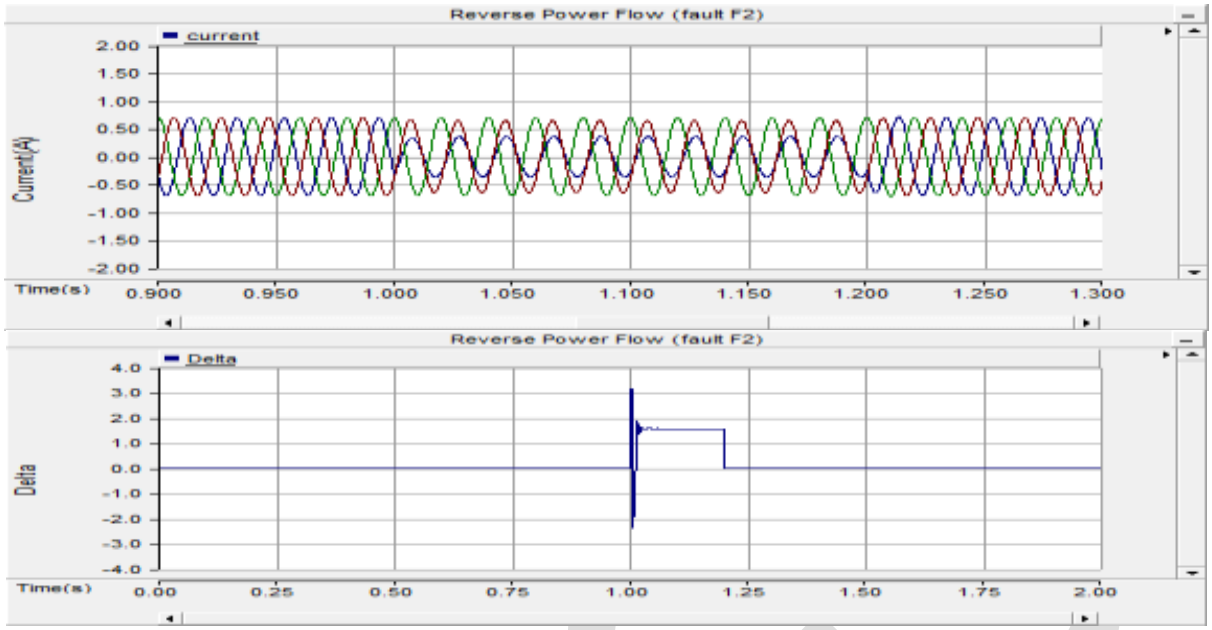

Fig. 4 Change in $Ø_{\Delta}$ and current with reverse power flow with L-G fault at F2.

Fig 3 and fig 4, show the graphs of current and value of delta during forward and reverse power flow with fault at F2. In both cases the value of delta is obtained as positive irrespective of the direction of power flow which indicates that the fault has occurred in the forward direction of relay.

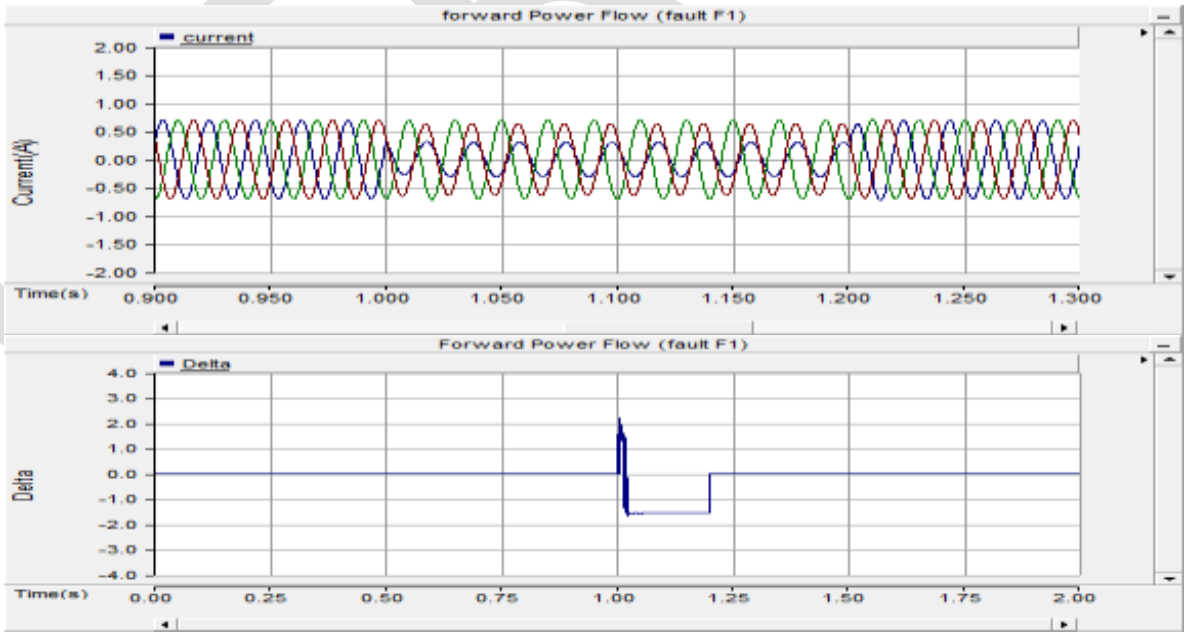

Fig. 5 Change in $Ø_{\Delta}$ and current with forward power flow with L-G fault at F1.

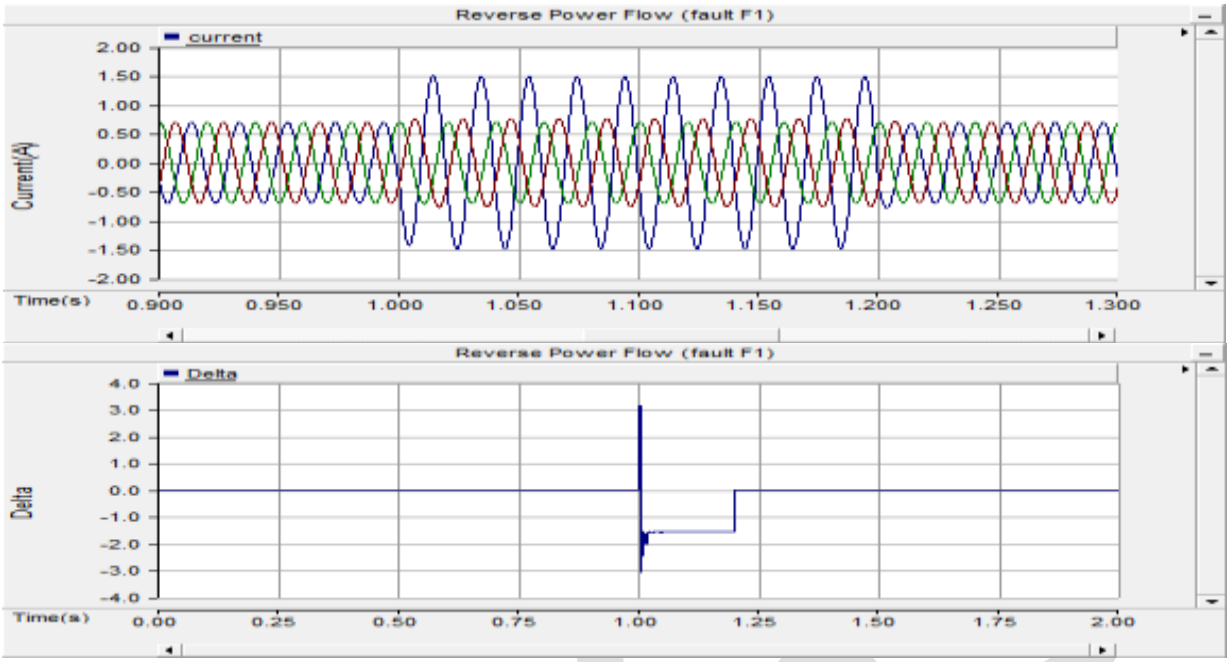

Fig. 6 Change $Ø_{\Delta}$ and current with reverse power flow with L-G fault at F1

Fig 5 and fig 6, show the graphs of current and value of delta during forward and reverse power flow with fault at F1. In both cases the value of delta is obtained as negative irrespective of the direction of power flow which indicates that the fault has occurred in the reverse direction of relay.

The reliable operation of protective relays may be affected by the fault resistance. The above system is evaluated with forward and reverse power flow against various faults in both directions with the fault resistances (R_f) between 1 to 10Ω.

TABLE 3

Effect of change in Fault Resistance.

POWER FLOW	FAULT TYPE	FAULT LOCATION	R_f (Ω)	$Ø_1$ (Rad)	$Ø_{ref}$ (Rad)	$Ø_{\Delta}$ (Rad)	FAULT DIRECTION
Forward	Ag	F2	2	-0.642	0.928	+1.57	Forward
Forward	Ag	F2	5	-0.377	1.193	+1.57	Forward
Forward	Ag	F2	10	-0.226	1.344	+1.57	Forward
Forward	Ag	F1	2	2.188	0.618	-1.57	Reverse
Forward	Ag	F1	5	2.297	0.727	-1.57	Reverse
Forward	Ag	F1	10	1.86	0.29	-1.57	Reverse
Reverse	Ag	F2	2	-0.98	0.59	+1.57	Forward
Reverse	Ag	F2	5	-0.872	0.698	+1.57	Forward
Reverse	Ag	F2	10	-1.23	0.33	+1.57	Forward
Reverse	Ag	F1	2	2.52	0.95	-1.57	Reverse
Reverse	Ag	F1	5	2.79	1.22	-1.57	Reverse
Reverse	Ag	F1	10	2.939	1.369	-1.57	Reverse

The results obtained show that the phase angle of postfault current ($Ø_1$) is affected by the change of fault resistance value. However as much as $Ø_1$ changes, the phase angle of reference current ($Ø_{ref}$) changes as well. Consequently, the phase angle, $Ø_{\Delta}$ remains fixed.

The distance to fault location from source 1 is calculated for L-G fault for both forward and reverse power flow. Here the Fast Fourier Transform (FFT) technique is used for calculating the pre and postfault phasors. Table 4 and 5 shows the results obtained for distance

calculation for L-G fault during forward and reverse power flow. Here by analyzing the results we can conclude that the accuracy of distance calculation is less when the fault is situated near source 1 or source 2. When the distance from sources increases the accuracy of locating the fault also increases.

TABLE 4

Fault distance Calculation for L-G fault during Forward Power Flow.

POWER FLOW	POSTFAULT CURRENT						DISTANCE TO FAULT FROM SOURCE 1		FAULT DIRECTION
	POSITIVE SEQUENCE		NEGATIVE SEQUENCE		ZERO SEQUENCE				
	MAGNITUDE	ANGLE	MAGNITUDE	ANGLE	MAGNITUDE	ANGLE	ACTUAL	CALCULATED	
Forward	0.582383	-1.60379	0.34418	-1.84468	0.372174	-1.89781	4	8.8187	Reverse
Forward	0.578514	-1.58226	0.337528	-1.81162	0.355314	-1.83811	6	9.2938	Reverse
Forward	0.574726	-1.56265	0.331345	-1.78112	0.340002	-1.7777	8	10.0767	Reverse
Forward	0.446439	-1.55125	0.20623	-1.89219	0.217195	-1.99365	10	10.8267	Reverse
Forward	0.448338	-1.53253	0.20539	-1.85041	0.205929	-1.90869	12	11.3145	Forward
Forward	0.450397	-1.5149	0.204983	-1.8105	0.196274	-1.81606	14	12.3507	Forward
Forward	0.452588	-1.49846	0.205024	-1.77268	0.188545	-1.71594	16	13.7447	Forward
Forward	0.454943	-1.48327	0.205521	-1.73721	0.183074	-1.60935	18	15.3317	Forward
Forward	0.457487	-1.46938	0.20648	-1.70432	0.180165	-1.49846	20	16.9962	Forward

TABLE 5

Fault distance Calculation for L-G fault during Reverse Power Flow.

POWER FLOW	POSTFAULT CURRENT						DISTANCE TO FAULT FROM SOURCE 1		FAULT DIRECTION
	POSITIVE SEQUENCE		NEGATIVE SEQUENCE		ZERO SEQUENCE				
	MAGNITUDE	ANGLE	MAGNITUDE	ANGLE	MAGNITUDE	ANGLE	ACTUAL	CALCULATED	
Reverse	0.189352	-2.75073	0.339935	-1.88802	0.367585	-1.94116	4	8.8189	Reverse
Reverse	0.177529	-2.72969	0.335277	-1.85386	0.352945	-1.88035	6	9.2937	Reverse
Reverse	0.166689	-2.71002	0.331023	-1.82226	0.339672	-1.81891	8	10.0767	Reverse
Reverse	0.137351	2.73065	0.204082	-1.85325	0.214934	-1.95471	10	10.8266	Reverse
Reverse	0.128696	2.72244	0.204417	-1.81037	0.204954	-1.86865	12	11.3144	Forward
Reverse	0.120332	2.71462	0.205182	-1.76935	0.196464	-1.77492	14	12.3508	Forward
Reverse	0.112288	2.70743	0.206399	-1.73044	0.189811	-1.67369	16	13.7446	Forward
Reverse	0.104561	2.70174	0.208086	-1.69386	0.185359	-1.566	18	15.3317	Forward
Reverse	0.0971501	2.69864	0.210255	-1.65987	0.18346	-1.45402	20	16.9960	Forward

CONCLUSION

A new protection philosophy is developed for identifying the direction of fault based on post fault current. The phase angle difference between reference current and current in each phase were calculated and based on the sign of this value the direction of fault is estimated. Also an algorithm to calculate distance of fault location during L-G fault is included in this system. Here post fault phase current phasors are required to calculate the distance to fault point. The reliability of the system for various operation conditions such as change in power flow direction and change in fault resistance were analysed for different fault positions. Also accuracy of distance calculation for line to ground were analyzed for fault at different lengths in both forward and reverse power flow conditions.

REFERENCES:

[1] Mario Vignolo and Raul Zeballos, "Transmission Networks or Distributed Generation?", Power, 1990.
[2] Angel Fernández Sarabia, "Impact of distributed generation on distribution system", Aalborg, Denmark, June 2011.
[3] Murari Mohan, Saha Ratan, Das Pekka Verho and Damir Novosel, "Review of Fault Location Techniques for Distribution Systems," Power Systems and Communications Infrastructures for the future, Beijing, September 2002.
[4] J. Sadeh, M. Bashir and E. Kamyab, "Effect of distributed generation capacity on the coordination of protection system of distribution network," Transmission and Distribution Conference and Exposition: Latin America (T&D-LA),IEEE/PES, Nov. 2010, pp. 110-115.
[5] A. Ituzaro, R. H. Douglin, and K. L. Butler-Purry, "Zonal overcurrent protection for smart radial distribution systems with distributed generation," in Proc. IEEE Power Energy Soc. Innovative Smart Grid Technol., Feb. 2013, pp. 1–6.
[6] S. M. Hashemi, M. T. Hagh, and H. Seyedi, "Transmission-line protection: A directional comparison scheme using the average of superimposed components," IEEE Trans. Power Del., vol. 28, no. 2, pp.955–964, Apr. 2013.
[7] P. Jafarian and M. Sanaye-Pasand, "High-speed superimposed-based protection of series-compensated transmission lines," Proc. Inst. Eng.Technol. Gen. Transm. Distrib., vol. 5, no. 12, pp. 1290–1300, 2011.
[8] K. Pradhan, A. Routray, and G. S. Madhan, "Fault direction estimation in radial distribution system using phase change in sequence current," IEEE Trans. Power Del., vol. 22, no. 4, pp. 2065–2071, Oct.2007

International Journal of Engineering Research and General Science Volume 3, Issue 5, September-October, 2015
ISSN 2091-2730

Investigation of Mechanical and Tribological Properties of Cu, Mg, Si, Zn Reinforced AA1100 Composite Fabricated By Stir Casting

Shubham Chitkara[1], Shivam Aeron[1], Kunal Sehrawat[1], Rajesh Khanna[2*], Neeraj Sharma[3]

[1] Student, B. Tech., Department of Mechanical Engineering, Maharishi Markandeshwar University (Mullana), India
[2]Professor, Department of Mechanical Engineering, Maharishi Markandeshwar University (Mullana), India
[3] Assistant Professor, Department of Mechanical Engineering, D.A.V. University, Jalandhar, India

Abstract— In the present work, a low cost stir casting process is used for the fabrication of Aluminium (AA 1100) based Metal Matrix Composites (MMC's) adding Copper (Cu), Magnesium (Mg), Silicon (Si) and Zinc (Zn) as the reinforcements. The objective of this work is production of Aluminium Matrix Composite (AMC) with better mechanical and tribological properties and relatively low manufacturing cost. Different wt% of Cu, Mg, Si and Zn are added to Aluminium (1100) to make the AMC and its mechanical and tribological properties have been investigated such as tensile strength, hardness, etc. These reinforcements showed improvements in the mechanical as well as tribological properties. These improvements in the properties are compared with the pure Aluminium (1100). It was found that tensile strength and hardness of the fabricated samples increased, with a maximum increase of 44.4% in tensile strength and 26.2% in hardness compared to pure Al 1100 but the percentage elongation decreased in each sample.

Keywords—Mechanical properties, Tensile Strength, Hardness, AMC, Tribological, Cu, Mg, Si, ,Zn

INTRODUCTION

Composite materials play a very vital role in the field of engineering as well as advance manufacturing in response to unprecedented demands from technology due to quickly advancing activities in aerospace, aviation and automobile industries. These materials have low specific gravity that makes their properties particularly superior in strength and modulus to many traditional engineering materials such as metals [1]. These innovative materials open up unlimited possibilities for modern material science and development. The characteristics of MMCs can be changed, depending on the applications.

However, the technology of MMCs is in competition with other modern technologies like powder metallurgy. Favorable properties of composites materials are high tensile strength, lower density, high electrical and thermal conductivity, corrosion resistance, improved wear resistance, etc. The advantages of composite materials are only realized when there is a reasonable cost equal to performance relationship in the component production. The use of composite material is obligatory if a special property can be achieved by application of these materials**.**

Aluminium alloy reinforced the discontinuous ceramic reinforcements is rapidly replacing conventional materials in various automotive, aerospace and automobile industries [2]. Due to light weight and high strength applications metal matrix composites has found increasing usage in industries found that aluminum matrix had poor fluidity compared with a casting of a aluminum alloy [3]. Silicon is the main alloying element in Al-Si alloys; it imparts high fluidity and low shrinkage, which result in good castability and weldability. Due to their excellent cast ability and good compromise between mechanical properties and lightness aluminum silicon alloys are most important and widely used casting alloys to cast components with complex shapes. Furthermore the applications of aluminum alloys in the automotive sector could be one of the economically sustainable innovations[4]. Al-Zn-Mg alloys can be used for both castings and wrought products, but because of the poor castability, the bulk is in the form of wrought products. Zinc is a tolerated impurity in many alloys, often up to 1.5-2% Zn, because it has no substantial effect on room-temperature properties. Interfacial bonding is improved by adding Mg. Additionally, the mechanical properties of composites are remarkably improved with the Mg content increasing [5]. Aluminium-magnesium alloys are both lighter than other aluminium alloys and much less flammable than alloys that contain a very high percentage of magnesium [6]. Density is reduced by magnesium and increased by all the other elements. The total amount of Zn + Mg + Cu controls the properties and consequently the uses. When the total is above 9%, high strength is paramount and corrosion resistance, formability and weldability are subordinated to it. With a total of from 6 to 8%, strength is still high, but formability and weldability are much better. Below a total of 5-6% fabricability becomes paramount and stress corrosion susceptibility tends to disappear [7]. Copper additions have a rather limited effect, which is approximately the same as that caused by the addition of the same amount of zinc. Thus, a copper-bearing alloy can be expected to have properties similar to those of a copper-free alloy with zinc content equal to the zinc plus copper content. This additive effect of copper applies up to 2.5% copper. The strength generally increases and ductility decreases with increase content of Cu and Mg [8,9].

The principal reasons for the use of these materials are light weight, low density and load bearing applications on account of their enhanced mechanical properties. Unreinforced Al shows the lowest wear resistance, while composites with the highest hardness and second-phase volume content are the most wear resistant, especially at high load [10]. Hardness was usually thought of as a wear controlling property, i.e. the higher the hardness, the greater is the wear resistance of the material. However, it should be emphasized

* Corresponding Author Email-ID: raajeshvkkhanna@rediffmail.com

that it is the hardness of the contacting asperities and not the bulk hardness that will control the wear rate. The addition of hard second phase particles to the matrix improves both wear resistance and mechanical properties [11].

MATERIALS AND EXPERIMENTAL PROCEDURE

Raw Materials

The materials identified for the experiment are:

- Aluminium alloy 1100

Table 1: Composition of Aluminium alloy (AA 1100)

Constituent	Aluminium	Copper	Mangenese	Zinc
% Composition	99	0.05	0.94	0.1

- Cu particulates of particle size 500 mesh (50 µm).
- Si particulates of particle size 500 mesh (50 µm).
- Mg particulates of particle size 500 mesh (50 µm).
- Zn particulates of particle size 500 mesh (50 µm).

Material Preparation

Different wt% of reinforcement was taken for the three samples fabricated. These wt% of reinforcements for the samples fabricated are shown in the table. These reinforcing particulates were then mixed according to their wt% for different samples and are preheated in oven to remove the moisture content present in it.

Fabrication of Composite by Stir Casting Process

Composite specimens are casted using the stir casting method. A muffle furnace is used for stir casting fabrication of MMC (line diagram shown in fig. 1). Mechanical stirring is used in stir casting liquid state method of composites materials fabrication, in which preheated reinforcement is mixed with a molten aluminium metal.
Factors considered in preparing metal matrix composites by stir casting method are:

- Maintaining a uniform distributed reinforced material.
- Wet ability of the substance.
- Porosity of the composites
- Chemical reaction between the reinforcement material and the matrix alloy.

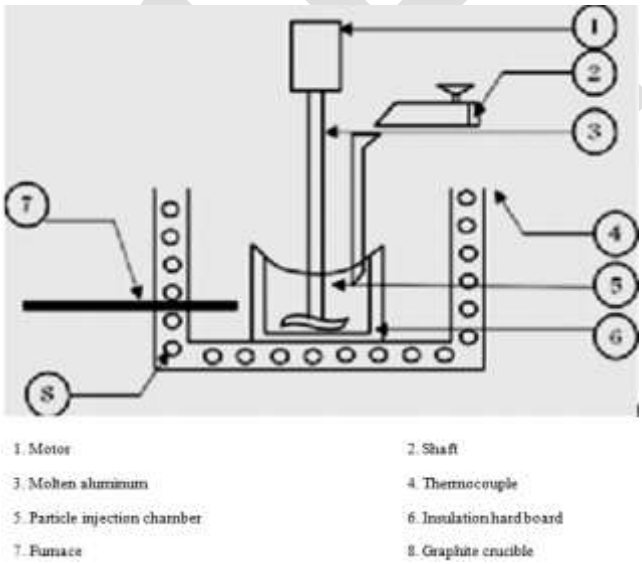

Figure 1: Schematic view of the Furnace [12]

Figure 2: Fabrication by stir Casting Process in a Muffle Furnace

Table 2: Different wt% of reinforcements used for the fabrication of AMC

Sample No.	Aluminium Alloy 1100 (By Wt.)	Cu Particlulates wt %	Mg Particlulates wt %	Si Particlulates wt%	Zn Particlulates wt %
1	1.8 Kg	1.5%	2 %	2.5%	0.5%
2	1.8 Kg	1.5%	4 %	5 %	1 %
3	1.8 Kg	3 %	2 %	2.5%	1 %

In the process, first, the Al matrix material is melted in a graphite crucible contained within a resistance-heated furnace and the liquid metal is heated to 910 ^{o}C and then Cu, Mg, Si & Zn particles are added into the molten Al material according to their volume fraction in nitrogen gas flow with a slow rate. The Cu, Mg, Si & Zn particles are stirred by a mixer at 750 rev/min. then again molten metal reheated in the stir casting furnace after completing the stirring process, the mixed material is cast into a metallic mould at 700-800^{o}c, and then quenched in water together with the mould. After that MMC is cooled in air. The fabricated MMC are shown in Figure 3.

Figure 3: Fabricated Samples of AMC.

Mechanical and Tribological Properties

The mechanical and tribological properties have been tested for the fabricated samples of the Aluminium Matrix Composite. The tests performed were tensile and elongation test, hardness test and wear test.

Tensile & Elongation Test Equipment: The testing machine used for tensile strength & elongation testing is the universal testing machine, UTE100 (Make: FIE, Capacity 100 kN, Resolution 0.01 kN).
Testing method used is IS 1608:2005. Temp. 25^{o}C and Rel. Humidity 40-60%. This test was performed at CITCO-IDFC Testing Laboratory, Chandigarh.

Hardness Testing Equipment: Vicker Hardness Tester (Make: FIE) is used for testing hardness of the fabricated composite samples. Testing method used is IS 1501:2002. Temp. 25^{o}C and Rel. Humidity 40-60%. This test was performed at CITCO-IDFC Testing Laboratory, Chandigarh.

Wear Testing Equipment: Sliding wear test was carried out using pin-on-disc apparatus. The disc is allowed to rotate at 1500 rpm. The pins which are held against the rotating disc are of 8 mm diameter and 30 mm length. The pressure on the specimen is applied by means of a precision dead weight pressure tester operated manually. In the experimentation, the specimens to be tested are taken in the form of a pin and are allowed to slide against a heat treated steel disc. The wear rate is calculated from weight loss measurements taken by weight balance machine (with accuracy 0.01 mg) before and after sliding. This test was performed at the Tribology Lab, MMEC, Mullana, Ambala.

RESULTS & DISCUSSION

Tensile & Elongation Test

Dumbell shaped specimens made for the tensile and elongation testing are shown in the figure 4.

Figure 4: Tested specimen for tensile and elongation test

1- Sample 1, 2- Sample 2, 3- Sample 3

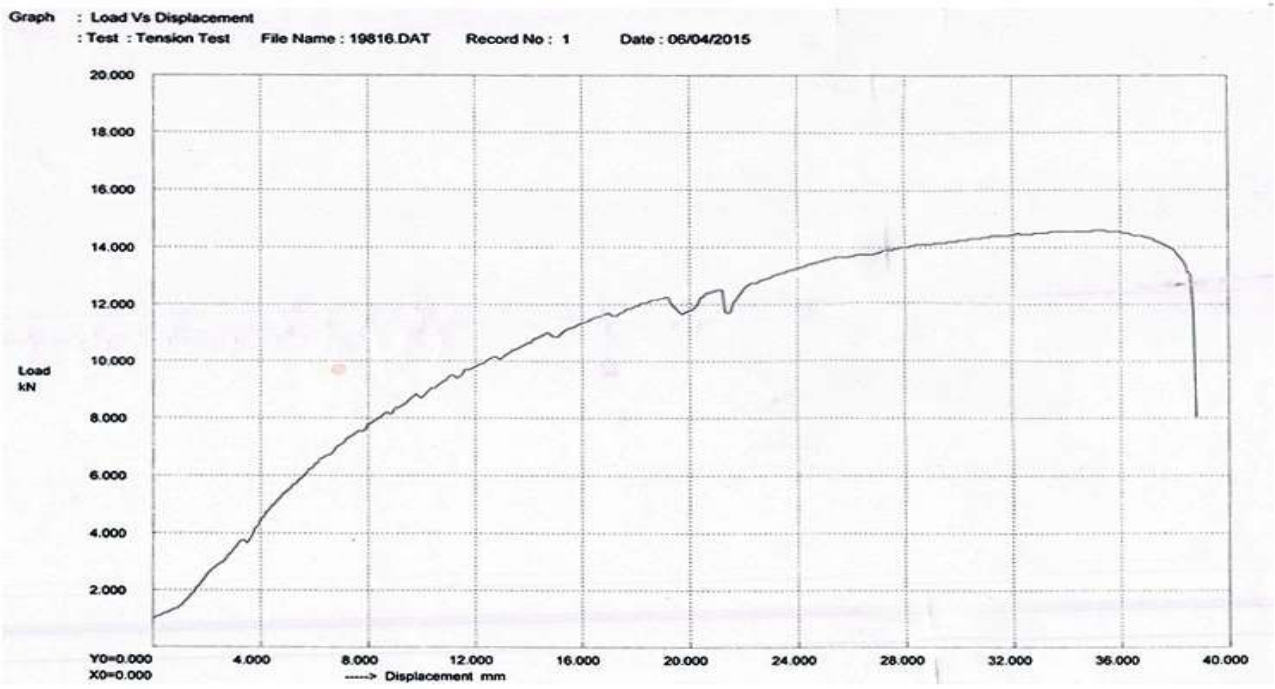

Figure 5: Stress v/s Displacement Graph for Sample 1

Figure 5 shows sample 1 which contain 1.5% Cu, 2% Mg, 2.5% Si & 0.5% Zn, can bear a maximum load of 14.70 kN and has a maximum displacement of about 38.5 mm.

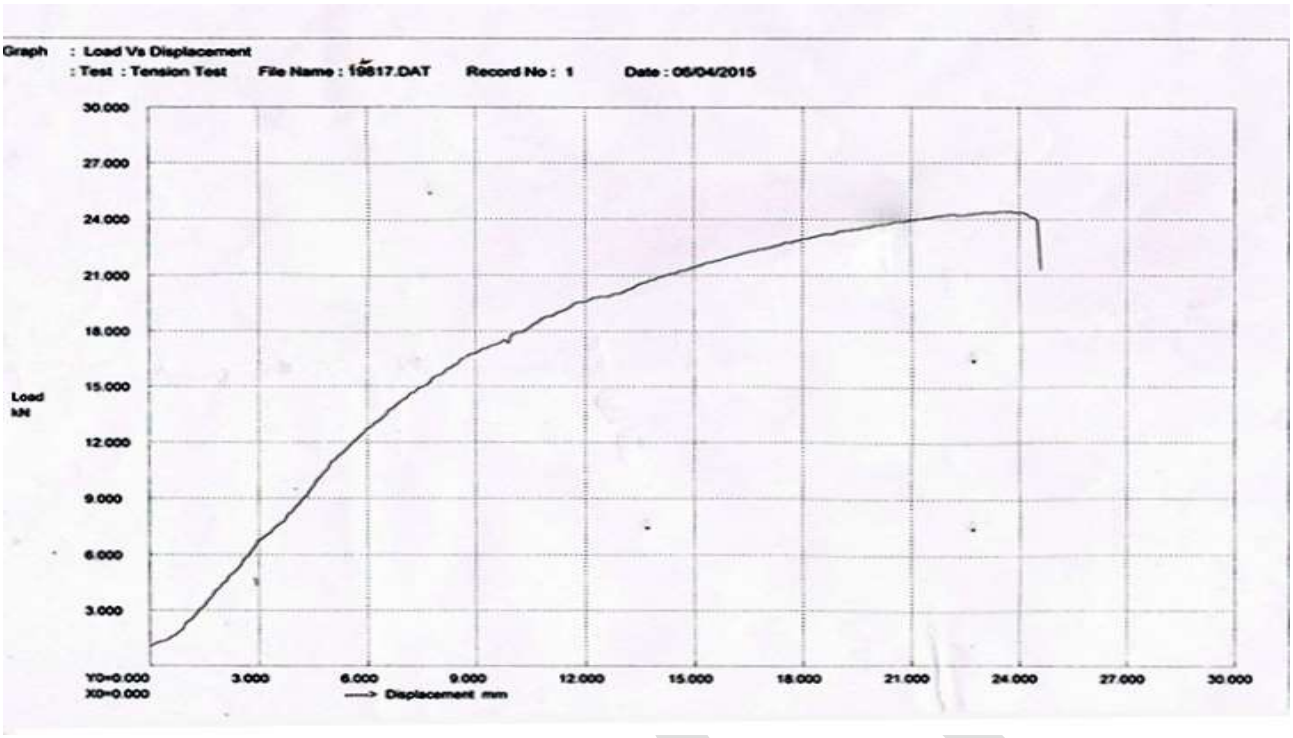

Figure 6: Stress v/s Displacement Graph for Sample 2

Figure 6 shows sample 2 which contain 1.5% Cu, 4% Mg, 5% Si & 1% Zn, can bear a maximum load of 21.30 kN and has a maximum displacement of about 24.5 mm.

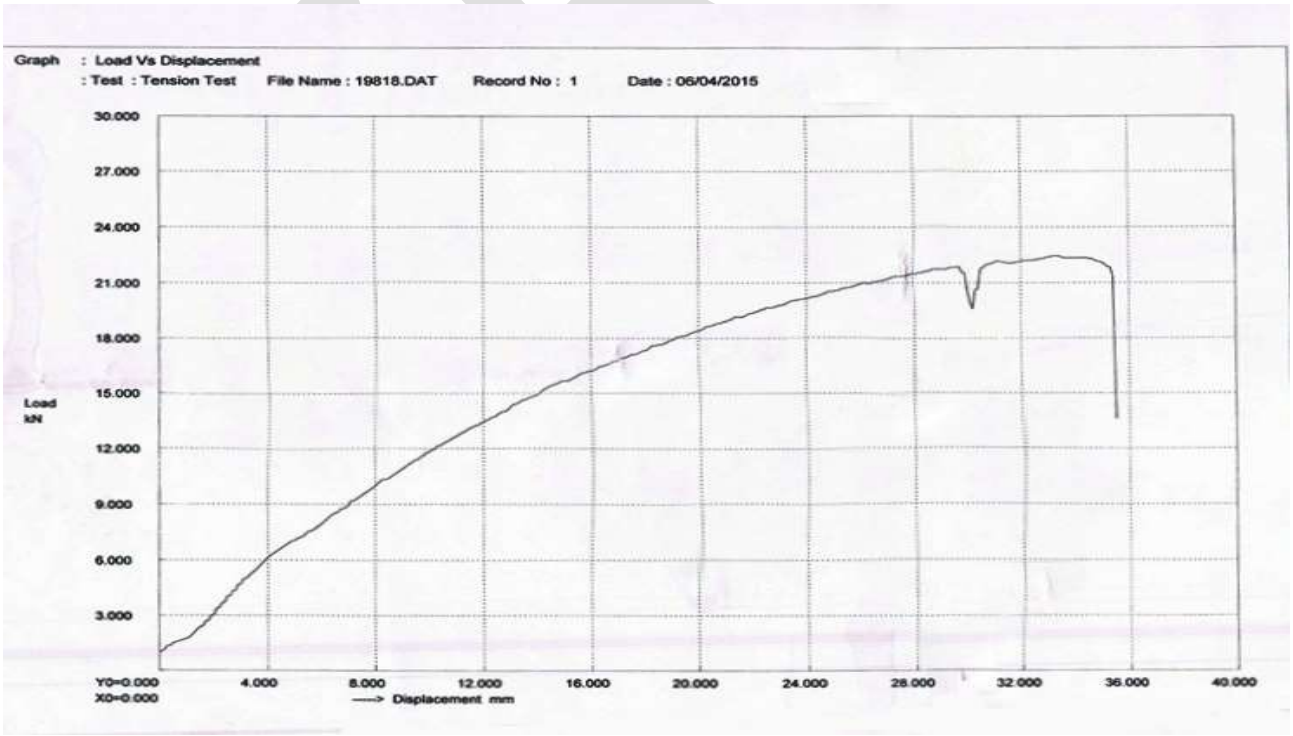

Figure 7: Stress v/s Displacement Graph for Sample 3

Figure 7 shows sample 3 which contain 3% Cu, 2% Mg, 2.5% Si & 1% Zn, can bear a maximum load of 22.50 kN and has a maximum displacement of about 35.5 mm.

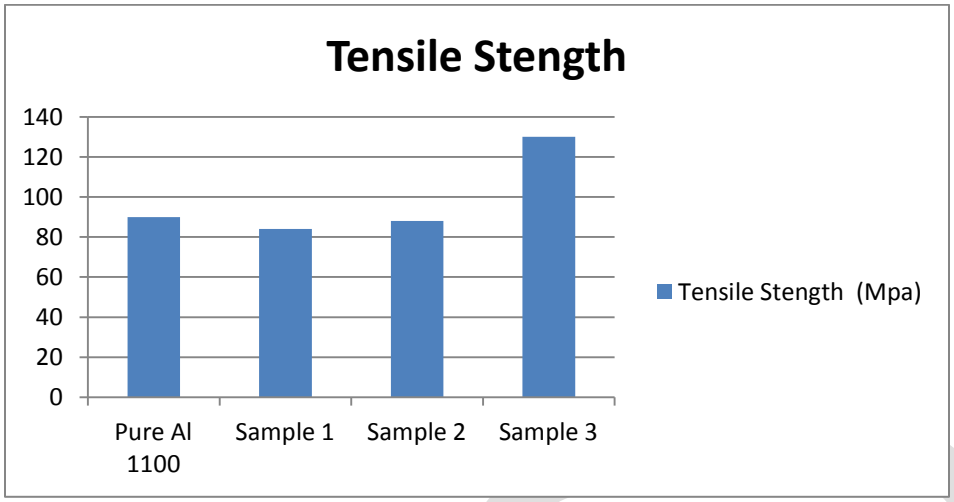

Figure 8: Tensile Strength Chart

The tensile strength for Aluminim Alloy 1100 is taken as 90 MPa [13]. The comparison of the fabricated samples with Pure Al 1100 is given in the Figure 8.

Table 3: Tensile & Elongation Test Results

Sample	Area (mm^2)	Tensile strength (MN/mm^2)	% Elongation
Sample 1	174.4	84	32.40
Sample 2	165.2	88	15.86
Sample 3	172.1	130	23.30

The results show that the maximum tensile strength is in sample 3 (130MPa) which is 44.4% more than the tensile strength of Pure Al 1100 which could be due to the increase in wt% of Cu and the additive effect of Cu & Zn which increases the tensile strength but decreases %elongation or ductility.

Hardness Test

The Vickers hardness for Pure Aluminium 1100 is taken as 35 HV [14]. The comparison hardness of Pure Al 1100 with fabricated samples is shown in Fig. 10. The maximum hardness is found in sample 2 (44.2 HV) which is 26.2% more than the hardness pure Al 1100 which could be due to the increase in wt% of Mg & Si from the other two samples.

Figure 9: Tested specimen of Hardness Test
1-Sample 1, 2- Sample 2, 3- Sample 3

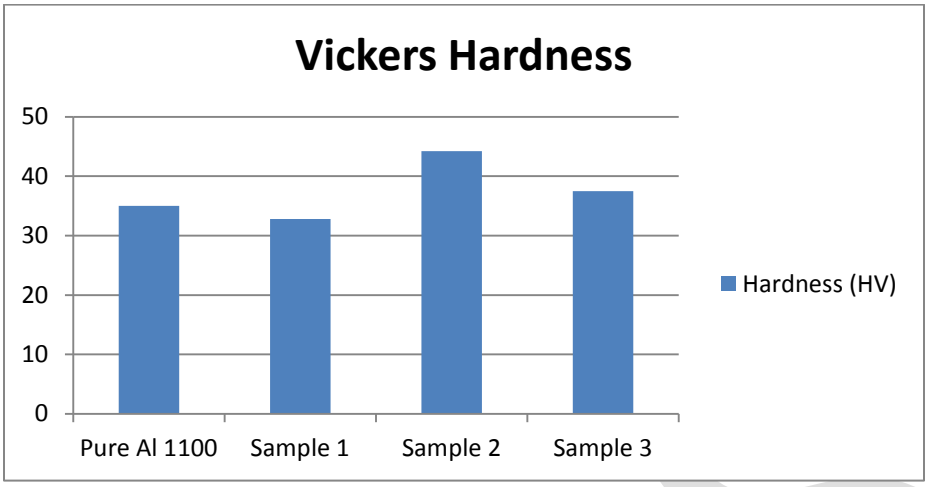

Figure 10: Hardness Chart

Table 4: Results of Vickers Hardness Test

Sample	HV (1)	HV (2)	HV (3)	HV (Average)
Sample 1	32	33.8	32.6	32.8
Sample 2	46.1	43.2	43.3	44.2
Sample 3	37.6	35.8	39.1	37.5

Wear Test

For analyzing the wear rate, 3 specimens were taken and held against the steel disc for 5 min time intervals. The weight loss during the wear process is measured by measuring the difference in the final and initial weight of the specimen thereby weighing the specimen before and after the wear test on the digital analytical weighing machine. The results of the wear test of the 3 fabricated samples are shown in Table 5.

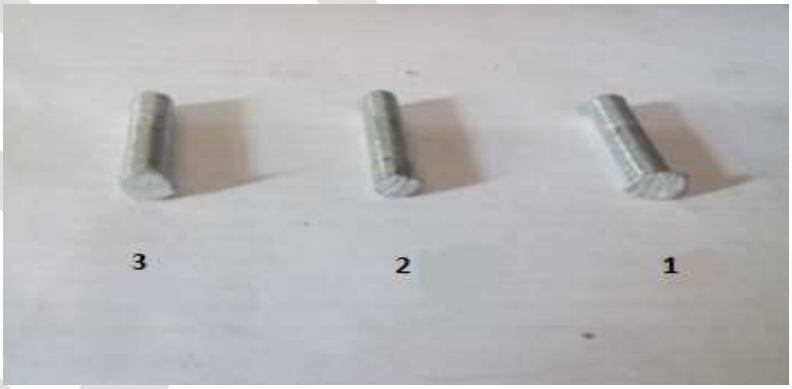

Figure 11: Tested specimen of Wear Test.

1-Sample 1, 2- Sample 2, 3- Sample 3

Table 5: Results of Wear Test.

Sample	Weight of the material before testing (g)	Weight of the material after testing (g)	Weight loss (g)
1	5.9980	5.9903	0.0077
2	5.0363	4.9565	0.0798
3	5.2003	-	-

The test on the third specimen failed in less than a minute because of the extreme amount of heat generation the specimen got stuck to the disc. The least amount of wear was found in the sample 1 with a weight loss of 0.0077g.

ACKNOWLEDGMENT

The authors are grateful to Dr. N.K. Batra, HOD, Mechanical Engineering Department, Maharishi Markandeshwar Engineering College, Mullana(Ambala), India, who gave abundance support to complete the research work. The authors would like to express profuse gratitude and appreciation to Mr. Shiv Kumar & Mr. Mukesh, Lab Technicians, MMEC, Mullana(Ambala) and all those who gave us support to make the research work accomplished and our Beloved Parents.

CONCLUSION

In the present work, Cu, Mg, Si & Zn are being reinforced in Aluminium Alloy 1100 at different weight percentages. Mechanical and Tribological properties of the fabricated AMC's are being investigated. The improvements in the mechanical properties are compared with the properties of pure Al 1100 which gives several conclusions:

Tensile & Elongation Test:

The improvements tensile strength observed in sample 3 (3% Cu, 2% Mg, 2.5% Si & 1% Zn) which is 44.4% more than the tensile strength of Pure Al 1100. But the % Elongation has decreased as compared to pure Al 1100.

Hardness Test:

The improvement in hardness is found in sample 2 (1.5% Cu, 4% Mg, 5% Si & 1% Zn) which is 26.2% more than the hardness pure Al 1100.

Wear Test:

The lowest weight loss observed at applied load 3 kg, 1500 rpm sliding speed and 100 mm track diameter is 0.0077 grams in sample 1 (1.5% Cu, 2% Mg, 2.5% Si & 0.5% Zn).

REFERENCES:

[1] L.M. Manocha and A.R. Bunsell, Advances in composite materials, Pergamon Press, Oxford, 1980.
[2] John E. Allison and Gerald S. Cole, 1993, Metal-matrix composites in the automotive industry: Opportunities and challenges.
[3] Young-Ho Seo and Chung-Gil Kang, The effect of applied pressure on particle-dispersion characteristics and mechanical properties in melt-stirring squeeze-cast SiCp/Al composites, Journal of materials processing Technology, 1995.
[4] M. Merlin et al., Journal of Materials Processing Technology, 2009.
[5] Lin GENG, Hong Wei ZHANG, Hao-Ze LI, Li-Na GUAN, Lu-Jung HUANG, Effects of Mg content on microstructure and mechanical properties of SiC_p/Al-Mg composites fabricated by semi-solid stirring technique, 2010.
[6] Kumai et al, 2005.
[7] Totalmateria.com, Article 77, Al-Mg-Cu alloys, 2003.
[8] C.H. Caceres, I.L. Svensson and J.A. Taylor, Strength-Ductility behavior of Al-Si-Cu-Mg Casting Alloys in T6 Temper, 2003.
[9] Hamid Reza Ezatpour, Seyed Abolkarim Sajjadi, Mohsen Haddad Sabzevar, Yizhong Huang, Investigation of microstructure and mechanical properties of Al6061-nanocomposite fabricated by stir casting, 2013.
[10] M.D Bermúdez, F.J Carrión, E.J Herrera Dry and lubricated wear resistance of mechanically-alloyed aluminium-base sintered composites, 2001.
[11] Basavakumar K.G., Mukunda P.G. and Chakraborty M., 'Dry sliding wear behavior of Al-12Si and Al-12Si-3Cu cast alloys', Materials & Design, 2009.
[12] Saravanakumr K., Venkatesh S., Harikumar P., Kannan K., Jayapal V., Studies on Aluminium-graphite by Stir Casting Technique, 2013.
[13] www.metalmensales.com, properties of Aluminium 1100.
[14] Valmir Martins Monteiro, Saulo Brinco Diniz, Bruna Godoi Meirelles, Luis Celso Da Silva, Andersan Dos Santos Paula, Microstructural And Mechanical Study Of Aluminium Alloys Submitted To Distinct Soaking Times During Solution Heat Treatment, 2014.

International Journal of Engineering Research and General Science Volume 3, Issue 5, September-October, 2015
ISSN 2091-2730

Implementing Dynamic Access Control in Openstack with Rbac using Token and Session Management

NITESH KUMAR

CH. Brahm Prakash Govt. Engineering College

Niteshks070@gmail.com

New delhi,India

Abstract— The emerging industry of Openstack brought us to an extent where security is of great importance .The model proposed in this paper implements dynamic access control in openstack using keystone ,this gives the finer granularity of authorization in openstack .The V model elaborates the flexible approach to attain the keystone identity service with the use of token and session management. The path followed by user to gain access to the system justify authenticity on every node .Therefore, providing a significant control mechanism.

Keywords—openstack ; Rbac ; token; session; V model ;session activation; token reallocation;

INTRODUCTION

As the cloud computing is new concept which enables the 2technologies such as web server ,network function virtualization and business models used to deliver IT capabilities(software ,platform ,hardware) as a service request, scalable and elastic[1].This is the new trend of computing where IT resources are dynamically scalable, virtualized and exposed as service on the internet[2].

This technology provide a well structured tool for the cloud management i.e Openstack, It is free and open source cloud software platform which can be used a infrastructure as a service[Iaas].All code is licensed under Apace 2 license. It is developed by NASA .

The main characteristics of openstack are as follows:

(i). Scalable: This solution is already developed worldwide in companies whose data volumes is measured in petabytes of distributed architecture and massively scalable upto 1 million physical machines, upto 60 million virtual machines and billion of stored objects[3].

(ii) Flexible: Openstack supports most virtualization solution of the market ESX. HYPER-V,KVM ,LXC,QEMU,UML,Xen andXenserver[2,4].

(iii). Opensource: It is the opensource technology so that it can be easily modified and changed but after going through a validation process. Many companies came forward to support the project and based on the code used by the NASA and Rackspace Cloud . It is written in python and currently implements two control APIs, the EC2 API and Rackspace.It uses different drivers to interface with a maximum no of hypervisors (Xen,KVM,HYPER-V,QEMU)[5].
Openstack components are as follows:

(1). Compute (Nova)

OpenStack Compute (Nova) is a cloud computing fabric controller, which is the main part of an IaaS system. It is designed to manage and automate pools of computer resources and can work with widely available virtualization technologies, as well as bare metal and high-performance computing (HPC)configurations. KVM, VMware, and Xen area available choices for hypervisor technology, together with Hyper-V and Linux container technology such as LXC.[6][7]
It is written in Python and uses many external libraries such as Eventlet (for concurrent programming), Kombu (for AMQP communication), and SQLAlchemy (for database access).[8] Compute's architecture is designed to scale horizontally on

standard hardware with no proprietary hardware or software requirements and provide the ability to integrate with legacy systems and third-party technologies.

(2) Image Service (Glance)

OpenStack Image Service (Glance) provides discovery, registration, and delivery services for disk and server images. Stored images can be used as a template. It can also be used to store and catalog an unlimited number of backups. The Image Service can store disk and server images in a variety of back-ends, including OpenStack Object Storage. OpenStack's image is an operating system installed on a virtual machine (VM).[14]
Glance—OpenStack's image service module—is a compute module, as it does not store images, variations, or instances—but rather catalogs them and holds their metadata from Swift or a storage backend datastore.[14]

(3) Object Storage (Swift)

OpenStack Object Storage (Swift) is a scalable redundant storage system. Objects and files are written to multiple disk drives spread throughout servers in the data center,with the OpenStack software responsible for ensuring data replication and integrity across the cluster. Storage clusters scale horizontally simply by adding new servers. Should a server or hard drive fail, OpenStack replicates its content from other active nodes to new locations in the cluster. Because OpenStack uses software logic to ensure data replication and distribution across different devices, inexpensive commodity hard drives and servers can be used. SwiftStack, an object storage software company, is currently the leading developer for Swift.[14]

(4) Dashboard (Horizon)

OpenStack Dashboard (Horizon) provides administrators and users a graphical interface to access, provision, and automate cloud-based resources. The design accommodates third party products and services, such as billing, monitoring, and additional management tools. The dashboard is also brandable for service providers and other commercial vendors who want to make use of it. The dashboard is one of several ways users can interact with OpenStack resources. Developers can automate access or build tools to manage resources using the native OpenStack API or the EC2 compatibility API.[14]

(5) Identity Service (Keystone)

OpenStack Identity (Keystone) provides a central directory of users mapped to the OpenStack services they can access. It acts as a common authentication system across the cloud operating system and can integrate with existing backend directory services like LDAP. It supports multiple forms of authentication including standard username and password credentials, token-based systems and AWS-style (i.e. Amazon Web Services) logins. Additionally, the catalog provides a queryable list of all of the services deployed in an OpenStack cloud in a single registry. Users and third-party tools can programmatically determine which resources they can access.[14]

(6) ACCESS CONTROL

Access is the ability to enter into a computer resource. An access control system enables an authority to control access to areas and resources in a given physical quantity or computer based system. With the rapid growth of information technologies, it is obviously convenient and efficient to provide good security services. Access control is a term for security practice that is supported by security systems and provides a way for security management [9] delivered via the Internet. Security issues are the major issue in the enterprise and e-management

Role Based Access Control (RBAC):

RBAC is considered a much more generalized model in compare to both the MAC & DAC, encompassing both the models as special cases providing a policy neutral framework which allows RBAC to be customized on a per-application basis. As the blend of the MAC & DAC models and integrity, RBAC is partially founded on principles showcased by Biba's .
RBAC dynamically assigns the roles to the users based on criteria defined by the manager or system administrator. Role-Based Access Control models are a set of fairly new models [10] first introduced in the ninety's. The RBAC92 model [11] introduces the concept of roles, and RBAC96 [12] refines RBAC92 thanks to the addition of the users notion (different from the subjects one) and a roles hierarchy defined as a partial order. RBAC also stands apart from the more traditional MAC and DAC by granted rights on transactions, not on underlying subjects. These rights are granted to roles, which at first glance appear to be a synonym for DAC groups. The difference lies in that groups consist of a collection of users while roles are a bridge between a collection of users and a collection of the Clark-Wilson model of transaction rights. While RBAC supports data abstraction through transactions, it cannot be

used to ensure permissions on sequences of operations need to be controlled .To do this, a less general and more sophisticated access control model must be used.

(B). Limitations in existing System:

(i) No centralized control: The OpenStack platform is divided into different services, like Nova for computing, Swift for storage, etc. Each service uses a configuration file with the corresponding security policy. For SDN controllers, there exists another control system. For the OPNFV platform, it lacks a synchronization mechanism between these configuration and control systems in order to build a consistent and End-to-End protection system[13].

(ii) No dynamic control: Currently, the authentication and authorization in OpenStack are achieved through the token mechanism, but there isn't any token revocation mechanism. Once a user gets an authorization token, we will not have any control over the user. It lacks dynamic control at runtime in OpenStack and/or SDN controllers[13].

(iii) No customization and flexibility: Each user of OpenStack and/or SDN controllers consumes their resource pool in their own manner, but it lacks customization for security management system integration. For example, in both OpenStack and OpenDaylight, user cannot define their own security policy for each VNF resource pool[13].

(iv) No fine-granularity: Finally, the granularity of authorization in OpenStack and/or SDN controllers is not enough fine. Currently, it's at the API-level. This means that we can authorize or deny a user from using an API like launch VM in OpenStack. But we need the granularity to be pushed to the resource-level, authorize or deny a user from using a specific resource through the API, e.g. allowing a user to launch a dedicated VNF VM. [13]

***(*C). METHODOLOGY PROPOSED**

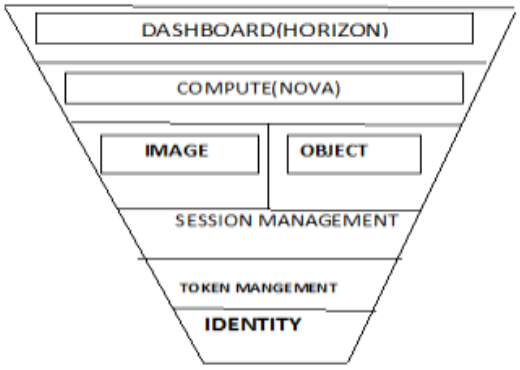

Fig.(i) V model

As per the given model V .this is more enhanced model for the openstack security system in which identity plays a major role in authentication.

The working of the model is as follows :-

Dashboard which is the major controlling center is at the top level and have the full view of the V components ,suppose a user wants to login then it enters through the UI of the dashboard and with the compute controller it register its image in the object storage and then it is logged in the session management and now it is binded with the time so that it verifies itself within the time allocated ,getting inside the token management, it mention its token and next in the identity it mention its role and access type and now the upward procedure follow again from the bottom i.e it gets its tokenid and then session Id means for which the token is valid,and then it is registered in the image service so that it have its backup and then get back to the compute. In this given model we actually overcome one of the flaws in the earlier system that is no dynamic control over the user after getting token from the keystone ,this is now

overcome by session management that is after getting the token from the keystone ,session will give a limited time to the user and in the image part we can apply token renewal system or in the session so that it can get again the session back.

(D).WORKING.

The working of the model is as follows:

According to the working diagram fig.(ii), When a user wants to login for the access it will interact with the UI based dashboard which give the Api based platform. Then user proceeds to the compute which is the controller part of the system, it guides through the all components of system. At the next step the login details ,time of activity and other details will be stored in the image which is for the backup data .Now it comes to the session management ,which will generate a session id and stored it in image ,now user is under the session i.e it have a limited time to enter its details ,in the next part it requests for the token according to its role and identity, keystone will authenticate it using its database ,now user will follow the reverse path that is gain a token from the token management and session id which contains the details about the session ,then registering through image and return to the dashboard with the access token and a session id .The administrator will have a look over to each part of system from the backend.

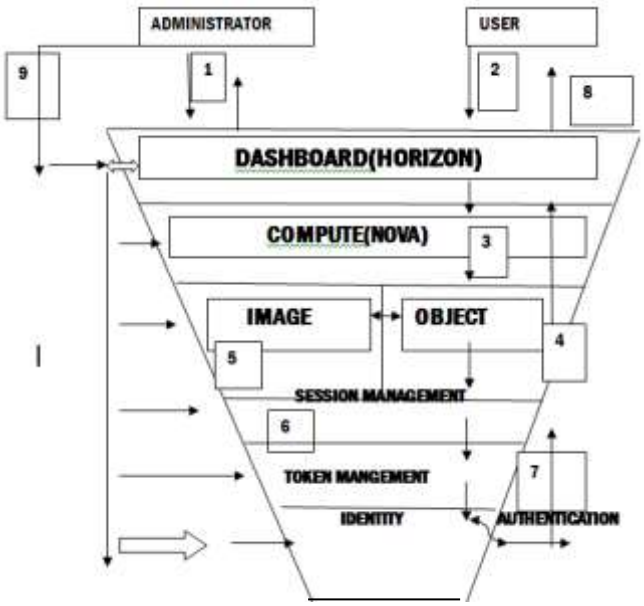

Fig.(ii) working of V model.

Working table of the diagram fig(ii).

S. NO. OPERATION

1. → admin operating at front end through user interface.
2 → user wants to gain access.
3 → manage the resources and user activity in the system.
4 → storing the temporary objects and files in multiple disk drives.
5 → containing backups about login credentials.
6 → provide session to the user before it takes the token and after taking the token.
7 → Manage the token granting ,token assessment, token reallocation and renewal.
8 → user comes out after authentication.
9 → Admin at the backend ,operates through dashboard , managing all components.

CONCLUSION

Finally ,customization of the dynamic access control has been made. Session and token management will keep track of user by token allocation, renewal and session activation[15]. Therefore the flaw that, no dynamic access control over the user ,has been fulfilled .Moreover the V model will provide finer granularity due to the deep authentication process which was at the api level earlier.

REFERENCES:

[1] Vaquero LM, Rodero-Merino L, Morn D (2011) "Locking the sky: a survey on IaaS cloud security. In Journal of computing Springer Verlag 91(1):93,1/2011 1-2.
[2] Keith J., Burkhard N.(2010).The future of cloud Computing.(expert group report).
[3] Ken pepple july 2011. Deploying OpenStack. OReilly Media, Inc., 1005 Gravenstein Highway North, Sebastopol,CA 95472
[4] Takako,P., Estcio,G., Kelner,J., Sadok,D. (2010) . ASurveyonOpensourceCloudComputingSolutions.WCGA-8thWorkshop on Clouds, Grids and Applications.Gramado:28May, 3-16. Teyssier,S. (2010).
[5] Openstack Open source software for building private and public clouds.
[6] *"OpenStack Compute: An Overview"* (PDF). openstack.org. 2010.
[7] *"HypervisorSupportMatrix"*
[8] *OpenStack — more than just software"*.
[9] A. Stoughton, " Access flow: A protection model which integrates access control and information Flow". Proc. of the IEEE Symposium on Security and Privacy, pages 9–18, Oakland,CA, 1981
[10] L. Habib , M. Jaume and C. Morisset , " A formal comparison of the Bell &LaPadula and RBAC models",HTTS Funded by the Macao Science and Tech. Development Fund,2008
[11] D. Ferraiolo and R. Kuhn ," Role Based Access Control ", In Proc of 15th NIST- National computer security conference , Pages 554-563,Baltimore, October 1992
[12] R.S. Sandhu ,E.J. Coyne ,H.L. Feinstein ,C.E. Youman ," Role Based access control models ",IEEE Computer , Volume 29 Issue-2,1996
[13] wiki.opnfv.org/moon.
[14] wikipedia.org/wiki/OpenStack.
[15] Shashank , Nitesh kumar ,"token and session compatibility in role based access control with priveleges management" ijert.org. vol 3 issue 11 nov 2014.

International Journal of Engineering Research and General Science Volume 3, Issue 5, September-October, 2015
ISSN 2091-2730

HYPERSONIC FLOW ANALYSIS ON AN ATMOSPHERIC RE-ENTRY MODULE

Dr. ROY N MATHEWS [a], SHAFEEQUE A P [b]

Department of Mechanical Engineering,

Mar Athanasius College of Engineering, Kothamangalam, Kerala, pin- 686 666, India.

Email:shafeeque.ap21@gmail.com, Tele: +91 9744060240

a-Professor ; b-M.Tech Scholar

Abstract—Atmospheric re-entry refers to the movement of human made objects as they enter the atmosphere of a planet from outer space. Re-entry capsules are blunt-bodies designed to withstand high heating loads experienced during entry into the atmosphere. Here conduct an external flow analysis on atmospheric re-entering vehicle called Apollo AS-202. Computational fluid dynamics is used to obtain the flow field that develops around reentry capsules. To evaluate the heat flux variation, velocity profile, temperature variation and pressure distribution at various locations of the capsules are presented. . The analysis is carried out for turbulent flow and standard flow properties available for Re-entry capsules in the literature using Navier-Stokes solver for different Mach numbers. The results of the simulation were discussed using velocity, temperature, heat flux and pressure contours.

Keywords—Re-entry vehicles, Atmospheric re-entry, Aerodynamic Heating, Thermal protection system, Hypersonic Flow, CFD, Heat fluxes.

INTRODUCTION

Re-entry capsules are used for space exploration applications due to their ability to withstand high heating loads during the re-entry phase. A re-entry capsule consists of a blunt fore body, followed by a conical after body with straight or rounded base [3]. A bow shock forms ahead of the vehicle to slow down the hypersonic flow. Apart from the blunt-shaped nose, the most recent re-entry vehicles are equipped with ablative Thermal Protection Systems (TPS) to avoid possible damage of the capsule and insulate the vehicles content.

In re-entry vehicles, during re-entry phase, the thermal loads play a major part. A re-entry capsule encounters a high temperature and chemically reacting flow during the re-entry phase [6]. Computational Fluid Dynamics is extensively used to simulate these flows, as high enthalpy and low density associated with the flight conditions are difficult to reproduce in wind tunnels or shock tunnels at each re-entry trajectory point. Wind and shock tunnel tests are difficult and are costly to conduct at high enthalpy conditions. CFD is a much more economical approach for studying such flows. Therefore CFD is extensively used as an analysis tool in the design of hypersonic vehicles. CFD is also used as a research tool to understand the complicated hypersonic effects.

Thermal analysis plays an important role in the design of atmospheric re-entry vehicles, which are subjected to severe aerodynamic heating. However, the thermal analysis is subject to a number of uncertainties. There can also be high uncertainty in the prediction of aerodynamic heat flux, due to factors such as scatter in the re-entry trajectory and highly complex phenomena that are difficult to analyze [2].

When a capsule reenters an atmospheric environment, a strong shock wave is formed in front of it. Behind the shock wave, a shock layer with very high temperature appears, where a high enthalpy fluid flows around a capsule, resulting in a severe heating

environment. Moreover, in an environment where the capsule velocity exceeds 8 km/s such as a super-orbit re-entry, there appear complicated phenomena accompanied by the radiation and/or the influence of turbulence [4].

The computed results are utilized to determine whether the aero-thermodynamic loads exceed the allowable values. If the loads are exceeding, then an optimized design is required to account for these loads. Moreover, if it is not exceeding, further analysis is done on the other components to ensure their reliability. By meshing the model, the re-entry vehicle is broken down into small components. When it is positioned into the CFD program, solutions to Navier-Strokes (N-S) equations are integrated across each of these small components and added up. It accounts for changes in temperature, density, and pressure of the surrounding atmosphere, and even includes viscous effects and shock waves [1].

Aerodynamic Heating

Atmospheric re-entry vehicles are subjected to aerodynamic heating during re-entry phase of their operation. Aerodynamic heating is the heating of a solid body produced by the passage of fluid over the body [5]. It is a form of forced convection in that the flow field is created by forces beyond those associated with the thermal processes. This process generates heat and consequently all external surfaces of the vehicle are heated.

Due to aerodynamic heating external surfaces of the re-entry vehicle gets heated. Thermal Protection Systems are necessary in order to protect the internal structure of the vehicle from the elevated heat fluxes occurring on the external surfaces. The design of a Thermal Protection System is based on the principle that the energy released by the aerodynamic heating must be absorbed or rejected by the Thermal Protection System.

METHODOLOGY

A CFD analysis on a launch vehicle can be broken down into few parts: (i). Creating a required model of re-entry vehicle in a computer program, (ii). Import the geometry into a meshing program, such as HYPERMESH, (iii). Analyse the meshed geometry in a CFD program by setting the design parameters and environmental conditions, (iv). Post-processing the output and evaluate the results.

AS-202 Flight Data

The flight data used for assessment/comparison of heat flux data on the capsule were taken from the AS-202 flight test which was performed as part of the Apollo program. Once the Apollo entry vehicle design was determined, two flight tests of the actual Command Module (AS-201 and AS-202) were conducted at super orbital entry velocities resulting from suborbital boosted trajectories with an intentional skip maneuver. Although AS-201 did not carry an on board inertial measurement unit (IMU), one was carried during the AS-202 flight, which enabled a reconstruction of the flight trajectory and vehicle orientation as a function of time.Figs. 1-3 and tables 1and 2are taken from Louis M.G.Walpot et.al[1][9][10].

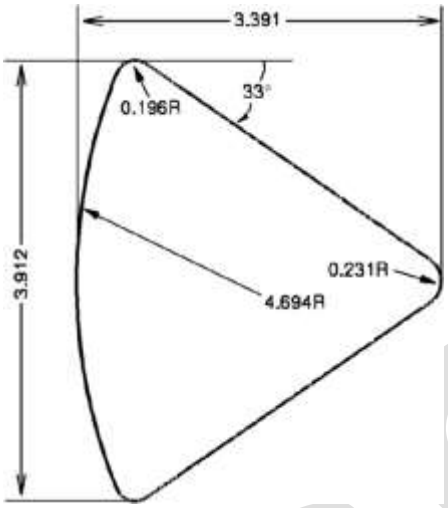

Fig.1 Schematic drawing of the outer mould line of AS-202 capsule

The afterbody heating environment for the Apollo Command Module shape as measured on the AS-202 mission is used as basis for comparison between CFD results and flight data.Fig.1 shows the outer mould line of the AS-202 as modeled for the CFD analyses. The re-entry trajectory of AS-202 in terms of velocity and altitude vs. time is shown in Fig.2.

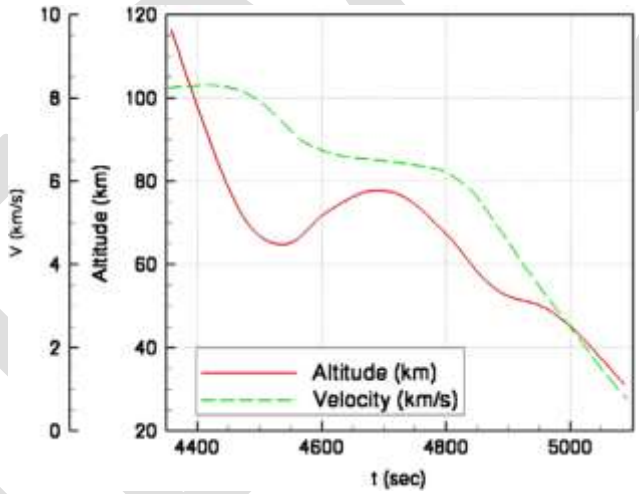

Fig.2 Altitude and velocity as a function of time from launch for AS-202.

Table 1 As-202 Trajectory Points And Freestream Conditions

Time[a] (s)	Alt. (km)	Re_D[b]	V (km/s)	M	ρ_∞ (kg/m^3)	T_∞ (K)	α	β (deg.)
4455	76.8	7.5×10^4	8.24	28.6	3.38e−5	205	18.2	2.0
4475	71.3	1.8×10^5	8.15	27.6	8.76e−5	217	17.9	2.5
4500	70.0	3.0×10^5	7.92	26.2	1.52e−4	227	17.8	2.5
4510	66.0	3.2×10^5	7.80	25.6	1.69e−4	230	17.8	2.5
4530	64.9	3.4×10^5	7.53	24.5	1.84e−4	234	17.9	2.5
4560	66.0	2.7×10^5	7.07	23.2	1.53e−4	231	18.1	2.5
4600	71.6	1.3×10^5	6.74	22.9	7.19e−5	215	18.3	2.5
4650	76.2	5.7×10^4	6.56	22.8	3.24e−5	206	18.5	2.0
4700	77.2	4.3×10^4	6.49	22.7	2.45e−5	203	18.5	2.0
4750	74.5	7.6×10^4	6.39	22.0	4.50e−5	210	18.4	2.0
4800	67.3	2.1×10^5	6.21	20.5	1.37e−4	210	18.4	2.0
4825	62.9	3.5×10^5	5.97	19.2	2.81e−4	239	18.3	2.0
4850	58.2	5.3×10^5	5.62	17.6	4.14e−4	252	18.3	2.5
4875	54.6	6.9×10^5	5.07	15.6	6.16e−4	262	18.4	2.5
4900	52.4	7.6×10^5	4.53	13.2	8.00e−4	268	18.6	2.5

[a] Seconds after launch.
[b] Freestream Reynolds number based on body diameter.

The points in time and the related freestream conditions used for comparison to flight data are tabulated in Table1. The small side slip angle has been neglected in the current simulations. The locations of calorimeters used to determine the heat fluxes on the AS-202 conical afterbody are depicted in Fig.3. The afterbody instrument package for AS-201 and AS-202 consisted of 23 surface-mounted calorimeters and 24 pressure transducers. Both flights were highly successful, with 16 of the calorimeters returning useful data on AS-201 and 19 on AS-202.Table 2 contains the exact coordinates of each calorimeter position. The afterbody heating rates for AS-201 were much higher than those for AS-202 because of the steeper entry angle (maximum heating rate of 25 vs 9 W/cm^2) [11].

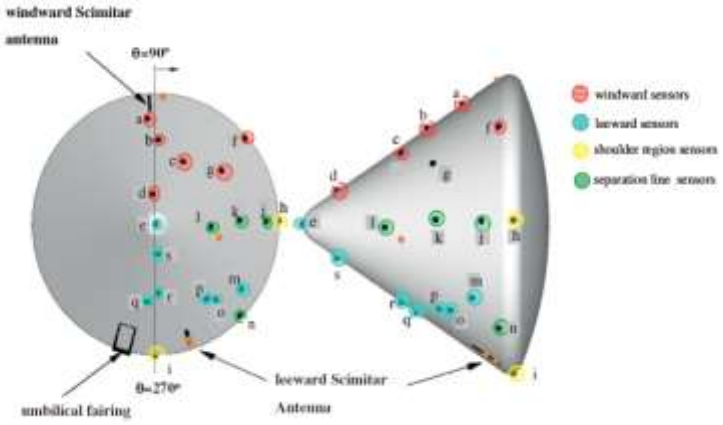

Fig.3 Locations of calorimeters on AS202 conical after body. Orange symbols indicate inoperative instruments. Letters correspond to the ID.

Table 2 Afterbody calorimeter locations for AS-202.

ID[a]	X^b (cm)	θ^b (deg.)	Range (W/cm^2)	ID[a]	X^b (cm)	θ^b (deg.)	Range (W/cm^2)
–	72.6	93.7	0–114	l	228.8	182.9	0–28
a	120.8	85.3	0–57	m	106.8	215.3	0–11.4
b	169.8	92.0	0–57	n	69.5	225.5	0–11.4
c	205.6	115.0	0–57	–	205.6	191.3	0–28
d	294.8	83.4	0–57	o	136.6	229.8	0–11.4
e	343.1	Apex	0–28	p	152.6	234.0	0–28
f	69.5	138.0	0–57	q	184.3	276.4	0–28
g	161.5	142.8	0–28	r	205.6	267.8	0–28
h	54.5	178.5	0–28	s	294.8	265.0	0–28
i	54.5	270.0	0–11.4	–	74.1	253.0	0–28
j	94.1	178.6	0–28	–	88.0	253.0	0–57
k	157.6	177.5	0–28				

Geometrical Modelling

The Apollo Command Module essentially consisted of a spherical section forebody and a 33^0 conical afterbody. The CM capsule was a 33^0 half-angle cone with the blunt after heat shield formed from a segment of a sphere of radius 4.694 m. A toroidal section with radius of 0.196 m provided the transition between the conical and spherical sections. The maximum capsule diameter of 3.91 m occurred in the toroidal section. To account for the fact that air flows around the launch vehicle, the area surrounding the re-entry vehicle model is meshed, rather than the re-entry vehicle itself.

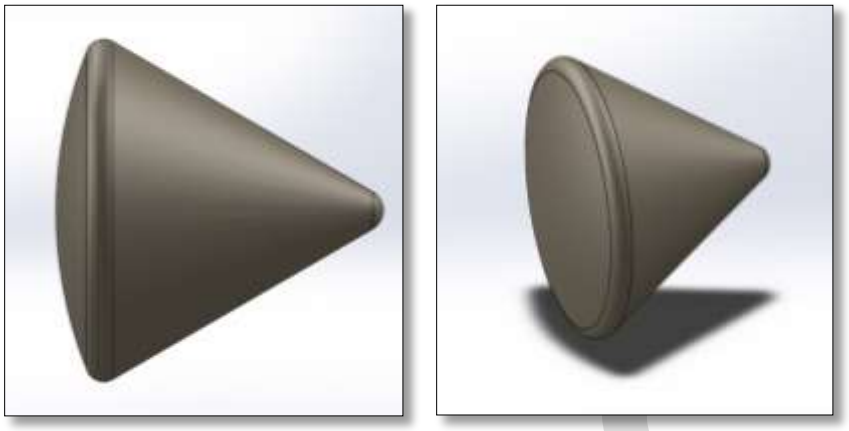

Fig.4 Three dimensional Apollo AS-202 model

Meshing

The suitable mesh has been computed using HYPERMESH over the surface of the capsule. The mesh should be very fine near the shoulder part and the far field also created around the body to created artificial environment as like experimental setup. Quadrilateral mesh inside capsule and triangular mesh outside with capsule model.Mesh is very fine near the surface of the reentry capsule, so that the results can be calculated accurately [16]. Minimum Orthogonal Quality = 9.8e-01, Maximum Aspect Ratio = 5.2e+00. Five layer boundary layer with growth ratio 1.1. First element size 0.01 cm.

As we know that one of the controlling factors of the flow simulation around the body is decided by the quality of mesh or the arrangement of the mesh. The arrangement of grid near Heat shield and shoulder is shown in Fig. 6. The grid is refined in the vicinity of the shock wave to capture the flow gradients accurately. Surface of the body is meshed very fine near very small faces when compare to large one. As the stagnation properties of flow act at the heat shield and the narrow face of the body, hence meshing near heat shield is to be most fine and accurate. The purpose of the heat shield is to transfer the heat energy to the atmosphere without conducting to the capsule.

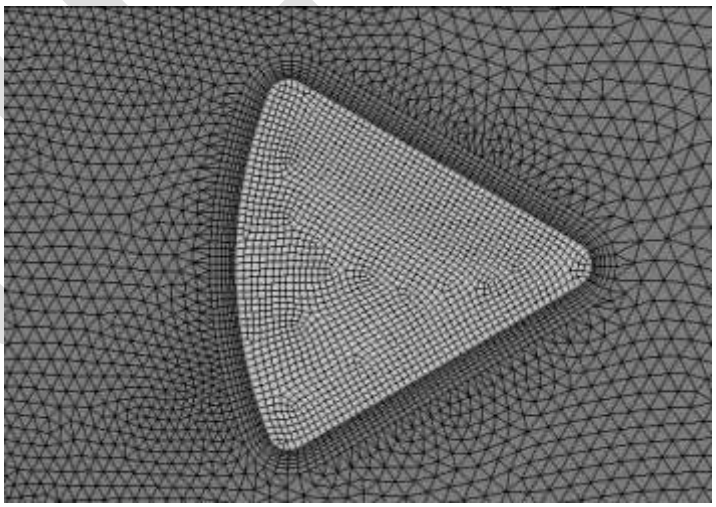

Fig.5 Two dimensional Meshing with capsule body

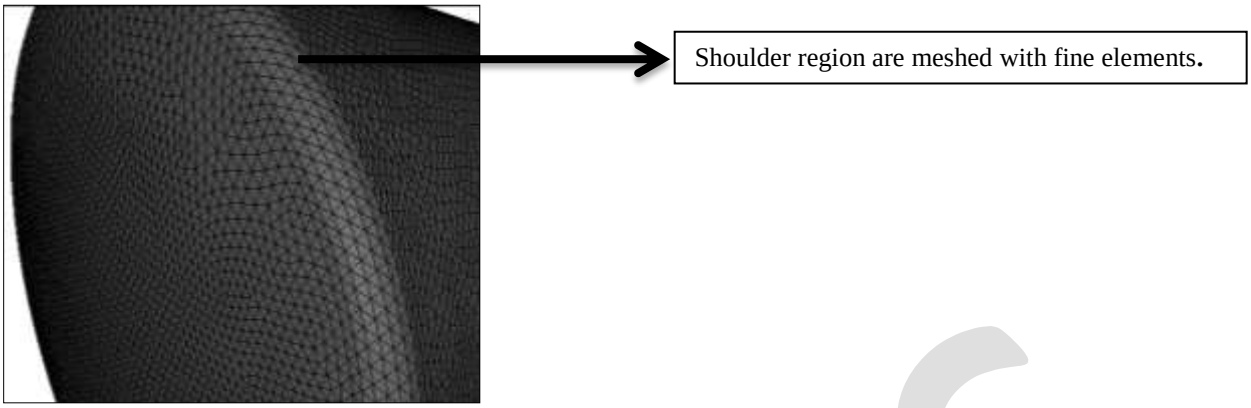

Fig.6 Enlarged view of Meshing of three dimensional model

Further imported the meshed file into FLUENT for analysis there the suitable boundary conditions and operating conditions are given to get all the performance parameter during the re-entering into the earth atmosphere.

Boundary Conditions

Table3:AS-202 trajectory points and free-stream conditions[4]

CASE	Altitude(km)	V(km/s)	M	ρ_∞ (kg/m^3)	T_∞(K)
1	70.0	7.92	26.2	$1.52*10^{-4}$	227
2	77.2	6.49	22.7	$2.45*10^{-5}$	203
3	54.6	5.07	15.6	$6.16*10^{-4}$	262

The simulation methodology used and the key points are highlighted. The freestream density, velocity, and temperature for the chosen condition are 0.000152 kg⁄m^3, 7920 m⁄s, and 227 K, respectively [8].

Turbulence modelling: For AS- 202, the Spalart–Allmaras model was used to cover turbulent flow situations. One-equation Spalart-Allmaras turbulence model is used to analyse hypersonic turbulent flow since this turbulence model is numerically robust and generally gives good predictions in hypersonic applications [12]. The governing equations are discretized using the finite volume approach. The method is second order accurate both in stream-wise and wall normal directions. The viscous fluxes and turbulent source terms are evaluated using second order accurate central differencing and implicit Data Parallel Line Relaxation is used to obtain steady-state solutions. No-slip, non-catalytic and isothermal wall boundary conditions are specified at the wall. Freestream conditions are specified at the outer boundary. The flow around the Apollo-shaped capsule at non-zero angle of attack is not axi-symmetric [13].

The far field around the body is at around below 90 km above sea level. The Fluid is considered as Ideal gas around the body [7]. The flow field around the re-entry configuration is simulated by solving the three-dimensional Navier- Stokes equations. The working medium, air, is taken as a perfect gas with molecular weight of 28.96 grams/mole and ratio of specific heat equal to 1.4. The temperature dependence of molecular viscosity is as per user defined function, and the conductivity is calculated using a Prandtl number of 0.72.

Equilibrium chemistry: Air is considered as a five species ideal gas mixture. air is modelled as a neutral mixture of five species (N_2, O_2, NO, N and O), with five finite rate chemical reactions [15]. No dissociation is observed in the solution and the mass fractions of

N_2 and O_2 remain at their freestream values throughout the flowfield. The temperature and pressure dependent equilibrium gas properties are modelled via appropriate fit functions. A temperature range between 50K and 20,000K and a density range between 10–12kg/m^3.

RESULTS AND DISCUSSIONS

The flowfield around the Apollo-shaped body is initialized to free-stream values all over the domain. As the simulation progresses the bow shock and the boundary layer on the vehicle are formed, followed by flow separation on the afterbody. As the separation bubble forms on the windward side. A large recirculation bubble is formed on the leeward side and the shear layer enclosing the separation bubble coalesces at the neck, where the recompression shock is formed. While the re-entry vehicle enters into the atmosphere, a bow shock is created at the base of the vehicle.

The absence of three dimensional flow field solution for the Apollo command module at zero angles of attack. The pressure measurements on the conical section generally agreed with the wind-tunnel predictions. The conical pressure measurements were low during maximum heating. Maximum pressure at fore body and its value is $1.945*10^6$ Pa. Minimum pressure $2*10^5$ Pa. It shows the severe pressure drag at the two edges of the module base. High static pressure is created in the base of the reentry vehicle as illustrated in Fig.7. Since, the pressure is high while re-entering in to the atmosphere due to the strong bow shock created. This bow shock will increase drag force acting on the re-entry vehicle and has the capability to decelerate the vehicle to low Mach numbers. The maximum static pressure is created at the far field of the re-entry vehicle because of the progressing bow shocks marching downstream of the vehicle. The increase in pressure is visualized exactly using the static pressure contour for 0^o angle of attack.

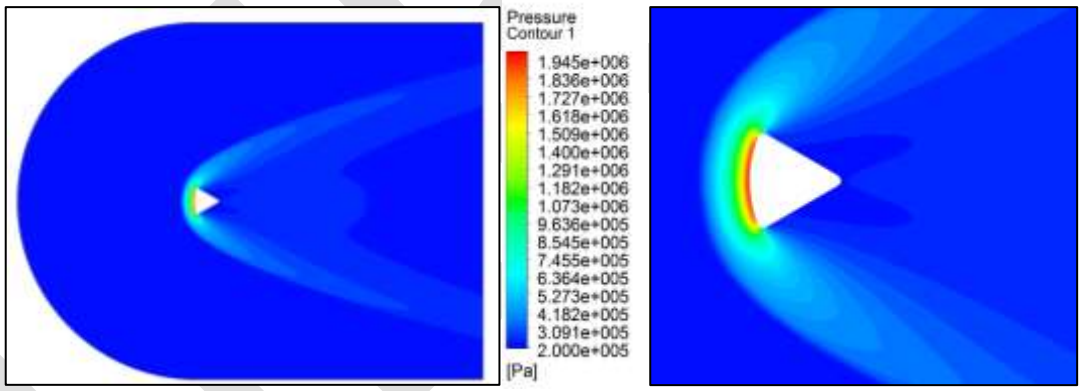

Fig.7 Pressure distribution of two dimensional model at Mach no =26.2

The fig.8 shows the simulation of the temperature contours over the capsule. Here we can see, the temperature is maximum at the heat shield and it is also observed that the potential as well as kinetic energy decreases. So according to the law of conservation, if some energy function decreases so in order to be conserved some other energy should be increasing. Here the kinetic and potential energy is decreasing and it is dissipating in the form of heat energy. Maximum temperature was at fore body section and its value $1.96*10^4$ K. Minimum temperature value $2.2*10^2$ K. Fig.9 shows velocity distribution of two dimensional model at Mach number =26.2. The maximum temperature is produced at the base of the re-entry vehicle and it is lowest amount at the edges. Fig.9 shows the velocity distribution of two dimensional model at Mach number =26.2. Zero velocity was at fore body section of re-entry capsule and maximum value was free stream velocity.

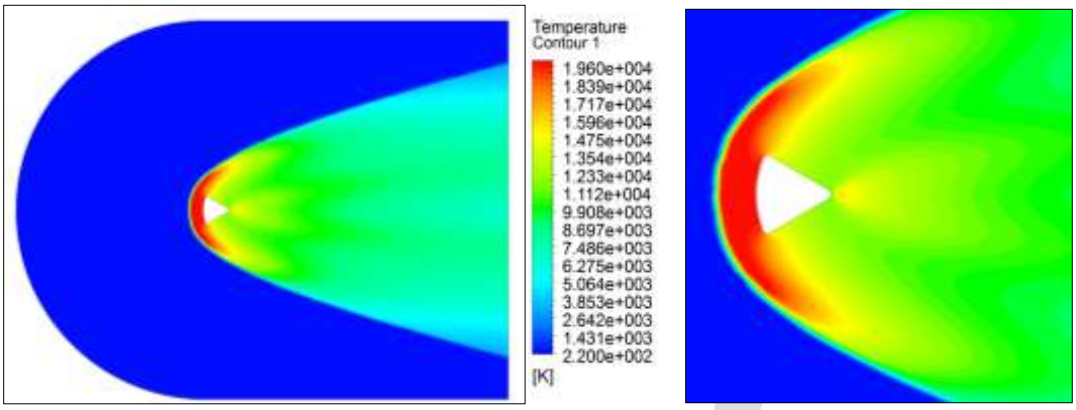

Fig.8 Temperature distribution of two dimensional model at Mach no. =26.2

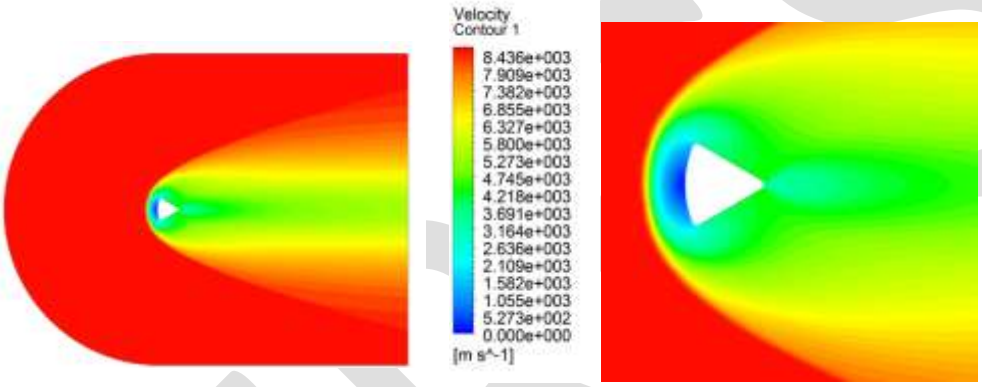

Fig.9 Velocity distribution of two dimensional model at Mach no =26.2

Two dimensional analysis without the capsule body not able to predict the wall flux properly. Next iteration, two dimensional analysis with capsule body, Fluid solid interface wall was created to have the heat transfer.All results were remain same, except for the heat flux.Two dimensional analysis with capsule body for the heat flux gives a value, and getting idea about the distribution.Three dimensional analysis is carried out to understand the heat flux distribution around the capsule body.

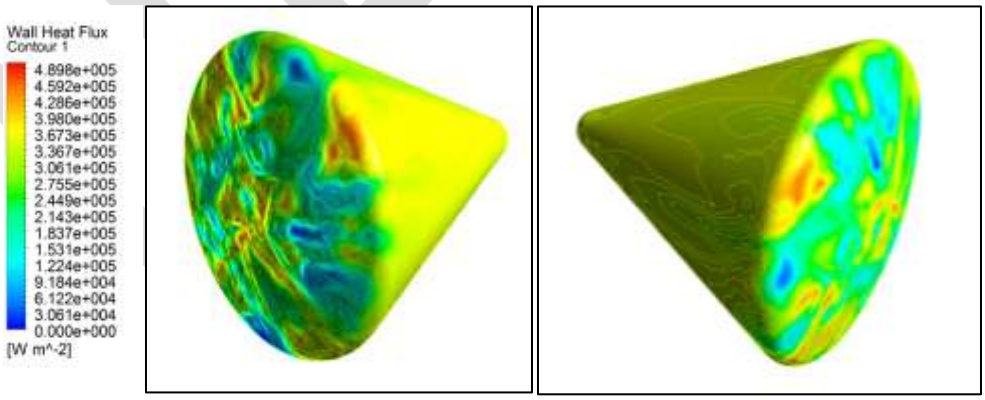

Fig.10 Heat flux distribution of three dimensional model at Mach no.=15.6

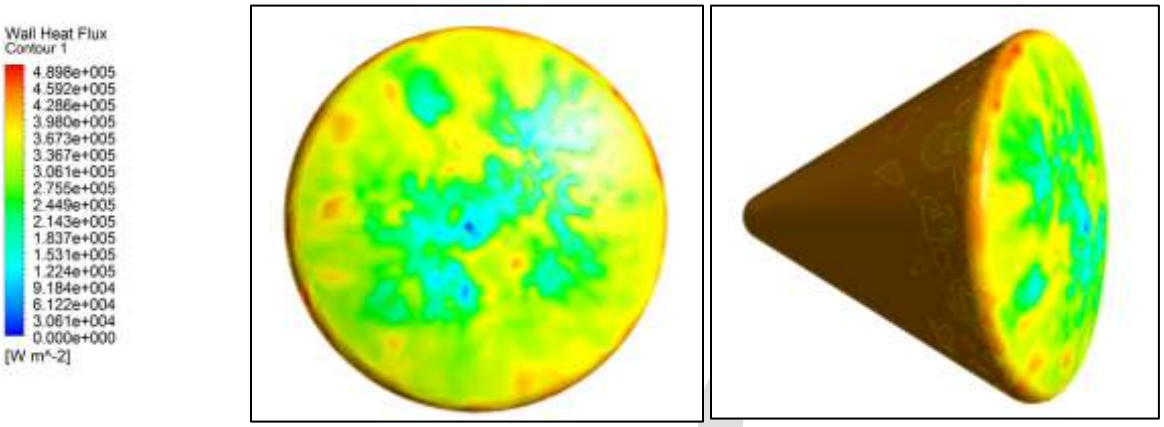

Fig.11 Heat flux distribution of three dimensional model at Mach no.=22.7

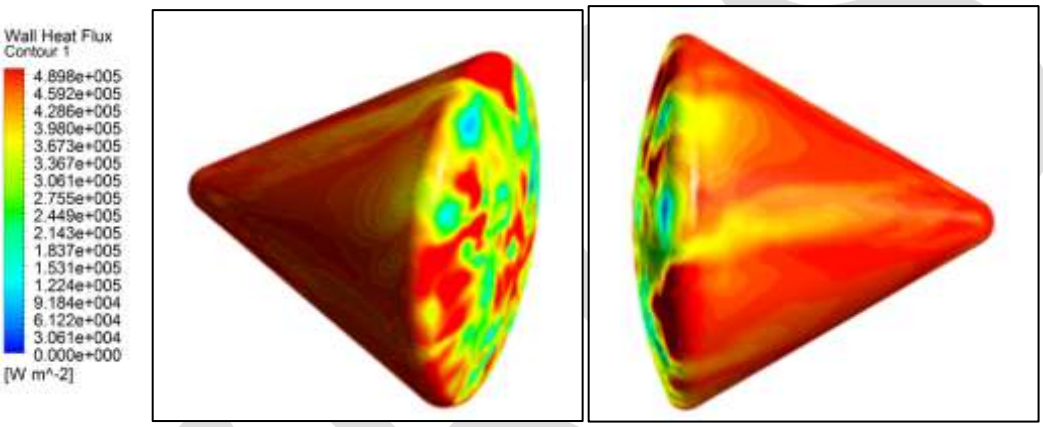

Fig.12 Heat flux distribution of three dimensional model at Mach no.=26.2

Figs. 10-12 shows the heat flux distribtion of three dimensional model at different Mach number.As Mach number increases the maximum heat flux surface also increases.It was clear that red region of the capsule at Mach number =26.2 was very higher than that of at Mach number =15.6.Maximum value of the heat flux was $4.898*10^5$ W/m^2. Fig.13 shows the heat Flux (W/m^2) at different locations of capsule at different Mach number. Maximum heat flux was generated at shoulder region of the capsule, it is the point where just before the maximum diameter point.ie, P3. In flight data maximum heat flux value is 57 W/cm^2 in table 2.

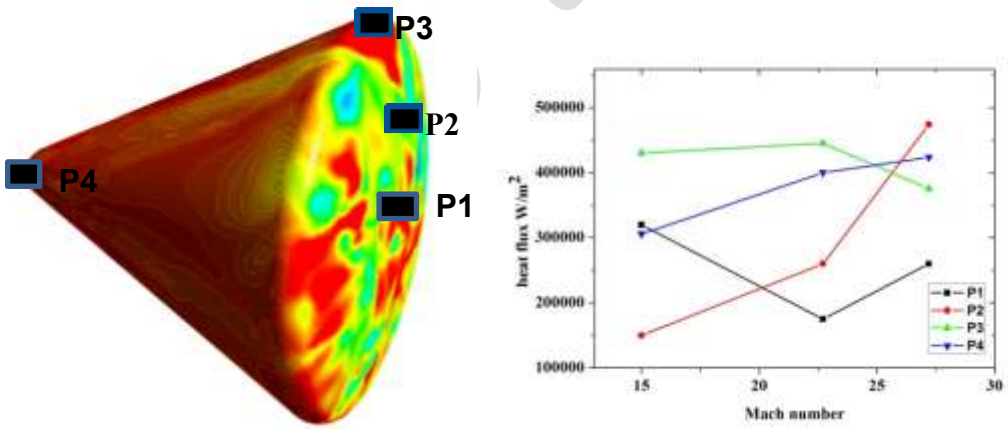

Fig.13 Heat Flux (W/m^2) at different locations of capsule at different Mach number

Table.4 Heat Flux (W/m^2) at different locations of capsule at different Mach number

Mach number	P1	P2	P3	P4
26.2	260000	474000	375688	423666
22.7	175000	260000	489800	400000
15.6	320000	150000	430000	306000

ACKNOWLEDGMENT

I acknowledge the support from Dr. Roy N Mathews and prof. Reji Mathew, Mar Athanasius College of Engineering, Kothamangalam (Affiliated to Mahatma Gandhi University , Kottayam, Kerala and AICTE, India). I express my deep sense of gratitude to R.Harikrishnan, Thermal Design Division, VSSC,Trivandrum,Kerala for the valuable guidance as well as timely advice which helped me a lot in doing my work successfully.

CONCLUSION

As observed in the figure above the velocity at the heat shield was minimum and increases as we move to the shoulder. This decrease in velocity results in increase in pressure gradient which results in the formation of shock wave. Major output parameters of the aero thermodynamic analysis are surface wall temperatures which are helpful in material selection for the survivability of the vehicle. Over the body for the decreasing Mach number conditions and wall outer surface temperature over the capsule is directly proportional to the Mach number. The shock wave formed comes closer to the body with increase in Mach number. This analysis gives the idea about the heat flux around the re-entry capsule body during re-entry phase at different Mach number. As the Mach number increases the temperature also increasing due to friction. As temperature increases heat flux increases. Calorimeters positioned at or very close to the shoulder, recorded higher heat flux levels. . In this work maximum value of the heat flux was $4.898*10^5$ W/m^2 it was slightly less than flight data.

From this investigation, it is proved that this method can offer aerodynamic information on a timely basis while keeping the cost and schedule of commercial programs. Wind tunnel tests are important in the validation of prediction methods if they are not available, validated the results with actual flight data. Right choice of material can avoid the localised heating. This method will help future research on reentry much easier than it was before. The CFD code will help future researcher to calculate reentry parameters for their research work.

REFERENCES:

1. Louis M.G.Walpot, Michael J.Wright, Peter Noeding, FerrySchrijer, “Base flow investigation of the Apollo AS-202 Command Module”, Progress in Aerospace Sciences 48–49 (2012) 57–74.

2. Jai Terry, Tracie Barber, “CFD and experimental study of an inflatable re-entry vehicle model at Mach 3 conditions”, Acta Astronautica 61 (2007) 854 – 865.

3. Krishnendu Sinha, “Computational Fluid Dynamics in Hypersonic Aerothermodynamics”, Defence Science Journal, Vol. 60, No. 6, (November 2010), pp. 663-671.

4. Y. Matsudaa, H. Kiharab, K. Abeb**,** “Numerical Study of Thermochemical Nonequilibrium Flow aroundReentry Capsule and Estimation of Aerodynamic Heating”, Procedia Engineering 67 (2013) 261 – 269.

5. N. S. Harshavardhan R, Sanjana K, Sai Sharan K, Srinivas.G, "Computational Flow Analysis Of Hypersonic Re-entry Blunt Body Using Fluent And Gambit", International Journal of Scientific & Engineering Research, Volume 5, Issue 5, (May-2014) ISSN 2229-5518.

6. Krishnendu Sinha, Siva Krishna Reddy, "Hypersonic Turbulent Reacting Flow Simulation of Fire II Re-entry Vehicle", 45th AIAA Aerospace Sciences Meeting and Exhibit 8 - 11 (January 2007).

7. Bruce Ralphin Rose. J, Saranya. P, "High Temperature Flow Characteristics over a Re-Entry Space Vehicle", International Journal of Latest Trends in Engineering and Technology (IJLTET).

8. D. Siva K. Reddy, Bijaylakshmi Saikia, Krishnendu Sinha, "Effect of High-Enthalpy Air Chemistry on Stagnation Point Heat Flux", Journal Of Thermophysics And Heat Transfer Vol. 28, No. 2, April–June (2014).

9. Dorothy B. Lee, "Apollo experience report: aerothermodynamics evaluation", NASA TN D-6843, (June 1972).

10. Ernest R Hillje, "Entry flight aerodynamics from Apollo Mission AS-202", NASA TN D-4185, (October 1967).

11. Roop N Gupta, Jerrold M Yos, Richard A. Thompson, "A review of reaction rates and thermodynamic and transport properties for an 11-species air model for chemical and thermal nonequilibrium calculations to 30,000K", NASA Technical Memorandum 101528. (February 1989).

12. Kushal S. Kedia, Krishnendu Sinha, "Effect Of Compressibility Corrections To Turbulence Models Applied To A Hypersonic Re-Entry Configuration", 33rd National and 3rd International Conference on Fluid Mechanics and Fluid Power December 7-9, (2006) NCFMFP2006-1221.

13. James N Moss, Christopher E Glass, Francis A Greene, "DSMC Simulations of Apollo Capsule Aerodynamics for Hypersonic Rarefied Conditions", 9th AIAA/ASM Thermophysics and Heat Transfer Conference 5-8 (June 2006).

14. Jose F. Padilla, Kun-Chang Tseng, Iain D. Boyd, "Analysis of Entry Vehicle Aerothermodynamics Using the Direct Simulation Monte Carlo Method", 38th AIAA Thermophysics Conference 6 - 9 (June 2005). AIAA 2005-4681.

15. Giuseppe Pezzella, AntonioViviani, "Aerodynamic analysis of a Mars exploration manned capsule", Acta Astronautica 69 (2011) 975–986.

16. Y. Zheng a, N.A. Ahmeda, W. Zhangb, "Heat dissipation using minimum counter flow jet ejection during spacecraft re-entry", Procedia Engineering 49 (2012) 271 – 279.

17. Chau-Lyan, Chang "Unsteady Aerothermodynamics Analysis of Hypersonic Flows over a Re entry Capsule", 42nd AIAA Joint Propulsion Conference and Exhibit.

International Journal of Engineering Research and General Science Volume 3, Issue 5, September-October, 2015
ISSN 2091-2730

IMAGE QUALITY ASSESSMENT FOR FAKE BIOMETRIC DETECTION: APPLICATION TO IRIS, FINGERPRINT, AND FACE RECOGNITION

Mohd Mujeed Uddin[1],S.V Altaf[2],Abdul Wasay Mudassir[3]

Mohd Mujeed Uddin[1],M.Tech student,ECE Department,Lords Institute of Engineering and Technology,Hyderabad,Telangana,India.mohdmujeebuddin2@gmail.com

S.V Altaf[2],Associate Professor,ECE Department,Lords Institute of Engineering and Technology,Hyderabad,Telangana,India.svaltaf@hotmail.com

Abdul Wasay Mudassir[3],Associate Professor,ECE Department,Lords Institute of Engineering and Technology,Hyderabad,Telangana,India.wasay403@gmail.com

Abstract— to ensure the actual presence of real legit i-mate in contrast to self manufactured or reconstructed sample is a significant problem in bio-metric authentication, which requires the development of new and efficient protection measures. In this paper, we present a novel software-based fake detection method that can be used in multiple bio-metric systems to detect different types of fraudulent access attempts. The objective of the proposed system is to enhance the security of bio-metric recognition frameworks, by adding liveness assessment in a fast, user-friendly, and non-intrusive manner, through the use of image quality assessment. The proposed approach presents a very low degree of complexity, which makes it suitable for real-time applications, using 25 general image quality features extracted from one image (i.e., the same acquired for authentication purposes) to distinguish between legitimate and impostor samples.[3] The experimental results, obtained on publicly available data sets of fingerprint, iris, and 2D face, show that the proposed method is highly competitive compared with other state-of-the-art approaches and that the analysis of the general image quality of real bio metric samples reveals highly valuable information that may be very efficiently used to discriminate them from fake traits.[9]

Index Terms— Image quality assessment, bio-metrics, security, attacks, countermeasures.

I.INTRODUCTION

A novel software-based multi-biometric and multi-attack protection method which targets to overcome part of these limitations through the use of image quality assessment (IQA). It is not only capable of operating with a very good performance under different biometric systems (multi-biometric) and for diverse spoofing scenarios, but it also provides a very good level of protection against certain non-spoofing attacks (multi-attack).[15] Moreover, being software-based, it presents the usual advantages of this type of approaches: fast, as it only needs one image (i.e., the same sample acquired for bio-metric recognition) to detect whether it is real or fake; non-intrusive; user-friendly (transparent to the user); cheap and easy to embed in already functional systems (as no new piece of hardware is required).

An added advantage of the proposed technique is its speed and very low complexity, which makes it very well suited to operate on real scenarios (one of the desired characteristics of this type of methods). As it does not deploy any trait-specific property (e.g., minutiae points, iris position or face detection),the computation load needed for image processing purposes is very reduced, using only general image quality measures fast to compute, combined with very simple classifiers. It has been tested on publicly available attack databases of iris, fingerprint and 2D face, where it has reached results fully comparable to those obtained on the same databases and following the same experimental protocols by more complex trait-specific top-ranked approaches from the state-of-the-art.[14]

II.SYSTEM ARCHITECTURE

The system makes use embedded board which makes use of less power consumptive and advanced micro controller like Raspberry Pi. Our ARM11 board comes with integrated peripherals like USB, ADC and Serial etc. On this board we are installing Linux operating system with necessary drivers for all peripheral devices .Mainly this system consists of peripherals like UVC driver camera and Fingerprint module.

After connecting all the devices, power uPs the device. When the device starts booting from flash, it first loads the Linux to the device and initializes all the drivers and the core kernel. After initialization of the kernel it first checks weather all the devices are working properly or not. After that it loads the file system and starts the start up scripts for running necessary processes and daemons. Finally it starts the main application.

This system captures image by means of web camera connected to ARM micro-controller through USB and the image is processed by using image processing technique. Image processing is any form of signal processing for which the input is an image, such as a photograph or video frame; the output of image processing may be either an image or a set of characteristics or parameters related to the image. Using algorithms child movement is monitored continuously like child position, child crying etc. And all these captured images are displayed on Display unit connected to ARM micro-controller.

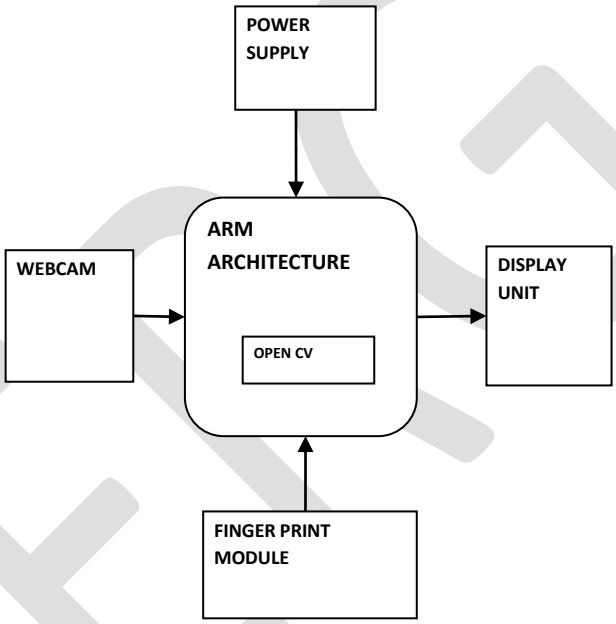

Fig.1: Block Diagram for Proposed System

When our application starts running it first check all the devices and resources which it needs are available or not. After that it checks the connection with the devices and gives control to the user.

The controller will recognize the face and iris of the particular person from the image. The finger print module will take the finger print from the person and send to controller. The controller will recognize the finger print of particular person from the data base. If they are matched then it will display the data on display unit.

III.HAAR CASCADE

Haar-like features are digital image features used in object recognition. They owe their name to their intuitive similarity with Haar wavelets and were used in the first real-time face detector. Here we will work with face detection. Initially, the algorithm needs a lot of positive images (images of faces) and negative images (images without faces) to train the classifier. Then we need to extract features from it. For this, haar features shown in below image are used. They are just like our convolutional kernel. Each feature is a single value obtained by subtracting sum of pixels under white rectangle from sum of pixels under black rectangle.

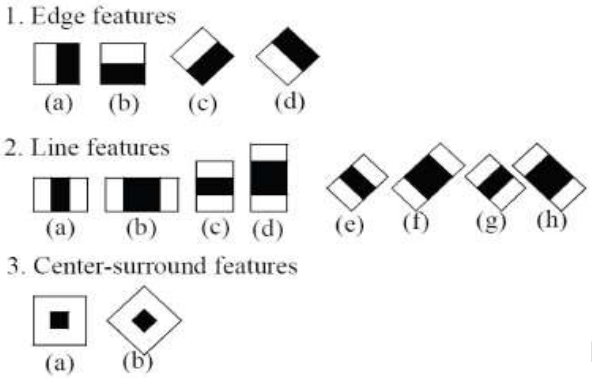

Fig.2: Haar Features

Now all possible sizes and locations of each kernel is used to calculate plenty of features. For each feature calculation, we need to find sum of pixels under white and black rectangles. To solve this, they introduced the integral images. It simplifies calculation of sum of pixels, how large may be the number of pixels, to an operation involving just four pixels.[1]

IV. PCA ALGORITHM:

PCA method (i.e., eigenface method) is M. Turk and A. Pent land proposed in the literature, the basic idea is: the image vector by KL transformation from high-dimensional vector is converted to low-dimensional vector, and the formation of low-dimensional linear vector space, that is, subspace, and then face the projector to the low dimensional space, with the resulting projection coefficients as the recognition feature vectors. Recognize faces, just the projection coefficient of samples to be identified in the target database sample set of projection coefficients were compared to determine what types of recently. PCA algorithm is divided into two steps: the core face database generation phase, the training phase and identification phase.

V.HARDWARE MODULES

A – ARM Architecture

The **Raspberry Pi** is a credit-card-sized single-board computer developed in the UK by the Raspberry Pi Foundation with the intention of promoting the teaching of basic computer science in schools. The Raspberry Pi is manufactured in two board configurations through licensed manufacturing deals with Newark element14 (Premier Farnell), RS Components and Ego-man. These companies sell the Raspberry Pi online. Ego-man produces a version for distribution solely in China and Taiwan, which can be distinguished from other Pi's by their red coloring and lack of FCC/CE marks.

Fig.3: Raspberry pi board

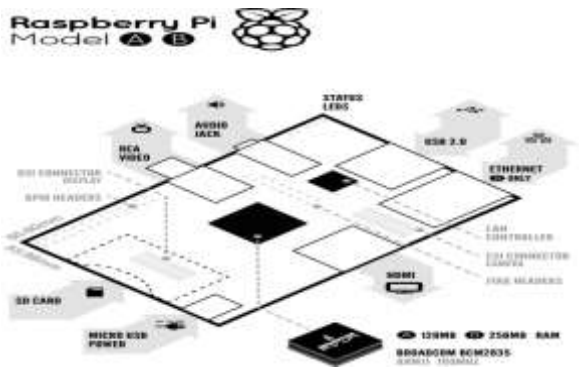

Fig.4: Board features

The hardware is the same across all manufacturers. The Raspberry Pi has a Broadcom BCM2835 system on a chip (SoC), which includes an ARM1176JZF-S 700 MHz processor, Video Core IV GPU, and was originally shipped with 256 megabytes of RAM, later upgraded to 512 MB. It does not include a built-in hard disk or solid-state drive, but uses an SD card for booting and persistent storage.[7]

The Foundation provides Debian and Arch Linux ARM distributions for download. Tools are available for Python as the main programming language, with support for BBC BASIC (via the RISC OS image or the Brandy Basic clone for Linux), C, Java and Perl.

B – Fingerprint Module

A fingerprint is an impression of the friction ridges on all parts of the finger. A friction ridge is a raised portion of the epidermis on the pal-mar (palm) or digits (fingers and toes) or plantar (sole) skin, consisting of one or more connected ridge units of friction ridge skin. These are sometimes known as "epidermal ridges" which are caused by the underlying interface between the dermal papillae of the dermis and the inter papillary (rete) pegs of the epidermis. These epidermal ridges serve to amplify vibrations triggered when fingertips brush across an uneven surface, better transmitting the signals to sensory nerves involved in fine texture perception. The ridges assist in gripping rough surfaces, as well as smooth wet surfaces.

Fig.5: Fingerprint Module

Fingerprints may be deposited in natural secretions from the eccrine glands present in friction ridge skin (secretions consisting primarily of water) or they may be made by ink or other contaminants transferred from the peaks of friction skin ridges to a relatively smooth surface such as a fingerprint card. The term fingerprint normally refers to impressions transferred from the pad on the last joint of fingers and thumbs, though fingerprint cards also typically record portions of lower joint areas of the fingers (which are also used to make identifications).[11][13]

C – Universal Video Camera

A UVC (or Universal Video Class) driver is a USB-category driver. A driver enables a device, such as your webcam, to communicate with your computer's operating system. And USB (or Universal Serial Bus) is a common type of connection that allows for high-speed data transfer. Most current operating systems support UVC. Although UVC is a relatively new format, it is quickly becoming common.[10]

There are two kinds of webcam drivers:

1. The one included with the installation disc that came with your product. For your webcam to work properly, this driver requires some time to install. It is specifically tuned for your webcam, designed by your webcam manufacturer and optimized for webcam performance.
2. A UVC driver:-You can only use one driver at a time, but either one will allow you to use your webcam with various applications.

It is a USB video camera using with laptop and Desktop computers.

The following Logitech webcams support UVC:

- Logitech® QuickCam® Pro 9000 for Business
- Logitech® QuickCam® Pro for Notebooks Business
- Logitech® QuickCam® Communicate MP for Business
- Logitech® QuickCam® Deluxe for Notebooks Business

Fig.6: UVC Driver Camera

VI. SOFTWARE REQUIREMENTS

A – Operating System

Linux or GNU/Linux is a free and open source software operating system for computers. The operating system is a collection of the basic instructions that tell the electronic parts of the computer what to do and how to work. Free and open source software (FOSS) means that everyone has the freedom to use it, see how it works, and changes it.

There is a lot of software for Linux, and since Linux is free software it means that none of the software will put any license restrictions on users. This is one of the reasons why many people like to use Linux.[6]

Projects that interface with the kernel provide much of the system's higher-level functionality. The GNU userland is an important part of most Linux-based systems, providing the most common implementation of the C library, a popular shell, and many of the common UNIX tools which carry out many basic operating system tasks. The graphical user interface (or GUI) used by most Linux systems is built on top of an implementation of the X Window System.

B – Integrated Development Environment (QT)

Qt is a cross-platform application framework that is widely used for developing application software with a graphical user interface (GUI) (in which cases Qt is classified as awidget toolkit), and also used for developing non-GUI programs such ascommand-line tools and consoles for servers.[8] Qt uses standard C++ but makes extensive use of a special code generator (called the Meta Object Compiler, or moc) together with several macros to enrich the language. Qt can also be used in several other programming languages via language bindings. It runs on the major desktop platforms and some of the mobile platforms. Non-GUI features include SQL database access, XML parsing, thread management, network support, and a unified cross-platform application programming interface for file handling.It has extensive internationalization support.

C – Opencv (image Processing library)

Open CV (Open Source Computer Vision) is a library of programming functions for real time computer vision. It is developed by Willow Garage, which is also the organization behind the famous Robot Operating System (ROS).[2]

Define abbreviations and acronyms the first time they are used in the text, even after they have been defined in the abstract. Abbreviations such as IEEE, SI, MKS, CGS, sc, dc, and rms do not have to be defined. Do not use abbreviations in the title or heads unless they are unavoidable.

Flow chart

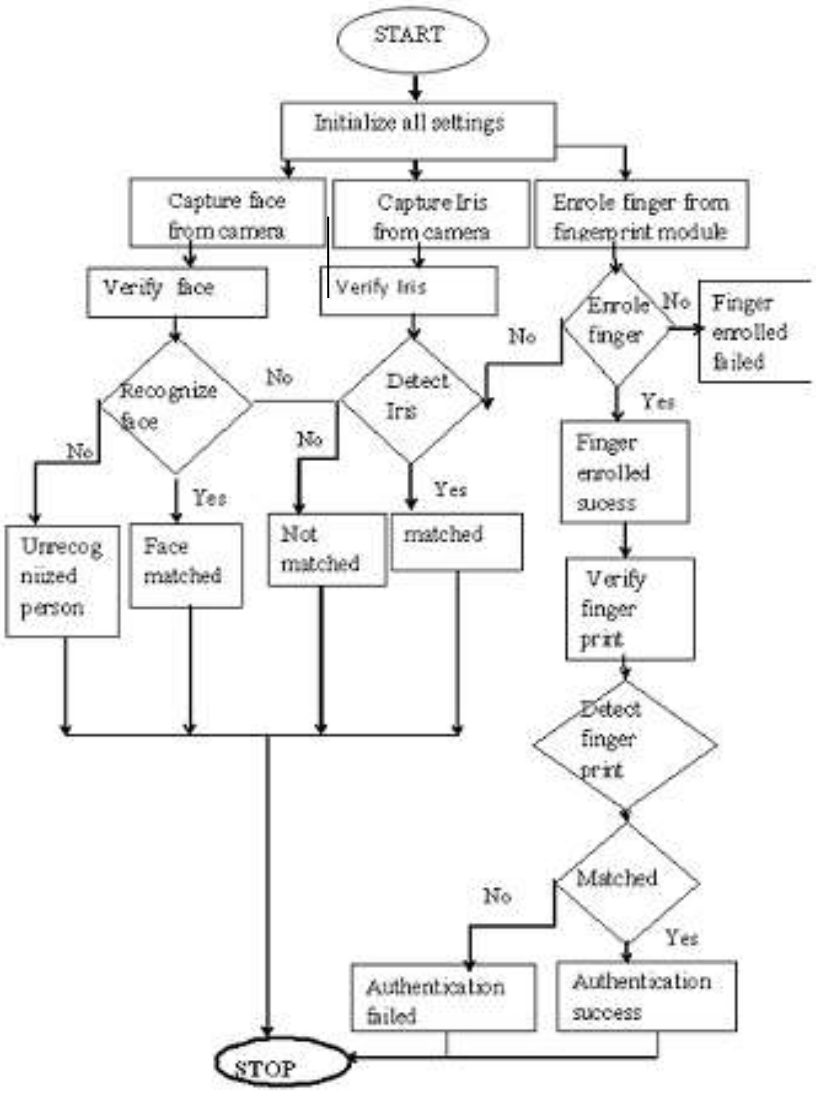

VII. RESULT

Fig.7:Overall view of the System

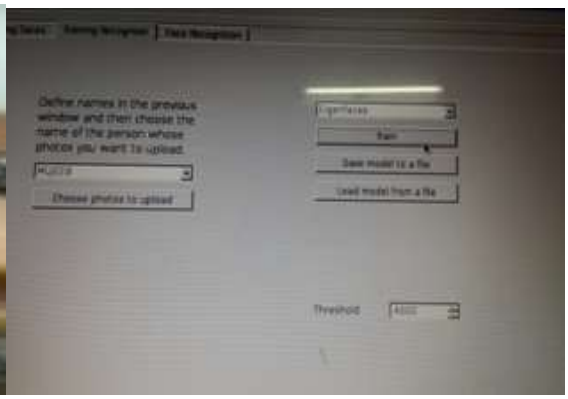

Fig.8:View of the Software

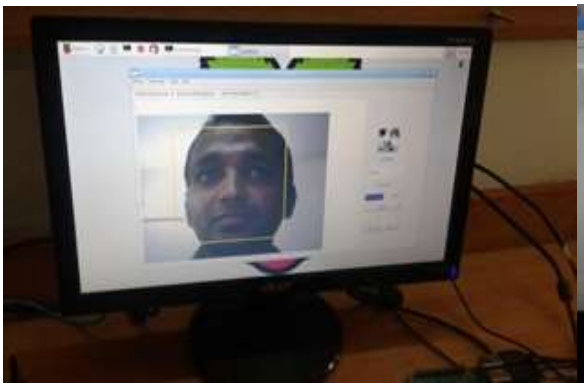

Fig.9:Identification of Person

Fig.10:Samples collection

After designing the system using Advance Raspberry Pi Board(BCM2835),Finger Print Module(R305),Web Camera etc as a Hardware Module and Qt Creator,Open CV library,Haar-cascade algorithm and Linux OS as Software Module the whole system is successfully designed and got the above results.

VIII. CONCLUSION

The project "Image Quality Assessment for Fake Biometric Detection: Application to Iris, Fingerprint, and Face Recognition" has been successfully designed and tested. It has been developed by integrating features of all the hardware components and software used. Presence of every module has been reasoned out and placed carefully thus contributing to the best working of the unit. Secondly, using highly advanced ARM9 board and with the help of growing technology the project has been successfully implemented.

REFERENCES:

[1] Dmitry Pertsau,AndreyUvarov " Face Detection Algorithm Using Haar-Like Feature for GPU Architecture" The 7th IEEE International conference on Intelligent Data Aquisation and Advanced Computing Systems: Technology and Applications 12-14 september 2013

[2].Paul Viola and Michael Jones in their paper "Rapid Object Detection using aBoosted Cascade of simple Features" The IEEE International conference on computer vision and pattern recognition.

[3]Dr. Sunil Kumar Singlain his paper " A Review of Image Based Fingerprint Authentication Algorithms". The International Journal of Advanced Research in Computer science and Software Engineering: Volume 3, issue 6, june 2013

[4]J. Galbally, J. Ortiz-Lopez, J. Fierrez, and J. Ortega-Garcia, "Iris liveness detection based on quality related features," in *Proc. 5th IAPR ICB*, Mar./Apr. 2012, pp. 271–276.

[5] J. Galbally, F. Alonso-Fernandez, J. Fierrez, and J. Ortega-Garcia,"A high performance fingerprint liveness detection method based on quality related features," Future Generat. Comput.Syst., vol. 28, no. 1, pp. 311–321, 2012.

[6]"Linux for Embedded and Real time Applications", by Doug Abbott .

[7]. Steve Furber, ARM SYSTEM-ON-CHIP ARCHITECTURE, Second Edition Person Education Limited, 2000.

[8].http://download.qt.io./learning/developerguides/qtquickappdevintro/QtQuickApp

[9]R. Cappelli, D. Maio, A. Lumini, and D. Maltoni, "Fingerprint imagereconstruction from standard templates," *IEEE Trans. Pattern Anal.Mach. Intell.*, vol. 29, no. 9, pp. 1489–1503, Sep. 2007.

[10]Liu Chun-cheng. USB Webcam Driver Development Based on Embedded Linux [J].Compter Engineering and Design, 2007, 28(8):1885-1888.

[11]J. Galbally, F. Alonso-Fernandez, J. Fierrez, and J. Ortega-Garcia, "A high performance fingerprint liveness detection method based on quality related features," *Future Generat. Comput. Syst.*, vol. 28, no. 1, ap.311–321, 2012.

[12]J. Galbally, J. Fierrez, F. Alonso-Fernandez, and M. Martinez-Diaz, "Evaluation of direct attacks to fingerprint verification systems,"*J. Telecommun. Syst.*, vol. 47, nos. 3–4, pp. 243–254, 2011.

[13]D. Maltoni, D. Maio, A. Jain, and S. Prabhakar, *Handbook of Fingerprint Recognition*. New York, NY, USA: Springer-Verlag, 2009.

[14]A. Liu, W. Lin, and M. Narwaria, "Image quality assessment based on gradient similarity," *IEEE Trans. Image Process.*, vol. 21, no. 4, ap.1500–1511, Apr. 2012.

[15]I. Chingovska, A. Anjos, and S. Marcel, "On the effectiveness of local binary patterns in face anti-spoofing," in *Proc. IEEE Int. Conf. Biometr. Special Interest Group*, Sep. 2012, pp. 1–7.

[16]H. R. Sheikh and A. C. Bovik, "Image information and visual quality," *IEEE Trans. Image Process.*, vol. 15, no. 2, pp. 430–444, Feb. 2006.

[17](2012). LIVE [Online]. Available: http://live.ece.utexas.edu/research/ Quality/index.htm

[18]J. Galbally, R. Cappelli, A. Lumini, G. G. de Rivera, D. Maltoni, J. Fierrez, *et al.*, "An evaluation of direct and indirect attacks using fake fingers generated from ISO templates," *Pattern Recognit. Lett.*, vol. 31, no. 8, pp. 725–732, 2010.

[19]M. M. Chakka, A. Anjos, S. Marcel, R. Tronci, B. Muntoni, G. Fadda, *et al.*, "Competition on countermeasures to 2D facial spoofing attacks," in *Proc. IEEE IJCB*, Oct. 2011, pp. 1–6.

[20]ISO/IEC 19792:2009, Information Technology—Security Techniques— Security Evaluation of Biometrics, ISO/IEC Standard 19792, 2009

International Journal of Engineering Research and General Science Volume 3, Issue 5, September-October, 2015
ISSN 2091-2730

Programmable Logic Controller and Its Applications

Tejas Kopte[1], Ankita Pai[2]

U.G. Student, Department of Electrical Engineering, Sardar Patel College of Engineering, Mumbai, India[1]

U.G. Student, Department of Electrical Engineering, Sardar Patel College of Engineering, Mumbai, India[2]

Email Id: koptetejas14@gmail.com

ABSTARCT: Since the industrial revolution took place in 18th century, various improvements have been done in the sector of industry. The sole principle behind it was to reduce the human efforts by means of automation. A Programmable Logic Controller(PLC) has created a huge impact in the field of automation because of its exceptional capabilities. It has transformed the industry into a new era and hence study of PLC need to be done in order to thrive in this competitive 21st century. This paper studies and analyses structure of a PLC, its components, programming, functioning and further discusses on how it is being used in present world.

KEYWORDS: PLC, Automation, Ladder logic, Input Output, Memory, Relays, Switches

I. INTRODUCTION

A programmable logic controller, commonly known as PLC is a specialized computer mainly used for automation in various industries. It is used in place of automation of a car manufacturing company where robotic arms are used, places where motors needs to be driven on reception of a command signal, in electrical power system for the operation of circuit breaker, etc. PLCs are programmable hence a single unit can be used for different kind of operations based on where it is used making it a versatile device. The major advantage of a PLC over the conventional controllers its robust nature. It has high fidelity in most dynamic environments. PLC is reluctant to noise from the peripherals and hence is a reliable device for automation where accuracy and correctness is prominent. Another major advantage of a PLC is its ability to handle multiple input and output ports which processes analog as well as digital signals.

Figure 1. SIEMENS S7-300 PLC

II. NEED FOR PLC

Earlier in all types of industries, relays were used for automation purpose. Relays are electromagnetic device which contains a coil and a mechanical action switches the relay between ON and OFF state. Various relays needed to be incorporated in a given system in

order to control its various parameters such as current or voltage for driving a motor. Thus in order to control a complete system multiple relays had to be used. It ultimately required lot of space and power because of bulky size of a relay due to its components. Also coordination between relays was a major issue because of their electromechanical operation. Thus development in the field of automation led to the invention of programmable logic controller. A PLC occupies very less space as compared to the conventional relay controller with high number of input and output ports included in one device. PLC is widely used in different kinds of industries because of its simplicity, user friendly operation, versatility, efficiency and compactness.

III. BUILDING BLOCKS OF PLC

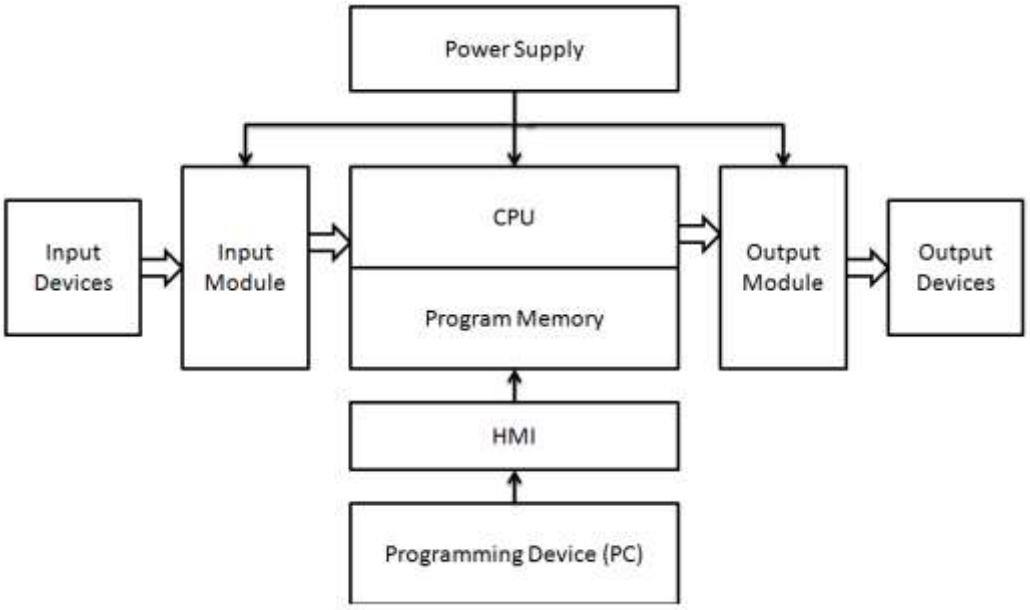

Figure 2. Block diagram of PLC

The major blocks constituting a programmable logic controller are 1)Power supply, 2)CPU, 3)Input Output system, 4) Memory, 5) Communication module

A. Power supply: The power supply module powers the controller including all its components with a standard 24V DC supply. It is generally placed at one end in the PLC rack. It converts the input power from 240V AC/ 120V AC to the rated 24V DC. It supplies an output current of 2A, 5A and 10A to the PLC modules.

B. CPU: It is the brain of the PLC controlling all the activities inside the controller. It resides typically adjacent to the power supply in the rack. The CPU is mainly composed of micro controllers and integrated circuits and is responsible for coordination between different units such as memory access, signal modules, I/O modules, etc. CPU has the following operating modes:

- Programming mode- In this mode a user program compiled on a PC is downloaded to the PLC for its execution.
- Run mode- In Run mode the PLC executes the downloaded program. It takes in the input values and produces the desired output as instructed in the program. In this mode PLC may also use the communication interfaces such as RS232, Profibus, SCADA or CC-Link.
- Stop mode- In this mode, the PLC stops executing the program. Hence no output is produced in this mode. Necessary input checks can be carried out for analysing or debugging.
- Reset mode- It resets the CPU and bring it back to its original position from where it started. If reset is done without deleting any data from the memory registers, such reset is called warm reset; and if reset is done erasing all the data from memory registers then such type of reset is called the cold reset.

C. Input Output System: The I/O modules in a PLC can be of two types namely, Analog modules or Digital modules. Depending on the application corresponding digital or analog input cards are placed in the PLC rack. The input cards basically does the function of collecting the data from external devices such as sensors, push buttons or communication devices, makes it compatible with PLC CPU by doing signal conditioning and sends it to the CPU for further execution. These input devices are connected to the PLC input module by the means of screw terminals on the card.

The output module performs the function of sending the control signal from CPU to corresponding output device for actual action. The hardware is similar to the input module. It can be digital module if has to send signals to devices accepting discrete signals such

as push buttons, micro switches, selector switches, etc. or it can be an analog module if the output devices are motors drives, alarm system, lamp, etc.

D. Memory: The memory block present in the PLC is majorly divided into three sections viz.

- Load memory
- Work memory
- System memory

- Load memory: It is used to store the user program. It can be ROM, ROM or EEPROM memory. In many PLCs the load memory can be extended by the means of memory card (RAM or EEPROM).
- Work memory: The work memory (Integrated RAM) is used to store the parts of the user program required for program processing.
- System memory:

a) PII and PIQ- Peripheral Image Input and Peripheral Image Output are the memory areas used to store and transfer data between input devices, PLC and output devices. These areas are checked in a cyclic manner during the execution of a program. The status signals from various input devices are stored in the PII region during program scan. At the end of program scan, the output signals stored in the PIQ region are transferred to the corresponding peripheral devices.
b) Timer/Counter area- This memory contains the 16-bit timers or counters. These timers/counters can be used by the programmer for various purposes. The number of timers and counters depends on the CPU.
c) Bit memory- This memory is used to store the intermediate results of a program execution. It is abbreviated by M. Size of this area depends upon the CPU.
d) Retentive memory- In PLC taking backup of certain memory is essential. This memory area is a non-volatile RAM which backs up the timer/counter, bit memory and data blocks without a backup battery.
e) Local stack- It is similar to bit memory in order to store the intermediate results, however it is not a global memory, that means it stores the data specific to a given block only.
f) Diagnostic area- It is used to store the diagnostic data such as ISTACK, BSTACK or Diagnostic buffer.

E. Communication module: A communication module in a PLC is used to establish a connection between PLC to PC or PLC to other PLC etc. With the advent of SCADA systems, ethernet module is widely used for communication. It uses TCP/IP protocol for communication over a network of other devices(PCs, PLCs). It is given an RJ-45 connector to establish connections with the help of a CAT-5 Ethernet cable.

IV. PLC PROGRAMMING

As seen before, the major advantage of PLC over the conventional devices is its ability to implement desired automation based on a user program. This program can be compiled by user on a PC and can be uploaded to the PLC. The manufacturer of PLC develops their own software to program the PLC, e.g, SIMATIC S7 by SIEMENS. The program can be written in following logics:

- Ladder Logic(LAD)- An ON-OFF switch and a relay coil are the basic components of these method. These symbols emulates the real life components used in an actual control system and thus LAD logic can be understood by person having little or no specific knowledge of programming. The switches used can be normally open type or normally closed type depending on their use. The entire program can be written using these symbols in separate lines. The complete program structure looks like a ladder hence the name.
- Statement Logic(STL)- In this method, logical statements are written as a program. Various keywords are used to represent various parameters in the program. Programmer need to have prior knowledge of these keywords in order to compile an acurate program to produce desired automation results.
- Functional Block Diagram(FBD)- This is a graphical programming language for a PLC. The block represents a function and is provided with input and output ports which can be connected to other blocks or input/output. The direction of signal through the blocks is fixed, i.e., from left to right.

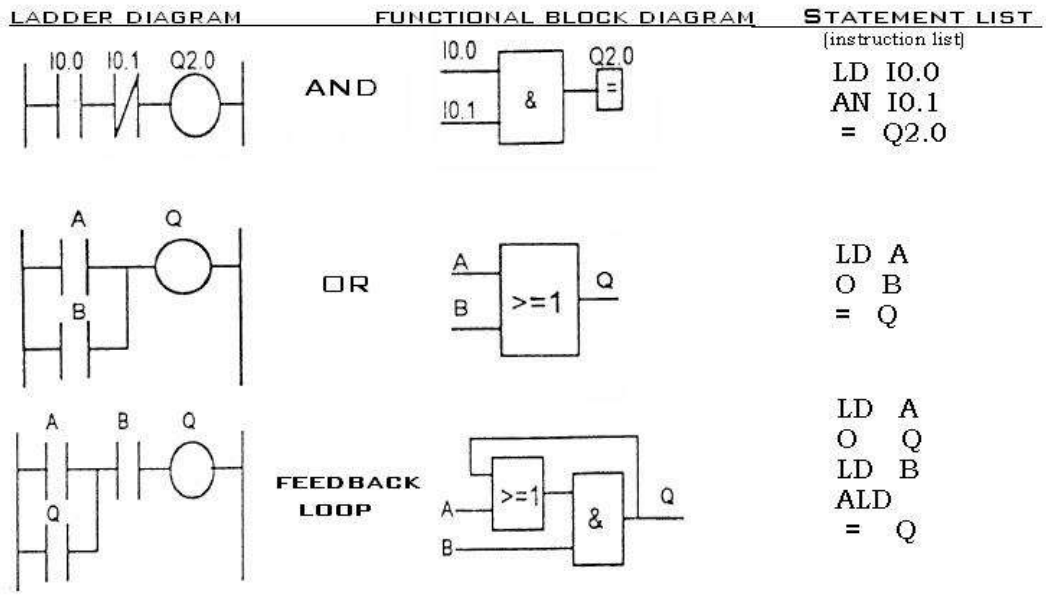

Figure 2. Comparison between PLC program logics

V. APPLICATIONS OF PLC

Because of the versatility of PLC, it is used in various places for automation. In industries various processes needs to be controlled at every instant of time such as valve control, pressure control, robotic action, etc. It becomes tedious and infeasible for humans to control all such activities on their own. Thus relays were used to perform those activities. However, a relay can be used only for a specific and limited operation which makes their use bulky and uneconomic. On the contrary PLC having the ability to perform number of tasks by simply modifying the program has become a prominent device for automation of such activities. There are various places where a PLC can be used. Some of those are listed as below:

- Robotic arm in car manufacturing
- Air compressors
- Airport runway lighting control
- Traffic signal control
- Smoke alarm control
- Process valve control
- Textile equipments
- Vacuum pump system

Apart from these applications, PLC is widely used in automation of electrical power system. At electrical substations automatic reclosing, circuit breaker tripping, capacitor switching, etc. can be controlled with PLCs.

VI. ADVANTAGES

1. Multiple devices such as timers, memory shells, etc. are embedded in one system which makes PLC very convenient and versatile to use
2. PLCs are robust in nature and can be operated effectively in adverse external conditions such as temperature, humidity, motion, etc.
3. PLCs are easily programmable and its programming language is easily understood
4. The interfacing between input and output is already done inside a PLC
5. Interfacing with HMI makes the monitoring of inputs and outputs of a PLC easy and convenient
6. Complex operations can be performed easily

VII. DISADVANTAGES

1. A lot of hard wiring is required for connection of input and output devices
2. Since PLC is a semiconductor device, it can't be operated over a level of temperature where it can't sustain it
3. Debugging with PLCs may become tedious as finding the fault is not very easy
4. Initial cost of PLC is high

VIII. CONCLUSION

A programmable logic controller has a huge potential in the field of automation because of its simplicity and effectiveness. In this century it is developing at a rapid rate in order to synchronize with the ever growing technology. PLC have become a must have in

industries dealing with automation. Along with that it has a lot of scope in functions at domestic level. Though it has certain disadvantage, these are certainly going to be solved in the near future because of increasing dominance of PLC. The use of ladder logic in PLC programming has made its much more easy to understand and requires very less training. In order to develop the automation field further, understanding of PLC is essential.

REFERENCE:

[1] Edward HRYNKIEWICZ, Mirosław CHMIEL, "About Programmable Logic Controller- step by step"- http://pe.org.pl/articles/2012/9a/66.pdf

[2] PLC History- http://www.machine-information-systems.com/PLC_History.html

[3] How PLCs Work- http://www.machine-information-systems.com/How_PLCs_Work.html

[4] PLC Manual, Basic guide to PLC- http://www.plcmanual.com/plc-programming

[5] PLC Applications- http://www.entertron.com/application.htm

[6] Siemens, SIMATIC S7-300 Module data Manual, February 2013.

[7] Siemens, SIMATIC Programming with STEP 7 Manual, March 2006.

[8] W. Bolton- "Programmable Logic Controllers, Sixth Edition"

[9] ANTONIO SORIN TASU- "PROGRAMMABLE LOGIC CONTROLLER"- http://www.idc-online.com/technical_references/pdfs/electronic_engineering/0305_0310.pdf

[10] L. A. Bryan, E. A. Bryan, "Programmable Controllers, Theory and Implementation, Second Edition"

[11] Frank Petruzella, "Programmable Logic Controllers, Third Edition"

[12] Industrial Manufacturing- Siemens, https://www.industry.usa.siemens.com/services/us/en/industry-services/training/self-study-courses/quick-step-courses/Documents/plcs.pdf

International Journal of Engineering Research and General Science Volume 3, Issue 5, September-October, 2015
ISSN 2091-2730

EXPERIMENTAL STUDY OF ERRORS IN GEARS BEFORE AND AFTER HEAT TREATMENT PROCESSES

[1] Manveen Kaur, [2]Abhishek Behera

[1]Final year, B.tech ADE, University Of Petroleum And Energy Studies, Dehradun.

[2]Final year, B.tech ADE, University Of Petroleum And Energy Studies, Dehradun

manveen.kaur25@gmail.com, 9568806329

ABSTRACT: This paper involves studying errors produced in the gear before and after heat treatment processes while manufacturing a spur gear. High torque load demands, low running noises and compact designs are basically the characteristics of modern gearboxes. In order to fulfill these requirements, profile specifications have to be controlled tightly. Heat treatment processes, hobbing, shaving, etc. leads to distortion in the profile, while manufacturing high accuracy gears. In this analysis two different blanks were taken to manufacture a spur gear of module 1.75mm , which went through a series of inspection at different stages of its manufacturing to get the gear within desired permissible limits. The present paper also deals with the finding of profile, lead and pitch errors before and after the heat treatment processes using Gear Testing Machine- TTi-300 N.

Keywords: Hobbing, Profile, lead, pitch error, gear testing machine.

[I]INTRODUCTION:

Gears are widely used in various mechanisms and devices to transmit power and motion positively (without slip) between parallel, intersecting (axis) or non-intersecting non parallel shafts. According to the requirements special attention needs to be paid while manufacturing of gears. The gear tooth flanks have a complex and precise shape demanding requirements of high surface finish. The starting product in gear manufacturing is called a gear blank. Machine, work fixture, cutter, arbor, machined blanks, and also the cutting parameters add some amount of errors to different gear elements. Heat treatment processes involved during formation of gears enhances its mechanical properties. But due to phase transformation as well as thermal stresses occurring during heat treatment processes, uncontrolled distortion of gears takes place causing deviation from required gear accuracy.

In this paper two blanks of the composition 16MnCr5H have been taken for experimental purpose. It went through the following processes to get the desired shape.

Blank -> Quality assurance ->hobbing -> Heat treatment -> tempering -> shot blasting -> honing ->washing -> Rolling-> Final inspection.

[II]LITERATURE REVIEW:

Nitin Haridas Mulay [4] presented a paper reviewing the current aspects of inspection metrology. He checked gear parameter errors by using different methods of inspection tester/instruments for getting good quality transmission gears. Isaich Paul Jenzen presented a thesis on modeling of heat treating processes for transmission gears in Dec.2009 to the faculty of Worcester Polytechnic Institute for the degree of Master in Science in Material Science and Technology. It provided a detailed review of the mass transfer, heat transfer and stress that occur during heat treatment. Raveen John, Dr. Y.S. Varadarjan & Paul Pereira[7] arrived at a solution for profile distortion problem encountered during heat treatment process of gear manufacturing using root cause analysis.

[III]DIFFERENT PROCESSES INVOLVED DURING MANUFACTURING OF GEARS:

1)Hobbing:- gear hobbing is a machining process. It is used for cutting teeth of a workpiece using a cutting tool called hob. It is inexpensive yet accurate maching process compared to other gear forming process.

2) Heat treatment process:-for transmission gears it is required that the surface of the tooth should be hard enough to resist wear while the core of the tooth should be soft for impact absorption without breakage during actual running.

Processes involved in surface hardening are as follows:-

a) Carburizing:- used to attain desired depth in the workpiece with carbon.

b) Quenching:- to induce hardness at the surface but not the core.

c) Tempering:- process relieves the structure of high residual stress to achieve improved toughness.

3) Shot blasting:- Shot blasting is a process in which the material is cleaned by removing the carbon content which remains after heat treatment process by bombarding round steel balls over the workpiece.

4) Honing:-it is a super finishing operation done on gears with bore. It is used to give super finish to the internal diameter of the gears, producing a precision surface by scrubbing an abrasive stone against it along a controlled path.

[IV]TERMINOLOGIES RELATED TO ERRORS IN GEARS:-

1) Profile inspection:- profile is the shape of the gear tooth curve measured from the root to the tip of the gear. Due to momentary disturbances of the rotational velocity ,profile errors results in the non- uniform motion transmission of the gears.

a) Profile form variation:-it is defined as the difference between the nominal involute form to the actual involute form.

b) Profile angle variation:-it is the distance between two nominal profiles that intersect the average profile at start and end points of the profile range.

c) Total profile variation:- it is the sum of the profile form variation and the profile angle deviation.

2) Helix or lead angle:-for parallel axis spur and helical gears, uniform loading across the full width of the teeth is required for this the pair of the meshing gears must have identical helix angles. The inadequate face width contact between the mating gears is caused due to lead error resulting in wear and noise of the gears.

a) Lead form variation:- it is defined as the difference between the nominal lead form line to the actual form line.

b) Lead angle variation:- it is defined as the result between the nominal and actual helix angle.

c) Total lead variation:- distance between two nominal leads enclosed within the lead inspection range.

3) Pitch error and run out :- due to these errors gears tends to make noise and also the motion transmission is non-uniform.

a) Run out variation (F_r):- it is defined as the maximum difference of the nominal radial position of all the teeth to the actual measured position.

b) Total pitch variation (F_p):- it is defined as the maximum difference between nominal angular position of each right and left flank to the actual measured position.

c) Single pitch variation (f_p) :- it is defined as the difference between the nominal angular position of each flank to the previous flank at the same side.

d) Difference between adjacent pitches (f_u):- difference between the actual dimensions of two successive right or left flank transverse position.

[V]METHODOLOGIES AND EXPERIMENTATIONS:

2 blanks of the composition 16 MnCr5H were taken. Its chemical composition was:-

% C-0.16/0.19

% Si- 0.25 max

% Mn- 1.0/1.3

% Cr- 0.8/1.1

% Mo- absent

% S- 0.015-0.035

% P- 0.035

% Cu- 0.30 max

% Al- 0.015/0.035

% Ti- 30 ppm max

% Ca- 10/20 ppm

The gear of the following specification was to be obtained:-

- No. of teeth -23
- Module- 1.75 mm
- Outside Ø- 45.60 /45.70
- MOT (between teeth)- 4 teeth
- MOT (soft)- 19.336/19.366
- MOT (hard)- 19.336/19.392

1) Inspection:- the bore size, parallelism and face run out of the blanks were measured using Air Unit, Height Gauge and Tapered Mandrel respectively.
These blanks were numbered 1 and 2 and the following observation was recorded:-

S.no.	Bore Size(mm)	Parallelism(microns)	Face run out(micron)
1.	16.990	20	20
2.	16.991	10	10

Where, Standard for bore size is: 16.990- 17.008 and maximum permissible error for parallelism and Face Run Out is 20 microns.

2) Hobbing:-

Now, these blanks were taken to the hobbing cell for cutting of tooth.

MACHINE DESCRIPTION:- Hobbing
MAKE :- LEIBHERR

S.NO.	PARAMETER	SPECIFICATION	MEAS. METHOD
1.	Material	16MnCr5H	Third party insp.
2.	Hardness	170 to 210 BHN	Harness tester
3.	OD	Φ45.6~45.7mm	Snap gauge
4.	Bore Size	Φ16.990~17.008	APG
5.	Dim	12.3~12.4mm	Snap gauge

6.	Dim	9.1~9.3mm	Snap gauge
7.	Surface Roughness	0.8Ra	Surface finish tester
8.	OD Runout	0.1mm	Mandrel & Dial
9.	perpendicularity	.020 mm	Between center mandrel and dial

MODEL :- LC150

INPUT MATERIAL CONDITIONS

PROCESS PARAMETERS:-
CUTTING SPEED:- 130~180m/min. (750~800 rpm)
FEED :- 1.3~1.8 mm/tr.
SHIFTING AMOUNT PER GEAR:- 5.515 mm

After Hobbing, these gears went to roll tester machine to find TCE and Micrometer to measure MOT :-

SAMPLE No.	TCE(microns)	MOT (mm)
1.	20	19.351
2.	20	19.357

3) Standard Room:-

After hobbing ,these samples went to the standard room to measure the pitch error , lead error and profile error using Gear Testing Machine- TTi-300 N.

Gear quality grades are standardized for different normal module/DP ranges and different ranges of reference diameters in AGMA, DIN, JIS and other standards. AGMA provides 8 grades from 15 to 8, where the higher grade number indicates the better gear accuracy. In DIN and JIS, a lower grade number means better gear accuracy. We have followed DIN 3962 standards.

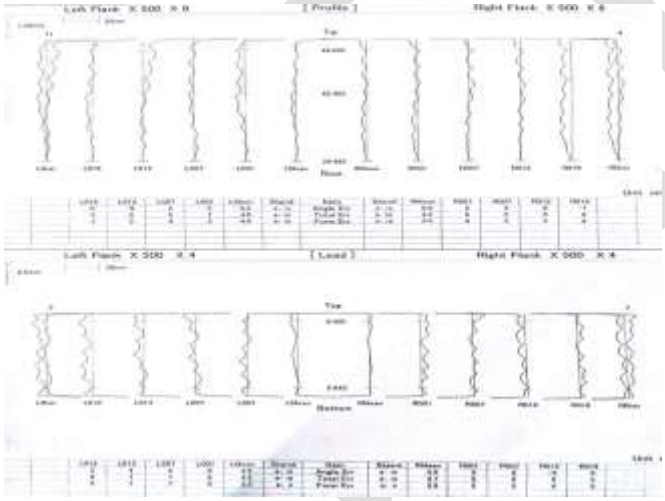

i)Profile and lead error of 1st piece

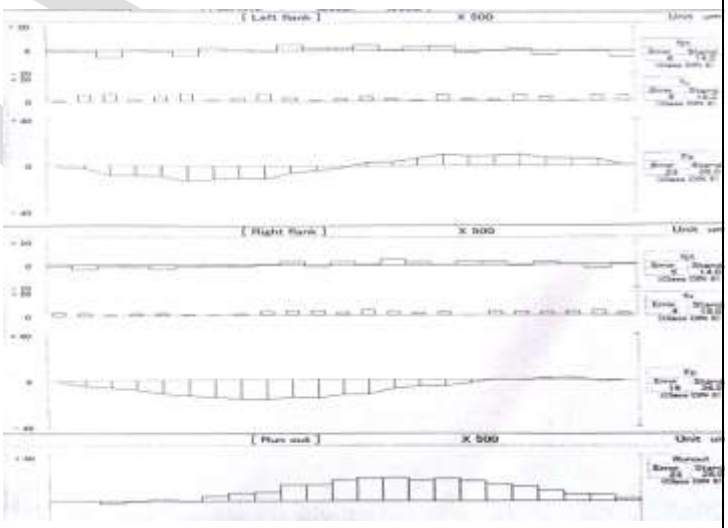

ii) pitch error of 1st piece

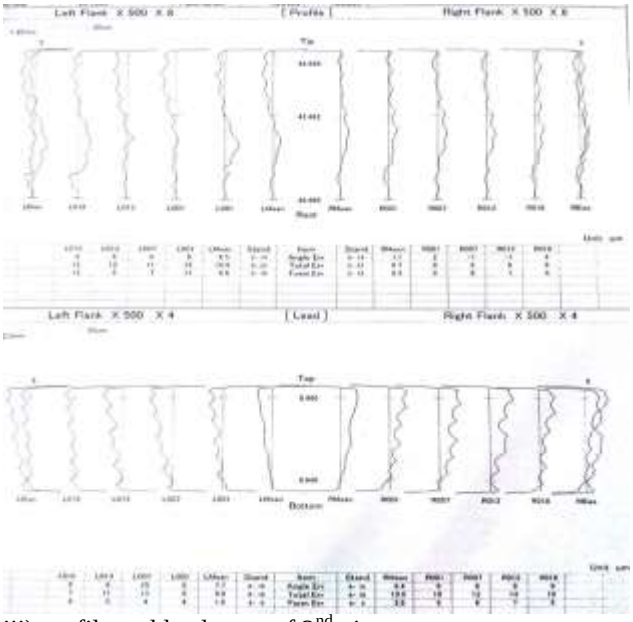

iii) profile and lead error of 2nd piece

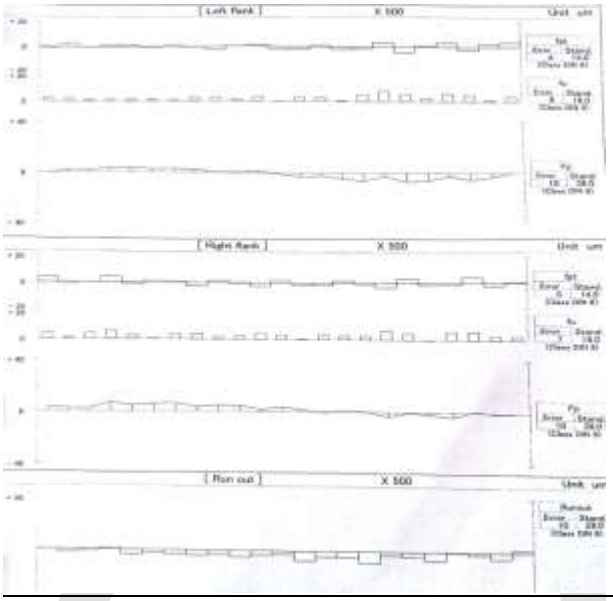

iv) pitch error of 2nd piece

4) HEAT TREATMENT:-

PROCESS PARAMETERS:

Parameters	temperature	CP/MV	Time(min)	Endo gas flow	Enrichment LPG flow
Pre wash(spraying)	70±5℃	--	15±5	--	--
Pre wash(drying)	70±10℃		15±5		
Pre heating	500±15℃	--	60±5		
Heating	850±15℃	0.7±.05%	15±5	8~10Nm^3/hr	50~250LPH
Carburizing	900±5℃	1±0.05%	90±5	8~10Nm^3/hr	50~250LPH
Diffusion	900±5℃	0.8±0.05%	30±5	8~10Nm^3/hr	50~250LPH
Hardening	840±5℃	0.7±0.05%	30±5	8~10Nm^3/hr	50~250LPH
Quenching	120±5℃	--	15	--	--
Post wash(Dunking)	70±5℃	--	15±5	--	--
Post wash(Spraying)	70±5℃	--	15±5	--	--
Post wash(Drying)	70±5℃	--	15±5	--	--
Tempering	160±10℃	--	120±10	--	--

PROCESS CONDITION:

Check item	Specification	Meas. method
Endo gas flow rate	8~10Nm^3/hr	Flow meter
Carbon potential(cp/mv)	As per cycle	Mv/Cp controller
Temp	As per cycle	Flow meter
Quench oil level	Pokayoke-no quenching happens if oil level is low or high	Level indicator
Quench media temperature	120±10℃	Temp controller
Roof fan	Zero speed switch or RPM monitoring	Alarm if fail
Air pressure & flow monitoring	5~7 kg/cm^2	Pressure switch
Pre wash & Post wash water	1.free of sludge 2.free of oil 3.PH- 8~12 4.cleaning media conc.- 3~5%	1.cleaning of water tank, every year 2.oil skimmer 3.PH test paper

	5.water pressure- 1.0 to 3 kg/cm^2	4.Refractories 5.pressure gauges

5)Testing lab:-
After heat treatment processes of these samples, they were taken to the testing lab to find the Surface and core hardness of the gears.

Rockwell hardness Tester(HRA)

Sample no.	Surface hardness
1.	81
2.	81

Core Hardness:- 38 HRC (Bainite + LCM)
Case Depth:- 0.47mm (micro Vickers hardness tester) (Tempered Martensite with R.A. ≤5%)

5) Standard Room:-
After heat treatment, these samples again went to the standard room to measure the pitch error ,lead error and profile error using Gear Testing Machine- TTi-300 N. The graphs of the following are shown below. These graphs shows the errors in the gears before and after heat treatment using light and dark lines respectively.

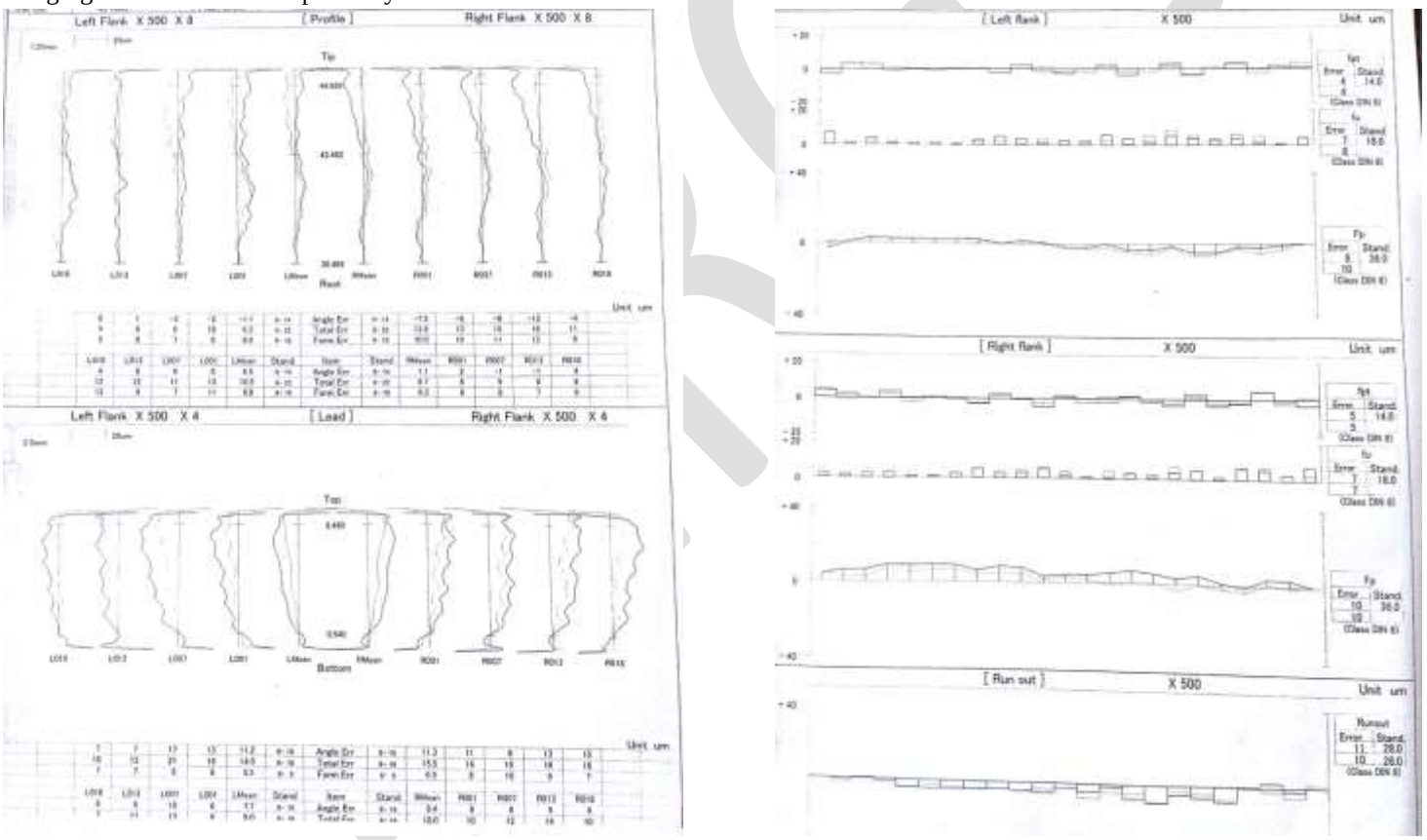

v) comparsion of profile, lead and pitch error of 2nd gear before and after heat treatment process

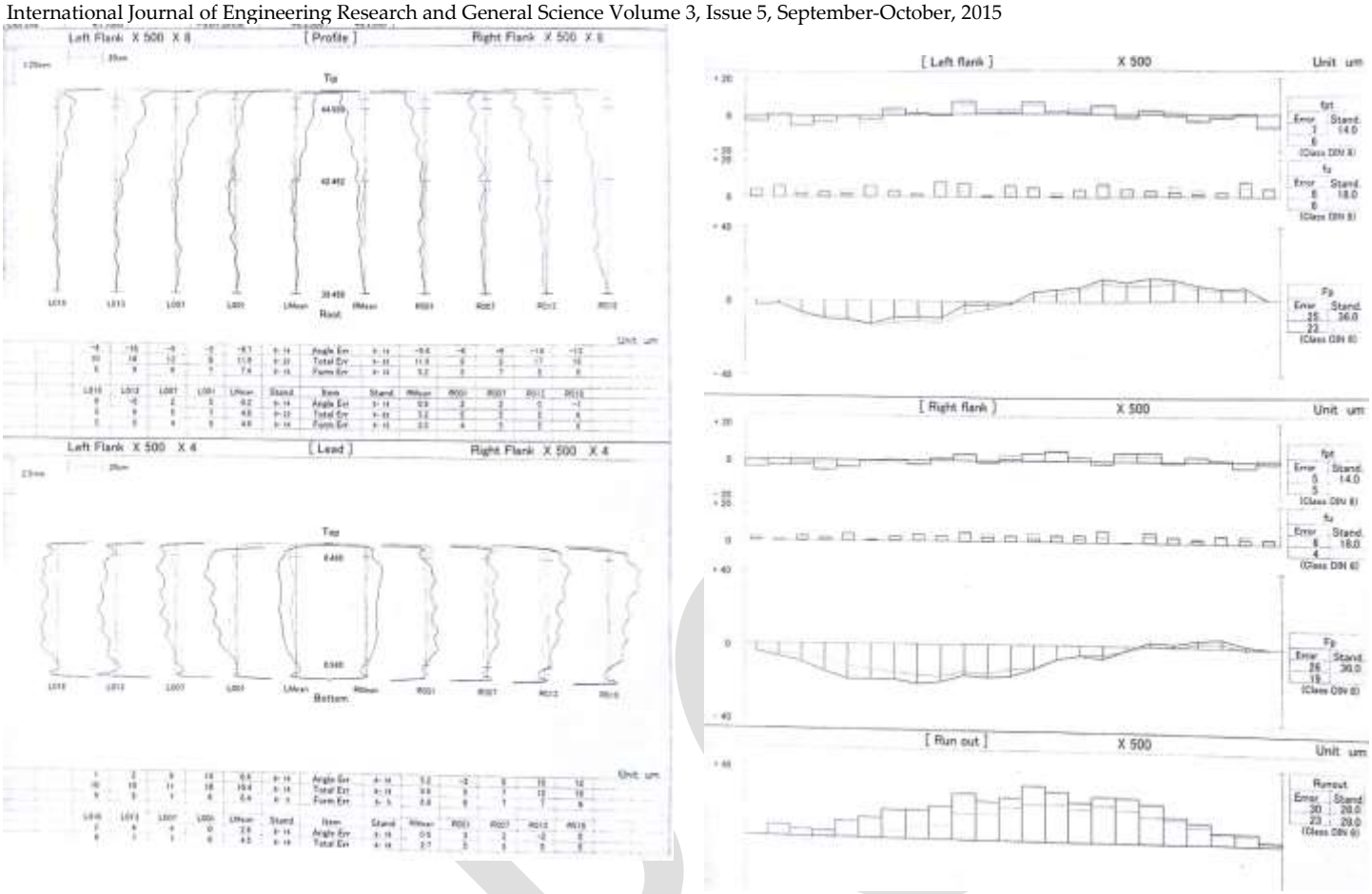

vi) comparison of profile, lead and pitch error of 1st gear before and after heat treatment process

6)FID:-

Finally after shot blasting and honing, TCC, TCE and MOT were measured:

Sample no.	TCC(microns)	TTE(microns)	MOT(mm)
1.	30	10	19.372
2.	30	10	19.379

[VI] CONCLUSION:-

Predictable and controlled dimensional and distortional changes can be achieved during the development work of heat treatment processes. Allowances can be provided at soft finishing stages, by establishing changes in the heat treatment processes and hence final dimensional tolerances can be achieved which are required for transmission gears.

REFERENCES:-

1)Welbourn D. B. 'Fundamental Knowledge of Gear Noise – A Survey' *Proc. Noise & Vibration of Eng. and Trans., I Mech E., Cranfield, UK, July 1979*, pp. 9–14.

2) B. Karpuschewski , H.-J. Knoche, M. Hipke, Gear finishing by abrasive processes.

3)Mayo, P. (1990). Gear Metrology. *proceedings of Australian society of sugarcane technologists* (p. 10). New Castle , NSW: A. Goninan & Co. Ltd.

4)mulay, n. h. (2012). Basic Concepts for Methods of Inspection of Gear Parameter. *AdMet 2012 Paper No. AI 002*, 2.

5)gear technology magazine

6)gear solutions magazine

7) Raveen John, D. Y. (2015, may). To arrive at solution for profile distortion problem encountered during heat treatment process of gear manufacuring using root cause analysis. *International Journal Of Innovative Research in Science , Engineering and Technology*, *4*(5), 11.

International Journal of Engineering Research and General Science Volume 3, Issue 5, September-October, 2015
ISSN 2091-2730

Integrated Biomass Gasification Combined Cycle

Neha Sharad Kotak
Final year, Mechanical Engineering, SIES GST Navi Mumbai
Maharashtra, India
nehaktk3@gmail.com

Abstract-- Acknowledging the limitations of numerous incumbent biofuel production technologies, in terms of resource potential, greenhouse gas savings and economic viability, there is considerable involvement in second generation routes. These offer the potential for a diversification of feedstocks to be used, lower greenhouse gas impacts, and lower costs. Gasification is a cardinal constituent of several of the proposed second generation paths, such as catalytic routes to diesel, gasoline, naphtha, methanol, ethanol and other alcohols, and syngas fermentation routes to ethanol. Prodigious technical procession are made that allows substantially augmented usage of biomass as a fuel. An appealing and executable possibility of biomass utilization for energy production is gasification integrated with a combined cycle. In biomass gasification, there is greater experience with gasifiers for heat and power applications than for fuels yield. This technology seems to have the hypothesis to reach utmost efficiencies based on fundamentally pristine and renewable fuel. The plants utilize low grade fuels at reasonable overall efficiencies of 35%-50% based on gross heating value. Integrated Biomass Gasification Combined Cycle (IBGCC) systems supplant the conventional combustor with a gasifier and gas turbine. Biomass gasifiers have the potency to be up to twice as efficient as using conventional boilers to generate electricity. Progressive gas turbine and combined cycle technology is commercially explicated and manifested with natural gas as well as solid fuels such as coal through the use of gasification technology. These melioration in efficiency can make environmentally clean biomass energy available at costs more competitive with fossil fuels. The gas and steam turbines operate together as a combined cycle

KEYWORDS-- Biomass gasification, biomass, Syngas, combined cycle, IBGCC, Gasifiers, Power generation

I. SIGNIFICANCE OF IBGCC

Profound concern exists over relatively high monetary value of electricity for citizens and businesses Worldwide, which enforces a financial in cumbrance and impairs countries ability to contend effectively. On the other hand, there is a prodigious cost to shield our environment and the starring factor of that cost is electricity. New environmentally favoured technologies and strategies are postulated to develop and deliver electricity at depressed cost and decreased environmental impacts. The potential problem is further compounded by a fact that systems reliableness and the price of electricity are adversely stricken by existing big inventory of superannuated steam power plants. Moreover, it is further amplified by a requirement for new cost-effective pollution control technologies needed to reduce the health and environmental impacts from power plant emissions. Therefore, an imperative demand

exists to evolve superior, but economical methods to produce electricity while scaling down the wood and green waste landfills with the state-of-the-art control emanation of fine particles and va por-phase toxics. The combination of progressive technology and meliorate fuel supply has in a way increased the feasible biomass power plant size into a range appealing to utilities, and thus inflate the market for biomass power beyond the independent power producers and co-generators who have, to date, been the master players in the biomass power industry.

II. INTRODUCTION

The Integrated biomass gasification combined cycle (IBGCC) produces electricity from biomass which can be expounded in two major parts as follows:

A. Biomass gasification

Biomass gasification implies partial combustion of biomass ensuing in production of combustible gases consisting of Carbon monoxide (CO), Hydrogen (H_2) and traces of Methane (CH_4). This mixture is called producer gas which can be used to run internal combustion engines , can be used as backup for furnace oil in upfront heat applications and can be used to produce, in an economically viable way, methanol – an exceedingly attractive chemical which can be used as a fuel for heat engines as well as chemical feedstock for industries. Since any biomass material can undergo gasification, this process is much more inviting than ethanol production or biogas where only selected biomass materials can produce the fuel. Besides, there is a problem that solid wastes are seldom in a form that can be readily utilized economically e.g. Wood wastes can be used in hog fuel boiler but the equipment is expensive and energy recovery is low. As a result it is often beneficial to commute this waste into more readily usable fuel from like producer gas and so the gasification process is victimized. However under present conditions, economic factors seem to provide the reinforced argument of considering gasification. In many situations where the cost of petroleum fuels is high or where provisions are unreliable the biomass gasification can be an economically viable system – provided the suitable biomass feedstock is easily accessible.

B. Combined cycle

The producer gas is commuted to electricity in a combined cycle power block comprising of a gas turbine process and a steam turbine process which also includes a heat recovery steam generator (HRSG).The combined cycle technology is connatural to the technology used in modern natural gas fired power plants.

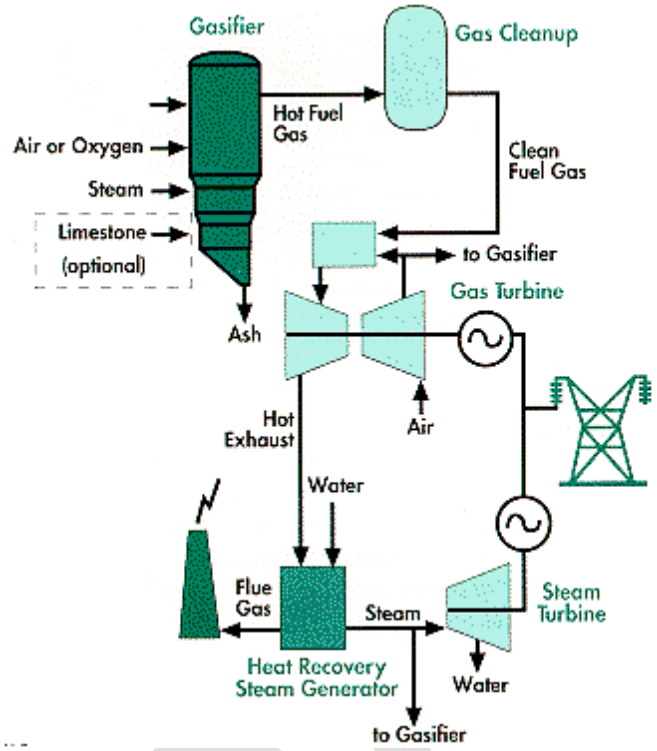

Figure1.Integrated Biomass Gasification Combined Cycle

III. CHARACTERISTICS OF IBGCC

The Integrated biomass gasification combined cycle offers distinctive features which the other competing technologies lack as:

1. It is environmentally superlative to conventional green biomass fired power plants and can be designed to meet the most rigorous ordinance;

2. Surmounts thermal efficiencies of the existing conventional technologies;

Also, IBGCC Power Generation technology proves its outstanding characteristic in a way that it has the potential applicability to a variety of fuels. The most pressing need for advanced gasification technology is for repowering of older coal-, and gas-fired boilers that typically have low efficiency and high discharge levels.

IV. WORKING OF IBGCC

IBGCC systems are antiseptic and it is based on an advanced technology - a gasifier used instead of the traditional combustor conjugated with a key enabling technology, the advanced gas turbine. The overall system is an integrated biomass gasification combined-cycle conformation that renders superior system efficiencies and ultra-low discharge levels.

4.1 Syngas formation

Syngas or the producer gas is the product of the gasification process which can be delineated as a thermochemical operation, denoting that the feedstock is ignited to high temperatures, producing gases which can undergo chemical reactions to form a synthesis gas. The biomass gasification process is a combination of four phases and the literal sequence depends on the gasification system applied. The phases of gasification are:

A. Drying

Biomass contains usually a large amount of water. Wood chips, for example, may easily achieve moisture values around 55% in weight. Drying is the gasification phase that occurs at lower temperature (100-150°C), ideally purely physical. At this temperature the water in the fuel evaporates and the steam diffuses towards the external atmosphere due to a negative gradient of concentration. In the case of gasification, if the drying process is retarded (low drying speed) the amount of unburnt carbon becomes larger, which is of course an unwanted effect. The drying speed is affected by thermal conductivity of the fuel and by the fuel packing.

B. Pyrolysis

It is a thermal process that converts the fuel, in the current case biomass, into char, ashes and volatiles. Pyrolysis evaporates the volatile ingreidient of the feedstock as it is heated. The volatile vapors contain hydrogen, carbon monoxide, carbon dioxide, methane, hydrocarbon gases, tar, and water vapors. As biomass feedstock's have more volatile components (70-86% on a dry basis) than coal (around 30%), pyrolysis plays a significant role in biomass gasification than in coal gasification. Byproducts also include solid char and ash.

C. Oxidation:

In the zones that are rich in oxygen, which is under-stoichiometric anyway, oxidation occurs between 700°C and 2000°C. Part of the char is combusted. Oxidation is the main source of energy for the gasification process, being strongly exothermic.

D. Reduction

It is the conversion of char into ash and gases, in a virtually oxygen-free atmosphere, thanks to carbon dioxide, water or hydrogen. Water may be inserted in the form of steam, mixed with the gasification agent flow.

4.2 TYPES OF GASIFIERS

Mainly the following five types of the gasifiers are used and they are:

A. Updraft gasifier (countercurrent)

In the countercurrent reactor the biomass is inserted from the top, while the gasification agent, usually steam and air, from the bottom, through the grate. The producer gas is extracted from the top.

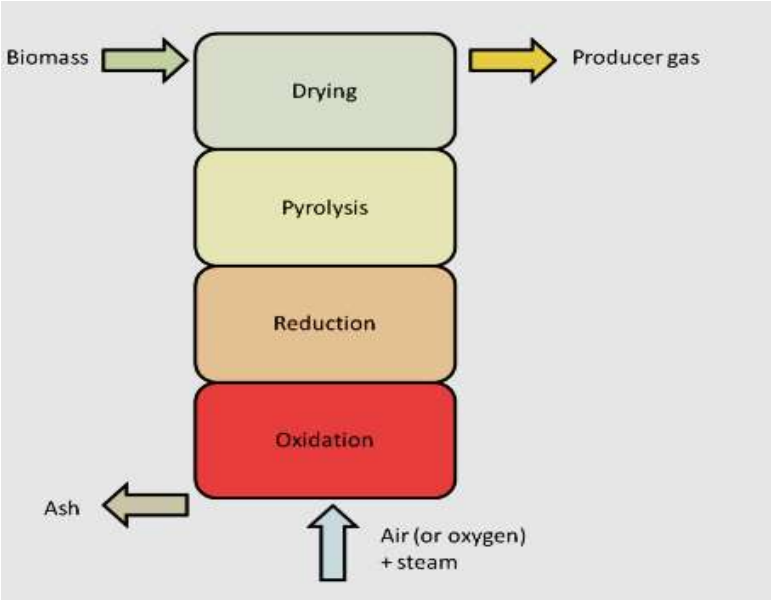

Figure 3. Updraft gasifier.

B. Downdraft fixed bed

The biomass along with air,oxygen or steam is fed from the top of the gasifier oxygen or steam, hence the biomass and gases move in the same direction. Some of the biomass is combusted, falling through the gasifier throat to form a bed of hot charcoal which the gases have to pass through the reactive zone. This ensures a fairly high quality syngas, which leaves at the base of the gasifier, with ash collected under the grate.

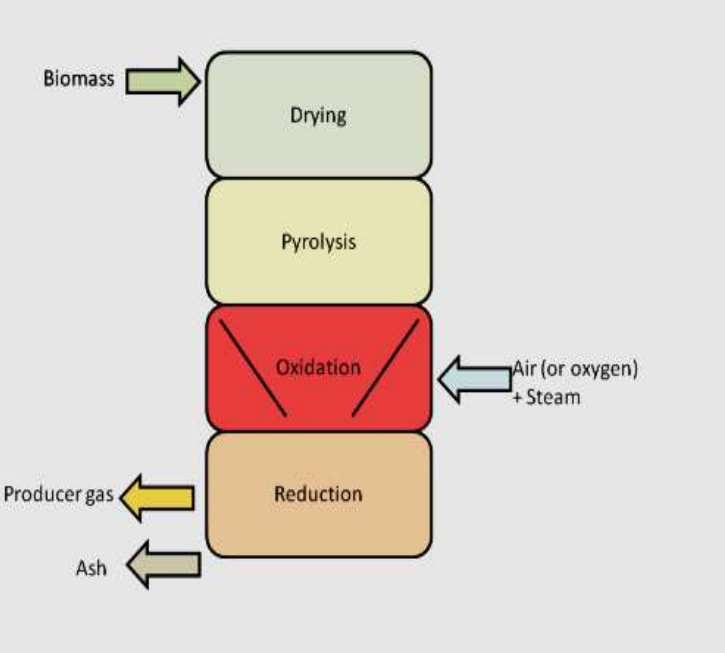

Figure 4. Downward gasifier .

C. Dual fluidized bed (Dual FB)

Dual fluidized bed system contains two chambers – a gasifier and a combustor. Biomass is fed into the CFB / BFB gasification chamber, and regenerated to nitrogen-free syngas and char using steam .The char is combusted in air in the CFB / BFB combustion chamber, heating the accompanying bed particles, further which is fed back into the gasification chamber, providing the indirect reaction heat .Cyclones remove any CFB chamber syngas or flue gas. It also operates at temperatures below 900°C to avoid ash melting and sticking and can be pressurized.

D. Circulating fluidized bed (CFB)

A bed of fine inert material has air, oxygen or steam blown upwards through it fast enough (5-10m/s) to set aside the material through the gasifier. Biomass is fed in from the side, is suspended, and ignites providing heat, or reacts to form syngas .The mixture of syngas and particles are isolated using a cyclone, with material returned into the basal part of the gasifier .

E. Fluidized bed gasifier

The fluidized bed gasifier is a completely different concept. The flowing gasification agent, which is blown at high velocity from the bottom, mixes biomass particles, oxidizer, hot gases and the bed material. The bed material consists of very small particles of inert material (a siliceous sand), which avoid sinterization, and catalysts, which decrease the tar amount and control the syngas composition. The temperature is very homogeneous and usually lower than in the fixed bed gasifiers, being around 750-900°C. The gasification phases are not spatially localized. This type of gasifier generates a high tar amount, due to the low temperature, difficulties in controlling the process and the need for creating a pressure in the reactor, usually. The main advantages are a very high heat transfer and high reaction velocity, thanks to the high turbulence, that assures compactness, useful especially in large scale plants. The carbon conversion is high and it is flexible to the changes in biomass moisture and fast to turn on and off.

4.3. POWER GENERATION

As it is fully customary, highly effective, combined cycle power plant is competent of reliable operation on natural gas or other fuel. The accession of the Integrated Biomass Gasification Combined Cycle (IBGCC) converts biomass to a clean fuel gas, which is burned in the progressive, high efficiency combustion turbine .The combined cycle concept includes the two main cycles that is the Brayton cycle (top cycle) and a Rankine cycle (bottom cycle), consists the recovery of the hot flue gas, which is generated by the Brayton cycle, through a Heat Recovery Steam Generator (HRSG) which is basically a set of heat exchangers that produces steam for the Rankine cycle. The steam generated by the HRSG is expanded in a steam turbine, generating power. Afterwards the steam, usually saturated, condensates and heat is released to the environment (or to the district heating system, if present). Finally the feed-water is compressed by a pump and sent again to the HRSG. Combining the two cycles and recovering part of the thermal energy of the flue gases result in high efficiency between 47% and 52%. A gas engine may also be combined with a Rankine cycle . Under this condition, since the flue gas temperature is lower than in the Brayton cycle, an additional firing helps to achieve the temperature required by the steam superheating.

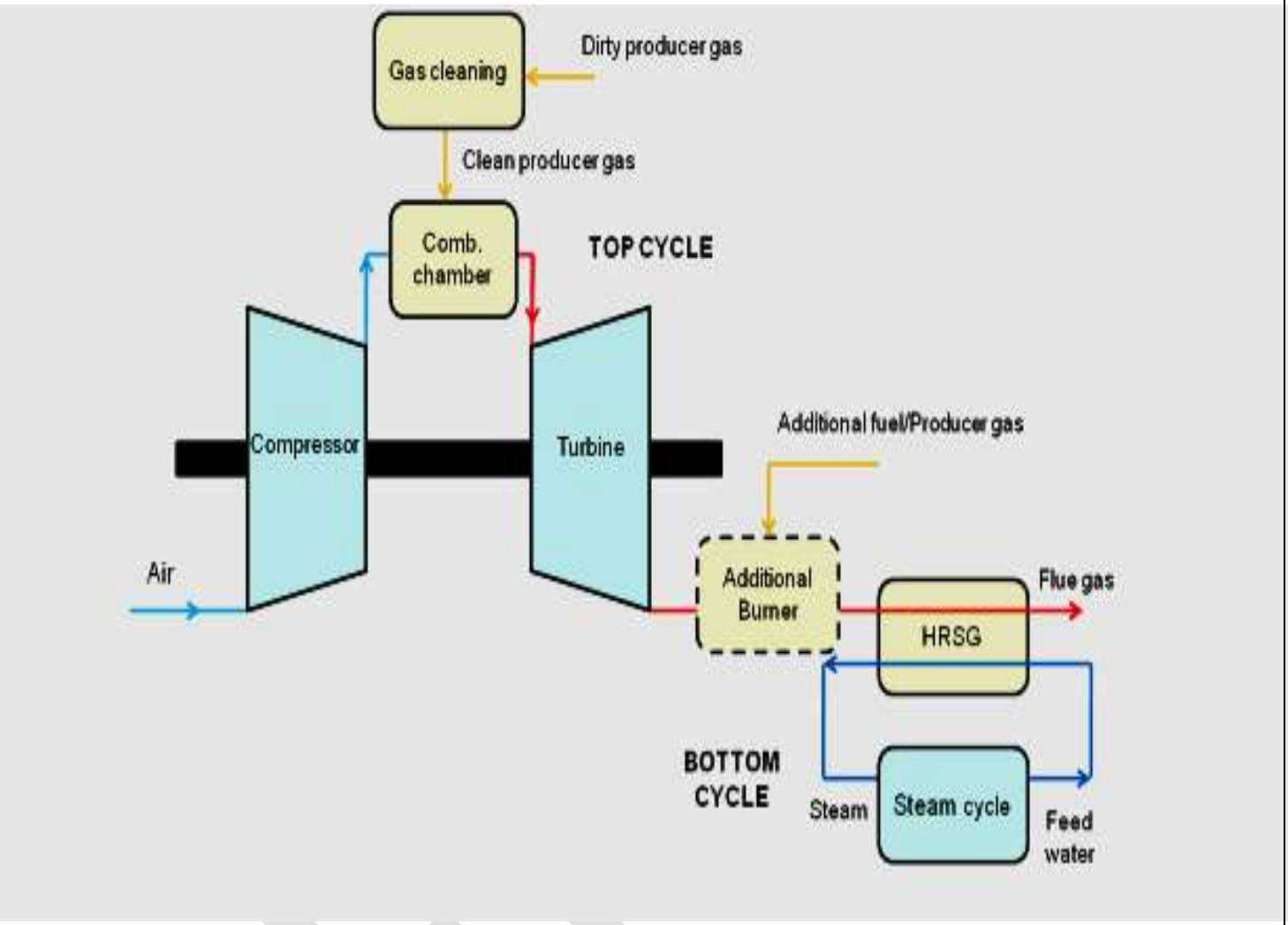

Figure 5. Combined plant with Brayton and Rankine cycle.

V. CONCLUSION

Moreover, these biomass power systems will further encourage research by directly and substantially benefitting from the technological procession being made by authorities and industry funded gas turbine and fuel cell development programs. These utilization technologies are the subject of substantial evolution endeavours, and are being showcased in integrated systems with coal gasifiers.

REFERENCES:

[1]. Report on "Review of Technologies for Gasification of Biomass and Wastes", June 2009.

[2]. Authors M. Worley and J. Yale *Harris Group Inc. Atlanta, Georgia ,report on* ' Biomass Gasification Technology Assessment'.

[3]. Authors Kevin R. Craig Margaret K. Mann, report on 'Cost and Performance Analysis of Biomass-Based Integrated (BIGCC) Power Systems'

[4]. Anil K. Rajvanshi Director, Nimbkar Agricultural Research Institute, ' BIOMASS GASIFICATION'.

[5]. Authors Matteo Carpentieri, Lidia Lombardi article on 'Life cycle assessment (LCA) of an integrated biomass gasification combined cycle (IBGCC) with CO2 removal'.

[6]. Authors Ke Liu, Chunshan Song and Velu Subramani book on 'Hydrogen and Syngas Production and Purification Technologies'

International Journal of Engineering Research and General Science Volume 3, Issue 5, September-October, 2015
ISSN 2091-2730

Pythagorean Tree Multiband Fractal Antenna

Renu Sharma[1], Dipa Nitin Kokane[2]

[1]M.Tech, [2]Senior Assistant Professor, ABES Engineering college, Ghaziabad (U.P.), Dept. of ECE

rsharma.joy@gmail.com, dipa.kokane@abes.ac.in

Abstract— In this paper the design and analysis of the Pythagorean tree fractal antenna is proposed, which uses a unique fractal geometry known as Pythagoras tree. It was simulated using IE3D electromagnetic simulator by which antenna properties such as return loss, gain, VSWR, Directivity and Bandwidth are analyzed. This antenna has a compact size of base patch 41.34*41.34*1.6 mm^3 .The antenna has been designed for the frequency ranges of 0 GHz to 6 GHz for which VSWR< 2 which includes the WLAN, Wi-Max & other wireless communication applications.

Keywords— Fractal, Multiband, Fractal antenna, Pythagorean tree, self-similarity, Iteration, Iterated function system.

INTRODUCTION

Antenna design is a very tricky problem. As the conventional antenna are intrinsically a very narrow band devices which does not helps to operate multiple applications with a single antenna and its behavior is depend on the size of antenna for their desired frequency. This has initiated antenna research in various directions, one of which is the fractal antenna [1]. The word fractal was derived from the Latin fractus meaning "broken" or "fractured" [2]. The concept of fractal was exposed by Benoit Mandelbrot the French mathematician during 1975 while conducting research on several naturally occurring irregular and fragmented geometries [3]. From this Fractal antenna was come and those provides the multiband behavior, self-similarity[4] & space filling properties[5], [6]. Fractal concept has emerged as novel method for designing multiband antennas[1][7]and which will expand the bandwidth and reduce the dimensions of the antenna [8]. Fractal engineering has the great ability in antenna miniaturization, multi-frequency and multiband application [9]. Fractal antenna is the field that uses the Fractal Geometries with iteration function system (IFS) for antenna design [10] [11]. The modern communication system has been developed to the broadband and integration; meanwhile people's needs for portable mobile communication are higher. This requires antenna development corresponding broadband technology, multifrequency technology and miniaturization.

In this paper, a fractal antenna using Pythagorean tree shape as the fractal geometry is design for multiband frequency bandwidth. The existence of infinite fractal geometries and their advantages opens the door to endless possibilities to accomplish the task at hand. The use of fractals provides us with a bigger set of parameters to control the antenna characteristics.

ANTENNA CONFIGURATION AND DESIGN

The procedure for designing the proposed antenna in IE3D software (ver. 14.10) is explained here. As, the Pythagorean shape Fractal tree is 2-D planar fractal antenna, constructed by squares patches [12], [13] and named after Greek mathematician Pythagoras. This antenna obey the Pythagoras theorem where each triple of touching of squares enclose a right triangle. If the base square (largest) has a size of L×L, the entire antenna fits inside a box of size 6L×4L. [13] Rest of the squares are iterated on the base square and each square is further scaled down by the factor of $(1/2)\times\sqrt{2}$. The proposed antenna is printed on RT/Duroid substrate with permittivity of 2.2 and loss tangent tanδ =.001 and thickness of substrate h=1.6 mm and compact dimension of 41.34*41.34*1.6mm^3. At centre of

each patch an etching is carried out which is approximate 25% of dimension of respected patch i.e. having a shape of two overlapped squares with a difference of 45^0 to each other.

If ' i ' is the iteration factor then, Number of squares in each iteration will be equal to 2^i. So size of patch scale down after i iteration will be $[1/\sqrt{2}]^i$. The microstrip patch antenna parameters helps for the calculation of basic patch for this antenna at frequency of 2.4 GHz. Antenna is feeded by the microstrip feeding of 13 mm length & 3 mm width to achieve 50Ω impedance characteristic [4]. Each square patch follows the Pythagoras theorem as they are iterated on the base patch making a right angle between two square patches touches base patch.

The designing of antenna consists of $L_1=W_1=$ 41.34 mm, $L_{E1}=W_{E1}=$10mm, $L_2=W_2=$29.23mm, $L_{E2}=W_{E2}=$7mm, $L_3=W_3=$20.66, $L_{E3}=W_{E3}=$5mm, and $W_f=$ 3 mm, $L_f=$13. Where L and W denotes the length and width of patch, L_E and W_E denotes the etching length and width, and L_f and W_f denotes the feeding length and width respectively.

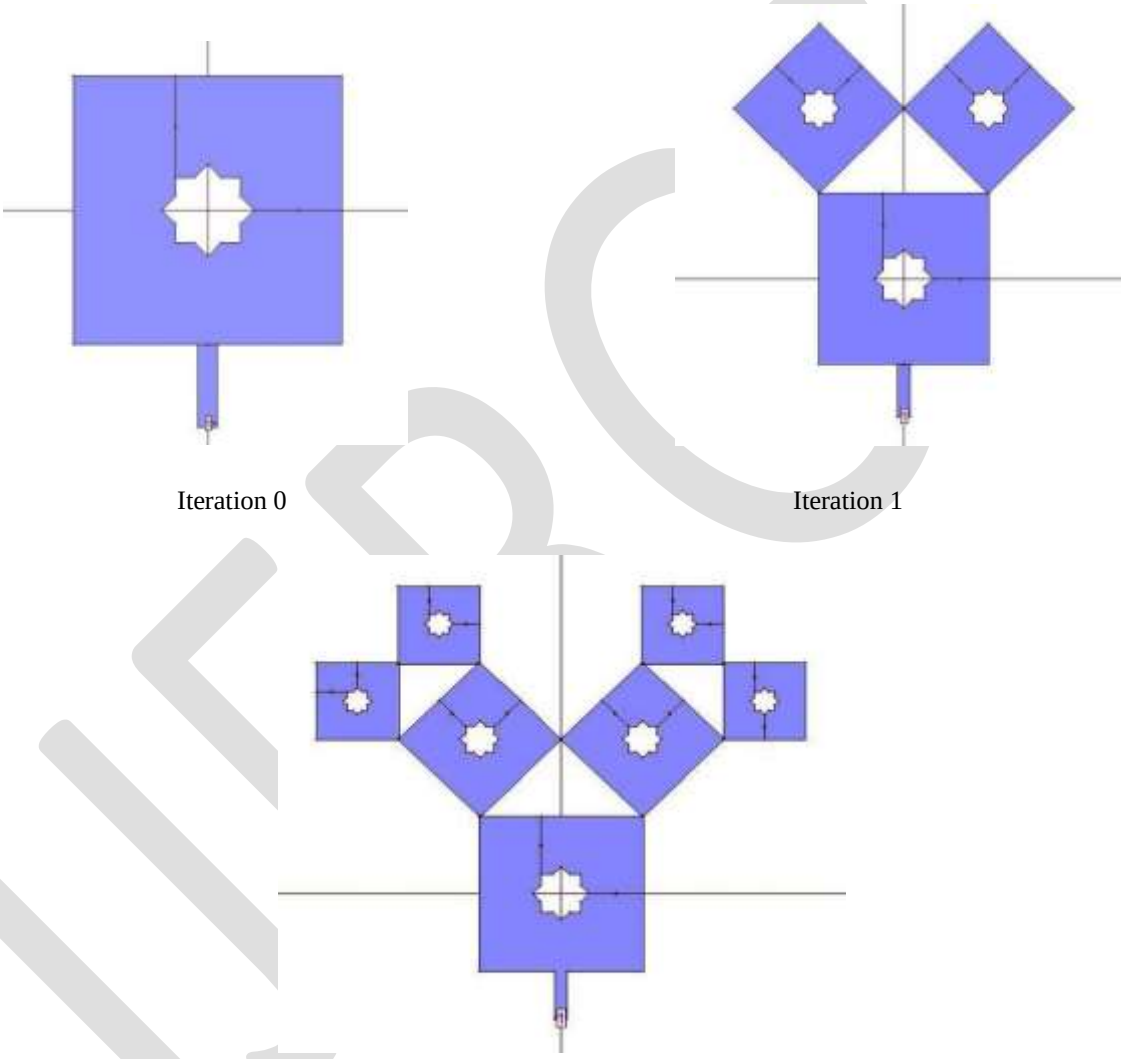

Fig:1 Proposed antenna design

RESULT AND DISCUSSION

The performance of the proposed antenna at different iterations haven been using integral Equation in three dimension (IE3D) software and characteristics have been analyze in term of return loss, VSWR, impedance bandwidth and radiation characteristic etc.

Fig:4 shows the Zero iteration, it is observed that at this the antenna resonates at frequency f = 4.692 GHz minimum value of return loss (RL)= -12.2824 dB means at this frequency antenna is capable to radiates its maximum value of energy towards the receiver and at f=5.23156 GHz value of return loss (RL)= -10.4231 dB. In First iteration the antenna resonates at frequency f = 4.67213

GHz minimum value of return loss (RL)= -11.5422dB , f=5.1332 GHz with RL= -10.1585 dB and at f=5.64 with RL=-13.5852. In iteration third the multiband behavior is achieved at frequency of 4.67213 GHz with return loss (RL) = -10.1427dB, second band is at 5.40369 GHz with RL = -24.4221dB, and third band at 5.80818 GHz with RL= -33.0563 and VSWR = 1.04853. Maximum Total Field gain = 6.58366 dBi.

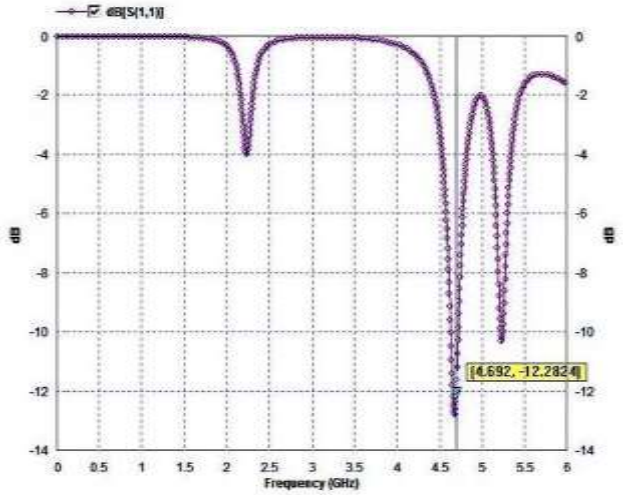

Fig 2: Return loss in case of iteration 0

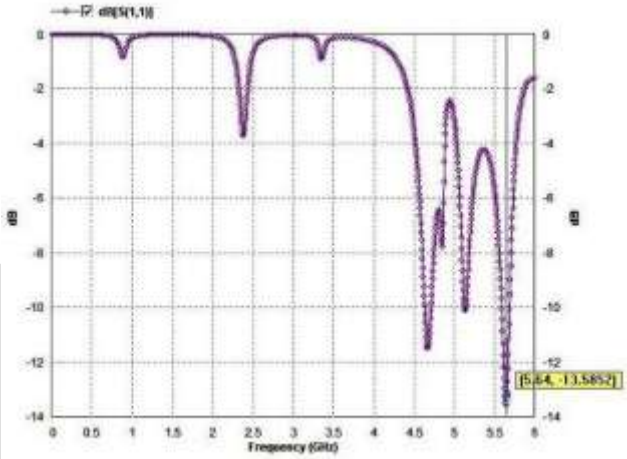

Fig 3: Return loss in case of iteration 1

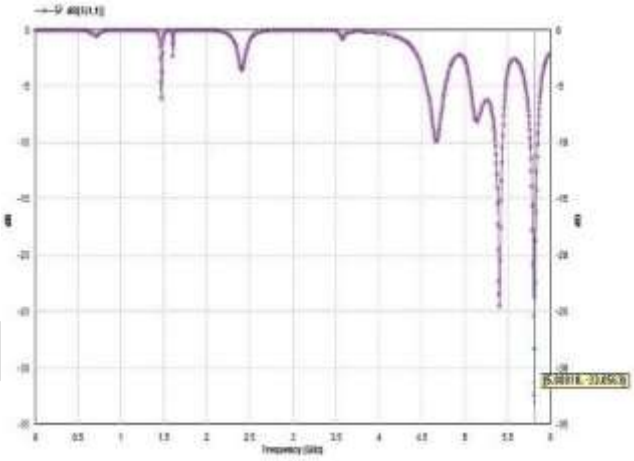

Fig 4: Return loss in case of iteration 2

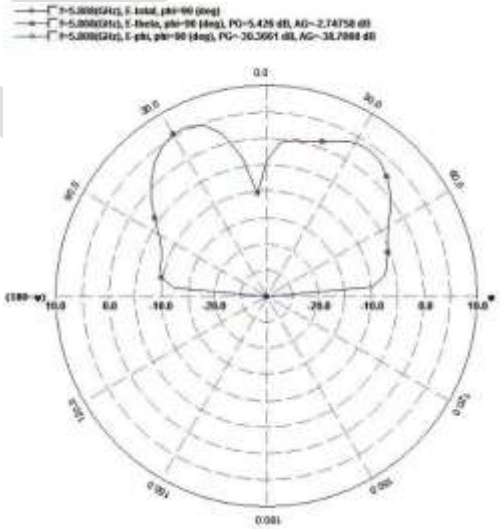

Fig5: 2D Radiation pattern of iteration 2

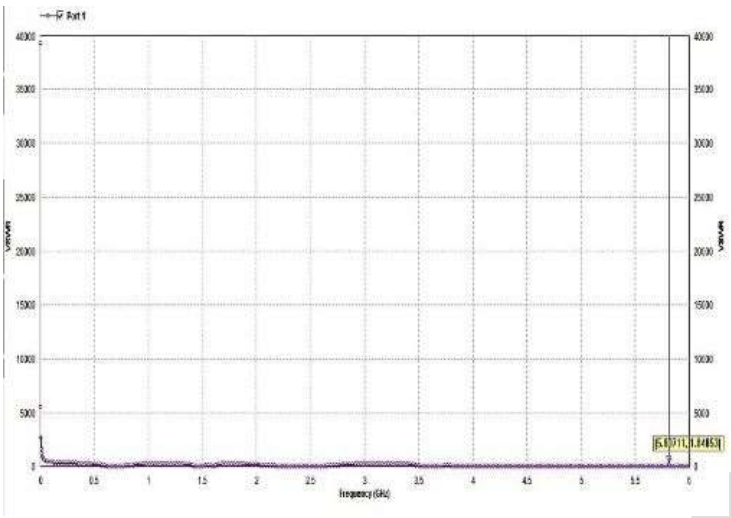

Fig 6: VSWR Pattern plot of iteration 2

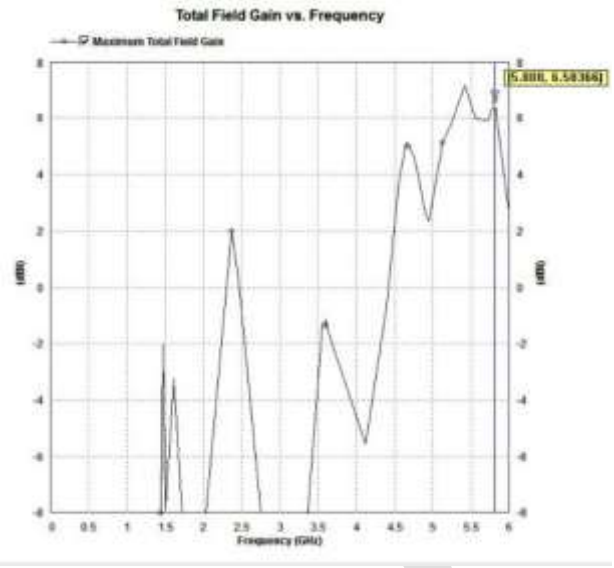

Fig7: Total Field Gain Vs Frequency of Iteration 2

ACKNOWLEDGMENT

The authors wish to great thank to their parents for their constant support and motivation without which this work would have never been completed. Also thanks to International Journal of Engineering Research and General Science team members to provide this type of a platform for researchers.

CONCLUSION

A Pythagorean Tree Fractal Antenna With Microstrip line feeding was investigated. It is observed that increasing the fractal iteration will generate the several bands and a good impedance matching was obtained. This particular antenna is capable to operate for WLAN (2.4 GHz) and also usable for the IEEE.11a (5.180-5.825 GHz). So the use of Pythagoras tree fractal geometry results in a multi-frequency and wide bandwidth operation of the antenna without employing any further modification.

REFERENCES:

[1] Vinoy, K. J., "Fractal shaped antenna elements for wide and multi-band wireless applications," Thesis, Pennsylvania, Aug. 2002.
[2] Briggs Johnl, Fractals "The Patterns of Chaos", pp. 148, 1992
[3] B B.Mandelbrot, "The Fractal Geometry of Nature", New York: W.H.Freeman, 1983
[4] J. Pourahmadazar, C. Ghobadi, J. Nourinia, and H. Shirzad, "Multiband ring fractal antenna for mobile devices," IEEE Antennas Wireless Propagate. Lett., vol. 9, pp. 863–866, 2010.
[5] Javad Pourahmadazar, Changiz Ghobadi, and Javad Nourinia, "Novel Modified Pythagorean Tree Fractal Monopole Antennas for UWB Applications "IEEE Antennas and Wireless Propagation Letters, Vol. 10, 2011
[6] Anirban Karmakar, Ustad Banerjee, Rowdra Ghatak and D Poddar, "Design and analysis of fractal based UWB Monopole antenna"IEEE,2013.
[7] K. J. Vinoy, J. K. Abraham, and V. K. Varadan, "Fractal dimension and frequency response of fractal shaped antennas, "in Proc. IEEE Antenna Propog. Soc. Int, Symp. Jun. 2003, vol. 4, pp.222-225.
[8] E. E. C. de Oliveira, P. H. da F. Silva, A. L. P. S. Campos, S. Gonc, A.D.Silva, "Overall Size Antenna Reduction using Fractal Geometry", Microwave and Optical Technology Letters, vol. 51, no. 3, March 2009, pp. 671 -674
[9] A. Aggarwal and M. V. Kartikeyan, "Pythagoras tree: a fractal patch antenna for multi-frequency and ultra-wide band-width operations" In Electromagnetics Research C, Vol. 16, 25-35, 2010

[10] Manas Ranjan Jena, B.B. Mangaraj and Debasis Mishra, "Bandwith and gain enhancement of multiband fractal antenna based on the sierpinski carpet geometry" ICTACT journal on communication technology, vol:04,issue 01,2013

[11] R.Uthayakumar, G.Arockia Prabakar "Creation of Fractal Objects By Using Iterated Function System," ICCCNT'12 An IEEE Sponsored, 26th -28th July, 2012

[12] Antenna Theory Design and analysis, 3rd edition by C.A. Balanis A john wily & sons.inc, Publication.

[13] G.Jacquenot, "Pythagoras tree", 2010 [online]. Available: http://www.mathworks.com/matlabcentral/fileexchange/26816Pythagoras-tree.

International Journal of Engineering Research and General Science Volume 3, Issue 5, September-October, 2015
ISSN 2091-2730

Cluster Based Routing Protocols for Target Tracking In WSN: A Survey

Mr. Ghule Shashikant M.[1], Prof. Ganjewar P.D.[2],

[1]Dept. of Computer Engg., MIT Academy of Engineering, Alandi, Email: shashikant.ghule@gmail.com,
[2]Dept. of Computer Engg., MIT Academy of Engineering, Alandi,Email: pdganjewar@comp.maepune.ac.in

Abstract— Wireless Sensor Network applications are attracting more and more research, especially in energy saving techniques that is the focus point of researchers in this area. One of the interesting and useful applications of Wireless Sensor Networks is the moveable target tracking. Wireless Sensor Networks that is used mainly to track movable targets in a monitored area and to report its location to the base station. Identification of exact position and path travelled by the movable object in an area is a major energy consumer process within Wireless Sensor Network. In this paper, we suggest a best cluster based routing protocol called *energy efficient target tracking protocol* (EETTP) for target tracking in Wireless Sensor Networks (WSNs), with the help of this protocol increase network lifetime of every node and reduce communication cost between nodes. Which integrates on-demand dynamic clustering into a cluster-based WSN for target tracking? By constructing on-demand dynamic clusters at boundary regions, nodes from different static clusters that detect the target can temporarily share information, and the tracking task can be handed over smoothly from one static cluster to another. As the target moves, static clusters and on-demand dynamic clusters alternately manage the target tracking task. The proposed protocol performs better in tracking the moving target when compared with other typical target tracking protocols. In particular, we systematically analyse a few important parameters of the cluster based routing protocols, and compare with these different approaches according to our taxonomy such as energy efficiency, communication cost. Finally, we summarize and conclude the paper with some future directions.

Keywords— WSN; target tracking; cluster; cluster head; boundary nodes; energy efficiency; static cluster; nodes; communication coast.

1. INTRODUCTION

Target tracking is considered important in WSNs, as it is a base for many practical applications, such as battlefield surveillance, emergency rescue, disaster response, and patient monitoring. Generally speaking, target tracking aims to detect the presence of a target and compute reliable estimates of its locations, while the target moves within an area of interest and forward these estimates to the base station in a timely manner.

Target tracking is believe to be as almost demanding applications in WSN because of application requirement that place a heavy burden on the network resources, such as it is energy consumption and communication cost between nodes. The main task of target tracking is identification of exact position and path travelled by the movable object reports to the base station, for this task wireless sensor network requires much more energy. Because of this reason it is necessary to develop energy efficient techniques that the application requirements of a target tracking system that reduce the total energy consumption and communication cost of the wireless sensor network.

Identification of exact position and path travelled by moveable object in an area uses the stable cluster for the network scalability and energy consumption. It uses a predictive mechanism to communicate with CH about the detecting the target to a node, and then the coherent cluster node send a message about the target to number of suitable neighbor nodes right before the arrival of the movable target. This problem can be solved as the target tracking task and transfer from one stable cluster to another stable clustering process. Therefore, stable cluster-based method is more appropriate for moveable target tracking in wireless sensor network. In any case, the static group nodes keep sensors in distinctive clusters from conveying and imparting their data to one another, which causes a boundary issue when the target moves crosswise over or along the boundaries of one cluster to another cluster. The boundary issue will bring about the increment of following vulnerability or the loss of the movable target.Therefore, a better protocol is required to solve the boundary problem, to decrease the use of node energy, decrease computation time of the node and local sensor communication in cluster based sensor networks. Several methods have been proposed in the outfit for information retrieval from sensor node in WSN.

2. RELATED WORK:

2.1. Techniques for target tracking in WSN:

In customary target tracking framework make utilization of unified approach in WSN. As the numerous sensor nodes are active in the system, more messages are forward towards the base station devours extra transmission capacity and energy. Hence, this methodology

is not blame tolerant as there is a solitary purpose of disappointment and needs adaptability. Also in conventional target following routines, a detecting undertaking is normally done by a node at once bringing about less precision and overwhelming reckoning weight on that node. In WSN every node has restricted energy; consequently traditional tracking methods based on complex signal processing algorithms are not useful [1].

To enhance the nature of target tracking, sensors need to make precise conjecture of the location of target. The imperative components of the WSN are versatility to expansive size of node arrangement, capacity to withstand intolerable ecological conditions, convenience and energy utilization. Target tracking application is cluster based, tree-based, and hybrid based strategies. In an target tracking application the sensor nodes that can sense the objective at a predetermined time are kept in active mode yet the remaining nodes are to be kept in rest mode, spared vitality until the objective reaches inside of their detecting range. The objective following assignment keeping up the harmony between system assets, for example, energy and data transfer capacity. In tree-based target tracking the nodes that distinguish the objective speaks with one another and chooses a root node. The root node gathers data from the entire node by means of a spanning tree. In the event that the root node is far from the objective, then the tree is reshaped. We require more exact target tracking in spanning tree-based methodologies, tree associations bring about high energy utilization. Hybrid techniques are the following calculations that perform the prerequisites of more than one sort of target tracking. In cluster based systems, nodes are either named group individuals or cluster heads. In cluster based target tracking, nodes identify the objective and send the data to their cluster head. Cluster heads gather all data from their cluster node and appraisal the position of the objective by utilizing confinement methods. After the position of the objective is figured, cluster head sends the position data to the sink. In the cluster based methodology, the essential advantages is the diminishing the energy utilization amid target tracking assignment.

2.2. Clustering :

So as to support preparing of information onto energy efficient network, sensor nodes can be separated into various little groups called clusters. The sensor nodes total into groups is called clustering. Each cluster has a solitary cluster head (CH). A cluster head is chosen from the sensor nodes with greatest remaining battery power and correspondence range. There are a few focal points of clustering the marvel. The essential favourable position is that, it backings system adaptability. That can likewise safeguard correspondence transfer speed. Clustering process can make stable WSN network topology at the level of sensor nodes network. The CH is likewise executing powerful administration procedures to extend the battery life of the individual sensors and to amplify the network lifetime. Every node, that works in three states. In the active state, that transmits bundles, get parcels, and sense the target. In Sensing state, that node performs a detecting operation. And in the sleep state, it sleeps for most of time and wakes up when it sense the target and listen to the message from another node. Since communication operations dominate the energy consumption, we mainly concentrate on energy consumption required for communication. The sensor nodes with the maximum residual energy is elected as the cluster head (CH) to take charge of signal processing from node CH. Fig.1 shows the basic clustering concept. The clustered sensor nodes detecting target & transfer their observations to the CH. The cluster head further process the information and transfer to the sink, referred to as the base station. Cluster-based target tracking approaches are classified into two types, such as static approach and dynamic approaches.

2.2.1. Benefits of clustering:

1. Provides useful energy consumption.
2. Provides scalability for large number of nodes.
3. Reduces communication overhead using prediction.

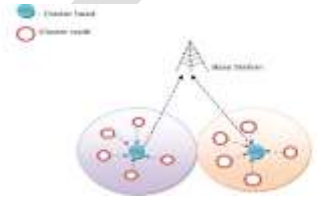

Fig 1: Clustering of sensors in network.

2.3. Classification Of Cluster based Target Tracking Methods:

WSN can be principally having two standard groupings, Hierarchal and matched frameworks. The hierarchal framework is a mesh based structure having multi bounce system among nodes that are passed on. The sensors that screen the goal and report back to the base station through cluster head. The hierarchal system is assembled into three essential orders exhibited in Fig. 2, Tree based, Cluster based and Hybrid based systems. Here in this paper we identify with review on the cluster based frameworks. The cluster based strategies can be again isolated into static cluster system and dynamic cluster approach [5].

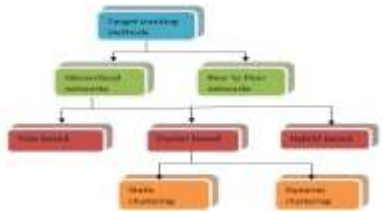

Fig 2: Classification Target Tracking Methods.

2.3.1. Static Cluster Based Target Tracking:

In static cluster based target tracking, at the time of network deployment stable clusters are generated. The clustering nodes and cluster head are characterized stable before and after target tracking. However, the static clustering has some drawbacks in spite of its simplicity. It is not robust because of its fixed clusters and cluster head. If the cluster head dies because of power depletion then the cluster provide uselessly. Because of the static cluster the sensor nodes from another cluster cannot share data and collaborate on data processing [5].

2.3.2. Dynamic Cluster Based Target Tracking:

In dynamic clustering sensor nodes that shape diverse cluster at distinctive times as per the movement of the objective as likes LEACH. Those nodes are the individuals from distinctive clusters at an alternate time and it minimizes the restriction mistake produced by that WSN network. Stand out cluster is in active state at every time as indicated by target movement in the WSN network. Hence, it decreases the energy utilization of sensors in the group. Dynamic clustering methodology is more protected and dependable than static grouping methodology. Likewise, the sensor hubs detecting and sending repetitive data has been decreased.

Parameters	Static Clustering	Dynamic Clustering
Localization error	Maximum	Minimum
Cluster head selection	Statically defined	Maximum residual energy
Cluster formation	Simple	Complex
Energy consumption	Low	High

Table1: Comparison of static and dynamic clustering

We have several methods in survey on cluster based target tracking in WSN to collect information from the WSN such as LEACH, HEED, TEEN, AFTEEN and HCTT. Here in this paper, I explain existing cluster based target tracking techniques with their advantages and disadvantages in this following part.

2.4. Low-Energy Adaptive Clustering Hierarchy (LEACH):

It is a cluster-based energy efficient routing protocol for a target tracking in wireless sensor network. LEACH consists of two working phases during network establishment. In the first set-up phase, sensor nodes select a local cluster head randomly among themselves, that the network may balance energy over consumption across the complete network. After the cluster head selection process, each cluster head broadcast their node id to all sensor nodes that these are the new cluster heads. Once the nodes receive the advertisement message from cluster head, each of them decides to which head it belongs to. In Second steady state phase, every sensor node sense and transmit data to the sink through their cluster head. After some period of time, the network again restarts the set-up phase. LEACH adopts multiple hops to communicate with node to base station, which makes it more practical than direct communication method. Besides, it is the assumption that all nodes have enough energy to communicate directly with the base station makes it difficult to apply in a large-scale network [2][3][8]. It is one of the limitations of LEACH when we used to track the movable target in large scale wireless sensor network.

2.5. Hybrid, Energy-Efficient Distributed Clustering (HEED):

HEED is believed to be as energy-efficient clustering algorithms that use the rest energy of the node to select the Cluster Heads (CHs). It is an updated version of LEACH routing protocol that considers residual energy and communication range as a selection criteria of the cluster head. The result of the HEED routing protocol is establish with better energy efficiency even as compare to LEACH, with

the better increasingthe network lifetime of WSN node. It uses residual energy as primary parameter. In this, all nodes are considered to be homogeneous i.e. all sensor nodes are deployed with same opening energy. As the lifetime of the sensor network is finite, there is need to re-energize the sensor network by adding more sensor nodes. These nodes will be furnished with more energy than the nodes that are already in use, which creates heterogeneity in terms of node energy [6][7][8][15].

2.5.1. The advantages of the HEED protocol [8]:

(1) It is superbly circulated clustering technique that advantages from the utilization of the two extensive constituents for CH determination, for example, node energy and correspondence range.
(2) Low power levels of cluster promote a development in spatial reuse while high power levels of cluster are important to use for middle cluster correspondence. This CH gives uniform dispersion past the system and equalizations the heap.
(3) Communications in a multi-hop trend between CHs and the BS warns more energy promotion and enhancement in difference with the single-hop trend, i.e., long-range communications directly from CHs to the sink, in the LEACH protocol.
Communications in a multi-hop pattern in the middle of CHs and the BS cautions more energy advancement and improvement in distinction with the single-hop pattern, i.e., long-run correspondences straightforwardly from CHs to the sink, in the LEACH convention.

2.5.2. Limitations with HEED [8]:

(1) The utilization of makeshift CHs that don't be extreme CHs abandons some uncovered nodes. As indicated by HEED execution, these nodes are considered to turn into a CH and these considered CHs may be in scope of different CHs or might not have any part connected with them. Therefore a bigger number of CHs are produced than the normal number and this likewise represents disequilibrium low energy drift in the system[9].
(2) Similar to LEACH, the work of cluster in every round forces critical measure of energy utilization in diminishing the network life time.
(3) HEED experiences a subsequent overhead since it needs a few reiterations to generate clusters. At every reiteration, considerable measures of parcels are telecast.
(4) Some CHs, particularly close to the sink, may kick the bucket prior on the grounds that these CHs have most extreme work load.

2.6. Threshold sensitive Energy Efficient sensor Network protocol (TEEN) :

TEEN [10] is a various levelled protocol whose primary target is to adapt to sudden changes in the detected properties, for example, spot of the objective. The convention consolidates the various levelled technique in accordance with an information driven viewpoint. The nodes sense their surroundings reliably, yet the energy utilization in this calculation can likely be substantially less than that in the proactive network, in light of the fact that information transmission is done less over and over.
TEEN uses a 2-level clustering topology is having two threshold values, hard threshold and delicate threshold. The prior threshold is starting limit esteem for the detected attribute. It is the ideal worth, past which the node detecting this quality must switch on its transmitter to transmit detected credits and report to its CH. The recent edge is a little contrast in the detected worth which begins the node transmitter and transmits that esteem to another hub.
In TEEN, a CH transmits its introductory qualities a hard limit and delicate edge to the nodes. Therefore the hard threshold tries to straightforwardness information correspondences by permit the node to transmit just when the detected worth is in the middle of hard and delicate limit esteem. The delicate threshold diminishes information interchanges when there is little or no adjustment in the detected worth. At the expense of expanded energy use, a littler estimation of the delicate threshold removes more correct data of the system. Consequently clients can deal with trade-off between energy proficiency and information. Besides, the delicate threshold can be differed and the clients can change the new parameters as needed at each group era time.

2.6.1. Advantages of TEEN:

(1) Based on the two threshold values, information transmission can be controlled excellently, i.e., just the sensitive information can be send to BS, so it lessens the energy needed for transmission and enhances the viability and ease of use of the accepting information.
(2) It supplements for vast changes in the sensed properties, which is suitable for time discriminating applications.

2.6.2. Drawbacks of TEEN:

1) It is not suitable for repeatable time discriminating applications since the client may not get any information at all if the estimations of the characteristics may not achieve the limit [11].
(2) TEEN has squandered time-slots and a plausibility that the BS will be unable to separate terminated nodes from live nodes, on the grounds that just when the information touch base at the hard threshold and has a variation higher than the delicate limit did the sensors reports the information to the BS.
(3) If CHs are not in the scope of one another the information may be lost, in light of the fact that data television is accomplished just by CHs [12].

2.7. Adaptive Threshold sensitive Energy Efficient sensor Network protocol:

The Adaptive Threshold sensitive energy efficient sensor network convention (APTEEN)[13], is an upgraded form of TEEN and goes for both transmitting time basic data and responding to time discriminating occasions. Then again, It is a hybrid protocol that progressions the periodicity or edge qualities utilized as a part of TEEN by prerequisite of user and the sort of the application. APTEEN is taking into account a query framework which has diverse sorts of queries, for example, verifiable, on-time, and steady which can be utilized as a part of a hybrid network.

All nodes sense the environment continuously, however just those nodes which sense an information esteem at or past the hard threshold endures transmitting. In the event that a node does not send information for a period equivalent to the tally time, it must sense and transmit the information once more. In APTEEN, each CH gathers the data from the node inside of its cluster and transmits the collected data to the BS. Amid the procedure of information accumulation, it is expected that the information got from the comparing node are connected, consequently it lessens a lot of repetition of the information to be send to the BS. Besides, an altered TDMA calendar is utilized to actualize the mixture arrange by relegating every node in the group a transmission opening. Moreover, APTEEN offers a ton of adaptability by permitting the client to set the CT interim and the limit values for vitality utilization can be controlled by changing the CT and in addition the threshold values.

2.7.1. Advantages of APTEEN:

(1) Based on the two edge values, information transmission can be controlled estimably, i.e., just the delicate information can be send to BS, with the goal that it diminishes the energy needed for transmission and enhances the viability and ease of use of the accepting information.

(2) It supplements for huge changes in the detected traits, which is suitable for time discriminating applications.

2.7.2. The main disadvantages of APTEEN are as follows:

(1) There exist additional complexity required to implement the threshold value and the count time.

(2) Actually, TEEN and APTEEN has similar drawbacks of additional overhead and complexity of cluster building in several levels, implementing threshold value based functions, and dealing with attribute based naming of queries [14].

2.8. Hybrid cluster-based target tracking (HCTT):

The objective following [16, 17, and 18] uses the steady cluster for the system versatility and energy efficiency. (The term of "stable cluster" does not imply that the cluster won't adjust amid the network lifetime. It implies that the cluster structure will keep unaltered for a moderately long time contrasted with a transiently created dynamic cluster, until the following round of grouping procedure begins. Along these lines, at this very moment the LEACH convention [19], every sensor nodes has the likelihood of turning into a cluster head to adjust the vitality load). It utilizes a prescient instrument to inform cluster heads about the hitting the objective and afterward the comparing cluster head awakens number of fitting nodes just before the entry of the objective. This work can be saved as the tracking task is handed over from one stable cluster to another without costly dynamic clustering processes. It likewise gives a versatile structure to facilitating and managing networks.Along these lines, stable cluster based methodologies are more suitable for target following in huge scale sensor network. In any case, the steady cluster enrolment stops sensors in distinctive groups from offering data to one another, which raises a boundary issue when the objective moves crosswise over or along the boundary of clusters. The boundary issue will bring about the increment of following incertitude or loss of the objective. In this way, another convention is important to take care of the boundary issue and understand the bargain between energy utilization and nearby sensor cooperation for cluster based sensor network.

ZhiboWang, Wei Lou, JunchaoMa, and Honglong Chen propose a hybrid cluster-based target tracking (HCTT) [4], for efficient target tracking in a large-scale cluster-based WSN. HCTT amalgamate on-demand dynamic clustering into a scalable cluster based WSN with the help of boundary nodes, which convenience sensor co-operation in clusters to find the solution to boundary problem. As shown in Figure 1**,**at the point when the objective is inside a static cluster, the cluster is skilled to track the objective; at this very moment moves close to the boundaries of cluster, an on-interest dynamic clustering procedure will be begin to deal with the following assignment to dodge the boundary issue. The on-demand dynamic cluster will stop rapidly after the objective moves separated from the boundaries. At the point when the objective moves, static clusters and on-demand dynamic clusters alternately manage the tracking task. By aggregate on-demand dynamic clusters into an adaptable cluster based structure, nodes fitting in with diverse static cluster can share data, which ensures effectively target following and clear up well bargain between energy utilization and nearby sensor co-operation.

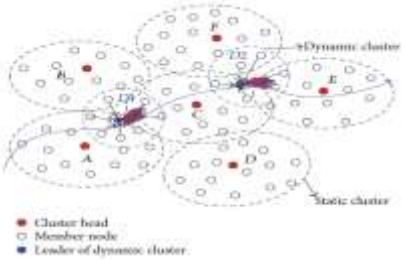

Figure 1: HCTT for target tracking in a cluster-based WSN.

2.8.1. *Advantage:*

With reference to above (3.5) HCTT has benefit over the LEACH, HEED, TEEN and AFTEEN protocol, it avoids boundary problem, transfer target smoothly from one static cluster to another cluster.

2.8.2. *Disadvantage:*

As per above discussion it has limitation about energy consumption. HCTT requires more energy in boundary region nodes for on demand cluster generation process.

3. PRAPOSED WORK:

In this paper, I speak to the suitable energy efficient protocol for target tracking and it is an enhanced form of LEACH, HEED, TEEN, AFTEEN and HCTT. With the assistance of proposed routing protocol increase the system lifetime of the each node and diminish correspondence overhead between two nodes.

3.1. Energy Efficient Target Tracking Protocol (EETTP):

In this section we propose an energy efficient target tracking protocol for wireless sensor network. With the help of this protocol we reduce energy usage using clustering algorithm and reduce communication cost. Work flow consists of a main task called cluster generation, boundary node formation, target tracking task.

3.1.1. Cluster Generation:

So as to support preparing of information onto energy efficient network, sensor nodes can be separated into various little groups called clusters. The sensor nodes total into groups is called clustering. Each cluster has a solitary cluster head (CH). A cluster head is chosen from the sensor nodes with greatest remaining battery power and correspondence range. In cluster based systems, clusters are identified using cluster heads. Clustering process can make stable WSN network topology at the level of sensor nodes network. The CH is likewise executing powerful administration procedures to extend the battery life of the individual sensors and to amplify the network lifetime.
In clustering process we consider parameters such as node energy (N_{TE}), communication range (R_N) of every node and time slot (T_s) of each and every node participated in cluster generation process. Each cluster within WSN consists of cluster head (CH_{Id}). In cluster formation first task is cluster head selection. In that process every node sends its node ID (N_{Id}), communication range (R_N) and node total energy (N_{TE}) to all neighbour node which are present in communication range. Every node compares his own communication range and node total energy with received parameters from his neighbour. If received communication range and node total energy greater than that node again broadcast his node ID as a cluster head (CH_{Id}) to its entire neighbour node otherwise it does not send any message to neighbour. Every node consist information in his buffer such as node ID, cluster head ID, communication range, node total energy along with its neighbour node information.

3.1.2. Internal Node/Boundary Node Formation:

At the point when following an target in a checking territory, number of nodes around the target co-work with one another to make the gathered data more complete, and exact. At the point when the target is inside a cluster, as every enacted sensor fit in with the same cluster, and they can correspond successfully with one another. Then again, when the target moves towards the boundaries of numerous clusters, the boundary issue happens. That is, the neighbourhood node co-operation gets to be inadequate and flawed on the grounds that sensor hubs that can screen the objective have a place with different cluster, which builds the vulnerability of the limitation of the objective or even results in the loss of the versatile focus because of the deficient detecting reports to the neighbour nodes and base station.
In a static cluster, a node is interprets as an internal node of its static cluster that means it does not have any information of node which belongs to another cluster. As each node is feel his own location and its neighbour information. Neighbour information consists N_{Id}, N_{TE}, R_N and CH_{Id} . It checks its neighbour list to determine whether a node is from another cluster within its sensing range. If obtained a neighbour node id with different cluster head, then it is a boundary node else it is as an internal node.

Definition 1.Boundary node of a static cluster

A node $V_i$is defined as a boundary node of its static cluster if there exists at least one of its neighbour nodes V_j, such that $(l_i, l_j) \leq r_s$and $(V_i) \neq C(V_j)$.

Interestingly, a node is characterized as an inside node of its static cluster on the off chance that it is not a boundary node. As every node is mindful of its own location and its neighbour data, it checks its neighbour rundown to figure out if there exists a node fitting in with another cluster inside of its detecting range. In the event that yes, it is a boundary node else, it is an inside node.

3.1.3. Target Tracking Task:

After all nodes deployed over an area, sensor nodes are organized into static clusters according to clustering algorithm such as HCTT. Each and every node works in two states active state, sleep state. In active state node is responsible to sense the target, send the message about target to the neighbour node, and cluster head. In sleep state node is only responsible to receive the message form neighbour. When the sleep state node receive message about target approaches in his neighbour node range that means it change its state from sleep to active state.

When the target is in the network, static cluster nodes sense the target. Static cluster nodes will send target ID, node id, time, cluster head id to neighbour node and cluster head, Wakes up neighbour node to track the target. When neighbour node receive message from his neighbour node, that node firstly check his buffered neighbour information, change its state from sleep state to active state and it is ready to track the target. This whole process requires more communication cost and it consumes energy of the node because continues monitoring and broadcasting and receiving nature. For reducing communication cost we use prediction method such as like TEEN and AFTEEN protocol.

In energy efficient routing protocol whenever node detects the target at that time node stores that value as limit value. This value consist attributes such as target id, node id, cluster head id and time (T_{id}, N_{id}, CH_{id}, T_s respectively). When node monitors target continuously, simultaneously in back end monitoring node compare his historical limit value with the new value. If node obtains different node id, with new time slot then broadcast that new values to the neighbour nodes and cluster head and that value is considered as a new limit value. Otherwise that node will not make any communication with neighbour and cluster head. In this way with the help of energy efficient routing protocol we reduce communication cost.

In second case, when target reach in boundary region. Boundary nodes in that region can detect the target and that node smoothly tracking the target because that node is responsible to communicate with boundary nodes of another cluster and with static nodes in his cluster. As the target moves across the boundaries, static clusters and boundary nodes are alternately manage the tracking task.

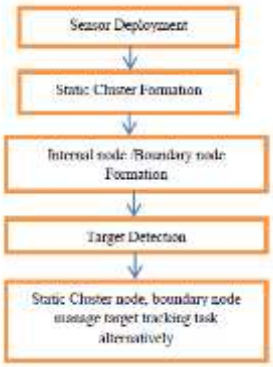

Fig 3. system workflow for energy efficient routing protocol

In grouping topology is manufactured as limit value, it is the introductory detected estimation of node. The edge is limit esteem for the detected quality. It is indisputably the estimation of the property past which, the node detecting this worth must switch on its transmitter and report to its CH. With the assistance of that we lessen correspondence cost between cluster head and target following node.

4. DISCUSSION:

From the above theory we observe that EETTP is more energy efficient algorithm for target tracking as compared to LEACH, HEED, TEEN, AFTEEEN, and HCTT. EETTP algorithm is more energy efficient because of the following reason.

1. LEACH, HEED, TEEN, AFTEEEN are requires more energy because cluster and cluster head selection process are implemented repeatedly in WSN. Whereas in EETTP cluster and cluster head selection process implemented only once. But this protocol is also implemented dynamic behaviour of cluster because if cluster head feels its total battery life is less than other nodes in cluster, then at that time cluster head selection process is again implemented by WSN network. That is one of the main reasons to require minimum energy for the EETTP to track the target.
2. LEACH, HEED requires more communication cost as compared to the TEEN, AFTEEN, and EETTP. Because in this protocol we consider threshold values such as past sensed value is compare with current values if that values are differed then and then communicate with cluster head and neighbour nodes.
3. Most important point regarding efficient and accurate target positioning task in WSN is implemented in HCTT and EETTP. When target move from one cluster region to another new cluster region at that time target is not tracked with the help of LEACH, TEEN etc. Because in these protocol there is not provision made for proper communication possible between two clusters, but it is possible in HCTT and EETTP. In HCTT, EETTP we create boundary nodes during cluster generation process, these nodes are responsible to make communication between two clusters inform exact position of the target to base station.

According to following comparison table EETTP is energy efficient for target tracking in WSN with minimum communication cost and track exact position of the target at given time.

Table 2: Comparison of the clustering algorithms.

Clustering Approach	Boundary Node Formation	Power Usage	Inter cluster connectivity	Communication cost	Target Detection accuracy
LEACH	No	Maximum	1-hope	Maximum	Moderate
HEED	No	Maximum	1-hope	Maximum	Moderate
TEEN	No	Moderate	1-hope	Moderate	Moderate
AFTEEN	No	Moderate	1-hope	Moderate	Moderate
HCTT	Yes	Moderate	1-hope	Maximum	Maximum
EETTP	Yes	Minimum	1-hope	Minimum	Maximum

5. CONCLUSION:

Network lifetime is the most important parameter in comparison of majority of WSN's applications such as target tracking using WSN. One of the main limitations of WSN is the limited power of sensor nodes. This limitation affords that saving energy and increasing network lifetime become two main issues in WSN's applications. In this paper we presented an cluster based Energy Efficient Target tracking protocol for reducing energy consumption and communication cost for target tracking in WSNs respectively. With the help of EETTP we solve boundary problem when we use more than one cluster in a WSN. Our proposed protocol considers both energy and communication range parameters for clustering. This method could be considered for improvement of LEACH, HEED, TEEN and AFTEEN protocols. In the future, the methods should be extended to track multiple moveable targets track in wireless sensor networks.

REFERENCES:

[1] K. Ramya[1], K. Praveen Kumar[2], and Dr. V. Srinivas Rao[3], "A Survey on Target Tracking Techniques in Wireless Sensor Networks", IJCSES, Vol.3, No.4, August 2012.

[2] ShengnanLia; b. Zheng Qinb, Laixiang Shana; "A survey on target tracking in well-deployed wireless sensor networks"jsw, VOL. 9, NO. 5, MAY 2014.

[3] W. R. Heinzelman[1], A. Chandrakasan[2], and H. Balakrishnan[3], "Energy-efficient communication protocol for wireless micro sensor networks", Proceedings of the 33rd Annual Hawaii International Conference on IEEE 2000.

[4] Zhibo Wang[1], Wei Lou[2], Junchao Ma[3],and Honglong Chen[4],"A Hybrid Cluster-Based Target Tracking Protocol for Wireless Sensor Networks", IJDSN Volume 2013 (2013), Article ID 494863.

[5] Karthika Gopal[1], Ramalakshmi Krishnamoorthy[2], " Analysis of Cluster based Target Tracking in Wireless Sensor etworks",International Journal of Computer Applications (0975 – 8887) Volume 62– No.7, January 2013.

[6] Wail Mardini[1], MuneerBani Yassein[2], Yaser Khamayseh[3], "Rotated Hybrid, energy-Efficient and Distributed (R-HEED) Clustering Protocol in WSN", WSEAS TRANSACTIONS on COMMUNICATIONS, E-ISSN: 2224-2864, Volume 13, 2014.

[7] Parvathi C[1], Dr. Suresha[2]," Existing Routing Protocols for Wireless Sensor Network – A study",IJCER, Vol. No. 4, Issue 7, July 2014.

[8] Xuxun Liu," A Survey on Clustering Routing Protocols in Wireless Sensor Networks", Sensors 2012, ISSN 1424-8220.

[9] Aslam, N.; Phillips, W.; Robertson, W.; Sivakumar, S. A multi-criterion optimization technique for energy efficient cluster formation in wireless sensor networks. Inf. Fusion 2011, 12, 202–212.

[10] Manjeshwar, E[1].;Agrawal, D.P.[2] " TEEN: A Routing Protocol for Enhanced Efficiency in Wireless Sensor Networks." In Proceedings of the 15th International Parallel and Distributed Processing Symposium (IPDPS), San Francisco, CA, USA, 23–27 April 2001; pp. 2009–2015.

[11] Kandris, D.[1]; Tsagkaropoulos, M.[2]; Politis, I.[3]; Tzes, A.; Kotsopoulos, S[4]. A Hybrid Scheme for Video Transmission over Wireless Multimedia Sensor Networks. In Proceedings of the 17th Mediterranean Conference on Control & Automation, Makedonia Palace, Thessaloniki, Greece, 24–26 June 2009; pp. 964–969.

[12] Kandris, D.[1]; Tsagkaropoulos, M.[2]; Politis, I.[3]; Tzes, A.; Kotsopoulos, S[4].Energy efficient and perceived QoS aware video routing over wireless multimedia sensor networks.Ad Hoc Netw.2011, 9, 591–607.

[13] Manjeshwar, A.; Agrawal, D. P. APTEEN: A Hybrid Protocol for Efficient Routing and Comprehensive Information Retrieval in Wireless Sensor Networks. In Proceedings of the 2nd International Workshop on Parallel and Distributed Computing Issues in Wireless Networks and Mobile computing, Lauderdale, FL, USA, 15–19 April 2002; pp. 195–202.

[14] Vidhyapriya, R.; Vanathi, P.T. Conserving energy in wireless sensor networks. IEEE Potentials 2007, 26, 37–42.

[15] Younis O., Fahmy S. HEED: A hybrid, energy-efficient, distributed clustering approach for *ad-hoc* sensor networks. IEEE Trans. Mobile Comput. 2004;3:366–379.

[16] H. Yang and B. Sikdar, "A protocol for tracking mobile targets using sensor networks," in Proceedings of the 1st IEEE International Workshop on Sensor Network Protocols and Applications, pp. 71–81, 2003.

[17] Z. B. Wang, H. B. Li, X. F. Shen, X. C. Sun, and Z. Wang, "Tracking and predicting moving targets in hierarchical sensor networks," in Proceedings of the IEEE International Conference on Networking, Sensing and Control, pp. 1169–1174, 2008.

International Journal of Engineering Research and General Science Volume 3, Issue 5, September-October, 2015
ISSN 2091-2730

A Survey to Automatic Summarization Techniques

Sherry
Computer Science Department
Thapar University
Patiala (Punjab), India

sherry.0989@gmail.com

Dr.Parteek Bhatia
Computer Science Department
Thapar University
Patiala (Punjab), India
parteek.bhatia@thapar.edu

Abstract- This paper presents a review for automatic text summarization techniques. Text Summarization is extraction of required information from the huge documents by ignoring the irrelevant details with the help of distinct approaches and provides the summary in compact way which reduces the effort and time of user. Due to the huge availability of data in all the fields the management and study of the information become difficult. Due to this the interest in the research of new automatic summarization techniques has been increased. Different approaches are used to determine summary. Plain text and multilingual text summarization play very important role in summary generation. This paper provides the review of all the existing text summarization techniques.

Keywords-Summary;UNL,NLization, UNLization;IAN; EUGENE;Multilingual.

INTRODUCTION

Automatic Text summarization has become very important part of our life due to huge volume of data that required to be compressed for people so, that it becomes possible to go through essential contents in short period of time. The research on the automatic text summarization has been started from 1950's.After a gap of decade's progress in the field of language processing was done due to the growing volume of online text. So, the large amount of electronic documents which are available in Internet has stimulated the development of excellent information retrieval systems. For example, Google always shows some part of the text corresponding to the query of the user. The user has to decide whether the document is interested or not only on the basis of extracted text. The user has to browse all the documents until a right document come. The solution is a use of automatic text summarizer which displays only the important and essential information about the document. Hence, it becomes very easy for the user to choose the right document.
The demand of the text summarization has observed in various domains like education, medical, government offices, research, business *etc*. So, the development of automatic summarization systems has importance due to research point of view. There are different approaches used for text summarization on the basis of single document, multi document summarization

APPLICATIONS OF TEXT SUMMRIES

Text Summarization is used is in medical field, in multimedia news summarization, in producing intelligent reports, in text for hand held devices, in text-to-Speech for blind people, in education and in summarizing meetings [1]. Many other scenarios use text summarization. For example, an information retrieval system uses automatic summarization to produce the list of retrievals. Now a day's summary of the email messages and news articles is sent to mobile devices as Short Message Service (SMS). Search engines also use summary mechanisms. The summary of the web pages is shown on the screen as a result of particular search.

SUMMARIZATION TECHNIQUES

a) Single Document Summarization

In single document summarization only one document is provided for summary generation. It is a simple and earliest approach for summarization. Extractive and abstractive both summaries methods can be applied on single document summarization.

b) Multi Document Summarization

Multi document summarization is also very important part of summarization. More than one information sources are provided for summary generation. Many web based clustering systems like news were inspired from multi document summary. But task of multi document technique is more difficult and complex than single document techniques. The real aim is not only to remove redundancy

and indentify correct text for summary but also to provide novelty and ensuring that final summary should be coherent and complete in itself. So it was a challenge for them to consider all the documents and relate the summary

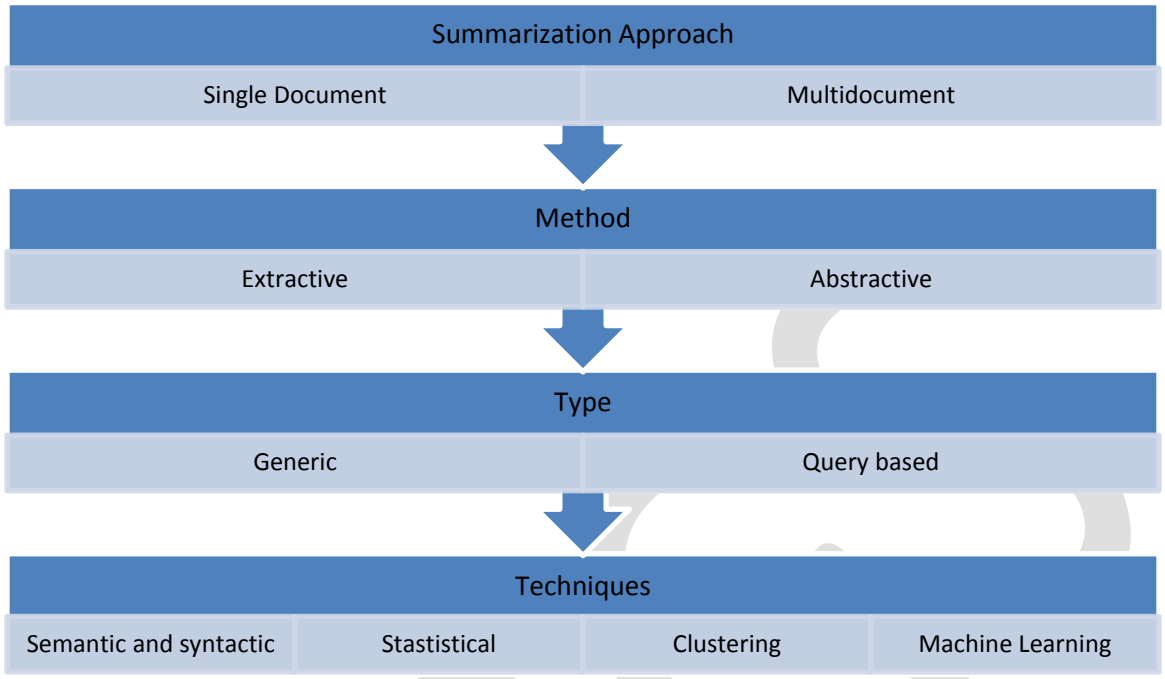

Figure 1.1: Summarization approaches

The work was initiated by the NLP group in the University of Columbia where summary system is called SUMMONS. At start procedures and challenges were different but later on people from different communities added their own perspective to the problem. Some approaches use clustering to indentify common themes and later on each cluster is represented by a sentence others produce more than one sentences from a cluster, while some uses maximal marginal relevance to work dynamically to include a passage if it is novel with the previous passages [2].

a) Extractive Summaries

Extractive summaries are simplest form of summaries. These approaches select the important information in the form of sentences, paragraphs *etc.* from the source document; combine them to generate short sentences. The selection of the sentences is made on the basis of different features like linguistic, statistical features *etc*. No synonyms of the words are used in extractive summaries for simplification [3]. Extractive summaries are not suitable for multi documents because sometimes these are biased towards some information sources.

b) Abstractive Summaries

Abstractive summaries are complex as compare to extractive summaries. These summaries consider the proper understanding of the source document and redefining it into new simple words [4].Actually it generates internal semantic representation; then use the natural language techniques for the summary creation which is close to human mind summary generation. Abstractive summaries add synonyms for the more simplification of the summaries.

c) Query based Summaries

Query based summaries are applicable in case of both single document and multi document summaries. Query based summaries are produced on the basis of is to retrieve sentences which satisfy user query. The score of the sentences are calculated on the basis of frequency of words in a document. A sentence with the query phrase provided a high score than others. The sentences with the high value of the score are extracted for summaries. Partial sentences may also be extracted and further union of them is carried out [5].

d) Generic Summaries

Generic summaries are not query based. Query based summaries are biased because they do not provide the overall review of the source document. They deal with the user queries only hence not suitable for content overview. To define the category of the

document and to describe the main key points of the document generic summaries are required. A best generic summary considers the main topics of the documents and tries to minimize the redundancy as less as possible [6].

e) Summary Techniques

There are four summary techniques which will be described as follows.

- Semantic and Syntactic (Rule-based)
- Statistical Technique
- Clustering Technique
- Machine Learning Technique

Semantic and Syntactic (Rule-based)
There are many semantic analysis techniques which are applied on text summarization to find the relation between different sentences. Following are the three semantic and syntactic summary techniques.

- Graph Representation
- Lexical Chains
- Natural language processing

In the graph representation lexical graphs, Graph matching, weighted graphs and unweighted graphs are used for summarization. In lexical chains word net, co-reference chains and lexical semantics *etc.* are used for summarization. Natural language processing used information extraction, part of speech tagger for the summarization. Summarization techniques under NLP are divided into two categories as follows.

- Plain Text Summarization
- Multilingual Summarization

In Plain text summaries resultant summary is in the same natural language but in multilingual text summarization resultant summary is in different natural language. Initial work in plain text summarization was started in 1950's. Most initial work on the text summarization was targeted on technical documents. Luhn (1958) proposed the first algorithm for text summarization at IBM. The author proposed text summarizer which was based upon frequency of a particular word in a document [7].The main motivation was to short the news information, biographical information. According to the Luhn summary has different categories, some of the summaries are difficult to generate than other. Different categories are Extractive, Abstractive, Indicative, Informative and Critical. Extractive summaries are simplest. These summaries contain the sentences which have already presented in text. Abstractive summaries contain some new text also. Indicative summaries represent the scope of the whole document without including whole content. Informative summaries represent the important factual content of the text document. Critical summaries represent reviews on scientific papers about their work and results. Baxendale (1958) also did work related to extractive summaries at IBM. The author more focused on the "sentence position". Approximately 200 documents are analyzed for research [8]. Edmundson (1969) proposed the system for document extraction. The proposed algorithm was the first algorithm for extractive summaries. Two previous features sentence frequency and position of the sentence were used along with the new features like cue words and skeleton. Cue words are words like hardly, significant etc. Skeleton define the heading of the document. After evaluation 44% results matched with the manual results [9].

Multilingual text summarization is come into existence in 2005. This technique is still in early stage but this different framework has many advantages in the newswire field in which information is combined from different foreign news agencies. Evans (2005) described the scenario in which there is always a preferred language in which summary is required, different multiple source documents are in demand and in different languages are available. They preferred English as a source language and documents are from the news articles in English language and Arabic. The logic was to generate the summary of English articles without discarding the details contains in Arabic. IBM's machine is used to do a transformation of Arabic language to English. The system checks the transformed document in Arabic corresponding to a document of English for each sentence. If match is found then sentence is found relevant for summary. Hence more grammatical summary is found this way, since machine translation is still not perfect of that. To find out the similarities between sentences Simfinder tool was used. This is a clustering based tool based upon similarity over different semantic and lexical features which is using long linear regression model. Universal Networking Language is mostly used in multilingual summarization.

Martins and Rino proposed algorithm for the text summarization using UNL. They presented UNLSumm model to prune the UNL text by means of heuristics that totally focus upon unnecessary binary relations. The system used decoder to produce corresponding

summary in Brazilian Portuguese. Their pruning heuristics are based upon the relations of UNL. Although each relation is not candidate for pruning because some relations like "agt" or "obj" convey important information [10]. Only some of the relations are candidates for pruning. According to this algorithm initially there was 84 heuristics were divided into two groups A and B shown by Figure 2.2 and Figure 2.3. Group A considers 39 heuristics. It also called as single pruning and removes the independent binary relations one by one. Group B heuristics are complex than the Group A heuristics. Group B heuristics are called chained pruning, *i.e.*, once the binary relation is excluded the interconnected binary relation is also excluded.

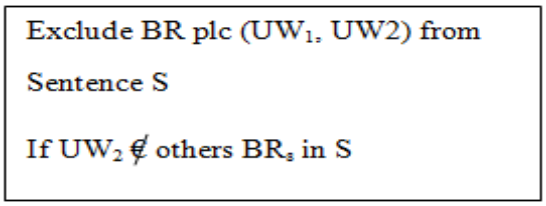

Figure 2.2: Group A heuristics

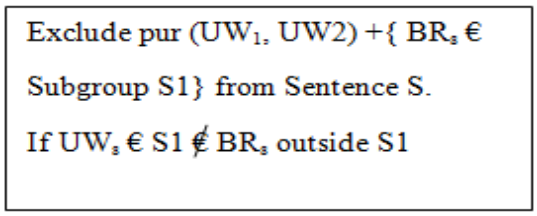

Figure 2.3: Group B heuristics

According to Figure 2.2 Group A heuristic delete the place relation from the UNL document, provided frequency of UW_2 is one means UW_2 should not be a part of any other relation in the same UNL sentence. While applying Group B heuristics frequency of UW_2 should be 2. These heuristics are more complicated because deleting a desired relation containing UW_1, UW_2 leaves blank [ ] in any other relation where UW_2 is placed. Hence to avoid this situation the relation containing [ ] is also removed from the UNL document. For example, if purpose relation as shown in Figure 2.3 is deleted containing UW_2 then any other relation in same UNL sentence containing UW_2 no more will the part of UNL document.

The serious problem regarding these heuristics is to decide the heuristics application order when considering both type of pruning. By default Group A heuristics are always applied and in case of interdependency when dangling of binary relations occurs, Group B are applied. However, Group A and B work on the same binary relations but sometimes after applying Group B heuristic results into more than one dangling relations. Hence, to give a priority to Group A or Group B heuristics is one of the major issues. The precision of the Heuristics is calculated represented by (2.1).

$$Precision(H) = Sat\_Num/Total\_Num \quad \ldots (2.1)$$

Sat_Num = No of applications of H leading to satisfactory results

$Total\_Num$ = Total No including satisfactory and unsatisfactory results

There are some limitations of approach which are as follows.

- Sometimes it covers non-relevant information.
- There is an upper bound to the number of heuristics applied for each entry.
- Application order is relevant and providing satisfactory results or not.

Managaikarasi and Gunasundari (2012) proposed an idea of text Summarization. The most important work they have done is improved methodology, which scans the document and transform into UNL graph. The system introduced UNL as a language for knowledge representation and information representation that can be describe in natural language conversation. They proposed method to find the summary of UNL document. The documents are collected from websites based upon the education domain. These documents contain images and unwanted information also. In the First Step stop words are removed. The sentence splitter is used to split document into sentences. The delimiter used is blank space here. In the next step sentences are again splitted into words. Then Morphological analyzer analyzes these words to find out the root word. These root words provide to UNL dictionary. Tenses and heuristic relations of the root words are indentified. The graph is constructed from given information. During graph construction counter field is also updated. Counter field is provided to find the important concepts, based upon threshold. Highest concepts sentences are finally picked for the resultant summary of the document. The system is tested on education domain document for summary. There was manually tested on the summary with experts. During summary preparation the data is collected from the news service providers. Each document includes the irrelevant information like images, tables *etc*. So, there is a need of creation of ideal summary for evaluation of results. For the ideal results the documents are distributed to three judges and rank is given to the sentences

according to their importance in text document. The future work for project is develop a well managed tool for evaluations and updating of UNL dictionaries with the help of root words provided by Morphological analyzer. It also identifies more and more UNL relations with the help of heuristic rules [11].

Pandian and Kalpana (2013) also proposed text Summarization mechanism using UNL. They focused on the tourism domain document which is UNL based. The Bengali UNL system is developed by them. UNL representation used by the system was for simple sentences not for complicated sentences. The main focus was mostly on DeConversion part which converts the universal networking language to Tamil language. The source document is scanned and it is converted into intermediate language. It further undergoes generation process for final output. For the summary process the source document undergoes a process of EnConversion which includes the steps like parts of speech tag, parts of speech parsing, identification of entity, and identification of relation, creation of dictionary and generation rules. Source document is converted into UNL document of UNL expressions. In the first phase parts of speech tagging and parts of speech parsing is carried out with the help of Stanford Parser. The outcome of the parser is used to find the entities and relationship between entities. Further rules are constructed and knowledge base is obtained for the generation of UNL expressions. UNL document containing UNL expressions are passed to the DeConvertor for the generation of the final summary and final output for three levels of users (level1 user, level2 user and level 3 users). The DeConversion module is constructed in such a way that it will perform the function of both summarizer and DeConvertor. To obtained the summary DeConversion module scan the word dictionary and find the relation between the different universal words, attributes of the universal words are collected and relation between universal words are taken. Further the unnecessary information like determiners, prepositions are reduced to obtained the final summary document. Final summary document is produced for the different levels of user's base upon the classification of ages. The distribution level of the summary document based upon the IQ level. DeConversion module produce summary in three steps which are as follows.

- Analysis and preparations of the dictionary information,
- Preparing DeConversion rules and
- DeConversion to produce the output summary document.

The experimental analysis is carried out using NetBeans IDE. The analysis obtained different levels of users based upon their level of IQ to access intelligence. The overall population is considered for experimental analysis. The performance of the overall system is analyzed and considered in the form of Decisiveness for all levels. It is defined by number of words compressed at different levels [12]. It is calculated for all the levels by using the given formula which is shown in 2.4.

$$\text{Decisiveness for the level User(DLU)} = \left\{100 - \frac{\text{No of words in level summarized document}}{\text{Total No of words in original document}} * 100\right\}$$

Decisiveness is find out and graph is plotted against decisiveness ratio and document. After plotting a graph it is observed that the compression for original document for level 1 user is more than rest level users. Same is true for rest two level users.
Sornlertlamvanich *et al.* proposed an approach for Summarization using Universal Networking Language. While producing summary this approach considers surface and semantic information of the UNL. The multilingualism can also be realized using DeConvertors from the summarized UNL document to the resultant target natural language document under the framework of UNL. Algorithm consists of four steps. In the first step the score of each UNL sentence is calculated. Score of the sentence is calculated by using weight of each universal word. Weight of each universal word is calculated by using the factor of frequency and inverse document frequency. After the score calculation some top most sentences based upon score are chosen for the future summary. By using the semantic information of the UNL the redundant words are removed from the summary in third step. This is mathematically calculated by using contribution function. The values obtained through contribution function are compared with the threshold value 1.5. To make summary more natural and real different sentences are merged based upon the head of the sentence and no of words in the sentence in fourth step. This algorithm is applicable for multiple document summarizations. Their experiment proved that use of the UNL improves the summary quality as compare to the plain text summarization. The semantic information of the UNL can also be applied to improve the naturalness in sentence level of summary [13].

Sherry and Parteek Bhatia (2015) also proposed an algorithm for multilingual text summarization technique. The algorithm was based upon the hybrid approach *i.e.* it extracts the best features of the previous algorithms and adds new features also. The system used UNL for language transformation. It was a six step algorithm. The overall complexity of an algorithm decreased due to removal of unnecessary relations in first step. Second step calculates the score for each UNL sentence. In the third step the best sentences are chosen for summary. Fourth step refine summary by calculating contribution functions on modifier relation. At the end sentences are merged and again UNL summary is processed for removing of unwanted words [14].

Statistical Technique

To extract relevant sentences for summary some summarization systems use statistical techniques. Binomial distribution, sentence compression and relevant scores these are statistical method used for summarization. Hidden Markov model also uses this approach.

Conroy and O'Leary (2001) applied hidden Markov model approach for plain text summarization. They used sequential model for the local independence. The system had three features: position of a particular sentence in document, number of different terns in a particular sentence, likeliness of particular sentence terms.

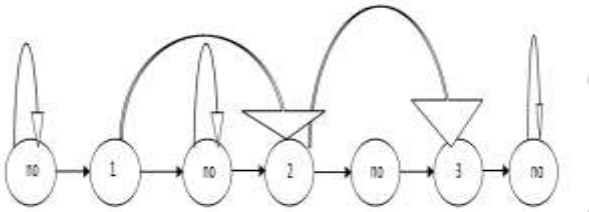

Figure 2.4: Markov model to extract the three summary sentences [23]

In Figure 2.4 Markov model is shown for $2s + 1$ states. Summary states and non summary states are alternated. In this "no" represents the non summary states and numerical numbers represents the summary states. There is a jump to next state in case of summary state. The Figure 2.4 represents the model with 7 nodes corresponds to $s = 3$.

2.7.3 Clustering Technique

Clustering is a process in which different objects are grouped based upon their properties, *i.e.*, objects with the similar properties belongs to same group. In a document different topics are arranged in a particular sequence. In cluster based summaries sentence selection is based upon the cluster Ci. The second factor is location of a particular sentence Li. The factor which increases the score of a particular sentence is its similarity to already present sentence in a document. The overall score of a sentence depend upon these three factors.

$$S_i = W1 * C_i + W2 * F_i + W3 * L_i \quad \ldots (2.5)$$

In this Si is score of sentence, C_i is cluster to which sentence belongs, Fi is document to which sentence belongs and L_i is location of a particular sentence.W1, W2 and W3 represents the weights [15].

Machine Learning Technique

Machine learning techniques are very effective for automatic text summarization. The some of the machine learning approaches are discuss as follows.

a) Naive Bayes Approach

Kupiec (1995) described a method for summarization. He described a classification function known as naïve Bayes classifier which is responsible for the each sentence to be a part of summary. If S denotes the total number of sentences and s denotes a particular sentence with a features F1 to Fk [16]. The formula of naïve Bayes is shown in 2.6:

$$P(s \in S|F1,F2,\ldots.Fk) = \frac{\left(\pi_1^k P(F_i s \in S).P(s \in S)\right)}{\pi_1^k P(F_i)}$$

The new features like sentence length and the uppercase words were added. Score is calculated for each sentence and based upon that top most n sentences were chosen. Aone *et al*. (1999) also describe a naïve Bayes classifier with more additional features. He introduced the terms "frequency" and "inverse document frequency" in plain text summaries. The corpus used in the experimental analysis was from newswire. The inverse document frequency was computed from a large corpus of the same area.

b) Rich features and Decision Trees

Lin and Hovy (1997) describe the importance of a feature "sentence position". According to this a weight is provided to sentence based upon its position in the text [17]. This method also called as position method. A newswire corpus was used for experimental

analysis. The authors measured the yield of every sentence position. They ranked the different sentence positions to produce the "Optimal Position Policy (OPP). They performed the two kinds of evaluations. They test on the unseen text. The first evaluation was exactly like the training documents and the second evaluation considered the word overlap for the manual abstracts was measured. Abstract windows and selected sentence windows were compared and precision, recall values were measured.

Lin (1999) broke away the assumption that the features are independent and tried to model the problem using decision trees instead of naïve-Bayes classifier. The system described lot of features in sentence extraction and their effects. The data set used was publicly available texts classified into various topics. The data set is divided into text fragments which are evaluated by human judges. Some important features were query signature (normalized score of the sentences depending on the number of query words), IR Signature (the salient word like the signature word), numerical data, proper name (Boolean value 1 is given to sentence that had a proper name), pronoun or adjective (Boolean value 1 is given if they appeared), weekday or month, Quotation, query and signature. The system experimented with different baselines like positional feature, simple combination of features. When machine extracted and human extracted sentences were matched, the decision tree was clearly the winner.

c) Log Linear Models

Osbrone (2002) described the Log Linear model approach for the plain text summarization. This approach is different than the previous approaches which always assumed feature independence. The system showed that this approach is better than naïve Bayes classifier approach [18]. The model can be stated mathematically as follows.

$$P(c|s) = \frac{1}{Z(s)} \exp\left(\Sigma_i \, \lambda_i F_i(c,s) \right) \qquad \ldots (2.7)$$

Where Z(S) is

$$Z(s) = \sum c \, (\sum i \, \lambda_i F_i(c,s))$$

In these equations c is a label, s is a item to be labeled, f_i is a feature (i-th feature) and λ_i is weight of the feature. There are two possible labels regarding whether the sentence is to be extracted from the document or not. The weights given to sentences are calculated from conjugate gradient descent. The non uniform prior is added to the model by authors. This model rejects too many sentences during processing. The features included by the authors were word paring, length and position of the sentence and discourse features like inside the introduction, part of conclusion.

d) Neural Networks

DUC (2001) applied the neural network technique for plain text summarization. The system produced a summary of single news article in 100 words. However the best systems in evaluations of experiments could not outperform the baseline analyzed by Nenkova in 2005. After 2002 the task for the single document summarization was dropped by DUC. Svore (2007) produced an algorithm based upon neural networks and used the third party features like dataset to resolve the problem of extractive summarization. The data set consists of 1365 documents collected from CNN.com. The datasets consists of human generated stories, articles, title and timestamp *etc*. For the evaluation two metrics were considered. The first one is to combine the system produced three highlights, combine the human generated three highlights and comparison of these two. The second take care about the ordering and the individual level comparison of the sentences [19].

Strove (2007) trained this model on the basis of labels and featured for each sentence that referred the ranking of each sentence in source document. Ranking was provided to the sentences on the basis of RankNet which was a paired based neural network algorithm. ROUGE-1 is used as a training set. The authors concluded that if a sentence contains keywords regarding new search engines and Wikipedia articles then the probability of a sentence in highlight is more.

ROUGH-1, ROUGH-2 was used for the evaluation purpose and statistically improvements were shown over baseline [20].

e) Other Approaches

Deep Natural Language Analysis Methods

Barzilay and Elhadad (1997) also described the technique for summarization. It is called Deep NLP analysis. The system described lexical chain that is formed using sequenced words in a given text, neighbor words called as spanning short and long distances. The following steps were used by them. First of all segmentation of the whole text, lexical chains identification, strong lexical chains are used for identification of the sentences. The system described cohesion in the document means togetherness of the different parts of the text. In the lexical cohesion semantically related words are used. For example, consider the sentence:

Amit bought a jag. *He loves the car* ... (2.9)

In (2.9) the word "car" refers to the word in the previous sentence "jag". It is lexical cohesion. The cohesion formula phenomenon occurs at word level as well as sentence level too. This results into lexical chains which are building blocks for summarization. Relation of the different words and their sequence was also find out which result into several chains and responsible for document representation. For the lexical chain determination Word net was used and three steps were applied.

1. Selection of candidate word set.
2. Find an appropriate chain for each candidate word.
3. If a chain is found word is inserted in a chain and then further updation is carried out.

Word net distance is used to measure relatedness. To find a desired set of candidate's simple nouns and compound nouns were used initially. At last summary is created by using strong lexical chains. The score was provided to them on the basis of length and homogeneity. Significant sentences were chosen on the basis of some heuristics.

Ono *et al.* (1994) put forward a computational model. They elaborated the procedure for extraction of rhetorical structure. To represent a relation between the different chunks of sentences binary trees were used. There were series of NLP steps used for the structure extraction they are analysis of sentences, rhetoric relation, text segmentation, generation of candidate and judgement. Evaluation was done on the basis of importance of different relations. Nodes of trees were pruned to reduce the sentence but the important information was always the part of the tree. Same procedure was applied to the paragraphs for summary generation. The data set used was 30 articles of Japanese newspaper [21].

Marco (1998) described a new approach without assuming as sentences in a document form a sequence which is flat. This approach was really different from other approaches. Rhetorical Structure Theory (RST) is used in the approach [22]. According to the system there are two non overlapping pieces of text spans known as nucleus and satellite. The purpose of the nucleus is to express the more essential part according to the writer but satellite did not do this. Satellite was dependent on nucleus but not vice versa.

The numbers inside the nodes represents the sentence number in the provided text. The text below the number is rhetorical relations in the selected text. There were different metrics used they were cluster based (in which each node was given a score on the basis of internal or external node. external nodes were always zero score nodes and the score of internal nodes depends upon the immediate children. Discourse tree is chosen when it has more score than other tree.), metric based upon the marker (a discourse structure A is chosen than B if A used more rhetorical relations than B), technique based upon clusters, metric based upon shape (prefer tree which is more skewed in shape),metric based upon connectivity (discourse structure is chosen if connectivity is higher than others), metrics based upon titles and positions.

There is also more different type of approaches for summary generation like short summaries, sentence compression and sequence document representation. Short summaries are headline style summaries. In a system there is a statistical relationship between headline and source text units. Statistical approach is used for sentence compression. The basic idea behind the system is compressing the sentence may be useful concept in single or multi document summarization

Research Gap

It has been analyzed that lot of research work has been done in plain text summarization. The various algorithm techniques have been proposed with different methodologies. Multilingual text summarization is a new research area in automatic summarization. A little work has been done in this research area. Mostly UNL is used for language translation. The various plain text summary techniques can be used to multilingual summarization for higher efficiency.

Conclusion and Future Scope

In this paper various approaches of summarization like single document, multi document, extractive, abstractive, generic and query based *etc*. has been described. The various summary techniques like machine learning, semantic and syntactic, clustering and statistical also have been discussed. Machine learning includes naïve Bayes, decision trees, and neural networks. Multilingual text summary approaches also have been described with detail procedures.

REFERENCES:

[1] Lal, Partha, and Stefan Ruger. "Extract-based summarization with simplification." Proceedings of the ACL. 2002

[2] Das, Dipanjan, and André FT Martins. "A survey on automatic text summarization." Literature Survey for the Language and Statistics II course at CMU 4 (2007): 192-195

[3] Cheung, Jackie CK. Comparing Abstractive and Extractive Summarization of Evaluative Text: Controversiality and Content Selection. Diss. UNIVERSITY OF BRITISH COLUMBIA, 2008

[4] Gupta, Vishal, and Gurpreet Singh Lehal. "A survey of text summarization extractive techniques." Journal of Emerging Technologies in Web Intelligence2.3 (2010): 258-268.

[5] Karmakar, Lad, and Chothani Hiten. "A Review Paper on Extractive Techniques of Text Summarization." (2015).

[6] Gong, Yihong, and Xin Liu. "Generic text summarization using relevance measure and latent semantic analysis." Proceedings of the 24th annual international ACM SIGIR conference on Research and development in information retrieval. ACM, 2001.

[7] Lal, Partha. "Text Summarization." (2002).

[8] Baxendale, Phyllis B. "Machine-made index for technical literature: an experiment." IBM Journal of Research and Development 2.4 (1958): 354-361.

[9] Edmundson, Harold P. "New methods in automatic extracting." Journal of the ACM (JACM) 16.2 (1969): 264-285.

[10] Martins, Camilla Brandel, and Lucia Helena Machado Rino. "Revisiting UNLSumm: Improvement through a case study." the Proceedings of the Workshop on Multilingual Information Access and Natural Language Processing. Vol. 1. 2002.

[11] Mangairkarasi, S., and S. Gunasundari. "Semantic based text summarization using universal networking language." Int. J. Appl. Inf. Syst 3.8 (2012): 18-23.

[12] Kalpana, S. "UNL based Document Summarization based on Level of Users."International Journal of Computer Applications 66.24 (2013).

[13] Sornlertlamvanich, Virach, Tanapong Potipiti, and Thatsanee Charoenporn. "UNL Document Summarization." Proceedings of the First International Workshop on Multimedia Annotation. 2001.

[14] Sherry, Parteek Kumar," Multilingual Text Summarizer" in "International Conference on Advances in Computer Engineering and Applications (ICACEA) IMS Engineering College, Ghaziabad, India 2015.

[15] Karmakar, Lad, and Chothani Hiten. "A Review Paper on Extractive Techniques of Text Summarization." (2015).

[16] Conroy, John M., and Dianne P. O'leary. "Text summarization via hidden markov models." Proceedings of the 24th annual international ACM SIGIR conference on Research and development in information retrieval. ACM, 2001.

[17] Das, Dipanjan, and André FT Martins. "A survey on automatic text summarization." Literature Survey for the Language and Statistics II course at CMU 4 (2007): 192-195.

[18] Osborne, Miles. "Using maximum entropy for sentence extraction."Proceedings of the ACL-02 Workshop on Automatic Summarization-Volume 4. Association for Computational Linguistics, 2002.

[19] Kaikhah, Khosrow. "Automatic text summarization with neural networks." (2004).

[20] Svore, Krysta Marie, Lucy Vanderwende, and Christopher JC Burges. "Enhancing Single-Document Summarization by Combining RankNet and Third-Party Sources." EMNLP-CoNLL. 2007.

[21] Barzilay, Regina, and Michael Elhadad. "Using lexical chains for text summarization." Advances in automatic text summarization (1999): 111-121.

[22] Flowerdew, Lynne. "An integration of corpus-based and genre-based approaches to text analysis in EAP/ESP: countering criticisms against corpus-based methodologies." English for Specific Purposes 24.3 (2005): 321-332

International Journal of Engineering Research and General Science Volume 3, Issue 5, September-October, 2015
ISSN 2091-2730

Review Paper on AJAX Comet and Websocket Uses for Web HMI/SCADA

Ayyaj .I .Nadaf [1], S. V. Kulkarni[2]. Dr. P. P. Shaha[3]. Dr. M. K. Bhanarkar[4]
Department of Electronics, Shivaji University, Kolhapur [1,4] ,
Department of Electronics, Devchand College, Nipani [2,3]
ayyaz.nadaf@gmail.com

Abstract— This paper presents review of Ajax Comet and Websocket technology and its uses for industrial control application. This could help for selecting the correct protocol in righteous application. AJAX is asynchronous JavaScript and Extensible Markup Language used for pushing data on a web. Comet is another dominant technology evolved for real time data access on web platform. Websocket is a new trend in which data is transferred in a bidirectional link established with lower layer model. Human Machine Interface (HMI) and Supervisory Control and Data Acquisition (SCADA) are the two major part in control application after Programmable Logic Controller (PLC).

Keywords— PROTOCOL, AJAX, COMET, WEBSOCKET, SCADA, PLC.

INTRODUCTION

IN Automated industry there are lots of process variable need to be controlled so as to get process under control. Simply saying there are lots of real time protocols available for real time monitoring of data. Prevalent manufacturer in the field of automation are Siemens, Allen-Bradley, Mitsubishi, Fanuc, Yamaha, Panasonic and much more stated their own protocols and dedicated hardware/software. New trend is of open source in this case they are building their platform for data interoperable. Same race found for the browser based technology. Basically they are platform independent. Some of supervisory control and data acquisition (SCADA) systems giving human interaction and data visualization for local and remote site using the html JavaScript functions. Websocket is evolution in server client web technology. It allows single TCP socket connection between server and client with little overhead. Advantage of using websocket is that it is full duplex bidirectional message sender receiver protocol with very low latency in transmission and reception. Websocket technology is now standardized which mean web technology is agreed standards for real time processing. Websockets are now reaching beyond for real time communication with cross platform standard. HTML5 is the key solution for modern platform independency. It is widely used in mobile and desktop applications. HTML5 with some advance add-on technic fulfill the job requirement.

BRIEF OVERVIEW.

Internet wasn't built for to be dynamic. It is gestated collection of Hyper Text Markup Language (HTML) pages. Over the time it became necessity to have rich components as a part of web designs like images, audio video etc. On the other hand server becomes more advance providing responses on the query basic leading this to dynamic HTML (DHTML) pages. Further development to this

leads developing of pages inbuilt with JavaScript. After few advances in DHTML requirement dynamic content updating took place by means of http polling within frames. Soon it is found that this technology is very hectic. As pages disappear and reappear for a little change. With reloading of complete page for minor update all information had to be resent which was already transmitted. This placed additional load on server with excess use of bandwidth. Things started to get exciting with introduction to live connect. Term Asynchronous JavaScript become familiar for very long period. The utility of page being updated in a background with background Hypertext Transmission protocol (HTTP) request remain obscure for very long time. In AJAX some Document Object Models (DOM), Cascaded Style Shit (CSS) and HTML is used. The term 'AJAX' was publicly stated on 18th Feb 2005 by Jesses James Garrett in article titled "AJAX: A New Approach to Web Application". The first draft officially published on 5th April 2006 by World Wide Web Consortium (W3C) standard specifying XMLHttpRequest.

Comet is a web application programing technology used for making communication between client and server with pushing data from server to client. Http long-held request allows server to push data to client without browsers explicit request. Comet approach is differing to original web technology where client request complete web page at a time. This approach has other names http server push, two way web, reverse Ajax, http streaming, Ajax push. Comet is not an acronym it is known as low latency data for web. Comet is helpful to minimize the latency between server clients by sustaining long lasting http connection. But holding connection till server's event is not worth. Browser may be blocked for new request until its previous query gets satisfied. This makes a question on browsers usability. Comet technology falls in streaming and long polling category. Many comet application uses long polling as it is very straight forward than streaming algorithm. XMLHttpRequest Hidden iframe and Ajax long polling are the measures in this technology.

Websocket became game changer for browser war .The websocket protocol was standardized by Internet Engineering task force (IETF) in 2011. Originally it was designed to be used by web technology but now it can be deployed in any client server application. Websocket protocol provides full duplex communication over single TCP connection. It takes http handshake connection and upgrades the connection to websocket. Instead of using new page for new information websocket allows to remain on the same page with updated information. Users need not to refresh the page or different pages to send receive information. Websocket provide raw socket capabilities to web that's why it is possible to use it any real time monitoring purposes. Custom protocol can be implemented on the top of basic architecture of websocket. Web tier application as well as embedded application can be built on the top of websocket. It is best for the real time monitoring.

RELATED WORK

HTML5 was designed to be platform independent, and can be used on an increasing number of mobile devices for creating both mobile websites and mobile applications [1]. This thesis presents a flexible and configurable database management system designated COMET, suitable for mbedded systems and in particular, vehicle control-systems. To be able to handle the varying requirements imposed by different systems, COMET emphasizes configurability and tailorability, by adopting a component-based architecture. The result of this research is the implementation of COMET BaseLine, which is an instance of COMET suited to a particular vehicle control-system [2]. One of the most familiar SCADA (supervisory control and data acquisition) application protocols now is OPC protocol. This interface is supported by almost all SCADA, visualization, and process control systems. There are many research efforts tried to design and implement an approach to access an OPC DA server through the Internet. To achieve this goal they used diverse of modern IT [3]. it is feasible to create a realtime Human Machine Interface, HMI, solution to a Command & Control System in HTML5. The conclusion is based on some HTML5 features that is of interest for a system of this kind, a comparison between some of the most relevant web server solutions and a prototype. It shows that it is possible to create a HMI in HTML5 for a Command & Control System but with some delimitations. A proposal would be to create a HMI in HTML5 as a supplement to the current instead of replacing it. The javaScript API used to present the map in the prototype is releasing an upcoming version with support for WebGL,

allowing smoother and graphical richer maps in the future [4]. Regarding the limitations of traditional web real-time communication solutions such as polling, long-polling, flash plug-in, propose that using new coming Web Socket technology in the web real-time communication field, introduce the features of Web Socket technology, analysis the difference between Web Socket protocol and HTTP protocol, offer an approach to implement the Web Socket both in client and server side, prove Web Socket can decrease network traffic and latency greatly by an experiment, made the prospect of future application of Web Socket in web real-time communication[5].

HOW IT WORKS AJAX COMET AND WEBSOCKET

All these technology were add-on to standard HTML. HTML5 version released with websocket Application Programming Interface (API) specifications. Polling, long-polling and streaming is done when HTTP request sent to server. Server then responds with web pages after acknowledgement. Many times when there is requirement of real time data for example medical instrument data readings, stock exchange, ticket sale, bookings update the client generally need to refresh the pages to updated information. But of course this is not the great solution. Real time communication attempts largely by polling and long polling by delaying the http connection completion. This is nothing but the comet based push technology. In comet push technology polling is done by method in which browser sends request at a regular interval and receive the response immediately. This is helpful if client and server have a scope of synchronization. Due to this approach unnecessarily application withdraws much bandwidth by opening new connection request and closes if data is not available. Streaming is done with connection kept open for definite time but streaming encapsulated in HTTP. Firewall and other filter mechanism chooses to buffer result; hence providing increase in latency to message delivery. Secure Socket Layer SSL provide additional shield for data security. All this push technology involve http request and response header which is unnecessary data forming latency. This adds overhead to bandwidth utilization.

With AJAX client can send and receive data in asynchronous manner without interfering existing display. Data is usually retrieved from XMLHttpRequest object need not to be a JavaScript Object Notation (JSON consumes less Bandwidth). DOM is accessed using JavaScript function and represents data to user on current page. JavaScript and XMLHttpRequest object both interchange data asynchronously between browser and server.

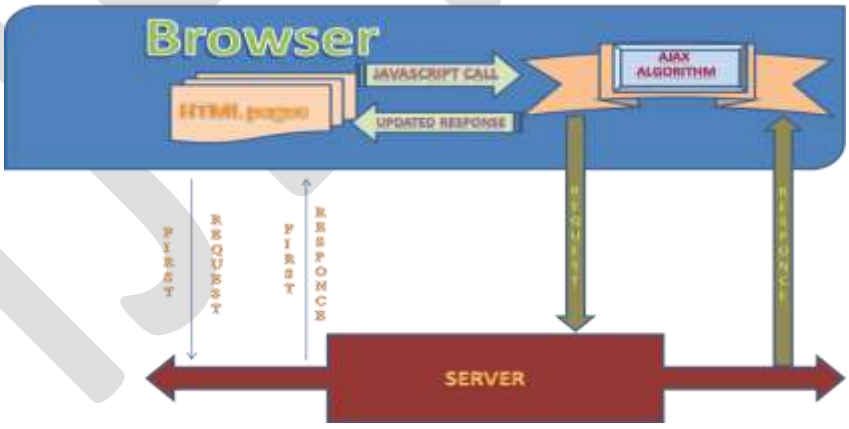

Figure 1: How Ajax works.

- Client browses pages from server and loads requested pages to client for first time.
- JavaScript function makes call to AJAX
- AJAX makes request to server asynchronously
- Server send information to AJAX

- Finally, Ajax respond back with updated information to the JavaScript call.

Simple jquery AJAX example:

```
var url='http://domainname/ajaxService';
jQuery.ajax(
url:url,
success:function(data)
{
        alert(data);
}
);
```

In Comet Based web Application long held http request generated by browser get data from server without further request. Comet application eliminates the traditional polling and page by page modeling by real time persistent HTTP connection. According to HTTP 1.1 specification browser should not have more than two simultaneous http connections to web server. Therefore keeping connection ON for real time server events can lead other problems. Browser might be kept idle and cant able to generate new request until previous request is satisfied. This is a negative impact on browsers usability. In streaming application comet opens a single persistent connection to all comet events. For every new comet event from server side client handle this incrementally without closing connection. Streaming has negative impact on all modern browsers.

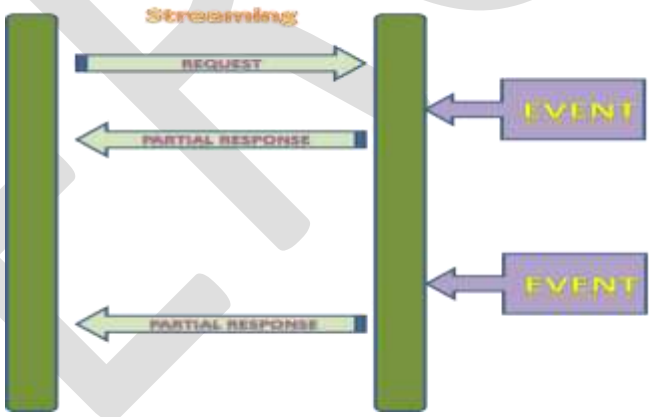

Figure 2: Streaming

Many implementation of comet application on different web browser uses long polling method. This is easier to deploy on any browser. It is very clear that from its name long polling involves client makes a polling request for comet events occur. This is similar to AJAX request style where browser keeps connection open until comet event occurs.

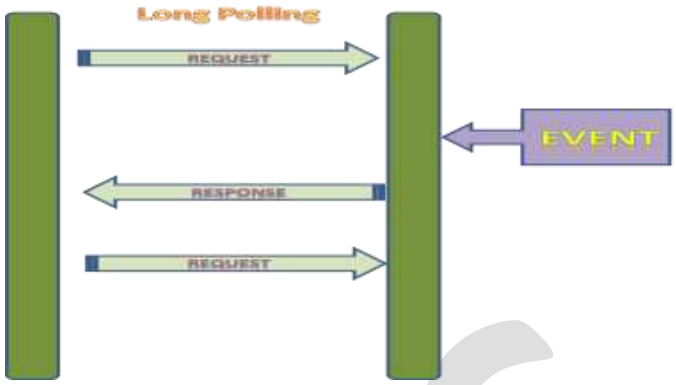

Figure 3: Long Polling

Advantage of this comet technology is that there is always a link between client and server; Server fetches the data to client as soon as it is available at client.

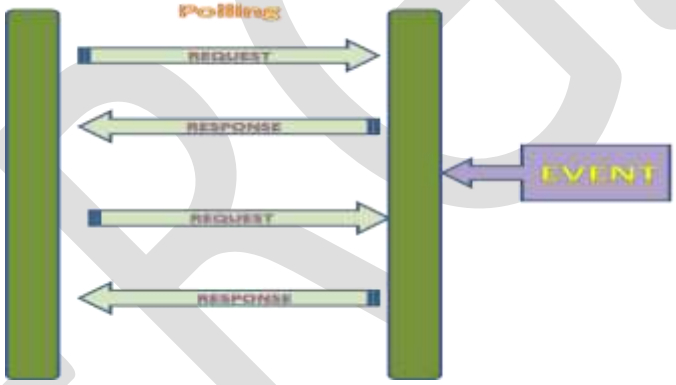

Figure 4: Polling

Websocket is a full duplex real time protocol over a single TCP connection. It provides few methods for data extraction and encapsulation. Following API creates websocket object and its associated event methods.

```
var url='http://domainname/ajaxService';
var Socket = new WebSocket(url);
Socket.onopen=function()
{
        //This method is called when socket connection is established.
}
Socket.onclose=function()
{
        //This method is called when socket is closed
}
Socket.onmessage=function()
```

```
{
        //This method is called when message is received
}

Socket.onerror=function()
{
        //This method is called when error occurred during communication
}
Socket.send(data)
{
        // This method is called to transfer the data from client.

}
```

CURRENT TREND OF DEVELOPING WEB SCADA

Basic process control application starts with sensing the physical process sending this information to controller then according to the controller algorithm outputs are generated. This is the basic close loop system. SCADA system is involved for user intervention and data logging. This should be in real time because SCADA client might be at distinct places and in distinct number. Human Machine Interface (HMI) is used for same expect for data logging. Unlike SCADA HMI requires special type of hardware and software. Basic features of HMI/SCADA should

- Provide real time access to plant floor parameters.
- Provide major alarms of the control system.
- Provide colourfully recognisable machine parts.
- Provide numerical display and input for user interaction.
- Provide multiple protocol support.
- Provide fail safe design

Industrial controller requires transferring the real time data to controller. In many case there is need of storing the real time information to server for like historical trends. Another example is that to view historical alarms it is necessary to store current alarms. Many industrial scada systems use these technologies.

OPC system .net is a scada software developer company providing SCADA solution for the smartphones like android and apple. The solution is based on AJAX technology design and development of SCADA for oil gas, nuclear, facilities management, food processing industry.

Figure 5: OPC SCADA https://www.opcsystems.com/help/ImagesExt/image5_34.jpg

Inductive automation serves ignition web based SCADA.

Figure 6: Inductive SCADA

https://inductiveautomation.com/static/images/product/webbased/wb3.png

Ignition's web-based architecture is platform independent browser based scada runs on any platform and it is powered by JAVA.

Another open source SCADA is SCADA BR is developed by open source community of OPEN SCADA and MANGO automation open source project of serotonin.

PVBROWSER is yet another open source web based SCADA framework developed in c and c++. All above support many industrial communication protocol but they are not yet supporting websocket.

CSWORK is yet another framework for browser based scada. Support variety of data protocol format for example BACnet, Modbus, SQL database, OPC data access server. Support real time historical trending, alarming.

CONCLUSION

Websocket is new trend in real time web based data communication. It must be a part of modules in PLC based protocol communication. Currently industry is using AJAX web based scada system. Some open source scada software are using their own framework for it. Internet browser is being used by many mobile and laptop. If web socket is used in industrial environment lot of additional cost and energy can be saved. Browser based solution (HTML5 and websocket) can be easily deploy on any platform.

REFERENCES:

[1] Jin-tae Park1 , Hyun-seo Hwang1 , Jun-soo Yun1 and Il-young Moon1 1 School of Computer Science and Engineering, Korea University of Technology and Education {wlsxo05, smilebear1, yuntn55, iymoon}@koreatech.ac.kr "Study of HTML5 WebSocket for a Multimedia Communication". International Journal of Multimedia and Ubiquitous Engineering Vol.9, No.7 (2014),pp.61-72 http://dx.doi.org/10.14257/ijmue.2014.9.7.06

[2] Dag Nystrom "COMET: A Component-Based Real-Time Database for Vehicle Control-Systems" Copyright Dag Nystr¨om, 2003 ISBN 91-88834-46-8 Printed by Arkitektkopia, V¨aster°as, Sweden Distribution: M¨alardalen University Press.

[3] Hosny A. Abbas & Ahmed M. Mohamed "Review on the Design of Web Based SCADA Systems Based on OPC DA Protocol " International Journal Of Computer Networks (IJCN), Volume (2) : Issue (6)

[4] Henrik Rydstedt "HTML5 as HMI in a Command &Control System" Tryckt av: Reprocentralen ITC ISSN: 1401-5749, UPTEC IT 14 004 Examinator: Lars-Åke Nordén Ämnesgranskare: Lars Oestreicher Handledare: Jakob Sagatowski

[5] Qigang Liu, Xiangyang Sun. Sydney Institute of Language & Commerce, ShangHai University, ShangHai, China. "Research of Web Real-Time Communication Based on Web Socket" 10.4236/ijcns.2012.512083 PP. 797-801.

[6] Dilip Kumar Sharma (G.L.A. Institute of Technology and Management, India), Gopalji Varshneya (G.L.A. Institute of Technology and Management, India) and Ashwani Kumar Upadhyay "AJAX in Development of Web-Based Architecture for Implementation of E-Governance" Volume 3, Issue 3. Copyright © 2007. 14 pages.

[7] Li-Jie Cui1 , Hui He2 and Hong-Wei Xuan1,Harbin, China 2Harbin Institute of Technology, Harbin, China andyclj1977@163.com, hehui@hit.edu.cn, henryxuan@hotmail.com "Analysis and Implementation of an Ajax-enabled Web Crawler" International Journal of Future Generation Communication and Networking Vol. 6, No. 2, April, 2013.

[8] D. G. Synodinos, "HTML 5 Web Sockets vs. Comet and Ajax,"2008. http://www.infoq.com/news/2008/12/websockets-vs-comet-ajax.

[9] Chwan-Hwa Wu, Senior Member, IEEE, J. David Irwin, Fellow, IEEE, and Fa Foster Dai, Senior Member, IEEE "Enabling Multimedia Applications for Factory Automation" IEEE TRANSACTIONS ON INDUSTRIAL ELECTRONICS, VOL. 48, NO. 5, OCTOBER 2001.

[10] Songchar Jiang "Wireless Communications and a Priority Access Protocol for Multiple Mobile Terminals in Factory Automation" IEEE TRANSACTIONS ON ROBOTICS AND AUTOMATION, VOL. 14, NO. 1, FEBRUARY 1998.

[11] Adnan Salihbegovic , Vlatko Marinković , Zoran Cico , Elvedin Karavdić b, Nina Delic ETF Sarajevo, Bosnia and Herzegovina b Bosna-S Oil Services Company, Bosnia and Herzegovina "Web based multilayered distributed SCADA/HMI system in refinery application" Computer Standards & Interfaces 31 (2009) 599–612.

[12] Bahram Ravani, Magomed Gabibulayev, Ty A. Lasky ,"Improvement of a Human-Machine Interface (HMI) for Driver Assistance Using an Event-Driven Prompting Display", IEEE transactions on control systems technology, vol. 19, no. 3, may 2011 page no 622-627.

[13] Angelos Amditis ,Luisa Andreone,Katia Pagle,Gustav Markkula,"Towards the Automotive HMI of the Future: Overview of the AIDE-Integrated Project" IEEE transactions on intelligent transportation systems, vol. 11, no. 3, september 2010 page no 567-578.

[14] Edwin Lughofer, James E. Smith, Muhammad Atif Tahir,"Human–Machine Interaction Issues in Quality Control Based on Online Image Classification", IEEE transactions on systems, man, and cybernetics—part a: systems and humans, vol. 39, no. 5, september 2009 page no 960-971.

[15] Doukas and Kleanthis Thramboulidis,"A Real Time Linux-Based Framework for Model-Driven Engineering in Control and Automation" IEEE transactions on industrial electronics, vol. 58, no. 3, march 2011 page no 914-924

International Journal of Engineering Research and General Science Volume 3, Issue 5, September-October, 2015
ISSN 2091-2730

PLC Based Control System for Brix Measurement.

Ayyaj .I .Nadaf [1], S. V. Kulkarni[2]. Dr. P. P. Shaha[3]. Dr. M. K. Bhanarkar[4]
Department of Electronics, Shivaji University, Kolhapur [1,4] ,
Department of Electronics, Devchand College, Nipani [2,3]
ayyaz.nadaf@gmail.com.

Abstract— This paper presents utilization of Programmable Control System (PLC) for sugar factory brix measurement. Brix is dissolved amount of sucrose crystal to clear syrup named after German mathematician and engineer Adolf Brix (symbol °Bx). Sugar industry use batch pans for boiling of clear syrup to form the sugar crystals. This pure crystal can only be developing in certain confined pan parameters. Pressure, temperature, vacuum and level are the main parameters of a pan system. One degree Brix is 1 gram of sucrose in 100 grams of solution and represents the strength of the solution as percentage by mass. PLC is a current trend in control system. In sugar industry PLC can be used for controlling parameter of the batch pan. PLC based control system can improve the results of this non-linear multi input multi output system.

Keywords— PLC, CONTROL SYSTEM, BRIX, CONDUCTIVITY, CRYSTALLIZER.

INTRODUCTION

INDIA is one of the largest sugar manufacturer country in the world. Cane farming is major source of income for the farmers in India. Process of sugar manufacturing starts from cane feeding to crushing unit where cane crushed and juice is extracted. This juice is then purified by various method and it is made available for evaporators. In evaporators the syrup is evaporates 75% to 85 % of water to 34% to 45% giving more viscous syrup to crystallizer pan hence leading to vacuum in crystallizer. Operators on pan floor control various valve by observing temperature, level, vacuum, pressure on gauges. For controlling of level workers looks at glass windows available on pan. Hence by observing various parameters operator controls the working of this crystallization process and bring the brix of syrup to 60% to 65%. Automation of such multi input multi output can give benefit of accurately measuring and controlling parameter over operator's judgement and fluctuations in the inputs hence minimizing error.

Brix increases with evaporation of water from syrup. This happens when heat transfer from steam to syrup. Evaporation rate depends on heat transfer in calandria walls from steam to syrup from tubes. Ratio can be defined as

$Q = T_c \cdot A \cdot \Delta T$

T_c: Heat Transfer Coeficient.

A: Area of heat exchange in m^2.

ΔT: Difference in temperatute of steam to boiling syrup.

Q: heat transfer quantity 1/(Kcal/kg/hr).

T_c depends on resistance to

1. Tube wall resistance (R_t).
2. Surface to syrup resistance (R_{s1}).
3. Steam to syrup resistance (R_{s2}).

$$Q= (A\cdot\Delta T)/(R_t + R_{s1}^{+} R_{s2}).$$

Some other factors which adversely affect the heat transfer are

1. Hydrostatic head.
2. Boiling Point elevation.
3. Incondensable gases.
4. Viscosity.
5. Surface tension.

Measurements of various parameters are done by different gauges and controlled by respective valves. Variable that to be controlled are

1. Juice input: Juice input to syrup crystallizer can be controlled by level controller. Level controller helps to control the rate of juice input to the pan.
2. Level: Level in syrup crystallizer can be controlled by regulating feed inlet.
3. Steam flow: Steam flow rate must be controlled in comparison with Temperature and vacuum.
4. Brix: Brix meter uses the conductivity of syrup and transmits signal to control vacuum and temperature percent of body.

RELATED WORK :-

Saravanan, V. Electron. & Instrum. Eng., M. Kumarasamy Coll. Zigbee based monitoring and control of melter process in sugar industry. The brix rate of the sugar masseicuite (semisolid state) has been measured using a micro-polar brix sensor. The objective of this paper is to monitor and control the brix in wireless manner using Zigbee network. The process has been designed using sensor networks and PIC controllers [1].

Rahim, A. Hashim, H.; Abdullah, N.E.; Hassan, S.L.M.; Shairah, I.; Halim, A.;Igol, F.A. "A numerical analysis of correlation between sucrose level measurementand near-infrared (NIR) for various grades of watermelon ripeness" This paper presents the determination of sucrose level content in various grades the relationship between the brix percentage value and the reflectance wavelength. Through the curve fitting line, the wavelength is successfully identified with respect to brix percentage value [2].

Elhaq, S.L.; Giri, F.; Unbehauen, H. "Experimental identification of five-effect evaporator in sugar industry " The dynamic behaviour of an industrial five-effect evaporator in sugar manufacturing is determined using the parameter identification approach. The purpose is to obtain an accurate mathematical model that can be used for advanced control design [3].

CONTROL ACTION:

Regulation of pressure (0 psi to 15 psi): It is done with controlling the steam flow rate inside the calandria. Opening the valve the flow rate of steam increased and by controlling flow valve down flow rate decreased.

Regulation of vacuum (-15 psi to15 psi): It is achieved by controlling input of finely sprayed cold water in condenser. Vapours evolving from pan is fed to condenser. Condenser is a closed chamber. This vapours condensate in condenser hence leading to vacuum in pan.

Regulation of Hot water and Syrup (0% to 100 %): this must be set by the operator on the concentration of syrup being heated in pan. On the basis of operator experience operator sets the boiling condition of pan. In order to increase and decrease concentration over time. This is used when crystal growth is taking place.

Level is maintained with control of Hot water valve once the syrup is being started heating. Conductivity is maintained with syrup control valve. Pressure and temperature is maintained with the controlling steam flow rate to calandria.

RESULT:-

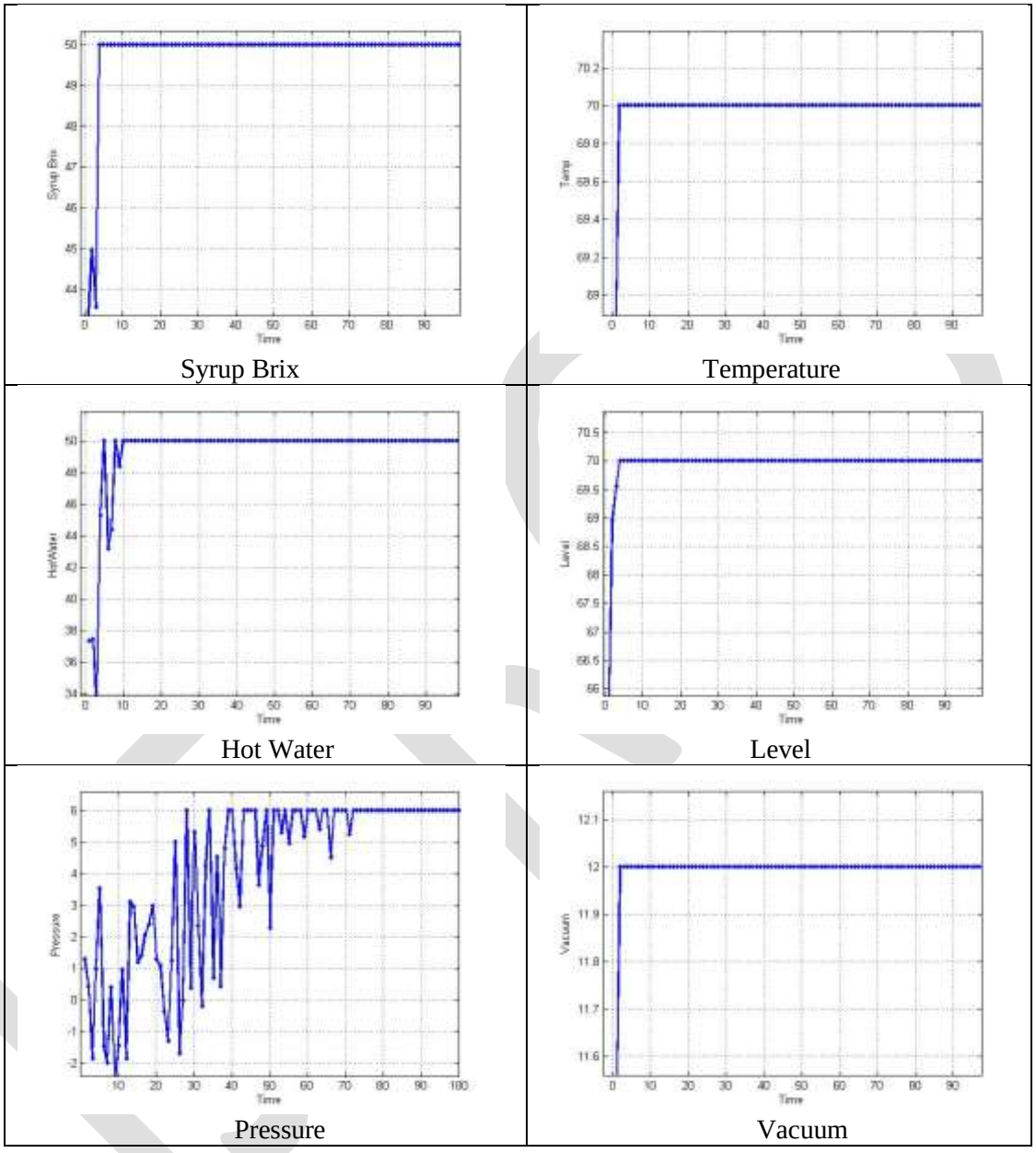

CONCLUSION

By controlling various valves or by maintain the set points of various parameters of syrup crystallizer good production can be achieved. Syrup crystallizer can be set in auto mode where all parameters managed by PLC based control system.

REFERENCES:

[1] Saravanan, V. ; Electron. & Instrum. Eng., M. Kumarasamy Coll. of Eng., Karur, India ; Arivoli, S. ; Valarmathi, K. "Zigbee based monitoring and control of melter process in sugar industry" Year: 2014. Pages: 1-4, DOI: 10.1109/ECS.2014.6892551 IEEE Conference Publications.

[2] Rahim, A.A.A.; Hashim, H.; Abdullah, N.E.; Hassan, S.L.M.; Shairah, I.; Halim, A.;Igol, F.A. "A numerical analysis of correlation between sucrose level measurementand near-infrared (NIR) for various grades of watermelon ripeness" Technology, Informatics, Management, Engineering, and Environment (TIME-E), 2013 International Conference on.Year: 2013. Pages: 180 – 185, DOI: 10.1109/TIME-E.2013.6611988 IEEE Conference Publications.

[3] Elhaq, S.L.; Giri, F.; Unbehauen, H. "Experimental identification of five-effect evaporator in sugar industry " Control Conference (ECC), 1997 European Year: 1997 Pages: 3532 – 3536. IEEE Conference Publications..

[4] Adnan Salihbegovic , Vlatko Marinković , Zoran Cico , Elvedin Karavdić b, Nina Delic ETF Sarajevo, Bosnia and Herzegovina Bosna-S Oil Services Company, Bosnia and Herzegovina "Web based multi-layered distributed SCADA/HMI system in refinery application" Computer Standards & Interfaces 31 (2009) 599–612.

[5] Chwan-Hwa Wu, Senior Member, IEEE, J. David Irwin, Fellow, IEEE, and Fa Foster Dai, Senior Member, IEEE "Enabling Multimedia Applications for Factory Automation" IEEE TRANSACTIONS ON INDUSTRIAL ELECTRONICS, VOL. 48, NO. 5,OCTOBER 2001.

[6] Hosny A. Abbas & Ahmed M. Mohamed "Review on the Design of Web Based SCADA Systems Based on OPC DA Protocol " International Journal Of Computer Networks (IJCN), Volume (2) : Issue (6).

[7] Mohamed Endi.,Y.Z.Elhalwagy.,Attalla hashad., "Three-Layer PLC/SCADA System Architecture in Process Automation and Data Monitoring" 978-1-4244-5586-7/10/C 2010 IEEE.

[8] YU Huiqun., "The Design and Realization of PID Liquid Level Control System",Based on S7-200 and EM235, 2010 International Conference on Intelligent Computation Technology and Automation, 978- 0769540771 /10 $26.00 © 2010 IEEE DOI10. 1109/ICICTA.2010.800.

[9] S. Da'na, A. Sagahyroon , A. Elrayes, A.R. Al-Ali, R. Al-Aydi, "Development of a monitoring and control platform for PLC-based applications", Computer Standards & Interfaces 30 (2008) 157–166.

[10] Vijay Kumar Khatri, Ahsan Javed Ghangro, Jetandar Kumar and Syed Jaad UI Haque.,"Industrial Data Acquisition and Control System using two PLCs' Networked over MPI Network", 2009 IEEE symposium on Industrial Electronics and Application (ISIEA2009), October46,2009,KualaLumpur,Malaysia.,978-1-4244-4/09/@2009IEEE.

[11] C D Johnson, "PLC Process Instrumentation and Technology", 8th Edition, Tata McGraw Hill.

[12] A.V. Pitteea, R.T.F. Ah King, and H.C.S. Rughooputh. Intelligent controller for multiple-effect evaporator in the sugar industry. In Proc. of the 2004 IEEE International conference on industrial technology, pages 1177– 1182, 2004.

[13] S.L. Elhaq, F.Giri, and H. Unbehauen. The development of controllers for a multiple-effect evaporator in sugar industry. In proc. of the 1997 European Control Conference, Brussels, Belgium, July 1997.

International Journal of Engineering Research and General Science Volume 3, Issue 5, September-October, 2015
ISSN 2091-2730

Review on Sigma-Delta Modulator

Vedanta Kuri[1], Dr. Abir Chattopadhyay[2]
Member IEEE[1] ,vedanta.kuri@gmail.com[1] , Mobile-08017102017 , Electronics and Communication Engineering Department[1], Adamas Institute of Technology, Barasat [1]
,FIETE[2] abir_chattopadhyay@yahoo.co.in[2] ,University Institute of Engineering and Management, Kolkata[2]

Abstract— In this paper detailed study of Sigma- Delta (Σ-Δ) modulator has been discussed and analyzed. Low power Σ-Δ ADC for various applications has been discussed. Use of oversampling ratio in designing of Σ-Δ ADC for reduction of noise as well as for better resolution has been analyzed theoretically and practically.

Keywords— Sigma- Delta (Σ-Δ) modulator, Oversampled ADC, Resolution.

INTRODUCTION

Emergence of powerful digital signal processors implemented in CMOS VLSI technology creates the need for high-resolution analog-to-digital converters that can be integrated in fabrication technologies optimized for digital circuits and systems. Depending on the ratio of sampling, the analog to digital converters can be divided into two categories. The first category is the Nyquist rate ADCs in which the input data is sampled at the Nyquist rate and the other type called oversampling ADCs, samples the signal at a rate much higher than the Nyquist rate.[1] The Block diagram of the Oversampling ADC is shown below.

Building Blocks of Oversampling ADC

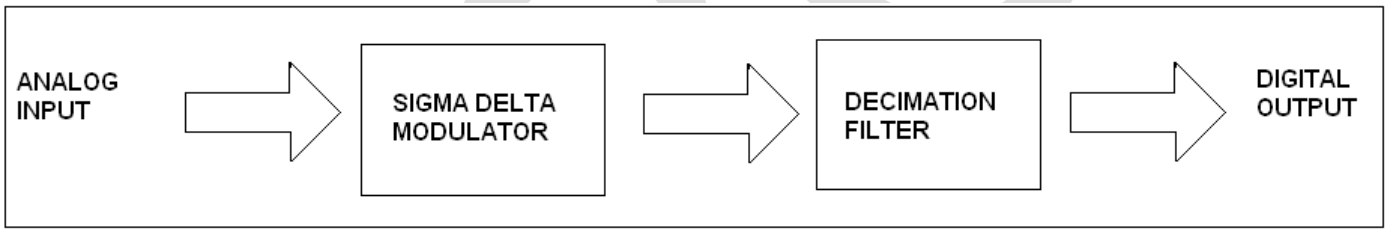

Fig. 1: Block Diagram of Oversampling ADC

OVERSAMPLING ADC

ADC can be separated into categories depending on the rate of sampling. The first category samples the input at the Nyquist rate,or fN =2F, where F is the bandwidth of the signal and fN is the sampling rate. The second type samples the signal at a rate much higher than the signal bandwidth. This type of converter is called an oversampling converter. Traditionally, successive approximation or dual slope converters are used when high resolution is desired. However, trimming is required when attempting to achieve higher accuracy. Dual slope converters require high speed, high accuracy integrators. That is only available using a high fT bipolar process. To design a high-precision sample and hold is another factor that limits the realization of a high resolution ADC using these architectures. The oversampling ADC is able to achieve much higher resolution than the Nyquist rate converters. This is because digital signal processing techniques are used in place of complex and precise analog components. The accuracy of the converter does not depend on the component matching, precise sample –and –hold circuitry, or trimming, and only a small amount of analog circuitry is required. Switched capacitor implementations are easily achieved, and as a result of the high sampling rate, only simplistic anti-aliasing circuitry needs to be used. However because of the amount of time required to sample the input signal, the throughput is considerably less than the Nuquist rate ADCs.[1]

BLOCK DIAGRAM

The block diagram of Low power Sigma-Delta Modulator ADC is given below.

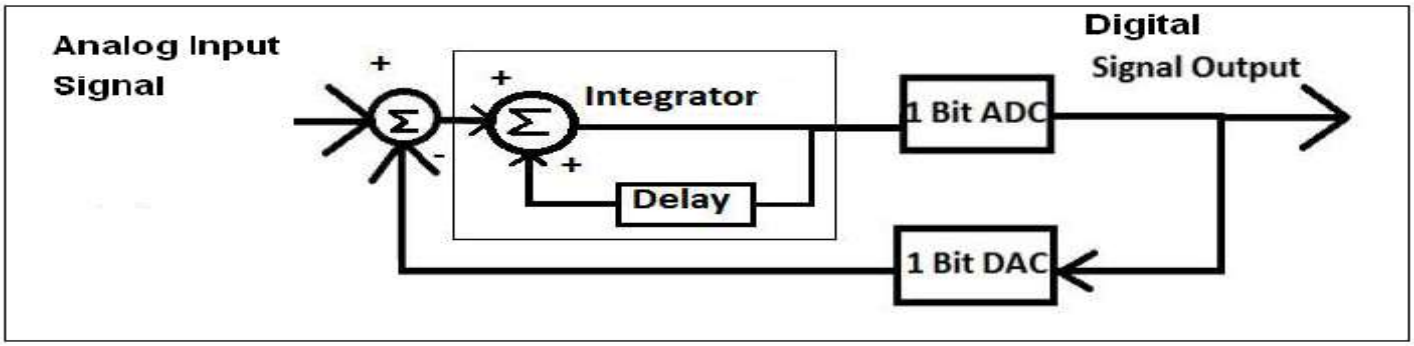

Fig 2. First-order Sigma-Delta Modulator.

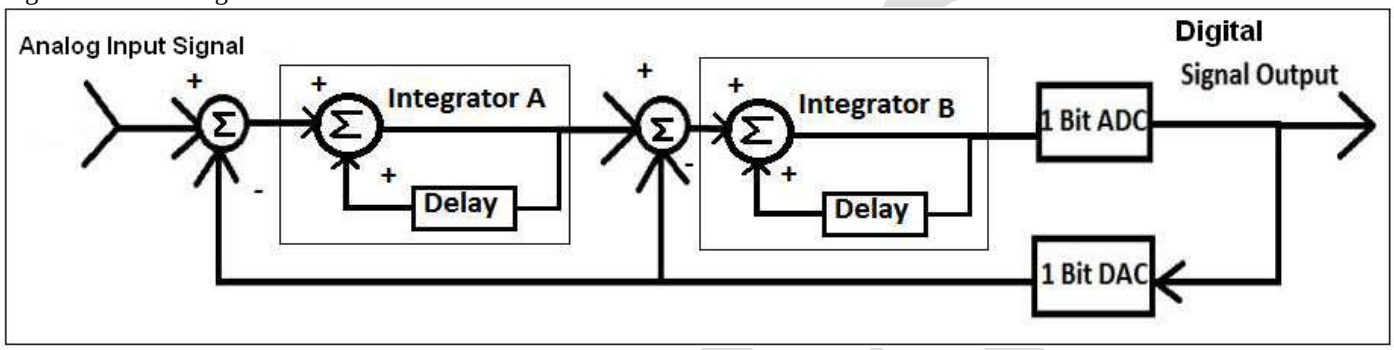

Fig 3. Second-order Sigma-Delta Modulator.

A comparative study of different Sigma-Delta modulator used for different applications designed and developed by different authors is shown below.

Paper Name	A 15 Bit 95 dB Low Power Discrete Time Sigma Delta Modulator	Bandpass Sigma-Delta Modulator for Sensor Signal Processing	First-Order Continuous-Time Sigma-Delta Modulator
Authors	1. Mohammed ArifuddinSohel 2. K. ChennaKeshava Reddy 3. Syed Abdul Sattar 4. Salma Jabeen	1. Lukáš Fujcik 2. Radimír Vrba	1. Yamei Li , San Jose State University, USA 2. Lili He , San Jose State University, USA
Abstract	In this paper high resolution low power sigma delta modulator over 5MHz at a sampling frequency of 1Ghz has been developed in which Signal to Quantization Noise Ratio (SQNR) of 95.3dB, leading to a 15 bit resolution of the ADC. A very low power consumption of 2.3mW at a supply voltage of 1.8V is achieved in 0.18micron CMOS technology. The 60 meter band or 5 MHz band is a relatively new amateur radio band that is useful for disaster management and this paper presents an ADC that can be used for this band.	Here, system architecture for sensor signal digitization utilizing a band pass sigma-delta modulator in 5V 0.7µm CMOS technology has been implemented for impedance spectroscopy, capacitive pressure sensor measurement and wireless applications.	In this paper first-order continuous-time sigma-delta modulator in 0.18 um CMOS technology that achieves a level of 60 dB SNR has been designed which operates at 1.8 V supply voltage. It can accept input signal bandwidth of 10 kHz with oversampling ratio of 250.
Paper Name	Sigma delta and multi-stage sigma delta modulation with inside loop dithering	Modeling and design of novel architecture of multibit switched-capacitor sigma-delta converter with two-step quantization process	A Mixed-Signal Architecture of Channel Select Filtering with Oversampled ADC for Multi-Standard RFID Reader Receiver
Authors	1.W. Chou , AT&T Bell Lab. 2.Murray Hill, NJ, USA	1.Lukas Fujcik , BUT FEEC, Udolni 53, CZ-602 00 Brno, Czech Republic 2.Jiri Haze , BUT FEEC, Udolni 53, CZ-602 00 Brno, Czech Republic RadimirVrba , BUT FEEC, Udolni 53, CZ-602 00 Brno, Czech Republic 3.ThibaultMougel , South Queensferry, Edinburgh EH30 9TG, Scotland	1.Hin-Tat Chan 2.Hong Kong Univ. of Sci. & Technol., Hong Kong 3.Wenting Wang ; Chi Fung Lok ; Lau, V.K. ; Chi-yingTsui ;

Abstract	In this paper dithering inside the loop of sigma-delta and multistage sigma-delta modulators is studied. For a multistage sigma-delta modulation system, inside-the-loop dithering makes the quantization error white for a system with three stages.	The two-step quantization technique was utilized to design of sigma-delta modulator. Parameters of decimation filter are derived from the specifications of the overall sigma-delta modulator. The architecture of switched-capacitor (SC) sigma -delta modulator was designed with sampling jitter, noise, and operational amplifier parameters such as white noise, finite dc gain, finite bandwidth, slew rate and saturation voltages.	In this paper a highly reconfigurable mixed-signal architecture for channel select filtering with the help of oversampled delta-sigma modulator is implemented which allows the RFID reader to support multi-standard operating environment with low power consumption and silicon area for single-chip implementation compared with pure analog or digital channel select filtering approach.
Paper Name	Oversampled ADC based on pulse frequency modulator and TDC	24-bit Low-Power Low-Cost Digital Audio Sigma-Delta DAC	A Continuous Time Sigma Delta Modulator With Operational Floating Integrator
Authors	1. Hernandez, L. Electron. Technol. Dept., Carlos III Univ., Madrid, Spain 2. Gutierrez, E.	1.LIU Yuyu 2.GAO Jun 3.YANG Xiaodong	1.DragosDucu*, 2.AncaManolescu** *Microchip Technology, Bucharest Romania E-mail: dragos.ducu@microchip.com **"POLITEHNICA" University of Bucharest E-mail: ammanolescu@yahoo.com
Abstract	In this paper the ring oscillator is replaced by a pulse frequency modulator (PFM) that provides improved linearity at the expense of feedback and analogue amplification is proposed. Compared to the equivalent continuous time sigma-delta modulators, the PFM may be more tolerant to circuit impairments. In addition, the output data of the proposed architecture is a multibit sequence through the use of a time-to-digital converter TDC instead of a Flash quantiser or a multibit digital-to-analogue converter. A high dynamic range can be achieved without severe constraints on analogue mismatch or clock jitter.	This paper presents a low-power low-cost 24-bit Σ-Δ digital-to-analog converter (DAC) in which a 15-level quantizer, third-order, single-stage Σ-Δ modulator is employed to reduce the passband quantization noise, relax the out-of-band filtering requirements, and enhance immunity to clock jitter for portable digital audio applications. A direct charge transfer switched-capacitor low-pass filter (DCT-SC LPF) is used to reconstruct the analog signal to reduce the kT/C noise and capacitor mismatch effect with a small increase of the power dissipation. The chip was fabricated in the SMIC 0.13 μm 1P5M CMOS process. The cell area of the digital part is 0.056 mm2 and the total area of the analog part is 0.34 mm2. The supply voltage is 1.2 V for the digital circuit and 3.3 V for the analog circuit. The power consumption of the analog part is 3.5 mW. The audio DAC achieves a 100 dB dynamic range and an 84 dB peak signal-to-noise-plus-distortion ratio over a 20 kHz passband.	In this sigma delta convertor for implementation of integrators in loop filter, operational floating conveyors are employed. The modulator is designed in 0.18um TSMC CMOS technology and features low power consumption (<3mW), low supply voltage (±1.8), and wide dynamic range (>70db).
Paper Name	A high-performance accelerometer with a fifth-order sigma–delta modulator	First Order Sigma-Delta Modulator Of An Oversampling Adc Design In Cmos Using Floating Gate MOSFETS	Design Of First Order And Second Order Sigma Delta Analog To Digital Converter
Authors	1.Yufeng Dong, 2.Michael Kraft, 3.Carsten Gollasch and 4.William Redman-White	1.Syam Prasad SBS Kommana Bachelor of Technology, Nagarjuna University, 2001 December 2004	1.Vineeta Upadhyay and 2.Aditi Patwa Department of ECE, Amrita School of Engineering, Bangalore, Karnataka, India.
Abstract	a micromachined accelerometer fabrication is mentioned. The in-plane sensor with fully differential structure has a mechanical noise floor below 1 μg $Hz^{-1/2}$, static sensitivity 16 pF g^{-1} and resonant frequency 325 Hz. FEM analyses are performed to verify these key parameters. The silicon-on-glass sensor is fabricated by deep reactive ion etching (DRIE) and anodic bonding. Compared with a second-order electromechanical ΣΔM, which only uses the sensing element as a loop filter, here it is cascaded with additional electronic integrators to form a fifth-order electromechanical ΣΔM, which leads to better signal to quantization noise ratio (SQNR). This novel approach is analysed	A new architecture for a sigma-delta oversampling ADC in which the first order modulator is realized using the floating gate MOSFETs at the input stage of an integrator and the comparator has been implemented. The first order modulator is designed using an 8 MHz sampling clock frequency and implemented in a standard 1.5μm n-well CMOS process. The decimator is an off-chip sinc-filter and is programmed using the VERILOG and tested with Altera Flex EPF10K70RC240 FPGA board. The ADC gives an 8-bit resolution with a 65 kHz bandwidth.	This paper presents the design of a first order and second order single bit Sigma-Delta Analog-to-Digital Converter (ADC) which is realized using CMOS technology. In this paper, a first Order and Second order Sigma-Delta ADC is designed which accepts an input signal of frequency 1 KHz, an OSR of128, and 256 KHz sampling frequency .It is implemented in a standard 90nm CMOS technology. The ADC operates at 0.5V reference voltage. The Design and Simulation of the Modulator is done using H-spice. This paper firstly elaborates Summer, Integrator, Comparator, D-Latch and DAC which is integrated together to form.

	and system level simulations are presented. A printed circuit board (PCB) prototype of this high-order ΣΔM loop was built and tested.		
Paper Name	A 1.8-V digital-audio sigma-delta modulator in 0.8-µm CMOS (1997)	Design of Low Power Sigma Delta ADC	Digital Power Amplification Using Sigma-Delta Modulation and Bit Flipping
Authors	1.Shahriar Rabii , 2.Shahriar Rabii , 3.Bruce A. Wooley , 4.Shahriar Rabii , 5.Shahriar Rabii , 6.Bruce A. Wooley	1Mohammed Arifuddin Sohel, 2.Chenna Kesava Reddy, 3.Syed Abdul Sattar	1. Anthony J Macgrath, 2.Mark B. Sandler
Abstract	Oversampling techniques based on sigma-delta (ΣΔ) modulation offer numerous advantages for the realization of high-resolution analog-to-digital (A/D) converters in a low-voltage environment. This paper examines the design and implementation of a CMOS ΣΔ modulator for digital-audio A/D conversion that operates from a single 1.8-V power supply. A cascaded modulator that maintains a large full-scale input range while avoiding signal clipping at internal nodes is intduced. The experimental modulator has been designed with fully-differential (ΣΔ)switched-capacitor integrators employing different input and output common-mode levels and boosted clock drivers in order to facilitate low voltage operation. Precise control of common-mode levels, high power supply noise rejection, and low power dissipation are obtained through the use of two-stage, class A/AB operational amplifiers. At a sampling rate of 4 MHz and an oversampling ratio of 80, an implementation of the modulator in a 0.8-µm CMOS technology with metal-to-polycide capacitors and NMOS and PMOS threshold voltages of +0.65-V and –0.75-V, respectively, achieves a dynamic range of 99 dB at a Nyquist conversion rate of 50 kHz. The modulator can operate from supply voltages ranging from 1.5 V to 2.5 V, occupies an active area of 1.5 mm 2, and dissipates 2.5 mW from a 1.8-V supply.	A Low power discrete time sigma delta ADC consisting of a second order sigma delta modulator and third order Cascaded Integrated Comb (CIC) filter is proposed. The second order modulator is designed to work at a signal band of 20K Hz at an oversampling ratio of 64 with a sampling frequency of 2.56 MHz. It achieves a signal to noise ratio of 85.2dB and a resolution of 14 bits. The CIC digital filter is designed to implement a decimation factor of 64, operating at a maximum sampling frequency of 2.56 MHz. A second order sigma delta modulator is implemented in 0.18micron CMOS technology using full custom design and the third order digital CIC decimation filter is implemented in verilog HDL. The complete Sigma Delta ADC, consisting of analog block of second order modulator and digital block of decimator consumes a total power 1.96mW.	A data conversion technique suitable for digital power amplifiers (DPAs) is described, based on a modified sigma-delta modulator. The pulse-repetition frequency (PRF) in the bit stream is reduced in order to increase the efficiency in the power output switching stage. The system offers PRFs comparable to pulse-width-modulation (PWM)-based DPAs, but with higher linearity and more than a thirty-fold reduction in bit-clock frequency.

Paper Name	Design and Development of Sigma-Delta Modulator	Linearization of Thermocouple Signals by ADC	Second Order Sigma-Delta Modulator-a Linearizing unit of Thermocouple

Authors	1Lalita Yadav, 2Vedanta Kuri, 3Abir Chattopadhyay	Vedanta Kuri Abir Chattopadhyay	Vedanta Kuri, Abir Chattopadhyay
Abstract	A low cost, highly resolution analog to digital converter is being designed and developed in our laboratory. Based on characteristics, a comparative study of different ADC is being made. Sigma delta modulator has been chosen for its better latency and throughput.	A novel linearizing circuit for linearization of thermocouple signals by ADC has been designed and developed. Sigma-Delta ADC has been considered in this proposed simpler circuit. Computational studies carried on material gives satisfactory results for the thermocouple.	Linearization is necessary when sensors produce voltage signal that are not linearly related to the physical measurement. It is the process of interpreting the signals from the transducer and can be done either with signal conditioning orthrough software. Different linearization mechanisms are available. In this paper a sigma delta ADC [1-3] is used for linearization of thermocouple signals. Thermocouple signal are of Non-linear type. To convert Non-linear form to linear form, a second order sigma-delta ADC has been introduced and developed for much better accuracy. Computational analysis has been fulfilled for J and K type thermocouple.
Paper Name	A low power Delta-Sigma Modulator Using a Charge-Pump Integrator	Incremental Data Converters at Low Oversampling Ratios	A 12-bit 3.125 MHz Bandwidth 0–3 MASH Delta-Sigma Modulator
Authors	Alireza Nilchi, Student Member, David A Johns, Fellow, IEEE	Trevor C. Caldwell, *Student Member, IEEE*, and David A. Johns, *Fellow, IEEE*	Ahmed Gharbiya, *Member, IEEE*, and David A. Johns, *Fellow, IEEE*
Abstract	In this paper a low-power switched-capacitor integrator based on a capacitive charge-pump (CP) is presented. The 0.13 m CMOS prototype of the CP based ADC achieves the same performance as a conventional ADC while consuming 66% lower OTA power in the front-end integrator. The CP based modulator realizes 87.8 dB SNDR, 89.2 dB SNR and 90 dB DR over a 10 kHz bandwidth with 148 W power consumption. The conventional ADC has similar performance but dissipates 241 W. The energy required per conversion-step for the CP based ADC (0.369 pJ/step) is almost 40% lower than that of the conventional ADC (0.607 pJ/step).	In this paper the use of incremental A/D converters with low oversampling ratios is proposed. Incremental A/D converters are able to achieve a higher SQNR than delta-sigma modulators at oversampling ratios below 4, allowing them to operate as higher bandwidth converters with medium resolution. The impact of removing the input S/H, as well as analyzing their behaviour at an OSR as low as 1 is explored. An eighth-order cascaded incremental A/D converter is analyzed and shown as an example.	In this paper a 12-bit 0–3MASHdelta-sigma modulator with a 3.125 MHz bandwidth in a 0.18 m CMOS technology is implemented. The modulator has an oversampling ratio of 8 (clock frequency of 50 MHz) and achieves a peak SNDR of 73.9 dB (77.2 dB peak SNR) and consumes 24mWfrom a 1.8 V supply. For comparison purposes, the modulator can be re-configured as a single-loop topology where a peak SNDR of 64.5 dB (66.3 dB peak SNR) is obtained with 22 mW power consumption. The energy required per conversion step for the 0–3MASHarchitecture (0.95 pJ/step) is less than half of that required by the feedback topology (2.57 pJ/step).
Paper Name	Combining Multipath and Single-Path Time-Interleaved Delta-Sigma Modulators	On The Implementation of Input-Feedforward Delta–Sigma Modulators	A Time-Interleaved Continuous-Time ΔΣ Modulator With 20-MHz Signal Bandwidth
Authors	Ahmed Gharbiya and David A. Johns	Ahmed Gharbiya, *Student Member, IEEE*, and D. A. Johns, *Fellow, IEEE*	Trevor C. Caldwell, *Student Member, IEEE*, and David A. Johns, *Fellow, IEEE*

Abstract	Here single-path time-interleaved delta-sigma modulators are analyzed and evaluated. It is found that finite opamp gain and bandwidth result in a mismatch between the noise transfer functions of the internal quantizers which degrades the performance of the architecture. A hybrid topology where the first stage uses multiple integrators while the rest of the modulator uses a single path of integrators is proposed to mitigate the mismatch problem.	Here some practical issues on the implementation of the input-feedforward delta–sigma modulators has been proposed. First, the timing constraint imposed by the input-feedforward path is identified and a possible method to relax the constraint is proposed. Second, the drawbacks of the analog adder needed before the quantizer are explained and a method to eliminate the adder is proposed.	In this paper the first implementation results for a time-interleaved continuous-time $\Delta\sum$modulator is implemented. The derivation of the time-interleaved continuous-time $\Delta\sum$ modulator from a discrete-time $\Delta\sum$ modulator is presented. With various simplifications, the resulting modulator has only a single path of integrators, making it robust to DC offsets. A time-interleaved by 2 continuous-time third-order low-pass $\Delta\sum$ modulator is designed in a 0.18- m CMOS technology with an oversampling ratio of 5 at sampling frequencies of 100 and 200 MHz. Experimental results show that a signal-to-noise-plus-distortion ratio (SNDR) of 57 dB and a dynamic range of 60 dB are obtained with an input bandwidth of 10 MHz, and an SNDR of 49 dB with a dynamic range of 55 dB is attained with an input bandwidth of 20 MHz. The power consumption is 101 and 103 mW, respectively.
Paper Name	High-Speed Oversampling Analog-To-Digital Converters	Time-Interleaved Oversampling A/D Converters: Theory and Practice	Design and Analysis of Delta-Sigma Based IIR Filters
Authors	Ahmed Gharbiya, Trevor C. Caldwell, And D. A. Johns Department of Electrical and Computer Engineering, University of Toronto 10 King's College Rd., Toronto, Ontario, CANADA, M5S 3G4	Ramin Khoini-Poorfard, *Member, IEEE,* Lysander B. Lim, *Member, IEEE,* and David A. Johns, *Senior Member, IEEE*	David A. Johns, and David M. Lewis, Member IEEE
Abstract	This paper is mainly tutorial in nature and discusses architectures for oversampling converters with a particular emphasis on those which are well suited for high frequency input signal bandwidths. The first part of the paper looks at various architectures for discrete-time modulators and looks at their performance when attempting high speed operation. The second part of this paper presents some recent advancement in time-interleaved oversampling converters. The next section describes the design and challenges in continuous-time modulators. Finally, conclusions are made and a brief summary of the recent state of the art of high-speed converters is presented.	In this paper, the design procedure and practical issues regarding the realization of time-interleaved oversampling converters are presented. Using the concept of block digital filtering, it is shown that arbitrary $\Delta\sum$ topologies can be converted into corresponding time-interleaved structures. Practical issues such as finite op amp gain, mismatching, and dc offsets are addressed, analyzed and practical solutions to overcome some of these problems are discussed. To verify the theoretical results, a discrete-component prototype of a second-order time-interleaved $\Delta\sum$ analog/digital (A/D) converter has been implemented and the design details as well as experimental results are presented.	This paper presents design techniques for IIR filters operating on oversampled delta-sigma ($\Delta\sum$) modulated signals. It is shown that $\Delta\sum$ -based IIR filters can be efficiently realized by eliminating all multibit multipliers through the use of re-modulating internal filter states. As well, noise results are presented showing that linear noise analysis gives excellent predictions of the noise performance over the frequency band of interest. Finally it is shown that latency and computational complexity can be reduced in some VLSI applications where digital representations of analog signals exists using oversampled $\Delta\sum$ converters.
Paper Name	Analysis of a sigma delta modulator with a multi-level quantizer and single-bit feedback.	A low power continuous time band pass sigma delta modulator using linearity enhanced OTA	Stable Delta-Sigma Modulator with Signal Dependent Forward Path Gain for Industrial Applications
Authors	1.S.J. Park , Dept. of Electr. Eng., Stanford Univ., CA, USA 2.R.M. Gray , Dept. of Electr. Eng., Stanford Univ., CA, USA 3.W. Chou , Electron. Res. Lab., Salisbury, SA, Australia	1.Sohel, M.A. ; 2.Keshava Reddy, K.C. ; 3. Naaz, M. ; 4. Naseeb, M.A.	1. K. Diwakar, 2. K. Aanandha Saravanan, 3. C. Senthilpari

Abstract	Quantization error of the single-loop single-stage sigma-delta modulator with a multilevel quantizer and single-bit feedback has been analysed.	In this paper a low power continuous-time bandpass fourth order sigma delta modulator over 5 MHz band has been implemented which is operating at a Sampling Frequency of 280MHz. Source degeneration technique is used to linearized the operational transconductance amplifier (OTA) . It is observed that Signal to Quantization Noise Ratio (SQNR) with a non-linear OTA is of 46.6dB and it is 55.07dB with a Source degenerated OTA showing a marked increase of 1.5 bits(9 dB) in resolution of modulator. Further, optimum transistor sizing leads to a very low power consumption of 10.9mW and a figure of merit of 2.445pJ/bit.	In this paper stable Delta-Sigma Modulator with Signal Dependent Forward Path Gain has been discussed. The existing second order, single stage, single bit, unity feedback gain , discrete DSM cannot be used for the normalized full range (-1 to +1) of an input signal since the DSM becomes unstable when the input signal is above ±0.55. The stability is also not guaranteed for input signals of amplitude less than ±0.55. In the present paper, the above mentioned second order DSM is modified with input signal dependent forward path gain. The proposed DSM is suitable for industrial applications where one needs the digital representation of the analog input signal, during each sampling period. The proposed DSM can operate almost for the full range of input signals (-0.95 to +0.95) without causing instability, assuming that the second integrator output should not exceed the circuit supply voltage, ±15 Volts.

CONCLUSION

Sigma-delta ADCs and DACs have proliferated into many modern applications including measurement, voice band, audio, etc. The technique takes full advantage of low cost CMOS processes and therefore makes integration with highly digital functions such as practical applications in DSP. Modern techniques such as the multi-bit data scrambled architecture minimize problems with idle tones which plagued early Σ-Δ products. Resolutions up to 24-bits are currently available and the requirements on analog anti-aliasing /anti-imaging filters are greatly relaxed due to oversampling. The internal digital filter in audio Σ-Δ ADCs can be designed for linear phase, which is a major requirement in those applications. High resolution Σ-Δ ADCs designed for measurement applications, the digital filter is generally designed so that zeros occur at the mains frequencies of 50 Hz and 60 Hz.

Many Σ-Δ converters offer a high level of user programmability with respect to output data rate, digital filter characteristics, and self-calibration modes. Multichannel Σ-Δ ADCs are now available for data acquisition systems, and most users are well-educated with respect to the settling time requirements of the internal digital filter in these applications.[1]

REFERENCES:

[1] Lalita Yadav, Vedanta Kuri, Abir Chattopadhyay, "Design and Development of Sigma-Delta Modulator",IJECT-VOL V ISSUE SPL II, JAN TO MARCH. 2014, ISSN : 2230-7109 (Online) | ISSN : 2230-9543 (Print)

[2] Vedanta Kuri, Abir Chattopadhyay, "Second Order Sigma-Delta Modulator-a Linearizing unit of Thermocouple", IJEECE-ISSN:0975-4814(Print),2014

[3] Ahmed Gharbiya, a student member, IEEE, and David A. Johns, Fellow, IEEE, "On The Implementation Of Input Feed Forward Delta Sigma Modulation", IEEE Transaction Circuits and systems, Express Briefs, Vol. 53, No. 6, June 2006.

[4] Aliriza Nilchi, a student member, IEEE, and David A.Johns, Fellow, IEEE, "A Low Power Delta Sigma Modulation Using A Charge Pump Integrator", IEEE Transaction Circuits and systems- Regular Papers, vol. 60, No. 5, May 2013.

[5] Ahmed Gharbiya, a student member, IEEE, and David A. Johns, Fellow, IEEE, "On The Implementation Of Input Feed Forward Delta Sigma Modulation", IEEE Transaction Circuits and systems, Express Briefs, Vol. 53, No. 6, June 2006.

[6] Sohel, M.A. ; Muffakham Jah Coll. of Eng. & Tech., Hyderabad, India ; Reddy, K.C.K. ; Sattar, S.A. ; Jabeen, S. , "A 15 Bit 95 dB Low Power Discrete Time Sigma Delta Modulator", International Conference on Computing Sciences (ICCS), 2012,Page(s):245 - 248 ,Print ISBN:978-1-4673-2647-6 ,INSPEC Accession Number:13221218 ,Conference Location :Phagwara DOI:10.1109/ICCS.2012.1 ,Publisher:IEEE

[7] Sohel, M.A. ; ECED, Muffakham Jah Coll. of Eng. & Technol., Hyderabad, India ; Keshava Reddy, K.C. ; Naaz, M. ; Naseeb, M.A., Microelectronics and Electronics (PrimeAsia), "A low power continuous time band pass sigma delta modulator using linearity enhanced OTA ", 2013 IEEE Asia Pacific Conference on Postgraduate Research in ,Page(s):1 - 6 ,Print ISBN:978-1-4799-2750-0,INSPECAccessionNumber:14080008,ConferenceLocation:Visakhapatnam ,DOI:10.1109/PrimeAsia.2013.6731168 ,Publisher:IEEE

[8] Fujcik, L. ; Dept. of Microelectron., Brno Univ. of Technol., Brno ; Vrba, R. , "Bandpass Sigma-Delta Modulator for Sensor Signal Processing", Fourth International Conference on Systems, 2009. ICONS '09.,Page(s):179 - 183 ,E-ISBN :978-0-7695-3551-7 ,Print ISBN:978-1-4244-3469-5 ,INSPEC Accession Number:10665837 ,DOI:10.1109/ICONS.2009.38 ,Publisher:IEEE

[9] K. DIWAKAR, C. SENTHILPARI and AJAY KUMAR SINGH, "Highly Stable Delta-Sigma Modulator for industrial applications", IEICE Electron.Express,Vol.5,No.15,pp.530-536,(2008) [CrossRef]

[10] Yamei Li and Lili He. San Jose State University. Department of Electrical Engineering. San Jose, CA. "*First-order Continuous-time Sigma-delta Modulator"*. 8th International Symposium on Quality Electronic Design, 2007. ISQED '07. Page(s):229 – 232,Print ISBN:0-7695-2795-7 ,INSPEC Accession Number:9454490 ,DOI:10.1109/ISQED.2007.77 ,Publisher:IEEE

[11] Chou, W. ; AT&T Bell Lab., Murray Hill, NJ, USA, "Sigma delta and multi-stage sigma delta modulation with inside loop dithering",International Conference on Acoustics, Speech, and Signal Processing, 1991. ICASSP-91., 1991 ,Page(s):1953 - 1956 vol.3 ,ISSN :1520-6149 ,Print ISBN:0-7803-0003-3,INSPEC Accession Number:4169218 .DOI:10.1109/ICASSP.1991.150771 ,Publisher:IEEE

[12] Fujcik, L. ; BUT FEEC, Udolni 53, CZ-602 00 Brno, Czech Republic ; Haze, J. ; Vrba, R. ; Mougel, T., "Modeling and design of novel architecture of multibit switched-capacitor sigma-delta converter with two-step quantization process", International Conference on Networking, International Conference on Systems and International Conference on Mobile Communications and Learning Technologies, 2006. ICN/ICONS/MCL 2006. ,Page(s):186 ,Print ISBN:0-7695-2552-0 ,DOI:10.1109/ICNICONSMCL.2006.149 ,Publisher:IEEE

[13] Hin-Tat Chan ; Hong Kong Univ. of Sci. & Technol., Hong Kong ; Wenting Wang ; Chi Fung Lok ; Lau, V.K. more authors, "A Mixed-Signal Architecture of Channel Select Filtering with Oversampled ADC for Multi-Standard RFID Reader Receiver", Published in: IEEE International Conference on RFID, 2007. Page(s):108 - 114 ,E-ISBN :1-4244-1013-4 ,Print ISBN:1-4244-1013-4 ,INSPEC Accession Number:9702158 ,DOI:10.1109/RFID.2007.346157 ,Publisher:IEEE

[14] Hernandez L. ; Electron. Technol. Dept., Carlos III Univ., Madrid, Spain ; Gutierrez E., "Oversampled ADC based on pulse frequency modulator and TDC", Published in:Electronics Letters (Volume:50 , Issue: 7) ,Page(s):498 - 499 ,ISSN :0013-5194 ,INSPEC Accession Number:14181196 ,DOI:10.1049/el.2013.3006 ,Date of Current Version :03 April 2014 ,Issue Date :March 27 2014 ,Sponsored by :Institution of Engineering and Technology ,Publisher:IET

[15] Liu, Yuyu; Gao, Jun; Yang, Xiaodong, "24-bit Low-Power Low-Cost Digital Audio Sigma-Delta DAC", TSINGHUA SCIENCE AND TECHNOLOGY,ISSN:1007-0214,12/17,pp74-82 ,Volume16,Number1,February2011

[16] Ducu, D.; Manolescu, A. , "A Continuous Time Sigma Delta Modulator With Operational Floating Integrator", 2012 International Semiconductor Conference (CAS),Year: 2012, Volume: 2 ,Pages: 463 - 466, DOI: 10.1109/SMICND.2012.6400729

[17] Yufeng Dong, Michael Kraft, Carsten Gollasch and William Redman-White, "A high-performance accelerometer with a fifth-order sigma–delta modulator", TB, RM, JMM/190438, 30/03/2005 INSTITUTE OF PHYSICS PUBLISHING JOURNAL OF MICROMECHANICS AND MICROENGINEERING, J. Micromech. Microeng. 15 (2005) 1–8 , doi:10.1088/0960-1317/15/0/000

[18] Syam Prasad SBS Kommana, Bachelor of Technology, Nagarjuna University, "First Order Sigma-Delta Modulator Of An Oversampling Adc Design In Cmos Using Floating Gate MOSFETS", 2001 December 2004,

[19] Vineeta Upadhyay and Aditi Patwa ,Department of ECE, Amrita School of Engineering, Bangalore, Karnataka, India., "Design Of First Order And Second Order Sigma Delta Analog To Digital Converter", International Journal of Advances in Engineering & Technology, July 2012. ©IJAET ,ISSN: 2231-1963

[20] Rabii, S. ; Center for Integrated Syst., Stanford Univ., CA, USA ; Wooley, B.A., "A 1.8-V digital-audio sigma-delta modulator in 0.8-µm CMOS (1997)",Published in:Solid-State Circuits, IEEE Journal of (Volume:32 , Issue: 6) ,Page(s):783 – 796,ISSN :0018-9200 ,INSPEC Accession Number:5598329 ,DOI:10.1109/4.585245 Date of Publication :Jun 1997 ,Date of Current Version :06 August 2002 Issue Date :Jun 1997 ,Sponsored by :IEEE Solid-State Circuits Society ,Publisher:IEEE .

[21] 1Mohammed Arifuddin Sohel, 2K. Chenna Kesava Reddy, 3Syed Abdul Sattar , "Design of Low Power Sigma Delta ADC", International Journal of VLSI design & Communication Systems (VLSICS) Vol.3, No.4, August 2012

1. Anthony J Macgrath, 2.Mark B. Sandler , "Digital Power Amplification Using Sigma-Delta Modulation and Bit Flipping", JAES Volume 45 Issue 6 pp. 476-487; June 1997

[22] Nilchi, A. ; Dept. of Electr. & Comput. Eng., Univ. of Toronto, Toronto, ON, Canada ; Johns, D.A., "A low power Delta-Sigma Modulator Using a Charge-Pump Integrator", IEEE Transactions on Circuits and Systems I: Regular Papers, (Volume:60 , Issue: 5) ,Page(s):1310 - 1321 ,ISSN :1549-8328 ,INSPEC Accession Number:14159165 ,DOI:10.1109/TCSI.2012.2220462 ,Date of Publication :21 December 2012 ,Date of Current Version :24 April 2013 ,Issue Date : May 2013 ,Sponsored by :IEEE Circuits and Systems Society ,Publisher:IEEE .

[23] Caldwell, T.C. ; Dept. of Electr. & Comput. Eng., Univ. of Toronto, Toronto, ON, Canada ; Johns, D.A., "Incremental Data Converters at Low Oversampling Ratios", IEEE Transactions on Circuits and Systems I: Regular Papers, (Volume:57 , Issue: 7) ,Page(s):1525 - 1537 ,ISSN :1549-8328 ,INSPEC Accession Number:11416856 ,DOI:10.1109/TCSI.2009.2034879 ,Date of Publication :31 December 2009 ,Date of Current Version :19 July 2010 ,Issue Date :July 2010 ,Sponsored by :IEEE Circuits and Systems Society ,Publisher:IEEE .

[24] Gharbiya, A. ; Dept. of Electr. & Comput. Eng., Univ. of Toronto, Toronto, ON ; Johns, D.A., "A 12-bit 3.125 MHz Bandwidth 0–3 MASH Delta-Sigma Modulator", 34th European Solid-State Circuits Conference, 2008. ESSCIRC 2008. ,Date of Conference:15-19 Sept. 2008 ,Page(s):206 - 209 ,ISSN :1930-8833 ,E-ISBN :978-1-4244-2362-0 ,Print ISBN:978-1-4244-2361-3 ,INSPEC Accession Number:10394723 ,Conference Location : Edinburgh ,DOI:10.1109/ESSCIRC.2008.4681828 ,Publisher:IEEE .

[25] Gharbiya, A. ; Dept. of Electr. & Comput. Eng., Univ. of Toronto, Toronto, ON ; Johns, D.A., "Combining Multipath and Single-Path Time-Interleaved Delta-Sigma Modulators", IEEE Transactions on Circuits and Systems II: Express Briefs, (Volume:55 , Issue: 12) ,Page(s):1224 - 1228 ,ISSN :1549-7747 ,INSPEC Accession Number:10362596 ,DOI:10.1109/TCSII.2008.2008062 ,Date of Publication : Dec. 2008 ,Date of Current Version : 22 December 2008 ,Issue Date : Dec. 2008 ,Sponsored by : IEEE Circuits and Systems Society ,Publisher:IEEE .

[26] Gharbiya, A. ; Dept. of Electr. & Comput. Eng., Toronto Univ., Ont. ; Johns, D.A., "On The Implementation of Input-Feedforward Delta–Sigma Modulators", IEEE Transactions on Circuits and Systems II: Express Briefs, (Volume:53 , Issue: 6) ,Page(s):453 - 457 ,ISSN :1549-7747 ,INSPEC Accession Number:8954931 ,DOI:10.1109/TCSII.2006.873829 ,Date of Publication :June 2006 ,Date of Current Version :19 June 2006 ,Issue Date :June 2006 ,Sponsored by :IEEE Circuits and Systems Society ,Publisher:IEEE .

[27] Caldwell, T.C. ; Dept. of Electr. & Comput. Eng., Toronto Univ., Ont. ; IEEE Journal of Johns, D.A., "A Time-Interleaved Continuous-Time ΔΣ Modulator With 20-MHz Signal Bandwidth", Solid-State Circuits, (Volume:41 , Issue: 7) ,Page(s): 1578 - 1588 ,ISSN :0018-9200 ,INSPEC Accession Number:9010804 ,DOI:10.1109/JSSC.2006.873889 ,Date of Publication :,July 2006 ,Date of Current Version :26 June 2006 ,Issue Date :July 2006 ,Sponsored by :IEEE Solid-State Circuits Society ,Publisher:IEEE .

[28] AHMED GHARBIYA, TREVOR C. CALDWELL, AND D. A. JOHNS, "High-Speed Oversampling Analog-To-Digital Converters", International Journal of High Speed Electronics and Systems,2005

[29] Khoini-Poorfard, R. ; Dept. of Electr. & Comput. Eng., Toronto Univ., Ont., Canada ; Lim, L.B. ; Johns, D.A., "Time-Interleaved Oversampling A/D Converters: Theory and Practice", IEEE Transactions on Circuits and Systems II: Analog and Digital Signal Processing, (Volume:44 , Issue: 8) ,Page(s):634 - 645 ,ISSN :1057-7130 ,INSPEC Accession Number:5682870 ,DOI:10.1109/82.618037 ,Date of Publication :Aug 1997 ,Date of Current Version :06 August 2002 ,Issue Date :Aug 1997 ,Sponsored by :IEEE Circuits and Systems Society ,Publisher:IEEE .

[30] Johns, D.A. ; Dept. of Electr. Eng., Toronto Univ., Ont., Canada ; Lewis, D.M., "Design and Analysis of Delta-Sigma Based IIR Filters", IEEE Transactions on Circuits and Systems II: Analog and Digital Signal Processing, (Volume:40 , Issue: 4) ,Page(s):233 - 240 ,ISSN :1057-7130 ,INSPEC Accession Number: 4492213 ,DOI:10.1109/82.224314 ,Date of Publication :Apr 1993 ,Date of Current Version :06 August 2002 ,Issue Date :Apr 1993 , Sponsored by : IEEE Circuits and Systems Society ,Publisher:IEEE .

[31] Sang Ju Park ; Dept. of Electr. Eng., Stanford Univ., CA, USA ; Gray, R.M. ; Chou, W., "Analysis of a sigma delta modulator with a multi-level quantizer and single-bit feedback.", International Conference on Acoustics, Speech, and Signal Processing, 1991. ICASSP-91., 1991 ,Date of Conference:14-17 Apr 1991 ,Page(s):1957 - 1960 vol.3 ,ISSN : 1520-6149 ,Print ISBN: 0-7803-0003-3 ,INSPEC Accession Number:4169219 ,Conference Location : Toronto, Ont. ,DOI:10.1109/ICASSP.1991.150773 ,Publisher:IEEE .

[32] Sohel, M.A. ; ECED, Muffakham Jah Coll. of Eng. & Technol., Hyderabad, India ; Keshava Reddy, K.C. ; Naaz, M. ; Naseeb, M.A., "A low power continuous time band pass sigma delta modulator using linearity enhanced OTA", Asia Pacific Conference on Postgraduate Research in Microelectronics and Electronics (PrimeAsia), 2013 IEEE ,Date of Conference: 19-21 Dec. 2013,Page(s):1 - 6 ,Print ISBN:978-1-4799-2750-0 ,INSPEC Accession Number:14080008 ,Conference Location :Visakhapatnam ,DOI: 10.1109/PrimeAsia.2013.6731168 ,Publisher:IEEE .

[33] W.L. Lee, C.G. Sodini,"A Topology for Higher-Order Interpolative Coders", ISCAS PROC. 1987.

[34] P.F. Ferguson, Jr., A. Ganesan, R. W. Adams,"One-Bit Higher Order Sigma-Delta A/D Converters", ISCAS PROC. 1990, Vol. 2, pp. 890-893.

[35] Wai Laing Lee,"A Novel Higher Order Interpolative Modulator Topology for High Resolution Oversampling A/D Converters, MIT Masters Thesis, June 1987.

[36] R. W. Adams,"Design and Implementation of an Audio 18-Bit Analogto-Digital Converter Using Oversampling Techniques", J. Audio Engineering Society, Vol. 34, March 1986, pp. 153-166.

[37] P. Ferguson, Jr., A. Ganesan, R. Adams, et. al.,"An 18-Bit 20-kHz Dual Sigma-Delta A/D Converter", ISSCC Digest of Technical Papers, February 1991.

[38] Robert Adams, Khiem Nguyen, Karl Sweetland,"A 113 dB SNR Oversampling DAC with Segmented Noise- Shaped Scrambling", ISSCC Digest of Technical Papers, Vol. 41, 1998, pp. 62, 63, 413. (describes a segmented audio DAC with data scrambling).

[39] Vedanta Kuri,Abir Chattopadhyay, "Linearization of Thermocouple Signals by ADC", ISSN: 2348-3385,International Journal: Adamas Technical Review, Vol. 1, No. 1, July 2014.

[40] [41] 1. K. Diwakar, 2.K. Aanandha Saravanan, 3. C. Senthilpari, "Stable Delta-Sigma Modulator with Signal Dependent Forward

[41] Path Gain for Industrial Applications", International Journal of Electrical, Computer, Energetic, Electronic and Communication

[42] Engineering Vol:8, No:9, 2014.

International Journal of Engineering Research and General Science Volume 3, Issue 5, September-October, 2015
ISSN 2091-2730

Architecture For Hiding Projected & Compressed Text In Digital Image Using Spread Spectrum Technique

Aditi Soni, Sujit K. Badodia

SVITS, Indore, India, aditisoni519@gmail.com, +917879633219

Abstract— The art of information hiding has received lots of attention in the recent years as security of information has become a big concern in this internet epoch. As sharing of sensitive information through a common communication channel has become unavoidable, Steganography is the science and art of hiding information. Steganography means hiding a secret message (the embedded message) within a file (source cover) in such a way that an observer will not be able to detect the presence of contents of the hidden message. In this paper, proposed data hiding method that utilizes Projection of the letters, then compression of that letters with spread spectrum image Steganography technique. Experimental results show that the proposed method can bury a large amount of secret data while keeping very high security, as when the message is decrypted.

Keywords— Steganography, Projection, Compression, Data hiding, Angle, Cover, Stego

INTRODUCTION

Steganography or Stego is often referred to in the IT community, which means, "covered writing" and it is derived from the Greek language. It is defined by Markus Kahn as follows, "Steganography is the science and art of communicating in a way which hides the existence of the message. In Cryptography, the enemy is allowed and able to detect, intercept and modify messages without being able to offend certain security premises guaranteed by a cryptosystem, the main aim of Steganography is to conceal messages inside other messages in a way that does not permit any enemy to even detect that there is a something fishy in message".

In a digital world, Steganography and Cryptography are both intended to secure information from the parties to which we don't want to share the information. Steganography can be used in a different types of data formats in the digital world of nowadays. The most well-liked data formats used are .bmp, .doc, .gif, .jpeg, .mp3, .txt and .wav. Used because of their fame on the Internet, ease of use of the steganographic tools that use these data formats and also due to the ease by which redundant or noisy data can be removed from them and replaced with a hidden message.

Steganography can be used to conceal important data inside another file so that the parties intended to get the message knows the presence of secret message. The general model of data hiding can be described in Fig 1. The embedded data is the message that one wants to send in secret.

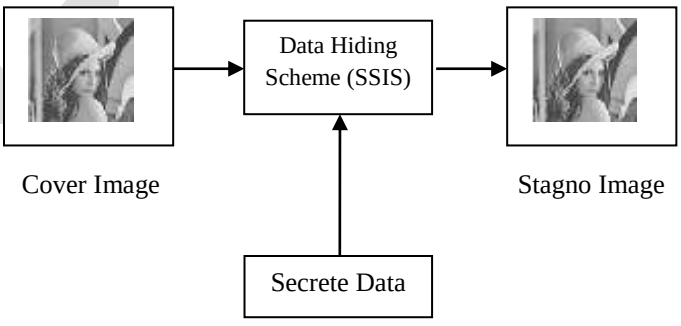

Fig 1. Data Hiding Scheme

CLASSIFICATION OF STEGANOGRAPHY METHODS

Steganography methods can be divided mainly into six categories.

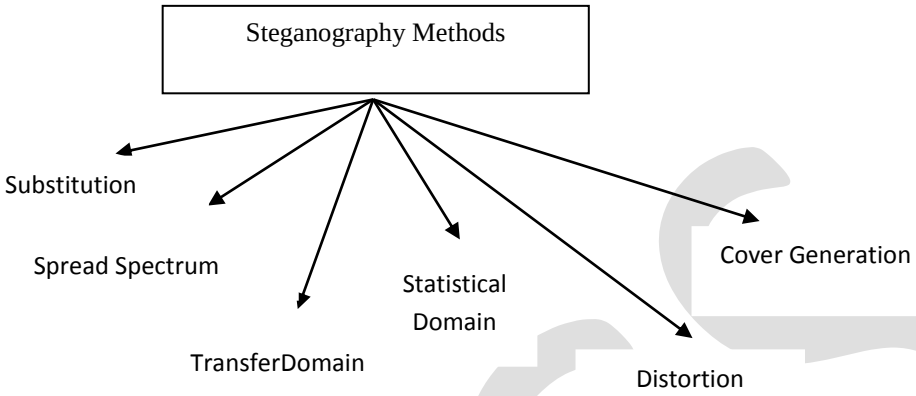

Fig 2 Classification of Steganography Methods

- Substitution methods substitute unneeded parts of a cover with a secret message (spatial domain).
- Transform domain techniques implant secret information in a transform space of the signal (frequency domain)
- Spread spectrum techniques takes the ideas from spread spectrum communication.
- Statistical methods encode information by varying several statistical properties of a Cover and utilize hypothesis testing in the withdrawal process.
- Distortion techniques stock up information by signal distortion and determine the deviation from the original cover in the decoding step.
- Cover generation methods encode information in the way a cover for secret communication is created.

The Spread Spectrum Image Steganography (SSIS) of the present discovery is a data hiding/secret communication steganographic system which uses digital imagery as a cover signal. The method on which we are doing survey i.e. Spread spectrum, it provides the ability to hide a significant abundance of information bits within digital images while avoiding detection by an observer. The message is recovered with lowest error probability due the use of error control coding. Spread spectrum image Steganography consignment is, at a minimum, an order of magnitude greater than of existing watermarking techniques. Furthermore, the original image is not necessary to extract the concealed message. The proposed receiver need only possess a key in order to reveal the secret message. The existence of the hidden information is virtually undetectable by human or computer analysis. At last, SSIS provides resiliency to transmission noise, like which found in a wireless environment and low levels of compression.

PROBLEM DEFINITION

There are many steganography techniques which are capable of hiding data within an image. These steganography techniques can be classified into two categories based on their algorithms: (1) spatial domain based techniques; (2) transform domain based techniques. Different methods were used for Hiding data. All the methods are used to increase the security. The most widely used technique to hide data is the usage of the LSB. The existing techniques are generally based on LSB (Least Significant Bit) where LSBs of the cover file are directly changed with message bits.

Ki-Hyun Jung et. al proposed the semi-reversible data hiding method based on interpolation and LSB substitution. Initially, interpolation methods are used to scale up and down the cover image before hiding secret data in it for a better capacity and quality. Secondly, the LSB substitution method is used to bury secret data. The most common Steganography techniques that used are least significant bit (LSB) substitution and pixel-value differencing (PVD). LSB substitution replaces the least significant bit with a secret bit stream. LSB matching is either added or subtracted randomly from the pixel value of the cover data when the embedding bit does

not match. The interpolation is a method of constructing new data points within the range of a different set of known data points in the mathematical field of numerical analysis. In the interpolation method, the size of the image is changed so that the hackers easily guess that something is fishy in that image. And the LSB technique is the common technique so that Robustness against statistical attacks and Robustness against image manipulation may destroy the hidden message. It is required for Steganography algorithms to be robust against malicious changes to the image.

LITERATURE REVIEW

- ☑ In Reference [1], **Ki-Hyun Jung et. al [2014]** this proposed the semi-reversible data hiding method based on interpolation and then LSB substitution. The interpolation method has been preprocessed before hiding secret data for aiming the higher capacity and good quality. Then, the LSB substitution method was applied for burying secret data. The cover image with the scaled down size and secret data could be extracted from the stego-image and any extra information is also not used. The experimental results showed that the average PSNR was 43.94 dB and the capacity was 393,216 bits when k=3. In the case of k=4, we demonstrated that the PSNR and capacity were 37.54 dB and 589,824 bits, respectively.
- ☑ In Reference [2], **Mehdi Hussain et.al. [2013]** gave an overview of different Steganography techniques and its major types and classification of Steganography which have been proposed in the literature during last few years. We have critical analyzed different intended techniques which show that visual quality of the image is degraded when hidden data increased from desired limit using LSB based methods. And many of them embedding techniques can be changed or shows indication of modification of image by careful analysis of the statistical properties of noise or perceptually analysis.
- ☑ In Reference [3], **Atallah M. et. al. [2012]** proposes a new Steganography technique which was presented, implemented and analyzed. The proposed method hides the secret message based on searching about the matching bits between the secret messages and image pixels values. The proposed method was compared with the LSB benchmarking method for hiding the secret message which hide the secret message directly in the least two significant bits of the image pixels.
- ☑ In Reference [4], **Mamta Juneja et. al. [2014]** proposed technique achieves the goal of an implementation of new steganography approach for images which integrates three new techniques a) Hybrid feature (line/edge/boundary/circle) detector technique integrating Canny and Enhanced Hough modify for bifurcating an image into edge and smooth areas b) Two Component based LSB Substitution Technique for hiding encrypted messages in edges of images c) Adaptive LSB substitution technique for hiding messages to smooth areas. It achieves the target of 50% hiding capacity and Imperceptibility(PSNR value) with minimum MSE(mean square error)while hiding more data on edges than smooth areas as edges being high in contrast, color, density, frequency and other noise disturbances can tolerate more changes in their pixel values than smooth areas.
- ☑ In Reference [6], **Chan CK et. Al. [2004]** proposed a data hiding scheme by simple LSB substitution. By applying an optimal pixel tuning process to the stego-image obtained by the simple LSB substitution method, the image quality of the stego-image can be seriously improved with low extra computational complexity. The worst case mean-square-error between the stego-image and the cover-image is derived.
- ☑ In Reference [7], Ming-Ni WuMin-Hui Lin proposed the LSB substitution and genetic algorithm (GA) to build up two different optimal substitution strategies: one is the worldwide optimal substitution strategy and the otherone is the local optimal substitution strategy. The experimental results confirm that our methods can provide superior image quality than the simple LSB and Wang et al.'s method do while provide large hiding capacity.

METHODOLOGY

A data hiding method that utilizes Projection of the letters, then compression of text and then data hiding using spread spectrum technique is proposed. The projection part is done by rotating the letters one by one by 85°. Then compression part can be done so that large amount of data can be hiding. Then at last Spread Spectrum Image Steganography (SSIS) is used. Spread spectrum

image Steganography payload is, at a minimum, an order of magnitude greater than of existing watermarking techniques. Furthermore, the original image is not needed to extract the hidden message. The proposed receiver need only possess a key in order to disclose the secret message. The existence of the hidden information is virtually untraceable by human or computer analysis. at last, SSIS provides resiliency to transmission noise, like which found in a wireless environment and low levels of compression

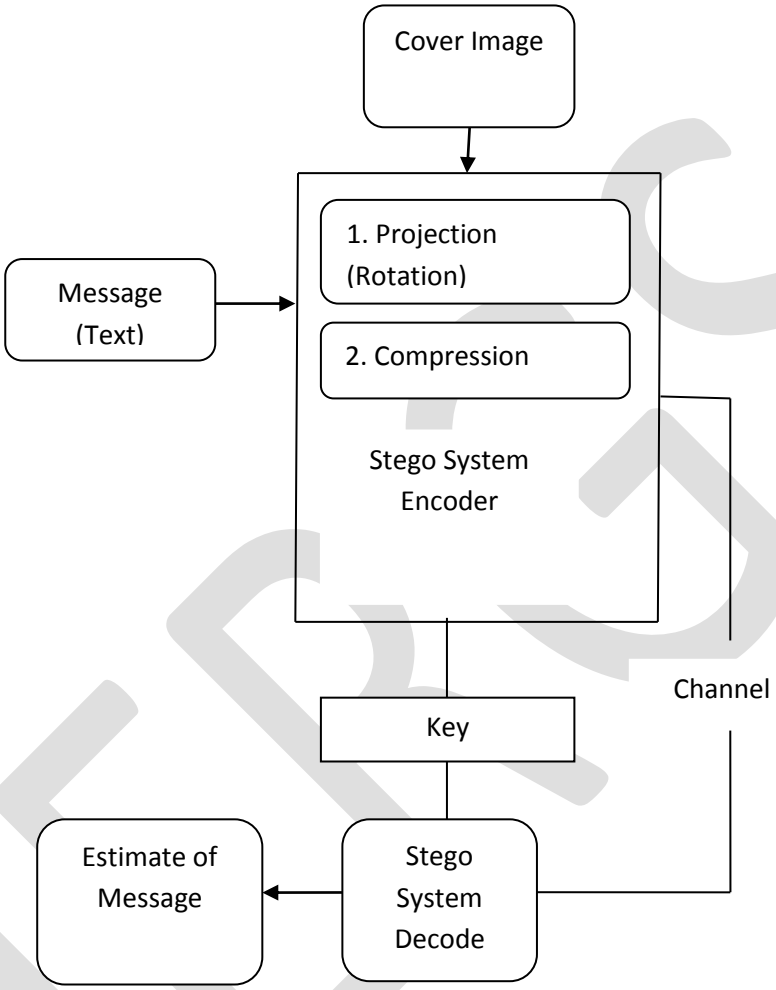

Fig 3 Block Diagram of Proposed System

Fig 3 shows that the sender initiate the message as text for appending on the cover image then it processed with the help of the projection which means that it will be rotated by 85^0 so that letters are tilted and meaning of the letters are change. It will helpful for our method and after this compression will be done. This data uploaded or merge with the cover image and that image not distorted in any manner. Send it to the receiver with the secure channel and at the end of the receiver key used for the decryption of the data and successfully receive the data.

CONCLUSION

In this paper, planned data hiding method that utilizes Projection of the letters, then compression of that letters and then Hiding the data with spread spectrum image Steganography technique. Also give an overview of different types of Steganography techniques, classification of Steganography which have been proposed in the journalism in last few years. Experimental results show that the proposed method can implant a huge amount of secret data while keeping very high security, as when the message is decrypted.

REFERENCES:

[1] Ki-Hyun Jung , Kee-Young Yoo "*Steganographic method based on interpolation and LSB substitution of digital images*" Springer Science+Business Media New York 2014 DOI 10.1007/s11042-013-1832-y.

[2] Mehdi Hussain and Mureed Hussain (2013) A survey of Image Steganography Techniques. International Journal of Advanced Science and Technology Vol. 54.

[3] Atallah M. Al-Shatnawi A New Method in Image Steganography with Improved Image Quality. Applied Mathematical Sciences, Vol. 6, 2012, no. 79, 3907 – 391

[4] Mamta. Juneja, and Parvinder S. Sandhu An Analysis of LSB Image SteganographyTechniques in Spatial Domain International Journal of Computer Science and Electronics Engineering (IJCSEE) Volume 1, Issue 2 (2013) ISSN 2320–401X (Print)

[5] Stefan Katzenbeiser & Fabien A.P.Petitcolas(1999), Information Hiding Techniques for Steganography and Digital Watermarking, Artech House, Computer Security series, Boston, London.

[6] Chan CK, Cheng LM (2004) Hiding data in images by simple LSB substitution. Pattern Recogn 37:469–474

[7] Ming-Ni WuMin-Hui Lin (2007), A LSB Substitution Oriented Image Hiding Strategy Using Genetic Algorithms

[8] Chang CC, Lin MH, Hu YC (2002) A fast and secure image hiding scheme based on LSB substitution. Int J Pattern Recog 16(4):399–416.

[9] Johnson, Neil F., "Steganography", 2000, URL: http://www.jjtc.com/stegdoc/index2.html

[10] Huang LC, Tseng LY, Hwang MS (2013) A reversible data hiding method by histogram shifting in high quality medical images. J Syst Software 86:716–727

[11] Johnson NF & Jajodia S (1998) Exploring steganography: seeing the unseen. Comput Pract 26–34

[12] Jung KH, Yoo KY (2009) Data hiding method using image interpolation. Comput Standards Interfaces 31: 465–470

[13] Jung KH & Yoo KY (2013) Data hiding using edge detector for scalable images. Multimedia Tools and Appl doi:10.1007/s11042-012-1293-84

[14] Lee CF, Huang YL (2012) An efficient image interpolation increasing payload in reversible data hiding. Expert Syst Appl 39:6712–6719

[15] Lee YP, Lee JC, Chen WK, Chang KC, Su IJ, Chang CP (2012) High-payload image hiding with quality recovery using tri-way pixel-value differencing. Information Sciences 191:214–225

[16] Lehmann TM, Gonner C, Spitzer K (1999) Survey: interpolation methods in medical image processing. IEEE Trans Med Imaging 18(11):1049–1075

[17] Mielikainen J (2006) LSB matching revisited. IEEE Signal Processing Letters 13:285–287

[18] Ni Z, Shi YQ, Ansari N, Su W (2006) Reversible data hiding. Circ Syst for Video Technol IEE 16:354–362 Swanson M, Kobayashi M, Tewfik A (1998) Multimedia data embedding and watermarking technologies. Proc IEEE 86(6):1064–1087

International Journal of Engineering Research and General Science Volume 3, Issue 5, September-October, 2015
ISSN 2091-2730

Large Capacity Constrained Multi Product, Multi Level Lot Sizing Optimization Using binary particle swarm optimization

V.V.D.Sahithi[1], P.Sai Krishna[2] , K.Lalith kumar[3] C.S.P.Rao[4]

1 Research assistant Professor, mechanical Engineering Department, VNR Vignana Jyothi Institute of Engineering And Technology, Hyderabad 500090, India

2 ,3 Research Student, mechanical Engineering Department, VNR Vignana Jyothi Institute of Engineering And Technology, Hyderabad 500090, India

4 Professor Department of Mechanical Engineering, National Institute of Technology Warangal, Warangal 506004, India

E-mail: Sahithi.vaka@gmail.com[1] , Saikrishna.parikirala@gmail.com [2] lalith.143143@gmail.com[3] csp_rao@rediffmail.com[4]

Abstract

Lot sizing is one of the most important and one of the most difficult to solve problems in production planning and belong to NP hard class of problems. The Capacity Constrained Multi Product, Multi Level Lot Sizing (CC-MPMLLS) belongs to those problems that production industries face in preparing material requirement planning (MRP) systems for executing their production plans is much more complex and is a combinatorial optimization problem aims to find the lot sizes that achieve cost effectiveness. It minimizes the total setup cost and holding cost by finding optimum lot sizes. As the costs of both dependent and independent items of all levels are varying with time. The subjects of single level lot sizing with variants have been addressed by several methods in the literature. Many heuristic methods have been developed to solve lot sizing problems, but most of them are applicable for small instances. Very few approaches are implemented for MPMLLS problems. In this paper we developed a Binary particle swarm optimization (BPSO) programming technique which can easily handle the large with complex product structures with in a reasonable CPU time .The effectiveness of algorithm is tested with variety of simulation experiments by taking both cost effectiveness and computational time into consideration. And Feasibility of BPSO algorithm is investigated by comparing results with binary genetic algorithm (BGA).

Keywords: Binary particle swarm optimization (BPSO), capacitated lot sizing, production planning

1. Introduction

In a Manufacturing production systems, as end products are usually made up of many intermediate items which consists in a combination of purchased parts and raw materials. The end item is therefore described by a bill of material (BOM), which is the recipe of product. For complex product structures number of levels in the BOM is more (multi level structures). So issue of satisfying external and inter demands becomes more complex which is taken care by Material Requirement Planning (MRP) which plays a very important role in coordinating replenishment decisions for complex goods in production system. Its basic philosophy is to ensure that the right numbers of components are available at right time. Lot sizing is one of the important decisions to be taken while preparing MRP.Lot sizing decisions give rise to the problem of identifying when and how much of product to produce such that setup, production and holding costs are minimized. Making the right decisions in lot sizing will affect directly the system performance and its productivity, which are important for manufacturing firm's ability to compete in the market [1].Therefore, developing and improving solutions for lot sizing problems, is very important.

Lot sizing problem attracted the attention because of its impact on the inventory levels and hence the total cost of production. It is basically concerned with finding order quantities of different items in the bill of material structure to minimize the setup cost and holding cost. Lot size might be the amount of production or purchase quantity depending on the demand at different time buckets to ensure and satisfy customer requirements. Minimizing total production cost is always a tradeoff decision between ordering and holding cost. So order quantity in particular period may be (i) requirement of that period or (ii) requirement of that period including with group of requirements of periods ahead or (iii) zero [2].

Lot sizing problems are mainly divided into 2 types like (a) single level lot sizing (SLLS), and (b) multi level lot sizing (MLLS). The number of final products in a production system is another important characteristic that affects the modeling and complexity of production planning problems. There are two principle types of production system in terms of number of products. In single item production planning there is only one end item (final product) for which the planning activity has to be organized, while in multi item production planning, there are several end items. The complexity of multi item problem is much higher than that of single item problems. Resources or capacities in a production planning systems include manpower, equipment, machines, budget, etc.when there is no restriction on resources, the problem is said to be uncapacitated, and when capacity constraints are explicitly stated, the problem

is named capacitated. Capacity restriction is important, and directly affects problem complexity. Problem solving will be more difficult when capacity constraints exist. Wagner and Whitin [3] proposed an algorithm in 1958 for single level lot sizing based on dynamic programming to find optimum lot size .a heuristic technique was proposed by silver and meal [4] in 1973 for minimizing the total cost. Mc Knew and Coleman [5] proposed a part period algorithm for minimizing setup and holding cost over different periods. Hernández, W. and G. Süer, [6] proposed a genetic algorithm (GA) for solving single level uncapacitated lot sizing problem with no shortages are allowed. And then they also implemented GA procedure for capacitated multi level problems successfully. N.Dellart, J.Jeunet, N.Jonard [7] successfully applied genetic algorithm for solving large multi level multi level lot sizing problems. Taˇsgetiren and Liang [8] presented a technique particle swarm optimization (2003) to minimize the inventory setup and holding cost for setup and holding cost minimization of simple product structures. Klorklear Wajanawichakon& Rapeepan Pitakaso [9] implemented binary PSO (2011) for multi level unconstrained problems of general product structures.

In this paper, the authors have considered a very large complex product structure of a multi product multi level lot sizing problem and Capacity constraints are also taken into consideration. Thus a class of CC-MPMLLS problems were considered and attempted to solve by modeling and simulations using Binary Particle Swarm Optimization Algorithm.

The Paper is organized in six sections: section2: mathematical formulation of CC-MPMLLS problem section3: Binary Particle Swarm Optimization (BPSO) model representation .section 4: numerical example .finally section5: problem illustration section6: conclusion.

2. Mathematical Formulation of CC-MPMLLS problem

The lot sizing problem in this can be described as follows. There are N items to be produced in T periods in a planning horizon such that a demand forecast would be attained. In multi stage production systems, the planning of each item depends on the production of other items, which are situated at lower hierarchical levels in bill of material structure. When we decided to produce one item a fixed cost and time is incurred. The resources for production and setup are limited. Lead times are assumed to be zero.

Let **N** be the number of types items to be produced (i=1, 2, 3…..n), **T** represents the number of periods in planning horizon (t=1, 2, 3…T). $\mathbf{C_{it}}$ is unit production cost of item **i** in period **t**, $\mathbf{S_{it}}$ means the setup cost of item **i** in period **t**,$\mathbf{H_{it}}$ the holding cost of item **i** in period **t**, $\mathbf{r_{ij}}$=number of units of item **i** required to produce 1 unit of j, $\mathbf{d_{it}}$=external demand for item i in period t, $\mathbf{C_{it}}$=unit production cost of item **i** in period **t**,$\mathbf{CA_{it}}$=available capacity of item **i** in period **t**. $\mathbf{X1_{it}}$ is the lot size of item **i** produced in period **t**. I_{it} is the inventory of item **I** in period **t**. $\mathbf{V_{ikt}}$ represents amount of item **k** required to produce item **i** in period **t**.$\mathbf{f_{it}}$ is fixed amount of item **i** required to produce in period **t**.

Min (Total cost) $= min[f(x)] = \sum_{i=1}^{n}\sum_{t=1}^{T}(C_{it}X1_{it} + S_{it}B_{it} + H_{it}I_{it})$ …… 1

$$I_{i,t-1} + X_{it} - I_{it} = d_{it} + \sum_{j\in S(i)} r_{ij} X_{jt}$$ ..…… 2

i=1, 2, 3…..N; t=1, 2, 3…T,

B_{it} =0 if $X1_{it}$=0

=1 if $X1_{it}$>0 ……..…..……. 3

$I_{it,}\ X1_{it} \geq 0$ ……..... 4

$$\sum_{i=1}^{N}(V_{ikt}X1_{it} + f_{ikt}B_{it}) \leq CA_{it}$$ .....…... 5

i=1, 2, 3…..N; t=1, 2, 3…T.

Here the objective function i.e.Equation-1 represents to minimize sum of production, setup, and inventory holding cost of all n items in **T** periods. Equation-2 represents an inventory balance constraints which describe the relation between inventory and production at the beginning and the end of periods. Equation-5 represents the capacity limitations of production and setup. Equation-3 is for binary variable which represents setup is made in period t or not for item i.e. Equation-6 represents that variables must be positive.

Several factors like ordering cost, holding cost, shortage cost, capacity constraints, minimum and maximum order quantity etc... Combination of these factors result in different models to be analyzed like capacitated or uncapacitated, single level or multi level, single item or multi item models.simple single product structures can be solved easily using mathematical equations .as CCMPMLLS problems are having very large solution space they are considered as NP-hard problems that does not have solution with polynomial time. So soft computing techniques are necessary to compute optimum values of lot sizes.

Taˇsgetiren and Liang [8] presented a technique particle swarm optimization (2004) to minimize the inventory setup and holding cost for setup and holding cost minimization of simple product structures. Klorklear Wajanawichakon& Rapeepan Pitakaso [9] implemented binary PSO (2011) for multi level unconstrained problems of general product structures.

In this paper authors have made an attempt to solve very large complex product structure of capacity constrained multi product multi level lot sizing problem. A binary PSO approach is used to model and simulate CC-MPMLLS problem and solved the same with time and solution efficiency. The authors have solved the same problem using Genetic Algorithm. The results of GA and BPSO are compared for the same set of problems under consideration.

3. Binary particle swarm optimization model representation

(a)Initial solution representation

Solution representation of particle p, X^{pk}_{id}, for BPSO $_{is}$ given in Table1.This representation is due to Hernández and Suer (1999). Where each swarm contains 'P' number of particles referring to d dimensions and 'i' items .here 'k' represents iteration number.

A population of binary values (0 or 1) are randomly assigned for't' dimensions of 'i' items in the MLLS problem for all 'p' particles which gives the information about where setups are made.

If $R_{id} > 0.5$ then $X_{id}=1$

Else $X_{id}=0$;

R_{id}=random value.

i= item number=1, 2, 3…n

k=iteration number=1, 2, 3…..k

d=period=1, 2, 3……t

For initial generation k=0, i.e. $X_{id} = X^0_{id}$

Table1.Representation of Particle

	1	**2**	**3**	**4**	**5**	**……..**	**12**
X^{pk}_{1d}	1	0	1	1	0	…….	1
X^{pk}_{2d}	-	-	-	-	-	…….	-
X^{pk}_{3d}	-	-	-	-	-	-	-
·	-	-	-	-	-	-	-

Lot size:

According to particle solution lot sizes are calculated as shown in Table 2.Time periods where demand is not "0" there set up has been made. So order quantity in particular period may be (i) requirement of that period or (ii) requirement of that period including with group of requirements of periods ahead or (iii) zero.

	1	**2**	**3**	**4**	**5**	**……..**	**12**
L^{pk}_{1d}	140	0	155	175	0	……	115
L^{pk}_{2d}	-	-	-	-	-	-	-
L^{pk}_{3d}	-	-	-	-	-	-	-
·	-	-	-	-	-	-	-

Table2. Lot size according to particle dimension

L^K_{id} =lot size of item i ordered in period d at iteration k of particle p.

(b) Velocity of initial generation particles

After assigning particle dimensions, velocity values need to be calculated as shown in Table3, to find next generation population. This velocity calculation is of 2 types i.e. 1) velocity calculation for initial generation (2) Velocity calculations for remaining generations.

Velocity values are restricted to some minimum and maximum namely

$V^{pk}_{id} = [V_{mini}, Vmaxi] = [-5, 5]$.

V^{pk}_{id} =velocity of particle of period d at iteration k

For initial genetaion velocity values are calculated using following formula

$$\mathbf{V^{0p}_{id} = V_{mini} + (V_{maxi} - V_{mini}) * R}$$

R=a random value within 0 to 1, which is generated using rand ().

Table 3. Velocity matrix of particle

	1	**2**	**3**	**4**	**5**	**……..**	**12**
V^{pk}_{1d}	-1.8	3.7	2.9	-0.69	-3.1	……..	1.2
V^{pk}_{2d}	-	-	-	-	-	-	-
V^{pk}_{3d}	-	-	-	-	-	-	-
V^{pk}_{id}	-	-	-	-	-	-	-

(c)Particle best and global best

Particle having best fitness value [$f(x^k_p)$] is assigned to global best .As it is the initial generation all particle best values are equal to particle values as shown in Table 4.

Table 4. Particle and global best matrices

	1	**2**	**3**	**4**	**5**	**……..**	**12**
$\mathbf{PB^{pk}_{1d}}$	1	0	1	1	0	…….	1
$\mathbf{PB^{pk}_{2d}}$	-	-	-	-	-	…….	-
$\mathbf{PB^{pk}_{3d}}$	-	-	-	-	-	-	-
$\mathbf{PB^{pk}_{id}}$ $\mathbf{PB^{K}_{id}}$	-	-	-	-	-	-	-

	1	**2**	**3**	**4**	**5**	**……..**	**12**
$\mathbf{GB^{k}_{1d}}$	1	0	1	1	0	…….	1

(d)Updating parameters for next generations:

(i)Updating velocity (V^{pk}_{id}):

(I) new velocity = V^{pk}_{id}=P ($V^{p,\,k-1}_{id}$ +$\Delta V^{p,\,k-1}_{id}$)

Where $\Delta V^{p,\,k-1}_{id}$= c1 R1 ($PB^{p,k-1}_{id}$ - $X^{p,k-1}_{id}$)+ c2 R2(GB^{K-1}_{id} - $X^{p,k-1}_{id}$)

C1, c2 are social and cognitive parameters, R1& R2 are uniform random numbers between (0, 1)

Here Piece wise linear function [P (V^{pk}_{id})]

P (V^{pk}_{id}) = Vmaxi if V^{pk}_{id} > Vmaxi

=V^{pk}_{id} if $|V^{pk}_{id}| <= V_{maxi}$

=Vmini if V^{pk}_{id} < Vmini

(ii)Updating position (X^{pk}_{id}) by sigmoid function:

X^{K}_{id}= 1 if R< S (V^{pk}_{id})

=0 otherwise

Sigmoid function S (V^{pk}_{id}):

This function forces velocity values to be in the limits of '0' to '1'.It helps to update next generation

X^{pk}_{id} values. $\mathbf{S\ (V^{pk}_{id}) = \frac{1}{1+e^{-Vpk\,id}}}$

(iii)Updating particle best and global best (PB^{pk}_{id} ,GB^{K}_{id})

After each and every iteration update particle best and global best values according to the fitness values of particles in the newly generated swarm.

(e) Terminination: If the number of iterations reaches a predetermined value, called maximum number of iterations then stop searching, other wise go to (d).

4. Numerical Example:

In this example two items are there in which item-2 is having independent demand and other item (i.e.item-1) demand depends on first one.Table5a and 5b represents the demands and also depicts different costs involved in the problem.

Figure 1 represents BOM structure.

Table 5a Product demand

Period	1	2	3	4	5	6
Demand	20	100	50	30	10	100

Table 5b setup and holding cost

Item No.	Setup cost	Holding cost
1	500	50
2	100	10

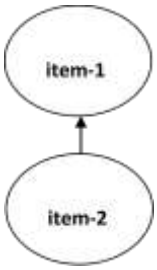

Figure 1.BOM structure

The problem is mapped and executed in terms of BPSO and the steps are given below:

Step1: initial generation

Particle 1

Item1	1	0	0	0	1	1
	200	0	0	0	10	100
	2.9	-1.8	3.5	-1.2	0.7	3.8
Item2	1	0	0	0	1	0
	200	0	0	0	110	0
	-1.5	1.6	-2.7	3.3	1.8	-3.9

Fitness fuction=f(x^0_1)=17200

Particle 2

Item1	1	1	1	0	0	1
	20	100	90	0	0	100
	-2.5	1.7	3	-4	1.6	2.3
Item2	1	0	0	0	0	1
	210	0	0	0	0	100
	2.2	-3.9	1.4	3	-4.6	2

Fitness function=f (x^0_2) =7500

Particle 3

Item1	1	0	1	0	1	1
	120	0	80	0	10	100
	3	-4.6	2	-1.2	0.7	3.8
Item2	1	0	1	0	1	0
	120	0	80	0	110	0
	-3	-4	1.6	2.9	-1.8	3.5

Fitness fuction=f(x^0_2) =9800

Step 2: As it is initial generation, assign each particle in the swarm to particle best (PB)

$PB^{1,0}_{1,1}=X^{1,0}_{1,1}$, $PB^{1,0}_{1,2}=X^{1,0}_{1,2}$..... $PB^{1,0}_{1,12}=X^{1,0}_{1,12}$

$PB^{1,0}_{2,1}=X^{1,0}_{2,1}$, $PB^{1,0}_{2,2}=X^{1,0}_{2,2}$..... $PB^{1,0}_{2,12}=X^{1,0}_{2,12}$

	D	1	2	3	4	5	6	Fitness
$PB^{1,0}_{id}$	i=1	1	0	0	0	1	1	17200
	i=2	1	0	0	0	1	0	
$PB^{2,0}_{id}$	i=1	1	1	1	0	0	1	7500
	i=2	1	0	0	0	0	1	
$PB^{3,0}_{id}$	i=1	1	0	1	0	1	1	9800

	i=2	1	0	1	0	1	0	

Assign best fitness particle to global best

	D	1	2	3	4	5	6	Fitness
GB_{id}^{0}	i=1	1	1	1	0	0	1	7500
	i=2	1	0	0	0	0	1	

Step 3: Updating velocity using piece wise function

Assume C1=C2=1, r1=r2=0.5;

Update particle dimension

$\Delta V^{1,0}_{12}$= c1 R1 ($PB^{1,0}_{12} - X^{1,0}_{12}$) + c2 R2($GB^{0}_{12} - X^{1,0}_{12}$)

$\Delta V^{1,0}_{12}$=1*0.5(0-0)+1*0.5(1-0)= 0.5

$V^{1,1}_{12}$=P ($V^{1,0}_{12}+\Delta V^{1,0}_{12}$)=P(-1.8+0.5)=-1.3

Updating particle position:

R (0, 1)=0.11 < Sigmoid(-1.3)=0.21

So new dimension value= X^{1}_{12}=1

- After completion of velocity calculations of all dimensions, particles are updated as follows

	D	1	2	3	4	5	6	fitness
$X^{1,1}_{id}$	i=1	1	1	1	1	0	1	6400
	$V^{1,1}_{1d}$	2.9	-1.3	4	-1.2	0.2	3.8	
	Sig($V^{1,1}_{1d}$)	0.94	0.21	0.98	0.23	0.54	0.97	
	Random	0.72	0.11	0.4	0.2	0.67	0.8	
	i=2	1	0	0	0	0	1	
	$V^{1,1}_{2d}$	-1.5	1.6	-2.7	3.3	1.3	3.3	
	Sig($V^{1,1}_{2d}$)	0.18	0.83	0.06	0.96	0.78	0.96	
	Random	0.10	0.91	0.10	0.99	0.80	0.91	
$X^{2,1}_{id}$	i=1	1	1	1	1	0	1	3500
	i=2	1	1	1	1	0	1	
$X^{3,1}_{id}$	i=1	1	0	0	0	1	1	9800
	i=2	1	0	0	0	1	0	

Updated particle best matrix

	D	1	2	3	4	5	6	Fitness
$PB^{1,1}_{id}$	i=1	1	1	1	1	0	1	6400
	i=2	1	0	0	0	0	1	
$PB^{2,1}_{id}$	i=1	1	1	1	1	0	1	3500
	i=2	1	1	1	1	0	1	
$PB^{3,1}_{id}$	i=1	1	0	1	0	1	1	9800
	i=2	1	0	1	0	1	0	

Global best matrix

	D	1	2	3	4	5	6	Fitness
GB_{id}^{1}	i=1	1	1	1	1	0	1	3500
	i=2	1	1	1	1	0	1	

Step 4: Termination

Repeat this procedure (step3) until iteration number k< max iteration.

5. Problem Illustration:

5.1. Problem

Problems shown in Figure 2a and 2b as M×T are taken for modeling and simulation of CC MLLS problem. Here M represents the total number of items involved in the BOM structure and T represents the number of periods. Table 6 represents different costs involved and Table 7and 8 carries information regarding demand and available capacity. Figure 2a is a BOM of single product where it contains 50×12 contains 50 different items in 9levels and, Figure 2b is a BOM of a multi product contains 39×12 structure with 39 different items in6 levels. Table 6 gives the information regarding the setup cost and holding costs of different items of both 50 ×12and39×12 problems. Table 7 gives the information regarding the demand and availability of end product of single product problem. Table 8 gives the information of demand and availability of end products of multi product problem.

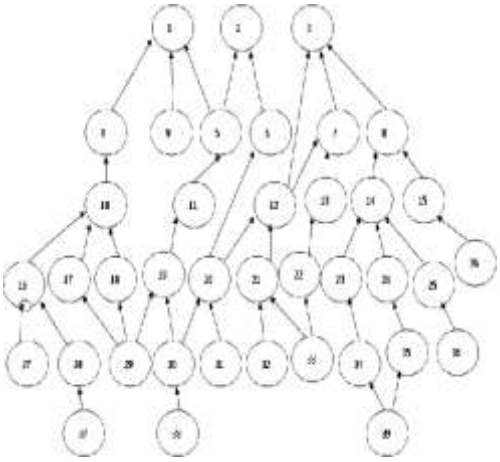

50×12

Figure 2a Product structures of a single product

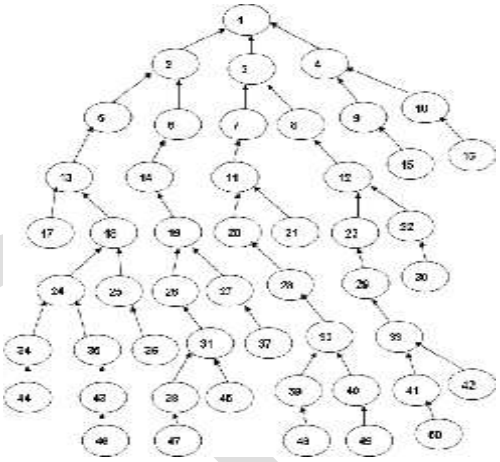

39×12

Figure2b Product structures of multi product

Table 6.Setup and Holding costs of different items in 50×12, 39×12 structures

S.No	50*12 problem		39*12 problem		S.NO	50*12 problem		39*12		S.NO	50*12		39*12	
	H.C	S.C	H.C	S.C		H.C	S.C	H.C	S.C		H.C	S.C	H.C	S.C
1	97.83	780	40.08	490	18	23.71	510	7.13	860	35	6.38	160	4.83	690
2	45.19	200	35.27	450	19	15.32	910	8.82	850	36	3.47	290	3.44	430
3	43.82	590	59.66	90	20	20.58	830	10.6	670	37	1.97	420	0.91	60
4	5.82	710	25.42	140	21	8.71	730	6.02	370	38	1.76	160	2.64	760
5	26.04	890	10.42	880	22	3.14	850	2.78	360	39	6.41	450	2.65	180
6	18.87	610	22.64	440	23	0.94	450	2.95	310	40	7.17	340		
7	27.03	920	22.31	70	24	13.02	370	9.32	440	41	2.97	750		
8	15.64	210	19.53	430	25	7.34	390	0.31	590	42	0.25	140		
9	2.67	490	1.34	930	26	7.53	540	1.45	580	43	3.22	430		
10	1.86	920	25.12	650	27	4.36	160	3.63	650	44	1.85	890		
11	23.5	520	9.46	740	28	18.52	480	4.35	450	45	3.84	610		
12	12.59	540	17.48	680	29	5.81	410	3.29	820	46	0.41	860		
13	25.13	510	4.32	800	30	1.93	140	5.04	620	47	0.37	860		
14	16.42	500	14.28	220	31	6.71	390	2.53	580	48	3.84	350		
15	0.84	300	2.56	850	32	15.35	370	3.3	340	49	3.95	610		
16	1.02	450	10.07	400	33	4.36	520	0.61	340	50	1.63	350		
17	0.62	440	4.59	650	34	3.28	700	2.52	80					

Table 7.Demand and Availability of end product in 50×12 problem

Period	1	2	3	4	5	6	7	8	9	10	11	12
Demand	15	5	15	110	65	165	125	25	90	15	140	115
Available	1000	2000	1000	0	5000	1000	0	500	800	500	1000	200

Table 8.Demand and Availability of end products in 39×12 problem

Period	1	2	3	4	5	6	7	8	9	10	11	12

Item1	10	100	10	130	115	150	70	10	65	70	165	125
available	1500	2000	0	1000	800	5000	0	800	500	1000	2000	200
Item2	175	15	85	90	85	90	75	150	75	10	150	15
available	0	1000	2000	1000	900	0	800	1200	500	500	1000	100
Item3	135	165	15	105	25	120	50	60	5	140	60	10
available	1000	2000	900	800	0	1000	1200	300	500	800	100	100

5.2. Experimental Parameters:

The Binary particle swarm optimization for capacitated large size lot sizing problem is coded in c language and run on Intel® Core™ Duo processors 667 MHz Front Side Bus and 2M Smart L2 Cache with 2GB RAM. Performance of BPSO is compared with a traditional Binary Genetic Algorithm.

Binary Genetic Algorithm Parameters:

In solving MLLS problems using Binary GA, multi point cross over is considered .Cross over of different types like product and periodic crossovers have been applied and single bit mutation is used. The cross over and mutation ratios considered are 0.80 and 0.10 respectively and 0.1 percentage of reproduction is taken.

Binary Particle swarm optimization:

For better convergence population size of BPSO should be at least twice the number of periods that are considered i.e. 24.In this paper population size is taken as 40 i.e. swarm size .means 40 different particles are considered ,as solution proceeds further particle fly around the solution space with different velocities and tries to reach optima.

Following Table 9 shows the effect of social cognitive parameters on the total cost i.e. fitness

Table 9.Effect of social cognitive parameters on cost

C1	C2	Avg cost
5	1	213882.63
1	1	207562.63
1	5	207507.96
3	2	202810.70
1	3	201254.17
2	5	201267.15
5	2	101047.38
5	1	201047.38
4	3	194724.83
3	5	191770.14
2	2	191520.84
3	3	190495.42

From this table 9 we can understand that the average cost obtained with different c_1, c2 values are more or less similar. So difference of various social cognitive values and the result of average total cost had no effect. Thus c1=c2=2 is chosen.

5.3. Simulation Results at different iterations tested in large –CCMPMLLS:

Table 10 shows the average total costs obtained by BPSO algorithm at different iterations of capacity constrained 39×12 MPMLLS problem.

Table 10.simulation results of different iterations

Particle No	300iterations	400 iterations	500 iterations	600 iterations
1	287163.81	296827.84	271354.18	252984.90
2	336654.96	367410.31	289081.71	315492.96
3	293118.93	269643.84	245523.12	284151.09
4	306763.81	302162.75	262019.62	243960.09
5	345834.90	248838.14	314560.21	329510.21
6	282012.65	266686.15	256661.42	281553.00
7	315013.18	272906.25	261492.73	352466.06
8	296122.84	348605.81	283168.21	288089.43
9	248314.07	301639.96	305530.84	254905.98
10	247896.62	257145.29	303904.59	243397.90
11	277441.78	269856.78	384417.81	292368.90
12	362870.81	306533.00	276282.09	298579.78
13	321958.31	371249.90	294672.75	275554.75
14	278471.87	271883.00	274612.28	296049.25
15	260861.73	311140.62	297362.34	272623.87
16	285929.62	286662.00	269972.37	299126.06
17	263018.00	289455.09	351597.21	266942.46
18	278906.21	264557.53	284343.62	267243.21
19	302362.43	298466.21	285951.65	253033.96
20	314437.37	274489.31	295188.09	240238.76
21	304807.06	304971.06	392710.34	266432.03
22	259932.62	261123.39	328282.68	284568.34
23	271942.18	259024.79	261638.71	357821.31
24	232535.56	267100.62	326993.50	294543.37
25	313567.40	259005.15	280591.90	306715.31
26	296707.34	268255.06	243848.54	358286.62
27	277164.31	281731.18	264352.62	276793.18
28	261792.07	274739.06	289422.71	299171.06
29	380921.25	256552.51	277678.18	258015.42
30	292137.40	266886.78	279697.71	256473.42
31	271272.21	280590.34	287545.06	319100.50
32	249626.34	265390.56	328519.46	262788.46
33	306842.96	251897.54	350235.21	315292.06
34	264361.06	294248.43	247796.82	241895.12
35	269949.12	326534.81	337587.68	248329.37
36	321372.84	248451.96	243114.26	241233.20
37	295246.15	261236.87	256835.37	219248.84
38	272370.71	296141.87	338252.03	323139.43
39	275238.12	346146.93	258783.17	285475.75
40	326699.65	259180.64	281134.03	283344.40
Avg	291241.00	285134.20	288971.5	282673.50

5.4. Comparison of results:

Following Tables11 and 12 shows the comparison of binary GA and PSO algorithms at different iterations of given CC-MLLS problems. Table 11 and Figure3 give the comparision of solution efficiency of single product problem between BGA and BPSO. Following table 12and Figure4 gives the comparision of solution efficiency of multi product problem between GA and BPSO.

Table 11.comparision 50×12 problem results between BGA and BPSO

Iteration No.(K)	**BGA**	**BPSO**

1	386785.09	250295.00
10	380891.31	243797.00
50	350503.75	203956.09
100	322136.16	193128.11
200	279484.72	192017.59
500	249875.41	189013.95
1000	234587.08	186579.11
2000	234587.08	186543.84
5000	234489.03	185042.16
10000	229484.6	184629.19
15000	229484.6	183973.11
20000	204240.90	181685.31
30000	204140.90	181685.31

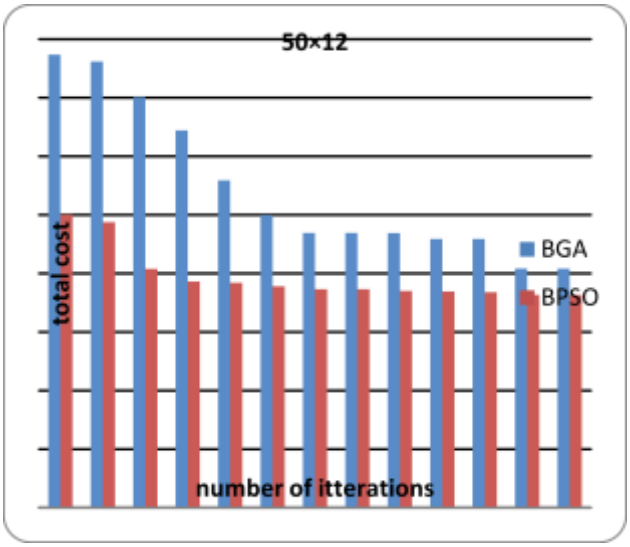

Figure3. BGA and BPSO comparison

Table 12.comparision 39×12 problem results between BGA and BPSO

Iteration No.(K)	BGA	BPSO
1	377421.19	246901.17
10	327867.12	217583.656
50	242463.20	204084.98
100	221525.29	202884.17
200	199022.79	194724.843
500	197410.34	193219.70
1000	197410.34	185691.15

2000	197410.34	185691.15
5000	197410.34	175684.78
10000	197410.34	172682.56
15000	197410.34	172682.56

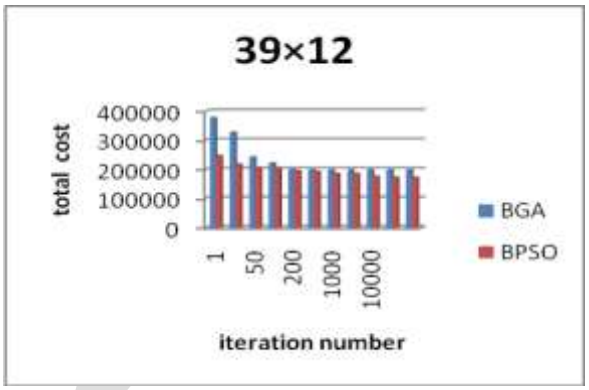

Figure4. BGA and BPSO comparison

Figure 5 represents the convergence of BPSO algorithm for two different problems of capacity constrained multi level lot sizing. The optimum solution i.e. totalcost for both single product (50×12) and Multi product (39×12) problems are given in Table 13and the following conclusions are drawn.

Figure 5. Convergence of BPSO

Following Table 13 gives the information about the Best solutions obtained for both single product & multi product problems of multi level using BGA and BPSO.

Table 13.Optimum solution Obtained by BPSO for MLLS problems

	BGA total cost	BPSO total cost	% of improvement
50 × 12	204,140.90	181,685.31	11
39 × 12	197,410.34	172,682.56	12.5

6. Conclusions

1. BPSO technique has been successfully employed to model and simulate CC-MPMLLS problem to minimize total cost. Two problems are single product with multi level multi item nature and other problem with three end products, multi item multi levels were considered and tested thoroughly with BPSO algorithm.BGA method is also implemented to solve the above problems and to compare with BPSO method
2. BPSO algorithm converges with in 10000 iterations for the problem under consideration and thus the developed algorithm is time efficient.

3.The solution obtained for the two problems under consideration by BGA and BPSO methods, it is observed that through both BGA and BPSO are successful methods in obtaining solutions, the solution obtained by BPSO is more efficient i.e. 11% improved in the case of 50×12 problem and 12.5% in39×12 problem

4. Computational experience show that the methodology can be implemented as a separate optimization module for solving all types of lot sizing problems in any MRP-II based package.

REFERENCES:

[1]B.Karimi, S.M.T. Fatemi Ghomi, J.M.Wilson," The capacitated lot sizing problem: a review of models and algorithms", the international journal of Management science, Omega 31(2003) 365-378.

[2] N.Dellart, J.Jeunet, Randomized multi-level lot-sizing heuristics for general product structures, European Journal of Operational Research 148 (2003) 211–228.

[3] Wagner, H. and Whitin, T. (2004). Dynamic version of the economic lot size model. Management Science, 50(12):1770–1774.

[4] Silver, E. and Meal, H. (1973). A heuristic for selecting lot size requirements for the case of a deterministic time-varying demand rate and discrete opportunities for replenishment. Production and Inventory Management, 14(2):64–74.

[5] Coleman, B.J., McKnew, M.A., 1991. An improved heuristic for multilevel lot sizing in material requirements planning. Decision Sciences 22, 136–156.

[6] Hernández, W. and G. Süer, "Genetic Algorithms in Lot Sizing Decisions", Proceedings of the Congress on Evolutionary Computing (CEC99), Washington DC, July 6-9, 1999.

[7] N.Dellart, J.Jeunet, A genetic algorithm to solve the general multi-level lot sizing problem with time varying costs. International journal of production Economics68 (2000)241-257.

[8]M.Fatih Tasgetiren and Yun-Chia Liang(2003),A binary particle swarm optimization algorithm for lot sizing problem, journal of Economic and Social Research5(2),1-20.

[9] Klorklear Wajanawichakon, Rapeepan Pitakaso, Solving large unconstrainted multi level lot-sizing problem by a binary particle swarm optimization. International Journal of Management Science and Engineering Management, 6(2): 134-141, 2011

International Journal of Engineering Research and General Science Volume 3, Issue 5, September-October, 2015
ISSN 2091-2730

An Iterative Improvement Search and Binary Particle Swarm Optimization for Large Capacitated Multi Item Multi Level Lot Sizing (CMIMLLS) Problem

V.V.D.Sahithi[1] ,P.Sai Krishna[2] ,K.Lalithkumar[3] ,C.S.P.Rao[4]

1 Research assistant Professor Department of mechanical engineering, VNR Vignana Jyothi Institute Of Engineering And Technology, Hyderabad 500090, India

2,3Research Student, Department mechanical Engineering, VNR Vignana Jyothi Institute of Engineering And Technology, Hyderabad 500090, India

4 Professor Department of Mechanical Engineering, National Institute of Technology Warangal, Warangal 506004, India

sahithi.vaka@gmail.com[1] lalith.143143@gmail.com[2] Saikrishna.parikirala@gmail.com [3] csp_rao@rediffmail.com[4]

Abstract

Lot sizing problem in Material Requirement Planning (MRP) systems belongs to those problems that industrial manufacturers face daily in organizing their overall production plans. Lot sizing plays an important role in minimization of totalcost (i.e. sum of setup and holding cost). When multiple levels, multiple items and capacity restrictions are involved in an inventory lot sizing problem, determination of optimum lot sizes becomes very complicated and may be treated as NP hard class of problems. However this combinatorial optimization problem can be solved by using soft computing techniques in a reasonable CPU time when small instances are considered. Many heuristic techniques were developed in the past to solve lot sizing problems but most of them were failed in successful implementation. In this paper the authors are presenting an Iterative improvement binary particle swarm optimization (IIBPSO) techniques for solving very large capacitated multi item multi level lot sizing problem (CMIMLLS). In the proposed algorithm first a set of initial solution is randomly choosen then, used the particles to find solution according to standard mechanism of binary particle swarm optimization (BPSO). After reaching a reasonable solution point, a hybrid selection with iterative improvement local search mechanism is applied to restart the algorithm. Hybrid selection is a kind of restart mechanism in BPSO, and finally a local search is used on the global best solution to improve the solution quality. The IIBPSO algorithm showed good experimental results and outperforms all other approaches in terms of quality of solution.

Keywords: inventory lot sizing, material requirement planning, hybrid particle swarm optimization.

1. Introduction

In most manufacturing and distribution companies, the highest individual cost is inventory. The cost of the inventory is directly related to the amount of inventory held and the bulk of manufacturers admit they consistently carry too much of it. Executives usually believe that the higher the service level is, the more stock is required. However, as demand forecasts are often inaccurate, inventory piles up, exposure to obsolescence increases, salable throughput decreases and customer service finally declines. Thus too much inventory further compounds service problems. But inventory reduction may be carried out at the expense of an increased cadence of orders. Unfortunately setup costs cannot come to zero even if they have been considerably reduced on grounds of just-in- time (JIT) guidelines. Thus critical to achieving a satisfactory trade-off between set-up costs and inventory holding costs is to implement proper lotsizing rules. But even the most comprehensive MRP systems do not provide an efficient methodology. In fact, commercially-available MRP software typically comes with the simplest yet suboptimal lot-sizing approaches [1].

Lot sizing problem attracted the attention because of its impact on the inventory levels and hence the total cost of production. It is basically concerned with finding order quantities of different items in the bill of material structure to minimize the setup cost and holding cost. Lot size might be the amount of production or purchase quantity depending on the demand at different time buckets to ensure and satisfy customer requirements [2]. Minimizing total production cost is always a tradeoff decision between ordering and holding cost. In the decision making, a number of factors need to be considered; carrying cost, setup cost, shortage cost, capacity restrictions, minimum order quantity, maximum order quantity, handling restrictions, quantity discounts, etc. All these factors can be combined to generate different models. For instance, some of the costs can be considered zero or infinity and some of the restrictions can be relaxed. Depending on the applicable model, different solution procedures exist. The model is complicated, along with its corresponding solution procedure, by the number of items considered, i.e., single item and multi item considerations. Another possible complication in the model is the inclusion of multi-levels consideration and capacity constraints. Hence the problem of lot sizing still stood as challenging problem of optimization and attracted research community.

The lot sizing problems can be mainly divided into Single level lot sizing problems (SLLS) and Multi-level lot sizing (MLLS) problems with and without capacity restrictions. SLLS problems without capacity restriction are simplest among them. Several heuristics were developed and successfully implemented on SLLS problems. In 1958, Wagner and Whitin (2004) introduced the SLLS model and developed a well-known exact algorithm based on dynamic programming]After that, Silver and Meal (1973) proposed the idea of minimizing average setup and inventory costs over several periods. Mc Knew and Coleman (1991) proposed a part period algorithm for minimizing setup and holding cost over different periods. Hernández, W. and G. Süer, proposed a genetic algorithm (GA) for solving single level uncapacitated lot sizing problem with no shortages. A few heuristics techniques were also developed to solve MLLS problems. N.Dellart, J.Jeunet successfully applied a Randomized multi-level lot-sizing heuristics for general product structures. Regina Berretta, Luiz Fernando Rodriguez proposed A memetic algorithm for a multi stage capacitated lot sizing problem .Taˇsgetiren and Liang presented particle swarm optimization (PSO) in 2003 to minimize the inventory setup and holding cost for minimization of simple product structures N.Dellart, J.Jeunet, N.Jonard successfully applied PSO for uncapacitated multi level lot sizing problem with flexible initial weight .Klorklear Wajanawichakon and Rapeepan Pitakaso implemented PSO (2011) for multi level unconstrained problems of general product structures.

In this paper, the authors have made an attempt to solve very large and complex product structure of capacity constrained multi item multi level lot sizing problem (MIMLLS). An iterative improvement search with BPSO approach is used to simulate CMIMLLS problem and solved several problems with time and solution efficiency. The authors have also solved the problems considered using Genetic Algorithm, BPSO and IIBPSO separately. The results of Binary GA, Iterative Improvement BGA (IIBGA) and BPSO are compared with the proposed method IIBPSO for the same set of problems under consideration. The Paper is organized in six sections: section2: mathematical formulation of CMIMLLS problem section3: IIBPSO procedure Section 4: numerical example section5: problem illustration and section6: conclusion is presented.

2. Mathematical Formulation of problem:

The lot sizing problem that we considered in this paper can be described as follows. We have 'N' items to be produced in 'T' periods in a planning horizon such that a demand forecast would be attained .In a multistage production systems ,the planning horizon of each item depends on the production of other items, which are situated at lower levels. The resources for production and setup are limited. Lead times are assumed to be zero.

Let N be the number of items, T the number of periods in the planning horizon the number of types of resources. C_{it} the unit production cost item I in period t, h_{it} the unit holding cost of item I in period t,S_{it} is the setup cost of item i in period t,d_{it} the demand for item I in period t,V_{ikt} the amount of resource k necessary to produce item i in period t, b_{kt} is the amount of resource k available in period t, M is the upper bound on X_{it} ,S(i) the set of immediate successor items to item I, and r_{ij} is the number of units of item i needed by one unit of item j, where jϵ S(i).

Decision variables are x_{ij} is the lot size of item i in period t, y_{it} is '1' if item is produced in period t and zero otherwise. I_{it} the inventory of item i in period t.

$$\text{Min (f(x))} = \sum_{i=1}^{N}\sum_{t=1}^{T}(C_{it}X_{it} + h_{it}I_{it} + S_{it}Y_{it}) \quad \text{.....(1)}$$

$$I_{i,t-1} + X_{it} - I_{it} = d_{it} + \sum_{j\epsilon S(i)} r_{ij}X_{jt} \quad \text{..... (2)}$$

i=1, 2,…….N ; T=1,2,……T

$$\sum_{i=1}^{N}(V_{ikt}X_{it} + f_{ikt}y_{it}) \leq b_{kt} \quad \text{..... (3)}$$

k=1, 2, 3,…….K; t=1,2,3,…….T

$$X_{it} \leq My_{it} \qquad \text{i=1,…..N; t=1,…..,T} \quad \text{.....(4)}$$

$$X_{it}, I_{it} \geq 0 \qquad \text{i=1,…..N; t=1,…..,T} \quad \text{.....(5)}$$

$$y_{it} \in \{0,1\} \qquad \text{i=1…N; t=1,…..,T} \quad \text{.....(6)}$$

The objective function (1) is to minimize the sum of production, inventory holding and setup cost in T periods. Equation (2) is inventory balance constraint, which describe the relationship between inventory and production at the beginning and the end of the period. Constraint (3) represents the capacity limitations of production and setup. Constraint(4) ensure that the solution will have setup when it has production .The last two constraints (5) and (6) require that variables must be positive and setup variables must be binary.

Several factors like ordering cost, holding cost, shortage cost, capacity constraints, minimum and maximum order quantity etc... Combination of these factors result in different models to be analyzed like capacitated or uncapacitated, single level or multi level, single item or multi item models.simple single product structures can be solved easily using mathematical equations .as CMIMLLS problems are having very large solution space they are considered as NP-hard problems that does not have solution with polynomial time. So soft computing techniques are necessary to compute optimum values of lot sizes.

In this paper authors have made an attempt to solve very large complex product structure of capacity constrained multi product multi level lot sizing problem. An iterative improvement binary PSO approach is used to simulate CMIMLLS problem and solved the same with time and solution efficiency. The authors have also solved similar problems using BGA, IIBGA, and BPSO. The results of BGA, IIBGA, BPSO, and IIBPSO are compared for the same set of problems under consideration.

3. Iterative Improvement Search Binary Particle Swarm Optimization (IIBPSO) Procedure:

Particle Swarm Optimization (PSO) is one of the evolutionary optimization methods inspired by nature which include evolutionary strategy (ES), evolutionary programming (EP), genetic algorithm (GA), and genetic programming (GP). PSO is distinctly different from other evolutionary-type methods in that it does not use the filtering operation (such as crossover and/or mutation) and the members of the entire population are maintained through the search procedure. In PSO algorithm, each member is called "particle", and each particle flies around in the multi-dimensional search space with a velocity, which is constantly updated by the particle's own experience and the experience of the particle's neighbors. Since PSO is basically developed through simulation of bird flocking in the two dimensional space and was first introduced by Kennedy and Eberhart (1995, 2001), it has been successfully applied to optimize various continuous nonlinear functions. Although the applications of PSO on combinatorial optimization problems are still limited, PSO has its merit in the simple concept and economic computational cost.

The main idea behind the development of PSO is the social sharing of information among individuals of a population. In PSO algorithms, search is conducted by using a population of particles, corresponding to individuals as in the case of evolutionary algorithms. Unlike GA, there is no operator of natural evolution which is used to generate new solutions for future generation. Instead, PSO is based on the exchange of information between individuals, so called particles, of the population, so called swarm. Each particle adjusts its own position towards its previous experience and towards the best previous position obtained in the swarm. Memorizing its best own position establishes the particle's experience implying a local search along with global search emerging from the neighboring experience or the experience of the whole swarm. Two variants of the PSO algorithm were developed, one with a global neighborhood, and other one with a local neighborhood. According to the global neighborhood, each particle moves towards its best previous position and towards the best particle in the whole swarm, called gbest model. If binary values (0 or 1) are used as particle dimensions it is called as Binary Particle Swarm Optimization (BPSO).

Even though we might find a good set of parameters for BPSO, Iterative Improvement search is still worth while trying to improve the performance of the solution. Local search algorithms move from solution to solution in the space of candidate solutions (the search space) by applying local changes, until a solution deemed optimal is found or a time bound is elapsed and helps to escape from local minima. Iterative Improvement search is one such local search algorithm which helps in improving solution efficiency.

(a) Initialization

In PSO algorithm, each member is called particle and each one represents one particular solution to the given problem. Group of particles is called as swarm.

(i) Initialization of particle

In multi level inventory problems each particle is represented by a matrix of m×n. where m represents the number of items involved in the problem, represents time buckets. And particle representation is X^{pt}_{id} .

Here p= particle number.

t=iteration number (represents row number)

i=item number (represents column number)

d=time period.

Example:

7 items and 6 periodic demands are involved in the problem then particle is represented by 7×6 matrix.

As it is initial generation, all dimentions of particle are assigned to "0" or "1" randomly.

If $R > 0.5$ then $X^{pt}_{id} = 1$.

Else $X^{pt}_{id} = 0$.

Here R represents a random number.

$$\text{Particle} = X^{pt}_{id} = \begin{bmatrix} 1 & 0 & 1 & 0 & 0 & 1 \\ 1 & 0 & 0 & 0 & 0 & 0 \\ 1 & 0 & 1 & 0 & 0 & 1 \\ 1 & 0 & 0 & 0 & 0 & 0 \\ 1 & 0 & 0 & 0 & 0 & 0 \\ 1 & 0 & 1 & 0 & 0 & 1 \\ 1 & 1 & 0 & 0 & 0 & 1 \end{bmatrix}$$

Figure. 1 Particle dimension representation

X^{pt}_{id} represents p^{th} particle of t^{th} iteration and swarm contains p different particles like this.

(ii) According to particle dimensions, fitness needs to be calculated for each and every particle, i.e. fitness (X^{pt}_{id}).

(iii) Initialization of particle velocities

After defining particle dimensions particle velocities needs to be calculated. For initial generation velocity calculation can be done using following formula

$$\mathbf{V^{p0}_{id} = V_{mini} + (V_{maxi} - V_{mini}) * R}$$

here $[V_{maxi}, V_{mini}] = [-x, x]$, here x is an integer.

Ex: let $[V_{maxi}, V_{mini}] = [-5, 5]$

$$V^{p0}_{id} = \begin{bmatrix} +1.5 & -2.4 & -3.8 & +2.5 & +4.3 & +1.5 \\ -0.6 & -1.4 & -1.4 & -0.9 & -3.6 & +4.4 \\ +2.5 & +0.6 & +0.2 & -1.4 & -1.2 & +3.2 \\ -1.1 & +0.5 & -3.5 & -1.9 & -2.0 & -0.9 \\ +2.2 & -2.5 & -3.9 & -1.3 & +3.6 & +4.0 \\ -1.3 & +0.0 & +1.2 & -1.6 & +4.3 & +0.3 \\ +0.7 & -3.4 & +0.2 & -4.2 & +1.2 & -1.7 \end{bmatrix}$$

Figure. 2 Particle velocity representation

(b) Updating Particle best and global best

After defining swarm i.e. all particle dimensions, fitness needs to be calculated. After calculating fitness value we need to assign global best value to the paticle containing best fitness value. As it is the initial generation all particle best($PB^{p,k}_{id}$) values are equal to particle values.

Here GB^{t}_{id} represents global best dimensions of t^{th} iteration .

Here PB^{pt}_{id} represents paticle best dimensions of p^{th} particle t^{th} iteration.

(c)Updating parameters for next generations

(i)Updating velocity of particle (V^{pt}_{id}):

$$\text{New velocity} = V^{pt}_{id} = P\left(V^{p,t-1}_{id} + \Delta V^{p,t-1}_{id}\right)$$

$$\Delta V^{p,t-1}_{id} = c1\ R1\ (PB^{p,t-1}_{id} - X^{p,t-1}_{id}) + c2\ R2\ (GB^{t-1}_{id} - X^{p,t-1}_{id})$$

C1, c2 are social and cognitive parameters, R1& R2 are uniform random numbers between (0, 1)

Here Piece wise linear function [$P(V^{pt}_{id})$]

$$P(V^{pt}_{id}) = V_{maxi} \quad \text{if } V^{pt}_{id} > V_{maxi}$$

$$= V^{pt}_{id} \quad \text{if } |V^{pt}_{id}| <= V_{maxi}$$

$$= V_{mini} \quad \text{if } V^{pt}_{id} < V_{mini}$$

(ii)Updating position (X^{pt}_{id}) by sigmoid function:

$$X^{pt}_{id} = 1 \quad \text{if} \quad R < S(V^{pt}_{id})$$

$$= 0 \quad \text{otherwise}$$

Sigmoid function $S(V^{pt}_{id})$:

This function forces velocity values to be in the limits of '0' to '1'.It helps to update next generation X^{pk}_{id} values.

$$S\left(V^{pt}{}_{id}\right) = \frac{1}{1+e^{-V_{id}^{pt}}}$$

(iii)Updating particle best and global best ($PB^{p,t}{}_{i,d}$,$GB^{t}{}_{i,d}$)

After each and every iteration update particle best and global best values according to the fitness values of particles in the newly generated swarm.

(d)Iterative Improvement Search Algorithm

Iterative Improvement Search Algorithm is a local search that moves from one solution S to another S' according to some neighborhood structure. Search procedure usually consists of the following steps.

(i) Initialization: Choose an initial schedule S to be the current solution and compute the value of the objective function F(S).

(ii) Neighbour Generation: Select a neighbour S' of the current solution S and compute F(S').

(iii) Acceptance Test: Iterative Improvement allows only strict improvement in the objective function value. It accepts a new solution S' only if $F(S') < F(S)$, where S is the current solution. Often instead of accepting the first neighbour with the value of the objective function smaller than $F(S)$ for the current solution, the algorithm constructs all neighbours (or a given number of Neighbours) and selects the best one.

(iv) Update particle best and global best values.

(e) Termination:

If the number of iterations reaches a predetermined value, called maximum number of iterations then stop searching, other wise go to (c) and repeat the procedure.

Pseudo code of IIBPSO is given in Figure3.

STEP1: Initialization phase

Initialize swarm
Assign velocities to all paticle
Fitness calculation
Particle best and global best

STEP2: Iteration phase with IIBPSO search

```
for (i=0; i<number of iterations; i++)
 {
        Update particles velocities
        Update dimensions of particles
        Calculate Fitness values
        Update Particle and global best values
        Iterative improvement local search
        Update Particle and global best
}
```

STEP3: Iteration phase by local search for global best value

```
for (i=0; i<number of iterations; i++)
 {
  Iterative improvement local search
}
```

Figure 3. Pseudo code of IIBPSO algorithm

4. Numerical Example:

A lot sizing problem of 7 items and 6 periods is taken from Jinxing Xie, Jiefang which is a general capacitated lot sizing problem (2002), and this example is also taken for the comparison with other problem considered in the paper.

M.Fatih Tasgetiren and Yun-Chia Liang (2003) say that if population size (number of particles in swarm) is at least double the number of periods in the planning horizon performance would be better. According to Yuhui Shi (2004), PSO with minimum population size 5 gives better performance.

But for the sake of convenience swarm size i.e. population size is taken as 3 in numerical example, even though all the problems are solved with population size of 40.

Step1: Swarm contains 3 particles, each of size 7×6

$$\text{Particle1} = \begin{bmatrix}1&0&1&0&0&1\\1&0&0&0&0&0\\1&0&1&0&0&1\\1&0&0&0&0&0\\1&0&0&0&0&0\\1&0&1&0&0&1\\1&1&0&0&0&1\end{bmatrix} = \begin{bmatrix}+4.3&-2.4&-3.8&+2.5&+4.3&+1.5\\-3.6&-1.4&-1.4&-0.9&-3.6&+4.4\\-1.2&+0.6&+0.2&-1.4&-1.2&+3.2\\-2.0&+0.5&-3.5&-1.9&-2.0&-0.9\\+3.6&-2.5&-3.9&-1.3&+3.6&+4.0\\+4.3&+0.0&+1.2&-1.6&+4.3&+0.3\\+1.2&-3.4&+0.2&-4.2&+1.2&-1.7\end{bmatrix} \rightarrow \text{Fitness} = 10948$$

$$\text{Particle2} = \begin{bmatrix}1&0&1&0&1&0\\1&0&1&0&1&0\\1&0&1&0&1&0\\1&1&0&0&1&0\\1&0&1&0&1&0\\1&0&1&0&0&0\\1&0&0&0&0&0\end{bmatrix} = \begin{bmatrix}+1.5&+3.4&-1.8&+2.5&+4.3&+1.5\\-0.6&-1.4&-1.4&-0.9&-3.6&+4.4\\+2.5&+1.6&+0.2&-1.4&-1.2&-3.2\\-1.1&+0.5&-3.5&-0.9&+2.0&+0.9\\+2.2&-2.5&-3.9&-1.3&+3.6&+4.0\\-1.3&+0.0&+1.2&-1.6&+4.3&+0.3\\+0.7&-3.4&+0.2&-4.2&+1.2&-1.7\end{bmatrix} \rightarrow \text{Fitness} = 11648$$

$$\text{Particle3} = \begin{bmatrix}1&0&1&0&1&0\\1&0&0&0&1&0\\1&0&1&0&0&0\\1&0&0&0&1&0\\1&0&0&0&1&0\\1&0&0&0&0&0\\1&0&1&0&0&0\end{bmatrix} = \begin{bmatrix}+0.5&+5.4&-1.8&+2.5&+3.3&+2.5\\-0.1&-2.4&-1.4&-0.9&-3.6&+1.4\\+2.5&+0.6&+1.2&-1.4&-3.2&-3.2\\-3.1&+0.5&-3.5&-1.9&+2.0&+0.9\\+2.2&-2.5&-3.9&-1.3&+3.6&+4.0\\-1.3&+0.0&+2.2&-1.6&+4.3&+0.3\\+0.7&-3.4&+0.2&-4.2&+1.2&-1.7\end{bmatrix} \rightarrow \text{Fitness} = 9376$$

Step2: As it is first generation assign all particle values to particle best, and best fitness particle dimensions to global best value

$$\text{PB}_1 = \begin{bmatrix}1&0&1&0&1&0\\1&0&0&0&1&0\\1&0&1&0&0&0\\1&0&0&0&1&0\\1&0&0&0&1&0\\1&0&0&0&0&0\\1&0&1&0&0&0\end{bmatrix} \quad PB_2 \begin{bmatrix}1&0&1&0&1&0\\1&0&1&0&1&0\\1&0&1&0&1&0\\1&1&0&0&1&0\\1&0&1&0&1&0\\1&0&1&0&0&0\\1&0&0&0&0&0\end{bmatrix} \quad PB_3 = \begin{bmatrix}1&0&1&0&1&0\\1&0&1&0&1&0\\1&0&1&0&1&0\\1&1&0&0&1&0\\1&0&1&0&1&0\\1&0&1&0&0&0\\1&0&0&0&0&0\end{bmatrix}$$

$$\text{Global Best} = \text{GB} = \begin{bmatrix}1&0&1&0&1&0\\1&0&0&0&1&0\\1&0&1&0&0&0\\1&0&0&0&1&0\\1&0&0&0&1&0\\1&0&0&0&0&0\\1&0&1&0&0&0\end{bmatrix}$$

Step3:

Update Velocity using standard procedure of Binary particle swarm optimization

$$\text{Particle1} = \begin{bmatrix}+4.3&-2.4&-3.8&+2.5&+4.3&+0.04\\-3.6&-1.4&-1.4&-0.9&-3.6&+4.4\\-1.2&+0.6&+0.2&-1.4&-1.2&+1.74\\-2.0&+0.5&-3.5&-1.9&-2.0&-0.9\\+3.6&-2.5&-3.9&-1.3&+3.6&+4.0\\+4.3&+0.0&+1.2&-1.6&+4.3&-1.16\\+1.2&-4.86&+1.66&-4.2&+1.2&-3.16\end{bmatrix} \rightarrow \begin{bmatrix}0.98&0.08&0.02&0.92&0.98&0.50\\0.02&0.19&0.19&0.28&0.02&0.98\\0.23&0.64&0.54&0.19&0.23&0.85\\0.11&0.62&0.02&0.13&0.11&0.28\\0.97&0.07&0.01&0.21&0.97&0.98\\0.98&0.50&0.76&0.16&0.98&0.23\\0.76&0.00&0.84&0.01&0.76&0.04\end{bmatrix}$$

$$\text{Sigmoid}(V + \Delta V) = \begin{bmatrix}0.98&0.08&0.02&0.92&0.98&0.50\\0.02&0.19&0.19&0.28&0.02&0.98\\0.23&0.64&0.54&0.19&0.23&0.85\\0.11&0.62&0.02&0.13&0.11&0.28\\0.97&0.07&0.01&0.21&0.97&0.98\\0.98&0.50&0.76&0.16&0.98&0.23\\0.76&0.00&0.84&0.01&0.76&0.04\end{bmatrix} R = \begin{bmatrix}0.0&0.5&0.09&0.90&0.99&0.71\\0.0&0.3&0.99&0.11&0.33&0.99\\0.0&0.72&0.81&0.89&0.54&0.89\\0.0&0.92&0.00&0.93&0.33&0.37\\0.0&0.10&0.80&0.10&0.98&0.99\\0.0&0.65&0.84&0.97&0.99&0.37\\0.0&0.5&0.98&0.70&0.85&0.35\end{bmatrix}$$

Update particle dimension matrix according new velocity matrix of paticle

$$\text{New Particle1} = \begin{bmatrix} 1 & 0 & 0 & 1 & 0 & 0 \\ 1 & 0 & 0 & 1 & 0 & 0 \\ 1 & 0 & 0 & 0 & 0 & 0 \\ 1 & 0 & 1 & 0 & 0 & 0 \\ 1 & 0 & 0 & 1 & 0 & 0 \\ 1 & 0 & 0 & 0 & 0 & 0 \\ 1 & 0 & 0 & 0 & 0 & 0 \end{bmatrix} = \rightarrow \text{Fitness} = 10300$$

As particle 1 fitness value is improved, so first particles, particle best (PB_1) value will be updated with current particle data. If fitness is not improved then particle best value will remain same.

Like this update particle best and global best values will be updated for all particles in the according to fitness values.

Step4: Repeat this procedure until iteration number k < max iteration.

Local Search:

$$\text{input Particle} = \begin{bmatrix} 1 & 0 & 0 & 1 & 0 & 0 \\ 1 & 0 & 0 & 1 & 0 & 0 \\ 1 & 0 & 0 & 0 & 0 & 0 \\ 1 & 0 & 1 & 0 & 0 & 0 \\ 1 & 0 & 0 & 1 & 0 & 0 \\ 1 & 0 & 0 & 0 & 0 & 0 \\ 1 & 0 & 0 & 0 & 0 & 0 \end{bmatrix} \rightarrow \text{new paticle} = \begin{bmatrix} 1 & 0 & 1 & 0 & 0 & 0 \\ 1 & 0 & 0 & 1 & 0 & 0 \\ 1 & 0 & 0 & 0 & 0 & 0 \\ 1 & 0 & 1 & 0 & 0 & 0 \\ 1 & 0 & 0 & 1 & 0 & 0 \\ 1 & 0 & 0 & 0 & 0 & 0 \\ 1 & 0 & 0 & 0 & 0 & 0 \end{bmatrix} \rightarrow \text{Fitness} = 9820$$

Fitness value of new particle is improved (10300>9820). As the solution is improved old particle (i.e. input particle) will be replaced with a new particle.

Step5:

After this goto step2 and repeat the procedure. If number of iterations are reached stop

5. Problem Illustration

Problems shown in Fig. 4a, 4b and 4c as M×T are taken for modeling and simulation of CMIMLLS problem. Here M represents the total number of items involved in the BOM structure and T represents the number of periods. Table 1 represents different costs involved and Table 2a,2b and 2c carries information regarding demand and available capacity. Figure 4a is a BOM of single product where it contains 50×12 structure with 50 different items, 12 periods in 9 levels, Figure 4b is a BOM of a multi product contains 39×12 structure with 39 different items, 12 periods in 6 levels and Figure 4c is a BOM of a multi product contains 75×36 structure with 75 different items, 36 periods in 10 levels. Table 1 gives the information regarding the setup cost (S.C.) and holding costs (H.C.) of different items of 50 ×12, 39×12 and 75×36 problems. Tables 2a, 2b and 2c give the information regarding demand and availability conditions.

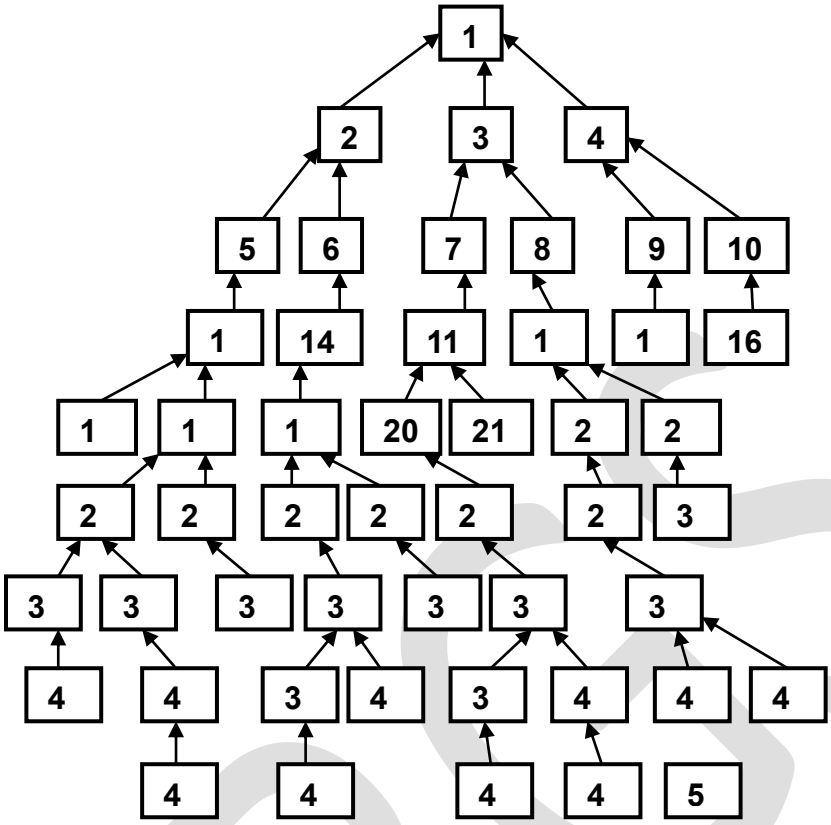

Figure 4a Product structures of 50×12 single product problem

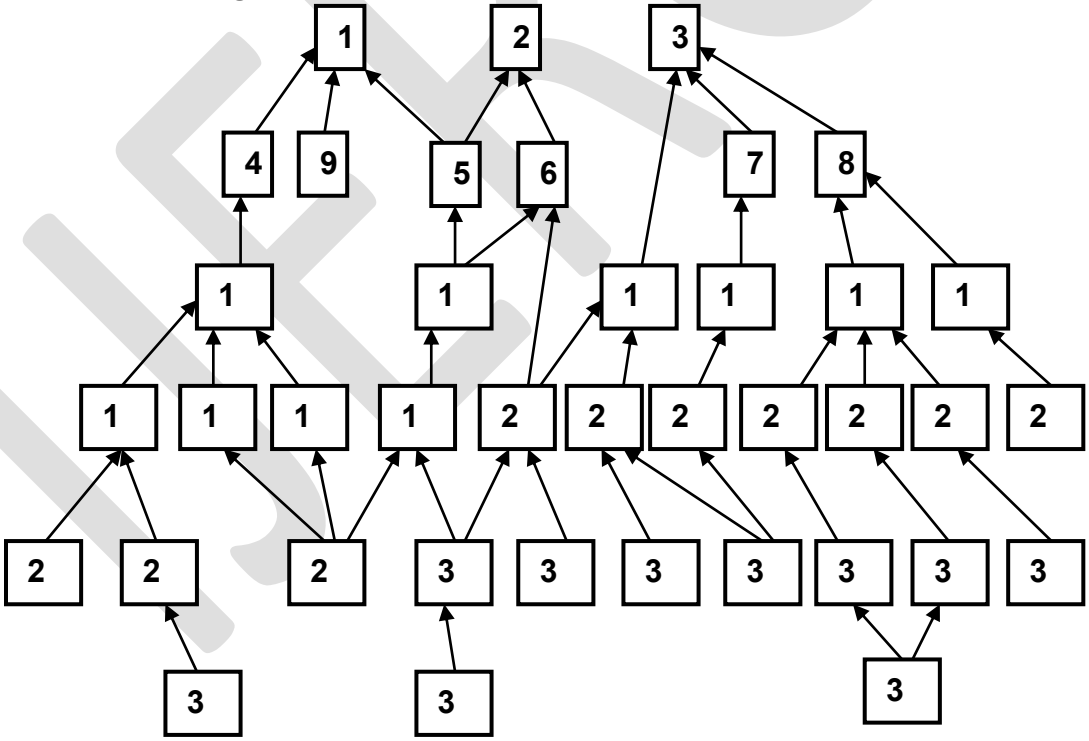

Figure 4b Product structures of 39×12 multi product problem

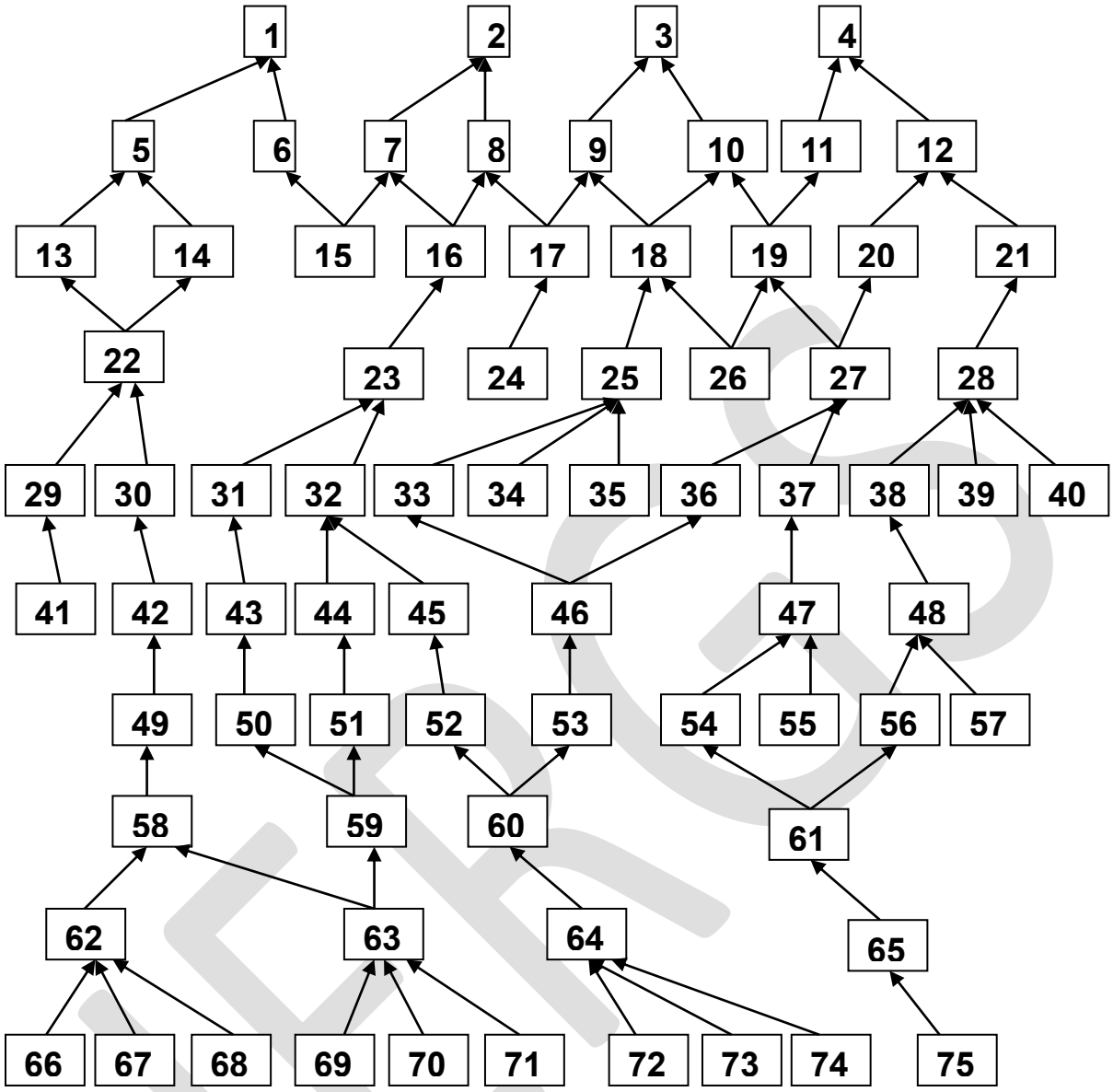

Figure 4c Product structures of 39×12 multi product problem

Table 1 Setup and Holding costs of different items in 50×12, 39×12,75×36 structures

S.No	50*12		39*12		75*36		S.No	50*12		39*12		75*36		S.No	75*36	
	H.C	S.C	H.C	S.C	H.C	S.C		H.C	S.C	H.C	S.C	H.C	S.C		H.C	S.C
1	97.83	780	40.08	490	50	410	26	7.53	540	1.45	580	30	580	51	18	800
2	45.19	200	35.27	450	49	450	27	4.36	160	3.63	650	31	620	52	17	410
3	43.82	590	59.66	90	50	430	28	18.52	480	4.35	450	30	610	53	16	350
4	5.82	710	25.42	140	48	420	29	5.81	410	3.29	820	30	490	54	15	320
5	26.04	890	10.42	880	47.2	250	30	1.93	140	5.04	620	30	300	55	14	280
6	18.87	610	22.64	440	46	300	31	6.71	390	2.53	580	29	200	56	13	280
7	27.03	920	22.31	70	42	500	32	15.35	370	3.3	340	29	200	57	12	180
8	15.64	210	19.53	430	42.5	800	33	4.36	520	0.61	340	25	100	58	11	680
9	2.67	490	1.34	930	40	400	34	3.28	700	2.52	80	25	120	59	10	190
10	1.86	920	25.12	650	40.5	500	35	6.38	160	4.83	690	25	300	60	9	100
11	23.5	520	9.46	740	37	200	36	3.47	290	3.44	430	27	400	61	8	480
12	12.59	540	17.48	680	36	330	37	1.97	420	0.91	60	27	200	62	7	200

13	25.13	510	4.32	800	45	480	38	1.76	160	2.64	760	25	800	63	6	270
14	16.42	500	14.28	220	40	450	39	6.41	450	2.65	180	25	100	64	5	600
15	0.84	300	2.56	850	37	380	40	7.17	340	-	-	25	250	65	4	210
16	1.02	450	10.07	400	40	200	41	2.97	750	-	-	27	450	66	3	700
17	0.62	440	4.59	650	36	100	42	0.25	140	-	-	28	100	67	3	100
18	23.71	510	7.13	860	35	100	43	3.22	430	-	-	26	200	68	3	200
19	15.32	910	8.82	850	35	120	44	1.85	890	-	-	25	800	69	3	100
20	20.58	830	10.6	670	34	280	45	3.84	610	-	-	26	100	70	3	150
21	8.71	730	6.02	370	33	270	46	0.41	860	-	-	24	500	71	3	200
22	3.14	850	2.78	360	35	290	47	0.37	860	-	-	24	480	72	2	100
23	0.94	450	2.95	310	35	320	48	3.84	350	-	-	22	250	73	2	200
24	13.02	370	9.32	440	33	380	49	3.95	610	-	-	21	600	74	2	100
25	7.34	390	0.31	590	30	560	50	1.63	350	-	-	19	100	75	1	100

H.C.=Holding Cost , S.C=Setup Cost

Table 2a Demand and Availability of end product in 50×12 problem

Period	1	2	3	4	5	6	7	8	9	10	11	12
Demand	15	5	15	110	65	165	125	25	90	15	140	115
Available	1000	2000	1000	0	5000	1000	0	500	800	500	1000	200

Table 2b Demand and Availability of end products in 39×12 problem

period	1	2	3	4	5	6	7	8	9	10	11	12
Item1	10	100	10	130	115	150	70	10	65	70	165	125
available	1500	2000	0	1000	800	5000	0	800	500	1000	2000	200
Item2	175	15	85	90	85	90	75	150	75	10	150	15
available	0	1000	2000	1000	900	0	800	1200	500	500	1000	100
Item3	135	165	15	105	25	120	50	60	5	140	60	10
available	1000	2000	900	800	0	1000	1200	300	500	800	100	100

Table 2c Demand and Availability of end products in 75×36 problem

period	1	2	3	4	5	6	7	8	9	10	11	12
Item1	10	100	10	10	70	10	20	10	10	50	10	70
available	∞	∞	∞	∞	0	∞	∞	∞	∞	∞	∞	∞
Item2	20	10	10	10	100	20	10	10	10	320	10	100
available	∞	∞	0	∞	5000	∞	∞	∞	∞	∞	∞	∞
Item3	30	10	10	100	10	10	20	10	40	100	10	10
available	∞	∞	∞	∞	∞	5000	∞	∞	∞	∞	∞	∞
Item4	40	10	10	30	10	10	10	10	100	10	10	120
available	∞	∞	∞	0	∞	∞	∞	∞	∞	∞	∞	∞
period	13	14	15	16	17	18	19	20	21	22	23	24
Item1	10	100	10	60	10	10	50	10	10	10	30	10
available	∞	∞	∞	∞	∞	0	∞	∞	∞	∞	∞	∞
Item2	10	20	10	170	10	10	50	10	10	10	210	10
available	∞	∞	0	∞	∞	∞	∞	∞	∞	∞	∞	∞
Item3	10	180	10	10	10	10	60	10	10	10	10	10

available	∞	∞	∞	∞	∞	∞	∞	∞	∞	∞	∞	∞
Item4	10	10	10	110	10	10	30	10	410	10	20	10
available	∞	∞	∞	0	∞	∞	∞	∞	∞	∞	∞	∞
period	25	26	27	28	29	30	31	32	33	34	35	36
Item1	20	10	90	10	10	310	10	250	10	10	90	10
available	∞	∞	∞	∞	0	∞	∞	∞	∞	1000	∞	∞
Item2	10	10	10	1000	10	10	10	10	10	10	80	10
available	∞	∞	∞	∞	800	0	∞	∞	500	∞	∞	∞
Item3	600	10	100	10	10	10	10	10	600	10	10	10
available	∞	∞	∞	∞	0	∞	∞	∞	0	∞	∞	∞
Item4	50	10	10	10	800	10	10	10	90	10	10	10
available	∞	∞	∞	∞	0	∞	∞	∞	∞	∞	∞	∞

6. Results

All capacitated large size lot sizing problems are coded in c language and run on Intel® Core™ Duo processors 667 MHz Front Side Bus and 2M Smart L2 Cache with 2GB RAM.

The authors have solved all the test problems using BGA, IIBGA, and BPSO, IIBPSO, and results are compared among them. A lot sizing problem of 7 items and 6 periods which is taken from Jinxing Xie, Jiefang (2002), is also taken for the comparison.

Following tables 3, 5, 7 and figures 5, 6, 7 show the comparison of binary BGA, IIBGA, BPSO and IIBPSO algorithms at different iterations of different problems under consideration. Table 4,6,8,9 gives the information about the optimum values obtained for different test problems for different programming techniques. Table10 gives the percentage of improvement of solutions of BGA, BPSO, IIBPSO techniques when compared to BGA technique solution for different problems under consideration.

Table 3 comparison 50×12 problem results among BGA, IIBGA, BPSO and IIBPSO

50×12				
Iteration	**BGA**	**IIBGA**	**BPSO**	**IIBPSO**
5	386,785.09	380,765.30	280,295.00	250295.00
25	380,891.31	352114.59	243,797.00	241009.15
50	350,503.75	330138.87	203,956.09	200037.17
100	322,136.16	321142.15	193,128.11	199121.89
200	279,484.72	290477.29	192,017.59	195192.04
500	249,875.41	250132.65	189,013.95	185013.09
1,000	234,587.08	230513.19	186,579.11	182599.11
2,000	234,587.08	232187.12	186,543.84	183450.08
5,000	234,489.03	223154.89	185,042.16	174057.32
10,000	229,484.6	219803.29	184,629.19	173753.29
15,000	229,484.6	214040.12	181,685.31	173753.29
20,000	204,240.90	213108.00	181,685.31	173753.29
30,000	204,140.90	191617.40	181,685.31	173753.29

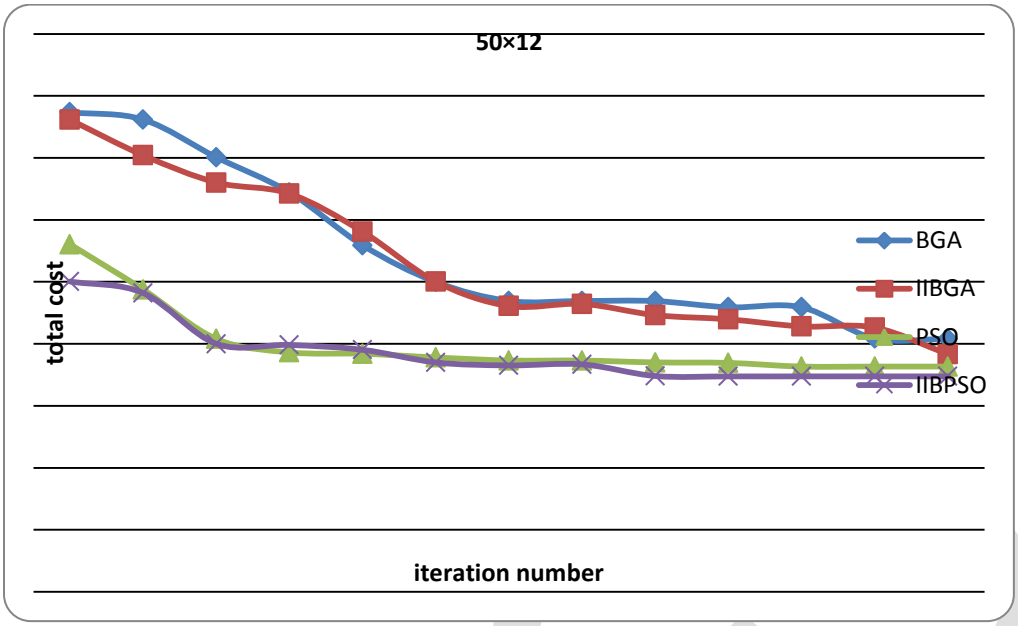

Figure. 5 BGA, IIBGA, BPSO, IIBPSO comparison at different iterations

Table 4 comparison 50×12 problem optimum results among BGA, IIBGA, BPSO and IIBPSO

50×12	BGA	IIBGA	BPSO	IIBPSO
	204,140.90	191617.40	181,685.31	173753.29

Table 5 comparison 39×12 problem results among BGA,IIBGA, BPSO and IIBPSO

39×12				
Iteration	**BGA**	**IIBGA**	**BPSO**	**IIBPSO**
5	377,421.19	350605.65	246,901.17	246,901.17
25	327,867.12	239426.79	217,583.65	213605.76
50	242,463.20	204744.77	204,084.98	197578.04
100	221,525.29	178650.31	202,884.17	191770.14
200	199,022.79	178346.06	194,724.84	191770.14
500	197,410.34	178244.00	193,219.70	186117.70
1,000	197,410.34	177609.65	185,691.15	142889.60
2,000	197,410.34	177609.65	185,691.15	142889.60
5,000	197,410.34	177609.65	172,684.78	142889.60
10,000	197,410.34	177609.65	172,682.56	142889.60
15,000	197,410.34	177609.65	172,682.56	142889.60

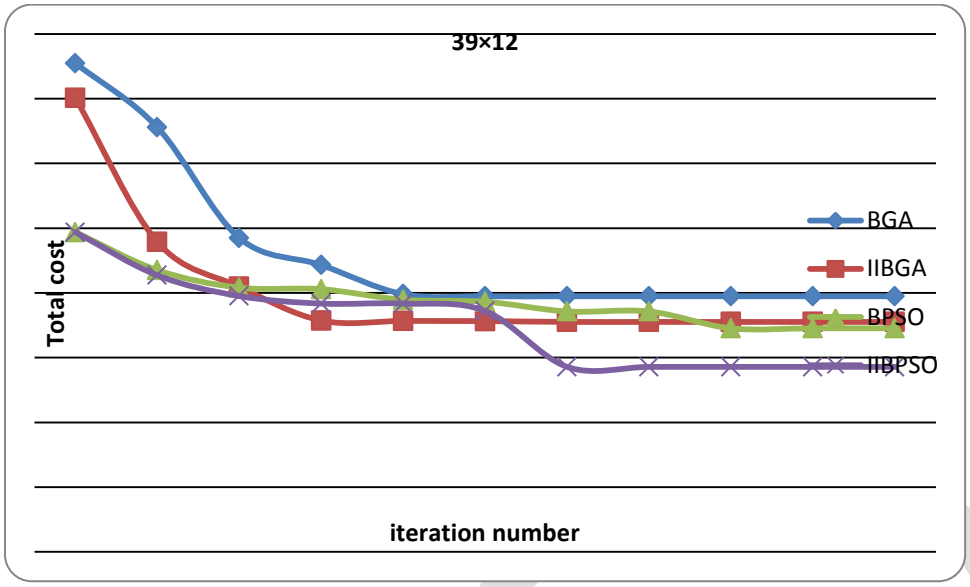

Figure. 6 BGA, IIBGA**,** BPSO, IIBPSO comparison at different iterations

Table 6 comparison 39×12 problem optimum results among BGA, IIBGA, BPSO and IIBPSO

39×12	BGA	IIBGA	BPSO	IIBPSO
	197,410.34	177609.65	172,682.56	142889.60

Table 7 comparison 75×36 problem results among BGA, IIBGA, BPSO and IIBPSO

75×36				
Iter No.	**BGA**	**IIBGA**	**BPSO**	**IIBPSO**
5	152174144	151074134	89866320	89866320
25	145240592	143150594	86317160	80226251
50	131999600	128899511	79341128	77312117
100	108485416	106374426	71873080	61752171
200	99614824	99919883	60409328	60409328
500	89866320	99614824	50344516	47817140
1,000	86317160	54844216	47819130	39071648
5,000	65511652	50344516	43816120	36459912
10,000	54344516	50344516	43816120	36291480
20,000	54344516	47444516	41817140	36205080
30,000	54344516	47344516	41817140	36205080

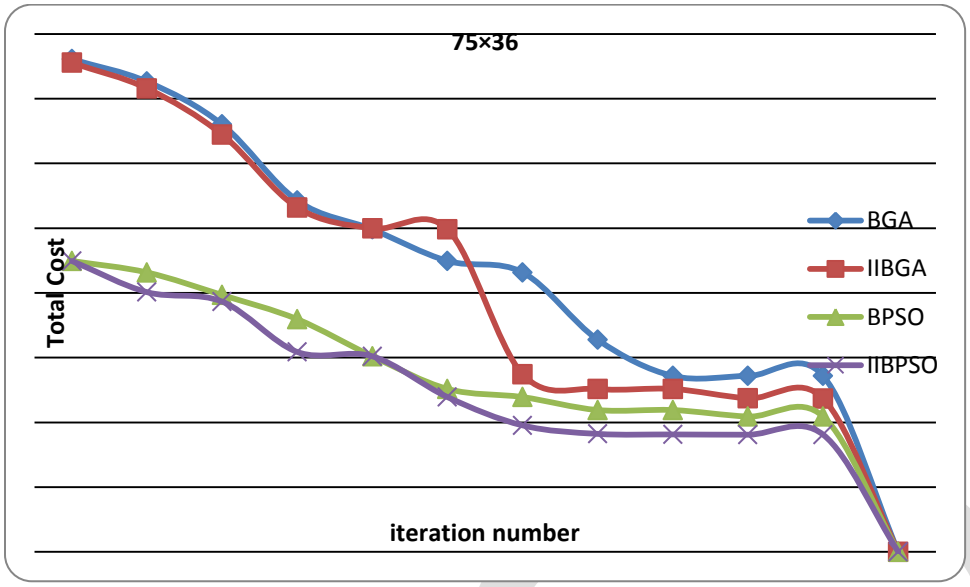

Figure 7 BGA, IIBGA, BPSO, IIBPSO comparison at different iterations

Table8 comparison 75×36 problem optimum results among BGA, IIBGA, BPSO and IIBPSO

75×36	BGA	IIBGA	BPSO	IIBPSO
	54344516	47344516	41817140	36205080

Table 9 comparisons 7×6, 50×12, 39×12, 75×36 problems optimum results among BGA, IIBGA, BPSO and IIBPSO

	BGA total cost	**IIBGA total cost**	**BPSO total cost**	**IIBPSO total cost**
7×6	9245	8320	8320	8320
50 × 12	204,140.90	191617.40	181,685.31	173753.29
39 × 12	197,410.34	177609.65	172,682.56	142889.60
75 × 36	54,344,516	47344516	41,817,140.0	36,205,080

Table 10 Percentage improvement in solution when compared to BGA Solution

	IIBGA	**BPSO**	**IIBPSO**
7×6	10	10	10
50 × 12	6.13	11	16
39 × 12	10	12.5	28
75 × 36	12.8	23.06	33.38

REFERENCES:

[1].N.P. Dellaert a, J. Jeunet b,*, Randomized multi-level lot-sizing heuristics for general product structures, European Journal of Operational Research 148 (2003) 211–228

[2]B.Karimi, S.M.T. Fatemi Ghomi, J.M.Wilson," The capacitated lot sizing problem: a review of models and algorithms", the international journal of Management science, Omega 31(2003) 365-378.

[3] Wagner, H. and Whitin, T. (2004). Dynamic version of the economic lot size model. Management Science, 50(12):1770–1774.

[4] Silver, E. and Meal, H. (1973). A heuristic for selecting lot size requirements for the case of a deterministic time-varying demand rate and discrete opportunities for replenishment. Production and Inventory Management, 14(2):64–74.

[5] Coleman, B.J., McKnew, M.A., 1991. An improved heuristic for multilevel lot sizing in material requirements planning. Decision Sciences 22, 136–156.

[6] Hernández, W. and G. Süer, "Genetic Algorithms in Lot Sizing Decisions", Proceedings of the Congress on Evolutionary Computing (CEC99), Washington DC, July 6-9, 1999.

[7] N.Dellart, J.Jeunet, A genetic algorithm to solve the general multi-level lot sizing problem with time varying costs. International journal of production Economics68 (2000)241-257.

[8].Regina Berretta, Luiz Fernando Rodriguez, A memetic algorithm for a multistage capacitated lot sizing problem, Int.j. Production Economics 87(2004)67-81.

[9]M.Fatih Tasgetiren and Yun-Chia Liang(2003),A binary particle swarm optimization algorithm for lot sizing problem, journal of Economic and Social Research5(2),1-20.

[10]Yi Hana, Jiafu Tanga, Iko Kakub, Lifeng Mua, Solving uncapacitated multilevel lot-sizing problems using a particle swarm optimization with flexible inertial weight, Computers and Mathematics with Applications 57 (2009) 1748_1755

[11] Klorklear Wajanawichakon, Rapeepan Pitakaso, Solving large unconstrainted multi level lot-sizing problem by a binary particle swarm optimization. International Journal of Management Science and Engineering Management, 6(2): 134-141, 2011.

[12] JINXING XIE AND JIEFANG DONG, Heuristic Genetic Algorithm for General Capacitated Lot Sizing problem, Computers and Mathematics with Applications 44(2002) 263-276

International Journal of Engineering Research and General Science Volume 3, Issue 5, September-October, 2015
ISSN 2091-2730

IMPORTANCE OF PSS AND SVC IN POWER OSCILLATION DAMPING

Feba Wilson[1], Jisha James[2]

PG Student [Power Systems], Dept. of EEE, Saintgits College of Engineering College, Pathamuttom, Kerala, India[1](E-mail-feba17@yahoo.com)

Assistant professor, Dept. of EEE, Saintgits College of Engineering College, Pathamuttom, Kerala, India[2]

Abstract— Low-area frequency oscillations are one of the major problems in the present power systems for smooth and reliable operation where power is essential to transfer from one area to another remote area through weak tie-lines. This kind of oscillations problem may result into system instability, cascade failure and even in blackouts, if they are not damp out quickly. It have been observed that local mode of oscillations can be damp out by using Power System Stabilizers (PSS) but damping inter-area mode of oscillations using PSS may not be possible always.Majority of the necessary damping torque is delivered by synchronous machines equipped with power system stabilizers (PSS). Nowadays, flexible AC transmission system (FACTS) devices are increasingly used in power systems. They have remarkable effects on increasing the damping of the system.

Keywords— Power system stabilizer,Automatic voltage regulator, Synchronous Generator,governing system, steady-state stability,transient stability,Static VAR compensator.

INTRODUCTION

Power System Stability is concerned as one of the main factors that affect the power system in its three main sectors: generation, transmission and distribution. There are several factors that can affect the stability of the system such as sudden load change, fault and generator shaft speed change. The instability problem is resulting in oscillatory behavior that, if undamped may eventually build up. Even undamped oscillations at low frequencies are undesirable because they limit power transfers in transmission lines and induce stress in the mechanical shaft. With proper design and compensation, the excitation system can be an effective means of enhancing stability in the dynamic range as well as in the first few cycles after a disturbance. The compensation by adding damping to the generator rotor oscillations is related to an auxiliary stabilizing signal and the device used to generate this signal is called Power System Stabilizer (PSS).

Stability can be controlled by controlling the excitation of the generator or its speed. In addition, the excitation can be controlled using Automatic Voltage regulator AVR. Nowadays, PSS becomes one of the main solutions to the instability behind the AVR. PSS is a device which provides additional supplementary control loops to the automatic voltage regulators system and/or the turbine governing system of a generating unit. It is considered as one of the most common ways of enhancing both small signal (steady-state) stability and large-signal (transient) stability. PSS are often used as an effective and economic means of damping such oscillations. The automatic voltage regulator (AVR) regulates the generator terminal voltage by controlling the amount of current supplied to the generator field winding by the exciter. It is mainly used to damp any oscillations accrued to the power system when load is changing. It keeps the terminal voltage of the generator constant so that the voltage on the load side will remains almost constant even the load is vary with time.

Power oscillations typically occur in large interconnected power systems, where two or more areas are interconnected through relatively weak alternating current (AC) transmission lines. These power oscillations are also referred to as inter area oscillations. If a power oscillation between two areas of a power system is excited, the rotor angles of synchronous machines in one area will start to oscillate in counter phase with synchronous machines in the other area and thereby force a flow of active power back and forth between the areas.

If the oscillation is sufficiently damped the oscillation will die out and the rotor angles return to a steady state. However, if there is in sufficient damping in the power system for this particular oscillation an ever increasing amount of active power is exchanged between the two areas until other security devices, e.g. synchronous machine or transmission line safety equipment, trip the unit or component. A cascading effect of equipment tripping and ultimately a system black out can be the consequence. Majority of the necessary damping torque is delivered by synchronous machines equipped with power system stabilizers (PSS).A basic concept of a known PSS is to add an auxiliary signal to the voltage reference of the exciter and thereby modulate the excitation voltage of the synchronous machine to damp the power oscillations.

II. POWER SYSTEM MODELLING

Synchronous Generator

The following assumptions are made:

1. Stator winding resistance is neglected.
2. Balancing conditions are assumed and saturation effects are neglected.
3. Damper winding effect is neglected.

The electrical system for each phase consists of a voltage source in series with an RL impedance, which implements the internal impedance of the machine. The value of R can be zero but the value of L must be positive.

The Simplified Synchronous Machine block implements the mechanical system described by

$$\Delta\omega(t) = \frac{1}{2H}\int_0^t (Tm - Te)\, dt - Kd\Delta\omega(t)$$

$$\omega(t) = \Delta\omega(t) + \omega_0,$$

where

$\Delta\omega$ = Speed variation with respect to speed of operation

H = constant of inertia

Tm = mechanical torque

Te = electromagnetic torque

Kd = damping factor representing the effect of damper windings

$\omega(t)$ = mechanical speed of the rotor

Static VAR Compensator (SVC)

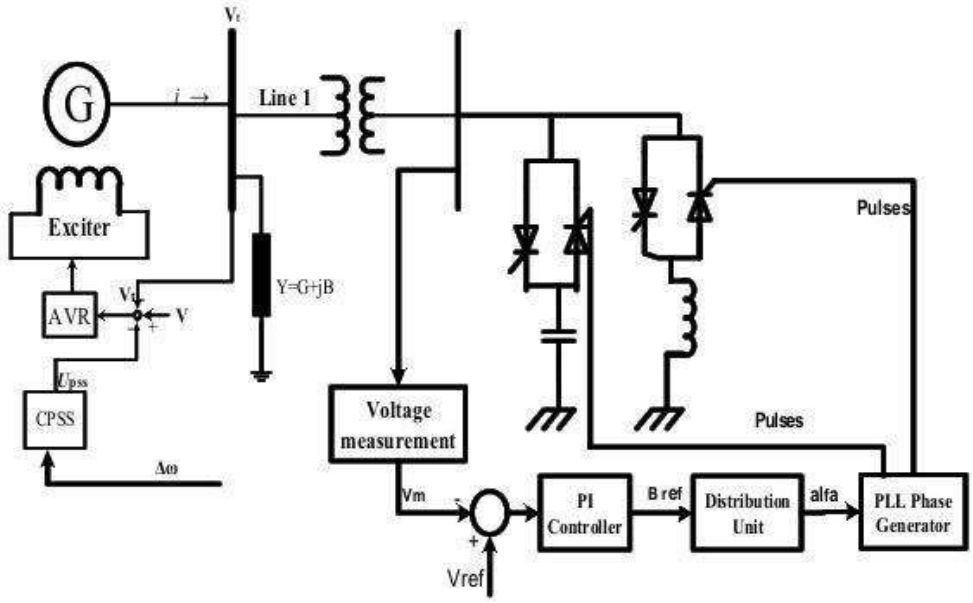

Fig. A single-line diagram of a SVC and a simplified block diagram of its control system.

The SVCs is a flexible and continuous reactive power compensator that has been used in power systems to regulate the reactive power and voltage to the actual system needs. It operates in two modes as capacitive and inductive. It consist of a thyristor-switched capacitor (TSC) and/or thyristor-controlled reactor (TCR). The current of SVC's reactor should be controlled in a way that a suitable control range between capacitive mode and inductive mode of SVC is determined. The SVC can be modelled as a first order linear differential equation model. This could be at the middle of a transmission line or at a load bus. When the SVC is operating in voltage regulation mode, its response speed to a change of system voltage depends on the voltage regulator gains (proportional gain Kp and integral gain Ki).

$B = (Kp+Ki/s).(VSVC-VSVC.ref)$ $\quad Bmin \leq B \leq Bmax$

III. SIMULATION RESULTS

CASE 1:SINGLE GENERATOR CONNECTED TO GRID(WITHOUT PSS)

Consider a single generator connected to grid. Without power system stabilizer, rotor angle deviation and rotor speed will be as follows.

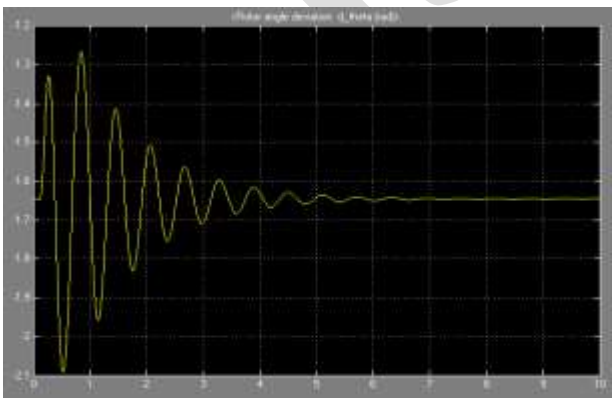

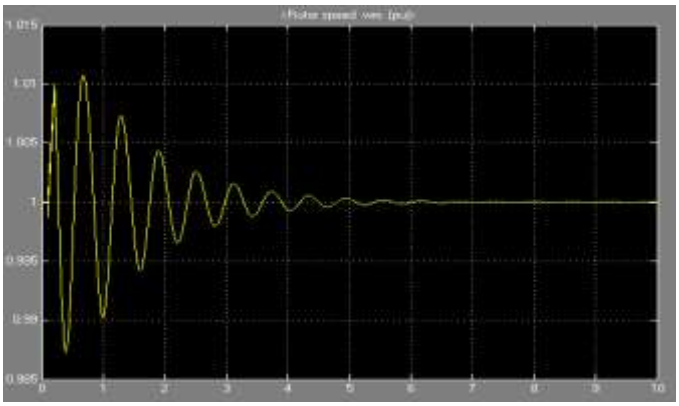

CASE 2: SINGLE GENERATOR CONNECTED TO GRID(WITH PSS)

With power system stabilizer, performance of system gets improved. Machine attains stability at faster rate.

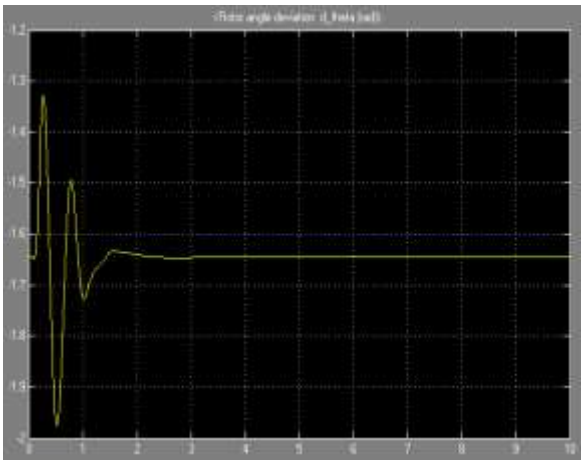

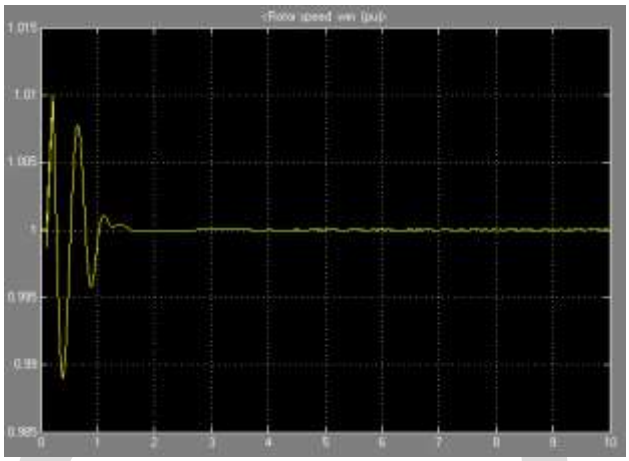

CASE 3: TWO MACHINE SYSTEM

Consider two machine system connected by a weak tie line. Static Var Compensator is one of a shunt connected FACTS devices, which is used to control the bus voltage at which it is connected to. It can also contribute to the stability of the system. Without SVC if a fault occur in the system, machines in the system may goes to unstable state. This can be understood by examining the rotor angle difference of the machines as well as speed of the machine which is nearer to the fault bus.

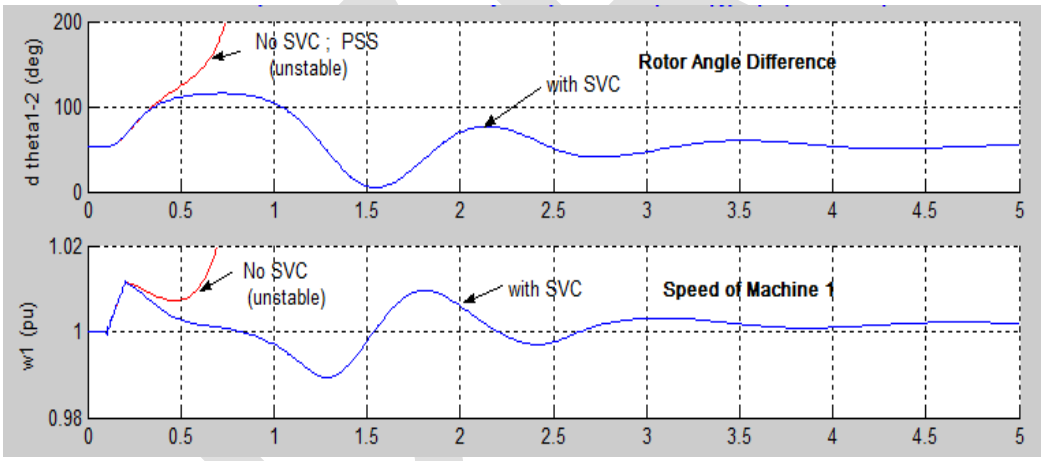

CONCLUSION

The power system is subjected to different types of disturbances such as small changes in the load that affects its efficiency and sometimes leads to unstable system. These disturbances cause oscillations at low frequencies that are undesirable since it affects the amount of transferred power through the transmission lines and leads to external stress to the mechanical shaft. To avoid such situation a power system stabilizer is added to the Automatic Voltage Regulator (AVR) to enhance stability in the dynamic range as well as in the first few cycles after a disturbance.

REFERENCES:

[1] Kundur, P., “Power System Stability and Control. Ontario,” McGraw-Hill, 1994.

[2] F. P. DeMello and C. Concordia, "Concepts of Synchronous Machine Stability as Affected by Excitation Control", IEEE Transactions on Power Apparatus and Systems, Vol. 88, 1969, pp. 316-329.
[3] P. Kundur, M. Klein, G. J. Rogers, and M. S. Zywno, "Application of Power System Stabilizers for Enhancement of Overall System Stability", IEEE Transactions on Power Systems, Vol. 4, 1989, pp. 614-626.
[4] J. H. Chow, J. J. Sanchez-Gasca, "Pole-placement Designs of Power System Stabilizers", IEEE Transactions on Power Systems, Vol. 4, No. 1, pp271-277
[5] Y. Y. Hsu and C. H. Cheng, "Design of Fuzzy Power System Stabilizers for Multimachine Power Systems", IEE Proceedings, Vol. 137, Part C, No.3, 1990, pp. 233-238.
[6] Yuan-Yih Hsu, Chao-Rong Chen, "Tuning of Power System Stabilizers Using an Artificial Neural Network", IEEE transactions on Energy Conversion, Vol. 8, 1992, pp. 612617.
[7] Jinyu Wen, Shijie Cheng and O.P. Malik, "A synchronous Generator Fuzzy Excitation Controller Optimally Designed with a Genetic Algorithm", IEEE Transactions on Power Systems, Vol. 13, 1998, pp 884-889
[8] M. A. Abido, "Hybridizing Rule-Based Power System Stabilizers with Genetic Algorithms", IEEE Transactions on Power Systems, Vol. 14, 1999, pp. 600-607
[9] Y.L. Abdel-Magid, M.A. Abido, S. Al-Baiyat and A.H. Mantawy, "Simultaneous Stabilization of Multimachine Power Systems via Genetic Algorithms", IEEE transactions on Power Systems, Vol. 14, 1999, 1428-1438.
[10] Y.L. Abdel-Magid, M.A. Abido and A.H. Mantawy, "Robust Tuning of Power System Stabilizers in Multimachine Power Systems", IEEE transactions on Power Systems, Vol. 15, 2000, pp 735-740.
[11] J. Lu, M.H. Nehrir and D.A. Pierre, "A Fuzzy Logic-based Adaptive Power System Stabilizer for Multi-machine Systems", Electric Power Systems Research, Vol. 60, 2001, pp115-pp121
[12] J. Lu, M.H. Nehrir and D.A. Pierre, "A Fuzzy Logic-based Adaptive Damping Controller for Static VAR Compensator", Electric Power Systems Research, Vol. 68, 2004, pp113-118

International Journal of Engineering Research and General Science Volume 3, Issue 5, September-October, 2015
ISSN 2091-2730

HARMONIC COMPENSATION USING FUZZY CONTROLLED DSTATCOM

Aswathy Anna Aprem, Fossy Mary Chacko

Department of Electrical Engineering, Saintgits College, Kerala, India

aswathyjy@gmail.com

Abstract— In this paper, a suitable controller for Distribution Static Compensator (DSTATCOM) is designed for improving the power quality. Power Quality has become a major issue in the present power system network. The network complexity is increasing more rapidly and most of the loads are inductive in nature which draws more reactive power. This causes harmonics and voltage variations in power system. To maintain the proper operation of inter-connected power system, we are using one of the FACTS devices such as DSTATCOM. It provides suitable compensation and thereby maintains the desired power factor, voltage and also reduce the harmonic content in distribution network. The fuzzy logic controlled block diagram for DSTATCOM which is optimized using GA is incorporated and also it has been simulated. A comparative study of PI controlled and Fuzzy Logic Controlled DSTATCOM is also made. The simulation is taken out by MATLAB/SIMULINK and the result shows the effectiveness of GA optimized Fuzzy controlled DSTATCOM for improvement of power quality.

Keywords— Distribution Static Compensator (DSTATCOM), Fuzzy Logic Controller(FLC), Proportional and Integral Controller (PI controller), Genetic algorithm (GA), Harmonics, Power Quality, scaling Factor.

1. INTRODUCTION

Due to insufficient reactive power support, the distribution power systems possess poor power quality and dynamic performance during disturbances. This can be due to harmonic pollution and load imbalance which causes extra stress on the networks and excessive voltage imbalance causing stress on other loads connected to the same network. Flexible AC Transmission Systems (FACTS) devices such as Static Synchronous Compensator (STATCOM) can be used to solve the power quality issues related to transmission lines while DSTATCOM can improve the power quality and dynamic performance in a distribution network. The Static Synchronous Compensator (STATCOM) is a shunt-connected reactive power compensation device that is capable of generating and/or absorbing reactive power at a given bus location and in which the output can be varied.

Generally, Proportional and Integral (PI) controllers are used to control the operation of the Distribution Static Compensator (DSTATCOM) in the distribution power system. However, the PI controlled DSTATCOM cannot provide optimal performance for different operating points since the power system is highly nonlinear and subject to various disturbances. More robust controllers such as the ones based on fuzzy logic approach are required for the DSTATCOM to provide adequate dynamic voltage control, stability and to solve power quality issues like voltage flicker, Harmonics etc. of the distribution power system.

According to the literature survey [1], the compensator is designed such that it not only cleans the distortion created by the load, but also improves the voltage quality at the point of common coupling (PCC). Specifically, a compensator-passive filter structure is proposed for this. The other aspect of the proposal is for a linear quadratic regulator (LQR)-based switching controller scheme that tracks reference using this compensator- filter structure.

A DSTATCOM is a shunt connected bidirectional converter based device which can provide adequate level of reactive power to improve the quality of electrical power featured as the voltage at the point of common coupling (PCC) in distribution network [2-4].

In this paper, the design of GA optimised FLCs for a 3MVA DSTATCOM for improving the power quality and transient behaviour of a distribution network is presented. PI controlled and fuzzy logic controlled DSTATCOM for improving the power quality and dynamic performance of a distribution power system is simulated using SimPowerSystem in MATLAB/Simulink environment and their comparison is made[5]. The dynamic performance, voltage flicker mitigation and Harmonic conditions are evaluated.

2. SYSTEM CONFIGURATION

Fig. 1 shows a configuration of a network where DSTATCOM is used as a shunt compensator to regulate voltage on a 25-kV distribution power system. 21 km and 2 km feeders are used to transmit power to loads at buses B2 and B3, respectively. A variable load producing continuously changing currents and voltage flicker is connected to bus B3 through a 25kV/600V transformer. The DSTATCOM uses Voltage Source Converter (VSC) to regulate voltage at PCC by absorbing or generating reactive power using power electronics to regulate three phase sinusoidal voltage at its terminal. The VSC uses forced commutated power electronic devices (GTOs, IGBTs or IGCTs) to synthesize the voltage on the secondary side of the coupling transformer from a DC voltage source. A DSTATCOM with VSC using PWM inverters has been used in this study.

3. CONTROL STRATEGY

In Fig. 2, PLL represents the phase-locked loop used to synchronize on the positive sequence component of the three phase (3Φ) primary voltage V_1. The output of the PLL is $\theta = \omega t$ and it is used to compute the direct-axis and quadrature-axis components of the AC (3Φ) voltages (*Vd* and *Vq*) and currents (*Id* and *Iq*). The DC measurement system in Fig. 2 provides the measurement of the DC voltage *Vdc*. The AC voltage measurement and current measurement systems in Fig. 2 measure the *d* and *q* components of AC positive-sequence voltage and currents to be controlled, respectively.

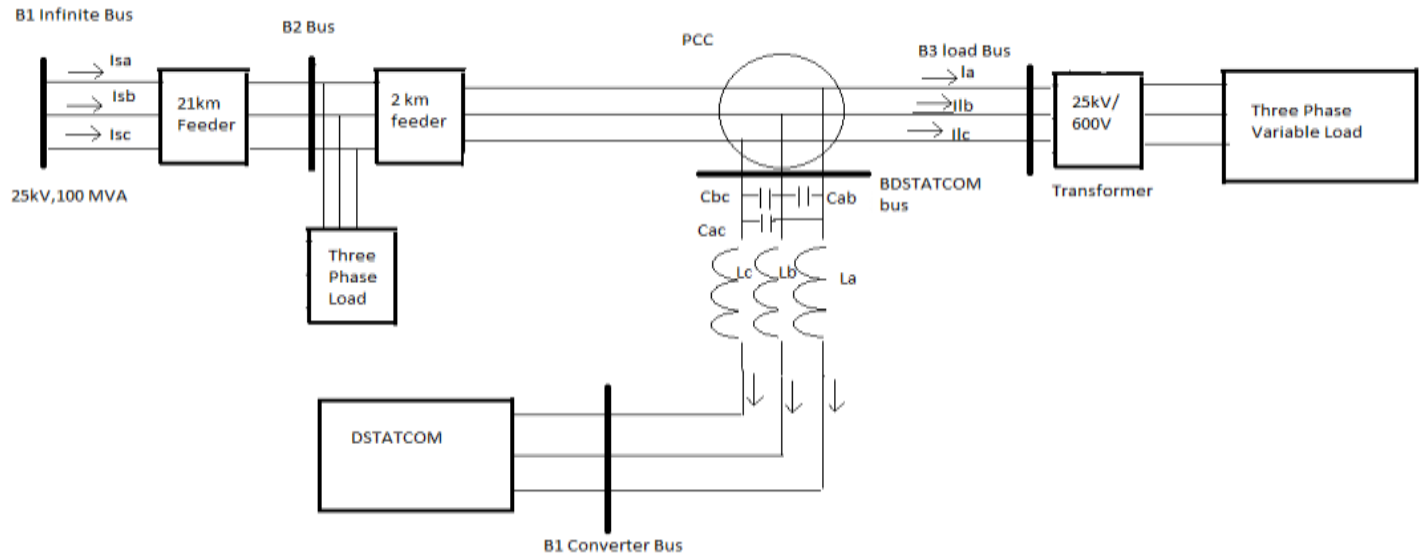

Fig.1. System Configuration of a Distribution Network.

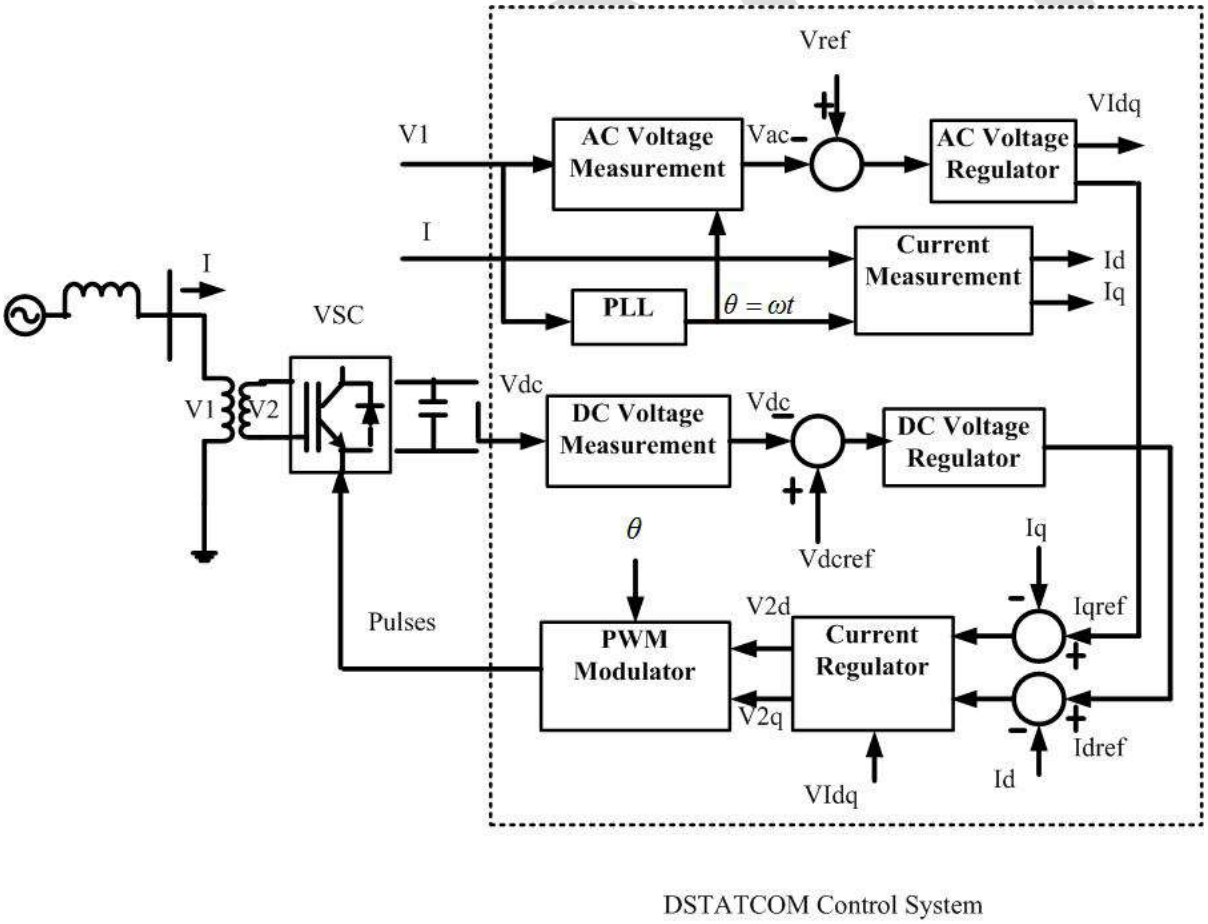

DSTATCOM Control System

Fig.2. DSTATCOM control system block diagram.

4. FUZZY LOGIC CONTROLLER DESIGN FOR THE DSTATCOM

A fuzzy logic controller (FLC) consists of four elements. These are a fuzzification interface, a rule base, an inference mechanism, and a defuzzification interface. A FLC has to be designed for the DC voltage regulator, the AC voltage regulator, and the current regulator. The design of the FLC for DC voltage regulator, AC voltage regulator and current regulators follows similar procedures. The PID-type FLC designed for DC voltage regulator has two inputs and one output. The ***error e*** (***e = Vdcref -Vdc***) and ***the rate of change of error*** e(t) are the inputs and the output of the FLC is *ΔId*. *ΔId*is integrated to produce *Idref*. In order to reduce the number of rules that is used in regular three-input PID-type FLC, two Sugeno-type FLC shown in Fig. 3 are used in this.

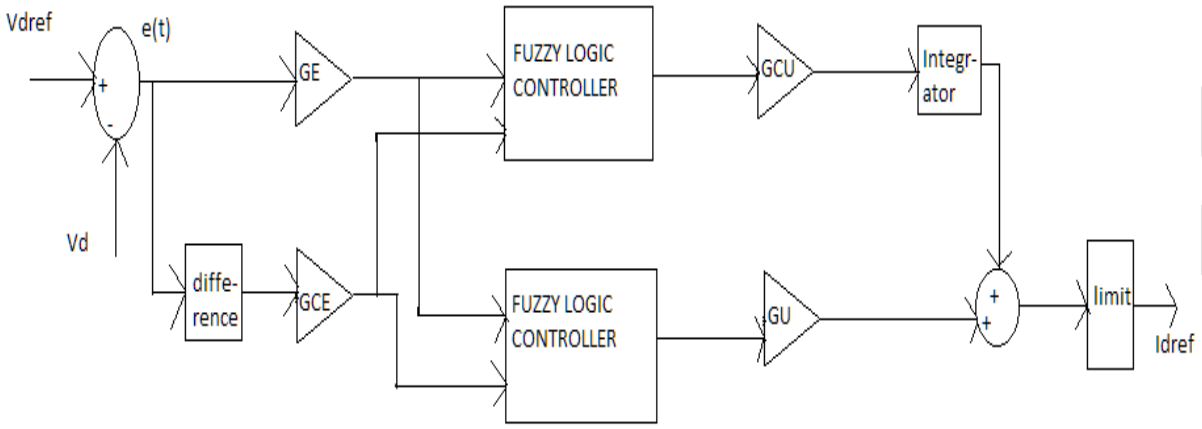

Fig.3. Block Diagram of Fuzzy Logic Controller based DC voltage Regulator.

As can be seen from Fig.3, four parameters need to be tuned using optimization methods. Namely, GE is the input error scaling factor, GCE is the input rate of change of error scaling factor, GCU is the PI-type FLC output scaling factor, and GU is the PD-type FLC output scaling factor respectively.

5. FUZZY LOGIC CONTROL OPTIMIZATION USING GA

Many real world problems involve multiple measures of performance, or objectives, which should be optimized simultaneously. In certain cases, objective functions may be optimized separately from each other and insight gained concerning the best that can be achieved in each performance dimension. However, suitable solutions to the overall problem can seldom be found in this way.

The Genetic Algorithm (GA) is a global search technique based on the principles of genetics and natural selection. Search parameters are represented as genes and these parameters evolve under specified rules in order to find the optimum solution .The basic structure of the GA consists of coding, selection, mating (crossover) and mutation.GA is easy to implement and it is a robust and reliable method.

Designing a fuzzy PID controller involves configuring the fuzzy inference system and setting the four scaling factors: GE, GCE, GCU and GU. We determine scaling factors GE, GCE, GCU and GU from the Kp, Ki, Kd gains used by the conventional PID controller. By comparing the expressions of the traditional PID and the linear fuzzy PID, the variables are related as:

- Kp = GCU * GCE + GU * GE
- Ki = GCU * GE
- Kd = GU * GCE

5.1 Optimization of Scaling Factors Using GA

By using the optimisation tool in the MATLAB, the tuning of the parameters can be done effectively. The following results shows the tuning using Genetic Algorithm. The DC voltage regulator, AC voltage regulator and Current regulator has been tuned. The main objective is to minimize the objective function.

DC VOLTAGE REGULATOR

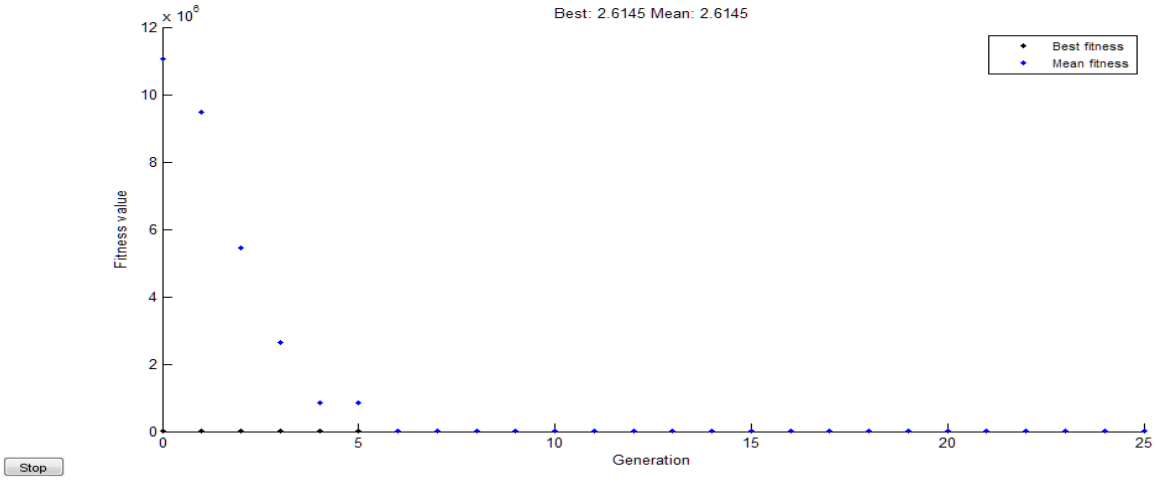

AC VOLTAGE REGULATOR

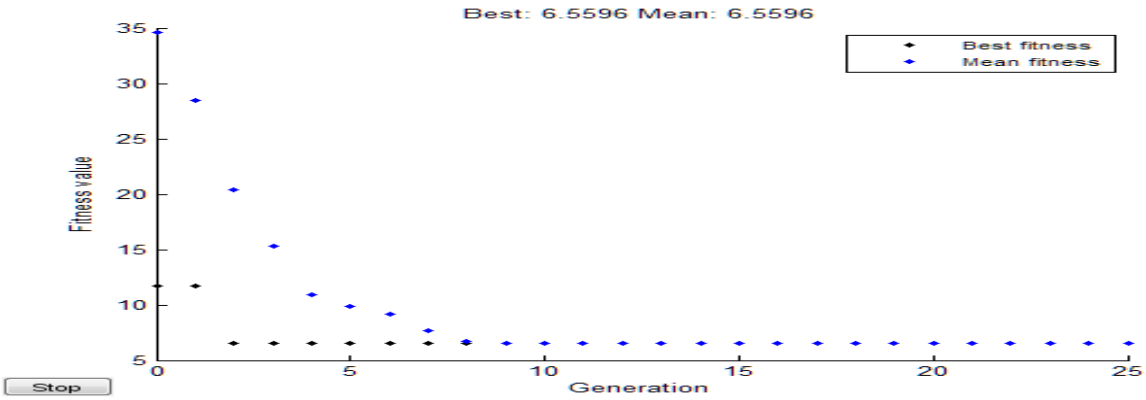

CURRENT REGULATOR

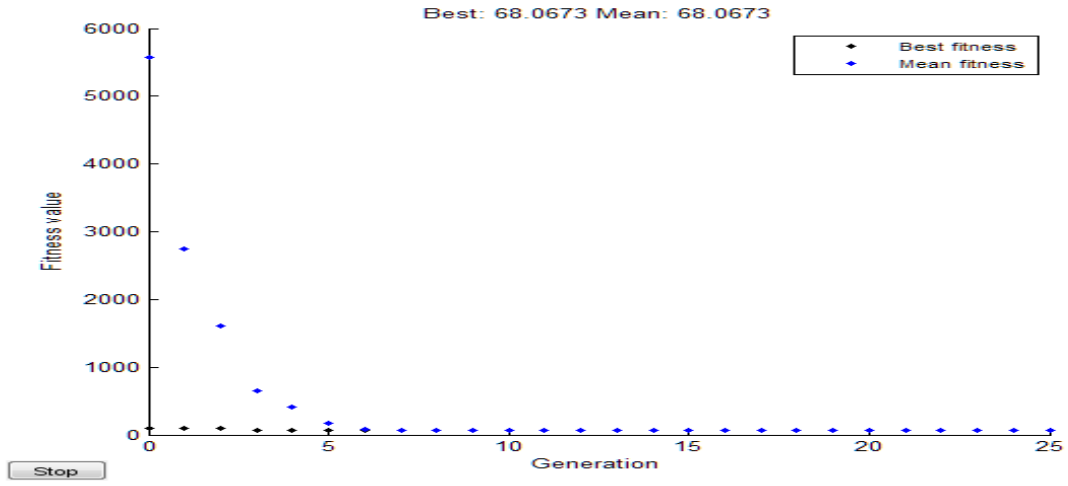

The tabular representation of the FLC rule base (with 49 rules) for the DC voltage regulator is shown in table below.

THE RULE TABLE WITH 49 RULES

Control Output		error						
		NL	**NM**	**NS**	**ZO**	**PS**	**PM**	**PL**
Rate of change of error	**PL**	ZO	PS	PM	PL	PL	PL	PL
	PM	NS	ZO	PS	PM	PL	PL	PL
	PS	NM	NS	ZO	PS	PM	PL	PL
	ZO	NL	NM	NS	ZO	PS	PL	PL
	NS	NL	NL	NM	NS	ZO	PS	PM
	NM	NL	NL	NL	NM	NS	ZO	PS
	NL	NL	NL	NL	NL	NM	NS	ZO

The size of inputs and output membership functions is chosen to be seven. The membership functions of the input variables for both the PI-type FLC and the PD-type FLC to be employed are of the triangular type and they are defined as shown in Figs. 4 and 5. The membership function of the output variable for both the PI-type FLC and the PD-type FLC are singletons as depicted in Fig. 6.

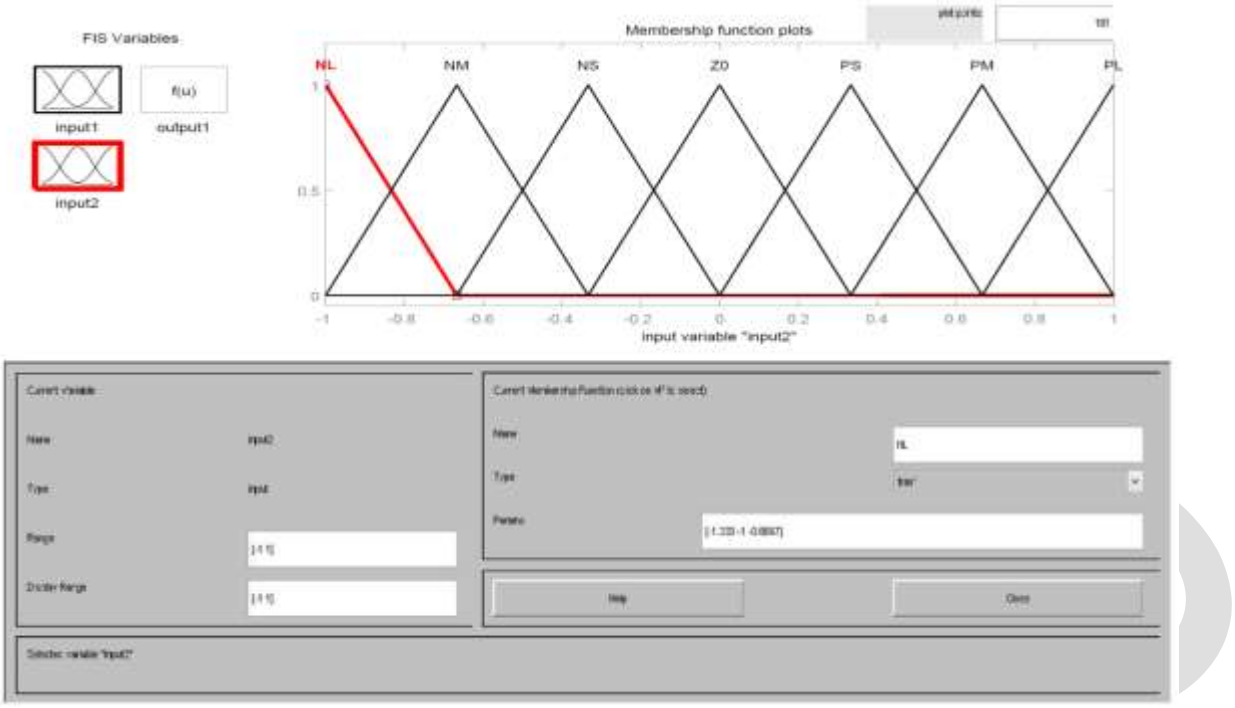

Fig.4. Membership function of the input error (e).

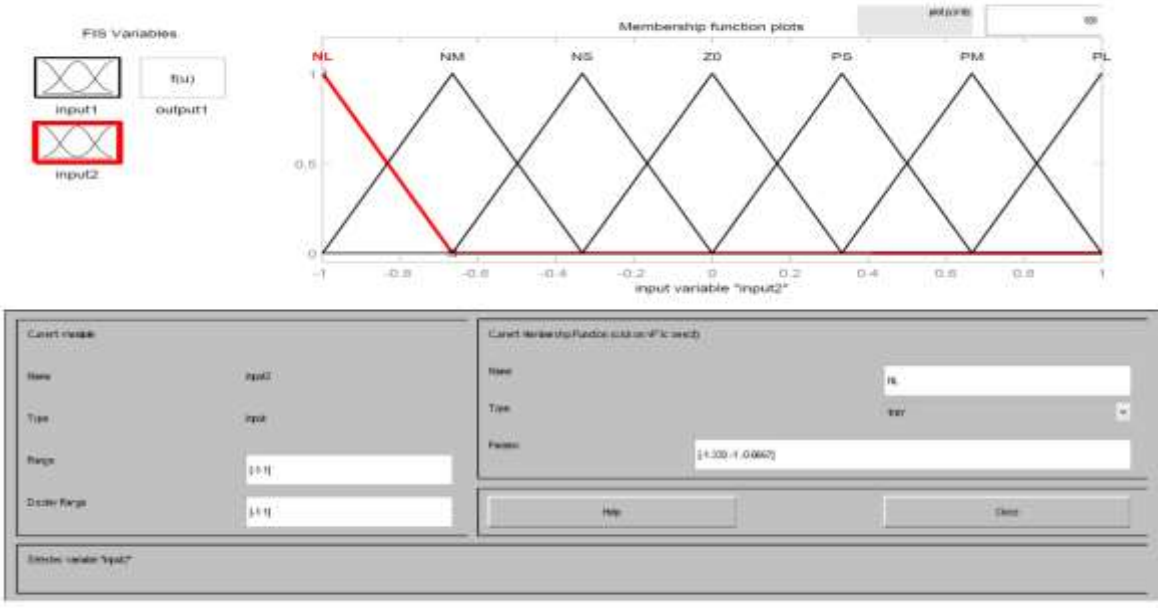

Fig.5. Membership function of the input rate of change of error e(t).

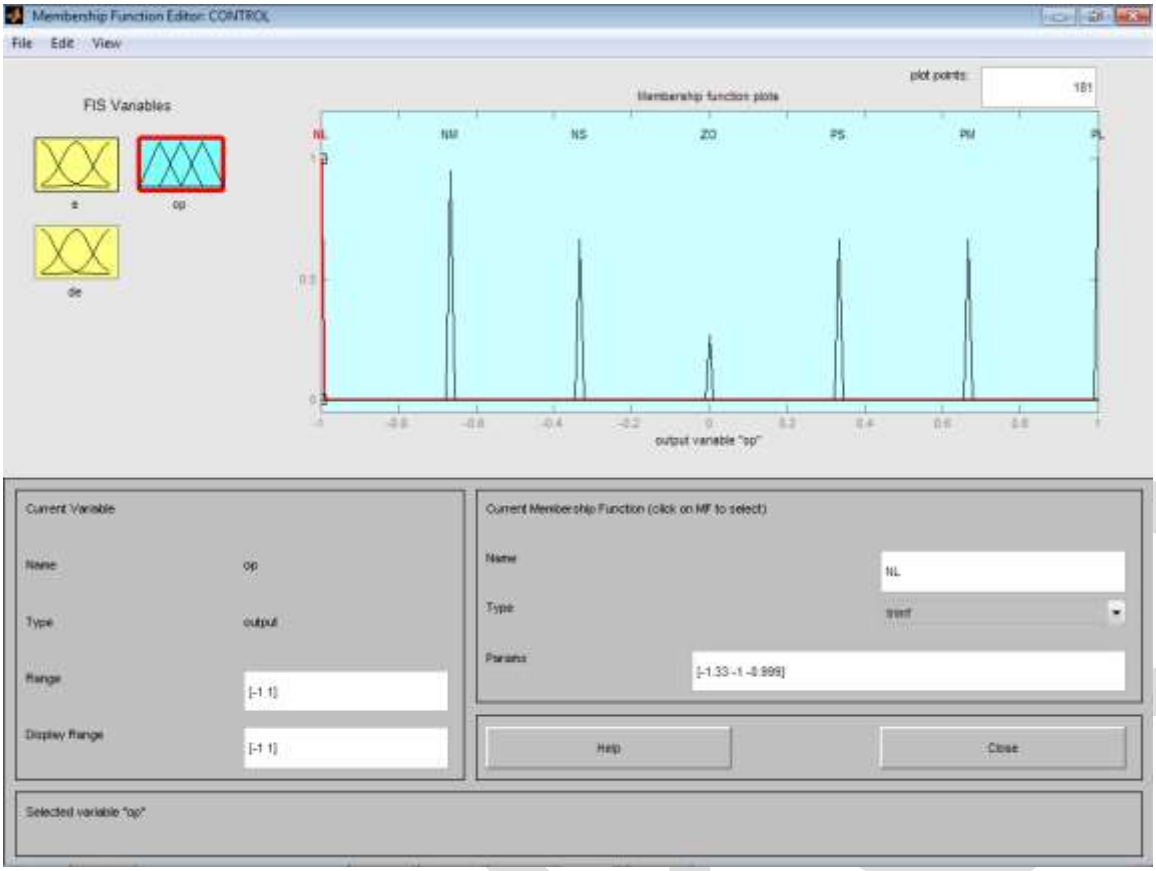

Figure 6: Membership function of the output of the FLC.

6. MATLAB BASED MODELLING OF THE SYSTEM

Comparative study of PI controlled and fuzzy logic controlled DSTATCOM for improving the power quality and dynamic performance of a distribution power system is simulated using SimPowerSystem in MATLAB/Simulink environment.

In this thesis, two control strategies of DSTATCOM are developed and compared:

1. PI controller

2. Fuzzy Logic Controller.

For analysis, different cases of the system are investigated.

1. Dynamic Response of both the PI controlled and Fuzzy controlled DSTATCOM.
   The dynamic response of a distributed power system subject to step changes in source voltage at the infinite bus is observed with the fuzzy controlled DSTATCOM and conventional PI controlled DSTATCOM. Fig. 9 shows the voltage at B3 when the source voltage has been changed by successively increasing the source voltage by 6%, decreasing it by 6% and bringing it back to its initial value at 0.2s, 0.3s, and 0.4s.
2. Mitigation of voltage flicker.
   The mitigation of voltage flicker with the fuzzy logic controlled and conventional PI controlled DSTATCOM can be observed when the load is varied.

3. Harmonic Analysis.

   By providing a non-linear load and imposing Harmonics into the system, the operation of DSTATCOM to reduce harmonics can be observed and compared.

7. SIMULATION RESULTS

The simulation result for the MATLAB models is investigated. Based on the results obtained, the comparison of both the controllers is done.

7.1. Uncompensated System

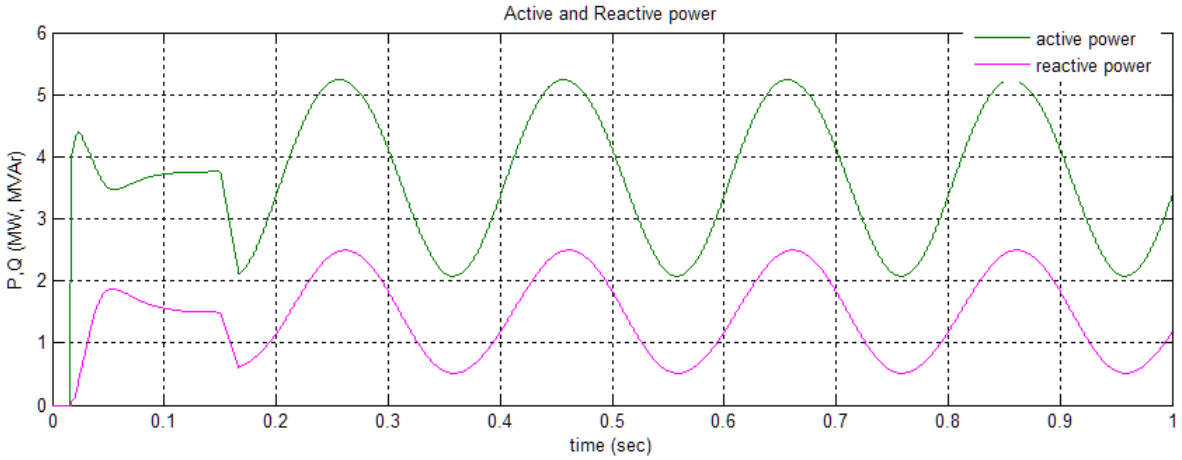

Fig.7. Active and Reactive power at Bus3 of distribution system without DSTATCOM

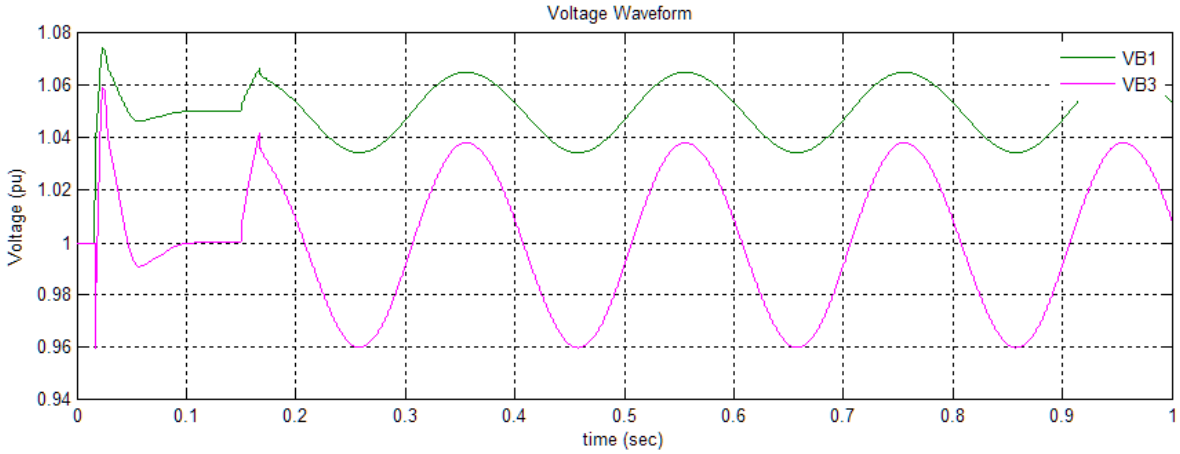

Fig.8. Voltage at Buses 1 and 3 of distribution system without DSTATCOM

7.2. System with PI and Fuzzy controlled DSTATCOM compensation.

1. Dynamic Response.

The dynamic response of a distributed power system subject to step changes in source voltage at the infinite bus is observed with the fuzzy controlled DSTATCOM and conventional PI controlled DSTATCOM.

PI CONTROLLER

Fig. 9 shows the voltage at B3 controlled by PI when the source voltage has been changed by successively increasing the source voltage by 6%, decreasing it by 6% and bringing it back to its initial value at 0.2s, 0.3s, and 0.4s.

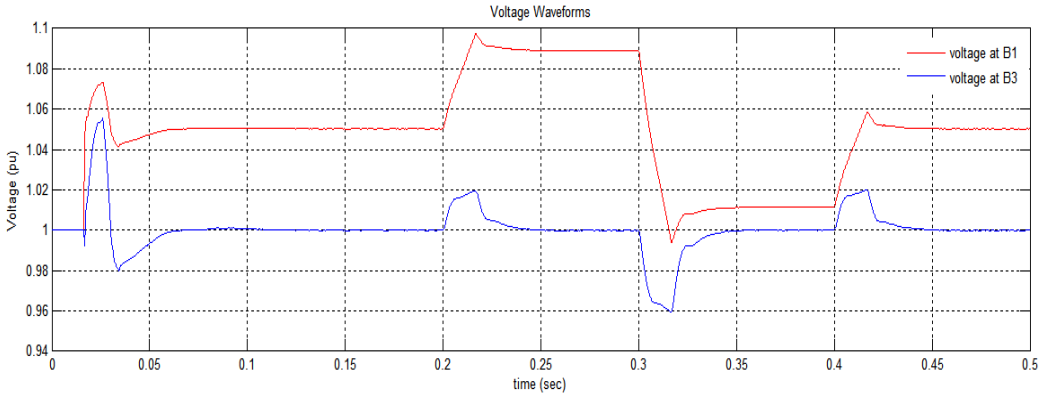

Fig.9. Simulation output of Voltages at buses B1 and B3.

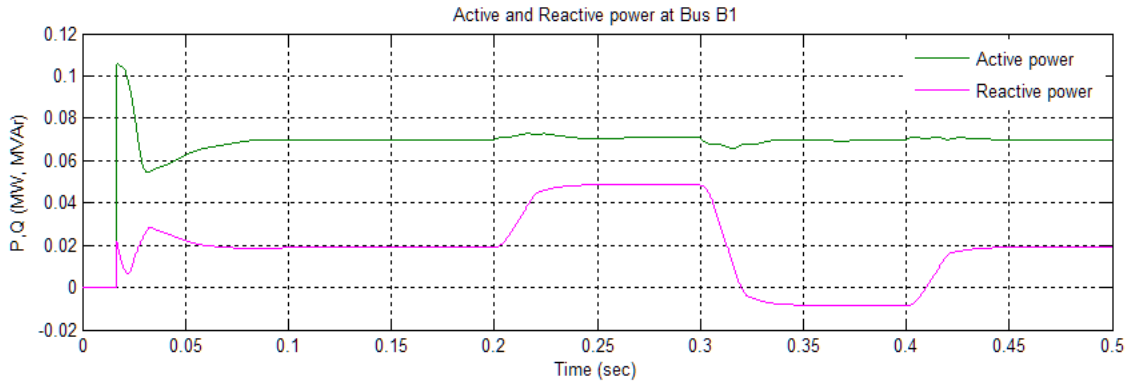

Fig.10. Simulation output of Active and reactive power at bus B1.

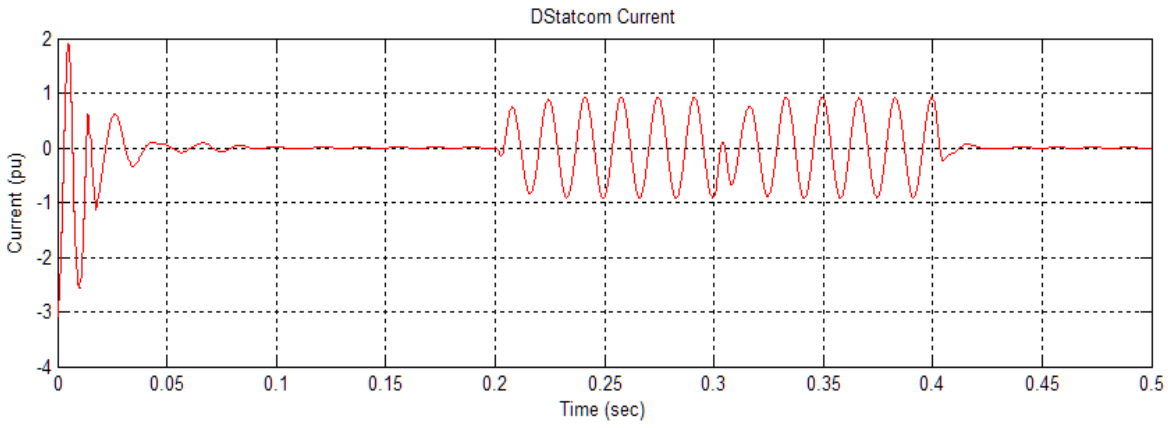

Fig.11. Simulation output of DSTATCOM current.

FUZZY LOGIC CONTROLLER

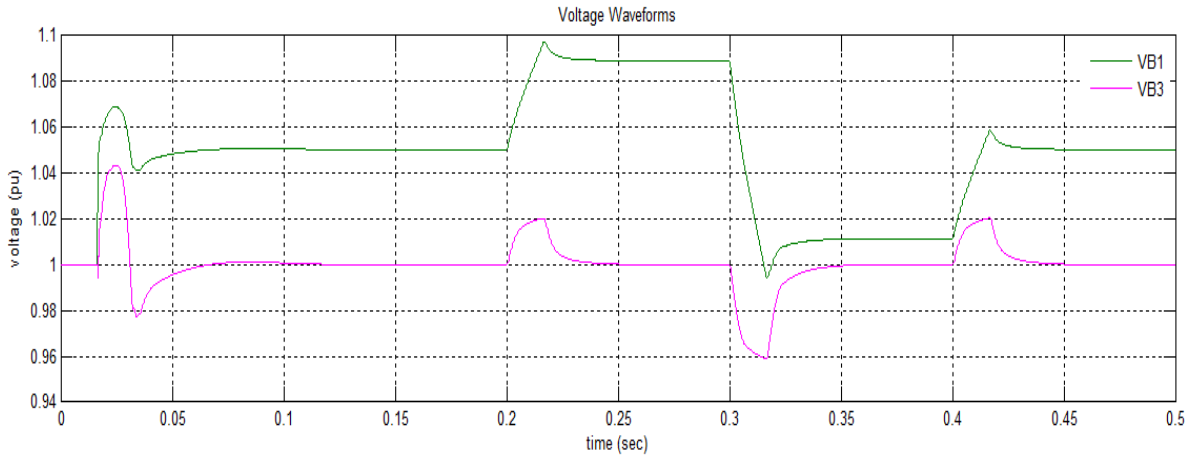

Fig.12. Simulation output of Voltages at buses B1 and B3.

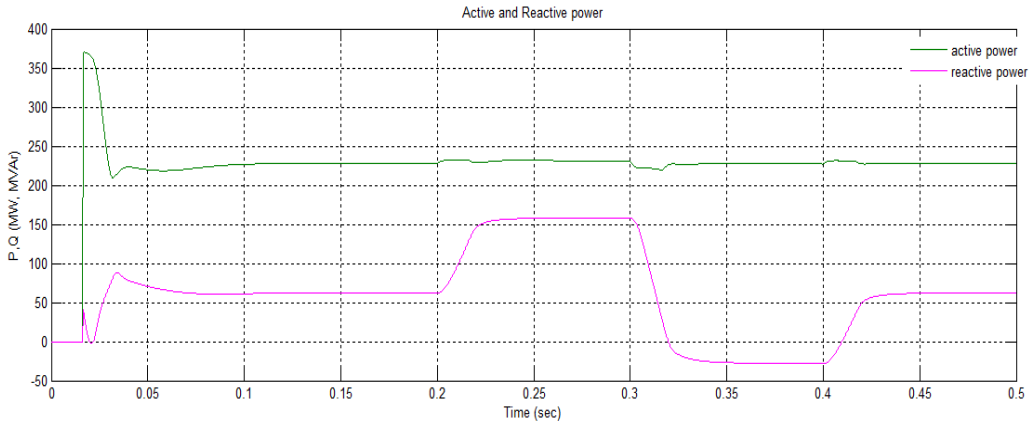

Fig.13. Simulation output of Active and reactive power at bus B1.

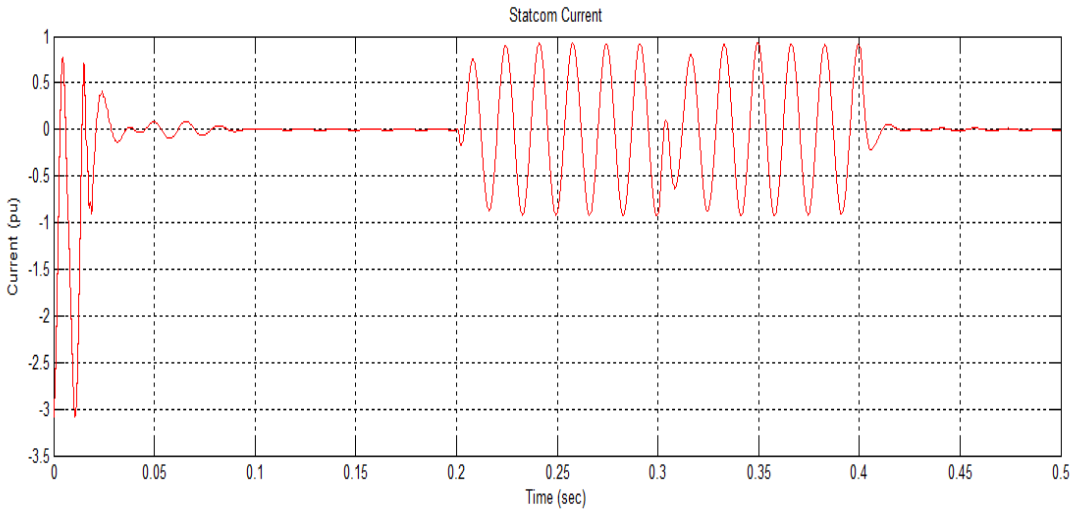

Fig.14. Simulation output of DSTATCOM current.

It can be deduced from the results that the dynamic response of the DSTATCOM can be improved much more by utilising FLCs instead of conventional PI controllers. The advantage of using the FLCs with the proposed structure is that PI-type part of the FLC can be used separately without any additional adjustment required.

After a transient lasting approximately 0.15 sec., the steady state is reached. Initially, the source voltage is such that the D-STATCOM is inactive. It does not absorb nor provide reactive power to the network. At t = 0.2 s, the source voltage is increased by 6%. The D-STATCOM compensates for this voltage increase by absorbing reactive power from the network (Q=+2.7 Mvar). At t = 0.3 s, the source voltage is decreased by 6% from the value corresponding to Q = 0. The D-STATCOM must generate reactive power to maintain a 1 pu voltage (Q changes from +2.7 MVAR to -2.8 MVAR).

2. Mitigation of voltage flicker.

The mitigation of voltage flicker with the fuzzy logic controlled and conventional PI controlled DSTATCOM can be observed when the load is varied.

PI CONTROLLER

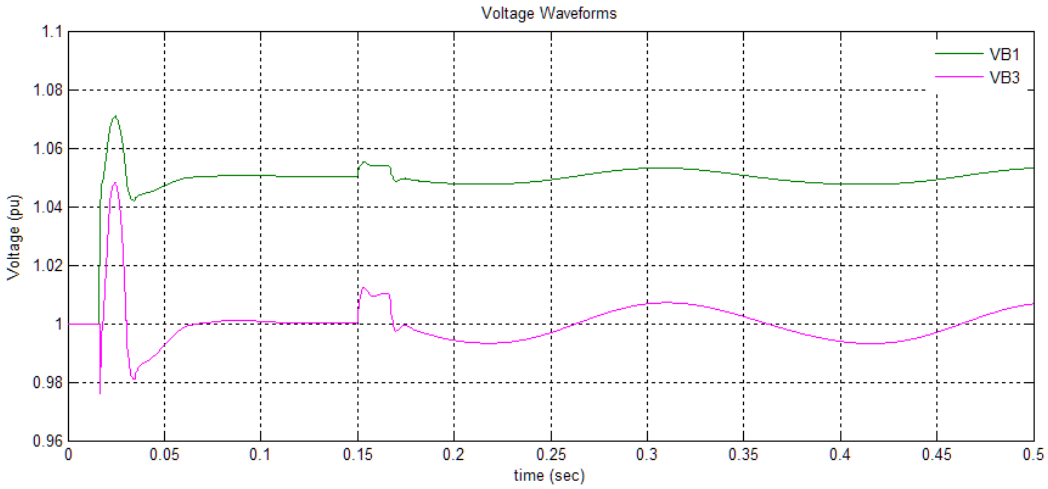

Fig.15. Simulation output of Voltages at buses B1 and B3.

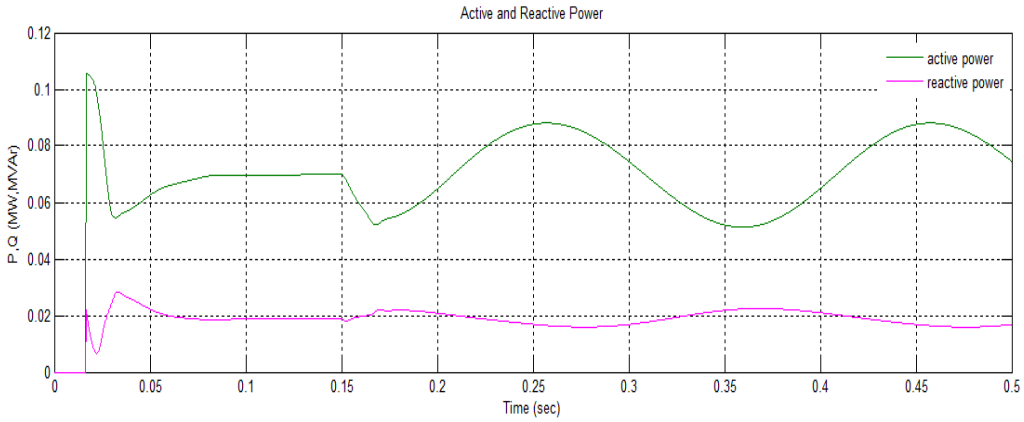

Fig.16. Simulation output of Active and reactive power at bus B1.

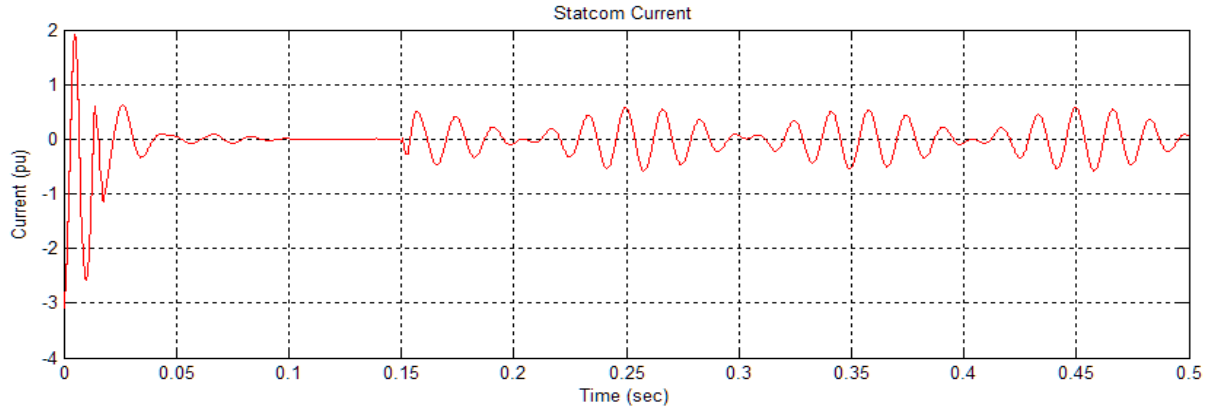

Fig.17. Simulation output of DSTATCOM current.

FUZZY LOGIC CONTROLLER

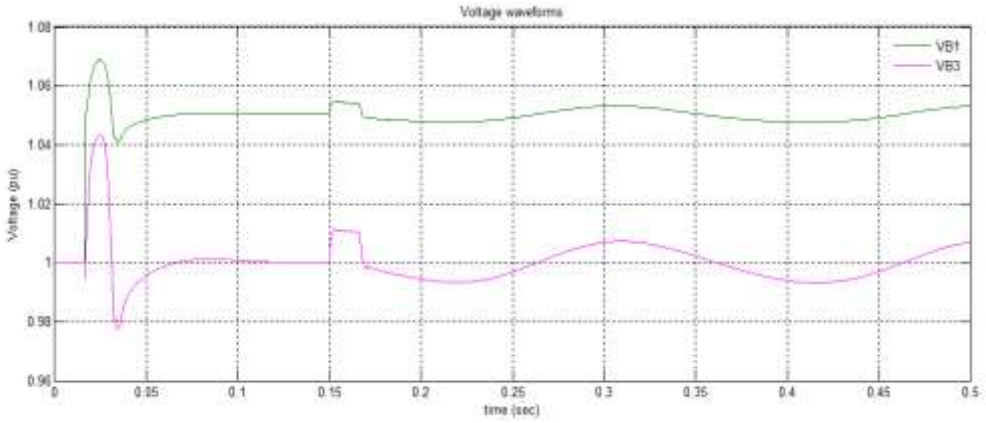

Fig. 18. Simulation output of Voltages at buses B1 and B3.

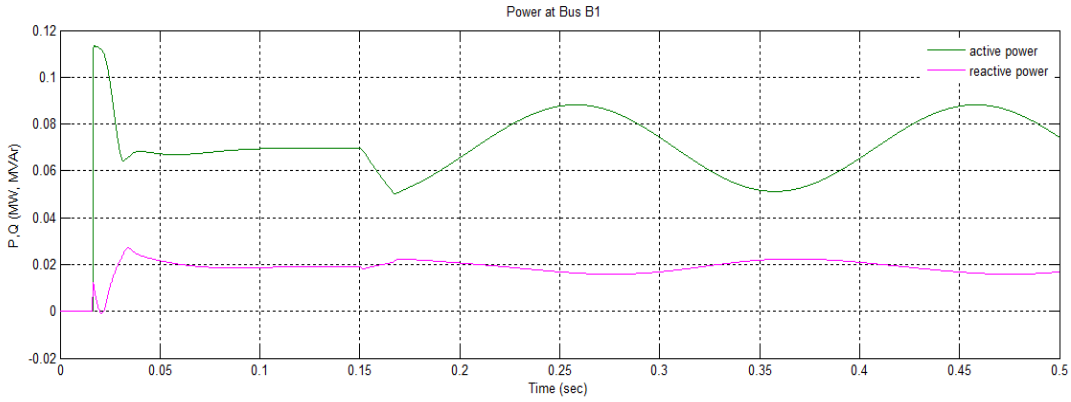

Fig.19. Simulation output of Active and reactive power at bus B1.

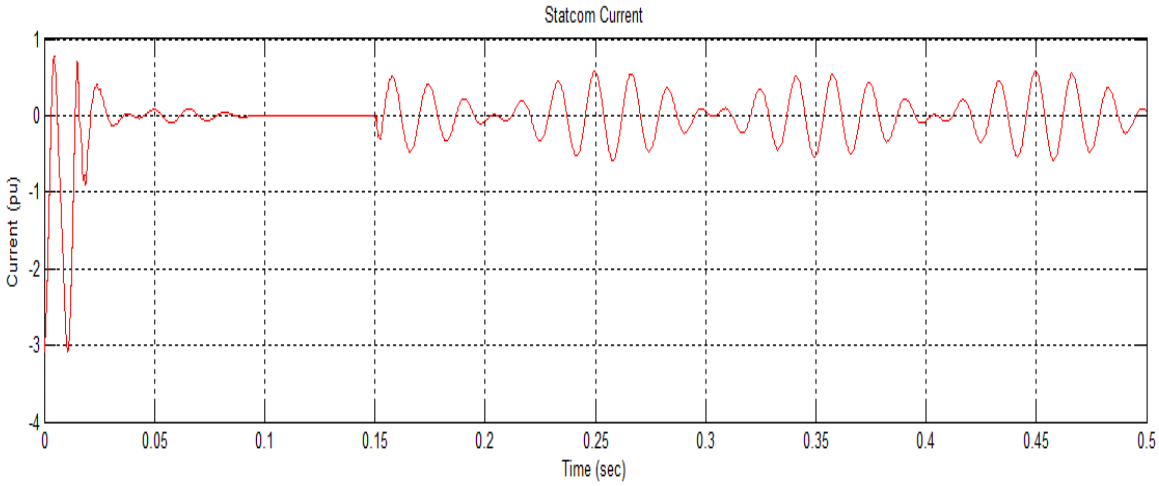

Fig.20. Simulation output of DSTATCOM current.

Fig. 15 and 18 shows the voltage at B3 with the fuzzy controlled DSTATCOM and conventional PI controlled DSTATCOM. It has been observed that voltage at B3 varies between 0.96 pu and 1.04 pu (±4% variation) without DSTATCOM in Fig.8. It is observed in Fig. 15 that the voltage fluctuation at bus B3 is reduced to ±0.7% with the PI controlled DSTATCOM. The voltage fluctuation at bus B3 is further reduced in Fig. 18 to ±0.6% with both the PI-type and PID-type fuzzy controlled DSTATCOM.

The D-STATCOM compensates voltage by injecting a reactive current modulated at 5 Hz and varying between 0.6 pu capacitive when voltage is low and 0.6 pu inductive when voltage is high.

3. Harmonic Mitigation.

   Inorder to obtain the THD analysis of the given system, the system is analysed without any compensation for non-linear load and the waveform distortions are analysed and THD values are measured using FFT analysis.

WITHOUT COMPENSATION

LOAD CURRENT

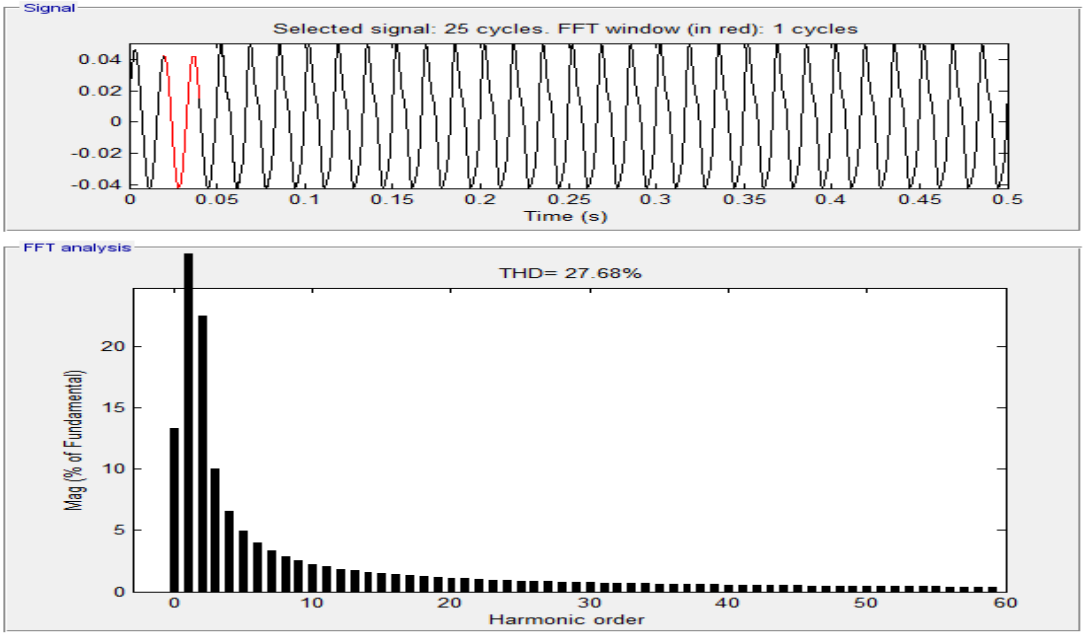

SOURCE CURRENT

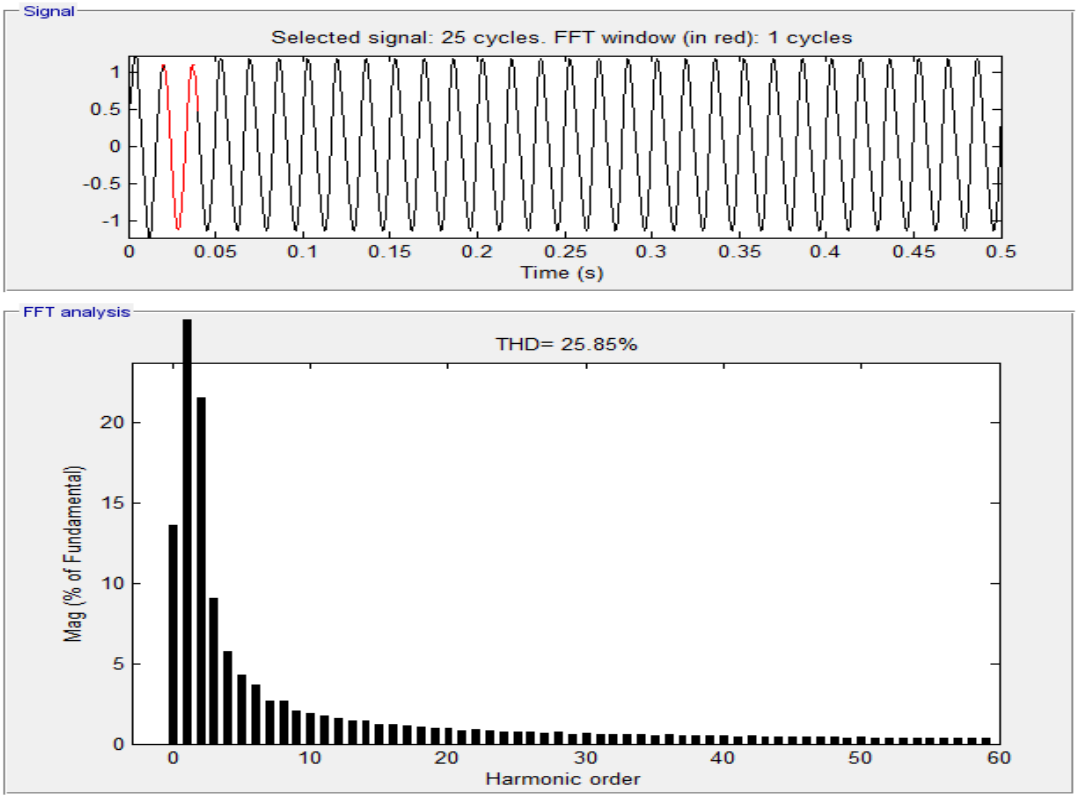

WITH PI CONTROLLER

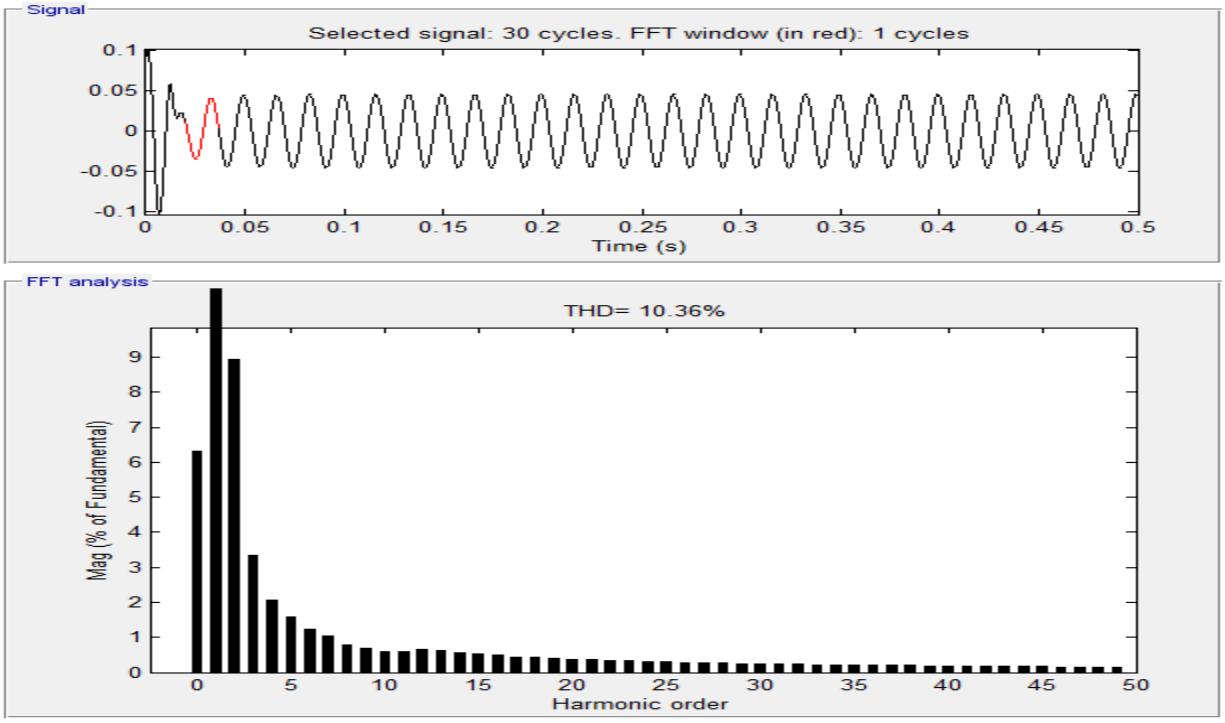

WITH FUZZY LOGIC CONTROLLER

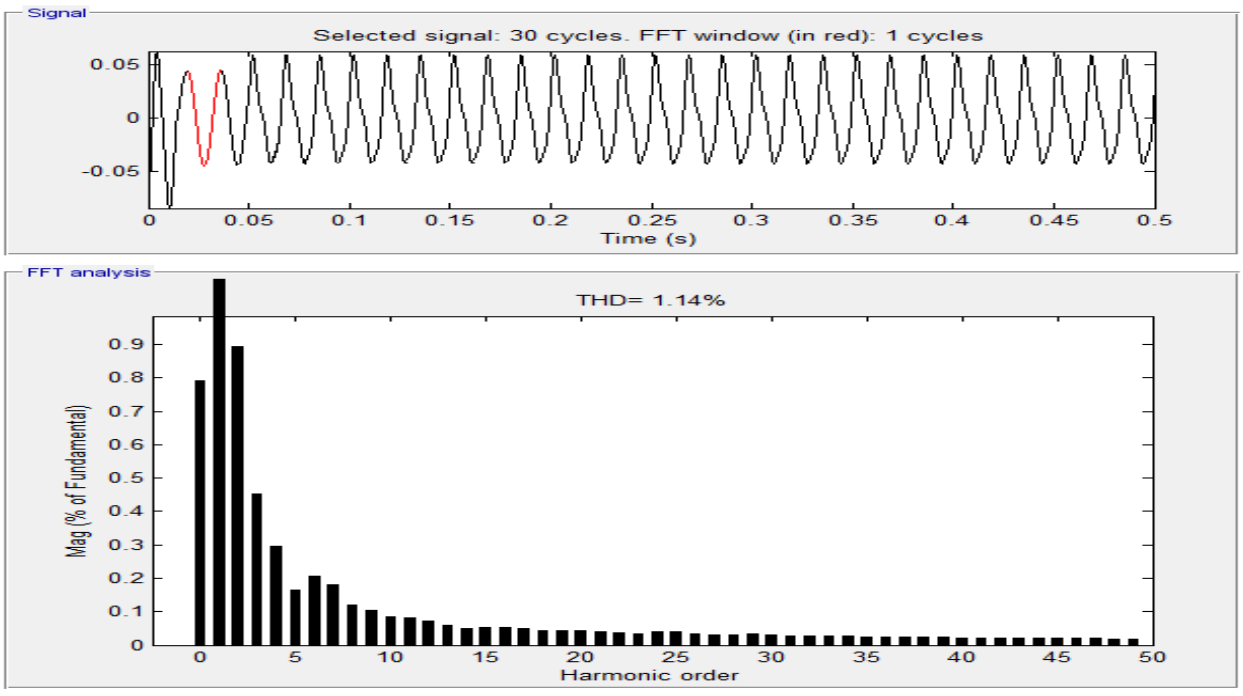

From the above figures, we can observe that the THD has considerably reduced in the case of Fuzzy logic controller. The table below shows the comparison of THD levels obtained after simulation.

	THD
Without DSTATCOM	25.85%
With PI controller	10.36%
With Fuzzy controller	1.14%

8. CONCLUSION

The design of FLCs for a DSTATCOM to improve power quality and dynamic performance of a distribution power system has done. FLC has to be designed for the DC voltage regulator, the AC voltage regulator, and the current regulator. The effect of Harmonic compensation using PI and Fuzzy Controller was evaluated. The results were compared with those of a conventional PI controlled DSTATCOM in the presence of source voltage variation and large load variations. The results show that the system's performance was dramatically improved by using FLC compared to the PI controller. The simulation results obtained in MATLAB/SimPowerSystems show that the DSTATCOM controlled by the GA optimised FLC provides better system dynamic response and hence improves power quality and transient behaviour for the distribution power system.

REFERENCES:

[1] A. Ghosh and G. Ledwich, "Load Compensating DSTATCOM in Weak AC Systems," *IEEE Trans. on Power Delivery*, vol. 18, no.4, October 2003.

[2] G. F. Reed, M. Takeda, F. Ojima, A. P. Sidell, R. E. Chervus and C. K. Nebecker, "Application of a 5MVA, 4.16kV D-STATCOM System for Voltage Flicker Compensation at Seattle Iron & Metals," *IEEE PES SM*, pp. 1605-1611, 2000.

[3] S. Kincic and A. Chandra, "Distribution Level STATCOM (DSTATCOMs) for Load Voltage Support," IEEE Proceedings of Power Engineering Conference on Large Engineering Systems, pp 30-37, 2003 .

[4] Juan Shi, AkhtarKalam, Amin Noshadi, Peng Shi "Genetic Algorithm Optimised Fuzzy Control of DSTATCOM for Improving Power Quality" *Australasian Universities Power Engineering Conference*, AUPEC 2014, Curtin University, Perth, Australia, 28 September – 1 October 2014

[5] D. Prasad, T. S. Kumar, B.V. Prasanth, and K.S.G.Sankar, "Fuzzy Logic Control of D-Statcom for Power Quality Improvement", *Int.Journal of Engineering Research and Applications*, ISSN: 2248- 9622, Vol. 3, Issue 6, pp.398-403, November-December 2013.

[6] N. Sreekanth, N. Pavan Kumar Reddy, "PI & Fuzzy Logic Based Controllers STATCOM For Grid Connected Wind Generator", *Int.Journal of Engineering Research and Applications*, ISSN: 2248- 9622, Vol. 2, Issue 5, pp.617-623, September- October 2012.

[7] N.M.G. Kumar1, P. SangameswaraRaju and P.Venkatesh, "Control Of DC Capacitor Voltage In A D-STATCOM Using Fuzzy Logic Controller", *Int. Journal of Advances in Engineering & Technology*,,ISSN: 2231-1963,Vol. 4, Issue 1, pp. 679-690, July 2012.

[8] RehanAbidi, Dr.MutasimNour, "Analysis Of A D-STATCOM In A 25 kV Power Distribution System Using Simulink", *Int.Journal of Electrical and Electronics Research*, ISSN: 2348-6988, Vol. 2, Issue 2, pp.26-34, April - June 2014.

[9] Mohit Bajaj, Vinay Kumar Dwivedi, Ankit Kumar, AnuragBansal, "Design And Simulation Of DSTATCOM For Power Quality Enhancement In Distribution Networks Under Various Fault Condition", *Int.Journal of Emerging Technology and Advanced Engineering*, ISSN:2250-2459, Vol. 3, Issue 4, April 2013.

[10] F. Herrera, M. Lozano, and J. L. Verdegay, "Tuning Fuzzy Logic Controllers By Genetic Algorithms", *Int.Journal ofApproximate Reasoning*.

[11] Y.T.R.Palleswari, B.Kali Prasanna And G.Lakshmi, "Multi Level Statcom For Harmonic Reduction", *International Journal Of Application Or Innovation In Engineering & Management (Ijaiem)*, Issn 2319 - 4847volume 2, Issue 10, October 2013

[12] N.G.Hingorani and L.Gyuyi, understanding FACTS-Concepts and technology of flexible AC Transmission Systems, IEEE Press, 1999.

International Journal of Engineering Research and General Science Volume 3, Issue 5, September-October, 2015
ISSN 2091-2730

Intrusion Detection For Different Distribution In Wireless Sensor Network

Miss. Samidha S. Davari

Department of Electronics Engineering

DKTE's Textile and Engineering Institute

Ichalkaranji

samidhashrikant@gmail.com

Mr. U. A. Patil

Assistant Professor, Department of Electronics Engineering

DKTE's Textile and Engineering Institute

Ichalkaranji

uapatil2002@yahoo.co.in

Abstract – Intrusion detection is one of the basic application in wireless sensor network. Intrusion detection is nothing but a mechanism for WSN to detect presence of incorrect or anomalous activities in the defined network. For intrusion detection a number of sensors are deployed in the area, which will monitored. In this paper there are different types of deployment strategies are discuss. In uniform distribution all the sensors are deployed uniformly and randomly in the network area. In Gaussian distribution sensors are deployed around a central important deployment point. Clustering algorithm is used for partitions the data set points into k-clusters. In this paper the distance between the data points is calculated by Euclidean distance. The results are compared with different model by varying different network parameter**.**

Key words – Wireless sensor network, Uniform deployment, Sensing range, Intrusion detection.

I. INTRODUCTION

Wireless sensor network (WSN) deals with many of the important fields like civil & tactical (military), health care, environmental monitoring, outdoor habitat monitoring, etc. Intrusion detection having good attention on network so, it is helpful for many application. Hence security of WSN in an important issue especially, if they have important information. The intruder detection is critical application in WSN. Failure in securing WSNs causes harmful effect in different types of application. An intrusion detection system (IDS) is one of an active process, that analyse system activity for unauthorized entry or malicious activity in deployed area. Intrusion detection problem considered into two ways. First, in view of a system component for monitoring the security of a WSN and ensure correct behaviour of the network as well as avoid false alarm. Second one is as monitoring system for detecting a malicious intruder that resides in deployed area [1].

The issue of tracking a moving intruder by power conserving operation as well as sensor collaboration two efficient sleep-awake schemes are developed to minimize the power consumption these are PECAS & MESH [2]. First derived the analysis of target detection and expectation and detection delay for stationary as well as mobile targets. This results are important for designers for energy efficient sensor network for monitoring the network with the help of this formulas prediction of detection performance [3]. Further the study of trade-off between the network lifetime as well as detection quality i.e how fast the intruder can be detected when the intruder will enters in field of interest[FoI]. The sensor coverage had to be designed according to the detection probability. The wave sensing scheduling protocol is proposed [4].

The intrusion detection problem will introduced in both homogeneous and heterogeneous WNS. Two detection models are used-Single sensing and Multiple sensing models for immediate detection of intruder. Characterizing intrusion detection probability with the help of parameters of intrusion distance and also network parameter [5].

Analytically evaluate the detection probability of mobile targets when the n sensors are deployed to monitor a field of interest. Showing the result of detection probability depend on the length of perimeters of the sensing areas of the sensors and not on their shape. Also the evaluation of mean free path whenever a target is first detected [6]. Coverage and Lifetime are two supreme problems in WSN. In the study of coverage and lifetime optimization and WSN with Gaussian distribution two types of dispersion $\sigma x=\sigma y$ & $\sigma x\neq\sigma y$ will considered. The proposed important deployment strategy in WSN & developed two algorithms for compute the optimal deployment strategy [7].

In this paper we proposed the different distribution model & the K-means algorithm for clustering the network. The intruder will be randomly chosen & an Euclidean distance will be calculated between two points. The different distribution model are compared by considering different network parameter. In this paper, we consider only single sensing detection in the network domain. At last comparison on the performance of intrusion detection in an uniform distribution with Gaussian distribution and provide guidelines in choosing a random sensor deployment strategy as well as the correct parameter.

The rest and this paper is arranged as follows. section 2 is network model, section 3 is result analysis, section 4 is conclude the paper.

II. NETWORK MODEL

The network models includes a different network deployment model, detection and sensing techniques, a clustering of network & calculation of Euclidean distance.

1. NETWORK DEPLOYMENT

1.1 UNIFORM

Wireless sensors are continuously report the sensed data to its main station. Study of Intrusion detection, gives the result for completely monitoring on the network and ensure the correct behavior of the network. For determining an intrusion detection capability of a Wireless sensor network a sensor deployment strategy is very much important. A random sensor deployment is usually adopted because of it having fast deployment strategy, easily scalable. In uniform distribution, the sensors are deployed randomly as well as uniformly in network domain. The intruder can be detected instantly after it enters in the field of interest (FoI) i.e. a network domain. ξ is the maximum allowable intrusion distance (MAD) is specified.

Suppose the intruder moves in the distance D. If $D<\xi$, the WSN gives good performance, otherwise, reconfiguration of the network will takes place.

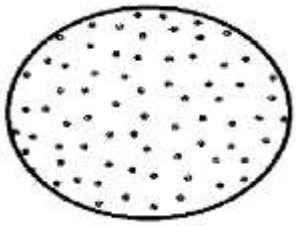

Fig. 1. Uniform distribution in circular area.

If the sensors are deployed in circular area. As shown in fig 1. Then the area is

$$A = \pi R^2$$

[1]

Intrusion detection means how instantly the intruder can be find out form the deployed sensor network. In fact, it shows the result that the intrusion detection capability of the WSN is rich means as early as the detection of intruder form the network domain.

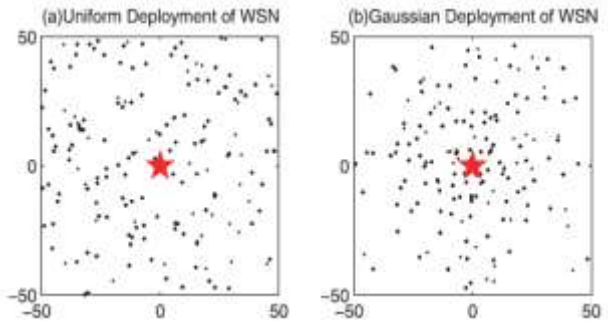

(a) (b)

Fig . 2. Uniform & Gaussian deployment in WSN

Fig.2. (a) shows the uniform deployment in WSN. In that the sensors are uniformly & randomly deploy in area is

$A = L \times L$ because, square in shape.

1.2 GAUSSIAN

If all of the sensors are deployed randomly and uniformly, in the network, that conforms to a uniform distribution. Also on the other hand, if all sensors are to protect an important entity as well as sensors are distributed to near great consequence, the resulting sensor network conforms to a Gaussian distribution [1]. Fig 2 (b) shows the Gaussian distribution. This distribution allows the placement of sensors in unbounded area. We assume the co-ordinates of the target point as G = (0, 0) and the standard deviation ($\sigma x = \sigma y = \sigma$). Then the probability density function (PDF) for point (x, y) is given by [7].

$$\mathbf{f}(\mathbf{x}, \mathbf{y}, \boldsymbol{\sigma}) = \frac{1}{2\pi\sigma^2} e^{-\frac{x^2+y^2}{2\sigma^2}}$$

[2]

In uniform sensor deployment, shows the detection probability is the same for any point in a WSN. But, some applications may require different degrees of detection probability at different locations. The Gaussian-distributed WSNs can provide differentiated detection capabilities at different locations. So we focus on the Gaussian distribution of the network.

Using MATLAB R2013a Simulink, area A=100 X 100 is predefined for the sensor deployment .The MATLAB simulink gives the better results as compare to WSN simulator developed in C++ [1].

1.3 SENSING & DETECTION TECHNIQUES

All sensors are assumed to be equipped with the same sensing range SR, and their sensing coverage is assumed to be circular [8]. In a WSN, there are two ways to detect an intruder: 1) single-sensing detection and 2) multiple-sensing detection [5]. In this paper our focus is on single-sensing detection, the intruder can be successfully detected by a single sensor when entering in sensors sensing range (SR). ξ is the maximal allowable distance. If $\xi = 0$, is called as immediate intrusion detection, that means the intruder has to be detected before it can travel some distance inside the network. On the other hand if, $\xi > 0$,the intruder is allowed to move some distance within the network.

2. CLUSTERING OF DEPLOYMENT SENSORS

For clustering the k- means clustering algorithm is used, which is aims to partition the n number of sensors into the k-clusters .In this paper. We considered 4 clusters that are shown by different colour. The uniform deployment of sensors is in 2D. In this paper we choose the sensors number. For the clustering algorithm we need the set of observations (x_1 ,x_2 ,……x_n) and also we choose randomly the value for k. Where the k < n. In the k-clustering algorithm the resulting clusters intra cluster similarity is high & inters cluster similarity is low. k-means algorithm follows following steps:

1. Arbitrarily generate k points (cluster centres),k being the number of clusters Desired.

2. Calculate the distance between each of the data points to each of the centres ,And assign each point to the closest centre.

3. Calculate the new cluster centre by calculating the mean value of all data Points in the respective cluster.

4. With the new centres, repeat step 2 If the assignment of cluster for the Data points changes, repeat step 2.3 else stop the process.

The distance between the data points is calculated using Euclidean distance as follows. The Euclidean distance between two points ,

X1 = (x11; x12: x1n)

X2 = (x21; x22: x2n)

$$\text{Distance}(X_{1i}, X_{2i}) = \sqrt{\sum_{X=i}^{n}(X_{1i}-X_{2i})^2} \quad [3]$$

$$E_{TX}(K,d) = KE_{elec} + K\epsilon_{fs}d^2, \text{ if } d<d_0 \quad [4]$$

$$= KE_{elec} + K\epsilon_{mp}d^2, \text{ if } d>d_0 \quad [5]$$

$$E_{RX}(d) = KE_{elec} \quad [6]$$

Where, E_{TX} is total energy used in transmitter of source node. E_{RX} represents energy used in receiver of destination node. ϵ_{mp} and ϵ_{fs} gives energy needed by transmit amplifier in case of multipath and free space. The energy consumption for transmitting K-bit packet over distance d. Where

$$d_0 = \sqrt{\epsilon_{fs} / \epsilon_{mp}} \quad [7]$$

III .RESULT ANALYSIS

The results in single-sensing detection cases indicate that the intrusion detection probability in a given Uniform and Gaussian-distributed WSN is determined from sets of network parameters that is Sensing range. The number of sensor N=500.The energy is fixed 2J. Using MATLAB R2013 simulink, the result for Uniform, Gaussian distribution is shown in fig. 3.The area is100 × 100 is selected. Partition of the distributed network into 4 cluster. So, here K=4. The Euclidean distance is calculated between two points in the network.

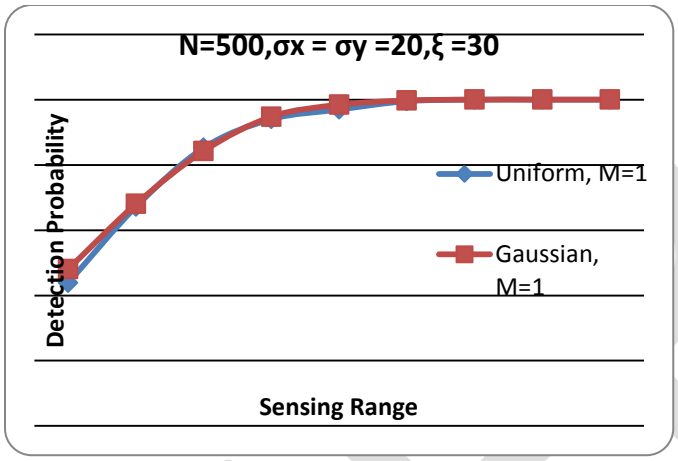

Fig. 3. Effect if sensing range SR on the detection probability in a distribution model. When $\xi > 0$.

We analyze the effect of sensing range and we set the number of deployed sensor maximal allowable intrusion distance, standard deviation and rounds as N = 500, $\xi = 30$, $\sigma = 20$, R = 50, respectively.

Fig. 3 shows the impact of sensing range on the intrusion detection probability in one-sensing detections in both Uniform and Gaussian WSNs. The detection probability is observed to improve as the sensing range increases, as a larger sensing range improves the network coverage, and higher network coverage tends to a quicker detection of the intruder in field of interest. The Gaussian WSNs are shown to outperform their uniform counterparts in one-sensing detection.

Moreover, Fig. 4 shows simulation outcomes for immediate intrusion detection. The immediate detection probability is much poor than if the intruder is allowed to travel some distance like 30 meters. So, in actual practice the implementation of full sensing coverage i.e an immediate detection of the intruder is not possible.

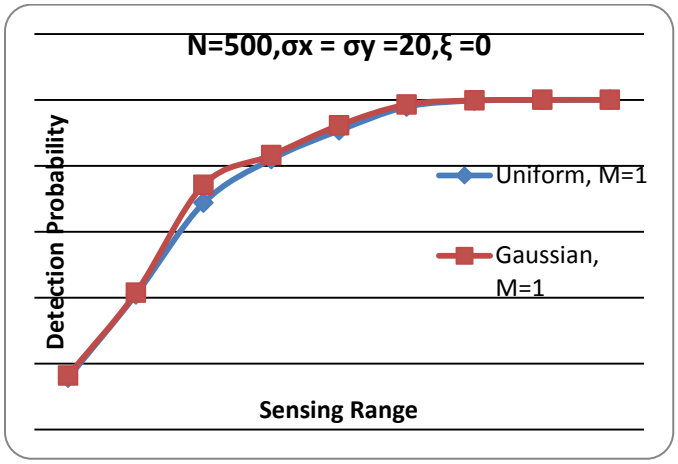

Fig. 4. Effect of sensing range SR on the detection probability in a distribution model. When ξ = 0.

We showing the network distribution for gaussian if N = 500, σx = σy =20, ξ =30 .The intruder is shown by astric sign in network domain. The four clusters are shown by different colours. The base station is at (0,0) position is shown in fig. 5

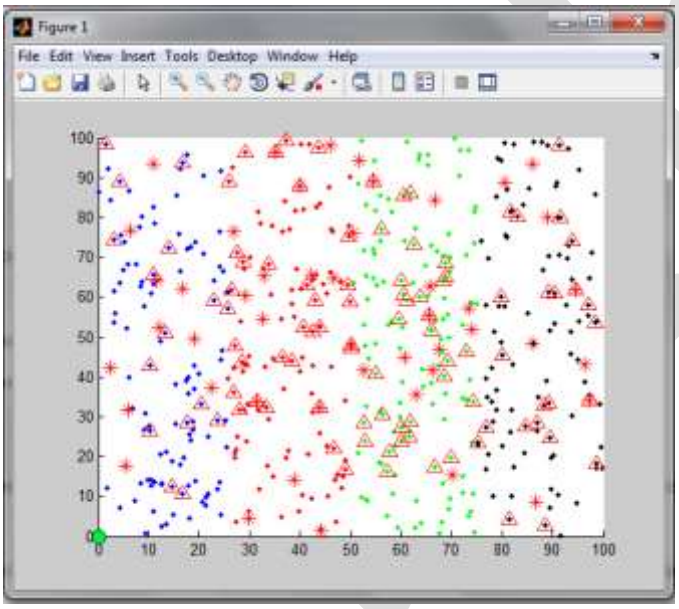

Fig. 5. Snapshot of Gaussian distribution for N = 500, σx = σy =20, ξ =30.

IV. CONCLUSION

This paper examines a uniformly and randomly deployment of the network, we call is an uniform distribution.

If all sensors are to protect an important entity as well as sensors are distributed to near great consequence, the resulting sensor network conforms to a Gaussian distribution. If the intruder can detect as early as possible, then the resulting intrusion detection probability is very rich. Using k- means clustering algorithm the randomly deployed network is divide into k cluster. In the k-clustering algorithm the resulting clusters intra cluster similarity is high & inters cluster similarity is low. Using single sensing detection, by varying network parameter like sensing range of sensor the result shows that the detection probability increases in both cases. While Gaussian distribution shows good results as compare to uniform distribution. Also the relaxed intrusion detection perform better as compare to immediate intrusion detection.

FUTURE SCOPE

We can focus on another sensing and detection techniques i.e. multiple sensing detection of sensors. Also we consider another network parameter like Standard Deviation, Number of sensors in both relaxed and immediate intrusion detection.

REFERENCES:

[1] Yun Wang, Weihuang Fu, and Dharma P. Agrawal, Life Fellow, IEEE"Gaussian versus Uniform Distribution for Intrusion Detection in Wireless Sensor Networks" IEEE parallel and distributed system vol 24, no.2 Feb 2013.
[2] I.F. Akyildiz, W. Su, Y. Sankarasubramaniam, and E. Cayirci, "A Survey on Wireless Sensor Networks," IEEE Comm. Magazine,vol. 40, no. 8, pp. 102-114, Aug. 2002.
[3] Q. Cao, T. Yan, J. Stankovic, and T. Abdelzaher, "Analysis of Target Detection Performance for Wireless Sensor Networks," Proc. First IEEE Int'l Conf. Distributed Computing in Sensor Systems, pp. 276-292, 2005.
[4] S. Ren, Q. Li, H. Wang, X. Chen, and X. Zhang, "Designand Analysis of Sensing Scheduling Algorithms under PartialCoverage for Object Detection in Sensor Networks," IEEETrans. Parallel and Distributed Systems, vol. 18, no. 3, pp. 334-350,Mar. 2007.
[5] Y. Wang, X. Wang, B. Xie, D. Wang, and D.P. Agrawal, "Intrusion Detection in Homogeneous and Heterogeneous Wireless Sensor Networks," IEEE Trans. Mobile Computing, vol. 7, no. 6, pp. 698-711, June 2008.
[6] L. Lazos, R. Poovendran, and J.A. Ritcey, "Probabilistic Detection of Mobile Targets in Heterogeneous Sensor Networks," IPSN '07: Proc. sixth Int'l Conf. Information Processing in Sensor Networks, pp. 519-528, 2007.
[7] D. Wang, B. Xie, and D.P. Agrawal, "Coverage and Lifetime Optimization of Wireless Sensor Networks with Gaussian Distribution," IEEE Trans. Mobile Computing, vol. 7, no. 12, pp. 1444-1458, Dec. 2008.
[8] C.-f. Hsin and M. Liu, "Network Coverage Using Low Duty- Cycle Sensors: Random & Coordinated Sleep Algorithms," Proc. Third Int'l Symp. Information Processing in Sensor Networks, pp. 433-442, 2004

MODIFICATION IN LSB METHOD OF IMAGE BASED STEGANOGRAPHY

*InduNehra, Student(M.Tech), RCEW, Jaipur
*Aishwary, Assistant Professor, RCEW Jaipur

ABSTRACT:LSB is well know method for stegnography. There are several changes suggested by different researchers time to time on LSB and stegnography. Most of the methods are by using enryption and in decryption of the message in different ways. This paper proposes the java APIs for encoding and decoding of messages which is to be staged.

Keywords: Stegnography, image based steganography, Efficiency consideration in LSB method, image encoding algorithm, image decoding algorithm.

I. INTRODUCTION

The proposed method is using very compact and effective APIs of java for implementation and understanding of encryption and decryption which is given in javax.crypto package.

Efficiency Considerations

Which working with the concept of LSB, three main issues which needs to be covered for efficiency and security of message which is hidden in the image.

- **Storing length of message: As per most of the references, the length is stored in first 31 pixels and data is stored in next each pixel. This is the general idea. So a malicious user can retrieve the first step of message by first 31 pixels.**

- **Storing message: After the length, the data is being stored in each pixel which can be easily retrieved by any malicious**

The proposed method is the implementation of the steganography method of LSB and they which is LSB and they APIs of Java Cryptography APIs of Java. Now the latest version of java we have used method for encoding and decoding for encryption and decryption.

A lots of researchers have worked on concept of LSB. Some of them have designed good algorithm. But a very few number of researchers have taken it to implementation level. Our focus of the work was to implement one of the best models, in which the data can be moved in secure and safe way. We tried to study various language specifications. Java has implemented one of the best security model so we used java security for designing t**he tool.**

user. We had idea of hide the message not in continuous pixel, this might be stored in even pixels or odd pixels or any arbitrary order like every 3th pixel. Its dependent on the size of message to be hidden behind the image. Also the pixel number can be retrieved dynamically by size of images and size of messages.

- Encoding messages: The first concen of study was to make message more and more secure. Any malicious user can retrieve the data easily if the structure of storage of message is known. So one more thought was to given on security of data/message.

We found that data should be stored in LSB after encryption so that this will be next layer of security. If working with java, java provides a good set of classes in package javax.crypto for encryption and decryption.

In the modified method following changes can be proposed:

- For better image after embedding of message, we used alternative pixel for storing the message. If each message is being stored in each pixel, the image quality degrades so we stored each bit of message in even or odd number of pixel. Like first bit will be stored in 12^{nd} pixel and then next bit to 14^{th} pixel and so on.

- For security of data, length is stored in some random pixel in the image. As per given in most of the standards, length is being stored in first 32 pixels which can easily be retrieved by any of the person for misuse. So we have used concepts that length is to be stored in any of the arbitrary location which is known only to sender and receiver. Agreed upon protocol will work and embed/decode the message accordingly

- Also for security of data, message can be encrypted by using java cryptography APIs which are available in javax.crypto package. So that the retrieval of exact message will be more tougher. The same is done by reverse at receiver end.

Comparison of Standard LSB method and Proposed Method

Standard LSB Method	**Our LSB Method**
Using sequence pixel of Cover Image.	Using Random pixel of Cover Image.
Message length is stored in first 31 bytes which is common and not safe.	Message length is stored in any arbitrary location.
Store 3 byte information per pixel	Store 1 byte information per pixel which will improve the result
Stego image looks almost same as the cover image.	Stego image looks same as the cover image, Better than Standard LSB.
The location of message in pixels are same	The location can be defined on the basis size of message to be embedded in the image

Image Encoding Algorithm in proposed method

Inputs: Hidden Message, Stego key and Cover Image

Output: Stego Image

Procedure

Step 1 calculate length of message and hide length in any 32-bit.

Step 2 extract the characters of Message.

Step 3 Encrypt message by using javax.crypto APIs.

Step 4 extract characters from stegokey .

Step 5 calculate pixel value from Cover Image.

Step 6 select LSB bit from pixel and select stego key characters and put into Image pixel.

Step 7 insert characters of message in pixels of Image.

Step 8 repeatestep 6 until characters has been embedded.

Step 9 repeatestep from 2 to 7 messsage length.

Step 10 output in Stego image.

Image Decoding Algorithm in proposed method

Inputs: Stego Image and Stego key

Output: Cover Image and Message

Procedure

Step 1 calculate length of message from given 32-bit pixel.

Step 2 extract pixels from Stego Image.

Step 3 start from 32 pixel and extract stego key characters from first component of the pixels..

Step 4 If this extracted key matches with the key entered by the receiver, then follow Step 5, otherwise terminate the program.

Step 5 If the key is correct, then go to next pixels and extract secret message characters from first component of next pixels. Follow Step 5 till up to terminating symbol, otherwise follow step 6.

Step 6 extract Characters from Stego Image.

Step 7 extract special bit from Characters.

Step 8 obtain message by decrypting using javax.crypto classes and Cover Image.

REFERENCES

- Ali-al, H. Mohammad, A. 2010. Digital Audio Watermarking Based on the Discrete Wavelets Transform and Singular Value Decomposition, European Journal Of Scientific Research, vol 39(1), pp 231-239.

- Aneesh Jain, IndranilSen Gupta, ―A JPEG Compression Resistant Steganography Scheme for Raster Graphics Images‖, TENCON 2007 - 2007 IEEE Region 10 Conference, vol.2
- Atallah M. Al-Shatnawi, "A New Method in Image ste-ganography with improved image quality", Applied mathe-matical science, Vol. 6, no79, 2012.

- A.Joseph Raphael et al(2012), Cryptography and Steganography – A Survey, Int. J. Comp. Tech. Appl., Vol 2 (3) pp 626-630

- BassamJamilMohd, Saed Abed and Thaier Al- Hayajneh, Computer Engineering Department Hashemite University, Zarqa, Jordan Sahel Alouneh,ComputerEngi-neering Department, German-Jordan University, Amman, Jordan, "FPGA Hardware of the LSB Steganography Meth-od" IEEE 2012.

- CHIN-CHEN CHANG, , H.W .TSENG. ,"A steganographic method for digital images using side match. Pattern Recognition Letters, 2004,vol. 25, p.1431-1437.
- Himanshu Gupta et al(2013), Enhanced Data Hiding Capacity Using LSB-Based Image Steganography Method, International Journal of Emerging Technology and Advanced Engineering, Volume 3, Issue 6 pp 212-214

- MamtaJuneja (2013), An Improved LSB based Steganography Technique for RGB Color Images, 2nd International Conference on Latest Computational Technologies (ICLCT'2013) June 17-18

- MasoudNosrati(2013), An introduction to steganography methods, World Applied Programming, Vol (1), No (3) pp 191-195

- Mehdi Kharrazi, Husrev T. Sencar, and NasirMemon,, Image Steganography and: Concepts and Practice", Depart-ment of Electrical and Computer Engineering Department of Computer and Information Science Polytechnic Universi-ty,Brooklyn, NY 11201, USA.
- Mrs. Kavitha, KavitaKadam, AshwiniKoshti, PriyaDunghav, "Steganography Using Least Significant Bit Algo-rithm", International Journal of Engineering Research and applications, vol.2, issue 3, pp. 338-341May-June2012.
- Nagham Hamid, AbidYahya, R. Badlishah Ahmad, Osamah M, "Image Steganography Techniques: An Over-view", International Journal of computer science and securi-ty, vol (6), Issue (3), 2012.

- R. Amirtharajan, R. Akila, P. Deepikachowdavarapu "A Comparative Analysis of Image Steganogra-phy",International Journal of computer Applications,Vol2- No3, May 2010.
- Shamim Ahmed Laskar(2012), High Capacity data hiding using LSB Steganography and Encryption, International Journal of Database Management Systems (IJDMS) Vol.4, No.6,

- SaeedMahmoudpour, SattarMirzakuchaki,"Hardware Architecture for a Message Hiding Algorithm with Novel Randomizers", International Journal of Computer Applica-tions (0975 – 8887) Volume 37– No.7, January 2012.

- Vijay kumarsharma, Vishal Shrivastava, "A Steganog-raphy algorithm for hiding image in image by improved LSB substitution by minimize technique", Journal of Theoretical and Applied Information Technology, Vol. 36 No.1, 15th February 2012.
- Java.oracle.com
- https://www.scribd.com/doc/48764974/Steganography-Data-hiding-using-LSB-algorithm

International Journal of Engineering Research and General Science Volume 3, Issue 5, September-October, 2015
ISSN 2091-2730

Effect of Induced Stress on the Corrosion Rate of Medium Carbon Steel in Saline Environment

Alo Oluwaseun[1] and Ibitoye Simeon[2]

[1]Department of Mechanical and Mechatronics Engineering, Afe Babalola University, Ado-Ekiti, Nigeria

[2]Department of Materials Science and Engineering, Obafemi Awolowo University, Ile-Ife, Nigeria

oluwaseunalo07@gmail.com; +2348038260969

Abstract-This study investigated how 0.33% medium carbon steel is affected by induced stress in a saline environment. Three geometries namely U-bend, C-ring and I-shape samples were formed representing varying degrees of stress level induced on the samples. The test specimens were subjected to static loading in saline environment containing 15.0 wt.%, 10.0 wt.% and 3.5 wt.% of sodium chloride (NaCl) for a typical exposure time of 31 days at ambient conditions of temperature and pressure. Weight loss method was used to estimate the corrosion rate in mils per year (mpy). The results of the experiment show that corrosion rate is maximum in samples with the highest stress level and in medium containing highest amount of dissolved chloride ions. The least corrosion rate occurred in samples with the least amount of chloride ions and in a non-stressed condition. It was inferred that the corrosion rate of 0.33 %C steels increased with increasing tensile stress and chloride ions content of the medium.

Key words: Stress corrosion cracking, medium carbon steel, saline environment, corrosion rate, chloride ion, induced stress, protective films

INTRODUCTION

Corrosion has persistently become a major problem and has attained a global nature in which there is no facet of human endeavour where its impact is not felt and recognized. Corrosion problems in production plants can increase substantially the operation and maintenance cost. For example, one of the most costly problems facing the oil companies is corrosion in crude oil systems. In their report, SPE stated that in the Nigeria oil and gas industry, the total pipeline breakage loss figure due to corrosion in 2004 alone is 396,000 metric tons while the financial losses is estimated to be 19.66 billion naira (#19.66billion) equivalent to US $154.4 million [1]. Generally, the shutdowns resulting from the failures of components due to corrosion are extremely expensive thus creating a great need for in-depth understanding of this insidious phenomenon.

Carbon steel is by far the most important alloy used as structural members [2]. Its behavior is a fundamental parameter in the design and application of structural steel such as reinforcement members in structures. This is because they can be readily bent or prestressed. They can also be used where small radii bend are necessary. Its high tensile strength, yield strength, percentage elongation and ductility are of great advantage in these applications. Unfortunately, corrosion has proved to be a major threat to its favourable mechanical properties.

Various studies have been carried out to investigate the corrosion mechanism and factors affecting the corrosion rates of steel alloys. For example, Ikpeseri [2] investigated the corrosion behaviour of mild steel in 0.5M H_2SO_4 and 3.5% NaCl solutions. His results showed that corrosion rate is higher in 0.5M H_2SO_4 environment than 3.5% NaCl throughout the entire period of investigation reaching a maximum of 22.2 mm/yr and 0.158 mm/yr respectively.

Stress corrosion cracking (SCC) is the cracking indicated from the combined influence of tensile stress and a corrosive environment [3]. The required tensile stresses may be in the form of directly applied stress or in the form of residual stress [4]. It has been reported that one of the most accepted mechanisms of SCC (*i.e.*, the "dissolution-repassivation" mechanism) requires recurrence of the steps of: (a) the stress-assisted disruption of the passive film at the crack-tip; (b) localized crack-tip dissolution at a high rate; and (c) repassivation at the crack-tip [5]-[7].

In the past it was thought by several investigators that SCC of a given alloy occurs only in limited range of specific environments [8]. However, subsequent researches have revealed that SCC occurs in wide range of environments including pure water [9]-[10]. It has been reported that the carbon steels are prone to SCC in carbonate, bicarbonate, acetates, phosphate and chloride environments [11-[12]. For example, studies on J-55 and N-80 steels have shown that H_2S containing chloride solutions promote SSC [13]. Also, synergistic effect of low concentration chloride in bicarbonate solutions and low concentration of sulfate causing SCC in low alloy steels has also been reported [14]-[15].

Various findings have also been reported on some variables affecting SCC of metallic materials in many media [16]-[18]. Also, Afolabi *et al*. [19] studied the stress corrosion cracking and microstructural analysis of a mild steel immersed in orange juice medium using weight loss technique and SEM analysis. Their results showed that SCC relative to mild steel is mainly a function of the acidity of the medium under study, and the corrosion rate increases with increase in exposure time throughout the exposure time. The SEM analysis revealed that the trans granular and inter granular attacks were visibly responsible for the corrosion of this material in this medium. Singh Raman and Wai [20] investigated the SCC of an austenitic stainless steel in nitrite-containing chloride solutions.

Their results showed that additions of NO_2 (1400–5600 ppm) accelerate susceptibility to chloride SCC. With increasing NO_2 content, SCC susceptibility increases in the order, 1400 ppm > 2800 ppm > 5600 ppm. This behaviour has been attributed to the increasing passivation characteristic with increasing NO_2 content. This work is concerned with the study of the effect of induced stress in the corrosion rate of 0.33% medium carbon steel in a saline environment.

MATERIALS AND METHODS

Materials for testing

The steel product (ST 44-2 plain) used in this study was a medium carbon steel in hot rolled condition of 0.33% C. The chemical composition of the steel is shown in Table 1. Table 2 shows the mechanical properties of the steel sample. The steel was obtained from Osogbo Steel Rolling Company (OSRC) in Osogbo, Nigeria

Table 1: Chemical Composition of Steel Sample (ST 44-2 plain)

Element	C	Mn	P	S	Ni	Cr	Mo	Sn	Fe	Others
Composition (%)	0.33	0.09	0.02	0.02	0.03	0.45	0.02	0.01	98.63	0.05

Table 2: Mechanical Properties of As-rolled 0.33%C Steel Sample

U.T.S (N/mm^2)	**Yield Strength (N/mm^2)**	**Elongation (%)**
318.0	258.0	26.0

Saline environment

The environment used for the corrosion testing was a saline-based one simulated in the laboratory. The saline environment was made up of three different compositions of sodium chloride (NaCl); 3.5 wt.%, 10.0 wt.% and 15.0 wt.% NaCl.

Sample preparation

One hundred and eight (108) medium steel samples were cut into three different geometries: 36 were cut into I-shape of 6 cm long, 36 cut into a U-bend of 12 cm long of small anchorage radius and the remaining 36 cut into a C-ring shape. Figures 1-3 shows the geometries of the samples. The radius of curvature (anchorage radius) distinguished the U- bend from the C-ring. The anchorage radius for the U-bend, C-ring and I-shape are 0.6 mm, 0.9 mm and 0 mm respectively. The I-shape samples were annealed between 650 ^oC – 670 ^oC for about 30 minutes and furnace cooled to room temperature in order to relieve internal stresses developed during solidification, rolling or machining and hence serve as control samples. The samples used have cylindrical geometry and each has a total surface area given by equation 1.

$$A = 2\pi rl + 2\pi r^2 \qquad \ldots\ldots\ldots\ldots\ldots 1$$

Quantifiable amount of tensile stress was induced in the samples by plastic deformation at various stress levels below the yield strength of the material. The expression to estimate the induced stress is given in equation 2.

$$L = \frac{0.95 f y_{\emptyset}}{4 f_{bu}} \qquad \ldots\ldots\ldots\ldots\ldots\ldots\ldots 2$$

Where L = anchorage radius in mm, f_y = characteristic strength of steel = tensile strength in N/mm^2, ϕ = diameter of the bar in mm, f_{bu} = induced stress in N/mm^2.

The calculated value for the induced stress for the U-Bend, C-Ring and I-Shape samples are 755.25 N/mm^2, 503.50 N/mm^2 and 0 N/mm^2 respectively. The U-bend and C-ring samples were statically loaded in such a way that a metal holder was placed through the legs of the samples which prevents stress-relaxation in the samples during corrosion process. The sample surfaces were then ground and polished to remove scales and oxide deposits on the steel surfaces. The I-shape samples were drilled in the center in other to make holes in them for proper suspension in the medium.

Measuring and weighing

After surface preparation, the specimens were carefully measured to permit calculation of the surface area needed in the formula for calculation the corrosion rate.

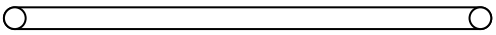

Figure 1: I-shape sample

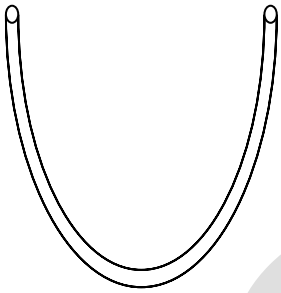

Figure 2: U-bend sample

Figure 3: C-ring sample

After measuring, the specimens were cleaned by washing in acetone and alcohol, then degreased in petroleum ether, dried in air and weighed. This was recorded as the initial weight of the specimen. The specimens were then stored in a desiccator before exposure to the corrosion environment to prevent reaction with the environment.

Immersion in saline environment

The I-shape samples were fully immersed in the medium while the U-bend and C-ring samples were partially immersed. The U-bend and C-ring samples were suspended in the medium through the holes bore in the metal holder. Partial immersion was adopted for the U-bend and C-ring in order to eliminate galvanic or two-metal corrosion as a result of a different metal used as the sample holder.

Determination of corrosion rate

The time of exposure to the corrosion medium during the experiment was 31 days (744 hours). However, after every 48 hours, samples were taken out of the environment, cleaned by holding under a stream of water, and scrubbing the surfaces with rubber stopper to remove corrosion products. They were then dried in warm air and re-weighed. The weight was recorded as the final weight. The weight loss was calculated using equation 3:

$W = W_o - W_f$ ……3

Where W = weight loss, W_o = initial weight and W_f = final weight

The change in weight of the specimens was then used to calculate the corrosion rate. The corrosion rate was determined through the mils per year method using equation 4:

Corrosion rate = $\frac{534W}{DAT}$ ……....4

Where W = weight loss in mg, D = density of specimen in g/cm^3, A = area of specimen in in^2 and T = exposure time in hours.

RESULTS

The variation of corrosion rate of I-shape, C-ring and U-bend samples at different concentrations of sodium chloride (NaCl) with increasing exposure time respectively is given in Figure 4-6.
Figures 7, 8 and 9 respectively show the corrosion behavior of the samples under varying stresses at 3.5 wt.%, 10.0 wt.% and 15.0 wt.% NaCl with increasing exposure time.

DISCUSSION OF RESULTS

The corrosion rate

As in all the figures, the corrosion rate of the samples in the saline environment increases as the experiment progresses over time. The graphs show that the samples underwent high corrosion rate in the first 48 hours of the corrosion testing period (Fig. 4-9). This may be due to the fact that the samples just like any other metals are unstable at high energy state; consequently, the metals want to achieve ra pid change to the low energy state where they become stable.

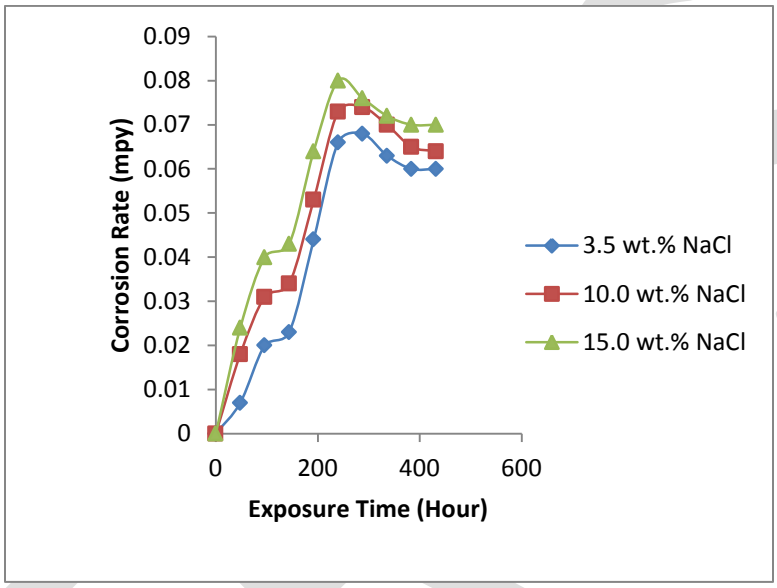

Fig. 4: Corrosion rate of I-shape samples at different concentration of sodium chloride (NaCl) with increasing exposure time

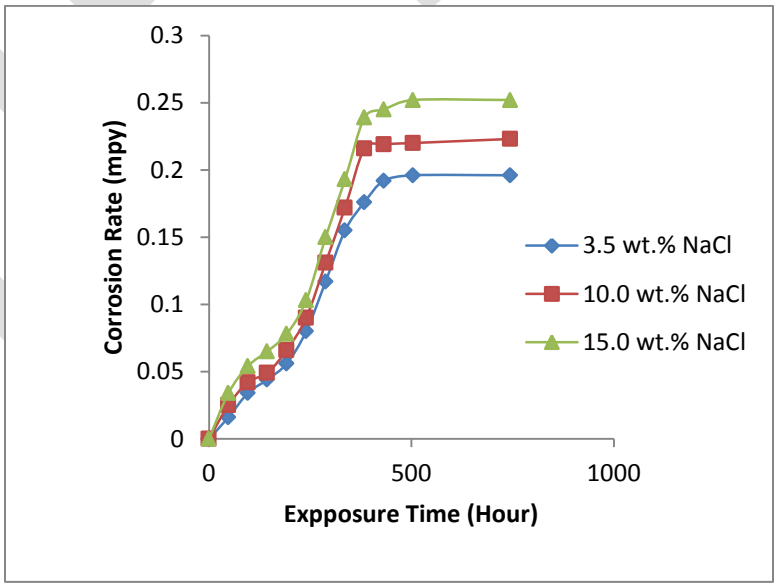

Fig 5: Corrosion rate of C-ring samples at different concentration of sodium chloride (NaCl) with increasing exposure time

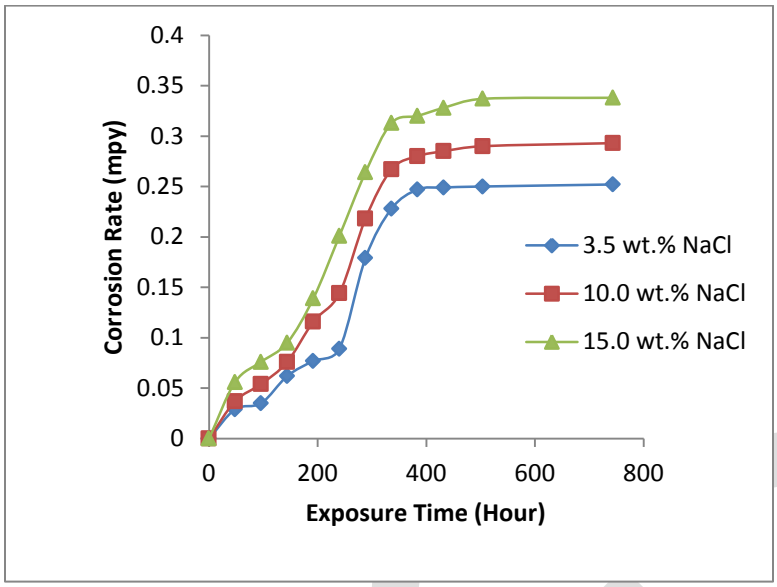

Fig. 6: Corrosion rate of U-bend samples at different concentration of sodium chloride (NaCl) with increasing exposure time

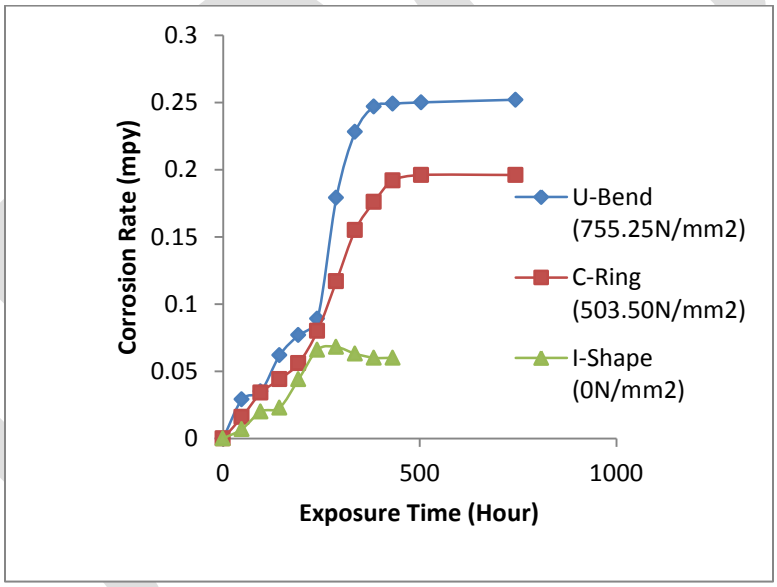

Fig. 7: Corrsosion behavior of the samples under varying tensile stress at 3.5 wt.% NaCl with increasing exposure time

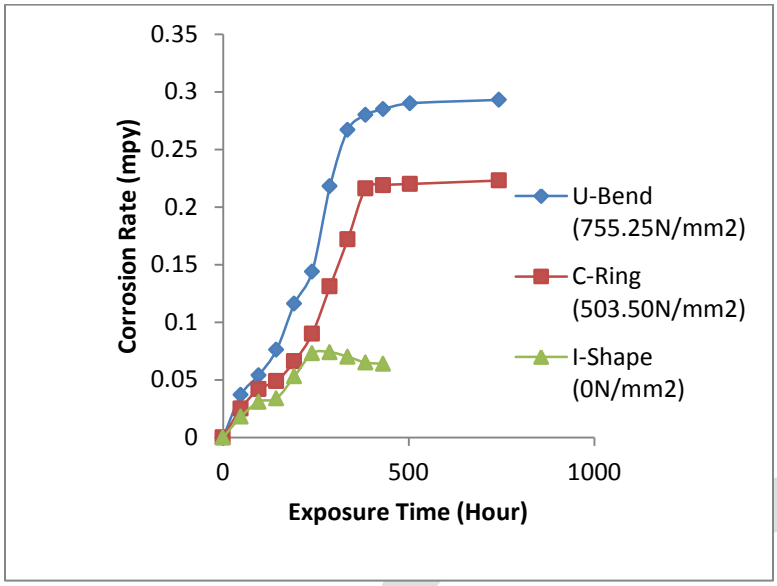

Fig. 8: Corrosion behavior of the samples under varying stress at 10.0 wt.% NaCl with increasing exposure time

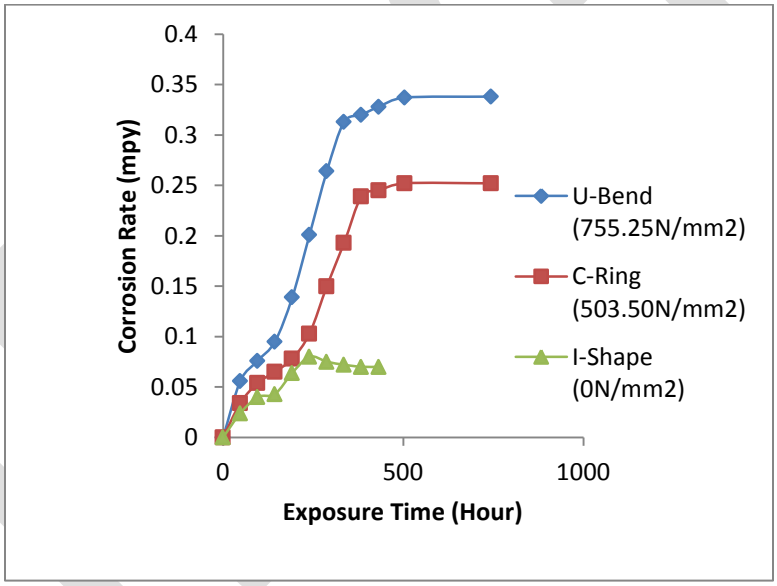

Fig. 9: Corrosion behavior of the samples under varying stress at 15.0 wt.% NaCl with increasing exposure time

Effect of chloride ions

Figure 4 shows that the corrosion rate of the I-shape medium carbon steel samples increased rapidly in the first 48 hours. The increase in the corrosion rate then became less rapid until it reached a peak and then started to decrease after five hundred and four (504) hours. As pointed out earlier, the initial rapid increase in corrosion rate is due to the rapid change of the metal samples to the low energy stat e where they become stable. However, the decrease in the corrosion rate at the end of the experiment could be attributed to formation of protective oxide film which shielded the metal from the environment. The corrosion rates of the C-ring and U-bend samples also in creased rapidly at the initial stage of the experiment (Fig. 5 and 6). However, towards the end of the experiment, the corrosion rates di d not decrease but were almost constant. This could be as a result of the increase in induced stress level in the C-ring and U-bend samp les which increased the proneness of the samples to corrosion.

The U-bend samples show the highest corrosion rate throughout the corrosion testing time in all concentrations of NaCl with the highest rate at 15.0 wt.% NaCl (Fig. 6). The C-ring test samples show characteristic corrosion behavior similar to the U-bend as the exposure time increases. In this regard, the highest corrosion rate occurred at 0.252 mpy while that of the U-bend rises up to 0.338 mpy. This behavior is associated with the combined effect of the tensile stress and concentration of corrosion medium being higher in the U-bend samples in 15.0 wt.% NaCl solution.

Chloride ion aggravates the degradation of materials in aqueous environment. It helps in breaking passive oxide layer, leading to localized corrosion [21]. The results of the experiment show that, for a particular level of induced stress, the corrosion rate of 0.33%C steel increases with time when in contact with chloride ions containing environment and the rate increases with increasing concentration of chloride ions, the highest being 15.0 wt.% followed by 10.0 wt.%. 3.5 wt.% NaCl solution shows the least corrosion rate effect (Figures. 4-6). The mechanism responsible for this increase is that there is an increase in the conductivity of the water thereby improving the mobility of ions between the metal/electrolyte interfaces as the chloride content increases.

Effect of induced tensile stress

The role of induced tensile stress could be shown to be important in rupturing protective films. The tensile stress is in fact the result of local corrosion processes in that when a metal is deformed beyond the elastic limit, a permanent or unrecoverable strain occurs in the stressed regions. This permanent plastic deformation causes an onset of plastic strain, thus creating high-energy sites in the microstructures of the metal. The higher the deformation, the higher the strain energy. This energy (strain) varies significantly within the molecules of the metals with the resulting highest energy occurring in the most stressed region (755.25 N/mm^2). Figure 7 shows that in the 3.5 wt.% NaCl solution, the I-shape samples exhibits the least corrosion rate being a non-stressed sample. The corrosion behavior in this case is due to the presence of chloride ions in the medium. The C-ring samples exhibit an increase in corrosion rate with increase in exposure time with the rate reaching a peak at about 0.252 mpy (Fig. 8). As shown in Figure 9, the U-sample shows the highest corrosion rate with a peak at about 0.388 mpy. The U-bend samples being highly stressed regions have the highest energy thereby showing more susceptibility to corrosion attack. This region is then preferentially attacked by the corrosive medium giving a high corrosion rate. The corrosion of the U-bend and C-ring can be attributed to the synergistic effect of induced tensile stress and corrosive medium. Corrosion in this case is seen to increase with increasing dissolved chloride where the medium corresponding to 15,0 wt.% NaCl has the highest corrosion rate and 3.5 wt.% NaCl the least.

CONCLUSION

Induced tensile stress increases the corrosion rate of medium carbon steels when they are in contact with chloride-ion environment. The highest corrosion rate (0.338 mpy) occurred in the U-bend samples, having the highest stress level of 755.25 N/mm^2, at 15.0 wt.% of NaCl which corresponds to the highest dissolved chloride ions concentration. This behavior was followed by the C-ring samples having about 503.5 N/mm^2 stress level and 0.252 mpy as the highest corrosion rate over the exposure time. The least corrosion rate occurred in the I-shape samples in their non –stressed condition. Therefore, the corrosion rate of 0.33 %C steels increased with increasing tensile stress and chloride ions content of the medium.

REFERENCES:

[1]. SPE (2008).Society of Petroleum Engineers Journal. Philips Publishing Inc. Company. 8:35.
[2]. Ikpeseni SC (2012). Corrosion Behaviour of Mild Steel in H_2SO_4 and NaCl Solutions. Journal of Science and Multidisciplinary Research. 4:10-15.
[3]. Saxena A, SinghRaman RK, Muddle BC, (2006). Slow Strain Rate for Monitoring Cracking of Mild Steels for Vessels and Pipes for Processing Using Caustic Solutions, International Journal of Pressure Vessels and Piping 83:399-404.
[4]. Afolabi AS (2007). Corrosion and Stress Corrosion Behaviors of Low and Medium Carbon Steels in Agro-Fluid Media. Leonardo Electronic Journal of Practices and Technologies. 10: 55-66
[5]. Jones DA (1992). Principles & Prevention of Corrosion, 2nd ed.; Prentice Hall: Upper Saddle River, NJ, USA. p. 239.
[6]. SinghRaman RK, Saxena A (2007). Role of Imposed Potential in Expanding the Regime of Strain Rates for Caustic Cracking. *J.* Electrochem. Soc. 154: C451–C457.
[7]. SinghRaman RK (2005). Evaluation of Caustic Embrittlement Susceptibility of Steels by Slow Strain Rate Testing. Metall. Mater. Trans. A 36A: 1817–1823.
[8]. Staehle RW, Forlty AJ, Van Rooyan D (1969) Fundamental Aspects of Stress Corrosion Cracking, Houston, TX, NACE. p.46.
[9]. Congleton J, Shoji T, Parkins RN (1985). Stress Corrosion Cracking of Reactor Pressure Vessel Steel in High Temperature Water Corrosion Sci. 25: 633.
[10]. Gangloff RP, Ives NB (1990). Environment induced cracking of metals. Houston, TX, NACE.
[11]. Parkins RN, Elices M, Sanchez-Gulvez V, Cabellare L (1982). Stress Corrosion Cracking and Hydrogen Embrittlement of Iron Base Alloys. Corrosion Sci. 22: 379.
[12]. Singheil ,D Garnor A (1987). Materials selection for bleached pulp washers. Material Performance, 26: 31.
[13]. Kerns GE (1986). Process industries corrosion, Houston, TX, NACE. p. 356.
[14]. Liu X, Mao X (1995). Electrochemical Polarization and SCC Behavior of a Pipeline Steel in Dilute Bicarbonate Solution with Chloride Ion. Scripta Metallurgical of Material. 33(1): 145-150.
[15]. Liu JY, Su CC (1994). Environment Effects in the SCC of Turbine Disc Steels. Corrosion Science. 36(12): 2017-2028.
[16]. Casales M, Salinas-Bravo VM, Martinez-Villafane A, Gonzalex-Rodriguez (2002). Effect of Heat Treatment on the Stress Corrosion Cracking of Alloy 690, Journal of Materials Science and Engineering A. 332(2002): 223-230.
[17]. SinghRaman RK, Muddle BC (2004). Stress Corrosion Cracking of Vessels and Pipes for Alumina Processing in Aggressive Caustic Solutions, International Journal of Pressure Vessels and Piping 81:557-561.

[18]. Rogante M, Battistella P, Cesari F (2006). Hydrogen Interaction and Stress Corrosion Cracking in Hydrocarbon Storage Vessel and Pipeline Weldings, International Journal of Hydrogen Energy. 31: 597-601.

[19]. Afolabi SA, Ogazi AC, Abdulkareem AS (2013). Comparative weight loss analyses of mild steel in agro fluid media, International Conference on Chemical, Mining and Metallurgical Engineering Nov. 27-28, 2013 Johannesburg (South Africa). pp. 217-220

[20]. SinghRaman RK, Wai HS (2014). Stress Corrosion Cracking of an Austenitic Stainless Steel in Nitrite-Containing Chloride Solutions Materials 2014(*7*): 7799-7808; http://dx.doi.org/10.3390/ma7127799

[21]. Subir P (2012). Modeling to Study the Effect of Environmental Parameters on Corrosion of Mild Steel in Seawater Using

Neural Network, International Scholarly Research Network Metallurgy 2012:1-6

International Journal of Engineering Research and general science is an open access peer review publication which is established for publishing the latest trends in engineering and give priority to quality papers which emphasis on basic and important concept through which there would be remarkable contribution to the research arena and also publish the genuine research work in the field of science, engineering and technologies

International Journal Of Engineering Research and General Science
ISSN 2091 - 2730